



## [LWT - Food Science and Technology](#)

ISSN: 0023-6438  
Elsevier Science

Volume 66 – Complete (March, 2016)

### [Investigation the effects of protein hydration states on the mobility water and fat in meat batters by LF-NMR technique](#)

Shao, Jun-Hua; Deng, Ya-Min; Song, Li; et al.  
p. 1 – 6

[  [Abstract](#)] [  [PDF Full Text](#)]

### [Escherichia coli O157:H7 and Salmonella Typhimurium inactivation by the effect of mandarin, lemon, and orange by-products in reference medium and in oat-fruit juice mixed beverage](#)

Sanz-Puig, Maria; Pina-Pérez, M.Consuelo; Martínez-López, Antonio; Rodrigo, Dolores  
p. 7 – 14

[  [Abstract](#)] [  [PDF Full Text](#)]

### [Mycelial biomass and intracellular polysaccharides yield of edible mushroom \*Agaricus blazei\* produced in wheat extract medium](#)

Zhai, Fei-Hong; Han, Jian-Rong  
p. 15 – 19

[  [Abstract](#)] [  [PDF Full Text](#)]

### [Prevalence, antimicrobial resistance and virulence traits in enterococci from food of animal origin in Turkey](#)

Yılmaz, Ebru Şebnem; Aslantaş, Özkan; Önen, Sevda Pehlivanlar; et al.  
p. 20 – 26

[  [Abstract](#)] [  [PDF Full Text](#)]

### [Effect of processing on the content and biological activity of polysaccharides from \*Pleurotus ostreatus\* mushroom](#)

Radzki, Wojciech; Ziaja-Sołtys, Marta; Nowak, Jakub; et al.  
p. 27 – 33

[  [Abstract](#)] [  [PDF Full Text](#)]

**[Refractance Window drying of pomegranate juice: Quality retention and energy efficiency](#)**

Baeghbali, Vahid; Niakousari, Mehrdad; Farahnaky, Asgar  
p. 34 – 40

[  [Abstract](#)] [  [PDF Full Text](#)]

**[Physicochemical properties of Alaska pollock \(\*Theragra chalcogramma\*\) surimi gels with oat bran](#)**

Alakhrash, Fatimah; Anyanwu, Ugochukwu; Tahergorabi, Reza  
p. 41 – 47

[  [Abstract](#)] [  [PDF Full Text](#)]

**[Influence of enzymatically produced sunflower oil based cocoa butter equivalents on the phase behavior of cocoa butter and quality of dark chocolate](#)**

Kadivar, Sheida; De Clercq, Nathalie; Mokbul, Mansura; Dewettinck, Koen  
p. 48 – 55

[  [Abstract](#)] [  [PDF Full Text](#)]

**[Changes in phenolic compounds and their antioxidant capacities in jujube \(\*Ziziphus jujuba\* Miller\) during three edible maturity stages](#)**

Wang, Bini; Huang, Qingyuan; Venkitasamy, Chandrasekar; et al.  
p. 56 – 62

[  [Abstract](#)] [  [PDF Full Text](#)]

**[Viscoelastic behavior and physico-chemical characteristics of heated swai-fish \(\*Pangasius hypophthalmus\*\) based emulsion containing fermented soybeans](#)**

Techarang, Jiranat; Apichartsrangkoon, Arunee; Pathomrungsinyounggul, Pattavara; et al.  
p. 63 – 71

[  [Abstract](#)] [  [PDF Full Text](#)]

**[Impact of cooking and germination on phenolic composition and dietary fibre fractions in dark beans \(\*Phaseolus vulgaris\* L.\) and lentils \(\*Lens culinaris\* L.\)](#)**

Dueñas, Montserrat; Sarmiento, Thaise; Aguilera, Yolanda; et al.  
p. 72 – 78

[  [Abstract](#)] [  [PDF Full Text](#)]

**[Optimization and rheological properties of chicken ball as affected by κ-carrageenan, fish gelatin and chicken meat](#)**

Yasin, Hazmi; Babji, Abdul Salam; Ismail, Hidayah  
p. 79 – 85

[  [Abstract](#)] [  [PDF Full Text](#)]

**[Monitoring of alcohol strength and titratable acidity of apple wine during fermentation using near-infrared spectroscopy](#)**

Peng, Bangzhu; Ge, Na; Cui, Lu; Zhao, Hui  
p. 86 – 92

[  [Abstract](#)] [  [PDF Full Text](#)]

**[Structure preservation of Aloe vera \(\*barbadensis\* Miller\) mucilage in a spray drying process](#)**

Medina-Torres, L.; Calderas, F.; Minjares, R.; et al.  
p. 93 – 100

[  [Abstract](#)] [  [PDF Full Text](#)]

**[Bioactive compounds from mustard flours for the control of patulin production in wheat tortillas](#)**

Saladino, Federica; Manyes, Lara; Luciano, Fernando B.; et al.  
p. 101 – 107

[  [Abstract](#)] [  [PDF Full Text](#)]

**[Inactivation of bacteria and murine norovirus in untreated groundwater using a pilot-scale continuous-flow intense pulsed light \(IPL\) system](#)**

Yi, Ji Yoon; Lee, Na-Hye; Chung, Myong-Soo  
p. 108 – 113

[  [Abstract](#)] [  [PDF Full Text](#)]

**[Effect of extrusion process on antinutritional factors and protein and starch digestibility of lentil splits](#)**

Rathod, Rahul P.; Annapure, Uday S.  
p. 114 – 123

[  [Abstract](#)] [  [PDF Full Text](#)]

**[Characterization of interphase volatile compounds in Chinese \*Luzhou\*-flavor liquor fermentation cellar analyzed by head space-solid phase micro extraction coupled with gas chromatography mass spectrometry \(HS-SPME/GC/MS\)](#)**

Ding, Xiaofei; Wu, Chongde; Huang, Jun; Zhou, Rongqing  
p. 124 – 133

[  [Abstract](#)] [  [PDF Full Text](#)]

**[Combined effect of prefermentative cold soak and SO<sub>2</sub> additions in Barbera D'Asti and Malbec wines: Anthocyanin composition, chromatic and sensory properties](#)**

Federico Casassa, L.; Bolcato, Esteban A.; Sari, Santiago E.; et al.  
p. 134 – 142

[  [Abstract](#)] [  [PDF Full Text](#)]

**[Effect of rotating magnetic field and flowing Ca<sup>2+</sup> solution on calcium uptake rate of fresh-cut apple](#)**

Jin, Yamei; Yang, Na; Tong, Qunyi; Xu, Xueming  
p. 143 – 150

[  [Abstract](#)] [  [PDF Full Text](#)]

**[Effects of adjustable parallel high voltage electrostatic field on the freshness of tilapia \(\*Oreochromis niloticus\*\) during refrigeration](#)**

Ko, Wen-Ching; Yang, Shang-Yan; Chang, Chao-Kai; Hsieh, Chang-Wei  
p. 151 – 157

[  [Abstract](#)] [  [PDF Full Text](#)]

**[Effect of indigenous \*Lactobacillus rhamnosus\* isolated from bovine milk on microbiological characteristics and aromatic profile of traditional yogurt](#)**

Innocente, Nadia; Biasutti, Marialuisa; Rita, Frisina; et al.  
p. 158 – 164

[  [Abstract](#)] [  [PDF Full Text](#)]

**[Combination of carboxymethyl cellulose-based coatings with calcium and ascorbic acid impacts in browning and quality of fresh-cut apples](#)**

Koushesh Saba, Mahmoud; Sogvar, Ommol Banin  
p. 165 – 171

[  [Abstract](#)] [  [PDF Full Text](#)]

**[Effect of processing factors on Shea \(\*Vitellaria paradoxa\*\) butter extraction](#)**

Yonas, G.A.; Shimelis, E.A.; Sisay, A.F.  
p. 172 – 178

[  [Abstract](#)] [  [PDF Full Text](#)]

**[Particle size distribution of soy flour affecting the quality of enriched gluten-free cakes](#)**

Dhen, Nahla; Román, Laura; Ben Rejeb, Ines; et al.  
p. 179 – 185

[  [Abstract](#)] [  [PDF Full Text](#)]

**[Gelatin from clown featherback skin: Extraction conditions](#)**

Kittiphattanabawon, Phanat; Benjakul, Soottawat; Sinthusamran, Sittichoke; Kishimura, Hideki  
p. 186 – 192

[  [Abstract](#)] [  [PDF Full Text](#)]

**[Modelling phenolic and volatile composition to characterize the effects of pre-fermentative cold soaking in Tempranillo wines](#)**

Aleixandre-Tudó, José L.; Álvarez, Inmaculada; Lizama, Victoria; et al.  
p. 193 – 200

[  [Abstract](#)] [  [PDF Full Text](#)]

**[Effects of dispersing media and heating rates on pasting profiles of wheat and gluten-free samples in relation to their solvent retention capacities and mixing properties](#)**

Mariotti, Manuela; Lucisano, Mara; Pagani, Maria Ambrogina; Ng, Perry K.W.  
p. 201 – 210

[  [Abstract](#)] [  [PDF Full Text](#)]

**[Effects of added inulin and wheat gluten on structure of rye porridge](#)**

Vázquez-Gutiérrez, José L.; Johansson, Daniel; Langton, Maud  
p. 211 – 216

[  [Abstract](#)] [  [PDF Full Text](#)]

**[A new milk-clotting enzyme produced by \*Bacillus\* sp. P45 applied in cream cheese development](#)**

Lemes, Ailton Cesar; Pavón, Yanina; Lazzaroni, Sandra; et al.  
p. 217 – 224

[  [Abstract](#)] [  [PDF Full Text](#)]

**[Anti-quorum sensing activity of spice oil nanoemulsions against food borne pathogens](#)**

Venkadesaperumal, Gopu; Rucha, Sambrey; Sundar, Kothandapani; Shetty, Prathapkumar Halady  
p. 225 – 231

[  [Abstract](#)] [  [PDF Full Text](#)]

**[Effects of tea polyphenols and different teas on pancreatic  \$\alpha\$ -amylase activity \*in vitro\*](#)**

Yang, Xiaoping; Kong, Fanbin  
p. 232 – 238

[  [Abstract](#)] [  [PDF Full Text](#)]

**[A comparison of the bactericidal effectiveness of hydrochloric and acetic acid on \*Staphylococcus aureus\* in silver carp during a pH-shift protein recovery process](#)**

Ronaghi, Maryam; Beamer, Sarah; Jaczynski, Jacek; Matak, Kristen E.  
p. 239 – 243

[  [Abstract](#)] [  [PDF Full Text](#)]

**[Antioxidant effect of spent, ground, and lyophilized brew from roasted coffee in frozen cooked pork patties](#)**

Jully, Katrina Maryse Malixi; Toto, Criselda S.; Were, Lilian  
p. 244 – 251

[  [Abstract](#)] [  [PDF Full Text](#)]

**[Influence of processing conditions on procyanidin profiles and antioxidant capacity of chocolates: Optimization of dark chocolate manufacturing by response surface methodology](#)**

Gültekin-Özgüven, Mine; Berktaş, İjlal; Özçelik, Beraat  
p. 252 – 259

[  [Abstract](#)] [  [PDF Full Text](#)]

**[Emulsifying properties of legume proteins at acidic conditions: Effect of protein concentration and ionic strength](#)**

Ladjal Ettoumi, Yakoub; Chibane, Mohamed; Romero, Alberto  
p. 260 – 266

[  [Abstract](#)] [  [PDF Full Text](#)]

**[Pasting, thermal, morphological, rheological and structural characteristics of \*Chenopodium\* \(\*Chenopodium album\*\) starch](#)**

Jan, Romee; Saxena, D.C.; Singh, Sukhcham  
p. 267 – 274

[  [Abstract](#)] [  [PDF Full Text](#)]

**[Characterization of lactic acid bacteria isolated from wheat bran sourdough](#)**

Manini, F.; Casiraghi, M.C.; Poutanen, K.; et al.  
p. 275 – 283

[  [Abstract](#)] [  [PDF Full Text](#)]

**[Rice starch and fructo-oligosaccharides as substitutes for phosphate and dextrose in whole muscle cooked hams: Sensory analysis and consumer preferences](#)**

Resconi, Virginia C.; Keenan, Derek F.; Barahona, Marta; et al.  
p. 284 – 292

[  [Abstract](#)] [  [PDF Full Text](#)]

**[Antioxidant activity of papaya seed extracts against H<sub>2</sub>O<sub>2</sub> induced oxidative stress in HepG2 cells](#)**

Salla, Swetha; Sunkara, Rajitha; Ogutu, Simon; et al.  
p. 293 – 297

[  [Abstract](#)] [  [PDF Full Text](#)]

**[Removal of \*Salmonella\* biofilm formed under meat processing environment by surfactant in combination with bio-enzyme](#)**

Wang, Huhu; Wang, Huawei; Xing, Tong; et al.  
p. 298 – 304

[  [Abstract](#)] [  [PDF Full Text](#)]

**[Effect of covalent modification by \(–\)-epigallocatechin-3-gallate on physicochemical and functional properties of whey protein isolate](#)**

Jia, Zhenbao; Zheng, Min; Tao, Fei; et al.  
p. 305 – 310

[  [Abstract](#)] [  [PDF Full Text](#)]

**[Phytochemical investigations and evaluation of antidiabetic potential of \*Prunus dulcis\* nuts](#)**

Qureshi, Muhammad Nasimullah; Numonov, Sodik; Abudurexiti, Ajigu; Aisa, Haji Akber  
p. 311 – 317

[  [Abstract](#)] [  [PDF Full Text](#)]

**[Effect of setting conditions on proteolysis and gelling properties of spotted featherback \(\*Chitala ornata\*\) muscle](#)**

Tachasirinukun, Piyawan; Chaijan, Manat; Riebroy, Siriporn  
p. 318 – 323

[  [Abstract](#)] [  [PDF Full Text](#)]

**[Effect of partially gelatinized corn starch on the rheological properties of wheat dough](#)**

Fu, Zong-qiang; Che, Li-ming; Li, Dong; et al.  
p. 324 – 331

[  [Abstract](#)] [  [PDF Full Text](#)]

**[Antimicrobial effect of essential oils in combinations against five bacteria and their effect on sensorial quality of ground meat](#)**

Ghabraie, Mina; Vu, Khanh Dang; Tata, Lina; et al.  
p. 332 – 339

[  [Abstract](#)] [  [PDF Full Text](#)]

**[Effects of different drying–solidification processes on physical properties, volatile fraction, and antioxidant activity of non-centrifugal cane brown sugar](#)**

Asikin, Yonathan; Hirose, Naoto; Tamaki, Hajime; et al.  
p. 340 – 347

[  [Abstract](#)] [  [PDF Full Text](#)]

**[The effect of milk fat substitution with palm fat on lactic acid bacteria counts in cheese-like products](#)**

Aljewicz, Marek; Cichosz, Grażyna; Nalepa, Beata; Bielecka, Marika  
p. 348 – 354

[  [Abstract](#)] [  [PDF Full Text](#)]

**[Microbiological and physico-chemical analysis of fermented protein-fortified cassava \(\*Manihot esculenta\* Crantz\) flour](#)**

Rosales-Soto, Maria U.; Gray, Peter M.; Fellman, John K.; et al.  
p. 355 – 360

[  [Abstract](#)] [  [PDF Full Text](#)]

**[Peach polyphenol and carotenoid content as affected by frozen storage and pasteurization](#)**

Oliveira, Ana; Alexandre, Elisabete M.C.; Coelho, Marta; et al.

p. 361 – 368

[  [Abstract](#)] [  [PDF Full Text](#)]

**[Analysis of the variability in microbial inactivation by acid treatments](#)**

Rodríguez, María R.; Aguirre, Juan S.; Lianou, Alexandra; et al.

p. 369 – 377

[  [Abstract](#)] [  [PDF Full Text](#)]

**[Fatty acid ethyl esters \(FAEE\) in extra virgin olive oil: A case study of a quality parameter](#)**

Gómez-Coca, Raquel B.; Fernandes, Gabriel D.; Pérez-Camino, María del Carmen; Moreda, Wenceslao

p. 378 – 383

[  [Abstract](#)] [  [PDF Full Text](#)]

**[Effect of stepwise baking on the structure, browning, texture, and \*in vitro\* starch digestibility of cookie](#)**

Kawai, Kiyoshi; Hando, Kana; Thuwapanichayanan, Ratiya; Hagura, Yoshio

p. 384 – 389

[  [Abstract](#)] [  [PDF Full Text](#)]

**[Comparison of carbonyl profiles from Czech and Spanish lagers: Traditional and modern technology](#)**

Andrés-Iglesias, Cristina; Nešpor, Jakub; Karabín, Marcel; et al.

p. 390 – 397

[  [Abstract](#)] [  [PDF Full Text](#)]

**[Melting release point of encapsulated phosphates and heating rate effects on control of lipid oxidation in cooked ground meat](#)**

Kılıç, B.; Şimşek, A.; Claus, J.R.; Atılğan, E.

p. 398 – 405

[  [Abstract](#)] [  [PDF Full Text](#)]

**[Simultaneous inoculation of yeasts and lactic acid bacteria: Effects on fermentation dynamics and chemical composition of Negroamaro wine](#)**

Tristezza, Mariana; di Feo, Luca; Tufariello, Maria; et al.

p. 406 – 412

[  [Abstract](#)] [  [PDF Full Text](#)]

**[Contribution of cross-links and proteoglycans in intramuscular connective tissue to shear force in bovine muscle with different marbling levels and maturities](#)**

Wang, Fulong; Zhang, Yawei; Li, Junke; et al.

p. 413 – 419

[  [Abstract](#)] [  [PDF Full Text](#)]

**[Development of a combined low-methoxyl-pectin and rice-bran-extract delivery system to improve the viability of \*Lactobacillus plantarum\* under acid and bile conditions](#)**

Chotiko, Arranee; Sathivel, Subramaniam  
p. 420 – 427

[  [Abstract](#)] [  [PDF Full Text](#)]

**[Probiotic characterization of lactic acid bacteria isolated from fermented foods and beverage of Ladakh](#)**

Angmo, Kunzes; Kumari, Anila; Savitri; Bhalla, Tek Chand  
p. 428 – 435

[  [Abstract](#)] [  [PDF Full Text](#)]

**[Microencapsulation of nisin in alginate beads by vibrating technology: Preliminary investigation](#)**

Maresca, Diamante; De Prisco, Annachiara; La Storia, Antonietta; et al.  
p. 436 – 443

[  [Abstract](#)] [  [PDF Full Text](#)]

**[Production of seafood flavour formulations from enzymatic hydrolysates of fish by-products](#)**

Peinado, I.; Koutsidis, G.; Ames, J.  
p. 444 – 452

[  [Abstract](#)] [  [PDF Full Text](#)]

**[Extraction and characterization of acid-soluble collagen from scales and skin of tilapia \(\*Oreochromis niloticus\*\)](#)**

Chen, Junde; Li, Long; Yi, Ruizao; et al.  
p. 453 – 459

[  [Abstract](#)] [  [PDF Full Text](#)]

**[Raspberry marc extracts increase antioxidative potential, ellagic acid, ellagitannin and anthocyanin concentrations in fruit purees](#)**

Bobinaitė, Ramunė; Viskelis, Pranas; Bobinas, Ąeslovas; et al.  
p. 460 – 467

[  [Abstract](#)] [  [PDF Full Text](#)]

**[Malolactic fermentation before or during wine aging in barrels](#)**

Izquierdo-Cañas, P.M.; Mena-Morales, A.; García-Romero, E.  
p. 468 – 474

[  [Abstract](#)] [  [PDF Full Text](#)]

**[Enhanced curcumin permeability by SLN formulation: The PAMPA approach](#)**

Righeschi, Chiara; Bergonzi, Maria Camilla; Isacchi, Benedetta; et al.  
p. 475 – 483

[  [Abstract](#)] [  [PDF Full Text](#)]

**[The influence of different the drying methods on chemical composition and antioxidant activity in chokeberries](#)**

Samoticha, Justyna; Wojdyło, Aneta; Lech, Krzysztof  
p. 484 – 489

[  [Abstract](#)] [  [PDF Full Text](#)]

**[Seabuckthorn as a novel prebiotic source improves probiotic viability in yogurt](#)**

Gunenc, Aynur; Khoury, Christina; Legault, Candace; et al.  
p. 490 – 495

[  [Abstract](#)] [  [PDF Full Text](#)]

**[Effect of ultrasound treatment on physico-chemical, nutraceutical and microbial quality of strawberry](#)**

Gani, Adil; Baba, Waqas N.; Ahmad, Mudasir; et al.  
p. 496 – 502

[  [Abstract](#)] [  [PDF Full Text](#)]

**[Effects of foam mat drying on physicochemical and microstructural properties of yacon juice powder](#)**

Franco, Talita Szlapak; Perussello, Camila Augusto; Ellendersen, Luciana Neves; Masson, Maria Lucia  
p. 503 – 513

[  [Abstract](#)] [  [PDF Full Text](#)]

**[Preparation of iron/zinc bound whey protein concentrate complexes and their stability](#)**

Shilpashree, B.G.; Arora, Sumit; Sharma, Vivek  
p. 514 – 522

[  [Abstract](#)] [  [PDF Full Text](#)]

**[Stability and quality of a bioactive peptide fraction incorporated orange juice](#)**

Khairallah, Mirna G.; Hettiarachchy, Navam S.; Rayaprolu, Srinivas J.  
p. 523 – 529

[  [Abstract](#)] [  [PDF Full Text](#)]

**[Correlation between physicochemical properties of \*japonica\* and \*indica\* rice starches](#)**

Jang, Eun-Hee; Lee, Su-Jin; Hong, Joo-Yeon; et al.  
p. 530 – 537

[  [Abstract](#)] [  [PDF Full Text](#)]

**[Study of two-stage microwave extraction of essential oil and pectin from pomelo peels](#)**

Chen, Qun; Hu, Zhuoyan; Yao, Fiona Yan-Dong; Liang, Hanhua  
p. 538 – 545

[  [Abstract](#)] [  [PDF Full Text](#)]

**[Development and validation of ELISA technique for early detection of rhizome rot in golden spice turmeric from different agroclimatic zones](#)**

Ray, Monalisa; Dash, Swagatika; Shahbazi, Sajad; et al.  
p. 546 – 552

[  [Abstract](#)] [  [PDF Full Text](#)]

**[Monitoring of spoilage and determination of microbial communities based on 16S rRNA gene sequence analysis of whole sea bream stored at various temperatures](#)**

Parlapani, Foteini F.; Boziaris, Ioannis S.  
p. 553 – 559

[  [Abstract](#)] [  [PDF Full Text](#)]

**[Inhibitory effects of lactic and malic organic acids on autoinducer type 2 \(AI-2\) quorum sensing of \*Escherichia coli\*O157:H7 and \*Salmonella\* Typhimurium](#)**

Almasoud, Ahmad; Hettiarachchy, Navam; Rayaprolu, Srinivas; et al.  
p. 560 – 564

[  [Abstract](#)] [  [PDF Full Text](#)]

**[Quality of the pre-cooked potato strips processed by Radiant Wall Oven](#)**

Kirmaci, Bilal; Singh, Rakesh K.  
p. 565 – 571

[  [Abstract](#)] [  [PDF Full Text](#)]

**[Characterization of kefir-like beverages produced from vegetable juices](#)**

Corona, Onofrio; Randazzo, Walter; Miceli, Alessandro; et al.  
p. 572 – 581

[  [Abstract](#)] [  [PDF Full Text](#)]

**[Colour stability of cooked ham packed under modified atmospheres in polyamide nanocomposite blends](#)**

Lloret, Elsa; Picouet, Pierre A.; Trbojevich, Raúl; Fernández, Avelina  
p. 582 – 589

[  [Abstract](#)] [  [PDF Full Text](#)]

**[Influence of microcrystalline cellulose on the microrheological property and freeze-thaw stability of soybean protein hydrolysate stabilized curcumin emulsion](#)**

Xu, Duoxia; Zhang, Jinjing; Cao, Yanping; et al.  
p. 590 – 597

[  [Abstract](#)] [  [PDF Full Text](#)]

**[Effect of ovalbumin on the quality of gluten-free rice flour bread made with soymilk](#)**

Nozawa, Masaaki; Ito, Seiko; Arai, Eiko

p. 598 – 605

[  [Abstract](#)] [  [PDF Full Text](#)]

**[Preparation of a coated Ti anode for producing acidic electrolyzed oxidizing water](#)**

Tang, Wenwei; Li, Yanfei; Li, Weihao; et al.

p. 606 – 614

[  [Abstract](#)] [  [PDF Full Text](#)]

**[Determination of phenolic acid decarboxylase produced by lactic acid bacteria isolated from shalgam \(ĀĀĀalgam\) juice using green analytical chemistry method](#)**

Okcu, Gozde; Ayhan, Kamuran; Gunes Altuntas, Evrim; et al.

p. 615 – 621

[  [Abstract](#)] [  [PDF Full Text](#)]

**[Study of the effect of microwave power coupled with hot air drying on orange peel by dielectric spectroscopy](#)**

Talens, Clara; Castro-Giraldez, Marta; Fito, Pedro J.

p. 622 – 628

[  [Abstract](#)] [  [PDF Full Text](#)]

**[Release of thymol from poly\(lactic acid\)-based antimicrobial films containing kenaf fibres as natural filler](#)**

Tawakkal, Intan S.M.A.; Cran, Marlene J.; Bigger, Stephen W.

p. 629 – 637

[  [Abstract](#)] [  [PDF Full Text](#)]

**[Morphological and \*in vitro\* antibacterial efficacy of quercetin loaded nanoparticles against food-borne microorganisms](#)**

Dinesh Kumar, V.; Verma, Priya Ranjan Prasad; Singh, Sandeep Kumar

p. 638 – 650

[  [Abstract](#)] [  [PDF Full Text](#)]

**[Physical decontamination of lupin \(\*Lupinus angustifolius\*\) protein isolates, seeds and flakes: Effects on microbiological status and micellar protein yield](#)**

Melde, Denise; Wiacek, Claudia; Braun, Peggy Gabriele

p. 651 – 656

[  [Abstract](#)] [  [PDF Full Text](#)]

**[Estimation of amino acids profile and escolar fish consumption risks due to biogenic amines content fluctuations in vacuum skin packaging/VSP during cold storage](#)**

ĀĀorĀĀević, ĀĀani; Buchtov, Hana; Borkovcov, Ivana

p. 657 – 663

[  [Abstract](#)] [  [PDF Full Text](#)]

**[Modelling the kinetics of \*Listeria monocytogenes\* in refrigerated fresh beef under different packaging atmospheres](#)**

Saraiva, C.; Fontes, M.C.; Patarata, L.; et al.

p. 664 – 671

[  [Abstract](#)] [  [PDF Full Text](#)]

**[Biocontrol of \*Listeria monocytogenes\* in fish by enterocin AS-48 and \*Listeria lytic\* bacteriophage P100](#)**

Baños, Alberto; García-López, José David; Núñez, Cristina; et al.

p. 672 – 677

[  [Abstract](#)] [  [PDF Full Text](#)]

**[Nutritional improvement and physicochemical evaluation of liver pâté formulations](#)**

Terrasa, A.M.; Dello Staffolo, Marina; Tomás, M.C.

p. 678 – 684

[  [Abstract](#)] [  [PDF Full Text](#)]

**[Hyperspectral imaging for real-time monitoring of water holding capacity in red meat](#)**

Kamruzzaman, Mohammed; Makino, Yoshio; Oshita, Seiichi

p. 685 – 691

[  [Abstract](#)] [  [PDF Full Text](#)]

**[Calendar](#)**

p. I

[  [Abstract](#)] [  [PDF Full Text](#)]

**[Editorial Board/Aims and Scope](#)**

p. IFC



# Investigation the effects of protein hydration states on the mobility water and fat in meat batters by LF-NMR technique



Jun-Hua Shao <sup>a,\*</sup>, Ya-Min Deng <sup>a</sup>, Li Song <sup>a</sup>, A. Batur <sup>b</sup>, Na Jia <sup>a</sup>, Deng-Yong Liu <sup>a</sup>

<sup>a</sup> College of Food Science and Technology, Bohai University, Jinzhou, Liaoning 121013, PR China

<sup>b</sup> College of Food Science and Pharmacy, Xinjiang Agricultural University, Wulumuqi 830052, PR China

## ARTICLE INFO

### Article history:

Received 22 May 2015

Received in revised form

15 September 2015

Accepted 2 October 2015

Available online 8 October 2015

### Keywords:

Meat batters

Proteins

LF-NMR

Water mobility

## ABSTRACT

The use of LF-NMR technique for assessing the influence of meat protein hydration states on the mobility water and fat in meat batters was investigated. Three relaxation components,  $T_{22}$  (50 ms),  $T_{2b}$  and  $T_{21}$  (lower than 10 ms) were found in meat group and fat group. The number of relaxation components in meat batters was not affected by water or fat addition, but the major component  $T_{22}$  clearly shifted to longer relaxation time (from 50 ms to 66 ms) with added water and fat. The relaxation time of heated meat emulsions was lowered, indicating that water and fat proton mobility was limited by heating. A new relaxation component  $T_{23}$  (200–300 ms) was observed after heating, which was deemed as attributing to free water and fat in emulsion gel. Besides, the effect of fat on relaxation time  $T_{22}$  of emulsion gel was higher than water. However, water presented higher influence on  $T_{23}$  in emulsion gel compared to fat. LF-NMR has been clearly demonstrated to be feasible to detect changes in the relaxation times of water and fat caused by different meat protein hydration states initially produced by meat batters with different treatments.

© 2015 Elsevier Ltd. All rights reserved.

## 1. Introduction

The water- and oil-binding properties of meat products can reflect the ability of combining water and fat of meat protein and influence the product quality, yield and cost (Rosenvold & Andersen, 2003). In addition, distributions of water and fat are also greatly correlated with juiciness of meat products. Finely comminuted meat products are a mixture of proteins, fat particles, water, salt and carbohydrates (Barbut, 1995). These components are held together by a variety of attractive forces acting between them in meat emulsion. Fats interact with proteins to develop texture, mouthfeel and assist in overall sensation of lubricity of food (Brewer, 2012; Rodriguez Furlán, Padilla, & Campderrós, 2014). Tolstoguzov (2003) considered that fat globules have a “ballbearing” effect, whereby the fat globules rotate relative to each other during shear conditions in the mouth and this creates a fluidity of mass that attenuates the forces on the palate. It has been well established that gels formed from meat products by heating may subsequently show synergetic effect (Wu, Xiong, Chen, Tang, & Zhou, 2009). And fat is known to contribute significantly to the

structure of meat emulsion gel and then to its water holding capacity (Einarsdóttir et al., 2014). Schmidt (1984), Shao, Zou, Xu, Wu, and Zhou (2011) observed that fat losses usually track moisture losses from the meat batters. The distribution and mobility of water in meat have a profound influence on essential meat quality attributes like juiciness, tenderness, firmness and appearance (Dhall, Halder, & Datta, 2012). The structure and physico-chemical properties of proteins and lipids influence the formation and stability of emulsions (Howell, Herman, & Li-Chan, 2001). A stable meat product is characterized by a minimum separation of water and fat from the product. Therefore it is important to understand the distribution of water in meat batters during the preparation of meat products.

LF-NMR can provide direct information about interactions between water protons and exchangeable protons in proteins and thereby reflecting the chemical–physical state of water in muscle and meat (Bertram, Purslow, & Andersen, 2002; Marcone et al., 2013). It has been implemented in the investigation of the distribution of water in muscle and proven to be a powerful tool for identifying water components (Marcone et al., 2013; Pearce, Rosenvold, Andersen, & Hopkins, 2011). By applying LF-NMR, proton relaxation time of water and fat can be obtained, which is influenced by the surrounding medium environment (Andersen, Frøst, & Viereck, 2010).

\* Corresponding author.

E-mail address: [shaohj024@163.com](mailto:shaohj024@163.com) (J.-H. Shao).

The preparation of meat batter goes through several stages. These stages include the salt-soluble proteins extractability, swelling of proteins, and formation of a matrix with homogeneous meat batters containing emulsified fat particles. A better understanding of the water distribution in meat batters during preparation by the addition of fat and water helps to elucidate their role in the protein matrix structure and the formation of a stable meat product (minimum separation of water and fat). In current study, different meat batters were prepared according to the stages mentioned above. The main objective was to investigate and assess the differences in the effects of fat and water on water holding capacity and water translational mobility in meat batters by LF-NMR, looking forward to evaluating the different stages of chopping through a way of analyzing water and fat distribution and mobility.

## 2. Materials and methods

### 2.1. Materials

Fresh pork longissimus dorsi (70.3% moisture, 22.2% protein, and 6.2% fat) and pork fat (89.9% fat, 8.1% moisture, 1.7% protein) were purchased from the local market (24–48 h postmortem, pH5.6 to 5.9). All visible connective tissue and fat were trimmed from the meat. The meat and fat were separately mixed and passed through a grinder (MM-12, Guangdong, China) using a 0.6 cm plate. Approximately 500 g samples were vacuum-packed in polyethylene bags and stored at  $-18^{\circ}\text{C}$  before using. Other ingredients and additives used were sodium chloride and sodium tripolyphosphate (STP).

### 2.2. Preparation of meat batters

The meat and fat were thawed ( $5^{\circ}\text{C}$  overnight). The preparation procedure according to Youssef and Barbut (2010) was as follows:

The lean meat (540 g) was chopped in a bowl chopper (Stephan UMC-5C, Germany), at the low speed setting for 30 s, followed by addition of 20 g salt and 3 g sodium tri-polyphosphate, while chopping at the high speed setting for 2 min, thus the meat group was obtained. If continued with a 1.5 min break (allowing time for protein extraction), 80 g ice water was added and the batter was chopped at the high speed setting for 1 min, then the meat + water group was obtained. Different with the two groups above, the obtaining of the group meat + water + fat was after the 1.5 min break, fat (200 g) and 1/3 ice water (79 g) were added and the batter chopped at the high speed setting for 1 min, followed by the addition of the left ice water (158 g) and chopping for another 2 min at the high-speed setting.

Final temperature of the batter did not exceed  $18^{\circ}\text{C}$ . Each batter was vacuum-packed to remove trapped air. Ten 35 g samples were stuffed into 50 mL polypropylene tubes, which were hermetically sealed. The plastic containers were centrifuged (Model 225, Fischer Scientific, Pittsburgh, PA, USA) at 500 g ( $4^{\circ}\text{C}$ ) setting for 3 min to remove any remaining air bubbles. Each of meat batters in the plastic containers was subjected to two different treatments. Half of the containers with each meat batter were chilled at  $4^{\circ}\text{C}$  and analyzed as raw (unheated) batters. The rest of the containers in each case were heated in a water-bath at  $75^{\circ}\text{C}$  for 30 min. Both unheated and heated samples were stored in a chiller at  $4^{\circ}\text{C}$  until analyzed.

### 2.3. LF-NMR spin–spin relaxation ( $T_2$ ) measurements

NMR relaxation measurements were performed on a Niumag Benchtop Pulsed NMR Analyzer PQ001 (Niumag Electric

Corporation, Shanghai, China) operating at a resonance frequency for protons of 22.6 MHz. Approximately 2 g sample was placed in a 15 mm glass tube and inserted in the NMR probe. Spin–spin relaxation time,  $T_2$ , was measured using the Carr–Purcell–Meiboom–Gill sequence. The  $T_2$  measurements were made with a  $\tau$ -value (time between  $90^{\circ}$  and  $180^{\circ}$  pulse) of 200  $\mu\text{s}$ . Data from 12,000 echoes were acquired as 32 scan repetitions. The repetition time between subsequent scans was 6.5 s. Each measurement was performed in triplicate.

### 2.4. Post-processing of NMR $T_2$ data

Distributed exponential fitting of CPMG decay curves were performed in MultiExp Inv Analysis software (Niumag Electric Corporation, Shanghai, China). For better fit, multi-exponential fitting analysis was performed on the relaxation data in the software algorithm. This analysis resulted in a plot of relaxation amplitude for individual relaxation processes versus relaxation time. By such analyses, time constants for each process were calculated from the peak position, and the area under each peak (corresponding to the proportion of water molecules exhibiting that relaxation time) was determined by cumulative integration. Additionally, the width of the relaxation population was calculated as the standard deviation of observed relaxation times for given peak.

### 2.5. Statistical analysis

The data were performed using SPSS for windows v13.0. Analysis of variance (one-way ANOVA) was performed taking as covariate the thermal treatment for each batter. Moreover, ANOVA's were carried out in order to evaluate the statistical significance ( $P < 0.05$ ) of the effect of chopping time in the meat batters. These variables were tested to the normalized Shapiro–Wilk normality test and to Bartlett's homogeneity test of variance. The Kruskal–Wallis test was used to test samples that did not fit the normal distribution.

## 3. Results and analyses

### 3.1. Relaxation time analysis of raw meat batters

The Low-field  $^1\text{H}$  NMR measurements describe the relaxation back to equilibrium of protons after perturbation by radiofrequency pulse train (Andersen et al., 2010). In heterogeneous systems, different NMR relaxation times can be obtained for water and lipids, as well as for structural elements such as gel pores or fat globules (Raffaella, Marco, Delfini, & Brosio, 2007). Discrete exponential fitting of all CPMG relaxation curves were performed to estimate  $T_2$  relaxation times of protons and the mobility of water and fat.

#### 3.1.1. Effect of water and fat on relaxation time $T_2$

$T_2$  distribution fitted is used to assess relaxation time of hydrogen protons. Three relaxation components were observed in meat batters (Figs. 1 and 2), showing that the meat proteins restricted the water mobility with different extents. The components with the shorter relaxation time,  $T_{2b}$  and  $T_{21}$  (0–10 ms), respectively corresponding to protons that are in macromolecular structures and that are combined closely with macromolecular. However, the main component  $T_{22}$  (40–70 ms), corresponding to the water or fat that are loosely combined in sol matrix of meat batters (Bertram et al., 2002; Shaarani, Nott, & Hall, 2006). Shorter relaxation time corresponded to a less mobile water fraction,

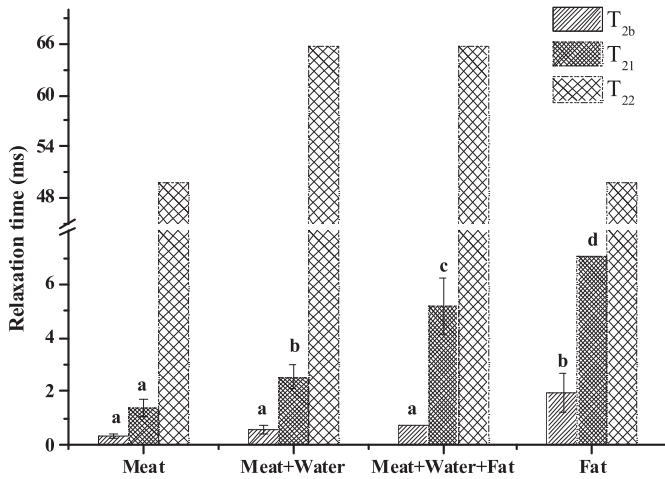


**Fig. 1.** Effect of water and fat on Relaxation time in meat batters. **a–d** Means related to relaxation time (above a bar) with different letters differ significantly ( $P < 0.05$ ). Error bars show the standard deviation.

whereas the longer relaxation time corresponded to a more mobile water fraction (Noronha, Duggan, Ziegler, O’Riordan, & O’Sullivan, 2008). The longer the relaxation time represents the less intense the water restriction by the proteins.

Firstly, Contrast the meat group with fat group, relaxation time  $T_{2b}$  and  $T_{21}$  of fat group were significantly higher ( $P < 0.05$ ) than meat group. However, the relaxation time  $T_{22}$  was not significantly different among treatments. Besides, the number of the relaxation components of meat group and fat group were both three, indicating that the relaxation components could be caused by water only or mixture of water and fat. Practically, it was difficult to distinguish between loosely bound fat and strongly restricted water. Therefore, both of them could be attributed to the protons which are tightly combined within macromolecules. Secondly, see the three relaxation time, there were no significant differences among different groups of meat batters compared  $T_{2b}$  ( $P > 0.05$ ). However, significant differences of  $T_{21}$  were observed by the addition of water and fat ( $P < 0.05$ ), which indicated that water and fat significantly affected the ability of protein binding the hydrogen protons. Moreover, the effect of fat was clearly higher than water ( $P < 0.05$ ). The reason could be related with the addition of fat which contributed more to the increase of  $T_{21}$  of meat batter system, as relaxation time  $T_{21}$  of fat group was significantly higher ( $P < 0.05$ ) than meat group. Besides, enhancement of water uptake and protein swelling, emulsification between protein and fat

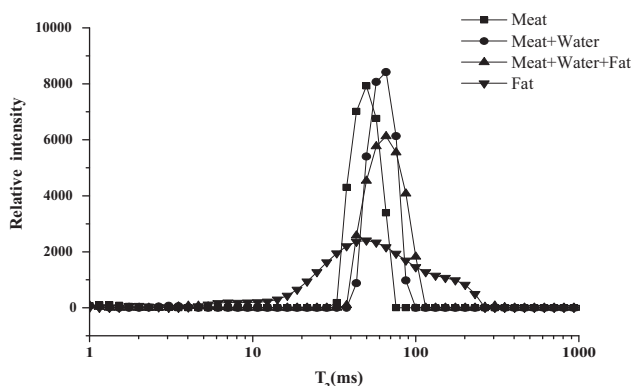


**Fig. 2.** Curves of Relaxation time ( $T_2$ ) in different meat batters.

during chopping all led to  $T_{21}$  increase. The result agreed with Andersen et al. (2010) who believed that higher fat content in the cream cheeses might influence the relaxation profiles.  $T_{22}$ , as a quite important index, dominantly reflects the water- and oil-binding properties. In this study,  $T_{22}$  of fat group and meat group was both 50 ms, so the fat protons and water protons were taken together as the factors that could influence the water- and oil-binding properties to be analyzed. On the other hand,  $T_{22}$  increased to 66 ms after adding water and fat, which suggested that the addition of water and fat influenced the mobility of the protons greatly.

**3.1.2. Effect of water and fat on peak area properties**

Comparing the group meat with fat group (Fig. 3), it could be observed that the peak area proportion of three relaxation times was not significantly different ( $P > 0.05$ ), so was the rate of relaxation time  $T_{22}$  and  $T_{21}$  which reflected the rate between liquid water and bound water of different systems (Fig. 4). This indicated that there were no significant differences of relaxation time  $T_2$  between protons of fat and water in meat batter ( $P > 0.05$ ). Actually it was very hard to distinguish loosely combined fat with closely combined water, thus relaxation time of water and fat in meat batter system could be considered as a whole to analyze.

For meat batter system, water and fat addition had no effects on the peak area proportion of relaxation time  $T_{2b}$  ( $P > 0.05$ ). However, the peak area proportion of  $T_{21}$  of meat emulsion showed a significant reduction after adding water and fat ( $P < 0.05$ ), indicated the drop of total amount of protons combining with macromolecular. The reason for this may be that protein is the main macromolecular that combine water and fat in meat batter system, and to meat emulsion of the same weight, once the content of water and fat increase, protein content would decrease accordingly. The protein that aimed to combine water and fat would also reduce, thus resulting in the decrease of this part of combined protons. Moreover, as shown in Fig. 4, by chopping and the addition of water and fat, the peak area ratio between  $T_{22}$  and  $T_{21}$  was increased meaning the content of liquid water or fat in meat batter was ascended.

**3.2. Relaxation time analysis of heated meat batters**

**3.2.1. Effect of water and fat on relaxation time  $T_2$**

After heating treatment, meat emulsion turned into emulsification gel. As presented (Figs. 5 and 6), four relaxation time  $T_{2b}$  (lower than 1 ms),  $T_{21}$  (1–10 ms),  $T_{22}$  (30–50 ms), and  $T_{23}$

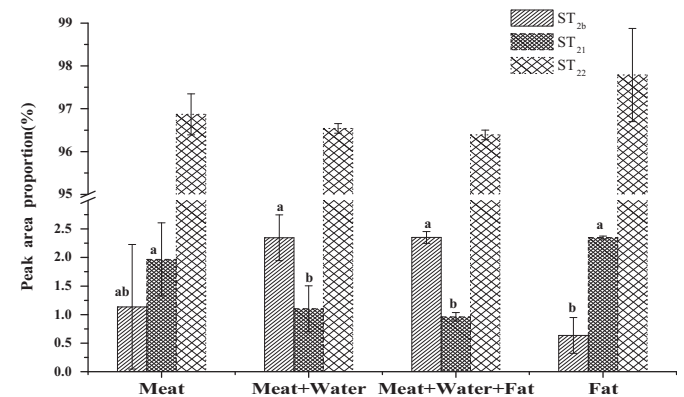


**Fig. 3.** Effect of water and fat on peaks area proportion in meat batters. **a, b** Means related to relaxation time (above a bar) with different letters differ significantly ( $P < 0.05$ ). Error bars show the standard deviation.

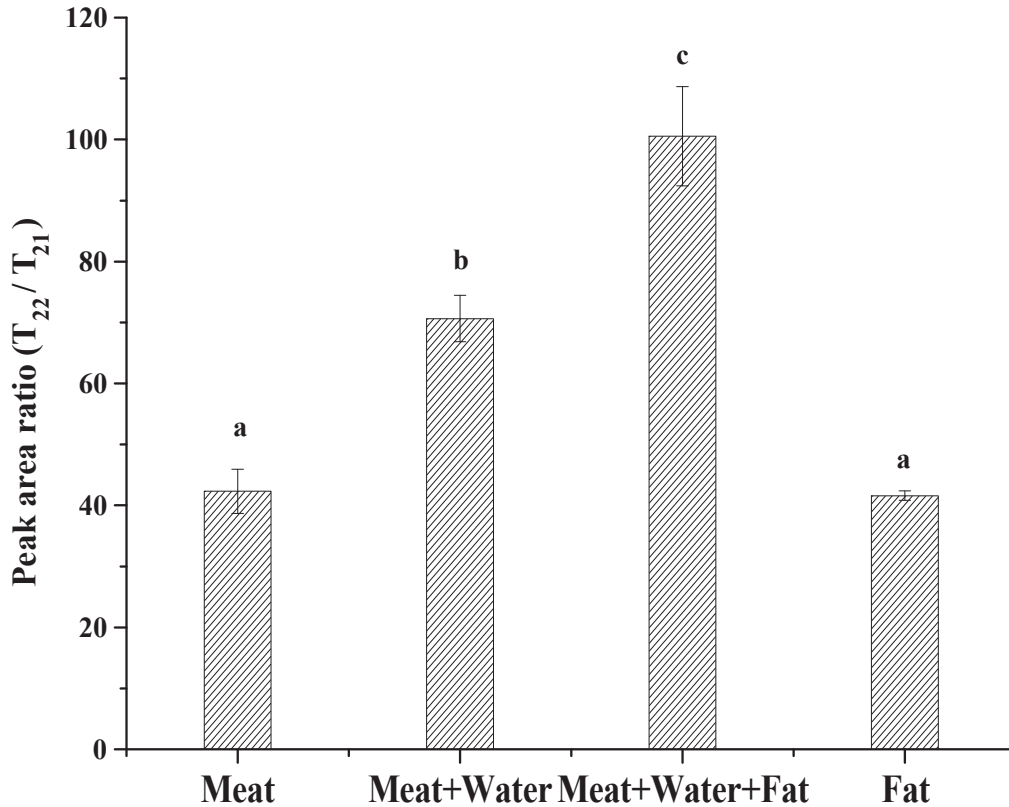


Fig. 4. Effect of water and fat on peaks area ratio in meat batters. a–c Means related to relaxation time (above a bar) with different letters differ significantly ( $P < 0.05$ ). Error bars show the standard deviation.

(200–300 ms) were observed in fitted  $T_2$  distribution of heated meat batters, respectively corresponding to the protons in protein macromolecular, that combine closely with macromolecular, the intercept water and fat, liquid water and fat. In the four relaxation components of different treatments of heated meat batters, only  $T_{22}$  existed significant differences. The relaxation time of water and fat that combine with protein was different which indicated that fat addition could significantly affect the combine state of protein with other components.

Compare the meat emulsion unheated with the heated meat batters, a new relaxation time  $T_{23}$  (200–300 ms) appeared by heating. This part of relaxation component corresponded to the liquid water in heated meat batter. The reason of this new peak may be due to that protein denaturation occurred and the gel was formed with precipitation of part of absorbed water that in state of

sol during heating process. In addition, heating could also result in fat melting deletion and turned into oil drops that mix in the precipitated water (Woo, Lee, & Kim, 1995). On the other hand, the relaxation time  $T_{2b}$ ,  $T_{21}$ , and  $T_{22}$  of heated meat batters all decreased, suggesting that protein denaturation by heating could constrain the motion of protons and make the combine closer of protein with water and fat.

### 3.2.2. Effect of water and fat on peak area properties

The most important motion of protons in heated batters was relaxation time  $T_{22}$ , whose peak area reached above 95% of the total peak area. However, there existed no significant ( $P > 0.05$ ) differences in peak area of the corresponding relaxation time in the three

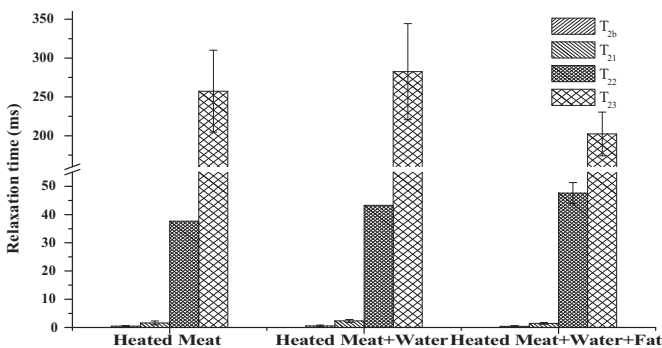


Fig. 5. Effect of water and fat on relaxation time ( $T_2$ ) in heated meat batters.

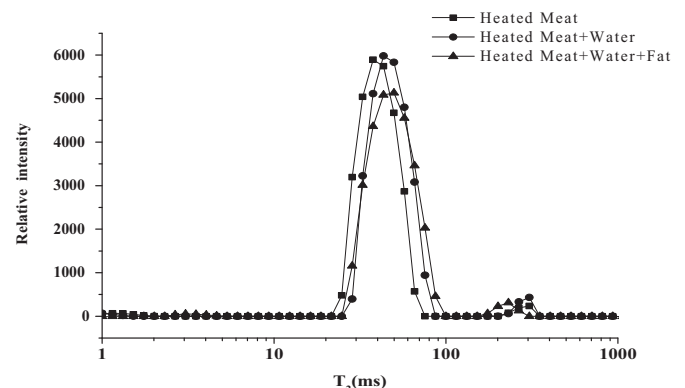


Fig. 6. Curves of relaxation time ( $T_2$ ) in different heated meat batters.

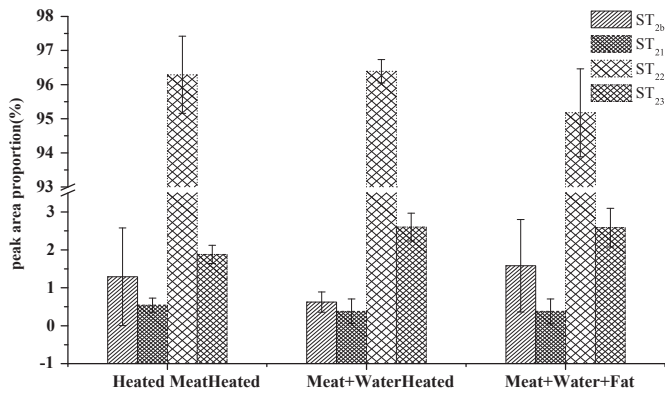


Fig. 7. Effect of water and fat on peaks area proportion in heated meat batters.

different treatments (Fig. 7). This indicated that addition of water and fat could not significantly affect the area percentage in their respective system of each peak in heated meat batters.

Chopping with water could not affect the ratio of relaxation time  $T_{22}$  and  $T_{21}$  (Fig. 8). There was a certain proportion between bound water in protein and water left in conformation of meat batters after adding water, and this just reflect the strong water retention of meat batters. On the other hand, compare this ratio of meat batters before and after heating, the value was elevated significantly. This suggested that protein that under swelling conditions could obviously combine more water or fat than the protein that form into emulsification gel, and heating has transformed part of combine water or fat into liquid water and fat in gel matrix.

## 4. Discussion

### 4.1. Distribution states of water and fat in raw meat batters

In this study, three relaxation components emerged in both meat and fat group.  $T_{2b}$  and  $T_{21}$  of fat group were higher than meat group, this suggested that the combination with macromolecules of fat protons was looser than that of water. Three peaks emerged in the relaxation time of protons in raw meat batters of different treatments, respectively represent the protons in protein structure, the protons that combined with protein macromolecules, the intercept water and fat protons in protein matrix. In chopping

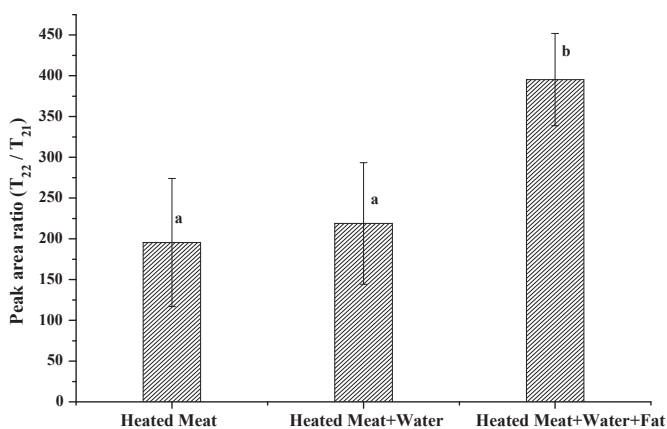


Fig. 8. Effect of water and fat on peaks area ratio in heated meat batters. **a**, **b** Means related to relaxation time (above a bar) with different letters differ significantly ( $P < 0.05$ ). Error bars show the standard deviation.

process of meat, the interaction of protein with salt ions makes ionic group electric double layer, reducing the electrostatic interactions between protein molecules and improving the solubility of protein to abstract the salt soluble proteins (Tornberg, 2005). Continue chopping after adding water,  $T_{21}$  and  $T_{22}$  of meat batters rose significantly accompanied by the increasing of the peak area ratio  $T_{22}/T_{21}$ . This indicated that the chemical exchange was accelerated between protons of protein and water or the water mobility enhanced (Hills, Takacs, & Belton, 1990), because fluid water the protein absorbed and the swelling degree was also increased. Continue chopping after adding fat, part of salt soluble proteins under state of swelling would emulsify with the chopped fat particles or fat drops, and well distributed emulsified fat were formed in protein matrix, then the combine state of total protein and protons was changed (Barbut, 1995). As results were presented in Fig. 1 that  $T_{21}$  of the meat group was lower than that of meat batter adding water (meat + water group), while  $T_{21}$  of meat batter adding water (meat + water group) was lower than that of meat batter adding water and fat (meat + water + fat group). These results could be interpreted by that  $T_{21}$  of fat group was significantly higher than that of the meat group and fat addition contributed more to  $T_{21}$  of the meat batter system. On the other hand, by absorption of water and emulsification with fat, the chemical exchange of proteins with water and fat protons was enhanced, and the mobility of water and fat was increased. In addition,  $T_{22}$  of meat group and fat group was both 50 ms, while  $T_{22}$  increased to 66 ms after water and fat were added to chop, suggesting that water and fat addition increased liquidity of this part of protons, and this would increase the possibility to loss fluid once undergoing heating or other external forces. To get meat products with high qualities, more need to be done to reduce the fluid loss by exploring the meat batters with different meat protein hydration states, and by LF-NMR we could obtain the intuitive analysis tentatively.

### 4.2. Distribution states of water and fat in emulsified gel

Heated meat batter turned into emulsified gel.  $T_{22}$  of emulsified gel was increased by the water and fat addition (Figs. 5 and 6), and  $T_{22}$  peak area proportion all reached above 95% of the total area (Fig. 7). This indicated the addition of water and fat increased chemical exchange of protein and water or fat protons in emulsified gel.  $T_{22}$  playing an important role in emulsified gel was consistent with the result of the unheated meat batters. Moreover,  $T_{22}/T_{21}$  of emulsified gel (heated meat group) and emulsified gel with water (heated meat + water group) existed no significant differences, revealing that protein had enough ability to absorb water to swell, resulting in strong water-holding capacity of protein. However,  $T_{22}/T_{21}$  increased significantly after adding fat, indicating that fat addition contributed more to liquid components the protein combined in emulsified gel.

Compare the unheated meat batters with the emulsified gel heated, a new relaxation time  $T_{23}$  came up by heating, and this component was corresponding to the fluid water in emulsified gel. About the formation of this new peak, it was analyzed that in heating process, protein denaturation and heat-induced shrinkage of the meat came up which resulting in a reduction in myofibrillar spacing, denaturation of structural proteins within the meat has been suggested to be responsible for heat-induced shrinkage of the fiber, and the associated loss of water due to the decreased water-holding capacity of denatured proteins, whatever the shrinkage was transverse or longitudinal to the fiber direction, it resulted cooking loss, so part of water that absorbed in sol state separated out (Christensen, Bertram, Aaslyng, & Christensen, 2011; Shao et al., 2011; Tornberg, 2005). It has been

reported that the water expelled from the structure may be caused by breakage of hydrogen bonds in the collagen which sustain its network. Hydroxyl groups stabilize the structure of collagen, and water forms hydrogen bonds between the hydroxyl groups and hydroxyproline, and consequently, thermal denaturation of collagen causes the breaking of bonds leading to shrinkage. Shrinkage of the collagen surrounding the myofibrils results in physical constraints on these structures and water is thereby forced out (Christensen et al., 2011). Heating may also result in the melt and the inflation of fat (Barbut, 1995), and then the fluid water content was increased by the mixture of the fat drops in the oozy water. On the other hand, relaxation time  $T_{2b}$ ,  $T_{21}$ , and  $T_{22}$  of the heated meat batters were all shortened, this indicated that protein denaturation by heating can constraint the motion of protons and make the combination of protein with water and fat more closer. As investigated, protein aggregated and formed the gel, then the relaxation time of the protons was lowered, the interaction between dipoles was no more acting by the average of turning effort.  $T_{22}/T_{21}$  was enhanced obviously after heating, indicating that water and fat combined by protein in swelling state were apparently higher than the protein that formed gel. Therefore, heating could transform part of combined water or fat into the fluid water and fat in gel matrix.

## 5. Conclusions

The effects of proteins with different hydration states on the mobility water and fat in processing of meat batters was investigated and assessed by LF-NMR technique in this study. There were three relaxation components in meat group and fat group, corresponding to the water or fat moderately bound ( $T_{22}$ , 50 ms) and tightly bound ( $T_{2b}$  and  $T_{21}$ , lower than 10 ms) within meat or fat matrix. Hence, relaxation time in meat batters can be assigned to the signals of water and fat. The addition of water and fat reduced the protein ability binding hydrogen protons and the effect of fat was greater than water. On the other hand, heat treatment increased the ability of protein binding hydrogen protons and limited water and fat proton mobility. Water could have higher effects on the juice loss of emulsion gel compared to that of fat. In conclusion, effects of meat protein hydration on the mobility water and fat in meat batters heated or not could be well measured by LF-NMR, proving the LF-NMR technique could be employed to predict the meat product comminuted conditions by reflecting the meat protein hydration states.

## Acknowledgments

This work was supported by the National Natural Science Foundation (31301510) and project no. BA2009007.

## References

- Andersen, C. M., Frøst, M. B., & Viereck, N. (2010). Spectroscopic characterization of low-and non-fat cream cheeses. *International Dairy Journal*, 20(1), 32–39.
- Barbut, S. (1995). Importance of fat emulsification and protein matrix characteristics in meat batter stability. *Journal of Muscle Foods*, 6, 161–167.
- Bertram, H. C., Purslow, P. P., & Andersen, H. J. (2002). Relationship between meat structure, water mobility, and distribution: a low-field nuclear magnetic resonance study. *Journal of Agricultural and Food Chemistry*, 50(4), 824–829.
- Brewer, M. S. (2012). Reducing the fat content in ground beef without sacrificing quality: a review. *Meat Science*, 91(4), 385–395.
- Christensen, L., Bertram, H. C., Aaslyng, M. D., & Christensen, M. (2011). Protein denaturation and water–protein interactions as affected by low temperature long time treatment of porcine Longissimus dorsi. *Meat science*, 88(4), 718–722.
- Dhall, A., Halder, A., & Datta, A. K. (2012). Multiphase and multicomponent transport with phase change during meat cooking. *Journal of Food Engineering*, 113(2), 299–309.
- Einarsdóttir, H., Nielsen, M. S., Miklos, R., Lametsch, R., Feidenhans'l, R., Larsen, R., et al. (2014). Analysis of micro-structure in raw and heat treated meat emulsions from multimodal X-ray microtomography. *Innovative Food Science & Emerging Technologies*, 24, 88–96.
- Hills, B. P., Takacs, S. F., & Belton, P. S. (1990). A new interpretation of proton NMR relaxation time measurements of water in food. *Food Chemistry*, 37(2), 95–111.
- Howell, N. K., Herman, H., & Li-Chan, E. C. (2001). Elucidation of protein-lipid interactions in a lysozyme-corn oil system by Fourier transform Raman spectroscopy. *Journal of Agricultural and Food Chemistry*, 49(3), 1529–1533.
- Marcone, M. F., Wang, S., Albabish, W., Nie, S., Somnarain, D., & Hill, A. (2013). Diverse food-based applications of nuclear magnetic resonance (NMR) technology. *Food Research International*, 51(2), 729–747.
- Noronha, N., Duggan, E., Ziegler, G. R., O'Riordan, E. D., & O'Sullivan, M. (2008). Investigation of imitation cheese matrix development using light microscopy and NMR relaxometry. *International Dairy Journal*, 18(6), 641–648.
- Pearce, K. L., Rosenfold, K., Andersen, H. J., & Hopkins, D. L. (2011). Water distribution and mobility in meat during the conversion of muscle to meat and ageing and the impacts on fresh meat quality attributes—a review. *Meat Science*, 89(2), 111–124.
- Raffaella, G., Marco, M., Delfini, M., & Brosio, E. (2007). A low-resolution and high-resolution nuclear magnetic resonance integrated approach to investigate the physical structure and metabolic profile of Mozzarella di Bufala Campana cheese. *International Dairy Journal*, 17(2), 167–176.
- Rodriguez Furlán, L. T., Padilla, A. P., & Campderrós, M. E. (2014). Development of reduced fat minced meats using inulin and bovine plasma proteins as fat replacers. *Meat Science*, 96(2), 762–768.
- Rosenfold, K., & Andersen, H. J. (2003). Factors of significance for pork quality—a review. *Meat Science*, 64(3), 219–237.
- Schmidt, G. R. (1984). Processing effects on meat product microstructure. *Food Microstructure*, 3, 33–39.
- Shaarani, S. M., Nott, K. P., & Hall, L. D. (2006). Combination of NMR and MRI quantitation of moisture and structure changes for convection cooking of fresh chicken meat. *Meat Science*, 72(3), 398–403.
- Shao, J. H., Zou, Y. F., Xu, X. L., Wu, J. Q., & Zhou, G. H. (2011). Evaluation of structural changes in raw and heated meat batters prepared with different lipids using Raman spectroscopy. *Food Research International*, 44(9), 2955–2961.
- Tolstoguzov, V. (2003). Some thermodynamic considerations in food formulation. *Food Hydrocolloids*, 17(1), 1–23.
- Tornberg, E. (2005). Effects of heat on meat proteins – implications on structure and quality of meat products. *Meat Science*, 70(3), 493–508.
- Woo, M. J., Lee, K. T., & Kim, C. J. (1995). Quality characteristics of emulsion-type sausage manufactured with cottonseed oil. *Korean Journal of Food Science Animal Resource*, 15(2), 187–191.
- Wu, M., Xiong, Y. L., Chen, J., Tang, X., & Zhou, G. H. (2009). Rheological and microstructural properties of porcine myofibrillar protein–lipid emulsion composite gels. *Journal of Food Science*, 74(4), E207–E217.
- Youssef, M. K., & Barbut, S. (2010). Physicochemical effects of the lipid phase and protein level on meat emulsion stability, texture, and microstructure. *Journal of Food Science*, 75(2), S108–S114.



## *Escherichia coli* O157:H7 and *Salmonella* Typhimurium inactivation by the effect of mandarin, lemon, and orange by-products in reference medium and in oat-fruit juice mixed beverage



Maria Sanz-Puig, M.Consuelo Pina-Pérez, Antonio Martínez-López, Dolores Rodrigo\*

Instituto de Agroquímica y Tecnología de Alimentos (IATA-CSIC), Av Catedratic Agustín Escardino Benlloch, 7, 46980, Paterna, València, Spain

### ARTICLE INFO

#### Article history:

Received 2 July 2015

Received in revised form

16 September 2015

Accepted 2 October 2015

Available online 9 October 2015

#### Keywords:

Citrus by-products

New ingredients

Antimicrobials

Bactericidal concentration

### ABSTRACT

The antimicrobial capability of three water extracts of citrus peels was evaluated against *Salmonella enterica* serovar Typhimurium and *Escherichia coli* O157:H7 at various concentrations (0.5, 1, 5, 10%) and temperatures (5, 10, 22 °C) in a reference medium. The best of them was mandarin by-product, achieving a maximum inactivation level against *S. Typhimurium* (8 log<sub>10</sub> cycles) with 5% at 5 °C. Also, this by-product had the highest total polyphenol content. Mandarin by-product showed a bactericidal effect in a food matrix also at 5 °C (≈2 log<sub>10</sub> cycles). All results were adjusted to the Weibull model and the *b* values indicated that the higher concentration of mandarin, the greater the inactivation rate in reference medium, without significant differences between 5 and 10%. Similarly, in the food matrix, the inactivation rate of *S. Typhimurium* was higher when the mandarin by-product was added. Therefore, the mandarin by-product could be used as a control measure of *S. Typhimurium* in pasteurized products, which are stored under refrigeration.

© 2015 Elsevier Ltd. All rights reserved.

### 1. Introduction

Citrus is the largest fruit crop worldwide, with an annual production of approximately 100 million tons. The main world producers are Brazil, the USA and Mediterranean countries (Djilas, 2009; Ghafar, Prasad, Weng, & Ismail, 2010). The industrial production of juices and other citrus derivatives generates approximately 15 million tons of citrus waste a year worldwide, which mainly consists of peel, seeds, and the fruit pulp. Citrus waste is usually consigned to landfill or incineration, which generates negative effects on the environment and a cost to the producers (O'Shea, Arendt, & Gallagher, 2012).

This valueless citrus waste can be considered as a renewable source of raw material whose use in various industrial fields could have a double benefit, economic and technological, as a result of its valorization (Martín-Luengo, Yates, Diaz, Saez Rojo, & Gonzalez Gil, 2011; Schieber, Stintzing, & Carle, 2001;). Since 2010 generalized agri-food by-product valorization has been a European Union requirement (EUROSTAT, 2010) and many research studies

nowadays are focused on recovering, revaluing, and recycling these by-products. One way of valorizing these by-products is the formulation of new products with added nutritional value. Citrus by-products are rich in functional compounds such as carotenoids and flavonoids, among others (O'Shea et al., 2012), whose antioxidant, anticarcinogenic, antiviral, and anti-inflammatory properties are well known. Citrus derivative compounds have an important nutritional and flavoring value, and an antimicrobial capability has also been attributed to some of them, mainly due to ferulic acid, hydrocinnamic acid, vanilidyl glucoside, hisperidin, vitamin C, carotenoid, and naringin (Ghafar et al., 2010). In this sense, they could be used like natural antimicrobials to control the growth of foodborne pathogens, replacing the chemical compounds which are used currently. Also, they could be used as an additional control measure of the microbial growth in situations of cold chain breakdown in pasteurized food that is stored in refrigeration (Sanz-Puig, Pina-Pérez, Rodrigo, & Martínez-López, 2015).

In this context, the aim of this study was to evaluate the antimicrobial effect of water extracts of by-products of citrus fruits – mandarin, orange, and lemon – against two of the foodborne pathogens of most concern that are found in low-acid beverages: *Salmonella enterica* serovar Typhimurium and *Escherichia coli* O157:H7.

\* Corresponding author.

E-mail address: [lolesra@iata.csic.es](mailto:lolesra@iata.csic.es) (D. Rodrigo).

## 2. Material and methods

### 2.1. Microbiology

Pure cultures of *S. Typhimurium* (CECT 443) and *E. coli* O157:H7 (CECT 5947) were provided freeze-dried by the Spanish Type Culture Collection. Both cultures were rehydrated with 10 mL of Tryptic Soy Broth (TSB) (Scharlab Chemie, Barcelona, Spain). After 20 min, the rehydrated culture was transferred to 500 mL of TSB and incubated at 37 °C with continuous shaking at 200 rpm for 14 h to obtain cells in a stationary growth stage. The cells were centrifuged twice at 4000 ×g at 4 °C for 15 min and then resuspended in TSB. After the second centrifugation, the cells were resuspended in 20 mL of TSB with 20% glycerol, and then dispensed in 2-mL vials with a final concentration of 108 colony forming units per milliliter (CFU/mL). The 2-mL samples were immediately frozen and stored at –80 °C until needed for the kinetic inactivation studies.

### 2.2. Citrus by-products

Dehydrated peel residues from mandarin (*Citrus reticulata*), orange (*Citrus sinensis*) and lemon (*Citrus limon*) were provided from primary production (Indulleida, S.A.). Each raw by-product was tested to screen its bacteriological quality. The bacteriological analysis determined the presence/absence of microbial contamination with *Listeria monocytogenes* and *Bacillus cereus* (Gram-positives), or *E. coli* O157:H7 and *S. Typhimurium* (Gram-negatives), and was carried out according to the procedures described by [Aycicek, Oguz, and Karci \(2006\)](#). No samples studied presented contamination with any of the microorganisms tested.

### 2.3. Total phenolic compounds

The total phenol content of the citrus by-products was determined spectrophotometrically according to the Folin–Ciocalteu colorimetric method ([Singleton & Rossi, 1965](#)). Gallic acid calibration standards with concentrations of 0, 100, 200, 300, 400, 500, 600, 700, 800, and 1000 ppm were prepared. Three mL of sodium carbonate solution (2% (w/v)) (Sigma–Aldrich Co. LLC, USA) and 100 µL of Folin–Ciocalteu reagent (1:1 (v/v)) (Sigma–Aldrich Co. LLC, USA) were added to an aliquot of 100 µL from each gallic acid standard (Sigma–Aldrich Co. LLC, USA) or sample tube. The mixture was shaken and allowed to stand at room temperature in the dark for 1 h. Absorbance was measured at 750 nm using a Lan Optics Model PG1800 spectrophotometer (Labolan, Spain), and the results were expressed as mg of gallic acid equivalents (GAE)/L.

### 2.4. Antimicrobial assay

Buffered peptone water (Scharlab Chemie, Barcelona, Spain) (0.1% (w/v)) was used as a reference substrate in the present study. For the assessment of citrus by-product antimicrobial capability, 1 mL of each vial of stock culture was added to reference substrate at a final concentration of 107 CFU/mL. The inoculated medium (buffered peptone water) was supplemented with dehydrated peel residues at different concentrations (0.5, 1, 5, and 10% (w/v)). All the samples were then incubated at different temperatures (5, 10, and 22 °C). At regular time intervals (hours), the cell suspension for each sample was evaluated by plate count in Tryptic Soy Agar (TSA) (Scharlab Chemie, Barcelona, Spain) after serial dilution with 0.1% (w/v) buffered peptone water. The plates were incubated at 37 °C for 24 h. Each dilution was plated in duplicate. The experiments were carried out in triplicate and the plate counts were used for CFU/mL enumeration.

A second set of experiments was conducted. The most effective antimicrobial of the three tested in the reference medium was evaluated against *S. Typhimurium* in various formulated beverages.

Finally, in order to compare the results, the behavior of both microorganisms under exposure to citrus by-product was characterized by estimating the minimal inhibitory concentration (MIC), being the lowest concentration of antimicrobial substance that is able to inhibit microbial growth ([Guillier, Nazer, & Dubois-Brissonnet, 2007](#)).

Also, the minimal bactericidal concentration (MBC) was estimated, being the lowest concentration of antimicrobial substance that is able to exert a bactericidal effect against the microorganism under study ([Bär, Både-Schumann, Krebs, & Cromme, 2009](#)).

### 2.5. Food matrix

The antimicrobial potential of the most bactericidal citrus by-product was tested against both pathogens in complex food matrices. Firstly, an oat beverage (OB) was used in this set of experiments. The beverage used was supplemented with the most effective citrus by-product and compared with the non-supplemented beverage. The concentration of the by-product was the minimum bactericidal concentration (MBC), and the incubation temperature was 5 °C, a typical temperature for storage of beverages of this kind. Secondly, an oat beverage containing 32.5% papaya, 10% mango, and 7.5% orange (OB-FM) was used. As in the case of the oat beverage, this beverage was supplemented with the most effective antimicrobial by-product using the minimum bactericidal concentration (MBC). The results were compared with those obtained in the non-supplemented OB-FM beverage.

The food matrices considered, OB (supplemented/not supplemented) and OB-FM (supplemented/not supplemented with the most bactericidal by-product), were inoculated with an initial microbial population of 108 CFU/mL. The bacterial growth/death during refrigerated storage was monitored by means of viable cell counts.

### 2.6. Modeling of microorganism inactivation

The microbial behavior was fitted to a Weibull equation ([Peleg & Cole, 1998](#)) to obtain a mathematical description of the kinetics of bacterial inactivation by the citrus by-product:

$$\log_{10}(S(t)) = -b \times t^n \quad (1)$$

where  $t$  is the time (hours),  $S$  is the survival fraction, i.e., the quotient between the cell concentration at time  $t$  ( $N_t$ ) (CFU/mL) and the initial cell concentration ( $N_0$ ) (CFU/mL);  $b$  is the scale factor and  $n$  is the form factor.

### 2.7. Data analysis and model evaluation

The statistical analysis was performed with STATGRAPHICS Centurion XV (version 15.1.03; STATGRAPHICS, Warrenton, VA).

This analysis included average and standard deviation calculations for the three repetitions and an ANOVA analysis to test significant differences depending on incubation conditions. The goodness of fit of the model was assessed by using the adjusted regression coefficient (*adjusted-R2*) ([López, 2004](#)).

### 3. Results and discussion

#### 3.1. Antimicrobial capacity of citrus by-products against *S. Typhimurium*

The antimicrobial effect of the mandarin, orange, and lemon by-products was evaluated against *S. Typhimurium* cells during 96 h of incubation at 5 and 10 °C and 24 h of incubation at 22 °C. Fig. 1 shows the log cycle reduction achieved for each combination.

With regard to the effect of temperature, *S. Typhimurium* growth was inhibited in non-supplemented reference medium (0%) with refrigerated incubation of 5 °C, while at 10 °C detectable growth was observed after 96 h, and it was higher at 22 °C. Therefore it can be concluded that low temperature acts as an effective bacterial proliferation barrier against *S. Typhimurium*,

which is in agreement with the findings of other authors (Okada, Ohnuku, Suzuki, & Igimi, 2013).

In general, all by-products tested reduced the microbial load of *S. Typhimurium* regardless of the incubation temperature, with a maximum reduction very close to 8 log<sub>10</sub> cycles at 5% and 10% mandarin by-product and 5 and 10 °C incubation temperature. We note that mandarin was the most effective by-product, followed by orange and lemon.

With regard to the by-product concentration, only 5 and 10% of orange and lemon by-products could be considered as an additional control measure for *S. Typhimurium* in the case of a cold chain break (22 °C), at least for 24 h. In contrast, for mandarin by-product, all concentrations tested could be used. In the case of temperature abuse (10 °C), 5 and 10% of by-product could also be considered as an additional control measure for this microorganism, at least for 96 h, although in orange by-product no significant differences ( $p \leq 0.05$ ) were observed among the concentrations studied.

An ANOVA analysis concluded that both incubation temperature and by-product concentration had a significant impact ( $p \leq 0.05$ ) on *S. Typhimurium* cell survival. As can be seen in Fig. 1, at all temperatures an increase in citrus by-product concentration was accompanied by greater microorganism growth inhibition or inactivation. However, no significant differences were observed between inactivation levels achieved when citrus by-product was added to the medium at 5–10%, with inactivation levels very close to 8 log<sub>10</sub> cycles at incubation temperatures of 5 and 10 °C in samples with mandarin by-product.

The antimicrobial potential of the by-products studied could be particularly relevant under the concept of hurdle barriers, acting as an additional measure to control bacterial proliferation in situations of abuse temperature (10 °C) or in the case of cold chain breakdown (22 °C) in pasteurized food products which must be storage at refrigeration temperatures. They can be added to this kind of products (fruit or vegetable creams or beverages) like an ingredient and control the microbial growth during their storage period. However, these by-products have a low but characteristic taste and odor that could not be accepted by the consumers at high concentrations. Therefore, is important to carry on a sensorial study with the aim to find the concentration of by-product with an antimicrobial capability and sensorial acceptance (Valero & Giner, 2006) and the food products where it could be added.

The minimum inhibitory concentration (MIC) and the minimum bactericidal concentration (MBC) for each citrus by-product in relation to incubation temperature were calculated (Table 1). *S. Typhimurium* is highly sensitive to contact with citrus by-products, with very low MIC and MBC values (0.5%). The microbiological sensitivity of *S. Typhimurium* depends on both the temperature and the citrus by-product type ( $p < 0.05$ ). The lowest MBC was obtained for mandarin at 5 and 22 °C; while lemon and orange

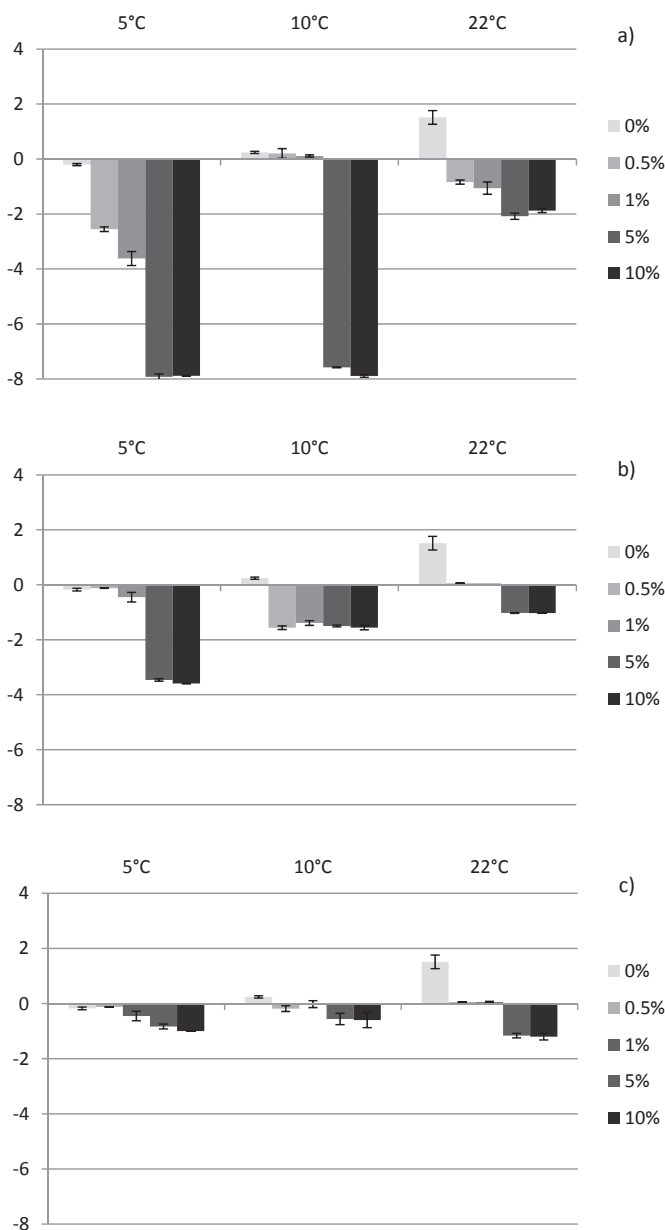


**Fig. 1.** Inactivation levels ( $\text{Log}_{10}(N_t/N_0)$ ) of *S. Typhimurium* in contact with various (0, 0.5, 1, 5, 10%) citrus by-products concentrations: mandarin (a), orange (b), and lemon (c) in buffered peptone water, incubated at different temperatures (5, 10, and 22 °C).

**Table 1**

Minimum inhibitory concentration (MIC) and Minimum bactericidal concentration (MBC) for *S. Typhimurium* in the conditions tested. No significant effects (–).

<i>S. Typhimurium</i>			
Temperature (°C)	By-product	MIC (%)	MBC (%)
5	Mandarin	–	0.5
	Orange	–	1
	Lemon	–	1
10	Mandarin	0.5	5
	Orange	–	0.5
	Lemon	–	0.5
22	Mandarin	–	0.5
	Orange	0.5	5
	Lemon	0.5	5

required a smaller MBC than mandarin to be effective against *S. Typhimurium* when the incubation temperature was 10 °C.

Generally, the MBC at refrigeration temperatures was lower than at room temperature (22 °C). This may be because refrigeration temperatures have a bacteriostatic capacity and exert a synergistic or additive effect with the by-product concentration. Other authors have shown the bacteriostatic capacity of refrigeration temperatures and have attributed it to a stress response mechanism that is activated in microorganisms at low temperatures (Shapiro & Cowen, 2012).

3.2. Antimicrobial capacity of citrus by-products against *E. coli* O157:H7

The results for the effect of the citrus by-products on *E. coli*

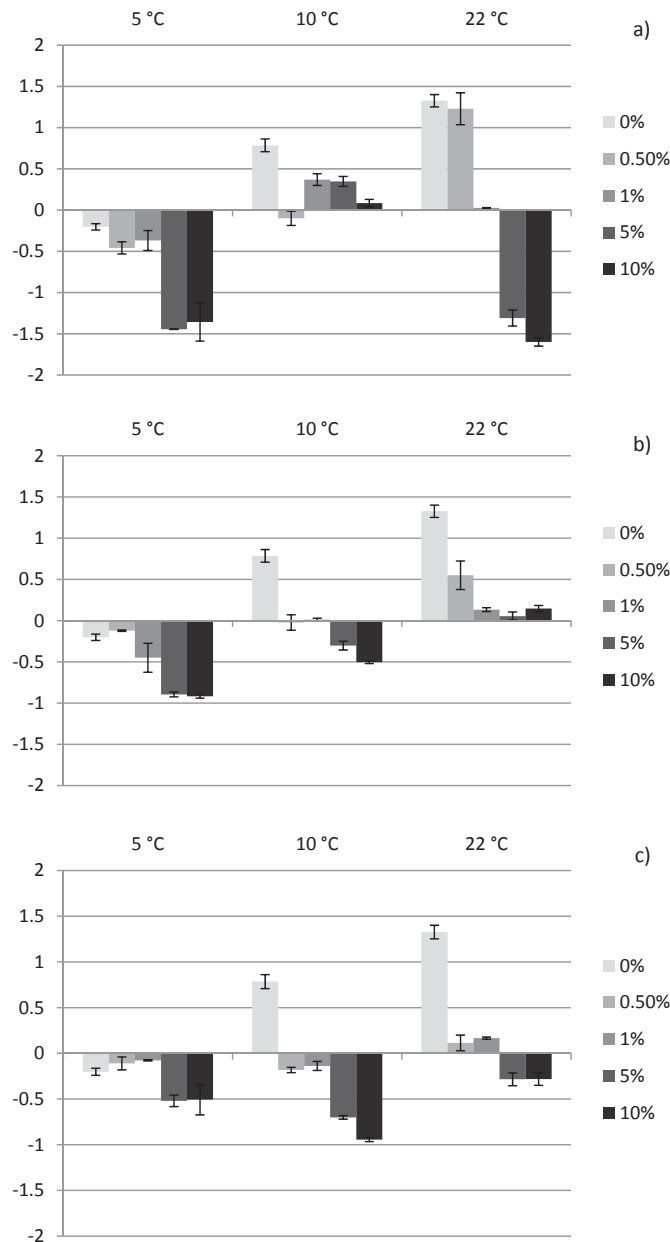


Fig. 2. Inactivation levels ( $\text{Log}_{10}(N_t/N_0)$ ) of *E. coli* O157:H7 in contact with various (0, 0.5, 1, 5, 10%) citric by-product concentrations: mandarin (a), orange (b), and lemon (c) in buffered peptone water, incubated at different temperatures (5, 10, and 22 °C).

O157:H7 are shown in Fig. 2.

As can be seen, low temperature (5 °C) inhibited *E. coli* O157:H7 cell growth in reference medium (0% by-product), while at 10 (abuse of temperature) and 22 °C (cold chain break) the microorganism was able to grow. Focusing on the effect of by-product concentration, 5 and 10% mandarin and orange by-product had a bactericidal effect ( $\geq 0.5 \text{ log}_{10}$  cycles), reducing *E. coli* O157:H7 counts by a maximum of 1.5  $\text{log}_{10}$  cycles. The effect of 5 and 10% concentrations on the bacteriostatic or bactericidal effect at temperatures other than 5 °C depended on the citrus by-product used. Concentrations lower than 5% appear to have a bacteriostatic effect, slowing down growth of the microorganisms. Note that at 10 °C *E. coli* O157:H7 started to grow and addition of the mandarin by-product showed a bacteriostatic capacity. In contrast, addition of the orange and lemon by-products did not have any antimicrobial (bacteriostatic or bactericidal) effect at this temperature. At 22 °C, the by-products studied had a bacteriostatic effect against *E. coli* O157:H7 when they were added at 5% (w/v), and addition of mandarin by-product at 10% (w/v) had a bactericidal effect, achieving a maximum reduction of 1.6  $\text{log}_{10}$  cycles.

The mandarin by-product also showed the highest antimicrobial potential against *E. coli* O157:H7, with reductions of 1.3 and 1.6  $\text{log}_{10}$  cycles at 5 and 22 °C, respectively. The orange and lemon by-products achieved a bactericidal effect, with reductions ranging from 0.5 to 1  $\text{log}_{10}$  cycles at refrigeration temperatures, and both exerted a bacteriostatic effect at 22 °C.

It is important to note that the effect of the by-products depended on the microorganism tested and the polyphenol structure (Taguri, Tanaka, & Koumo, 2004; Daglia, 2011). In our case, *S. Typhimurium* was more sensitive than *E. coli* O157:H7 to the various by-products used. This might indicate that each antimicrobial could be specific against a particular microorganism or group of microorganisms.

An ANOVA analysis of data for *E. coli* O157:H7 revealed that for all the by-products studied both incubation temperature and by-product concentration had a significant influence on the antimicrobial activity against *E. coli* O157:H7 ( $p < 0.05$ ), achieving the highest antimicrobial effect by 5 and 10% by-product addition, without significant differences between them.

Table 2 shows the MIC and MBC of the citrus by-products against *E. coli* O157:H7 for each combination of the factors (temperature – concentration) tested. The MIC values are 0.5% at all the temperatures studied, and the MBC values are between 1 and 5%, both being influenced by the incubation temperature and the type of citrus by-product added.

The mandarin by-product had a bactericidal effect at 5 °C, a bacteriostatic effect at 10 °C, and both at 22 °C. However, although the orange and lemon by-products have the same MIC and MBC values as the mandarin by-product at 10 and 22 °C, they showed a

Table 2 Minimum inhibitory concentration (MIC) and Minimum bactericidal concentration (MBC) for *E. coli* O157:H7 in the conditions tested. No significant effects (–).

<i>E. coli</i> O157:H7			
Temperature (°C)	By-product	MIC (%)	MBC (%)
5	Mandarin	–	5
	Orange	–	1
	Lemon	–	5
10	Mandarin	0.5	–
	Orange	0.5	5
	Lemon	–	5
22	Mandarin	0.5	5
	Orange	0.5	–
	Lemon	–	5

lower antimicrobial capacity expressed as  $\log_{10}$  cycle reduction. Therefore, under the conditions studied, it is possible to conclude that *E. coli* O157:H7 has less sensitivity to the citrus by-products studied than *S. Typhimurium*.

It is well known that the antimicrobial effect of many natural products in a real or buffered medium is influenced by environmental factors (e.g., pH and temperature conditions), the concentration of the natural ingredient, and the sensitiveness of the microbe (e.g., strain, virulence) (Bajpai, Baek, & Kang, 2012).

Table 3 shows the pH values for the citrus by-products tested at concentrations of 5 and 10%. Although it has traditionally been accepted that pH plays an important part in inhibiting cellular activity, the table shows that the citrus by-product with the lowest pH value is lemon, while the by-product with the best antimicrobial effect against the microorganisms under study is mandarin. This result appears to indicate that pH is not the most important factor that influences citrus by-product antimicrobial activity.

### 3.3. Polyphenol concentration of citrus by-products

The bacteriostatic and bactericidal capacities of citrus by-products could be significantly influenced by their composition, mainly because of their polyphenol content. Numerous studies show that they have many bioactive compounds such as polyphenols, including ferulic acid, hydrocinnamic acid, cyaniding glucoside, hisperidin, carotenoid, and naringin, in their peel and seeds, which have antioxidant and antimicrobial properties (Ghafar et al., 2010). Table 4 shows the polyphenol content measured for each citrus by-product under study. As can be seen in the table, the mandarin by-product has the highest total polyphenol content, followed by orange and then lemon. In this case, the total polyphenol content coincides with the antimicrobial capacity of the by-products: the citrus by-product with the highest polyphenol content, mandarin, is the one with the greatest antimicrobial capacity, followed by the orange and lemon by-products. Therefore we can conclude that polyphenol content may be directly related to antimicrobial activity, in accordance with other studies (Devi, Suganthi, Kesika, & Pandian, 2008).

### 3.4. Mathematical modeling of *S. Typhimurium* and *E. coli* O157:H7 inactivation

The experimental curves obtained for *S. Typhimurium* and *E. coli* O157:H7 were fitted to a Weibull distribution function, owing to its simplicity and robustness for describing inactivation kinetics (De Oliveira, Soares, & Piccoli, 2011).

The results of the fitting are shown in Tables 5 and 6. The *b* value is related to inactivation rate: the higher the *b* value, the faster the microorganism dies. The Weibull kinetic *b* values for *S. Typhimurium* (Table 5) increase with higher by-product concentrations, achieving the maximum inactivation rate at 5% by-product concentration, without significant differences ( $>0.05$ ) between the *b* values at 5 and 10% by-product concentration.

The same pattern occurs in the *E. coli* O157:H7 inactivation kinetics. As can be seen in Table 6, at lower by-product concentrations the *b* values are close to 0 or negative, owing to microorganism growth. However, at higher citrus by-product

**Table 4**  
Total polyphenol content in by-product extracts.

Citrus by-product	Polyphenol content (mg gallic acid/L)
Mandarin 10%	5111.50 ± 201.93
Orange 10%	4809.72 ± 287.47
Lemon 10%	4600.00 ± 20.00

concentrations the *b* value increases, without significant differences between 5 and 10% (w/v) addition.

Therefore the concentration of citrus by-product added affects the inactivation rate of the two Gram-negative microorganisms studied. In contrast, there does not appear to be a relationship between incubation temperature and *b* value, and, therefore, with the rate of microorganism inactivation.

### 3.5. Antimicrobial potential of mandarin by-product incorporated in an oat-based beverage

According to the results in the previous sections, mandarin (MND) had the highest antimicrobial potential among the citrus by-products studied in reference medium.

Table 7 shows the inactivation levels reached in *S. Typhimurium* and *E. coli* O157:H7 in oat beverage (OB) supplemented or not supplemented with mandarin during the refrigerated storage period of 144 h at 5 °C. Although temperature produces some log reductions in the microbial load, an additive effect can be attributed to the mandarin by-product added to the real beverages, producing an additional reduction for *S. Typhimurium* of 0.47  $\log_{10}$  cycles when MND was incorporated in OB and 0.68  $\log_{10}$  cycles when MND was added to oat-based beverage with fruit juice mixture (OB + FM); and for *E. coli* O157:H7 additional reductions close to 1.18  $\log_{10}$  cycles were achieved when MND was incorporated in OB, and 0.65  $\log_{10}$  cycles when MND was added to OB + FM. Although MND had higher effectiveness against *S. Typhimurium* in reference medium, *E. coli* O157:H7 was more sensitive when MND was added to the food matrices studied. It can be observed that the inactivation levels achieved for both microorganisms in OB + FM were significantly ( $p \leq 0.05$ ) higher than those achieved in OB. Some research studies have shown that many fruits are rich in bioactive compounds with antioxidant properties, such as polyphenols, which could also have additional antimicrobial properties against foodborne pathogens (Ghasemi, Ghasemi, & Ebrahimzadeh, 2009; Mandalari et al., 2007).

According to the results obtained, the bactericidal effect of mandarin on both microorganisms was higher in reference medium than in food matrix. When the mandarin by-product was added to a real matrix, its antimicrobial effectiveness against *S. Typhimurium* was 75% less than when it was added to the reference medium. The interference of the real substrate was remarkable in the case of the *S. Typhimurium* growth/death pattern under refrigeration using OB as the food matrix. The addition of MND (5% (w/v)) in reference medium resulted in a reduction of 8  $\log_{10}$  cycles for *S. Typhimurium*, while incorporation of this by-product in OB only produced a reduction close to 1  $\log_{10}$  cycle under the same time and temperature storage conditions (96 h, 5 °C). Several authors attribute to food matrix complexity a

**Table 3**  
pH values measured for mandarin, orange, and lemon by-products at concentrations of 5 and 10%.

	Mandarin		Orange		Lemon	
	5%	10%	5%	10%	5%	10%
pH	4.39 ± 0.02	4.24 ± 0.01	4.85 ± 0.04	4.54 ± 0.02	3.92 ± 0.06	3.77 ± 0.06

**Table 5**  
Weibull kinetic values for *S. Typhimurium* inactivation under the citrus by-product effect at various concentrations (% (w/v)) and temperatures (°C).

% By-product			0%	0.5%	1%	5%	10%
Mandarin	5 °C	b	0.013 ± 0.017	0.008 ± 0.004	0.132 ± 0.077	1.019 ± 0.118	0.915 ± 0.126
		n	0.804 ± 0.434	1.277 ± 0.144	0.776 ± 0.148	0.420 ± 0.027	0.445 ± 0.040
		R <sup>2</sup>	0.904	0.998	0.956	0.965	0.957
	10 °C	b	-0.005 ± 0.054	-0.103 ± 0.153	-0.007 ± 0.022	1.935 ± 0.100	1.668 ± 0.151
		n	0.285 ± 0.159	0.580 ± 0.668	0.558 ± 0.174	0.273 ± 0.010	0.333 ± 0.019
		R <sup>2</sup>	0.908	0.905	0.913	0.951	0.958
	22 °C	b	-0.005 ± 0.001	0.036 ± 0.024	0.005 ± 0.004	0.428 ± 0.026	0.300 ± 0.001
		n	1.796 ± 0.053	1.0395 ± 0.265	1.774 ± 0.313	0.510 ± 0.030	0.554 ± 0.012
		R <sup>2</sup>	0.948	0.952	0.979	0.979	0.960
Orange	5 °C	b	0.009 ± 0.011	0.004 ± 0.005	0.068 ± 0.045	0.350 ± 0.009	0.285 ± 0.010
		n	0.804 ± 0.362	1.839 ± 0.874	1.226 ± 1.274	0.512 ± 0.011	0.561 ± 0.012
		R <sup>2</sup>	0.928	0.948	0.960	0.940	0.941
	10 °C	b	-0.098 ± 0.139	0.349 ± 0.141	0.409 ± 0.001	0.303 ± 0.036	0.008 ± 0.005
		n	0.814 ± 1.035	0.387 ± 0.081	0.301 ± 0.013	0.382 ± 0.057	1.178 ± 0.153
		R <sup>2</sup>	0.905	0.941	0.951	0.901	0.959
	22 °C	b	-0.005 ± 0.001	-0.014 ± 0.009	-0.034 ± 0.005	0.414 ± 0.009	0.421 ± 0.019
		n	1.796 ± 0.053	0.674 ± 0.200	0.337 ± 0.464	0.301 ± 0.012	0.294 ± 0.020
		R <sup>2</sup>	0.948	0.961	0.949	0.964	0.937
Lemon	5 °C	b	0.026 ± 0.012	0.011 ± 0.011	0.057 ± 0.015	0.007 ± 0.004	0.033 ± 0.030
		n	0.418 ± 0.183	0.784 ± 0.175	0.519 ± 0.086	1.090 ± 0.125	0.798 ± 0.223
		R <sup>2</sup>	0.940	0.953	0.931	0.935	0.948
	10 °C	b	-0.039 ± 0.039	0.023 ± 0.011	0.027 ± 0.012	0.030 ± 0.026	0.003 ± 0.004
		n	0.458 ± 0.130	0.570 ± 0.142	0.608 ± 0.155	0.701 ± 0.131	1.265 ± 0.396
		R <sup>2</sup>	0.934	0.910	0.913	0.951	0.942
	22 °C	b	-0.005 ± 0.001	-0.014 ± 0.009	-0.041 ± 0.004	0.478 ± 0.113	0.384 ± 0.040
		n	1.796 ± 0.053	0.674 ± 0.200	0.170 ± 0.228	0.320 ± 0.092	0.416 ± 0.057
		R <sup>2</sup>	0.948	0.961	0.954	0.941	0.916

The *b* value is negative when the microorganism grows and positive when the microorganism dies.

**Table 6**  
Weibull kinetic values for *E. coli* O157:H7 inactivation under the citrus by-product effect at various concentrations (% (w/v)) and temperatures (°C).

% By-product			0%	0.5%	1%	5%	10%
Mandarin	5 °C	b	0.017 ± 0.008	0.027 ± 0.013	0.033 ± 0.011	0.107 ± 0.016	0.090 ± 0.010
		n	0.561 ± 0.067	0.548 ± 0.230	0.855 ± 0.074	0.613 ± 0.044	0.652 ± 0.018
		R <sup>2</sup>	0.925	0.921	0.928	0.938	0.931
	10 °C	b	-0.001 ± 0.001	-0.009 ± 0.016	-0.027 ± 0.037	-0.001 ± 0.001	-0.018 ± 0.006
		n	1.460 ± 0.284	0.663 ± 0.497	0.859 ± 0.561	3.796 ± 0.968	0.344 ± 0.230
		R <sup>2</sup>	0.960	0.949	0.955	0.930	0.953
	22 °C	b	-0.036 ± 0.002	-0.015 ± 0.021	-0.116 ± 0.037	0.358 ± 0.178	0.291 ± 0.036
		n	1.138 ± 0.026	1.798 ± 0.912	0.180 ± 0.253	0.450 ± 0.188	0.544 ± 0.041
		R <sup>2</sup>	0.973	0.921	0.953	0.942	0.912
Orange	5 °C	b	0.005 ± 0.006	0.001 ± 0.001	0.014 ± 0.019	0.001 ± 0.001	0.001 ± 0.002
		n	1.013 ± 0.547	1.385 ± 0.501	1.849 ± 0.470	1.843 ± 0.051	1.532 ± 0.569
		R <sup>2</sup>	0.941	0.945	0.965	0.957	0.921
	10 °C	b	-0.001 ± 0.001	0.029 ± 0.028	0.033 ± 0.007	0.023 ± 0.009	0.079 ± 0.013
		n	1.457 ± 0.280	0.403 ± 0.239	0.437 ± 0.035	0.559 ± 0.130	0.438 ± 0.060
		R <sup>2</sup>	0.960	0.966	0.939	0.963	0.921
	22 °C	b	-0.036 ± 0.002	-0.038 ± 0.010	-0.051 ± 0.057	0.020 ± 0.028	0.029 ± 0.069
		n	1.138 ± 0.026	1.012 ± 0.071	0.647 ± 0.154	1.078 ± 1.265	0.347 ± 0.490
		R <sup>2</sup>	0.973	0.922	0.970	0.939	0.925
Lemon	5 °C	b	0.017 ± 0.006	0.008 ± 0.005	0.017 ± 0.011	0.003 ± 0.003	0.001 ± 0.001
		n	0.526 ± 0.049	0.785 ± 0.091	0.349 ± 0.212	1.137 ± 0.257	1.485 ± 0.007
		R <sup>2</sup>	0.935	0.913	0.939	0.927	0.915
	10 °C	b	-0.001 ± 0.001	0.038 ± 0.029	0.014 ± 0.019	0.032 ± 0.018	0.839 ± 0.121
		n	1.378 ± 0.168	0.460 ± 0.132	0.808 ± 0.337	0.669 ± 0.093	0.037 ± 0.038
		R <sup>2</sup>	0.952	0.933	0.925	0.935	0.985
	22 °C	b	-0.036 ± 0.002	-0.018 ± 0.018	-0.019 ± 0.017	0.035 ± 0.001	0.001 ± 0.001
		n	1.138 ± 0.026	0.961 ± 0.645	0.769 ± 0.344	0.672 ± 0.094	2.905 ± 1.919
		R <sup>2</sup>	0.973	0.961	0.954	0.923	0.965

The *b* value is negative when the microorganism grows and positive when the microorganism dies.

protective effect that reduces the effectiveness of many control treatments (Gutierrez, Barry-Ryan, & Bourke, 2008). The protective effect of a lipid-rich substrate such as oat milk could affect the antimicrobial potential of mandarin against *S. Typhimurium* (Di Pascua, Hoskins, Betts, & Mauriello, 2006).

The addition of a papaya, mango, and orange juice mixture to the beverage studied significantly increased the inactivation values

at each storage point recorded for both microbial populations. After the complete storage period, *S. Typhimurium* inactivation was almost doubled (increasing from 0.74 log<sub>10</sub> cycles in OB to 1.25 in OB + FM) by the additional effect of the fruit juices. This may be because mango, orange, and papaya are fruits rich in bioactive substances such as polyphenol compounds (Tomás-Barberán & Espín, 2001), which might produce an antimicrobial effect against

**Table 7**

Inactivation levels ( $\log_{10}$  cycles) achieved in the food matrices studied for both *S. Typhimurium* and *E. coli* O157:H7 by the intervention of mandarin (MND) by-product added at MBC 5% during a refrigerated storage period of 144 h at 5 °C.

Microorganism	Storage time (h)	OB	OB + MND	OB + FM	OB + FM + MND
<i>E. coli</i> O157:H7	0	0	0	0	0
	24	-0.10 ± 0.00	-0.92 ± 0.05	-0.91 ± 0.05	-1.75 ± 0.12
	48	-0.15 ± 0.04	-0.96 ± 0.04	-0.96 ± 0.07	-1.92 ± 0.06
	96	-0.72 ± 0.06	-1.12 ± 0.08	-1.06 ± 0.05	-1.73 ± 0.06
	144	-0.83 ± 0.06	-2.01 ± 0.13	-1.57 ± 0.07	-2.22 ± 0.23
<i>S. Typhimurium</i>	0	0	0	0	0
	24	-0.10 ± 0.00	-0.77 ± 0.03	-0.59 ± 0.02	-1.20 ± 0.11
	48	-0.15 ± 0.02	-0.94 ± 0.02	-0.64 ± 0.05	-1.32 ± 0.07
	96	-0.48 ± 0.01	-0.98 ± 0.05	-0.85 ± 0.05	-1.54 ± 0.06
	144	-0.65 ± 0.06	-1.12 ± 0.08	-1.17 ± 0.06	-1.85 ± 0.10

OB: Oat beverage; OB + MND: Oat beverage supplemented with 5% (w/v) mandarin; OB + FM: Oat beverage and fruit juice (papaya, mango, and orange) mixture; OB + FM + MND: Oat beverage and fruit juice mixture supplemented with 5% (w/v) mandarin.

**Table 8**

Weibull kinetic parameters of *E. coli* O157:H7 and *S. Typhimurium* inactivation in Oat beverage and Oat beverage – fruit juice mixture when supplemented/not supplemented with 5% (w/v) mandarin by-product under refrigerated storage (144 h, 5 °C).

Beverage		OB	OB + MND	OB + FM	OB + FM + MND
<i>S. Typhimurium</i>	b	0.014 ± 0.003	0.461 ± 0.015	0.137 ± 0.002	0.571 ± 0.006
	n	0.746 ± 0.012	0.179 ± 0.022	0.419 ± 0.025	0.219 ± 0.011
	Adj-R <sup>2</sup>	0.903	0.968	0.962	0.983
	RMSE	0.071	0.051	0.055	0.002
<i>E. coli</i> O157:H7	b	0.018 ± 0.003	0.121 ± 0.011	0.261 ± 0.001	0.802 ± 0.026
	n	0.767 ± 0.025	0.541 ± 0.023	0.325 ± 0.031	0.221 ± 0.021
	Adj-R <sup>2</sup>	0.946	0.887	0.915	0.993
	RMSE	0.091	0.062	0.022	0.001

OB: Oat beverage; OB + MND: Oat beverage supplemented with 5% (w/v) mandarin; OB + FM: Oat beverage and fruit juice (papaya, mango, and orange) mixture; OB + FM + MND: Oat beverage and fruit juice mixture supplemented with 5% (w/v) mandarin.

the microorganisms studied. Also, the acid pH of the beverage (pH 4.6) might contribute to the antimicrobial effect shown when the fruit juice mixture was added. The supplementation of OB + FM with 5% (w/v) MND increased the final *S. Typhimurium* inactivation level to a maximum of 1.85  $\log_{10}$  cycles compared with the 1.12  $\log_{10}$  cycles achieved in OB + MND, and it increased the maximum *E. coli* O157:H7 inactivation level to 2.22  $\log_{10}$  cycles compared with the 2.01  $\log_{10}$  cycles achieved in OB + MND.

### 3.6. Mathematical modeling of antimicrobial effect of mandarin by-product addition in an oat-based beverage

The results obtained for microbial inactivation in the oat-based beverage and oat-based beverage with fruit juice mixture, both supplemented/not supplemented with mandarin by-product addition, were fitted to a Weibull distribution function and their kinetic parameters were obtained. The *b* and *n* values obtained are shown in Table 8. In all cases the *n* values are below 0, indicating a concave survival pattern for the microorganisms studied in the beverage. With regard to the scale factor, the *b* values in the fruit juice mixture were higher than those obtained in the oat beverage, indicating the influence of the juice mixture on the microbial inactivation response. The addition of mandarin increased inactivation rates in both OB and OB + FM, with a maximum of  $0.571 \pm 0.006$  for *S. Typhimurium* inactivation and  $0.802 \pm 0.026$  for *E. coli* O157:H7 inactivation in OB + FM supplemented with mandarin by-product.

## 4. Conclusions

In conclusion, the three citrus by-products under study showed an antimicrobial effect against *S. Typhimurium*. The maximum reduction level was achieved by the mandarin by-product, followed by the orange and lemon by-products.

The same order can be observed in their polyphenol content, so there may be a relationship between the polyphenol content of the citrus by-products and their antimicrobial activity.

Also, the mandarin by-product was able to exert an antimicrobial effect both on a reference medium (8  $\log_{10}$  cycles for *S. Typhimurium* and 1.6  $\log_{10}$  cycles for *E. coli* O157:H7) and on a real food matrix, an oat-based beverage supplemented/not supplemented with a fruit juice mixture ( $\approx 2 \log_{10}$  cycle reductions for *S. Typhimurium* and *E. coli* O157:H7). Therefore this by-product could be used as an ingredient for technological purposes owing to its potential to act as an additional control measure inhibiting bacterial proliferation, e.g., in pasteurized foods, which have limited refrigerated storage.

## Acknowledgments

M. Sanz-Puig is grateful to the CSIC for providing a contract as a researcher working actively on the projects with reference IPT-2011-1724-060000 and AGL 2013-48993-C2-2-R, funded by the Ministry of Economy and Competitiveness and with FEDER funds. M.C. Pina-Pérez is grateful to the CSIC for providing a doctoral contract. We are also grateful to INDULLEIDA, S.A. company that has provided to us the by-products which we have worked with.

## References

- Aycicek, H., Oguz, U., & Karci, K. (2006). Determination of total aerobic and indicator bacteria on some raw eaten vegetables from wholesalers in Ankara, Turkey. *International Journal of Hygiene and Environmental Health*, 209, 197–201.
- Bajpai, V. K., Baek, K. H., & Kang, S. Ch (2012). Control of Salmonella in foods by using essential oils: a review. *Food Research International*, 45(2), 722–734.
- Bär, W., Bäder-Schumann, U., Krebs, A., & Cromme, L. (2009). Rapid method for detection of minimal bactericidal concentration of antibiotics. *Journal of Microbiological Methods*, 77(1), 85–89.
- Daglia, M. (2011). Polyphenols as antimicrobial agents. *Current Opinion in Biotechnology*, 23(2), 174–181.
- De Oliveira, T. L. C., Soares, R. A., & Piccoli, R. H. (2011). A Weibull model to describe

- antimicrobial kinetics of oregano and lemongrass essential oils against *Salmonella* Enteritidis in ground beef during refrigerated storage. *Meat Science*, 93, 3645–3651.
- Devi, K. P., Suganthi, N., Kesika, P., & Pandian, S. K. (2008). Bioprotective properties of seaweeds: in vitro evaluation of antioxidant activity and antimicrobial activity against food borne bacteria in relation to polyphenolic content. *BMC Complementary and Alternative Medicine*, 8, 38.
- Di Pascua, R., Hoskins, N., Betts, G., & Mauriello, G. (2006). Changes in membrane fatty acids composition of microbial cells induced by addiction of thymol, carvacrol, limonene, cinnamaldehyde, and eugenol in the growing media. *Journal of Agricultural and Food Chemistry*, 54(7), 2745–2749.
- Djilas, S. (2009). By-products of fruits processing as a source of phytochemicals. *Chemical Industry & Chemical Engineering Quarterly*, 15(4), 191–202.
- EUROSTAT data. (2010). *Preparatory study on food waste across EU 27 October 2010*. European Commission (DG ENV). Available at: [http://ec.europa.eu/environment/eusssd/pdf/bio\\_foodwaste\\_report.pdf](http://ec.europa.eu/environment/eusssd/pdf/bio_foodwaste_report.pdf).
- Ghafar, M. F. A., Prasad, K. N., Weng, K. K., & Ismail, A. (2010). Flavonoid, hesperidine, total phenolic contents and antioxidant activities from Citrus species. *African Journal of Biotechnology*, 9(3), 326–330.
- Ghasemi, K., Ghasemi, Y., & Ebrahimpzadeh, M. A. (2009). Antioxidant activity, phenol and flavonoid contents of 13 citrus species peels and tissues. *Pakistan Journal of Pharmaceutical Sciences*, 22(3), 277–281.
- Guillier, L., Nazer, A. I., & Dubois-Brissonnet, F. (2007). Growth response of *Salmonella typhimurium* in the presence of natural and synthetic antimicrobials: estimation of MICs from three different models. *Journal of Food Protection*, 70(10), 2243–2250.
- Gutierrez, J., Barry-Ryan, C., & Bourke, P. (2008). The antimicrobial efficacy of plant essential oil combinations and interactions with food ingredients. *International Journal of Food Microbiology*, 124(1), 91–97.
- López, C. P. (2004). *Técnicas de Análisis Multivariante de Datos. Aplicaciones con el SPSS*. ISBN: 84-205-4104-4.
- Mandalari, G., Bennett, R. N., Bisignano, G., Trombetta, D., Saija, A., Faulds, C. B., et al. (2007). Antimicrobial activity of flavonoids extracted from bergamot (*Citrus bergamia* Risso) peel, a byproduct of the essential oil industry. *Journal of Applied Microbiology*, 103, 2056–2064.
- Martín-Luengo, M. A., Yates, M., Diaz, M., Saez Rojo, E., & Gonzalez Gil, L. (2011). Renewable fine chemicals from rice and citric subproducts: ecomaterials. *Applied Catalysis B: Environmental*, 106, 488–493.
- Okada, Y., Ohnoku, I., Suzuki, H., & Igimi, S. (2013). Growth of *Listeria monocytogenes* in refrigerated ready-to-eat foods in Japan. *Food Additives & Contaminants: Part A*, 30(8), 1446–1449.
- O'Shea, N., Arendt, E. K., & Gallagher, E. (2012). Dietary fibre and phytochemical characteristics of fruit and vegetable by-products and their recent applications as novel ingredients in food products. *Innovative Food Science and Emerging Technologies*, 16, 1–10.
- Peleg, M., & Cole, M. B. (1998). Reinterpretation of microbial survival curves. *Critical Reviews in Food Science and Nutrition*, 38(5).
- Sanz-Puig, M., Pina-Pérez, M. C., Rodrigo, D., & Martínez-López, A. (2015). Antimicrobial activity of cauliflower (*Brassica oleracea* var. *Botrytis*) by-product against *Listeria monocytogenes*. *Food Control*, 50, 435–440.
- Schieber, A., Stintzing, F. C., & Carle, R. (2001). By-products of plant food processing as a source of functional compounds – recent developments. *Trends in Food Science & Technology*, 12, 401–413.
- Shapiro, R. S., & Cowen, L. E. (2012). Thermal control of microbial development and virulence: molecular mechanisms of microbial temperature sensing. *mBIO*, 3(5).
- Singleton, V. L., & Rossi, J. A. (1965). Colorimetry of total phenolics with phosphomolybdic-phosphotungstic acid reagents. *American Journal of Enology and Viticulture*, 16(3), 144–158.
- Taguri, T., Tanaka, T., & Koumo, I. (2004). Antimicrobial activity of 10 different plant polyphenols against bacteria causing food-borne disease. *Biological and Pharmaceutical Bulletin*, 27(12), 1965–1969.
- Tomás-Barberán, F. A., & Espín, J. C. (2001). Phenolic compounds and related enzymes as determinants of quality in fruits and vegetables. *Journal of the Science of Food and Agriculture*, 81(9), 853–876.
- Valero, M., & Giner, M. J. (2006). Effects of antimicrobial components of essential oils on growth of *Bacillus cereus* INRA L2104 in and the sensory qualities of carrot broth. *International Journal of Food Microbiology*, 106(1), 90–94.



# Mycelial biomass and intracellular polysaccharides yield of edible mushroom *Agaricus blazei* produced in wheat extract medium



Fei-Hong Zhai, Jian-Rong Han\*

School of Life Science, Shanxi University, Taiyuan, 030006, China

## ARTICLE INFO

### Article history:

Received 20 June 2015

Received in revised form

26 August 2015

Accepted 2 October 2015

Available online 8 October 2015

### Keywords:

*Agaricus blazei*

Intracellular polysaccharides

Mycelial biomass

Wheat extract medium

## ABSTRACT

The aim of this work was to evaluate the potential of wheat extract as basal medium for the submerged fermentation of *Agaricus blazei* Murrill (ABM) and optimize the medium and fermentation conditions to obtain maximal mycelial biomass and intracellular polysaccharides (IPS) yield of this fungus. In the basal medium, the mycelial biomass and IPS yield of ABM was respectively 2.01 g/L and 93.42 mg/L. Supplementation of peptone and maltose to the basal medium caused a significant increase in either mycelial biomass or IPS yield as compared with control ( $P < 0.05$ ). Through response surface methodology, the optimum wheat extract medium for the submerged fermentation of ABM was the following: 1000 mL wheat extract, 3.44 g peptone, 43.00 g maltose, 1.00 g  $\text{KH}_2\text{PO}_4$  and 0.50 g  $\text{MgSO}_4$ . Through orthogonal experiments, the optimum fermentation conditions were the following: inoculation volume of 10% (v/v), medium volume of 70 mL per flask and rotation speed of 170 rpm. By the optimization of medium and fermentation conditions, the mycelial biomass and IPS yield of ABM reached their maximum values of 16.02 g/L and 1041.32 mg/L, respectively.

© 2015 Elsevier Ltd. All rights reserved.

## 1. Introduction

*Agaricus blazei* Murrill (ABM) has been traditionally used as medicine (Mizuno, 1995). It is particularly rich in polysaccharides and has shown positive effects in preventing and treating cancer (Ebina & Fujiyama, 1998). Its polysaccharides have stronger anti-tumor activity against sarcoma 180 in mice than other edible-medicinal fungus, such as *Ganoderma lucidum*, *Lentinus edodes*, and *Coriolus versicolor* (Zou, 2005). Moreover, many reports indicated that there were available antioxidant properties in the fruit bodies of ABM (Izawa & Inoue, 2004; Soares et al., 2009; Tsai, Tsai, & Mau, 2007). Further functions include liver protection, antigenotoxicity and antidiabetes and so on (Barbisan et al., 2002; Su, Hwang, Kuo, Shu, & Sheen, 2008).

The most common utilization of ABM was cultivating it on solid substrates and collecting the fruit bodies, which could be used for direct consumption or as medicines indirectly. The fruit bodies of ABM are relatively expensive due to the low yields. The utilization of many edible and medicinal mushrooms is limited because it is difficult to cultivate their fruit bodies. Production of mushrooms in

submerged cultures has recently become attractive. There are some reports indicated that the fermentation products of ABM also have immunomodulation, antitumor, antioxidation and antivirus effects like the fruit bodies (Ker et al., 2005; Sorimachi et al., 2001; Su et al., 2008). The protein and polysaccharides contents in ABM mycelia were equal to or even higher than that of fruit bodies. The mycelia could also be used to extract some functional components. Compared with the cultivation of fruit bodies, submerged fermentation of edible and medicinal mushrooms has some advantages, such as short fermentation time, easy controllability and lesser chances of contamination (Shih, Pan, & Hsieh, 2006). So submerged fermentation is a good choice to produce the mycelia and extract beneficial substances of edible mushrooms.

Some reports indicated that the components of medium, especially nitrogen and carbon sources, had significant effects on the mycelial biomass and polysaccharides yield of *Pleurotus ostreatus* or *A. blazei* (Camelini et al., 2013; Gern, Wisbeck, Rampinelli, Ninow, & Furlan, 2008; Hamed, Ghanati, & Vahidi, 2012). Kossen (2000) reported that the morphological characteristics of mycelium pellet of filamentous fungi would be influenced by fermentation medium, inoculum volume and so on. Besides, the submerged fermentation conditions, such as medium volume and rotation speed, could also influence the metabolism and growth of mycelia. However, the effects of wheat extract medium on mycelial biomass

\* Corresponding author.

E-mail address: [hjr@sxu.edu.cn](mailto:hjr@sxu.edu.cn) (J.-R. Han).

and intracellular polysaccharides (IPS) yield of ABM have not been reported.

In China, large amounts of wheat extract are produced in the process of preparing wheat spawn as inoculum for the cultivation of mushrooms, and generally, these wheat extract is considered to be useless residue and discarded, which is a waste of this resource. The wheat extract could be the basal medium for the submerged fermentation of ABM. In the present study, the potential of wheat extract as the basal medium for the submerged fermentation of ABM was assessed. Further, the wheat extract medium and fermentation conditions were optimized to obtain the maximal mycelial biomass and IPS yield of ABM.

## 2. Materials and methods

### 2.1. Microorganisms and media

*A. blazei* Murrill SH26 was obtained from the Institute of Edible Fungi, Shanghai Academy of Agricultural Science, China, and routinely maintained on potato dextrose agar (PDA) slants.

The basal medium for the submerged fermentation of ABM consisted of 1000 mL wheat extract, 1 g  $\text{KH}_2\text{PO}_4$  and 0.5 g  $\text{MgSO}_4$ . The wheat extract was obtained by cooking 200 g wheat for 20 min in 1 L of distilled water; filter, bring volume to 1 L. The initial pH of the medium was adjusted to 6.5. The saccharides and nitrogen sources being added to the basal medium were described in the text (Table 1 and Table 2). Then 50 mL of medium was dispensed into each Erlenmeyer flask of 250 mL capacity.

### 2.2. Submerged fermentation

In this experiment, the mycelial pellet suspension was used as inoculum. It was obtained by culturing mycelium in 250 mL shaken flasks containing 50 mL basal medium (25 °C, 150 rpm, 7 days) inoculated with five discs of mycelium and agar, 10 mm in diameter, from agar plate cultures of this fungus on PDA medium. After sterilization, each flask was inoculated with the inoculum (5%, v/v) and incubated at 25 °C in a rotatory shaker at 150 rpm for 10 days.

### 2.3. Determination of mycelial biomass and IPS yield

The mycelial pellets were collected by centrifuging the fermentation broth at 8000 rpm for 10 min and washing the precipitate three times with distilled water, then drying at 60 °C to constant weight to determine their biomass.

The dried mycelial pellets were ground at 4 °C, and extracted three times with distilled water at 100 °C for 4.5 h. The filtrate was collected after the mixture was centrifuged at 5000 rpm for 10 min and treated with cooled ethanol (8 °C) at a volume ratio of 1:4 (sample: ethanol). After six hours under refrigeration (4 °C), the

**Table 1**

Effects of supplementary saccharides and nitrogen sources in wheat extract medium on mycelial biomass and IPS yield of *Agaricus blazei* Murrill.

Adjuvant	Mycelial biomass (g/L)	IPS yield (mg/L)
Control	2.01 ± 0.18 <sup>a</sup>	93.42 ± 8.12 <sup>a</sup>
Peptone	3.02 ± 0.27 <sup>d</sup>	152.21 ± 13.21 <sup>e</sup>
Yeast extract	2.96 ± 0.26 <sup>d</sup>	148.71 ± 11.56 <sup>de</sup>
( $\text{NH}_4$ ) <sub>2</sub> SO <sub>4</sub>	2.42 ± 0.22 <sup>b</sup>	113.43 ± 10.33 <sup>b</sup>
Glucose	2.77 ± 0.25 <sup>c</sup>	142.12 ± 12.45 <sup>d</sup>
Sucrose	2.54 ± 0.23 <sup>b</sup>	129.27 ± 10.32 <sup>c</sup>
Maltose	3.06 ± 0.29 <sup>d</sup>	162.31 ± 14.87 <sup>f</sup>

Data represent means ± standard deviation (n = 5).

Values in the same column with different superscripts are significantly different (P < 0.05).

**Table 2**

Effects of peptone and maltose concentrations in wheat extract medium on mycelial biomass and IPS yield of *Agaricus blazei* Murrill.

Adjuvant	Concentration (g/L)	Mycelial biomass (g/L)	IPS yield (mg/L)
Peptone	1.0	3.11 ± 0.29 <sup>a</sup>	156.22 ± 13.33 <sup>a</sup>
	2.0	3.94 ± 0.31 <sup>b</sup>	201.31 ± 18.21 <sup>b</sup>
	3.0	4.21 ± 0.36 <sup>c</sup>	216.72 ± 20.01 <sup>c</sup>
	4.0	4.24 ± 0.41 <sup>c</sup>	219.33 ± 17.98 <sup>c</sup>
	5.0	4.31 ± 0.39 <sup>c</sup>	218.72 ± 18.66 <sup>c</sup>
Maltose	10	2.51 ± 0.22 <sup>a</sup>	101.81 ± 9.63 <sup>a</sup>
	20	3.11 ± 0.27 <sup>b</sup>	160.33 ± 14.43 <sup>b</sup>
	30	3.97 ± 0.33 <sup>c</sup>	192.83 ± 17.66 <sup>c</sup>
	40	4.44 ± 0.36 <sup>d</sup>	203.12 ± 18.54 <sup>d</sup>
	50	4.52 ± 0.41 <sup>d</sup>	206.76 ± 19.43 <sup>d</sup>

Data represent means ± standard deviation (n = 5).

Values in the same column with different superscripts are significantly different (P < 0.05).

water-ethanol mixture was centrifuged at 5000 rpm for 10 min. By dissolving the precipitation with distilled water, the IPS solution was obtained (Wang, Wang, & Han, 2013). The IPS content was determined by the phenol-sulfuric acid method (Hsieh, Hsu, & Yang, 2005).

### 2.4. Optimization of wheat extract medium

In order to further optimize the wheat extract medium, response surface methodology (RSM) using Central Composite design experiment was applied to identify the concentrations of supplemented saccharide and nitrogen source in the basal medium. The RSM was designed based on the results of single factor experiments (Tables 1 and 2) using Minitab software (version 15, USA). Finally, the ultimate optimal medium components amounts were computed using the Minitab Response Surface Optimizer function, which enabled us to distinguish the best combination of each constituent. The designed matrix for the two independent variables is exhibited in Table 3. For forecasting the optimal point, a second order polynomial function was fitted to correlate the relationship between the mycelial biomass and medium components (nitrogen source and saccharide) amounts. The equation is:

$$Y = \beta_0 + \beta_1 X_1 + \beta_2 X_2 + \beta_{11} X_1^2 + \beta_{22} X_2^2 + \beta_{12} X_1 X_2.$$

Where Y is the predicted response variable,  $\beta_0$  is the model constant,  $\beta_1$  and  $\beta_2$  are linear coefficients,  $\beta_{11}$  and  $\beta_{22}$  are quadratic coefficients,  $\beta_{12}$  is the cross product coefficient,  $X_1$  and  $X_2$  are independent variables,  $X_1 X_2$  is the interaction term  $X_1$  with  $X_2$ . The

**Table 3**

Central Composite design matrix and the response of mycelial biomass of *Agaricus blazei* Murrill.

Trials	$X_1$ (g/L)	$X_2$ (g/L)	Mycelial biomass (g/L)	
			Measured	Predicted
1	-1 (2)	-1 (30)	8.22	7.9916
2	1 (4)	-1 (30)	10.21	10.1786
3	-1 (2)	1 (50)	8.73	8.7739
4	1 (4)	1 (50)	10.93	11.1709
5	-1.4142 (1.60)	0 (40)	7.27	7.4031
6	1.41421 (4.41)	0 (40)	10.79	10.6444
7	0 (3)	-1.4142 (25.86)	9.22	9.4063
8	0 (3)	1.41421 (54.14)	10.86	10.6612
9	0 (3)	0 (40)	11.74	11.6260
10	0 (3)	0 (40)	11.62	11.6260
11	0 (3)	0 (40)	11.47	11.6260
12	0 (3)	0 (40)	11.53	11.6260
13	0 (3)	0 (40)	11.77	11.6260

**Table 4**  
Statistical analysis of the Central Composite design.

Variable	Coefficient	SE-coefficient	T value	p value
Constant	11.6260	0.12379	99.919	0.000
X <sub>1</sub>	1.0960	0.09786	15.828	0.000
X <sub>2</sub>	0.3937	0.09786	6.128	0.005
X <sub>1</sub> <sup>2</sup>	-1.2761	0.10495	-16.757	0.000
X <sub>2</sub> <sup>2</sup>	-0.7711	0.10495	-10.253	0.000
X <sub>1</sub> X <sub>2</sub>	0.1525	0.13840	0.513	0.307

quality of fit of the equation was presented by the coefficient of determination  $R^2$ . The obtained data from the experiment were analyzed by linear multiple regression using Minitab 15 and presented in Table 4. The analysis of ANOVA for the fitted quadratic polynomial model was listed in Table 5.

### 2.5. Optimization of fermentation conditions

The optimum fermentation conditions were studied through an orthogonal experimental design, where the inoculation volume, medium volume and rotation speed were changed from 5 to 15% (v/v), 50–70 mL per flask, and 150–170 rpm (Table 6). The variance analysis of orthogonal experiment was listed in Table 7.

### 2.6. Experimentation and analysis

All the experiments were replicated in five flasks and the data are presented as the mean and standard error of five independent experiments. Duncan's multiple range test (Du, 1985) was used to determine the significant differences among mean values at the  $P < 0.05$  level. Analysis of variance of the orthogonal experimental results was carried out using the Statistical Analysis System software (SAS version 9.00, SAS Institute, Inc., 2000), the sources of variance being inoculation volume, medium volume and rotation speed.

## 3. Results

### 3.1. Effects of supplementary saccharides and nitrogen sources on mycelial biomass and IPS yield

Due to the nitrogen and carbon deficiency, addition of nitrogen and carbon sources to the basal medium was required for increasing the mycelial biomass and IPS yield. We examined the effects of supplementary saccharides and nitrogen sources on mycelial biomass and IPS yield (Table 1). In this experiment, the basal medium served as control. Among three kinds of nitrogen sources, peptone gave the highest IPS yield (152.21 mg/L) and mycelial biomass (3.02 g/L) respectively, followed by yeast extract. Among three kinds of saccharides, maltose gave the highest IPS yield (162.31 mg/L) and mycelial biomass (3.06 g/L) respectively, followed by glucose. Table 2 showed that addition of 3.0 g/L

peptone to the basal medium was sufficient to cause a significant increase ( $P < 0.05$ ) in either mycelial biomass or IPS yield as compared with control. Similarly, supplementation of 40 g/L maltose to the basal medium caused a significant increase in either mycelial biomass or IPS yield ( $P < 0.05$ ).

### 3.2. Optimization of wheat extract medium using RSM

The Central Composite design and the corresponding data were listed in Table 3. The statistical analysis of the Central Composite design was listed in Table 4. After the regression analysis, the second-order response model was founded. The polynomial model for mycelial biomass ( $Y_{biomass}$ ) was expressed by Eq. (1).

$$Y_{biomass} = 11.63 + 1.10X_1 + 0.40X_2 - 1.28X_1^2 - 0.77X_2^2 + 0.15X_1X_2 \quad (1)$$

Where  $Y$  is the predicted response and  $X_1, X_2$  are the coded values of the concentration of peptone and maltose. As illustrated in Table 5, relatively high  $F$  value and very low  $p$  value indicated that the experimental model was in excellent conformity with the experiment for the response. Data in Table 5 show low value of  $F$  test and high  $p$  value ( $P > 0.01$ ) for lack of fit, which was non-significant indicating that the model is fit. The linear regression coefficient  $R^2$  of mycelial biomass was 97.89%, and the adjusted determination coefficient  $R_{adj}^2$  was 96.38%, which showed accuracy of the model for the Central Composite design. The regression analysis showed that both peptone ( $x_1$ ) and maltose ( $x_2$ ) concentrations in the basal medium had significant effects on mycelial biomass, and the effect of peptone concentration was more significant than maltose concentration. Moreover, the positive coefficient of  $x_1$  and  $x_2$  indicated a linear effect to increase  $Y_{biomass}$ . Quadratic terms ( $X_1^2$  and  $X_2^2$ ) had negative effects to  $Y_{biomass}$  and interactive term ( $X_1X_2$ ) didn't have a significant influence ( $P > 0.05$ ) on response.

Three-dimensional response surface plot (Fig. 1a) and 2D contour plot (Fig. 1b) to graphically represent regression equations are generally used to demonstrate the relative effect of peptone and maltose. Fig. 1a and b showed that the growth of ABM was sensitive even when peptone and maltose concentrations were subject to small alteration. An increase in mycelial biomass could be significantly achieved with the increases of peptone and maltose concentrations.

The final optimum concentrations of peptone and maltose were calculated by means of Minitab Response Surface Optimizer function. Optimized values of the two factors were found to be: peptone 3.4428 g/L, maltose 42.9998 g/L. And this model forecasted a maximum mycelial biomass of 11.9468 g/L.

In the verification experiment, the peptone and maltose concentrations in the medium were respectively set as 3.44 g/L and 43.00 g/L. Under this condition, the mycelial biomass of ABM was 11.88 g/L, which were very close to the predicted values, suggesting

**Table 5**  
Analysis of ANOVA for the fitted quadratic polynomial model.

Source	Degree of freedom	Sum of squares	Mean of squares	F value	p value
Regression	5	24.8588	4.97176	64.89	0.000
Linear	2	10.8496	5.42478	70.80	0.000
Square	2	13.9162	6.95810	90.82	0.000
Interaction	1	0.0930	0.09302	1.21	0.307
Residual error	7	0.5363	0.07662		
Lack-of-fit	3	0.4690	0.15633	9.29	0.028
Pure error	4	0.0673	0.01683		
Total	12	25.3951			

**Table 6**  
Results of orthogonal experiment to assess optimal submerged fermentation conditions for *Agaricus blazei* Murrill.

Experimental no.	Inoculation volume (v/v, %)	Medium volume (mL)	Rotation speed (rpm)	Mycelial biomass (g/L)
1	5	50	150	11.32
2	5	60	160	12.33
3	5	70	170	12.46
4	10	50	160	13.07
5	10	60	170	15.76
6	10	70	150	14.43
7	15	50	170	10.66
8	15	60	150	10.98
9	15	70	160	12.93

that the model about mycelial biomass were adoptable. And in this medium, the IPS yield reached 782.46 mg/L.

### 3.3. Optimization of submerged fermentation conditions

In order to make good use of the wheat extract medium, the submerged fermentation conditions were optimized. The preliminary study indicated that the inoculation volume, medium volume and rotation speed had significant influences on the mycelial biomass of ABM (data not shown). So, the three factors were chosen to carry out the orthogonal experiments to optimize the fermentation conditions according to the mycelial biomass. The orthogonal experiment results (Table 6) indicated that the theoretical optimum fermentation conditions were the following: inoculation volume of 10%, medium volume of 70 mL per flask and rotation speed of 170 rpm. A verification experiment was carried out and the results showed that under the optimum conditions, the mycelial biomass of ABM was 16.02 g/L, which was 6.97 times higher than that of control. The IPS yield was also determined under the optimum conditions, reached 1041.32 mg/L, which was 10.14 times higher than that of control. The results of variance analysis (Table 7) showed that the factor inoculation volume had a more significant impact on the mycelial biomass than other two factors.

## 4. Discussion

It had been reported that the mycelial biomass of *Agaricus bisporus* in ram horn hydrolysate was about 10.8 g/L (Kurbanoglu, Algur, & Zulkadir, 2004), and the maximum mycelial biomass of ABM in an optimized medium consisted of glucose, yeast extract and peptone was 13.91 g/L (Liu & Wang, 2007). In our experiment, the highest mycelial biomass was 16.02 g/L. The results suggest that wheat extract has the potential to produce ABM mycelia. Cost effective production of ABM mycelia depends on the reliability, availability and cost of medium ingredients. Based on yield and cost, it appears that wheat extract is an economically viable alternative. Development of alternative media with higher mycelial biomass capacity would lower the production cost of ABM mycelia. The question arose whether the use of grains other than wheat (such as corn, rice, sorghum, millet and broomcorn millet), would result in higher mycelial biomass than wheat extract. So, the

**Table 7**  
Variance analysis of orthogonal experiment.

Variation source	Degree of freedom	Sum of squares	F value	$F_{0.05}$	$F_{0.01}$
Inoculation volume	2	14.3345	7.2838	19	99
Medium volume	2	4.3862	2.2288		
Rotation speed	2	0.8317	0.4226		
Error	2	1.9680			
Sum	8				

importance of further studies on more cereals extracts to increase the mycelial biomass of ABM can readily be seen.

Shih et al. (2006) reported that the IPS yield of *Antrodia cinnamomea* would decline when prolonged the fermentation time. The probable cause of this situation was the secretion of polysaccharide degrading enzymes. Liu et al. (2010) reported that the extraction conditions, such as ultrasonic treating time, extraction temperature, extraction time and ethanol concentration, would influence the extraction rate of *Pleurotus* sp. IPS. In our pre-experiments, the mycelial biomass of ABM could reach the highest after fermentation of 10 days. So, in this experiment, the fermentation time of ABM was set as 10 days. Perhaps a further research on the effects of different fermentation time on IPS yield of ABM should be conducted.

The nutritional values and taste components of ABM mycelia have been studied (Ker et al., 2005). In addition to their nutritional value, ABM mycelia are of high gastronomic value (Su et al., 2008).

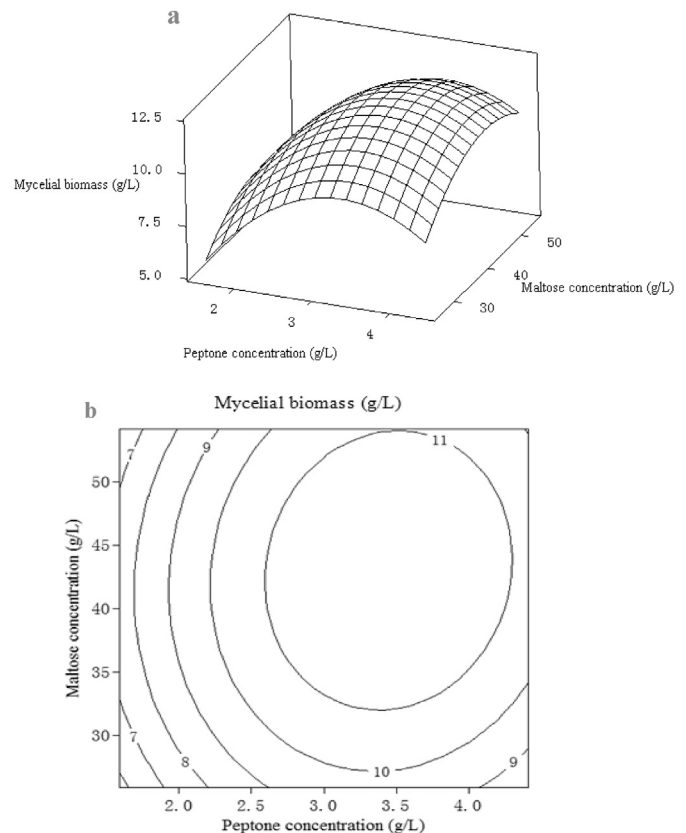


**Fig. 1.** Response surface plot (a) and 2D contour plot (b) of the combined effects of peptone and maltose concentrations in wheat extract medium on mycelial biomass of *Agaricus blazei* Murrill.

In this experiment, the IPS of mycelia was a physiologically active substance. Certainly, the possibility that the mycelia of ABM contain some physiologically active substances besides the polysaccharides cannot be ruled out. This implied that mycelia of ABM could be processed into many special functional foods containing some bioactive substances. Functional foods as a marketing term was initiated in the 1980s and was used to describe foods fortified with ingredients capable of producing health benefits. This concept is becoming increasingly popular with consumers because of a heightened awareness of the link between health, nutrition, and diet. Food manufacturers are enthusiastic about developing such products because the added ingredients give increased value to food (Hilliam, 1998). In this case, all bioactive components present in the mycelia should be assayed. The importance of further studies on submerged fermentation of ABM in wheat extract or other cereals extracts can readily be seen. The submerged fermentation of ABM is still far from being thoroughly studied.

## 5. Conclusions

This study was the first to evaluate the potential of wheat extract as the basal medium for the submerged fermentation of ABM. The following conclusions could be drawn: 1) the wheat extract can be used to produce mycelia of ABM; 2) through response surface methodology, the optimum wheat extract medium for the submerged fermentation of ABM was obtained. In the optimized medium, the mycelial biomass and IPS yield were respectively 4.91 times and 7.38 times higher than control; 3) through orthogonal experiments, the optimum fermentation conditions were the following: inoculation volume of 10% (v/v), medium volume of 70 mL per flask and rotation speed of 170 rpm; 4) by the optimization of medium and fermentation conditions, the mycelial biomass and IPS yield of ABM reached their maximum values of 16.02 g/L and 1041.32 mg/L, respectively, which were 6.97 and 10.14 times higher than control.

## Acknowledgments

Support for this research by the Shanxi Province Coal Fund (Grant No.FT2014–03) is gratefully acknowledged.

## References

- Barbisan, L. F., Miyamoto, M., Scolastici, C., Salvadori, D. M., Ribeiro, L. R., Eira, A. F., et al. (2002). Influence of aqueous extract of *Agaricus blazei* on rat liver toxicity induced by different doses of diethylnitrosamine. *Journal of Ethnopharmacology*, 83, 25–32.
- Camelini, C. M., Gomes, A., Cardozo, F. T. G. S., Simões, C. M. O., Rossi, M. J., Giachini, A. J., et al. (2013). Production of polysaccharide from *Agaricus subrufescens* Peck on solid-state fermentation. *Applied Microbiology and Biotechnology*, 97, 123–133.
- Du, R. J. (1985). *Biological statistics*. Beijing: Higher Education Press.
- Ebina, T., & Fujiyama, Y. (1998). Antitumor effect of a peptide-glucan preparation extracted from *Agaricus blazei* in a double grafted tumor system in mice. *Biotherapy*, 11, 259–265.
- Gern, R. M. M., Wisbeck, E., Rampinelli, J. R., Ninow, J. L., & Furlan, S. A. (2008). Alternative medium for production of *Pleurotus ostreatus* biomass and potential antitumor polysaccharides. *Bioresource Technology*, 99, 76–82.
- Hamed, A., Ghanati, F., & Vahidi, H. (2012). Study on the effects of different culture conditions on the morphology of *Agaricus blazei* and the relationship between morphology and biomass or EPS production. *Annals of Microbiology*, 62, 699–707.
- Hilliam, M. (1998). The market for functional foods. *International Dairy Journal*, 8, 349–353.
- Hsieh, C. Y., Hsu, T. H., & Yang, F. C. (2005). Production of polysaccharides of *Ganoderma lucidum* (CCRC36021) by reusing thin stillage. *Process Biochemistry*, 40, 909–916.
- Izawa, S., & Inoue, Y. (2004). A screening system for antioxidants using thioredoxin-deficient yeast: discovery of thermostable antioxidant activity from *Agaricus blazei* Murill. *Applied Microbiology and Biotechnology*, 64, 537–542.
- Ker, Y. B., Chen, K. C., Chyau, C. C., Chen, C. C., Guo, J. H., Hsieh, C. L., et al. (2005). Antioxidant capability of polysaccharides fractionated from submerged-cultured *Agaricus blazei* mycelia. *Journal of Agricultural and Food Chemistry*, 53, 7052–7058.
- Kossen, N. W. F. (2000). The morphology of filamentous fungi. *Advances in Biochemical Engineering/Biotechnology*, 70, 1–33.
- Kurbanoglu, E. B., Algur, O. F., & Zulkadir, A. (2004). Submerged production of edible mushroom *Agaricus bisporus* mycelium in ram horn hydrolysate. *Industrial Crops and Products*, 19, 225–230.
- Liu, G. Q., & Wang, X. L. (2007). Optimization of critical medium components using response surface methodology for biomass and extracellular polysaccharides production by *Agaricus blazei*. *Applied Microbiology and Biotechnology*, 74, 78–83.
- Liu, X. N., Zhou, B., Lin, R. S., Jia, L., Deng, P., Fan, K. M., et al. (2010). Extraction and antioxidant activities of intracellular polysaccharide from *Pleurotus* sp. mycelium. *International Journal of Biological Macromolecules*, 42, 116–119.
- Mizuno, T. (1995). Bioactive biomolecules of mushrooms: food, function and medical effect of mushroom fungi. *Food Reviews International*, 11, 7–21.
- Shih, I. L., Pan, K., & Hsieh, C. (2006). Influence of nutritional components and oxygen supply on the mycelial growth and bioactive metabolites production in submerged culture of *Antrodia cinnamomea*. *Process Biochemistry*, 41, 1129–1135.
- Soares, A. A., de Souza, C. G. M., Daniel, F. M., Ferrari, G. P., da Costa, S. M. G., & Peralta, R. M. (2009). Antioxidant activity and total phenolic content of *Agaricus brasiliensis* (*Agaricus blazei* Murril) in two stages of maturity. *Food Chemistry*, 112, 775–781.
- Sorimachi, K., Akimoto, K., Ikehara, Y., Inafuku, K., Okubo, A., & Yamazaki, S. (2001). Secretion of TNF-alpha, IL-8 and nitric oxide by macrophages activated with *Agaricus blazei* Murill fractions in vitro. *Cell Structure and Function*, 26, 103–108.
- Su, Z. Y., Hwang, L. S., Kuo, Y. H., Shu, C. H., & Sheen, L. Y. (2008). Black soybean promotes the formation of active components with antihepatoma activity in the fermentation product of *Agaricus blazei*. *Journal of Agricultural and Food Chemistry*, 56, 9447–9454.
- Tsai, S. Y., Tsai, H. L., & Mau, J. L. (2007). Antioxidant properties of *Agaricus blazei*, *Agrocybe cylindracea*, and *Boletus edulis*. *LWT-Food Science and Technology*, 40, 1392–1402.
- Wang, J. T., Wang, Q., & Han, J. R. (2013). Yield, polysaccharides content and antioxidant properties of the mushroom *Agaricus subrufescens* produced on different substrates based on selected agricultural wastes. *Scientia Horticulturae*, 157, 84–89.
- Zou, X. (2005). Effects of Zn supplementation on the growth, amino acid composition, polysaccharide yields and anti-tumour activity of *Agaricus brasiliensis*. *World Journal of Microbiology and Biotechnology*, 21, 261–264.



## Prevalence, antimicrobial resistance and virulence traits in enterococci from food of animal origin in Turkey



Ebru Şebnem Yılmaz<sup>a</sup>, Özkan Aslantaş<sup>b</sup>, Sevda Pehlivanlar Önen<sup>c</sup>, Süheyla Türkyılmaz<sup>d</sup>, Cemil Kürekci<sup>c,\*</sup>

<sup>a</sup> Department of Biology, Faculty of Art and Science, Mustafa Kemal University, Hatay, Turkey

<sup>b</sup> Department of Microbiology, Faculty of Veterinary Medicine, Mustafa Kemal University, Hatay, Turkey

<sup>c</sup> Department of Food Hygiene and Technology, Faculty of Veterinary Medicine, Mustafa Kemal University, Hatay, Turkey

<sup>d</sup> Department of Microbiology, Faculty of Veterinary Medicine, Adnan Menderes University, Aydın, Turkey

### ARTICLE INFO

#### Article history:

Received 18 June 2015

Received in revised form

18 August 2015

Accepted 2 October 2015

Available online 8 October 2015

#### Keywords:

*Enterococcus* spp.

Multi-drug resistance

Chicken meat

Virulence genes

### ABSTRACT

The objective of this work was to investigate the antibiotic susceptibility, the mechanisms implicated and the potential virulence genes (gelatinase [*gelE*], cytolysins [*cylA*, *cylM*, *cylB*], cell wall adhesins [*efaAfs* and *efaAfm*], enterococcal surface protein [*esp*], sex pheromones [*cpd*, *cob*, *ccf*], enhanced expression of pheromone [*eep*], aggregation substance [*aggA*]) in enterococci isolated from retail chicken and beef meat samples in Hatay, Turkey. Hundred-one (96%) isolates from chicken meat and sixty-three (63%) from minced meat isolates showed resistance to at least one of the 12 antimicrobial agents tested. The highest frequency of resistance was against tetracycline (89.5% and 53%), erythromycin (59% and 2%), ciprofloxacin (35.2% and 12%) and trimethoprim/sulfamethoxazole (34.3% and 7%) for isolates from chicken and beef samples, respectively. The *ermB*, *tetM* and *tetL* genes were predominantly detected by PCR. Five enterococci from chicken meat were found to be phenotypically resistant to vancomycin and carried the *vanA* gene. The presence of virulence genes including *gelE*, *ccf*, *cpd*, *efaAfs*, and *aggA* were frequently detected. The results of this study show that retail chicken and beef meat is source of concern for public health due to having high prevalence of antibiotic resistance and as well as harbouring virulence factors.

© 2015 Elsevier Ltd. All rights reserved.

## 1. Introduction

Enterococci are Gram-positive, facultative anaerobe bacteria that normally widespread in the intestine of animals and humans. In addition, enterococci are present in a variety of fermented meat and dairy products as a starter culture without affecting human health (Foulquié Moreno, Sarantinopoulos, Tsakalidou, & De Vuyst, 2006). Moreover, some enterococci are able to produce bacteriocins called as enterocins which have already been reported to have antimicrobial activity against food spoilage bacteria such as *Listeria monocytogenes* (Ahmadova et al., 2013). Enterococci have, however, been recognised as an emerging cause of nosocomial infections (Leavis, Bonten, & Willems, 2006) including bacteraemia, septicaemia, endocarditis and urinary tract infections (Hidron et al., 2008) which could be life threatening in immunocompetent and severely ill individuals.

Enterococci have an intrinsic antibiotic resistance to semi-synthetic penicillins, aminoglycosides (low level), vancomycin (low level resistant in *E. gallinarum*, *E. casseliflavus*/*E. flavescens*), lincosamides (mostly), polymyxines and streptogramins (*Enterococcus faecalis*) (Klare, Konstabel, Badstübner, Werner, & Witte, 2003). Enterococci can also develop acquired resistance to many other antibiotics by carrying various resistant traits through plasmids, integrons and transposons (Hollenbeck & Rice, 2012). Enterococcal infections have been traditionally treated with glycopeptides antibiotics, mostly vancomycin, since it was approved for human use. However, because of extensive clinical use of vancomycin in hospitals, frequency of vancomycin resistance ( $Va^R$ ) was dramatically increased (Kirst, Thompson, & Nicas, 1998). In addition to this extensive usage in hospitals, using growth promoters in livestock could potentially lead to the development of resistant strains. For example, in 1986, avoparcin, a glycopeptide analog, was approved to use as a growth promoter of food animals in Norway (Borgen et al., 2000). There was evidence to show an association between

\* Corresponding author.

E-mail address: [ckurekci@hotmail.com](mailto:ckurekci@hotmail.com) (C. Kürekci).

injudicious use of this class of antibiotics in food animals and a substantial rise in the prevalence of Va<sup>R</sup> Enterococci (VRE) recovered from farm animals, foods of animal origin including chicken meat, pork, and beef and from infected humans. Resistance was found to be plasmid-borne and could be transferred to other enterococci (Flannagan et al., 2003). These authors suggested that use of avoparcin in livestock allowed for selection and persistence of resistant strains. Because of the increase prevalence of Va<sup>R</sup> in *Enterococcus* isolates, the use of avoparcin as a feed additive in food animals was banned in 1997 in all European Union countries (Borgen et al., 2000).

Besides antibiotic resistance, enterococci are able to produce potential virulence factors that may enhance their pathogenicity, in another word responsible for causing diseases (Biswas, Dey, Adhikari, & Sen, 2014). These include haemolysin, gelatinase, enterococcal surface protein (Esp), aggregation substance, serine protease, capsule, cell wall polysaccharide and superoxide (Elsner et al., 2000). For example, several studies suggest that haemolysin is important for *Enterococcus* infectivity in animals and humans (Chow et al., 1993; Johnson, 1994). Gelatinase has been shown to be an important virulence factor for aiding to endocarditis in an animal model (Thurlow et al., 2010). It has been shown that *E. faecalis* producing Enterococcal surface protein Esp is more persistence in urinary bladder in experimentally infected animals (Shankar et al., 2001). Enterococci from food of animal origin have been shown to produce these abovementioned virulence factors suggesting that these animal products could act as potential reservoirs for human infections.

There is little data about the incidence of microbial resistance of *Enterococcus* strains in foods of animal origin in Turkey. Therefore, monitoring antimicrobial sensitivity is not only necessary for choosing appropriate antimicrobial agents but also important to monitor antimicrobial resistance development. In this view, the aim of the current study was to investigate the prevalence of enterococci in retail meat samples (chicken and beef) and their antimicrobial resistance profile. The detection of virulence genes and antimicrobial resistance genes were also examined.

## 2. Materials and methods

### 2.1. Sample collection, isolation and identification of *Enterococcus* species

A total of 200 samples of chicken (100) and beef (100) were collected from butcher shops and supermarkets in and around Hatay province in Turkey. All samples were collected in sterile plastic bags, stored in ice packs and transported immediately to the laboratory within 2 h for microbiological analysis. Each sample was screened for the presence of *Enterococcus* spp. using previously published protocols with some modifications (Hayes et al., 2003; Klibi et al., 2013). Meat samples (25 g) were placed in sterile plastic bags containing 225 mL buffered peptone water and mixed with stomacher for 3 min. Rinsate samples (50 mL) were then incubated at 37 °C for 24 h. Following incubation, 10 µl was subcultured into Enterococcosel Broth and further incubated at 37 °C for 24 h. After enrichment, a loopful of broth culture was aseptically streaked on VRE agar and VRA agar including 6 mg/L vancomycin. Plates were incubated at 37 °C for 24 h after which one colony per sample with typical enterococci morphology was then transferred onto blood agar plates in order to obtain pure culture. These isolates were then subjected to Gram staining and catalase test. Identification of the isolates was done by 16S rRNA sequencing. Bacterial 16S rRNA was amplified by using universal primers 16S 20 (5'-AGA GTT TGA TCC TGG CTC AG-3') and 1390 (5'-GAC GGG CGG TGT GTA CAA-3') (Sghir, Antonopoulos, & Mackie, 1998; Suau et al., 1999). The PCR

products were sequenced and analysed with the BLAST program available at the National Center for Biotechnology Information (NCBI).

### 2.2. Antibiotic sensitivity testing

Antimicrobial susceptibility was determined using disc diffusion method according to the Clinical Laboratory Standards Institute (CLSI, 2012) recommendations. Mueller Hinton Agar (MHA) was used for susceptibility testing and the plates were incubated in incubator at 37 °C for 20–24 h. The isolates were screened for susceptibility to 10 antibiotics including penicillin (P; 10 U/disc), ampicillin (AMP; 10 µg/disc), vancomycin (VA; 30 µg/disc), teicoplanin (TEC; 30 µg/disc), erythromycin (E; 15 µg/disc), tetracycline (TE; 30 µg/disc), ciprofloxacin (CIP; 5 µg/disc), chloramphenicol (C; 30 µg/disc), gentamycin (CN; 10 µg/disc) and trimethoprim/sulfamethoxazole (SXT; 1.25–23.75 µg/disc). Antibiotics tested in this study were selected based on their usage in veterinary practice among those classified as “critically important” (P, AMP, VA, TEC, CIP, CN and E) or “highly important” (SXT, C and TE) in human medicine (WHO, 2011). The minimum inhibitory concentration (MIC) values for vancomycin and teicoplanin were determined for Va<sup>R</sup> strains using E-Test (Oxoid UK).

### 2.3. Screening of antibiotic resistance genes

The presence of genetic determinants in isolates showing antimicrobial resistance by disc assay conferring resistance to macrolide and tetracycline (*ermA*, *ermB*, *mefA/E*, *tetK*, *tetL*, *tetM* and *tetO*) (Malhotra-Kumar, Lammens, Piessens, & Goossens, 2005), to aminoglycosides (*aac(6)-Ie-aph(2)-Ia*, *aph(2)-Ib*, *aph(2)-Ic*, *aph(2)-Id*, *aph(3)-IIIa*, *ant(4)-Ia* (Vakulenko et al., 2003) and chloramphenicol (*cat*) (Aarestrup, Agrees, Gerner-Smith, Madsen, & Jensen, 2000) was determined by PCR. The presence of vancomycin resistance genes (*vanA*, *vanB*, *vanC1/2*, *vanD*, *vanE*, *vanG*) was also analysed as previously described (Depardieu, Perichon, & Courvalin, 2004). Antibiotic resistance genes, primer sequences and lengths of products are listed in Table 1.

### 2.4. Detection of genetic determinants related to virulence

The presence of the genes responsible for the expression of gelatinase (*gelA*), cytolysin (*cylA*, *cylM* and *cylB*), cell wall adhesins (*efaAfs* and *efaAfm*), enterococcal surface protein (*esp*), sex-pheromones (*cpd*, *cob*, *ccf* and *eep*), and the aggregation substance (*aggA*) were investigated in all enterococci isolates (Eaton & Gasson, 2001; Marques & Suzart 2004; Shankar, Baghdayan, Huycke, Lindahl, & Gilmore, 1999). Virulence markers and PCR primers are listed in Table 2.

### 2.5. Statistical analysis

Pearson's chi-square ( $\chi^2$ ) test was used to determine if there were significant differences ( $P < 0.05$ ) in frequency of antimicrobial resistance profiles, resistance genes and virulence traits among *Enterococci* isolates obtained from different meat species.

## 3. Results

A total of 205 isolates were obtained from chicken ( $n = 105$ ) and beef samples ( $n = 100$ ). Three different species including *E. faecalis* ( $n = 103$ ), *E. hirae* ( $n = 1$ ) and *Enterococcus faecium* ( $n = 1$ ) were isolated from chicken meat, while only *E. faecalis* was identified from beef samples. A total of five VRE, including four *E. faecalis* and one *E. faecium* isolates, were isolated from one-hundred chicken meats.

**Table 1**  
PCR primers, products and references for the detection of antibiotic resistance genes.

Primer	Sequence (5' to 3')	Product size (bp)	References
<i>erm(A)</i>	CCC GAA AAA TAC GCA AAA TTT CAT CCC TGT TTA CCC ATT TAT AAA CG	590	Malhotra-Kumar et al. 2005
<i>erm(B)</i>	TGG TAT TCC AAA TGC GTA ATG CTG TGG TAT GGC GGG TAA GT	745	
<i>meff(A/E)</i>	CAA TAT GGG CAG GGC AAG AAG CTG TTC CAA TGC TAC GG	317	
<i>tet(K)</i>	GAT CAA TTG TAG CTT TAG GTG AAG G TTT TGT TGA TTT ACC AGG TAC CAT T	155	
<i>tet(M)</i>	GTG GAC AAA GGT ACA ACG AG CGG TAA AGT TCG TCA CAC AC	406	
<i>tet(O)</i>	AAC TTA GGC ATT CTG GCT CAC TCC CAC TGT TCC ATA TCG TCA	515	
<i>tet(L)</i>	TGG TGG AAT GAT AGC CCA TT CAG GAA TGA CAG CAC GCT AA	229	
<i>aac(6)-le-aph(2)-la</i>	CAG GAA TTT ATC GAA AAT GGT AGA AAA G CAC AAT CGA CTA AAG AGT ACC AAT C	369	Vakulenko et al. 2003
<i>aac(6)-le-aph(2)-la</i>	CAG AGC CTT GGG AAG ATG AAG CCT CGT GTA ATT CAT GTT CTG GC	348	
<i>aph(2)-Ib</i>	CTT GGA CGC TGA GAT ATA TGA GCA C GTT TGT AGC AAT TCA GAA ACA CCC TT	867	
<i>aph(2)-Ic</i>	CCA CAA TGA TAA TGA CTC AGT TCC C CCA CAG CTT CCG ATA GCA AGA G	444	
<i>aph(2)-Id</i>	GTG GTT TTT ACA GGA ATG CCA TC CCC TCT TCA TAC CAA TCC ATA TAA CC	641	
<i>aph(3)-IIIa</i>	GGC TAA AAT GAG AAT ATC ACC GG CTT TAA AAA ATC ATA CAG CTC GCG	523	
<i>ant(4)-Ia</i>	CAA ACT GCT AAA TCG GTA GAA GCC GGA AAG TTG ACC AGA CAT TAC GAA CT	294	
CatpIP 501	GGA TAT GAA ATT TAT CCC TC CAA TCA TCT ACC CTA TGA AT	505	Aarestrup et al. 2000
<i>vanA</i>	GGG AAA ACG ACA ATT GC GTA CAA TGC GGC CGT TA	732	Depardieu et al. 2004
<i>vanB</i>	ACG GAA TGG GAA GCC GA TGC ACC CGA TTT CGT TC	647	
<i>vanC1/2</i>	ATG GAT TGG TAY TKG TAT TAG CGG GAG TGM CYM GTA A	815/827	
<i>vanD</i>	TGT GGG ATG CGA TAT TCA A TGC AGC CAA GTA TCC GGT AA	500	
<i>vanE</i>	TGT GGT ATC GGA GCT GCA G ATA GTT TAG CTG GTA AC	430	
<i>vanG</i>	CGG CAT CCG CTG TTT TTG A GAA CGA TAG ACC AAT GCC TT	941	

**Table 2**  
PCR primers, products and references for the detection of virulence genes.

Primer name	Sequence (5' to 3')	Product size (bp)	References
<i>gelE</i>	ACC CCG TAT CAT TGG TTT ACG CAT TGC TTT TCC ATC	419	Eaton and Gasson (2001)
<i>cylA</i>	TGG ATG ATA GTG ATA GGA AGT TCT ACA GTA AAT CTT TCG TCA	517	Eaton and Gasson (2001)
<i>ccf</i>	GGG AAT TGA GTA GTG AAG AAG AGC CGC TAA AAT CGG TAA AAT	543	Eaton and Gasson (2001)
<i>efaAfs</i>	GAC AGA CCC TCA CGA ATA AGT TCA TCA TGC TGC TGT AGT A	705	Eaton and Gasson (2001)
<i>efaAfm</i>	AAC AGA TCC GCA TGA ATA CAT TTC ATC ATC TGA TAG TA	735	Eaton and Gasson (2001)
<i>cylM</i>	CTG ATG GAA AGA AGA TAG TAT TGA GTT GGT CTG ATT ACA TTT	742	Eaton and Gasson (2001)
<i>cpd</i>	TGG TGG GTT ATT TTT CAA TTC TAC GGC TCT GGC TTA CTA	782	Eaton and Gasson (2001)
<i>cylB</i>	ATT CCT ACC TAT GTT CTG TTA AAT AAA CTC TTC TTT TCC AAC	843	Eaton and Gasson (2001)
<i>esp</i>	TTG CTA ATG CTA GTC CAC GAC C GCG TCA ACA CTT GCA TTG CCG AA	933	Shankar et al. (1999)
<i>eep</i>	GAG CGG GTA TTT TAG TTC GT TAC TCC AGC ATT GGA TGC T	937	Marques and Suzart (2004)
<i>cob</i>	AAC ATT CAG CAA ACA AAG C TTG TCA TAA AGA GTG GTC AT	1405	Eaton and Gasson (2001)
<i>aggA</i>	AAG AAA AAG TAG ACC AAC AAC GGC AAG ACA AGT AAA TA	1553	Eaton and Gasson (2001)

All isolates were tested against twelve antibiotics. Hundred-one (96%) strains from chicken meat and sixty-three isolates (63%) from beef presented resistance to at least one of the twelve antimicrobial drugs tested. Among all *E. faecalis* isolates from chicken carcasses, resistance was observed to tetracycline (89.3%), ciprofloxacin (34.9%), erythromycin (59.2%), trimethoprim/sulfamethoxazole (33%) and chloramphenicol (18.4%). One strain of *E. faecium* isolated from chicken meats had resistance to all antimicrobials tested except chloramphenicol, while *E. hirae* strain was found to be resistance to penicillin, tetracycline and trimethoprim/sulfamethoxazole. Only one isolate from minced meat were resistant to chloromphenicol. For beef isolates, the highest frequency of resistance was against tetracycline (53%), ciprofloxacin (12%) and trimethoprim/sulfamethoxazole (7%). No resistance to ampicillin, vancomycin, chloramphenicol and gentamycin were observed. The rates of resistance to penicillin (3%) and erythromycin (2%) were low, while only one isolates was found to be resistance to chloramphenicol (Table 3). Overall, 40% of chicken meat isolates were found to be resistant to three or more separate classes of antimicrobials (the multidrug resistance), whereas only 3% of minced meat isolates displayed the multidrug resistance. The antibiotic sensitivity test showed that  $Va^F$  enterococci were all resistant to tetracycline, erythromycin, trimethoprim/sulfamethoxazole, ampicillin and penicillin. The proportion of isolates from retail chicken resistant to tetracycline, erythromycin, trimethoprim/sulfamethoxazole, ciprofloxacin and chloramphenicol were significantly higher ( $P < 0.05$ ) than those isolated from retail beef.

In the chicken meat samples, the *ermB* gene was found in 79 (75.2%) isolates and the *mefA/E* gene was found in only one (0.95%) isolate while the *ermA* gene was not detected in any of the isolates. For beef isolates, only three (3%) harboured the *ermB* gene. Among tested aminoglycosides resistance genes; *aph(3')-IIIa*, *ant(6)-Ia* and *aac(6')-Ie-aph(2'')-Ia* were observed in six (5.7%), one (0.95%) and one (0.95%) isolates from chicken meat, respectively, whereas none of the isolates from beef samples had these genes. Detection of the *cat* gene encodes resistance to chloramphenicol was confirmed in 5 (4.8%) isolates from chicken meat samples. In addition, the *tetL* gene was the most common, found in 85 (81%) isolates, the *tetM* gene in 80 (76.2%), the *tetO* gene in 18 (17.1%) and the *tetK* gene in one isolate from chicken meat samples. For beef isolates, the *tetM* gene was found in 17 (17%) isolates, the *tetL* gene in 10 (10%), the *tetK* gene in one and the *tetO* gene in one isolate. Sixty isolates carried two and fifteen isolates carried three *tet* genes while twenty four isolates only carried one *tet* genes in chicken isolates. For beef isolates, six isolates carried two and one isolate carried three *tet* genes, however fourteen isolates carried only one *tet* gene. A total of 3 isolates that were resistant to tetracycline did not contain any of the tested genes. All these chicken VRE possessed the *vanA* genotype, *ermB*, *tetM* and *tetL*, but the *vanB*, *vanC1* and *vanC2/3* genes

were not detected (Table 4).

Fig. 1 shows the percentage of virulence genes in the isolates recovered from chicken and beef meat samples. The most prevalent virulence determinants were *cpd* (100% and 92.4%), followed by *ccf* (98% and 99%) and *afs* (95% and 95.2%) in isolates obtained from beef and chicken, respectively. The *gelE* and *eep* genes were detected in 82.9% and 88.6% of chicken isolates, and 75% and 84% of beef isolates, respectively. Enterococci from chicken meat samples also carried virulence genes including the *aggA* and *cob* (both genes, 26.7%), which was encountered only in one isolate (both genes, 1%) obtained from beef samples. The *efaAfm* and *cylM* were not detected in beef isolates and the *cylB* was not detected in chicken isolates. The enterococci isolates that harboured the *cpd*, *cylA*, *cylM* and *aggA* genes were greater ( $P < 0.05$ ) in retail chicken than in beef. There was no association found between phenotypic antibiotic resistance and the virulence genes detected.

#### 4. Discussion

Even though it is known that enterococci are ubiquitous organism in the gut, it is one of the emerging organism causing nosocomial infections in humans. Recent studies confirmed enterococci contamination in a wide range of foods including cheese, sausages, meat, milk, and cereals due to improper handling (Kolman, Akan, & Akiroglu, 2009). Studies conducted by Olsen, Schønheyder, Christensen, and Bisgaard (2012) have provided strong evidence that enterococci originating from foods of animal origin had a remarkable degree of similarity in virulence characteristics with human isolates implicating animal meat as an important source for virulent enterococci strains for human colonization. To our best knowledge, this is the first report on the presence of virulence and antibiotic resistance genes in enterococci from retail meat samples in Turkey, even though there are some reports available on the prevalence and antimicrobial resistance of enterococci in meat, cheese and fermented Turkish foods (Çitak, Yucel, & Orhan, 2004; Kolman et al., 2009; Togay, Keskin, Acik, & Temiz, 2010). Enterococci strains were isolated from all samples tested and five chicken samples were contaminated with VRE strains. Among serotypes isolated in this study, *E. faecalis* was the most prevalent, while only one *E. faecium* and *E. hirae* were isolated from chicken samples. The level of contamination and the species distribution found in this study is consistent with the recent reports from Canada and Tunisia where *E. faecalis* is the most commonly reported from chicken meat samples (Aslam, Diarra, Checkley, Bohaychuk, & Masson, 2012; Klibi et al., 2013). Authors also indicated a negligible prevalence in poultry carcasses for *E. faecium* and *E. hirae* (2%). In Tunisia, *E. faecalis* was also reported to be the most frequently reported species from foods of animal origin but there were other species also detected including *E. gallinarum*, *E. casseliflavus*, *E. mundtii*, and *E. sulfureus* (Klibi et al., 2013).

It is well known fact that the percentage of multiple antibiotic resistant enterococci strains is much lower among environmental strains when compared to clinical strains (Abriouel et al., 2008). Enterococci strains are also naturally resistant to aminoglycoside, lincomycine and quinupristin/dalfopristin. In the current study, resistance to three or more class of antibiotics (multidrug resistance) was found to be 40% for chicken derived enterococci isolates and only 3% for beef derived isolates which is in agreement with a recent study in Canada in which multidrug resistance was found in 91% of chicken *E. faecalis* and 14% beef *E. faecalis* isolates (Aslam et al., 2012). A high percentage of enterococcal isolates from chicken and beef samples were resistant to critically important antibiotics including ciprofloxacin and erythromycin, as well as tetracycline. A high frequency of resistance to erythromycin and tetracycline in enterococci from various foods was also reported in

**Table 3**  
Distribution of antimicrobial resistance among the enterococci.

Antimicrobials	Chicken meat	Minced meat
	<i>E. faecalis</i> , %	<i>E. faecalis</i> , %
Ampicillin	4.9	0
Penicillin	4.9	3
Vancomycin	3.9	0
Teicoplanin	3.9	0
Erythromycin	59.2	2
Tetracycline	89.3	53
Gentamycin	4.9	0
Ciprofloxacin	34.9	12
Chloramphenicol	18.4	1
Trimethoprim/sulfamethoxazole	33.0	7
<b>Total (n)</b>	<b>103</b>	<b>100</b>

**Table 4**  
Main features of VRE isolated in the present study.

Isolate	Source	Virulence traits	Antimicrobial resistance <sup>a</sup>	Resistance gene Variants	MIC (µg/mL)	
					Vancomycin	Teicoplanin
<i>E. faecium</i>	Chicken	<i>afm</i> , <i>ccf</i> , <i>cob</i> , <i>gelE</i>	TE, E, SXT, AMP, P, CIP	<i>vanA</i> , <i>ermB</i> , <i>tetM</i> , <i>tetL</i>	>256	64
<i>E. faecalis</i>	Chicken	<i>afs</i> , <i>ccf</i> , <i>esp</i>	TE, E, SXT, AMP, P, CIP	<i>vanA</i> , <i>ermB</i> , <i>tetM</i> , <i>tetL</i>	>256	64
<i>E. faecalis</i>	Chicken	<i>afs</i> , <i>ccf</i>	TE, E, SXT, AMP, P	<i>vanA</i> , <i>ermB</i> , <i>tetM</i> , <i>tetL</i>	>256	64
<i>E. faecalis</i>	Chicken	<i>afs</i> , <i>ccf</i>	TE, E, SXT, AMP, P, CIP	<i>vanA</i> , <i>ermB</i> , <i>tetM</i> , <i>tetL</i>	>256	64
<i>E. faecalis</i>	Chicken	<i>afs</i> , <i>ccf</i>	TE, E, SXT, AMP, P, CIP	<i>vanA</i> , <i>ermB</i> , <i>tetM</i> , <i>tetL</i>	>256	64

<sup>a</sup> TE, tetracycline; E, erythromycin; STX, trimethoprim-sulfamethoxazole; AMC, ampicillin; P, penicillin; CIP, ciprofloxacin.

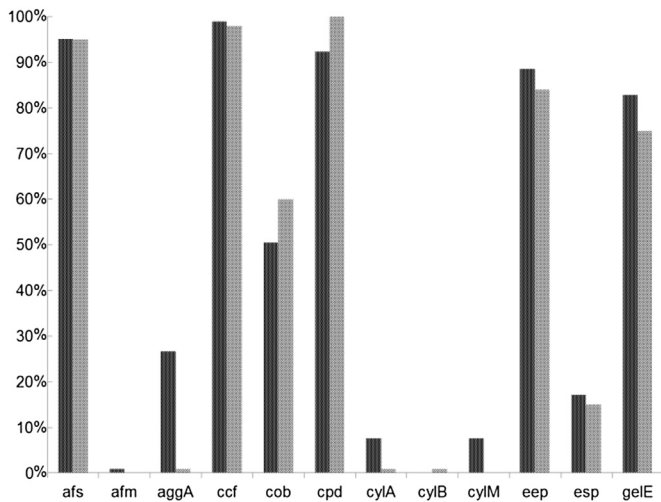


**Fig. 1.** Distribution of virulence genes in enterococci. Dark bars and grey bars represent the percentage of isolates obtained from chicken and beef meat samples, respectively. Vertical bar represents percentage of isolates, horizontal bar represents virulence genes.

Canada, Turkey and Tunisia (Aslam et al., 2012; Hammad, Shimamoto, & Shimamoto, 2014; Klibi et al., 2013; Koluman et al., 2009; Togay et al., 2010). 37% and 12% of isolates of enterococci obtained from chicken and beef samples were also found to be resistant to ciprofloxacin in this study. However, there was no enterococcal isolates found to be resistant to ciprofloxacin in Canada (Aslam et al., 2012), suggesting that this class of antibiotics might be still used in animal production in Turkey. In this study, there was no enterococci showed high level aminoglycoside resistance. However, high level of aminoglycoside resistant isolates were obtained from chicken isolates and this situation was attributed to the use of this antibiotics in poultry breeding in Tunisia (Klibi et al., 2013). Chicken isolates showed significantly higher rates of resistance ( $P < 0.05$ ) to tetracycline, erythromycin, trimethoprim/sulfamethoxazole, ciprofloxacin and chloramphenicol than did beef isolates, suggesting that antibiotic resistance profile of food borne pathogens in broiler and chicken meat samples has to be regularly monitored in Turkey.

Vancomycin, which is one of the few alternatives in treating enterococcal infections is ranked as critically important in human medicine and the presence of  $Va^R$  strains in foods is of great importance (WHO, 2011). There is significant evidence showing the reduced number of VRE were isolated since 1995 when avoparcin was first banned for use in livestock (Borgen et al., 2000; Bortolaia, Mander, Jensen, Olsen, & Guardabassi, 2015). In our study, 5% of chicken meat samples were found to have VRE strains. This is similar to results of a recent study from Spain in which 4.7% of chicken samples at retail level were also found to harbour VRE enterococci with acquired mechanisms of resistance ten years after

the ban (Lopez et al., 2009). The continuance of  $Va^R$  was attributed to the co-existence of the *ermB* gene encoding erythromycin resistance and vancomycin resistance genes on the same plasmid (Lopez et al., 2009). This observation was also obtained in our study as all  $Va^R$  isolates carried the both *vanA* and *ermB* genes together. In comparison, no VRE was detected in food of animal origins in studies done in Canada which can be explained with the implementation of strict no vancomycin usage in livestock.

In this study, the *tet(M)* or *tet(L)* genes encoding tetracycline resistance were found to be the most common resistance traits detected in enterococci isolates. Other earlier studies from Canada (Aslam et al., 2012) and Tunisia (Klibi et al., 2013) were also reported that tetracycline resistant Enterococci isolates from meat samples harboured the *tet(M)* or *tet(L)* genes mostly. A number of tetracycline resistance determinants including the *tet(M)*, *tet(L)*, *tet(K)*, *tet(O)* have been described so far. Several studies from all around the worlds showed that the *tet(M)* gene is the most frequently detected in tetracycline resistant enterococci isolates due to the transfer of Tn916-type transposons (Wilcks, Andersen, & Licht, 2005). In the current study, the *ermB* gene conferring erythromycin resistance was most frequently determined in Enterococci isolates, and none of the erythromycin resistant isolates harboured the *ermA*, *ermC* and *msrC* genes. There are also reports of the *ermB* gene in erythromycin resistant enterococci from foods of animal origin, animal and humans (Aslam et al., 2012; Diarra et al., 2010). Only 4.8% of isolates were found to carry the *cat* gene in chloramphenicol resistant chicken isolates. The *aph(3')-IIIa*, *ant(6)-Ia* and *aac(6')-Ie-aph(2'')-Ia* gene encoding aminoglycosides were only detected in chicken isolates in low frequency.

The presence of virulence factors does not necessarily mean that the strains isolated from the foods of animal origin cause diseases in humans, but may have pathogenic potential as these factors have been found to contribute to the severity of infection (Biswas et al., 2014; Elsner et al., 2000; Thurlow et al., 2010). A number of genes including *gelE*, *ccf*, *cpd*, *cob*, *afs*, and *aggA* were frequently detected in enterococci strains isolated from chicken and beef samples, which is similar to previous studies (Aslam et al., 2012; Jahan & Holley, 2014; Klibi et al., 2013). The genes, *gelE* and *cpd*, associated with toxin production and sex pheromones were also reported to be commonly found in commensal isolates (Nuevo-Palop & Narbad, 2011). Virulence traits (*cylA*, *cyLB* and *cyLM*) associated with the production of the active cytolysin were reported to be the most important genes and were present in small number of isolates. Of the twenty nine enterococcal strains from raw and fermented meat, only two harboured the *cylA* gene (Jahan & Holley, 2014). Domann et al., (2007) reported that virulence trait for aggregation (*aggA*) may support the strain's probiotic characters. The *esp* gene is known to be associated with the biofilm production, endocarditis and nosocomial infections (Hayes, English, Carr, Wagner, & Joseph, 2004; Heikens et al., 2011) were detected in both chicken and beef isolates at low frequency which is in agreement with a previous study carried by Olsen et al., (2012). It was also previously speculated that this gene might play a role in the attachment to the equipment in the slaughter

house which might cause the contamination of meat products (Hayes et al., 2004). A recent report found that virulence genes carried by enterococci isolates in human and poultry isolates had similar gene sequences, supporting the zoonotic potential of this organism (Olsen et al., 2012). A recent study found an association between the genes encoding aggregation substances and cytolysin and the *tetM* resistance genes (Aslam et al., 2012). However, there were no such an association detected in our study. Moreover, some virulence traits (*cylA*, *cylM* and *aggA*) were statistically more prevalent in chicken isolates which was also demonstrated by Aslam et al., (2012).

In conclusion, the current study reveals the presence of  $Va^R$  enterococci in chicken carcasses in Turkey. The presence of  $Va^R$  enterococci on meats creates a major risk for public health which might cause severe infections due to consumption of this contaminated product. In addition, a high level of resistance against clinically important class of antibiotics was found in enterococci which is also important concern for the effective treatment of infections and the potential transfer of this resistance to other intestinal organisms. Further research is needed to establish the risk of transmission of these organisms from foods of animal origin to humans and also to monitor the increasing antimicrobial resistance as well as virulence and resistance genes.

### Acknowledgements

This project is financially supported by MKU Scientific Research Project Fund (Project Number: BAP-413). We thank Dr. Errol Hassan (The University of Queensland) for his valuable comments on the manuscript.

### References

- Aarestrup, F. M., Agrees, Y., Gerner-Smith, P., Madsen, M., & Jensen, L. B. (2000). Comparison of antimicrobial resistance phenotypes and resistance genes in *Enterococcus faecalis* and *Enterococcus faecium* from humans in the community, broilers and pigs in Denmark. *Diagnostic Microbiology and Infectious Disease*, 37, 127–137.
- Abriouel, H., Omar, N. B., Molinos, A. C., López, R. L., Grande, M. J., Martínez-Viedma, P., et al. (2008). Comparative analysis of genetic diversity and incidence of virulence factors and antibiotic resistance among enterococcal populations from raw fruit and vegetable foods water and soil and clinical samples. *International Journal of Food Microbiology*, 123, 38–49.
- Ahmadova, A., Todorov, S. D., Choiset, Y., Rabesona, H., Zadi, T. M., Kuliyeu, A., et al. (2013). Evaluation of antimicrobial activity, probiotic properties and safety of wild strain *Enterococcus faecium* AQ71 isolated from Azerbaijani Motal cheese. *Food Control*, 30, 631–641.
- Aslam, M., Diarra, M. S., Checkley, S., Bohaychuk, V., & Masson, L. (2012). Characterization of antimicrobial resistance and virulence genes in *Enterococcus* spp. isolated from retail meats in Alberta, Canada. *International Journal of Food Microbiology*, 156, 222–230.
- Biswas, P. P., Dey, S., Adhikari, L., & Sen, A. (2014). Virulence markers of vancomycin resistant enterococci isolated from infected and colonized patients. *Journal of Global Infectious Diseases*, 6, 157–163.
- Borgen, K., Simonsen, G. S., Sundsfjord, A., Wasteson, Y., Olsvik, E., & Kruse, H. (2000). Continuing high prevalence of VanA-type vancomycin-resistant enterococci on Norwegian poultry farms three years after avoparcin was banned. *Journal of Applied Microbiology*, 89, 478–485.
- Bortolaia, V., Mander, M., Jensen, L. B., Olsen, J. E., & Guardabassi, L. (2015). Persistence of vancomycin resistance in multiple clones of *Enterococcus faecium* isolated from Danish broilers 15 years after the ban of avoparcin. *Antimicrobial Agents and Chemotherapy*, 59, 2926–2929.
- Chow, J. W., Thal, L. A., Perri, M. B., Vazquez, J. A., Donabedian, S. M., Clewell, D. B., et al. (1993). Plasmid-associated hemolysin and aggregation substance production contribute to virulence in experimental enterococcal endocarditis. *Antimicrobial Agents and Chemotherapy*, 37, 2474–2477.
- Çitak, S., Yuçel, N., & Orhan, S. (2004). Antibiotic resistance and incidence of *Enterococcus* species in Turkish white cheese. *International Journal of Dairy Technology*, 57, 27–31.
- Clinical and Laboratory Standards Institute (CLSI). (2012). CLSI document, M100-S22. *Performance standards for antimicrobial susceptibility testing; twenty-second informational supplement* (Vol. 32(3)). Wayne, PA.
- Depardieu, F., Perichon, B., & Courvalin, P. (2004). Detection of the van alphabet and identification of enterococci and staphylococci at the species level by multiplex PCR. *Journal of Clinical Microbiology*, 42, 5857–5860.
- Diarra, M. S., Rempel, H., Champagne, J., Masson, L., Pritchard, J., & Topp, E. (2010). Distribution of antimicrobial resistance and virulence genes in *Enterococcus* spp. and characterization of isolates from broiler chickens. *Applied and Environmental Microbiology*, 76(8249), 8033–8043.
- Domann, E., Hain, T., Ghai, R., Billion, A., Kuenne, C., Zimmermann, K., et al. (2007). Comparative genomic analysis for the presence of potential enterococcal virulence factors in the probiotic *Enterococcus faecalis* strain Symbioflor 1. *International Journal of Medical Microbiology*, 297, 533–539.
- Eaton, T. J., & Gasson, M. J. (2001). Molecular screening of *Enterococcus* virulence determinants and potential for genetic exchange between food and medical isolates. *Applied and Environmental Microbiology*, 67, 1628–1635.
- Elsner, H. A., Sobottka, I., Mack, D., Claussen, M., Laufs, R., & Wirth, R. (2000). Virulence factors of *Enterococcus faecalis* and *Enterococcus faecium* blood culture isolates. *European Journal of Clinical Microbiology and Infectious Diseases*, 19, 39–42.
- Flannagan, S. E., Chow, J. W., Donabedian, S. M., Brown, W. J., Perri, M. B., Zervos, M. J., et al. (2003). Plasmid content of a Vancomycin-Resistant *Enterococcus faecalis* isolate from a patient also colonized by *Staphylococcus aureus* with a VanA phenotype. *Antimicrobial Agents and Chemotherapy*, 47, 3954–3959.
- Foulquié Moreno, M. R., Sarantinopoulos, P., Tsakalidou, E., & De Vuyst, L. (2006). The role and application of enterococci in food and health. *International Journal of Food Microbiology*, 106, 1–24.
- Hammad, A. M., Shimamoto, T., & Shimamoto, T. (2014). Genetic characterization of antibiotic resistance and virulence factors in *Enterococcus* spp. from Japanese retail ready-to-eat raw fish. *Food Microbiology*, 38, 62–66.
- Hayes, J. R., English, L. L., Carr, L. E., Wagner, D. D., & Joseph, S. W. (2004). Multiple antibiotic resistance of *Enterococcus* spp. isolated from commercial poultry production environments. *Applied and Environmental Microbiology*, 70, 6005–6011.
- Hayes, J. R., English, L. L., Carter, P. J., Proescholdt, T., Lee, K. Y., Wagner, D. D., et al. (2003). Prevalence and antimicrobial resistance of *Enterococcus* species isolated from retail meats. *Applied and Environmental Microbiology*, 69, 7153–7160.
- Heikens, E., Singh, K. V., Jacques-Palaz, K. D., Van Luit-Asbroek, M., Oostdijk, E. A. N., Bonten, M. J. M., et al. (2011). Contribution of the enterococcal surface protein Esp to pathogenesis of *Enterococcus faecium* endocarditis. *Microbes and Infection*, 13, 1185–1190.
- Hidron, A. I., Edwards, J. R., Patel, J., Horan, T. C., Sievert, D. M., Pollock, D. A., et al. (2008). NHSN annual update: antimicrobial resistant pathogens associated with healthcare-associated infections: annual summary of data reported to the national healthcare safety network at the centers for disease control and prevention, 2006–2007. *Infection Control and Hospital Epidemiology*, 29, 996–1011.
- Hollenbeck, B. L., & Rice, L. B. (2012). Intrinsic and acquired resistance mechanisms in enterococcus. *Virulence*, 3, 421–433.
- Jahan, M., & Holley, R. A. (2014). Incidence of virulence factors in enterococci from raw and fermented meat and biofilm forming capacity at 25 °C and 37 °C. *International Journal of Food Microbiology*, 170, 65–69.
- Johnson, A. P. (1994). The pathogenicity of enterococci. *Journal of Antimicrobial Chemotherapy*, 33, 1083–1089.
- Kirst, H. A., Thompson, D. G., & Nicas, T. I. (1998). Historical yearly usage of vancomycin. *Antimicrobial Agents and Chemotherapy*, 42, 1303–1304.
- Klare, I., Konstabel, C., Badstübner, D., Werner, G., & Witte, W. (2003). Occurrence and spread of antibiotic resistances in *Enterococcus faecium*. *International Journal of Food Microbiology*, 88, 269–290.
- Klibi, N., Said, L. B., Jouini, A., Slama, K. B., López, M., Sallem, R. B., et al. (2013). Species distribution, antibiotic resistance and virulence traits in enterococci from meat in Tunisia. *Meat Science*, 93, 675–680.
- Koluman, A., Akan, L. S. C., & Akiroglu, F. P. (2009). Occurrence and antimicrobial resistance of enterococci in retail foods. *Food Control*, 20, 281–283.
- Leavis, H. L., Bonten, M. J., & Willems, R. J. (2006). Identification of high-risk enterococcal clonal complexes: global dispersion and antibiotic resistance. *Current Opinion in Microbiology*, 9, 454–460.
- Lopez, M., Saenz, Y., Rojo-Bezares, B., Martinez, S., Del Campo, R., Ruiz-Larrea, F., et al. (2009). Detection of vanA and vanB2-containing enterococci from food samples in Spain, including *Enterococcus faecium* strains of CC17 and the new singleton ST425. *International Journal of Food Microbiology*, 133, 172–178.
- Malhotra-Kumar, S., Lammens, C., Piessens, J., & Goossens, H. (2005). Multiplex PCR for simultaneous detection of macrolide and tetracycline resistance determinants in streptococci. *Antimicrobial Agents and Chemotherapy*, 49, 4798–4800.
- Marques de Bittencourt, E., & Suzart, S. (2004). Occurrence of virulence-associated genes in clinical *Enterococcus faecalis* strains isolated in Londrina, Brazil. *Journal of Medical Microbiology*, 53, 1069–1073.
- Nueno-Palop, C., & Narbad, A. (2011). Probiotic assessment of *Enterococcus faecalis* CP58 isolated from human gut. *International Journal of Food Microbiology*, 145, 390–394.
- Olsen, R. H., Schönheyder, H. C., Christensen, H., & Bisgaard, M. (2012). *Enterococcus faecalis* of human and poultry origin share virulence genes supporting the zoonotic potential of *E. faecalis*. *Zoonoses and Public Health*, 59, 256–263.
- Sghir, A., Antonopoulos, D., & Mackie, R. I. (1998). Design and evaluation of a lactobacillus group-specific ribosomal RNA-targeted hybridization probe and its application to the study of intestinal microecology in pigs. *Systematic and Applied Microbiology*, 21, 291–296.
- Shankar, V., Baghdadyan, A. S., Huycke, M. M., Lindahl, G., & Gilmore, M. S. (1999). Infection-derived *Enterococcus faecalis*, infection-derived *Enterococcus faecalis* strains are enriched in esp, a gene encoding a novel surface protein. *Infection*

- and Immunity, 67, 193–200.
- Shankar, N., Lockatell, C. V., Baghdayan, A. S., Drachenberg, C., Gilmore, M. S., & Johnson, D. E. (2001). Role of *Enterococcus faecalis* surface protein Esp in the pathogenesis of ascending urinary tract infection. *Infection and Immunity*, 69, 4366–4372.
- Suau, A., Bonnet, R., Sutren, M., Godon, J. J., Gibson, G., Collins, M. D., et al. (1999). Direct rDNA community analysis reveals a myriad of novel bacterial lineages within the human gut. *Applied and Environmental Microbiology*, 65, 4799–4807.
- Thurlow, L. R., Thomas, V. C., Narayanan, S., Olson, S., Fleming, S. D., & Hancock, L. E. (2010). Gelatinase contributes to the pathogenesis of endocarditis caused by *Enterococcus faecalis*. *Infection and Immunity*, 78, 4936–4943.
- Togay, S. O., Keskin, A. C., Acik, L., & Temiz, A. (2010). Virulence genes, antibiotic resistance and plasmid profiles of *Enterococcus faecalis* and *Enterococcus faecium* from naturally fermented Turkish foods. *Journal of Applied Microbiology*, 109, 1084–1092.
- Vakulenko, S. B., Zervos, M. J., Donabedian, S. M., Lerner, S. A., Voskresenskiy, A. M., & Chow, J. W. (2003). Multiplex PCR for detection of aminoglycoside resistance genes in enterococci. *Antimicrobial Agents and Chemotherapy*, 47, 1423–1426.
- Wilcks, A., Andersen, S. R., & Licht, T. R. (2005). Characterization of transferable tetracycline resistance genes in *Enterococcus faecalis* isolated from raw food. *FEMS Microbiology Letters*, 243, 15–19.
- World Health Organization (WHO). (2011). *Critically important antimicrobials for human medicine-3rd revision*. WHO Advisory Group on Integrated Surveillance of Antimicrobial Resistance (AGISAR). Geneva, Switzerland: WHO Press, ISBN 978924 1504485.



## Effect of processing on the content and biological activity of polysaccharides from *Pleurotus ostreatus* mushroom



Wojciech Radzki<sup>a,\*</sup>, Marta Ziąja-Sołtys<sup>b</sup>, Jakub Nowak<sup>c</sup>, Jolanta Rzymowska<sup>b</sup>,  
Jolanta Topolska<sup>b</sup>, Aneta Stawińska<sup>a</sup>, Monika Michalak-Majewska<sup>a</sup>,  
Marta Zalewska-Korona<sup>a</sup>, Andrzej Kuczumow<sup>d</sup>

<sup>a</sup> Department of Fruits, Vegetables and Mushrooms Technology, University of Life Sciences in Lublin, 20-704, Lublin, Poland

<sup>b</sup> Department of Biology and Genetics, Medical University of Lublin, 20-093, Lublin, Poland

<sup>c</sup> Department of Chemistry, Lublin Catholic University, 20-718, Lublin, Poland

<sup>d</sup> Institute of Environmental Engineering, Lublin Catholic University, 37-450, Stalowa Wola, Poland

### ARTICLE INFO

#### Article history:

Received 12 February 2015

Received in revised form

19 August 2015

Accepted 5 October 2015

Available online 8 October 2015

#### Keywords:

Oyster mushroom

Polysaccharides

Antioxidant

Antiproliferative

### ABSTRACT

Water soluble polysaccharides (WSP) were isolated from processed and non-processed fruiting bodies of oyster mushroom (*Pleurotus ostreatus*). The processing methods involved: blanching, boiling and blanching followed by fermenting with a strain of lactic acid bacteria (*Lactobacillus plantarum*). The yields of WSP ranged from  $78.7 \pm 1.5$  mg/g to  $120.1 \pm 4.9$  mg/g dry weight of sample. Blanching did not affect the content of WSP. Boiling for 15 min, led to the substantial decrease in the amount of WSP (34.7% decline). The isolated samples differed in carbohydrate, protein and phenolics content. FTIR spectroscopy of the WSP samples confirmed the presence of both  $\alpha$ - and  $\beta$ -glycosidic linkages. Gel permeation chromatography showed the presence of compounds having the molecular weight of 198.3, 11.9, 3.1 kDa. The samples possessed antioxidant capacity measured by ABTS method ( $14.14 \pm 0.63$  to  $29.48 \pm 1.12$   $\mu$ moles of Trolox per 1 g dw) and FRAP assay ( $2.49 \pm 0.54$  to  $16.52 \pm 0.55$   $\mu$ moles of Trolox equivalents per 1 g dw). The antioxidant potential was decreased by the processing. Similarly, anti-proliferative activity of WSP towards human breast cell lines (MCF-7 and T-47D) was lower due to the processing.

© 2015 Elsevier Ltd. All rights reserved.

### 1. Introduction

Mushrooms are abundant source of polysaccharides which are the part of their cell walls. They differ greatly in molecular weight, structure, conformation and physical properties (Wasser, 2002). Additionally, some of them are reported to exert beneficial effect on health and can be used in the treatment of some diseases. Biological activity of mushroom polysaccharides is mainly related to their immunomodulating and anticancer properties. Moreover, they are also known to exhibit antiviral effect, lower blood lipids or possess antioxidant and antiproliferative activity (Roupas, Keogh, Noakes, Margetts, & Taylor, 2010; Stachowiak & Reguła, 2012).

*Pleurotus ostreatus* (known as oyster mushroom) is a popular, widely cultivated edible fungus, known for its hypocholesterolemic

properties. A few different polysaccharides were isolated from fruiting bodies of this species, including pleuran, a high molecular weight  $\beta$ -(1  $\rightarrow$  3) (1  $\rightarrow$  6)-glucan. These polysaccharides are reported to demonstrate immunomodulating, antioxidant, anti-proliferative or prebiotic activity. Number of studies revealed that they vary in their chemical structure in terms of molecular weight, glycosidic bond conformation, branching, tertiary conformation or sugar composition. Moreover, the chemical structure of mushroom polysaccharides affect their biological activity (Zhang, Cui, Cheung, & Wang, 2007). High molecular weight (2200–2900 kDa),  $\beta$ -(1  $\rightarrow$  3) (1  $\rightarrow$  6)-glucan possessing prebiotic activity was obtained by Synytsya, Míčková, Jablonský, Sluková, and Čopíková (2008). Other authors isolated proteoglycans of lower molecular weight (1–31 kDa) which were capable of inhibiting proliferation of various cancer cell lines (Lavi, Friesem, Geresh, Hadar, & Schwartz, 2006; Martin & Brophy, 2010; Tong et al., 2009). Antiproliferative effect results from the induction of apoptosis of cancer cells. Antioxidant activity of *P. ostreatus* polysaccharides was demonstrated by

\* Corresponding author.

E-mail address: [wpradzki@gmail.com](mailto:wpradzki@gmail.com) (W. Radzki).

proteoglycans described by other researchers (Sun & Liu, 2009; Xia, Fan, Zhu, & Tong, 2011).

Mushrooms are rarely eaten raw and they require to be processed before the consumption. Most often thermal or hydrothermal treatments are applied. It is well known that processing of food may cause substantial changes in its chemical composition and thus affect nutritional and health properties. However, few studies describe the effect of processing on mushrooms-derived biologically active polysaccharides. Fan, Li, Deng, and Ai (2012) investigated how different drying techniques affect antioxidant activity of polysaccharides that were isolated from the medicinal mushroom *Ganoderma lucidum*. Thetsrimuang, Khammuang, Chiablaem, Srisomsap, and Sarnthima (2011) compared antioxidant and antiproliferative activities of polysaccharides obtained from fresh and dried *Lentinus polychrous* fungus. So far, however, no studies focused on the influence of hydrothermal processing on the biologically active mushrooms-derived polysaccharides. Therefore, the present paper aims to verify the impact of some processing methods on the content, chemical composition, antioxidant and antiproliferative activity of water soluble polysaccharides (WSP) obtained from *P. ostreatus* fruiting bodies. The applied processing used in this work included boiling, blanching and fermenting with lactic acid bacteria (*Lactobacillus plantarum*). Lactic acid fermentation is a process which allows to develop food probiotic products with improved nutritional quality (Beena Divya, Kulangara Varsha, Madhavan Nampootheri, Ismail, & Pandey, 2012).

## 2. Materials and methods

### 2.1. Mushroom samples

Fresh fruiting bodies of *P. ostreatus* were purchased directly from a producer (in 2013) and belonged to the same crop. After a harvest they were kept at 5 °C and were subjected to processing within 5 h.

### 2.2. Processing of mushrooms

The mushrooms were divided into four groups (500 g per group) and were further submitted to processing technologies: blanching in water containing 0.5% (w/v) citric acid (5 min, 95 °C); boiling in water (15 min, 100 °C); blanching in water (as reported above) and fermenting with lactic acid bacteria (see below). The fourth group was not processed (control).

The fermented mushrooms were prepared as follows. Fruiting bodies after blanching were washed with cool water and put tightly into screw-capped plastic vessels (PET). The brine solution was added which consisted of sucrose (10 g/l kg of blanched mushrooms) and 3% (w/v) NaCl. The mixture was then inoculated with 5 mL of bacterial suspension ( $10^6$  cfu/mL). The mushrooms were fermented for 10 days at 21–22 °C and then stored 20 days at 5 °C. The final pH of the product was 3.7.

All the samples were then subjected to freeze-drying with an Alpha 1-2LD plus freeze dryer (Christ, Germany) and ground to fine powder.

### 2.3. Extraction of water soluble polysaccharides

Four grams of powdered mushrooms were suspended in 200 mL of 80% ethanol and extracted in a rotary shaker at 80 °C for 60 min. The ethanolic extract containing low molecular weight compounds was removed by centrifugation ( $3755 \times g$ , 20 min) and the solid residue was washed twice with 80% ethanol and centrifuged. The alcohol insoluble fraction was then re-suspended in deionised water (ratio 1:50 w/v) and autoclaved at 115 °C for 180 min. The obtained slurry was cooled and centrifuged ( $3755 \times g$ , 20 min) and

the supernatant was concentrated with a rotary evaporator and precipitated with three volumes of 2-propanol (24 h, at 5 °C). The precipitate was then centrifuged, washed twice with 80% methanol, re-dissolved in hot deionised water, lyophilised and weighed. The extraction process was done in triplicate.

### 2.4. Chemical characteristics of polysaccharides

#### 2.4.1. Determination of total carbohydrate, protein and phenolics content

The content of carbohydrates in water soluble polysaccharides was measured with phenol-sulphuric acid method, using glucose as a standard (Dubois, Gilles, Hamilton, Rebers, & Smith, 1956). The amount of protein was determined according to the method developed by Bradford (1976), using bovine serum albumin as a standard. Total phenolics content was measured according to the method of Singleton and Rossi (1965) with gallic acid used as a standard.

#### 2.4.2. FTIR spectroscopy

FTIR spectra of lyophilised water soluble polysaccharides were recorded on Nicolet NXR 9650 spectrometer (Thermo, USA). The data was collected in the range of  $4000\text{--}600\text{ cm}^{-1}$  and ATR technique was applied.

#### 2.4.3. Gel permeation chromatography

The molecular weight of the isolated polysaccharides was determined with gel permeation chromatography, according to the modified method described by other authors (Malinowska, Krzyckowski, Łapienis, & Herold, 2009). The samples were dissolved in aqueous solution of  $\text{NaN}_3$  (0.1%, w/v) and were applied to three TSK-GEL columns: G5000PWXL, G3000PWXL and G2500PWXL ( $7.8 \times 300$  mm, Tosoh, Japan). The chromatographic system was equipped with K-501 pump (Knauer, Germany) and Refracto Monitor IV refractive index detector (LDC Analytical, USA). The flow of the mobile phase (0.1% (w/v)  $\text{NaN}_3$ ) was set at 1 mL/min. Pullulans of different molecular weight were used to construct a standard curve.

### 2.5. Antioxidant activity

#### 2.5.1. ABTS radical scavenging activity

The assay was done according to the method described by Re et al. (1999). ABTS reagent was prepared by incubating 7 mM ABTS solution with 2.45 mM potassium persulfate solution for 16 h at room temperature. The ABTS<sup>+</sup> solution was then brought to an absorbance of 0.7 (at 734 nm). The samples (25  $\mu\text{L}$ , 1 mg/mL) were mixed with 975  $\mu\text{L}$  of ABTS<sup>+</sup> solution and left to stand for 15 min at room temperature. The absorbance was measured at 734 nm against a blank sample. The calibration curve was done with different concentrations of Trolox (20–200  $\mu\text{M}$ ) and the results were expressed as micromoles of Trolox equivalent (TE) per 1 g of mushroom dry weight.

#### 2.5.2. Ferric reducing antioxidant power (FRAP)

The ability of polysaccharides to reduce ferric ions was analysed according to the method described by Benzie and Strain (1996). Fresh FRAP reagent was prepared daily by mixing 300 mM acetate buffer (pH 3.6) with 10 mM 2,4,6-tripyridyl-striazine (TPTZ) solution in 40 mM HCl and 20 mM  $\text{FeCl}_3 \cdot 6\text{H}_2\text{O}$  (10:1:1 ratio). The reagent was incubated at 37 °C for 90 min before an analysis. Aliquots of the samples (100  $\mu\text{L}$ ) were mixed with FRAP reagent (final volume, 2 mL) and were then incubated at 37 °C for 90 min. The change in the absorbance was measured at 593 nm. Trolox aqueous solutions (20–200  $\mu\text{M}$ ) were used to construct the calibration curve

and the results were reported as micromoles of Trolox equivalent (TE) per 1 g of mushroom dry weight.

## 2.6. Antiproliferative activity

Antiproliferative activity was tested on MCF-7 human breast adenocarcinoma cell line (ATCC HTB-22) and T-47D human ductal breast (epithelial tumour) carcinoma cell line (ECACC Catalog, No. 85102201). MCF-7 cell line was grown in RPMI 1640 medium (Sigma) supplemented with 10% fetal bovine serum (FBS, Sigma), 50 µg/mL bovine insulin (Sigma), 100 U/mL penicillin (Polfa, Poland) and 100 µg/mL streptomycin, (Polfa, Poland). The complete growth medium for T47D was RPMI 1640 medium (Sigma) supplemented with 10% fetal bovine serum (FBS, Sigma) and antibiotics (100 U/mL penicillin (Polfa, Poland)), 100 µg/mL streptomycin, (Polfa, Poland). Both cell lines were grown at 37 °C in humidified atmosphere with 5% CO<sub>2</sub> (standard conditions).

Antiproliferative activity of the tested polysaccharides was measured with MTT assay developed by Mosmann (1983). T47D and MCF-7 cells were seeded on 96-well plates at concentrations of  $3 \times 10^5$  cells/mL and  $2 \times 10^5$  cells/mL, respectively. After 24 h incubation at standard conditions (37 °C, 5% CO<sub>2</sub> flow, 95% air humidity), when cells in each well reached about 75%–80% confluence, the growth medium was replaced with dilutions of the tested polysaccharides dissolved in RPMI medium containing 2% FBS (at the concentrations ranging from 25 µg/mL to 250 µg/mL). Cells were incubated with polysaccharides for 24 h, followed by addition of 25 µL of MTT (Sigma) solution (5 mg/mL in PBS) per well. After 3 h incubation at 37 °C formazan crystals were solubilised by adding 100 µL of lysis buffer (10% SDS in 0.01 M HCl) per well. Plates were incubated overnight at standard conditions. The absorbance was read at 540 nm with a plate reader (680XR, Bio-Rad), and the mean value for each concentrations was calculated. The percentage of viable cells were calculated from the absorbance.

## 2.7. Statistical analysis

All measurements were carried out in triplicate and the obtained data was expressed as mean ± SD (standard deviation). The data was evaluated using unidirectional analysis of variance ANOVA with a level of significance set at  $\alpha = 0.05$ . Statistically different data was compared by Fisher's least significant difference (LSD) test.

## 3. Results and discussion

### 3.1. Water soluble polysaccharides content

The amount of WSP obtained from non-processed *P. ostreatus* was  $78.7 \pm 1.5$  mg/g dw, as shown in Fig. 1a. The processing of the fruiting bodies caused marked changes in the content of WSP. Blanching resulted in the increase of WSP ( $120.1 \pm 4.9$  mg/g dw). This could be explained by the fact that blanching leads to an extraction of soluble low molecular weight compounds and thus increasing the percentage of the fraction containing high molecular weight compounds. The similar effect was observed in blanched potatoes in which the content of pectin, cellulose and hemicellulose was increased (Gołubowska, 2005). Furthermore, Zivanovic and Buescher (2004) reported that blanching of *Agaricus bisporus* fruiting bodies caused the increase of total polysaccharides and protein content. Fruiting bodies that were cooked for 15 min also contained higher amount of WSP ( $100.4 \pm 4.7$  mg/g dw), comparing to control group. This fact could be still attributed to the change of the proportion of easily soluble substances to difficultly soluble compounds. This has been noted before by Dikeman, Bauer, Flickinger, and Fahey (2005) who observed substantial

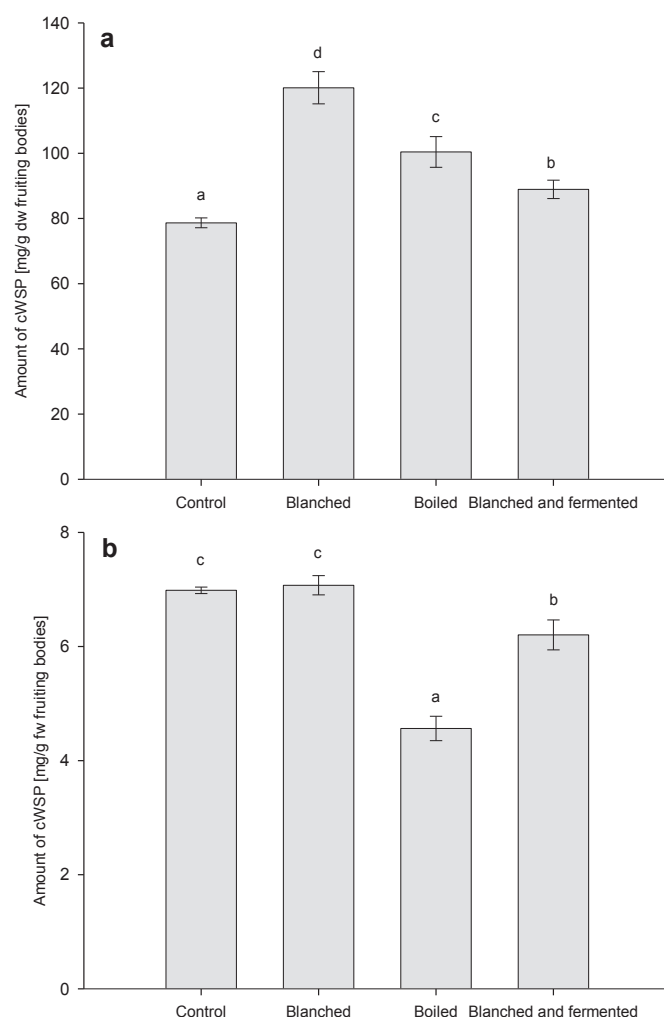


**Fig. 1.** The content of polysaccharides isolated from *P. ostreatus* fruiting bodies calculated on **dry** weight basis (A) and the **fresh** weight basis (B). Error bars indicate mean ± standard deviation (n = 3). Different letters indicate significant differences among the treatments according to LSD test (p < 0.05).

concentration of the fibre in various mushroom species, following the cooking process. The level of WSP in blanched and fermented samples (88.9 mg/g dw) was higher compared to non-processed fruiting bodies, but lower than in fruiting bodies that were solely blanched or cooked.

In order to investigate whether or not the applied processing techniques had a negative impact on the content of WSP, the results were calculated on the fresh weight basis, taking into consideration the loss of the mass (Fig. 1b). As can be seen from the graph, blanching did not affect negatively the content of WSP. However, boiling for 15 min, led to the substantial decrease in the amount of WSP (34.7% decline, comparing to the control). The observed loss could be attributed to the water extraction of the polysaccharides during the cooking procedure. With respect to the blanched and fermented mushrooms, the observed decrease was lower (14.7%). Because blanching alone did not influence the content of WSP it is possible that the presence of bacteria could be responsible for the loss. Additionally, two weeks storage could have caused WSP to diffuse into brine.

### 3.2. Chemical characteristics of water soluble polysaccharides

#### 3.2.1. Carbohydrate, protein and phenolics content

The amount of total carbohydrates, protein and phenolics is

**Table 1**

The amount of total carbohydrate, proteins and polyphenolics in the isolated water soluble polysaccharides of *P. ostreatus*. Mean values  $\pm$  standard deviation ( $n = 3$ ) with different letters indicate significant differences among the treatments according to LSD test ( $p < 0.05$ ).

Treatment	Total carbohydrate (% dw)	Protein content (% dw)	Total phenolics content (% dw)
Control	58.0 $\pm$ 3.9a	7.8 $\pm$ 0.5c	0.77 $\pm$ 0.04d
Blanched	76.3 $\pm$ 5.6b	3.9 $\pm$ 0.2b	0.41 $\pm$ 0.03b
Boiled	71.3 $\pm$ 2.9b	7.1 $\pm$ 0.5c	0.53 $\pm$ 0.06c
Blanched and fermented	89.2 $\pm$ 3.5c	3.0 $\pm$ 0.2a	0.29 $\pm$ 0.06a

presented in Table 1. The total carbohydrate content in the WSP extracted from non-processed fruiting bodies was 58.0  $\pm$  3.9% dw. This value was similar to that reported by other authors (62.8  $\pm$  7.7%), who isolated polysaccharides from *P. ostreatus* using similar method (Mitra, Khatua, & Acharya, 2013). The extracts obtained from blanched, boiled, blanched and fermented mushrooms contained higher level of carbohydrates (76.3  $\pm$  5.6%, 71.3  $\pm$  2.9, 89.2  $\pm$  3.5%, respectively).

Regarding to the protein content, its quantity in the control samples reached 7.8  $\pm$  0.5% dw. This amount was much higher comparing to those reported by Zhang, Dai, Kong, and Chen (2012) who found that the protein content ranged from 0.84% to 1.23%, depending on the method of isolation. This huge discrepancy could be attributed to the use of DAE resin by these researchers during the isolation procedure. On the other hand, other studies demonstrated much higher protein content in polysaccharides isolated from *P. ostreatus* ranging from 15% (Mitra et al., 2013) to 24% (Xia et al., 2011). The processing of mushrooms caused significant change in the protein content of WSP. In the samples isolated from blanched mushrooms its amount decreased approximately two times, relative to the control and reached 3.9  $\pm$  0.2%. Boiling resulted in rather negligible loss of protein level (7.1  $\pm$  0.5%) in relation to control samples. The greatest decline in the protein content was observed in WSP extracted from blanched and fermented mushrooms where its value reached 3.0  $\pm$  0.2%. It could be

possible that the lowest amount of protein in WSP obtained from blanched and fermented mushrooms could result from the presence of bacteria which released enzymes which caused degradation of protein (Dallagnol, Pescuma, DeValdez, & Rollán, 2013).

With regard to the phenolics, they were found in the smallest amount (below 1% dw) comparing to other WSP constituents. Total phenolics content of polysaccharides isolated from non-processed fruiting bodies was 0.77  $\pm$  0.04% dw. This data does not support the findings by Vamanu (2012) in which polyphenolics quantity was approximately ten times higher. This huge difference probably resulted from slightly different extraction procedure because the authors have omitted the stage of alcoholic extraction. Besides, the polysaccharides were obtained from mycelium, not from fruiting bodies. The fact that mushroom polysaccharides contain polyphenolic compounds is well established (Klaus et al., 2011). Polyphenolics tend to bind with polysaccharides with hydrogen bonds, hydrophobic interactions or even covalent bonds (Renard, Baron, Guyot, & Drilleau, 2001). Bound polyphenolics contribute to antioxidant activity of polysaccharides and their presence is highly beneficial. They are slowly released from the matrix by intestine microbes and are absorbed by an organism (Saura-Calixto, 2011). The processing of fruiting bodies led to substantial changes in the phenolics content and a similar trend to protein was observed. The rapid, 46% decline was noticed as the result of blanching and 31% in the case of cooking. A possible explanation for this is that hydrothermal processes may lead to solubilisation and releasing of phenolics (Martínez-Hernández, Artés-Hernández, Gómez, & Artés, 2013). Another possible explanation for this effect is thermal degradation due to the elevated temperature (Martínez, Pérez, Carballo, & Franco, 2013; Sikora, Cieślík, Leszczyńska, Filipiak-Florkiewicz, & Pisulewski, 2008). Lactic acid fermentation caused the highest (63%) decrease in phenolics content. This could be explained by diffusion of soluble phenolics into brine. This process could possibly have been enhanced by bacterial enzymes (Ciska, Karamać, & Kosińska, 2005).

### 3.2.2. FTIR spectroscopy

The FTIR spectra of isolated WSP are depicted in Fig. 2. They are

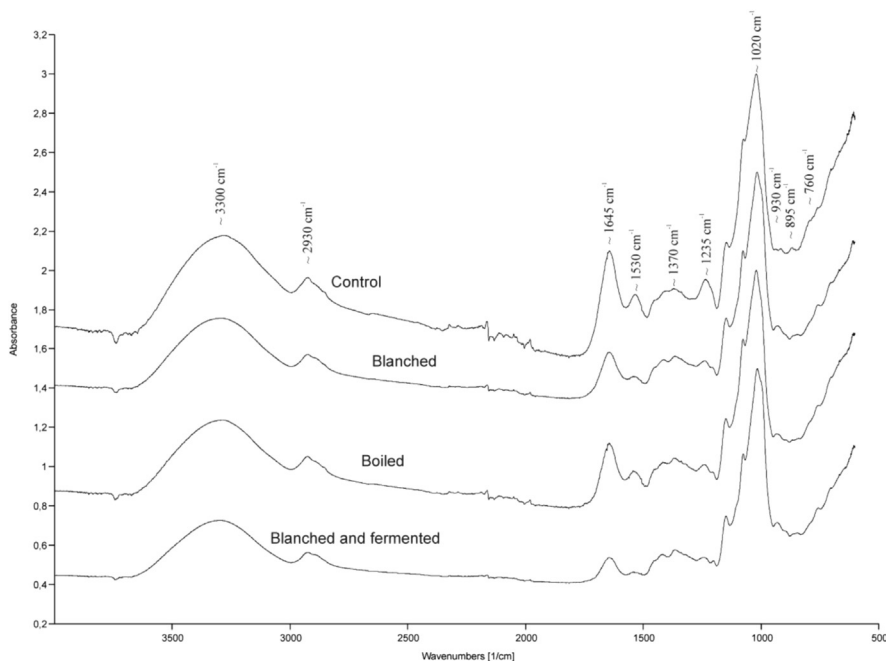


Fig. 2. FTIR spectra of water soluble polysaccharides obtained from non-processed (control) and processed fruiting bodies of *P. ostreatus*.

generally similar to that obtained by other authors (Gutiérrez, Prieto, & Martínez, 1996) and they show bands characteristic of the presence of polysaccharides and protein molecules. The broad peak in the region of  $3000\text{--}3500\text{ cm}^{-1}$  could be attributed to O–H and N–H stretching vibrations, while the band at  $\sim 2930\text{ cm}^{-1}$  is the result of C–H stretching. The absorption at  $\sim 1645\text{ cm}^{-1}$  (amide I) is indicative of C=O stretching mode, whereas the signal at  $1530\text{ cm}^{-1}$  corresponds to the presence of bending vibrations of N–H groups. These two bands indicate the presence of protein. In the region of  $1450\text{--}1300\text{ cm}^{-1}$  there are signals related to bending vibrations of  $\text{CH}_2$ , O–H and C–O–H (Mohaček-Grošev, Božac, & Puppels, 2001). Intense peaks observed at  $950\text{--}1190\text{ cm}^{-1}$  result from stretching vibrations of C–O–C, COH and C–C (Larkin, 2011). Analysis of  $700\text{--}950\text{ cm}^{-1}$  region can give information on the type of glycosidic links present in the sample. Signal at  $\sim 895\text{ cm}^{-1}$  may suggest the presence of  $\beta$ -glucans (Mohaček-Grošev et al., 2001), while bands at  $\sim 930\text{ cm}^{-1}$ ,  $\sim 850\text{ cm}^{-1}$ ,  $\sim 760\text{ cm}^{-1}$  are indicative of  $\alpha$ -glucans (Novák et al., 2012; Wiater et al., 2011).

### 3.2.3. Gel permeation chromatography

Gel permeation chromatography was performed to identify molecular weight of main WSP components. All the spectra showed sharp, symmetrical peak at  $18.1\text{--}19.1\text{ mL}$ . It corresponds to a compound having molecular weight of  $198.3\text{ kDa}$  (Fig. 3). The chromatogram of the extracted WSP from the control samples possessed also intense signals at  $22.4\text{ mL}$  and  $24.68\text{ mL}$  which can be attributed to the compounds of the lower molecular mass ( $11.9$  and  $3.1\text{ kDa}$ , respectively). These signals were not recorded in the samples obtained from the processed mushrooms. The presence of  $198.3\text{ kDa}$  fraction is in agreement with the results of other authors who extracted *P. ostreatus* polysaccharides (using similar isolation method) which had molecular mass  $187\text{ kDa}$  (Maity et al., 2011). Other researchers obtained the fractions of the lower molecular weight:  $1\text{--}10\text{ kDa}$  (Lavi et al., 2006) and  $10.5\text{ kDa}$  (Synytsya et al., 2009). The processing of fruiting bodies, regardless of the method applied, caused  $3.1\text{ kDa}$  fraction to disappear. Probably it could be eluted during the applied processes. Additionally, blanching led to diminishing of  $11.9\text{ kDa}$  fraction. Further studies should be undertaken to investigate the chemical composition of each fraction and the role they play in exerting antioxidant and antiproliferative activities.

### 3.3. Antioxidant capacity

Water soluble polysaccharides isolated from both processed and non-processed fruiting bodies displayed ABTS scavenging activity ranging from  $14.14 \pm 0.63$  to  $29.48 \pm 1.12\ \mu\text{moles of Trolox per } 1\text{ g dw}$  (Fig. 4). The control sample showed the highest value ( $29.48 \pm 1.12\ \mu\text{moles of Trolox per } 1\text{ g dw}$ ), which was rapidly decreased due to the processing. As the result of blanching approximately 26% decline was noticed, whereas boiling led to approximately 12% decrease. The highest drop in activity (approximately 52%) demonstrated the samples that were obtained from the blanched and fermented mushrooms. Our data are in qualitative agreement with other studies that investigated antioxidant capacity of fermented *A. bisporus* and *P. ostreatus* fruiting bodies and reported substantial decline in ABTS radical scavenging activity (approximately 60% and 90%, respectively) (Skąpska et al., 2008).

With respect to the FRAP assay, the activity values were lower comparing with ABTS assay and varied from  $2.49 \pm 0.54$  to  $16.52 \pm 0.55\ \mu\text{moles of Trolox equivalents per } 1\text{ g dw}$  (Fig. 4). However, the similar trend was observed in terms of the decrease of the antioxidant activity. The highest value was observed in the control samples ( $16.52 \pm 0.55\ \mu\text{moles of Trolox equivalents per } 1\text{ g dw}$ ) and the processing methods had a negative impact on the

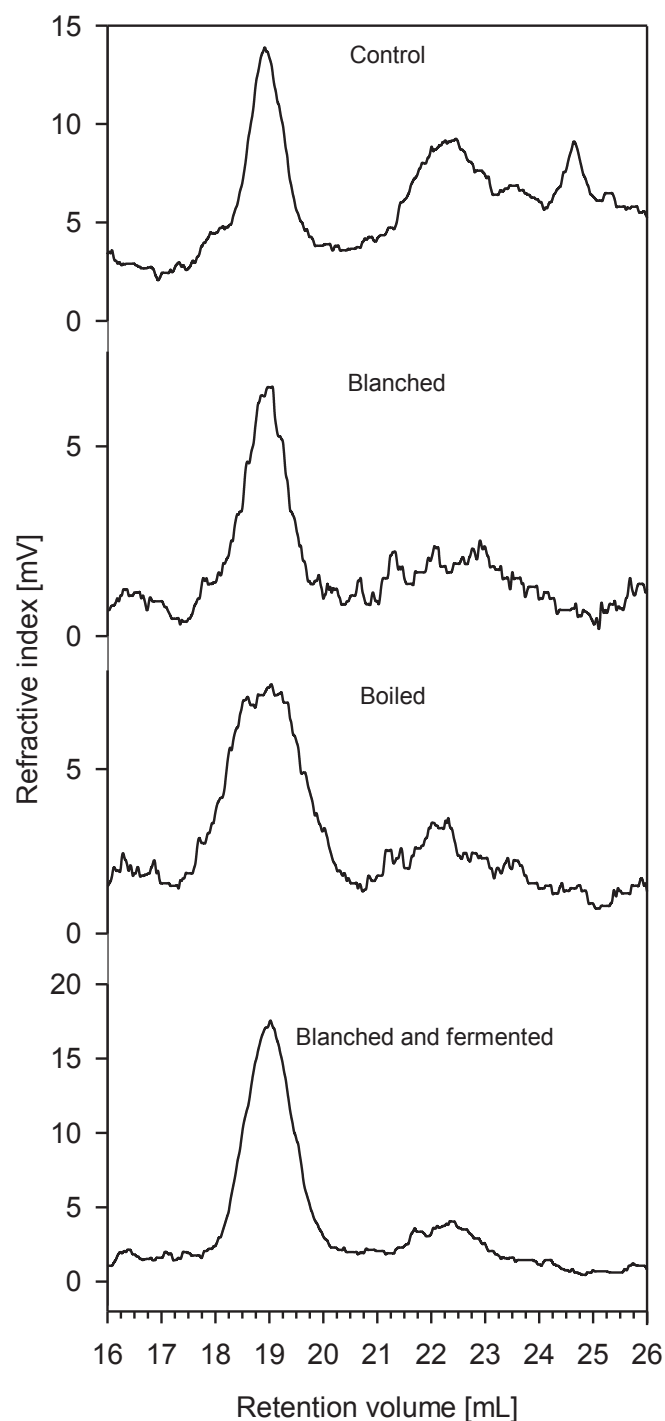
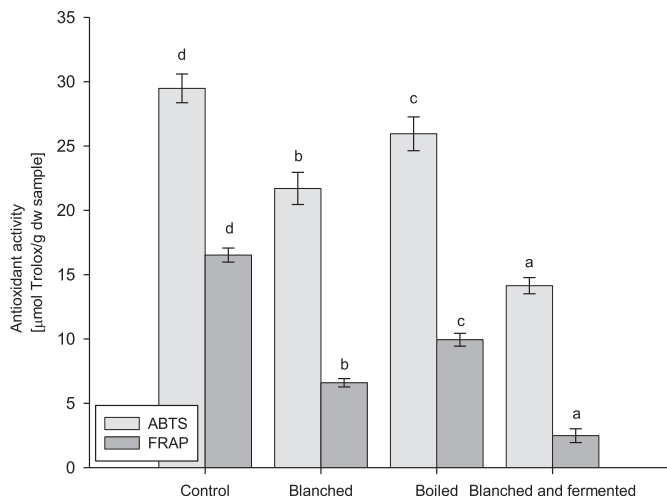


Fig. 3. Gel permeation chromatography of water soluble polysaccharides extracted from non-processed (control) and processed fruiting bodies.

activity. Blanching resulted in approximately 60% decrease, while boiling caused approximately 40% decline. The highest decrease (approximately 85%) was noticed for WSP isolated from blanched and fermented fruiting bodies.

Previous studies has shown that hydrothermal treatments leads to the decrease of total antioxidant potential of mushrooms (Nguyen, Nagasaka, & Ohshima, 2012; Soler-Rivas, Ramírez-Anguiano, Reglero, & Santoyo, 2009). The current study found that the applied processing altered antioxidant activity of the obtained



**Fig. 4.** Antioxidant capacity of water soluble polysaccharides extracted from non-processed (control) and processed mushrooms. Error bars indicate mean  $\pm$  standard deviation ( $n = 3$ ). Different letters indicate significant differences among the treatments according to LSD test ( $p < 0.05$ ).

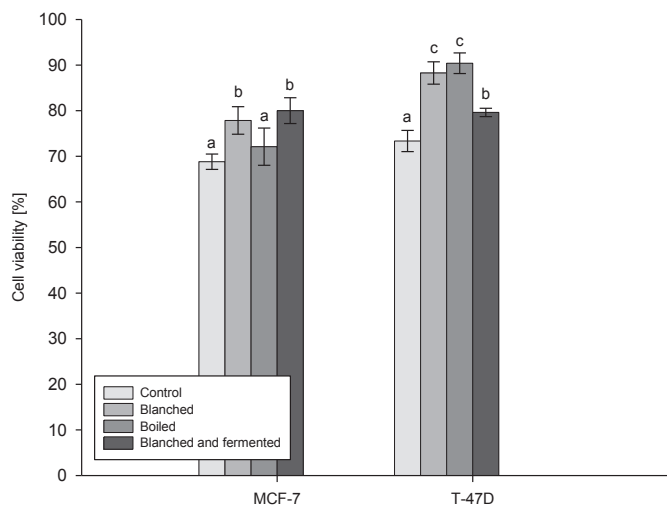


**Fig. 5.** Cell viability (%) of MCF-7 and T-47D human adenocarcinoma cell line after treatment with water soluble polysaccharides (250  $\mu\text{g/mL}$ ) obtained from non-processed (control) and processed *P. ostreatus* fruiting bodies. Error bars indicate mean  $\pm$  standard deviation ( $n = 3$ ). Different letters indicate significant differences among the treatments according to LSD test ( $p < 0.05$ ).

polysaccharides. As a consequence, this may affect their health-promoting properties.

### 3.4. Antiproliferative activity

The extracted water soluble polysaccharides were analysed in terms of their antiproliferative activity against MCF-7 and T-47D breast cancer cell lines. The results showed that WSP displayed slight inhibitory action on both cells lines (Fig. 5). The effect was most evident at the concentrations of 250  $\mu\text{g/mL}$ . The strongest activity was displayed by the samples derived from non-processed fruiting bodies (cell viability reached  $68.8 \pm 1.7\%$ ). As the result of processing, the drop of the activity was noticed and the cell viability amounted to  $77.9 \pm 3.0\%$ ,  $72.1 \pm 4.1\%$  and  $80.0 \pm 2.8\%$  for blanched, boiled, blanched and fermented samples, respectively. With regard to the T-47D cell line, the antiproliferative activity was generally

lower comparing to MCF-7 line. The lowest cell viability was found in non-processed samples ( $73.4 \pm 2.3\%$ ) and similarly to MCF-7 line, the processing led to the statistically relevant decrease in the activity.

Current literature does not provide information on the impact of hydrothermal processing on antiproliferative activity of food-derived polysaccharides. However, some studies were conducted on rich in phenolics methanolic extracts. Chatthongpisut, Schwartz, and Yongsawatdigul (2015) showed that cooking procedures leads to substantial decline in antiproliferative activity of purple rice. Also other authors reported that lotus roots and white onions cooked for 10 min possessed lower antiproliferative potential (Im et al., 2012).

## 4. Conclusions

Water soluble polysaccharides were extracted from both processed and non-processed mushrooms, giving different yields. The processing (boiling and blanching followed by fermenting) led to the decrease of polysaccharides content. Therefore, the real intake of these macromolecules can differ between raw and processed form. Moreover, all the processes caused substantial changes in chemical composition of polysaccharides (protein and phenolics contents were decreased). Along with the changes of chemical composition caused by the processing, antioxidant and antiproliferative activities were decreased which may affect nutritional and health values. Therefore, hydrothermal processing, especially long, should not be applied in order to fully retain health promoting properties of *P. ostreatus*. Further work would be suggested to investigate the impact of different processing techniques like microwave cooking, steaming or frying on bioactive polysaccharides from *P. ostreatus*. Moreover, since mushrooms polysaccharides are known to exert immunomodulating effect, more research is required to determine the impact of processing on this effect.

## References

- Beena Divya, J., Kulangara Varsha, K., Madhavan Nampoothiri, K., Ismail, B., & Pandey, A. (2012). Probiotic fermented foods for health benefits. *Engineering in Life Sciences*, 12, 377–390.
- Benzie, I. F. F., & Strain, J. J. (1996). The ferric reducing ability of plasma (FRAP) as a measure of 'antioxidant power': the FRAP assay. *Analytical Biochemistry*, 239, 70–76.
- Bradford, M. M. (1976). A rapid and sensitive method for the quantitation of microgram quantities of protein utilizing the principle of protein dye binding. *Analytical Biochemistry*, 72, 248–254.
- Chatthongpisut, R., Schwartz, S. J., & Yongsawatdigul, J. (2015). Antioxidant activities and antiproliferative activity of Thai purple rice cooked by various methods on human colon cancer cells. *Food Chemistry*, 188, 99–105.
- Ciska, E., Karamač, M., & Kosińska, A. (2005). Antioxidant activity of extracts of white cabbage and sauerkraut. *Polish Journal of Food and Nutrition Sciences*, 14/55, 367–373.
- Dallagnol, A. M., Pescuma, M., De Valdez, G. F., & Rollán, G. (2013). Fermentation of quinoa and wheat slurries by *Lactobacillus plantarum* CRL 778: proteolytic activity. *Applied Microbiology and Biotechnology*, 97, 3129–3140.
- Dikeman, C. L., Bauer, L. L., Flickinger, E. A., & Fahey, G. C., Jr. (2005). Effects of stage of maturity and cooking on the chemical composition of select mushroom varieties. *Journal of Agricultural and Food Chemistry*, 53, 1130–1138.
- Dubois, M., Gilles, K. A., Hamilton, J. K., Rebers, P. A., & Smith, F. (1956). Colorimetric method for determination of sugars and related substances. *Analytical Chemistry*, 28, 350–356.
- Fan, L., Li, J., Deng, K., & Ai, L. (2012). Effects of drying methods on the antioxidant activities of polysaccharides extracted from *Ganoderma lucidum*. *Carbohydrate Polymers*, 87, 1849–1854.
- Golubowska, G. (2005). Changes of polysaccharide content and texture of potato during French fries production. *Food Chemistry*, 90, 847–851.
- Gutiérrez, A., Prieto, A., & Martínez, A. T. (1996). Structural characterization of extracellular polysaccharides produced by fungi from the genus *Pleurotus*. *Carbohydrate Research*, 281, 143–154.
- Im, M. H., Park, Y. S., Ham, K. S., Kang, S. G., Heo, B. G., Leontowicz, H., et al. (2012). Effects of cooking on the bioactivity of lotus roots and white onions. *International Journal of Food Properties*, 15, 49–59.
- Klaus, A., Kozarski, M., Niksic, M., Jakovljevic, D., Todorovic, N., & Van

- Griensven, L. J. L. D. (2011). Antioxidative activities and chemical characterization of polysaccharides extracted from the basidiomycete *Schizophyllum commune*. *LWT – Food Science and Technology*, 44, 2005–2011.
- Larkin, P. (2011). *Infrared and Raman spectroscopy principles and spectral interpretation*. Elsevier.
- Lavi, I., Friesem, D., Geresh, S., Hadar, Y., & Schwartz, B. (2006). An aqueous polysaccharide extract from the edible mushroom *Pleurotus ostreatus* induces anti-proliferative and pro-apoptotic effects on HT-29 colon cancer cells. *Cancer Letters*, 244, 61–70.
- Maity, K. K., Patra, S., Dey, B., Bhunia, S. K., Mandal, S., Das, D., et al. (2011). A heteropolysaccharide from aqueous extract of an edible mushroom, *Pleurotus ostreatus* cultivar: structural and biological studies. *Carbohydrate Research*, 346, 366–372.
- Malinowska, E., Krzyczkowski, W., Łapienis, G., & Herold, F. (2009). Improved simultaneous production of mycelial biomass and polysaccharides by submerged culture of *Herichium erinaceum*: optimization using a central composite rotatable design (CCRD). *Journal of Industrial Microbiology and Biotechnology*, 36, 1513–1527.
- Martin, K. R., & Brophy, S. K. (2010). Commonly consumed and specialty dietary mushrooms reduce cellular proliferation in MCF-7 human breast cancer cells. *Experimental Biology and Medicine*, 235, 1306–1314.
- Martínez-Hernández, G. B., Artés-Hernández, F., Gómez, P. A., & Artés, F. (2013). Quality changes after vacuum-based and conventional industrial cooking of kailan-hybrid broccoli throughout retail cold storage. *LWT – Food Science and Technology*, 50, 707–714.
- Martínez, S., Pérez, N., Carballo, J., & Franco, I. (2013). Effect of blanching methods and frozen storage on some quality parameters of turnip greens (“grelós”). *LWT – Food Science and Technology*, 51, 383–392.
- Mitra, P., Khatua, S., & Acharya, K. (2013). Free radical scavenging and nos activation properties of water soluble crude polysaccharide from *Pleurotus ostreatus*. *Asian Journal of Pharmaceutical and Clinical Research*, 6, 67–70.
- Mohaček-Grošev, V., Božac, R., & Puppels, G. J. (2001). Vibrational spectroscopic characterization of wild growing mushrooms and toadstools. *Spectrochimica Acta – Part A: Molecular and Biomolecular Spectroscopy*, 57, 2815–2829.
- Mosmann, T. (1983). Rapid colorimetric assay for cellular growth and survival: application to proliferation and cytotoxicity assays. *Journal of Immunological Methods*, 65, 55–63.
- Nguyen, T. H., Nagasaka, R., & Ohshima, T. (2012). Effects of extraction solvents, cooking procedures and storage conditions on the contents of ergothioneine and phenolic compounds and antioxidative capacity of the cultivated mushroom *Flammulina velutipes*. *International Journal of Food Science and Technology*, 47, 1193–1205.
- Novák, M., Synytsya, A., Gedeon, O., Slepíčka, P., Procházková, V., Blahovec, J., et al. (2012). Yeast  $\beta(1\text{-}3),(1\text{-}6)\text{-d}$ -glucan films: preparation and characterization of some structural and physical properties. *Carbohydrate Polymers*, 87, 2496–2504.
- Renard, C. M. G. C., Baron, A., Guyot, S., & Drilleau, J. F. (2001). Interactions between apple cell walls and native apple polyphenols: quantification and some consequences. *International Journal of Biological Macromolecules*, 29, 115–125.
- Re, R., Pellegrini, N., Proteggente, A., Pannala, A., Yang, M., & Rice-Evans, C. (1999). Antioxidant activity applying an improved ABTS radical cation decolorization assay. *Free Radical Biology and Medicine*, 26, 1231–1237.
- Roupas, P., Keogh, J., Noakes, M., Margetts, C., & Taylor, P. (2010). Mushrooms and agaritine: a mini-review. *Journal of Functional Foods*, 2, 91–98.
- Saura-Calixto, F. (2011). Dietary fiber as a carrier of dietary antioxidants: an essential physiological function. *Journal of Agricultural and Food Chemistry*, 59, 43–49.
- Sikora, E., Ciešlik, E., Leszczyńska, T., Filipiak-Florkiewicz, A., & Pisulewski, P. M. (2008). The antioxidant activity of selected cruciferous vegetables subjected to aquathermal processing. *Food Chemistry*, 107, 55–59.
- Singleton, V. L., & Rossi, J. A. (1965). Colorimetry of total phenolics with phosphomolybdic acid–phosphotungstic acid reagents. *American Journal of Enology and Viticulture*, 16, 144–158.
- Skąpska, S., Owczarek, L., Jasińska, U., Hałasinska, A., Danielczuk, J., & Sokotowska, B. (2008). Zmiany pojemności przeciwutleniającej grzybów jadalnych w procesie kiszenia. *Żywność Nauka Technologia Jakość*, 59, 243–250.
- Soler-Rivas, C., Ramírez-Anguiano, A. C., Reglero, G., & Santoyo, S. (2009). Effect of cooking, in vitro digestion and Caco-2 cells absorption on the radical scavenging activities of edible mushrooms. *International Journal of Food Science and Technology*, 44, 2189–2197.
- Stachowiak, B., & Reguła, J. (2012). Health-promoting potential of edible macrofungi under special consideration of polysaccharides: a review. *European Food Research and Technology*, 234, 369–380.
- Sun, Y., & Liu, J. (2009). Purification, structure and immunobiological activity of a water-soluble polysaccharide from the fruiting body of *Pleurotus ostreatus*. *Bioresource Technology*, 100, 983–986.
- Synytsya, A., Míčková, K., Jablonský, I., Sluková, M., & Čopíková, J. (2008). Mushrooms of genus *Pleurotus* as a source of dietary fibres and glucans for food supplements. *Czech Journal of Food Sciences*, 26, 441–446.
- Synytsya, A., Míčková, K., Jablonský, I., Spěváček, J., Erban, V., Kovářiková, E., et al. (2009). Glucans from fruit bodies of cultivated mushrooms *Pleurotus ostreatus* and *Pleurotus eryngii*: structure and potential prebiotic activity. *Carbohydrate Polymers*, 76, 548–556.
- Thetsrimuang, C., Khammuang, S., Chiablaem, K., Srisomsap, C., & Sarntitha, R. (2011). Antioxidant properties and cytotoxicity of crude polysaccharides from *Lentinus polychrous* Lévl. *Food Chemistry*, 128, 634–639.
- Tong, H., Xia, F., Feng, K., Sun, G., Gao, X., Sun, L., et al. (2009). Structural characterization and in vitro antitumor activity of a novel polysaccharide isolated from the fruiting bodies of *Pleurotus ostreatus*. *Bioresource Technology*, 100, 1682–1686.
- Vamanu, E. (2012). Biological activities of the polysaccharides produced in submerged culture of two edible *Pleurotus ostreatus* mushrooms. *Journal of Biomedicine and Biotechnology*, 2012.
- Wasser, S. (2002). Medicinal mushrooms as a source of antitumor and immunomodulating polysaccharides. *Applied Microbiology and Biotechnology*, 60, 258–274.
- Wiater, A., Paduch, R., Pleszczyńska, M., Próchniak, K., Choma, A., Kandeferszerzeń, M., et al. (2011).  $\alpha\text{-}(1 \rightarrow 3)\text{-d}$ -glucans from fruiting bodies of selected macrofungi and the biological activity of their carboxymethylated products. *Biotechnology Letters*, 33, 787–795.
- Xia, F., Fan, J., Zhu, M., & Tong, H. (2011). Antioxidant effects of a water-soluble proteoglycan isolated from the fruiting bodies of *Pleurotus ostreatus*. *Journal of the Taiwan Institute of Chemical Engineers*, 42, 402–407.
- Zhang, M., Cui, S. W., Cheung, P. C. K., & Wang, Q. (2007). Antitumor polysaccharides from mushrooms: a review on their isolation process, structural characteristics and antitumor activity. *Trends in Food Science and Technology*, 18, 4–19.
- Zhang, Y., Dai, L., Kong, X., & Chen, L. (2012). Characterization and in vitro antioxidant activities of polysaccharides from *Pleurotus ostreatus*. *International Journal of Biological Macromolecules*, 51, 259–265.
- Zivanovic, S., & Buescher, R. (2004). Changes in mushroom texture and cell wall composition affected by thermal processing. *Journal of Food Science*, 69, SNQ44–SNQ49.



# Refractance Window drying of pomegranate juice: Quality retention and energy efficiency



Vahid Baeghbali<sup>a</sup>, Mehrdad Niakousari<sup>a, b, \*</sup>, Asgar Farahnaky<sup>a, c</sup>

<sup>a</sup> Department of Food Science and Technology, Faculty of Agriculture, Shiraz University, Shiraz, Iran

<sup>b</sup> Advanced Technologies Research Institute, Shiraz University, Shiraz, Iran

<sup>c</sup> School of Biomedical Sciences and Graham Centre for Agricultural Innovation, Charles Sturt University, Wagga Wagga, New South Wales 2678, Australia

## ARTICLE INFO

### Article history:

Received 1 March 2015

Received in revised form

28 September 2015

Accepted 5 October 2015

Available online 9 October 2015

### Keywords:

Refractance window drying

Pomegranate juice

Anthocyanins

Antioxidant activity

Energy efficiency

## ABSTRACT

Refractance Window (RW) drying system utilizes circulating hot water as a means to carry thermal energy to materials to be dehydrated. Products are spread on a transparent plastic conveyer belt that moves over circulating water in a shallow trough. In this study the quality retention characteristics of pomegranate juice (PJ) concentrate dried in a continuous pilot scale RW drying system were evaluated against freeze drying and spray drying methods. Samples of PJ concentrate (Brix 64) mixed with Gum Arabic as a carrier (35%, dry basis) were dried by the RW drying, freeze drying and spray drying methods. Physicochemical properties including moisture content, solubility, bulk density and color parameters of samples dried using different methods were compared. Chemical analysis and color measurements of reconstituted samples showed that RW dryer can produce high-quality products with anthocyanins content, anthocyanins color and antioxidant activity equal or greater than those of the freeze dried and spray dried samples. Energy consumption of the RW dryer was about one third and 1/40 of those of spray drying and freeze drying systems, respectively.

© 2015 Elsevier Ltd. All rights reserved.

## 1. Introduction

Refractance Window™ (RW)<sup>1,2,3</sup> as a relatively new film drying technique is characterized by short time exposure of foods to relatively low temperatures (Magoon, 1986; Nindo, Feng, Shen, Tang, & Kang, 2003). For drying a similar amount of a product, the cost of the RW equipment is estimated about one-third of the cost of a freeze-dryer, whereas the energy consumption of a RW is less than half of a freeze-dryer (Nindo & Tang, 2007). RW drying system utilizes circulating water at 95–97 °C as a means to carry

thermal energy to materials to be dehydrated. Pureed products are spread on a transparent Mylar plastic conveyer belt that moves over circulating water in a shallow trough and the unused thermal energy in the circulating water is recycled (Fig. 1). The actual product temperature is usually between 70 °C and 80 °C (Abonyi, Feng et al. 2002). Previous studies on RW technology have shown a high retention of product quality (color, vitamins and antioxidants) as compared to other conventional drying methods including freeze drying (Abonyi, Feng et al. 2002; Abonyi, Tang, & Edwards, 1999; Nindo & Tang, 2007). A study on the effect of RW drying, freeze drying, hot-air oven drying and natural convective drying on color characteristics of paprika showed that the freeze dried and RW dried paprika had better reflected color characteristics and there was no significant difference in browning index between freeze dried and RW dried samples (Topuz, Feng, & Kushad, 2009); however further studies on the influence of drying methods on carotenoids and capsaicinoids of paprika showed that natural convective drying method, due to an ongoing synthesis, resulted in higher carotenoids and capsaicinoids contents than those of other methods (Topuz, Dincer, Özdemir, Feng, & Kushad, 2011). Another study on drying of tomato juice using a batch Refractance window dryer and a laboratory freeze dryer,

*Abbreviations:* RW, Refractance Window; PJ, pomegranate juice; FD, freeze dryer; SD, spray dryer.

\* Corresponding author. Department of Food Science and Technology, Faculty of Agriculture, Shiraz University, Shiraz, Iran.

*E-mail addresses:* [baeghbali@shirazu.ac.ir](mailto:baeghbali@shirazu.ac.ir) (V. Baeghbali), [niakosar@shirazu.ac.ir](mailto:niakosar@shirazu.ac.ir) (M. Niakousari), [farahnak@shirazu.ac.ir](mailto:farahnak@shirazu.ac.ir), [afarahnaky@csu.edu.au](mailto:afarahnaky@csu.edu.au) (A. Farahnaky).

<sup>1</sup> RW™ is a trademark used exclusively for Refractance Window® drying and evaporation. Their mention in this paper is solely for correctness and does not imply endorsement of the technology over other systems performing similar function. Unless otherwise stated, RW will refer to Refractance Window® or RW™.

<sup>2</sup> Refractance Window.

<sup>3</sup> Pomegranate Juice.

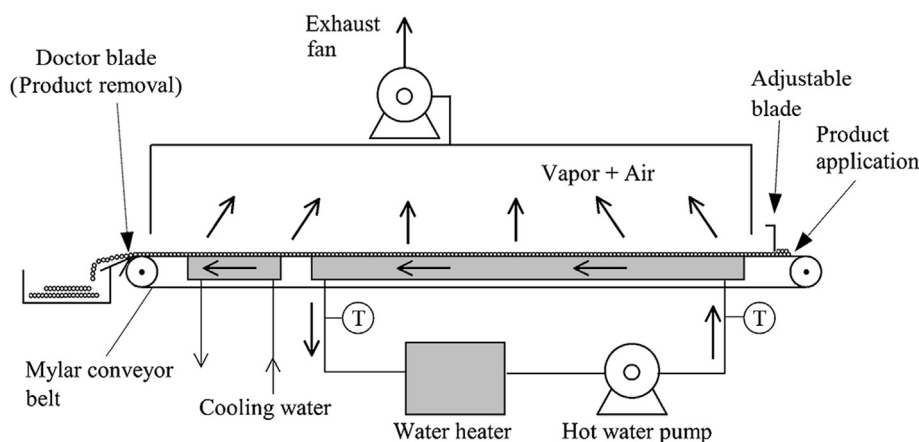


Fig. 1. Schematic of Refractance Window drying system (adapted from Abony et al. 2002).

showed no significant difference between ascorbic acid content and color parameters of RW and freeze dried samples (Baeghbali, Niakosari, & Kiani, 2010). In a recent study haskap berry puree was dried using an RW dryer in industrial scale and the anthocyanin content of the product was determined using pH-differential method and HPLC analysis. The results showed that the RW dried haskap berries retained more than 90% of anthocyanins (Celli, Khattab, Ghanem, & Brooks, 2016).

The pomegranate (*Punica granatum*, Punicaceae) is a native seasonal fruit of Iran; however, its high nutritional value and appealing taste make it desirable to have a pomegranate product available throughout the year and drying is regarded as a suitable tool to achieve this goal (Yousefi, Emam-Djomeh, & Mousavi, 2011). Pomegranate juice (PJ) concentrate is currently being produced in industrial scale and used for production of various fruit juices, nectars, drinks and sauces. Dried PJ has better storability and a longer shelf life than PJ concentrate. Studies have shown the health benefits of phytochemicals in PJ, primarily polyphenols including anthocyanin pigments, flavonol glycosides, procyanidins, phenolic acids and ellagic acid derivatives (Negi & Jayaprakasha, 2003). Red color is the most important quality criteria for fruit juices containing anthocyanin but unfortunately, anthocyanins are susceptible to degradation (Somers & Evans, 1986). Various factors affect the stability of anthocyanins, including the temperature of processing, the chemical nature of anthocyanins, pH, ascorbic acid, hydrogen peroxide, sugars, light and metals (Turfan, Türkyılmaz, Yemis, & Özkan, 2011). The antioxidant capacity of commercial PJ is three times higher than those of red wine and green tea (Gil, Tomas-Barberan, Hess-Pierce, Holcroft, & Kader, 2000).

The present study aims to investigate the potential to produce PJ powder using a pilot scale continuous RW dryer, a batch freeze dryer and a pilot scale spray dryer and to compare the powders obtained from the three methods in terms of physiochemical characteristics of the powders, including moisture content, solubility, yield, bulk density, color, anthocyanin color, total anthocyanins content, antioxidant activity and total phenolic compounds. The three drying systems were also analyzed for specific energy consumption and energy efficiency.

## 2. Materials and methods

PJ concentrate ( $^{\circ}\text{Brix} = 64$ ) was purchased from a commercial supplier (Green Farm, Neyriz, Iran); it was produced in industrial

scale by evaporation of clarified fresh pomegranate juice. PJ concentrate was dried by a pilot scale continuous Refractance Window dryer, a batch freeze drier (Dena Vacuum Industry, Teheran, Iran) and a pilot scale spray drying unit (Maham Sanat, Neyshabur, Iran). In preliminary tests, it was established that the PJ concentrate could not be dried to a powder without supplementing the feed with certain amount of a drying aid (antiplasticizing agent); due to its high sugar and organic acid contents. Thus, the feed was supplemented with gum Arabic prior to drying process. Gum Arabic has high water solubility, relatively low viscosity (compared to other gums e.g. xanthan gum) and high stability in acidic solutions (Montenegro, Boiero, Valle, & Borsarelli, 2012). Based on the previous studies, the minimum amount of gum Arabic needed to yield a reasonable quantity of powder with the lowest particle stickiness, was 35% of the total soluble solid of the PJ concentrate (35% gum Arabic in the feed dry matter). In all drying methods, the total soluble solid of the feed under investigation was adjusted to 50% ( $^{\circ}\text{Brix} = 50$ ) by adding distilled water. The total soluble solids ( $^{\circ}\text{Brix}$ ) were determined at 25  $^{\circ}\text{C}$  using an Abbe refractometer (CETi, Belgium). All tests were conducted in triplicate. The experimental conditions of the drying methods are explained in the following sections.

### 2.1. Dryers

#### 2.1.1. Refractance Window drying

A continuous pilot scale RW dryer with an effective length of 1.95 m was designed and fabricated in the Department of Food Science and Technology at Shiraz University. Because of operation of the exhaust fan, air at 28  $^{\circ}\text{C}$  and 30% relative humidity (RH) was forced over the bed at an average air velocity of 0.1 m/s to remove the moisture. Air velocity was measured using an AM-4201 anemometer (Lutron, Taipei, Taiwan). The hot water temperature was 91  $^{\circ}\text{C}$  and the cooling water temperature was 20  $^{\circ}\text{C}$ . The hot water and the cooling water flow rates were 2.5  $\text{m}^3/\text{hr}$  and 1  $\text{m}^3/\text{hr}$ , respectively. The Mylar belt speed was 3.9 mm/s. The thickness of the PJ concentrate applied to the polymer belt was set to be approximately 0.5 mm, using an adjustable blade. Flow rate of the feed was regulated at 0.5 L per hour using a peristaltic pump. Residence time of material on the drying belt was set to 8.5 min by adjusting the belt speed. The feed (a mixture of PJ concentrate and gum Arabic) was dried to 5.3% moisture content (wb). Dried product was removed from the belt, using a doctor blade (Figs. 1 and 2).

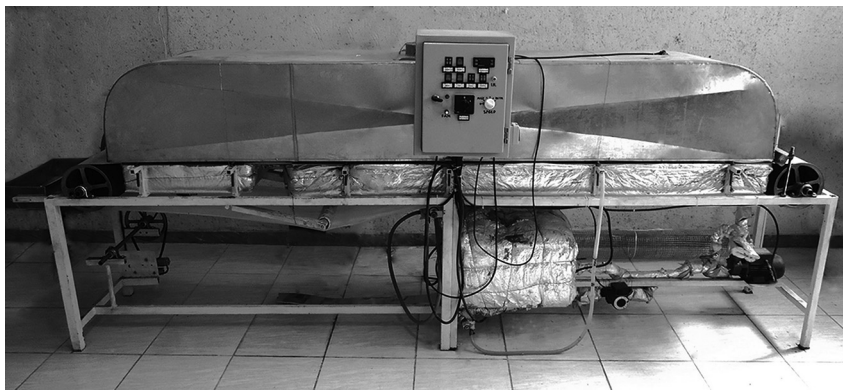


Fig. 2. Refractance Window drying system used in this study (manufactured in Department of Food Science and Technology at Shiraz University).

### 2.1.2. Spray drying

A pilot-scale mixed flow spray dryer (Maham Sanat, Neyshabur, Iran) was used in spray drying experiment. Inner diameter of the dryer chamber was 115 cm and its height was 165 cm. A two-fluid nozzle was used to atomize the sample pneumatically by high-velocity compressed air at 1 bar pressure. Feed rate was 0.75 L per hour and the feed temperature was 40 °C. The inlet and outlet air temperatures were  $140 \pm 1$  °C and  $75 \pm 1$  °C, respectively. Samples were dried to moisture content of 2.9% (wb).

### 2.1.3. Freeze drying

The PJ concentrate samples were quick-frozen at  $-80$  °C. The freeze dryer (Dena Vacuum Industry, Tehran, Iran) was operated at an absolute pressure of 3.0 kPa. The heat plate temperature of the freeze dryer was 20 °C and the condenser temperature was  $-40$  °C. Initial weight of each sample was 100 g and the drying time to reduce moisture content to 8.5% (wb) was 24 h. Some researchers have chosen long periods of time (up to 8 days) for freeze drying in order to obtain powders with lower moisture content; e.g., Topaz et al., 2009 and 2011. In this study freeze drying time was selected to be 24 h in order to have practical energy efficiency comparison with pilot scale RW and spray dryers. Freeze drying was included because it is frequently used as a high quality drying standard against other drying systems in producing dehydrated fruits and vegetables (Nindo & Tang, 2007).

After drying, the products were vacuum packed in polyethylene bags, sealed using a DZ-400 vacuum packing machine (Wenzhou Zhonghuan Packaging Machine Co., Ltd, China) and stored at 4 °C for further analysis.

## 2.2. Moisture content determination

Moisture content of the dried PJ samples was determined using oven method ( $103 \pm 1$  °C) according to the approved method of Association of Official Analytical Chemists (AOAC, 2002).

## 2.3. Solubility

Solubility was determined according to Eastman and Moore (1984) with some modifications. First, 100 mL of distilled water was transferred into a blender jar. The powder sample (1 g, dry basis) was carefully added to the blender operating at 15,000 rpm for 5 min. The solution was poured into a tube and centrifuged at  $3000 \times g$  for 5 min. An aliquot of 25 mL of the supernatant was then transferred to a pre-weighed petri dishes and immediately oven-dried at 105 °C for 5 h. The solubility (%) was calculated as the weight difference (Cano-Chauca, Stringheta, Ramos, & Cal-Vidal,

2005).

## 2.4. Yield

Weight of the dry material of the produced powders and weight of the feeds consumed were used to determine the spray dryer and RW dryer yields according to the Equation (1).

$$\text{Yield} = \frac{P \times S_P}{L \times S_F} \times 100 \quad (1)$$

where P is the rate of powder production (g/min),  $S_P$  is the percent of total solids of the powder, L is the feed flow rate (g/min), and  $S_F$  is the percent of total solids of the feed (Chegini & Ghobadian, 2007). The freeze drying was performed in a batch system therefore its yield was calculated using the same equation where P is the weight of dried product (g),  $S_P$  is the percentage of total solids of the powder, L is the weight of sample before drying (g), and  $S_F$  is the percentage of total solids of the sample.

## 2.5. Bulk density

To determine the (tapped) bulk density, 20 g of each powder was weighed into a 100 mL graduated cylinder then gently dropped 10 times on a rubber mat from a height of 15 cm. The bulk density was calculated by dividing the mass of the powder by the volume of the cylinder occupied by the powder (Goula, Karapantsios, Achilias, & Adamopoulos, 2008).

## 2.6. Pomegranate juice reconstitution

Dehydrated samples were rehydrated at room temperature with deionized water. The amount of water used to reconstitute the PJ powders was calculated based on the moisture content of the dried samples to reach a soluble solid content of 20% (g solid/g water) in the mixture. According to the Codex general standard for fruit juices and nectars, minimum pomegranate soluble solids level (Brix) for reconstituted PJ is 12.0% (Codex Standard 247, 2005). In the present study pomegranate soluble solids in reconstituted samples were adjusted to 13.0%. Since the dried samples contained 35% gum Arabic (in dry matter), a reconstituted sample with 20% soluble solids, was consisted of 13% pomegranate soluble solids (and 7% gum Arabic). The control sample was prepared by adding deionized water and gum Arabic to PJ concentrate to reach a soluble solid content of 20% in the mixture similar to the reconstituted samples.

## 2.7. Chemical analysis

In this study, the influences of different drying methods on pH, titratable acidity, anthocyanin color, total anthocyanins content, antioxidant activity and total phenolic compounds of reconstituted PJs were investigated.

The pH was determined using a pH/mV/temperature meter (Keison, UK). Titratable acidity was determined according to the AOAC (2002), and expressed as percentage of the citric acid.

Total anthocyanins content of samples was determined by pH differential method using two buffer systems: potassium chloride buffer, pH 1.0 (0.025 M) and sodium acetate buffer, pH 4.5 (0.4 M) (Cam, Hisil, & Durmaz, 2009). Briefly, 0.4 mL of PJ sample was mixed with 3.6 mL of corresponding buffers and read against water as a blank at 510 nm ( $A_{510}$ ) and 700 nm ( $A_{700}$ ). The Equation (2) was used to calculate absorbance (A):

$$A = (A_{510} - A_{700})_{\text{pH}1.0} - (A_{510} - A_{700})_{\text{pH}4.5} \quad (2)$$

Total anthocyanin content (TAC) of samples (mg cyanidin-3-glucoside/100 mL of PJ) was evaluated using equation (3):

$$\text{TAC} = (A \times \text{MW} \times \text{DF} \times 100) / \text{MA} \quad (3)$$

where A: absorbance; MW: molecular weight (449.2); DF: dilution factor (10); MA: molar absorptivity of cyanidin-3-glucoside (26,900).

Anthocyanin color (AC) was determined by spectrophotometry (Alper, Savas, & Acar, 2005) using Equation (4):

$$\text{AC} = [(Abs_{533-a} - Abs_{700}) - (Abs_{533-b} - Abs_{700})] \times \text{DF} \quad (4)$$

where  $Abs_{533-a}$  is the reading in a sample without bisulfite application, and  $Abs_{533-b}$  is the reading in sample with bisulfite application and DF is dilution factor.

Antioxidant activity was determined according to the method of Cam et al. (2009); 0.1 mL of samples was mixed with 0.9 mL of 100 mM Tris-HCl buffer (pH 7.4) to which 1 mL of DPPH (0.500  $\mu\text{M}$  in ethanol) was added. The control sample was prepared in similar way by adding 0.1 mL of water instead of sample. The mixtures were shaken vigorously and left to stand for 30 min. Absorbance of the resulting solution was measured at 517 nm by a Unico UV-2100 UV-vis spectrophotometer (South Brunswick, USA). The reaction mixture without DPPH was used for the background correction. The Equation (5) was applied to assess the antioxidant activity:

$$\text{Antioxidant activity (\%)} = [1 - (A_{\text{Sample}} / A_{\text{Control}})] \times 100 \quad (5)$$

where  $A_{\text{Sample}}$  is PJ sample absorbance in 517 nm and  $A_{\text{Control}}$  is control sample absorbance at 517 nm (Cam et al., 2009).

The Folin-Ciocalteu assay was used for the determination of total phenol content in PJs (Vinson, Dabbagh, Mamdouh, & Jang, 1995).

## 2.8. Color measurement

The color of dried samples and reconstituted PJ samples (L, a, and b) was measured using digital imaging and Photoshop software (Adobe Systems Inc., San Jose, California, USA) (Afshari-Jouybari & Farahnaky, 2011). Color difference ( $\Delta E$ ) was evaluated based on the Equation (6):

$$\Delta E = [(L_i - L_0)^2 + (a_i - a_0)^2 + (b_i - b_0)^2]^{1/2} \quad (6)$$

where  $L_i$ ,  $a_i$  and  $b_i$  are color measurement values for reconstituted sample and  $L_0$ ,  $a_0$  and  $b_0$  are color measurement values for the control sample.

## 2.9. Energy efficiency assessment

1 kg of PJ concentrate (with 35% gum Arabic in dry matter and Brix = 50), was used in three replica tests to evaluate the energy consumption of each dryer (Pilot scale RW, spray dryer and freeze dryer). Total energy consumption of each test was measured after water temperature of the RW dryer reached 91 °C, inlet air temperature of the spray dryer reached  $140 \pm 1$  °C and condenser temperature of the freeze dryer reached  $-40$  °C. The measurement was done using a digital single phase kWh meter with 0.01 kWh accuracy connected to the main power cable of each dryer so the measurements included energy consumption of all parts of the dryer (heaters, pumps, fans, etc.). Energy efficiency (EE) of each drying experiment was evaluated by the ratio of the energy needed for dehydration of 1 kg PJ sample ( $Q_T$ ) to the measured energy consumption ( $Q_M$ ). Basic energy efficiency calculation was performed using the following equations:

$$Q_T = (mc\Delta T) + (mL_v) \quad (7)$$

$$\text{EE} = Q_T / Q_M \quad (8)$$

where m is mass and c is specific heat of the sample;  $\Delta T$  is the temperature difference;  $L_v$  is the latent heat of vaporization in RW and spray dryer and the latent heat of sublimation in the freeze dryer;  $Q_M$  is the measured energy consumption by digital kWh meter and EE is energy efficiency.

## 2.10. Statistical analysis

All experiments were conducted in triplicate and an analysis of variance was performed. The least significant difference at  $p < 0.05$  was calculated using the Duncan test on PASW Statistics 18 software (PASAW 18; SPSS Inc., Chicago, USA). The data were expressed as mean  $\pm$  SD.

## 3. Results and discussion

### 3.1. Moisture content, solubility and color measurement of dried samples (powders)

Final moisture content, solubility and the color changes in samples as affected by different drying methods are shown in Table 1. Moisture content of the freeze dried and spray dried powders were highest and lowest, respectively. Higher moisture content of the freeze dried samples was probably due to the short time of the process; Topaz et al. (2009 and 2011) used eight days to freeze dry paprika puree to 4.6% moisture content. Pavan, Schmidt, & Feng (2012) in a study on drying açai juice using RW dryer, freeze dryer and hot air dryer, stated that moisture content of the products followed the order: RW dried > freeze dried > hot air dried. No significant difference in powder solubility for powders obtained from RW dryer and spray dryer was observed ( $p < 0.05$ ) (Table 1). The results were in good agreement with those reported by Yousefi et al. (2011). However, the solubility of the freeze dried powders was significantly lower. This was probably due to relatively high moisture content of the freeze dried sample causing the particles to stick together.

Color measurements showed no significant difference in lightness (L value) and yellowness (b) values among the freeze-dried and RW-dried samples and lightness of spray dried samples were significantly higher ( $p < 0.05$ ). Color measurement results for strawberry puree (without carrier) dried using RW dryer and freeze dryer showed the same pattern for lightness values, redness and yellowness of dried samples of the present study (Abonyi, Feng,

**Table 1**  
Moisture content, yield, bulk density, solubility and color measurement results of powders produced by spray, freeze and Refractance Window drying methods.

Sample	Moisture content (% wet basis)	Yield (%)	Bulk density (kg/m <sup>3</sup> )	Solubility (%)	Color measurement		
					L	a	b
Freeze dried	8.55 ± 0.57 <sup>a,*</sup>	96.7 ± 0.3 <sup>a</sup>	430.1 ± 8.9 <sup>a</sup>	89.1 ± 0.5 <sup>b</sup>	44.0 ± 0.9 <sup>b</sup>	24.3 ± 0.5 <sup>a</sup>	19.7 ± 0.3 <sup>a</sup>
RW dried	5.38 ± 0.57 <sup>b</sup>	95.2 ± 0.3 <sup>a</sup>	343.1 ± 8.9 <sup>b</sup>	92.9 ± 0.5 <sup>a</sup>	41.7 ± 0.9 <sup>b</sup>	17.3 ± 0.5 <sup>b</sup>	19.6 ± 0.3 <sup>a</sup>
Spray dried	2.92 ± 0.57 <sup>c</sup>	78.1 ± 0.3 <sup>b</sup>	322.1 ± 8.9 <sup>b</sup>	93.5 ± 0.5 <sup>a</sup>	50.3 ± 0.9 <sup>a</sup>	13.7 ± 0.5 <sup>c</sup>	16.7 ± 0.3 <sup>b</sup>

\*Different letters in each column indicate a significant difference ( $p \leq 0.05$ ).

et al., 2002). In another study, Nindo and Tang reported the same trend in comparison of lightness of dried strawberry puree using spray dryer, RW dryer and freeze dryer (Nindo & Tang, 2007). Freeze dried samples had the highest redness (a value) and spray dried samples had the lowest; this was probably due to greater loss of anthocyanins in spray dried samples; the results of anthocyanin measurement of the samples, support this conclusion.

### 3.2. Yield

Drying yields of freeze dryer, spray dryer and RW dryer are presented in Table 1. Spray drying PJ causes the materials to adhere to the wall chamber and cyclone (Yousefi et al., 2011) and some of the small particles were lost in the exhaust air; but the doctor blade installed on the RW was able to scrape off almost all of the dried product, therefore RW yield is much higher.

### 3.3. Tapped bulk density

Tapped density is the mass of the solid particles plus moisture divided by the total volume occupied by the particles, surface moisture and all pores, closed or open, in the surrounding atmosphere and is generally used to characterize the final product obtained by milling or drying (Onwulata, 2005). Bulk density of PJ powders dried by different methods are shown in Table 1. The RW dried sample had a less-packed structure formed in the measurement tube, with lower bulk density because of the flaky shape of its particles. Because of the fine structure of the spray dried sample, its bulk density was higher. Caparino, Sablani, Tang, Syamaladevi, and Nindo (2013) described the microstructure of RW dried mango puree as “smooth flakes with nearly uniform thickness” based on scanning electron micrographs (SEM) of mango powders and stated that “the uniformity of the flake thickness was the result of a controlled feeding of mango puree using a spreader bar at the inlet section of the RW dryer”. Bulk density of freeze dried sample was the highest; this could be due to higher moisture content of the dried product. Koc, Ern, & Ertekin (2008) also reported that bulk density of freeze dried samples with higher moisture content were considerably higher.

## 3.4. Chemical analysis of reconstituted samples

### 3.4.1. pH and titratable acidity

Results shown in Table 2 indicate that drying method did not have a significant effect on pH and titratable acidity of the reconstituted samples ( $p < 0.05$ ). The pH of all samples were slightly higher than usual range of natural PJ (2.93–3.20 according to US FDA/CFSAN 2007); this was probably due to presence of gum Arabic in the powder. The pH of a 35% (w/v) gum Arabic solution in water was measured to be  $5.89 \pm 0.13$ .

### 3.4.2. Anthocyanin color

The anthocyanin color in reconstituted PJ samples dried by different methods are shown in Table 3. Anthocyanin color in the

RW dried sample was higher but not significantly different from that of spray dried samples. Anthocyanin color in RW dried samples was slightly lower but not significantly different from that of freeze dried samples ( $p \leq 0.05$ ). Decrease in anthocyanin color of spray dried samples could be due to using heat in the process; Alper et al. (2005) reported a decrease in anthocyanin color of PJ samples after pasteurization.

### 3.4.3. Total anthocyanins content

Total anthocyanins content in reconstituted PJ samples dried by different methods are shown in Table 3. Total anthocyanins content in RW dried samples were significantly higher from that of freeze and spray dried samples ( $p < 0.05$ ). Celli, Khattab, Ghanem, & Brooks (2016) in a study on RW dried haskap berries concluded that RW drying method can retain above 90% of the haskap berry anthocyanins. Maximum anthocyanin content reduction was observed in spray dried sample which was probably due to thermal damage to anthocyanins. Lohachoompol, George & Craske, (2004) reported a decrease in anthocyanin content of cabin dried blueberries due to thermal drying process.

### 3.4.4. Antioxidant activity

Free radical species play a critical role in cardiovascular and inflammatory diseases as well as in neurodegenerative disorders, cancer and aging. Diets rich in antioxidants could help prevent many diseases affecting not only the heart, immune system and cancer but also the eyes (Varela-Santos et al., 2012). Antioxidant activity of reconstituted PJ samples dried by different methods is shown in Table 3. Antioxidant activity of RW dried samples was slightly higher but not significantly different from that of freeze dried samples ( $p < 0.05$ ). Antioxidant activity of RW dried samples was significantly higher than spray dried sample.

### 3.4.5. Total phenolic compounds

Total phenolic compounds in reconstituted PJ samples dried by different methods are also shown in Table 3. Total anthocyanins content in RW dried samples were significantly higher from spray dried samples but lower from freeze dried samples ( $p < 0.05$ ). This was probably due to use of heat in RW and spray drying methods. Alper et al. (2005) observed a decrease in total phenolic compounds of clarified and non-clarified PJ samples after pasteurization.

## 3.5. Color measurement

The color changes in reconstituted PJ as affected by different drying methods are shown in Table 2. In comparison to the control sample, the freeze-dried sample had a brighter color (highest L) than the spray and RW-dried samples. No significant difference was found in values among the freeze-dried, RW-dried, and control samples ( $p < 0.05$ ). Spray drying darkened the reconstituted product color as indicated by low L values. Overall, RW and freeze-dried samples were more red but slightly darker than the control sample as evidenced by lower L values. These results are compatible with the color measurement results of the sample powders,

**Table 2**

pH and titratable acidity (%citric acid), color measurement results in L a b, and color difference ( $\Delta E$ ) values of reconstituted samples from powders dried by spray, freeze and Refractance Window drying methods and the control sample.

Sample	pH	Titratable acidity (% citric acid)	Color measurement			
			L	a	b	$\Delta E$
Control	3.45 ± 0.21 <sup>a*</sup>	1.51 ± 0.12 <sup>a</sup>	31.7 ± 0.5 <sup>a</sup>	31.3 ± 0.3 <sup>a</sup>	37.7 ± 0.4 <sup>a</sup>	—
Freeze dried	3.50 ± 0.21 <sup>a</sup>	1.49 ± 0.12 <sup>a</sup>	30.0 ± 0.5 <sup>b</sup>	32.0 ± 0.3 <sup>a</sup>	36.3 ± 0.4 <sup>b</sup>	2.3 ± 0.5 <sup>c</sup>
Refractance window	3.53 ± 0.21 <sup>a</sup>	1.48 ± 0.12 <sup>a</sup>	28.3 ± 0.5 <sup>c</sup>	32.6 ± 0.3 <sup>a</sup>	34.3 ± 0.4 <sup>c</sup>	5.1 ± 0.5 <sup>b</sup>
Spray dried	3.68 ± 0.21 <sup>a</sup>	1.37 ± 0.12 <sup>a</sup>	26.7 ± 0.5 <sup>d</sup>	29.7 ± 0.3 <sup>b</sup>	33.0 ± 0.4 <sup>d</sup>	7.0 ± 0.5 <sup>a</sup>

\*Different letters in each column indicate a significant difference ( $p \leq 0.05$ ).

**Table 3**

Anthocyanin color, total anthocyanins content, antioxidant activity and total phenolic compounds of control sample and samples dried by spray, freeze and Refractance Window drying methods.

Sample	AC	TAC	AA	TPC
Control	0.387 ± 0.018 <sup>a*</sup>	12.670 ± 0.447 <sup>a</sup>	16.619 ± 2.113 <sup>a</sup>	580.3 ± 5.044 <sup>a</sup>
Freeze dried	0.247 ± 0.018 <sup>b</sup>	9.017 ± 0.447 <sup>c</sup>	12.656 ± 2.113 <sup>b</sup>	571.0 ± 5.044 <sup>a</sup>
Refractance window	0.232 ± 0.018 <sup>b,c</sup>	10.771 ± 0.447 <sup>b</sup>	12.947 ± 2.113 <sup>b</sup>	534.2 ± 5.044 <sup>b</sup>
Spray dried	0.183 ± 0.018 <sup>c</sup>	7.723 ± 0.447 <sup>c</sup>	9.979 ± 2.113 <sup>c</sup>	511.9 ± 5.044 <sup>c</sup>

AC: Anthocyanin color, TAC: Total anthocyanins content (mg cyanidin-3-glucoside/100 mL of PJ), AA: Antioxidant activity (%), TPC: Total phenolic compounds (mg equivalent gallic acid).

\*Different letters in each column indicate a significant difference ( $p \leq 0.05$ ).

stated above.

### 3.6. Energy efficiency

Overall energy efficiencies of the drying methods compared in this study are shown in Table 4. Abony, Tang, & Edwards (1999) calculated overall energy efficiency of a RW dryer in drying of carrot puree and strawberry puree samples 37.9% and 27.9%, respectively which is similar to the calculated efficiency in this study. Overall energy efficiency of the freeze dryer and spray dryer in this study was relatively low; although freeze drying has always been considered an expensive drying method, the spray dryer energy efficiency was found lower than expected and this was probably due to un-optimized conditions of the test.

Regarding environmental impact, as shown in Table 4, the calculated quantity of carbon dioxide emission to the atmosphere in case of freeze dryer and spray dryer was higher than RW dryer. These calculations have been made according to the literature: to obtain 1 kWh electricity from coal or fuel, 800 g of CO<sub>2</sub> will be rejected to the atmosphere during combustion of fossil fuel (Ferhat, Meklati, Smadja, & Chemat, 2006).

## 4. Conclusion

Quality of reconstituted pomegranate juice dried with the Refractance Window (RW) system was comparable to the freeze-dried product. Total anthocyanins content, anthocyanin color and antioxidant activity in the reconstituted pomegranate juice after RW drying were similar to the freeze-dried sample and higher than

the spray-dried product. RW-dried pomegranate juice had higher total anthocyanins content than freeze dried and spray dried samples and higher total phenolic compounds than spray dried samples. The color alterations in dried samples depended on the drying method and Refractance Window drying caused less color changes in the sample in comparison with spray dryer. Energy efficiency of Refractance Window dryer obtained from tests was comparable to spray dryer and considerably higher than freeze dryer. The results obtained in this study show that the Refractance Window dryer is an energy efficient drying technique and has good quality retention ability. Although RW showed some advantages over other drying technologies, further research is required to investigate scaling up of RW technology for drying fruit products.

## Acknowledgment

The authors wish to thank the INSF (Iran National Science Foundation) for their support.

## References

- Abonyi, B. I., Feng, H., Tang, J., Edwards, C. G., Mattinson, D. S., & Fellman, J. K. (2002). Quality retention in strawberry and carrot purees dried with refractance Window™ System. *Journal of Food Science*, 67, 1051–1056.
- Abonyi, B. I., Tang, J., & Edwards, C. G. (1999). *Evaluation of energy efficiency and quality retention for the refractance Window™ drying system*. Research Report. Pullman, WA: Washington State University.
- Afshari-Jouybari, H., & Farahnaky, A. (2011). Evaluation of photoshop software potential for food colorimetry. *Journal of Food Engineering*, 106(2), 170–175.
- Alper, N., Savas, K. B., & Acar, J. (2005). Influence of processing and pasteurization on color values and total phenolic compounds of pomegranate juice. *Journal of Food Processing and Preservation*, 29, 357–368.
- AOAC. (2002). *Official methods of analysis*. Gaithersburg, Maryland (17th ed.). Washington, D.C: Association of Official Analytical Chemists.
- Baeghbal, V., Niakosari, M., & Kiani, M. (2010). Design, manufacture and investigating functionality of a new batch refractance window system. In *Proceedings of 5th international conference on innovations in food and bioprocess technology*. Pathumthani, Thailand: Asian Institute of Technology.
- Cam, M., Hisil, Y., & Durmaz, G. (2009). Classification of eight pomegranate juices based on antioxidant capacity measured by four methods. *Journal of Food Chemistry*, 112, 721–726.
- Cano-Chauca, M., Stringheta, P. C., Ramos, A. M., & Cal-Vidal, J. (2005). Effect of carriers on the microstructure of mango powder obtained by spray drying and its functional characterization. *Innovative Food Science and Emerging Technologies*, 6, 420–428.
- Caparino, O. A., Sablani, S. S., Tang, J., Syamaladevi, R. M., & Nindo, C. I. (2013). Water sorption, glass transition, and microstructures of refractance window and

**Table 4**

Overall energy efficiency of spray, freeze and Refractance Window dryers.

Dryer	Calculated energy needed for drying 1 kg sample (kWh)	Energy consumption for drying 1 kg sample (kWh)	Overall energy efficiency (%)	CO <sub>2</sub> emission for drying 1 kg sample (kg)
Freeze dryer	1.46	130.65 ± 0.82 <sup>a*</sup>	1.12	104.52
RW dryer	1.36	4.31 ± 0.82 <sup>c</sup>	31.56	3.45
Spray dryer	1.42	11.01 ± 0.82 <sup>b</sup>	12.92	8.81

\*Different letters in each column indicate a significant difference ( $p \leq 0.05$ ).

- freeze-dried mango (Philippine "Carabao" Var.) powder. *Drying Technology*, 31, 1969–1978.
- Celli, G. B., Khattab, R., Ghanem, A., & Brooks, M. S. (2016). Refractance Window™ drying of haskap berry – preliminary results on anthocyanin retention and physicochemical properties. *Food Chemistry*, 194, 218–221.
- Chegini, G. R., & Ghobadian, B. (2007). Spray dryer parameters for fruit juice drying. *World Journal of Agricultural Sciences*, 3(2), 230–236.
- Codex Alimentarius Commission. (2005). General standard for fruit juices and nectars. *Codex Standard*, 247.
- Eastman, J.E., & Moore, C.O. (1984). Cold water soluble granular starch for gelled food composition. US Patent: 4465702.
- Ferhat, M. A., Meklati, B. Y., Smadja, J., & Chemat, F. (2006). An improved microwave cleverger apparatus for distillation of essential oils from orange peel. *Journal of Chromatography A*, 1112, 121–126.
- Gil, M. I., Tomas-Barberan, F. A., Hess-Pierce, B., Holcroft, D. M., & Kader, A. A. (2000). Antioxidant activity of pomegranate juice and its relationship with phenolic composition and processing. *Journal of Agricultural Food Chemistry*, 48, 4581–4589.
- Goula, A. M., Karapantsios, T. D., Achilias, D. S., & Adamopoulos, K. G. (2008). Water sorption isotherms and glass transition temperature of spray dried tomato pulp. *Journal of Food Engineering*, 85, 73–83.
- Koc, B., Ern, I., & Ertekin, F. K. (2008). Modelling bulk density, porosity and shrinkage of quince during drying: the effect of drying method. *Journal of Food Engineering*, 85, 340–349.
- Lohachoompol, V., George, S., & Craske, J. (2004). The change of total anthocyanins in blueberries and their antioxidant effect after drying and freezing. *Journal of Biomedicine and Biotechnology*, 5, 248–252.
- Magoon, R.E. (1986). Method and apparatus for drying fruit pulp and the like. US Patent: 4631837.
- Montenegro, M. A., Boiero, M. L., Valle, L., & Borsarelli, C. D. (2012). Gum arabic: more than an Edible Emulsifier. In C. J. R. Verbeek (Ed.), *Products and applications of biopolymers* (pp. 3–26). <http://dx.doi.org/10.5772/33783>. InTech, ISBN: 978-953-51-0226-7.
- Negi, P. S., & Jayaprakasha, G. K. (2003). Antioxidant and antibacterial activities of *Punica granatum* peel extracts. *Journal of Food Science*, 68, 1473–1477.
- Nindo, C. I., Feng, H., Shen, G. Q., Tang, J., & Kang, D. H. (2003). Energy utilization and microbial reduction in a new film drying system. *Journal of Food Processing and Preservation*, 27(2), 117–136.
- Nindo, C. I., & Tang, J. (2007). Refractance window dehydration technology: a novel contact drying method. *Drying Technology*, 25(1), 37–48.
- Onwulata, C. (2005). *Encapsulated and powdered foods* (pp. 39–71, 331–361). Boca Raton, USA: Taylor and Francis.
- Pavan, A. M., Schmidt, S. J., & Feng, H. (2012). Water sorption behavior and thermal analysis of freeze-dried, refractance window-dried and hot-air dried açai (*Euterpe oleracea Martius*) juice. *LWT - Food Science and Technology*, 48, 75–81.
- Somers, T. C., & Evans, M. E. (1986). Evolution of red wines I. Ambient influences on colour composition during early maturation. *Vitis*, 25, 31–39.
- Topuz, A., Dincer, C., Özdemir, K. S., Feng, H., & Kushad, M. (2011). Influence of different drying methods on carotenoids and capsaicinoids of paprika (Cv. Jalapeno). *Food Chemistry*, 129, 860–865.
- Topuz, A., Feng, H., & Kushad, M. (2009). The effect of drying method and storage on color characteristics of paprika. *LWT - Food Science and Technology*, 42, 1667–1673.
- Turfan, O., Türkyılmaz, M., Yemis, O., & Özkan, M. (2011). Anthocyanin and colour changes during processing of pomegranate (*Punica granatum* L., cv. Hicaznar) juice from sacs and whole fruit. *Food Chemistry*, 129, 1644–1651.
- US FDA/CFSAN. (2007). *Approximate pH of foods and food products*. USA: FDA/Center for Food Safety & Applied Nutrition.
- Varela-Santos, E., Ochoa-Martinez, A., Tabilo-Munizaga, G., Reyes, J. E., Pérez-Won, M., Briones-Labarca, V., et al. (2012). Effect of high hydrostatic pressure (HHP) processing on physicochemical properties, bioactive compounds and shelf-life of pomegranate juice. *Innovative Food Science and Emerging Technologies*, 13, 13–22.
- Vinson, J. A., Dabbagh, Y. A., Mamdouh, M. S., & Jang, J. (1995). Plant flavonoids, especially tea flavonols are powerful antioxidants using an in vitro oxidation model for heart disease. *Journal of Agricultural and Food Chemistry*, 43, 2800–2802.
- Yousefi, S., Emam-Djomeh, Z., & Mousavi, S. M. (2011). Effect of carrier type and spray drying on the physicochemical properties of powdered and reconstituted pomegranate juice (*Punica Granatum* L.). *Journal of Food Science and Technology*, 48(6), 677–684.



# Physicochemical properties of Alaska pollock (*Theragra chalcogramma*) surimi gels with oat bran



Fatimah Alakhrash, Ugochukwu Anyanwu, Reza Tahergorabi\*

North Carolina Agricultural and Technical State University, Greensboro, NC, USA

## ARTICLE INFO

### Article history:

Received 2 June 2015

Received in revised form

29 September 2015

Accepted 4 October 2015

Available online 9 October 2015

### Keywords:

Surimi

Dietary fiber

Oat bran

Texture

Color

## ABSTRACT

Oat bran is a gluten-free dietary fiber that may reduce the risk of heart disease and diabetes. Currently, surimi, a derivative of seafood, is neither produced with fiber, nor has the effect of fiber on the physicochemical properties of surimi gels been thoroughly studied. In this context therefore, the purpose of this study was to address the physicochemical properties of surimi gels formulated with variable levels of oat bran while maintaining constant levels of protein and water. Oat bran and SiO<sub>2</sub> incorporated in inverse concentrations were used in developing treatments of 0–8 g/100 g oat bran. Incorporation of oat bran up to 6 g/100 g greatly enhanced ( $P < 0.05$ ) gel texture (Kramer shear force and texture profile analysis). Protein content that was rather elevated appears not affecting the pH. Surimi gels with oat bran would apparently reduce ( $P < 0.05$ ) the whiteness, coincidental with L\* but with increasing b\* values. Water holding capacity concurrent with texture would likely improve ( $P < 0.05$ ) with cooking loss probably due to the absorbent nature of oat bran. This study suggests that incorporating oat bran into surimi products would likely not compromise quality, which may be useful to manufacturers for marketing surimi products with added health benefits.

© 2015 Elsevier Ltd. All rights reserved.

## 1. Introduction

In the USA as well as many Western countries, coronary artery disease and blood cholesterol respectively stand among major causes of death and risk factor. Reductions in total and low-density lipoprotein (LDL) cholesterol decrease the risk of the malady (Kerckhoffs, Hornstra, & Mensink, 2003). Increasing dietary fiber has been recommended as a safe and practical approach for cholesterol reduction. However, Americans seem not yet attaining the recommended amounts of dietary fiber reflected by the reported intake of about 15 g per day. The recommended adequate intake for fiber stands at 25 g per day for women and 38 g per day for men (Dietary Guidelines Advisory Committee, 2010). Dietary fiber is found predominantly in plant foods. It is the remnant of the edible part of plants that is resistant to human digestion (American Association of Cereal Chemists, 2001). It consists of both soluble and insoluble fiber. The soluble fiber from oat bran is very effective in lowering blood cholesterol, normalizing blood sugar levels, and lowering the risk of cardiovascular disease, obesity, and type 2

diabetes (Brand-Miller et al., 2012). Oat is an important food grain in temperate regions of the world (Butt, Tahir-Nadeem, Khan, Shabir, & Butt, 2008). Bran is the edible, outermost layer of the oat kernel and is produced by grinding clean groats or rolled oats to separate the resulting flour by sieving, bolting, and other suitable means into fractions such that the oat bran is not more than 50% of the starting material. Oat bran contains a heart-healthy soluble fiber called  $\beta$ -glucan. Oat bran contains 17.1 g/100 g protein, 66 g/100 g carbohydrates, 7 g/100 g fat, 11 g/100 g dietary fiber, 10.4 g/100 g  $\beta$ -glucan, 1.3 mg niacin, 171 mg magnesium, 6.4 mg iron, 0.17 mg copper, 441 mg potassium, and less than 0.5 mg  $\alpha$ -tocopherol (Feng et al., 2013). By including the oat bran in food products, the antioxidant-rich portion of the grain is retained. On the basis of numerous clinical studies, the US Food and Drug Administration (FDA) permitted the use of a claim that oat soluble fiber has the ability to reduce the risk of heart disease (Daou & Zhang, 2012).

In addition to health benefits, dietary fiber possesses hydrocolloidal properties that can be useful in food manufacturing as well as when fiber is added as an ingredient in final food products. Oat products such as oat bran have also been used in meat systems to improve functional properties (e.g., water absorption). Specifically, oat bran and oat fiber appears to be suitable fat replacements

\* Corresponding author.

E-mail address: [rtahergo@ncat.edu](mailto:rtahergo@ncat.edu) (R. Tahergorabi).

in ground beef and pork sausage products due to their ability to retain water and emulate particle definition in ground meat in terms of both color and texture (Özvural & Vural, 2008). Advantages of oat bran may include its savory taste, which imitates fat, the lack of cereal flavor, and the way it retains the natural flavorings of meat. It also reduces fat absorption, slows carbohydrate absorption, and aids satiety (Modi, Mahendrakar, Sachindra, & Rao, 2004). Oat bran was used as a fat substitute in meatballs, and it has been reported that meatballs containing oat bran had lower concentrations of total fat and trans fatty acids compared to control samples (Yılmaz & Dağlıoğlu, 2003). Meatballs made with 20 g/100 g oat bran present increases in protein, ash content, lightness, and yellowness, but reducing moisture and redness. Sensory attributes of meatballs may show no significant difference amidst the increases in acceptability. In these applications, oat bran potentially cements desirable functional properties. These properties make oat bran a functional ingredient for potential incorporation into surimi seafood products.

Surimi is minced and deboned fish meat that has been washed of lipids, water-soluble or sarcoplasmic proteins, and other impurities for use in the manufacture of imitation seafood products such as imitation crab legs. Park and Lin (2005) indicated that surimi consumption in the United States has steadily increased over the years. The popularity remains high and continues to grow, possibly due to the low cholesterol, low fat, and high nutrient content of surimi seafood. Due to its low fat content, nutritional quality, and highly functional proteins, surimi is a logical candidate for functional additives. Nonetheless, fiber is not traditionally added to surimi seafood. Previous studies on fiber in surimi have utilized soluble fibers such as carrageenan, chicory root inulin, garrofin, guar, and xanthan (Cardoso, Mendes, Pedro, & Nunes, 2008; Sánchez-Alonso, Haji-Maleki, & Borderias, 2007). These soluble fibers had detrimental effects on the gelation of surimi proteins, resulting in a loss of gel elasticity and strength coupled with gel hardening and increased brittleness. Different seafood species and the type of fiber probably caused these varied results. Importantly, in the design of previous studies, the protein concentration of surimi gels decreased proportionally with the increased concentration of added fiber, making both protein content and fiber content experimental variables. Surimi with a lower protein concentration shows poorer thermal gelation characteristics, yielding gels with poorer textural properties (Kristinsson, Lanier, Halldorsdottir, Geirsdottir, & Park, 2013). Thus, the lower protein concentration probably confounded the experiment results that were attributed only to the added fiber. The objectives of this study were to determine (1) proximate composition and pH (2) textural (Kramer shear force, and texture profile analysis) and color ( $L^*a^*b^*$  tristimulus color values) properties (3) expressible water and water holding capacity and (4) cooking loss of Alaska pollock surimi gels formulated with constant protein and water contents, but variable contents of oat bran.

## 2. Materials and methods

### 2.1. Surimi

Frozen Alaska pollock surimi grade A was purchased from Trident Seafoods Corp. (Seattle, WA). The surimi contained cryoprotectants (4 g/100 g of sorbitol and 4 g/100 g of sucrose as well as 0.15 g/100 g respective of sodium tripolyphosphate, and 0.15 g/100 g of tetrasodium pyrophosphate) that were delivered in tight boxes surrounded with ice. The frozen surimi was divided into 600 g weight of blocks from total weight of 1000 g used for this study and vacuum sealed. It was then stored at  $-80^{\circ}\text{C}$  until needed.

### 2.2. Preparation of surimi paste

The surimi paste was prepared according to the process described by Jaczynski and Park (2004). The first step was to thaw the frozen surimi at  $4^{\circ}\text{C}$  overnight. The surimi was then chopped at low speed for 1 min in a universal food processor (Model UMC5, Stephan Machinery Corp., Columbus, OH). The universal food processor is equipped with a two-layer cooling jacket and a temperature probe which enables to control the temperature between 1 and  $4^{\circ}\text{C}$  during chopping. The surimi paste was obtained by extracting surimi myofibrillar protein with 2 g/100 g of NaCl (non-iodized Morton salt, Morton International Inc., Chicago, IL) and chopping at low speed for 0.5 min. Final moisture of the surimi gels was adjusted to 78 g/100 g by adding chilled water ( $4^{\circ}\text{C}$ ) to the paste according to the batter formulation in Table 1. In order to maintain the same protein concentration and moisture content for all treatment groups but variable concentration of soluble fiber, silicon dioxide ( $\text{SiO}_2$ ) was added to surimi gels as inert filler (Taherogorabi, Beamer, Matak, & Jaczynski, 2012). Oat bran (Old Fashioned Quaker Oat Bran, Chicago, IL) and  $\text{SiO}_2$  (silicon dioxide crystalline 325 mesh, Spectrum Chemical, Gardena, CA) were added to the surimi paste in four combinations to a total final concentration of 8 g/100 g. One treatment without added fiber (with 8 g/100 g silicon dioxide) was a control. Treatments included 0 g/100 g fiber (0 g/100 g oat bran, 8 g/100 g silicon dioxide – control), 2 g/100 g fiber (2 g/100 g oat bran, 6 g/100 g silicon dioxide), 4 g/100 g fiber (4 g/100 g oat bran, 4 g/100 g silicon dioxide), 6 g/100 g fiber (6 g/100 g oat bran, 2 g/100 g silicon dioxide), and 8 g/100 g fiber (8 g/100 g oat bran, 0 g/100 g silicon dioxide). All ingredients in each treatment were chopped at low speed for 1 min. Additional chopping was performed at high speed under vacuum (0.5 bar) for 3 min. Surimi pastes were prepared in 1 kg batches. Pastes prepared in this manner were used to develop heat-set surimi gels.

### 2.3. Preparation of heat-set surimi gels

A surimi paste was stuffed through plastic hotdog casings (Lem Products Direct; West Chester, OH) (diameter: 2.6 cm, length: 17.5 cm), and the casings were tightened from both sides. Surimi pastes were cooked in a water bath at  $90^{\circ}\text{C}$  for 30 min, cooled in an ice bath for approximately 20 min, and the hotdog casings were peeled. Heat-set surimi gels prepared in this manner were used for evaluation of proximate composition (ash, moisture, and protein content), pH, color (tristimulus color values), texture (texture profile analysis and Kramer shear force), water holding capacity, and cooking loss.

### 2.4. Proximate composition of surimi gels

The levels of moisture content, crude protein content and ash content were determined for surimi gels. Moisture was determined by placing a 2 g sample on an aluminum dish (Fisher Scientific Co., Fairlawn, NJ), spreading it evenly across the dish, and oven-drying it at  $105^{\circ}\text{C}$  for 24 h (AOAC, 1995). Crude protein was analyzed by means of a Kjeldahl assay and expressed as g/100 g (AOAC, 1995). Ash content was determined through incinerating samples in a muffle furnace at  $550^{\circ}\text{C}$  for 24 h and expressed as g/100 g (AOAC, 1995).

### 2.5. pH

pH was measured according to Xu, Xia, Yang, & Nie, 2010 using a hand-held pH meter (Oakton, Vernon Hills, IL) and the probe was calibrated before each measurement.

**Table 1**

Final surimi batter formulations. Batters with different levels of fiber were formulated to contain 78% moisture and constant amounts of protein, water, and salt by using inert filler (silicon dioxide – SiO<sub>2</sub>). Batch size was 1000 g.

Fiber (g/1000 g)	Inert filler – SiO <sub>2</sub> (g/1000 g)	Surimi (g/1000 g)	Water (g/1000 g)	Salt (g/1000 g)	Batch weight (g)
0.0 <sup>a</sup>	80.0	480.0	420.0	20.0	1000.0
20.0	60.0	480.0	420.0	20.0	1000.0
40.0	40.0	480.0	420.0	20.0	1000.0
60.0	20.0	480.0	420.0	20.0	1000.0
80.0	0.0	480.0	420.0	20.0	1000.0

<sup>a</sup> Control.

## 2.6. Texture properties of surimi gels

Two different methods were applied to determine the surimi texture properties: the Kramer shear test and texture profile analysis (TPA). Cylindrical surimi gels (height = 8.0 cm, diameter = 2 cm) were used for the Kramer shear test (Model TA-XT2, Texture Technologies Corp., Scarsdale, NY) with a Kramer cell attachment (Tahergorabi, Beamer, Matak, & Jaczynski, 2011). The Kramer shear cell contained five 3.0-mm thick and 70-mm wide shear blades passing through a cell with a corresponding number of slots. Individual samples were weighed and placed under the blades in the Kramer cell. Shear force was measured at 127-mm/min crosshead speeds and expressed as maximum peak force (N) per g of sample.

$$\text{Expressible water} = \frac{\text{Pre - pressed weight (g)} - \text{Post - pressed weight (g)}}{\text{Pre - pressed weight (g)}}$$

The TPA method was performed according to Tahergorabi et al. (2011). Cylindrical gels (height = 2.5 cm, diameter = 2 cm) were used for the TPA measurement. Surimi samples were exposed to two cycles at 50% compression using the texture analyzer with a 70-mm TPA compression plate attachment moving at a speed of

$$\text{Water holding capacity} = \frac{\text{Total Moisture Content (g)} - \text{Expressible Water Content (g)}}{\text{Total Moisture Content (g)}} \times 100$$

127 mm/min. From the resulting force–time curves, hardness, springiness, cohesiveness, gumminess, chewiness, and resilience were determined. Springiness, cohesiveness, gumminess, chewiness, and resilience do not have units.

## 2.7. Color properties of surimi gels

The surimi gels were equilibrated to room temperature before color measurements. The color properties of surimi gels were determined by using a Minolta Chroma Meter CR-400/410 colorimeter (Minolta Camera Co. Ltd., Osaka, Japan). Cylindrical gels (height = 2.5 cm, diameter = 2 cm) were used for color measurements. The values of the CIE (Commission Internationale d'Eclairage of France) color method using L\*a\*b\* tristimulus color values were determined. The whiteness of surimi gels was calculated based on the following equation (Park & Lin, 2005).

$$\text{Whiteness} = 100 - \left[ (100 - L^*)^2 + a^{*2} + b^{*2} \right]^{1/2}$$

## 2.8. Expressible water and water holding capacity of surimi gels

The expressible water of surimi gels was calculated according to Park, Graves, Draves, and Yongsawatdigul (2013): a slice of surimi gel (2 cm diameter, 0.3 cm thick, and about 1 g in weight) was placed between two filter papers and pressed by oil pressure equipment under a fixed pressure (980 kPa) for 20 s. Expressible water was calculated with the following formula. Three samples were tested, and the average value was used.

The water holding capacity (WHC) of surimi gels was calculated as a percentage as the ratio of the water remaining to the initial water content of the sample:

## 2.9. Cooking loss of surimi gels

Cooking loss was determined by weighing 5 g of surimi from each treatment before cooking (initial weight) and after cooking (final weight). Cooking loss was calculated as a percentage:

$$\text{Cooking loss} = \frac{\text{Initial Weight} - \text{Final Weight}}{\text{Initial Weight}} \times 100$$

## 2.10. Statistical analysis

The data obtained from this study were subjected to one-way analysis of variance (ANOVA) to establish significant differences between the measured parameters of treatments compared to

**Table 2**  
Effect of fiber on proximate composition\* and pH\* of surimi gels.

Fiber concentrations (g/100 g)	0**	2	4	6	8
Moisture (g/100 g)	76.95 ± 0.3 <sup>b</sup>	77.56 ± 0.1 <sup>ab</sup>	78.49 ± 0.2 <sup>a</sup>	77.45 ± 0.93 <sup>ab</sup>	78.3 ± 0.2 <sup>a</sup>
Protein (g/100 g)	9.03 ± 0 <sup>c</sup>	9.22 ± 0.2 <sup>bc</sup>	9.07 ± 0.1 <sup>bc</sup>	10.94 ± 0.8 <sup>ab</sup>	12.38 ± 0.6 <sup>a</sup>
Ash (g/100 g)	10.45 ± 0.3 <sup>a</sup>	8.38 ± 0.2 <sup>b</sup>	6.24 ± 0.1 <sup>c</sup>	4.62 ± 0.1 <sup>d</sup>	1.99 ± 0 <sup>e</sup>
pH	6.85 ± 0.64 <sup>a</sup>	6.88 ± 0.02 <sup>a</sup>	6.87 ± 0 <sup>a</sup>	6.88 ± 0.02 <sup>a</sup>	6.71 ± 0.04 <sup>a</sup>

\*Data are given as mean values ± standard deviation (SD, n = 3). Different letters within the same row indicate significant differences (Fisher's Least Significant Difference, P < 0.05) between mean values. \*\*Control.

control. A significant difference was determined at the 0.05 probability level and differences between means were resolved using the Least Significant Difference (LSD) test (Ott & Longnecker, 2008). The statistical analyses of data were performed using SAS (2002). The data are reported as mean values ± standard deviation (SD). The experiments were independently triplicated (n = 3).

### 3. Results and discussion

#### 3.1. Proximate composition of surimi gels

##### 3.1.1. Moisture content

Moisture content of surimi gels developed with different concentrations of oat bran resembled in all the treatments except for the control (Table 2). Although the moisture content of the control sample was significantly different (P < 0.05) from the other treatments, yet numerically lower but slightly. This might be due to the fact that the amount of water added to different treatments in this study was equal. However, in contrast to this study, Yilmaz and Dağlıoğlu (2003) found that the moisture content of meatballs could decrease with the addition of oat bran. This moisture reduction was probably due to the different levels of fat and water used in their study.

##### 3.1.2. Protein content

Addition of oat bran from 2 to 8 g/100 g resulted in an increase (P < 0.05) in protein contents of surimi gels. The 8 g/100 g oat bran treatment obtained considerable increases in protein value (P < 0.05) compared to the control (Table 2). The oat bran used in this study contained 3.7 g/100 g protein according to the information provided at the label of product. Therefore, this might have contributed to the increases in the protein values. Kumar, Kaur, Singh, and Rastogi (2010) also showed that the protein content of Chevon (goat) meat was enhanced with the addition of 20 g/100 g oat bran; that could be considered an added effect.

##### 3.1.3. Ash content

Ash content of the samples was found to be affected by the addition of oat bran. Apparently, incorporating oat bran appears to decrease the ash content of surimi gels with each increment of added fiber. The result tends not to completely agree with findings of Yilmaz and Dağlıoğlu (2003) wherein ash content was found to increase with the incorporation of oat bran onto the meatballs, even up to 20 g/100 g oat bran, given that the least ash contents were found at the control meatballs. The use of inert filler (SiO<sub>2</sub>) incorporated inversely with oat bran as well as improved concentration of SiO<sub>2</sub> at control may, presumably, consolidate the increases regards to the ash content.

#### 3.2. pH

The pH values of surimi gels were not affected by the addition of oat bran (Table 2). Similar to these results, Serdaroglu (2006) found

that the addition of oat bran had no significant effect (P > 0.05) on pH in beef patties. Gelling properties of the myofibrillar proteins (MPs) depend upon pH. At the isoelectric point (pI), proteins have a net charge of zero and retain the least amount of water. Most proteins aggregate and are least soluble at their pI. This results in poor gels or even prevents gel formation. Aggregation of proteins prior to heating inhibits gel formation by MPs, and its extent depends basically upon the electrostatic charge on the molecules, which in turn is affected by pH and ionic strength. The optimum pH for gelation is reported to be within the range of 6.5–7.5 (Park et al., 2013) and the pH for this study was found to lie between these ranges.

#### 3.3. Texture properties of surimi gels

Two different methods were employed to determine texture: Kramer shear test and texture profile analysis (TPA). Although these texture measurements are commonly employed for determination of textural properties, each method provides slightly different information. The most comprehensive understanding of textural properties is provided by a combination of these methods. Kramer shear force and TPA are considered empirical tests that are often used to evaluate texture properties of gelled meat products including surimi-based seafood (Jaczynski & Park, 2004). Therefore, these two different tests were employed in the present study.

The Kramer shear test is a measure of gel strength; the results are shown in Fig. 1. Fortification of surimi with 6 and 8 g/100 g of fiber resulted in gels that required the highest (P < 0.05) force to shear them; i.e., had the highest gel strength. In the case of Chevon (goat) meat patties, however, the addition of oat bran resulted in a decrease in shear force with increased fiber (Kumar et al., 2010). The product containing 50 g/100 g oat bran had much lower shear force values than the control and the product with 15 g/100 g oat bran. This might be due to the increasing amount of water added to different treatments; in our study, the added water and protein content were maintained at constant levels.

Similar to Kramer test, texture profile analysis (TPA) is an empirical method to assess texture. TPA allows determination of six parameters: hardness, springiness, cohesiveness, gumminess, chewiness, and resilience (Cardoso et al., 2008). TPA hardness confirmed Kramer shear force; i.e., it increased (P < 0.05) with each increment of added fiber (Fig. 2). Yilmaz and Dağlıoğlu (2003) used oat bran in the production of meatballs and indicated that hardness of meatballs increased with the addition of more oat bran. The meatballs produced with the addition of 20 g/100 g oat bran had the highest (P < 0.05) hardness value. Table 3 shows the results for TPA measurements. Treatments with 4, 6, and 8 g/100 g oat bran caused a significant increase (P < 0.05) in springiness, cohesiveness, gumminess, chewiness, and resilience of the surimi gels. TPA resilience with 6 and 8 g/100 g fiber resulted in the most (P < 0.05) resilient gels.

In general, the results of the Kramer shear test, and TPA were supportive of each other. The control treatment showed the

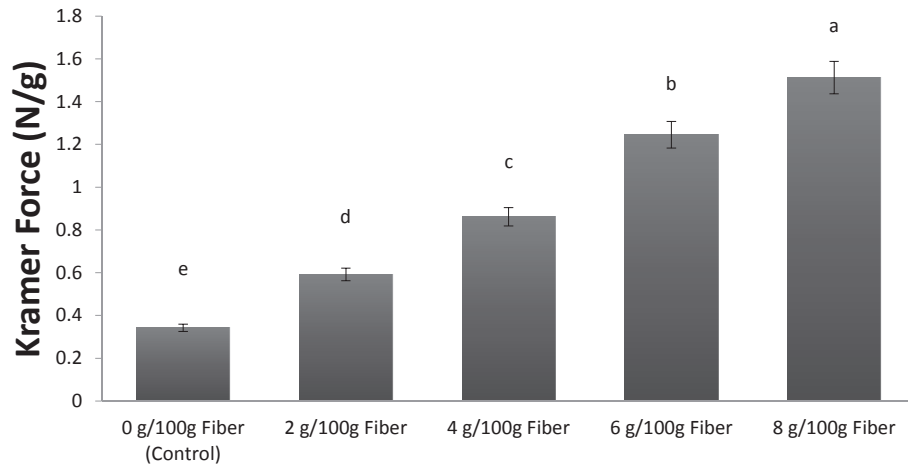


**Fig. 1.** Effect of fiber on Kramer shear force\* of surimi gels. \*Data are given as mean values  $\pm$  standard deviation (SD,  $n = 3$ ). Small bars on the top of data bars indicate SD. Different letters on the top of SD bars indicate significant differences (Fisher's Least Significant Difference,  $P < 0.05$ ) between mean values.

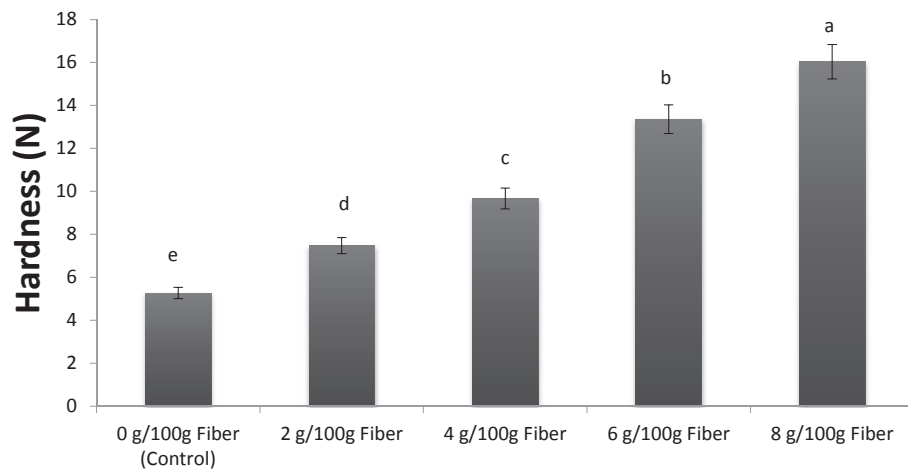


**Fig. 2.** Effect of fiber on hardness (TPA)\* of surimi gels. \*Data are given as mean values  $\pm$  standard deviation (SD,  $n = 3$ ). Small bars on the top of data bars indicate SD. Different letters on the top of SD bars indicate significant differences (Fisher's Least Significant Difference,  $P < 0.05$ ) between mean values.

weakest gel; whereas the 8 g/100 g fiber treatment formed a gel with great hardness, chewiness, cohesiveness and gumminess. Based on these results, fortification of surimi with 6 g/100 g of fiber results in the most optimal gel texture; while providing the highest fortification with this health beneficial nutrient. Previous studies of fiber incorporation in surimi showed mixed results, with some reporting a decrease in gel strength and hardness, and others reporting an increase in these measures (Cardoso, Mendes, & Nunes, 2007; Cardoso et al., 2008; Cardoso, Mendes, Vaz-Pires, &

Nunes, 2009). These differences depend on the type of fiber used as well as fortification level and the aquatic species from which surimi was manufactured. It is also important to maintain the same protein and moisture content in the tested surimi gels (Kerr, Wang, & Choi, 2005). In the present study, protein and moisture content remained constant.

### 3.4. Color properties of surimi gels

Table 4 shows the tristimulus color values ( $L^*$ ,  $a^*$ , and  $b^*$ ), and whiteness of surimi gels. Incorporating between 2 and 8 g/100 g oat bran, lightness ( $L^*$ ) showed palpable decreases ( $P < 0.05$ ). The addition of oat bran to surimi, in all treatments, resulted in more negative  $a^*$  values, indicating a slightly greater green hue in these treatments. It was found that with incorporating oat bran proportionally from 2 to 8 g/100 g, while lightness decreases with increasing greenness and yellowness, the overall whiteness of the surimi samples decreases. However, no difference ( $P > 0.05$ ) was observed by addition of 6 and 8 g/100 g of fiber. The increase in yellow color of the samples could be contributed to the carotenoid pigments present in oat bran (Yılmaz & Dağlıoğlu, 2003). These results tended to agree with the report of Yılmaz and Dağlıoğlu

**Table 3**  
Effect of fiber on texture profile analysis (TPA)\* of surimi gels.

	Fiber concentrations (g/100 g)				
	0**	2	4	6	8
Springiness	0.9 $\pm$ 0.5 <sup>b</sup>	0.9 $\pm$ 0.5 <sup>b</sup>	1.1 $\pm$ 0.4 <sup>a</sup>	1.1 $\pm$ 0.4 <sup>a</sup>	1.1 $\pm$ 0.4 <sup>a</sup>
Cohesiveness	0.6 $\pm$ 0 <sup>c</sup>	0.6 $\pm$ 0 <sup>c</sup>	0.7 $\pm$ 0 <sup>b</sup>	0.7 $\pm$ 0 <sup>b</sup>	0.8 $\pm$ 0 <sup>a</sup>
Gumminess	3.0 $\pm$ 0.5 <sup>e</sup>	4.6 $\pm$ 0.2 <sup>d</sup>	6.5 $\pm$ 0.3 <sup>c</sup>	9.7 $\pm$ 0.6 <sup>b</sup>	12.3 $\pm$ 0.5 <sup>a</sup>
Chewiness	2.7 $\pm$ 0.6 <sup>e</sup>	4.4 $\pm$ 0.2 <sup>d</sup>	7.7 $\pm$ 0.4 <sup>c</sup>	9.4 $\pm$ 0.7 <sup>b</sup>	11.3 $\pm$ 0.6 <sup>a</sup>
Resilience	0.2 $\pm$ 0 <sup>c</sup>	0.3 $\pm$ 0 <sup>b</sup>	0.3 $\pm$ 0 <sup>b</sup>	0.4 $\pm$ 0 <sup>a</sup>	0.4 $\pm$ 0 <sup>a</sup>

\*Data are given as mean values  $\pm$  standard deviation (SD,  $n = 3$ ). Different letters within the same row indicate significant differences (Fisher's Least Significant Difference,  $P < 0.05$ ) between mean values. \*\*Control.

**Table 4**  
Effect of fiber on color properties\* of surimi gels.

	Fiber concentrations (g/100 g)				
	0**	2	4	6	8
L*	88.6 ± 0.4 <sup>a</sup>	87.50 ± 0.4 <sup>b</sup>	85.7 ± 0.3 <sup>c</sup>	83.4 ± 0.7 <sup>d</sup>	83.4 ± 0.7 <sup>d</sup>
a*	-0.9 ± 0.1 <sup>a</sup>	-1.2 ± 0 <sup>b</sup>	-1.3 ± 0.1 <sup>b</sup>	-1.6 ± 0.1 <sup>c</sup>	-1.6 ± 0.1 <sup>c</sup>
b*	5.5 ± 0.5 <sup>d</sup>	6.7 ± 0.4 <sup>c</sup>	7.4 ± 0.3 <sup>b</sup>	8.8 ± 0.5 <sup>a</sup>	8.8 ± 0.5 <sup>a</sup>
Whiteness	87.27 ± 0.2 <sup>a</sup>	85.78 ± 0.4 <sup>b</sup>	83.88 ± 0.2 <sup>c</sup>	81.16 ± 0.3 <sup>d</sup>	81.16 ± 0.3 <sup>d</sup>

\*Data are given as mean values ± standard deviation (SD, n = 3). Different letters within the same row indicate significant differences (Fisher's Least Significant Difference, P < 0.05) between mean values. \*\*Control.

**Table 5**  
Effect of fiber on water holding capacity (WHC)\* and expressible water (EW)\* of surimi gels.

Fiber (g/1000 g)	WHC (g/100 g)	EW (g)
0.0**	92.00 ± 0.0 <sup>e</sup>	6.1 ± 0.0 <sup>a</sup>
20.0	94.79 ± 0.0 <sup>c</sup>	4.0 ± 0.0 <sup>c</sup>
40.0	92.43 ± 0.0 <sup>de</sup>	5.9 ± 0.0 <sup>b</sup>
60.0	95.87 ± 0.2 <sup>b</sup>	3.1 ± 0.0 <sup>d</sup>
80.0	96.61 ± 0.0 <sup>a</sup>	2.5 ± 0.0 <sup>e</sup>

\*Data are given as mean values ± standard deviation (SD, n = 3). Different letters within the same column indicate significant differences (Fisher's Least Significant Difference, P < 0.05) between mean values. \*\*Control.

(2003), who added 5, 10, 15, or 20 g/100 g of oat bran to meatballs. They found that meatballs made with 20 g/100 g oat bran had the highest b\*, and the lowest a\* values. However, Hughes, Cofrades, and Troy (1997) found that the addition of oat fiber to frankfurters had no effect on the color, regardless of the fat level. Because of the significance of whiteness in surimi gels, studies have been performed to increase the intensity of whiteness by the addition of external agents to it. Moisture content is the component generally used to increase whiteness. In addition to moisture, components such as titanium dioxide or oils can be added to improve the whiteness of the surimi gels (Tahergorabi et al., 2011).

### 3.5. Expressible water and water holding capacity of surimi gels

The results for expressible water (EW) and water holding capacity (WHC) of the surimi gels are shown in Table 5. WHC also known as hydration of meat, is closely related to taste, tenderness/juiciness, color, and other features of meat quality. WHC is the

ability of meat muscle to retain moisture in meat (Abdullah, Mason, Cullen, & Al-Shamma'a, 2013). There was an increase in WHC by addition of fiber up to 2 g/100 g but decreased with 4 g/100 g fiber. Fortification of surimi with 6 and 8 g/100 g increased the ability of fish protein to retain its moisture. WHC is a particularly important quality attribute. During the production of comminuted meat products, due to the mincing process of the meat, the structure of the meat proteins that hold water is destroyed, and therefore, the ability of the meat to hold water is decreased (Schmidt, Scheier, & Hopkins, 2013). These results showed that the addition of fiber may improve the WHC which consequently enhance the quality of surimi products.

The expressible water (EW) refers to the amount of liquid squeezed from a protein by the application of force (Nielsen, 2010). The EW decreased (P < 0.05) with addition of fiber to surimi gels which indicates the amount of moisture lost by the application of force. In general, the results of WHC and EW were supportive of each other.

### 3.6. Cooking loss of surimi gels

Results for cooking loss is shown in Fig. 3. The addition of 6 and 8 g/100 g oat bran showed decreases (P < 0.05) in cooking loss. This result is in line with Talukder and Sharma (2010), who found that increasing the amount of added oat bran decreased cooking loss, due to the absorbent nature of oat bran. This could be due to the presence of β-glucan, a component of oat bran that is hydrophilic and consequently binds free water. Cooking loss indicates the amount of water which is lost during cooking, and therefore, it is associated with water holding capacity of the meat. When meat is heated, if the meat has lower cooking loss, it will be understood

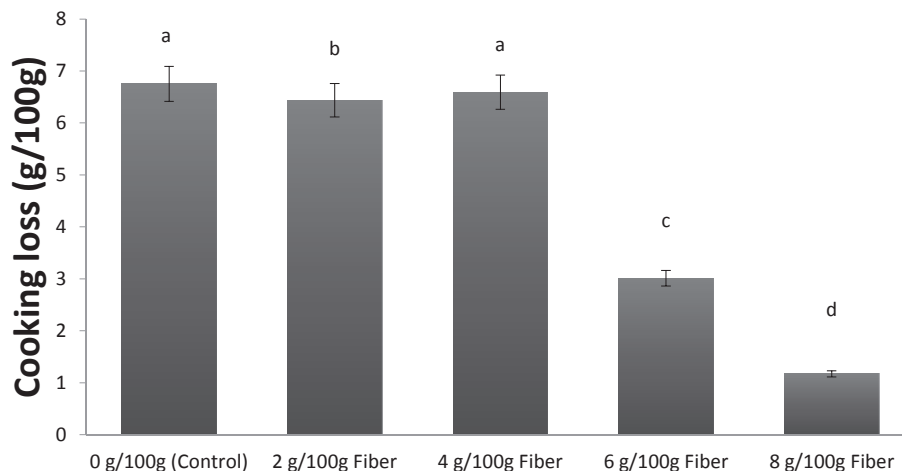


**Fig. 3.** Effect of fiber on cooking loss\* of surimi gels. \*Data are given as mean values ± standard deviation (SD, n = 3). Small bars on the top of data bars indicate SD. Different letters on the top of SD bars indicate significant differences (Fisher's Least Significant Difference, P < 0.05) between mean values.

that the meat has a higher ability to hold water, and therefore, it has greater WHC. This was similar to the present study. If the water holding capacity of a meat product is low, the meat will lose a larger amount of water during cooking, leading to production of a drier product that may be unacceptable to consumers (Park et al., 2013). This may explain the beneficial effect of adding oat bran to improve WHC and cooking loss of the surimi products.

#### 4. Conclusion

This study demonstrated that oat bran as a dietary fiber can be used to fortify surimi seafood. American diet is deficient in this health-beneficial nutrient. Fortification of surimi with dietary fiber up to 6 g/100 g improved textural properties; although it resulted in slightly lower color values, these values are still acceptable in premium grade surimi. Textural results support water holding capacity, which indicated the ability of surimi to retain more water by oat bran addition. Cooking loss was also reduced significantly. These results are promising for the future implications of manufacturing and marketing a surimi product with potential health benefits from added oat bran. Although these results are promising, sensory evaluation is recommended to assess consumer acceptance of the product.

#### References

- Abdullah, B. M., Mason, A., Cullen, J. D., & Al-Shamma'a, A. (2013). Water-holding capacity assessment of meat using an electromagnetic sensing method. In *Paper presented at the RF and Microwave Conference (RFM), 2013 IEEE International*.
- American Association of Cereal Chemists, AACC. (2001). The definition of dietary fiber. *Cereal Foods World*, 46(3), 112–126.
- Association of Official Analytical Chemists. (1995). *Official methods of analysis of AOAC International*.
- Brand-Miller, J. C., Atkinson, F. S., Gahler, R. J., Kacinik, V., Lyon, M. R., & Wood, S. (2012). Effects of added PGX<sup>®</sup>, a novel functional fibre, on the glycaemic index of starchy foods. *British Journal of Nutrition*, 108(02), 245–248.
- Butt, M. S., Tahir-Nadeem, M., Khan, M. K. I., Shabir, R., & Butt, M. S. (2008). Oat: unique among the cereals. *European Journal of Nutrition*, 47(2), 68–79.
- Cardoso, C., Mendes, R., & Nunes, M. L. (2007). Dietary fibers' effect on the textural properties of fish heat-induced gels. *Journal of Aquatic Food Product Technology*, 16(3), 19–30.
- Cardoso, C., Mendes, R., Pedro, S., & Nunes, M. L. (2008). Quality changes during storage of fish sausages containing dietary fiber. *Journal of Aquatic Food Product Technology*, 17(1), 73–95.
- Cardoso, C., Mendes, R., Vaz-Pires, P., & Nunes, M. L. (2009). Effect of dietary fibre and MTGase on the quality of mackerel surimi gels. *Journal of the Science of Food and Agriculture*, 89(10), 1648–1658.
- Daou, C., & Zhang, H. (2012). Oat beta-glucan: its role in health promotion and prevention of diseases. *Comprehensive Reviews in Food Science and Food Safety*, 11(4), 355–365.
- Dietary Guidelines Advisory Committee. (2010). *Report of the Dietary Guidelines Advisory Committee on the dietary guidelines for Americans, 2010, to the Secretary of Agriculture and the Secretary of Health and Human Services*. Agricultural Research Service.
- Feng, B., Ma, L. J., Yao, J. J., Fang, Y., Mei, Y. A., & Wei, S. M. (2013). Protective effect of oat bran extracts on human dermal fibroblast injury induced by hydrogen peroxide. *Journal of Zhejiang University Science B*, 14(2), 97–105.
- Hughes, E., Cofrades, S., & Troy, D. J. (1997). Effects of fat level, oat fibre and carrageenan on frankfurters formulated with 5, 12 and 30% fat. *Meat Science*, 45(3), 273–281.
- Jaczynski, J., & Park, J. W. (2004). Microbial inactivation and electron penetration in surimi seafood during electron beam and heat. *Journal of Food Science*, 68(5), 1788–1792, 69(1), 53–57.
- Kerckhoffs, D., Hornstra, G., & Mensink, R. (2003). Cholesterol-lowering effect of  $\beta$ -glucan from oat bran in mildly hypercholesterolemic subjects may decrease when  $\beta$ -glucan is incorporated into bread and cookies. *American Journal of Clinical Nutrition*, 78, 221–227.
- Kerr, W. L., Wang, X., & Choi, S. G. (2005). Physical and sensory characteristics of low-fat italian sausage prepared with hydrated oat. *Journal of Food Quality*, 28(1), 62–77.
- Kristinsson, H. G., Lanier, T. C., Halldorsdottir, S. M., Geirsdottir, M., & Park, J. W. (2013). Fish protein isolate by pH shift. In J. W. Park (Ed.), *Surimi and surimi seafood* (3rd ed., pp. 3–23). Boca Raton, FL: CRC Press.
- Kumar, A., Kaur, M., Singh, P., & Rastogi, A. (2010). Effect of oat bran on nutritional quality of chevon patties. *Indian Journal of Small Ruminants*, 16(2), 284–286.
- Modi, V. K., Mahendrakar, N. S., Sachindra, N. M., & Rao, D. N. (2004). Quality of nuggets prepared from fresh and smoked spent layer chicken meat. *Journal of Muscle Foods*, 15(3), 195–204.
- Nielsen, S. S. (2010). *Food analysis* (p. 550). New York, NY, USA: Springer.
- Ott, R., & Longnecker, M. (2008). *An introduction to statistical methods and data analysis*. Cengage Learning.
- Özvural, E. B., & Vural, H. (2008). Utilization of interesterified oil blends in the production of frankfurters. *Meat Science*, 78(3), 211–216.
- Park, J. W., Graves, D., Draves, R., & Yongsawatdigul, J. (2013). Manufacture of surimi harvest to frozen block. In J. W. Park (Ed.), *Surimi and surimi seafood* (3rd ed., pp. 55–96). Boca Raton, FL: CRC Press.
- Park, J. W., & Lin, T. M. (2005). Surimi: manufacturing and evaluation. In J. W. Park (Ed.), *Surimi and surimi seafood* (2nd ed., pp. 33–106). Boca Raton, FL: Taylor & Francis Group.
- Sánchez-Alonso, I., Haji-Maleki, R., & Borderias, A. J. (2007). Wheat fiber as a functional ingredient in restructured fish products. *Food Chemistry*, 100(3), 1037–1043.
- SAS Institute. (2002). *SAS/STAT guide for personal computers, version 8.1*. Cary (NC): SAS Institute.
- Schmidt, H., Scheier, R., & Hopkins, D. L. (2013). Preliminary investigation on the relationship of Raman spectra of sheep meat with shear force and cooking loss. *Meat science*, 93(1), 138–143.
- Serdaroglu, M. (2006). The characteristics of beef patties containing different levels of fat and oat flour. *International Journal of Food Science & Technology*, 41(2), 147–153.
- Tahergorabi, R., Beamer, S. K., Matak, K. E., & Jaczynski, J. (2011). Effect of isoelectric solubilization/precipitation and titanium dioxide on whitening and texture of proteins recovered from dark chicken-meat processing by-products. *LWT-Food Science and Technology*, 44(4), 896–903.
- Tahergorabi, R., Beamer, S. K., Matak, K. E., & Jaczynski, J. (2012). Salt substitution in surimi seafood and its effects on instrumental quality attributes. *LWT-Food Science and Technology*, 48(2), 175–181.
- Talukder, S., & Sharma, D. P. (2010). Development of dietary fiber rich chicken meat patties using wheat and oat bran. *Journal of Food Science And Technology*, 47(2), 224–229.
- Xu, Y., Xia, W., Yang, F., & Nie, X. (2010). Physical and chemical changes of silver carp sausages during fermentation with *Pediococcus pentosaceus*. *Food Chemistry*, 122(3), 633–637.
- Yılmaz, I., & Dağlıoğlu, O. (2003). The effect of replacing fat with oat bran on fatty acid composition and physicochemical properties of meatballs. *Meat Science*, 65(2), 819–823.



# Influence of enzymatically produced sunflower oil based cocoa butter equivalents on the phase behavior of cocoa butter and quality of dark chocolate



Sheida Kadivar\*, Nathalie De Clercq, Mansura Mokbul, Koen Dewettinck

Laboratory of Food Technology and Engineering, Ghent University, Coupure Links 653, B-9000 Ghent, Belgium

## ARTICLE INFO

### Article history:

Received 24 June 2015

Received in revised form

28 September 2015

Accepted 2 October 2015

Available online 8 October 2015

### Keywords:

Cocoa butter equivalent

Iso-solid diagram

Melting behavior

Dark chocolate

## ABSTRACT

The two enzymatically produced sunflower oil based cocoa butter equivalents (CBEs) were blended with cocoa butter (CB) at varying concentrations (g/100 g). The peak maximum decreased significantly upon the addition more CBE due to the presence of the low-melting TAGs. However, the melting heat and the melting onset temperature were comparable to CB up to 25 g CBE/100 g blend. The iso-solid diagram showed monotectic behavior with softening effect proportional to CBE increase. A significant decrease in SFC was observed at all temperatures for the blends in which the CBE ratio was above 25 g/100 g blend. The second part of this study was set out to determine the performance of CBE replacement in chocolates and compounds at 20 °C. All the chocolates and compounds even in the level of 5 g CBE/100 g blend had significantly lower Casson yield stress than reference chocolate. However, the viscosity of the chocolate with 5 g HSHO CBE/100 g blend was comparable with the reference chocolate. Higher amounts of CBE slightly decreased the peak maximum however up to 5 g CBE/100 g blend, the melting behavior did not significantly change compared to the reference chocolate without CBE. The hardness of the reference chocolate was comparable with chocolate with 5 g CBE/100 g blend up to 2 weeks.

© 2015 Elsevier Ltd. All rights reserved.

## 1. Introduction

Enzymatic modification of fats and oils for the production of specific structured triacylglycerols (TAGs) is showing lots of attention for a long time (Rozenaal & Macrae, 1997). Nowadays, different industries are using enzymatic interesterification techniques with sn-1,3 specific lipases for the production of cocoa butter equivalents (CBE), human milk fat substitutes, and so on. Specific structured TAGs are TAGs that are stereospecifically modified or reformulated to obtain specific functions for nutrition, food, and pharmaceutical applications. Using chemical interesterification in the production of these types of TAGs is usually not applicable because of deficiency in positional specificity (Xu, 2000).

**Abbreviations:** CB, cocoa butter; CBE, cocoa butter equivalent; DAG, diacylglycerols; FA, fatty acids; FFA, free fatty acids; HOSO, high oleic sunflower oil; HSHO, high stearic high oleic sunflower oil; POP, 1,3-dipalmitoyl-2-oleoyl-glycerol; POST, 1(3)-palmitoyl-3(1)stearoyl-2-oleoyl-glycerol; PLM, Polarized light microscope; SOO, saturated-oleoyl-oleoyl; SOS, saturated-oleoyl-saturated; SSS, Trisaturated; SFC, solid fat content; TAG, triacylglycerols.

\* Corresponding author.

E-mail address: [sheida.kadivar@UGent.be](mailto:sheida.kadivar@UGent.be) (S. Kadivar).

Functional and nutritional properties of modified oils and fats depend not only on fatty acid (FA) profiles but also on FA distributions in the glycerol backbone. Cocoa butter (CB) for instance, is an essential ingredient in chocolate as it forms the continuous phase and is responsible for the gloss, texture and typical melting behavior of chocolate. These distinctive physical properties are the result of its special TAG composition, which consists of three major TAGs, namely, 1,3-dipalmitoyl-2-oleoyl-glycerol (POP), 1(3)-palmitoyl-3(1)stearoyl-2-oleoyl-glycerol (POST), and 1,3-distearoyl-2-oleoyl-glycerol (StOSt), with oleic acid at the sn-2 position of the glycerol backbone. The melting point of CB is between 32 and 35 °C and it can re-crystallize during tempering process to a stable crystal form (Foubert, Vanrolleghem, Thas, & Dewettinck, 2004).

Although CB is the ideal ingredient in chocolate and other confectionary products, an increasing demand for chocolate products, high price of CB and uncertainty in the supply leads the researchers and manufacturer to look for alternatives such as CBE (Tchobo et al., 2009). A CBE is a non-lauric fat that can replace CB with preservation of its chemical and physical characteristics (Verstringe, De Clercq, Nguyen, Kadivar, & Dewettinck, 2012). By using lipase-catalyzed reactions, all the three main TAGs can be

produced with oils in which the sn-2 position is mainly occupied by oleic acid (Rozendaal & Macrae, 1997).

While vegetable fats, other than illipe, palm, sal, shea, kokum and mango are not allowed for use as CBE in chocolate (Union, 2000), the improved physical properties of enzymatically produced CBE may make it a suitable partial replacement ingredient for CB in chocolate and other confectionary products. However, when developing a structured lipid for this purpose, it is important to consider how the novel fat will compare physically with CB. Melting, crystallization, and microstructure are the main properties that are used for the evaluation of an enzymatically produced CBE (Çiftçi, Kowalski, Göğüş, & Fadiloğlu, 2009).

High Oleic Sunflower Oil (HOSO) contains high levels of oleic acid (~80 g/100 g), mainly in the form of triolein (OOO) (>60 g/100 g). It has a very low solid content at room temperature. Instead, High Stearic High Oleic (HSHO) sunflower oil contains considerable amount of stearic acid (~15 g/100 g) but it is still liquid at high temperature. These types of oils are promising sources to produce CBE through enzymatic acidolysis by 1,3 specific enzyme since their TAGs are rich in oleic acid in the sn-2 position of their glycerol backbones. The present work involves formulating several potential CBEs by blending the stearin fraction of two enzymatically produced sunflower oil rich in SOS TAGs with CB and further studying their compatibility with CB through iso-solid diagrams. Subsequently, the formulated CBEs were used as fat phase of dark chocolate in order to evaluate their influence on quality parameters of dark chocolate. The results from this study could help the fats and oils industries to extend their knowledge on the compatibility of two enzymatically produced sunflower oil based CBEs with CB and their influence on the quality of chocolate products.

## 2. Materials and methods

### 2.1. Materials

Refined HOSO and FAs were provided from Oleon (Oelegem, Belgium). FAs consisted of a mixture of stearic acid (53.4 g/100 g), palmitic acid (44.8 g/100 g), myristic acid (1.2 g/100 g) and arachidic acid (0.6 g/100 g). HSHO was provided by Nutrisun Business Unit of Advanta Seeds. Immobilized lipase from *Rhizomucor miehei* (Lipozyme RMIM, Novozymes, immobilized on ion-exchange resin, sn-1,3 specific) was purchased from Sigma–Aldrich (Schnelldorf, Germany). All other reagents and solvents were of analytical or chromatographic grade.

### 2.2. Methods

#### 2.2.1. CBE production

**2.2.1.1. Enzymatic acidolysis.** Acidolysis reaction with lipase was carried out in a 1 kg batch reactor under optimized conditions. Details of the production of CBE and its isolation from the reaction mixture and the analyses have been reported previously (Kadivar, De Clercq, Van de Walle, & Dewettinck, 2014). The acidolyzed product was distilled in a short path distillation unit (VTA, Degendorf, Germany) at  $P = 0.3$  Pa and  $T = 200$  °C. At these conditions, free fatty acids were almost removed ( $FFA < 0.3$  g/100 g).

**2.2.1.2. Fractionation.** The method of Chong, Hoh, and Wang (1992) was adopted for the fractionation. The distilled product was dissolved in hexane (1:10 g/ml) and left at 4 °C for 24 h. The precipitated fat was filtered off, and the filtrate was evaporated to dryness. The mother liquor was then dissolved in acetone (1:10 g/ml) and cooled at 4 °C for 24 h. The second precipitated fat fraction was obtained and dried under nitrogen for 4 h at 60 °C.

#### 2.2.2. Blend preparation

CB and enzymatically produced CBEs were melted at 70 °C and blended at proportions of 100:0, 75:25, 50:50, 95:05 and 0:100 (g/100 g).

#### 2.2.3. Fatty acid composition

The AOCS official method Ce 2–66 (Firestone, 1998) was used for preparing methyl esters for further analysis by GC according to the AOCS Official Methods Ce 1–62 (Firestone, 1998).

#### 2.2.4. Triacylglycerol composition

TAGs were analyzed with an optimized method developed by Rombaut, De Clercq, Foubert, and Dewettinck (2009). Separation of TAG species was performed on a Shimadzu HPLC system (Shimadzu, Japan). The details of the system was reported in our previous study (Kadivar et al., 2014). The results of TAG composition are presented in Table 1.

#### 2.2.5. Pulsed nuclear magnetic resonance (pNMR)

Solid fat content (SFC) was measured by pulsed NMR (pNMR) with a Bruker Minispec pc 20 (Bruker, Karlsruhe, Germany). Melted CB and CBEs were placed in NMR tubes (three replicates) and submitted to the tempering treatments of the IUPAC 2.150 serial tempering method. SFC was determined in the range of 5–40 °C at 5 °C intervals following 60 min incubations at each temperature.

#### 2.2.6. Differential scanning calorimetry (DSC)

The DSC experiments were performed with a Q1000 DSC with a refrigerated cooling and an auto-sampler system (TA Instruments, New Castle, USA). Nitrogen was used to purge the system. Samples were sealed in hermetic pans and an empty pan was used as a reference. Non-isothermal crystallization and melting experiments were performed. Samples were initially heated from room temperature to 65 °C and held at this temperature for 10 min to destroy crystal memory; cooled to –20 °C at 5 °C/min and held for 5 min; and heated to 65 °C at 5 °C/min to determine the melting profile. Results were presented using the TA Universal Analysis 2000 software (TA Instruments).

#### 2.2.7. Chocolate production

Standard dark chocolate products with the formulation of 48 g fine sugar/100 g chocolate (BarryCallebaut Belgium, Wieze, Belgium) with particle size distribution of around 0.1 mm, 30.90 g CB/100 g chocolate, 20.5 g cocoa powder/100 g chocolate and 0.6 g soy lecithin/100 g chocolate (Unimills, Zwijndrecht, the Netherlands) were prepared at UGent Cacaolab. The cocoa powder was lightly alkalinized dark brown with pH in the range of 6.8–7.2. The fat and moisture content were 11 g/100 g cocoa powder and 5 g/100 g cocoa powder, respectively. The soy lecithin had the moisture content of 0.19 g/100 g with acetone insolubles value of 64.25 g/100 g. Different chocolate and compound products with different amounts of CBEs (5 g, 25 g, 50 g and 100 g in 100 g fat blend) were produced and stored at 20 °C. Chocolate production started with mixing all the ingredients. The mixture of sugar, cocoa powder and CB/CBE needed to be refined to a particle size <35 µm. After refining the mixture was transferred to the conche. This process is carried out in two different stages: dry conching and liquid conching following the tempering process.

### 2.3. Quality parameters of chocolate

#### 2.3.1. Flow behavior

The flow behavior of chocolate and compounds were analyzed using TA Instruments AR 2000 (TA Instruments, New Castle, Delaware, USA). Chocolate and compound samples were melted at 50 °C

**Table 1**  
Overview of TAGs in blends.<sup>a</sup>

	CB	<sup>b</sup> CBE:CB (5:95)		CBE:CB (25:75)		CBE:CB (50:50)		CBE:CB (100:0)	
		HOSO	HSHO	HOSO	HSHO	HOSO	HSHO	HOSO	HSHO
SSS	0.4c	1.1bc	0.5c	0.5bc	0.9b	0.2c	1.2b	0.6bc	2.0a
SOS	96.0a	94.7a	95.9a	89.4b	94.8a	86.0c	89.4b	74.6e	78.0d
SOO	3.0f	4.2e	3.0f	5.7d	3.9e	10.8c	7.5d	19.4a	13.1b
DAG	–	–	–	–	–	1.0d	1.4c	2.2b	2.9a
∑others	0.6	0.0	0.6	4.4	0.4	2.0	0.5	3.2	4.0

<sup>a</sup> Values indicated with the same letters are not significantly different ( $\alpha = 0.05$ ).

<sup>b</sup> For abbreviations see "List of abbreviations".

for 1 h and 20 g of the sample was placed into a preheated cup. The measurement procedure was based on ICA (2000) method. Temperature was set at 40 °C. Shear rate of the bob was increased logarithmically from 2 s<sup>-1</sup> to 50 s<sup>-1</sup> followed by holding at 50 s<sup>-1</sup> and finally decreased to 2 s<sup>-1</sup>. Meanwhile, shear stress and viscosity were measured. Each sample was analyzed in triplicate. The Casson model was fitted to the shear rate (from 0.1 to 65 s<sup>-1</sup>)-shear stress data.

### 2.3.2. Melting profile

The surface of the chocolate was scraped off with a scalpel and 5–10 mg of the chocolate flakes were transferred to an aluminum pan for subsequent analysis in a 2010 CE DSC with refrigerated cooling system (TA Instruments, New Castle, USA). When the system reached the equilibrium conditions at 20 °C, the pan was put in the DSC cell and the melting profile was recorded by heating at 5 °C/min to 65 °C.

### 2.3.3. Texture analysis

A penetration test was performed on Texture Analyzer (Instron Model 5942, USA) together with 500 N load cell and penetration probe (needle). The chocolates and compounds were placed on the table of the texture analyzer at 20 °C. The penetration probe descended with a speed of 2 mm/s, the measurements started at a trigger of 0.2 N. The probe penetrated 5 mm into the chocolates and compounds. The hardness (N) is the maximum force required to penetrate the sample.

### 2.3.4. Statistical analysis

IBM SPSS Statistics software (version 22, SPSS inc., Chicago, USA) was used for statistical analysis. The variables were compared with One-Way ANOVA. Then Tukey test was performed in case of variances were equal to identify the significant differences at 95% confidence level. In case of unequal variances, Dunnett T3 test was applied.

## 3. Results and discussion

### 3.1. Physicochemical characterization of the formulated CBEs

#### 3.1.1. Fatty acid composition

The fatty acid (FA) profiles of the different blends are presented in Table 2. CB contains three main FA, palmitic (C16:0), stearic (C18:0) and oleic (C18:1) acid at levels of 28.1 g/100 g, 34.5 g/100 g and 33.2 g/100 g, respectively which is in agreement with previous studies (Kang, Jeon, Kim, & Kim, 2013; Shukla, 2005). There is no significant difference in the amount of palmitic and stearic acid between 5 g CBE/100 g blends and CB however, they contain significantly higher oleic acid than CB ( $P < 0.05$ ). It was observed that by adding more than 5 g CBEs in the blend, oleic acid content was significantly increased along with a gradual decrease in palmitic and stearic acid. Comparing the two sunflower CBEs, they are

significantly different in the concentration of all types of FA.

#### 3.1.2. Iso-solid diagrams and thermal properties of the blends

The functionality of fats in food products depends on their melting behavior and as a result, solid fat content (SFC) can be a good indicator of the melting behavior of fats. By determining the SFC profile of the oils and fats or their blends their suitability for a certain application can be identified (NorAini, Embong, Aminah, Md. Ali, & Maimon, 1995). Since CB is considered as a stabilizing fat, the blends were tempered according to the official IUPAC tempering procedure, before recording the SFC profile as function of temperature. The results of the measurements are provided in Fig. 1. CB showed a high SFC up to 20 °C, followed by a steep decrease between 25 and 35 °C and no solid fat was detected above body temperature. When more than 25 g CBE was added to 100 g blend, the SFC in the temperature range 15 °C–25 °C, related to the hardness of a fat, gradually decreased. All the blends, except 5 g CBE/100 g blend, had a lower heat resistance (SFC between 25 and 30 °C) compared to CB. Only HSHO CBE showed residual amounts of solid fat (3.1 g solid fat/100 g blend) above body temperature (Fig. 1) which is still acceptable and would not be an issue to cause a waxy mouth feel. This finding is attributed to the presence of the high-melting TAGs. A significant decrease ( $P < 0.05$ ) in SFC was observed at all temperatures (5–30 °C) for blends in which the CBE ratio was above 25 g/100 g blend. These variations in the SFC are mainly due to differences in the TAG contents of CB and CBEs. The SFC of a soft CB is approximately 63 g solid fat/100 g oil and 20 g solid fat/100 g oil at 20 °C and 30 °C, respectively (Shukla, 1995). This is in case for the blends up to 25 g CBE/100 g blend. However, 50 g CBE/100 g blends and both sunflower oil based CBEs had significantly lower SFC at those mentioned temperatures.

The phase behavior of lipids can be explained by iso-solid phase (Humphrey & Narine, 2005). Iso-solid curves have been used to show eutectic and diluents effects in mixed fats systems (Wang, Liu, Jin, Meng, & Wang, 2011) and they provide worthwhile information for a manufacturer who wants to know the state of a mixture at a given temperature. Furthermore, it offers critical information regarding the compatibility of fat mixtures. Different fats in a blend can be compatible (monotectic), partial compatible and incompatible (eutectic). Two types of fats are not compatible (eutectic) when the theoretical iso-solid line joining the pure fats cannot be fit to a linear interpolation (Timms, 1984).

The CBEs/CB blends show monotectic behavior with softening effect proportional to CBE increase (Fig. 2). The absence of eutectic in Fig. 2 reveals that on one hand there is no incompatibility between CBEs and CB and on the other hand there is similarity in molecular volume, shape and polymorphs between CB and CB/CBEs mixtures (Mat Dian, Sundram, & Idris, 2006) and this is more pronounced for HSHO CBEs. However, addition of CBEs higher than 25 g CBEs/100 g blend are not recommended because of the strong softening effect, particularly at low temperatures. Better compatibility between CBEs and CB was observed at temperature ranges of

**Table 2**  
Fatty acid composition of the blends.<sup>a</sup>

	CB	<sup>b</sup> CBE:CB (5:95)		CBE:CB (25:75)		CBE:CB (50:50)		CBE:CB (100:0)	
		HOSO	HSHO	HOSO	HSHO	HOSO	HSHO	HOSO	HSHO
C16:0	28.1a	28.0a	28.1ab	27.1b	27.6b	26.2c	26.8c	25.2d	24.0e
C18:0	34.5ab	34.2abc	34.3a	33.0d	33.6bc	31.6e	32.5cd	29.9f	31.4e
C18:1	33.2h	33.8g	33.6g	35.8e	34.8f	38.2c	36.8d	41.2a	39.5b
C18:2	2.9d	3.0c	3.0cd	3.2b	3.1cd	3.3ab	3.2d	3.3a	3.0cd
C20:0	1.0a	1.0b	1.0a	0.9c	0.9a	0.7d	0.7a	0.4e	1.0b
C22:0	0.0b	0.0b	0.0b	0.0b	0.0b	0.0b	0.0b	0.0b	0.8a
Others	0.2	0.0	0.0	0.0	0.0	0.0	0.0	0.0	0.3

<sup>a</sup> Values indicated with the same letters are not significantly different ( $\alpha = 0.05$ ); All measurements were performed in duplicate and the standard error for each sample was below 1.5%.

<sup>b</sup> For abbreviations see “List of abbreviations”.

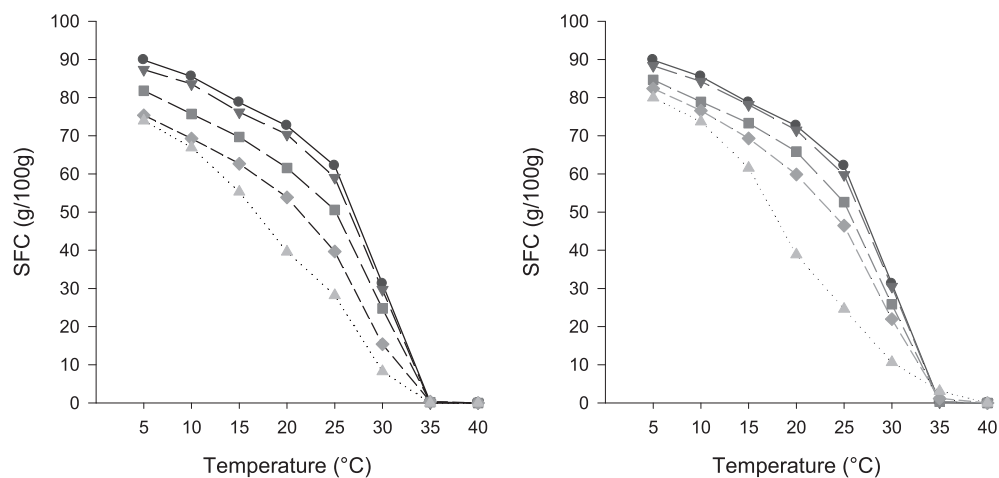


**Fig. 1.** Solid fat content of the high oleic sunflower oil cocoa butter equivalent blends (left) and high stearic high oleic sunflower oil cocoa butter equivalent blends (right). —●— CB, —■— 5 g CBE/100 g blend, —△— 25 g CBE/100 g blend, —◇— 50 g CBE/100 g blend, —○— CBE.

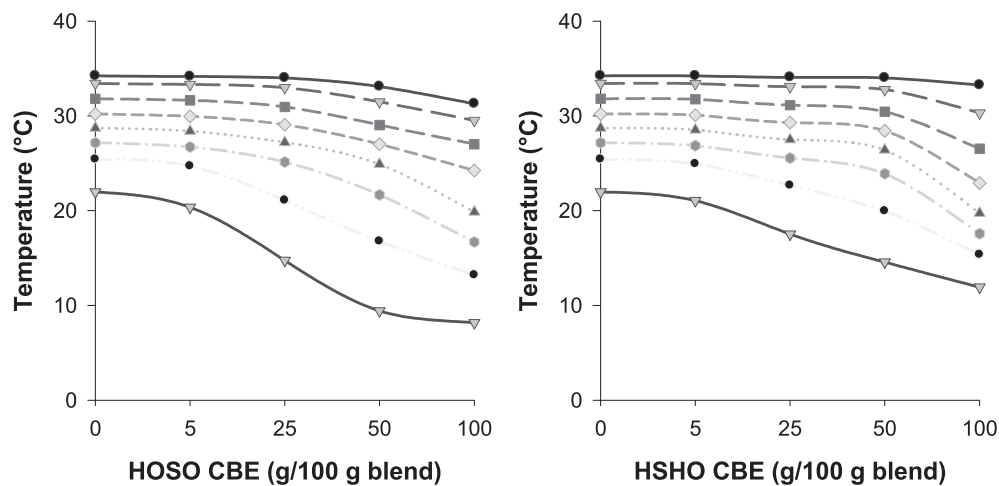


**Fig. 2.** Binary iso-solid phase diagram for high oleic sunflower oil cocoa butter equivalent (HOSO CBE) and high stearic high oleic sunflower oil cocoa butter equivalent (HSHO CBE) blends (—●— 5 g solid fat/100 g blend, —■— 10 g solid fat/100 g blend, —△— 20 g solid fat/100 g blend, —◇— 30 g solid fat/100 g blend, —○— 40 g solid fat/100 g blend, —□— 50 g solid fat/100 g blend, —◇— 60 g solid fat/100 g blend, —▽— 70 g solid fat/100 g blend).

30 °C and over for all the blends meaning that in the mouth (at body temperature), the blends will not cause mouth feel significantly.

The relative proportions of the three main TAGs, POP, POST and StOSt in CB and other fats that can be used as CBEs, can be exemplified on a ternary triangular composition diagram. The objective

of the CBE formulations is to achieve a composition similar to the composition of these three TAGs of CB. Phase diagrams of the binary and ternary mixtures of these three pure TAGs and from different fat blends were previously reported (Smith, Bhaggan, & Talbot, 2013; Wesdorp et al., 2005). Fig. 3 illustrates the ternary diagram reported with eutectic, miscible-like and miscible areas

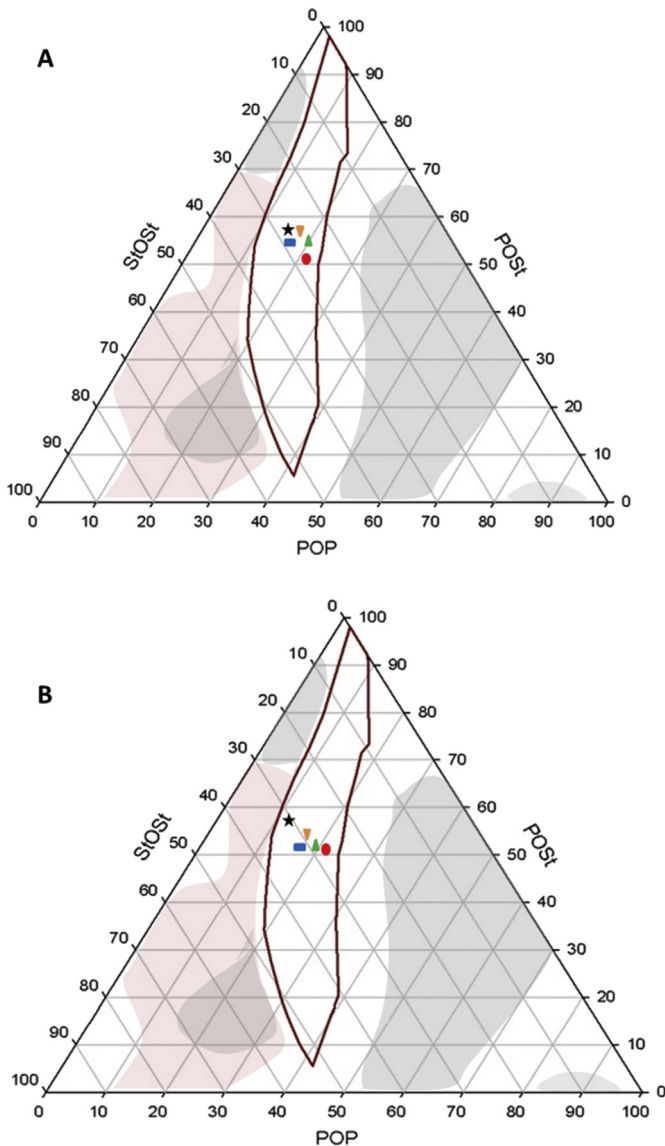


**Fig. 3.** Ternary and phase behavior diagrams of the POP/POST/StOSt composition of the high oleic sunflower oil cocoa butter equivalent blends (A) and high stearic high oleic sunflower oil cocoa butter equivalent blends (B) (after (Padley et al., 1981)). ● CB, ▲ 5 g CBE/100 g blend, ■ 25 g CBE/100 g blend, ▼ 50 g CBE/100 g blend, ★ CBE, □ Miscible, ■ Miscible-like, ▭ Eutectic.

where the CBE blends can be included. As it is clear in the figure, all the blends spread along the miscible areas. It should be noted that the ternary diagram is made for pure TAGs and in this study other TAGs species interactions can be interfered. However, there are no data about the influence of other TAGs on the behavior of confectionary fats in these diagrams. Nevertheless, the location of these blends within the ternary diagrams was in good agreement with the pNMR data, where partial miscibility was found between CB and CBEs. Padley, Paulussen, Soeters, and Tresser (1981) have previously reported in their patent a composition area (red line) in the ternary phase diagram of three major TAGs which represented same physical properties and tempering characteristics as CB. All of the blends are located in the reported region (Fig. 3).

The melting curves of CBEs blends changed with increasing amounts of CBEs (Fig. 4). At higher CBE additions, the increase of the proportion of SOO motivated a decrease of the melting point and the melting enthalpy (Table 3). As it is shown in Fig. 4, for HSHO CBE the DSC melting curve exhibited small shoulders before and

after the main melting peak over a wide temperature range probably caused by the considerable content of tri-saturated (2 g/100 g) and mono-saturated TAGs (13.1 g/100 g) (Fig. 4). The HOSO CBE displayed melting curves in a similar pattern but in a less pronounced size. This can be explained by the presence of tri-saturates in CBEs that resulted in polymorphic transformation up on heating of CBE at the end of the trace. Similar polymorphic transformation on heating of CBE at higher tri-saturated TAG levels was also observed by Cebula (1992). Regarding the other blends, the highest SOS content showed a single high-melting peak at around 20–22 °C but with different melting enthalpy compared with CB (Table 3). Up to addition of 25 g HOSO CBE/100 g blend and 50 g HSHO CBE/100 g blend had no influence on onset temperature of CB however the melting temperature of all the blends was significantly lower than CB ( $p < 0.05$ ). Due to the higher stearic acid content of HSHO CBE, this CBE showed higher onset and peak maximum temperature than the HOSO CBE.

### 3.2. Influence of sunflower oil based cocoa butter equivalents on quality of chocolate

The CBE/CB blends characterized in previous part were used in the production of the chocolate and compounds as described in Section 2.2.7. The tempering was performed by hand on a marble table. The temper index before moulding varied between 4 and 6 for the different chocolates and compounds.

#### 3.2.1. Flow behavior

The Casson model was fitted to the flow curves to obtain the Casson yield stress ( $\sigma_{Ca}$ ) and viscosity ( $\eta_{Ca}$ ). Table 4 presents the two Casson parameters as function of the CBE concentration. There is a decreasing trend in Casson yield stress and Casson plastic viscosity with increasing CBE concentration. All the chocolates and compounds had significantly lower Casson yield stress than the reference chocolate ( $p < 0.05$ ). This can be an interesting finding since chocolate flow properties can be adjusted by adding the CBEs. The higher yield stress of reference chocolate can be due to the presence of FFA (1.1 g/100 g). De Clercq et al. (2012) discussed that, when FFA are present a higher yield stress is necessary before the chocolate start to flow. Moreover, comparing the two types of CBEs, all the samples produced from HSHO CBE had significantly lower Casson yield stress than samples made from HOSO CBE. This can be due to the higher PSD of HSHO CBE. PSD and rheological parameters are highly linked. The yield stress decreases when particle size increases because fewer surfaces are available to interact. Another reason especially for 50 g HSHO CBE/100 g blend and HSHO CBE can be due to their DAGs. DAGs have emulsifying properties so they will interact at the interface together with the lecithin molecules to coat the sugar particles and the cocoa particles therefore yield stress correspondingly decreased when more DAGs were present in the chocolate.

In contrast, all the chocolates and compounds (except chocolate with 5 g HSHO CBE/100 g blend and compound with 50 g HSHO CBE/100 g blend) showed significantly lower viscosity than the reference chocolate ( $p < 5\%$ ). Furthermore, all HSHO CBE replacements are more viscous than HOSO CBE. The higher viscosity of HSHO chocolate and compounds could also be related to their higher PSD value (31.9  $\mu\text{m}$ ). In lower PSD, higher amount of surface area is available to interact. In contrast, for samples with higher PSD, the surface area for interaction is lower which leads to higher viscosity (Aidoo, De Clercq, Afoakwa, & Dewettinck, 2014).

#### 3.2.2. Melting behavior

The chocolates were stored at 20 °C and sampled after 1 day, 2 and 4 weeks to record a melting profile. The DSC melting profiles

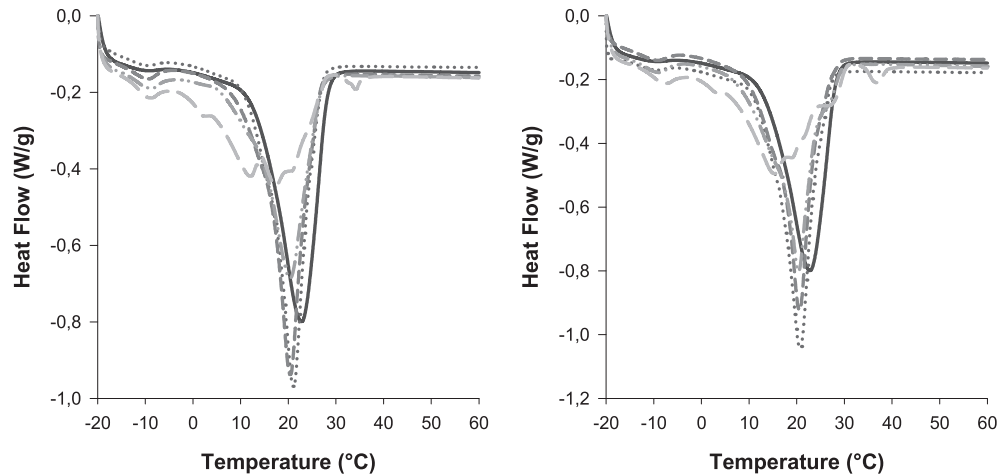


**Fig. 4.** DSC melting curves for high oleic sunflower oil cocoa butter equivalent blends (left) and high stearic high oleic sunflower oil cocoa butter equivalent blends (right). — CB, — 5 g CBE/100 g blend, — 25 g CBE/100 g blend, — 50 g CBE/100 g blend, — CBE.

**Table 3**

Overview of  $T_{\text{onset}}$ ,  $T_{\text{peak}}$  and melting heat of CBEs/CB blends.<sup>a</sup>

	CB	<sup>b</sup> CBE:CB (5:95)		CBE:CB (25:75)		CBE:CB (50:50)		CBE:CB (100:0)	
		HOSO	HSHO	HOSO	HSHO	HOSO	HSHO	HOSO	HSHO
$T_{\text{onset}}$ (°C)	14.0 ± 0.3b	15.0 ± 0.1ab	14.8 ± 0.0ab	15.0 ± 0.0ab	15.5 ± 0.1a	12.8 ± 0.6c	15.1 ± 0.0ab	5.2 ± 0.1e	7.9 ± 0.1d
$T_{\text{max}}$ (°C)	22.3 ± 0.6a	21.0 ± 0.1b	21.0 ± 0.2b	20.5 ± 0.1bc	20.6 ± 0.0bc	20.2 ± 0.3c	20.4 ± 0.2bc	15.3 ± 0.2e	17.6 ± 0.1d
Melting heat (J/g)	76.7 ± 1.4ab	77.5 ± 0.5a	77.1 ± 1.8ab	72.3 ± 0.4bcd	73.5 ± 0.2abc	64.0 ± 0.4f	69.2 ± 0.2cde	68.1 ± 2.0def	63.9 ± 3.2ef

<sup>a</sup> Values indicated with the same letters are not significantly different ( $\alpha = 0.05$ ).

<sup>b</sup> For abbreviations see "List of abbreviations".

**Table 4**

Casson yield stress and Casson viscosity chocolate and compounds.<sup>a</sup>

	CB	<sup>b</sup> CBE:CB (5:95)		CBE:CB (25:75)		CBE:CB (50:50)		CBE:CB (100:0)	
		HOSO	HSHO	HOSO	HSHO	HOSO	HSHO	HOSO	HSHO
$\sigma_{\text{CA}}$ (Pa)	16.5 ± 0.2a	15.4 ± 0.1b	13.4 ± 0.1ef	14.2 ± 0.1c	13.7 ± 0.1de	14.0 ± 0.2cd	13.2 ± 0.1f	13.4 ± 0.2ef	12.2 ± 0.2g
$\eta_{\text{CA}}$ (Pa.s)	1.47 ± 0.0a	1.40 ± 0.0bc	1.46 ± 0.0ab	1.40 ± 0.0c	1.41 ± 0.0bc	1.39 ± 0.0c	1.47 ± 0.0a	1.26 ± 0.0e	1.33 ± 0.0d

<sup>a</sup> Values indicated with the same letters are not significantly different ( $\alpha = 0.05$ ).

<sup>b</sup> For abbreviations see "List of abbreviations".

were analyzed to derive the melting characteristics as described in Section 2.3.4. The results of DSC parameters of two representative chocolates (with 5 g CBEs/100 g blend) and compound (with full fat replacement) are presented in Fig. 5.

As it is clear from Fig. 5, no significant differences were found between the  $T_{\text{onset}}$  of the reference chocolate and the other chocolates and compounds after 24 h after tempering ( $T_{\text{onset}}$  reference chocolate = 28.2 °C). However, after four weeks, the  $T_{\text{onset}}$  of the reference chocolate was significantly higher than  $T_{\text{onset}}$  of all the other chocolate and compounds ( $p < 0.05$ ). The higher onset temperature of the reference chocolate can be explained by the typical narrow melting peak of tempered chocolate. Replacing the CB with CBE leads to the chocolate and compound containing more SOO TAGs (low melting TAGs) giving rise to a lower  $T_{\text{onset}}$ . The same explanation can be given regarding the peak maximum. The compounds with only CBE had significantly lower melting temperature ( $T_{\text{peak}} = 30.8$  °C for HOSO CBE and  $T_{\text{peak}} = 31.7$  °C for HSHO CBE) in comparison to the reference chocolate. Lower peak maximum of these compounds can be due to the presence of  $\beta_{\text{IV}}$  crystals. CBEs have slow crystal growth property. However, there was no difference between the reference chocolate and the chocolate with 5 g CBEs/100 g blend after 4 weeks of storage indicating the existence of the stable  $\beta_{\text{V}}$  crystals.

The melting profile of chocolate is characterized by a sharp, narrow melting range leading to a quick melt at body temperature, producing a cool sensation and giving rise of flavors release (Schlichter-Aronhime & Garti, 1988). The peak width at half height can be determined in order to evaluate this behavior (De Clercq et al., 2014). No significant differences were observed between the reference chocolate and the other chocolates and compounds after 1 day of storage. However, upon prolonging time some differences appeared between the samples. The width at half height was significantly higher for all the compounds produced with both types of CBEs and chocolate with 5 g HSHO CBE/100 g blend over four weeks of storage (Fig. 5). The melting profile of these compounds had a lower  $T_{\text{onset}}$  and a broader peak. This can be explained by the higher amount of SOO present. The broader melting profile can lead to waxy mouth feel, less cooling sensation and less intense flavor release.

It can be seen from the Fig. 5 that, the peak area of the other chocolate and compounds slightly increased during storage. This can be due to the post crystallization. Consequently, the shift to higher peak area was probably the result of the re-crystallization of  $\beta_{\text{IV}}$  to  $\beta_{\text{V}}$ . Addition of CBE seemed to slow down this post crystallization process. The peak area for all the compounds even after 4 weeks was still quite low, indicating that  $\beta_{\text{IV}}$  crystals were present.

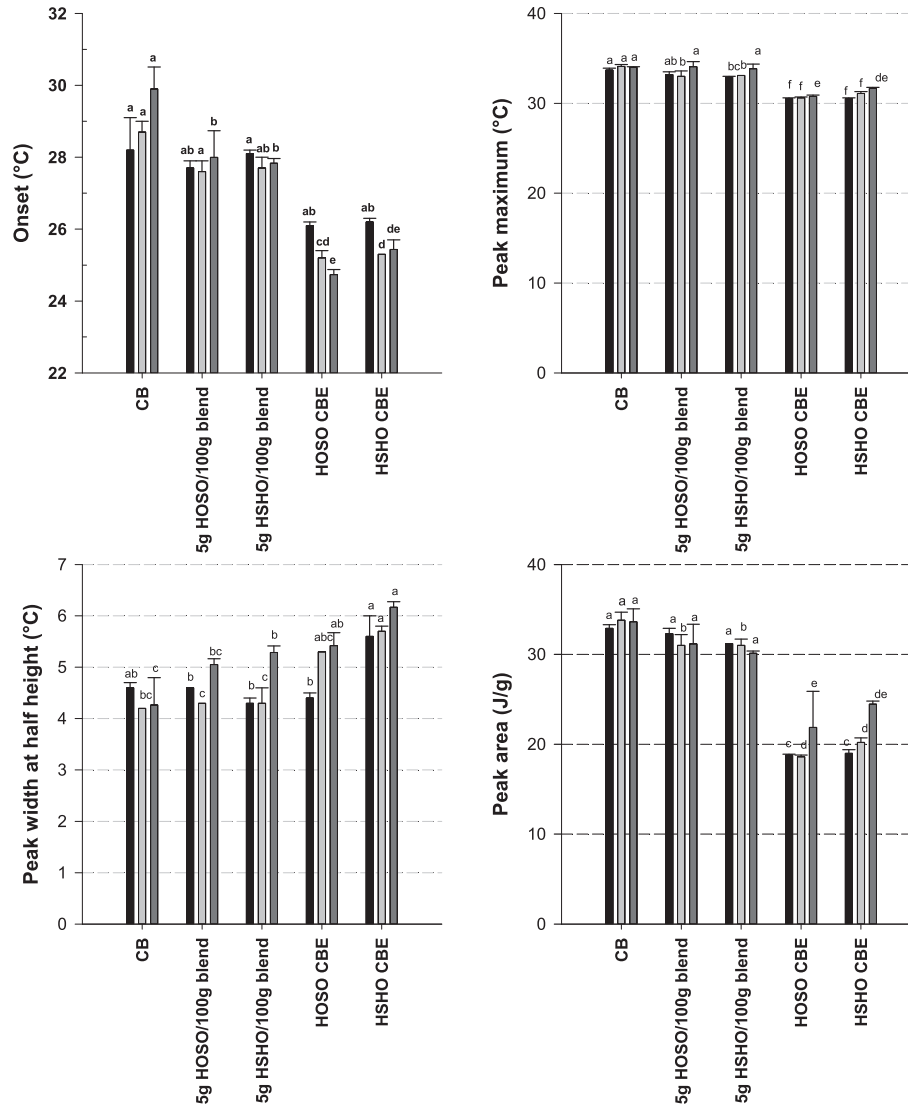


Fig. 5. Melting behavior of chocolates and compounds after 1 day, 2 weeks and 4 weeks; values indicated with the same letters are not significantly different ( $\alpha = 0.05$ ). ■ 1 Day, ▒ 2 Weeks, □ 4 Weeks.

Up to 5 g CBE/100 g blend, the influence was limited as peak maximum and area were not significantly different. It could be concluded that up to 5 g CBE/100 g blend addition, the melting behavior did not significantly change compared to the reference chocolate without CBE.

### 3.2.3. Hardness

A good quality chocolate is a solid product with a good snap at room temperature and a shiny appearance along with an easy melting in the mouth bringing a pleasant mouth feel (E.O. Afoakwa, 2011). The macroscopic properties were evaluated by measuring the hardness of the chocolate after 1 day, 2 and 4 weeks of production. It can be seen from the graph in Fig. 6 that the hardness of reference chocolate was similar to the chocolate with 5 g CBE/100 g blend up to 2 weeks. However, a linear decrease was observed when more CB was replaced. This can be explained by TAG composition of CBEs as they contain higher SOO TAGs leading to softening of CB and the chocolates and compounds afterwards. As discussed in Section 3.1.2, the iso-solid diagrams of the blends containing more CBEs showed softening effect (Fig. 2) which results in lower hardness of compounds in comparison to the reference chocolate and chocolates with 5 g CBE/100 g blend. As observed in

the DSC profiles, chocolates showed post-crystallization beyond two weeks of storage that led to the higher hardness of the samples. However, as can be seen from the figure this is not the fact for the chocolate with 5 g HOSO CBE/100 g blend and compound with 25 g HSHO CBE/100 g blend. In both samples the hardness significantly decrease upon 4 weeks of the storage at 20 °C ( $p < 0.05$ ). Brunello, McGauley, and Marangoni (2003) also observed a drastic decrease in hardness of CB after a longer period of storage at 20 °C, which they linked with a completed polymorphic transition from  $\beta'$  to  $\beta$ . They claimed that polymorphic transformations involve solid-state as well as melt mediated processes which latter surprisingly have large effects on mechanical properties. Within this research, the samples were tempered. The decrease in hardness can be an indication that the samples were not completely in the  $\beta_V$  polymorphic form after tempering. During storage, the polymorphic transition proceeded and while this transition was completing, the hardness dropped. It can be expected that the network formation in the under-tempered chocolate with 5 g HOSO CBE/100 g bend and compound with 25 g HSHO CBE/100 g blend is weaker, less efficient in comparison to the well-tempered chocolate and compounds, resulting in a lower maximum force required to penetrate the sample (E. O. Afoakwa, Paterson, Fowler, & Vieira, 2009).

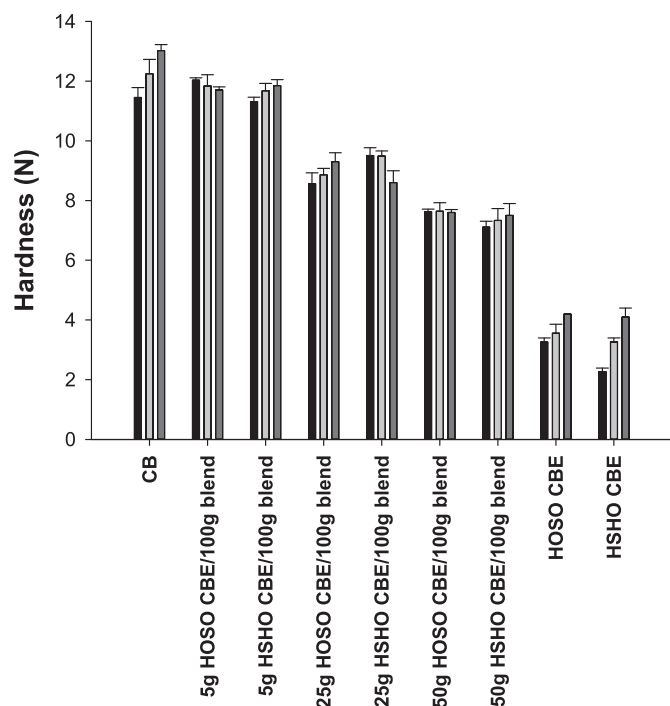


**Fig. 6.** Hardness of tempered samples stored at 20 °C measured by penetration test; values indicated with the same letters are not significantly different ( $\alpha = 0.05$ ). ■ 1 Day, □ 2 Weeks.

#### 4. Conclusion

Two enzymatically produced sunflower oil based CBEs were formulated by blending them with CB to screen their possible applicability in confectionary products. Iso-solid phase diagram of mixtures of CBEs with CB in different proportions showed satisfactory compatibility with no eutectic behavior that is more pronounced for HSHO CBE blends. The SFC profiles of the blends were reduced by increasing the CBE level in the blends due to the mixing effect of the lower melting SOO. Only HSHO CBE showed a residual amount of solid fat above body temperature that is still acceptable and would not be an issue to cause a waxy mouth feel. In the second part of this research, the CBE blends were applied in a dark chocolate. Up to 5 g CBE/100 g blend, the physical characteristics of the chocolates were not significantly influenced. Higher amounts of CBEs decreased the peak maximum and the Casson yield stress significantly. The latter may be of practical interest as this implies that the chocolate flow properties can be adjusted by adding a CBE. Comparing two different CBEs in dark chocolate and compounds revealed that the chocolate and compounds produced from HSHO CBE had higher particle size distribution and viscosity along with lower yield stress. The overall characterization suggested that the CBEs formulated from the second stearin of HOSO and HSHO with CB can be potentially utilized as alternative fats in confectionary application. Comparing the physicochemical properties of the two sunflower oil CBEs revealed that HSHO CBE was a more promising source than HOSO CBE as an alternative to CB.

#### Acknowledgments

The authors acknowledge Nutrisun Business Unit of Advanta Seeds for providing high stearic high oleic sunflower oil.

#### References

Afoakwa, E. O. (2011). *Chocolate science and technology*. Wiley.

- Afoakwa, E. O., Paterson, A., Fowler, M., & Vieira, J. (2009). Influence of tempering and fat crystallization behaviours on microstructural and melting properties in dark chocolate systems. *Food Research International*, 42(1), 200–209.
- Aidoo, R. P., De Clercq, N., Afoakwa, E. O., & Dewettinck, K. (2014). Optimisation of processing conditions and rheological properties using stephan mixer as conche in small-scale chocolate processing. *International Journal of Food Science & Technology*, 49(3), 740–746. <http://dx.doi.org/10.1111/ijfs.12360>.
- Brunello, N., McGauley, S. E., & Marangoni, A. G. (2003). Mechanical properties of cocoa butter in relation to its crystallization behavior and microstructure. *LWT – Food Science and Technology*, 36(5), 525–532.
- Cebula, D., & Smith, K. (1992). Differential scanning calorimetry of confectionary fats: part II—effects of blends and minor components. *Journal of the American Oil Chemists' Society*, 69(10), 992–998.
- Chong, C., Hoh, Y., & Wang, C. (1992). Fractionation procedures for obtaining cocoa butter-like fat from enzymatically interesterified palm olein. *Journal of the American Oil Chemists' Society*, 69(2), 137–140.
- Çiftçi, O. N., Kowalski, B., Gögüş, F., & Fadiloğlu, S. (2009). Effect of the addition of a cocoa butter—like fat enzymatically produced from olive pomace oil on the oxidative stability of cocoa butter. *Journal of Food Science*, 74(4), E184–E190.
- De Clercq, N., Depypere, F., Delbaere, C., Nopens, I., Bernaert, H., & Dewettinck, K. (2014). Influence of cocoa butter diacylglycerols on migration induced fat bloom in filled chocolates. *European Journal of Lipid Science and Technology*, 1388–1399.
- De Clercq, N., Moens, K., Depypere, F., Vila Ayala, J., Calliauw, G., De Greyt, W., et al. (2012). Influence of cocoa butter refining on the quality of milk chocolate. *Journal of Food Engineering*, 111(2), 412–419.
- Firestone, D. (1998). *Official methods and recommended practices of the AOCS*. American Oil Chemists' Society.
- Foubert, I., Vanrolleghem, P. A., Thas, O., & Dewettinck, K. (2004). Influence of chemical composition on the isothermal cocoa butter crystallization. *Journal of Food Science*, 69(9), E478–E487.
- Humphrey, K. L., & Narine, S. S. (2005). *Lipid phase behavior fat crystal networks* (pp. 83–115).
- Kadivar, S., De Clercq, N., Van de Walle, D., & Dewettinck, K. (2014). Optimisation of enzymatic synthesis of cocoa butter equivalent from high oleic sunflower oil. *Journal of the Science of Food and Agriculture*, 94(7), 1325–1331.
- Kang, K., Jeon, H., Kim, I. H., & Kim, B. H. (2013). Cocoa butter equivalents prepared by blending fractionated palm stearin and shea stearin. *Food Science and Biotechnology*, 22(2), 347–352.
- Mat Dian, N. L. H., Sundram, K., & Idris, N. A. (2006). DSC study on the melting properties of palm oil, sunflower oil, and palm kernel olein blends before and after chemical interesterification. *Journal of the American Oil Chemists' Society*, 83(8), 739–745.
- NorAini, I., Embong, M. S., Aminah, A., Md Ali, A. R., & Maimon, C. H. C. (1995). Physical characteristics of shortenings based on modified palm oil, milkfat and low melting milkfat fraction. *Lipid/Fett*, 97(7–8), 253–260.
- Padley F. B., Paulussen C. N., Soeters C., & Tresser D. (1981). *Chocolate having defined hard fat*: google patents.
- Rombaut, R., De Clercq, N., Foubert, I., & Dewettinck, K. (2009). Triacylglycerol analysis of fats and oils by evaporative light scattering detection. *Journal of the American Oil Chemists' Society*, 86(1), 19–25.
- Rozendaal, A., & Macrae, A. R. (1997). Interesterification of oils and fats. In F. D. Gunstone, & F. B. Padley (Eds.), *Lipid technologies and applications* (pp. 223–263). New York: CRC Press.
- Schlichter-Aronhime, J., & Garti, N. (1988). Solidification and polymorphism in cocoa butter and the blooming problems. In N. Garti, & K. Sato (Eds.), *Crystallization and polymorphism of fats and fatty acids* (Vol. 31, pp. 363–393).
- Shukla, V. K. S. (1995). Cocoa butter properties and quality. *Lipid Technology*, 7(3), 54–57.
- Shukla, V. K. S. (2005). *Confectionery lipids Bailey's industrial oil and fat products*. John Wiley & Sons, Inc.
- Smith, K. W., Bhagga, K., & Talbot, G. (2013). Phase behavior of symmetrical monounsaturated triacylglycerols. *European Journal of Lipid Science and Technology*, 115(8), 838–846.
- Tchobo, F. P., Piombo, G., Pina, M., Soumanou, M. M., Villeneuve, P., & Sohounhloue, D. C. K. (2009). Enzymatic synthesis of cocoa butter equivalent through transesterification of *Pentadesma butyracea* butter. *Journal of Food Lipids*, 16(4), 605–617.
- Timms, R. E. (1984). Phase behaviour of fats and their mixtures. *Progress in Lipid Research*, 23(1), 1–38.
- Union, E. (2000). *Directive 2000/36/EC of the European parliament and of the council relating to cocoa and chocolate products intended for human consumption* (pp. 19–25).
- Verstringe, S., De Clercq, N., Nguyen, M. T., Kadivar, S., & Dewettinck, K. (2012). Enzymatic and other modification techniques to produce cocoa butter alternatives. In N. Garti, & N. Widlak (Eds.), *Cocoa butter and related compounds* (pp. 443–474). AOCS Press.
- Wang, F., Liu, Y., Jin, Q., Meng, Z., & Wang, X. (2011). Characterization of cocoa butter substitutes, milk fat and cocoa butter mixtures. *European Journal of Lipid Science and Technology*, 113(9), 1145–1151.
- Wesdorp, L. H., Van Meeteren, J. A., De Jong, S., Giessen, R. V. D., Overbosch, P., Grootsholten, P. A. M., & de Loos, T. H. (2005). Liquid-multiple solid phase equilibria in fats: theory and experiments. *Fat Crystal Networks*, 481–709.
- Xu, X. (2000). Production of specific-structured triacylglycerols by lipase-catalyzed reactions: a review. *European Journal of Lipid Science and Technology*, 102(4), 287–303.



## Changes in phenolic compounds and their antioxidant capacities in jujube (*Ziziphus jujuba* Miller) during three edible maturity stages



Bini Wang<sup>a,b,\*</sup>, Qingyuan Huang<sup>a</sup>, Chandrasekar Venkitasamy<sup>b</sup>, Hongkang Chai<sup>a</sup>, Hui Gao<sup>a</sup>, Ni Cheng<sup>a</sup>, Wei Cao<sup>a</sup>, Xingang Lv<sup>a</sup>, Zhongli Pan<sup>b,c,\*\*</sup>

<sup>a</sup> Department of Food Science and Engineering, College of Chemical Engineering, Northwest University, Xi'an, Shaanxi 710069, China

<sup>b</sup> Department of Biological and Agricultural Engineering, University of California, Davis, One Shields Avenue, Davis, CA 95616, USA

<sup>c</sup> Healthy Processed Foods Research Unit, USDA-ARS-WRRC, 800 Buchanan St., Albany, CA 94710, USA

### ARTICLE INFO

#### Article history:

Received 10 April 2015

Received in revised form

9 September 2015

Accepted 2 October 2015

Available online 9 October 2015

#### Keywords:

*Ziziphus*

Insoluble-bound phenolic

Antioxidant activity

Maturity stage

#### Chemical compounds studied in this article:

Gallic acid (PubChem CID:370)

Protocatechuic acid (PubChem CID:72)

*p*-Hydroxybenzoic acid (PubChem CID:135)

Chlorogenic acid (PubChem CID:1794427)

Caffeic acid (PubChem CID:689043)

*p*-Coumaric acid (PubChem CID:637542)

Ferulic acid (PubChem CID:445858)

Rosmarinic acid (PubChem CID:5281792)

Ellagic acid (PubChem CID:5281855)

Quercetin (PubChem CID:5280343)

Syringic acid (PubChem CID:10742)

Hesperetin (PubChem CID:72281)

Rutin (PubChem CID:5280805)

### ABSTRACT

This study investigated the changes in total phenolic content (TPC), total flavonoid content (TFC), individual phenolic compound content, DPPH radical scavenging activity and antioxidant capacity measured by FRAP assay of four phenolic fractions (free, esterified, glycosided and insoluble-bound) from jujube during three edible maturity stages. The maturity stages of jujubes were established as white maturity (WM), half-red maturity (HM) and red maturity (RM). The free fraction in jujube at WM stage had the highest TPC, TFC, total phenolic acid contents, and antioxidant capacities. The phenolic contents and their activities greatly decreased with the increasing maturity stage. Caffeic acid was the most predominant in all detected phenolic compounds at WM stage, while rutin dominated at HM and RM stages. Even though most of phenolic compounds with antioxidant activity in jujube existed at the WM stage as the free form, the insoluble-bound fractions also contained a large number of phenolic compounds.

© 2015 Elsevier Ltd. All rights reserved.

## 1. Introduction

Jujube is the fruit of *Ziziphus jujuba* Miller, a thorny rhamnaceous plant widely cultivated in subtropical and tropical regions of

\* Corresponding author (B.N. Wang). Department of Food Science and Engineering, College of Chemical Engineering, Northwest University, Xi'an, Shaanxi 710069, China.

\*\* Corresponding author (Z.L. Pan). Department of Biological and Agricultural Engineering, University of California, Davis, One Shields Avenue, Davis, CA 95616, USA.

E-mail address: [wangbini@nwu.edu.cn](mailto:wangbini@nwu.edu.cn) (B. Wang).

Asia, especially in China, America and Europe. China is the largest producer contributing over 90% of the world jujube production and the only country exporting jujube fruits. The total annual yield of fresh jujube fruits in 2009 was 600 million kilograms (Lu, Lou, Zheng, Hu, & Li, 2012) and has been increasing in the recent years in China. Globally, jujube is popularly consumed as fresh or dried fruit and has been used to prepare compotes, jams, beverages and cakes.

The color of jujube peel changes from green to yellow, then to reddish and finally to red during maturation. These peel colors represent maturity stages typically called green fruit stage, white

maturity (WM), half-red maturity (HM), and red maturity (RM) stage, respectively. The fruit is unsuitable for eating or processing until it ripens to WM stage. Production of various processed products prefers jujube at a specific maturity stage. For example, fresh consumption or most processed products require jujube at HM or RM stage, dried products require jujube at RM stage and processing into saccades needs jujube at WM stage. There is an increased interest in the potential health benefits of jujube to human beings. An ancient Chinese book on herbal medicine named *Huangdi Neijing* (475–221 BC) showed that jujube was one of five most valuable fruits (peach, pear, apricot, plum, and jujube) in China. It has a high nutritional value and potential health benefits including antioxidant activity (Gao, Wu, & Wang, 2013). It has been widely used as food, a functional food additive, and a traditional Chinese medicine for several thousands of years and attracted research on its bioactive substances, such as phenolic compounds (Du et al., 2013; Chen et al., 2013; Choi, Ahn, Kozukue, Levin, & Friedman, 2011; Wang, Cao, Gao, Fan, & Zheng, 2010).

Phenolic compounds are secondary metabolites of plants that play an important role in the pigmentation, growth, reproduction of plants as well as plant resistance to pathogens (Ghasemzadeh & Ghasemzadeh, 2011). Their content in fruit is largely affected by genotype (cultivar), pre-harvest environmental conditions, post-harvest storage conditions, processing and the degree of maturity at harvest (Shahidi & Naczk, 2004). During fruit maturation, the phenolic compounds undergo a series of complex biosynthesis process, leading to the changes in their composition and content in plant and plant-derived foods (Prasanna, Prabha, & Tharanathan, 2007). They have received increased attention due to their potent antioxidant capacities and their remarkable health benefits in the prevention of various oxidative stresses associated diseases, such as cancer, cellular aging, cardiovascular diseases and inflammation (Dai & Mumper, 2010). Several studies revealed that the phenolic compounds and their bioactivities in jujube could be influenced by its maturity (Wu, Gao, Guo, Yu, & Wang, 2012; Chen et al., 2013; Choi et al., 2012). Those studies evaluated the phenolic compounds in soluble extracts alone and ignored the insoluble-bound ones in residues, leading to the underestimation of real phenolic content of jujube and their corresponding antioxidant activities. In general, the phenolic compounds in food are classified as soluble (extractable) and insoluble (non-extractable) compounds based on the location of phenolic compounds in the plant together with the chemical structure of these substances (Reis Giada, 2013). The former can typically be extracted by organic solvents, while the latter is bound to cell wall polysaccharides or proteins forming insoluble stable complexes. Interestingly, these insoluble phenolics are also very important in health effects from the nutritional viewpoint and they exert their antioxidant effects to protect the body against oxidative stress (Liyana-Pathirana & Shahidi, 2006; Pérez-Jiménez & Torres, 2011). Though the insoluble phenolic compounds cannot be extracted by organic solvents, they may be released from the complexes by the action of intestinal enzymes or colonic microbiota and thereby transformed into small phenolics and metabolites that are subsequently absorbed. Therefore, the insoluble compounds should also be well studied.

In our previous study, we found that the major fraction of phenolic acids in different tissues of jujube is insoluble-bound (Wang, Liu, Zheng, Fan, & Cao, 2011). However, there is no information available related to the effect of maturity stages on the soluble and insoluble phenolic compounds of jujube and their antioxidant capacities, which is important to ensure that jujube is harvested at right maturity with high antioxidants content. Furthermore, producers and industrialists also need the valuable information on bioactive compounds in jujube and their antioxidant activities at different maturity stages for marketing purpose.

Thus, the aim of the present study was to evaluate the changes in phenolic compounds (in free, esterified, glycosided and insoluble-bound forms) and their antioxidant activities of jujube at three edible maturity stages. The results of this study could lead to identification of the optimal maturity stage for the harvest of jujube with high composition of polyphenols targeting increased antioxidant activities.

## 2. Materials and methods

### 2.1. Samples of jujube fruits

Fresh jujubes (*Ziziphus jujube* cv. Jishanbanzao) used in this study were obtained from a local farm in Jishan County, south-western part of Shanxi Province, North China. No pesticide was used in the jujube crop. Jujube samples were harvested from July 25th to October 5th of 2014 at three edible stages of maturity determined based on the surface color. The three maturity stages were established as white maturity (WM), yellow skin color; half-red maturity (HM), representing jujube with red surface area of 40%–60%; and red maturity (RM), having 100% red surface area. Jujubes were picked up randomly from different parts of several trees of the same species and were free from visible blemishes and disease. Jujubes were frozen and stored in airtight polyethylene bags at  $-18^{\circ}\text{C}$  in a freezer until they were analyzed.

### 2.2. Chemicals

Gallic acid, protocatechuic acid, *p*-hydroxybenzoic acid, syringic acid, caffeic acid, *p*-coumaric acid, ferulic acid, chlorogenic acid, rosmarinic acid, ellagic acid, rutin, hesperetin, 2,2-diphenyl-1-picryl-hydrazyl (DPPH), and 2,4,6-tripyridyl-*s*-triazine (TPTZ) were purchased from Sigma–Aldrich (Steinheim, Germany). All other chemicals were also analytical grade and were obtained from Xi'an Chemical Co. (Xi'an, China). HPLC grade methanol was purchased from Merck (Darmstadt, Germany). Analytical grade acetic acid was supplied by Beijing Reagent Co. Ltd (Beijing, China) and HPLC grade water was purified by Milli-Q system (Millipore Bedford, MA, USA).

### 2.3. Preparation of crude jujube extracts

The frozen jujube fruits were thawed and cleaned with tap water. The seeds were removed from jujubes and the edible portion was homogenized in a blender for 1 min. A sample of 100 g of homogenized jujube was lyophilized, milled and sieved through a standard sieve of 100 mesh. The powdered samples (2 g) of jujube at different maturity stages were extracted with 15 mL of 80% (v/v) aqueous methanol at room temperature. The solution was sonicated for 30 min and then centrifuged at 2000 g for 10 min to collect supernatant. The supernatant extraction was repeated for three times and the accumulated supernatants were used for the fractionation of free phenolic compounds, soluble glycosides and esters of phenolic compounds. The residue left after the extraction of supernatant was saved for the determination of insoluble-bound phenolic compounds.

### 2.4. Fractionation of free and bound phenolic compounds

Phenolic compounds in crude extracts were fractionated into free and bound forms following our previously established methods (Wang et al., 2011) as described below. The crude extract (supernatants) obtained after the methanol extraction from jujube as described in the previous step was evaporated under vacuum at  $35^{\circ}\text{C}$  to about 10 mL. The aqueous suspension was acidified to pH 2

using 6 M hydrochloric acid (HCl), and extracted for five times with ethyl acetate at a solvent to water phase ratio of 1: 1. The ethyl acetate extracts were referred to as the free phenolic compounds (F1). The aqueous phase remained after the ethyl acetate extraction was treated by alkaline hydrolysis (4 M sodium hydroxide (NaOH) containing 10 mM ethylenediaminetetraacetic acid (EDTA) and 1% ascorbic acid) under nitrogen for 4 h at room temperature. After acidification to pH 2 with 6 M HCl, phenolic compounds (F2) released from soluble esters were extracted from the hydrolysate for five times using the procedure as described above. Following this, the aqueous phase remained after the F2 separation was hydrolyzed with 5 mL 6 M HCl for 30 min at 85 °C under nitrogen. Phenolic compounds (F3) released from soluble glycosides were separated from the hydrolysate for five times following the procedure as described above. The residues from the 80% methanol extractions were hydrolyzed directly with 8 mL of 4 M NaOH (containing 10 mM EDTA and 1% ascorbic acid) under the same conditions as the ester. After acidification to pH 2 using 6 M HCl, phenolic compounds (F4) released from methanol-insoluble ester-bound phenolics were extracted from the hydrolysate for five times as described above. Extraction was done for triplicate samples. Each of the phenolic fractions, obtained as described above, was dehydrated with anhydrous sodium sulfate, filtered, and evaporated to dryness under vacuum at 35 °C. The dry residues were dissolved into 5 mL of methanol, and these solutions were used for the determination of phenolic contents and antioxidant activities as described below.

### 2.5. Determination of total phenolic contents

Total phenolic contents (TPC) in each fraction of jujube extract were determined according to a previously described laboratory procedure of the modified Folin-Ciocalteu colorimetric method (Wang et al., 2011). TPC was evaluated at 760 nm by adding Folin-Ciocalteu reagent to the sample. The average value of triplicate data was expressed as the gallic acid equivalents in mg per 100 g dry weight (mg GAE/100 g DW).

### 2.6. Determination of total flavonoids content

Total flavonoids content (TFC) in each fraction of jujube extract was measured colorimetrically at 510 nm following a previously reported method (Jia, Tang, & Wu, 1999). TFC was expressed as rutin equivalents in mg per 100 g dry weight (mg RE/100 g DW). The absorbance was measured for triplicate samples.

### 2.7. HPLC-ECD analysis

The phenolic compounds in the four phenolic fractions from jujube were separated and quantified using a HPLC fitted with an electrochemical detector (ECD) as described by Wang et al. (2011) with minor revision. HPLC analysis of phenolic compounds were carried out using an Agilent 1100 HPLC System (Agilent, USA) equipped with a vacuum degasser, a quaternary solvent delivery pump, a manual chromatographic valve, a thermostated column compartment, and a HP1049A programmable ECD (HP, USA). A Zorbax SB-C18 column (150 × 4.6 mm, 5.0 μm) connected with a Zorbax SB-C18 guard column (20 × 4.0 mm, 5 μm). The mobile phase adopted was methanol (A) and 0.15% aqueous formic acid (B) (v/v) using a linear gradient elution of 5–8% A at 0–6 min, 8–15% A at 6–10 min, 15–35% A at 10–15 min, 35–55% A at 15–20 min, 55–65% A at 20–25 min and 65–80% A at 25–30 min. The flow-rate was kept at 1.0 mL min<sup>-1</sup> at all times. The column was operated at 30 °C and the injection volume was 10.0 μL. The electrochemical detector was set at 800 mV in the oxidative mode. Re-equilibration

duration was set as 6 min by using the starting condition before injection of the next individual sample. Quantification of phenolic acids was carried out by an external standard method using calibration curves. The amount of each phenolic acid was expressed as microgram per gram dry weight (μg/g DW).

### 2.8. Radical DPPH scavenging activity

Scavenging activity on DPPH free radicals by each phenolic acid fraction was assessed according to the method reported by Wang et al. (2011).

### 2.9. Ferric reducing antioxidant power (FRAP)

FRAP assay of each sample was performed following a previously described laboratory procedure (Wang et al., 2011).

### 2.10. Statistical analysis

The results presented in the tables are the mean value ± SD (standard deviation) from three replicates. Data analysis was carried out using SAS software, version 8.1. Statistically significant difference between the samples was evaluated by the Tukey's test. Difference at  $p < 0.05$  was considered to be significant. The correlation analysis between phenolics and antioxidant activity was made using standard Pearson correlation.

## 3. Results and discussion

### 3.1. Total phenolics of jujube at three edible maturity stages

The TPCs in four phenolic fractions of jujube at three edible maturity stages are shown in Table 1. The maturity stages had a significant influence on the TPCs in jujube. The TPC in each phenolic fraction significantly decreased ( $p < 0.05$ ) with the increase in maturity stages. All fractions extracted from WM stage were observed to have several folds (1.8–12 folds) higher amounts of TPC than those at RM stage. The sum of TPC in four fractions of jujube sharply decreased from 1515.35 mg GAE/100 g DW at WM stage to 362.68 mg GAE/100 g DW at RM stage ( $p < 0.05$ ). Previous studies (Wu et al., 2012; Zozio et al., 2014) reported only the TPC values of the soluble extracts obtained from jujube during ripening and ignored the TPC of insoluble extracts. The TPC of the soluble extracts decreased with maturity stage, which was in agreement with those reported previously for jujube and other fruits (Zozio et al., 2014; Wang, Cheng, Cao, & Jiang, 2013; Wu et al., 2012; Kondo, Tsuda, Muto, & Ueda, 2002; Gruz, Ayaz, Torun, & Strnad, 2011). However, the quantities of TPC obtained from this study were lower than the previously published results (Wang et al., 2011; Wu et al., 2012). This might be mainly attributed to the differences in the cultivar and sources of the materials, as well as the regional differences (Gull et al., 2012). In the four phenolic fractions, F1 was the major fraction constituting 57.1% and 42.5% of the sum of the TPC at WM and HM stages of jujube, respectively. The F2 and F4 dominated at RM stage, comprising 29.0% and 28.4% of TPC, respectively. These results indicated that the TPC was clearly dependent on maturity stages, and the maturation process increased the bound phenolics content.

### 3.2. Total flavonoids in jujube at three maturity stages

Most previous studies revealed that jujube contained considerable amounts of flavonoids including rutin (Pawłowska, Camangi, Bader, & Braca, 2009; Zhang, Jiang, Ye, Ye, & Ren, 2010; Wu et al., 2012; Du et al., 2013; Gao et al., 2012), and mainly examined TFC

**Table 1**  
TPC (mg GAE/100 g DW) in four phenolic fractions of jujube during maturity.

Maturity stages	Phenolic fractions			
	Free (F1)	Esterified (F2)	Glycosided (F3)	Insoluble-bound (F4)
White maturity (WM)	864.73 ± 3.27 <sup>a</sup>	190.30 ± 2.44 <sup>a</sup>	197.83 ± 5.92 <sup>a</sup>	262.49 ± 5.22 <sup>a</sup>
Half-red maturity (HM)	259.00 ± 7.14 <sup>b</sup>	75.31 ± 3.11 <sup>b</sup>	122.11 ± 6.79 <sup>b</sup>	152.83 ± 3.06 <sup>b</sup>
Red maturity (RM)	71.67 ± 1.99 <sup>c</sup>	105.13 ± 5.67 <sup>b</sup>	82.78 ± 6.16 <sup>c</sup>	103.10 ± 2.81 <sup>c</sup>

Different lower case letters correspond to significant differences at  $p < 0.05$ .

in ethanol or methanol extracts of jujube. Flavonoids has also been found in the insoluble (non-extractable) fraction and associated with dietary fiber in tomato peel and roselle tea (Arranz, Silván, & Saura-Calixto, 2010; Kapasakalidis, Rastall, & Gordon, 2009; Navarro-Gonzalez, García-Valverde, García-Alonso, & Periago, 2011; Sáyago-Ayerdi, Arranz, Serrano, & Goñi, 2007). Little information has been reported on TFC in the insoluble fraction in jujube.

In the present study, the TFC in soluble and insoluble fractions of jujube at three maturity stages were determined (Table 2). Results showed that the TFC in all four phenolic fractions of jujube rapidly decreased with the progress of maturity. The rapidest decrease in TFC occurred for F1, and the TFC was significantly reduced by 6 folds from WM to RM stage ( $p < 0.05$ ). The sum of TFC in four fractions exhibited a continuously decreasing trend similar to TPC and decreased from 1692.66 mg RE/100 g DW at WM stage to 483.47 mg RE/100 g DW at RM stage, which was consistent with those reported for pear-jujube (Wu et al., 2012). The TFC values obtained for the soluble fraction of jujube (422.43–1525.43 mg RE/100 g DW) were within the ranges reported by Zhang et al. (2010), from 276.43 to 1851.96 mg QE/100 g DW and by Gao et al. (2012), from 62.0 to 284.9 mg RE/100 g FW in ethanol or methanol extracts of different jujube cultivars. With the increase of jujube maturity, the percentage of TFC in F1 continuously decreased from 65.7% to 34.6%, while the TFC in F4 continuously increased from 16.3% to 36.7%. As jujube became fully ripen (RM stage), F1 and F4 were the major fractions constituting 34.6% and 36.9% of the sum of TFC, respectively. Therefore, the TFC in the insoluble fraction (F4) cannot be ignored, and further research is required to identify the association or binding of these flavonoids with other compounds of jujube.

### 3.3. Individual phenolic compounds

Thirteen phenolic compounds, including hydroxybenzoic acids (gallic, protocatechuic, *p*-hydroxybenzoic and syringate), hydroxycinnamic acids (caffeic, *p*-coumaric, and ferulic), other phenolic acids (chlorogenic, rosmarinic, and ellagic) and flavonoid (rutin, quercetin and hesperetin) were well separated and quantified by HPLC-ECD. But syringate and hesperetin were not found in jujube at all three maturity stages. The distribution of the phenolic compounds in the four fractions obtained from jujube at the three maturity stages is presented in Table 3. The results showed that free phenolic compounds were the most abundant at all of the maturity stages.

Free phenolic compounds comprised of 80.0%, 53.5% and 85.9%

of the total phenolic compounds in jujube at WM, HM and RM, respectively (Fig. 1). The content of free phenolic compounds in jujube was much higher at WM (1698.29  $\mu\text{g/g}$  DW) than those at HM and RM stages (794.50 and 1165.66  $\mu\text{g/g}$  DW, respectively). Rutin was reported as a common component in jujube extracts (Pawlowska et al., 2009), and was the most predominant phenolic compound at any maturity stages in this work. The levels of rutin decreased from 925.83  $\mu\text{g/g}$  DW (WM) to 602.04  $\mu\text{g/g}$  DW (HM), and then increased to 670.63  $\mu\text{g/g}$  DW (RM). This change is consistent with the results reported by Wu et al. (2012), but the obtained values in this research were more than 10 times higher. Choi et al. (2012) also found rutin content continuously decreased as the fruits matured, and epicatechin was the most prevalent flavonoid during the maturity stages which was not observed in our study. Caffeic acid was the dominant phenolic compounds at WM stage, while chlorogenic acid, an ester of caffeic acid, was mostly present in the free form at RM stage. The *p*-coumaric acid was detected only at HM stage and ferulic acid was detected only at RM stage. In addition, quercetin, gallic and rosmarinic acids were not detected at any maturity stages.

Phenolic compounds released from soluble esters constituted from 3.4% (at RM) to 18.6% (at HM) of the total quantified phenolic compounds in jujube (Fig. 1). At HM stage, the total content of phenolic compounds released from soluble esters was 275.92  $\mu\text{g/g}$  DW, which was 2-fold higher than that at WM stage and 5-fold higher than that at RM stage. The *p*-coumaric acid was the principal phenolic presented as soluble esters at WM stage, whereas rutin dominated at RM stage. Each of rutin and chlorogenic acid constituted for more than 36% of the total phenolic compounds content at HM stage. However, gallic and rosmarinic acids were not detected in this fraction at any maturity stages.

Glycosided phenolic compounds ranged from 3.8% (at RM) to 24.6% (at HM) of the total phenolic compounds presented in jujube (Fig. 1). The total contents of glycosided phenolics in jujube at WM and HM stage were 260.02  $\mu\text{g/g}$  DW and 365.88  $\mu\text{g/g}$  DW, respectively, which were about 5-fold and 7-fold higher than that at RM (52.08  $\mu\text{g/g}$  DW), respectively. Glycosided gallic acid presented mostly at WM stage and HM stage and was not detected at RM stage. The percentage of glycosided gallic acid at WM and HM were 76.4% and 56.8% of the total glycosided phenolics, respectively. Though chlorogenic and protocatechuic acids were the principal phenolics at RM, they were at very low levels of 15.15  $\mu\text{g/g}$  DW and 10.89  $\mu\text{g/g}$  DW, respectively.

The insoluble-bound phenolic compounds constituted 3.5%,

**Table 2**  
TFC (mg Rutin/100 g DW) in four phenolic fractions of jujube during maturity.

Maturity stages	Phenolic fractions			
	F1	F2	F3	F4
White maturity (WM)	1002.00 ± 10.60 <sup>a</sup>	274.94 ± 15.46 <sup>a</sup>	167.23 ± 22.97 <sup>a</sup>	248.49 ± 6.27 <sup>a</sup>
Half-red maturity (HM)	956.39 ± 9.17 <sup>b</sup>	125.72 ± 7.97 <sup>b</sup>	137.88 ± 14.10 <sup>a</sup>	258.69 ± 6.90 <sup>a</sup>
Red maturity (RM)	167.45 ± 18.79 <sup>c</sup>	77.42 ± 11.93 <sup>c</sup>	61.05 ± 7.31 <sup>b</sup>	177.56 ± 7.63 <sup>b</sup>

Different lower case letters correspond to significant differences at  $p < 0.05$ .

**Table 3**  
Composition of phenolic compounds in jujube during maturity ( $\mu\text{g/g DW}$ ).

Phenolics	White maturity				Half-red maturity				Red maturity			
	F1	F2	F3	F4	F1	F2	F3	F4	F1	F2	F3	F4
Phenolic acids												
Gallic	0.00	0.00	198.66	0.00	0.00	51.57	207.86	8.41	0.00	0.00	0.00	0.00
Protocatechuic	6.57	7.89	5.37	7.30	8.22	6.89	21.01	2.16	9.72	1.62	10.89	3.18
p-hydroxybenzoic	71.35	0.90	7.21	4.41	12.54	1.36	2.60	5.39	0.14	0.34	2.83	1.29
Caffeic	637.88	10.18	1.05	15.56	138.68	1.82	0.93	5.61	76.79	9.52	2.87	17.52
p-coumaric	0.00	34.70	7.64	16.94	18.08	10.64	7.55	19.10	0.00	2.50	5.23	32.92
Ferulic	0.00	0.70	6.29	0.00	0.00	1.86	8.85	0.00	41.84	1.65	0.00	6.33
Chlorogenic	47.55	15.42	21.39	10.58	8.01	100.00	39.52	1.26	366.53	10.42	15.15	26.27
Rosmarinic acid	0.00	0.00	0.63	0.03	0.00	0.00	6.62	0.00	0.00	0.00	0.90	0.07
Ellagic acid	9.11	3.56	5.94	18.04	6.93	0.00	13.08	2.06	0.00	0.00	1.51	0.00
$\Sigma$ TPA	772.46	73.33	254.18	72.86	192.46	174.14	308.03	43.99	495.03	26.06	39.38	87.58
Flavonoids												
Rutin	925.83	17.73	0.00	0.86	602.04	101.74	51.14	4.79	670.63	20.59	8.07	4.71
Quercetin	0.00	0.63	0.00	0.00	0.00	0.04	6.71	0.00	0.00	0.12	4.63	0.00
$\Sigma$ TP	1698.29	91.69	260.02	73.72	794.50	275.92	365.88	48.78	1165.66	46.77	52.08	92.29

3.3%, and 6.8% of total phenolics in jujube at WM, HW and RW stages, respectively (Fig. 1). Insoluble-bound *p*-coumaric acid was one of the major phenolic compounds in jujube found at the three maturity stages, and represented 23.0%, 39.1% and 35.7% of the total insoluble-bound phenolics at WM, HM and RM stages, respectively. Furthermore, ellagic acid mainly presented in insoluble-bound form and caffeic acid was the major phenolic compounds at WM stage, while *p*-coumaric and chlorogenic acids dominated this fraction at RM stage.

The total content of quantified phenolic compounds in the four fractions from jujube continuously decreased from 2123.72  $\mu\text{g/g DW}$  to 1356.80  $\mu\text{g/g DW}$  as the fruits matured. The total detected phenolic acid and flavonoid contents decreased by 38.7% and 30.1% from WM to HM stage, respectively, and then slightly decreased (by 9.8% and 8.6%) as the fruit ripening progressed. Moreover, both contents were almost equal at any maturity stage.

The level of total individual phenolic compound contents in jujube at different maturity stages was calculated as a sum of individual phenolic compound present in all four fractions. Apparently, rutin was the dominant phenolic compound in jujube at any maturity stage, comprising 44.5%, 51.2% and 51.9% of the total phenols at WM, HM and RM stages, respectively (Fig. 2). Caffeic and chlorogenic acids were the principal phenolic compounds in jujube with 31.3% and 30.8% of the total phenols at WM and RM stages, respectively, while gallic acid was also in a large quantity at HM stage.

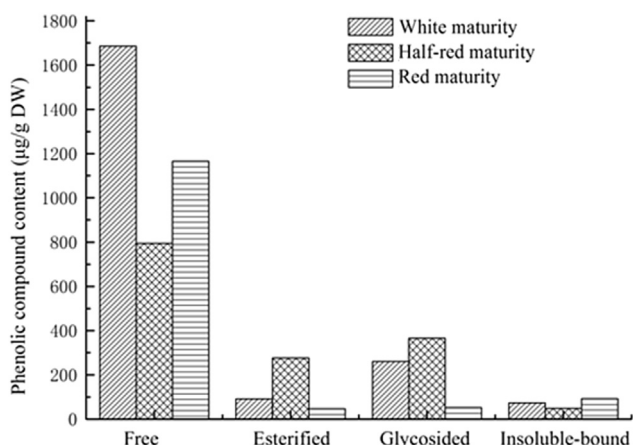


**Fig. 1.** Phenolic compound contents in four fractions of jujube at three maturity stages.

### 3.4. DPPH radical scavenging activity

The scavenging capabilities against DPPH radicals of the four phenolic fractions from jujube at three maturity stages are presented in Fig. 3. Overall, during the maturity process the DPPH radical scavenging activities decreased from WM to RM stage, with very high scavenging activity for F1 and F4 at each maturity stage and low activity in F3. The F1 and F4 at WM stage, F1 at HM stage and F2 at RM stage showed the highest scavenging activity (about 90%) in the all phenolic fractions, in spite of low TPC and TFC in these fractions except for F1 at WM stage. The results might be due to other phytochemicals with high scavenging activity in the fractions. An unknown peak in the fractions (not shown) was found and considered as one such compound responsible for high scavenging activity, which needs to further investigated. Similar results of decrease in DPPH radical scavenging activity with the increasing maturity stage were also reported by others (Lu et al., 2012; Zozio et al., 2014).

### 3.5. Antioxidant activity

The antioxidant activities of the four phenolic fractions from

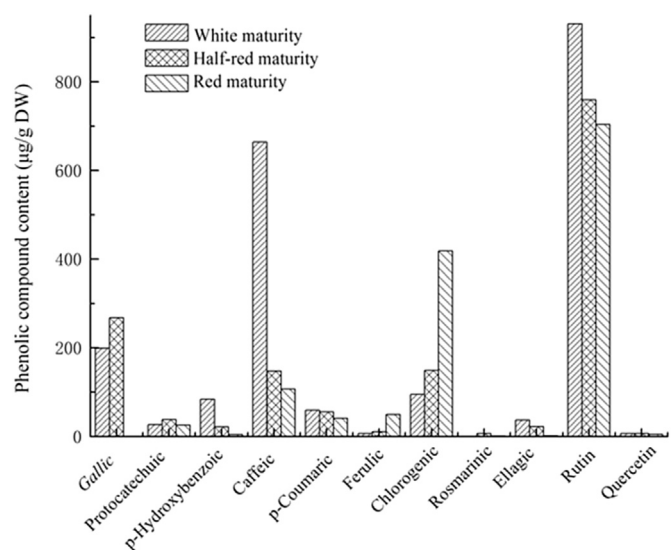


**Fig. 2.** Total contents of individual phenolic compounds in four fractions of jujube at three maturity stages.

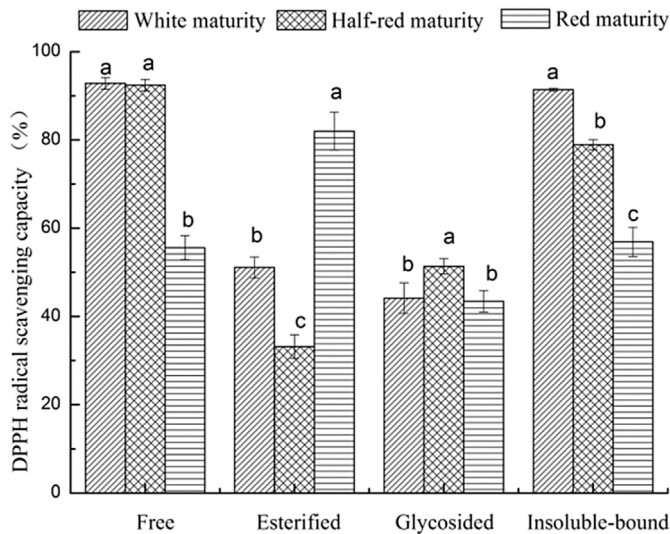


**Fig. 3.** DPPH radical scavenging activities of four phenolic fractions from jujube at three maturity stages. Different lower case letters correspond to significant differences for maturity stages in one group at  $p < 0.05$ .

jujube at the three ripening stages were quantified by FRAP assay, as shown in Fig. 4. The FRAP values in the four fractions mostly displayed the same trend similar to TPC and decreased from WM to RM stage, which was in accordance with the results reported previously (Wu et al., 2012; Zozio et al., 2014; Choi et al., 2012). The sharp increase in FRAP values observed in F4 at HM stage might be due to the increased content of other antioxidants at this maturity stage. It was also found that F4 showed higher antioxidant activities than F2 and F3 because they had more total phenols, total flavonoids as well as phenolic compounds. These results suggested that the insoluble-bound phenolics present in the residues of jujube (F4) constituted an important portion of the phenolic compounds in jujube with non-negligible antioxidant capacity. In our previous study (Wang et al., 2011), F4 in jujube pulp was also found to be the strongest antioxidant activity by DPPH and FRAP assays. Therefore, the composition of phenolic compounds of this fraction needs to be investigated further, which might result in the identification of some new antioxidant components with high bioactivities.

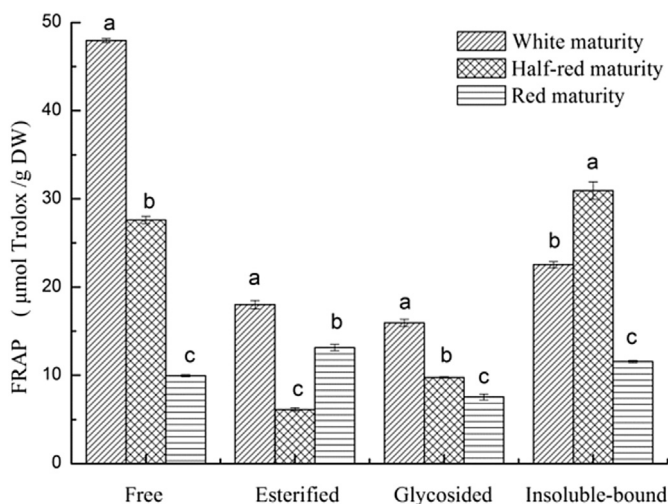


**Fig. 4.** FRAP values of four phenolic fractions of jujube at three maturity stages. Different lower case letters correspond to significant differences for maturity stages in one group at  $p < 0.05$ .

**Table 4**  
Correlation coefficients ( $r$ ) of phenolics and antioxidant activity.

	TFC	DPPH	FRAP	HPLC
TPC	0.799**	0.565	0.871*	0.336
TFC		0.654*	0.836**	0.536
DPPH			0.581*	0.180
FRAP				0.431

\*\* $p < 0.01$ ; \* $p < 0.05$ .

### 3.6. Correlations

The correlations between the antioxidant activities measured by DPPH and FRAP assays and the TPC, TFC and sum of phenolic contents by HPLC of each fraction are reported in Table 4 along with Pearson product-moment correlation coefficients ( $r$ ) and  $p$  values. The data from Table 4 were used to explore the relationship of phenolics in each fraction from jujube at different maturity stages and their antioxidant activities. The DPPH radical scavenging activity was correlated significantly with TFC and the antioxidant activity measured by FRAP assay ( $p < 0.05$ ), but not significantly with the TPC and the sum of detected phenolic content by HPLC ( $p > 0.05$ ). The FRAP value was significantly and positively correlated to the TPC and TFC ( $p < 0.05$  and  $p < 0.01$ , respectively), suggesting that these phenolic compounds might be responsible for a large proportion of the antioxidant activity. The results are well in agreement with previously reported findings (Xue, Feng, Cao, Cao, & Jiang, 2009; Zhang et al., 2010; Choi et al., 2011; Wang et al., 2011). Moreover, the TPC had significant and positive correlation ( $p < 0.01$ ) with the TFC. This indicated that the flavonoids might be responsible for the most of the phenolics in the samples. However, the total detected phenolic content by HPLC was not significantly correlated with all others ( $p > 0.05$ ).

## 4. Conclusions

The data obtained from this study suggested that there were great changes in TPC, TFC, individual phenolics, and antioxidant activity of free, esterified, glycosided, and insoluble-bound phenolic fractions of jujube during its maturity. Both TPC and TFC decreased with the increasing maturity from WM to RM stage. All quantified phenolic acids in the four fractions were mainly in jujube at WM stage and greatly decreased with the increase of maturity; while rutin was mostly present at HM and RM stages. The antioxidant activity determined by FRAP was significantly correlated with TPC, TFC and DPPH radical scavenging activity. The phenolic fractions at WM stage exhibited the highest antioxidant activity. In addition, the insoluble-bound phenolic fractions from jujube contained a large number of phenolic compounds and showed high activities and therefore they should not be ignored. Consequently, WM stage was considered as a proper harvesting period for jujube to have high antioxidant ingredients and for development of potential natural antioxidants. But further studies are still needed to identify the unknown antioxidant substances and the major phenolic compounds present in jujube at different maturities.

## Acknowledgments

This work is financially supported by the National Natural Science Foundation of China (31101325) and the Science & Technology Project of Shaanxi Province (2012K02-06).

## References

Arranz, S., Silván, J. M., & Saura-Calixto, F. (2010). Nonextractable polyphenols,

- usually ignored, are the major part of dietary polyphenols: a study on the Spanish diet. *Molecular Nutrition & Food Research*, 54, 1646–1658.
- Chen, J. P., Li, Z. G., Maiwulanjiang, M., Zhang, W. L., Zhan, J. Y. X., Lam, C. T. W., et al. (2013). Chemical and biological assessment of *Ziziphus jujuba* fruits from China: different geographical sources and developmental stages. *Journal of Agricultural and Food Chemistry*, 61, 7315–7324.
- Choi, S. H., Ahn, J. B., Kim, H. J., Im, N. K., Kozukue, N., Levin, C. E., et al. (2012). Changes in free amino acid, protein, and flavonoid content in jujube (*Ziziphus jujuba*) fruit during eight stages of growth and antioxidative and cancer cell inhibitory effects by extracts. *Journal of Agricultural and Food Chemistry*, 60, 10245–10255.
- Choi, S. H., Ahn, J. B., Kozukue, N., Levin, C. E., & Friedman, M. (2011). Distribution of free amino acids, flavonoids, total phenolics, and antioxidative activities of jujube (*Ziziphus jujuba*) fruits and seeds harvested from plants grown in Korea. *Journal of Agricultural and Food Chemistry*, 59, 6594–6604.
- Dai, J., & Mumper, R. J. (2010). Plant Phenolics: extraction, analysis and their antioxidant and anticancer properties. *Molecules*, 15, 7313–7352.
- Du, L. J., Gao, Q. H., Ji, X. L., Ma, Y. J., Xu, F. Y., & Wang, M. (2013). Comparison of flavonoids, phenolic acids, and antioxidant activity of explosion-puffed and sun-dried jujubes (*Ziziphus jujuba* Mill.). *Journal of Agricultural and Food Chemistry*, 61, 11840–11847.
- Gao, Q. H., Wu, C. S., & Wang, M. (2013). The jujube (*Ziziphus jujuba* Mill.) fruit: a review of current knowledge of fruit composition and health benefits. *Journal of Agricultural and Food Chemistry*, 61, 3351–3363.
- Gao, Q. H., Wu, C. S., Yu, J. G., Wang, M., Ma, Y. J., & Li, C. L. (2012). Textural characteristic, antioxidant activity, sugar, organic acid, and phenolic profiles of 10 promising jujube (*Ziziphus jujuba* Mill.) selections. *Journal of Food Science*, C1218–C1225.
- Ghasemzadeh, A., & Ghasemzadeh, N. (2011). Flavonoids and phenolic acids: role and biochemical activity in plants and human. *Journal of Medicinal Plants Research*, 5, 6697–6703.
- Gruz, J., Ayaz, F. A., Torun, H., & Strnad, M. (2011). Phenolic acid content and radical scavenging activity of extracts from medlar (*Mespilus germanica* L.) fruit at different stages of ripening. *Food Chemistry*, 124, 271–277.
- Gull, J., Sultana, B., Anwar, F., Naseer, R., Ashraf, M., & Ashrafuzzaman, M. (2012). Variation in antioxidant attributes at three ripening stages of guava (*Psidium guajava* L.) fruit from different geographical regions of Pakistan. *Molecules*, 17, 3165–3180.
- Jia, Z., Tang, M., & Wu, J. (1999). The determination of flavonoid contents in mulberry and their scavenging effects on superoxide radicals. *Food Chemistry*, 64, 555–599.
- Kapasakalidis, P. G., Rastall, R. A., & Gordon, M. H. (2009). Effect of a cellulase treatment on extraction of antioxidant phenols from black currant (*Ribes nigrum* L.) pomace. *Journal of Agricultural and Food Chemistry*, 57, 4342–4351.
- Kondo, S., Tsuda, K., Muto, N., & Ueda, J. (2002). Antioxidative activity of apple skin or flesh extracts associated with fruit development on selected apple cultivars. *Scientia Horticulturae*, 96, 177–185.
- Liyana-Pathirana, C. M., & Shahidi, F. (2006). Importance of insoluble-bound phenolics to antioxidant properties of wheat. *Journal of Agricultural and Food Chemistry*, 54, 1256–1264.
- Lu, H., Lou, H., Zheng, H., Hu, Y., & Li, Y. (2012). Nondestructive evaluation of quality changes and the optimum time for harvesting during jujube (*Ziziphus jujuba* Mill. cv. Changhong) fruits development. *Food and Bioprocess Technology*, 5, 2586–2595.
- Navarro-Gonzalez, I., García-Valverde, V., García-Alonso, J., & Periago, M. J. (2011). Chemical profile, functional and antioxidant properties of tomato peel fiber. *Food Research International*, 44, 1528–1535.
- Pawlowska, A. M., Camangi, F., Bader, A., & Braca, A. (2009). Flavonoids of *Ziziphus jujuba* L. and *Ziziphus spina-christi* (L.) Willd (Rhamnaceae) fruits. *Food Chemistry*, 112, 858–862.
- Pérez-Jiménez, J., & Torres, J. L. (2011). Analysis of nonextractable phenolic compounds in foods: the current state of the art. *Journal of Agricultural and Food Chemistry*, 59, 12713–12724.
- Prasanna, V., Prabha, T. N., & Tharanathan, R. N. (2007). Fruit ripening phenomena—an overview. *Critical Reviews in Food Science and Nutrition*, 47, 1–19.
- Reis Giada, M. L. (2013). In J. A. Morales-Gonzalez (Ed.), *Food phenolic compounds: Main classes, sources and their antioxidant power, oxidative stress and chronic degenerative diseases — A role for antioxidants*. ISBN: 978-953-51-1123-8, In Tech.
- Sáyago-Ayerdi, S. G., Arranz, S., Serrano, J., & Goñi, I. (2007). Dietary fiber content and associated antioxidant compounds in roselle flower (*Hibiscus sabdariffa* L.) beverage. *Journal of Agricultural and Food Chemistry*, 55, 7886–7890.
- Shahidi, F., & Naczk, M. (2004). *Phenolic compounds in fruits and vegetables. In phenolics in food and nutraceutical* (pp. 131–156). Tulsa, OK, USA: CRC Press.
- Wang, B. N., Cao, W., Gao, H., Fan, M. T., & Zheng, J. B. (2010). Simultaneous determination of six phenolic compounds in jujube by LC-ECD. *Chromatographia*, 71, 703–707.
- Wang, C., Cheng, D., Cao, J., & Jiang, W. (2013). Antioxidant capacity and chemical constituents of Chinese jujube (*Ziziphus jujuba* Mill.) at different ripening stages. *Food Science and Biotechnology*, 22, 639–644.
- Wang, B. N., Liu, H. F., Zheng, J. B., Fan, M. T., & Cao, W. (2011). Distribution of phenolic acids in different tissues of jujube and their antioxidant activity. *Journal of Agricultural and Food Chemistry*, 59, 1288–1292.
- Wu, C. S., Gao, Q. H., Guo, X. D., Yu, J. G., & Wang, M. (2012). Effect of ripening stage on physicochemical properties and antioxidant profiles of a promising table fruit 'pear-jujube' (*Ziziphus jujuba* Mill.). *Scientia Horticulturae*, 148, 177–184.
- Xue, Z., Feng, W., Cao, J., Cao, D., & Jiang, W. (2009). Antioxidant activity and total phenolic contents in peel and pulp of Chinese jujube (*Ziziphus jujuba* mill) fruits. *Journal of Food Biochemistry*, 33, 613–629.
- Zhang, H., Jiang, L., Ye, S., Ye, Y. B., & Ren, F. Z. (2010). Systematic evaluation of antioxidant capacities of the ethanolic extract of different tissues of jujube (*Ziziphus jujuba* Mill.) from China. *Food and Chemical Toxicology*, 48, 1461–1465.
- Zozio, S., Servent, A., Casal, G., Mbéguié-A-Mbéguié, D., Ravion, S., Pallet, D., et al. (2014). Changes in antioxidant activity during the ripening of jujube (*Ziziphus mauritiana* Lamk). *Food Chemistry*, 150, 448–456.



# Viscoelastic behavior and physico-chemical characteristics of heated *swai*-fish (*Pangasius hypophthalmus*) based emulsion containing fermented soybeans



Jiranat Techarang<sup>a</sup>, Arunee Apichartsrangkoon<sup>b,\*</sup>, Pattavara Pathomrungsyounggul<sup>c</sup>, Pittaya Chaikham<sup>d</sup>, Katekan Dajanta<sup>e</sup>

<sup>a</sup> Science and Technology Research Institute, Chiang Mai University, Chiang Mai 50200, Thailand

<sup>b</sup> Postharvest Technology Research Institute, Chiang Mai University, Chiang Mai 50200, Thailand

<sup>c</sup> Division of Food Engineering, School of Agro-Industry, Chiang Mai University, Chiang Mai 50100, Thailand

<sup>d</sup> Faculty of Science and Technology, Phranakorn Si Ayutthaya Rajabhat University, Phranakorn Si Ayutthaya 13000, Thailand

<sup>e</sup> Faculty of Food and Agricultural Technology, Pibulsongkram Rajabhat University, Phitsanulok, Thailand

## ARTICLE INFO

### Article history:

Received 25 June 2015

Received in revised form

1 October 2015

Accepted 5 October 2015

Available online 13 October 2015

### Keywords:

*Swai*-fish sausage

*Thua nao*

Rice-*koji* miso

Isoflavones

Oscillatory test

Creep test

### Chemical compounds studied in this article:

Boron trifluoride (PubChem CID: 6356)

Flavones (PubChem CID: 10680)

Acetonitrile (PubChem CID: 6342)

Acetic acid (PubChem CID: 176)

Diadzin (PubChem CID: 9261)

Glycitin (PubChem CID: 187808)

Genistin (PubChem CID: 5281377)

Daidzein (PubChem CID: 5281708)

Glycitein (PubChem CID: 5317750)

Genistein (PubChem CID: 5280961)

## ABSTRACT

Various proportions of fermented soybeans i.e. *thua nao* and rice-*koji* miso were added into the *swai*-fish emulsion to improve the health potential of the products. Accordingly, the physico-chemical, microbiological properties and sensory attributes of the fish-based emulsions as well as the main ingredients were determined. The results showed that fatty acid profile of the *swai*-fish fillet consisted mainly of saturated and monounsaturated fatty acids, while isoflavone profiles of the fermented soybeans illustrated that *thua nao* contained more aglycones than rice-*koji* miso. For physical properties, the profiles of storage and loss moduli, creep parameters and gel strength depicted that samples added *thua nao* gave rise to stronger gel structure than those added rice-*koji* miso or the whole fish emulsion. Microbiological examination indicated that the fish emulsion with *thua nao* addition showed high total plate or spore counts.

© 2015 Elsevier Ltd. All rights reserved.

## 1. Introduction

*Swai*-fish (*Pangasius hypophthalmus*) is one of the most popular oily fresh-waterfish sold in Thailand. It has white and tender flesh, low cholesterol (21–39 mg/100 g<sup>-1</sup>), less fishy odor and good flavor when cooked (Na-Nakorn & Moeikum, 2009; Urban et al., 2008).

Because of its low price compared to other fish, *swai*-fish is frequently available on the local markets for being supplied to the health conscious consumers. To develop health comminuted-fish emulsion, high quality products of fermented soy protein such as *thua nao* (*natto*) or *miso* were incorporated in this study. *Thua nao* (*natto*) is well-known for its highly essential amino acids and phenolic compounds especially isoflavone in the forms of aglycones e.g. daidzein, glycitein and genistein, or glucosides e.g. daidzin, glycitin and genistin, which are largely produced during

\* Corresponding author.

E-mail address: [arunee.a@cmu.ac.th](mailto:arunee.a@cmu.ac.th) (A. Apichartsrangkoon).

fermentation (Dajanta, Chukeatirote, Apichartsrangkoon, & Frazier, 2009). It is believed that these phytoestrogens could improve health protective effects such as reducing the risk of cardiovascular disease, lower breast and colon cancers and promoting bone health (Murphy, Barua, & Hauck, 2002). Therefore, including these phytochemicals in food would definitely add value to the products. Despite this alkaline fermented soybean provides high nutrients, it is unlikely that common consumers would accept its strong unique odor. *Miso* giving an umami flavor is frequently fermented by *Aspergillus oryzae*, *Aspergillus sojae* or, *Aspergillus awamori* for the preparation of rice-*koji* (Giri, Osako, Okamoto, Okazaki, & Ohshima, 2011). *Miso* is another fermented soy protein which contains several hydrolyzed amino acids and isoflavones. Yamabe, Kobayashi-Hattori, Kaneko, Endo, and Takita (2007) fermented rice-*koji* miso by *A. oryzae* for 6 months and found that the glycoside contents decreased from 86.4 to 44.9%, whereas aglycones increased from 9.6 to 53.3%.

Rheology is extensively used to characterize the physical structure of food biopolymers which can form either viscoelastic true or weak gels (coagulant type gel). Various gels have weak viscoelastic characteristic. For instance, gluten heated at 90 °C for 30 min upto 6 h were characterized as weak viscoelastic gel, since their storage modulus ( $G'$ ) essentially dominated the loss modulus ( $G''$ ) and both modulus-profiles were slightly frequency dependent (Apichartsrangkoon, 2002). Another example of weak viscoelastic characterization was the pressurized gels of ostrich-meat sausages which  $G'$  was larger than  $G''$  with small  $\tan\delta$  values (0.23). The difference between  $G'$  and  $G''$  plots was essentially 1 log cycle, depicting that these gels exhibited strong elasticity with solid-like behavior (Chattong & Apichartsrangkoon, 2009). Apart from the oscillatory measurement, other rheological techniques such as creep and relaxation tests were also frequently used to characterize the structure of gels. Chattong, Apichartsrangkoon, and Bell (2007) compared the measuring procedures between oscillatory and creep tests by using pressurized ostrich-meat gel containing xanthan gum as the specimens and found that creep testing better demonstrated the textural changes than oscillatory testing. However, this wasn't with the case of pressurized ostrich-meat sausages without gum additive, since the oscillatory results were well coincident with the creep parameters (Chattong & Apichartsrangkoon, 2009).

The aim of this study was to develop *swai*-fish emulsion with the addition of *thua nao* and rice-*koji miso* to improve the health-promoting effect. Accordingly, their rheological, physical, chemical and microbiological qualities were assessed.

## 2. Materials and methods

### 2.1. Experimental materials

*Swai*-fish (*P. hypophthalmus*) fillet was purchased from a local market in Chiang Mai province, Thailand. *Thua nao* was produced following a modified method of Dajanta, Apichartsrangkoon, Chukeatirote, and Frazier (2011) using soybean cultivar CM60 and *Bacillus subtilis* TISTR 001 (Thailand Institute of Science and Technological Research, Thailand) as a starter culture. Rice-*koji miso* (Ken Co. Ltd., Japan) was purchased from a local market in Chiang Mai, Thailand.

### 2.2. Preparation of *swai*-fish based emulsions containing fermented soybeans

The *swai*-fish fillet was chopped with *thua nao* and rice-*koji miso* with various proportion according to the formula in Table 1. The mixture of each formula was then blended for 6 min with 10 g  $\text{kg}^{-1}$

**Table 1**  
Formulation of *swai*-fish based batters containing fermented soybeans.

Major raw materials	Control	Treatments				
		1	2	3	4	5
<i>Swai</i> -fish fillet (g $\text{kg}^{-1}$ batter)	1000	900	900	900	900	900
<i>Thua nao</i> (g $\text{kg}^{-1}$ batter)	–	100	–	70	50	30
Rice- <i>koji miso</i> (g $\text{kg}^{-1}$ batter)	–	–	100	30	50	70

sodium chloride and 3 g  $\text{kg}^{-1}$  sodium tripolyphosphate by a household blender. The final temperature of the batter was maintained at around 10 °C. The batters were then stuffed in collagen casing 2.3 cm in diameter (Food EQ Ltd., Thailand) and heated at 72 °C for 30 min in a water bath (Techarang & Apichartsrangkoon, 2015).

### 2.3. Proximate analysis

The *swai*-fish based emulsion and the ingredients such as *swai*-fish fillet, *thua nao* and rice-*koji miso* were analyzed for crude protein, crude fat and moisture content according to the standard AOAC methods (AOAC, 2000). The pH was also measured using a pH meter (Sartorius PB-20, Germany). The analysis was done in triplication (n = 6).

### 2.4. Color measurement

A colorimeter (Minolta Chroma Meter, CR-300, Japan) was used to measure the color parameters ( $L$ ,  $a^*$  and  $b^*$ ) of *swai*-fish fillet, *thua nao*, rice-*koji miso* and the finished products. The parameters in term of  $L$ ,  $a^*$  and  $b^*$  were used to calculate the browning index (BI) following Equation (1) (Ferrari, Maresca, & Ciccarone, 2010).

$$\text{BI} = [100(x - 0.31)]/0.172 \quad (1)$$

$$\text{where } x = (a^* + 1.75L)/(5.645L + a^* - 3.012b^*).$$

The analysis was done in triplication (n = 9).

### 2.5. Determination of isoflavones in fermented soybean

*Thua nao* or rice-*koji miso* was extracted separately following a modified method of Murphy et al. (2002). One gram of each freeze-dried samples included 110  $\mu\text{L}$  flavones (Sigma-Aldrich Co. Ltd., UK) as an internal standard were extracted with 5 mL acetonitrile, 10 mL of 0.1 mol  $\text{L}^{-1}$  HCl and 5 mL distilled water. The supernatant was centrifuged at 1677  $\times$  g for 5 min, then filtered through 0.45  $\mu\text{m}$  membrane filter for HPLC analysis.

HPLC analysis was performed following a modified method of Klejduš et al. (2005). The Shimadzu HPLC systems were equipped with Inersil ODS-3 C18 column (4.6  $\times$  250 mm, 5.0  $\mu\text{m}$ ) and SPD-M20A photodiode array detector. The mobile phase consisted of 0.1 mL 100  $\text{mL}^{-1}$  acetic acid in filtered MilliQ water (solvent A) and 80 mL 100  $\text{mL}^{-1}$  methanol (solvent B). The injection volume was 20  $\mu\text{L}$  with gradient elution. Flow rate of the mobile phase was 1 mL  $\text{min}^{-1}$  and temperature of the column was 40 °C. The eluted isoflavones were detected at  $\lambda_{\text{max}}$  255 nm. Concentration of each component was achieved from the corresponding calibration curves after adjustment with the internal standard. Typical chromatogram of the detected isoflavones are shown in Fig. 1a and b. The analysis was done in triplication (n = 6).

### 2.6. Determination of fatty acid in *swai*-fish fillet

*Swai*-fish fillet was the major proportion (900 g  $\text{kg}^{-1}$ ) of the formulas, hence only fatty acids of this ingredient were determined. The fatty acid profile of *swai*-fish fillet was determined following a

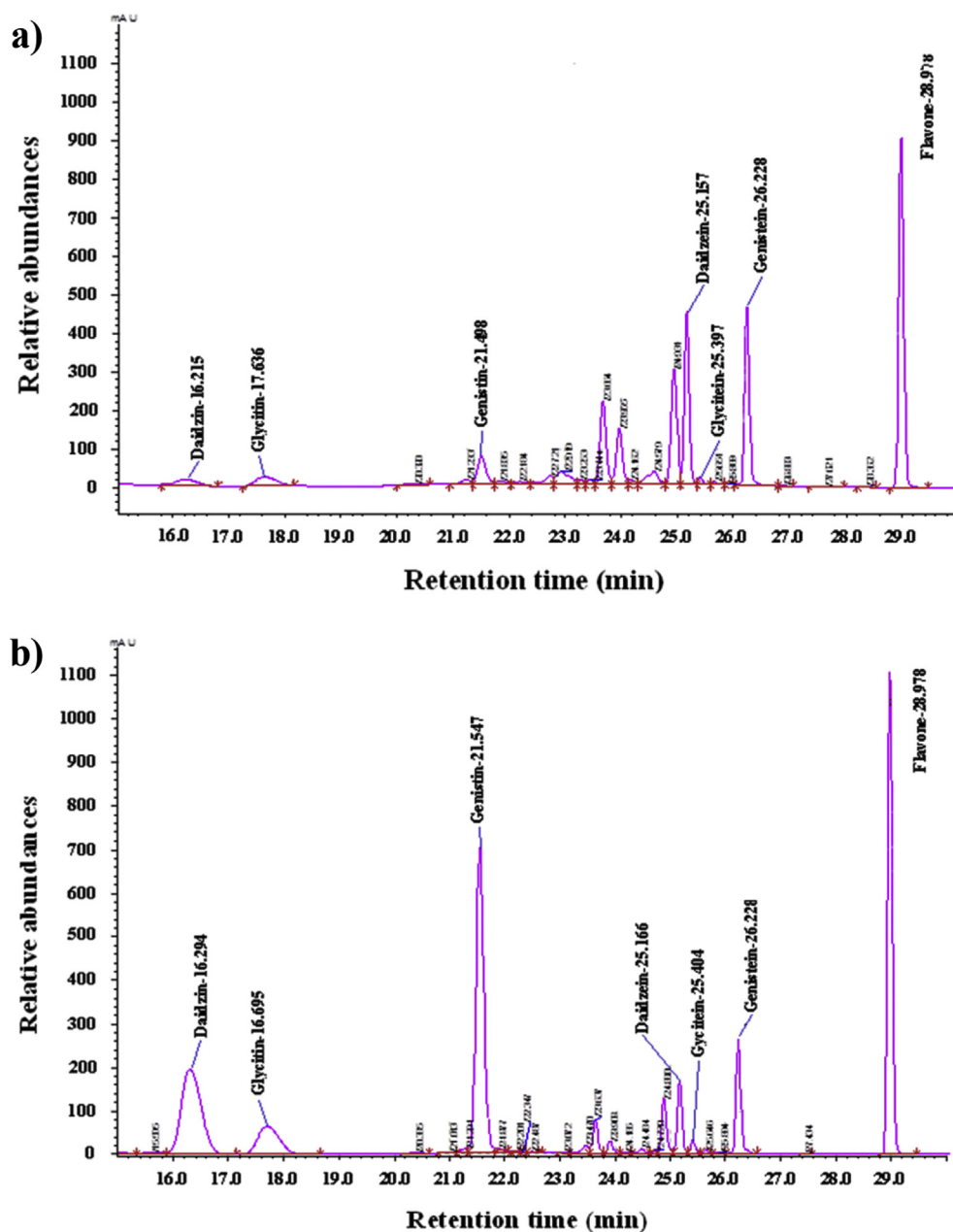


Fig. 1. Chromatograms of isoflavones found in *thua nao* (a) and rice-*koji miso* (b).

modified method of AOAC 996.06 (2005) as follows.

The fat was extracted by adding 100 mg pygallic acid, 10.0 mL of 8.3 mol L<sup>-1</sup> HCl and 2 mL ethanol into 2 g of ground *swai*-fish fillet. After hydrolysis, the fat portion was separated, and mixed with 3 mL chloroform and 3 mL diethylether. Subsequently, 2 mL of 7 g boron trifluoride in 100 g methanol and 1 mL toluene were added into the remained fat, then heated at 100 °C for 45 min. A volume of 5 mL distilled water, 1 mL hexane, and 1 g sodium sulfate were added into the mixture. Top layer of fatty acid methyl esters (FAMES) was filtered through a membrane filter for GC experiment. Gas chromatographic system using an Agilent Technologies 6890NGC (Santa Clara, CA, USA) equipped with a FID detector and a fused-silica capillary column with 100 m × 0.25 mm diameter, 0.2 μm film thickness (SupelcoSP-2560). Helium with a flow rate of 0.75 mL min<sup>-1</sup> was used as a carrier gas. One μL injection of the FAME mixture was set for a split ratio of 200:1. The temperatures of

the injector and the detector were 250 and 285 °C, respectively. The program of oven temperature was commencing at 140 °C, held for 5 min, then set the temperature program for 3 °C min<sup>-1</sup> to 250 °C and held for 17 min. The total running time was 55 min. Concentration of each component was achieved from the calibration curves of corresponding standard fatty acids. Typical chromatogram of total fatty acid is shown in Fig. 2. The analysis was done in triplication (n = 6).

## 2.7. Determination of gel strength

Gel strength of the fish emulsions was determined using a Texture Analyser TA-XT Plus (Stable Micro Systems Ltd., Surrey, UK) with a 50 kg load cell. The samples were cut into pieces of 23 mm diameter × 20 mm height. During measurement, a Warner Blatzler blade was cut through a piece of sample with sharing cross-head

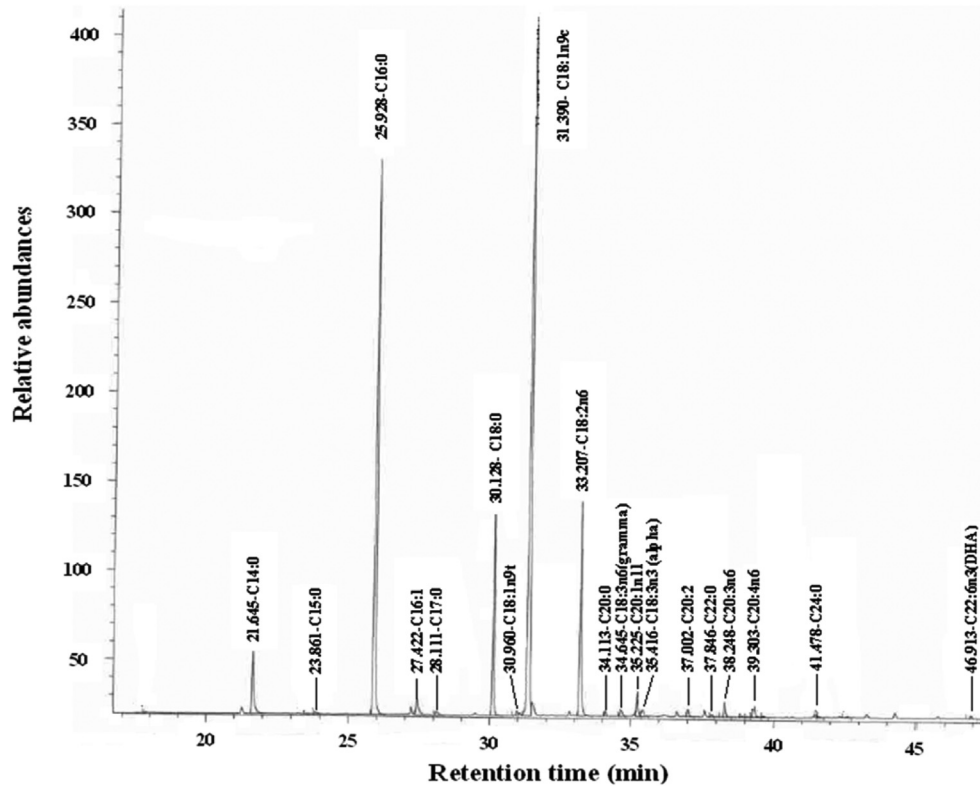


Fig. 2. Chromatogram of fatty acids of swai-fish fillet.

speed of 10 mm/s. Peaks of the shear force were recorded and the gel strength was then calculated by multiplying shear force (N) with the distance of shearing (m) (Techarang & Apichartsrangkoon, 2015).

The measurement was performed in triplication ( $n = 15$ ).

### 2.8. Determination of water holding capacity

Percentage of water holding capacity which is the ability of emulsion to hold the entire water in the system can be assessed from the released water plus expressible water subtracted from 1 ( $\times 100$ ) (Techarang & Apichartsrangkoon, 2015). Released water is the weight of sample left after blotting water from the surface, while expressible water is the weight of the sample left after the water in the sample being discharged under compression (Funami, Yada, & Nakao, 1998). The measurement was performed in triplication ( $n = 9$ ).

### 2.9. Dynamic viscoelastic characterization

The viscoelastic behavior of the fish based emulsions was determined following a procedure of Techarang and Apichartsrangkoon (2015). A controlled stress rheometer (AR2000, TA Instruments-Waters LLC, New Castle, USA) equipped with a parallel plate of 25 mm diameter and a gap width of 1 mm was used. This is the most appropriate gap for avoiding slipperiness. Initially stress-amplitude sweeps were performed at a frequency of 1 Hz to search for a linear viscoelastic region (Fig. 3). Accordingly, a stress amplitude of 20 Pa was chosen for further frequency-sweep and creep tests. Oscillatory frequency-sweeps were carried out at 25 °C scanned across a frequency range of 0.1–10 Hz. Subsequently, storage ( $G'$ ), loss ( $G''$ ) moduli and loss tangent ( $\tan \delta$ ) were recorded. Creep measurement was performed

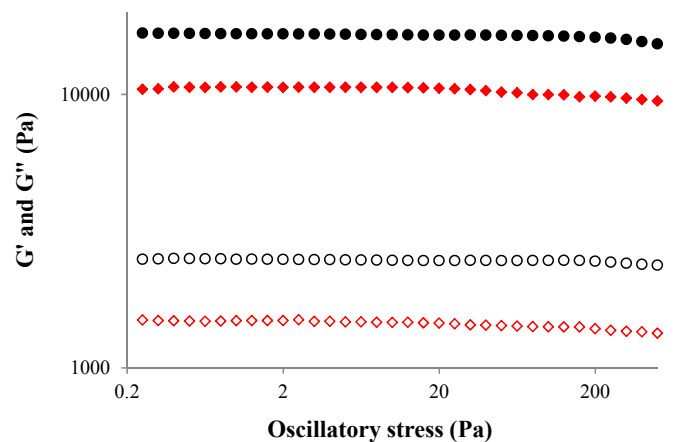


Fig. 3. Stress amplitude sweep (0.1–500 Pa) at a frequency of 1 Hz for heated swai-fish emulsion ( $\blacklozenge, \blacklozenge$  control) and heated swai-fish emulsion containing 10% *thua nao* ( $\bullet, \circ$  treatment 1)  $G'$  = filled symbols and  $G''$  = unfilled symbols.

for 300 s and the recovery testing was instantaneously undertaken for 900 s. The mathematical models of the creep curves were calculated following Equation (2). A four-element “Burgers” model (Steffe, 1996) was then fitted as shown in Fig. 4.

$$J(t) = J_0 + J_1[1 - \exp(-t/\lambda_{ret})] + t/\mu_0 \quad (2)$$

where  $J_0$  (the instantaneous elastic compliance,  $\text{Pa}^{-1}$ ).

$J_1$  (retarded compliance for Kelvin–Voigt model,  $\text{Pa}^{-1}$ ).

$\lambda_{ret}$  (retardation time for Kelvin–Voigt model, s).

$\mu_0$  (Newtonian viscosity,  $\text{Pa s}$ ) and  $t$  (time, s).

The measurement was performed in triplication ( $n = 9$ ).

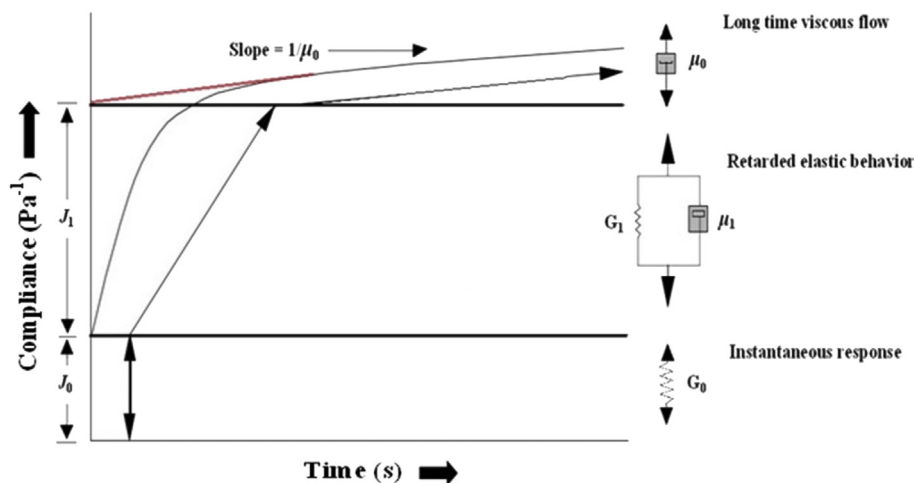


Fig. 4. Standard creep curve of the compliance versus deformation time with an indication of the four-element Burger's model.

### 2.10. Microbiological assessment

A standard plate count of *swai*-fish fillet, *thua nao*, rice-*koji miso* and the fish-based emulsions was carried out following the AOAC method (AOAC, 2000). Purposely, 1 g of the sample was added into 9 mL of 0.1 g 100 mL<sup>-1</sup> peptone water for the preparation of series of dilution. A volume of 1 mL dilutions was then transferred to the plate count agar, and incubated at 37 °C for 2 days. The spore count was applied the same procedure as standard plate count, excepting that series of peptone dilution were heated at 80 °C for 10 min prior to transferring to the plate count agar (Siemer, Toepfl, & Heinz, 2014). Viable cell and spore quantification were expressed as colony-forming units per g (CFU/g). The determination was performed in triplication (n = 6).

### 2.11. Sensory evaluation

For sample presentation, 5 formulas of fish-based emulsions and the control with size of 23 mm diameter × 1 cm height were served to the panelists by completely randomized order (Macfie, Bratchell, Greenhoff, & Vallis, 1989). Fifty untrained panelists evaluated for color, flavor, odor, firmness, air cells and overall acceptability and provided judgments according to 5-point hedonic scale (where, 1 = extremely dislike; 5 = extremely like). The assessment was performed in duplication.

### 2.12. Statistical analysis

The treatments and the control in this study were carried out with triplication. Analysis of variance (ANOVA) was done by using SPSS Version 22 (SPSS Inc., Chicago, USA), and determination of significant differences among treatment means was applied Duncan's multiple range tests ( $P \leq 0.05$ ).

## 3. Results and discussion

### 3.1. Physical, chemical and microbiological qualities of main ingredients

#### 3.1.1. Color parameters

The main ingredients used in this study comprised *swai*-fish fillet, *thua nao* which was fermented by *B. subtilis* TISTR 001 and rice-*koji miso*. Their physical and chemical qualities are shown in Table 2. Color parameters in Table 2 illustrated that *swai*-fish fillet

and rice-*koji miso* had the equivalent lightness, while *thua nao* displayed darker color reflected by the  $L$  parameter, which might be due to significantly highest intensity ( $P \leq 0.05$ ) of redness and yellowish of *thua nao*. In overall, *swai*-fish fillet was the lightest ingredient followed by rice-*koji miso* and *thua nao*, respectively depicted by the browning index. A study by Dajanta, Chukeatirote, and Apichartsrangkoon (2012) determined color of different Thai commercial *thua nao* supported that the products had lightness ( $L$ ) in the range of 38.63–47.18, while  $a^*$  and  $b^*$  were 6.91–9.10 and 14.79–23.12, respectively.

#### 3.1.2. Chemical properties

*Thua nao* is an alkaline fermented soybean having high pH in turn, whereas rice-*koji miso* has lower pH. However, both ingredients contain various isoflavones which are phytoestrogens in the forms of glucosides and aglycones. Table 2 and Fig. 1a and b showed the detected isoflavones in the fermented soybeans consisting of daidzin, glycitin, genistin, daidzein, glycitein and genistein. It is interesting that *thua nao* contained much more aglycones than glucosides, whereas rice-*koji miso* had more glucosides than aglycones. In *thua nao*, the aglycones: daidzein, genistein and glycitein were the major components, while daidzin, genistin and glycitin were the predominant glucosides in rice-*koji miso*. This result was also coincident with the study of Xu, Du, and Xu (2015) revealed that the isoflavones in *natto* were very much higher than those in rice-*koji miso*. Obviously, the aglycone form provides better health potential than the glucoside form. Since the glucoside form conjugating with glucose moiety has greater molecular weight and higher hydrophilicity than the free aglycone form. These characteristics of glucoside triggered off poor absorption into small intestine (Izumi et al., 2000; Kano, Takayanagi, Harada, Sawada, & Ishikawa, 2006). However, this bioactivity of glucoside could be improved by an enzyme such as  $\beta$ -glucosidase transforming the glucoside to aglycone (Malashree, Mudgil, Dagar, Kumar, & Puniya, 2012; Uzzan & Abuza, 2004).

Despite, *swai*-fish fillet had lower protein and fat contents than *thua nao* and rice-*koji miso*, the characteristic of fat (97 g kg<sup>-1</sup>) in *swai*-fish fillet would reflect the overall product quality. Because *swai*-fish fillet is the main ingredient (900 g kg<sup>-1</sup>) in the formula, other fermented soybeans (100 g kg<sup>-1</sup>) were the trivial contribution. Table 3 and Fig. 2 show that the principle fatty acids in the fat of *swai*-fish fillet comprised of saturated fatty acids (SFAs) and monounsaturated fatty acids (MUFAs). The majorities of such fatty acids were palmitic acid (C16:0), stearic acid (C18:0) and cis-9-

**Table 2**  
Physico-chemical and microbiological properties of swai-fish fillet, *thua nao* and rice-koji miso.

Properties	Major raw materials		
	Swai-fish fillet	<i>Thua nao</i>	Rice koji-miso
Color parameters			
<i>L</i>	53.16 ± 1.10 <sup>a</sup>	42.91 ± 2.39 <sup>b</sup>	52.92 ± 2.19 <sup>a</sup>
<i>a</i> *	0.73 ± 0.07 <sup>c</sup>	5.69 ± 0.45 <sup>a</sup>	4.24 ± 0.35 <sup>b</sup>
<i>b</i> *	2.95 ± 0.53 <sup>b</sup>	14.45 ± 0.99 <sup>a</sup>	14.66 ± 0.74 <sup>a</sup>
Browning index	6.49 ± 0.85 <sup>c</sup>	49.55 ± 1.21 <sup>a</sup>	37.33 ± 0.95 <sup>b</sup>
Chemical compositions			
Moisture (g 100 g <sup>-1</sup> )	75.50 ± 1.02 <sup>a</sup>	46.63 ± 2.26 <sup>b</sup>	45.21 ± 1.65 <sup>b</sup>
Protein (g 100 g <sup>-1</sup> )	15.88 ± 1.23 <sup>c</sup>	39.75 ± 2.27 <sup>a</sup>	27.04 ± 1.66 <sup>b</sup>
Fat (g 100 g <sup>-1</sup> )	9.69 ± 0.85 <sup>c</sup>	16.68 ± 0.42 <sup>a</sup>	11.07 ± 0.32 <sup>b</sup>
pH	7.38 ± 0.04 <sup>b</sup>	8.43 ± 0.22 <sup>a</sup>	6.74 ± 0.15 <sup>c</sup>
Isoflavones			
Total-glucosides (μg g <sup>-1</sup> )	–	214.72 ± 19.98 <sup>b</sup>	1778.96 ± 82.40 <sup>a</sup>
Daidzin (μg g <sup>-1</sup> )	–	51.78 ± 8.67 <sup>bc</sup>	703.59 ± 27.98 <sup>ab</sup>
Glycitin (μg g <sup>-1</sup> )	–	96.00 ± 8.24 <sup>ba</sup>	120.95 ± 13.77 <sup>ac</sup>
Genistin (μg g <sup>-1</sup> )	–	66.94 ± 3.07 <sup>bb</sup>	954.42 ± 40.65 <sup>aa</sup>
Total-aglycones (μg g <sup>-1</sup> )	–	729.33 ± 53.37 <sup>a</sup>	348.40 ± 16.92 <sup>b</sup>
Diadzein (μg g <sup>-1</sup> )	–	295.08 ± 19.70 <sup>aa</sup>	152.52 ± 8.24 <sup>ba</sup>
Glycitein (μg g <sup>-1</sup> )	–	178.20 ± 16.65 <sup>ac</sup>	43.67 ± 2.57 <sup>bb</sup>
Genistein (μg g <sup>-1</sup> )	–	256.05 ± 17.02 <sup>ab</sup>	152.21 ± 6.11 <sup>ba</sup>
Microbiological qualities			
Standard plate count (CFU g <sup>-1</sup> )	2.14 ± 0.19 × 10 <sup>3c</sup>	5.08 ± 0.95 × 10 <sup>8a</sup>	5.19 ± 0.59 × 10 <sup>3b</sup>
Spore count (CFU g <sup>-1</sup> )	<10 <sup>b</sup>	4.22 ± 0.83 × 10 <sup>8a</sup>	<10 <sup>b</sup>

Means followed the same small or capital letters in each row or in each column are not significantly different ( $P > 0.05$ ).

**Table 3**  
Fatty acid profile of swai-fish fillet

Type of fatty acids	Contents (g kg <sup>-1</sup> )
Myristic acid (C14:0)	3.49 ± 0.014
Pentadecanoic acid (C15:0)	0.21 ± 0.023
Palmitic acid (C16:0)	28.31 ± 0.041
Heptadecanoic acid (C17:0)	0.28 ± 0.010
Stearic acid (C18:0)	8.80 ± 0.014
Arachidic acid (C20:0)	0.32 ± 0.025
Behenic acid (C22:0)	0.09 ± 0.014
Lignoceric acid (C24:0)	0.12 ± 0.013
<b>Total saturated fatty acids</b>	<b>41.62 ± 0.054</b>
Palmitoleic acid (C16:1n7)	1.20 ± 0.112
trans-9-Elaidic acid (C18:1n9t)	0.23 ± 0.013
cis-9-Oleic acid (C18:1n9c)	39.56 ± 0.140
cis-11-Eicosenoic acid (C20:1n11)	1.24 ± 0.010
<b>Total monounsaturated fatty acids</b>	<b>42.23 ± 0.133</b>
cis-9,12-Linoleic acid (C18:2n6)	10.43 ± 0.131
γ-Linolenic acid (C18:3n6)	0.47 ± 0.011
α-Linolenic acid (C18:3n3)	0.46 ± 0.014
cis-11,14-Eicosadienoic acid (C20:2)	0.40 ± 0.103
cis-8,11,14-Eicosatrienoic acid (C20:3n6)	0.80 ± 0.015
Arachidonic acid (C20:4n6)	0.76 ± 0.102
4,7,10,13,16,19-Docosahexaenoic acid (DHA) (C22:6n3)	0.22 ± 0.013
<b>Total polyunsaturated fatty acids</b>	<b>13.54 ± 0.113</b>
<b>trans fats</b>	<b>0.22 ± 0.013</b>
<b>Omega-3</b>	<b>0.95 ± 0.024</b>
<b>Omega-6</b>	<b>12.53 ± 0.102</b>
<b>Omega-9</b>	<b>39.81 ± 0.133</b>

The bold numbers are the high quantities.

oleic acid (C18:1n9c). On the other hands, cis-9,12-linoleic acid (C18:2n6) was the major polyunsaturated fatty acid (PUFA) present with the lesser extent. Fortunately, only little trans fats were found in swai-fish fillet, while omega-9 (n-9) fatty acids existed with high concentration, followed by omega-6 (n-6) and omega-3 (n-3) fatty acids, respectively. Therefore, 97 g fat kg<sup>-1</sup> flesh in swai-fish fillet could provide some extent of health potential to such fish fillet, besides the beneficial fish protein. Other studies, for instance, Maqsood and Benjakul (2010) reported that total 92 g fat kg<sup>-1</sup> flesh of Thai striped catfish (*P. hypophthalmus*) contained 42.60 g MUFAs

100 g<sup>-1</sup> fat, followed by 33.87 g SFAs 100 g<sup>-1</sup> fat and 21.95 g PUFAs 100 g<sup>-1</sup> fat. Earlier, Orban et al. (2008) found 44.77 g SFAs 100 g<sup>-1</sup> fat in frozen Vietnamese *sutchi* catfish (*P. hypophthalmus*) fillets, followed by 34.68 g MUFAs 100 g<sup>-1</sup> fat and 15.55 g PUFAs 100 g<sup>-1</sup> fat with the ratio of n-3/n-6 being 0.40.

### 3.1.3. Microbiological qualities

The microbiological qualities in Table 2 depicted that *thua nao* exhibited highest standard plate and spore counts. Since *thua nao* contained vegetative cells and spores of *B. subtilis* TISTR 001 which were fairly tolerant to heat and could be present in the standard plate and spore counts. On the other hand, the standard plate count of swai-fish fillet was roughly 3 log CFU g<sup>-1</sup> which was considered as an acceptable benchmark (ICMSF, 1986). The standard plate count for rice-koji miso also exhibited around 3 log CFU g<sup>-1</sup> which could be the remained lactic-acid bacteria from pasteurization as mentioned earlier.

### 3.2. Physical, chemical, microbiological properties and sensory scores of heated swai-fish based emulsions containing *thua nao* and rice-koji miso

#### 3.2.1. Color parameters

Table 4 shows the physical properties of swai-fish based emulsion with various treatment conditions as shown in Table 1. Usually, heated fish emulsions had white opaque color, when incorporating fermented soybeans, color of the treated samples would change to light yellowish. Accordingly, *L* parameter for lightness indicated that the control was significantly lightest ( $P \leq 0.05$ ), followed sequentially by treatments 1, 3, 4, 2 and 5. For *a*\* parameter, treatments 1 and 3 had the positive *a*\*, while other treatments and the control showed negative *a*\*. Because of treatments 1 and 3 containing higher amount of *thua nao*, slight red color from this ingredient would trigger off *a*\* parameter to appear in positive direction. In overall, the control had significantly lower *b*\* parameter (yellowish) and browning index ( $P \leq 0.05$ ) than other treatments.

**Table 4**Physico-chemical, microbiological properties and sensory attributes of heated swai-fish emulsions containing *thua nao* and rice-koji miso.

Characteristics	Control	Treatments				
		1	2	3	4	5
<b>Physical properties</b>						
<b>Color parameters</b>						
<i>L</i>	86.20 ± 1.09 <sup>a</sup>	80.37 ± 0.61 <sup>b</sup>	78.49 ± 0.54 <sup>c</sup>	79.96 ± 0.61 <sup>b</sup>	79.93 ± 0.37 <sup>b</sup>	77.90 ± 1.93 <sup>bc</sup>
<i>a</i> *	-2.14 ± 0.13 <sup>d</sup>	0.34 ± 0.13 <sup>a</sup>	-0.38 ± 0.04 <sup>c</sup>	0.31 ± 0.14 <sup>a</sup>	-0.19 ± 0.04 <sup>b</sup>	-0.32 ± 0.05 <sup>c</sup>
<i>b</i> *	5.84 ± 0.52 <sup>b</sup>	20.14 ± 0.67 <sup>a</sup>	20.81 ± 0.43 <sup>a</sup>	20.23 ± 0.58 <sup>a</sup>	20.37 ± 0.51 <sup>a</sup>	20.83 ± 0.64 <sup>a</sup>
Browning index	4.95 ± 0.67 <sup>b</sup>	28.16 ± 1.14 <sup>a</sup>	29.33 ± 0.61 <sup>a</sup>	28.43 ± 0.75 <sup>a</sup>	28.20 ± 0.82 <sup>a</sup>	29.68 ± 0.47 <sup>a</sup>
Water holding capacity (g 100 g <sup>-1</sup> )	93.06 ± 0.47 <sup>a</sup>	91.83 ± 0.34 <sup>b</sup>	92.81 ± 0.25 <sup>a</sup>	92.42 ± 0.54 <sup>ab</sup>	92.55 ± 0.41 <sup>ab</sup>	92.74 ± 0.47 <sup>a</sup>
Gel strength (N m)	0.57 ± 0.05 <sup>b</sup>	0.79 ± 0.04 <sup>a</sup>	0.64 ± 0.04 <sup>b</sup>	0.75 ± 0.07 <sup>ab</sup>	0.69 ± 0.07 <sup>ab</sup>	0.65 ± 0.03 <sup>b</sup>
<b>Chemical properties</b>						
Moisture content (g 100 g <sup>-1</sup> )	86.05 ± 0.50 <sup>a</sup>	83.04 ± 0.65 <sup>c</sup>	84.70 ± 0.49 <sup>b</sup>	83.38 ± 0.39 <sup>c</sup>	83.61 ± 0.27 <sup>c</sup>	84.52 ± 0.34 <sup>b</sup>
pH	7.30 ± 0.04 <sup>d</sup>	7.80 ± 0.05 <sup>a</sup>	7.02 ± 0.02 <sup>e</sup>	7.70 ± 0.02 <sup>b</sup>	7.49 ± 0.02 <sup>c</sup>	7.23 ± 0.03 <sup>d</sup>
<b>Rheological parameters</b>						
Loss tangent ( <i>G''/G'</i> ) at 1 Hz	0.13 ± 0.01 <sup>b</sup>	0.19 ± 0.02 <sup>a</sup>	0.14 ± 0.02 <sup>b</sup>	0.19 ± 0.02 <sup>a</sup>	0.18 ± 0.01 <sup>a</sup>	0.17 ± 0.03 <sup>ab</sup>
<i>J</i> <sub>0</sub> × 10 <sup>-4</sup> (Pa <sup>-1</sup> )	2.70 ± 0.22 <sup>a</sup>	2.18 ± 0.15 <sup>b</sup>	2.58 ± 0.11 <sup>a</sup>	2.32 ± 0.10 <sup>b</sup>	2.40 ± 0.12 <sup>ab</sup>	2.44 ± 0.15 <sup>ab</sup>
<i>J</i> <sub>1</sub> × 10 <sup>-4</sup> (Pa <sup>-1</sup> )	5.98 ± 0.26 <sup>a</sup>	1.45 ± 0.10 <sup>e</sup>	4.56 ± 0.18 <sup>b</sup>	2.19 ± 0.17 <sup>d</sup>	3.03 ± 0.28 <sup>c</sup>	4.18 ± 0.33 <sup>b</sup>
<i>λ</i> <sub>ret</sub> (s)	50.58 ± 2.48 <sup>a</sup>	33.24 ± 1.53 <sup>e</sup>	45.36 ± 2.06 <sup>b</sup>	38.04 ± 1.60 <sup>d</sup>	41.53 ± 1.76 <sup>c</sup>	43.60 ± 2.97 <sup>bc</sup>
<i>η</i> <sub>0</sub> × 10 <sup>5</sup> (Pa s)	4.75 ± 0.19 <sup>e</sup>	16.65 ± 1.32 <sup>a</sup>	5.54 ± 0.36 <sup>d</sup>	13.83 ± 1.02 <sup>b</sup>	8.28 ± 0.29 <sup>c</sup>	5.60 ± 0.33 <sup>d</sup>
<b>Microbiological qualities</b>						
Total plate count (CFU g <sup>-1</sup> )	<10 <sup>f</sup>	1.58 ± 0.23 × 10 <sup>4a</sup>	4.39 ± 1.02 × 10 <sup>2e</sup>	7.23 ± 0.65 × 10 <sup>3b</sup>	4.88 ± 0.37 × 10 <sup>3c</sup>	2.08 ± 0.23 × 10 <sup>3d</sup>
Spore count (CFU g <sup>-1</sup> )	<10 <sup>e</sup>	1.21 ± 0.10 × 10 <sup>4a</sup>	<10 <sup>e</sup>	6.67 ± 0.72 × 10 <sup>3b</sup>	4.01 ± 0.59 × 10 <sup>3c</sup>	1.78 ± 0.28 × 10 <sup>3d</sup>
<b>Sensory attributes</b>						
Color	2.21 ± 0.20 <sup>d</sup>	3.19 ± 0.16 <sup>c</sup>	3.58 ± 0.13 <sup>b</sup>	<b>3.86 ± 0.15<sup>a</sup></b>	3.54 ± 0.17 <sup>b</sup>	<b>3.70 ± 0.15<sup>ab</sup></b>
Flavor	2.69 ± 0.18 <sup>c</sup>	2.97 ± 0.19 <sup>bc</sup>	3.16 ± 0.16 <sup>b</sup>	<b>3.56 ± 0.17<sup>a</sup></b>	<b>3.52 ± 0.19<sup>a</sup></b>	3.21 ± 0.20 <sup>ab</sup>
Odor	2.59 ± 0.19 <sup>b</sup>	<b>2.88 ± 0.22<sup>ab</sup></b>	<b>3.13 ± 0.17<sup>a</sup></b>	<b>3.21 ± 0.16<sup>a</sup></b>	<b>3.17 ± 0.20<sup>a</sup></b>	<b>3.10 ± 0.20<sup>a</sup></b>
Firmness	<b>3.44 ± 0.18<sup>a</sup></b>	3.08 ± 0.16 <sup>b</sup>	3.10 ± 0.16 <sup>b</sup>	<b>3.35 ± 0.14<sup>ab</sup></b>	<b>3.21 ± 0.19<sup>ab</sup></b>	2.84 ± 0.16 <sup>b</sup>
Air cells	3.42 ± 0.19 <sup>ab</sup>	3.32 ± 0.18 <sup>b</sup>	3.30 ± 0.19 <sup>b</sup>	<b>3.74 ± 0.16<sup>a</sup></b>	<b>3.73 ± 0.17<sup>a</sup></b>	3.24 ± 0.21 <sup>b</sup>
Overall acceptability	2.81 ± 0.20 <sup>c</sup>	3.05 ± 0.15 <sup>bc</sup>	3.30 ± 0.16 <sup>b</sup>	<b>3.64 ± 0.13<sup>a</sup></b>	<b>3.42 ± 0.16<sup>ab</sup></b>	3.17 ± 0.16 <sup>b</sup>

Means followed the same letter in each row are not significantly different ( $P > 0.05$ ). The bold numbers in sensory attributes were the most acceptable scores.

### 3.2.2. Water holding capacity, gel strength, moisture content and pH

Water holding capacity of the emulsions was insignificantly different ( $P > 0.05$ ) among treatments and the control (Table 4) which could be the effect of adding salt and phosphate in the emulsified formula masking this characteristic. Therefore, the water holding capacities were not treatment sensitive in the presence of these additives. Usually, salt enhances more soluble myofibrillar proteins which then migrate to the fat globule surface, concentrate and form protein matrix at the fat/water interface (Youssef & Barbut, 2010). Apart from salt, mechanical emulsification of protein and fat in the batter could affect water holding capacity of the product. When the protein is improperly emulsified from mechanical overheating during blending process and the fat separates to the product surface, these could lead to lowering emulsifying property of the batter, consequently, lowering water holding capacity of the product (Liu, Callahan, & Solomon, 2009).

Gel strength of the treatments was significantly higher ( $P \leq 0.05$ ) than that of the control, presumably, due to lower moisture content of the treated samples than the control. In addition, Table 4 shows that treatments 1 and 3 which contained higher amount of *thua nao* (an alkaline fermented soybean) than other treatments had significantly highest pH and gel strength ( $P \leq 0.05$ ). Since the slimy mucilage in *thua nao* which was composed of levan ( $\beta$ -2,6-fructan) and polyglutamic acid had binding potential, resulting firmer product structure was achieved (Donot, Fontana, Baccou, & Schorr-Galindo, 2012; Zhang et al., 2014).

### 3.2.3. Rheological behavior

**3.2.3.1. Geometrically oscillatory measurement.** Dynamic oscillatory measurement is a popular physical characterization of bio polymeric gels. In this context, the profiles of storage ( $G'$ ) and loss ( $G''$ ) moduli of the control and the fish-based emulsions were illustrated in Fig. 5. The plots of  $G'$  and  $G''$  as a function of frequency for treatment 1 were depicted for the strongest sample, while those of

the controls were the weakest, due to the former displaying highest  $G'$  and  $G''$  and vice versa for the weak samples. It is noteworthy that these two viscoelastic geometries increased with the increase of *thua nao* addition which could be associated with the reduction of moisture contents and the effect of the slimy mucilage in *thua nao* as mentioned earlier. Moreover, the gel strength (Table 4) also agreed with the viscoelastic behaviors. In overall,  $G'$  was bigger than  $G''$  across the frequency range with small loss tangent ( $G''/G' = 0.13$ – $0.19$ ) as shown in Table 4 and the difference between  $G'$  and  $G''$  of each plot was around one log cycle. This was a mirror of weak viscoelastic or coagulant gel types with some crosslink density (Chattong & Apichartsrangkoon, 2009). Moreover, these results were also complied with the study of Apichartsrangkoon (2002) demonstrating that  $G'$  and  $G''$  plots of the heated gluten and soy mixed-gels were little frequency dependence and  $G'$  was bigger than  $G''$ . This reflected of solid-like characteristic with high crosslink density.

**3.2.3.2. Creep and recovery testing.** The creep curves for the control and the treated emulsions were best fitted by the four-element Burgers model which comprised Kelvin-Voigt model connected in series to a spring and a dashpot elements as shown in Fig. 4. Other finding of the viscoelastic behavior of O/W model-system meat emulsions and chicken meat frankfurters was also characterized using the Burgers model (Dzadzal, Markowski, Sadowski, Jakóbczak, & Janulin, 2015; Yilmaz, Karaman, Dogan, Yetim, & Kayacier, 2012).

Fig. 6 illustrated the creep and recovery curves of the fish based emulsions and the control. It is apparent that the creep curve of the treatment 1 laid on the lowest position or having lowest instantaneous elastic compliance ( $J_0$ ), while the control curve laid on the highest position suggesting that treatment 1 was the strongest gel and vice versa for the control. In addition, the creep parameters in Table 4 such as  $J_0$ ,  $J_1$  and  $\lambda_{ret}$  increased with the reduction of gel rigidity, accordingly, treatment 1 had the highest gel rigidity,

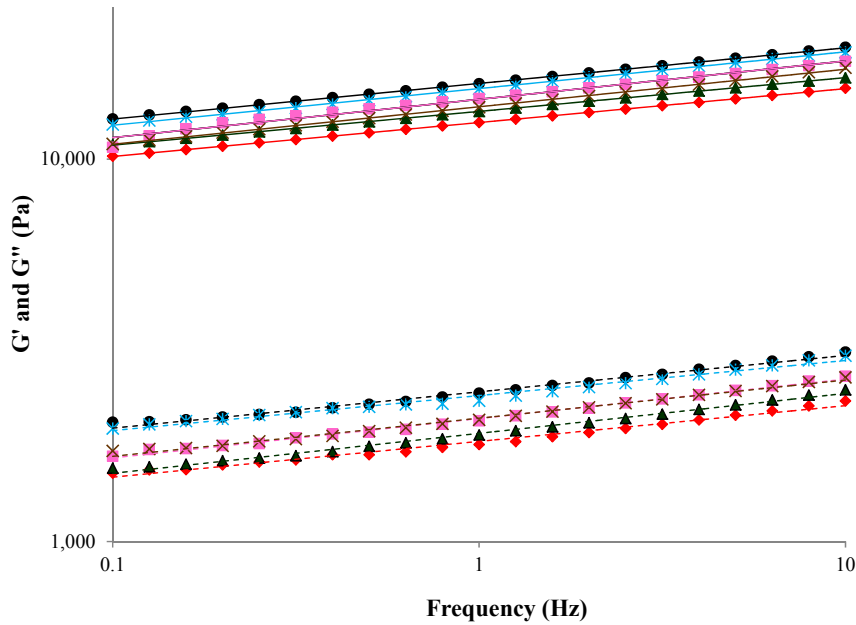


Fig. 5. Plots of storage ( $G'$ ) and loss ( $G''$ ) moduli versus frequency (0.1–10 Hz) of the heated control (*swai*-fish emulsion) and the heated *swai*-fish emulsions containing *thua nao* or rice-*koji* miso ( $G'$  = straight lines and  $G''$  = dotted lines;  $\blacklozenge$  = control,  $\bullet$  = treatment 1,  $\blacktriangle$  = treatment 2,  $\ast$  = treatment 3,  $\blacksquare$  = treatment 4 and  $\times$  = treatment 5).

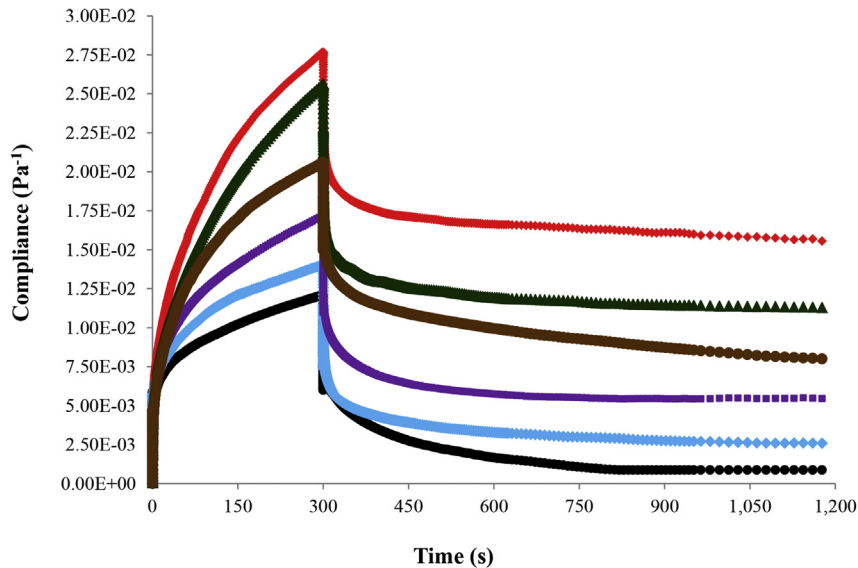


Fig. 6. Creep-recovery curves of the heated control (*swai*-fish emulsion) and the heated *swai*-fish emulsions containing *thua nao* or rice-*koji* miso ( $\blacklozenge$  = control,  $\bullet$  = treatment 1,  $\blacktriangle$  = treatment 2,  $\blacklozenge$  = treatment 3,  $\blacksquare$  = treatment 4 and  $\bullet$  = treatment 5).

sequentially followed by treatment 3, 4, 5, 2 and the control, respectively. These results were also well complied with the oscillatory profiles (Fig. 5) and the gel strength (Table 4). The viscosity or  $\mu_0$  referred to the final steady-state of a Newtonian flow has a reversed meaning from  $J_0$ ,  $J_1$  and  $\lambda_{ret}$  (Chattong & Apichartsrangkoon, 2009; Chattong et al., 2007).

#### 3.2.4. Microbiological qualities

Table 4 illustrated that every treatment exhibited total plate count in the range of 2–4 log CFU  $g^{-1}$  and spore count in the range of 3–4 log CFU  $g^{-1}$  except treatment 2 (spore count) and the control without adding *thua nao*. It is obvious that the spore of *B. subtilis* TISTR 001 was fairly resistant to heat treatment (72 °C/30 min),

thus some of this bacteria and spore could survive after heating and were present in the total plate and spore counts. Since the total plate and spore counts of the control were less than 1 log CFU  $g^{-1}$ , this might imply that general microbes in the corresponding treatments were also satisfactorily inhibited. Other investigations, for instance, Scheldeman, Herman, Foster, and Hendrickx (2006) noted that *Bacillus* species such as *Bacillus cereus*, *Bacillus coagulans*, *B. subtilis*, and *Bacillus sporothermodurans* were likely to form highly heat resistant spores which could survive from normal heat treatment. Kort et al. (2005) also stated that a temperature of more than 100 °C was needed to inhibit *Bacillus* spores to 1 log CFU  $g^{-1}$ . Therefore, a temperature of 70 °C in this study was certainly insufficient to inactivate the spore of *B. subtilis*.

### 3.2.5. Sensory evaluation

Sensory evaluation was performed by 50 untrained panelists to judge six essential attributes following 5-point hedonic scale. The mean scores of each attribute of 5 treatments and the control are shown in Table 4. It was found that treatment 3 received significantly highest scores ( $P \leq 0.05$ ) for all attributes, consecutively followed by treatments 4, 2, 5, 1 and the control, respectively. It is noticeable that the control had less flavor, while treatment 1 had strong odor as well as treatments 2 and 5 with high amount of additional rice-*koji* miso were rather salty. Therefore, these treatments were scored for lower overall acceptability, only treatments 3 and 4 gained high sensorial scores.

## 4. Conclusions

Fatty acid profile of the *swai*-fish fillet was composed mainly of saturated and monounsaturated fatty acids with the ratio of  $n-3/n-6$  being 0.08, while isoflavone profiles of the fermented soybeans revealed that *thua nao* contained more aglycones such as diadzein, glycitein and genistein than rice-*koji* miso, which could provide better health supplements. The physico-chemical properties of fish based emulsions varied 5 treatments condition could be clarified as follows. Browning indices of all treatments were higher than those of the control. In addition, the oscillatory and creep testing illustrated that treatment 1 was the strongest gel followed by treatments 3, 4, 5, 2 and the control, while the gel strengths increased with the increase of *thua nao* in the formula. For microbiological quality, total plate or spore counts showed that fish based emulsions with *thua nao* addition retained high viable cells and spores of *B. subtilis*. In overall, treatments 3 and 4 received the highest sensorial scores.

## Acknowledgments

The authors wish to thank Chiang Mai University for their financial support.

## References

- AOAC. (2000). *Official methods of analysis* (17th ed.). Washington, DC: Association of Official Analytical Chemists.
- AOAC. (2005). *Official methods of analysis* (18th ed.). Washington, DC: Association of Official Analytical Chemists.
- Apichartsrangkoon, A. (2002). Dynamic viscoelastic properties of heated gluten/soy protein gels. *Journal of Food Science*, 67(2), 653–657.
- Chatotong, U., & Apichartsrangkoon, A. (2009). Dynamic viscoelastic characterisation of ostrich-meat yor (Thai sausage) following pressure, temperature and holding time regimes. *Meat Science*, 81(3), 426–432.
- Chatotong, U., Apichartsrangkoon, A., & Bell, A. E. (2007). Effects of hydrocolloid addition and high pressure processing on the rheological properties and microstructure of a commercial ostrich meat product "Yor" (Thai sausage). *Meat Science*, 76(3), 548–554.
- Dajanta, K., Apichartsrangkoon, A., Chukeatirote, E., & Frazier, R. A. (2011). Free-amino acid profiles of *thua nao*, a Thai fermented soybean. *Food Chemistry*, 125(2), 342–347.
- Dajanta, K., Chukeatirote, E., & Apichartsrangkoon, A. (2012). Nutritional and physicochemical qualities of *thua nao* (Thai traditional fermented soybean). *Chiang Mai Journal of Science*, 39(4), 562–574.
- Dajanta, K., Chukeatirote, E., Apichartsrangkoon, A., & Frazier, R. A. (2009). Enhanced aglycone production of fermented soybean products by *Bacillus* species. *Acta Biologica Szegediensis*, 53(2), 93–98.
- Donot, F., Fontana, A., Baccou, J. C., & Schorr-Galindo, S. (2012). Microbial exopolysaccharides: main examples of synthesis, excretion, genetics and extraction. *Carbohydrate Polymers*, 87(2), 951–962.
- Dzadzil, L., Markowski, M., Sadowski, P., Jakóbczak, A., & Janulin, M. (2015). Creep and recovery characteristics of chicken meat frankfurters. *Journal of Agricultural Science and Technology*, 17, 827–835.
- Ferrari, G., Maresca, P., & Ciccarone, R. (2010). The application of high hydrostatic pressure for the stabilization of functional foods: pomegranate juice. *Journal of Food Engineering*, 100(2), 245–253.
- Funami, T., Yada, H., & Nakao, Y. (1998). Thermal and rheological properties of curdlan gel in minced pork gel. *Food Hydrocolloids*, 12(1), 55–64.
- Giri, A., Osako, K., Okamoto, A., Okazaki, E., & Ohshima, T. (2011). Antioxidative properties of aqueous and aroma extracts of squid miso prepared with *Aspergillus oryzae*-inoculated koji. *Food Research International*, 44(1), 317–325.
- ICMSF. (1986). *International Commission on Microbiological Specifications for Foods, sampling for microbiological analysis: Principles and scientific application* (2nd ed., Vol. 2). Toronto: University of Toronto Press.
- Izumi, T., Piskula, M. K., Osawa, S., Obata, A., Tobe, K., Saito, M., et al. (2000). Soy isoflavone aglycones are absorbed faster and in higher amounts than their glucosides in humans. *The Journal of Nutrition*, 130(7), 1695–1699.
- Kano, M., Takayanagi, T., Harada, K., Sawada, S., & Ishikawa, F. (2006). Bioavailability of isoflavones after ingestion of soy beverages in healthy adults. *The Journal of Nutrition*, 136(9), 2291–2296.
- Klejduš, B., Mikelová, R., Petřilová, J., Potěšil, D., Adam, V., Stiborová, M., et al. (2005). Determination of isoflavones in soy bits by fast column high-performance liquid chromatography coupled with UV-visible diode-array detection. *Journal of Chromatography A*, 1084(1–2), 71–79.
- Kort, R., O'Brien, A. C., van Stokkum, I. H. M., Oomes, S. J. C. M., Crielgaard, W., Hellingwerf, K. J., et al. (2005). Assessment of heat resistance of bacterial spores from food product isolates by fluorescence monitoring of dipicolinic acid release. *Applied and Environmental Microbiology*, 71(7), 3556–3564.
- Liu, M. N., Callahan, J. A., & Solomon, M. B. (2009). Meat products, processed meat ingredients. In *Kirk-Othmer encyclopedia of chemical technology*. John Wiley & Sons, Inc.
- Macfie, H. J., Bratchell, N., Greenhoff, K., & Vallis, L. V. (1989). Designs to balance the effect of order of presentation and first-order carry-over effects in hall tests. *Journal of Sensory Studies*, 4(2), 129–148.
- Malashree, L., Mudgil, P., Dagar, S. S., Kumar, S., & Puniya, A. K. (2012).  $\beta$ -Glucosidase activity of *Lactobacilli* for biotransformation of soy isoflavones. *Food Biotechnology*, 26(2), 154–163.
- Maqsood, S., & Benjakul, S. (2010). Comparative studies of four different phenolic compounds: *in vitro* antioxidative activity and the preventive effect on lipid oxidation of fish oil emulsion and fish mince. *Food Chemistry*, 119(1), 123–132.
- Murphy, P. A., Barua, K., & Hauck, C. C. (2002). Solvent extraction selection in the determination of isoflavones in soy foods. *Journal of Chromatography B*, 777(1–2), 129–138.
- Na-Nakorn, U., & Moeikum, T. (2009). Genetic diversity of domesticated stocks of striped catfish, *Pangasianodon hypophthalmus* (Sauvage 1878), in Thailand: relevance to broodstock management regimes. *Aquaculture*, 297(1–4), 70–77.
- Orban, E., Nevigato, T., Lena, G. D., Masci, M., Casini, I., Gambelli, L., et al. (2008). New trends in the seafood market. Sutchi catfish (*Pangasius hypophthalmus*) fillets from Vietnam: nutritional quality and safety aspects. *Food Chemistry*, 110(2), 383–389.
- Scheldeman, P., Herman, L., Foster, S., & Hendrickx, M. (2006). *Bacillus sporothermodurans* and other highly heat-resistant spore formers in milk. *Journal of Applied Microbiology*, 101(3), 542–555.
- Siemer, C., Toepfl, S., & Heinz, V. (2014). Inactivation of *Bacillus subtilis* spores by pulsed electric fields (PEF) in combination with thermal energy – I. Influence of process- and product parameters. *Food Control*, 39(0), 163–171.
- Steffe, J. F. (1996). *Rheological methods in food process engineering* (2nd ed.). East Lansing, USA: Freeman Press.
- Techarang, J., & Apichartsrangkoon, A. (2015). Physical, chemical and rheological parameters of pressurized *swai*-fish (*Pangasius hypophthalmus*) emulsion incorporating fermented soybeans. *Food and Bioprocess Processing*, 94(0), 649–656.
- Uzzan, M., & Abuza, T. P. L. (2004). Critical issues in R&D of soy isoflavone-enriched foods and dietary supplements. *Journal of Food Science*, 69(3), CRH77–CRH86.
- Xu, L., Du, B., & Xu, B. (2015). A systematic, comparative study on the beneficial health components and antioxidant activities of commercially fermented soy products marketed in China. *Food Chemistry*, 174(0), 202–213.
- Yamabe, S., Kobayashi-Hattori, K., Kaneko, K., Endo, H., & Takita, T. (2007). Effect of soybean varieties on the content and composition of isoflavone in rice-*koji* miso. *Food Chemistry*, 100(1), 369–374.
- Yilmaz, M. T., Karaman, S., Dogan, M., Yetim, H., & Kayacier, A. (2012). Characterization of O/W model system meat emulsions using shear creep and recovery tests based on mechanical simulation models and their correlation with texture profile analysis (TPA) parameters. *Journal of Food Engineering*, 108(2), 327–336.
- Youssef, M. K., & Barbut, S. (2010). Physicochemical effects of the lipid phase and protein level on meat emulsion stability, texture, and microstructure. *Journal of Food Science*, 75(2), S108–S114.
- Zhang, T., Li, R., Qian, H., Mu, W., Miao, M., & Jiang, B. (2014). Biosynthesis of levan by levansucrase from *Bacillus methylotrophicus* SK 21.002. *Carbohydrate Polymers*, 101(0), 975–981.



# Impact of cooking and germination on phenolic composition and dietary fibre fractions in dark beans (*Phaseolus vulgaris* L.) and lentils (*Lens culinaris* L.)



Montserrat Dueñas<sup>b</sup>, Thaise Sarmento<sup>a</sup>, Yolanda Aguilera<sup>a</sup>, Vanesa Benitez<sup>a</sup>, Esperanza Mollá<sup>a</sup>, Rosa M. Esteban<sup>a</sup>, María A. Martín-Cabrejas<sup>a,\*</sup>

<sup>a</sup> Departamento de Química Agrícola y Bromatología, Facultad de Ciencias, Instituto de Ciencias de la Alimentación (CIAL), Campus Universidad Autónoma de Madrid (UAM), 28049 Madrid, Spain

<sup>b</sup> Grupo de Investigación de Polifenoles, Unidad de Nutrición y Bromatología, Facultad de Farmacia, Universidad de Salamanca, Campus Miguel Unamuno, 37007 Salamanca, Spain

## ARTICLE INFO

### Article history:

Received 5 June 2015

Received in revised form

6 October 2015

Accepted 8 October 2015

Available online 19 October 2015

### Keywords:

Beans  
Lentils  
Cooking  
Germination  
Phenolic compounds  
Dietary fibre fractions

## ABSTRACT

The impact of cooking and germination on dietary fibre and phenolic compound composition was studied in beans (*Phaseolus vulgaris* L.) and lentils (*Lens culinaris* L.). An investigation on phenolic compounds in dietary fibre fractions was carried out due to the scarce literature on the behaviour of these compounds during legume processing. A general decrease in the concentration of insoluble and soluble fibre fractions were observed in processed bean and lentil flours, although an increase in the content of insoluble and soluble fibre fractions in sprouts and cooked beans, respectively, was found. Hydroxybenzoic and hydroxycinnamic compounds, flavan-3-ols, procyanidins, flavonols and flavones were identified in dietary fibre fractions in cooked and germinated beans and lentils. Phenolic compound constituents of the different dietary fibre fractions accounted from 73% to 97% in insoluble dietary fibre fraction (IDF) flours and from 3% to 25% in soluble dietary fibre fraction (SDF) in raw and processed bean and lentil flours. These processing techniques may produce positive changes in the dietary fibre and phenolic compound composition and its association could improve phytochemical and nutritional quality and maximize the health-promoting properties of legumes.

© 2015 Elsevier Ltd. All rights reserved.

## 1. Introduction

The role of legumes in health promotion is gaining interest in developing countries because of close association between their consumption and their effects against chronic diseases, as obesity, cardiovascular disease, type 2 diabetes and large intestine cancer (Vaz-Patto et al., 2015). Beneficial effects of legumes are due to their excellent nutritional value. Legumes present high content in proteins, carbohydrates, dietary fibre, minerals and vitamins, but they also are rich source of natural antioxidants such as phenolic compounds, vitamin C and tocopherols. Phenolic compounds can play a key role by scavenging harmful reactive oxygen agents and protect cells from oxidative damage related to aging and age-related disorders (Thériault, Caillet, Kermasha, & Lacroix, 2006). In addition,

*in vitro* and *in vivo* studies have demonstrated that phenolic compounds may exhibit anti-atherosclerotic and anti-inflammatory properties, and they are able to inhibit the growth of human cancer cell lines (Del Rio et al., 2013). On the other hand, dietary fibre has an essential role in intestinal health and prevention of diseases from different origins (Philips, 2013). Recently, it has also been suggested that the presence of polyphenols associated with dietary fibre may significantly affect the physiological properties and health effects of dietary fibre (Saura-Calixto, 2011). Pérez-Jiménez et al., (2008, 2009) demonstrated that polyphenols present in a rich dietary fibre matrix results in a significant increase in plasma antioxidant capacity, and reductions of total cholesterol, LDL cholesterol, triacylglycerols in plasma and blood pressure. Çelik, Gökmen, and Fogliano (2013) revealed that the antioxidant capacity of compounds chemically bound to dietary fibre structure could be reconstituted in the presence of other hydrogen-donating substances in liquid phase.

Legume seeds before their consumption need to be processed to

\* Corresponding author.

E-mail address: [maria.martin@uam.es](mailto:maria.martin@uam.es) (M.A. Martín-Cabrejas).

improve nutritional profile and decrease the non-nutritional factors (Martín-Cabrejas et al., 2009). Heat treatment such as cooking is the most common method of processing of legumes, which mainly results in significant reductions in phytic acid, oligosaccharides, minerals, tannins and phenolic compounds content (Wang, Hatcher, Toews, & Gawalko, 2009; Wang, Hatcher, Tyler, Toews, & Gawalko, 2010). Many studies confirm that heat treatment significantly improves protein quality and soluble dietary fibre (SDF) and decreases the insoluble dietary fibre fraction (IDF) (Martín-Cabrejas et al., 2008; Wang et al., 2010).

Germination is an economic, inexpensive and effective process that provides a source of bioactive compounds (Donkor, Stojanovska, Ginn, Ashton, & Vasiljevic, 2012; López-Amorós et al., 2013). Legume sprouting has also been suggested as powerful strategy to increase antioxidant activity (Świeca, Gawlik-Dziki, Kowalczyk, & Złotek, 2012). However, phenolic compounds composition and content associated to their antioxidant properties depend on the germination conditions and type of legumes (Dueñas, Martínez-Villaluenga, Limón, Peñas, & Frias, 2015; López-Amorós, Hernández, & Estrella, 2006). Thus, germination has shown to have a significant impact on both dietary fibre fractions, promoting an improvement of IDF/SDF ratio, which is important both for healthy properties and for technological characteristics (Benítez et al., 2013).

The objective of this study was to evaluate the impact of cooking and germination on dietary fibre fractions in dark beans (*Phaseolus vulgaris* L.) and lentils (*Lens culinaris* L.). Due to scarce literature on the profile of phenolic compounds that is associated to the dietary fibre in processing legumes, an investigation on the behaviour of these compounds in dietary fibre fractions during processing of bean and lentil flours has been carried out. Results from this study will provide valuable information on phytochemical composition of dark bean seeds and lentils in order to develop functional ingredients from these legumes.

## 2. Materials and methods

### 2.1. Plant material

Dark bean seeds (*P. vulgaris* var. Tolosa) and lentils (*L. culinaris* var. Rubia de la Armaña) were kindly provided by Institute of Food Science, Technology and Nutrition (ICTAN-CSIC). Seeds were stored in polyethylene containers at 4 °C and cleaned before germination process.

### 2.2. Processing methods

**Cooking.** Legume seeds (500 g) were soaked in water (3 L) for 18 h, at room temperature. The water was then discarded and seeds were boiled at atmospheric pressure for 60 min for dark beans and for 20 min for lentils, with water (3 L); seeds were then separated from water, freeze-dried, milled and passed through a 0.5 mm sieve. The obtained flours were stored under vacuum conditions in desiccators at 4 °C in the dark until further analysis.

**Germination.** 200 g of seeds were soaked in 0.07% sodium hypochlorite solution (1000 mL) for 30 min. Then, seeds were drained and washed with distilled water (1000 mL) until they reached a neutral pH. Afterward, seeds were soaked in distilled water for an additional 5.5 h and shaken very 30 min. Finally, hydrated seeds were placed in trays where a wet filter paper was extended, and were then covered. The trays were introduced into a pilot scale germinator G-120 model (ASL Snijders International S.L., Holland). Seeds were maintained wet by capillarity. Germination was performed in darkness at 20 °C for 7 days. Sprouts were freeze-dried, milled, passed through a 0.5 mm sieve; the obtained flours

were stored under vacuum conditions in desiccators at 4 °C in the dark until further analysis.

### 2.3. Chemical composition analysis

Proximate chemical composition analysis of the seed flours including total ash, crude fat, and crude protein were performed according to official AOAC procedures (AOAC, 1995).

### 2.4. Dietary fibre determination

Dietary fibre (DF) was determined according to Mes-Tris AOAC method 991.43 (AOAC, 1995). The principle of the method was based on the use of three enzymes (heat stable  $\alpha$ -amylase, protease and amyloglucosidase) under different incubation conditions in order to remove starch and protein components. Dietary fibre fractions were obtained as indigestible residues after enzymatic digestion of non-dietary fibre components. The insoluble residues were isolated by filtration and soluble fibre was precipitated with ethanol. Dried residues correspond to insoluble dietary fibre (IDF) and soluble dietary fibre (SDF), respectively. Determination of residual ash and proteins (as Kjeldahl N 6.25) was carried out on the residues for corresponding corrections. Total dietary fibre (TDF) calculated as sum of IDF and SDF (AOAC, 1995).

### 2.5. Extraction of phenolic compounds from dietary fibre fractions of legume flours

Dietary fibre fractions of legume flours (2.0 g) were macerated with 3 × 20 mL of a solution of methanol-HCl (1%)/water (80:20, v/v) using an orbital shaker at room temperature, and the supernatants were separated by centrifugation (4000g and 5 °C for 20 min). The extracts were combined and concentrated at 30 °C under vacuum for methanol evaporation. The residue was dissolved in methanol:water (1:1 v/v), according to Dueñas, Hernández, Estrella, and Fernández (2009). The obtained extracts were analysed by HPLC-DAD-MS analysis. The extractions were performed in duplicate. The phenolic compounds present in dietary fibre fractions were analysed by HPLC-DAD-MS.

### 2.6. HPLC-DAD-MS analysis of phenolic compounds

The extracts (100  $\mu$ l) that were previously filtered through a 0.45  $\mu$ m membrane were injected onto a Waters system (Milford, Mass, USA) chromatograph equipped with autoinjector, a quaternary pump, diode array detector (DAD), according to Dueñas et al. (2009). Briefly, the chromatographic system was comprised of auto-injector, quaternary pump, photodiode-array detector 2001 and Millennium 32 chromatography manager software (waters, Milford, Mass, USA). Separation of phenolic compounds was achieved on a reverse phase C<sub>18</sub> column (Nova-Pak, 300 × 3.9 mm, particle size 4  $\mu$ m). The mobile phase was comprised of two solvents, A: water/acetic acid (98:2, v/v) and B: water/acetonitrile/acetic acid (78:20:2, v/v/v). The gradient profile was 0–55 min, 100–20% A; 55–70 min, 20–10% A; 70–80 min, 10–5% A; 80–110 min, 100% B. The flow rate was 1 mL/min from the beginning to 55 min and 1.2 mL/min from this point to the end.

Detection was carried out by scaling the absorption between 210 and 400 nm with an acquisition speed of 1 s. Mass spectra were obtained using a Hewlett Packard 100 MS (Palo Alto, CA) chromatogram equipped with an API source and electrospray ionization (ESI) interface. The solvent gradient and column employed were identical to those for HPLC-DAD analyses. The ESI conditions were as follows: negative-ion mode analysis: 2 as the nebulizer gas at 275 kPa, drying gas flow rate and temperature of 10 L/min and

340 °C, respectively; voltage the capillary entrance set at 4000 V; and variable fragmentation voltage at 100 V ( $m/z$  200–1000) and 250 V ( $m/z$  1000–2500). Mass spectra were recorded from a  $m/z$  of 100–2500.

The phenolic compounds were characterized according to their UV and mass spectra and retention times, and comparison with authentic standards when available. For quantitative analysis, calibration curves were prepared by injection of known concentrations of different standard compounds. However, compounds for which a commercial standard was not available were quantified through the calibration curve of a compound from the same phenolic group. Samples were in triplicate and the results expressed in  $\mu\text{g}$  per g dry weight.

### 2.7. Statistical analysis

Data were subjected to one-way analysis of variance (ANOVA) and significant differences between samples were determined by the least significant differences (LSD) test at  $p \leq 0.05$  probability level, using PASW Statistics 18.0 software (IBM, Armonk, NY, USA).

## 3. Results and discussion

### 3.1. Impact of thermal treatment and germination of beans and lentils on proximate composition

Table 1 shows the proximate composition of raw and processed bean and lentil flours. Protein content of raw lentil flours (22.0 g/100 g DM) was higher than bean flours (17.7 g/100 g DM), and also higher than those reported for other lentil varieties and other legumes (19.5 g/100 g DM in lentil variety Pardina, 20.8 g/100 g DM in chickpea) (Aguilera et al., 2010; Masood, Shah, & Zeb, 2014). Cooking resulted in a significant ( $p < 0.05$ ) increase in protein content (by 6% and 8% in beans and lentils, respectively) compared to control (raw legumes), but ash content was reduced significantly ( $p < 0.05$ ). The increases in protein content in cooked beans and lentils were attributed to solubilisation of components and, consequently, as a concentration effect (Pujolá, Farreras, & Casañas, 2007; Wang et al., 2009). The significant decrease in ash content during cooking would result from diffusion of minerals into the boiling water. Similar results have been reported for peas, lentils, beans and chickpeas (Aguilera et al., 2010; Wang, Hatcher, & Gawalko, 2008, 2009, 2010). Thus, the cooked flours revealed higher energy levels than control due to their high protein contents. However, germination process produced a significant ( $p < 0.05$ ) decrease of protein and increase in ash and carbohydrate contents. The protein concentration decreased significantly with respect to raw flours (by 11% and 14% in beans and lentils, respectively). Germinated seeds exhibit increased proteolytic activity, which results in hydrolysis of storage proteins (Ghavidel & Prakash, 2007).

**Table 1**  
Proximate Composition of raw and processed lentil and bean flours (g/100 g dry matter).<sup>a</sup>

Sample	Ash	Fat	Protein	Total carbohydrates	Energy (kJ/100 g)
<b>Beans</b>					
Raw	3.8 ± 0.0 <sup>b</sup>	1.1 ± 0.1 <sup>a</sup>	17.7 ± 0.5 <sup>b</sup>	77.4	1629.6
Cooking	2.6 ± 0.1 <sup>a</sup>	1.2 ± 0.1 <sup>a</sup>	18.7 ± 0.4 <sup>c</sup>	77.5	1651.8
Germinated	4.3 ± 0.0 <sup>c</sup>	2.0 ± 0.2 <sup>b</sup>	15.7 ± 0.4 <sup>a</sup>	78.2	1643.5
<b>Lentils</b>					
Raw	3.4 ± 0.1 <sup>b</sup>	0.8 ± 0.0 <sup>a</sup>	22.0 ± 0.8 <sup>b</sup>	73.8	1630.0
Cooking	2.1 ± 0.1 <sup>a</sup>	1.4 ± 0.1 <sup>c</sup>	23.7 ± 0.9 <sup>c</sup>	72.9	1666.0
Germinated	3.6 ± 0.0 <sup>c</sup>	1.1 ± 0.1 <sup>b</sup>	18.9 ± 0.4 <sup>a</sup>	76.4	1633.0

<sup>a</sup> Mean values of each column followed by different superscript letter significantly differ when subjected to Duncan's multiple range test ( $p < 0.05$ ). Mean ± SD ( $n = 6$ ). Total carbohydrates are calculated by difference.

### 3.2. Impact of thermal treatment and germination of beans and lentils on dietary fibre

Insoluble dietary fibre (IDF) (Table 2) was the main fraction of total dietary fibre (TDF), since it represented from 79% in beans to 91% in lentils. The SDF fraction constituted 21% in beans and 9% in lentils of the dietary fibre of these legumes. Likewise, the content of IDF in lentils (245 mg/g) was higher than in beans (215 mg/g) and the content of SDF in lentils (24 mg/g) was smaller than in beans. These results of dietary fibre were higher than in other varieties, such as lentil var. Pardina that presented 216 mg/g in IDF (Martín-Cabrejas et al., 2006) and beans var. Carilla containing 171 mg/g in IDF (Martín-Cabrejas et al., 2004).

The process of cooking impacted the IDF fraction differently in the two legumes, showing a significant decrease in lentil (14%), whereas beans did not show changes compared to raw samples. In addition, the SDF fraction in cooked beans exhibited a slight increase; however, SDF content decreased significantly (27%) in cooked lentils compared to raw lentils. This reduction in SDF due to cooking was also reported in peas (Wang et al., 2008), lentils (Wang et al., 2009), due to the solubilisation of polysaccharide contents that constitute the SDF fraction.

Germination produced important differences in dietary fibre fractions; a notable increase in the level of IDF (34%) and TDF (26%) in beans was observed with respect to raw legume. On the contrary, germinated lentils showed a decrease of TDF (25%), as a consequence of the marked decrease (23%) of IDF (from 245 mg/g to 186 mg/g). Likewise, SDF fractions decreased in the two studied legumes, and this reduction was more pronounced in germinated lentils (47%). This decrease in SDF level are not in concordance with the results obtained by other authors who demonstrated an increase in SDF content during the germination process (Chang, Sang, Eun, & Young, 2006; Martín-Cabrejas et al., 2008), as consequence mainly of the rise of cellulosic glucose due to the metabolic reactions undergone by seeds during germination.

The decrease of SDF detected could be due to possible degradation of SDF of high molecular weight to smaller fragments and

**Table 2**  
Dietary fibre content in raw and processed bean and lentil flours (mg/g dry matter).<sup>a</sup>

Sample	IDF	SDF	TDF	IDF:SDF
<b>Beans</b>				
Raw	214.6 ± 3.4 <sup>a</sup>	57.8 ± 1.1 <sup>b</sup>	272.4	4:1
Cooking	218.6 ± 2.3 <sup>a</sup>	59.7 ± 0.7 <sup>c</sup>	278.3	4:1
Germinated	288.6 ± 11.3 <sup>b</sup>	55.3 ± 1.4 <sup>a</sup>	343.9	5:1
<b>Lentils</b>				
Raw	244.6 ± 2.0 <sup>c</sup>	24.0 ± 3.5 <sup>c</sup>	268.6	10:1
Cooking	210.1 ± 3.8 <sup>b</sup>	17.6 ± 2.7 <sup>b</sup>	228.0	12:1
Germinated	188.5 ± 1.6 <sup>a</sup>	12.8 ± 1.8 <sup>a</sup>	201.3	15:1

<sup>a</sup> Mean values within a column and legume followed by different superscript letters were significantly different at  $p < 0.05$ . Means ± SD ( $n = 6$ ).

depending on the extent of depolymerization, a fraction of SDF could be incompletely recovered by ethanolic precipitation in the fibre analysis (Martín-Cabrejas et al., 2004). These modifications promoted by germination produced an improvement in IDF/SDF ratio with respect to non-treated legumes. This fact might exert an influence on the physiological effects and physicochemical properties of dietary fibre. Thus, the effect of germination was dependent on the type of legume (López-Amorós et al., 2006; Mahadevamma & Tharanathan, 2004). The studied legumes exhibited different behaviours during processing due to the different structures and compositions of the cell wall network.

### 3.3. Effect of thermal treatment and germination on phenolic compounds in dietary fibre fractions of beans and lentils

At present, there is scarce literature on the profile of phenolic compounds that are associated with dietary fibre. Because of the role of phenolic compounds in this complex matrix of the plant cell wall, these components were studied in the dietary fibre fractions in cooked and germinated beans and lentils. Their levels were determined by HPLC-DAD-MS, as is shown in Tables 3 and 4. The retention time,  $\lambda_{\text{max}}$ , molecular ion and their fragment ion pattern allowed the identification of hydroxybenzoic and hydroxycinnamic, flavan-3-ol, procyanidins, flavonols and flavones phenolic classes.

Hydroxybenzoic, hydroxycinnamic compounds and flavonols were the phenolic compounds identified in the IDF and SDF fractions in raw and processed bean flours (Table 5). Hydroxybenzoic compounds were the most abundant phenolic class detected in IDF and SDF fractions in raw and processed flours accounting for approximately 90% in the dietary fibre fractions in raw and cooked beans, with protocatechuic acid and aldehyde occurring in higher concentrations. However, no hydroxybenzoic compounds were identified in IDF fractions in sprouted beans, and free hydroxycinnamic acids (*trans-p*-coumaric, *trans*-ferulic and sinapic acids) were only identified in IDF fraction. The percentage of hydroxycinnamics in SDF for sprouts accounted for approximately 73% while hydroxybenzoics accounted for 27% of the total identified phenolics in this fraction. In contrast, hydroxybenzoics accounted for approximately 85–90% of the total identified phenolics in SDF of raw and cooked beans.

Bean seeds also included hydroxycinnamic compounds linked to hydroxyacids (aldaric acid), as was observed in raw and processed extracts, with feruloyl aldaric acids the main compounds in this group in SDF fractions in sprouts. However, it is noteworthy that *trans-p*-coumaric and *trans*-ferulic acids were present in higher concentration in IDF for sprouts beans (8.18  $\mu\text{g/g}$  and 25.9  $\mu\text{g/g}$ ).

These acids were found either free or bound to cell walls (or dietary fibre) such as cellulose, lignin and protein in plant foods and beverages (Goñi, Díaz-Rubio, Pérez-Jiménez, & Saura-Calixto, 2009). In addition, it has been observed that the majority of phenolics in wheat are present in the insoluble bound form, and are involved in crosslinking polymers, particularly arabinoxylans in the grain cell walls (Saulnier, Sado, Branlard, Charmet, & Guillon, 2007).

The flavonol compounds in the form of kaempferol glycosides and quercetin derivative were only found in the IDF fractions in raw and germinated beans, accounting for a low proportion (1–5%) with respect to total phenolic compounds identified in this fraction.

The total phenolic compounds concentration in each fraction was higher in IDF fraction in raw and sprout beans (22.8  $\mu\text{g/g}$ –37.2  $\mu\text{g/g}$ ), except for SDF fraction in boiled beans whose total phenolic compounds content was higher than IDF fraction. This behaviour could be related to increase of SDF content in boiled beans with respect to raw beans as was shown in Table 2. Similarly, the total of phenolic compounds content in IDF fraction in sprouts could be related to enhanced IDF content in this sample. The sum of total phenolic concentration in IDF and SDF fractions in germinated beans was higher (45.2  $\mu\text{g/g}$ ) in comparison to raw beans. The observed pronounced reduction of total phenolic compounds concentration in germinated beans (61%) could be due to the possible association of these compounds to dietary fibre fractions.

Similarly to bean samples, hydroxybenzoic compounds were the most abundant phenolic compounds identified mainly in IDF fraction of raw and processed lentils samples, accounting for between 73% in sprouts and ~90% in raw and boiled samples, with *p*-vanillin the main compound of this group in raw lentils and protocatechuic acid in sprouts lentils (Table 6). The detection of *p*-vanillin could be due to release from depolymerisation of the lignin components (Vanbeneden, Gils, Delvaux, & Delvaux, 2008). It has been demonstrated that ferulic acid in very severe conditions may decompose to other chemicals such as vanillin (Arrieta-Baez et al., 2012).

Flavonoids present in the dietary fibre fraction were catechins, procyanidins, flavonols and flavones groups. Flavan-3-ol compounds in the form of (+)-catechin-3-O-hexoside and (+)-catechin were only found in the IDF fraction in raw seeds. On the contrary, procyanidin dimer was only identified in the IDF fraction in raw seeds and SDF fraction in boiled flours, with this group of compounds the only identified in this dietary fibre fraction.

The flavonol compounds in the form of kaempferol and quercetin glycosides were mainly identified in the IDF fraction in raw and processed flours, accounting for approximately 6% of total phenolic compounds identified in this fraction; however, flavonol

**Table 3**

Wavelength of maximum UV absorption and molecular ions of the identified phenolics in dietary fibre fractions of raw and processed beans.

Compounds	$\lambda_{\text{max}}$ (nm)	Molecular ion [M-H] <sup>-</sup> (m/z)	MS <sup>2</sup> (m/z)
<b>Hydroxybenzoic compounds</b>			
Gallic aldehyde	302	153	–
Protocatechuic acid	257, 294	153	–
Protocatechuic aldehyde	278, 310	137	–
<i>p</i> -Hydroxybenzoic acid	250	137	–
<i>p</i> -Hydroxybenzaldehyde	312	121	–
<b>Hydroxycinnamic compounds</b>			
<i>trans</i> -Feruloyl aldaric acid	233, 326	285	209, 193
Sinapoyl aldaric acid	235, 326	415	209, 223
<i>trans</i> -Ferulic acid	235, 322	193	–
<i>trans-p</i> -Coumaric acid	233, 314	173	–
Sinapic acid	237, 323	223	–
<b>Flavonols</b>			
Kaempferol rhamnoside-dihexoside	348	755	609,431,285
Quercetin derivative	352	–	301
Kaempferol-O-acylhexaside	350	489	285

**Table 4**  
Wavelength of maximum UV absorption and molecular ions of the identified phenolics in dietary fibre fractions of raw and processed lentils.

Compounds	$\lambda$ max (nm)	Molecular ion [M–H] <sup>–</sup> (m/z)	MS <sup>2</sup> (m/z)
<b>Hydroxybenzoic compounds</b>			
Gallic acid	270	169	–
Gallic aldehyde	302	153	–
Protocatechuic acid	257, 294	153	–
Protocatechuic aldehyde	278, 310	137	–
<i>p</i> -Hydroxybenzoic acid	250	137	–
<i>p</i> -Hydroxybenzaldehyde	312	121	–
<i>p</i> -vanillin	280, 309	151	–
Vanillic acid	252, 290	167	–
<b>Catechins and Procyanidins</b>			
(+)-Catechin 3- <i>O</i> -hexoside	280	451	289
(+)-Catechin	280	289	–
Procyanidin dimer B2	278	577	289
Procyanidin dimer	279	577	289
Gallate procyanidin dimer (P <sub>2</sub> G <sub>1</sub> )	280	729	289
<b>Flavonols and Flavones</b>			
Kaempferol dihexoside	346	609	285
Kaempferol 3- <i>O</i> -rutinoside	348	593	285
Quercetin 3- <i>O</i> -glucoside	355	463	301
Luteolin rhamnose hexose	338	593	431, 285
Kaempferol rhamnose-dihexoside	348	755	593, 285
Kaempferol 3- <i>O</i> -glucoside	265, 347	447	285
Kaempferol	267, 367	285	–

**Table 5**  
Concentration ( $\mu\text{g/g}$  dry matter) of phenolic compounds in dietary fibre fractions of raw and processed beans.

Compounds	Raw beans		Cooked beans		Germinated beans	
	Insoluble fibre	Soluble fibre	Insoluble fibre	Soluble fibre	Insoluble fibre	Soluble fibre
<i>Hydroxybenzoic compounds</i>						
Gallic aldehyde	nd	nd	0.87 ± 0.10	2.58 ± 0.49	nd	0.23 ± 0.10
Protocatechuic acid	7.10 ± 0.94	1.18 ± 0.12	t	6.30 ± 0.61	nd	1.07 ± 0.03
Protocatechuic aldehyde	7.23 ± 0.30	2.38 ± 0.26	nd	1.02 ± 0.20	nd	nd
<i>p</i> -Hydroxybenzoic acid	2.86 ± 0.75	2.20 ± 0.06	0.89 ± 0.09	5.46 ± 0.59	nd	0.53 ± 0.06
<i>p</i> -Hydroxybenzoic aldehyde	3.25 ± 0.01	1.54 ± 0.20	1.96 ± 0.20	6.30 ± 0.87	nd	0.34 ± 0.08
<b>Total</b>	<b>20.4</b>	<b>7.3</b>	<b>3.7</b>	<b>21.7</b>	<b>nd</b>	<b>2.2</b>
<i>Hydroxycinnamic compounds</i>						
<i>trans</i> -Feruloyl aldaric acid	0.37 ± 0.02	0.50 ± 0.01	nd	0.56 ± 0.03	nd	0.41 ± 0.01
<i>trans</i> -Feruloyl aldaric acid	nd	0.70 ± 0.09	nd	nd	nd	4.39 ± 0.07
<i>trans</i> -Feruloyl aldaric acid	nd	nd	nd	nd	nd	0.21 ± 0.01
Sinapoyl aldaric acid	0.34 ± 0.05	nd	nd	0.70 ± 0.11	nd	0.13 ± 0.00
<i>trans</i> - <i>p</i> -Coumaric acid	0.22 ± 0.01	nd	nd	nd	8.18 ± 0.56	nd
<i>trans</i> -Ferulic acid	nd	nd	nd	0.88 ± 0.23	25.90 ± 1.21	0.76 ± 0.09
Sinapic acid	0.37 ± 0.05	nd	nd	nd	2.60 ± 0.05	nd
<b>Total</b>	<b>1.3</b>	<b>1.2</b>	<b>nd</b>	<b>2.1</b>	<b>36.7</b>	<b>5.9</b>
<i>Flavonols</i>						
Kaempferol dihexoside-rhamnoside	1.06 ± 0.04	nd	nd	nd	nd	nd
Quercetin derivative	nd	nd	nd	nd	0.36 ± 0.02	nd
Kaempferol- <i>O</i> -acylhexoside	nd	nd	nd	nd	0.12 ± 0.00	nd
<b>Total</b>	<b>1.1</b>	<b>nd</b>	<b>nd</b>	<b>nd</b>	<b>0.5</b>	<b>nd</b>

t: traces; nd: not detected.

group in IDF fraction in germinated flours accounted for a higher percentage (26%).

Similar behaviour to beans flours, the total phenolic concentration in IDF fractions in lentils was higher in comparison to SDF fractions in raw and processed lentils. Lower concentration of total phenolic compounds was observed in dietary fibre fraction of cooked lentil flours (12.1  $\mu\text{g/g}$ ) compared to the dietary fibre fraction of raw lentils flours (80.8  $\mu\text{g/g}$ ).

These results show a general trend of greater proportion of phenolic compound constituents in IDF fractions compared to SDF. In dietary fibre fractions of raw and processed bean and lentil flours, phenolic compound constituents ranged from 73% to 97% in IDF flours and from 3% to 25% in SDF fractions. Cooked beans seemed to be an exception where phenolic compound percentage

in SDF was higher (86%) than in the IDF fraction (14%).

This fact is in concordance with the results obtained by other authors who demonstrated that phenolic compounds occur in substantial amounts especially in IDF, with the highest proportion found in fruits, followed by vegetables and cereals (Goñi et al., 2009; Saura-Calixto & Díaz-Rubio, 2007). However, polyphenols associated with SDF may present different structures, including soluble flavonoids and phenolic acids (Goñi et al., 2009).

Therefore, these results confirm the notable presence of phenolic compounds in dietary fibre fractions, mainly in IDF in raw and processed bean and lentil flours. A possible association in the behaviour of these compounds in dietary fibre fractions during processing with total phenolic compounds and dietary fibre contents could be observed.

**Table 6**  
Concentration ( $\mu\text{g/g}$  dry matter) of phenolic compounds in dietary fibre fractions of raw and processed lentils.

Compounds	Raw lentils		Cooked lentils		Germinated lentils	
	Insoluble fibre	Soluble fibre	Insoluble fibre	Soluble fibre	Insoluble fibre	Soluble fibre
<i>Hydroxybenzoic compounds</i>						
Gallic acid	2.54 $\pm$ 0.03	nd	1.07 $\pm$ 0.10	nd	1.75 $\pm$ 0.41	nd
Gallic aldehyde	2.23 $\pm$ 0.06	nd	0.58 $\pm$ 0.03	nd	0.62 $\pm$ 0.00	nd
Protocatechuic acid	4.27 $\pm$ 0.73	nd	1.93 $\pm$ 0.24	nd	2.10 $\pm$ 0.05	nd
Protocatechuic aldehyde	8.84 $\pm$ 1.20	nd	2.27 $\pm$ 0.09	nd	5.69 $\pm$ 0.63	nd
<i>p</i> -Hydroxybenzoic acid	2.48 $\pm$ 0.05	1.27 $\pm$ 0.39	0.85 $\pm$ 0.03	nd	nd	1.27 $\pm$ 0.02
<i>p</i> -Hydroxybenzoic aldehyde	1.45 $\pm$ 0.13	0.77 $\pm$ 0.18	1.80 $\pm$ 0.32	nd	1.11 $\pm$ 0.00	0.62 $\pm$ 0.03
<i>p</i> -vanillin	51.36 $\pm$ 1.32	nd	nd	nd	nd	nd
Vanillic acid	nd	nd	nd	nd	2.25 $\pm$ 0.04	nd
<b>Total</b>	<b>73.2</b>	<b>2.0</b>	<b>8.5</b>	<b>nd</b>	<b>13.5</b>	<b>1.9</b>
<i>Catechins and Procyanidins</i>						
(+)-Catechin-3- <i>O</i> -hexoside	0.84 $\pm$ 0.09	nd	nd	nd	nd	nd
(+)-Catechin	0.53 $\pm$ 0.04	nd	nd	nd	nd	nd
Procyanidin dimer B2	0.49 $\pm$ 0.05	nd	nd	nd	nd	nd
Procyanidin dimer	0.54 $\pm$ 0.02	nd	nd	0.72 $\pm$ 0.18	nd	nd
Procyanidin dimer	nd	nd	nd	1.10 $\pm$ 0.01	nd	nd
Procyanidin dimer	nd	nd	nd	0.68 $\pm$ 0.06	nd	nd
Gallate procyanidin dimer (P <sub>2</sub> G <sub>1</sub> )	nd	nd	nd	0.54 $\pm$ 0.03	nd	nd
<b>Total</b>	<b>2.4</b>	<b>nd</b>	<b>nd</b>	<b>3.0</b>	<b>nd</b>	<b>nd</b>
<i>Flavonols and Flavones</i>						
Kaempferol dihexoside	1.37 $\pm$ 0.20	nd	nd	nd	nd	nd
Kaempferol rutinoside	0.30 $\pm$ 0.10	t	nd	nd	nd	nd
Quercetin-3- <i>O</i> -glucoside	1.00 $\pm$ 0.06	nd	nd	nd	nd	nd
Luteolin rhamnoside-hexoside	0.36 $\pm$ 0.00	nd	nd	nd	nd	nd
Kaempferol rhamnoside dihexoside	nd	nd	0.19 $\pm$ 0.01	nd	2.45 $\pm$ 0.09	nd
Kaempferol-3- <i>O</i> -glucoside	0.61 $\pm$ 0.03	0.56 $\pm$ 0.02	nd	nd	nd	nd
Kaempferol diglucoside	nd	nd	nd	nd	nd	0.51 $\pm$ 0.02
Kaempferol	1.64 $\pm$ 0.42	nd	0.36 $\pm$ 0.07	nd	nd	nd
<b>Total</b>	<b>5.3</b>	<b>0.6</b>	<b>0.5</b>	<b>nd</b>	<b>2.5</b>	<b>0.5</b>

t: traces; nd: not detected.

#### 4. Conclusions

Cooking and germination process resulted in important changes and phenolic distribution within dietary fibre fractions of beans and lentils. A general decrease in the concentration of insoluble and soluble fibre fractions was observed in processed bean and lentil flours, although an increase in the content of insoluble and soluble fibre fractions in sprouts and cooked beans, respectively, was found. Phenolic compounds such as no-flavonoids and flavonoids were identified in dietary fibre fractions in processed beans and lentils. Some compounds identified in dietary fibre fractions could be associated to depolymerisation of the lignin components, such as vanillin identified in IDF in lentils. A general enhancement in the total phenolic concentration was found in IDF in both legumes. Therefore, processing legumes may produce positive changes in the dietary fibre and phenolic compound composition and its association could improve phytochemical and nutritional quality and maximize the health-promoting properties of legumes.

#### Acknowledgements

This study was supported by Ministerio de Ciencia e Innovación (AGL2008-05673-C02-02/ALI). M.D. thanks the Spanish “Ramon y Cajal” Program for financial support.

#### References

- Aguilera, Y., Dueñas, M., Estrella, I., Hernández, T., Benítez, V., Esteban, R. M., et al. (2010). Evaluation of phenolic profile and antioxidant properties of pardina lentil as affected by industrial dehydration. *Journal of Agricultural and Food Chemistry*, 58(18), 10101–10108.
- AOAC. (1995). *Official methods of analysis* (16th ed.). Washington, D.C.: Association of Official Analytical Chemists.
- Arrieta-Baez, D., Dorantes-Alvarez, D., Martinez-Torres, R., Zepeda-Vallejo, G.,

- Jaramillo-Flores, M. E., Ortiz-Moreno, A., et al. (2012). Effect of thermal sterilization on ferulic, coumaric and cinnamic acids: dimerization and antioxidant activity. *Journal of the Science of Food and Agriculture*, 92(13), 2715–2720.
- Benítez, V., Cantera, S., Aguilera, Y., Mollá, E., Esteban, R. M., Diaz, M. F., et al. (2013). Impact of germination on starch, dietary fiber and physicochemical properties in non-conventional legumes. *Food Research International*, 50(1), 64–69.
- Çelik, E. E., Gökmen, V., & Fogliano, V. (2013). Soluble antioxidant compounds regenerate the antioxidants bound to insoluble parts of food. *Journal of Agricultural and Food Chemistry*, 61(43), 10329–10334.
- Chang, H. L., Sang, H. O., Eun, J. Y., & Young, S. K. (2006). Effects of raw, cooked and germinated small black soybean powders on dietary fibre content and gastrointestinal functions. *Food Science and Biotechnology*, 15(4), 635–638.
- Del Rio, D., Rodríguez-Mateos, A., Spencer, J. P. E., Tognolini, M., Borges, G., & Crozier, A. (2013). Dietary (poly)phenolics in human health: structures, bioavailability, and evidence of protective effects against chronic diseases. *Antioxidants & Redox Signaling*, 18(14), 1818–1892.
- Donkor, O. N., Stojanovska, L., Ginn, P., Ashton, J., & Vasiljevic, T. (2012). Germinated grains-sources of bioactive compounds. *Food Chemistry*, 135(3), 950–959.
- Dueñas, M., Hernández, T., Estrella, I., & Fernández, D. (2009). Germination as a process to increase the polyphenol content and antioxidant activity of lupin seeds (*Lupinus angustifolius* L.). *Food Chemistry*, 117(4), 599–607.
- Dueñas, M., Martínez-Villaluenga, C., Limón, R. I., Peñas, E., & Frias, J. (2015). Effect of germination and elicitation on phenolic composition and bioactivity of kidney beans. *Food Research International*, 70, 55–63.
- Ghavidel, R. A., & Prakash, J. (2007). The impact of germination and dehulling on nutrients, antinutrients, in vitro iron and calcium bioavailability and in vitro starch and protein digestibility of some legume seeds. *LWT—Food Science and Technology*, 40(7), 1292–1299.
- Goñi, I., Díaz-Rubio, M. E., Pérez-Jiménez, J., & Saura-Calixto, F. (2009). Towards an updated methodology for measurement of dietary fiber, including associated polyphenols in food and beverages. *Food Research International*, 42(7), 840–846.
- López-Amorós, M. L., El-Nagggar, T., Dueñas, M., Ortega, T., Estrella, Hernández, T., et al. (2013). Effect of cooking and germination on phenolic composition and biological properties of dark beans (*Phaseolus vulgaris* L.). *Food Chemistry*, 138(1), 547–555.
- López-Amorós, M. L., Hernández, T., & Estrella, I. (2006). Effect of germination on legume phenolic compounds and their antioxidant activity. *Journal Food Composition and Analysis*, 19(4), 277–283.
- Mahadevamma, S., & Tharanathan, R. N. (2004). Processing of legumes: resistant starch and dietary fiber contents. *Journal of Food Quality*, 27(4), 289–303.
- Martín-Cabezas, M. A., Aguilera, Y., Benítez, V., Mollá, E., López-Andreu, F. J., & Esteban, R. M. (2006). Effect of industrial dehydration on the soluble carbohydrates and dietary fiber fractions in legumes. *Journal of Agricultural and Food*

- Chemistry*, 54(20), 7652–7657.
- Martín-Cabrejas, M. A., Aguilera, Y., Pedrosa, M. M., Cuadrado, C., Hernández, T., Díaz, S., et al. (2009). The impact of dehydration process on antinutrients and protein digestibility of some legume flours. *Food Chemistry*, 114(3), 1063–1068.
- Martín-Cabrejas, M. A., Díaz, M. F., Aguilera, Y., Benítez, V., Mollá, E., & Esteban, R. M. (2008). Influence of germination on the soluble carbohydrates and dietary fibre fractions in non-conventional legumes. *Food Chemistry*, 107(3), 1045–1052.
- Martín-Cabrejas, M. A., Sanfiz, B., Vidal, A., Molla, E., Esteban, R., & Lopez-Andreu, F. J. (2004). Effect of fermentation and autoclaving on dietary fiber fractions and anti-nutritional factors of beans (*Phaseolus vulgaris* L.). *Journal of Agricultural and Food Chemistry*, 52(2), 261–266.
- Masood, T., Shah, H. U., & Zeb, A. (2014). Effect of sprouting time on proximate composition and ascorbic acid level of mung bean (*Vigna radiata* L.) and chickpea (*Cicer Arietinum* L.) seeds. *The Journal of Animal & Plant Sciences*, 24(3), 850–859.
- Pérez-Jiménez, J., Serrano, J., Tabernero, M., Arranz, S., Díaz-Rubio, M. E., García-Diz, L., et al. Saura-Calixto, F. (2008). Effects of grape antioxidant dietary fiber on cardiovascular disease risk factors. *Nutrition*, 24(7–8), 646–653.
- Pérez-Jiménez, Serrano, J., Tabernero, M., Arranz, S., Díaz-Rubio, E., García-Diz, L., et al. Saura-Calixto, F. (2009). Bioavailability of phenolic antioxidants associated with dietary fiber: plasma antioxidant capacity after acute and long-term intake in humans. *Plant Foods for Human Nutrition*, 64(2), 102–107.
- Philips, G. O. (2013). Dietary fibre: a chemical category or a health ingredient? *Bioactive Carbohydrates and Dietary Fibre*, 1(1), 3–9.
- Pujolá, M., Farreras, A., & Casañas, F. (2007). Protein and starch content of raw, soaked and cooked beans (*Phaseolus vulgaris* L.). *Food Chemistry*, 102(4), 1034–1041.
- Saulnier, L., Sado, P. E., Branlard, G., Charmet, G., & Guillon, F. (2007). Wheat arabinoxylans: exploiting variation in amount and composition to develop enhanced varieties. *Journal of Cereal Science*, 46(3), 261–281.
- Saura-Calixto, F. (2011). Dietary fiber as a carrier of dietary antioxidants: an essential physiological function. *Journal of Agricultural and Food Chemistry*, 59(1), 43–49.
- Saura-Calixto, F., & Díaz-Rubio, M. E. (2007). Polyphenols associated with dietary fibre in wine: a wine polyphenols gap? *Food Research International*, 40(5), 613–619.
- Świeca, M., Gawlik-Dziki, U., Kowalczyk, D., & Złotek, U. (2012). Impact of germination time and type of illumination on the antioxidant compounds and antioxidant capacity of *Lens culinaris* sprouts. *Scientia Horticulturae*, 140(1), 87–95.
- Thériault, M., Caillet, S., Kermasha, S., & Lacroix, M. (2006). Antioxidant, antiradical and antimutagenic activities of phenolic compounds present in maple products. *Food Chemistry*, 98(3), 490–501.
- Vanbeneden, N., Gils, F., Delvaux, F., & Delvaux, F. R. (2008). Formation of 4-vinyl and 4-ethyl derivatives from hydroxycinnamic acids: occurrence of volatile phenolic flavour compounds in beer and distribution of Pad1-activity among brewing yeast. *Food Chemistry*, 107(1), 221–230.
- Vaz-Patto, M., Amarowicz, R., Aryee, A. N. A., Boye, J. I., Chung, H. J., Martín-Cabrejas, M. A., et al. (2015). Achievements and challenges in improving the nutritional quality of food legumes. *Critical Reviews in Plant Sciences*, 34(1–3), 105–143.
- Wang, N., Hatcher, D. W., & Gawalko, E. J. (2008). Effect of variety and processing on nutrients and certain anti-nutrients in field peas (*Pisum sativum*). *Food Chemistry*, 111(1), 132–138.
- Wang, N., Hatcher, D. W., Toews, R., & Gawalko, E. J. (2009). Influence of cooking and dehulling on nutritional composition of several varieties of lentils (*Lens culinaris*). *LWT—Food Science and Technology*, 42(4), 842–848.
- Wang, N., Hatcher, D. W., Tyler, R. T., Toews, R., & Gawalko, E. J. (2010). Effect of cooking on the composition of beans (*Phaseolus vulgaris* L.) and chickpeas (*Cicer arietinum* L.). *Food Research International*, 43(2), 589–594.



## Optimization and rheological properties of chicken ball as affected by $\kappa$ -carrageenan, fish gelatin and chicken meat



Hazmi Yasin\*, Abdul Salam Babji, Hidayah Ismail

School of Chemical Sciences and Food Technology, Faculty of Science and Technology, Universiti Kebangsaan Malaysia, 43600 Bangi, Selangor, Malaysia

### ARTICLE INFO

#### Article history:

Received 23 May 2015

Received in revised form

3 October 2015

Accepted 5 October 2015

Available online 13 October 2015

#### Keywords:

Optimization

Chicken ball

Carrageenan

Gelatin

Meat concentration

### ABSTRACT

A Central Composite Rotatable Design (CCRD) was adopted in the optimization of chicken ball with the addition of fish gelatin (1–5 g/100 ml), carrageenan (1–4 g/100 ml), and chicken breast meat (55–65 g/100 g) on textural properties (hardness, elasticity, cohesiveness, and chewiness), cooking gain, and water holding capacity (WHC). For each response, a second-order polynomial model was developed using multiple linear regression analysis. Applying desirability function method, optimum conditions for chicken ball were found to be carrageenan concentration of 1.28 g/100 ml, fish gelatin concentration of 4.62 g/100 ml, and chicken meat concentration of 60.52 g/100 g. At this optimum point, hardness, elasticity, cohesiveness, chewiness, cooking gain, and WHC were found to be 62.59 N, 0.79 mm, 0.625, 30.495 N mm, 106.345, and 5.14 g/100 g, respectively.  $G'$  value of control on dynamic rheological properties was the highest among chicken ball samples with addition of carrageenan and gelatin. The higher the mixture concentrations of carrageenan, gelatin and meat, the higher  $G'$  value of chicken ball.

© 2015 Elsevier Ltd. All rights reserved.

### 1. Introduction

Today's consumers are health and nutrition-conscious and tend to avoid food products with high fat content. Comminuted meat products contained approximately 20–30 g/100 g fat; therefore it is essential for the meat industry to reduce the fat contents of their products (Candogan & Kolsarici, 2003).

Biopolymers or hydrocolloids are in general used in a variety of applications as thickeners, stabilisers, fat substitute, taste release and structural components. In food applications biopolymers will be mixed with fat, minerals, vitamins and water, and there is usually more than one type of biopolymer present in a product. Mixed biopolymer systems are important because physical properties can be more finely controlled. When biopolymers or polyelectrolytes are mixed it is accepted that the systems will phase separate. Oppositely charged polyelectrolytes will associate into complexes, while equally charged polyelectrolytes will segregate into different phases (Piculell, Bergfeldt, & Nilsson, 1995). When these systems gel, complex morphologies can be developed, as described by Morris (1986) and Tolstoguzov and Braudo (1983).

Addition of hydrocolloids such as gelatin, carrageenan and

pectin in meat products, such as chicken ball, would result in beneficial outcome. These hydrocolloids have been widely used singly or as mixtures in a variety of meat products to improve the quality especially the textural and rheological characteristics related to sensory acceptance. Mixtures of hydrocolloids are commonly used to impart novel and improved rheological characteristics to food products and added benefits include fat reduction and reduction in costs. The nature of the synergy can be due to association of the different hydrocolloid molecules. If two hydrocolloids associate then precipitation or gelation can occur (Phillips & Williams, 2009). Oppositely charged hydrocolloids are likely to associate and form a precipitate while there is evidence to show that for some stiff polysaccharide molecules association results in gel formation.

By mixing fish gelatin and kappa-carrageenan one might be able to identify new and improved gelling systems (Haug, Draget, & Smidsrod, 2003). Before such a system can be developed and commercialized it is important to know the behavior of the mixtures with different composition in meat products (chicken ball).

Finding the optimum critical values of the processing variables that maximize the mixture of hydrocolloids properties should be a high priority process. Response Surface Methodology has been reported to be an effective and powerful tool for optimization of a process when the independent variables have a combined effect on the desired response. RSM is a collection of statistical and

\* Corresponding author.

E-mail address: [hzm111@gmail.com](mailto:hzm111@gmail.com) (H. Yasin).

mathematical system that has been successfully used for developing, improving and optimizing such processes (Bostan, Razavi, & Farhoosh, 2008; Cui, Mazza, Oomah, & Billiaderis, 1994; Koocheki et al., 2008; Myers & Montgomery, 1995; Sariçoban, Yilmaz, & Karakaya, 2009; Wu, Cui, Tang, & Gu, 2007).

This research is proposed to study the optimization of the synergistic effects of the selected hydrocolloids (fish gelatin and  $\kappa$ -carrageenan) in improving the quality of the processed meat products (chicken ball), resulting in a novel range of gelled comminuted meat system replacing typical meat emulsions. The rheological properties of chicken ball with various concentrations of  $\kappa$ -carrageenan and fish gelatin are also studied to evaluate the dynamic rheological properties of chicken ball with the addition of  $\kappa$ -carrageenan, fish gelatin and meat concentrations.

## 2. Materials and methods

### 2.1. Materials

All the biopolymers were food grade samples. Fish gelatin samples were a first-extract acid-process sample obtained from skin of freshwater fish species and provided by Bagus baking solutions center, Malaysia. The kappa-carrageenan ( $\kappa$ -carrageenan) sample was kindly provided by R&M Chemical, Essex, UK. The  $\kappa$ -carrageenan was contained breaking strength 780–880 g, syneresis >1.0 g/100 g, pH (0.5 g/100 ml solution) 7–10, loss on drying >12.0 g/100 g, aerobic plate count 5000 CFU/g, and yeast and mould 200 CFU/g.

### 2.2. Chicken balls preparation

Chicken breast meat is the main ingredient in the production of chicken balls. Frozen chicken breast meat was purchased from the Econ Save market in Selangor, Malaysia. Meat and chicken fat were ground, weighed and kept in the chiller ( $5 \pm 1^\circ\text{C}$ ) until processing time. Food ingredients such as salt (1 g/100 g), soy protein isolate (ISP) (4.5 g/100 g), potato starch (3 g/100 g), carrageenan (1–4 g/100 ml), and gelatin (1–5 g/100 ml) were weighed according to the specified composition before processing carried out. The minced meat (55–65 g/100 g), ice water (3.9–20.9 g/100 g), ISP and salt were mixed together in mixer (National Model MK-K77, Tokyo, Japan) for 1 min. After that chicken and shortening (15 g/100 g) were put into the batter and mixed for 30 s. Finally, carrageenan and gelatin were mixed for 30 s until the batter was well mixed. The batter was shaped into balls and cooked in water at a temperature of 90–95 °C for 5 min.

### 2.3. Texture profile analysis (TPA)

After cooking (90–95 °C) and cooling to room temperature (22 °C), three whole chicken balls of 5.5 mm diameter and 2.5 cm height were subjected to texture profile analysis using the texture analyzer AGS-J 500N (Shimadzu, Japan) as described by Bourne (2002). The chicken ball was placed on the platform of the texture analyzer. A cylinder plunger of 6 mm diameter was attached to a 50 kg load cell and the sample was compressed to 75% of its original height at a cross head speed of 60 mm/min, twice in two cycles. The following parameters were employed:

Hardness (N): breaking force of the product at the first loading cycle in texture profile analysis,

Cohesiveness: the ratio of storage work to total work in the second loading cycle in texture profile analysis.

Elasticity (mm): the ratio of storage deformation to total deformation in the second loading cycle in texture profile analysis.

Chewiness (N mm): hardness  $\times$  cohesiveness  $\times$  elasticity.

### 2.4. Cooking gain

Cooking gain of chicken ball was determined from the known weight of chicken ball before and after cooking (AOAC, 1995).

### 2.5. Water holding capacity (WHC)

A centrifuge technique was used to determine water holding capacity (WHC) of cooked chicken balls with slight modification. About 10 g of chicken ball sample was centrifuged at  $12,000 \times g$  for 30 min at 4 °C. Lower values indicate better WHC (Serदारoglu, Yıldız-Turp, & Abrodímov, 2005). Values of WHC were based on ratio between weight before centrifuge ( $W_1$ ) and weight after centrifuge ( $W_2$ )  $((W_1 - W_2)/W_1) \times 100$  (Ramírez, DelÁngel, Uresti, Velazquez, & Vazquez, 2007).

### 2.6. Dynamic rheological properties

The rheological behavior of the fish gelatin and  $\kappa$ -carrageenan mixture in chicken ball was characterized using a Physica MCR 501 (Anton Paar Shape Tech GmbH, Austria) using a cone-plate geometry (0.01 mm gap).

Temperature ramps was run over the range from 20 °C to 90 °C with constant strain amplitude of 10% chosen from the linear viscoelastic region of the samples at 1 Hz. Storage modulus ( $G'$ ) as a function of heating temperature was recorded as described by Li-kang et al. (2013) with slight modification.

### 2.7. Response surface methodology (RSM)

Central Composite Rotatable Design (CCRD) was adopted in the optimization of chicken ball with the addition of gelatin and carrageenan with various concentrations. CCRD in the experimental design consists of  $2^3$  factorial points. Carrageenan concentration (g/100 ml,  $X_1$ ), gelatin concentration (g/100 ml,  $X_2$ ) and meat concentration (g/100 g,  $X_3$ ) were chosen as independent variables. The range and central point values of these three independent variables were based on the results of preliminary experiments (Table 1). The hardness (N,  $Y_1$ ), elasticity (mm,  $Y_2$ ), cohesiveness ( $Y_3$ ), chewiness (N.mm,  $Y_4$ ), cooking gain (g/100 g,  $Y_5$ ), and Water Holding Capacity (WHC) (g/100 g,  $Y_6$ ) were selected as the dependent variables for the combination of the independent variables (Table 2).

The Response Surface Methodology (RSM) with Central Composite Rotatable Design (CCRD) was analyzed using Design Expert 7 (Stat-Ease Inc., USA). Where  $Y$  is the dependent variable (hardness, elasticity, cohesiveness, chewiness, cooking gain, and WHC),  $\beta_0$  is the constant,  $\beta_i$ ;  $\beta_{ii}$  and  $\beta_{ij}$  are regression coefficients and  $X_i$ ,  $X_j$  are levels of the independent variables. The  $R^2$  value and the lack of fit value were determined.

$$Y = \beta_0 + \sum_{i=1}^3 \beta_i X_i + \sum_{i=1}^3 \beta_{ii} X_i^2 + \sum_{i=1}^2 \sum_{j=i+1}^3 \beta_{ij} X_i X_j$$

After the multifactor analysis of variance and the second-order model prediction determinations, the optimal pre-treatment condition was obtained by the desirability function approach and the response surface plots were developed using Design Expert 7 (Stat-Ease Inc., USA).

Based on the experimental design suggested by Design-Expert® Software version 7, 16 runs with 2 blocks of experiments were conducted. Experimental results of the 3-factors, 5-levels central composite design are shown in Table 2. The response surface

**Table 1**

Experimental range and values of the independent process variables in the design for processing of chicken ball.

Independent variables	Symbol	Coded levels				
		–1.414	–1	0	1	1.414
Carrageenan concentration (g/100 ml)	X <sub>1</sub>	0.38	1	2.5	4	4.62
Gelatin concentration (g/100 ml)	X <sub>2</sub>	0.17	1	3	5	5.83
Meat concentration (g/100 g)	X <sub>3</sub>	52.93	55	65	65	67.07

**Table 2**

Responses of dependent variables for production of chicken ball.

Exp no	Variable levels			Responses					
	X <sub>1</sub>	X <sub>2</sub>	X <sub>3</sub>	Y <sub>1</sub>	Y <sub>2</sub>	Y <sub>3</sub>	Y <sub>4</sub>	Y <sub>5</sub>	Y <sub>6</sub>
1	–1.000	–1.000	–1.000	57.6	0.74	0.66	30.29	111.8	0.994
2	0.000	0.000	0.000	62.65	0.88	0.56	30.37	106.5	6.039
3	1.000	1.000	–1.000	49.37	0.88	0.42	18.64	102.4	0.892
4	0.000	0.000	0.000	57.6	0.84	0.57	28.81	103.6	3.175
5	1.000	–1.000	1.000	77.1	0.73	0.63	45.14	104.6	10.02
6	–1.000	1.000	1.000	55.44	0.79	0.59	20.13	104.3	2.786
7	0.000	0.000	0.000	59.70	0.79	0.56	28.66	106.8	1.497
8	0.000	0.000	0.000	67.40	0.82	0.61	35.5	108.6	0.595
9	0.000	0.000	–1.414	58.77	0.63	0.55	23.76	108.8	2.487
10	0.000	0.000	1.414	56.25	0.81	0.59	30.51	105.6	3.276
11	0.000	–1.414	0.000	39.75	0.78	0.39	10.38	105.4	1.186
12	–1.414	0.000	0.000	32.80	0.82	0.53	14.88	105	3.708
13	1.414	0.000	0.000	70.30	0.79	0.62	34.93	109.9	2.167
14	0.000	0.000	0.000	63.72	0.78	0.58	30.38	108.4	1.161
15	0.000	0.000	0.000	43.58	0.79	0.48	15.58	108.1	1.980
16	0.000	1.414	0.000	79.25	0.85	0.67	40.84	109.8	3.128

Y<sub>1</sub>: hardness; Y<sub>2</sub>: elasticity; Y<sub>3</sub>: cohesiveness; Y<sub>4</sub>: chewiness; Y<sub>5</sub>: cooking gain and Y<sub>6</sub>: WHC.

regression (RSREG) procedure for Design-Expert® software was employed to fit the quadratic polynomial equation to the experimental data.

### 3. Results and discussion

The R<sup>2</sup> values of models for this study were higher than 0.70, indicating a good fit, as shown in Table 3. All of the lacks of fit tests were not significant, which also showed a good fit between the experimental data and the model. The R<sup>2</sup> value reflects the suitability of the model to represent the real relationship between the selected reaction parameters. Many statistical analyses were used for fitting the model, to judge the experimental error, the statistical significance of the terms in the model, and the suitability of the model (Sanaei, Mahmoodani, See, Yusop, & Babji, 2013). However, there is no reference value stating that higher R<sup>2</sup> suggests a good model and lower R<sup>2</sup> suggests a poor model.

According to the analysis of variance (ANOVA), models were significant on different characteristics of chicken ball with the addition of various concentrations of carrageenan, gelatin and meat concentration. In many studies, the optimum point was determined based on the highest desirability to the responses. The input to the procedure was the range of process parameters as used in experimental runs, whereas the target factors were chosen as the minimized condition for carrageenan, maximized condition for gelatin, and in range condition for meat concentration. The reason of the variables were to be maximized, minimized or in range in order to know what the “best” proportions of the factors are so as to maximize (or minimize) a response.

On this study, the analysis indicated that optimum value for the responses of chicken ball processing with the addition of carrageenan and gelatin can be achieved using a carrageenan concentration of 1.28 g/100 ml, gelatin concentration of 4.62 g/100 ml and

meat concentration of 60.52 g/100 g. The responses for hardness, elasticity, cohesiveness, chewiness, cooking gain and WHC, were predicted at 62.59 N; 0.79 mm; 0.625; 30.495 N mm; 106.345 g/100 g; and 5.14 g/100 g respectively, with a desirability value of 1. The desirability value of 1 or close to 1 indicated that the setting seems to achieve favorable results for all responses as a whole.

#### 3.1. Texture profile analysis (TPA)

Figs. 1 and 2 illustrate the effects of carrageenan, gelatin and meat concentrations as three-dimensional graphs where direction of these effects can be seen. Fig. 1(A) and (D) indicates that increasing carrageenan and gelatin concentrations level increased ( $P \leq 0.05$ ) hardness and chewiness values where meat concentration was left to be constant at 60 g/100 g.

As stated before, optimal conditions for each response on this study had been determined. Fig. 1(A) and (D) show the response surface for the interaction between carrageenan concentration and gelatin concentration at constant meat concentration (60 g/100 g). For Fig. 1(A), hardness increased when concentration of gelatin increased up to optimum point at each of carrageenan concentration. Similar condition appeared on chewiness. Somboon, Karrila, Kaewmanee, & Karrila, 2014 reported when concentration of fish gelatin increased, hardness and elasticity of both fish gelatin and  $\kappa$ -carrageenan increased significantly. Yi, Kim, Bae, Whiteside, and Park (2006) and Pranoto, Lee, and Park (2007) also reported that gel strength (hardness) can be improved by mixing with enzymic modification and suitable gelling agent such as  $\kappa$ -carrageenan. Serdaroglu et al. (2005) stated that the textural properties in comminuted meat proteins could be affected by the degree of the extraction of myofibrillar protein, stromal protein content, the degree of comminuting and the types and levels of non-meat ingredients such as fat and starch.

#### 3.2. Cooking gain and WHC

Cooking gain is the most important factor for the meat industry in predicting the behavior of products during cooking due to non-meat ingredients or other factors (Pietrasik & Li-Chan, 2002). In this study, the results have high cooking gain (due to the weight of after cooking being more than the weight of before cooking, cooking gain results then multiply with 100). The average results of cooking gain (g/100 g) are presented in Fig. 2(A). On Fig. 2(A), cooking gain decreased when gelatin and carrageenan concentrations increased where meat concentration was left to be constant at 60 g/100 g. The highest cooking gain value in this study occurred at the lowest concentration of carrageenan, gelatin and meat (1 g/100 ml carrageenan, 1 g/100 ml gelatin and 55 g/100 g meat concentration).

Gelatin has the property to absorb all liquid. Pietrasik (2003) stated that addition of  $\kappa$ -carrageenan significantly decreased the percentage of water loss indicating that the hydrocolloid improved water retention of meat gels. The formulations containing gelatin has interior micelles in the chicken ball that can hold water and maintain the juiciness of chicken balls. As seen in Fig. 2(B), WHC

**Table 3**  
Response surface model for processing condition of chicken ball.

Response	Model equation	Model significance	Lack of fit	R <sup>2</sup>
Hardness	<u>Coded equation</u> 58.40 + 13.26X <sub>1</sub> + 13.97X <sub>2</sub> - 0.89X <sub>3</sub> - 7.28X <sub>12</sub> + 21.44X <sub>13</sub> + 9.90X <sub>23</sub>	0.0113 <sup>a</sup>	0.9112 <sup>b</sup>	0.8209
	<u>Actual equation</u> 614.80 - 155.38X <sub>1</sub> - 46.35X <sub>2</sub> - 10.29X <sub>3</sub> - 2.43X <sub>12</sub> + 2.85X <sub>13</sub> + 0.10X <sub>23</sub>			
Elasticity	<u>Coded equation</u> 0.82 - 0.011X <sub>1</sub> + 0.025X <sub>2</sub> + 0.064X <sub>3</sub> - 1.687E-003X <sub>11</sub> + 3.313E-003X <sub>22</sub> - 0.0044X <sub>33</sub> + 0.089X <sub>12</sub> - 0.025X <sub>13</sub> - 0.031X <sub>23</sub>	0.0443 <sup>a</sup>	0.5924 <sup>b</sup>	0.9012
	<u>Actual equation</u> 7.16 + 0.11X <sub>1</sub> + 0.11X <sub>2</sub> + 0.02X <sub>3</sub> - 7.49774E-004X <sub>11</sub> + 8.28252E-004X <sub>22</sub> - 1.76748E-003X <sub>33</sub> + 0.029547X <sub>12</sub> - 3.36684E-003X <sub>13</sub> - 3.06066E-003X <sub>23</sub>			
Cohesiveness	<u>Coded equation</u> 0.56 + 0.032X <sub>1</sub> + 0.099X <sub>2</sub> + 0.014X <sub>3</sub> - 0.021X <sub>12</sub> + 0.17X <sub>13</sub> + 0.082X <sub>23</sub>	0.0037 <sup>a</sup>	0.8734 <sup>b</sup>	0.8674
	<u>Actual equation</u> 4.99 - 1.30X <sub>1</sub> - 0.42X <sub>2</sub> - 0.07X <sub>3</sub> - 6.95262E-003X <sub>12</sub> + 0.02X <sub>13</sub> + 8.18198E-003X <sub>23</sub>			
Chewiness	<u>Coded equation</u> 27.58 + 7.09X <sub>1</sub> + 10.77X <sub>2</sub> + 2.39X <sub>3</sub> - 1.70X <sub>12</sub> + 19.93X <sub>13</sub> + 3.75X <sub>23</sub>	0.0085 <sup>a</sup>	0.9950 <sup>b</sup>	0.8345
	<u>Actual equation</u> 432.89 - 153.04X <sub>1</sub> - 15.69X <sub>2</sub> - 7.29X <sub>3</sub> - 0.56X <sub>12</sub> + 2.65X <sub>13</sub> + 0.37X <sub>23</sub>			
Cooking gain	<u>Coded equation</u> 106.75 + 1.73X <sub>1</sub> + 1.56X <sub>2</sub> - 1.13X <sub>3</sub> + 0.20X <sub>12</sub> + 3.99X <sub>13</sub> + 4.03X <sub>23</sub>	0.0012 <sup>a</sup>	0.8653 <sup>b</sup>	0.9012
	<u>Actual equation</u> 267.97 - 30.96X <sub>1</sub> - 23.58X <sub>2</sub> - 2.76X <sub>3</sub> + 0.06X <sub>12</sub> + 0.53X <sub>13</sub> - 0.40X <sub>23</sub>			
WHC	<u>Coded equation</u> 2.91 - 0.54X <sub>1</sub> + 0.69X <sub>2</sub> + 0.28X <sub>3</sub> - 2.45X <sub>12</sub> + 2.52X <sub>13</sub> - 2.33X <sub>23</sub>	0.0221 <sup>a</sup>	0.7929 <sup>b</sup>	0.7847
	<u>Actual equation</u> 1.81 - 18.08X <sub>1</sub> + 16.36X <sub>2</sub> - 0.08X <sub>3</sub> - 0.82X <sub>12</sub> + 0.34X <sub>13</sub> - 0.23X <sub>23</sub>			

<sup>a</sup> Significant ( $p \leq 0.05$ ).

<sup>b</sup> Not significant ( $p \geq 0.05$ ).

decreased when gelatin concentration increased up to optimum point at each carrageenan concentration. But subsequently, decreased in gelatin and carrageenan showed a slight increase in WHC.

The result in this study is high cooking gain. This result indicates that during cooking, some of the moisture is lost, but due to the ability of  $\kappa$ -carrageenan and gelatin to absorb water during cooking, it has resulted high cooking gain in chicken ball. Moreover, this cooking gain in this study was also the highest (>100 g/100 g) when compared with the cooking gains of meatballs containing legume flours as extenders: 93.2 g/100 g (lentil flour), 92.8 g/100 g (black eye bean flour), 88.6 g/100 g (chickpea flour) and 85.2 g/100 g (rusk) (Serdaroglu et al., 2005). This result was also higher when compared with the cooking gain of meatballs prepared using wheat flour, whey protein concentrate and soy protein isolate and their effect on the oxidative processes and textural properties of cooked meatballs, as reported by Ulu (2004).

Ulu (2006) in his previous study reported that gain was significantly higher for the carrageenan series. Particularly in the low fat meatballs with added carrageenan, gain and fat retention were higher ( $p < 0.05$ ). Meanwhile Bater, Descamps, and Maurer (1993) reported that addition of 0.5 g/100 ml  $\kappa$ -carrageenan to a restructured turkey meat significantly increased product gain.

### 3.3. Dynamic rheological properties

Study for dynamic rheological test has been used extensively for heat-induced gelation of myofibrillar proteins (Hamann, 1992; Visessanguan, Ogawa, Nakai, & An, 2000). Changes in the storage modulus ( $G'$ ) of the chicken ball during heating were determined for the preparations having different ratios of gelatin and carrageenan (Figs. 3 and 4). Elastic modulus (storage modulus,  $G'$ ) value in this study was higher than loss modulus ( $G''$ ). If  $G'$  is much greater than  $G''$ , the material will behave more like a solid; that is, the deformations will be essentially elastic. However, if  $G''$  is much greater than  $G'$ , the energy used to deform the material is

dissipated viscously and the material's behavior is liquid-like (Rao, 1999, chap. 3 and 5).

Elastic modulus can be used to measure increase indicates of the formation of elastic gel network (Tahergorabi, Sivanandan, & Jaczynski, 2012; Venugopal et al., 2002). In Fig. 3,  $G'$  showed a typical initial decrease to about 45 °C, slight increase at 45–50 °C and followed by a rapid increase to about 85 °C and stabilization for control (chicken breast meat). For gelatin (3 g/100 ml fish gelatin concentration with 60 g/100 g chicken breast meat concentration) and carrageenan (2.5 g/100 ml  $\kappa$ -carrageenan with 60 g/100 g chicken breast meat concentration),  $G'$  showed a typical initial decrease to about 55 °C and followed by increase to about 80 °C for gelatin and 85 °C for carrageenan (Fig. 3). The increase at 45–55 °C indicates the initial stages of gel network formation due to partial un-folding of myosin (Sano, Noguchi, Tsuchiya, & Matsumoto, 1988). Similar results have been reported by Xiong and Brekke (1990) and Li-kang et al. (2013), who found that gelation was initiated at 45–50 °C being dependent upon protein-protein interaction. This study showed that generally  $G'$  value of carrageenan was higher than  $G'$  value of gelatin.

Similar results also occurred when chicken ball (55 g/100 g and 60 g/100 g chicken breast meat) was added with carrageenan and gelatin at various concentrations (Fig. 4). All mixtures showed a typical initial decrease of  $G'$  to about 45–55 °C except for M2. Mixture of M2 showed initial decrease of  $G'$  to about 60 °C and also has lower  $G'$  values than M1, M3 and M4. The lowest value of  $G'$  occurred at initial decrease was M5, but at rapid increase of  $G'$  from 55 to 90 °C,  $G'$  values of M5 were higher than M1 and M2 which much higher in carrageenan and gelatin concentrations.

Egelandsdal, Martinsen, and Autio (1995) reported that a decrease on  $G'$  value is a temperature where protein denaturation occurred. The  $G'$  values increase markedly from 60 °C to 80 °C, where the major transition from 60 °C was due to protein aggregation and gelation (Owen, Tung, & Paulson, 1992). This is evidence of the transformation from a viscous sol to an elastic gel network (Alvarez, Xiong, Castillo, Payne, & Garrido, 2012; Cofrades, Serrano,

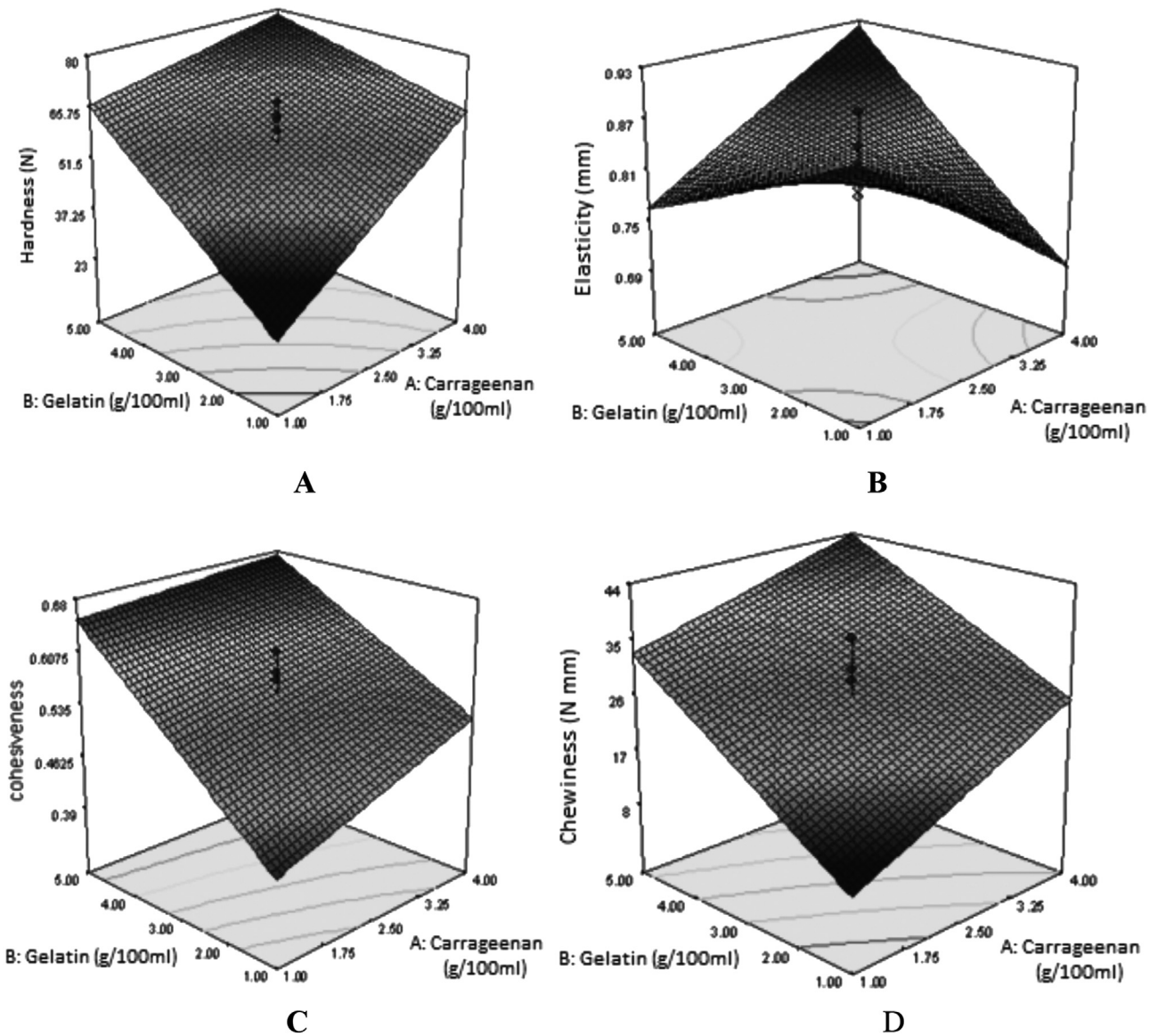


Fig. 1. Effect of carrageenan concentration, gelatin concentration and meat concentration on: (A) hardness; (B) elasticity; (C) cohesiveness; and (D) chewiness of chicken ball.

Ayo, Carballo, & Jimenez-Colmenero, 2008). A high  $G'$  usually indicates that the product more rigid and less ductile, whereas a low  $G'$  indicates a soft texture (Li Kang et al., 2013).

Carrageenan and gelatin are known to have a strong, rigid gel (high elastic modulus) which adopt a disordered conformation at high temperatures but on cooling undergo a conformation change and stiff ordered helices are formed which self-associate to form a gel (Vasile & Zaikov, 2009).

In this study (Fig. 4), M4 was the highest value of  $G'$ . It can be seen from 20 to 70 °C that generally the higher the mixture concentrations of carrageenan, gelatin and meat, the higher  $G'$  values. All mixtures weakened as the temperature increase (until 55 °C). For M1 which has high carrageenan concentration (4 g/100 ml) and gelatin concentration (5 g/100 ml) but low in meat concentration (55 g/100 g),  $G'$  values was higher at 20–60 °C than M2, M3 and M5, but then  $G'$  values lower than M3 and M5 at 60–90 °C. Michon, Cuvelier, Launay, and Parker (1996) correlated the temperature increase on  $G'$  of iota carrageenan and gelatin mixture, whereas the temperature increased, the system (iota-carrageenan and gelatin mixture) weakened regularly and at all higher temperatures,  $G'$  for

the mixture were higher than for either of the biopolymers alone.

In general, the maximum  $G'$  value of all chicken ball samples was found above 75 °C where the value did not exceed 30 kPa. The highest  $G'$  value occurred when there were no carrageenan and gelatin added. Addition of various concentrations of carrageenan and gelatin made the chicken ball samples become less rigid and tender.

#### 4. Conclusions

It is noted that gelatin and carrageenan are hydrocolloid which formed defined structures that undergo various changes during cooking and freezing, resulting in different cooking gain, texture profile analysis values (hardness, elasticity, cohesiveness and chewiness), WHC, and rheological properties of chicken ball. Results in this study showed that the effects of carrageenan, gelatin, and meat concentrations were statistically significant for optimization of chicken ball, improving the quality of the processed meat product (chicken ball). Second-order polynomial models were obtained for predicting texture profile analysis (hardness, elasticity,

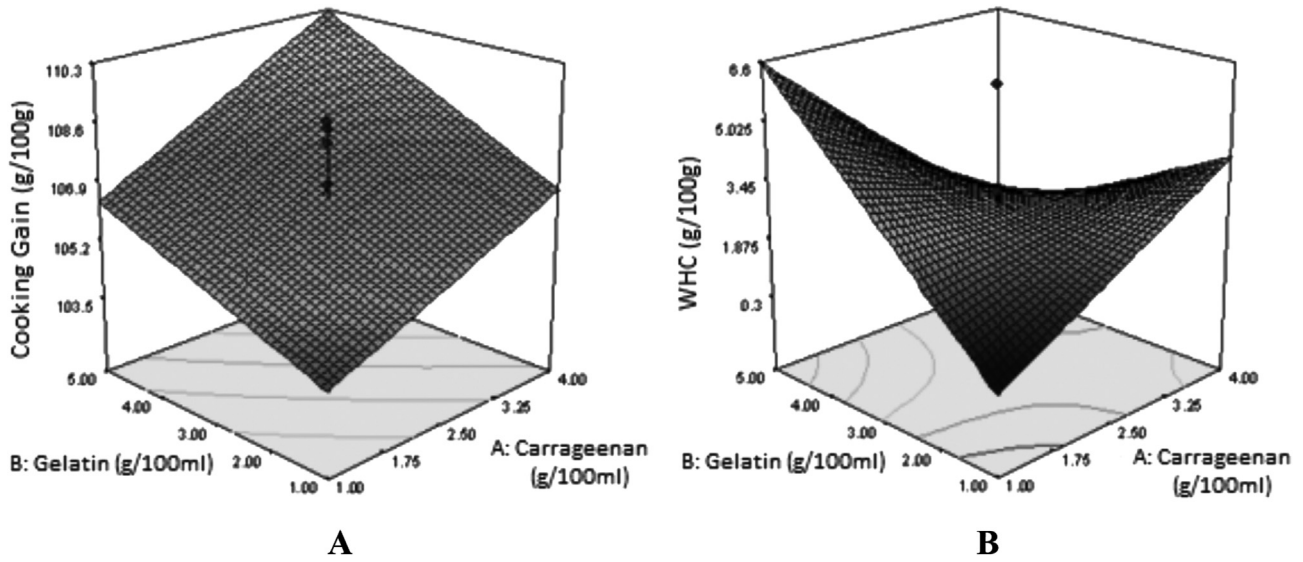


Fig. 2. Effect of carrageenan, gelatin concentration and meat concentration on: (A) cooking gain and (B) WHC.

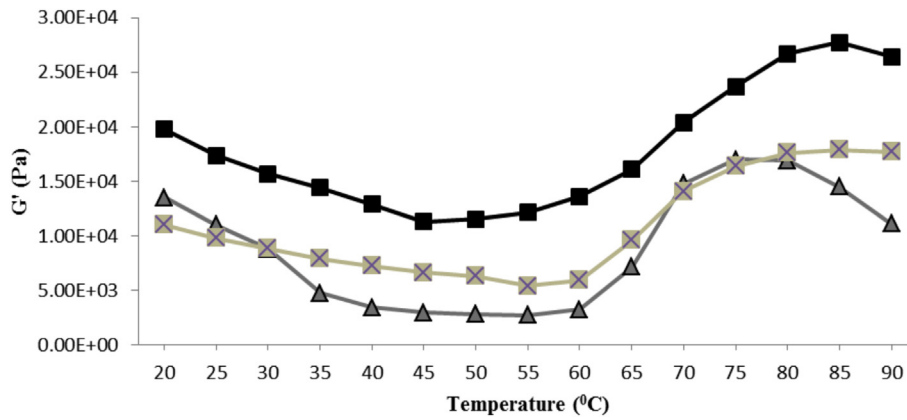


Fig. 3. Changes in dynamic storage modulus ( $G'$ , Pa) and temperature ( $T$ , °C) for each of the different carrageenan and gelatin concentrations on chicken ball (60 g/100 g chicken breast meat). C: carrageenan & G: gelatin. ■ control, ▲ 3 g/100 ml gelatin and ✕ 2.5 g/100 ml carrageenan.

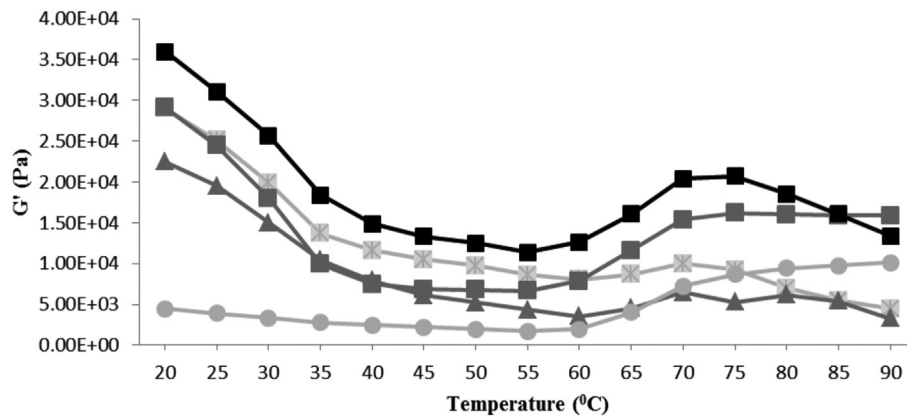


Fig. 4. Changes in dynamic storage modulus ( $G'$ , Pa) and temperature ( $T$ , °C) for each of the different carrageenan, gelatin and meat concentrations on chicken ball. — M1 (C: 4 g/100 ml; G: 5 g/100 ml & M: 55 g/100 g), — M2 (C: 2.5 g/100 ml; G: 3 g/100 ml & M: 60 g/100 g), — M3 (C: 2.5 g/100 ml; G: 5.83 g/100 ml & M: 60 g/100 g), — M4 (C: 4.62 g/100 ml; G: 3 g/100 ml & M: 60 g/100 g), & — M5 (C: 1 g/100 ml; G: 1 g/100 ml & M: 55 g/100 g). C: carrageenan, G: gelatin & M: meat.

cohesiveness, and chewiness), cooking gain, and WHC. Optimum conditions for chicken ball with addition of carrageenan, gelatin, and chicken meat would be as follows: carrageenan concentration 1.28 g/100 ml, gelatin concentration 4.62 g/100 ml, and meat concentration 60.52 g/100 g. For dynamic rheological properties,  $G'$  value of control on dynamic rheological properties was the highest among chicken ball samples with addition of carrageenan and gelatin alone. The higher the mixture concentrations of carrageenan, gelatin and meat, the higher  $G'$  value of chicken ball.

## Acknowledgments

The authors are grateful to UKM-GUP-2011-196 (Malaysia) for the financial support of this work.

## References

- Alvarez, D., Xiong, Y. L., Castillo, M., Payne, F. A., & Garrido, M. D. (2012). Textural and viscoelastic properties of pork frankfurters containing canola-olive oils, rice bran, and walnut. *Meat Science*, 92, 8–15.
- AOAC. (1995). *Official method of analysis* (16th ed.). Washington, DC: Association of the Official Analytical Chemists.
- Bater, B., Descamps, O., & Maurer, A. J. (1993). Quality characteristics of hydrocolloid added oven-roasted turkey breasts. *Poultry Science*, 72, 349–354.
- Bostan, A., Razavi, S. M. A., & Farhoosh, R. (2008). *Optimization of extraction process of crude hydrocolloid from wild sage seed (Salvia macrosiphon) and evaluation of its time-independent rheological properties*. MSc thesis. Iran: Ferdowsi University of Mashhad (abstract in English).
- Bourne, M. C. (2002). *Food texture and viscosity: Concept and measurement* (2nd ed.). Waltham, MA: Academic Press.
- Candogan, K., & Kolsarici, N. (2003). Storage stability of low-fat beef Frankfurters formulated with carrageenan or carrageenan with pectin. *Meat Science*, 64, 207–214.
- Cofrades, S., Serrano, A., Ayo, J., Carballo, J., & Jimenez-Colmenero, F. (2008). Characteristics of meat batters with added native and preheated defatted walnut. *Food Chemistry Journal*, 107, 1506–1514.
- Cui, W., Mazza, G., Oomah, B. D., & Billiaderis, C. G. (1994). Optimization of an aqueous extraction process for flaxseed gum by response surface methodology. *LWT – Food Science and Technology*, 27, 363–369.
- Egeland, B., Martinsen, B., & Autio, K. (1995). Rheological parameters as predictors of protein functionality: a model study using myofibrils of different fibre-type composition. *Meat Science*, 39, 97–111.
- Hamann, D. D. (1992). Rheological studies of fish proteins. In *International conference and industrial exhibition on food hydrocolloids* (p. 4e49). Tokyo, Japan: Japanese Society of Food Hydrocolloids.
- Haug, I. J., Draget, K. I., & Smidsrod, O. (2003). Physical behavior of fish gelatin – kappa – carrageenan mixtures. *Carbohydrate Polymers*, 56, 11–19.
- Koocheki, A., Mortazavi, S. A., Shahidi, F., Razavi, S. M. A., Kadkhodae, R., & Mohamadzadeh Milani, J. (2008). Optimization of mucilage extraction from *Qodume shirazi* seed (*Alyssum homolocarpum*) using response surface methodology. *Journal of Food Process Engineering*. <http://dx.doi.org/10.1111/j.1745-4530.2008.00312.x>.
- \* Li-kang, Z., Zou, Y. F., Xu, X. L., Zhu, C. Z., Wang, P., & Zhou, G. H. (2013). Effect of various amounts of pork and chicken meat on the sensory and physicochemical properties of Chinese-style meatball. *Journal of Food Science and Technology International*, 19(6), 963–970 (\*This reference is a key reference. It describes the condition of rheological properties when temperature changed).
- Michon, C., Cuvelier, G., Launay, B., & Parker, A. (1996). Viscoelastic properties of t-carrageenan/gelatin mixtures. *Carbohydrate Polymers*, 30(14)–8617(96), 00108–117.
- Morris, V. J. (1986). Multicomponent gels. In G. O. Phillips, D. J. Wedlock, & P. A. Williams (Eds.), *Gums and stabilisers for the food industry 3* (pp. 87–99). New York, London: Elsevier.
- Myers, R. H., & Montgomery, D. C. (1995). *Response surface methodology, process and product optimization using designed experiments* (2nd ed.). New York, NY: John Wiley and Sons.
- Owen, S. R., Tung, M. A., & Paulson, A. T. (1992). Thermorheological studies of food polymer dispersions. *Journal of Food Engineering*, 16, 39–53.
- Phillips, O., & Williams, P. A. (2009). *Handbook of hydrocolloids*. In *Woodhead publishing series in food science, technology and nutrition*. Amsterdam: Elsevier.
- Piculell, L., Bergfeldt, K., & Nilsson, S. (1995). Factors determining phase behaviour of multi component polymer systems. In S. E. Harding, S. E. Hill, & J. R. Mitchell (Eds.), *Biopolymer mixtures* (pp. 13–35). Nottingham: Nottingham University Press.
- \* Pietrasik, Z. (2003). Binding and textural properties of beef gels processed with kappa-carrageenan, egg albumin and microbial transglutaminase. *Meat Science*, 3(63), 317–324 (\*This reference is a key reference. This reference stated that addition of kappa-carrageenan as one of hydrocolloid, improved water retention of meat gels).
- Pietrasik, Z., & Li-Chan, E. C. Y. (2002). Binding and textural properties of beef gels as affected by protein, carrageenan and microbial transglutaminase addition. *Food Research International*, 35, 91–98.
- \* Pranoto, Lee, C. M., & Park, H. J. (2007). Characterizations of fish gelatin films added with gellan and kappa-carrageenan. *LWT – Food Science and Technology*, 40, 766–774. \* This reference is a key reference. This reference reported that gel strength (hardness) can be improved by mixing with enzymic modification and suitable gelling agent such as kappa-carrageenan.
- Ramirez, J. A., Del Angel, A., Uresti, R. M., Velazquez, G., & Vazquez, M. (2007). Low-salt restructured products from striped mullet (*Mugil cephalus*) using microbial transglutaminase or whey protein concentrate as additives. *Food Chemistry*, 102, 243–249.
- Rao, M. A. (1999). Rheological behavior of processed fluid and semisolid foods (Chapter 3 and 5). In M. A. Rao (Ed.), *Rheology of fluid and semisolid foods: Principles and applications* (pp. 105–108), 244–254.
- Sanaei, A. V., Mahmoodani, F., See, S. F., Yusop, S. M., & Babji, A. S. (2013). Optimization of gelatin extraction and physico-chemical properties of catfish (*Clarias gariepinus*) bone gelatin. *International Food Research Journal*, 20(1), 423–430.
- \* Sano, T., Noguchi, S. F., Tsuchiya, T., & Matsumoto, J. J. (1988). Dynamic viscoelastic behavior of natural actomyosin and myosin during thermal gelation. *Journal of Food Science*, 53, 924–928 (\*This reference is a key reference. It describes the condition of rheological properties when temperature changed).
- Sarıçoban, C., Yilmaz, M. T., & Karakaya, M. (2009). Response surface methodology study on the optimization of effects of fat, wheat bran and salt on chemical, textural and sensory properties of patties. *Meat Science*, 83, 610–619.
- Serdaroglu, M., Yildiz-Turp, G., & Abrodimov, K. (2005). Quality of low-fat meatballs containing legume flours as extenders. *Meat Science*, 70, 99–105.
- Somboon, N., Karrila, T. T., Kaewmanee, T., & Karrila, S. J. (2014). Properties of gels from mixed agar and fish gelatin. *International Food Research Journal*, 21(2), 485–492.
- Tahergorabi, R., Sivanandan, L., & Jaczynski, J. (2012). Dynamic rheology and endothermic transitions of proteins recovered from chicken-meat processing by-products using isoelectric solubilization/precipitation and addition of TiO<sub>2</sub>. *LWT – Food Science and Technology*, 46, 148–155.
- Tolstoguzov, V. B., & Braudo, E. E. (1983). Fabricated foodstuffs as multicomponent gels. *Journal of Texture Studies*, 14, 183–212.
- Ulu, H. (2004). Effect of wheat flour, whey protein concentrate and soya protein isolate on oxidative process and textural properties of cooked meatballs. *Food Chemistry Journal*, 87, 523–529.
- Ulu, H. (2006). Effects of carrageenan and guar gum on the cooking and textural properties of low-fat meatballs. *Food Chemistry Journal*, 95, 600–605.
- Vasile, C., & Zaikov, G. E. (2009). *Environmentally degradable materials based on multicomponent polymeric systems*. Boca Raton: CRC Press.
- Venugopal, V., Kakatkar, A., Bongirwar, D. R., Karthikeyan, M., Mathew, S., & Shamasundar, B. A. (2002). Gelation of shark meat under mild acidic conditions: physicochemical and rheological characterization of the gel. *Journal of Food Science*, 67, 2681–2686.
- Visessanguan, W., Ogawa, M., Nakai, S., & An, H. (2000). Physiological changes and mechanism of heat induced gelation of arrowtooth flounder. *Journal of Agricultural and Food Chemistry*, 48, 1016–1023.
- Wu, Y., Cui, S. W., Tang, J., & Gu, X. (2007). Optimization of extraction process of crude polysaccharides from boat-fruited sterculia seeds by response surface methodology. *Food Chemistry*, 105, 1599–1605.
- Xiong, Y. L., & Brekke, C. J. (1990). Thermal transitions of salt soluble proteins from pre- and post-rigor chicken muscles. *Journal of Food Science*, 55, 1540–1543.
- \* Yi, J. B., Kim, Y. T., Bae, H. J., Whiteside, W. S., & Park, H. J. (2006). Influence of transglutaminase-induced cross-linking on properties of fish gelatin films. *Journal of Food Science*, 71, 376–383. \*This reference is a key reference. This reference reported that gel strength (hardness) can be improved by mixing with enzymic modification and suitable gelling agent such as kappa-carrageenan.



# Monitoring of alcohol strength and titratable acidity of apple wine during fermentation using near-infrared spectroscopy



Bangzhu Peng<sup>a,\*</sup>, Na Ge<sup>a</sup>, Lu Cui<sup>b</sup>, Hui Zhao<sup>b</sup>

<sup>a</sup> Key Laboratory of Environment Correlative Dietology, Ministry of Education, College of Food Science & Technology, Huazhong Agricultural University, 430070, Wuhan, Hubei, China

<sup>b</sup> College of Food Science & Engineering, Northwest A & F University, 712100, Yangling, Shaanxi, China

## ARTICLE INFO

### Article history:

Received 25 May 2015

Received in revised form

29 September 2015

Accepted 5 October 2015

Available online 9 October 2015

### Keywords:

Near-infrared spectroscopy

Apple wine

Monitoring

Fermentation

Process control

## ABSTRACT

Rapid development in apple wine industry has raised a growing need for effective fermentation process monitoring. The alcohol strength and titratable acidity have been used as indicators for process control and optimization in apple wine making. The objective of this study was to investigate the efficacy of using near-infrared (NIR) spectroscopy to monitor and assess the process parameters during apple wine fermentation. A simple and rapid NIR spectroscopy method was developed for simultaneous determination of alcohol strength and titratable acidity in apple wine. The selected spectral regions of 6101.9–5446.2  $\text{cm}^{-1}$ , and 11,995.4–7498.1  $\text{cm}^{-1}$  were pretreated by second derivative (SD) and straight line subtraction (SLS) for alcohol strength and titratable acidity, respectively, prior to developing calibration models using partial least squares (PLS) regression with cross-validation. The highest  $R_c^2$  and the lowest RMSECV in the calibration set were obtained for the alcohol strength (0.923 and 4.63 mL/L) and for the titratable acidity (0.930 and 0.264 g/L). The NIR calibration models showed good correlation of determination and low predictive errors. Application of the NIR calibration models demonstrated the feasibility of NIR spectroscopy to be used as a quality control tool for monitoring the apple wine fermentation process.

© 2015 Elsevier Ltd. All rights reserved.

## 1. Introduction

Apple wine is widely used as a fermented alcoholic beverage in most countries. The steadily-growing diversity of commercial apple wine, coupled with increasing consumer demand, has prompted a need to monitor their major chemical composition changes for process control and quality assessment in order to better manage fermentation process. Alcohol strength and titratable acidity have been used as indicators during apple wine fermentation process for quality control and optimization in apple wine industry; hence, it is of great importance to monitor the changes of alcohol strength and titratable acidity in fermentation process for improving apple wine quality. A variety of methods have been developed for monitoring the parameters of alcohol strength and titratable acidity in previous research, including chemical assays, pH meters, and high pressure liquid chromatography, etc. (S.A.C., 2008; Satora, Tarko, Sroka, & Blaszczyk, 2014; Wilson, Maguer, Duitschaever, Buteau, & Allen,

2003; Ye, Yue, Yuan, & Li, 2014; Zhang, Fang, & Li, 2011), but these methods generally had the disadvantages of sample preparation, reagent consumption and complicated operation with time-consuming that might hamper the quality of final apple wine. With the development of brewing technology and the demand of quality control, it is important to perform fast and accurate determination of target composition for cost saving and online monitoring product quality (Blanco, Peinado, & Mas, 2004).

Nowadays, apple wine brewing industry needs to introduce and develop more advanced analysis method online in order to get reliable feedback data in time, which applied to guide the fermentation process. The monitoring of a fermentation process often requires fast and frequent measurements, which makes Near-infrared (NIR) spectroscopy an excellent candidate for online analysis to provide rapid determination and straightforward monitoring. Bioprocess monitoring is becoming one of the most challenging applications of NIR spectroscopy (Lachenmeier, 2007). With the application of chemometric techniques, a single spectrum can be subjected to many different calibration models, to measure many compositions in various types of food (Shen et al., 2010). NIR spectroscopy is a widely used rapid and non-destructive technique

\* Corresponding author.

E-mail address: [bzpeng@mail.hzau.edu.cn](mailto:bzpeng@mail.hzau.edu.cn) (B. Peng).

for quality measurements and control in food and agricultural product analyses (Antonucci et al., 2011; Chen, Ding, Cai, Sun, & Zhao, 2012; Chen, Zhao, Fang, & Wang, 2007; Grassi, Amigo, Lyndgaard, Foschino, & Casiraghi, 2014; Pouliot, Paquin, Martel, Gauthier, & Pouliot, 1997; Xie, Ye, Liu, & Ying, 2011), and is currently an ideal alternative to traditional analytical techniques for monitoring bioprocess (McLeod et al., 2009). With the application of chemometric techniques, a single spectrum can be subjected to many different calibration models, to measure many compositions (McLeod et al., 2009), and this modern analytical technology has been used as a well-suited method for general process real-time monitoring, which is of great interest for many wine makers to conduct process control. Di Egidio, Sinelli, Giovanelli, Moles, and Casiraghi (2010) obtained good calibration models for the prediction of the main compositional changes with FT-NIR to evaluate alcoholic fermentation online in red wine. Buratti et al. (2011) demonstrated that the non-destructive method of NIR are suitable for the monitoring of must-wine fermentation giving crucial information about the quality of the final product in agreement with chemical parameters. Giovenzana, Beghi, and Guidetti (2014) carried out a preliminary study to verify the possibility of employing a device based on NIR spectroscopy, directly on the production line of craft beer. Grassi et al. (2014) investigated the capability of FT-NIR spectroscopy to monitor and assess process parameters in beer fermentation with two different yeast strains at different temperatures, and the results showed that FT-NIR spectroscopy demonstrated to be a perfectly suitable quantitative method to be implemented in the production of beer. NIR spectroscopy has already shown promise as a rapid and non-destructive method for determining various compounds simultaneously in the fermentation industry (Liang et al., 2013). Nevertheless, less research exists on the application of NIR spectroscopy for monitoring and assessment of changes in relevant physico-chemical parameters in the apple wine fermentation process. Therefore, much more intensive work is needed to really evaluate the feasibility of NIR spectroscopy in monitoring apple wine fermentation process. The objectives of this study were to develop fourier transform near infrared (FT-NIR) spectroscopy calibration models for predicting alcohol strength and titratable acidity of apple wine in order to monitor fermentation process. In addition, the feasibility of using FT-NIR spectroscopy to monitor these two indicators simultaneously during the fermentation of apple wine was explored.

## 2. Materials and methods

### 2.1. Apple wine fermentation and sampling

Ripe Fuji apples used in this study were harvested from different commercial orchards located at Luochuan county in northwest China, and stored in a cold room at 4 °C until use. Apple juice was obtained by squeezing the mixed apples from different orchards from LZ juice extractor with a vacuum pressing and filtration system in room temperature (Gongda company, Wenzhou, China), during which the sodium bisulfite of 100 mg/L was added to apple juice in order to inhibit the bacteria growth immediately (Peng, Yue, & Yuan, 2008). The total sugar and pH of all juice samples for fermentation were then adjusted to 200 g/L with saccharose and 3.4 with 0.5 M hydrochloric acid, respectively. A total of nine apple wine fermentation trials were conducted using three different yeasts (*Saccharomyces cerevisiae* 1750, PF12 and WP45) at three temperatures of 17, 20 and 23 °C according to dry type brewing technology in laboratory. The apple wine samples were collected right after yeast inoculation (0 h, starting time), and then every 12 h until the 10th day of fermentation in each trial. When sampling,

about 30 mL of samples were discharged out directly from fermented supernatant. One hundred and sixty samples were collected from eight trials for developing the models of quantifying the alcoholic strength and titratable acidity, while another trial with twenty collected samples was used to evaluate the feasibility of FT-NIR spectroscopy in monitoring apple wine fermentation process.

### 2.2. Chemical analysis

The performance of a quantitative NIR model is mainly dependent on the performance of reference method (Bock & Connelly, 2008). Poor precision and accuracy of the reference method will limit the performance of the NIR model. Therefore, it is important to ensure the targeted parameter as close to the true value as possible. In this study, samples were centrifuged at 5000 rpm for 5 min and supernatants were collected for chemical analysis. Alcoholic strength was measured by using an PT-1 alcoholmeter (Pute company, Beijing, China), immersed in a distillate at a temperature of 20 °C; titratable acidity was determined by acid–base titration method according to SAC standard GB/T 15038 (S.A.C., 2008) and the results were expressed as malic acid. All reagents used were of analytical grade, and related solutions were prepared by ultrapure water produced with a millipore purification system (Millipore, Mississauga, Canada) in the experiments. All analyses were done in triplicate.

### 2.3. Spectrum collection

FT-NIR spectra collected directly from the supernatant of apple wine samples using a MPA FT-NIR spectrometer (Bruker Optics, Germany) in the range of 12,000 to 4000  $\text{cm}^{-1}$ , which equipped with an InGaAs detector and a liquid fiber optic probe with a 2 mm path length. An air background was employed as a probe reference, and the liquid probe directly immersed into samples for collecting the spectra at 25 °C. The spectral resolution was set at 8  $\text{cm}^{-1}$  with an interval of 2  $\text{cm}^{-1}$  and the spectra were recorded performing 20 scans for both the reference and tested samples. The spectra were recorded in triplicate and an average spectrum was collected to ensure an adequate signal-to-noise ratio for the subsequent analysis. The NIR instrument control, spectra scanning, and initial data processing were performed by using OPUS software version 5.5 (Bruker Optics, Germany).

### 2.4. Preprocessing of spectra and chemometric analysis

NIR spectra preprocessing in multivariate calibration is still trial and error due to the lack of sufficient prior information and an incomplete knowledge of the raw data (Xu et al., 2008). How to select a proper preprocessing method depends largely on the expertise and experience of practitioners. To establish best calibration model, spectra data from samples need to conduct different treatments for reducing noise interference and increasing the resolution of small absorbance bands (Huang, Yu, Xu, & Ying, 2008). Chemometric analysis is usually used as a tool to correlate the effective information in the NIR spectra signal to a number of latent variables or factors, constrained by a set of calibration reference data (Massart et al., 1997). Partial least squares (PLS) regression is a well-established chemometric technique whereby factors are derived by taking into account the variation in the spectral data that is relevant for explaining variation in the characteristics of interest in the original samples (Williams, 2001).

In this study, spectra preprocessing was made by straight line subtraction (SLS), first derivative (FD), second derivative (SD), vector normalization (VN), min–max normalization (MMN),

**Table 1**  
Analysis for chemical reference values of alcohol strength and titratable acidity in samples.

Parameter	Set	n	Range	Mean	CV (%)	PSE
Alcohol strength (mL/L)	Calibration	120	0–126.3	6.63	67.6	1.92
	Prediction	40	0–117.5	6.13	58.7	1.63
Titratable acidity (g/L)	Calibration	120	2.08–8.92	5.35	32.7	0.161
	Prediction	40	3.07–6.80	4.60	24.3	0.172

n: the number of samples; CV: coefficient of variation; PSE: pooled standard error.

multiplicative scattering correction (MSC), and the combination of every two methods using OPUS software (v.5.5 Bruker Optics, Germany). The number of latent factors used in the calibration models is of critical importance to avoid under or over fitting of the data and to ensure that the models are optimized for the intended purpose of the procedure (Inon, Llarío, Garrigues, & de la Guardia, 2005; Valderrama, Braga, & Poppi, 2007).

### 2.5. Establishment and evaluation of NIRS models

For establishment of NIRS model, calibration is generally performed by developing a calibration model that relates target composition concentration to absorbance spectra for a set of reference samples in calibration set (Cozzolino, Parker, Damberg, Herderich, & Gishen, 2006). In this study, the calibration models of alcohol strength and titratable acidity were developed using PLS regressions with leave-one-out cross validation, which it makes a subset of the samples leaving one out and trying to predict the one that was left out (Norgaard et al., 2000). The performance of calibration models was evaluated in terms of determination coefficient ( $R^2$ ) and root mean square error of cross-validation ( $RMSECV$ ), among which the  $R^2$  is a way of describing the strength of the relationship between two variables, and the larger the  $R^2$  is, the more variability is explained by the calibration model; the  $RMSECV$  is usually defined as the standard deviation of differences between spectral data and reference values in the cross-validation sample set (Di Egidio, Olivieri, Woodcock, & Downey, 2011; Williams, 2001). Generally, a better model should have higher  $R^2$  and smaller  $RMSECV$ . In addition, to evaluate the predictive capability of the calibration model, root mean square error of prediction ( $RMSEP$ ), which indicates the total error in prediction, should be acceptable when the model is applied to generate predictions outside the calibration set. Moreover, the ratio of standard deviation to the standard error of prediction ( $RPD$ ) was also employed as an indicator of NIRS predictions in this study. And higher  $RPD$  values usually indicate better NIR predictions (Williams, 2001). Generally, a good model should possess higher values of  $R^2$  and  $RPD$ , and lower values of  $RMSEC$  and  $RMSEP$  (Bao et al., 2014). Only optimal models are selected and discussed in this study.

The related equations defined as

$$R^2 = \left( 1 - \frac{\sum_{i=1}^n (y_{Ti} - y_{Pi})^2}{\sum_{i=1}^n (y_{Ti} - y_a)^2} \right);$$

$$RMSECV = \sqrt{\frac{\sum_{i=1}^n (y_{Ti} - y_{Pi})^2}{n}}; \quad RMSEP = \sqrt{\frac{\sum_{i=1}^m (y_{Ti} - y_{Pi})^2}{m}}$$

where  $y_{Ti}$  is the reference value of the parameter for the  $i$ th sample of the calibration set or prediction set;  $y_{Pi}$  is the predicted value obtained by NIRS model;  $y_a$  is the average value of reference;  $n$ ,  $m$  are the number of samples in calibration set and prediction set, respectively.

## 3. Results and discussion

### 3.1. Chemical analysis

Samples for establishing NIRS model should be representative of the commercial fermentation process of apple wine, and have the expected variability within the scope of the NIR calibration procedure. The calibration and prediction sets contained 120 and 40 samples, respectively, which were selected by the Kennard–Stone algorithm in each set that covered the whole range of each chemical parameter (Kennard & Stone, 1969; Valderrama et al., 2007). The samples of prediction set were selected as external validation (not used in calibration procedures) to evaluate the prediction ability of calibration models.

The range, mean, coefficient of variation (CV) and pooled standard error (PSE) for the alcohol strength and titratable acidity measured in both calibration and prediction sets were listed in Table 1. A calibration set containing 120 samples was used for model development in the ranges from 0 to 126.3 mL/L for alcohol strength, and from 2.08 to 8.92 g/L for titratable acidity, respectively. The ranges in values measured were in accordance with typical values expected in apple wines (Satora et al., 2014; Ye et al., 2014). Concentration spots of alcohol strength and titratable acidity in samples were plotted in Fig. 1. As can be seen from the Fig. 1, there is a positive relationship between alcohol strength and titratable acidity. This is because both of the two substances are yeast metabolites in fermentation process, and can thus accumulate continuously in apple wine samples. The statistics data showed a considerable degree of variations in the content of alcohol strength and titratable acidity, as indicated by the range and CV

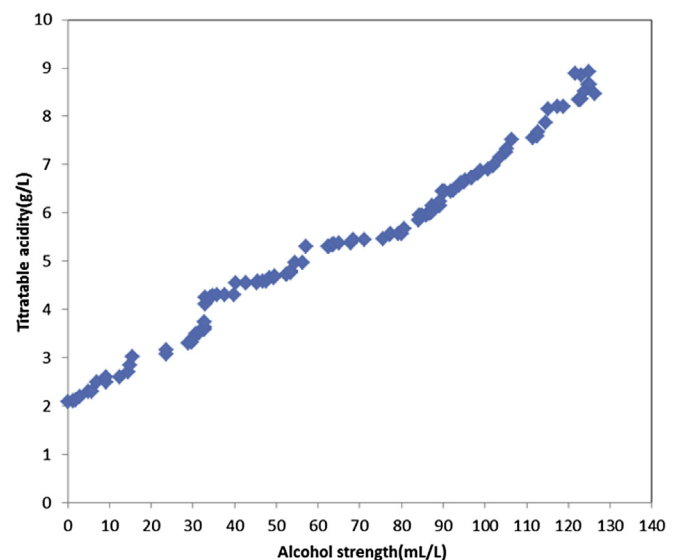


**Fig. 1.** Concentration spots of alcohol strength and titratable acidity in samples for developing FT-NIRS models of alcohol strength and titratable acidity in order to monitor apple wine fermentation process.

**Table 2**  
Statistics of calibration models of alcohol strength and titratable acidity in apple wine samples.

Parameter	Spectral region	Preprocessing method	Rank	Calibration set			Prediction set			
				<i>n</i>	<i>RMSECV</i>	$R_c^2$	<i>n</i>	<i>RMSEP</i>	$R_p^2$	<i>RPD</i>
Alcohol strength (mL/L)	6101.9–5446.2 $\text{cm}^{-1}$	SD	6	115	4.63	0.923	40	4.25	0.993	7.12
Titratable acidity (g/L)	11,995.4–7498.1 $\text{cm}^{-1}$	SLS	6	114	0.264	0.931	40	0.213	0.973	6.86

SD: second derivative; SLS: straight line subtraction; *RMSECV*: root mean square error of cross validation;  $R_c^2$ : determination coefficient for calibration set;  $R_p^2$ : determination coefficient for prediction set; *RPD*: residual predictive deviation.

values in Table 1. The large CV values of alcohol strength (67.6%, 58.7%, respectively for calibration and prediction sets) and titratable acidity (32.7%, 24.3%, respectively for calibration and prediction sets) were possibly related to different fermentation conditions being studied. Therefore, the variability of sample data in both calibration and prediction sets was considered suitable for developing stable and reliable NIR calibrations for alcohol strength and titratable acidity.

### 3.2. Selection and preprocessing of NIR spectra

Preprocessing of raw near-infrared spectra (NIRS) is indispensable because the measured spectra are subject to significant noises, baselines and other irrelevant information, which may affect the predictive ability of NIRS model (Blanco et al., 2004). Hence, it is imperative to perform the spectral range selection and pretreatment for visualizing and extracting relevant information from the spectra best suited for calibration model. In this study, the automation optimization function of the OPUS-QUANT2 software was used to optimize the calibration conditions for developing best calibration models of alcohol strength and titratable acidity. The

best conditions including the spectral region, preprocessing method and rank, were selected based on the smaller rank value and *RMSECV* for the calibration models according to PLS algorithm. The statistics of optimal conditions are given in Table 2. The best spectral regions selected for developing calibration models of alcohol strength and titratable acidity were 6101.9–5446.2  $\text{cm}^{-1}$ , 11,995.4–7498.1  $\text{cm}^{-1}$ , respectively. The profiles of selected spectral regions preprocessed by second derivative (SD) and straight line subtraction (SLS) for alcohol strength and titratable acidity, respectively, are shown in Figs. 2 and 3. From Figs. 2 and 3, more positive information and less noise were identified and extracted from the differences of the spectra pretreated by SD or SLS, and thus these pretreatments had contributed most to precision of each model.

### 3.3. Calibration and validation of models

The calibration models of alcohol strength and titratable acidity were developed using PLS regressions with leave-one-out cross validation. The PLS regression is a technique that constructs new predictor factors derived by taking into account the variation in

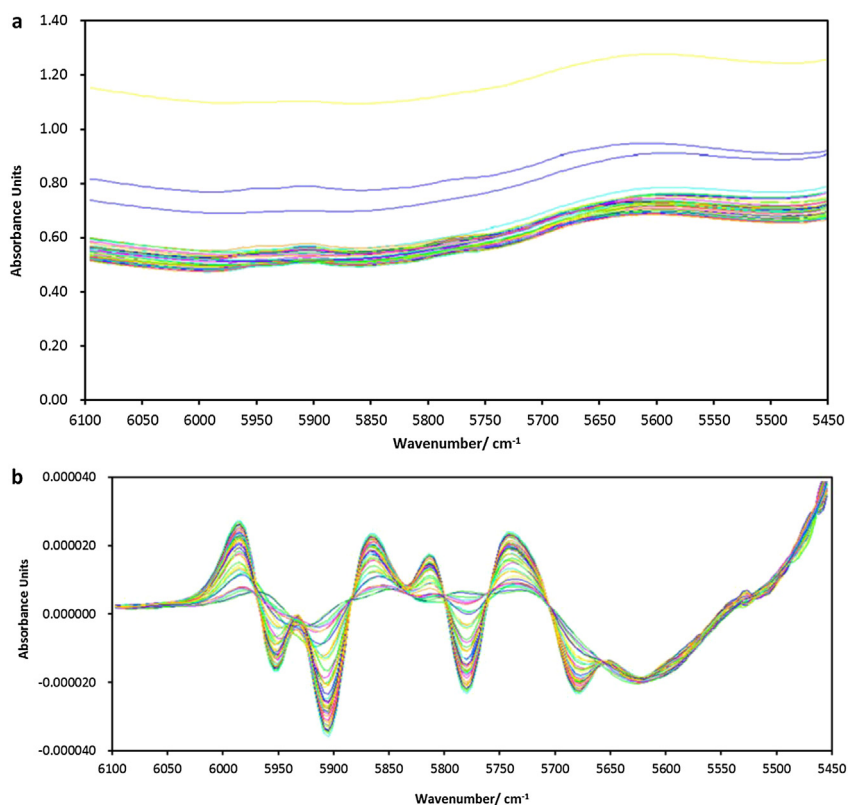


**Fig. 2.** The profile of selected spectral regions of 6101.9 ~ 5446.2  $\text{cm}^{-1}$  before and after pretreatment by second derivative (SD) for developing calibration model of alcohol strength in apple wine fermentation process (a: the original selected spectra; b: the spectra after pretreatment by SD).

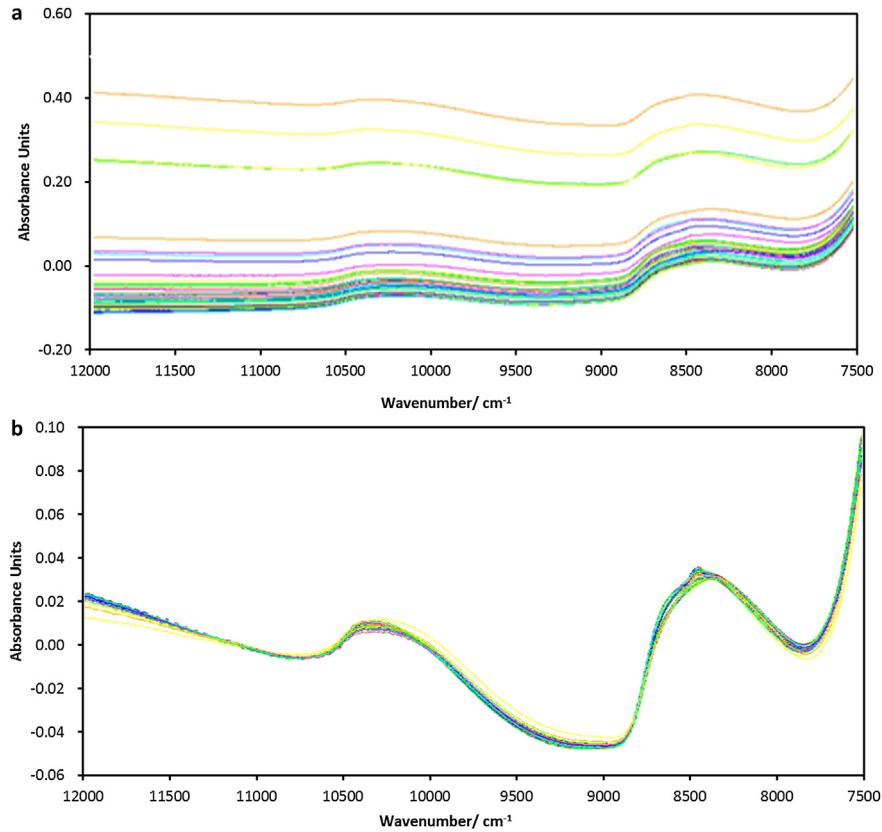


**Fig. 3.** The profile of selected spectral regions of 11995.4–7498.1  $\text{cm}^{-1}$  before and after pretreatment by straight line subtraction (SLS) for developing calibration model of titratable acidity in apple wine fermentation process (a: the original selected spectra; b: the spectra after pretreatment by SLS).

spectral data that is relevant for explaining variation in the characteristics of interest in original samples (Li, Zhang, & Atungulu, 2014; Williams, 2001), and it is also one of the standard methods used to develop calibration equations to predict chemical compositions of a sample from NIR spectra (Reeves, 2001).

Statistics for the calibration models developed for alcohol strength and titratable acidity in apple wines using FT-NIR spectra are shown in Table 2. Outliers in the calibration set were identified and excluded based on extreme leverages (Lillhonga & Geladi,

2005). The lowest  $RMSECV$  and the highest  $R_c^2$  in the calibration set were obtained for alcohol strength (4.63 mL/L and 0.923) with removal of 5 outliers, and titratable acidity (0.264 mg/L and 0.930) with removal of 6 outliers. Generally, values of  $R^2$  greater than 0.9 indicate excellent quantitative information for calibration model (Shenk & Westerhaus, 1996). To improve the stability of the models, the rank must be appropriately chosen to avoid overfit during calibration. Fig. 4 shows the correlation between  $RMSECV$  and Rank in calibration by PLS regression with leave-one-out validation, and

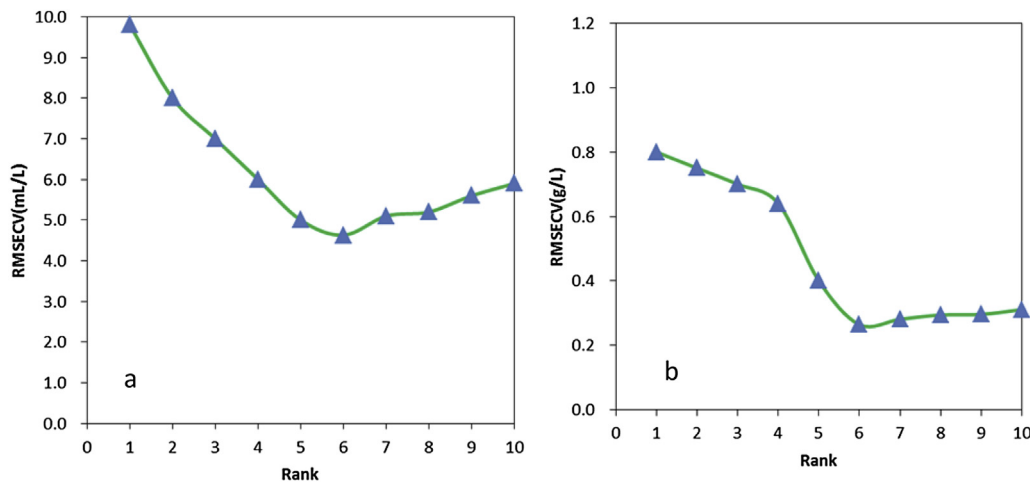


**Fig. 4.** Correlation between  $RMSECV$  and Rank in calibration set by PLS regression with leave-one-out cross validation for developing FT-NIRS models (a: for alcohol strength; b: for titratable acidity).

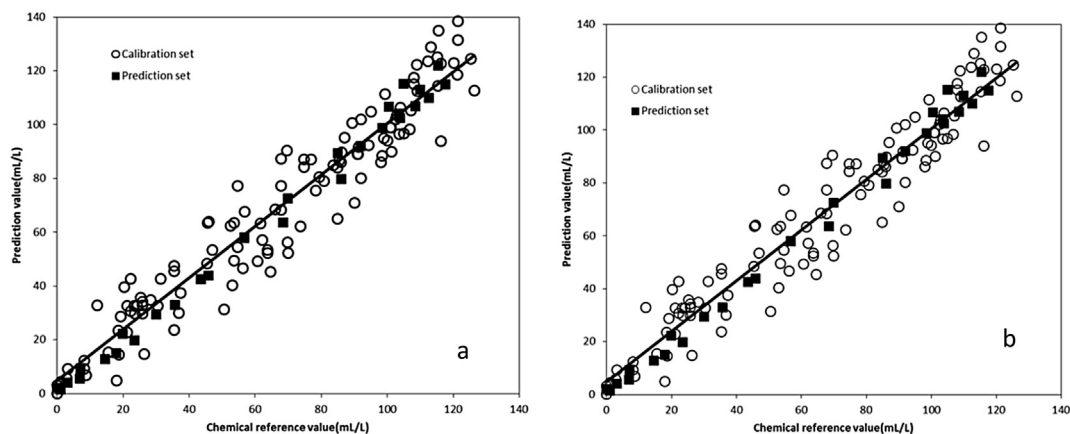


**Fig. 5.** Correlation statistics between chemical reference value and FT-NIRS prediction value in calibration and prediction sets. The FT-NIRS models were developed by PLS regression with leave-one-out cross validation using selected spectral regions of 11,995.4 ~ 7498.1  $\text{cm}^{-1}$  pretreated by SLS, and 6101.9 ~ 5446.2  $\text{cm}^{-1}$  pretreated by SD for alcohol strength (a) and titratable acidity (b), respectively.

the optimum ranks are both 6 for alcohol strength and titratable acidity calibration models. The correlation plots between chemical reference value and FT-NIR prediction value for the two parameters of apple wine in calibration set are shown in Fig. 5. The results show that the NIRS calibration models have excellent precision. Therefore, these two physicochemical parameters in apple wine might be measured by FT-NIR spectroscopy.

In order to further evaluate the prediction capability of the models, an external validation was conducted by applying FT-NIRS models to the 40 samples of prediction set. Table 2 shows that adequate small  $RMSEP$  values were obtained for alcohol strength and titratable acidity (4.25 mL/L and 0.213 mg/L), meanwhile the  $R_p^2$  values (0.993 and 0.973) are closed to 1. The rate of prediction to deviation ( $RPD$ ) could be an indicator of model validation and a higher  $RPD$  would be deemed better for prediction capability of model. A good calibration model should have a  $RPD$  value higher than 3.0 (Williams, 2001). A  $RPD$  value of 6.5–8.0 is generally considered as good for quality control purpose (Botelho, Mendes, & Sena, 2013). As shown in Table 2,  $RPD$  for the calibration models of alcohol strength and titratable acidity (7.12 and 6.86) were considered satisfactory. Additionally, the correlation plots between chemical reference value and FT-NIR prediction value for the two parameters of apple wine in prediction set are shown in Fig. 5. The results indicate that the calibration models are adequate as a tool to determine the alcohol strength and titratable acidity with accurate performance during apple wine fermentation. Similar results were obtained by Ye et al. (2014) for the determination of total acidity with the determination coefficients of 0.98 and the  $RMSEP$  of 0.021 in apple wine by FT-NIRS transmission mode.

### 3.4. Application of models

In order to check the feasibility of NIRS method developed in this study, one apple wine fermentation trail was monitored by the calibration models. The alcohol strength and titratable acidity with time during the apple wine fermentation were predicted using NIRS calibration and also measured by the chemical reference methods. The analyses of results are presented in Fig. 6. Fig. 6 shows that the  $R^2$  for the predicted versus measured values of the alcohol strength and titratable acidity were 0.962 and 0.972, respectively. The  $RMSEP$  of the alcohol strength and titratable acidity were 3.6 mL/L and 0.22 g/L, respectively. The predicted and measured values of the alcohol strength and titratable acidity showed similar variations over the entire fermentation period. All these results

suggest that the calibration models have good predictive capacity for alcohol strength and titratable acidity during apple wine fermentation, and this rapid NIR method could be taken to monitor the apple wine fermentation process with sufficient feasibility.

## 4. Conclusion

This study developed a simple and rapid NIRS method for simultaneous determination of alcohol strength and titratable acidity content in apple wine. The NIRS models showed a good agreement between calibration and prediction data with adequate high correlation of determination of  $R^2$  and relatively low predictive errors of  $RMSEP$ . The results demonstrated that NIR spectroscopy can be used as an alternative method to rapidly analyze alcohol strength and titratable acidity, with a very high applicability for monitoring apple wine fermentation process in order to improve the quality of apple wine.

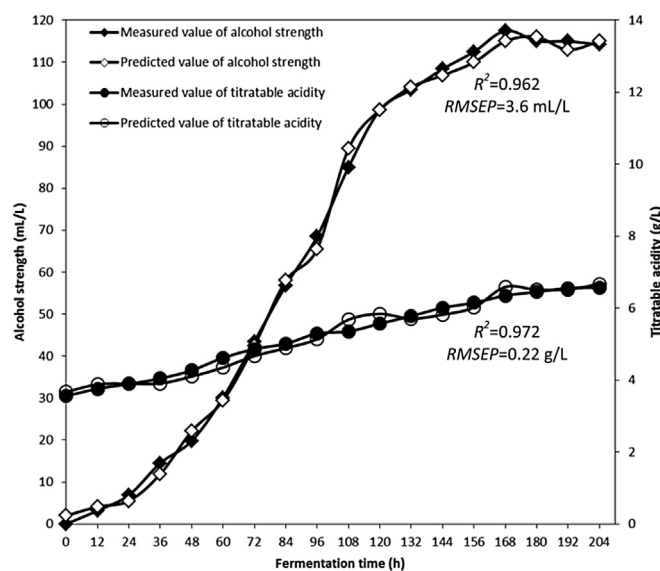


**Fig. 6.** Evolution of alcohol strength and titratable acidity in one fermentation run of apple wine at 20 °C with *S. cerevisiae* PF12, the predicted versus measured values of alcohol strength ( $R^2 = 0.962$ ,  $RMSEP = 3.6$  mL/L), and titratable acidity ( $R^2 = 0.972$ ,  $RMSEP = 0.22$  g/L) using the FT-NIRS models to monitor the fermentation process.

## Acknowledgments

This research was partially supported by the Fundamental Research Funds for the Central Universities (2662015BQ019) and National Natural Science Foundation of the Republic of China (20806062, 31301498). The authors acknowledge the anonymous reviewers very much for their valuable comments and improvements. R. Symoneaux, S. Chollet, R. Bauduin, J.M. Le Quéré, A. Baron. Impact of apple procyanidins on sensory perception in model cider (part 2): Degree of polymerization and interactions with the matrix components. *LWT – Food Science and Technology*, Volume 57, Issue 1, June 2014, Pages 28–34.

## References

- Antonucci, F., Pallottino, F., Paglia, G., Palma, A., Aquino, S., & Menesatti, P. (2011). Non-destructive estimation of mandarin maturity status through portable VIS-NIR spectrophotometer. *Food and Bioprocess Technology*, 4(5), 809–813.
- Bao, Y., Liu, F., Kong, W., Sun, D., He, Y., & Qiu, Z. (2014). Measurement of soluble solid contents and pH of white vinegars using VIS/NIR spectroscopy and least squares support vector machine. *Food and Bioprocess Technology*, 7(3), 54–61.
- Blanco, M., Peinado, A. C., & Mas, J. (2004). Analytical monitoring of alcoholic fermentation using NIR spectroscopy. *Biotechnology and Bioengineering*, 88, 536–542.
- Bock, J. E., & Connelly, R. K. (2008). Innovative uses of near-infrared spectroscopy in food processing. *Journal of Food Science*, 73(7), 91–98.
- Botelho, B. G., Mendes, B. A. P., & Sena, M. S. (2013). Development and analytical validation of robust near-infrared multivariate calibration models for the quality inspection control of mozzarella cheese. *Food Analytical Methods*, 6, 881–891.
- Buratti, S., Ballabio, D., Giovanelli, G., Dominguez, C. M. Z., Moles, A., Benedetti, S., et al. (2011). Monitoring of alcoholic fermentation using near infrared and mid infrared spectroscopies combined with electronic nose and electronic tongue. *Analytica Chimica Acta*, 697, 67–74.
- Chen, Q., Ding, J., Cai, J., Sun, Z., & Zhao, J. (2012). Simultaneous measurement of total acid content and soluble saltfree solids content in Chinese vinegar using near-infrared spectroscopy. *Journal of Food Science*, 77(2), 222–227.
- Chen, Q., Zhao, J., Fang, C., & Wang, D. (2007). Feasibility study on identification of green, black and oolong teas using near-infrared reflectance spectroscopy based on support vector machine (SVM). *Spectrochimica Acta A*, 66, 568–574.
- Cozzolino, D., Parker, M., Damberg, R. G., Herderich, M., & Gishen, M. (2006). Chemometrics and visible-near infrared spectroscopic monitoring of red wine fermentation in a pilot scale. *Biotechnology and Bioengineering*, 95, 1101–1107.
- Di Egidio, V., Olivieri, P., Woodcock, T., & Downey, G. (2011). Confirmation of brand identity in foods by near infrared transmittance spectroscopy using classification and class-modelling chemometric techniques—the example of a Belgian beer. *Food Research International*, 44, 544–549.
- Di Egidio, V., Sinelli, N., Giovanelli, G., Moles, A., & Casiraghi, E. (2010). NIR and MIR spectroscopy as rapid methods to monitor red wine fermentation. *European Food Research and Technology*, 230, 947–955.
- Giovenzana, V., Beghi, R., & Guidetti, R. (2014). Rapid evaluation of craft beer quality during fermentation process by vis/NIR spectroscopy. *Journal of Food Engineering*, 142, 80–86.
- Grassi, S., Amigo, J. M., Lyndgaard, C. B. G., Foschino, R., & Casiraghi, E. (2014). Beer fermentation: monitoring of process parameters by FTNIR and multivariate data analysis. *Food Chemistry*, 155, 279–286.
- Huang, H., Yu, H., Xu, H., & Ying, Y. (2008). Near infrared spectroscopy for on/in-line monitoring of quality in foods and beverages: a review. *Journal of Food Engineering*, 87(3), 303–313.
- Inon, F. A., Llarío, R., Garrigues, S., & de la Guardia, M. (2005). Development of a PLS based method for determination of the quality of beers by use of NIR spectral ranges and sample-introduction considerations. *Analytical and Bioanalytical Chemistry*, 382, 1549–1561.
- Kennard, R. W., & Stone, L. A. (1969). Computer aided design experiments. *Technometrics*, 11, 137–148.
- Lachenmeier, D. W. (2007). Rapid quality control of spirit drinks and beer using multivariate data analysis of Fourier transform infrared spectra. *Food Chemistry*, 101, 825–832.
- Liang, J., Zhang, D., Guo, X., Xu, Q., Xie, X., Zhang, C., ... Chen, N. (2013). At-line near-infrared spectroscopy for monitoring concentrations in temperature-triggered glutamate fermentation. *Bioprocess and Biosystems Engineering*, 36, 1879–1887.
- Lillhonga, T., & Geladi, P. (2005). Replicate analysis and outlier detection in multivariate NIR calibration, illustrated with biofuel analysis. *Analytica Chimica Acta*, 544, 177–183.
- Li, X., Zhang, A., & Atungulu, G. (2014). Characterization and multivariate analysis of physical properties of clingstone peaches. *Food and Bioprocess Technology*, 7, 1756–1766.
- Massart, D. L., Vandeginste, B. G. M., Buydens, L. M. C., de Jong, S., Lewi, P. L., & Smeyers-Verbeke, J. (1997). *Handbook of chemometrics and qualimetrics: Part B*. Amsterdam: Elsevier.
- McLeod, G., Clelland, K., Tapp, H., Kemsley, E. K., Wilson, R. H., & Poulter, G. (2009). A comparison of variate pre-selection methods for use in partial least squares regression: a case study on NIR spectroscopy applied to monitoring beer fermentation. *Journal of Food Engineering*, 90, 300–307.
- Norgaard, L., Saudland, A., Wagner, J., Nielsen, J. P., Munck, L., & Engelsen, S. B. (2000). Interval partial least-squares regression (iPLS): a comparative chemometric study with an example from near infrared spectroscopy. *Journal of Applied Spectroscopy*, 54, 413–419.
- Peng, B., Yue, T., & Yuan, Y. (2008). A fuzzy comprehensive evaluation for selecting yeast for cider making. *International Journal of Food Science Technology*, 43(1), 140–144.
- Pouliot, M., Paquin, P., Martel, R., Gauthier, S. F., & Pouliot, Y. (1997). Whey changes during processing determined by near infrared spectroscopy. *Journal of Food Science*, 62(3), 475–479.
- Reeves, J. B. (2001). Near-infrared diffuse reflectance spectroscopy for the analysis of poultry manures. *Journal of Agricultural and Food Chemistry*, 49, 2193–2197.
- S.A.C. (2008). *GB/T 15038. Analytical methods of wine and fruit wine* (pp. 20–41). China Standards Press.
- Satora, P., Tarko, T., Sroka, P., & Blaszczyk, U. (2014). The influence of *Wickerhamomyces anomalus* killer yeast on the fermentation and chemical composition of apple wines. *FEMS Yeast Research*, 14, 729–740.
- Shenk, J. S., & Westerhaus, M. O. (1996). Calibration the ISI way. In A. M. C. Davies, & P. Williams (Eds.), *Near infrared spectroscopy: The future waves* (pp. 198–202). Chichester: NIR Publications.
- Shen, F., Niu, X., Yang, D., Ying, L. B., Zhu, G., & Wu, J. (2010). Determination of amino acids in Chinese rice wine by fourier transform near-infrared spectroscopy. *Journal of Agricultural and Food Chemistry*, 58, 9809–9816.
- Valderrama, P., Braga, J. W. B., & Poppi, R. J. (2007). Variable selection, outlier detection, and figures of merit estimation in a partial least-squares regression multivariate calibration model. A case study for the determination of quality parameters in the alcohol industry by near infrared spectroscopy. *Journal of Agricultural and Food Chemistry*, 55, 8331–8338.
- Williams, P. C. (2001). Implementation of near-infrared technology. In P. C. Williams, & K. H. Norris (Eds.), *Near infrared technology: In the agricultural and food industries* (pp. 145–171). St. Paul: American Association of Cereal Chemists, Inc.
- Wilson, S. M., Maguer, M. L., Duitschaever, C., Buteau, C., & Allen, O. B. (2003). Effect of processing treatments on the characteristics of juices and still ciders from Ontario-grown apples. *Journal of the Science of Food and Agriculture*, 54, 215–224.
- Xie, L., Ye, X., Liu, D., & Ying, Y. (2011). Prediction of titratable acidity, malic acid, and citric acid in bayberry fruit by near-infrared spectroscopy. *Food Research International*, 44(7), 2198–2204.
- Xu, L., Zhou, Y., Tang, L., Wu, H., Jiang, J., Shen, G., et al. (2008). Ensemble pre-processing of near-infrared (NIR) spectra for multivariate calibration. *Analytica Chimica Acta*, 616(2), 138–143.
- Ye, M., Yue, T., Yuan, Y., & Li, Z. (2014). Application of FT-NIR spectroscopy to apple wine for rapid simultaneous determination of soluble solids content, pH, total acidity, and total ester content. *Food and Bioprocess Technology*, 7, 3055–3062.
- Zhang, A., Fang, Y., & Li, X. (2011). Occurrence and estimation of trans-resveratrol in one-year-old canes from seven major Chinese grape producing regions. *Molecules*, 6, 2846–2861.



## Structure preservation of Aloe vera (*barbadensis* Miller) mucilage in a spray drying process



L. Medina-Torres<sup>a,\*</sup>, F. Calderas<sup>b</sup>, R. Minjares<sup>c</sup>, A. Femenia<sup>c</sup>, G. Sánchez-Olivares<sup>b</sup>,  
F.R. González-Laredo<sup>d</sup>, R. Santiago-Adame<sup>d</sup>, D.M. Ramirez-Nuñez<sup>e</sup>,  
J. Rodríguez-Ramírez<sup>f</sup>, O. Manero<sup>g</sup>

<sup>a</sup> Facultad de Química, Universidad Nacional Autónoma de México (UNAM), México, D.F. 04510, Mexico

<sup>b</sup> CIATEC, A.C., Omega 201, León Gto., 37545, Mexico

<sup>c</sup> Ingeniería Agroalimentaria, Departamento de Química, Universitat de les Illes Balears, Spain

<sup>d</sup> Departamento de Ingenierías Química y Bioquímica, Instituto Tecnológico de Durango, Blvd. Felipe Pescador 1830 Ote., 34080, Durango, Dgo., Mexico

<sup>e</sup> Facultad de Ciencias Químicas, Universidad Juárez del Estado de Durango (UJED), Avenida veterinaria, s/n, Circuito Universitario, C.P. 34120, Durango, Dgo., Mexico

<sup>f</sup> Centro Interdisciplinario de Investigación para el Desarrollo Integral Regional Unidad Oaxaca, Hornos No. 1003, Col. Noche Buena, Santa Cruz Xoxocotlán, C.P. 71230, Oaxaca, Mexico

<sup>g</sup> Instituto de Investigaciones en Materiales, Universidad Nacional Autónoma de México (UNAM), México, D.F. 04510, Mexico

### ARTICLE INFO

#### Article history:

Received 9 April 2015

Received in revised form

5 October 2015

Accepted 6 October 2015

Available online 19 October 2015

#### Keywords:

Rheology

Molecular-weight

Viscoelastic properties

Viscosity

Polysaccharides

### ABSTRACT

Aloe vera (*barbadensis* Miller) mucilage in powder form was obtained by spray-drying following by suspension in aqueous solution, to enable microstructure recovery. The rheological behavior of the reconstituted mucilage was evaluated as a function of mucilage concentration, temperature, pH and ionic-strength. Mucilage solutions exhibited shear-thinning non-Newtonian behavior. The viscosity was found dependent on ionic-strength. This dependence is more evident when divalent cations are used, although a strong rise in viscosity upon increasing pH is observed. Linear viscoelastic data show a predominant viscous behavior, but with a crossover point (storage module  $G'$  = loss module  $G''$ ) suggesting a change in molecular conformation to a random-coil arrangement of the mucilage microstructure. The spray-dried powders were compared with fresh mucilage, with regard to chemical composition and mechanical flow behavior. Results reveal a small structure modification during the spray-drying process, evidencing preservation of the mucilage microstructure when optimum spray-drying conditions are used, i.e., 1.5 L/h inlet flow, temperature of 150 °C and atomization rate of 27,500 rpm.

© 2015 Elsevier Ltd. All rights reserved.

### 1. Introduction

Polysaccharides are used in the food industry for their ability to modify the functional properties of food systems (Medina-Torres, Brito-de La Fuente, Torrestiana-Sánchez, & Katthain, 2000). Since polysaccharides impart a functional property to a specific product, the economics and availability of polysaccharides are important in the final formulation (Whistler, 1993). A very popular plant in the Cactaceae family is Aloe vera (AV) (*barbadensis* Miller) which has been widely studied due to its healing properties. AV is a heteropolysaccharide (it is formed by several polysaccharides) of high

molecular weight.

Spray-drying (SD) is a process widely used to produce powders due to several advantages such as capacity to produce powders of a specific particle size and moisture content, continuous operation, short production times, cost effectiveness, and flexibility (Keshani, Daud, Nourozi, Namvar, & Ghasemi, 2015 and references therein). Examples of recent studies of SD food products are: Blackberry (Ferrari, Germer, & de Aguirre, 2012), coffee oil (Frascarelli, Silva, Tonon, & Hubinger, 2012), Yoghurt (Sakin-Yilmazer, Koç, Balkir, & Kaymak-Ertekin, 2014), among others. However, the relative high temperatures used in the SD process can negatively affect the properties of the powders causing degradation and oxidation of the product. Thus, finding the best process conditions is of paramount importance to obtain powders with optimum properties. For example, it was found that the increase in inlet air-temperature

\* Corresponding author.

E-mail address: [luismt@unam.mx](mailto:luismt@unam.mx) (L. Medina-Torres).

leads to a decrease of efficiency and oil retention in the encapsulation process of coffee oil by SD (Frascareli et al., 2012). Ferrari et al., (2012) reported that a high inlet air-temperature (180 °C) leads to particles with smoother surface, lower moisture contents and higher hygroscopicity for the case of SD blackberry powders. Whereas, in the case of *Opuntia* fruits (Gandia-Herrero, Jimenez-Atenzar, Cabanes, Garcia-Carmona, & Escribano, 2010), low inlet air-temperature (120 °C) was associated with a large degree of particle shrinkage and deformation. With regard to shear-viscosity, Sakin-Yilmazer et al., (2014) reported that an increase in inlet air-temperature caused a decrease in apparent viscosity of reconstituted powders of SD yoghurt, which was related to the denaturalization of proteins and destruction of the protein network. With respect to studies on how SD process conditions affect the product structure, Paudel, Loyson, and Van de Mooter (2013) studied spray dried naproxen–polyvinylpyrrolidone (PVP) K25 amorphous solid dispersions. They found that a high inlet temperature or feed-flow lead to the formation of phase-separated dispersions with strong hydrogen-bonded fractions and higher amorphous drug fractions (resulted from fast evaporation conditions) leading to superior physical stability, while lower inlet temperature generated more homogeneous systems. Moreover, in the case of the AV mucilage, Cervantes-Martínez et al (2014) reported that the increase of inlet temperature and atomization speed led to a decrease in shear-viscosity of reconstituted AV-powder, which was attributed to sample degradation. A combination of high atomization speed and low inlet temperature were reported as key factors in reducing sample degradation which was inferred from rheological measurements (viscoelasticity and first normal-stress difference). In this regard, there are few studies about the rheological properties of reconstituted mucilage after a (SD) process.

The purpose of this study is to characterize the flow-thickening properties of the reconstituted AV-mucilage powders obtained by SD to obtain the optimum conditions to avoid sample degradation, maintaining the molecular weight of the AV powders.

## 2. Materials and methods

### 2.1. Raw materials

AV leaves were collected from a dry area of northern Mexico (Durango, Dgo.), from a cultivated area of 2500 m<sup>2</sup>, with a production of 2.5 tons per year under controlled irrigation and constant organic fertilizer every two months. These plants have a thick and short herbaceous stem with a diameter of 10 cm and height of 20–25 cm on average, prior to the stage of flourishing. The leaves have S shape towards the tip (center are erect or slightly curved and thinner) with 70–90 cm on average height and 8 cm thick. Only the bright green leaves without brown spots with 24–30 months-old on average that grew in the outer part of the plant were cut.

### 2.2. Extraction of the AV mucilage

The tip, base, thorns and bark on both sides of the leaves were separated after cutting, washing and cooling. Semi-frozen pulp was placed in a commercial juice extractor Hamilton Beach<sup>®</sup> Health-Smart; then the juice was clarified in a tabletop centrifuge brand Heraeus Labofuge model 400/400 R to remove suspended solids; the juice was stored in sterilized jars at low temperatures (−4 °C). pH (AOAC, 1990), degrees Brix, refractometer (model RF-10-CAT), moisture (OHAUS, thermo-balance MB2000), and total solids (NMX-F-510-1998) were measured in the mucilage samples.

### 2.3. Chemicals

The monosaccharide standards: L-Rhamnose, L-Fucose, L-Arabinose, D-Xylose, D-Mannose, D-Galactose, D-Glucose grade reactive and 2-Deoxy-Glucose (>99%) were used as internal standards, and sodium nitrate was purchased from Sigma–Aldrich. Reagent-grade Sulfuric acid and dichloromethane were supplied by Scharlab S. L. (Spain).

### 2.4. Physicochemical characterization of fresh AV mucilage

#### 2.4.1. Moisture content fresh samples

The moisture content of raw samples was determined with an automatic thermo-balance (model Sartorius<sup>®</sup> MA35), with a 0.01% error, automatic selection of time (0.1–99 min), with a temperature range of 1–150 °C and infrared heating-system. The thermo-balance was programmed at 90 °C for 40 min during the initial processing of the samples (non-destructive). Subsequently, in the development of this process, second and third treatments were applied, reaching 30 min at 110 °C. Results are expressed in g/kg of wet sample.

### 2.5. Spray Drying (SD)

A Mobile Minor parallel-flow spray-dryer (model Niro, Copenhagen, Denmark) equipped with a rotary atomizer (Minor TS M02/A) was used to dry the AV-mucilage solution. SD conditions (see Table 1) were used according to previous reports (Cervantes-Martínez et al., 2014) to obtain the optimum mechanical and functional properties of the SD process (inlet: 150 °C, 1.5 L/h and 27,500 rpm).

#### 2.5.1. Moisture content of the SD powders

The moisture content of the SD powder was determined with an infrared thermo-balance AD-4714<sup>a</sup>, at a temperature of 110 °C for a period of 60 min and a weight of 5 g per sample for each test, performed in duplicate. Results were expressed in percentage of dry matter.

### 2.6. Analytical determinations

#### 2.6.1. Total Phenolic Content (TFC)

The TFC was determined by the Folin-Ciocalteu method modified by Heimler, Vignolini, Dini and Romani (2005). To prepare the reference sample, dry powders of mucilage (1 mg) were dissolved in de-ionized water (1 mL), homogenized in a Vortex analog mixer (Fisher Scientific) for 10 min, until a homogeneous mixture was obtained. In the presence of dim light, 125 µL of the standard sample, 500 µL of distilled water and 125 µL of Folin-Ciocalteu reagent were mixed in test tubes. The mixture reacted for 6 min. Then 1250 µL of sodium carbonate (7 g/L) and 1 mL of distilled water were added to the reaction mixture. This mixture was incubated for 90 min at room temperature and in total absence of light; finally, absorbance was measured at 760 nm with water as blank. The TPC was expressed as mg of gallic acid equivalent (GAE, GAE/g of spray dried powder) through the calibration curve of gallic acid.

#### 2.6.2. Antioxidant capacity measured by trapping free radicals (DPPH method, 2,2-diphenyl-1-picrylhydrazyl)

Antioxidant capacity was measured in terms of the radical scavenging capacity (RSC) using the DPPH method\* (2, 2-diphenyl-1-picrylhydrazyl) (Brand-Williams, Cuvelier, & Berset, 1995). In this study 0.025 mg/mL of DPPH were used as a standard reagent and dried samples were dissolved in methanol/water (1:1 in volume), which were also used as target. Samples were prepared in duplicate

**Table 1**

Spray drying conditions, yield (Y) and Humidity (Hum) content for all treatments including fresh mucilage sample. Ti=Inlet temperature, To = Outlet temperature, Tw = wall temperature, Ff = Inlet flow, Y = yield, M = Moisture.

Treatment	Ti (°C)	To (°C)	Tw (°C)	Ff (L/h)	As (rpm)	Y (g/kg)	M (g/kg)
T1	170	98	55.12	1.5	23,000	0.090	0.08
T2	170	98	46.3	1.5	27,500	0.120	0.10
T3	170	98	55.12	1.7	23,000	0.080	0.080
T4	170	95	46.3	1.7	27,500	0.130	0.110
T5	150	67	48.63	1.5	23,000	0.060	0.080
<b>T6</b>	<b>150</b>	<b>98</b>	<b>40.85</b>	<b>1.5</b>	<b>27,500</b>	<b>0.110</b>	<b>0.120</b>
T7	150	75	48.63	1.7	23,000	0.160	0.080
T8	150	78	40.85	1.7	27,500	0.160	0.110
T9, Freeze drying	<b>-40</b>	<b>25</b>	—	—	—	<b>0.180</b>	<b>0.100</b>
T10, Fresh mucilage	—	—	—	—	—	—	90

Bold letters indicate the best spray drying conditions and the commercial freeze dried sample for comparison.

\*(P < 0.05).

considering five concentrations within a range of 100–2500 mg/mL. In presence of dim light, 0.5 mL of each sample was added to test tubes and then 3.5 mL of the DPPH solution were added, previously adjusted to an absorbance of 0.78 at a wavelength of 515 nm. The absorbance of the mixtures was measured 7 times every 5 min, up to a reaction time of 30 min. The free-radical scavenging capacity is expressed as a percentage according to the following Equation (1):

$$\%(\text{RSC}) = \left\{ 1 - \left( \frac{\text{Abs}_{515 \text{ sample}}}{\text{Abs}_{515 \text{ DPPH solution}^*}} \right) \right\} \times 100 \quad (1)$$

#### 2.6.3. Analysis of carbohydrate composition

Carbohydrate analysis was performed as described by Simões, Nunes, Domingues, Coimbra, and Domingues (2012) for neutral sugars. Sugars were released from residues by acid hydrolysis. Approximately 5 mg of fresh and dried AV-mucilage were dispersed in 12 mol/L H<sub>2</sub>SO<sub>4</sub> solution for 3 h followed by dilution to 1 mol/L and hydrolyzed at 100 °C for 2.5 h (Saeman, Moore, Mitchell, & Millett, 1954). A second sample was hydrolyzed only with 1 mol/L H<sub>2</sub>SO<sub>4</sub> (100 °C for 2.5 h). The cellulose content was estimated by the difference in glucose obtained by Saeman hydrolysis and the second (mild) hydrolysis method. The neutral sugars as alditol acetate derivatives were separated with dichloromethane and analyzed by gas chromatography with a flame ionization detector equipped with a 30 m column DB-225 (J&W Scientific, Folsom, CA, USA) with internal diameter and film thickness of 0.25 mm and 0.15 μm, respectively. The oven temperature program included an initial temperature of 200 °C, a rise in temperature at a rate of 40 °C/min up to 220 °C, keeping this temperature for 7 min, followed by a rate of 20 °C/min up to 230 °C and maintaining this temperature for 1 min. The injector and detector temperatures were 220 and 230 °C, respectively. The flow rate of the carrier gas (He) was set at 1.7 mL/min. Uronic acids were determined by colorimetry, as total uronic acid (Blumenkrantz & Asboe-Hansen, 1973) using a hydrolyzed sample (3 h at 20 °C in 12 mol/L H<sub>2</sub>SO<sub>4</sub>, followed by heating at 100 °C for 1 h in 1 mol/L H<sub>2</sub>SO<sub>4</sub>).

#### 2.6.4. Molecular weight

The molecular weight of mucilage was measured using HPLC (Perkin–Elmer Model 250) equipped with a G 2000 SW column (TSK-GEL), a IR refractive index detector (Perkin–Elmer series 1000) and an integrator (Spectra-Physics, SP4270 model). Sodium nitrate (50 mg mol/L) was eluted at 50 °C with a flow rate of 0.7 mL/min. Dextrans (commercial grade, Sigma EE.UU, *Leuconostoc mesenteroides*: B-152 strain and dextran T70 produced by Pharmacia Biotechnology, Sweden) with molecular weights from 5000 to

87,000 were used as standards.

#### 2.7. Morphology by scanning electron microscopy (SEM)

The sample was placed in copper seats, fixed with conductive tape and coated with gold at 1 kPa during 90s (model Desk II, Denton Vacuum, NJ, USA). Samples were observed in a scanning electron microscope (JEOL Mod. JSM6300 Jeol, Japan) with voltage of 20 kV and 1000× magnification.

#### 2.8. Rheological properties

##### 2.8.1. Mucilage reconstituted solutions

SD powder mucilage samples were re-suspended in de-ionized water using a magnetic stirrer (Thermo Scientific, Telesystem 15) at 500 rpm at 24 ± 1 °C for 90 min. Samples with 0.06 g/mL were prepared to study the effects of changes in pH, temperature and ionic strength on the rheological behavior of mucilage. All rheological measurements were performed in a stress controlled rheometer (AR-G2, TA Instruments) using a cone and plate geometry (d = 60 mm, 1° angle) with a Peltier plate system attached to a circulating water bath (Haake, Germany, Mod. F3T). Samples were characterized under simple shear flow. The viscoelastic properties, storage (G') and loss modulus (G'') were measured under small-amplitude oscillatory with frequency range from 0.1 to 200 rad/s.

Finally, the first normal stress difference under steady-shear (N1) was measured to determine the elastic properties under shear flow.

#### 2.9. Experimental design

The experimental design is shown in Table 1. Experiments were performed according to a 2<sup>3</sup> factorial design: two different inlet air-temperatures (Ti = 150 and 170 °C), two inlet flows (Ff = 1.5 and 1.7 L/h) and two atomization speeds (As = 23,000 and 27,500 rpm). Outlet (To) and wall temperatures (Tw) were measured but not controlled in the SD process. A freeze-dried sample (T9) and fresh mucilage (T10) are used for comparison (see Table 1). Three replications were performed for each test for a total of 24 SD runs. Data were analyzed by ANOVA with statistical significance of P < 0.05.

### 3. Results and discussion

#### 3.1. Analytical determinations

##### 3.1.1. Physical characteristics of powders obtained by SD

The process conditions, yield and moisture content of SD powders (T1–T8), freeze-dried powder (T9, used for comparison

purposes) and fresh mucilage (T10), the latter with 3 °Brix, pH of 4.6 and total solids content of 0.12 g/kg, are shown in Table 1. According to the operation conditions of SD, the time that the particles remain inside the dryer (residence time) related to the inlet flow ( $F_i$ ) and spraying speed (rotary atomizer velocity) has ample influence on the moisture content (Hum) and degree of particle agglomeration (stickiness) (Chiou & Langrish, 2007). For example, sample T5 reveals the lowest-attainable yield, which is related to the low inlet-flow (1.5 L/h) which represents a long residence time combined with a high temperature gradient  $\Delta T = T_i - T_o$  (150 – 67 °C). Sample T6 in comparison, reveals a higher yield, attributable to the lower temperature gradient and larger atomization speed ( $A_s = 27,500$  rpm), as compared to sample T5 (23,000 rpm).

### 3.1.2. Total Phenolic Content (TPC)

Table 2 shows the TPC expressed in mg of gallic-acid equivalent for the 10 samples (sample identification, same as Table 1). According to Wang et al. (2013) a major decrease in TPC is found in the low-temperature dehydrated product probably due to long residence times required to reach the pre-set final moisture. This is confirmed with sample T2, where a combination of high inlet-temperature (170 °C) and low inlet-flow (1.5 L/h, see Table 1) leads to long residence times with high temperature, and hence the lowest phenol content (Table 2). A higher temperature in conjunction with high feed-flow reduces the particle residence-time and improves the retention of functional groups, as the particles stay shorter periods at high temperatures. This is the case of samples T3 and T4 (see Table 1).

### 3.1.3. Antioxidant capacity measured by trapping free radicals (DPPH method, 2,2-diphenyl-1-picrylhydrazyl)

In general, the high phenolic content implies a high antioxidant capacity, which is strongly linked to the molecular structure. The use of the DPPH technique was made according to Brand-Williams et al. (1995) providing a straightforward way to evaluate the antioxidant activity of trapping radicals; however, some care must be taken when interpreting the data. In Table 2, the percentage of trapping free radicals for all samples is presented. A widely-used parameter to estimate the antioxidant capacity is the median effective concentration ( $EC_{50}$ ) (Cuvelier, Richard, & Berset, 1992; Sánchez-Moreno, Larrauri, and Saura-Calixto, 1998).  $EC_{50}$  is the concentration that inhibits 50% of the DPPH\* radicals in solution; the lower the  $EC_{50}$ , a higher antioxidant activity is found.

Treatments T1 and T3 show the lowest % RSA (<0.06 g/mL) with concentrations higher than 5000 mg/mL. This may be due to the degradation of the molecule caused by high drying temperatures; while in treatments T7 and T8, low antioxidant levels are caused by

high feed-flow and low atomizing pressure, accompanied with high residence times within the drying chamber, leading to degradation of the biopolymer (through chain scission). Sample T9 also shows a low percentage of trapped free-radicals due to the drying process (freeze-drying). According to these results, interaction with DPPH depends on the presence and preservation of the conformational structure of mucilage.

### 3.1.4. Analysis of the carbohydrate composition

Experimental results for the samples with the highest monosaccharide contents (T6 and T10) are summarized in Table 3. Sample T6 shows the highest monosaccharide content in comparison to fresh mucilage (T10), evidencing the optimum drying conditions according to total phenolic content and antioxidant activity (Table 2). Rodríguez-González et al., (2011) reported that the high mannose and glucose contents suggest the occurrence of the acemannan polymer, the main bioactive ingredient of AV. Femenia, García-Pascual, Simal, and Rosselló (2003) evaluated the effect of dehydration at different air-drying temperatures on the bioactive polysaccharides of AV.

In general, carbohydrate analysis revealed that the AV-mucilage mainly contains mannose and significant amounts of uronic acids, arabinose, and xylose. Acemannan, the main active component of AV originates from mannose, which has been reported to occur in large quantities in AV (McAnalley, 1993).

### 3.1.5. Molecular weight

From elution profiles using HPLC, the molecular weight of the SD-mucilage was determined; a value of  $4.18 \times 10^4$  for sample T6 was found, while for fresh mucilage amounts to  $5.96 \times 10^4$ . The reduction in Mw is expected due to the thermal treatment and high shear-forces present in the SD chamber. However, the difference is less than 10% of the reference Mw, which evidences the structure preservation achieved using the optimum drying conditions while preserving the antioxidant activity. Also, the reduction in monosaccharide content (see Table 3) of sample T6 as compared with the fresh mucilage (T10) is a remarkable result of the mild degradation caused by the SD process, since the reductions for all monosaccharide samples range in the order of 10% or less.

## 3.2. Scanning Electron Microscopy (SEM)

Fig. 1 shows micrographs of powders obtained by the SD process (A) and the lyophilized sample (B), where the morphology of the SD micro-particles consists of semi-spherical shapes (sample T6 see Table 1 for SD process conditions). Furthermore, freeze-dried micro-particles (sample T9) have rough surfaces with cavities and, sometimes, structural cracks. These morphological irregularities are possibly due to the removing water process during drying. Ball-struck type particles were observed in SD samples (T6) similar to those reported by Alamilla-Beltrán, Chanona-Pérez, Jiménez-

**Table 2**

Total phenolic content expressed by mg of gallic acid equivalents and antioxidant activity (free radical method) for all treatments including fresh mucilage sample (Data at 25 °C, pH = 4).

Treatment	Gallic acid equivalents (mg)	%, Radical scavenging activity
T1	137 ± 10	7 ± 3
T2	15 ± 1	52 ± 5
T3	85 ± 5	7.5 ± 0.3
T4	91 ± 3	47 ± 5
T5	88 ± 4	51 ± 6
T6	87 ± 3	52 ± 5
T7	98 ± 6	12 ± 2
T8	60 ± 5	6 ± 2
T9	88 ± 5	6 ± 3
T10	356 ± 15	55 ± 7

\*(P < 0.05).

**Table 3**

Sugar composition of the mucilage of the Aloe vera (*barbadensis* Miller).

Composition, % mol	Fresh, (T10)	SD, (T6)
Mannose	47 ± 2	43 ± 2
Glucose	41 ± 2	37 ± 3
Uronic acids	6.1 ± 0.5	4.8 ± 0.5
Galactose	4.5 ± 0.4	2.1 ± 0.2
Xylose	7.0 ± 1.1	0.70 ± 0.05
Arabinose	1.9 ± 0.1	1.6 ± 0.1
Rhamnose	0.90 ± 0.03	0.7 ± 0.1
Fucose	0.80 ± 0.02	N.D

\*(P < 0.05).

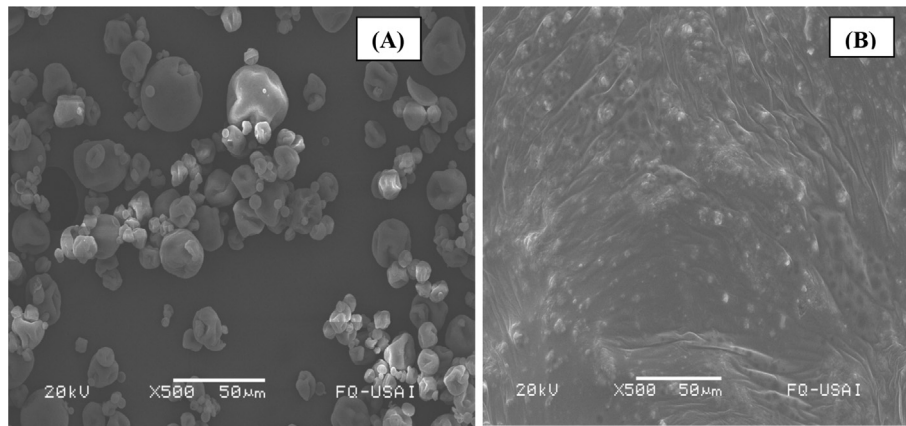


**Fig. 1.** Micrographs of spray dried Aloe vera powders: A) Sample T6 (Spray dried at 150 °C inlet temperature, 1.5 L/h inlet flow and 27,500 rpm atomization speed) and, B) Sample T9 (Freeze dried at –40 °C inlet temperature, used for comparison purposes).

Aparicio, and Gutiérrez-López (2005). Using air at low temperature in the SD process leads to irregular micro-particles with folds on its surface, while air at high temperature results in more rigid porous surfaces and micro-particles. In this study, using the SD process (T6) leads to semi-spherical micro-particles, with no apparent cracks without agglomerations or tack processes.

### 3.3. Rheological behavior. Steady-state simple-shear

#### 3.3.1. Concentration effect

Shear viscosity as a function of mucilage concentration is shown in Fig. 2. The sample with treatment T6 is used here at two different concentrations (0.03 and 0.06 g/mL) and compared with either fresh mucilage, freeze-dried mucilage and xantham gum. In general, mucilage solutions behave as shear-thinning fluids ( $n < 1$ ) i.e., the viscosity decreases with increasing shear-rate.

The shear-viscosity of polysaccharide solutions in a wide range of strain-rates has been modeled with a power-law model (Equation (2)):

$$\eta = K \dot{\gamma}^n \quad (2)$$

where  $\eta$  is the shear viscosity (Pa s) and  $\dot{\gamma}$  is the shear strain rate (1/

s),  $K$  is the consistency index ( $\text{Pa s}^n$ ) and  $n$  is the shear-thinning index.

Morris, Cutler, Ross-Murphy, Rees, and Price (1981) empirically found a value of 0.76 for the slope of the viscosity ( $\eta$ ) vs shear rate ( $\dot{\gamma}$ ) at high shear rates for “random-coil” polysaccharides in solutions with high polydispersity. Note that the flow properties of commercial biopolymers (xanthan gum) are similar to those of the AV-mucilage 0.06 g/mL (Fig. 2). Viscosity values of a solution of 0.06 g/mL mucilage are comparable to those of a xanthan solution (0.03 g/mL).

#### 3.3.2. Temperature effect

The influence of temperature on the viscous properties of fresh, spray-dried and lyophilized mucilage is shown in Fig. 3. The curve shape is not affected by temperature, suggesting temperature stability in the analyzed range. Dependence of viscosity on temperature can be represented by the Arrhenius equation (Lewis, 1987):

$$\eta = A \exp \left[ \frac{Ea}{R(1/T - 1/T_0)} \right] \quad (3)$$

where  $Ea$  is the activation energy ( $\text{kcal mol}^{-1}$ ),  $R$  is the gas constant:  $1.987207 \text{ cal mol}^{-1} \text{ K}^{-1}$ ,  $A$  is the constant related to the

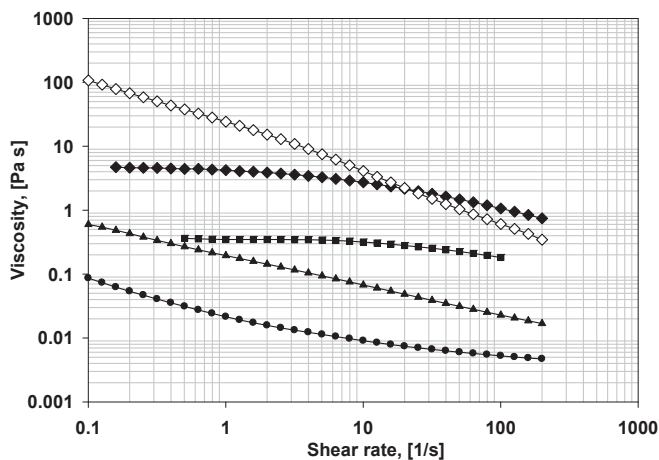


**Fig. 2.** Effect of mucilage concentration on steady-shear viscosity at 25 °C of fresh Aloe vera mucilage at 3 °Brix (sample T1 ●), Freeze dried at 0.03 g/mL (T9 ▲), Spray Drying sample (T6) reconstituted at two concentrations 0.03 (■) and 0.06 (◆) g/mL, and Xanthan gum at 0.03 g/mL (◇) (for comparison purposes).

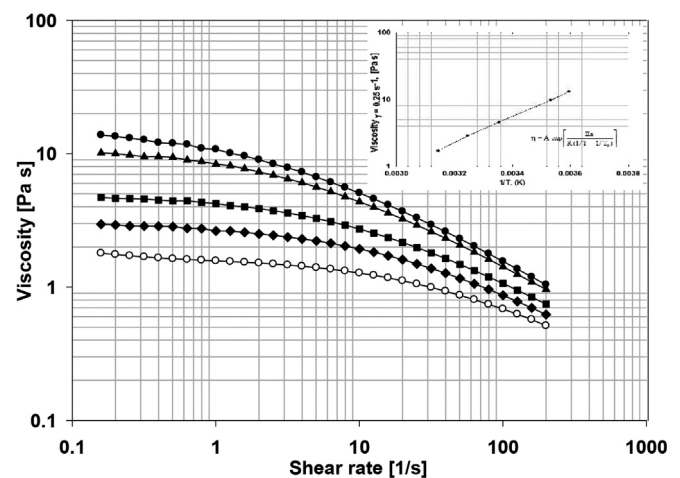


**Fig. 3.** Effect of the temperature on the steady shear viscosity of reconstituted spray dried Aloe vera mucilage powders 5 °C (●), 10 °C (▲), 25 °C (■), 35 °C (◆), 45 °C (○).

molecular collision frequency between T and T<sub>0</sub> (K). The reference temperature T<sub>0</sub> is 273.15 K for data shown in Fig. 3.

Values obtained from the linear regression are: E<sub>a</sub> = 124.35 J/mol for the fresh mucilage, 790.5 J/mol for the reconstituted freeze-dried mucilage, and with the SD process 1831.3 J/mol with 0.03 g/mL and 3.824 kcal/mol with 0.06 g/mL (correlation of R<sup>2</sup> = 0.9998). It is interesting to note that several biopolymers such as xanthan gum have revealed fairly stable viscous properties with respect to temperature (Rajinder, 1995) similarly to the value obtained with low AV concentrations (0.03 g/mL).

3.3.3. Effect of ionic strength

Experimental results regarding the effect of ionic strength on the viscous properties of mucilage (concentration of 0.06 g/mL) are shown in Fig. 4. Viscosity values are taken from the flow curve at a shear rate of 0.25 s<sup>-1</sup>. The effect of the ionic concentration on the viscosity is important to determine the dependence of rheological properties on the presence of functional ions. Charged molecules show a strong viscosity dependence of ionic strength. Medina-Torres et al., (2000) represented this functionality by using the following Equation (4):

$$\eta = \eta_{\infty} + SI^{-1/2} \tag{4}$$

where, η<sub>∞</sub> is the extrapolation of η to infinite ionic-strength. S is the slope of the function of η versus I<sup>-1/2</sup> related to the rigidity of the polymer chain.

Predictions of Equation (4) are also shown in Fig. 4 (dotted line). It is clear that for increasing ion concentration η decreases, as expected for polyelectrolyte solutions composed of several polysaccharides such as the AV-mucilage. Typical values of the slope (S) for xanthan samples are in the range of 0.55 and 0.66 (Lillford & Norton, 1991). S-values of the AV-mucilage range from 0.335 to 0.360, revealing that S depends on the ionic strength. According to data shown in Fig. 4, the viscosity reduction depends more on the Na<sup>+</sup> ions concentration than that of Ca<sup>++</sup> ions.

Ionic strength (or a negative charge) produces a strong intermolecular repulsion, which explains the high mucilage viscosity in

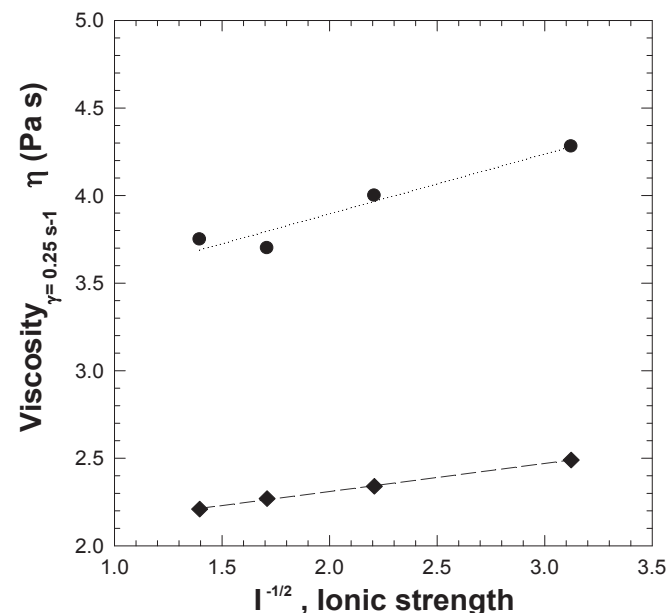


Fig. 4. Dependence of viscosity on ion strength for sample T6 at 0.06 g/mL reconstituted mucilage solution, at 25 °C. For two ions: Ca<sup>++</sup> (●) and Na<sup>+</sup> (◆).

de-ionized water. Otherwise, the addition of positive ions causes a reduction in the repulsion forces. These results are similar to those previously reported by Trachtenberg and Mayer (1982).

3.3.4. pH effect

The effect of pH on viscosity in simple-shear flow is shown in Fig. 5, where viscosity values are taken from the flow curve at a shear rate of 0.25 s<sup>-1</sup>. Upon increasing pH causes an increase in the viscosity. In the alkaline region, the viscosity tends to a plateau (saturation effect). Moreover, a sharp increase is observed between pH 4 and 6. The ionization of the carboxyl groups of the mucilage molecule above pH 4.0 may explain this sharp increase in viscosity.

A similar argument was reported by Trachtenberg and Mayer (1982) to explain the increase in the intrinsic viscosity of mucilage with pH (to almost zero-shear conditions). Consequently, it is clear that both pH and ionic strength influence the hydrodynamic volume of the AV-molecule. Conformational changes in the molecule should be considered to determine the functional properties of the AV-mucilage.

3.4. Elastic properties of simple shear flow

The first normal stress difference under simple-shear flow (N<sub>1</sub>) is a material function that allows the evaluation of the elastic properties of the material under flow. Fig. 6 shows N<sub>1</sub> as a function of shear stress τ<sub>12</sub>, revealing that aqueous solutions of mucilage are elastic under flow.

In comparison, a standard solution of polyisobutylene is shown in Fig. 6 (with the slope of 2 at low shear-rates). These results are represented by the following equation suggested by Broadbent and Lodge (1971):

$$N_1 = m'[\tau_{12}]^{n'} \tag{5}$$

where: m' is the characteristic consistency index, τ<sub>12</sub> is the shear stress (Pa) and n' is the flow behavior index (which can vary between 0 and 2). For the mucilage concentration studied in this work, N<sub>1</sub> is reasonably predicted by Equation (5), where m' and n' are given in the caption of Fig. 6. Values of N<sub>1</sub> are higher in the case of SD-mucilage as compared to fresh mucilage but the slope remains the same. This is expected since the total solid content between the samples is different. Similar trends were observed in the literature for a wide range of synthetic biopolymers (Ait-Kadi, Choplin, & Carreau, 1989).

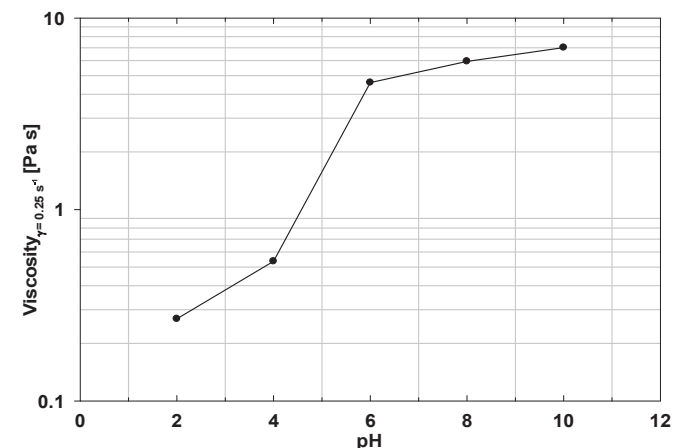
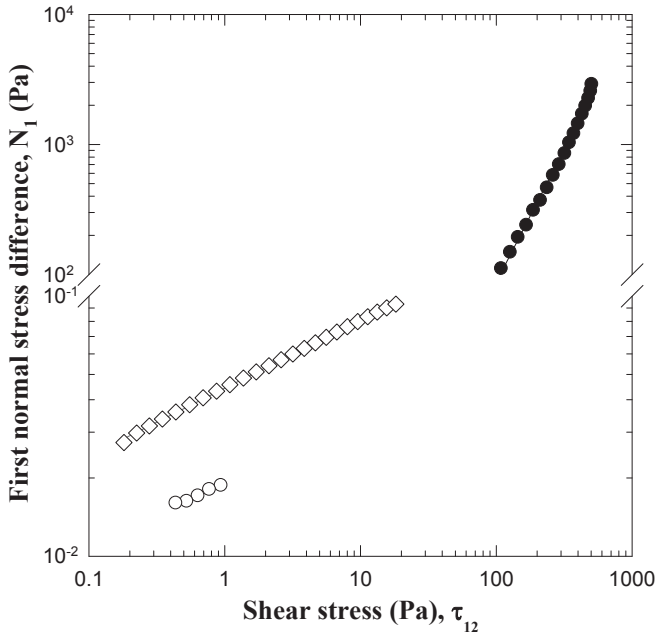


Fig. 5. pH dependence of the steady shear viscosity for mucilage 0.06 g/mL mucilage solution, and 25 °C.



**Fig. 6.** First normal stress difference ( $N_1$ ) as a function of shear stress  $\tau_1$  and the values of  $m'$  and  $n'$  are given for fresh Aloe vera ( $\circ$ ) ( $n' = 0.2181$ ,  $m' = 0.1787 \text{ Pa}^{1-n'}$ ), Spray dried reconstituted at 0.06 g/mL sample (T6,  $\diamond$ ) ( $n' = 0.2613$ ,  $m' = 0.2582 \text{ Pa}^{1-n'}$ ), and standard solution of polyisobutylene ( $\bullet$ ) ( $n' = 2.04$ ,  $m' = 0.1177 \text{ Pa}^{1-n'}$ ) this polymer used for comparison purposes only.

3.5. Rheological behavior of oscillatory shear flow at steady state

3.5.1. Concentration effect

Typical oscillatory flow curves of small amplitude strain as a function of concentration of mucilage in de-ionized water at 25 °C are shown in Fig. 7. The storage ( $G'$ ) and viscous modulus ( $G''$ ) are calculated from an oscillatory shear-flow according to the following equations:

$$G' = (\tau_0/\varepsilon_0)\cos\theta \tag{6}$$

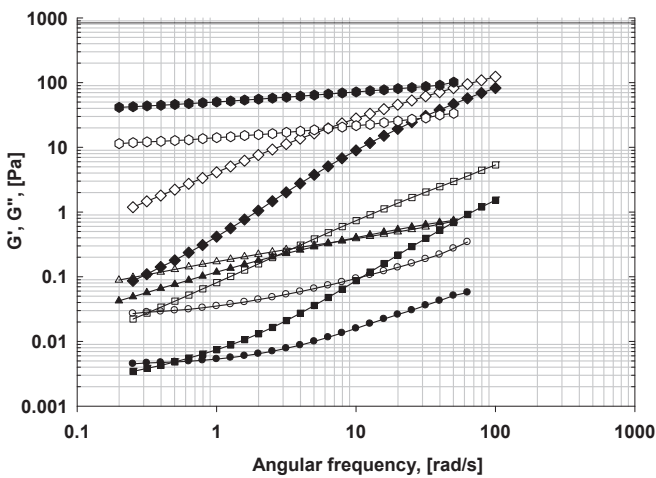


**Fig. 7.** Frequency dependence of the storage modulus  $G'$  (filled symbols) and loss modulus  $G''$  (empty symbols) for fresh Aloe vera at 3 °Brix ( $\bullet$ ,  $\circ$  small circle), freeze dried AV mucilage at 0.03 g/mL ( $\blacksquare$ ,  $\blacktriangle$ ), reconstituted spray dried Aloe vera mucilage at 0.03 g/mL ( $\blacksquare$ ,  $\square$ ) and 0.06 g/mL ( $\blacklozenge$ ,  $\lozenge$ ) and xanthan gum solutions ( $\bullet$ ,  $\circ$  large circle) in deionized water at 25 °C.

$$G'' = (\tau_0/\varepsilon_0)\sin\theta \tag{7}$$

where  $\tau_0$  is the oscillatory stress,  $\varepsilon_0$  is the strain and  $\theta$  is the phase angle between the stress and strain oscillatory signals.

The spectrum shows a typical mechanical behavior of a random-coil configuration (Morris et al., 1981). Mucilage solutions show viscoelastic properties of a predominant viscous behavior  $G'' > G'$  (Clark & Ross-Murphy, 1987). This behavior depends on the mucilage concentration in the dilute region (<0.06 g/mL).

Upon increasing the mucilage content,  $G'$  becomes larger than  $G''$ , indicating increasing elasticity due to macromolecular network formation. This behavior has been observed for xanthan gum for concentrations above 0.03 g/mL (Rajinder, 1995). In Fig. 4, data for xanthan 0.03 g/mL are presented for comparative purposes. Results suggest that mucilage solutions with 0.06 g/mL exhibit similar viscoelastic properties than xanthan solutions with 0.03 g/mL content.

3.5.2. Temperature effect

The effect of temperature on the viscoelastic properties of SD-reconstituted mucilage is presented in Fig. 8, for a concentration of 0.06 g/mL in de-ionized water. The dependence of both dynamic moduli  $G'$  and  $G''$  on frequency is observed at 5 and 35 °C. A similar trend has been reported by Morris et al. (1981) for random-coil polysaccharide conformations. It is important to note that at 5 °C, the point of intersection between  $G'$  and  $G''$  occurs at high frequency (short times), which suggest a conformational change in the mucilage structure.

Furthermore, the elastic and viscous responses under simple-shear are also dependent on both pH and ionic strength (data not shown here), revealing that the rheological properties of mucilage are dependent on molecular conformation.

4. Conclusions

Aloe vera mucilage powders were produced by spray-drying under different process conditions; they were analyzed in relation to their moisture content, total phenolic content, antioxidant capacity, carbohydrate composition, molecular weight and morphology. Reconstituted powders were evaluated by rheological techniques.

The rheological behavior of fresh AV-mucilage, lyophilized and

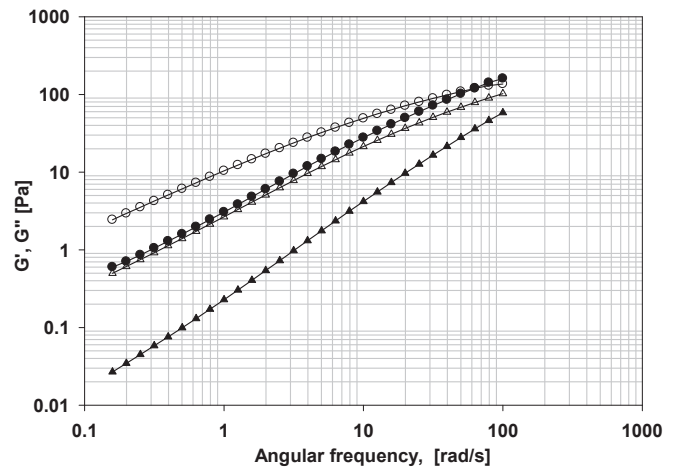


**Fig. 8.** Effect of temperature on the mechanical spectrum (viscoelastic moduli) of reconstituted SD AV mucilage at 0.06 g/mL. Storage  $G'$  (filled symbols) and loss modulus  $G''$  (empty symbols). 5 °C ( $\bullet$ ,  $\circ$ ) and 35 °C ( $\blacktriangle$ ,  $\triangle$ ).

re-suspended in aqueous medium after SD in powder form reveals shear thinning behavior ( $n < 1$ ).

Viscous AV-mucilage solutions are found unstable to temperature changes at concentrations higher than 0.03 g/mL. Furthermore, the shear viscosity depends on the ionic strength in the same way as a common poly-electrolyte molecule; this behavior is more pronounced with divalent ions.

Viscosity depends on solution-pH and a sharp viscosity increase is found in the range 4–6 of pH.

Elastic properties under shear flow were analyzed through measurements of  $N_1$  in SD-reconstituted mucilage samples. Similar trends as those reported in the literature were found, signaling the possibility of substitution of some commercial gums by these systems.

Results evidence the possibility to preserve the physical properties and structure of the SD-powders of Aloe vera if specific process conditions that minimize the effect of the thermal processing are employed. It is important to note that the total phenolic content and antioxidant capacity of mucilage powders show a remarkable response, scavenging free radicals in the samples processed at lower temperatures, low temperature difference  $\Delta T$  (inlet and outlet) and low inlet flow. High expectations of the use of SD in natural biopolymers for possible use in the food industry are envisaged.

## Acknowledgments

We acknowledge the financial support of CONACYT through Project CB-2014/235880.

## References

- Ait-Kadi, A., Choplin, L., & Carreau, P. J. (1989). On correlations of primary normal stresses in polymer solutions. *Polymer Engineering & Science*, *29*, 1265–1272.
- Alamilla-Beltrán, L., Chanona-Pérez, J., Jiménez-Aparicio, A., & Gutiérrez-López, G. (2005). Description of morphological changes of particles along spray drying. *Journal of Food Engineering*, *67*, 179–184.
- AOAC. (1990). *Official methods of analysis*. Arlington, USA: Association of Official Analytical Chemists.
- Blumenkrantz, N., & Asboe-Hansen, G. (1973). New method for quantitative determination of uronic acids. *Analytical Biochemistry*, *54*, 484–489.
- Brand-Williams, W., Cuvelier, M. E., & Berset, C. (1995). Use of a free radical method to evaluate antioxidant activity. *LWT—Food Science and Technology*, *28*, 25–30.
- Broadbent, J. M., & Lodge, A. S. (1971). Determination of normal-stress differences in steady shear flow: III. A wide-gap concentric cylinder apparatus. *Rheologica Acta*, *10*, 557–558.
- Cervantes-Martínez, C. V., Medina-Torres, L., González-Laredo, R. F., Calderas, F., Sánchez-Olivares, G., Herrera-Valencia, E. E., et al. (2014). Study of spray drying of the Aloe vera mucilage (Aloe vera barbadensis Miller) as a function of its rheological properties. *LWT—Food Science and Technology*, *55*, 426–435.
- Chiou, D., & Langrish, T. A. G. (2007). Development and characterization of novel nutraceuticals with spray drying technology. *Journal of Food Engineering*, *82*, 84–91.
- Clark, A. H., & Ross-Murphy, S. B. (1987). Structural and mechanical properties of biopolymer gels. In *Advances in polymer science* (Vol. 83, pp. 57–192). Germany: Cuvelier, M. E., Richard, H., & Berset, C. (1992). Comparison of the antioxidative activity of some acid-phenols: structure activity relationship. *Bioscience Biotechnology and Biochemistry*, *56*, 324–325.
- Femenia, A., García-Pascual, P., Simal, S., & Rosselló, C. (2003). Effects of heat treatment and dehydration on bioactive polysaccharide acemannan and cell wall polymers from Aloe barbadensis Miller. *Carbohydrate Polymers*, *51*, 397–405.
- Ferrari, C. C., Germer, S. P. M., & de Aguirre, J. M. (2012). Effects of spray-drying conditions on the physicochemical properties of blackberry powder. *Drying Technology*, *30*, 154–163.
- Frascarelli, E. C., Silva, V. M., Tonon, R. V., & Hubinger, M. D. (2012). Effect of process conditions on the microencapsulation of coffee oil by spray drying. *Food and Bioprocess Processing*, *90*, 413–424.
- Gandia-Herrero, F., Jimenez-Atenzar, M., Cabanes, J., Garcia-Carmona, F., & Escribano, J. (2010). Stabilization of the bioactive pigment of opuntia fruits through maltodextrin encapsulation. *Journal of Agricultural and Food Chemistry*, *58*, 10646–10652.
- Heimler, D., Vignolini, P., Dini, M., & Romani, A. (2005). Rapid tests to assess the antioxidant activity of Phaseolus vulgaris L. dry beans. *Journal of Agricultural and Food Chemistry*, *53*, 3053–3056.
- Keshani, S., Daud, W. R. W., Nourozi, M. M., Namvar, F., & Ghasemi, M. (2015). Spray drying: an overview on wall deposition, process and modeling. *Journal of Food Engineering*, *146*, 152–162.
- Lewis, M. J. (1987). *Physical properties of foods and food processing systems* (pp. 465–468). Chichester, UK: Ellis Horwood Ltd.
- Lillford, P. J., & Norton, I. T. (1991). Food Hydrocolloids: an end user's viewpoint. In G. O. Phillips, P. A. Williams, & D. J. Wedlock (Eds.), *Gums and stabilizers for the food industry* (Vol. 3, pp. 3–12). Oxford, UK: IRL.
- McAnalley, B. H. (1993). *Process for preparation of Aloe products*. European Patent WO 89/06539.
- Medina-Torres, L., Brito-de La Fuente, E., Torrestiana-Sánchez, B., & Katthain, R. (2000). Rheological properties of the mucilage gum (*Opuntia ficus indica*). *Chemistry Hydrocolloid*, *14*, 417–424.
- Morris, E. R., Cutler, A. N., Ross-Murphy, S. B., Rees, D. A., & Price, J. (1981). Concentration and shear dependence of viscosity in random coil polysaccharide solutions. *Carbohydrate Polymers*, *1*, 5–21.
- Paudel, A., Loyson, Y., & Van de Mooter, G. (2013). An investigation into the effect of Spray drying temperature and atomizing conditions on miscibility, physical stability, and performance of Naproxen-PVP K 25 solid dispersions. *Journal of Pharmaceutical Sciences*, *102*, 1249–1267.
- Rajinder, P. (1995). Oscillatory, creep and steady flow behavior of Xanthan-thickened oil-in-water emulsions. *AIChE Journal*, *41*, 783–794.
- Rodríguez-González, V. M., Femenia, A., González-Laredo, R. F., Rocha-Guzmán, N. E., Gallegos-Infante, J. A., Candelas-Cadillo, M. G., et al. (2011). Effects of pasteurization on bioactive polysaccharide acemannan and cell wall polymers from Aloe barbadensis Miller. *Carbohydrate Polymers*, *86*, 1675–1683.
- Saeman, J. F., Moore, W. E., Mitchell, R. L., & Millett, M. A. (1954). Techniques for the determination of pulp constituents by quantitative paper chromatography. *TAPPI Journal*, *34*, 336–365.
- Sakin-Yilmazer, M., Koç, B., Balkir, P., & Kaymak-Ertekin, F. (2014). Rheological behavior of reconstituted yoghurt powder—An optimization study. *Powder Technology*, *266*, 433–439.
- Sánchez-Moreno, C., Larrauri, J. A., & Saura-Calixto, F. (1998). A procedure to measure the antiradical efficiency of polyphenols. *Journal of the Science of Food and Agriculture*, *76*, 270–276.
- Simões, J., Nunes, F. M., Domingues, P., Coimbra, M. A., & Domingues, M. R. (2012). Mass spectrometry characterization of an Aloe vera mannan presenting immunostimulatory activity. *Carbohydrate Polymers*, *90*, 229–236.
- Trachtenberg, S., & Mayer, A. M. (1982). Biophysical properties of *Opuntia ficus-indica* mucilage. *Phytochemistry*, *21*, 2835–2843.
- Wang, Y. F., Liu, Y. Y., Huo, J. L., Zhao, T. T., Ren, J., & Wei, X. L. (2013). Effect of different drying methods on chemical composition and bioactivity of tea polysaccharides. *International Journal of Biological Macromolecules*, *62*, 714–719.
- Whistler, R. L. (1993). Industrial gums: polysaccharides and their derivatives. In R. L. Whistler, & N. B. James (Eds.), *Introduction to industrial gums* (pp. 1–19). USA: Academic Press Inc.



## Bioactive compounds from mustard flours for the control of patulin production in wheat tortillas



Federica Saladino<sup>a</sup>, Lara Manyes<sup>a</sup>, Fernando B. Luciano<sup>b</sup>, Jordi Mañes<sup>a</sup>,  
Mónica Fernandez-Franzon<sup>a</sup>, Giuseppe Meca<sup>a,\*</sup>

<sup>a</sup> Laboratory of Food Chemistry and Toxicology, Faculty of Pharmacy, University of Valencia, Av. Vicent Andrés Estellés s/n, 46100 Burjassot, Spain

<sup>b</sup> School of Agricultural Sciences and Veterinary Medicine, Pontificia Universidade Católica do Paraná, BR 376 Km 14, São José dos Pinhais, PR 83010-500, Brazil

### ARTICLE INFO

#### Article history:

Received 9 July 2015

Received in revised form

18 September 2015

Accepted 2 October 2015

Available online 9 October 2015

#### Keywords:

Glucosinolates

Isothiocyanates

*Penicillium expansum*

Chemical control

PAT

### ABSTRACT

Patulin (PAT) is a toxic fungal metabolite produced by *Penicillium*, *Aspergillus* and *Byssoschlamys* growing especially in fruit and cereals. PAT exhibits a number of toxic effects in animals and its presence in food is undesirable. In this study the reduction of the mycotoxin PAT produced by a strain of *Penicillium expansum*, on wheat tortillas was studied using volatile bioactive compounds present in the oriental and yellow mustard flour and also using the standard solution of the antifungal compound allyl isothiocyanate (AIT), developing an active packaging with two different systems of release of those bioactive compounds. Also the kinetic of volatilization of the compounds used in the bioactive packaging was evaluated using the technique of the gas chromatography (GC) coupled to the flame ionization detector (FID). The PAT was extracted from the samples using the QUECHERS methodology and was determined using the technique of the liquid chromatography (LC) coupled to the mass spectrometry detector in tandem (MS/MS). The maximum of volatilization of the AIT in the bioactive packaging is produced between 1 and 24 h depending on the volatilization technique and is stable during two months, whereas the reduction of PAT evidenced in the samples treated ranged from 80 to 100%.

© 2015 Elsevier Ltd. All rights reserved.

### 1. Introduction

Patulin (Fig. 1) (PAT) is a toxic secondary metabolite produced by a wide range of fungal species of the genera *Penicillium*, *Aspergillus* and *Byssoschlamys*. Among the different genera, the most important PAT producer is *Penicillium expansum* (Moake, Padilla-Zakour, & Worobo, 2005). PAT has been found as a contaminant in many moldy fruits, vegetables, cereals and other foods. However, the major sources of contamination are apples and apple products, which are also the most important source of PAT in the human diet (Baert et al., 2007; Murillo-Arbizu, Amézqueta, González-Peñas, & de Cerain, 2009; Reddy et al., 2010).

PAT has been classified in Group 3 by IARC that means not classifiable as to its carcinogenicity to humans, although it has been shown to cause neurotoxic and mutagenic effects in animals (IARC,

2002). In 1995, the Joint Food and Agriculture Organization/World Health Organization Expert Committee on Food Additives (JECFA, 1995) recommended a provisional tolerable daily intake (pTDI) of 0.4 µg PAT/kg body weight/day based on long-term exposure (JECFA, 1995). As a result, the levels of PAT in fruits are subjected to legislative control. The Codex Alimentarius recommends levels of PAT in fruits and fruit juices to be lower than 0.05 mg/kg.

PAT causes gastrointestinal effects as distension, ulceration and hemorrhage in acute and short-term *in vivo* studies. Recent studies have also demonstrated that PAT alters the intestinal barrier function. PAT has electrophilic properties and high reactivity to cellular nucleophiles. At cellular level it can cause enzyme inhibition and chromosomal damage. PAT causes cytotoxic and chromosome-damaging effects mainly by forming covalent adducts with essential cellular thiols (Fliege & Metzler, 2000; Glaser & Stopper, 2012).

Vegetables like broccoli, cauliflower, cabbage, Brussels sprouts, belong to the Brassica genus and are widely consumed. A healthy diet should include Brassica vegetables because these vegetables are rich in health-promoting compounds like ascorbic acid, soluble fiber, selenium, glucosinolates (GLS), etc. Among these compounds,

\* Corresponding author. Laboratory of Food Chemistry and Toxicology, Faculty of Pharmacy, University of Valencia, Av. Vicent Andrés Estellés s/n, 46100 Burjassot, Spain.

E-mail address: [giuseppe.meca@uv.es](mailto:giuseppe.meca@uv.es) (G. Meca).

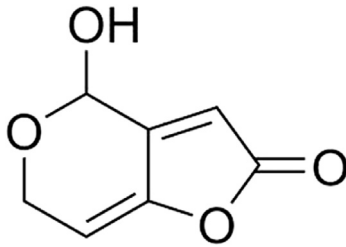


Fig. 1. Patulin chemical structure.

GLS have been extensively studied in the past decades. GLS are secondary metabolites that can be classified as aliphatic, aromatic or indolic depending on their side chain (Fahey, Zalcmann, & Talalay, 2001). GLS are hydrolyzed by a group of endogenous  $\beta$ -glucosidases termed myrosinase (Fig. 2). Myrosinase (MYR) is stored separately from GLS in the plants, but will mix with GLS upon tissue damage (Kissen, Rossiter, & Bones, 2009). Hydrolysis of the thioglucosidic bond by myrosinases releases an aglycone that can either rearrange into an isothiocyanate or be converted to other products such as nitriles, epithionitriles or organic thiocyanates depending on the presence of specific proteins and certain structural prerequisites.

Fungi growth inhibition by isothiocyanates has been reported since the late 1930's (Luciano & Holley, 2009). These compounds are very unique in comparison to other essential oils, since they are only formed when the plant cell suffers some kind of injury such as insect bite, grinding, milling or fungi contamination in the presence of water (Luciano & Holley, 2009). Then, the isothiocyanate precursors, called GLS, are transformed by the enzyme myrosinase. Therefore, isothiocyanates are not present in dry mustard flour, unless water is added to it.

ITCs exhibit biocidal activity against microorganisms including fungi (Nielsen & Rios, 2000) and bacteria (Luciano & Holley, 2011), as well as insects (Tsao, Yu, Potter, & Chiba, 2002) and nematodes (Flemming, Turner, & Hunt, 2006). In particular, it has been demonstrated that AIT effectively inhibits the growth of a variety of pathogenic microorganisms at low concentrations (Lin, Preston, &

Wei, 2000; Luciano & Holley, 2009). The potential of AIT as a natural antimicrobial in different food matrices, including chicken breast (Shin, Harte, Ryser, & Selke, 2010), ground beef (Nadarajah, Han, & Holley, 2005), dry-cured ham (Graumann & Holley, 2007), fermented dry sausages (Chacon, Muthukumarasamy, & Holley, 2006), and tuna meet (Hasegawa, Matsumoto, Hoshino, & Iwashita, 1999) has been studied.

The aims of this study were to study a) the quantity of the GLS present in yellow and oriental mustard flours b) the kinetic of volatilization of the antimicrobial AIT present in two active packaging and c) the inhibition of the *P. expansum* growth and PAT production in wheat tortillas treated with AIT.

## 2. Materials and methods

### 2.1. Materials and chemicals

PAT, sinalbin and sinigrin (98% purity), formic acid (HCOOH), AIT (94% purity), para-hydroxybenzylisothiocyanate (PHBITC), tetrabutylammonium hydrogen sulfate (TBA), ammonium formate, and sodium chloride (NaCl) were obtained from Sigma–Aldrich (St. Louis, USA). Oriental (*Brassica juncea*) and yellow mustard (*Brassica alba*) flours were provided by G.S. Dumm dry mustard millers (Hamilton, Ontario, Ca). Methanol was purchased from Fisher Scientific (New Hampshire, USA). Deionized water (<18 M $\Omega$  cm resistivity) was obtained from a Milli-Q water purification system (Millipore, Bedford, MA, USA). Chromatographic solvents and water were degassed for 20 min using a Branson 5200 (Branson Ultrasonic Corp., CT, USA) ultrasonic bath. The strain of *P. expansum* CECT 2278, was obtained from the Spanish Type Culture Collection (CECT, Valencia, Spain). The plastic trays used for the experiments were composed by multilayer polyethylene (13"  $\times$  9.6" clear, rectangular, with an oxygen transmission of 6509 cm<sup>3</sup>/mil/m<sup>2</sup>/24 h) and were provided by Saplex (Barcelona, Spain).

### 2.2. GLS extraction and determination

GLS from oriental and yellow mustard flours were extracted using the method of Prestera et al. (1996) with modifications. Twenty grams of each flour were placed in a 50 mL glass tube and autoclaved at 115 °C during 15 min to inactivate the enzyme

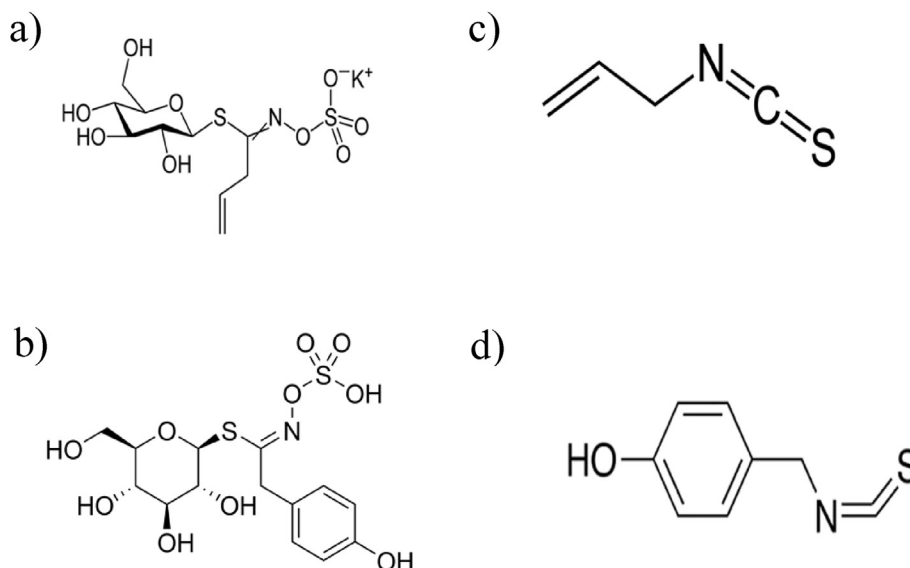


Fig. 2. Chemical structure of the bioactive GLSs a) sinigrin and b) sinalbin c) and of the ITCs c) AIT and d) PHBITC.

myrosinase. Then, the samples were added with 200 mL of boiling distilled water in a 500 mL Erlenmeyer flask and the mixture was stirred for 10 min at 350 rpm. The mixtures were cooled at room temperature, centrifuged at 2500 rpm for 5 min at 4 °C and filtered through Whatman no. 4 filter paper into 50 mL screw-capped tubes. The extracts were filtered again through a 0.22 µm filter. Separation and quantification of GLS were performed using a Shimadzu LC system (Shimadzu, Japan), equipped with a Gemini C18 column (4.6 × 150 mm i.d. 5 µm; Phenomenex, Palo Alto, CA). Elution was carried out isocratically for 20 min at a flow rate of 1 mL/min, using a solvent system containing 20% (v/v) acetonitrile and 80% water+0.02 M tetrabutylammonium hydrogen sulfate (pH 5.5). The injection volume used was 20 µL. A UV detector was used to measure the absorbance at 227 nm in order to verify and quantify the presence of GLS sinigrin (SN) and sinalbin (SA) with reference retention time of 2.23 and 1.83 min respectively.

### 2.3. Headspace analysis of AIT

The study of the release of the AIT used to preserve the wheat tortillas (stored in plastic trays) against *P. expansum* growth and PAT production was carried out performing two different sets of experiments and in particular:

- 1) It was evaluated the AIT released in the plastic tray by the conversion of the GLS contained in the oriental mustard flour into AIT through myrosinase conversion in presence of water. The flour (4 g) was weighted and placed in a small plastic bag containing 3 mL of water, and after the homogenization of the mustard flours matrices were pasted on the cover tray.
- 2) It was evaluated the AIT released by the evaporation of a 50 µL of the standard solution of the AIT placed on a 2.5 × 2.5 cm paper-filter plastic and pasted on the cover tray.

The AIT evaporated in the headspace of the plastic trays described above was determined using a gas chromatograph (GC) equipped with flame ionization detector (FID) (GC 6890, Agilent Technologies Inc., Santa Clara, Calif., U.S.A.), equipped with a 30 m × 0.25 mm CP-SIL 88 fused capillary column (Varian, Middelburg, Netherlands). The inlet temperature was set at 200 °C, whereas the detector temperature was 250 °C. H<sub>2</sub> served as carrier gas (5 ml/min), and the FID gasses were H<sub>2</sub> (40 mL/min), and purified air (450 mL/min). The temperature program was as follow: initial temperature of 60 °C was held for 1 min, raised at 8 °C/min until 100 °C and held for 5 min, then raised at 15 °C/min until 200 °C, totalizing 16.6 min per sample analysis. Identification and quantification of AIT was carried out comparing the samples areas with points standards curve (1–100 mg/kg).

Test trays were stored at room temperature (0–2 months) and then 100 µL of the head space was injected in the chromatograph through a septum applied in the tray cover (Fig. 4). Three replicates were carried out for each test condition.

### 2.4. Wheat tortillas food system experiments

In a multilayer plastic tray of 1L (Saplex, Barcelona, Spain) was inserted a sample of wheat tortilla (10 g). The samples were treated with:

- a) Three quantities of oriental and yellow mustard flours (0.5, 1 and 2 g) placed in a small plastic bag with the same quantity of water to promote the reaction of conversion of the GLS into ITCs and pasted on the tray plastic cover.

- b) Three different quantities of the standard solution of the AIT (50–100–200 µL/L) placed on a 2.5 × 2.5 cm paper-filter pasted on the plastic tray cover.

The wheat tortillas (50 g) were contaminated with one mL of *P. expansum* CECT 2681 grown in Potato Dextrose Broth (PDB) (Oxoid, UK) medium containing 10<sup>6</sup> conidia/mL. Conidial concentration was measured by optical density at 600 nm in sterile water and adjusted to 10<sup>6</sup> conidia/ml in PDB as reported Kelly, Grimm, Bendig, Hempel, and Krull (2006). The control group did not receive any mustard flours or AIT treatments. The plastic trays were closed and incubated at 23 °C during 30 days.

### 2.5. PAT extraction

For wheat tortilla samples 10 ± 0.01 g test portion was weighed into a 50 mL Falcon polypropylene tube (Becton Dickinson, Le Pont de Claix, France). Ten milliliters of acetonitrile were added in all samples, and the resulting slurry was vigorously hand-mixed and placed onto an automated shaker for 5 min.

Partitioning Step: A magnesium sulfate (MgSO<sub>4</sub>)/sodium chloride (NaCl) salt mixture (4:1, w/w) (5.0 ± 0.2) was added to the slurry, which was immediately and vigorously hand shaken for a few seconds before centrifugation at room temperature at 4000 g for 15 min.

Cleanup by Dispersive Solid-Phase Extraction (dSPE): The resulting acetonitrile-based supernatant (6 mL) was transferred to a 15 mL Falcon polypropylene tube already filled with 400 mg of Primary Secondary Amine (PSA), 400 mg of C<sub>18</sub>, and 1200 mg of MgSO<sub>4</sub>, and the tubes were vigorously hand-shaken for about 30 s. After centrifugation (4000 g at room temperature for 10 min), the supernatant (1 mL) was transferred into a new 15 mL Falcon polypropylene tube filled beforehand with 10 µL of a 5% formic acid solution in water (v/v). Sample was mixed and evaporated to dryness at 40 °C under a stream of nitrogen.

Final Treatment of the Extract: The residue was reconstituted in H<sub>2</sub>O (200 µL) before being filtered over a Polytetrafluoroethylene (PTFE) syringe filter, 0.2 µm, 13 mm, and collected into a amber glass vial for further liquid chromatography tandem mass spectrometry (LC-MS/MS) analysis (Desmarchelier, Mujahid, Racault, Perring, & Lancova, 2011).

### 2.6. LC-MS/MS PAT determination

LC analysis was performed on a 150 mm × 4.6 mm, 2.1 mm i.d., 2.5 µm, Gemini C18 column (Phenomenex, Palo Alto, CA) using an Agilent 1100 binary pump system. The mobile phase was constituted by H<sub>2</sub>O (A), and acetonitrile (B). A linear gradient program was set up with 0.2 min, 5% B; 2.5 min, 95% B; a hold at 95% B for 2 min; and a return to 5% B in 0.5 min (the LC column was reconditioned at 5% B for an additional 10 min). The flow rate was 0.3 mL/min, and 20 µL of the extract were injected. MS detection was performed using an 4000 QTrap (Applied Biosystems, Toronto, CA) equipped with a Turbo Ion Spray ionization source. MS tuning was performed in positive electrospray ionization (ESI) by syringe-infusing separately a 10 µg/mL solution of PAT. The block source temperature was maintained at 500 °C, and the gas set values were as follows: curtain gas, 40 psi; nebulizer gas, 30 psi; turbo gas, 30 psi; collision gas, 1.2 × 10<sup>4</sup> psi. The entrance potential and the collision exit potential were settled at 10 and 15 V, respectively, and the electrospray capillary voltage was set at +4 kV. Quantitative analysis was performed using tandem MS in selected reaction monitoring (SRM) mode using as quantification transition the ion with a *m/z* of 153, whereas as analyte confirmation the ions with a *m/z* of 109 and 81. Data processing was carried out using Analyst

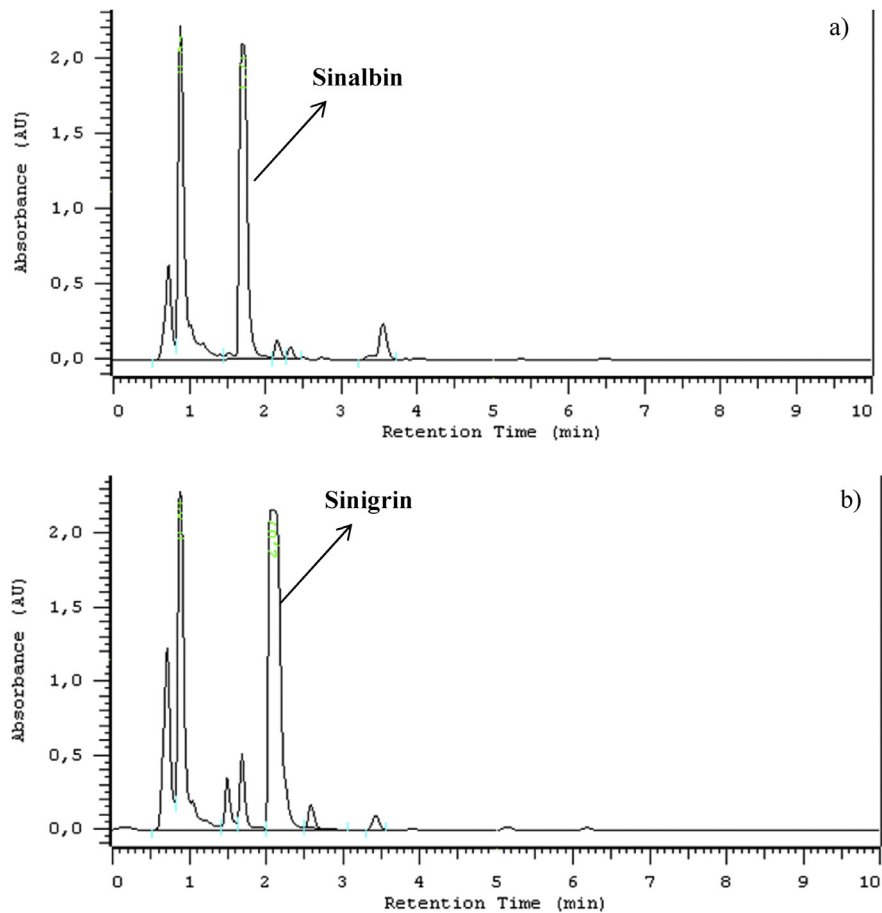


**Fig. 3.** LC-DAD chromatograms of the a) sinialbin and b) sinigrin presents in the yellow and oriental mustard flours respectively. (For interpretation of the references to colour in this figure legend, the reader is referred to the web version of this article.)

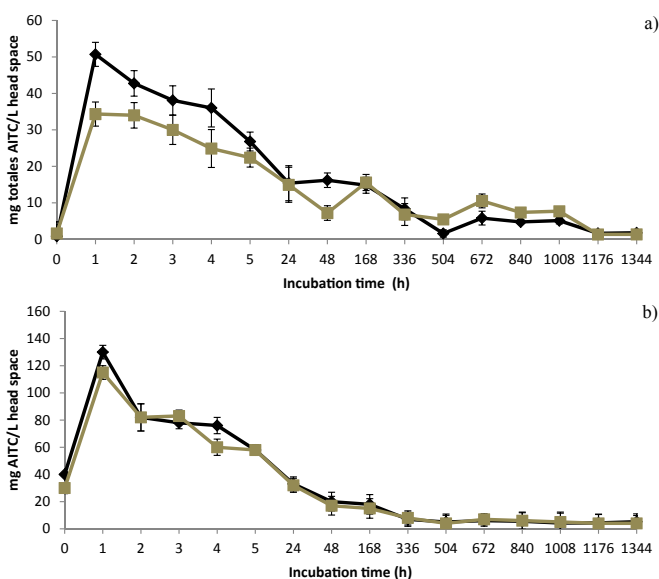


**Fig. 4.** Volatilization kinetics of the AIT contained in the plastic trays a) employing 4 g of oriental mustard placed in a small plastic bag containing 3 mL of water to promote the sinigrin conversion in AIT, b) employing the AIT released by the evaporation of a 100  $\mu$ L of the standard solution of the bioactive compound placed on a 2.5  $\times$  2.5 cm paper-filter and pasted on the cover tray (Black = with food, grey = without food). (For interpretation of the references to colour in this figure legend, the reader is referred to the web version of this article.)

software 1.5. PAT was quantitated by means of an external calibration curve (Desmarchelier et al., 2011).

### 3. Results and discussion

#### 3.1. GLS evaluation in yellow and oriental mustard flours

The GLS presents in the yellow and oriental mustard flours were analytically characterized to know the total amount of the GLS that can be converted in ITCs through the action of the enzyme myrosinase. Both flour matrices were extracted with an aqueous extraction and analyzed using the LC-DAD technique (Fig. 3). The principal GL present in the oriental mustard flour was the sinigrin (SN), with a retention detected in the quantity of 46 g/Kg, whereas the yellow mustard flour was characterized for the presence of the GL sinialbin (SA) in the concentration of 42 g/Kg. These two GLS, SN and SA, are the precursor of the antimicrobial compounds AIT and parahydroxybenzyl isothiocyanate (PHITC) respectively that are the compounds that through the reaction with the enzyme myrosinase were used to reduce the growth of the strain of *P. expansum* inoculated on wheat tortillas.

To improve the safety of bakery products, the addition of other agents during manufacture to control the presence of the myco-toxigenic fungi is of great interest. One alternative to the synthetically antimicrobial compounds with promise is the mustard flour, which has natural antimicrobial properties. All plants in the Brassicaceae family contain GLS as secondary metabolites, and yellow (*B. juncea*) and oriental (*B. alba*) mustards contains the GLS SN and

SA. Upon physical damage of the plant tissue, hydrolysis of GLS is catalyzed by the endogenous enzyme myrosinase in the presence of moisture to produce the antimicrobial compounds AIT and PHBITC (Delaquis & Mazza, 1995; Ekanayake et al., 2006). The mechanism of action of these antimicrobial compounds is uncertain, but it may inhibit essential enzymes and cause membrane damage (Lin et al., 2000).

### 3.2. Gas chromatography evaluation of the AIT volatilization

The volatilization of the bioactive compound AIT employed to reduce the growth of the strain of *P. expansum* CECT 2278 in wheat tortillas samples was studied using three different methodologies. The first methodology was based on the employment of the oriental mustard flour inserted in a small plastic bag with water that catalyze the reaction conversion of the GL SN in the AIT mediated by the enzyme myrosinase, whereas the second methodology was developed absorbing 50  $\mu$ L of the AIT standard solution on a paper filter pasted under the plastic tray cover used for the wheat tortillas storage. The volatilization of the bioactive compound AIT was studied with and without the presence of the food matrix employed in this study at room temperature during two months storage.

In particular as shown in Fig. 4a, using the oriental mustard flour, the maximum level of AIT detected in the headspace with and without the sample were of 34.3 and 50.7 mg/L respectively. This difference on the AIT volatilization could be related to several factors:

- During the incubation time studied the concentration of the AIT decrease until 15 mg/L evidenced at 24 h incubation, and then continue to decrease probably due to the absorption of the AIT in the plastic matrix that compose the tray and also for the absorption of the bioactive compound in the food matrix tested.
- Another important aspect that has to be considered is that the AIT during the volatilization can be converted in other compounds with less antimicrobial activity as thiocyanates and nitrils (Meca, Luciano, Zhou, Tsao, & Mañes, 2012).

Employing the second AIT volatilization system (50  $\mu$ L of AIT standard solution absorbed on a paper filter) the maximum AIT dispersion in the headspace was detected during the first incubation hour and was of 130 and 115 mg/L considering the presence and the absence of the food matrix present in the plastic tray (Fig. 4b). The concentration of the bioactive compound in the headspace decrease between the second and the fifth incubation hour arriving at 20 mg/L at 48 h incubation and remain constant to 5 mg/L until the end of the experiments. Employing this AIT volatilization system the concentration of the AIT present in the headspace in the first 48 h was 2.0 fold highest than the data evidenced using the oriental flour as AIT generation system. This application of the AIT has the advantage to promote a more rapid AIT volatilization in the first incubation hours reducing the possibility of growth/germination of the mycotoxigenic fungi in food matrices. Considering the data evidenced in our study the presence of the food matrix does not influence significantly the vaporization of the AIT.

### 3.3. PAT reduction in wheat tortillas

The sample preparation for PAT analysis in wheat tortillas was based on the QuEChERS procedures described in AOAC International official method 2007.01 and CEN standard method (2008). All the parameters optimized for LC-MS/MS analysis are described below:

The limit of detection (LOD) was defined as the lowest

concentration producing a chromatographic peak with a signal-to-noise ratio (S/N)  $\geq 3$ .

Despite closely depending on the cleanliness of the MS source, and thus submitted to small variations over the time, the LOD was broadly estimated within a 0.2  $\mu$ g/kg for the food matrix studied. The limit of quantitation (LOQ) was arbitrarily defined as the lowest fortification level, that was, 5  $\mu$ g/kg.

Internal standard corrected recoveries were within a 94–104% range, whereas precision data, that is, RSD<sub>r</sub> and RSD<sub>IR</sub>, were of 1.3 and 3.3%, respectively.

All of these results were compliant with the analytical requirements of the European Committee for Standardization (2010).

The bioactive compound AIT used in this study was tested for the reduction of the *P. expansum* growth in wheat tortillas samples and also the production by the microorganism of the mycotoxin PAT was evaluated to understand if the fungal growth reduction can influence the mycotoxin reduction. The wheat tortillas were treated with two different AIT applications as explained in the material and method section.

The PAT present in the food products treated with those two methodologies was analyzed using the technique of the LC-MS/MS (Fig. 5).

As evidenced in Fig. 6, the mean reduction of the PAT observed using the two different AIT applications was of 92.58%. The highest PAT reduction was evidenced in the experiments carried out using 2.0 g of yellow mustard flour with a 99.1%, whereas the lowest was observed using the 0.5 g of oriental mustard flour with 85.5%. Comparing the results obtained using the two mustard flours no significative differences were detected using 0.5 and 1.0 g of both flours, whereas using 2.0 g, the PAT reduction observed using the yellow and oriental mustard flour were of 99.1 and 92.9% respectively. The results obtained using the standard solutions of the AIT were comparable with the data obtained with the two flours matrices employed.

This article can be considered the first where a chemical approach based on the use of the bioactive compounds ITCs was employed to reduce the PAT produced by *P. expansum* in food matrices, whereas the use of other strategies to reduce the PAT present in food products was evaluated by many authors.

In particular Drusch, Kopka, and Keading (2007) studied the stability of PAT in an aqueous juice-like model system. At acidic pH, the presence of ascorbic acid reduced the stability of PAT. After 34 days, PAT was reduced to 30% of its initial concentration in the presence of ascorbic acid compared to 68–71% in samples without ascorbic acid. Conditions during storage (presence of light, oxygen and/or metal ions) influenced the stability of PAT. Furthermore, it was possible to induce degradation of PAT by either generating hydroxyl radicals or by adding the rather stable radical diphenyl-1-picrylhydrazyl (DPPH). The data evidenced by the authors indicate that PAT is decomposed by free radicals generated by oxidation of ascorbic acid to dehydroascorbic acid. The percentages of PAT reduction evidenced in this study are 0.5 fold lower than the data evidenced in our study.

Yun et al. (2008), studied the effects of organic acids, amino acids, and ethanol on the radio-degradation of PAT by gamma irradiation in an aqueous model system. The PAT, dissolved in distilled water at a concentration of 50 ppm, was practically degraded by the gamma irradiation at the dose of 1.0 kGy, while 33% of the PAT remained in apple juice. In the aqueous model system, the radio-degradation of PAT was partially inhibited by the addition of organic acids, amino acids, and ethanol. The proportions of remaining PAT after irradiation with the dose of 1.0 kGy in the 1% solution of malic acid, citric acid, lactic acid, acetic acid, ascorbic acid, and ethanol were 31.4%, 2.3%, 31.2%, 6.1%, 50.8%, and 12.5%, respectively. During 30 days of storage, the remaining PAT was

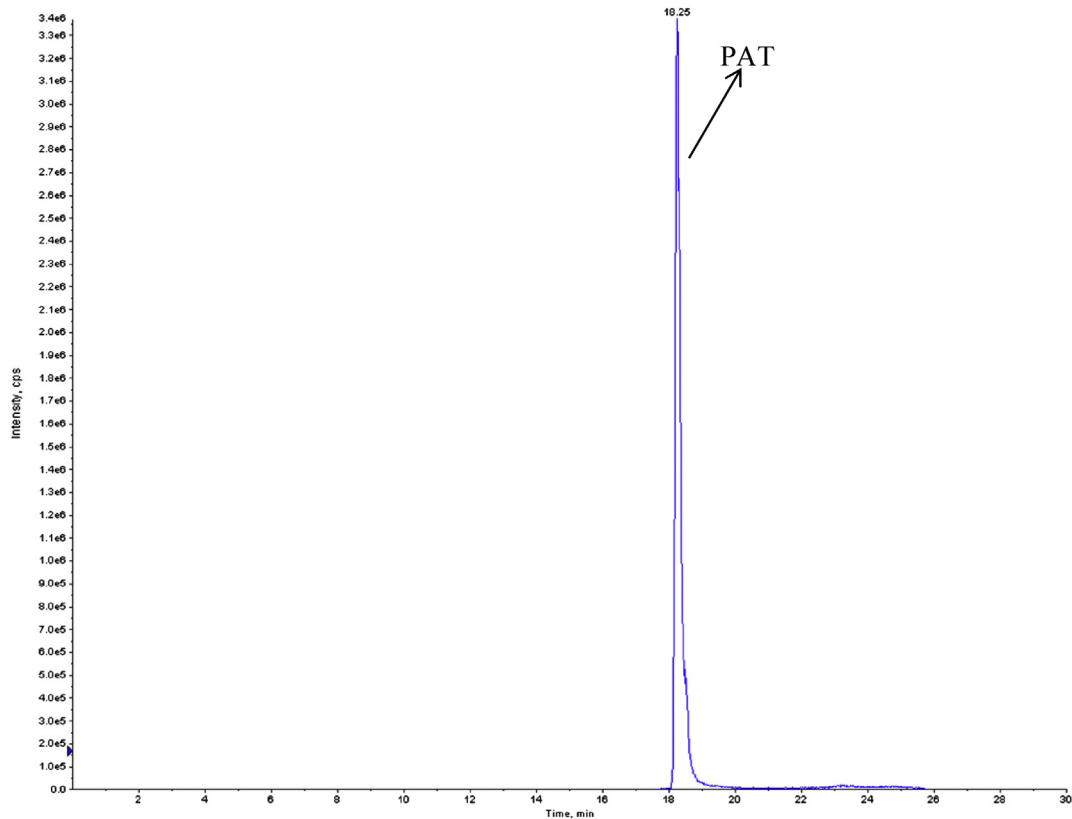


Fig. 5. LC-MS/MS chromatogram of the patulin present in the control wheat tortilla treated without AIT treatment.

reduced gradually in the solution of ascorbic acid and malic acid compared to being stable in other samples. The amino acids, serine, threonine, and histidine, inhibited the radio-degradation of PAT. It was suggested that 1 kGy of gamma irradiation (recommended radiation doses for radication and/or quarantine in fruits) is effective for the reduction of PAT, but the nutritional elements should be considered because the radio-degradation effects are environment dependent.

Gao, Yue, Yuan, Fu, and Peng (2009), evaluated the ultrasonic degradation technology of PAT to reduce the content of this bioactive compound in apple juice and improve the security of the food product. Based on the single-factor test, the optimum condition of ultrasonic was developed through orthogonal design. The results showed that the best process parameters of PAT ultrasonic

degradation in apple juice is power 420 W, time 90 min, frequency 28 kHz, temperature 30 °C, with the PAT degradation rate of 69.43%. There is minor impact on the key quality parameters of apple juice. The data evidenced in this study are 30% lowest than the data evidenced in our study.

Zhu, Koutchma, Warriner, Shao, and Zhou (2013) evaluated the feasibility of monochromatic ultraviolet (UV) radiation at 253.7 nm as a possible commercial application for the reduction of PAT in fresh apple cider and juice. It was shown that 56.5%, 87.5%, 94.8% and 98.6% reduction of PAT can be achieved, respectively, in the model solution, apple cider, apple juice without ascorbic acid addition and apple juice with ascorbic acid addition in 2-mm thickness sample initially spiked by 1 mg/L of PAT after UV exposure for 40 min at UV irradiance of 3.00mWcm<sup>2</sup>.

Funes, Gómez, Resnik, and Alzamora (2013) investigated the effect of pulsed light (PL) dose on PAT degradation in McIlvaine buffer, apple juice and apple purée. The exposure of all samples to PL doses between 2.4 and 35.8 J/cm<sup>2</sup> resulted in a significant decrease in PAT levels. PAT reduction in McIlvaine buffer did not depend markedly on the initial concentration of the mycotoxin. At the maximum dose tested, the remaining average PAT level dissolved in McIlvaine buffer ranged from 5 to 15%, while in apple juice the values declined up to 22%. In apple purée naturally contaminated with 29 mg/kg of PAT, exposure to a PL dose of 12 J/cm<sup>2</sup> provoked a 51% reduction in PAT concentration, while no residual contamination was detected for higher irradiation times. These results suggested that PL treatment would be a potential alternative method to reduce PAT contamination in apple products. However, further investigations need to be conducted to evaluate toxicological safety of PAT degradation product(s). The results evidenced in this study are 1.0 fold lower than the data produced in our study.

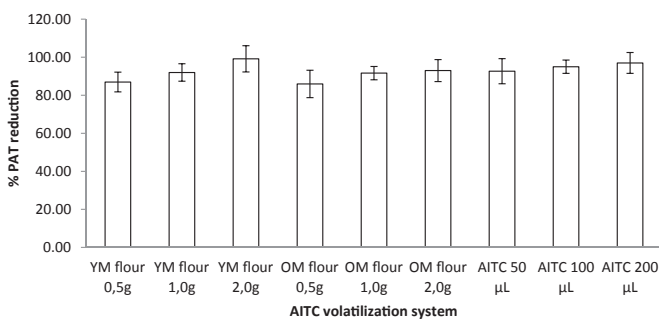


Fig. 6. Patulin reduction in wheat tortillas contaminated with the strain of *Penicillium expansum* CECT 2278 (patulin producer) and treated with yellow (YM) and oriental (OM) mustard flours and also with three different quantities of the standard solution of the AIT.

#### 4. Conclusion

The results evidenced in this study demonstrate that the bioactive compounds present in yellow and oriental mustard flours can reduce the growth of the strain of *P. expansum*, PAT producer in wheat tortillas samples. No significant differences were observed on the reduction of PAT produced by the strain tested using the two different methodologies of the release of the ITCs. Also the results obtained by the kinetic of the ITCs volatilization demonstrate that this isothiocyanates are stable in the bioactive packaging maintaining antifungal concentration during two months. The results obtained in this study could be considered of particular interest considering the potential application that those bioactive compounds could have in the industries to improve the shelf life of many food products.

#### Acknowledgments

This research was supported by the Ministry of Economy and Competitiveness (AGL2013-43194-P) and by the PhD program of the Valencian Community Santiago Grisolia.

#### References

- Baert, K., Devlieghere, F., Flyps, H., Oosterlinck, M., Ahmed, M. M., & Rajkovic, A. (2007). Influence of storage conditions of apples on growth and patulin production by *Penicillium expansum*. *International Journal Food Microbiology*, 119, 170–181.
- Chacon, P. A., Muthukumarasamy, P., & Holley, R. A. (2006). Elimination of *Escherichia coli* O157:H7 from fermented dry sausages at an organoleptically acceptable level of microencapsulated allyl isothiocyanate. *Applied and Environmental Microbiology*, 72, 3096–3102.
- Delaquis, P. J., & Mazza, G. (1995). Antimicrobial properties of isothiocyanates in food preservation. *Food Technology*, 49, 73–84.
- Desmarchelier, A., Mujahid, A., Racault, L., Perring, L., & Lancova, K. (2011). Analysis of patulin in pear- and apple-based foodstuffs by liquid chromatography electrospray ionization tandem mass spectrometry. *Journal of Agriculture and Food Chemistry*, 59, 7659–7665.
- Drusch, S., Kopka, S., & Keadling, J. (2007). Stability of patulin in a juice-like aqueous model system in the presence of ascorbic acid. *Food Chemistry*, 100, 192–197.
- Ekanayake, A., Kester, J. J., Li, J. J., Zehentbauer, G. N., Bunke, P. R., & Zent, J. B. (2006). Isoguard TM: a natural anti-microbial agent derived from white mustard seed. *Acta Horticulturae*, 709, 101–108.
- European Committee for Standardization (CEN). (2008). *EN 15662: 2008. Foods of plant origin- determination of pesticide residues using GC-MS and/or LC-MS/MS following acetonitrile extraction/partitioning and clean-up by dispersive SPE-QuEChERS-method.*
- European Committee for Standardization (CEN). (2010). *CEN/TR 16059: 2010. Food analysis- performance criteria for single laboratory validated methods of analysis for the determination of mycotoxins.*
- Fahey, J. W., Zalcmann, A. T., & Talalay, P. (2001). The chemical diversity and distribution of glucosinolates and isothiocyanates among plants. *Phytochemistry*, 56, 5–51.
- Flemming, C. C., Turner, S. J., & Hunt, M. (2006). Management of root knot nematodes in turfgrass using mustard formulations and biostimulants. *Communications in Agriculture and Applied Biological Sciences*, 71, 653–658.
- Fliege, R., & Metzler, R. M. (2000). Electrophilic properties of patulin. N-acetylcysteine and glutathione adducts. *Chemical Research in Toxicology*, 13, 373–381.
- Funes, G. J., Gómez, P. L., Resnik, S. L., & Alzamora, S. M. (2013). Application of pulsed light to patulin reduction in Mcllvaine buffer and apple Products. *Food Control*, 30, 405–410.
- Gao, Z., Yue, T., Yuan, Y., Fu, X., & Peng, B. (2009). Ultrasonic degradation of patulin in apple juice. *Chinese Society for Agriculture Machinery*, 40, 138–142.
- Glaser, N., & Stopper, H. (2012). Patulin: mechanism of genotoxicity. *Food and Chemical Toxicology*, 50, 1796–1801.
- Graumann, G. H., & Holley, R. A. (2007). Survival of *Escherichia coli* O157:H7 in needle tenderized dry cured Westphalian ham. *International Journal of Food Microbiology*, 118, 173–179.
- Hasegawa, N., Matsumoto, Y., Hoshino, A., & Iwashita, K. (1999). Comparison of effects of *Wasabia japonica* and allyl isothiocyanate on the growth of four strains of *Vibrio parahaemolyticus* in lean and fatty tuna meat suspensions. *International Journal of Food Microbiology*, 49, 27–34.
- IARC. (2002). Some traditional herbal medicines, some mycotoxins, naphthalene and styrene. In *Monographs on the evaluation of carcinogenic risks to humans* (Vol. 82). Lyon: International Agency for Research on Cancer.
- JECFA. (1995). *Evaluation of certain food additives and contaminants: Forty-fourth report of the joint FAO/WHO expert committee on food additives*. Geneva: WHO. Technical Report Series No. 859, 9241208597.
- Kelly, S., Grimm, L. H., Bendig, C., Hempel, D. C., & Krull, R. (2006). Effects of dynamic induced shear stress on fungal growth and morphology. *Process Biochemistry*, 41, 2113–2117.
- Kissen, R., Rossiter, J. T., & Bones, A. M. (2009). The 'mustard oil bomb': not so easy to assemble?! Localization, expression and distribution of the components of the myrosinase enzyme system. *Phytochemical Reviews*, 8, 69–86.
- Lin, C. M., Preston, J. F., & Wei, C. I. (2000). Antibacterial mechanism of allyl isothiocyanate. *Journal of Food Protection*, 63, 727–734.
- Luciano, F. B., & Holley, R. A. (2009). Enzymatic inhibition by allyl isothiocyanate and factors affecting its antimicrobial action against *Escherichia coli* O157:H7. *International Journal of Food Microbiology*, 131, 240–245.
- Luciano, F. B., & Holley, R. A. (2011). Bacterial degradation of glucosinolates and its influence on the growth of *E. coli* O157:H7 in a dry-fermented sausage model – Part 2. *Fleischwirtschaft International*, 26, 78–81.
- Meca, G., Luciano, F. B., Zhou, T., Tsao, R., & Mañes, J. (2012). Chemical reduction of the mycotoxin beauvericin using allyl isothiocyanate. *Food and Chemical Toxicology*, 50, 1755–1762.
- Moake, M. M., Padilla-Zakour, O. I., & Worobo, R. W. (2005). Comprehensive review of patulin control methods in foods. *Comprehensive Review in Food Science and Food Safety*, 4, 8–21.
- Murillo-Arbizu, M., Amézqueta, S., González-Peñas, E., & de Cerain, A. L. (2009). Occurrence of patulin and its dietary intake through apple juice consumption by the Spanish population. *Food Chemistry*, 113, 420–423.
- Nadarajah, D., Han, J. H., & Holley, R. A. (2005). Inactivation of *Escherichia coli* O157:H7 in package ground beef by allyl isothiocyanate. *International Journal of Food Microbiology*, 99, 269–279.
- Nielsen, P. V., & Rios, R. (2000). Inhibition of fungal growth on bread by volatile components from spices and herbs, and the possible application in active packaging, with special emphasis on mustard essential oil. *International Journal of Food Microbiology*, 60, 219–229.
- Prester, T., Fahey, J. W., Holtzclaw, W. D., Abeygunawardana, C., Kachinski, J. L., & Talalay, P. (1996). Comprehensive chromatographic and spectroscopic methods for the separation and identification of intact glucosinolates. *Analytical Biochemistry*, 239, 168–179.
- Reddy, K. R. N., Salleh, B., Saad, B., Abbas, H. K., Abel, C. A., & Shier, W. T. (2010). An overview of mycotoxin contamination in foods and its implications for human health. *Toxin Reviews*, 29, 3–26.
- Shin, J. M., Harte, B., Ryser, E., & Selke, S. (2010). Active packaging of fresh chicken breast, with allyl isothiocyanate (AIT) in combination with modified atmosphere packaging (MAP) to control the growth of pathogens. *Journal of Food Science*, 75, 65–71.
- Tsao, R., Yu, Q., Potter, J., & Chiba, M. (2002). Direct and simultaneous analysis of sinigrin and allyl isothiocyanate in mustard samples by high-performance liquid chromatography. *Journal of Agricultural and Food Chemistry*, 50, 4749–4753.
- Yun, H. J., Lim, S. Y., Yang, S. H., Lee, W. Y., Kwon, J. H., Lim, B. L., et al. (2008). Effect of gamma irradiation on the growth and patulin production of *Penicillium griseofulvum* in an apple model system. *Food Science and Biotechnology*, 17, 723–727.
- Zhu, Y., Koutchma, T., Warriner, K., Shao, S., & Zhou, T. (2013). Kinetics of patulin degradation in model solution, apple cider and apple juice by ultraviolet radiation. *Food Science and Technology International*, 19, 291–303.



Contents lists available at ScienceDirect

## LWT - Food Science and Technology

journal homepage: [www.elsevier.com/locate/lwt](http://www.elsevier.com/locate/lwt)

# Inactivation of bacteria and murine norovirus in untreated groundwater using a pilot-scale continuous-flow intense pulsed light (IPL) system



Ji Yoon Yi<sup>1</sup>, Na-Hye Lee<sup>1</sup>, Myong-Soo Chung<sup>\*</sup>

Department of Food Science and Engineering, Ewha Womans University, Seoul 120-750, South Korea

## ARTICLE INFO

### Article history:

Received 2 June 2015

Received in revised form

30 September 2015

Accepted 8 October 2015

Available online 19 October 2015

### Keywords:

Microbial inactivation

Pilot-scale intense pulsed light (IPL) system

Untreated groundwater

*Escherichia coli* C600

Murine norovirus

## ABSTRACT

The objective of this study was to characterize the inactivation effects of a pilot-scale continuous-flow intense pulsed light (IPL) system on microorganisms in untreated groundwater used in the food industry. The inactivation effects of laboratory- and pilot-scale IPL systems on murine norovirus (MNV), a human norovirus surrogate, were also investigated. Flow rates of 40, 32, 20 and 12 l/min were tested (corresponding to 89, 113, 179, and 290 s of treatment time in a chamber, respectively). A 290-s pilot-scale IPL treatment at an energy dose of 14.02 J/cm<sup>2</sup> resulted in a 4.79-log reduction of *Escherichia coli* C600 in water with an initial count of 10<sup>5</sup>–10<sup>6</sup> CFU/ml, while a 270-s treatment at an energy dose of 13.05 J/cm<sup>2</sup> resulted in a 2.91-log inactivation of aerobic and facultative anaerobic heterotrophs in untreated groundwater with the initial count of 4.5 × 10<sup>4</sup> CFU/ml. An 89-s treatment at a dose of 4.30 J/cm<sup>2</sup> resulted in a 3.35-log inactivation of MNV in water with the initial count of 10<sup>3</sup>–10<sup>4</sup> PFU/ml. The energy dose and the inactivation level showed linearity for this system. These trends should form the basis of a large-scale IPL-based water management system with improved energy efficiency.

© 2015 Elsevier Ltd. All rights reserved.

## 1. Introduction

Intense pulsed light (IPL) is currently receiving considerable interest as an excitation source in nonthermal sterilization applications. This novel technology treats both vegetative cells and spores on the surface of foods or in water, and uses short-duration and high-frequency pulses of broad-spectrum light that is rich in ultraviolet radiation of the shortest wavelengths (UV–C), with corresponding germicidal effects (Dunn, Ott, & Clark, 1995; Farrell, Garvey, Cormican, Laffey, & Rowan, 2010). IPL technology is regarded as a reliable alternative to conventional continuous UV–C treatment because of its ability to inactivate microorganisms more rapidly and effectively with relatively high penetration depth and emission power (Cheigh, Hwang, & Chung, 2013). It has potential applications in the treatment of materials and devices used in the pharmaceutical, medical, food, and water industries.

The inactivation efficacy of IPL is influenced by various factors, including the distance of the sample from the lamp, size and

growth state of the bacteria, light intensity, sample thickness, treatment time, and electrical input (Artíguez, Lasagabaster, & de Marañón, 2011; Gómez-López et al., 2005). The lethality of IPL can be attributed to its broad-spectrum UV–C content, short duration, and high peak power (Dunn et al., 1995). Many studies have been conducted to illuminate the diverse mechanisms underlying IPL-induced microbial inactivation, and all have stressed the key role of the UV component of the pulsed spectrum in combination with other secondary photochemical and photo-thermal effects (Anderson, Rowan, MacGregor, Fouracre, & Farish, 2000; Wang, MacGregor, Anderson, & Woolsey, 2005).

Untreated groundwater is widely consumed as drinking water or as a water supply in industrial food production. However, microbial contamination of untreated groundwater is a serious environmental problem. Humans can be infected by contact with contaminated water, by ingestion of spoiled foods, and even by inhalation (Hassen et al., 2000). Agents contaminating untreated groundwater include pathogenic bacteria, protozoa, and viruses from wastewater, surface water, or leaking sewage pipes. Among those agents, the main hazards are from *Cryptosporidium*, bacterial pathogens, and enteroviruses (Schijven & Hassanizadeh, 2000).

According to the Centers for Diseases Control and Prevention (2011), human norovirus is the leading agent among food-borne

<sup>\*</sup> Corresponding author.

E-mail address: [mschung@ewha.ac.kr](mailto:mschung@ewha.ac.kr) (M.-S. Chung).

<sup>1</sup> These authors contributed equally to this work.

pathogens. It is highly infectious, since merely 10–100 virions can cause disease (Caul, 1994). This nonenveloped virus possesses an outer shell with a highly stable capsid that protects the single-stranded positive-sense RNA inside (Feng, Divers, Ma, & Li, 2011). It is spread through various routes, including consumption of contaminated water and food, person-to-person transmission, or contact with polluted surfaces (Kukkula, Maunula, Silvennoinen, & von Bonsdorff, 1999; Said, Perl, & Sears, 2008). Since human norovirus is pervasive in drinking or food-related water sources, it is a considerable public health concern.

Human norovirus cannot be propagated in cell culture (Duizer et al., 2004), so several animal caliciviruses that are cultivable and morphologically similar to human norovirus have been used as models to investigate the efficacy of chemical and physical inactivation methods (Duizer et al., 2004; Park, Boston, Kase, Sampson, & Sobsey, 2007). Murine norovirus (MNV) is one of the most common surrogates for human norovirus because it possesses similar characteristics, such as its genetic structure and the fecal-oral transmission route (Wobus, Thackray, & Virgin, 2006; Bae & Schwab, 2008). Green (2007) and Wobus et al. (2006) have demonstrated that the size (28–35 nm in diameter), buoyant density ( $1.37 \pm 0.04 \text{ g/cm}^3$ ), shape (small, rounded, icosahedral structure), and genome organization of MNV-1 are similar to those of human norovirus.

Numerous studies have demonstrated the inactivation effects of IPL on various food surfaces, food packaging materials, and related equipment (Belliot et al., 2013; Dunn et al., 1995; Ozer et al., 2006). However, there are limited data related to the application of a pilot-scale continuous-flow IPL system for the inactivation of contaminated water. Most of the research conducted on the decontamination of water in large-scale systems has thus far focused on UV-based inactivation systems. For example, Hassen et al. (2000) investigated the efficacy of pilot-scale UV treatment of wastewater, and Jolis, Lam, and Pitt (2001) used a pilot-scale UV system to irradiate coliform bacteria in recycled water. Moreover, while IPL has been widely used for bacterial inactivation, there is a dearth of literature on virus inactivation by IPL. The most common method of MNV inactivation studied to date employs UV light (Park, Linden, & Sobsey, 2011) or a laboratory-scale IPL (Vimont, Fliss, & Jean, 2015), whereas inactivation of MNV using a pilot-scale IPL has not been evaluated previously.

The aim of this study was to determine the efficacy of a pilot-scale continuous-flow IPL system for the inactivation of *Escherichia coli* C600, aerobic and facultative anaerobic heterotrophs, and MNV in water. Inactivation of *E. coli*-C600-contaminated water was conducted prior to untreated groundwater treatment, since the initial microbial population of untreated groundwater was uncontrollable. For virus treatment, a laboratory-scale IPL system was first investigated rather than the direct application of the pilot-scale IPL system so that the effect of system size could be identified. A critical evaluation of the effect of various essential parameters on IPL, such as energy dose and treatment time, was performed. A pilot-scale version of a nonthermal technology was thus designed and determined to be an alternative to conventional thermal technology for providing safe foods to customers.

## 2. Materials and methods

### 2.1. IPL systems

#### 2.1.1. Laboratory-scale IPL system

A laboratory-scale IPL system was designed and set up in our laboratory. This system consisted of two parts: a pulse generator and a treatment chamber (Fig. 1). The pulse generator comprised a power supply and a pulse-control device, and was the same

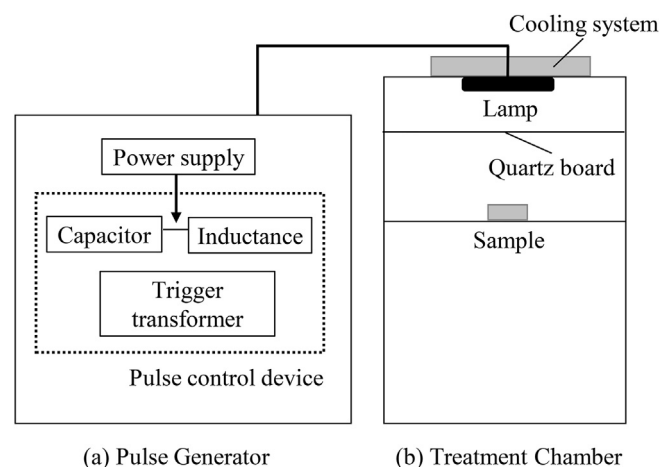


Fig. 1. Schematic layout of the laboratory-scale intense pulsed light system: pulse generator (a) and treatment chamber (b).

apparatus described in our previous paper (Cheigh et al., 2013). The height of the lamp above the movable rack in the treatment chamber was adjustable. The light source was positioned 9 cm from samples. The spectral distribution of the laboratory-scale IPL system was determined using a radiospectrometer (ILT-900, International Light Technologies, Peabody, MA, USA) throughout the experiments. The emission spectrum of this lamp ranges from UV to the infrared region, and its intensity depends on the voltage level. Fig. 2 displays the instantaneous spectral distribution of this xenon lamp. The IPL intensity for each sample was calculated by integrating the average irradiance over the wavelength range, and the IPL dose (expressed in  $\text{J/cm}^2$ ) was calculated based on the intensity multiplied by the treatment time. The cooling system of the treatment chamber included an air fan for removing the heat generated by the pulse-producing device.

#### 2.1.2. Pilot-scale continuous-flow IPL system

A pulse generator and a treatment chamber for the pilot-scale IPL system were also designed and set up. This pilot-scale continuous-flow IPL system comprised an IPL power source, a pump to draw water, filters to remove impurities such as sand and dust, a flow-rate controller to regulate a flow, a treatment chamber, and an air compressor to circulate the sample in the chamber, as shown schematically in Fig. 3.

The power source comprised a rectifier, a capacitor, and a trigger control. This system can activate multiple lamps simultaneously.

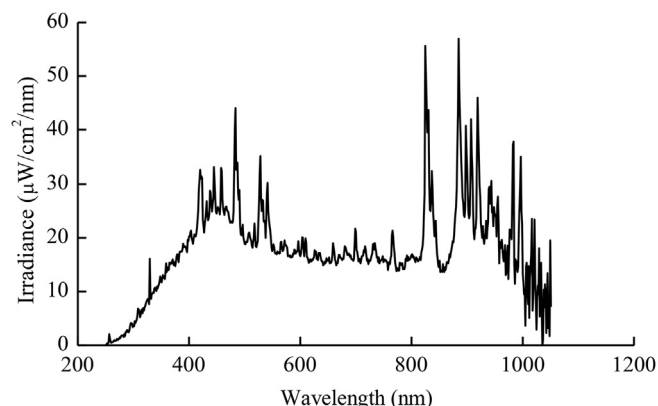


Fig. 2. Instantaneous spectral distribution of the xenon lamp used in this study.

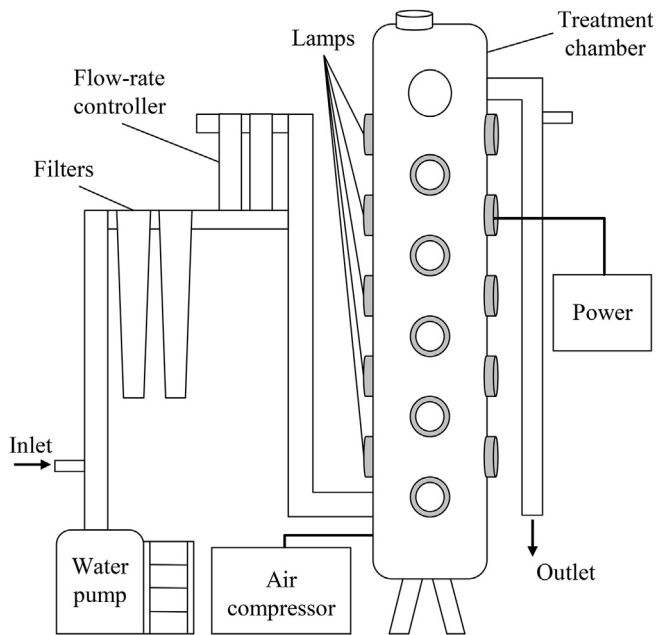


Fig. 3. Schematic layout of the pilot-scale continuous-flow intense pulsed light system.

The pulsed power source uses power compression technology to transport preserved electrical energy to the xenon flash lamp for a brief duration but with strong peak power. The power supply produced a maximum voltage of 30 kV. The input power of the 220-V AC supply source at 25 A was rectified, converted to the maximum permissible voltage, and then supplied to a 0.12- $\mu$ F capacitor. When the required electrical energy had accumulated in the capacitor, it was released to the lamp to enable it to emit light energy.

The cylindrical lamps used in this pilot-scale system were 145-mm long with an external diameter of 7.14 mm (Type NL 4006, Heraeus Noblelight, Cambridge, UK). Each lamp was filled with xenon at a pressure of 450 torr and had an emission spectrum ranging from UV to infrared similar with the laboratory-scale IPL system. Ten 2.5-cm-diameter quartz tubes that intersect the chamber seal the lamps to protect them. The spectral distribution of the pilot-scale IPL system was also determined using a spectroradiometer (ILT-900, International Light Technologies). The IPL intensity and dose of each sample was calculated in the same way as described in Section 2.1.1.

The cylindrical treatment chamber was constructed from stainless steel, with an inner diameter of 31 cm and a height of 93 cm. The volumetric space of the chamber, excluding the quartz tube, was roughly 66 l. The water sample entered the chamber through the lower side inlet, and after reaching the other, upper side of the chamber, it could be drained. After each treatment, the inner part of the chamber was washed with 0.5% sodium hypochlorite solution to remove any pollutants.

The treatment time of this pilot-scale IPL system was set by controlling the flow rate. Flow rates of 40, 32, 20, and 12 l/min were tested, corresponding to 89, 113, 179, and 290 s of treatment time in the chamber, respectively.

## 2.2. Sample preparation

### 2.2.1. Cultivation of *E. coli* C600 and MNV

The microorganism used prior to the untreated groundwater experiment was *E. coli* C600. *E. coli* C600 cultures were prepared by

transferring one or two colonies of the organisms to 15 ml of sterile Nutrient Broth (NB; Difco, Sparks, MD, USA) and cultured at 37 °C for 24 h with shaking in order to attain the late stationary phase. A 10-ml aliquot of prepared fluid was transferred to a conical flask containing 1 l of NB and incubated with shaking at 37 °C for 5 h to allow the cells to grow to early stationary phase.

MNV was provided by the Molecular Virology Laboratory at Yonsei University (Seoul, Korea) and propagated in RAW 264.7 macrophage cells (provided by the same laboratory). RAW 264.7 cells were cultured in complete Dulbecco's modified Eagle's medium (DMEM) supplemented with 10% (v/v) fetal bovine serum, 1% (v/v) nonessential amino acids, 1% (v/v) penicillin streptomycin, and 1% (v/v) 100-mM sodium pyruvate (all from Gibco, New York, NY, USA) at 37 °C with 5% CO<sub>2</sub>. For virus propagation, cell lines were inoculated in cell culture dishes with MNV and incubated at 37 °C for 48 h. The viruses were gathered from infected cell lysates by centrifugation at 1500  $\times$  g, 4 °C for 5 min (Gyrozen, Seoul, Korea), separating the cell sediment from the fluid medium. The titers of MNV were 10<sup>6</sup>–10<sup>7</sup> plaque-forming units (PFU)/ml. They were kept frozen in aliquots at –70 °C.

### 2.2.2. Sampling untreated groundwater from food processing plants

Untreated groundwater samples were collected during April 2014 from three different food processing plants (400 l from each) into 20-l plastic containers that had been cleaned with distilled water. The containers were moved to our laboratory from these plants within 6 h of collection, and immediately stored at 4 °C. The samples were used for experiments within 12–24 h after collection.

## 2.3. IPL treatments

For both scales of the IPL system, pulsed light was set at 0.15 ms duration and 5 Hz. All experiments were conducted at a room temperature of 24  $\pm$  2 °C.

### 2.3.1. The pilot-scale IPL treatments of *E. coli* C600 and untreated groundwater

Cultivated *E. coli* C600 cells were seeded into 100 l of water to produce a viable cell count of roughly 10<sup>5</sup>–10<sup>6</sup> colony-forming units (CFU)/ml. A plastic container holding 100 l of inoculated water was mixed carefully with a plastic stick in order to make a homogeneous suspension. The treatment was applied using 5, 10, or 15 lamps at 1200 V for 89, 113, 179, or 290 s (i.e., the number of lamps and the treatment time were varied between experiments).

The untreated groundwater samples were treated with 15 lamps at 1200 V for 90, 108, or 270 s (i.e., only the treatment time was varied between experiments).

### 2.3.2. Inactivation of MNV by the laboratory-scale IPL systems

The viral lethality of the IPL treatment system under different conditions was evaluated by treating a predetermined number of viruses inoculated in phosphate-buffered saline (PBS) solution and then enumerating the survivors (expressed in terms of PFU/ml). MNV suspensions were prepared in PBS solution. For the laboratory-scale treatment, propagated cells were seeded separately into 5 ml of PBS solution and virus suspensions, with a depth of 2 mm, and treated in a sterile Petri dish (50  $\times$  15 mm) placed immediately below the lamp without a cover. Untreated virus solutions were used as positive control samples. The samples were treated using various lamp voltages (800, 1200, and 1800 V) and treatment times (10, 20, 30, 40, and 50 s).

For the pilot-scale treatment, MNV were seeded into 100 l of untreated groundwater, resulting in approximately 10<sup>3</sup>–10<sup>4</sup> PFU/ml. Inoculated water was mixed using the same method described in 2.3.1 to make homogenous suspension and treated using

15 lamps at 1200 V for 89, 113, or 179 s (i.e., only the treatment time was varied between experiments).

#### 2.4. Assays

The lethality of the various treatments is expressed as a log reduction value, showing the relative number of individuals surviving the inactivation. All tests were conducted in triplicate.

For *E. Coli* C600 assays, two samples of 20–30 ml were collected into sterile conical tubes before and after the treatment. The samples were serially diluted in sterile 0.85% saline solution and spread onto Nutrient Agar plates (Difco). After incubating the plates at 37 °C for 48 h, plates with 30–300 colonies were used to determine viable counts. Aerobic and facultative anaerobic heterotrophs were targeted for the microbiological examination in untreated groundwater. They were counted using the Methods of Officially Determined Quality Test for Drinking Water proposed by the Korean Ministry of Environment (2007). In the case of psychrophilic bacteria, 0.1 ml of undiluted sample and tenfold serial dilutions were spread onto R2A Agar plates (Difco), and incubated at 21 °C for 72 h. The counts of mesophilic bacteria were conducted on Plate Count Agar (Difco), and the plates were incubated at 35 °C for 24 h.

MNV infectivity was quantified using a plaque assay. The MNV titer was measured by assaying serial dilutions in six-well tissue culture plates containing  $2 \times 10^6$  cells/well. Thereafter, 1-ml aliquots of virus suspension treated with IPL were inoculated into RAW 264.7 cells, incubated for 1 h for virus adsorption, and then overlaid with 3 ml of 1% (w/v) agarose in DMEM at 37 °C with 5% CO<sub>2</sub>. After infection for 48 h, the cells were stained with neutral red in PBS solution. Plates with 10–100 plaques were counted, and the virus titer was calculated from the sample dilution and the number of plaques, and expressed in PFU/ml.

#### 2.5. Statistical analysis

The log reduction value  $\log(N/N_0)$  was used to quantify the inactivation, where  $N_0$  is the number of pathogens inoculated and  $N$  is the number of pathogens surviving after the treatment. IBM SPSS Statistics (version 22, IBM SPSS, Chicago, IL, USA) was used for the statistical analysis. The data are expressed as mean and SE values. The results were analyzed statistically by one-way analysis of variance and the Duncan test to determine differences among the various mean values, with a probability value of  $p < 0.05$  considered to be indicative of a significant difference. Linear regressions were performed to fit the energy dose–response of *E. coli* C600 in the pilot-scale and MNV in the laboratory-scale IPL system, respectively. The goodness-of-fits were determined with  $R^2$  value and their significances were examined with analyses of variance. Standardized residuals were calculated to find out outliers.

### 3. Results and discussion

#### 3.1. Inactivation of *E. coli* C600 by the pilot-scale IPL system

Application of the pilot-scale continuous-flow IPL system successfully reduced the *E. coli* C600 population in water. As mentioned in Section 1, the efficacy of that microbial reduction can be affected by various factors, including the characteristics of the bacterial population, sample, light source, exposure duration, and energy source. The variable parameters selected for this study were the number of lamps and the treatment time. Fig. 4 shows the inactivation trends for the pilot-scale IPL treatment of bacterial infected water using 5, 10, and 15 lamps. The initial *E. coli* C600 count was  $10^6$  CFU/ml; the bacterial lethality for this system varied

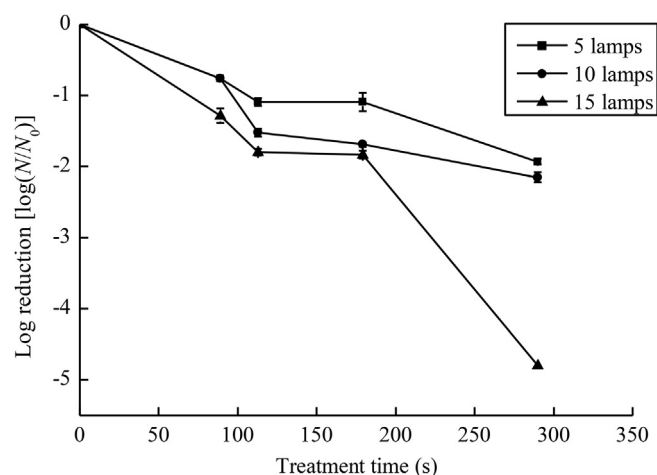


Fig. 4. Pilot-scale continuous-flow intense pulsed light inactivation of *Escherichia coli* C600 in water with various numbers of lamps as a function of treatment time at 1200 V. The error bars represent the standard error of mean ( $p < 0.05$ ,  $n = 3$ ). The initial count was  $10^5$ – $10^6$  CFU/ml. Plates with 30–300 colonies were used to determine viable counts for the detection limit.

with both the treatment time and the energy dose, with the results showing that a longer treatment time and higher energy dose resulted in more effective inactivation of *E. coli* C600. Treatment for 290 s using 5, 10, and 15 lamps (corresponding to energy doses of 8.64, 11.27, and 14.02 J/cm<sup>2</sup>, respectively) induced 2.21-, 2.88-, and 4.79-log reductions in *E. coli* C600, respectively. These values are not as high as those obtained by a laboratory-scale pulsed UV radiation system described in the literature (0.43-log reduction per mJ/cm<sup>2</sup>) (Wang et al., 2005), suggesting that the system tested in this study was less powerful. While water has a high transmittance of pulsed light, a certain threshold energy dose is required to sterilize large amounts of water due to a shading effect that makes it very difficult to destroy organisms distant from the lamps (Gómez-López et al., 2005). However, since the pilot-scale IPL system treats water continuously at the flow rate of 720 l/h, it would be a foundation for handling extremely large amounts of untreated groundwater, i.e. over 17 tons with 24 h of operation per day.

The energy dose had an inverse linear relationship with the log reduction of *E. coli* C600 in the pilot-scale IPL system and can be described by the equation presented in Fig. 5, with  $R^2 = 0.9130$ . This

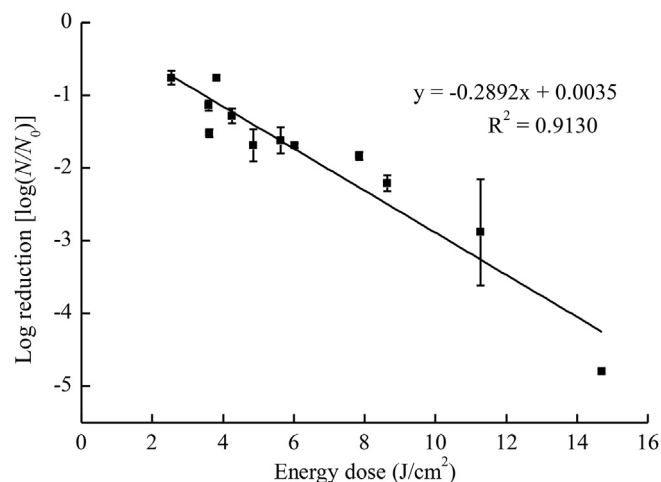


Fig. 5. Energy dose–response curve of inactivation of *Escherichia coli* C600 in the pilot-scale intense pulsed light system. The error bars represent the standard error of mean ( $p < 0.05$ ,  $n = 3$ ).

result showed that *E. coli* C600 treated at a higher energy dose was more likely to satisfy the inactivation approach. The linear pattern is consistent with the findings from a previous study (Hassen et al., 2000).

### 3.2. Treatment of untreated groundwater by the pilot-scale IPL system

The variable parameter set for the pilot-scale IPL treatment of untreated groundwater was the treatment time. Since the samples were collected from different locations, they possessed various initial microbial populations, which could change the sterilization efficacy due to the shading effect. Gómez-López et al. (2005) noted that with higher population, bacteria in the upper part shade the others below them from being treated by IPL. Table 1 lists the changes in the level of microbial inactivation relative to the initial number of total cells (i.e., before treatment). Untreated groundwater collected from food processing plants A and B were contaminated at initial levels of  $7.0 \times 10^1$  and  $4.0 \times 10^2$  CFU/ml, respectively, and all cells were inactivated after a treatment time of <2 min. Untreated groundwater collected from food processing plant C was contaminated at the initial level of  $4.5 \times 10^4$  CFU/ml, and treatment for 270 s (corresponding to an energy dose of  $13.05 \text{ J/cm}^2$ ) induced a 2.91-log reduction in the microbial population. Thus, the characteristics of the initial microbial population exerted a considerable effect on the susceptibility to the IPL treatment: microbial numbers reduced more rapidly when the initial population was lower. All bacteria were inactivated in water with initial cell populations of  $\leq 10^4$  CFU/ml at shorter treatment time, while the bacteria were more resistant to IPL with higher initial cell populations. Farrell et al. (2010) also reported that the lower the initial population treated, the better the inactivation achieved. They demonstrated that higher initial populations cause heterogeneous sample seeding, so that cells in the bottom part are not exposed to the lamps due to shading effect. Although the samples were homogeneously mixed in this study, bacteria still show shading effect due to their high population. Also, our pilot-scale IPL system treats samples in the continuous manner but since the flow of samples is slow due to the large diameter of chamber, bacteria could still show shading effect.

### 3.3. Inactivation of MNV by the laboratory-scale IPL system

MNV inactivation was tested at various voltages and treatment times. Higher energy doses and longer treatment times induced greater levels of MNV inactivation in PBS solution. The general trends of these data are depicted clearly in Fig. 6. The initial count of  $10^6$ – $10^7$  PFU/ml was all inactivated after the treatment of 1800 V at 30 s. Thus, we stopped the treatment for 1800 V at 30 s regarding inactivation efficiency and compared the results at 30 s. Treatment conditions with energy doses of  $0.64 \text{ J/cm}^2$  (800 V),  $1.45 \text{ J/cm}^2$  (1200 V), and  $3.43 \text{ J/cm}^2$  (1800 V) for 30 s, resulted in 2.59-, 3.77-, and 6.69-log reductions in the MNV population, respectively. These values suggest a slightly higher efficacy than in a previous study in

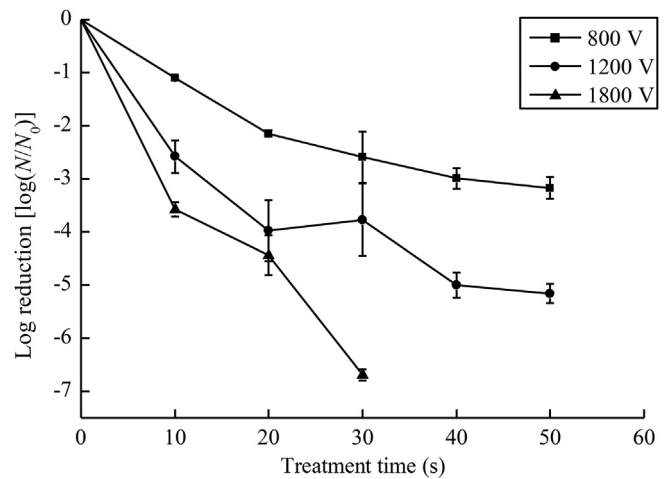


Fig. 6. Laboratory-scale intense pulsed light inactivation of murine norovirus in phosphate-buffered saline solution as a function of treatment time at various voltages. The error bars represent the standard error of mean ( $p < 0.05$ ,  $n = 3$ ). The initial count was  $10^6$ – $10^7$  PFU/ml. Plates with 10–100 plaques were used to determine viable counts for the detection limit.

which a 3-log reduction in MNV was attained with a pulsed-light device at an energy dose of  $3.45 \text{ J/cm}^2$  (Vimont et al., 2015). The results imply the high sensitivity of MNV in PBS solution to IPL inactivation, and suggest that IPL would be effective for the inactivation of human norovirus. Moreover, pathogenic particles in suspension were nearly all inactivated after irradiation at  $3.43 \text{ J/cm}^2$ . The virus-inactivation mechanism of IPL has not been fully characterized, but it is thought that the irradiation is detrimental to the virus capsid and damages its nucleic acids (Belliot et al., 2013). Since MNV is a single-stranded, positive-sense RNA virus enclosed by a virus capsid protein (Feng et al., 2011), damage to its RNA genome would prove to be fatal for the virus.

The energy dose–response curve for MNV in this system is presented in Fig. 7. The linear equation was calculated with  $R^2 = 0.9057$ . This result showed that MNV was more likely to satisfy the inactivation approach with a higher energy dose. This inverse linear pattern is consistent with that found in a previous study (Park et al., 2011).

### 3.4. Inactivation of MNV by the pilot-scale IPL system

As indicated in Table 2, MNV was inactivated in a treatment-time-dependent manner by the pilot-scale IPL system. A 3.35-log reduction was achieved with the 89-s treatment (corresponding to an energy dose of  $4.30 \text{ J/cm}^2$ ), and all cells were inactivated after a treatment time of >113 s. The reduction of MNV achieved using the pilot-scale IPL system is thus far less than that achieved using the laboratory-scale system. However, it can still be suggested that the pilot-scale IPL system is capable of inactivating MNV in water, since the pilot-scale continuous-flow IPL system can treat larger

**Table 1**  
Bactericidal efficacy of the pilot-scale continuous-flow intense pulsed light system with 15 lamps for aerobic and facultative anaerobic heterotrophs in untreated groundwater.

Food-processing plant	Total initial bacteria counts (CFU/ml)	Treatment time (s)	Result (log reduction)
A	$7.0 \times 10^1$	90	TR
B	$4.0 \times 10^2$	108	TR
C	$4.5 \times 10^4$	270	2.91

CFU: colony-forming units. ( $n = 3$ ). TR: total reduction means no colonies were formed.

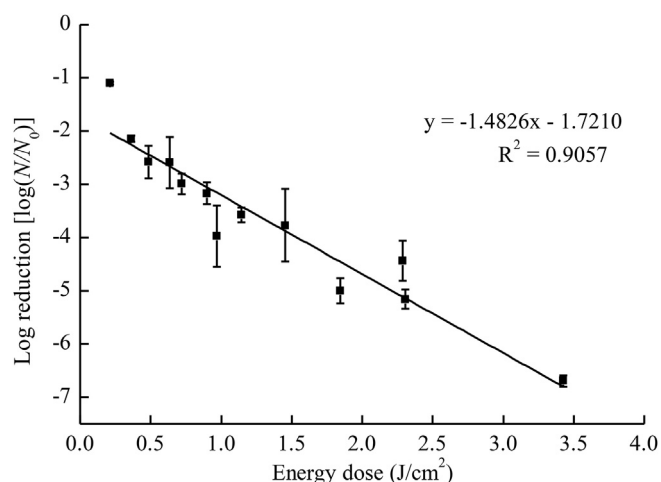


**Fig. 7.** Energy dose–response curve of inactivation of murine norovirus in the laboratory-scale intense pulsed light system. The error bars represent the standard error of mean ( $p < 0.05$ ,  $n = 3$ ).

**Table 2**

Inactivation of murine norovirus in water for the pilot-scale continuous-flow intense pulsed light system with 15 lamps.

Total initial virus counts (PFU/ml)	Treatment time (s)	Result (log reduction)
$2.3 \times 10^3$	89	3.35
$2.3 \times 10^3$	113	TR
$2.3 \times 10^3$	179	TR

PFU: plaque-forming units. ( $n = 3$ ). TR: total reduction means no plaques were formed.

amounts of water much more rapidly and in a continuous manner, compared to the laboratory-scale system.

#### 4. Conclusions

This study examined the inactivating effect of self-designed IPL systems on water samples contaminated with various types of pathogens. Through the scale-up, it was shown that the pilot-scale continuous-flow IPL system can inactivate diverse pathogens, from microbes to viruses, i.e. *E. coli* (maximum 4.79-log reduction), aerobic and facultative anaerobic heterotrophs (maximum 2.91-log reduction), and MNV (maximum 3.35-log reduction) in a large amount of water. This system treats contaminated water continuously at the flow rate of 720 l/h so that it can cover over 17 tons with 24 h of operation per day. Since this study shows the inactivation efficacy being well with the scaled-up continuous IPL system, it could be applied to the food industry immediately although further research for the life time of lamps is needed. It is also highly efficient because the system has low running costs and requires little maintenance in comparison to other nonthermal techniques such as chlorine treatment. Overall, results of this research serve as a starting point for investigating an industrial-scale IPL system for the decontamination of untreated groundwater at food processing industries with respect to diverse pathogens, from microbes to viruses. This type of system would benefit food processing industries by providing guaranteed safety with less expense and fewer side effects.

#### Acknowledgment

This research was supported by a grant (10162KFDA995) from the Korean Ministry of Food & Drug Safety and a grant (313031-3)

from the High Value-added Food Technology Development Program, Ministry of Agriculture, Food and Rural Affairs.

#### References

- Anderson, J. G., Rowan, N. J., MacGregor, S. J., Fouracre, R. A., & Farish, O. (2000). Inactivation of food-borne enteropathogenic bacteria and spoilage fungi using pulsed-light. *IEEE Transactions on Plasma Science*, 28, 83–88.
- Artíguez, M. L., Lasagabaster, A., & de Marañón, I. M. (2011). Factors affecting microbial inactivation by pulsed light in a continuous flow-through unit for liquid products treatment. *Procedia Food Science*, 1, 786–791.
- Bae, J., & Schwab, K. J. (2008). Evaluation of murine norovirus, feline calicivirus, poliovirus, and MS2 as surrogates for human norovirus in a model of viral persistence in surface water and groundwater. *Applied and Environmental Microbiology*, 74, 477–484.
- Belliot, G., Loutreul, J., Estienney, M., Cazeaux, C., Nicorescu, I., Aho, S., et al. (2013). Potential of pulsed light to inactivate bacteriophage MS2 in simple liquid medium and on complex foodstuffs. *Food and Environmental Virology*, 5, 176–179.
- Caul, E. O. (1994). Small round structured viruses: airborne transmission and hospital control. *Lancet*, 343, 1240–1242.
- Centers for Disease Control and Prevention. (2011). Surveillance for foodborne disease outbreaks – United States, 2008. *MMWR*, 60, 1197–1202.
- Cheigh, C. I., Hwang, H. J., & Chung, M. S. (2013). Intense pulsed light (IPL) and UV–C treatments for inactivating *Listeria monocytogenes* on solid medium and seafoods. *Food Research International*, 54, 745–752.
- Duizer, E., Bijkerk, P., Rockx, B., De Groot, A., Twisk, F., & Koopmans, M. (2004). Inactivation of caliciviruses. *Applied and Environmental Microbiology*, 70, 4538–4543.
- Duizer, E., Schwab, K. J., Neill, F. H., Atmar, R. L., Koopmans, M. P., & Estes, M. K. (2004). Laboratory efforts to cultivate noroviruses. *Journal of General Virology*, 85, 79–87.
- Dunn, J., Ott, T., & Clark, W. (1995). Pulsed-light treatment of food and packaging. *Food Technology*, 49, 95–98.
- Farrell, H. P., Garvey, M., Cormican, M., Laffey, J. G., & Rowan, N. J. (2010). Investigation of critical inter-related factors affecting the efficacy of pulsed light for inactivating clinically relevant bacterial pathogens. *Journal of Applied Microbiology*, 108, 1494–1508.
- Feng, K., Divers, E., Ma, Y., & Li, J. (2011). Inactivation of a human norovirus surrogate, human norovirus virus-like particles, and vesicular stomatitis virus by gamma irradiation. *Applied and Environmental Microbiology*, 77, 3507–3517.
- Gómez López, V. M., Devlieghere, F., Bonduelle, V., & Debever, J. (2005). Factors affecting the inactivation of micro-organisms by intense light pulses. *Journal of Applied Microbiology*, 99, 460–470.
- Green, K. Y. (2007). Caliciviridae: the noroviruses. In D. M. Knipe, & P. M. Howley (Eds.), *Fields virology* (5th ed., pp. 949–979). Pennsylvania: Lippincott Williams & Wilkins.
- Hassen, A., Mahrouk, M., Ouzari, H., Cherif, M., Boudabous, A., & Damelincourt, J. J. (2000). UV disinfection of treated wastewater in a large-scale pilot plant and inactivation of selected bacteria in a laboratory UV device. *Bioresource Technology*, 74, 141–150.
- Jolis, D., Lam, C., & Pitt, P. (2001). Particle effects on ultraviolet disinfection of coliform bacteria in recycled water. *Water Environmental Research*, 73, 233–236.
- Korean Ministry of Environment. (2007). *Methods of officially determined quality test for drinking water*. Retrieved from <http://Water.nier.go.kr> Accessed 15.05.15.
- Kukkula, M., Maunula, L., Silvennoinen, E., & von Bonsdorff, C. H. (1999). Outbreak of viral gastroenteritis due to drinking water contaminated by Norwalk-like viruses. *Journal of Infectious Diseases*, 180, 1771–1776.
- Ozer, N. P., & Demirci, A. (2006). Inactivation of *Escherichia coli* O157: H7 and *Listeria monocytogenes* inoculated on raw salmon fillets by pulsed UV-light treatment. *International Journal of Food Science & Technology*, 41, 354–360.
- Park, G. W., Boston, D. M., Kase, J. A., Sampson, M. N., & Sobsey, M. D. (2007). Evaluation of liquid-and fog-based application of sterilox hypochlorous acid solution for surface inactivation of human norovirus. *Applied and Environmental Microbiology*, 73, 4463–4468.
- Park, G. W., Linden, K. G., & Sobsey, M. D. (2011). Inactivation of murine norovirus, feline calicivirus and echovirus 12 as surrogates for human norovirus (NoV) and coliphage (F+) MS2 by ultraviolet light (254 nm) and the effect of cell association on UV inactivation. *Letters in Applied Microbiology*, 52, 162–167.
- Said, M. A., Perl, T. M., & Sears, C. L. (2008). Gastrointestinal flu: norovirus in health care and long-term care facilities. *Clinical Infectious Diseases*, 47, 1202–1208.
- Schijven, J. F., & Hassanizadeh, S. M. (2000). Removal of viruses by soil passage: overview of modeling, processes, and parameters. *Critical Reviews in Environmental Science and Technology*, 30, 49–127.
- Vimont, A., Fliss, I., & Jean, J. (2015). Efficacy and mechanisms of murine norovirus inhibition by pulsed-light technology. *Applied and Environmental Microbiology*, 81, 2950–2957.
- Wang, T., MacGregor, S. J., Anderson, J. G., & Woolsey, G. A. (2005). Pulsed ultraviolet inactivation spectrum of *Escherichia coli*. *Water Research*, 39, 2921–2925.
- Wobus, C. E., Thackray, L. B., & Virgin, H. W. (2006). Murine norovirus: a model system to study norovirus biology and pathogenesis. *Journal of Virology*, 80, 5104–5112.



# Effect of extrusion process on antinutritional factors and protein and starch digestibility of lentil splits



Rahul P. Rathod, Uday S. Annapure\*

Food Engineering and Technology Department, Institute of Chemical Technology, Matunga, Mumbai 400 019, India

## ARTICLE INFO

### Article history:

Received 7 May 2015

Received in revised form

8 October 2015

Accepted 9 October 2015

Available online 22 October 2015

### Keywords:

Extruded product

Antinutritional factor

RSM

Protein digestibility

Lentil

## ABSTRACT

Lentil contains substantial amount of protein, carbohydrate, fiber and other nutrients like folate and iron but their bioavailability and utilization by human is relatively low and less explored, this is due to the presence of various antinutritional factors such as trypsin inhibitor, phytic acid and tannins. The present study was aimed to evaluate the physicochemical and sensory properties of extruded product by using response surface methodology (RSM), effect of different moisture content in raw material and the temperature of extrusion processing on the inactivation of these antinutritional factors in lentil. The attempts were also made to assess in vitro protein and starch digestibility. The die temperature has been varied from 140 to 180 °C with screw speed of 150–250 rpm at constant feed rate 16 rpm (340 g/min) and the feed moisture of the raw material was in the range of 14–22%. It was observed that extrusion was the best method to abolish trypsin inhibitors (99.54%), phytic acid (99.30%) and tannin (98.83%) without altering the protein content. Furthermore, it was also found that the associated thermal treatment was most effective in improving protein and starch digestibility (up to 89% and 96%, respectively) when it was compared with traditional thermal processes.

© 2015 Elsevier Ltd. All rights reserved.

## 1. Introduction

Lentil (*Lens culinaris* Medikus) is excellent source of proteins, carbohydrates, dietary fiber and essential minerals (Bishnoi and Khetarpaul, 1994). However, antinutritional factors such as phytic acid, trypsin inhibitors and tannins, which are present in lentil was considered undesirable for obstructing the bioavailability of minerals (Reddy, Sathe, & Salunkhe, 1982) and they compromise the protein digestibility, harming the nutritional value of this food (Sgarbieri and Whitaker, 1982). Therefore, it must be substantial reduction or complete elimination of these antinutrients before they can be safely consumed. The effects of processing on antinutritional factor (which is majorly carried out by extrusion process) vary notably, depending on the techniques and conditions, including time, temperature and moisture content, which in turn can enhance the bioavailability of proteins and minerals (Nestares, Barrionuevo, Urbano, López-Frías, 1999; Nestares, Lopez-Frias, Barrionuevo, & Urbano, 1996). A wide range of processing techniques could improve the protein and starch digestibility of

legumes and therefore their utilization (Alonso, Oruae, & Marzo, 1998). However, it is already known and understood that some of the treatments could make physicochemical changes in proteins, starch and other components of legume seeds affecting their overall nutritional properties (De Pilli, Fiore, Giuliani, Derossi, & Severini, 2011; Valle, Quillien, & Gueguen, 1994). In India, and many other countries, lentils are generally processed and consumed in different forms, depending on culture, source and taste preferences. The processing methods include ordinary and pressure cooking or microwave cooking methods are generally used for cooking of lentil, however, there was less reduction of antinutritional factor occurred in this common processing methods (Alonso, Aguirre, & Marzo, 2000).

In recent years, the demand for snacks with improved nutritional and functional properties has been increased. Among these, expanded product has gained preference among both consumers and producers (Ernault, Moraru, & Kokini, 2002). Extrusion of food is an emerging technology for the food industries to process and produced large number of products of varying size, shape, texture and taste (Kaur, Panday, & Mishra, 2007). Extrusion cooking is used worldwide for the production of expanded snack foods, as there is a huge demand of healthy and nutritious ready-to-eat products from all age groups of consumer. Krokida and Lazou (2010) studied that

\* Corresponding author.

E-mail address: [udayannapure@gmail.com](mailto:udayannapure@gmail.com) (U.S. Annapure).

for consumer acceptability structural and textural properties as well as quality of expanded products proven to be more vital. Extrusion conditions such as feed moisture content, extrusion temperature and screw speed were controlled to obtain optimized product quality (Meng, Threinen, Hansen, & Driedger, 2010). Therefore, the aim of this study was to investigate the effects of extrusion processing on the level of antinutritional factor such as trypsin inhibitor, phytic acid, tannins as well as in vitro protein and starch digestibility of lentil extruded product. The present investigations were also carried out to explore the possibility of lentil as a candidate for production of protein rich extruded product and study the effect of feed moisture and extrusion temperature on the antinutritional factors to increases the bioavailability of proteins and starch.

## 2. Materials and methods

### 2.1. Materials

Commercial lentil (*Lens culinaris* Medik) was purchased from agriculture produce market committee (APMC), Vashi, Mumbai, India. The lentil was cleaned ground to obtain flour and passed through 60 mesh sieve to obtain uniform particle size. All the chemicals used for the study were of AR grade.

### 2.2. Methods

#### 2.2.1. Proximate composition

Proximate composition of lentil flour was determined in accordance with the AOAC (1980, 2006) methods. Lentil flour contain 1.03% fat, 23.86% protein, 65.52% carbohydrate, 9.06% moisture and 0.53% ash content and are fairly rich in starch with 54.78%. Starch is the most influential component of lentil seed affecting the structural and functional properties of extrudates. Total fiber contain in lentil flour was 10.84%. The proximate composition, on a dry basis, of lentil flours is depicted in Table 2 as mean values ( $\pm$ standard deviation) of at least three replicates and the mean values are expressed as g per 100 g of sample.

#### 2.2.2. Preparation of sample

Samples were prepared by adding calculated amount of distilled water to obtain the different desired moisture levels (14, 18, and 22%) and allowed to equilibrate for 24 h before extrusion process.

**Table 2**

Proximate composition of lentil seeds.

Sr.no.	Proximate constituents	Content (g/100 g)
1	Moisture	9.06 $\pm$ 0.19
2	Fat	1.03 $\pm$ 0.06
3	Protein	23.86 $\pm$ 0.11
4	Total carbohydrate	65.52 $\pm$ 0.32
5	Ash content	0.53 $\pm$ 0.04
6	Starch	54.78 $\pm$ 0.12
7	Fiber	10.84 $\pm$ 0.06

All the values are Mean  $\pm$  SD of three individual determinations.

#### 2.2.3. Extrusion process

The lentil flour was extruded in a co-rotating twin screw extruder (KETSE 20/40 Brabender GmbH and Co. KG, Duisburg, Germany) with four independent heating zones. Twin screw extruder has screw diameter of 2 cm and screw length of 40 cm (L/D ratio of 20:1). Screw speed range is up to 900 rpm. The die diameter was 4 mm and feed rate was kept constant at 16 rpm (20.4 kg/hr). The temperature during extrusion was adjusted according to the experimental design by using electric heaters. Extrudates were produced using temperatures in the range of 140–180 °C and three levels of screw speeds (150, 200 and 250 rpm). Temperatures for different zone were Conveying zone (95, 115 and 135 °C), Mixing zone (110, 130 and 150 °C), Cooking zone (125, 145 and 165 °C), High pressure zone (die) (140, 160 and 180 °C). The extrudates were cooled to room temperature, dried in tray dryer at 45 °C for 2 h, packed in polyethylene bags and stored in a desiccator till further analysis.

#### 2.2.4. Experimental design

The response surface methodology was applied using a central composite design (CCD) for three independent variables (Barros-Neto, Scarminio, & Bruns, 2010), namely: the moisture content of the raw material, the extrusion temperature (die temperature) and the screw speed. The dependent variables used were the overall expansion, bulk density, water soluble index, water absorption index and hardness for each compound individually and in total for all the compounds. Twenty tests were performed: eight tests of factorial points ( $2^3$ ) (three levels for each factor), six axial points (two for each variable) and six repetitions of the central point (Table 1).

The results from the dependent variables were subjected to multiple regression analysis using design expert software 7.0.0 full version (Stat-Ease, Minneapolis, USA) and coefficients with p values

**Table 1**

Variables and their levels employed in Central Composite Design.

Experiment	Feed moisture content (X1)		Die temperature (X2)		Screw speed (X3)	
	Coded value	Uncoded value	Coded value	Uncoded value	Coded value	Uncoded value
1	-1	14	-1	140	-1	150
2	1	22	-1	140	-1	150
3	-1	14	1	180	-1	150
4	1	22	1	180	-1	150
5	-1	14	-1	140	1	250
6	1	22	-1	140	1	250
7	-1	14	1	180	1	250
8	1	22	1	180	1	250
9	-1.68	11.27	0	160	0	200
10	1.68	24.73	0	160	0	200
11	0	18	-1.68	126.36	0	200
12	0	18	1.68	193.64	0	200
13	0	18	0	160	-1.68	115.91
14	0	18	0	160	1.68	284.09
15–20	0	18	0	160	0	200

below 0.05 were considered significant. Linear and quadratic models were tested to explain the influence of independent variables on the response variables, because in Response Surface Methodology, the relationship between these variables is unknown and, therefore, it is necessary to find an adequate approximation to the true relationship between the response and the independent variables.

#### 2.2.5. Overall expansion

Overall expansion was calculated as the ratio of bulk (apparent) specific volume and true specific volume.

Bulk specific volume =  $1/\text{Bulk density}$

True specific volume =  $1/\text{True density}$

#### 2.2.6. Bulk density

As per the reported data, for expanded products bulk density is vital physical property of products as well as bulk density is very important quality attribute from the view of commercial production of extruded products. The bulk density was determined from 10 random measurements on the diameter (D, cm) and length (L, cm) of the extrudates using digital calipers, and the weight (m, g) was determined on an analytical balance. The bulk density was obtained from following formula (Ding, Ainsworth, Tucker, & Marson, 2005),

Bulk Density =  $4 \times m / (\pi \times D^2 L)$

#### 2.2.7. Expansion index (EI)

The diameters of 10 extruded products were measured using Vernier calipers (Absolute Digimatic Caliper, Series-500, Innox, Japan). Expansion index of the samples was determined by dividing the average diameter of the products by the diameter of the die nozzle (Ding et al., 2005).

#### 2.2.8. Porosity

The porosity of extrudates was determined from the bulk and apparent volumes. Porosity was calculated using the equation:

Porosity =  $(\text{Bulk volume} - \text{Apparent volume}) / \text{Bulk volume}$

where, Bulk volume =  $(1/\rho_b)$  and Apparent volume =  $(1/\rho_s)$

#### 2.2.9. Water solubility index (WSI) and water absorption index (WAI)

Extrudates were ground to powder and passed through the 60 mesh sieve for uniform size distribution. 2.5 g ground powder was suspended in 25 ml water at room temperature for 30 min, with intermediate stirring and then centrifuged at  $3000 \times g$  for 15 min. The supernatant was decanted into the reweighed evaporating dish and water was evaporated till constant weight to get dry solids. The WSI is the weight of dry solids in the supernatant expressed as a percentage of the original weight of sample where as WAI is the weight of residue obtained after removal of the supernatant per unit weight of original dry solids (Ding et al., 2005).

#### 2.2.10. Hardness

Hardness of the extrudate was determined using a Stable Micro System TAXT2i texture analyzer (Serial No.4650, TEE version

no.2.64 UK) fitted with a 50 kg load cell. Ten samples of approximately 5 cm in length were placed transversally on a platform over a 1 cm thick metal sheet and penetrating perpendicularly by the probe (2 mm cylindrical) (Ding et al., 2005). Probe was set to move at a test speed of 3 mm/s for a distance of 50 mm from the sample and penetrate about 5 mm in sample. Maximum force needed to break the sample was recorded and analysed by Texture Exponent software associated with the texture analyser. Measurements are reported as an average of all replicates.

#### 2.2.11. Phytic acid

Phytic acid was extracted in lentil and extruded samples with 2.4% HCl (1:20 w/v). The obtained mixture was centrifuged at 17,300 g (Sorvalle1 RC-5B) for 30 min at 15 °C and the supernatants collected. Glass barrel Econo-columns 0.7\*15 cm (Bio Rad Laboratories) were filled with 0.5 g of AG 1\*4 anion-exchange resin to effect phytate purification. To assess total phytic acid content, the simple procedure based on the reaction between ferric chloride and sulfosalicylic acid was followed (Fruehbeck, Alonso, Marzo, & Santidriaan, 1995).

#### 2.2.12. Condensed tannins

Condensed tannins were extracted with HCl:Methanol (1:100 v/v) for 7 h in lentil and extruded sample with mechanical stirring at room temperature and centrifuged at 5000 g at 15 °C for 15 min. Aliquots were immediately analyzed for tannin using the 0.5% vanillin assay (Broadhurst & Jones, 1978).

#### 2.2.13. Trypsin inhibitors

Trypsin inhibitor was analyzed as described by Kakade, Rackis, McGhee, and Puski (1974), using a-N-benzoyl-DL-arginine-p-nitro-anilidehydrochloride (BAPNA) as the substrate for trypsin. 1 g of finely ground lentil and extruded sample was extracted with 10 ml of 0.15 M phosphate buffer pH 8.1 at 4 °C overnight. Extracts were incubated with 250 ml of trypsin solution (0.004% trypsin in 0.025 M glycine HCl buffer) and diluted to 1 ml with buffer phosphate (pH 8.1). 2.5 ml of 0.001 M BAPNA solution in pH 8.1 buffer phosphates was added and warmed to 37 °C for 10 min reaction stopped by adding 1 ml of 30% acetic acid. Trypsin inhibitor was calculated from the absorbance read at 410 nm against a reagent blank.

#### 2.2.14. Polyphenols

The method of the Association of Official Analytical Chemists with some modifications (Christensen, 1974) was used. Total phenols were extracted in a sample of 1 g flour with 75 ml of water. An internal standard curve was prepared by adding 10 ml of 0–0.01% tannic acid to the flasks. The contents were heated for 30 min at 70 °C with constant shaking. Clear supernatants were collected after centrifuging the contents at 2500 g for 15 min and filtering them. Polyphenols were determined using the Folin-Denis reagent.

#### 2.2.15. In vitro protein digestibility

A system consisting, 100 mg (0.1 g) dry and defatted samples incubated at 1.5 mg pepsin in 15 ml of 0.1N HCl at 37 °C for 3 h, neutralize with 7.5 ml 0.2N NaOH, Add 4 mg pancreatin in 7.5 ml phosphate buffer (pH 8) incubated for 37 °C for 24 h, then add 5 mg of TCA, centrifugate at 5000 rpm for 10 min. After that discard supernatant dry residue at 40–50 °C and carried out Microkjhaldaal. The percent in vitro protein digestibility (IVPD) was calculated using the following equation.

In vitro protein digestibility % =  $\{(\text{total protein} - \text{residue protein}) / \text{total protein}\} * 100$

### 2.2.16. *In vitro* starch digestibility

The *in vitro* starch digestibility (IVSD) was determined in flours (50 mg/ml of 0.2 M phosphate buffer, pH 6.9) after amylolysis with 0.5 ml of pancreatic amylase (1260 U/mg) suspension (0.4 mg/ml of 0.2 M phosphate buffer, pH 6.9) at 20 °C for 2 h according to the method of Singh, Kherdekar, and Jambunathan (1982). At the end of the incubation period, 2 ml of 3,5-dini-trosalicylic acid reagent were added and the mixture boiled for 5 min. After cooling, the absorbance of the filtered solution was measured at 550 nm with maltose used as standard. IVSD was expressed as mg of maltose released per gram of sample on a dry weight basis. Values were corrected for the background.

### 2.2.17. Sensory analysis

Ten trained students from food engineering department evaluated the extruded snacks for appearance, flavor, texture, taste and overall acceptability in triplicate. Panelists were instructed to eat and swallow each sample and rate the intensity of each attribute using a nine-point scale (1 = dislike extremely and 9 = like extremely) (ISO 11136:2014). The sessions were performed on the same day (with a minimum 2-h break between the sessions) at the sensory laboratory of the Food Engineering and Technology Department (Mumbai, India) designed in accordance with ISO guidelines (ISO International Organization for Standardization, 2007). Assessors were asked not to smoke, eat or drink anything, except water, at least 1 h before the tasting sessions. For each sample, panelists received a sample served in plate coded with a digit number. Participants were provided with mineral water to clean their mouth between tastings. Presentation orders were systematically varied over assessors and replicates in order to balance the effects of serving order and carryover (MacFie, Bratchell, Greenhoff, & Vallis, 1989).

## 3. Results and discussion

### 3.1. Overall expansion (OE) and bulk density (BD)

The OE and BD of the extrudates varied between 1.98 to 4.26 and

0.1218 to 0.3864 respectively as shown in Figs. 1 and 2. BD is a measure of how much expansion has occurred as a result of extrusion. The heat developed during extrusion can increase the temperature of the moisture above the boiling point so that when the extrudate exits from the die, a part of the moisture would quickly flash-off as steam and result in an expanded structure with large alveoli and low density. On the other hand, if not enough heat is generated to flash-off enough of the moisture (because of low die temperature and high feed moisture), less expansion occurs resulting in a high BD product with collapsed cells which usually disintegrates on cooling. High density product is an indication of more uniform and continuous protein matrix and therefore, the extrudate is dense with parallel layers, no air pockets and is not spongy upon hydration (Filli, 2009).

From ANOVA, results show that the process variables, singularly or in combination, had a significant influence on the physical properties of extrudate ( $p < 0.001$ ). The feed moisture (A) and die temperature (B) were found to the highest coefficients and had the most significant effect on the expansion ( $p \leq 0.02$ ) and inverse significant effect on BD ( $p \leq 0.001$ ) of extrudate while screw speed ( $p > 0.05$ ) had no such significant effect on the extrudate OE and BD. A high OE is desirable in a production of expanded snacks. As the temperature of extrusion cooking increased, starch becomes more fully cooked and thus better able to expand (Baladrán-quintana, Barbosa-cánovas, Zazueta-morales, Anzaldúa-morales, & Quintero-ramos, 1998). Coefficient of determination  $R^2$  for OE and BD are 0.9823, 0.9775 respectively. Response model equations are,

$$\text{overall expansion} = +4.26 - 0.13 * A + 0.036 * B - 0.028 * C - 0.032 * A * B - 0.040 * A * C - 0.19 * B * C - 0.79 * A^2 - 1.05 * B^2 - 0.17 * C^2$$

$$\text{Bulk density} = +0.12 + 0.016 * A - 0.011 * B - 0.015 * C - 6.930E - 004 * A * B + 4.518E003 * A * C + 0.010 * B * C + 0.095 * A^2 + 0.10 * B^2 + 4.663E - 003 * C^2$$

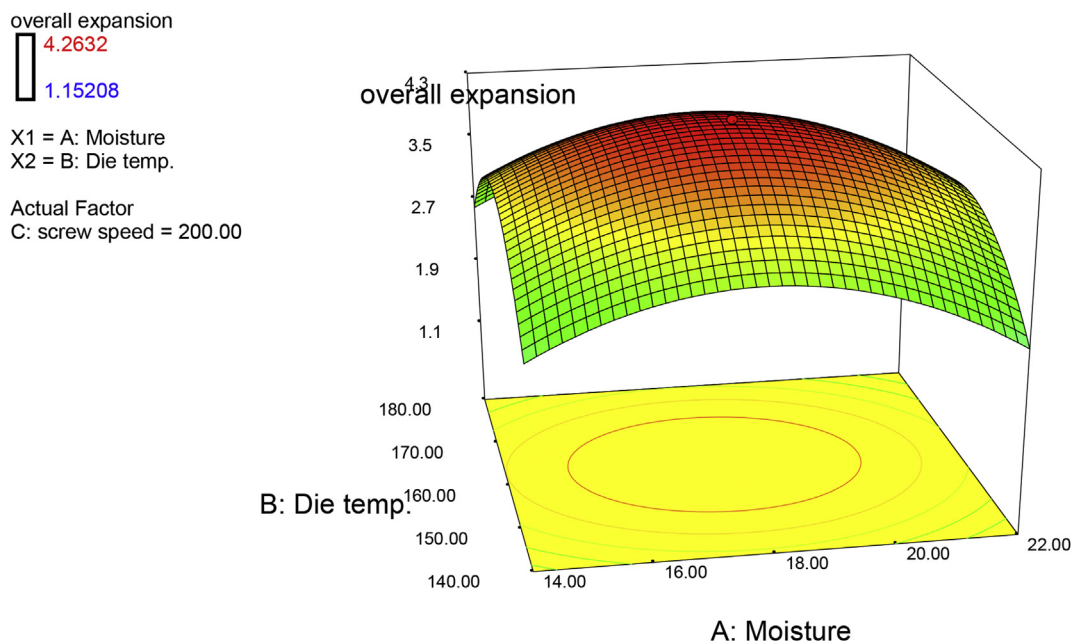


Fig. 1. The 3-D response surface plots of overall expansion significant interactions between moisture and die temperature.

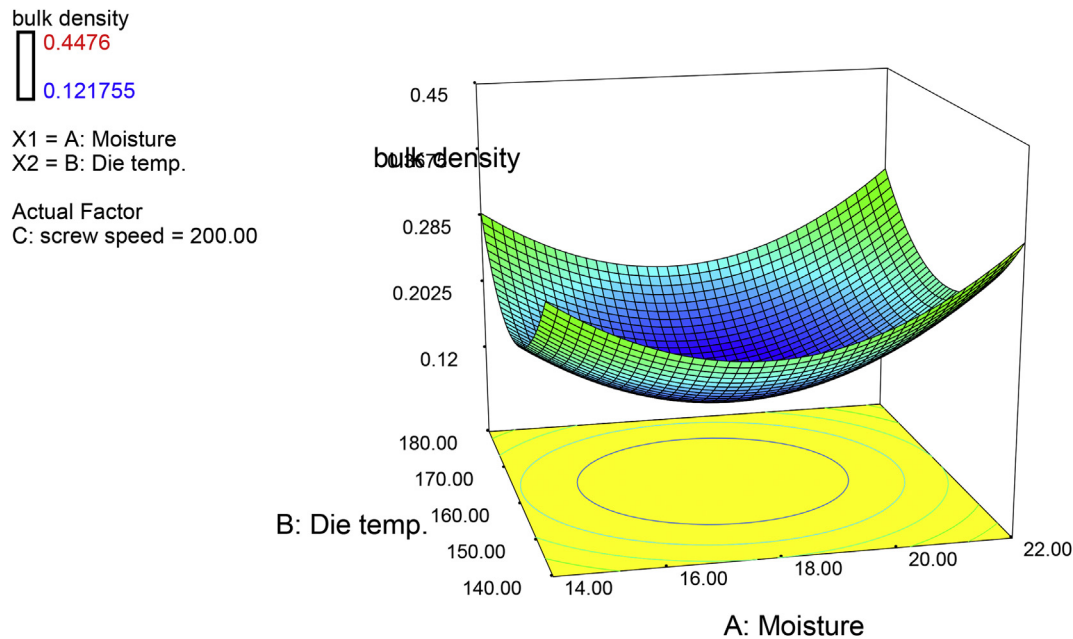


Fig. 2. The 3-D response surface plots of bulk density significant interactions between moisture and die temperature.

### 3.2. Expansion index (EI)

The EI of extrudates describes the degree of puffing undergone by the material as it exits the extruder. Sectional EI considers expansion only in the direction perpendicular to extrudate flow, while BD considers expansion in all directions. Several researchers have demonstrated that the EI of extruded depends on the degree of starch gelatinization (Case, Hanna, & Schwartz, 1992). As well proteins act as diluents and reduce expansion due to their ability to affect water distribution in the matrix, and to the fact that their macromolecular structure and conformation affect the extensional properties of extruded.

Fig. 3 showed the effect of moisture and die temperature on EI. Die temperature is one of the most important factors that contribute to starch modification during extrusion although excessive starch degradation decreases expansion. An increase in die temperature increased EI. The measured EI of lentil extrudates varied from 1.91 to 3.27. The feed moisture (A) and die temperature (B) were found to have significant effect on the expansion of extrudate. Response model equation with  $R^2$  (0.9892) is,

$$\text{Expansion Index} = +3.27 - 0.022 * A + 0.029 * B + 0.046 * C + 0.014 * A * B + 7.292E - 003 * A * C - 9.375E - 003 * B * C - 0.39 * A^2 - 0.47 * B^2 - 0.19 * C^2$$

### 3.3. Porosity

Air cells were created during extrusion giving expanded products with variable pore size and number. Porosity created during extrusion can be used to describe the expansion properties of the extruded products (Thymi, Krokida, Pappa, & Maroulis, 2005). Fig. 4 showing increasing feed moisture (14%–22%) caused an increased porosity whereas increased temperature showing inverse effect resulted on decreased porosity because high temperature resulted to increase dextrinization and weakening of structure while it was not significantly dependent on screw speed ( $p > 0.05$ ). Response

model equation with  $R^2$  (0.9892) is,

$$\text{Porosity} = +77.08 - 2.11 * A + 1.59 * B + 0.27 * C - 1.47 * A * B - 0.11 * A * C - 2.33 * B * C - 7.40 * A^2 - 19.86 * B^2 + 1.11 * C^2$$

### 3.4. Water absorption index (WAI) and water solubility index (WSI)

The extrudates exhibited WAI in the range of 2.1–4.1 shown in Fig. 5 with coefficient of determination ( $R^2 = 0.9972$ ). Positive correlation was demonstrated by the significant effects of moisture content ( $p < 0.01$ ) and die temperature ( $p < 0.01$ ) towards WAI. The result shows that an increase in moisture (A) and die temperature (B) was significant at  $p < 0.01$  and the screw speed led to a decrease in WAI. The comminution of starch molecules as a result of degradation caused by high die temperature may have made it imperative for the extrudates to hold less water, hence a lesser WAI. Similar observations were registered by Singh and Smith (1997). The negative correlation between WAI and screw speed can be attributed to the extended time of stay of the feed formulation inside the barrel of the extruder resulting in extensive cooking, ergo an increased WAI.

The corresponding second-order response model equation is,

$$\text{WAI} = +4.10 - 0.063 * A + 0.070 * B + 0.043 * C + 0.14 * A * B - 0.093 * A * C - 6.875E - 003 * B * C - 0.25 * A^2 - 0.73 * B^2 - 0.088 * C^2$$

WSI measures the amount of soluble components released during extrusion (Kirby, Ollett, Parker, & Smith, 1988). It is often used as an indicator of the starch degradation (Ding, Ainsworth, Plunkett, Tucker, & Marson, 2006), since this process leads to the generation of smaller and more water soluble molecules. Jones, Chinnaswamy, Tan, and Hanna (2000) reported that dietary fiber, starch and protein contents affect WSI. Besides changes in starch, WSI also be influenced by structural changes of other components during extrusion, such as proteins (undergo denaturation) and

Design-Expert® Software

Expansion Index



X1 = A: Moisture

X2 = B: Die temp.

Actual Factor

C: Screw speed = 200.00

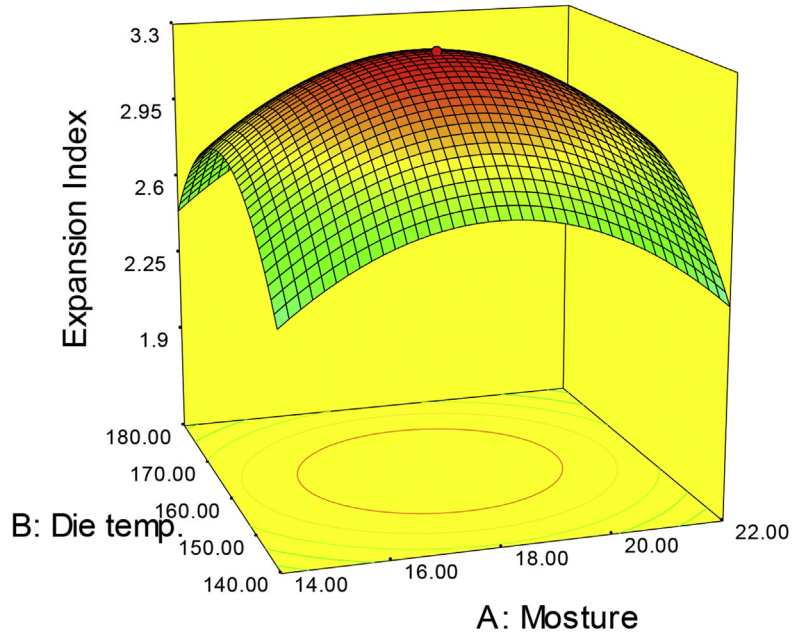


Fig. 3. The 3-D response surface plots of Expansion Index significant interactions between moisture and die temperature.

Design-Expert® Software

Porosity



X1 = A: Moisture

X2 = B: Die temp.

Actual Factor

C: Screw speed = 200.00

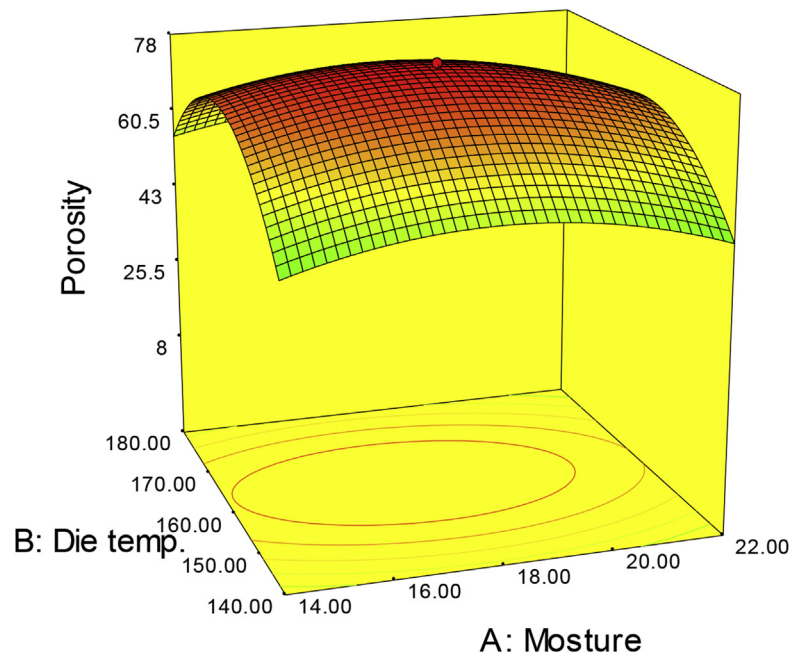


Fig. 4. The 3-D response surface plots of porosity significant interactions between moisture and die temperature.

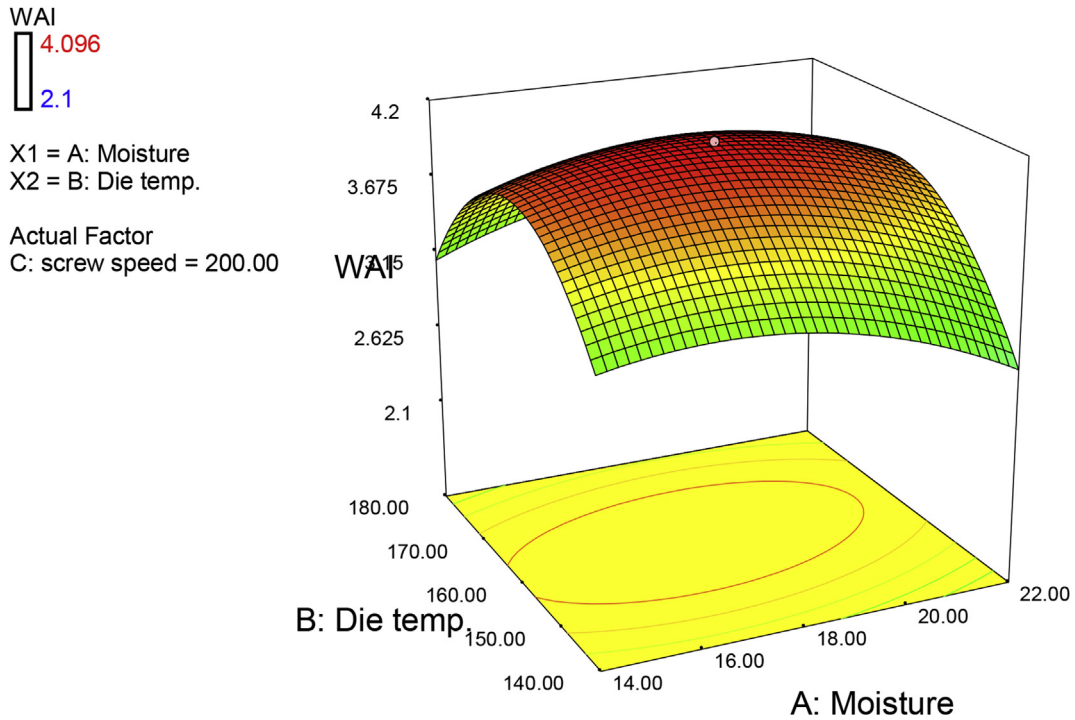


Fig. 5. The 3-D response surface plots of Water absorption index significant interactions between moisture and die temperature.

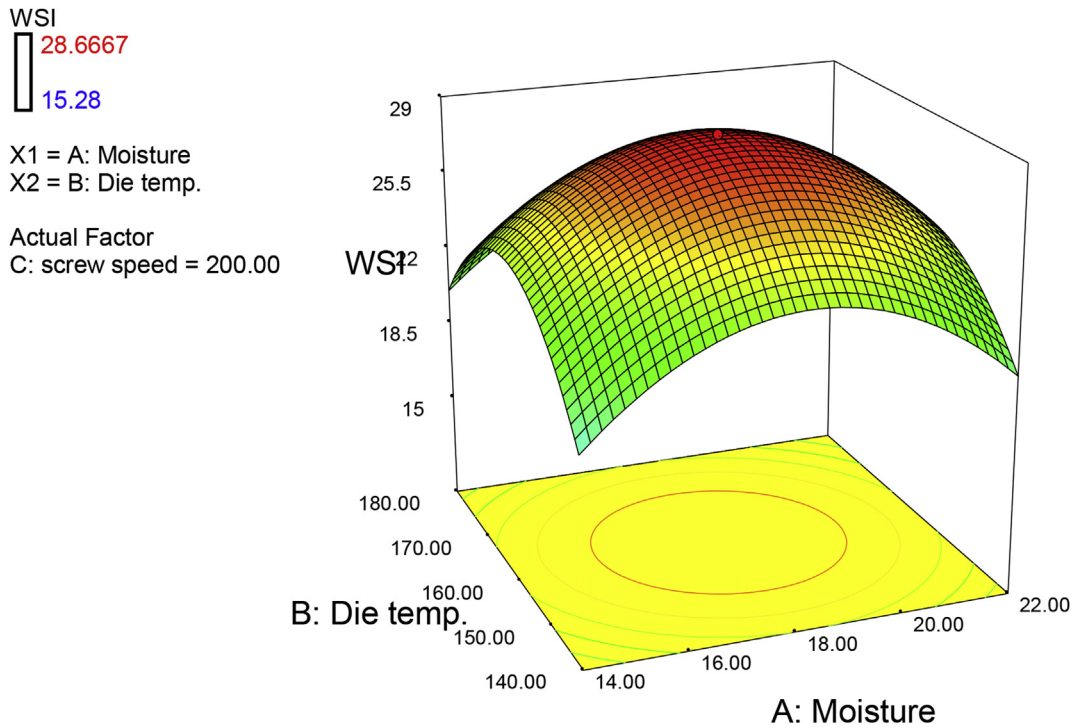


Fig. 6. The 3-D response surface plots of Water soluble index significant interactions between moisture and die temperature.

fibers which affecting its solubility. The extrudates exhibited WSI in the range of 18.30–28.67% shown in Fig. 6 with coefficient of determination ( $R^2 = 0.977$ ).

Response model equation is,

$$WSI = +28.66 - 0.024 * A + 3.163E - 003 * B - 0.044 * C - 0.32 * A * B + 0.19 * A * C + 0.44 * B * C - 4.31 * A^2 - 4.59 * B^2 - 0.56 * C^2$$

It was observed that the moisture content (A) and die temperature (B) had the most significant effect on the WSI of extrudates. WSI was significantly affected by the quadratic term of feed

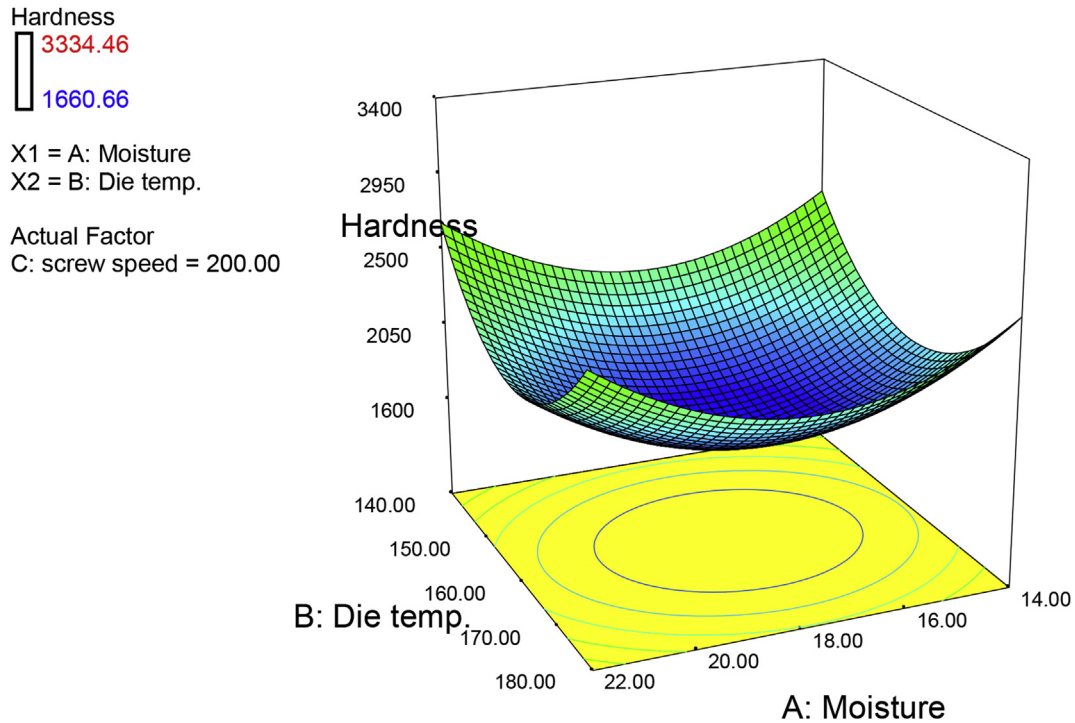


Fig. 7. The 3-D response surface plots of Hardness significant interactions between moisture and die temperature.

moisture (A) and die temperature (B) ( $p \leq 0.001$ ) but was not significantly dependent on screw speed (C) ( $p > 0.05$ ).

### 3.5. Hardness

The effect of extrusion conditions on hardness is shown in Fig. 7. Feed moisture (A) ( $P < 0.001$ ) was found to have the most significant effect on hardness of extrudates. Result showed that extrudates with higher overall expansion with low density had lower hardness. Previous studies have also reported that hardness of extrudate increased as the feed moisture content increased (Liu, Hsieh, Heymann, & Huff, 2000). Hardness of extrudates increased with increase in die temperature at low feed moisture while it decreased with increase in die temperature at higher feed moisture content. Hardness of extrudates ranges from 1660.66 to 3334.46. Response model equation with  $R^2$  (0.9882) is,

$$\text{Hardness} = +1665.26 + 38.56 * A - 22.27 * B - 2.51 * C - 5.91 * A * B + 10.07 * A * C - 17.15 * B * C + 398.00 * A^2 + 544.11 * B^2 + 37.23 * C^2$$

Table 3

Predicted and experimental values of the responses at optimum conditions 18% moisture content, 160 °C die temperature and 200 rpm screw speed.

Responses	Predicted value	Experimental value <sup>a</sup>
Overall expansion	4.26	4.26 ± 0.10
Bulk density	0.12	0.12 ± 0.01
WSI	28.12	28.67 ± 0.16
WAI	4.1	4.10 ± 0.07
Hardness	1652.86	1660.66 ± 46

<sup>a</sup> All the values are mean ± SD of ten individual determinations.

### 3.6. Verification of results

The suitability of the model developed for predicting the optimum response values was tested using the recommended optimum conditions of the variables and was also used to validate experimental and predicted values of the responses. Table 3 shows the predicted and experimental values of the responses at optimum conditions.

### 3.7. Phytic acid, condensed tannins and polyphenols

Data on phytic acid, condensed tannins and polyphenol contents of raw material (raw lentil seed) and extruded product at different temperature and different moisture are summarized in Table 4. Extrusion cooking significantly reduced the levels of phytic acid, condensed tannins and polyphenols. The data agree with those found by Alonso et al. (1998) in other legume seeds.

Extrusion cooking caused a significant reduction in phytic acid content compared to raw lentil as well as condensed tannins and polyphenols were also significantly reduced due to extrusion processing method. Thermal degradation of these molecules, as well as changes in their chemical reactivity or the formation of insoluble complexes, could explain the significant reduction of the anti-nutrients by thermal processing (Kataria, Chauhan, & Punia, 1989).

The effect of increase in extrusion temperature from 140 to 180 °C caused to decrease in antinutritional factors more than 93%, such as phytic acid upto 99.30% and tannin upto 98.83%. Also there is considerable change of total polyphenol (upto 65%).

Study also observed that, there was significant change occurred when moisture is increased from 14 to 22% during extrusion process. More moisture contain is resulted as high reduction of phytic acid, tannin and polyphenol as compare to less moisture which is shown in Fig. 4. Thus, these results show the importance of the extrusion process to degrade the antinutritional factors.

**Table 4**  
Phytic acid, tannin, trypsin inhibitor, total polyphenols content, in vitro protein and starch digestibility in raw lentil and extrudates made from lentil using different extrusion temperature and feed moisture.<sup>a</sup>

Extrusion temperature (°C)	Feed moisture (%)	Phytic acid (g/100 g dry matter)	Tannin (mg eq. cat/100 g dry matter)	Trypsin inhibitor (IU/mg dry mater)	Total polyphenols (mg GAE/g)	Protein digestibility %	Starch digestibility %
140	14	0.057 ± 0.02 (95.01%)	0.065 ± 0.04 (93.08%)	0.049 ± 0.02 (98.26%)	5.1 ± 0.8 (27.14%)	70.62 ± 0.14	77.52 ± 0.11
	18	0.054 ± 0.01 (95.27%)	0.062 ± 0.01 (93.40%)	0.046 ± 0.05 (98.37%)	4.8 ± 0.13 (31.43%)	73.08 ± 0.17	78.37 ± 0.15
	22	0.052 ± 0.01 (95.45%)	0.059 ± 0.02 (93.72%)	0.044 ± 0.04 (98.44%)	4.6 ± 0.12 (34.28%)	75.38 ± 0.55	80.13 ± 0.22
160	14	0.030 ± 0.03 (97.38)	0.040 ± 0.01 (95.74%)	0.030 ± 0.02 (98.94%)	3.7 ± 0.6 (47.14%)	78.31 ± 0.20	85.22 ± 0.27
	18	0.027 ± 0.01 (97.64%)	0.038 ± 0.03 (95.96%)	0.026 ± 0.01 (99.07%)	3.5 ± 0.16 (50%)	80.22 ± 0.10	86.15 ± 0.05
	22	0.026 ± 0.01 (97.73%)	0.035 ± 0.01 (96.28%)	0.020 ± 0.02 (99.29%)	3.2 ± 0.11 (54.28%)	81.06 ± 0.26	87.20 ± 0.09
180	14	0.011 ± 0.02 (99.04%)	0.020 ± 0.01 (97.87%)	0.017 ± 0.01 (99.39%)	2.9 ± 0.1 (58.57%)	86.23 ± 0.12	91.94 ± 0.09
	18	0.010 ± 0.001 (99.13%)	0.018 ± 0.02 (98.08%)	0.014 ± 0.03 (99.50%)	2.5 ± 0.09 (64.29%)	87.12 ± 0.25	94.64 ± 0.07
	22	0.008 ± 0.01 (99.30%)	0.011 ± 0.02 (98.83%)	0.013 ± 0.01 (99.54%)	2.4 ± 0.4 (65.71%)	88.64 ± 0.11	96.04 ± 0.18
Lentil seed (Control)		1.1436 ± 0.10	0.94 ± 0.09	2.823 ± 0.12	7.0 ± 0.7	39.39 ± 0.08	60.68 ± 0.05

<sup>a</sup> All the values are mean ± SD of three individual determinations. Figures in the parenthesis indicate % reduction in phytic acid, tannin, trypsin inhibitor and total polyphenols, and increased % of protein and starch digestibility.

### 3.8. Trypsin inhibitor

Table 4 shows that a reduction of trypsin inhibitor in the raw lentil and extruded product significantly by extrusion process using different temperatures. These results are in agreement with previous findings (Alonso et al., 1998). Extrusion is the most effective method for reducing trypsin inhibitor activity when compared with the other treatments. Extrusion cooking drastically reduced trypsin inhibitor of the extrudates by 98%. As Adams (2007) suggests, reactions involving deamidation splitting of covalent bonds, such as hydrolysis of peptide bonds at aspartic acid residues, and interchange or destruction of disulfide bonds, might be involved in the thermal inactivation.

There is also role of moisture content for the inactivation of trypsin inhibitor. From this study it is observed that, increase in moisture content during extrusion process caused the increase in removal of trypsin inhibitor.

### 3.9. Protein and starch digestibility

Table 4 show that both IVPD and IVSD of raw lentil and extruded were increased significantly by extrusion process. The results agree with those of Bishnoi and Khetarpaul (1994) in legume seeds. Compared with control, extrusion cooking produced a more significant improvement of IVPD and IVSD in extrudate. The increase of digestibility produced by the extrusion processing was higher in starch than in protein. Improvement of protein digestibility after extrusion processing could be attributable to the reduction or elimination of different antinutritional factor. Phytic acid, trypsin inhibitor as well as condensed tannins and polyphenols are known to interact with protein to form complexes. This interaction increased the degree of cross-linking, decreasing the solubility of proteins and making protein complexes less susceptible to proteolytic attack than the same protein alone (Reddy, Pierson, Sathé, & Salunkhe, 1985).

An increase in IVPD was observed in extruded products compared to the other processing methods such as traditional

cooking methods (ordinary cooking and microwave cooking). This can be related to the higher efficiency of this thermal treatment in reduction of trypsin inhibitory activities. IVPD and IVSD were increased upto 89% and 96% respectively. It was also observed that, there was significant effect of moisture on IVPD and IVSD, which increased with higher in feed moisture. That means higher the feed moisture used for extrusion process gave higher IVPD and IVSD.

### 3.10. Sensory evaluation

The sensory scores obtained for extrudates with different trial are summarized in Table 5. The sensory scores for overall acceptance obtained for lentil extrudates were 7.13, 7.01, 7.17, 6.07 and 7.87 for runs (14%, 140 °C, 150 rpm), (22%, 180 °C, 150 rpm), (14%, 180 °C, 250 rpm), (18%, 127 °C, 200 rpm) and (18%, 160 °C, 200 rpm) respectively. From these results, it is very clear that extrudates with good sensory acceptability can be produced from lentil. Extrudate with moisture content of 18% with a die temperature of 160 °C at 200 rpm was found to be most acceptable using both sensory evaluation and statistical analysis.

## 4. Conclusions

The present studies show the ability of extrusion processing on reducing antinutritional factor such as phytic acid, tannin, trypsin inhibitor and total polyphenol levels and the efficiency of improving IVPD and IVSD. Extrusion caused the significant reduction of protein antinutritional factors and appeared to be the most effective process with improving both IVPD and IVSD. Further, it is revealed that lentil has a great potential for extrusion to produce ready-to-eat snacks with good acceptance. The physicochemical properties and sensory characteristics of lentil-based extrudate were highly dependent on process variables, feed moisture content, die temperature and screw speed. RSM was used to establish the correlation between these process variables, and physical properties of extruded product. It was proved that extrusion process increased nutritional value of extruded product due to the

**Table 5**  
Sensory results for lentil-based extrudates.

Trial no.	Appearance	Taste	Flavor	Texture	Overall acceptability
1	7.1 ± 0.1	6.45 ± 0.18	7.32 ± 0.14	7.65 ± 0.30	7.13 ± 0.10
4	6.89 ± 0.14	6.32 ± 0.22	7.34 ± 0.16	7.49 ± 0.12	7.01 ± 0.14
7	6.52 ± 0.16	6.53 ± 0.12	7.19 ± 0.26	6.93 ± 0.14	7.17 ± 0.20
11	6.2 ± 0.24	5.8 ± 0.09	7.2 ± 0.28	5.08 ± 0.08	6.07 ± 0.11
15	8.1 ± 0.18	7.86 ± 0.32	7.60 ± 0.21	7.92 ± 0.22	7.87 ± 0.16

All the values are mean ± SD of ten individual determinations.

significant reduction in antinutritional factors. The overall best quality product was optimized and obtained at 18% moisture, 160 °C die temperature and 200 rpm screw speed. The sensory evaluation showed that the optimized extrudate was the most acceptable. Thus, results indicate that lentil may be the good candidate to be used as an industrial raw material for the production of extruded snacks with great nutritional value.

## Acknowledgment

The authors gratefully acknowledge University Grant Commission (UGC) for financial support in carrying out this work.

## References

- Adams, J. B. (2007). Review: enzyme inactivation during heat processing of food-stuffs. *International Journal of Food Science & Technology*, 26(1), 1–20. <http://dx.doi.org/10.1111/j.1365-2621.1991.tb01136.x>.
- Alonso, R., Aguirre, E., & Marzo, F. (2000). Effects of extrusion and traditional processing methods on antinutrients and in vitro digestibility of protein and starch in faba and kidney beans. *Food Chemistry*, 68, 159–165.
- Alonso, R., Orua, E., & Marzo, F. (1998). Effects of extrusion and conventional processing methods on protein and antinutritional factor contents in pea seeds. *Food Chemistry*, 63, 505–512.
- Association of Official Analytical Chemists (AOAC). (1980). *Official methods of AOAC* (Vol. II). Washington: Association of Official Chemists.
- Association of Official Analytical Chemists (AOAC). (2006). *Official methods of AOAC, International* (18th ed.). Gaithersburg, MD, USA.
- Balandrán-quintana, R. R., Barbosa-cánovas, G. V., Zazueta-morales, J. J., Anzaldúa-morales, A., & Quintero-ramos, A. (1998). Functional and nutritional properties of extruded whole pinto bean meal (*Phaseolus Vulgaris* L.). *Journal of Food Science*, 63(1), 113–116.
- Barros-Neto, B., Scarmínio, I. S., & Bruns, R. E. (2010). *Como fazer experimentos: pesquisa e desenvolvimentonaciência e naindústria* (4th ed.). Porto Alegre: Bookman.
- Bishnoi, S., & Khetarpaul, N. (1994). Effect of domestic processing and cooking methods on in-vitro starch digestibility of different pea cultivars (*Pisum sativum*). *Food Chemistry*, 47, 177–182.
- Broadhurst, R. B., & Jones, W. T. (1978). Analysis of condensed tannins using acidified vanillin. *Journal of the Science of Food and Agriculture*, 29(9), 788–794. <http://dx.doi.org/10.1002/jsfa.2740290908>.
- Case, S. E., Hanna, M. A., & Schwartz, S. J. (1992). Effect of starch gelatinization on physical properties of extruded wheat and corn based products. *Cereal Chemistry*, 69, 401–404.
- Christensen, K. D. (1974). *Improving the plant proteins by nuclear techniques*. Vienna: International Atomic Energy Agency.
- De Pilli, T., Fiore, A. G., Giuliani, R., Derossi, A., & Severini, C. (2011). Functional food produced by extrusion: cooking technology (Book chapter). In L. M. Salander, & D. N. Alwell (Eds.), *Food production: New research* (pp. 1–44). Nova Science Publishers.
- Ding, Q. B., Ainsworth, P., Plunkett, A., Tucker, G., & Marson, H. (2006). The effect of extrusion conditions on the functional and physical properties of wheat-based expanded snacks. *Journal of Food Engineering*, 73, 142–148.
- Ding, Q.-B., Ainsworth, P., Tucker, G., & Marson, H. (2005). The effect of extrusion conditions on the physicochemical properties and sensory characteristics of rice-based expanded snacks. *Journal of Food Engineering*, 66(3), 283–289. <http://doi.org/10.1016/j.jfoodeng.2004.03.019>.
- Ernault, V., Moraru, C. I., & Kokini, J. L. (2002). Influence of fat on expansion of glassy amylopectin extrudates by microwave heating. *Cereal Chemistry*, 79(2), 265–273. <http://dx.doi.org/10.1094/CCHEM.2002.79.2.265>.
- Filli, K. B. (2009). *Production, optimization and characterization of extruded fura from pearl millet and grain legume flour mixtures*. Maiduguri, Nigeria: University of Maiduguri (Unpublished PhD Thesis).
- Fruehbeck, G., Alonso, R., Marzo, F., & Santidriaan, S. (1995). A modified method for indirect quantitative analysis of phytate in foodstuffs. *Analytical Biochemistry*, 72, 248–254.
- ISO International Organization for Standardization. (2007). *Sensory analysis – general guidance for the design of test rooms (ISO 8589:2007)*. Geneva, Switzerland.
- Jones, D., Chinnaswamy, R., Tan, Y., & Hanna, Y. (2000). Physico-chemical properties of ready-to-eat breakfast cereals. *Cereal Food World*, 45, 164–168.
- Kakade, M. L., Rackis, J. L., McGhee, J. E., & Puski, G. (1974). Determination of trypsin inhibitor activity of soy bean products: a collaborative analysis of an improved procedure. *Cereal Chemistry*, 51, 376–382.
- Kataria, A., Chauhan, B. M., & Punia, D. (1989). Antinutrients and protein digestibility (in vitro) of mung bean as affected by domestic processing and cooking. *Food Chemistry*, 32, 9–17.
- Kaur, M., Panday, H., & Mishra, H. N. (2007). Recent advances in food extrusion. *Beverage and Food World*, 46–49.
- Kirby, A. R., Ollett, A. L., Parker, R., & Smith, A. C. (1988). An experimental study of screw configuration effects in the twin-screw extrusion-cooking of maize grits. *Journal of Food Engineering*, 8, 247–272.
- Krokida, M., & Lazou, A. (2010). Functional properties of corn and corn–lentil extrudates. *Food Research International*, 43(2), 609–616.
- Liu, Y., Hsieh, F., Heymann, H., & Huff, H. E. (2000). Effect of process conditions on the physical and sensory properties of extruded oat–corn puff. *Journal of Food Science*, 65, 1253–1259.
- MacFie, H. J. H., Bratchell, N., Greenhoff, K., & Vallis, L. V. (1989). Designs to balance the effect of order of presentation and first order carry-over effects in hall tests. *Journal of Sensory Studies*, 4, 129–148. <http://dx.doi.org/10.1111/j.1745-459X.1989.tb00463.x>.
- Meng, X., Threinen, D., Hansen, M., & Driedger, D. (2010). Effects of extrusion conditions on system parameters and physical properties of a chickpea flour-based snack. *Food Research International*, 43, 650–658.
- Nestares, T., Barrionuevo, M., Urbano, G., & López-Frías, M. (1999). Effect of processing methods on the calcium, phosphorus, and phytic acid contents and nutritive utilization of chickpea (*Cicer arietinum* L.). *Journal of Agricultural and Food Chemistry*, 47(7), 2807–2812. <http://dx.doi.org/10.1021/jf9808325>.
- Nestares, T., Lopez-Frias, M., Barrionuevo, M., & Urbano, G. (1996). Nutritional assessment of raw and processed chickpea (*Cicer arietinum* L.) protein in growing rats. *Journal of Agriculture and Food Chemistry*, 44, 2760–2765.
- Reddy, N. R., Pierson, M. D., Sathe, S. K., & Salunkhe, D. K. (1985). Dry bean tannins: a review of nutritional implications. *Journal of American Oil Chemistry Society*, 62, 541–549.
- Reddy, N. R., Sathe, S. K., & Salunkhe, D. K. (1982). Phytates in cereals and legumes. *Advances in Food Research*, 28, 1–92.
- Sgarbieri, V. C., & Whitaker, J. R. (1982). Physical, chemical and nutritional properties of common bean (*Phaseolus*) proteins. *Advances in Food Research*, 28, 93–166.
- Singh, U., Kherdekar, M. S., & Jambunathan, R. (1982). Studies on Desi and Kabuli chickpea (*Cicer arietinum* L.) cultivars. The levels of amylase inhibitors, levels of oligosaccharides and in vitro starch digestibility. *Journal of Food Science*, 47, 510–512.
- Singh, N., & Smith, A. C. (1997). A comparison of wheat starch, whole wheat meal and oat flour in the extrusion cooking process. *Journal of Food Engineering*, 34(1), 15–32.
- Thymi, S., Krokida, M. K., Pappa, A., & Maroulis, Z. B. (2005). Structural properties of extruded corn starch. *Journal of Food Engineering*, 68, 519–526.
- Valle, G. D., Quillien, L., & Gueguen, J. (1994). Relationships between processing conditions and starch and protein modifications during extrusion cooking of pea flour. *Journal of the Science of Food and Agriculture*, 64, 509–517.



# Characterization of interphase volatile compounds in Chinese *Luzhou*-flavor liquor fermentation cellar analyzed by head space-solid phase micro extraction coupled with gas chromatography mass spectrometry (HS-SPME/GC/MS)

Xiaofei Ding<sup>a, b</sup>, Chongde Wu<sup>a, b</sup>, Jun Huang<sup>a, b</sup>, Rongqing Zhou<sup>a, b, c, \*</sup>

<sup>a</sup> College of Light Industry, Textile & Food Engineering, Sichuan University, Chengdu 610065, China

<sup>b</sup> Key Laboratory of Leather Chemistry and Engineering, Ministry of Education, Sichuan University, Chengdu 610065, China

<sup>c</sup> National Engineering Research Center of Solid-State Manufacturing, Luzhou 646000, China

## ARTICLE INFO

### Article history:

Received 12 September 2015

Received in revised form

30 September 2015

Accepted 7 October 2015

Available online 22 October 2015

### Keywords:

Interphase volatile compounds

Fermentation cellar

HS-SPME/GC/MS

PCA

PLS-DA

### Chemical compounds studied in this article:

Ammonium molybdate (PubChem CID:

16211167)

Sodium hydroxide (PubChem CID: 14798)

Sodium chloride (PubChem CID: 5234)

Boric acid (PubChem CID: 7628)

Ascorbic acid (PubChem CID: 54670067)

Potassium dichromate (PubChem CID:

24502)

Potassium iodide (PubChem CID: 4875)

Potassium sodium tartrate (PubChem CID:

165453)

Methyl octanoate (PubChem CID: 8091)

2-Octanol (PubChem CID: 20083)

## ABSTRACT

This study aimed to investigate volatile compounds characteristics of Pit mud (PM), *Zaopei* (ZP), *Huangshui* (HS) in Chinese *Luzhou*-flavor liquor fermentation cellar by HS-SPME/GC/MS. Results indicated that pit age and spatial position had a stronger effect on volatiles than physicochemical properties. A total of 59 volatiles had been identified, and phenylethyl alcohol, butyric acid, pentanoic acid, hexanoic acid, heptanoic acid, ethyl lactate, ethyl hexanoate, ethyl hexadecanoate, ethyl linoleate and ethyl elaidate were dominant, accounting for roughly 66.30%. Additionally, the total level of volatiles significantly increased from upper layer (U) to under layer (D), except for 2-year-MPM and 40-year-MZP, and 40-year-DPM (834.14 mg/kg) had the highest content. PCA explanation plane primarily revealed the main differentiation based on their loading plot values. Results of PLS-DA showed 4-methylphenol and gamma-nonanolactone were correlated with 2-year-PM. In addition to ethyl phenylacetate, ethyl hexanoate, furfuryl hexanoate, ethyl nonanoate, perhydrofarnesyl acetone and 2-acetyl furan were associated with 40-year-PM. Isoamyl hexanoate, octyl octanoate, benzaldehyde and 2-nonenal were with 10-year-PM. 3-methyl-1-butanol, ethyl lactate, ethyl hydrocinnamate and 3-furancarboxaldehyde were related to 2-year-ZP, while ethyl decanoate and ethyl linolenate were relevant to 10-year-ZP. No specific compounds for 40-year-ZP and HS samples were found.

© 2015 Elsevier Ltd. All rights reserved.

## 1. Introduction

Chinese liquor is one of the oldest distillates in the world and has higher ethanol content (normally 38–68% vol.) contrasted

\* Corresponding author. College of Light Industry, Textile and Food Engineering, Sichuan University, Chengdu 610065, China.

E-mail address: [zhourqing@scu.edu.cn](mailto:zhourqing@scu.edu.cn) (R. Zhou).

with other spirits such as vodka, whiskey and brandy. The south of Sichuan province is the main region of producing liquor in China, where long-term annual precipitation is 1200–1400 mm and long-term annual mean air temperature is 16.0–17.5 °C. Here, *Luzhou*-flavor liquor, also known as strong-flavor liquor, is one of the famous Chinese distilled spirits. Cellar, constructed with special clay, provides a suitable habitat for fermentation. There are three indispensable phases during the fermentation process, including PM, ZP and HS. PM, a solid phase, is domesticated for many years

and contains abundant organics and mineral components. ZP is a mixture of *Daqu*, streamed grains, fermented grains and rice husk, and the major biochemical reaction occurred in this phase. In consideration of a large number of voids in the ZP, thus ZP is regarded as a micro-aerobic phase. Moreover, during the process, large liquid metabolites and free water are accumulated in the bottom of cellar, which are called as HS, a liquid phase. In the past, we had investigated interphase microbial community characteristics by two molecular tools and proved that the community characteristics in the PM and ZP simply determined the unique feature of HS (Ding, Wu, Huang, & Zhou, 2015). It is noted that interphase mass transfer affects not only material metabolism and community diversity, but also flavor compounds. Additionally, by GC–MS paired with multiple analysis approaches, different kinds (Fenggu and Jiannanchun) and pit ages (new cellar and 50-year cellar) of raw liquors were compared and results demonstrated that the differences in microbial community could lead to the discrepancy of flavors (Zheng, Liang, Wu, Zhou, & Liao, 2014). However, until now, only Xia, Wu, Huang, and Zhou (2014) had selected and applied potential whole-cell enzymes in the esterification of HS based on physicochemical analysis in combination with volatile profile analysis. Therefore, it is essential to exploit interphase volatile compounds characteristics and differences in the cellar for further improving the production and quality of Luzhou-flavor liquor.

Recently, multivariate statistical techniques such as PCA and PLS-DA have provided possibility to extract and use information based on overall properties of the sample, and performed a classification without the need for additional compositional data (Cynkar, Damberg, Smith, & Cozzolino, 2010), and been successfully used in wines (Consonni, Cagliani, Guantieri, & Simonato, 2011; Daniel et al., 2006; Liu, Cozzolino, Cynkar, Gishen, & Colby, 2006; Serrano-Lourido, Saurina, Hernandez-Cassou, & Checa, 2012). For example, different French brandies: Armagnac, Cognac, Calvados and Mirabelle were compared by using PLS-DA based on their volatile profiles (Ledauphin, Le Milbeau, Barillier, & Hennequin, 2010).

The aim of this study was to investigate interphase volatile compounds and differences in Chinese Luzhou-flavor liquor cellar of different pit ages and positions by HS-SPME/GC/MS. To our knowledge, this is the first report to uncover the discrepancies and shifts of interphase flavors by multivariate statistical method.

## 2. Materials and methods

### 2.1. Sampling

Samples were obtained from different cellars in liquor company (Xufu Co., Ltd, Yibin City, Sichuan Province, China), which were used persistently for 2, 10 and 40 years, respectively. The sampling method was according to previous literature (Ding et al., 2015), and sampling sites were depicted in Fig. 1. As shown in Table 1, PM and ZP samples were collected from upper, middle and under layer of each cellar, respectively, and four subsamples were collected in each layer, and well mixed, then transferred to sterile polyethylene bags and stored at  $-20^{\circ}\text{C}$  until analyzed. For each HS sample, approximately 100 mL was collected from the bottom of the cellar after fermentation and immediately poured into glass bottles, then sealed storing at  $4^{\circ}\text{C}$  until analyzed.

### 2.2. Determination of basic physicochemical properties

Moisture content was determined by oven drying method, and pH was determined by pH meter. Available phosphorus was extracted with sodium bicarbonate and determined by ammonium

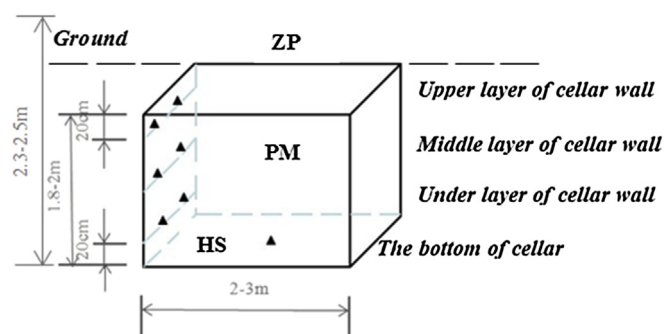


**Fig. 1.** Sampling sites of PM, ZP and HS. PM and ZP samples were collected from three different positions of each cellar, and four subsamples were collected in each layer; while HS sample was collected from the bottom of cellar.

**Table 1**  
Sampling numbers and their related positions in the fermentation cellar.

Pit age	Fermentation cellar			
	Upper layer (U)	Middle layer (M)	Under layer (D)	Bottom
2-year	UPM, UZP	MPM, MZP	DPM, DZP	HS
10-year	UPM, UZP	MPM, MZP	DPM, DZP	HS
40-year	UPM, UZP,	MPM, MZP,	DPM, DZP	HS

molybdate method (Ding et al., 2015), and reducing sugar was determined by dinitrosalicylic acid (DNS) method (Breuil & Saddler, 1985). Total acid was determined by alkali titration method (Kim & Lee, 2008).  $\text{NH}_4^+-\text{N}$  in the PM was determined by potassium iodide mercury method (Ding et al., 2015), while  $\text{NH}_4^+-\text{N}$  in the ZP and HS was determined by formol titration method (Cui, Zheng, Wu, & Zhou, 2014). Additionally, alcohol strength was determined by dichromate oxidation method (Crowell & Ough, 1979) and total ester was determined according to spectrophotometrical method (Feng, Zhan, Wang, Zhang, & Lin, 2012).

### 2.3. HS-SPME sampling and GC/MS analysis

A 50/30  $\mu\text{m}$  DVB/CAR/PDMS fiber (Supelco, Inc., Bellefonte, PA) was used for aroma extraction. The conditions for HS-SPME were based on the reported method with slight modifications (Du, Fan, & Xu, 2011). The extracting volatile compounds were carried out on Trace GC Ultra gas chromatograph-DSQ II mass spectrometer (Thermo Electron Corporation, Waltham, USA) equipped with an HP-INNOWAX capillary column (30.0 m  $\times$  0.25 mm  $\times$  0.25  $\mu\text{m}$ , Agilent Technology, USA) and a flame ionization detector (FID). Mass spectrum was generated in the electron impact (EI) mode at 70 eV ionization energy using the full scan mode (45–400 amu). The GC operation condition was achieved according to the protocols reported previously (Zheng, Liang, et al., 2014). The constituents were tentatively identified by matching mass spectrum with NIST05 spectrum database and verified by comparison of their Kováts retention indices (RI) with the RI reported in literatures, which was calculated by using  $\text{C}_8-\text{C}_{20}$  n-alkanes. The odor description of compounds in this paper was reported at [www.flavornet.org](http://www.flavornet.org). The relative concentration of volatile compound was estimated as:

$$C_2 = C_1 \times S_2 / S_1$$

Where  $C_2$  was the relative volatile compounds of sample (mg/kg),  $C_1$  was the concentration of internal standard (mg/kg; internal standard: 10  $\mu\text{L}$  2-octanol [0.93 mg/mL] and 10  $\mu\text{L}$  methyl octanoate [0.88 mg/mL] for alcohols and the rest, respectively),  $S_2$  was the

relative peak area of analyte,  $S_1$  was the peak area of internal standard.

#### 2.4. Data analysis

All assays were conducted in triplicate and results were expressed as mean  $\pm$  standard deviation. The analysis of variance (ANOVA) was used to test the significance of assay ( $p < 0.05$ ) with software SPSS 17.0. Likewise, PCA was performed with software SPSS 17.0. PLS-DA was conducted by SIMCA-P 11.5 software (UMETRICS, Sweden).

In multivariate data analysis, PCA is a well-known technique frequently applied to reduce the dimensionality and complexity of original data matrix while retained the maximum amount of variability (Malherbe, Watts, Nieuwoudt, Bauer, & Du Toit, 2009). It therefore possibly discriminated the differences between various samples and allowed visualization of clusters and outliers. In this study, PCA aimed to derive the first two principal components from volatile compounds data and examined the probable grouping of samples. After that, PLS-DA method allowed to combine variables in the data set to maximize the separation between classes and minimized the distance between intragroup clustering (Bigot, Meile, Kapitan, & Montet, 2015). In our case, the X and Y matrix consisted of volatile composition data of observations and dummy variables, respectively.

As for the PLS weight plot, composition variables of which could reveal the variables contributing to the separation. Volatiles that were close to dummy variables of class membership contributed strongly to the separation of classes (Ledauphin et al., 2010).

### 3. Results and discussion

#### 3.1. The changing pattern of physicochemical properties

The physicochemical properties of PM, ZP and HS of Chinese Luzhou-flavor liquor were shown in Table 2. The content of moisture,  $\text{NH}_4^+-\text{N}$  and available phosphorus generally increased in the PM with the depth of cellar, except for pH. In contrast, the reducing sugar, total acid and  $\text{NH}_4^+-\text{N}$  of HS sharply decreased from 7.83 g/100 g to 3.71 g/100 g, from 6.24 g/100 g to 4.18 g/100 g, and from

0.256 g/100 g to 0.199 g/100 g with pit age, respectively. Moreover, the moisture,  $\text{NH}_4^+-\text{N}$  and total ester of ZP did not fluctuate much with values maintaining at around 63.52%, 0.43 g/100 g and 2.40 g/100 g, respectively, which was consistent with previous study (Ding et al., 2015). Meanwhile, the total acid presented an increasing trend from upper layer to under layer as a whole.

#### 3.2. Volatile compounds data analysis

A total number of 59 volatile compounds identified in various samples were shown in Table 3 and Table 4, including alcohols (6), acids (12), esters (28), phenols (4) and aldehyde (4), furans (1), ketones (4). Overall, the proportion of each group showed the following order: esters > acids > alcohols > phenols, aldehydes and ketones > furans. Of them, ten aroma compounds were detected in each sample, and accounted for an average of 66.30% of the total aroma compounds. These constituents were phenylethyl alcohol, butyric acid, pentanoic acid, hexanoic acid, heptanoic acid, ethyl lactate, ethyl hexanoate, ethyl hexadecanoate, ethyl linoleate and ethyl elaidate. Differences of volatile constituents among samples were also discovered. For instance, decanoic acid and six kinds of ester constituents (phenethyl butyrate, butyl hexanoate, isoamyl hexanoate, ethyl heptanoate, ethyl octanoate and ethyl pentadecanoate) had high concentrations in the PM, while four kinds of esters (ethyl heptanoate, ethyl octanoate, ethyl hydrocinnamate and ethyl myristate) had high level in the ZP.

The total concentration of volatile compounds in the samples was calculated according to the data mentioned in Tables 3 and 4. The total content of volatiles always significantly increased from upper layer to under layer, except for 2-year-MPM and 40-year-MZP (Fig. 2). It suggested that the volatile of interphase intermediates exhibited distinct space-time feature. This could be caused by the divergence of metabolite profiles, since physicochemical properties and microbial community structure varied along with pit age and spatial position (Zheng, Wu, Huang, Zhou, & Liao, 2014). Furthermore, the content of dissolved oxygen in the under layer was lower than upper layer and the quantity of anaerobic microbes detected in the former were much higher. As a consequence, the ability of producing volatiles in the under layer of cellar would be better. Tables 3 and 4 also illustrated that the

**Table 2**  
The changes of physicochemical properties of PM, ZP and HS samples.

Sample	Moisture (%)	$\text{NH}_4^+-\text{N}$ (g/100 g)	pH	Available phosphorus (mg/100 g)
2-year-UPM	27.04 $\pm$ 0.68	0.101 $\pm$ 0.009	3.66	23.28 $\pm$ 0.32
2-year-MPM	25.74 $\pm$ 0.24	0.138 $\pm$ 0.008	4.32	24.50 $\pm$ 0.33
2-year-DPM	27.91 $\pm$ 1.61	0.145 $\pm$ 0.012	3.81	37.61 $\pm$ 0.51
10-year-UPM	33.90 $\pm$ 0.50	0.561 $\pm$ 0.007	5.16	29.66 $\pm$ 0.56
10-year-MPM	35.86 $\pm$ 0.74	0.307 $\pm$ 0.003	3.68	36.59 $\pm$ 0.87
10-year-DPM	37.30 $\pm$ 2.78	0.556 $\pm$ 0.010	3.96	37.22 $\pm$ 0.12
40-year-UPM	19.28 $\pm$ 0.29	0.162 $\pm$ 0.009	3.89	14.50 $\pm$ 0.10
40-year-MPM	33.06 $\pm$ 0.92	0.245 $\pm$ 0.011	4.13	33.01 $\pm$ 0.39
40-year-DPM	33.77 $\pm$ 1.12	0.207 $\pm$ 0.009	3.74	31.47 $\pm$ 3.19

Sample	Moisture (%)	Reducing sugar (g/100 g)	Total acid (g/100 g)	$\text{NH}_4^+-\text{N}$ (g/100 g)	Alcoholic strength (mL/100 g)	Total ester (g/100 g)
2-year-HS	84.68 $\pm$ 0.20	7.83 $\pm$ 0.13	6.24 $\pm$ 0.06	0.256 $\pm$ 0.001	4.50 $\pm$ 0.00	3.48 $\pm$ 0.00
10-year-HS	87.44 $\pm$ 0.19	5.75 $\pm$ 0.04	4.26 $\pm$ 0.02	0.260 $\pm$ 0.003	4.00 $\pm$ 0.00	3.60 $\pm$ 0.00
40-year-HS	88.77 $\pm$ 0.29	3.71 $\pm$ 0.02	4.18 $\pm$ 0.00	0.199 $\pm$ 0.001	5.50 $\pm$ 0.00	4.30 $\pm$ 0.02
2-year-UZP	64.24 $\pm$ 0.05	0.63 $\pm$ 0.01	12.25 $\pm$ 0.00	0.489 $\pm$ 0.000	11.19 $\pm$ 0.00	2.97 $\pm$ 0.02
2-year-MZP	63.36 $\pm$ 0.94	1.12 $\pm$ 0.01	14.52 $\pm$ 0.22	0.567 $\pm$ 0.016	12.88 $\pm$ 0.00	2.74 $\pm$ 0.05
2-year-DZP	64.39 $\pm$ 0.53	1.43 $\pm$ 0.02	15.69 $\pm$ 0.02	0.549 $\pm$ 0.005	13.83 $\pm$ 0.00	2.48 $\pm$ 0.12
10-year-UZP	63.55 $\pm$ 0.24	2.47 $\pm$ 0.04	8.64 $\pm$ 0.00	0.320 $\pm$ 0.000	8.68 $\pm$ 0.00	1.48 $\pm$ 0.03
10-year-MZP	63.75 $\pm$ 1.20	3.90 $\pm$ 0.12	9.03 $\pm$ 0.07	0.312 $\pm$ 0.008	8.67 $\pm$ 0.00	2.27 $\pm$ 0.03
10-year-DZP	65.20 $\pm$ 0.48	2.88 $\pm$ 0.03	18.95 $\pm$ 0.00	0.414 $\pm$ 0.006	9.67 $\pm$ 0.00	2.96 $\pm$ 0.14
40-year-UZP	59.67 $\pm$ 1.27	6.12 $\pm$ 0.14	6.31 $\pm$ 0.02	0.257 $\pm$ 0.005	7.76 $\pm$ 0.00	1.34 $\pm$ 0.02
40-year-MZP	63.54 $\pm$ 0.52	3.95 $\pm$ 0.06	16.03 $\pm$ 0.07	0.426 $\pm$ 0.000	8.28 $\pm$ 0.00	2.98 $\pm$ 0.11
40-year-DZP	64.03 $\pm$ 0.20	3.97 $\pm$ 0.01	14.80 $\pm$ 0.07	0.534 $\pm$ 0.008	8.39 $\pm$ 0.00	2.35 $\pm$ 0.06

**Table 3**

Mean values (mg/kg) with standard deviations (SD, n = 3) of volatile compounds in the PM and HS samples.

Number	Compounds				
		2-year-UPM	2-year-MPM	2-year-DPM	10-year-UPM
1	3-furanmethanol	0.1392 ± 0.0321	0.1515 ± 0.0123	0.1763 ± 0.0067	0.0069 ± 0.0015
2	n-butyl alcohol	0.0129 ± 0.0033	0.0112 ± 0.0041	0.0123 ± 0.0006	0.0631 ± 0.0153
3	3-methyl-1-butanol	0.0150 ± 0.0021	0.1657 ± 0.2333	0.0910 ± 0.0188	0.0063 ± 0.0004
4	2-pentanol	0.0126 ± 0.0007	0.2666 ± 0.0567	0.0611 ± 0.0169	0.0523 ± 0.0149
5	1-hexanol	0.7040 ± 0.1070	1.6902 ± 0.7755	1.4453 ± 0.7627	4.3572 ± 0.4404
6	Phenylethyl alcohol	1.8027 ± 0.1280	6.0764 ± 1.3592	3.4460 ± 1.0980	3.0555 ± 1.3391
7	Acetic acid	0.9464 ± 0.1469	0.6645 ± 0.0887	0.5650 ± 0.2527	0.6988 ± 0.1597
8	Isobutyric acid	0.0890 ± 0.0165	0.3336 ± 0.1257	0.2103 ± 0.0417	0.7928 ± 0.1779
9	Butyric acid	4.1435 ± 0.7803	9.0135 ± 0.8300	2.5012 ± 0.8975	4.6686 ± 1.0292
10	3-methyl, butyric acid	0.2972 ± 0.0597	0.8300 ± 0.1208	0.8920 ± 0.1810	3.0767 ± 1.0600
11	Pentanoic acid	1.3372 ± 0.2618	8.3921 ± 6.2276	2.1767 ± 0.3888	6.1249 ± 0.8191
12	Hexanoic acid	38.3966 ± 6.0903	189.5290 ± 42.5157	128.3196 ± 9.8900	45.1497 ± 11.0030
13	Heptanoic acid	4.3445 ± 1.2765	38.1572 ± 6.1641	8.4972 ± 2.6412	10.3819 ± 0.5506
14	Decanoic acid	1.0375 ± 0.2233	7.5708 ± 1.2233	3.1610 ± 1.2599	6.9010 ± 4.1130
15	Benzeneacetic acid	0.3655 ± 0.1256	0.3432 ± 0.1098	0.5536 ± 0.2099	1.0073 ± 0.0786
16	Hydrocinnamic acid	0.2270 ± 0.0509	0.1491 ± 0.0662	0.4683 ± 0.1089	0.7012 ± 0.0269
17	Myristic acid	0.1139 ± 0.0291	0.0048 ± 0.0019	0.1246 ± 0.0765	0.0818 ± 0.0091
18	Hexadecanoic acid	0.1121 ± 0.0023	0.1767 ± 0.0038	0.1902 ± 0.0067	0.0043 ± 0.0012
19	Hexyl acetate	0.0280 ± 0.0058	0.0616 ± 0.0257	0.0224 ± 0.0186	0.1887 ± 0.0754
20	Ethyl phenylacetate	0.9730 ± 0.1065	1.0073 ± 0.0423	0.5816 ± 0.3468	1.3746 ± 0.5295
21	Ethyl lactate	1.4602 ± 0.2183	2.5650 ± 0.3797	2.2763 ± 0.2806	0.2127 ± 0.0816
22	Phenethyl butyrate	6.4025 ± 0.9147	12.8856 ± 8.0103	8.3371 ± 3.0701	6.1254 ± 0.5150
23	Ethyl hydrogen succinate	0.3896 ± 0.0523	1.3910 ± 0.4528	0.4315 ± 0.1647	0.2886 ± 0.0166
24	Ethyl pentanoate	0.0508 ± 0.0202	0.6973 ± 0.5047	0.0744 ± 0.0122	0.0644 ± 0.0059
25	Ethyl hexanoate	19.6550 ± 3.0770	107.1367 ± 44.3113	99.0323 ± 8.3454	24.7569 ± 1.5613
26	Butyl hexanoate	5.6477 ± 1.3852	4.2297 ± 1.4879	1.4582 ± 0.7004	10.0734 ± 4.7572
27	Propyl hexanoate	0.3438 ± 0.0615	2.6272 ± 2.7273	0.6513 ± 0.3602	0.6860 ± 0.0441
28	Isoamyl hexanoate	10.8018 ± 0.9414	28.7472 ± 7.1116	12.9508 ± 6.1585	2.6677 ± 1.0611
29	Furfuryl hexanoate	0.3737 ± 0.0312	1.4031 ± 0.0630	0.4776 ± 0.0889	0.0027 ± 0.0012
30	Ethyl heptanoate	4.2426 ± 1.0325	24.1596 ± 9.0490	4.4087 ± 2.9000	2.1139 ± 0.1752
31	Furfuryl heptanoate	0.0081 ± 0.0015	0.2384 ± 0.1021	0.0052 ± 0.0024	0.0071 ± 0.0025
32	Ethyl octanoate	16.4678 ± 4.2089	70.2022 ± 10.1011	121.0708 ± 9.3320	33.5947 ± 9.3827
33	Octyl octanoate	0.0127 ± 0.0022	0.7072 ± 0.2022	0.0171 ± 0.0164	0.0270 ± 0.0023
34	Ethyl nonanoate	2.1589 ± 0.0725	3.6223 ± 1.2524	1.2035 ± 0.3415	1.2046 ± 0.2042
35	Ethyl decanoate	0.6448 ± 0.1378	0.6612 ± 0.4620	0.0172 ± 0.0088	0.0216 ± 0.0054
36	Ethyl undecanoate	0.3024 ± 0.0147	0.4353 ± 0.0764	0.3534 ± 0.1211	0.2706 ± 0.1328
37	Ethyl hydrocinnamate	2.1174 ± 0.3345	0.1627 ± 0.0200	1.5700 ± 0.5221	2.0109 ± 0.2308
38	Ethyl tridecanoate	0.4294 ± 0.0339	5.3531 ± 0.6581	0.4618 ± 0.2218	0.3245 ± 0.1102
39	Ethyl myristate	0.0025 ± 0.0006	0.0403 ± 0.0186	0.0203 ± 0.0067	0.0571 ± 0.0242
40	Ethyl pentadecanoate	7.9476 ± 0.8171	23.0405 ± 6.3588	10.9272 ± 1.1337	3.1573 ± 0.6189
41	Ethyl hexadecanoate	34.4714 ± 4.5120	27.6568 ± 4.6102	15.3403 ± 12.7503	11.4191 ± 1.5755
42	Ethyl heptadecanoate	0.1601 ± 0.0250	0.1404 ± 0.0267	0.1357 ± 0.0556	0.0554 ± 0.0006
43	Ethyl oleate	0.0142 ± 0.0017	0.0645 ± 0.0293	0.0021 ± 0.0004	0.0011 ± 0.0002
44	Ethyl linoleate	10.7123 ± 2.4416	5.9750 ± 0.9042	4.3957 ± 0.7056	0.2647 ± 0.0122
45	Ethyl elaidate	8.8070 ± 1.7752	3.1692 ± 0.3089	2.4835 ± 1.8686	0.5278 ± 0.0371
46	Ethyl linolenate	0.1583 ± 0.0404	0.0880 ± 0.0030	0.0790 ± 0.0459	0.0126 ± 0.0090
47	4-ethyl-2-methoxyphenol	0.0894 ± 0.0220	0.0721 ± 0.0101	0.0671 ± 0.0032	0.0114 ± 0.0071
48	4-methylphenol	1.6553 ± 0.2574	2.8449 ± 0.1098	2.3738 ± 0.2571	0.7762 ± 1.2738
49	4-ethylphenol	0.5752 ± 0.5487	0.0951 ± 0.0145	1.4447 ± 0.3324	0.0479 ± 0.0009
50	2,4-di-tert-butylphenol	0.0036 ± 0.0011	0.0809 ± 0.1070	0.3328 ± 0.0597	0.0023 ± 0.0007
51	3-furancarboxaldehyde	0.1526 ± 0.0353	0.6177 ± 0.8188	0.1021 ± 0.0039	0.0511 ± 0.0174
52	Benzaldehyde	0.5917 ± 0.0540	0.5276 ± 0.0212	0.4123 ± 0.0563	2.2217 ± 1.6782
53	2-nonenal	0.0339 ± 0.0099	0.0042 ± 0.0028	0.0164 ± 0.0076	0.0100 ± 0.0045
54	Gamma-nonanolactone	0.0688 ± 0.0075	0.8734 ± 0.3553	0.0516 ± 0.0109	0.0345 ± 0.0084
55	2-acetyl furan	0.1691 ± 0.0450	0.3473 ± 0.0037	0.1668 ± 0.0334	0.1213 ± 0.0099
56	3-hydroxy-2-butanone	0.0024 ± 0.0007	0.0086 ± 0.0051	0.0072 ± 0.0011	0.0009 ± 0.0001
57	Acetophenone	0.0442 ± 0.0119	0.0788 ± 0.0467	0.2014 ± 0.0221	0.0045 ± 0.0009
58	2-pentadecanone	0.1012 ± 0.0393	0.3645 ± 0.0916	0.5444 ± 0.3119	0.1294 ± 0.0525
59	Perhydrofarnesyl acetone	0.0657 ± 0.0099	0.0654 ± 0.0016	0.0041 ± 0.0011	0.1818 ± 0.0416

concentration of PM and ZP were distinctly higher than HS. Simultaneously, in our present research, we had proved that the PLFA-based total biomass was extremely low in the HS compared with PM and ZP (Ding et al., 2015). Specially, 40-year-DPM sample had the highest total level of volatile compounds with the concentration of 834.14 mg/kg, followed by 2-year-MPM (597.98 mg/kg), 10-year-DPM (577.24 mg/kg), 10-year-MPM (499.46 mg/kg), 2-year-DPM (447.40 mg/kg), 40-year-MPM (401.68 mg/kg), 40-year-DZP (275.39 mg/kg), etc. It was in agreement with that good liquor

depended on old cellars, which uninterruptedly employed for several decades or even hundreds years.

Tables 3 and 4 summarized that esters composed the majority of volatiles in the cellar, such as low molecular weight ethyl esters (C6–C11), high molecular weight ethyl esters C13–C20, acetate esters and isoamyl esters. It formed from the esterification of alcohols with fatty acids during fermentation and was closely related to yeast species and enzymatic activity (de la Roza, Laca, Garcia, & Diaz, 2003). Currently, the role and contribution of non-

PM					HS	
10-year-MPM	10-year-DPM	40-year-UPM	40-year-MPM	40-year-DPM	2-year-HS	10-year-HS
0.0183 ± 0.0238	0.1587 ± 0.0609	0.2066 ± 0.0441	0.2013 ± 0.0300	0.0489 ± 0.0066	0.1080 ± 0.0034	0.1427 ± 0.0205
0.0024 ± 0.0010	0.0175 ± 0.0028	0.0192 ± 0.0081	0.0453 ± 0.0022	0.0465 ± 0.0022	0.0187 ± 0.0021	0.0010 ± 0.0003
0.0106 ± 0.0076	0.0271 ± 0.0047	0.0330 ± 0.0003	0.0929 ± 0.0287	0.4800 ± 0.2373	0.1651 ± 0.0523	0.2755 ± 0.0529
0.0525 ± 0.0070	0.2639 ± 0.0117	0.0119 ± 0.0060	0.1480 ± 0.0114	0.1778 ± 0.0193	0.0918 ± 0.0153	0.0788 ± 0.0369
4.4881 ± 0.1361	4.5943 ± 0.2982	0.5249 ± 0.0703	3.5212 ± 0.3192	4.7460 ± 1.2346	0.1766 ± 0.0081	0.1739 ± 0.0421
6.5909 ± 3.4143	0.4617 ± 0.2011	1.1822 ± 0.1432	6.9298 ± 0.5847	1.8107 ± 0.4638	1.0071 ± 0.2099	1.6958 ± 0.6458
1.5856 ± 0.0191	1.2803 ± 0.2125	0.4487 ± 0.0233	0.7261 ± 0.3254	1.3005 ± 0.2531	0.3172 ± 0.1452	0.6009 ± 0.1002
0.4853 ± 0.0803	1.0120 ± 0.2801	0.1867 ± 0.0051	0.4114 ± 0.0042	1.2616 ± 0.7381	0.1708 ± 0.0173	0.5152 ± 0.1622
7.8182 ± 0.6765	8.2033 ± 2.1676	6.4376 ± 0.3262	8.9730 ± 1.0809	8.9820 ± 1.2373	1.2581 ± 0.0344	4.9336 ± 1.7536
5.0828 ± 1.8032	4.6659 ± 1.1484	0.5197 ± 0.0356	3.0280 ± 0.0398	0.6650 ± 0.0563	0.4044 ± 0.0255	1.2599 ± 0.4761
7.6862 ± 1.5749	7.9256 ± 1.7453	1.7693 ± 0.1812	8.9420 ± 0.3796	9.5441 ± 3.4172	1.1237 ± 0.0081	2.9628 ± 1.0675
94.4627 ± 12.8045	81.0445 ± 8.8046	23.1394 ± 1.8436	51.4577 ± 5.7402	244.6067 ± 54.5064	12.0738 ± 1.3604	29.7048 ± 7.1723
21.0060 ± 5.3534	65.6432 ± 2.4243	2.5767 ± 0.1691	28.4236 ± 1.2598	43.8380 ± 5.9656	1.5230 ± 0.3690	3.3619 ± 1.2120
23.4079 ± 7.0028	11.1073 ± 0.6699	0.3172 ± 0.0181	12.7497 ± 0.1349	1.1903 ± 0.2032	0.0990 ± 0.0205	0.1704 ± 0.0184
0.9156 ± 0.0279	1.9580 ± 0.5719	0.2514 ± 0.0922	1.2076 ± 0.2444	2.0239 ± 1.4747	0.1583 ± 0.0318	0.1445 ± 0.1812
1.0253 ± 0.0060	1.3572 ± 0.4696	0.3021 ± 0.0657	1.1243 ± 0.0879	0.9122 ± 0.5399	0.0878 ± 0.0018	0.0879 ± 0.0855
0.2822 ± 0.2366	0.0940 ± 0.0044	0.0882 ± 0.0064	0.1136 ± 0.0380	0.0450 ± 0.0053	0.1320 ± 0.1056	0.1945 ± 0.0611
0.0045 ± 0.0011	0.0054 ± 0.0015	0.0437 ± 0.0068	0.0140 ± 0.0011	0.2630 ± 0.0598	0.0609 ± 0.0107	0.0029 ± 0.0012
0.1128 ± 0.0052	0.0897 ± 0.0010	0.0211 ± 0.0036	0.1248 ± 0.0064	0.2037 ± 0.0628	0.0016 ± 0.0009	0.0043 ± 0.0016
2.2519 ± 1.5350	1.6963 ± 0.1207	0.6061 ± 0.1071	1.8707 ± 0.3097	3.6194 ± 0.7820	0.2271 ± 0.0073	1.1042 ± 0.1367
2.9473 ± 0.0705	3.3566 ± 0.1651	0.6914 ± 0.0215	2.4791 ± 0.1876	7.1329 ± 1.9882	2.7278 ± 0.4046	6.7900 ± 1.6391
19.3274 ± 4.5068	21.1642 ± 0.6805	1.6657 ± 0.1785	15.2339 ± 1.3642	44.6771 ± 5.5661	0.2061 ± 0.0113	0.5016 ± 0.1689
1.4059 ± 0.4303	1.8952 ± 0.1554	0.1417 ± 0.0207	0.8605 ± 0.0282	1.3207 ± 0.0808	0.0332 ± 0.0010	0.0698 ± 0.0256
0.2688 ± 0.0668	0.1607 ± 0.0081	0.0153 ± 0.0040	0.3996 ± 0.0290	0.7337 ± 0.1865	0.0485 ± 0.0471	0.1889 ± 0.0284
109.1357 ± 5.0405	75.9201 ± 2.0319	7.4450 ± 1.3302	102.1343 ± 7.0102	171.2828 ± 40.7473	6.1893 ± 0.1981	10.2393 ± 1.2620
10.6416 ± 1.5435	10.5125 ± 1.0150	4.2118 ± 0.3972	5.9756 ± 0.8760	9.6220 ± 3.0786	0.0495 ± 0.0099	0.0300 ± 0.0089
1.5901 ± 0.0203	2.7699 ± 0.1341	0.3084 ± 0.0310	2.1310 ± 0.2230	3.0679 ± 0.7795	0.0349 ± 0.0099	0.0671 ± 0.0301
30.1863 ± 3.9629	19.9303 ± 2.6641	3.4154 ± 0.4329	1.9518 ± 0.0210	1.9838 ± 0.5145	0.0106 ± 0.0033	0.0236 ± 0.0077
0.8244 ± 0.0193	0.0188 ± 0.0125	0.2179 ± 0.0475	0.6878 ± 0.0613	1.8098 ± 0.1617	0.0231 ± 0.0033	0.2331 ± 0.0108
14.2083 ± 1.0546	13.0165 ± 0.5900	1.1526 ± 0.1465	11.5318 ± 1.4450	25.6429 ± 4.2354	0.1763 ± 0.0401	0.2429 ± 0.0283
0.0261 ± 0.0291	0.5903 ± 0.1819	0.2061 ± 0.0227	0.0018 ± 0.0008	0.3487 ± 0.0775	0.0006 ± 0.0001	0.0007 ± 0.0001
78.1290 ± 9.2303	180.4767 ± 0.6407	16.2122 ± 1.3948	75.2039 ± 7.4040	127.4805 ± 28.7855	0.1616 ± 0.0322	0.1215 ± 0.0269
0.0089 ± 0.0105	1.5251 ± 0.4407	0.0018 ± 0.0002	0.4322 ± 0.0115	0.1818 ± 0.0759	0.0765 ± 0.0029	0.1122 ± 0.0146
6.7428 ± 0.6313	0.7252 ± 0.3212	0.9713 ± 0.1272	4.4374 ± 0.3272	9.9752 ± 0.3212	0.0092 ± 0.0034	0.0110 ± 0.0035
0.1835 ± 0.1987	0.0151 ± 0.0144	2.4193 ± 0.4359	0.0440 ± 0.0266	1.4741 ± 1.2096	0.0387 ± 0.0064	0.1534 ± 0.0238
0.4753 ± 0.0023	0.0178 ± 0.0066	0.2796 ± 0.0066	0.4404 ± 0.0178	1.0651 ± 0.3736	0.0027 ± 0.0001	0.0035 ± 0.0011
0.4544 ± 0.0231	0.2522 ± 0.0166	3.1764 ± 0.6301	2.5358 ± 0.2354	0.5701 ± 0.0212	0.3264 ± 0.0156	0.8134 ± 0.0628
0.9011 ± 0.2008	0.1099 ± 0.0371	0.2999 ± 0.0437	0.0616 ± 0.0204	2.0256 ± 0.1088	0.0389 ± 0.0045	0.0490 ± 0.0055
0.8432 ± 0.2191	0.0465 ± 0.0070	5.9686 ± 0.7312	3.9130 ± 0.7962	3.4523 ± 0.4667	0.1050 ± 0.0056	0.4174 ± 0.0676
13.2874 ± 2.3965	13.0907 ± 1.7749	5.8889 ± 0.6862	5.8523 ± 1.3644	32.7422 ± 4.0312	0.0354 ± 0.0061	0.4604 ± 0.1033
22.4095 ± 4.7707	32.8366 ± 0.9678	15.6929 ± 1.5741	23.2884 ± 0.7698	46.9977 ± 9.2164	3.7404 ± 1.9993	9.1148 ± 2.7088
0.1442 ± 0.0388	0.1488 ± 0.0010	0.0923 ± 0.0149	0.1654 ± 0.0180	0.6824 ± 0.0477	0.0121 ± 0.0052	0.0260 ± 0.0048
0.0434 ± 0.0012	0.0232 ± 0.0023	0.0029 ± 0.0011	0.0013 ± 0.0002	0.8520 ± 1.0867	0.0066 ± 0.0013	0.0079 ± 0.0032
1.0715 ± 0.1644	1.6860 ± 0.0532	3.1989 ± 0.1533	2.4745 ± 0.1050	4.0129 ± 2.6688	3.9494 ± 0.5877	0.5706 ± 0.1046
0.8630 ± 0.1966	1.9020 ± 0.0730	2.7093 ± 0.2088	2.7829 ± 0.0830	1.7407 ± 1.1899	2.7110 ± 0.3243	3.7811 ± 0.5099
0.3010 ± 0.0080	0.3311 ± 0.0548	0.0679 ± 0.0064	0.1132 ± 0.0134	0.2101 ± 0.0676	0.0948 ± 0.0237	0.0764 ± 0.0330
0.0549 ± 0.0119	0.0375 ± 0.0065	0.0280 ± 0.0033	0.1189 ± 0.0042	0.0454 ± 0.0112	0.1002 ± 0.0316	0.0165 ± 0.0088
0.8940 ± 0.4059	0.9695 ± 0.0194	1.8087 ± 0.1457	1.8880 ± 0.3966	2.4445 ± 0.4990	0.6044 ± 0.0315	2.0957 ± 0.4055
0.1821 ± 0.0250	0.1801 ± 0.0249	0.0289 ± 0.0029	0.1451 ± 0.0243	0.2165 ± 0.0499	0.0408 ± 0.0134	0.0475 ± 0.0100
0.0043 ± 0.0008	0.0217 ± 0.0049	0.2220 ± 0.0228	0.2061 ± 0.0414	0.0290 ± 0.0031	0.0179 ± 0.0061	0.3035 ± 0.3065
0.0094 ± 0.0124	0.0191 ± 0.0046	0.0619 ± 0.0074	0.0034 ± 0.0030	0.9391 ± 0.4344	0.0210 ± 0.0009	0.3605 ± 0.0178
3.0193 ± 0.8208	0.1607 ± 0.0173	0.5459 ± 0.0749	1.7872 ± 0.1918	0.6162 ± 0.1223	0.0411 ± 0.0218	0.3291 ± 0.0891
0.0653 ± 0.0086	0.4391 ± 0.1652	0.2596 ± 0.0324	0.0027 ± 0.0019	0.0007 ± 0.0010	0.0210 ± 0.0062	0.0004 ± 0.0001
0.7217 ± 0.7341	0.0104 ± 0.0021	0.0859 ± 0.0044	0.1077 ± 0.0066	0.1998 ± 0.0559	0.0686 ± 0.0207	0.1053 ± 0.0432
0.1417 ± 0.0067	0.1617 ± 0.0282	0.0832 ± 0.0157	0.0901 ± 0.0330	1.6162 ± 0.1002	0.0717 ± 0.0010	0.0980 ± 0.0020
0.0226 ± 0.0006	0.0330 ± 0.0076	0.0014 ± 0.0002	0.0048 ± 0.0001	0.0046 ± 0.0062	0.0069 ± 0.0037	0.0393 ± 0.0100
0.0089 ± 0.0009	0.0008 ± 0.0001	0.1450 ± 0.0257	0.9617 ± 0.2578	0.0039 ± 0.0040	0.3112 ± 0.0099	0.4543 ± 0.2101
0.4390 ± 0.1079	0.8657 ± 0.0332	0.0360 ± 0.0038	0.8705 ± 0.6278	0.3836 ± 0.4931	0.0017 ± 0.0005	0.0170 ± 0.0142
0.1910 ± 0.2010	0.2130 ± 0.0370	0.1007 ± 0.0057	0.2580 ± 0.1718	0.7863 ± 0.1471	0.0047 ± 0.0009	0.0327 ± 0.0110

*Saccharomyces* yeasts (presented mostly during the initial stages of spontaneous wine fermentation) in the final wine product, including *Rhodotorula*, *Pichia*, *Candida*, *Metschnikowia*, *Kloeckera*, and *Hansenula* had been investigated. Some of non-*Saccharomyces* yeasts produced metabolites, such as esters, higher alcohols, acetic acid and 3-hydroxy-2-butanone (Reid, Theron, du Toit, & Divol, 2012). The amount of esters in the ZP ranging from 92.73 to 224.79 mg/kg, occupied for 77.63–88.13% of the total volatiles, which was evidently higher than PM (52.81–70.04%) an HS (41.22–55.59%). We had found that PM, ZP and HS had relatively

high concentrations of fungal biomarkers (18:1 $\omega$ 9 and 18:2 $\omega$ 6,9) and these fungal were affiliated with five different genera (*Aspergillus*, *Geotrichum*, *Galactomyces*, *Pichia*, and *Zygosaccharomyces*) by combined PLFA and DGGE (Ding et al., 2015). *Daqu* was not only a crucial fermentation starter, involving various hydrolases (amylase enzyme, protease enzyme, redox enzyme and cellulose enzyme) and primary microbial sources, but also an essential material for liquor brewing. *Daqu* could promote the formation of volatiles by enzymatic and non-enzymatic reaction when added into ZP, especially esters. Therefore, as the matrix of raw liquor distillation,

**Table 4**  
Mean values (mg/kg) with standard deviations (SD, n = 3) of volatile compounds in the HS and ZP sample.

Number	Compounds	HS		ZP							
		40-year-HS	2-year-UZP	2-year-MZP	2-year-DZP	10-year-UZP	10-year-MZP	10-year-DZP	40-year-UZP	40-year-MZP	40-year-DZP
1	3-furanmethanol	0.3690 ± 0.1083	0.2122 ± 0.1090	0.3265 ± 0.0122	0.3628 ± 0.0323	0.1857 ± 0.0257	0.2271 ± 0.0061	0.2461 ± 0.0016	0.1608 ± 0.0694	0.3278 ± 0.0321	0.1659 ± 0.0045
2	n-butyl alcohol	0.0033 ± 0.0011	0.0701 ± 0.0230	0.0690 ± 0.0203	0.0678 ± 0.0189	0.1559 ± 0.0365	0.0024 ± 0.0011	0.0004 ± 0.0002	0.1368 ± 0.0201	0.0117 ± 0.0034	0.0711 ± 0.0158
3	3-methyl-1-butanol	0.3056 ± 0.4308	0.1642 ± 0.0548	0.1991 ± 0.0153	0.1897 ± 0.0301	0.1890 ± 0.0328	0.1317 ± 0.0077	0.1667 ± 0.0156	0.0480 ± 0.0006	0.0840 ± 0.0082	0.1961 ± 0.0142
4	2-pentanol	0.1205 ± 0.0657	0.0066 ± 0.0017	0.0079 ± 0.0079	0.0101 ± 0.0043	0.0225 ± 0.0039	0.0063 ± 0.0001	0.0265 ± 0.0056	0.0181 ± 0.0020	0.0022 ± 0.0005	0.2447 ± 0.0360
5	1-hexanol	3.0710 ± 0.5800	0.2977 ± 0.0549	0.3907 ± 0.0420	1.2561 ± 0.0510	0.1127 ± 0.0090	0.2456 ± 0.0174	0.8769 ± 0.0703	0.8753 ± 0.1716	0.4995 ± 0.0738	3.4548 ± 0.2378
6	Phenylethyl alcohol	4.5125 ± 1.2305	2.5436 ± 0.0498	0.0243 ± 0.0105	1.9149 ± 0.1641	1.4702 ± 0.3160	1.5183 ± 0.0493	1.9696 ± 0.0625	1.5172 ± 0.1354	2.0239 ± 0.0847	1.5087 ± 0.3098
7	Acetic acid	0.7975 ± 1.0643	0.7066 ± 0.2088	1.3736 ± 0.2908	0.3802 ± 0.0481	0.5433 ± 0.0742	0.8022 ± 0.3011	0.4301 ± 0.0839	0.5717 ± 0.1152	0.8132 ± 0.0050	0.2305 ± 0.1041
8	Isobutyric acid	0.6757 ± 0.1270	0.0232 ± 0.0020	0.1967 ± 0.0190	0.2002 ± 0.0038	0.0241 ± 0.0042	0.0347 ± 0.0023	0.1177 ± 0.0080	0.1175 ± 0.0074	0.0701 ± 0.0014	0.2533 ± 0.0066
9	Butyric acid	5.7218 ± 3.0618	0.5055 ± 0.1023	0.6603 ± 0.0339	1.8194 ± 0.1516	0.8630 ± 0.1934	0.7500 ± 0.0132	1.0530 ± 0.0558	0.7503 ± 0.6593	1.0429 ± 0.1487	3.9055 ± 0.9265
10	3-methyl, butyric acid	1.6092 ± 0.5038	0.1089 ± 0.0020	0.2538 ± 0.0556	0.3412 ± 0.1543	0.0759 ± 0.0146	0.0869 ± 0.0045	0.3191 ± 0.0336	0.4741 ± 0.0215	0.2728 ± 0.0151	0.7088 ± 0.1553
11	Pentanoic acid	4.5829 ± 1.1616	0.3044 ± 0.1077	0.4079 ± 0.0918	0.9989 ± 0.4737	0.1315 ± 0.0249	0.2180 ± 0.0050	0.7239 ± 0.0609	2.0163 ± 0.1631	0.7046 ± 0.0152	2.7558 ± 0.6502
12	Hexanoic acid	44.0865 ± 1.4145	16.3784 ± 0.2708	24.5929 ± 3.4923	26.8529 ± 6.9905	5.5857 ± 1.1121	11.4404 ± 0.0278	26.6167 ± 1.1504	18.0881 ± 3.5393	14.2709 ± 0.3367	36.8855 ± 6.8877
13	Heptanoic acid	9.3864 ± 0.3663	0.6104 ± 0.0299	1.0100 ± 0.0946	1.1261 ± 0.2998	0.2740 ± 0.0598	0.3215 ± 0.0120	1.0179 ± 0.2038	2.8754 ± 0.0116	0.9301 ± 0.0771	5.2556 ± 1.0953
14	Decanoic acid	0.4550 ± 0.1326	0.2033 ± 0.0202	0.2089 ± 0.0500	0.4065 ± 0.0018	0.2922 ± 0.0487	0.2728 ± 0.0149	0.4879 ± 0.0662	0.2140 ± 0.0853	0.2453 ± 0.0527	0.4952 ± 0.1271
15	Benzeneacetic acid	0.8099 ± 0.4195	0.0898 ± 0.0220	0.1698 ± 0.0220	0.2048 ± 0.0304	0.0748 ± 0.0239	0.0819 ± 0.0594	0.3132 ± 0.0907	0.1330 ± 0.0828	0.2735 ± 0.0588	0.5943 ± 0.1648
16	Hydrocinamic acid	0.5072 ± 0.1501	0.1165 ± 0.0300	0.2544 ± 0.0330	0.2974 ± 0.0156	0.2772 ± 0.0700	0.3213 ± 0.0521	0.6452 ± 0.0037	0.1580 ± 0.0960	0.2342 ± 0.0574	0.4181 ± 0.0195
17	Myristic acid	0.3106 ± 0.2059	0.1321 ± 0.0383	0.1574 ± 0.0482	0.1453 ± 0.0668	0.1498 ± 0.0352	0.2124 ± 0.0105	0.2477 ± 0.0172	0.1163 ± 0.0407	0.1476 ± 0.0289	0.1725 ± 0.0343
18	Hexadecanoic acid	1.0591 ± 0.3562	0.6089 ± 0.0030	1.2333 ± 0.2144	0.7318 ± 0.0401	0.6913 ± 0.2128	0.6459 ± 0.0776	0.9382 ± 0.0226	0.3655 ± 0.1937	0.8553 ± 0.0734	0.5140 ± 0.0189
19	Hexyl acetate	0.0695 ± 0.0558	0.0583 ± 0.0029	0.0737 ± 0.0165	0.0796 ± 0.0120	0.0140 ± 0.0012	0.0122 ± 0.0019	0.0092 ± 0.0007	0.0588 ± 0.0195	0.0520 ± 0.0074	0.1794 ± 0.0065
20	Ethyl phenylacetate	1.3908 ± 0.5856	1.0504 ± 0.0737	1.8855 ± 0.0945	0.8120 ± 0.0337	0.5160 ± 0.0705	0.5820 ± 0.0329	1.9815 ± 0.0262	0.5842 ± 0.0834	1.2242 ± 0.0543	1.1534 ± 0.0533
21	Ethyl lactate	0.1374 ± 0.0524	6.5971 ± 1.3019	7.1535 ± 0.6234	7.5584 ± 1.4002	1.4109 ± 0.2675	3.1342 ± 0.1304	9.2010 ± 0.7156	0.6140 ± 0.0005	3.1700 ± 0.3209	2.1795 ± 0.5152
22	Phenethyl butyrate	1.0850 ± 0.0061	0.6877 ± 0.1085	2.0418 ± 0.5712	1.0682 ± 0.0030	0.2921 ± 0.0396	0.4064 ± 0.0207	1.9873 ± 0.3696	1.5371 ± 0.2312	1.1596 ± 0.2203	2.1539 ± 0.3002
23	Ethyl hydrogen succinate	0.1958 ± 0.0910	0.0545 ± 0.0088	0.0699 ± 0.0110	0.0787 ± 0.0454	0.0416 ± 0.0108	0.0660 ± 0.0063	0.1381 ± 0.0284	0.0627 ± 0.0236	0.1075 ± 0.0215	0.0865 ± 0.0611
24	Ethyl pentanoate	0.5409 ± 0.1489	0.1814 ± 0.0378	0.2362 ± 0.0161	0.1375 ± 0.0057	0.0743 ± 0.0157	0.1040 ± 0.0201	0.3902 ± 0.0708	0.3725 ± 0.0405	0.3111 ± 0.0153	0.5122 ± 0.0172
25	Ethyl hexanoate	41.1321 ± 0.6081	23.1340 ± 2.9674	34.4660 ± 3.0601	60.4678 ± 2.1121	17.3775 ± 1.7813	26.8446 ± 1.0773	65.7368 ± 5.1035	33.7288 ± 8.4248	26.7396 ± 9.2704	83.4260 ± 5.8721
26	Butyl hexanoate	0.6022 ± 0.2231	1.9202 ± 0.2204	1.6622 ± 0.0873	2.1989 ± 0.1328	1.2122 ± 0.1465	0.5250 ± 0.0469	0.3358 ± 0.0149	9.4947 ± 1.6586	1.1843 ± 0.0700	10.5818 ± 0.1037
27	Propyl hexanoate	0.1919 ± 0.0552	0.1973 ± 0.0180	0.2081 ± 0.0238	0.2755 ± 0.0118	0.1679 ± 0.0311	0.1374 ± 0.0078	0.4101 ± 0.0478	1.0234 ± 0.1730	0.2201 ± 0.0216	1.2245 ± 0.0020
28	Isoamyl hexanoate	0.1659 ± 0.0821	0.0003 ± 0.0001	2.9428 ± 0.7358	3.2022 ± 0.6308	2.4221 ± 0.3167	3.4232 ± 0.2922	13.3891 ± 0.5905	4.1847 ± 0.6093	5.1418 ± 0.1407	18.3679 ± 1.0091
29	Furfuryl hexanoate	0.0638 ± 0.0366	0.1532 ± 0.0304	0.2854 ± 0.0608	0.2446 ± 0.0116	0.0249 ± 0.0002	0.1271 ± 0.0110	0.5182 ± 0.0406	0.1743 ± 0.0351	0.2282 ± 0.0217	0.6378 ± 0.0091
30	Ethyl heptanoate	1.2196 ± 0.0663	1.9530 ± 0.0732	3.7269 ± 0.2558	2.0427 ± 0.0183	1.3636 ± 0.1483	1.8075 ± 0.0892	3.7629 ± 0.2073	6.2683 ± 1.2267	3.1700 ± 0.3265	7.8971 ± 0.1607
31	Furfuryl heptanoate	0.0005 ± 0.0002	0.0048 ± 0.0011	0.0180 ± 0.0022	0.0052 ± 0.0037	0.0010 ± 0.0004	0.0019 ± 0.0003	0.0054 ± 0.0011	0.0303 ± 0.0125	0.0104 ± 0.0066	0.0094 ± 0.0003
32	Ethyl octanoate	0.1715 ± 0.0543	10.0051 ± 0.0013	10.0080 ± 0.0041	18.1022 ± 0.0023	12.1657 ± 1.4271	16.2763 ± 0.9858	19.4831 ± 0.7913	73.3753 ± 16.4606	11.6981 ± 0.2776	35.5653 ± 1.7811
33	Octyl octanoate	0.5782 ± 0.0908	0.0542 ± 0.0232	0.0637 ± 0.0381	0.0886 ± 0.0038	0.0460 ± 0.0120	0.0676 ± 0.0123	0.0898 ± 0.0101	0.2420 ± 0.0022	0.0564 ± 0.0093	0.1844 ± 0.0302
34	Ethyl nonanoate	0.0171 ± 0.0031	2.0011 ± 0.0413	1.8604 ± 0.1391	0.4074 ± 0.0084	0.5822 ± 0.0788	0.8290 ± 0.0838	0.5677 ± 0.0331	7.5837 ± 1.0235	0.5497 ± 0.0368	0.9494 ± 0.0425
35	Ethyl decanoate	0.2739 ± 0.0220	0.3551 ± 0.4266	0.7813 ± 0.1271	1.4356 ± 0.1143	2.6199 ± 0.3003	3.7688 ± 0.3275	3.7467 ± 0.1887	2.6347 ± 0.3755	1.6049 ± 0.1109	3.0561 ± 0.0361
36	Ethyl undecanoate	0.0081 ± 0.0042	0.4550 ± 0.1141	0.5927 ± 0.0526	0.0578 ± 0.0045	0.0295 ± 0.0052	0.0234 ± 0.0189	0.0592 ± 0.0079	0.1073 ± 0.0978	0.0888 ± 0.0485	0.0366 ± 0.0005
37	Ethyl hydrocinamate	1.1944 ± 0.0742	2.0267 ± 0.1304	5.1871 ± 0.6528	1.2495 ± 0.0281	1.6001 ± 0.2119	1.8230 ± 0.0800	4.2054 ± 0.2576	3.5921 ± 0.7196	1.8984 ± 0.0958	4.0482 ± 0.2669
38	Ethyl tridecanoate	0.2431 ± 0.0008	0.1569 ± 0.0279	0.3161 ± 0.0628	0.0587 ± 0.0082	0.0420 ± 0.0067	0.0830 ± 0.0077	0.0751 ± 0.0177	0.0484 ± 0.0144	0.0548 ± 0.0087	0.0638 ± 0.0107
39	Ethyl myristate	3.7717 ± 0.1133	8.3779 ± 1.3910	13.4874 ± 4.3456	4.4667 ± 3.0536	4.5939 ± 0.7772	5.2063 ± 0.1813	10.4880 ± 1.9267	2.1279 ± 1.8319	4.8742 ± 0.8557	4.0692 ± 0.7253
40	Ethyl pentadecanoate	0.6815 ± 0.0082	1.9640 ± 0.2454	4.0928 ± 0.8973	0.7153 ± 0.2133	0.6833 ± 0.1226	0.6975 ± 0.0258	1.1645 ± 0.2187	0.3935 ± 0.1591	0.7536 ± 0.1619	0.6379 ± 0.1319
41	Ethyl hexadecanoate	34.1089 ± 0.8575	36.3948 ± 2.8819	51.1791 ± 15.9875	36.9435 ± 1.3648	22.7996 ± 3.8259	25.2141 ± 0.7579	43.4470 ± 4.1759	14.0530 ± 6.5875	22.2633 ± 2.7272	25.6917 ± 5.8816
42	Ethyl heptadecanoate	0.1119 ± 0.0023	0.1608 ± 0.0192	0.2767 ± 0.0984	0.1093 ± 0.0101	0.0789 ± 0.0164	0.0809 ± 0.0058	0.1548 ± 0.0179	0.0412 ± 0.0205	0.0913 ± 0.0186	0.0643 ± 0.0174
43	Ethyl oleate	0.0109 ± 0.0014	0.5380 ± 0.2927	0.1541 ± 0.0951	0.0053 ± 0.0006	0.0111 ± 0.0021	0.0074 ± 0.0003	0.0159 ± 0.0008	0.0127 ± 0.0069	0.0331 ± 0.0085	0.0316 ± 0.0027
44	Ethyl linoleate	3.0138 ± 0.2308	12.5465 ± 11.3575	28.9872 ± 11.5493	19.7374 ± 1.1736	13.2638 ± 3.3450	11.9700 ± 1.1267	24.4025 ± 1.8578	2.4112 ± 1.2635	6.8179 ± 2.2098	5.3945 ± 1.9670
45	Ethyl elaidate	14.4074 ± 0.5638	11.2100 ± 0.0033	15.9013 ± 0.5654	12.7230 ± 0.5724	9.0786 ± 2.1852	9.1197 ± 0.5510	18.5801 ± 0.9507	2.3992 ± 1.3273	6.1348 ± 1.8012	5.5412 ± 1.6531
46	Ethyl linolenate	0.4648 ± 0.0580	0.1123 ± 0.0077	0.1435 ± 0.0099	0.4580 ± 0.0241	0.2136 ± 0.0586	0.1745 ± 0.0230	0.4417 ± 0.0567	0.0257 ± 0.0124	0.0909 ± 0.0323	0.0403 ± 0.0100
47	4-ethyl-2-methoxyphenol	0.1636 ± 0.0307	0.2011 ± 0.0405	0.2159 ± 0.0359	0.2979 ± 0.1273	0.1440 ± 0.0251	0.1973 ± 0.0039	0.1955 ± 0.0199	0.1282 ± 0.0218	0.3466 ± 0.0324	0.2794 ± 0.0090
48	4-methylphenol	3.9417 ± 0.3238	0.5159 ± 0.3021	0.8283 ± 0.1211	1.1697 ± 0.3302	0.3431 ± 0.0844	0.4090 ± 0.0078	1.5283 ± 0.0825	0.7551 ± 0.1557	1.2004 ± 0.1055	2.1654 ± 0.4050
49	4-ethylphenol	0.0674 ± 0.0046	1.0322 ± 0.0219	1.2023 ± 0.3030	1.0417 ± 0.3289	0.0662 ± 0.0183	0.0571 ± 0.0018	0.0826 ± 0.0098	0.0221 ± 0.0052	0.0623 ± 0.0079	0.0847 ± 0.0159
50	2,4-di-tert-butylphenol	0.1033 ± 0.0065	0.1179 ± 0.0248	0.2439 ± 0.0702	0.1139 ± 0.0829	0.0499 ± 0.0131	0.0419 ± 0.0073	0.0652 ± 0.0113	0.0113 ± 0.0067	0.0340 ± 0.0120	0.0422 ± 0.0229
51	3-furan-carboxaldehyde	0.5588 ± 0.0062	1.4120 ± 0.3181	1.2957 ± 0.6058	0.0870 ± 0.0041	0.1888 ± 0.0385	0.1719 ± 0.0043	0.7426 ± 0.0637	0.2337 ± 0.0502	0.2225 ± 0.0020	0.1372 ± 0.0020
52	benzaldehyde	0.3638 ± 0.1374	0.2240 ± 0.0100	0.2390 ± 0.0900	0.2991 ± 0.0188	0.3376 ± 0.0654	0.3517 ± 0.0136	0.3773 ± 0.0240	3.5886 ± 0.4934	0.6266 ± 0.0212	0.8259 ± 0.0094

(continued on next page)

Table 4 (continued)

Number Compounds	HS		ZP								
	40-year-HS	2-year-HS	2-year-UZP	2-year-MZP	2-year-DZP	10-year-UZP	10-year-MZP	10-year-DZP	40-year-UZP	40-year-MZP	40-year-DZP
53	0.0005 ± 0.0001	0.0001	0.0005 ± 0.0001	0.0006 ± 0.0001	0.0210 ± 0.0045	0.0334 ± 0.0091	0.0803 ± 0.0046	0.0568 ± 0.0006	0.0421 ± 0.0068	0.0187 ± 0.0016	0.0394 ± 0.0043
54	0.1904 ± 0.0039	0.1213 ± 0.0290	0.1213 ± 0.0290	0.1442 ± 0.0203	0.1363 ± 0.0127	0.1397 ± 0.0378	0.1312 ± 0.0026	0.1243 ± 0.0027	0.1071 ± 0.0181	0.1153 ± 0.0135	0.0735 ± 0.0131
55	0.2512 ± 0.0997	0.0056 ± 0.0006	0.0056 ± 0.0006	0.0047 ± 0.0009	0.0062 ± 0.0002	0.0040 ± 0.0004	0.0063 ± 0.0008	0.0094 ± 0.0001	0.0061 ± 0.0032	0.0140 ± 0.0008	0.0169 ± 0.0009
56	0.0025 ± 0.0018	0.0007 ± 0.0001	0.0007 ± 0.0001	0.0008 ± 0.0001	0.0129 ± 0.0060	0.0004 ± 0.0001	0.0002 ± 0.0001	0.0596 ± 0.0053	0.0036 ± 0.0006	0.0055 ± 0.0010	0.0186 ± 0.0046
57	0.4456 ± 0.0366	0.1020 ± 0.0021	0.1020 ± 0.0021	0.1105 ± 0.0203	0.2161 ± 0.2133	0.0024 ± 0.0005	0.0013 ± 0.0007	0.0025 ± 0.0004	0.0111 ± 0.0047	0.0022 ± 0.0004	0.0104 ± 0.0014
58	0.0254 ± 0.0009	0.2160 ± 0.0139	0.2160 ± 0.0139	0.3596 ± 0.0478	0.0458 ± 0.0007	0.0169 ± 0.0023	0.0167 ± 0.0014	0.0269 ± 0.0044	0.0163 ± 0.0069	0.0245 ± 0.0056	0.0297 ± 0.0067
59	0.0565 ± 0.0064	0.1034 ± 0.0133	0.1034 ± 0.0133	0.1532 ± 0.0706	0.0596 ± 0.0232	0.0439 ± 0.0085	0.0455 ± 0.0022	0.0549 ± 0.0132	0.0395 ± 0.0254	0.0556 ± 0.0107	0.0519 ± 0.0087

the scale of esters in the ZP was the highest. Moreover, the percentage of low molecular weight ethyl esters (C6–C11), including ethyl hexanoate, ethyl heptanoate, ethyl octanoate, ethyl nonanoate, ethyl decanoate, ethyl undecanoate and ethyl hydrocinnamate, enhanced from upper layer to under layer, except for 40-year-UZP. It was worth noting that among these compounds, ethyl hexanoate, the most important aroma contributor with apple peel and fruit odors, had low threshold concentrations (Pino & Queris, 2011), whereas possessed high level in each sample. It was in accordance with that the characteristic of Luzhou-flavor liquor was mainly determined by the content of ethyl hexanoate. Conversely, a clear effect was not found on the proportion of high molecular weight ethyl esters (C13–C20) with respect to pig age and position. The ratios of this group in the PM on the whole were lower than HS and ZP. In addition, acetate esters were catalyzed by alcohol acetyltransferases, which utilized acetyl-CoA to acetylate higher alcohols formed from the degradation of amino acids or carbohydrates (Shalit et al., 2001). Phenethyl acetate and isoamyl acetate, possessed sensory impact described as “banana and apple”, and only phenethyl acetate was detected in all samples. The concentration of isoamyl esters, for example isoamyl hexanoate, was low in the HS, which produced by yeast during fermentation and had been identified with fruity aroma (Arrieta-Garay et al., 2014). Furthermore, apparently differences were found for isoamyl hexanoate between samples. Hydroxy esters were formed from the esterification of the corresponding hydroxyl fatty acids and responsible for fruity-floral fragrance, which could be produced from the reduction of keto acids (Pino & Queris, 2011), but none was observed in this study.

Twelve organic acids contributed to fruity, cheesy, fatty and rancid notes, were identified and produced in the cellar by lipid oxidation, among which butyric acid, pentanoic acid, hexanoic acid, heptanoic acid and decanoic acid were abundant. Contents of acetic acid, isobutyric acid, benzenoacetic acid and hydrocinnamic acid were not changed much in each PM sample. Interesting, the gap between the proportion of esters and acids in the PM (esters: 52.81–70.04%; acids: 26.72–42.67%) and ZP (esters: 77.63–88.13%; acids: 8.54–18.95%) was much greater, while was not in the HS (esters: 41.22–55.59%; acids: 36.76–51.44%). It was due to that HS was rich in organic acids especially hexanoic acid. Additionally, it was widely considered that hexanoic acid was a saturated fatty acid that had six carbons and one carboxylic group (Jeon et al., 2013) and could be converted into other useful materials such as ethyl hexanoate and hexanol via esterification and hydrogenation. In this study, the concentration of hexanoic acid reached 244.61 mg/kg in the 40-year-DPM. Previous study had reported that *Clostridium kluyveri* produced hexanoic acid from ethanol upon growing with methane-producing bacterium (Barker & Beck, 1942). Genthner, Davis, and Bryant (1981) revealed that the methanol-utilizing bacterium, *Eubacterium limosum* produced hexanoic acid from methanol. Actually, family *Clostridiaceae*, as an important group in the liquor fermentation, converted organic substances into organic acids, such as butyric and hexanoic acids, alcohols, CO<sub>2</sub>/H<sub>2</sub> and minerals, forming ethyl butyrate and ethyl hexanoate (Hahnke, Elvert, Striesow, Mollar, & Klocke, 2014). Previous research concerning microbial distribution of new and old cellar indicated that the relative steady physiochemical environment and microbial structure were formed through long term domestication process, and might result in the orthogenesis of microorganism and *Clostridiales* dominated. The methanol-utilizing bacterium in the cellar incorporated four families: *Methanocorpusculaceae*, *Methanobacteriaceae*, *Methanomicrobiaceae* and *Methanosetaeaceae*. Consequently, the syntrophic relationship between hydrogen-producing bacteria and hydrogen-consuming methanogens formed flavor constituents as well as maintained the stability of

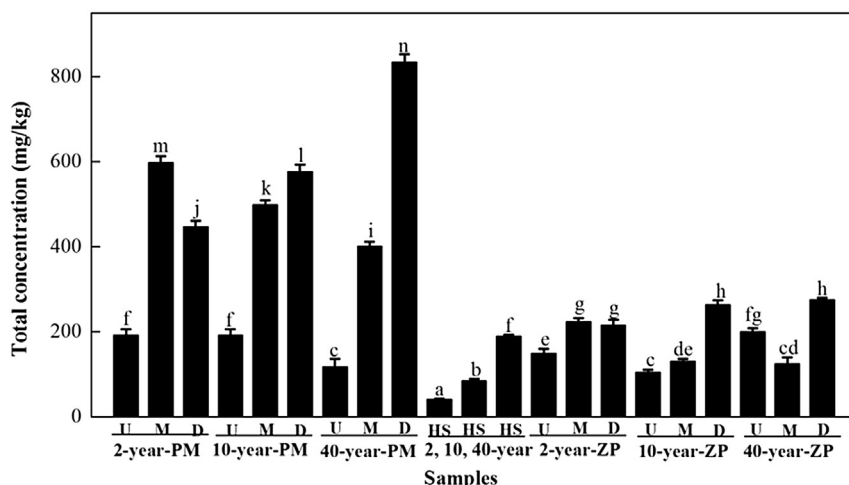


Fig. 2. Variation of total concentration of volatiles of PM, ZP and HS. Different letters indicate significant differences ( $P < 0.05$ ).

community structure (Ding et al., 2015).

Routinely, alcohols were formed from the degradation of carbohydrates in the fermentation cellar by Embden-Meyerhof-Parnas metabolic pathway (EMP). Within them, phenylethyl alcohol and 1-hexanol were produced in the greater amounts. Phenylethyl alcohol was characterized by a rose-like odor while 1-hexanol was responsible for resinous, flowery, green odor; 3-methyl-1-butanol imparted a whiskey, malt, burnt odor; 2-pentanol impacted a green odor; n-butyl alcohol had a woody-alcohol odor; 3-furanmethanol owned a caramel-like, sweet, fruity, nutty, meaty and burnt odor.

Undoubtedly, four phenols constituents, namely 4-methyl phenol, 4-ethyl-2-methoxyphenol, 2,4-di-tert-butylphenol and 4-ethylphenol were found. With regard to furans, 3-furancarboxaldehyde was solely detected, which was formed from thermal degradation of sugars by caramelization, and arisen from the decomposition of polysaccharides. The aldehydes such as 3-furancarboxaldehyde, benzaldehyde, 2-nonenal and gamma-nonanolactone had low concentrations, representing 0.11–1.98% of the total volatiles. Intriguingly, gamma-nonanolactone gave a potato odor and had a relatively stable content (0.12 mg/kg) in the ZP. Moreover, four volatile ketones, 3-hydroxy-2-butanone, acetophenone, 2-pentadecanone and perhydrofarnesyl acetone existed in each sample.

### 3.3. PCA analysis

The number of values for each sample was quite high, and a statistical analysis was necessary. PCA analysis was implemented on the whole data matrix (21 samples  $\times$  59 volatile compounds). Generally, the data were all auto-scaled to avoid variables with high intensities being considered as more important than those with low intensities, that is, each variable was centered in its mean and divided by its sample standard deviation (Wagner et al., 2006). Fig. 3(A) showed the score plot of the first two principal components explained 87.03% of total variance in raw data (PC1 = 44.33% and PC2 = 42.70%). In the bi-dimensional plot of sample scores, a legible separation between samples could be separated via the loading plot values on PC1 axis. Only samples from 2-year-UPM and 40-year-DZP mixed with HS samples, while sample from 40-year-UZP overlapped with PM samples. However, no visible separation between samples from various pit ages was acquired in the PCA score plot.

The loading values of the first two principal components were also investigated to explain the basis of separation (Fig. 3(B)). Hexanoic acid, ethyl phenylacetate, phenethyl butyrate, ethyl hexanoate, propyl hexanoate, furfuryl hexanoate, ethyl heptanoate, ethyl pentadecanoate, ethyl heptadecanoate, 2-acetyl furan and perhydrofarnesyl acetone were positioned toward the highest

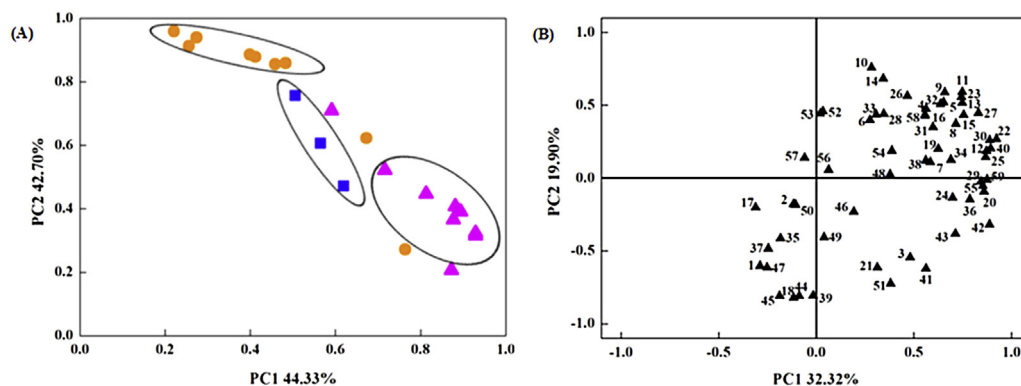
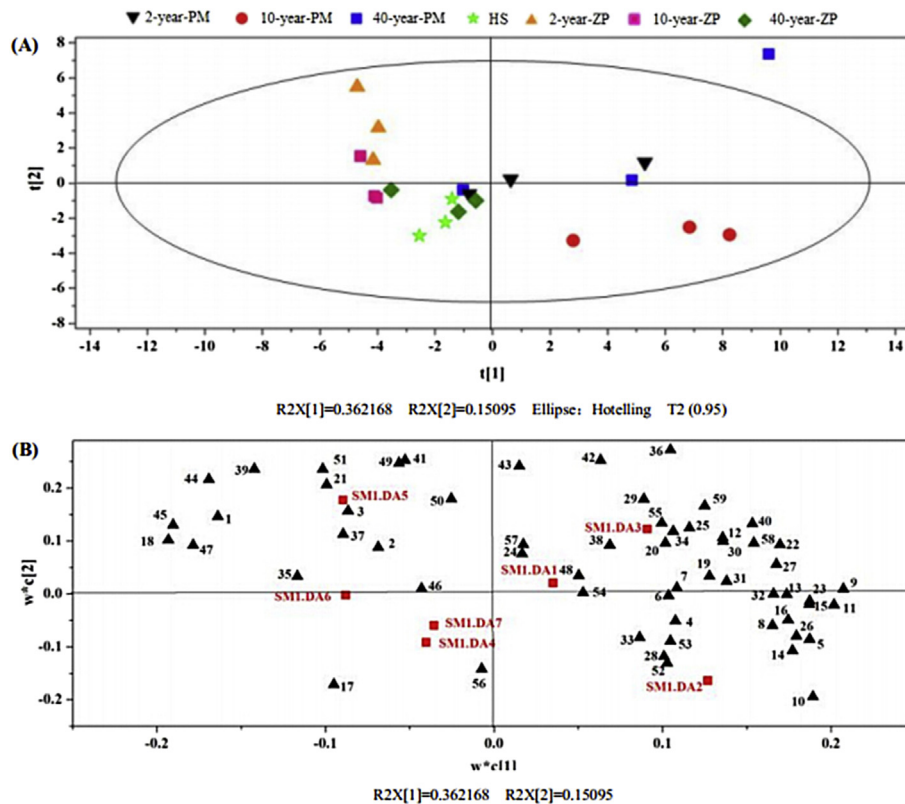


Fig. 3. (A) score and (B) loading plot of PCA according to volatile compositions in the PM, ZP and HS samples. Purple triangles, blue squares and orange circles represented PM, HS and ZP, respectively. Each number in the atlas represented one compound listed in Tables 3 and 4. (For interpretation of the references to color in this figure legend, the reader is referred to the web version of this article.)



**Fig. 4.** (A) PLS-DA of the volatile components of all the PM, ZP and HS samples given as a two-dimensional representation of the scores ( $t[1]$  and  $t[2]$ ) on the first and second PLS components. The first PLS ( $R^2X[1]$ ) component explains 36.22% and the second PLS ( $R^2X[2]$ ) component explained 15.10% of the variation of the X data. (B) PLS-DA weight plot of composition variables,  $w^*c[1]$  and  $w^*c[2]$ , for all the samples, respectively, on the first and second compounds. Each number in the atlas represented one compound listed in Tables 3 and 4. SMI.DA1, 2, 3, 4, 5, 6 and 7 represented 2-year-PM, 10-year-PM, 40-year-PM, HS, 2-year-ZP, 10-year-ZP and 40-year-ZP, respectively.

weight on PC1. What's more, hexadecanoic acid, ethyl myristate, ethyl linoleate and ethyl elaidate were situated toward the highest weight on second PC. Nevertheless, the result was preliminary and represented a potential ability to distinguish the samples. Hence, PLS-DA was employed to get more insights into the separation.

### 3.4. PLS-DA analysis

PLS-DA was performed to sharpen the separation between samples and build classification models. As shown in Fig. 4(A), the results explained 51.3% of the total variance with  $R^2X = 51.3%$ ,  $R^2Y = 22.3%$  and three groups could be clearly defined: one group for the sample dots of PM (first and four quadrant), a group for the sample dots of HS (third quadrant), and another group for the sample dots of ZP (second and third quadrant). This was similar to that obtained by PCA model with improved classification. It might be ascribed to the fact that the direction that most explained the variability in X was the same as that which described the maximum covariance with class membership matrix (Pereira, Reis, Saraiva, & Marques, 2010).

In Fig. 4(B), the results of PLS-DA highly coincided with the comparison result of concentration. For example, compounds including 4-methylphenol and gamma-nonanolactone were strongly correlated with 2-year-PM. This tended to confirm the fact that concentrations of 4-methylphenol and gamma-nonanolactone in the 2-year-PM were higher. In addition to compounds ethyl phenylacetate, ethyl hexanoate, furfuryl hexanoate, ethyl nonanoate, perhydrofarnesyl acetone and 2-acetyl furan were extremely associated with 40-year-PM, which also indicated a high concentration of these compounds. Isoamyl hexanoate, octyl

octanoate, benzaldehyde and 2-nonenal were with 10-year-PM. It tended to indicate isoamyl hexanoate, octyl octanoate, benzaldehyde and 2-nonenal were particularly highly concentrated in the 10-year-PM. Importantly, volatile markers could also extend the discrimination to other samples. 3-methyl-1-butanol, ethyl lactate, ethyl hydrocinnamate and 3-furancarboxaldehyde were related to 2-year-ZP, while ethyl decanoate and ethyl linolenate were relevant to 10-year-ZP. Whereas, no specific compounds for 40-year-ZP and HS samples toward others were found.

## 4. Conclusion

Interphase volatile constituents in Chinese Luzhou-flavor liquor fermentation cellar from different pit ages and spatial positions were extracted and semi quantified by HS-SPME/GC/MS technique. Results showed that pit age and spatial position had a stronger effect on volatiles than physicochemical properties. PM, ZP and HS had a semblable volatile constituents, which had an extremely close relationship with interphase microbial community structure, and the deviation of concentrations contributed to the discrimination. Multivariate method was proved to be efficient to differentiate samples in relation with the variance of concentrations of volatile compounds, and clearly depicted the volatile makers.

## Acknowledgments

This work was financially supported by the National Science Foundation of China (31171742) and Sichuan Province Science and Technology Support Program (2014SZ0129).

## References

- Arrieta-Garay, Y., Blanco, P., Lopez-Vazquez, C., Rodriguez-Bencomo, J. J., Perez-Correa, J. R., Lopez, F., et al. (2014). Effects of distillation system and yeast strain on the aroma profile of Albariño (*Vitis vinifera* L.) grape pomace spirits. *Journal of Agricultural and Food Chemistry*, 62(43), 10552–10560.
- Barker, H., & Beck, J. (1942). *Clostridium aciduri* and *Clostridium cylindrosporium*, organisms fermenting uric acid and some other purines. *Journal of Bacteriology*, 43(3), 291–304.
- Bigot, C., Meile, J. C., Kapitan, A., & Montet, D. (2015). Discriminating organic and conventional foods by analysis of their microbial ecology: an application on fruits. *Food Control*, 48, 123–129.
- Breuil, C., & Saddler, J. N. (1985). Comparison of the 3,5-dinitrosalicylic acid and Nelson-Somogyi methods of assaying for reducing sugars and determining cellulase activity. *Enzyme and Microbial Technology*, 7(7), 327–332.
- Consonni, R., Cagliani, L. R., Guantieri, V., & Simonato, B. (2011). Identification of metabolic content of selected Amarone wine. *Food Chemistry*, 129(2), 693–699.
- Crowell, E., & Ough, C. (1979). A modified procedure for alcohol determination by dichromate oxidation. *American Journal of Enology and Viticulture*, 30(1), 61–63.
- Cui, R. Y., Zheng, J., Wu, C. D., & Zhou, R. Q. (2014). Effect of different halophilic microbial fermentation patterns on the volatile compound profiles and sensory properties of soy sauce moromi. *European Food Research and Technology*, 239(2), 321–331.
- Cynkar, W., Damberg, R., Smith, P., & Cozzolino, D. (2010). Classification of Tempranillo wines according to geographic origin: combination of mass spectrometry based electronic nose and chemometrics. *Analytica Chimica Acta*, 660(1–2), 227–231.
- Daniël, P., Pascale, L., Georges, C., Roger, C., Odile, L., & Guillaume, S. (2006). Discrimination of Cognacs and other distilled drinks by mid-infrared spectroscopy. *Journal of Agricultural and Food Chemistry*, 54(15), 5220–5226.
- Ding, X., Wu, C., Huang, J., & Zhou, R. (2015). Interphase microbial community characteristics in the fermentation cellar of Chinese Luzhou-flavor liquor determined by PLFA and DGGE profiles. *Food Research International*, 72, 16–24.
- Du, H., Fan, W., & Xu, Y. (2011). Characterization of geosmin as source of earthy odor in different aroma type Chinese liquors. *Journal of Agricultural and Food Chemistry*, 59(15), 8331–8337.
- Feng, J., Zhan, X. B., Wang, D., Zhang, L. M., & Lin, C. C. (2012). Identification and analysis of the metabolic functions of a high-salt-tolerant halophilic aromatic yeast *Candida etchellsii* for soy sauce production. *World Journal of Microbiology and Biotechnology*, 28(4), 1451–1458.
- Genthner, B., Davis, C., & Bryant, M. P. (1981). Features of rumen and sewage sludge strains of *Eubacterium limosum*, a methanol- and H<sub>2</sub>-CO<sub>2</sub>-utilizing species. *Applied and Environmental Microbiology*, 42(1), 12–19.
- Hahnke, S., Elvert, M., Striesow, J., Mollar, X. P., & Klocke, M. (2014). *Clostridium bornimense*, sp. nov., isolated from a mesophilic two-phase lab-scale biogas reactor. *International Journal of Systematic and Evolutionary Microbiology*, 64(8), 2792–2797.
- Jeon, B. S., Moon, C., Kim, B. C., Kim, H., Um, Y., & Sang, B. I. (2013). In situ extractive fermentation for the production of hexanoic acid from galactitol by *Clostridium* sp. BS-1. *Enzyme and Microbial Technology*, 53(3), 143–151.
- Kim, J. S., & Lee, Y. S. (2008). A study of chemical characteristics of soy sauce and mixed soy sauce: chemical characteristics of soy sauce. *European Food Research and Technology*, 227(3), 933–944.
- Ledauphin, J., Le Milbeau, C., Barillier, D., & Hennequin, D. (2010). Differences in the volatile compositions of French labeled brandies (Armagnac, Calvados, Cognac, and Mirabelle) using GC-MS and PLS-DA. *Journal of Agricultural and Food Chemistry*, 58(13), 7782–7793.
- Liu, L., Cozzolino, D., Cynkar, W. U., Gishen, M., & Colby, C. B. (2006). Geographic classification of Spanish and Australian tempranillo red wines by visible and near-infrared spectroscopy combined with multivariate analysis. *Journal of Agricultural and Food Chemistry*, 54(18), 6754–6759.
- Malherbe, S., Watts, V., Nieuwoudt, H. H., Bauer, F. F., & Du Toit, M. (2009). Analysis of volatile profiles of fermenting grape must by headspace solid-phase dynamic extraction coupled with gas chromatography–mass spectrometry (HS-SPDE GC-MS): novel application to investigate problem fermentations. *Journal of Agricultural and Food Chemistry*, 57(12), 5161–5166.
- Pereira, A. C., Reis, M. S., Saraiva, P. M., & Marques, J. C. (2010). Analysis and assessment of Madeira wine ageing over an extended time period through GC-MS and chemometric analysis. *Analytica Chimica Acta*, 660(1–2), 8–21.
- Pino, J. A., & Queris, O. (2011). Analysis of volatile compounds of mango wine. *Food Chemistry*, 125(4), 1141–1146.
- Reid, V. J., Theron, L. W., du Toit, M., & Divol, B. (2012). Identification and partial characterization of extracellular aspartic protease genes from *Metschnikowia pulcherrima* IWBT Y1123 and *Candida apicola* IWBT Y1384. *Applied and Environmental Microbiology*, 78(19), 6838–6849.
- de la Roza, C., Laca, A., Garcia, L. A., & Diaz, M. (2003). Ethanol and ethyl acetate production during the cider fermentation from laboratory to industrial scale. *Process Biochemistry*, 38(10), 1451–1456.
- Serrano-Lourido, D., Saurina, J., Hernandez-Cassou, S., & Checa, A. (2012). Classification and characterisation of Spanish red wines according to their appellation of origin based on chromatographic profiles and chemometric data analysis. *Food Chemistry*, 135(3), 1425–1431.
- Shalit, M., Katzir, N., Tadmor, Y., Larkov, O., Burger, Y., Shalekhet, F., et al. (2001). Acetyl-CoA: alcohol acetyltransferase activity and aroma formation in ripening melon fruits. *Journal of Agricultural and Food Chemistry*, 49(2), 794–799.
- Wagner, S., Scholz, K., Donegan, M., Burton, L., Wingate, J., & Völkel, W. (2006). Metabonomics and biomarker discovery: LC-MS metabolic profiling and constant neutral loss scanning combined with multivariate data analysis for mercapturic acid analysis. *Analytical Chemistry*, 78(4), 1296–1305.
- Xia, Q., Wu, C., Huang, J., & Zhou, R. (2014). Selection and application of potential whole-cell enzymes in the esterification of Huangshui, a by-product formed during Chinese liquor-making. *Journal of the Institute of Brewing*, 120(1), 45–51.
- Zheng, J., Liang, R., Wu, C., Zhou, R., & Liao, X. (2014). Discrimination of different kinds of Luzhou-flavor raw liquors based on their volatile features. *Food Research International*, 56, 77–84.
- Zheng, J., Wu, C., Huang, J., Zhou, R., & Liao, X. (2014). Spatial distribution of bacterial communities and related biochemical properties in Luzhou-flavor liquor-fermented grains. *Journal of Food Science*, 79(12), M2491–M2498.



# Combined effect of prefermentative cold soak and SO<sub>2</sub> additions in Barbera D'Asti and Malbec wines: Anthocyanin composition, chromatic and sensory properties



L. Federico Casassa<sup>a, b, \*</sup>, Esteban A. Bolcato<sup>a</sup>, Santiago E. Sari<sup>a</sup>, Martín L. Fanzone<sup>c</sup>, Viviana P. Jofré<sup>c</sup>

<sup>a</sup> Centro de Estudios de Enología, Instituto Nacional de Tecnología Agropecuaria (INTA), San Martín 3853, 5507 Luján de Cuyo, Mendoza, Argentina

<sup>b</sup> Wine & Viticulture Department, California Polytechnic State University, San Luis Obispo, CA 93407, USA

<sup>c</sup> Laboratorio de Aromas y Sustancias Naturales, Instituto Nacional de Tecnología Agropecuaria (INTA), San Martín 3853, 5507 Luján de Cuyo, Mendoza, Argentina

## ARTICLE INFO

### Article history:

Received 7 March 2015

Received in revised form

6 October 2015

Accepted 8 October 2015

Available online 22 October 2015

### Keywords:

Cold soak

Sulfur dioxide

Anthocyanins

Wine color

Sensory analysis

## ABSTRACT

The effects of prefermentative cold soak (CS) combined with two SO<sub>2</sub> additions (50 and 100 mg L<sup>-1</sup>) on the anthocyanin composition, chromatic properties and sensory attributes of Barbera D'Asti and Malbec wines were studied. Cold soak had no effect on the basic chemistry of the wines. The cultivar factor affected anthocyanins, tannins, total phenolics and the chromatic features of the wines, favoring Malbec over Barbera D'Asti wines. Cold soak combined with 50 mg L<sup>-1</sup> SO<sub>2</sub> failed to increase the phenolic content of the wines relative to a control, but combined with 100 mg L<sup>-1</sup> SO<sub>2</sub>, CS increased anthocyanins, saturation and the red color component of the wines. Cold soak + 100 mg L<sup>-1</sup> also increased the sensory attributes color intensity, violet hue, jammy aroma and astringency in Barbera D'Asti wines but there was no effect of any treatment on the sensory properties of Malbec wines. Overall, CS combined with an SO<sub>2</sub> addition of 100 mg L<sup>-1</sup> appears to have a positive effect but only from the perspective of wine phenolics and color.

© 2015 Elsevier Ltd. All rights reserved.

## 1. Introduction

Many winemaking practices that are recognized as traditional techniques in specific winegrowing regions are being incorporated to the pool of global winemaking practices thereby emerging as new trends in regions where such practices were not commonplace. One example is the use of prefermentative cold soak (CS) as a part of the production scheme for red winemaking. Red wines own their sensory properties to the maceration process in which phenolics and flavor components are solubilized and migrate by diffusion from the skins and seeds into the fermenting must/wine. The maceration process entails in itself the combination of maceration and alcoholic fermentation (AF), whereby the fermentation process produces heat needed for phenolic extraction (Boulton, Singleton, Bisson, & Kunkee, 1998) while favoring the occurrence chemical reactions

such as the formation of polymeric pigments (Casassa & Harbertson, 2014). During active AF, dissolved oxygen levels are typically low, ensuring low or lack thereof of enzymatic coupled oxidations, which are detrimental for wine color and flavor (Boulton et al., 1998). The CS technique, which consists on allowing the maceration of grape solids (skins and seeds) with the must prior to the onset of AF, entails conditions of temperature and dissolved oxygen different from that of a traditional maceration (Casassa & Sari, 2014; Delteil, 2004). First, low temperatures during CS prevent the onset of AF and, as a result, there is no heat generation (Casassa & Sari, 2014; Parenti, Spugnoli, Calamai, Ferrari, & Gori, 2004; Stefanini & Pantani, 2013). The onset AF is delayed by keeping the must temperature at 5–10 °C for a period of 3–5 h up to 10 days (Álvarez, Aleixandre, García, & Lizama, 2006; Casassa & Sari, 2014; Gil-Muñoz et al., 2009; Ortega-Heras, Pérez-Magariño, & González-Sanjosé, 2012). Solid CO<sub>2</sub>, also known as dry ice, is sometimes used during CS with that end. Second, while low levels of dissolved oxygen are typically encountered during the maceration process, during CS dissolved oxygen levels are higher as a result of crushing operations and so it is the potential risk for enzymatic oxidations (Casassa & Sari, 2014). In this regard, sulfur

\* Corresponding author. Wine & Viticulture Department, California Polytechnic State University, San Luis Obispo, CA 93407, USA.

E-mail address: [lcasassa@calpoly.edu](mailto:lcasassa@calpoly.edu) (L. Federico Casassa).

dioxide at the additions normally used for red winemaking (30–80 mg L<sup>-1</sup>), can reduce polyphenol-oxidase activity up to 90% (Boulton et al., 1998). Additionally, SO<sub>2</sub> in the range of 40–150 mg kg<sup>-1</sup> increases the extraction of phenolics and, specifically, that of anthocyanins (Bakker et al., 1998; Pateraki et al., 2014). Since one of the intended goals of CS is to favor anthocyanin extraction prior to the onset of AF, the combination of CS with higher additions of SO<sub>2</sub> represent an option for minimizing polyphenol-oxidase reactions and increasing the retention of anthocyanins.

Prefermentative CS has gained widespread adoption and, accordingly, a rising body of research involving CS has paralleled this growth. Reported chemical and sensory outcomes of CS are inconsistent across different cultivars, growing regions and specific variations of this technique, precisely as a result of this vast array of assorted conditions. For phenolic compounds, some reports indicate a null effect (Ortega-Heras et al., 2012; Pérez-Lamela, García-Falcón, Simal-Gándara, & Orriols-Fernández, 2007) or even a decrease in the retention of phenolic after CS (Budic-Leto, Tomislav, & Vrhovsek, 2003; González-Neves, Gil, Favre, & Ferrer, 2012). Likewise, one study in Cabernet Sauvignon wines showed that the volatile composition of control and CS wines as determined by SPME GC–MS was statistically undistinguishable for 31 out of 33 volatiles (Gardner, Zoeklein, & Mallikarjunan, 2011). These results are at odds with what CS is supposed to bring to red winemaking.

Because the occurrence of enzymatic oxidations during CS can outweigh its positive effects on phenolic extraction (Casassa & Sari, 2014), the working hypothesis of this study was that the potential benefits of CS may be realized when combined with higher SO<sub>2</sub> additions. To test this hypothesis, we combined CS with two SO<sub>2</sub> additions, one considered standard (50 mg L<sup>-1</sup>), and the other considered above-average (100 mg L<sup>-1</sup>) in two red wine cvs., Barbera D'Asti and Malbec, which have very distinctive anthocyanin concentrations.

## 2. Materials & methods

### 2.1. Grapes

Own-rooted Barbera D'Asti and Malbec grapes (*Vitis vinifera* L.) were obtained from a commercial vineyard located in Luján de Cuyo, Mendoza, Argentina (33° 00' S, 68° 51' W). For each cv., a total of 900 kg were manually harvested to 18-kg plastic boxes (Table 1). For the grape basic analysis, four independent samples, each of 30 berries, were taken at harvest for each cv. and analyzed for berry weight and volume, seeds/berry, Brix (Atago, Tokyo, Japan), pH (Orion model 701-A, Thermo Scientific, Waltham, MA, USA), titratable acidity, and laccase activity (Dubourdieu, Grassin, Deruche, & Ribereau-Gayon, 1984).

### 2.2. Winemaking

Grapes were transported to the Wine Research Center experimental winery. Upon reception, grapes crushed and destemmed

(Metal Liniers model MTL 12, Mendoza, Argentina), and the musts pumped into 100-L stainless steel tanks. The experimental design consisted of three maceration treatments for each of the 2 cvs., replicated three times (n = 3). Control wines were produced with a standard SO<sub>2</sub> addition of 50 mg L<sup>-1</sup>, and a maceration length of 15 days at 24.5 ± 2.5 °C; cap management consisted of two daily full-volume pump-overs followed by two daily punch downs (morning and afternoon, 1 min each). Cold soak (CS) with solid CO<sub>2</sub> (dry ice) consisted of 3 days of CS at 9 ± 3 °C achieved by periodic additions of CO<sub>2</sub>. During crushing, SO<sub>2</sub> was added at two doses: 50 mg L<sup>-1</sup> (CS + 50 mg L<sup>-1</sup>) and 100 mg L<sup>-1</sup> (CS + 50 mg L<sup>-1</sup>) together with an addition of 13 kg of CO<sub>2</sub> pellets (Praxair SA, Mendoza, Argentina) per 100 kg of destemmed grapes. Afterwards, CO<sub>2</sub> was added at a rate of 5 kg tank day<sup>-1</sup> followed by two daily punch-downs (1 min each). The 3-day CS was followed by a 12-day maceration period under the same conditions as those of control wines. All tanks were inoculated 5 h after crushing with a commercial yeast (EC-1118; Lallemand Inc., Copenhagen, Denmark) at a rate of 0.3 g L<sup>-1</sup> (Casassa & Sari, 2014). The titratable acidity (TA) of all musts was adjusted to 7 g L<sup>-1</sup> with food-grade tartaric acid. After maceration was completed, malolactic fermentation (MLF) was induced with a commercial *Oenococcus Oeni* culture (VP-41, Lallemand Inc., Copenhagen, Denmark). After MLF (malic acid < 0.20 g L<sup>-1</sup>), the wines were racked off the lees, adjusted to 30 mg L<sup>-1</sup> of free SO<sub>2</sub>, and stored at 1 °C for 45 days to allow tartaric stabilization. After this period, the wines were racked and brought to room temperature for 48 h. Prior to bottling, free SO<sub>2</sub> was adjusted to 0.5 mg L<sup>-1</sup> of molecular SO<sub>2</sub>. The bottles were stored horizontally in a cellar (12 ± 1 °C).

### 2.3. Wine basic analysis

Alcohol content, titratable acidity (TA), volatile acidity (VA), pH, and glycerol content were obtained using a FOSS Wine-Scan (FT-120) rapid-scanning infrared Fourier-transform spectrometer (FOSS, Hillerød, Denmark). During fermentation, density at 20 °C was measured with a densimeter (Fite, Buenos Aires, Argentina). Reducing sugars were determined following a reference method (INV, 2013). Malic acid was determined enzymatically (Vintessential Laboratories, Victoria, Australia).

### 2.4. Spectrophotometric analysis

Spectrophotometric measurements to evaluate wine phenolics and color were performed after MLF. Total phenols (expressed as gallic acid equivalents (GAE), mg L<sup>-1</sup>), anthocyanins (mg L<sup>-1</sup> malvidin-3-glucoside) and tannins (mg L<sup>-1</sup> (+)-catechin) were measured as described (Porter, Hrstich, & Chan, 1985; Ribereau-Gayon, Glories, Maujean, & Dubourdieu, 2006). Wine color was determined with the Cie–Lab system using the MSCV™ software (Grupo de Color de La Rioja, Logroño, Spain) in a Perkin–Elmer Lambda 3B spectrophotometer (Norwalk, CT, USA).

**Table 1**

Harvest date and basic physical and chemical composition of Barbera D'Asti and Malbec grapes used for the winemaking treatments. Values represent the mean (±SEM) of four independent sample replicates taken at harvest (n = 30 berries).

Cultivar	Harvest date	Berry weight (g)	Berry volume (cm <sup>3</sup> )	Seeds per berry	Laccase activity (U mL <sup>-1</sup> )	Brix	pH	Titratable acidity (g L <sup>-1</sup> tartaric acid)
Barbera D'Asti	30-III-2009	2.05 ± 0.05 a <sup>a</sup>	1.75 ± 0.07 a	1.94 ± 0.04 b	2.82 ± 0.36 a	27.13 ± 0.15 b	3.48 ± 0.01 a	5.98 ± 0.19 b
Malbec	17-III-2009	1.95 ± 0.03 a	1.79 ± 0.05 a	1.61 ± 0.18 a	3.06 ± 0.29 a	25.83 ± 0.15 a	3.76 ± 0.02 b	4.93 ± 0.26 a
p-value	–	0.1648 <sup>b</sup>	0.6281	<b>0.0148</b>	0.6281	<b>0.0321</b>	<b>0.0030</b>	<b>0.0298</b>

<sup>a</sup> Different letters within a column indicate significant differences for the Student t-Test and p < 0.05.

<sup>b</sup> Significant p-values (p < 0.05) are shown in bold.

### 2.5. HPLC-DAD analysis of grapes and wines

Anthocyanins in grapes and wines were measured as previously described (Fanzone, Peña-Neira, Jofre, Assof, & Zamora, 2010). The chromatographic system consisted on a PerkinElmer Series 200 high-performance liquid chromatograph equipped with a diode array detector (DAD), a quaternary pump and an autosampler (HPLC-DAD; PerkinElmer, Shelton, CT, USA). Separation was performed on a reverse-phase Nova-Pak C18 column (150 mm × 3.9 mm i.d., 4 μm) at room temperature (Waters Corp., Milford, MA), using a gradient consisting of solvent A (water/formic acid, 90:10, v/v) and solvent B (acetonitrile) applied at a flow rate of 1.1 mL min<sup>-1</sup> from 0 to 22 min and at flow rate of 1.5 mL min<sup>-1</sup> from 22 to 35 min as follows: 96–85% A and 4–15% B from 0 to 12 min, 85–85% A and 15–15% B from 12 to 22 min, 85–70% A and 15–30% B from 22 to 35 min. Photodiode array detection (DAD) was performed from 210 to 600 nm. For quantification, DAD-chromatograms were extracted at 520. The identification of anthocyanin pigments was carried out by comparison of their spectra and retention time with those of standards and quantified using malvidin-3-glucoside chloride as external standard (Extrasynthèse, Lyon, France), as previously detailed (Fanzone et al., 2010) and a standard calibration curve [Concentration (mg/L) = 0.769683 + (0.0000683547 × Area); R<sup>2</sup> = 0.98]. The confirmation of these compounds was performed by HPLC-DAD/ESI-MS as described by Gomes Rebello et al. (2013).

### 2.6. Sensory analysis

Two trained panels, one of 12 individuals, and the other of 14 individuals, with ages ranging from 25 to 65 years of age, all of which had experience on training protocols for wine sensory analysis were convened. Wines were analyzed after MLF and all the replicates (n = 3) of each cv. were included in the evaluation design. Two formal evaluation sessions were held throughout the experiment, one for each wine cv., with three additional introductory sessions devoted to terminology development and attribute definition. During the first introductory session, panelists were presented with the wines. During the second introductory session, panelists defined by consensus two color attributes (color intensity and violet hue), two aroma attributes (jammy and red fruit), one taste attribute (bitterness) and one mouthfeel attribute (astringency) to characterize the wines. During the third introductory session, a definition and a standard, if applicable, were provided for each attribute, and the panelists underwent training with the standards. Specifications for these standards are provided in Table 6. The intensity of each attribute was assessed using a non-structured 120 mm line scale containing two reference points located at 12 mm of each end of the line. Wines were presented in triplicate in ISO wine glasses (ISO, 1977) covered with plastic lids to trap volatiles, following a balanced, complete block design. To minimize sensory carry-over, panelists were asked to rinse their mouth with mineral water and eat a cracker between samples following a sip and spit protocol (Colonna, Adams, & Noble, 2004).

### 2.7. Data analysis

Fruit physical and chemical compositions were analyzed by a Student t-test for independent samples ( $p < 0.05$ ). The basic, phenolic, anthocyanin, and chromatic composition of the wines were analyzed by a fixed-effect two-way analysis of variance (ANOVA) with interactions, including as main effects the grape cv. (Barbera D'Asti and Malbec), and the maceration technique (control, CS + 50 mg L<sup>-1</sup> and CS + 100 mg L<sup>-1</sup>), as well as their interaction. In addition, the full data set was reevaluated by one-way

ANOVA on a cv. and maceration technique basis (Supplemental Tables 1 to 3). The data generated by the sensory analysis were analyzed by one-way ANOVA. In all cases, Fisher's LSD test was used as a *post-hoc* comparison of means with a 5% level for rejection of the null hypothesis. Data analysis was performed using XLSTAT (Addinsoft, Paris, France). The relationship between the anthocyanin and chromatic composition was evaluated by Partial Least Square Regression (PLSR), using the anthocyanin composition data as predictors (X matrix) and the chromatic data as responses (Y matrix). This analysis was performed using the Unscrambler statistical package (Unscrambler version 10.3, Camo Software, Oslo, Norway).

## 3. Results & discussion

### 3.1. Basic physical and chemical composition of the grapes

Table 1 shows the basic composition of the Barbera D'Asti and Malbec grapes. Barbera D'Asti grapes had higher number of seeds per berry, Brix and TA than Malbec grapes, whereas pH was lower. Additionally, the detailed anthocyanin profile of both grape cvs. was determined to establish potential qualitative and quantitative differences between the cvs. and the wines to be produced. There were obvious quantitative differences between the anthocyanin profile of Barbera D'Asti and Malbec grapes (Table 2). For example, total glucosylated, acetylated, and coumaroylated anthocyanins were 22, 26 and 260% higher in Malbec than in Barbera D'Asti grapes. Qualitatively, the anthocyanin profile was identical in Barbera D'Asti and Malbec grapes, with the only exception of cyanidin-3-(6-coumaroyl)-glucoside, which was not detected in Barbera D'Asti grapes. Interestingly, Barbera D'Asti grapes were particularly high in cyanidin-3-glucoside and peonidin-3-glucoside, with malvidin-3-glucoside representing 47% of the total anthocyanin content. In contrast, malvidin-3-glucoside accounted for 56% of the total anthocyanin profile in Malbec grapes.

### 3.2. Sugar consumption and temperature profiles during cold soak and alcoholic fermentation

Fig. 1 shows the evolution of temperature (Fig. 1a and c) and sugar consumption (Fig. 1b and d) during AF. Temperatures during CS ranged from 8 to 14 °C and from 4 to 10 °C in Barbera D'Asti and Malbec wines, respectively. For control wines, temperatures ranged from 18 to 28 °C and from 20 to 28 °C in Barbera D'Asti and Malbec wines, respectively. There was no apparent sugar consumption during CS for both cvs. Three previous independent studies have demonstrated that the use of solid CO<sub>2</sub> avoids sugar consumption during CS (Casassa, Bolcato, & Sari, 2015; Casassa & Sari, 2014; Hierro, González, Mas, & Guillamón, 2006), probably due to the combined effect of low temperature and low dissolved oxygen achieved by the CO<sub>2</sub>. There was a minor effect of the initial SO<sub>2</sub> addition on the kinetic of sugar consumption during AF in Barbera D'Asti wines, with the treatment CS + 100 mg L<sup>-1</sup> showing a slower rate of sugar consumption between days 6–9. Nevertheless, by day 14 residual sugar levels were essentially the same in the three treatments. For Malbec wines, sugar consumption was not affected by the initial SO<sub>2</sub> additions.

### 3.3. Basic chemical composition of the wines

Table 3 shows a two-way ANOVA performed on the basic chemical composition of the wines considering two factors: the cv. (Barbera D'Asti and Malbec), and the three maceration techniques (control, CS + 50 mg L<sup>-1</sup> and CS + 100 mg L<sup>-1</sup>). When the two cvs. were contrasted, Barbera D'Asti wines had higher ethanol levels

**Table 2**

Concentration (mg kg<sup>-1</sup> berry fresh weight) of the detailed anthocyanin composition of Barbera D'Asti and Malbec grapes used for the winemaking treatments. Values represent the mean ( $\pm$ SEM) of four independent sample replicates taken at harvest (n = 30 berries).

Anthocyanin	Barbera D'Asti	Malbec	p-value
Delphinidin-3-glucoside	91.6 $\pm$ 14.5 a <sup>a</sup>	104.8 $\pm$ 6.7 a	0.4561 <sup>b</sup>
Cyanidin-3-glucoside	109.2 $\pm$ 21.1 b	25.1 $\pm$ 8.8 a	<b>0.0078</b>
Petunidin-3-glucoside	136.7 $\pm$ 8.1 a	152.6 $\pm$ 12.2 a	0.2708
Peonidin-3-glucoside	164.5 $\pm$ 7.9 b	82.3 $\pm$ 11.5 a	<b>0.0035</b>
Malvidin-3-glucoside	702.3 $\pm$ 23.3 a	1103.8 $\pm$ 11.5 b	<b>0.0001</b>
Total glucosylated	1204.2 $\pm$ 66.6 a	1468.6 $\pm$ 44.1 b	<b>0.0295</b>
Delphinidin-3-(6-acetyl)-glucoside	19.1 $\pm$ 2.6 a	22.6 $\pm$ 1.8 a	0.3003
Cyanidin-3-(6-acetyl)-glucoside	19.2 $\pm$ 13.8 a	16.1 $\pm$ 2.9 a	0.3809
Petunidin-3-(6-acetyl)-glucoside	31.1 $\pm$ 3.5 a	32.2 $\pm$ 1.5 a	0.7818
Peonidin-3-(6-acetyl)-glucoside	26.4 $\pm$ 2.9 a	29.5 $\pm$ 1.5 a	0.3934
Malvidin-3-(6-acetyl)-glucoside	155.5 $\pm$ 3.2 a	217.2 $\pm$ 1.8 b	<b>0.0001</b>
Total acetylated	251.3 $\pm$ 1.48 a	317.5 $\pm$ 8.1 b	<b>0.0171</b>
Delphinidin-3-(6-coumaroyl)-glucoside	5.7 $\pm$ 0.5 a	13.9 $\pm$ 0.5 b	<b>0.0002</b>
Cyanidin-3-(6-coumaroyl)-glucoside	nd <sup>c</sup>	0.3 $\pm$ 0.3	–
Petunidin-3-(6-coumaroyl)-glucoside	1.9 $\pm$ 0.4 a	8.2 $\pm$ 0.4 b	<b>0.0004</b>
Peonidin-3-(6-coumaroyl)-glucoside	5.3 $\pm$ 0.5 a	8.7 $\pm$ 0.5 b	<b>0.0085</b>
Malvidin-3-(6-coumaroyl)-glucoside	33.6 $\pm$ 0.4 a	135.7 $\pm$ 0.3 b	<b>&lt; 0.0001</b>
Total coumaroylated	46.6 $\pm$ 1.7 a	166.7 $\pm$ 0.2 b	<b>&lt; 0.0001</b>
Total anthocyanins	1502.1 $\pm$ 82.8 a	1952.8 $\pm$ 53.5 b	<b>0.0103</b>

<sup>a</sup> Different letters within a row indicate significant differences for the Student t-Test and  $p < 0.05$ .

<sup>b</sup> Significant  $p$ -values ( $p < 0.05$ ) are shown in bold.

<sup>c</sup> Not detected.

than Malbec wines, in line with initial sugar contents. The TA was higher in Barbera D'Asti wines as a result of  $\sim 0.5$  g L<sup>-1</sup> of residual malic acid. Volatile acidity was also higher in Barbera D'Asti wines likely due to a lengthy MLF in these wines (data not shown).

Alcoholic fermentation arrested spontaneously in Barbera D'Asti wines at about 6 g L<sup>-1</sup> of residual sugars due to high ethanol levels (16.70% v/v). The cv. had no influence on the glycerol content of the wines. As for maceration technique, CS had no effect on the basic

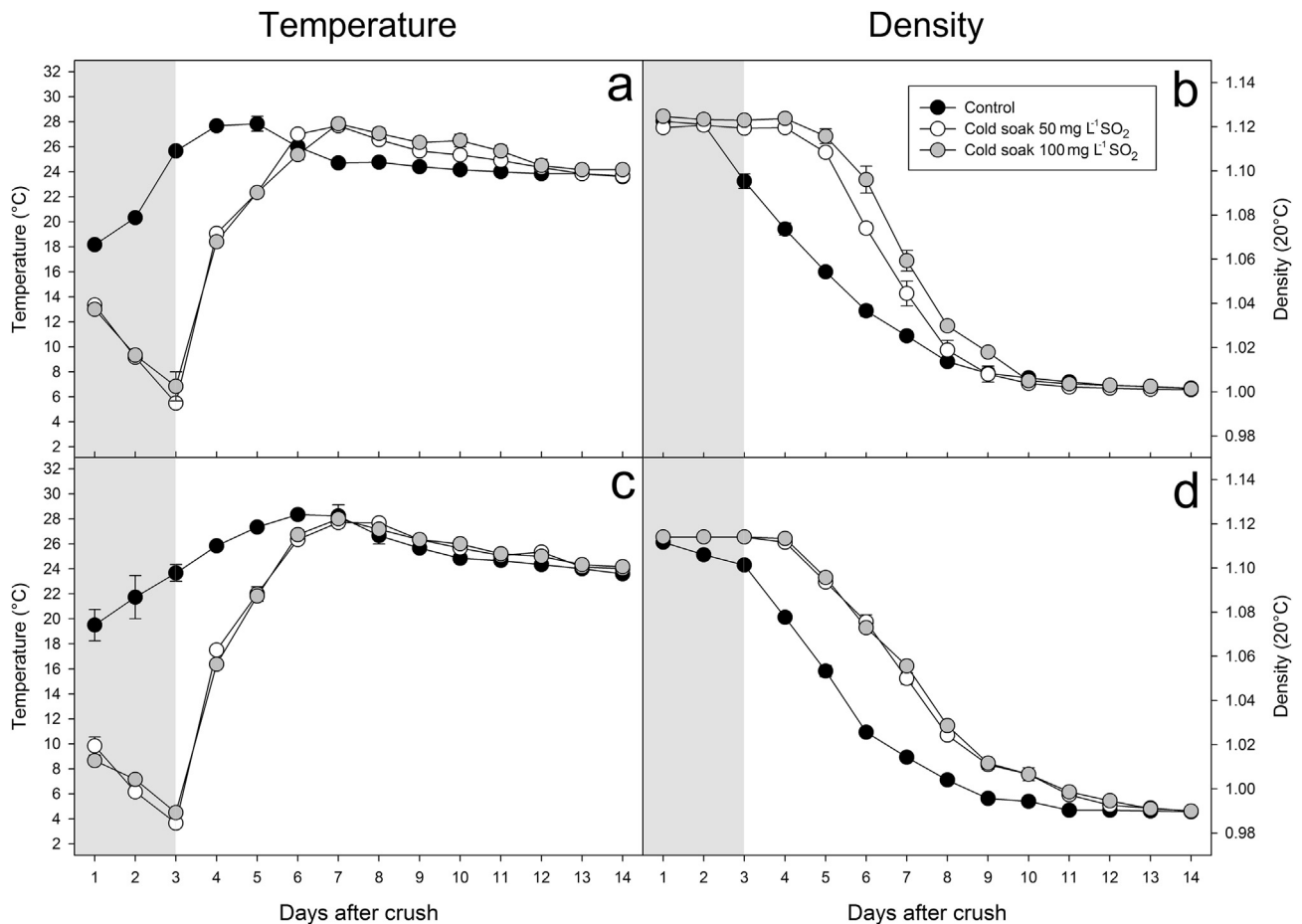


**Fig. 1.** Evolution of temperature (a and c), and sugar consumption (b and d) during cold soak and alcoholic fermentation for the control, CS + 50 mg L<sup>-1</sup> and CS + 100 mg L<sup>-1</sup> treatments in: a and b, Barbera D'Asti; c and d, Malbec. The cold soak period is shown in grey color. If not shown, error bars are obscured by the treatment symbol.

**Table 3**  
Two-way ANOVA of basic analysis of Barbera D'Asti and Malbec wines produced applying cold soak (CS) with two SO<sub>2</sub> additions at crushing (50 and 100 mg L<sup>-1</sup>), and a control treatment. Values represent the mean ( $\pm$ SEM) of three tank replicates.

ANOVA parameter	Ethanol (% v/v)	Titrateable acidity (g L <sup>-1</sup> tartaric acid)	Volatile acidity (g L <sup>-1</sup> acetic acid)	Malic acid (g L <sup>-1</sup> )	pH	Residual sugars (g L <sup>-1</sup> )	Glycerol (g L <sup>-1</sup> )
Cultivar (cv.)							
Barbera D'Asti	16.70 $\pm$ 0.11 b <sup>a</sup>	5.69 $\pm$ 0.16 b	0.81 $\pm$ 0.02 b	0.52 $\pm$ 0.10 b	3.62 $\pm$ 0.02 a	5.95 $\pm$ 0.60 b	9.46 $\pm$ 0.05 a
Malbec	15.19 $\pm$ 0.05 a	4.78 $\pm$ 0.07 a	0.51 $\pm$ 0.02 a	0.14 $\pm$ 0.04 a	3.87 $\pm$ 0.01 b	3.15 $\pm$ 0.07 a	9.34 $\pm$ 0.04 a
p-value	<b>&lt; 0.0001</b> <sup>b</sup>	<b>&lt; 0.0001</b>	<b>&lt; 0.0001</b>	<b>0.0011</b>	0.7915	<b>0.0012</b>	0.1174
Maceration technique (MT)							
Control	16.00 $\pm$ 0.30 a	5.42 $\pm$ 0.30 a	0.68 $\pm$ 0.07 a	0.34 $\pm$ 0.12 a	3.76 $\pm$ 0.02 a	4.85 $\pm$ 1.15 a	9.32 $\pm$ 0.06 a
CS + 50 mg L <sup>-1</sup> SO <sub>2</sub>	15.91 $\pm$ 0.19 a	5.08 $\pm$ 0.15 a	0.68 $\pm$ 0.06 a	0.22 $\pm$ 0.06 a	3.75 $\pm$ 0.02 a	3.94 $\pm$ 0.39 a	9.43 $\pm$ 0.05 a
CS + 100 mg L <sup>-1</sup> SO <sub>2</sub>	15.93 $\pm$ 0.23 a	5.21 $\pm$ 0.26 a	0.63 $\pm$ 0.07 a	0.44 $\pm$ 0.16 a	3.73 $\pm$ 0.02 a	4.87 $\pm$ 0.83 a	9.45 $\pm$ 0.07 a
p-value	0.6248	0.2087	0.4933	0.1676	0.3956	0.4059	0.3325
cv. $\times$ MT interaction							
p-value	0.0884	0.1157	0.8125	0.0681	0.6322	0.2072	0.8322

<sup>a</sup> Different letters within a column and ANOVA parameter indicate significant differences for Fisher's LSD Test and  $p < 0.05$ .

<sup>b</sup> Significant  $p$ -values ( $p < 0.05$ ) are shown in bold.

chemical composition of the wines. This null effect of CS on the basic chemistry of red wines had already been put in evidence in Malbec and Barbera D'Asti wines (Casassa et al., 2015; Casassa & Sari, 2014), as well as in Cabernet Sauvignon, Merlot, Pinot Noir and Syrah (Casassa et al., 2015).

#### 3.4. Phenolic and chromatic composition of the wines

A summary of the phenolic and chromatic composition of the wines is shown in Table 4. Total phenols were higher in Malbec, but tannins were at comparable amounts in both Barbera D'Asti and Malbec wines. As one of the main drivers of tannin content in red wines is the number of seeds per berry (Harbertson, Kennedy, & Adams, 2002), the higher tannin levels in Barbera D'Asti wines were expected based on a higher number of seeds per berry, but those in Malbec were at odds with the lower number of seeds per berry observed in Malbec grapes (Table 1). This suggests that Malbec seeds may be unusually high in tannins, but these results need to be confirmed. Malbec wines had lower lightness (thus they were darker), and were more saturated and with a lower hue than Barbera D'Asti wines.

The CS + 50 mg L<sup>-1</sup> treatment failed to increase the total phenolic and tannin content of the wines relative to the control wines. Only when CS was conducted with a SO<sub>2</sub> addition of 100 mg L<sup>-1</sup> an extractive effect on total phenolics and tannins, albeit moderate, was observed. This extractive effect could be solely attributed to the addition of SO<sub>2</sub> applied in the CS + 100 mg L<sup>-1</sup> treatment, as both control and CS + 50 mg L<sup>-1</sup> wines were produced using the same addition of 50 mg L<sup>-1</sup> SO<sub>2</sub>. It could be argued

that a treatment of the form control + 100 mg L<sup>-1</sup> should have been included in our experimental design. However, the goal of this study was not to explore the effect of different SO<sub>2</sub> additions but rather to uncover potential beneficial effects of SO<sub>2</sub> additions higher than those conventionally applied during CS. The motivation for this was the realization that under standard CS conditions, in which SO<sub>2</sub> additions range from 30 to 80 mg L<sup>-1</sup> SO<sub>2</sub>, CS alone has little or no positive effect on phenolic extraction when the length of CS extends for more than 4 days (Casassa et al., 2015; Casassa & Sari, 2014; Ortega-Heras et al., 2012; Pérez-Lamela et al., 2007). The hypothesis put forth was that coupled enzymatic oxidations may oxidize phenolic and flavor compounds during CS, thus outweighing the positive extractive effect on phenolics achieved by this technique. To test this hypothesis, the length of CS was herein set to 3 days and combined with 100 mg L<sup>-1</sup> SO<sub>2</sub> addition. The results presented here seem to confirm this hypothesis, thereby highlighting the positive effect of a short CS combined with a SO<sub>2</sub> addition of 100 mg L<sup>-1</sup>. Similar results have also been reported in Pinot Noir whereby CS conducted with SO<sub>2</sub> produced wines higher in color and polymeric pigments relative to CS conducted without SO<sub>2</sub> (Parley, Vanhanen, & Heatherbell, 2001).

For the chromatic composition, CS at both SO<sub>2</sub> additions increased saturation (C\*), and the red component of wine color (a\*), while decreasing hue (H\*) relative to control wines. Moreover, the significance of the interactive effects between the cv. and the maceration technique factors for most phenolic and chromatic measurements suggests that the effect of CS is contingent upon the grape cv. to which the technique is applied, an otherwise well-known empirical observation.

**Table 4**  
Two-way ANOVA of the phenolic and chromatic composition of Barbera D'Asti and Malbec wines produced applying cold soak (CS) with two SO<sub>2</sub> additions at crushing (50 and 100 mg L<sup>-1</sup>), and a control treatment. Values represent the mean ( $\pm$ SEM) of three tank replicates.

ANOVA parameter	Phenolic composition			Chromatic composition (Cie-Lab units)				
	Anthocyanins (mg L <sup>-1</sup> )	Total phenols (mg L <sup>-1</sup> GAE)	Tannins (mg L <sup>-1</sup> )	L*	C*	H*	a*	b*
Cultivar (cv.)								
Barbera D'Asti	156 $\pm$ 12 a <sup>a</sup>	2140 $\pm$ 95 a	872 $\pm$ 46 a	56.8 $\pm$ 2.2 b	44.2 $\pm$ 2.1 a	6.5 $\pm$ 0.6 b	43.9 $\pm$ 2.1 a	4.9 $\pm$ 0.3 b
Malbec	380 $\pm$ 34 b	2533 $\pm$ 53 b	970 $\pm$ 37 a	39.6 $\pm$ 0.7 a	60.4 $\pm$ 0.7 b	2.9 $\pm$ 0.6 a	60.2 $\pm$ 0.3 b	2.1 $\pm$ 1.1 a
p-value	<b>&lt; 0.0001</b> <sup>b</sup>	<b>0.0004</b>	0.0517	<b>&lt; 0.0001</b>	<b>&lt; 0.0001</b>	<b>&lt; 0.0001</b>	<b>&lt; 0.0001</b>	<b>0.0257</b>
Maceration technique (MT)								
Control	215 $\pm$ 51 a	2215 $\pm$ 139 a	853 $\pm$ 65 a	50.9 $\pm$ 5.4 b	49.3 $\pm$ 5.1 a	6.4 $\pm$ 1.2 b	49.1 $\pm$ 5.2 a	3.4 $\pm$ 1.8 a
CS + 50 mg L <sup>-1</sup> SO <sub>2</sub>	305 $\pm$ 72 b	2315 $\pm$ 142 ab	933 $\pm$ 51 ab	47.6 $\pm$ 4.3 ab	53.1 $\pm$ 3.6 b	4.3 $\pm$ 0.6 a	53.0 $\pm$ 3.6 b	3.9 $\pm$ 0.5 a
CS + 100 mg L <sup>-1</sup> SO <sub>2</sub>	283 $\pm$ 44 ab	2490 $\pm$ 62 b	978 $\pm$ 37 b	45.9 $\pm$ 2.6 a	54.5 $\pm$ 2.6 b	3.4 $\pm$ 1.1 a	54.4 $\pm$ 2.6 b	3.1 $\pm$ 0.9 a
p-value	0.117	<b>0.0449</b>	0.1174	0.0811	<b>0.0283</b>	<b>0.0038</b>	<b>0.0212</b>	0.8263
cv. $\times$ MT interaction								
p-value	0.593	<b>0.0353</b>	<b>0.0301</b>	<b>0.0151</b>	<b>0.0119</b>	0.0731	<b>0.0102</b>	0.2916

<sup>a</sup> Different letters within a column and ANOVA parameter indicate significant differences for Fisher's LSD Test and  $p < 0.05$ .

<sup>b</sup> Significant  $p$ -values ( $p < 0.05$ ) are shown in bold.

The anthocyanin composition was also determined in the wines after MLF (Table 5). There were no qualitative but rather quantitative differences between Barbera D'Asti and Malbec wines, which largely favored Malbec wines, with an overall 3-fold increase in the total anthocyanin content relative to Barbera D'Asti wines. Furthermore, the comparison of the anthocyanin profile of the grapes and that of the resulting wines highlighted some interesting relationships. For example, Barbera D'Asti grapes were particularly abundant in cyanidin-3-glucoside (Table 2), yet in the Barbera D'Asti wines the concentration of cyanidin-3-glucoside did not differ from that of Malbec wines, suggesting the high reactivity and potential instability of cyanidin-3-glucoside once extracted into wine.

When the three maceration techniques were considered, 7 out of 14 anthocyanins showed significant differences. In general, these differences followed the same trend uncovered for total phenolics and tannins. That is, CS + 50 mg L<sup>-1</sup> failed to increase the concentration of anthocyanins and a positive effect on anthocyanin extraction was only observed in the CS + 100 mg L<sup>-1</sup> treatment. Nevertheless, the improvement of the anthocyanin content in CS + 100 mg L<sup>-1</sup> was moderate, as it was only 28% higher than in control wines. In addition, this positive effect of CS + 100 mg L<sup>-1</sup> on anthocyanins was more evident for Malbec than for Barbera D'Asti wines. There were no significant cv. × maceration technique interactions for any of the anthocyanins and vitisins.

### 3.5. Partial Least Square Regression (PLSR)

As one of the main goals of CS is to improve chromatic features of red wines, the PLSR analysis was undertaken to understand how individual anthocyanins influence wine color when mediated by the CS technique. The PLSR scores, showing the position of the wines of both cvs., including their replicates (n = 3), are shown in Fig. 2a. The PLSR correlation loadings indicating the relative position of the variables are shown in Fig. 2b. Factor 1, which explained 99% of the variance of the anthocyanin composition and 78% of the variance of the chromatic composition, separated the Malbec from the Barbera D'Asti wines, which clustered in the negative and positive portion, respectively, of Factor 1. Factor 2, which only explained 4% of the residual variance of the chromatic attributes, was inconclusive in separating the wines as a function of the winemaking treatments, because most of the variance of the data was concentrated in factor 1. The PLSR correlation loadings showed specific relationships between the anthocyanin and chromatic variables. For example, saturation (C\*) and the red color component (a\*) were predicted by malvidin-3-glucoside and its derivatives, and by peonidin-, petunidin- and delphinidin-3-glucosides. In turn, these variables were related with Malbec wines produced with the CS + 100 mg L<sup>-1</sup> treatment. Lightness (L\*), hue (H\*) and the yellow color component were predicted mainly by Vitisin B. Vitisin B is a pyranoanthocyanin derived from the condensation of anthocyanins and acetaldehyde that displays orange–brick/orange-brown color hues (Bakker & Timberlake, 1997). In turn, the content of Vitisin B was related with the control wines of Barbera D'Asti that were characterized by high hue and lightness, and thus lower saturation. Overall, the PLSR analysis suggests a stronger effect of the wine cv. over the maceration technique. It also suggest that 100 mg L<sup>-1</sup> SO<sub>2</sub> had a positive effect on preserving anthocyanins in Malbec wines, which in turn contributed to the saturation and red color component of these wines.

### 3.6. Sensory analysis

The wines were assessed by two trained panels (Fig. 3),

**Table 5**  
Two-way ANOVA of the detailed anthocyanin composition and concentration (mg L<sup>-1</sup>) at pressing of Barbera D'Asti and Malbec wines produced applying cold soak (CS) with two SO<sub>2</sub> additions at crushing (50 and 100 mg L<sup>-1</sup>), and a control treatment. Values represent the mean (±SEM) of three tank replicates.

ANOVA parameter	Delphinidin-3-glucoside	Cyanidin-3-glucoside	Petunidin-3-glucoside	Peonidin-3-glucoside	Malvidin-3-glucoside	Delphinidin-3-(6-acetyl)-glucoside	Petunidin-3-(6-acetyl)-glucoside	Peonidin-3-(6-acetyl)-glucoside	Malvidin-3-(6-acetyl)-glucoside	Delphinidin-3-(6-coumaroyl)-glucoside	Petunidin-3-(6-coumaroyl)-glucoside	Peonidin-3-(6-coumaroyl)-glucoside	Malvidin-3-(6-coumaroyl)-glucoside	Vitisin A	Vitisin B	Total anthocyanins
Cultivar (cv.)																
Barbera D'Asti	4.2 ± 0.5 a <sup>a</sup>	2.3 ± 0.4 a	7.6 ± 0.9 a	6.9 ± 0.7 a	34.4 ± 2.4 a	1.4 ± 0.2 a	1.4 ± 0.2 a	2.7 ± 0.3 a	2.5 ± 0.3 a	6.5 ± 0.6 a	0.2 ± 0.0 a	0.1 ± 0.0 a	2.6 ± 0.4 a	3.1 ± 0.3 a	3.7 ± 0.4	74.1 ± 6.5 a
Malbec	9.4 ± 0.8 b	2.8 ± 0.2 a	22.3 ± 1.5 b	20.7 ± 0.9 b	129.3 ± 5.6 b	2.5 ± 0.3 b	2.5 ± 0.3 b	8.2 ± 0.7 b	8.2 ± 0.7 b	24.2 ± 1.4 b	1.8 ± 0.1 b	0.9 ± 0.1 b	14.1 ± 0.7 b	6.4 ± 0.3 b	n.d. <sup>c</sup>	252.8 ± 11.9 b
p-value	< 0.0001 <sup>b</sup>	0.9783	< 0.0001	< 0.0001	< 0.0001	0.0066	0.0006	< 0.0001	< 0.0001	< 0.0001	< 0.0001	< 0.0001	< 0.0001	< 0.0001	< 0.0001	< 0.0001
Maceration technique (MT)																
Control	6.0 ± 1.3 a	2.6 ± 0.2 a	13.2 ± 3.0 a	12.5 ± 2.9 a	74.4 ± 20.3 a	1.8 ± 0.3 a	1.8 ± 0.3 a	5.4 ± 1.6 a	4.8 ± 1.2 a	13.2 ± 3.4 a	0.9 ± 0.3 a	0.4 ± 0.1 a	7.0 ± 2.4 a	4.9 ± 0.9 a	1.7 ± 0.8 a	146.8 ± 37.9 a
CS + 50	6.2 ± 1.6 a	2.6 ± 0.6 a	13.3 ± 3.4 a	13.1 ± 3.4 a	78.6 ± 20.2 a	1.6 ± 0.4 a	1.6 ± 0.4 a	5.8 ± 2.1 a	5.2 ± 1.7 a	14.4 ± 3.9 a	1.1 ± 0.4 b	0.5 ± 0.2 ab	8.6 ± 2.8 ab	4.2 ± 0.9 a	1.5 ± 0.8 a	155.9 ± 40.8 a
SO <sub>2</sub>																
CS + 100	8.1 ± 1.3 a	3.1 ± 0.1 a	18.4 ± 3.9 b	15.7 ± 3.2 b	92.6 ± 24.1 b	2.4 ± 0.3 a	2.4 ± 0.3 a	6.1 ± 1.3 a	6.1 ± 1.3 a	18.4 ± 4.7 b	1.2 ± 0.4 b	0.6 ± 0.2 b	9.4 ± 2.6 b	5.2 ± 0.7 a	2.3 ± 1.1 a	187.7 ± 44.1 b
SO <sub>2</sub>																
p-value	0.1983	0.6161	0.0085	0.0366	0.0185	0.2424	0.4321	0.9501	0.4163	0.0019	0.0214	0.2497	0.0276	0.1773	0.1774	0.0285
cv. × MT interaction																
p-value	0.9953	0.8064	0.3999	0.8064	0.1805	0.9806	0.8303	0.726	0.7203	0.0562	0.4722	0.1488	0.6682	0.7977	0.1774	0.534

<sup>a</sup> Different letters within a column and ANOVA parameter indicate significant differences for Fisher's LSD Test and  $p < 0.05$ .

<sup>b</sup> Significant  $p$ -values ( $p < 0.05$ ) are shown in bold.

<sup>c</sup> Not detected.

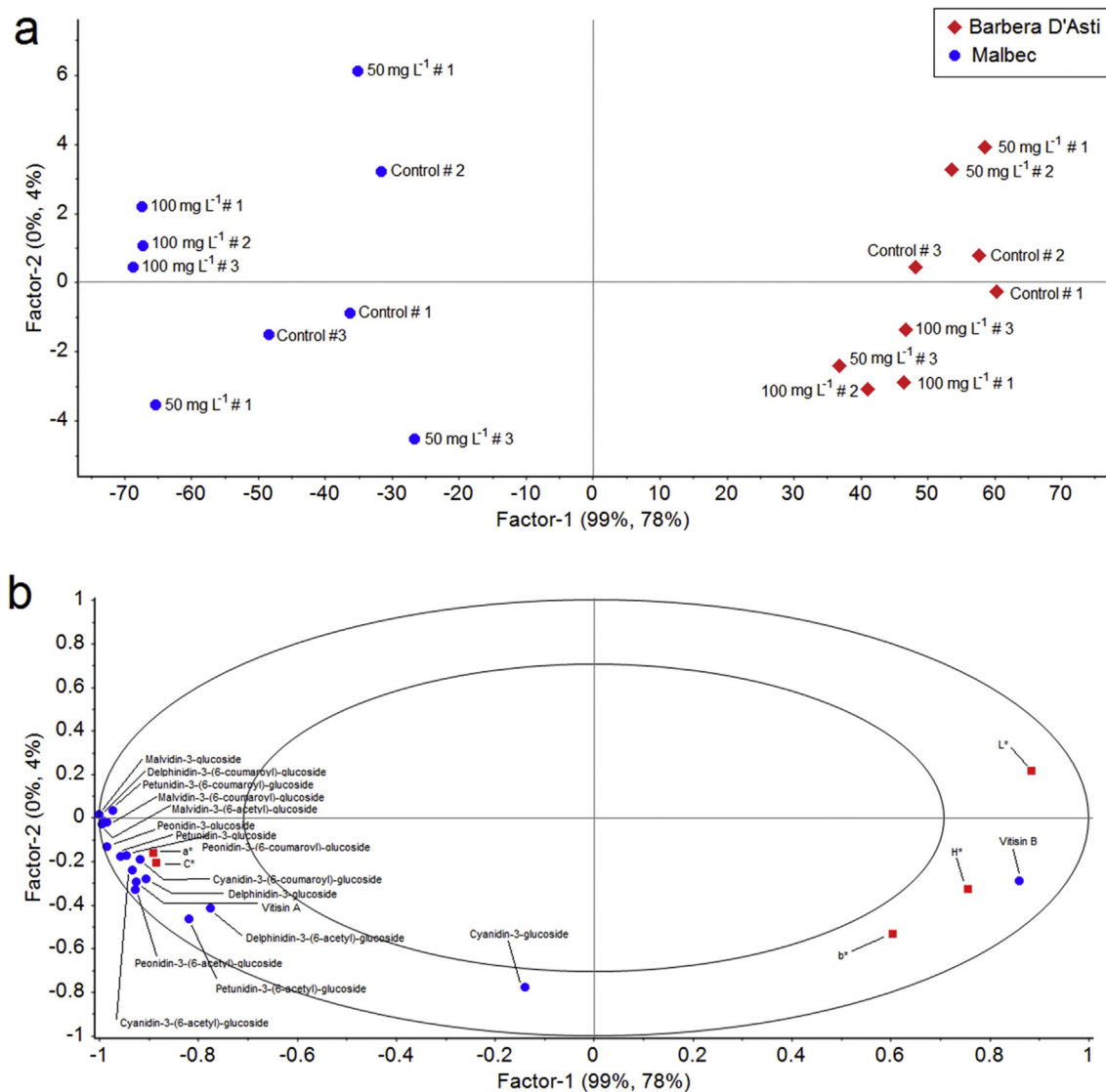


**Fig. 2.** Partial Least Squares Regression analysis: (a) wine scores, and (b) correlation loadings of the relationship between monomeric anthocyanins (X matrix, predictors, in blue circles) and Cie-Lab parameters (Y matrix, predicted, in red squares). Factor 1 (horizontal) explained 99% of wines' anthocyanin composition and 78% of wines' Cie-Lab chromatic parameters, while factor 2 (vertical) explained 0 and 4%, respectively. (For interpretation of the references to colour in this figure legend, the reader is referred to the web version of this article.)

including sensory descriptors pertaining to color, aroma, taste and mouthfeel (tactile) sensations, which were defined by consensus (Table 6). For Barbera D'Asti wines, CS + 50 mg L<sup>-1</sup> had no effect on the sensory profile relative to the control wines. A previous report also in Barbera D'Asti produced with CS (4 days at 9 ± 2.5 °C) found that this technique had no impact on perceived aroma, bitterness and astringency, but it impacted positively color intensity (Casassa et al., 2015). However, in the latter study CS was combined with an SO<sub>2</sub> addition of 80 mg L<sup>-1</sup>, which is closer to the 100 mg L<sup>-1</sup> addition performed in the present study. In fact, CS + 100 mg L<sup>-1</sup> SO<sub>2</sub> increased both perceived color intensity and violet hue in Barbera D'Asti wines (Fig. 3a). Furthermore, CS + 100 mg L<sup>-1</sup> also increased the jammy aroma and astringency relative to the other two treatments. For Malbec wines, there was no effect of any of the three maceration techniques on the sensory profile of the wines. Previous report in Malbec produced with CS (7 days at 5 ± 1.25 °C) reported either minor sensory changes relative to a control after 24 months of bottle aging (Casassa & Sari, 2014) or no effect on aroma, taste and mouthfeel properties (Casassa et al., 2015). Taken together, these results suggest that Malbec does not benefit from

the application of CS with CO<sub>2</sub> regardless of the CS length or the SO<sub>2</sub> doses in the range of 50–100 mg L<sup>-1</sup>.

#### 4. Conclusions

The chemical and sensory effects of CS combined with two additions of SO<sub>2</sub>, 50 and 100 mg L<sup>-1</sup>, were studied in Barbera D'Asti and Malbec wines. Cold soak had no effect on the basic chemistry of the wines, but the two SO<sub>2</sub> additions had a measurable effect on the chromatic and phenolic composition of the wines. In addition to expected differences due to the cv., CS impacted positively color and phenolics only when combined with a SO<sub>2</sub> addition of 100 mg L<sup>-1</sup>. Although the increase in anthocyanin concentration caused by CS + 100 mg L<sup>-1</sup> in Barbera D'Asti wines was moderate, it was enough to positively impact color intensity and violet hue. In Malbec wines, CS produced no measurable sensory changes. PLSR results suggested a positive effect of CS + 100 mg L<sup>-1</sup> on anthocyanins, saturation, and the red color component of Malbec wines but this effect was less prominent for the CS + 100 mg L<sup>-1</sup> counterpart of Barbera D'Asti wines. Yet the sensory analysis suggested

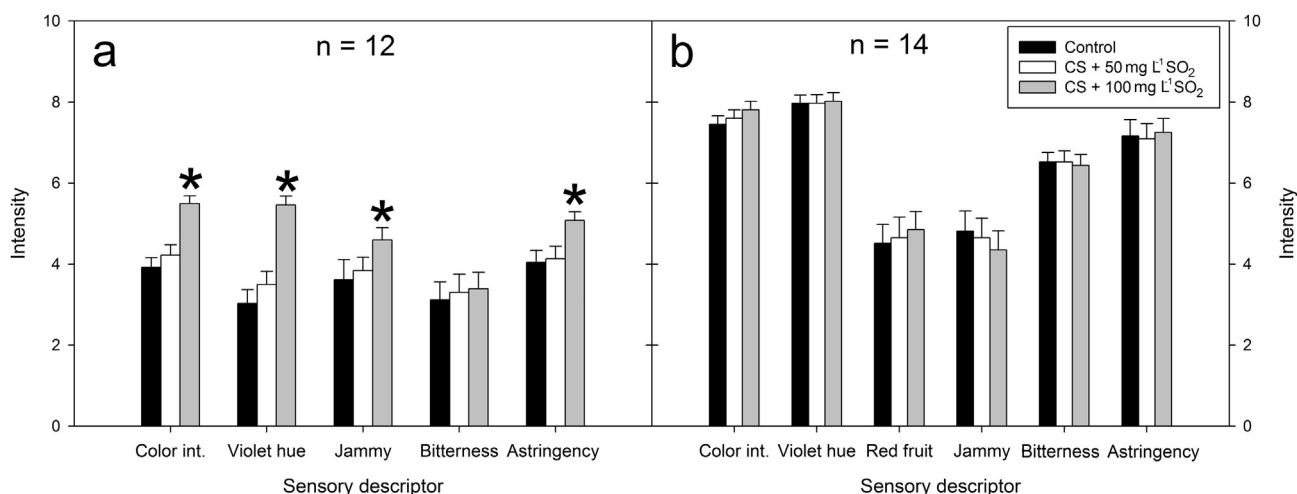


**Fig. 3.** Sensory analysis of control, CS + 50 mg L<sup>-1</sup> and CS + 100 mg L<sup>-1</sup> treatments of a) Barbera D'Asti; b) Malbec. "n" indicates the number of panelist that participated in each analysis. (\*) indicates significant differences for Fisher's LSD test and  $p < 0.05$ .

**Table 6**

Attribute definition and standards used during the training and formal sensory evaluations of the wines.

Attribute	Definition	Standard
Color intensity	The overall intensity of wine color observed when tilting the glass 45° against a white background.	NA
Violet hue	The overall amount of violet hue of wine color observed when tilting the glass 45° against a white background.	NA
Red fruit	Overall red fruity aroma of the wine.	5 crushed fresh strawberries/L + 100 mL brine of canned cherries/L <sup>a</sup>
Jammy	Overall jammy character of the wine.	20 g/L of plum jam (Emeth, Buenos Aires, Argentina) <sup>a</sup>
Bitterness	The feeling of bitterness immediately after expectoration of the wine.	200 mg/L quinine sulfate (Sigma–Aldrich, Buenos Aires, Argentina) <sup>a</sup>
Astringency	The feeling of puckeriness or lack of lubrication sensation around the gums immediately after expectoration of the wine.	2.5 g/L tannic acid (Sigma–Aldrich, Buenos Aires, Argentina) <sup>a</sup>

NA: Not applicable.

<sup>a</sup> Standards prepared using as a base wine a 2008 Malbec wine.

otherwise, i.e. a positive sensory effect of CS + 100 mg L<sup>-1</sup> in color intensity and violet hue in Barbera D'Asti wines. This discrepancy pertains to the disagreement sometimes observed between chemical measurements of a given set of wines and the sensory response elicited by them. In this regard, new approaches such as sensomics appears as promising tools towards uncovering which chemical components of the wine matrix have a measurable sensory impact. From a practical standpoint, the use of higher SO<sub>2</sub> additions during CS seems advisable, notwithstanding the rather moderate sensory impact of CS. Furthermore, the application of CS would have to consider cost-related constraints as well as those imposed by current marketing and technological trends of low-input enology, and, in particular, lower additions of SO<sub>2</sub>.

## Appendix A. Supplementary data

Supplementary data related to this article can be found at <http://dx.doi.org/10.1016/j.lwt.2015.10.026>.

## References

- Álvarez, I., Aleixandre, J. L., García, M. J., & Lizama, V. (2006). Impact of pre-fermentative maceration on the phenolic and volatile compounds in Monastrell red wines. *Analytica Chimica Acta*, 563(1–2), 109–115.
- Bakker, J., Bridle, P., Bellworthy, S. J., Garcia-Viguera, C., Reader, H. P., & Watkins, S. J. (1998). Effect of sulphur dioxide and must extraction on colour, phenolic composition and sensory quality of red table wine. *Journal of the Science of Food and Agriculture*, 78(3), 297–307.
- Bakker, J., & Timberlake, C. F. (1997). Isolation, identification, and characterization of new color-stable anthocyanins occurring in some red wines. *Journal of Agricultural and Food Chemistry*, 45(1), 35–43.
- Boulton, R. B., Singleton, V. L., Bisson, L. F., & Kunkee, R. E. (1998). *Principles and practices of winemaking*. New York: Kluwer, Springer.
- Budic-Leto, I., Tomislav, L., & Vrhovsek, U. (2003). Influence of different maceration techniques and ageing on proanthocyanidins and anthocyanins of red wine cv. Babic (*Vitis vinifera* L.). *Food Technology and Biotechnology*, 41, 299–303.
- Casassa, L. F., Bolcato, E. A., & Sari, S. E. (2015). Chemical, chromatic, and sensory attributes of 6 red wines produced with prefermentative cold soak. *Food Chemistry*, 174(0), 110–118.
- Casassa, L. F., & Harbertson, J. F. (2014). Extraction, evolution, and sensory impact of phenolic compounds during red wine maceration. *Annual Review of Food Science and Technology*, 5(1), 83–109.
- Casassa, L. F., & Sari, S. E. (2014). Sensory and chemical effects of two alternatives of prefermentative cold soak in Malbec wines during winemaking and bottle ageing. *International Journal of Food Science & Technology*, 50(4), 1044–1055.
- Colonna, A. E., Adams, D. O., & Noble, A. C. (2004). Comparison of procedures for reducing astringency carry-over effects in evaluation of red wines. *Australian Journal of Grape and Wine Research*, 10(1), 26–31.
- Delteil, D. (2004). La Macération Préfermentaire à Froid (MPF) des raisins méditerranéens et rhodaniens. *Revue des Œnologues*, 112(112), 29–32.
- Dubourdieu, D., Grassin, C., Deruche, C., & Ribereau-Gayon, P. (1984). Mise au point d'une mesure rapide de l'activité laccase dans les moûts et dans les vins par la méthode à la syringaldazine. Application à l'appréciation de l'état sanitaire des vendanges. *Connaissance de la Vigne & du Vin*, 18, 237–252.
- Fanzone, M., Peña-Neira, A. L., Jofre, V., Assof, M., & Zamora, F. (2010). Phenolic characterization of Malbec wines from Mendoza province (Argentina). *Journal of Agricultural and Food Chemistry*, 58(4), 2388–2397.
- Gardner, D. M., Zoecklein, B. W., & Mallikarjunan, K. (2011). Electronic nose analysis of Cabernet Sauvignon (*Vitis vinifera* L.) grape and wine volatile differences during cold soak and postfermentation. *American Journal of Enology and Viticulture*, 62(1), 81–90.
- Gil-Muñoz, R., Moreno-Pérez, A., Vila-López, R., Fernández-Fernández, J., Martínez-Cutillas, A., & Gómez-Plaza, E. (2009). Influence of low temperature prefermentative techniques on chromatic and phenolic characteristics of Syrah and Cabernet Sauvignon wines. *European Food Research and Technology*, 228(5), 777–788.
- Gomes Rebello, L. P., Lago-Vanzela, E. S., Teixeira Barcia, M., Mota Ramos, A.,

- Stringheta, P. C., Da-Silva, R., et al. (2013). Phenolic composition of the berry parts of hybrid grape cultivar BRS Violeta (BRS Rubea × IAC 1398-21) using HPLC–DAD–ESI–MS/MS. *Food Research International*, 54(1), 356–366.
- González-Neves, G., Gil, G., Favre, G., & Ferrer, M. (2012). Influence of grape composition and winemaking on the anthocyanin composition of red wines of Tannat. *International Journal of Food Science & Technology*, 47(5), 900–909.
- Harbertson, J. F., Kennedy, J. A., & Adams, D. O. (2002). Tannin in skins and seeds of Cabernet Sauvignon, Syrah, and Pinot Noir berries during ripening. *American Journal of Enology and Viticulture*, 53(1), 54–59.
- Hierro, N., González, Á., Mas, A., & Guillamón, J. M. (2006). Diversity and evolution of non-Saccharomyces yeast populations during wine fermentation: effect of grape ripeness and cold maceration. *FEMS Yeast Research*, 6(1), 102–111.
- Instituto Nacional de Vitivinicultura (INV) - Argentinean Government. (2013). *Resolución mayo de 1938-Dirección Nacional de Química*.
- ISO. (1977). *Sensory analysis-apparatus: Wine tasting glass*, 3591 C.F.R.
- Ortega-Heras, M., Pérez-Magariño, S., & González-Sanjosé, M. L. (2012). Comparative study of the use of maceration enzymes and cold pre-fermentative maceration on phenolic and anthocyanic composition and colour of a Mencía red wine. *LWT – Food Science and Technology*, 48(1), 1–8.
- Parenti, A., Spugnoli, P., Calamai, L., Ferrari, S., & Gori, C. (2004). Effects of cold maceration on red wine quality from Tuscan Sangiovese grape. *European Food Research and Technology*, 218(4), 360–366.
- Parley, A., Vanhanen, L., & Heatherbell, D. (2001). Effects of pre-fermentation enzyme maceration on extraction and colour stability in Pinot Noir wine. *Australian Journal of Grape and Wine Research*, 7(3), 146–152.
- Pateraki, C., Paramithiotis, S., Doulgeraki, A., Kallithraka, S., Kotseridis, Y., & Drosinos, E. (2014). Effect of sulfur dioxide addition in wild yeast population dynamics and polyphenolic composition during spontaneous red wine fermentation from *Vitis vinifera* cultivar Agiorgitiko. *European Food Research and Technology*, 1–9.
- Pérez-Lamela, C., García-Falcón, M. S., Simal-Gándara, J., & Orriols-Fernández, I. (2007). Influence of grape variety, vine system and enological treatments on the colour stability of young red wines. *Food Chemistry*, 101(2), 601–606.
- Porter, L. J., Hrstich, L. N., & Chan, B. G. (1985). The conversion of procyanidins and prodelphinidins to cyanidin and delphinidin. *Phytochemistry*, 25(1), 223–230.
- Ribéreau-Gayon, P., Glories, Y., Maujean, A., & Dubourdieu, D. (2006). Handbook of enology. In *The chemistry of wine stabilization and treatments* (2nd ed., Vol. 2). Chichester, West Sussex, England: John Wiley & Sons Ltd.
- Stefanini, F. M., & Pantani, O. L. (2013). Bayesian model to compare vinification procedures. *Biometrical Letters*, 50(2), 61–80.



# Effect of rotating magnetic field and flowing $\text{Ca}^{2+}$ solution on calcium uptake rate of fresh-cut apple



Yamei Jin <sup>a, b</sup>, Na Yang <sup>b</sup>, Qunyi Tong <sup>b</sup>, Xueming Xu <sup>a, b, c, \*</sup>

<sup>a</sup> State Key Laboratory of Food Science and Technology, Jiangnan University, Wuxi 214122, Jiangsu Province, China

<sup>b</sup> School of Food Science and Technology, Jiangnan University, Wuxi 214122, Jiangsu Province, China

<sup>c</sup> Synergetic Innovation Center of Food Safety and Nutrition, Jiangnan University, Wuxi 214122, China

## ARTICLE INFO

### Article history:

Received 10 July 2015

Received in revised form

8 October 2015

Accepted 10 October 2015

Available online 22 October 2015

### Keywords:

Magnetic flux density

Reynolds number

Frequency

Calcium fortification

Fresh-cut apple

## ABSTRACT

The combination of a rotating perpendicular magnetic field and a flowing  $\text{Ca}^{2+}$  solution accelerated the calcium uptake of fresh-cut apple cubes and shortened the time needed for calcium equilibration between the  $\text{Ca}^{2+}$  solution and samples. The influence of operational parameters (Reynolds number of the flowing  $\text{Ca}^{2+}$  solution, magnetic flux density of the magnetic field, rotating frequency of the magnetic field, and temperature) on the calcium uptake rate were investigated. Negative exponential models were used to sufficiently describe the calcium uptake rate of samples. Magnetic flux density and temperature positively affected the calcium uptake rate. Higher Reynolds number and rotating frequency both accelerated the calcium diffusion, but excessively high levels (turbulent flowing at  $\text{Re} = 4134$  or rotating frequency at 10 Hz) decreased the calcium content. Neither the flowing  $\text{Ca}^{2+}$  solution alone, nor the magnetic field alone, accelerated the calcium diffusion. This study provides an alternative methodology for the mineral fortification of fresh-cut fruits under the joint action of a rotating magnetic field and a flowing electrolyte solution.

© 2015 Elsevier Ltd. All rights reserved.

## 1. Introduction

Calcium, an abundant essential mineral for life, plays an important role in physiological activities such as maintaining the normal muscle contraction, prevention of osteoporosis, and rickets (Ebashi & Endo, 1968; Ross, Taylor, Yaktine, & Del Valle, 2011). However, calcium deficiency is nearly a worldwide problem, due to either a lower intake than the recommended amount or incomplete absorption (Looker, 2006; Weaver, 2013). The mineral-fortification of foods has been considered as the most effective and safest approach for the supplement of calcium so far (Hurrell, 1997).

Fresh-cut fruits and vegetables have been popular in developed countries, and are also increasingly consumed in some developing countries for their convenience, attractive appearance, and nutritional value (Barrett, Beaulieu, & Shewfelt, 2010).

Vacuum impregnation has been widely used as a technique to obtain these mineral-fortified vegetables and fruits products rapidly (Fito et al., 2001; Zhao & Xie, 2004). Calcium enrichment of

fresh apple can be realized using vacuum impregnation, with a diluted high-fructose corn syrup containing calcium gluconate and calcium lactate, which improves the firmness of apple samples (Xie & Zhao, 2003). According to Moraga, Moraga, Fito, and Martínez-Navarrete (2009), the shelf-life of grapefruit is extended by impregnation with a calcium lactate solution, since the dehydration decreased the cellular respiration rate. Park, Kodihalli, and Zhao (2005) report that both the color and firmness of fresh-cut apple are excellently retained during 3-week of cold storage after fortification with  $10 \text{ g L}^{-1}$  calcium caseinate. Gras, Vidal, Betoret, Chiralt, and Fito (2003) find that calcium can significantly modify the mechanical behavior of eggplant and carrot with vacuum impregnation treatment, although no notable change is observed in oyster mushrooms. In order to obtain high-quality Ca-fortified fruits and vegetables, carbohydrates such as sucrose (Gras et al., 2003; Perez-Cabrera, Chafer, Chiralt, & Gonzalez-Martinez, 2011), fructose corn syrup (Lin, Leonard, Lederer, Traber, & Zhao, 2006), and honey (Park et al., 2005) can be added into the impregnating solutions.

A porosity range of 2%–30% is reported for most plant tissues (Derossi, De Pilli, & Severini, 2012). This porous structure allows ions and some small molecules to easily diffuse from the impregnating solution into plant materials. As an electrolyte solution flows

\* Corresponding author. State Key Laboratory of Food Science and Technology, Jiangnan University, Wuxi 214122, Jiangsu Province, China.

E-mail address: [xmxu@jiangnan.edu.cn](mailto:xmxu@jiangnan.edu.cn) (X. Xu).

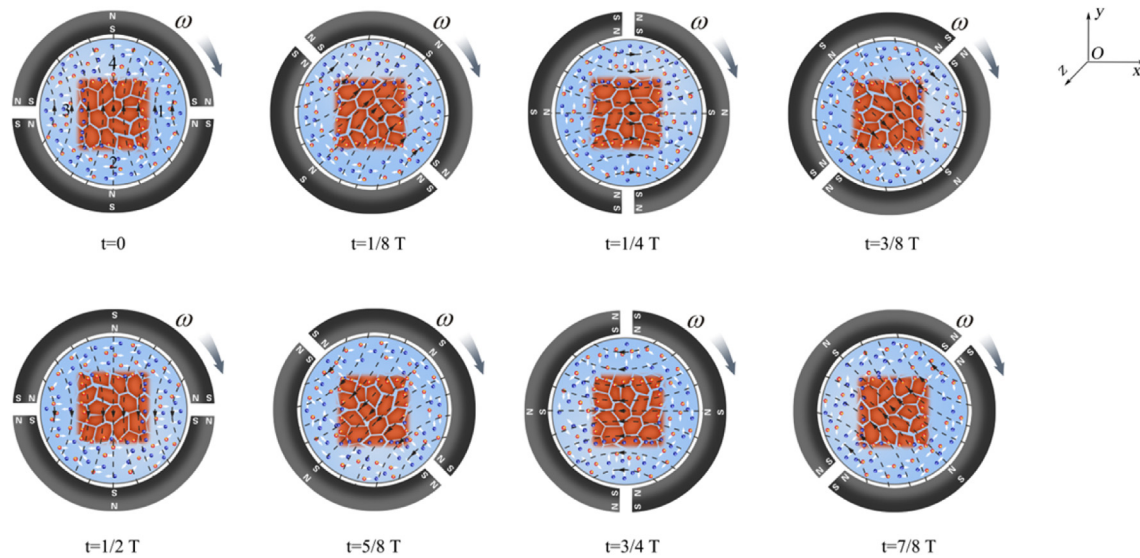


Fig. 1. The direction of Lorentz force on ions in one rotating period of the perpendicular magnetic field.

through a perpendicular magnetic field, the charged ions will experience Lorentz force,  $F_L$ , quantitatively expressed as  $F_L = qvB$ , where  $q$  is net ion charge,  $v$  is the ion velocity, and  $B$  is the magnetic flux density (Wright & Van Der Beken, 1972). In other words, under the action of a perpendicular magnetic field, orientation movement of free ions will occur, which could enhance mass transfer efficiency (Oshitani, Uehara, & Higashitani, 1999). As reported, induced voltage could be detected by a special detector as NaCl solution moved through a perpendicular magnetic field (Wright & Van Der Beken, 1972), indicating the existence of separation and orientation migration of cations and anions. That chemical reactions (e.g. electrolysis and electrolytic deposition) kinetic parameters were significantly influenced by the magnetic field were also observed. It was demonstrated that the effects of magnetic field on ionic conduction is related to ion variety, fluid flowing state (described by Reynolds number), magnetic flux density of magnetic field, and rotating frequency of magnetic field (Devos et al., 2000; Monzon & Coey, 2014).

Few data on the calcium fortification of fruits and vegetables with the combination of magnetic field and flowing minerals solution have been reported, which promises to be an important area of study. Therefore, the objective of this study was to propose an alternative method that combined a perpendicular magnetic field with a flowing  $\text{Ca}^{2+}$  solution to accomplish the calcium fortification of fresh-cut apple cubes. The effects of operating parameters (Reynolds number of the flowing  $\text{Ca}^{2+}$  solution, magnetic flux

density of the magnetic field, rotating frequency of the magnetic field, and temperature) on calcium content of fresh-cut apples were investigated, and calcium uptake of fresh-cut apples was also analyzed by the negative exponential equation to verify the effectiveness of this method.

## 2. Materials and methods

### 2.1. Experimental principle and instruments

In one period,  $T$ , of the rotating magnetic field, the Lorentz force of moving ions and the movement direction of ions are summarized in Fig. 1 and Table 1. Hypothesizing that the electrolyte solution flows in  $z$ -direction and the magnets rotate in a clockwise direction; charged ions will experience the Lorentz force with varying directions, which can be predicted using Fleming's left hand rule. For example, when  $t = 0$ , cations are subject to the Lorentz force in  $-x$ -direction and then forced to gather towards side 1 of the sample. On the contrary, anions are subject to the Lorentz force in  $x$ -direction and forced to gather towards side 3 (Fig. 1  $t = 0$ ). As a whole, both the cations and anions can diffuse and accumulate on each side of samples as the  $\text{Ca}^{2+}$  solution flows through the rotating magnetic field. When a static magnetic field is applied on the flowing electrolyte solution, cations and anions will be forced to accumulate only on fixed sides of samples rather than on each side consecutively.

Table 1  
The direction of Lorentz force of free ions in one rotating period.

Time	Cations		Anions	
	The direction of Lorentz force	Ionic gathering sides of sample	The direction of Lorentz force	Ionic gathering sides of sample
$t = 0$	$-x$	1	$x$	3
$t = 1/8 T$	$(-x, y)$	1,2	$(x, -y)$	3,4
$t = 1/4 T$	$y$	1,2	$-y$	3,4
$t = 3/8 T$	$(x, y)$	2,3	$(-x, -y)$	1,4
$t = 1/2 T$	$x$	3	$-x$	1
$t = 5/8 T$	$(x, -y)$	3,4	$(-x, y)$	1,2
$t = 3/4 T$	$-y$	3,4	$y$	1,2
$t = 7/8 T$	$(-x, -y)$	1,4	$(x, y)$	2,3

$T$ , period of the rotating magnetic field.

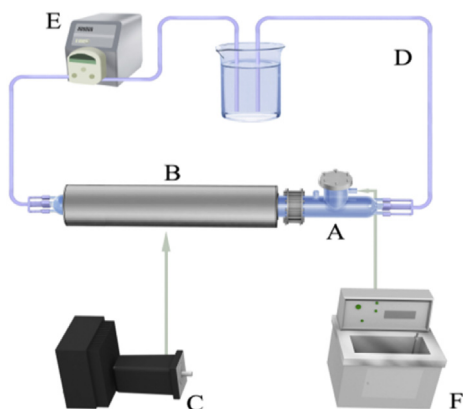


**Fig. 2.** The apparatus of magnetic-field-assisted calcium fortification system: (A) glass chamber, (B) perpendicular magnetic field, (C) servomotor, (D) the supporting pipeline, (E) peristaltic pump, (F) constant-temperature circulating water bath.

The experimental system, illustrated in Fig. 2, consists of a glass chamber (A), perpendicular magnetic field (B), a servomotor (C), a supporting pipeline (D), a peristaltic pump (E), and a constant-temperature circulating water bath (F). The perpendicular magnetic field was generated by eight semicircle neodymium magnets with inner diameter of 70 mm, external diameter of 90 mm (Fig. 3a), and individual length of 80 mm. The magnetic field lines distribution in one pair of magnets (Fig. 3b) was modeled using the simulation software at the AC/DC module of Comsol Multiphysics 4.4b (COMSOL Co. Ltd., Shanghai, China). Samples were placed in the area of the uniform magnetic field.

## 2.2. Raw materials and treatments

Fresh 'Fuji' apples ( $12.16 \pm 0.35$  °Brix) with similar diameter and apparent ripeness were purchased from Wal-Mart supermarket (Wuxi, China). The central section of the apples was removed and the remaining parts were washed, peeled, and then cut into square cubes ( $20 \text{ mm} \times 20 \text{ mm} \times 20 \text{ mm}$ ). An isotonic solution (11.2 g sucrose and 4.4 g calcium lactate per 100 g  $\text{H}_2\text{O}$ ) was used as the impregnating solution (Barrera, Betoret, & Fito, 2004).

About 200 g of apple cubes were collected in two mesh bags and placed in the center of the glass chamber inside the perpendicular magnetic field (Fig. 4). Then, under the drive of the peristaltic pump (BT100S, Baoding Lead Fluid Technology Co. Ltd., Baoding, China), 6000 g of the  $\text{Ca}^{2+}$  solution filled the pipeline and chamber. The treatment parameters in the apple-cube calcium fortification were set as follows: Reynolds number of the flowing  $\text{Ca}^{2+}$  solution ( $Re = 563, 1127, \text{ and } 4134$ ), magnetic flux density of the magnetic field ( $B = 0.09 \text{ and } 0.13 \text{ T}$ ), rotating frequency of the magnetic field ( $f = 1, 5, \text{ and } 10 \text{ Hz}$ ), and temperature ( $T = 5, 10, 15, \text{ and } 30 \text{ }^\circ\text{C}$ ). Specific Reynolds number was regulated by changing the rotation rate of the peristaltic pump.  $B = 0.09 \text{ T}$  and  $0.13 \text{ T}$  was controlled by N38-type and N50-type magnets, respectively. The rotating frequency of the magnetic field was controlled by the operating speed of the servomotor. Processing temperature was maintained by the constant-temperature circulating water bath.

Reynolds number was calculated according to Equation (1) (Miller, 1989).

$$Re = \rho \bar{v} D / \eta \quad (1)$$

where  $Re$  is Reynolds number,  $\rho$  is the density of the fluid ( $\text{kg m}^{-3}$ ),  $\bar{v}$  is the mean velocity of the fluid ( $\text{m s}^{-1}$ ),  $D$  is the inner diameter of

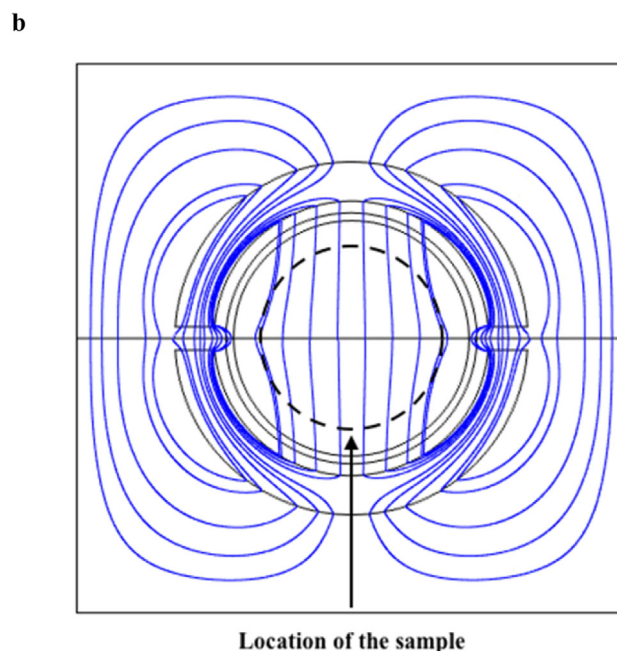


**Fig. 3.** Layout of the magnetic field area, (a) neodymium magnet; (b) magnetic field lines distribution and magnetic flux density in the opposing pole magnets.

the supporting pipeline (m), and  $\eta$  is the dynamic viscosity of the fluid ( $\text{kg} \cdot (\text{m s})^{-1}$ ).  $\bar{v}$  was converted by the volume flow rate,  $\rho$  was calculated as the ratio of mass to volume and  $\eta$  was measured using a Brookfield viscometer (LVDV-C, Brookfield, Stoughton, USA).

As a control process, the apple samples were just statically immersed in the  $\text{Ca}^{2+}$  solution. All the variables and levels for treatments are shown in Table 2.

## 2.3. Calcium content measurements and modeling

The calcium content in apple cubes was determined after 0, 30, 60, 90, 120, 150, 180, 240, 300, 420, and 540 min treatments referring to the method described by Park et al. (2005). The Ca-fortified products were cut into pieces in ceramic crucibles and previously dried at  $105 \text{ }^\circ\text{C}$  for 18 h in a forced-air oven. Then the

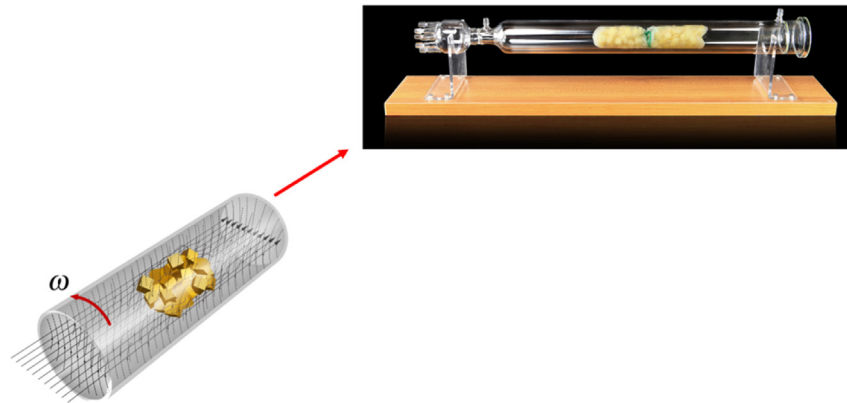


Fig. 4. The location of samples in a glass chamber for calcium fortification.

**Table 2**  
Variables and levels for calcium fortification treatments of fresh-cut apple.

Treatments	Variables				
	Re	B (T)	f (Hz)	T (°C)	
Static immersion	–	–	–	5, 10, 15, 30	
Flowing Ca <sup>2+</sup> solution	563	–	–	5, 10, 15, 30	
	1127	–	–	5, 10, 15, 30	
	4134	–	–	5, 10, 15, 30	
	–	–	–	5, 10, 15, 30	
Magnetic field	–	0.09	–	5, 10, 15, 30	
	–	0.13	–	5, 10, 15, 30	
	–	0.09	1	5, 10, 15, 30	
	–	0.09	5	5, 10, 15, 30	
	–	0.09	10	5, 10, 15, 30	
	–	0.13	1	5, 10, 15, 30	
	–	0.13	5	5, 10, 15, 30	
	–	0.13	10	5, 10, 15, 30	
	–	0.13	–	5, 10, 15, 30	
	–	0.13	–	5, 10, 15, 30	
Combination of rotating magnetic field and flowing Ca <sup>2+</sup> solution	563	0.09	–	5, 10, 15, 30	
	563	0.13	–	5, 10, 15, 30	
	1127	0.09	–	5, 10, 15, 30	
	1127	0.13	–	5, 10, 15, 30	
	4134	0.09	–	5, 10, 15, 30	
	4134	0.13	–	5, 10, 15, 30	
	563	0.09	1	5, 10, 15, 30	
	563	0.09	5	5, 10, 15, 30	
	563	0.09	10	5, 10, 15, 30	
	563	0.13	1	5, 10, 15, 30	
	563	0.13	5	5, 10, 15, 30	
	563	0.13	10	5, 10, 15, 30	
	1127	0.09	1	5, 10, 15, 30	
	1127	0.09	5	5, 10, 15, 30	
	1127	0.09	10	5, 10, 15, 30	
	1127	0.13	1	5, 10, 15, 30	
	1127	0.13	5	5, 10, 15, 30	
	1127	0.13	10	5, 10, 15, 30	
	Combination of rotating magnetic field and flowing Ca <sup>2+</sup> solution	4134	0.09	1	5, 10, 15, 30
		4134	0.09	5	5, 10, 15, 30
4134		0.09	10	5, 10, 15, 30	
4134		0.13	1	5, 10, 15, 30	
4134		0.13	5	5, 10, 15, 30	
4134		0.13	10	5, 10, 15, 30	
4134		0.13	–	5, 10, 15, 30	
4134		0.13	–	5, 10, 15, 30	

Re, Reynolds number of the flowing Ca<sup>2+</sup> solution; B, magnetic flux density of the magnetic field; f, rotating frequency of the magnetic field; T, temperature. Re = 563 and 1127 (Laminar flowing), Re = 4134 (Turbulent flowing).

dried samples were digested at 550 °C in a muffle furnace for 5 h. After cooling, the ashes were dissolved in 20 g L<sup>-1</sup> lanthanum oxide solutions for analysis by atomic absorption spectrometry (TAS-986, Beijing Purinje General Instrument Co. Ltd., Beijing, China) at wavelength of 422.7 nm.

The calcium uptake of apple cubes was modeled by a negative exponential model (Ørskov & McDonald, 1979; Quintero-Chávez

et al., 2012).

$$Y(t) = a + b[1 - \exp(-kt)] \quad (2)$$

where  $Y(t)$  is the calcium content (10<sup>-2</sup> mg g<sup>-1</sup>) in apple cubes estimated at the processing time,  $t$ .  $a$  is the initial calcium content (10<sup>-2</sup> mg g<sup>-1</sup>) in the samples at  $t = 0$ .  $b$  is the potential calcium

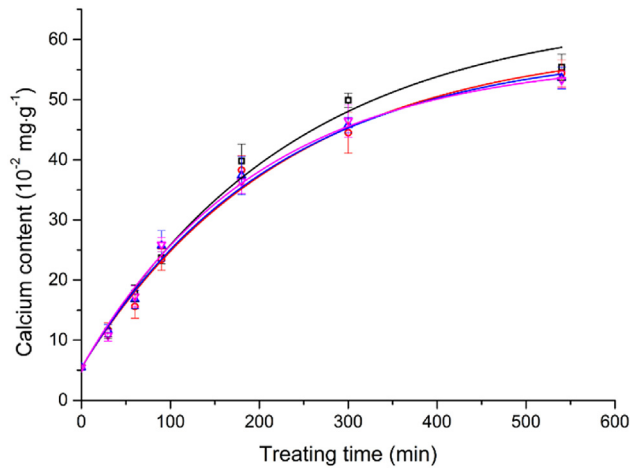


**Fig. 5.** Calcium content in fresh-cut apple cubes treated with Static immersion (■) or flowing  $\text{Ca}^{2+}$  solution ( $Re = 563$  (●);  $Re = 1127$  (▲);  $Re = 4134$  (▼)) at temperature of  $15\text{ }^{\circ}\text{C}$ .  $Re$  is Reynolds number of the flowing  $\text{Ca}^{2+}$  solution.

content ( $10^{-2}\text{ mg g}^{-1}$ ) in the samples.  $k$  is the rate constant ( $\text{min}^{-1}$ ) of the calcium uptake. Determination coefficient  $R^2$  and root mean square error RMSE ( $10^{-2}\text{ mg g}^{-1}$ ) were used for judging the qualities of models.

#### 2.4. Statistical analysis

Every parallel experiment was run in triplicate. The results were analyzed using SPSS 16.0 software (SPSS, Inc., Chicago, IL, USA). One-way analysis of variance was used to analyze data, and Duncan's multiple range tests were conducted to determine differences between the means. Results were considered statistically significant at  $P < 0.05$ .

### 3. Results and discussion

Fig. 5 shows the changes of calcium content in the apple cubes treated by flowing  $\text{Ca}^{2+}$  solution without magnetic field, with the static immersion treatment as comparison ( $T = 15\text{ }^{\circ}\text{C}$ ). The model parameters of the treatments for calcium uptake in apple samples calculated by the negative exponential regressions are summarized in Table 3. Relatively high  $R^2$  and low RMSE indicated a desirable quality of the model to describe the mass transport. The calcium uptake rate constants of flowing  $\text{Ca}^{2+}$  immersion treatment were lower than that of static immersion treatment, which indicated that the flowing of  $\text{Ca}^{2+}$  solution had a negative effect on calcium diffusion into apple tissues. This phenomenon was similar to the interference of rollover or high-speed agitation on vegetables pickling. According to Capaccioni, Casales, and Yeannes (2011), the agitation at 50 rpm significantly decreases the salt content of the marinated *Engraulis anchoita* filets and much too high hydrodynamic power impedes the ion diffusion.

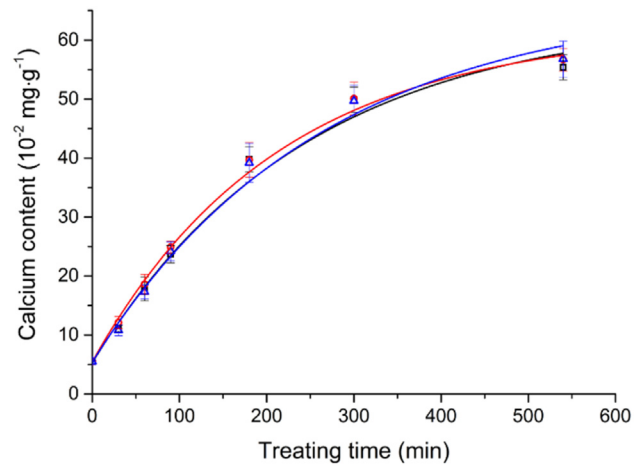


**Fig. 6.** Calcium content in fresh-cut apple cubes treated with static immersion (■) or magnetic field (static magnetic field,  $B = 0.13\text{ T}$  (●); rotating magnetic field,  $B = 0.13\text{ T}$ ,  $f = 5\text{ Hz}$  (▲)) at temperature of  $15\text{ }^{\circ}\text{C}$ .  $B$  is the magnetic flux density of the magnetic field, and  $f$  is the rotating frequency of the magnetic field.

The calcium content in apple cubes that were treated by static immersion, static magnetic field, and rotating magnetic field at temperature of  $15\text{ }^{\circ}\text{C}$  are illustrated in Fig. 6. The model parameters for calcium uptake of samples are listed in Table 4. No significant difference in calcium content of apple samples occurred during these three processes. The magnetic field treatment alone did not accelerate the mass transfer significantly.

Fig. 7 and Table 5 present the changes of calcium content and the parameters for calcium uptake models of the apple cubes that were treated by the combination of magnetic field and flowing  $\text{Ca}^{2+}$  solution ( $T = 15\text{ }^{\circ}\text{C}$ ). Higher calcium uptake rate constants and more rapid calcium equilibriums between samples and solutions were achieved under the joint action of magnetic field and flowing  $\text{Ca}^{2+}$  solution, in comparison with the static immersion treatment. The calcium uptake rate constants of these process were  $5.17 \times 10^{-3}\text{ min}^{-1}$ ,  $6.05 \times 10^{-3}\text{ min}^{-1}$ ,  $7.56 \times 10^{-3}\text{ min}^{-1}$ ,  $8.35 \times 10^{-3}\text{ min}^{-1}$  and  $13.30 \times 10^{-3}\text{ min}^{-1}$ , respectively. The rotating magnetic field compared with a static one resulted in a significant rise in increase of the calcium uptake rate. The reason for this rise is that the electromotive force, induced by the directional variation of the magnetic flux density, enhanced the ionic conduction in the sample-solution system (Dehel, Dickinson, Lorge, & Startzel, 2007; Oshitani et al., 1999; Volpe & Eremenko, 2007). In addition, the larger magnetic flux density a magnetic field had, the higher the calcium uptake rate constant was. According to equation  $F_L = qvB$  (Wright & Van Der Beken, 1972), a larger Lorentz force,  $F_L$ , was induced by a greater magnetic flux density to force the orientation of moving free ions to change drastically.

On the basis of the above results, the combination of a rotating magnetic field and the flowing  $\text{Ca}^{2+}$  solution was effective to accelerate the diffusion of  $\text{Ca}^{2+}$  into apple tissues. Then the effects

**Table 3**

Parameters of the negative exponential models for calcium uptake of apple cubes treated with static immersion or flowing  $\text{Ca}^{2+}$  solution at temperature of  $15\text{ }^{\circ}\text{C}$ .

Fortification treatments ( $T = 15\text{ }^{\circ}\text{C}$ )	$a$ ( $10^{-2}\text{ mg g}^{-1}$ )	$b$ ( $10^{-2}\text{ mg g}^{-1}$ )	$k$ ( $10^{-3}\text{ min}^{-1}$ )	$R^2$	RMSE ( $10^{-2}\text{ mg g}^{-1}$ )
Static immersion	3.82	56.41	5.17	0.96	1.46
$Re = 563$	3.68	54.08	5.04	0.95	1.58
$Re = 1127$	5.31	51.78	5.11	0.98	1.86
$Re = 4134$	3.12	52.66	4.91	0.95	1.08

$Re$ , Reynolds number of the flowing  $\text{Ca}^{2+}$  solution;  $T$ , temperature;  $a$ , the initial calcium content in the samples at  $t = 0$ ;  $b$ , the potential calcium content;  $k$ , the rate constant of the calcium uptake;  $R^2$ , determination coefficient; RMSE, root mean square error.

**Table 4**

Parameters of the negative exponential models for calcium uptake of apple cubes treated with static immersion or magnetic field at temperature of 15 °C.

Fortification treatments ( $T = 15\text{ }^{\circ}\text{C}$ )	$a$ ( $10^{-2}\text{ mg g}^{-1}$ )	$b$ ( $10^{-2}\text{ mg g}^{-1}$ )	$k$ ( $10^{-3}\text{ min}^{-1}$ )	$R^2$	RMSE ( $10^{-2}\text{ mg g}^{-1}$ )
Static immersion	3.82	56.41	5.17	0.96	1.46
$B = 0.13\text{ T}$	4.41	56.46	5.13	0.94	1.10
$B = 0.13\text{ T}, f = 5\text{ Hz}$	4.59	56.63	5.24	0.95	2.11

$B$ , magnetic flux density of the magnetic field;  $f$ , rotating frequency of the magnetic field;  $T$ , temperature;  $a$ , the initial calcium content in the samples at  $t = 0$ ;  $b$ , the potential calcium content;  $k$ , the rate constant of the calcium uptake;  $R^2$ , determination coefficient; RMSE, root mean square error.

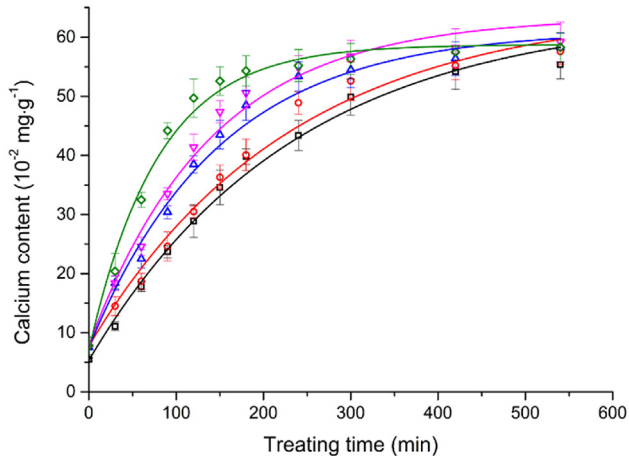


**Fig. 7.** Comparison of calcium fortification effectiveness between joint actions of 1) static magnetic field and flowing  $\text{Ca}^{2+}$  solution and 2) rotating magnetic field and flowing  $\text{Ca}^{2+}$  solution at temperature of 15 °C: Static immersion ( $\blacksquare$ );  $B = 0.09\text{ T}$ ,  $Re = 563$  ( $\bullet$ );  $B = 0.13\text{ T}$ ,  $Re = 563$  ( $\blacktriangle$ );  $B = 0.09\text{ T}$ ,  $Re = 563$ ,  $f = 5\text{ Hz}$  ( $\blacktriangledown$ );  $B = 0.13\text{ T}$ ,  $Re = 563$ ,  $f = 5\text{ Hz}$  ( $\blacklozenge$ ).  $B$  is the magnetic flux density of the magnetic field,  $f$  is the rotating frequency of the magnetic field, and  $Re$  is Reynolds number of the flowing  $\text{Ca}^{2+}$  solution.

of rotating frequency of the rotating magnetic field, Reynolds number of the flowing  $\text{Ca}^{2+}$  solution, and the treatment temperature on the calcium uptake of apple samples were explored, with the results presented in Fig. 8 and Table 6.

Fig. 8a shows an increase in calcium content in the samples with the rotating frequency of magnetic field rising from 1 Hz to 5 Hz. However, lower calcium contents were observed at 10 Hz. Accordingly, the calcium uptake constants at 1 Hz, 5 Hz, and 10 Hz were  $8.95 \times 10^{-3}$ ,  $16.0 \times 10^{-3}$ , and  $6.75 \times 10^{-3}\text{ min}^{-1}$  (Table 6), respectively, when the magnetic flux density was 0.13 T, Reynolds number was 1127, and temperature was 15 °C. According to Faraday's law of electromagnetic induction, the electromotive force is positively correlated with the varying rate of magnetic flux density, which enhances ionic conduction effect and diffusion coefficient. However, as a large amount of charged solutes were subjected to overlarge electromotive force, turbulence in a laminar flow solution

would occur and reduce the effectiveness of mass transfer, thereby lowering the calcium uptake rate constant (Dehel et al., 2007; Oshitani et al., 1999; Volpe & Eremenko, 2007).

A similar effect of frequency of the electric field on the diffusion coefficients of beet dye during their brining with a moderate electric field is described by Kulshrestha and Sastry (2003). The diffusion coefficient increased initially and then decreased with the frequency increasing from 0 to 5000 Hz. The most rapid diffusion was obtained at the frequency of 10 Hz and at the electric field intensity of 23.9 V/cm.

The calcium contents in apple cubes at different Reynolds number,  $Re$ , are presented in Fig. 8b. Under operating conditions of  $B = 0.13\text{ T}$ ,  $f = 5\text{ Hz}$ , and  $T = 15\text{ }^{\circ}\text{C}$ ,  $Re = 563$  and 1127 (but not 4134) both resulted in significant increase ( $P < 0.05$ ) of calcium content in fresh-cut apples (Fig. 8b) and the calcium uptake rate constant (Table 6), in comparison to the conventional static immersion. Too high hydrodynamic force interfered with the diffusion of  $\text{Ca}^{2+}$  into the samples. Thus, we supposed that there was a threshold Reynolds number, below which higher velocity of the  $\text{Ca}^{2+}$  solution could accelerate calcium diffusion much more significantly.

Increasing temperature from 5 to 30 °C led to increase in both mass transfer efficiency and equilibrium calcium content (Fig. 8c and Table 6). These increments were attributed to the high ionic mobility at high temperature. Other vegetable materials, such as potato and Chinese water chestnut, also have higher salt diffusion coefficients when they are brined at higher temperature (Liu, 1992; Sarang & Sastry, 2007). As a whole, the calcium uptake rate was maximized to  $17.2 \times 10^{-3}\text{ min}^{-1}$  at following conditions:  $Re = 1127$ ,  $f = 5\text{ Hz}$ ,  $B = 0.13\text{ T}$ , and  $T = 30\text{ }^{\circ}\text{C}$ .

#### 4. Conclusions

The combination of a rotating perpendicular magnetic field and a flowing  $\text{Ca}^{2+}$  solution on fresh-apples led to an increased calcium uptake rate and a shorter calcium equilibration time, according to the negative exponential modeling results. Thus, this study provides an alternative methodology for ion enrichment in porous food materials under the joint action of a rotating perpendicular magnetic field and a flowing electrolyte solution. Analysis of processing efficiency and economic benefits of this methodology will be considered in further application.

**Table 5**Comparison of calcium fortification effectiveness between joint treatments with 1) static magnetic field and flowing  $\text{Ca}^{2+}$  solution and 2) rotating magnetic field and flowing  $\text{Ca}^{2+}$  solution at temperature of 15 °C.

Fortification treatments ( $T = 15\text{ }^{\circ}\text{C}$ )	$a$ ( $10^{-2}\text{ mg g}^{-1}$ )	$b$ ( $10^{-2}\text{ mg g}^{-1}$ )	$k$ ( $10^{-3}\text{ min}^{-1}$ )	$R^2$	RMSE ( $10^{-2}\text{ mg g}^{-1}$ )
Static immersion	3.82	56.41	5.17	0.96	1.46
$B = 0.09\text{ T}$ , $Re = 563$	5.95	56.92	6.05	0.96	1.95
$B = 0.13\text{ T}$ , $Re = 563$	6.31	53.68	7.56	0.95	2.16
$B = 0.09\text{ T}$ , $Re = 563$ , $f = 5\text{ Hz}$	6.59	54.32	8.35	0.98	2.16
$B = 0.13\text{ T}$ , $Re = 563$ , $f = 5\text{ Hz}$	5.99	52.30	13.30	0.94	2.33

$B$ , magnetic flux density of the magnetic field;  $f$ , rotating frequency of the magnetic field;  $Re$ , Reynolds number of the flowing  $\text{Ca}^{2+}$  solution;  $T$ , temperature;  $a$ , the initial calcium content in the samples at  $t = 0$ ;  $b$ , the potential calcium content;  $k$ , the rate constant of the calcium uptake;  $R^2$  is determination coefficient; RMSE is root mean square error.

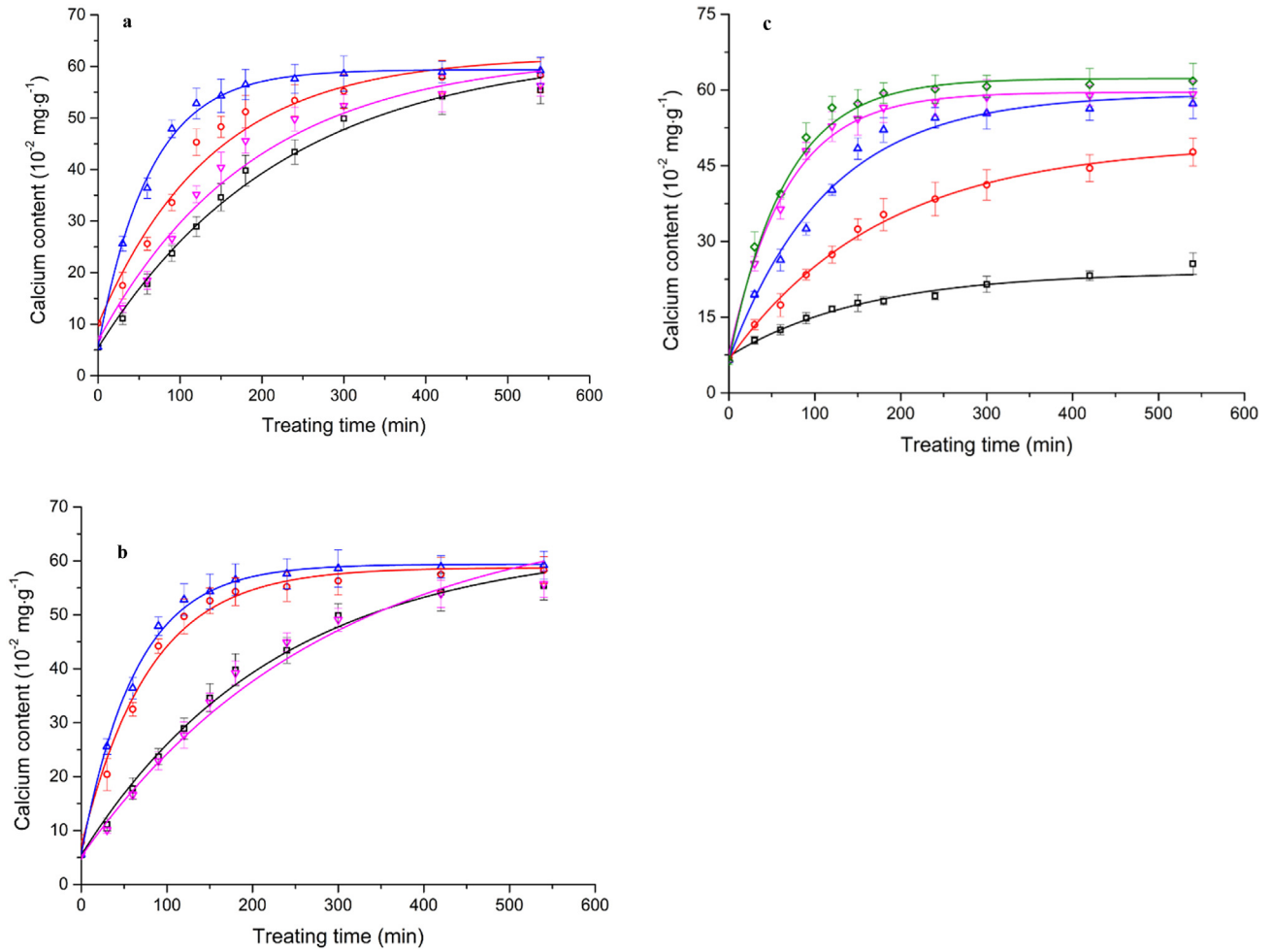


**Fig. 8.** Calcium content in fresh-cut apple cubes under the joint treatments of rotating magnetic field and flowing  $\text{Ca}^{2+}$  solution. (a) Effect of frequency,  $f$  (static immersion,  $T = 15\text{ }^\circ\text{C}$  ( $\blacksquare$ ):  $f = 1\text{ Hz}$ ,  $B = 0.13\text{ T}$ ,  $Re = 1127$ ,  $T = 15\text{ }^\circ\text{C}$  ( $\circ$ );  $f = 5\text{ Hz}$ ,  $B = 0.13\text{ T}$ ,  $Re = 1127$ ,  $T = 15\text{ }^\circ\text{C}$  ( $\blacktriangle$ );  $f = 10\text{ Hz}$ ,  $B = 0.13\text{ T}$ ,  $Re = 1127$ ,  $T = 15\text{ }^\circ\text{C}$  ( $\blacktriangledown$ )). (b) Effect of Reynolds number,  $Re$  (static immersion,  $T = 15\text{ }^\circ\text{C}$  ( $\blacksquare$ );  $Re = 563$ ,  $B = 0.13\text{ T}$ ,  $f = 5\text{ Hz}$ ,  $T = 15\text{ }^\circ\text{C}$  ( $\circ$ );  $Re = 1127$ ,  $B = 0.13\text{ T}$ ,  $f = 5\text{ Hz}$ ,  $T = 15\text{ }^\circ\text{C}$  ( $\blacktriangle$ );  $Re = 4134$ ,  $B = 0.13\text{ T}$ ,  $f = 5\text{ Hz}$ ,  $T = 15\text{ }^\circ\text{C}$  ( $\blacktriangledown$ )). (c) Effect of temperature,  $T$  (static immersion,  $T = 5\text{ }^\circ\text{C}$  ( $\blacksquare$ );  $B = 0.13\text{ T}$ ,  $f = 5\text{ Hz}$ ,  $Re = 1127$ ,  $T = 5\text{ }^\circ\text{C}$  ( $\circ$ );  $B = 0.13\text{ T}$ ,  $f = 5\text{ Hz}$ ,  $Re = 1127$ ,  $T = 10\text{ }^\circ\text{C}$  ( $\blacktriangle$ );  $B = 0.13\text{ T}$ ,  $f = 5\text{ Hz}$ ,  $Re = 1127$ ,  $T = 15\text{ }^\circ\text{C}$  ( $\blacktriangledown$ );  $B = 0.13\text{ T}$ ,  $f = 5\text{ Hz}$ ,  $Re = 1127$ ,  $T = 30\text{ }^\circ\text{C}$  ( $\blacklozenge$ )).  $B$  is the magnetic flux density of the magnetic field,  $f$  is the rotating frequency of the magnetic field,  $Re$  is Reynolds number of the flowing  $\text{Ca}^{2+}$  solution and  $T$  is temperature.

**Table 6**  
Regression coefficients for calcium uptake of apple cubes treated with the combination of rotating magnetic field and flowing  $\text{Ca}^{2+}$  solution.

Fortification treatments	$a$ ( $10^{-2}\text{ mg g}^{-1}$ )	$b$ ( $10^{-2}\text{ mg g}^{-1}$ )	$k$ ( $10^{-3}\text{ min}^{-1}$ )	$R^2$	RMSE ( $10^{-2}\text{ mg g}^{-1}$ )
$B = 0.13\text{ T}$ , $f = 1\text{ Hz}$ , $Re = 1127$ , $T = 15\text{ }^\circ\text{C}$	7.41	52.19	8.95	0.94	3.13
$B = 0.13\text{ T}$ , $f = 5\text{ Hz}$ , $Re = 1127$ , $T = 15\text{ }^\circ\text{C}$	5.18	54.09	16.0	0.97	1.25
$B = 0.13\text{ T}$ , $f = 10\text{ Hz}$ , $Re = 1127$ , $T = 15\text{ }^\circ\text{C}$	4.19	54.84	6.75	0.96	2.93
$B = 0.13\text{ T}$ , $f = 5\text{ Hz}$ , $Re = 563$ , $T = 15\text{ }^\circ\text{C}$	5.99	52.30	13.3	0.94	2.33
$B = 0.13\text{ T}$ , $f = 5\text{ Hz}$ , $Re = 1127$ , $T = 15\text{ }^\circ\text{C}$	5.18	54.09	16.0	0.97	1.25
$B = 0.13\text{ T}$ , $f = 5\text{ Hz}$ , $Re = 4134$ , $T = 15\text{ }^\circ\text{C}$	3.19	57.82	4.98	0.98	1.91
Static immersion, $T = 5\text{ }^\circ\text{C}$	7.65	18.23	5.01	0.94	0.63
$B = 0.13\text{ T}$ , $f = 5\text{ Hz}$ , $Re = 1127$ , $T = 5\text{ }^\circ\text{C}$	6.18	42.76	5.88	0.95	0.91
$B = 0.13\text{ T}$ , $f = 5\text{ Hz}$ , $Re = 1127$ , $T = 10\text{ }^\circ\text{C}$	5.56	53.18	9.35	0.97	1.41
$B = 0.13\text{ T}$ , $f = 5\text{ Hz}$ , $Re = 1127$ , $T = 15\text{ }^\circ\text{C}$	5.18	54.09	16.0	0.97	1.25
$B = 0.13\text{ T}$ , $f = 5\text{ Hz}$ , $Re = 1127$ , $T = 30\text{ }^\circ\text{C}$	6.10	55.46	17.2	0.97	1.32

$B$ , magnetic flux density of the magnetic field;  $f$ , rotating frequency of the magnetic field;  $Re$ , Reynolds number of the flowing  $\text{Ca}^{2+}$  solution;  $T$ , temperature;  $a$ , the initial calcium content in the samples at  $t = 0$ ;  $b$ , the potential calcium content;  $k$ , the rate constant of the calcium uptake;  $R^2$  is determination coefficient; RMSE is root mean square error.

**Acknowledgments**

This work was financially supported by National “Twelfth Five-Year” Plan for Science & Technology Support of China (Nos.

2012BAD37B01), the Doctor Candidate Foundation of Jiangnan University (Nos. KYLX\_1166).

## References

- Barrera, C., Betoret, N., & Fito, P. (2004).  $\text{Ca}^{2+}$  and  $\text{Fe}^{2+}$  influence on the osmotic dehydration kinetics of apple slices (var. Granny Smith). *Journal of Food Engineering*, 65(1), 9–14.
- Barrett, D. M., Beaulieu, J. C., & Shewfelt, R. (2010). Color, flavor, texture, and nutritional quality of fresh-cut fruits and vegetables: desirable levels, instrumental and sensory measurement, and the effects of processing. *Critical Reviews in Food Science and Nutrition*, 50(5), 369–389.
- Capaccioni, M. E., Casales, M. R., & Yeannes, M. I. (2011). Acid and salt uptake during the marinading process of *Engraulis anchoita* filets influence of the solution: fish ratio and agitation. *Food Science and Technology (Campinas)*, 31(4), 884–890.
- Dehel, T. F., Dickinson, M., Lorge, F., & Startzel, R. (2007). Electric field and Lorentz force contribution to atmospheric vortex phenomena. *Journal of Electrostatics*, 65(10), 631–638.
- Derossi, A., De Pilli, T., & Severini, C. (2012). The application of vacuum impregnation techniques in food industry. In B. Valdez (Ed.), *Scientific, health and social aspects of the food industry* (pp. 25–56). Croatia: InTech.
- Devos, O., Aaboubi, O., Chopart, J. P., Olivier, A., Gabrielli, C., & Tribollet, B. (2000). Is there a magnetic field effect on electrochemical kinetics? *The Journal of Physical Chemistry A*, 104(7), 1544–1548.
- Ebashi, S., & Endo, M. (1968). Calcium and muscle contraction. *Progress in Biophysics and Molecular Biology*, 18, 123–183.
- Fito, P., Chiralt, A., Betoret, N., Gras, M., Chafer, M., Martínez-Monzo, J., et al. (2001). Vacuum impregnation and osmotic dehydration in matrix engineering: application in functional fresh food development. *Journal of Food Engineering*, 49, 175–183.
- Gras, M. L., Vidal, D., Betoret, N., Chiralt, A., & Fito, P. (2003). Calcium fortification of vegetables by vacuum impregnation interactions with cellular matrix. *Journal of Food Engineering*, 56, 279–284.
- Hurrell, R. F. (1997). Preventing iron deficiency through food fortification. *Nutrition Reviews*, 55(6), 210–222.
- Kulshrestha, S., & Sastry, S. (2003). Frequency and voltage effects on enhanced diffusion during moderate electric field (MEF) treatment. *Innovative Food Science and Emerging Technologies*, 4(2), 189–194.
- Lin, D. S., Leonard, S. W., Lederer, C., Traber, M. G., & Zhao, Y. (2006). Retention of fortified vitamin E and sensory quality of fresh-cut pears by vacuum impregnation with honey. *Journal of Food Science*, 71(7), S553–S559.
- Liu, H. (1992). A kinetic study of salt diffusion in potato at high temperature. *International Journal of Food Science and Technology*, 27(4), 443–455.
- Looker, A. C. (2006). Dietary calcium intake. In C. M. Weaver, & R. P. Heaney (Eds.), *Calcium in human health* (pp. 105–127). Totawa: Humana Press.
- Miller, R. W. (1989). *Flow measurement engineering handbook* (2nd ed.). New York: McGraw-Hill.
- Monzon, L. M., & Coey, J. M. D. (2014). Magnetic fields in electrochemistry: the Lorentz force. A mini-review. *Electrochemistry Communications*, 42, 38–41.
- Moraga, M. J., Moraga, G., Fito, P. J., & Martínez-Navarrete, N. (2009). Effect of vacuum impregnation with calcium lactate on the osmotic dehydration kinetics and quality of osmodehydrated grapefruit. *Journal of Food Engineering*, 90(3), 372–379.
- Ørskov, E. R., & McDonald, I. (1979). The estimation of protein degradability in the rumen from incubation measurements weighted according to rate of passage. *The Journal of Agricultural Science*, 92(02), 499–503.
- Oshitani, J., Uehara, R., & Higashitani, K. (1999). Magnetic effects on electrolyte solutions in pulse and alternating fields. *Journal of Colloid and Interface Science*, 209, 374–379.
- Park, S., Kodihalli, I., & Zhao, Y. (2005). Nutritional, sensory, and physicochemical properties of vitamin E- and mineral-fortified fresh-cut apples by use of vacuum impregnation. *Journal of Food Science*, 70(9), S593–S599.
- Perez-Cabrera, L., Chafer, M., Chiralt, A., & Gonzalez-Martinez, C. (2011). Effectiveness of antibrowning agents applied by vacuum impregnation on minimally processed pear. *LWT-Food Science and Technology*, 44, 2273–2280.
- Quintero-Chávez, R., Quintero-Ramos, A., Jiménez-Castro, J., Barnard, J., Márquez-Meléndez, R., Zazueta-Morales, et al. (2012). Modeling of total soluble solid and NaCl uptake during osmotic treatment of bell peppers under different infusion pressures. *Food and Bioprocess Technology*, 5(1), 184–192.
- Ross, A. C., Taylor, C. L., Yaktine, A. L., & Del Valle, H. B. (2011). *Dietary reference intakes for calcium and vitamin D*. Washington, DC: National Academies Press (Chapter 2).
- Sarang, S., & Sastry, S. K. (2007). Diffusion and equilibrium distribution coefficients of salt within vegetable tissue: effects of salt concentration and temperature. *Journal of Food Engineering*, 82(3), 377–382.
- Volpe, P., & Eremenko, T. (2007). Mechanisms of the target response to magnetic fields and their correlation with the biological complexity. *The Environmentalist*, 27(4), 387–393.
- Weaver, C. M. (2013). Calcium is not only safe but important for health. In P. Burckhardt, B. Dawson-Hughes, & C. M. Weaver (Eds.), *Nutritional influences on Bone Health* (pp. 359–363). London: Springer.
- Wright, J. J., & Van Der Beken, S. (1972). The hall effect in a flowing electrolyte. *American Journal of Physics*, 40, 245.
- Xie, J., & Zhao, Y. (2003). Nutritional enrichment of fresh apple (Royal Gala) by vacuum impregnation. *International Journal of Food Sciences and Nutrition*, 54(5), 387–398.
- Zhao, Y., & Xie, J. (2004). Practical applications of vacuum impregnation in fruit and vegetable processing. *Trends in Food Science and Technology*, 15, 434–451.



# Effects of adjustable parallel high voltage electrostatic field on the freshness of tilapia (*Oreochromis niloticus*) during refrigeration



Wen-Ching Ko <sup>a</sup>, Shang-Yan Yang <sup>a</sup>, Chao-Kai Chang <sup>b</sup>, Chang-Wei Hsieh <sup>b, c, \*</sup>

<sup>a</sup> Department of Bioindustry Technology, Da-Yeh University, 168 University Rd, Dacun, Chang-Hua, Taiwan

<sup>b</sup> Biotechnology Research Center, Da-Yeh University, 168 University Rd, Dacun, Chang-Hua, Taiwan

<sup>c</sup> Department of Medicinal Botanicals and Health Applications, Da-Yeh University, 168 University Rd, Dacun, Chang-Hua, Taiwan

## ARTICLE INFO

### Article history:

Received 27 May 2015

Received in revised form

2 October 2015

Accepted 5 October 2015

Available online 9 October 2015

### Keywords:

Adjustable parallel high voltage electrostatic field (AP-HVEF)

Tilapia meat

Preserving freshness

Fish freshness indicators

## ABSTRACT

Our preliminary findings indicated that at 4 °C, a High Voltage Electrostatic Field (HVEF) of 100 kV/m can effectively extend the shelf life of fish for up to 2 days. This study further investigated changes in the freshness of tilapia meat after using various HVEF treatments: 300, 600, or 900 kV/m. Both the VBN and K-values of the untreated tilapia meat increased during the storage period, eventually exceeding the hygienic standard on the 6th day, with values of 60% and 25 mg/100 g, respectively. However, in fish treated with 600 kV/m HVEF, the K value approached 60% around the 8th day; fish treated with 300 kV/m HVEF had a VBN of only 20.47 mg/100 g. This demonstrated the effectiveness of HVEF in preserving freshness. In untreated fish, the total plate counts (TPC) reached  $4.02 \times 10^5$  CFU/g meat by the 8th day, while fish treated with an HVEF of 900 kV/m still had not exceeded the sanitary standard in that same time period ( $3.45 \times 10^5$  CFU/g meat). In summary, an HVEF with 600 kV/m electric field strength or more can enhance food preservation, as it effectively delays ATP degradation, protein denaturation, lipid oxidation, and microbiological growth.

© 2015 Elsevier Ltd. All rights reserved.

## 1. Introduction

While seafood has very high economic and nutritional value, its perishable nature requires proper handling and preservation to maintain its safety, quality, and nutritional benefits (Soares & Gonçalves, 2012). Autolytic, microbial spoilage, and lipid oxidation are dependent upon the temperature and oxygen levels at which fish are stored; therefore, most deteriorative factors can be delayed by controlling the temperature or modifying the atmosphere in order to inhibit enzymes and microorganism activity (Alfaro, Hernández, Baliño-Zuazo, & Barranco, 2013).

High-voltage electrostatic field (HVEF) treatment is a non-thermal technology that processes food without leaving any residual chemicals or radiation. Current research indicates that the electric field effect will produce ozone (Karaca & Velioglu, 2014a) and affect cell membrane permeability (Markov, 1988) and enzyme activity (Chapman, 1994), thereby inhibiting microbes (Hsieh, Lai, Lee, & Ko, 2011) and extending the shelf life of agricultural

products (Atungulu, Nishiyama, & Koide, 2004; Hsieh & Ko, 2008; Hsieh et al., 2011). In addition, more studies confirmed that HVEF could be applied to produce higher quality frozen products by controlled ice nucleation, such as pork and chicken (Hsieh, Lai, Ho, Huang, & Ko, 2010; Orłowska, Havet, & Le-Bail, 2009; Xanthakis, Havet, Chevallier, Abadie, & Le-Bail, 2013). These studies show that HVEF is suitable for the preservation and processing of agricultural products.

Tilapia (*Oreochromis niloticus*) is one of the most common freshwater fish in the aquaculture industry, prized for its neutral flavor and economic value (Liu et al., 2015). The traditional use of ice or refrigeration to store fish products during their distribution and marketing results in a short shelf life of 5–10 days (depending on species, harvest location, and season) and heavy economic losses (Pedrosa-Menabrito & Regenstein, 1990).

Our previous study showed that 4 °C, an HVEF of 100 kV/m has the potential to slow the rate of deterioration in tilapia during storage (microbial, VBN and K-value), and extend its shelf life by up to 2 days (Hsieh et al., 2011). The main objective of this study is to investigate the effects of the electric field strength on the freshness indicators of tilapia during storage (microbial, VBN, TBA and K-value) by employing an adjustable parallel high voltage

\* Corresponding author. Department of Medicinal Botanicals and Health Applications, Da-Yeh University, 168 University Rd, Dacun, Chang-Hua, Taiwan.

E-mail address: [welson@mail.dyu.edu.tw](mailto:welson@mail.dyu.edu.tw) (C.-W. Hsieh).

electrostatic field (AP-HVEF), ultimately leading to the development of more effective fish preservation techniques.

## 2. Materials and methods

### 2.1. AP-HVEF experimental apparatus

Live tilapia were purchased from a local retail market (Changhua, Taiwan) and kept on ice prior to sample preparation. The tilapia was dissected into pieces and skinned fish steaks resized into 3 cm × 2 cm × 1 cm portions at the laboratory (Da-Yeh University, Changhua, Taiwan). The fish were then stored in a refrigerator at 4 °C, 75% RH, and treated with HVEF (300, 600, or 900 kV/m) for 8 days; while the control group had no HVEF treatment (0 kV/m). The AP-HVEF equipment consisted of an electrostatic generator with an output voltage of 50 kV DC (SC-PME 50, COSMI, Taiwan), and the schematic diagram of the experimental HVEF system is as show in Fig. 1; the adjustable parallel electric field strength formula is, as follows (1) (Orlowska et al., 2009):

$$E = V/d \quad (1)$$

Where E is the electric field strength; V, the voltage (kV) input to the plate; and d is the distance (m) between the two plates.

### 2.2. Measurement of pH

A tilapia sample of 10 g was thoroughly homogenized with 45 ml of distilled water. The pH value of the homogenate was analyzed using a pH meter (TOA Electronics Ltd. HM-20S, Japan) (Ngapo, Babare, Reynolds, & Mawson, 1999).

### 2.3. Measurement of hunter color and color differences

A color meter (ZE-2000, Nippon Denshoku Co., Tokyo, Japan) was used to measure the surface color of the tilapia meat during storage. In addition, CIE L, a, b values were used to calculate the total color difference ( $\Delta E$ ). Observations were made for triplicate samples (Sathivel, 2005).

### 2.4. Measurement of total plate counts

The total aerobic bacterial plate counts were determined by using the spread plates of Standard Plate Count Agar (PCA, Difco™, USA), and incubating the samples for 48 h at 37 °C. The results were expressed as log CFU/g meat actual mass (Alfaro et al., 2013).

### 2.5. Measurement of total volatile basic nitrogen (VBN)

A minced sample of 10 g was diluted 10 – fold when transferred into a distillation flask containing 100 ml of distilled water. It was then filtered after shaking frequently for 30 min; 2 g of magnesium oxide and an antifoaming agent were added, and the mixture was distilled using the micro Kjeldahl distillation apparatus. Distillate was placed into 25 ml 4% boric acid with five drops of Tashero indicator added (1: 5, methyl red - ethanol and bromocresol green) and left for 25 min. The solution was then titrated using 0.1 M HCl to calculate the sample's total volatile basic nitrogen in terms of mg VBN/100 g meat (He, Liu, Nirasawa, Zheng, & Liu, 2013).

### 2.6. Thiobarbituric acid value (TBA)

1 g of the sample was added to 5 ml TBA reagent (0.375%) [TBA and 15% TCA (trichloroacetic acid) dissolved in 0.25 N HCl solution], and the two were mixed in a boiling water bath for 10 min; the sample was then cooled under tap water. Finally, the sample was centrifuged at 3380 g for 25 min, and the resulting supernatant measured at 532 nm absorbance ( $A_{532}$ ) (2) (Jayasingh & Cornforth, 2004).

$$\text{TBA number (mg MDA/Kg fish meat sample)} = \frac{\text{sample } (A_{532})}{\times 2.77} \quad (2)$$

### 2.7. K- value

ATP and its related compounds (ADP, AMP, IMP, HxR and Hx) were measured, as follows; 10 g of ordinary muscle sample were

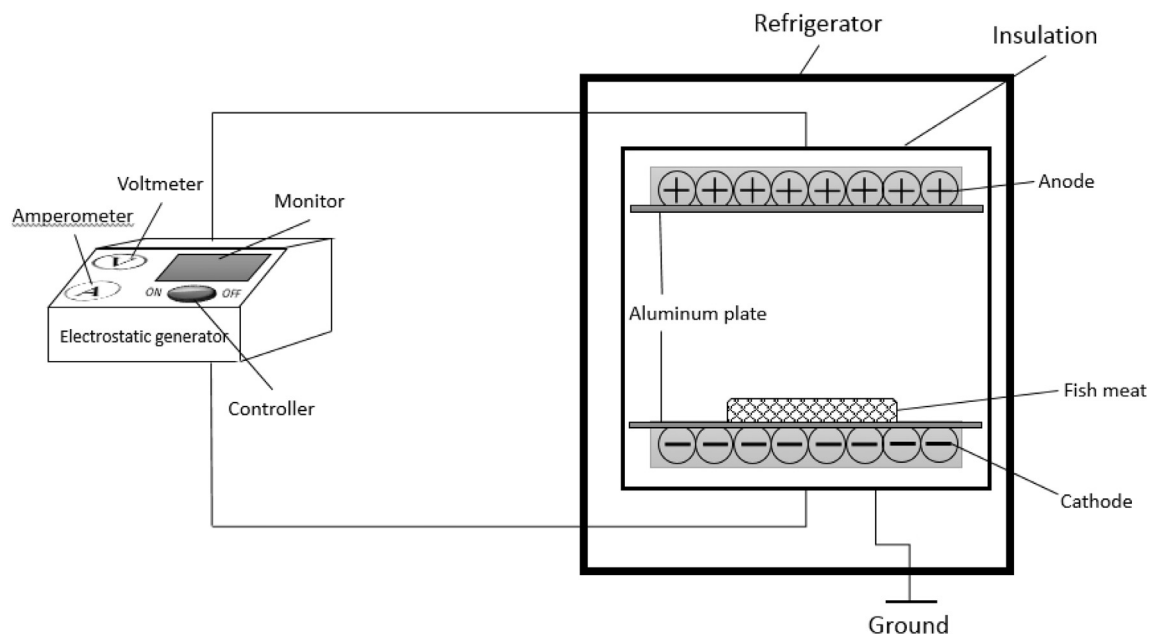


Fig. 1. Schematic diagram of the HVEF treatment system.

pre-treated, as per our previous study, and an analysis of ATP and its related compounds was performed using HPLC (HP 1100 series, Hewlett–Packard Co. Palo Alto, CA, USA). The separation was performed using an RP-18 column (5  $\mu$ m, 250–4.6 mm endcapped, Hewlett–Packard Co. Palo Alto, CA, USA) with a mobile phase consisting of 0.06 M  $K_2HPO_4$  – 0.04 M  $KH_2PO_4$ . The flow rate was 1.0 ml/min sample, and the detection wavelength was set to 254 nm. K-values were defined by the amount of ATP, and each related compound was calculated based on the standard ATP, ADP, AMP, IMP, inosine (HxR), and hypoxanthine (Hx) according to the following Eq. (3) (Yoneda, Kasamatsu, Hatae, & Watabe, 2002):

$$K \text{ value}(\%) = \frac{HxR - Hx}{ATP + ADP + AMP + IMP + HxR + Hx} \times 100 \quad (3)$$

### 2.8. Sensory assessment

A total of 20 fish samples were kept whole, stored in a refrigerator (4 °C, 75% RH), and taken out at regular intervals for visual appearance assessment in order to observe the grade of clarity (clear, slightly cloudy, and cloudy) under selected electric field strengths. The assessment was carried out by a minimum of 20 trained panelists (twenty to thirty years old), who were trained in fish quality assessment before the experiment. (Stone & Sidel, 2004).

### 2.9. Statistical analysis

Date analysis and statistical computations for analysis of variance (ANOVA) and Duncan's test by Statistical Analysis System (SAS Inst. Inc., Cary, NC, USA) were carried out. Significant difference was defined as  $p < 0.05$ . The differences among treatments were verified by their least significant difference.

## 3. Results and discussion

### 3.1. pH value

Some studies reported that an increased pH value during storage may be attributed to the production of basic compounds, such as ammonia and trimethylamine, as well as other biogenic amines (Masniyom, Benjakul, & Visessanguan, 2002; Ruiz-Capillas & Moral, 2001). Table 1 shows that HVEF has the ability to delay the increase in pH value, a phenomenon consistent with the results of our previous study (Hsieh et al., 2011). However, HVEF had no significant effect when the electric field strength was only 300 kV/m. Compared to the control (0 kV/m); the pH inhibition nearly doubled when the HVEF electric field strength was at 600 kV/m; however, there was no significant difference when the field strength was increased from 600 to 900 kV/m. In summary, an increased HVEF electric field strength is effective in delaying the

decline in fish freshness. However, the electric field strength has threshold characteristics, i.e. a larger electric field effect is not necessarily better for preservation.

### 3.2. Hunter color and color difference

The myofibrillar protein structure of the fish denatured during storage was due to factors, such as enzymes, microorganisms, and oxidation, resulting in a changed appearance, such as cloudy, green, and browning meat (Young & Whittle, 1985); such changes are important indicators of freshness during storage (Joo, Kauffman, Kim, & Park, 1999; Wagner & AÑÓN, 1986).

The results of HEVF on fish appearance are as shown in Table 1. Each group exhibited a strong downward trend. The electric field strength had no significant influence on *L*, *a* or *b* values, and the color gradually shifted towards green as storage time increased. However, selected electric field strengths can delay the *L* value and  $\Delta E$  increase by 0.7–0.8 fold after the 8th day. The *a* value decreased the degree of selected HVEFs strengths treatment (300, 600, and 900 kV/m) by 5.6, 4.2, and 5.1 times, respectively, and was lower than the control group (6 times) by about 0.8–0.6 times after the 8th day. Moreover, the HVEF treatment showed the ability to delay the increased level of *b* values, as compared to the control group, by about 1.24–1.34 times at the 8th day. These results are the same as in our previous study, demonstrating that HVEF has the potential to inhibit microbial growth, protein denaturation, and lipid peroxidation.

### 3.3. Volatile basic nitrogen (VBN)

During fish corruption, as the activation of microorganisms, protein, and nitrogen-containing compounds degrade into volatile basic nitrogen (VBN), it is primarily comprised of ammonia and secondary and tertiary amines (Feng, Jiang, Wang, & Li, 2012). VBN is an important indicator of fish freshness during storage; a value reaching 35–40 mg/100 g is the standard for evaluating spoilage (Ruiz-Capillas & Moral, 2001).

Fig. 2 shows the influence of different electric field strengths on VBN. The VBN content of each group increased over time. Tilapia meat that did not receive electric field treatment reached the initial spoilage standard on the 7th day (35.34 mg/100 g). Under the same storage conditions, tilapia meat that received different electric field treatments: 300, 600, and 900 kV/m, had VBN values of 29.23, 24.15, and 26.62 mg/100 g, respectively, which are all less than the spoilage standard, thereby demonstrating that the rate of VBN generation was suppressed by up to 0.7 times. Our results show that HVEF treatment has the potential to inhibit enzymes and bacteria, delaying the decomposition of tilapia meat during storage; similar results were found in previous studies (He et al., 2013; Hsieh et al., 2011). This study confirms that increasing the electric field effect contributes to the inhibition of VBN.

**Table 1**  
Effects of HVEF on the pH value and hunter color values of tilapia during storage at 4 °C.

	pH		<i>L</i> value		<i>a</i> value		<i>b</i> value		$\Delta E$	
	Day 4	Day 8	Day 2	Day 8	Day 2	Day 8	Day 2	Day 8	Day 2	Day 8
0 kV/m	6.70 $\pm$ 0.02 <sup>d</sup>	7.30 $\pm$ 0.02 <sup>a</sup>	42.48 $\pm$ 0.04 <sup>b</sup>	44.25 $\pm$ 0.04 <sup>a</sup>	0.26 $\pm$ 0.04 <sup>a</sup>	–1.55 $\pm$ 0.03 <sup>a</sup>	3.95 $\pm$ 0.04 <sup>a</sup>	5.8 $\pm$ 0.04 <sup>a</sup>	1.00 $\pm$ 0.08 <sup>a</sup>	3.14 $\pm$ 0.04 <sup>a</sup>
300 kV/m	6.74 $\pm$ 0.06 <sup>c</sup>	7.28 $\pm$ 0.03 <sup>b</sup>	42.50 $\pm$ 0.02 <sup>a</sup>	43.50 $\pm$ 0.05 <sup>b</sup>	0.22 $\pm$ 0.04 <sup>c</sup>	–1.23 $\pm$ 0.06 <sup>b</sup>	3.52 $\pm$ 0.05 <sup>b</sup>	5.0 $\pm$ 0.04 <sup>b</sup>	0.54 $\pm$ 0.02 <sup>b</sup>	2.52 $\pm$ 0.02 <sup>b</sup>
600 kV/m	6.78 $\pm$ 0.06 <sup>b</sup>	7.12 $\pm$ 0.04 <sup>c</sup>	42.52 $\pm$ 0.03 <sup>a</sup>	43.12 $\pm$ 0.06 <sup>c</sup>	0.25 $\pm$ 0.05 <sup>b</sup>	–1.05 $\pm$ 0.05 <sup>c</sup>	3.48 $\pm$ 0.03 <sup>c</sup>	5.0 $\pm$ 0.03 <sup>b</sup>	0.48 $\pm$ 0.06 <sup>c</sup>	2.33 $\pm$ 0.04 <sup>c</sup>
900 kV/m	6.84 $\pm$ 0.03 <sup>a</sup>	7.08 $\pm$ 0.06 <sup>d</sup>	42.47 $\pm$ 0.03 <sup>b</sup>	43.15 $\pm$ 0.03 <sup>c</sup>	0.20 $\pm$ 0.04 <sup>d</sup>	–1.02 $\pm$ 0.06 <sup>d</sup>	3.22 $\pm$ 0.02 <sup>d</sup>	4.8 $\pm$ 0.02 <sup>c</sup>	0.45 $\pm$ 0.06 <sup>d</sup>	2.31 $\pm$ 0.02 <sup>d</sup>

$n = 5$ .

Means within the same with different superscripts (a, b, c, d) are significantly different at  $p < 0.05$ .

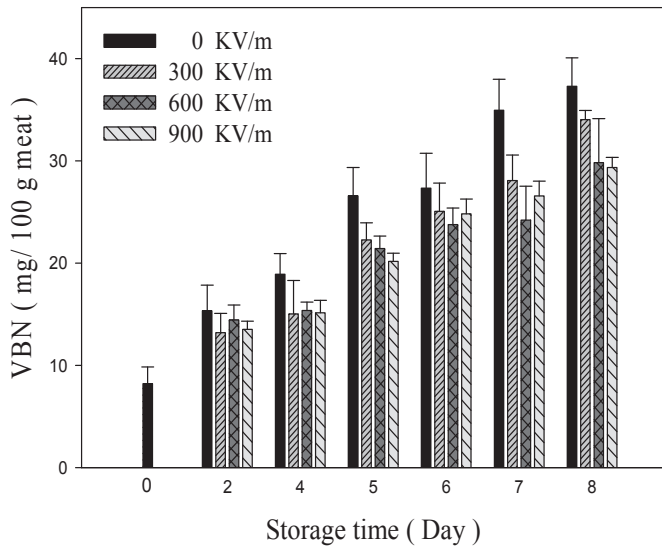


Fig. 2. Effects of HVEF on the VBN of tilapia meat during storage at 4 °C. Error bars represent  $\pm$  SD (n = 3).

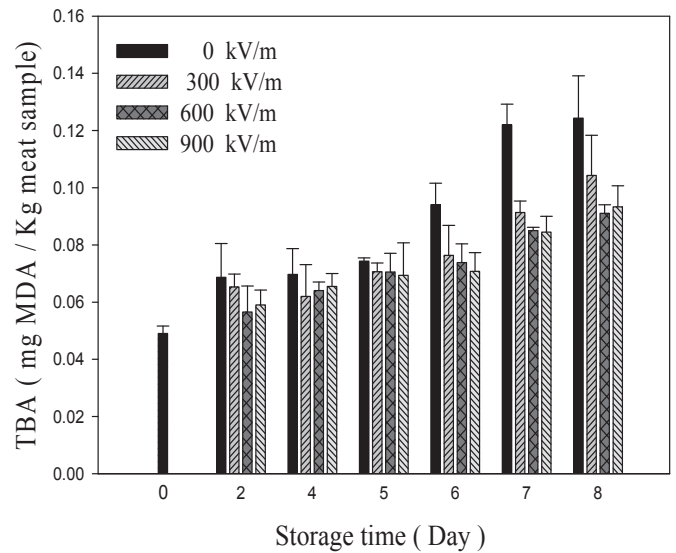


Fig. 4. Effects of HVEF on the TBA value of tilapia meat during storage at 4 °C. Error bars represent  $\pm$  SD (n = 3).

### 3.4. Microbiological analyses

Our previous study confirmed that, after the 8th day of storage at 4 °C, an HVEF of 100 kV/m can effectively inhibit the growth of microorganisms in fish by 0.65 times (Hsieh et al., 2011). Moreover, previous studies have proven that a pulsed electric field can be useful in the sterilization of fruit juice under various conditions (Guo et al., 2014; Gurtler, Rivera, Zhang, & Geveke, 2010). Therefore, increasing the electric field strength should improve the inhibition of microorganism growth in tilapia during storage.

Fig. 3 shows the effects of HVEF strength on aerobic microbes in tilapia meat. The initial total plate counts observed in the tilapia meat were about  $8.14 \times 10^3$  CFU/g meat; a level of  $10^7$  CFU/g meat is regarded as spoilage. Viable bacteria count in the control group (0 kV/m) increased over time and reached  $3.51 \times 10^6$  CFU/g after the 8th day of storage. However, the viable microbial population in the 300 kV/m, 600 kV/m and 900 kV/m samples increased less than

$10^6$  CFU/g during the 8th day of storage, which is significantly less than the control group ( $P < 0.05$ ) (Fig. 3). Related studies indicate that the total viable count of Atlantic horse mackerel (*Trachurus trachurus*) fillets treated by modified atmosphere was  $10^6$  CFU/g after the 7th day of storage at 4 °C (Alfaro et al., 2013), and our research shows that HVEF can better inhibit the bacteria growth rate, approaching a factor of 10 – fold. This phenomenon is similar to our previous results (Hsieh et al., 2011), in which HVEF either caused oxygen to leave the samples, nitrogen to cover the samples, or an interaction between ozone and negative air ions, ultimately resulting in the inhibition of aerobic microbe growth (Fan, Song, Hildebrand, & Forney, 2002; Karaca & Velioglu, 2014b). HVEF treatment could effectively decrease the microbe growth rate in refrigerated (4 °C) tilapia meat; this inhibitory effect increases 10 – fold as the electric field strength increases from 0 kV/m to 900 kV/m (Fig. 3).

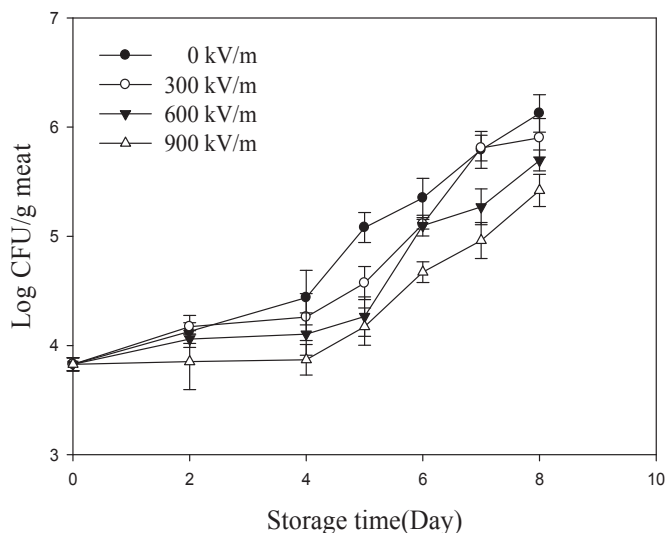


Fig. 3. Changes in the total plate counts of tilapia meat after HVEF treatment. Error bars represent  $\pm$  SD (n = 3).

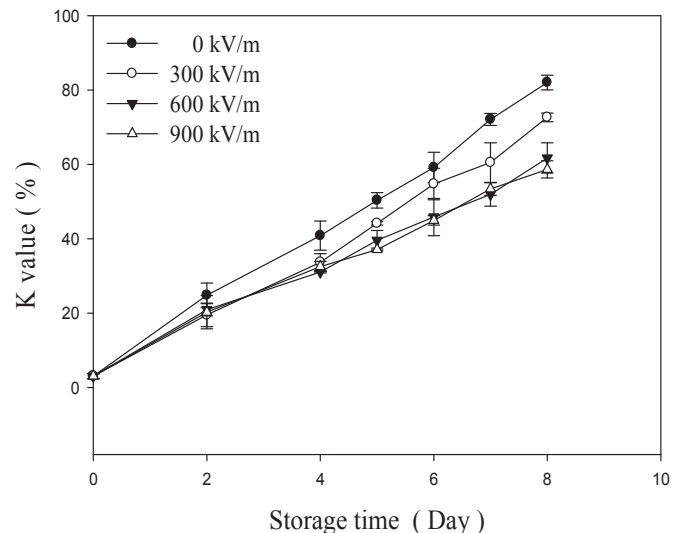


Fig. 5. Effects of HVEF on the K-value of tilapia meat during storage at 4 °C. Error bars represent  $\pm$  SD (n = 3).

3.5. Thiobarbituric acid value (TBA)

Thiobarbituric acid value is an indicator of the oxidative deterioration of fish meat oil. The results showed the same trend as the other freshness indicators. The TBA value of fillets treated with various HVEF was significantly lower than the control sample (without HVEF treatment). Moreover, by the 8th day, the TBA of the control group (0.124 mg MDA/Kg fish meat sample) was higher than the HVEF treatment groups (0.09–0.11) by about 1.2 times

(Fig. 4). Related studies indicate that blocking oxygen in direct contact with fish, whether by polymer materials or modified atmosphere packaging, could reduce the fish meat lipid oxidation (Masniyom et al., 2002; Sathivel, 2005). The electrostatic induction phenomenon of HVEF charges the material's surface, thus, reducing the frequency of the fish's contact with the surrounding oxygen and slowing the rate of fish meat lipid oxidation. Similar results have already been shown in our previous study (Hsieh & Ko, 2008) and other studies examining the application of HVEF to fresh

Day 0	Electric field strength(kV/m)	Day 8
	0kV/m/	
	300 kV/m	
	600 kV/m	
	900 kV/m	

Fig. 6. Effects of HVEF on the appearance of tilapia eyes during storage at 4 °C.

agricultural products (Shivashankara, Isobe, Al-Haq, Takenaka, & Shiina, 2004). Moreover, this result is similar to the previous results regarding the use of modified atmosphere packaging to inhibit fish oil oxidative deterioration (Masniyom et al., 2002). The current results prove that HVEF has the ability to decelerate the oxidative deterioration of perishable foods.

### 3.6. K-value evaluation

The increased K-values of the control group were significantly higher than in any of the HVEF treatment groups (Fig. 5). The K-values for the control group increased continuously throughout the storage period and reached 59.16% on the 6th day, a value approaching the rejection point (60%) (Mohan, Ravishankar, Gopal, & Kumar, 2009). Conversely, the K-value for both the 600 kV/m and 900 kV/m groups was less than 45% on the 6th day. The K-value for the 300 kV/m group was 55.54%, better than the control group, but still approaching the rejection point. The K-values for the 600 kV/m and 900 kV/m groups approached the rejection point on the 8th day, while the K-value for the 300 kV/m group reached the rejection point on the 6th day. This demonstrated that HVEF treatment can slow the increase of K-values, and has greater benefit when the electric field strength is 600 kV/m and 900 kV/m.

Related studies indicate that ozone water combined with antioxidants can inhibit the fish ATP degradation phenomenon due to inactivation of microorganisms (Feng et al., 2012). In addition, chemical gradients (changes in concentration) and potential gradients (changes in membrane potential) drive aqueous ions to the inside and outside of the cell membrane *in vivo*. This mechanism determines the cell membrane penetration and the direction of biological metabolic reactions (Markov, 1988). Therefore, applying an electric field to an organism will affect its metabolic reactions and decrease ATP degradation. This shows that HVEF is beneficial in inhibiting ATP degradation, protein denaturation, microbial growth, and oxidative deterioration. Furthermore, increasing HVEF strength is effective in extending the storage life of fish samples.

### 3.7. Sensory assessment

Fig. 6 shows the eye changes in tilapia after treatment with selected HVEF strengths, and after 8 days storage at 4 °C. The cloudy appearance of the eyes was significantly higher in the control group than in the HVEF treatment groups overall, indicating the progressive loss of freshness in all groups. However, increasing the electric field strength delayed the eyes becoming cloudy. In fact, the eyes were still clear in the 600 and 900 kV/m storage groups, even after 8 days storage. Compared to our preliminary study (Hsieh et al., 2011), the storage period may be extended by more than one day when the HVEF is increased. Based on these findings, HVEF treatment might be a useful process for preserving the storage quality of tilapia meat, and provide even greater benefits when the electric field strength is 600 kV/m or more.

## 4. Conclusions

The current study showed that HVEF has good potential for use in food preservation, as it effectively maintains fish freshness; the benefits increased when the electric field strength was 600 kV/m or more. Furthermore, this approach has the advantage of not using any additives, as it is a form of physical preservation. Storage methods that prohibit the use of chemical preservatives will create a big niche in the future, and HVEF has the potential to serve as a viable means of preservation without reagent residue. That said the denaturation of fish protein is another important indicator of fish

quality. Therefore, the next phase in our studies will focus on exploring the effects of HVEF on fish protein and Ca<sup>2+</sup>-ATPase.

## Acknowledgments

The financial support from the National Science Council, Republic of China (grant Nos. 103-2221-E-212-012, 104-2221-E-212-010-MY2) is acknowledged.

## References

- Alfaro, B., Hernández, I., Balaño-Zuazo, L., & Barranco, A. (2013). Quality changes of Atlantic horse mackerel fillets (*Trachurus trachurus*) packed in a modified atmosphere at different storage temperatures. *Journal of the Science of Food and Agriculture*, 93(9), 2179–2187. <http://dx.doi.org/10.1002/jsfa.6025>.
- Atungulu, G., Nishiyama, Y., & Koide, S. (2004). Electrode configuration and polarity effects on physicochemical properties of electric field treated apples post harvest. *Biosystems Engineering*, 87(3), 313–323. <http://dx.doi.org/10.1016/j.biosystemseng.2003.11.011>.
- Chapman, D. (1994). The role of water in biomembrane structures. *Journal of Food Engineering*, 22(1–4), 367–380. doi:[http://dx.doi.org/10.1016/0260-8774\(94\)90040-X](http://dx.doi.org/10.1016/0260-8774(94)90040-X).
- Fan, L., Song, J., Hildebrand, P. D., & Forney, C. F. (2002). Interaction of ozone and negative air ions to control micro-organisms. *Journal of Applied Microbiology*, 93(1), 144–148. <http://dx.doi.org/10.1046/j.1365-2672.2002.01683.x>.
- Feng, L., Jiang, T., Wang, Y., & Li, J. (2012). Effects of tea polyphenol coating combined with ozone water washing on the storage quality of black sea bream (*Sparus macrocephalus*). *Food Chemistry*, 135(4), 2915–2921. doi:<http://dx.doi.org/10.1016/j.foodchem.2012.07.078>.
- Guo, M., Jin, T., Geveke, D., Fan, X., Sites, J., & Wang, L. (2014). Evaluation of microbial stability, bioactive compounds, physicochemical properties, and consumer acceptance of pomegranate juice processed in a commercial scale pulsed electric field system. *Food and Bioprocess Technology*, 7(7), 2112–2120. <http://dx.doi.org/10.1007/s11947-013-1185-6>.
- Gurtler, J. B., Rivera, R. B., Zhang, H. Q., & Geveke, D. J. (2010). Selection of surrogate bacteria in place of *E. coli* O157:H7 and *Salmonella* Typhimurium for pulsed electric field treatment of orange juice. *International Journal of Food Microbiology*, 139(1–2), 1–8. <http://dx.doi.org/10.1016/j.ijfoodmicro.2010.02.023>.
- He, X., Liu, R., Nirasawa, S., Zheng, D., & Liu, H. (2013). Effect of high voltage electrostatic field treatment on thawing characteristics and post-thawing quality of frozen pork tenderloin meat. *Journal of Food Engineering*, 115(2), 245–250. <http://dx.doi.org/10.1016/j.jfoodeng.2012.10.023>.
- Hsieh, C.-W., & Ko, W.-C. (2008). Effect of high-voltage electrostatic field on quality of carrot juice during refrigeration. *LWT – Food Science and Technology*, 41(10), 1752–1757. <http://dx.doi.org/10.1016/j.lwt.2008.01.009>.
- Hsieh, C. W., Lai, C. H., Ho, W. J., Huang, S. C., & Ko, W. C. (2010). Effect of thawing and cold storage on frozen chicken thigh meat quality by high-voltage electrostatic field. *Journal of Food Science*, 75(4), M193–M197. <http://dx.doi.org/10.1111/j.1750-3841.2010.01594.x>.
- Hsieh, C. W., Lai, C. H., Lee, C. H., & Ko, W. C. (2011). Effects of high-voltage electrostatic fields on the quality of tilapia meat during refrigeration. *Journal of Food Science*, 76(6), M312–M317. <http://dx.doi.org/10.1111/j.1750-3841.2011.02218.x>.
- Jayasingh, P., & Cornforth, D. P. (2004). Comparison of antioxidant effects of milk mineral, butylated hydroxytoluene and sodium tripolyphosphate in raw and cooked ground pork. *Meat Science*, 66(1), 83–89. doi:[http://dx.doi.org/10.1016/S0309-1740\(03\)00018-4](http://dx.doi.org/10.1016/S0309-1740(03)00018-4).
- Joo, S. T., Kauffman, R. G., Kim, B. C., & Park, G. B. (1999). The relationship of sarcoplasmic and myofibrillar protein solubility to colour and water-holding capacity in porcine longissimus muscle. *Meat Science*, 52(3), 291–297. doi:[http://dx.doi.org/10.1016/S0309-1740\(99\)00005-4](http://dx.doi.org/10.1016/S0309-1740(99)00005-4).
- Karaca, H., & Velioglu, Y. S. (2014a). Effects of ozone treatments on microbial quality and some chemical properties of lettuce, spinach, and parsley. *Postharvest Biology and Technology*, 88, 46–53. <http://dx.doi.org/10.1016/j.postharvbio.2013.09.003>.
- Karaca, H., & Velioglu, Y. S. (2014b). Effects of ozone treatments on microbial quality and some chemical properties of lettuce, spinach, and parsley. *Postharvest Biology and Technology*, 88(0), 46–53. doi:<http://dx.doi.org/10.1016/j.postharvbio.2013.09.003>.
- Liu, Y., Ma, D.-h., Wang, X.-c., Liu, L.-p., Fan, Y.-x., & Cao, J.-x. (2015). Prediction of chemical composition and geographical origin traceability of Chinese export tilapia fillets products by near infrared reflectance spectroscopy. *LWT – Food Science and Technology*, 60(2), 1214–1218. <http://dx.doi.org/10.1016/j.lwt.2014.09.009>.
- Markov, M. (1988). Electromagnetic fields — a new ecological factor. In M. Markov, & M. Blank (Eds.), *Electromagnetic fields and biomembranes* (pp. 135–140). Springer US.
- Masniyom, P., Benjakul, S., & Visessanguan, W. (2002). Shelf-life extension of refrigerated seabass slices under modified atmosphere packaging. *Journal of the Science of Food and Agriculture*, 82(8), 873–880. <http://dx.doi.org/10.1002/jsfa.1108>.
- Mohan, C. O., Ravishankar, C. N., Gopal, T. K. S., & Kumar, K. A. (2009). Nucleotide

- breakdown products of seer fish (*Scomberomorus commerson*) steaks stored in O<sub>2</sub> scavenger packs during chilled storage. *Innovative Food Science & Emerging Technologies*, 10(2), 272–278. doi:<http://dx.doi.org/10.1016/j.ifset.2008.11.012>.
- Ngapo, T. M., Babare, I. H., Reynolds, J., & Mawson, R. F. (1999). Freezing and thawing rate effects on drip loss from samples of pork. *Meat Science*, 53(3), 149–158. doi:[http://dx.doi.org/10.1016/S0309-1740\(99\)00050-9](http://dx.doi.org/10.1016/S0309-1740(99)00050-9).
- Orlowska, M., Havet, M., & Le-Bail, A. (2009). Controlled ice nucleation under high voltage DC electrostatic field conditions. *Food Research International*, 42(7), 879–884. doi:<http://dx.doi.org/10.1016/j.foodres.2009.03.015>.
- Pedrosa-Menabrito, A., & Regenstein, J. M. (1990). Shelf-life extension of fresh fish—a review part II—preservation of fish. *Journal of Food Quality*, 13(2), 129–146. <http://dx.doi.org/10.1111/j.1745-4557.1990.tb00013.x>.
- Ruiz-Capillas, C., & Moral, A. (2001). Residual effect of CO<sub>2</sub> on hake (*Merluccius merluccius* L.) stored in modified and controlled atmospheres. *European Food Research and Technology*, 212(4), 413–420. <http://dx.doi.org/10.1007/s002170000270>.
- Sathivel, S. (2005). Chitosan and protein coatings affect yield, moisture loss, and lipid oxidation of pink Salmon (*Oncorhynchus gorboscha*) fillets during frozen storage. *Journal of Food Science*, 70(8), e455–e459. <http://dx.doi.org/10.1111/j.1365-2621.2005.tb11514.x>.
- Shivashankara, K. S., Isobe, S., Al-Haq, M. I., Takenaka, M., & Shiina, T. (2004). Fruit antioxidant activity, ascorbic acid, total phenol, quercetin, and carotene of Irwin mango fruits stored at low temperature after high electric field pretreatment. *Journal of Agricultural and Food Chemistry*, 52(5), 1281–1286. <http://dx.doi.org/10.1021/jf030243l>.
- Soares, K. M. d. P., & Gonçalves, A. A. (2012). Qualidade e segurança do pescado. *Revista do Instituto Adolfo Lutz (Impresso)*, 71, 1–10. Retrieved from [http://periodicos.ses.sp.bvs.br/scielo.php?script=sci\\_arttext&pid=S0073-98552012000100001&nrm=iso](http://periodicos.ses.sp.bvs.br/scielo.php?script=sci_arttext&pid=S0073-98552012000100001&nrm=iso).
- Stone, H., & Sidel, J. L. (2004). Preface. In H. Stone, & J. L. Sidel (Eds.), *Sensory evaluation practices (Third edition)* (3rd ed., pp. xiii–xiv). San Diego: Academic Press.
- Wagner, J. R., & AÑÓN, M. C. (1986). Effect of frozen storage on protein denaturation in bovine muscle. *International Journal of Food Science & Technology*, 21(2), 547–558. <http://dx.doi.org/10.1111/j.1365-2621.1986.tb00393.x>.
- Xanthakis, E., Havet, M., Chevallier, S., Abadie, J., & Le-Bail, A. (2013). Effect of static electric field on ice crystal size reduction during freezing of pork meat. *Innovative Food Science & Emerging Technologies*, 20, 115–120. <http://dx.doi.org/10.1016/j.ifset.2013.06.011>.
- Yoneda, C., Kasamatsu, C., Hatae, K., & Watabe, S. (2002). Changes in taste and textural properties of the foot of the Japanese cockle (*Fulvia mutica*) by cooking and during storage. *Fisheries Science*, 68(5), 1138–1144. <http://dx.doi.org/10.1046/j.1444-2906.2002.00544.x>.
- Young, K. W., & Whittle, K. J. (1985). Colour measurement of fish minces using hunter L, a, b values. *Journal of the Science of Food and Agriculture*, 36(5), 383–392. <http://dx.doi.org/10.1002/jsfa.2740360511>.



# Effect of indigenous *Lactobacillus rhamnosus* isolated from bovine milk on microbiological characteristics and aromatic profile of traditional yogurt



Nadia Innocente<sup>\*</sup>, Marialuisa Biasutti, Frisina Rita, Romina Brichese, Giuseppe Comi, Lucilla Iacumin

Department of Food Science, University of Udine, Udine, Italy

## ARTICLE INFO

### Article history:

Received 14 July 2015

Received in revised form

21 September 2015

Accepted 12 October 2015

Available online 22 October 2015

### Keywords:

Yogurt

Probiotic bacteria

Aroma profile

## ABSTRACT

The indigenous *Lactobacillus rhamnosus* DSA LR1 was isolated from milk that was obtained from a restricted geographical area in northeast Italy and it was chosen, among other isolated strains on the bases of its resistance to the pH of gastric juices, the bile salts, the antibiotics and its lipolytic and proteolytic activities. The indigenous isolated potential probiotic bacteria were then added in combination with starter bacteria to the milk used for yogurt production. The results showed that *L. rhamnosus* DSA LR1 was able to maintain its viability for the entire shelf-life period without affecting on the viability or acidification capacity of starter culture.

At the end of the fermentation period, the yogurt that had been co-fermented with *L. rhamnosus* DSA LR1 presented an aroma profile that was qualitatively similar to the control yogurt but less intense from a quantitative point of view. However, all of the major volatile compounds tended to increase during storage at 4 °C for 20 days, yogurt with *L. rhamnosus* had absolute areas larger than the areas of the control yogurt for all major carbonyl compounds.

© 2015 Elsevier Ltd. All rights reserved.

## 1. Introduction

Yogurt is a cultured dairy product that is widely consumed as a healthful and nutritious food and for its sensory properties. Chemically, yogurt is a complex gel system that incorporates protein, polysaccharides, and lipids in its structure. Yogurt is commonly made by fermenting cow's milk using a symbiotic culture of the bacteria *Lactobacillus delbruekii* ssp. *bulgaricus* and *Streptococcus thermophilus* under controlled temperature and environmental conditions (Marshall, 1993). The role of these two starter bacteria in yogurt manufacturing can be summarized as milk acidification and the synthesis of aromatic compounds. Milk acidification denatures casein micelles resulting in the formation of the coagulated gel. Also whey proteins are incorporated in the gel and contribute to give yogurt its texture and characteristic tang. Volatile compounds that contribute to the final aroma of yoghurt may be divided into four categories: nonvolatile carboxylic acids

(lactic or pyruvic), volatile carboxylic acids (butyric or acetic), carbonyl compounds (acetaldehyde or diacetyl), diketones (2,3-butanedione and 2,3-pentanedione) and miscellaneous organic compounds (amino acids or products formed by thermal degradation) (Guler & Park, 2011). More than 90 different volatiles have been identified in yogurt. The occurrence and concentration of these volatiles are affected by the chemical composition of the milk base, the processing conditions (e.g., heat treatment, homogenization), the ratio, activity and strains of the starter culture used and the incubation period (Kneifel, Ulbert, Erhard, & Jaros, 1992; Ott, Fay, & Chaintreau, 1997; Ott, Germond, Baumgartner, & Chaintreau, 1999). Thus, the analysis of volatile organic compounds can be used for quality monitoring during yogurt production (Cheng, 2010).

Yogurts are also considered the most popular food carriers of probiotic microorganisms that may confer many health benefits. The consumer preference for yogurt as a vehicle for probiotic cultures is related to the reputation of a naturally healthful product (Cruz et al., 2012). Probiotic bacteria are able to tolerate acid and bile and are able to survive in the intestinal tract; thus, they have a beneficial effect on intestinal function and promote good health

<sup>\*</sup> Corresponding author. Department of Food Science, Via Sondrio, 2/A, University of Udine, Italy.

E-mail address: [nadia.innocente@uniud.it](mailto:nadia.innocente@uniud.it) (N. Innocente).



formation as previously described (Ercolini, Moschetti, Blaiotta, & Coppola, 2001). One millilitre of each bulk suspension was centrifuged at  $14,000 \times g$  for 10 min at  $4^\circ\text{C}$  to pellet the cells, and the pellet was subjected to RNA extraction. RNA was then subjected to molecular analysis using reverse transcription and PCR-DGGE technique (Iacumin et al., 2009). As a result of the “bulk” molecular analysis, different fingerprints were obtained. Analysis of the patterns and their corresponding dilutions gives information about the dominant species occurring and allows us to ascertain the ratio of concentration among the inoculated species.

#### 2.4. pH, titratable acidity and lactose content

The pH of the yogurt samples was measured at  $20^\circ\text{C}$  using a digital pH meter (Crison pH electrode, Crison Instruments, SA, Alella, Spain; Hanna Instruments pH meter, mod. pH 301, Hanna Instruments, Inc., RI, USA). Titratable acidity was measured by titrating a sample (25 mL of yogurt added to 2.5 mL of distilled water) with 0.25 N NaOH following the IDF standard method (IDF, 1991). The results were expressed as grams lactic acid  $100\text{ g}^{-1}$  yogurt (Segat, Biasutti, Iacumin, Carboni, & Innocente, 2014).

The lactose content determination was performed using high-performance liquid chromatography (HPLC) according to the procedure reported by Jeon, Galitzer, and Kenesly (1984).

#### 2.5. Analysis of volatile compounds

Analysis of the aroma compounds of yogurt samples was performed using headspace solid-phase microextraction (HS-SPME) coupled to gas chromatography with mass spectrometric detection (GC/MS).

The isolation and concentration of the headspace volatile flavour compounds were carried out using a DVB/CAR/PDMS (divinylbenzene/carboxen/polydimethylsiloxanate) fibre, 50/30  $\mu\text{m}$  film thickness, according to the method reported by Conurso, Verzera, Romeo, Ziino, and Conte (2008).

The GC/MS system consisted of a Model 3400 Varian gas chromatograph coupled to a model ion trap detector (ITD) Varian Saturn mass spectrometer (Varian Instruments, Walnut Creek, CA). The thermal desorption of the analytes from the fibre was performed in the injector port (set at  $230^\circ\text{C}$ ) in splitless mode for high-boiling compounds (the split valve was opened 3 min after injection) and in split mode for low-boiling compounds (Innocente, Marchesini, & Biasutti, 2011; Innocente, Munari, & Biasutti, 2013; Innocente, Marchesini, & Biasutti, 2014). Separation was performed on an Econo-CAP EC-Wax column (30 m long, 0.25 mm inner diameter, 0.25  $\mu\text{m}$  film thickness, Alltech, State College, PA). The oven temperature was held at  $50^\circ\text{C}$  for 5 min, then raised to  $230^\circ\text{C}$  ( $10^\circ\text{C min}^{-1}$ , held 10 min) to a final temperature of  $250^\circ\text{C}$  ( $10^\circ\text{C min}^{-1}$ , held 10 min). The ITD mass spectrometer conditions were as follows: the temperatures of the manifold and the transfer line were  $170^\circ\text{C}$  and  $250^\circ\text{C}$ , respectively, electron ionization mass spectra were recorded at 70 eV, the ionization current was 10  $\mu\text{A}$  and the scan rate was  $1.5\text{ scans s}^{-1}$  (Innocente, Biasutti, & Comuzzo, 2007; Innocente, Biasutti, & Marchesini, 2009). Compounds were identified by comparing their mass spectrum with the spectra of the mass spectral library Wiley 5. Moreover, the Kovats retention indexes were determined and compared with the retention indexes of the compounds. The absolute peak area of each compound was used for comparing and interpreting the data.

#### 2.6. Statistical analysis

Between groups design with one independent variable (presence/absence of *L. rhamnosus* DSA LR1) was used in this research.

The experimental group (treatment group) consisted of three samples of yogurt made on three different days with the addition of *L. rhamnosus* DSA LR1; the control group consisted of three samples of yogurt made on three different days without the addition of *L. rhamnosus* DSA LR1. In all sample considered chemical and microbiological analyses were performed three times. Then, all results were averages of at least six measurements and were reported as the mean  $\pm$  standard deviation (SD). Student's *t*-test was used to compare 2 means, and one-way ANOVA (*F*-test) and Tukey's Honestly Significant Difference test were used for multiple comparisons. In both cases, the differences between the means were considered statistically significant for *P*-values  $<0.05$ . All statistical analyses were conducted using the software Statistical Discovery JMP 3.0 for Windows (SAS Institute Inc., Cary, NC).

### 3. Results and discussion

#### 3.1. Physicochemical and microbiological characterization of yogurt samples

Sixty (60) out of the 300 isolates from the milk from a restricted geographical area of northeast Italy resulted to belong to the *L. rhamnosus* specie. The genetic characterization by Random Amplified Polymorphic DNA (RAPD) –PCR technique allowed the identification of 11 different genotypes of *L. rhamnosus*. One strain per each genotypes was further investigated for resistance to the pH and bile salts, for the ability to grow at different temperatures, for the lipolytic and proteolytic activity, for the antibiotic resistance and the capacity to produce biogenic amines. Based on these results, the *L. rhamnosus* DSA LR1 strain that was able to grow at pH 2 and 8 and in MRS broth supplemented with 0.3% bile salts was chosen. This strain was also characterized by the presence of moderate lipolytic and high proteolytic activity but was not capable of producing biogenic amines and resistant only to Kanamycin and Tobramycin. The *L. rhamnosus* DSA LR1 also showed a good growth capacity at the fermentation temperature ( $40^\circ\text{C}$ ) and at the storage temperature of the yogurt ( $4^\circ\text{C}$ ). These information allowed us to consider the *L. rhamnosus* DSA LR1 strain as a candidate probiotic bacteria. Indeed, according to recent Food and Agriculture Organization (FAO) and WHO guidelines (FAO WHO, 2002), probiotic organisms used in food must retain viability during transit through the gastrointestinal tract and therefore they must have the ability to resist gastric juices and exposure to bile in the stomach and small intestine (Saad et al., 2013). Furthermore, they must be able to tolerate different stress during food processing and maintain their effectiveness and potency for the duration of the shelf-life of the product (Hutkins, 2006).

The indigenous isolated potential probiotic bacteria were then added in combination with starter cultures to the milk used in the production of experimental yogurt. Table 1 shows the microbial loads of control (CTR) and experimental (SP) yogurts that were monitored at the end of production (0 days) and during storage at  $4^\circ\text{C}$  (10 and 20 days). It was not possible to detect statistically significant differences (Student *t* test,  $P > 0.05$ ) in the lactic acid bacteria content between the CTR and SP samples. Both samples presented a load in lactic acid bacteria exceeding  $8\text{ log CFU mL}^{-1}$  throughout the storage period. However, yeasts were able to grow during the period of storage, but their counts remained really low till the end of the storage period, after 20 days (maximum value observed was  $2.66\text{ log CFU mL}^{-1}$  for sample CTR).

Using PCR-DGGE, it was possible to obtain the fingerprint of the different viable lactic acid bacteria species present in yogurts and to determine the relative concentrations of *L. delbrueckii* subsp. *bulgaricus*, *St. thermophilus* and *L. rhamnosus* DSA LR1. The results allowed us to establish that *L. rhamnosus* DSA LR1 was able to

**Table 1**Microbial counts ( $\pm$ SD) monitored during storage at 4 °C of control yogurt (CTR) and experimental yogurt (SP).

	Days	Total mesophil count (log CFU mL <sup>-1</sup> )	Lactic acid bacteria (log CFU mL <sup>-1</sup> )	Yeast (log CFU mL <sup>-1</sup> )
CTR	0	2.60 $\pm$ 0.23 a	8.39 $\pm$ 0.07 a	<10*
	10	2.66 $\pm$ 0.13 a	8.92 $\pm$ 0.62 a	<10*
	20	2.51 $\pm$ 0.18 a	8.44 $\pm$ 0.49 a	2.66 $\pm$ 0.76 a
SP	0	1.98 $\pm$ 0.22 b	9.13 $\pm$ 0.23 a	<10
	10	1.85 $\pm$ 0.19 b	8.82 $\pm$ 0.11 a	1.60 $\pm$ 0.08 a
	20	2.01 $\pm$ 0.03 b	8.72 $\pm$ 0.31 a	1.74 $\pm$ 0.32 a

Within a column, values followed by the same letter are not significantly different according to Tuckey test ( $P \leq 0.05$ ).

\*Data were expressed as CFU mL<sup>-1</sup>.

maintain its viability throughout the shelf-life period. Indeed, after 20 days of storage, *L. rhamnosus* DSA LR1 was present at an average value of approximately 7 log CFU mL<sup>-1</sup>, which still satisfied the minimum recommended level (not less than 6.0 log CFU g<sup>-1</sup>) to ensure their potential health-promoting effects (Alamprese, Foschino, Rossi, Pompei, & Corti, 2005; Granato et al., 2010; Lee & Salminen, 1995; Oliveira, Sodini, Remeuf, & Corrieu, 2001). Additionally, the two starter species *L. delbrueckii* subsp. *bulgaricus* and *St. thermophilus* remained nearly stable throughout the 20-day storage period in both the CTR and SP samples.

The main physicochemical parameters of the CTR and SP yogurt samples are reported in Table 2. The SP yogurt showed amounts of residual lactose, titratable acidity (expressed as % equivalent lactic acid) and pH values that were always comparable to the CTR sample either at the end of fermentation (0 days) or during the refrigerated storage (10 and 20 days at 4 °C).

### 3.2. Aromatic profile of yogurt samples

Overall, in the headspace of the yogurt samples, 15 volatile compounds were identified and grouped according to the following chemical classes: short-chain free fatty acids, aldehydes and ketones. Below, the behaviour of those compounds that have been reported to be the most representative and significant in defining the flavour profile of yogurt was discussed. The carbonyl compounds are the major volatile compounds that are commonly reported to be responsible for giving a desirable flavour to yogurt (Cheng, 2010; Ulberth & Kneifel, 1992). Among these volatile compounds acetaldehyde is reported to contribute most to the typical flavour of yogurt since this compound imparts yogurt its characteristic green apple or nutty notes (Cheng, 2010).

The behaviours of the absolute peak areas of acetaldehyde during storage for both the (CTR and SP) samples are reported in Fig. 1. In the CTR sample at the end of the fermentation period, acetaldehyde was characterized by a high absolute peak area that was subsequently lowered during storage. The reduction of acetaldehyde in yogurt stored for 10 days at 4 °C has also been reported by other authors (Cheng, 2010; Ott et al., 1999; Tamine & Robinson, 2007). In SP, the absolute quantity of acetaldehyde was found to show a low absolute peak area at the end of fermentation. Then, this compound increased during storage and, after 20 days, reached

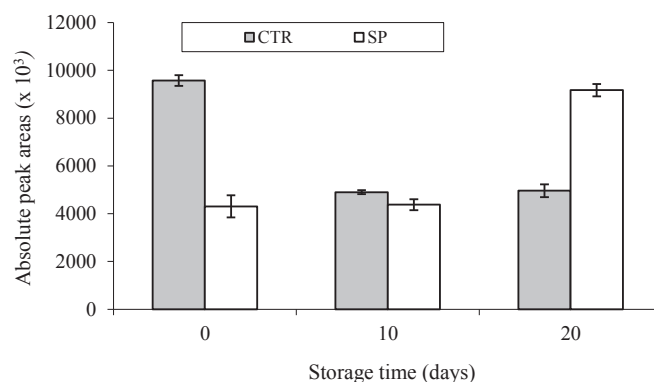


**Fig. 1.** Profile of acetaldehyde (expressed as the mean value of the absolute peak area) during storage of the experimental (SP) and the control (CTR) yogurt samples.

a very high signal, which was comparable with the results obtained for the CTR sample at the beginning of the conservation. The formation of acetaldehyde in yogurt is known to occur during fermentation, and the final levels are dependent on the presence of specific enzymes that are able to catalyse the formation of this compound from different milk constituents.

Diacetyl is another important aroma compound that gives the yogurt a buttery flavour. Diacetyl is a diketone that is derived by the fermentation of citrate present in milk (Cheng, 2010; Vedamuthu, 2006). During the storage period, the absolute peak area of this diketone remained low and almost constant in the CTR sample, whereas the absolute peak area of diacetyl reached very high values in the SP sample (Fig. 2). Under the operation conditions adopted, *L. rhamnosus* DSA LR1 is believed to be characterized by a strong citrate degradation capacity, and this activity may slowly continue during the storage at 4 °C such that the highest absolute values would be reached at the end of this period. This ability of *L. rhamnosus* DSA LR1 may also be proved by the highest absolute peak areas of CO<sub>2</sub>, which were detected in the headspace of the experimental sample after 20 days of storage (Fig. 3). This compound is well known to be produced in high amount by these two metabolic pathways.

Fig. 4 shows the behaviours of acetone (A) and acetoin (B). Acetoin derives from the enzymatic degradation of diacetyl and

**Table 2**Mean values ( $\pm$ SD) of lactose content, pH and titratable acidity of the control (CTR) and the experimental (SP) yogurt samples stored at 4 °C for 20 days.

	Days	Lactose (g/100 g)	pH	Titratable acidity (g lactic acid/100 g)
CTR	0	2.95 $\pm$ 0.12 a	4.09 $\pm$ 0.01 a	1.10 $\pm$ 0.01 c
	10	n.d.	3.95 $\pm$ 0.01 c	1.18 $\pm$ 0.01 b
	20	n.d.	3.73 $\pm$ 0.04 d	1.22 $\pm$ 0.01 a
SP	0	3.04 $\pm$ 0.09 a	4.11 $\pm$ 0.04 a	1.05 $\pm$ 0.01 c
	10	n.d.	3.92 $\pm$ 0.02 c	1.19 $\pm$ 0.03 a,b
	20	n.d.	3.80 $\pm$ 0.01 d	1.21 $\pm$ 0.01 a

Within a column, values followed by the same letter are not significantly different according to Tuckey test ( $P \leq 0.05$ ).

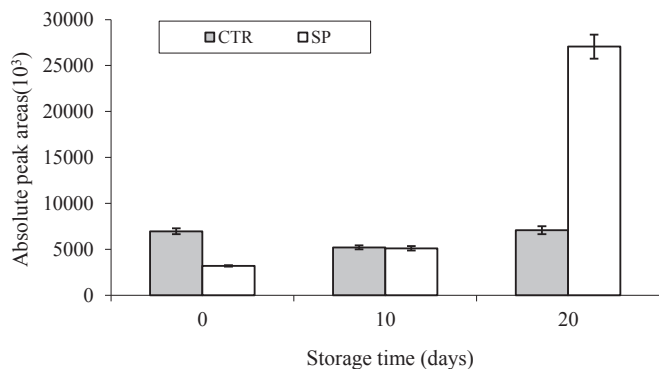


Fig. 2. Trends of diacetyl during storage of the experimental (SP) and the control (CTR) yogurt samples.

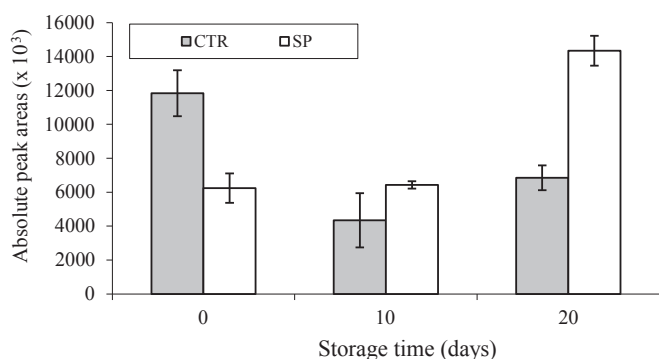


Fig. 3. Trends of CO<sub>2</sub> during storage of the experimental (SP) and the control (CTR) yogurt samples.

imparts buttery notes similar to those of its precursor, whereas acetone gives fruity notes (Tamime & Robinson, 2007; Cheng, 2010). For both of these compounds, a decrease in the CTR sample and an increase in the SP sample during the storage period could be observed; moreover, after 20 days of storage, the yogurt co-fermented with *L. rhamnosus* DSA LR1 was characterized by the highest absolute peak areas for both these ketones.

Fig. 5 reports the behaviour of the absolute peak areas of 2-heptanone and 2-nonanone, two methylketones derived from  $\beta$ -oxidation of octanoic acid and decarboxylation of decanoic acid, respectively (McSweeney & Sousa, 2000). Both of these compounds were found to have a significantly higher absolute peak area (Student t test,  $P \leq 0.05$ ) in the SP yogurt than in the CTR sample, possibly because the *L. rhamnosus* DSA LRA1 might have a slower but more prolonged capacity for oxidation and decarboxylation of fatty acids compared with the starters in the CTR sample. Gallardo-Escamilla, Kelly, and Delahunty (2005) reported that these compounds were significant for eliciting yogurt odour and contributes to the “fruity” flavour.

However, regarding the possible influence of the changes in metabolite concentrations on consumer appeal it is important to consider that although each of carbonyl compounds detected constitutes a recognizable aroma alone, yogurt flavour is determined by a corrected balanced mixture of the important volatile compounds. For example, 1:1 acetaldehyde and diacetyl ratio would give a preferred typical yogurt flavour, while too much acetaldehyde compared to diacetyl would lead to a green off-flavour. Also the ratio of acetaldehyde to acetone plays a significant role in the development of yogurt flavour, and a ratio of 2.8:1 results in the desired fullness flavor (Cheng, 2010).

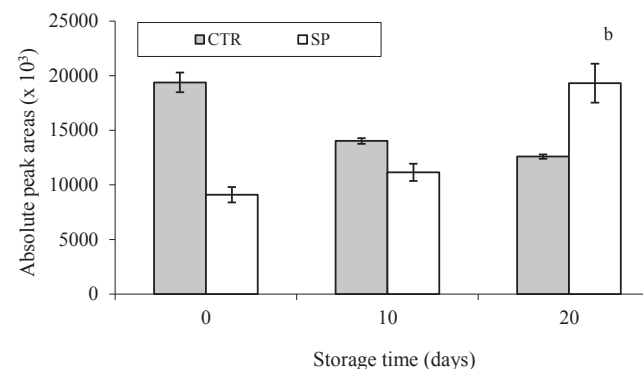
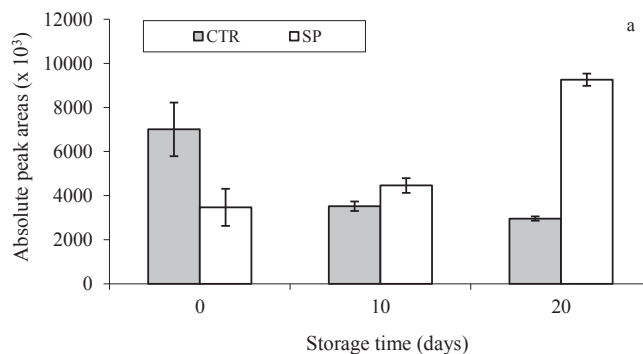


Fig. 4. Trends of acetone (a) and acetoin (b) during storage of the experimental (SP) and the control (CTR) yogurt samples.

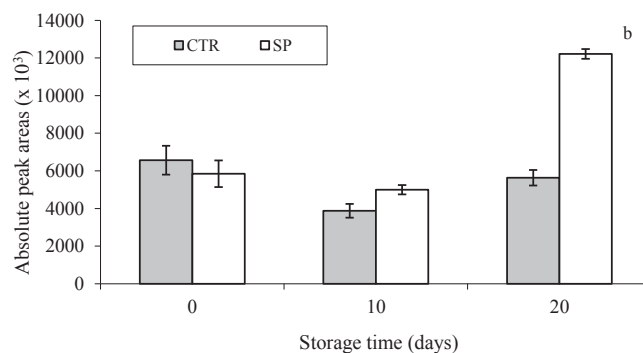
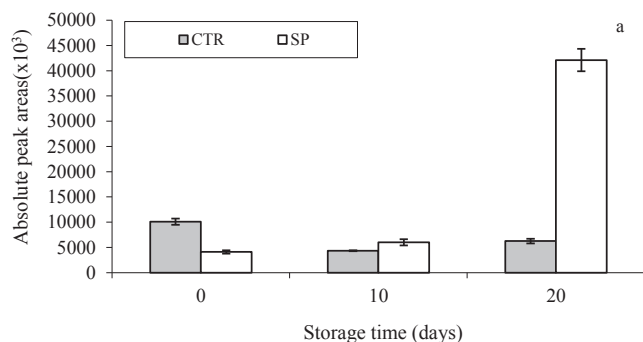


Fig. 5. Trends of 1,2-heptanone (a) and 2-nonanone (b) during storage of the experimental (SP) and the control (CTR) yogurt samples.

**Table 3**

Average values ( $\pm$ SD) of the absolute peaks area ( $\times 10^6$ ) of the fatty acid compounds determined in the head space of the control (CTR) and experimental (SP) samples stored at 4° C for 20 days.

Days	Absolute peak area $\times 10^6$				
	Acetic acid	Butanoic acid	Hexanoic acid	Octanoic acid	
0	CTR	34.44 $\pm$ 3.61 a	17.82 $\pm$ 1.53 a	31.42 $\pm$ 5.21 a	7.33 $\pm$ 0.63 a
	SP	24.38 $\pm$ 4.74 b	13.96 $\pm$ 1.67 b	25.40 $\pm$ 2.51 a	4.09 $\pm$ 1.19 b
10	CTR	38.98 $\pm$ 7.46 a	15.51 $\pm$ 3.72 a	22.04 $\pm$ 4.50 a	3.74 $\pm$ 0.79 a
	SP	29.06 $\pm$ 3.96 a	11.59 $\pm$ 1.72 a	20.26 $\pm$ 3.07 a	4.14 $\pm$ 1.44 a
20	CTR	45.50 $\pm$ 2.67 a	18.52 $\pm$ 0.40 a	26.25 $\pm$ 1.05 a	4.46 $\pm$ 0.28 b
	SP	51.81 $\pm$ 4.21 a	18.16 $\pm$ 1.19 a	26.35 $\pm$ 2.21 a	5.96 $\pm$ 0.54 a

For a same storage time, different letters indicate significant differences from the statistical point of view between the average values of the samples (Student t test,  $P \leq 0.05$ ).

Finally, the yogurt samples were characterized by the volatile profile of the following short-chain fatty acids: acetic, butanoic, hexanoic, and octanoic acid. These compounds are known to be produced during yogurt fermentation by both lipolytic processes ( $C_4$ – $C_{20}$ ) and lactic acid starter fermentation ( $C_2$ – $C_4$ ) (Tamime & Robinson, 2007). Generally, these compounds are reported to be present in yogurt in low amounts. They were found to have a relatively high absolute peak area in both of the yogurt samples (Table 3). Differences in the fatty acid profile between the CTR and the SP sample were determined only at the end of fermentation. These differences disappeared during yogurt storage. Therefore, the presence of *L. rhamnosus* DSA LR1 did not appear to affect the short-chain fatty acid profile of yogurt.

#### 4. Conclusions

From eleven different genotypes of *L. rhamnosus* isolated from the milk of a restricted geographical area in the northeast of Italy, the *L. rhamnosus* DSA LR1 was chosen for its ability to grow at the pH of gastric juices and in presence of bile salts.

Physicochemical and microbiological analysis of yogurt samples suggested no obvious interference from the addition of indigenous *L. rhamnosus* DSA LR1 on the growth, viability and acidification capacity of yogurt starters. The viability of the indigenous probiotic bacteria decreased slightly (approximately 1 log reduction) throughout the storage period such that after 20 days, *L. rhamnosus* DSA LR1 was present at an average value of approximately 7 log CFU mL<sup>-1</sup>, which still satisfied the minimum recommended level to ensure the potential health-promoting effects.

However, the co-fermentation with *L. rhamnosus* DSA LR1 influenced the aromatic profile of yogurt and allowed us to obtain a functional product that had a close link with the production area and was characterized by a more rich volatile profile at the end of the shelf-life.

Future studies should assess the effects of the different analytical aromatic profiles on the sensory characteristics of products. Indeed, a better understanding of how consumer acceptance is affected by the presence of aroma compounds can be obtained through determining the correlations of yogurt sensory properties with the volatile compound compositions. It should be considered that the volatile compounds–matrix interactions, the release mechanisms of volatile compound and their synergistic actions are some of the factors that could affect the aromatic contribution of different volatile compounds. Therefore, an affective test based on consumer perception should be performed to evaluate the changes in sensory characteristics of the yogurt caused by the addition of indigenous *L. rhamnosus* DSA LR1.

#### References

- Alamprese, C., Foschino, R., Rossi, M., Pompei, C., & Corti, S. (2005). Effects of *Lactobacillus rhamnosus* GG addition in ice-cream. *International Journal of Dairy Technology*, 58, 200–205.
- Biasutti, M., Venir, E., Marchesini, G., & Innocente, N. (2010). Rheological properties of model dairy emulsions as affected by high pressure homogenization. *Innovative Food Science and Emerging Technologies*, 11, 580–586.
- Cheng, H. (2010). Volatile flavor compounds in yogurt: a review. *Critical Reviews in Food Science and Nutrition*, 50, 938–950.
- Condurso, C., Verzera, A., Romeo, V., Ziino, M., & Conte, F. (2008). Solid-phase microextraction and gas chromatography mass spectrometry analysis of dairy product volatiles for the determination of shelf-life. *International Dairy Journal*, 18, 819–825.
- Corcoran, B. M., Stanton, C., Fitzgerald, G., & Ross, R. P. (2008). Life under stress: the probiotic stress response and how it may be manipulated. *Current Pharmaceutical Design*, 14, 1382–1399.
- Cruz, A. G., Castro, W. F., Faria, J. A. F., Lollo, P. C. B., Amaya-Farfán, J., Freitas, M. Q., et al. (2012). Probiotic yogurts manufactured with increased glucose oxidase levels: postacidification, proteolytic patterns, survival of probiotic microorganisms, production of organic acid and aroma compounds. *Journal Dairy Science*, 95, 2261–2269.
- Ercolini, D., Moschetti, G., Blaiotta, G., & Coppola, S. (2001). The potential of a polyphasic PCR-DGGE approach in evaluating microbial diversity of natural whey cultures for Water-Buffered Mozzarella cheese production: bias of culture-dependent and culture-independent analyses. *Systematic Applied Microbiology*, 24, 610–617.
- FAO WHO. (2002). *Guidelines for the evaluation of probiotics in food* (pp. 1–11). London, Ontario: Food and Agriculture Organization of the United Nations and World Health Organization Working Group Report.
- Gallardo-Escamilla, F. J., Kelly, A. L., & Delahunty, C. M. (2005). Influence of starter culture on flavour and headspace volatile profiles of fermented whey and whey produced from fermented milk. *Journal Dairy Science*, 88, 3745–3753.
- Granato, D., Branco, G. F., Cruz, A. G., de Assis Fonseca Faria, J., & Shah, N. P. (2010). Probiotic dairy products as functional foods. *Comprehensive Reviews in Food Science and Food Safety*, 9, 455–470.
- Guler, Z., & Park, Y. W. (2011). Characteristics of physico-chemical properties, volatile compounds and free fatty acid profiles of commercial set-type Turkish yoghurts. *Journal of Animal Sciences*, 1, 1–9.
- Hutkins, R. W. (2006). *Microbiology and technology of fermented foods* (1st ed.). Ames, Iowa, USA: Blackwell Publishing Professional Ed.
- Iacumin, L., Cecchini, F., Manzano, M., Osualdini, M., Boscolo, D., Orlic, S., et al. (2009). Description of the microflora of sourdoughs by culture-dependent and culture-independent methods. *Food Microbiology*, 26, 128–135.
- Iacumin, L., Comi, G., Cantoni, C., & Coccolin, L. (2006). Molecular and technological characterization of *Staphylococcus xylosum* isolated from naturally fermented Italian sausages by RAPD, Rep-PCR and Sau-PCR analysis. *Meat Science*, 74, 281–288.
- Iacumin, L., Ginaldi, F., Manzano, M., Anastasi, V., Reale, A., Zotta, T., et al. (2015). High resolution melting analysis (HRM) as a new tool for the identification of species belonging to the *Lactobacillus casei* group and comparison with species-specific PCRs and multiplex PCR. *Food Microbiology*, 46, 357–367.
- IDF. (1991). *Yogurt – Determination of titrable acidity. IDF standard 150*. Brussels, Belgium: International Dairy Federation.
- Innocente, N., Biasutti, M., & Comuzzo, G. (2007). Characterization of a traditional semi-hard Italian cheese produced by soaking in wine. *Food Chemistry*, 105, 1452–1456.
- Innocente, N., Biasutti, M., & Marchesini, G. (2009). Aroma retention capacity of different whey protein concentrates. *Milchwissenschaft-Milk Science International*, 64, 304–307.
- Innocente, N., Marchesini, G., & Biasutti, M. (2011). Feasibility of the SPME method for the determination of aroma retention capacity of the proteose-peptone milk protein fraction at different pH values. *Food Chemistry*, 124, 1249–1257.
- Innocente, N., Marchesini, G., & Biasutti, M. (2014). Effect of high-pressure homogenisation on the retention of selected aroma compounds in model dairy emulsions. *International Journal of Food Science & Technology*, 49, 1992–2000.
- Innocente, N., Munari, M., & Biasutti, M. (2013). Characterization by solid phase microextraction-gas chromatography of the volatile profile of protected designation of origin Montasio cheese during ripening. *Journal Dairy Science*, 96, 1–7.
- Innocente, N., Segat, A., Manzocco, L., Marino, M., Mifreni, M., Bortolomeoli, I., et al. (2014). Effect of pulsed light on total microbial count and alkaline phosphatase activity of raw milk. *International Dairy Journal*, 39, 108–112.
- Jeon, I. J., Galitzer, S. J., & Kenney, K. J. (1984). Rapid determination of lactose and its hydrolyzates in whey and whey permeate by high performance liquid chromatography. *Journal Dairy Science*, 67, 884–887.
- Kneifel, W., Ulbert, F., Erhard, F., & Jaros, D. (1992). Aroma profiles and sensory properties of yoghurt and yoghurt related products. I. Screening of commercially available starter cultures. *Milchwissenschaft*, 47, 362–365.
- Lee, Y. K., & Salminen, S. (1995). The coming of age of probiotics. *Trends in Food Science and Technology*, 6, 241–244.
- Maifreni, M., Frigo, F., Bortolomeoli, I., Innocente, N., Biasutti, M., & Marino, M. (2013). Identification of the enterobacteriaceae in Montasio cheese and assessment of their amino acid decarboxylase activity. *Journal Dairy Research*, 80, 122–127.

- Marshall, V. M. (1993). Starter cultures for milk fermentation and their characteristics. *International Journal Dairy Technology*, 46, 49–56.
- Mattila-Sandholm, T., Myllarinen, P., Crittenden, R., Mogensen, G., Fonden, R., & Saarela, M. (2002). Technological challenges for future probiotic foods. *International Dairy Journal*, 12, 173–182.
- McSweeney, P. L. H., & Sousa, M. J. (2000). Biochemical pathways for the production of flavour compounds in cheeses during ripening: a review. *Lait*, 80, 293–324.
- National Committee for Clinical Laboratory Standards. (1993). *Performance standards for antimicrobial disk and dilution susceptibility tests for bacteria isolated from animals; approved standard. NCCLS document M31A*. Wayne, Pennsylvania: National Committee for Clinical Laboratory Standards.
- Oliveira, M. N., Sodini, I., Remeuf, F., & Corrieu, G. (2001). Effect of milk supplementation and culture composition on acidification, textural properties and microbiological stability of fermented milks containing probiotic bacteria. *International Dairy Journal*, 11, 935–942.
- Ott, A., Fay, L. B., & Chaintreau, A. (1997). Determination and origin of the aroma impact compounds of yogurt flavor. *Journal Agricultural. Food Chemistry*, 45, 850–858.
- Ott, A., Germond, J., Baumgartner, M., & Chaintreau, A. (1999). Aroma comparisons of traditional and mild yogurts: headspace gas chromatography quantification of volatiles and origin of  $\alpha$ -diketones. *Journal Agricultural. Food Chemistry*, 47, 2379–2385.
- Pennacchia, C., Ercolini, D., Blaiotta, G., Pepe, O., Mauriello, G., & Villani, F. (2004). Selection of *Lactobacillus* strains from fermented sausages for their potential use as probiotics. *Meat Science*, 67, 309–317.
- Saad, N., Delattre, C., Urdaci, M., Schmitter, J. M., & Bressolier, P. (2013). An overview of the last advances in probiotic and prebiotic field. *LWT-Food Science and Technology*, 50, 1–16.
- Sanders, M. E. (1999). Probiotics. *Food Technology*, 53, 67–77.
- Segat, A., Biasutti, M., Iacumin, L., Carboni, C., & Innocente, N. (2014). Use of ozone in production chain of high moisture Mozzarella cheese. *LWT-Food Science and Technology*, 55, 513–514.
- Settachaimongkon, S., van Valenberg, H. J. F., Winata, V., Wang, X., Nout, M. J. R., van Hooijdonk, T. C. M., et al. (2015). Effect of sublethal preculturing on the survival of probiotics and metabolite formation in set-yogurt. *Food Microbiology*, 49, 104–115.
- Tamine, A. Y., & Robinson, R. K. (2007). *Yogurt: Science and technology* (2nd ed.). Boca Raton, FL: CRC Press.
- Ulberth, F., & Kneifel, W. (1992). Aroma profiles and sensory properties of yogurt and yogurt-related products. II. Classification of starter cultures by means of cluster analysis. *Milchwissenschaft*, 47, 432–434.
- Vedamuthu, E. R. (2006). Starter cultures for yogurt and fermented milk. In R. C. Chandan, C. White, A. Kilara, & Y. H. Hui (Eds.), *Manufacturing yogurt and fermented milks* (pp. 89–116). Ames, IA: Blackwell Publishing Professional Ed.
- Vinderola, C. G., & Reinheimer, J. A. (1999). Culture enumeration of *Bifidobacterium bifidum* and *Lactobacillus acidophilus* in the presence of yoghurt bacteria. *International Dairy Journal*, 9, 497–505.



# Combination of carboxymethyl cellulose-based coatings with calcium and ascorbic acid impacts in browning and quality of fresh-cut apples



Mahmoud Koushesh Saba<sup>a, \*</sup>, Ommol Banin Sogvar<sup>b</sup>

<sup>a</sup> Department of Horticultural Science, University of Kurdistan, Sanandaj, P.O.Box: 416, Iran

<sup>b</sup> Department of Horticultural Science, University of Kurdistan, Sanandaj, Iran

## ARTICLE INFO

### Article history:

Received 22 July 2015

Received in revised form

26 September 2015

Accepted 6 October 2015

Available online 22 October 2015

### Keywords:

Edible coating

Minimally processed fruit

Anti-browning agents

Polyphenol oxidase

## ABSTRACT

Fresh cut apples have a short shelf-life due to their high rate of deterioration, water loss and cut-surface browning that can rapidly reduce fruit quality. In this study the effects of carboxymethyl cellulose (CMC) coatings in combination with CaCl<sub>2</sub> and ascorbic acid (AA) has been studied. Apple slices were dipped for 5 min in distilled water (uncoated), CMC (1% w/v) + CaCl<sub>2</sub> (0.5%), or CMC (1%) + CaCl<sub>2</sub> (0.5%) + AA (2%), and then stored at 4 °C, 90–95% (RH). The treatments suppressed browning, retained flesh firmness, and reduced soluble solid content, titratable acidity and pH changes of the slices. Browning incidence with CMC in combination with AA was lower than that of CMC solely. Vitamin C and antioxidant capacity in treatments was higher than that of uncoated. Coating treatments generally reduced total phenolic and flavonoid concentrations and polyphenol oxidase and peroxidase activity changes of slices during storage. These findings suggest that the combination use of CMC + AA may be useful for maintaining quality and reducing surface browning of fresh cut apples.

© 2015 Elsevier Ltd. All rights reserved.

## 1. Introduction

Recently, there has been an increasing market demand for minimally processed fruits and vegetables. Fresh cut apples in particular are desired as a convenient snack for catering services to salad-bars, schools, and company cafeterias (Saftner, Abbott, Bhagwat, & Vinyard, 2005). However minimally processed products became more perishable because processing results in quality deterioration associated with water loss, softening, microbial contamination, increased respiration, and cut-surface browning (Rolle & Chism, 1987). Enzymatic browning is one of the most important reactions occur in many fresh-cut fruits and vegetables. The reaction in which phenolic compounds are oxidized is related to polyphenol oxidase (PPO) activity, the amount of phenolics, and the presence of oxygen (Koukounaras, Diamantidis, & Sfakiotakis, 2008). However, antioxidants are involved in browning and maintaining the commercial value of fresh cut products (Rojas-Grau, Sobrino-Lopez, Tapia, & Martin-Belloso, 2006).

Many compounds may be used to reduce browning in foods (McGhie, Hunt, & Barnett, 2005). Ascorbic acid (AA) is known as

one of the most widely used compounds, since it is very effective in reducing browning, generally recognized as safe, inexpensive, and consumer friendly (Robles-Sánchez, Rojas-Graü, Odriozola-Serrano, González-Aguilar, & Martin-Belloso, 2013a). AA treatments reduce cut surface browning and increase apple slice shelf life, but only for a short period of time, since use of AA soften the tissue and promotes microbial growth (Gil, Gorny, & Kader, 1998) and subsequent fruit deterioration. Moreover, once the AA has been completely oxidized to dehydro-ascorbic acid, the reaction lead to convert back quinones to phenolic compounds, quinones again can be accumulated and undergo browning (Sarpers, 1993).

Edible coatings have been used to reduce the deleterious effect brought about by minimal processing. The semipermeable barrier provided by edible coatings is aimed to extend shelf life by reducing moisture and solute migration, gas exchange, respiration, and oxidative reaction rates, as well as suppress physiological disorders on fresh-cut fruits (Rojas-Graü, Tapia, Rodríguez, Carmona, & Martin-Belloso, 2007; Rojas-Grau, Tapia, & Martin-Belloso, 2008). Carboxymethyl cellulose (CMC) is a linear, long-chain, water-soluble, anionic polysaccharide that can be used as fruit coating (Gol, Patel, & Rao, 2013). Purified CMC is a white to cream-colored, tasteless, odorless, free-flowing powder (Hattori, Abe, Yoshida, & Cuculo, 2004; Keller, 1986). Treatment with CMC can extend strawberry (Gol et al., 2013) and cucumber (Oluwaseun, Kayode,

\* Corresponding author.

E-mail address: [m.saba@uok.ac.ir](mailto:m.saba@uok.ac.ir) (M. Koushesh Saba).

Bolajoko, & Bunmi, 2013) shelf life and maintain quality of fruit. Edible coatings can also serve as carriers of food additives, e.g. anti-browning and antimicrobials agents, colorants, flavors, nutrients, and spices (Pranoto, Salokhe, & Rakshit, 2005).

Until recently, there have been few researches that investigated the effect of the combination of CMC and anti-browning agents for minimally processed products to inhibit enzymatic browning. The objective of this study was to develop procedures for the use of CMC coatings in combination with anti-browning agent and to extend the shelf-life of minimally processed apple slices.

## 2. Materials and methods

### 2.1. Fruit slicing and treatments

Apples (*Malus domestica* Borkh L.) of approximately same size and maturity were harvested from a commercial orchard and stored at 1 °C until processing. These fruits were rinsed gently with 200 µL L<sup>-1</sup> sodium hypochlorite solution, dried naturally and cut into eight equal slices using a sharp stainless steel knife and seed cavity was removed.

Coating solutions were prepared by dissolving CMC powder in distilled water (1% w/v) and heated at 85 °C for 30 min while stirring until the solution became clear and 2.5 mL 100<sup>-1</sup> mL glycerol was added as plasticizer. Fruit slices were divided in three groups and were dipped in the following solutions for 4 min, T1: distilled water as uncoated control, T2: CMC +0.5% CaCl<sub>2</sub> and T3: CMC +0.5% CaCl<sub>2</sub> +2% AA. Temperature of all solutions was 24 °C. Following, all fruit were air-dried at room temperature and then placed in polystyrene boxes, each containing 10 apple slices, and stored at 4 °C with 95% relative humidity. Three boxes were sampled at 0, 1, 3, 6, 9 and 12 days for each treatment.

### 2.2. Measurement of browning index

Evaluation of slices surface browning was subjectively based on a numeral scoring index (Lin et al., 2013) using a scale of 0–4, where 0 = none, 1 = slight (up to 5% surface affected), 2 = moderate (5–20% surface affected), 3 = moderately severe (20–50% surface affected) and 4 = extreme (>50% surface affected) for individual slices. Severity index of flesh browning determined as follows: ((% fruit with slight browning × 1) + (% fruit with moderate browning × 2) + (% fruit with moderately severe browning × 3) + (% fruit with extreme browning × 4))/5.

### 2.3. Fruit quality measurements

Fruit slice firmness was evaluated using a texture analyzer (Santam, STM-1, Iran), fitted with an 8 mm probe with constant speed of 20 mm min<sup>-1</sup>. Values were expressed as Newton (N). A wedge-shaped slice of flesh taken from each fruit slice was pooled and juiced. Soluble solids content (SSC) was measured using a temperature-compensated refractometer (Brix 0–32%, Atago, Japan). Titratable acidity (TA) was measured by titrating 10 mL of juice with 0.1 N NaOH to an end point of pH 8.2 and expressed as % malic acid. The pH of fruit juice was measured using a pH meter (Metrohm 827, Switzerland).

### 2.4. Vitamin C assay

Vitamin C content was determined by titration with 2,6-dichlorophenolindophenol (DCPIP) (AOAC, 2000), using different AA concentrations for the standard curve, and expressed in mg of vitamin C per 100 g fresh weight (FW).

### 2.5. Total phenol (TP) and total flavonoid (TF) concentration

TP concentrations were measured by homogenizing 1 g of frozen tissue from each replicate with 3 mL ice cold 1% HCl–methanol solution and then centrifuged at 4 °C for 15 min at 12,000× g. The supernatant was collected and used for phenol determination. TP concentration in the extracts were determined according to the Folin–Ciocalteu procedure (Orthofer & Lamuela-Raventos, 1999), using gallic acid for the standard curve. Results are expressed as mg of gallic acid equivalent (GAE) per 100 g of FW.

TF concentrations were measured according to Bouayed, Hoffmann, and Bohn (2011). One mL aliquot of catechin standard solution (0–100 mg/L) or samples were added to 10 mL volumetric flasks containing 4 mL water. Initially 0.3 mL of 5% NaNO<sub>2</sub> was added to the flask, following 0.3 mL of 10% AlCl<sub>3</sub> was added after 5 min, and then 2 mL of 1 M NaOH was added to the mixture. Immediately, the solution was diluted to a final volume of 10 mL with water and mixed thoroughly. The absorbance was measured at 510 nm, using a spectrophotometer (Unico UV-2100, USA). TF was expressed as mg catechin equivalents per 100 g FW.

### 2.6. Total antioxidant activity (TAA)

TAA was determined by the 2,2-Diphenyl-1-picryl-hydrazil (DPPH) radical-scavenging method according to Sanchez Moreno, Larrauri, and Saura-Calixto (1999). The absorbance was measured at 517 nm, using a spectrophotometer. Total antioxidant activity was expressed as the percentage inhibition of the DPPH radical and was determined using the following equation:

$$\text{TAA}(\%) = \frac{\text{Abs}_{\text{sample}} - \text{Abs}_{\text{control}}}{\text{Abs}_{\text{sample}}} \times 100$$

### 2.7. Enzyme activities

The activity of peroxidase (POX) and superoxide dismutase (SOD) was measured using 1 g of sample homogenized in 2 mL of freshly prepared 100 mM phosphate buffer (pH 7). The homogenate was centrifuged and the supernatant was used as a source of crude enzyme. All steps to obtain enzyme preparations were carried out at 4 °C.

POX activity was determined by the rate of guaiacol oxidation in the presence of hydrogen peroxide at 470 nm for 1 min, as described previously (Ghanati, Morita, & Yokota, 2002). The reaction mixture contained 50 mM phosphate buffer (pH 7), 28 mM guaiacol, and enzyme extract in a 3 mL assay volume, and the reaction was initiated by adding hydrogen peroxide at a final concentration of 5 mM. The enzyme activity was expressed as units of enzyme per milligram of protein. SOD activity was determined by measuring the ability of SOD to inhibit the photochemical reduction of nitroblue tetrazolium (NBT) at 560 nm after exposure to a light for 30 min (Giannopolitis & Ries, 1977), as described previously (Koushesh Saba, Arzani, & Barzegar, 2012). A total of 1 unit of SOD activity is defined as the amount of enzyme that inhibits the NBT photoreduction by 50% under the assay conditions.

PPO enzyme was extracted by blending 1 g of frozen sample in freshly prepared 100 mM phosphate buffer (pH 6.8) containing polyvinylpyrrolidone (PVP), followed by centrifugation at 16000g for 20 min, as described previously. Aliquots of the supernatant were added to solution containing catechol at a final concentration of 0.05 M. The increase in absorbance was monitored at 410 nm for 2 min at 25 °C. PPO activity was expressed as units per milligram of protein of the homogenate (Koushesh Saba et al., 2012).

The protein concentration in each sample was determined by the method described in the literature using bovine serum albumin (BSA) as a standard.

## 2.8. Statistical analysis

Data for the analytical determinations were subjected to analysis of variance (ANOVA) with the SAS 8.0 software (SAS Institute Inc., Cary, USA). Sources of variation were storage life (days) duration and treatments. Mean values were calculated and reported as the mean  $\pm$  standard error ( $n = 3$ ). The least significant difference (LSD) test at  $P$  value 0.05 was used to compare means among treatments.

## 3. Results

### 3.1. Browning index (BI)

The sign of browning was first detected at 1 day storage; thereafter, BI incidence and severity increased with a longer storage in uncoated or coated apple slices. However, BI was strongly suppressed in fruit coated with CMC coating or CMC in combination with AA. The effect of CMC + AA on BI was greater than that for CMC alone (Fig. 1).

### 3.2. Fruit quality

Fruit firmness of uncoated fruit decreased from 23.40 to 17.00 N during storage but coated fruit retain firmness. Uncoated fruit loss 27.24% of their firmness, while coated fruit with CMC and CMC + AA in combination with  $\text{CaCl}_2$  retained 99.52 and 99.88% of firmness, respectively, after 12 days of storage (Fig. 2A).

SSC progressively increased regardless of treatments during storage; but SSC of uncoated slices increased greater than CMC +  $\text{CaCl}_2$  alone or + AA – coated fruit (Fig. 2B). SSC in uncoated fruit was greater than coated fruit in all sampling time while there was no difference between CMC alone or in combination with AA.

TA decreased during storage for all samples (Fig. 2C). Fruit coated with CMC had a significant lower loss of TA than the uncoated fruits. Fruit pH increased during storage in either coated or uncoated but it was greater in uncoated than coating treatments.

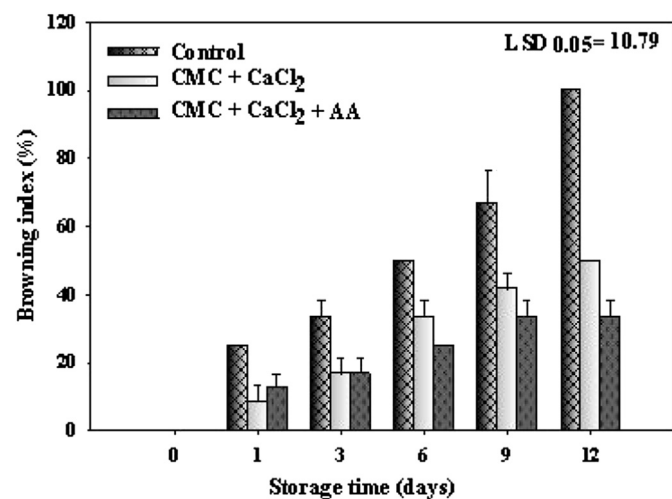


Fig. 1. Browning index of fresh-cut apples in fruit either uncoated or coated with CMC alone or in combination with AA. Fruit were stored at 4 °C for up to 12 days. Vertical bars represent standard error ( $n = 3$ ).

### 3.3. Vitamin C content

Vitamin C content decreased over 12 days storage time at 4 °C in coated and uncoated apple slices, however CMC coating maintained higher vitamin C content during storage (Fig. 2D). Initial vitamin C content was 15 mg 100 g<sup>-1</sup> FW. Over the storage vitamin C content decreased to 1.30, 4 and 4.90 mg 100 g<sup>-1</sup> FW in uncoated, CMC +  $\text{CaCl}_2$  and CMC +  $\text{CaCl}_2$  + AA, respectively.

### 3.4. TP and TF content

TP concentration decreased regardless of treatments; but TP of CMC +  $\text{CaCl}_2$  alone or + AA – coated fruit were greater than that of uncoated fruit. The effect of coating in combination with AA was greater than that for CMC alone (Fig. 3B).

TF concentration decreased in both coated and uncoated slices during storage. Although the difference among treatments were not significant but the overall flavonoids content were 10.48, 11.08 and 11.60 mg 100 g<sup>-1</sup> FW in uncoated, CMC +  $\text{CaCl}_2$  and CMC +  $\text{CaCl}_2$  + AA treatments (Fig. 3C).

### 3.5. Total antioxidant activity (TAA)

TAA decreased in uncoated but were relatively stable in coated fruit slices during the 12 days of cold storage. There was no difference in fruit TAA after treatment with either CMC alone or CMC combination with AA (Fig. 3A).

### 3.6. Enzyme activities

PPO and POX enzymes activities in all apple slices increased continuously along storage times. However, coated apple slices showed relatively lowered PPO and POX activities as compared to the uncoated during storage. PPO and POX activities in uncoated samples were 2.16 and 17.56 U mg<sup>-1</sup> protein at the end of storage, respectively, while PPO and POX activities in CMC +  $\text{CaCl}_2$  + AA were 1 and 12.00 U mg<sup>-1</sup> protein at same time, respectively (Fig. 4A, B).

SOD activity was 2.50 U mg<sup>-1</sup> protein at first day and decreased to 0.10, 0.70 and 1 U mg<sup>-1</sup> protein in uncoated, CMC +  $\text{CaCl}_2$  and CMC +  $\text{CaCl}_2$  + AA treatments, respectively. The SOD activity in CMC +  $\text{CaCl}_2$  + AA was significantly greater than other treatment over storage time (Fig. 3D).

## 4. Discussion

Apple fruits are undergoing browning during minimally processing. In the current study the incidence of browning was evidence after 1 day storage at 4 °C and increased thereafter. However, coating treatments markedly reduce BI to about 41.55% of uncoated levels after 12 days of storage. BI index in CMC + AA treatment was lower than in CMC treatment alone, so that BI incidence of CMC treatment on day 12 was 16.67% higher than CMC + AA treatment. Fruit coatings have been reported to act protectively in minimally processed fruit and prevented BI in apple (Chauhan, Raju, Singh, & Bawa, 2011; Li-Qin, Jie, Shu-Hua, & Lai-Hui, 2009; Perez-Gago, Serra, & Del Rio, 2006; Qi, Hu, Jiang, Tian, & Li, 2011; Wu & Chen, 2013), pear (Oms-Oliu, Soliva-Fortuny, & Martín-Belloso, 2008a) and papaya (Tapia et al., 2008). AA also has been used as a highly effective inhibitor of enzymatic browning in peach slice (Li-Qin et al., 2009) and apple (Gil et al., 1998) because of a reduction in phenolic compound oxidation and its ability to reduce quinones back to phenolic compounds (Perez-Gago et al., 2006). Olivas, Rodriguez, and Barbosa-Canovas (2003) reported the positive effect of the incorporation of some additives (ascorbic acid, calcium

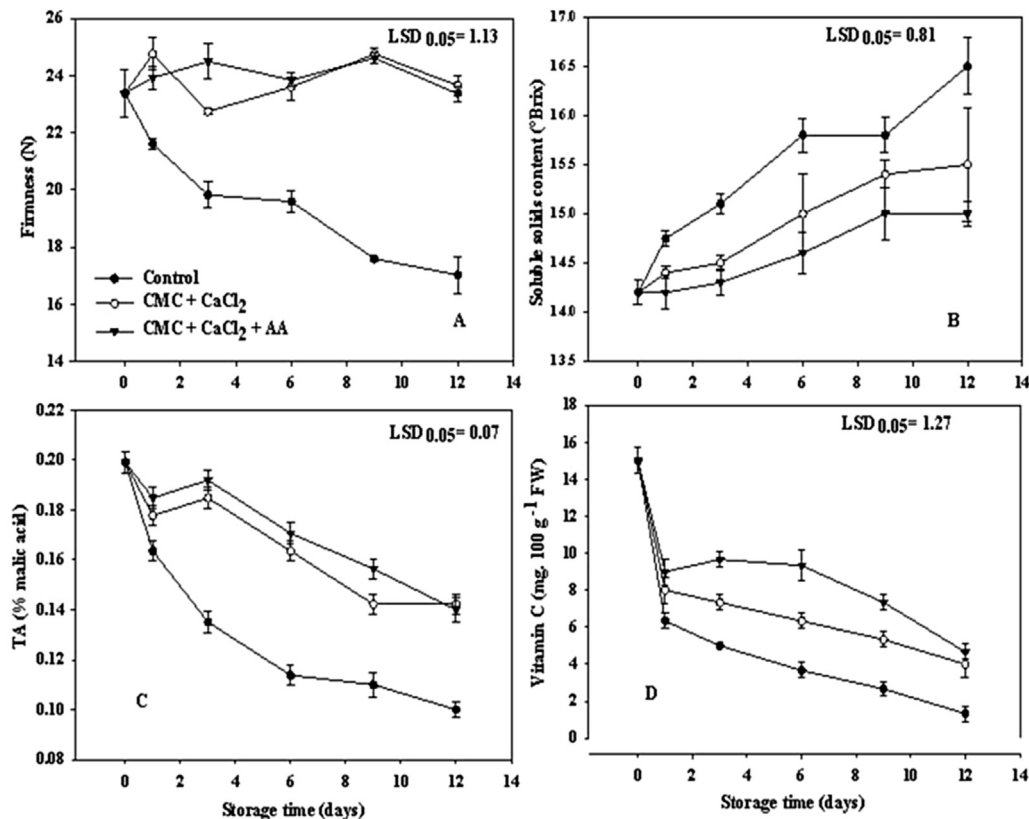


Fig. 2. Firmness (N) (A), Soluble solids content ( $^{\circ}$ Brix) (B), TA (% malic acid) (C) and Vitamin C ( $\text{mg } 100 \text{ g}^{-1} \text{ FW}$ ) (D) in fresh-cut apples either uncoated or coated with CMC alone or in combination with AA. Fruit were stored at  $4^{\circ}\text{C}$  for up to 12 days. Vertical bars represent standard error ( $n = 3$ ).

chloride and sorbic acid) into methylcellulose coatings on the browning control of fresh-cut 'Anjou' pears. Recent work confirmed that CMC coatings have the potential to carry and hold additives as anti-browning agents on the surface of cut tissues, and in this way aid in being more effective for control of browning.

It has been reported that fresh cut coated with edible coating enhanced or retain fruit firmness (Oluwaseun et al., 2013; Qi et al., 2011; Rojas-Grau et al., 2008). Apple slices firmness was also retained by CMC coating in the current study (Fig. 2A). The softening observed in apple fresh cuts may be due to the pectic acid undergoing acid hydrolysis. Calcium chloride treatments firm fruit tissue by reacting with pectic acid in the cell wall to form calcium pectate which strengthens molecular bonding between constituents of cell wall (Gorny, Gil, & Kader, 1996; King & Bolin, 1989). Treating apple fruits slices with chitosan coating +0.5%  $\text{CaCl}_2$  has been reported that significantly retained slice firmness and reduced cut surface browning (Qi et al., 2011). In agreement to previous reports on fruit coating, CMC combination with  $\text{CaCl}_2$ , effectively retain apple slice firmness.

Vitamin C content of apple slices decreased significantly in uncoated and coated fruit during first day of processing, however treatments delayed vitamin C losses thereafter. Vitamin C is lost due to the activities of phenol oxidase and ascorbic acid oxidase enzymes during storage (Salunkhe, Boun, & Rddy, 1991). It has been reported that CMC coating was effective in reducing the vitamin C loss in cucumber fruit during storage (Oluwaseun et al., 2013). Vitamin C losses were also delayed by CMC coating in current study (Fig. 2D). The reduction of ascorbic acid loss in coated fruit may be due to the low oxygen permeability of CMC coating (Freire, Lebrun, Ducamp, & Reynes, 2005), which lowered the activity of the enzymes and prevented oxidation of ascorbic acid. In recent work the

reduction in vitamin C in CMC + AA was slower than that of CMC alone (Fig. 2D). These results are similar to those who found that fresh cut coated with AA led to delay vitamin losses (Robles-Sánchez, Rojas-Grau, Odriozola-Serrano, González-Aguilar, & Martín-Belloso, 2013b; Sun, Liang, Xie, Lei, & Mo, 2010).

During the storage of fresh cut apple, both TP and TF concentration decreased however, those of coated fruit was greater than that of uncoated in all sampling times (Fig. 3B, C). These findings are in agreement to those found that tomato fruit coated with gum arabic maintained total antioxidant capacity and total phenolics during storage as compared to the uncoated fruit (Ali, Maqbool, Alderson, & Zahid, 2013). Although CMC alone was effective to decline TP and TF reduction, but the combination of CMC and AA was more effective to maintain both TP and TF in apple slices (Fig. 3B, C). It has been reported that AA treatments (Gil et al., 1998) or other antioxidants (Oms-Oliu et al. 2008a), which act as efficient reducing agents, are able to prevent phenolic compounds decline.

Antioxidant activity of 'Jonagold' and 'Sampion' apples increased (Leja, Mareczek, & Ben, 2003), while that of 'Golden' apple reduced during storage (Bouayed et al., 2011). It has been reported that fruit coating were effective to maintain antioxidant capacity in either whole fruit (Ali et al., 2013) or fresh cuts (Oms-Oliu, Soliva-Fortuny, & Martín-Belloso, 2008b). In current study, antioxidant capacity markedly reduced during apple slice storage in uncoated but CMC coating alone or in combination with AA retained antioxidant capacity as same levels as the first day (Fig. 3A). Similarly AA treatments maintain the antioxidant capacity in apple slices (Javdani, Ghasemnezhad, & Zare, 2013). It has been suggested ascorbic acid exerts protection by: (1) acting as an oxygen scavenger, removing molecular oxygen and avoiding polyphenol oxidase-catalyzed reactions (Rico, Martín-Diana, Barat, &

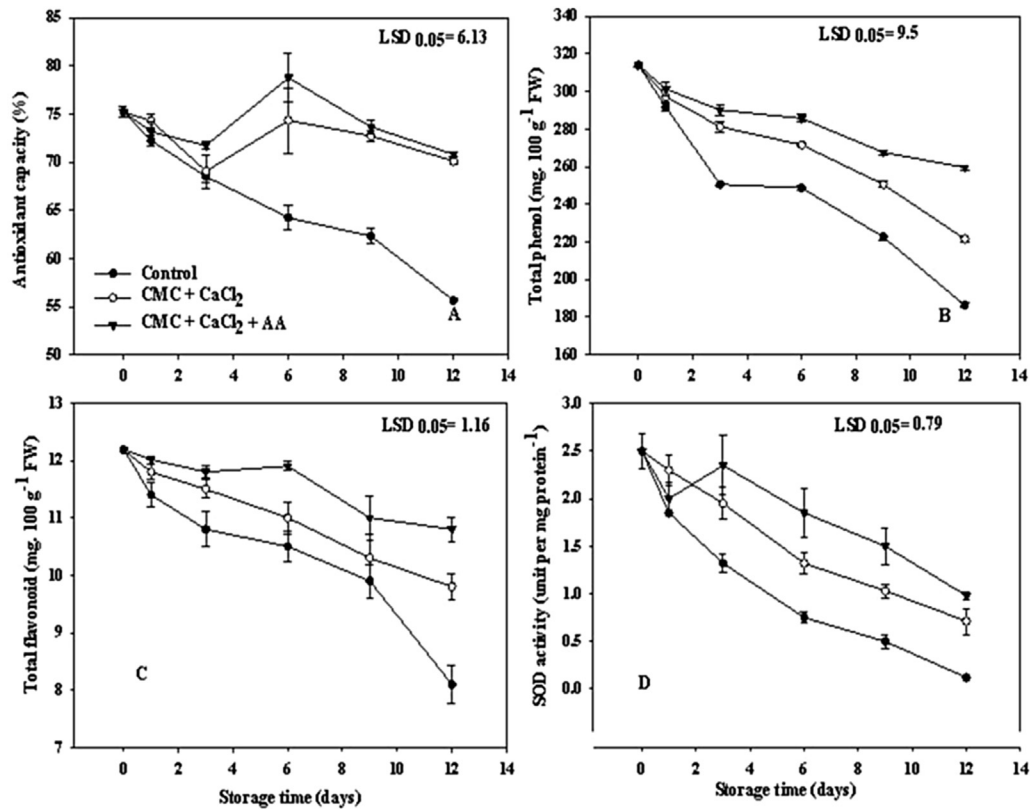


**Fig. 3.** Antioxidant capacity (%) (A), Total phenol (mg 100 g<sup>-1</sup> FW) (B), Total flavonoid (mg 100 g<sup>-1</sup> FW) (C) and SOD activity (unit per mg protein<sup>-1</sup>) (D) in fresh-cut apples either uncoated or coated with CMC alone or in combination with AA. Fruit were stored at 4 °C for up to 12 days. Vertical bars represent standard error (n = 3).

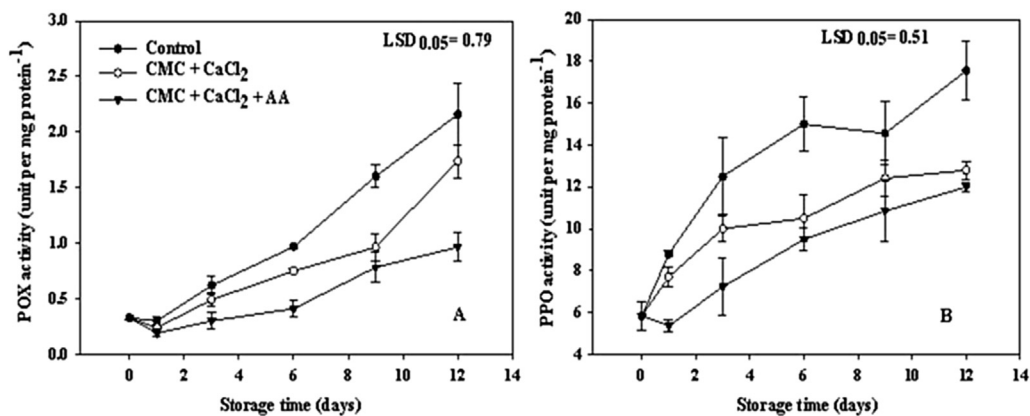


**Fig. 4.** POX activity (unit per mg protein<sup>-1</sup>) (A) and PPO activity (unit per mg protein<sup>-1</sup>) (B) in fresh-cut apples either uncoated or coated with CMC alone or in combination with AA. Fruit were stored at 4 °C for up to 12 days. Vertical bars represent standard error (n = 3).

Barry-Ryan, 2007) and (2) self-oxidation to avoid oxidation of phenol compounds or reduction of enzymatically formed o-quinones to their precursor diphenols (Mayer & Harel, 1979). Therefore, it is possible the AA treatment reduced cut surface browning by increasing antioxidant capacity in apple slices.

PPO is considered to be the key enzyme in cut surface browning on fresh-cut fruits and vegetables (Javdani et al., 2013; Sun et al., 2010; Tapia et al., 2008). It is generally assumed that minimal processing operations cause disruption of compartmentalization in apple, allowing substrates and PPO to come into contact to result in browning. It is also necessary to study the changes in POX enzymes as they can contribute to the discoloration in fresh-cut products

(Jang & Moon, 2011). The overall PPO and POX activity increased in either uncoated or coated apple slices but, PPO and POX enzymes activity in coating treatments, especially CMC + AA was always lower than the uncoated slices (Fig. 4A, B). In agreement to these results it has been reported that chitosan + AA decreased PPO activity (Sun et al., 2010) while in contrast, PPO activity was unaffected by AA in fresh-cut cantaloupe melon (Lamikanra & Watson, 2001).

The effects of AA on POX are in agreement with those of Jang & Moon, (2011), who reported that the presence of ascorbic acid effectively reduced the POX activity in the fresh cut apple. The reduced POX activity in the AA-coated fruit could be the result of a

lower oxidative stress on the fruit surface, because of the antioxidant nature of molecular AA, or the utilization of POX enzyme-hydrogen donor complex formation.

The SOD enzyme is the first line of cell defense against free radicals, and its greater activity in fruits has been related to a higher resistance to stress and a longer commercial life. High SOD activity has been associated with stress tolerance in plants because it neutralizes the reactivity of the superoxide radical, which is over produced under stress (Bowler, Montagu, & Inze, 1992). In recent work, although enzyme activity decreased during apple fresh cut storage but, SOD activity in CMC treatments, especially CMC + AA was always higher than the uncoated (Fig. 3D). These results were in agreement with Sun et al. (2010) who reported that the coated litchi fruits with chitosan and AA showed a relative higher value of SOD than the uncoated.

## 5. Conclusions

The present research findings indicated that a combination of CMC and AA seemed to have a synergistic effect for control of surface browning of fresh-cut apple during storage. Coatings retarded tissue softening, maintained vitamin C and antioxidant capacity greater than the uncoated in minimally processed apple slices during storage. Also, in this study coating treatments significantly decreased PPO and POX activity that are related to browning in fresh cut apple. The effect of AA on PPO and POX could be related to its preservative action on apple cut surface. These results suggest that CMC plus AA treatments may be a useful way for maintaining fresh cut apples fruit quality without browning and extending their postharvest life rather than coating treatment alone.

## Acknowledgment

We thank University of Kurdistan for providing facilities and financial support. Furthermore, we express our thanks to Professor Christopher B. Watkins, Cornell University, Ithaca, NY, for his valuable comments on the manuscript and English revision.

## References

- Ali, A., Maqbool, M., Alderson, P. G., & Zahid, N. (2013). Effect of gum arabic as an edible coating on antioxidant capacity of tomato (*Solanum lycopersicum* L.) fruit during storage. *Postharvest Biology and Technology*, 76, 119–124.
- AOAC. (2000). Vitamin C (ascorbic acid) in vitamin preparations and juices: 2, 6 titrimetric method final action. *Association of Official Analytical Chemists Official Method*, 4(967), 21.
- Bouayed, J., Hoffmann, L., & Bohn, T. (2011). Total phenolics, flavonoids, anthocyanins and antioxidant activity following simulated gastro-intestinal digestion and dialysis of apple varieties: bioaccessibility and potential uptake. *Food Chemistry*, 128(1), 14–21.
- Bowler, C., Montagu, M. V., & Inze, D. (1992). Superoxide dismutase and stress tolerance. *Annual Review of Plant Biology*, 43(1), 83–116.
- Chauhan, O. P., Raju, P. S., Singh, A., & Bawa, A. S. (2011). Shellac and aloe-gel-based surface coatings for maintaining keeping quality of apple slices. *Food Chemistry*, 126(3), 961–966.
- Freire, M., Lebrun, M., Ducamp, M. N., & Reynes, M. (2005). Evaluation of edible coatings in fresh cuts mango fruits. *Alimentaria*, 369, 85–91.
- Ghanati, F., Morita, A., & Yokota, H. (2002). Induction of suberin and increase of lignin content by excess boron in tobacco cells. *Soil Science and Plant Nutrition*, 48(3), 357–364.
- Giannopolitis, C. N., & Ries, S. K. (1977). Superoxide dismutases I. Occurrence in higher plants. *Plant Physiology*, 59(2), 309–314.
- Gil, M. I., Gorny, J. R., & Kader, A. A. (1998). Responses of 'Fuji' apple slices to ascorbic acid treatments and low-oxygen atmospheres. *HortScience*, 33(2), 305–309.
- Gol, N. B., Patel, P. R., & Rao, T. V. R. (2013). Improvement of quality and shelf-life of strawberries with edible coatings enriched with chitosan. *Postharvest Biology and Technology*, 85(1), 185–195.
- Gorny, J. R., Gil, M. I., & Kader, A. A. (1996). Postharvest physiology and quality maintenance of fresh-cut pears. *Acta Horticulture*, 464, 231–236.
- Hattori, K., Abe, E., Yoshida, T., & Cuculo, J. A. (2004). New solvents for cellulose. II. Ethylenediamine/thiocyanate salt system. *Polymer*, 36(2), 123–130.
- Jang, J.-H., & Moon, K.-D. (2011). Inhibition of polyphenol oxidase and peroxidase activities on fresh-cut apple by simultaneous treatment of ultrasound and ascorbic acid. *Food Chemistry*, 124(2), 444–449.
- Javdani, Z., Ghasemnezhad, M., & Zare, S. (2013). A comparison of heat treatment and ascorbic acid on controlling enzymatic browning of fresh-cuts apple fruit. *International Journal of Agriculture and Crop Sciences*, 5(3), 186–193.
- Keller, J. D. (1986). Sodium carboxymethylcellulose (CMC). In M. Glicksman (Ed.), *Food hydrocolloids* (pp. 43–109). Boca Raton FL, USA: CRC Press, Inc.
- King, A. D., & Bolin, H. R. (1989). Physiological and microbiological storage of stability of minimally processed fruits and vegetables. *HortScience*, 3043(1), 132–139.
- Koukounaras, A., Diamantidis, G., & Sfakiotakis, E. (2008). The effect of heat treatment on quality retention of fresh-cut peach. *Postharvest Biology and Technology*, 48(1), 30–36.
- Koushesh Saba, M., Arzani, K., & Barzegar, M. (2012). Postharvest polyamine application alleviates chilling injury and affects apricot storage ability. *Journal of Agricultural and Food Chemistry*, 60, 8947–8953.
- Lamikanra, O., & Watson, M. A. (2001). Effects of ascorbic acid on peroxidase and polyphenoloxidase activities in fresh-cut cantaloupe melon. *Journal of Food Science*, 66(9), 1283–1286.
- Leja, M., Mareczek, A., & Ben, J. (2003). Antioxidant properties of two apple cultivars during long-term storage. *Food Chemistry*, 80(3), 303–307.
- Li-Qin, Z., Jie, Z., Shu-Hua, Z., & Lai-Hui, G. (2009). Inhibition of browning on the surface of peach slices by short-term exposure to nitric oxide and ascorbic acid. *Food Chemistry*, 114(1), 174–179.
- Lin, Y. F., Hu, Y. H., Lin, H. T., Liu, X., Chen, Y. H., Zhang, S., et al. (2013). Inhibitory effects of propyl gallate on tyrosinase and its application in controlling pericarp browning of harvested longan fruits. *Journal of Agricultural and Food Chemistry*, 61, 2889–2895.
- Mayer, A. M., & Harel, E. (1979). Polyphenol oxidases in plants. *Phytochemistry*, 18(2), 193–215.
- McGhie, T. K., Hunt, M., & Barnett, L. E. (2005). Cultivar and growing region determine the antioxidant polyphenolic concentration and composition of apples grown in New Zealand. *Journal of Agricultural and Food Chemistry*, 53(8), 3065–3070.
- Olivas, G. I., Rodriguez, J. J., & Barbosa-Canovas, G. (2003). Edible coatings composed of methylcellulose, stearic acid, and additives to preserve quality of pear wedges. *Journal of Food Processing and Preservation*, 27(4), 299–320.
- Oluwaseun, A. C., Kayode, A., Bolajoko, F. O., & Bunmi, A. J. (2013). Effects of coatings on storability of carrot under evaporative coolant system. *Albanian Journal of Agricultural Sciences*, 12(3), 485.
- Oms-Oliu, G., Soliva-Fortuny, R., & Martín-Belloso, O. (2008a). Edible coatings with antibrowning agents to maintain sensory quality and antioxidant properties of fresh-cut pears. *Postharvest Biology and Technology*, 50(1), 87–94.
- Oms-Oliu, G., Soliva-Fortuny, R., & Martín-Belloso, O. (2008b). Using polysaccharide-based edible coatings to enhance quality and antioxidant properties of fresh-cut melon. *LWT - Food Science and Technology*, 41(10), 1862–1870.
- Orthofer, R., & Lamuela-Raventos, R. M. (1999). Analysis of total phenols and other oxidation substrates and antioxidants by means of Folin–Ciocalteu, s reagent. *Methods in Enzymology*, 299(8), 152–178.
- Perez-Gago, M. B., Serra, M., & Del Rio, M. A. (2006). Color change of fresh-cut apples coated with whey protein concentrate-based edible coatings. *Postharvest Biology and Technology*, 39(1), 84–92.
- Pranoto, Y., Salokhe, V. M., & Rakshit, S. K. (2005). Physical and antibacterial properties of alginate-based edible film incorporated with garlic oil. *Food Research International*, 38(3), 267–272.
- Qi, H., Hu, W., Jiang, A., Tian, M., & Li, Y. (2011). Extending shelf-life of fresh-cut "Fuji" apples with chitosan-coatings. *Innovative Food Science & Emerging Technologies*, 12(1), 62–66.
- Rico, D., Martín-Diana, A. B., Barat, J. M., & Barry-Ryan, C. (2007). Extending and measuring the quality of fresh-cut fruit and vegetables: a review. *Trends in Food Science & Technology*, 18(7), 373–386.
- Robles-Sánchez, R. M., Rojas-Graü, M. A., Odriozola-Serrano, I., González-Aguilar, G., & Martín-Belloso, O. (2013a). Influence of alginate-based edible coating as carrier of antibrowning agents on bioactive compounds and antioxidant activity in fresh-cut Kent mangoes. *LWT - Food Science and Technology*, 50(1), 240–246.
- Robles-Sánchez, R. M., Rojas-Graü, M. A., Odriozola-Serrano, I., González-Aguilar, G., & Martín-Belloso, O. (2013b). Influence of alginate-based edible coating as carrier of antibrowning agents on bioactive compounds and antioxidant activity in fresh-cut Kent mangoes. *LWT-Food Science and Technology*, 50(1), 240–246.
- Rojas-Grau, M. A., Sobrino-Lopez, A., Tapia, M. S., & Martín-Belloso, O. (2006). Browning inhibition in fresh-cut Fuji apple slices by natural antibrowning agents. *Journal of Food Science - Chicago*, 71(1), 59–65.
- Rojas-Grau, M. A., Tapia, M. S., & Martín-Belloso, O. (2008). Using polysaccharide-based edible coatings to maintain quality of fresh-cut Fuji apples. *LWT-Food Science and Technology*, 41(1), 139–147.
- Rojas-Graü, M. A., Tapia, M. S., Rodríguez, F. J., Carmona, A. J., & Martín-Belloso, O. (2007). Alginate and gellan-based edible coatings as carriers of antibrowning agents applied on fresh-cut Fuji apples. *Food Hydrocolloids*, 21(1), 118–127.
- Rolle, R. S., & Chism, G. W. (1987). Physiological consequences of minimally processed fruits and vegetables. *Journal of Food Quality*, 10(3), 157–177.
- Saftner, R. A., Abbott, J., Bhagwat, A. A., & Vinyard, B. (2005). Quality measurement of intact and fresh cut slices of Fuji, Granny Smith, Pink Lady, and GoldRush apples. *Journal of Food Science*, 70(5), 317–324.
- Salunkhe, D. K., Boun, H. R., & Rddy, N. R. (1991). *Storage processing and nutritional*

- quality of fruits and vegetables (vol. 1). CRC Press Inc. Fresh Fruits and Vegetables.
- Sanchez Moreno, C., Larrauri, J. A., & Saura-Calixto, F. (1999). A procedure to measure the antiradical efficiency of polyphenols. *Journal of the Science of Food and Agriculture*, 76, 270–276.
- Sarpers, G. M. (1993). Browning of foods: control by sulfates, antioxidants, and other means. *Food Technology*, 47(10), 75–84.
- Sun, D., Liang, G., Xie, J., Lei, X., & Mo, Y. (2010). Improved preservation effects of litchi fruit by combining chitosan coating with ascorbic acid treatment during postharvest storage. *African Journal of Biotechnology*, 9(22), 3272–3279.
- Tapia, M. S., Rojas-Graü, M. A., Carmona, A., Rodriguez, F. J., Soliva-Fortuny, R., & Martin-Belloso, O. (2008). Use of alginate-and gellan-based coatings for improving barrier, texture and nutritional properties of fresh-cut papaya. *Food Hydrocolloids*, 22(8), 1493–1503.
- Wu, S., & Chen, J. (2013). Using pullulan-based edible coatings to extend shelf-life of fresh-cut “Fuji” apples. *International Journal of Biological Macromolecules*, 55, 254–257.



Contents lists available at ScienceDirect

## LWT - Food Science and Technology

journal homepage: [www.elsevier.com/locate/lwt](http://www.elsevier.com/locate/lwt)

# Effect of processing factors on Shea (*Vitellaria paradoxa*) butter extraction

G.A. Yonas<sup>a,\*</sup>, E.A. Shimelis<sup>b</sup>, A.F. Sisay<sup>c</sup><sup>a</sup> School of Chemical and Food Engineering, Bahir Dar University, P.O. Box 26, Bahir Dar, Ethiopia<sup>b</sup> School of Chemical and Bio-Engineering, Addis Ababa University, P.O. Box 385, Addis Ababa, Ethiopia<sup>c</sup> Ethiopian Environment and Forest Research Institute, P.O. Box 2322, Addis Ababa, Ethiopia

## ARTICLE INFO

## Article history:

Received 27 June 2015

Received in revised form

10 October 2015

Accepted 13 October 2015

Available online 19 October 2015

## Keywords:

Butter yield

Conditioning duration

Die temperature

Moisture content

Optimization

## Chemical Compounds Studied in this Article:

Hexane (PubChem CID: 8058)

Hydrochloric acid (PubChem CID: 313)

Nitric acid (PubChem CID: 944)

Calcium standard for AAS (PubChem CID:

24963)

Copper standard for AAS (PubChem CID:

23978)

Lead standard for AAS (PubChem CID:

24924)

Zinc standard for AAS (PubChem CID:

23994)

## ABSTRACT

The objective of this work was to evaluate the effect of processing factors on butter yield and mineral concentration of Shea butter (*Vitellaria paradoxa*) subspecies *nilotica* extracted using screw expeller. The significant effect of conditioning duration (CD), kernel moisture content (MC) and die temperature (DT) were investigated by a 3<sup>3</sup> full factorial design combined with response surface methodology. Butter yield, fines particles (foot), Ca and Zn concentration were selected as response variables. The model enabled to identify the optimum operating settings (MC = 6.5 g/100 g w.b and DT = 65.5 °C) for maximize butter yield, under which it predicted 42.05 g/100 g d.w. While considering other response, in allover optimization, CD of 30 min, MC of 9 g/100 g w.b and DT of 65 °C were obtained.

© 2015 Elsevier Ltd. All rights reserved.

## 1. Introduction

The Shea tree (*Vitellaria paradoxa* C. F. Gaertn, Sapotaceae family), is a major tree species of African agroforestry systems. The native range of this long-lived (over 200 years) savannah tree species is a large belt approximately 5000 km long by 500 km wide in areas receiving 600–1400 mm of rainfall. *V. paradoxa* is divided into two subspecies: subspecies *paradoxa* extends from Senegal

eastwards to the Central African Republic whilst the other named *nilotica* occurs in Uganda, Northeast Zaire, Southern Sudan and Ethiopia (Davrieux et al., 2010; Hall, Aebischer, Tomlinson, Osei-Amaning, & Hindle, 1996). In Ethiopia the trees found in Gambella region at an altitude 600 m a.s.l, in areas receiving an annual rainfall of about 900–1400 mm (Deribe, 2005).

The tree is generally found in semi-arid to arid areas north of the humid forest zone and blossom from February to March; fruits from May to August and mature from June to July. The fruit annual production is from 15 to 30 kg/tree (Honfo, Akissoe, Linnemann, Soumanou, & Van Boekel, 2013). Shea butter extracted using traditional boiling, semi-mechanized, mechanical and solvent extraction. Traditional method is labor-intensive, inefficient (20%) and inconsistency. Fully mechanized system like screw oil expeller

Abbreviation: CD, conditioning duration; MC, Moisture content; DT, die temperature of screw expeller.

\* Corresponding author.

E-mail address: [yonassefa@gmail.com](mailto:yonassefa@gmail.com) (G.A. Yonas).

achieves extraction rates of 42–50% (USAID, 2004; FAO and CFC, 2004). Traditionally Shea butter used as food accompaniment, skin protectant, moisturizer and therapeutic; internationally it used in chocolate, cosmetics and pharmaceutical industries (Ferris, Collinson, Wanda, Jagwe, & Wright, 2001; USAID, 2004).

The variability in butter yield mainly depends on the origin, pretreatments, processing factors and methods of extraction (Honfo et al., 2013). Davrieux et al., (2010) noticed that the average fat content of East African Shea kernels (52.92 g/100 g) was significantly higher ( $P < 0.05$ ) than West African (48.03 g/100 g). Yield variability ranged from 43.9 to 58.4 g/100 g within Uganda also reported by Gwali et al., (2013). Pretreatment like soaking of nuts at room temperature for two weeks achieved higher (55 g/100 g) butter yield (Nde Bup, Kapseu, Matos, Mabilia, & Mouloungui, 2011). Heating (70–160 °C) of kernels for 25 min results higher butter yield (Adeeko & Ajibola, 1990). Analysis of the butter extracted from 4 mm thick slices dried at 45 °C showed highest yield (Kapseu et al., 2007). Processing factors such as particle size, heating temperature, screw speed, nozzle size and their interaction on the butter yield of mechanically expressed oil were reported (Adeeko & Ajibola, 1990; Nagre, Ellis, & Oduro, 2012; Olaniyan & Oje, 2011).

There is no report regarding the fines particles (foot) content of Shea butter. However, Martínez, Mattea, and Maestri (2008) and Evangelista, Isbell, and Cermak (2012) determine the effect of processing factors on foot content of walnut and palm kernel oil respectively. The presence of some minerals in Shea butter has been reported by various authors. Some minerals were assessed by using atomic absorption spectroscopy and neutron activation analysis. Ca value varies from 0.2 to 34.1 mg/100 g d.w, Zn from 1.9 to 3.4 and Cu from 0 to 1.5 (Honfo et al., 2013; Megnanou, Niamke, & Diopoh, 2007). These heavy metal ions actively catalyze lipid oxidation. Their presence even in trace amounts has long been recognized as potentially detrimental to the shelf life of fats and oils. They can activate molecular oxygen by producing superoxides and lead to the formation of hydroxyl free radicals (Szefer & Nriagu, 2007).

Variations in Shea butter have often been attributed to origin, extraction methods and processing factors. In view of, variability this research work is aimed to evaluate the effect of processing factors on butter yield and mineral concentration of Shea butter from Phugnido district using screw expeller. A model equation that would predict and determine the optimum conditions for butter yield, foot and mineral concentration was developed. Which is very important with regards to butter manufacturing, moreover the overall optimization of the process is also addressed for the first time.

---


$$\text{Extracted Butter (g/100g)} = (\text{Butter in Kernel} - \text{Butter in Press cake}) \quad (2)$$


---

## 2. Materials and methods

### 2.1. Sample collection and pretreatments

Shea nuts, which are not damaged and spoiled, were collected from selected mother tree in Phugnido district, Gambella, Ethiopia. After, the pulp was removed by both scraping and boiling the nuts parboiled and dried using sunlight for a week. The dried nuts then cracked and the resulting kernels were manually sorted, washed and then dried using drying cabinet (Model: AS 100, 2003, Italy) at 50 °C and 15% relative humidity. The cleaned kernels were manually grinded (3–5 mm), then conditioned using autoclave (Model: KORIMAT KA 160, 2006, Germany) at 95 °C and 2 MPa for 0, 15 and

30 min with saturated steam. The batches were put in drying cabinet at 50 °C and 15% relative humidity to reach uniform moisture content of 3 g/100 g. Considering the initial moisture content and the mass of Shea kernel in each jar, the required mass of distilled water was added to reach the target moisture content of 3, 9 and 15 g/100 g (w.b) using Eq. (1) as research performed by Zewdu and Solomon (2007).

$$Q = W_i(M_f - M_i) / (100 - M_f) \quad (1)$$

where: Q is the mass of water to be added in kg;  $W_i$  is the initial mass of the sample in kg;  $M_i$  and  $M_f$  are the initial and final moisture content of the sample in g/100 g (w.b) respectively. The required amount of distilled water were added to each glass jars, then the samples were kept in refrigerator at 5 °C ( $\pm 1$ ) for 5 days for the moisture to distribute uniformly throughout the sample. The jars were shaken at regular interval to facilitate internal moisture stabilization.

### 2.2. Extraction of Shea butter

The pretreated kernels were pressed in a single step using screw oil expeller (Model: CA 59 G, 2011, Germany). The expeller was set using 4 mm restriction die, 20 rpm screw speed. The screw press was first run for 15 min without input material while heating via an electrical heating ring attached around the press barrel, to the desired temperature. The running temperature, both the butter and outgoing material (press cake) were constantly checked with a digital thermometer inserted into the restriction die. Between each run the press chamber components were dismantled, washed and dried. Each run was warmed in air tight jar at its perspective die temperature for 30 min just before pressing. The resulted butter was collected and filtered using low speed centrifuge (Model: L-530 Tabletop, 2012, China) at 5030 g for 30 min. The filtered butter was labeled and frozen at –16 °C till analyses performed.

### 2.3. Methods of analysis

According to Ixtaina et al., (2011) the initial butter content in the kernel and the residual butter content in the press cake was extracted with hexane, gravimetrically determined and expressed in dry basis. The butter yield from each run was calculated considering the initial butter content in the kernel and the residual butter content in the press cake using Eq. (2) (Martinez et al., 2012). Butter yield was expressed as a ratio between the respective run butter yields to initial butter content using Eq. (3).

$$\text{Butter Yield (g/100g)} = (\text{Extracted Butter} / \text{Butter in Kernel}) \times 100\% \quad (3)$$

As performed by Martínez et al., (2012), the fines particles were separated by centrifugation at 5030 g for 30 min, washed with hexane, filtered using Qualitative filter paper (Whatman grade 1, 2012, USA), dried for 30 min at 105 °C, and then gravimetrically determined and expressed as weight percentage of the butter content. In mineral analysis, 0.25 g butter sample was subjected to acid digestion with 8 mL of nitric acid (65%), using high

performance Microwave digester (Model: ETHOS One-CAT288EN-003, 2008, Italy), then diluted to 100 mL using deionized water and analyzed for Ca, Cu, Pb and Zn using atomic absorption spectrophotometer (Model: ZEE nit 700 P, 2012, Germany) equipped with a flame and graphite furnace with the Zeeman background corrector.

#### 2.4. Experimental design and statistical data analysis

Processing factors that are conditioning duration, moisture content and die temperature were varied into three levels (Table 1) to obtain second-order and robust optimization model as described by Lazic (2004). According to Montgomery (2005) a combination of response surface methodology (RSM) with full factorial design ( $3^3$ ) was developed to evaluate contribution of each factors, their interaction and for optimization. The butter yield, foot and Ca and Zn concentration were chosen as responses (dependent variables). Response surface methodology with miscellaneous design and 5 center points were used to evaluate 32 experimental runs (means of triplicate). The adequacy of the model was determined by evaluating the lack of fit, coefficient of determination ( $R^2$ ) and the Fisher test value (F-value) obtained from the analysis of variance that was generated by "Design-Expert<sup>®</sup>" Version 7.0.0 (Stat-Ease, Inc., Minneapolis, MN, USA) software.

Statistical significance of the model and variables were determined at 5% probability level ( $P < 0.05$ ). Each model was expressed in terms of coded factors and regardless of statistical insignificant terms. In spite of insignificance, factors that exhibit interaction was not eliminated from the models in order to support hierarchy.

### 3. Results and discussion

#### 3.1. Response surface modeling and optimization of butter yield

As presented in Table 2, the highest extracted butter (41.63 g/100 g d.w) and butter yield (82.20 g/100 g d.w); and lowest extracted butter (18.50) and butter yield (36.53) were obtained at 0 min CD, 3 g/100 g MC, DT 70 °C and at 0 min CD, 15 g/100 g MC, 30 °C DT respectively. The ANOVA results highlight the regression is statistically significant ( $p < 0.05$ ) with a satisfactory determination coefficient of  $R^2 = 0.9923$ . That is the coefficient of determination was able to explain 99.23% of the data variability.

$$\begin{aligned} \text{Butter yield} = & 76.45 + 0.68CD - 14.99MC + 4.15DT + 2.29CD \\ & \times MC - 2.00MC \times DT + 1.26CD^2 - 17.60MC^2 \\ & - 2.82DT^2 \end{aligned} \quad (4)$$

Eq. (4) shows the linear coefficient of MC is about 4 times of DT, this implies MC is more effective in regulating butter yield than DT. Moreover, the negative value in both quadratic terms leads to maximum extraction efficient (83.25%) around 6.5 g/100 g MC and 65 °C DT (Fig. 1). The lower butter yield in less moisture kernel was probably due to the low moisture to displace the butter from the

cell wall structures. In contrast, higher MC above the optimal value (6.5) was the cause for the discrepancy of butter droplets not to form continuous phase to flow out and resulted insufficient friction during pressing (Martinez et al., 2012; Nagre et al., 2012). The optimum value is lower than 12–15 g/100 g recommended by Fintrac (1999) for use of simple manual presses, which operates at less expelling pressure than screw expeller.

Butter yield show increment as DT raise; however interaction with other factors improved only up to 65 °C. The high butter viscosity at low temperature, which makes difficult to seeps through the cake structure, might be the cause for low yield. On the other hand, high temperature evaporates the moisture within kernels, which makes insufficient to displace the butter from the cell wall structure (Nagre et al., 2012). The finding was much similar with the report by Tacoronte (2010) who suggested between 60 and 62 °C using hydraulic jack press, and to Obeng, Adjaloo, and Donkor (2010) who found 60 °C using low pressure manual screw press. However, it was lower than 82.24 °C reported by Olaniyan and Oje (2011) using an instrumented piston-cylinder rig.

#### 3.2. Response surface modeling and optimization of foot (fines particles)

The highest foot of 32.32% was obtained at 0 min CD, 3 g/100 g MC and 30 °C DT, while the lowest (3.63) was obtained at 15 min CD, 3 g/100 g MC and 70 °C DT. The regression is statistically significant ( $p < 0.05$ ) with a satisfactory determination coefficient of  $R^2 = 0.9989$ .

$$\begin{aligned} \text{Foot} = & 12.47 - 0.23CD - 4.90MC - 6.59DT + 0.53CD \times MC \\ & + 6.90MC \times DT + 1.00MC^2 - 0.83DT^2 \end{aligned} \quad (5)$$

As indicated in Eq. (5) all factors had negative coefficients that imply indirect proportion; and the higher magnitude in DT makes it much effective in decreasing foot content. High interaction between MC and DT indicates reduction of foot at less moisture with high temperature and at high moisture with less temperature (Fig. 2). In the former case the press cake less disintegrated by water evaporation and the high temperature coagulates the protein that did compact the press cake FAO, (2001). While at less die temperature more moisture needed to soften the press cake to reduce the fine particles diverted to the barrel openings. Similar to Evangelista et al., (2012) conditioning duration was insignificant.

The optimization result gives a minimum (3.4 g/100 g) foot values around 30 min CD, 3 g/100 g MC and 70 °C DT. At lowest foot percentage, the press cake became compact and lesser amount diverted to the barrel openings. Whereas at highest, the press cake become soft, fragile and greater amount of sediments diverted to the barrel openings. The finding was similar to Walnut seed oil extraction report by Martinez et al., (2008). Generally, as the press cake flexibility increases foot that will goes into the butter shows reduction.

#### 3.3. Response surface modeling and optimization of minerals

As presented in Table 2, The highest concentration of both Ca (21.99 mg/100 g d.w) and Zn (0.647) in the butter occurred at 30 min CD, 9 g/100 g MC and 30 °C DT; the lowest were found around 30 min CD, 15 g/100 g MC and 70 °C DT for both Ca (8.02) and Zn (0.607 mg/100 g d.w). The values in this finding were similar to other reports that stated from 0.2 to 34.1 and 1.9 to 3.4 (mg/100 g d.w) for both Ca and Zn respectively (Honfo et al., 2013).

Relatively concentration of Zn is lesser than Ca; this caused

**Table 1**  
Experimental design of the study.

No.	Processing factors	Levels		
		1	2	3
1	Conditioning duration (min)	0	15	30
2	Moisture content (g/100 g w.b)	3	9	15
3	Die temperature (°C)	30	50	70

**Table 2**  
Butter yield, extracted butter, foot and minerals compositions of Shea butter at different processing factors.

Run	Independent variables			Butter yield (g/100 g d.w)	Extracted butter (g/100 g d.w)	Foot (g/100 g)	Minerals (mg/100 g d.w)		
	Conditioning duration (min)	Moisture content (w.b)	Die temperature (°C)				Ca	Zn	Cu Pb
1	0	3	30	65.14 ± 4.07	32.99 ± 5.11	32.23 ± 4.52	12.29 ± 0.42	0.646 ± 0.03	ND ND
2	0	3	50	76.91 ± 4.70	38.95 ± 5.39	18.80 ± 3.84	13.24 ± 0.46	0.612 ± 0.01	ND ND
3	0	3	70	82.20 ± 2.64	41.63 ± 3.17	4.76 ± 1.04	14.58 ± 0.11	0.652 ± 0.02	ND ND
4	15	3	30	65.08 ± 2.15	32.96 ± 3.20	30.67 ± 1.10	19.77 ± 0.85	0.653 ± 0.01	ND ND
5	15	3	50	74.24 ± 2.07	37.60 ± 2.85	18.75 ± 1.30	16.77 ± 0.26	0.618 ± 0.05	ND ND
6	15	3	70	76.90 ± 4.30	38.94 ± 4.99	3.63 ± 1.32	14.78 ± 0.80	0.654 ± 0.01	ND ND
7	30	3	30	65.34 ± 3.02	33.09 ± 4.07	30.47 ± 1.52	21.46 ± 0.55	0.662 ± 0.01	ND ND
8	30	3	50	73.76 ± 3.97	37.35 ± 4.76	17.54 ± 2.42	16.90 ± 0.23	0.628 ± 0.02	ND ND
9	30	3	70	75.68 ± 2.61	38.32 ± 3.34	3.54 ± 3.03	10.35 ± 0.32	0.659 ± 0.01	ND ND
10	0	9	30	70.73 ± 2.06	35.82 ± 2.95	18.47 ± 5.62	13.75 ± 0.50	0.656 ± 0.01	ND ND
11	0	9	50	78.39 ± 3.40	39.70 ± 4.04	12.92 ± 1.30	14.75 ± 1.03	0.610 ± 0.01	ND ND
12	0	9	70	76.57 ± 4.17	38.78 ± 4.92	5.63 ± 1.25	15.76 ± 0.05	0.636 ± 0.03	ND ND
13	15	9	30	70.89 ± 2.01	35.90 ± 2.89	17.78 ± 2.20	19.75 ± 1.04	0.655 ± 0.03	ND ND
14	15	9	50	77.41 ± 1.99	39.20 ± 2.67	12.78 ± 1.02	16.66 ± 0.90	0.615 ± 0.02	ND ND
15	15	9	50	77.41 ± 1.30	39.20 ± 1.62	12.54 ± 2.50	16.66 ± 0.90	0.612 ± 0.02	ND ND
16	15	9	50	75.42 ± 1.14	38.19 ± 2.03	12.60 ± 2.50	15.76 ± 1.05	0.612 ± 0.01	ND ND
17	15	9	50	76.56 ± 1.90	38.77 ± 1.75	12.40 ± 1.50	17.56 ± 1.03	0.613 ± 0.01	ND ND
18	15	9	50	74.28 ± 1.22	37.62 ± 2.00	12.53 ± 2.20	16.77 ± 1.03	0.612 ± 0.02	ND ND
19	15	9	50	77.41 ± 0.26	39.20 ± 1.67	12.16 ± 1.25	16.66 ± 0.90	0.612 ± 0.01	ND ND
20	15	9	70	76.49 ± 0.25	38.73 ± 1.34	4.86 ± 1.57	14.56 ± 0.59	0.636 ± 0.01	ND ND
21	30	9	30	71.41 ± 2.46	36.16 ± 3.33	17.70 ± 2.22	21.99 ± 0.18	0.647 ± 0.01	ND ND
22	30	9	50	77.86 ± 0.36	39.43 ± 1.02	12.34 ± 2.50	16.75 ± 0.29	0.614 ± 0.05	ND ND
23	30	9	70	80.15 ± 1.20	40.59 ± 1.80	4.87 ± 1.20	9.75 ± 0.34	0.637 ± 0.03	ND ND
24	0	15	30	36.53 ± 0.24	18.50 ± 1.73	7.23 ± 1.92	12.67 ± 0.60	0.664 ± 0.02	ND ND
25	0	15	50	40.04 ± 0.18	20.28 ± 2.45	7.76 ± 1.57	14.46 ± 0.93	0.615 ± 0.01	ND ND
26	0	15	70	44.30 ± 0.05	22.43 ± 1.73	7.87 ± 3.17	14.46 ± 1.46	0.625 ± 0.01	ND ND
27	15	15	30	37.82 ± 0.14	19.15 ± 1.73	7.67 ± 3.57	18.46 ± 1.38	0.655 ± 0.01	ND ND
28	15	15	50	45.92 ± 0.07	23.25 ± 1.56	8.69 ± 1.35	15.69 ± 1.16	0.606 ± 0.02	ND ND
29	15	15	70	42.01 ± 3.25	21.27 ± 5.76	7.88 ± 2.06	13.88 ± 0.25	0.616 ± 0.02	ND ND
30	30	15	30	44.43 ± 0.55	22.50 ± 2.22	7.87 ± 2.08	20.58 ± 0.97	0.646 ± 0.01	ND ND
31	30	15	50	46.71 ± 2.62	23.65 ± 4.24	8.76 ± 0.87	14.14 ± 0.53	0.596 ± 0.01	ND ND
32	30	15	70	47.69 ± 1.62	24.15 ± 3.20	8.41 ± 0.88	8.02 ± 0.65	0.607 ± 0.01	ND ND

Values are means ± SD (n = 3) and ND denotes "Not Detected".

higher sensitivity in the model used for Zn. Moreover their chemical properties vary, hence the ANOVA results show little different between two minerals.

As expressed in Eqs. (6) and (7) both models are statistically significant (p < 0.05) with a determination coefficient of R<sup>2</sup> = 0.9805 and 0.9894 respectively.

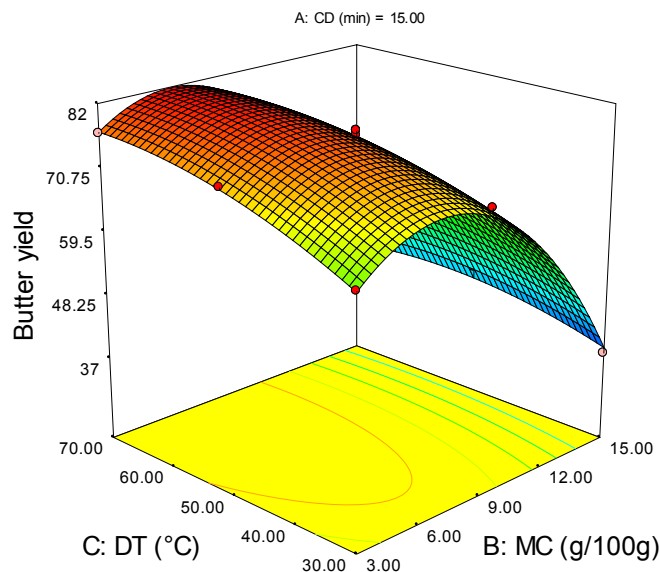


**Fig. 1.** Response surface plot showing the interaction effect of die temperature-moisture content on butter yield.

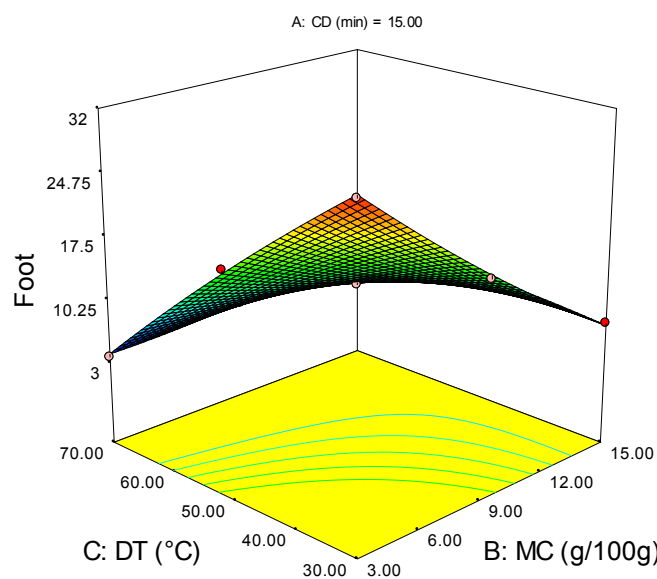


**Fig. 2.** Response surface plot showing the interaction effect of die temperature-moisture content on foot.

$$Ca = 16.98 + 0.78CD - 0.43MC - 2.48DT - 0.62CD \times MC - 3.5CD \times DT - 1.76 \times CD^2 - 0.67MC^2$$

(6)

$$\begin{aligned} Zn = & 0.61 - (1.19 \times 10^3)CD - (8.75 \times 10^3)MC \\ & - (9.01 \times 10^3)DT - (7.83 \times 10^3)CD \times MC \\ & - (0.01 \times 10^3)MC \times DT + (0.03)DT^2 \end{aligned} \quad (7)$$

Eq. (6) indicates DT is more determinant factor compared to others. The negative value of the quadratic term in both CD and MC leads to a maximum Ca concentration at 19.5 min CD and 8.0% respectively (Fig. 3). The response surface for minimum Ca concentration (8.3) shows the optimum 30 min CD, 15 g/100 g MC and 70 °C DT. In Eq. (7) DT and MC have the highest influence on Zn concentration. As well, the negative value in the quadratic term of DT leads to a maximum Zn concentration around 52 °C DT. Hence, the response surface for minimum Zn concentration (0.59) obtained at 30 min CD, 15 g/100 g MC and around 55 °C DT (Figs. 4 and 5).

Proportional increase of Ca concentration with CD, up to the peak, might be due to the effect of high temperature and pressure used for conditioning. As explained by FAO (2001) conditioning results rupture of cell walls and coagulation of protein in the kernel. This might be the cause for the release of Ca available within the kernel and to be mixed with the butter. However, longer CD showed decline of Ca concentration, this is possibly due to the high solubility of Ca in water to be washed-out by the steam used for conditioning (Damodaran, Parkin, & Fennema, 2008).

Regardless of factors interaction, it can be concluded that MC is indirectly proportional to minerals concentration. This is possibly due to high water available in the kernel to solubilize the minerals than letting to precipitate into the butter (Damodaran et al., 2008).

DT raises exhibit reduction of minerals concentration (Fig. 3). This might be due to the change in chemical dissociation of molecules that resulted the release of minerals in ions form that makes them more soluble in the water available than being expelled with the butter extracted. This finding is similar to the statement by Singh, Gamlath, and Wakeling (2007) that, the possibility of phytate hydrolysis at high extrusion temperature, also the modification of fiber components reduces their chelating activity, which favors the availability of minerals to be solubilized easily. However, for Zn

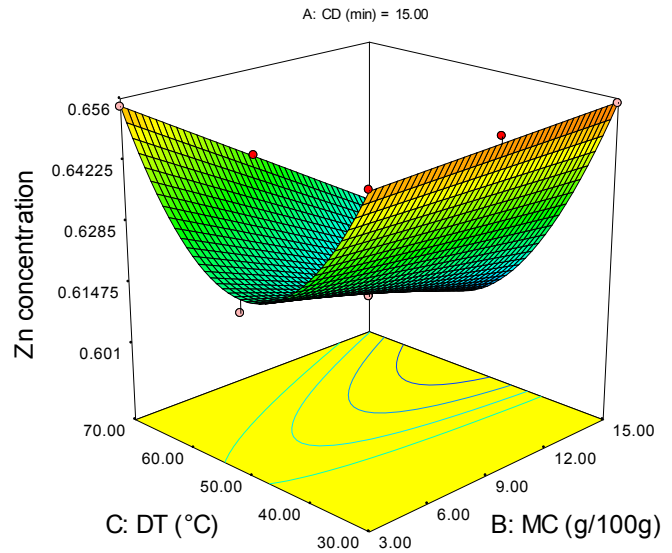


Fig. 4. Response surface plot showing the interaction effect die temperature-moisture content on Zn concentration.

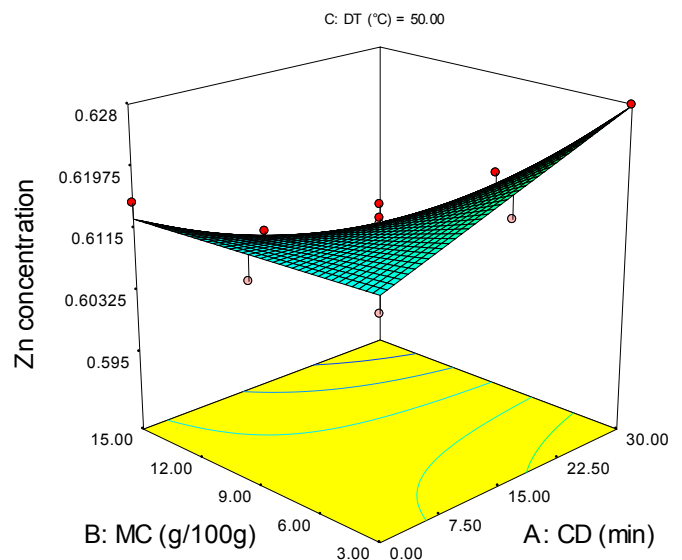


Fig. 5. Response surface plot showing the interaction effect of moisture content-conditioning duration on Zn concentration.

beyond 55.77 °C the concentration showed increment (Fig. 4), this might be a result of high  $Zn^{2+}$  reactivity to form insoluble compound that would be precipitated into the butter (Damodaran et al., 2008). In addition, the water evaporation from the kernel at high die temperature would causes saturation of  $Zn^{2+}$  where a revers mechanism might occur.

Higher DT (70 °C) resulted reduction of Ca concentration than lower DT (30 °C). This reduction might be explained by the fact that, high temperature favors the dissociation effect of molecules in the kernel and the modification of fiber components that reduced their chelating effect, this favors the availability of minerals to mobilize easily and solubilize in the water than to the butter extracted. However, lower temperature is not enough to alter the structure of molecules and fibers, the minerals which are not in hydrolyzed form easily precipitate in the butter. Further, longer CD will favor the release of minerals by rupturing cell walls and coagulating the

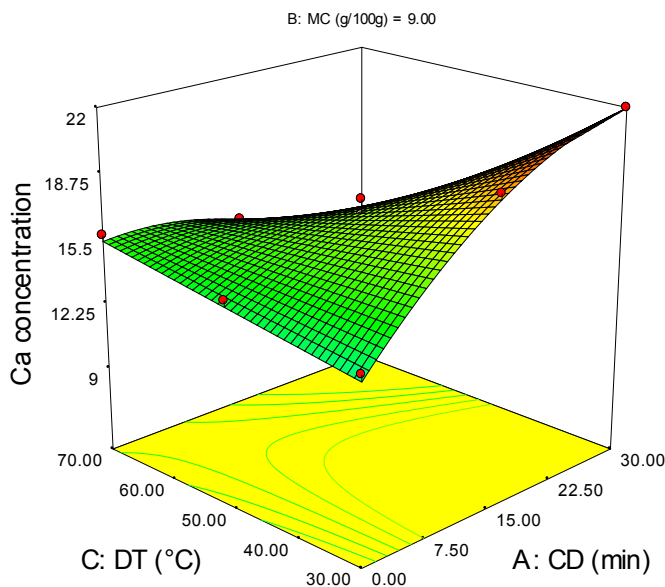


Fig. 3. Response surface plot showing the interaction effect of die temperature-conditioning duration on Ca concentration.

protein in the kernel (Singh et al., 2007; FAO, 2001).

Higher moist kernels (15 g/100 g) resulted relatively lower Zn concentration in the butter than lower (3) moist kernel. This might be the presence of higher moisture to diffuse Zn (water-soluble) to the press cake (Damodaran et al., 2008). Moreover, high factor interaction between conditioning duration and moisture content indicates that cell structure disintegration by conditioning was not sufficient to minimize the Zn concentration, unless enough moisture is available to solubilize the minerals than letting to precipitate in the butter (FAO, 2001). The slight increase of Zn concentration as MC increases at low DT (30 °C); might be due to low temperature that is not enough to hydrolyze molecules that bind Zn and to make it available to be solubilize in water and expelled out with the press cake.

While at high (70 °C) DT the rise in MC resulted reduction of Zn concentration, this might be due to the hydrolysis of molecules at high die temperature that yield Zn<sup>2+</sup> to be solubilize in water and expelled out with the press cake (Damodaran et al., 2008; Singh et al., 2007).

### 3.3.1. Copper and lead

As presented in Table 2 copper and lead were not detected. Since they are toxic and accelerate the oxidation reaction their absence preferred. Nevertheless, the presence of Cu in Shea butter was reported by Honfo et al., (2013) where it varies from 0 to 1.5 mg/100 g d.w.

### 3.4. Overall optimal conditions

As discussed in previous sections optimal conditions for each response were discovered separately. Yet, it can be observed that the optimal values of the factors do not match for all responses. Hence, to find an overall optimal condition, a response surface optimization covering all the four responses (butter yield, foot, Ca and Zn concentration) was applied. From manufacturing perspective of Shea butter, butter yield was given higher weight than foot content and minerals concentration. Since butter with reasonable foot content and minerals concentration can be further filtered and used for soap making and other products, it is more appropriate to prioritize butter yield than other response variables in overall optimization. Optimization criteria were as follows: maximize butter yield and minimize others, all responses given one weight while butter yield given two. Optimal 30 min CD, around 9 g/100 g MC and 65 °C DT were discovered.

## 4. Conclusion

In this study the developed model equations can be used to predict butter yield and other response variables, as influenced by conditioning duration, moisture content and die temperature. Different model equations were used to express each response; and all three factors were not necessarily significant in all cases. The highest butter yield (82.20 g/100 g d.w) obtained at 6.5 g/100 g moisture content and 65.5 °C die temperature, while conditioning duration was insignificant. In both foot and minerals concentration die temperature had more influence relative to other factors. Less foot content (3.4 g/100 g) in Shea butter was achieved at 30 min CD, 3 g/100 g MC and 70 °C DT. The response surface for minimum Ca (8.3 mg/100 g d.w) and Zn (0.59 mg/100 g d.w) concentration shows the optimum values of 30 min CD, 15 g/100 g MC and 70 °C DT and 30 min CD, 15 g/100 g MC and 55 °C DT respectively. Whereas Cu and Pb not detected in the extracted Shea butter. In overall all optimization, favoring butter yield 30 min conditioning duration, 9 g/100 g moisture content and 65 °C die temperature were obtained. Hence, Shea butter produced around these

processing conditions will produce highest butter yield with lowest foot and mineral concentration of Ca and Zn.

## Acknowledgments

The authors wish to thank Addis Ababa University and Ethiopian Environment and Forest Research Institute for funding this research. In a special way, we would like to thank Mr. Omar Sherif from Forestry Research Center, Phugnido Shea Butter Cooperative, Gambella Agriculture Research Institute and School of Chemical and Food Engineering at Bahir Dar University, Ethiopia.

## References

- Adeeko, K. A., & Ajibola, O. O. (1990). Processing factors affecting yield and quality of mechanically expressed groundnut oil. *Journal of Agricultural Engineering Research*, 45, 31–43.
- Damodaran, S., Parkin, K. L., & Fennema, O. R. (Eds.). (2008). *Fennema's food chemistry* (4th ed.). Boca Raton, FL: CRC Press Taylor & Francis Group.
- Davrieux, F., Allal, F., Piombo, G., Kelly, B., Okulo, J. B., Thiam, M., et al. (2010). Near infrared spectroscopy for high-throughput characterization of Shea tree (*Vitellaria paradoxa*) nut fat profiles. *Journal of Agricultural and Food Chemistry*, 58, 7811–7819. <http://dx.doi.org/10.1021/jf100409v>.
- Deribe, G. B. (2005). *Ecology and phenotypic variations of Vitellaria paradoxa subspecies nitolica (Kotschy), A. N. Henry et al., in Ethiopia*. PhD thesis. Universiti Putra Malaysia.
- Evangelista, R. L., Isbell, T. A., & Cermak, S. C. (2012). Extraction of pennycress (*Thlaspi arvense* L.) seed oil by full pressing. *Industrial Crops and Products*, 37(2012), 76–81. <http://dx.doi.org/10.1016/j.indcrop.2011.12.003>.
- FAO (2001). Small-scale palm oil processing in Africa. (Agricultural Services Bulletin 148). Author: Geoffrey Mrema, Agricultural Support Systems Division.
- FAO and CFC. (2004). In *International workshop on processing and marketing of shea products in Africa. (cfc technical paper no. 21). Dakar (Senegal), 4–6 Mar 2002*. Rome (Italy): FAO.
- Ferris, R. S. B., Collinson, C., Wanda, K., Jagwe, J., & Wright, P. (2001). *Evaluating the marketing opportunities for Shea nut and Shea nut processed products in Uganda*. Natural Resources Institute. Submitted by USAID in October 2001.
- Fintrac. (1999). *Market and technical survey: Shea nuts. Prepared for USAID*. Washington DC: Fintrac. Inc.
- Gwali, S., Nakabonge, G., Okullo, J. B. L., Eilu, G., Forestier-Chiron, N., Piombo, G., et al. (2013). Fat content and fatty acid profiles of Shea tree (*Vitellaria paradoxa* subspecies *nitolica*) ethno-varieties in Uganda. *Forests, Trees and Livelihoods*. <http://dx.doi.org/10.1080/14728028.2012.755810>.
- Hall, J. B., Aebischer, P. D., Tomlinson, H. F., Osei-Amaning, E., & Hindle, J. R. (1996). *Vitellaria paradoxa: a monograph* (p. 105). Bangor, UK: School of Agricultural and Forest Sciences, University of Wales.
- Honfo, F. G., Akissoe, N., Linnemann, A. R., Soumanou, M., & Van Boekel, M. A. J. S. (2013). Nutritional composition of Shea products and chemical properties of Shea butter. *Critical Reviews in Food Science and Nutrition*, 54(5), 673–686. <http://dx.doi.org/10.1080/10408398.2011.604142>.
- Ixtaina, V. T., Martinez, M. L., Spotorno, V., Mateo, C. M., Maestri, D. M., Diehl, B. W. K., et al. (2011). Characterization of chia seed oils obtained by pressing and solvent extraction. *Journal of Food Composition and Analysis*, 24(2011), 166–174. <http://dx.doi.org/10.1016/j.jfca.2010.08.006>.
- Kapseu, C., Nde Bup, D., Tchiegang, C., Abi, C. F., Broto, F., & Parmentier, M. (2007). Effect of particle size and drying temperature on drying rate and oil extracted yields of *Bucchozia coriacea* (MVAN) and *Butyrospermum parkii* ENGL. *International Journal of Food Science and Technology*, 42, 573–578. <http://dx.doi.org/10.1111/j.1365-2621.2006.01277.x>.
- Lazic, Z. R. (2004). *Design of experiments in chemical engineering*. Weinheim: WILEY-VCH Verlag GmbH & Co. KGaA.
- Martinez, M. L., Marín, M. A., Faller, C. M. S., Revol, J., Penci, M. C., & Ribotta, P. D. (2012). Chia (*Salvia hispanica* L.) oil extraction: study of processing parameters. *LWT – Food Science and Technology*, 47(1), 78–82. <http://dx.doi.org/10.1016/j.lwt.2011.12.032>.
- Martinez, M. L., Mattea, M. A., & Maestri, D. M. (2008). Pressing and supercritical carbon dioxide extraction of walnut oil. *Journal of Food Engineering*, 88(2008), 399–404. <http://dx.doi.org/10.1016/j.jfoodeng.2008.02.026>.
- Megnanou, R. M., Niamke, S., & Diopoh, J. (2007). Physicochemical and microbiological characteristics of optimized and traditional Shea butters from Côte d'Ivoire. *African Journal of Biochemistry Research*, 1(4), 041–047.
- Montgomery, D. (2005). *Design and analysis of experiments*. New York: John Wiley & Sons Inc.
- Nagre, R. D., Ellis, W. O., & Odoro, I. (2012). Yield and quality of *Pycnanthus kombo* kernel butter as affected by temperature-moisture interactions. *African Journal of Food Science*, 6(8), 224–231, 30 April, 2012.
- Nde Bup, D., Kapseu, C., Matos, L., Mabilia, B., & Mouloungui, Z. (2011). Influence of physical pretreatments of Shea nuts (*Vitellaria paradoxa* Gaertn) on butter quality. *European Journal of Lipid Science and Technology*, 113, 1152–1160. <http://dx.doi.org/10.1002/ejlt.201100005>.

- Obeng, G. Y., Adjaloo, M. K., & Donkor, P. (2010). Effect of temperature, moisture content, particle size and roasting on shea butter extraction efficiency. *International Journal of Food Engineering*, 6(2), 1556–3758. <http://dx.doi.org/10.2202/1556-3758.1848>. ISSN (Online).
- Olaniyan, A. M., & Oje, K. (2011). Development of model equations for selecting optimum parameters for dry process of shea butter extraction. *Journal of Cereals and Oilseeds*, 2(4), 47–56.
- Singh, S., Gamlath, S., & Wakeling, L. (2007). Nutritional aspects of food extrusion: a review. *International Journal of Food Science and Technology*, 42, 916–929. <http://dx.doi.org/10.1111/j.1365-2621.2006.01309.x>.
- Szefer, P., & Nriagu, J. O. (2007). In *Mineral components in foods. Chemical and functional properties of food components series* (p. 136). Boca Raton, FL: CRC Press.
- Tacoronte, L. C. (2010). *Putting the press to the test: Effects of temperature on Shea nut oil output*. Bachelor's thesis. Boston, USA: Massachusetts Institute of Technology. Retrieved from URI <http://hdl.handle.net/1721.1/60205>.
- USAID. (2004). In P. Lovett (Ed.), *The Shea butter value chain: Production, transformation and marketing in West Africa. (The West African trade hub report no. 2.)*. Shea Butter Consultant for WATH. Submitted to USAID November, 2004.
- Zewdu, A. D., & Solomon, W. K. (2007). Moisture-dependent physical properties of tef seed. *Biosystems Engineering*, 96(1), 57–63. <http://dx.doi.org/10.1016/j.biosystemseng.2006.09.008>.



## Particle size distribution of soy flour affecting the quality of enriched gluten-free cakes



Nahla Dhen<sup>a, b</sup>, Laura Román<sup>b</sup>, Ines Ben Rejeb<sup>a</sup>, Mario M. Martínez<sup>b</sup>, Mohamed Garogouri<sup>a</sup>, Manuel Gómez<sup>b, \*</sup>

<sup>a</sup> Biocatalysis and Industrial Enzymes Group, Laboratory of Microbial Ecology and Technology, Carthage University, National Institute of Applied Sciences and Technology, BP 676, 1080 Tunis, Tunisia

<sup>b</sup> Food Technology Area, College of Agricultural Engineering, University of Valladolid, Avda. Madrid 44, 34004 Palencia, Spain

### ARTICLE INFO

#### Article history:

Received 28 August 2015

Received in revised form

11 October 2015

Accepted 12 October 2015

Available online 19 October 2015

#### Keywords:

Celiac

Sponge

Layer

Batter

Texture

### ABSTRACT

In this study, soy flour of three particle sizes (<132, 132–156 and >156 μm) were used to substitute 15% and 30% of starch in layer and sponge cakes formulations. Batter microstructure, density and viscosity, and cake specific volume, texture and colour were evaluated. Results showed that soy flour incorporation in layer cakes decreased batter density as its particle size increased and also increased batter viscosity. However, batter prepared with intermediate flour particle size led to the lowest viscosity while the coarse fraction presented the highest viscosity. In sponge cakes, soy flour incorporation increased batter density. At 30%, the fraction with the larger particle size had the lower density. Batter viscosity was only affected in the case of 30% soy flour substitution, being significantly decreased with the use of the fine fraction. Enrichment of layer cakes did not affect their specific volumes but a flattened shape was obtained. Soy flour incorporation decreased layer cakes hardness. In contrast, its incorporation reduced the sponge cake specific volume as the addition percentage and the particle size increased. Soy flour incorporation prevented cakes from staling during storage.

© 2015 Elsevier Ltd. All rights reserved.

## 1. Introduction

In recent years, there has been an increasing interest towards gluten-free bakery products. Pathologies related to gluten intake such as celiac disease has an estimated prevalence of 1–2% worldwide (Rodrigo, 2006) while wheat allergy and gluten sensitivity affect 0.2–0.5 and 6% of USA population, respectively (Rosell, Barro, Sousa, & Mena, 2014). Therefore, the consumption of gluten-free products is higher and more frequent. Nevertheless, the quality of gluten-free products is still deficient and their nutritional value is poorer compared to those containing gluten (Matos & Rosell, 2011).

Most gluten-free products available on the market are made from starches, which leads to products with low fiber and protein content in comparison with similar products containing gluten. Leguminous flours have always been very popular featuring as supplementary ingredients in bakery products due to their high protein content and because their amino acids are well

complemented with those present in cereals (Chavan & Kadam, 1993). Soybean meal also has nutritional benefits as it possesses anticancer power, reduces the risk of cardiovascular diseases and prevents from aging diseases (Friedman & Brandon, 2001; McCue & Shetty, 2004). However, although some researchers have studied the incorporation of soy protein in cakes or muffins made with starch, wheat flour (Majzoobi, Ghiasi, Habibi, Hedayati, & Farahnaky, 2014; Ronda, Oliete, Gomez, Caballero, & Pando, 2011; Sung, Park, & Chang, 2006) or rice flour (Matos, Sanz, & Rosell, 2014), or even the addition of soy flour to microwaved cakes (Sakiyan, 2015), studies about the incorporation of soy flour in cakes as well as the influence of the flour particle size on cakes have not been carried out.

It is well known that the type of flour has a significant effect on cake quality (Gomez, Oliete, Rosell, Pando, & Fernandez, 2008; Oliete et al., 2010), and that flour particle size is one of the most influential factors both in wheat (Gaines, 1985; Gomez, Ruiz-Paris, & Oliete, 2010) and gluten-free cakes (de la Hera, Martínez, Oliete, & Gomez, 2013).

The present work aims to study corn starch cake enrichment with soy flour and to evaluate the effect of its particle size on the

\* Corresponding author.

E-mail address: [pallares@iaf.uva.es](mailto:pallares@iaf.uva.es) (M. Gómez).

cake quality. Therefore, layer and sponge cakes were made by partially replacing corn starch by soy flour of three different particle sizes at percentages of substitution of 15 and 30%. Both flour composition and microstructure were assessed and batter microstructure, density and viscosity were characterized. The volume and texture of the final products were also evaluated.

## 2. Materials and methods

### 2.1. Materials

Soy flour enzymatically inactive used in this work was from Harinera Polo (Zaragoza, Spain). The composition, provided by the supplier, was: 10 g/100 g humidity, 4 g/100 g ash, 38 g/100 g protein, 22 g/100 g fat and 2 g/100 g lecithin. Different particle sizes were obtained by sieving the flour in a Bühler MLI 300B sifter (Uzwil, Switzerland). Thus, three fractions were separated; >156  $\mu\text{m}$  (coarsest), 132–156  $\mu\text{m}$  (intermediate, representing circa 40% of the original flour) and <132  $\mu\text{m}$  (finest). Native corn starch was provided by Daesang Corp (Seoul, Korea). The baking powder “25x1” and the emulsifier “SuperMixo T500” were both from Puratos (Gerona, Spain). Sugar, sunflower oil, milk, powdered milk and liquid pasteurized whole eggs were purchased from local market.

### 2.2. Methods

#### 2.2.1. Proximate composition and particle size distribution of soy flours

Moisture (method 925.10), ash (method 923.03), fat (method 920.85), protein (method 945.18B) and fiber (method 920.86) contents were determined in triplicate according to AOAC procedures (AOAC, 1990). The nitrogen content was calculated and multiplied by 6.25 to obtain the crude protein content. The carbohydrate content was calculated by difference.

The volume fraction-length mean diameter ( $d_{4,3}$ ) of the three particle sized flours were determined using a laser diffraction technique with a Malvern Mastersizer 3000 E (Malvern Instruments Ltd., Malvern, Worcestershire, UK).

#### 2.2.2. Microstructure of soy flour determined by environmental scanning electron microscopy (ESEM)

ESEM of the three fractions of soy flour was carried out using a microscope Quanta 200 F, (Hillsboro, Oregon, USA). The sample was placed on a specimen holder with the help of double-sided scotch tape. Experiments were carried out under high vacuum space and a Back Scattered Electron detector. The magnification and accelerating voltage are showed on each SEM image.

#### 2.2.3. Cakes preparation

Two types of cake were made, layer and sponge cakes. Formulations and recipes of different cakes are given in Table 1. Layer cakes were made with a single-bowl mixing procedure. All ingredients were mixed for 1 min at speed 4 (135 rpm), and 9 min at speed 6 (180 rpm) using a Kitchen-Aid Professional mixer; KPM5 (KitchenAid, St. Joseph, Michigan, USA). Then, 185 g of cake batter were placed into baking aluminum pans (109 × 159 × 38 mm) and baked. Sponge cakes were made with a creaming–mixing procedure. Sugar, liquid pasteurized egg, water and emulsifier were mixed using a Kitchen-Aid Professional mixer (Kitchen Aid, St. Joseph, MI, USA) for 2 min at speed 6 (180 rpm). After that, the powdered milk, soy flour and corn starch were added and the mixing process was continued for 3 min at speed 8 (225 rpm). Cake batter (100 g) was placed into oil-coated aluminum pans (109 × 159 × 38 mm), and baked. For both cakes, baking was performed at 190 °C for 25 min in a preheated electric oven (Salva,

**Table 1**

Formulation of layer and sponge cakes made replacing corn starch by soy flour at different percentages (0, 15 and 30%).

	Layer cake			Sponge cake		
	0	15	30	0	15	30
Corn starch	350	297.5	245	245	208.25	171.5
Soy flour <sup>a</sup>	–	52.5	105	–	36.75	73.5
Sugar	315	315	315	240.5	240.5	240.5
Milk	210	210	210	–	–	–
Powdered milk	–	–	–	25	25	25
Liquid egg	175	175	175	344	344	344
Sunflower oil	105	116.7	116.7	–	–	–
emulsifier	–	–	–	14	14	14
Water	–	–	–	55	55	55
Baking powder	10.5	10.5	10.5	–	–	–

<sup>a</sup> Soy flour of three different particle sizes was used.

Lezo, Spain). After baking, cakes were left to cool for 60 min at room temperature. Then, they were removed from the pans and were packaged in polyethylene bags and finally stored at 20 °C until further analyses. For each type of cake, a control cake was prepared (100% corn starch) and each of the three different particle sizes of the soy flour was used to replace the corn starch at levels of 15% and 30%. Two replicates of each preparation were made.

#### 2.2.4. Batter characterization

Batter measurements were performed twice immediately after their preparation. Batter density was measured using a pycnometer Elcometer 1800 (Elcometer, Manchester, UK). Viscosity of batter was determined using a Rapid Viscoanalyser (RVA-4) (Newport Scientific model 4-SA, Warriewood, Australia). Sample batter (15 g for sponge cake batter and 25 g for layer batter) was placed in the RVA aluminum canister with a plastic paddle. The viscosity of the batter was recorded at 30 °C after stirring for 3 min at 160 rpm.

Batter bubbles were examined using a DM750 microscope (Leica Microsystems, Wetzlar, Germany) with 40 and 100× magnification, and fitted with an EC3 video camera and images were captured using LAS EZ software (Leica Microsystems, Wetzlar, Germany). In order to visualize bubbles, a drop of batter was placed on a microscope slide and covered with a coverslip. The slides were then compressed under a 1 kg weight to create a layer of uniform thickness.

#### 2.2.5. Cake quality evaluation

Cake quality was assessed on two cakes from each type 24 h after baking. Cake volume was determined using a laser sensor with the Volscan Profiler volume analyser (Stable Microsystems, Surrey, UK). The specific volume was calculated as the ratio between the volume of the cake and its weight. Weight loss was calculated as the ratio between weight of batter in the pan before baking and the weight of the cake after baking, expressed as a percentage.

The textural properties of the cake were measured with a TA, XT2 Texture Analyzer (Stable Micro Systems, Godalming, U.K.) and the Texture Expert Exceed software for data analysis. Texture Profile Analysis (TPA) test was carried out using a cylindrical aluminium probe (25 mm diameter) and a double compression test to compress crumb samples to 50% of their original height at a speed of 2 mm/s. Measurements were carried out on two slices (20 mm thickness) taken from the centre of each cake. The textural parameters considered were hardness (peak force of the first compression cycle, in N), cohesiveness (ratio of positive force area during the second compression to that during the first compression area, dimensionless), and springiness (ratio of the time duration of force input during the second compression to that during the first

compression, dimensionless). After seven days of storage, the increase in hardness ( $\Delta$  hardness) was also measured in order to evaluate the staling of the cakes.

Hedonic sensory evaluation of cakes was conducted with 68 cake-usual consumer volunteers: staff and students of the Agricultural Engineering College (Palencia, Spain). Cakes were evaluated on the basis of acceptance of their appearance, odour, taste, texture and overall acceptability on a nine-point hedonic scale. The scale of values ranged from “dislike extremely” (score 1) to “like extremely” (score 9). Samples were analysed one day after baking.

### 2.2.6. Statistical analysis

Analysis of variance (ANOVA) was used to study differences between the batters and cakes measurements. Fisher's least significant difference (LSD) test was used to describe means within 95% confidence intervals. The statistical analysis was performed using Statgraphics Centurion XVI software (Statpoint Technologies, Warrenton, USA).

## 3. Results and discussion

### 3.1. Flour characterization

#### 3.1.1. Flour proximate composition and particle size distribution

Raw material analysis was carried out in order to characterize the three fractions of the soy flour. Results were depicted in Table 2. The coarsest flours exhibit the highest moisture content. Ash and protein content was higher for the finest soy flour, and lower for the intermediate and coarse, which could indicate that some part of the grain, richer in ash and protein content, was broken in the form of small particles. Concerning the fat content, the finest flour displayed the highest content, whereas the largest particle size showed the lowest fat content, as was previously observed by Russin, Arcand, and Boye (2007). However, these authors did not find differences either in the ash or protein content between the different particle sizes studied. These differences can be due to a different milling procedure or down to the fact that the soy flour used in this study was enzymatically inactive. On the contrary, the coarser the particle size is, the higher the carbohydrate content in the flour.

#### 3.1.2. Microstructure

ESEM was conducted in order to identify the microstructural properties of soy flour from different particle sizes. Fig. 1 shows SEM images of fine (<132  $\mu\text{m}$ ) and coarse (>156  $\mu\text{m}$ ) soy flours. No differences were found between fine and intermediate particle size of soy flour (images not shown). SEM images exhibited that soy flour with particle <132  $\mu\text{m}$  (a,b) was organized in a large number of small particles with irregular shapes containing starch granules, which appeared with a smooth clean surface in a very compact structure within the protein matrix (b). Nevertheless, more flattened and loose particles are also observed, where no starch granules are noticed. These fragments correspond mainly to protein fractions, which agree with that observed in the chemical

composition of the flours. The fact that the finer fractions are richer in such fragments with higher protein content is common in legume flours (Pelgrom, Vissers, Boom, & Schutyser, 2013; Wu & Nichols, 2005). Images of coarse soy flour (c,d) displayed a larger compact structure of flour particles showing a rougher surface, which could be related to their lower fat content, and loose starch granules. Nevertheless, the presence of some fine flour particles was also observed.

Overall both flours presented a very similar structure, so its influence on the characteristics of batters and cakes should be principally attributed to their different chemical composition or surface area instead of the structural differences between them.

### 3.2. Batter characteristics

The properties of all batters analyzed are summarized in Table 3. The results showed that in the case of layer cakes, soy flour incorporation decreased batter density. It is known that batter density depends on the amount of gas bubbles incorporated during mechanical mixing which also affects the cake quality. Thus, soy flour would promote air incorporation during mixing, with no significant differences between batters at 15% or 30% of soy flour substitution. Wilderjans, Pareyt, Goesaert, Brijs, and Delcour (2008) also observed a decrease in batter density for pound cakes, similar to layer cakes when the starch content was reduced in the formulation and replaced by proteins. However, in our study, the results showed that despite the fact that the finest fractions have higher protein content and a lower carbohydrate content, the coarser the particle size, the lower the batter density, allowing greater air incorporation. These results were already observed by Gomez et al. (2010) and de la Hera et al. (2013) when using wheat or rice flours of different particle sizes in layer cakes preparation, but in these cases the composition of the different fractions was similar, so the effect must only be linked to the particle size. Photomicrographs in Fig. 2a showed a greater number of bubbles in soy layer batters compared to the control. These bubbles had a larger diameter, especially in batters with the coarsest particle sizes, which is in agreement with those observed by de la Hera et al. (2013) in rice flours. From these results it could be expected that, despite a less air incorporation, layer cakes prepared using soy flour <132  $\mu\text{m}$  could have a softer texture and higher volume, since a small bubble size is preferred for a good texture, volume, shape and grain of cake (Hicsasmaz, Yazgan, Bozoglu, & Katnas, 2003), as these depend on the capability of the batter to trap the air during baking process (Stauffer, 1990). Regarding the viscosity, results showed that soy flour incorporation made it increase, as previously reported by Wilderjans et al. (2008) when starch was replaced by protein in pound cakes. Results displayed that particle size significantly affected the viscosity for both levels of soy flour substitution. Batters prepared using the coarsest fraction had the highest viscosity. It should be noted that a high batter viscosity aids in incorporating and retaining more air bubbles, providing more stable and voluminous cakes (Lebesi & Tzia, 2011). However, as long as the batter viscosity is considered, not only the viscosity of the liquid that

**Table 2**

Characterization of coarsest, intermediate and finest particle sizes of soy flours.

Soy flour sample	Moisture (g/100 g)	Ash (g/100 g)	Fat (g/100 g)	Fiber(g/100 g)	Protein (g/100 g)	Carbohydrate (g/100 g)	$d_{(4,3)}$ ( $\mu\text{m}$ )
<132 $\mu\text{m}$	5.1a	5.68c	28b	1.02a	33.8c	27a	40.2a
132–156 $\mu\text{m}$	4.9a	5.31b	27b	1.00a	29.6b	32a	101.0b
>156 $\mu\text{m}$	5.8b	4.96a	13a	0.93a	19.3a	55b	313.0c
Standard error	0.2	0.04	2	0.06	0.8	2	16

Different letters in the same column indicate significant differences (95% level) (Fisher's test). Data are mean values (n = 3).

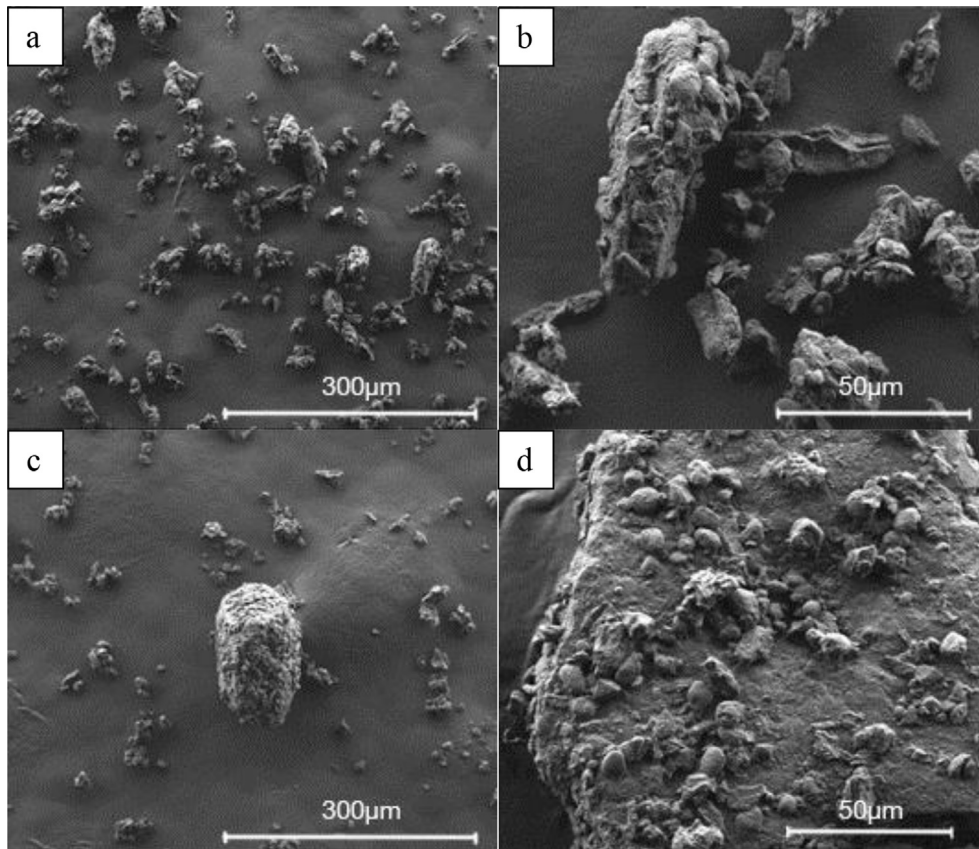


Fig. 1. Scanning Electron micrographs (500× magnification) of soy flour with <132 μm (a,b) and >156 μm (c,d) particle sizes. Arrows show starch granules.

**Table 3**  
Effect of soy flour replacement and particle size on batter viscosity and density.

Sample	Batter viscosity 30 °C (10 <sup>-3</sup> Pa s)		Batter density (g/mL)	
	Layer cake	Sponge cake	Layer cake	Sponge cake
<b>Control</b>	711a	3139bcd	1.12d	0.30a
<b>15% Soy flour</b>				
<132 μm	1355c	3630cd	1.08c	0.33 ab
132–156 μm	948b	3566cd	1.03b	0.33 ab
>156 μm	1864d	4054d	1.03 ab	0.33 ab
<b>30% Soy flour</b>				
<132 μm	2321f	1727a	1.05bc	0.32 ab
132–156 μm	2194e	2405 ab	1.03b	0.35b
>156 μm	2548 g	2787bc	1.00a	0.31a
Standard error	579	312	0.01	0.01

Different letters in the same column indicate significant differences (95% level) (Fisher's test).

Data are mean values (n = 2).

surrounds the bubbles influenced its value, but also the amount and distribution of air incorporated.

Conversely to that observed in layer batters, a slight increase in the density after the addition of soy flour was found in sponge batters with no significant differences in the two of replacement. Therefore, this result suggested that less air was incorporated during mixing. The same trend was reported by Gomez et al. (2008) for a substitution of wheat flour by chickpea flour (with a less starch content in its composition) in sponge cakes. The effect of particle size is only seen in the case of 30% soy flour incorporation, where the fraction with the largest particle size had the lowest density. Just like it happened in layer batter, a coarse particle size could help

air entrapment during mixing. This finding was observed by de la Hera et al. (2013) when studying the impact of flour particle size on gluten-free rice cakes.

Micrographs in Fig. 2b showed that soy flour incorporation caused a reduction in the amount of air in the form of bubbles into the batter. A coalescence phenomenon was clearly observed between batter bubbles in the case of intermediate and coarse soy flours indicating less stability of the batter, and therefore less gas retention capacity when baking. Thus, it seems that the particles of soy flour with a larger size interfere with the formation of the emulsion. Concerning batter viscosity, results showed that there is no effect when the incorporation of 15% soy flour was carried out. Nevertheless, at 30% substitution, a decrease in the viscosity was noted which was only significant in the case of the fine and intermediate particle sizes. These differences are possibly associated with the amount of incorporated air and the way in which this incorporation occurred, but also with the chemical composition of flour, since protein compared to starch has a lower thickening capacity. Results showed that viscosity for sponge batter was higher than for layer batter. This difference between the types of cakes can be related to differences in their internal structure and in the interaction between ingredients. In fact, sponge batters incorporate more air during mixing (de la Hera et al., 2013).

### 3.3. Cake characteristics

The characteristics of enriched cakes with soy flours of different particle sizes are displayed in Table 4. Results indicated no significant differences in specific volume between control and soy flour layer cakes. Nevertheless, it was observed that enriched layer cakes have a flattened shape (Fig. 3) especially when using coarse soy

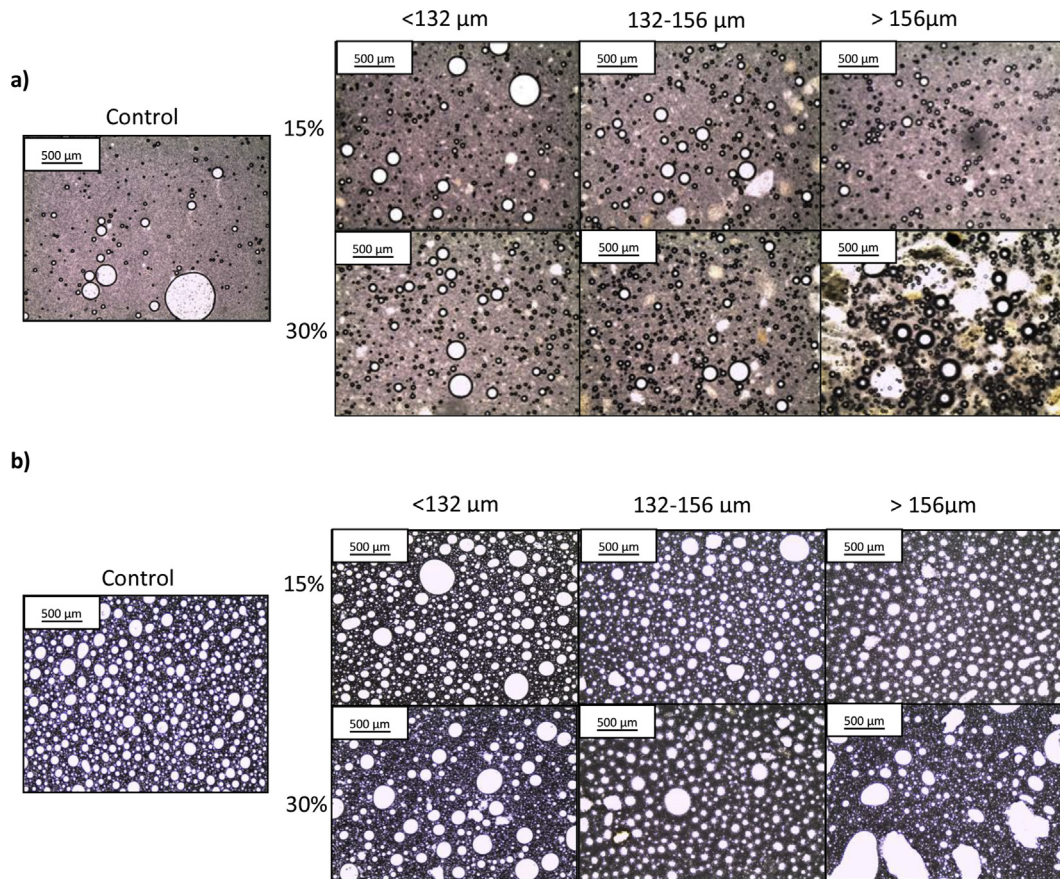


**Fig. 2.** Photomicrograph of batters from layer cakes (a) and sponge cakes (b). Three levels of replacement (0, 15 and 30%) and particle sizes (<132, 132–156 and > 156 μm) of soy flour are shown.

**Table 4**  
Effect of soy flour replacement and particle size on specific volume, weight loss and textural properties of gluten-free cakes.

Sample	Specific volume (mL/g)		Weight loss (g/100 g)		Hardness (N)		Springiness (mm)		Cohesiveness		Δ hardness	
	LC	SC	LC	SC	LC	SC	LC	SC	LC	SC	LC	SC
<b>Control</b>	2.27 ab	4.59d	14.3d	21.0c	10.0f	3.3a	0.69 ab	0.87a	0.35bc	0.43 ab	93c	70b
<b>15% soy flour</b>												
<132 μm	2.41b	4.03c	11.4bc	18.7 ab	6.5c	4.5b	0.72bc	0.91b	0.33 ab	0.41 ab	67bc	54 ab
132–156 μm	2.16a	3.74b	11.9c	17.3a	4.2a	4.5b	0.79d	0.92b	0.39 e	0.42 ab	63 ab	38a
>156 μm	2.37b	3.47 ab	10.8 ab	18.0 ab	5.1b	5.0bc	0.67a	0.91b	0.33 ab	0.39a	59 ab	38 ab
<b>30% soy flour</b>												
<132 μm	2.13a	3.48 ab	10.1a	17.6 ab	8.2e	5.3bc	0.72bc	0.92b	0.36cd	0.48c	38a	36a
132–156 μm	2.09a	3.34a	10.3a	18.4 ab	7.4de	5.2bc	0.74c	0.93b	0.37de	0.50c	38a	28a
>156 μm	2.17a	3.20a	10.3a	19.0b	7.0cd	5.7c	0.71abc	0.90 ab	0.31a	0.45bc	40 ab	30a
Standard error	0.06	0.08	0.2	0.5	0.3	0.4	0.01	0.01	0.01	0.02	9	21

Different letters in the same column indicate significant differences (95% level) (Fisher's test).

Data are mean values (n = 2).

LC:Layer cake; SC:Sponge cake.

flours. This may indicate a slight drop in the height of cakes in the final stages of baking or cooling. This effect is clearer in the case of sponge cakes, where a decline in cake height and specific volume can be seen with the increase in both the incorporation of soy flour, and the particle size. These results could be related to the larger size of the bubbles and the coalescence phenomenon in these cakes. In fact, [Majzoubi, Hedayati, Habibi, Ghiasi and Farahnaky \(2014\)](#) reported that large size bubbles in the batter may burst in the oven causing the collapse of the cake. [Gomez, Ruiz, and Oliete \(2011\)](#) while studying the effect of the freeze process of the batters on

the quality of cakes observed that an increase in the bubble size led to a flatter shape for layer cakes, and to an important reduction in the specific volume for sponge cakes. Nevertheless, no correlation has been observed between the amount of air incorporated (batter density) and the specific volume of the cakes, for neither of these two types.

This may be due to the fact that the cake volume not only depends on the air incorporated into the batter, but also on the air retained, on the air produced by the baking agents during processing, and on the formation of a stable structure during baking

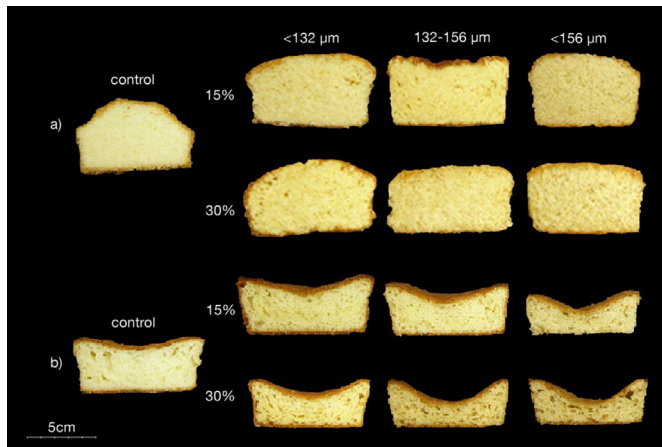


**Fig. 3.** Cross-section of cakes made from different particle sizes (<132, 132–156 and >156  $\mu\text{m}$ ) and levels of soy flour (0, 15 and 30%). Layer cake (a) and sponge cake (b) are shown.

(Stauffer, 1990). Therefore, it seems that the effect of the addition of soy flour influenced the batter structure and the size of the bubbles, especially for sponge cakes, in which no leavening agent is included and the increase in volume depends more on the good air incorporation, in quantity, but especially in terms of bubble size and foam stability. The higher protein content and lower starch content of soy flours may also influence the development of the cake, since starch is responsible for achieving the final structure, gelatinizing and increasing the consistency of the dough during baking. Actually, Gomez et al. (2008) already found that a higher amount of ingredients with higher protein content in the cake formulation resulted in a volume decrease, especially owing to the collapse of the structure during the final stages of baking process or during cooling. Regarding the particle size of the flours, the results are in agreement with those observed by de la Hera et al. (2013) for rice cakes. These authors observed that the particle size of the flour had a greater influence on the specific volume of the sponge cakes in comparison with layer cakes, preferring the flours with a finer particle size as they resulted in a better air distribution in the batter. In this study, these results are also observed even though the weight of soy flour in the formulation is much smaller, so it seems that the influence of the particle size is greater than the differences in the composition of the different flours.

Some of the differences could also be attributed to differences between the viscosities of the batters since this is related to the ability to retain air during baking (Lakshminarayan, Rathinam, & KrishnaRau, 2006). Actually, Lebesi and Tzia (2011) stated that a good cake batter must have a sufficient viscosity to prevent the incorporated air bubbles from rising to the surface and being lost during initial heating. However, in this study an increase in viscosity for layer cakes is observed as soy flour is incorporated, which does not result in differences in the specific volume. Meanwhile, for sponge cakes, no clear trend is observed in the viscosity values, but clear differences are shown in the volume of the cakes. It should be taken into account that despite the fact that a higher viscosity of the materials surrounding the air bubbles can increase the emulsion stability, when the batter viscosity is measured, the distribution as well as the amount of incorporated air make a great influence on it.

Results presented in Table 4 showed that the addition of soy flour led to weight loss in both types of cakes, but any clear trend is observed as far as the particle size of the flour is concerned. Weight loss is a consequence of water evaporation during baking and it depends on cake volume, when the volume increases, the surface in contact with air increases hence the evaporation of water rise (de la

Hera et al., 2013). This effect can explain the observations found for sponge cakes, where the addition of soy flour promoted a decrease of the specific volume and weight loss, although the lower volume of the cakes made with the coarser flours did not lead to a lower loss of volume. Meanwhile, for layer cakes, the incorporation of soy flour slightly modified the specific volume but reduced the weight loss, which may be related to the different chemical composition of the soy flour as compared with the starch, especially to its higher protein content, with greater oil and water absorption capacity.

Textural properties of prepared cakes are presented in Table 4. In the case of layer cakes, results showed a clear decrease in the hardness after incorporation of soy flour, clearer in cakes with 15% of addition. This effect was lower when using the finest flour compared to the coarsest one. This reduction cannot be entirely justified by differences in the volume of cakes, as usual (Gomez, Ruiz-París, Oliete, & Pando, 2010), but the differences between the two levels (15% and 30%) can be partly due to this effect. Conversely, in this case, the effect of the changes in the structure of the crumb (Rodríguez-García, Sahi, & Hernando, 2014) and especially the higher content in fat, fiber and protein of soy flour and the higher water content of the final cake can predominate. Regarding the cohesiveness and springiness, slight differences are displayed and without any clear trend.

In the case of sponge cakes, the incorporation of soy flour increased its hardness independently of the particle size and the percentage added. This increase is more evident as the level of soy addition is enhanced. Thus, these differences can be attributed to the lower specific volume of the enriched cakes, although the greater percentage of fat and protein of the soy flours could minimize this effect. The soy flour incorporation also caused an increase of springiness, regardless of the added level, and cohesiveness only at 30% of substitution but no effect due to particle size was observed in these two textural parameters. The increase in hardness of the cakes was reduced with the addition of soy flour in both types of cakes. In general, it is known that a higher specific volume minimizes the consequent changes to the staling (Gomez et al., 2010). Nevertheless, this effect was not observed in this study, which could be related to the fact that hardening phenomenon in cakes during time of storage are attributed to crumb dehydration, which was avoided in this study by packaging the cakes, and to starch retrogradation (Gujral, Rosell, Sharma, & Singh, 2003). Logically, when replacing starch by soy flour, less starch is available in the formulation, reducing the retrogradation and thus, the staling of cakes.

In the case of sensory analysis, results showed a slight decline in the score with soy cakes in almost all parameters, mainly in taste evaluation and in those cakes made with coarser flours. This trend is to be expected when a “strange” ingredient is introduced in the formulation. A lower score of all the sponge cakes was observed which is expected due to the greater dryness of these cakes, usually eaten together with chocolate, creams or jams. As for the particle size of the soy flour, sponge cakes with smaller particle size obtained a better score, with no significant differences with the control sample in appearance, texture and overall acceptability, something quite logical in view of the volume data and images. Meanwhile, in layer cakes, no differences were observed among the different particle sizes studied.

#### 4. Conclusion

The incorporation of soy flour into the formulations of cakes could be a good alternative for the enrichment of gluten-free cakes because of its nutritional properties. Nonetheless, both the quantity of soy flour and the particle size of this flour remarkably influenced the characteristics of the cakes elaborated, especially sponge cakes.

The enrichment of starch cakes with soy flours decreased the hardness of the cakes and the staling during storage. However, the inclusion of soy flour gave rise to cakes with a flatter shape, and in the case of the sponge cakes, led to a greater reduction on the specific volume, which can be minimized if soy flours with a finer particle size are used.

### Acknowledgment

Nahla Dhen thanks Tunisian Ministry of Higher Education and Scientific Research for the financial support. MM Martínez would like to thank predoctoral fellowship from Spanish Ministry of Education, Culture and Sport.

### References

- AOAC. (1990). *Official methods of analysis* (12th ed.). Washington DC: Association of Official Analytical Chemists.
- Chavan, J. K., & Kadam, S. S. (1993). Nutritional enrichment of bakery products by supplementation with nonwheat flours. *Critical Reviews in Food Science and Nutrition*, 33, 189–226.
- Friedman, M., & Brandon, D. L. (2001). Nutritional and health benefits of soy proteins. *Journal of Agricultural and Food Chemistry*, 49, 1069–1086.
- Gaines, C. S. (1985). Associations among soft wheat flour particle size, protein content, chlorine response, kernel hardness, milling quality, white layer cake volume, and sugar-snap cookie spread. *Cereal Chemistry*, 62, 290–292.
- Gomez, M., Oliete, B., Rosell, C. M., Pando, V., & Fernandez, E. (2008). Studies on cake quality made of wheat-chickpea flour blends. *LWT-Food Science and Technology*, 41, 1701–1709.
- Gomez, M., Ruiz-Paris, E., & Oliete, B. (2010a). Influence of flour mill streams on cake quality. *International Journal of Food Science and Technology*, 45, 1794–1800.
- Gomez, M., Ruiz-Paris, E., Oliete, B., & Pando, V. (2010b). Modelling of texture evolution of cakes during storage. *Journal of Texture Studies*, 41, 17–33.
- Gomez, M., Ruiz, E., & Oliete, B. (2011). Effect of batter freezing conditions and resting time on cake quality. *LWT-Food Science and Technology*, 44, 911–916.
- Gujral, H. S., Rosell, C. M., Sharma, S., & Singh, S. (2003). Effect of sodium lauryl sulphate on the texture of sponge cake. *Food Science and Technology International*, 9, 89–95.
- de la Hera, E., Martínez, M., Oliete, B., & Gomez, M. (2013). Influence of flour particle size on quality of gluten-free rice-cakes. *Food and Bioprocess Technology*, 6, 2280–2288.
- Hicsasmaz, Y., Yazgan, F., Bozoglu, S., & Katnas, Z. (2003). Effect of polydextrose-substitution on the cell structure of the high-ratio cake system. *LWT-Food Science and Technology*, 36, 441–450.
- Lakshminarayan, S. M., Rathinam, V., & KrishnaRau, L. (2006). Effect of maltodextrin and emulsifiers on the viscosity of cake batter and on the quality of cakes. *Journal of the Science of Food and Agriculture*, 86, 706–712.
- Lebesi, M., & Tzia, C. (2011). Effect of the addition of different dietary fiber and edible cereal bran sources on the baking and sensory characteristics of cupcakes. *Food and Bioprocess Technology*, 4, 710–722.
- Majzoubi, M., Ghiasi, F., Habibi, M., Hedayati, S., & Farahnaky, A. (2014a). Influence of soy protein isolate on the quality of batter and sponge cake. *Journal of Food Processing and Preservation*, 38, 1164–1170.
- Majzoubi, M., Hedayati, S., Habibi, M., Ghiasi, F., & Farahnaky, A. (2014b). Effects of corn resistant starch on the physicochemical properties of cake. *Journal of Agricultural Science and Technology*, 16, 569–576.
- Matos, M. E., & Rosell, C. M. (2011). Chemical composition and starch digestibility of different gluten-free breads. *Plant Food for Human Nutrition*, 66, 224–230.
- Matos, M. E., Sanz, T., & Rosell, C. M. (2014). Establishing the function of proteins on the rheological and quality properties of rice based gluten free muffins. *Food Hydrocolloids*, 35, 150–158.
- McCue, P., & Shetty, K. (2004). Health benefits of soy isoflavonoids and strategies for enhancement: a review. *Critical Reviews in Food Science and Nutrition*, 44, 361–367.
- Oliete, B., Perez, G. T., Gomez, M., Ribotta, P. D., Moiraghi, M., & Leon, A. E. (2010). Use of wheat, triticale and rye flours in layer cake production. *International Journal of Food Science and Technology*, 45, 697–706.
- Pelgrom, P. J. M., Vissers, A. M., Boom, R. M., & Schutyser, M. A. I. (2013). Dry fractionation for production of functional pea protein concentrates. *Food Research International*, 53, 232–239.
- Rodrigo, L. (2006). Celiac disease. *World Journal of Gastroenterology*, 12, 6585–6593.
- Rodríguez-García, J., Sahi, S. S., & Hernando, I. (2014). Functionality of lipase and emulsifiers in low-fat cakes with inulin. *LWT-Food Science and Technology*, 58, 173–182.
- Ronda, F., Oliete, B., Gomez, M., Caballero, P. A., & Pando, V. (2011). Rheological study of layer cake batters made with soybean protein isolate and different starch sources. *Journal of Food Engineering*, 102, 272–277.
- Rosell, C. M., Barro, F., Sousa, C., & Mena, M. C. (2014). Cereals for developing gluten-free products and analytical tools for gluten detection. *Journal of Cereal Science*, 59, 354–364.
- Russin, T. A., Arcand, Y., & Boye, J. I. (2007). Particle size effect on soy protein isolate extraction. *Journal of Food Processing and Preservation*, 31, 308–319.
- Sakiyan, O. (2015). Optimization of formulation of soy-cakes baked in infrared-microwave combination oven by response surface methodology. *Journal of Food Science and Technology-Mysore*, 52, 2910–2917.
- Stauffer, C. E. (1990). *Functional additives for bakery foods*. New York: Van Nostrand Reinhold.
- Sung, M. J., Park, Y. S., & Chang, H. G. (2006). Quality characteristics of sponge cake supplemented with soy protein concentrate. *Food Science and Biotechnology*, 15, 860–865.
- Wilderjans, E., Pareyt, B., Goesaert, H., Brijs, K., & Delcour, J. A. (2008). The role of gluten in a pound cake system: a model approach based on gluten-starch blends. *Food Chemistry*, 110, 909–915.
- Wu, Y. V., & Nichols, N. N. (2005). Fine grinding and air classification of field pea. *Cereal Chemistry*, 82, 341–344.



## Gelatin from clown featherback skin: Extraction conditions



Phanat Kittiphattanabawon <sup>a,\*</sup>, Soottawat Benjakul <sup>b</sup>, Sittichoke Sinthusamran <sup>b</sup>, Hideki Kishimura <sup>c</sup>

<sup>a</sup> Department of Food Science and Technology, Faculty of Technology and Community Development, Thaksin University, Phatthalung Campus, Phatthalung 93210, Thailand

<sup>b</sup> Department of Food Technology, Faculty of Agro-Industry, Prince of Songkla University, Hat Yai, Songkhla 90112, Thailand

<sup>c</sup> Laboratory of Marine Products and Food Science, Research Faculty of Fisheries Sciences, Hokkaido University, Hakodate, Hokkaido 041-8611, Japan

### ARTICLE INFO

#### Article history:

Received 30 June 2015

Received in revised form

8 October 2015

Accepted 9 October 2015

Available online 23 October 2015

#### Keywords:

Gelatin

Extraction time

Extraction temperature

Clown featherback

*Chitala ornata*

### ABSTRACT

Gel properties of gelatin from clown featherback skin as affected by different extraction temperatures (45, 65 and 85 °C) and times (6 and 12 h) were determined. The gelatin recovery was found in the range of 73.99–95.85 g/100 g. Gelatin had glycine as major amino acid, followed by alanine and proline. Gel strength generally decreased as extraction temperature and time increased. With increasing temperature and time, band intensity of  $\alpha$ -,  $\beta$ - and  $\gamma$ -chains decreased. Gelling temperature (15.53–24.71 °C) and gelling time (11.62–49.27 min) varied, depending on extraction condition. All gelatin could set at 25 °C, except those extracted at 65 °C for 12 or at 85 °C for 6 and 12 h. Gelatin extracted at 45 °C for 6 and 12 h showed higher gel strength, compared bovine gelatin ( $P < 0.05$ ). Therefore, properties of gelatin from clown featherback skin could be influenced by extraction condition.

© 2015 Elsevier Ltd. All rights reserved.

### 1. Introduction

Clown featherback (*Chitala ornata*) is freshwater fish, which is commonly found in Thailand. It has been generally used for fish ball and fish cake production since its meat is white and has good gel forming ability. During dressing, skins (17–22 g/100 g of total weight) are removed. Currently, the skin has been processed as the crispy fried fish skin. However, the market value is still low. The production of high-value products could pave the way for gaining the higher benefit or revenue. The skins are rich in collagen can serve as raw material for production of gelatin (Foegeding, Lanier, & Hultin, 1996; Wong, 1989). Gelatin is biopolymer obtained from partial denaturation of collagen. It has a wide range of applications in food and non-food (photographic, cosmetic and pharmaceutical) industries (Regenstein & Zhou, 2007). Generally, the skin and bone of bovine and porcine are the major sources for gelatin production. Due to the religious restrictions of Muslim, Jew and Hindu, an alternative source for gelatin production, especially from skin, bone and scale from fish processing by-products, have gained attention (Benjakul, Kittiphattanabawon, & Regenstein, 2012). However, fish gelatin has limited applications owing to some limitations. Fish

gelatin has been known to show poorer gel properties than mammalian counterparts. Additionally, fish gelatin is not able to set at room temperature. The gel properties are mainly governed by imino acid content (proline and hydroxyproline contents) and molecular weight distribution, chain length of  $\alpha$ -,  $\beta$ - and  $\gamma$ -chains (Muyonga, Cole, & Duodu, 2004a). When harsh extraction condition was implemented, gelatin with higher content of imino acid content might show the poor gel properties (Cho, Gu, & Kim, 2005). However, gelatin extracted with milder condition with the superior gel properties mostly shows the low yield (Kittiphattanabawon, Benjakul, Visessanguan, & Shahidi, 2010). As a consequence, the extraction conditions for gelatin production should be optimised. So far, gelatin from the skin of freshwater fish has been extracted at varying temperatures and times from African catfish (Alfaro, Biluca, Marquetti, Tonial, & de Souza, 2014), seabass (Sinthusamran, Benjakul, & Kishimura, 2014), wami tilapia (da Trindade Alfaro, Fonseca, Balbinot, de Souza, & Prentice, 2014), farmed giant catfish (Jongjareonrak et al., 2010) and channel catfish (Yang et al., 2007). Nevertheless, there is no information regarding gelatin from the skin of clown featherback, a freshwater fish widely used for fish ball production in Thailand, as influenced by extraction conditions. Therefore, the aim of this study was to extract and characterise gelatin from skin of clown featherback using different extraction temperatures and times.

\* Corresponding author.

E-mail address: [kphanat@gmail.com](mailto:kphanat@gmail.com) (P. Kittiphattanabawon).

## 2. Materials and methods

### 2.1. Chemicals

All chemicals were of analytical grade. Sodium dodecyl sulphate (SDS), Coomassie Blue R-250, and *N,N,N',N'*-tetramethylethylenediamine (TEMED) were procured from Bio-Rad Laboratories (Hercules, CA, USA). High-molecular-weight marker was purchased from GE Healthcare UK Limited (Buckinghamshire, UK). Food grade bovine bone gelatin with the gel strength of 150–250 g was obtained from Halagel (Thailand) Co., Ltd., (Bangkok, Thailand).

### 2.2. Preparation of clown featherback skin

Skin of clown featherback (*C. ornata*) with the weight of 0.7–1.5 kg was obtained from a local fish ball and fish cake processing plant at Talaadthai in Pathumthani province, Thailand. The skin was prepared following the method of Kittiphattanabawon et al. (2010). The prepared skin was placed in polyethylene bags (50–100 g/bag) and stored at –20 °C until used but not longer than 3 months. The moisture content of prepared skin was 65.72 g/100 g as determined by AOAC method (AOAC, 2000). Prior to collagen extraction, the frozen skin was thawed with running water until the core temperature of the skin reached 8–10 °C.

### 2.3. Extraction of gelatin from clown featherback skin

Gelatin from the skin was extracted following the method of Kittiphattanabawon et al. (2010). Firstly, the skin was mixed with 0.1 mol/L NaOH at a sample to solution ratio of 1:10 (mass/volume ratio) and the mixture was stirred for 2 h at 15–20 °C to remove non-collagenous proteins. The alkali solution was changed every 40 min. The pretreated skin was washed with tap water until the neutral pH of wash water was obtained. The skin was subsequently swollen by mixing with 0.05 mol/L acetic acid at a sample to solution ratio of 1:10 (mass/volume ratio) and stirred for 30 min at room temperature (26–28 °C). Stirring was carried out using an overhead stirrer (model W20.n, IKA®-Werke GmbH & CO.KG, Stanfen, Germany) at a speed of 250 rpm. After swelling process, the residue was washed thoroughly with tap water until pH of wash water became neutral.

To extract the gelatin, the swollen skin was mixed with distilled water at different temperatures (45, 65 and 85 °C) using a sample to water ratio of 1:2 (mass/volume ratio). The mixtures were continuously stirred using an overhead stirrer at a speed of 150 rpm for 6 h and 12 h under designated temperatures, followed by filtration with two layers of cheesecloth. Then, 100 mL of filtrates were mixed with 1 g of activated carbon. The mixtures were then filtered using a Buchner funnel with Whatman No.4 filter paper (Whatman International, Ltd., Maidstone, England), followed by freeze-drying using a freeze-dryer (CoolSafe 55, ScanLaf A/S, Lyngø, Denmark). The obtained gelatin samples were calculated for recovery and subjected to analysis.

### 2.4. Recovery of gelatin

Recovery of gelatin obtained was calculated based on the weight of starting raw material using the following equation:

$$\text{Recovery (g/100 g)} = \frac{\text{Hyp content in skin (mg/g skin)} \times \text{skin used for extraction (g)}}{\text{Hyp content in gelatin (mg/g gelatin)} \times \text{gelatin obtained (g)}} \times 100$$

Hydroxyproline (Hyp) contents in the skin and gelatin were determined according to the method of Bergman and Loxley (1963).

### 2.5. Characterisation of gelatin

#### 2.5.1. SDS-polyacrylamide gel electrophoresis (SDS-PAGE)

SDS-PAGE was performed by the method of Laemmli (1970). The sample preparation and electrophoretic conditions were performed according to the method of Kittiphattanabawon et al. (2010). High-molecular-weight protein markers (GE Healthcare UK Limited, Buckinghamshire, UK) were used to estimate the molecular weight of proteins.

#### 2.5.2. Fourier transform infrared (FTIR) spectroscopic analysis

FTIR spectra of samples were obtained using a Bruker model EQUINOX 55 FTIR spectrometer (Bruker, Ettlingen, Germany). The measuring condition and analysis of data were performed by the method of Kittiphattanabawon et al. (2010).

#### 2.5.3. Amino acid analysis

Gelatin samples were hydrolysed under reduced pressure in 4.0 mol/L methane sulphonic acid containing 2 g/L 3-2(2-aminoethyl)indole at 115 °C for 24 h. The hydrolysates were neutralised with 3.5 mol/L NaOH and diluted with 0.2 mol/L citrate buffer (pH 2.2). An aliquot of 0.4 mL was applied to an amino acid analyser (MLC-703; Atto Co., Tokyo, Japan).

### 2.6. Determination of gel properties

#### 2.6.1. Colour of gel

The colour of gelatin gels (66.7 g/L) was measured with a Hunter lab colourimeter (Color Flex, Hunter Lab Inc., Reston, VA, USA) in term of  $L^*$ ,  $a^*$  and  $b^*$  values.

#### 2.6.2. Turbidity

Gelatin solution (66.7 g/L) was poured into 1 cm cuvette at room temperature. The turbidity of gelatin solution was measured using spectrophotometer (model UV-1800, Shimadzu, Kyoto, Japan) at 600 nm against distilled water.

#### 2.6.3. Gel strength

Gel strength was determined according to the British Standard 757: 1975 method (BSI, 1975).

#### 2.6.4. Gelling temperature and time

Gelatin solution (66.7 g/L) was prepared in the same manner as described in the method of Sinthusamran et al. (2014). The gelling time and temperature were measured using a controlled stress rheometer (HAAKE RheoStress 1, Karlsruhe, Germany) equipped with a cone/plate geometry (diameter of 35 mm, 1°).

The gelling temperatures of the gelatin samples were measured following the method of Sinthusamran et al. (2014) with a slight modification. For gelling time measurement, the temperature of gelatin solution was fixed at 25 °C and the same measurement conditions for gelling temperature were used.

Plot of phase angle as a function of temperature and time was prepared and used for determination gelling temperature and time,

respectively. The gelling temperatures and time were calculated, where  $\tan \delta$  became 1 or  $\delta$  was  $45^\circ$ .

### 2.6.5. Microstructure of gelatin gel

Microstructure of gelatin gel was visualised using a scanning electron microscopy (SEM) according to the method of [Sinthusamran et al. \(2014\)](#).

### 2.7. Statistical analysis

The experiments were carried out in triplicate using three different lots of samples. The difference between means were tested by Duncan's multiple range ([Steel & Torrie, 1980](#)). The data were presented as means  $\pm$  standard deviation. Statistical analysis was performed using the statistical Package for Social Sciences (SPSS for windows: SPSS Inc., Chicago, IL, USA).

## 3. Results and discussion

### 3.1. Recovery of gelatin

Recovery of gelatin from the skin of clown featherback extracted with water at different extraction temperatures (45, 65 and  $85^\circ\text{C}$ ) and times (6 and 12 h) is shown in [Table 1](#). The recovery of gelatin extracted with different conditions ranged from 74 to 95.9 g/100 g, whilst that of gelatin from unicorn leatherjacket skin extracted at 65 and  $75^\circ\text{C}$  was in the range of 15.4–27.9 g/100 g ([Kaewruang, Benjakul, Prodpran, & Nalinanon, 2013](#)). It was noted that the structure of unicorn leatherjacket skin was more compact than that of clown featherback skin. The looser skin could favour the extraction of gelatin as indicated by the higher recovery of gelatin from clown featherback skin. The recovery of gelatin was generally increased as extraction temperature and time increased ( $P < 0.05$ ). With increasing extraction temperature and time, the bondings between  $\alpha$ -chains in the native mother collagen were more destabilised, in which more free  $\alpha$ - or  $\beta$ -chains were released from the skin complex ([Sinthusamran et al., 2014](#)). As a consequence, gelatin was more extracted as shown by higher recovery. The result was in accordance with gelatin from the skin of other freshwater fish, tilapia and seabass ([Sinthusamran et al., 2014](#); [da Trindade Alfaro et al., 2014](#)). Although gelatin extracted at harsher condition had higher recovery, the properties of gelatin might be diminished. [da Trindade Alfaro et al. \(2014\)](#) reported that gelatin from wami tilapia skin extracted at higher temperature and longer time had higher yield, but poorer viscosity and gel strength was obtained.

### 3.2. Protein patterns

Protein patterns of gelatin from clown featherback skin

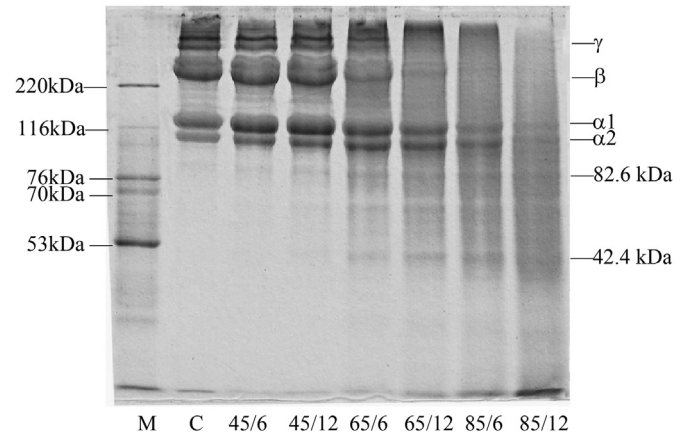


**Fig. 1.** SDS-PAGE patterns of gelatin from the skin of clown featherback extracted at different temperatures for various times. M and C denote high molecular weight markers and acid soluble collagen, respectively. The numbers before and after “/” denote extraction temperature and extraction time, respectively.

extracted under different conditions in comparison with its acid soluble collagen (ASC) are shown in [Fig. 1](#). No marked differences in protein patterns were observed between gelatin extracted at  $45^\circ\text{C}$  and ASC.  $\alpha$ - and  $\beta$ -chains were found as the dominant constituents in gelatin extracted at  $45^\circ\text{C}$ , regardless of extraction time. When the extraction temperature was higher than  $45^\circ\text{C}$ , bands of  $\alpha$ -,  $\beta$ - and  $\gamma$ -chains were more degraded particularly with increasing extraction time. Peptides with MW of 82.6 and 42.4 kDa were found as extraction temperature and time increased. Moreover, increasing small peptides were also noticed at the dye front of each well. The result suggested that those peptides were degradation products from  $\alpha$ -,  $\beta$ - and  $\gamma$ -chains induced by the thermal process. The result was in accordance the report of [Nagarajan, Benjakul, Prodpran, Songtipya, and Kishimura \(2012\)](#) and [Kaewruang et al. \(2013\)](#). Therefore, the extraction at high temperature directly induced the degradation of gelatin components, thereby affecting the properties of gelatin.

### 3.3. Fourier transform infrared (FTIR) spectra

FTIR spectra of gelatin from clown featherback skin extracted under different conditions, compared with ASC are depicted in [Fig. 2](#). The similar patterns in FTIR spectra, including amide I, amide II, amide III, amide A and amide B, between ASC and all gelatin samples were observed. Amide I, which was associated with C=O stretching vibration ([Payne & Veis, 1988](#)), of gelatin extracted at  $45^\circ\text{C}$  for 6 and 12 h,  $65^\circ\text{C}$  for 6 and 12 h and  $85^\circ\text{C}$  for 6 and 12 h was detected at wavenumbers of 1630, 1631, 1630, 1634, 1631 and  $1635\text{ cm}^{-1}$ , respectively. It was noticed that amide I peak was

**Table 1**

Recovery, gel colour and solution turbidity of gelatin from the skin of clown featherback extracted at different temperatures for various times.

Extraction conditions	Recovery (g/100g)	Colour value			Turbidity
		$L^*$	$a^*$	$b^*$	
Bovine <sup>a</sup>	—	$65.17 \pm 0.09^a$	$0.82 \pm 0.06^a$	$29.54 \pm 0.09^a$	$0.0566 \pm 0.0035^a$
$45^\circ\text{C}$ for 6 h	$74.0 \pm 1.1^d$	$66.94 \pm 0.21^a$	$-0.96 \pm 0.05^e$	$10.92 \pm 0.90^d$	$0.0634 \pm 0.0020^b$
$45^\circ\text{C}$ for 12 h	$75.1 \pm 4.1^{cd}$	$62.30 \pm 0.40^b$	$-0.71 \pm 0.10^d$	$11.07 \pm 0.48^d$	$0.0828 \pm 0.0021^c$
$65^\circ\text{C}$ for 6 h	$81.6 \pm 2.1^b$	$61.70 \pm 3.62^b$	$-0.61 \pm 0.09^d$	$11.08 \pm 0.48^d$	$0.1259 \pm 0.0058^d$
$65^\circ\text{C}$ for 12 h	$83.6 \pm 1.2^b$	$61.62 \pm 1.44^b$	$0.29 \pm 0.10^b$	$11.25 \pm 0.67^d$	$0.1549 \pm 0.0049^e$
$85^\circ\text{C}$ for 6 h	$94.5 \pm 6.4^a$	$61.46 \pm 2.15^b$	$-1.55 \pm 0.17^f$	$15.65 \pm 0.78^c$	$0.1793 \pm 0.0020^f$
$85^\circ\text{C}$ for 12 h	$95.9 \pm 9.0^a$	$51.87 \pm 0.57^c$	$0.01 \pm 0.02^c$	$19.59 \pm 0.61^b$	$0.5136 \pm 0.0027^g$

Values are presented as mean  $\pm$  SD ( $n = 3$ ).

Different superscripts in the same column indicate significant difference ( $P < 0.05$ ).

<sup>a</sup> Food grade bovine bone gelatin.

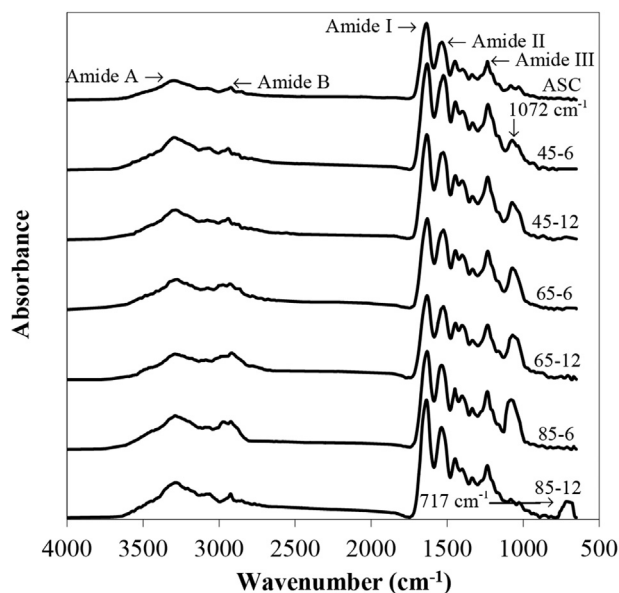


Fig. 2. FTIR spectra of acid soluble collagen and gelatins from the skins of clown featherback extracted at different temperatures for various times.

shifted to higher wavenumber as increasing extraction temperature and time. This indicated the greater loss of triple helix due to the enhanced disruption of inter chain interaction induced by harsher condition (Kaewruang et al., 2013). The result was in accordance the report of Kittiphattanabawon et al. (2010) who reported that gelatins extracted at the higher temperature generally contained a higher amount of low molecular weight components, in which the reactive group (C=O) could be more exposed and became more reactive between  $\alpha$ -chains. This coincided with the higher degradation of  $\alpha$ -,  $\beta$ - and  $\gamma$ -chains at high extraction temperature (Fig. 1). Amide II band of gelatin was found at wavenumber ranging from 1524 to 1536  $\text{cm}^{-1}$ . Amide II arises from bending vibration of N–H groups and stretching vibrations of C–N groups (Nagarajan et al., 2012). Amide III of gelatin (1231–1235  $\text{cm}^{-1}$ ) had lower amplitude when extraction temperature and time increased. These changes were indicative of a greater disorder from an  $\alpha$ -helical to a random coil structure (Muyonga, Cole, & Duodu, 2004b). Amide A band was shifted to higher wavenumber when ASC (3263  $\text{cm}^{-1}$ ) transformed to gelatin (3274–3296  $\text{cm}^{-1}$ ). The amide A band associated with the N–H stretching vibration showed the existence of hydrogen bonds. Normally, a free N–H stretching vibration occurs in the range of 3400–3440  $\text{cm}^{-1}$ . When the N–H group of a peptide is involved in a hydrogen bond, the position is shifted to lower frequency (Doyle, Blout, & Bendit, 1975). The result suggested that hydrogen bonds stabilised collagen structure were broken by thermal hydrolysis during gelatin extraction, particularly at higher temperature.

The ratio between amplitude of amide III and 1454  $\text{cm}^{-1}$  peak of ASC was closer to 1, whilst that of the corresponding gelatin (0.88–0.99) was lower. The gelatin extracted at temperature below 65  $^{\circ}\text{C}$  (0.99) showed the higher ratio, compared with those extracted at 85  $^{\circ}\text{C}$  (0.88–0.97). Generally, the ratio of amide III to 1454  $\text{cm}^{-1}$  of approximately 1.0 reveals the triple-helical structure of collagens (Plepis, Goissis, & Das-Gupta, 1996). The result indicated that the triple-helical structure of collagen could be destroyed by thermal hydrolysis during extraction, especially gelatin extracted under harsh condition (85  $^{\circ}\text{C}$ ). On the other hand, gelatin had the higher amplitude at wavenumber of 1072  $\text{cm}^{-1}$ , compared with that of ASC and the amplitude increased as

extraction temperature and time increased, except for gelatin extracted at 85  $^{\circ}\text{C}$  for 12 h. However, the wavenumber of 717  $\text{cm}^{-1}$  was only noticed in gelatin extracted at 85  $^{\circ}\text{C}$  for 12 h Jackson, Choo, Watson, Halliday, and Mantsch (1995) reported that these bands (717 and 1072  $\text{cm}^{-1}$ ) were associated with the C–O stretching vibrations of the short peptide chains. The result reconfirmed the higher degradation of gelatin extracted at higher temperatures. The result indicated that the primary structure ( $\alpha$ -chain), secondary structures (triple-helical structure) and functional group of gelatins from clown featherback skin were affected by extraction temperature and time.

### 3.4. Amino acid composition

Amino acid composition of gelatin from the skin of clown featherback extracted at 45  $^{\circ}\text{C}$  for 6 h, exhibiting the highest gel strength is shown in Table 2. In generally, amino acid composition of gelatin extracted at different temperatures for various times did not show significant differences in amino acid composition (Sinthusamran et al., 2014). Glycine is a major amino acid in gelatin from clown featherback skin (334 residues/1000 residues), followed by alanine (123 residues/1000 residues), proline (122 residues/1000 residues) and hydroxyproline (85 residues/1000 residues), respectively. Low amounts of cysteine (1 residue/1000 residues), histidine (4 residues/1000 residues), tyrosine (4 residues/1000 residues) and hydroxylysine (6 residues/1000 residues) were observed. Generally, glycine occurs every third position in the  $\alpha$ -chain and represents nearly one third of total residues (Benjakul, Oungbho, Visessanguan, Thiansilakul, & Roytrakul, 2009). The imino acid content of gelatin from clown featherback skin (207 residues/1000 residues) was slightly lower than that of gelatin from calf skin (219 residues/1000 residues) (Jongjareonrak et al., 2010). However, it was comparable to that of gelatin from seabass skin (199–202 residues/1000 residues) and giant catfish (211 residues/1000 residues) (Jongjareonrak et al., 2010; Sinthusamran et al., 2014). Imino acid content is an important factor for determining gel strength of gelatin. Benjakul et al. (2012) reported that imino acid, especially hydroxyproline, involve in gel formation by acting as H-donor, in which hydrogen bond can be formed with adjacent chain possessing H-acceptor.

Table 2  
Amino acid compositions of gelatin from the skin of clown featherback extracted at 45  $^{\circ}\text{C}$  for 6 h (residues/1000 residues).

Amino acids	Content (residues/1000 residues)
Alanine	123
Arginine	52
Aspartic acid/Asparagine	42
Cysteine	1
Glutamine/Glutamic acid	71
Glycine	334
Histidine	5
Isoleucine	10
Leucine	19
Lysine	16
Hydroxylysine	16
Methionine	12
Phenylalanine	14
Hydroxyproline	85
Proline	122
Serine	34
Threonine	24
Tyrosine	4
Valine	17
<b>Total</b>	<b>1000</b>
Imino acid	207

### 3.5. Gel properties

#### 3.5.1. Colour and turbidity of gel

The colour of gel from gelatin extracted at different extraction temperatures for various times is shown in Table 1. The colour of gel was expressed as the lightness ( $L^*$ ), redness ( $a^*$ ) and yellowness ( $b^*$ ). The lightness of gelatin gel slightly decreased as extraction temperature and time increased ( $P < 0.05$ ). Sharp decrease in lightness was observed in the gel of gelatin extracted at 85 °C for 12 h ( $P < 0.05$ ). Increase in redness of gel was also found when the extraction time increased ( $P < 0.05$ ). In general, gel of gelatin with extraction temperature of 85 °C showed the higher yellowness than those with extraction temperature of 45 and 65 °C ( $P < 0.05$ ). Occurrence of non-enzymatic browning reaction during extraction at higher temperature for longer time might contribute to the increased yellowness. When comparing the colour of gel with that of the food-grade bovine bone gelatin, there were some difference in lightness and redness. However, the much higher yellowness was noticeable in gelatin gel from bovine bone. Bone had more complex structure than the skin, in which the harsher extraction condition was required to obtain the higher yield, leading to the formation of colouring components mediated by several reactions.

The turbidity of gelatin solution from clown featherback skin increased as extraction temperature and time increased ( $P < 0.05$ ) (Table 1). The highest turbidity was observed in gelatin solution from gelatin extracted at 85 °C for 12 h ( $P < 0.05$ ). The result was in accordance with the report of Kittiphattanabawon et al. (2010). Random aggregation of protein from gelatin was more pronounced when extraction was performed at higher temperature for longer time, leading to the increased turbidity (Johnson & Zabik, 1981; Kittiphattanabawon et al., 2010).

#### 3.5.2. Gel strength of gelatin gel

Gel strength of gelatin extracted at different extraction temperatures for different times is shown in Fig. 3A. Gelatin gel is a reversibly crosslinked biopolymer network stabilised mainly by hydrogen bonded junction zones (Benjakul et al., 2012). Gel strength of gelatin decreased as extraction temperature and time increased, especially when extraction temperature was performed at 85 °C ( $P < 0.05$ ). The result was in accordance in gelatin from skin of wami tilapia (da Trindade Alfaro et al., 2014). Very low gel strength was also found in gelatin from brownbanded bamboo shark (56–111 g) and blacktip shark (10–17 g) extracted at high temperature (75 °C) (Kittiphattanabawon et al., 2010). The lower gel strength was associated with the presence of small peptides as indicated by the degradation of  $\alpha$ -,  $\beta$ - and  $\gamma$ -chains (Fig. 1). Normand, Muller, Ravey, and Parker (2000) reported that higher extraction temperature caused more protein degradation, thereby producing protein fragments and lowering gelling ability. Gelatin molecules with the shorter chain are not able to form the strong inter-junction zone, especially via hydrogen bond or other weak bonds such as hydrophobic interaction or ionic interaction. In contrast to the gelatin molecules with longer chain length are capable of alignment or self-aggregation more effectively (Benjakul et al., 2012). Similar phenomenon was reported for gelatin from the skins of seabass (Sinthusamran et al., 2014), splendid squid (Nagarajan et al., 2012) and channel catfish (Yang et al., 2007). When comparing gel strength with that of bovine bone gelatin, gelatin from clown featherback skin extracted at 45 and 65 °C (225–284 g) exhibited the higher gel strength than bovine bone gelatin (185 g) ( $P < 0.05$ ). Therefore, both extraction temperature and time play a crucial role in gel forming ability of resulting gelatin from skin of clown featherback.

#### 3.5.3. Gelling temperature and time

Gelling temperature and time were the temperature and time required for gel formation as indicated by phase angle of sample at

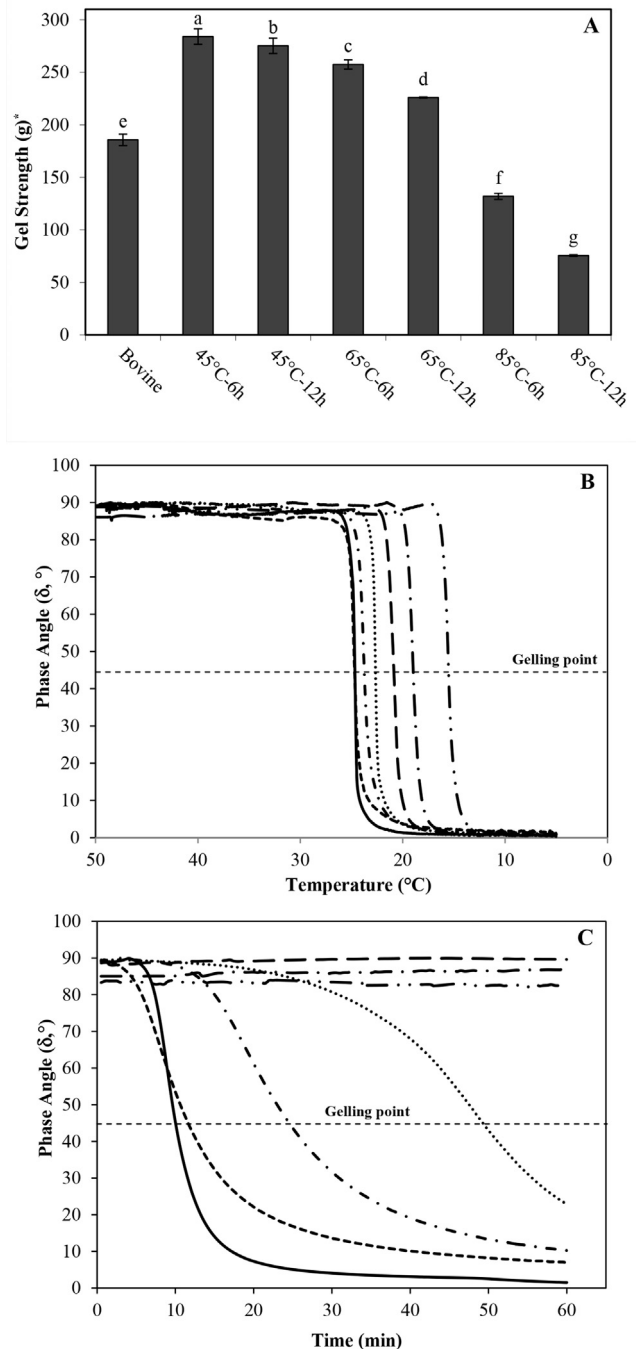


Fig. 3. Gel strength of gels (A) and changes in phase angle ( $\delta$ ) of solution as a function of temperature (B) and time (C) of gelatin from the skin of clown featherback extracted at different temperatures for various times. Different letters on the bars denote the significant differences ( $P < 0.05$ ). — Bovine, - - - 45 °C for 6 h, - · - 45 °C for 12 h, ····· 60 °C for 6 h, - - - 60 °C for 12 h, - · - 85 °C for 6 h, - · - 85 °C for 12 h. The unit of gel strength was shown in term of g-force, which could be converted to Pa by multiply with 98.0665.

45 °C, respectively (Fig. 3B and C). Changes in phase angle indicated the rapid transition, in which the formation of junction zones in the three-dimensional network took place with subsequent development of strong gel matrix (Sinthusamran et al., 2014). The gelling temperature of bovine gelatin and gelatin extracted at 45 °C for 6 and 12 h, 65 °C for 6 and 12 h and 85 °C for 6 and 12 h was 24.67, 24.71, 23.76, 22.66, 20.87, 18.98 and 15.53 °C, respectively (Fig. 3B). It was noticed that the higher extraction temperature and longer

extraction time resulted in the decreases in gelling temperature of gelatin ( $P < 0.05$ ). The marked decrease in gelling temperature was noticed in the gelatin solution obtained from gelatin extracted at 85 °C for 12 h. Eysturskarð, Haug, Elharfaoui, Djabourov, and Draget (2009) reported that gelling temperature of gelatin from saithe skins was more or less unaffected by increasing the extraction temperature from 22 to 45 °C, whilst a drop in gelling temperature was found by increasing extraction temperature to 65 °C. Additionally, gelatin from silver carp skin extracted at 50 °C for 3 h had gelling temperature of 18.7 °C (Boran, Mulvaney, & Regenstein, 2010). Thus, gelling temperature of gelatin from clown

featherback was higher than gelatin from saithe and silver carp skins. It might be caused by the difference in habitat temperature of those fishes. No difference in gelling temperature between gelatin extracted at 45 °C for 6 h (24.71 °C) and bovine gelatin (24.67 °C) was observed ( $P > 0.05$ ).

Gelling time is time required for the gel formation. In this study, the gelling time was measured at 25 °C. Gel of bovine gelatin set within 10.02 min. Clown featherback gelatin extracted at 45 °C for 6 and 12 h and 65 °C for 6 h were able to set at 25 °C within 11.62, 24.53 and 49.27 min, respectively, whilst that of the clown featherback gelatin extracted at 65 °C for 12 h and 85 °C was not able to

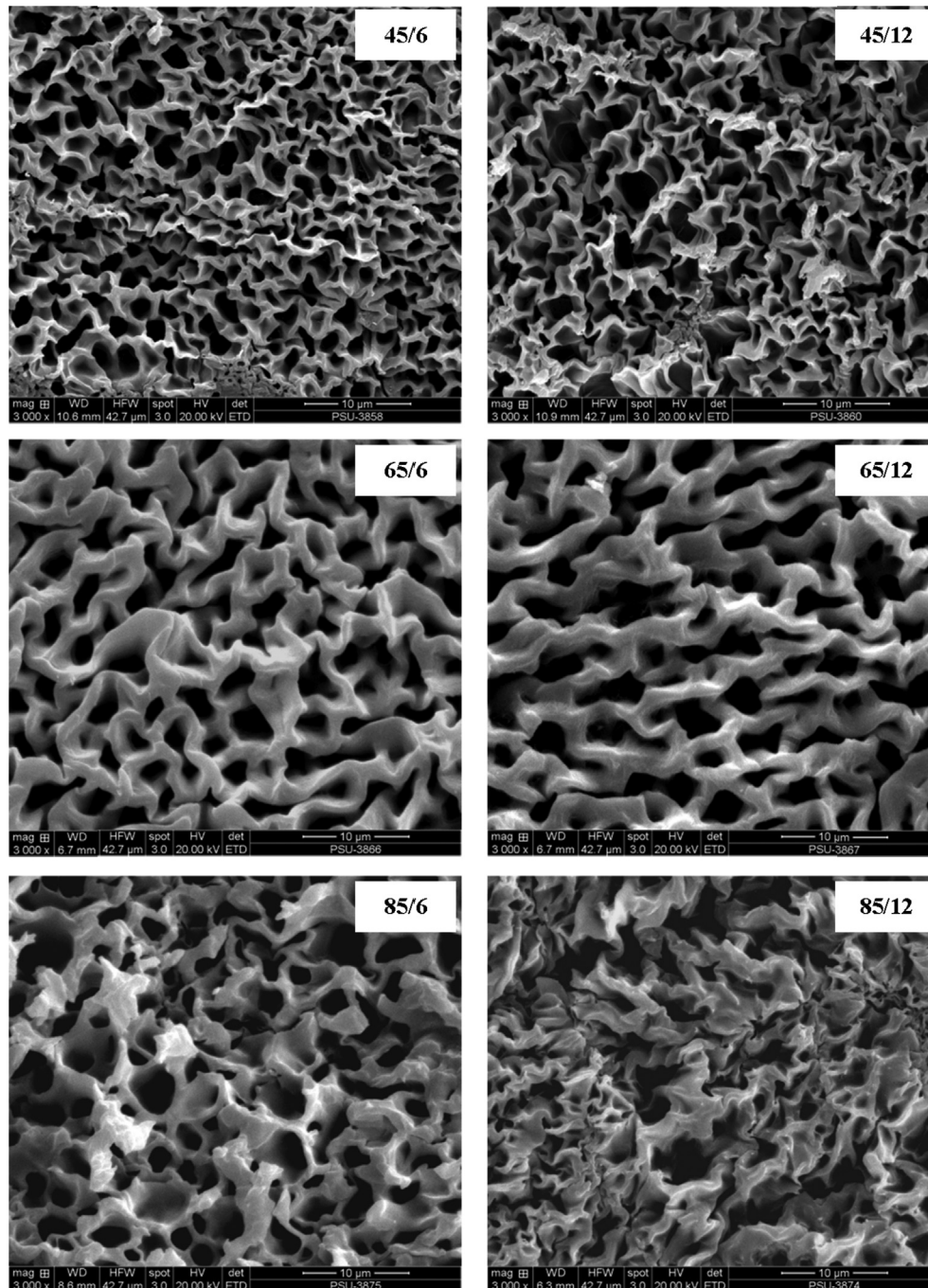


**Fig. 4.** Microstructure of gels from gelatin from the skin of clown featherback extracted at different temperatures for various times. Magnification: 3000 ×. The numbers before and after “/” denote extraction temperature and extraction time, respectively.

set at 25 °C (Fig. 3C). It was suggested that gelatin obtained from the milder extraction required less time for gel setting than that obtained from harsher extraction. It was noted that gelatin obtained from very harsh extraction was not able to set. This result was in agreement with the previous report (Kittiphattanabawon et al., 2010; Muyonga et al., 2004a; Sinthusamran et al., 2014).

The differences in gelling temperature and time amongst gelatin extracted under different conditions and bovine gelatin might be caused by differences in molecular weight distributions (Muyonga et al., 2004a). On the other hand, lower gelling temperature and longer gelling time were coincidental with lower molecular weight distribution (Fig. 1) and gel strength (Fig. 3A). Thus, gelling behaviour of gelatin was determined by extraction condition.

#### 3.5.4. Microstructure of gelatin gel

Microstructure of gel from gelatin extracted under different conditions is illustrated in Fig. 4. Generally, all gelatin gels showed a uniform network, which had different thickness of strand and size of void. The network with thinnest strands and smallest voids was found in the gel from gelatin extracted at 45 °C for 6 h. However, gel from gelatin extracted at 85 °C not only had thicker strands and larger voids, but also showed the disordered network. Sinthusamran et al. (2014) reported that gel having finer network with smaller voids indicated the uniform distribution of water in the fine and ordered gel matrix. The microstructure of gel correlated well with gel strength (Fig. 3A). The gel network with finer strand and smaller void could be resistant to the force applied. Furthermore, gelatin extracted under milder conditions had more amount of  $\alpha$ -,  $\beta$ - and  $\gamma$ -chains than those extracted with harsher condition (Fig. 1). As a consequence, the gelatin extracted using milder condition had the higher connected strands with stronger network as indicated by higher gel strength.

## 4. Conclusions

Gel property of gelatin depended on extraction temperature and time. Gelatin extracted at higher temperature for longer time had higher recovery but the poorer gel strength. Gelatin extracted at 45 °C for 6 or 12 h showed the higher gel strength, compared with bovine gelatin. Moreover, gel of those gelatins could be set at 25 °C and was transparent. Therefore, gelatin from clown featherback skin should be extracted at 45 °C for 6 or 12 h to obtain gelatin with gel properties equivalent to or better those commercial bovine gelatin.

## Acknowledgement

This work was supported by The Thailand Research Fund and Thaksin University for contract No. TRG5780036 to Dr. Phanat Kittiphattanabawon. The TRF Distinguished Research Professor Grant was also acknowledged. Thanks to Faculty of Agro-industry, Prince of Songkla University for the permission to use facilities for this research.

## References

Alfaro, A. T., Biluca, F. C., Marquetti, C., Toniai, I. B., & de Souza, N. E. (2014). African catfish (*Clarias gariepinus*) skin gelatin: extraction optimization and physico-chemical properties. *Food Research International*, 65(PC), 416–422.

AOAC. (2000). *Official methods of analysis*. Arlington: Association of Official Analytical Chemists Inc.

Benjakul, S., Kittiphattanabawon, P., & Regenstien, J. M. (2012). Fish gelatin. In B. K. Simpson, G. Paliyath, L. M. L. Nollet, S. Benjakul, & F. Toldrá (Eds.), *Food*

*biochemistry and food processing* (pp. 388–405). Iowa: John Wiley & Sons, Inc.

Benjakul, S., Oungbho, K., Visessanguan, W., Thiansilakul, Y., & Roytrakul, S. (2009). Characteristics of gelatin from the skins of bigeye snapper, *Priacanthus tayenus* and *Priacanthus macracanthus*. *Food Chemistry*, 116(2), 445–451.

Bergman, I., & Loxley, R. (1963). Two improved and simplified methods for the spectrophotometric determination of hydroxyproline. *Analytical Chemistry*, 35(12), 1961–1965.

Boran, G., Mulvaney, S. J., & Regenstien, J. M. (2010). Rheological properties of gelatin from silver carp skin compared to commercially available gelatins from different sources. *Journal of Food Science*, 75(8), E565–E571.

BSI. (1975). *Methods for sampling and testing gelatin (Physical and chemical methods)*. London: BSI.

Cho, S. M., Gu, Y. S., & Kim, S. B. (2005). Extracting optimization and physical properties of yellowfin tuna (*Thunnus albacares*) skin gelatin compared to mammalian gelatins. *Food Hydrocolloids*, 19(2), 221–229.

Doyle, B. B., Blout, E. R., & Bendit, E. G. (1975). Infrared spectroscopy of collagen and collagen like polypeptides. *Biopolymers*, 14(5), 937–957.

Eysturskarð, J., Haug, I. J., Elharfaoui, N., Djabourov, M., & Draget, K. I. (2009). Structural and mechanical properties of fish gelatin as a function of extraction conditions. *Food Hydrocolloids*, 23(7), 1702–1711.

Foegeding, E. A., Lanier, T. C., & Hultin, H. O. (1996). Characteristics of edible muscle tissues. In O. R. Fennema (Ed.), *Food chemistry* (pp. 879–942). New York: Marcel Dekker, Inc.

Jackson, M., Choo, L. P., Watson, P. H., Halliday, W. C., & Mantsch, H. H. (1995). Beware of connective tissue proteins: assignment and implications of collagen absorptions in infrared spectra of human tissues. *Biochimica et Biophysica Acta – Molecular Basis of Disease*, 1270(1), 1–6.

Johnson, T. M., & Zabik, M. E. (1981). Egg albumin proteins interactions in an angel food cake system. *Journal of Food Science*, 46(4), 1231–1236.

Jongjareonrak, A., Rawdkuen, S., Chaijan, M., Benjakul, S., Osako, K., & Tanaka, M. (2010). Chemical compositions and characterisation of skin gelatin from farmed giant catfish (*Pangasianodon gigas*). *LWT – Food Science and Technology*, 43(1), 161–165.

Kaewruang, P., Benjakul, S., Prodpran, T., & Nalinanon, S. (2013). Physicochemical and functional properties of gelatin from the skin of unicorn leatherjacket (*Aluterus monoceros*) as affected by extraction conditions. *Food Bioscience*, 2, 1–9.

Kittiphattanabawon, P., Benjakul, S., Visessanguan, W., & Shahidi, F. (2010). Comparative study on characteristics of gelatin from the skins of brownbanded bamboo shark and blacktip shark as affected by extraction conditions. *Food Hydrocolloids*, 24(2–3), 164–171.

Laemmli, U. K. (1970). Cleavage of structural proteins during the assembly of the head of bacteriophage T4. *Nature*, 227(5259), 680–685.

Muyonga, J. H., Cole, C. G. B., & Duodu, K. G. (2004a). Extraction and physico-chemical characterisation of Nile perch (*Lates niloticus*) skin and bone gelatin. *Food Hydrocolloids*, 18(4), 581–592.

Muyonga, J. H., Cole, C. G. B., & Duodu, K. G. (2004b). Fourier transform infrared (FTIR) spectroscopic study of acid soluble collagen and gelatin from skins and bones of young and adult Nile perch (*Lates niloticus*). *Food Chemistry*, 86(3), 325–332.

Nagarajan, M., Benjakul, S., Prodpran, T., Songtipya, P., & Kishimura, H. (2012). Characteristics and functional properties of gelatin from splendid squid (*Loligo formosana*) skin as affected by extraction temperatures. *Food Hydrocolloids*, 29(2), 389–397.

Normand, V., Muller, S., Ravey, J. C., & Parker, A. (2000). Gelation kinetics of gelatin: a master curve and network modeling. *Macromolecules*, 33(3), 1063–1071.

Payne, K. J., & Veis, A. (1988). Fourier transform infrared spectroscopy of collagen and gelatin solutions: Deconvolution of the amide I band for conformational studies. *Biopolymers*, 27(11), 1749–1760.

Plepis, A. M. D. G., Goissis, G., & Das-Gupta, D. K. (1996). Dielectric and pyroelectric characterization of anionic and native collagen. *Polymer Engineering and Science*, 36(24), 2932–2938.

Regenstien, J. M., & Zhou, P. (2007). Collagen and gelatin from marine by-products. In F. Shahidi (Ed.), *Maximising the value of marine by-products* (pp. 279–303). Cambridge: Woodhead Publishing Limited.

Sinthusamran, S., Benjakul, S., & Kishimura, H. (2014). Characteristics and gel properties of gelatin from skin of seabass (*Lates calcarifer*) as influenced by extraction conditions. *Food Chemistry*, 152, 276–284.

Steel, R. G. D., & Torrie, J. H. (1980). *Principles and procedures of statistics: A biometrical approach*. New York: McGraw-Hill.

da Trindade Alfaro, A., Fonseca, G. G., Balbinot, E., de Souza, N. E., & Prentice, C. (2014). Yield, viscosity, and gel strength of wami tilapia (*Oreochromis urolepis hornorum*) skin gelatin: optimization of the extraction process. *Food Science and Biotechnology*, 23(3), 765–773.

Wong, D. W. S. (1989). *Mechanism and theory in food chemistry*. New York: Van Nostrand Reinhold Company Inc.

Yang, H., Wang, Y., Jiang, M., Oh, J. H., Herring, J., & Zhou, P. (2007). 2-Step optimization of the extraction and subsequent physical properties of channel catfish (*Ictalurus punctatus*) skin gelatin. *Journal of Food Science*, 72(4), C188–C195.



## Modelling phenolic and volatile composition to characterize the effects of pre-fermentative cold soaking in Tempranillo wines



José L. Aleixandre-Tudó<sup>a, c, \*</sup>, Inmaculada Álvarez<sup>c</sup>, Victoria Lizama<sup>c</sup>,  
Hélène Nieuwoudt<sup>a, b</sup>, María J. García<sup>c</sup>, José L. Aleixandre<sup>c</sup>, Wessel J. du Toit<sup>a</sup>

<sup>a</sup> Department of Viticulture and Oenology, Stellenbosch University, Private Bag X1, Matieland 7602, South Africa

<sup>b</sup> Institute for Wine Biotechnology, Stellenbosch University, Private Bag X1, Matieland 7602, South Africa

<sup>c</sup> Departamento de Tecnología de Alimentos, Universitat Politècnica de Valencia, Camino de Vera s/n, 46022 Valencia, Spain

### ARTICLE INFO

#### Article history:

Received 13 July 2015

Received in revised form

17 September 2015

Accepted 12 October 2015

Available online 22 October 2015

#### Keywords:

Cold soak

Dry ice

Phenolics

Volatiles and OPLS-DA

### ABSTRACT

The impact of pre-fermentative cold soak, alone or in combination with dry ice addition, on colour, phenolic and volatile composition of Tempranillo wines at 12 months after bottling was studied. A control wine without cold soak was also evaluated. A sample set consisting of 66 wines was investigated. The results from ANOVA and PCA analysis showed significant treatment-related differences for a number of chemical measurements, as well as overlapping effects. Orthogonal projections to latent structures discriminant analysis (OPLS-DA) of the data showed that the dry ice addition treatment had a major effect on the anthocyanin fraction and on the levels of ethyl decanoate, 2-phenylethyl acetate and decanoic acid. In comparison, the cold soak treatment only had a slight effect on the bisulphite bleaching anthocyanins and volatile composition.

© 2015 Elsevier Ltd. All rights reserved.

### 1. Introduction

Polyphenols and volatiles are essential for wine colour, mouth-feel and flavour. The relative proportions of anthocyanins and tannins can be adjusted during skin maceration to achieve a wine capable of undergoing good evolution during aging (Glories & Galvin, 1990). Therefore, when fruit and full bodied red wines are required, pre-fermentative cold maceration appears as an alternative for winemakers (Cai et al., 2014). However, the effects of pre-fermentative techniques are highly dependent on grape sanitary status and phenolic ripeness (Alvarez, Aleixandre, García, & Lizama, 2006), as well as on the aromatic nature of the variety (Moreno-Pérez, Vila-López, & Fernández-Fernández, 2013).

Skin polyphenols and volatile compounds are extracted throughout the pre-fermentative cold soak in the absence of ethanol (Gómez-Míguez, González-Miret, & Heredia, 2007). Dry ice (solid carbon dioxide) addition appears as a common method to obtain the cold temperatures required for this technique (Heredia

et al., 2010). After crushing and dry ice addition, grape skin cells are broken and disorganized through freezing, which facilitates aroma and phenolic extraction (Álvarez, Aleixandre, García, Lizama, & Aleixandre-Tudó, 2009).

Contradictory results have been observed in the literature regarding the effect of pre-fermentative cold soak techniques on chemical wine composition. Several studies have shown that cold soak has either no effect, while a decrease in phenolic levels was also observed (De Beer, Joubert, Marais, & Manley, 2006; Heatherbell, Dicey, Goldsworthy, & Vanhanen, 1997; Marais, 2003; Okubo, Goto-Yamamoto, & Okazaki, 2003). Other authors noticed an increased phenolic content and higher sensory scores when wines were cold soaked before fermentation (Gil-Muñoz et al., 2009; Gordillo, López-Infante, Ramírez-Pérez, González-Miret, & Heredia, 2010; Heredia et al., 2010; Koyama, Goto-Yamamoto, & Hashizume, 2007). During the cold soak step numerous reactions between grape phenolics also occur, which may influence wine sensory properties (Parenti, Spugnoli, Calamai, Ferrari, & Gori, 2004). Moreover, other compounds (proteins and polysaccharides) are also extracted, which may participate in condensation reactions (Gómez-Plaza, Gil-Muñoz, López-Roca, Martínez-Cutillas, & Fernández-Fernández, 2001).

Pre-fermentative techniques have been used extensively in the

\* Corresponding author. Department of Viticulture and Oenology, Stellenbosch University, Private Bag X1, Matieland 7602, South Africa.

E-mail address: [joaltu@sun.ac.za](mailto:joaltu@sun.ac.za) (J.L. Aleixandre-Tudó).

production of white and rosé wines and have been recommended as a means for enhancing wine aroma (Sánchez Palomo, González-Viñas, Díaz-Maroto, Soriano-Pérez, & Pérez-Coello, 2007). Cold soak has also been tested in red winemaking (Sacchi, Bisson, & Adams, 2005). However, little is known about its effect on the volatile composition. Moreno-Pérez et al. (2013) cited differences between cold soak treated red wines and conventional winemaking after six months of bottling, although no differences between pre-treatments (cold soak, freezing grapes and dry ice addition) were observed. Moreover, in Monastrell wines increased volatile compound levels were reported for Monastrell wines produced by dry ice addition after 6 months of bottle storage (Alvarez, Aleixandre, García, & Lizama, 2006).

Based on these contradictory reports, the aim of this work was thus to evaluate the impact of cold soak techniques on color, phenolic and volatile composition of red Tempranillo wines at 12 months of bottle storage. Tempranillo is one of the most widely planted grape cultivars in Spain and wines made from this cultivar are increasingly being accepted in new world wine producing countries such as Australia and the United States (Cynkar, Damberg, Smith, & Cozzolino, 2010; USDA, 2014).

## 2. Materials and methods

### 2.1. Wine samples

Tempranillo grapes from a commercial vineyard (Utiel-Requena, Valencia, Spain) were harvested in 2008. At harvest, the grapes had  $221.33 \pm 9.29$  g/L of total sugar content, total acidity of  $6.1 \pm 0.2$  g/L as tartaric acid, pH of  $3.34 \pm 0.12$  and potential alcohol of  $13.07 \pm 0.64\%$  vol. ( $N = 3$ ). Wines were produced at an experimental wine production centre (Universitat Politècnica de València (UPV)). 40 kg of grapes were destemmed, crushed, mixed and divided into closed 50 L stainless steel tanks. Potassium bisulphite was added at 100 mg/kg before fermentation. Treatments consisted of traditional vinification wines (T–V) without cold soak (control); cold soaked wines at 6 to 8 °C for four days (C–S); and dry ice addition (0 to 2 °C) followed by cold soak at 6 to 8 °C for four days (D–I). Twenty-two small scale vinifications were made for each treatment. After the cold soak period wines were left to warm up in the fermentation room and commercial yeasts were inoculated at 20 g/hL (*Saccharomyces cerevisiae* strain EP 841, Agrovín, Spain). The highest temperature during fermentation was 25 °C. Manual punching down was carried out twice a day. T–V wines were left on the skins for 15 days to ensure that sugar levels were lower than 2 g/L. Following the same workflow, C–S and D–I wines were also left on the skins for 15 days after the four days cold soak treatment. After fermentation wines were pressed and the first 5 L were mixed with 20 L free-run wine. *Oenococcus oeni* strain OE 104 (Agrovín, Spain) lactic acid bacteria was inoculated and malolactic fermentation (MLF) was conducted at room temperature (~20 °C). Potassium bisulphite was added at 50 mg/L before bottling. Wines were stored at room temperature ( $15 \pm 2$  °C) and cork closures were used.

### 2.2. Analytical methods

A UV–Visible JASCO V-530 spectrophotometer, and a JASCO MD-2010 Plus high-performance liquid chromatography instrument coupled with a diode array detector (DAD) (JASCO LC-Net II/ADC, Tokyo, Japan) were used for phenolic measurements. All the spectrophotometric measurements were performed in triplicate. Using the analytical methods described by Glories (1984) colour intensity, hue, gelatin (astringency) and EtOH (tannin-polysaccharide molecules) indexes were estimated. The Ribéreau-Gayon and

Stronestreet (1965) method was used for the determination of bisulphite bleached anthocyanins. Catechins were quantified using the method reported by Sun, Ricardo Da Silva, and Spranger (1998). The modified version of the MCP tannin assay reported by Mercurio, Damberg, Herderich, and Smith (2007) was used for tannin quantification. The method reported by Boulton (1996) was used to analyze the contribution of the copigmented, free and polymeric anthocyanins to the total wine colour. PVPP (anthocyanin-tannin complexes) and DMACH (tannin degree of polymerization) indexes were calculated according to Vivas and Glories (1995). The Folin-Ciocalteu index was determined using the method developed by Singleton and Rossi (1965).

HPLC was used to quantify individual phenolic compounds using the method reported by Jensen, Blachez, Egebo, and Meyer (2007). Gallic acid, (+)-catechin and (–)-epicatechin were quantified at 280 nm. Flavan-3-ols were defined as the sum of (+)-catechin and (–)-epicatechin. Hydroxycinnamic acids were quantified at 316 nm. Phenolic acids were calculated as the sum of gallic and caffeic, coumaric, *p*-coumaric and caftaric acid. Flavonols (quercetin rutinoside, quercetin glucoside, myricetin, quercetin and kaempferol) were quantified at 365 nm. Delphinidin, cyanidin, peonidin, petunidin and malvidin acetyl and coumaryl glucosides resulted in the derivated anthocyanins. Total anthocyanins were calculated as the sum of anthocyanidin-3-glucosides and derivated anthocyanins. Within each phenolic group, compounds were identified based on their intrinsic spectral features and retention times. Commercially available standards were used to build the calibration curves for phenolics quantifications: gallic acid (Fluka, Milwaukee, WI, USA), (+)-catechin (Fluka, Milwaukee, WI, USA) for flavan-3-ols, caffeic acid (Fluka, Milwaukee, WI, USA) for hydroxycinnamic acids, rutin (Sigma–Aldrich, St Louis, MO) for flavonols and malvidine-3-glucoside (Sigma–Aldrich, St Louis, MO) for anthocyanins. 20 µL of the wine sample were injected twice after centrifugation (5000 rpm) and filtration (0.45 µm membrane Millipore filter). Separation was carried out on a Gemini NX (Phenomenex, Torrance, CA) 5 µm, 250 mm × 4.6 mm i.d. column at 40 °C. Acetonitrile and *o*-phosphoric acid were used as solvents. Solvents composition and the elution gradient were reported elsewhere (Jensen et al., 2007).

An Agilent gas chromatograph (GC) (Agilent Technologies, Waldbronn, Germany) equipped with a split/splitless capillary injection port and flame ionization detector (FID) was used for the analysis of the wine aroma composition. Separations were performed on a ZB- WAX Plus column (50 m × 0.25 mm i.d., 0.25 µm film thickness) from Phenomenex (Aschaffenburg, Germany). Duplicate injections were performed using the following conditions: injector temperature, 250 °C; detector temperature, 300 °C; carrier gas flow (N<sub>2</sub>), 1 mL/min. Injections were made in split mode (split ratio, 1/60; sample size, 1 µL). The oven temperature was maintained at 40 °C for 7 min, from 40 to 110 °C at 4 °C/min, from 110 to 170 °C at 10 °C/min, and then held for 10 min. The comparison of retention times with those of standard compounds was used to identify volatile compounds. Preparation of the samples was carried out following the method proposed by Hernanz, Heredia, Beltran, and Recamales (1999). Twenty volatile compounds were quantified with 2-octanol as internal standard.

### 2.3. Statistical analysis

Statgraphics Plus 5.1 software was used for the ANOVA treatment of the data. Principal component analysis (PCA) and orthogonal projections to latent structures discriminant analysis (OPLS-DA) (Trygg & Wold, 2002) was performed using SIMCA version 13.0.3 software ([www.umetrics.com](http://www.umetrics.com)). Chemical measurements

were Pareto ( $1/\sqrt{\text{Standard Deviation}}$ ) scaled. The advantages of Pareto scaling have been defined as a means of reducing the impact of noise and artefacts in the models (Wiklund et al., 2008).

### 3. Results and discussion

#### 3.1. Effect of pre-fermentative maceration techniques on wine phenolic composition

ANOVA results showed no differences between the control and pre-fermentative treated wines in colour density and hue after 12 months of bottling (Table 1). Bisulphite bleaching anthocyanins showed higher values in cold soaked (C–S) and dry ice added (D–I) wines. Higher levels of malvidine-3-monoglucoside, sum of anthocyanidins and total anthocyanins were found in D–I wines. These results are in accordance with those obtained by Alvarez et al. (2006) and Gil-Muñoz et al. (2009) which indicate an increase in the anthocyanin concentrations due to cold soak with dry ice addition. The higher anthocyanin derivatives values observed might support the idea that dry ice addition is capable of increasing not only the free anthocyanin fraction. The extraction of other low molecular weight phenolics that could react with free anthocyanins might give rise to more complex anthocyanin moieties (Alexandre-Tudó et al., 2013). Gil-Muñoz et al. (2009) also reported increased phenolic extraction and an improvement on the chromatic characteristics in cold soaked wines.

Pre-fermentative cold soak techniques have been reported to influence the presence of phenolic compounds with high copigmentation potential (Álvarez, Alexandre, García, Lizama, & Alexandre-Tudó, 2009; Heredia et al., 2010). Despite the reported results no differences in the copigmentation fraction were observed. Copigmented anthocyanins account for almost half of the observed colour in young red wines and it is thought that anthocyanins may take part in future condensation reactions. Moreover, it is also believed that at early stages of fermentation the anthocyanin-copigment molecules can prevent anthocyanin

oxidation, favouring further covalent tannin-anthocyanin interaction (Boulton, 2001).

The colour resulting from the free non-copigmented anthocyanins and the flavan-3-ol concentration was also higher in D–I wines. Parenti et al. (2004) reported increased flavan-3-ol, tannin and anthocyanin concentrations in cold soaked wines after bottling, which led to more anthocyanin-tannin interactions. Contrarily to what was reported, anthocyanin-tannin interactions (PVPP index and % of colour due to polymeric anthocyanins) were not increased in this study at 12 months of bottling.

#### 3.2. Effect of pre-fermentative cold soak techniques on wine volatile composition

The ANOVA results showed that pre-fermentative cold soak techniques caused significant differences (Table 2) in fatty acids (octanoic and decanoic acid), ethyl esters (ethyl hexanoate and ethyl decanoate), an ester (2-Phenylethyl acetate), a volatile phenol (4-vinylphenol) and a lactone ( $\gamma$ -butyrolactone). The concentration of octanoic acid was lower in C–S and D–I wines, while the opposite was found for decanoic acid, although only significant for D–I wines. Moreover, no trends were observed in the esters and ethyl esters levels found for the different treatments. The levels of 4-vinylphenol were lower for D–I wines when compared to T–V and C–S treatments. Finally  $\gamma$ -butyrolactone levels seem to be diminished by cold soak treatments, with T–V wines having the highest levels of this compound. Moreno-Pérez et al. (2013) were not able to discriminate between the volatile composition of cold soaked Monastrell, Cabernet Sauvignon and Syrah cold soaked wines (freezing grapes, dry ice and cold soak) and concluded that these effects were variety dependent.

The large within treatment variations (as indicated by high standard deviations), probably caused by the large number of small scale fermentations, could possibly explain why non-significant differences were observed for some compounds (Table 2). Contrarily to univariate techniques such as ANOVA that

**Table 1**

Colour and phenolic profile of Tempranillo wines after 12 month of bottle aging. Mean  $\pm$  standard deviation values of the phenolic measurement.

		T–V (n = 22)	C–S (n = 22)	D–I (n = 22)	p-value
Color density (1)	CDe	12.71 $\pm$ 1.55	12.52 $\pm$ 0.88	12.21 $\pm$ 1.06	0.39
Hue (2)	Hue	71.20 $\pm$ 2.63	69.93 $\pm$ 2.28	70.84 $\pm$ 2.28	0.20
Bisulphite bleaching ant. (mg/L) (3)	BBA	271.85 $\pm$ 27.83 a	297.59 $\pm$ 38.96 b	287.27 $\pm$ 30.64 b	0.04*
Delphinidin-3-glucoside (mg/L) (4)	Del	33.10 $\pm$ 2.84	32.21 $\pm$ 1.85	33.58 $\pm$ 1.73	0.19
Cyanidin-3-glucoside (mg/L) (5)	Cya	2.17 $\pm$ 2.15	2.15 $\pm$ 0.25	2.33 $\pm$ 0.03	0.65
Petunidin-3-glucoside (mg/L) (6)	Pet	30.67 $\pm$ 31.93	31.93 $\pm$ 1.90	32.61 $\pm$ 2.42	0.08
Peonidin-3-glucoside (mg/L) (7)	Peo	5.13 $\pm$ 1.01	5.20 $\pm$ 0.87	5.49 $\pm$ 0.90	0.49
Malvidin-3-glucoside (mg/L) (8)	Mal	255.42 $\pm$ 18.40 a	257.34 $\pm$ 26.61 a	280.43 $\pm$ 25.88 b	0.00*
Anthocyanidins (mg/L) (9)	Ant	326.49 $\pm$ 24.64 a	328.83 $\pm$ 30.30 a	354.45 $\pm$ 29.36 b	0.00*
Anthocyanin derivatives (mg/L) (10)	ADe	46.84 $\pm$ 3.69 a	48.33 $\pm$ 7.28 a	53.34 $\pm$ 8.63 b	0.00*
Total anthocyanins (mg/L) (11)	ToA	373.33 $\pm$ 25.24 a	377.16 $\pm$ 34.48 a	407.78 $\pm$ 32.23 b	0.00*
% Copigmented anthocyanins (12)	%CA	10.48 $\pm$ 2.65	10.61 $\pm$ 2.39	10.48 $\pm$ 2.25	0.91
% Free anthocyanins (13)	%FA	39.49 $\pm$ 1.21 a	40.72 $\pm$ 2.91 ab	41.98 $\pm$ 2.76 b	0.04*
% Polymerized anthocyanins (14)	%PA	50.03 $\pm$ 7.62	48.67 $\pm$ 3.54	47.54 $\pm$ 4.70	0.77
PVPP index (15)	PVI	32.02 $\pm$ 3.07	32.79 $\pm$ 2.90	33.92 $\pm$ 2.98	0.07
Folin index (16)	Fol	46.22 $\pm$ 2.23	45.65 $\pm$ 1.95	45.56 $\pm$ 1.95	0.50
Phenolic acids (mg/L) (17)	PhA	146.74 $\pm$ 29.40	148.56 $\pm$ 26.35	137.98 $\pm$ 26.56	0.34
Flavonols (mg/L) (18)	Flo	61.27 $\pm$ 20.59	57.19 $\pm$ 20.87	63.38 $\pm$ 19.34	0.59
Catechin assay (mg/L) (19)	Cat	85.49 $\pm$ 17.59	84.93 $\pm$ 15.05	85.49 $\pm$ 13.88	0.99
Flavan-3-ols (mg/L) (20)	Fla	65.45 $\pm$ 19.01 a	70.16 $\pm$ 20.00 ab	80.89 $\pm$ 18.34 b	0.03*
Tannins (g/L) (21)	Tan	2.15 $\pm$ 0.25 b	2.01 $\pm$ 0.20 a	2.03 $\pm$ 0.23 a	0.03*
DMACH index (22)	DMI	43.41 $\pm$ 4.23	43.76 $\pm$ 3.21	44.82 $\pm$ 3.99	0.29
Ethanol index (23)	Etl	21.75 $\pm$ 5.89	23.96 $\pm$ 4.39	22.78 $\pm$ 4.83	0.25
Gelatin index (24)	Gel	64.97 $\pm$ 5.96	65.45 $\pm$ 10.12	65.53 $\pm$ 8.65	0.96

n: number of samples involved in the analysis from each treatment. T–V: traditional vinification; C–S: cold soak; D–I: dry ice.\*Statistical analysis ANOVA at 95% confidence level with same letters indicating no significant difference for Tukey's test.

**Table 2**  
Volatile composition of Tempranillo wines after 12 month of bottle aging. Mean  $\pm$  standard deviation values ( $\mu\text{g/L}$ ) of the quantified volatile compounds.

		T–V (n = 22)	C–S (n = 22)	D–I (n = 22)	p-value	PT <sup>a,b</sup>
Isoamyl acetate (25)	IsA	449.55 $\pm$ 221.45	704.91 $\pm$ 349.04	675.18 $\pm$ 550.59	0.07	30(I) <sup>#</sup>
Ethyl hexanoate (26)	EHe	173.27 $\pm$ 125.21 b	105.48 $\pm$ 34.87 a	85.90 $\pm$ 19.71 a	0.00*	50(I) <sup>#</sup>
Ethyl lactate (27)	ELa	12797.10 $\pm$ 10021.19	23283.53 $\pm$ 19508.42	21629.45 $\pm$ 20015.09	0.10	14000(II) <sup>‡</sup>
Cis-3-hexen-1-ol (28)	C3H	26.30 $\pm$ 19.55	18.22 $\pm$ 9.84	21.14 $\pm$ 17.22	0.25	400(III) <sup>‡</sup>
Ethyl 3-hydroxybutyrate (29)	EHB	21.21 $\pm$ 11.84	21.79 $\pm$ 9.90	22.33 $\pm$ 15.42	0.96	20000(III) <sup>p</sup>
Isobutyric acid (30)	IbA	2731.74 $\pm$ 1398.11	2998.24 $\pm$ 1646.48	3032.73 $\pm$ 2053.87	0.82	2300(IV) <sup>§</sup>
4-Vinylphenol (31)	4Vp	27.29 $\pm$ 22.48 b	26.58 $\pm$ 18.69 b	8.43 $\pm$ 9.04 a	0.00*	180(III) <sup>§</sup>
Butyric acid (32)	BtA	6.60 $\pm$ 4.54	7.45 $\pm$ 4.78	7.27 $\pm$ 5.65	0.84	173(III) <sup>‡</sup>
Ethyl decanoate (33)	EDe	425.89 $\pm$ 228.45 b	190.63 $\pm$ 68.13 a	573.95 $\pm$ 119.04 c	0.00*	200(I) <sup>‡</sup>
$\gamma$ -Butyrolactone (34)	Btl	40.58 $\pm$ 23.75 b	26.77 $\pm$ 10.83 a	23.77 $\pm$ 9.69 a	0.00*	35(III) <sup>p</sup>
Isopentanoic acid (35)	IpA	3.69 $\pm$ 1.63	3.86 $\pm$ 2.44	4.03 $\pm$ 2.68	0.89	30(III) <sup>‡</sup>
Diethyl succinate (36)	DeS	535.60 $\pm$ 317.26	614.19 $\pm$ 299.84	713.82 $\pm$ 170.98	0.10	200000(III) <sup>‡</sup>
2-Phenylethyl acetate (37)	2 PA	163.38 $\pm$ 74.92 a	213.14 $\pm$ 50.23 a	306.31 $\pm$ 140.36 b	0.00*	250(IV) <sup>#</sup>
Hexanoic acid (38)	HeA	3121.63 $\pm$ 1459.38	3161.95 $\pm$ 1632.91	2717.16 $\pm$ 1619.91	0.59	420(V) <sup>§</sup>
2-Methoxyphenol (39)	2 MP	197.77 $\pm$ 68.82	249.24 $\pm$ 77.78	247.83 $\pm$ 111.20	0.09	9.5(III) <sup>‡</sup>
2-Phenylethanol (40)	2Pe	40792.84 $\pm$ 30714.08	47685.85 $\pm$ 29690.71	50851.00 $\pm$ 30873.27	0.54	14000(IV) <sup>‡</sup>
4-Ethylguaiaacol (41)	4 Eg	283.54 $\pm$ 97.22	238.30 $\pm$ 64.57	209.23 $\pm$ 150.89	0.09	33(IV) <sup>#</sup>
Octanoic acid (42)	OcA	576.25 $\pm$ 259.34 b	422.5 $\pm$ 233.28 a	350.92 $\pm$ 185.84 a	0.01*	500(III) <sup>‡</sup>
4-Ethylphenol (43)	4Ep	51.40 $\pm$ 19.30	39.36 $\pm$ 15.64	43.57 $\pm$ 21.57	0.11	440(IV) <sup>§</sup>
Decanoic acid (44)	DeA	308.73 $\pm$ 104.77 a	340.20 $\pm$ 66.34 ab	408.89 $\pm$ 170.14 b	0.03*	1000(III) <sup>‡</sup>

n: number of samples involved in the analysis from each treatment. T–V: traditional vinification; C–S: cold soak; D–I: dry ice. PT: perception threshold. \*Statistical analysis ANOVA at 95% confidence level with same letters indicating no significant difference for Tukey's test.

<sup>a</sup>The reference from which the value was obtained is given in parentheses: I (Swiegers, Bartowsky, Henschke, & Pretorius, 2005); II (Li, Tao, Wang, & Zhang, 2008); III (Culleré, Escudero, Cacho, & Ferreira, 2004); IV (Francis & Newton, 2005); V (Ferreira, López, & Cacho, 2000).

<sup>b</sup>Symbols correspond to different matrices from which the PT was obtained: <sup>#</sup>10% ethanol/water solution; <sup>‡</sup>12% ethanol/water solution; <sup>§</sup>12% ethanol/water solution with 8 g/L glycerol and different salts; <sup>p</sup>10% ethanol/water solution with 5 g/L of tartaric acid at pH 3.2; <sup>q</sup>11% ethanol/water solution with 7 g/L glycerol and 5 g/L tartaric acid; <sup>r</sup>10% ethanol/water solution with 7 g/L glycerol at pH 3.0.

compare only one variable at the time, multivariate techniques include more than one statistical variable and include the effect of all variables on the responses of interest. PCA and OPLS-DA were thus performed to explore the parameters that could contribute to the variation between treatments.

### 3.3. Multivariate data analysis

In order to investigate the relationship between chemical composition and treatments in a more holistic approach, PCA was performed on the 66 samples and 44 variables (24 phenolic measurements and 20 volatile compounds). The bi-plot (Fig. 1 (a)) showed that the first two principal components captured 93.7% of the explained variance (PC1 = 60.6% and PC2 = 33.1%) in the dataset. Although some differences were shown in the ANOVA, no clear trend based on treatments was observed in the PCA plot (i.e. no grouping of samples), thereby making it difficult to understand which chemical compounds were correlated to the applied pre-fermentative techniques.

As has been reported by several authors, cold pre-fermentative techniques might initially increase anthocyanin and phenolic extraction (Gil-Muñoz et al., 2009), although the reactions that occur during storage could reduce or even negate this effect. In a study reported by Ortega-Heras, Pérez-Magariño, and González-Sanjosé (2012) the higher extraction of some phenolic compounds induced by cold soak was no longer evident at the end of bottle aging (12 months). Other authors reported that the effect might depend on the vintage, which could be related to the phenolic maturity of the grapes (Álvarez, Alexandre, García, & Lizama, 2006; De Beer et al., 2006). The discrepancies in the above mentioned studies indicated that the effect could also depend on the variety used (Bussé-Valverde et al., 2010; Gil-Muñoz et al., 2009; ).

With the aim of further investigating the differences between treatments, the OPLS-DA technique was applied to the data. OPLS-DA removes variability in X (chemical data) that is orthogonal to Y (treatments), by separating systematic variation into predictive

components and orthogonal components (Lee, Hong, & Lee, 2009).

Fig. 1 (B) shows OPLS-DA bi-plot of pre-fermentative cold soaked (C–S and D–I) and control wines (T–V) using the complete set of 66 wines and 44 variables (chemical data). The model resulted in two predictive components and five orthogonal components, with cross-validated predictive ability  $Q^2(Y) = 52.3\%$ , total explained variance  $R^2(X) = 98.7\%$ , and variance related to treatment effect  $R^2_p(X) = 7\%$ . Compared to the results obtained with PCA, OPLS-DA exhibited an improved separation of cold soaked and control wines (Fig. 1 (b)). C–S and D–I wines were mostly located towards the negative end of PC1, and T–V wines towards the positive end. Moreover, a differentiation between C–S and D–I wines was observed on PC2, with C–S wines located towards the positive end, and D–I towards the negative end.

In order to further investigate the effect of cold soak treatments on the chemical composition of the wines, only the statistically significant compounds identified in the ANOVA were considered. In addition, pairwise comparisons of the chemical composition of T–V, C–S wines and D–I wines were performed. Fig. 2 shows the cross-validated OPLS-DA scores plots (a.1, b.1 and c.1) and the S-plots (a.2, b.2 and c.2) that were constructed on the pair-wise comparisons. S-plots are scatter plots of the predictive values obtained by cross validation vs. the correlation vectors. The S-plot often takes an "S" shape if the X variables are scaled to Pareto variance. X variables located far out of the "S" wings combine high covariance and correlation and are therefore important contributors to the differences between treatments.

The comparison of significant variables in T–V and C–S wines is shown in Fig. 2(a.1 and a.2), and a clear separation between samples of the different treatments was not observed (Fig. 2(a.1)). The volatile compounds ethyl decanoate (EDe), ethyl hexanoate (EHe) and octanoic acid (OcA) appeared located on the lower edge of the "S" wing and are therefore highly correlated with T–V wines. On the other hand, looking at the opposite side of the S-plot, the volatile compounds decanoic acid (DeA) and 2-phenylethyl acetate (2 PA) together with the bisulphite bleaching anthocyanins (BBA) were important contributors to C–S wines (Fig. 2(A.2)).

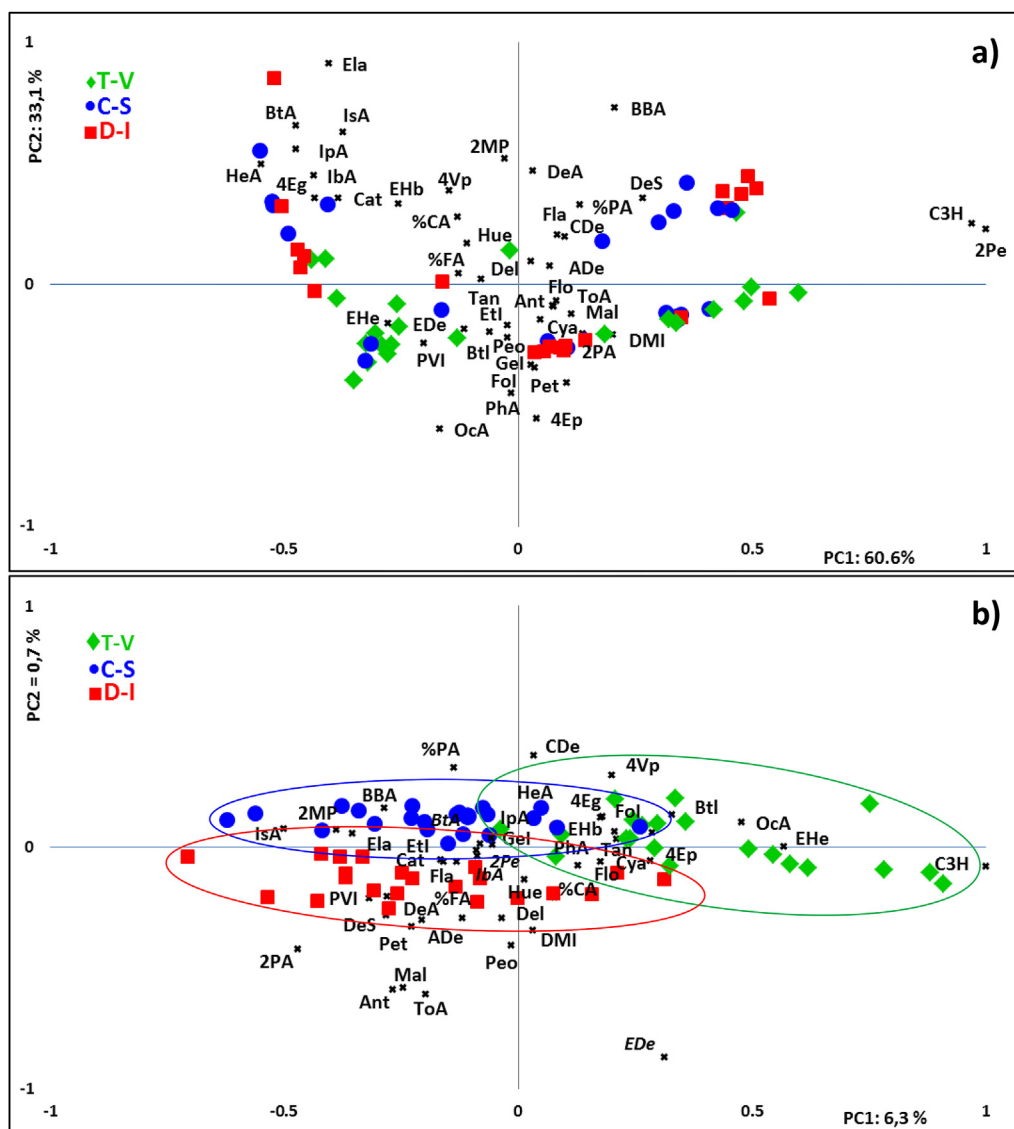


**Fig. 1.** Principal component analysis bi-plot (PCA) (A) and orthogonal projections on latent structures discriminant analysis bi-plot (OPLS-DA) (B) of phenolic determinations and volatile compounds of wines elaborated with pre-fermentative cold maceration techniques. ◆ T–V wines; ● C–S wines; ■ D–I wines. Phenolic and volatile abbreviations correspond to Tables 1 and 2.

Fig. 2(b.1 and b.2) also show the cross-validated OPLS-DA scores plot and the S-plot for the pair T–V vs. D–I. A better separation between samples was clearly observed, which could be interpreted as bigger differences in chemical composition between wines, than those observed between C–S and T–V treatments (Fig. 2(b.1)). For the D–I and T–V pair, the volatile compounds octanoic acid (Oca), ethyl hexanoate (EHe),  $\gamma$ -butirolactone (Btl) and 4-vinilphenol (4VP) appeared to be correlated with T–V wines, while ethyl decanoate (Ede), 2-phenylethyl acetate (2 PA) and decanoic acid (DeA), together with the parameters related with the anthocyanin fraction (malvidine (Mal), anthocyanidins (Ant), anthocyanin derivates (ADe), total anthocyanins (TAn), bisulfite bleaching anthocyanins (BBA) and % free anthocyanins (%FA)) and the parameter flavan-3-ols (Fla) appeared highly related with dry D–I wines (Fig. 2(b.2)).

Finally, the direct comparison between pre-fermentative techniques (C–S vs. D–I) is shown in Fig. 2(c.1 and c.2). A clear separation between treatments was also observed (Fig. 2(c.1)). These results suggested that the dry ice addition treatment (D–I wines) had the biggest influence on the volatile and phenolic composition

of Tempranillo wines after 12 months of bottle aging. C–S wines also differed from T–V wines, although the variation in phenolic and volatile composition was less pronounced. The volatile compounds ethyl decanoate (Ede), 2-phenylethyl acetate (2 PA) and decanoic acid (DeA), together with some of the mentioned anthocyanin related parameters, were strongly correlated with the D–I wines. On the other hand, volatile compounds such as octanoic acid (Oca), ethyl hexanoate (EHe),  $\gamma$ -butirolactone (Btl) and 4-vinilphenol (4VP) were correlated with C–S wines (Fig. 2(C.2)).

### 3.4. OPLS-DA classification

Classification models were established using half of the samples ( $N = 33$ ) for the calibration set, while the other 33 samples were used to validate the models. The classification results are shown in Table 3. In order to investigate which group of chemical compounds had the biggest influence on the differences between cold soak treatments the parameters were grouped based on the corresponding phenolic family and also on their aromatic chemical

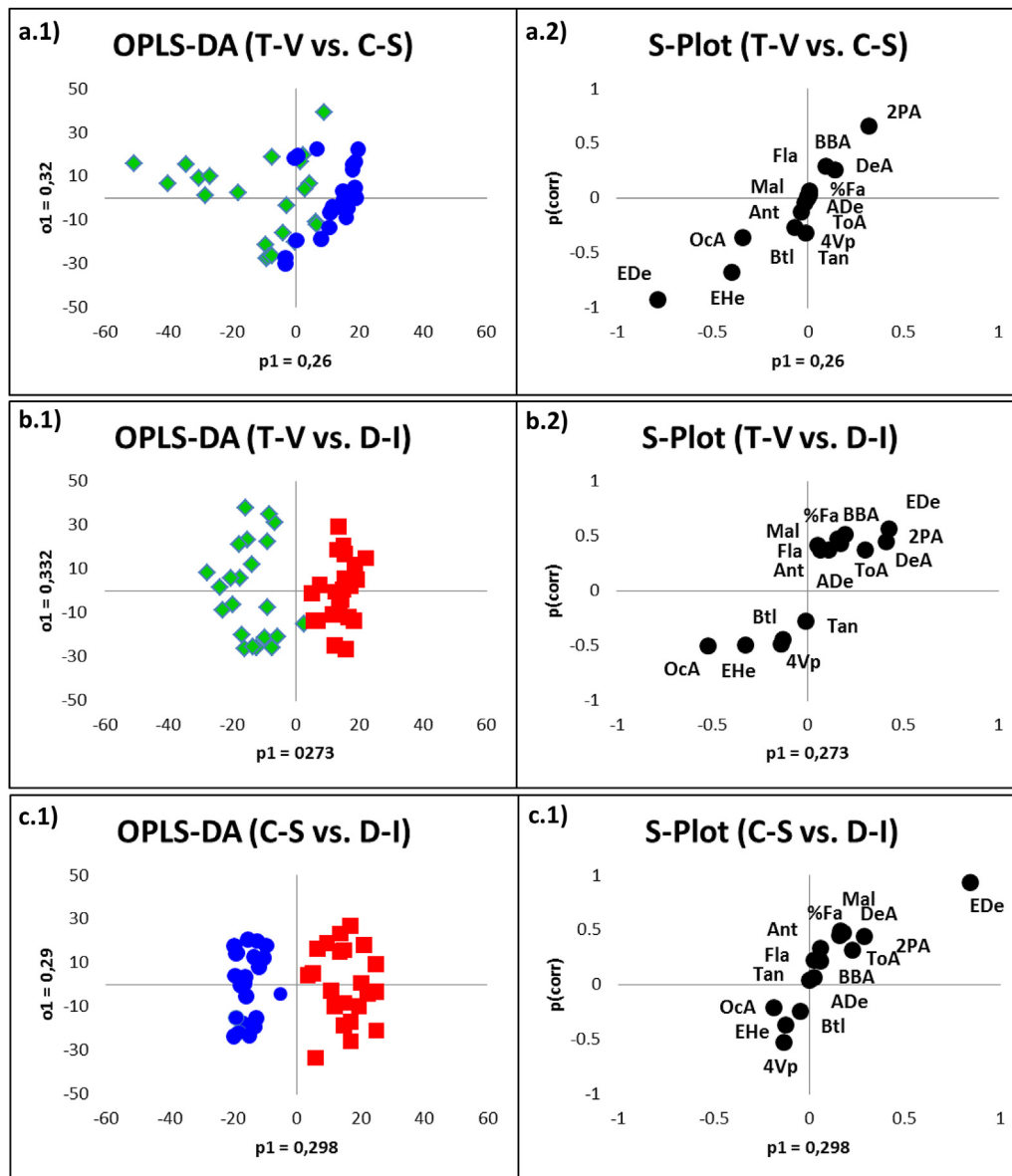


**Fig. 2.** OPLS-DA scores plots and S-Plots considering the significant phenolic and volatile parameters identified in the ANOVA of wines elaborated with pre-fermentative cold maceration techniques. Comparison among T–V and C–S wine (A.1 and A.2), T–V and D–I wines (B.1 and B.2) and C–S and D–I wines (C.1 and C.2). ◆ T–V wines, ● C–S wines, ■ D–I wines. Phenolic and volatile abbreviations correspond to Tables 1 and 2.

families (esters, higher alcohols, volatile phenols, fatty acids and lactones). Therefore groups containing anthocyanin (BBA, Del, Cya, Pet, Peo, Mal, Ant, Ade, ToA, %CA, %FA, %PA, PVI), tannin (PVI, Cat, Fla, Tan, DMI, Etl, Gel), phenolic acids (PhA) and flavonol (Flo) related parameters were tested. Two additional groups, one including the total phenolics parameter (Fol) and another considering the two wine colour related parameters (CDe and Hue) were also performed. Two groups including all the phenolic measurement and all the volatile compounds were also considered. Finally the classification was again performed taking into account all the variables included in the study (phenolic + volatiles). This last model showed a validation accuracy of 87.88% in classifying the cold soak techniques, thus highlighting the impact that pre-fermentative cooling techniques have on wine chemical composition.

Within phenolic compounds, anthocyanin related parameters were 60.61% accurately classified in validation showing the effect of

these techniques on the anthocyanin fraction. Finally when all the phenolic measurements were included in the model 54.55% of the samples were accurately classified.

Regarding volatile compounds, the ester group appeared as the group of compounds with the better ability to classify samples, with 63.64% of validation accuracy. Otherwise other groups of volatile compounds showed lower accuracy in classifying Tempranillo wines (Table 3). An important increase in ester levels has also been observed in cold soaked and dry ice added pre-fermentative macerated wines (Table 2). Compounds such as ethyl decanoate (soap, floral, grape, fruity, fatty, and pleasant) and 2-phenylethyl acetate (rose, honey, tobacco, fruity, flowery, pleasant) were identified as important contributors of D–I wines aroma. In addition, when the volatile compounds were all included in the prediction model, 81.82% of the samples were correctly classified.

**Table 3**

Summary of orthogonal projection to latent structures discriminant analysis (OPLS-DA) classification results.

Model	Parameters included <sup>a</sup>	Cold soak	
		Calibration (%) N = 33	Validation (%) N = 33
Color	1,2	39,39	27,27
Total phenolics	16	39,39	39,39
Anthocyanins	3–15	63,64	60,61
Tannins	15,19–24	45,45	39,39
Phenolic acids	17	36,36	33,33
Flavonols	18	48,48	27,27
Phenolics	1–24	69,70	54,55
Esters	25–27,29,33,36,37	84,85	63,64
Higher alcohols	28,40	42,42	42,42
Fatty acids	30,32,35,38,42,44	45,45	42,42
Volatile phenols	31,39,41,43	66,67	48,48
Lactones	34	45,45	42,42
Volatile compounds	25–44	100	81,82
Phenolics + Volatiles	1–44	100	87,88

<sup>a</sup> Parameters included in each model, numbers correspond to Tables 1 and 2 33 random selected samples were included in the calibration set while the remaining 33 were used for model validation.

#### 4. Conclusions

Dry ice addition led to significant effects on anthocyanins and flaval-3-ols levels. However an increased formation of tannins and polymeric pigments was not observed. Dry ice also influenced volatile composition with increased levels of ethyl decanoate, 2-phenylethyl acetate and decanoic acid. Pre-fermentative cold soak caused minor changes in the anthocyanins and volatile fraction. An extended cold soak period might cause larger effects, but in this case economic reasons need to be considered. Moreover from the classification analysis cold soak treatments seem to strongly influence the volatile composition, especially esters, together with the anthocyanin fraction. Finally it is important to mention that these results should be confirmed with further investigations which include at least three seasons due to our study only being conducted on a single vintage.

#### Acknowledgements

The research reported here is a project financially supported by the Spanish Government (AGL 2006-10723-C02-02) which the authors gratefully acknowledge.

#### References

- Aleixandre-Tudó, J. L., Álvarez, I., Lizama, V., García, M. J., Aleixandre, J. L., & du Toit, W. J. (2013). Impact of caffeic acid addition on phenolic composition of Tempranillo wines from different winemaking techniques. *Journal of Agricultural and Food Chemistry*, 61, 11900–11912.
- Álvarez, I., Aleixandre, J. L., García, M. J., Lizama, V., & Aleixandre-Tudó, J. L. (2009). Effect of the prefermentative addition of pigments on the polyphenolic composition of Tempranillo wines after malolactic fermentation. *European Food Research and Technology*, 228, 201–210.
- Alvarez, I., Aleixandre, J. L., García, M. J., & Lizama, V. (2006). Impact of pre-fermentative maceration on the phenolic and volatile compounds in Monastrell red wines. *Analytica Chimica Acta*, 563, 109–115.
- Boulton, R. B. (1996). Methods for the assessment of copigmentation in red wines. In *Presented at the 47th Annual Meeting of the American Society for Enology and Viticulture, Reno, NV*.
- Boulton, R. (2001). The copigmentation of anthocyanins and its role in the color of red wine: a critical review. *American Journal of Enology and Viticulture*, 52, 67–87.
- Bussé-Valverde, N., Gómez-Plaza, E., López-Roca, J. M., Gil-Muñoz, R., Fernández-Fernández, J. I., & Bautista-Ortín, A. (2010). Effect of different enological practices on skin and sees proanthocyanidins in three varietal wines. *Journal of Agricultural and Food Chemistry*, 58, 11333–11339.
- Cai, J., Zhu, B. Q., Wang, Y. H., Lu, L., Lan, Y. B., Reeves, M. J., & Duan, C. Q. (2014). Influence of pre-fermentation cold maceration treatment on aroma compounds of Cabernet Sauvignon wines fermented in different industrial scale fermenters. *Food Chemistry*, 154, 217–229.
- Culleré, L., Escudero, A., Cacho, J., & Ferreira, V. (2004). Gas chromatography–olfactometry and chemical quantitative study of the aroma of six premium quality Spanish aged red wines. *Journal of Agricultural and Food Chemistry*, 52(6), 1653–1660.
- Cynkar, W., Damberg, R., Smith, P., & Cozzolino, D. (2010). Classification of Tempranillo wines according to geographic origin: combination of mass spectrometry based electronic nose and chemometrics. *Analytica Chimica Acta*, 660(1–2), 227–231.
- De Beer, D., Joubert, E., Marais, J., & Manley, M. (2006). Maceration before and during fermentation: effect on Pinotage wine phenolic composition, total antioxidant capacity and objective colour parameters. *South African Journal of Enology and Viticulture*, 27, 137–150.
- Ferreira, V., López, R., & Cacho, J. F. (2000). Quantitative determination of the odorants of young red wines from different grape varieties. *Journal of the Science of Food and Agriculture*, 80, 1659–1667.
- Francis, I. L., & Newton, J. L. (2005). Determining wine aroma from compositional data. *Australian Journal of Grape and Wine Research*, 11, 114–126.
- Gil-Muñoz, R., Moreno-Pérez, A., Vila-López, R., Martínez-Cutillas, A., Fernández-Fernández, J. I., & Gómez-Plaza, E. (2009). Influence of low temperature prefermentative techniques on chromatic and phenolic characteristics of Syrah and Cabernet sauvignon wines. *European Food Research and Technology*, 228, 777–788.
- Glories, Y. (1984). La couleur des vins rouges. Mesure, origine et interpretation. *Connaissance de la Vigne et du Vin*, 18(4), 253–271.
- Glories, Y., & Galvin, C. (1990). Les complexes tanin-anthocyanes en présence d'éthanal. Conditions de leur formation. *Actualités œnologiques*, 89, 408–413.
- Gómez-Míguez, M., González-Miret, M., & Heredia, F. (2007). Evolution of color and anthocyanin composition of Syrah wines elaborated with pre-fermentative cold maceration. *Journal of Food Engineering*, 79, 271–278.
- Gómez-Plaza, E., Gil-Muñoz, R., López-Roca, J. M., Martínez-Cutillas, A., & Fernández-Fernández, J. I. (2001). Phenolic compounds and color stability of red wines: effect of skin maceration time. *American Journal of Enology and Viticulture*, 52(3), 266–270.
- Gordillo, B., López-Infante, M. I., Ramírez-Pérez, P., González-Miret, M., & Heredia, F. (2010). Influence of prefermentative cold maceration on the color and anthocyanin copigmentation of organic Tempranillo wines elaborated in warm climate. *Journal of Agricultural and Food Chemistry*, 58, 6797–6803.
- Heatherbell, D., Dicey, M., Goldsworthy, S., & Vanhanen, L. (1997). Effect of pre-fermentation cold maceration on the composition, color and flavor of Pinot noir wine. In G. F. Steans (Ed.), *Proceedings of the New Zealand Grape & Wine Symposium* (pp. 30–42). New Zealand Society for Viticulture and Oenology, P.O. Box 90-276, Auckland Mail Centre, Auckland 1, New Zealand.
- Heredia, F. J., Escudero-Gilete, M. L., Hernanz, D., Gordillo, B., Meléndez-Martínez, A. J., Vicario, I. M., & González-Miret, M. L. (2010). Influence of the refrigeration technique on the color and phenolic composition of Syrah wines obtained with pre-fermentative cold maceration. *Food Chemistry*, 118, 377–383.
- Hernanz, D., Heredia, F. J., Beltran, R., & Recamales, M. A. F. (1999). Optimization of an extraction method of aroma compounds in white wine using ultrasound. *Talanta*, 50, 413–421.
- Jensen, J. S., Blachez, B., Egebo, M., & Meyer, A. S. (2007). Rapid extraction of polyphenols from red grapes. *American Journal of Enology and Viticulture*, 58(4), 451–461.
- Koyama, K., Goto-Yamamoto, N., & Hashizume, K. (2007). Influence of maceration temperature in red wine vinification on extraction of phenolics from berry skins

- and seed of grape (*Vitis Vinifera*). *Bioscience Biotechnology Biochemistry*, 71(4), 958–965.
- Lee, J. E., Hong, Y. S., & Lee, C. H. (2009). Characterization of fermentative behaviors of lactic acid bacteria in grape wines through <sup>1</sup>H NMR- and GC-based metabolic profiling. *Journal of Agricultural and Food Chemistry*, 57, 4810–4817.
- Li, H., Tao, Y. S., Wang, H., & Zhang, L. (2008). Impact odorants of Chardonnay dry white wine from Changli County (China). *European Food Research and Technology*, 227(1), 287–292.
- Marais, J. (2003). Effect of different wine-making techniques on the composition and quality of Pinotage wine I. Low-temperature skin contact prior to fermentation. *South African Journal of Enology and Viticulture*, 24, 70–75.
- Mercurio, M. D., Damberg, R. G., Herderich, M. J., & Smith, P. A. (2007). High throughput analysis of red wine and grape phenolics: adaptation and validation of methyl cellulose precipitable tannin assay and modified Somers color assay to a rapid 96 well plate format. *Journal of Agricultural and Food Chemistry*, 55(12), 4651–4657.
- Moreno-Pérez, A., Vila-López, R., & Fernández-Fernández, J. I. (2013). Influence of cold pre-fermentation treatments on the major volatile compounds of three wine varieties. *Food Chemistry*, 139(1–4), 770–776.
- Okubo, K., Goto-Yamamoto, N., & Okazaki, N. (2003). Effect of prefermentative cold soak on extraction of anthocyanin during red wine making. *Journal of the Brewing Society of Japan*, 98, 193–200.
- Ortega-Heras, M., Pérez-Magariño, S., & González-Sanjosed, M. (2012). Comparative study of the use of maceration enzymes and cold prefermentative maceration on phenolic and anthocyanic composition and color of a Mencia red wine. *LWT - Food Science and Technology*, 48, 1–8.
- Parenti, A., Spugnoli, P., Calamai, L., Ferrari, S., & Gori, C. (2004). Effects of cold maceration on red wine quality from Tuscan Sangiovese grape. *European Food Research and Technology*, 218, 360–366.
- Ribéreau-Gayon, P., & Stronestreet, E. (1965). Le dosage des anthocyanes dans le vin rouge. *Bulletin de la Société Chimique de France*, 9, 119–142.
- Sacchi, K., Bisson, L., & Adams, D. (2005). A review of the effect of winemaking techniques on phenolic interaction in red wines. *American Journal of Enology and Viticulture*, 53(3), 197–206.
- Sánchez Palomo, E., González-Viñas, M. A., Díaz-Maroto, M. C., Soriano-Pérez, A., & Pérez-Coello, M. S. (2007). Aroma potential of Albillo wines and effect of skin-contact treatment. *Food Chemistry*, 103, 631–640.
- Singleton, V. L., & Rossi, J. (1965). A Colorimetry of total phenolics with phosphomolybdic-phosphotungstic acid reagents. *American Journal of Enology and Viticulture*, 16, 144–158.
- Sun, B., Ricardo Da Silva, J. M., & Spranger, I. (1998). Critical factors of vanillin assay for catechins and proanthocyanidins. *Journal of Agricultural and Food Chemistry*, 46, 4267–4274.
- Swiegers, J. H., Bartowsky, E. J., Henschke, P. A., & Pretorius, I. S. (2005). Yeast and bacterial modulation of wine aroma and flavour. *Australian Journal of Grape and Wine Research*, 11, 139–173.
- Trygg, J., & Wold, S. (2002). Orthogonal projections to latent structures (O-PLS). *Journal of Chemometrics*, 16, 119–128.
- USDA. (2014). *National Agricultural Statistics Service. California grape Crush report. Washington, DC.*
- Vivas, N., & Glories, Y. (1995). Ranking of red wines matured in barrels. A tentative classification of racking techniques. *Australian and New Zealand Wine Industry Journal*, 10, 241–243.
- Wiklund, S., Johansson, E., Sjöström, L., Mellerowicz, E. J., Edlund, U., Shockcor, J. P., Gottfries, J., Moritz, T., & Trygg, J. (2008). Visualization of GC/TOF-MS-based metabolomics data for identification of biochemically interesting compounds using OPLS class models. *Analytical Chemistry*, 80, 115–122.



# Effects of dispersing media and heating rates on pasting profiles of wheat and gluten-free samples in relation to their solvent retention capacities and mixing properties



Manuela Mariotti <sup>a, \*</sup>, Mara Lucisano <sup>a</sup>, Maria Ambrogina Pagani <sup>a</sup>, Perry K.W. Ng <sup>b</sup>

<sup>a</sup> Department of Food, Environmental and Nutritional Sciences (DeFENS), Università degli Studi di Milano, Via G. Celoria 2, 20133, Milan, Italy

<sup>b</sup> Department of Food Science and Human Nutrition, Michigan State University, 135 GM Trout FSHN Building, East Lansing, MI, 48824-1224, USA

## ARTICLE INFO

### Article history:

Received 4 June 2015

Received in revised form

18 September 2015

Accepted 24 September 2015

Available online 14 October 2015

### Keywords:

Wheat flour

Gluten-free

Solvent Retention Capacity

Rapid Visco-Analyser

Confocal Laser Scanning Microscopy

## ABSTRACT

Four commercial wheat flours and two commercial GF bread mixtures were investigated in this study. The main aim was to find time-, cost- and sample-saving methods able to determine the quality characteristics of these materials in relation to their end-use and to the interactions taking place in the various systems. Samples were mainly characterized by Solvent Retention Capacity (SRC) and Rapid Visco-Analyser (RVA) tests. Mixogram and Confocal Laser Scanning Microscopy were adopted to investigate dough networking. In particular, RVA tests were performed adopting various heating rates and dispersing media, to: *i*) investigate how different heating/cooling rates could affect samples' pasting properties; *ii*) evaluate the role of alpha-amylase activity in controlling RVA profiles; *iii*) determine the contribution of proteins to RVA profiles. Interesting results were obtained in particular from SRC and RVA, suggesting that going beyond their conventional use as standard methods was feasible and very profitable. In fact, both the approaches well differentiated not only common and durum wheat flours but also the GF mixtures (e.g. WRC values ranged from  $53.7 \pm 0.1$  to  $152.1 \pm 0.8$  g/100 g db, and peak viscosity – measured at a heating rate of  $3 \text{ }^\circ\text{C}/\text{min}$  – from  $682 \pm 72$  cP to  $4026 \pm 11$  cP).

© 2015 Elsevier Ltd. All rights reserved.

## 1. Introduction

Wheat flour is used in the production of a wide range of foods that results from different ingredient formulae and/or different processing conditions. Not every flour type is equally suitable for producing a specific end-product, and variations in levels and

properties of flour constituents result in end-products having different quality: important differences in processing and/or end-product quality can arise, even if flour specifications are met. Therefore the determination of flour quality is of great importance, as it relates to the desired end-product and its manufacturing process (Duyvejonck, Lagrain, Pareyt, Courtin, & Delcour, 2011). Rapid tests, able to save time and money, and requiring only small quantities of sample would be preferable. Various methods are available, such as chemical–physical analyses, rheological tests, and baking tests (Duyvejonck, Lagrain, Dornez, Delcour, & Courtin, 2012). However, all these analyses do not always take into account the contribution or functionality of specific flour constituents in a given process.

The situation is even more complex when gluten-free (GF) mixtures are used. Gluten can be considered as the essential structure-building component in bread, and it provides structure and texture in other bakery products: its removal impairs the dough's capacity to properly develop during kneading, leavening and baking (Mariotti, Lucisano, Pagani, & Ng, 2009), and its replacement in GF baked products represents a major technological challenge. As alternatives to wheat flour, other flours, pseudocereals (Mariotti, Lucisano, Pagani, & Iametti, 2008), dairy proteins,

*Abbreviations:* AA, alpha-amylase; ANOVA, analysis of variance; BU, Brabender Unit; CLSM, Confocal Laser Scanning Microscopy; DS, damaged starch; DWS, commercial re-milled durum wheat semolina; FITC, fluorescein isothiocyanate; FN, falling number; GF, gluten-free; GFM1, commercial gluten-free bread mixture; GFM2, commercial gluten-free bread mixture; GG, guar gum; GPI, gluten performance index; HPMC, hydroxyl-propyl-methyl-cellulose; HWF1, commercial hard wheat flour; HWF2, commercial hard wheat flour containing malt; LASRC, lactic acid solvent retention capacity; LBG, locust bean gum; LSD, least significant difference; MVAG, Micro Visco-Amylo-Graph; ODT, farinographic optimum development time; PSY, psyllium; RVA, Rapid Visco-Analyser; SCSRC, sodium carbonate solvent retention capacity; SN, aqueous AgNO<sub>3</sub> (silver nitrate) solution; SRC, solvent retention capacity; SuSRC, sucrose solvent retention capacity; SWF, commercial soft wheat flour; TS, total starch; WA, farinographic water absorption; WRC, water retention capacity.

\* Corresponding author.

E-mail addresses: [manuela.mariotti@unimi.it](mailto:manuela.mariotti@unimi.it), [mariotti.manu@gmail.com](mailto:mariotti.manu@gmail.com) (M. Mariotti).

non-gluten vegetable proteins, gums, fibres and many other ingredients have been recently incorporated in GF bread formulations aiming to increase both the nutritional and technological quality (Mariotti et al., 2009). Therefore, the setting up of tests able to quickly help in the formulation and evaluation of GF mixtures is another interesting challenge.

The Rapid Visco Analyser (RVA) and the Micro Visco-Amylo-Graph (MVAG) are instruments widely used to test flour or starch performance: a flour or starch suspension is subjected to a defined heating and cooling program, and the viscosity is recorded as a function of temperature and time. Even if they have been traditionally used for measuring starch pasting properties, essentially for screening/routine purposes, they could be used – when proper testing conditions are developed – as informative and rapid instruments to reveal the extent of interactions among a mixture of food components. This could be of specific importance for GF mixtures, where many ingredients at different ratios and having various functionalities are present. Although studies on two-component interactions (starch-proteins, starch-lipids, protein-lipids) are common in the literature, only few relate with the functionality (i.e. chemical–physical properties, interrelationships, etc.) of food ingredients in a food system with more than two components. Alternative uses of RVA and MVAG have been little investigated up to now, as well (Cappa, Lucisano, & Mariotti, 2013; Derycke et al., 2005; Mariotti, Zardi, Lucisano, & Pagani, 2005; Onwulata, Tunick, & Thomas-Gahring, 2013; Turner & Bason, 1997; Zhang & Hamaker, 2003).

Another method, commonly used in the USA for predicting the functionality of different soft wheat flour constituents, is Solvent Retention Capacity (SRC) testing. The SRC methodology is based on quantifying the swelling behaviour of flour polymers networks and, hence, their ability to retain a given solvent, relating flour functionality to specific constituents (Slade & Levine, 1994). Water retention capacity has been associated with the overall water holding capacity of all flour constituents; sodium carbonate SRC with damaged starch characteristics (Duyvejonck et al., 2011); sucrose SRC (SuSRC) with flour arabinoxylan characteristics; lactic acid SRC (LASRC) with glutenin network formation and gluten strength (Slade & Levine, 1994). A practical functionality profile of soft wheat flour, useful for predicting its performance in specific baking applications (Duyvejonck et al., 2012), could be thus obtained. However, despite its origin, the SRC could be also tested on other wheat samples, or, at an extreme level, on GF bread mixtures.

Different wheat flours (two hard wheat flours, one soft wheat flour, a re-milled durum wheat semolina) and two commercial GF bread mixtures (completely different in terms of ingredients) were considered in this study. They were mainly characterized by SRC and RVA, to test the ability of these rapid methods for the assessment of the quality of such different samples. Mixograms and Confocal Laser Scanning Microscopy (CLSM) were adopted, too, to gain information on the various doughs' networking and their relationships with their respective RVA and SRC features. In particular, RVA tests were performed adopting various heating rates and dispersing media, aiming to: *i*) investigate how different heating and cooling rates can affect pasting properties; *ii*) evaluate the role of alpha-amylase activity in controlling RVA profiles; *iii*) determine the contribution of proteins to RVA profiles. The main purpose was to identify time- and cost-saving as well as informative methods able to describe the quality profiles of various samples.

## 2. Materials and methods

### 2.1. Materials

Two commercial hard wheat flours (HWF1, containing malt;

HWF2), one commercial soft wheat flour (SWF), one commercial re-milled durum wheat semolina (DWS) and two commercial gluten-free bread mixtures (GFM1 and GFM2) were used in this research. As reported on the labels, GFM1 was made of corn starch, sugar, chicory fibres (inulin), fibres of psyllium seeds (PSY), guar gum (GG), and corn maltodextrins, while GFM2 was made of rice flour, potato starch, sugar, E464 (hydroxyl-propyl-methyl-cellulose, HPMC), locust bean gum (LBG), salt, and E471 (mono- and diglycerides of fatty acids). The actual percent of each ingredient was not provided on the labels.

### 2.2. Chemical–physical evaluations

The moisture content of the samples was determined according to the AACCI Standard Method 44-15 (AACCI, 2000). Results ( $n = 3$ ) are expressed as g/100 g.

The total nitrogen content was determined according to the AOAC Standard Method 920.87 (AOAC, 2000). The protein content was calculated adopting 5.70 as a conversion factor for the wheat flours and 6.25 for the GF mixtures. Results ( $n = 3$ ) are given as g/100 g d.b.

The total starch (TS) content was determined enzymatically using the “Total Starch Assay Kit” by Megazyme International Ireland Ltd. (Wicklow, Ireland). Results ( $n = 4$ ) are given as g/100 g d.b.

The damaged starch (DS) content was determined enzymatically using the “Starch Damage Assay Kit” by Megazyme International Ireland Ltd. (Wicklow, Ireland). Results ( $n = 4$ ) are expressed as g/100 g d.b., and as a percentage of the total starch content ( $DS^*/100/TS$ ).

The alpha-amylase (AA) activity was measured using the “Alpha Amylase Assay Procedure” by Megazyme International Ireland Ltd. (Wicklow, Ireland). Results ( $n = 4$ ) are expressed as IU/g d.b.

The Falling Number (FN) was evaluated according to the AACCI Standard Method 56-81 (AACCI, 2000). Results ( $n = 5$ ) are expressed in seconds (s).

### 2.3. RVA measurements

#### a) Use of different heating/cooling rates

The pasting properties of the samples were measured ( $n \geq 2$ ) using the RVA-4 controlled by ThermoLine for Windows software v. 2.2 (Newport Scientific Pty Ltd., Warriewood, NSW, Australia). The suspensions (3.50 g of sample, on a 14 g/100 g moisture basis, in 25 mL of distilled water) were subjected to the following standard temperature profile: heating from 50 °C up to 95 °C, holding at 95 °C for 5 min, cooling from 95 °C down to 50 °C. Four different temperature rates were applied to the slurries (STD1: 12.0 °C/min, STD2: 6.0 °C/min, STD3: 3.0 °C/min, STD4: 1.5 °C/min), with stirring at 160 rpm, and the viscosity (cP) was recorded as a function of temperature and time. The total running times were: 13 min (STD1), 23 min (STD2), 38 min (STD3), and 68 min (STD4). The following indices were considered: peak viscosity (cP), breakdown viscosity (cP), setback viscosity (cP), and final viscosity (cP).

All the above mentioned tests were also carried out ( $n \geq 2$ ) in the presence of an alpha-amylase inhibitor: 25 mL of 1 mmol/L aqueous AgNO<sub>3</sub> solution (silver nitrate, SN), instead of distilled water (Crosbie & Lambe, 1993; Mariotti et al., 2005).

#### b) Use of different dispersing media

The suspensions (15 g of sample at 14 g/100 g moisture basis in 25 mL of 0.1 mol/L lactic acid) were subjected ( $n \geq 2$ ) to the following testing conditions in the ‘acidulated testing profile’ (cold

method): 5 min at 25 °C, heating from 25 °C up to 50 °C in 2 min, holding at 50 °C for 3 min; stirring: 160 rpm; total running time: 10 min (Turner & Bason, 1997).

The suspensions (3 g of sample at 14 g/100 g moisture basis in 3.50 mL of ethanol plus 20 mL of distilled water) were subjected ( $n \geq 2$ ) to the following testing conditions in the 'baking testing profile' (hot method): 2 min at 50 °C, heating from 50 °C up to 85 °C in 4.5 min, holding at 85 °C for 2 min, cooling from 85 °C down to 20 °C in 7.5 min, holding at 20 °C for 4 min; stirring: 160 rpm; total running time: 20 min (Turner & Bason, 1997).

Results are given as viscosity profiles (average curves;  $n \geq 2$ ).

#### 2.4. Solvent Retention Capacity

The solvent retention capacity (SRC) of the various samples was determined according to the AACCI Standard Method 56-11 (AACCI, 2000). SRC is the weight of solvent (water; 5 g/100 g Na<sub>2</sub>CO<sub>3</sub>; 5 g/100 g lactic acid; 50 g/100 g sucrose) held by flour after centrifugation (WRC, water retention capacity; SCSRC, sodium carbonate solvent retention capacity; LASRC, lactic acid solvent retention capacity; SuSRC, sucrose solvent retention capacity, respectively). Results ( $n = 3$ ) are expressed as percent of flour weight, on a 14 g/100 g moisture basis. A predictive SRC parameter, the gluten performance index (GPI), was calculated as follows: [LASRC/(SCSRC + SuSRC)] (Kweon, Slade, & Levine, 2011).

#### 2.5. Mixograph

Mixograph analyses were performed according to the AACCI Standard Method 54-40A (AACCI, 2000). The mixing process was recorded for 10 min. Results are given as mixograms.

#### 2.6. Confocal Laser Scanning Microscopy

A confocal laser scanning microscope (CLSM, LSM5 Pascal, Zeiss, Thornwood, NY) was used to observe the ultrastructure of the doughs during their development in a farinograph bowl (50 g). First, wheat flour samples were submitted to the farinographic test (ICC 115/1; 1992) in order to obtain water absorption (WA, %; optimal consistency: 500 Brabender Units, BU) and optimum development time (ODT, min) indices. GF mixtures were treated as reported by Mariotti et al. (2009) (optimal consistency: 200 BU). Subsequently, the tests were repeated, and samples were collected for CLSM: at the ODT and after 10 min mixing, for the wheat samples; just after 10 min mixing for the GF mixtures. CLSM doughs preparation and observations were performed as reported by Mariotti et al. (2009). At least two replicates were made for each sample.

#### 2.7. Statistical analysis

Analysis of variance (ANOVA) and significant correlations were performed on the data, adopting the least significant difference (LSD) and Pearson correlation analysis procedure, respectively, to test the statistical significance of the differences between means at a  $P < 0.05$  confidence level (Statgraphics Plus v. 5.01; StatPoint, Inc., Herndon, Virginia, USA).

### 3. Results and discussion

Different commercial flours were selected for this study, taking into account their final utilization. Generally, in fact, HWFs are used for breadmaking, SWFs for biscuit making, and DWs for pasta

making, while GF mixtures must take into account both the nutritional and sensory needs of celiac people and the technological needs of the food industry for their final destination. All of these samples were commercial, i.e., identifications and origins of material sources were unknown.

#### 3.1. Chemical–physical properties

Samples were first characterized for their chemical–physical properties (Table 1). Significantly different ( $P < 0.05$ ) moisture levels were found among the samples. Among the wheat flours, SWF had the lowest protein and the highest total starch (TS) values. HWF1, HWF2 and DWS were not significantly different ( $P > 0.05$ ) in terms of total starch, while significant differences were recorded in terms of proteins (HWF1 > HWF2 > DWS). As regards the GF mixtures, no proteins were detected in GFM1, in agreement with the fact that this sample is sold as a 'low-protein' GF bread mixture.

In terms of damaged starch (DS), the lowest value among the wheat flours (both in absolute terms or as a percentage of TS) was obtained for SWF, despite its highest TS content. The highest DS values were exhibited by HWF1 and DWS, which is a re-milled durum wheat semolina (DS values can be influenced, in fact, both by the hardness of the kernel and by the conditions adopted during the milling process). DS in GFM1 came from corn starch, this ingredient being the only source of starch in the formulation. DS was higher for GFM2. DS is a very important index, since it determines a marked modification in a sample's hydration and mixing properties; furthermore, DS granules can be rapidly hydrolysed by alpha- and beta-amylases, producing fermentable sugars, very useful in particular in long-fermentation procedures (Donald, 2004).

The amount of endogenous alpha-amylase (AA) is another key quality parameter in the commercial utilization of most cereals. In baking, it is essential that the AA level is adequate (to originate fermentable sugars), but not so high as to result in excessive starch dextrinization during the baking process, to avoid sticky doughs (McCleary, McNally, & Monaghan, 2002). As expected, GFM1 exhibited the lowest value (no detectable protein), and a very low value was also obtained for GFM2. Increasing AA values were found among the wheat flours, following this order: SWF < DWS < HWF2 < HWF1. Since HWF1 contained malt, its high AA value was not surprising.

Significant differences ( $P < 0.05$ ) were found among the samples in terms of FN, too. The lowest value was exhibited by HWF1, enriched with malt, while the highest one was for DWS, among the wheat flours. A value of  $532 \pm 16$  s was found for GFM2: despite the presence of hydrocolloids (hydroxypropylmethylcellulose, HPMC; locust bean gum, LBG), it was within the range of values found for the wheat flours. On the contrary, values higher than 900 s were exhibited by GFM1, in which psyllium (PSY) and guar gum (GG) played a major role, producing a very stiff gel in which the stirrer barely penetrated. While HPMC solutions exhibit a pseudoplastic behaviour (they have some interfacial activities and can form films; BeMiller, 2009), PSY has extremely strong gelling and water-absorbing abilities (Mariotti et al., 2009). However, as the hydrocolloids functionality is usually determined in model systems, in a real food it may change because of interactions with the other food components (Mariotti et al., 2009). Therefore, simple and rapid tests such as DS, AA, FN, able to give information (even indirectly) on the properties of complex systems, were very useful even when GF samples were considered.

**Table 1**  
Chemical–physical properties of the various samples (n.d. = not detectable).

Sample	Moisture (g/100 g)	Protein (g/100 g db)	Total starch (TS) (g/100 g db)	Damaged starch (DS) (g/100 g db)	DS*100/TS	Alpha-amylase activity (AA) (IU/g db)	Falling number (db) (s)
HWF1	12.90 <sup>cd</sup> ± 0.04	14.62 <sup>e</sup> ± 0.36	76.90 <sup>b</sup> ± 0.45	7.90 <sup>f</sup> ± 0.12	10.27	1.587 <sup>f</sup> ± 0.008	320 <sup>a</sup> ± 5
HWF2	11.17 <sup>b</sup> ± 0.33	12.16 <sup>d</sup> ± 0.10	77.68 <sup>b</sup> ± 0.76	6.43 <sup>d</sup> ± 0.16	8.28	0.554 <sup>e</sup> ± 0.006	568 <sup>d</sup> ± 21
SWF	12.63 <sup>c</sup> ± 0.01	7.40 <sup>b</sup> ± 0.14	80.78 <sup>c</sup> ± 0.56	3.32 <sup>b</sup> ± 0.08	4.10	0.323 <sup>c</sup> ± 0.004	424 <sup>b</sup> ± 20
DWS	13.83 <sup>e</sup> ± 0.07	11.12 <sup>c</sup> ± 0.26	77.48 <sup>b</sup> ± 1.14	7.67 <sup>e</sup> ± 0.20	9.90	0.500 <sup>d</sup> ± 0.017	665 <sup>e</sup> ± 18
GFM1	10.28 <sup>a</sup> ± 0.38	n.d.	83.22 <sup>d</sup> ± 0.96	1.49 <sup>a</sup> ± 0.03	1.78	0.026 <sup>a</sup> ± 0.003	>900
GFM2	13.30 <sup>d</sup> ± 0.06	3.42 <sup>a</sup> ± 0.14	69.00 <sup>a</sup> ± 1.14	4.19 <sup>c</sup> ± 0.08	6.08	0.106 <sup>b</sup> ± 0.002	532 <sup>c</sup> ± 16

Note: Values followed by different letters in the same column are significantly different ( $P < 0.05$ ).

Abbreviations: HWF1: hard wheat flour; HWF2: hard wheat flour containing malt; SWF: soft wheat flour; DWS: re-milled durum wheat semolina; GFM1 and GFM2: gluten-free bread mixtures; DS\*100/TS, ratio between damaged starch and total starch.

### 3.2. Viscosity profiles as determined by different heating/cooling rates

The viscosity profiles of the four wheat flours (Fig. 1a–d) and of the two GF mixtures (Fig. 1e–f), at the four different heating/cooling rates adopted (STD1 = 12.0 °C/min; STD2 = 6.0 °C/min; STD3 = 3.0 °C/min; STD4 = 1.5 °C/min), in the presence of distilled water or AgNO<sub>3</sub> (silver nitrate, SN), are depicted in Fig. 1. A univocal trend could not be observed for the breakdown and the setback. On the contrary, the peak viscosity and the final viscosity generally significantly decreased ( $P < 0.05$ ) with the decrease in the heating rate (especially when SN was not present) (Table 2). Many factors, acting simultaneously, could have determined this general trend.

During the RVA test, starch damage promoted by shear should also be taken into account. The RVA paddle can have some mechanical effects on the slurry undergoing the test: the longer the test, the higher the mechanical damage to starch, the lower the viscosity profile. The extent of the mechanical damage can depend also on the fine molecular starch structure (the more compact it is, the lower the swelling of the granules). Some mechanical damage can be also determined by starch granule size and morphology (e.g. the larger the size of the granule, the higher its swelling, the more probable its disruption due to shear) (Mariotti et al., 2005). Among the starches commonly used for foods, potato starch granules are the largest (15–75 µm) and those of rice starch the smallest (granule 3–8 µm). In GFM2, potato starch and rice starch, as well as hydrocolloids and mono- and di-glycerides of fatty acids, are all present and it is very interesting to highlight how the lower RVA heating/cooling rates resulted in up to three unresolved viscosity peaks. Independent of all the above mentioned factors and of the different types of investigated materials, significant correlations ( $P < 0.05$ ) were found between DS and PV (peak viscosity) indices: STD1,  $r = -0.877$ ; STD2,  $r = -0.882$ ; STD3,  $r = -0.910$ ; STD4,  $r = -0.911$ . DS/TS index was also significantly ( $P < 0.05$ ) correlated to PV indices.

The presence of certain endogenous AA activity strongly affected the pasting profile of the samples. The action of AA rapidly reduces the size of the starch molecules, and thereby the viscosity of the slurry. Moreover, the lower the heating rate, the longer the time the endogenous AA can act on starch granules, the lower the viscosities recorded during the whole test (Table 2). AA activity, in fact, modifies starch in a way that decreases the viscosity after cooling, i.e. the retrogradation tendency (Mariotti et al., 2005). Significant correlations ( $P < 0.05$ ) were found between AA and PV indices: STD1,  $r = -0.914$ ; STD2,  $r = -0.854$ ; STD3,  $r = -0.864$ ; STD4,  $r = -0.859$ .

RVA tests were also performed in the presence of AgNO<sub>3</sub>, an efficacious AA inhibitor (Crosbie & Lambe, 1993). The corresponding viscosity profiles have been reported in Fig. 1, and the RVA indices in Table 2.

Generally, the higher the AA activity, the larger the variations in the viscosity profiles between samples with or without AA inhibitor. For example, AA was at its maximum level in HWF1, and the PV increases recorded in the presence of AgNO<sub>3</sub> were the largest: from 133% for STD1 (12 °C/min) up to 725% for STD4 (1.5 °C/min). Moreover, the highest variations due to AA inhibition were recorded when the lowest heating rate was applied, and this was not unexpected, due to all the above-mentioned reasons. Within the same temperature profile, PV variations due to AA inhibition were always statistically significant ( $P < 0.05$ ). Only in the case of GFM1, in which AA was practically absent, variations in PV, in relation to the heating rates adopted, were limited in the presence of water, and not significant ( $P < 0.05$ ) in the presence of AgNO<sub>3</sub>. Significant correlations ( $P < 0.05$ ) were found between AA and PV increases due to AgNO<sub>3</sub>: STD1,  $r = 0.940$ ; STD2,  $r = 0.964$ ; STD3,  $r = 0.958$ ; STD4,  $r = 0.963$ .

Adopting different heating/cooling rates, in the absence or presence of AgNO<sub>3</sub>, came out to be therefore a quick and useful way to gain indirect information on the properties of different samples, GF ones included, undergoing various thermal processes. Important correlations were also found between PV and DS, and between PV and AA; this is very interesting, as DS and AA are two key quality indices in the cereal sector.

### 3.3. Viscosity profiles as determined by different dispersing media

Since a significant ( $P < 0.05$ ) correlation was found between the protein content of the samples and their PV values (STD1,  $r = -0.978$ ; STD2,  $r = -0.983$ ; STD3,  $r = -0.978$ ; STD4,  $r = -0.973$ ), more investigations were performed to better understand the contributions of proteins of various sources to RVA profiles.

Results of the 'acidulated testing profile' are depicted in Fig. 1g. The method was readily able to discriminate among different samples with a range of quality. The higher viscosity values recorded at the beginning of the test (at 25 °C), in comparison to those recorded in the standard RVA test (at 50 °C) were due to the higher amount of sample suspended in the medium (15 g/25 mL vs. 3.5 g/25 mL). Despite this common fact, very different viscosity profiles were observed. Lactic acid causes proteins to coagulate, thickening the slurry and giving a higher viscosity. Actually, the wheat flours could be ordered as follows, in terms of viscosity profiles: HWF1 > HWF2 > DWS > SWF. This order perfectly reflected the protein contents of the samples. Going on with the test, a general viscosity decrease was observed, due to temperature increase. After reaching 50 °C, a new increase in viscosity was detected, due to starch beginning to swell. Similar trends were observed for GFM2. Despite its lack of gluten and its very low protein content, this sample exhibited the highest initial viscosity, due to the presence of hydrocolloids and sugar that compete for water with the protein and starches present in the mixture. A different behaviour was

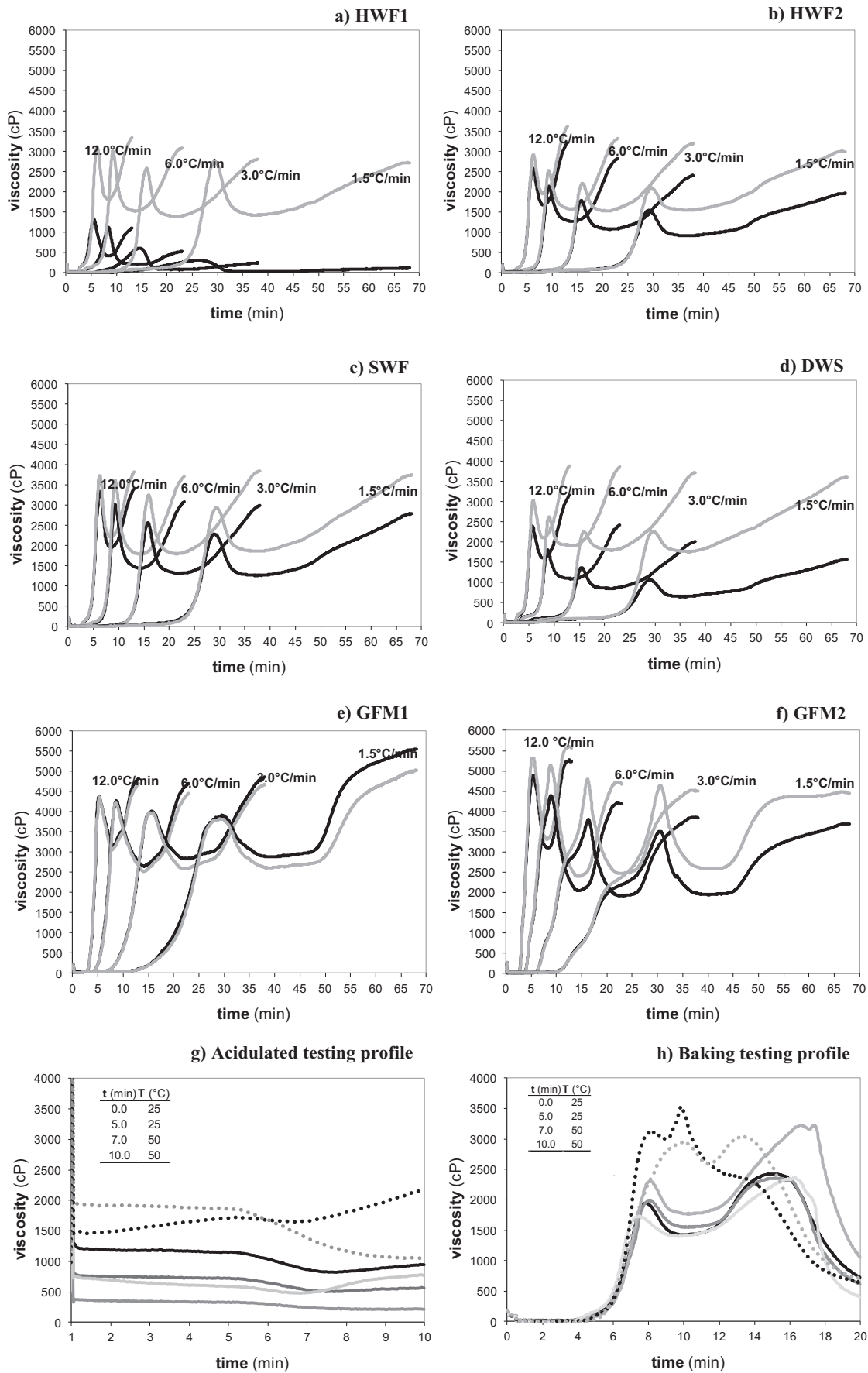


**Fig. 1.** (a)–(f) Influence of the heating rate and of the endogenous enzymatic activity on the pasting profiles of the various samples (*black profiles*: in the presence of distilled water; *grey profiles*: in the presence of  $\text{AgNO}_3$ ; *profiles*: average curves). (g) RVA acidulated testing profiles (*cold method*) of the various samples. *Key symbols*: — HWF1, — HWF2, — SWF, — DWS, .... GFM1, .... GFM2. (h) RVA baking testing profiles (*hot method*) of the various samples (*profiles*: average curves). *Key symbols*: — HWF1, — HWF2, — SWF, — DWS, .... GFM1, .... GFM2. *Abbreviations*: HWF1: hard wheat flour; HWF2: hard wheat flour containing malt; SWF: soft wheat flour; DWS: re-milled durum wheat semolina; GFM1 and GFM2: gluten-free bread mixtures.

**Table 2**  
Influence of the heating rate and of the endogenous enzymatic activity on the RVA indices.

	Testing conditions	Peak viscosity (cP)	Breakdown (cP)	Setback (cP)	Final viscosity (cP)	
HWF1	STD1	1350 <sup>d</sup> ± 11 <sup>X</sup>	948 <sup>d</sup> ± 20 <sup>X</sup>	675 <sup>d</sup> ± 8 <sup>X</sup>	1077 <sup>d</sup> ± 29 <sup>X</sup>	
	STD1 + AgNO <sub>3</sub>	3143 <sup>C</sup> ± 18 <sup>Y</sup>	1317 <sup>B</sup> ± 10 <sup>Y</sup>	1545 <sup>B</sup> ± 17 <sup>Y</sup>	3370 <sup>D</sup> ± 24 <sup>Y</sup>	
	STD2	1110 <sup>c</sup> ± 22 <sup>X</sup>	912 <sup>c</sup> ± 10 <sup>X</sup>	318 <sup>c</sup> ± 3 <sup>X</sup>	516 <sup>c</sup> ± 16 <sup>X</sup>	
	STD2 + AgNO <sub>3</sub>	3019 <sup>B</sup> ± 8 <sup>Y</sup>	1493 <sup>C</sup> ± 16 <sup>Y</sup>	1575 <sup>B</sup> ± 22 <sup>Y</sup>	3101 <sup>C</sup> ± 35 <sup>Y</sup>	
	STD3	682 <sup>b</sup> ± 72 <sup>X</sup>	541 <sup>b</sup> ± 8 <sup>X</sup>	168 <sup>b</sup> ± 7 <sup>X</sup>	309 <sup>b</sup> ± 70 <sup>X</sup>	
	STD3 + AgNO <sub>3</sub>	2663 <sup>A</sup> ± 100 <sup>Y</sup>	1236 <sup>A</sup> ± 62 <sup>Y</sup>	1421 <sup>A</sup> ± 12 <sup>Y</sup>	2848 <sup>B</sup> ± 50 <sup>Y</sup>	
	STD4	334 <sup>a</sup> ± 23 <sup>X</sup>	280 <sup>a</sup> ± 11 <sup>X</sup>	96 <sup>a</sup> ± 5 <sup>X</sup>	149 <sup>a</sup> ± 40 <sup>X</sup>	
	STD4 + AgNO <sub>3</sub>	2756 <sup>A</sup> ± 13 <sup>Y</sup>	2625 <sup>D</sup> ± 2 <sup>Y</sup>	2592 <sup>C</sup> ± 8 <sup>Y</sup>	2723 <sup>A</sup> ± 3 <sup>Y</sup>	
	HWF2	STD1	2608 <sup>d</sup> ± 15 <sup>X</sup>	899 <sup>b</sup> ± 18 <sup>X</sup>	1529 <sup>b</sup> ± 18 <sup>X</sup>	3237 <sup>d</sup> ± 16 <sup>X</sup>
		STD1 + AgNO <sub>3</sub>	2913 <sup>D</sup> ± 22 <sup>Y</sup>	952 <sup>B</sup> ± 6 <sup>Y</sup>	1656 <sup>A</sup> ± 3 <sup>Y</sup>	3617 <sup>D</sup> ± 19 <sup>Y</sup>
STD2		2144 <sup>c</sup> ± 7 <sup>X</sup>	880 <sup>b</sup> ± 8 <sup>X</sup>	1550 <sup>b</sup> ± 16 <sup>X</sup>	2814 <sup>c</sup> ± 31 <sup>X</sup>	
STD2 + AgNO <sub>3</sub>		2558 <sup>C</sup> ± 25 <sup>Y</sup>	974 <sup>C</sup> ± 11 <sup>Y</sup>	1783 <sup>B</sup> ± 35 <sup>Y</sup>	3367 <sup>C</sup> ± 49 <sup>Y</sup>	
STD3		1811 <sup>b</sup> ± 24 <sup>X</sup>	712 <sup>a</sup> ± 1 <sup>X</sup>	1342 <sup>a</sup> ± 21 <sup>X</sup>	2441 <sup>b</sup> ± 45 <sup>X</sup>	
STD3 + AgNO <sub>3</sub>		2244 <sup>B</sup> ± 34 <sup>Y</sup>	688 <sup>A</sup> ± 1 <sup>X</sup>	1671 <sup>A</sup> ± 11 <sup>Y</sup>	3227 <sup>B</sup> ± 24 <sup>Y</sup>	
STD4		1561 <sup>a</sup> ± 10 <sup>X</sup>	1445 <sup>c</sup> ± 3 <sup>X</sup>	1873 <sup>c</sup> ± 16 <sup>X</sup>	1989 <sup>a</sup> ± 23 <sup>X</sup>	
STD4 + AgNO <sub>3</sub>		2101 <sup>A</sup> ± 4 <sup>Y</sup>	1999 <sup>D</sup> ± 4 <sup>Y</sup>	2906 <sup>C</sup> ± 6 <sup>Y</sup>	3008 <sup>A</sup> ± 6 <sup>Y</sup>	
SWF		STD1	3340 <sup>d</sup> ± 12 <sup>X</sup>	1397 <sup>b</sup> ± 14 <sup>X</sup>	1447 <sup>a</sup> ± 14 <sup>X</sup>	3389 <sup>e</sup> ± 22 <sup>X</sup>
		STD1 + AgNO <sub>3</sub>	3694 <sup>C</sup> ± 49 <sup>Y</sup>	1519 <sup>B</sup> ± 29 <sup>Y</sup>	1609 <sup>A</sup> ± 4 <sup>Y</sup>	3784 <sup>AB</sup> ± 39 <sup>Y</sup>
	STD2	3041 <sup>c</sup> ± 14 <sup>X</sup>	1594 <sup>c</sup> ± 5 <sup>X</sup>	1661 <sup>b</sup> ± 15 <sup>X</sup>	3109 <sup>b</sup> ± 25 <sup>X</sup>	
	STD2 + AgNO <sub>3</sub>	3629 <sup>C</sup> ± 8 <sup>Y</sup>	1857 <sup>C</sup> ± 8 <sup>Y</sup>	1934 <sup>B</sup> ± 15 <sup>Y</sup>	3706 <sup>A</sup> ± 24 <sup>Y</sup>	
	STD3	2635 <sup>b</sup> ± 65 <sup>X</sup>	1265 <sup>a</sup> ± 9 <sup>X</sup>	1681 <sup>b</sup> ± 16 <sup>X</sup>	3051 <sup>b</sup> ± 60 <sup>X</sup>	
	STD3 + AgNO <sub>3</sub>	3272 <sup>B</sup> ± 16 <sup>Y</sup>	1456 <sup>A</sup> ± 4 <sup>Y</sup>	2053 <sup>C</sup> ± 4 <sup>Y</sup>	3869 <sup>B</sup> ± 16 <sup>Y</sup>	
	STD4	2301 <sup>a</sup> ± 17 <sup>X</sup>	2181 <sup>d</sup> ± 9 <sup>X</sup>	2676 <sup>c</sup> ± 3 <sup>X</sup>	2797 <sup>a</sup> ± 5 <sup>X</sup>	
	STD4 + AgNO <sub>3</sub>	2995 <sup>A</sup> ± 73 <sup>Y</sup>	2898 <sup>D</sup> ± 52 <sup>Y</sup>	3708 <sup>D</sup> ± 51 <sup>Y</sup>	3805 <sup>B</sup> ± 71 <sup>Y</sup>	
	DWS	STD1	2399 <sup>d</sup> ± 8 <sup>X</sup>	798 <sup>c</sup> ± 5 <sup>X</sup>	1560 <sup>c</sup> ± 11 <sup>X</sup>	3162 <sup>d</sup> ± 15 <sup>X</sup>
		STD1 + AgNO <sub>3</sub>	3028 <sup>D</sup> ± 7 <sup>Y</sup>	932 <sup>C</sup> ± 4 <sup>Y</sup>	1792 <sup>A</sup> ± 5 <sup>Y</sup>	3888 <sup>C</sup> ± 9 <sup>Y</sup>
STD2		1839 <sup>c</sup> ± 47 <sup>X</sup>	697 <sup>b</sup> ± 27 <sup>X</sup>	1380 <sup>b</sup> ± 44 <sup>X</sup>	2522 <sup>c</sup> ± 87 <sup>X</sup>	
STD2 + AgNO <sub>3</sub>		2658 <sup>C</sup> ± 28 <sup>Y</sup>	731 <sup>B</sup> ± 15 <sup>Y</sup>	1985 <sup>C</sup> ± 21 <sup>Y</sup>	3912 <sup>C</sup> ± 34 <sup>Y</sup>	
STD3		1410 <sup>b</sup> ± 55 <sup>X</sup>	520 <sup>a</sup> ± 8 <sup>X</sup>	1178 <sup>a</sup> ± 21 <sup>X</sup>	2068 <sup>b</sup> ± 50 <sup>X</sup>	
STD3 + AgNO <sub>3</sub>		2266 <sup>B</sup> ± 1 <sup>Y</sup>	474 <sup>A</sup> ± 13 <sup>X</sup>	1920 <sup>B</sup> ± 13 <sup>Y</sup>	3712 <sup>B</sup> ± 25 <sup>Y</sup>	
STD4		1089 <sup>a</sup> ± 26 <sup>X</sup>	940 <sup>d</sup> ± 21 <sup>X</sup>	1429 <sup>b</sup> ± 7 <sup>X</sup>	1578 <sup>a</sup> ± 12 <sup>X</sup>	
STD4 + AgNO <sub>3</sub>		2236 <sup>A</sup> ± 45 <sup>Y</sup>	2089 <sup>D</sup> ± 45 <sup>Y</sup>	3433 <sup>D</sup> ± 33 <sup>Y</sup>	3580 <sup>A</sup> ± 34 <sup>Y</sup>	
GFM1		STD1	4347 <sup>b</sup> ± 62 <sup>X</sup>	1215 <sup>a</sup> ± 19 <sup>X</sup>	1646 <sup>a</sup> ± 35 <sup>X</sup>	4778 <sup>a</sup> ± 78 <sup>X</sup>
		STD1 + AgNO <sub>3</sub>	4305 <sup>A</sup> ± 96 <sup>X</sup>	1247 <sup>A</sup> ± 102 <sup>X</sup>	1650 <sup>A</sup> ± 6 <sup>X</sup>	4708 <sup>AB</sup> ± 11 <sup>X</sup>
	STD2	4307 <sup>b</sup> ± 47 <sup>X</sup>	1569 <sup>b</sup> ± 71 <sup>X</sup>	2041 <sup>b</sup> ± 16 <sup>X</sup>	4778 <sup>a</sup> ± 102 <sup>X</sup>	
	STD2 + AgNO <sub>3</sub>	4225 <sup>A</sup> ± 1 <sup>X</sup>	1683 <sup>B</sup> ± 39 <sup>X</sup>	1957 <sup>B</sup> ± 26 <sup>X</sup>	4499 <sup>A</sup> ± 64 <sup>X</sup>	
	STD3	4026 <sup>a</sup> ± 11 <sup>X</sup>	1225 <sup>a</sup> ± 65 <sup>X</sup>	1993 <sup>b</sup> ± 47 <sup>X</sup>	4794 <sup>a</sup> ± 101 <sup>X</sup>	
	STD3 + AgNO <sub>3</sub>	4086 <sup>A</sup> ± 151 <sup>X</sup>	1391 <sup>A</sup> ± 5 <sup>X</sup>	2064 <sup>C</sup> ± 44 <sup>X</sup>	4760 <sup>B</sup> ± 112 <sup>X</sup>	
	STD4	3981 <sup>a</sup> ± 87 <sup>X</sup>	2990 <sup>c</sup> ± 46 <sup>X</sup>	4734 <sup>c</sup> ± 209 <sup>X</sup>	5725 <sup>b</sup> ± 250 <sup>X</sup>	
	STD4 + AgNO <sub>3</sub>	3958 <sup>A</sup> ± 186 <sup>X</sup>	3070 <sup>C</sup> ± 98 <sup>X</sup>	4195 <sup>D</sup> ± 11 <sup>X</sup>	5083 <sup>C</sup> ± 77 <sup>X</sup>	
	GFM2	STD1	4396 <sup>d</sup> ± 57 <sup>X</sup>	1819 <sup>a</sup> ± 23 <sup>X</sup>	2144 <sup>c</sup> ± 8 <sup>X</sup>	5261 <sup>d</sup> ± 26 <sup>X</sup>
		STD1 + AgNO <sub>3</sub>	5322 <sup>C</sup> ± 4 <sup>Y</sup>	1994 <sup>A</sup> ± 17 <sup>Y</sup>	2272 <sup>B</sup> ± 28 <sup>Y</sup>	5598 <sup>C</sup> ± 48 <sup>Y</sup>
STD2		4436 <sup>c</sup> ± 57 <sup>X</sup>	2373 <sup>b</sup> ± 35 <sup>X</sup>	2180 <sup>c</sup> ± 51 <sup>X</sup>	4243 <sup>c</sup> ± 73 <sup>X</sup>	
STD2 + AgNO <sub>3</sub>		5125 <sup>C</sup> ± 30 <sup>Y</sup>	2739 <sup>D</sup> ± 4 <sup>Y</sup>	2314 <sup>B</sup> ± 74 <sup>X</sup>	4700 <sup>B</sup> ± 47 <sup>Y</sup>	
STD3		3812 <sup>b</sup> ± 23 <sup>X</sup>	1876 <sup>a</sup> ± 2 <sup>X</sup>	1924 <sup>b</sup> ± 2 <sup>X</sup>	3860 <sup>b</sup> ± 18 <sup>X</sup>	
STD3 + AgNO <sub>3</sub>		4841 <sup>B</sup> ± 47 <sup>Y</sup>	2334 <sup>B</sup> ± 6 <sup>Y</sup>	2004 <sup>A</sup> ± 35 <sup>X</sup>	4511 <sup>A</sup> ± 18 <sup>Y</sup>	
STD4		3584 <sup>a</sup> ± 102 <sup>X</sup>	1671 <sup>a</sup> ± 149 <sup>X</sup>	1750 <sup>a</sup> ± 5 <sup>X</sup>	3663 <sup>a</sup> ± 42 <sup>X</sup>	
STD4 + AgNO <sub>3</sub>		4536 <sup>A</sup> ± 146 <sup>Y</sup>	2463 <sup>C</sup> ± 88 <sup>Y</sup>	2316 <sup>B</sup> ± 16 <sup>Y</sup>	4390 <sup>A</sup> ± 73 <sup>Y</sup>	

Note: Within the same sample, in the absence of AgNO<sub>3</sub>, values followed by different small letters in the same column are significantly different ( $P < 0.05$ ) (influence of the heating/cooling rate); within the same standard profile, in the presence of AgNO<sub>3</sub>, values followed by different capital letters in the same column are significantly different ( $P < 0.05$ ) (influence of the heating/cooling rate); within the same samples, for the same heating/cooling rate, values followed by different capital letters (X or Y) are significantly different ( $P < 0.05$ ) (influence of the endogenous enzymatic activity).

Abbreviations: HWF1: hard wheat flour; HWF2: hard wheat flour containing malt; SWF: soft wheat flour; DWS: re-milled durum wheat semolina; GFM1 and GFM2: gluten-free bread mixtures; for STD meanings, see Section 2.3a.

observed for GFM1, which exhibited a continuous viscosity increase, probably due to the progressive hydration of the fibres and hydrocolloids present in the mixture.

Results of the 'baking testing profile' have been reported in Fig. 1h. HWF1 and HWF2 exhibited very similar profiles, in relation to temperature variations. A higher viscosity profile was observed for SWF and a lower one for DWS. Therefore, the method was readily able to discriminate among different samples with a range of quality. Differences among samples usually indicate differences in degree of wheat hardness, and the lower viscosity of the HWFs could reflect lower solubility or unfolding of the glutenin fraction, which is associated with good breadmaking quality (Turner & Bason, 1997). Although GFM2's viscosity curve resembled in some way those of the wheat samples, GFM1's curve – in

which no protein was present – was completely different. An unresolved double peak was observed, again, during the hot stage, and a progressive decrease in viscosity was recorded during cooling. The mechanisms behind this are still under investigation, but what is interesting to highlight here is that the RVA baking test profile was able to quickly differentiate not only the various commercial wheat flours but also the two GF commercial bread mixtures.

Therefore, differentiating while performing RVA tests (*i.e.*, different heating/cooling rates; different dispersing media) could be a strategic way to carry out time-, cost- and sample-saving tests able to give information on the quality profiles of various materials, GF ones included.

**Table 3**  
Solvent retention capacity (SRC) of the various samples.

Sample	WRC (g/100 g db)	SCSRC (g/100 g db)	LASRC (g/100 g db)	SuSRC (g/100 g db)	GPI
HWF1	68.8 <sup>c</sup> ± 0.5	80.1 <sup>c</sup> ± 0.3	115.8 <sup>e</sup> ± 0.8	103.7 <sup>c</sup> ± 0.1	0.628 <sup>f</sup>
HWF2	61.8 <sup>b</sup> ± 0.1	71.4 <sup>b</sup> ± 0.2	94.1 <sup>d</sup> ± 1.4	93.1 <sup>b</sup> ± 0.2	0.578 <sup>e</sup>
SWF	53.7 <sup>a</sup> ± 0.1	69.1 <sup>a</sup> ± 0.4	79.2 <sup>a</sup> ± 0.4	86.2 <sup>a</sup> ± 0.1	0.508 <sup>c</sup>
DWS	68.2 <sup>c</sup> ± 0.5	84.4 <sup>d</sup> ± 0.2	87.6 <sup>c</sup> ± 0.1	97.8 <sup>bc</sup> ± 2.3	0.481 <sup>b</sup>
GFM1	152.1 <sup>e</sup> ± 0.8	127.4 <sup>f</sup> ± 0.6	134.8 <sup>f</sup> ± 0.1	128.5 <sup>d</sup> ± 1.3	0.527 <sup>d</sup>
GFM2	78.3 <sup>d</sup> ± 0.1	88.9 <sup>e</sup> ± 0.2	83.7 <sup>b</sup> ± 1.0	101.7 <sup>c</sup> ± 0.6	0.439 <sup>a</sup>

Note: Values followed by different letters in the same column are significantly different ( $P < 0.05$ ).

Abbreviations: HWF1: hard wheat flour; HWF2: hard wheat flour containing malt; SWF: soft wheat flour; DWS: re-milled durum wheat semolina; GFM1 and GFM2: gluten-free bread mixtures; variables: WRC, water retention capacity; SCSRC, sodium carbonate solvent retention capacity; LASRC, lactic acid solvent retention capacity; SuSRC, sucrose solvent retention capacity; GPI, gluten performance index, calculated as follows:  $[LASRC/(SCSRC + SuSRC)]$ .

### 3.4. Solvent retention capacity (SRC)

Despite its 'origin', SRC profiling was applied to various samples to test its potential differentiating abilities. Actually, statistically significant differences ( $P < 0.05$ ) were found among the samples

(Table 3): HWF1, HWF2, SWF, DWS and the two GF mixtures were well differentiated by SRC testing.

Among the wheat flours, SWF exhibited the lowest SRC values, which was consistent with its chemical composition. Significant differences ( $P < 0.05$ ) were also exhibited by the two

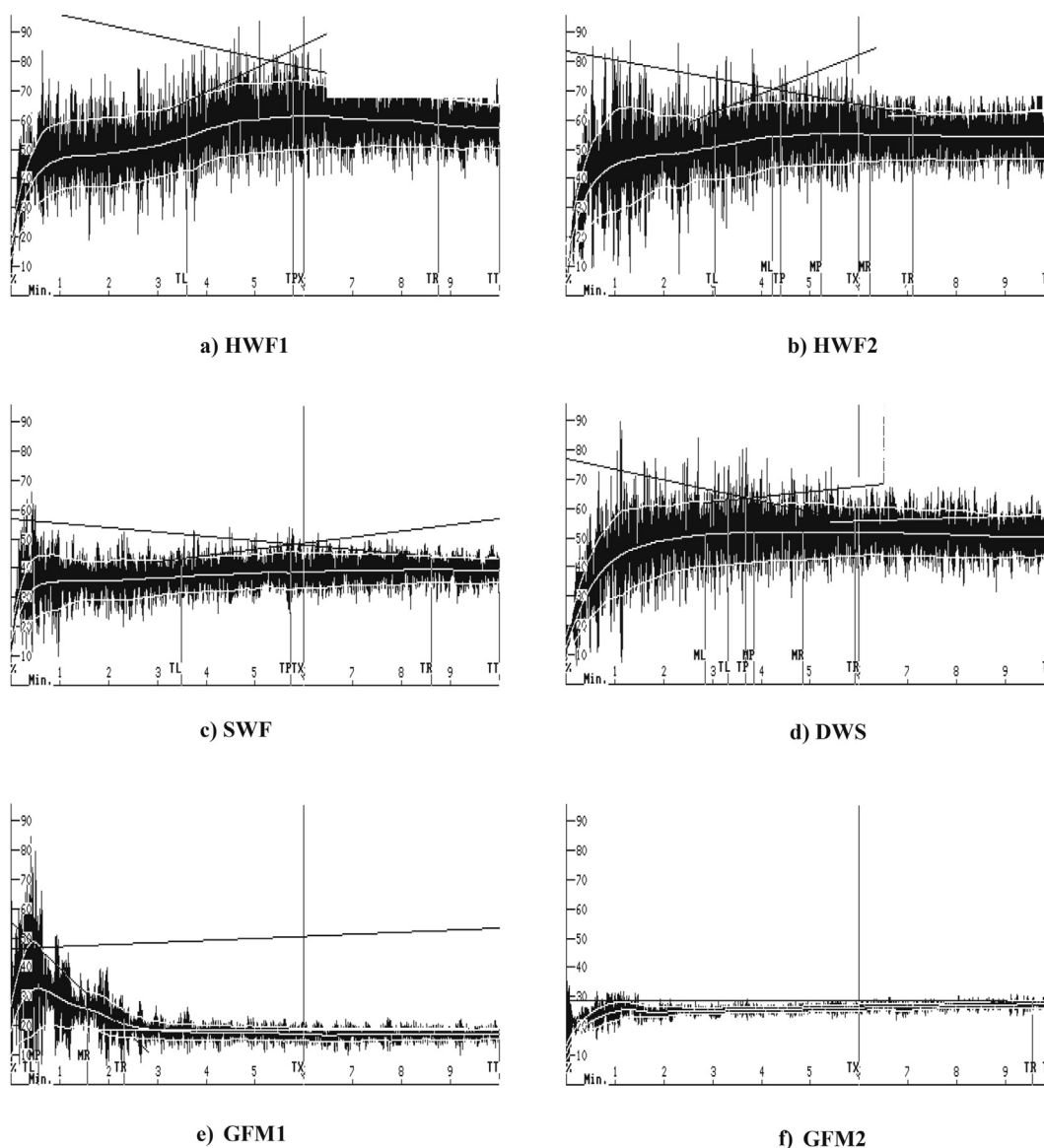


**Fig. 2.** Mixograms of the four wheat flours (a–d) and of the two commercial gluten-free bread mixtures (e–f). Abbreviations: HWF1: hard wheat flour; HWF2: hard wheat flour containing malt; SWF: soft wheat flour; DWS: re-milled durum wheat semolina; GFM1 and GFM2: gluten-free bread mixtures.

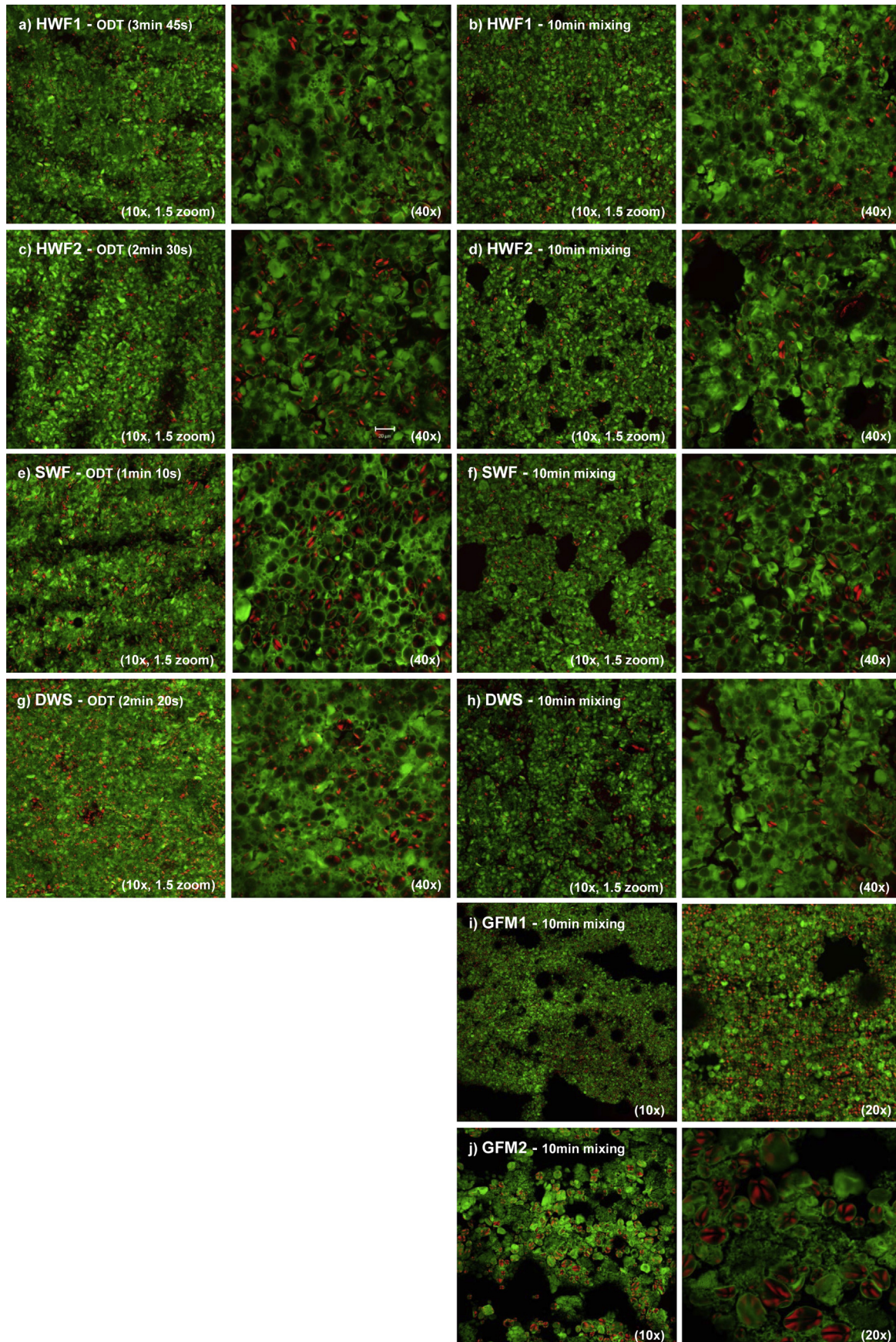


**Fig. 3.** CLSM images of the various doughs at their optimal development time and after 10 min mixing. *Abbreviations:* ODT: optimum development time; HWF1: hard wheat flour; HWF2: hard wheat flour containing malt; SWF: soft wheat flour; DWS: re-milled durum wheat semolina; GFM1 and GFM2: gluten-free bread mixtures.

hard wheat flours: HWF1 had a higher SRC profile (in accordance with its higher DS and protein levels) in comparison to HWF2. DWS also stood out for its SRC profile. The gluten performance index (GPI), also was significantly different ( $P < 0.05$ ) among all the samples. Therefore, the importance of this rapid test in differentiating practical functionality profiles of wheat samples was confirmed.

An interesting aspect was its ability in differentiating the two commercial GF samples, even if apparently a 'nonsense' because of their lack of gluten. Significant differences ( $P < 0.05$ ) were evidenced between the two GF mixtures. GFM1 had the highest SRC values, probably due to the strong water absorption and cold swelling/gelling abilities of psyllium (Mariotti et al., 2009) as well as to the emulsifying, thickening, and stabilizing properties of guar gum (Mariotti, Pagani, & Lucisano, 2013). Certainly, data interpretation has to be different when dealing with GF samples, but the discriminating abilities of the test are still evident.

High positive correlations were observed among the different SRCs (both including or excluding the GF samples). In particular, the followings were found (GF samples included): WRC and SCSRC ( $r = 0.986$ ,  $P < 0.005$ ), WRC and SuSRC ( $r = 0.975$ ,  $P < 0.005$ ), SCSRC and SuSRC ( $r = 0.964$ ,  $P < 0.005$ ), LASRC and SuSRC ( $r = 0.855$ ,  $P < 0.05$ ). Water is necessary for gluten development and to hydrate the various ingredients of GF mixtures. It also has a strategic role in determining dough workability as well as the performance of the end-products. Therefore, understanding key constituents in determining water absorption in gluten-based or gluten-free materials is crucial, and the SRC profile could be a very informative and proper test.

### 3.5. Mixing properties

In order to test if the differences highlighted with the previous rapid and simple methods were confirmed when going on into the simulation of a real process, some mixograms were recorded (Fig. 2). During food processing, in fact, one of the first steps is generally the mixing of various raw materials according to a specific recipe. A Mixograph records the increase in stress as dough is mixed to its maximum resistance, and the subsequent decrease in stress upon over-mixing. Mixograms were actually different among the samples, and those of the four wheat flours were easily distinguished and typical of their commercial category. The information obtained from the tests carried out in the first part of the study was thus confirmed. Mixograms of the two commercial GF mixtures were also recorded. Despite both GF samples being destined for breadmaking, they had different behaviours during mixing, not only in comparison to the wheat flour samples but also between them. Among many others, the specific prolonged stability during mixing and over-mixing was a distinctive aspect: it took time to fully hydrate the many different components of the GF mixture, but when hydration was complete, dough resistance to mixing remained constant.

### 3.6. Ultrastructural features

Confocal Laser Scanning Microscopy (CLSM) was performed to visualize dough networking during mixing. Fig. 3 delineates the overlay of the images obtained by simple polarized light and fluorescence of the same area: in red (in web version), the starch granules; in green (in web version), the protein matrix. Fig. 3a, c, e, and g refer to 'gluten-based' doughs at their optimum development time (ODT). Starch granules were well enveloped into the gluten-matrix, which appeared homogeneous and continuous, in particular in SWF (Fig. 3e) and DWS (Fig. 3g) doughs. However, differences were observed in the samples when mixing was prolonged

up to 10 min (Fig. 3b, d, f, h): while HWF1 matrix was still homogeneous and continuous, holes and tears appeared in HWF2, SWF and DWS. Actually, the mixing stabilities of the samples (as determined by the farinographic test) were as follows: HWF1, 14 min; HWF2, 8 min; SWF, 1.5 min; DWS, 3.5 min, and their resistances to mixing were 16 min, 9.5 min, 2.5 min, 5 min, respectively. These results could easily explain why HWF1 still maintained its optimal network after 10 min mixing.

In contrast to that of wheat doughs, a continuous matrix could not be found in GF samples. Psyllium seemed to provide stability to the dough matrix, and GFM1 dough ultrastructure appeared quite homogeneous and regular, likely because of the presence of a single source of starch in the recipe (Fig. 3i). The presence of potato and rice starch granules completely enveloped by proteins, and of different 'structures' attributable to hydrocolloids, made GFM2 dough ultrastructure quite inhomogeneous (Fig. 3j); however, its mixing behaviour was very stable, probably due to the well-balanced properties of the different ingredients used in its recipe.

## 4. Conclusions

Different materials (both from wheat and from non-gluten mixtures) were involved in this study, and it was highlighted that methods such as SRC or RVA beyond being used as standard tests, can be properly modified/adapted to take into account the contribution or functionality of specific flour/mixture constituents in a given process. They also save time, money and require small quantities of sample. If the observed relationships here highlighted will be confirmed using a higher number of samples, these methods could really be very useful for Quality Control and Research and Development purposes: they could be used not only singly as standard methods to routinely characterize raw materials, but they can also be modified or combined in order to produce quality profiles for different materials, including GF samples. Certainly, data interpretation has to be different when dealing with GF samples, but the discriminating abilities of these tests are still impressive.

## References

- AACCI. (2000). *AACC 44-15, moisture, air-oven method; AACC 54-40, mixograph method; AACC 56-11, solvent retention capacity profile; AACC 56-81, determination of falling number. Approved methods of the American association of cereal chemists* (10th ed.). St. Paul, MN, USA: The American Association of Cereal Chemists.
- AOAC. (2000). *AOAC 920.87, Kjeldahl method. Official methods of analysis of AOAC international* (17th ed.). Gaithersburg, MD, USA: Association of Analytical Communities.
- BeMiller, J. N. (2009). Hydrocolloids. In E. K. Arendt, & F. Dal Bello (Eds.), *Gluten-free cereal products and beverages* (pp. 203–215) (AP).
- Cappa, C., Lucisano, M., & Mariotti, M. (2013). Influence of psyllium, sugar beet fibre and water on gluten-free dough properties and bread quality. *Carbohydrate Polymers*, 98(2), 1657–1666.
- Crosbie, G. B., & Lambe, W. J. (1993). The application of the flour swelling volume test for potential noodle quality to wheat breeding lines affected by sprouting. *Journal of Cereal Science*, 18, 267–276.
- Derycke, V., Veraverbeke, W. S., Vandeputte, G. E., De Man, W., Hosney, R. C., & Delcour, J. A. (2005). Impact of proteins on pasting and cooking properties of nonparboiled and parboiled rice. *Cereal Chemistry*, 82(4), 468–474.
- Donald, A. M. (2004). Understanding starch structure and functionality. In A. C. Eliasson (Ed.), *Starch in food: Structure, function and applications* (pp. 156–184). Cambridge, England: Woodhead Publishing Limited.
- Duyvejonck, A. E., Lagrain, B., Dornez, E., Delcour, J. A., & Courtin, C. M. (2012). Suitability of solvent retention capacity tests to assess the cookie and bread making quality of European wheat flours. *LWT – Food Science and Technology*, 47, 56–63.
- Duyvejonck, A. E., Lagrain, B., Pareyt, B., Courtin, C. M., & Delcour, J. A. (2011). Relative contribution of wheat flour constituents to solvent retention capacity profiles of European wheats. *Journal of Cereal Science*, 53, 312–318.
- ICC. (1992). *ICC 115/1, method for using the brabender farinograph. ICC standard methods*. Vienna: International Association for Cereal Science and Technology.

- Kweon, M., Slade, L., & Levine, H. (2011). Solvent retention capacity (SRC) testing of wheat flour: principles and value in predicting flour functionality in different wheat-based food processes and in wheat breeding – a review. *Cereal Chemistry*, 88(6), 537–552.
- Mariotti, M., Lucisano, M., Pagani, M. A., & Iametti, S. (2008). Macromolecular interactions and rheological properties of buckwheat dough obtained from differently processed grains. *Journal of Agricultural and Food Chemistry*, 56(11), 4258–4267.
- Mariotti, M., Lucisano, M., Pagani, M. A., & Ng, P. K. W. (2009). The role of corn starch, amaranth flour, pea isolate and psyllium flour on the rheological properties of gluten-free dough. *Food Research International*, 42(8), 963–975.
- Mariotti, M., Pagani, M. A., & Lucisano, M. (2013). The role of buckwheat and HPMC on the breadmaking properties of some commercial gluten-free bread mixtures. *Food Hydrocolloids*, 30, 393–400.
- Mariotti, M., Zardi, M., Lucisano, M., & Pagani, M. A. (2005). Influence of the heating rate on the pasting properties of various flours. *Starch/Stärke*, 57, 564–572.
- McCleary, B., McNally, M., & Monaghan, D. (2002). Measurements of  $\alpha$ -amylase activity in white wheat flour, milled malt, and microbial enzyme preparations, using the ceralpha assay: a collaborative study. *Journal of AOAC International*, 85(5), 1096–1102.
- Onwulata, C. I., Tunick, M. H., & Thomas-Gahring, A. E. (2013). Rapid visco analysis of food protein pastes. *Journal of Food Processing and Preservation*, 38, 2083–2089.
- Slade, L., & Levine, H. (1994). Structure-function relationships of cookie and cracker ingredients. In H. Faridi (Ed.), *The science of cookie and cracker production* (pp. 23–141). New York, NY, USA: Chapman & Hall.
- Turner, N., & Bason, M. (1997). Assessing the functional properties of wheat flour properties. *RVA World*, 12, 2–4.
- Zhang, G., & Hamaker, B. (2003). A three component interaction among starch, protein and free fatty acids revealed by pasting profiles. *Journal of Agricultural and Food Chemistry*, 51, 2797–2800.



# Effects of added inulin and wheat gluten on structure of rye porridge



José L. Vázquez-Gutiérrez\*, Daniel Johansson, Maud Langton

Department of Food Science, SLU – Swedish University of Agricultural Sciences, PO Box 7051, SE-750 07 Uppsala, Sweden

## ARTICLE INFO

### Article history:

Received 1 July 2015

Received in revised form

10 October 2015

Accepted 13 October 2015

Available online 19 October 2015

### Keywords:

Rye

Starch

Microscopy

Fructan

Viscosity

## ABSTRACT

The aim was to study the microstructure and distribution of components of rye porridge enriched with different inulin and gluten proportions (0:0, 3:9, 6:6, 9:3), and their relationship with texture. Inulin was labeled with fluorescein isothiocyanate (FITC) prior to its addition to the porridges, and multiple staining was applied to cryosections in order to also observe other components of the porridges. Porridge structure consisted of grain fragments and a continuous phase formed by released amylose, starch granules and protein. Addition of inulin and gluten to rye porridge partly hindered starch gelatinization due to their water binding capacity. The green fluorescence from FITC-labeled inulin was brighter in detached starch granules in the continuous phase, indicating greater interaction of inulin with starch than with protein. Viscosity was lower in those porridges with high inulin content and low gluten content. Solubilized inulin created a protective layer around starch granules limiting their swelling and amylose release, which may explain the differences in viscosity between the porridges and could have further influence in starch digestibility.

© 2015 Elsevier Ltd. All rights reserved.

## 1. Introduction

Consumers are demanding healthier food products with improved functionalities and an increasing number of new food formulations are being developed to satisfy this need. The compatibility or incompatibility between ingredients in new food formulations can affect both texture and structure (Icoz, Moraru, & Kokini, 2005). These structural changes could also have later implications in the intended functionality of the product (McClements, Decker, Park, & Weiss, 2009). When it comes to porridge, the rheological properties are of great importance for quality control and consumer acceptance (Sai Manohar, Urmila Devi, Bhattacharya, & Venkateswara Rao, 2011). Moreover, it can also have influence on the satiating properties of the product (Mars, Hogenkamp, Gosses, Stafleu, & De Graaf, 2009). Rye foods, which are important elements in the healthy Nordic diet, have shown favorable effects on appetite (Isaksson et al., 2012), as well as beneficial effects on postprandial insulin responses and inflammatory biomarkers (Fung et al., 2002; Landberg et al., 2010; Rosén, Östman, & Björck, 2011). Addition of plant protein and fermentable dietary fiber could possibly enhance the appetite suppressing effect of whole-grain rye porridge. Such effects may in part be due to

alterations in the microstructure of the product (Lundin, Golding, & Wooster, 2008).

Inulin is an oligo-fructose polymer of interest in human nutrition due to its ability to act as dietary fiber and prebiotic (Roberfroid, 2007). Due to its structure, inulin resists digestion in the human intestine and is fermented by bacteria in the colon, which has been suggested to affect appetite (Cani, Dewever, & Delzenne, 2004). Little work has been done to investigate the effects of inulin on food structure. Microstructural studies of inulin-enriched products have been carried out on cereal and dairy products (Aravind, Sissons, Fellows, Blazek, & Gilbert, 2012; Guardoño, Vázquez-Gutiérrez, Hernando, & Quiles, 2013; Guggisberg, Cuthbert-Steven, Piccinali, Bütikofer, & Eberhard, 2009; Rodríguez-García, Puig, Salvador, & Hernando, 2012; Sotowiej et al., 2015). However, the studies do not provide a detailed localization of solubilized inulin in the structure and only insolubilized inulin crystals have been detected by light microscopy (Guardoño et al., 2013). Interactions between inulin and the protein structural network in yogurt have been suggested (Guggisberg et al., 2009; Kip, Meyer, & Jellema, 2006), but such interactions have neither been properly described nor confirmed by microstructural observations.

Gluten is found in the endosperm of cereals such as wheat, barley, and rye and is an important by-product from wet milling of wheat flour. Wheat gluten is a common food ingredient in bakery products such as hamburger buns (Esteller, Pitombo, & Lannes,

\* Corresponding author.

E-mail address: [jose.luis.vazquez.gutierrez@slu.se](mailto:jose.luis.vazquez.gutierrez@slu.se) (J.L. Vázquez-Gutiérrez).

2005), meat products as binding and enriching ingredient (Zhang, Xiao, Samaraweera, Lee, & Ahn, 2010), breakfast cereals, and pasta (Day, 2011). Wheat gluten is marketed in two forms: 'non-vital' and 'vital'. Nonvital wheat gluten has undergone irreversible denaturation, while vital dry gluten in contact with water rehydrates rapidly and regains its intrinsic functionality (Esteller et al., 2005). Therefore, vital gluten constitutes a desired additive in baked and meat products due to its ability to form a viscoelastic mass through the interaction with water (Esteller et al., 2005; Zhang et al., 2010). Interactions between gluten and starch have been reported and supported by microscopy observation (Chen, Deng, Wu, Tian, & Xie, 2010). It has also been suggested that there could be interactions between gluten and inulin but this has not been confirmed by microstructural observation (Morris & Morris, 2012; Peressini & Sensidoni, 2009; Rubel, Pérez, Manrique, & Genovese, 2015; Wang, Rosell, & Benedito de Barber, 2002).

Labeling of inulin with fluorescein isothiocyanate (FITC) has been successfully used for studies of the phase behavior of inulin-waxy maize starch systems (Zimeri & Kokini, 2003a). To our knowledge, the method has so far only been used for model systems and this is the first time that FITC labeling and localization of inulin by confocal microscopy is performed in a complex food system. Previously only inulin crystals could be identified and the location of soluble inulin could only be suggested in such systems, not proven by fluorescence signal as in this study.

The aim of this study was to analyze the effect of partial substitution of rye flakes for inulin and gluten on the microstructure and texture of whole grain rye flake porridge to obtain a better understanding of the functionality of the product.

## 2. Materials and methods

### 2.1. Sample preparation

Rye porridge was made from whole grain rye flakes, produced by steaming, cutting and rolling rye kernels (Lantmännen Cerealia, Järna, Sweden). Four different samples were prepared, one with 40 g rye flakes and the rest contained 40 g rye flakes with different combinations of inulin (Orafti®GR inulin, purity 90%; Beneo, Mannheim, Germany) and gluten (Vital Wheat Gluten, purity 77%; Arrowhead Mills, Boulder, USA). The combined additions were recalculated to compensate for impurities to ensure ratios inulin/gluten of 1:3 (3 g inulin and 9 g gluten, 3I9G), 1:1 (6 g inulin and 6 g gluten, 6I6G) and 3:1 (9 g inulin and 3 g gluten, 9I3G), as well as similar total weight of all the porridges. Samples were prepared by adding boiling water (150 g) to the rye flakes/inulin/gluten mixtures and manually stirred for 30 s. The samples were then left to rest for 2 min and manually stirred again for another 30 s. The samples were left to rest for another 2 min, and then deposited in aluminum caps and frozen with liquid nitrogen. Short-chain inulin (degree of polymerization between 10 and 20) was chosen as it would have greater solubility than long-chain inulin (Tárrega, Torres, & Costell, 2011) and would be expected to have less effect on the viscosity of the product (Morris & Morris, 2012; Tárrega et al., 2011).

### 2.2. Labeling method

Inulin was covalently labeled with fluorescein isothiocyanate (FITC, Sigma–Aldrich Co. LLC., St Louis, MO) following the procedure described by Zimeri and Kokini (2003a) with modifications. Briefly, inulin (1 g) was dissolved in dimethyl sulfoxide (10 mL) containing two drops of pyridine. FITC (0.04 g) was added, followed by addition of the catalyst dibutyltin dilaurate (20 mg). The mixture

was heated for 3 h at 50 °C using a water bath. Several precipitations in ethanol were performed to remove the free dye. FITC-inulin was filtered using a filter paper No. 3 (Whatman, Wand R Balston Ltd, England), dried overnight in a vacuum oven at 85 °C, and stored in the dark under refrigeration to prevent loss of fluorescence. In order to prepare the porridges, an amount of FITC-labeled inulin (1% of the total inulin amounts described in Section 2.1) was added before the mixing with hot water and the sample preparation procedure outlined in Section 2.1 was followed.

### 2.3. Microscopy

The frozen samples were transferred to a cryostat, and 8 µm cryosections were obtained and placed in glass slides. Multiple staining was applied to cryosections, lugol's solution (0.05 g/L iodine) to detect starch and protein (Groves, 2006), 0.1 g/L Calcofluor White for β-glucan (Dornez et al., 2011), and 0.02 g/L Texas Red for protein (Johansson, Krona, & Stading, 2012). A Nikon Eclipse Ni–U research microscope coupled to a HGFI mercury lamp (Nikon, Tokyo, Japan) was used to visualize the microstructure of the porridges. Bright field and epifluorescence images were obtained using CFI Plan 4× objective (N.A. 0.20, W.D. 20 mm) and CFI Plan Fluor 10× (N.A. 0.30, W.D. 16 mm) and 20× (N.A. 0.75, W.D. 1 mm) objectives. Blue (Epi-FL Filterset DAPI, excitation wavelength 382–393 nm, emission 417–477), green (Epi-FL Filterset FITC, excitation wavelength 465–500 nm, emission 516–556 nm), and red (Epi-FL Filterset Texas Red, excitation 540–580 nm, emission 600–660 nm) light fluorescence filters were used to observe the fluorescence of Calcofluor, FITC-inulin, and Texas Red, respectively. Images were captured with a Nikon Digital Sight DS-Fi2-U3 digital camera.

### 2.4. Texture analysis

A RVA (Rapid Visco Analyzer, Newport Scientific Pvt. Ltd., Australia) with an impeller–cup combination was used to measure the viscosity of the porridges. Since rye porridge includes particles in the millimeter range it is impossible to use rheometry with gap distances which would give controlled shear rates and absolute measurements. For the RVA measurement the average temperature, as measured with a thermocouple connected to a digital readout during the preparation process described in Section 2.1, was used. The rate profile was set to simulate the stirring with an extra measurement period at the end of the run (Table 1). For each different formulation, approximately 35 g of the sample were introduced in a stainless steel cylinder and analyzed in the RVA in triplicate. The average viscosity during the last 15 s of each measurement period was used to derive a viscosity profile for each product. The first 15 s of the measurement periods were not included to avoid the initial instabilities.

### 2.5. Statistical analysis

Differences between viscosity profiles were evaluated using a mixed effect model suitable for repeated measurements with PROC mixed in SAS, version 9.4 (SAS Institute Inc, Cary, NC, USA). Time,

**Table 1**  
Conditions for the RVA test on the porridge samples (total duration 330 s).

Step	1	2	3	4	5
Temperature (°C)	75	75	75	75	75
Duration (s)	30	120	30	120	30
Agitation (rpm)	30	0	30	0	30

product and a time  $\times$  product interaction term were included as fixed effects with time as a repeated variable. Sample was included as a random effect. When a significant time  $\times$  product interaction was found, Tukey's honest significance test was performed for each time point.

### 3. Results and discussion

#### 3.1. Characterization of porridge structure by iodine staining

After the addition of hot water to the whole grain rye flakes, starch granules swelled and collapsed leading to gelatinization. The structure of the rye porridges, as visualized with iodine staining, consisted of kernel fragments and an aqueous continuous phase with released amylose (blue) and amylopectin (brown/purple), small fragments of starch granules (dark blue/violet) and protein (yellow). Iodine staining, further allowed for visualization of the aleurone and subaleurone cells, both rich in protein, as shown in yellow color (Fig. 1A and B). Amylose and amylopectin seen in the continuous phase were released from starch granules at the edge of the grain fragments as these had more access to water and therefore underwent greater swelling. A few detached starch granules could be distinguished in the aqueous phase, showing great level of distortion (Fig. 1C).

Starch granules in porridges containing inulin and gluten appeared to be less swollen than the ones in the control product (Fig. 1D–F). This may be due to inulin and gluten competing for water against the starch, owing to their water binding capacity, as has previously been suggested in white sauces formulated with soy protein and inulin (Guardeño et al., 2013). With no inulin and gluten added, more water was available for the starch, leading to greater swelling of the granules.

The porridge with the highest amount of inulin (9I3G) showed smaller and less distorted starch granules in the continuous phase compared with the sample with the highest amount of gluten (3I9G). Moreover, the 9I3G presented less amount of released amylose/amylopectin in the aqueous phase, which appeared less stained than in the other samples.

According to Bishay (1998) and Manno et al. (2009), inulin has a greater affinity for the water than starch polysaccharides and gluten. The water that is bound to inulin chains is more mobile than when it is bound to the starch; this is simply due to inulin having shorter, more mobile molecules (Lobato, Grossmann, & Benassi, 2009). The inulin's preferential properties for hydrating, aggregating, and forming a matrix encase starch granules in a semi-solid gel (Tolstoguzov, 2003). This encasing of the starch granules would possibly limit water movement to the starch granules, reducing swelling and gelatinization (Brennan, Kuri, & Tudorica, 2004).

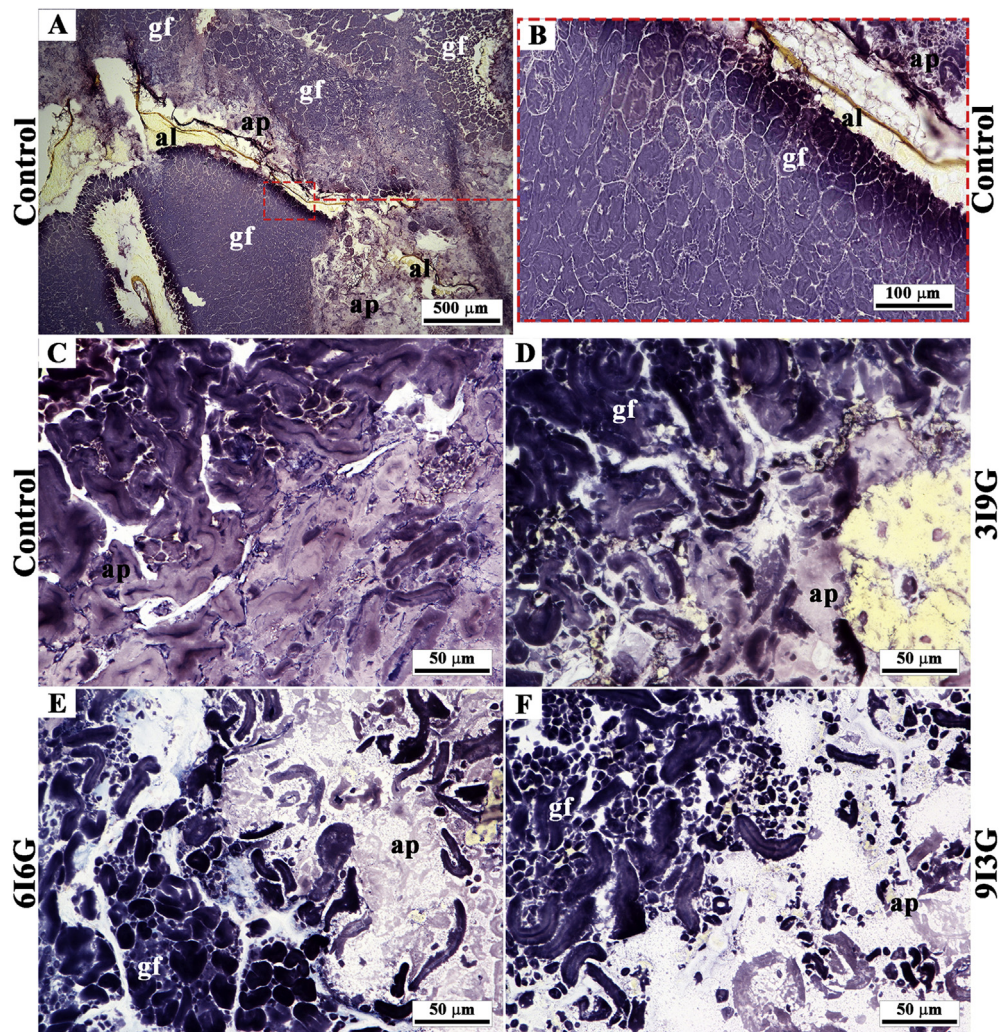


**Fig. 1.** Light microscopy images of different porridge cryosections stained with lugol's solution. A–C) Control; D) 3:9 inulin/gluten (3I9G); E) 6:6 inulin/gluten (6I6G); F) 9:3 inulin/gluten (9I3G). gf: grain fragment; al: aleurone; ap: aqueous phase.

### 3.2. Location of inulin by epifluorescence

When samples were observed under epifluorescence, inulin labeled with FITC could be detected as green fluorescence. The control sample, which did not contain inulin, presented faint green autofluorescence from proteins and cell walls (Fig. 2A). However, strong green autofluorescence was detected in the pericarp due to the high concentration of phenolic acids in that area (Dornez et al., 2011). Therefore, the pericarp area appeared in light blue-turquoise color in all the samples after combining blue and green fluorescence signals (Fig. 2A–D). Calcofluor staining allowed detecting  $\beta$ -glucan as blue fluorescence. High concentration of  $\beta$ -glucan was observed in the aleurone and subaleurone layers, where thick and relatively intact cell walls were observed. The blue fluorescence lost continuity and became thinner towards deeper layers of the starch endosperm, indicating that cell walls were damaged and  $\beta$ -glucan content was lower in those areas (Fig. 2A). Fragments of cell walls with  $\beta$ -glucan could also be found in the aqueous phase among detached starch granules and protein aggregates (Fig. 2B–D).

Green fluorescence signal from FITC-labeled inulin was observed heterogeneously distributed in the aqueous phase and it was brighter as the amount of added inulin increased. In the sample with lower amount of added inulin (319G), the green fluorescence appeared to be slightly brighter in specific areas (Fig. 2B). These areas were stained in black-dark blue color after lugol staining (Fig. 2F), corresponding to non-gelatinized starch granules and aggregates of released amylose. In the samples with equal amount of added inulin and gluten (616G), the fluorescence from the amylose aggregates became brighter (Fig. 2C). Bright green fluorescence could also be observed around the gluten aggregates, which were stained in yellow with lugol (Fig. 2G), which could

indicate interactions between inulin and gluten protein. The formulation with the highest amount of inulin (913G) presented the brightest green fluorescence overall, especially located in the starchy areas rich in amylose (Fig. 2D and H).

Some studies have not found evidence of interaction between inulin and amylopectin (Icoz & Kokini, 2008; Zimeri & Kokini, 2003b). Therefore, it was concluded that the green fluorescence observed in the starchy areas was due to interaction between inulin and amylose or with starch granule-associated proteins.

When samples were observed at higher magnification, bluish precipitates could be observed around gluten aggregates after iodine staining in the porridges with medium and high amount of inulin (616G and 913G), as shown in Fig. 3A. These precipitates could correspond to released amylose, which would be interacting with the gluten protein. In the same way, bright green fluorescence surrounding the gluten aggregates, which could be detected as red fluorescence after Texas Red staining, could be observed (Fig. 3B). This indicated the presence of inulin in similar areas where the amylose was located. Both amylose and inulin could interact with gluten protein.

### 3.3. Texture analysis

A statistically significant interaction between product  $\times$  time was detected on the viscosity profiles ( $P < 0.05$ ). Therefore, Tukey's honest significance test was performed for each time-point. All porridges exhibited increasing viscosity during the measurement (Fig. 4). This increase in viscosity was likely due to a series of changes taking place in the structure of the porridges. The starch granules swell and amylose and amylopectin leach from the granules resulting in increased viscosity. Simultaneously, granules

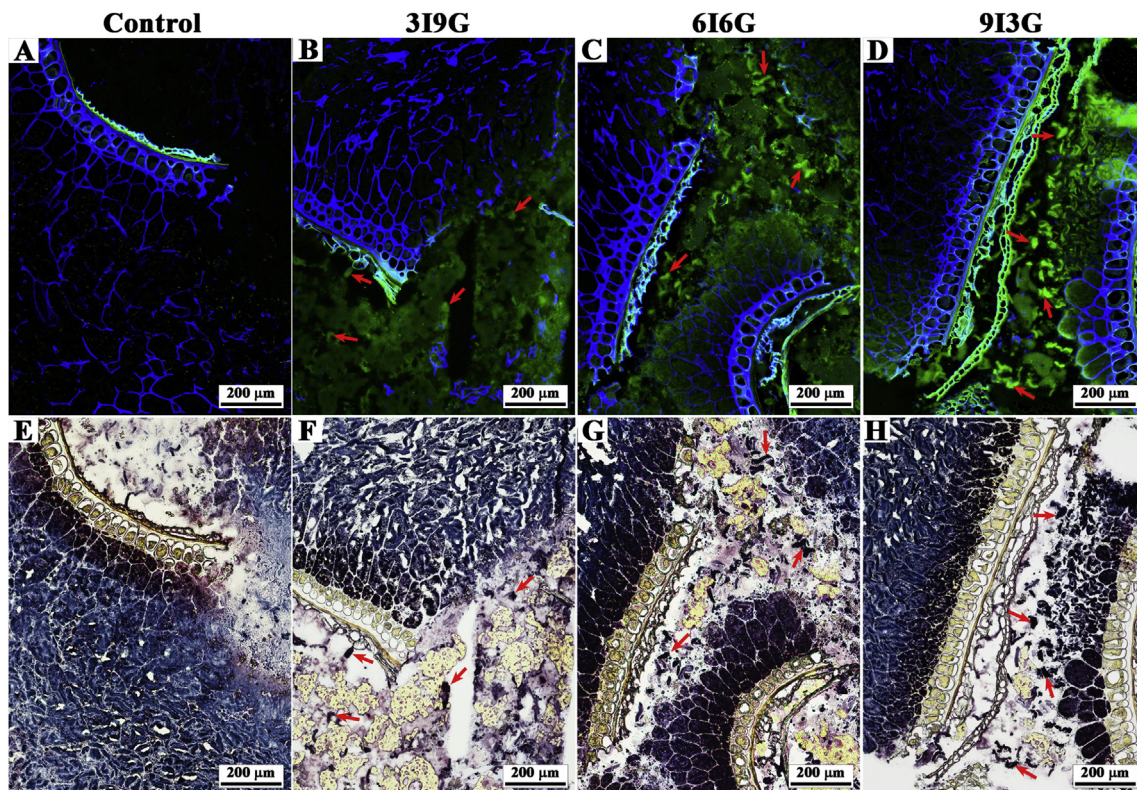


**Fig. 2.** Microstructure of porridge with different inulin and gluten proportions: 0:0 (control), 3:9 (319G), 6:6 (616G), 9:3 (913G). Epifluorescence images (top row) with Calcofluor White staining (blue fluorescence for  $\beta$ -glucan and green fluorescence for FITC-labeled inulin) and bright field images (bottom row) with iodine staining (protein in yellow, amylose in blue, amylopectin in purple). Red arrows: inulin rich areas (top row) colocalized with starch areas (bottom row). Same areas are shown in both rows. (For interpretation of the references to color in this figure legend, the reader is referred to the web version of this article.)

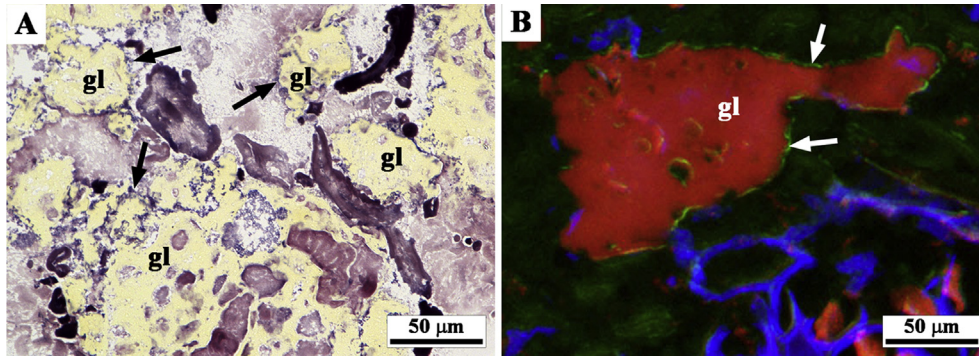


**Fig. 3.** Microstructure of rye porridge with equal amounts of added gluten and inulin (616G). A) Bright field with iodine staining; B) Epifluorescence with Calcofluor and Texas Red staining. Black arrows: amylose precipitates; white arrows: inulin; gl: gluten aggregate.

rapture and amylose and amylopectin chains align, contributing to decreased viscosity. Among the enriched porridges, the final viscosity values significantly decreased ( $P < 0.05$ ) with increasing inulin content and decreasing gluten content (Fig. 4). A similar trend was also seen at the two first time points. Since the enriched porridges contained higher amount of dry matter compared to the control porridge (more than 52 g for the enriched versus 40 g for the control), all the enriched porridges would be expected to have higher viscosity values. However, all enriched porridges, except the porridge with highest gluten content (319G), had significantly lower ( $P < 0.05$ ) viscosity than the control one at all time points.

The high water binding capacity of inulin and gluten decrease the water available for starch gelatinization. Moreover, as observed in the microstructural study, inulin was located preferentially around detached starch granules. The significantly lower ( $P < 0.05$ ) final viscosity measured in the samples with higher inulin content (913G and 616G) could also be due to the additional effect of inulin, encasing the starch granules, as observed in the epifluorescence images (Fig. 2B–D). This would limit the release of amylose from the granules and result in a smaller contribution from the starch network to the viscosity. Gluten aggregates could also interfere with the starch network thereby decreasing the viscosity. Chen et al. (2010) reported that type and amount of added gluten had considerable influence on the mechanisms involved in the pasting

properties of starch, such as transportation of available water and transmission of gelatinization energy. However, since the viscosity reached in the porridges decreased with increasing inulin content, it seems that inulin had greater influence on the viscosity of the porridge than gluten (Fig. 4). Moreover, as shown in the microstructural study, gluten occurs as bigger particles while inulin seems to accumulate at surfaces with amylose. The higher content of particles in the porridge with the highest gluten content could contribute to the increase in viscosity and would explain the differences in viscosity observed between the porridges.

Unlike what has been previously reported in white sauces (Guardeño, Hernando, Llorca, Hernández-Carrión, & Quiles, 2012; Guardeño et al., 2013), no signs of inulin insolubility or recrystallization could be observed in porridges. Kim, Faqih, and Wang (2001) reported that low concentrations of inulin such as 0.5 g/L do not lead to gel network formation after heating at 80 °C. The concentration of inulin in the porridge with highest inulin content (913G) was 0.67 g/L. According to Kim et al. (2001), approximately 2.5 g/L inulin can be dissolved at 80 °C. Furthermore, short-chain inulin, as the one used in this study, is more likely to remain solubilized than long-chain inulin (Tárrega et al., 2011). Therefore, it could be concluded that inulin was completely dissolved in all the porridges and that concentration was not sufficient for gel formation.

The protective effect of inulin on starch granules to reduce swelling and resist degradation has previously been reported for inulin-enriched white sauces, leading to a less compact and cohesive continuous phase (Guardeño et al., 2012, 2013). Since the concentration of inulin reached in the porridges was relatively low, the density of inulin chains would not be able to reach a critical crowding effect. Therefore, inulin would act as diluent in the porridges without interacting synergistically with starch, as has been reported for mashed potato (Alvarez, Fernández, Solas, & Canet, 2011). Contrarily, other studies on inulin-enriched products, such as yoghurt, have reported a marked increase in the consistency with the addition of inulin, which has been attributed to the generation of a second network supporting the one of casein (Guggisberg et al., 2009). Kip et al. (2006) concluded that inulin may also be partially involved in the formation of the protein structural network during yoghurt fermentation by complexation with protein aggregates. Differential scanning calorimetry analyses on potato starch-inulin gels have also suggested that gelatinization of potato starch with inulin produced binary gel of common network that could result from the competition of both components for water (Krystyjan, Ciesielski, Khachatryan, Sikora, & Tomasik, 2015). Aravind et al. (2012) hypothesized that relatively small amounts of inulin, similar to those added to rye porridge in this study, support formation of a well-developed protein–fiber

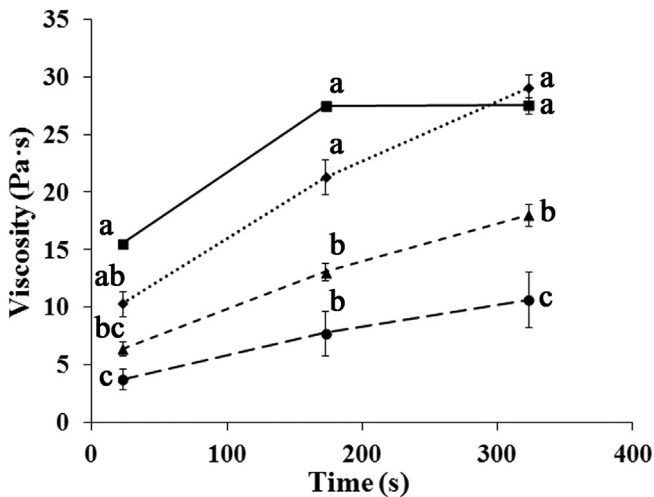


**Fig. 4.** Viscosity profiles of rye porridge with different inulin and gluten proportions derived from measurement periods in the RVA. Control (—■—), 3:9 (··◆··), 6:6 (—▲—), 9:3 (—●—). Values are least square means ± standard errors. Different letters at specific time points indicate statistically significant differences between products ( $P < 0.05$ ).

matrix subsequently acting as a physical barrier to starch-degrading enzymes based on *in vitro* starch digestion tests. In this way, the addition of inulin to rye porridge could limit starch digestibility and have later implications for the glycemic response. Consequently it could potentially be utilized for the development of products with reduced glycemic index.

#### 4. Conclusions

Addition of inulin and gluten to rye porridge partly hindered starch gelatinization due to their water binding capacity. Inulin was completely solubilized and preferentially located in detached starch granules of the aqueous phase of the porridge, which could be due to interaction between inulin and amylose molecules. The solubilized inulin would create a protective layer around the starch granules limiting their swelling and the amylose release. This protective matrix around the starch granules, together with the water binding capacity of inulin and gluten, would explain the lower viscosity values observed in the porridges with added inulin and gluten. On the other hand, the presence of gluten particles would contribute to increased viscosity and could explain the higher viscosity observed for the porridge with highest gluten content compared to the other enriched porridges. This feature may lead to limited accessibility of starch-degrading enzymes, which could affect starch digestibility *in vivo* and glycemic index.

#### Acknowledgments

The authors thank Dr. Rikard Landberg for discussions and comments related to the current work, Isabella Lee for her input on ingredients and sample preparation, and Lantmännen for providing the products for the study.

#### References

- Alvarez, M. D., Fernández, C., Solas, M. T., & Canet, W. (2011). Viscoelasticity and microstructure of inulin-enriched mashed potatoes: influence of freezing and cryoprotectants. *Journal of Food Engineering*, *102*, 66–76.
- Aravind, N., Sissons, M. J., Fellows, C. M., Blazek, J., & Gilbert, E. P. (2012). Effect of inulin soluble dietary fibre addition on technological, sensory, and structural properties of durum wheat spaghetti. *Food Chemistry*, *132*, 993–1002.
- Bishay, I. E. (1998). Rheological characterization of inulin. In P. A. Williams, & G. O. Phillips (Eds.), *Gums and stabilizers for the food industry*. London: Royal Society of Chemistry.
- Brennan, C. S., Kuri, V., & Tudorica, C. M. (2004). Inulin-enriched pasta: effects on textural properties and starch degradation. *Food Chemistry*, *86*, 189–193.
- Cani, P. D., Dewever, C., & Delzenne, N. M. (2004). Inulin-type fructans modulate gastrointestinal peptides involved in appetite regulation (glucagon-like peptide-1 and ghrelin) in rats. *British Journal of Nutrition*, *92*, 521–526.
- Chen, J.-s., Deng, Z.-y., Wu, P., Tian, J.-c., & Xie, Q.-g. (2010). Effect of gluten on pasting properties of wheat starch. *Agricultural Sciences in China*, *9*, 1836–1844.
- Day, L. (2011). Wheat gluten: production, properties and application. In G. O. Phillips, & P. A. Williams (Eds.), *Handbook of food proteins* (pp. 267–288). Woodhead Publishing.
- Dornez, E., Holopainen, U., Cuyvers, S., Poutanen, K., Delcour, J. A., Courtin, C. M., et al. (2011). Study of grain cell wall structures by microscopic analysis with four different staining techniques. *Journal of Cereal Science*, *54*, 363–373.
- Esteller, M. S., Pitombo, R. N. M., & Lannes, S. C. S. (2005). Effect of freeze-dried gluten addition on texture of hamburger buns. *Journal of Cereal Science*, *41*, 19–21.
- Fung, T. T., Hu, F. B., Pereira, M. A., Liu, S., Stampfer, M. J., Colditz, G. A., et al. (2002). Whole-grain intake and the risk of type 2 diabetes: a prospective study in men. *The American Journal of Clinical Nutrition*, *76*, 535–540.
- Groves, K. (2006). Microscopy: a tool to study ingredient interactions in foods. In A. G. Gaonkar, & A. McPherson (Eds.), *Ingredient interactions: Effects on food quality*. Boca Raton: CRC Press.
- Guardoño, L. M., Hernando, I., Llorca, E., Hernández-Carrión, M., & Quiles, A. (2012). Microstructural, physical, and sensory impact of starch, inulin, and soy protein in low-fat gluten and lactose free white sauces. *Journal of Food Science*, *77*, C859–C865.
- Guardoño, L. M., Vázquez-Gutiérrez, J. L., Hernando, I., & Quiles, A. (2013). Effect of different rice starches, inulin, and soy protein on microstructural, physical, and sensory properties of low-fat, gluten, and lactose free white sauces. *Czech Journal of Food Sciences*, *31*, 575–580.
- Guggisberg, D., Cuthbert-Steven, J., Piccinali, P., Bütikofer, U., & Eberhard, P. (2009). Rheological, microstructural and sensory characterization of low-fat and whole milk set yoghurt as influenced by inulin addition. *International Dairy Journal*, *19*, 107–115.
- Icoz, D. Z., & Kokini, J. L. (2008). Theoretical analysis of predictive miscibility of carbohydrate polymers – software calculations for inulin–amylopectin systems. *Carbohydrate Polymers*, *72*, 52–59.
- Icoz, D. Z., Moraru, C. I., & Kokini, J. L. (2005). Polymer–polymer interactions in dextran systems using thermal analysis. *Carbohydrate Polymers*, *62*, 120–129.
- Isaksson, H., Tillander, I., Andersson, R., Olsson, J., Fredriksson, H., Webb, D.-L., et al. (2012). Whole grain rye breakfast – Sustained satiety during three weeks of regular consumption. *Physiology & Behavior*, *105*, 877–884.
- Johansson, D., Krona, A., & Stading, M. (2012). Influence of surface lipids in commercial zein on microstructure and rheological properties of gluten-free dough. *Annual Transactions of the Nordic Rheology Society*, *20*, 247–251.
- Kim, Y., Faqih, M. N., & Wang, S. S. (2001). Factors affecting gel formation of inulin. *Carbohydrate Polymers*, *46*, 135–145.
- Kip, P., Meyer, D., & Jellema, R. H. (2006). Inulins improve sensoric and textural properties of low-fat yoghurts. *International Dairy Journal*, *16*, 1098–1103.
- Krystyan, M., Ciesielski, W., Khachatryan, G., Sikora, M., & Tomasik, P. (2015). Structure, rheological, textural and thermal properties of potato starch – inulin gels. *LWT – Food Science and Technology*, *60*, 131–136.
- Landberg, R., Andersson, S.-O., Zhang, J.-X., Johansson, J.-E., Stenman, U.-H., Adlercreutz, H., et al. (2010). Rye whole grain and bran intake compared with refined wheat decreases urinary C-peptide, plasma insulin, and prostate specific antigen in men with prostate cancer. *The Journal of Nutrition*, *140*, 2180–2186.
- Lobato, L. P., Grossmann, M. V. E., & Benassi, M. T. (2009). Inulin addition in starch-based dairy desserts: Instrumental texture and sensory aspects. *Food Science and Technology International*, *15*, 317–323.
- Lundin, L., Golding, M., & Wooster, T. J. (2008). Understanding food structure and function in developing food for appetite control. *Nutrition & Dietetics*, *65*, S79–S85.
- Manno, D., Filippo, E., Serra, A., Negro, C., De Bellis, L., & Miceli, A. (2009). The influence of inulin addition on the morphological and structural properties of durum wheat pasta. *International Journal of Food Science & Technology*, *44*, 2218–2224.
- Mars, M., Hogenkamp, P. S., Gosses, A. M., Stafleu, A., & De Graaf, C. (2009). Effect of viscosity on learned satiation. *Physiology & Behavior*, *98*, 60–66.
- McClements, D. J., Decker, E. A., Park, Y., & Weiss, J. (2009). Structural design principles for delivery of bioactive components in nutraceuticals and functional foods. *Critical Reviews in Food Science and Nutrition*, *49*, 577–606.
- Morris, C., & Morris, G. A. (2012). The effect of inulin and fructo-oligosaccharide supplementation on the textural, rheological and sensory properties of bread and their role in weight management: a review. *Food Chemistry*, *133*, 237–248.
- Peressini, D., & Sensidoni, A. (2009). Effect of soluble dietary fibre addition on rheological and breadmaking properties of wheat doughs. *Journal of Cereal Science*, *49*, 190–201.
- Roberfroid, M. B. (2007). Inulin-type fructans: functional food ingredients. *The Journal of Nutrition*, *137*, 2493S–2502S.
- Rodríguez-García, J., Puig, A., Salvador, A., & Hernando, I. (2012). Optimization of a sponge cake formulation with inulin as fat replacer: structure, physicochemical, and sensory properties. *Journal of Food Science*, *77*, C189–C197.
- Rosén, L. A. H., Östman, E. M., & Björck, I. M. E. (2011). Effects of cereal breakfasts on postprandial glucose, appetite regulation and voluntary energy intake at a subsequent standardized lunch; focusing on rye products. *Nutrition Journal*, *10*, 7–7.
- Rubel, I. A., Pérez, E. E., Manrique, G. D., & Genovese, D. B. (2015). Fibre enrichment of wheat bread with Jerusalem artichoke inulin: effect on dough rheology and bread quality. *Food Structure*, *3*, 21–29.
- Sai Manohar, R., Urmila Devi, G. R., Bhattacharya, S., & Venkateswara Rao, G. (2011). Wheat porridge with soy protein isolate and skimmed milk powder: rheological, pasting and sensory characteristics. *Journal of Food Engineering*, *103*, 1–8.
- Solowiej, B., Glibowski, P., Muszyński, S., Wydrych, J., Gawron, A., & Jeliński, T. (2015). The effect of fat replacement by inulin on the physicochemical properties and microstructure of acid casein processed cheese analogues with added whey protein polymers. *Food Hydrocolloids*, *44*, 1–11.
- Tárrega, A., Torres, J. D., & Costell, E. (2011). Influence of the chain-length distribution of inulin on the rheology and microstructure of prebiotic dairy desserts. *Journal of Food Engineering*, *104*, 356–363.
- Tolstoguzov, V. (2003). Thermodynamic considerations of starch functionality in foods. *Carbohydrate Polymers*, *51*, 99–111.
- Wang, J., Rosell, C. M., & Benedito de Barber, C. (2002). Effect of the addition of different fibres on wheat dough performance and bread quality. *Food Chemistry*, *79*, 221–226.
- Zhang, W., Xiao, S., Samaraweera, H., Lee, E. J., & Ahn, D. U. (2010). Improving functional value of meat products. *Meat Science*, *86*, 15–31.
- Zimeri, J. E., & Kokini, J. L. (2003a). Morphological characterization of the phase behavior of inulin–waxy maize starch systems in high moisture environments. *Carbohydrate Polymers*, *52*, 225–236.
- Zimeri, J. E., & Kokini, J. L. (2003b). Phase transitions of inulin–waxy maize starch systems in limited moisture environments. *Carbohydrate Polymers*, *51*, 183–190.



## A new milk-clotting enzyme produced by *Bacillus* sp. P45 applied in cream cheese development



Ailton Cesar Lemes<sup>a</sup>, Yanina Pavón<sup>b</sup>, Sandra Lazzaroni<sup>b</sup>, Sergio Rozycki<sup>b</sup>, Adriano Brandelli<sup>c</sup>, Susana Juliano Kalil<sup>a,\*</sup>

<sup>a</sup> EQA, Universidade Federal do Rio Grande, Rio Grande, Brazil

<sup>b</sup> ITA, Universidad Nacional del Litoral, Santa Fé, Argentina

<sup>c</sup> ICTA, Universidade Federal do Rio Grande do Sul, Porto Alegre, Brazil

### ARTICLE INFO

#### Article history:

Received 22 June 2015

Received in revised form

8 September 2015

Accepted 15 October 2015

Available online 19 October 2015

#### Keywords:

Keratinase

Proteases

Chia

Quinoa

Cream cheese

### ABSTRACT

The growing demand for natural coagulants led to an increased necessity for rennet substitutes, promoting a search for new sources of proteases with coagulant properties. The aim of this study was to investigate the application of a bacterial enzyme as a novel milk-clotting protease in the development of cream cheese enriched with chia and quinoa flour. At the concentration of 30 mg/mL, the milk-clotting strength was similar to that observed for commercial chymosin, demonstrating the enzyme ability to catalyze the hydrolysis of milk casein. The cheese developed showed high water retention ( $\geq 99.0\%$ ) and consequently low syneresis process. The results indicate that the product made using the enzyme showed adequate sanitary conditions and technological characteristics indicated that the product is highly stable and viable.

© 2015 Elsevier Ltd. All rights reserved.

### 1. Introduction

Obtaining natural milk coagulants is a challenge since rennet availability is limited compared with the increasing demand of the dairy industry. Natural coagulants of animal origin are expensive, and their consumption has been restricted due to religious or dietary reasons. This scenario has led to a growing demand for novel rennet substitutes, promoting a search for new sources of proteases with coagulant properties (Ahmed, Morishima, Babiker, & Mori, 2009; Jacob, Jaros, & Rohm, 2011; Mazorra-Manzano et al., 2013).

Different proteases have been used for this purpose, including those extracted from vegetables (Corrons, Bertucci, Liggieri, Lopez, & Bruno, 2012; Galán, Cabezas, & Fernández-Salguero, 2012) and animals (Rolet-Repecaud et al., 2013; Shamtsyan, Dmitriyeva, Kolesnikov, & Denisova, 2014; Trujillo, Guamis, Laencina, & Lopez, 2000), but their applications may be limited by factors, such as cultivation and climatic variations, which can affect their production and supply.

Thus, microbial enzymes are attractive and have been tested in

milk coagulation (Daroit et al., 2012). *Bacillus* sp. P45, isolated from the intestine of Jaraqui fish (*Piaractus mesopotamicus*) originating from the Amazon basin (Sirtori, Cladera-Olivera, Lorenzini, Tsai, & Brandelli, 2006), produces an enzyme that presents great potential for protein hydrolysis (Daroit, Correa, & Brandelli, 2009). A keratinolytic protease was purified and characterized as a subtilisin-like serine protease of about 26 kDa that hydrolyses casein at high rates (Daroit, Corrêa, Segalin, & Brandelli, 2010). This enzyme also produces bioactive hydrolysates during proteolysis of ovine casein (Daroit et al., 2012). Therefore, this protease may be useful for development of dairy products through milk-clotting processes.

Dairy products enriched with bioactive compounds have attracted increased consumer interest. Quinoa (*Chenopodium quinoa* Willd.) is a seed recognized for its high content of essential amino acids, protein, fiber and minerals (Madl, Sterk, & Mittelbach, 2006; Nsimba, Kikuzaki, & Konishi, 2008). Also, chia (*Salvia hispanica* L.) presents high contents of protein, fiber (Capitani, Spotorno, Nolasco, & Tomas, 2012; Marineli et al., 2014) and elevated amount of  $\alpha$ -linolenic acids (Ayerza & Coates, 2011). Both seeds have a high antioxidant activity (Capitani et al., 2012), associated with protection against lipid oxidation, inflammatory processes, cancer and other diseases related to oxidative stress (Gawlik-Dziki et al., 2013). This suggests that quinoa and chia can be useful as functional ingredients in food

\* Corresponding author.

E-mail address: [dqmsjk@furg.br](mailto:dqmsjk@furg.br) (S.J. Kalil).

formulations (Marineli et al., 2014).

The aim of this study was to investigate the milk-clotting ability of a protease obtained from *Bacillus* sp. P45 and apply the enzyme in the development of cream cheese enriched with chia and quinoa flour.

## 2. Materials and methods

### 2.1. Microorganism, inoculum, cultivation and enzyme purification

The enzyme was produced by submerged cultivation of *Bacillus* sp. P45 using feather meal as a substrate (Daroit, Correa, & Brandelli, 2011), and then purified using aqueous two-phase system integrated into the diafiltration process (Sala et al., 2014). The enzyme preparation containing the partially purified protease with molecular mass around 26–28 kDa (Daroit et al., 2010; Sala et al., 2014) was lyophilized and stored at 4 °C for use in later steps.

### 2.2. Milk-clotting enzyme activity (MCA)

The MCA was examined by the method of Berridge (1952) using the crude enzyme, purified enzyme, and commercial chymosin (Agrolac Parana<sup>®</sup>) as standard. Milk aliquots were incubated at 30 °C and 1 mL of the enzyme solution (10 to 50 mg/mL), was added. The clotting time was determined from the clot formation in the tube wall. MCA is defined as the amount of enzyme that clots 10 mL of reconstituted skim milk in 100 seconds at 30 °C (Eq. (1)). The correlation between the inverse of the enzyme concentration and the MCA was done to predict the coagulation time and the coagulant activity of the enzymes.

$$MCA = \frac{10 \cdot \text{volume of milk}}{\text{clotting time (s)} \cdot \text{coagulant volume}} \quad (1)$$

### 2.3. Cream cheese development

The cream cheese enriched with chia and quinoa flour was produced in the Dairy Institute of the UNL (Santa Fé, Argentina) using the purified protease obtained from *Bacillus* sp. P45 that was standardized in relation to the milk-clotting activity of commercial chymosin enzyme. The cheese was obtained by mixing milk powder, cream and water at 50 °C for 5 min (Fig. 1). Then, the milk was pasteurized (75 °C/15 s) and homogenized (150 atm). Milk was pasteurized again (75 °C/15 s), adjusted to 50 °C and added espina corona, chia and quinoa flour, whey protein concentrate, milk powder and potassium sorbate. The mixture was stirred for 10 min, pasteurized (75 °C/15 s) and cooled (45 °C) for calcium citrate addition. Milk was placed in a thermostatic bath at 40 °C and a starter culture containing *Streptococcus thermophilus* and *Lactobacillus delbrueckii* subsp. *bulgaricus*, and the purified enzyme were added. After the clotting process, the curd mass was homogenized (50 atm) and cooled (15 °C). The formulations were stored in sealed packages at 4 °C. The product was evaluated in relation to pH and acidity (every 5 days), texture profile and water retention (days 1, 13 and 25 of storage), water activity and total solids (13th day of storage). The chemical composition and microbiological analyses were performed on the 25th day of storage. All samples were made by the same process, however, presented different relative concentrations of cream, chia and quinoa flour (Table 1), as previously established by the research group.

### 2.4. Cream cheese profile

#### 2.4.1. pH and acidity determination during cream cheese storage

The pH was measured potentiometrically and the acidity by

direct titration with 0.1 mol/L NaOH (AOAC, 2005). The results were determined as Dornic degrees and converted to lactic acid concentration (mol/L).

#### 2.4.2. Water retention and water activity

Water retention (%WR) analyses were performed during samples storage by centrifugation and gravimetry. The %WR was determined by centrifugation of the samples (1000× g, 20 min, at 4 °C) stored at 4 °C in suitable containers containing 50 g of cheese. After centrifugation, the supernatant was drained and weighed to determine the water retention (Eq. (2)).

$$\%WR = 100 - \left( \frac{\text{Initial weight} - \text{final weight}}{\text{initial weight}} \right) \times 100 \quad (2)$$

The %WR by gravity was determined by weighing the tubes containing the samples stored under the same conditions. The supernatant fluids present on the surface were drained and weighed to determine the parameters. The water activity was determined at 2 °C using Aqua Lab CX-2T equipment.

#### 2.4.3. Texture profile

The texture profile was determined using an Instron Bluehill<sup>®</sup> texturometer from a stress curve in Newton (N) versus time (s). The following mechanical properties were determined: hardness, adhesiveness, springiness, cohesiveness, gumminess, chewiness and resilience. The parameters used in the tests were double penetration of 30 mm into the samples, speed penetration of 1 mm/s, bristle of 10 N, penetrometer diameter of 12 mm and cylinder diameter of 36 mm at 10 °C (Pons & Fiszman, 1996; Santini et al., 2007).

#### 2.4.4. Chemical and microbiological analyses

The chemical composition (moisture, ash, protein, fiber and lipids) was determined by standard procedures and carbohydrates were calculated by difference (AOAC, 2005). Caloric values were calculated using conversion factors based on the chemical composition from the sum of the protein content × 4, lipids × 9 and carbohydrates × 4 (Horwitz, 1997). Microbiological analyses were performed for *Staphylococcus aureus*, *Salmonella* spp., *Listeria monocytogenes*, total and fecal coliforms, aerobic mesophilic, molds and yeasts, following standard protocols (Doores, Salfinger, & Tortorello, 2013).

### 2.5. Statistical analysis

Data were subjected to analysis of variance to detect significant differences between treatments by Tukey's test. Differences were considered significant when  $P < 0.05$ .

## 3. Results and discussion

### 3.1. Milk-clotting activity

Both crude and purified enzyme at the concentration of 30 mg/mL showed similar milk-clotting capability to that observed for commercial coagulant (Table 2), demonstrating the potential to be used as an alternative coagulant. The results indicated that MCA was dependent of the enzyme concentration; the milk-clotting time decreased as the enzyme concentration increased, similar to that observed for plant enzymes (Ahmed et al., 2009; Beka et al., 2014; Chazarra, Sidrach, Lopez-Molina, & Rodriguez-Lopez, 2007). A clear linear correlation between the inverse of the enzyme

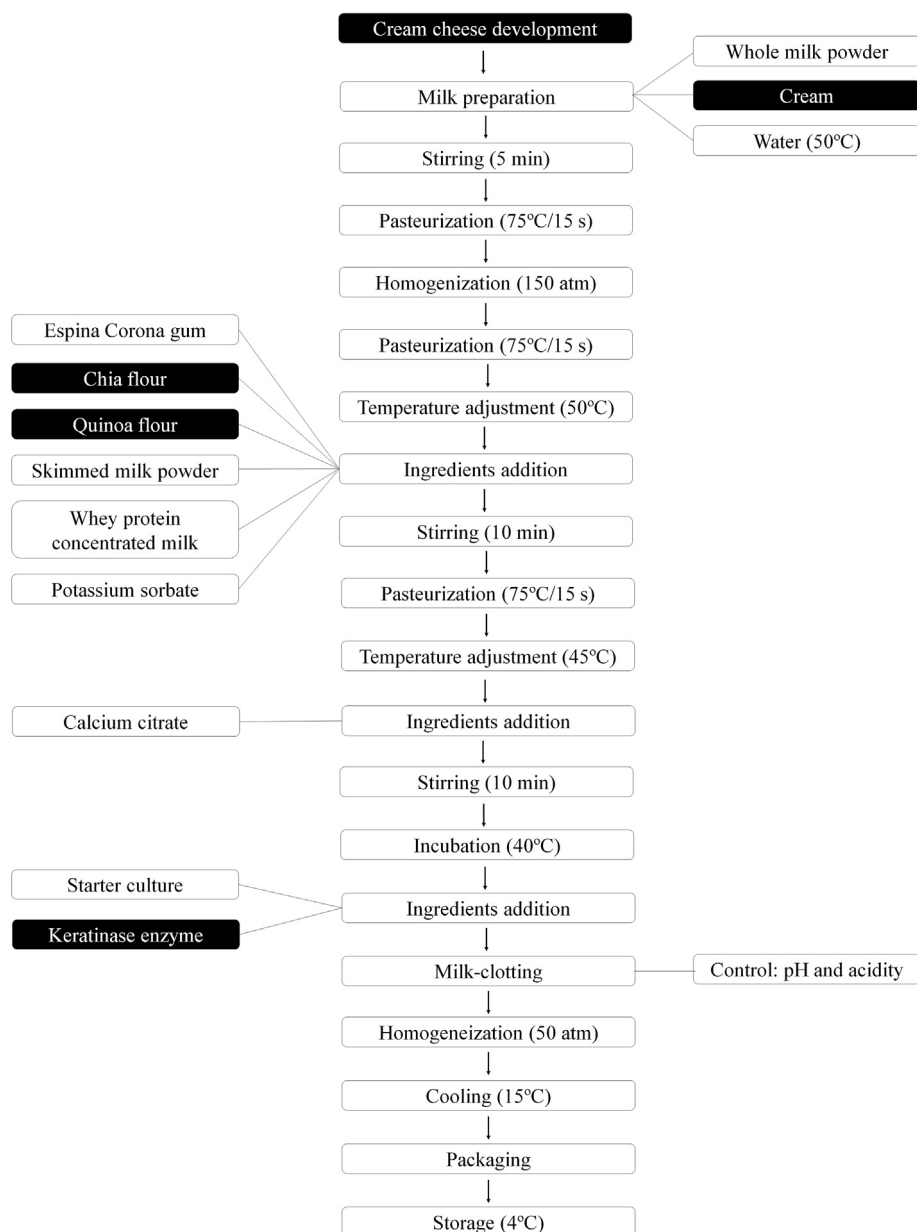


Fig. 1. Flowchart of cream cheese development.

Table 1

Cream cheese formulations made from purified enzyme.

Ingredients (%)	Formulations				
	1	2	3	4	5
Cream	6.0	10.0	6.0	10.0	8.0
Chia flour	4.0	4.0	1.0	1.0	2.5
Quinoa flour	1.0	1.0	4.0	4.0	2.5

concentration and the MCA values was verified for the crude and the purified enzyme (Crude enzyme =  $36.1 + 2034.9^*x$ ,  $r^2 = 0.9994$ ; Purified enzyme =  $23.9 + 2390.6^*x$ ,  $r^2 = 0.9995$ ), thus making it possible to predict the coagulation time and the coagulant activity of the enzyme. The clots formed by the three enzymes (crude, purified and commercial) showed the same characteristics: stability and transparent whey exudate. These results showed that both the purified and crude enzyme could be used as alternative milk coagulants.

Table 2

Milk-clotting activity of crude, purified and commercial enzyme.

Enzyme	(mg/mL)	Clotting time (s)	Chymosin unit
Crude	10	$239 \pm 7.2^e$	$0.42 \pm 1.10^{-2e}$
	20	$140 \pm 2.0^d$	$0.71 \pm 1.10^{-2d}$
	30	$105 \pm 1.7^c$	$0.95 \pm 2.10^{-2c}$
	40	$85 \pm 1.5^b$	$1.17 \pm 2.10^{-2b}$
	50	$76 \pm 2.6^a$	$1.32 \pm 5.10^{-2a}$
Purified	10	$264 \pm 4^e$	$0.38 \pm 5.10^{-3e}$
	20	$141 \pm 3^d$	$0.71 \pm 0.01^d$
	30	$105 \pm 2^c$	$0.96 \pm 0.02^c$
	40	$82 \pm 2^b$	$1.22 \pm 0.02^b$
	50	$74 \pm 2^a$	$1.36 \pm 0.03^a$
Commercial	1 mL	$106 \pm 1^c$	$0.96 \pm 0.01^c$

The statistical analysis of the means was conducted using Tukey's test. The same letters in the columns represent no significant differences at the significance level of 5%.

The optimal coagulant activity for dairy product development is crucial because of its influence on the technological properties of the product, including the texture parameters (Børsting, Stallknecht, Vogensen, & Ardö, 2015) and the sensory attributes (Galán, Prados, Pino, Tejada, & Fernández-Salguero, 2008). Despite the similarity in the MCA, the use of purified enzyme could be advantageous since that preliminary sensory tests, conducted by trained evaluators, indicated that the crude enzyme caused intense acetic odor and brown coloration, affecting the color and aroma of the final product, and therefore, consumer acceptance. Thus, the purified enzyme was chosen to be applied in the cream cheese development.

### 3.2. Cream cheese profile

#### 3.2.1. pH and acidity

A decline of pH and proportional increase in lactic acid production was observed in all samples (Fig. 2). The pH ranged from 6.6 to 6.3 at the beginning to 5.3 at the end of fermentation process. The lactic acid concentration ranged from 0.02 to 0.03 at the initial phase, reaching 0.06–0.1 mol/L at the end of fermentation process, lasting approximately 5 h.

The pH reduction and increase in acidity occurs due to lactic acid fermentation that is initiated when the starter culture is added. The microorganisms perform the hydrolysis of lactose into glucose and galactose, and the monosaccharides are subsequently transformed

into lactic acid. The lactic acid production causes a drop in the pH during fermentation and storage because most of the enzymes remain active and the microorganisms remain viable. However, this effect is less marked during the storage, as low temperatures are used (Rojas-Castro, Chacón-Villalobos, & Pineda-Castro, 2007). In addition to provide specific sensory characteristics, pH reduction is important to prevent the growth of pathogenic bacteria. The pH variation during storage also depends on the buffering capacity of the cheese, which is related to the amount of protein and minerals, ammonium formation, and/or lactic acid catabolism (Lawrence, Heap, & Gilles, 1984; Merheb-Dini, Garcia, Penna, Gomes, & da Silva, 2012).

A reduction in pH (Fig. 3A) and an increase of acidity (Fig. 3B) was observed in all formulations during the storage period. During the first ten days, the pH decreased and lactic acid production was more pronounced than in subsequent periods, with a tendency to stabilize at the end of storage. This could be due to several factors, including the inhibition of the enzymatic activity present in the lactic culture, the viability of the microbial load, represented by the starter culture employed, and the lactose depletion combined with low temperature (Rojas-Castro et al., 2007).

The pH stabilizing effect at the end of the storage is a natural and desirable phenomenon during the development of fermented dairy products and has been previously described in several studies. Additionally, the pH values and acidity observed in this study are comparable with those reported by other authors (Deegan, Holopainen, McSweeney, Alatossava, & Tuorila, 2014; Olmedo,

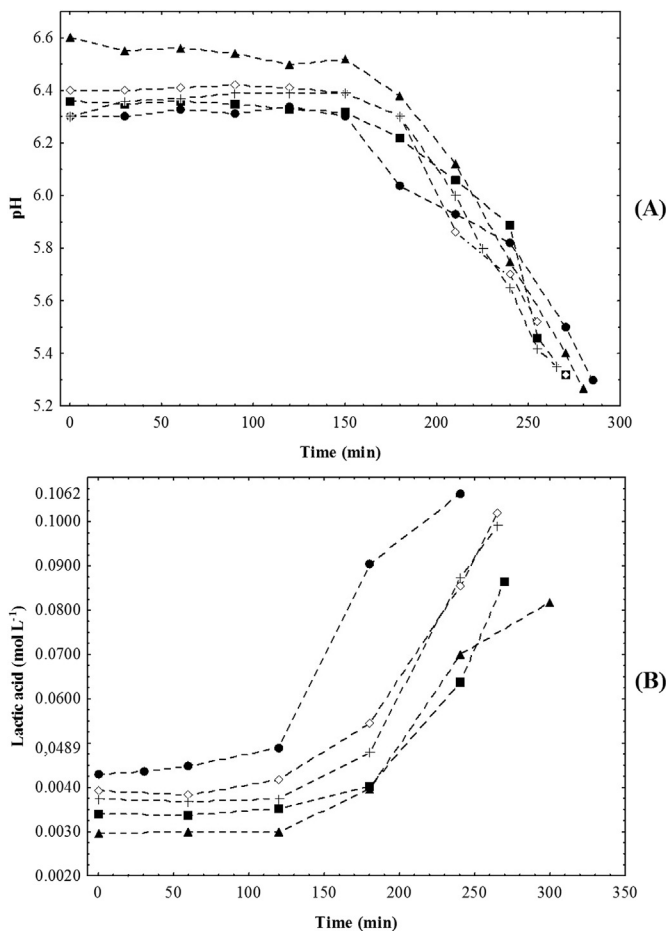


Fig. 2. pH (A) and acidity (B) of the formulations prepared from purified enzyme during the fermentation process. (●)1, (■)2, (◇)3, (▲)4 and (+)5.

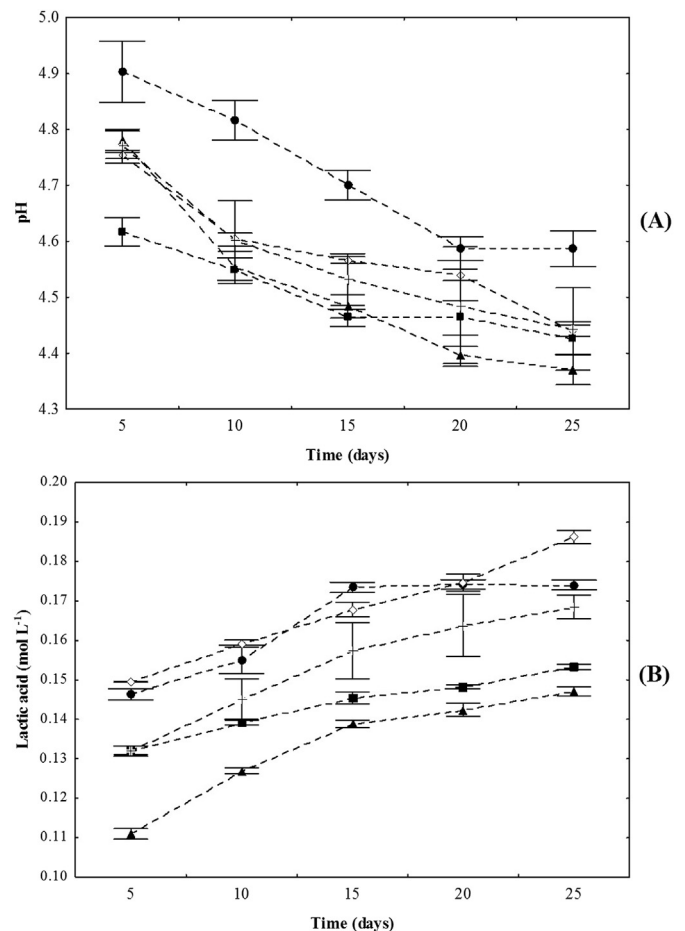


Fig. 3. pH (A) and acidity (B) of the five formulations prepared from purified keratinase enzyme during the storage by 25 days. (●)1, (■)2, (◇)3, (▲)4 and (+)5.

Nepote, & Grosso, 2013) and are consistent with those typically expected for this product.

### 3.2.2. Water activity and chemical composition

The chemical composition of the formulations (Table 3) was similar to other cream cheeses described in the literature (Souza, Carneiro, Pinto, Souza, & Stephani, 2012; Zulkurnain, Goh, Karim, & Liong, 2008). The lipid concentration was proportional to the content of cream added during the development and was significantly higher for formulations 2, 4 and 5. These formulations presented 10% lipids, while samples 1 and 3 showed 7.0 and 5.5% lipids, respectively. The moisture content of all samples was greater than 70.0%, and is characterized by specific legislation (ANVISA, 2001) as a product of very high humidity.

The  $a_w$  values were similar for all samples, regardless the amount of cream, chia or quinoa flour used. The  $a_w$  determination is important because it is related to the available water, which can be used for deteriorative reactions or microbial metabolism (Ostrowska-Ligeza & Lenart, 2015). The  $a_w$  values, approximately 0.96, indicate that the product would be susceptible to most bacteria and fungi, but the acidic pH of the cheese protects against several pathogenic bacteria.

The fiber content varied from 3.00 to 4.96% and formulation 3 showed the highest value. The US Food and Drug Administration allows foods to be labeled as 'a good source of fiber' or 'high fibre' if they contain more than 2.5 g or 5.0 g of dietary fibre per serving, respectively (Jin, Hsien, & Huff, 1994). Development of products with high sensory acceptance and high fiber contents could minimize dietary disturbances and stimulate a healthy lifestyle. The increase in life expectancy has generated a great interest in foods that are rich in fibers, which may prevent some diseases such as diabetes mellitus, cardiovascular diseases, obesity and colon cancer (Tharanathan & Mahadevamma, 2003).

The protein content ranged from 5.4 to 7.4% and was significantly higher for formulations 1 and 3, with lower quantities of cream and lower amounts of chia and quinoa flour, respectively. The incorporation of these products may be indicated as a protein source, especially with regard to the contribution of the essential amino acids contained in the seeds of chia and quinoa (Madl et al., 2006).

### 3.2.3. Water retention

Regarding the water retention, no significant differences were observed among the formulations for the initial period of storage. The values were identical when evaluated by gravity (Fig. 4A) and very similar by centrifugation (Fig. 4B).

A decrease in the water retention causes the syneresis process, which refers to the serum that is released from the gel structure of the cheese and accumulates on the surface. An increase in the

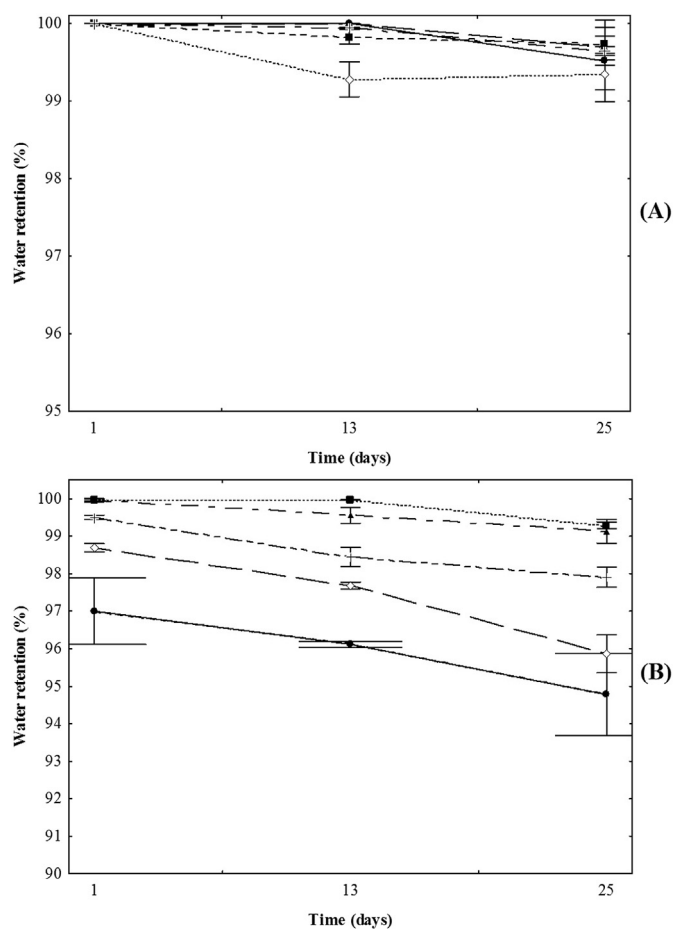


Fig. 4. Water retention (%) determined by gravity (A) and centrifugation (B) of the five formulation: (●) 1, (■) 2, (◇) 3, (▲) 4 and (+) 5.

syneresis process was observed in the 13th day of storage, with a significant elevation ( $P \leq 0.05$ ) during storage for 25 days, which can be verified by reduction of water retention values (Fig. 4). This occurrence was more evident when the samples were evaluated by centrifugation, indicating a greater water release from the cheese matrix.

Despite the increase in water release, the syneresis process verified by gravity analysis that simulates the product exposure under normal storage conditions was practically null, indicating a low risk of syneresis process and consequently absence of serum on the cheese surface. This allows us to assume that the enzyme application, in combination with the components used in the cheese, produces clots with high stability and water retention. The

Table 3  
Chemical composition of cream cheese developed.

Components (%) <sup>a</sup>	Formulations				
	1	2	3	4	5
Moisture	72.24 ± 0.46 <sup>bc</sup>	73.42 ± 0.32 <sup>ab</sup>	72.04 ± 0.52 <sup>c</sup>	74.2 ± 0.51 <sup>a</sup>	73.01 ± 0.1 <sup>abc</sup>
Protein	7.4 ± 0.21 <sup>a</sup>	5.7 ± 0.37 <sup>c</sup>	6.9 ± 0.62 <sup>ab</sup>	5.4 ± 0.42 <sup>c</sup>	6.2 ± 0.27 <sup>bc</sup>
Lipids	7.0 ± 0.72 <sup>b</sup>	10.0 ± 0.47 <sup>a</sup>	5.5 ± 0.62 <sup>b</sup>	10.0 ± 0.25 <sup>a</sup>	10.0 ± 0.82 <sup>a</sup>
Fiber	3.54 ± 0.32 <sup>b</sup>	3.0 ± 0.81 <sup>b</sup>	4.96 ± 0.09 <sup>a</sup>	3.44 ± 0.07 <sup>b</sup>	4.08 ± 0.68 <sup>ab</sup>
Ash	1.69 ± 0.02 <sup>a</sup>	1.29 ± 0.04 <sup>d</sup>	1.59 ± 0.02 <sup>b</sup>	1.23 ± 0.00 <sup>d</sup>	1.37 ± 0.03 <sup>cd</sup>
Carbohydrate	8.13	6.59	9.01	5.7	5.34
Water activity	0.962 ± 0.004 <sup>a</sup>	0.962 ± 0.002 <sup>a</sup>	0.958 ± 0.001 <sup>a</sup>	0.962 ± 0.004 <sup>a</sup>	0.961 ± 0.002 <sup>a</sup>
Calories (kcal)	125.12	139.16	113.14	134.4	136.16

The statistical analysis of the means employed Tukey's test, and different letters in the same row represent significant differences at the significance level of 5%.

<sup>a</sup> Except for water activity and caloric value.

stability may also be favored by the addition of quinoa and chia because they also present a high water retention capacity (Bhargava, Shukla, & Ohri, 2006; Capitani et al., 2012), especially due to the high protein content. In addition, stabilizers used in the samples, such as espina corona gum tend to “bind” water in the gel structure, generally improving the hydration of proteins. Despite the reduction of the %WR values during storage ( $P < 0.05$ ), the lower value obtained with respect to gravity (99.3%) was insignificant and does not affect this quality attribute. The high protein and fat contents contribute to a stable structure, retaining water during storage (Zulkurnain et al., 2008). The formulations 2 and 4, with the highest cream concentration, showed the highest water retention when measured by centrifugation, and, consequently, a lower syneresis process during the storage, mainly due to the emulsifying properties (Mateo et al., 2009). The opposite was also observed; samples with less cream addition showed the greatest water release from the cheese matrix.

### 3.2.4. Texture profile

The texture profile of the formulations was evaluated in different storage times (Table 4). In general, all parameters showed significant differences ( $P < 0.05$ ) as a function of time and the formulations studied. The elasticity was the only parameter that showed no significant difference, suggesting no change in the recovery of initial cheese dimensions after the removal of the deforming force (Santini et al., 2007).

Formulation 3, with the highest quinoa and less cream content, had the highest hardness. This suggests that the high capacity of quinoa to absorb water, combined with a lower fat concentration, which is responsible for creaminess and smoothness, can contribute to a greater resistance to deformation (Santini et al., 2007). Formulations 1, 2 and 5 showed an increase in hardness on the 13th day of storage, while formulations 3 and 4 showed an increase in hardness on the 25th day of storage.

The adhesiveness was higher for samples with higher quinoa contents, indicating the formation of a resistant structure that requires a greater force for removing the cheese from the contact surface of the mouth (Bryant, Ustunol, & Steffe, 1995; Karaman & Akalin, 2013). Formulations 1, 2 and 3 showed no significant variation in adhesiveness during the 25 days of storage. However, formulations 4 and 5 showed an increase in adhesiveness on the 13th day of storage.

The cohesiveness was significantly higher for formulation 1, where higher chia and lower cream contents were used. These conditions favored the production of a more elastic gel that requires

a greater effort to deform the cream cheese. There was no change in the cohesiveness parameter for formulations 1 and 5. However, this parameter was significantly altered in formulations 2, 3 and 4 on the 25th day of storage.

The gumminess and chewiness showed the same behavior. The highest values were found for samples with higher quinoa contents, demonstrating their influence on the texture profile. Both gumminess and chewiness remained equal in formulation 3 during 25 days of storage. However, there was significant difference for formulations 1, 2 and 5 on the 13th day and a significant change in these attributes for formulation 4 on the 25th day of storage.

Changes in the texture profile during the storage can be triggered by proteolysis, glycolysis, lipolysis, and pH changes. These alterations, in addition to the full solubility of the cheese constituents and the continuous enzymatic activities cause a change in the texture (Lucy, Johnson, & Horne, 2003). Furthermore, the increase in acidity during the storage may also cause changes in the characteristics of protein aggregates and in the texture profile (Queiroga et al., 2013).

In general, the different formulations showed no significant variations on the parameters evaluated during development and storage. Thus, it is possible to designate the formulations with lower cream contents, once consumers seek products with healthier and more functional properties. Furthermore, a high cream content may not be desirable, as it has been associated with increased health risk (Andrade, Mattos, Carvalho, Machado, & de Oliveira, 2013).

Therefore, taking into account the desirable final characteristics of the product, especially acceptability by consumers, two products with reduced cream contents could be suggested for marketing: formulations 1 and 3 (high chia and quinoa content, respectively). The properties of these seeds suggest their use as functional ingredients with a high potential for application in this type of product by improving food quality and nutritional enrichment. In addition, products containing chia or quinoa represent new products that satisfy a new market demand. Furthermore, the addition of components that have human health benefits and present nutritional and technological advantages, such as increases in moisture retention, texture and elasticity, justify the use of chia and quinoa seeds as enrichments.

### 3.2.5. Microbiological analyses

The cheese formulations showed suitable sanitary conditions during storage, compatible with current Brazilian regulations (ANVISA, 2001; MAPA, 1996). *Staphylococcus aureus* was absent in

**Table 4**  
Texture profile of cream cheeses developed.

Storage (Days)	Samples	Hardness (N)	Adhesiveness (N × s)	Cohesiveness	Gumminess (N)	Chewiness (N)	Resilience
1	1	0.15 ± 0.01 <sup>dA</sup>	0.37 ± 0.13 <sup>dA</sup>	0.82 ± 0.05 <sup>aA</sup>	0.13 ± 0.00 <sup>aA</sup>	0.13 ± 0.00 <sup>dA</sup>	0.07 ± 0.05 <sup>aA</sup>
	2	0.24 ± 0.01 <sup>cA</sup>	1.62 ± 0.10 <sup>cA</sup>	0.72 ± 0.02 <sup>bA</sup>	0.17 ± 0.01 <sup>aA</sup>	0.17 ± 0.01 <sup>cA</sup>	0.01 ± 0.00 <sup>abA</sup>
	3	0.35 ± 0.02 <sup>aA</sup>	4.38 ± 0.33 <sup>aA</sup>	0.73 ± 0.01 <sup>bA</sup>	0.41 ± 0.28 <sup>aA</sup>	0.26 ± 0.02 <sup>aA</sup>	0.01 ± 0.00 <sup>bA</sup>
	4	0.31 ± 0.00 <sup>bA</sup>	3.57 ± 0.22 <sup>bAB</sup>	0.74 ± 0.01 <sup>bA</sup>	0.23 ± 0.00 <sup>aA</sup>	0.23 ± 0.00 <sup>bA</sup>	0.01 ± 0.00 <sup>bA</sup>
	5	0.32 ± 0.01 <sup>bA</sup>	3.56 ± 0.36 <sup>bA</sup>	0.70 ± 0.02 <sup>bA</sup>	0.22 ± 0.00 <sup>aA</sup>	0.22 ± 0.00 <sup>bA</sup>	0.01 ± 0.00 <sup>bA</sup>
13	1	0.16 ± 0.01 <sup>dA</sup>	0.26 ± 0.16 <sup>cA</sup>	0.87 ± 0.05 <sup>aA</sup>	0.14 ± 0.00 <sup>bB</sup>	0.14 ± 0.01 <sup>cB</sup>	0.05 ± 0.04 <sup>aA</sup>
	2	0.28 ± 0.01 <sup>cB</sup>	2.33 ± 0.28 <sup>bA</sup>	0.80 ± 0.02 <sup>bC</sup>	0.22 ± 0.01 <sup>cB</sup>	0.22 ± 0.01 <sup>bB</sup>	0.01 ± 0.00 <sup>bB</sup>
	3	0.34 ± 0.02 <sup>abA</sup>	2.91 ± 0.52 <sup>bA</sup>	0.72 ± 0.01 <sup>cA</sup>	0.25 ± 0.01 <sup>aA</sup>	0.25 ± 0.01 <sup>abA</sup>	0.01 ± 0.00 <sup>bA</sup>
	4	0.33 ± 0.02 <sup>bA</sup>	3.17 ± 0.34 <sup>bB</sup>	0.75 ± 0.02 <sup>bcA</sup>	0.25 ± 0.01 <sup>aA</sup>	0.25 ± 0.01 <sup>abA</sup>	0.01 ± 0.00 <sup>bB</sup>
	5	0.38 ± 0.02 <sup>aB</sup>	4.26 ± 0.30 <sup>aAB</sup>	0.69 ± 0.01 <sup>cA</sup>	0.26 ± 0.01 <sup>abB</sup>	0.26 ± 0.01 <sup>aB</sup>	0.01 ± 0.00 <sup>abB</sup>
25	1	0.17 ± 0.01 <sup>cA</sup>	0.15 ± 0.08 <sup>cA</sup>	0.84 ± 0.03 <sup>aA</sup>	0.14 ± 0.00 <sup>cB</sup>	0.14 ± 0.00 <sup>cB</sup>	0.04 ± 0.01 <sup>aA</sup>
	2	0.29 ± 0.01 <sup>bB</sup>	1.93 ± 0.49 <sup>bA</sup>	0.74 ± 0.04 <sup>abB</sup>	0.21 ± 0.00 <sup>bB</sup>	0.21 ± 0.00 <sup>bB</sup>	0.01 ± 0.00 <sup>bB</sup>
	3	0.40 ± 0.01 <sup>aB</sup>	3.74 ± 0.88 <sup>aA</sup>	0.68 ± 0.02 <sup>bcB</sup>	0.27 ± 0.01 <sup>aA</sup>	0.27 ± 0.01 <sup>aA</sup>	0.01 ± 0.00 <sup>bB</sup>
	4	0.40 ± 0.03 <sup>aB</sup>	4.55 ± 0.61 <sup>aC</sup>	0.66 ± 0.01 <sup>cB</sup>	0.27 ± 0.01 <sup>aB</sup>	0.27 ± 0.01 <sup>aB</sup>	0.00 ± 0.00 <sup>bC</sup>
	5	0.40 ± 0.01 <sup>aB</sup>	4.74 ± 0.20 <sup>abB</sup>	0.69 ± 0.01 <sup>bcA</sup>	0.28 ± 0.01 <sup>abB</sup>	0.28 ± 0.01 <sup>abB</sup>	0.00 ± 0.00 <sup>abA</sup>

The same lowercase letters in the same column indicate no significant differences among the formulations for the same storage time ( $P < 0.05$ ). The same uppercase letters in the same column indicate no significant differences among the storage times for the same formulation ( $P < 0.05$ ).

the samples. The absence of *Salmonella* spp. and *L. monocytogenes* was found in 25 g. The results for total and fecal coliform were <0.3 MP N/g. Total counts of aerobic mesophilic were approximately  $1.0 \times 10^4$  CFU/g, and yeasts and molds were approximately  $3.6 \times 10^3$  CFU/g. Therefore, the preservatives and the manufacturing process were sufficient to ensure the satisfactory sanitary conditions and microbial stability during the storage.

#### 4. Conclusion

A novel protease from *Bacillus* sp. P45 after purification showed a high coagulating activity and the ability to hydrolyze milk proteins. The enzyme was efficiently used in the development of cream cheese enriched with chia and quinoa flour. The technological parameters demonstrated that formulations were highly stable and viable. The product was very stable, presenting a high level of water retention and showed high fiber contents, suggesting that the product may be consumed as a fiber source with health benefits. Moreover, the results indicate the feasibility of the purified enzyme as an alternative coagulant for the development of innovative biotechnological processes, such as the development of new dairy products with functional ingredients.

#### Acknowledgments

This work was supported by CAPES (CAPES-MINCYT 004/12) and CNPq, Brazil.

#### References

- Ahmed, I. A. M., Morishima, I., Babiker, E. E., & Mori, N. (2009). Characterisation of partially purified milk-clotting enzyme from *Solanum dubium* Fresen seeds. *Food Chemistry*, *116*, 395–400. <http://dx.doi.org/10.1016/j.foodchem.2008.11.072>.
- Andrade, J. P., Mattos, L. A. P. E., Carvalho, A. C., Machado, C. A., & de Oliveira, G. M. M. (2013). National physician qualification program in cardiovascular disease prevention and integral care. *Arquivos Brasileiros de Cardiologia*, *100*, 203–211. <http://dx.doi.org/10.5935/Abc.20130061>.
- ANVISA. (2001). Technical regulation microbiological standards for foods. *Brasília: Official Daily of Federative Republic of Brazil*, 1–18. Available: [www.portal.anvisa.gov.br](http://www.portal.anvisa.gov.br).
- AOAC. (2005). *Official methods of analysis of the association analytical chemists* (18th ed.). Gaithersburg, MD: Association of Official Analytical Chemists International.
- Ayerza, R., & Coates, W. (2011). Protein content, oil content and fatty acid profiles as potential criteria to determine the origin of commercially grown chia (*Salvia hispanica* L.). *Industrial Crops and Products*, *34*, 1366–1371. <http://dx.doi.org/10.1016/j.indcrop.2010.12.007>.
- Beka, R. G., Krier, F., Botquin, M., Guiama, V. D., Donn, P., Libouga, D. G., et al. (2014). Characterisation of a milk-clotting extract from *Balanites aegyptiaca* fruit pulp. *International Dairy Journal*, *34*, 25–31. <http://dx.doi.org/10.1016/j.idairyj.2013.06.013>.
- Berridge, N. J. (1952). An improved method of observing the clotting of milk containing rennin. *Journal of Dairy Research*, *19*, 328–329.
- Bhargava, A., Shukla, S., & Ohri, D. (2006). *Chenopodium quinoa* – an Indian perspective. *Industrial Crops and Products*, *23*, 73–87. <http://dx.doi.org/10.1016/j.indcrop.2005.04.002>.
- Børsting, M. W., Stallknecht, M. K., Vogensen, F. K., & Ardó, Y. (2015). Influence of proteolytic *Lactococcus lactis* subsp. *cremoris* on ripening of reduced-fat Cheddar cheese made with camel chymosin. *International Dairy Journal*, *41*, 38–45. <http://dx.doi.org/10.1016/j.idairyj.2014.09.002>.
- Bryant, A., Ustunol, Z., & Steffe, J. (1995). Texture of cheddar cheese as influenced by fat reduction. *Journal of Food Science*, *60*, 1216–1219. <http://dx.doi.org/10.1111/j.1365-2621.1995.tb04559.x>.
- Capitani, M. I., Spotorno, V., Nolasco, S. M., & Tomas, M. C. (2012). Physicochemical and functional characterization of by-products from chia (*Salvia hispanica* L.) seeds of Argentina. *LWT – Food Science and Technology*, *45*, 94–102. <http://dx.doi.org/10.1016/j.lwt.2011.07.012>.
- Chazarra, S., Sidrach, L., Lopez-Molina, D., & Rodriguez-Lopez, J. (2007). Characterization of the milk-clotting properties of extracts from artichoke (*Cynara scolymus* L.) flowers. *International Dairy Journal*, *17*, 1393–1400. <http://dx.doi.org/10.1016/j.idairyj.2007.04.010>.
- Corrons, M. A., Bertucci, J. I., Liggieri, C. S., Lopez, L. M. I., & Bruno, M. A. (2012). Milk clotting activity and production of bioactive peptides from whey using *Maclura pomifera* proteases. *LWT – Food Science and Technology*, *47*, 103–109. <http://dx.doi.org/10.1016/j.lwt.2011.12.028>.
- Daroit, D. J., Correa, A. P. F., & Brandelli, A. (2009). Keratinolytic potential of a novel *Bacillus* sp P45 isolated from the Amazon basin fish *Piaractus mesopotamicus*. *International Biodeterioration & Biodegradation*, *63*, 358–363. <http://dx.doi.org/10.1016/j.ibiod.2008.11.008>.
- Daroit, D. J., Correa, A. P. F., & Brandelli, A. (2011). Production of keratinolytic proteases through bioconversion of feather meal by the Amazonian bacterium *Bacillus* sp P45. *International Biodeterioration & Biodegradation*, *65*, 45–51. <http://dx.doi.org/10.1016/j.ibiod.2010.04.014>.
- Daroit, D. J., Corrêa, A. P. F., Canales, M. M., Coelho, J. G., Hidalgo, M. E., Tichota, D. M., et al. (2012). Physicochemical properties and biological activities of ovine caseinate hydrolysate. *Dairy Science and Technology*, *92*, 335–351.
- Daroit, D. J., Corrêa, A. P. F., Segalin, J., & Brandelli, A. (2010). Characterization of a keratinolytic protease produced by the feather-degrading Amazonian bacterium *Bacillus* sp. P45. *Biocatalysis and Biotransformation*, *28*, 370–379. <http://dx.doi.org/10.3109/10242422.2010.532549>.
- Deegan, K. C., Holopainen, U., McSweeney, P. L. H., Alatossava, T., & Tuorila, H. (2014). Characterisation of the sensory properties and market positioning of novel reduced-fat cheese. *Innovative Food Science & Emerging Technologies*, *21*, 169–178. <http://dx.doi.org/10.1016/j.ifset.2013.10.003>.
- Doores, S., Salfinger, Y., & Tortorello, M. L. (2013). *Compendium of methods for the microbiological examination of foods* (4th ed.). Washington DC: American Public Health Association.
- Galán, E., Cabezas, L., & Fernández-Salguero, J. (2012). Proteolysis, microbiology and sensory properties of ewes' milk cheese produced with plant coagulant from cardoon *Cynara cardunculus*, calf rennet or a mixture thereof. *International Dairy Journal*, *25*, 92–96. <http://dx.doi.org/10.1016/j.idairyj.2012.02.001>.
- Galán, E., Prados, F., Pino, A., Tejada, L., & Fernández-Salguero, J. (2008). Influence of different amounts of vegetable coagulant from cardoon *Cynara cardunculus* and calf rennet on the proteolysis and sensory characteristics of cheeses made with sheep milk. *International Dairy Journal*, *18*, 93–98. <http://dx.doi.org/10.1016/j.idairyj.2007.06.003>.
- Gawlik-Dziki, U., Swieca, M., Sulkowski, M., Dziki, D., Baraniak, B., & Czyn, J. (2013). Antioxidant and anticancer activities of *Chenopodium quinoa* leaves extracts – in vitro study. *Food and Chemical Toxicology*, *57*, 154–160. <http://dx.doi.org/10.1016/j.fct.2013.03.023>.
- Horwitz, W. (1997). *Official methods of analysis of the association of official analytical chemists* (16th ed.). Gaithersburg: AOAC.
- Jacob, M., Jaros, D., & Rohm, H. (2011). Recent advances in milk clotting enzymes. *International Journal of Dairy Technology*, *64*, 14–33. <http://dx.doi.org/10.1111/j.1471-0307.2010.00633.x>.
- Jun, Z., Hsien, F., Huff, H. E. (1994). Extrusion cooking of corn meal with soy fiber, salt, and sugar. *Cereal Chemistry*, *71*, 227–233.
- Karaman, A. D., & Akalin, A. S. (2013). Improving quality characteristics of reduced and low fat Turkish white cheeses using homogenized cream. *LWT – Food Science and Technology*, *50*, 503–510. <http://dx.doi.org/10.1016/j.lwt.2012.08.017>.
- Lawrence, R. C., Heap, H. A., & Gilles, J. (1984). A controlled approach to cheese technology. *Journal of Dairy Science*, *67*, 1632–1645.
- Lucey, J. A., Johnson, M. E., & Horne, D. S. (2003). Invited review: perspectives on the basis of the rheology and texture properties of cheese. *Journal of Dairy Science*, *86*, 2725–2743. [http://dx.doi.org/10.3168/jds.S0022-0302\(03\)73869-7](http://dx.doi.org/10.3168/jds.S0022-0302(03)73869-7).
- Madl, T., Sterk, H., & Mittelbach, M. (2006). Tandem mass spectrometric analysis of a complex triterpene saponin mixture of *Chenopodium quinoa*. *Journal of the American Society for Mass Spectrometry*, *17*, 795–806. <http://dx.doi.org/10.1016/j.jasms.2006.02.013>.
- MAPA. (1996). *General technical regulation for fixing the cheese microbiological requirements*. Brasília: Official Daily of Federative Republic of Brazil.
- Marineli, R. D., Moraes, E. A., Lenquiste, S. A., Godoy, A. T., Eberlin, M. N., & Marostica, M. R. (2014). Chemical characterization and antioxidant potential of Chilean chia seeds and oil (*Salvia hispanica* L.). *LWT – Food Science and Technology*, *59*, 1304–1310. <http://dx.doi.org/10.1016/j.lwt.2014.04.014>.
- Mateo, M. J., Everard, C. D., Fagan, C. C., O'Donnell, C. P., Castillo, M., Payne, F. A., et al. (2009). Effect of milk fat concentration and gel firmness on syneresis during curd stirring in cheese-making. *International Dairy Journal*, *19*, 264–268. <http://dx.doi.org/10.1016/j.idairyj.2008.10.014>.
- Mazorra-Manzano, M. A., Moreno-Hernandez, J. M., Ramirez-Suarez, J. C., Torres-Llanez, M. D., Gonzalez-Cordova, A. F., & Vallejo-Cordoba, B. (2013). Sour orange *Citrus aurantium* L. flowers: a new vegetable source of milk-clotting proteases. *LWT – Food Science and Technology*, *54*, 325–330. <http://dx.doi.org/10.1016/j.lwt.2013.07.009>.
- Merheb-Dini, C., Garcia, G. A. C., Penna, A. L. B., Gomes, E., & da Silva, R. (2012). Use of a new milk-clotting protease from *Thermomucor indicae-seudatae* N31 as coagulant and changes during ripening of Prato cheese. *Food Chemistry*, *130*, 859–865. <http://dx.doi.org/10.1016/j.foodchem.2011.07.105>.
- Nsimba, R. Y., Kikuzaki, H., & Konishi, Y. (2008). Antioxidant activity of various extracts and fractions of *Chenopodium quinoa* and *Amaranthus* spp. seeds. *Food Chemistry*, *106*, 760–766. <http://dx.doi.org/10.1016/j.foodchem.2007.06.004>.
- Olmedo, R. H., Nepote, V., & Grosso, N. R. (2013). Preservation of sensory and chemical properties in flavoured cheese prepared with cream cheese base using oregano and rosemary essential oils. *LWT – Food Science and Technology*, *53*, 409–417. <http://dx.doi.org/10.1016/j.lwt.2013.04.007>.
- Ostrowska-Ligeza, E., & Lenart, A. (2015). Influence of water activity on the compressibility and mechanical properties of cocoa products. *LWT – Food Science and Technology*, *60*, 1054–1060. <http://dx.doi.org/10.1016/j.lwt.2014.10.040>.

- Pons, M., & Fiszman, S. M. (1996). Instrumental texture profile analysis with particular reference to gelled systems. *Journal of Texture Studies*, 27, 597–624. <http://dx.doi.org/10.1111/j.1745-4603.1996.tb00996.x>.
- Queiroga, R. C. R. E., Santos, B. M., Gomes, A. M. P., Monteiro, M. J., Teixeira, S. M., de Souza, E. L., et al. (2013). Nutritional, textural and sensory properties of Coalho cheese made of goats', cows' milk and their mixture. *LWT – Food Science and Technology*, 50, 538–544. <http://dx.doi.org/10.1016/j.lwt.2012.08.011>.
- Rojas-Castro, W. N., Chacón-Villalobos, A., & Pineda-Castro, M. L. (2007). Características del yogurt batido de fresa derivadas de diferentes proporciones de leche de vaca y cabra. *Agronómica Mesoamérica*, 18, 221–237.
- Rolet-Repecaud, O., Berthier, F., Beuvier, E., Gavoye, S., Notz, E., Roustel, S., et al. (2013). Characterization of the non-coagulating enzyme fraction of different milk-clotting preparations. *LWT-Food Science and Technology*, 50, 459–468. <http://dx.doi.org/10.1016/j.lwt.2012.08.021>.
- Sala, L., Gautério, G. V., Younan, F. F., Brandelli, A., Moraes, C. C., & Kalil, S. J. (2014). Integration of ultrafiltration into an aqueous two-phase system in the keratinase purification. *Process Biochemistry*, 49, 2016–2024. <http://dx.doi.org/10.1016/j.procbio.2014.07.013>.
- Santini, Z. G., Alsina, D. A., Sthaus, R., Meinardi, C., Freyre, M., Díaz, J. R., et al. (2007). Evaluación de la textura en quesos de oveja. Aplicaciones del análisis factorial discriminante. *Fave*, 5/6, 1–2.
- Shamtsyan, M., Dmitriyeva, T., Kolesnikov, B., & Denisova, N. (2014). Novel milk-clotting enzyme produced by *Coprinus lagopides* basidial mushroom. *LWT – Food Science and Technology*, 58, 343–347. <http://dx.doi.org/10.1016/j.lwt.2013.10.009>.
- Sirtori, L. R., Cladera-Olivera, F., Lorenzini, D. M., Tsai, S. M., & Brandelli, A. (2006). Purification and partial characterization of an antimicrobial peptide produced by *Bacillus* sp. strain P45, a bacterium from the Amazon basin fish *Piaractus mesopotamicus*. *Journal of General and Applied Microbiology*, 52, 357–363. <http://dx.doi.org/10.2323/jgam.52.357>.
- Souza, V. R., Carneiro, J. D. S., Pinto, S. M., Souza, A. B., & Stephani, R. (2012). Effect of starter culture and inulin addition on microbial viability, texture, and chemical characteristics of whole or skim milk Kefir. *Revista do Instituto de Laticínios Cândido Tostes*, 67, 20–28.
- Tharanathan, R. N., & Mahadevamma, S. (2003). Grain legumes – a boom to human nutrition. *Trends in Food Science & Technology*, 14, 507–518. <http://dx.doi.org/10.1016/j.tifs.2003.07.002>.
- Trujillo, A. J., Guamis, B., Laencina, J., & Lopez, M. B. (2000). Proteolytic activities of some milk clotting enzymes on ovine casein. *Food Chemistry*, 71, 449–457. [http://dx.doi.org/10.1016/S0308-8146\(00\)00170-9](http://dx.doi.org/10.1016/S0308-8146(00)00170-9).
- Zulkurnain, M., Goh, M. H., Karim, A. A., & Liong, M. T. (2008). Development of a soy-based cream cheese. *Journal of Texture Studies*, 39, 635–654. <http://dx.doi.org/10.1111/j.1745-4603.2008.00163.x>.



# Anti-quorum sensing activity of spice oil nanoemulsions against food borne pathogens



Gopu Venkadesaperumal, Sambrey Rucha, Kothandapani Sundar, Prathapkumar Halady Shetty\*

Department of Food Science and Technology, Pondicherry University, Pondicherry 605014, India

## ARTICLE INFO

### Article history:

Received 25 May 2015

Received in revised form

1 October 2015

Accepted 18 October 2015

Available online 21 October 2015

### Keywords:

Quorum quenching

Nanoemulsion

Ultrasonic emulsification

Anti-biofilm

Essential oil

## ABSTRACT

Quorum sensing (QS) mechanism plays a vital role in many bacterial species, which is found to be implicated in various factors including bacterial pathogenicity and food spoilage. Therefore interrupting the QS mechanism may be an attractive strategy to develop novel QS-based anti-bacterial drugs. Here, we investigated the quorum sensing inhibitory activity of spice oil nanoemulsions (NE) and its anti-biofilm property against selected food pathogens using the biosensor strain *Chromobacterium violaceum* CV026. Essential oil nanoemulsions were formulated by ultrasonic emulsification of Tween80 and water. The emulsification method for nanoformulations was standardized with Tween80 concentration and sonication time to attain high physical solidity and minimum droplet diameter. Stable cumin (*Cuminum cyminum*), pepper (*Piper nigrum*), and fennel (*Foeniculum vulgare*) oil nanoemulsions with respective droplet diameters of 52.89 nm, 82.08 nm and 59.52 nm were formulated by ultrasonic emulsification. Nanoemulsions at all tested concentrations inhibited the production of violacein pigment in *C. violaceum* CV026 below their minimum inhibitory concentration (MIC) level. In addition, the upshot of the current investigation reveals that all three nanoemulsions strongly interferes with quorum regulated phenotypes like biofilm formation and exopolysaccharide (EPS) production.

Above findings lay a solid foundation for the utilization of nanoemulsions as QS-based antibacterial/anti-biofilm agents to manage food borne pathogens and biofilm formation in food industries.

© 2015 Elsevier Ltd. All rights reserved.

## 1. Introduction

Many bacterial species communicate with each other in a population-dependent manner through a mechanism called quorum sensing (QS) to regulate their physiological functions. The quorum sensing signaling mechanism is mediated through the release of small, diffusible signaling molecules called as auto-inducers (Miller & Bassler, 2001; Waters & Bassler, 2005). N-acyl homoserine lactones (AHLs) act as signaling molecules in Gram-negative bacteria, whereas peptide based compounds act as signaling molecules in Gram-positive bacteria (Li et al., 2007). A major worry that persists in various health departments worldwide is the formation of biofilms by infectious bacteria which is a QS regulated phenomenon (Kalia, 2013). The efforts to disrupt these biofilms led to the identification of molecules that were able to

quench the QS mechanism, thereby inhibiting the biofilm formation.

Even though a large spectrum of quorum inhibitors were identified, plant-based compounds have been significantly used for a long time to treat microbial infections and have earned more attention as a source of anti-QS compounds for the treatment of biofilms (Gibot, 2004). Essential oils are complex mixtures of volatile compounds that are isolated from plant materials. The essential oils of *Salvia sclarea*, *Juniperus communis*, *Citrus lemon*, and *Origanum majorana* were proved to exhibit anti-QS and biofilm inhibitory activity (Kerekes et al., 2013). Similarly, the essential oils of *Cinnamomum verum* (Niu, Alfre, & Gilbert, 2006) and *Syzygium aromaticum* (Khan, Zahin, Hasan, Husain, & Ahmad, 2009) were also proved to exhibit quorum sensing inhibitory (QSI) potential. It was observed that essential oils exhibit antimicrobial activity at a higher concentration than that of needed by cells in the media (Valero & Giner, 2006) and they lose their bactericidal activity after certain dilutions due to the changes in droplet structures (Teixeria et al., 2007). These limitations can be overcome by using

\* Corresponding author.

E-mail address: [pkshalady@yahoo.co.uk](mailto:pkshalady@yahoo.co.uk) (P.H. Shetty).

nanoemulsion since the concentration of essential oil in the nano formulation is lower. Moreover, nanoemulsions are suitable for efficient delivery of active ingredients, and their large surface area enables rapid penetration of actives. To the best of our knowledge, this is the first time that we have investigated the quorum-quenching activity of stable nanoemulsion prepared from essential oils against Gram-negative bacterial pathogens.

## 2. Materials and methods

### 2.1. Bacterial strains and culture conditions

A mutant strain of *Chromobacterium violaceum* CV026 (CECT5999) procured from Spanish type culture collection, a derivative of wild-type unable to synthesize its AHLs was used as reporter strain. Cultures used in this study also include *Salmonella typhimurium* (ATCC 14028), *Escherichia coli* (MTCC 727), *Klebsiella pneumoniae* (MTCC 12202), and *C. violaceum* MTCC 2656. All the cultures were grown in the nutrient broth, except CECT 5999 and MTCC 2656, which were routinely cultured aerobically in Luria–Bertani (LB) broth supplemented with kanamycin (20 µg/ml). Bacterial cultures were stored as 40% glycerol stock at –80 °C. Bacterial cultures with an optical density of 0.1 at 600 nm were used for all studies. N-hexanoyl-DL-homoserine lactone (Sigma, Aldrich) was added to the medium to induce the violacein production in CECT5999 when required.

### 2.2. Nanoemulsion preparation

The essential oils of cumin, fennel and pepper were purchased from Cyrus Enterprises, India, and the nanoemulsions were formulated using Tween80 and water (Ghosh, Mukherjee, & Chandrasekaran, 2013). Coarse emulsions were prepared in the ratios (v/v) 1:1, 1:2, 1:3 and 1:4 where the concentration of essential oil was fixed constant (6% v/v). The coarse emulsion was then subjected to ultrasonic homogenization for 15 min each with a pulse of 30 s on and 30 s off in an ultrasonic homogenizer (Sonic-Vibracell, USA) with a maximum power output of 750 W. The probe with a diameter of 13 mm was used for homogenization; heat generated during the process was nullified by placing the emulsion in a beaker containing ice. Formulated nanoemulsions were characterized and investigated for their stability at room temperature.

### 2.3. Determination of particle size and polydispersion index

Polydispersity index (PDI) and particle size of the formulated nanoemulsions were determined by using a particle size analyzer (Zetasizer, UK). Brownian motion of the nanoemulsion formulation leads to a fluctuation in the intensity of scattered light. This fluctuation in the scattered light intensity was measured by the dynamic light scattering technique (DLS). The droplet radius ( $R$ ) was calculated from Stokes–Einstein equation (Tadros, Izquierdo, Esquena, & Solans, 2004) as follows:

$$D = kT/6\eta R$$

where  $D$  is the translational diffusion coefficient ( $m^2/s$ ),  $k$  is the Boltzmann's constant ( $JK^{-1}$ ),  $T$  is the absolute temperature in Kelvin, and  $\eta$  is the viscosity of the medium ( $kg/ms$ ). All the formulations were diluted with milli-Q (Seimens, Germany) double-distilled water prior to experiment to eliminate the effect of viscosity caused due to ingredients and also to reduce multiple scattering effect. The particle diameter was determined from the particle radius. Concentration of nanoemulsion with the lowest droplet size in nanometer range was used for further studies.

### 2.4. Stability of nanoemulsion

The resistance of formulated emulsions to centrifugation was studied by centrifuging at 10,000 rpm for 30 min at room temperature. Further nanoemulsions were stored at room temperature for its intrinsic stability and observed for phase separation or creaming respectively (Ghosh et al., 2013).

### 2.5. Kinetics of killing

Emulsion formulations with the lowest droplet diameter were selected for the kinetics of killing. Briefly, overnight bacterial cultures were centrifuged at 5000 g for 10 min. The obtained pellet was washed thrice with phosphate buffered saline, and a test inoculum was prepared. Test bacterial cultures prepared (1% v/v) were challenged against preferred nanoemulsion formulations. For viable counts, 0.1 ml of the sample was taken from each tube and spread onto nutrient agar plates. Viable colonies were counted after incubation at 37 °C for 24 h (Al-Adham, Khalil, Al-Hmoud, Kierans, & Collier, 2000).

### 2.6. Minimal inhibitory concentration of nanoemulsions

Anti-microbial activities of nanoemulsions against selected pathogens were determined by MIC. Briefly 12-well microtiter plates containing nutrient broth supplemented with different concentrations of the nanoemulsion (10–200 µL) were inoculated with 1% of the overnight bacterial culture. Microtiter plates (MTP) were then incubated for 24 h, before and after incubation, the absorbance of the medium was measured at the wavelength of 600 nm. The lowest concentration of formulations, which showed complete inhibition of visible growth, represented the MIC. Growth curve experiments were also conducted to demonstrate the anti-bacterial effect of formulated nanoemulsions with 1% inoculum in nutrient broth at both MIC and sub-MIC levels. The bacterial growth was monitored for 24 h at 37 °C by measuring the absorbance at 600 nm using a microplate reader (Biotek, USA). All further experiments were carried out only at the sub-MIC level.

### 2.7. QSI bioassay

Disc diffusion assay was carried out to detect the anti-QS activity of nanoemulsions. Briefly exogenous HHL (N-hexanoyl-DL-homoserine lactone) was added to 100 ml of sterilized LB agar at an appropriate temperature and was then gently mixed and poured into the Petriplates. The overnight culture of *C. violaceum* CV026 was swabbed evenly onto a solidified agar surface. Sterile discs were loaded with appropriate volumes of formulations and placed onto the agar plates, which were then incubated at 37 °C for 24 h. QSI activity was scored as an obscure, colorless, but doable halo around the discs. Sonicated Tween80 and water were used as control.

Similarly, the flask incubation assay was carried out for the quantitative determination of violacein inhibition by nanoemulsions. Inoculated LB broth supplemented with HHL (5 µM) and nanoemulsions at different concentrations (30–50 µl/ml) was incubated for 24 h at 30 °C. Violacein extraction was carried out as described by Choo, Rukayadi, and Hwang (2006). Briefly, 1 ml of culture from each flask was centrifuged at 10,000 g for 5 min to precipitate violacein. The pellet was dissolved in 1 ml of dimethyl sulfoxide (DMSO) and vortexed robustly to solubilize the violacein completely. Above mixture was centrifuged again to remove the cells and was quantified at 585 nm using a microplate reader (Biotek, USA). The experiment was repeated for triplicate values and the percentage of inhibition was calculated by the formula as

follows:

$$\frac{\text{control OD585 nm} - \text{test OD585 nm}}{\text{control OD585 nm}} \times 100$$

### 2.8. Reduction in EPS production

LB broth with and without formulated spice oil nanoemulsions (30–50  $\mu\text{l/ml}$ ) were inoculated with 1% of test bacterial cultures and incubated at 30 °C. Biofilms that adhered to the walls of test tubes were harvested to obtain crude EPS. Briefly, late-log phase cells were removed by centrifugation at 5000 g for 30 min at 2 °C. Filtered supernatant was added to three volumes of chilled ethanol and incubated overnight at 2 °C to precipitate the dislodged EPS. The precipitated EPS was collected by centrifugation at 5000 g for 30 min, then dissolved in 1 ml of deionized water, and finally stored at –40 °C until further use. Total carbohydrate content in the EPS was quantified by the phenol-sulfuric acid method using glucose as a standard (Huston, Methe, & Deming, 2004).

### 2.9. Effect of formulated nanoemulsions on biofilm formation

Microtiter plate assay was performed to quantify the effect of nanoemulsions on the biofilm formation of test bacterial pathogens (Limsuwan & Voravuthikunchai, 2008). LB broth with and without formulations (30–50  $\mu\text{l/ml}$ ) was inoculated with 1% of bacterial cultures and incubated at 30 °C. After incubation, plates were carefully rinsed with double-distilled water to remove loosely attached cells. Adhered cell on the walls were stained with 100  $\mu\text{l}$  of 0.2% crystal violet solution (HiMedia, India) for 10 min. Excess stain was removed by rinsing with distilled water and washed with 100  $\mu\text{l}$  of 95% ethanol. Intensity was measured at OD<sub>650 nm</sub> by using a microplate reader (Biotek, USA), for quantification of biofilm biomass.

### 2.10. Statistical analysis

All the experimental data represents the mean of triplicate values. Differences between control and test samples were analyzed by one way ANOVA.

## 3. Results and discussion

### 3.1. Formulation and characterization of nanoemulsions

The droplet sizes of all three formulated nanoemulsions after 15 min of ultrasonic emulsification are shown in Table 1. Formulations that exhibited the lowest droplet diameter with a uniform distribution were selected for further screening. For cumin, fennel, and pepper oil, nanoemulsions with ratios of 1:1, 1:2, and 1:3 exhibited the lowest droplet diameters of 52.89  $\pm$  0.32, 59.52  $\pm$  0.43, and 82.08  $\pm$  0.24 nm, respectively (Fig. 1). It was observed that there was an increase in the droplet diameter with the increase in the ratio of oil and surfactant. Our results are in agreement with the fact that minimum droplet size is achieved at

lower oil to surfactant ratios (Gutiérrez et al., 2008). On further increasing the concentration of surfactant, much decrease in the droplet diameter was not observed and hence formulations on above mentioned ratios were optimized and used for further screening. The particle size distributions of the nanoemulsions that were formulated at each ratio are shown in the Supplementary Fig. 1. In this preparation, Tween80 was selected as the surfactant, as it posses the high hydrophilic-lipophilic balance and its effect on minimizing droplet diameters when compared with polymers (Qian & McClement, 2011).

### 3.2. Stability of formulated nanoemulsions

All three formulations that had been prepared by 10 min of sonication were stable even after 60 days. Neither phase separation nor creaming was observed. As sonication time increases, the stability of nanoemulsions was also increased. A similar trend of decrease in the droplet diameter of sunflower oil nanoemulsion with the increase in sonication time was stated by Leong, Wooster, Kentish, and Ashok kumar (2009). All the formulations were found to be stable even after centrifugation at 10,000 rpm for 30 min.

### 3.3. Kinetics of killing

Antimicrobial activity of formulated spice oil nanoemulsions was evaluated against test pathogens. No viable cells were noticed after 5 min of interaction with undiluted formulations (cumin oil 1:1; pepper oil 1:3, and fennel oil 1:2). Our results are in accordance with Zhang et al. (2009) who reported that emulsions in the nanometer range causes 6 log reductions in viable bacterial cells in 1 min. At a twofold dilution, cumin and fennel oil exhibited around 3 log reductions in the cell viability of all tested pathogens (Fig. 2). Tested formulations at a 10-fold dilution did not exhibit much difference in their cell viability even after 1-h incubation. This correlates with the minimum inhibitory level of nanoemulsions against test pathogens. More than 50% reductions in cell viability were observed at a 5-fold dilution within 60 min of exposure. Bacterial pellets dissolved in PBS were maintained as controls and no significant decrease in cell count was observed during the experimental period. Results showed that nanoemulsions at even 5-fold and 10-fold dilutions exhibited significant antibacterial activity, whereas microemulsions lose their bactericidal activity on dilution (Teixeria et al., 2007).

### 3.4. Minimal inhibitory concentration

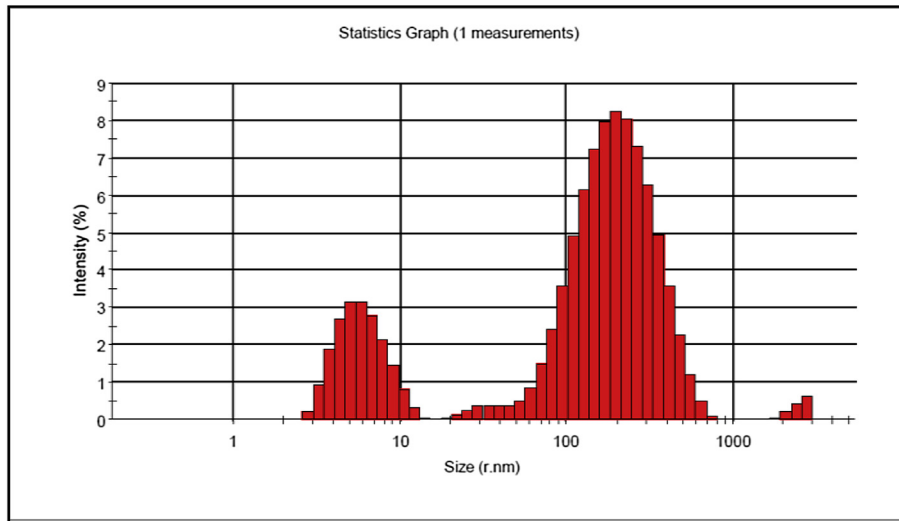
Minimum inhibitory concentration of nanoemulsion formulations were determined against the bio-sensor strain *C. violaceum* as well as against all three test pathogens. MIC was determined as the lowest concentration that showed complete inhibition of visible growth. The MIC of cumin nanoemulsion was 70  $\mu\text{l/ml}$  for *K. pneumoniae*, 60  $\mu\text{l/ml}$  for *C. violaceum*, *S. typhimurium*, and *E. coli*. Fennel oil nanoemulsion exhibited MIC against *C. violaceum* at the concentration of 60  $\mu\text{l/ml}$  and 80  $\mu\text{l/ml}$  for *K. Pneumoniae*, *S. typhimurium*, and *E. coli* respectively. Pepper exhibited a relatively higher concentration of MIC against *C. violaceum* at the

**Table 1**

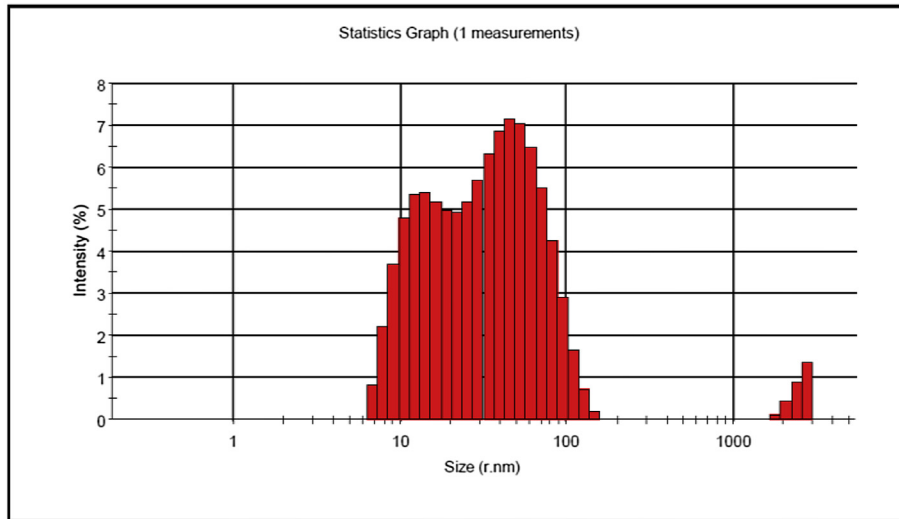
Physiochemical characterization of formulated spice oil nanoemulsions. Data represented were mean of triplicate values with standard deviation.

Nanoemulsions	Particle size (nm)	Polydispersion index (PDI)	Oil: Surfactant ratio (v/v)
Cumin oil	52.89 $\pm$ 0.32	0.385 $\pm$ 0.001	1:1
Pepper oil	82.08 $\pm$ 0.24	1.00 $\pm$ 0.001	1:3
Fennel oil	59.52 $\pm$ 0.43	0.248 $\pm$ 0.001	1:2

A



B



C

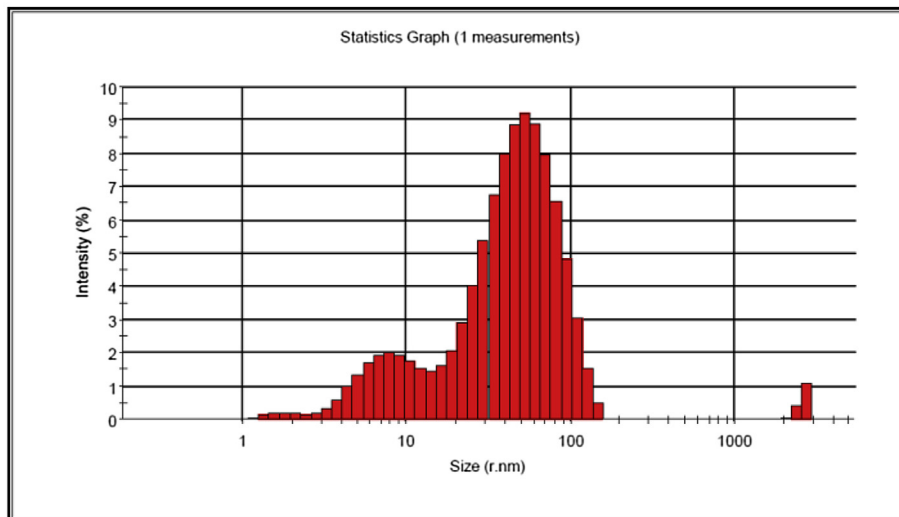


**Fig. 1.** Particle size distribution of nanoemulsion: *C. cyminum* oil NE prepared in the ratio of 1:1 (a), *P. nigrum* oil NE in the ratio of 1:3 (b), and *F. vulgare* oil NE prepared in the ratio of 1:2 (c) as measured by dynamic light scattering (DLS) method.

concentration of 110  $\mu\text{l/ml}$  and 90  $\mu\text{l/ml}$  for all other tested bacteria. Hence, all the experiments were carried out at sub-MIC levels of 20 and 50  $\mu\text{l/ml}$ . This would not probably impose a selective pressure for the development of resistance. In addition, bacterial growth curve experiments evidenced that at the sub-MIC level there are no

significant changes in the growth pattern of the test bacterial strains; however, at their respective MIC levels, a notable reduction was observed in the bacterial cell density, as evidenced in [Supplementary Fig. 2](#).

### 3.5. QSI bioassay

In the disc diffusion method, nanoemulsions exhibited anti-QS activity against the reporter strain *C. violaceum* CV026, which was indicated by the loss of purple pigmentation. Cumin oil and fennel oil emulsion at the concentration of 50  $\mu\text{l}$  exhibited anti-QS activity through violacein inhibition around the discs. Tested emulsion showed the immediate zone of clearance, which may be because of the bactericidal effect that is followed by the opaque, halo zone of clearance; this indicates the inhibition of violacein production ([Fig. 3](#)). In quantitative analysis by the flask incubation assay, nanoemulsions at all tested concentrations significantly reduced violacein production in tests when compared with control. It was interesting to note that fennel and cumin nanoemulsions revealed a strong QSI potential by inhibiting violacein pigment production in *C. violaceum* CECT5999 when compared to that of pepper. Our results are true to the fact that the potential advantages of nanoemulsion like high stability, low turbidity, and high solubility over conventional ones make them excellent systems ([McClements & Rao, 2011](#); [Silva, Cerqueira, & Vicente, 2012](#); [Solans, Izquierdo, Nolla, Azemar, & Garcia-Celma, 2005](#)). At the concentration of 50  $\mu\text{l/ml}$ , fennel emulsion exhibited 75.69% of inhibition as highest and pepper emulsion at the concentration of 30  $\mu\text{l/ml}$  inhibited 32.89% of violacein production when compared to that of control ([Fig. 4](#)). It was reported that essential oils of thyme, ginger and turmeric inhibited violacein inhibition up to the level of 41% ([Vattem, Mihalik, Crixell, & McLean, 2007](#)). In this study nano formulation of fennel oil inhibited violacein production up to 75.69% which indicates that essential oils blended into nanoemulsions can act as strong quorum quenchers than the corresponding essential oils or methanol extracts.

### 3.6. Inhibition of biofilm formation and EPS production

An important phenotypic expression responsible for the virulence of the pathogenic bacteria is the production of exo-

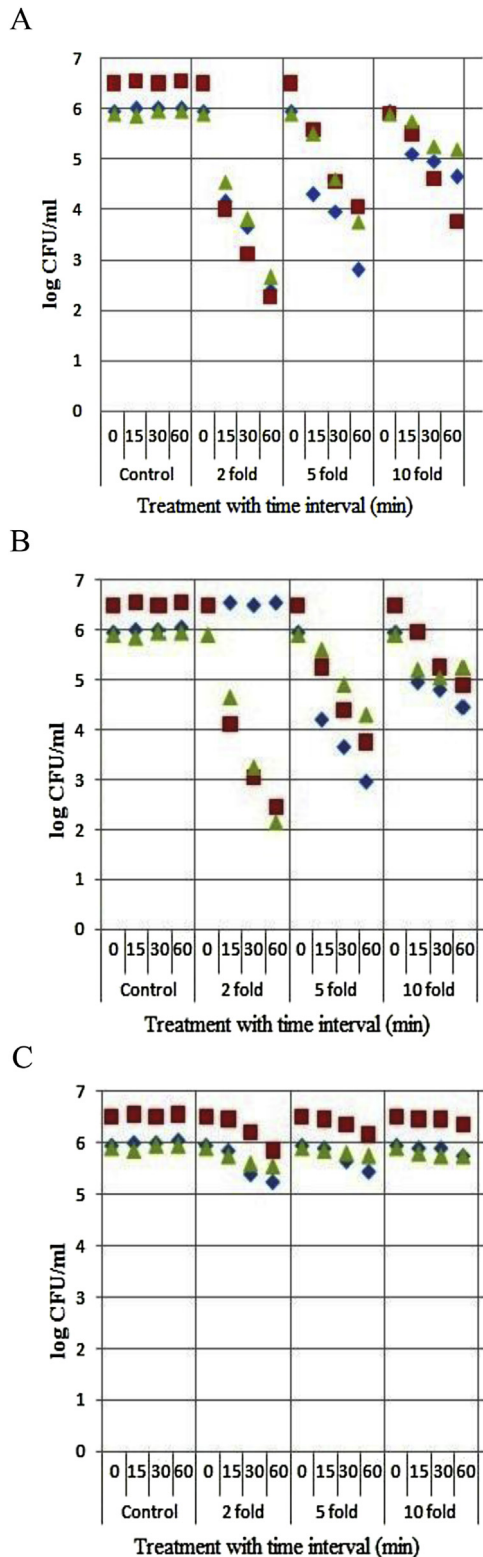


**Fig. 2.** Effect of spice oil nanoemulsions on cell viability of test pathogens against time and concentration.

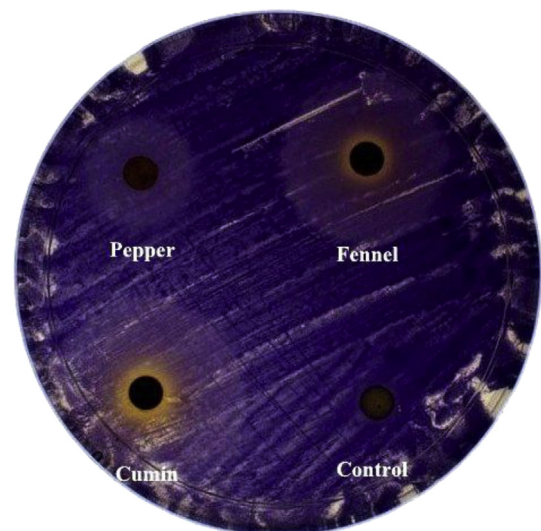


**Fig. 3.** Quorum sensing inhibitory bioassay of spice oil nanoemulsions showing inhibition of HHL mediated violacein production in *C. violaceum* CV026.

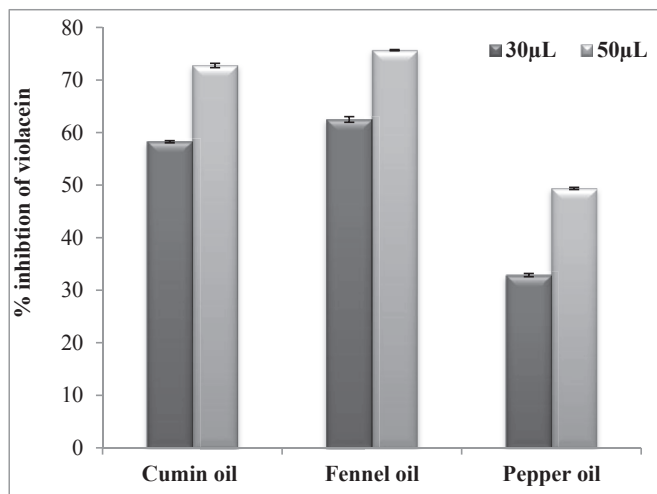


**Fig. 4.** Inhibition of violacein production in *C. violaceum* CV026 by spice oil nanoemulsions. Vertical bars represent the mean values of triplicates with a standard deviation.

polysaccharide which plays an important role in laying down the biofilm architecture and also in maturation (You et al., 2007). In our study, EPS was extracted from treated and untreated cultures of test pathogens. The spectrometric analysis revealed that there is a concentration-dependent increase/decrease in EPS production. A maximum of 60.6% inhibition was recorded by fennel oil nanoemulsion at the concentration of 50 µl/ml in *E. coli* and minimum of 1.3% inhibition was observed at 30 µl/ml pepper oil nanoemulsion in *K. pneumoniae* (Fig. 5). The enhanced effect of nanoemulsion over essential oil may be due to its large surface area and smallest droplet size which allowed the active components of spices to interact more efficiently.

Biofilms act as a key component by pathogens to nullify the efficacy of antibiotics and anti-biofilm agents. As EPS production is also correlated with biofilm forming potential of the bacterium, effect of nanoemulsion on biofilm formation by test pathogens were tested (Fig. 6). In anti-biofilm assay, cumin formulation exhibited maximum inhibition of biofilm formation up to 53.06% in *K. pneumoniae* at the concentration of 50 µl/ml; whereas 11.14% inhibition of biofilm formation was recorded against *K. pneumoniae* by fennel nanoemulsion at 50 µl/ml. Bacterial pathogens that are

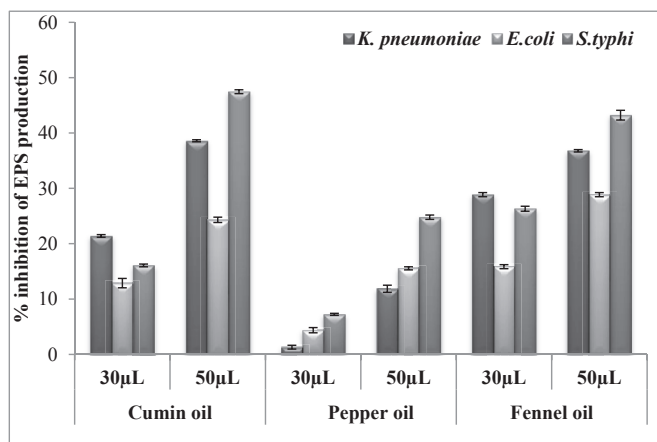


**Fig. 5.** Effect of formulated spice oil nanoemulsions on EPS production against food borne pathogens. Vertical bars represent the mean values of triplicates with a standard deviation.

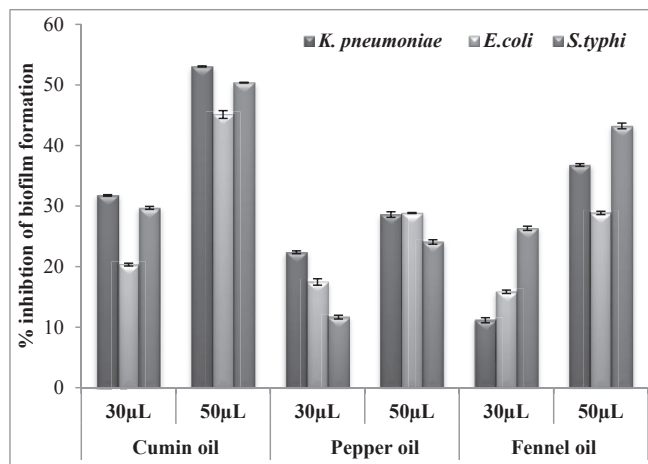


**Fig. 6.** Effect of formulated spice oil nanoemulsions on biofilm formation against food borne pathogens. Vertical bars represent the mean values of triplicates with a standard deviation.

resistant to conventional antibiotics by a wide range of mechanisms, adhere to the surface of food processing equipments. Even though effective treatments like using nanoparticles producing nitric acid (Mihu et al., 2010) seems to give the positive result, its usage in food industries and its potential side effect needs further investigation. Hence, food based nanoemulsions containing spice oil and surfactant may act as good alternatives to manage food borne pathogens.

#### 4. Conclusion

To this end, we have evaluated the quorum quenching activity of stable food-grade spice oil nanoemulsions against QS-dependent phenotypes of selected food borne pathogens. The obtained results exhibited that the formulated spice oil nanoemulsions effectively regulated bacterial phenotypes like violacein pigmentation, biofilm formation, and EPS production when compared with untreated controls. Among the three formulations, cumin and fennel oil nanoemulsions exhibited pronounced activity in all tests when compared with pepper oil nanoemulsion. Hence, by this study, we lay a solid foundation for the use of spice oil nanoformulations as a suitable alternative over conventional antimicrobials. Formulated nanoemulsions were tested for stability proves its candidature for field utilization. Tested nanoemulsions are ideal for treatment and/or for surface decontamination of bacterial infections with the aid of QS-based antibacterial drugs.

#### Conflict of interest

Authors declare that they have no conflict of interest.

#### Acknowledgments

Authors acknowledge, Pondicherry University for providing necessary facilities. Venkadesaperumal G, thankfully acknowledges ICMR for providing financial assistance in the form of "ICMR-Senior Research Fellowship" (3/1/2/14/2013-Nut).

#### Appendix A. Supplementary data

Supplementary data related to this article can be found at <http://dx.doi.org/10.1016/j.lwt.2015.10.044>.

## References

- Al-Adham, I. S. I., Khalil, E., Al-Hmoud, N. D., Kierans, M., & Collier, P. J. (2000). Microemulsions are membrane-active, antimicrobial, self-preserving systems. *Journal of Applied Microbiology*, *89*, 32–39.
- Choo, J. H., Rukayadi, Y., & Hwang, J. K. (2006). Inhibition of bacterial quorum sensing by vanilla extract. *Letters in Applied Microbiology*, *42*, 637–641.
- Ghosh, V., Mukherjee, A., & Chandrasekaran, N. (2013). Ultrasonic emulsification of food-grade nanoemulsion formulation and evaluation of its bactericidal activity. *Ultrasonics Sonochemistry*, *20*, 338–344.
- Gibot, S. (2004). Fighting the enemy properly. *Critical Care Medicine*, *32*, 1223–1224.
- Gutiérrez, J. M., González, C., Maestro, A., Solè, I., Pey, C. M., & Nolla, J. (2008). Nanoemulsions: new applications and optimization of their preparation. *Current Opinion in Colloid & Interface Science*, *13*, 245–251.
- Huston, A. L., Methe, B., & Deming, J. W. (2004). Purification, characterization, and sequencing of an extracellular cold-active aminopeptidase produced by marine psychrophile *Colwellia psychrerythraea* strain 34H. *Applied and Environmental Microbiology*, *70*, 3321–3328.
- Kalia, V. C. (2013). Quorum sensing inhibitors: an overview. *Biotechnology Advances*, *31*, 224–245.
- Kerekes, E. B., Deák, É., Takó, M., Tserennadmid, R., Petkovits, T., Vágvölgyi, C., et al. (2013). Anti-biofilm forming and anti-quorum sensing activity of selected essential oils and their main components on food-related microorganisms. *Journal of Applied Microbiology*, *115*, 933–942.
- Khan, M. S. A., Zahin, M., Hasan, S., Husain, F. M., & Ahmad, I. (2009). Inhibition of quorum sensing regulated bacterial functions by plant essential oils with special reference to clove oil. *Letters in Applied Microbiology*, *49*, 354–359.
- Leong, T. S. H., Wooster, T. J., Kentish, S. E., & Ashokkumar, M. (2009). Minimising oil droplet size using ultrasonic emulsification. *Ultrasonics Sonochemistry*, *16*, 721–727.
- Li, M., Lai, Y., Villaruz, A., Cha, D., Sturdevant, D., & Otto, M. (2007). Gram-positive three-component antimicrobial peptide-sensing system. *Proceedings of the National Academy of Sciences United States of America*, *104*, 9469–9474.
- Limsuwan, S., & Voravuthikunchai, S. P. (2008). *Boesenbergia pandurata* (Roxb.) Schltr., *Eleutherine americana* Merr. and *Rhodomyrtus tomentosa* (Aiton) Hassk. as antibiofilm producing and antiquorum sensing in *Streptococcus pyogenes*. *FEMS Immunology and Medical Microbiology*, *5*, 429–436.
- McClements, D. J., & Rao, J. (2011). Food-grade nanoemulsions: formulation, fabrication, properties, performance, biological fate, and potential toxicity. *Critical Reviews in Food Science and Nutrition*, *51*, 285–330.
- Mihu, M. R., Sandkovsky, U., Han, G., Friedman, J. M., Nosanchuk, J. D., & Martinez, L. R. (2010). The use of nitric oxide releasing nanoparticles as a treatment against *Acinetobacter baumannii* in wound infections. *Virulence*, *1*, 62–67.
- Miller, M., & Bassler, B. (2001). Quorum sensing in Bacteria. *Annual Review Microbiology*, *55*, 165–199.
- Niu, C., Alfre, S., & Gilbert, E. S. (2006). Subinhibitory concentrations of cinnamaldehyde interfere with quorum sensing. *Letters in Applied Microbiology*, *43*, 489–494.
- Qian, C., & McClement, D. J. (2011). Formation of nanoemulsions stabilized by model food-grade emulsifiers using high-pressure homogenization: factors affecting particle size. *Food Hydrocolloids*, *25*, 1000–1008.
- Silva, H. D., Cerqueira, M. A., & Vicente, A. A. (2012). Nanoemulsions for food applications: development and characterization. *Food Bioprocess Technology*, *5*, 854–867.
- Solans, C., Izquierdo, P., Nolla, J., Azemar, N., & Garcia-Celma, M. J. (2005). Nanoemulsions. *Current Opinion in Colloid and Interface Science*, *10*, 102–110.
- Tadros, T., Izquierdo, P., Esquena, J., & Solans, C. (2004). Formation and stability of nanoemulsions. *Advances in Colloid and Interface Science*, 303–318.
- Teixeira, P. C., Leite, G. M., Domingues, R. J., Silva, J., Gibbs, P. A., & Ferreira, J. P. (2007). Antimicrobial effects of a microemulsion and a nanoemulsion on enteric and other pathogens and biofilms. *International Journal of Food Microbiology*, *118*, 15–19.
- Valero, M., & Giner, M. J. (2006). Effects of antimicrobial components of essential oils on growth of *Bacillus cereus* INRA L2104 in and the sensory qualities of carrot broth. *International Journal of Food Microbiology*, *106*, 90–94.
- Vattem, D. A., Mihalik, K., Crixell, S. H., & McLean, R. J. C. (2007). Dietary phytochemicals as quorum sensing inhibitors. *Fitoterapia*, *78*, 302–310.
- Waters, C. M., & Bassler, B. L. (2005). Quorum sensing: cell-to-cell communication in bacteria. *Annual Review Cell Biology*, *21*, 319–346.
- You, J., Xue, X., Cao, L., Lu, X., Wang, J., Zhang, L., et al. (2007). Inhibition of *Vibrio* biofilm formation by a marine actinomycete strain A66. *Applied Microbiology and Biotechnology*, *76*, 1137–1144.
- Zhang, H., Shen, Y., Weng, P., Zhao, G., Feng, F., & Zheng, X. (2009). Antimicrobial activity of a food-grade fully dilutable microemulsion against *Escherichia coli* and *Staphylococcus aureus*. *International Journal of Food Microbiology*, *135*, 211–215.



## Effects of tea polyphenols and different teas on pancreatic $\alpha$ -amylase activity *in vitro*



Xiaoping Yang <sup>a, b</sup>, Fanbin Kong <sup>b, \*</sup>

<sup>a</sup> Key Laboratory of Horticultural Plant Biology (Huazhong Agricultural University), Ministry of Education, Wuhan, 430070, PR China

<sup>b</sup> Department of Food Science and Technology, College of Agricultural and Environmental Sciences, The University of Georgia, Athens, GA, 30602-2610, United States

### ARTICLE INFO

#### Article history:

Received 5 July 2015

Received in revised form

10 October 2015

Accepted 13 October 2015

Available online 23 October 2015

#### Keywords:

Tea polyphenols

Tea

$\alpha$ -amylase

Enzyme inhibition

Antioxidant

### ABSTRACT

The effects of tea polyphenols (TP) and different types of teas (green, black and oolong tea) processed from the same fresh leaves on pancreatic  $\alpha$ -amylase activity were studied using potato starch and cooked potato as substrates. The results showed that, with the both substrates, low concentration of TP significantly increased  $\alpha$ -amylase activity while high concentration inhibited it by non-competitive fashion. In addition, the extents of enzymatic activation and inhibition were different when TP was pre-incubated with  $\alpha$ -amylase or starch, respectively. The interaction of TP with enzyme/starch led to decreased antioxidant capacity. Results also showed that all the three types of teas significantly enhanced  $\alpha$ -amylase activity for a wide range of concentrations (0.34–27.14 mg/mL), and green tea showed the highest activation effect. It is concluded that high concentration of TP exhibits mild inhibitory effect against  $\alpha$ -amylase, while green tea, black tea and oolong tea enhance  $\alpha$ -amylase activity, which may be due to other constituents in the tea, enhancing  $\alpha$ -amylase activity that counteracts the inhibitory effect of TP.

© 2015 Elsevier Ltd. All rights reserved.

## 1. Introduction

Tea is a popular drink around the world, as it is the second most commonly consumed beverage worldwide only behind water. Tea has many health benefits such as lowering cholesterol levels, preventing cancer, and improving the immune system function (Sinija & Mishra, 2008). Studies have also shown that tea may help regulate the digestion and drinking tea benefits digestive health. In fact, tea has been used for thousands of years as a postprandial digestive aid in India and China (Underwood, 2012). The beneficial effects of tea on the digestive system may be related to tea polyphenols (TP, mainly containing catechins). Studies have shown that epigallocatechin-3-gallate (EGCG), a catechin, may help regulate the digestive system as it reduces inflammation in the gastrointestinal tract and colitis models (Oz, Chen, & de Villiers, 2013).

Despite the consensus that tea improves digestive health, the effects of tea and TP on digestive enzymes, especially  $\alpha$ -amylase, are not yet agreed upon. For example, Hara and Honda (1990) found that TP inhibited  $\alpha$ -amylase in a noncompetitive fashion, while

other researchers found that TP and green tea extract had little or no inhibition of  $\alpha$ -amylase (Gao, Xu, Wang, Wang, & Hochstetter, 2013; Kwon, Apostolidis, & Shetty, 2008). In addition, the inhibition of  $\alpha$ -amylase seems to be dependent on the type of tea. It has been reported that black tea had substantial inhibitory effect against  $\alpha$ -amylase whereas green tea had low or no inhibitory effect (Koh, Wong, Loo, Kasapis, & Huang, 2010; Quesille-Villalobos, Torrico, & Ranilla, 2013). In another study, Wu, Ding, Xia, and Tu (2010) found that TP increased the activity of pancreatic  $\alpha$ -amylase. Liu, Wang, Peng, and Zhang (2011) also found that green TP increased the digestion rate of corn starch. From these findings, it is difficult to draw a conclusion on how TP and teas affect  $\alpha$ -amylase activity. It was noted that some studies investigated purified TP, and others used teas extracts. Since the effects of TP and tea on  $\alpha$ -amylase activity might be different due to the existence of other components in the tea, a study comparing TP and tea extract should help obtain insight information about the role of tea in modulating the enzyme activity. It was also noted that different materials and experimental conditions were involved in the existing studies, such as source of teas, incubation order (i.e. the sequence of adding substrate and enzyme to TP/tea extract.) and the concentrations of TP/tea extract tested.

\* Corresponding author.

E-mail address: [fkong@uga.edu](mailto:fkong@uga.edu) (F. Kong).

To compare the effect of different types of teas on the enzyme activity, it is important to have the teas processed from the same fresh tea leaves because the composition and total phenolic content in different fresh tea leaves maybe markedly different, thus affecting the composition and total phenolic content in tea extracts (Lin, Tsai, Tsay, & Lin, 2003). It was noted that the teas were mostly obtained from local stores in the existing researches. It was difficult to ensure the same fresh tea leaves were used. Moreover, teas used in some studies were in the form of tea bag, which could contain additives that might affect enzyme activity. Similarly, different concentrations of TP and tea extracts were used in existing studies making it difficult to compare the results. A study covering a wide scope of the concentration of TP and tea extracts should give more comprehensive information about the impact of tea on enzyme. In addition, the incubation order of TP and tea extracts might also affect  $\alpha$ -amylase activity because polyphenol can interact with both proteins and polysaccharides forming a binary or ternary complex (Luck et al., 1994), but there is no published information found about the effect of the incubation order on  $\alpha$ -amylase activity.

The objective of this study was to systematically investigate the effect of TP and different types of tea extracts on the  $\alpha$ -amylase activity as affected by concentration of TP/tea extracts and incubation orders. The study aimed to provide comprehensive information regarding the impact of tea on  $\alpha$ -amylase activity. In this study, three types of teas, including green tea, black tea and oolong tea, were processed with the same fresh tea leaves. TP and these teas were compared for their influence on the  $\alpha$ -amylase activity, covering a wide range of concentrations and different incubation orders. In addition, the change in the antioxidant capacity of TP in the enzyme hydrolysis system was also studied to understand the interactions among TP, starch and enzyme.

## 2. Materials and methods

### 2.1. Materials

Tea polyphenols (TP) from green tea (purity of 98 g/100g) was purchased from Nanjing Qingze Medical Technological Development Co. Ltd (Nanjing, China). Porcine pancreatic  $\alpha$ -amylase (EC 3.2.1.1), potato starch, 3, 5-dinitrosalicylic acid were purchased from Sigma Chemical Co. (St. Louis, MO). All reagents and chemicals used were of analytical grade.

### 2.2. Processing of tea

Green tea, black tea and oolong tea were respectively processed at the tea factory of Huazhong Agricultural University (HZAU), Wuhan, China. Briefly, fresh tea leaves were picked from *Camellia sinensis* bushes in tea garden at HZAU. Then, with these fresh leaves, green tea was processed by fixing, rolling and drying, and black tea was processed by withering, rolling, fermenting and drying, and oolong tea was processed by sunshine withering, tedding fresh leaves, rocking green, stir-fry green, rolling and drying (Shi, 1997). These teas were crushed, sieved through 0.42 mm pore size sieve and stored at  $-20\text{ }^{\circ}\text{C}$  for further use.

### 2.3. Effect of TP on $\alpha$ -amylase activity

#### 2.3.1. Influence of TP concentration

The  $\alpha$ -amylase inhibition assay was conducted with potato starch as substrate using the method of Zhao, Iyer, Flores, Donhowe, and Kong (2013). TP was dissolved in phosphate buffer (pH 6.9, 20 mmol/L). Potato starch solution (3.0 g/100 mL) was prepared by dissolving potato starch in phosphate buffer (pH 6.9, 20 mmol/L) and gelatinized for 20 min at  $80\text{ }^{\circ}\text{C}$ . A series of tubes was added

with 300  $\mu\text{L}$  serial 2-fold dilutions of TP solution, including 0.16, 0.31, 0.63, 1.25, 2.50, 5.00, 10.00, and 20.00 mg/mL, respectively, and 300  $\mu\text{L}$  of  $\alpha$ -amylase (100 U/mL) in phosphate buffer (pH 6.9, 20 mmol/L). The tubes were incubated in a water bath at  $37\text{ }^{\circ}\text{C}$  for 20 min, and added with 1 mL 3.0 g/100 mL potato starch solution. The reaction mixture was incubated at  $37\text{ }^{\circ}\text{C}$  for 20, 60, 120 min and then the reaction were stopped with 1.5 mL of dinitrosalicylic acid reagent. Thereafter, the mixture was boiled for 5 min and cooled to room temperature. Then the reaction mixture was diluted by adding 6 mL of deionized water and the absorbance was measured at 540 nm using a UV-vis spectrophotometer (Evolution 300, Thermo Fisher Scientific Inc., USA). The  $\alpha$ -amylase activity was expressed as U/mL, where one unit was defined as the amount of enzyme required to release one mol glucose equivalent per minute under the above assay condition. The inhibitory effect was calculated using following formula: Inhibitory effect (%) = (the  $\alpha$ -amylase activity of control - the  $\alpha$ -amylase activity of sample)/the  $\alpha$ -amylase activity of control  $\times 100$ .

#### 2.3.2. Influence of pre-incubation of TP and starch

The effect of incubation order on  $\alpha$ -amylase activity was tested with potato starch as substrate using the same method as described above, except that 300  $\mu\text{L}$  of TP solution and 1 mL of potato starch solution were mixed first and incubated at  $37\text{ }^{\circ}\text{C}$  for 20 min, followed by the addition of 300  $\mu\text{L}$  of  $\alpha$ -amylase solution.

### 2.4. Inhibition mode of TP on the $\alpha$ -amylase

The catalysis kinetics of  $\alpha$ -amylase in the presence of TP at different concentrations (0, 10, and 20 mg/mL) were performed using the method of Chethan, Sreerama, and Malleshi (2008). 300  $\mu\text{L}$  of TP solution and different amounts of  $\alpha$ -amylase solution (100 U/mL, 50, 100, 150, 200, 250, and 300  $\mu\text{L}$ ) were added to a series of tubes, followed by the addition of phosphate buffer to make the final volume 600  $\mu\text{L}$ . The tubes were incubated at  $37\text{ }^{\circ}\text{C}$  for 20 min, and added with 1 mL of potato starch solution (3.0 g/100 mL). The reaction mixture was incubated at  $37\text{ }^{\circ}\text{C}$  for 30 min. Lineweaver–Burk (LB) analysis of  $\alpha$ -amylase in the presence of TP (0, 10, and 20 mg/mL) was performed according to the methods of Chethan et al. (2008). The inhibition was measured with increasing concentrations of potato starch as a substrate (0.5, 1.0, 2.0, and 3.0 g/100 mL). 300  $\mu\text{L}$  of TP solution and 300  $\mu\text{L}$  of  $\alpha$ -amylase solution (100 U/mL) were mixed first and incubated at  $37\text{ }^{\circ}\text{C}$  for 20 min, followed by the addition of 1 mL of different concentrations of potato starch solution for 30 min at  $37\text{ }^{\circ}\text{C}$ . The type of inhibition was determined by LB plot analysis of the data, which were calculated from the results according to Michaelis–Menten kinetics.

### 2.5. Change in the antioxidant capacity of TP during enzymatic hydrolysis

Similar to above, 300  $\mu\text{L}$  of TP solution was incubated with 300  $\mu\text{L}$  of  $\alpha$ -amylase solution (100 U/mL) in phosphate buffer at  $37\text{ }^{\circ}\text{C}$  for 20 min. Then the mixture was added with 1 mL 3.0 g/100 mL potato starch solution, and incubated at  $37\text{ }^{\circ}\text{C}$  for 120 min. The ferric-reducing antioxidant capacity (FRAP) of TP in the supernatant during enzymatic hydrolysis was measured using the method of Benzie and Strain (1996), and results were expressed as mmol/L  $\text{Fe}^{2+}$  equivalents. The 1,1-diphenyl-2-picrylhydrazyl radical (DPPH $\cdot$ ) scavenging activity was determined according to the method described by Zhu, Hackman, Ensunsa, Holt, and Keen (2002), and results were expressed as ascorbic acid equivalent antioxidant capacity (AEAC). The hydroxyl radical ( $\cdot\text{OH}$ ) scavenging activity was measured by the deoxyribose method (Aruoma, 1994)

modified by Hagerman et al. (1998), and results were expressed as scavenging percentage (%).

### 2.6. Preparation of tea extracts and determination of total phenolic contents

25.0 g of green tea, black tea and oolong tea were respectively soaked in 100 mL boiling deionized water for 30 min (Zhong, 1989). The mixtures were centrifuged and the supernatants were collected and diluted to obtain 100 mL tea extracts. The tea extracts were further diluted 1.0-fold, 1.25-fold, 1.67-fold, 2.5-fold, 5-fold, and 25-fold to obtain a series of tea extracts. Total phenolic contents in them were measured with Folin-Ciocalteu's method using gallic acid for the standard curve, and results were expressed as mg of gallic acid equivalents (GAEs) per millilitre of tea extract (mg GAEs/mL).

### 2.7. Effect of tea extracts on $\alpha$ -amylase activity

The effects of tea extracts on  $\alpha$ -amylase activity were measured according to the method described above in Section 2.3.1. 300  $\mu$ L of the above tea extracts was incubated with 300  $\mu$ L of  $\alpha$ -amylase, then added with 1 mL of potato starch solution. The activation effect (%) was calculated using following formula: Activation effect (%) = (the  $\alpha$ -amylase activity of sample – the  $\alpha$ -amylase activity of control)/the  $\alpha$ -amylase activity of control  $\times$  100.

### 2.8. Change of antioxidant capacity in tea extracts during enzymatic hydrolysis

The change of antioxidant capacity of different tea extracts in the supernatant during enzymatic hydrolysis was measured as described in Section 2.5.

### 2.9. Statistical analyses

All data were expressed as the mean  $\pm$  SD of three replications of the experiment. Statistical analysis was performed by one-way analysis of variance followed by LSD test. Significant difference was considered at  $p < 0.05$ .

## 3. Results

### 3.1. Effect of TP on $\alpha$ -amylase activity

As shown in Fig. 1, TP concentration and incubation order significantly affected  $\alpha$ -amylase activity. When pre-incubated with  $\alpha$ -amylase prior to addition of potato starch (Fig. 1a), TP significantly increased  $\alpha$ -amylase activity at low concentrations. The activation effect increased with the increase of TP concentration and gradually reached a peak at 2.50 mg/mL of TP (0.47 mg/mL in reaction mixture), and the maximum activation magnitude of the activity was above 200%. After that, the enzyme activation magnitude gradually decreased with increasing TP concentration. TP significantly inhibited  $\alpha$ -amylase activity in a dose-dependent manner when its concentration was more than 10.00 mg/mL (1.88 mg/mL in reaction mixture). When TP was pre-incubated with starch (Fig. 1b), the initial increase in enzyme activity at low concentrations of TP was also observed but within a much lower concentration limit of 1.25 mg/mL (0.23 mg/mL in reaction mixture), and the increase in enzyme activity was also very limited (max. about 12.5%). TP started to significantly inhibit  $\alpha$ -amylase activity in a dose-dependent manner at TP concentration over 2.50 mg/mL (0.47 mg/mL in reaction mixture). As an indicator of inhibitory potency, the concentrations required for 50%

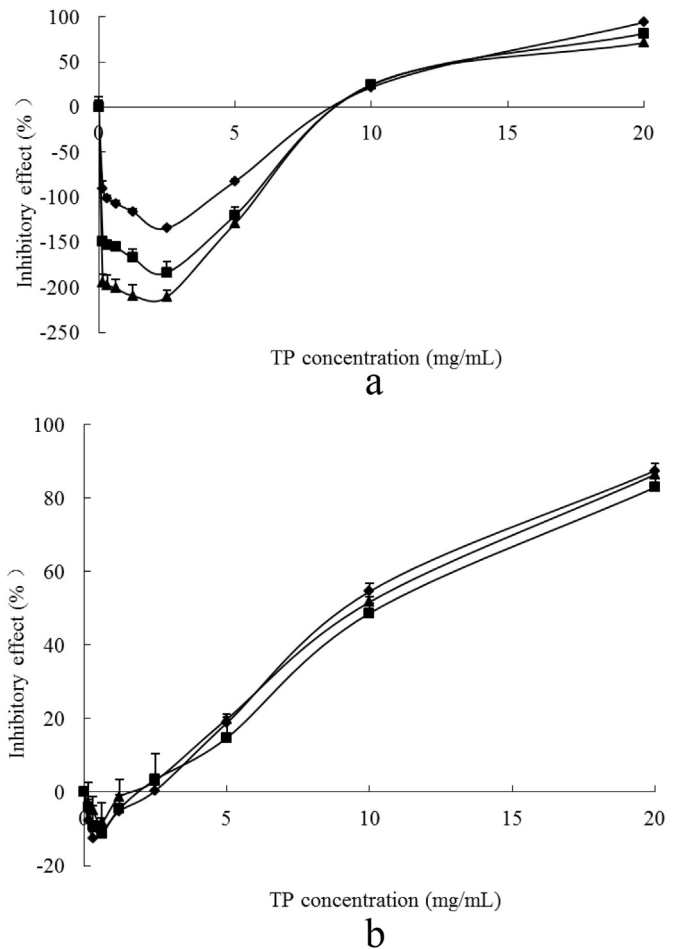


Fig. 1. Effect of TP on  $\alpha$ -amylase activity. a) 300  $\mu$ L of TP was pre-incubated with 300  $\mu$ L of  $\alpha$ -amylase solution (100 U/mL) at 37  $^{\circ}$ C for 20 min, followed by the addition of 1 mL 3.0 g/100 mL starch solution at 37  $^{\circ}$ C for 20, 60, 120 min; b) 300  $\mu$ L of TP was pre-incubated with 1 mL 3.0 g/100 mL starch solution at 37  $^{\circ}$ C for 20 min, followed by the addition of 300  $\mu$ L of  $\alpha$ -amylase solution (100 U/mL) at 37  $^{\circ}$ C for 20 ( $\blacklozenge$ ), 60 ( $\blacksquare$ ), 120 ( $\blacktriangle$ ) minutes.

inhibition of enzyme activity ( $IC_{50}$ ) were calculated from the dose–response curves, and the  $IC_{50}$  value was 13.78 mg/mL (2.58 mg/mL in reaction mixture) when TP was pre-incubated with  $\alpha$ -amylase, and 9.83 mg/mL (1.84 mg/mL in reaction mixture) with starch, respectively.

### 3.2. Inhibition kinetics of TP on $\alpha$ -amylase

Fig. 2a depicts the catalysis kinetics of  $\alpha$ -amylase in the presence and absence of TP. It shows that the lines intersect at the origin with different slopes, and the higher the TP concentration, the smaller the slope of the line is, which shows that TP is a reversible inhibitor against  $\alpha$ -amylase because it only decreases the catalysis velocity of  $\alpha$ -amylase as indicated by the change of the slope.

It is well-known that an inhibitor is noncompetitive when increasing the concentration of substrate results in a family of lines with a common intercept on the  $1/V$  axis but with different slopes (Zhao et al., 2013). Fig. 2b depicts the effect of TP on  $\alpha$ -amylase activity as presented in Lineweaver–Burk type plots, which suggests that the inhibition of  $\alpha$ -amylase by TP is noncompetitive.

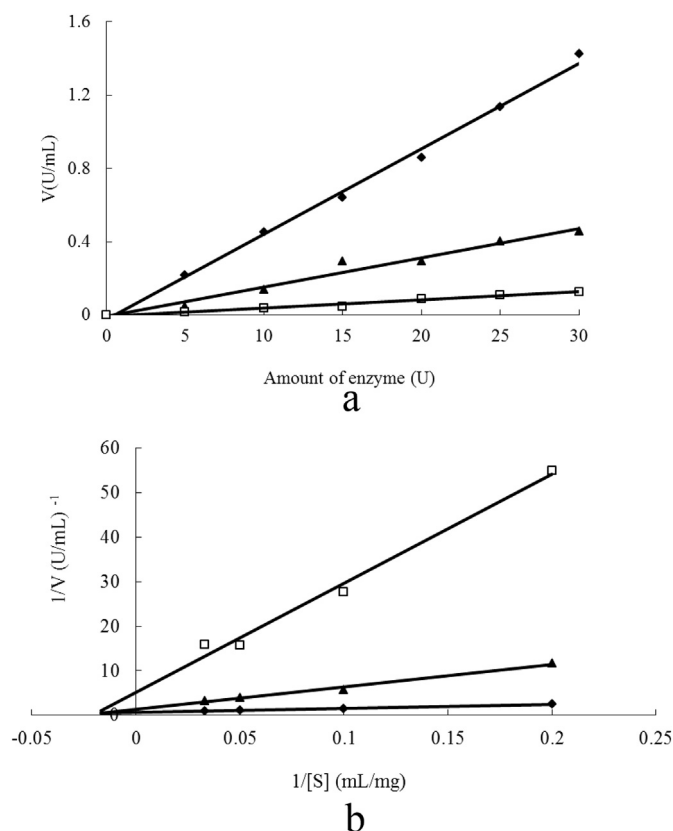


**Fig. 2.** The inhibition mode of TP on  $\alpha$ -amylase. a) the catalysis kinetics of  $\alpha$ -amylase in the presence and absence of TP [0 (◆), 10 (▲), 20 (□) mg/mL]. 300  $\mu$ L of TP solution and different amounts of  $\alpha$ -amylase solution (100 U/mL, 50, 100, 150, 200, 250, and 300  $\mu$ L) were mixed first and incubated at 37 °C for 20 min, followed by the addition of 1 mL of 3.0 g/100 mL potato starch solution at 37 °C for 30 min b) Lineweaver–Burk analysis of  $\alpha$ -amylase in the presence and absence of TP. 300  $\mu$ L of TP solution and 300  $\mu$ L of  $\alpha$ -amylase solution (100 U/mL) were mixed first and incubated at 37 °C for 20 min, followed by the addition of 1 mL of different concentrations of potato starch solution (0.5, 1.0, 2.0, and 3.0 g/100 mL) at 37 °C for 30 min.

### 3.3. Change in the antioxidant capacity of TP during enzymatic hydrolysis

The antioxidant capacity of TP in the supernatant during enzymatic hydrolysis was measured. The pre-incubation with  $\alpha$ -amylase significantly decreased the antioxidant capacity of TP in the supernatant. However, the subsequent enzymatic hydrolysis significantly increased the antioxidant capacity in the supernatant although it was still significantly lower than that of untreated TP. The antioxidant capacity of TP after 60 min of enzymatic hydrolysis was significantly higher than that after 20 min and 120 min of

enzymatic hydrolysis. The TP content in the supernatant was also measured and a similar changing trend was observed (data not shown). A strong positive linear correlation (FRAP:  $R^2 > 0.996$ ; DPPH $\cdot$  scavenging activity:  $R^2 > 0.738$ ;  $\cdot$ OH scavenging activity:  $R^2 > 0.906$ ) existed between the concentration and the antioxidant capacity of TP.

### 3.4. Effect of tea extracts on $\alpha$ -amylase activity

In this study, the effect of three types of teas processed from the same fresh tea leaves on  $\alpha$ -amylase activity was studied as a comparison of that of TP. A series of concentrations of the extracts of green tea, black tea and oolong tea was prepared with different total phenolic contents. As expected, total phenolic contents in green tea extract was significantly higher than that in oolong tea extract, and that in oolong tea was significantly higher than that in black tea (Table 1).

As shown in Fig. 3a and b, all the tea extracts significantly increased  $\alpha$ -amylase activity for all the test concentrations, and the activation effect was dependent on their concentration and the type of tea. Green tea extract showed the highest activation effect, and the activation magnitude increased with the increasing extract concentration until reaching a maximum, and then gradually decreased. Oolong tea extract showed a similar trend but the activation magnitude was significantly lower. The activation magnitude of black tea extract increased continually and leveled off with the increasing concentration.

Like TP, the incubation order of tea extract also had significant effect on  $\alpha$ -amylase activity. Fig. 3c shows the effect of incubation order for green tea extract with potato starch as substrate. It can be seen when green tea extract was pre-incubated with starch, the maximum activation magnitude of the activity was 405%, where tea extract was diluted 1.67-fold and total phenolic content was 16.03 mg/mL (3.01 mg/mL in reaction mixture). For the case where tea extract was pre-incubated with  $\alpha$ -amylase, the maximum activation magnitude was 367%, which was obtained by tea extract with 2.5-fold dilution and the phenolic content 10.44 mg/mL (1.96 mg/mL in reaction mixture).

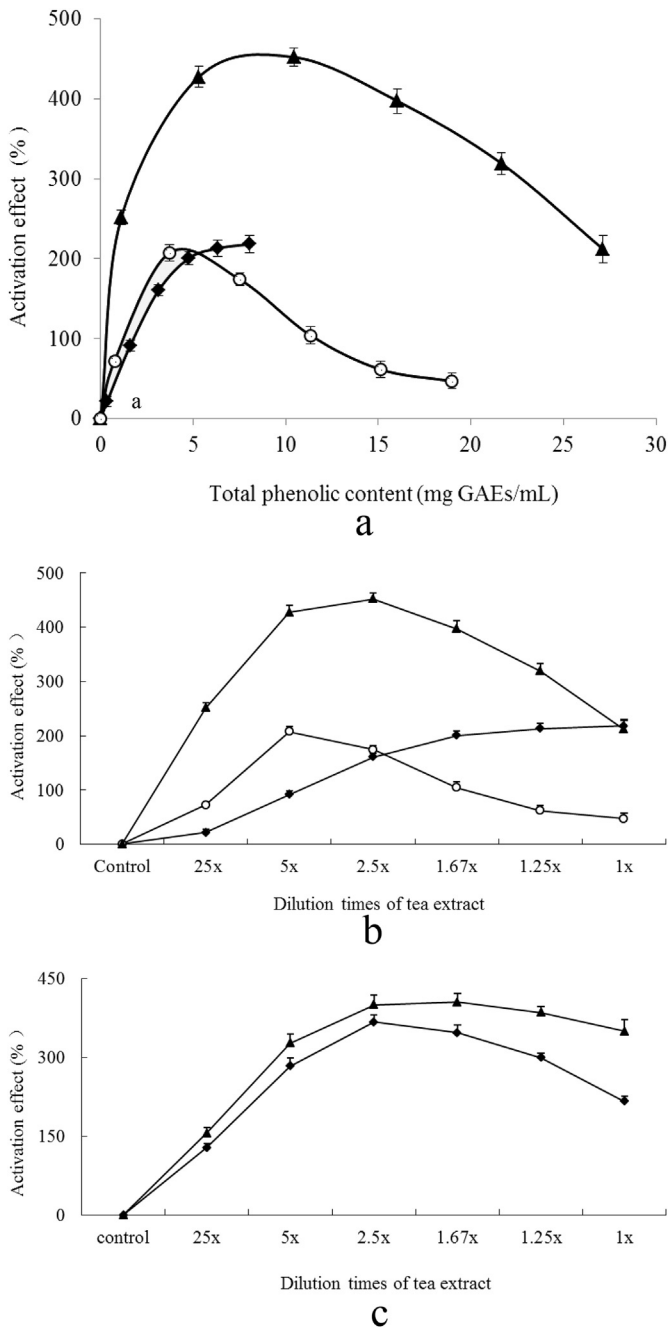
### 3.5. Antioxidant capacity of different teas during enzymatic hydrolysis

Table 1 shows the total phenolic content and antioxidant capacity for the three tea extracts without dilution. The total phenolic contents follow the order: green tea > oolong tea > black tea. The antioxidant capacities, as expressed by the FRAP and the radical scavenging activity against DPPH $\cdot$  and  $\cdot$ OH, were well correlated with their total phenolic contents. The antioxidant capacities of the three tea extracts and their total phenolic contents in the supernatant were also measured during enzymatic hydrolysis (data not shown). The results showed that the change of the antioxidant

**Table 1**  
Total phenolic content and antioxidant capacity of TP and tea extracts.<sup>a</sup>

	TP (20 mg/mL)	Green tea	Black tea	Oolong tea
Total phenolic content (mg GAEs/mL)	18.44 $\pm$ 0.05b	27.14 $\pm$ 0.94a	8.05 $\pm$ 0.71c	18.98 $\pm$ 0.88b
FRAP (mmol/L Fe <sup>2+</sup> )	8.23 $\pm$ 0.49c	16.83 $\pm$ 0.65a	6.29 $\pm$ 0.37d	13.58 $\pm$ 0.58b
DPPH $\cdot$ scavenging activity ( $\mu$ g/mL AEAC)	21.37 $\pm$ 1.25b	41.06 $\pm$ 1.37a	21.28 $\pm$ 1.97b	40.40 $\pm$ 1.20a
$\cdot$ OH scavenging activity (%)	87.71 $\pm$ 1.62a	86.49 $\pm$ 1.28a	75.71 $\pm$ 1.71c	80.67 $\pm$ 1.92b

<sup>a</sup> 25.0 g of green tea, black tea and oolong tea was respectively extracted with 100 mL boiling deionized water for 30 min, centrifuged and diluted to obtain 100 mL tea extract. Total phenolic contents in the tea extracts were measured with Folin-Ciocalteu's method, and results were expressed as mg of gallic acid equivalents per millilitre of tea extract (mg GAEs/mL). 20.00 mg/mL of TP was also expressed as mg GAEs/mL with Folin-Ciocalteu's method. Total antioxidant capacities of TP and these tea extracts were measured. The FRAP was expressed as mmol/L Fe<sup>2+</sup> equivalents. The DPPH $\cdot$  scavenging activity was expressed as ascorbic acid equivalent antioxidant capacity (AEAC). The  $\cdot$ OH scavenging activity was expressed as scavenging percentage (%). Different letters in the same row indicate significant differences at  $P < 0.05$ .



**Fig. 3.** Effect of tea extracts (a: total phenolic content; b: dilution times) and pre-incubation order (c) of green tea extract on  $\alpha$ -amylase activity. 25.0 g of green tea (▲), black tea (◆) and oolong tea (○) was respectively extracted with 100 mL boiling deionized water for 30 min, centrifuged and diluted to obtain 100 mL tea extract. The tea extract was further diluted 1-fold, 1.25-fold, 1.67-fold, 2.5-fold, 5-fold, and 25-fold to obtain a series of tea extracts. (◆) Tea extract was pre-incubated with  $\alpha$ -amylase; (▲) Tea extract was pre-incubated with starch.

capacities of the three tea extracts showed a similar trend to that of their total phenolic contents in the supernatant during enzymatic hydrolysis: a significant decrease when enzyme was just added followed by a gradual increase with continued enzymatic hydrolysis. Strong positive linear correlations were also observed between the antioxidant capacity and total phenolic content in the extracts of green tea (FRAP:  $R^2 > 0.992$ ; DPPH· scavenging activity:  $R^2 > 0.765$ ; ·OH scavenging activity:  $R^2 > 0.977$ ), black tea (FRAP:  $R^2 > 0.996$ ; DPPH· scavenging activity:  $R^2 > 0.663$ ; ·OH scavenging

activity:  $R^2 > 0.992$ ) as well as oolong tea (FRAP:  $R^2 > 0.989$ ; DPPH· scavenging activity:  $R^2 > 0.734$ ; ·OH scavenging activity:  $R^2 > 0.964$ ).

#### 4. Discussion

Chinese people have consumed tea for thousands of years, holding the belief that drinking tea can help digestion, and some studies have shown that tea increases digestive enzyme activity and can be used as digestion aid (Tagliacuzzi, Verzelloni, & Conte, 2005; Wu et al., 2010). However, some recently published studies imply that drinking tea hinders digestion (Forester, Gu, & Lambert, 2012; He, Lv, & Yao, 2006) because TP is capable of binding and precipitating protein through non-covalent interaction (Dreosti, 2000), and the interaction between TP and digestive enzyme can change the molecular configuration of enzyme, leading to the loss of enzyme activity and thereby reducing food digestibility. The disagreement within literature about the effect of TP and teas on enzyme activity might be related to the different TP concentrations and incubation orders involved in these studies. The source of tea was also responsible for the contradictory results because most of the existing research were conducted with teas purchased from market. It is also noted that tea extracts and purified TP may possess different effect due to the existence of other components in teas. In this project, we tested the effect of TP and the extracts of green tea, black tea as well as oolong tea processed with the same fresh tea leaves on  $\alpha$ -amylase activity *in vitro*. A wide range of concentrations of TP and tea extracts were tested, comparing two different incubation orders and using potato starch as substrate.

The results from this study showed that the effects of TP and tea extracts on  $\alpha$ -amylase activity were complex, and concentration, incubation order as well as tea type all significantly affected  $\alpha$ -amylase activity. When the ratio of starch to enzyme remained unchanged, TP at low concentrations (below about 8 mg/mL, 1.50 mg/mL in reaction mixture) increased  $\alpha$ -amylase activity, whereas high concentrations (over 10 mg/mL, 1.88 mg/mL in reaction mixture) inhibited enzyme activity. The  $IC_{50}$  value against  $\alpha$ -amylase was 13.78 mg/mL (2.58 mg/mL in reaction mixture) when TP was pre-incubated with  $\alpha$ -amylase, and 9.83 mg/mL (1.84 mg/mL in reaction mixture) with starch, respectively, which was similar to the report of Gao et al. (2013), who showed that the  $IC_{50}$  value of TP against  $\alpha$ -amylase was 1.37 mg/mL. We also tested the effect of TP with cooked potato as substrate, and found the similar effect (data not shown), and the maximum increase in enzyme activity was 84.75% for 20 min of enzymatic hydrolysis, which was lower than that with potato starch (134.3%) as substrate. These results suggested that TP only had a mild inhibitory effect against  $\alpha$ -amylase at high concentrations. Hara and Honda (1990) reported a strong inhibition effect of TP against  $\alpha$ -amylase with an  $IC_{50}$  value ranging 0.5–120  $\mu$ g/mL. The disagreement may be due to different experimental conditions: a relatively low content of starch was used in their test to react with TP before enzyme was added. The starch might have been bound to TP leading to reduced hydrolysis efficiency.

The results also showed that the extracts of green tea, black tea and oolong tea increased the enzyme activity for all the test concentrations (Fig. 3a and b) despite of the high total phenolic contents they contained (maximum concentration was 27.14 mg/mL in green tea extract, 8.05 mg/mL in black tea extract and 18.98 mg/mL in oolong tea extract). The strong enzyme activation effect of tea extracts might be explained by the composition of teas. Although polyphenols were the major component of tea extracts, other components, such as ions and caffeine, were also present in tea extracts and might affect the activity of  $\alpha$ -amylase. Several studies have reported that ions such as  $Cl^-$  (Aghajari, Feller, Gerday, &

Haser, 2002),  $\text{Co}^{2+}$ ,  $\text{Ca}^{2+}$  (Saboury, 2002) and  $\text{Ba}^{2+}$  (Usha, Krishna, Muni, & Hemalatha, 2011) can enhance  $\alpha$ -amylase activity and tea extracts contain ions in abundance (Cabrera, Artacho, & Giménez, 2013). It was also reported that caffeine could enhance  $\alpha$ -amylase activity (Kashani-Amin, Yaghmaei, Larijani, & Ebrahim-Habibi, 2013). The content of caffeine in the tea extracts of green tea, black tea and oolong tea was tested with HPLC, which were 0.37, 0.29 and 0.32 mg/mL, respectively. Therefore, we speculate that the ions and caffeine in tea extracts promote the activity of  $\alpha$ -amylase and retard the mild inhibitory effect of polyphenols against  $\alpha$ -amylase. Fig. 3a showed that the effect of the three tea extracts on  $\alpha$ -amylase activity was different at the same total phenolic contents, which also confirmed that the different effects were due to the other components in these tea extracts in addition to polyphenols.

The green tea, black tea and oolong tea were processed with the same fresh leaves and extracted in the same condition. The stronger enzyme activation effect of green tea extract than black tea extract and oolong tea extract on the same dilution (Fig. 3b) might be also related to the different components in these tea extracts. Green tea (non-fermented tea), black tea (fully-fermented tea) and oolong tea (semi-fermented tea) are processed through attaining different levels of oxidation, and green tea possesses the highest total phenolic content and black tea possesses the highest content of polyphenol oxidation products (Jain, Manghani, Kohli, Nigam, & Rani, 2013; Yi et al., 2015). It is also known that the polyphenol oxidation products are more easily to bind and precipitate caffeine and metal cations than TP (Liang, Lu, & Zhang, 2002). Therefore, green tea extract should contain relatively high contents of polyphenols, caffeine and metal cations, and eventually demonstrate a strong effect of activation. The activation effect of green tea extract increased at low concentration and gradually reached a peak, then gradually decreased at high concentration, which is well correlated to the effect of TP (Fig. 1) which enhanced enzyme activity at low concentrations and inhibited it at high concentrations. The activation effect of oolong tea extract showed a similar trend to that green tea extract, but the activation magnitude was lower, which might be related to its lower content of caffeine and metal cations. Black tea extract also showed an increasing activation effect with the concentration but had no decreasing phase, which is probably because the black tea extract contained much lower total phenolic content: the maximum total phenolic content was 8.05 mg/mL (1.51 mg/mL in reaction mixture) for 1-fold diluted extract where TP has no obvious inhibition or activation effect on  $\alpha$ -amylase.

The incubation order also significantly influenced  $\alpha$ -amylase activity. Our study showed that when TP was pre-incubated with  $\alpha$ -amylase prior to addition of starch, the increase in enzyme activity was significantly higher and occurred over a wider TP concentration range (up to about 8 mg/mL) than that with starch (up to 1.25 mg/mL) (Fig. 1), and the  $\text{IC}_{50}$  values were also significantly different in the two incubation orders. A similar effect of incubation order for TP with cooked potato as substrate and for green tea extract with the both substrates was also observed (data not shown). The study revealed that TP might not only bind and precipitate  $\alpha$ -amylase but also bind to starch, and that the binding with starch might have reduced the available binding sites for the enzyme, thus affecting the  $\alpha$ -amylase activity. This result is consistent with the findings of Liu et al. (2011), who reported the interaction between TP and amylose, and of Xiao et al. (2013), who also reported that the highly reactive hydroxyl (OH) groups in TP interacted with the OH groups of starches leading to the formation of hydrogen bonds. Luck et al. (1994) reported that polyphenol might not only form a binary complex with protein or polysaccharide, but also form a ternary complex with both protein and polysaccharide, and the complexes could be reversible depending

on pH, temperature, and their concentrations, etc., leading to enzyme regeneration.

The influence of incubation order on  $\alpha$ -amylase activity was different for tea extracts, where the increase in enzyme activity was significantly lower when green tea extract was pre-incubated with  $\alpha$ -amylase than that with starch (Fig. 3b). The reason for the difference is not clear; but we speculate that it may also be caused by other components present in tea extract. This difference may suggest that drinking tea after a meal is more beneficial for the starch digestion than before a meal, which is consistent with Chinese belief of that drinking tea after a meal helps digestion.

The antioxidant capacity of TP in the supernatant was significantly decreased right after enzyme was added, then increased when enzymatic hydrolysis was continued, and the change of TP content in the supernatant had a similar trend to that of the antioxidant capacity (data not shown). The initial decrease was attributed to the binding reaction of TP to enzyme, and the subsequent increase might be a result of enzyme regeneration (Luck et al., 1994). It was noted that the antioxidant capacity after 120 min of enzymatic hydrolysis was lower than that after 60 min, which might be due to that the enzymatic hydrolysis for a long time has caused the degradation of TP that decreased the antioxidant capacity. Similar phenomenon was observed by Chen et al. (2013) who reported decreased antioxidant capacity of tea juice during *in vitro* digestion. The change in the antioxidant capacity of tea extracts during enzymatic hydrolysis also showed a similar trend to that of TP, and strong positive linear correlations between the antioxidant capacity and total phenolic contents of tea extracts were also observed, which confirmed the reaction had occurred among polyphenols, enzyme and/or starch, indicating that the activation effect was due to other components present in tea extract.

## 5. Conclusions

This study showed that TP has mild inhibitory effect against  $\alpha$ -amylase at high concentration and both TP concentration and incubation order had significant effects on  $\alpha$ -amylase activity. Green tea, black tea and oolong tea all increased  $\alpha$ -amylase activity and green tea has the highest activation effect. The activation effect of tea extracts on  $\alpha$ -amylase activity may be related to other constituents such as ions and caffeine present in teas that counteract the mild inhibition effect of TP. The interaction between TP and enzyme/starch also led to changed antioxidant capacity. To our knowledge, this is the first study comparing the effect of TP and different teas processed from the same fresh tea leaves on  $\alpha$ -amylase activity and confirming the activation effect of teas on  $\alpha$ -amylase activity.

## Acknowledgments

This work was financially supported by the Fundamental Research Funds for the Central Universities, China (grant no. 2013PY091) and the Natural Science Foundation of Hubei Province, China (grant no. 2011CDB136).

## References

- Aghajari, N., Feller, G., Gerday, C., & Haser, R. (2002). Structural basis of  $\alpha$ -amylase activation by chloride. *Protein Science*, *11*, 1435–1441.
- Aruoma, O. I. (1994). Deoxyribose assay for detecting hydroxyl radicals. *Methods in Enzymology*, *233*, 57–66.
- Benzie, I. F. F., & Strain, J. J. (1996). The ferric reducing ability of plasma (FRAP) as a measure of "antioxidant power": the FRAP assay. *Analytical Biochemistry*, *239*, 70–76.
- Cabrera, C., Artacho, R., & Giménez, R. (2013). Beneficial effects of green tea-A review. *Journal of the American College of Nutrition*, *25*, 79–99.

- Chen, G. L., Hu, K., Zhong, N. J., Guo, J., Gong, Y. S., Deng, X. T., et al. (2013). Antioxidant capacities and total polyphenol content of nine commercially available tea juices measured by an *in vitro* digestion model. *European Journal of Food Research and Technology*, 236, 303–310.
- Chethan, S., Sreerama, Y. N., & Malleshi, N. G. (2008). Mode of inhibition of finger millet malt amylases by the millet phenolics. *Food Chemistry*, 111, 187–191.
- Dreosti, I. E. (2000). Antioxidant polyphenols in tea, cocoa, and wine. *Nutrition*, 16, 692–694.
- Forester, S. C., Gu, Y. Y., & Lambert, J. D. (2012). Inhibition of starch digestion by the green tea polyphenol, (-)-epigallocatechin-3-gallate. *Molecular Nutrition & Food Research*, 56, 1647–1654.
- Gao, J. J., Xu, P., Wang, Y. F., Wang, Y. Q., & Hochstetter, D. (2013). Combined effects of green tea extracts, green tea polyphenols or epigallocatechin gallate with acarbose on inhibition against  $\alpha$ -amylase and  $\alpha$ -glucosidase *in vitro*. *Molecules*, 18, 11614–11623.
- Hagerman, A. E., Riedl, K. M., Jones, G. A., Sovik, K. N., Ritchard, N. T., Hartzfeld, P. W., et al. (1998). High molecular weight plant polyphenolics (tannins) as biological antioxidants. *Journal of Agricultural and Food Chemistry*, 46, 1887–1892.
- Hara, Y., & Honda, M. (1990). The inhibition of  $\alpha$ -amylase by tea polyphenols. *Agricultural and Biological Chemistry*, 54, 1939–1945.
- He, Q., Lv, Y. P., & Yao, K. (2006). Effects of tea polyphenols on the activities of alpha-amylase, pepsin, trypsin and lipase. *Food Chemistry*, 101, 1178–1182.
- Jain, A., Manghani, C., Kohli, S., Nigam, D., & Rani, V. (2013). Tea and human health: the dark shadows. *Toxicology Letters*, 220, 82–87.
- Kashani-Amin, E., Yaghmaei, P., Larijani, B., & Ebrahim-Habibi, A. (2013). Xanthine derivatives as activators of alpha-amylase: Hypothesis on a link with the hyperglycemia induced by caffeine. *Obesity Research & Clinical Practice*, 7, 487–493.
- Koh, L. W., Wong, L. L., Loo, Y. Y., Kasapis, S., & Huang, D. (2010). Evaluation of different teas against starch digestibility by mammalian glycosidases. *Journal of Agricultural and Food Chemistry*, 58, 148–154.
- Kwon, Y., Apostolidis, E., & Shetty, K. (2008). Inhibitory potential of wine and tea against  $\alpha$ -amylase and  $\alpha$ -glucosidase for management of hyperglycemia linked to type 2 diabetes. *Journal of Food Biochemistry*, 32, 15–31.
- Liang, Y. R., Lu, J. L., & Zhang, L. Y. (2002). Comparative study of cream in infusions of black tea and green tea [*Camellia sinensis* (L.) O. Kuntze]. *International Journal of Food Science and Technology*, 37, 627–634.
- Lin, Y. S., Tsai, Y. J., Tsay, J. S., & Lin, J. K. (2003). Factors affecting the levels of tea polyphenols and caffeine in tea leaves. *Journal of Agricultural and Food Chemistry*, 51, 1864–1873.
- Liu, J., Wang, M. Z., Peng, S. L., & Zhang, G. Y. (2011). Effect of green tea catechins on the postprandial glycemic response to starches differing in amylose content. *Journal of Agricultural and Food Chemistry*, 59, 4582–4588.
- Luck, G., Liao, H., Murray, J., Grimmer, H., Warminski, E., Williamson, M., et al. (1994). Polyphenols, astringency and proline-rich proteins. *Phytochemistry*, 37, 357–371.
- Oz, H. S., Chen, T., & de Villiers, W. J. (2013). Green tea polyphenols and sulfasalazine have parallel anti-inflammatory properties in colitis models. *Frontiers in Immunology*, 4, 1–10.
- Quesille-Villalobos, A. M., Torrico, J. S., & Ranilla, L. G. (2013). Phenolic compounds, antioxidant capacity, and *in vitro*  $\alpha$ -amylase inhibitory potential of tea infusions (*Camellia sinensis*) commercialized in Chile. *CyTA-Journal of Food*, 11, 60–67.
- Saboury, A. A. (2002). Stability, activity and binding properties study of  $\alpha$ -amylase upon interaction with  $\text{Ca}^{2+}$  and  $\text{Co}^{2+}$ . *Biologia (Bratislava)*, 57, 221–228.
- Shi, Z. P. (1997). *Tea processing science*. Beijing: China Agriculture Press.
- Sinija, V. R., & Mishra, H. N. (2008). Green tea: health benefits. *Journal of Nutritional & Environmental Medicine*, 17, 232–242.
- Tagliazucchi, D., Verzelloni, E., & Conte, A. (2005). Effect of some phenolic compounds and beverages on pepsin activity during simulated gastric digestion. *Journal of Agricultural and Food Chemistry*, 53, 8706–8713.
- Underwood, C. (2012). *Green tea: Digestion and metabolism*. Comment <http://www.safealternativemedicine.co.uk/greenteadigestionmetabolism.html> Accessed in September 2012.
- Usha, B., Krishna, V. G., Muni, K. D., & Hemalatha, K. P. J. (2011). Partial characterization of  $\alpha$ -amylase from germinating little millets (panicum sumatrense). *Journal of Phytology*, 3, 1–8.
- Wu, Y. Y., Ding, L., Xia, H., & Tu, Y. Y. (2010). Analysis of the major chemical compositions in Fuzhuan brick-tea and its effect on activities of pancreatic enzymes *in vitro*. *African Journal of Biotechnology*, 9, 6748–6754.
- Xiao, H. X., Lin, Q. L., Liu, G. Q., Wu, Y., Wei, W., & Fu, X. J. (2013). Inhibitory effects of green tea polyphenols on the retrogradation of starches from different botanical sources. *Food and Bioprocess Technology*, 6, 2177–2181.
- Yi, T., Zhu, L., Peng, W. L., He, X. C., Chen, H. L., Li, J., et al. (2015). Comparison of ten major constituents in seven types of processed tea using HPLC-DAD-MS followed by principal component and hierarchical cluster analysis. *LWT-Food Science and Technology*, 62, 194–201.
- Zhao, W., Iyer, V., Flores, F. P., Donhowe, E., & Kong, F. B. (2013). Microencapsulation of tannic acid for oral administration to inhibit carbohydrate digestion in the gastrointestinal tract. *Journal of Functional Foods*, 4, 899–905.
- Zhong, L. (1989). *Physicochemical analysis on tea quality*. Shanghai: Shanghai Science and Technology Press (in Chinese).
- Zhu, Q. Y., Hackman, R. M., Ensunsa, J. L., Holt, R. R., & Keen, C. L. (2002). Antioxidative activities of oolong tea. *Journal of Agricultural and Food Chemistry*, 50, 6929–6934.



# A comparison of the bactericidal effectiveness of hydrochloric and acetic acid on *Staphylococcus aureus* in silver carp during a pH-shift protein recovery process



Maryam Ronaghi, Sarah Beamer, Jacek Jaczynski, Kristen E. Matak\*

Animal and Nutritional Sciences, PO Box 6108, West Virginia University, Morgantown, WV 26506, USA

## ARTICLE INFO

### Article history:

Received 24 August 2015  
Received in revised form  
25 September 2015  
Accepted 18 October 2015  
Available online 21 October 2015

### Keywords:

*Staphylococcus aureus*  
Silver carp  
Organic acid  
pH-shift  
Protein recovery

## ABSTRACT

The bactericidal effectiveness of a pH-shift protein recovery process was tested against *Staphylococcus aureus*. Protein from ground silver carp inoculated with *S. aureus* was solubilized at pH 2.5, 3.0, 11.5, or 12.5 with the addition of glacial acetic acid (AA), hydrochloric acid (HCl) or sodium hydroxide. Lipid and other insoluble components (bone, skin and so on) were removed by centrifugation. Solubilized protein was brought to the isoelectric point (pH 5.5) with the addition of acid or base. Microbial analysis was performed on all fractions and survivors were enumerated on Baird Parker and Tryptic Soy Agar media. No significant differences in recovery were observed ( $P > 0.05$ ) between media in the protein, lipid and water fractions. The main effect of acid type did not have a significant ( $P > 0.05$ ) impact on microbial reductions for any fraction; however, significant reductions occurred as a function of protein solubilization pH ( $P < 0.0001$ ) with basic solubilization strategies being most effective. The greatest reductions ( $P < 0.05$ ) occurred in the protein fraction when protein was solubilized at pH 12.5 and precipitated with acetic acid for a 2.50 log reduction in the protein fraction. These results show that the pH-shift protein recovery process will significantly reduce *S. aureus*.

© 2015 Elsevier Ltd. All rights reserved.

## 1. Introduction

Isoelectric solubilization and precipitation (ISP) processing is a non-thermal method used to recover protein and lipid from by-products of fish processing. This is achieved by using extremely acidic or basic pH shifts to solubilize proteins so that insoluble components (skin, bones, insoluble protein, scales, etc.) may be separated from them by centrifugation. Proteins precipitate when the solution is returned to the isoelectric point of the protein and then the protein is recovered from the process water by a second centrifugation. Since this is a non-thermal process, it is important to determine the extent at which the process will reduce bacterial load in the recovered protein. When hydrochloric acid (HCl) is used as the processing acid, this process is effective at significantly reducing *Listeria innocua* and *Escherichia coli* in ISP-recovered fish protein (Lansdowne, Beamer, Jaczynski & Matak, 2009a, 2009b); however, microbial reductions did not provide a 6-log reduction, which is the reduction amount needed to be considered a pasteurization effect (FDA, 2011).

The pKa is an indicator of the strength of an acid on a logarithmic scale and the strength of an acid is defined by the tendency of the acid to give up its proton to water and become dissociated. Strong acids, like HCl, have a low pKa, which means they are mostly in their dissociated form in solutions and consequently, outside of the bacterial cell. However, acid shock or acid stress will occur in bacterial cells when H<sup>+</sup> ions cross the cell membrane and lower intracellular pH. On the other hand, weak organic acids, like citric and acetic acid, have a higher pKa and are present in both dissociated and undissociated forms in solution. Organic acids freely enter the cell in their undissociated form. Since the pH of the cytoplasm is generally more alkaline than the surrounding medium, the weak acid dissociates once inside the cell, releasing a proton which contributes to acidification of the cytoplasm (Cotter & Hill, 2003). An indicator of bactericidal effectiveness of an acid is the amount of dissociation that occurs within the bacterial cell. The bacterial cell must actively remove the free protons released by the acid and a high concentration of protons will cause cell death by ATP depletion (Jay, Loessner & Golden, 2005). Otto, Paker, et al. (2011) explored the bactericidal effectiveness of using citric or acetic acids instead of HCl acid as the pH-shift processing acid. When protein was solubilized under acidic processing conditions,

\* Corresponding author.

E-mail address: [Kristen.Matak@mail.wvu.edu](mailto:Kristen.Matak@mail.wvu.edu) (K.E. Matak).

they reported greater reductions in *L. innocua* populations when citric or acetic acid was used as the processing acid when compared to HCl. They also reported a total net pasteurization effect (6-log reduction in microbial populations) in the recovered fractions when acetic acid was used as the pH-shift processing acid at protein solubilization pH 3.0 (Otto, Paker, et al., 2011).

*Staphylococcus aureus* is a facultative anaerobic Gram-positive coccid bacterium that is mostly found in the nostrils and on the skin and hair of warm-blooded animals (Doyle, Beuchat & Montville, 2001). Most food contaminations by *S. aureus* can be traced back to human carriers as well as contaminated equipment that were involved in the preparation process. These bacteria have the ability to tolerate a wide range of temperatures, pH environments, salt concentrations, and are able to survive for extended periods in a dry state (Doyle et al., 2001). Food poisoning by *S. aureus* is a common cause of gastroenteritis which is not due to the ingestion of the live organism but rather is a result of the production of enterotoxin in the staphylococci-contaminated food (Doyle et al., 2001). Symptoms of food poisoning include nausea, violent vomiting, abdominal cramping, sweating, headache, prostration, diarrhea and sometimes a drop in body temperature. Occasional hospitalization is possible for elderly and infants, but the mortality rate is very low (Bore, Langsrud, Langsrud, Rode & Holck, 2007). It is possible that *Staphylococci* exist, at least in low numbers, in all or most animal origin food products or products that have been handled directly by humans and have not been heat processed properly (Bore et al., 2007). Therefore, the objective of this study was to compare the effectiveness of hydrochloric acid to acetic acid on the reduction of *S. aureus* during the pH-shift protein recovery process.

## 2. Material and methods

### 2.1. Fish preparation

Fresh silver carp (*Hypophthalmichthys molitrix*) was headed, gutted and sanitized by dipping in a 50 ppm bleach solution for 10 s (Clorox Regular Bleach, Clorox, Oakland, CA, USA). After draining for an additional 10 s, fish were placed in a sanitized food processor (BIRO, Marblehead, model 12, Ohio, USA) and ground into a thick paste. All equipment (i.e., food processor, utensils, beakers, etc.) were sanitized by spraying with 70% ethanol and exposed to UV light (254 nm) for 15 min. The paste was divided and 155 g was placed into freezer bags and stored at  $-80\text{ }^{\circ}\text{C}$  (Lansdowne et al., 2009a).

### 2.2. Bacterial strain, inoculum preparation and inoculation of fish paste

*S. aureus* lab strain (ATCC 25923) was revived in 100 mL sterile brain heart infusion broth in a sterile 250 mL flask (BHI; Becton, Dickinson & Co., Sparks, MD) and incubated at  $37\text{ }^{\circ}\text{C}$  for 18–24 h in a rotary incubator (Barnstead lab-line, model 305, Melrose Park, IL) at 50 rpm. The initial culture was transferred by loop to a second sterile flask containing 100 mL brain heart infusion and the same process was repeated. The initial culture was spread onto slants of trypticase soy agar (TSA; Acumedia, Lansing, MI), incubated for 18–24 h at  $37\text{ }^{\circ}\text{C}$  and stored at  $4\text{ }^{\circ}\text{C}$ .

*S. aureus* from working stock slant was twice transferred by loop inocula into 100 mL sterile BHI flasks and incubated at  $37\text{ }^{\circ}\text{C}$  for 18–24 h at 50 rpm in a rotary incubator. Contents were transferred to sterile centrifuge bottles and centrifuged at  $10,000 \times G$  for 10 min at  $4\text{ }^{\circ}\text{C}$  (Otto, Beamer, Jaczynski, Matak, 2011; Otto, Paker, et al., 2011). Supernatant was removed and pellet was used to inoculate fish paste.

Fish paste (155 g) was thawed at  $4\text{ }^{\circ}\text{C}$  for 18–24 h and emptied into an autoclaved ceramic dish (473 mL). The *S. aureus* pellet was mixed into the paste using an autoclaved spatula to produce an average initial inoculum level of  $7.6 \times 10^7$  CFU/g. The inoculated paste was immediately used for pH-shift protein recovery processing (Otto, Beamer, et al., 2011; Otto, Paker, et al., 2011).

### 2.3. Isoelectric solubilization/precipitation

After inoculation, 155 g of fish paste was placed in an autoclaved beaker and homogenized with 930 mL distilled (1:6 wt/vol), deionized water. Homogenizer (BIRO, Marblehead, model 12, Ohio, USA) was sanitized by spraying with 70% ethanol and placing under UV light for 15 min. Glacial acetic acid (Fischer Scientific, Fairlawn, N.L., U.S.A.), 6 N hydrochloric acid (HCl) or 10 N sodium hydroxide (NaOH) was added to the mixture until the target pH (2.5, 3.0, 11.5 or 12.5) was reached. Once pH was adjusted, homogenization was continued for an additional 10 min to allow protein solubilization. The homogenized mixture was poured into autoclaved centrifuge bottles and centrifuged at  $10,000 \times G$  for 10 min at  $4\text{ }^{\circ}\text{C}$  (Otto, Beamer, et al., 2011; Otto, Paker, et al., 2011). The supernatant (solubilized protein) was poured through autoclaved cheesecloth to collect the lipid. Lipid and insoluble portions remaining on the bottom of the centrifuge tubes were retained in sterile containers for microbial analysis. The supernatant was brought to its isoelectric point (pH 5.5) by the addition of 10 N NaOH, glacial acetic acid or 6 N HCl and homogenized for an additional 5 min. The solution was poured into autoclaved centrifuge bottles and was centrifuged at  $10,000 \times G$  for 10 min at  $4\text{ }^{\circ}\text{C}$  (Otto, Beamer, et al., 2011; Otto, Paker, et al., 2011). Both supernatant and precipitated proteins were retained separately in sterile containers for microbial analysis.

### 2.4. Microbial analysis

Microbial load was determined on uninoculated fish paste (background), inoculated fish paste (initial), and recovered fractions (protein, lipid, insoluble and water). An aliquot (1 g) was placed into separate stomacher bags with 9 mL sterile peptone buffer and hand-pummeled for 2 min. Pummeled samples were serially diluted (10-fold) and spread-plated onto TSA (non-selective) and Baird Parker medium (BP; selective) plates and incubated at  $37\text{ }^{\circ}\text{C}$  for 24 h. The detection limit for non-inoculated fish paste was  $<10^3$  CFU/g, for lipid, protein and insoluble fractions it was  $<10^2$  CFU/g and for water it was  $<10$  CFU/g (Otto, Beamer, et al., 2011; Otto, Paker, et al., 2011). The log CFU/g reduction in each fraction was calculated by subtracting the number of recovered bacterial from the initial inoculum:  $\log(\text{initial inoculum}) - \log(\text{survivors in specific fraction})$  (Lansdowne et al., 2009a, 2009b).

### 2.5. Statistical analysis

This study was replicated three times for each acid type and each solubilization pH value. Microbial counts (CFU/g) were converted into logarithmic units and recovered cells were expressed as log CFU/g. Data were analyzed by analysis of variance and differences in means were determined using Turkey's honestly significant differences test ( $P \leq 0.05$ ) (JMP 11, SAS Institute, Cary, NC).

## 3. Results and discussion

For all trials, the mean background flora of the initial fish paste was  $3.4 \times 10^3$  CFU/g on TSA and there was no growth of *S. aureus* detected ( $<10^2$  CFU/g) on BP. There were no differences ( $P > 0.05$ ) in cell recovery on TSA and BP for the protein, lipid, and water fractions, which indicates that microbial death due to the pH-shift

process was an “all-or-nothing event” for *S. aureus* (Table 1). When bacterial cells are exposed to a chemical or physical process that inflicts injury but does not kill them, characteristic growth capabilities are often diminished and the cells are unable to form visible colonies under selective conditions. However, when conditions are favorable like when grown on non-selective media, cells are able to repair themselves and form visible colonies (Wesche, Gurtler, Marks & Ryser, 2009). In this study, cells in the protein, lipid and water fractions that sustained injury were unable to repair themselves on TSA, a nutrient rich growth medium. This is consistent with Lansdowne et al. (2009a) and Otto, Beamer, et al. (2011), Otto, Paker, et al. (2011) who found that when Gram-positive *Listeria monocytogenes* and *L. innocua* were exposed to the pH-shift process, there were no differences in recovery on selective or non-selective media. The morphology of Gram-positive bacterial cell walls include a thick peptidoglycan layer which provides structure and support against both mechanical and osmotic lysis. It is possible that these components prolonged the internal homeostasis of the bacterium which allowed it to better survive in the extreme acidic or basic pH-shift processing environment. Although, if the cell wall ruptured or was compromised it was beyond the repair capabilities of the organism, as indicated by the similar growth outputs on the two types of media.

Gram-positive cells utilize a combination of strategies to maintain intracellular pH including cytoplasmic buffering by synthesizing intracellular metabolites for the production of alkali by the arginine deiminase (ADI) system or urease system to neutralize the microenvironment in and around the cell, altering the composition of the cell envelope, producing shock proteins and chaperones, changing the way cells communicate with one another, altering metabolic pathways, and so on (Bore et al., 2007; Cotter & Hill, 2003). Utilizing proton pumps are perhaps the most well-known mechanism of acid resistance associated with Gram-positive bacteria. Proton pumps like  $F_1F_0$ -ATPase and glutamate decarboxylase (GAD) systems are used by bacterial cells to move protons ( $H^+$ ) out of the cytoplasm in response to increasingly acidic environments. Ideally, bacteria would first detect slight changes in environmental factors to allow them to mobilize necessary strategies. However, during the pH-shift protein recovery process it is likely that the cells that were unable to avoid or escape the harsh conditions were forced to rely heavily on the proton pumps to

maintain intracellular pH at the expense of ATP synthase activity (Cotter & Hill, 2003). The *S. aureus* cells that survived likely did so without injury because they were able to keep the cytoplasmic pH stable long enough to mobilize the other strategies described above that would increase their rate of survival in extremely acidic environments. It is also possible that *S. aureus* utilized the ability to up-regulate certain proteins that alter the structure of the cell membrane and therefore, increased the ability of the cell to maintain intracellular pH. For example, the resistance of *S. aureus* to extreme shifts in pH may be due to the presence of sigma factors ( $\sigma^B$ ) which are protein subunits seen in Gram-positive bacteria (including *S. aureus*) that contribute to acid tolerance by regulating genes that exhibit stress responses to acidic environments (Raengpradub, Wiedmann, & Boor, 2008).

According to the U.S. Food and Drug Administration, pasteurization is defined as a 6-log reduction in microbial populations. A net pasteurization effect was not observed at any of the pH processing conditions. Table 2 shows that the main effect of acid type did not have a significant ( $P > 0.05$ ) impact on microbial reductions for any of the fractions; however, significant reductions occurred as a function of protein solubilization pH ( $P < 0.0001$ ) with basic solubilization strategies being most effective. The greatest reductions ( $P < 0.05$ ) occurred in the protein fraction when protein was solubilized at pH 12.5 and precipitated with acetic acid for a 2.50 log CFU/g reduction in the protein fraction (Table 1). For all pH and acid combinations, the greatest reductions were seen in the water fraction, with a range of 4.16–5.18 log CFU/g reduction, likely due to cells being removed with the denser fractions via centrifugation. These results are consistent with Lansdowne et al. (2009a) when they tested the bactericidal effectiveness of HCl as a processing acid in the pH shift process against *L. innocua*, there was a 2.01 log CFU/g reduction in the protein fraction and 4.92 log CFU/g reduction in the water fraction at protein solubilization pH 12.5; however, the greatest microbial reductions were seen when protein was precipitated at pH 2.0 for all fractions (Lansdowne et al., 2009a). In addition, Otto, Paker, et al. (2011) reported that when acetic acid was used to solubilize protein at pH 3.0 they exceeded a 6-log reduction of *L. innocua* in the protein fraction; however, they were only able to produce a 3.53 log CFU/g reduction in *L. monocytogenes* (Otto, Beamer, et al., 2011). The results of this current study showed that protein solubilization at pH 12.5 was

**Table 1**

Log reduction of *S. aureus* by the pH-shift protein recovery process with acetic and hydrochloric acids in silver carp. Values were determined by subtraction of the log CFU/g of recovered cells within a fraction from the log of the actual initial inoculation (average 7.88 log CFU/g).

Fraction	pH	Acid	Log reduction (mean log CFU/g $\pm$ SD, n = 3)		Fraction	pH	Acid	Log reduction (Mean log CFU/g $\pm$ SD, n = 3)	
			BP	TSA				BP	TSA
<b>Protein</b>	2.5	Acetic	0.58 $\pm$ 0.17 <sup>bc</sup>	0.73 $\pm$ 0.23 <sup>c</sup>	<b>Lipid</b>	2.5	Acetic	1.05 $\pm$ 0.14 <sup>b</sup>	1.06 $\pm$ 0.21 <sup>b</sup>
		HCl	0.97 $\pm$ 0.12 <sup>bc</sup>	1.13 $\pm$ 0.19 <sup>c</sup>			HCl	1.80 $\pm$ 0.13 <sup>b</sup>	2.00 $\pm$ 0.29 <sup>b</sup>
	3.0	Acetic	0.31 $\pm$ 0.27 <sup>c</sup>	0.36 $\pm$ 0.32 <sup>c</sup>		3.0	Acetic	1.09 $\pm$ 0.17 <sup>b</sup>	1.26 $\pm$ 0.36 <sup>b</sup>
		HCl	0.93 $\pm$ 0.29 <sup>bc</sup>	0.90 $\pm$ 0.33 <sup>c</sup>			HCl	1.83 $\pm$ 0.14 <sup>b</sup>	1.79 $\pm$ 0.11 <sup>b</sup>
	11.5	Acetic	1.03 $\pm$ 0.39 <sup>bc</sup>	1.23 $\pm$ 0.21 <sup>c</sup>		11.5	Acetic	1.35 $\pm$ 0.60 <sup>b</sup>	1.60 $\pm$ 0.44 <sup>b</sup>
		HCl	1.04 $\pm$ 0.14 <sup>bc</sup>	1.42 $\pm$ 0.41 <sup>bc</sup>			HCl	0.77 $\pm$ 0.44 <sup>b</sup>	1.46 $\pm$ 0.85 <sup>b</sup>
	12.5	Acetic	2.22 $\pm$ 0.54 <sup>a</sup>	2.77 $\pm$ 0.60 <sup>a</sup>		12.5	Acetic	4.17 $\pm$ 0.60 <sup>a</sup>	4.25 $\pm$ 0.78 <sup>a</sup>
		HCl	1.46 $\pm$ 0.35 <sup>ab</sup>	2.34 $\pm$ 0.60 <sup>ab</sup>			HCl	3.64 $\pm$ 0.82 <sup>a</sup>	3.96 $\pm$ 0.68 <sup>a</sup>
<b>Insoluble</b>	2.5	Acetic	0.99 $\pm$ 0.21 <sup>bc</sup>	0.99 $\pm$ 0.09 <sup>bc</sup>	<b>Water</b>	2.5	Acetic	4.10 $\pm$ 0.51 <sup>a</sup>	4.15 $\pm$ 0.08 <sup>a</sup>
		HCl	1.64 $\pm$ 0.06 <sup>b</sup>	2.02 $\pm$ 0.37 <sup>b</sup>			HCl	4.39 $\pm$ 0.36 <sup>a</sup>	4.05 $\pm$ 0.89 <sup>a</sup>
	3.0	Acetic	1.13 $\pm$ 0.05 <sup>bc</sup>	1.25 $\pm$ 0.22 <sup>bc</sup>		3.0	Acetic	4.09 $\pm$ 0.97 <sup>a</sup>	4.16 $\pm$ 1.03 <sup>a</sup>
		HCl	1.37 $\pm$ 0.20 <sup>bc</sup>	1.32 $\pm$ 0.15 <sup>bc</sup>			HCl	4.38 $\pm$ 0.39 <sup>a</sup>	4.02 $\pm$ 0.35 <sup>a</sup>
	11.5	Acetic	<b>0.70 <math>\pm</math> 0.21<sup>cd</sup></b>	<b>1.20 <math>\pm</math> 0.07<sup>bc</sup></b>		11.5	Acetic	4.03 $\pm$ 0.61 <sup>a</sup>	3.93 $\pm$ 0.35 <sup>a</sup>
		HCl	0.10 $\pm$ 0.17 <sup>d</sup>	0.58 $\pm$ 0.34 <sup>c</sup>			HCl	4.16 $\pm$ 0.20 <sup>a</sup>	4.52 $\pm$ 0.23 <sup>a</sup>
	12.5	Acetic	3.46 $\pm$ 0.62 <sup>a</sup>	4.42 $\pm$ 1.08 <sup>a</sup>		12.5	Acetic	5.15 $\pm$ 0.77 <sup>a</sup>	5.63 $\pm$ 1.16 <sup>a</sup>
		HCl	<b>2.72 <math>\pm</math> 0.35<sup>a</sup></b>	<b>4.07 <math>\pm</math> 0.49<sup>a</sup></b>			HCl	4.68 $\pm$ 0.16 <sup>a</sup>	5.27 $\pm$ 0.40 <sup>a</sup>

<sup>a, b, c</sup> Values designated with different letters within a column in a fraction are significantly different ( $P < 0.05$ ) as determined by Tukey's HSD. Values in **bold** indicate a significant difference in recovery between **BP** and **TSA** ( $P < 0.05$ ).

**Table 2**

Log reduction of *S. aureus* exposed to several pH shifts in different fractions of headed and gutted silver carp. Values were determined by subtraction of the log of recovered cells within a fraction from the log CFU/g of the actual initial inoculation (average 7.88 log CFU/g). For all fractions except for the insoluble fraction there were no significant differences in recovery between TSA and BP ( $P > 0.05$ ); therefore, data were combined.

	Log reduction (mean log CFU/g $\pm$ SEM)				
	Protein	Lipid	Water	Insoluble (BP)	Insoluble (TSA)
HCl	1.27 $\pm$ 0.11	2.16 $\pm$ 0.23	4.43 $\pm$ 0.11	1.46 $\pm$ 0.25	2.27 $\pm$ 0.51
AA	1.15 $\pm$ 0.19	1.98 $\pm$ 0.28	4.41 $\pm$ 0.18	1.57 $\pm$ 0.28	1.84 $\pm$ 0.41
pH 12.5	2.20 $\pm$ 0.19 <sup>a</sup>	4.00 $\pm$ 0.19 <sup>a</sup>	5.18 $\pm$ 0.21 <sup>a</sup>	3.09 $\pm$ 0.25 <sup>a</sup>	4.62 $\pm$ 0.40 <sup>a</sup>
pH 11.5	1.18 $\pm$ 0.09 <sup>b</sup>	1.29 $\pm$ 0.18 <sup>b</sup>	4.16 $\pm$ 0.12 <sup>b</sup>	0.40 $\pm$ 0.15 <sup>c</sup>	0.89 $\pm$ 0.17 <sup>b</sup>
pH 3.0	0.63 $\pm$ 0.12 <sup>c</sup>	1.50 $\pm$ 0.11 <sup>b</sup>	4.16 $\pm$ 0.19 <sup>b</sup>	1.25 $\pm$ 0.08 <sup>b</sup>	1.29 $\pm$ 0.07 <sup>b</sup>
pH 2.5	0.85 $\pm$ 0.08 <sup>bc</sup>	1.48 $\pm$ 0.14 <sup>b</sup>	4.18 $\pm$ 0.21 <sup>b</sup>	1.32 $\pm$ 0.16 <sup>b</sup>	1.51 $\pm$ 0.25 <sup>b</sup>
P-value acid	0.2864	0.1988	0.8738	0.3639	0.9411
P-value pH	<0.0001	<0.0001	<0.0001	<0.0001	<0.0001
P-value acid*pH	0.0038	0.0024	0.4298	0.0018	0.0779

<sup>a,b,c</sup> Different letters indicate significant differences between different solubilization pH values (two-way ANOVA, Tukey's HSD,  $P < 0.05$ ). There were no significant differences between processing acids.

most effective at reducing *S. aureus*, regardless of acid type (Table 2). Adaptive strategies to highly basic environments are similar to responses to highly acidic environments and include mechanisms to increase production of metabolic acid, increase ATP synthase activity to increase  $H^+$  entry into the cell, changes in cell surface properties and increased activity of monovalent cation/proton antiporters (Padan, Bibi, Ito & Krulwich, 2005). However, highly basic environments may have also facilitated the solubilization of the bacterial membrane protein and lipids leading to the exposure of hydrophobic sites of adjacent lipids to the environment and ultimately causing irreparable damage to the cell wall (Jacobsohn, Lehman & Jacobsohn, 1992). Recall that the pH of the fish slurry was adjusted to pH 11.5 and 12.5 using NaOH, a commonly used sanitizer that would impact microbial outcome. When the insoluble fraction was removed via centrifugation the slurry was still under basic conditions (at pH 11.5 or 12.5) and had not yet been exposed to either acid. Therefore, when the insoluble data were combined for each of the basic protein solubilization pHs the differences in microbial recovery between the TSA and BP were statistically significant ( $P \leq 0.05$ ). These differences in recovery show that NaOH caused cell injury and that the damaged cells were able to repair themselves on the nutrient-rich TSA media.

Fig. 1 shows that when protein was solubilized under basic conditions there were no significant differences in microbial reductions in the protein fraction between HCl and acetic acids when TSA and BP data were combined; however, when protein was solubilized under acidic conditions there were significant differences ( $P < 0.05$ ) in microbial reductions, with the greater reductions occurring when HCl was used as the processing acid. These results are in contrast to previously reported studies where reductions of *L. innocua* in the protein fraction when acetic acid was used to solubilize protein at pH 3.0 exceeded a 6.0 log CFU/g reduction (Otto, Beamer, et al., 2011), compared to a 1.10 log CFU/g reduction when HCl was used (Lansdowne et al., 2009a). The authors attributed the inhibitory effect of acetic acid to its ability to passively diffuse into the cytoplasm of the bacterium where it would then dissociate and overwhelm the buffering capacity of the cell. Weak organic acids exist in a pH-dependent equilibrium between the dissociated and undissociated state in solutions. The dissociation of an acid depends on temperature, pH and the dissociation constant of the acid (Rode et al., 2010). Once inside the cell, the organic acid molecules dissociate and release charged anions and protons which do not freely cross the cellular membrane. The accumulation of these protons and anions will eventually cause membrane disruption. On the other hand, strong acids such as HCl completely

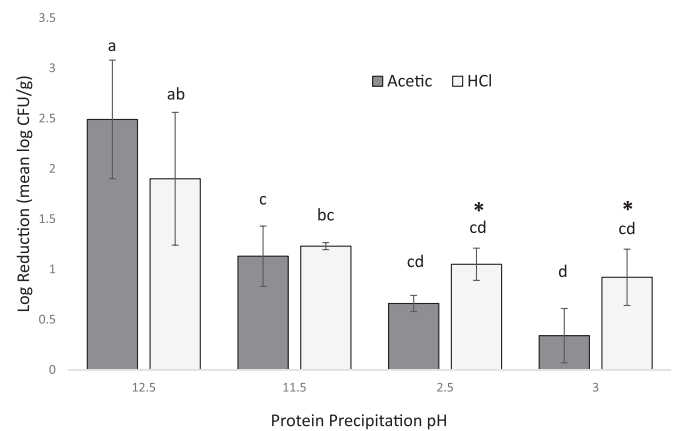


**Fig. 1.** Log CFU/g reduction of *S. aureus* in the recovered protein fraction when exposed to several pH shifts during pH-shift protein recovery process. Values were determined by subtraction of the log of recovered cells within the recovered protein fraction from the log of the actual initial inoculation (average 7.88 log CFU/g). There were no significant difference in microbial recovery on selective media therefore data were combined ( $n = 6$ ). <sup>a,b,c,d</sup> Different letters indicate significant differences between all solubilization pH values and processing acid combinations. \*Asterisk indicates significant differences in recovery between processing acids.

dissociate in solutions. The protons tend to pass through the membrane by interacting with the systems that control the proton flow in and out of the cell, such as the electron transport system. Therefore, in extreme acidic or basic conditions, bacterial cells must either keep protons from entering or expel them as fast as they enter. Perhaps increasing the exposure time of *S. aureus* to these acids could result in greater log reductions and would allow us to better differentiate between the effectiveness of acids used during the pH-shift process.

#### 4. Conclusion

The results indicate that the pH-shift process will not eliminate *S. aureus* populations, however populations were significantly reduced when protein was solubilized under basic conditions. The collected data shows that acetic acid is as effective as HCl when used to precipitate protein during the pH-shift process at reducing *S. aureus*; however, HCl was a better antimicrobial than acetic acid when it was used to solubilize the protein during the pH-shift process. Basic protein solubilization conditions were more

effective at reducing *S. aureus* during the pH-shift process. These results show that while the pH shift process will significantly reduce *S. aureus*, further processing or other hurdles are required to achieve a net pasteurization effect.

### Acknowledgment

This work was funded by the HATCH Program Project # (WVA 00622) and the USDA Cooperative State Research Education and Extension Service (2010- 34386- 21745).

### References

- Bore, E., Langsrud, S., Langsrud, O., Rode, T. M., & Holck, A. (2007). Acid-shock responses in *Staphylococcus aureus* investigated by global gene expression analysis. *Microbiology*, *153*, 2289–2303.
- Cotter, P. D., & Hill, C. (2003). Surviving the acid test: responses of Gram-positive bacteria to low pH. *Microbiology and Molecular Biology Reviews*, *67*, 429–453.
- Doyle, M. P., Beuchat, L. R., & Montville, T. J. (Eds.). (2001). *Food microbiology: Fundamentals and frontiers*. Washington, D.C.: ASM Press.
- [FDA] Food and Drug Administration. (2011). *Fish and fisheries products hazards and controls guidance* (chapter 16). Available from: [http://google2.fda.gov/search?q=Pasteurization&client=FDAGov&site=FDAGov&lr=&proxystyle=FDAGov&requiredfields=-archive%3AYes&output=xml\\_no\\_dtd&getfields=\\*](http://google2.fda.gov/search?q=Pasteurization&client=FDAGov&site=FDAGov&lr=&proxystyle=FDAGov&requiredfields=-archive%3AYes&output=xml_no_dtd&getfields=*) Accessed 10.06.15.
- Jacobsohn, M. K., Lehman, M. M., & Jacobsohn, G. M. (1992). Cell membranes and multilamellar vesicles: influence of pH on solvent-induced damage. *Lipids*, *27*, 694–700.
- Jay, J., Loessner, M., & Golden, D. (2005). Food protection with chemicals, and by biocontrol. p. 301–350. In D. Heldman (Ed.), *Modern food microbiology* (7th ed.). New York: Springer.
- Lansdowne, L. R., Beamer, S., Jaczynski, J., & Matak, K. E. (2009a). Survival of *Listeria innocua* after isoelectric solubilization and precipitation of fish protein. *Journal of Food Science*, *74*(4), M201–M205.
- Lansdowne, L. R., Beamer, S., Jaczynski, J., & Matak, K. E. (2009b). Survival of *Escherichia coli* after isoelectric solubilization and precipitation of fish protein. *Journal of Food Protection*, *7*, 1398–1403.
- Otto, R. A., Beamer, S., Jaczynski, J., & Matak, K. E. (2011). The effect of using citric or acetic acid on survival of *Listeria monocytogenes* during fish protein recovery by isoelectric solubilization and precipitation process. *Journal of Food Science*, *76*(8), M579–M583.
- Otto, R. A., Paker, I., Bane, L., Beamer, S., Jaczynski, J., & Matak, K. E. (2011). Survival of *Listeria innocua* in rainbow Trout protein recovered by isoelectric solubilization and precipitation with acetic and citric acids.
- Padan, E., Bibi, E., Ito, M., & Krulwich, T. A. (2005 November 30). Alkaline pH homeostasis in bacteria: new insights. *Biochimica et Biophysica Acta*, *1717*(2), 67–88.
- Raengpradub, S., Wiedmann, M., & Boor, K. J. (2008). Comparative analysis of the  $\sigma_B$ -dependent stress responses in *Listeria monocytogenes* and *Listeria innocua* strains exposed to selected stress conditions. *Applied and Environmental Microbiology*, *74*(1), 158–171.
- Rode, T. M., Møretro, T., Langsrud, S., Vogt, G., & Holck, A. (2010). Responses of *Staphylococcus aureus* exposed to HCl and organic acid stress. *Can. J. Microbiol.*, *56*, 777–792.
- Wesche, A. M., Gurtler, J. B., Marks, B. P., & Ryser, E. T. (2009). Stress, sublethal injury, resuscitation, and virulence of bacterial foodborne pathogens. *Journal of Food Protection*, *72*(5), 1121–1138.



# Antioxidant effect of spent, ground, and lyophilized brew from roasted coffee in frozen cooked pork patties



Katrina Maryse Malixi July<sup>a</sup>, Criselda S. Toto<sup>b</sup>, Lilian Were<sup>a,\*</sup>

<sup>a</sup> Food Science Program, Schmid College of Science and Technology, Chapman University, 1 University Drive, Orange, CA 92866, USA

<sup>b</sup> Mathematics and Computer Science, Chapman University, 1 University Drive, Orange, CA 92866, USA

## ARTICLE INFO

### Article history:

Received 28 July 2015

Received in revised form

2 October 2015

Accepted 19 October 2015

Available online 21 October 2015

### Keywords:

Coffee

Cooked pork

Frozen storage

Oxidation

## ABSTRACT

The ability of light and dark roasted coffee (1 g/kg) in varying application forms (spent ground [SCG], whole ground [WGC], or lyophilized brew [LBC]) to inhibit lipid and protein oxidation in cooked pork patties stored at  $-18^{\circ}\text{C}$  was monitored over 3 months. Malondialdehyde (MDA) for the negative control (NC) increased from 0.31 to 1.11 mg MDA/kg pork over 3 months, while pork with coffee or rosemary oleoresin had lower values at month 3 (0.054–0.40 mg MDA/kg pork). The NC had the highest values for hexanal, octanal, and nonanal (2.59, 0.10, and 0.13 mg/kg pork, respectively), while light and dark LBC in pork inhibited hexanal (0.37 and 0.39 mg/kg pork), octanal (0.017 and 0.021 mg/kg pork), and nonanal (0.036 and 0.048 mg/kg pork) to the same extent as rosemary oleoresin at month 3 (0.30, 0.015, 0.036 mg aldehyde/kg pork, respectively). Thiol content for all treatments remained relatively stable from month 0–3 (0.56–0.96 to 0.67–1.02), while metmyoglobin slightly increased (49–55% to 55–56%) over 3 months. The results suggest that adding coffee neither inhibited nor promoted protein oxidation in cooked pork patties but inhibited lipid oxidation resulting in comparable values to pork with added rosemary oleoresin.

© 2015 Elsevier Ltd. All rights reserved.

## 1. Introduction

The efficiency and convenience offered by precooking products makes precooked pork appealing in today's fast-paced lifestyle (Nolan, Bowers, & Kropf, 1989). While the convenience appeals to consumers, precooking before packaging and storing can accelerate oxidation, deteriorating product quality (Dai, Lu, Wu, Lu, Han, Liu, et al., 2014; Kingston, Monahan, Buckley, & Lynch, 1998; Salminen, Estevez, Kivikari, & Heinonen, 2006; Sasse, Colindres, & Brewer, 2009). Cooking destroys the integrity of cell membranes releasing phospholipids, and inactivates several protective antioxidants e.g. catalase (Rhee, Anderson, & Sams, 1996). In addition, hemoproteins such as myoglobin are denatured allowing the release of the prooxidant iron, which can result in the warmed-over flavor (WOF). The WOF becomes predominant with precooking and is characterized by undesirable organoleptic qualities (Rojas & Brewer, 2007). These adverse qualities are due to the secondary products of lipid oxidation (LOX) such as hexanal, octanal, and nonanal. Destruction of cell membranes, decreased

catalase activity, and the increase in nonheme iron can elevate the rate of LOX in cooked pork, therefore, it is important to apply strategies to prolong the shelf-life of cooked pork products (Fernandez-Lopez et al., 2003; Rhee et al., 1996).

Multiple preservation methods are applied to maintain meat quality, including storage temperature and antioxidants. Frozen storage is an effective method since low temperatures slow down oxidative reactions. However, freezing does not completely inhibit physical and chemical reactions causing discoloration and oxidative rancidity over time. Antioxidants (AOXs) can be added to combat LOX and protein oxidation (POX). Rosemary has become the industry natural AOX based on overall effectiveness in pork and other meat matrices (Georgantelis, Ambrosiadis, Katikou, Blekas, & Georgakis, 2007; Kim, Cadwallader, Kido, & Watanabe, 2013). The key bioactive antioxidant rosemary compounds are carnosol, carnosic and rosmarinic acid which readily donate their hydrogens acting as free radical scavengers. Recently, roasted coffee was shown to inhibit LOX as effectively as rosemary oleoresin in refrigerated beef with added salt, a known prooxidant of LOX (Lin, Toto, & Were, 2015). The bioactivity of roasted coffee is attributed to a combination of hydroxycinnamic chlorogenic acids (CGAs), and Maillard reaction products (MRPs), which scavenge free radicals

\* Corresponding author.

E-mail address: [were@chapman.edu](mailto:were@chapman.edu) (L. Were).

and chelate metal catalysts of LOX and POX (Del Pino-Garcia, Gonzalez-Sanjose, Rivero-Perez, & Muniz, 2012; Delgado-Andrade, Rufian-Henares, & Morales, 2005; Farah, 2012). Concentrations of AOX compounds differ in whole ground coffee (WGC), lyophilized brew coffee (LBC), or spent coffee ground (SCG) and by roast degrees. Spent coffee, from home or restaurant preparations, are of particular interest since substantial bioactive compounds may remain due to short brewing time and coffeemaker filter (Ludwig et al., 2012). Furthermore, SCG are considered waste products hence repurposing into a sustainable preservation method can result in economic gain for the meat and coffee industry, while still producing a safe, quality pork product.

To our knowledge, no studies have investigated the effectiveness of SCG as an antioxidant in food and limited studies have reported the effects of roasted coffee in food matrices: Nissen, Byrne, Bertelsen, and Skibsted (2004) in cooked frozen pork, Budryn and Nebesny (2013) in cookies and chocolate, and Lin et al. (2015) in raw refrigerated beef. The experimental objective was to determine the optimal combination of roast degree (light or dark) with application form (SCG, WGC, LBC) for the greatest AOX effect to preserve shelf life and quality in frozen precooked pork.

## 2. Material and methods

### 2.1. Chemicals

Aldehyde and 4-heptanone standards, bovine albumin serum, biuret reagent, HPLC grade methanol, water, formic acid, acetonitrile, ferrous sulfate heptahydrate and sodium phosphate dibasic anhydrous were purchased from Fisher Scientific (Tustin, CA, USA). Sodium phosphate monobasic was from Spectrum Chemical (Gardena, CA, USA). Ellman's reagent 5, 5'-dithiobis(2-nitrobenzoic acid), EDTA, ferrozine, trichloroacetic acid (TCA), 2-Thiobarbituric acid (TBA), and 1, 1, 3, 3-tetramethoxypropane (TMP) were purchased from Sigma–Aldrich (St. Louis, MO, USA).

### 2.2. Preparation of coffee and pork treatments

Green Colombia Primeval coffee beans obtained from Rose Park Roasters (Long Beach, CA, USA) were roasted to produce a light (10 min 32 s to 210 °C) and dark (12 min 8 s to 235 °C) roast. Whole coffee beans were ground (Cuisinart “Grind Central” Coffee Grinder, East Windsor, NJ, USA) and passed through a 1.0 mm sieve (18-mesh size) resulting in WGC. Lyophilized brewed coffee was prepared following the methods indicated by Budryn and Nebesny (2013) with modifications. Coffee brew was prepared by heating water to 90 °C, then adding ground coffee to water at a 1 to 6 ratio. The solution was held at 90 °C for five min with constant stirring, filtered with a paper coffee filter to yield liquid brew, which was then lyophilized (Dura-Dry mP manifold lyophilizer, FTS Systems, model #FD2085C0000, Stone Ridge, NY, USA) to yield LBC. The remaining solid grounds from coffee brew extraction was lyophilized and used as SCG. Coffee was stored at <0 °C before use. Before incorporation into minced pork, all coffee forms were passed through a 1.0 mm sieve (18-mesh size).

Meat was prepared in accordance to AOAC Official method 983.18 (AOAC, 2010) with modifications. Minced sirloin pork chops from Butcher hogs, averaging 6 months in age, 95.34 kg live weight at the time of slaughter, was supplied and prepared at Farmer John<sup>®</sup> facilities (Vernon, CA, USA). Pork meat was minced in an industrial-sized chopper, and refrigerated (<4 °C) overnight prior to addition of coffee or rosemary oleoresin the following day. All treatments, negative control (NC), rosemary oleoresin [RO; Herbalox<sup>®</sup> HT-25 from Kalsec Inc. (Kalamazoo, MI, USA); (2 g/kg)], SCG, WGC, and LBC of light (1 g/kg) and dark (1 g/kg) roasts were mixed using a

Hobart Legacy HL200 20 Qt mixer (Troy, OH, USA) for two min resulting in eight different treatment samples with uniform processing. This process was repeated per treatment in order to achieve true duplicates. The pork was transferred to polyethylene plastic bags, placed into cardboard boxes, and transported 56 km from Vernon to Orange, CA, USA.

### 2.3. Cooked pork preparation

Pork meat was stored at 4 °C until ready to be formed into pork patties (~3 h). Pork was prepared and cooked following the Research Guidelines for Cookery, Sensory Evaluation, and Instrumental Tenderness Measurements of Fresh Meat (AMSA, 1995) with modifications. Pork patties (100 ± 1 g) were molded (11.5 cm diameter, 1.25 cm thickness) then cooked on two electric griddles (ToastMaster<sup>®</sup>, Model #TG21W & # TM161GR, St. Louis, MO, USA) set to 205 °C for 3.5 min on each side or until internal temperature reached a minimum of 72 °C in the center of the patty. Patties were cooled at 22–25 °C before being individually placed into oxygen permeable zipper bags (polyethylene, 16.5 cm × 14.9 cm). Patties were stored at –18 °C until ready to be analyzed. Patties from each treatment were transferred from –18 °C to 4 °C to thaw for 12 h, and were hand mixed for 30 s prior to analysis.

### 2.4. Chlorogenic, Maillard reaction products, and iron chelating ability quantification

Spent, ground, and lyophilized brew of light, medium, and dark roasted coffee were added to deionized water at 1 g/100 mL to test MRPs and 0.1 g/100 mL to test iron chelating ability and CGA, then incubated for 2 h at 22 °C. Quantification of CGA in the various forms of coffee were measured via HPLC following protocols by Lin et al. (2015). A C18 column (Kinetex, 2.6u C18 100A, 100 × 4.60 mm, Phenomenx, Torrance, CA, USA) was used at 30 °C using a flow rate of 1.5 mL/min with mobile phase (A) 1 mg/mL formic acid in HPLC water and (B) HPLC grade acetonitrile. Sample was injected (5 µL) with starting conditions of A/B, 95/5 held for 10 min. Solvent A was linearly decreased to 85% within 1 min and held for 0.5 min before returning back to starting conditions within 2.5 min. A standard curve of chlorogenic acid (0–0.6 mM) was used to quantify chlorogenic acid detected at 330 nm. Quantification of MRPs and ferrous iron chelating ability were measured following protocols by Teets and Were (2008).

### 2.5. Thiobarbituric acid reactive substances (TBARS) measurement

The TBARS assay was prepared as described by Lin et al. (2015) with modifications. The supernatant (5 mL) was reacted with 5 mL of 0.02 M TBA solution in glass test tubes. Recovery values were determined by spiking additional meat samples (randomly chosen each testing day) with 0.5 mL of 0.15 or 0.45 mM TMP solution to achieve final TMP concentration of 0.006 and 0.018 mM after 12.0 mL of TCA had been added. These mixtures were vortexed and centrifuged alongside the other samples. A TMP standard curve (0–7.5 nmol MDA/mL) was used to quantify MDA after 16 h incubation at 22–25 °C in the dark. Absorbance was measured at 532 nm and 600 nm, with the latter accounting for any potential turbidity, using a FLUOstar Omega multimode microplate reader (Cary, NC, USA).

### 2.6. Purge and trap gas chromatography measurement of volatile aldehydes

Volatile compounds from pork samples were extracted via distillation and measured by gas chromatography (GC) using

internal standard 4-heptanone (50 µL/L) following protocols by Lin et al. (2015). Samples were analyzed in duplicate and hexanal, octanal, and nonanal concentrations were expressed as mg/kg based on internal response factor of the internal standard and each respective aldehyde.

### 2.7. Free thiol content measurement

Free thiol content was measured following method by Eymard, Baron, and Jacobsen (2009) with modifications. Protein was extracted from pork (5.0 ± 0.1 g) and vortexed for 30 s with 25 mL of 0.1 M phosphate buffer (pH 7.4) in 50 mL centrifuge tubes. After centrifugation (3000 rpm/127.8 g) for 15 min at 4 °C, the supernatant was filtered through eight layers of cheesecloth to obtain protein homogenates. For each treatment, 400 µL of homogenate, 600 µL DI water, and 14.3 µL of 0.01 M DTNB in 0.2 M EDTA was added to a microcentrifuge tube and incubated in a water bath (40 °C) for 15 min. The Biuret method was used to determine average protein extracted using 0.1 M phosphate buffer. The protein concentration in solution was determined to be 0.037 g/mL. Concentration of free thiol content expressed in µmol thiol/g protein was read in triplicates at 412 nm using a molar extinction coefficient of 13,600 M<sup>-1</sup> cm<sup>-1</sup>.

### 2.8. Quantification of metmyoglobin formation

Metmyoglobin concentration was calculated as described by Tang, Faustman, and Hoagland (2004). Extracted proteins from Section 2.7 for each treatment were aliquoted in triplicate and absorbance was measured at 503, 525, 557, and 582 nm. Percent metmyoglobin was calculated by the equation:

$$[\% \text{ metmyoglobin}] = (-0.159 R_1 - 0.085 R_2 + 1.262 R_3 - 0.520) \times 100$$

where  $R_1 = A_{582}/A_{525}$ ,  $R_2 = A_{557}/A_{525}$ ,  $R_3 = A_{503}/A_{525}$ .

### 2.9. Statistical analysis

Duplicates frozen cooked pork patties with coffee in pork treatments (1 g/kg of each coffee combination), positive control (2 g/kg Herbalox<sup>®</sup> HT-25), and negative control (no AOXs added) were monitored over 3 months. General linear model procedure in Statistical Analysis 9.3 Software (SAS Institute, 2011) was used to determine the differences in means between treatments per month for TBARS, GC, free thiol content, and percent metmyoglobin (MetMb). Analysis of variance (ANOVA) and Duncan's multiple

range test were performed to determine whether a statistical significance existed. In addition, Pearson's correlation coefficients between each assay were determined. A level of significance of  $\alpha = 0.05$  was used throughout analysis.

## 3. Results and discussion

### 3.1. Antioxidants in coffee

The LBC form for all roast degrees had the highest CGA amongst all application forms, while SCG had the least (Table 1), attributed to the higher solubility of low molecular weight compounds extracted from coffee grounds into the brew. The majority of CGAs remained in the brew, however, extraction of all CGA was incomplete as noted by the amount left in the SCG. Ludwig et al. (2012) reported that brew time and temperature affects the final concentration of CGA extracted. The incomplete removal of phenolic compounds into the brew supports the hypothesis that spent coffee could be utilized as an AOX. Increasing roast degree decreased concentrations of CGA as expected since roasting degrades CGAs or incorporates them into MRPs (Nicolli, Anese, Manzocco, & Lerici, 1997).

The MRPs in lyophilized brew increased by 23% from light to medium roast coffee, whereas dark roasted coffee showed similar values of MRPs to the medium roast (Table 1). With the exception of light SCG, all roasts of SCG and WGC forms reported similar values of MRPs, since the majority of water soluble MRPs are also extracted into the brew form (Bravo, Juaniz, Monente, Caemmerer, Kroh, Paz De Pena et al., 2012). Due to the extraction of water soluble MRPs into the brew, this also resulted in higher levels of metal chelation values for LBC compared to the spent and ground form. However, there was a decreasing trend with increasing roast degree in regards to LBC, which was consistent with Lin et al. (2015). In regards to the other application forms, there was an increase in metal chelation with increasing roast degree for SCG, while WGC maintained similar values with increasing roast degree.

### 3.2. Extent of lipid oxidation measured by thiobarbituric acid reactive substances

The TBARS values reached the highest levels in month 2, increasing from 0.031 to 0.31 mg MDA/kg pork in month 0 to 0.070–1.15 mg MDA/kg pork in month 2 (Fig 1). In month 3 amongst treatments, TBARS levels remained the same (light and dark LBC, light and dark WGC, and negative control) or decreased (light and dark SCG, rosemary oleoresin) from month 2. Despite the decrease observed from month 2–3 for some treatments, there was

**Table 1**  
Maillard reaction products, metal chelation and chlorogenic acid concentration for spent ground, whole ground, and lyophilized brew form coffee solutions.

	MRPs <sup>a</sup> (absorbance intensity units)	Metal chelation <sup>b</sup> (µmol EDTA/g coffee equivalents)	3-CGA <sup>c</sup> (Mg/g coffee)	Total 3-CGA <sup>c</sup> (mg/g coffee)
Light				21.00
Spent	0.73 ± 0.012	14.05 ± 1.48	1.98	
Ground	1.23 ± 0.012	24.00 ± 6.96	4.70	
Lyophilized Brew	4.80 ± 0.14	58.38 ± 2.29	14.32	
Medium				16.13
Spent	1.42 ± 0.024	21.43 ± 0.70	2.01	
Ground	1.47 ± 0.017	24.23 ± 0.76	6.83	
Lyophilized Brew	5.91 ± 0.15	43.67 ± 2.83	7.28	
Dark				12.16
Spent	1.75 ± 0.019	30.97 ± 1.65	1.86	
Ground	2.22 ± 0.013	26.79 ± 1.95	4.40	
Lyophilized Brew	5.83 ± 0.47	35.94 ± 1.02	5.90	

<sup>a</sup> Brown nitrogenous Maillard reaction products from hot brewed coffee at 1 g coffee/100 mL measured at 420 nm.

<sup>b</sup> Metal chelation by ferrozine assay for hot brewed coffee at 0.1 g coffee/100 mL measured at 562 nm.

<sup>c</sup> Chlorogenic acid content by HPLC analysis for cold brewed coffee at 0.1 g/100 mL.

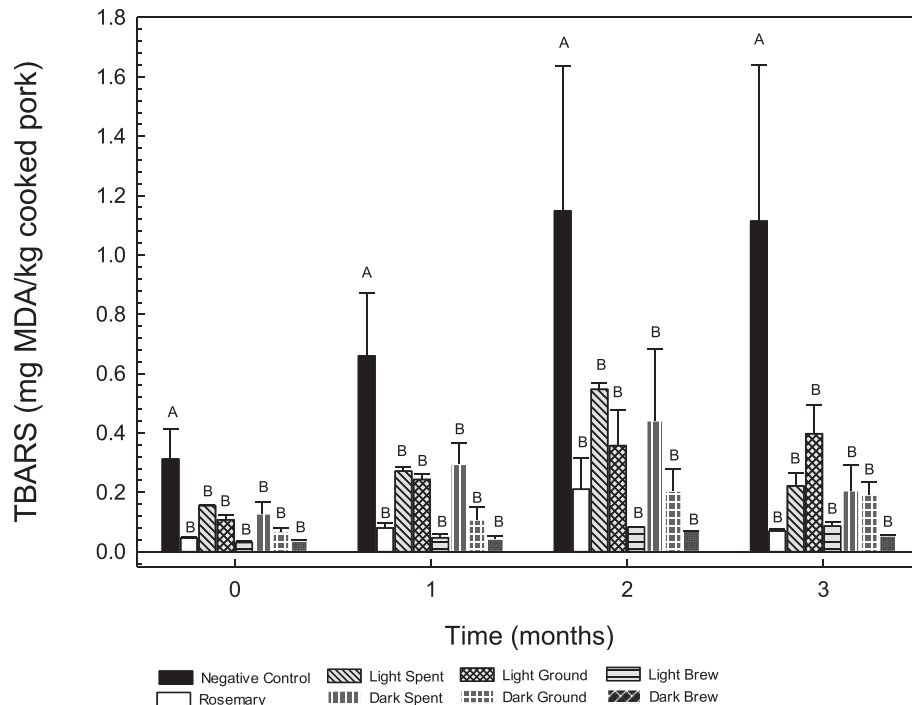


**Fig. 1.** Thiobarbituric acid reactive substances/TBARS (mg MDA/kg pork)  $\pm$  standard deviation with negative control (no antioxidants added), coffee in pork treatments (1 g/kg light and dark roasts of spent, whole, lyophilized brewed) and rosemary oleoresin (2 g/kg) in cooked pork patties analyzed monthly over 3 months of frozen storage. Means followed by the same letter between samples for each month are not significantly different (Duncan's multiple range test  $p \leq 0.05$ ).

an overall increase from initial to end of storage with increases ranging from 43 to 270%. This trend was similar to the results reported by Sasse et al. (2009) and Abd El-Alim, Lugasi, Hovari, and Dworschak (1999). While oxidative reactions are significantly inhibited in frozen storage, LOX reactions can still occur, although at slower rates as noted by the overall increase during storage (Rhee et al., 1996; Sasse et al., 2009). The decrease from month 2–3 could be attributed to (1) MDA decomposition to other organic by-products such as alcohols and acids, or (2) decomposition by bacteria such as *Pseudomonas*, which attack carbonyl compounds like MDA (Georgantelis et al., 2007). The former is the most probably pathway since growth of *Pseudomonas*, a psychrotrophic bacteria, would be negligible at frozen conditions. Furthermore, secondary products of LOX, including MDA, can react with free amino groups from proteins. Since the TBARS assay measures only free MDA, the MDA-protein interaction can result in lower TBARS values (Viljanen, Kivikari, & Heinonen, 2004).

Negative control exhibited higher TBARS values throughout storage compared with other treatments ( $p \leq 0.05$ ), suggesting that AOX compounds from rosemary oleoresin and coffee inhibited MDA formation. By month 3, all pork samples with added coffee presented similar TBARS values (0.054–0.22 mg MDA/kg pork) to rosemary oleoresin (0.070 mg MDA/kg pork), with the exception of light WGC which reported slightly higher MDA concentrations by the end of storage (0.40 mg MDA/kg pork). Despite the overall increase over time in TBARS, all coffee treated pork, with the exception of light SCG, never exceeded the threshold of when rancidity can be detected; 0.5 mg MDA/kg of pork (Gray & Pearson, 1987; Sheard et al., 2000). Negative control surpassed the threshold value after the first month of storage with TBARS value of 0.660 mg MDA/kg pork. In month 2, light SCG (0.55 mg MDA/kg pork) reached the highest value of TBARS for all coffee treated pork for the entirety of testing.

The results in the present study contradict those by Nissen et al.

(2004) who reported that coffee provided little to no protection against LOX in comparison to rosemary extracts. This may be due to the 20-fold difference between coffee extract concentration in the previous study (0.05 g/kg) compared with the present study (1 g/kg), and use of a different rosemary extract. The present study shows that all coffee combinations were as effective as rosemary oleoresin at inhibiting MDA production.

### 3.3. Extent of lipid oxidation measured by gas chromatography

Pork samples in the last 2 months of analysis exhibited the highest concentrations of hexanal with values ranging from 0.30 to 2.59 mg hexanal/kg pork, compared to octanal (0.015–0.12 mg octanal/kg pork) and nonanal (0.036–0.13 mg nonanal/kg pork) (Fig 2). Hexanal, the main aldehyde formed, was consistent with literature (Meynier, Genot, & Gandemer, 1998), as it forms from oxidation of n-6 fatty acids, specifically linoleic acid, the predominant polyunsaturated fatty acid in pork (14.3 g/100 g). By month 3, the negative control (2.59 mg/kg pork) had the highest hexanal, while both light and dark roasts of LBC (0.37 and 0.39 mg/kg pork, respectively), inhibited hexanal production to the same extent as rosemary oleoresin (0.30 mg/kg pork) ( $p \leq 0.05$ ).

There was no significant difference for both octanal and nonanal from month 2–3, which was consistent with a study done on beef by Lin et al. (2015). Despite the differences in study parameters (muscle types investigated and storage temperatures), octanal and nonanal displayed similar trends in both studies. Nonanal and octanal forms from oxidation of n-9 fatty acids, such as oleic acid. Although oleic acid (34.3 g/100 g) is present in higher quantities in pork than linoleic acid (14.3 g/100 g), monounsaturated fatty acids are more stable against oxidation than polyunsaturated fatty acids (Meynier et al., 1998). Amongst the coffee in pork treatments, there was no significant difference observed with the exception of month 3 for octanal. In month 3, the negative control displayed the highest

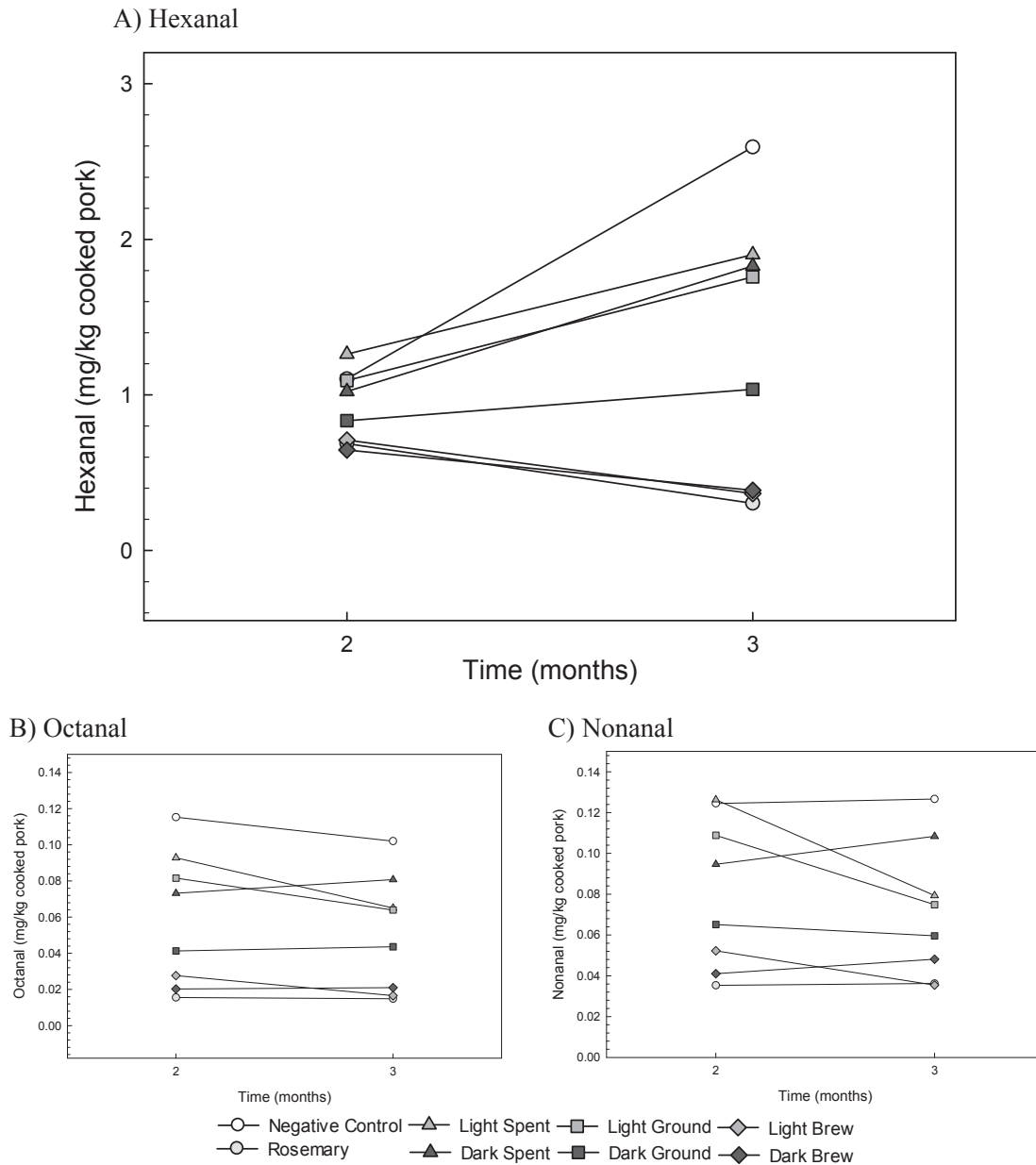


**Fig. 2.** Key volatile aldehyde (mg/kg cooked pork) for negative control (no antioxidants added), coffee in pork treatments (1 g/kg light and dark roasts of spent, whole, lyophilized brewed), and rosemary oleoresin (2 g/kg) in cooked pork patties analyzed after 2 months of frozen storage.

octanal (0.10 mg/kg pork), while light LBC and rosemary oleoresin inhibited octanal formation (0.017 and 0.015 mg/kg pork, respectively). Volatile aldehydes are considered to be one of the most important products of LOX since they have such low threshold values for detection (Ladikos & Lougovois, 1990). The rancidity thresholds for hexanal reported by Shahidi and Pegg (1994) can range from 0.0045 to 0.15 mg/kg cooked pork. Although MDA flavor thresholds for rancidity were not surpassed (Section 3.2), hexanal thresholds were exceeded by month 2 of storage by all treatments, with the lowest value for hexanal being observed by dark brew (0.65 mg/kg pork).

Based on results from Section 3.1, differing CGA levels had no effect on MDA formation since all added coffee in pork treatments produced similar results to rosemary oleoresin. However, CGA and MRP levels correlated with greater AOX effect against volatile aldehydes in frozen cooked pork. The ranking for application form

effectiveness against hexanal, octanal, and nonanal was as follows: LBC > WGC > SCG, corresponding with CGA and MRP concentrations found in Table 1.

#### 3.4. Protein oxidation measured by thiol content

Thiol content increased from month 0–1 ( $p < 0.05$ ) ranging in values from 0.56 to 0.96 to 0.82–1.10  $\mu\text{mol/g}$  protein, respectively. In month 2, all treatments decreased in thiol content from month 1 ranging in values from 0.59 to 0.90  $\mu\text{mol/g}$  protein. From month 2–3, thiol content for negative control, rosemary oleoresin, and dark WGC increased, light LBC, dark SCG and LBC decreased, while light SCG and WGC remained relatively the same (Fig. 3). Thiol content was expected to gradually decrease or remain stable over the frozen storage period (Lund, Hviid, & Skibsted, 2007; Nieto, Jongberg, Andersen, & Skibsted, 2013). Despite unexpected

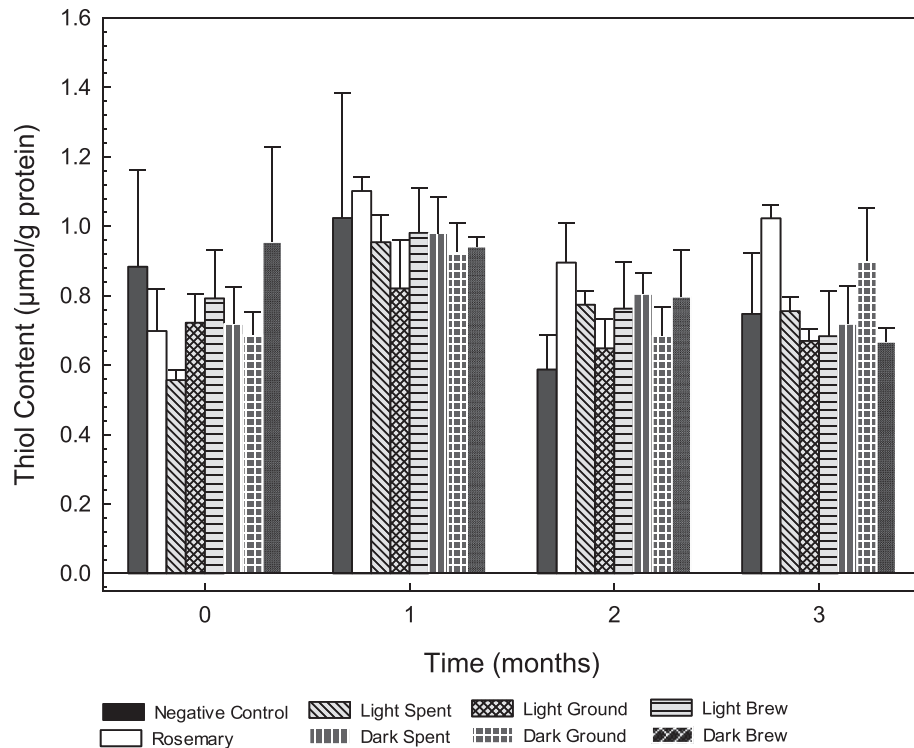


**Fig. 3.** Thiol content ( $\mu\text{mol thiol/g pork}$ )  $\pm$  standard deviation for negative control (no antioxidants added), coffee in pork treatments (1 g/kg light and dark roasts of spent, whole, lyophilized brewed), and rosemary oleoresin (2 g/kg) in cooked pork patties analyzed monthly over 3 months of frozen storage.

increases in certain coffee in pork treatments, no significant difference amongst treatments were observed across the storage period ( $p \geq 0.05$ ), indicating added coffee and Herbalox<sup>®</sup> HT-25 may not have a significant effect on POX.

Haak, Raes, and De Smet (2009) found that 0.005–0.02% rosemary extract, tocopherols, and green tea extract did not influence POX in frozen cooked pork until day 8 of frozen storage. Whereas, Nieto et al. (2013) found that 0.05% and 0.4% of rosemary essential oil was able to protect against thiol loss in chilled raw pork throughout the 9 day storage. Lara, Gutierrez, Timon, and Andres (2011) found that 0.03% rosemary and 0.1% lemon balm extracts in cooked meat exerted a protective effect against POX throughout storage. While these studies differ in design, which influences the extent of effectiveness of AOXs, our results correspond to other studies which indicate that rosemary oleoresin does not have an effect in inhibiting the loss of sulfhydryl content.

### 3.5. Extent of protein oxidation measured by metmyoglobin formation

An increase in metmyoglobin (MetMb) formation by 1–14% over 3 months was observed (Fig 4). Significant differences were found amongst treatments for all testing months with the exception of month 1, which had % MetMb range of 55.25–56.24%. By month 3, rosemary oleoresin had lower MetMb (54.47%) ( $p \leq 0.05$ ), while pork with added coffee were more similar to the negative control and ranged in values from 56.20 to 56.37%, which indicates that coffee may not inhibit MetMb to the same extent as Herbalox<sup>®</sup> HT-25 in frozen cooked pork patties.

The overall range for MetMb for the entire study was 49.33–57.18%. Fernandez-Lopez et al. (2003) found with fresh meat, values for MetMb initially ranged from 25 to 30%. After cooking, these values increased to 32–45%. At the end of the 8 day

testing of chilled storage, Fernandez-Lopez et al. (2003) detected a distinct difference between control samples and added AOX samples with MetMb ranging from 70 to 75% and 42–48%, respectively. In the present study, MetMb values for all treatments were higher on the initial day of testing (49.33–55.36%). However, the range of MetMb formed stayed relatively stable throughout frozen storage. The difference in results could have been due to frozen storage versus refrigerated storage.

Myoglobin oxidation in pork meat is predominantly affected by temperature and time (Faustman, Sun, Mancini, & Suman, 2010). The pork in the present study was cooked prior to  $-18^\circ\text{C}$  storage. The cooking could explain why MetMb values were initially higher. Greene, Hsin, and Zipser (1971) found that MetMb levels exceeding 40% were rejected by consumers as a poor quality raw product, however, since these pork products are cooked, there is a wider range of acceptance since browning is expected with cooking. Denaturation of myoglobin unravels intact proteins, exposes heme iron. Oxidation of the centrally located iron, accounts for the higher MetMb values observed initially, which is expected to increase with extended storage periods. The reactive products of LOX, such as peroxides, promote myoglobin oxidation (Fernandez-Lopez et al., 2003; Rhee et al., 1996). The stable MetMb values could be explained by the slowing of oxidative reactions due to frozen storage.

## 4. Conclusion

The use of light and dark roasted coffee in spent ground, whole ground, and lyophilized brewed form at 1 g coffee/kg pork lowered MDA and hexanal in frozen cooked pork patties to the same extent as rosemary oleoresin, showing potential as an alternative AOX for LOX. In regards to POX, coffee AOXs neither had a positive nor negative impact on free thiol content or MetMb formation. The

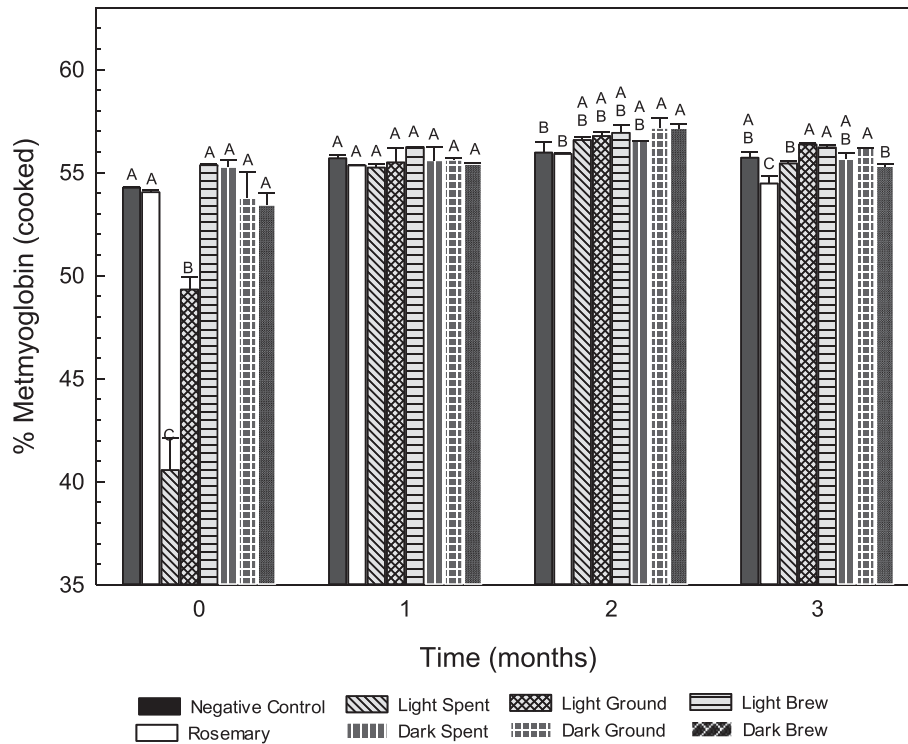


**Fig. 4.** Percent metmyoglobin for negative control (no antioxidants added), coffee in pork treatments (1 g/kg light and dark roasts of spent, whole, lyophilized brewed), and rosemary oleoresin (2 g/kg) in cooked pork patties analyzed monthly over 3 months of frozen storage. Means followed by the same letter between the samples for each month are not significantly different (Duncan's multiple range test  $p \leq 0.05$ ). Error bars represent standard deviation.

results show that all forms of both roast degrees could extend the shelf life of frozen cooked pork patties.

### Acknowledgments

The authors would like to thank Tiffany Hashimoto for assistance with data collection, Andrew and Nathan at Rose Park Roasters for roasting the coffee, Mandeep Saini and Elizabeth Lawton at Farmer John® for providing the pork and assisting in preparing samples, and Chapman University for funding the research.

### References

- Abd El-Alim, S. S. L., Lugasi, A., Hovari, J., & Dworschak, E. (1999). Culinary herbs inhibit lipid oxidation in raw and cooked minced meat patties during storage. *Journal of the Science of Food and Agriculture*, 79(2), 277–285.
- AMSA. (1995). *Research guidelines for cookery, sensory evaluation, and instrumental tenderness measurements of fresh meat*. Chicago, IL: American Meat Science Association.
- AOAC. (2010). *Official methods of analysis* (18th ed.). Arlington, VA: Association of Official Analysis Chemists International.
- Bravo, J., Juaniz, I., Monente, C., Caemmerer, B., Kroh, L. W., Paz De Pena, M., et al. (2012). Evaluation of spent coffee obtained from the most common coffee-makers as a source of hydrophilic bioactive compounds. *Journal of Agricultural and Food Chemistry*, 60(51), 12565–12573.
- Budryn, G., & Nebesny, E. (2013). Effects of green and roasted coffee antioxidants on quality and shelf life of cookies and chocolates. *Journal of Food Processing and Preservation*, 37(5), 835–845.
- Dai, Y., Lu, Y., Wu, W., Lu, X. M., Han, Z. P., Liu, Y., et al. (2014). Changes in oxidation, color and texture deteriorations during refrigerated storage of ohmically and water bath-cooked pork meat. *Innovative Food Science and Emerging Technologies*, 26, 341–346.
- Del Pino-García, R., Gonzalez-SanJose, M. L., Rivero-Perez, M. D., & Muniz, P. (2012). Influence of the degree of roasting on the antioxidant capacity and genoprotective effect of instant coffee: contribution of the melanoidin fraction. *Journal of Agricultural and Food Chemistry*, 60(42), 10530–10539.
- Delgado-Andrade, C., Rufian-Henares, J. A., & Morales, F. J. (2005). Assessing the antioxidant activity of melanoidins from coffee brews by different antioxidant methods. *Journal of Agricultural and Food Chemistry*, 53(20), 7832–7836.
- Eymard, S., Baron, C. P., & Jacobsen, C. (2009). Oxidation of lipid and protein in horse mackerel (*Trachurus trachurus*) mince and washed minces during processing and storage. *Food Chemistry*, 114(1), 57–65.
- Farah, A. (2012). Coffee constituents. In Y.-F. Chu (Ed.), *Coffee: Emerging health effects and disease prevention* (1st ed., pp. 21–58). Blackwell Publishing Ltd.
- Faustman, C., Sun, Q., Mancini, R., & Suman, S. P. (2010). Myoglobin and lipid oxidation interactions: mechanistic bases and control. *Meat Science*, 86(1), 86–94.
- Fernandez-Lopez, J., Sevilla, L., Sayas-Barbera, E., Navarro, C., Marin, F., & Perez-Alvarez, J. A. (2003). Evaluation of the antioxidant potential of hyssop (*Hyssopus officinalis* L.) and rosemary (*Rosmarinus officinalis* L.) extracts in cooked pork meat. *Journal of Food Science*, 68(2), 660–664.
- Georgantelis, D., Ambrosiadis, I., Katikou, P., Blekas, G., & Georgakis, P. A. (2007). Effect of rosemary extract, chitosan and alpha-tocopherol on microbiological parameters and lipid oxidation of fresh pork sausages stored at 4 degrees C. *Meat Science*, 76(1), 172–181.
- Gray, J. I., & Pearson, A. M. (1987). Rancidity and warmed-over flavor. In *Handbook of meat, poultry and seafood quality* (pp. 221–269). New York: Van Nostrand Reinhold Co.
- Greene, B. E., Hsin, I. M., & Zipser, M. W. (1971). Retardation of oxidative color changes in raw ground beef. *Journal of Food Science*, 36(6), 940–942.
- Haak, L., Raes, K., & De Smet, S. (2009). Effect of plant phenolics, tocopherol and ascorbic acid on oxidative stability of pork patties. *Journal of the Science of Food and Agriculture*, 89(8), 1360–1365.
- Kim, H., Cadwallader, K. R., Kido, H., & Watanabe, Y. (2013). Effect of addition of commercial rosemary extracts on potent odorants in cooked beef. *Meat Science*, 94(2), 170–176.
- Kingston, E. R., Monahan, F. J., Buckley, D. J., & Lynch, P. B. (1998). Lipid oxidation in cooked pork as affected by vitamin E, cooking and storage conditions. *Journal of Food Science*, 63(3), 386–389.
- Ladikos, D., & Lougovois, V. (1990). Lipid oxidation in muscle foods: a review. *Food Chemistry*, 35(4), 295–314.
- Lara, M. S., Gutierrez, J. I., Timon, M., & Andres, A. I. (2011). Evaluation of two natural extracts (*Rosmarinus officinalis* L. and *Melissa officinalis* L.) as antioxidants in cooked pork patties packed in MAP. *Meat Science*, 88(3), 481–488.
- Lin, C., Toto, C., & Were, L. (2015). Antioxidant effectiveness of ground roasted coffee in raw ground top round beef with added sodium chloride. *LWT - Food Science and Technology*, 60(1), 29–35.
- Ludwig, I. A., Sanchez, L., Caemmerer, B., Kroh, L. W., Paz De Pena, M., & Cid, C. (2012). Extraction of coffee antioxidants: Impact of brewing time and method. *Food Research International*, 48(1), 57–64.
- Lund, M. N., Hviid, M. S., & Skibsted, L. H. (2007). The combined effect of

- antioxidants and modified atmosphere packaging on protein and lipid oxidation in beef patties during chill storage. *Meat Science*, 76(2), 226–233.
- Meynier, A., Genot, C., & Gandemer, G. (1998). Volatile compounds of oxidized pork phospholipids. *Journal of the American Oil Chemists Society*, 75(1), 1–7.
- Nicoli, M. C., Anese, M., Manzocco, L., & Lerici, C. R. (1997). Antioxidant properties of coffee brews in relation to the roasting degree. *LWT-Food Science and Technology*, 30(3), 292–297.
- Nieto, G., Jongberg, S., Andersen, M. L., & Skibsted, L. H. (2013). Thiol oxidation and protein cross-link formation during chill storage of pork patties added essential oil of oregano, rosemary, or garlic. *Meat Science*, 95(2), 177–184.
- Nissen, L. R., Byrne, D. V., Bertelsen, G., & Skibsted, L. H. (2004). The antioxidative activity of plant extracts in cooked pork patties as evaluated by descriptive sensory profiling and chemical analysis. *Meat Science*, 68(3), 485–495.
- Nolan, N. L., Bowers, J. A., & Kropf, D. H. (1989). Lipid oxidation and sensory analysis of cooked pork and turkey stored under modified atmospheres. *Journal of Food Science*, 54(4), 846–849.
- Rhee, K. S., Anderson, L. M., & Sams, A. R. (1996). Lipid oxidation potential of beef, chicken, and pork. *Journal of Food Science*, 61(1), 8–12.
- Rojas, M. C., & Brewer, M. S. (2007). Effect of natural antioxidants on oxidative stability of cooked, refrigerated beef and pork. *Journal of Food Science*, 72(4), S282–S288.
- Salminen, H., Estevez, M., Kivikari, R., & Heinonen, M. (2006). Inhibition of protein and lipid oxidation by rapeseed, camelina and soy meal in cooked pork meat patties. *European Food Research and Technology*, 223(4), 461–468.
- SAS Institute. (2011). *The SAS system for Windows (Version 9.3)*. Cary, NC, USA.
- Sasse, A., Colindres, P., & Brewer, M. S. (2009). Effect of natural and synthetic antioxidants on the oxidative stability of cooked, frozen pork patties. *Journal of Food Science*, 74(1), S30–S35.
- Shahidi, F., & Pegg, R. B. (1994). Hexanal as an indicator of the flavor deterioration of meat and meat-products. *Lipids Food Flavors*, 558, 256–279.
- Sheard, P. R., Enser, M., Wood, J. D., Nute, G. R., Gill, B. P., & Richardson, R. I. (2000). Shelf life and quality of pork and pork products with raised n-3 PUFA. *Meat Science*, 55(2), 213–221.
- Tang, J., Faustman, C., & Hoagland, T. A. (2004). Krzywicki revisited: Equations for spectrophotometric determination of myoglobin redox forms in aqueous meat extracts. *Journal of Food Science*, 69(9), C717–C720.
- Teets, A. S., & Were, L. M. (2008). Inhibition of lipid oxidation in refrigerated and frozen salted raw minced chicken breasts with electron beam irradiated almond skin powder. *Meat Science*, 80, 1326–1332.
- Viljanen, K., Kivikari, R., & Heinonen, M. (2004). Protein-lipid interactions during liposome oxidation with added anthocyanin and other phenolic compounds. *Journal of Agricultural and Food Chemistry*, 52(5), 1104–1111.



# Influence of processing conditions on procyanidin profiles and antioxidant capacity of chocolates: Optimization of dark chocolate manufacturing by response surface methodology



Mine Gültekin-Özgülven, İjlal Berktaş, Beraat Özçelik\*

Department of Food Engineering, Faculty of Chemical and Metallurgical Engineering, Istanbul Technical University, Maslak, TR-34469, Istanbul, Turkey

## ARTICLE INFO

### Article history:

Received 8 May 2015

Received in revised form

15 October 2015

Accepted 19 October 2015

Available online 21 October 2015

### Keywords:

Dark chocolate

Polyphenols

Process

Antioxidant

RSM

## ABSTRACT

Dark chocolate is a good source of dietary flavonoids, mainly comprised of (+)-catechin, (–)-epicatechin, and their oligomeric and polymeric procyanidins. Nevertheless, flavonoid content and antioxidant capacity are affected during chocolate manufacturing. In this study, the influence of manufacturing process of dark chocolate, particularly, roasting of cocoa beans (115–135 °C), conching (60–80 °C), and alkalinization treatment (pH 7–9) was studied and the process conditions were optimized via Response Surface Methodology (RSM). Validation of the model accomplished applying the conditions generated by RSM. Considering the data obtained from the model; chocolate manufacturing process, particularly increasing alkalization degree and roasting temperature significantly reduced phenolics and related antioxidant capacity ( $p < 0.05$ ). Nevertheless, increasing conching temperature was insignificant ( $p > 0.05$ ) since higher temperature leads to a shorter required processing time.

© 2015 Elsevier Ltd. All rights reserved.

## 1. Introduction

Cocoa bean, and its derivative products (dark chocolate and cocoa powder) are rich polyphenol sources which have beneficial effects for health such as anti-ulcer, anti-carcinogenic, anti-thrombotic, anti-microbial effects and they exhibit antioxidant activity (Jonfia-Essien, West, Alderson, & Tucker, 2008). Cocoa bean polyphenols consist of catechins or flavan-3-ols (37%), proanthocyanidins (58%) and anthocyanins (4%) (Cooper et al., 2007; Miller et al., 2008; Wollgast & Anklam, 2000). However, phenolic content of cocoa beans depends on botanical variety, genetic and agronomical factors such as postharvest handling, fermentation and drying conditions (Tomas-Barberan et al., 2007).

Fermentation, drying, and roasting are essential for characteristic flavour development in cocoa beans. During fermentation, polyphenols undergo oxidation to condensed high molecular insoluble tannins catalysed by polyphenol oxidase enzyme. Then, cocoa beans are dried to decrease the moisture content below 8% which is the critical moisture content for mould growth (Wollgast & Anklam, 2000). Meanwhile, water activity of cocoa beans must

be below 0.70 for microbiological stability (Sandoval & Barreiro, 2002). After drying, beans are roasted at 100–150 °C for maximum 120 min to develop further typical chocolate flavour. The final nib (broken beans) is ground to obtain “chocolate liquor” by releasing cocoa butter from the broken-down cell walls (Wollgast & Anklam, 2000).

Chocolate liquor and cocoa butter are the main ingredients of chocolate manufacturing with others such as sugar and emulsifiers. After mixing all ingredients in mixers, obtained chocolate paste is refined by roll refiners. For the final texture and flavour, refined chocolate paste is conched with varied temperature-time conditions. During conching, moisture is reduced, volatile substances are removed and all particles are dispersed in continuous fat phase. Meanwhile, phenolic content is expected to be reduced due to high temperature and oxygen in roasting and conching steps. Moreover, if alkalization treatment (Dutching) which relies on neutralization of acetic acid is present, phenolic content decreases sharply (McShea et al., 2008). In Dutching, colour and flavour are modified by raising pH from 5.5 up to 8.2 with potassium or sodium bicarbonate. Finally, melted chocolate is cooled by agitation in tempering step where small stable cocoa butter crystals occur and give glossy appearance, snap, good texture, bloom resistance and contraction to the chocolate (Afoakwa, Paterson, Fowler, & Vieira, 2008; Tanabe & Hofberger, 2006).

\* Corresponding author.

E-mail address: [ozcelik@itu.edu.tr](mailto:ozcelik@itu.edu.tr) (B. Özçelik).

In the literature, some researchers studied phenolics and antioxidant capacity of cocoa beans (Arlorio et al., 2008; de Brito et al., 2000; Jonfia-Essien et al., 2008; Niemenak, Rohsius, Elwers, Omokolo Ndoumou, & Lieberei, 2006; Othman, Ismail, Ghani, & Adenan, 2007) cocoa powder (Lee, Kim, Lee, & Lee, 2003; Miller et al., 2008), different types of chocolates (Pimentel, Nitzke, Klipel, & de Jong, 2010; Sulistyowati & Misnawi, 2008; Wollgast & Anklam, 2000), and cocoa liquor (Jinap, Jamilah, & Nazamid, 2005). Considering their findings, it is possible to say that choosing cocoa beans rich in phenolics, reducing temperature and/or time in roasting or conching may conserve polyphenols.

On the other hand, there are *in vivo* antioxidant studies related to health benefits of chocolate consumption (Pearson et al., 2002; Rein et al., 2000; Schramm et al., 2001; Serafini et al., 2003). Finally, some studies about probiotic, prebiotic, and synbiotic chocolate development were performed (Cardarelli, Aragon-Alegro, Alegro, de Castro, & Saad et al., 2008; Erdem et al., 2014; Patel, Parekh, & Subhash, 2008). All those studies mentioned the functional properties of cocoa beans, cocoa powder and chocolate. Nevertheless, this study has focused on determination of optimum chocolate manufacturing conditions by using Response Surface Methodology (RSM) since possible modifications in processing conditions regarding roasting, conching and alkalization treatment may reduce the loss of phenolics and antioxidant capacity. To our knowledge, there is limited number of studies investigating the effect of industrial chocolate manufacturing on procyanidin profile, and antioxidant capacity. For this purpose, the aim of the present study was to investigate the changes in procyanidin profile, and antioxidant capacity during roasting, conching, alkalization treatment to optimize the chocolate manufacturing.

## 2. Materials and methods

### 2.1. Chemicals and reagents

Epicatechin (EC), epigallocatechin gallate (EGCG), epigallocatechin (EGC), epicatechin gallate (ECG), Trolox (6-hydroxy-2,5,7,8-tetramethylchroman-2-carboxylic acid), 2,2-azobis(2-amidinopropane) dihydrochloride (AAPH), fluorescein, Folin–Ciocalteu reagent were purchased from Sigma–Aldrich Chemie GmbH & Co. KG (Steinheim, Germany). Other chemicals and reagents were of analytical or high-performance liquid chromatography grade. To identify and quantify procyanidins, a composite procyanidin oligomer standard containing monomers through decamers was purified from cocoa beans.

### 2.2. Chocolate manufacturing

Ingredients such as roasted cocoa beans and alkalized chocolate liquor were provided from Altinmarka Inc. and dark chocolate samples were kindly produced by Nestle Turkey Inc. Recipe of dark chocolate contained cocoa liquor (43.20%), cocoa butter (5.50%), sugar (47.52%), soy lecithin (0.25%), milk fat (3.50%) and vanilla extract (0.03%). Cocoa liquor, sugar and vanilla extract were mixed in a mixer for 5 min. After pre-refining, the batch was fed to the five roller refiner lasting 3 h. After addition of cocoa butter and milk fat to the chocolate paste, conching was performed at 80 °C for 11 h, at 70 °C for 12 h, and at 60 °C for 13 h, respectively. As the last step of conching, lecithin is added to the mass and mixed for 30 min more. Then, chocolate paste was tempered with a continuous process heat exchanger to be ready for deposition. Finally, dark chocolate samples were cooled and demoulded. Chocolate samples were analysed in a week after manufacturing. Until then, they were stored in plastic bucket at room temperature.

### 2.3. Extraction of phenolics

The samples were extracted following the method described by Wollgast (2004). 1 g of milled samples were defatted twice with 10 ml n-hexane for 5 min in an ultrasonic bath at 30 °C and was subsequently centrifuged for 10 min at 3000× g. Polyphenols were extracted from the air-dried sample with 10 ml of a mixture of methanol and water (80:20 v/v) for 10 min at 30 °C in the ultrasonic bath.

### 2.4. Extraction of procyanidins

All defatted samples were dissolved in acetone: Milli-Q water: acetic acid (70: 29.5: 0.5, v/v/v) at a ratio of 1: 5. After vortexing for 5 min and centrifuged at 12,000 rpm, the supernatant was filtered through 0.45 µm syringe filters (Adamson et al., 1999).

### 2.5. Preparation of semi-purified oligomers from cocoa beans

A composite procyanidin oligomer standard containing monomers through decamers was purified from cocoa beans previously described by Adamson et al. (1999) and Gu, House, Wu, Ou, and Prior (2006). The fresh seeds were ground in a high-speed laboratory mill with liquid nitrogen until the particle size was reduced to approximately 90 µm. Lipids were removed from 220 g of the ground seeds by extracting with 1000 mL of hexane three times. The lipid free solids were air-dried to yield approximately 100 g of fat free material. A fraction containing procyanidins was obtained by extraction with 1000 mL of 70 vol% acetone in water. The suspension was centrifuged for 10 min at 1500 g. The acetone layer was decanted through a funnel with glass wool. The aqueous acetone was then re-extracted with hexane (75 mL) to remove residual lipids. The hexane layer was discarded, and the aqueous acetone was rotary evaporated under partial vacuum at 40 °C to a final volume of 200 mL. The aqueous extract was freeze-dried to yield approximately 19 g of acetone extract material (Adamson et al., 1999).

Approximately, 2 g of acetone extract was suspended in 10 mL of 70% aqueous methanol and centrifuged at 1500 g. The supernatant was semipurified on a Sephadex LH-20 column (6 × 1.5 cm) that had previously been equilibrated with 30% (v/v) aqueous methanol for over 4 h before use. After the sample had been loaded, the column was washed with 40 mL of 30% methanol/water to remove sugars and other phenols. Proanthocyanidins were recovered from the column by elution with 70 mL of 70% (v/v) aqueous acetone (Gu et al., 2006).

Approximately 0.7 g of semipurified acetone extract was dissolved in 7 mL of acetone/water/acetic acid in a ratio by volume of 70: 29.5: 0.5, respectively (Adamson et al., 1999). Semi-purified fractions were analysed by UFLC/MS–MS using the parameters described by Lazarus, Adamson, Hammerstone, and Schmitz (1999).

### 2.6. Total phenolic and flavonoid content

Total phenolic content (TPC) was measured using Folin–Ciocalteu assay (Wollgast, 2004) while total flavonoid content (TFC) was performed according to the method described by Lee et al. (2003). Results were expressed as mg of catechin equivalents (CE) per kg of defatted samples. All samples were analysed in triplicate.

### 2.7. UFLC-MS/MS analysis of catechins

Six major catechins were determined [(+)-catechin,

(–)-epicatechin, GC, EGC, ECG and EGCG)] by UFLC-MS/MS system which is equipped with a ultra fast liquid chromatography (Prominence Liquid Chromatography LC-20AD, Shimadzu), a micro vacuum degasser (Prominence Degasser DGU-20A3, Shimadzu), an autosampler (Prominence AutoSampler SIL-20AHT, Shimadzu), a column oven (Prominence Column Oven CTO-10ASVP, Shimadzu), a controller (Prominence Controller CBM-20A Lite, Shimadzu) and an MS detector with electrospray ion source (ESI) and triple quadrupole analyzer (API-2000 Liquid Chromatography/Tandem Mass Spectrometry System, ABSciex, USA).

In this study, chromatographic separations were performed on an Inertsil C8 column (150 mm × 2.1 mm, 3 μm). A gradient of mobile phase A (7.5 mM formic acid) and mobile phase B (Acetonitrile) was used for the chromatographic separation. The gradient profile was set as follows: 10 min 95% B eluent, 11 min 15% B and 13 min it was stopped. The flow rate was 0.5 mL min<sup>-1</sup> and the injection volume was 20 μl for each standard mixture and the column temperature was set to 40 °C.

API 2000 was operated in the triple quadrupole mass spectrometry mode using an electrospray ionization (ESI) source operating in the negative (–) ion mode with Multiple Reaction Monitoring (MRM) in the experiments presented here. MS interface conditions were set as follows: ion spray voltage of –4500 V, source temperature of 525 °C, gas 1 temperature of 20 °C. Declustering potential (DP), entrance potential (EP), collision energy (CE) and collision cell exit potential (CXP) parameters were optimized for all of the phenolic compounds.

## 2.8. UFLC analysis of procyanidins

Separation of the compounds up to trimers was achieved by reversed phase UFLC with PDA detector previously described by Adamson et al. (1999) and Rios et al. (2002). Chromatographic separation was performed by using a Inertsil C18 (250 mm × 4.6 mm, 5 μm) column at 30 °C with a 20 μL injection volume. The binary mobile phase consisted of water: tetrahydrofuran: trifluoroacetic acid (98: 2: 0.1, by vol) (A) and acetonitrile (B). Flow rate of 0.5 mL/min as follows: 10 min. 15–17% B; 5 min. 17% B; 15 min. 17–40% B; 5 min. 40–50% B; 10 min. 50–60% B; 5 min. 60–90% B. Detection was performed at 280 nm.

## 2.9. Antioxidant capacity analysis

Antioxidant analysis were performed with ORAC and DPPH assays. All samples were analysed in triplicate.

### 2.9.1. ORAC assay

Both hydrophilic and lipophilic oxygen radical absorbance capacity (H-ORAC and L-ORAC) assays were carried out on a Synergy™ HT Multi-Detection Microplate Reader (BioTek Instruments, Winooski, VT at 37 °C, described by Huang, Ou, Hampsch-Woodill, Flanagan, and Deemer (2002) and Huang, Ou, and Prior (2005), respectively. Results were expressed as micromoles of Trolox equivalents (TE) per gram of defatted samples.

For hydrophilic ORAC, samples (0.3 g) were extracted with 25 mL of 70:29.5:0.5 acetone/water/acetic acid by sonication at 30 °C for 10 min. For lipophilic ORAC assay, 1 g sample was dissolved in 20 ml acetone. An aliquot of sample solution was diluted with 7% randomly methylated beta-cyclodextrin (RMCD) (w/v) solvent in a 50% acetone–water (v/v) mixture and was shaken for 1 h at room temperature on a orbital shaker at 400 rpm (Wu et al., 2011).

### 2.9.2. DPPH assay

DPPH radical scavenging activities of the samples were

determined according to Lee et al. (2003). 0.1 ml of diluted phenolic extract was mixed with 2.9 ml of  $6 \times 10^{-5}$  mM DPPH radical solution in methanol. Then the mixture was shaken vigorously and allowed to stand for 30 min at room temperature in the dark. Decrease in absorbance at 517 nm was measured.

## 2.10. Experimental design and statistical analysis

A three-level central composite rotatable design (CCD) was used for the response surface methodology (RSM) studies, and 17 experimental settings were generated with three factors by using Design Expert 9.0 (Stat-Ease, Inc., MN, USA) software. The three factors chosen were roasting temperature, (115–155 °C); alkalinization concentration and conching temperature (60–80 °C). The independent variables and experimental design are presented in Table 1. All experiments were run randomly, and duplicate reactions were carried out at all design points. A total of 17 runs with three centre points (0, 0, 0) were generated. Experiments were randomly run. The regression analyses, statistical significance, and response surfaces were analysed using Design Expert 9.0 software.

## 3. Results and discussion

### 3.1. Total phenolic and flavonoid content

In the present study, TPC changed between 2.07 and 8.22 mg kg<sup>-1</sup> while TFC varied from 1.64 to 6.64 mg kg<sup>-1</sup> (Table 1). Reduction in TPC and TFC was observed depending on roasting temperature and alkali treatment ( $p < 0.05$ ). Andres-Lacueva et al. (2008) observed that alkalization treatment resulted in 60% loss of the mean total flavonoid content during cocoa powder manufacturing. In another study, Jolic, Redovnikovic, Markovic, Sipusic, and Delonga (2011) also demonstrated that the process of roasting and cocoa nib alkalisation influenced phenolic compounds and antioxidant capacity during cocoa bean processing. They reported that roasting and alkalization treatment resulted in 14% and 64% loss of the total phenolics content, respectively.

On the other hand, conching temperature did not decrease TPC and TFC significantly ( $p > 0.05$ ). It is suggested that higher conching temperature requires shorter conching times. However, there is limited information about the influence of conching process on phenolics. Only, Sulistyowati and Misnawi (2008) reported that polyphenol reduction was triggered more by the presence of alkali than conching temperature. In a recent study, Di Mattia et al. (2014) determined that long time conching process (6 h before and 6 h after lecithin addition, at 60 °C) caused a slight but not significant reduction of the total procyanidin content while short time conching process (6 h before lecithin addition, at 90 °C and 1 h after lecithin addition, at 60 °C) caused a slight but not significant increase of the total procyanidin content compared to unconched initial raw chocolate mass. We also detected that conching process did not affect phenolic compounds.

### 3.2. Antioxidant capacity

The antioxidant capacity of the samples was measured using ORAC and DPPH assays. Since cocoa and cocoa products contain hydrophilic antioxidants more than 90%, usually H-ORAC is employed, and L-ORAC is omitted in the literature. In this study, both lipophilic and hydrophilic antioxidant capacities were measured and total antioxidant capacity (TAC) combining hydrophilic (H-ORAC) and lipophilic (L-ORAC) antioxidant compounds was determined for all samples. TAC (H-ORAC + L-ORAC) values of the samples were found to be between 126.34 and 206.25 μmol TE

**Table 1**  
Experimental design with factors and responses.

Exp.No	RT (°C)	pH	CT (°C)	TPC (mg CE/g)	TFC (mg CE/g)	H-ORAC (μmol TE/g)	L-ORAC (μmol TE/g)	TAC (μmol TE/g)	EC <sub>50</sub> (mg/100 g)	C (mg/100 g)	EC (mg/100 g)	Dimer B2 (mg/100 g)	Trimer C1 (mg/100 g)
1	155	9	60	2.94 ± 0.28	1.64 ± 0.17	143.51 ± 20.80	5.50 ± 0.65	149.01	0.047 ± 0.001	12.64 ± 0.67	146.00±10.21	98.90 ± 10.52	13.58 ± 1.25
2	155	7	60	5.59 ± 0.44	3.65 ± 0.18	162.18 ± 27.04	4.92 ± 0.41	167.10	0.035 ± 0.001	25.51 ± 0.23	180.66 ± 21.23	77.91 ± 10.58	25.78 ± 1.32
3	135	8	60	4.88 ± 0.23	3.21 ± 0.16	144.91 ± 5.51	5.77 ± 0.07	150.68	0.041 ± 0.001	24.45 ± 0.25	189.46 ± 32.89	80.19 ± 1.85	20.76 ± 2.25
4	115	7	80	8.22 ± 0.79	6.28 ± 0.32	200.50 ± 13.02	5.75 ± 0.70	206.25	0.024 ± 0.001	37.77 ± 0.32	213.50 ± 21.58	160.78 ± 10.50	32.07 ± 2.63
5	135	9	70	3.28 ± 0.34	1.83 ± 0.20	120.60 ± 19.30	5.74 ± 0.79	126.34	0.055 ± 0.001	16.08 ± 0.25	141.05 ± 11.12	86.90 ± 12.30	17.38 ± 2.87
6	135	8	70	3.12 ± 0.52	2.65 ± 0.32	148.16 ± 29.70	5.63±0.85	153.79	0.037 ± 0.001	25.56 ± 0.53	159.66 ± 15.45	72.92 ± 15.78	26.58 ± 2.89
7	135	7	70	6.83 ± 0.30	4.23 ± 0.07	184.99 ± 5.92	5.31 ± 0.26	190.30	0.028 ± 0.001	32.62 ± 0.41	156.01 ± 12.36	97.24 ± 17.45	26.60 ± 2.00
8	135	8	70	3.32 ± 0.14	2.66 ± 0.20	151.19 ± 20.33	4.18 ± 0.24	155.37	0.038 ± 0.001	13.76 ± 0.52	125.50 ± 15.14	78.57 ± 18.54	19.15 ± 2.21
9	155	8	70	3.03 ± 0.11	2.73 ± 0.02	121.9 ± 8.64	5.21 ± 0.59	127.11	0.044 ± 0.001	15.67 ± 0.25	121.37 ± 12.15	73.02 ± 18.52	15.60 ± 2.58
10	155	7	80	4.60 ± 0.12	2.85 ± 0.10	143.54 ± 25.97	5.38 ± 1.17	148.92	0.035 ± 0.001	13.51 ± 0.56	135.17 ± 14.87	88.90 ± 12.45	20.87 ± 2.54
11	115	7	60	8.79 ± 0.30	6.61 ± 0.05	191.0 ± 16.01	4.95 ± 1.10	195.95	0.023 ± 0.001	25.95±0.32	197.82 ± 15.62	111.02 ± 12.41	25.67 ± 1.54
12	115	8	70	6.65 ± 0.47	4.06 ± 0.44	114.98 ± 18.83	5.87±0.47	120.85	0.036 ± 0.001	28.00 ± 0.89	132.60 ± 25.45	95.80 ± 12.45	20.69 ± 1.01
13	155	9	80	2.07 ± 0.77	1.56 ± 0.25	94.82 ± 11.67	5.99 ± 1.11	100.81	0.050 ± 0.001	14.97 ± 0.19	122.00 ± 17.87	90.75 ± 12.12	15.15 ± 2.32
14	115	9	60	4.92 ± 0.45	2.88 ± 0.02	124.96 ± 2.87	5.90 ± 1.41	130.86	0.044±0.001	15.28 ± 0.96	161.64 ± 21.87	92.76 ± 16.14	28.21 ± 2.54
15	135	8	80	3.72 ± 0.26	2.75 ± 0.36	179.09 ± 16.10	5.86 ± 0.40	184.95	0.038 ± 0.001	22.00 ± 0.95	188.23 ± 26.54	85.00 ± 12.41	26.85 ± 2.53
16	115	9	80	4.52 ± 0.39	1.79 ± 0.12	178.0 ± 9.18	5.79 ± 0.09	183.79	0.041 ± 0.001	24.00 ± 0.76	185.23 ± 28.74	86.00 ± 16.75	13.00 ± 3.24
17	135	8	70	4.65 ± 1.48	2.04 ± 0.19	175.52 ± 18.30	5.79 ± 0.04	181.31	0.028 ± 0.001	15.60 ± 0.87	132.55 ± 35.74	75.21 ± 15.10	27.04 ± 3.33

RT: roasting temperature; CT: conching temperature; TPC: total phenolic content; TFC: total flavonoid content; C: catechin; EC: epi-catechin.

TAC: total antioxidant capacity; H-ORAC: hydrophilic ORAC; L-ORAC: lipophilic ORAC.

per g. In previous studies, H-ORAC value was reported to be 131.2 μmol TE per g by Adamson et al. (1999) while TAC was found to be in the range of 161 and 349 μmol TE per g by Gu et al. (2006). Our results are in agreement with these reported results. In addition, results of ORAC assay showed a strong correlation between total phenolics and antioxidant capacity ( $R^2 = 0.83$ ), and between total flavonoids and antioxidant capacity ( $R^2 = 0.80$ ). In terms of DPPH assay, EC<sub>50</sub> values ranged from 0.023 to 0.047. Similar to ORAC assay, DPPH assay was highly correlated to total phenolics ( $R^2 = 0.85$ ) and total flavonoids ( $R^2 = 0.86$ ). As in the agreement of TPC and TFC, roasting of cocoa beans and alkali treatment affected the antioxidant capacity significantly ( $p < 0.05$ ) (Table 1). Arlorio et al. (2008) also showed that roasted cocoa bean samples had lower antioxidant capacity than unroasted beans. Similarly, Jolic et al. (2011) demonstrated that the antioxidant capacity of roasted cocoa bean was decreased for approximately 10%. Loss of phenolics and antioxidant activity may vary with the degree of alkalization such as light and heavy alkalization (Miller et al., 2008). In addition, Sulistyowati and Misnawi (2008) suggested that reduction of the antioxidant capacity in milk chocolate due to alkali improvement from 1 g to 15 g at conching temperature of 40 °C and 80 °C was calculated to be 7 and 18%, respectively. This reduction was caused by heat and alkali, synergistically. Nevertheless, in the current study it was found that conching was statistically insignificant ( $p > 0.05$ ) in dark chocolate manufacturing. Since conching temperature-time parameters can vary depending on the type of chocolate, dark chocolate is conched at higher temperatures (in the range of 60–80 °C) than milk chocolate. Regarding this narrow conching parameters range, our data is not compatible with the findings of Sulistyowati and Misnawi (2008). Di Mattia et al. (2014) also determined that a high temperature-short time conching process did not affect antioxidant capacity due to prevented procyandin degradation.

### 3.3. Analysis of catechins by LC-MS-MS

Methanolic extracts of epicatechin (EC), C (catechin), EGC (epigallocatechin), ECG (epicatechingallate), EGCG (epigallocatechingallate) were investigated by LC-MS-MS. Concentrations of EC, C, EGC, GC, ECG and EGCG were shown in Table 2. EC content was in the range of 47.77 and 93.30 mg per kg

**Table 2**  
Quantification of catechins in chocolate extracts by LC-MS-MS.

	EC (mg/kg)	C (mg/kg)	EGC (mg/kg)	GC (mg/kg)	ECG (mg/kg)	EGCG (mg/kg)
1	47.77 ± 2.25	27.10 ± 2.48	1.00 ± 0.050	ND	ND	ND
2	76.63 ± 2.32	43.00 ± 3.74	3.97 ± 0.060	ND	ND	ND
3	79.67 ± 3.45	48.43 ± 3.59	3.98 ± 0.036	ND	ND	ND
4	93.30 ± 2.15	69.00 ± 1.42	3.62 ± 0.095	ND	ND	ND
5	46.33 ± 2.87	25.80 ± 6.75	1.00 ± 0.065	ND	ND	ND
6	74.10 ± 5.98	42.53 ± 4.52	4.12 ± 0.023	ND	ND	ND
7	72.47 ± 5.87	40.40 ± 5.45	4.09 ± 0.014	ND	ND	ND
8	70.83 ± 2.78	39.17 ± 5.87	4.04 ± 0.043	ND	ND	ND
9	56.87 ± 2.34	48.43 ± 6.74	3.58 ± 0.099	ND	ND	ND
10	59.57 ± 2.68	35.03 ± 6.54	4.07 ± 0.036	ND	ND	ND
11	71.73 ± 4.41	50.23 ± 4.45	3.81 ± 0.054	ND	ND	ND
12	52.73 ± 9.54	36.60 ± 4.86	3.58 ± 0.047	ND	ND	ND
13	46.80 ± 7.87	24.27 ± 5.84	1.00 ± 0.078	ND	ND	ND
14	78.20 ± 4.87	38.20 ± 5.89	1.00 ± 0.065	ND	ND	ND
15	70.83 ± 2.74	41.87 ± 1.89	3.99 ± 0.045	ND	ND	ND
16	68.13 ± 3.65	47.47 ± 7.46	1.00 ± 0.041	ND	ND	ND
17	58.87 ± 5.48	28.87 ± 3.51	4.01 ± 0.077	ND	ND	ND

ND: Not detected, C: catechin, EC:epi-catechin, EGC: epigallocatechin, GC: galloca-

techin. ECG: epi-catechin gallate, EGCG: epigallocatechingallate.

while C content changed between 24.27 and 69.00 mg per kg. EGc was detected in trace amounts, ranging from 1.00 to 4.12 mg per kg.

### 3.4. Analysis of procyanidins by UFLC

Procyanidins were extracted by acetone: Milli-Q water: acetic acid (70: 29.5: 0.5, v/v/v) since this mixture was determined as the most efficient solvent mixture for dark-chocolate procyanidins (Counet & Collin, 2003). RP-LC analysis of procyanidins were carried out to detect EC, C, Dimer B2, Trimer C1. By using reversed phase, it is only possible to determine oligomers up to trimers (Rios et al., 2002). As presented in Table 1, EC content ranged between 121 and 197 mg/100 g while C content was in the range of 12.64 and 37.77 mg per 100 g. Dimer B2 content changed from 72.92 to 160.78 and Trimer C1 content varied from 13.00 to 32.07 mg per 100 g. These findings are consistent with the previous data obtained from similar extraction procedure (Cooper et al., 2007; Gu et al., 2006).

In our study, we found that roasting and alkalization treatment affected catechin, epicatechin, dimer B2 and trimer C1. Conching process was also involved this impact in case of EC and dimer B2 (Models 1–8). Payne, Hurst, Miller, Rank, and Stuart (2010) suggested that roasting in excess of 70 °C generated significant amounts of (–)-catechin, probably due to epimerization of (–)-epicatechin. Nevertheless, alkalization treatment resulted in a loss in both epicatechin and catechin (Andres-Lacueva et al., 2008; Payne et al., 2010). Such decline was also determined for di-, tri-, and tetrameric procyanidins (Andres-Lacueva et al., 2008; Di Mattia et al., 2014). Di Mattia et al. (2014) also reported that procyanidin pattern was affected by different processing conditions. A higher amount of monomers were formed after high temperature-short time conching while a higher amount of polymers were formed after low temperature-long time conching.

### 3.5. Model fitting

The results of TPC, TFC, EC<sub>50</sub> and TAC (responses) of the chocolate formulations all the experiments are shown in Table 1. The experimental data was used to calculate the coefficients of the equations, which were used to predict the responses. Analysis of variance (ANOVA) in Table 3 indicated that the models showed no lack of fit for TPC, TFC, EC<sub>50</sub> and TAC values since *p* values of were higher than *p* > 0.05 (0.844, 0.538, 0.772, 0.435, 0.751, 0.828, 0.095, 0.634) and coefficients of multiple determinations, R<sup>2</sup>, being 0.955, 0.971, 0.776, 0.838, 0.5034, 0.907, 0.937, and 0.663 all indicate that models fit the experimental data points, which means that models are appropriate for prediction. *p*-values smaller than 0.05 for any of the terms in the models indicate that term has a more significant effect on the respective responses.

The model equations for the responses can be written as follows:

$$\text{TPC} = 111.611 - 0.501\text{RT} - 15.587\text{pH} \quad (1)$$

$$\text{TFC} = 96.774 - 0.611\text{RT} - 8.517\text{pH} + 0.051\text{RT}^2 + 1.391 \cdot 10^{-3}\text{RT}^2 \quad (2)$$

$$\text{EC}_{50} = -0.061 + 1.863 \cdot 10^{-4}\text{RT} + 9.729 \cdot 10^{-3}\text{pH} \quad (3)$$

$$\text{TAC} = -478.304 - 205.184\text{pH} - 0.079\text{RT}^2 \quad (4)$$

$$\text{C} = +0.90287 - 2.43542 \cdot 10^{-3}\text{RT} - 0.052394\text{pH} \quad (5)$$

**Table 3**  
Regression coefficients and *p*-values for significant responses.

Responses	Factors <sup>a</sup>	Coefficient	<i>p</i> -value	Model fit
TPC	RT (L)	−0.501	0.0001 <sup>(b)</sup>	R <sup>2</sup> = 0.9549 F = 16.46 p = 0.0006
	RT (Q)	1.283	0.2136	
	pH (L)	−15.587	<0.0001 <sup>b</sup>	
	pH (Q)	0.731	0.0925	
	CT (L)	0.039	0.0791	
	CT (Q)	−2.608	0.9425	
	RT X pH	0.0149	0.2120	
	RT X CT	−5.621*10 <sup>−4</sup>	0.6206	
	CT X pH	3.579*10 <sup>−3</sup>	0.8737	
	Intercept	111.611		
Lack of Fit			0.8436	
TFC	RT (L)	−0.611	<0.0001 <sup>b</sup>	R <sup>2</sup> = 0.9712 F = 26.20 p = 0.0001
	RT (Q)	1.391*10 <sup>−3</sup>	0.0427 <sup>b</sup>	
	pH (L)	−8.517	<0.0001 <sup>b</sup>	
	pH (Q)	0.192	0.4220	
	CT (L)	−0.271	0.1546	
	CT (Q)	1.410*10 <sup>−3</sup>	0.5509	
	RT X pH	0.0251	0.0062 <sup>b</sup>	
	RT X CT	−2.258*10 <sup>−4</sup>	0.7390	
	CT X pH	0.011	0.4371	
	Intercept	96.774		
Lack of Fit			0.5375	
EC <sub>50</sub>	RT (L)	1.863	0.0325 <sup>b</sup>	R <sup>2</sup> = 0.7758 F = 15.00 p = 0.0002
	pH (L)	9.729	<0.0001 <sup>b</sup>	
	CT (L)	−7.493	0.6384	
	Intercept	−0.061		
Lack of Fit			0.7723	
TAC	RT (L)	28.263	0.0628	R <sup>2</sup> = 0.8382 F = 4.03 p = 0.0399
	RT (Q)	−0.0796	0.0247 <sup>b</sup>	
	pH (L)	−205.183	0.0117 <sup>b</sup>	
	pH (Q)	13.008	0.2823	
	CT (L)	−10.087	0.3256	
	CT (Q)	0.185	0.1416	
	RT X pH	−0.054	0.8719	
	RT X CT	−0.099	0.0177 <sup>b</sup>	
	CT X pH	−0.217	0.7465	
	Intercept	−478.603		
Lack of Fit			0.4349	
C	RT (L)	−3.1833*10 <sup>−4</sup>	0.0360 <sup>b</sup>	R <sup>2</sup> = 0.5034 F = 6.23 p = 0.0242
	pH (L)	−7.4833*10 <sup>−3</sup>	0.0166 <sup>b</sup>	
	CT (L)	1.0667*10 <sup>−4</sup>	0.7015	
	Intercept	0.13575		
Lack of Fit			0.7507	
EC	RT (L)	0.16096	0.0035 <sup>b</sup>	R <sup>2</sup> = 0.9065 F = 7.54 p = 0.0072
	RT (Q)	−4.8506*10 <sup>−4</sup>	0.0518	
	pH (L)	−0.86752	0.0209 <sup>b</sup>	
	pH (Q)	0.02143	0.8034	
	CT (L)	−53.516	0.4874	
	CT (Q)	4.2456*10 <sup>−3</sup>	0.0014 <sup>b</sup>	
	RT X pH	1.0383*10 <sup>−3</sup>	0.6871	
	RT X CT	−6.7975*10 <sup>−4</sup>	0.0252 <sup>b</sup>	
	CT X pH	3.6745*10 <sup>−3</sup>	0.4687	
	Intercept	14.014		
Lack of Fit			0.8275	
Dimer B2	RT (L)	−0.0746	0.0033 <sup>b</sup>	R <sup>2</sup> = 0.9374 F = 11.64 p = 0.0019
	RT (Q)	1.4529	0.2561	
	pH (L)	−2.8816	0.0088 <sup>b</sup>	
	pH (Q)	0.1547	0.0133 <sup>b</sup>	
	CT (L)	0.0559	0.1471	
	CT (Q)	3.994*10 <sup>−4</sup>	0.4235	
	RT X pH	6.555*10 <sup>−3</sup>	0.0019 <sup>b</sup>	
	RT X CT	−3.1972*10 <sup>−4</sup>	0.0510	
	CT X pH	−8.0832*10 <sup>−3</sup>	0.0207 <sup>b</sup>	
	Intercept	15.94669		
Lack of Fit			0.0947	
Trimer C1	RT (L)	−1.9321*10 <sup>−3</sup>	0.0131 <sup>b</sup>	R <sup>2</sup> = 0.6629 F = 8.52 p = 0.0022
	pH (L)	−0.0537	0.0015 <sup>b</sup>	
	CT (L)	−1.6057*10 <sup>−3</sup>	0.2543	
	Intercept	1.02909	0.6002	
Lack of Fit			0.6335	

L: Linear; Q: Quadratic.

<sup>a</sup> RT = Roasting temperature (°C); CT = Conching temperature (°C); RTXpH represent the interaction term of roasting temperature and pH; RTXCT represent the interaction term of roasting temperature and conching temperature; CTXpH represent the interaction term of conching temperature and pH.

<sup>b</sup> Statistically significant at *p* < 0.05.

$$EC = +14.01427 + 0.16096*RT - 0.86752*pH - 6.79750*10^{-4}RT CT + 4.24561*10^{-3}CT^2 \quad (6)$$

$$Dimer B2 = 15.94669 - 0.074579*RT - 2.88163*pH + 6.5548*10^{-3}RT pH - 8.08317*10^{-3}pH CT + 0.15469 pH^2 \quad (7)$$

$$Trimer C1 = 1.02909 - 1.93206*10^{-3}RT - 0.053676*pH \quad (8)$$

where RT is the roasting temperature, and CT is the conching temperature.

Regarding significant terms obtained from equations, the first order-variables, RT and pH had negative effects on the TPC, TFC, C, EC, Dimer B2 and Trimer C1 values. Meanwhile, the first order-variable of pH only affected the TAC value in a negative way. In contrast, EC<sub>50</sub> value was positively correlated by the first order-

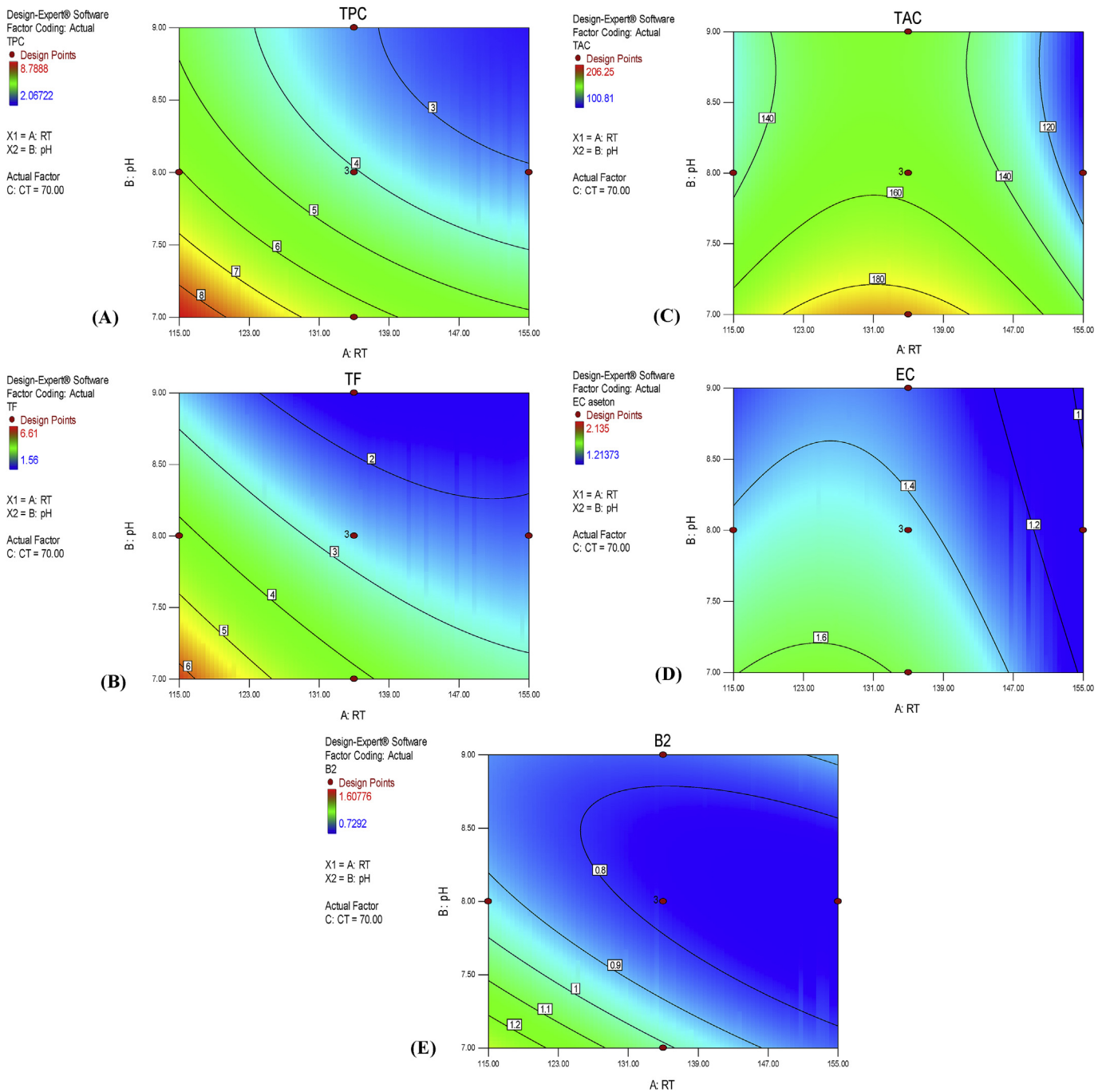


**Fig. 1.** Contour plots of TPC (A), TF (B), TAC (C), EC (D), and Dimer B2 (E) as function of RT, pH and CT. Where TPC; total phenolic content, TFC; total flavonoid content, TAC; total antioxidant capacity; EC, epi-catechin, RT; roasting temperature, CT; conching temperature.

**Table 4**  
Optimum formulations, predicted results and experimental results used in the validation of model.

	RT	pH	CT	Predicted scores				Experimental scores			
				TPC	TFC	EC50	TAC	TPC	TFC	EC50	TAC
Opt 1	115	7.0	78.7	8.42	6.13	0.023	206.26	8.00	5.73	0.023	205.0
Opt 2	115	7.0	75.5	8.53	6.14	0.023	189.17	8.03	5.73	0.023	195.2

Opt: optimum formulation, TPC: total phenolic content, TFC: total flavonoid content, TAC: total antioxidant capacity.

variables of RT and pH.

The interaction of term of RT and pH (RT\*pH) had a positive effect on the TFC and Dimer B2 values, whereas TAC and EC values were negatively affected by (RT\*pH). Meanwhile, the Dimer B2 value was correlated negatively by the interaction of term of pH and CT (pH\*CT). In addition, there was a negative correlation between the interaction term of CT and pH (CT\*pH) and the Dimer B2 value.

The second-order variable of RT (RT<sup>2</sup>) had a positive effect on the TFC value whereas it had a negative effect on the TAC value. While the second-order variable of CT (CT<sup>2</sup>) affected the EC value, the second-order variable of pH (pH<sup>2</sup>) affected the Dimer B2 value positively.

### 3.5.1. Response surface plots

The impact of RT, pH and CT levels on TPC, TF, EC<sub>50</sub>, TAC, and EC, C, Dimer B2 and Trimer C1 can be seen in Fig. 1. Fig. 1A showed that mutual increase in pH and RT resulted in a decrease in TPC. As the pH increased from 7 to 8 and RT increased from 115 °C to 135 °C, TPC was reduced sharply. Exceeding 135 °C, a slight TPC reduction was observed with increasing pH to 9.0. Similarly, TFC significantly decreased as RT increased from 115 °C to 135 °C and pH increased from 7 to 8 (Fig. 1B). According to Fig. 1C, an increase in pH resulted in TAC reduction. However, increase in RT did not change the TAC value. This reduction was more intense as pH exceeded 8 while RT exceeded 155 °C. Based on Fig. 1D, as the pH increased from 115 to 139 °C and pH from 7 to 8, a reduction was observed in EC. As RT exceeded 147 °C, this reduction was progressive without considering pH. pH increased from 8 to 9 resulted in a decrease in EC, which was independent of RT. Fig. 1E showed that increasing pH up to 8 with increasing RT up to 147 °C caused a decrease in B2. As the pH value exceeded 8, further decrease was observed with increasing RT.

### 3.5.2. Validation of model

Design Expert 9.0 software generated optimum formulations for targeted responses. Two optimum formulations were produced. Optimum formulations, predicted scores and experimental results for responses are summarized in Table 4. Optimization results showed that at minimum roasting temperature (115 °C) and minimum pH value (7), conching temperature should change between 75.5 and 78.7. Compared to Table 1, it is possible to say that total phenolics, flavonoids and antioxidant capacity (TAC and EC<sub>50</sub>) exhibited the maximum results at these optimal conditions. The experimental scores were satisfactorily close to the values predicted by the model. These results confirm the validation of the model generated by Design Expert 9.0 software.

## 4. Conclusion

Chocolate manufacturing process, particularly pH and roasting temperature significantly changed the procyanidin profile and antioxidant capacity ( $p < 0.05$ ). Increasing pH and roasting temperature affected the phenolic content and related antioxidant capacity, negatively. In contrast, conching temperature did not have a significant effect ( $p > 0.05$ ). This may be explained by selecting a

narrow range of conching temperature (between 60 and 80 °C) and time–temperature relation. In addition, the optimum process conditions were determined by using the model. The experimental scores were satisfactorily close to the values predicted by the model which confirms the validation of the model.

## Acknowledgements

We would like to thank the technical staff of Nestle Turkey Inc., Özlem Bahtiyar, Adnan Özkıranartlı, and Şirin Yılmaz for the manufacturing of chocolate samples.

## References

- Adamson, G. E., Lazarus, S. A., Mitchell, A. E., Prior, R. L., Cao, G., Jacobs, P. H., et al. (1999). HPLC method for the quantification of procyanidins in cocoa and chocolate samples and correlation to total antioxidant capacity. *Journal of Agricultural and Food Chemistry*, 47, 4184–4188.
- Afoakwa, E. O., Paterson, A., Fowler, M., & Vieira, J. (2008). Effects of tempering and fat crystallisation behaviour on microstructure, mechanical properties and appearance in dark chocolate systems. *Journal of Food Engineering*, 89, 128–136.
- Andres-Lacueva, C., Monagas, M., Khan, N., Izquierdo-Pulido, M., Urpi-Sarda, M., Permany, J., et al. (2008). Flavanol and flavonol contents of cocoa powder products: influence of the manufacturing process. *Journal of Agricultural and Food Chemistry*, 56, 3111–3117.
- Arlorio, M., Locatelli, M., Travaglia, F., Coisson, J., Grosso, E. D., Minassi, A., et al. (2008). Roasting impact on the contents of clovamide (N-caffeoyl-L-DOPA) and the antioxidant capacity of cocoa beans (*Theobroma cacao* L.). *Food Chemistry*, 106, 967–975.
- de Brito, E. S., Pezoa García, N. H., Gallão, M., Cortelazzo, A. L., Fevreiro, P. S., & Braga, M. R. (2000). Structural and chemical changes in cocoa (*Theobroma cacao* L.) during fermentation, drying and roasting. *Journal of the Science of Food and Agriculture*, 81, 281–288.
- Cardarelli, H. R., Aragon-Alegro, L. C., Alegro, J. H., de Castro, I. A., & Saad, S. M. (2008). Effect of inulin and *Lactobacillus paracasei* on sensory and instrumental texture properties of functional chocolate mousse. *Journal of the Science of Food and Agriculture*, 88, 1318–1324.
- Cooper, K. A., Campos-Gimenez, E., Alvares, D. J., Nagy, K., Donovan, J. L., & Williamson, G. (2007). Rapid reversed phase ultra-performance liquid chromatography analysis of the major cocoa polyphenols and inter-relationships of their concentrations in chocolate. *Journal of Agricultural and Food Chemistry*, 55, 2841–2847.
- Counet, C., & Collin, S. (2003). Effect of the number of flavanol units on the antioxidant capacity of procyanidin fractions isolated from chocolate. *Journal of Agricultural and Food Chemistry*, 51, 6816–6822.
- Di Mattia, C., Martuscelli, M., Sacchetti, G., Beheydt, B., Mastrocola, D., & Pittia, P. (2014). Effect of different conching processes on procyanidin content and antioxidant properties of chocolate. *Food Research International*, 63, 367–372.
- Erdem, Ö., Gültekin-Özgüven, M., Berktaş, I., Erşan, S., Tuna, H. E., Karadağ, A., et al. (2014). Development of a novel synbiotic dark chocolate enriched with *Bacillus indicus* HU36, maltodextrin and lemon fiber: optimization by response surface methodology. *LWT Food Science and Technology*, 56, 187–193.
- Gu, L., House, S. E., Wu, X., Ou, B., & Prior, R. L. (2006). Procyanidin and catechin contents and antioxidant capacity of cocoa and chocolate products. *Journal of Agricultural and Food Chemistry*, 54, 4057–4061.
- Huang, D., Ou, B., Hampsch-Woodill, M., Flanagan, J., & Deemer, E. (2002). Development and validation of oxygen radical absorbance capacity assay for lipophilic antioxidants using randomly methylated beta-cyclodextrin as the solubility enhancer. *Journal of Agricultural and Food Chemistry*, 50, 1815–1821.
- Huang, D., Ou, B., & Prior, R. L. (2005). The chemistry behind antioxidant capacity assays. *Journal of Agricultural and Food Chemistry*, 53, 1841–1856.
- Jinap, S., Jamilah, B., & Nazamid, S. (2005). Changes in polyphenol ability to produce astringency during roasting of cocoa liquor. *Journal of the Science of Food and Agriculture*, 85, 917–924.
- Jolic, S. M., Redovnikovic, I. R., Markovic, K., Sipusic, D. I., & Delonga, K. (2011). Changes of phenolic compounds and antioxidant capacity in cocoa beans processing. *International Journal of Food Science and Technology*, 46, 1793–1800.
- Jonfia-Essen, W. A., West, G., Alderson, P. G., & Tucker, G. (2008). Phenolic content

- and antioxidant capacity of hybrid variety cocoa beans. *Food Chemistry*, 108, 1155–1159.
- Lazarus, S. A., Adamson, G. E., Hammerstone, J. F., & Schmitz, H. H. (1999). High performance liquid chromatography/mass spectrometry analysis of proanthocyanidins in food stuffs. *Journal of Agricultural and Food Chemistry*, 47, 3693–3701.
- Lee, K. W., Kim, Y. J., Lee, H. J., & Lee, C. Y. (2003). Cocoa has more phenolic phytochemicals and a higher antioxidant capacity than teas and red wine. *Journal of Agricultural and Food Chemistry*, 51, 7292–7295.
- McShea, A., Ramiro-Puig, E., Munro, S. B., Casadesus, G., Castel, M., & Smith, M. A. (2008). Clinical benefit and preservation of flavonols in dark chocolate manufacturing. *Nutrition Reviews*, 66, 630–641.
- Miller, K. B., Hurst, W. J., Payne, M. J., Stuart, D. A., Apgar, J., Sweigart, D. S., et al. (2008). Impact of alkalization on the antioxidant and flavanol content of commercial cocoa powders. *Journal of Agricultural and Food Chemistry*, 56, 8527–8533.
- Niemenak, N., Rohsius, C., Elwers, S., Omokolo Ndoumou, D., & Lieberei, R. (2006). Comparative study of different cocoa (*Theobroma cacao* L.) clones in terms of their phenolics and anthocyanins contents. *Journal of Food Composition and Analysis*, 19, 612–619.
- Othman, A., Ismail, A., Ghani, N. A., & Adenan, I. (2007). Antioxidant capacity and phenolic content of cocoa beans. *Food Chemistry*, 100, 1523–1530.
- Patel, P., Parekh, T., & Subhash, R. (2008). Development of probiotic and synbiotic chocolate mousse: a functional food. *Biotechnology*, 7, 769–774.
- Payne, M. J., Hurst, W. J., Miller, K. B., Rank, C., & Stuart, D. A. (2010). Impact of fermentation, drying, roasting, and Dutch processing on epicatechin and catechin content of cacao beans and cocoa ingredients. *Journal of Agricultural and Food Chemistry*, 58, 10518–10527.
- Pearson, D. A., Paglieroni, T. G., Rein, D., Wun, T., Schramm, D. D., Wang, J. F., et al. (2002). The effects of flavanol-rich cocoa and aspirin on ex vivo platelet function. *Thrombosis Research*, 106, 191–197.
- Pimentel, F. A., Nitzke, J. A., Klipel, C. B., & de Jong, E. V. (2010). Chocolate and red wine - a comparison between flavonoid content. *Food Chemistry*, 120, 109–112.
- Rein, D., Lotito, S., Holt, R. R., Keen, C. L., Schmitz, H. H., & Fraga, C. G. (2000). Epicatechin in human plasma: *in vivo* determination and effect of chocolate consumption on plasma oxidation status. *Journal of Nutrition*, 130, 2109–2114.
- Rios, L. Y., Bennett, R. N., Lazarus, S. A., Rémésy, C., Scalbert, A., & Williamson, G. (2002). Cocoa procyanidins are stable during gastric transit in humans. *The American Journal of Clinical Nutrition*, 76, 1106–1110.
- Sandoval, A. J., & Barreiro, J. A. (2002). Water sorption isotherms of non-fermented cocoa beans (*Theobroma cacao*). *Journal of Food Engineering*, 51, 119–123.
- Schramm, D. D., Wang, J. F., Holt, R. R., Ensunsa, J. L., Gonsalves, J. L., Lazarus, S. A., et al. (2001). Chocolate procyanidins decrease the leukotriene-prostacyclin ratio in humans and human aortic endothelial cells. *American Journal of Clinical Nutrition*, 73, 36–40.
- Serafini, M., Bugianesi, R., Maiani, G., Valtuena, S., de Santis, S., & Crozier, A. (2003). Plasma antioxidants from chocolate. *Nature*, 424, 1013–1013.
- Sulistyowati, E., & Misnawi, J. S. (2008). Effects of alkali concentration and conching temperature on antioxidant capacity and physical properties of chocolate. *International Food Research Journal*, 15, 297–304.
- Tanabe, N. A., & Hofberger, R. (2006). Chocolate. In Y. H. Hui (Ed.), *Handbook of food science, technology, and engineering* (Vol. 4, pp. 1–11). Boca Raton: CRC Press.
- Tomas-Barberan, F. A., Cienfuegos-Jovellanos, E., Marin, A., Muguerza, B., Gil-Izquierdo, A., Cerdaa, B., et al. (2007). A new process to develop a cocoa powder with higher flavonoid monomer content and enhanced bioavailability in healthy humans. *Journal of Agricultural and Food Chemistry*, 55, 3926–3935.
- Wollgast, J. (2004). *The contents and effects of polyphenols in chocolate, doctoral dissertation*. Retrieved from <http://geb.uni-giessen.de/geb/volltexte/2005/2239/pdf/WollgastJan-2005-06-10.pdf>.
- Wollgast, J., & Anklam, E. (2000). Review on polyphenols in *Theobroma cacao*: changes in composition during the manufacture of chocolate and methodology for identification and quantification. *Food Research International*, 33, 423–447.
- Wu, X., Liang, L., Zou, Y., Zhao, T., Zhao, J., Li, F., et al. (2011). Aqueous two-phase extraction, identification and antioxidant capacity of anthocyanins from mulberry (*Morus atropurpurea* Roxb.). *Food Chemistry*, 129, 443–453.



# Emulsifying properties of legume proteins at acidic conditions: Effect of protein concentration and ionic strength



Yakoub Ladjal Ettoumi <sup>a,\*</sup>, Mohamed Chibane <sup>b</sup>, Alberto Romero <sup>c</sup>

<sup>a</sup> Département des Sciences Alimentaires, FSNV, Université Abderahman Mira, Bejaia, Route Targa Ouzemour, Bejaia 06000, Algeria

<sup>b</sup> Laboratoire de Gestion et Valorisation des Ressources Naturelles Assurance Qualité, Université Akli Mohand Oulhadj de Bouira, 10000 Bouira, Algeria

<sup>c</sup> Departamento de Ingeniería Química, Facultad de Química, Universidad de Sevilla, 41012 Sevilla, Spain

## ARTICLE INFO

### Article history:

Received 7 June 2015

Received in revised form

7 August 2015

Accepted 19 October 2015

Available online 21 October 2015

### Keywords:

Acidic emulsions

Legume protein

Protein concentration

Ionic strength

Microstructure

## ABSTRACT

This work is focused on emulsifying properties of pea, chickpea and lentil protein isolates at acidic conditions (pH 3), as affected by protein concentration and ionic strength. Emulsions characteristics and stability (droplet size distribution, flocculation, coalescence and creaming) were determined. The microstructure of selected emulsions was also studied. Results indicated that emulsifying properties (ability and stability) are dependent to protein concentration and highly sensitive to ionic strength. In our conditions, the best emulsifying properties are found around 1.5% of protein, and at less than 50 mM of NaCl. Clearly, ionic strength affects emulsions microstructure. Thus, this study indicated that pea, chickpea and lentil proteins would have great potential as emulsifiers in acidic food formulations.

© 2015 Elsevier Ltd. All rights reserved.

## 1. Introduction

In the time being, the consumer demands originated from health concerns, allergenicity, religious limitations (Halal) and rising trend of vegetarianism have increased the interest of food industry in use of functional plant proteins as alternative to animal proteins (Aydemir & Yemenicioglu, 2013; Carbonaro, Maselli, & Nucara, 2014). The production of plant protein isolates is of growing interest to industry because of the increasing applications of plant proteins in food and non-food markets (Zhang, Bo, Wanmeng, & Zhang, 2009). Nevertheless, these applications in the food trade are almost limited to proteins from soybean and wheat, whereas other vegetable proteins are available and less used. Thus, searchers, food manufacturers and consumers are looking for alternative protein sources (Boye et al., 2010; Liang & Tang, 2014; Shen & Tang, 2014; Taherian et al., 2011; Toews & Wang, 2013). Among these are those from dry legumes that are extensively grown in different parts of the world and, in particular, in the Mediterranean region.

There is increased interest in legume proteins as they can be used as good substitute for animal and soybean proteins (Joshi

et al., 2012; Liang & Tang, 2014; Shen & Tang, 2014; Zhang et al., 2009). In this regard, the understanding of factors affecting the functional properties of legume proteins enables better control of these properties, which will facilitate the novel application of these proteins. The functional properties such as solubility, water and oil absorption capacity, gelation, foam and emulsion formation of legume protein isolates were studied to some extent previously (Aydemir & Yemenicioglu, 2013; Boye et al., 2010; Makri, Papalamprou, & Doxastakis, 2005). However, there is lack of fundamental knowledge and supporting data on the emulsifying properties of legumes proteins. Particularly, studies on emulsifying properties of legumes protein, taking into account, protein concentration, pH, ionic strength and relationship between structure and functionality are scarce.

In general, the emulsifying properties of plant proteins are dependent on the physicochemical properties of proteins, including, composition (e.g. vicilin/legume ratio), solubility, conformational stability and Hydrophobicity (Kaushal, Kumar, & Sharma, 2012; Lestari, Mulderb, & Sanders, 2011; Liang & Tang, 2014). Also, environmental conditions, including, pH, ionic strength, protein concentration and oil fraction have an effect (Liang & Tang, 2014; Yu, Ahmedna & Goktepelpek, 2007).

Our previous study (Ladjal E., Boudries, Chibane & Romero, 2015) demonstrated that legume protein isolates have good

\* Corresponding author.

E-mail address: [yakoblajel@hotmail.fr](mailto:yakoblajel@hotmail.fr) (Y. Ladjal Ettoumi).

emulsifying ability and stability at pH 3; suggesting their use in acidic formulation, such as, salad dressing and mayonnaise. Thus, the present study is aimed to investigate the effect of protein concentration and ionic strength on emulsifying properties of protein stabilized emulsions at pH 3 using protein isolates derived from three legumes (pea, chickpea and lentil). The microstructure of the selected emulsions is also studied.

## 2. Material and method

### 2.1. Preparation of legume protein isolates

Whole flours of pea (*Pisum sativum*), chickpea (*Cicer arietinum*) and lentil (*Lens culinaris*) were prepared as previously (Ladjal & Chibane, 2015). Legume protein isolates was prepared according to the method of Papalamprou, Doxastakis, and Kiosseoglou (2010) with slight modification. In brief, flour (100 g) was mixed with distilled water at a 1:10 ratio (w/v), adjusted to pH 8.0 using 1 M NaOH and stirred at 500 rpm for 45 min at room temperature (20–22 °C). The suspension was then centrifuged at  $4500 \times g$  for 20 min at 4 °C to collect the supernatant. The resulting pellet was re-suspended in distilled water at a ratio of 1:5 (w/v), adjusted to pH 8.0, stirred for an additional 45 min, followed by centrifugation ( $4500 \times g$ , 20 min, 4 °C). Both supernatants were pooled and adjusted to pH = 4.0 (pea) or pH = 4.5 (chickpea and lentil) using 0.1 M HCl to precipitate the protein. The protein was recovered by centrifugation and collected (Karaca, Low, & Nickerson, 2011). The pH adjustment values are deduced from our previous study on the protein solubility (Ladjal & Chibane, 2015). The obtained precipitate was washed twice with distilled water (4 °C) and re-dispersed in distilled water with pH adjusted to pH 7 with 1 M NaOH, and freeze-dried (Boye et al., 2010). The protein contents were determined in quadruplicate as %N  $\times 6.25$  using a Leco CHNS-932 nitrogen micro analyser (Leco Corporation, St. Joseph, MI, USA) (Etheridge, Pesti, & Foster, 1998). Their protein contents were  $85.7 \pm 0.6\%$ ,  $85.9 \pm 0.2\%$  and  $84.8 \pm 0.1\%$  (fresh matter) for pea protein (PP), chickpea protein (CP) and lentil protein (LP), respectively.

### 2.2. Emulsions preparation

Three protein solutions with a different protein concentration (0.5–2%, w/v) were prepared at pH adjusted to 3, stirred using a magnetic stirrer for 2 h at room temperature and, then, stored overnight at 4 °C to allow complete hydration. Each protein solution or dispersion was mixed with sunflower oil at oil fraction ( $\phi$ ) = 0.1, and pre-homogenized using the high-speed dispersing and emulsifying unit (model IKA-ULTRA-TURRAX-T25 basic, IKA Works, Inc., Germany) at 17,000 rpm for 1 min. Then, the pre-homogenized dispersions were further homogenized by a high pressing emulsificator (Emulsiflex-C5, Canada) for one pass at a pressure level of 40 MPa. To investigate the effect of ionic strength, we used the same parameters with protein concentration of 1.5% and the salt concentration (salt dissolved in deionised water) varied from 0 mM to 200 mM of NaCl. The fresh emulsions were stored for various periods of time (e.g., 24 h) prior to further analysis. All other materials and chemicals used were purchased from regular suppliers and were of analytical grade.

### 2.3. Emulsions characterization

Droplet-size distribution ( $d_{4,3}$ ), flocculation and coalescence indices (FI and CI) as well as creaming indices of prepared emulsions were evaluated as reported by Liang and Tang (2013).

### 2.4. Emulsion microstructure

The microstructure of the selected emulsions was determined by means of confocal scanning laser microscopy a ZEISS LSM 7 DUO (Germany). A small aliquot of freshly prepared emulsion was placed on a microscope slide and covered with a cover slip prior to analysis. Emulsions were colored by Nile bleu. The emission of Nile bleu was detected in the 633 nm). This technique provides images of dark fat droplets and a bright water phase where proteins were found. a 63 $\times$  objective was used. The microstructure images were analyzed using image analysis software (ZEN\_2012SP1\_black\_SP2\_blue).

### 2.5. Statistical analysis

Statistical analysis was carried out using analysis of variance (ANOVA) and the significant difference between the samples was determined using LSD test at  $p < 0.05$ .

## 3. Result and discussion

### 3.1. Effect of protein concentration on emulsifying properties

#### 3.1.1. Droplet size distribution

The effects of protein concentration on emulsifying properties were measured at pH 3.0 and an oil fraction of 0.1, at various protein concentrations (0.5, 1, 1.5 and 2%, (w/v)). The  $d_{4,3}$  of the droplets, diluted in 1% SDS or deionized water, was calculated and summarized in Table 1. In general, the smaller the droplet sizes of protein-stabilized emulsions, the better the emulsifying ability of the protein is (Shen & Tang, 2014).

Generally, with the exception of PP-stabilized emulsions, CP and LP-stabilized emulsions exhibited the best emulsifying ability (corresponding to the lowest diameter) at 2% concentration. But the other concentrations did not display significant difference in their emulsifying ability. This trend was noted both in SDS and water dilutions. For PP emulsion, the smallest droplet size was found at 1.5% in water dilution and at 1% and 1.5% in SDS dilution. From this concentration, there was a slight increase in droplets size indicating an excess of non adsorbing protein which promote droplets flocculation by depletion phenomenon. The high  $d_{4,3}$  values of the emulsions containing 0.5% protein suggested that protein content may not be enough to cover the oil droplets and form sufficiently dense adsorption layer (Sanchez & Patino, 2005). As a result, protein acted as bridges among the oil droplets and led to droplets aggregation (Guo & Mu, 2011; Sun & Gunasekaran, 2009). Our results are in agreement with those reported by Sun and Gunasekaran (2009), and corroborate well with those of Joshi et al. (2012), which suggest that the higher the protein concentration (lentil protein), the greater was the reduction in interfacial tension, displaying stabilized emulsion with high turbidity and small oil droplet.

#### 3.1.2. Flocculation in fresh emulsions

The flocculated state of oil droplets was evaluated in terms of flocculation index (FI), as shown in Table 1. The FI (0 h) varied with type and concentration of protein. Basically, the FI (0 h) varied considerably from 0.88 in 1.5% LP emulsion to 3.72 in 1% PP emulsion. PP-stabilized emulsion exhibited the lowest FI (1.19) at 2% concentration. Whereas, 1.5% concentrations displayed the lowest FI in CP and LP emulsions (1.82 and 0.88 respectively). At any concentration (except to 2% PP emulsion), LP-stabilized emulsions exhibited lower flocculation phenomenon than PP and CP emulsions, which might be due to its lower content of SH and SS bounds (Ladjal, Boudries, Chibane, & Romero, 2015). Thus, SH groups can

**Table 1**  
Emulsion characteristics, including volume-mean droplet size ( $d_{4,3}$ ), flocculation and coalescence indices (FI and CI) of legume protein-stabilized emulsions at various protein concentration, freshly prepared or after a storage of 24 h. FI and CI are calculated using mean values of droplet size ( $d_{4,3}$ ).

Emulsion	Protein % (w/v)	$d_{4,3}$ ( $\mu\text{m}$ )				Indices		
		0 h		24 h		FI		CI (%)
		Water	SDS	Water	SDS	0 h	24 h	
PP emulsions	0.5	9.10 $\pm$ 0.56 <sup>a</sup>	2.69 $\pm$ 0.07 <sup>b</sup>	9.94 $\pm$ 0.69 <sup>a</sup>	3.00 $\pm$ 0.13 <sup>b</sup>	2.38	2.31	11.52
	1.0	8.12 $\pm$ 0.24 <sup>b</sup>	1.72 $\pm$ 0.01 <sup>d</sup>	9.02 $\pm$ 0.81 <sup>ab</sup>	1.83 $\pm$ 0.01 <sup>d</sup>	3.72	3.40	19.18
	1.5	6.14 $\pm$ 0.70 <sup>c</sup>	2.06 $\pm$ 0.14 <sup>c</sup>	6.22 $\pm$ 0.67 <sup>c</sup>	2.61 $\pm$ 0.15 <sup>c</sup>	1.98	1.37	27.02
	2.0	8.15 $\pm$ 0.27 <sup>b</sup>	3.72 $\pm$ 0.18 <sup>a</sup>	8.48 $\pm$ 0.04 <sup>b</sup>	4.23 $\pm$ 0.03 <sup>a</sup>	1.19	1.00	13.70
CP emulsions	0.5	8.48 $\pm$ 0.08 <sup>a</sup>	2.51 $\pm$ 0.14 <sup>a</sup>	8.98 $\pm$ 0.7 <sup>a</sup>	3.64 $\pm$ 0.00 <sup>a</sup>	2.37	1.46	45.01
	1.0	8.00 $\pm$ 1.85 <sup>ab</sup>	2.75 $\pm$ 0.03 <sup>a</sup>	7.50 $\pm$ 2.07 <sup>a</sup>	3.56 $\pm$ 0.07 <sup>a</sup>	1.91	1.10	29.45
	1.5	7.41 $\pm$ 0.14 <sup>ab</sup>	2.62 $\pm$ 0.29 <sup>a</sup>	8.15 $\pm$ 0.25 <sup>a</sup>	2.69 $\pm$ 0.17 <sup>b</sup>	1.82	1.92	6.48
	2.0	6.83 $\pm$ 0.31 <sup>b</sup>	1.97 $\pm$ 0.02 <sup>b</sup>	6.96 $\pm$ 0.31 <sup>a</sup>	2.24 $\pm$ 0.13 <sup>c</sup>	2.46	2.11	13.51
LP emulsions	0.5	6.69 $\pm$ 0.25 <sup>a</sup>	2.85 $\pm$ 0.08 <sup>a</sup>	8.94 $\pm$ 0.97 <sup>a</sup>	2.98 $\pm$ 0.12 <sup>b</sup>	1.34	2.00	4.31
	1.0	6.38 $\pm$ 0.83 <sup>a</sup>	2.66 $\pm$ 0.12 <sup>b</sup>	8.11 $\pm$ 0.34 <sup>a</sup>	3.65 $\pm$ 0.11 <sup>a</sup>	1.39	1.21	37.46
	1.5	5.26 $\pm$ 0.20 <sup>b</sup>	2.79 $\pm$ 0.13 <sup>ab</sup>	5.59 $\pm$ 0.19 <sup>b</sup>	2.87 $\pm$ 0.17 <sup>b</sup>	0.88	0.94	2.98
	2.0	5.19 $\pm$ 0.12 <sup>b</sup>	2.05 $\pm$ 0.03 <sup>c</sup>	5.62 $\pm$ 0.62 <sup>b</sup>	3.01 $\pm$ 0.2 <sup>b</sup>	1.52	0.86	46.51

Values expressed are mean  $\pm$  standard deviation. Means in the column (in the same protein emulsion) with different superscript are significantly different at  $p < 0.05$ . PP: Pea protein; CP: Chickpea protein; LP: Lentil protein.

form bridge and enhance droplets flocculation. In general, FI% progressively decreased to a minimal value, as the concentration increased from 0.5 to 1.5%, while a further increase in concentration (2%) contrarily led to a gradual increase in FI%. An increase in protein concentration enhanced protein adsorption and surface coverage of oil droplets, which effectively inhibited droplet aggregation (Sun & Gunasekaran, 2009). However, further increase in protein concentration (up to 1.5% in our case), could promote depletion flocculation. Interestingly, protein stabilized emulsions showed low FI at 1.5% concentration, suggesting that the oil–water interface is saturated by protein molecules. Joshi and collaborators (2012) suggest a concentration of 1% as interface saturation point in lentil protein stabilized emulsion with oil fraction of 10%. According to Liang and Tang (2014), the flocculated state of droplets displayed inverse trend in pea proteins stabilized emulsions, where FI% progressively increased up to a maximal value, as the concentration increased from 0.25 to 1.0 g/100 ml, while a further increase in concentration contrarily led to a gradual decrease in FI%.

### 3.1.3. Flocculation and coalescence stability

Emulsions are inclined to break down over time through a variety of physicochemical mechanisms, including gravitational separation, flocculation, coalescence and Ostwald ripening. The stability of various emulsions formed at various concentrations upon storage of 24 h was evaluated in terms of flocculation (FI) and coalescence indexes (CI).

The FI (24 h) varied with concentration and type of proteins. PP-stabilized emulsion exhibited high FI at 0.5 and 1.0% concentration, and low FI at 1.5 and 2% concentrations. In the contrary, CP emulsion showed high flocculation index at 2% concentration, but the other concentration displayed low values. In the case of LP emulsion, the FI decreased when concentration increased to reach the minimal value at 2.0% concentration.

Regarding coalescence, there was also great variation in the results, depending to the type and concentration of protein. CI% values diverged from 2.98% in 1.5% LP emulsion to 46.51% in 2% LP emulsion. PP-stabilized emulsions showed low CI at 0.5% and 2% concentrations, while CI was more or less high at 1% and 1.5% concentrations respectively. In the case of CP emulsions, the lowest CI value was obtained at 1.5% concentration, and the highest value was obtained at 0.5% concentration. Differently, LP-stabilized emulsions displayed very low CI at 0.5% and 1.5% concentrations, and high values at 1% and 2% concentrations. Basically, protein-stabilized emulsions showed good emulsifying stability at 1.5%

and 2% concentrations.

This divergence between protein emulsification behaviors might be due to the difference in physicochemical properties, such as, molecular weight, hydrophobicity, free SH and SS bounds as determined previously (Ladjal E. et al., 2015). Clearly, LP-stabilized emulsions are the most stable comparing to the others. According to our results, the underlying mechanism for emulsion instability was by means of droplet flocculation and coalescence. Stable emulsions can be prepared when the interface is completely covered with particles. However, upon insufficient loading of the interface, droplet coalescence cannot be fully prevented, and partial coalescence may take place (Scholten, Moschakis, & Biliaderis, 2014). The thickness of the interfacial layer determines the magnitude and range of the steric repulsion between droplets. Droplet flocculation can be inhibited if the range of the steric repulsion is longer than the range of any attractive interactions, such as van der Waals or hydrophobic (Chung & McClements, 2014). Hence, emulsion stability at high protein concentration can be attributed to the formation of multilayered protein shell around oil droplet which successfully prevents the coalescence of oil droplets Joshi et al. (2012).

### 3.1.4. Creaming stability

The creaming index of the three protein emulsions at different protein concentrations, upon quiescent storage up to 7 days was investigated. As expected, various emulsions showed different creaming behaviors, depending on the type of proteins and the applied concentration. Clearly, for any emulsion at 0.5% concentration, the creaming index was the highest. It increased with storage to reach the maximum values on the 7th day. It should be noted that there was no creaming in 2% CP emulsion and 1.5% and 2% LP emulsion even after 7 days of storage. In the contrary, low concentration (0.5%) displayed clear creaming even after one day of storage (in the case of PP and LP emulsions).

These observations indicated that increasing the concentration progressively improved the creaming stability of these emulsions. The improvement of the creaming stability could be in part due to the progressive decreases in  $d_{4,3}$  (water dilution; Table 1). A similar improvement of creaming stability upon increasing protein concentration has been observed for emulsions stabilized by pea proteins (Liang & Tang, 2014). Higher protein concentration lowered creaming rate possibly due to the unadsorbed protein in the aqueous phase which increase the viscosity (Sun & Gunasekaran, 2009). Hence, higher protein concentration may facilitate the

adsorption of protein to the interface of oil droplets, slightly increase their density, and consequently prevent gravitational separation (Piorkowski & McClements, 2013). In addition, increasing protein concentration enhanced the surface coverage of oil droplets against flocculation and reduced the scope for protein bridging, leading to decreased creaming (Sun & Gunasekaran, 2009).

For each system, there is a critical concentration of proteins, above which the droplet size and emulsion stability, may be independent of concentration (at constant oil fraction). Under the investigated conditions of the present work, and taking into account emulsifying ability and stability, we can approximately see that this critical concentration was about 1.5%.

### 3.2. Effects of ionic strength on emulsifying properties

Another factor that plays a role in protein-emulsifying properties is salt presence. NaCl affects the protein-emulsifying properties mainly by two mechanisms: (1) salts reduce the electrostatic repulsion between droplets through electrostatic screening and (2) high concentrations of electrolytes alter the structural organization of water molecules, which alters the strength of the hydrophobic interactions between non-polar groups (Zhang et al., 2009).

To investigate the effect of ionic strength on emulsifying properties of pea, chickpea and lentil protein, we fixed the same parameters (pH 3, oil fraction 0.1) using the critical protein concentration (1.5%), and then we tested different ionic strengths (0–200 mM).

#### 3.2.1. Droplet size distribution

Emulsifying properties of various legume proteins (PP, CP and LP) at different ionic strength (0, 50, 100, 150 and 200 mM NaCl) were evaluated at pH 3, protein concentration of 1.5% and an oil fraction of 0.1 using droplet-size analysis. The  $d_{4,3}$  of the droplets, diluted in 1% SDS or deionized water, was calculated and summarized in Table 2.

Emulsions were highly sensitive to changes in ionic strength. Although the particle size in SDS dilution was approximately in the same range (ranging from  $\approx 1.5$  to  $4 \mu\text{m}$ ), the mean particle diameter in water dilution significantly increased with NaCl addition, indicating that salt addition promoted droplet aggregation without affecting the initial droplet size. At ionic strength of 0 and 50 mM, the particle diameter of emulsions remained relatively

small and emulsions were more stable against aggregation. At relatively high ionic strength ( $\geq 100$  mM), emulsions were unstable manifesting droplet aggregation, maintaining relatively small droplet sizes in SDS dilution. The large diameter in water dilutions, at high ionic strength, is due to the screening of the surface charges that encouraged protein–protein interaction, but, however, reduced protein–oil interaction (Zhang et al., 2009). The most likely stabilization mechanism preventing droplet aggregation of protein stabilized emulsion is, hence, electrostatic repulsion (Joye & McClements, 2014). For example, at pH 3, the droplets had a high net charge, which would generate a strong electrostatic repulsion that prevents droplet aggregation. By increasing the ionic strength, the net charge on the droplets is decreased and the proteins tend to aggregate (solubility decrease), as a result, emulsion is destabilized by flocculation (Joye & McClements, 2014).

#### 3.2.2. Flocculation in fresh emulsions

High flocculation was observed even though droplet size distribution (SDS dilution at 0 h) was not clearly affected by ionic strength. All emulsions were destabilized by salt addition and displayed extensive aggregation behavior expressed as FI (0 h). FI (0 h) values varied from 0.88 to 7.09 in 0 mM LP and 200 mM CP-stabilized emulsions, respectively. Basically, the higher the ionic strength, the higher the FI is. Where, low ionic strength exhibited the lowest FI and vice versa. Interestingly, there was a positive correlation between ionic strength and FI (0 h). Flocculation is due to “electrostatic screening” phenomenon, which occurs when the ionic strength of the aqueous phase is increased (Piorkowski & McClements, 2013) (i.e. the accumulation of counter-ions around the surfaces, Salminen & Weiss, 2014). Inducing the neutralization of the protein external charge, as a result, the electrostatic repulsions will be reduced, encouraging the protein aggregation.

#### 3.2.3. Flocculation and coalescence stability

Regarding results in Table 2, it can be seen that, after 24 h of storage, the flocculation increased with ionic strength increase. An extensive flocculation (FI, 24 h) was observed at high ionic strengths. Markedly, for the three protein emulsions, the FI increased with ionic strength increase, to reach the maximal values at 150 mM of ionic strength. This finding corroborate with Joye and McClements (2014)'s suggestions, indicating that by increasing the ionic strength, the net charge on the droplets is shielded or

**Table 2**

Emulsion characteristics, including volume-mean droplet size ( $d_{4,3}$ ), flocculation and coalescence indices (FI and CI) of legume protein-stabilized emulsions at various ionic strength, freshly prepared or after a storage of 24 h. FI and CI are calculated using mean values of droplet size ( $d_{4,3}$ ).

Emulsion	Ionic strength (mM NaCl)	$d_{4,3}$ ( $\mu\text{m}$ )				Indices		
		0 h		24 h		FI		CI (%)
		Water	SDS	Water	SDS	0 h	24 h	
PP emulsions	0	6.14 $\pm$ 0.70 <sup>c</sup>	2.06 $\pm$ 0.14 <sup>c</sup>	6.22 $\pm$ 0.67 <sup>c</sup>	2.61 $\pm$ 0.15 <sup>b</sup>	1.98	1.37	27.02
	50	6.21 $\pm$ 0.18 <sup>c</sup>	2.33 $\pm$ 0.10 <sup>c</sup>	7.06 $\pm$ 0.36 <sup>c</sup>	2.53 $\pm$ 0.09 <sup>b</sup>	1.65	1.78	8.55
	100	10.48 $\pm$ 0.23 <sup>b</sup>	3.58 $\pm$ 0.52 <sup>a</sup>	14.86 $\pm$ 1.06 <sup>b</sup>	4.20 $\pm$ 0.72 <sup>a</sup>	1.82	2.33	20.16
	150	13.91 $\pm$ 0.62 <sup>a</sup>	2.70 $\pm$ 0.04 <sup>bc</sup>	16.44 $\pm$ 1.21 <sup>ab</sup>	3.44 $\pm$ 0.10 <sup>ab</sup>	4.14	3.77	27.17
	200	14.05 $\pm$ 0.73 <sup>a</sup>	3.32 $\pm$ 0.67 <sup>ab</sup>	17.19 $\pm$ 0.98 <sup>a</sup>	4.72 $\pm$ 1.50 <sup>a</sup>	3.06	2.63	36.56
CP emulsions	0	7.41 $\pm$ 0.14 <sup>d</sup>	2.46 $\pm$ 0.12 <sup>a</sup>	8.49 $\pm$ 0.33 <sup>c</sup>	2.71 $\pm$ 0.15 <sup>b</sup>	2.01	2.13	10.16
	50	7.67 $\pm$ 0.15 <sup>cd</sup>	1.56 $\pm$ 0.11 <sup>c</sup>	8.47 $\pm$ 1.23 <sup>c</sup>	2.04 $\pm$ 0.09 <sup>c</sup>	3.91	3.14	30.70
	100	8.11 $\pm$ 0.09 <sup>c</sup>	1.68 $\pm$ 0.01 <sup>c</sup>	10.27 $\pm$ 2.31 <sup>bc</sup>	2.01 $\pm$ 0.07 <sup>c</sup>	3.81	4.10	19.36
	150	10.64 $\pm$ 0.56 <sup>b</sup>	1.90 $\pm$ 0.00 <sup>b</sup>	13.03 $\pm$ 3.34 <sup>b</sup>	2.26 $\pm$ 0.26 <sup>c</sup>	4.60	4.76	18.94
	200	12.70 $\pm$ 0.37 <sup>a</sup>	1.57 $\pm$ 0.01 <sup>c</sup>	17.83 $\pm$ 1.61 <sup>a</sup>	4.03 $\pm$ 0.43 <sup>a</sup>	7.09	3.42	156.68
LP emulsions	0	5.26 $\pm$ 0.20 <sup>d</sup>	2.79 $\pm$ 0.13 <sup>b</sup>	5.59 $\pm$ 0.19 <sup>d</sup>	2.87 $\pm$ 0.17 <sup>cd</sup>	0.88	0.94	2.86
	50	5.61 $\pm$ 0.32 <sup>d</sup>	2.95 $\pm$ 0.22 <sup>b</sup>	6.78 $\pm$ 0.29 <sup>d</sup>	3.41 $\pm$ 0.21 <sup>b</sup>	0.89	0.98	15.55
	100	9.35 $\pm$ 0.62 <sup>c</sup>	4.28 $\pm$ 0.10 <sup>a</sup>	11.24 $\pm$ 0.71 <sup>c</sup>	5.07 $\pm$ 0.20 <sup>a</sup>	1.18	1.21	18.35
	150	12.49 $\pm$ 0.59 <sup>b</sup>	2.05 $\pm$ 0.0 <sup>c</sup>	20.43 $\pm$ 1.78 <sup>b</sup>	2.55 $\pm$ 0.18 <sup>d</sup>	5.09	7.00	24.55
	200	17.13 $\pm$ 2.34 <sup>a</sup>	2.31 $\pm$ 0.08 <sup>c</sup>	25.09 $\pm$ 1.95 <sup>a</sup>	3.23 $\pm$ 0.24 <sup>bc</sup>	6.41	6.76	39.82

Values expressed are mean  $\pm$  standard deviation. Means in the column (in the same protein emulsion) with different superscript are significantly different at  $p < 0.05$ . PP: Pea protein; CP: Chickpea protein; LP: Lentil protein.

decreased and the emulsion is destabilized by flocculation.

The coalescence phenomenon also was determined as coalescence index (CI %) (Table 2). For example, CI% was ranging from 2.88% to 156% in 0 mM LP and 200 mM CP emulsions, respectively. For any emulsion, the highest CI% was found at the highest ionic strength (200 mM). It is well known that, coalescence rate can be reduced if the protein, in addition to decreasing the interfacial tension, can form a film with good viscoelastic properties in the oil–water interface, to resist droplet–droplet collision (Lestari et al., 2011). Based on our results, we can deduce that, at high ionic strength, legume proteins form films with insufficient steric repulsion and weak viscoelastic properties at the interface, which accelerate emulsion destabilization.

### 3.2.4. Creaming stability

Table 3 shows the creaming index of the three protein emulsions at different ionic strengths (from 0 to 200 mM), upon quiescent storage up to 7 days. As expected, emulsions showed different creaming behaviors, depending to the type of proteins and the applied ionic strength. Clearly, for any emulsion, the creaming index increase when the ionic strength increase. It increased with storage to reach the maximum values on the 7th day. Interestingly, creaming was the lowest at the lowest ionic strength (0 and 50 mM). LP emulsions exhibited the most stable state comparing to PP and CP stabilized emulsion. The ability of an emulsion to resist creaming is highly dependent on the droplet size, density difference between the dispersed and continuous phases, and the viscosity of the continuous phase. Emulsions with smaller droplets, a lower density contrast between phases, and higher viscosity are more stable to creaming (Karaca et al., 2011).

As reported in Joshi et al. (2012), low salt concentrations enhance solubility because hydrated salt ions especially the anions weakly bind to the charged group of proteins. This phenomenon is known by “the salting-in effect” of proteins resulting into high solubility in the presence of low concentration of salt (Yuliana, Truong, Huynh, Ho, & Ju, 2014). At low concentrations, salts can stabilize proteins through non specific electrostatic interactions, dependent only on the ionic strength of the medium (Hamada, Arakawa, & Shiraki, 2009), and the increased solubility of proteins comes from the water bound with the ions (Joshi et al., 2012). However, at high concentrations, salts exert specific effects on

proteins depending on the type and concentration of the salts (Hamada et al., 2009; Molina-Bolivar, Galisteo-Gonzalez, & Hidalgo-Alvarez, 2001). When NaCl concentration increase (above 0.15 mM), it can rather reduce the protein solubility (Joshi et al., 2012). Since, the monovalent Na<sup>+</sup> ions are counterions for the negatively charged protein molecules, whereas the monovalent Cl<sup>-</sup> ions are counterions for the positively charged (Rao, Chen, & Chen, 2009), leading to a decrease in electrostatic repulsion, thus enhancing hydrophobic interactions (Yuliana et al., 2014). When net charge of protein molecules is screened sufficiently, molecules will be able to approach closely enough together to aggregate (Chantrapornchai & McClements, 2002). This can be also attributed to the increase of interfacial tension between the protein surface and bulk solvent (Hamada et al., 2009). In the other hand, the decrease in emulsion stability at high ionic strengths can be attributed also to the hydration of adsorbed counterions (Fiscaro, Compari, & Braibanti, 2011). This phenomenon is known by “the salting-out effect”. Proteins can interact with water through hydrogen bonding with greater or comparable strength to water–water interactions. This is because the water molecules prefer to form strong hydrogen bonds with the ions instead of weaker bonds with the hydrated biopolymers (proteins) (Salminen & Weiss, 2014). This promotes protein–protein interaction and protein aggregate formation, which ultimately results into slow diffusion of protein molecules into oil–water interface at high salt concentration (Joshi et al., 2012). Furthermore, it has also been suggested that salt at its high concentrations can compete with protein for water to ionize itself. This competition effectively reduces the availability of water and increases the protein dehydration (Joshi et al., 2012). When the hydration repulsion becomes negligible compared with the van der Waals attraction, the particles will aggregate (Salminen & Weiss, 2014), encouraging creaming.

Likewise, the ionic strength has an effect on protein hydrophobicity. Zhang et al. (2009) reported that the emulsifying activity and hydrophobicity of chickpea proteins take the same trend as function of ionic strength; they decrease first and then increase with the increase of ionic strength, the lowest values (both parameters) occurred at ionic strength 0.1 M. The ionic strength seems also to have an effect on the conformational structure of legume proteins (Zhang et al., 2009).

Under the investigated conditions of the present work, and taking into account emulsifying ability and stability, we can approximately see that the critical ionic strength was in the range of 0–50 mM NaCl.

### 3.2.5. Emulsion microstructure

According to the results of emulsifying properties of the investigated emulsions, we selected two emulsions for each protein; 0 mM and 50 mM NaCl (at 1.5% protein concentration). Fig. 1 shows the CLSM microstructural observations of various fresh emulsions formed at 0 mM and 50 mM of NaCl. Proteins are stained in green and oil droplets appear as dark bubbles.

In emulsions at 0 mM, it can be observed that most of the droplets were present in the separated and unflocculated form. However, in emulsions with 50 mM NaCl, droplets were in flocculated state. The results confirmed that emulsions at 0 mM were stable to aggregation, however, emulsions at 50 mM showed even bigger aggregates. This can be explained by the electrostatic screening and dehydration effects of ionic strength on proteins, thus increasing the attractive interactions of protein–protein as detailed above. Herein, these results evidence that emulsions instability in presence of salt was related to protein aggregation, leading to physical separation (coalescence and creaming). It should be noted that LP-stabilized emulsion was more sensitive to

**Table 3**

Creaming index of various legume protein emulsions formed at various ionic strengths, upon storage up to 7 days. Each data is means of at least duplicate measurements.

Emulsion	Ionic strength (mMNaCl)	Creaming index		
		1 day	4 days	7 days
PP	0	0.00	24.50 ± 1.50	29.00 ± 1.00
	50	13.33 ± 5.77	25.22 ± 1.34	27.27 ± 2.36
	100	26.69 ± 7.84	34.67 ± 2.27	35.47 ± 2.82
	150	26.21 ± 3.35	32.20 ± 5.78	33.00 ± 6.45
	200	31.92 ± 2.98	37.01 ± 5.92	37.54 ± 5.48
CP	0	±	±	+
	50	+	29.00 ± 0.00	34.00 ± 0.00
	100	29.00 ± 0.00	29.00 ± 0.00	29.00 ± 0.00
	150	30.00 ± 0.00	31.00 ± 0.00	32.00 ± 0.00
	200	22.72 ± 3.85	23.63 ± 5.14	23.63 ± 5.14
LP	0	0.0 ± 0.0	0.0 ± 0.0	ND
	50	0.0 ± 0.0	0.0 ± 0.0	ND
	100	11.87 ± 0.88	16.87 ± 2.65	ND
	150	16.31 ± 0.85	20.76 ± 1.08	ND
	200	29.86 ± 10.80	36.38 ± 7.45	ND

Values expressed are mean ± standard deviation. PP: pea protein, CP: chickpea protein and LP: lentil protein. ±: Slight creaming not objectively evaluated; +: clear creaming not objectively evaluated; ND: not determined.

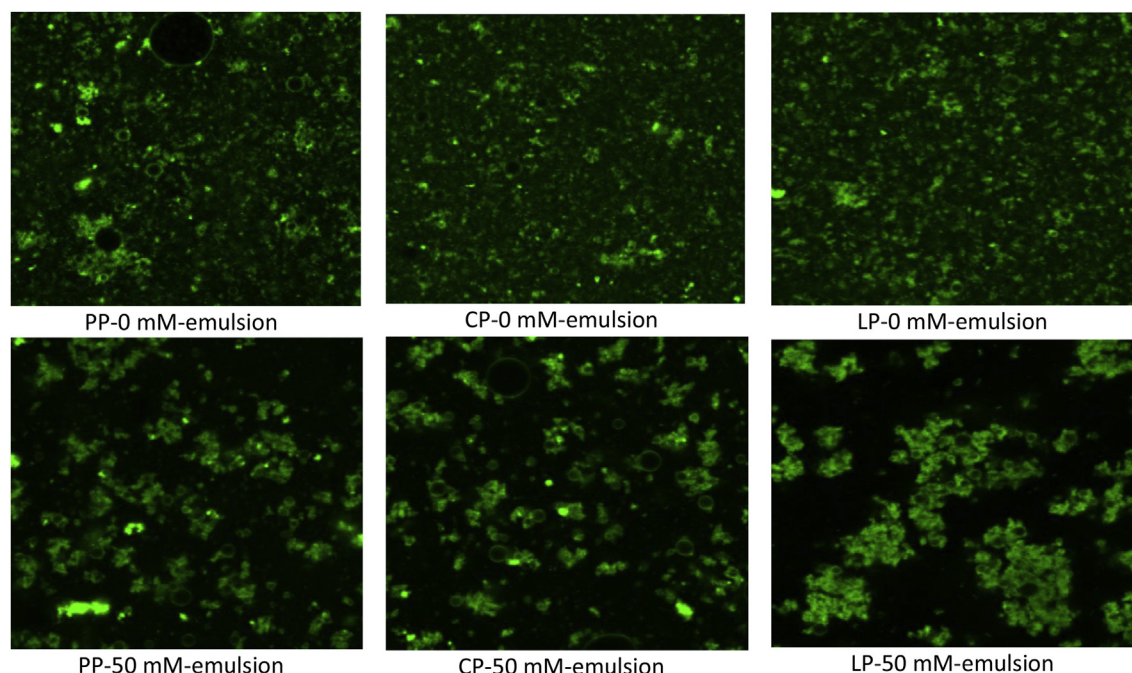


Fig. 1. CLSM images of legume protein-stabilized emulsions at 0 and 50 mM NaCl. PP: Pea protein, CP: Chickpea protein and LP: Lentil protein.

ionic strength, showing intensive aggregation at 50 mM of NaCl. Our results are in agreement with those reported on whey protein stabilized emulsions containing various concentrations of  $\text{CaCl}_2$  (Ye & Singh, 2000). Equally, Shao and Tang (2014) reported the same remark about the effect of NaCl on the microstructure of soy protein-stabilized emulsions.

#### 4. Conclusion

This study confirms that, at pH 3, protein concentration and ionic strength (sodium chloride) have a major influence on the characteristics of legume protein-stabilized emulsions, including, droplet size distribution, flocculation, coalescence creaming and microstructure. Basically, it was found that 1.5% (w/v) of protein and 0 mM to < 50 mM of NaCl are the best conditions to produce stable emulsions with legume proteins. It should be noted that high ionic strength ( $\geq 50$  mM) promotes flocculation and accelerates destabilization of legume protein emulsions, whilst, high protein concentration improves their stability. Our results suggest the use of these proteins as emulsifiers in acid food formulation, such as, mayonnaise and salad dressing.

#### Acknowledgments

The authors wish to thank Béjaia University and the Universidad de Seville for the valorous technical support. The authors acknowledge also to the Microscopy Service (CITIUS-Universidad de Sevilla) for providing full access and assistance.

#### References

- Aydemir, L. Y., & Yemenicioglu, A. (2013). Potential of Turkish Kabuli type chickpea and green and red lentil cultivars as source of soy and animal origin functional protein alternatives. *LWT - Food Science and Technology*, 50, 686–694.
- Boye, J. I., Aksay, S., Roufik, S., Ribéreau, S., Mondor, M., Farmworth, E., ... Rajamohamed, S. H. (2010). Comparison of the functional properties of pea, chickpea and lentil protein concentrates processed using ultrafiltration and isoelectric precipitation techniques. *Food Research International*, 43(2), 537–546.

- Carbonaro, M., Maselli, P., & Nucara, A. (2014). *Structural aspects of legume proteins and nutraceutical properties*. Food Research International. <http://dx.doi.org/10.1016/j.foodres.2014.11.007>.
- Chantrapomchai, W., & McClements, D. J. (2002). Influence of NaCl on optical properties, large strain rheology and water holding capacity of heat induced whey protein isolates gels. *Food Hydrocolloids*, 16, 467–476.
- Chung, C., & McClements, D. J. (2014). Structure-function relationships in food emulsions: Improving food quality and sensory perception. *Food Structure*, 1, 106–126.
- Etheridge, R. D., Pesti, G. M., & Foster, E. H. (1998). A comparison of nitrogen values obtained utilizing the Kjeldahl and Dumas combustion methodologies (Leco CNS) on samples typical of an animal nutrition analytical laboratory. *Animal Feed Science and Technology*, 73, 21–23.
- Fisicaro, E., Compari, C., & Braibanti, A. (2011). Hydrophobic hydration processes: thermal and chemical denaturation of proteins. *Biophysical Chemistry*, 156, 51–67.
- Guo, Q., & Mu, T. H. (2011). Emulsifying properties of sweet potato protein: effect of protein concentration and oil volume fraction. *Food Hydrocolloids*, 25, 98–106.
- Hamada, H., Arakawa, T., & Shiraki, K. (2009). Effect of additives on protein aggregation. *Current Pharmaceutical Biotechnology*, 10, 400–407.
- Joshi, M., Adhikari, B., Aldred, P., Panozzo, J. F., Kaspis, S., & Barrow, C. J. (2012). Interfacial and emulsifying properties of lentil protein isolate. *Food Chemistry*, 134, 1343–1353.
- Joye, I. J., & McClements, D. J. (2014). Emulsifying and emulsion-stabilizing properties of gluten hydrolysates. *Journal of Agricultural and Food Chemistry*, 62, 2623–2630.
- Karaca, A. C., Low, N., & Nickerson, M. (2011). Emulsifying properties of chickpea, faba bean, lentil and pea proteins produced by isoelectric precipitation and salt extraction. *Food Research International*, 44, 2742–2750.
- Kaushal, P., Kumar, V., & Sharma, H. K. (2012). Comparative study of physico-chemical, functional, antinutritional and pasting properties of taro (*Colocasia esculenta*), rice (*Oryza sativa*) flour, pigeonpea (*Cajanus cajan*) flour and their blends. *LWT - Food Science and Technology*, 48(1), 59–68.
- Ladjal, E. Y., Boudries, H., Chibane, M., & Romero, A. (2015). Pea, chickpea and lentil protein isolates: physicochemical characterization and emulsifying properties. *Food Biophysics*. Accepted manuscript <http://dx.doi.org/10.1007/s11483-015-9411-6>.
- Ladjal, E. Y., & Chibane, M. (2015). Some physicochemical and functional properties of pea, chickpea and lentil whole flours. *International Food Research Journal*, 22(3), 987–996.
- Lestari, D., Mulderb, W. J., & Sanders, J. P. M. (2011). Jatropha seed protein functional properties for technical applications. *Biochemical Engineering Journal*, 53, 297–304.
- Liang, H.-N., & Tang, C.-H. (2013). pH-dependent emulsifying properties of pea [*Pisum sativum* (L.)] proteins. *Food Hydrocolloids*, 33, 309–319.
- Liang, H.-N., & Tang, C.-H. (2014). Pea protein exhibits a novel pickering stabilization for oil-in-water emulsions at pH 3.0. *LWT - Food Science and Technology*, 58, 463–469.
- Makri, E., Papalamprou, E., & Doxastakis, G. (2005). Study of functional properties of

- seed storage proteins from indigenous European legume crops (lupin, pea, broad bean) in admixture with polysaccharides. *Food Hydrocolloids*, 19, 583–594.
- Molina-Bolivar, J. A., Galisteo-Gonzalez, F., & Hidalgo-Alvarez, R. (2001). Specific adsorption on protein-covered particles and its influence on colloidal stability. *Colloids and Surfaces B: Biointerfaces*, 21, 125–135.
- Papalamprou, E. M., Doxastakis, G. I., & Kiosseoglou, V. (2010). Chickpea protein isolates obtained by wet extraction as emulsifying agents. *Journal of the Science of Food and Agriculture*, 90(2), 304–313.
- Piorowski, D. T., & McClements, D. J. (2013). Beverage emulsions: recent developments in formulation, production, and applications: Review. *Food Hydrocolloids*, 1–37. <http://dx.doi.org/10.1016/j.foodhyd.2013.07.009>.
- Rao, J.-J., Chen, Z.-M., & Chen, B.-C. (2009). Modulation and stabilization of silk fibroin-coated oil-in-water emulsions. *Food Technology and Biotechnology*, 47(4), 413–420.
- Salminen, H., & Weiss, J. (2014). Electrostatic adsorption and stability of whey protein-pectin complexes on emulsion interfaces. *Food Hydrocolloids*, 35, 410–419.
- Sanchez, C. C., & Patino, J. M. R. (2005). Interfacial, foaming and emulsifying characteristics of sodium caseinate as influenced by protein concentration in solution. *Food Hydrocolloids*, 19, 407–416.
- Scholten, E., Moschakis, T., & Biliaderis, C. G. (2014). Biopolymer composites for engineering food structures to control product functionality. *Food Structure*, 1, 39–54.
- Shao, Y., & Tang, C.-H. (2014). Characteristics and oxidative stability of soy protein-stabilized oil-in-water emulsions: influence of ionic strength and heat pretreatment. *Food Hydrocolloids*, 37, 149–158.
- Shen, L., & Tang, C.-H. (2014). Emulsifying properties of vicilins: dependence on the protein type and concentration. *Food Hydrocolloids*, 36, 278–286.
- Sun, C., & Gunasekaran, S. (2009). Effects of protein concentration and oil-phase volume fraction on the stability and rheology of menhaden oil-in-water emulsions stabilized by whey protein isolate with xanthan gum. *Food Hydrocolloids*, 23, 165–174.
- Taherian, A. R., Mondor, M., Labranche, J., Drolet, H., Ippersiel, D., & Lamarche, F. (2011). Comparative study of functional properties of commercial and membrane processed yellow pea protein isolates. *Food Research International*, 44, 2505–2514.
- Toews, R., & Wang, N. (2013). Physicochemical and functional properties of protein concentrates from pulses. *Food Research International*, 52, 445–451.
- Ye, A., & Singh, H. (2000). Influence of calcium chloride addition on the properties of emulsions stabilized by whey protein concentrate. *Food Hydrocolloids*, 14, 337–346.
- Yu, J., Ahmedna, M., & Goktepe, I. (2007). Peanut protein concentrate: production and functional properties as affected by processing. *Food Chemistry*, 103, 121–129.
- Yuliana, M., Truong, C. T., Huynh, L. H., Ho, Q. P., & Ju, Y.-H. (2014). Isolation and characterization of protein isolated from defatted cashew nut shell: influence of pH and NaCl on solubility and functional properties. *LWT – Food Science and Technology*, 55, 621–626.
- Zhang, T., Bo, J., Wanmeng, M., & Zhang, W. (2009). Emulsifying properties of chickpea protein isolates: Influence of pH and NaCl. *Food Hydrocolloids*, 23, 146–152.



# Pasting, thermal, morphological, rheological and structural characteristics of *Chenopodium album* starch



Romee Jan\*, D.C. Saxena, Sukhcham Singh

Department of Food Engineering and Technology, Sant Longowal Institute of Engineering & Technology, Longowal, Sangrur, Punjab, India

## ARTICLE INFO

### Article history:

Received 22 June 2015

Received in revised form

13 October 2015

Accepted 17 October 2015

Available online 21 October 2015

### Keywords:

*Chenopodium*

*Amaranth*

Starch

Dynamic rheology

Physicochemical properties

## ABSTRACT

*Chenopodium album* is an annual fast-growing underutilized pseudo cereal with high percentage of starch content. The aim of present study was to analyze the isolated starch for its physicochemical, morphological, pasting, thermal, rheological and FTIR spectrometric characteristics. Amylose content of *C. album* V1 and *C. album* V2 starches was found 16.75 g/100 g and 19.11 g/100 g. The starch showed polygonal shape and granule size was found to vary from 1.021 to 1.033  $\mu\text{m}$ , respectively. Peak gelatinization temperature ( $T_p$ ) for *C. album* V1 was found to be 63.20 °C while for *C. album* V2 it was 61.05 °C. Peak viscosity of the starch varied from 1812 cP for *C. album* V1 to 4012 cP for *C. album* V2, respectively. Thus *C. album* starch showed higher paste viscosity and unique viscoelastic behavior that might enhance their potential usage in different product formulations. FTIR spectrometric analysis revealed almost similar structural components within *C. album* V1 and *C. album* V2 starches. However, morsel variability was observed with *Amaranthus* starch.

© 2015 Elsevier Ltd. All rights reserved.

## 1. Introduction

*Chenopodium album* belongs to the family *chenopodiaceae* with *Chenopodium* as the generic name and grows as an annual wild plant at an altitude of 4700 m above sea level. The plant is cultivated widely in Europe, North America, Iran and Asia with Western Rajasthan, Kulu and Shimla acting as the prominent cultivators of the crop within the India. The weedy plant is known as “pigweed” in English while as its popular Hindi name is “Bathua”. The plant is relatively inexpensive, commonly available in India during summer and winter seasons in the fields of wheat, barley, mustard and gram. The seeds generally go to waste due to non availability of processing techniques for the crop. The valuable underutilized pseudo-cereals like the *Chenopodium* are regarded like the true cereals, rich in mealy material enabling their elaborative utilization in different types of flour, bread, noodles and other starch related products. The starch from *Chenopodium* can be isolated in saponin-free form. The main constituent of grain is the small sized (<1  $\mu\text{m}$ ) starch granule with an amylose content of about 11% that creates unique applications in food industries and being a major

constituent of grains it can confer to structure, texture, consistency and appeal to many food systems (Lorenz, 1990).

Studies on new natural starches are essential for their best use and also to increase the utilization of starchy flours. A growing demand for starch from the food industry has created the need for new sources of this polysaccharide. The research on separation and characterization of starch from *C. album* grain is scanty and these grains can be explored as a new source of starch for various food formulations. However keeping in view of above, the present study aims to explore the pasting, thermal, morphological, rheological and structural properties of the starch extracted from different cultivars of *C. album* and compared to the starch isolated from other pseudocereal.

## 2. Materials and methods

### 2.1. Raw material

The grains of *C. album* (V1) are not commonly available in market. Hence, the grains of *C. album* var. IC415477 (V1) were procured from National Bureau of Plant Genetic Resources (NBPGR), Shimla, Himachal Pradesh, India. The grains of *C. album* var. local Punjab (V2) and *Amaranthus cholai* var. local Punjab (V3) was locally procured. The samples were analyzed for carbohydrate and protein by standard methods of analysis AOAC (992-23, 1995).

\* Corresponding author.

E-mail addresses: [romeegan12@gmail.com](mailto:romeegan12@gmail.com) (R. Jan), [sukhcham@yahoo.com](mailto:sukhcham@yahoo.com) (S. Singh).

## 2.2. Isolation of starch

The starch was isolated from different cultivars using the pre-standardized process of starch extraction. Grains (100 g) were steeped in 100 ml of NaOH (0.25 g/100 ml) at 4 °C for 24 h. The supernatant was decanted, and fresh volume of sodium hydroxide was added to the solid part and stirred for another 1 h at ambient temperature, double deionized water was used during steeping. The steeped grains were ground in a grinder (wet grinding) and the paste obtained was mixed with (1:5 ratio) water to form the slurry. The slurry was filtered through 200, 300 and 400 mesh sieve, respectively. The filtrate was centrifuged at  $3830 \times g$  for 10 min. The process of washing and centrifugation were repeated six times until the white starchy layer was obtained. The starch was dried for 6 h at 40 °C and passed through a mesh of 100 BSS (149  $\mu\text{m}$ ).

## 2.3. Physicochemical properties

### 2.3.1. Color determination

The color values of starches from three varieties was measured using Hunter colorimeter (Model I5 Green Macbeth, USA) in terms of lightness ( $L^*$ ). Whiteness index (WI) was calculated according to Hsu, Chen, Weng, & Tseng, (2003) as per the following equation:

$$WI = 100 - \sqrt{(100 - L)^2 + a^2 + b^2}$$

where: L, a, and b were Hunter L, a, and b values.

### 2.3.2. Amylose content

Amylose content of the samples was examined by the method of Morrison and Laignelet (1983). Starch sample of 70 mg was mixed with 10 ml of urea and DMSO (Dimethyl Sulfoxide) solution in 1:9 ratio and heated for 10 min at 100 °C with continuous stirring. The mixed sample was incubated at 100 °C for 1 h and then cooled to room temperature. Addition of 0.5 ml solution of above mixed incubated sample was taken with subsequent addition of 25 ml distilled water and 1 ml solution of iodine (I) and potassium iodide (KI). Blank sample was also prepared and absorbance was taken at 635 nm.

$$\text{Amylose Content (\%)} = (28.414 \times \text{Blue value}) - 6.218$$

where blue value (BV) is the absorbance at 635 nm of starch and I<sub>2</sub>/KI solution.

### 2.3.3. Swelling power and solubility

The procedure of Bello-Prez, Acevedo, Zamudio-Flores, Mendez-Montealov, and Rodriguez-Ambriz (2010) with few modifications was used for determination of swelling power and solubility of starches. These were determined over a temperature range of 55–95 °C. Starch slurry (2 g/100 ml, starch dry basis) in centrifuge tubes was heated at 55, 65, 75, 85 and 95 °C for 30 min. The tubes after cooling were centrifuged at  $112 \times g$  for 20 min (C24, BL; M/s. Remi Laboratory Industries, Mumbai, India). The supernatant was carefully decanted in petriplates, evaporated and dried at 105 °C for 5 h till constant weight is achieved and were weighed to calculate the g/100 g Solubility. The residue was weighed for swelling power estimation. The experiment was conducted in triplicates. Swelling power and solubility was calculated as:

$$\text{Swelling Power} = \frac{\text{Weight of sediment paste (g)}}{\text{Weight of sample (dry basis, g)}}$$

$$\text{Solubility (g/100g)} = \frac{\text{Weight of soluble (g)}}{\text{Weight of sample (dry basis)}} \times 100$$

## 2.4. Pasting properties

The pasting properties of the starches were evaluated with the Rapid Visco Analyser (RVA, Starch Master TM; Model N17133; Newport Scientific Pvt. Ltd., Warriewood, Australia). A programmed heating and cooling cycle was used, where the samples were held at 50 °C for 1 min, heated to 95 °C at 12 °C/min, held at 95 °C for 2.5 min, before cooling from 95 to 50 °C at 12 °C/min and holding at 50 °C for 2 min. Parameters recorded were pasting temperature, peak viscosity, final viscosity (viscosity at 50 °C), breakdown viscosity (peak trough viscosity) and setback viscosity (final trough viscosity).

## 2.5. Thermal properties

The gelatinization characteristics of the starches were studied using a differential scanning calorimeter (DSC-7, PerkinElmer, and Norwalk, CT). Starch (2 mg, dry basis) was loaded into aluminum pan and distilled water was added to achieve a starch – water suspension containing 70 g/100 g water. Samples were hermetically sealed and allowed to equilibrate for 1 h at room temperature before analysis. The DSC analyzer was calibrated using indium and the sample pans were heated at a rate of 10 °C/min from 20 to 140 °C. The temperature at the onset of gelatinization ( $T_o$ ), at the peak ( $T_p$ ), at conclusion the ( $T_c$ ) and the enthalpy ( $\Delta H$ ) were calculated automatically (Sandhu & Singh, 2007).

## 2.6. Rheological properties

Dynamic rheology of starches was analyzed wherein temperature sweep oscillatory test was performed with Modular Compact Rheometer (MCR102, M/s. Anton Paar, Austria), equipped with parallel plate system (50 mm diameter) and PP50-SN32770 (dia. = 0.5 mm) probe. The gap size was set at 0.5 mm; strain and frequency was set to 0.5% and 1 Hz, respectively. About 2 ml of starch suspension (20 g/100 g) was loaded on the ram of Rheometer and the edge of sample was covered with a thin layer of low density silicon oil to minimize evaporation losses. The starch sample was subjected to temperature sweep test with a temperature ramp from 50 to 90 °C at a heating rate of 2 °C/min. The dynamic rheological properties of starches in terms of storage modulus ( $G'$ ), loss modulus ( $G''$ ) and loss factor ( $\tan \delta$ ) were determined as a function of temperature.

## 2.7. Morphological properties

The granule shape as a major morphological characteristic of the sample was analyzed at a moisture content of 5–6 g/100 g. Scanning electron micrographs (SEMs) were taken with a JEOL, Tokyo, Japan, Model No. JSM 6610LV. The Starch samples were mounted on aluminum stub using a double backed cellophane tape, coated in auto finer coater, JEOLJFC1600, with gold palladium (60:40, g:g). The starch samples were examined at magnifications of 5000 and 10,000 $\times$ .

## 2.8. X-ray diffraction analysis

The crystallinity of the powdered starch samples was determined using an X-ray diffractometer, PAN analytical, Phillips,

Holland, Model No. X" Pert PRO with the following conditions: target Cu-anode X-ray, 30 kV, 40 mA and scanning speed of 0.5°/min. Origin Pro software package was used for determining the total area under the curve and the area under each prominent peak. The percentage crystallinity was calculated using formula below:

$$\%Crystallinity = \frac{(\text{Area under peaks})}{\text{Total area}} \times 100$$

### 2.9. FTIR spectroscopy

Infrared spectra were recorded using an Agilent Technologies Cary 660 FTIR spectrometer. The samples were analyzed by preparing KBr pellets using anhydrous potassium bromide. The proportion of sample was taken as 1:15 g/g of KBr and the granular mixture were ground vigorously in a pestle mortar until pulverized into fine powder. Small quantity of this powder was carefully put into pellet-forming mould, pressed under hydraulic pressure and then used for obtaining IR spectrum. The IR region measured was between 4000 cm<sup>-1</sup> and 400 cm<sup>-1</sup> representing the average of 64 scans. All spectra's were recorded at room temperature under ambient conditions.

### 2.10. Statistical evaluation

All the analysis were determined in triplicates and Statistical analysis was performed using Statistica-log software package version 7 (M/s. StatSoft Inc., OK, USA). The significant differences were obtained by a one-way analysis of variance (ANOVA) followed by Duncan's multiple range test (DMRT) at significance level of P < 0.05.

## 3. Results and discussion

The carbohydrate content of *C. album* V1 and *C. album* V2 was found 51.18 and 53.65 g/100 g, while protein content of *C. album* V1 and *C. album* V2 was 13.83 and 13.12 g/100 g, respectively.

### 3.1. Starch yield, purity and color value

The starch yield, purity and color values of *C. album* V1, *C. album* V2, and *A. cholai* V3 starches are shown in Table 1. Significant variation (p < 0.05) in yield of starches was observed among *C. album* V1, *C. album* V2 and *A. cholai* V3, respectively. This variation in observed yield may be due to the varietal difference among the sources used for extraction. Purity of starches was observed in the range of 99.12–99.65 g/100 g. However, significant differences were not observed in the purity of *C. album* V1 and *C. album* V2 starch. While significantly highest purity was noted in *A. cholai* V3 starch. This might be due to the compositional changes (protein, fat and fiber content) of the starches. The L\* value of extracted starches varied significantly (p ≤ 0.05) from 95.95 to 96.83. While as the whiteness of the starches ranged from 94.14 to 94.61, respectively. Lowest L\* value was observed for *C. album* V1 starch and the highest

value was observed for *A. cholai* V3. However higher whiteness was observed for *A. cholai* V3 starch and lower whiteness was noticed for *C. album* V1 starch. The observed values of lightness were found greater than 90, which gives a satisfactory whiteness for starch purity as reported previously by Boudries et al., (2009).

### 3.2. Physico-chemical properties of starch

#### 3.2.1. Amylose content

Amylose content of *C. album* starches differ significantly (p ≤ 0.05) with higher mean value of 19.11 g/100 g in *C. album* V2 followed by 16.75 g/100 g in *C. album* V1 (Table 1). Amylose content affects the functional and physicochemical properties of starch, including its pasting, gelatinization, retrogradation and swelling characteristics (Svegmark et al., 2002). Also the factors such as botanical sources, climatic conditions, harvest time and different types of soil during cultivation affects the variability in amylose and amylopectin ratio within the same specie (Noda et al., 2004).

#### 3.2.2. Swelling power and solubility

Swelling power of the *C. album* V2 starch ranged from 1.5 to 1.48 g/g, where as solubility varied from 6.66 to 60.0 g/100 g within the temperature range of 55–95 °C, as shown in Fig. 1(a) and (b). While in case of *C. album* V1 and *A. cholai* V3, the swelling power was found to be 1.63–1.85 g/g and 2.85–8.41 g/g, whereas the solubility values ranged from 5.0 to 50 g/100 g and 4–36 g/100 g, respectively. The trend showed by the curves related to swelling power and solubility of starches was found similar upon increase in the temperature. *C. album* V1 and *C. album* V2 starches showed similar increasing trend in early hours of heating that changed towards the decreasing trend thereafter in late periods of the study. Starch aqueous suspension when heated above gelatinization temperature results in the distraction of starch crystalline structure and exposure of water molecules to hydroxyl groups of amylose and amylopectin through hydrogen bonding, resulting in swelling of starch molecules, and increased solubility due to leaching of some soluble starch into liquid. A strongly bonded micellar structure of the starch granule may render it relatively defiant to swelling, also Sasaki, Yasui, Matsuki, and Satake (2003) suggested that amylose reinforced the internal network within the granule that restricts the swelling and the waxy starch swell to a greater extent than normal amylose starch. Contrarily to it *A. cholai* V3 showed a significantly different behavior whose starch granules continued to swell with further increase in temperature as shown in Fig. 1(a) and (b). It might be due to the presence of low amylose content in *A. cholai* V3 starch, as reported by Tester and Morrison (1990) that amylose dominates the solubility of starch whereas amylopectin mainly influences the starch swelling power. Thus the ratio of amylose and amylopectin in the starch granule and the way in which they are arranged inside the granule affect the swelling and solubility of the starch.

#### 3.2.3. Pasting properties

Pasting properties provide imminent information about the cooking behavior of starches during heating and cooling cycles.

**Table 1**

Purity, yield and amylose content of starches along with the lightness coordinate (L\*) and whiteness of color.

Sources	Starch yield (g/100 g)	Purity of starch (g/100 g)	Amylose content (g/100 g)	L* value	Whiteness (W)
<i>C. album</i> (V1)	47.3 ± 0.51 <sup>a</sup>	99.20 ± 1.11 <sup>b</sup>	16.75 ± 0.80 <sup>b</sup>	95.95 ± 0.99 <sup>b</sup>	94.14 ± 0.66 <sup>b</sup>
<i>C. album</i> (V2)	37.59 ± 1.10 <sup>b</sup>	99.12 ± 1.04 <sup>b</sup>	19.11 ± 0.56 <sup>a</sup>	96.2 ± 1.7 <sup>b</sup>	94.05 ± 1.35 <sup>b</sup>
<i>A. cholai</i> (V3)	31.47 ± 0.97 <sup>c</sup>	99.65 ± 1.40 <sup>a</sup>	1.87 ± 0.11 <sup>c</sup>	96.83 ± 0.12 <sup>a</sup>	94.61 ± 0.02 <sup>a</sup>

Results are expressed as mean values ± standard deviation of three determinations. Means in rank with different superscripts differ significantly (p ≤ 0.05).

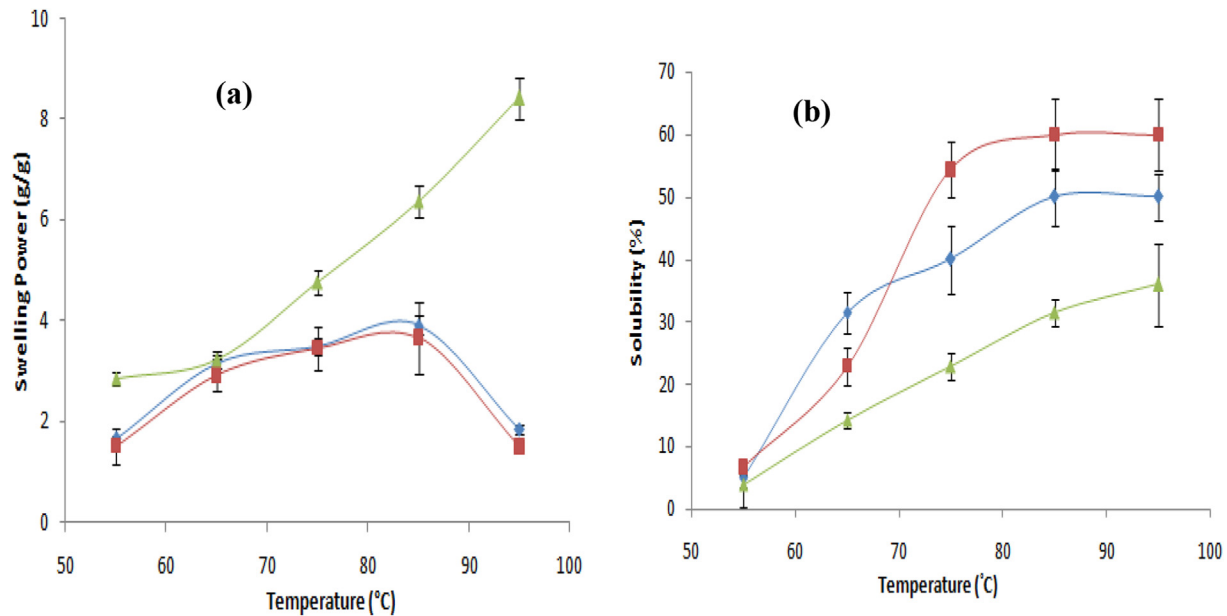


Fig. 1. Effect of temperature on (a) swelling power (b) solubility of the starches obtained from *C. album* V1 *C. album* V2 and *A. cholai* V3.

Viscosity of starches was found to increase with an increase in temperature with the *C. album* V2 exhibiting significantly higher peak viscosity (PV) (4012 cP) in comparison to *C. album* V1 and *A. cholai* V3 starches. Peak viscosity is regarded as the maximum viscosity attained by the sample and tendency of starch granules to swell freely before physical breakdown. The increase in viscosity with increase in temperature may be accredited to the removal of water from the exuded amylose of granules as they swell (Ghiasi, Marston, & Hosney, 1982). Pasting temperature is the minimum temperature required to cook the starch. *C. album* V2 starch showed a lower pasting temperature of 76.65 °C than *C. album* V1 and *A. cholai* V3 starches. The high pasting temperature of starch indicates the higher resistance of starch granules towards the swelling. The break down viscosity (BD) and set back viscosity values (SV) of starch paste varied significantly ( $p \leq 0.05$ ) with respective mean values of 331 cP and 1190 cP for *C. album* V2 starch which was found to be higher than *A. cholai* V3 and lower than *C. album* V1 starch.

Breakdown viscosity, measure of resistance of starch paste to heat and shear, indicates the stability of the paste and Setback reflects the degree of retrogradation that is expected to correlate positively with the amylose content of starch (Abdel-Aal, Hucl, Chibbar, Han, & Demeke, 2002). Final viscosity indicates a gelling tendency that gives an insight of stability to cooled-cooked starch paste under low shear. *C. album* V2 showed a higher final viscosity

(FV) of 4871 cP followed by *C. album* V1 and *A. cholai* V3 as shown in Table 2. The viscosity of *C. album* V2 and *C. album* V1 continued to ascend quite sharply on cooling as compared to *A. cholai* V3 which may be attributed to the higher amylose content and water binding capacity of these starches.

### 3.2.4. Thermal properties

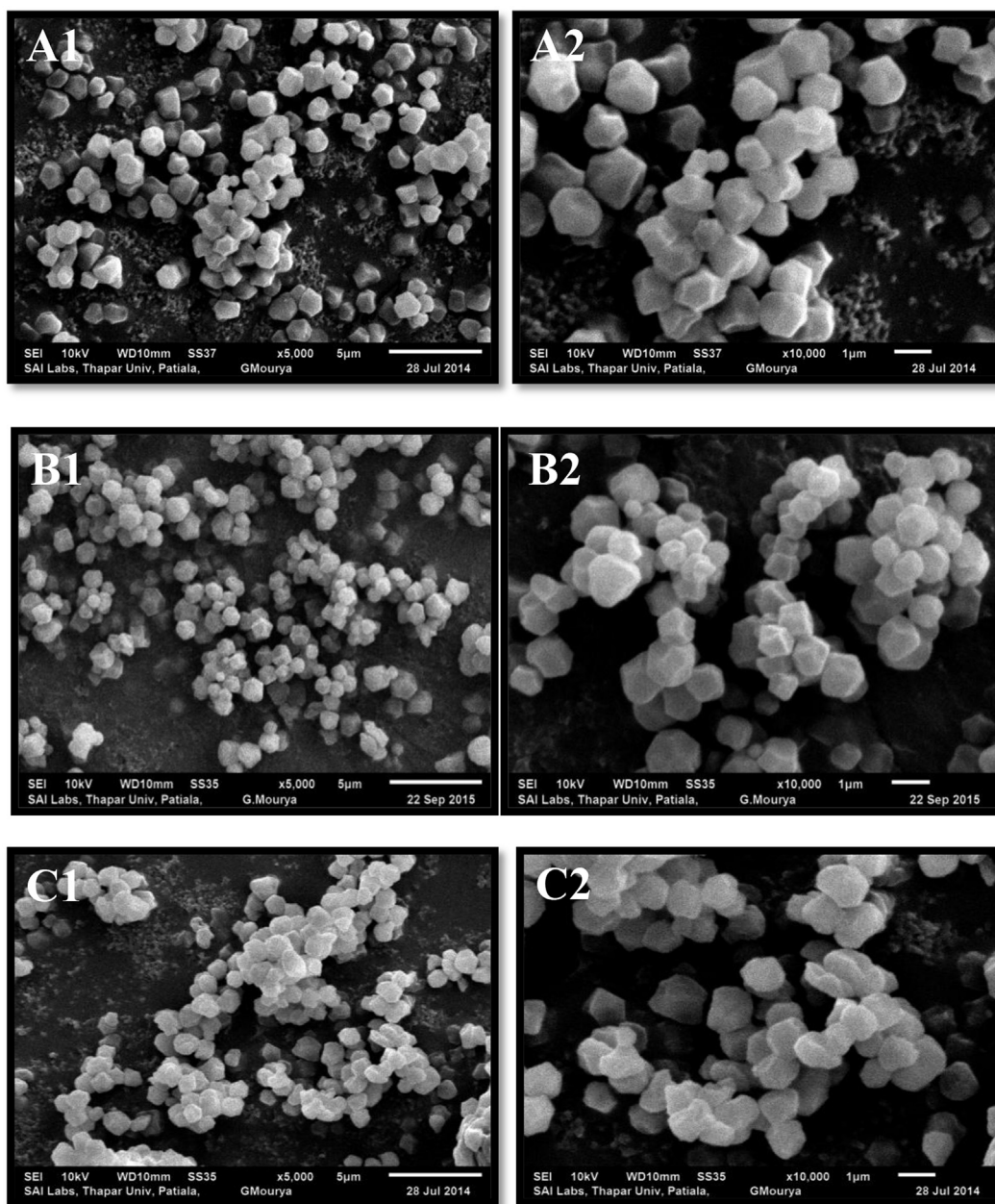
Thermal transition temperatures ( $T_0$ ,  $T_p$ ,  $T_c$ ) along with enthalpy of gelatinization ( $\Delta H_{gel}$ ) and gelatinization temperature range ( $T_R = T_c - T_0$ ) are presented in Table 2. *C. album* V2 starch showed significantly ( $p \leq 0.05$ ) lower  $T_0$ ,  $T_c$  and  $\Delta H_{gel}$  values of 41.75, 63.87 °C and 12.81 J/g, respectively, in contrary to the higher range observed in *C. album* V1 and *A. cholai* V3 starch. The lower gelatinization temperatures of starch indicated lesser energy usage requirement to instigate starch gelatinization and vice versa. Fredriksson, Silverio, Anderson, Eliasson, and Aman (1998) reported starch crystallinity increases with amylopectin content and for this reason; higher amylopectin content containing starches (i.e. lower amylose content) would be expected to have higher onset, peak, and conclusion temperatures. Furthermore starches from various botanical sources diverge in compositions that reveal different transition temperatures and gelatinization enthalpies (Singh, Singh, Kaur, Sodhi, & Gill, 2003). The values of thermal transitions are in close conformity with the annotations of thermal values observed by Steffolani, Leon, and Perez (2013).

Table 2  
Pasting and thermal properties of starches from *C. album* (V1), *C. album* (V2) and *A. cholai* (V3).

	<i>C. album</i> (V1)	<i>C. album</i> (V2)	<i>A. cholai</i> (V3)		<i>C. album</i> (V1)	<i>C. album</i> (V2)	<i>A. cholai</i> (V3)
PV (cP)	1812 ± 12.50 <sup>b</sup>	4012 ± 21.0 <sup>a</sup>	1086 ± 29.51 <sup>c</sup>	$T_0$ (°C)	54.64 ± 0.65 <sup>b</sup>	41.75 ± 0.43 <sup>c</sup>	58.02 ± 0.76 <sup>a</sup>
BV (cP)	421 ± 23.50 <sup>a</sup>	331 ± 13.50 <sup>b</sup>	318 ± 27.50 <sup>c</sup>	$T_p$ (°C)	63.20 ± 0.04 <sup>b</sup>	61.05 ± 0.04 <sup>c</sup>	73.30 ± 0.10 <sup>a</sup>
FV (cP)	2865 ± 20.00 <sup>b</sup>	4871 ± 45.03 <sup>a</sup>	970 ± 28.00 <sup>c</sup>	$T_c$ (°C)	82.67 ± 1.11 <sup>b</sup>	63.87 ± 1.05 <sup>c</sup>	86.70 ± 0.89 <sup>a</sup>
SV (cP)	1474 ± 19.51 <sup>a</sup>	1190 ± 10.5 <sup>b</sup>	211 ± 22.00 <sup>c</sup>	$\Delta H_{gel}$ (J/g)	14.10 ± 1.21 <sup>b</sup>	12.81 ± 0.60 <sup>c</sup>	16.50 ± 0.30 <sup>a</sup>
P Temp (°C)	76.70 ± 1.76 <sup>b</sup>	76.65 ± 1.10 <sup>b</sup>	76.74 ± 0.95 <sup>a</sup>	$T_c - T_0$ ( $T_R$ )	28.03 ± 0.85 <sup>b</sup>	22.12 ± 0.54 <sup>c</sup>	28.68 ± 1.27 <sup>a</sup>

PV, peak viscosity; TV, trough viscosity; BV, breakdown viscosity; FV, final viscosity; SV, setback viscosity; P Temp, pasting temperature;  $T_0$ , onset temperature;  $T_p$ , peak temperature;  $T_c$ , conclusion temperature;  $\Delta H_{gel}$  (J/g), enthalpy of gelatinization;  $T_R$ , Gelatinization temperature range.

Results are expressed as mean values ± standard deviation of three determinations. Means in rank with different superscripts differ significantly ( $p \leq 0.05$ ).



**Fig. 2.** SEM micrographs of starches: (A1, A2) top two images representing *C. album* (V2) at magnification level of 5000 $\times$  and 10,000 $\times$ . the middle two micrographs (B1, B2) belong to *C. album* (V1) at 5000 $\times$  and 10,000 $\times$ , while the last two micrographs (C1, C2) are from *A. cholai* (V3) at 5000 $\times$  and 10,000 $\times$ .

### 3.2.5. Morphological characteristics

The scanning electron micrograph of the starches has revealed that the starch granules are polygonal and angular in shape. Morphological examination of the starches showed the varying size of starch granules with average granule size of 1.021  $\mu\text{m}$  and 1.033  $\mu\text{m}$  found in *C. album* V2 and *C. album* V1, respectively. Microscopic observations (Fig. 2, A–C) of the starch samples reveal the established organization of starch granules in form of clusters, which may be due to the aggregation of starch granules natively in the starchy perisperm. The size and shapes of the observed granules are in close agreement with Villarreal, Ribotta, and Iturriaga (2013).

### 3.2.6. X-ray diffraction analysis

The X-ray diffraction pattern of starches is shown in Fig. 3. *C. album* V2 starch displayed “A” type diffraction pattern with peak

intensities observed at 15.23, 17.13, 18.19 and 23.32 $^\circ$  that are comparable with the findings of Manek et al., (2005) on cereal starches. *C. album* V1 and *A. cholai* V3 starches showed similar diffractograms as that of *C. album* V2 starch. X-ray diffractometry has been used to reveal the presence and characteristics of the crystalline structure of the starch granules. The percentage starch crystallinity of *C. album* V2 was found to be 29.58%, while as *C. album* V1 and *A. cholai* V3 starches showed an average value of 37.47 and 33.88%, respectively. The starch crystallinity varies with crystal size and amount of crystalline region, whereas the amylose chain is responsible for the amorphous region and orientation of double helices within the crystalline domain with degree of interaction involving double helices (Singh, McCarthy, & Singh, 2006).

### 3.2.7. FTIR spectroscopy

Interpretation of the infrared (IR) absorption bands is achieved

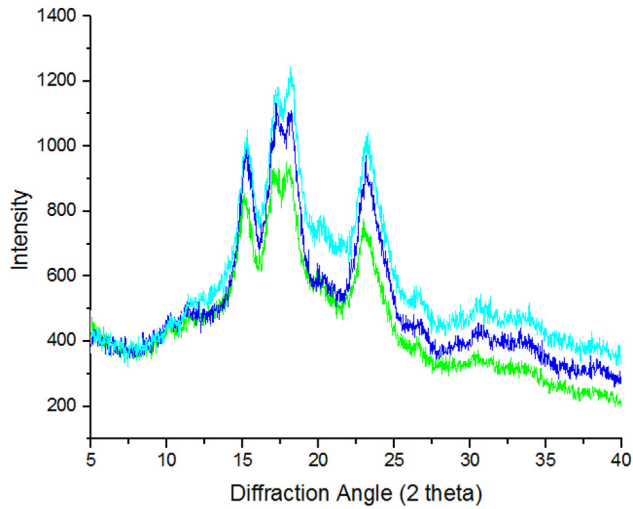


Fig. 3. X-ray diffraction (XRD) pattern of starch granules obtained from *C. album* (V1) *C. album* (V2) *A. cholai* (V3).

in the light of earlier investigation (Yadav, Mahadevamma, Tharanathan, & Ramteke, 2007). The IR spectra of starch samples exhibited bands that originate mainly from the vibrational modes of amylose and amylopectin. Infra red spectral patterns of *C. album* V1 and *C. album* V2 starches were found consistent to each other although spectra of *A. cholai* V3 starch powder was found to be up shifted in comparison to *C. album* V1 and *C. album* V2 starches shown in Fig. 4. The stretching frequency at about  $3200\text{ cm}^{-1}$ – $3400\text{ cm}^{-1}$  were assigned to the O–H group for both *C. album* V1 and *C. album* V2 starches, while as the hydroxyl peak for *A. cholai* V3 was found up shifted at  $3552.166\text{ cm}^{-1}$  due to the less significant hydrogen bonding.

Similarly the peaks at  $2931.329\text{ cm}^{-1}$  and  $2886.590$  are due to the symmetric stretching of C–H group and bands appearing at  $2361.163\text{ cm}^{-1}$  are ascribed to the bending vibrational modes of glycosidic linkage. The absorption band at  $1637.913\text{ cm}^{-1}$  in *C. album* V1 and *C. album* V2 is attributed to the O–H related vibration that indicate the inter and intra-molecular hydrogen bonding between the amorphous region of starch and water molecules. The above mentioned band appeared sharply at about  $1652.052\text{ cm}^{-1}$  in case of *A. cholai* V3 which again confirms the absence of hydrogen bonding (O–H) in its starch. Besides this the

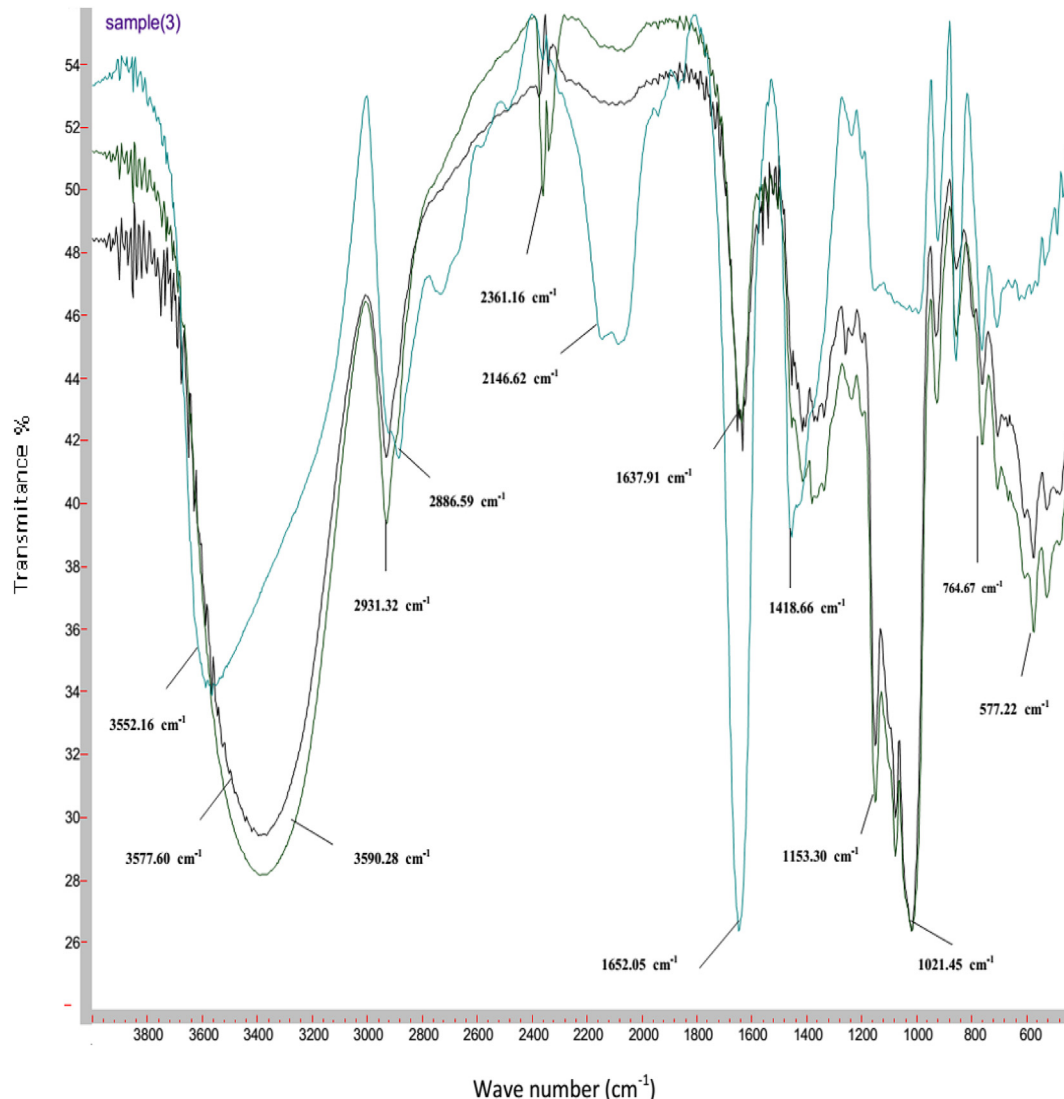


Fig. 4. FTIR spectrometric analysis of starch acquired from *C. album* (V1), *C. album* (V2) and *A. cholai* (V3).

**Table 3**  
Rheological characteristics of starch gels during heating obtained from *C. album* (V1), *C. album* (V2) and *A. cholai* (V3).

Sources	TG' (°C)	Peak G' (Pa)	Peak G'' (Pa)	Peak tan δ
<i>C. album</i> (V1)	90.14 ± 1.52 <sup>a</sup>	48,670 ± 95.77 <sup>a</sup>	5437 ± 74.21 <sup>b</sup>	0.111 ± 0.05 <sup>c</sup>
<i>C. album</i> (V2)	87.3 ± 1.12 <sup>b</sup>	41,500 ± 93.60 <sup>c</sup>	7590 ± 63.97 <sup>a</sup>	0.182 ± 0.50 <sup>b</sup>
<i>A. cholai</i> (V3)	69.7 ± 0.31 <sup>c</sup>	4571.35 ± 53.05 <sup>b</sup>	990 ± 21.46 <sup>c</sup>	0.216 ± 0.10 <sup>a</sup>

G', storage modulus; G'', loss modulus; Peak tan δ, damping factor G'/G''.

Results are expressed as mean values ± standard deviation of three determinations. Means in rank with different superscripts differ significantly ( $p \leq 0.05$ ).

*A. cholai* V3 starch showed a broad band of C=N and C=C asymmetric stretching due to presence of glycosidic linkage skeleton in the region of 1200–900 cm<sup>-1</sup>. The broad bands in the region of 800 cm<sup>-1</sup> to 400 cm<sup>-1</sup> are bending vibrational modes of the glucose pyranose ring.

### 3.2.8. Rheological properties

The rheological properties of starches during heating are shown in Table 3. Storage modulus (G') and loss modulus (G'') of *C. album* V1 and *C. album* V2 starch suspensions increased steeply to maxima and still tend to increase further with incessant heating indicating their granule resistance to deformation, whereas the parameters for *A. cholai* V3 starch increased initially upon heating reaching a maximum and thereafter decreasing upon continuous heating. This reduction in G' and G'' values of *A. cholai* V3 may be due to the disintegration of starch granules leading to the melting of remaining crystallites and increasing the molecular mobility. The temperature (T<sub>G'max</sub>) of *C. album* V2 starch at which the storage modulus (G') loss modulus (G'') reached the highest value was found to be 87.3 °C which was found to be higher than *A. cholai* V3 but lower than the *C. album* V1 starch (Table 3). This increase in both storage and loss moduli before T<sub>G'max</sub> is due to swelling of starch granules and leaching of amylose chains, contributing to the formation of a composite network of solvated materials supporting partially disintegrated starch granules (Arocas, Sanz, & Fiszman, 2009; Huang, Lu & Hsu, 2000). The G' value of 41,500 Pa, G'' value of 7590 Pa was observed with a damping factor (Tan δ<sub>Peak</sub>) of 0.182 in *C. album* V2 starch suspension. The variation in G', G'' and tan δ during heating cycle may be due to the difference in starch granule structure and its amylose content (Svegmark & Hermansson, 1993). The results are in close proximity with the study of Kong, Kasapis, Bao, and Corke (2012) on amaranth.

## 4. Conclusion

The carbohydrate content of *C. album* varieties V1 and V2 was found to be 51.18 and 53.65 g/100 g, respectively. The starch obtained was found 47.30 and 37.59 g/100 g being higher than *A. cholai* V3 with higher purity values of 99.12 and 99.20 g/100 g, respectively. *Chenopodium* starches showed lower swelling power, mean granule diameter, pasting temperature and gelatinization temperature, whereas higher values were noticed for amylose content, pasting viscosity and solubility when compared to *A. cholai* V3 starch. A typical A-type X-ray diffraction pattern with crystallinity of 29.58%, 37.47% was found for *C. album* V1 and V2 starches. The *C. album* starches showed higher Peak G' and G'' than *A. cholai* V3. The analysis of various properties of *C. album* starches will provide valuable information associated with the functional properties of starch, as desirable functional properties can be used in various food industries due to its impending applications for the development of various products viz., in high viscous foods, as a good gelling agent, in dessert and other food formulations and could replace chemically modified starches that are currently being used in a number of products. Moreover due to small granule size,

starches may find wide applications in edible biodegradable films, as fat substitutes (due to smooth creamy structure), as a binder with orally active ingredients. The above all interesting and unique rheological behavior of these starches can be beneficially exploited in the formulation of specialty food products.

## References

- Abdel-Aal, E. S. M., Hucl, P., Chibbar, R. N., Han, H. L., & Demeke, T. (2002). Physicochemical and structural characteristics of flours and starches from waxy and nonwaxy wheats. *Cereal Chemistry*, 79, 458–464.
- AOAC. (1995). *Official methods of analysis* (15th ed.). Washington, D. C., USA: Association of Official Analytical Chemists.
- Arocas, A., Sanz, T., & Fiszman, S. M. (2009). Influence of corn starch type in the rheological. Properties of a white sauce after heating and freezing. *Food Hydrocolloids*, 23, 901–907.
- Bello-Prez, L. A., Acevedo, E. A., Zamudio-Flores, P. B., Mendez-Montealvo, G., & Rodriguez-Ambriz, S. (2010). Effect of high acetylation degree in the morphological, physicochemical and structural characteristics of barley starch. *LWT-Food Science and Technology*, 43, 1434–1440.
- Boudries, N., Belhaneche, N., Nadjemi, B., Deroanne, C., Mathlouthi, M., Roger, B., et al. (2009). Physicochemical and functional properties of starches from sorghum cultivated in the Sahara of Algeria. *Carbohydrate Polymers*, 78(3), 475–480.
- Fredriksson, H., Silverio, J., Anderson, R., Eliasson, A. C., & Aman, P. (1998). The influence of amylose and amylopectin on gelatinization and retrogradation properties of different starches. *Carbohydrate Polymers*, 35, 119–134.
- Ghiasi, K., Marston, V. K., & Hosney, R. C. (1982). Gelatinization of wheat starch. II starch–surfactant interaction. *Cereal Chemistry*, 59(2), 86–88.
- Hsu, C. L., Chen, W., Weng, Y. M., & Tseng, C. Y. (2003). Chemical composition, physical properties, and antioxidant activities of yam flours as affected by different drying methods. *Food Chemistry*, 83, 85–92.
- Huang, C., Lu, S., & Hsu, S. (2000). Viscoelastic changes of rice starch suspensions during gelatinization. *Journal of Food Science*, 65, 215–220.
- Kong, X., Kasapis, S., Bao, J., & Corke, H. (2012). Influence of acid hydrolysis on thermal and rheological properties of amaranth starches varying in amylose content. *Journal of the Science of Food and Agriculture*, 92, 1800–1807.
- Lorenz, K. (1990). Quinoa (*Chenopodium quinoa*) starch: physicochemical properties and functional characteristics. *Starch*, 42, 81–86.
- Manek, R. V., Kunle, O. O., Emeje, M. O., Builders, P., Rao, R. G. V., & Lopez, G. P. (2005). Physical, thermal and sorption profiles of starch obtained from *Tacca leontopetaloides*. *Starch*, 57, 55–61.
- Morrison, W. R., & Laignelet, B. (1983). An improved colorimetric procedure for determining apparent amylose and total amylose in cereal and other starches. *Journal of Cereal Science*, 1, 9–20.
- Noda, T., Tsuda, S., Mori, M., Takigawa, S., Matsuura-Endo, C., & Saito, K. (2004). The effect of harvest dates on the starch properties of various potato cultivars. *Food Chemistry*, 86, 119–125.
- Sandhu, K. S., & Singh, N. (2007). Some properties of corn starches II: physicochemical, gelatinization, retrogradation, pasting and gel textural properties. *Food Chemistry*, 101, 1499–1507.
- Sasaki, T., Yasui, T., Matsuki, J., & Satake, T. (2003). Comparison of physical properties of wheat starch gels with different amylose contents. *Cereal Chemistry*, 80, 861–866.
- Singh, J., McCarthy, O., & Singh, H. (2006). Physico-chemical and morphological characteristics of new Zealand Taewa (Maori potato) starches. *Carbohydrate Polymers*, 64, 569–581.
- Singh, N., Singh, J., Kaur, L., Sodhi, N. S., & Gill, B. S. (2003). Morphological, thermal and rheological properties of starches from different botanical sources. *Food Chemistry*, 81, 219–231.
- Steffolani, M. E., Leon, A. E., & Perez, G. T. (2013). Study of the physicochemical and functional characterization of quinoa and kaniwa starches. *Starch/Stärke*, 65, 976–983.
- Svegmark, K., Helmersson, K., Nilsson, G., Nilsson, P. O., Andersson, R., & Svensson, E. (2002). Comparison of potato amylopectin starches and potato starches. Influence of year and variety. *Carbohydrate Polymers*, 47, 331–340.
- Svegmark, K., & Hermansson, A. M. (1993). Microstructure and rheological properties of composites of potato starch granules and amylose: a comparison of observed and predicted structure. *Food Structure*, 12, 181–193.

Tester, R. F., & Morrison, W. R. (1990). Swelling and gelatinization of cereal starches. Effect of amylopectin, amylose and lipid. *Cereal Chemistry*, *67*, 551–557.

Villarreal, M. E., Ribotta, P. D., & Iturriaga, B. L. (2013). Comparing methods for extracting amaranthus starch and the properties of the isolated starches. *LWT-Food Science and Technology*, *51*(2), 441–447.

Yadav, R. A., Mahadevamma, S., Tharanathan, R. N., & Ramteke, R. S. (2007). Characteristics of acetylated and enzyme-modified potato and sweet potato flours. *Food Chemistry*, *103*, 1119–1126.



## Characterization of lactic acid bacteria isolated from wheat bran sourdough



F. Manini<sup>a</sup>, M.C. Casiraghi<sup>a,\*</sup>, K. Poutanen<sup>b,c</sup>, M. Brasca<sup>d</sup>, D. Erba<sup>a</sup>, C. Plumed-Ferrer<sup>b</sup>

<sup>a</sup> Dept. of Food, Environmental and Nutritional Science, University of Milan, Milan, Italy

<sup>b</sup> University of Eastern Finland, Institute of Public Health and Clinical Nutrition, PO Box 1627, FI-70211 Kuopio, Finland

<sup>c</sup> VTT Technical Research Centre of Finland, PO Box 1000, FI-02044, VTT, Finland

<sup>d</sup> Institute of Sciences of Food Production, Italian National Research Council, Milan, Italy

### ARTICLE INFO

#### Article history:

Received 28 April 2015

Received in revised form

24 September 2015

Accepted 18 October 2015

Available online 21 October 2015

#### Keywords:

Lactic acid bacteria

Probiotic

Wheat bran sourdough

Starter cultures

### ABSTRACT

Spontaneously fermented foods, such as sourdough, represent a source of lactic acid bacteria with potential interesting functional and technological properties as well as a potential source of probiotics. The choice of the starter cultures has a critical impact on the palatability, processability and nutritional attributes of fermented products. The aim of this study was to characterize the predominant microbial species previously isolated from a sourdough-like spontaneous fermented wheat bran. Lactic acid bacteria, such as *Leuconostoc mesenteroides*, *Leuconostoc citreum*, *Lactobacillus brevis*, *Lactobacillus curvatus*, *Lactobacillus sakei*, *Lactobacillus plantarum* and *Pediococcus pentosaceus*, were phenotypically characterized by their growth and acidification rate, carbohydrate metabolism, antifungal activity, exopolysaccharide production, as well as safety. The strains were also tested for xylan- and phytate-degrading activities. Moreover, probiotic properties, such as acid and bile tolerance, anti-listeria activity and adhesion ability to Caco-2 cells were examined. *L. plantarum* CE42, CE60 and *P. pentosaceus* CE65, CE23 showed interesting technological application potential due to their antifungal activity and exopolysaccharide production. Some strains also exhibited phytate degrading activity and could be exploited to improve mineral bioavailability of fermented products. Moreover, *P. pentosaceus* CE65 seems to be a candidate for use as probiotic.

© 2015 Elsevier Ltd. All rights reserved.

### 1. Introduction

The demand for faster, more efficient, controllable and large-scale fermentation has resulted in a careful selection of starter microorganisms to guarantee the reproducibility of fermentation at industrial scale and to obtain a product with specific properties (Carnevali, Ciati, Leporati, & Paese, 2007). The choice of starter culture has critical impact on the final quality of fermented foods. Fermentation with well-characterized cultures, yeast or lactic acid bacteria (LAB), could be a potential tool to improve the palatability, processability and the nutritional value of fermented cereal products or high-fiber ingredients, such as sourdough bread, fermented wheat bran and whole-meal flours (Salmenkallio-Marttila, Katina, & Autio, 2001).

The main criteria used to select microbial starters are desirable technological, sensory and nutritional aspects. Technological factors of interest for fermentation are growth and acidification rate (Coda et al., 2010), synthesis of antimicrobial compounds (Messens & De Vuyst, 2002), antifungal activity (Coda et al., 2013) and exopolysaccharide production (e.g. glucan and fructan) (Galle & Arendt, 2014). Among nutritional properties, degradation of anti-nutritional factors (e.g. phytic acid) and increased availability of functional compounds (e.g. soluble fiber, soluble arabinoxylans, free phenolic acids, bioactive peptides) are desirable (Katina & Poutanen, 2013). Technologically interesting potential starter strains are usually selected from the food matrix they are going to be used for. Some recent studies have shown that the use of selected autochthonous LAB to ferment sourdough is a suitable biotechnological approach to exploit the potential of cereals and pseudo-cereals in bread making (Coda et al., 2010). Moreover, fermentation of bran with yeasts and LAB or with enzymes has been shown to improve loaf volume, crumb structure and shelf life, as well as nutritional properties of bread supplemented with

\* Corresponding author. Dept. of Food, Environmental and Nutritional Science, University of Milan, Via G. Celoria 2, 20133 Milan, Italy.

E-mail address: [maria.casiraghi@unimi.it](mailto:maria.casiraghi@unimi.it) (M.C. Casiraghi).

fermented bran (Katina et al., 2012; Salmenkallio-Marttila et al., 2001).

LAB could also be exploited because of their probiotic properties in order to contribute to the health and wellbeing of the hosts by maintaining or improving their intestinal microbial balance (Asahara et al., 2004). In the case of baked products, the probiotic cultures should be added to the final product and/or their survival and viability should be guaranteed throughout the process steps involved in the manufacture and during the storage conditions (Soukoulis et al., 2014). The aim of the current study was to characterize the 13 LAB strains previously isolated from a spontaneous fermented sourdough-like wheat bran (Manini et al., 2014) for their potential use as starter cultures in food applications such as wheat bran fermentation and sourdough bread, and as potential probiotics.

## 2. Materials and methods

### 2.1. Microorganisms

Thirteen LAB strains were previously isolated from spontaneously fermented wheat bran sourdough-like and identified by phenotypic and molecular techniques (Manini et al., 2014). The following species were found: *Lactobacillus brevis* (n = 2), *Lactobacillus plantarum* (n = 3), *Lactobacillus curvatus* (n = 1), *Lactobacillus sakei* (n = 1), *Leuconostoc mesenteroides* (n = 2), *Leuconostoc citreum* (n = 2), and *Pediococcus pentosaceus* (n = 2) (Table 1). As control, *Lactobacillus rhamnosus* GG was used as well as two recently isolated potential probiotic strains *L. plantarum* Q823 and *Lactobacillus casei* Q11 (unpublished results).

### 2.2. Growth and acidification rate

The fermentation capacity of the strains was evaluated measuring microbial counts, pH and Total Titratable Acidity (TTA) using wheat bran (raw, untreated) (mean particle size 475–633 µm -Molino Quaglia, Vighizzolo D'Este, PD, Italy) as a substrate.

An overnight culture (1% v/v) of each test strain was individually inoculated into a sample (100 g) of wheat bran dough (15% w/v of bran and 85% of water) and incubated for 8 h at 30 °C. The microbial counts were evaluated before and after fermentation. The LAB were determined on de Man, Rogosa and Sharpe agar (MRS agar) (LAB M, Lancashire, UK) and the yeasts were evaluated on Plate Count Agar (PCA) (LAB M). Plates were incubated at 30 °C for 48–72 h pH and TTA developments were measured during fermentation. A sample (10 g) of bran was taken every 2 h and suspended in 100 mL of

distilled water. For the determination of TTA, this suspension was titrated with 0.1 M NaOH to a final pH of 8.5, detected by a pHmeter (PHM 250, Radiometer, Copenhagen); TTA was expressed as mL of 0.1 M NaOH needed to achieve the final pH of 8.5. All samples were analyzed in duplicate.

### 2.3. Technological properties and antibiotic resistance

#### 2.3.1. Carbohydrate metabolism and gas production assessment

Carbohydrate fermentation profiles of the strains were determined by using API 50 CH system (BioMérieux, Marcy-l'Etoile, France). The test was performed according to the Manufacturer's instructions. Moreover, each pure culture was further characterized by Durham tube method in MRS broth at 30 °C for 24 h for detecting gas production.

#### 2.3.2. Phytase activity

The LAB strains were preliminary inoculated in MRS broth and incubated at 30 °C for 24 h. Strains were then grown at 30 °C for 24–48 h in modified Chalmers broth without neutral red and with 1% of sodium phytate (Sigma–Aldrich, Milan, Italy). The phytase activity was determined on modified Chalmers agar plates without CaCO<sub>3</sub> and with 1% of phytic acid calcium or sodium salt (Sigma–Aldrich) as described by Anastasio et al. (2010).

#### 2.3.3. Xylanase activity

For the screening of xylanase producing microorganisms, an agar medium was prepared by adding 0.1% (w/v) of the dyed substrate (Remazolbrilliant Blue R treated Azo-Xylan – birchwood), (Megazyme International Ireland Ltd, Co. Wicklow, Ireland), as the only carbon source, to a sodium phosphate buffer, 100 mM, pH 6 and/or a sodium acetate buffer, 100 mM, pH 4.5 (to test the activity at different pH).

LAB were preliminary inoculated in MRS broth and incubated at 30 °C for 24 h. The cell cultures were inoculated in wells made in triplicate in the agar plates and examined, after 48 h of incubation at 30 °C, for clearing zones around the holes.

#### 2.3.4. Antifungal activity

The antifungal activity of the strains was determined using the overlay method described by Magnusson and Schnürer (2001), slightly modified.

The molds *Aspergillus oryzae* ATCC 66222 and *Aspergillus niger* 25541 were used for this test. A spore suspension was prepared by growing the molds on PCA at 30 °C for 3–4 days and then collecting the conidia by vigorously shaking the slants with sterile peptone water.

LAB were inoculated as two 2-cm-long lines on MRS plates and incubated at 30 °C for 48 h. The plates were then overlaid with 10 mL of malt extract soft agar (3% malt extract, 1.5% bacto peptone, 0.75% agar) inoculated with fungal spore suspension. After solidification, the plates were incubated aerobically at 30 °C for 48 h. The plates were examined for zones of inhibition around the bacterial streaks.

#### 2.3.5. Exopolysaccharides

LAB strains were plated on different MRS agar plate with glucose, sucrose, raffinose, maltose, lactose and starch as the only carbon source. Plates were incubated for 2 days at 30 °C. Duplicate plates containing 25–250 colonies were scored for mucoid properties (scale of ++ = excess EPS to – = no visible mucoid). Colonies were scored as ropy if strings of 5 mm or more were detected when the colony was touched once with a wire inoculating loop (Ruas-Madiedo & De Los Reyes-Gavilán, 2005).

**Table 1**

Lactic acid bacteria isolated from a sourdough-like fermented wheat bran.

Microorganism	Strain	Isolation source
<i>L. brevis</i>	CE94	Wheat bran sourdough
<i>L. brevis</i>	CE85	Wheat bran sourdough
<i>L. plantarum</i>	CE42	Wheat bran sourdough
<i>L. plantarum</i>	CE60	Wheat bran sourdough
<i>L. plantarum</i>	CE84	Wheat bran sourdough
<i>L. curvatus</i>	CE83	Wheat bran sourdough
<i>L. sakei</i>	CE47	Wheat bran sourdough
<i>Ln. mesenteroides</i>	CE52	Wheat bran sourdough
<i>Ln. mesenteroides</i>	CE48	Wheat bran sourdough
<i>Ln. citreum</i>	CE88	Wheat bran sourdough
<i>Ln. citreum</i>	CE54	Wheat bran sourdough
<i>P. pentosaceus</i>	CE65	Wheat bran sourdough
<i>P. pentosaceus</i>	CE23	Wheat bran sourdough
<i>L. rhamnosus</i> GG (control)	GG	GIT of a healthy human
<i>L. plantarum</i> (control)	Q823	Quinoa seeds
<i>L. casei</i> (control)	Q11	Quinoa seeds

### 2.3.6. Antibiotic resistance

The minimum inhibitory concentrations (MICs) of ten antibiotics (gentamicin, kanamycin, streptomycin, tetracycline, erythromycin, clindamycin, chloramphenicol, ampicillin, neomycin, vancomycin) were determined by the microdilution method as reported by the ISO 10932:2010 standard method (ISO 10932/IDF 223, 2010).

Briefly, strains were prepared by suspending single colonies (picked up from fresh cultures on LSM agar plates incubated for 48 h at 37 °C) in a tube with 3 mL of 0.85% saline suspension and the density was adjusted spectrophotometrically to an OD<sub>625</sub> of 0.16–0.20 and subsequently diluting them 1:500 in the medium. This suspension density corresponds approximately to McFarland standard 1 (Mcf 1),  $3 \times 10^8$  CFU/mL.

Inoculation of manually pre-made MIC microtiter test plates (containing the different antibiotic concentrations in 50 µl of LSM broth per well), with the standardized strain suspensions, was performed to obtain a final LAB inoculum of  $10^2$  bacteria mL<sup>-1</sup>. The microtiter plates were subsequently incubated anaerobically either at 28 °C or at 32 °C (*P. pentosaceus*) for 24 h. The MICs were evaluated as the lowest concentration of a given antibiotic at which no growth of the test organism was observed.

Epidemiological cut-off values were defined according to the FEEDAP Panel (EFSA-FEEDAP, 2012).

## 2.4. Potential probiotic properties

### 2.4.1. Growth at 30 °C and 37 °C

The growth performances at 30 °C and 37 °C for 24 h in MRS broth were monitored using a Thermo Bioscreen C automatic turbidometer (Labsystems Oy, Helsinki, Finland). Growth was measured using 100-well Honeycomb microplates (TermoLabsystems, Helsinki, Finland). Each strain was tested in five replicates in a total volume of 300 µL per well.

### 2.4.2. Acid tolerance

The ability of the strains to survive at low pH was evaluated in triplicate as described by Lee et al. (2011), in acidified MRS broth (final pH 2.5). The pH-adjusted MRS broth was inoculated with an overnight culture of the different LAB strains (1% v/v) to a final cell concentration of approximately  $1.0 \times 10^7$  CFU/mL. pH tolerance was evaluated by measuring survival after 2 h of incubation at 37 °C to simulate intestinal conditions. Bacterial counts were determined in duplicate, on MRS agar plates and incubated at 30 °C for 48 h.

### 2.4.3. Bile tolerance

Bile tolerance was measured in triplicate by means of the method described by Sabir, Beyatli, Cokmus, and Onal–Darilmaz (2010) in MRS broth containing 0.3% oxgall (Sigma–Aldrich, Steinheim, Germany), inoculated (1% v/v) and incubated at 37 °C. Samples were taken at 24 h and plated on duplicate MRS agar plates. The survival rate was determined after a 48 h incubation at 30 °C.

### 2.4.4. Adhesion to human colon carcinoma cell-line Caco-2

The human colon carcinoma cell-line Caco-2 cells (ATTC HTB-37) were grown in 75 cm<sup>3</sup> cell culture bottles (Sarstedt, Inc., Newton, NC, USA) using DMEM supplemented with 10% (v/v) heat inactivated fetal bovine serum, 2 mM L-glutamine, 1% (v/v) non-essential amino acids and 100 IU penicillin/mL and 100 µg streptomycin/mL (EuroClone, Sizio, Italy). Caco-2 cells were subsequently seeded to 24-well culture plates at a concentration of  $2.5 \times 10^5$  cells per well. Cells were differentiated for 2 weeks, changing medium every 2–3 days. Cells were always incubated at 37 °C in a 5% CO<sub>2</sub> atmosphere.

Four bacterial strains were chosen for this test based on the results obtained in previous tests. *L. curvatus* CE83, *L. plantarum* CE84, *L. brevis* CE85, *P. pentosaceus* CE65 were grown overnight at 37 °C in MRS broth. After incubation, bacterial cells were collected by centrifugation, washed twice with PBS and suspended in PBS to an appropriate dilution (Abs<sub>625nm</sub> of 0.2, approx.  $2 \times 10^8$  CFU/mL) then added to each well and incubated for 2 h. After incubation, the cells were washed four times and lysed with 0.1% Triton X-100 (Sigma–Aldrich). Cell lysates were serially diluted, plated in duplicate on MRS agar and then incubated at 37 °C for 2 days. The adhesion capacity of the strains was calculated as percentage of the bacteria counted from the cell lysates divided by the total bacteria added to the well. Three biological replicates made in different days and four replicates for each biological replicates were used for this test.

### 2.4.5. Anti-listeria activity

The capacity of the strains to inhibit *Listeria* was determined using the agar spot test described by Jacobsen et al. (1999), with some modifications. The assayed strains included *Listeria innocua*, *L. monocytogenes* and *L. welshimeri*, isolated respectively from food, animal and human.

A 100-µl of an overnight culture of the pathogen strains was plated on PCA and dried. The LAB strains were then spotted (10 µl) in triplicate on the surface of the PCA plate and incubated at 37 °C to develop the spots. After 48 h the inhibition zones were evaluated. A clear zone of more than 1 mm around a spot was scored as positive. Each test was performed in duplicate.

## 3. Results and discussion

### 3.1. Growth and acidification rate

The growth of all the tested LAB increased substantially after 8 h of bran fermentation (average increase approximately 2.7 log CFU g<sup>-1</sup>, Table 2). In particular, *L. sakei* CE47 and *Ln. mesenteroides* CE48 showed the highest growth (3.6 and 3.7 log CFU g<sup>-1</sup> respectively), while the lowest growth was observed with *Ln. citreum* CE54 (1.6 log CFU g<sup>-1</sup>). *L. plantarum* CE84, CE42, CE60, *L. curvatus* CE83, *L. sakei* CE47, and *P. pentosaceus* CE65, CE23 showed the highest acidification rate, the smallest pH reached being pH 4. The lowest acidification rate was obtained with obligate heterofermentative *L. brevis* CE94, CE85, in which pH reached values 5.6 and 5.5 respectively.

### 3.2. Technological properties and antibiotic resistance

#### 3.2.1. Carbohydrate metabolism and gas production assessment

The carbohydrate metabolism profiles of the LAB are shown in Table 3. All the tested strains were able to ferment D-galactose, D-glucose, D-fructose, D-maltose and N-acetylglucosamine. Mixtures of strains with different carbohydrate metabolism are frequently used because they may guarantee optimal acidification and sensory properties (Gobbetti, 1998). Among the tested strains, *Ln. citreum* CE88, *Ln. mesenteroides* CE48, *L. curvatus* CE83, *L. brevis* CE94, CE85 and *P. pentosaceus* CE65 were able to use both L-arabinose and D-xylose confirming similar findings reported before (Gobbetti et al., 1999). Among *L. plantarum* strains, only CE60 was able to use L-arabinose and to a lesser extent also D-arabinose.

Despite that none of the *L. plantarum* tested metabolized xylose, these strains showed the widest carbohydrate utilization spectrum. This species is commonly found in sourdoughs ecosystems and its prevalence in cereal fermentations has been mainly attributed to the versatile metabolism of carbohydrates (Minervini et al., 2010).

Gas production was observed by *Ln. mesenteroides* CE48, CE52 and *Ln. citreum* CE88, CE54.

**Table 2**  
pH, Total Titratable Acidity (TTA) and microbial counts measured every 2 h of wheat bran fermentation.

Bacterial culture		0 h	2 h	4 h	6 h	8 h
CE94 <i>L. brevis</i>	pH	6.5 ± 0.1	6.3 ± 0.0	6.3 ± 0.1	6.0 ± 0.0	5.6 ± 0.0
	TTA	1.8 ± 0.2	2.2 ± 0.0	2.7 ± 0.1	3.6 ± 0.2	4.4 ± 0.1
	log CFU g <sup>-1</sup>	7.8	n.d.	n.d.	n.d.	10.5
CE85 <i>L. brevis</i>	pH	6.4 ± 0.0	6.3 ± 0.0	6.2 ± 0.0	5.9 ± 0.0	5.5 ± 0.0
	TTA	1.9 ± 0.1	2.4 ± 0.0	3.1 ± 0.1	3.6 ± 0.0	4.4 ± 0.1
	log CFU g <sup>-1</sup>	7.9	n.d.	n.d.	n.d.	10.7
CE84 <i>L. plantarum</i>	pH	6.3 ± 0.0	6.2 ± 0.1	5.7 ± 0.1	4.5 ± 0.0	4.0 ± 0.0
	TTA	2.1 ± 0.1	2.7 ± 0.0	4.0 ± 0.0	6.9 ± 0.0	8.6 ± 0.0
	log CFU g <sup>-1</sup>	8.3	n.d.	n.d.	n.d.	11.1
CE42 <i>L. plantarum</i>	pH	6.4 ± 0.0	6.3 ± 0.0	6.1 ± 0.0	5.3 ± 0.0	4.2 ± 0.0
	TTA	1.8 ± 0.1	2.5 ± 0.1	3.5 ± 0.1	5.0 ± 0.1	7.8 ± 0.1
	log CFU g <sup>-1</sup>	8.3	n.d.	n.d.	n.d.	11.0
CE60 <i>L. plantarum</i>	pH	6.2 ± 0.0	6.1 ± 0.0	5.6 ± 0.0	4.5 ± 0.0	4.0 ± 0.0
	TTA	2.2 ± 0.1	3.1 ± 0.1	4.5 ± 0.1	6.8 ± 0.0	10.2 ± 0.4
	log CFU g <sup>-1</sup>	8.6	n.d.	n.d.	n.d.	11.3
CE83 <i>L. curvatus</i>	pH	6.4 ± 0.1	6.2 ± 0.0	5.8 ± 0.0	4.8 ± 0.0	4.2 ± 0.0
	TTA	1.7 ± 0.0	2.4 ± 0.1	3.3 ± 0.1	5.9 ± 0.1	7.5 ± 0.3
	log CFU g <sup>-1</sup>	8.3	n.d.	n.d.	n.d.	11.1
CE47 <i>L. sakei</i>	pH	6.3 ± 0.0	6.1 ± 0.0	5.5 ± 0.0	4.5 ± 0.0	4.1 ± 0.0
	TTA	2.0 ± 0.1	2.9 ± 0.1	4.5 ± 0.1	6.4 ± 0.0	9.0 ± 0.0
	log CFU g <sup>-1</sup>	8.0	n.d.	n.d.	n.d.	11.6
CE52 <i>Ln. mesenteroides</i>	pH	6.3 ± 0.0	6.3 ± 0.1	6.0 ± 0.0	5.4 ± 0.0	4.8 ± 0.0
	TTA	1.9 ± 0.1	2.5 ± 0.0	3.6 ± 0.1	5.0 ± 0.1	6.5 ± 0.1
	log CFU g <sup>-1</sup>	8.0	n.d.	n.d.	n.d.	10.6
CE48 <i>Ln. mesenteroides</i>	pH	6.4 ± 0.1	6.3 ± 0.1	6.0 ± 0.0	5.3 ± 0.0	4.4 ± 0.0
	TTA	1.9 ± 0.2	2.5 ± 0.2	3.1 ± 0.2	5.2 ± 0.2	7.0 ± 0.2
	log CFU g <sup>-1</sup>	7.5	n.d.	n.d.	n.d.	11.2
CE88 <i>Ln. citreum</i>	pH	6.4 ± 0.0	6.2 ± 0.0	5.9 ± 0.0	4.9 ± 0.0	4.4 ± 0.0
	TTA	1.8 ± 0.1	2.7 ± 0.2	3.8 ± 0.0	6.4 ± 0.0	8.2 ± 0.1
	log CFU g <sup>-1</sup>	8.3	n.d.	n.d.	n.d.	11.0
CE54 <i>Ln. citreum</i>	pH	6.4 ± 0.0	6.3 ± 0.1	5.7 ± 0.1	4.7 ± 0.0	4.4 ± 0.0
	TTA	2.0 ± 0.0	2.7 ± 0.2	4.2 ± 0.1	8.4 ± 0.4	8.6 ± 0.3
	log CFU g <sup>-1</sup>	8.5	n.d.	n.d.	n.d.	10.1
CE65 <i>P. pentosaceus</i>	pH	6.3 ± 0.0	6.2 ± 0.0	5.8 ± 0.0	4.5 ± 0.0	4.1 ± 0.0
	TTA	2.1 ± 0.0	2.9 ± 0.2	4.4 ± 0.1	6.8 ± 0.1	9.4 ± 0.1
	log CFU g <sup>-1</sup>	8.4	n.d.	n.d.	n.d.	11.0
CE23 <i>P. pentosaceus</i>	pH	6.3 ± 0.0	6.2 ± 0.0	5.7 ± 0.0	4.6 ± 0.3	4.0 ± 0.0
	TTA	1.8 ± 0.2	2.4 ± 0.1	3.7 ± 0.1	7.3 ± 0.1	9.5 ± 0.0
	log CFU g <sup>-1</sup>	7.8	n.d.	n.d.	n.d.	10.8

Microbial in counts are expressed log CFU g<sup>-1</sup>. TTA is measured in mL of 0.1 M NaOH per 10 g. n.d. = not determined.

### 3.2.2. Enzymatic activities

The indigenous microbiota of sourdough is a source of considerable genetic diversity representing different enzymatic activities useful in biotechnological applications (Pepe et al., 2004). Enzymes, such as xylanase and phytase are examples of the technological and nutritional potential of the microbial biomass of sourdough.

None of the tested strains showed endo-xylanase activity in the plate assay (Table 4). Xylanolytic enzymes are involved in the hydrolysis of xylan and arabinoxylan polymers, and consequently in their solubilization (Gruppen, Kormelink, & Voragen, 1993). Moreover, in bread and bakery industry, xylanases are used to increase the dough viscosity, bread volume and shelf life (Poutanen, Flander, & Katina, 2009).

Considering the nutritional importance of this enzymatic activity, related to “solubilization” of bran dietary fiber, further investigation has been planned to evaluate the presence and the expression of genes codifying for this activity.

Regarding phytate activity, the ability to degrade sodium phytate was prevalent among all the LAB tested, except for *L. plantarum* CE60. This is consistent with a study of De Angelis et al. (2003) in which phytase activity was prevalent in all the 12 species representing LAB isolated from sourdough. Moreover, 8 out of 13 LAB strains tested were able to hydrolyze both hexacalcium and sodium phytate (phy<sup>+</sup>), the most abundant phytate forms in cereals and legume-based foods. In particular, *Ln. citreum* CE54 exhibited

potent activity both on calcium and sodium phytates. Although some *P. pentosaceus* strains have been reported to be able to degrade both sodium and calcium phytate (De Angelis et al., 2003), in the present study the two *P. pentosaceus* strains degraded only one of the phytate types, reflecting a variability among strains of phytase activity. The strains that have shown phytate degrading ability could be exploited as starter cultures in fermented foods to improve mineral bioavailability and thus upgrading the nutritional quality of phytate-rich foods.

### 3.2.3. Antifungal activity

The culture overlay assay carried out on the LAB strains showed different levels of inhibition against the two fungal target strains *A. oryzae* and *A. niger* (Table 5), which are capable of rapid growth on the surface of bakery products (Smith, Daifas, El-Khoury, Koukoutsis, & El-Khoury, 2004).

*L. plantarum* CE42, CE60, CE84, *L. curvatus* CE83 and *P. pentosaceus* CE65, CE23 showed the highest activity against *A. oryzae* and a moderate activity against *A. niger*. The latter was particularly inhibited by *Ln. mesenteroides* CE52 and *L. brevis* CE94. In previous studies, some *L. plantarum* have been shown to possess antifungal activity due to the formation of lactic acid, acetic acid, and hydrogen peroxide, to the competition for nutrients and the production of bacteriocins (Gupta & Srivastava, 2014). During the last few years, there has been a growing interest in the use of

**Table 3**  
Carbohydrate metabolism of lactic acid bacteria tested by API 50 CH system.

	CE94 <sup>a</sup>	CE85 <sup>a</sup>	CE42 <sup>b</sup>	CE60 <sup>b</sup>	CE84 <sup>b</sup>	CE83 <sup>c</sup>	CE48 <sup>d</sup>	CE88 <sup>e</sup>	CE65 <sup>f</sup>	CE23 <sup>f</sup>
Glycerol	–	–	+	+	+	–	–	–	+	+
Erythritol	–	–	–	+	–	–	–	–	–	–
D-arabinose	–	–	–	+	–	–	–	–	–	–
L-arabinose	+++	+++	–	+++	–	+++	+++	+++	+++	+++
D-ribose	+++	+++	+++	+++	+++	+++	+++	–	+++	+++
D-xylose	+++	+++	–	–	–	+++	+++	++	+++	–
L-xylose	–	–	–	–	–	–	–	–	–	–
D-adonitol	–	–	–	–	–	–	–	–	–	–
Methyl-βD-xYlopiranoside	–	–	–	–	–	–	–	–	–	–
D-galactose	+++	++	+++	+++	+++	++	++	++	+++	+++
D-glucose	+++	++	+++	+++	+++	+++	+++	+++	+++	+++
D-fructose	++	++	+++	+++	+++	++	++	+++	+++	+++
D-mannose	–	–	+++	+++	+++	–	–	+++	+++	+++
L-sorbose	–	–	–	–	–	–	–	–	–	–
L-rhamnose	–	–	–	–	+	–	–	–	–	++
Dulcitol	–	–	–	–	–	–	–	–	–	–
Inositol	–	–	–	–	–	–	–	–	–	–
D-mannitol	+	–	+++	+++	+++	+	+	++	–	–
D-sorbitol	–	–	+++	+++	+++	–	–	–	–	–
Methyl-αD-mannopyranoside	–	–	+++	+++	–	–	–	–	–	–
Methyl-αD-glucopyranoside	++	++	–	–	–	++	++	++	–	–
N-acetylglucosamine	+	++	+++	+++	+++	++	++	+++	+++	+++
Amigdaline	–	+++	+++	+++	+++	–	–	+	+++	+++
Arbutin	–	–	+++	+++	+++	–	–	++	+++	+++
Esculin	+	+	+	+	+	+	+	+	+	+
Salicin	–	–	+++	+++	+++	–	–	+++	+++	+++
D-cellobiose	+	+++	+++	+++	+++	+	+	–	+++	+++
D-maltose	+++	+++	+++	+++	+++	++	+++	+++	+++	+++
D-lactose	–	–	+++	+++	+++	–	–	–	+++	++
D-melibiose	–	++	+++	+++	+++	–	–	+++	–	+++
D-saccharose	–	–	+++	+	+++	–	–	+++	–	+++
D-trehalose	–	–	+++	+++	+++	–	–	+++	+++	+++
Inulin	–	–	–	–	–	–	–	–	+	–
D-melezitose	–	+++	–	+++	+++	–	–	–	–	–
D-raffinose	–	+++	+++	+++	+++	–	–	+++	–	+++
Amidon	–	–	–	–	–	–	–	–	–	–
Glycogen	–	–	–	–	–	–	–	–	–	–
Xylitol	–	–	–	–	–	–	–	–	–	–
Gentiobiose	–	–	+++	+++	+++	–	–	–	+++	+++
D-turanose	–	+++	–	+++	+++	–	–	+++	–	–
D-lyxose	–	–	–	–	–	–	–	–	–	–
D-tagatose	–	–	–	–	–	–	–	–	+++	+++
D-fucose	–	–	–	–	–	–	–	–	–	–
L-fucose	–	–	–	–	–	–	–	–	–	–
D-arabitol	–	++	++	++	+	–	–	–	–	–
L-arabitol	–	–	–	–	–	–	–	–	–	–
Potassium gluconate	++	++	++	–	++	++	+	++	++	++
Potassium 2-ketogluconate	–	–	–	–	–	–	–	++	–	–
Potassium 5-ketogluconate	++	++	–	–	–	+	+	++	–	–

Interpretation of LAB growth in API 50 CH system +++ = high growth (yellow); ++ = quite growth (green); + = little growth (dark green); – = not growth (blue).

<sup>a</sup> *L. brevis*.

<sup>b</sup> *L. plantarum*.

<sup>c</sup> *L. curvatus*.

<sup>d</sup> *Ln. mesenteroides*.

<sup>e</sup> *Ln. citreum*.

<sup>f</sup> *P. pentosaceus*.

microorganisms and/or their metabolites to prevent spoilage and to extend the shelf-life of bakery products (Garofalo et al., 2012).

### 3.2.4. Exopolysaccharide production

An interesting property of sourdough LAB is their ability to synthesize a large structural variety of exopolysaccharides (EPS), such as glucan and/or fructans (Galle & Arendt, 2014). EPS have a positive effect on the texture, mouthfeel, taste perception, and stability of fermented food and for certain EPS, prebiotic effects have also been described (Dal Bello et al., 2001).

In accordance to Tiekink and Gänzle (2005), who postulated that any sourdough microbiota contains at a high probability at least one EPS producing strain, only 3 out of 13 LAB strains studied here

did not produce EPS (CE47; CE52; CE85), the major EPS producers being *L. plantarum* and *P. pentosaceus*. As shown in Table 6, the two *P. pentosaceus* strains were able to produce EPS while growing both on maltose and sucrose, CE65 also growing on glucose and CE23 on raffinose. The *L. plantarum* tested produced EPS with different carbohydrates, indicating that in each case the most suitable carbohydrate is largely strain-dependent. *L. plantarum* CE84 was able to produce EPS in presence of different carbon sources, such as sucrose, raffinose, maltose and in particular lactose, while *L. plantarum* CE42 and CE60 were able to produce EPS in presence of starch, usually the most abundant carbon source in cereal products. *Ln. mesenteroides* CE48 produced EPS using glucose and maltose as carbon source and probably synthesized dextran as reported in

**Table 4**  
Phytase and endo-xylanase activities of lactic acid bacteria.

Bacterial culture		Phytase activity		Xylanase activity
		Phytic acid calcium salt	Phytic acid sodium salt	
CE94	<i>L. brevis</i>	+	+++	–
CE85	<i>L. brevis</i>	+	+++	–
CE42	<i>L. plantarum</i>	+	+++	–
CE60	<i>L. plantarum</i>	++	–	–
CE84	<i>L. plantarum</i>	+	++	–
CE83	<i>L. curvatus</i>	–	++	–
CE47	<i>L. sakei</i>	+	+	–
CE52	<i>Ln. mesenteroides</i>	++	++	–
CE48	<i>Ln. mesenteroides</i>	–	++	–
CE88	<i>Ln. citreum</i>	++	+	–
CE54	<i>Ln. citreum</i>	+++	+++	–
CE65	<i>P. pentosaceus</i>	–	+	–
CE23	<i>P. pentosaceus</i>	–	+	–
Q11	<i>L. casei</i>	+++	++	–
2	<i>Clostridium</i>	nd	nd	+++

Interpretation of zone diameter of inhibition: – = no inhibition; + = 0.01–0.1 cm; ++ = 0.1–0.3 cm; +++ = >0.3 cm. nd, not determined.

**Table 5**  
Antifungal activity of lactic acid bacteria.

Bacterial culture		<i>Aspergillus oryzae</i> ATCC 66222	<i>Aspergillus niger</i> 25541
CE94	<i>L. brevis</i>	++	+++
CE85	<i>L. brevis</i>	++	+
CE42	<i>L. plantarum</i>	+++	++
CE60	<i>L. plantarum</i>	+++	++
CE84	<i>L. plantarum</i>	+++	++
CE83	<i>L. curvatus</i>	+++	++
CE47	<i>L. sakei</i>	+	–
CE52	<i>Ln. mesenteroides</i>	++	+++
CE48	<i>Ln. mesenteroides</i>	++	+
CE88	<i>Ln. citreum</i>	+	–
CE54	<i>Ln. citreum</i>	++	+
CE65	<i>P. pentosaceus</i>	+++	++
CE23	<i>P. pentosaceus</i>	+++	++
Q823	<i>L. plantarum</i>	++	+
Q11	<i>L. casei</i>	++	–
GG	<i>L. rhamnosus</i>	+++	+

Interpretation of zone diameter of inhibition – = no inhibition; + = 0.01–0.3 cm; ++ = 0.3–0.6 cm; +++ = > 0.6 cm.

other studies (Lacaze, Wick, & Cappelle, 2007); in Panettone, a traditional Italian sweet bread, dextran from *Ln. mesenteroides* is responsible for the long storage stability (Decock & Cappelle, 2005). Differently, *Ln. mesenteroides* CE52 did not show any EPS production.

### 3.2.5. Antibiotic resistance

Although LAB have been generally recognized as safe (GRAS), it has been shown that genes coding for antibiotics resistance can be transferred among bacteria of different genera and thus to human commensal flora and to pathogenic bacteria, temporarily residing

**Table 6**  
Exopolisaccharides production of lactic acid bacteria in MRS medium with different carbon source.

Bacterial culture		GLU	SUC	RAF	MAL	LAC	ST
CE94	<i>L. brevis</i>	–	–	–	+	–	–
CE85	<i>L. brevis</i>	–	–	–	–	–	–
CE42	<i>L. plantarum</i>	–	–	–	–	–	+
CE60	<i>L. plantarum</i>	++	–	–	–	–	+
CE84	<i>L. plantarum</i>	–	+	+	+	++	–
CE83	<i>L. curvatus</i>	–	–	–	++	–	–
CE47	<i>L. sakei</i>	–	–	–	–	–	–
CE52	<i>Ln. mesenteroides</i>	–	–	–	–	–	–
CE48	<i>Ln. mesenteroides</i>	+	–	–	+	–	–
CE88	<i>Ln. citreum</i>	–	–	+	–	–	–
CE54	<i>Ln. citreum</i>	+	–	–	–	–	–
CE65	<i>P. pentosaceus</i>	++	+	–	+	–	–
CE23	<i>P. pentosaceus</i>	–	+	++	++	–	–
Q823	<i>L. plantarum</i>	+	++	++	++	+	++
Q11	<i>L. casei</i>	–	–	–	–	–	–

– = no sticky; + = sticky; ++ = very sticky. Abbreviations: GLU = glucose; SUC = sucrose; RAF = raffinose; MAL = maltose; LAC = lactose; ST = starch.

in the hosts, which consequently cannot be treated with previously successful antibiotics (Adimpong, Nielsen, Sørensen, Derkx, & Jespersen, 2012).

The results of antibiotic susceptibility testing are shown in Table 7. The bacteria were considered resistant to a particular antibiotic when the MIC ( $\mu\text{g/mL}$ ) values obtained were higher than the recommended breakpoint value, defined at species level by the FEEDAP Panel (EFSA-FEEDAP, 2012). In the present study, *L. plantarum* CE84, *L. curvatus* CE83 and *L. brevis* CE94, CE85 were resistant to Clindamycin. This antibiotic is used to treat infections caused by anaerobic bacteria but also aerobic gram-positive cocci such as *Staphylococcus* or *Streptococcus*. However, cases of clindamycin-resistant and methicillin-resistant *Staphylococcus aureus* are being reported (Cadena et al., 2012) and thus these strains may require further molecular investigation to find out the cause of these resistance patterns and they should not be used as starter cultures in foods, unless the type of resistance can be shown to be non-transmissible. The investigated strains had MIC values for vancomycin of 64 or 128  $\mu\text{g mL}^{-1}$ , which can be expected in the case of *Lactobacillus*, *Pediococcus* and *Leuconostoc* species (MIC values 128  $\mu\text{g mL}^{-1}$ ) because this is due to the absence of D-Ala-D-lactate in their cell wall (Ammor, Belén Flórez, & Mayo, 2007). Thus, the resistance mechanisms observed among these strains are probably inherent or intrinsic to their species and could therefore not be attributed to acquisition of resistance genes. No other strain showed to be resistant to the antibiotic tested and thus these strains are safe for the use as starter cultures and/or probiotics.

### 3.3. Screening for probiotic properties

Spontaneously fermented foods, such as sourdough, may constitute a reservoir for new LAB strains with potential probiotic characteristics. The LAB strains were screened for their ability to survive to the passage through the gastro-intestinal tract (GIT), to adhere to epithelial surfaces and for their antagonistic activity towards pathogens.

#### 3.3.1. Growth at 30 °C and 37 °C

All the tested strains have grown both at 30 °C and 37 °C, except for *Ln. mesenteroides* CE52 that did not grow at 37 °C (Table 8).

#### 3.3.2. pH and bile resistance

According to Fuller (1992), bile, even at low concentrations, can inhibit the growth of microorganisms. Gilliland, Staley, and Bush (1984) reported that 0.3% is considered to be a critical concentration for screening for resistant strains. All strains were able to survive in 0.3% (w/v) bile and *L. plantarum* CE60, CE84, *L. curvatus* CE83, *Ln. mesenteroides* CE48 and *L. brevis* CE94, CE85 were even able to replicate in presence of bile salt after 24 h (Table 8). In accordance with Delgado, O'sullivan, Fitzgerald, and Mayo (2007), the acidic condition (pH 2.5) seemed to be more damaging to the bacteria, with only 6 out of 13 strains surviving 2 h of exposure and none of them growing.

In conclusion, *L. curvatus* CE83, *Ln. mesenteroides* CE48, *L. brevis* CE94, CE85 and *P. pentosaceus* CE65, CE23 were able to survive when exposed to the conditions resembling those of the GIT, in terms of the low pH and the presence of bile salts.

Our study showed that the acidic tolerance is not necessarily related to the species of LAB, but may also be strain-specific; in fact, differences were observed among strains belonging to the same species, such as *L. plantarum*, *Ln mesenteroides* and *P. pentosaceus*, in terms of acid and bile tolerance. Moreover, although strains of *L. plantarum* have previously been shown to survive gastric transit (Mathara et al., 2008), our results indicate that *L. plantarum* may have strong bile tolerance but lower ability to survive at low pH.

**Table 7**  
Minimal inhibitory concentration (MICs) of tested antibiotics in lactic acid bacteria.

	<i>L. brevis</i>			<i>L. plantarum</i>			<i>L. curvatus</i>			<i>L. sakei</i>			<i>Ln. mesenteroides</i>			<i>Ln. citreum</i>			<i>P. pentosaceus</i>		
	CE94	CE85	FEEDAP breakpoint ( $\mu\text{g mL}^{-1}$ )	CE42	CE60	CE84	FEEDAP breakpoint ( $\mu\text{g mL}^{-1}$ )	CE83	CE47	FEEDAP breakpoint ( $\mu\text{g mL}^{-1}$ )	CE52	CE48	CE88	CE54	FEEDAP breakpoint ( $\mu\text{g mL}^{-1}$ )	CE65	CE23	FEEDAP breakpoint ( $\mu\text{g mL}^{-1}$ )	MIC ( $\mu\text{g mL}^{-1}$ )	MIC ( $\mu\text{g mL}^{-1}$ )	MIC ( $\mu\text{g mL}^{-1}$ )
GEN	4	4	16	4	4	4	16	4	4	16	4	4	4	4	4	4	4	16	4	4	16
KAN	16	16	32	16	16	64	64	16	16	64	16	16	16	16	16	16	64	64	16	64	64
STREP	4	4	64	4	16	32	n.r.	4	4	64	4	4	4	64	4	4	16	64	4	16	64
TET	8	8	8	8	8	8	32	8	1	8	1	1	1	8	4	4	4	8	4	4	8
ERY	<0.25	<0.25	1	<0.25	0.5	<0.25	1	<0.25	<0.25	1	<0.25	<0.25	0.5	0.5	1	<0.25	0.5	1	<0.25	0.5	1
CLIN	8	8	1	0.25	0.25	8	2	8	0.25	1	0.25	0.25	0.25	0.25	1	0.25	0.25	1	0.25	0.25	1
CHL	1	1	4	4	4	4	8	4	4	4	1	1	1	4	4	1	1	4	4	1	4
AMP	0.25	0.25	2	0.25	0.25	0.25	2	0.25	1	4	0.25	0.25	0.25	2	0.25	1	1	4	1	1	4
NEO	4	4	n.r.	4	4	4	n.r.	4	4	4	4	4	4	n.r.	4	4	4	4	4	4	4
VAN	128	128	n.r.	128	128	128	n.r.	128	64	n.r.	128	128	128	128	n.r.	128	128	n.r.	128	128	n.r.

Abbreviations: GEN, Gentamicin; KAN, Kanamycin; STREP, Streptomycin; TET, Tetracycline; ERY, Erythromycin; CLIN, Clindamycin; CHL, Chloramphenicol; AMP, Ampicillin; NEO, Neomycin; VAN, Vancomycin. FEEDAP Breakpoint (EFSA Journal 2012), n.r. = not required.

**Table 8**  
Tolerance to temperature, low pH conditions (pH 2.5 for 2 h of incubation) and to bile salt (0.3% Oxgall for 24 h of incubation) and adhesion to human colon carcinoma cell line Caco-2.

Bacterial culture	Temperature		pH 2.5		Oxgall 0.3%		Adhesion to Caco-2 cell-line <sup>b</sup>
	30 °C	37 °C	0 h log CFU mL <sup>-1</sup>	2 h log CFU mL <sup>-1</sup>	0 h log CFU mL <sup>-1</sup>	24 h log CFU mL <sup>-1</sup>	
CE94 <i>L. brevis</i>	+	+	7.3 ± 0.1	6.0 ± 0.7	5.8 ± 0.5	7.3 ± 1.2	nd
CE85 <i>L. brevis</i>	+	+	7.3 ± 0.1	3.4 ± 1.1	5.6 ± 0.5	6.6 ± 1.1	6.1 ± 0.0/76.4%
CE42 <i>L. plantarum</i>	+++	+++	5.8 ± 0.8	0.0 ± 0.0	7.0 ± 0.6	5.3 ± 1.5	0.0 ± 0.0
CE60 <i>L. plantarum</i>	++	+++	7.8 ± 0.3	0.0 ± 0.0	7.0 ± 0.6	8.2 ± 0.3	nd
CE84 <i>L. plantarum</i>	+++	+++	8.1 ± 0.2	0.0 ± 0.0	6.5 ± 0.7	8.2 ± 0.3	6.5 ± 0.0/81.4%
CE83 <i>L. curvatus</i>	++	+++	7.5 ± 0.2	3.7 ± 0.2	7.1 ± 0.0	8.1 ± 0.0	6.3 ± 0.1/79.4%
CE47 <i>L. sakei</i>	+	++	6.7 ± 0.2	0.0 ± 0.0	3.2 ± 1.0	1.0 ± 1.4	nd
CE52 <i>Ln. mesenteroides</i>	+	–	7.2 ± 0.8	0.0 ± 0.0	7.2 ± 0.3	0.5 ± 0.8	nd
CE48 <i>Ln. mesenteroides</i>	+	+	7.8 ± 0.2	4.6 ± 1.0	7.3 ± 0.2	8.4 ± 0.0	nd
CE88 <i>Ln. citreum</i>	+	+	7.8 ± 0.4	0.0 ± 0.0	6.7 ± 0.5	4.5 ± 0.7	nd
CE54 <i>Ln. citreum</i>	+	+	7.9 ± 0.6	0.0 ± 0.0	5.9 ± 0.5	3.4 ± 0.2	nd
CE65 <i>P. pentosaceus</i>	++	+++	7.4 ± 0.1	3.4 ± 0.9	7.1 ± 0.1	3.9 ± 0.7	6.5 ± 0.1/81.6%
CE23 <i>P. pentosaceus</i>	+	++	7.7 ± 0.1	1.3 ± 0.9	6.0 ± 0.0	2.7 ± 0.4	nd
Q823 <i>L. plantarum</i>	+++	+++	7.3 ± 0.1	7.2 ± 0.2	7.3 ± 0.0	7.4 ± 0.1	5.9 ± 0.4/73.7%
Q11 <i>L. casei</i>	+++	+++	7.2 ± 0.3	1.5 ± 0.3	7.1 ± 0.2	5.3 ± 0.5	7.4 ± 0.3/92.5%
GG <i>L. rhamnosus</i>	+++	+++	7.2 ± 0.3	7.4 ± 0.0	7.1 ± 0.2	6.3 ± 0.2	5.5 ± 0.2/69.3%

LAB growth in MRS broth at 30 °C and 37 °C measured as Abs 420–580 nm at the beginning of stationary phase: +++ = >2.0; ++ = 1.9–1.7; + = 1.7–1.0; – = <1.0 <sup>b</sup>Average log no. of adhering lactobacilli in Caco-2 cell after 2 h incubation. Initial inoculums at approximately 1 × 10<sup>8</sup> CFU/mL (log 8.0). nd, not determined.

These tests are, however, rather qualitative, and the resistances of probiotic cultures to low pH and bile in food matrices during passage through the GIT might be greater than those seen in the physiological solutions used in the present study.

### 3.3.3. Adhesion to Caco-2 cells

The capacity of bacteria to adhere to the intestinal mucosa is a key factor in a strain's ability to function as desired in the intestine and thus have probiotic effects.

The adhesion ability to Caco-2 cells, which simulates the morphological and physiological characteristics of human enterocytes (Blum et al., 1999), was evaluated for 4 LAB strains (Table 8), belonging to different species, selected according to their ability to survive to the conditions resembling those of the GIT: *L. curvatus* CE83, *L. brevis* CE85, *P. pentosaceus* CE65, and also *L. plantarum* CE84 was tested despite its poor resistance to low pH. *L. rhamnosus* GG, *L. plantarum* Q823 and *L. plantarum* CE42 were used as positive and negative control, respectively. All the tested strains strongly adhered to the Caco-2 cells with adhesive properties even higher than those assessed in the positive control. *L. curvatus* CE83, *L. brevis* CE85 and *P. pentosaceus* CE65, due to their ability to survive to the conditions of the GIT and their capacity to adhere to the intestinal mucosa, could be suitable candidates to be used as probiotics.

**Table 9**  
Anti-listeria activity of lactic acid bacteria.

Bacterial culture	<i>L. innocua</i>	<i>L. monocytogenes</i>	<i>L. welshimeri</i>
CE94 <i>L. brevis</i>	–	–	–
CE85 <i>L. brevis</i>	–	–	–
CE42 <i>L. plantarum</i>	++	++	++
CE60 <i>L. plantarum</i>	++	++	++
CE84 <i>L. plantarum</i>	++	++	++
CE83 <i>L. curvatus</i>	–	–	–
CE47 <i>L. sakei</i>	–	+	+
CE52 <i>Ln. mesenteroides</i>	+	+	+
CE48 <i>Ln. mesenteroides</i>	–	–	–
CE88 <i>Ln. citreum</i>	–	+	–
CE54 <i>Ln. citreum</i>	–	+	–
CE65 <i>P. pentosaceus</i>	++	++	++
CE23 <i>P. pentosaceus</i>	+	–	++

Interpretation of zone diameter of inhibition – = no inhibition; + = 0.1–0.2 cm; ++ = 0.2–0.3 cm.

### 3.3.4. Anti-listeria activity

The inhibition of pathogenic bacteria, causing diarrhea or other diseases in the human intestine, is a desirable property for probiotic bacteria (Delgado et al., 2007) in order to balance the intestinal environment, and thereby improve host health. *L. plantarum* CE42, CE60, CE84 and *P. pentosaceus* CE65 showed high inhibitory activity against the *Listeria* species tested (*L. innocua*, *L. monocytogenes*, *L. welshimeri*) (Table 9). *Ln. citreum* CE88, CE54 were able to inhibit only *L. monocytogenes*, and *L. sakei* CE47 showed activity against *L. monocytogenes* and *L. welshimeri*. This inhibition could be due to the production of inhibitory substances, such as organic acids, bacteriocins or peroxide hydroxide (Juven, Schved, & Lindner, 1992).

## 4. Conclusions

Wheat bran sourdough proved a good source of several interesting microbial strains with potential for future applications. Excluding the strains resistant to clindamycin, *L. plantarum* CE42, CE60 and *P. pentosaceus* CE65, CE23 could have interesting technological applications due to their antifungal activity and EPS production. These strains also shown phytate-degrading activity on calcium and/or sodium phytate salts and could thus also be useful to improve mineral bioavailability of fermented products. Moreover, *P. pentosaceus* CE65 seems to be a suitable candidate for use as

probiotic. Further studies will be needed in order to test the effectiveness of these strains in improving the quality of fermented products and to better determine their suitability for specific applications.

## References

- Adimpong, D. B., Nielsen, D. S., Sørensen, K. I., Derckx, P. M., & Jespersen, L. (2012). Genotypic characterization and safety assessment of lactic acid bacteria from indigenous African fermented food products. *BMC Microbiology*, *12*, 75–86.
- Ammor, M. S., Belén Flórez, A., & Mayo, B. (2007). Antibiotic resistance in non-enterococcal lactic acid bacteria and bifidobacteria. *Food Microbiology*, *24*, 559–570.
- Anastasio, M., Pepe, O., Cirillo, T., Palomba, S., Blaiotta, G., & Villani, F. (2010). Selection and use of phytate-degrading LAB to improve cereal-based products by Mineral solubilization during dough fermentation. *Journal of Food Science*, *75*, M28–M35.
- Asahara, T., Shimizu, K., Nomoto, K., Hamabata, T., Ozawa, A., & Takeda, Y. (2004). Probiotic bifidobacteria protect mice from lethal infection with Shiga toxin-producing *Escherichia coli* O157: H7. *Infection and Immunity*, *72*, 2240–2247.
- Blum, S., Reiner, R., Schiffrin, E. J., Crittenden, R., Mattila-Sandholm, T., Ouwehand, A. C., et al. (1999). Adhesion studies for probiotics: need for validation and refinement. *Trends in Food Science & Technology*, *10*, 405–410.
- Cadena, J., Sreeramouju, P., Nair, S., Henao-Martinez, A., Jorgensen, J., & Patterson, J. E. (2012). Clindamycin-resistant methicillin-resistant *Staphylococcus aureus*: epidemiologic and molecular characteristics and associated clinical factors. *Diagnostic Microbiology and Infectious Disease*, *74*, 16–21.
- Carnevali, P., Ciati, R., Leporati, A., & Paese, M. (2007). Liquid sourdough fermentation: industrial application perspectives. *Food Microbiology*, *24*, 150–154.
- Coda, R., Nionelli, L., Rizzello, C. G., De Angelis, M., Tossut, P., & Gobbetti, M. (2010). Spelt and emmer flours: characterization of the lactic acid bacteria microbiota and selection of mixed autochthonous starters for bread making. *Journal of Applied Microbiology*, *108*, 925–935.
- Coda, R., Rizzello, C. G., Di Cagno, R., Trani, A., Cardinali, G., & Gobbetti, M. (2013). Antifungal activity of *Meyerozyma guilliermondii*: identification of active compounds synthesized during dough fermentation and their effect on long-term storage of wheat bread. *Food Microbiology*, *33*, 243–251.
- Dal Bello, F. D., Walter, J., Hertel, C., & Hammes, W. P. (2001). In vitro study of prebiotic properties of levan-type exopolysaccharides from lactobacilli and non-digestible carbohydrates using denaturing gradient gel electrophoresis. *Systematic and Applied Microbiology*, *24*, 232–237.
- De Angelis, M., Gallo, G., Corbo, M. R., Mc Sweeney, P. L. H., Faccia, A., Giovine, M., et al. (2003). Phytase activity in sourdough lactic acid bacteria: purification and characterization of a phytase from *Lactobacillus sanfranciscensis* CB1. *International Journal of Food Microbiology*, *87*, 259–270.
- Decock, P., & Cappelle, S. (2005). Bread technology and sourdough technology. *Trends in Food Science & Technology*, *16*, 113–120.
- Delgado, S., O'sullivan, E., Fitzgerald, G., & Mayo, B. (2007). Subtractive screening for probiotic properties of *Lactobacillus* species from the human gastrointestinal tract in the search for new probiotics. *Journal of Food Science*, *72*, M310–M315.
- EFSA-FEEDAP. (2012). Guidance on the assessment of bacterial susceptibility to antimicrobials of human and veterinary importance. *EFSA Journal*, *10*, 2740–2749.
- Fuller, R. (1992). *Probiotics: The scientific basis* (Vol. 1). London: Chapman and Hall.
- Galle, S., & Arendt, E. K. (2014). Exopolysaccharides from sourdough lactic acid bacteria. *Critical Reviews in Food Science and Nutrition*, *54*, 891–901.
- Garofalo, C., Zannini, E., Aquilanti, L., Silvestri, G., Fierro, O., Picariello, G., et al. (2012). Selection of sourdough lactobacilli with antifungal activity for use as biopreservatives in bakery products. *Journal of Agricultural and Food Chemistry*, *60*, 7719–7728.
- Gilliland, S. E., Staley, T. E., & Bush, L. J. (1984). Importance in bile tolerance of *Lactobacillus acidophilus* used as a dietary adjunct. *Journal of Dairy Science*, *67*, 3045–3051.
- Gobbetti, M. (1998). Interactions between lactic acid bacteria and yeasts in sourdoughs. *Trends in Food Science & Technology*, *9*, 267–274.
- Gobbetti, M., De Angelis, M., Arnault, P., Tossut, P., Corsetti, A., & Lavermicocca, P. (1999). Added pentosans in breadmaking: fermentations of derived pentoses by sourdough lactic acid bacteria. *Food Microbiology*, *16*, 409–418.
- Gruppen, H., Kormelink, F. J. M., & Voragen, A. G. J. (1993). Enzymic degradation of waterunextractable cell wall material and arabinoxylans from wheat flour. *Journal of Cereal Science*, *18*, 129–143.
- Gupta, R., & Srivastava, S. (2014). Antifungal effect of antimicrobial peptides (AMPs LR14) derived from *Lactobacillus plantarum* strain LR14 and their applications in prevention of grain spoilage. *Food Microbiology*, *42*, 1–7.
- International Standard ISO 10932/IDF 223. (2010). *Milk and milk products – Determination of the minimal inhibitory concentration (MIC) of antibiotics applicable to bifidobacteria and non-enterococcal lactic acid bacteria (LAB)*.
- Jacobsen, C. N., Nielsen, V. R., Hayford, A. E., Møller, P. L., Michaelsen, K. F., Paerregaard, A., et al. (1999). Screening of probiotic activities of forty-seven strains of *Lactobacillus* spp. by in vitro techniques and evaluation of the colonization ability of five selected strains in humans. *Applied and Environmental Microbiology*, *65*, 4949–4956.
- Juven, B. J., Schved, F., & Lindner, P. (1992). Antagonistic compounds produced by a chicken intestinal strain of *Lactobacillus acidophilus*. *Journal of Food Protection*, *55*, 157–161.
- Katina, K., Juvonen, R., Laitila, A., Flander, L., Nordlund, E., Kariluoto, S., et al. (2012). Fermented wheat bran as a functional ingredient in baking. *Cereal Chemistry*, *89*, 126–134.
- Katina, K., & Poutanen, K. (2013). Nutritional aspects of cereal fermentation with lactic acid bacteria and yeast. In M. Gobbetti, & M. Gänzle (Eds.), *Handbook on sourdough biotechnology* (pp. 229–242). New York: Springer Science + Business Media.
- Lacaze, G., Wick, M., & Cappelle, S. (2007). Emerging fermentation technologies: development of novel sourdoughs. *Food Microbiology*, *24*, 155–160.
- Lee, J., Yun, H. S., Cho, K. W., Oh, S., Kim, S. H., Chun, T., et al. (2011). Evaluation of probiotic characteristics of newly isolated *Lactobacillus* spp.: immune modulation and longevity. *International Journal of Food Microbiology*, *148*, 80–86.
- Magnusson, J., & Schnürer, J. (2001). *Lactobacillus coryniformis* subsp. *coryniformis* strain Si3 produces a broad-spectrum proteinaceous antifungal compound. *Applied and Environmental Microbiology*, *67*, 1–5.
- Manini, F., Brasca, M., Plumed-Ferrer, C., Morandi, S., Erba, D., & Casiraghi, M. C. (2014). Study of the chemical changes and evolution of microbiota during sourdough like fermentation of wheat bran. *Cereal Chemistry*, *91*, 342–349.
- Mathara, J. M., Schillinger, U., Kutima, P. M., Mbugua, S. K., Guigas, C., Franz, C., et al. (2008). Functional properties of *Lactobacillus plantarum* strains isolated from Maasai traditional fermented milk products in Kenya. *Current Microbiology*, *56*, 315–321.
- Messens, W., & De Vuyst, L. (2002). Inhibitory substances produced by *Lactobacilli* isolated from sourdoughs – a review. *International Journal of Food Microbiology*, *72*, 31–43.
- Minervini, F., De Angelis, M., Di Cagno, R., Pinto, D., Siragusa, S., Rizzello, C. G., et al. (2010). Robustness of *Lactobacillus plantarum* starters during daily propagation of wheat flour sourdough type I. *Food Microbiology*, *27*, 897–908.
- Pepe, O., Blajotta, G., Anastasio, M., Moschetti, G., Ercolini, D., & Villani, F. (2004). Technological and molecular diversity of *Lactobacillus plantarum* strains isolated from naturally fermented sourdoughs. *Systematic and Applied Microbiology*, *27*, 443–453.
- Poutanen, K., Flander, L., & Katina, K. (2009). Sourdough and cereal fermentation in a nutritional perspective. *Food Microbiology*, *26*, 693–699.
- Ruas-Madiedo, P., & De Los Reyes-Gavilán, C. G. (2005). *Invited review: methods for the screening, isolation, and characterization of exopolysaccharides produced by lactic acid bacteria*. *Journal of Dairy Science*, *88*, 843–856.
- Sabir, F., Beyatli, Y., Cokmus, C., & Onal-Darilmaz, D. (2010). Assessment of potential probiotic properties of *Lactobacillus* spp., *Lactococcus* spp., and *Pediococcus* spp. strains isolated from kefir. *Journal of Food Science*, *75*, M568–M573.
- Salmenkallio-Marttila, M., Katina, K., & Autio, K. (2001). Effect of bran fermentation on quality and microstructure of high-fibre wheat bread. *Cereal Chemistry*, *78*, 429–435.
- Smith, J. P., Daifas, D. P., El-Khoury, W., Koukoutsis, J., & El-Khoury, A. (2004). Shelf life and safety concerns of bakery products—a review. *Critical Reviews in Food Science and Nutrition*, *44*, 19–55.
- Soukoulis, C., Yonekura, L., Gan, H. H., Behboudi-Jobbehdar, S., Parmenter, C., & Fisk, I. (2014). Probiotic edible films as a new strategy for developing functional bakery products: the case of pan bread. *Food Hydrocolloids*, *39*, 231–242.
- Tiekink, M., & Gänzle, M. G. (2005). Exopolysaccharides from cereal-associated lactobacilli. *Trends in Food Science & Technology*, *16*, 79–84.



Contents lists available at ScienceDirect

## LWT - Food Science and Technology

journal homepage: [www.elsevier.com/locate/lwt](http://www.elsevier.com/locate/lwt)

# Rice starch and fructo-oligosaccharides as substitutes for phosphate and dextrose in whole muscle cooked hams: Sensory analysis and consumer preferences



Virginia C. Resconi<sup>a</sup>, Derek F. Keenan<sup>a</sup>, Marta Barahona<sup>a</sup>, Luis Guerrero<sup>b</sup>,  
Joseph P. Kerry<sup>c</sup>, Ruth M. Hamill<sup>a,\*</sup>

<sup>a</sup> Teagasc, Food Research Centre Ashtown, Dublin 15, Ireland

<sup>b</sup> IRTA, Finca Camps i Armet, 17121 Monells, Girona, Spain

<sup>c</sup> School of Food and Nutritional Sciences, UCC, Cork, Ireland

## ARTICLE INFO

### Article history:

Received 23 July 2015

Received in revised form

15 October 2015

Accepted 19 October 2015

Available online 22 October 2015

### Keywords:

Clean label

Pork

Response surface methodology

Triangle test

## ABSTRACT

Sensory characteristics and visual acceptability of cooked hams with rice starch (RS) and fructo-oligosaccharides (FOS) as substitutes for, respectively, sodium tripolyphosphate (STPP) and dextrose (Dex), were evaluated. Replacement of STPP with RS is associated with hams being less juicy, salty and springy, but more adhesive and could negatively affect appearance; but replacement of Dex by FOS had minimal sensory influence. The relative importance of product appearance, pack labels and price information cues in simulated purchasing decisions was also investigated. Consumer purchase choices were more influenced by product appearance than by pack labels referring to additives or price. Including labelling information regarding reduction or exclusion of phosphates may be more important than labels regarding a reduction in salt. For the Irish consumers studied here, the use of phosphates in cooked hams sounds artificial, unhealthy and unknown, whereas dietary fibre was perceived as healthy, natural and improving of the eating quality.

© 2015 Elsevier Ltd. All rights reserved.

## 1. Introduction

Many European consumers perceive processed meats as unhealthy and as containing high levels of harmful chemicals, fat and salt (Hauggaard, Hansen, Jensen, & Grunert, 2014). Furthermore, excess consumption of processed meat is associated with increased risk of developing coronary heart diseases and diabetes (Micha, Michas, & Mozaffarian, 2012). However, at the same time, many of these products are traditional and are regularly consumed as part of the typical diets of European consumers. Therefore, novel approaches to develop healthier versions of processed meat products, taking into consideration nutritional advice and legislation, are needed. Possible approaches include reducing and/or replacing artificial additives with clean label ingredients, or the inclusion of new healthy ingredients. Phosphate reduction and addition of fibre are two approaches that have potential to improve the perception and health profile of meat products. Research has shown that

dietary fibre can be successfully added to meat products to improve their healthiness (Fernández-Ginés, Fernández-López, Sayas-Barberá, & Pérez-Alvarez, 2005) and some products were/are available in the market generally (Jiménez-Colmenero, Reig, & Toldrá, 2006). If added in sufficient quantities, a health claim, such as “contains dietary fibre” could be included on the label (Regulation (EC) No 1924/2006).

Modification of traditional formulations to improve their health profile could, however, negatively impact technological and sensory characteristics of the traditional product. While instrumental, chemical and microbiological studies are useful to characterize the safety and can help to predict the organoleptic characteristics of the novel products, only sensory analysis can predict their sensory acceptability to consumers. For example, cooked hams prepared with two salt replacers (Ocean's Flavor: OF45, OF60) were found to have acceptable instrumental and safety characteristics, but had a low acceptability in flavour and aftertaste due to bitterness and further flavour optimization would be required before product launch (Pietrasik & Gaudette, 2014).

In a previous study aimed at improving the health profile of

\* Corresponding author.

E-mail address: [ruth.hamill@teagasc.ie](mailto:ruth.hamill@teagasc.ie) (R.M. Hamill).

**Table 1**  
Definitions of the descriptors used in the sensory analysis of the cooked ham.

Descriptor	Definition
Tenderness	Force required during the first bite between molars to deform the sample (0 = very hard to 10 = very tender).
Juiciness	Amount of perceived juice released from the product during mastication (0 = dry to 10 = very juicy).
Springiness	Degree and rapidity of recovery from a deforming force (compression by molar teeth, 0 = non-elastic to 10 = extremely springy).
Adhesiveness	Force required to remove material that adheres to the mouth (0 = non-adhesive to 10 = very adhesive)
Salty taste	Intensity of the taste characterised by sodium chloride (0 = non-salty to 10 = very salty)
Ham flavour	Intensity of the typical ham flavour (0 = non-flavour to 10 = very intense flavour)

traditional cooked ham, rice starch (RS) and fibre (fructo-oligosaccharides, FOS) were proposed as substitutes for phosphates (STPP) and sugar (dextrose, Dex) (Resconi et al., 2015) to assess the potential of cooked ham containing FOS as a source of fibre. Instrumental and chemical analysis demonstrated that the healthier products had acceptable technological characteristics but differed from the conventional product in certain aspects. Since STPP substitution with RS affected water retention and instrumental texture (Resconi et al., 2015), the sensorially perceived juiciness and texture of a ham with total or partial substitution of phosphates could also change with respect to a traditional cooked ham formulation (with 0.3% added phosphates). RS inclusion could further affect the acceptability of the appearance since starch gel pockets were visible in the hams (Resconi et al., 2015). It is also important to establish consumer attitudes and acceptance of modifications to traditional products for example, addition of fibre in cooked ham products. Previous studies suggest that consumers readily accept bioactive compounds in dairy products (Tobin, O'Sullivan, Hamill, & Kerry, 2014), such as yoghurt with added oligosaccharides/fibre or omega-3 fatty acids. However, is still uncertain if consumers accept similar compounds in traditional meat based products.

In an initial study, the effect of different brine ingredient components (STPP, RS, FOS and Dex) on instrumental and chemical quality of cooked ham (Resconi et al., 2015) was investigated and now we aim to study their effects on sensory characteristics and visual acceptability. The second objective is to evaluate the relative importance of appearance, ingredient labels and price cues in simulated purchasing decisions. A questionnaire was also conducted to obtain the socio-demographic and consumption habits information of consumers and to describe their views and concerns related to cooked ham.

## 2. Materials and methods

### 2.1. Ham preparation

Hams were manufactured in the Meat Industry Development Unit (Teagasc, Food Research Centre, Ashdown, Ireland). Four ingredients, STPP (Na<sub>5</sub>P<sub>3</sub>O<sub>10</sub>, Redbrook Ingredient Services Ltd., Ireland), RS (Remyline XS, Beneo, Belgium), Dex (Roquette Freres, Lestrem, France) and FOS (Beneo ORAFIT<sup>®</sup> Synergy1, Beneo, Belgium) were used for each formulation according to the experimental design. Pickling salt at 2.5% and sodium ascorbate at 0.05% w/w in injected muscle was also included in all the hams. Two pork muscles, *Biceps femoris* (BF) and *Semimembranosus* (SM) from female carcasses (Rosderra Irish Meats Group, Edenderry, Ireland) were pumped to 120%, using a 20-needle brine injector and then tumbled for 12 h (6 rpm: 30 min on/off). Tumbled muscles were netted, vacuum packed, heat shrink-wrapped and steam cooked at 85 °C, 85% RH, to a core temperature of 72 °C. After cooking, hams were chilled to 2–4 °C for 24 h, sliced at 2.5 mm thickness, vacuum packed and stored at 2–4 °C.

### 2.2. Sensory analysis (trained panelists)

#### 2.2.1. Triangular test

For the triangular test, three pairs of cooked hams with different combination of the four ingredients (STPP, RS, Dex, FOS) from *B. femoris* and *Semimembranosus* muscles were compared:

- control vs. RS 0.30 (STPP 0%, RS 0.3%, Dex 0.2%, FOS 0%).
- control vs. RS 1.17 (STPP 0%, RS 1.17%, Dex 0.2%, FOS 0%).
- control vs. FOS (STPP 0.3%, RS 0%, Dex 0.2%, FOS 3%).

A triangular test for the 'no difference hypothesis' was performed according to the British Standard ISO 4120 (ISO, 2004). A 16 member panel, from a pool of screened assessors selected for their sensory performance (ISO-8586-1, 1993), evaluated two triads (one for each muscle) per pair comparison in individual booths under red light. Muscles from the left and the right side from the same animal were compared.

#### 2.2.2. Descriptive test

A response surface methodology (RSM) based on d-optimal experiment was designed using Design Expert software (v. 7.6.1, Stat-Ease Inc.). This is described in detail in Resconi et al. (2015), where instrumental and chemical data is presented. Briefly, four

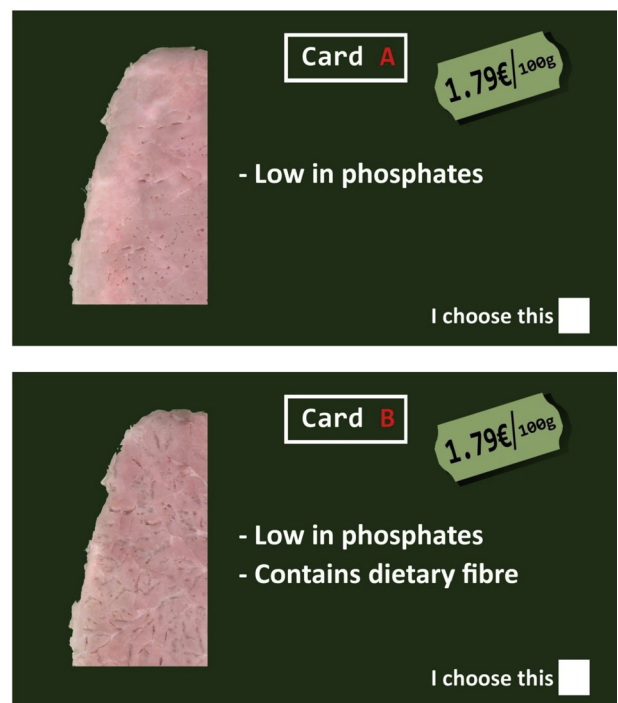


**Fig. 1.** Example of the pair comparison used in the choice based conjoint analysis. Card A shows an image with a ham without gel pockets (Image 1) and in the card B, the gel pockets are visible (Image 2).

**Table 2**  
Triangular test for 'no difference hypothesis' in cooked hams prepared with different formulations.

	control vs. RS 0.30%	control vs. RS 1.17%	control vs. FOS 3%
<b>Biceps femoris</b> (n = 16)			
Correct responses	31.25%	75.00%	75.00%
P value	>0.200	0.001	0.001
<b>Semimembranosus</b> (n = 16)			
Correct responses	81.25%	68.75%	31.25%
P value	<0.001	0.010	>0.200
<b>Both muscles</b> (n = 32)			
Correct responses	56.25%	71.88%	53.13%
P value	0.010	<0.001	<0.050

Control: phosphate 0.3%. RS: phosphate 0%, rice starch 0.30%/1.17%, respectively. FOS: phosphate 0.3%, fructo-oligosaccharides 3.00%. All expressed by weight in the injected muscle (picking salt at 2.5%, dextrose at 0.2% and sodium ascorbate at 0.05% were also included in each ham).

**Table 3**  
Response surface models for eating quality characteristics of whole cooked hams prepared with different ingredients and muscles (25 runs per muscle).

	Tenderness	Juiciness	Springiness	Adhesiveness	Salty taste	Ham flavour
Model	Linear	Linear	Linear	2FI	Linear	2FI
p model	0.017	<0.001	0.003	<0.001	0.001	0.037
p lack of fit	ns	0.033	ns	ns	ns	ns
R <sup>2</sup>	0.114	0.440	0.224	0.512	0.250	0.286
F values						
STPP		15.19***		21.27***	8.47**	
RS		4.23*		0.02 ns		0.10 ns
Dex				0.67 ns		0.44 ns
FOS			3.55 ns	0.79 ns		0.06 ns
Muscle	6.17*	17.34***	10.05**	2.95 ns	7.22**	0.23 ns
STPP × Dex				8.46**		
RS × Dex						2.72 ns
RS × FOS				2.51 ns		9.43**
Dex × Muscle				3.32 ns		3.22 ns

Ns:  $p > 0.05$ , \* $p \leq 0.05$ , \*\* $p \leq 0.01$ , \*\*\* $p \leq 0.001$ . 2FI: two level full factorial.

numerical factors (ingredients) were included: STPP (0–0.3% w/w in injected muscle), RS (0–1.2%), Dex (0–0.2%) and FOS (0–3%), with the following constraints: STPP + RS  $\geq$  0.3%; Dex + FOS  $\geq$  0.2%; STPP + RS + Dex + FOS  $\leq$  3.3%. The 25 brine formulations generated by the software were used to inject the *B. femoris* and *Semimembranosus* muscles for ham manufacturing. The preparation of the hams was carried out in 25 sequential formulations (runs) over six weeks (4–5 runs per week). Control hams (STPP 0.3, RS 0, Dex 0.2, FOS 0) were also prepared every week to ensure consistency between the preparations.

The panel (8 members) was chosen from a pool of screened assessors selected for their sensory performance (ISO-8586-1, 1993). They were experienced in sensory analyses of meat products, and three training sessions were conducted to familiarise the panelists with the specific characteristics of the hams under study.

The sensory profile was developed in 2 additional sessions. The resultant descriptors are described in Table 1. Scores of the samples

per plate were indicated in a 10 cm structured lineal scale, transformed into a numerical scale (0–100) for the statistical analysis. The quantitative descriptive test was performed in individual cabins with controlled environmental conditions under red light (ISO-8589, 1988). The test comprised 6 sessions, 4 plates per session (2 plates per muscle) and 3 samples per plate (2 runs + control), except in the last session in which 2 of the 4 plates had 4 samples (3 runs + control).

Cross-sectional slices of each ham, 2 mm thick, were cut into three portions, wrapped in aluminium foil and marked with a random 3-digit code. To avoid the possible effects of the order of presentation and first-order carryover effects, the samples were presented in a balanced order (Macfie, Bratchell, Greenhoff, & Vallis, 1989). To cleanse their palate between samples, panelists were given bottled water and unsalted crackers. Samples were analysed fresh on day 7 after cooking. The mean per muscle per run was obtained and results were analysed using Design Expert

**Table 4**  
Pearson's correlations coefficients between responses from the trained<sup>1</sup> and consumer<sup>2</sup> sensory panels and factors for whole muscle cooked hams (n = 50).

	STPP	RS	Dex	FOS	Muscle
Tenderness <sup>1</sup>	0.070 ns	0.146 ns	0.182 ns	-0.118 ns	0.338*
Juiciness <sup>1</sup>	0.421**	0.208 ns	0.099 ns	-0.173 ns	-0.460***
Springiness <sup>1</sup>	0.184 ns	-0.094 ns	0.186 ns	-0.242 ns	-0.407**
Adhesiveness <sup>1</sup>	-0.521***	0.068 ns	0.057 ns	0.234 ns	0.183 ns
Salty taste <sup>1</sup>	0.367**	0.181 ns	0.141 ns	-0.240 ns	-0.339*
Ham flavour <sup>1</sup>	-0.189 ns	0.163 ns	-0.063 ns	0.018 ns	0.058 ns
Overall visual liking <sup>2</sup>	0.236 ns	0.009 ns	-0.053 ns	-0.094 ns	
Colour acceptability <sup>2</sup>	0.152 ns	0.144 ns	0.043 ns	-0.050 ns	
Visual texture acceptability <sup>2</sup>	0.273 ns	0.044 ns	-0.089 ns	-0.228 ns	
Willingness to buy (%) <sup>2</sup>	0.087 ns	0.279 ns	-0.099 ns	-0.084 ns	

ns: not significant; \* $p \leq 0.05$ ; \*\* $p \leq 0.01$ ; \*\*\* $p \leq 0.001$ .

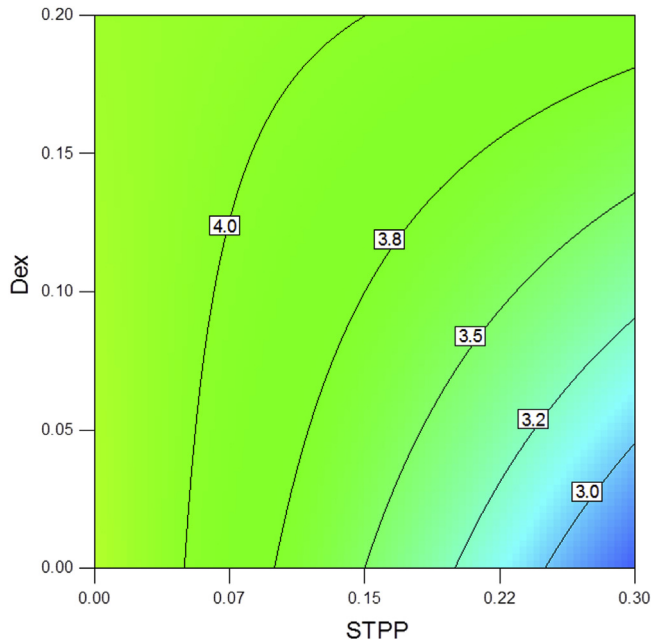


**Fig. 2.** Contour of the response surface model for the sensory attribute 'adhesiveness' in whole muscle cooked hams, as affected by the inclusion of dextrose (Dex) and sodium tripolyphosphates (STPP). The remaining factors were fixed at the following settings: RS: 0.30, FOS: 0.20, M: average. RS: rice starch; FOS: fructo-oligosaccharides; M: muscle. The levels of the ingredients are expressed in % by weight of the injected muscle.

software. The data on the sensory attributes along with the technological and instrumental characteristics published in Resconi et al. (2015) were subjected to a Principal Component Analysis using the statistical software XLStat (version 2013.2.04). Pearson correlations between responses and the factors were conducted using SPSS (version 18.0).

### 2.3. Consumer analysis

The target was 100 Irish (or resident of Ireland for more than 10

years) residents from the province of Leinster, regular consumers of cooked ham, women and men, aged 20–64 years. The survey was divided into three sections: the visual acceptability study, a choice-based conjoint analysis and a questionnaire.

#### 2.3.1. Visual acceptability

**2.3.1.1. Image acquisition.** The image acquisition was performed on *B. femoris* muscles, the same day of slicing. Slices were held at room temperature for 30 min; removed from the vacuum package, blotted dry with tissue paper, individually placed in on the glass plate of the scanner (HPscanjet 5590 flatbed scanner with HP Photo & Imaging Gallery software, version 1.1) together with a graduated colour card (QPCard 201) and covered with a laminated green sheet of paper for colour contrast. The scanner was cover to exclude external light sources. The system used ensured consistent illumination.

**2.3.1.2. Experimental design and evaluation.** The images obtained were colour corrected (QPcolorsoft 501 software, version 2.0) and Adobe Photoshop CS6 (version 13.0) was used to homogenize the background and size the images for printing the jpeg files, ensuring the size of the ham slices was controlled. Ham images with 3-digit random number codes were randomly presented and consumers were asked to indicate the level of acceptability using a seven-point scale between *I dislike extremely* and *I like extremely* for overall visual appearance, colour and texture, and their willingness to buy the hams (yes or no). The balanced incomplete block design (Cochran & Cox, 1978) consisted of 25 runs (as described in Section 2.2.2), 4 treatments for each consumer and 16 repetitions. A control slice of cooked ham was included in each of the 100 comparisons. The mean and the percentage of consumers willing to buy the hams were obtained for the 25 runs and statistical analysis were performed with Design Expert software.

#### 2.3.2. Choice-based conjoint analysis

The choice-based conjoint analysis was designed and analysed using the XLStat software (version 2013.2.04), using a quarter factorial design with 12 profiles, 10 comparisons per consumer (presented randomly), and 2 options/cards per comparison (Fig. 1).

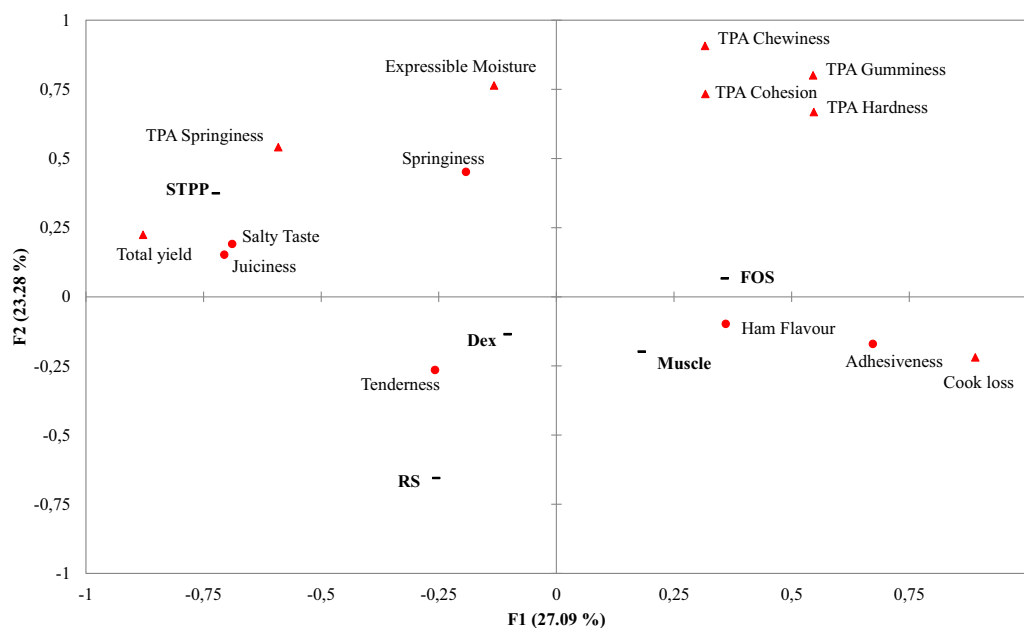


**Fig. 3.** Principal component analysis of the sensory attributes and technological and instrumental analysis of cooked hams (Resconi et al., 2015), as affected by ingredients: phosphates (STPP), rice starch (RS), dextrose (Dex) and fructo-oligosaccharides (FOS); and muscle type: *Semimembranosus* and *Biceps femoris*.

Detail of the design is presented in the [Supplementary material \(Tables A1 and A2\)](#). Five factors were studied:

- Appearance: a cooked ham image without perceptible starch gel pockets (Image 1) or with perceptible starch gels pockets (Image 2). The images obtained were edited with Adobe Photoshop to give an appearance of a similar size, colour and level of external fat.
- Phosphate label: *No added phosphates*; *Low in phosphates*; no label
- Fibre label: *Contains dietary fibre*; no label
- Salt label: *Low in salt*; no label
- Price label: 1.79 €/100 g; 1.99 €/100 g. The prices were between the ranges found at commercial level for high quality hams in Dublin in March 2013.

### 2.3.3. Questionnaire

The questionnaire consisted of 18 questions (see section B in the [Supplementary material](#)) in relation to the characteristics of the consumer, consumption habits of cooked ham and perceptions on the product in general and the ingredients studied in particular. The frequency of responses was obtained to analyses the data.

## 3. Results and discussion

### 3.1. Sensory analysis

The triangular test showed differences in the eating characteristics between control hams and hams containing RS at 0.3% without phosphates in SM (Table 2). Similar results were observed in the two muscles (SM and BF) when comparing controls with hams at higher levels of RS (1.17%). The results of the descriptive sensory analysis (Tables 3 and 4, Figs. 2 and 3) could help to explain the differences found by the triangular test, since particularly STPP, but also RS, affected some attributes (juiciness, adhesiveness and salty taste). At the same time, results of the processing and instrumental analysis (cook loss, expressible moisture, texture profile analysis) published earlier also reflected these results (Fig. 2, Resconi et al., 2015). The addition of FOS at 3% modified the sensory characteristics of the *B. femoris* hams compared to controls (Table 2), with the most commonly cited panelists' comments referring to changes in texture, juiciness and intensity of salty taste.

The response surface models for the descriptive sensory analysis showed  $R^2$  lower than 0.3 for tenderness, springiness, salty taste and ham flavour, while lack of fit was significant for juiciness, which means a low prediction and validity of these models (Table 3). Adhesiveness produced a two-factor interaction model with a  $R^2$  higher than 0.50, which indicates an evident decrease with the addition of STPP when no dextrose is added and a less pronounced decrease when it is included (Fig. 2). With the exception of adhesiveness, the response surface models were not able to identify clear effects of the ingredients (STPP, RS, Dex and FOS) and muscle type on the sensory responses, as the triangular test had shown. It should be considered that in the triangular test only extreme treatments were compared and that in discrimination tests subtle differences are better perceived than in descriptive methods (Meilgaard, Carr, & Civille, 1991).

A principal component analysis (PCA) analysis was carried out to permit visualisation of relationships and trends within the sensory data, and to compare the sensory attributes with previously published (Resconi et al., 2015) processing and instrumental data. Phosphates were positively correlated with juiciness, salty taste and springiness (instrumental and sensory measurements), and negatively with adhesiveness (Fig. 3), as confirmed by the Pearson

**Table 5**

Socio-demographic characteristics of consumers (N: number of answers obtained) residents from the province of Leinster (Ireland).

<b>Gender (N 100)<sup>a</sup></b>	
Male	49.0%
Female	51.0%
<b>Age (N 100)<sup>a</sup></b>	
20–34	47.0%
35–49	25.0%
50–64	28.0%
<b>Nationality (N 100)<sup>a</sup></b>	
Irish	95.0%
Other	5.0%
<b>Population (N 97)<sup>a</sup></b>	
≥100,000 inhabitants	76.3%
<100,000 inhabitants	23.7%
<b>Level of education (N 100)<sup>a</sup></b>	
Some primary degree (not complete)	1.0%
Primary or equivalent	2.0%
Intermediate/Junior/Group Certificate or equivalent	4.0%
Leaving certificate or equivalent	15.0%
Diploma/Certificate	29.0%
Primary degree/Nursing Qualification	13.0%
Postgraduate/Higher Degree	32.0%
Other	4.0%
<b>Employment status (N 100)<sup>a</sup></b>	
Working for payment or profit	77.0%
Working in the home	4.0%
Retired	3.0%
Unemployed	2.0%
Student	11.0%
Government/employment training scheme	1.0%
Unable to work due to permanent sickness/disability	1.0%
Other	1.0%
<b>Occupation (N 94)<sup>b</sup></b>	
Administrative and secretarial occupations	12.4%
Associate professional and technical occupations	7.9%
Caring, leisure and other service occupations	5.6%
Elementary occupations	5.6%
Managers, directors and senior officials	13.5%
Professional	36.0%
Sales and customer service occupations	7.9%
Skilled trades occupations	9.0%
Unemployed	2.2%

<sup>a</sup> Percentages from total answers.

<sup>b</sup> Percentage from total answers subtracting students.

correlations (Table 4). These results could be explained by the effect of phosphates in enhancing the retention of water and weakening the myofibrillar structure (Keenan, Desmond, Hayes, Kenny, & Kerry, 2010; Sheard, Nute, Richardson, Perry, & Taylor, 1999). Saltiness perception could be due to the added salt (sodium tripolyphosphates), but could also be related to a higher release of sodium in the

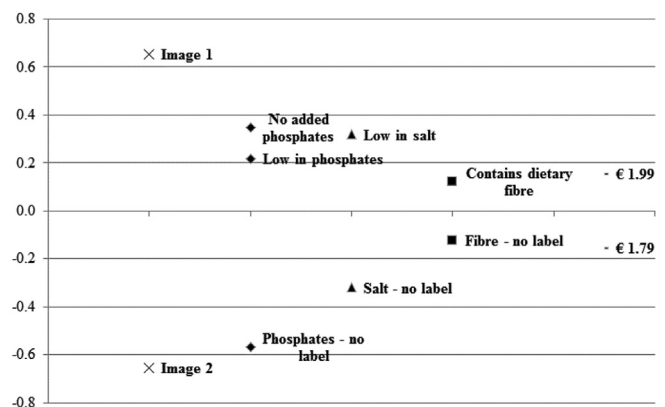


**Fig. 4.** Utility values for each level of the factors studied in the choice based conjoint analysis.

**Table 6**

Cooked ham consumption habits (N: number of answers obtained).

Frequency of consumption (N 97)		
Few times per week	10.3%	
Once per month	10.3%	
Two-three times per month	23.7%	
Once a week	20.6%	
Two-four times per week	32.0%	
Once a day	3.1%	
Manner of consumption (multiple choice, 97 consumers)		
	Yes	No
Sandwich/snack	92.8%	7.2%
Main meal lunch/dinner	54.6%	45.4%
Other (salads, etc.)	6.2%	93.8%
Type of cooked ham usually bought (multiple choice, 97 consumers)		
	Yes	No
Cooked ham slices tray-packed	78.4%	21.6%
Cooked ham slices in a deli counter	45.4%	54.6%
Whole piece of cooked pork ham	25.8%	74.2%
Whole piece of raw pork ham and cook it at home	54.6%	45.4%
Usually cooked ham at home is bought by (N 97)		
Themselves	66.0%	
Others	34.0%	
Wife	40.0%	
Husband	13.3%	
Mother	20.0%	
Parents	26.7%	

mouth due to the effects of phosphate on texture, e.g. increased juiciness (Engel, Nicklaus, Septier, Salles, & Quéré, 2000; Lawrence et al., 2012). RS was positively related to sensory tenderness and negatively to most of the instrumental texture parameters (Fig. 3), probably due to the increased retention of the loosely bound water (Resconi et al., 2015). Dextrose is usually added to improve cooked ham flavour (Toldrà, Mora, & Flores, 2010), however no such effect was found in our study. Although FOS co-localised on the PCA plot with ham flavour intensity (Fig. 3), their correlation was not significant ( $p > 0.05$ ). Other studies also found no effect of FOS on flavour in meat products (Cáceres, García, Toro, & Selgas, 2004; dos Santos, Campagnol, Pacheco, & Pollonio, 2012; García, Cáceres, & Selgas, 2006). Finally, muscle type was related to juiciness, springiness, saltiness and tenderness (Fig. 3, Table 4), with the *Biceps femoris* hams less tender (mean value 5.9), springier (5.2), saltier (6.2) and juicier (5.1) compared to *Semimembranosus* (mean values of 6.5, 4.6, 5.5, 4.2, respectively for each attribute), which could be explained partially by the higher cross-sectional fibre area and thicker peri- and endomy- sium of the *Biceps femoris* muscle (Lachowicz, Sobczak, Gajowiecki, & Żych, 2003).

### 3.2. Consumer analysis

#### 3.2.1. Visual acceptability

Table 5 shows the socio-demographic characteristics of the consumers studied. While in our survey there was a lower percentage of consumers from middle age compared with the Central

Statistics Office (CSO) data from the province of Leinster, Ireland (2011), the differences were not abrupt, and therefore gender, population share and age were quite well represented in the study (20–34 years: 39.6%, 35–49 years: 35.7%, 50–64: 24.8%), according to CSO (2011). Regarding education level and occupation, while most of the groups were present, more professionals and higher educated people were sampled compared to the actual population of Leinster.

Changes in L, a\* and b\* have been reported with FOS inclusion in mortadela, but similarly to this study FOS did not affect colour liking (Cáceres et al., 2004). In fact, response surface models were not significant for the acceptability of any visual appearance (overall, colour and texture) scores or for the consumers' willingness to buy ( $p > 0.05$ ), which means that none of the ingredients evaluated had a statistical effect on the appearance of the hams. The ingredients tested in this work were previously studied for instrumental colour and they showed significant effects (Resconi et al., 2015), but these changes were not perceived as important for consumers. Because slices from entire muscles were used, images differed in multiple visual characteristics, such as shape, marbling or presence of spots, etc.; which were not included in the models. This potentially diluted any subtle differences due to the experimental variables and possibly affected acceptability scores. However, this is reflective of normal variation in commercially produced artisanal ham. Consumers differing sensitivities and the high variability and complexity of ham samples was likely a factor. In fact, a previous study reached a similar conclusion, since

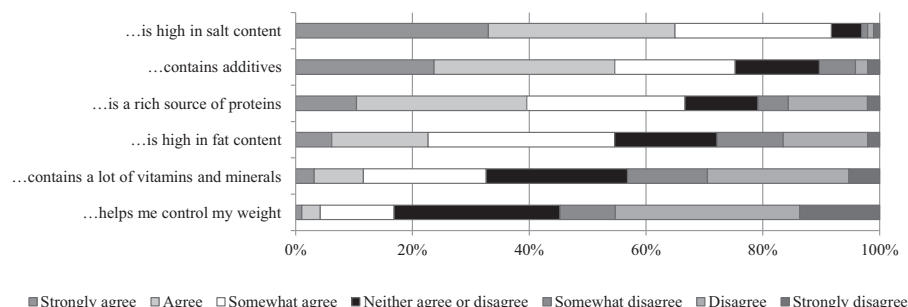


Fig. 5. Level of agreement with the following statements. Cooked ham...

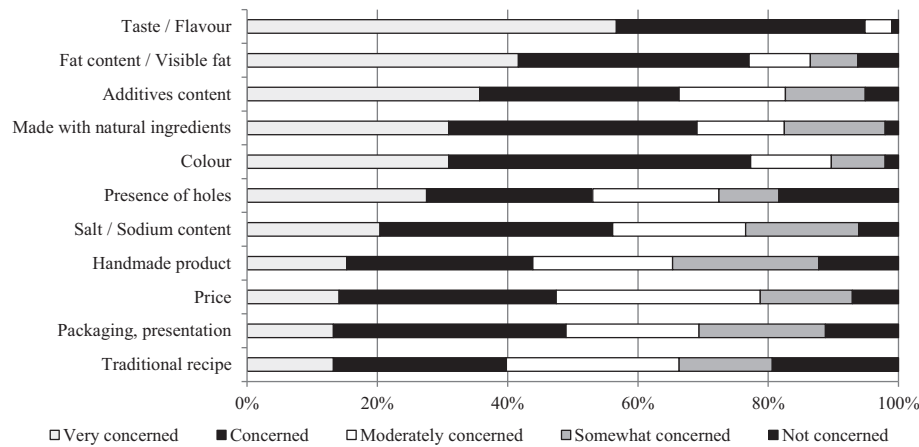


Fig. 6. Any concerns regarding aspects of cooked ham.

digitized colour and texture features permitted ham classification by technological quality (yield and processing characteristics), but not by sensory appearance or visual acceptability (Iqbal, Valous, Mendoza, & Da-Wen Sun, 2010).

### 3.2.2. Choice-based conjoint analysis

The results of the conjoint analysis show not only that Irish consumers prefer to choose images without gel pockets (Image 1, Fig. 4), but also that for them this cue was more important in the simulated purchase decision compared to extrinsic cues, i.e., labels regarding the use of additives and price. The relative importance of the factors was as follows: appearance 38.2%; phosphate label, 26.8%; salt label, 18.7%; price, 9.0%; and finally, dietary fibre-related label (7.3%). In the study of González-Viñas, Caballero, Gallego, and García Ruiz (2004), the appetizing aspect (illustration) of a frankfurter was also considered the most important criteria for Spanish consumers when purchasing. The lack of knowledge of what causes observed gel pockets could be a cause of concern by consumers, as Cilla et al. (2006) found for white spots in cured hams.

The use of labels “low in phosphates” and particularly “no added phosphates” in cooked hams did, however, positively influence choices (Fig. 4). The utilities for phosphates “no label” are  $-0.57$ , whereas  $-0.32$  correspond to “no label” regarding salt. Therefore, in a simulated market situation, a ham packed without information about a reduction or an exclusion of phosphates, could strongly

affect consumer choice, even more than the absence of labels regarding a reduction of salt, despite the fact that consumers are generally aware of the harmful effect of diets high in sodium/salt (Kim, Lopetcharat, Gerard, & Drake, 2012) and are perhaps less familiar with the term phosphate.

For the factor ‘price’, the most expensive was preferred (Fig. 4), probably because it was perceived as an indication of quality, as found by Bello Acebrón and Calvo Dopico (2000). However, it should be taken into account that consumers could be reluctant to state the real influence of price on their choices (Morales, Guerrero, Claret, Guàrdia, & Gou, 2008).

To the best of our knowledge there are no cooked hams with added dietary fibre available at commercial level. Higher quality hams are generally considered to be those with lower addition of brine (water and additives) and minor processing (Iqbal et al., 2010), such as those studied here, and the inclusion of fibre in such products could be unfamiliar to consumers and may be perceived as damaging the traditional character of the product (Guerrero et al., 2009). However, although they weren't familiar with the inclusion of fibre in ham, the product was perceived positively by Irish consumers. Other studies have also shown that the addition of healthy ingredients in meat products and generally in foods could be appealing to consumers (Haugard et al., 2014; Kim et al., 2012; Tobin et al., 2014), especially for health conscious consumers (Baixauli, Salvador, Hough, & Fiszman, 2008). Even though in our study, fibre was perceived favourably, the importance compared with other cues evaluated was low, and therefore, commercial decisions to produce this novel and healthy type of hams should be carefully considered, due to the additional costs involved in production. It should be taken into account that although consumers might be willing to buy healthier meat products, they are not always keen to pay more for them (Tobin et al., 2014). The results of the present study reflect the average decision made by consumers. Perhaps within the population, there might be a niche market much more interested in this type of product.

### 3.2.3. Questionnaire

In Ireland, sausages and cooked ham are the most commonly eaten meats every day (SAFEFOOD, 2008). Cooked ham consumption habits of the population sampled are shown in Table 6. It was a pre-requisite to be a consumer of cooked ham, and most of those surveyed consumed ham frequently in sandwiches or snacks and/or as a main meal. It is traditional in Ireland to buy whole raw pork hams to cook at home for lunch or dinner, and this style of ham consumption was reflected in this study (55% of responses).

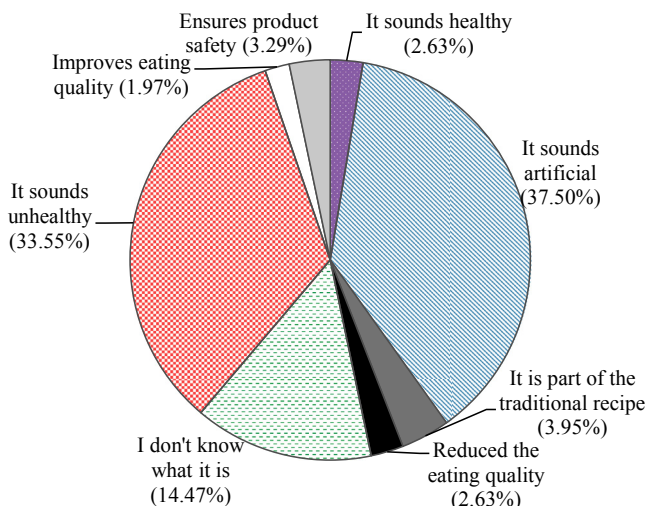


Fig. 7. Consumers' perceptions of the use of phosphates in cooked ham.

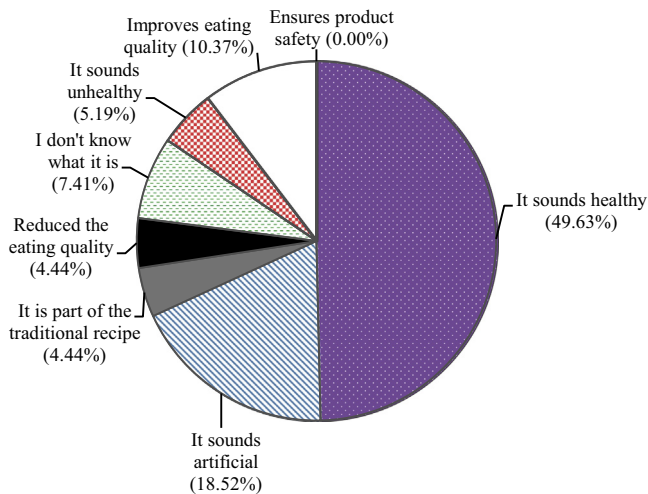


Fig. 8. Consumers' perceptions of the use of dietary fibre in cooked ham.

However, most interviewed consumers buy cooked ham slices tray-packed.

Perception of cooked ham ranged from slightly unhealthy to slightly healthy for 85% of the survey respondents, perhaps due to their perception of ham as a product high in salt and additives (Fig. 5). Most recognized is that cooked ham is a rich source of protein, but more than 50% also perceive it as being high in fat, although this is not actually the case for this meat product (Vandendriessche, 2008). Meat products are generally considered unhealthy by 36–40 year old women and people that consume few or no meat products, although more than 50% considers them healthy as part of an overall balanced diet (Tobin et al., 2014). However, ham is considered healthier or less processed compared to other meat products (SAFEFOOD, 2008).

Overall the responses in our study showed that consumers are health conscious; in fact they asserted they tried to follow a healthy diet frequently (74% of respondents) or always (20%), and 83% considered their health status good or very good. According to the study of Tobin et al. (2014) concerns around meat products were related mainly to the use of salts (80%), fat (60%) and chemicals (50%). In our study, apart from fat and additives, other highly important concerns were the taste and colour of cooked ham, and almost 20% of respondents were not concerned at all by the presence of holes, even though it is considered a defect unappealing to consumers by Hullberg, Johansson, and Lundström (2005) or by the use of a traditional recipe (Fig. 6). The negative view of consumers about the use of phosphates (Fig. 7) in cooked ham was because it sounds artificial, unhealthy and is unknown, whereas the use of dietary fibre (Fig. 8) was perceived as healthy, and although some consumers perceived it as artificial, some also think that it could improve the eating quality of the product. Previous studies have shown that labelling could affect consumer perceptions (Baixauli et al., 2008; Morales, Aguiar, Subiabre, & Realini, 2013). This could mean that, regardless a real effect on sensory parameters, the acceptability could improve by using the label “contains dietary fibre” in cooked hams. In fact, Baixauli et al. (2008), found an increase in liking scores of wholemeal muffins when information was given to the consumers compared to a blind tasting.

#### 4. Conclusion

Due to the negative attitude of consumers toward the term phosphates, further efforts should be conducted in order to reduce

or exclude this additive in meat products. The substitute proposed in this study, rice starch, could negatively affect the appearance of whole cooked hams and modified slightly the eating characteristics of the traditional product. However, at the same time if more information about the product is provided, it could mean that the product is perceived to be trustworthy. Consumers value positively the inclusion of novel healthy ingredients in cooked ham, such as fibre (fructo-oligosaccharides), that could be used also to replace sugars and showed subtle/null sensory influence in terms of visual acceptability and eating quality.

#### Acknowledgements

Research funding was provided under the National Development Plan, through the Food Institutional Research Measure (08/RD/TAFRC/671), administered by the Department of Agriculture, Food and the Marine, Ireland. We acknowledge the technical support of Eugene Vesey, Sophie Gough and Hamza Chakhman, and the advice of Maeve Henchion and Sinéad McCarthy in designing the consumer questionnaire and to Sergi Real Vidal for designing the cards for the choice-based conjoint study. We are also grateful to panelists and consumers for their voluntary participation in the study.

#### Appendix A. Supplementary data

Supplementary data related to this article can be found at <http://dx.doi.org/10.1016/j.lwt.2015.10.048>.

#### References

- Baixauli, R., Salvador, A., Hough, G., & Fiszman, S. M. (2008). How information about fibre (traditional and resistant starch) influences consumer acceptance of muffins. *Food Quality and Preference*, 19(7), 628–635.
- Bello Acebrón, L., & Calvo Dopico, D. (2000). The importance of intrinsic and extrinsic cues to expected and experienced quality: an empirical application for beef. *Food Quality and Preference*, 11(3), 229–238.
- Cáceres, E., García, M. L., Toro, J., & Selgas, M. D. (2004). The effect of fructooligosaccharides on the sensory characteristics of cooked sausages. *Meat Science*, 68(1), 87–96.
- Cilla, I., Martínez, L., Guerrero, L., Guàrdia, M. D., Arnau, J., Altarriba, J., et al. (2006). Consumer beliefs and attitudes towards dry-cured ham and protected designation of origin Teruel Ham in two Spanish regions differing in product knowledge. *Food Science and Technology International*, 12(3), 229–240.
- Cochran, W., & Cox, G. (1978). *Diseños experimentales*. Mexico: Trillias.
- CSO. (2011). *Central Statistics Office*.
- Engel, E., Nicklaus, S., Septier, C., Salles, C., & Quéré, J. L. L. (2000). Taste active compounds in a goat cheese water-soluble extract. 2. Determination of the relative impact of water-soluble extract components on its taste using omission tests. *Journal of Agricultural and Food Chemistry*, 48(9), 4260–4267.
- Fernández-Ginés, J. M., Fernández-López, J., Sayas-Barberá, E., & Pérez-Alvarez, J. A. (2005). Meat products as functional foods: a review. *Journal of Food Science*, 70(2), R37–R43.
- García, M. L., Cáceres, E., & Selgas, M. D. (2006). Effect of inulin on the textural and sensory properties of mortadella, a Spanish cooked meat product. *International Journal of Food Science & Technology*, 41(10), 1207–1215.
- González-Viñas, M. A., Caballero, A. B., Gallego, I., & García Ruiz, A. (2004). Evaluation of the physico-chemical, rheological and sensory characteristics of commercially available Frankfurters in Spain and consumer preferences. *Meat Science*, 67(4), 633–641.
- Guerrero, L., Guàrdia, M. D., Xicola, J., Verbeke, W., Vanhonacker, F., Zakowska-Biemans, S., et al. (2009). Consumer-driven definition of traditional food products and innovation in traditional foods. A qualitative cross-cultural study. *Appetite*, 52(2), 345–354.
- Haugaard, P., Hansen, F., Jensen, M., & Grunert, K. G. (2014). Consumer attitudes toward new technique for preserving organic meat using herbs and berries. *Meat Science*, 96(1), 126–135.
- Hullberg, A., Johansson, L., & Lundström, K. (2005). Effect of tumbling and RN genotype on sensory perception of cured-smoked pork loin. *Meat Science*, 69(4), 721–732.
- Iqbal, A., Valous, N. A., Mendoza, F., & Da-Wen Sun, P. A. (2010). Classification of pre-sliced pork and Turkey ham qualities based on image colour and textural features and their relationships with consumer responses. *Meat Science*, 84(3), 455–465.
- ISO-8586-1. (1993). *Sensory analysis methodology. General guidance for the selection*

- and training and monitoring of assessors. Part 1. Selected assessors. International Standards Organisation Publications.
- ISO-8589. (1988). *Sensory analysis. General guidance for the design of test rooms*. International Standards Organisation Publications.
- ISO. (2004). *Sensory analysis – Methodology – Triangle test. ISO 4120:2004*. British Standard.
- Jiménez-Colmenero, F., Reig, M., & Toldrá, F. (2006). New approaches for the development of functional meat products. In L. M. L. Nollet, & F. Toldrá (Eds.), *Advanced technologies for meat processing*. CRC Press.
- Keenan, D. F., Desmond, E. M., Hayes, J. E., Kenny, T. A., & Kerry, J. P. (2010). The effect of hot-boning and reduced added phosphate on the processing and sensory properties of cured beef prepared from two forequarter muscles. *Meat Science*, *84*(4), 691–698.
- Kim, M. K., Lopetcharat, K., Gerard, P. D., & Drake, M. A. (2012). Consumer awareness of salt and sodium reduction and sodium labeling. *Journal of Food Science*, *77*(9), S307–S313.
- Lachowicz, K., Sobczak, M., Gajowiecki, L., & Żych, A. (2003). Effects of massaging time on texture, rheological properties, and structure of three pork ham muscles. *Meat Science*, *63*(2), 225–233.
- Lawrence, G., Buchin, S., Achilleos, C., Bérodiér, F., Septier, C., Courcoux, P., et al. (2012). *In vivo* sodium release and saltiness perception in solid lipoprotein matrices. 1. Effect of composition and texture. *Journal of Agricultural and Food Chemistry*, *60*(21), 5287–5298.
- Macfie, H. J., Bratchell, N., Greenhoff, K., & Vallis, L. V. (1989). Designs to balance the effect of order presentation and first-order and carryover effects in hall tests. *Journal of Sensory Studies*, *4*, 129–148.
- Meilgaard, M. C., Carr, B. T., & Civille, G. V. (1991). *Sensory evaluation techniques*. Boca Raton, FL: CRC Press.
- Micha, R., Michas, G., & Mozaffarian, D. (2012). Unprocessed red and processed meats and risk of coronary artery disease and type 2 diabetes – an updated review of the evidence. *Current Atherosclerosis Reports*, *14*(6), 515–524.
- Morales, R., Aguiar, A. P. S., Subiabre, I., & Realini, C. E. (2013). Beef acceptability and consumer expectations associated with production systems and marbling. *Food Quality and Preference*, *29*(2), 166–173.
- Morales, R., Guerrero, L., Claret, A., Guàrdia, M. D., & Gou, P. (2008). Beliefs and attitudes of butchers and consumers towards dry-cured ham. *Meat Science*, *80*(4), 1005–1012.
- Pietrasik, Z., & Gaudette, N. J. (2014). The impact of salt replacers and flavor enhancer on the processing characteristics and consumer acceptance of restructured cooked hams. *Meat Science*, *96*(3), 1165–1170.
- Resconi, V. C., Keenan, D. F., Gough, S., Doran, L., Allen, P., Kerry, J. P., et al. (2015). Response surface methodology analysis of rice starch and fructooligosaccharides as substitutes for phosphate and dextrose in whole muscle cooked hams. *LWT – Food Science and Technology*, *64*(2), 946–958.
- SAFEFOOD. (2008). *Consumer focused review of the Pork Supply Chain*.
- dos Santos, B. A., Campagnol, P. C. B., Pacheco, M. T. B., & Pollonio, M. A. R. (2012). Fructooligosaccharides as a fat replacer in fermented cooked sausages. *International Journal of Food Science & Technology*, *47*(6), 1183–1192.
- Sheard, P. R., Nute, G. R., Richardson, R. I., Perry, A., & Taylor, A. A. (1999). Injection of water and polyphosphate into pork to improve juiciness and tenderness after cooking. *Meat Science*, *51*(4), 371–376.
- Tobin, B. D., O'Sullivan, M. G., Hamill, R., & Kerry, J. P. (2014). European consumer attitudes on the associated health benefits of neutraceutical-containing processed meats using Co-enzyme Q10 as a sample functional ingredient. *Meat Science*, *97*(2), 207–213.
- Toldrá, F., Mora, L., & Flores, M. (2010). Chapter 16. Cooked Ham. In F. Toldrá (Ed.), *Handbook of meat processing* (pp. 301–311). Iowa, USA: Wiley-Blackwell.
- Vandendriessche, F. (2008). Meat products in the past, today and in the future. *Meat Science*, *78*(1–2), 104–111.



## Antioxidant activity of papaya seed extracts against H<sub>2</sub>O<sub>2</sub> induced oxidative stress in HepG2 cells



Swetha Salla<sup>a</sup>, Rajitha Sunkara<sup>a</sup>, Simon Ogutu<sup>b</sup>, Lloyd T. Walker<sup>b</sup>, Martha Verghese<sup>a,\*</sup>

<sup>a</sup> Nutritional Biochemistry and Food Toxicology Laboratory, Department of Food Science, Alabama A & M University, Normal, AL, 35762, United States

<sup>b</sup> Food Chemistry Laboratory, Department of Food Science, Alabama A & M University, Normal, AL, 35762, United States

### ARTICLE INFO

#### Article history:

Received 19 March 2015

Received in revised form

27 August 2015

Accepted 2 September 2015

Available online 8 September 2015

#### Keywords:

Papaya seeds  
Oxidative stress  
Antioxidants

### ABSTRACT

Phytochemicals protect major biomolecules from oxidation caused by free radicals thus, prevent the onset of many chronic diseases. Papaya seeds are discarded after consuming the fruit, but they contain many bioactive compounds. The objective of this study was to determine the *in-vitro* antioxidant activity of papaya seeds and their effect on endogenous antioxidant enzymes in HepG2 cells. Papaya seeds were extracted in methanol and hexane. Total polyphenols, flavonoids and the antioxidant capacity of methanol extracts (ME) and hexane extracts (HE) of seeds were determined. Modulation of endogenous glutathione (GSH), superoxide dismutase (SOD), catalase (CAT) and glutathione peroxidase (GPx) by ME & HE in oxidative stress induced cells were also evaluated in this study. Polyphenols and flavonoids in ME were 5.5 and 1.3 folds higher ( $p \leq 0.05$ ) compared to HE respectively. *In-vitro* antioxidant potential of ME was higher ( $p \leq 0.05$ ) compared to HE. Inducing oxidative stress, significantly ( $p \leq 0.05$ ) lowered SOD, CAT, GPx activities and GSH levels in HepG2 cells. However, treating cells with ME induced CAT, GSH and GPx whereas, HE induced SOD, GPx and GSH. Overall, papaya seed extracts were effective in protecting HepG2 cells from oxidative stress.

© 2015 Published by Elsevier Ltd.

### 1. Introduction

Reactive oxygen species (ROS) are generated in the human body during various metabolic processes. They play an important role in cell signaling, neurotransmission and also maintains homeostasis in normal tissues (Yamamoto, 2000). In a healthy human being generation of ROS are kept in check by antioxidative defense mechanisms such as superoxide dismutase (SOD), catalase (CAT), glutathione peroxidase (GPx) (Michiels, Raes, Toussaint, & Remacle, 1994) and glutathione (GSH) (Fang, Yang, & Wu, 2002). However, an imbalance in this mechanism favoring the over production of ROS results in oxidative stress, which has major implications in the etiology of many chronic diseases such as cancer, diabetes and obesity (Ames & Gold, 1991; Ames, Shigenaga, & Gold, 1993).

Recently, much attention has been focused on dietary polyphenols, as they inhibits oxidation of biomolecules by scavenging free radicals (Heinonen, Meyer, & Frankel, 1998; Urquiaga & Leighton, 2000) or by inducing endogenous antioxidant enzymes (Balogun et al., 2003; Chen, Yu, Owuor, & Kong, 2000; La Marca et al., 2012) thus protect humans from the onset of various chronic diseases.

*Carica papaya* L. is a tropical plant belongs to caricaceae and it is widely known for its nutritive value. Papaya fruits are a rich source of polyphenols, carotenoids and vitamin C (Gayosso-García Sancho, Yahia, & González-Aguilar, 2011). Papaya is a unique fruit in caricaceae family, containing benzyl isothiocyanates (BITC). In papayas, benzyl glucosinolates and myrosinase are compartmentalized. Upon tissue rupture, glucotropaeolin come in contact with myrosinase, which hydrolyses glucotropaeolin to benzyl-isothiocyanates (BITC) (Matusheski, Juvik, & Jeffery, 2004). In the papaya fruit pulp, benzyl-isothiocyanates decreases but increases in the seeds as it matures (Tang, 1971). Papaya seeds also contain alkaloids, saponins, tannins and phenolics (Okoye, 2011). Papaya seeds have hypoglycemic, (Adeneye & Olagunju, 2009), hypo-lipidemic (Nwangwa & Ekhoje, 2013) and nephroprotective (Olagunju et al., 2009) properties. Antioxidant effect of papaya

**Abbreviations:** ME, methanol extracts; HE, hexane extracts; DPPH, 2,2 diphenyl 1-picrylhydrazyl radical scavenging ability; FRAP, ferric reducing antioxidant potential; TAC, total antioxidant capacity; NORs, nitric oxide radical scavenging ability; SOD, superoxide dismutase; CAT, catalase; GPx, glutathione peroxidase; GSH, glutathione; ROS, reactive oxygen species; H<sub>2</sub>O<sub>2</sub>, hydrogen peroxide; IC<sub>50</sub>, inhibitory concentration 50%; DMSO, dimethyl sulfoxide.

\* Corresponding author.

E-mail address: [martha.verghese@aamu.edu](mailto:martha.verghese@aamu.edu) (M. Verghese).

seeds might be one of the underlying mechanisms for these protective effects. Therefore, we investigated *in-vitro* antioxidant capacity of papaya seeds extracts and their role in protecting hepatoma cells from hydrogen peroxide induced oxidative stress.

## 2. Materials and methods

Fresh mature papaya fruits (variety Caribbean red) were obtained from a local health food store, Huntsville, AL. The fruits were washed and cut into two halves, seeds were collected, washed under running water and freeze dried (VirTis Genesis 35L Sp Scientific, Warminster, PA). The seeds were crushed into a fine powder using a laboratory blender prior to extraction.

For preparation of methanol extracts, freeze dried seed powder was soaked in 80% methanol for 48 h with continuous shaking. The extracts were filtered using whatman filter paper and filtrate was evaporated in a rotary evaporator (Rotavapor R-215 Buchi, Zurich, Switzerland) at 40 °C and 240 rpm. The residue was re-suspended in 80% methanol and stored at –80 °C until use.

For preparation of hexane extracts, 5 g of seed powder was collected in a thimble and extracted in a soxhlet apparatus by refluxing with hexane. Hexane was evaporated and residue was re-suspended in DMSO and stored at –80 °C until use.

### 2.1. Total polyphenols, flavonoids and BITC

Total polyphenols were determined according to Singleton and Rossi, (1965) using gallic acid as standard. About 12.5 µL of Folin-Ciocalteu's reagent was added to 12.5 µL of sample and 50 µL of distilled water. After 5 min 125 µL of 7% sodium carbonate was added and absorbance was measured at 750 nm after incubating for 90 min at room temperature.

Flavonoid content was determined according to Marinova, Ribarova, & Atanassova, (2005) using catechin as a standard. About 25 µL of extracts and 7.5 µL of 7.5% sodium nitrite was added followed by the addition of 15 µL 10% aluminum chloride, 50 µL of 1 M NaOH and 40 µL of water. The reaction mixture was incubated for 5 min and absorbance was measured at 520 nm.

Papaya seed extracts obtained from above were filtered through a 0.45 µm whatmann filter unit and 10 µL of sample was injected into HPLC (Shimadzu LC-20 AD Prominence, Maryland, USA) with biobasic 18 column (Thermoelectron Corporation, 250 × 4.6, 5 µm). For the mobile phase, acetonitrile: water: trifluoroacetic acid (40%:60%:0.1%) was used at 1 mL/min flow rate. BITC were quantified with respect to pure standard at 254 nm (Nakamura et al., 2007).

### 2.2. Antioxidant assays

#### 2.2.1. DPPH (2,2-diphenyl-1-picrylhydrazyl) radical scavenging activity

The DPPH assay was done according to Brand-Williams, Cuvelier, & Berset, (1995) with slight modifications. Briefly, 210 µL of DPPH (0.1 mM) was added to 40 µL of samples and blank. The absorbance was recorded at 517 nm for 90 min at 30 min interval. Percentage of DPPH inhibition was calculated by

$$\% \text{ DPPH} = (A_C - A_S/A_C) \times 100$$

$A_C$  = absorbance of control,  $A_S$  = absorbance of sample.

#### 2.2.2. Ferric reducing antioxidative potential (FRAP)

FRAP was determined according to Benzie and Strain, (1996) with slight modifications using  $\text{FeSO}_4 \cdot 7\text{H}_2\text{O}$  standard.

Reagent A: 300 mM acetate buffer, pH 3.6 (16 mL glacial acetic acid and 3.1 gm sodium acetate trihydrate), reagent B: 10 mM 2,4,6-Tris(2-pyridyl)-s-triazine (TPTZ) in 40 mM HCl and reagent C: 20 mM  $\text{FeCl}_3 \cdot 6\text{H}_2\text{O}$  were prepared. The FRAP reagent was prepared by mixing reagents A:B:C in 10:1:1 just before use. Approximately 30 µL of FRAP reagent was added to 10 µL of standards and samples. The absorbance was recorded at 593 nm for 6 min at 1 min interval.

#### 2.2.3. Total antioxidative capacity by phosphomolybdenum method (TAC)

Total antioxidative capacity was determined according to (Prieto, Pineda, & Aguilar, 1999) using ascorbic acid standard. About 3 mL of reagent (0.6 M sulfuric acid, 28 mM sodium phosphate and 4 mM ammonium molybdate) was added to 300 µL of extracts and incubated at 95 °C for 90 min. The absorbance was recorded at 695 nm after cooling the reaction mixture to room temperature.

#### 2.2.4. Nitric oxide radical scavenging activity (NORS)

The nitric oxide radical scavenging activity was determined according to (Sakat, Juvekar, & Gambhire, 2010). The reaction mixture contained 1 mL of 10 mM sodium nitroprusside and 1 mL of extracts or ascorbic acid standard in phosphate buffer (pH 7.4) was incubated at 25 °C for 150 min. After incubation, 1 mL from the reaction mixture was taken out and 1 mL of Griess reagent (1% sulphanilamide, 2% phosphoric acid and 0.1% naphthyl ethylene diamine dihydrochloride) was added to it. The ability of extracts to inhibit nitric oxide formation was measured at 546 nm.

### 2.3. Cell culture

Human hepatoma cell lines (HepG2) were obtained from ATCC (American Type Culture Collection, Manassas, VA). Cells were maintained in DMEM supplemented with 10% FBS, 100 µl/ml of streptomycin and penicillin at 37 °C in a humidified 5%  $\text{CO}_2$  atmosphere.

Cells were treated with different concentrations (50, 100, 250, 500 µg/ml) of ME and HE for 24 h. Oxidative stress was induced by treating cells with 500 µM  $\text{H}_2\text{O}_2$  for another 2 h at 37 °C. Cells were then lysed in ice cold solubilization buffer and centrifuged at 10,000 g for 15 min at 4 °C. The supernatant was collected and antioxidant enzyme activities were analyzed.

### 2.4. Cell viability

The effect of ME and HE on cell viability was determined using Abnova MTT (3-[4, 5-dimethyl thiazol-2yl]-2, 5-diphenyl tetrazoliumbromide) cell viability assay kit (Walnut, CA). Cell viability was expressed as percentage relative to control cells.

### 2.5. SOD, CAT, GPx activities and glutathione (GSH) levels

SOD, CAT, GPx activities and GSH levels in cell extracts were measured using Cayman Chemicals assay kits (Ann Arbor, MI).

### 2.6. Statistical analysis

All experiments were performed in triplicates and the data were recorded as means ± SD. One way ANOVA was performed using SAS 9.2 version. Means separation was done by t test and  $p \leq 0.05$  was regarded as significant.

### 3. Results

#### 3.1. Total polyphenols, flavonoids and BITC content

Total polyphenolic and flavonoid content in papaya seeds were significantly affected by the solvent used (Table 1). Total polyphenols and flavonoids in ME were 5.5 and 1.3 folds higher ( $p \leq 0.05$ ) compared to HE. BITC content in HE was  $4.47 \mu\text{M}/100 \text{ g DW}$ , whereas BITC were not detected in ME.

#### 3.2. Antioxidant activity of papaya seed extracts

Methanol extracts at  $1 \text{ mg/ml}$  concentration inhibited at least 50% of DPPH radical, however, HE even at  $0.25 \text{ g/ml}$  concentration inhibited only 13.09% of DPPH radical. FRAP, TAC and NORS ability of ME was 37, 4.4 and 21 times higher compared to ( $p \leq 0.05$ ) HE respectively (Table 2).

#### 3.3. Cell viability

Increasing concentrations of ME and HE lowered cell viability (Fig. 1). Hexane extracts were effective in lowering cell viability compared to ME. At the highest concentrations of ME & HE ( $500 \mu\text{g/ml}$ ), 76% and 62% were viable.

#### 3.4. Papaya seed extracts on antioxidant enzyme (SOD, CAT, GPx) activities and GSH levels

SOD, CAT, GPx, activities and GSH levels were significantly lower ( $p \leq 0.05$ ) in cells treated with  $500 \mu\text{M H}_2\text{O}_2$  by 67%, 25%, 44% and 13% compared to control cells respectively (Fig. 2).

Methanol and hexane extracts at all selected concentrations were effective in restoring SOD activity in the cells that was lowed due to  $\text{H}_2\text{O}_2$ , except in cells treated with  $500 \mu\text{g/ml}$  of ME. SOD activity in cells at ME 50, 100 &  $250 \mu\text{g/ml}$  was 2.4, 2.2 and 1.6 folds higher compared to  $\text{H}_2\text{O}_2$  treated cells respectively. SOD activity was higher significantly ( $p \leq 0.05$ ) in cells treated HE compared to cells treated with ME and  $\text{H}_2\text{O}_2$ . SOD activity in cells at  $100 \mu\text{g/ml}$  HE was 3.4 folds higher ( $p \leq 0.05$ ) compared to  $\text{H}_2\text{O}_2$  treated cells (Fig. 2a).

CAT activity was significantly ( $p \leq 0.05$ ) high in cells treated with 250 &  $500 \mu\text{g/ml}$  of ME. CAT activity in these cells was 1.8 fold higher compared to  $\text{H}_2\text{O}_2$  treated cells. CAT activity was significantly ( $p \leq 0.05$ ) lower in the cells treated with HE when compared to ME treated cells, however did not differ significantly ( $p \leq 0.05$ ) from  $\text{H}_2\text{O}_2$  treated cells (Fig. 2b).

GPx activity was significantly ( $p \leq 0.05$ ) higher in the cells at  $250 \mu\text{g/ml}$  of ME and there was no significant ( $p \leq 0.05$ ) difference between cells at  $500 \mu\text{g/ml}$  of ME and HE. Cells treated with  $250 \mu\text{g/ml}$  of ME,  $500 \mu\text{g/ml}$  of ME & HE exhibited 3.5 & 2.8 folds higher GPx activity compared to  $\text{H}_2\text{O}_2$  treated cells. In cells treated with 50, 100 &  $250 \mu\text{g/ml}$  of HE, enhanced GPx activity was observed when compared to  $\text{H}_2\text{O}_2$  treated cells (Fig. 2c).

**Table 1**  
Polyphenols, flavonoids and benzyl isothiocyanate content in papaya seed extracts.

	ME	HE
Polyphenols (mg GAE/100 g DW)	$62.27 \pm 2.27^{\text{a}}$	$3.40 \pm 1.40^{\text{p}}$
Flavonoids (mg CE/100 g DW)	$11.26 \pm 0.40^{\text{a}}$	$2.68 \pm 0.40^{\text{p}}$
BITC ( $\mu\text{M}/100 \text{ g DW}$ )	ND	$4.47 \pm 0.04$

Values are means  $\pm$  SD; Means in a same row with superscripts without a common letter differ significantly at  $p \leq 0.05$ . ME-methanol extracts, HE-hexane extracts, GAE-gallic acid equivalents, CE-catechin equivalents, BITC-benzyl isothiocyanates, DW- dry weight basis, ND-not detected.

**Table 2**  
Antioxidant capacities of papaya seed methanol and hexane extracts.

	Methanol extracts	Hexane extracts
DPPH ( $\text{IC}_{50} \text{ mg/ml}$ )	1	ND
FRAP ( $\mu\text{M FeSO}_4/100 \text{ g}$ )	$667.18 \pm 8.49^{\text{a}}$	$17.78 \pm 2.15^{\text{b}}$
TAC (mM AA/100 g)	$2485.53 \pm 23.21^{\text{a}}$	$568.46 \pm 9.72^{\text{b}}$
NORS (mg AA/100 g)	$517.79 \pm 13.81^{\text{a}}$	$24.63 \pm 3.57^{\text{b}}$

Values are means  $\pm$  SD; Means in a row with superscripts without a common letter differ  $p \leq 0.05$  ME-methanol extracts, HE-hexane extracts, DPPH- 2,2-diphenyl-1-picrylhydrazyl, FRAP- ferric reducing antioxidant potential, TAC-total antioxidant capacity, NORS- nitric oxide, radical scavenging ability,  $\text{IC}_{50}$ - inhibitory concentration; ND-not detected; AA-ascorbic acid.

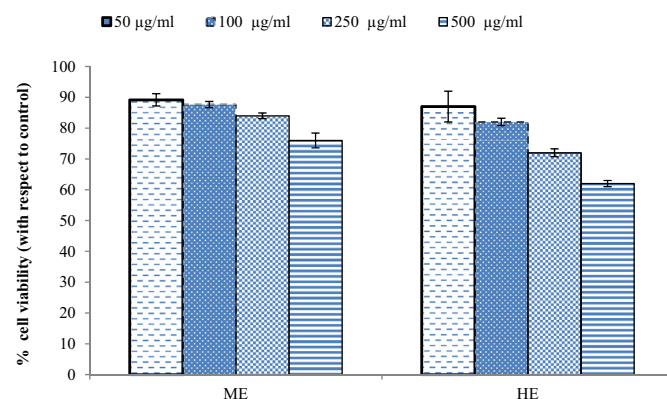


**Fig. 1.** Papaya seed extracts on HepG2 cell viability. Values are means  $\pm$  SD; ME- methanol extracts, HE- hexane extracts.

GSH levels were significantly ( $p \leq 0.05$ ) enhanced by 28, 17.3 & 34% in cells treated with  $250 \mu\text{g/ml}$  of ME, 100 &  $250 \mu\text{g/ml}$  of HE compared to  $\text{H}_2\text{O}_2$  treated cells respectively (Fig. 2d). GSH levels in the cells treated with  $100 \mu\text{g/ml}$  ME and 50 &  $500 \mu\text{g/ml}$  HE did not differ significantly ( $p \leq 0.05$ ) from control cells, however significantly ( $p \leq 0.05$ ) higher compared to  $\text{H}_2\text{O}_2$  treated cells.

### 4. Discussion

Polyphenols act as antioxidants by neutralizing ROS and by chelating metal ion. Due to this, polyphenols may possess positive effect against certain diseases including cancer, diabetes, atherosclerosis and coronary heart diseases. Polyphenols may also enhance the activity of endogenous antioxidants including SOD, CAT, GPx and GSH, which act as first line of defense against oxidative stress in cells. Earlier studies have demonstrated the presence of polyphenols in papaya seed (Afolabi & Ofobrukweta, 2011; Maisarah, Asmah, & Fauziah, 2014), however, the difference in polyphenolic content reported in this study might be due to different stage of maturity or the nature of solvent used to extracts. In the present study, polarity of solvent used played a major role in extracting polyphenols. Aqueous methanol due to its polar nature has resulted in higher amount of polyphenols compared to non-polar hexane, indicating polyphenols in papaya seeds are more hydrophilic than hydrophobic. Similar results were reported by Ng, Ang, Khoo, and Yim (2012), where polyphenolic content of papaya seeds was higher in water extracts (polar nature) and lower in hexane extracts (non-polar nature). In that study authors also reported that, polyphenolic content depend on duration of extraction as shorter time may not extract completely whereas longer duration might result in the breakdown of extracted compounds.

Non-polar BITC were detected only in hexane extracts. BITC content of papaya seeds reported in study was lower compared to those reported by Lee, Lee, and Su (2011) and Nakamura et al.

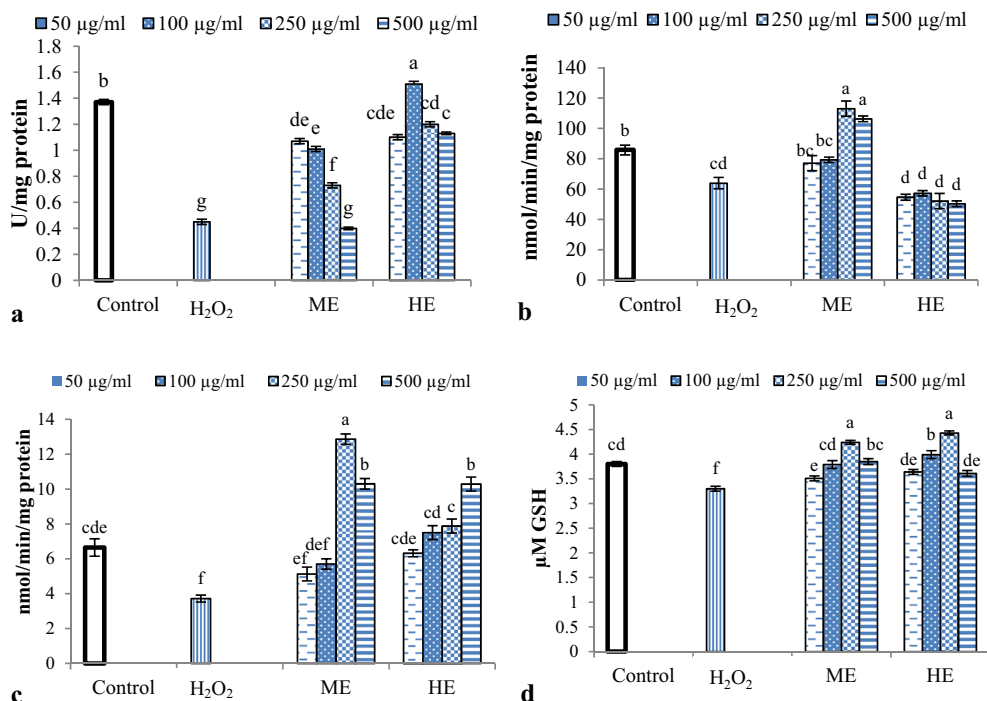


**Fig. 2.** Papaya seed extracts on a. superoxide dismutase activity b. catalase activity c. glutathione peroxidase activity and d. glutathione levels in oxidative stress induced HepG2 cells.

Values are means  $\pm$  SD. Bars within a figure without a common superscript differ significantly at  $p \leq 0.05$ . ME- methanol extracts, HE- hexane extracts, GSH- glutathione.

(2007). This might be due to varietal difference, stage of maturity, different extracting conditions or inactivation of myrosinase during extraction using soxhlet.

Methanol extracts exhibited higher *in-vitro* antioxidant potential compared to hexane extracts, which was determined by measuring DPPH radical scavenging ability, nitric oxide radical scavenging ability, ferric reducing antioxidant potential and total antioxidant capacity. Methanol extracts due to the presence of higher polyphenolic and flavonoid content might have higher antioxidant potential compared to HE. Kothari and Seshadri (2010) have reported that chloroform-methanol extracts of papaya seeds (polar nature) exhibited higher antioxidant capacity compared to acetone extracts (less polar), which correlated to their polyphenolic content. Polyphenols act as antioxidants by stabilizing free radical by donating hydrogen atom or single electron or by chelating the pro-oxidant metal ions (Rice-Evans, Miller, & Paganga, 1997). Many earlier studies have also confirmed the antioxidant capacity of polyphenols (Kumaran & Karunakaran, 2007; Nagendra Prasad et al., 2009; Razali, Razab, Junit, & Aziz, 2008; Siddhuraju, 2007).

The cell viability assay is dependent on the conversion of yellow colored MTT to purple color formazan crystal by mitochondrial dehydrogenases in the living cells (Twentyman & Luscombe, 1987). At higher selected concentrations, papaya seed extracts might cause damage to the cell membrane and lowered cell viability.

In a normal cell, SOD destroys highly reactive superoxides to oxygen and hydrogen peroxide. Peroxides are further neutralized by CAT or GPx in to water and oxygen. GPx neutralize hydrogen peroxide by utilizing GSH as a substrate (Fridovich, 1995; Sandalio, López-Huertas, Bueno, & Del Río, 1997; Teixeira, Schumacher, & Meneghini, 1998). Collectively, these antioxidant enzymes provide first line of defense to the cells against oxidative stress.

Hydrogen peroxide was utilized in this study to induce oxidative stress as, it is one of the most abundantly generated ROS. Moreover,

H<sub>2</sub>O<sub>2</sub> is readily transported through lipid bilayer and then initiate Fenton reaction by reacting with metal ions to form extremely toxic hydroxyl radicals, leading to oxidative stress (Halliwell, 2001). This might have caused reduction in SOD, CAT, GPx activities and GSH levels in H<sub>2</sub>O<sub>2</sub> treated cells. Some earlier studies have also reported the reduction in cellular antioxidants by inducing oxidative stress (Ju et al., 2012; Martín, González-Burgos, Carretero, & Gómez-Serranillos, 2011).

Dose response decrease in SOD activity in cells treated with ME might be due to the neutralization of superoxides to hydrogen peroxides by polyphenols present in the extracts. Methanol extracts enhanced CAT, GPx activities and GSH levels, suggesting ROS scavenging ability of extracts may be related to increase in antioxidant enzyme activity. Significantly higher SOD activity in cells treated with HE might be due to the synergistic effect of polyphenols and lipophilic antioxidants such as tocopherol in the papaya seeds (Maisarah et al., 2014; Malacrida, Kimura, & Jorge, 2011). Hexane extracts did not enhance CAT activity that was lowered by inducing oxidative stress. However HE enhanced GPx activity and GSH levels compared to H<sub>2</sub>O<sub>2</sub> treated cells, thus cells may detoxify H<sub>2</sub>O<sub>2</sub>. Besides CAT, GPx is also a predominant cellular enzyme in neutralizing H<sub>2</sub>O<sub>2</sub> utilizing GSH as substrate. In this process, GSH is oxidized to glutathione disulfide (GSSG). However, increased GSH levels in cells treated with ME and HE might be due to the induction of glutathione reductase (GR) by the extracts as GR reduces GSSG back to GSH (Fang et al., 2002). Earlier studies also demonstrated that polyphenols in white tea (Yen et al., 2013) and coriandrum (Hashim, Lincy, Remya, Teena, & Anila, 2005) protected cells from H<sub>2</sub>O<sub>2</sub> induced oxidative stress by restoring SOD, CAT, GSH and GPx activities.

Overall, the protective effect of papaya seed extracts on HepG2 cells might be: by directly scavenging free radicals or by chelating metal ions thus inhibiting Fenton reactions as shown by various antioxidant assays (Table 2). Moreover, phytochemicals in papaya

seed extracts might activate the transcription factor that stimulates antioxidant response elements on the genes finally leading to the expression of antioxidant enzymes.

In conclusion, ME had higher levels of polyphenols and *in-vitro* antioxidant capacities compared to HE. However, both ME and HE offered protection in HepG2 cells against oxidative stress. In this regard, molecular mechanisms by which papaya seed extracts induced antioxidant enzymes need to be evaluated.

## Acknowledgments

This research was funded by The Alabama Agricultural Research Experiment Station, USDA/NIFA ALAX-012-0412 Alabama A&M University, Normal, AL 35762.

## References

- Adeneye, A., & Olagunju, J. (2009). Preliminary hypoglycemic and hypolipidemic activities of the aqueous seed extract of *Carica papaya* Linn in Wistar rats. *Biology and Medicine*, 1, 1–10.
- Afolabi, I., & Ofobrukwa, K. (2011). Physicochemical and nutritional qualities of *Carica papaya* seed products. *Journal of Medicinal Plants Research*, 5(14), 3113–3117.
- Ames, B. N., & Gold, L. S. (1991). Endogenous mutagens and the causes of aging and cancer. *Mutation Research/Fundamental and Molecular Mechanisms of Mutagenesis*, 250(1), 3–16.
- Ames, B. N., Shigenaga, M. K., & Gold, L. S. (1993). DNA lesions, inducible DNA repair, and cell division: three key factors in mutagenesis and carcinogenesis. *Environmental Health Perspectives*, 101(Suppl. 5), 35.
- Balogun, E., Hoque, M., Gong, P., Killeen, E., Green, C., Foresti, R., et al. (2003). Curcumin activates the haem oxygenase-1 gene via regulation of Nr2 and the antioxidant-responsive element. *Biochemical Journal*, 371, 887–895.
- Benzie, I. F., & Strain, J. (1996). The ferric reducing ability of plasma (FRAP) as a measure of “antioxidant power”: the FRAP assay. *Analytical Biochemistry*, 239(1), 70–76.
- Brand-Williams, W., Cuvelier, M., & Berset, C. (1995). Use of a free radical method to evaluate antioxidant activity. *LWT-Food Science and Technology*, 28(1), 25–30.
- Chen, C., Yu, R., Owuor, E. D., & Kong, A. N. T. (2000). Activation of antioxidant-response element (ARE), mitogen-activated protein kinases (MAPKs) and caspases by major green tea polyphenol components during cell survival and death. *Archives of Pharmacological Research*, 23(6), 605–612.
- Fang, Y. Z., Yang, S., & Wu, G. (2002). Free radicals, antioxidants, and nutrition. *Nutrition*, 18(10), 872–879.
- Fridovich, I. (1995). Superoxide radical and superoxide dismutases. *Annual Review of Biochemistry*, 64(1), 97–112.
- Gayosso-García Sancho, L. E., Yahia, E. M., & González-Aguilar, G. A. (2011). Identification and quantification of phenols, carotenoids, and vitamin C from papaya (*Carica papaya* L., cv. Maradol) fruit determined by HPLC-DAD-MS/MS-ESI. *Food Research International*, 44(5), 1284–1291.
- Halliwell, B. (2001). Role of free radicals in the neurodegenerative diseases. *Drugs & Aging*, 18(9), 685–716.
- Hashim, M., Lincy, S., Remya, V., Teena, M., & Anila, L. (2005). Effect of polyphenolic compounds from *Coriandrum sativum* on H<sub>2</sub>O<sub>2</sub>-induced oxidative stress in human lymphocytes. *Food Chemistry*, 92(4), 653–660.
- Heinonen, I. M., Meyer, A. S., & Frankel, E. N. (1998). Antioxidant activity of berry phenolics on human low-density lipoprotein and liposome oxidation. *Journal of Agricultural and Food Chemistry*, 46(10), 4107–4112.
- Ju, H. Y., Chen, S. C., Wu, K. J., Kuo, H. C., Hseu, Y. C., Ching, H., et al. (2012). Antioxidant phenolic profile from ethyl acetate fraction of *Fructus Ligustri Lucidi* with protection against hydrogen peroxide-induced oxidative damage in SH-SY5Y cells. *Food and Chemical Toxicology*, 50(3), 492–502.
- Kothari, V., & Seshadri, S. (2010). Antioxidant activity of seed extracts of *Annona squamosa* and *Carica papaya*. *Nutrition & Food Science*, 40(4), 403–408.
- Kumaran, A., & Karunakaran, R. J. (2007). In vitro antioxidant activities of methanol extracts of five *Phyllanthus* species from India. *LWT-Food Science and Technology*, 40(2), 344–352.
- La Marca, M., Beffy, P., Della Croce, C., Gervasi, P., Iori, R., Puccinelli, E., et al. (2012). Structural influence of isothiocyanates on expression of cytochrome P450, phase II enzymes, and activation of Nr2f2 in primary rat hepatocytes. *Food and Chemical Toxicology*, 50(8), 2822–2830.
- Lee, W. J., Lee, M. H., & Su, N. W. (2011). Characteristics of papaya seed oils obtained by extrusion–expelling processes. *Journal of the Science of Food and Agriculture*, 91(13), 2348–2354.
- Maisarah, A., Asmah, R., & Fauziah, O. (2014). Proximate analysis, antioxidant and antiproliferative activities of different parts of *carica papaya*. *Journal of Nutrition and Food Science*, 4, 267.
- Malacrida, C. R., Kimura, M., & Jorge, N. (2011). Characterization of a high oleic oil extracted from papaya (*Carica papaya* L.) seeds. *Food Science and Technology (Campinas)*, 31(4), 929–934.
- Marinova, D., Ribarova, F., & Atanassova, M. (2005). Total phenolics and total flavonoids in Bulgarian fruits and vegetables. *Journal of the University of Chemical Technology and Metallurgy*, 40(3), 255–260.
- Martín, S., González-Burgos, E., Carretero, M. E., & Gómez-Serranillos, M. P. (2011). Neuroprotective properties of Spanish red wine and its isolated polyphenols on astrocytes. *Food Chemistry*, 128(1), 40–48.
- Matusheski, N. V., Juvik, J. A., & Jeffery, E. H. (2004). Heating decreases epithiospecifier protein activity and increases sulforaphane formation in broccoli. *Phytochemistry*, 65(9), 1273–1281.
- Michiels, C., Raes, M., Toussaint, O., & Remacle, J. (1994). Importance of Se-glutathione peroxidase, catalase, and Cu/Zn-SOD for cell survival against oxidative stress. *Free Radical Biology and Medicine*, 17(3), 235–248.
- Nagendra Prasad, K., Yang, B., Yang, S., Chen, Y., Zhao, M., Ashraf, M., et al. (2009). Identification of phenolic compounds and appraisal of antioxidant and anti-tyrosinase activities from litchi (*Litchi sinensis* Sonn.) seeds. *Food Chemistry*, 116(1), 1–7.
- Nakamura, Y., Yoshimoto, M., Murata, Y., Shimoishi, Y., Asai, Y., Park, E. Y., et al. (2007). Papaya seed represents a rich source of biologically active isothiocyanate. *Journal of Agricultural and Food Chemistry*, 55(11), 4407–4413.
- Ng, L., Ang, Y., Khoo, H., & Yim, H. (2012). Influence of different extraction parameters on antioxidant properties of *Carica papaya* peel and seed. *Research Journal of Phytochemistry*, 6(3).
- Nwangwa, E., & Ekhoeye, E. (2013). Anti-hyperlipidemic activity of aqueous extract of *Carica papaya* seed in albino rats fed with high fat diet.
- Okoye, E. (2011). Preliminary phytochemical analysis and antimicrobial activity of seeds of *Carica papaya*. *J. Basic Physics Research*, 2(1), 66–69.
- Olagunju, J., Adeneye, A., Fagbohunka, B., Bisuga, N., Ketiku, A., Benebo, A., et al. (2009). Nephroprotective activities of the aqueous seed extract of *Carica papaya* Linn. in carbon tetrachloride induced renal injured Wistar rats: a dose- and time-dependent study. *Biology and Medicine*, 1(1), 11–19.
- Prieto, P., Pineda, M., & Aguilar, M. (1999). Spectrophotometric quantitation of antioxidant capacity through the formation of a phosphomolybdenum complex: specific application to the determination of vitamin E. *Analytical Biochemistry*, 269(2), 337–341.
- Razali, N., Razab, R., Junit, S. M., & Aziz, A. A. (2008). Radical scavenging and reducing properties of extracts of cashew shoots (*Anacardium occidentale*). *Food Chemistry*, 111(1), 38–44.
- Rice-Evans, C., Miller, N., & Paganga, G. (1997). Antioxidant properties of phenolic compounds. *Trends in Plant Science*, 2(4), 152–159.
- Sakat, S., Juvekar, A. R., & Gambhire, M. N. (2010). In vitro antioxidant and anti-inflammatory activity of methanol extract of *Oxalis corniculata* Linn. *International Journal of Pharmacy and Pharmacology Sciences*, 2(1), 146–155.
- Sandalio, L. M., López-Huertas, E., Bueno, P., & Del Río, L. A. (1997). Immunocytochemical localization of copper, zinc superoxide dismutase in peroxisomes from *Wihermelon* (*Citrullus vulgaris* Schrad.) Cotyledons. *Free Radical Research*, 26(3), 187–194.
- Siddhuraju, P. (2007). Antioxidant activity of polyphenolic compounds extracted from defatted raw and dry heated *Tamarindus indica* seed coat. *LWT-Food Science and Technology*, 40(6), 982–990.
- Singleton, V., & Rossi, J. A. (1965). Colorimetry of total phenolics with phosphomolybdic-phosphotungstic acid reagents. *American Journal of Enology and Viticulture*, 16(3), 144–158.
- Tang, C. S. (1971). Benzyl isothiocyanate of papaya fruit. *Phytochemistry*, 10(1), 117–121.
- Teixeira, H. D., Schumacher, R. I., & Meneghini, R. (1998). Lower intracellular hydrogen peroxide levels in cells overexpressing CuZn-superoxide dismutase. *Proceedings of the National Academy of Sciences*, 95(14), 7872–7875.
- Twentyman, P., & Luscombe, M. (1987). A study of some variables in a tetrazolium dye (MTT) based assay for cell growth and chemosensitivity. *British Journal of Cancer*, 56(3), 279.
- Urquiaga, I., & Leighton, F. (2000). Plant polyphenol antioxidants and oxidative stress. *Biological Research*, 33(2), 55–64.
- Yamamoto, Y. Y. (2000). *Free radicals in chemistry, biology and medicine*. UK: OICA International.
- Yen, W. J., Chyau, C. C., Lee, C. P., Chu, H. L., Chang, L. W., & Duh, P. D. (2013). Cytoprotective effect of white tea against H<sub>2</sub>O<sub>2</sub>-induced oxidative stress in vitro. *Food Chemistry*, 141(4), 4107–4114.



## Removal of *Salmonella* biofilm formed under meat processing environment by surfactant in combination with bio-enzyme



Huhu Wang<sup>a, b</sup>, Huawei Wang<sup>a, b</sup>, Tong Xing<sup>a, b</sup>, Na Wu<sup>a, b</sup>, Xinglian Xu<sup>a, b, \*</sup>, Guanghong Zhou<sup>a, b</sup>

<sup>a</sup> National Center of Meat Quality and Safety Control, Nanjing Agricultural University, Nanjing 210095, PR China

<sup>b</sup> Synergetic Innovation Center of Food Safety and Nutrition, Nanjing Agricultural University, Nanjing 210095, PR China

### ARTICLE INFO

#### Article history:

Received 11 July 2015

Received in revised form

23 September 2015

Accepted 19 October 2015

Available online 22 October 2015

#### Keywords:

*Salmonella*

Biofilm

Removal

CTAB

Cellulase

### ABSTRACT

*Salmonella* outbreaks are commonly linked to consumption of contaminated food, its outbreaks have been associated with the biofilm formed on food processing surfaces, due to the acquired resistance that this bacterium possesses. In this study, four surfactants and five bio-enzymes were individually and conjunctively tested to remove the biofilm formed on stainless steel surfaces by a seven-strain cocktail of *Salmonella* grown in meat thawing-loss broth (MTLB). The results showed that cetyltrimethyl ammonium bromide (CTAB) and sodium dodecyl sulfate (SDS) reduced greater numbers of biofilm cells than tween-80 and rhamnolipid. 1 mg/mL of CTAB and 10 mg/mL of SDS could remove 100% cells of biofilm at irreversible attachment phase (about 5.39 Log CFU/cm<sup>2</sup>). Compared to proteinase K, dispasell, glucoside amylase and subtilisin, cellulase reached greater reduction (85%, about 5.6 Log CFU/cm<sup>2</sup>) of cells in mature biofilm, but still remaining a huge number of residual biofilm cells. The combination of cellulase following CTAB immersion was effective in removal mature biofilm (100%, about 6.2 Log CFU/cm<sup>2</sup> cells), which was supported by the observation of fluorescence microscopy. This study indicated that CTAB combined with cellulase can apply as an alternative strategy to drastically remove mature biofilm of *Salmonella* exposed to meat processing environments.

© 2015 Elsevier Ltd. All rights reserved.

## 1. Introduction

*Salmonella* spp. is recognized as a globally widespread food-borne pathogen and is considered to be the second most common cause (behind *Campylobacter* spp.) of food-borne bacterial illness all over the world (CDC, 2014; Vieira et al., 2009); In 2013, *Salmonella* was responsible for an estimated 82,694 human cases and 59 deaths in the EU, resulting in notification rate of 20.4 cases per 100,000 population (EFSA-ECDC, 2015). The two most commonly reported *Salmonella* serovars were still Enteritidis and Typhimurium, representing 39.5% and 20.2%, respectively, of all reported serovars in confirmed human cases (EFSA-ECDC, 2015). *Salmonella* was frequently detected in a variety of animal-food products such as meat, poultry and eggs. Consumption of these raw and undercooked corresponding food contaminated with *Salmonella* may lead to development of acute gastroenteritis

characterized by emesis, diarrhea, etc. It is now commonly accepted that food-borne pathogens such as *Salmonella* may grow predominantly as biofilm on solid surfaces, in most of their growth habitats in natural and industrial settings, rather than in planktonic mode (Shi & Zhu, 2009; Thallinger, Prasetyo, Nyanhongo, & Guebitz, 2013). Biofilm of food-borne pathogens were wide present in a variety of food processing sites, including dairy, fish processing, poultry, and ready-to-eat foods (Srey, Jahid, & Ha, 2013), and many food-borne outbreaks have been associated with biofilm (Simoes, Simoes, & Vieira, 2010). An example of this is the *Salmonella* outbreak in Spanish, which resulted in 2138 cases due to consumption of pre-cooked chicken contaminated by the biofilm of *Salmonella* Hadar formed on a bend of a pipe transporting gravy in the processing site (Perez-Rodriguez, Valero, Carrasco, Garcia, & Zurera, 2008).

The biofilm cells can be resistant to environmental stresses, antibiotics and disinfectants (Hoiby, Bjarnsholt, Givskov, Molin, & Ciofu, 2010; Mah & O'Toole, 2001), and as a consequence are extremely difficult to eradicate in food industry. Therefore, much effort has been devoted for developing strategies to interfere with

\* Corresponding author. National Center of Meat Quality and Safety Control, Nanjing Agricultural University, Nanjing 210095, PR China.

E-mail address: [xlxu@njau.edu.cn](mailto:xlxu@njau.edu.cn) (X. Xu).

biofilm formation. Srey et al. (2013) and Jahid and Ha (2012) have reviewed the conventional control strategies of biofilm used to gain more proximity to efficiently maintain good hygiene throughout food industries, including sodium hypochlorite, hydrogen peroxide, ozone, and peracetic acid. Giaouris et al. (2014) also have discussed several novel control methods of pathogens biofilm, such as essential oils and bacteriophages. Additionally, the metabolite molecules of microbial interactions such as N-acylhomoserine lactone (AHL), autoinducer-2 and c-di-GMP, have been successfully evaluated as an alternative means for preventing from biofilm formation (Park, Lim, & Choi, 2015; Wang, Ye, Zhang, Dong, Xu, & Zhou, 2013). However, recent concerns have been raised over the effectiveness, safety and convenience of these approaches, consequently many approaches studied in lab conditions were limited in actual food processing. Current measures of biofilm removal in food industry, in particular of chemical-based disinfectants, were commonly applied by directly spraying or/and immersing. This application can enable the pathogens to survive and proliferate under higher concentration of disinfectants. Bremer, Fillery, and McQuillan (2006) reported that a standard clean-in-place regime (water rinse, 1% sodium hydroxide at 65 °C for 10 min, water rinse, 1.0% nitric acid at 65 °C for 10 min, water rinse) did not ensure the removal of bacteria biofilm formed under dairy processing environments. In addition, similar type of control measures have some other well-known drawbacks, such as the limit permeability into EPS of biofilm, the possible toxicity of residues, the promotion of genetic exchange between different bacteria and the resistance to disinfectants. Therefore, new approaches to control biofilm in the food industry should be focused according to the dynamical processes or steps of biofilm formation, including initial irreversible attachment, rudimentary, maturation and dispersion (Mizan, Jahid, & Ha, 2015). The novel two-step approaches should be explored, the adhesion cells in biofilm are firstly detached and removed based on the reduction of hydrophobicity between attachment cells and solid surface, and the degradation of EPS of biofilm, then all the planktonic cells (detachment from surfaces) are disinfected by bactericides or other control approaches.

The environments involving in biofilm formation such as food-borne isolates, room or lower temperature, variety of contacted-surfaces and residues of food liquid, which could be commonly encountered during food processing, were critical for biofilm removal. The existing studies about controlling biofilm were focused on the biofilm of *Salmonella* grown in some standard lab growth conditions (Burgos, Lopez, Aguayo, Pulido, & Galvez, 2013; Islam et al., 2014), there is little information about the removal of *Salmonella* biofilm grown in meat-based substrate under meat processing environments. The residual of meat liquid on processing contact-surfaces may protect the cells in biofilm, and then weaken the cleaning efficiency of control strategies. Therefore, In this study, meat-borne isolates, stainless steel surfaces and a meat-based growth substrate were tested to simulate the conditions probably found in the meat processing plants, and the focus was highlighted on the effect of single tested surfactant, single tested bio-enzyme, and the combination of special surfactant and bio-enzyme on biofilm removal of *Salmonella*.

## 2. Materials and methods

### 2.1. Strains and incubation medium

Seven *Salmonella* strains (*S. Typhimurium*, *S. Enteritidis*, *S. Infantis*, *S. Stanley*, *S. Agona*, *S. Derby* and *S. Indiana*) isolated from meat processing surfaces and poultry meat, were used in this study. Each strain stored in 40% glycerol at –70 °C was twice separately cultured in Trypticase Soy Broth (TSB) at 37 °C for 20 h, resulting in

early stationary phase culture, then a seven-strain cocktail of *Salmonella* strains was prepared as following: 5 mL of each strain was centrifuged at 10,000 g, 4 °C for 5 min, and then the cell pellets were washed with 0.85% of NaCl solution twice and were re-suspended in NaCl solution. The concentrations of cell suspension were determined with OD<sub>600nm</sub>. The ratio of each strain in the cocktail was 1:1:1:1:1:1:1, and the final concentration of cocktail was approximate 8 Log CFU/mL.

A meat-based growth medium (chicken meat thawing-loss broth, MTLB) was used for biofilm formation. The MTLB was prepared as described previously (Midelet & Carpentier, 2002). The final concentration of protein in MTLB was 1 mg/mL confirmed by the Biuret protein assay.

### 2.2. Biofilm formed on stainless steel

Stainless steel plates (50 × 20 × 1 mm, food grade 304, 2B finish), a material commonly used in the manufacture of meat-processing equipments, were used for biofilm formation. Prior to use, the plates were cleaned as previously described by Poimenidou et al. (2009). For biofilm formation, 100 µL of cocktail suspension prepared as described above was transferred into a centrifuge tube (40 mL) containing 10 mL of MTLB loading a stainless steel plate. The stainless steel plates were partly (10 cm<sup>2</sup>) submerged into MTLB fluid, and part of each plate was exposed to the air-liquid interphase (Chorianopoulos, Giaouris, Kourkoutas, & Nychas, 2010), and then the tubes were incubated at 20 °C, and the biofilm were obtained at 36 h and 132 h.

### 2.3. Removal of biofilm by individual and combination measures

Four surfactants (the cetyltrimethyl ammonium bromide (CTAB, BioSharp), sodium dodecyl sulfate (SDS, BioSharp), rhamnolipid and tween-80 (SunShineBio)), three proteases (proteinase K, dispase and subtilisin, Sigma) and two glycosidases (cellulase (R-10), Yakult; glucoside amylase, Sigma), were used for biofilm removal. The detail of experiment design was shown in Table 1. A single stainless steel plate loading biofilm was rinsed three times with 0.85% NaCl solution to remove non-attached cells, and then the plates were immersed in appropriate surfactant or bio-enzyme solutions under special conditions (Table 1).

### 2.4. Cells numeration of the biofilm removal

The plates treated by variety treatments described in Table 1, were rinsed three times with 0.85% NaCl solution to remove residual surfactants, bio-enzymes and planktonic cells, then the residual cells in biofilm on stainless steel plates were determined by swabbing and plate counting method. The residual cells of biofilm were removed with sterile cotton swabs and the swabs were transferred to tubes containing 0.85% NaCl solution, vortexed with beads for about 5 min, and then serial dilutions were prepared (Winkelstroter, Gomes, Thomaz, Souza, & De Martinis, 2011). Results were expressed as the Log CFU/cm<sup>2</sup> (total of 10 cm<sup>2</sup>), four replicates were tested for each treatment. The percentage of reduction biofilm cells (%) was calculated as following: (the cells numbers in control group – the cells numbers in treatment group)/the cells numbers in control group × 100.

### 2.5. Fluorescence microscopy analysis

Stainless steel plates incubated in MTLB at 20 °C for 36 h and 132 h were aseptically rinsed three times with 0.85% NaCl solution to remove planktonic cells. The procedure of fluorescence microscopy was followed as previously described by Wang, Ding, Dong,

**Table 1**  
The experiment design and removal procedures used in this study.

Measures	Treatment groups	Concentrations (mg/mL)			Treatment time (h)	Temperature (°C)
		A (weak)	B (medium)	C (strong)		
Single surfactant	CTAB	0.5	1	10	1	20
	SDS	5	10	100		
	Tween-80	5	10	100		
	Rhamnolipid	5	10	100		
	Control	Immersion with water				
Single bio-enzyme	Proteinase K	0.2	0.4	4	2	40
	Dispase II	1	2	20		
	Cellulase	1	2	20		
	Glucoside amylase	1	2	20		
	Subtilisin	0.5	1	10		
	Control	Immersion with water				
Combined removal	Control	Immersion with distilled water 3 h				40
	I	Immersion with CTAB 1 h, followed by water immersion 2 h				
	II	Immersion with cellulase 2 h, followed by water immersion 1 h				
	III	Immersion with CTAB 1 h, followed by cellulase immersion 2 h				
	IV	Immersion with cellulase 2 h, followed by CTAB immersion 1 h				
CTAB: 1 mg/mL	V	Immersion with mixture solution (Cellulase + CTAB) 2 h				
Cellulase: 20 mg/mL						

Ye, Xu, & Zhou (2013): the biofilm on stainless steel plate was stained with 4, 6-diamidino-2-phenylindole (DAPA, 5 µg/mL, Beyotime, Ltd., China) in the dark at room temperature for 5 min. Subsequently, the plates were rinsed three times with sterile deionized water to remove excess stain. Images of attached cells and biofilm were obtained with fluorescence microscopy (AX10, Zeiss, German) using a 100× oil immersion objective.

## 2.6. Statistical analysis

The results were expressed as mean ± standard deviation (n = 4). Statistical significance was determined by a one-way Duncan's ANOVA procedure of SPSS 13.0. The level of statistical significance was  $p < 0.05$ .

## 3. Results

### 3.1. Effect of single surfactant on biofilm removal

The initial cells numbers in biofilm grown in MTLB for 36 h were approximate 5.39 Log CFU/cm<sup>2</sup>, which was confirmed by XLD plates. As shown in Fig. 1, there were great differences in the reduction of cells numbers between each surfactant, and the reduction were also significantly ( $p < 0.05$ ) affected by the concentrations of tested surfactants. More cells were detached by CTAB and SDS compared with tween-80 and rhamnolipid. The removal of biofilm cells treated with tween-80 and rhamnolipid significantly increased ( $p < 0.05$ ) in a concentration-dependent manner, whereas no difference was observed in reduction for CTAB when the concentrations increasing from 1 mg/mL to 10 mg/mL. Tween-80 and rhamnolipid only removed less than 60% of biofilm cells, even when the concentration increased at 100 mg/mL. Notably, the CTAB at 1 mg/mL and the SDS at 100 mg/mL could thoroughly detach 100% of the biofilm cells adhered on stainless steel surface (about 5.39 Log CFU/cm<sup>2</sup>), indicating that CTAB and SDS may be used as ideal approach to removal the biofilm grown in meat-based substrate at irreversible attachment phase (about 36 h).

### 3.2. Effect of single bio-enzyme on biofilm removal

The initial cells numbers in biofilm grown in MTLB for 132 h (mature phase) were 6.15 ± 0.14 Log CFU/cm<sup>2</sup>. Great differences in reduction of mature biofilm were observed between each enzyme

(Fig. 2), with cellulase and subtilisin removing more numbers of biofilm than other tested enzymes, the proteinase K and glucoside amylase showed weak detachment ability (less than 55%), even at the high concentrations. The reduction of biofilm was obviously increased ( $p < 0.05$ ) along with the concentrations of each enzyme rising. Compared to the reduction of biofilm treated with surfactants, less numbers of biofilm cells were detached after treated with tested enzymes in this study, only reaching less than 85%.

### 3.3. Effect of combination approaches on removal of mature biofilm

Combination measures were applied to remove mature biofilm in this study, since single enzyme could not thoroughly detach mature biofilm from stainless steel surface. Our design was based on a hypothesis that the skeleton structure of EPS of mature biofilm may be cleaved and degraded by the cellulase (20 mg/mL), and then the CTAB (1 mg/mL) easily permeated into the EPS of biofilm and altered the hydrophobicity of cells surface, conjunctively resulting in biofilm removal. The reduction population of mature biofilm treated with the cleaning groups is illustrated in Fig. 3. The group I (biofilm treated with single CTAB) could remain about 2.8 Log CFU/cm<sup>2</sup> cells of mature biofilm, almost removing half of the cells numbers in mature biofilm. The reduction of biofilm cells treated with group II (treated with single cellulase) reached more than 5.0 Log CFU/cm<sup>2</sup> of residual biofilm cells. The group III (biofilm treated with CTAB following by cellulase) yielded great biofilm reductions ( $p < 0.05$ ) that were significant more than those observed for group I and group II. Similarly, group V (biofilm treated with a mixture solution of CTAB and cellulase) remained about 2.7 Log CFU/cm<sup>2</sup> of biofilm cells, which was significant ( $p < 0.05$ ) more than group III but less than group I and II. Expectedly, treating plates loading mature biofilm with group IV (biofilm treated with cellulase, then following by CTAB) could significantly reduce the 6.22 ± 0.16 Log CFU/cm<sup>2</sup> of biofilm cells, which was the maximum numbers of mature biofilm formed in our tested conditions, indicating that the group IV could completely remove all of the cells in mature biofilm.

### 3.4. Fluorescence microscopy analysis

Fluorescence microscopy was performed for the visualization of mature biofilm and to confirm the effect of combination approaches on biofilm removal (Fig. 4). A typical structure of mature biofilm in control group was observed, characterized by a complex

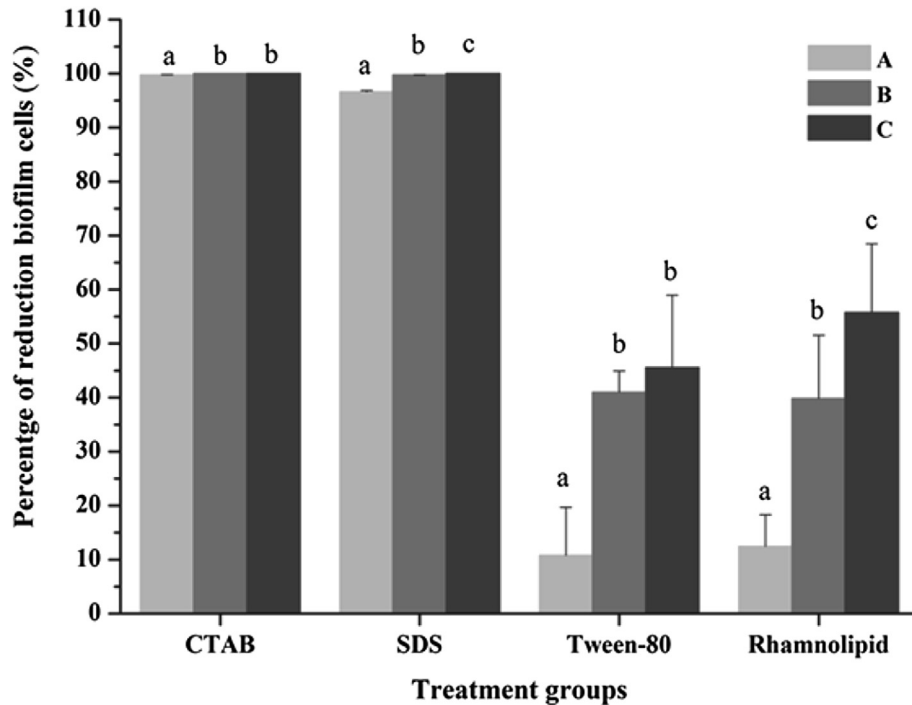


**Fig. 1.** Removal of biofilm cells treated with surfactants. Each symbol indicates the mean  $\pm$  standard deviation of four independent experiments ( $n = 4$ ). A, B and C represent the low, medium and high concentrations of each surfactant. Different lowercase letters for the same surfactant indicated a significant difference ( $p < 0.05$ ).

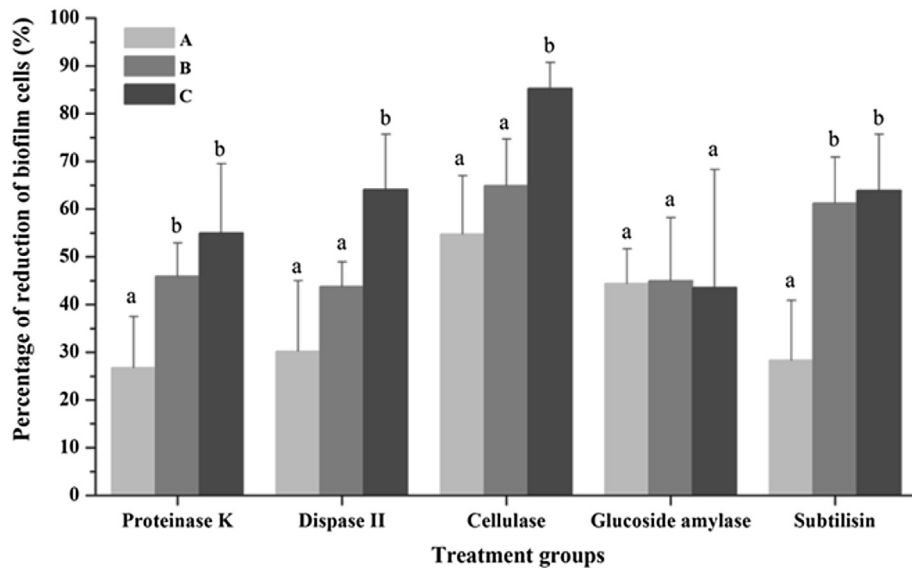


**Fig. 2.** Removal of biofilm cells treated with enzymes. Each symbol indicates the mean  $\pm$  standard deviation of four independent experiments ( $n = 4$ ). A, B and C represent the low, medium and high concentration of each enzyme. Different lowercase letters for the same enzyme indicated a significant difference ( $p < 0.05$ ).

three-dimensional structure formed by many cells aggregates held together by a network of extracellular matrix, covering more than 80% of the surface of the substratum. As observed in Fig. 4, many large cells clusters held together by a great quantity of EPS were also observed after treated by group II approach, and an architectural feature of mature biofilm was still retained, whereas small cells clusters (less than 10  $\mu\text{m}$  in width) scattered over the surface were found in group I, III and V, the results were in agreement with the cells enumeration in Fig. 3, where the cells numbers of residual biofilm were nearly close among the three treatments. Expectedly, there were only few single cells distributed over the stainless steel

surface treated with group II, which was also in line with the numeration observation in Fig. 3.

#### 4. Discussion

Biofilm formation of food-borne pathogens on food processing surfaces was widely concerned in food industry due to the serious cross-contamination. It is clear that use of more efficient and eco-friendly procedures for cleaning and disinfection of biofilm are required. In this study, the differences in solubility and cleaning efficiency of each tested surfactants ranged from 0.1 to 100 mg/mL

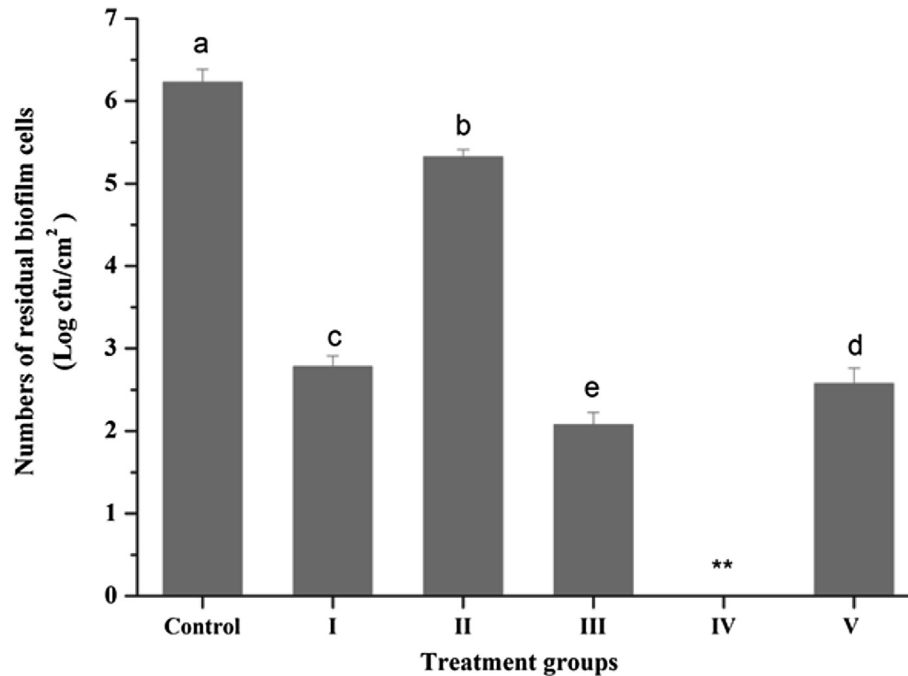


**Fig. 3.** Numbers of residual biofilm cells treated with combination measures. Each symbol indicated the mean  $\pm$  standard deviation of four independent experiments ( $n = 4$ ). \*\* indicated that the residual biofilm cells were not detected by the plate count method. Different lowercase letters in the different groups indicated a significant difference ( $p < 0.05$ ).

were tested in our primary experiments (data not shown). The CTAB was insoluble beyond 15 mg/mL, other three surfactants exhibited good solubility even at 100 mg/mL. Based on the removal efficiency and economy of surfactants, the tested concentrations were applied in this study (Table 1). Developing a practical disinfectant will be our final research goal, so the economy of tested surfactants must be considered. Similarly, according to the removal efficiency and economy of tested bio-enzymes, where the primary tested concentrations of enzymes ranged from 0.2 to 20 mg/mL in the primary experiments, three concentrations of each bio-enzyme (initial concentration, two times and the ten times) were also

finally chosen to applied in this study (Table 1). In order to determine a better surfactant, four types of surfactants, cationic (CTAB), anionic (SDS), nonionic (tween-80) and bio-surfactant (rhamnolipid) were tested. The CTAB and SDS showed greater reduction of biofilm than rhamnolipid and tween-80 (Fig. 1), even the CTAB at 0.5 mg/mL still obtained >98% reduction of biofilm cells at irreversible attachment phase. A similar observation has been reported by Simoes, Simoes, and Vieira (2009), who found that more than 95% of *Pseudomonas fluorescens* biofilm cells was removed after exposure to about 0.33 mg/mL CTAB. Simoes, Simoes, Cleto, Pereira, and Vieira (2008) also emphasized that independent application of

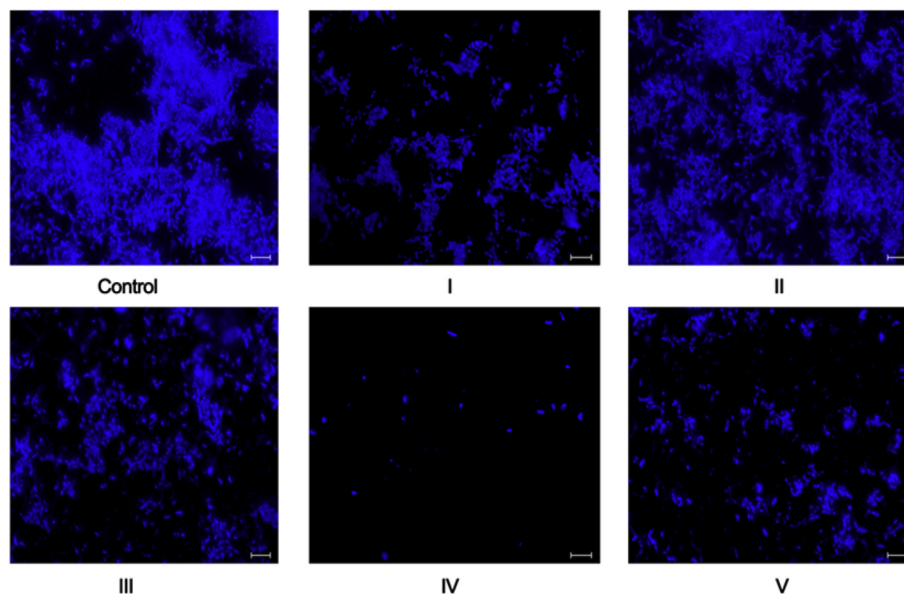


**Fig. 4.** Representative fluorescence microscopy images of residual biofilm treated with different combination measure (IV groups, CTAB + cellulase). Cell communities were stained with 4, 6-diamidino-2-phenylindole (DAPI, 5  $\mu$ g/mL). Bar scale is 10  $\mu$ m, magnification 1000 $\times$ .

CTAB were markedly effective in removing attached *P. fluorescens* (6 Log CFU/cm<sup>2</sup>). Less than 60% reduction of biofilm exposed to tween-80 and rhamnolipid were observed in this study, our finding was also supported by another observation (Schreiberova, Hedbavna, Cejkova, Jirku, & Masak, 2009). When bacteria biofilm was under the irreversible attachment stage, the quantity of EPS formation was few, and the interaction between cells and stainless steel surfaces primarily depend on the hydrophobicity of cells and solid surfaces (Donlan, 2002). The decrease in hydrophobicity on contacted-surfaces showed a significant decrease in cells attachment. Pre-conditioning of contacted-surface with surfactants have been reported to prevent cells adhesion (Chen, 2012; Choi, Park, Lee, Park, & Kim, 2011). The emphasis of cleaning biofilm from stainless steel surface using surfactants was associated with the hydrophobicity of cells surface. Splendiani, Livingston, and Nicoletta (2006) have evaluated the potential of twenty-two surfactants for the reduction of *Burkholderia* sp. biofilm, revealing that the surfactants could increase bacterial negative charge and reduce the attachment capability of cells. It has been demonstrated that *P. fluorescens* treated with CTAB become positively charged, indicating that CTAB cements the cells to, rather than removing them from the negatively charged solid surface (Azeredo, Pacheco, Lopes, Oliveira, & Vieira, 2002). Besides promoting the surface changes of cells, CTAB may also rupture the lipid components of cell membrane with cell lysis being a secondary effect (Gilbert, Allison, & McBain, 2002; Simoes, Pereira, Machado, Simoes, & Vieira, 2006). In our study, tween-80, SDS and rhamnolipid displayed certain removal ability, at least reducing 40% of the biofilm cells. Meanwhile, Mireles, Toguchi, and Harshey (2001) noted that addition of tween-80, SDS and rhamnolipid to a preformed biofilm could accelerate the biofilm dispersal of *Salmonella enteric* without affecting cell growth. However, a weak reduction of rhamnolipid (1%, w/v) on *S. Enteritidis* and mixed biofilm after 2 h contact were observed by Gomes and Nitschke (2012), still remaining 86.5% and 69.8% residue cells after cleaning, respectively. Only less than 0.5 Log CFU/coupon reduction of *Salmonella* Typhimurium biofilm formed on stainless steel was observed by Chen, Zhao, and Doyle (2015) when coupon was exposed to 2% SDS for 10 min, this discrepancy can be explained by the differences in the exposure time between different studies.

An effective cleaning procedure should break up or dissolve the EPS matrix associated with the biofilm so that disinfectants can gain access to the viable cells. Therefore, five bio-enzymes were tested to break up the EPS matrix and clean the mature biofilm of *Salmonella* grown in MTLB for 132 h. Tested enzymes caused great differences in the reduction of mature biofilm (Fig. 2), showing a concentration-depend manner. Amylase enzymes have been found to be less effective in the degradation of EPS of *P. fluorescens* biofilm as compared to protease enzymes (Molobela, Cloete, & Beukes, 2010); this finding was also in agreement with our study where protease enzymes including proteinase K, dispase and subtilisin were more effective in reduction of cells than glucoside amylase. A similar finding was also reported by Chai, Wang, Tao, and Mou (2014) who observed that only about 80% of the biofilm cells preformed by *Klebsiella* sp. were eliminated after treatment with polysaccharide depolymerase enzyme from bacteriophage. In our study, subtilisin, which is a serine protease that cleave proteins in which serine serves as the nucleophilic amino acid, showed greater reduction of biofilm than glucoside amylase, this finding was also supported by the reports of Lequette, Boels, Clarisse, and Faille (2010), who observed that subtilisin was more efficient in removing biofilm cells than enzyme mixture with cellulase,  $\alpha$ -amylase and  $\beta$ -glucanase. However, cellulase showed the greater reduction biofilm in our study, this apparent discrepancy could partly be explained by the different structural composition of EPS of

different biofilm. There were great differences in the proportions of proteins and carbohydrates in EPS of biofilm formed by bacteria. The proteases hydrolyze the proteins in EPS, and amylases break the bond of carbohydrates associated with the EPS. Therefore, the enzymes efficiency on biofilm removal may vary according to the species of bacteria.

Although the tested bio-enzymes displayed obvious reduction of biofilm cells, there were still a fair amount of residual biofilm cells on stainless steel surfaces. Several combined treatments with CTAB and cellulase were used to remove the mature biofilm, the synergistic effect was shown in Fig. 3. As expected, the treatment of group II displayed the least reduction of biofilm, which was in agreement with the observation in Fig. 2. In group I and group III, where the CTAB was first directly applied, resulting that the surfactant cannot penetrate into the inside of biofilm due to the protection of EPS. The group IV (the tested plates were first immersed with cellulase, then immersed with CTAB) was found to be effective in mature biofilm removal, this finding was further supported by the results of fluorescence microscopy analysis (Fig. 4). The observation of combination measures in this study proved our hypothesis that the skeleton structure of EPS of *Salmonella* biofilm were firstly broken by the cellulase, then it facilitated the CTAB to contact the inner cells of biofilm. Hence, the combination of surfactant and bio-enzyme could be used as a new and improved environmental friendly alternative strategy to remove mature biofilm of *Salmonella*. Frankly, it must be recognized that the use of bio-enzymes in biofilm control is still limited due to the high commercial costs of the enzymes, even though they were known as environmental-friendly “green cleanser”.

## 5. Conclusion

CTAB and SDS were shown to be more effective than tween-80 and rhamnolipid in the reduction of *Salmonella* biofilm (at an irreversible attachment phase) formed on stainless steels surfaces under a simulating meat processing environment. Although five tested bio-enzymes (protease, dispase II, cellulase, glucoside amylase and subtilisin) displayed great abilities of removal mature biofilm, many residue biofilm cells were still present on stainless steel surface. A combination treatment of 20 mg/mL of cellulase following by 1 mg/mL of CTAB immersion had a better reduction of mature biofilm than single treatment. The combination approach could thoroughly remove the mature biofilm, which was also supported by the fluorescence microscopy. According to the two-step strategy of control biofilm as mentioned in introduction section, further study should be focused on the “second step”, disinfecting all of the planktonic cells from the “first removal step” with eco-friendly disinfectants such as acidic electrolyzed water and bacteriophages.

## Acknowledgments

This study was supported by the project funded by the grant from the Natural Science Foundation of Jiangsu Province (BK20150678) and the Priority Academic Program Development of Jiangsu Higher Education Institutions (PAPD, 080-809001).

## References

- Azeredo, J., Pacheco, A. P., Lopes, I., Oliveira, R., & Vieira, M. J. (2002). Monitoring cell detachment by surfactants in a parallel plate flow chamber. In *Proceedings of the International Specialised Conference on Biofilm Monitoring, Porto* (pp. 62–65).
- Bremer, P. J., Fillery, S., & McQuillan, A. J. (2006). Laboratory scale clean-in-place (CIP) studies on the effectiveness of different caustic and acid wash steps on the removal of dairy biofilms. *International Journal of Food Microbiology*, 106, 254–262.

- Burgos, M. J. G., Lopez, R. L., Aguayo, M. D. C. L., Pulido, R. P., & Galvez, A. (2013). Inhibition of planktonic and sessile *Salmonella enterica* cells by combinations of enterocin AS-48, polymyxin B and biocides. *Food Control*, 30, 214–221.
- CDC. (2014). *Foodborne diseases active surveillance network (FoodNet): FoodNet surveillance report for 2012 (final report)*. Atlanta, Georgia: U.S. Department of Health and Human Services, CDC.
- Chai, Z., Wang, J., Tao, S., & Mou, H. (2014). Application of bacteriophage-borne enzyme combined with chlorine dioxide on controlling bacterial biofilm. *LWT-Food Science and Technology*, 59, 1159–1165.
- Chen, G. (2012). *Escherichia coli* adhesion to abiotic surfaces in the presence of nonionic surfactants. *Journal of Adhesion Science and Technology*, 17, 2131–2139.
- Chen, D., Zhao, T., & Doyle, M. P. (2015). Control of pathogens in biofilms on the surface of stainless steel by levulinic acid plus sodium dodecyl sulfate. *International Journal of Food Microbiology*, 207, 1–7.
- Choi, N. C., Park, S. J., Lee, C. G., Park, J. A., & Kim, S. B. (2011). Influence of surfactants on bacterial adhesion to metal oxide-coated surfaces. *Environmental Engineering Research*, 16, 219–225.
- Chorianopoulos, N. G., Giaouris, E. D., Kourkoutas, Y., & Nychas, G. J. E. (2010). Inhibition of the early stage of *Salmonella enterica* serovar Enteritidis biofilm development on stainless steel by cell-free supernatant of a *Hafnia alvei* culture. *Applied and Environmental Microbiology*, 76, 2018–2022.
- Donlan, R. M. (2002). Biofilms: microbial life on surfaces. *Emerging Infectious Diseases*, 8, 881–890.
- EFSA-ECDC (European Food Safety Authority and European Centre for Disease Prevention and Control). (2015). The European Union summary report on trends and sources of zoonoses, zoonotic agents and food-borne outbreaks in 2013. *EFSA Journal*, 13, 3991.
- Giaouris, E., Heir, E., Hebraud, M., Chorianopoulos, N., Langsrud, S., Moretto, T., et al. (2014). Attachment and biofilm formation by foodborne bacteria in meat processing environments: causes, implications, role of bacterial interactions and control by alternative novel methods. *Meat Science*, 97, 298–309.
- Gilbert, P., Allison, D. G., & McBain, A. J. (2002). Biofilms in vitro and in vivo: do singular mechanisms influx cross-resistance. *Journal of Applied Microbiology*, 92, 98S–110S.
- Gomes, M. Z. V., & Nitschke, M. (2012). Evaluation of rhamnolipid and surfactin to reduce the adhesion and remove biofilms of individual and mixed cultures of food pathogenic bacteria. *Food Control*, 25, 441–447.
- Hoiby, N., Bjarnsholt, T., Givskov, M., Molin, S., & Ciofu, O. (2010). Antibiotic resistance of bacterial biofilms. *International Journal of Antimicrobial Agents*, 35, 322–332.
- Islam, M. T., Oishi, A., Machida, C., Ogura, A., Kin, S., Honjoh, K. I., et al. (2014). Combined effects of selected food additives on adhesion of various foodborne pathogens onto microtiter plate and cabbage leaves. *Food Control*, 46, 233–241.
- Jahid, I. K., & Ha, S. D. (2012). A review of microbial biofilms of produce: future challenge to food safety. *Food Science and Biotechnology*, 21, 299–316.
- Lequette, Y., Boels, G., Clarisse, M., & Faille, C. (2010). Using enzymes to remove biofilms of bacterial isolates sampled in the food-industry. *Biofouling*, 26, 421–431.
- Mah, T. F. C., & O'Toole, G. A. (2001). Mechanisms of biofilm resistance to antimicrobial agents. *Trends in Microbiology*, 9, 34–39.
- Midelet, G., & Carpentier, B. (2002). Transfer of microorganisms, including *Listeria monocytogenes*, from various materials to beef. *Applied and Environmental Microbiology*, 68, 4015–4024.
- Mireles, J. R., Toguchi, A., & Harshey, R. M. (2001). *Salmonella enterica* serovar Typhimurium swarming mutants with altered biofilm-forming abilities: surfactin inhibits biofilm formation. *Journal of Bacteriology*, 183, 5848–5854.
- Mizan, M. F. R., Jahid, I. K., & Ha, S. D. (2015). Microbial biofilms in seafood: a food-hygiene challenge. *Food microbiology*, 49, 41–55.
- Molobela, I. P., Cloete, T. E., & Beukes, M. (2010). Protease and amylase enzymes for biofilm removal and degradation of extracellular polymeric substances (EPS) produced by *Pseudomonas fluorescens* bacteria. *Journal of Microbiology*, 4, 1515–1524.
- Park, J. H., Lim, J. G., & Choi, S. H. (2015). Effects of elevated intracellular cyclic di-GMP levels on biofilm formation and transcription profiles of *Vibrio vulnificus*. *Food Science and Biotechnology*, 24, 771–776.
- Perez-Rodriguez, F., Valero, A., Carrasco, E., Garcia, R. M., & Zurera, G. (2008). Understanding and modeling bacterial transfer to foods: a review. *Trends in Food Science & Technology*, 19, 131–144.
- Poimenidou, S., Belessi, C. A., Giaouris, E. D., Gounadaki, A. S., Nychas, G. J. E., & Skandamis, P. N. (2009). *Listeria monocytogenes* attachment to and detachment from stainless steel surfaces in a simulated dairy processing environment. *Applied and Environmental Microbiology*, 75, 7182–7188.
- Schreiberova, O., Hedbavna, P., Cejkova, A., Jirku, V., & Masak, J. (2009). Effect of surfactants on the biofilm of *Rhodococcus erythropolis*, a potent degrader of aromatic pollutants. *New Biotechnology*, 30, 62–68.
- Shi, X. M., & Zhu, X. N. (2009). Biofilm formation and food safety in food industries. *Trends in Food Science & Technology*, 20, 407–413.
- Simoës, M., Pereira, M. O., Machado, I., Simoes, L. C., & Vieira, M. J. (2006). Comparative antibacterial potential of selected aldehyde-based biocides and surfactants against planktonic *Pseudomonas fluorescens*. *Journal of Industrial Microbiology and Biotechnology*, 33, 741–749.
- Simoës, M., Simoes, L. C., Cleto, S., Pereira, M. O., & Vieira, M. J. (2008). The effects of a biocide and a surfactant on the detachment of *Pseudomonas fluorescens* from glass surfaces. *International Journal of Food Microbiology*, 121, 335–341.
- Simoës, M., Simoes, L. C., & Vieira, M. J. (2009). Species association increases biofilm resistance to chemical and mechanical treatments. *Water Research*, 43, 229–237.
- Simoës, M., Simoes, L. C., & Vieira, M. J. (2010). A review of current and emergent biofilm control strategies. *LWT-Food Science and Technology*, 43, 573–583.
- Splendiani, A., Livingston, A. G., & Nicoletta, C. (2006). Control membrane-attached biofilms using surfactants. *Biotechnology and Bioengineering*, 94, 15–23.
- Srey, S., Jahid, I. K., & Ha, S. D. (2013). Biofilm formation in food industries: a food safety concern. *Food Control*, 31, 572–585.
- Thallinger, B., Prasetyo, E. N., Nyanhongo, G. S., & Guebitz, G. M. (2013). Antimicrobial enzymes: an emerging strategy to fight microbes and microbial biofilms. *Biotechnology Journal*, 8, 97–109.
- Vieira, A., Jensen, A. R., Pires, S. M., Karlslose, P. S., Wegener, H. C., & Wong, D. L. F. (2009). WHO global food-borne infections network country databank – a resource to link human and non-human sources of *Salmonella* [C]. In *Proceeding of the 12th Symposium of the International Society for Veterinary Epidemiology and Economics, Durban, South Africa*.
- Wang, H. H., Ding, S. J., Dong, Y., Ye, K. P., Xu, X. L., & Zhou, G. H. (2013). Biofilm formation of *Salmonella* serotypes in simulated meat processing environments and its relationship to cell characteristics. *Journal of Food Protection*, 76, 1784–1789.
- Wang, H. H., Ye, K. P., Zhang, Q. Q., Dong, Y., Xu, X. L., & Zhou, G. H. (2013). Biofilm formation of meat-borne *Salmonella enterica* and inhibition by the cell-free supernatant from *Pseudomonas aeruginosa*. *Food Control*, 32, 650–658.
- Winkelstroter, L. K., Gomes, B. C., Thomaz, M. R. S., Souza, V. M., & De Martinis, E. C. P. (2011). *Lactobacillus sakei* 1 and its bacteriocin influence adhesion of *Listeria monocytogenes* on stainless steel surface. *Food Control*, 22, 1404–1407.



# Effect of covalent modification by (–)-epigallocatechin-3-gallate on physicochemical and functional properties of whey protein isolate



Zhenbao Jia<sup>a</sup>, Min Zheng<sup>b</sup>, Fei Tao<sup>c</sup>, Wenwei Chen<sup>c</sup>, Guangrong Huang<sup>a</sup>, Jiaxin Jiang<sup>a,\*</sup>

<sup>a</sup> Key Laboratory of Marine Food Quality and Hazard Controlling Technology of Zhejiang Province, China Jiliang University, Hangzhou 310018, China

<sup>b</sup> Department of Basic Medical, Jiangxi Medical College, Shangrao 334000, China

<sup>c</sup> National & Local United Engineering Lab of Quality Controlling Technology and Instrumentation for Marine Food, China Jiliang University, Hangzhou 310018, China

## ARTICLE INFO

### Article history:

Received 1 July 2015

Received in revised form

16 October 2015

Accepted 21 October 2015

Available online 23 October 2015

### Keywords:

Whey protein isolate

(–)-Epigallocatechin-3-gallate

Modification

Functional property

## ABSTRACT

The physicochemical and functional properties of covalently modified whey protein isolate (WPI) by (–)-epigallocatechin-3-gallate (EGCG) were investigated. WPI was chemically modified by EGCG under alkaline conditions. The effect of modification on foaming and emulsifying properties was evaluated. The results of SDS-PAGE and size exclusion chromatography indicated that modification by EGCG induced cross-linking on proteins of WPI. Fourier transform infrared spectroscopy (FT-IR) analysis illustrated the incorporation of phenolic groups into the modified WPI and the changes in protein secondary structure. Intrinsic fluorescence spectra revealed that modified WPI had a more compact tertiary structure compared to unmodified WPI. The modified WPI exhibited better foaming and emulsifying properties than unmodified WPI. These results suggest that EGCG modification is a potential method for improving the functional properties of WPI.

© 2015 Elsevier Ltd. All rights reserved.

## 1. Introduction

Whey proteins and their products are important food ingredients that are extensively utilized in manufacturing of food due to their high nutritional quality and versatile functional properties. WPI, one of the most important whey protein products, is a spray-dried powder with high protein content. Functional properties for WPI are particularly important in relation to the texture and structure of processed food. Therefore, increasing interest is directed toward modifying WPI to enhance functionality and thereby add value to the protein. Chemical modification is an effective way to improve the functional properties of WPI. During the past decade, a number of chemical modifications such as phosphorylation, glycation, deamidation, succinylation, and Maillard reaction have been proposed to improve the functional properties of WPI (Li, Enomoto, Ohki, Ohtomo, & Aoki, 2005; Liu & Zhong, 2012; Ma, Forssell, Partanen, Buchert, & Boer, 2011; Morand, Guyomarç'h, Legland, & Famelart, 2012).

Phenolic compounds represent the largest group of secondary plant metabolites and are widely distributed in plants. Dietary

phenolic substances have received much attention due to their ability to scavenge reactive oxygen species. Additionally, dietary phenolic compounds are known to interact with proteins in the food matrix. The details of the interactions between target proteins and phenolic compounds are not well understood, but covalent interactions of food proteins with phenolic compounds have been proposed. Phenolic compounds may be oxidized in an alkaline solution to their corresponding quinones (Hurrell & Finot, 1984). The electron-deficient quinones represent a species of highly reactive substances that normally react further with nucleophilic amino acid residues in a protein chain (Kroll, Rawel, & Rohn, 2003; Rawel, Rohn, Kruse, & Kroll, 2002). Many food proteins such as whey proteins, myoglobin, lysozyme, bovine serum albumin, and soy proteins could interact with phenolic compounds in this manner. Covalent modification by phenolic compounds produces food protein derivatives that have different physicochemical and conformational properties compared with unmodified proteins. Rawel, Czajka, Rohn and Kroll (2002) reported that soy protein derivatives exhibited different characteristics compared with unmodified soy protein, including isoelectric points, solubility, digestibility, secondary structure, and thermal stability. Ali, Homann, Khalil, Kruse, and Rawel (2013) reported that modification of  $\beta$ -lactoglobulin with coffee-specific phenolic compounds resulted in

\* Corresponding author.

E-mail address: [cjlujiaxinjiang@gmail.com](mailto:cjlujiaxinjiang@gmail.com) (J. Jiang).

changed structural properties, and alteration in solubility, surface hydrophobicity, and emulsifying properties were observed.

Tea is one of the most widely consumed beverages in the world, and is a rich source of health protective phenolic compounds (Kim et al., 2011; Thielecke & Boschmann, 2009). The predominant bioactive phenolic component of green tea, (–)-epigallocatechin-3-gallate (EGCG) is known to possess antioxidant, anti-inflammatory, and anti-cancer cell proliferation properties (Katiyar, Afaq, Azizuddin, & Mukhtar, 2001; Lestringant, Guri, Gülseren, Relkin, & Corredig, 2014; Zhong, Chiou, Pan, & Shahidi, 2012). On the basis of previous literature, we hypothesized that EGCG could covalently bind to nucleophilic amino acid residues in whey protein under alkaline conditions, which could lead to conformational changes. It is well known that the functional properties of food proteins are closely related to their physicochemical and structural characteristics. Accordingly, functional properties of whey protein may be altered by modification with EGCG through covalent reaction. However, to our knowledge, no studies have investigated the effects of covalent modification by EGCG on functional properties of WPI, particularly the foaming and emulsifying properties. Therefore, the main objective of the present study was to investigate the effect of covalent modification by EGCG on the physicochemical characteristics of WPI. Furthermore, the foaming and emulsifying properties of modified WPI were evaluated and compared.

## 2. Material and method

### 2.1. Chemicals

WPI was obtained from Hilmar Cheese Co. (Hilmar, CA, USA). According to the product bulletin, the typical composition of the WPI was 89% protein, 1.5% lactose, 0.5% fat, 2.5% ash, and 4.5% moisture. EGCG, KBr, and electrophoresis reagent were purchased from Sigma–Aldrich (Shanghai) Trading Co., Ltd. (Shanghai, China). Corn oil was purchased from Wumart Stores, Inc. (Hangzhou, China). All other chemicals were of reagent grade and obtained from Mike Chemical Co., Ltd. (Hangzhou, China).

### 2.2. Preparation of modified WPI with EGCG

WPI powder was dispersed in deionized water (35 g into 900 mL), and the pH value of the protein dispersion was adjusted to 9.0 using 0.5 M NaOH. EGCG solution (50 mL of 5 mg/mL) was mixed with the protein dispersion and then the volume was adjusted to 1000 mL with deionized water. After 12 h of reaction time under continuous stirring at 25 °C, the pH value of the protein dispersion was adjusted to 6.8 using 0.5 M HCl. To remove the free phenolic compounds in the protein dispersion, an ultrafiltration was performed using a Millipore Pellicon cassette module (Bedford, MA, USA), containing Biomax-5 membrane with a molecular weight cut-off (MWCO) of 5 kDa, with a membrane area of 0.1 m<sup>2</sup>. The ultrafiltration was operated in the mode of batch ultrafiltration with full recycle of the retentate. Until the final volume reduced to 200 mL, 800 mL of deionized water was added into the retentate. The ultrafiltration was repeated five times, and then the retentate was lyophilized. In addition, a control experiment was performed to obtain the unmodified WPI without EGCG during the same period.

### 2.3. Sodium dodecyl sulfate-polyacrylamide gel electrophoresis (SDS-PAGE)

SDS-PAGE was performed by a slab gel made from 5% stacking gel and 12% separating gel, according to the method of Laemmli (1970). WPI samples were dissolved in loading buffer (50 mM

Tris–Cl, pH 6.8, with 2% SDS, 10% glycerol and 0.1% bromophenol blue). Each well in the SDS-PAGE gel was loaded with 10 µg of WPI sample. Middle range unstained protein standard (catalog no. BM525, Sangon Biotech, Shanghai, China) was applied. The gel was stained with Coomassie Blue R-250, destained, and scanned.

### 2.4. Size exclusion chromatography (SEC)

Size exclusion chromatography (SEC) experiments were performed using the GE Healthcare ÄKTA Purifier 100 FPLC system equipped with a monitor UV-900 (Uppsala, Sweden) on a column of Sephacryl S-100 HR (1.6 × 70 cm). The column was equilibrated and eluted with 100 mM phosphate buffer (pH 7.8) at a flow rate of 1 mL/min. A 500 µL aliquot of WPI solution (5 mg/mL) was loaded on the column. The absorbance at 280 nm was used for detection of protein elution.

### 2.5. FT-IR spectroscopy

Infrared spectra were recorded at room temperature using a Thermo Scientific Nicolet 380 spectrometer (Madison, WI, USA) equipped with a deuterated triglycine sulfate detector. The WPI samples were mixed with KBr and then laminated. The resolution and scanning time were 4 cm<sup>-1</sup> and 32 times, respectively.

### 2.6. Intrinsic fluorescence spectroscopy

The fluorescence spectra were recorded using a Shimadzu RF-5301PC spectrofluorometer (Tokyo, Japan) in a 1 cm path length quartz cell. The excitation wavelength was 285 nm. Both the excitation and emission slit widths were set at 5 nm. The concentration of sample solutions prepared in 50 mM phosphate buffer (pH 7.0) was adjusted to 0.3 mg/mL. The emission spectra were collected between 300 and 450 nm.

### 2.7. Determination of foaming properties

Foaming properties were determined by using the method described by Aewsiri, Benjakul, and Visessanguan (2009) with some modifications. WPI dispersions (5, 20 and 35 mg/mL) were prepared in graduated test tubes by dispersing WPI powder in 20 mL of 100 mM phosphate buffer (pH 6.8). Whipping treatment was conducted at 12,000 rpm for 2 min at 25 °C using the IKA T25 homogenizer (Staufen, Germany). The sample was allowed to stand for 15 min at 25 °C. Both foaming capacity (FC) and foaming stability (FS) were calculated from the following equations:

$$FC (\%) = \frac{V_1}{V_0} \times 100$$

$$FS (\%) = \frac{V_2}{V_1} \times 100$$

where,  $V_0$  is the liquid volume before whipping,  $V_1$  is the initial foam volume after whipping and  $V_2$  is the final foam volume after leaving at 25 °C for 15 min.

### 2.8. Emulsion preparation and particle size determination

WPI dispersions (10, 20, and 40 mg/mL) were prepared in beakers by dispersing WPI powder in 150.0 mL of 100 mM phosphate buffer (pH 6.8) containing sodium azide (0.1 mg/mL). The emulsion was formed by transferring 50.0 mL of corn oil into the sample dispersion. The mixture was then pre-homogenized with the IKA T25 homogenizer (Staufen, Germany) at 12,000 rpm for 1 min at

25 °C. The crude emulsions were then homogenized with GEA Niro Soavi NS1001L2K high pressure homogenizer (Parma, Italy) for three passes at 40 MPa. After 0 and 28 days of storage at room temperature, a 30  $\mu$ L aliquot of the emulsion sample was transferred into 50 mL of SDS solution (1 mg/mL) and mixed. Then, the average droplet size was measured with Malvern Nano S90 Zeta-sizer (Worcestershire, U.K.), and expressed as the volume-surface average droplet size ( $d_{32}$ ) of emulsion.

### 2.9. Statistical analysis

Determinations of foaming and emulsifying properties were carried out in triplicate and the data was expressed in mean  $\pm$  standard deviation. Differences between means were assessed using a one-way analysis of variance (ANOVA). Values of  $P < 0.05$  were considered to be statistically significant. Statistical analysis was performed using SPSS statistical software version 13.0 (SPSS Inc, Chicago, USA).

## 3. Results and discussion

### 3.1. Profile of modified WPI by EGCG

SDS-PAGE run under reducing conditions was used to study change in the protein profile of WPI as a result of modification by EGCG. As shown in Fig. 1, the SDS-PAGE pattern of unmodified WPI showed three main bands attributed to  $\alpha$ -lactalbumin ( $\alpha$ -La),  $\beta$ -lactoglobulin ( $\beta$ -Lg), and bovine serum albumin (BSA), respectively (Lane 1). The SDS-PAGE pattern of modified WPI (Lane 2) revealed the formation of protein complexes, demonstrated by the dark stains at the top of the separating gel. Additionally, the formation of a new broad band with an estimated average molecular weight of around 36 kDa was observed at the middle of the separating gel, suggesting that the oligomer of whey proteins was obtained. The intensities of  $\alpha$ -La, BSA, and  $\beta$ -Lg bands in modified WPI decreased by comparison to those of unmodified WPI, suggesting that the proteins corresponding to these bands could be involved in the formation of cross-linked products. The SDS-PAGE results

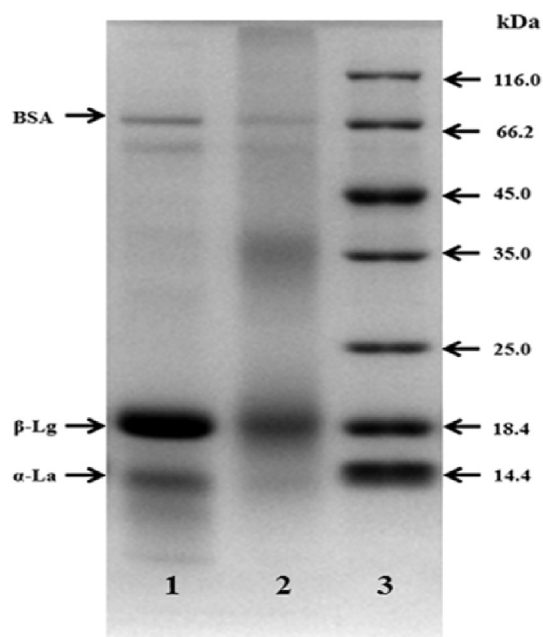


**Fig. 1.** SDS-PAGE patterns of unmodified and modified WPI. Lane 1, Unmodified WPI; Lane 2, Modified WPI; Lanes 3, Molecular weight standard.

demonstrated that the reaction by EGCG caused covalent cross-linking of whey proteins.

To support this finding, we used size exclusion chromatography (SEC) to analyze the unmodified and modified WPI. Fig. 2 shows the elution profiles of samples. Peaks 1, 2, and 3 in the elution profile of unmodified WPI were attributed to BSA,  $\beta$ -Lg, and  $\alpha$ -La, respectively. In the elution profile of modified WPI, a new peak appeared between peak 1 and peak 2, supporting the hypothesis that a cross-linking reaction occurred. Furthermore, the intensities of peaks 2 and 3 decreased and the intensity of peak 1 increased, which indicated that the whey protein components were polymerized to form protein complexes with high molecular weight. The results of SDS-PAGE and SEC illustrated that EGCG induced a cross-linking reaction and caused the change of profile for WPI. Our findings were not in agreement with the results of previous literature. Ishii et al. (2008) investigated the interaction between proteins and EGCG, and showed that EGCG can covalently bind to proteins through autoxidation, generating protein-EGCG conjugates. Meanwhile, Ali et al. (2013) also reported that the interaction between  $\beta$ -Lg and chlorogenic acid under alkaline conditions resulted in the attachment of phenolic derivatives to protein chains, leading to the formation of adducts. We speculated that the characteristics of both the protein and the phenolic compounds played crucial roles in the formation of reaction products.

### 3.2. FT-IR

Determining a protein's structure is essential for fully understanding its functional properties. FT-IR is a sensitive tool for detecting conformational changes of protein secondary structure (Jackson & Mantsch, 1995). Fig. 3 shows the FT-IR spectra of unmodified and modified WPI. In the spectrum of unmodified WPI, we observed three strong bands at 3294.2, 1648.0, and 1541.4  $\text{cm}^{-1}$ , corresponding to the vibrations for the amide A, amide I, and amide II of protein, respectively. As compared to the spectrum of unmodified WPI, a new absorption band at 3399.0  $\text{cm}^{-1}$  appeared in the EGCG-modified WPI spectrum, attributed to the O–H stretching vibration of the phenolic groups. The new band confirmed the binding of phenolic groups to the protein components in WPI via the covalent bond. Therefore, we speculated that some EGCG derivatives were incorporated into the cross-linked protein as bridging agents. The role of phenolic compounds as bridging agents in laccase-catalyzed cross-linking of protein has been proved in previous reports (Mattinen et al., 2005; Steffensen, Andersen, Degn, & Nielsen, 2008).

The amide I band represents the vibration of C=O stretching of the peptide bond, whereas the amide II band is primarily due to the vibrations of N–H bending and C–N stretching. Both amide I and amide II bands consist of overlapping bands at characteristic frequencies corresponding to different secondary structure elements (e.g.,  $\alpha$ -helices,  $\beta$ -sheets, turns, and disordered structures). Therefore, the frequencies of amide I and amide II bands are highly sensitive to the secondary structure of the polypeptide chain (Carton, Böcker, Ofstad, Sørheim, & Kohler, 2009). There have been a large amount of experimental and theoretical studies on these vibrations, especially with regard to their frequencies in relation to the secondary structures of polypeptide chains (Pelton & McLean, 2000; Torii, 2012). As shown in Fig. 3, the frequencies of amide I and amide II for modified WPI shifted to 1651.1 and 1538.2  $\text{cm}^{-1}$ , respectively. This indicated that the secondary structure of WPI was changed after modification.

### 3.3. Intrinsic fluorescence emission spectrum

The intrinsic fluorescence emission spectrum of protein is

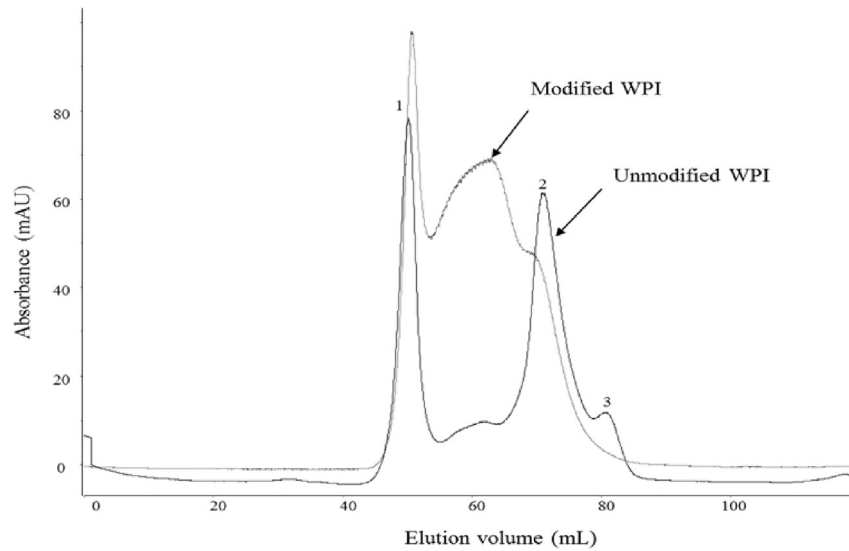


Fig. 2. SEC elution profiles of unmodified and modified WPI on the column of Sephacryl S-100 HR.

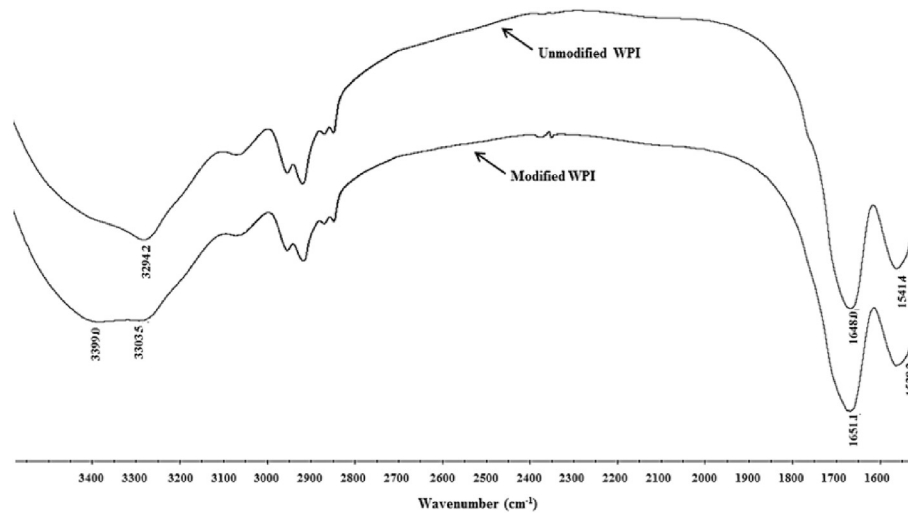


Fig. 3. The FT-IR spectra of unmodified and modified WPI.

usually dominated by tryptophan (Trp) and provides sensitive detection of tertiary conformation of the protein involved. The main proteins in WPI were  $\beta$ -lactoglobulin and  $\alpha$ -lactalbumin, which contained two and four Trp residues, respectively. To gain more insight into the conformational changes caused by the reaction of WPI with EGCG, the intrinsic Trp fluorescence assay was performed. Fig. 4 shows the intrinsic emission fluorescence spectra of unmodified and modified WPI with EGCG. The maximum fluorescence emission for modified WPI shifted from 336 nm to 339 nm, and the fluorescence intensity dramatically decreased. The red shift of the emission maximum indicated that the major fluorophore Trp was exposed to a more hydrophilic environment after modification, as a result of perturbation of protein tertiary structure (Kristo, Hazizaj, & Corredig, 2012). The decrease in the fluorescence intensity reflects that the Trp residues are less exposed in the modified WPI as compared to the control. A more compact protein molecule may allow deeper burial of its fluorophores in the protein core than a less compact molecule (Withana-Gamage, Hegedus, Qiu, McIntosh, & Wanasundara, 2013); therefore, the low

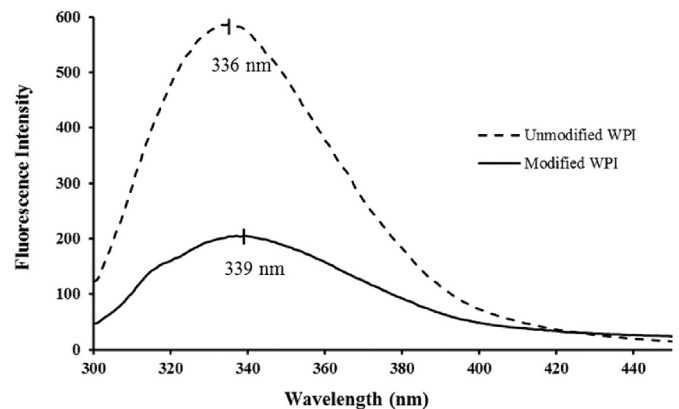


Fig. 4. Intrinsic fluorescence spectra of unmodified and modified WPI.

**Table 1**

The foaming capacity (FC) and foaming stability (FS) of modified and unmodified WPI at different concentrations.

	5 mg/mL		20 mg/mL		35 mg/mL	
	FC (%)	FS (%)	FC (%)	FS (%)	FC (%)	FS (%)
Unmodified WPI	27.2 ± 4.98 <sup>a</sup>	27.0 ± 7.36 <sup>a</sup>	157.8 ± 2.42 <sup>a</sup>	14.2 ± 0.58 <sup>a</sup>	159.2 ± 3.48 <sup>a</sup>	15.4 ± 1.45 <sup>a</sup>
Modified WPI	50.0 ± 1.32 <sup>b</sup>	25.5 ± 1.68 <sup>a</sup>	187.7 ± 14.67 <sup>b</sup>	23.4 ± 4.69 <sup>b</sup>	208.6 ± 1.79 <sup>b</sup>	30.1 ± 2.41 <sup>b</sup>

Results are expressed as the mean ± standard deviation; n = 3. Different letters within the same column are statistically different ( $P < 0.05$ ).

fluorescence intensity may indirectly indicate a high degree of molecule compactness for modified WPI. Another possible cause for the decrease in the intensity of intrinsic fluorescence may have been the attachment of phenolic moieties to protein, which led to a quenching effect, thereby reducing the emission intensity (Feroz, Mohamad, Bujang, Malek, & Tayyab, 2012).

### 3.4. Foaming properties

Foaming properties, estimated through FC and FS, are presented in Table 1. In the range of 5–35 mg/mL, the FC of modified WPI was significantly higher than those of unmodified WPI ( $P < 0.05$ ). At the low concentration (5 mg/mL), FS of modified WPI was comparable to that of unmodified WPI ( $P > 0.05$ ), but at the higher concentrations (25 mg/mL and 35 mg/mL), FS was significantly higher than those of unmodified WPI ( $P < 0.05$ ). The results revealed that the foaming properties of WPI were greatly improved by EGCG modification.

As described above, we found that the WPI was significantly modified by the cross-linking reaction induced by EGCG. The focus of previous studies were on the manipulation of foaming behavior of proteins by means of cross-linking treatment (Foegeding, Luck, & Davis, 2006; Moro, Báez, Busti, Ballerini, & Delorenzi, 2010). Molecular size of food protein was a crucial factor influencing foaming properties. It has been observed that whey protein polymers exhibited higher intrinsic viscosity compared with native whey protein, which generated more stabilized foams by the effective deceleration of drainage rate (Davis & Foegeding, 2004; Vardhanabhuti & Foegeding, 1999). Partanen et al. (2009) reported that the foaming capacity of sodium caseinate was improved due to the cross-linking reaction catalyzed by transglutaminase. Furthermore, the authors indicated that the cross-linking treatment changed the interfacial elasticity and enhanced the foam formation by means of suppressing coalescence and disproportionation. Additionally, it has been demonstrated by Kuan, Bhat, and Karim (2011) that the cross-linking and polymerization of egg white protein improved the foaming properties, because the cross-linked structure effectively enhanced the unfolding of the protein during foam forming and formation of more elastic foam networks at the air–water interfaces. Therefore, the improved foaming properties of modified WPI might be explained by the increased molecular size due to the cross-linking reaction.

### 3.5. Emulsifying properties

In the present study, the original  $d_{32}$  of emulsions (day 0) were

measured as the indicator of emulsifying ability, and the increases of  $d_{32}$  after 28 days of storage were followed to evaluate the emulsion stability. The results are presented in Table 2. At low concentrations (10 and 20 mg/mL), the modified WPI exhibited significantly lower original  $d_{32}$  values than unmodified WPI ( $P < 0.05$ ). But as the concentration rose to 40 mg/mL, there was no significant difference between the original  $d_{32}$  values of modified and unmodified WPI ( $P > 0.05$ ). The results implied that the emulsifying ability of WPI was increased after the modification. At all concentrations assayed, the increases of  $d_{32}$  values of modified WPI emulsions were lower than those of unmodified WPI emulsions after 28 days of storage, indicating EGCG modification improved the emulsion stability of WPI. This finding was consistent with the results in previous literature, which revealed that  $\alpha$ -La-polyphenol covalent complexes had better emulsion stability than  $\alpha$ -La (Wang et al., 2015).

WPI is considered to be a surface-active agent and can adsorb to the surfaces of oil droplets to form an interfacial film and stabilize the oil/water emulsion against flocculation or coalescence. The emulsifying properties of proteins depend on their abilities to diffuse to the oil/water interface, and then undergo partial unfolding and rearrangement at the interface. Conformational characteristic of food protein is particularly important in relation to the emulsifying properties of protein. According to Jambak, Lelas, Mason, Kresić, and Badanjak (2009), the changes of the protein conformational structure could influence surface hydrophobicity and subsequently lead to better adsorption of the oil/water emulsion system. Afizah and Rizvi (2014) stated that the improvement in the emulsifying activity of texturized whey protein concentrate was caused by the increase of exposed aromatic residues, which resulted in the increased affinity of the proteins towards the oil-water interface. They also explained that the aggregated whey protein formed a thicker protein membrane, thus providing better emulsifying stability for the oil droplets. EGCG-induced protein conformational changes were indicated by the results obtained from SDS-PAGE, FT-IR, and intrinsic Trp fluorescence assay. Therefore, the results suggested that the conformational changes on the surface properties of WPI upon EGCG modification led to the improvement of the emulsifying properties.

## 4. Conclusion

In summary, our results indicated the possibility of using EGCG modification to improve the functional properties of WPI. The EGCG modification caused cross-linking and conformational structure changes of proteins in WPI. Furthermore, we found that

**Table 2**The average droplet size ( $d_{32}$ ) of emulsion with modified and unmodified WPI at different concentrations during storage.

	0 day			28 days		
	10 mg/mL	20 mg/mL	40 mg/mL	10 mg/mL	20 mg/mL	40 mg/mL
Unmodified WPI	689.8 ± 42.31 <sup>a</sup>	423.9 ± 30.78 <sup>a</sup>	301.3 ± 12.62 <sup>a</sup>	804.4 ± 40.84 <sup>a</sup>	509.5 ± 31.41 <sup>a</sup>	337.2 ± 17.42 <sup>a</sup>
Modified WPI	506.9 ± 31.78 <sup>b</sup>	350.2 ± 17.33 <sup>b</sup>	288.6 ± 7.17 <sup>a</sup>	596.2 ± 26.73 <sup>b</sup>	409.4 ± 20.16 <sup>b</sup>	299.4 ± 12.35 <sup>b</sup>

Results are expressed as the mean ± standard deviation; n = 3. Different letters within the same column are statistically different ( $P < 0.05$ ).

the foaming and emulsifying properties of WPI were enhanced by EGCG modification. This study provides valuable information on the potential application of modified WPI by EGCG. Further research is needed to evaluate the effect of EGCG modification on other functionalities of WPI, in order to develop their applications in food industries.

## Acknowledgments

We gratefully acknowledge the financial support from the National Natural Science Foundation of China (31101319).

## References

- Aewsiri, T., Benjakul, S., & Visessanguan, W. (2009). Functional properties of gelatin from cuttlefish (*Sepia pharaonis*) skin as affected by bleaching using hydrogen peroxide. *Food Chemistry*, *115*, 243–249.
- Afizah, M. N., & Rizvi, S. S. H. (2014). Functional properties of whey protein concentrate texturized at acidic pH: effect of extrusion temperature. *LWT – Food Science and Technology*, *57*, 290–298.
- Ali, M., Homann, T., Khalil, M., Kruse, H. P., & Rawel, H. (2013). Milk whey protein modification by coffee-specific phenolics: effect on structural and functional properties. *Journal of Agricultural and Food Chemistry*, *61*, 6911–6920.
- Carton, I., Böcker, U., Ofstad, R., Sørheim, O., & Kohler, A. (2009). Monitoring secondary structural changes in salted and smoked salmon muscle myofiber proteins by FT-IR microspectroscopy. *Journal of Agricultural and Food Chemistry*, *57*, 3563–3570.
- Davis, J. P., & Foegeding, E. A. (2004). Foaming and interfacial properties of polymerized whey protein isolate. *Journal of Food Science*, *69*, C404–C410.
- Feroz, S. R., Mohamad, S. B., Bujang, N., Malek, S. N. A., & Tayyab, S. (2012). Multi-spectroscopic and molecular modeling approach to investigate the interaction of flavokawain B with human serum albumin. *Journal of Agricultural and Food Chemistry*, *60*, 5899–5908.
- Foegeding, E. A., Luck, P. J., & Davis, J. P. (2006). Factors determining the physical properties of protein foams. *Food Hydrocolloids*, *20*, 284–292.
- Hurrell, R. F., & Finot, P. A. (1984). Nutritional consequences of the reactions between proteins and oxidized polyphenolic acids. *Advances in Experimental Medicine and Biology*, *177*, 423–435.
- Ishii, T., Mori, T., Tanaka, T., Mizuno, D., Yamaji, R., Kumazawa, S., et al. (2008). Covalent modification of proteins by green tea polyphenol (–)-epigallocatechin-3-gallate through autoxidation. *Free Radical Biology & Medicine*, *45*, 1384–1394.
- Jackson, M., & Mantsch, H. H. (1995). The use and misuse of FTIR spectroscopy in the determination of protein structure. *Critical Reviews in Biochemistry and Molecular Biology*, *30*, 95–120.
- Jambrak, A. R., Lelas, V., Mason, T. J., Kresić, G., & Badanjak, M. (2009). Physical properties of ultrasound treated soy proteins. *Journal of Food Engineering*, *93*, 386–393.
- Katiyar, S. K., Afaq, F., Azizuddin, K., & Mukhtar, H. (2001). Inhibition of UVB-induced oxidative stress-mediated phosphorylation of mitogen-activated protein kinase signaling pathways in cultured human epidermal keratinocytes by green tea polyphenol (–)-Epigallocatechin-3-gallate. *Toxicology and Applied Pharmacology*, *176*, 110–117.
- Kim, A., Chiu, A., Barone, M. K., Avino, D., Wang, F., Coleman, C. I., et al. (2011). Green tea catechins decrease total and low-density lipoprotein cholesterol: a systematic review and meta-analysis. *Journal of the American Dietetic Association*, *111*, 1720–1729.
- Kristo, E., Hazizaj, A., & Corredig, M. (2012). Structural changes imposed on whey proteins by UV irradiation in a continuous UV light reactor. *Journal of Agricultural and Food Chemistry*, *60*, 6204–6209.
- Kroll, J., Rawel, H. M., & Rohn, S. (2003). Reactions of plant phenolics with food proteins and enzymes under special consideration of covalent bonds. *Food Science and Technology Research*, *9*, 205–218.
- Kuan, Y. H., Bhat, R., & Karim, A. A. (2011). Emulsifying and foaming properties of ultraviolet-irradiated egg white protein and sodium caseinate. *Journal of Agricultural and Food Chemistry*, *59*, 4111–4118.
- Laemmli, U. K. (1970). Cleavage of structural proteins during the assembly of the head of bacteriophage T4. *Nature*, *227*, 680–685.
- Lestringant, P., Guri, A., Gülseren, I., Relkin, P., & Corredig, M. (2014). Effect of processing on physicochemical characteristics and bioefficacy of  $\beta$ -lactoglobulin-epigallocatechin-3-gallate complexes. *Journal of Agricultural and Food Chemistry*, *62*, 8357–8364.
- Li, C. P., Enomoto, H., Ohki, S., Ohtomo, H., & Aoki, T. (2005). Improvement of functional properties of whey protein isolate through glycation and phosphorylation by dry heating. *Journal of Dairy Science*, *88*, 4137–4145.
- Liu, G., & Zhong, Q. (2012). Glycation of whey protein to provide steric hindrance against thermal aggregation. *Journal of Agricultural and Food Chemistry*, *60*, 9754–9762.
- Ma, H., Forssell, P., Partanen, R., Buchert, J., & Boer, H. (2011). Charge modifications to improve the emulsifying properties of whey protein isolate. *Journal of Agricultural and Food Chemistry*, *59*, 13246–13253.
- Mattinen, M., Kruus, K., Buchert, J., Nielsen, J. H., Andersen, H. J., & Steffensen, C. L. (2005). Laccase-catalyzed polymerization of tyrosine-containing peptides. *FEBS Journal*, *272*, 3640–3650.
- Morand, M., Guyomarc'h, F., Legland, D., & Famelart, M. H. (2012). Changing the isoelectric point of the heat-induced whey protein complexes affects the acid gelation of skim milk. *International Dairy Journal*, *23*, 9–17.
- Moro, A., Báez, G. D., Busti, P. A., Ballerini, G. A., & Delorenzi, N. J. (2010). Effects of heat-treated  $\beta$ -lactoglobulin and its aggregates on foaming properties. *Food Hydrocolloids*, *25*, 1009–1015.
- Partanen, R., Paananen, A., Forssell, P., Linder, M. B., Lille, M., Buchert, J., et al. (2009). Effect of transglutaminase-induced cross-linking of sodium caseinate on the properties of equilibrated interfaces and foams. *Colloids and Surfaces A, Physicochemical and Engineering Aspects*, *344*, 79–85.
- Pelton, J. T., & McLean, L. R. (2000). Spectroscopic methods for analysis of protein secondary structure. *Analytical Biochemistry*, *277*, 167–176.
- Rawel, H. M., Czajka, D., Rohn, S., & Kroll, J. (2002a). Interactions of different phenolic acids and flavonoids with soy proteins. *International Journal of Biological Macromolecules*, *30*, 137–150.
- Rawel, H. M., Rohn, S., Kruse, H. P., & Kroll, J. (2002b). Structural changes induced in bovine serum albumin by covalent attachment of chlorogenic acid. *Food Chemistry*, *78*, 443–455.
- Steffensen, C. L., Andersen, M. L., Degn, P. E., & Nielsen, J. H. (2008). Cross-linking proteins by laccase-catalyzed oxidation: importance relative to other modifications. *Journal of Agricultural and Food Chemistry*, *56*, 12002–12010.
- Thielecke, F., & Boschmann, M. (2009). The potential role of green tea catechins in the prevention of the metabolic syndrome – a review. *Phytochemistry*, *70*, 11–24.
- Torii, H. (2012). Mechanism of the secondary structure dependence of the infrared intensity of the amide II mode of peptide chains. *Journal of Physical Chemistry Letters*, *3*, 112–116.
- Vardhanabhuti, B., & Foegeding, E. A. (1999). Rheological properties and characterization of polymerized whey protein isolates. *Journal of Agricultural and Food Chemistry*, *47*, 3649–3655.
- Wang, X., Liu, F., Liu, L., Wei, Z., Yuan, F., & Gao, Y. (2015). Physicochemical characterization of  $\beta$ -carotene emulsion stabilized by covalent complexes of  $\alpha$ -lactalbumin with (–)-epigallocatechin gallate or chlorogenic acid. *Food Chemistry*, *173*, 564–568.
- Withana-Gamage, T. S., Hegedus, D. D., Qiu, X., McIntosh, T., & Wanasundara, J. P. D. (2013). Structural and physicochemical property relationships of cruciferin homohexamers. *Journal of Agricultural and Food Chemistry*, *61*, 5848–5859.
- Zhong, Y., Chiou, Y. S., Pan, M. H., & Shahidi, F. (2012). Anti-inflammatory activity of lipophilic epigallocatechin gallate (EGCG) derivatives in LPS-stimulated murine macrophages. *Food Chemistry*, *134*, 742–748.



## Phytochemical investigations and evaluation of antidiabetic potential of *Prunus dulcis* nuts



Muhammad Nasimullah Qureshi<sup>a, b, c</sup>, Sodik Numonov<sup>a, b, d</sup>, Ajigu Abudurexiti<sup>b</sup>,  
Haji Akber Aisa<sup>a, b, \*</sup>

<sup>a</sup> Key Laboratory of Plant Resources and Chemistry in Arid Regions, Xinjiang Technical Institute of Physics and Chemistry, Chinese Academy of Sciences, Urumqi 830011, PR China

<sup>b</sup> Key Laboratory of Xinjiang Indigenous Medicinal Plants Resource Utilization, Xinjiang Technical Institute of Physics and Chemistry, Chinese Academy of Sciences, Urumqi 830011, PR China

<sup>c</sup> Department of Chemistry, Abdul Wali Khan University Mardan, Mardan 23200, Pakistan

<sup>d</sup> State Scientifically-Experimental and Production Organization Academy of Sciences of the Republic of Tajikistan, Dushanbe 734063 Tajikistan

### ARTICLE INFO

#### Article history:

Received 11 May 2015

Received in revised form

28 August 2015

Accepted 30 August 2015

Available online 2 September 2015

#### Keywords:

*Prunus dulcis* nuts

Column chromatography

LC-MS/MS

<sup>1</sup>H and <sup>13</sup>C NMR

Antidiabetic activity

#### Chemical compounds studied in this article are:

Dihydroquercetin glucoside (PubChem CID 71587141)

Eriodictyol glucoside (PubChem CID 13254473)

Kaempferol rutinoside (PubChem CID 20055286)

Isorhamnetin rutinoside (PubChem CID 5481663)

Kaempferol hexoside (PubChem CID 5282102)

Catechin hexoside (PubChem CID 14282767)

Eriodictyol (PubChem CID: 440735)

Quercetin (PubChem CID: 5280343)

Kaempferol (PubChem CID: 5280863)

Isorhamnetin (PubChem CID: 5281654).

### ABSTRACT

*Prunus dulcis* has long been known as a source of nutrients in many traditional foods and healthy snack. Presence of various biologically active compounds, such as phenolic compounds including flavonoids, phenolic acids, tannins etc and vitamin E, bases for their antioxidant and other health promoting activities. The present study is focused on the phytochemical characterization through chromatographic isolation and purification, and mass spectrometric identification of various compounds along with evaluation of antidiabetic activity of various extracts of *P. dulcis* nuts. Stigmasitosterol-3-O-β-D-glucoside and α-D-Glucopyranosyl-(1 → 2)-β-D-fructofuranoside were isolated for the first time along with a known compound isolated previously from the skin of the almond. Mass spectrometric analysis delivered some compounds like catechin dihexoside, caffeoyl-6'-secologanoside and (epi)catechin-ethyl trimer which were detected for the first time in almond along with other compounds which have been identified in the skin of almond. Highest antidiabetic activity has been determined for 70% ethanol extract, even more than the control sample, among the other extracts evaluated. The published literature showed no such detailed study of the whole almond nuts as the main focus was on the brown almond skin, and is presented for the first time.

© 2015 Elsevier Ltd. All rights reserved.

### 1. Introduction

Plants associated with food including nuts, fruits, vegetables and spices have been the primary source of naturally occurring pharmacologically active metabolites for human (Alasalvar & Shahidi, 2009; Qureshi, Stecher, & Bonn, 2014). These plants have been

\* Corresponding author. Key Laboratory of Plant Resources and Chemistry in Arid Regions, Xinjiang Technical Institute of Physics and Chemistry, Chinese Academy of Sciences, 40-1 South Beijing Road, Urumqi 830011, PR China.

E-mail address: [haji@ms.xjb.ac.cn](mailto:haji@ms.xjb.ac.cn) (H.A. Aisa).

used to cure different diseases since ancient time, employing raw plant material and pure compounds extracted from these plants (Monagas, Garrido, Lebrón-Aguilar, Bartolome, & Gómez-Cordovés, 2007; Qureshi et al., 2014). Increasing trend has been observed in using the crude extracts of these nuts, fruits, vegetables and spices by the food, pharmaceutical and cosmetic industries based on their various proven pharmacological properties (Qureshi, Stecher, Qureshi, Sultana, & Bonn, 2012; Sultana et al., 2008). *Prunus dulcis*, the cultivated sweet almond, belongs to the family Rosaceae and is one of the most popular tree nuts worldwide. Almond nuts have been used in various forms as in the form of raw nuts or the processed foods, such as snack foods and in a variety of bakery and confectionery products. It has long been known as a source of nutrients in many traditional foods and healthy snack (Esfahlan, Jamei, & Esfahlan, 2010; Jamshed & Gilani, 2014; Monagas et al., 2007). Antioxidant and other health promoting activities of almonds are due to the presence of various biologically active compounds, such as phenolic compounds: flavonoids, phenolic acids, tannins etc and vitamin E (Rao, 2012; Xie, Roto, & Bolling, 2012).

Various pharmacological activities such as lowering of blood pressure, decreasing of cholesterol level, anti-inflammatory effects, anticarcinogenic, reducing the risk of cardiovascular disease and obesity related problems, have been attributed to the regular moderate use of almond nuts (Monagas et al., 2007; Rao, 2012). It has been shown that polyphenolic compounds present in almond skin act synergistically with vitamin C and E, thus enhancing the antioxidant protection by safeguarding the low density lipoprotein (LDL) from oxidation (Esfahlan et al., 2010; Jamshed & Gilani, 2014). Procyanadin present in the skin have a proven hepatoprotective effect besides other properties such as antioxidant, antiatherogenic, and anticarcinogenic (de Pascual-Teresa, Moreno, & García-Viguera, 2010; Truong et al., 2014; Wijeratne, Abou-Zaid, & Shahidi, 2006; Xie et al., 2012).

Type 2 diabetes mellitus is a metabolic disorder characterized by the insulin resistance due to inadequate insulin action in the human resulting defects in insulin signaling, thus causes hyperglycemia in blood. It has been shown that an enzyme named protein tyrosine phosphatase 1B (PTP1B) is responsible for the negative regulation of insulin signaling in human (Koren & Fantus, 2007). Therefore, inhibition of such negative regulator is necessary for the treatment of type 2 diabetes mellitus (Baumgartner et al., 2010; Zhang & Lee, 2003). Chemical compounds capable of inhibiting this enzyme PTP1B from negative regulation of insulin are beneficial for curing type 2 diabetes mellitus (Zhang & Lee, 2003). In spite of enormous efforts for targeting the PTP1B enzyme to inhibit its action in creating defects in insulin signaling, there is still need to identify safe, selective and effective PTP1B inhibitor (Kasibhatla, Wos, & Peters, 2007). Polyphenolic compounds especially flavonoids and their glycosides, in the pure form as well as extracts containing these compounds, have shown promising results as PTP1B inhibitor and can be used in pharmaceutical formulations against type 2 diabetes mellitus (Zhang et al., 2010; Na et al., 2015).

Among the various analytical techniques, liquid chromatography hyphenated to UV or PDA and mass spectrometry has been mostly employed for the characterization of compounds in foods and phyto-pharmaceuticals. Numerous studies have focused on the characterization of polyphenols in almonds (Bolling, Dolnikowski, Blumberg, & Oliver Chen, 2009; Frison-Norrie & Sporns, 2002; Frison & Sporns, 2002; Hughey et al., 2012, 2008; Mandalari et al., 2010; Milbury, Chen, Dolnikowski, & Blumberg, 2006; Monagas et al., 2007; Wijeratne et al., 2006). Almond skin contains hydroxybenzoic acids and aldehydes, phenolic acids, flavan-3-ols, flavonol glycosides, flavonol aglycones, flavanones, flavonone glycosides, flavonone aglycones, isoflavones and lignans which comprise 0.2–0.8% of the dry weight of almond skins (Garrido,

Monagas, Gómez-Cordovés, & Bartolomé, 2008; Monagas et al., 2007; Monagas et al., 2009). Flavanol and flavonol glycosides are the most abundant phenolic compounds in almond skin, particularly catechin, epicatechin, isorhamnetin-3-O-rutinoside, isorhamnetin-3-O-glucoside, naringenin-7-O-glucoside and kaempferol-3-O-rutinoside (Bolling, Dolnikowski, Blumberg, & Chen, 2010; Hughey et al., 2012; Milbury et al., 2006; Monagas et al., 2007; Monagas et al., 2009).

It appears from the literature that much of the work so far has been performed on almond, is focused on the almond skin, which is 3–4% of the almond nut, containing antioxidant polyphenolic compounds in major. To our knowledge, literature regarding the chemical characterization, pharmacological activities of the whole almond seed, and isolation and purification of the active metabolites is very scarce. The present study deals with the characterization of polyphenolic compounds in 70% ethanol extract of the almond nuts through LC-MS in negative ionization mode and determination of antidiabetic activity of different extracts of whole almond shelled seed. Further, isolation of active compounds through chromatographic procedures was carried out producing pure compounds.

## 2. Materials and methods

### 2.1. General section

HPLC grade acetonitrile, methanol and formic acid were obtained from Merck KGaA (Darmstadt, Germany). Petroleum ether (60–90 °C), hexane, chloroform, ethyl acetate, methanol, absolute ethanol were of analytical grade purchased from Tianjinshi Baishi Chemicals Company (pvt) Urumqi, China. For HPLC-UV and LC-MS analyses HPLC grade solvents were used. Silica gel (mesh size 100–200; surface area 200–300 m<sup>2</sup>) and sphenadex LH-20 were used for column chromatography. Double distilled water obtained through Millipore water system was used through out the experiments.

<sup>1</sup>H (400 and 600 MHz), <sup>13</sup>C (100 and 150 MHz), and 2D NMR spectra were obtained on Varian AM-600 and AM-400 NMR spectrometers. Pre-coated silica (HSGF 254) TLC plates (2.5 × 10 cm; thickness 0.2 mm) were used for developing the TLC profile of the fractions, with compounds visualized by spraying with 5% (v/v) H<sub>2</sub>SO<sub>4</sub> in ethanol solution and UV light.

### 2.2. Collection of the almond fruit

Almond fruits (*P. dulcis*) were obtained from almond farm in Kashghar, China. The fruits were authenticated and voucher sample has been deposited in the herbarium of the Xinjiang Technical Institute of Physics and Chemistry, Chinese Academy of Sciences, Urumqi 830011, P. R. China. Shells were removed and shelled nuts were ground to powder with particle size 50–300 mesh through grinder (Model: 500A) from AO LI BANG, P. R. China.

### 2.3. Extraction and isolation

Fig. 1 shows the flow sheet diagram of the extraction and chromatographic procedure. 2.5 kg of almond seed powder were added 7.5 L of petroleum ether:hexane (1:1) in a steel extractor for 24 h at room temperature to defat the seed powder and to extract the oil. Extraction was repeated three times. Solvent was recovered using rotary evaporator (Büchi, Japan) at 30–35 °C affording 52% oil. After extracting the oil, the seeds powder was dried at room temperature and extracted with 70% ethanol (10 L) for 24 h. Extraction was repeated three time and all the extracts were combined and filtered. Solvent was recovered using rotary evaporator producing dry extract (232 g). The dry extract was suspended

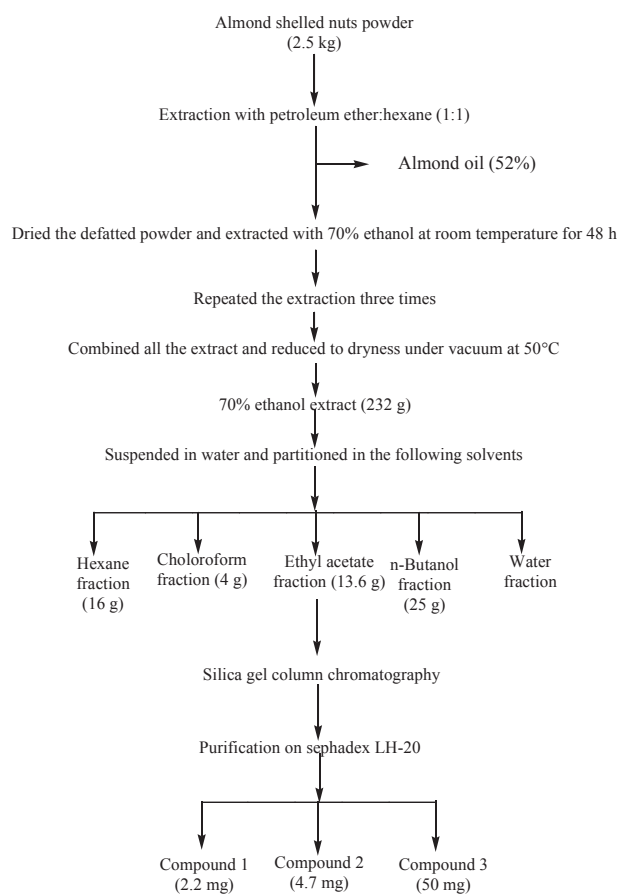


Fig. 1. Flow sheet diagram of the extraction and chromatographic procedure.

in water (500 mL) and partitioned successively with hexane (3 × 500 mL), chloroform (3 × 500 mL), ethyl acetate (3 × 500 mL) and n-butanol (3 × 500 mL) yielding gummy fractions of hexane (16 g), chloroform (4 g), ethyl acetate (13.6 g) and n-butanol (25 g). The remaining was the aqueous extract.

Eleven gram of ethyl acetate fraction was mixed thoroughly with about 25 g of dry silica gel. The mixture was dried in the oven at 45 °C. The mixture was then subjected to silica gel column chromatography in a uniform layer. Elution was performed in a gradient mode starting with petroleum ether:ethyl acetate (9:1). Polarity of the eluent was gradually increased as petroleum ether:ethyl acetate (4:1–1:1) - ethyl acetate - ethyl acetate:methanol (9:1–1:1) - methanol and ended with methanol:water (4:1). Similar fractions were combined after developing their TLC profile.

Fractions 8 to 12 were combined together (38 mg) and subjected to sephadex LH-20 column chromatography (25 × 1.6 cm) with methanol:chloroform (1:1) producing 10 fractions. Fractions 7–8 were combined (9.9 mg) and re-subjected to sephadex LH-20 column chromatography (25 × 1.6 cm) with methanol delivering a pure compound (**1**) 2.2 mg.

Fraction 16 was divided into methanol soluble and methanol:chloroform (1:1) soluble part 16b. Fraction 16b was washed three times with methanol producing a pure compound (**2**) 4.7 mg. Fractions 46 resulted in crystallization on standing without further processing. The crystals were separated and washed giving a pure crystalline compound (**3**). The spectra of the isolated compounds were recorded with <sup>1</sup>H and <sup>13</sup>C NMR along with HMBC, HSQC and DEPT analysis to characterize these compounds.

## 2.4. Spectral identification of isolated compounds

**Compound 1**; Catechin: <sup>1</sup>H NMR (600 MHz, MeOH-*d*<sub>4</sub>) δ<sub>H</sub> 4.51 (1H, d, *J* = 7.5 Hz, H-2), 3.93 (1H, m, H-3), 2.47 (1H, dd, *J* = 16.1; 8.1 Hz, H-4a), 2.80 (1H, dd, *J* = 16.1; 5.4 Hz, H-4b), 5.88 (1H, d, *J* = 2.2 Hz, H-6), 5.80 (1H, *J* = 2.2 Hz, H-8), 6.72 (1H, d, *J* = 8.1 Hz, H-5'), 6.67 (1H, dd, *J* = 8.1; 1.8 Hz, H-6'), 6.79 (1H, d, *J* = 1.7 Hz, H-2').

**Compound 2**; Stigmasitosterol-3-O-β-D-glucoside: <sup>1</sup>H NMR (600 MHz, Pyridine-*d*<sub>5</sub>) δ<sub>H</sub> 0.67 (3H, s, H-18), 0.87 (3H, s, H-26), 0.89 (3H, s, H-27), 0.91 (3H, t, *J* = 7.4 Hz, H-29), 0.95 (3H, s, H-19), 1.00 (3H, d, *J* = 6.4 Hz, H-21), 3.96 (1H, d, *J* = 5.6 Hz, H-3), 5.37 (1H, d, *J* = 4.6 Hz, H-22), 5.10 (1H, d, *J* = 7.7 Hz, H-23). Glucose ring: 4.04 (1H, m, H-3), 4.34 (1H, d, *J* = 5.4 Hz, H-5), 4.10 (1H, t, *J* = 7.1 Hz, H-2), 4.30 (1H, m, H-4), 4.61 (d, *J* = 11.4 Hz, H-6a); 4.46 (1H, dd, *J* = 11.4 Hz, H-6b), 5.03 (1H, br. s, H-1).

**Compound 3**; α-D-Glucopyranosyl-(1 → 2)-β-D-fructofuranoside: <sup>1</sup>H NMR (400 MHz, D<sub>2</sub>O) δ<sub>H</sub> 5.37 (1H, d, *J* = 3.8 Hz, H-1), 3.51 (1H, d, *J* = 3.8 Hz, H-2), 3.70 (1H, d, *J* = 9.6 Hz, H-3), 3.42 (1H, t, *J* = 9.4 Hz, H-4), 3.86 (1H, m, H-5), 3.78 (4H, *J* = 2.7 Hz, H-6, H-6'), 3.63 (2H, br. s, H-1'), 3.50 (1H, d, *J* = 3.8 Hz, H-2'), 4.17 (1H, d, *J* = 8.8 Hz, H-3'), 4.0 (1H, t, *J* = 8.5 Hz, H-4'), 3.82 (1H, m, H-5'). <sup>13</sup>C NMR (100 MHz, D<sub>2</sub>O) δ<sub>C</sub> 94.9 (C-1), 73.8 (C-2), 73.8 (C-2), 75.3 (C-3), 72.0 (C-4), 75.1 (C-5), 62.8 (C-6), 64.1 (C-1'), 106.4 (C-2'), 79.1 (C-3'), 76.7 (C-4'), 84.1 (C-5'), 65.1 (C-6').

## 2.5. HPLC-MS/MS analysis

LC system coupled to a linear ion trap mass spectrometer (4000 Q TRAP) from AB Sciex equipped with column oven, a solvent delivery pump and an auto-sampler. Analyst 1.5 software was used to control LC-ESI-MS. The chromatographic separation was performed on a reversed stationary phase column (XBridge™ C18, particle size 5 μm, 4.6 × 150 mm with guard column). Gradient elution was carried out using mobile phase A: 1% formic acid in water and B: 1% formic acid in acetonitrile. Column temperature was kept as ambient and a flow rate of 0.5 ml per minute was used. Zero time condition was 5% B and a linear gradient to 60% B was applied up to 30 min. Then a linear gradient to 100% B up to 35 min was applied and the column was equilibrated at 100% B for 5 min. The whole analysis took 40 min. MS was used in negative ionization mode and the scanning was performed in the mass range *m/z* values from 100 to 2000. Twenty microliters (20 μL) of sample was injected into the chromatographic column.

## 2.6. Antidiabetic activity: PTP1B (protein tyrosine phosphatase-1B) inhibitory assay

The inhibition activity of the plant extracts against human recombinant PTP1B was evaluated using pNPP as a substrate, according to PTP1B pNPP hydrolysis of the phosphate group and produces a color reaction measured the activity of PTP1B. Dried extracts (0.1 g) were dissolved in 1 mL of DMSO and were preincubated with the enzyme at room temperature for 5 min. 178 μL of buffer [containing 20 mM HEPES (4-(2-Hydroxyethyl)-1-piperazineethanesulfonic acid), 150 mM NaCl and 1 mM EDTA (ethylenediaminetetraacetic acid)] were added to 96 well plate. One microliter of PTP1B protein solution (0.115 mg/mL) and 1 μL of the test sample or positive control sample or DMSO were added to the buffer solution and mixed them well. The 96 well plate was preincubated at room temperature for 10 min, and then 20 μL of pNPP solution (35 mM) were added. Following incubation at 25 °C for 30 min in dark, the reaction was terminated with the addition of 10 μL of 3 M NaOH solution. The absorbance was determined at 405 nm wavelength using SpectraMax MD5 (USA Molecular Devices) and was corrected by measuring the increase in absorbance

at 405 nm of sample from the nonenzymatic hydrolysis of 35 mM pNPP obtained in the absence of PTP1B enzyme (Bozorov et al., 2014; Yili et al., 2014). Inhibition percentage (%) and IC<sub>50</sub> value was calculated. PTP1B inhibitor was used as a control sample.

### 3. Results and discussion

#### 3.1. Isolation and purification of compounds

It has been shown that most of the biologically active compounds present in plants like polyphenolic compounds and their glycosides, which are responsible for various pharmacological activities such as PTP1B inhibition activity, antioxidant activity, antimicrobial activity (Ajileye, Obuotor, Akinkunmi, & Aderogba, 2015; Jiang et al., 2015; Sang et al., 2002; Sang, Lapsley, Rosen, & Ho, 2002), are extracted in ethyl acetate during their extraction and fractionation. Based on the previous literature published and the significant PTP1B activity shown in this experiment, ethyl acetate fraction was selected for the isolation of the following pure compounds.

**Compound 1;** Catechin: white crystals, MF C<sub>15</sub>H<sub>14</sub>O<sub>6</sub> (Fig. 2). The <sup>1</sup>H NMR spectrum showed three aromatic protons signals at δ<sub>H</sub> 6.79 (1H, d, *J* = 1.7 Hz, H-2'), δ<sub>H</sub> 6.72 (1H, d, *J* = 8.1 Hz, H-5') and δ<sub>H</sub> 6.67 (1H, dd, *J* = 8.1; 1.8 Hz, H-6') in the form of an ABD spin-system, which indicated that 3', 4' were substituted on the B-ring and showed a pair of meta coupling protons signals at δ<sub>H</sub> 5.88 (1H, d,

*J* = 2.2 Hz, H-6) and δ<sub>H</sub> 5.80 (1H, *J* = 2.2 Hz, H-8) for the A ring. Two doublet–doublet signals at δ<sub>H</sub> 2.47 (1H, dd, *J* = 16.1; 8.1 Hz, H-4a) and δ<sub>H</sub> 2.80 (1H, dd, *J* = 16.1; 5.4 Hz, H-4b) correspond to methylene protons. One doublet signal centered at δ<sub>H</sub> 4.51 (1H, d, *J* = 7.5 Hz) and one multiplet signal at δ<sub>H</sub> 3.93 ppm were seen due to the methine nucleus H-2 and H-3. Compound 1 was identified as catechin based on similarities of spectral data with the published literature (Hye, Taher, Ali, Ali, & Zaman, 2009; Numonov, Usmanova, & Aisa, 2013a, 2013b).

**Compound 2;** Stigmasitosterol-3-O-β-D-glucoside: white powder, MF C<sub>35</sub>H<sub>58</sub>O<sub>6</sub> (Fig. 2). In the <sup>1</sup>H NMR spectrum, olefinic protons H22 & H23 (δ<sub>H</sub> 5.37 (1H, d, *J* = 4.6 Hz; 5.10 (1H, d, *J* = 7.7 Hz) and an oxygenated methine (δ<sub>H</sub> 3.96 (1H, d, *J* = 5.6 Hz, H-3) signals were observed. Also, a number of methylenes and methines signals (δ<sub>H</sub> 2.75–1.01) appeared. The four singlet methyl [(δ<sub>H</sub> 0.67 (3H, s, H-18), 0.87 (3H, s, H-26), 0.95 (3H, s, H-19) and 0.89 (3H, s, H-27)], one doublet methyl (δ<sub>H</sub> 1.00 (3H, d, *J* = 6.4 Hz, H-21) and a triplet methyl (δ<sub>H</sub> 0.91 (3H, t, *J* = 7.4 Hz, H-29) signals were observed. It was confirmed from the appearance of the anomeric proton (δ<sub>H</sub> 5.03 br. s) signal in the <sup>1</sup>H NMR spectrum, that the glucose ring has β-glycosidic linkage. In the <sup>13</sup>C-NMR spectrum, 29 carbon signals consisting of a quaternary carbon (δ<sub>C</sub> 141.3), an olefinic methine (δ<sub>C</sub> 122.4), an oxygenated methine (δ<sub>C</sub> 78.56) and six methyl (δ<sub>C</sub> 19.9, 19.4, 19.6, 20.4, 12.6 and 12.4) signals were seen. Thus, we concluded that compound 1 was a sterol compound composed of two double bonds and one hydroxyl group. In the <sup>13</sup>C NMR

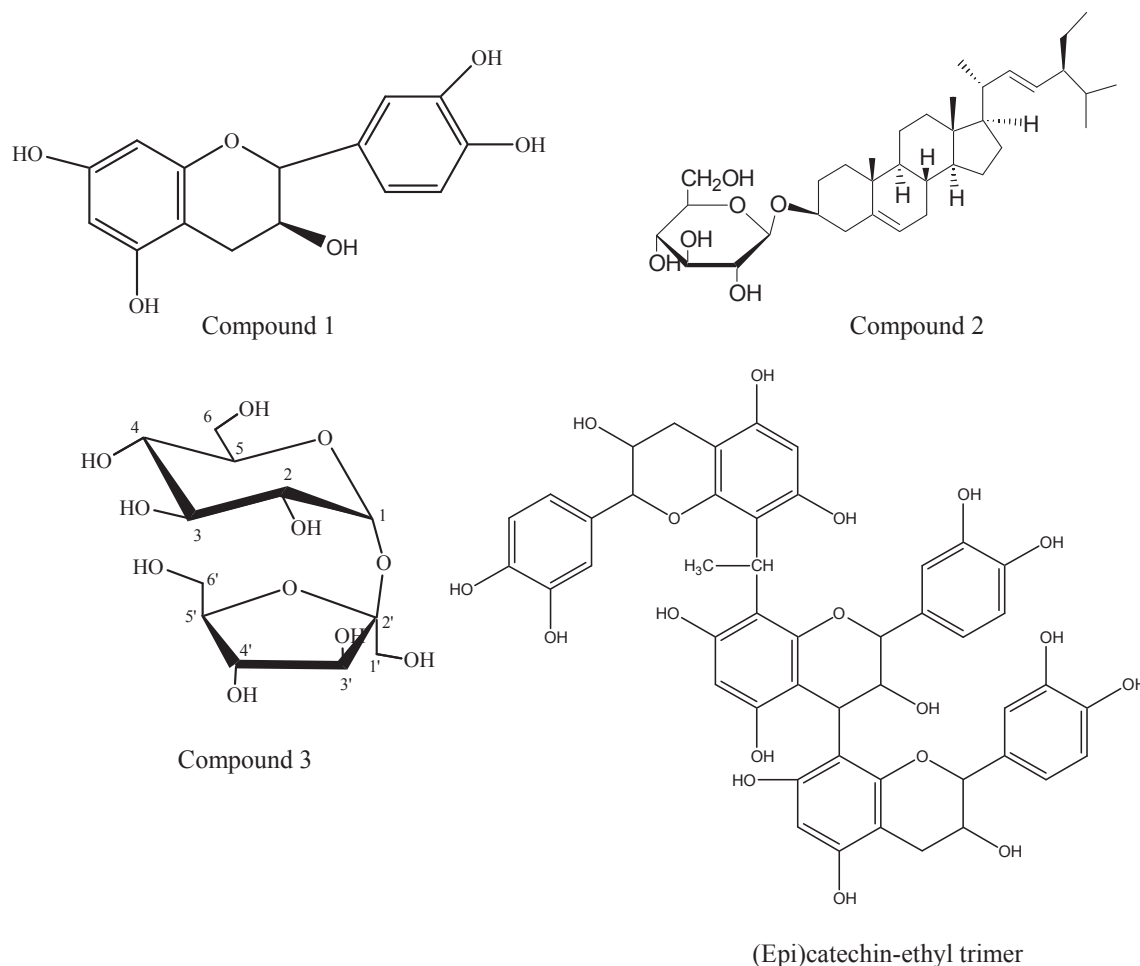


**Fig. 2.** Chemical structure of compound 1: (+)-catechin; compound 2: stigmasitosterol-3-O-β-D-glucoside; compound 3: α-D-Glucopyranosyl-(1 → 2)-β-D-fructofuranoside and (epi)catechin-ethyl trimer.

spectrum, the sugar signals were identified as D-glucoside. Compound **2** was finally identified as stigmasterol-3-O- $\beta$ -D-glucoside through the comparison of physical and spectroscopic data.  $^1\text{H}$  NMR and  $^{13}\text{C}$  NMR spectral data are in well agreement with the reported spectral data (Goat, 1991; Khatun, Billah, & Quader, 2012; Kobayashi, Tsuru, Todo, & Mitsuhashi, 1973).

Compound **3**;  $\alpha$ -D-Glucopyranosyl-(1  $\rightarrow$  2)- $\beta$ -D-fructofuranoside: white color needle like crystals, MF  $\text{C}_{12}\text{H}_{22}\text{O}_{11}$  (Fig. 2). The  $^1\text{H}$  NMR spectrum of compound **3** showed the presence of disaccharides units, exhibited signals for anomeric protons at  $\delta$  5.37 and 3.63 indicating the presence of  $\alpha$ -glucopyranosyl and  $\beta$ -fructofuranoside units, respectively, and these proton signals were correlated with anomeric carbon signals at  $\delta$  92.6 and 106.4 in the HMQC experiment. On the basis of NMR (1D, 2D) experiments and comparison of the spectral data with the published literature (Hyun, Min, & Choi, 2010) the compound was finally identified as  $\alpha$ -D-Glucopyranosyl-(1  $\rightarrow$  2)- $\beta$ -D-fructofuranoside. From the literature it appears that  $\alpha$ -D-Glucopyranosyl-(1  $\rightarrow$  2)- $\beta$ -D-fructofuranoside has not been isolated nor detected in almond and it is isolated in pure form and the presented for the first time.

### 3.2. HPLC-MS/MS analysis

The crude 70% ethanol extract of the whole almond seed without shell was analyzed through LC-MS/MS which was operated in negative ionization mode. The experiment was performed in triplicate, delivering the signals for different compounds at various  $m/z$  values. Fig. 3 shows the total ion chromatogram obtained from LC-MS analysis of 70% ethanol extract of almond nuts. All the compounds identified through LC-MS/MS analysis along with their peaks retention times, fragmentation pattern and the references, on the basis of which they have been assigned the names, are tabulated in Table 1. Peak at 8.45 min showed  $[\text{M}-\text{H}]^-$  ion at the  $m/z$  value 613.1 and at 8.662 min with  $[\text{M}-\text{H}]^-$  ion at  $m/z$  value 451 were assigned to catechin dihexoside and catechin hexoside respectively after comparing their fragmentation pattern with the published literature. Catechin hexoside has already been identified in the skin of almond but catechin dihexoside is detected for the first time. Peaks at 9.663 min, 11.631 min and 13.59 min gives fragmentation pattern similar to (epi)catechin dimer and this dimeric (epi)catechin has already been detected in almond skin. Peak at 10.661 min confirmed the presence of dihydroquercetin glucoside while those at 10.728 min and 12.547 min clarify the fragmentation pattern of (epi)catechin trimer. (epi)Catechin was detected at 11.082, 12.825 and 15.195 min and fragments arose from the peak at 11.363 were

similar to the dimer named as (epi)afzelchin-(epi)catechin present in the skin of almond. Two peaks at retention time 12.264 min and 15.811 min showed similar fragmentation pattern to that of eriodictyol glucoside. Peak for caffeoyl-6'-secologanoside arose at 12.33 min in the LC chromatogram with  $[\text{M}-\text{H}]^-$  ion at  $m/z$  value 551.2. To our knowledge from the previous literature regarding almond, this has not been detected and is presented for the first time in almond.

Compound at 14.429 min with  $[\text{M}-\text{H}]^-$  ion at  $m/z$  893 was assigned to (epi)catechin-ethyl trimer. This is a condensed products of (epi)catechin with acetaldehyde, corresponding to three (epi)catechin units with one ethyl-bridge (Fig. 2). As fragment ions, vinyl-catechin adducts with a signal at  $m/z$  315 (as observed in (epi)catechin-ethyl dimer fragmentation,  $m/z$  605), ions resulted from RDA fragmentation of trimers, and characteristic fragmentation pattern ions of procyanidin dimers were observed. This assignment was made after comparing the fragmentation pattern with published pattern in the literature. To our knowledge, this is the first time that (epi)catechin-ethyl trimer has been identified in almond. Thus, the presence of (epi)catechin-ethyl trimer in the seeds of almond constitutes a new element to take into account in their structural analysis. Peaks at 15.811 min, 15.881 min, 16.156 min and 17.40 min were assigned to the eriodictyol hexoside, kaempferol rutinoside, isorhamnetin rutinoside and kaempferol hexoside respectively based on their similar fragmentation pattern with the corresponding flavonoid glycosides. Eriodictyol, quercetin, kaempferol and isorhamnetin gave peaks at 18.952 min, 21.507 min, 24.306 min and 24.73 min respectively. Peak assignments to the corresponding compounds in all the cases were based on comparison of the fragments arose with the already published literature. Further, from our literature review it appears that this is first time to present such a detailed study of whole almond seed without shell using LC-MS-MS as a separation and detection technique. Until now most of the research work performed on the brown skin of almond and a comprehensive literature is available regarding the chemical composition of the skin of almond.

### 3.3. Antidiabetic activity

Antidiabetic activity was determined using protein tyrosine phosphatase-1B (PTP1B) inhibition procedure. PTP1B is an enzyme that belongs to the protein tyrosine phosphatase family and a negative regulator of the insulin signaling pathway (Tiong et al., 2013). Among the seven samples alcoholic extract showed strong anti diabetic (PTP1B inhibition) activity with an  $\text{IC}_{50}$  0.46  $\mu\text{g}/\text{mL}$ .

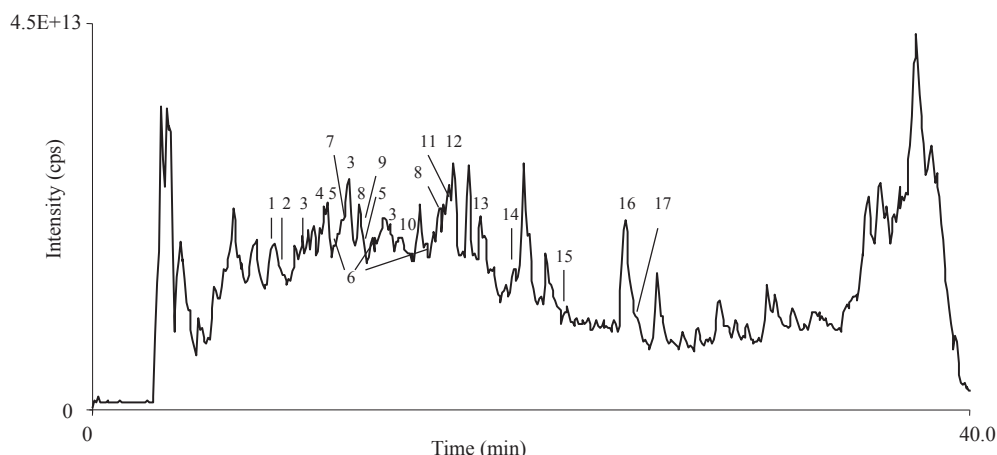


Fig. 3. LC-MS chromatogram of the *Prunus dulcis* nuts 70% ethanol extract.

**Table 1**  
Results of the LC-MS/MS analysis of 70% ethanol extract of almond nuts.

No	RT	Compound name	[M-H] <sup>-</sup> ion	Fragmentation	Reference
1	8.45	Catechin dihexoside	613	613.1, 289.2	(Quifer-Rada et al., 2015)
2	8.662	Catechin hexoside	451	451, 313.1, 289.2, 109.4	(Ojwang, Yang, Dykes, & Awika, 2013)
3	9.663, 11.631, 13.59	(epi)Catechin-(epi)catechin	577	577.1, 451, 425.2, 407.2, 289.1	(Monagas et al., 2007; Ojwang et al., 2013; de Souza, Cipriani, Iacomini, Gorin, & Sasaki, 2008)
4	10.661	Dihydroquercetin glucoside	465	465.1, 303, 285.1	(Monagas et al., 2007)
5	10.728, 12.547	(epi)Catechin-(epi)catechin-(epi)catechin	865	865.3, 739.2, 713,695.2, 577.2, 451.1, 425.8, 407.2, 289.2, 289.1	(Monagas et al., 2007; Ojwang et al., 2013)
6	11.082, 12.825, 15.195	(epi)Catechin	289	289.1	(Monagas et al., 2007)
7	11.363	(epi)Afzelchin-(epi)catechin	561	561.1, 543, 435, 425, 407.2, 289.1	(Monagas et al., 2007; Verardo et al., 2010)
8	12.264, 15.811	Eriodictyol glucoside	449	449, 287.2	(Monagas et al., 2007)
9	12.33	Caffeoyl-6'-secologanoside	551	551.2, 389.2, 341.2	(Obied, Bedgood, Prenzler, & Robards, 2007)
10	14.429	(epi)Catechin-ethyl trimer	893	893.2, 723, 603, 577, 451, 433.2, 425, 407, 315.4, 289.2	(Rockenbach et al., 2012)
11	15.881	Kaempferol rutinoside	593	592.9, 302.8, 285.2	(Monagas et al., 2007)
12	16.156	Isorhamnetin rutinoside	623	623.35, 315.5	(Monagas et al., 2007)
13	17.4	Kaempferol hexoside	447	447.1, 285.1	(Monagas et al., 2007)
14	18.952	Eriodictyol	287	287	(Monagas et al., 2007)
15	21.507	Quercetin	301	301	(Monagas et al., 2007)
16	24.306	Kaempferol	285	285	(Monagas et al., 2007)
17	24.73	Isorhamnetin	315	315.1, 300.1	(Monagas et al., 2007)

which is more than that of the PTP1B inhibitor with an IC<sub>50</sub> 1.46 µg/mL. Remaining extracts showed lower anti diabetic activity with a decreasing order as: hexane extract > ethyl acetate extract > chloroform extract > n-butanol extract. Water extract and oil delivered IC<sub>50</sub> value > 50. The experimental results (Table 2) from our study clarified the strong inhibitory effect of 70% ethanol extract of the defatted almond for PTP1B without further processing for the development of phytopharmaceuticals and food for diabetic patient. Higher activity of the alcoholic extract in comparison to PTP1B inhibitor showed the synergistic relationship between analytes present in the defatted almond seed. This relationship is unified by the low PTP1B inhibiting activity after the successive fractionation of the alcoholic extract with different solvents.

#### 4. Conclusions

Presence of various bioactive metabolites has been confirmed proving the almond nuts as a healthy nutritional source. Isolation of stigmatosterol-3-O-β-D-glucoside and α-D-Glucopyranosyl-(1 → 2)-β-D-fructofuranoside from ethyl acetate fraction along with mass spectrometric identification of catechin dihexoside, caffeoyl-6'-secologanoside and (epi)catechin-ethyl trimer were reported for the first time in almond along with other compounds which have been isolated and identified previously in the skin of almond. Highest antidiabetic activity showed by the almond extract lends the credence to the use of almond crude alcoholic extract in anti-diabetic formulations in comparison to further fractionation or semi purification of the crude extracts. Although ethyl acetate

fraction has been studied the most in the literature, our study clearly showed that other fractions also have activities and deserve further investigation in the future. The published literature showed no such detailed study of the whole almond nuts, as the main focus has been on the brown almond skin, and is presented for the first time.

#### Acknowledgments

This study was funded by the Projects of the International Cooperation and Exchange of the National Natural Science Foundation of China (NO. 31110103908) and the Central Asian Drug Discovery & Development Centre of Chinese Academy of Sciences.

Chinese Academy of Sciences is acknowledged for providing the scholarship during this study.

#### References

- Ajileye, O. O., Obuotor, E. M., Akinkunmi, E. O., & Aderogba, M. A. (2015). Isolation and characterization of antioxidant and antimicrobial compounds from *Anacardium occidentale* L. (Anacardiaceae) leaf extract. *Journal of King Saud University-Science*, 27(3), 244–252.
- Alasalvar, C., & Shahidi, F. (2009). Natural antioxidants in tree nuts. *European Journal of Lipid Science and Technology*, 111(11), 1056–1062.
- Baumgartner, R. R., Steinmann, D., Heiss, E. H., Atanasov, A. G., Ganzera, M., & Stuppner, H. (2010). Bioactivity-guided isolation of 1,2,3,4,6-Penta-O-galloyl-d-glucopyranose from *Paeonia lactiflora* roots as a PTP1B inhibitor. *Journal of Natural Products*, 73(9), 1578–1581.
- Bolling, B. W., Dolnikowski, G., Blumberg, J. B., & Chen, C.-Y. O. (2010). Polyphenol content and antioxidant activity of California almonds depend on cultivar and harvest year. *Food Chemistry*, 122(3), 819–825.
- Bolling, B. W., Dolnikowski, G., Blumberg, J. B., & Oliver Chen, C. (2009). Quantification of almond skin polyphenols by liquid chromatography-mass spectrometry. *Journal of Food Science*, 74(4), C326–C332.
- Bozorov, K., Ma, H.-R., Zhao, J.-Y., Zhao, H.-Q., Chen, H., & Bobakulov, K. (2014). Discovery of diethyl 2, 5-diaminothiophene-3, 4-dicarboxylate derivatives as potent anticancer and antimicrobial agents and screening of anti-diabetic activity: synthesis and in vitro biological evaluation. Part 1. *European Journal of Medicinal Chemistry*, 84, 739–745.
- Esfahlan, A. J., Jamei, R., & Esfahlan, R. J. (2010). The importance of almond (*Prunus amygdalus* L.) and its by-products. *Food Chemistry*, 120(2), 349–360.
- Frison-Norrie, S., & Sporns, P. (2002). Identification and quantification of flavonol glycosides in almond seed coats using MALDI-TOF MS. *Journal of Agricultural and Food Chemistry*, 50(10), 2782–2787.
- Frison, S., & Sporns, P. (2002). Variation in the flavonol glycoside composition of almond seed coats as determined by MALDI-TOF mass spectrometry. *Journal of Agricultural and Food Chemistry*, 50(23), 6818–6822.
- Garrido, I., Monagas, M., Gómez-Cordovés, C., & Bartolomé, B. (2008). Polyphenols

**Table 2**  
Results of inhibitory effect of extracts on enzyme PTP1B.

Sample	PTP1B inhibition assay IC <sub>50</sub> (µg/ml)
70% Ethanol extract	0.46 ± 0.05
Ethyl acetate fraction	1.89 ± 0.19
Hexane fraction	1.83 ± 0.16
Chloroform fraction	4.53 ± 0.34
n-Butanol fraction	38.25 ± 3.91
Water fraction	>50
Almond oil	>50
PTP1B inhibitor	1.46 ± 0.40

- and antioxidant properties of almond skins: influence of industrial processing. *Journal of Food Science*, 73(2), C106–C115.
- Goad, L. J. (1991). Phytosterols. *Methods in Plant Biochemistry*, 7, 369–434.
- Hughey, C. A., Januszewicz, R., Minardi, C. S., Phung, J., Huffman, B. A., & Reyes, L. (2012). Distribution of almond polyphenols in blanch water and skins as a function of blanching time and temperature. *Food Chemistry*, 131(4), 1165–1173.
- Hughey, C. A., Wilcox, B., Minardi, C. S., Takehara, C. W., Sundararaman, M., & Were, L. M. (2008). Capillary liquid chromatography–mass spectrometry for the rapid identification and quantification of almond flavonoids. *Journal of Chromatography A*, 1192(2), 259–265.
- Hye, M., Taher, M., Ali, M., Ali, M., & Zaman, S. (2009). Isolation of (+)-catechin from *Acacia catechu* (Cutch tree) by a convenient method. *Journal of Scientific Research*, 1(2), 300–305.
- Hyun, S. K., Min, B. S., & Choi, J. S. (2010). Isolation of phenolics, nucleosides, saccharides and an alkaloid from the root of *Aralia cordata*. *Natural Product Sciences*, 16(1), 20–25.
- Jamshed, H., & Gilani, A. H. (2014). Almonds inhibit dyslipidemia and vascular dysfunction in rats through multiple pathways. *The Journal of Nutrition*, 144(11), 1768–1774.
- Jiang, L., Numonov, S., Bobakulov, K., Qureshi, M. N., Zhao, H., & Aisa, H. A. (2015). Phytochemical profiling and evaluation of pharmacological activities of *Hypericum scabrum* L. *Molecules*, 20(6), 11257–11271.
- Kasibhatla, B., Wos, J., & Peters, K. G. (2007). Targeting protein tyrosine phosphatase to enhance insulin action for the potential treatment of diabetes. *Current Opinion in Investigational Drugs*, 8(10), 805–813.
- Khatun, M., Billah, M., & Quader, M. A. (2012). Sterols and sterol glucoside from *Phyllanthus* species. *Dhaka University Journal of Science*, 60(1), 5–10.
- Kobayashi, M., Tsuru, R., Todo, K., & Mitsuhashi, H. (1973). Marine sterols—II: Asterosterol, a new C26 sterol from *Asterias amurensis* lütken. *Tetrahedron*, 29(9), 1193–1196.
- Koren, S., & Fantus, I. G. (2007). Inhibition of the protein tyrosine phosphatase PTP1B: potential therapy for obesity, insulin resistance and type-2 diabetes mellitus. *Best Practice & Research Clinical Endocrinology & Metabolism*, 21(4), 621–640.
- Mandalari, G., Tomaino, A., Arcoraci, T., Martorana, M., Turco, V. L., & Cacciola, F. (2010). Characterization of polyphenols, lipids and dietary fibre from almond skins (*Amygdalus communis* L.). *Journal of Food Composition and Analysis*, 23(2), 166–174.
- Milbury, P. E., Chen, C.-Y., Dolnikowski, G. G., & Blumberg, J. B. (2006). Determination of flavonoids and phenolics and their distribution in almonds. *Journal of Agricultural and Food Chemistry*, 54(14), 5027–5033.
- Monagas, M., Garrido, I., Lebrón-Aguilar, R., Bartolome, B., & Gómez-Cordovés, C. (2007). Almond (*Prunus dulcis* (Mill.) DA Webb) skins as a potential source of bioactive polyphenols. *Journal of Agricultural and Food Chemistry*, 55(21), 8498–8507.
- Monagas, M., Garrido, I., Lebron-Aguilar, R., Gómez-Cordovés, M. C., Rybarczyk, A., & Amarowicz, R. (2009). Comparative flavan-3-ol profile and antioxidant capacity of roasted peanut, hazelnut, and almond skins. *Journal of Agricultural and Food Chemistry*, 57(22), 10590–10599.
- Na, B., Nguyen, P.-H., Zhao, B.-T., Vo, Q.-H., Min, B. S., & Woo, M. H. (2015). Protein tyrosine phosphatase 1B (PTP1B) inhibitory activity and glucosidase inhibitory activity of compounds isolated from *Agrimonia pilosa*. *Pharmaceutical Biology*, 2015, 1–7.
- Numonov, S., Usmanova, S., & Aisa, H. (2013a). Chemical composition of *Dracocephalum heterophyllum*. *Chemistry of Natural Compounds*, 49(3), 511–513.
- Numonov, S., Usmanova, S., & Aisa, H. (2013b). A triterpenoid and flavonoids from *Dracocephalum heterophyllum*. *Chemistry of Natural Compounds*, 48(6), 1109–1110.
- Obied, H. K., Bedgood, D. R., Prenzler, P. D., & Robards, K. (2007). Chemical screening of olive biophenol extracts by hyphenated liquid chromatography. *Analytica Chimica Acta*, 603(2), 176–189.
- Ojwang, L. O., Yang, L., Dykes, L., & Awika, J. (2013). Proanthocyanidin profile of cowpea (*Vigna unguiculata*) reveals catechin-O-glucoside as the dominant compound. *Food Chemistry*, 139(1), 35–43.
- de Pascual-Teresa, S., Moreno, D. A., & García-Viguera, C. (2010). Flavonols and anthocyanins in cardiovascular health: a review of current evidence. *International Journal of Molecular Sciences*, 11(4), 1679–1703.
- Quifer-Rada, P., Vallverdú-Queralt, A., Martínez-Huélamo, M., Chiva-Blanch, G., Jáuregui, O., & Estruch, R. (2015). A comprehensive characterisation of beer polyphenols by high resolution mass spectrometry (LC–ESI-LTQ–Orbitrap-MS). *Food Chemistry*, 169, 336–343.
- Qureshi, M. N., Stecher, G., & Bonn, G. K. (2014). Determination of total polyphenolic compounds and flavonoids in *Juglans regia* leaves. *Pakistan Journal of Pharmaceutical Science*, 27(4), 865–869.
- Qureshi, M. N., Stecher, G., Qureshi, M. U., Sultana, T., & Bonn, G. K. (2012). Determination of dicaffeoylquinic acid in selected medicinal plants using HPLC-PDA and LC-ESI-MS/MS. *Journal of the Chemical Society of Pakistan*, 34(1), 168–172.
- Rao, H. J. (2012). Therapeutic applications of almonds (*Prunus amygdalus* L.): a review. *Journal of Clinical and Diagnostic Research*, 6(1), 130–135.
- Rockenbach, I. I., Jungfer, E., Ritter, C., Santiago-Schübel, B., Thiele, B., & Fett, R. (2012). Characterization of flavan-3-ols in seeds of grape pomace by CE, HPLC-DAD-MS n and LC-ESI-FTICR-MS. *Food Research International*, 48(2), 848–855.
- Sang, S., Lapsley, K., Jeong, W.-S., Lachance, P. A., Ho, C.-T., & Rosen, R. T. (2002). Antioxidative phenolic compounds isolated from almond skins (*Prunus amygdalus* Batsch). *Journal of Agricultural and Food Chemistry*, 50(8), 2459–2463.
- Sang, S., Lapsley, K., Rosen, R. T., & Ho, C.-T. (2002). New prenylated benzoic acid and other constituents from almond hulls (*Prunus amygdalus* Batsch). *Journal of Agricultural and Food Chemistry*, 50(3), 607–609.
- de Souza, L. M., Cipriani, T. R., Iacomini, M., Gorin, P. A., & Sasaki, G. L. (2008). HPLC/ESI-MS and NMR analysis of flavonoids and tannins in bioactive extract from leaves of *Maytenus ilicifolia*. *Journal of Pharmaceutical and Biomedical Analysis*, 47(1), 59–67.
- Sultana, T., Stecher, G., Mayer, R., Trojer, L., Qureshi, M. N., & Abel, G. (2008). Quality assessment and quantitative analysis of flavonoids from tea samples of different origins by HPLC-DAD-ESI-MS. *Journal of Agricultural and Food Chemistry*, 56, 3444–3453.
- Tiong, S. H., Looi, C. Y., Hazni, H., Arya, A., Paydar, M., & Wong, W. F. (2013). Antidiabetic and antioxidant properties of alkaloids from *Catharanthus roseus* (L.) G. Don. *Molecules*, 18(8), 9770–9784.
- Truong, V.-L., Bak, M.-J., Jun, M., Kong, A.-N. T., Ho, C.-T., & Jeong, W.-S. (2014). Antioxidant defense and hepatoprotection by procyanidins from almond (*Prunus amygdalus*) skins. *Journal of Agricultural and Food Chemistry*, 62(34), 8668–8678.
- Verardo, V., Arráez-Román, D., Segura-Carretero, A., Marconi, E., Fernández-Gutiérrez, A., & Caboni, M. F. (2010). Identification of buckwheat phenolic compounds by reverse phase high performance liquid chromatography–electrospray ionization–time of flight–mass spectrometry (RP-HPLC-ESI-TOF-MS). *Journal of Cereal Science*, 52(2), 170–176.
- Wijeratne, S. S., Abou-Zaid, M. M., & Shahidi, F. (2006). Antioxidant polyphenols in almond and its coproducts. *Journal of Agricultural and Food Chemistry*, 54(2), 312–318.
- Xie, L., Roto, A. V., & Bolling, B. W. (2012). Characterization of ellagitannins, gallo-tannins, and bound proanthocyanidins from California almond (*Prunus dulcis*) varieties. *Journal of Agricultural and Food Chemistry*, 60(49), 12151–12156.
- Yili, A., Yimamu, H., Ghulameden, S., Qing, Z. H., Aisa, H. A., & Morlock, G. E. (2014). Determination of antidiabetic polysaccharides of *Ocimum basilicum* seeds indigenous to Xinjiang of China by high-performance thin-layer chromatography–UV/Vis-mass spectrometry. *JPC-Journal of Planar Chromatography-Modern TLC*, 27(1), 11–18.
- Zhang, Z.-Y., & Lee, S.-Y. (2003). PTP1B inhibitors as potential therapeutics in the treatment of type 2 diabetes and obesity. *Expert Opinion on Investigational Drugs*, 12(2), 223–233.
- Zhang, J., Shen, Q., Lu, J.-C., Li, J.-Y., Liu, W.-Y., & Yang, J.-J. (2010). Phenolic compounds from the leaves of *Cyclocarya paliurus* (Batal.) Ijinskaja and their inhibitory activity against PTP1B. *Food Chemistry*, 119(4), 1491–1496.



## Effect of setting conditions on proteolysis and gelling properties of spotted featherback (*Chitala ornata*) muscle



Piyawan Tachasirinukun<sup>a</sup>, Manat Chaijan<sup>b</sup>, Siriporn Riebroy<sup>a,\*</sup>

<sup>a</sup> Food and Nutrition Program, Faculty of Agriculture, Kasetsart University, Bangkok 10900, Thailand

<sup>b</sup> Department of Food Technology, School of Agricultural Technology, Walailak University, Thasala, Nakhon Si Thammarat 80160, Thailand

### ARTICLE INFO

#### Article history:

Received 25 March 2015

Received in revised form

7 September 2015

Accepted 19 October 2015

Available online 22 October 2015

#### Keywords:

Spotted featherback (*Chitala ornata*)

Proteolysis

Setting temperature

Gel properties

### ABSTRACT

Gels from spotted featherback (SF) muscle were prepared by different setting conditions including 4 °C/18 h, 25 °C/30 min, 25 °C/2 h, 40 °C/30 min and 60 °C/30 min followed by cooking at 90 °C/20 min. Directly cooked gel was used as a control. SF gels set at 4 °C/18 h and 60 °C/30 min exhibited higher proteolytic degradation than did by other setting temperatures and control ( $P < 0.05$ ) as evidenced by TCA-soluble peptides and the marked decrease in myosin heavy chain (MHC) under SDS-PAGE. For gelling properties, setting at 60 °C/30 min showed the gel with lowest breaking force and highest expressible drip whereas setting at 25 °C/30 min rendered the gel with highest breaking force ( $P < 0.05$ ). Indeed, the higher the setting temperature applied the lower the  $a^*$  value was observed ( $P < 0.05$ ). However, the  $L^*$  and  $b^*$  values were varied among setting conditions. A finer structure of SF gel correlated well with the breaking force, particularly at medium setting temperature (25 °C/30 min). Therefore, the setting regimes strongly influenced the proteolysis and gel properties of SF muscle. Setting at 25 °C for 30 min was the best suit to prevent the proteolysis and hence strengthen the gel of SF muscle.

© 2015 Elsevier Ltd. All rights reserved.

### 1. Introduction

Gelation is one of important functional properties of fish mince, surimi (washed fish mince) and ground meat. Basically, gelation is the cross-linking of randomly dispersed polymer chains to form a three-dimensional network (Smith, 1991) which including initial denaturation to cause protein unfolding, protein–protein interactions and aggregation giving rise to matrices capable of holding water, fat or other components through physico-chemical forces (Mulvihill & Kinsella, 1987; Sikorski, 2001). However, protein–protein interaction, known as association, aggregation and polymerization, are dependent upon temperatures, pH, and the type of muscle proteins used (Deng, Andrews, & Laursen, 1997). The three-dimensional structure is responsible for the elasticity and the textural strength of the gel (Sikorski, 2001). Myofibrillar proteins, particularly myosin and actomyosin, which are composed of multiple cooperative domains, are able to form highly viscoelastic and rigid gels (Xiong, 1997). In general, protein gelation has been traditionally achieved by heating (Totosaus, Montejano, Salazar, & Guerrero, 2002). Upon heating, the denaturation and degradation

of muscle proteins can occur with varying degrees depending on temperature and time. The influence of setting phenomenon on gel properties of surimi has been reported (Benjakul, Visessanguan, Riebroy, Ishizaki, & Tanaka, 2002). The setting temperature can affect enzymatic activities, protein degradation and gelation (Huang, Seguro, Motoki, & Tawada, 1992). In the case of surimi, incubation the sol at 0–40 °C prior to heating is generally used for gel strengthening (Lanier, 1992). Setting can be performed at low temperatures (0–4 °C), medium temperatures (25 °C) and high temperatures (40 °C) (Lanier, 1992), whereas protein degradation caused by proteinases, commonly found at 50–60 °C (Lee et al., 1990; Kamath, Lanier, Foegeding, & Hamann, 1992) leading to gel structure disintegration or softening (Benjakul, Visessanguan, & Chantarasuwan, 2004; Jiang, 2000). Benjakul, Chantarasuwan, & Visessanguan, (2003) suggested that setting at different temperatures produces different gel characteristics and setting at low temperature usually takes a longer time.

Spotted featherback (*Chitala ornata*, SF) is an important freshwater fish in economic value of Thailand. In general, SF meat has been used to produce many kinds of foods such as fish ball, fried curry-fish cake and som-fug (fermented fish sausage). SF is commonly sold in the form of scraped meat in plastic bags and kept on ice during transportation and distribution. For nutritional value,

\* Corresponding author.

E-mail address: [agrsrpr@ku.ac.th](mailto:agrsrpr@ku.ac.th) (S. Riebroy).

spotted featherback meat is a good source of protein (Puwastein et al., 1999).

Generally, heating is usually applied for SF meat processing. SF meat can be mixed with other adjunct ingredients (salt, sugar, chili paste, etc.) and kept on ice overnight (18–24 h) before cooking. This preparation can be considered as low temperature setting of SF meat. In this traditional preparation, proteolysis and biochemical changes of muscle can be taken place to some degrees during iced storage. Those changes would associate with poorer gelling characteristics of final products. However, many products and recipes from SF mince were directly cooked (without setting). For instance, Thai green curry with fish ball (Kang-Keaw-Wan) production, the SF meat is knead with a pinch of salt (about 0.33%) and the ball-shaped of mixture is boiled without setting. From point of view, SF meat is popularly used as a raw material for production of food product with high quality in textural properties. However, no information regarding the degradation of muscle proteins and gel-forming ability of SF meat as affected by different setting conditions has been reported. Therefore, the objective of this study was to investigate the effect of setting conditions on proteolysis and gel properties of SF meat.

## 2. Materials and methods

### 2.1. Chemicals

Sodium chloride (NaCl) and bromophenol blue were obtained from Carlo Erba (Milan, Italy). Trichloroacetic acid (TCA), methanol and bis-acrylamide were purchased from Merck (Darmstadt, Germany). Acetic acid, glutaraldehyde, ethanol, and  $\beta$ -mercaptoethanol ( $\beta$ ME) was obtained from Sigma (Steinheim, Germany). N,N,N',N'-tetramethylethylenediamine (TEMED) was obtained from AMRESCO (Solon, OH, USA). Coomassie brilliant blue R-250 was obtained from Panreac (Barcelona, Spain).

### 2.2. Fish samples and preparation

Fresh SF (body length about 60–65 cm and an average weight of 1.5–2.0 kg) were obtained from Bangpakong River, Prachin Buri, Thailand. After capture within 12 h, fish were transported in ice with a fish/ice ratio of 1:2 (w/w) to Food and Nutrition Laboratory, Faculty of Agriculture, Kasetsart University within 1 h. The whole fish were immediately washed, filleted and manually scraped into meat. The meat was kept on ice (2 h) during preparation and analysis. The pH value of SF meat was measured as described by the method of Benjakul, Seymour, Morrissey, and An (1997).

### 2.3. Gel preparation

Before gel preparation, SF meat was manually mixed to uniformity. Moisture content of sample was measured according to the method of AOAC (2000) and adjusted to 80%. Then, the sample were added with 2.5 g/100 g NaCl and chopped for 5 min to obtain the homogenous sol. The sol was stuffed into polyvinylidene casing with a diameter of 2.5 cm and both ends of the casing were sealed tightly. To prepare gel, the sols were incubated at several conditions including 4 °C/18 h, 25 °C/30 min, 25 °C/2 h, 40 °C/30 min, 60 °C/30 min prior heating at 90 °C/20 min. The gel without setting was heated directly and used as the control. The gels were cooled in ice-water for 30 min and stored for 24 h at 4 °C prior to analyses.

### 2.4. Determination of TCA-soluble peptides

TCA-soluble peptides were determined according to the method of Morrissey, Wu, Lin, & An (1993). Gel samples (3 g) were

homogenised with 27 ml of TCA (5 g/100 ml) at speed no.2 (11,000 rpm) using a homogeniser (T18 basic, IKA, Staufen, Germany). The homogenate were kept on ice for 1 h and centrifuged at 8000  $\times$ g for 5 min using a refrigerated centrifuge (Allegra X-15R centrifuge, Beckman Coulter, California, USA). The soluble peptides in the supernatant were measured by the Lowry method (Lowry, Rosebrough, Farr, & Randall, 1951) and expressed as  $\mu$ mol tyrosine/g dry weight.

### 2.5. SDS–polyacrylamide gel electrophoresis (SDS-PAGE)

SDS-PAGE was carried out according to the method of Leammli (1970) using 10 g/100 ml running gel and 4 g/100 ml stacking gel. Gel sample (3 g) were mixed with 27 ml of 5 g/100 ml SDS and homogenised for 1 min. The homogenate were incubated at 85 °C for 1 h to dissolve the proteins, followed by centrifuged at 8500  $\times$ g for 5 min at room temperature using a centrifuge (Allegra X-15R centrifuge, Beckman Coulter, USA). Protein concentrations were determined according to the Biuret method (Robinson & Hodgen, 1940) using bovine serum albumin as a standard. Solubilized samples were mixed at a 1:1 (v/v) ratio with the sample buffer (0.5 M Tris–HCl, pH 6.8, containing 4 g/100 ml SDS and 20 g/100 ml glycerol) in the presence of 10 ml/100 ml  $\beta$ ME. Samples (10  $\mu$ g protein) were loaded onto polyacrylamide gels. The electrophoresis was carried out at 15 mA per gel using a vertical gel electrophoresis unit (Mini-Protean II; Bio-Rad Laboratories, Richmond, California, USA). After separation, protein bands were stained with 0.05% (w/v) Coomassie Blue R-250 in 15 ml/100 ml methanol and 5 ml/100 ml acetic acid and destained with 30 ml/100 ml methanol and 10 ml/100 ml acetic acid.

### 2.6. Determination of expressible drip

Expressible drip was measured according to the method of Ng (1978). A gel sample with a thickness of 0.5 cm were weighed and placed between two pieces of Whatman filter paper no. 1 at the top and three pieces of the same type of filter paper at the bottom. The standard weight (5 kg) were placed on the top of the sample and maintained for 2 min. The sample were then removed and weighed again. Expressible drip were calculated and expressed as percentage of sample weight.

### 2.7. Determination of textural properties

Texture analysis, breaking force and deformation, of the gel were performed using a Texture Analyzer (TA-XT plus, Stable Micro System, Surrey, UK). Gels were equilibrated and evaluated at room temperature (25–28 °C). Five cylinder-shaped samples with a length of 2.5 cm were prepared and subjected to determination. Breaking force (gel strength) and deformation (elasticity and deformability) were measured using the texture analyser equipped with a spherical plunger (diameter 5 mm, depression speed of 60 mm/min).

### 2.8. Determination of colour

The colour of sample was measured in L\* (lightness), a\* (redness/greenness) and b\* (yellowness/blueness) the using a ColorFlex (Colorflex, HunterLab, USA).

### 2.9. Determination of microstructure

Microstructure of gels with different setting temperatures and direct heating were determined as described by Jones and Mandigo (1982). Samples with a thickness of 2–3 mm were fixed with

2.5 ml/100 ml glutaraldehyde in 0.2 mol/L phosphate buffer (pH 7.2) for 2 h. The samples were then rinsed for 1 h in distilled water before being dehydrated in ethanol with serial concentrations of 50, 70, 80, 90 and 100 ml/100 ml. Dried samples were mounted on a bronze stub and sputter-coated with gold. The specimens were visualised using a scanning electron microscope (JSM-5410LV, Jeol, Tokyo, Japan) at an acceleration voltage of 15 kV.

## 2.10. Statistical analysis

The data were subjected to analysis of variance (ANOVA) and mean comparison was performed by Duncan's Multiple Range Test (Steel & Torrie, 1980). Statistical analysis was performed using SPSS statistical analysis program (version 19.0).

## 3. Results and discussion

### 3.1. Proteolysis of spotted featherback (SF) gel as influenced by different setting conditions

#### 3.1.1. TCA-soluble peptides

Generally, TCA-soluble peptides of SF gels with prior setting at 4 °C for 18 h and 60 °C for 30 min were greater than those setting at other conditions ( $P > 0.05$ ) (Fig. 1). The results indicated that the degradation of muscle proteins obviously occurred during setting at 4 °C and 60 °C. Proteases are found in the soluble sarcoplasmic component of muscle tissue, in association with cellular organelles, connective tissues and myofibrils, and in the interfiber space (Ashie & Simpson, 1997). Kamath et al. (1992) found that proteolysis in croaker paste increased with increasing temperature of setting between 40 and 50 °C. The presence of proteolytic enzymes in fish muscle might be activated at 60 °C, while both endogenous and microbial proteases (particularly psychrophilic bacteria) might contribute to the proteolysis at 4 °C with longer incubation time. No differences in TCA-soluble peptides of gels setting at 25 °C for 2 h and the control were found ( $P > 0.05$ ). The setting at 25 °C for 30 min exhibited the lowest TCA-soluble peptides ( $P < 0.05$ ). This result was in agreement with Benjakul, Chantarasuwan, et al. (2003) who reported that suwari gel from some tropical fish, prepared by setting at 25 °C, showed lower degradation, although the setting time increased up to 8 h Toyohara, Kinoshita, and Shimizu

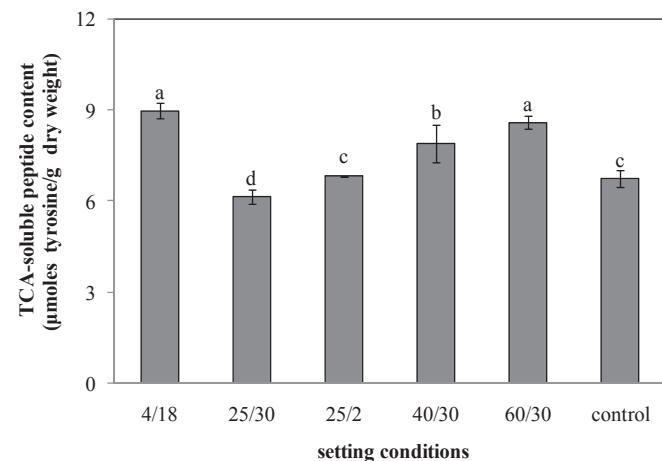


**Fig. 1.** TCA-soluble peptides of gels from SF meat prepared by different setting conditions; 4/18: 4 °C/18 h, 25/30: 25 °C/30 min, 25/2: 25 °C/2 h, 40/30: 40 °C/30 min, 60/30: 60 °C/30 min and without setting (control) followed by cooking at 90 °C/20 min. Bars represent the standard deviation from triplicate determinations. Different letters indicated significant differences ( $P < 0.05$ ).

(1990) reported that proteolytic degradation of fish gels could be classified into two types according to the localization of the gel degradation-inducing factor (GIF) in muscle cells which can be induced by sarcoplasmic GIF. From the results, the protein degradation can be occurred during setting, especially 60 °C for 30 min and 4 °C for 18 h. Thus, the setting condition was strongly affected SF protein degradation.

### 3.1.2. Protein patterns

Based on protein patterns (Fig. 2), myosin heavy chain (MHC) band intensity markedly decreased when SF gel was subjected to setting at 60 °C for 30 min. However, no marked changes in actin bands of all samples were observed. Setting at 25 °C, the longer the setting time applied, the lower the MHC band intensity was observed. Generally, optimum temperature for setting among species may be determined by the heat-stability of myosin and the rate of cross-linking may be dependent on the conformation of the substrate myosin at a given temperature rather than on the optimum temperature of transglutaminase activity (Benjakul, Chantarasuwan, et al., 2003; Kamath et al., 1992). The result was in accordance with Takeda and Seki (1996) and Ando, Tsukamasa, and Makinodan (1998), who found degradation products with molecular weights of 150 and 170 kDa during setting of walleye pollack surimi paste at 25 °C and 30 °C, respectively. Furthermore, Benjakul et al. (2004) found degradation products with molecular weights of 120 and 150 kDa during setting of surimi from threadfin bream, bigeye snapper, barracuda and bigeye croaker. From the result, setting at 25 °C for 30 min showed the gel with greater polymerization of MHC and it was coincidental with the lowered TCA-soluble peptide content in this gel (Fig. 1). The setting temperatures would affect the proteinase activity. From the results, the proteolysis of SF muscle proteins occurred during setting at 4 °C for 18 h and 60 °C for 30 min, however the MHC was lowered obviously in latter setting condition. Thus, the SF meat could set at 25 °C for 30 min prior to heating at 90 °C for 20 min to minimize the protein degradation.

### 3.2. Properties of spotted featherback (SF) gel as influenced by different setting conditions

#### 3.2.1. Expressible drip

The expressible drip of SF gels is shown in Table 1. SF gel

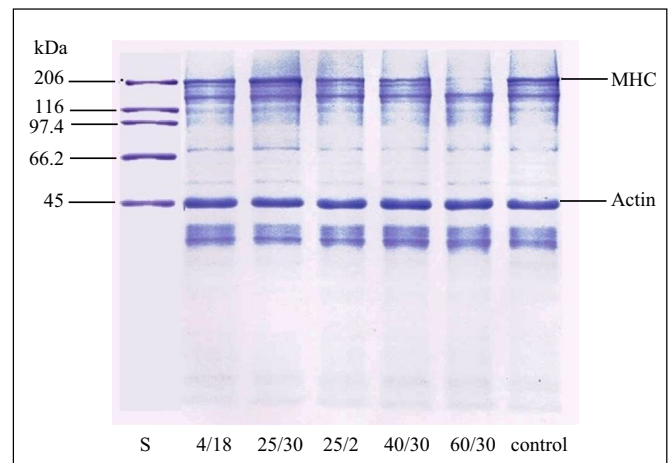


**Fig. 2.** SDS-polyacrylamide gel electrophoresis (SDS-PAGE) protein pattern of SF gels prepared by different setting conditions; 4/18: 4 °C/18 h, 25/30: 25 °C/30 min, 25/2: 25 °C/2 h, 40/30: 40 °C/30 min, 60/30: 60 °C/30 min and without setting (control) followed by cooking at 90 °C/20 min. MHC: myosin heavy chain.

**Table 1**  
Expressible drip (%) of gels from SF meat prepared by different setting conditions.

Setting conditions		Expressible drip (%)
4 °C 18 h	90 °C 20 min	4.02 ± 0.07 <sup>a,b**</sup>
25 °C 30 min	90 °C 20 min	4.00 ± 0.06 <sup>bc</sup>
25 °C 2 h	90 °C 20 min	3.89 ± 0.07 <sup>c</sup>
40 °C 30 min	90 °C 20 min	3.62 ± 0.01 <sup>d</sup>
60 °C 30 min	90 °C 20 min	4.81 ± 0.08 <sup>a</sup>
90 °C 20 min (control)		3.97 ± 0.32 <sup>c</sup>

\* Values are given as mean ± S.D. from five determinations.  
\*\* Different superscripts indicate the significant differences ( $P < 0.05$ ).

underwent setting at 60 °C for 30 min revealed the highest expressible drip ( $P < 0.05$ ). No differences in expressible drip of SF gels setting at 4 °C for 18 h, 25 °C for 30 min or 2 h were observed ( $P > 0.05$ ). SF gel setting at 40 °C for 30 min exhibited the lowest expressible drip ( $P < 0.05$ ). Niwa (1992) suggested that the more water retained in the gel network when gels had low expressible drip. Gradual alignment of protein molecules at medium temperature contributed to more ordered-network, which could imbibe more water (Benjakul, Chantarasuwan, et al., 2003). Chaijan, Panpipat, and Benjakul (2010) reported that gel of Indian

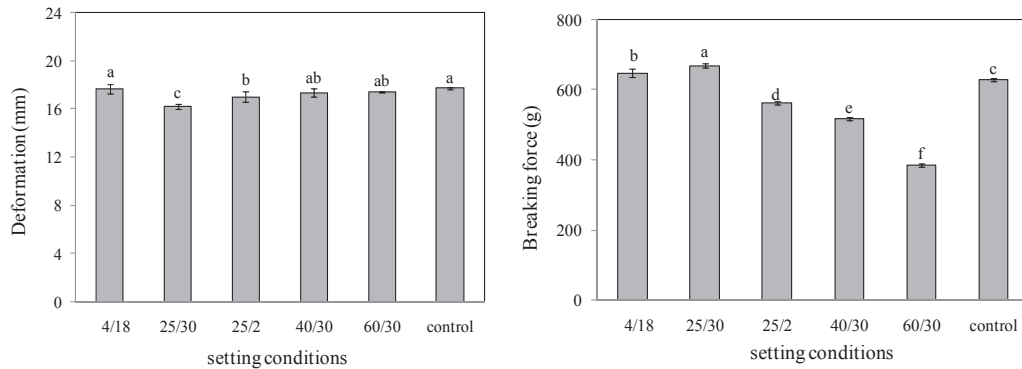


**Fig. 3.** Breaking force and deformation of gels from SF meat prepared by different setting conditions; 4/18: 4 °C/18 h, 25/30: 25 °C/30 min, 25/2: 25 °C/2 h, 40/30: 40 °C/30 min, 60/30: 60 °C/30 min and without setting (control) followed by cooking at 90 °C/20 min. Bars indicated standard deviation from five determinations. Different letters indicated significant differences ( $P < 0.05$ ).

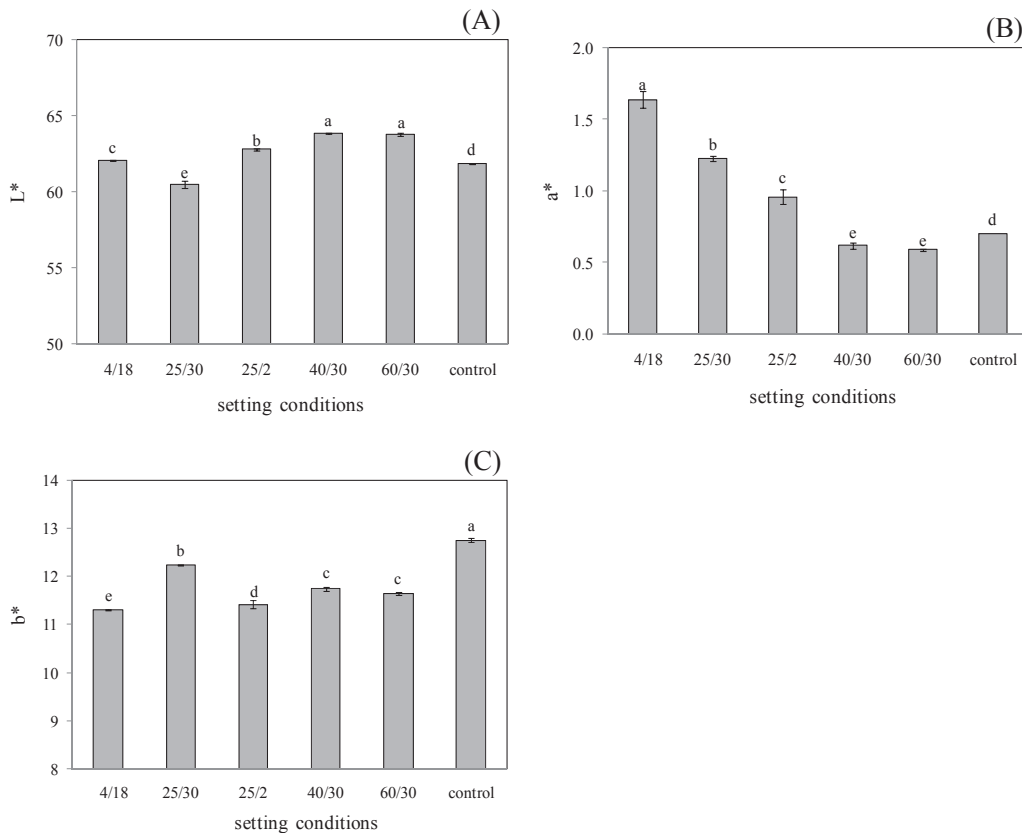


**Fig. 4.** L\* (A), a\* (B) and b\* (C) of gels from SF meat prepared by different setting conditions; 4/18: 4 °C/18 h, 25/30: 25 °C/30 min, 25/2: 25 °C/2 h, 40/30: 40 °C/30 min, 60/30: 60 °C/30 min and without setting (control) followed by cooking at 90 °C/20 min. Bars represent the standard deviation from five determinations. Different letters indicated significant differences ( $P < 0.05$ ).

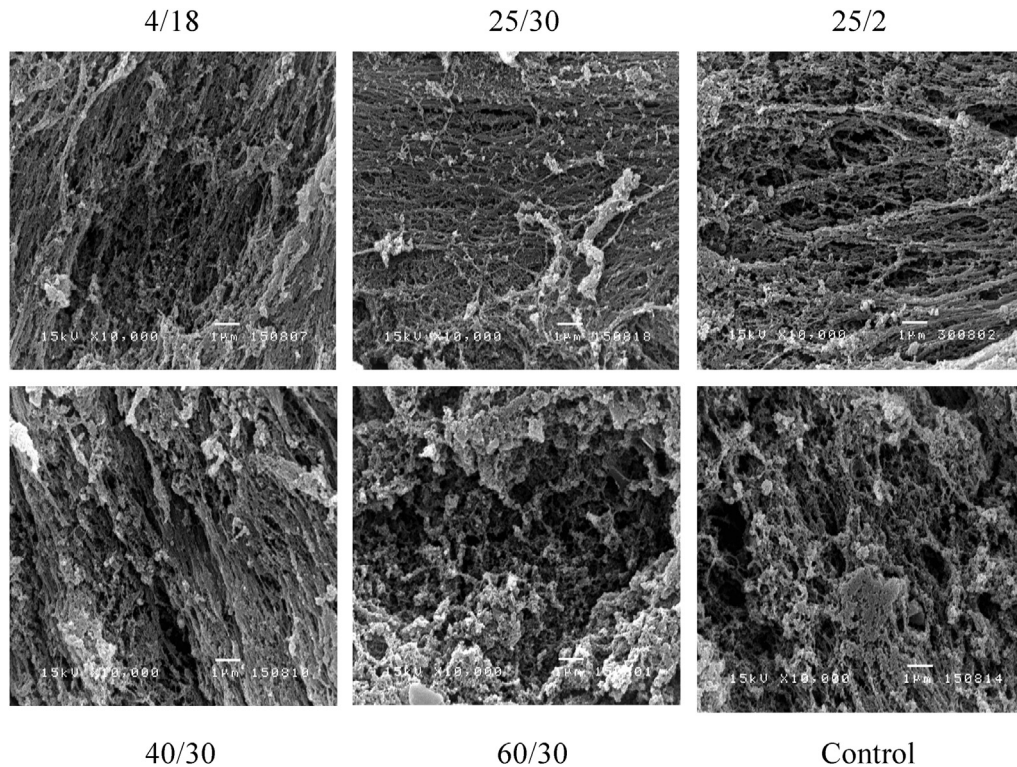


**Fig. 5.** Microstructure of SF gels from SF meat prepared by different setting conditions; 4/18: 4 °C/18 h, 25/30: 25 °C/30 min, 25/2: 25 °C/2 h, 40/30: 40 °C/30 min, 60/30: 60 °C/30 min and without setting (control) followed by cooking at 90 °C/20 min.

mackerel, short-bodied mackerel and frigate mackerel surimi set at 60 °C for 30 min prior heating had the highest expressible drip. During heating at 90 °C for 20 min, rapid unfolding of proteins results in more intense coagulation (Niwa, 1992; Tammattinna, Benjakul, Visessanguan, & Tanaka, 2007). Therefore, the appropriate setting could be used to improve gel forming ability via non-disulfide covalent bonds. Different expressible moisture content suggested the differences in water holding capacity of gel network (Tammattinna et al., 2007). Low expressible moisture content of the gels suggested the more water retained in gel network (Niwa, 1992). From the results, expressible drip of SF gel was influenced by setting temperatures, particularly setting at 60 °C for 30 min. Therefore, setting at low and medium temperatures could be used to improve the water holding capacity of SF gel.

### 3.2.2. Textural properties

The breaking force and deformation of SF gels set under different conditions are shown in Fig. 3. SF gels set at 25 °C for 30 min prior to heating at 90 °C for 20 min exhibited the highest breaking force ( $P < 0.05$ ), while gel set at 60 °C for 30 min showed the lowest breaking force ( $P < 0.05$ ). Generally, gelling properties of surimi were affected by the setting condition (Jiang, 2000; Lanier, 1992). Different setting temperatures resulted in the different breaking force of SF gel. During setting, several bonds induced protein aggregation particularly hydrophobic interaction and disulfide bonds were established (Benjakul, Visessanguan, Ishizaki, & Tanaka, 2001). Formation of large aggregates is presumably a prerequisite for formation of a good elastic gel (Chan, Gill, & Paulson, 1992). Also, heat-activated proteinases were associated with the degradation of surimi protein and gel softening (Benjakul, Visessanguan, & Tueksuban, 2003; Niwa, 1992). Proteolytic activity in fish muscle is associated with gel weakening in surimi (An, Peters, & Seymour, 1996; Benjakul et al., 2004). Chaijan et al.

(2010) found that the modori gel (set at 60 °C) of Indian mackerel, short-bodied mackerel and frigate mackerel surimi exhibited the lowest breaking force compared to other setting conditions. Surimi gels from bigeye snapper, barracuda and bigeye croaker set at high temperature (40 °C) showed higher protein degradation, compared with those set at medium temperature (25 °C) (Benjakul, Visessanguan, et al., 2003, 2004). This phenomenon was induced by endogenous heat activated proteases, which can degrade myosin (Jiang, 2000). The lowest breaking force of SF gel set at 60 °C for 30 min was in agreement with the highest TCA-soluble peptide content (Fig. 1) and protein degradation in SDS-PAGE pattern (Fig. 2). The high breaking force was concomitant with the decrease in MHC band intensity and the formation of high molecular weight polymerised protein band (Fig. 2). Gels set at 25 °C for 30 min prior to heating at 90 °C for 20 min showed the lowest deformation ( $P < 0.05$ ) and no differences in deformation were observed among the other samples. From the results, breaking force of SF gel was governed by setting conditions. Furthermore, the proteolysis also contributed to poorer gel quality, particularly SF gel setting at 60 °C for 30 min (Figs. 1 and 2).

### 3.2.3. Color

$L^*$ ,  $a^*$  and  $b^*$  values of SF gels set under different conditions are shown in Fig. 4. The SF gel set at 40 °C for 30 min and 60 °C for 30 min had higher  $L^*$  value than other samples ( $P < 0.05$ ) (Fig. 4A). The water release caused by denaturation and aggregation of muscle proteins might be taken place to a greater extent with high temperature setting (Table 1). Released water, especially at the gel surface, would increase the degree of light scattering. As a consequence, the  $L^*$  value was increased. However, decrease in  $L^*$  of the control (without setting) was observed ( $P > 0.05$ ). This phenomenon can be influenced by temperature and possibly due to the greater denaturation, degradation and oxidation of pigments or

other muscle proteins. Lower  $a^*$  value of sample prepared by setting at 40 °C for 30 min and 60 °C for 30 min was observed ( $P < 0.05$ ) (Fig. 4B). The results indicated that oxidation of myoglobin possibly occurred to a greater extent during heat-induced gelation. Myoglobin and haemoglobin play an essential role in the whiteness of gel (Chaijan, Benjakul, Visessanguan, & Faustman, 2007; Chen, 2000). Therefore, setting temperatures directly affected on colour of SF gels.

#### 3.2.4. Microstructure

Microstructures of gels from SF meat set under different conditions are illustrated in Fig. 5. The gels set at 4 °C for 18 h, 25 °C for 30 min, 25 °C for 2 h and 40 °C for 30 min showed finer and longer strands than those set at 60 °C for 30 min and direct heating (control). When setting at 60 °C for 30 min was applied, the gel network was disorganized and the three dimensional gel network was destroyed, corresponding to the very weak gel. This disruption of gel network was related to the degradation of MHC by proteases (Cao et al., 1999; Ngo, Katsuji, & Yoshiaki, 2010). The microstructure of gel has correlated well with the gel strength. As a result, setting at 25 °C for 30 min enhanced the gel formation and induced a fine with a smaller and compact gel network, correlated with the highest gel strength.

#### 4. Conclusion

The setting conditions directly affected the proteolysis and gel properties of SF meat. The proteolysis significantly occurred during setting at 4 °C for 18 h and 60 °C for 30 min, contributing to the lowered water holding capacity and gel weakening of SF meat. From the results, setting at medium temperatures (25 °C) could be used for SF gel production showing better gel quality than other setting regimes. Therefore, this setting condition is a promising means to improve gel quality of SF meat.

#### Acknowledgements

This study was financially supported from the research scholarship for international publication, the Graduate School, Kasetsart University, Bangkok, Thailand.

#### References

- Ando, M., Tsukamasa, Y., & Makinodan, Y. (1998). Identification of 170 k component which appears in the setting process of surimi gel. *Fisheries Science*, 64, 497–498.
- An, H., Peters, M. Y., & Seymour, T. A. (1996). Roles of endogenous enzymes in surimi gelation. *Journal of Food Science and Technology*, 7(10), 321–326.
- AOAC. (2000). *Official method of analysis of AOAC international* (17th ed.). Washington, DC: Association of Official Analytical Chemists.
- Ashie, I. N. A., & Simpson, B. K. (1997). Proteolysis in food myosystems – a review. *Journal of Food Biochemistry*, 21, 91–123.
- Benjakul, S., Chantarasuwan, C., & Visessanguan, W. (2003). Effect of medium temperature setting on gelling characteristic of surimi from some tropical fish. *Journal of Food Chemistry*, 82, 567–574.
- Benjakul, S., Seymour, T. A., Morrissey, M. T., & An, H. (1997). Physicochemical changes in Pacific whiting muscle proteins during iced storage. *Journal of Food Science*, 62, 729–733.
- Benjakul, S., Visessanguan, W., & Chantarasuwan, C. (2004). Effect of high-temperature setting on gelling characteristic of surimi from some tropical fish. *Journal of Food Science and Technology*, 39, 671–680.
- Benjakul, S., Visessanguan, W., Ishizaki, S., & Tanaka, M. (2001). Differences in gelation characteristics of natural actomyosin from two species of bigeye snapper, *Priacanthus tayenus* and *Priacanthus macracanthus*. *Journal of Food Science*, 66, 1311–1318.
- Benjakul, S., Visessanguan, W., Riebroy, S., Ishizaki, S., & Tanaka, M. (2002). Gel-forming properties of surimi produced from bigeye snapper, *Priacanthus tayenus* and *P. macracanthus*, stored in ice. *Journal of the Science of Food and Agriculture*, 82, 1142–1451.
- Benjakul, S., Visessanguan, W., & Tueksuban, J. (2003). Heat activated proteolysis in lizardfish (*Saurida tumbil*) muscle. *Food Research International*, 36, 1021–1028.
- Cao, M. J., Hara, K., Osatomi, K., Tachibana, K., Izumi, T., & Ishihara, T. (1999). Myofibril-bound serine proteinase (MBP) and its degradation of myofibrillar proteins. *Journal of Food Science*, 64, 644–647.
- Chaijan, M., Benjakul, S., Visessanguan, W., Lee, S., & Faustman, C. (2007). The effect of freezing and aldehydes on the interaction between fish myoglobin and myofibrillar proteins. *Journal of Agricultural and Food Chemistry*, 55, 4562–4568.
- Chaijan, M., Panpipat, W., & Benjakul, S. (2010). Physicochemical properties and gel-forming ability of surimi from three species of mackerel caught in Southern Thailand. *Food Chemistry*, 121, 85–92.
- Chan, J. K., Gill, T. A., & Paulson, A. T. (1992). Cross-linking of myosin heavy chains from cod, herring and silver hake during thermal setting. *Journal of Food Science*, 57(4), 906–912.
- Chen, H. H. (2000). Decoloration and gel-forming ability of horse mackerel mince by air-flotation washing. *Journal of Food Science*, 67, 2970–2975.
- Deng, G. J., Andrews, D. W., & Laursen, R. A. (1997). Amino acid sequence of a new type of antifreeze protein from the longhorn sculpin *Myoxocephalus octodecimspinosus*. *Federation of European Biochemical Societies Letters*, 402, 17–20.
- Huang, Y. P., Seguro, K., Motoki, M., & Tawada, K. (1992). Cross-linking of contractile proteins from skeletal muscle by treatment with microbial transglutaminase. *Journal of Biochemistry of Tokyo*, 112, 229–234.
- Jiang, S. T. (2000). Enzymes and their effects on seafood texture. In N. F. Haard, & B. K. Simpson (Eds.), *Seafood enzymes: Utilization and influence on postharvest seafood quality* (pp. 411–450). New York: Marcel Dekker, Inc.
- Jones, K. W., & Mandigo, R. W. (1982). Effects of chopping temperature on the microstructure of meat emulsions. *Journal of Food Science*, 47, 1930–1935.
- Kamath, G. G., Lanier, T. C., Foegeding, E. A., & Hamann, D. D. (1992). Nondisulfide covalent cross-linking of myosin heavy chain in "setting" of Alaska pollock and Atlantic croaker surimi. *Journal of Food Biochemistry*, 16(2), 151–172.
- Lanier, T. C. (1992). Measurement of surimi composition and functional properties. In T. C. Lanier, & C. M. Lee (Eds.), *Surimi technology* (pp. 123–166). New York: Marcel Dekker, Inc.
- Leammler, U. K. (1970). Cleavage of structure protein during the assembly of head bacteriophage T4. *Nature*, 227, 680–685.
- Lee, N. H., Seki, N., Kato, N., Nakagawa, N., Terui, S., & Arai, K. (1990). Gel forming ability and cross-linking ability of myosin heavy chain in salted meat paste from threadfin bream. *Nippon Suisan Gakkaishi*, 56, 329–336.
- Lowry, O. H., Rosebrough, N. J., Farr, L. A., & Randall, R. J. (1951). Protein measurement with the Folin phenol reagent. *Journal of Biological Chemistry*, 193, 256–275.
- Morrissey, M. T., Wu, J. W., Lin, D., & An, H. (1993). Protease inhibitor effects on torsion measurements and autolysis of Pacific whiting surimi. *Journal of Food Science*, 58, 1054–1059.
- Mulvihill, D. M., & Kinsella, J. E. (1987). Gelation characteristics of whey proteins and  $\beta$ -lactoglobulin. *Food Technology*, 102–111.
- Ng, C. S. (1978). Measurement of free and expressible drips. In H. Hasegawa (Ed.), *Laboratory manual on analytical methods and procedure for fish and fish products* (pp. 1–2). New York, USA: Marcel Dekker.
- Ngo, V. P., Katsuji, M., & Yoshiaki, I. (2010). Microstructure of white croaker surimi protein gels set at low temperature under the inhibition of the polymerization and degradation of protein. *Journal of Biological Sciences*, 10, 499–506.
- Niwa, E. (1992). Chemistry of surimi gelation. In T. C. Lanier, & C. M. Lee (Eds.), *Surimi technology* (pp. 389–428). New York: Marcel Dekker, Inc.
- Puwastein, P., Judprosong, K., Kettwan, E., Vasanachitt, K., Nakngamanong, Y., & Bhattacharjee, L. (1999). Proximate composition of raw and cooked Thai freshwater and marine fish. *Journal of Food Composition and Analysis*, 12, 9–12.
- Robinson, H. W., & Hodgen, C. G. (1940). The biuret reaction in the determination of serum protein I. A study of the condition necessary for the production of the stable color which bears a quantitative relationship to the protein concentration. *Journal of Biological Chemistry*, 135, 707–725.
- Sikorski, Z. E. (2001). *Chemical and functional properties of food components*. New York: CRC Press LLC.
- Smith, D. M. (1991). Factors influencing heat induced gelation of muscle proteins. In N. Paris, & R. Bradford (Eds.), *Interactions of food proteins*. USA: Washington DC: American Chemical Society.
- Steel, R. G. D., & Torrie, J. H. (1980). *Principle and procedure of statistics: A biomaterial approach* (2nd ed.). New York: MacGraw-Hill.
- Takeda, H., & Seki, N. (1996). Enzyme-catalyzed crosslinking and degradation of myosin heavy chain in walleye pollack surimi paste during setting. *Fisheries Science*, 62, 462–467.
- Tammattinna, A., Benjakul, S., Visessanguan, W., & Tanaka, M. (2007). Gelling properties of white shrimp (*Penaeus vannamei*) meat as influenced by setting condition and microbial transglutaminase. *LWT-Food Science & Technology*, 40, 1489–1497.
- Totosaus, A., Montejo, J. G., Salazar, J. A., & Guerrero, I. (2002). A review of physical and chemical protein-gel induction. *International Journal of Food Science and Technology*, 37, 589–601.
- Toyohara, H., Kinoshita, M., & Shimizu, Y. (1990). Proteolytic gel degradation of threadfin-bream meat gel. *Journal of Food Science*, 55, 259–260.
- Xiong, Y. L. (1997). Structure-function relationships of muscle proteins. In S. Damodaran, & A. Paraf (Eds.), *Food proteins and their applications* (pp. 341–392). New York: Marcel Dekker.



# Effect of partially gelatinized corn starch on the rheological properties of wheat dough



Zong-qiang Fu <sup>a,1</sup>, Li-ming Che <sup>b,1</sup>, Dong Li <sup>a,\*\*</sup>, Li-jun Wang <sup>c,\*</sup>, Benu Adhikari <sup>d</sup>

<sup>a</sup> College of Engineering, National Energy R & D Center for Non-food Biomass, China Agricultural University, P. O. Box 50, 17 Qinghua Donglu, Beijing 100083, China

<sup>b</sup> College of Chemistry and Chemical Engineering, Xiamen University, Xiamen, China

<sup>c</sup> College of Food Science and Nutritional Engineering, Beijing Key Laboratory of Functional Food from Plant Resources, China Agricultural University, Beijing, China

<sup>d</sup> School of Applied Sciences, RMIT University, Melbourne City Campus, VIC 3001, Australia

## ARTICLE INFO

### Article history:

Received 23 June 2015

Received in revised form

18 October 2015

Accepted 20 October 2015

Available online 23 October 2015

### Keywords:

Rheological properties

Viscosity

Creep

Recovery

Partially gelatinized starch

## ABSTRACT

Ten, twenty and thirty percent (g/100 g) of wheat flour was substituted with partially gelatinized corn starch or ungelatinized corn starch and the rheological properties of the resultant dough samples were investigated. The apparent viscosity of dough increased with the increase in the concentration and degree of gelatinization of partially gelatinized starch samples except in the case of dough substituted with starch sample with high gelatinization degree (96.78%) at 30 g/100 g concentration. The presence of partially gelatinized starch increased the storage ( $G'$ ) and loss ( $G''$ ) moduli values and decreased the frequency sensitivity of dough samples. The dough prepared from wheat flour alone (control) showed the highest creep compliance and the lowest elastic recovery. In brief, the rheological properties of dough were influenced by the degree of substitution more than by the degree of gelatinization of substitutes.

© 2015 Elsevier Ltd. All rights reserved.

## 1. Introduction

Starch is the main component of wheat flour (about 80 g/100 g) and contributes to the formation of texture and quality of dough (Yang, Song, & Zheng, 2011). In many food applications, functional properties of starch can have important implication on the quality of end-use products (Hung & Morita, 2005). The different amylose/amylopectine ratio (Lee, Swanson, & Baik, 2001), granule structure (Goesaert et al., 2005) and granule size (Šebečić & Šebečić, 1996) of starch in wheat flour influences the texture, stability and elasticity of dough and bread.

In order to meet some specific requirements dough is commonly mixed with modified starches (Hung & Morita, 2004; Korus, Witczak, Ziobro, & Juszczak, 2009; Miyazaki, Maeda, & Morita, 2008). Pregelatinized starch is a physically modified starch which can reconstitute in cold water directly and provides desirable

pasting and texturizing characteristics (Miyazaki, Van Hung, Maeda, & Morita, 2006). Due to these advantages, pregelatinized starch is commonly used in dough. Onyango, Mutungi, Unbehend, and Lindhauer (2011) added pregelatinized starch to the gluten-free dough and they found the presence of pregelatinized starch increased the viscosity of the liquid phase and enhanced the network created by the native starch granules. Xue, Sakai, and Fukuoka (2008) used microwave heating to partially gelatinize starch in dough for making noodles. They found that the cooking time of noodles produced by using partially gelatinized dough was reduced significantly compared to the un-gelatinized noodles.

From the results of these studies, addition of pregelatinized starch can modify the properties of dough and the quality of the products. However, these studies did not show clearly about a relationship between the addition of partially gelatinized starch and the rheological properties of dough.

Pregelatinized starch is a modified starch in which the crystalline zones in the starch granules are partially or completely destroyed. Different degrees of gelatinization in the partially gelatinized starch give rise to a diverse granule structure having different degree of crystallinity (Fu, Wang, Li, & Adhikari, 2012). This difference in degree of crystallinity in partially gelatinized

\* Corresponding author.

\*\* Corresponding author.

E-mail addresses: [dongli@cau.edu.cn](mailto:dongli@cau.edu.cn) (D. Li), [wj@cau.edu.cn](mailto:wj@cau.edu.cn) (L.-j. Wang).

<sup>1</sup> These authors contributed equally to this work.

starch is expected to influence the performance of dough. However, research on the effects of residual crystallinity and the characteristics of partially gelatinized starch granules on the rheological properties of dough is not reported.

In these contexts, the objective of this work was to study the effect of partially gelatinized corn starch on the rheological properties of wheat dough. The rheological tests included steady shear flow, frequency sweep and creep-recovery. This would provide better understanding of the rheological properties of wheat dough containing partially gelatinized starch.

## 2. Materials and methods

### 2.1. Materials

Wheat flour was obtained from Beijing Guchuan Flour Group Co., Ltd. (Beijing, China). Its protein and moisture contents were 10.8 g/100 g and 7.3 g/100 g, respectively. Commercial gluten powder was obtained from Juancheng Jianfa Flour Co., Ltd. (Shandong, China). Its moisture content was 5.9 g/100 g. Native corn starch having 10.0 g/100 g moisture content was obtained from Hebei Zhangjiakou Yujin Food Co., Ltd. (Hebei, China). Partially gelatinized starch samples were obtained by controlled gelatinization of starch at 64 °C (S64), 68 °C (S68) and 70 °C (S70) as previously reported (Fu et al., 2012). Corn starch suspension at a starch concentration of 10.0 g/100 g was prepared by adding 20.0 g of pre-dried corn starch into deionized water at 24 ± 1 °C. Each batch of dispersion was thoroughly stirred at 300 rpm (in beakers) for 15 min using a thermostated water bath maintained at 64 °C, 68 °C and 70 °C. These partially gelatinized starch dispersions were spray dried using a bench-top spray drier (GPW120- II, Shandong Tianli Drying Equipment Inc., China). The inlet temperature, exhaust aspiration level, the flow rate of the air and feed rate used in the spray drying process were set at 200 °C, 95%, 0.375 m<sup>3</sup>/h and 7.2 mL/min, respectively. Partially gelatinized starch was also prepared at 25 °C (S25) by stirring corn starch slurry for 15 min at 25 °C followed by spray drying. The degree of gelatinization of S25, S64, S68 and S70 samples was determined using a differential scanning calorimeter (DSC-Q10, TA Instruments, New Castle, USA) and was found to be 32.30%, 47.75%, 69.40% and 96.78%, respectively.

### 2.2. Dough preparation

In each formulation, 10, 20 and 30 g/100 g of native and partially gelatinized corn starch containing 10.8 g/100 g of gluten powder was substituted for wheat flour. A fixed amount of water was added to each sample to attain 42 g/100 g moisture content on wet basis. The dough samples were mixed for about 10 min and allowed to stabilize for 20 min in a sealed container before further tests. The dough formulations containing the mixture of native corn starch and gluten powder and only wheat flour (100 g/100 g) were used as control.

### 2.3. Rheological tests

Rheological measurements were performed using AR2000ex rheometer (TA Instruments Ltd., Crawley, UK). The temperature was maintained at 30 °C using a water bath connected to a Peltier system. An aluminum parallel plate geometry was chosen to conduct steady shear flow tests (20 mm diameter, 1 mm gap). The frequency sweep tests and creep-recovery tests were conducted using parallel plate geometry having 40 mm diameter and 1 mm gap. A thin layer of silicone oil was applied on the rim of the samples in order to prevent evaporation. The linear viscoelastic region was determined for each sample through strain sweep tests

at 0.1, 1 and 100 Hz, respectively (data not shown). Viscoelastic properties (storage moduli  $G'$  and loss moduli  $G''$ ) of all the samples were determined within the linear viscoelastic region. A stabilization time of 15 min was applied to all the samples before measuring.

#### 2.3.1. Steady shear flow tests

The steady shear flow tests were performed over a shear rate range of 0.01–10 s<sup>-1</sup> to measure the apparent viscosity. The apparent viscosity versus shear rate data were fitted by using the Cross model (Moreira, Chenlo, & Torres, 2011) as given by Eq. (1):

$$\eta = \eta_{\infty} + \frac{\eta_0 - \eta_{\infty}}{1 + (k\dot{\gamma})^{(1-n)}} \quad (1)$$

where  $\eta$  (Pa s) is the apparent viscosity,  $\dot{\gamma}$  (s<sup>-1</sup>) is the shear rate,  $\eta_0$  and  $\eta_{\infty}$  (Pa s) are the viscosity values at zero and infinite shear rates, respectively. Similar,  $k$  (s) is the time constant and  $n$  is the flow behavior index. The value of  $\eta_{\infty}$  can be obtained from the experimental results corresponding to the equilibrium viscosity obtained at the end of shearing. In the cases where  $\eta_0 \gg \eta_{\infty}$  and  $\eta \gg \eta_{\infty}$ , it can be assumed that  $\eta_0 - \eta_{\infty} \approx \eta_0$  and  $\eta_{\infty} \rightarrow 0$  the Eq. (1) can be rewritten as Eq. (2) (Ravi & Bhattacharya, 2004).

$$\eta = \frac{\eta_0}{1 + (k\dot{\gamma})^{(1-n)}} \quad (2)$$

#### 2.3.2. Frequency sweep tests

The frequency sweep tests were performed over the frequency range of 0.1–100 Hz (angular frequency range of 0.6283–628.3 rad/s). The strain amplitude for these frequency sweep tests was selected as 0.25% based on the strain sweep results (data not shown) in order to confine these tests within linear viscoelastic region. Experimental  $G'$  and  $G''$  were fitted by using Eq. (3) and Eq. (4), respectively.

$$\log G' = \log a' + b' \log \omega \quad (3)$$

$$\log G'' = \log a'' + b'' \log \omega \quad (4)$$

where  $\omega$  (rad/s) is the angular frequency and  $a'$ ,  $a''$ ,  $b'$  and  $b''$  are the fitting parameters.

#### 2.3.3. Creep-recovery tests

Creep-recovery tests were carried out using a constant shear stress of 50 Pa. The variation in shear strain as a function of the applied stress was measured for 3 min. The applied stress was then removed and change in strain was recorded for further 5 min. Creep data was described with creep compliance rheological parameters,  $J(t)_C$  (Pa<sup>-1</sup>) =  $\gamma/\sigma$  where  $\gamma$  is the strain and  $\sigma$  is the constant shear stress during creep test. The creep compliance data of dough samples was fitted to the Burgers model by Eq. (5) and Eq. (6) for creep and recovery phases, respectively (Moreira et al., 2011):

$$J(t)_C = J_0 + J_m(1 - \exp(-t/\lambda)) + t/\eta_0 \quad (5)$$

$$J(t)_R = J_{\max} - J_0 - J_m(1 - \exp(-t/\lambda)) \quad (6)$$

where,  $J_0$  (Pa<sup>-1</sup>),  $J_m$  (Pa<sup>-1</sup>) and  $J_{\max}$  (Pa<sup>-1</sup>) are the instantaneous, viscoelastic and maximum creep compliance values, respectively.  $t$  (s) and  $\lambda$  (s) are the phase and mean retardation time values, respectively.  $\eta_0$  (Pa s) is the zero-shear viscosity. The percentage recovery of dough was represented by the elastic recovery (%) given by Eq. (7).

$$J_e(\%) = (S_m - S_f) / S_m \quad (7)$$

where,  $S_m$  and  $S_f$  are the maximum and final strain values, respectively.

#### 2.4. Statistical analyses

All the tests were carried out at least in triplicate and results are reported as the mean and standard deviation of these measurements. Duncan's multiple comparison tests were used to determine the significant effect of partially gelatinized starch on the rheological properties of dough samples. A 95% ( $p < 0.05$ ) confidence level was used in all cases and the SPSS statistical package (LEAD Technologies, US) was used for data analysis.

### 3. Results and discussion

#### 3.1. Effect of substitution on apparent shear viscosity of dough

The steady shear flow curves of dough samples are shown in Fig. 1. The apparent viscosity values of all the samples decreased with increase in the shear rate indicating that all the samples exhibited shear-thinning behavior albeit at different levels. The weakening of molecular network in these pastes due to applied shear is responsible for the observed shear thinning behavior (Ravi & Bhattacharya, 2004). The increase of the proportion of partially gelatinized starch in the formulation resulted in the increase of apparent viscosity (Fig. 1B,C,D, and E). As can be seen from Fig. 1, the apparent viscosity values of dough samples partially substituted with S68 and S70 were higher than that of the control samples. The apparent viscosity values of dough samples partially substituted with S68 and S70 were also higher than the apparent viscosity values of the dough samples partially substituted with S25 and S64, which means that apparent shear viscosity of dough also depends on the degree of gelatinization of partially gelatinized starch. The cross model was used to predict the apparent viscosity of the dough. It fitted the testing apparent viscosity very well.

The Cross model parameters for dough samples are summarized in Table 1. As the concentration of the partially gelatinized starch in the dough increased, the values of zero-shear viscosity ( $\eta_0$ ) increased significantly ( $p < 0.05$ ). The values of  $\eta_0$  were also influenced by the degree of gelatinization of substitutes. However, it seems that the concentration of substitutes played a more important role to modify the properties of dough. The values of the parameter ( $k$ ) of all the dough samples decreased significantly ( $p < 0.05$ ) with increase in the concentration of the partially gelatinized starch. A decrease in  $k$  values due to the increase in the concentration of partially gelatinized starch indicated a lower rate of breakdown of starch granule network in substituted dough samples (Ravi & Bhattacharya, 2004). The flow behavior index ( $n$ ) is the reflection of the shear-thinning behavior. As the concentration of the substitute increased, the  $n$  value decreased significantly ( $P < 0.05$ ). When the degree of gelatinization of the substitutes increased, the  $n$  value also decreased indicating to the increased shear-thinning behavior of these samples. However, the  $n$  value of dough sample substituted by S70 was lower than that of the dough sample substituted by S68 when the percentage of substitute was 30 g/100 g.

Gelatinized starch can be rehydrated at room temperature and it produces great viscosity and smooth texture (Singh & Singh, 2003). Therefore, it can be used as thickeners in foods and as adhesives in the textile industry (Anastasiades, Thanou, Loulis, Stapatoris, & Karapantsios, 2002). When the wheat flour was judiciously

substituted with partially gelatinized starch and gluten, the starch granules in dough were made to adhere to one another. The attractive force among the granules increased with the increase in the concentration and the degree of gelatinization of substituted starch. As a result, the mobility of starch granules decreased which was reflected in the increase in the apparent viscosity values. We have shown in our earlier study that the swelling power of partially gelatinized starch has a relationship with the degree of gelatinization. For example, the degree of gelatinization of S70 was 96.78% which was higher than that of other partially gelatinized starches and the swelling power of S70 was found to be 7.14 which was the highest among all the partially gelatinized starch samples at 30 °C (Fu et al., 2012). The S70 with enhanced water absorption could absorb more water from dough sample. The highest degree of gelatinization of S70 leads to the weakest structure. The large swelling granules of S70 tend to break into small pieces during the shearing process which may play the role of a lubricant. As the percentage of substitution increased, this effect will play an increasingly important role in the rheological properties of dough samples. Consequently, the apparent viscosity of dough sample substituted by S70 was not as high as that of the dough sample substituted by S68 when the percentage of substitute was 30 g/100 g.

#### 3.2. Effect of substitution on viscoelastic characteristics of dough

Fig. 2 shows the variation in storage ( $G'$ ) and loss ( $G''$ ) moduli of dough samples. All the tested dough samples showed  $G' > G''$  throughout the frequency range indicating to a more elastic (than viscous) gel structure. It can also be observed that the moduli ( $G'$  and  $G''$ ) of all dough samples increased with increase in the frequency from 0.1 to 100 Hz. The  $G'$  and  $G''$  of control and dough samples substituted by S25 were lower than those of other dough samples.

The values parameters  $a'$ ,  $a''$ ,  $b'$  and  $b''$  for all the dough samples are given in Table 2. The values of these parameters indicate that the substitutes significantly ( $P < 0.05$ ) altered the dynamic rheological properties of dough samples compared with the control. The  $a' > a''$  in all the dough samples supported the fact that these dough samples are predominantly elastic than viscous. The values  $a'$  and  $a''$  increased significantly ( $P < 0.05$ ) with increase in the concentration of the partially gelatinized starch. When the degree of gelatinization of the substitutes increased, the values  $a'$  and  $a''$  changed a little. This observation indicates that when a dough sample is substituted with higher concentration of substitutes, it results in to stronger elastic structure. However, the values  $a'$  and  $a''$  of S70 were lower than those of S68 when the percentage of substitute was 30 g/100 g which is in accordance with the observation made earlier in apparent viscosity data. Regarding the  $b'$  and  $b''$  parameters, the control samples had higher values than other dough samples suggesting that the substitutes decreased the frequency sensitivity of dough samples.

As described in Section 3.1., partially gelatinized starch can produce a paste when rehydrated compared to the native starch. Partially gelatinized starch behaves similar to a gum and exhibits similar characteristics (Yu & Ngadi, 2006). Like gums, the partially gelatinized starch imparts greater water holding characteristics to dough which ultimately results into more elastic and firmer consistency. At given moisture content, the storage modulus increased as the concentration of the partially gelatinized starch was increased. The wheat flour dough can be regarded as a composite material where the starch granules act as filler in the continuous gluten matrix (Miyazaki et al., 2006; Sikora et al., 2010). In such a material, the modulus of the composite depends on the ratio of the modulus of the two materials (Larsson & Eliasson, 1997). The starch

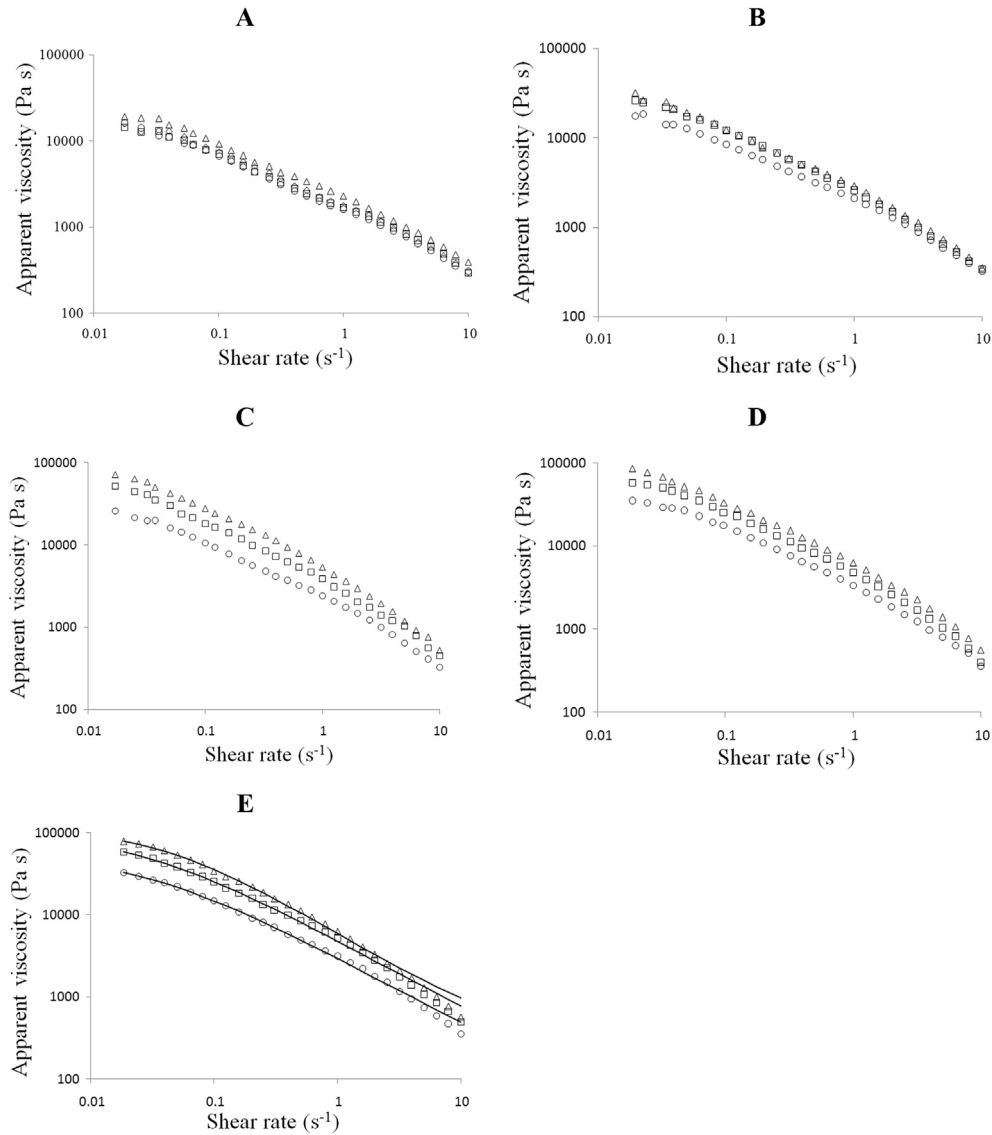


**Fig. 1.** Experimental steady-shear flow curves for wheat dough with different additives at different concentrations. (A) Native corn starch; (B) S25; (C) S64; (D) S68; (E) S70. ( $\diamond$  Control;  $\circ$  10 g/100 g;  $\square$  20 g/100 g;  $\triangle$  30 g/100 g; — predicted line).

**Table 1**

Parameters of steady shear flow for wheat dough substituted by different partially gelatinized starch at different concentrations.

Additives	Ratio (g/100 g)	Parameters				$R^2$
		$\eta_0$ ( $\times 10^4$ Pa s)	$k$ (s)	$n$		
Control	—	$3.26 \pm 0.19^a$	$47.85 \pm 1.52^h$	$0.27 \pm 0.02^h$	0.991	
Native corn starch	10	$3.04 \pm 0.15^a$	$50.53 \pm 1.88^i$	$0.30 \pm 0.01^i$	0.999	
Native corn starch	20	$3.07 \pm 0.16^a$	$49.28 \pm 1.50^{hi}$	$0.29 \pm 0.02^{hi}$	0.996	
Native corn starch	30	$3.77 \pm 0.17^b$	$39.88 \pm 1.59^g$	$0.24 \pm 0.01^g$	0.994	
S25	10	$3.19 \pm 0.17^a$	$47.91 \pm 1.58^h$	$0.28 \pm 0.01^{hi}$	0.997	
S25	20	$5.40 \pm 0.19^d$	$32.31 \pm 1.42^e$	$0.20 \pm 0.01^e$	0.999	
S25	30	$6.56 \pm 0.10^e$	$29.51 \pm 0.71^d$	$0.16 \pm 0.01^d$	0.994	
S64	10	$4.01 \pm 0.11^b$	$37.77 \pm 1.03^g$	$0.23 \pm 0.01^{fg}$	0.998	
S64	20	$6.44 \pm 0.13^e$	$30.55 \pm 1.00^{de}$	$0.18 \pm 0.01^d$	0.997	
S64	30	$8.92 \pm 0.14^g$	$21.29 \pm 1.59^{ab}$	$0.08 \pm 0.01^b$	0.998	
S68	10	$4.89 \pm 0.15^c$	$35.11 \pm 1.11^f$	$0.21 \pm 0.01^{ef}$	0.999	
S68	20	$7.84 \pm 0.13^f$	$25.30 \pm 1.64^c$	$0.12 \pm 0.01^c$	0.999	
S68	30	$11.05 \pm 0.49^h$	$19.73 \pm 1.10^a$	$0.04 \pm 0.00^a$	0.999	
S70	10	$4.88 \pm 0.22^c$	$35.06 \pm 0.95^f$	$0.21 \pm 0.01^{ef}$	0.999	
S70	20	$7.79 \pm 0.24^f$	$25.00 \pm 0.89^c$	$0.12 \pm 0.01^c$	0.999	
S70	30	$8.97 \pm 0.07^g$	$22.17 \pm 0.92^b$	$0.07 \pm 0.00^b$	0.999	

Values are mean  $\pm$  standard deviation ( $n = 3$ ). Values in the same column followed by different lowercase letters indicate to the significant difference ( $P < 0.05$ ).

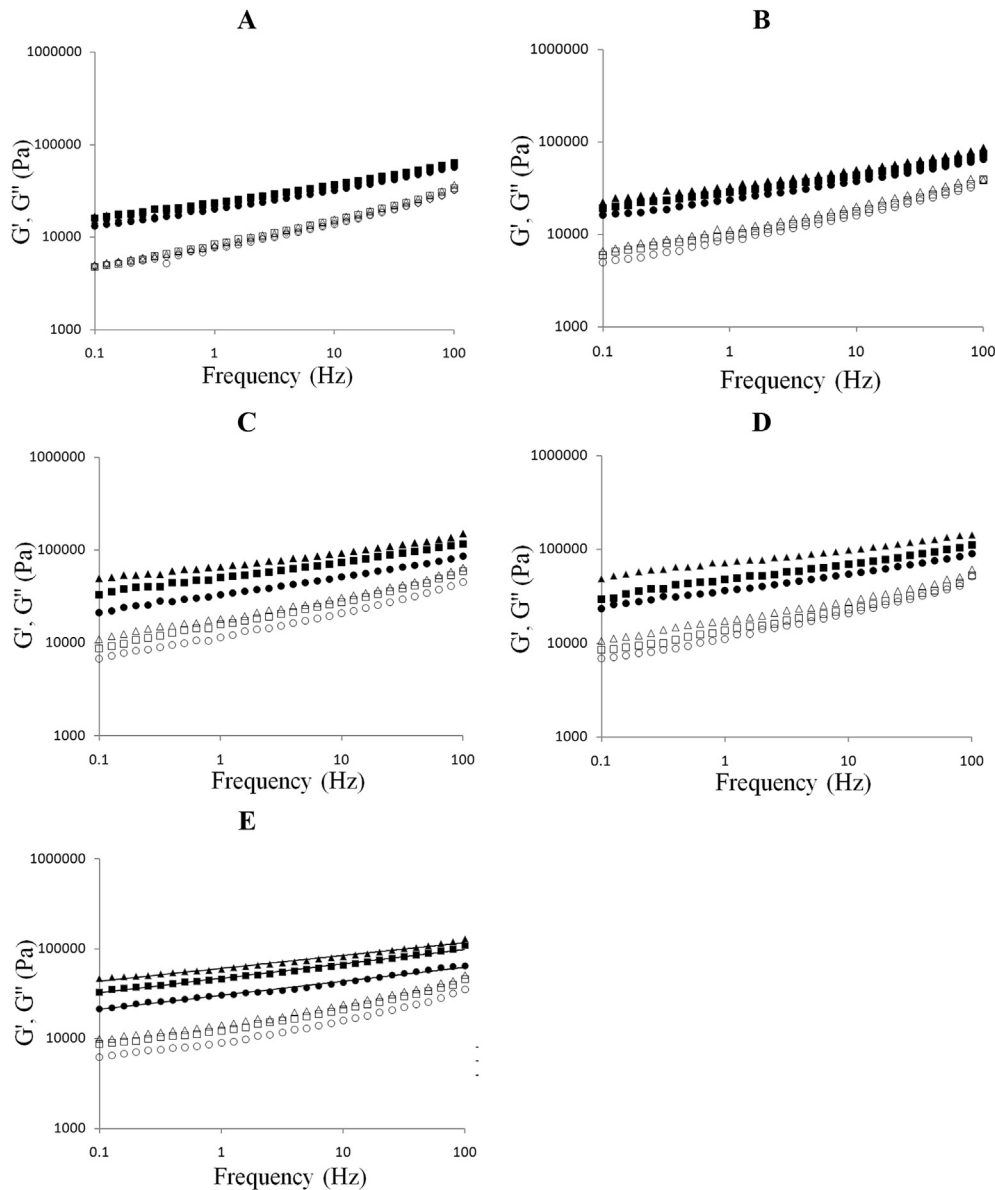


**Fig. 2.** Experimental  $G'$  and  $G''$  data for wheat dough with different additives at different concentrations. (A) Native corn starch; (B) S25; (C) S64; (D) S68; (E) S70. ( $G'$ :  $\blacklozenge$  Control;  $\bullet$  10 g/100 g;  $\blacksquare$  20 g/100 g;  $\blacktriangle$  30 g/100 g; — predicted line;  $G''$ :  $\diamond$  Control;  $\circ$  10 g/100 g;  $\square$  20 g/100 g;  $\triangle$  30 g/100 g).

sample S70 with high water binding capacity may inhibit the development of gluten which lowers the consistency of the gluten network leading the dough to be less resistance to strains (Fustier, Castaigne, Turgeon, & Biliaderis, 2008; Yang et al., 2011).

### 3.3. Effect of substitution on creep-recovery of dough

The creep-recovery curves of dough samples are presented in Fig. 3. As the concentration of substitutes increased, the maximum creep compliance decreased significantly ( $P < 0.05$ ). As can be seen from this figure, the degree of gelatinization of substitutes also significantly ( $P < 0.05$ ) altered the maximum creep compliance of dough samples. Wang and Sun (2002) suggested that the maximum creep compliance could be used to characterize the rigidity (firmness) of dough samples. They reported that stronger dough samples which had greater resistance to deformation had smaller creep compliance than softer dough samples. The fact that the dough samples substituted with S68 and S70 exhibited greater

resistance to deformation and showed smaller creep compliance than other dough samples agrees with Wang and Sun (2002)'s observation.

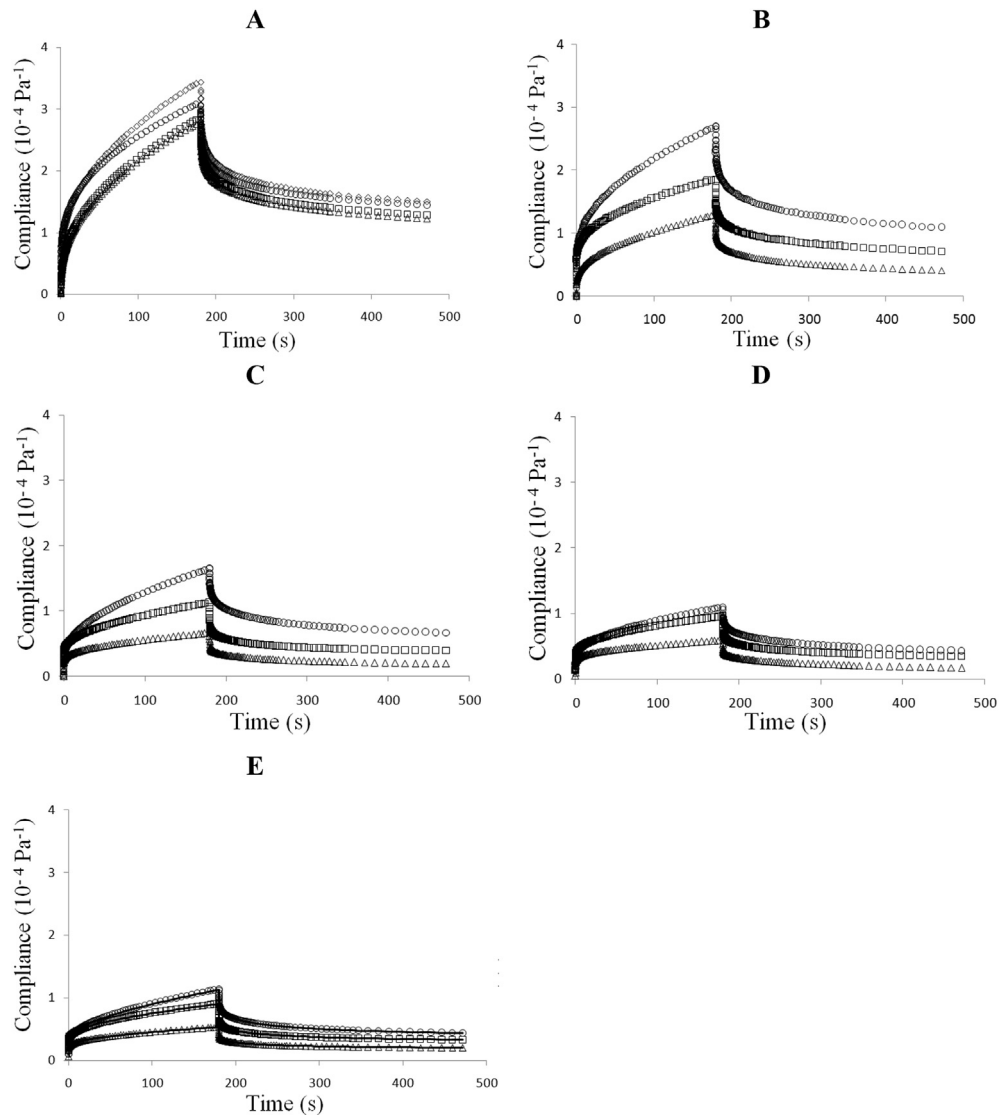
The Burgers model parameters for creep-recovery phase calculated using Eq. (5) and Eq. (6) are presented in Fig. 4. The instantaneous, viscoelastic and maximum creep compliance ( $J_0$ ,  $J_m$  and  $J_{max}$ ) all decreased with the increase in the concentration of substitutes. The values of creep compliance for control samples were higher than those for other samples, indicating that control samples were softer. The retardation time ( $\lambda$ ) is the time required for the applied stress to decrease to  $1/e$  (approximately 36.8%) of its initial value under constant deformation (Jiménez-Avalos, Ramos-Ramírez, & Salazar-Montoya, 2005). As can be seen from Fig. 4C, the retardation time of control samples is higher than those of other samples. Zero-shear viscosity ( $\eta_0$ ) reflects on the flowability of a material at the end of applied stress. The values of the zero-shear viscosity increased with the increase in the degree of gelatinization of substitutes. This observation indicated that the dough

**Table 2**

Parameters of frequency sweep for wheat dough substituted by different partially gelatinized starch at different concentrations.

Additives	Ratio (g/100 g)	$G'$			$G''$		
		$a'(\times 10^4 \text{ Pa s}^n)$	$b'(\times 10^{-1})$	$R^2$	$a''(\times 10^3 \text{ Pa s}^n)$	$b''(\times 10^{-1})$	$R^2$
Control	—	1.37 ± 0.13 <sup>a</sup>	2.12 ± 0.05 <sup>g</sup>	0.998	4.39 ± 0.35 <sup>a</sup>	2.82 ± 0.06 <sup>gh</sup>	0.993
Native corn starch	10	1.34 ± 0.09 <sup>a</sup>	2.14 ± 0.04 <sup>g</sup>	0.997	4.34 ± 0.24 <sup>a</sup>	2.92 ± 0.05 <sup>h</sup>	0.993
Native corn starch	20	1.54 ± 0.14 <sup>a</sup>	2.04 ± 0.06 <sup>hi</sup>	0.996	4.76 ± 0.45 <sup>a</sup>	2.85 ± 0.08 <sup>gh</sup>	0.991
Native corn starch	30	1.51 ± 0.14 <sup>a</sup>	1.98 ± 0.02 <sup>gh</sup>	0.995	4.61 ± 0.35 <sup>a</sup>	2.85 ± 0.06 <sup>gh</sup>	0.992
S25	10	1.51 ± 0.13 <sup>a</sup>	2.10 ± 0.08 <sup>ig</sup>	0.998	4.81 ± 0.46 <sup>a</sup>	2.86 ± 0.07 <sup>h</sup>	0.992
S25	20	2.12 ± 0.20 <sup>b</sup>	1.91 ± 0.04 <sup>g</sup>	0.995	6.08 ± 0.52 <sup>b</sup>	2.76 ± 0.05 <sup>efg</sup>	0.991
S25	30	2.57 ± 0.24 <sup>c</sup>	1.82 ± 0.06 <sup>f</sup>	0.994	7.09 ± 0.43 <sup>c</sup>	2.72 ± 0.04 <sup>ef</sup>	0.990
S64	10	2.37 ± 0.13 <sup>bc</sup>	1.91 ± 0.06 <sup>g</sup>	0.996	6.73 ± 0.11 <sup>bc</sup>	2.75 ± 0.04 <sup>efg</sup>	0.992
S64	20	3.49 ± 0.16 <sup>d</sup>	1.71 ± 0.02 <sup>de</sup>	0.995	8.76 ± 0.59 <sup>d</sup>	2.61 ± 0.09 <sup>bcd</sup>	0.989
S64	30	4.78 ± 0.23 <sup>e</sup>	1.55 ± 0.03 <sup>b</sup>	0.992	10.81 ± 0.28 <sup>e</sup>	2.51 ± 0.03 <sup>ab</sup>	0.986
S68	10	2.68 ± 0.23 <sup>c</sup>	1.78 ± 0.09 <sup>ef</sup>	0.996	6.90 ± 0.42 <sup>bc</sup>	2.69 ± 0.08 <sup>de</sup>	0.990
S68	20	3.76 ± 0.35 <sup>d</sup>	1.64 ± 0.06 <sup>cd</sup>	0.993	8.47 ± 0.56 <sup>d</sup>	2.58 ± 0.03 <sup>bc</sup>	0.990
S68	30	5.27 ± 0.27 <sup>f</sup>	1.45 ± 0.03 <sup>a</sup>	0.992	10.35 ± 0.58 <sup>e</sup>	2.42 ± 0.07 <sup>a</sup>	0.986
S70	10	2.53 ± 0.19 <sup>c</sup>	1.79 ± 0.06 <sup>ef</sup>	0.996	6.49 ± 0.53 <sup>bc</sup>	2.67 ± 0.04 <sup>de</sup>	0.989
S70	20	3.73 ± 0.26 <sup>d</sup>	1.63 ± 0.03 <sup>bc</sup>	0.994	8.64 ± 0.73 <sup>d</sup>	2.51 ± 0.12 <sup>ab</sup>	0.982
S70	30	4.83 ± 0.26 <sup>e</sup>	1.46 ± 0.03 <sup>a</sup>	0.992	9.37 ± 0.72 <sup>d</sup>	2.48 ± 0.07 <sup>a</sup>	0.990

Values are mean ± standard deviation (n = 3). Values in the same column followed by different lowercase letters indicate to the significant difference (P &lt; 0.05).

**Fig. 3.** Creep and recovery curves for wheat dough with different additives at different concentrations. (A) Native corn starch; (B) S25; (C) S64; (D) S68; (E) S70. ( $\diamond$  Control;  $\circ$  10 g/100 g;  $\square$  20 g/100 g;  $\triangle$  30 g/100 g; — predicted line).

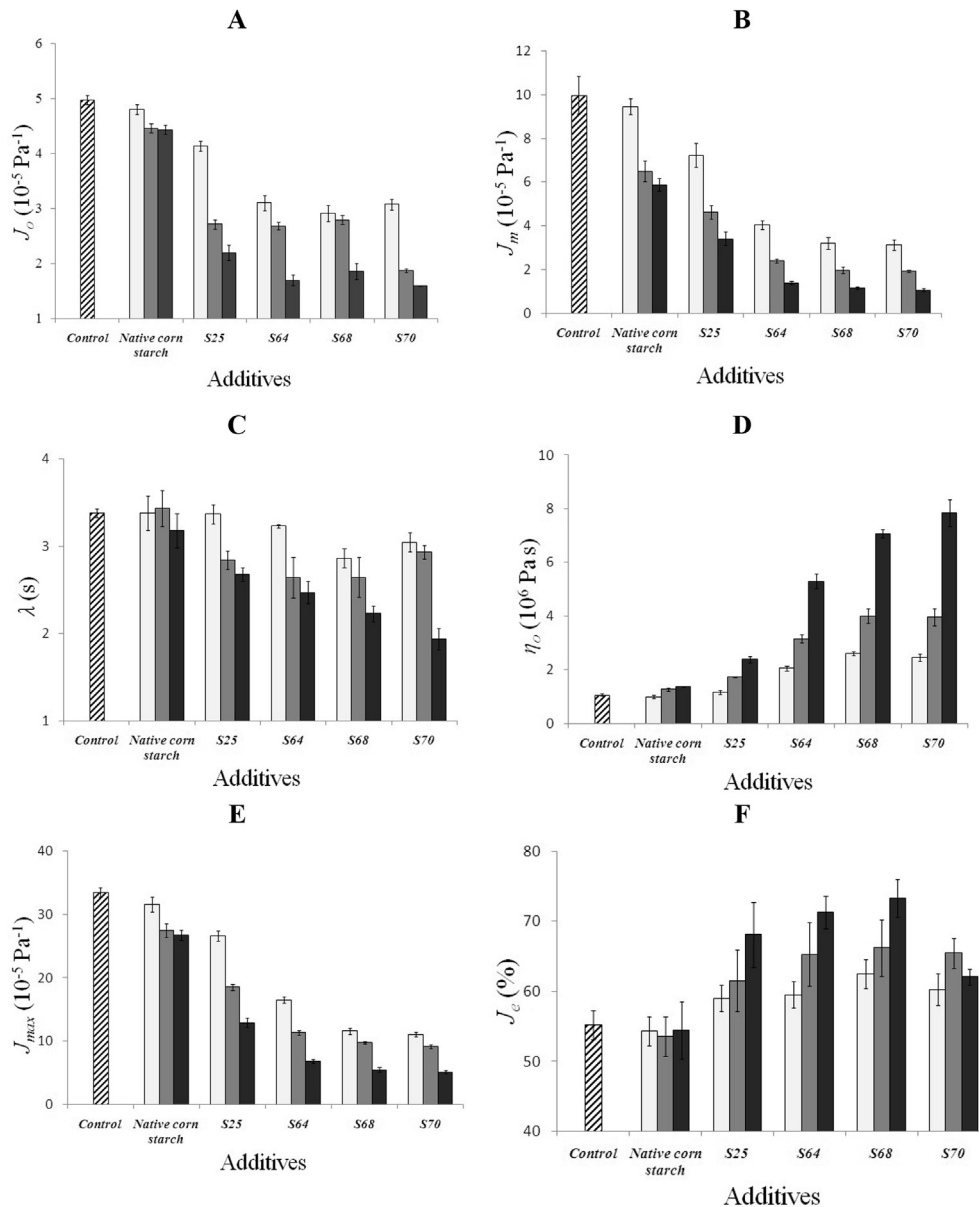


**Fig. 4.** Creep-recovery parameters for wheat dough with different additives at different concentrations. Creep phase: (A)–(D); Recovery phase: (E). (▨) Control; □ 10 g/100 g; ■ 20 g/100 g; ■ 30 g/100 g.

samples substituted with starch with higher degree of gelatinization exhibited more viscous behavior and greater resistance to flow. The elastic recovery ( $J_e$ ) reflects the extent of bonding among the constituents of dough samples. As can be seen from Fig. 4F, the values of  $J_e$  changed a lot as the concentration of substitutes increased which indicated less deformation or breakage of the composite network, while the values of  $J_e$  changed a little as the degree of gelatinization of substitutes increased. The elastic recovery of dough sample substituted with S70 decreased when the percentage of substitute increased from 20 g/100 g to 30 g/100 g.

The dough samples substituted with partially gelatinized starch at different gelatinization degree and different level of substitution showed different rheological properties. This can be attributed to the fact that the starch fraction plays an important role for the viscoelastic properties of flour dough (Khatkar & Schofield, 2002). The effect of starch in dough characteristics is largely related to its physical properties, such as size and shape of granules and water

binding capacity (Witczak, Juszcak, Ziobro, & Korus, 2012). The swelling ability of partially gelatinized starch granules during rehydration process greatly increases with increase in the degree of gelatinization (Fu et al., 2012). The enlarged granules occupy the free space and alter the consistency of dough which increases the resistance of dough against deformation (Witczak et al., 2012). In this regard, Hüttner, Bello, and Arendt (2010) also reported that the increased elasticity of dough was primarily related to the water hydration capacity of starch.

#### 4. Conclusions

Dough samples substituted with partially gelatinized starch (at different degree of gelatinization and different degree of substitution) exhibited different rheological properties. The apparent viscosity of dough increased with the increase in the concentration and degree of gelatinization of the partially gelatinized starch

samples except dough sample substituted with S70 at 30 g/100 g concentration. All the dough samples substituted with partially gelatinized starch showed increase in storage ( $G'$ ) and loss ( $G''$ ) moduli. The wheat dough (control) had higher creep compliance compared to those dough samples substituted with partially gelatinized starch. The elastic recovery ( $J_e$ ) of control dough samples was the lowest. The rheological data of dough samples were fitted to different models. It is found that the experimental results were in good agreement with the model predictions. In a word, the rheological properties of dough were influenced by the degree of substitution more than by the degree of gelatinization of substitutes.

## Acknowledgments

This research was supported by Chinese Universities Scientific Fund (No. 2015SP001), High Technology Research and Development Program of China (No. 2011AA100802) and Science and Technology Support Project of China (No. 2013BAD10B03).

## References

- Anastasiades, A., Thanou, S., Loulis, D., Staporis, A., & Karapantsios, T. D. (2002). Rheological and physical characterization of pregelatinized maize starches. *Journal of Food Engineering*, 52(1), 57–66.
- Fustier, P., Castaigne, F., Turgeon, S. L., & Biliaderis, C. G. (2008). Flour constituent interactions and their influence on dough rheology and quality of semi-sweet biscuits: a mixture design approach with reconstituted blends of gluten, water-solubles and starch fractions. *Journal of Cereal Science*, 48, 144–158.
- Fu, Z.-Q., Wang, L.-J., Li, D., & Adhikari, B. (2012). Effects of partial gelatinization on structure and thermal properties of corn starch after spray drying. *Carbohydrate Polymers*, 88(4), 1319–1325.
- Goesaert, H., Brijs, K., Veraverbeke, W. S., Courtin, C. M., Gebruers, K., & Delcour, J. A. (2005). Wheat flour constituents: how they impact bread quality, and how to impact their functionality. *Trends in Food Science & Technology*, 16, 12–30.
- Hung, P. V., & Morita, N. (2004). Dough properties and bread quality of flours supplemented with cross-linked corn starch. *Food Research International*, 37(5), 461–467.
- Hung, P. V., & Morita, N. (2005). Thermal and rheological properties of dough and bread as affected by various cross-linked corn starch substitutions. *Starch/Stärke*, 57, 540–546.
- Hüttner, E. K., Bello, F. D., & Arendt, E. K. (2010). Rheological properties and bread making performance of commercial wholegrain oat flours. *Journal of Cereal Science*, 52(1), 65–71.
- Jiménez-Avalos, H. A., Ramos-Ramírez, E. G., & Salazar-Montoya, J. A. (2005). Viscoelastic characterization of gum Arabic and maize starch mixture using the Maxwell model. *Carbohydrate Polymers*, 62(1), 11–18.
- Khatkar, B. S., & Schofield, J. D. (2002). Dynamic rheology of wheat flour dough. I. Non-linear viscoelastic behaviour. *Journal of the Science of Food and Agriculture*, 82, 827–829.
- Korus, J., Witczak, M., Ziobro, R., & Juszcak, L. (2009). The impact of resistant starch on characteristics of gluten-free dough and bread. *Food Hydrocolloids*, 23, 988–995.
- Larsson, H., & Eliasson, A. C. (1997). Influence of the starch granule surface on the rheological behavior of wheat flour dough. *Journal of Texture Studies*, 28(5), 487–501.
- Lee, M. R., Swanson, B. G., & Baik, B. K. (2001). Influence of amylose content on properties of wheat starch and breadmaking quality of starch and gluten blends. *Cereal Chemistry*, 78(6), 701–706.
- Miyazaki, M., Maeda, T., & Morita, N. (2008). Bread quality of frozen dough substituted with modified tapioca starches. *European Food Research and Technology*, 227(2), 503–509.
- Miyazaki, M., Van Hung, P., Maeda, T., & Morita, N. (2006). Recent advances in application of modified starches for breadmaking. *Trends in Food Science & Technology*, 17(11), 591–599.
- Moreira, R., Chenlo, F., & Torres, M. D. (2011). Effect of sodium chloride, sucrose and chestnut starch on rheological properties of chestnut flour doughs. *Food Hydrocolloids*, 25, 1041–1050.
- Onyango, C., Mutungi, C., Unbehend, G., & Lindhauer, M. G. (2011). Rheological and textural properties of sorghum-based formulations modified with variable amounts of native or pregelatinized cassava starch. *LWT – Food Science and Technology*, 44(3), 687–693.
- Ravi, R., & Bhattacharya, S. (2004). Flow behaviour of chickpea (*Cicer arietinum* L.) flour dispersions: effect of additives. *Journal of Food Engineering*, 65, 619–624.
- Šebecić, B., & Šebecić, B. (1996). Wheat flour starch granule-size distribution and rheological properties of dough. Part 4. Farinographic measurements. *Food/Nahrung*, 40(5), 256–260.
- Sikora, M., Kowalski, S., Krystyan, M., Ziobro, R., Wrona, P., Curic, D., et al. (2010). Starch gelatinization as measured by rheological properties of the dough. *Journal of Food Engineering*, 96, 505–509.
- Singh, J., & Singh, N. (2003). Studies on the morphological and rheological properties of granule cold water soluble corn and potato starches. *Food Hydrocolloids*, 17, 63–72.
- Wang, F. C., & Sun, X. S. (2002). Creep-recovery of wheat flour doughs and relationship to other physical dough tests and breadmaking performance. *Cereal Chemistry*, 79(4), 567–571.
- Witczak, M., Juszcak, L., Ziobro, R., & Korus, J. (2012). Influence of modified starches on properties of gluten-free dough and bread. Part I: Rheological and thermal properties of gluten-free dough. *Food Hydrocolloids*, 28, 353–360.
- Xue, C., Sakai, N., & Fukuoka, M. (2008). Use of microwave heating to control the degree of starch gelatinization in noodles. *Journal of Food Engineering*, 87, 357–362.
- Yang, Y., Song, Y., & Zheng, Q. (2011). Rheological behaviors of doughs reconstituted from wheat gluten and starch. *Journal of Food Science and Technology*, 48(4), 489–493.
- Yu, L. J., & Ngadi, M. O. (2006). Rheological properties of instant fried noodle dough as affected by some ingredients. *Journal of the Science of Food and Agriculture*, 86(4), 544–548.



# Antimicrobial effect of essential oils in combinations against five bacteria and their effect on sensorial quality of ground meat



Mina Ghabraie, Khanh Dang Vu, Lina Tata, Stéphane Salmieri, Monique Lacroix\*

Research Laboratories in Sciences Applied to Food, Canadian Irradiation Center, INRS-Institut Armand-Frappier, Institute of Nutraceutical and Functional Foods, 531, Boulevard des Prairies, Laval, Québec, H7V 1B7, Canada

## ARTICLE INFO

### Article history:

Received 17 June 2015

Received in revised form

22 September 2015

Accepted 21 October 2015

Available online 24 October 2015

### Keywords:

Essential oil (EO)

Food pathogen

Spoilage bacteria

Interaction of EO

Food model

## ABSTRACT

The antibacterial activity of 32 Essential Oils (EOs) was assessed against four pathogenic bacteria (*Escherichia coli*, *Listeria monocytogenes*, *Staphylococcus aureus*, and *Salmonella* Typhimurium) and one spoilage bacterium (*Pseudomonas aeruginosa*). Agar diffusion, micro-atmosphere and microbroth assays were used to evaluate the antibacterial activity in solid, vapour and liquid phase, respectively. In solid phase, Red thyme, Red bergamot, Ajowan, Summer savory, Chinese cinnamon, and Cinnamon bark had higher inhibitory zone (20–40 mm) against five target bacteria as compared with other EOs. Red thyme, Red bergamot, Ajowan, Summer savory inhibited *S. aureus* by more than 60 mm. In vapour phase, at 30 µl of tested EOs, Chinese cinnamon and Red bergamot were the only EOs that inhibited all target bacteria with the inhibition zone from 20 to more than 60 mm depending on target bacteria. In liquid phase, Chinese cinnamon showed the best antibacterial activity among all EOs and it inhibited *S. aureus* and *E. coli* at low minimum inhibitory concentration (MIC) of 470 ppm. In checkerboard method, combined Chinese cinnamon and Cinnamon bark EOs showed additive antibacterial effects against all bacteria. Sensory evaluation of combined Chinese cinnamon and Cinnamon bark EOs used in cooked meat was conducted and an EO level of 0.05% was the highest organoleptically acceptable.

© 2015 Elsevier Ltd. All rights reserved.

## 1. Introduction

Elimination of foodborne pathogenic and spoilage bacteria is important for food companies. Food spoilage includes physical damage and/or chemical changes which are due to contamination of food by yeast or bacteria (Cueva et al., 2011). Consumption of contaminated food with pathogenic bacteria causes foodborne illness which is one of the big concerns of public health. According to Thomas et al. (2013), it is estimated that each year in Canada, there are 4.0 million episodes of domestically acquired foodborne illnesses.

Food and food products can be contaminated during production, processing, distribution, and preparation (Gaulin, Nguon, Leblanc, Ramsay, & Roy, 2013). Foodborne pathogens such as *Salmonella* sp., *Staphylococcus aureus*, *Listeria monocytogenes* and *Escherichia coli* are responsible for numerous illnesses and death (Oussalah, Caillet, Saucier, & Lacroix, 2007). *Pseudomonas aeruginosa* is a food spoilage organism that can cause off-flavor and discoloration

of refrigerated meat (Gutierrez, Barry-Ryan, & Bourke, 2009).

The shelf life, nutrition and microbial quality of food products are important aspects that food companies critically consider. In fact, synthetic preservatives have been widely used to eliminate bacteria and prolong the shelf-life of food products. However, synthetic preservatives may cause health problems for consumers in a long term period. Thus, searching for new and potential natural antimicrobial agents from different sources such as microbial metabolites, plant and spice extracts for food application has been increasing significantly (Cueva et al., 2011).

It has been identified that due to co-evolution, plants produce secondary metabolites such as essential oil (EOs) as defense systems against predators (fungi, insects, etc.). EOs have proven biological properties such as antibacterial, antiparasitic, antifungal, antioxidant and, insecticidal and they have served since ancient times (Solorzano-Santos & Miranda-Novales, 2012). EOs have an oily consistency, and are produced by organs of plants such as buds, flowers, leaves, stems, seeds, fruits, and roots etc. (Bakkali, Averbeck, Averbeck, & Idaomar, 2008). They are mostly extracted from nonwoody organs and are liquid at room temperature (Dorman & Deans, 2000). Over 1340 plants having antimicrobial

\* Corresponding author.

E-mail address: [Monique.Lacroix@iaf.inrs.ca](mailto:Monique.Lacroix@iaf.inrs.ca) (M. Lacroix).

compounds have been identified (Tajkarimi, Ibrahim, & Cliver, 2010). According to Burt (2004), out of 3000 EOs which are already recognized, 300 EOs are commercially important. It is mentioned in several studies that spices and EOs are generally recognized as safe (GRAS) (Burt, 2004; Goñi et al., 2009). Both major and minor compounds can contribute to the antimicrobial properties of EOs because some minor compounds may have synergistic or additive activity with the major ones or cause the synergy between major compounds (Burt, 2004).

Due to their antimicrobial properties and their safety, EOs are known as one of the best candidates to be used as preservatives; however, application is limited due to their taste and odor impacts, especially at high concentrations (Goñi et al., 2009). Therefore, it is necessary to determine their lowest concentration with acceptable sensorial level in order to use them in food without any changes in smell and taste (Turgis, Vu, Dupont, & Lacroix, 2012). It has been demonstrated that EOs have antimicrobial activity against pathogenic bacteria at the range of 0.05–0.1% in food systems (Tajkarimi et al., 2010). In fact, the organoleptically acceptable concentration depends on individual EO, the specific food systems, the method of application and food product cooking methods. Indeed, it would be changed when other compounds are added to the food too.

Thus, the objective of this study was to assess the antimicrobial activities of 32 different EOs against 5 different foodborne pathogens and spoilage bacteria using three methods including agar diffusion assay, micro-atmosphere diffusion assay and microbroth dilution assay. Further, to select the best combined EOs with high antimicrobial effects for food application, the combined effects (synergistic, additive, no interaction, or antagonist effect) of different EOs were evaluated using the checkerboard method. Moreover, sensorial analysis was performed to determine the organoleptically acceptable concentration of selected EOs combination on ground meat as a food model.

## 2. Materials and methods

### 2.1. Preparation of EOs

The list of evaluated EOs and their main constituents is presented in Table 1. EOs were prepared as oil-in-water emulsion before utilization for evaluation of their antimicrobial properties. The emulsion of EOs consisted of 2.5% EO (v/v), 5.0% Tween 80 (w/v) (Sigma–Aldrich Ltd), and 92.5% water (w/w), and was homogenized for 4 min at 15000 rpm using an Ultra Turrax (TP18/1059 homogenizer).

The emulsion of EOs was used for microbroth dilution and checkerboard assays while EOs (without emulsion) were used directly for agar diffusion assay and micro-atmosphere diffusion assay.

### 2.2. Preparation of bacterial cultures

Five bacterial strains, two Gram-positive (*L. monocytogenes* HPB 2812 and *S. aureus* ATCC 29213) and three Gram-negative (*E. coli* O157:H7 EDL933, *Salmonella* Typhimurium SL 1344 and *P. aeruginosa* ATCC 15422) were used as target bacteria in antimicrobial tests. All the bacteria were stored at  $-80^{\circ}\text{C}$  in Tryptic Soy Broth (TSB) medium (TSB; BD, Franklin Lakes, NJ, USA) containing glycerol (10% v/v). Before experiment, stock cultures were propagated through two consecutive 24 h growth cycles in TSB at  $37^{\circ}\text{C}$  to reach the concentration of approximately  $10^9$  CFU/ml and at the same day of experiment, the grown cultures were diluted in saline solution to obtain a working culture of approximately  $10^6$  CFU/ml.

### 2.3. Antimicrobial activity of EOs against target bacteria using agar diffusion assay

The tryptic soy agar (TSA) plates were inoculated with a target bacterium (approximately  $10^6$  CFU/ml) on the agar surface. Then, a sterile 6-mm diameter cellulose test disc was put on the middle of the agar surface and 4  $\mu\text{l}$  of EO were applied on it. For control, 4  $\mu\text{l}$  of sterile water was used. Each plate was sealed well with Parafilm to prevent vapor transfer from the samples as well the loss of volatile components of EOs (Cardiet, Fuzeau, Barreau, & Fleurat-Lessard, 2012; Dussault, Vu, & Lacroix, 2014). Plates were incubated for 72 h at  $37^{\circ}\text{C}$ . The inhibition diameter (colony-free perimeter) around the cellulose disc was measured with a precise ruler (Traceable<sup>®</sup> Carbon Fiber Digital Caliper, resolution: 0.1 mm/0.01, accuracy:  $\pm 0.2$  mm/0.01, Fisher Scientific, Canada).

### 2.4. Evaluation of antimicrobial activity of EOs using micro-atmosphere diffusion assay

To evaluate the antimicrobial activity of volatile compounds of EOs against target bacteria, micro-atmosphere diffusion assay was performed using inverse Petri dish method (Cardiet et al., 2012). The TSA plates were inoculated with a target bacterium using the same method as mentioned in the agar diffusion assay. The Petri dishes were inverted and 30  $\mu\text{l}$  was deposited on a cellulose disc (20 mm in diameter) which was placed in the middle of the lid of Petri dish. For control, 30  $\mu\text{l}$  of sterile water was used. The Petri dishes were hermetically sealed with Parafilm to prevent vapor transfer between samples as well the loss of volatile components of EOs. Samples were incubated for 24 h at  $37^{\circ}\text{C}$ . The inhibition diameter was measured with a Traceable<sup>®</sup> Carbon Fiber Digital Caliper.

### 2.5. Determination of minimum inhibitory concentration (MIC) of EOs against target bacteria using broth microdilution assay

The emulsion of each EO was prepared according to modified protocol of Turgis et al. (2012). Serial dilutions were performed from 10000 ppm to 10 ppm using Mueller–Hinton (MH) broth. From each concentration, 125  $\mu\text{l}$  of the emulsified EO were taken and filled into wells of columns 1 to 11 of a 96-well microplate (Sarstedt, Montreal, QC, Canada). Then, 15  $\mu\text{l}$  of working culture bacteria (approximately  $10^6$  CFU/ml) were dispensed into all the wells. For each bacterium, three rows of a microplate were used. In the blank or negative control (2 rows of the microplate), 15  $\mu\text{l}$  of saline solution was used instead of the working culture bacteria. The positive control (without antimicrobial agent) in the column 12 of a microplate consisted of 125  $\mu\text{l}$  of MH broth and 15  $\mu\text{l}$  of working culture bacteria (Turgis et al., 2012). In this test, the final concentration of each EO was ranged from 10 ppm to 10000 ppm. It should be mentioned that the sterile Tween 80 solution (5%, w/v) that used for emulsification of EOs did not have any antibacterial activity. The microplate was incubated under aerobic condition and agitated at 80 rpm in a shaker for 24 h at  $37^{\circ}\text{C}$ . The absorbance was measured at 595 nm in a BioTek ELx800<sup>®</sup> absorbance microplate reader (BioTek Instruments Inc., Winooski, VT, USA). The MIC is the lowest concentration of antimicrobial agent demonstrating the complete growth inhibition of bacterial strain and showing equal absorbance as blank.

### 2.6. Determination of antimicrobial effects of combined EOs using checkerboard method

The checkerboard method was chosen to assess the efficacy of possible interaction between EOs which could be synergistic, additive, or exhibiting no interaction or antagonist against the pathogens. In this method, Fractional Inhibitory Concentration (FIC)

**Table 1**  
Selected essential oils<sup>a</sup> for evaluation their antimicrobial activity against five pathogens.

No.	Latin name	Common name	Origin	Distilled part	Composition (%) <sup>b</sup>
1	<i>Melissa officinalis</i> L.	Lemon balm/common balm	Quebec	Aerial part	β-Caryophyllene (23.31), geranial (11.58), germacrene-D (11.49), neral (6.76), geraniol (6.01)
2	<i>Juniperus communis</i> L.	Common juniper	Quebec	Twigs-Berries	α-Pinene (75.61), δ-3-carene (5.46), β-pinene (3.88), myrcene (3.18)
3	<i>Mentha x Piperita</i> L.	Chocolate mint	Quebec	Aerial part	Menthol (40.12), mentone (25.29), 1,8-cineole (5.90)
4	<i>Cuminum cyminum</i> L.	Cumin	Egypt	Seeds	Cuminic aldehyde (39.16), β-pinene (15.69), γ-terpinene (15.63), <i>p</i> -cymene (12.47), <i>p</i> -menthadiene (8.11)
5	<i>Satureja hortensis</i> L.	Summer savory	Hungary	Flower top	Carvacrol (26.8), <i>p</i> -cymene (23.6), thymol (14.4)
6	<i>Laurus nobilis</i> L.	Bay laurel	Hungary	Leaves	1,8-Cineole (48.1), α-terpineol (6.8), sabinene (6.4), α-pinene (6.3), β-pinene (5.8)
7	<i>Monarda didyma</i> L.	Red bergamot	Quebec	Flower top	Carvacrol (48.21), <i>p</i> -cymene (13.98), γ-terpinene (12.69)
8	<i>Curcuma longa</i> L.	Tumeric	Madagascar	Root	β-Turmerone (36.14), α-turmerone (28.60), myrcene + α-phellandrene (7.90)
9	<i>Cinnamomum cassia</i> (Nees & T. Nees) J.Presl.	Chinese cinnamon	Vietnam	Bark	<i>Trans</i> -cinnamaldehyde (87.58), cinnamyl acetate (7.53)
10	<i>Rosmarinus officinalis</i> L.	Rosemary	Morocco	Aerial part	1,8-Cineole (44.48), α-pinene (12.45), camphor (10.70)
11	<i>Ledum groenlandicum</i> (Oeder) Kron & Judd	Labrador tea	Quebec	Flower top	Limonene (9.94), sabinene (4.72), 1,4-terpinenol (4.36), β-pinene (3.95), mirtental (3.83), α-pinene (3.60)
12	<i>Thymus vulgaris</i> L.	Common thyme	Bolivia	Aerial part	Thymol (34.70), γ-terpinene (19.87), <i>p</i> -cymene (19.47)
13	<i>Thymus zygis</i> L.	Red thyme	Spain	Aerial part	Thymol (48.03), <i>p</i> -cymene (16.60), γ-terpinene (8.18)
14	<i>Origanum vulgare v. kaliteria</i>	Oregano/Greek oregano	Bolivia	Aerial part	Carvacrol (21.01), 1,4-terpinenol (18.68), 4-thujanol (12.14)
15	<i>Cinnamomum verum</i> J.Presl.	Cinnamon bark	Madagascar	Bark	<i>Trans</i> -cinnamaldehyde (40.71), cinnamyl acetate (14.25), β-phellandrene (9.02), β-caryophyllene (7.41)
16	<i>Melaleuca quinquenervia</i> (Cav.) S.T.Blake	Niaouli/punk tree	Madagascar	Leaves	1,8-Cineole (53.39), α-pinene + α-thujene (9.16), limonene (7.93), α-terpineol + terpenyl acetate (7.81)
17	<i>Salvia officinalis</i> L.	Common sage	Spain	Aerial part	α-Thujone (35.37), camphor (11.05), 1,8-cineole (8.31), β-thujone (6.93)
18	<i>Eugenia caryophyllus</i> (Spreng.) Bullock & S. G. Harrison	Clove	Madagascar	Floral buds	Eugenol (83–95), eugenyl acetate (9.96), β-caryophyllene (4.01)
19	<i>Tsuga Canadensis</i> (L.) Carrière	Hemlock spruce/Canadian hemlock	Quebec	Branches-Needles	Bornyl acetate (38.44), α-pinene (17.64), camphene (14.05)
20	<i>Monarda fistulosa</i> L.	Wild bergamot	France	Flower top	Geraniol (91.71)
21	<i>Cymbopogon martini</i> (Roxb.) Wats	Palmarosa/Gingergrass	India	Aerial part	Geraniol (80.14), geranyl acetate (9.10)
22	<i>Cinnamomum camphora</i> (L.) J.Presl.	Camphor tree	Madagascar	Leaves	1,8-Cineole (57.13), sabinene (14.46), α-terpineol (8.76)
23	<i>Abies balsamea</i> (L.) Mill.	Balsam fir	Quebec	Needles	β-Pinene (31.41), δ-3-carene (15.47), α-pinene (13.00), bornyl acetate (9.20), limonene (8.40)
24	<i>Thuja occidentalis</i> L.	Eastern white cedar	Quebec	Branches	α-Thujone (45.65), fenchone (12.11), β-thujone (8.37), sabinene (4.00)
25	<i>Picea mariana</i> (Mill.) Britton, Sterns & Poggenburg	Black spruce	Quebec	Branches-Needles	Bornyl acetate (31.01), camphene (18.16), α-pinene (14.00), δ-3-carene (6.42)
26	<i>Picea glauca</i> (Moench) Voss	White spruce	Quebec	Branches-Needles	Bornyl acetate (17.81), β-pinene (13.77), camphor (13.26), α-pinene (12.16), camphene (11.47), β-phellandrene (11.28)
27	<i>Solidago Canadensis</i> L.	Canada Golden-rod	Quebec	Flower top	β-Germacrene (28.59), α-pinene (15.90), limonene (12.65), myrcene (7.92)
28	<i>Daucus carota</i> L.	Wild carrot	Quebec	Seeds	Sabinene (31.72), geranyl acetate (15.23), α-pinene (14.58), myrcene (4.90)
29	<i>Pinus resinosa</i> Sol. ex Aiton	Red pine	Quebec	Twigs-Buds	α-Pinene (49.49), β-pinene (32.26), myrcene (5.90)
30	<i>Pinus strobus</i> L.	White pine	Quebec	Twigs-Buds	α-Pinene (29.82), β-pinene (26.60), δ-3-carene (9.62), myrcene (8.59), limonene (8.52)
31	<i>Pinus sylvestris</i> L.	Scots pine	Quebec	Twigs-Buds	δ-3-carene (30.52), α-pinene (26.91), limonene (7.37), β-pinene (5.78)
32	<i>Trachyspermum ammi</i> L.	Ajowan	India	Seeds	γ-terpinene (36.40), thymol (32.35), <i>p</i> -cymene (24.72), camphene (2.71)

<sup>a</sup> Essential oils were provided by Aliksir inc. (Grondines, QC, Canada).

<sup>b</sup> Composition determined by gas chromatography analysis using 2 capillary columns (30 m × 0.25 mm): Supelcowax 10 (polar) and DB-5 (apolar).

index of EOs in combinations were used (Gutierrez, Barry-Ryan, & Bourke, 2008; Gutierrez et al., 2009; Turgis et al., 2012). Each of the two selected EOs was two-fold diluted with Mueller–Hinton in two separate microplates of 96 wells. Then the EOs were transferred into the main microplate which contained a serial concentration of 50 µl of essential oil 'a' (EOa) along the X axis and the serial concentration of same volume of essential oil 'b' (EOb) along the Y axis. In the last 2 rows of the microplate there were only EOa at serial concentrations and in two columns (7 and 8 of the microplate) there were only EOb at serial concentrations. In total, there were a 6 × 6 matrix in which there was a combination of EOa and EOb at different concentrations in each well. Subsequently, 100 µl of Mueller–Hinton (MH) medium containing approximately 2 × 10<sup>6</sup> CFU/ml of one target bacterium were added to the wells. In the last column of the microplate there was MH medium with a target bacterium and was considered as a positive control. The combinations of EOs without bacteria were filled in other empty columns and were considered as a negative control or blank. Plates

were incubated at 37 °C for 24 h on the shaker at 80 rpm. The optical density (OD) of the wells containing combined EOs which had same OD of the wells in the blank was used to calculate the FIC. The FIC was calculated by the following formula ((Gutierrez et al., 2008; 2009; Turgis et al., 2012).):

$$FICa = (MICa\ combined / MICa\ alone)$$

$$FICb = (MICb\ combined / MICb\ alone)$$

$$FIC = FICa + FICb$$

Where

'MICa alone' is the MIC value of EOa tested alone; 'MICb alone' is the MIC value of EOb tested alone; 'MICa combined' is the MIC value of EOa tested in combination with EOb; 'MICb combined' is the MIC value of EOb tested in combination with EOa.

The results are considered as synergistic when FIC ≤ 0.5, additive

when  $0.5 < \text{FIC} \leq 1$ , no interaction for  $1 < \text{FIC} \leq 4$  and antagonist for the  $\text{FIC} > 4$  (Gutierrez et al., 2008; 2009; Turgis et al., 2012).

### 2.7. Sensorial analysis of selected EOs in cooked meat

The most active combination of EOs against target bacteria was chosen for sensorial evaluation in ready-to-cooked meat. To find the highest organoleptically accepted concentration, a panel of 10 individuals (research team) evaluated the smell and taste of the samples following the standard sensorial evaluation protocol (Poste, Mackie, Butler, & Larmond, 1991). Some panelists have extensive experience in conducting sensory assessments of different food products. The members who had no experience were trained in a training session with the use of hedonic scale and the quality attributes that are used for sensory analysis. Several concentrations (0.2, 0.1, 0.05, 0.025 and, 0.0125%) of the selected combination of EOs were applied on ready to cook meat (Kafta, Adonis, Laval, Canada) and also applied on lean ground beef (26% of fat) (IGA, Laval, Canada). Both meat models were cooked for 15 min at 205 °C and when the temperature inside reached 80 °C, they were cooked for another 30 s. The samples were served in separate cups with closed lids and they were identified by 3 random digits. The evaluation was carried out with 9-point hedonic scale: 9 = Like extremely, 8 = Like very much, 7 = Like moderately, 6 = Like slightly, 5 = Neither like nor dislike, 4 = Dislike slightly, 3 = Dislike moderately, 2 = Dislike very much, 1 = Dislike extremely.

### 2.8. Statistical analysis

All the experiments were performed at least two independent times. Each independent time was conducted with three replications. One-way analysis of variance (ANOVA) tests was conducted using SPSS program (IBM Corporation, Somers, NY, USA). Duncan's multiple range tests was used to compare the mean values. Differences between mean values at  $p \leq 0.05$  was considered significantly.

## 3. Results

### 3.1. Antimicrobial effects of EOs against foodborne and spoilage bacteria in agar diffusion assay

The results of antibacterial effects of 32 EOs against foodborne and spoilage bacteria using the agar diffusion method are presented in Table 2.

Chinese cinnamon and Ajowan EOs caused the highest inhibition diameter of approximately 35 mm against *L. monocytogenes*. Summer savory, Red bergamot, red thyme, and Ajowan EOs were very active against *S. aureus*, causing more than 65 mm of inhibition (Table 2). Red thyme and Red bergamot EOs inhibited the growth diameter of *E. coli* by 64.3 and 55.9 mm, respectively; while other EOs caused the inhibition zone less than 35 mm or no inhibition. Similarly, Red thyme was the most effective EO against *S. Typhimurium*, causing an inhibition diameter of 34.1 mm; follow was Red bergamot EO, causing 30.6 mm of inhibition. It is of interest to see that there were only six EOs consisting of Red thyme, Red bergamot, Ajowan, Summer savory, Chinese cinnamon, and Cinnamon bark showed better inhibitory activity against the five target bacteria as compared with other tested EOs and these 6 EOs could inhibited the growth diameter of *P. aeruginosa* by 10–19.5 mm (Table 2).

### 3.2. Antimicrobial effects of EOs against foodborne and spoilage bacteria in micro-atmosphere assay

The antibacterial effects (inhibition diameter) of 32 EOs against 5 foodborne and spoilage bacteria are presented in Table 3.

There were 7 EOs could inhibit totally the growth of *L. monocytogenes*. They were Lemon balm, Chocolate mint, Red bergamot, Red thyme, Wild bergamot, Palmarosa (gingergrass) and Ajowan EOs. Chinese cinnamon, Summer savory and Cinnamon bark EOs were also high active against *L. monocytogenes*, causing more than 50 mm of inhibition diameter (Table 3). The growth of *S. aureus* was totally inhibited by 9 EOs consisting of Lemon balm, Chocolate mint, Summer savory, Red bergamot, Common thyme, Red thyme, Oregano, Hemlock spruce, Wild bergamot, and Ajowan EOs (Table 3). Chinese cinnamon EO was the most effective EO against *E. coli*, causing 67.5 mm of inhibition diameter. Summer savory, Red bergamot, Red thyme, and Cinnamon bark EOs also showed rather high antibacterial effects against *E. coli*, causing the inhibition diameter in the range from 42.8 to 47 mm (Table 3). Red bergamot EO was the most active against *S. Typhimurium*, causing 40.3 mm of inhibition diameter while Chinese cinnamon also showed rather high active with 32.7 mm of inhibition (Table 3). Red bergamot and Chinese cinnamon were only two EOs showing their capacity in inhibiting the growth diameter of *P. aeruginosa* by approximately 27 mm and they were also the only 2 EOs that had antibacterial effects against 5 target bacteria (Table 3).

### 3.3. Antibacterial effects of EOs and combined EOs against five foodborne and spoilage bacteria in broth and checkerboard assays

The antibacterial effects of 32 EOs against 5 foodborne and spoilage bacteria in liquid phase (MIC values) are presented in Table 4. Chinese cinnamon showed the best activity among all the EOs. This EO inhibited the growth of *S. aureus* and *E. coli* at the concentration of 470 ppm (~0.05%) which was the lowest MIC we detect in this study while there were several EOs such as Common juniper, Bay laurel and, Curcuma which couldn't inhibit the bacterial growth even at 10000 ppm (or 1%, w/v).

The antibacterial effects of combined EOs by checkerboard method against five foodborne and spoilage bacteria are presented in Table 5. This test was conducted to assess the interaction of two EOs in liquid phase for which the most efficient EOs inhibiting each bacterium were chosen according to their MIC values for this test. Red bergamot, Chinese cinnamon, Red thyme, Cinnamon bark, Clove and Wild bergamot were chosen as the most effective EOs in liquid phase against *L. monocytogenes*, *S. aureus*, *E. coli* and *S. Typhimurium* due to their overall lower MIC values against these pathogenic bacteria as compared to the other EOs. Among all the tested combinations, the combinations of Red bergamot and Clove, Red bergamot and Wild bergamot, Chinese cinnamon and Red thyme showed better antimicrobial efficiency as they showed additive effect against 3 out of 4 tested bacteria. Results showed that the combination of Chinese cinnamon and Cinnamon bark showed additive effect against all tested bacteria. Based on broth microdilution results, Chinese cinnamon, Cinnamon bark and Wild bergamot EOs could also inhibit the *P. aeruginosa*. So the combination of Chinese cinnamon with Cinnamon bark and Chinese cinnamon with Wild bergamot were selected to assess their combined antimicrobial effect against *P. aeruginosa* using the checkerboard method and the results were  $0.64 \pm 0.09$  (additive) and  $1.29 \pm 0.19$  (not interactive), respectively. Based on overall results, Chinese cinnamon and cinnamon bark EOs were selected as a mixture of EOs for evaluation of their sensorial effects in a meat model.

### 3.4. Sensorial properties of selected combined EOs in meat products

The results of sensorial analysis are presented in Table 6. The results were the average of scores which the examiners gave to each sample. Based on 9-point hedonic scale the values more than 5 were considered organoleptically acceptable. It can be observed

**Table 2**  
Antibacterial effects of EOs against five foodborne and spoilage bacteria in agar diffusion assay\*\*.

No.	EOs (Common name)	<i>L. monocytogenes</i>	<i>S. aureus</i>	<i>E. coli</i>	<i>S. Typhimurium</i>	<i>P. aeruginosa</i>
1	Lemon balm	–*	–	–	–	–
2	Common juniper	10.7 ± 1.3 h	–	–	–	–
3	Chocolate mint	12.4 ± 1.1 fgh	22.7 ± 2.5 fg	13.8 ± 2.3 g	–	–
4	Cumin	–	–	10.1 ± 1.5 i	–	–
5	Summer savory	31.7 ± 3.9 b	65.0 ± 6.7 c	34.7 ± 6.2 c	28.9 ± 0.3 bc	10.7 ± 0.2 d
6	Bay laurel	–	–	10.5 ± 1.7 hi	–	–
7	Red bergamot	25.3 ± 0.8 cd	71.5 ± 6.0 b	55.9 ± 0.4 b	30.6 ± 2.9 b	10.0 ± 1.8 d
8	Tumeric	–	–	–	–	–
9	Chinese cinnamon	34.2 ± 2.8 a	33.0 ± 0.5 e	25.7 ± 4.3 e	21.0 ± 3.4 d	19.5 ± 4.9 a
10	Rosemary	11.2 ± 3.1 gh	–	10.4 ± 0.6 hi	–	–
11	Labrador tea	10.1 ± 2.7 h	11.9 ± 0.5 ij	10.7 ± 2.2 ghi	–	–
12	Common thyme	23.3 ± 2.2 d	35.6 ± 0.4 e	20.5 ± 0.4 f	18.1 ± 0.1 e	–
13	Red thyme	13.2 ± 3.1 efg	70.8 ± 3.1 b	64.3 ± 4.9 a	34.1 ± 6.4 a	16.8 ± 2.6 b
14	Oregano/Greek oregano	–	57.5 ± 2.9 d	11.5 ± 0.4 ghi	16.8 ± 1.8 e	–
15	Cinnamon bark	27.8 ± 0.6 c	25.5 ± 3.0 f	17.6 ± 1.9 f	22.2 ± 1.4 d	13.2 ± 0.4 c
16	Niaouli/punk tree	15.2 ± 0.5 e	14.6 ± 3.3 hi	12.7 ± 0.6 ghi	–	–
17	Common sage	–	12.6 ± 2.2 hij	13.6 ± 2.7 gh	–	–
18	Clove	14.8 ± 0.3 ef	19.9 ± 1.3 g	–	12.0 ± 0.8 f	–
19	Hemlock spruce	–	–	–	–	–
20	Wild bergamot	–	15.8 ± 2.0 h	–	–	–
21	Gingergrass/Palmarosa	10.9 ± 0.7 gh	15.7 ± 0.5 h	–	–	–
22	Camphor tree	12.0 ± 1.8 gh	–	11.7 ± 1.6 ghi	–	–
23	Balsam fir	–	–	–	–	–
24	Eastern white cedar	–	12.5 ± 1.0 hij	–	–	–
25	Black spruce	–	11.0 ± 1.9 j	–	–	–
26	White spruce	–	10.2 ± 0.5 j	–	–	–
27	Canada Golden-rod	–	–	–	–	–
28	Wild carrot	–	–	–	–	–
29	Red pine	–	–	–	–	–
30	White pine	–	–	–	–	–
31	Scots pine	–	–	–	–	–
32	Ajowan	35.7 ± 3.7 a	77.0 ± 1.7 a	29.0 ± 3.8 d	27.7 ± 3.2 c	20.4 ± 1.9 a

\*(-) no inhibition or inhibition less than 10 mm.

\*\*In each column, numbers with the same lower case letters are not significantly different ( $P > 0.05$ ).

that 0.05% (v/v) of combined EOs (Chinese cinnamon and Cinnamon bark) was acceptable in term of smell and taste in both ground beef and ready to cook (RTC) ground meat.

#### 4. Discussion

In this study the antimicrobial activity of 32 EOs and the combination effect of them were evaluated. According to the results EOs such as Red bergamot, Chinese cinnamon, Red thyme, Cinnamon bark, Clove and Wild bergamot generally demonstrated higher antimicrobial activity with all the assay methods. The combination of Chinese cinnamon and Cinnamon bark at 0.05% in meat model was organoleptic acceptable.

The effectiveness of EOs in vapour phase could be completely different from direct contact in solid and liquid phase (Goñi et al., 2009). In direct contact, hydrophilic components of EOs are more critical than volatile substances whereas in vapour phase the volatile components could be both hydrophilic and hydrophobic (Goñi et al., 2009). Depend on composition of EOs, some can inhibit bacteria in vapour phase more efficiency than liquid phase. This may occur due to forming micelles which decrease the attachment of EOs to microorganisms in liquid phase while in vapour phase there can be free attachment (Laird & Phillips, 2012). Also due to high amount of monoterpenes in vapour of EOs, they can attack the bacteria easily compare to liquid phase. They can be used as air decontaminants in storage rooms and they can be good candidates to be used in active packaging. Also due to their volatility they will not change organoleptic properties of foods (Laird & Phillips, 2012).

It is recognized that carvacrol, thymol and cinnamaldehyde were the main compounds of some EOs such as Summer savory, Red bergamot, Chinese cinnamon, Red thyme, and Ajowan. These

compounds already demonstrated their antibacterial effects in other studies (Gill & Holley, 2004; Gutiérrez-Larraínzar et al., 2012). The EOs contain these compounds also demonstrated medium or high inhibitory activity against four pathogenic bacteria which showed higher antimicrobial activity in vapour phases as well as in solid phase. In case of antibacterial activity in solid phase, it is possible to use EOs on the surface of foods to derive benefit of their antimicrobial activity. Also such EOs can be used as coating solution for food products, such as, vegetables or fruits. Edible films such as methylcellulose, chitosan, alginate, etc. can be used as carriers for EOs. (Severino et al., 2014).

In the liquid phase, Red bergamot, Chinese cinnamon, Cinnamon bark, Clove and, Wild bergamot generally showed high antimicrobial activity against tested bacteria due to their low MIC values. As compared with other results, Red bergamot, Chinese cinnamon and Cinnamon bark showed higher antimicrobial activity in solid phases as well; however, Clove and Wild bergamot worked better in liquid phase rather than solid phase.

By comparing all the antibacterial effects of the different performed assays (solid phase, vapour phase and liquid phase) against the tested bacteria, *S. aureus* was the most sensitive bacterium to the tested EOs, followed by *L. monocytogenes*, *E. coli*, *S. Typhimurium*; and finally *P. aeruginosa* was the least sensitive bacteria to tested EOs.

Due to the lipophilic characteristic, EOs can permeabilize bacterial membrane and cause the loss of ions and ATP, collapse of proton pumps and finally release of macromolecules and causing bacterial cell lysis (Bakkali et al., 2008; Turgis et al., 2012). By accumulating in the cytoplasm, they could also damage lipids and proteins (Bakkali et al., 2008). The majority of EOs eliminate bacteria by affecting their cell membrane in various ways and cause cell death. If two EOs

**Table 3**  
Antibacterial effects of EOs against five foodborne and spoilage bacteria in micro-atmosphere assay.

No.	EOs (common name)	<i>L. monocytogenes</i>	<i>S. aureus</i>	<i>E. coli</i>	<i>S. Typhimurium</i>	<i>P. aeruginosa</i>
1	Lemon balm	78.0 ± 0.0 a**	78.0 ± 0.0 a	–*	–	–
2	Common juniper	–	–	–	–	–
3	Chocolate mint	78.0 ± 0.0 a	78.0 ± 0.0 a	–	–	–
4	Cumin	–	26.6 ± 3.6 f	–	–	–
5	Summer savory	59.2 ± 2.6 c	78.0 ± 0.0 a	42.8 ± 6.5 b	22.9 ± 0.2 d	–
6	Bay laurel	–	–	–	–	–
7	Red bergamot	78.0 ± 0.0 a	78.0 ± 0.0 a	45.6 ± 2.5 b	40.3 ± 0.4 a	28.1 ± 1.6 a
8	Tumeric	–	–	–	–	–
9	Chinese cinnamon	66.4 ± 2.0 b	73.0 ± 4.2 b	67.5 ± 3.6 a	32.7 ± 3.4 b	27.8 ± 3.2 a
10	Rosemary	–	–	–	–	–
11	Labrador tea	27.9 ± 1.5 g	54.0 ± 2.3 c	–	–	–
12	Common thyme	37.2 ± 0.4 f	78.0 ± 0.0 a	34.6 ± 6.4 c	15.2 ± 2.3 f	–
13	Red thyme	78.0 ± 0.0 a	78.0 ± 0.0 a	47.0 ± 1.4 b	25.4 ± 1.1 c	–
14	Oregano/Greek oregano	46.0 ± 1.8 e	78.0 ± 0.0 a	36.1 ± 2.2 c	15.7 ± 2.1 f	–
15	Cinnamon bark	52.8 ± 0.4 d	35.4 ± 3.8 e	45.0 ± 2.4 b	12.3 ± 1.0 g	–
16	Niaouli/punk tree	26.8 ± 6.5 g	29.8 ± 4.6 f	–	–	–
17	Common sage	–	28.6 ± 2.7 f	–	–	–
18	Clove	26.8 ± 5.6 g	42.4 ± 0.6 d	28.1 ± 4.0 d	20.7 ± 0.0 e	–
19	Hemlock spruce	–	78.0 ± 0.0 a	–	–	–
20	Wild bergamot	78.0 ± 0.0 a	78.0 ± 0.0 a	20.1 ± 2.6 e	–	–
21	Palmarosa/Gingergrass	78.0 ± 0.0 a	–	–	–	–
22	Camphor tree	–	–	–	–	–
23	Balsam fir	–	–	–	–	–
24	Eastern white cedar	–	27.6 ± 3.5 f	–	–	–
25	Black spruce	–	–	–	–	–
26	White spruce	–	–	–	–	–
27	Canada Golden-rod	36.1 ± 5.7 f	30.1 ± 2.2 f	–	–	–
28	Wild carrot	–	–	–	–	–
29	Red pine	–	–	–	–	–
30	White pine	–	–	–	–	–
31	Scots pine	–	–	–	–	–
32	Ajowan	78.0 ± 0.0 a	78.0 ± 0.0 a	26.4 ± 3.7 d	26.6 ± 0.8 c	–

\* (–) Indicate there was no inhibition activity.

\*\* In each column, numbers with the same lower case letters are not significantly different ( $P > 0.05$ ).**Table 4**  
Minimum inhibitory concentration (MIC, ppm) of EOs against five foodborne and spoilage bacteria.

No.	EOs	<i>L. monocytogenes</i>	<i>S. aureus</i>	<i>E. coli</i>	<i>S. Typhimurium</i>	<i>P. aeruginosa</i>
1	Lemon balm/common balm	3125	5000	– <sup>a</sup>	–	–
2	Common juniper	–	–	–	–	–
3	Chocolate mint	1880	7500	8750	4375	–
4	Cumin	1250	5000	10000	–	–
5	Summer savory	5000	2500	5000	5000	–
6	Bay laurel	–	–	–	–	–
7	Red bergamot	1250	2500	1250	5000	–
8	Tumeric	–	–	–	–	–
9	Chinese cinnamon	625	470	470	940	1250
10	Rosemary	4380	–	–	10000	–
11	Labrador tea	–	–	–	–	–
12	Common thyme	–	–	–	–	–
13	Red thyme	10000	1250	1250	–	–
14	Oregano/Greek oregano	–	6250	5000	3330	–
15	Cinnamon bark	780	1250	780	1250	2500
16	Niaouli/punk tree	3880	10000	–	–	–
17	Common sage	–	–	–	–	–
18	Clove	3750	1875	1875	3750	–
19	Hemlock spruce/Canadian hemlock	–	–	–	–	–
20	Wild bergamot	3125	1875	1250	1875	10000
21	Palmarosa/Gingergrass	3750	7500	5000	5000	–
22	Camphor tree	10000	–	–	–	–
23	Balsam fir	–	–	–	–	–
24	Eastern white cedar	–	10000	–	–	–
25	Black spruce	–	–	–	–	–
26	White spruce	–	–	–	–	–
27	Canada Golden-rod	–	–	–	–	–
28	Wild carrot	10000	–	–	–	–
29	Red pine	10000	–	–	–	–
30	White pine	10000	–	–	–	–
31	Scots pine	–	–	–	–	–
32	Ajowan	5000	3750	5000	–	–

<sup>a</sup> (–): MIC > 10000 ppm.

**Table 5**  
Fractional Inhibitory Concentration (FIC) of combined EOs against target bacteria.

	<i>L. monocytogenes</i>	Act <sup>a</sup>	<i>S. aureus</i>	Act	<i>E. coli</i>	Act	<i>S. Typhimurium</i>	Act
Red bergamot + Chinese cinnamon	0.66 ± 0.13	AD	0.67 ± 0.12	AD	1.06 ± 0.00	I	1.12 ± 0.10	I
Red bergamot + Red thyme	1.12 ± 0.10	I	0.59 ± 0.05	AD	1.07 ± 0.04	I	0.76 ± 0.25	AD
Red bergamot + Cinnamon bark	1.12 ± 0.11	I	1.11 ± 0.11	I	1.11 ± 0.11	I	1.03 ± 0.02	I
Red bergamot + Clove	0.91 ± 0.15	AD	1.26 ± 0.22	I	0.51 ± 0.03	AD	0.63 ± 0.10	AD
Red bergamot + Wild bergamot	0.63 ± 0.10	AD	0.64 ± 0.09	AD	1.14 ± 0.09	I	0.59 ± 0.05	AD
Chinese cinnamon + Red thyme	1.05 ± 0.06	I	0.47 ± 0.09	AD	0.74 ± 0.00	AD	0.53 ± 0.02	AD
Chinese cinnamon + Cinnamon bark	0.64 ± 0.09	AD	0.60 ± 0.03	AD	0.74 ± 0.00	AD	0.82 ± 0.00	AD
Chinese cinnamon + Clove	1.08 ± 0.03	I	1.10 ± 0.03	I	0.70 ± 0.06	AD	1.20 ± 0.06	I
Chinese cinnamon + Wild bergamot	1.14 ± 0.09	I	0.70 ± 0.0	AD	1.12 ± 0.12	I	0.82 ± 0.14	AD
Red thyme + Cinnamon bark	1.07 ± 0.04	I	1.04 ± 0.01	I	0.64 ± 0.09	AD	1.14 ± 0.09	I
Red thyme + Clove	0.94 ± 0.17	AD	1.22 ± 0.23	I	1.12 ± 0.13	I	0.94 ± 0.17	AD
Cinnamon bark + Clove	1.05 ± 0.05	I	1.09 ± 0.05	I	1.08 ± 0.03	I	1.08 ± 0.03	I
Cinnamon bark + Wild bergamot	1.06 ± 0.05	I	0.64 ± 0.09	AD	1.04 ± 0.01	I	1.08 ± 0.03	I

<sup>a</sup> Act = Activity; FIC ≤ 0.5: synergic effect (S); 0.5 < FIC ≤ 1: additive effect (AD); 1 < FIC ≤ 4: no interactive effect (I); FIC > 4: antagonistic effect (A).

**Table 6**  
Sensorial evaluation of two kinds of meat with a series concentration of combined EOs (Chinese cinnamon and Cinnamon bark).

Properties	Smell		Taste	
	RTC <sup>a</sup> meat	Ground beef	RTC meat	Ground beef
Control	6.40 ± 1.95 <sup>b</sup>	6.75 ± 1.28 <sup>bc</sup>	6.88 ± 2.02 <sup>c</sup>	6.66 ± 1.75 <sup>c</sup>
0.0125%	6.00 ± 1.94 <sup>ab2</sup>	5.37 ± 0.91 <sup>bc</sup>	6.33 ± 1.11 <sup>bc</sup>	5.16 ± 2.48 <sup>bc</sup>
0.025%	6.40 ± 1.42 <sup>b</sup>	5.00 ± 1.69 <sup>abc</sup>	6.33 ± 2.34 <sup>bc</sup>	5.83 ± 1.60 <sup>c</sup>
0.05%	6.00 ± 2.05 <sup>b</sup>	5.25 ± 2.12 <sup>bc</sup>	5.88 ± 2.47 <sup>bc</sup>	5.00 ± 2.00 <sup>bc</sup>
0.1%	5.60 ± 2.50 <sup>b</sup>	3.75 ± 1.75 <sup>ab</sup>	4.55 ± 2.24 <sup>ab</sup>	3.50 ± 1.51 <sup>ab</sup>
0.2%	3.00 ± 1.41 <sup>a</sup>	3.37 ± 1.59 <sup>a</sup>	3.22 ± 2.33 <sup>a</sup>	2.33 ± 1.21 <sup>a</sup>

<sup>1</sup>RTC = ready-to-cook.

<sup>2</sup>In each column, numbers with the same lower case letters are not significantly different ( $p > 0.05$ ).

have similar compositions, it is more probable to show additive effect rather than synergistic effect (Gutierrez et al., 2008). Both Chinese cinnamon and Cinnamon bark possess trans-cinnamaldehyde and they exhibit additive effect against all tested bacteria.

## 5. Conclusion

In this study, Red thyme, Red bergamot, Summer savory, Chinese cinnamon and Cinnamon bark are 5 among 32 tested EOs that overall show high antibacterial activity against all tested bacteria. Among all EOs, Chinese cinnamon showed the best antibacterial activity and it inhibited *S. aureus* and *E. coli* at low MIC value of 470 ppm in microbroth dilution assay. In checkerboard assay, the combination of Red bergamot and Clove, Red bergamot and Wild bergamot, Chinese cinnamon and Red thyme showed better antibacterial activity as they showed additive effect against at least 3 tested bacteria. Combination of Chinese cinnamon and Cinnamon bark showed additive effect against all pathogenic and spoilage bacteria. The combined EOs formulation of Chinese cinnamon and Cinnamon bark was selected for sensorial evaluation and it was organoleptically acceptable at the concentration 0.05% in both cooked meats (ready-to-cook and ground beef). Further studies on application of this selected EOs alone or in combination with other natural antimicrobial agents such as nisin, nitrite, organic acids, etc. (as a hurdle technology) against pathogenic and spoilage bacteria will be conducted to evaluate their potential in food preservation.

## Acknowledgments

The Québec Ministry of Agriculture, Fisheries and Food are particularly acknowledged for their financial support through the PSIA program (Programme de Soutien à l'Innovation en

Agroalimentaire) (911064). Alikir Inc. is acknowledged for providing us the Essential Oils and financial support as well. Finally, the authors sincerely thank the trainees, Héma Fritz and Virginie Geslain, for their technical contributions.

## References

- Bakkali, F., Averbeck, S., Averbeck, D., & Idaomar, M. (2008). Biological effects of essential oils – a review. *Food and Chemical Toxicology*, 46(2), 446–475.
- Burt, S. (2004). Essential oils: their antibacterial properties and potential applications in foods—a review. *International Journal of Food Microbiology*, 94(3), 223–253.
- Cardiet, G., Fuzeau, B., Barreau, C., & Fleurat-Lessard, F. (2012). Contact and fumigant toxicity of some essential oil constituents against a grain insect pest *Sitophilus oryzae* and two fungi, *Aspergillus westerdijkiae* and *Fusarium graminearum*. *Journal of Pest Science*, 85(3), 351–358.
- Cueva, C., Moreno-Arribas, M. V., Bartolome, B., Salazar, O., Vicente, M. F., & Bills, G. F. (2011). Antibiosis of vineyard ecosystem fungi against food-borne microorganisms. *Research in Microbiology*, 162(10), 1043–1051.
- Dorman, H. J., & Deans, S. G. (2000). Antimicrobial agents from plants: antibacterial activity of plant volatile oils. *Journal of Applied Microbiology*, 88(2), 308–316.
- Dussault, D., Vu, K. D., & Lacroix, M. (2014). In vitro evaluation of antimicrobial activities of various commercial essential oils, oleoresin and pure compounds against food pathogens and application in ham. *Meat Science*, 96(1), 514–520.
- Gaulin, C., Nguon, S., Leblanc, M. A., Ramsay, D., & Roy, S. (2013). Multiple outbreaks of gastroenteritis that were associated with 16 funerals and a unique caterer and spanned 6 days, 2011, Quebec, Canada. *Journal of Food Protection*, 76(9), 1582–1589.
- Gill, A. O., & Holley, R. A. (2004). Mechanisms of bactericidal action of cinnamaldehyde against *Listeria monocytogenes* and of eugenol against *L. monocytogenes* and *Lactobacillus sakei*. *Applied and Environmental Microbiology*, 70(10), 5750–5755.
- Goñi, P., López, P., Sánchez, C., Gómez-Lus, R., Becerril, R., & Nerín, C. (2009). Antimicrobial activity in the vapour phase of a combination of cinnamon and clove essential oils. *Food Chemistry*, 116(4), 982–989.
- Gutiérrez-Larraínzar, M., Rúa, J., Caro, I., de Castro, C., de Arriaga, D., García-Armesto, M. R., et al. (2012). Evaluation of antimicrobial and antioxidant activities of natural phenolic compounds against foodborne pathogens and spoilage bacteria. *Food Control*, 26(2), 555–563.
- Gutierrez, J., Barry-Ryan, C., & Bourke, P. (2008). The antimicrobial efficacy of plant essential oil combinations and interactions with food ingredients. *International Journal of Food Microbiology*, 124(1), 91–97.
- Gutierrez, J., Barry-Ryan, C., & Bourke, P. (2009). Antimicrobial activity of plant essential oils using food model media: efficacy, synergistic potential and interactions with food components. *Food Microbiology*, 26(2), 142–150.
- Laird, K., & Phillips, C. (2012). Vapour phase: a potential future use for essential oils as antimicrobials? *Letters in Applied Microbiology*, 54(3), 169–174.
- Oussalah, M., Caillet, S., Saucier, L., & Lacroix, M. (2007). Inhibitory effects of selected plant essential oils on the growth of four pathogenic bacteria: *E. coli* O157:H7, *Salmonella Typhimurium*, *Staphylococcus aureus* and *Listeria monocytogenes*. *Food Control*, 18(5), 414–420.
- Poste, L. M., Mackie, D. A., Butler, G., & Larmond, E. (1991). *Laboratory methods for sensory evaluation of food*. Canada Department of Agriculture. ©Minister of Supply and Services Canada.
- Severino, R., Vu, K. D., Donsi, F., Salmieri, S., Ferrari, G., & Lacroix, M. (2014). Antimicrobial effects of different combined non-thermal treatments against *Listeria monocytogenes* in broccoli florets. *Journal of Food Engineering*, 124(0), 1–10.
- Solorzano-Santos, F., & Miranda-Navales, M. G. (2012). Essential oils from aromatic herbs as antimicrobial agents. *Current Opinion in Biotechnology*, 23(2), 136–141.
- Tajkarimi, M. M., Ibrahim, S. A., & Cliver, D. O. (2010). Antimicrobial herb and spice

- compounds in food. *Food Control*, 21(9), 1199–1218.
- Thomas, M. K., Murray, R., Flockhart, L., Pintar, K., Pollari, F., Fazil, A., et al. (2013). Estimates of the burden of foodborne illness in Canada for 30 specified pathogens and unspecified agents, Circa 2006. *Foodborne Pathogens and Disease*, 0(0), 1–10. <http://dx.doi.org/10.1089/fpd.2012.1389>.
- Turgis, M., Vu, K. D., Dupont, C., & Lacroix, M. (2012). Combined antimicrobial effect of essential oils and bacteriocins against foodborne pathogens and food spoilage bacteria. *Food Research International*, 48(2), 696–702.



# Effects of different drying–solidification processes on physical properties, volatile fraction, and antioxidant activity of non-centrifugal cane brown sugar



Yonathan Asikin <sup>a</sup>, Naoto Hirose <sup>b</sup>, Hajime Tamaki <sup>c</sup>, Satoru Ito <sup>d</sup>, Hirosuke Oku <sup>a</sup>, Koji Wada <sup>c,\*</sup>

<sup>a</sup> Tropical Biosphere Research Center, University of the Ryukyus, 1 Senbaru, Nishihara, Okinawa 903-0213, Japan

<sup>b</sup> Regional Agricultural System Section, Okinawa Prefectural Agricultural Research Center, 820 Makabe, Itoman, Okinawa 901-0336, Japan

<sup>c</sup> Department of Bioscience and Biotechnology, Faculty of Agriculture, University of the Ryukyus, 1 Senbaru, Nishihara, Okinawa 903-0213, Japan

<sup>d</sup> Product Development Division, Mitsui Sugar Co., Ltd., 36-2 Nihonbashi-Hakozakicho, Chuo-ku, Tokyo, 103-8423, Japan

## ARTICLE INFO

### Article history:

Received 26 June 2015

Received in revised form

14 October 2015

Accepted 16 October 2015

Available online 23 October 2015

### Keywords:

Non-centrifugal cane brown sugar

Drying–solidification process

Volatile aroma components

Odor detection frequency

Antioxidant activity

## ABSTRACT

Three drying–solidification processes, namely open pan (OP), horizontal thin-film (HTF), and vertical thin-film (VTF) methods, produced non-centrifugal cane brown sugars with different quality profiles, represented by physical properties, volatile fractions, and antioxidant activities. The OP brown sugar had lighter color due to the lower temperature used in its drying–solidification process, and a larger open-surface design to facilitate evaporation in its processing line made the brown sugar contains much smaller amount of volatile aroma components. On the other hand, higher evaporation temperature in the drying–solidification processes for HTF and VTF enhanced the accumulation of volatile fractions. The brown sugars predominantly comprised sweet-caramel aroma, and to a less extent, nutty-roasted, acidic, and grassy characteristics owing to the presence of acidic aroma components such as butanoic and 3-methyl butanoic acids, along with 2,3-dihydro-3,5-dihydroxy-6-methyl-4H-pyran-4-one, 5-methyl-2-pyrazinylmethanol, and 2,5-dimethyl-pyrazine. The production lines discriminated their aroma profiles due to the odor detectability of these aroma compounds wherein ketones and pyrazines were highly detected in OP brown sugar, acids and sulfurs in HTF brown sugar, and alcohols in VTF brown sugar. Additionally, the higher temperatures used in thin-film evaporation processes enhanced total phenolic content of brown sugar, and consequently its antioxidant activity.

© 2015 Elsevier Ltd. All rights reserved.

## 1. Introduction

Non-centrifugally processed cane brown sugar is widely produced in many countries and regions under different local names. The process lacks the removal of molasses components that are responsible for their brown appearance. They are called kokuto or kurozato in Japan, jaggery or gur in South Asia, panela or rapadura in South America. The solidified forms of this sugar contain various phytochemicals that are derived from the extracted raw material from the sugarcane and are responsible for their biological potential (Jaffé, 2012). Hence, brown sugars possess beneficial food functions such as antioxidation, antiangiogenesis, cytoprotection,

and skin damage protection (Nayaka, Sathisha, Manohar, Chandrashekar, & Dharmesh, 2009; Sumiyoshi, Hayashi, & Kimura, 2009). Furthermore, the non-centrifugation process in producing brown sugar imparts this product with distinct phenolic acids and volatile phenolics, as well as non-enzymatic Maillard reaction products (Asikin et al., 2014; Payet, Sing, & Smadja, 2005).

The processing method is considered one of the predominant factors affecting the product quality attributes in the manufacturing of sugar products (Jaeger, Janositz, & Knorr, 2010; Naknean & Meenune, 2015). The Okinawan brown sugar manufacturers generally practice three different types of production methods (Fig. 1). The main difference between these production lines is in the finishing evaporation process of drying–solidification, wherein the concentrated sugar syrup is transformed into solid brown sugar product. The evaporation processes consist of open pan (OP), horizontal thin-film (HTF), and vertical

\* Corresponding author.

E-mail address: [kojiwada@agr.u-ryukyuu.ac.jp](mailto:kojiwada@agr.u-ryukyuu.ac.jp) (K. Wada).

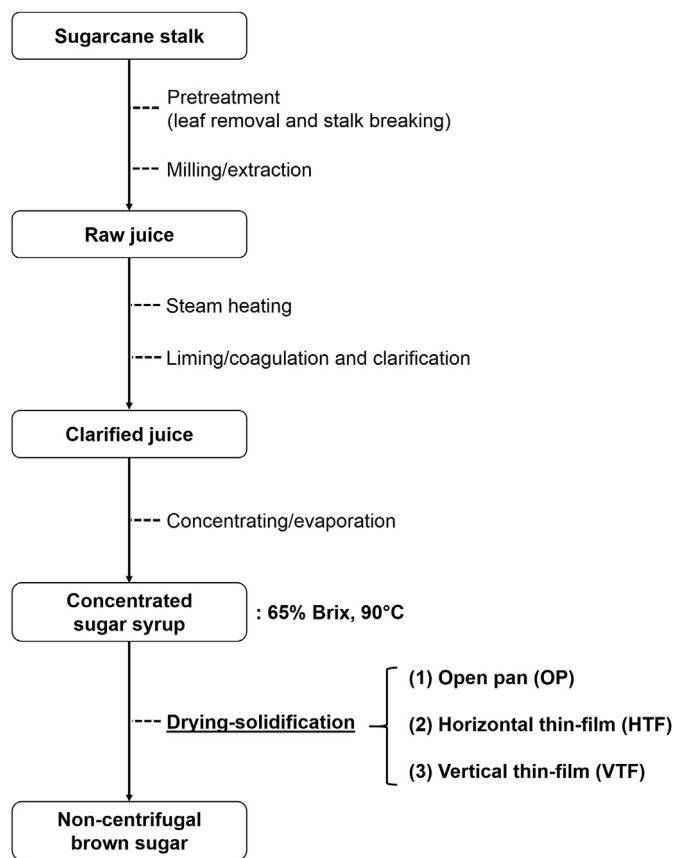


**Fig. 1.** General scheme of the production line of non-centrifugal brown sugar. The drying–solidification processes are (1) open pan, (2) horizontal thin-film, and (3) vertical thin-film.

thin-film (VTF) methods with different evaporation characteristics and procedures (Table 1). The OP drying–solidification technique evaporates moisture from concentrated sugar syrup in a series of pans located above a furnace, while the other two methods perform continuous agitation in the cylindrical heating tube (either horizontal or vertical) to form solidified thin-film surface from high-pressure drops of sugar syrup, and thus vaporize the moisture. These processes are considered to affect the quality attributes of brown sugar products such as physical, flavor, and functionality traits.

Volatile aroma compounds are among the micro-components that greatly influence the quality of food, including brown sugar (Asikin et al., 2014). Their presence is involved in the development of flavor, as they alter acceptability and palatability of the foods (Legako et al., 2015). On the other hand, antioxidation is an

**Table 1**

Process parameter of drying–solidification in non-centrifugal brown sugar production.

Description	OP	HTF	VTF
Process type	Batch <sup>a</sup>	Continuous	Continuous
Syrup-mass flow (ton/h)	2.56	0.81	0.49
Temperature (°C)	128–132	132–135	132–135
Heat transfer area (m <sup>2</sup> )	18.50	8.00	6.15
Pressure	Atmospheric	Atmospheric	Atmospheric

The drying–solidification processes are open pan (OP), horizontal thin-film (HTF), and vertical thin-film (VTF).

<sup>a</sup> One batch produces 160 kg brown sugar in a process sequence of 4–5 min.

essential quality parameter for food preservation, packaging, storage, and transport; antioxidant property of brown sugar has also been intensively studied in terms of its functional and health promoting effects (Asikin et al., 2014; Jaffé, 2012; Payet et al., 2005).

Therefore, the present study aimed at the evaluation of the profile of volatile aroma component and the antioxidant activity of non-centrifugal brown sugars from three different production lines, which differed in their drying–solidification processes. Additionally, physical properties of the brown sugars such as color, moisture content, and water activity ( $a_w$ ) were also evaluated.

## 2. Materials and methods

### 2.1. Standards and reagents

Chemicals used for the identification of volatile aroma components were purchased from Sigma–Aldrich (St Louis, MO, USA) and Tokyo Chemical Industry (Tokyo, Japan). Cyclohexanol, gallic acid, 2,2'-azobis(2-amidinopropane) dihydrochloride (AAPH), and 1,1-diphenyl-2-picrylhydrazyl (DPPH) were obtained from Wako Pure Chemical Industries (Osaka, Japan). Folin–Ciocalteu reagent was obtained from Kanto Chemical Co., Inc. (Tokyo, Japan). 6-Hydroxy-2,5,7,8-tetramethylchroman-2-carboxylic acid (Trolox) was purchased from Calbiochem (San Diego, CA, USA) and fluorescein sodium salt from Sigma–Aldrich. All other reagents were of analytical grade.

### 2.2. Samples

Brown sugars were collected from three factories with different types of drying–solidification methods, namely Taramatougyou (OP), Iriomotetougyou (HTF), and Iheyatougyou (VTF), in Okinawa, Japan, in February 2013. The newly produced brown sugar blocks (3 kg) were immediately crushed into powder, and then were vacuum packaged and stored at  $-30\text{ }^{\circ}\text{C}$  prior to analysis.

### 2.3. Color, moisture content, and water activity ( $a_w$ ) analyses

The color of brown sugar was evaluated in terms of the International Commission for Uniform Methods of Sugar Analysis (ICUMSA) by using the ICUMSA GS1/3–7 protocol (ICUMSA, 2003) and the CIE  $L^*a^*b^*$  color space using an NFF 333 spectrophotometer (Nippon Densoku Industries, Tokyo, Japan). Moisture content and  $a_w$  were determined using moisture content (MX-50, A&D, Tokyo, Japan) and  $a_w$  analyzers (LabSwift-AW, Novasina, Lachen, Switzerland), respectively. All analyses were carried out in triplicate.

### 2.4. Volatile aroma components analysis

The volatile aroma components of brown sugar were extracted using an organic solvent followed by solvent-assisted flavor evaporation (SAFE) technique (Engel, Bahr, & Schieberle, 1999). Briefly, 30 g of sample, 200 mL of diethyl ether, and 10  $\mu\text{L}$  of the internal standard cyclohexanol (1%) were placed into a round-bottomed flask, and the mixture was shaken for 24 h at  $5\text{ }^{\circ}\text{C}$ . The extract containing volatile aroma components was filtered using an Advantec No. 2 filter paper (Toyo Roshi Kaisha, Tokyo, Japan), and the non-volatile fraction was separated through the SAFE method under vacuum at  $40\text{ }^{\circ}\text{C}$ . Afterwards, the extract was dehydrated over 5 g anhydrous sodium sulfate for 12 h at  $5\text{ }^{\circ}\text{C}$ . The volume was then reduced to 50  $\mu\text{L}$  using Vigreux column followed by Kuderna–Danish concentrator under gentle nitrogen stream. The volatile aroma component extract was stored at  $-30\text{ }^{\circ}\text{C}$  until analysis.

The volatile aroma component profile was analyzed using

Agilent 7890A gas chromatography (GC) coupled with a flame ionization detector (FID) and an Agilent 5975C mass spectrophotometry (MS) system (Agilent J&W, Santa Clara, CA, USA) (Asikin et al., 2014). The aroma extract (1  $\mu\text{L}$ ) was injected into a DB-Wax column (60 m  $\times$  0.25 mm i.d., film thickness 0.25  $\mu\text{m}$ , Agilent J&W) at a split ratio of 1:10, and the linear velocity of the helium carrier gas was 32 cm/s. The temperatures of GC injector and FID were both set at 250 °C. The temperature of the oven was initially set at 40 °C for 2 min, then raised to 200 °C at a rate of 2 °C/min, and held constant at 200 °C for 38 min. For MS detection, the ion source and interface were both programmed at 230 °C, electron-impact ionization at 70 eV, acquisition range ( $m/z$ ) at 29–450 amu, and scan rate at 1.77 scans/s.

Peak identification was performed through comparison of the MS fragmentation patterns with the National Institute of Standards and Technology (NIST) MS Spectral Library, Version 2008, and the spectra of co-injected aroma standards. Identification was further confirmed by comparing their linear retention indices (RIs) towards a homologous series of *n*-alkanes (C7–C28). The resulting peak was calibrated by FID response of the internal standard, and the content of aroma compounds was expressed as milligrams per 100 g of brown sugar. All analyses were carried out in triplicate.

### 2.5. Odor description and detection analyses

The odor of volatile aroma components of brown sugar was described via GC-olfactometry (GC-O) with an Agilent 7890A GC coupled with FID (Agilent J&W) and olfactory detection port (ODP) (Gerstel, Mülheim, Germany). The detection frequency of each peak was determined by four trained assessors (1 male and 3 females, 21–32 years old) in triplicate (Arena, Guarrera, Campisi, & Asmundo, 2006). An assessor was asked to detect and describe the odor in 37.5 min per day. The GC column and conditions were the same as described above except that the injection split ratio was 1:5. The split ratio for the FID and ODP was 1:1, and the ODP was supplied with humidified air. The relative percentages of odor detection were determined based on aroma component groups and assessed odors.

### 2.6. Total phenolic content assay

Total phenolic content of brown sugar was determined according to previously described method (Asikin et al., 2013). Briefly, various concentrations of sample (20  $\mu\text{L}$ ; 5–30 mg/mL) were introduced in a Nunc 96-well microplate (Roskilde, Denmark), followed by distilled water (60  $\mu\text{L}$ ) and 2-fold diluted Folin–Ciocalteu reagent (15  $\mu\text{L}$ ). The mixture was agitated, and the reaction was allowed to occur for 5 min at room temperature, and then 2% sodium carbonate solution (75  $\mu\text{L}$ ) were added to each well. Subsequently, the microplate was placed in a PowerWave XS2 microplate reader (BioTek, Winooski, VT, USA), agitated, and allowed to stand for 15 min before absorbance measurement at 750 nm. The phenolic content of the sample was calibrated using gallic acid (5–100  $\mu\text{g/mL}$ ) and expressed as milligrams of gallic acid equivalents (GAE) per 100 g of brown sugar. All analyses were carried out in triplicate.

### 2.7. Oxygen radical absorbance capacity (ORAC) assay

The ORAC assay was determined according to a previously modified method (Asikin et al., 2013). Briefly, various concentrations of sample (25  $\mu\text{L}$ ; 200–500  $\mu\text{g/mL}$ ) in 75 mM pH 7.0 phosphate buffer and 90-nM fluorescein solutions (150  $\mu\text{L}$ ) were transferred to a black Nunc 96-well microplate. The microplate was gently agitated and incubated for 10 min at 37 °C in a Synergy HT

microplate reader (BioTek). Afterwards, 160-mM AAPH solution containing peroxy radicals (25  $\mu\text{L}$ ) were added to each well. The radical-scavenging reaction was maintained at 37 °C, and the fluorescence intensity was recorded every minute for 30 min at 485 nm (excitation) and 530 nm (emission) wavelengths. The area under the curve (AUC) of relative fluorescence value was calculated using the equation:  $\text{AUC} = 0.5 + f_1/f_0 + \dots + f_i/f_0 + \dots + f_{29}/f_0 + 0.5(f_{30}/f_0)$ , where  $f_0$  is the initial relative fluorescence intensity at 0 min and  $f_i$  is the relative fluorescence intensity at time  $i$ . The ORAC value of the sample was calibrated using Trolox (5–40  $\mu\text{M}$ ) and expressed as micromoles of Trolox equivalents (TE) per 100 g of brown sugar. All analyses were carried out in triplicate.

### 2.8. DPPH radical-scavenging activity assay

The DPPH radical-scavenging activity of brown sugar was determined according to a previously described method (Rockenbach et al., 2011) with slight modifications. Briefly, various concentrations of sample (50  $\mu\text{L}$ ; 5–10 mg/mL), 0.1 mM DPPH solution (50  $\mu\text{L}$ ), and 200 mM pH 6.0 MES buffer (100  $\mu\text{L}$ ) were transferred to a Nunc 96-well microplate, and mixed. After 30-min incubation, the reduction of DPPH radicals by the sample was monitored through absorbance measurement at 517 nm in a PowerWave XS2 microplate reader (BioTek). The DPPH radical-scavenging activity of the sample was calibrated using Trolox (40–200  $\mu\text{M}$ ) and expressed as micromoles of Trolox equivalents (TE) per 100 g of brown sugar. All analyses were carried out in triplicate.

### 2.9. Statistical analysis

The mean values of physical properties, volatile aroma components, and antioxidant capabilities of brown sugars were subjected to analysis of variance with Fisher's least significant difference post-hoc test ( $p < 0.05$ ) using Microsoft Office Excel 2007 (Microsoft Corp., Redmond, WA, USA).

## 3. Results and discussion

### 3.1. Characteristics of drying–solidification processes and physical properties of non-centrifugal brown sugar

Drying–solidification processes in non-centrifugal brown sugar manufacturing are important evaporation procedures where most of the moisture in concentrated sugar syrup is removed by various heating techniques, resulting in solidified brown sugar products (Fig. 1). The OP drying–solidification method evaporated moisture of 65% Brix-concentrated sugar syrup at an average mass flow of 2.56 ton/h over constant temperature of 128–132 °C in a batch processing system (Table 1). On the other hand, in the agitated thin-film evaporation method, which is comprised of HTF and VTF systems, solidified brown sugar was produced continuously in smaller volumes (0.81 and 0.49 ton/h, respectively) at higher temperature ranges. The OP method requires much more surface area for performing heat transfer and vaporizing moisture from the sugars than that of HTF and VTF evaporation processes (18.50 versus 8.00 and 6.15  $\text{m}^2$ , respectively). On the other hand, agitated thin-film evaporators benefit from the action of dispersing rotor in the cylindrical heating tube (either horizontal or vertical) on forming a thin-film surface from high-pressure drops of sugar syrup inlet over centrifugal forces of blades mounted on shaft placed coaxially with the tube to solidify the brown sugar. These drying–solidification processes affected the quality attributes of non-centrifugal brown sugar, including their physical properties (color, moisture content, and  $a_w$ ), volatile aroma components, and antioxidant capabilities.

The brown sugars from different production lines varied significantly ( $p < 0.05$ ) according to their physical traits, including color, moisture content, and water activity (Table 2). Regarding ICUMSA color, the difference follows the rank order: HTF > VTF > OP (IU 29529, 19343, and 12410, respectively). Moreover, there was no trend line between color unit (IU) value and  $L^*$  color space of these brown sugars, but to their reddish color spaces of (+)  $a^*$  value, ensuring the differentiating impact of production line to their brown color properties. The two thin-film evaporation systems, which produce darker brown sugars at higher temperatures, are certainly beneficial in terms of colored compounds such as phenolics and melanoidins that remain in the brown sugar if compared to the remaining colored compounds in OP brown sugar. This result confirms that the formation of dark-colored pigment compounds is enhanced by the increase of temperature used during the heating process (Fogliano, Monti, Musella, Randazzo, & Ritieni, 1999). Then, compared to HTF method, vertical-inlet feed line produces a lighter product due to gravitational fall advantage in conveying the concentrated sugar syrup at a lower mass transfer capacity while transforming it into solidified brown sugar (0.81 versus 0.49 ton/h, Table 1). On the other hand, a lower-temperature constant heating process and a greater amount of mass transfer in OP batch-line made the brown sugar much lighter in color. However, the color of non-centrifugal brown sugar from these three different drying–solidification processes had lighter appearance comparing to previously reported commercial dark brown sugar produced in India (IU 37080) but much darker than that of Brazilian brown sugars (IU 157 to 575) (Generoso et al., 2009; Singh, Bharose, Verma, & Singh, 2013).

Moreover, the evaporation method affected the moisture content in solidified brown sugar: OP brown sugar had higher moisture content and  $a_w$  values than those of thin-film evaporation methods. In this matter, it is clearly observed that the heat exposure in OP batch method is less effective in evaporating moisture over large amount of concentrated sugar syrup inlet than in thin-film evaporators. Hence, the analyzed brown sugars had similar levels of moisture contents as previously reported for commercial brown sugars (2.13–6.02%) (Generoso et al., 2009). However, the three different evaporation processes ensured appropriate moisture removal to produce solidified brown sugars with  $a_w$  values within a particular range for food quality and safety necessary to be protected from common bacterial deterioration and oxidative spoilage (Maltini, Torreggiani, Venir, & Bertolo, 2003).

### 3.2. Volatile aroma components and odor detection profiles of non-centrifugal brown sugar from different drying–solidification processes

A total of 38 volatile aroma components were determined in the

**Table 2**

Color (ICUMSA color unit and CIE  $L^*a^*b^*$  color spaces), moisture content, and water activity ( $a_w$ ) of non-centrifugal brown sugars from different drying–solidification processes.

Properties <sup>a</sup>	OP	HTF	VTF
ICUMSA color unit (IU)	12410 ± 255 c <sup>b</sup>	29529 ± 665 a	19343 ± 244 b
$L^*$ value	35.61 ± 3.18 a	31.08 ± 0.12 b	26.26 ± 0.21 c
$a^*$ value	6.33 ± 0.10 c	7.47 ± 0.02 a	6.73 ± 0.05 b
$b^*$ value	20.01 ± 0.18 a	19.41 ± 0.15 b	17.15 ± 0.29 c
Moisture content (%)	4.16 ± 0.22 a	3.90 ± 0.19 a	3.53 ± 0.10 b
Water activity ( $a_w$ )	0.644 ± 0.002 a	0.612 ± 0.003 b	0.550 ± 0.001 c

The drying–solidification processes are open pan (OP), horizontal thin-film (HTF), and vertical thin-film (VTF).

<sup>a</sup> Each value is expressed as the mean ± standard deviation ( $n = 3$ ).

<sup>b</sup> Means in the same row followed by the same letter are not significantly different ( $p < 0.05$ ).

evaluated non-centrifugal brown sugars (Table 3). HTF and VTF drying–solidification production lines present greater amount of aroma components in its solidified product (2.47 and 2.58 mg/100 g, respectively) than in OP brown sugar (1.88 mg/100 g). Higher heating process in the continuous thin film evaporators could be responsible for enhancing the release of volatile fractions from sugar syrup inlet. For instance, the formation of Maillard reaction products such as pyrazines, furans, and pyranones from their precursors is favored at higher temperatures as the ones used in the HTF and VTF drying–solidification processes (Fogliano et al., 1999; Osada & Shibamoto, 2006) since the cylindrical evaporation tubes in these evaporators could entrap more aroma compounds from vaporization into solidified brown sugar products. On the other hand, the release of aroma component is enhanced during moisture evaporation of the batch OP method due to the larger upper surface of heated sugar syrup being directly exposed to the atmosphere.

The predominant volatile aroma fractions extracted from these brown sugars were alcohols (0.61–1.53 mg/100 g, 6 compounds), acids (0.59–0.77 mg/100 g, 9 compounds), and ketones (0.34–0.73 mg/100 g, 12 compounds). Additionally, the brown sugars contained 6 pyrazine, 2 sulfuric, 2 phenol, and 1 aldehyde compounds. The mixture of these compounds contributes to the entire aroma profile of each brown sugar providing different kinds of odors with discriminable detection frequencies. Moreover, VTF evaporation method yielded significantly higher ( $p < 0.05$ ) amounts of alcohol stereoisomers [R-(R\*,R\*)]-2,3-butanediol and [S-(R\*,R\*)]-2,3-butanediol (0.32 and 0.95 mg/100 g, respectively), causing its solidified product much different than other two brown sugars for comprising approximately double amount of alcohol components (1.53 versus 0.61–0.69 mg/100 g, respectively). In the acid group, OP brown sugar contained significantly higher 2-propenoic, dodecanoic, and 2-methyl-propenoic acids (0.23, 0.05, and 0.02 mg/100 g, respectively) than that of brown sugars produced by thin-film evaporation methods. Besides being originated from sugarcane stalks as raw material, the acid compounds in brown sugar could also be derived from the fermentation process which occurred in raw sugarcane juice prior to steam heating and liming treatments (Qureshi, Bhongale, & Thorave, 2011), yielding high detectable acidic fermentation products such as butanoic, and 3-methyl butanoic acids (detection frequency 12 of all 12 repetitions), and providing strong dairy, foul smell, and acidic odors in all evaluated brown sugars.

Moreover, particular ketone compounds with moderate to high detectabilities such as 2,3-dihydro-3,5-dihydroxy-6-methyl-4H-pyran-4-one, 2-pyrrolidinone, and 2,5-pyrrolidinedione could generate a specific pleasant sweet, cotton candy/maple-like, and caramel characteristics. On the other hand, alcohol and phenol groups like 5-methyl-2-pyrazinylmethanol, 5-methyl-2-furanmethanol, and 2-methoxy-phenol might supplement acidic, medicinal, minty, and herbaceous odors to the pleasant predominantly sweet characteristic odor of brown sugars. The aroma profile of brown sugar might be complemented by the presence of pyrazine compounds such as 2,5-dimethyl-pyrazine, 2,6-dimethyl-pyrazine, and 2,3,5-trimethyl-pyrazine derived from Maillard reaction for providing nutty, roasted, and coffee-like odors (Asikin et al., 2014; Jousse, Jongen, Agterof, Russell, & Braat, 2002). The evaporation process also distinguished its solidified brown sugar product for generating heat-related sulfuric compounds such as dimethyl sulfoxide and dimethyl sulfone (Segurel, Razungles, Riou, Trigueiro, & Baumes, 2005; Xu, Zhang, Fang, Sun, & Wang, 2014). Various volatile aroma compounds such as alcohol stereoisomers of 2,3-butanediol, along with benzoic and dodecanoic acids, 2,3-dihydro-3,5-dihydroxy-6-methyl-4H-pyran-4-one, and vanillin, are also reported to be present in about eight commercial brown sugars at different concentrations, indicating these aroma

**Table 3**  
Volatile aroma components of non-centrifugal brown sugars from different drying–solidification processes.

No.	RI <sup>a</sup>	Compound	Content (mg/100 g) <sup>b</sup>			Detection frequency <sup>c</sup>			Odor description <sup>c</sup>	Identification <sup>d</sup>
			OP	HTF	VTF	OP	HTF	VTF		
1	931	Ethanol	0.209 ± 0.021 a <sup>e</sup>	0.169 ± 0.028 a	0.233 ± 0.066 a	3	–	–	Alcoholic, solvent	RI, MS, PC
2	1540	[R-(R*,R*)]-2,3-butanediol	0.094 ± 0.003 c	0.162 ± 0.035 b	0.322 ± 0.013 a	3	3	4	Sweet, grassy, fruity	RI, MS, PC
3	1579	[S-(R*,R*)]-2,3-butanediol	0.339 ± 0.004 b	0.215 ± 0.043 c	0.953 ± 0.043 a	5	4	7	Sweet, flowery, rancid	RI, MS, PC
4	1656	2-Furanmethanol	0.020 ± 0.001 ab	0.035 ± 0.012 a	0.013 ± 0.001 b	3	4	6	Roasted, nutty, fruity	RI, MS, PC
5	1720	5-Methyl-2-furanmethanol	0.005 ± 0.000 b	0.012 ± 0.003 a	0.008 ± 0.000 ab	5	9	8	Sweet, fruity, minty	RI, MS
6	2069	5-Methyl-2-pyrazinylmethanol	0.001 ± 0.000 b	0.020 ± 0.004 a	0.005 ± 0.001 b	11	11	10	Acidic, sweat-like, sweet	RI, MS
		Total alcohols	0.668	0.614	1.534					
7	1256	4,5-Dihydro-2-methyl-3(2H)-furanone	0.004 ± 0.001 a	0.009 ± 0.004 a	0.003 ± 0.000 a	–	4	4	Toasted, buttery	RI, MS, PC
8	1278	3-Hydroxy-2-butanone	0.006 ± 0.001 a	0.008 ± 0.003 a	0.007 ± 0.000 a	7	3	5	Sweet, nutty, dairy-like	RI, MS, PC
9	1292	1-Hydroxy-2-propanone	0.052 ± 0.005 b	0.119 ± 0.039 a	0.087 ± 0.010 ab	6	7	5	Sweet, grassy, coffee-like	RI, MS, PC
10	1614	Butyrolactone	0.011 ± 0.001 b	0.025 ± 0.007 a	0.008 ± 0.000 b	4	–	3	Cooked, sweet	RI, MS, PC
11	1746	2(5H)-Furanone	0.010 ± 0.001 a	0.015 ± 0.003 a	0.011 ± 0.000 a	8	7	4	Pungent, cheesy	RI, MS
12	1826	3-Methyl-1,2-cyclopentanedione	0.003 ± 0.001 b	0.013 ± 0.003 a	0.002 ± 0.001 b	8	8	5	Sweet, maple-like, medicinal	RI, MS, PC
13	1966	2-Acetyl pyrrole	0.010 ± 0.000 b	0.019 ± 0.006 a	0.003 ± 0.000 b	3	4	–	Herbaceous, metallic, sweet	RI, MS, PC
14	2027	Pantolactone	0.024 ± 0.001 a	0.023 ± 0.005 a	0.022 ± 0.000 a	5	7	4	Sweet, caramel	RI, MS, PC
15	2035	2,5-Dimethyl-4-hydroxy-3(2H)-furanone	0.002 ± 0.000 b	0.004 ± 0.000 a	0.002 ± 0.000 b	7	6	7	Sweet, cotton candy-like, caramel	RI, MS, PC
16	2044	2-Pyrrolidinone	0.008 ± 0.001 b	0.013 ± 0.001 a	0.005 ± 0.000 c	11	7	9	Sweet, cotton candy-like, caramel	RI, MS, PC
17	2268	2,3-Dihydro-3,5-dihydroxy-6-methyl-4H-pyran-4-one	0.164 ± 0.017 b	0.359 ± 0.038 a	0.207 ± 0.011 b	11	12	10	Sweet, maple-like, caramel	RI, MS
18	2467	2,5-Pyrrolidinedione	0.040 ± 0.003 b	0.126 ± 0.021 a	0.026 ± 0.001 b	5	9	4	Sweet, cotton candy-like, caramel	RI, MS, PC
		Total ketones	0.336	0.731	0.383					
19	1262	2-Methyl-pyrazine	0.008 ± 0.001 ab	0.022 ± 0.011 a	0.004 ± 0.000 b	3	–	6	Sweet, grassy, acidic	RI, MS, PC
20	1321	2,5-Dimethyl-pyrazine	0.052 ± 0.001 ab	0.073 ± 0.035 a	0.012 ± 0.000 b	7	10	8	Nutty, earthy, roasted	RI, MS, PC
21	1327	2,6-Dimethyl-pyrazine	0.010 ± 0.000 a	0.020 ± 0.010 a	0.010 ± 0.000 a	8	7	3	Nutty, sweet	RI, MS, PC
22	1345	2,3-Dimethyl-pyrazine	0.002 ± 0.000 b	0.007 ± 0.003 a	0.001 ± 0.000 b	3	4	–	Nutty, roasted, coffee-like	RI, MS, PC
23	1407	2,3,5-Trimethyl-pyrazine	0.007 ± 0.000 a	0.010 ± 0.002 a	0.003 ± 0.000 b	12	4	7	Nutty, earthy, roasted	RI, MS, PC
24	1458	2-Ethyl-3,6-dimethyl-pyrazine	0.001 ± 0.000 a	0.004 ± 0.001 a	tr.	9	9	10	Nutty, earthy, coffee-like	RI, MS, PC
		Total pyrazines	0.080	0.136	0.029					
25	1528	Propanoic acid	0.047 ± 0.004 b	0.097 ± 0.026 a	0.059 ± 0.003 ab	5	5	4	Rancid, acidic	RI, MS, PC
26	1560	2-Methyl-propanoic acid	0.016 ± 0.003 a	0.009 ± 0.004 b	0.008 ± 0.001 b	–	–	–	–	RI, MS
27	1618	Butanoic acid	0.017 ± 0.001 c	0.137 ± 0.040 b	0.223 ± 0.014 a	12	12	12	Cheesy, yogurt-like, acidic	RI, MS, PC
28	1622	2-Propenoic acid	0.234 ± 0.019 a	0.091 ± 0.017 b	0.042 ± 0.009 c	4	4	–	Baked, vinegar-like	RI, MS, PC
29	1664	3-Methyl-butanoic acid	0.023 ± 0.004 a	0.014 ± 0.005 ab	0.009 ± 0.001 b	12	12	12	Cheesy, foul smell, acidic	RI, MS, PC
30	1735	Pentanoic acid	0.002 ± 0.001 a	0.001 ± 0.000 b	tr.	7	6	–	Rancid, buttery	RI, MS, PC
31	2176	2-Hydroxy-propanoic acid	0.097 ± 0.035 b	0.208 ± 0.047 a	0.147 ± 0.030 ab	–	3	–	Grassy, sweat-like	RI, MS, PC
32	2417	Benzoic acid	0.132 ± 0.003 b	0.186 ± 0.036 a	0.082 ± 0.003 b	5	10	9	Sweet, caramel	RI, MS, PC
33	2482	Dodecanoic acid	0.045 ± 0.007 a	0.025 ± 0.005 b	0.016 ± 0.002 b	3	3	–	Dairy-like, caramel	RI, MS, PC
		Total acids	0.614	0.768	0.587					
34	1581	Dimethyl sulfoxide	0.132 ± 0.021 a	0.159 ± 0.018 a	tr.	–	3	–	Rancid, pungent, metallic	RI, MS, PC
35	1895	Dimethyl sulfone	0.017 ± 0.003 a	0.018 ± 0.004 a	0.009 ± 0.001 b	4	5	4	Sweet, waxy, sulfuric	RI, MS, PC
		Total sulfurs	0.148	0.177	0.009					
36	1852	2-Methoxy-phenol	0.012 ± 0.003 a	0.017 ± 0.006 a	0.011 ± 0.001 a	11	11	12	Sweet, medicinal, herbaceous	RI, MS, PC
37	2263	2,6-Dimethoxy-phenol	0.005 ± 0.000 ab	0.007 ± 0.002 a	0.003 ± 0.000 b	4	–	–	Sweet, maple-like, caramel	RI, MS, PC
38	2549	Vanillin	0.016 ± 0.001 a	0.015 ± 0.003 a	0.019 ± 0.001 a	6	7	6	Sweet, cotton candy-like	RI, MS, PC
		Total phenols and aldehyde	0.033	0.039	0.033					
		Total identified/detected	1.878	2.465	2.575	220	220	188		

The drying–solidification processes are open pan (OP), horizontal thin-film (HTF), and vertical thin-film (VTF).

<sup>a</sup> Retention indices relative to *n*-alkanes on a polar DB-Wax column.

<sup>b</sup> Each value is expressed as the mean ± standard deviation (*n* = 3); tr: trace amount (<0.01%).

<sup>c</sup> Detection frequency and odor description based on the aroma sniffing determination of 4 panelists in 3 replications using GC-O.

<sup>d</sup> RI: identification based on retention index; MS: identification based on the NIST MS library; PC: identification based on pure standards analyzed by mass spectrometry.

<sup>e</sup> Means in the same row followed by the same letter are not significantly different (*p* < 0.05).

components as characteristic volatile fractions in the non-centrifugal cane brown sugar despite cane plant origin and manufacturing process and storage variations (Asikin et al., 2014; Payet et al., 2005).

It is noteworthy that the drying–solidification process used for the production of non-centrifugal brown sugars also affected the detection ratio of their volatile aroma components, as well as the resulting aroma profile (Fig. 2). In detail, among the six aroma component groups, ketones showed the highest odor detectability (31.91–34.09%), followed by acids, alcohols, and pyrazines (Fig. 2a), and each brown sugar remarkably varied on the detectability of such aroma components. In detail, ketones and pyrazines were detected higher in OP brown sugar (34.09 and 19.09%, respectively); acids and sulfurs in HTF brown sugar (25.00 and 3.64%, respectively); and alcohols in VTF brown sugar (18.62%). Furthermore, the detection variability of volatile aroma components also altered their aroma profiles, wherein HTF brown sugar possessed higher assessed sweet-caramel odor (34.64%) but had lower detectability of other aromas than the other two brown sugars (Fig. 2b). OP brown sugar had higher nutty-roasted, acidic, dairy, and earthy characteristics (13.27, 13.01, 11.73, and 7.14%, respectively), as well as predominant sweet and caramel odor, while VTF brown sugar presented a higher grassy aroma (12.03%). However, the variation of these aroma profiles was not only related to the relative odor detection frequency of these six aroma component groups, but also to the content and detectability of various aroma compounds from different functional groups. For instance, detectability of Maillard reaction products such as pyrazines clearly provided greater assessed nutty-roasted odor, and the occurrence of various acids enhanced acidic and dairy-like aromas in OP brown sugar. Additionally, superior sweet-caramel characteristic in HTF brown sugar was provided by 2,3-dihydro-3,5-dihydroxy-6-methyl-4H-pyran-4-one and 2,5-pyrrolidinedione compounds, which were found in significantly higher amounts ( $p < 0.05$ ) (Table 3).

Data on aroma component profile discrimination among non-centrifugal brown sugars with regards to their drying–solidification processes should provide useful insights when these brown sugars are used as ingredients in various food and beverage products. For instance, regarding total content of volatile aroma compounds, the preference options of brown sugar formulation uses may follow the intensity order: VTF > HTF > OP. Then, besides the provision of basic sweet odor, the differentiation needs of specific nutty, roasted, acidic, and grassy aroma characteristics in food product development could also be provided by brown sugars from different production lines.

### 3.3. Antioxidant profiles of non-centrifugal brown sugar from different drying–solidification processes

Non-centrifugation procedures caused the brown sugars to retain a large amount of antioxidative phenolics and flavonoids from the sugarcane stalks (Payet et al., 2005). Consistent with the differences on formation of dark-colored substances in the brown sugar (Table 2), high-temperature thin-film evaporation processes liberate more phenolic compounds compared with brown sugar from OP drying–solidification line (Fig. 3). Practices of thermal heating in food processing such as evaporation, roasting, and extrusion could initiate the development of antioxidant-related polyphenol compounds, as well as Maillard reaction derivatives such as furosine and hydroxymethylfurfural, which are preferably formed by increasing the process temperature up to certain levels (Chandrasekara & Shahidi, 2011; Osada & Shibamoto, 2006).

Accordingly, brown sugar from HTF drying–solidification method was found to contain significantly higher ( $p < 0.05$ ) total

phenolics (264.2 mg GAE/100 g), followed by VTF and OP brown sugars (217.8 and 210.5 mg GAE/100 g, respectively) (Fig. 3a). The total phenolic contents of the evaluated brown sugars are higher than that of previously reported industrial brown sugars (10.8–41.8 mg GAE/100 g) and other cane sugar manufacturing products but lower than jaggery sugar (383.7 mg GAE/100 g) (Nayaka et al., 2009; Payet et al., 2005), revealing their potential benefits for comprising polyphenol functional components. HTF brown sugar also could scavenge peroxy radical more effectively, as represented by its higher ORAC value (5743.5  $\mu\text{mol TE}/100\text{ g}$ ), than other evaluated brown sugars (Fig. 3b). However, there are no significant differences of total phenolic contents and ORAC values between VTF and OP brown sugars. In consideration to the similar evaporation temperature process in the two thin film evaporation lines, the higher mass transfer of the HTF process might be responsible for retaining these antioxidation properties in its solidified brown sugar, whilst certain antioxidants might be vaporized during the evaporation process in slower sugar syrup inlet of gravitational fall-aided VTF drying–solidification method (0.81 versus 0.49 ton/h, Table 1). In addition, the brown sugars could scavenge DPPH radical at a similar level, ranging from 1494.7 to 1698.3  $\mu\text{mol TE}/100\text{ g}$ , and it was also discovered that the total phenolic content of non-centrifugal brown sugar had a more relevant correlation with its ORAC value than with DPPH radical-scavenging activity. These phenolic–antioxidation correlation findings, particularly relating to the ability to scavenge free radicals

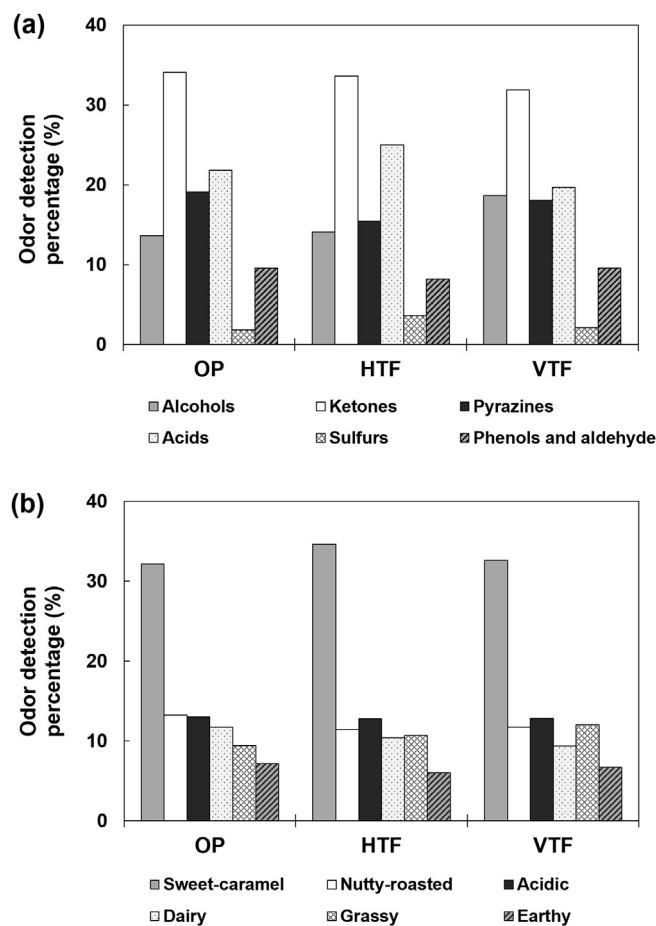


Fig. 2. Detection percentage of (a) aroma component groups and (b) assessed odors of non-centrifugal brown sugars from different drying–solidification processes: open pan (OP), horizontal thin-film (HTF), and vertical thin-film (VTF), determined through GC-O analysis.

as signified by ORAC values, were in agreement with previously reported works (Payet et al., 2005; Xu, Li, Lu, Beta, & Hydamaka, 2009).

The information of antioxidant activity in brown sugar is important for enhancing its functional and beneficial health promoting effects and for defining the necessary packaging and storage conditions in order to delay oxidative damage during their commercial distribution. Additionally, these findings can be used as an important basis for further enhancing quality attributes of non-centrifugal brown sugars according to process parameter optimization on drying–solidification processes.

#### 4. Conclusion

Drying–solidification process is a key source of variation that contributes to the quality attribute differentiation in non-centrifugally processed cane brown sugar. The OP drying–solidification line produced lighter color of solidified brown sugar due to its lower–temperature process, and a larger OP-surface design to facilitate evaporation produced smaller amount of volatile aroma components. Moreover, the odors of ketone and pyrazine compounds were highly detected in OP brown sugar. On the other hand, VTF and HTF brown sugars from thin-film evaporation lines had a greater content of volatile fractions in different mixtures of aroma profiles of sweet-caramel, nutty-roasted, acidic-dairy, and grassy characteristics. Enhanced heating drying–solidification process in brown sugar manufacturing also affected phenolic

content and antioxidant activity levels, wherein HTF brown sugar provided the highest total phenolic content and ORAC values. These findings also indicate that drying–solidification process is a vital process in non-centrifugal brown sugar manufacture affecting antioxidant potentials of its solidified form of brown sugar, together with their physical and aroma profiles. These quality attribute distinctions in non-centrifugal brown sugar of different drying–solidification processes may distinguish the specific use of each brown sugar product.

#### Acknowledgments

We are grateful to the Japan Society for the Promotion of Science for the International Research Fellowship, awarded to Y.A (ID No.P14075). We thank Sawako Takahara and Ai Tomimura (University of the Ryukyus) for their excellent technical assistance. This work was partially supported by a Grant-in-Aid for Scientific Research (No.26350095) from Japan Society for the Promotion of Science.

#### References

- Arena, E., Guarrera, N., Campisi, S., & Asmundo, C. N. (2006). Comparison of odour active compounds detected by gas-chromatography-olfactometry between hand-squeezed juices from different orange varieties. *Food Chemistry*, *98*, 59–63.
- Asikin, Y., Kamiya, A., Mizu, M., Takara, K., Tamaki, H., & Wada, K. (2014). Changes in the physicochemical characteristics, including flavour components and Maillard reaction products, of non-centrifugal cane brown sugar during storage. *Food Chemistry*, *149*, 170–177.
- Asikin, Y., Takahashi, M., Mishima, T., Mizu, M., Takara, K., & Wada, K. (2013). Antioxidant activity of sugarcane molasses against 2,2'-azobis(2-amidinopropane) dihydrochloride-induced peroxy radicals. *Food Chemistry*, *141*, 466–472.
- Chandrasekara, N., & Shahidi, F. (2011). Effect of roasting on phenolic content and antioxidant activities of whole cashew nuts, kernels, and testa. *Journal of Agricultural and Food Chemistry*, *59*, 5006–5014.
- Engel, W., Bahr, W., & Schieberle, P. (1999). Solvent assisted flavour evaporation – a new and versatile technique for the careful and direct isolation of aroma compounds from complex food matrices. *European Food Research and Technology*, *209*, 237–241.
- Fogliano, V., Monti, M. S., Musella, T., Randazzo, G., & Ritieni, A. (1999). Formation of coloured Maillard reaction products in a gluten–glucose model system. *Food Chemistry*, *66*, 293–299.
- Generoso, W. C., Borges, M. T. M. R., Ceccato-Antonini, S. R., Marino, A. F., Silva, M. V. M., Nassu, R. T., et al. (2009). Physical-chemical and microbiological evaluation of commercial brown sugar. *Revista do Instituto Adolfo Lutz*, *68*, 259–268.
- ICUMSA. (2003). *ICUMSA methods book supplement 2002*. Berlin: Verlag Dr. Albert Bartens KG.
- Jaeger, H., Janositz, A., & Knorr, D. (2010). The Maillard reaction and its control during food processing. The potential of emerging technologies. *Pathologie Biologie*, *58*, 207–213.
- Jaffé, W. R. (2012). Health effects of non-centrifugal sugar: a review. *Sugar Tech*, *14*, 87–94.
- Jousse, F., Jongen, T., Agterof, W., Russell, S., & Braat, P. (2002). Simplified kinetic scheme of flavor formation by the Maillard reaction. *Journal of Food Science*, *67*, 2534–2542.
- Legako, J. F., Brooks, J. C., O'Quinn, T. G., Hagan, T. D. J., Polkinghorne, R., Farmer, L. J., et al. (2015). Consumer palatability scores and volatile beef flavor compounds of five USDA quality grades and four muscles. *Meat Science*, *100*, 291–300.
- Maltini, E., Torreggiani, D., Venir, E., & Bertolo, G. (2003). Water activity and the preservation of plant foods. *Food Chemistry*, *82*, 79–86.
- Naknean, P., & Meenune, M. (2015). Impact of clarification of palm sap and processing method on the quality of palm sugar syrup (*Borassus flabellifer* Linn.). *Sugar Tech*, *17*, 195–203.
- Nayaka, M. A. H., Sathisha, U. V., Manohar, M. P., Chandrashekar, K. B., & Dharmesh, S. M. (2009). Cytoprotective and antioxidant activity studies of jaggery sugar. *Food Chemistry*, *115*, 113–118.
- Osada, Y., & Shibamoto, T. (2006). Antioxidative activity of volatile extracts from Maillard model systems. *Food Chemistry*, *98*, 522–528.
- Payet, B., Sing, A. S. C., & Smadja, J. (2005). Assessment of antioxidant activity of cane brown sugars by ABTS and DPPH radical scavenging assays: determination of their polyphenolic and volatile constituents. *Journal of Agricultural and Food Chemistry*, *53*, 10074–10079.
- Qureshi, M. S., Bhongale, S. S., & Thorave, A. K. (2011). Determination of organic acid impurities in lactic acid obtained by fermentation of sugarcane juice. *Journal of Chromatography A*, *1218*, 7147–7157.
- Rockenbach, I. I., Gonzaga, L. V., Rizelio, V. M., Gonçalves, A. E. S. S., Genovese, M. I.,

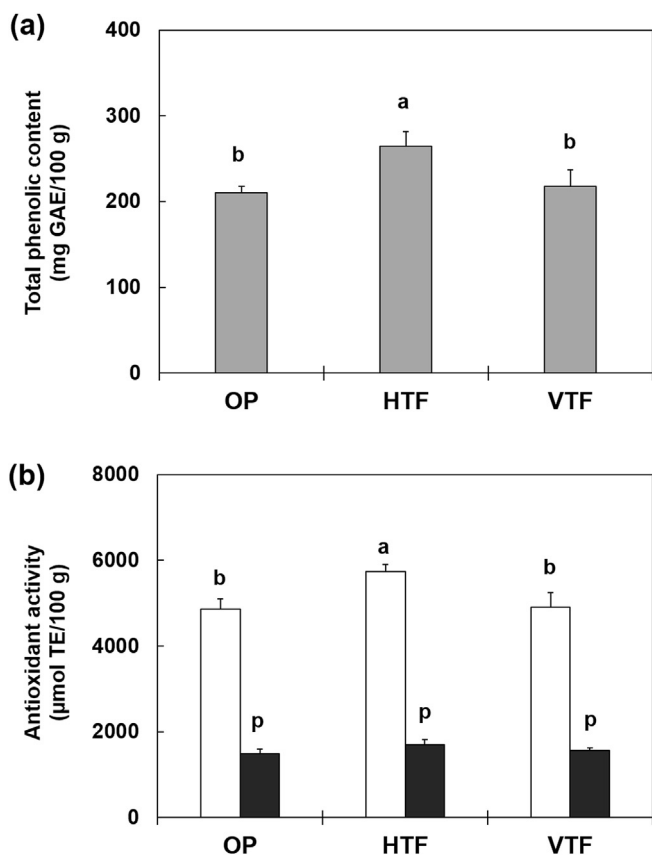


**Fig. 3.** (a) Total phenolic content (mg GAE/100 g) and (b) antioxidant profiles represented by ORAC value (□) and DPPH radical-scavenging activity (■) (μmol TE/100 g) of non-centrifugal brown sugars from different drying–solidification processes: open pan (OP), horizontal thin-film (HTF), and vertical thin-film (VTF). Each value is expressed as the mean ± standard deviation ( $n = 3$ ). Means in the same group followed by the same letter are not significantly different ( $p < 0.05$ ).

- & Fett, R. (2011). Phenolic compounds and antioxidant activity of seed and skin extracts of red grape (*Vitis vinifera* and *Vitis labrusca*) pomace from Brazilian winemaking. *Food Research International*, 44, 897–901.
- Segurel, M. A., Razungles, A. J., Riou, C., Trigueiro, M. G., & Baumes, R. L. (2005). Ability of possible DMS precursors to release DMS during wine aging and in the conditions of heat-alkaline treatment. *Journal of Agricultural and Food Chemistry*, 53, 2637–2645.
- Singh, K., Bharose, R., Verma, S. K., & Singh, V. K. (2013). Potential of powdered activated mustard cake for decolorising raw sugar. *Journal of the Science of Food and Agriculture*, 93, 157–165.
- Sumiyoshi, M., Hayashi, T., & Kimura, Y. (2009). Effects of the nonsugar fraction of brown sugar on chronic ultraviolet B irradiation-induced photoaging in melanin-possessing hairless mice. *Journal of Natural Medicines*, 63, 130–136.
- Xu, X., Li, W., Lu, Z., Beta, T., & Hydamaka, A. W. (2009). Phenolic content, composition, antioxidant activity, and their changes during domestic cooking of potatoes. *Journal of Agricultural and Food Chemistry*, 57, 10231–10238.
- Xu, Y. X., Zhang, M., Fang, Z. X., Sun, J. C., & Wang, Y. Q. (2014). How to improve bayberry (*Myrica rubra* Sieb. et Zucc.) juice flavour quality: Effect of juice processing and storage on volatile compounds. *Food Chemistry*, 151, 40–46.



# The effect of milk fat substitution with palm fat on lactic acid bacteria counts in cheese-like products



Marek Aljewicz<sup>a,\*</sup>, Grażyna Cichosz<sup>a</sup>, Beata Nalepa<sup>b</sup>, Marika Bielecka<sup>a</sup>

<sup>a</sup> Department of Dairy Science and Quality Management, Faculty of Food Science, University of Warmia and Mazury in Olsztyn, 10-719 Olsztyn, Poland

<sup>b</sup> Department of Industrial and Food Microbiology, Faculty of Food Sciences, University of Warmia and Mazury, Plac Cieszyński 1, 10-726 Olsztyn, Poland

## ARTICLE INFO

### Article history:

Received 31 May 2015

Received in revised form

6 October 2015

Accepted 18 October 2015

Available online 23 October 2015

### Keywords:

Cheese-like products

Gouda

Probiotic

*Lactobacillus*

Viability

Fingerprinting

## ABSTRACT

This study evaluated the influence of complete substitution of milk fat with palm fat on the growth of lactic acid bacteria in Gouda-type cheese-like products, as compared with Gouda cheeses of the same type. Cheese-like products and ripened cheeses were produced in industrial plants with or without the addition of probiotic cultures. The analysed products were evaluated during ripening and storage based on the counts of starter lactic acid bacteria (SLAB), non-starter lactic acid bacteria and the viability of *Lactobacillus acidophilus* NCFM and *Lactobacillus paracasei* LPC-37 probiotic cultures.

The highest SLAB counts were determined in control and experimental Gouda cheeses. SLAB were significantly less abundant in cheese-like products. During ripening, a greater reduction in SLAB counts was observed in control ripened cheeses than in control cheese-like products. *Lactococcus* sp. counts were lower in experimental products containing *L. acidophilus* NCFM than in products with *L. paracasei* LPC-37.

The viability of *L. acidophilus* NCFM was significantly correlated with product type and the time of ripening and storage. The counts of *L. acidophilus* NCFM were higher in ripened cheeses than in cheese-like products. *L. paracasei* LPC-37 cultures were characterised by higher viability rates in products than *L. acidophilus* NCFM.

© 2015 Elsevier Ltd. All rights reserved.

## 1. Introduction

Growing awareness about the significance of diet and nutrition for health has increased consumer interest in functional foods. A wide assortment of functional foods are available on the dairy market. Yoghurt is a major functional dairy product because its chemical composition can be easily modified, and it can be enhanced with probiotic cultures. Most of the probiotic cultures were isolated from human or animal digestive tract, but one culture used in the experiment - *Lactobacillus paracasei* LPC-37 was isolated from dairy products.

Cheese constitutes environment more suitable for long-term viability of lactic acid bacteria and probiotic bacteria, than yogurts due to higher buffering capacity, lower titratable acidity, higher pH value, lower oxygen content, higher fat content and higher nutrient availability. One of main differences among probiotic dairy products and probiotic cheeses is that in the first products probiotic

bacteria should maintain their viability during relatively long ripening-storage period (Madureira et al., 2008; Karimi, Mortazavian, & Cruz, 2011).

When consumed on a regular basis, probiotic bacteria regulate the quantitative and qualitative composition of the gut microflora and/or modify the immune system to deliver health benefits for both humans and animals (Lahtinen et al., 2012; Vasiljevic & Shah, 2008; Wang et al., 2012). Yet for probiotic bacteria to modulate health, their minimum content in food products should be 6–7 log CFU g<sup>-1</sup>, and daily yoghurt consumption should not be less than 100 g. Ripened cheeses are consumed in smaller daily amounts than fermented milks due to their higher fat content and relatively high price. For this reason, cheeses should contain minimum 8–9 log CFU g<sup>-1</sup> probiotic bacteria to deliver health benefits. Due to significantly higher counts of probiotic bacteria in the product, health-promoting effects can be achieved already when ripened cheese is consumed in the daily amount of 20 g.

The survival of probiotic cultures in fresh cheese (Masuda, Yamanari, & Itoh, 2005), fresh cheese with inulin (Buriti, Cardarelli, Filisetti, & Saad, 2007), soft ripened cheese (Coetret, Gueguen, & Vernoux, 2004) and hard cheese (Bergamini, Hynes,

\* Corresponding author. Tel.: +48 89 524 5179; fax: +48 89 523 3402.

E-mail address: [marek.aljewicz@uwm.edu.pl](mailto:marek.aljewicz@uwm.edu.pl) (M. Aljewicz).

Palma, Sabbag, & Zalazar, 2009; Sharp, McMahon, & Roadbent, 2008) has been investigated by numerous authors. Cheese like-products, due to lower prices than regular cheeses are an integral part of the dairy market in Poland and Eastern European countries. In contrast to original dairy products, very little is known about the viability of probiotic bacteria in Gouda-type cheese-like products where milk fat was completely substituted with palm fat. To compensate for this knowledge gap, the aim of this study was to evaluate the effect of milk fat substitution with palm fat on the viability of starter bacteria (SLAB), non-starter bacteria (NSLAB) and *Lactobacillus acidophilus* NCFM and *L. paracasei* LPC-37 probiotic cultures in Gouda-type cheese-like products and Gouda cheeses during ripening and storage.

## 2. Materials and methods

### 2.1. Production of ripened cheeses and cheese-like products

The experimental material comprised ripened Gouda-type cheese-like products and Gouda-type cheese manufactured in an industrial plant in Giżycko, Poland. Gouda-type cheese-like products and Gouda-type cheese were manufactured as described by Aljewicz and Cichosz (2015).

### 2.2. Chemical composition

Samples of representative cheeses were collected as indicated by AOAC 955.30 (AOAC, 2005). Cheeses were grated using a Santos 2 grater (Lyon, France). Grated cheese samples were analysed in triplicate to determine their salt content by the AOAC 975.20 Volhard method (AOAC, 2005), fat content by the Van Gulik method (ISO, 2008) and moisture content by the AOAC 926.08 procedure of oven drying at 102 °C (AOAC, 2005). Total nitrogen and protein content was determined by the Kjeldahl method (ISO, 2011). The pH of cheese slurry, prepared by blending 10 g of grated cheese with 10 mL of deionised H<sub>2</sub>O, was measured with a pH meter (Elmetron CP 501, Zabrze, Poland, electrode: Inode, Zabrze, Poland) after calibration with pH 4.0 and pH 7.0 buffers (Merck, Darmstadt, Germany).

### 2.3. Microbiological analysis

Cheese samples were prepared according to PN-EN ISO (2010). A cheese sample of 10 g was added to a 90 mL of sodium citrate solution (20 g L<sup>-1</sup>, POCh, Gliwice, Poland) with a temperature of 40 °C. Samples were homogenised in a stomacher (BagMixer 400W, Saint Nom, France) to produce a uniform suspension. *L. acidophilus* NCFM was determined according to ISO (2006). Total *L. paracasei* LPC-37 counts were determined on MRS agar modified through the addition of 30.0 g of sodium chloride (POCh). pH was adjusted to 5.8 ± 0.1. All ingredients were dissolved in distilled water and sterilised by autoclaving at 118 °C for 15 min. After melting and cooling, they were supplemented with filter-sterilised vancomycin (Applichem, Darmstadt, Germany) to final concentration of 30 µg mL<sup>-1</sup>. Samples were incubated anaerobically at 37 °C for 72 h with the use of the AnaeroGen system (Oxoid, Poznan, Poland). Total non-starter lactobacilli counts were determined in control and experimental cheeses on Rogosa agar (Merck). Samples were incubated anaerobically at 37 °C for 72 h with the use of the AnaeroGen system (Oxoid).

The total counts of starter bacteria were determined in control and experimental cheeses on M17 agar (Merck, Darmstadt, Germany). Samples were incubated aerobically at 30 °C for 48 h (mesophilic cultures).

### 2.4. Confirmation of strains belonging to the *L. acidophilus* and *L. paracasei* DNA isolation

In order to confirm the belonging to the *Lactobacillus* genus, *L. acidophilus* and *L. paracasei* species and *L. acidophilus* NCFM and *L. paracasei* LPC37 strains randomly selected bacterial colonies were checked in the Gram stain test (Olympus BX51, Japan). Then, the material from the collected colonies was grown in MRS broth at 37 °C for 24 h under anaerobic conditions. Next, total genomic DNA was extracted with the Genomic Mini kit (A&A Biotechnology, Poland) according to the manufacturer.

**species-specific PCR.** Amplification was carried out using a thermal cycler MJmini (Bio-rad, Poland) and two pair species-specific primers: Laci-1 (5'-TGCAAAGTGGTAGCGTAAGC-3') and 23-10C (5'-CCTTCCCTCACGGTACTG-3') for the identification of *L. acidophilus* (Song et al., 2000) or Y2 (5'-CCCAGCTGCCTCCCGTAGGAGT-3') and para (5'-CACCGAGATCAACATGG-3') for *L. paracasei* (Ward & Timmins, 1999). The reaction mixture (20 µl) contained 1xTaq buffer with 2.0 mM MgCl<sub>2</sub>, 0.25 mM of species-specific primers, 0.2 mM of each dNTPs, 20–40 ng of bacterial DNA and 1 U of Taq DNA Polymerase (Thermo Scientific, Lithuania). DNA fragments were amplified as follows: *L. acidophilus* – 35 cycles consisting of denaturation at 95 °C for 20 s, annealing at 68 °C for 2 min, extension at 72 °C for 2 min, and a 5 min final extension step at 74 °C; *L. paracasei* – initial denaturation at 94 °C for 3 min, followed by 30 cycles consisting of denaturation at 94 °C for 45 s, annealing at 45 °C for 45 s, extension at 72 °C for 1 min, and a 5 min final extension step at 72 °C.

**rep-PCR.** Amplifications were performed with 1 U of Dream Taq DNA polymerase (Thermo Scientific), 2.5 mM MgCl<sub>2</sub>, 0.2 mM of each dNTPs, and 0.1 mM of primer GTG<sub>5</sub> (5'-GTGGTGGTGGTGGTGG-3') (Markiewicz, Biedrzycka, Wasilewska, & Bielecka, 2010). An initial denaturation at 94 °C for 4 min was followed by 35 cycles of denaturation at 94 °C for 30 s, annealing at 42 °C for 30 s, and elongation at 72 °C for 30 s, and a final extension at 72 °C for 4 min.

All amplicons were analysed in a 1.0 or 1.5% × TBE agarose gel electrophoresis containing 10 mg/ml ethidium bromide, visualized under UV illumination and photographed.

### 2.5. Statistical analysis

The results were verified for normal distribution and homogeneity of variance. The significance of differences between means was analysed by Duncan's test. The interactions between factors were determined by ANOVA for the completely randomized design. The results were processed in Statistica 10.0 PL software (Statsoft 2011, Krakow, Poland) at P < 0.05 for n = 3 (physicochemical and biochemical parameters) and at P < 0.05 for n = 3 (microbiological analysis in duplicate). All data were presented as means ± standard error of mean. Each repetition of the experience has been manufactured the same day from the same milk.

## 3. Results

### 3.1. Chemical composition of cheese-like products and Gouda cheeses

The average water content of Gouda cheeses was determined at 42.00%, and it did not differ significantly (P > 0.05) from that of Gouda-type cheese-like products (44.0%). The protein content of ripened cheeses and Gouda-type cheese-like products was similar (P > 0.05) at 24%. The analysed product groups differed significantly (P < 0.05) in their average fat content which reached 27% in ripened Gouda cheeses and 28% in Gouda-type cheese-like products (Table A.1). The average content of sodium chloride was determined at

**Table A.1**  
Composition of control and experimental Gouda cheeses and Gouda-type cheese-like products.

Composition	Gouda cheese			Gouda-type cheese-like products		
	Control	NCFM	LPC-37	Control	NCFM	LPC-37
Moisture	41.65 ± 0.02 <sup>c</sup>	42.88 ± 0.20 <sup>ab</sup>	42.37 ± 0.28 <sup>a</sup>	44.18 ± 0.17 <sup>ad</sup>	43.02 ± 0.30 <sup>ab</sup>	44.44 ± 0.18 <sup>c</sup>
Protein	23.54 ± 0.05 <sup>c</sup>	24.15 ± 0.05 <sup>ab</sup>	24.15 ± 0.05 <sup>ab</sup>	23.50 ± 0.01 <sup>d</sup>	24.05 ± 0.16 <sup>db</sup>	24.25 ± 0.06 <sup>e</sup>
Fat	26.50 ± 0.00 <sup>h</sup>	27.73 ± 0.16 <sup>bc</sup>	27.07 ± 0.19 <sup>a</sup>	28.34 ± 0.17 <sup>f</sup>	27.51 ± 0.21 <sup>g</sup>	28.17 ± 0.25 <sup>e</sup>
FDM	45.42 ± 0.02 <sup>a</sup>	48.54 ± 0.28 <sup>b</sup>	46.97 ± 0.15 <sup>f</sup>	50.76 ± 0.31 <sup>e</sup>	48.27 ± 0.15 <sup>a</sup>	50.7 ± 0.37 <sup>d</sup>
MFFS	56.67 ± 0.03 <sup>c</sup>	59.33 ± 0.26 <sup>b</sup>	58.09 ± 0.25 <sup>a</sup>	61.64 ± 0.25 <sup>a</sup>	59.34 ± 0.26 <sup>a</sup>	61.87 ± 0.21 <sup>d</sup>
Salt	1.42 ± 0.01 <sup>c</sup>	1.24 ± 0.01 <sup>e</sup>	1.53 ± 0.01 <sup>d</sup>	1.69 ± 0.01 <sup>a</sup>	1.33 ± 0.01 <sup>bc</sup>	1.72 ± 0.01 <sup>d</sup>
P/F	0.89 ± 0.01 <sup>a</sup>	0.88 ± 0.01 <sup>ab</sup>	0.90 ± 0.01 <sup>a</sup>	0.83 ± 0.01 <sup>e</sup>	0.88 ± 0.02 <sup>d</sup>	0.87 ± 0.01 <sup>f</sup>

Abbreviations are: FDM, fat in dry matter; MFFS, moisture in the fat free substance; SDM, salt in dry matter P/F, protein/fat ratio. Analyses were conducted after brining of Gouda cheeses and Gouda-type cheese-like products. Values (%) are means ± standard error of mean; means in rows with the same superscript letters are not significantly different ( $P < 0.05$ ).

1.40% in Gouda cheeses, and it did not differ significantly from that of Gouda-type cheese-like products (1.58%).

### 3.2. Changes in the acidity of cheese-like products and Gouda cheeses

Immediately after salting, average acidity reached pH 5.41 in ripened Gouda cheeses, and it was significantly ( $P < 0.05$ ) higher than in Gouda-type cheese-like products (pH 5.52) (Fig. A1). A gradual drop in acidity was noted in both Gouda cheeses and Gouda-type cheese-like between weeks 2 and 6 of ripening, and the observed decrease was greater in control than in experimental products. During three months of storage, acidity decreased gradually in both Gouda cheeses and Gouda-type cheese-like products (control and experiment), and the noted drop was always greater in ripened Gouda cheeses (control:  $\Delta$ pH 0.18; NCFM:  $\Delta$ pH 0.25; LPC-37:  $\Delta$ pH 0.30) than in Gouda-type cheese-like products (control:  $\Delta$ pH 0.14; NCFM:  $\Delta$ pH 0.15; LPC-37:  $\Delta$ pH 0.16). Gouda-type cheese-like products were significantly less acidic ( $P < 0.05$ ) than ripened cheeses after three months of storage.

Control Gouda cheeses were characterised by a greater decrease in SLAB counts ( $1.92 \log_{10} \text{CFU g}^{-1}$ ) than control Gouda-type cheese-like products ( $0.88 \log_{10} \text{CFU g}^{-1}$ ) during ripening and storage. The decrease in SLAB counts after six weeks of ripening and three months of storage was greater in products containing *L. acidophilus* NCFM ( $1.90 \log_{10} \text{CFU g}^{-1}$ ) than in products containing *L. paracasei* LPC-37 ( $0.17 \log_{10} \text{CFU g}^{-1}$ ). After ripening and storage, a significant decrease in SLAB counts was noted in control Gouda-type cheese-like products then in Gouda cheeses.

### 3.4. Changes in the counts of non-starter lactic acid bacteria

The counts of non-starter lactic acid bacteria (NSLAB) were also determined by the substitution of milk fat with palm fat, the time of ripening and the applied probiotic culture (Table. C.1). Immediately after salting, NSLAB counts in control Gouda-type cheese-like products reached  $6.21 \log_{10} \text{CFU g}^{-1}$  and were significantly higher ( $P < 0.05$ ) than in control Gouda cheese ( $3.85 \log_{10} \text{CFU g}^{-1}$ ). Immediately after salting, the average NSLAB counts were determined at  $7.59 \log_{10} \text{CFU g}^{-1}$  in experimental Gouda-type cheese-

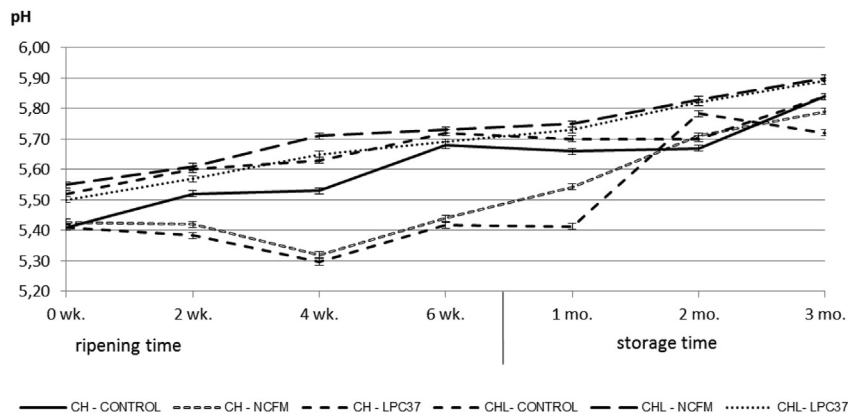


**Fig. A1.** Change the pH value during ripening and storage period of Gouda cheeses and Gouda-type cheese-like products. Abbreviation: CH- Gouda cheese; CHL- Gouda-type cheese-like products; NCFM – cheese/ cheese-like products with *L. acidophilus* NCFM, LPC37 – cheese/ cheese-like products with *L. paracasei* LPC37. Values are means ± standard error of mean ( $n = 3$  sets of data analysed in duplicate).

### 3.3. Changes in the counts of mesophilic starter lactic acid bacteria

The counts of mesophilic starter lactic acid bacteria (SLAB) were influenced by the substitution of milk fat with palm fat, the time of ripening and storage, and the applied probiotic culture (Table. B.1). Immediately after salting, the average SLAB counts in control and experimental Gouda-type cheese-like products were determined at  $9.28 \log_{10} \text{CFU g}^{-1}$  and were significantly lower ( $P < 0.05$ ) than in Gouda cheeses ( $9.22 \log_{10} \text{CFU g}^{-1}$ ).

like products and Gouda cheeses containing *L. acidophilus* NCFM and were significantly lower than in the corresponding products containing *L. paracasei* LPC-37 ( $9.38 \log_{10} \text{CFU g}^{-1}$ ).

After six weeks of ripening, a significant increase in NSLAB counts was noted in control Gouda-type cheese-like products and Gouda cheeses, and it was greater in Gouda cheeses (by  $4.62 \log_{10} \text{CFU g}^{-1}$ ) than in Gouda-type cheese-like products (by  $1.96 \log_{10} \text{CFU g}^{-1}$ ). Similarly to control, Gouda cheeses and Gouda-type cheese-like products, a significant increase ( $0.12 \log_{10} \text{CFU g}^{-1}$ ) in

**Table B.1**Average count (log cfu g<sup>-1</sup>) of starter microorganisms during ripening and storage of Gouda cheeses and Gouda-type cheese-like products.

Sample		Viable counts log CFU g <sup>-1</sup>						
		Ripening [wk.]				Storage [mo.]		
		0	2	4	6	1	2	3
Gouda cheese	Mezophilic culture starter							
	Control cheese	9.4 ± 0.08 <sup>a</sup>	9.26 ± 0.03 <sup>b</sup>	8.93 ± 0.02 <sup>c</sup>	8.46 ± 0.08 <sup>a</sup>	8.37 ± 0.02 <sup>a</sup>	7.81 ± 0.03 <sup>d</sup>	7.45 ± 0.05 <sup>e</sup>
	NCFM	9.65 ± 0.03 <sup>a</sup>	8.89 ± 0.01 <sup>b</sup>	8.69 ± 0.08 <sup>c</sup>	9.36 ± 0.18 <sup>d</sup>	7.91 ± 0.04 <sup>e</sup>	7.51 ± 0.21 <sup>f</sup>	7.36 ± 0.09 <sup>g</sup>
	LPC37	8.61 ± 0.34 <sup>a</sup>	8.35 ± 0.06 <sup>a</sup>	8.55 ± 0.06 <sup>a</sup>	9.24 ± 0.00 <sup>b</sup>	9.19 ± 0.07 <sup>bc</sup>	9.12 ± 0.06 <sup>bc</sup>	8.70 ± 0.09 <sup>a</sup>
Gouda-type cheese-like products	Control cheese	9.05 ± 0.08 <sup>ac</sup>	9.05 ± 0.03 <sup>a</sup>	9.18 ± 0.04 <sup>bc</sup>	8.47 ± 0.06 <sup>d</sup>	8.39 ± 0.05 <sup>e</sup>	8.65 ± 0.05 <sup>f</sup>	8.17 ± 0.09 <sup>g</sup>
	NCFM	9.40 ± 0.09 <sup>a</sup>	8.60 ± 0.09 <sup>b</sup>	8.33 ± 0.12 <sup>c</sup>	8.88 ± 0.16 <sup>d</sup>	8.53 ± 0.27 <sup>d</sup>	7.54 ± 0.26 <sup>e</sup>	7.90 ± 0.03 <sup>f</sup>
	LPC37	9.39 ± 0.23 <sup>a</sup>	9.21 ± 0.04 <sup>b</sup>	8.74 ± 0.04 <sup>c</sup>	8.73 ± 0.18 <sup>d</sup>	9.17 ± 0.05 <sup>bc</sup>	9.29 ± 0.08 <sup>a</sup>	8.96 ± 0.03 <sup>e</sup>

Abbreviation: NCFM – cheese/cheese-like products with *L. acidophilus* NCFM, LPC37 – cheese/cheese-like products with *L. acidophilus* LPC37. Values are means ± standard error of mean (n = 3 sets of data analysed in duplicate); means in a row with the same superscript letters are not significantly different (P < 0.05).

**Table C.1**Average count (log cfu g<sup>-1</sup>) of nonstarter lactic acid bacteria (lactobacilli) during ripening and storage of Gouda cheeses and Gouda-type cheese-like products.

Sample		Viable counts log CFU g <sup>-1</sup>						
		Ripening [wk.]				Storage [mo.]		
		0	2	4	6	1	2	3
Gouda cheese	Control cheese	3.85 ± 0.05 <sup>a</sup>	5.69 ± 0.02 <sup>b</sup>	8.93 ± 0.26 <sup>c</sup>	8.47 ± 0.08 <sup>d</sup>	8.08 ± 0.00 <sup>e</sup>	8.32 ± 0.06 <sup>f</sup>	8.70 ± 0.09 <sup>c</sup>
	NCFM	7.59 ± 0.02 <sup>a</sup>	7.90 ± 0.01 <sup>b</sup>	7.34 ± 0.06 <sup>c</sup>	7.47 ± 0.02 <sup>d</sup>	7.26 ± 0.03 <sup>e</sup>	7.76 ± 0.04 <sup>f</sup>	7.62 ± 0.07 <sup>a</sup>
	LPC37	9.32 ± 0.03 <sup>a</sup>	9.47 ± 0.01 <sup>b</sup>	10.10 ± 0.19 <sup>c</sup>	9.35 ± 0.01 <sup>d</sup>	9.06 ± 0.08 <sup>e</sup>	8.83 ± 0.03 <sup>f</sup>	8.61 ± 0.10 <sup>g</sup>
	Gouda-type cheese-like products	Control cheese	6.21 ± 0.23 <sup>a</sup>	8.14 ± 0.03 <sup>b</sup>	8.23 ± 0.10 <sup>b</sup>	8.17 ± 0.09 <sup>b</sup>	9.11 ± 0.05 <sup>c</sup>	8.72 ± 0.08 <sup>d</sup>
	NCFM	7.58 ± 0.10 <sup>a</sup>	7.56 ± 0.29 <sup>ace</sup>	8.26 ± 0.05 <sup>b</sup>	7.32 ± 0.09 <sup>c</sup>	7.98 ± 0.06 <sup>d</sup>	7.81 ± 0.08 <sup>e</sup>	7.79 ± 0.10 <sup>e</sup>
	LPC37	9.44 ± 0.24 <sup>a</sup>	9.20 ± 0.16 <sup>b</sup>	8.70 ± 0.16 <sup>c</sup>	7.56 ± 0.16 <sup>d</sup>	9.87 ± 0.07 <sup>e</sup>	9.67 ± 0.19 <sup>e</sup>	9.68 ± 0.20 <sup>e</sup>

Abbreviation: NCFM – cheese/cheese-like products with *L. acidophilus* NCFM, LPC37 – cheese/cheese-like products with *L. paracasei* LPC37. Values are means ± standard error of mean (n = 3 sets of data analysed in duplicate); means in a row with the same superscript letters are not significantly different (P < 0.05).

NSLAB counts was observed in experimental products containing *L. paracasei* LPC-37. Unlike in control Gouda cheeses and Gouda-type cheese-like products, a significant decrease (P < 0.05) in NSLAB counts was noted in experimental products containing *L. acidophilus* NCFM at 0.12 log<sub>10</sub> CFU g<sup>-1</sup> and 0.26 log<sub>10</sub> CFU g<sup>-1</sup>, respectively.

After three months of storage, NSLAB counts increased significantly (0.62 log<sub>10</sub> CFU g<sup>-1</sup>; P < 0.05) in control Gouda cheeses, whereas no changes in this parameter were noted in control Gouda-type cheese-like products. In experimental Gouda cheeses and Gouda-type cheese-like products containing *L. acidophilus* NCFM, NSLAB counts increased by 0.15 log<sub>10</sub> CFU g<sup>-1</sup> and 0.47 log<sub>10</sub> CFU g<sup>-1</sup>, respectively. A significant increase (2.12 log<sub>10</sub> CFU g<sup>-1</sup>) in NSLAB counts was also observed in experimental Gouda-type cheese-like products with *L. paracasei* LPC-37. In contrast, NSLAB counts decreased by 0.74 log<sub>10</sub> CFU g<sup>-1</sup> in experimental Gouda cheeses containing *L. paracasei* LPC-37 (Table. C.1).

### 3.5. Changes in the counts of probiotic bacteria

Immediately after salting, the average counts of *L. acidophilus* NCFM probiotic bacteria were determined at 7.67 log<sub>10</sub> CFU g<sup>-1</sup> in

experimental Gouda-type cheese-like products and Gouda cheeses (Table. D.1). After six weeks of ripening, a minor decrease of approximately 0.5 log<sub>10</sub> CFU g<sup>-1</sup> (P < 0.05) in *L. acidophilus* NCFM counts was noted in Gouda-type cheese-like products. The counts of *L. acidophilus* NCFM remained stable in Gouda cheeses. The counts of *L. acidophilus* NCFM decreased in both Gouda-type cheese-like products and Gouda cheeses after three months of storage. The observed drop was lower in Gouda-type cheese-like products (approximately 0.70 log<sub>10</sub> CFU g<sup>-1</sup>) than in cheeses (1.20 log<sub>10</sub> CFU g<sup>-1</sup>) (P < 0.05) (Table. D.1).

In experimental Gouda-type cheese-like products and Gouda cheeses containing *L. paracasei* LPC-37, the average counts of probiotic bacteria were determined at 9.21 log<sub>10</sub> CFU g<sup>-1</sup> immediately after salting and underwent only minor changes during ripening. After six weeks of ripening, *L. paracasei* LPC-37 counts in the evaluated Gouda-type cheese-like products and ripened cheeses were comparable at approximately 9.22 log<sub>10</sub> CFU g<sup>-1</sup>. After three months of storage, a decrease in the counts of *L. paracasei* LPC-37 was noted in both Gouda-type cheese-like products and Gouda cheeses. The observed drop was significantly lower (0.20 log<sub>10</sub> CFU g<sup>-1</sup>) in Gouda-type cheese-like products than in Gouda

**Table D.1**Average count (log cfu g<sup>-1</sup>) of probiotic bacteria during ripening and storage of Gouda cheeses and Gouda-type cheese-like products.

	Viable counts log CFU g <sup>-1</sup>						
	Ripening [wk.]				Storage [mo.]		
	0	2	4	6	1	2	3
Gouda cheese							
with <i>L. acidophilus</i> NCFM	7.55 ± 0.04 <sup>aA</sup>	7.65 ± 0.04 <sup>bA</sup>	7.53 ± 0.06 <sup>aB</sup>	7.55 ± 0.04 <sup>aB</sup>	6.97 ± 0.02 <sup>cB</sup>	6.74 ± 0.1 <sup>cB</sup>	5.76 ± 0.11 <sup>dB</sup>
with <i>L. paracasei</i> LPC-37	9.32 ± 0.11 <sup>aB</sup>	9.42 ± 0.04 <sup>aC</sup>	9.69 ± 0.03 <sup>bC</sup>	9.3 ± 0.05 <sup>cC</sup>	9.03 ± 0.05 <sup>dB</sup>	8.87 ± 0.08 <sup>cA</sup>	8.62 ± 0.08 <sup>fA</sup>
Gouda-type cheese-like products							
with <i>L. acidophilus</i> NCFM	7.79 ± 0.08 <sup>aB</sup>	7.59 ± 0.22 <sup>bAB</sup>	7.94 ± 0.03 <sup>cC</sup>	7.31 ± 0.29 <sup>bdB</sup>	7.17 ± 0.07 <sup>dC</sup>	7.15 ± 0.05 <sup>dC</sup>	6.46 ± 0.14 <sup>eC</sup>
with <i>L. paracasei</i> LPC-37	9.1 ± 0.08 <sup>acA</sup>	9.12 ± 0.05 <sup>acA</sup>	9.14 ± 0.02 <sup>aA</sup>	9.14 ± 0.04 <sup>aA</sup>	9.29 ± 0.03 <sup>bC</sup>	9.08 ± 0.06 <sup>aB</sup>	9.09 ± 0.09 <sup>cB</sup>

Values are means ± standard error of mean (n = 3 sets of data analysed in duplicate); means in a row and column with the same superscript letters are not significantly different (P < 0.05).

cheeses ( $0.41 \log_{10} \text{CFU g}^{-1}$ ) ( $P < 0.05$ ) (Table D.1).

State the number of isolated strains that were identified by PCR and rep-PCR with the GTG5 primer as *L. acidophilus* (93.4% - confirmation to the genus) and *L. paracasei* (93.9% - confirmation to the genus). Fig. B1 and Fig. B2 shows the gel images for randomly selected rep-PCR fingerprints obtained from the two probiotic strains *L. acidophilus* NCFM and *L. paracasei* LPC-37. Although the *Lactobacillus* isolates were subjected to multiple culture conditions, the rep-PCR fingerprints of each strain appeared stable and reproducible. The average similarity of the replicate fingerprints of *L. acidophilus* NCFM was 93% and for *L. paracasei* LPC-37 it was 97%.

#### 4. Discussion

The analysed cheese-like products and Gouda cheeses were characterised by minor differences in chemical composition. The chemical composition of Gouda-type cheese-like products and

ripened cheeses is determined by various factors, including the microbiological quality of ingredients, the presence of native enzymes in raw milk and, most importantly, the rate of lactic acid fermentation. Bacterial adjuncts have an insignificant impact on a product's chemical composition and may only influence the metabolic activity of acidifying cultures. The production of ripened Gouda cheeses and Gouda-type cheese-like products with identical chemical composition is virtually impossible (even under industrial conditions) due to variations and complexity of microbiological, biochemical and physicochemical processes.

The acidity of cheese-like products and Gouda cheeses is shaped mainly in early stages of production (curd cutting and drying). Significantly lower (by pH 0.1) acidity of Gouda-type cheese-like products than Gouda cheeses can probably be attributed to a drop in the acidifying activity of starter cultures (used in the production process) resulting from the substitution of milk fat with palm fat. During ripening and storage, the rate of changes in the acidity of

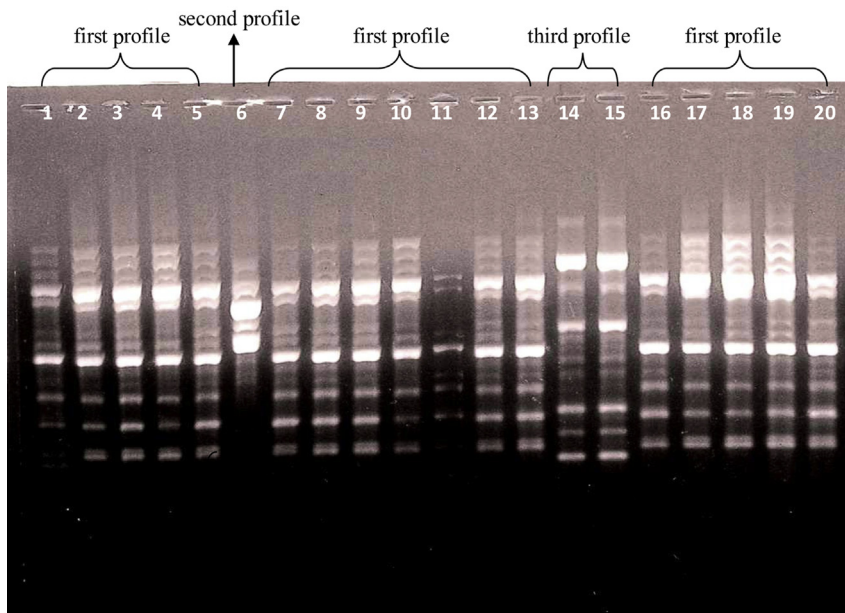


Fig. B1. rep-PCR fingerprinting patterns of *L. acidophilus* isolates. Lanes: 1–19 – isolates; 20 – *L. acidophilus* NCFM (explanation within the text).

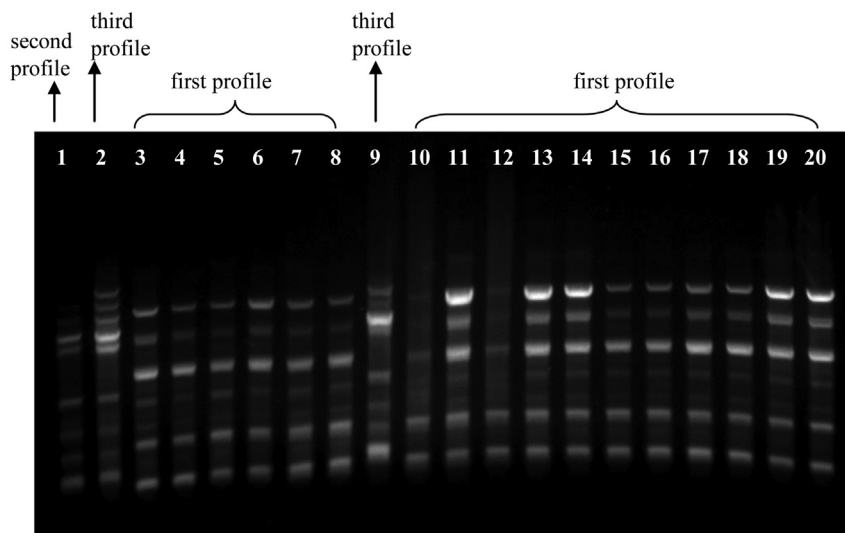


Fig. B2. rep-PCR patterns of *L. paracasei* isolates. Lanes: 1–19 – isolates; 20 – *L. paracasei* LPC-37 (explanation within the text).

both control and experimental cheese-like products and ripened cheeses was typical and characteristic of secondary fermentation. The much greater drop in the acidity of cheese-like products during ripening and storage resulted from faster degradation of lactates by highly abundant NSLAB.

Significantly higher counts of *Lactococcus* sp. starter cultures in experimental ripened Gouda cheeses and Gouda-type cheese-like products can probably be explained by inhibited growth of the accompanying microflora (data not shown) which had to compete with *Lactococcus* sp. for the same sources of carbon and nitrogen (Bzducha & Obiedziński, 2007; Vinderola, Mocchiutti, & Reinheimer, 2002). Higher counts of starter cultures in experimental cheeses could also result from the peptidolytic activity of *L. paracasei* LPC-37. Low-molecular-weight peptides produced by hydrolysis and free amino acids are used by proliferating *Lactococcus* sp. as a source of easily available nitrogen. The stimulating or antagonistic effect of *Lactococcus* sp. on starter cultures is determined mainly by the biochemical activity of secondary microflora and, to a lesser extent, by the product's chemical composition and the temperature of ripening and storage (Ziarno, Zaręba, & Bzducha-Wróbel, 2010).

The acidifying activity of starter cultures is one of the key factors determining the quality of the end product. Higher NSLAB counts ( $2.4 \log \text{CFU g}^{-1}$ ) in control Gouda-type cheese-like products than in control ripened Gouda cheeses resulted from significantly lower acidity (by pH 0.1) in the examined products immediately after salting. *Lactobacillus* counts were higher in experimental Gouda-type cheese-like products and Gouda cheeses because *L. paracasei* LPC-37 and *L. acidophilus* NCFM probiotic cultures were used in the production process. Immediately after salting, *Lactobacillus* counts were higher in experimental Gouda-type cheese-like products and Gouda cheeses than in control products, by  $2.3 \log \text{CFU g}^{-1}$  and  $4.6 \log \text{CFU g}^{-1}$ , respectively. Control Gouda-type cheese-like products and Gouda cheeses contained only NSLAB. Despite thermisation, bacteriostatic and pasteurisation of milk, ripened cheeses always contain NSLAB, mainly *Lactobacillus plantarum*, *L. paracasei*, *Lactobacillus rhamnosus*, *Lactobacillus brevis*, *Lactobacillus fermentum*, *Lactobacillus casei* and *Lactobacillus delbrueckii* (De Angelis et al., 2004; Immonen, Karjalainen, Sirviö, & Tanskanen, 2008). The presence of NSLAB in ripened cheeses and, most probably, cheese-like products is associated with the protective effects of fat and bacteria's resistance to short-term thermal processing (Jordan & Cogan, 1999).

The survival of *L. paracasei* LPC-37 and *Lactobacillus acidophilus* NCFM probiotic cultures was determined by the availability of substrates such as organic acids and their salts, sugars, peptides and free amino acids which are produced by milk-coagulating enzymes, native enzymes, and extracellular and intracellular bacterial enzymes which are released during autolysis of bacterial cells. Our findings corroborate the results of other studies where various strains of *Lactobacillus* sp. were characterised by high survival rates in Pategrás cheese (Bergamini et al., 2009), white-brined cheese (Özer, Kirmaci, Senel, Atamer, & Hayaloğlu, 2008), Gouda (Gomes, Malcata, Klaver, & Grande, 1995) and cheddar (Sharp et al., 2008). The minor drop in the counts of *L. paracasei* LPC-37 and *L. acidophilus* NCFM probiotic cultures as well as starter cultures in Gouda cheeses and Gouda-type cheese-like products during three months of storage resulted from much lower temperature ( $4^\circ\text{C}$ ) and sublethal stress response of some bacteria. High bacterial survival rates throughout the entire period of storage can probably be attributed to the synthesis of low-molecular-weight ( $\sim 7 \text{ kDa}$ ) peptides (CspA-CspE) which facilitate RNA transcription at low temperatures (Graumann, Wendrich, Weber, Schroder, & Marahiel, 1997). When exposed to stress, lactic acid bacteria can synthesize cyclopropane fatty acids – lactobacillic acid (C19cyc11) and dehydrosterculic acid

(C19cyc9) – which are responsible for maintaining the physicochemical properties of cells, such as cytoplasm liquidity (Montanari, Sado-Kamdem, Serrazanetti, Etoa, & Guerzoni, 2010). The synthesis of intracellular fatty acids is determined by the acidity of the product matrix. This observation was confirmed by higher survival rates of SLAB and NSLAB in Gouda-type cheese-like products than in Gouda cheeses. It should also be noted that the adaptive abilities of bacterial cells, including the synthesis of protective peptides and intracellular fatty acids, are strain-specific traits which are determined by the availability of carbon sources (Hosseini, Hussain, & Britz, 2015).

Apart from genetic factors, the survival of bacterial cultures in ripened and stored cheese is also determined by the type of fat used. Similarly to starter cultures, lower counts of probiotic cultures during the ripening of Gouda-type cheese-like products resulted from their lower metabolic activity. The use of palm fat in the production of Gouda-type cheese-like products modified the profile of free fatty acids (FFAs) released during ripening. This is an important consideration because *Lactobacillus* sp. counts during the ripening of semi-hard cheeses are determined by the presence of medium-chain and long-chain saturated fatty acids (Rodrigues, Rocha-Santos, Gomes, Goodfellow, & Freitas, 2012) which are released due to damage to the membrane of milk fat globules (slurry heating and evaporation) and under the influence of bacterial lipases and esterases during ripening and storage (Collins, McSweeney, & Wilkinson, 2003; Rodrigues et al., 2011).

Oxidative changes in FFAs require the presence of oxygen which is produced in small quantities by metabolizing NSLAB. The resulting oxylipids and short-chain aldehydes contribute to the elimination of bacterial cells by making cell walls partially permeable, inhibiting intracellular enzymes and blocking ion channels that transport nutrients to bacterial cells. The accumulation of FFAs in a product leads to a drop in SLAB and NSLAB counts. The antibacterial effects of FFAs are determined by the number of unsaturated bonds, acid structure and chain length, and they can differ within the same genus or even species of bacteria. Differences in the sensitivity of bacterial cells to FFAs and/or their oxidation products could be attributed to the bacteria's ability to quickly change the surface charge of a cell wall. As a result, the cell wall becomes less susceptible to FFAs and their oxidation products (Desbois & Smith, 2010).

Gouda-type cheese-like products where milk fat was completely substituted with palm fat were characterised by a significantly higher content of fatty acids C16:0, C18:1 and C18:2, and a lower content of C12:0 and C18:0 in comparison with Gouda cheeses (data not shown). Unlike cheeses, cheese-like products did not contain fatty acids C8:0 or C10:0 (Bockisch, 1998). During ripening, the insignificantly greater decrease in SLAB and NSLAB counts in Gouda-type cheese-like products than in ripened Gouda cheeses may be attributed to the inhibitory effect of FFAs on the enzymatic activity of the bacterial cell membrane (Hamel, 2009; Won et al., 2007; Zheng et al., 2005). Unlike in the ripening period, the decrease in probiotic counts was significantly lower in Gouda-type cheese-like products than in Gouda cheeses during storage. The higher survival rates of probiotic bacteria in lower temperatures resulted most probably from a decrease in their metabolic activity.

## 5. Conclusions

In this study, the substitution of milk fat with palm fat reduced the counts of *Lactococcus* sp. as well as *L. acidophilus* NCFM and *L. paracasei* LPC-37 probiotic cultures in Gouda-type cheese-like products during ripening. Mesophilic *L. paracasei* LPC-37 bacteria were characterised by higher survival rates than thermophilic *L. acidophilus* NCFM in Gouda cheeses and Gouda-type cheese-like

products. The survival rates of SLAB, NSLAB and *Lactobacillus* sp. probiotic cultures were significantly determined by the type of fat (fatty acid profile) and temperature applied in the production process. All Gouda-type cheese-like products were characterised by lower counts of mesophilic lactic acid bacteria, NSLAB, and *L. acidophilus* NCFM and *L. paracasei* LPC-37 probiotic cultures. The decrease in the counts of lactic acid bacteria was smaller during the storage of the analysed Gouda cheeses and Gouda-type cheese-like products than during their ripening.

## Acknowledgements

We express our thanks to the Dairy Plant in Giżycko (Poland) and the LabMlek Dairy Laboratory in Olsztyn (Poland) for assistance in performing the experiment. We gratefully acknowledge financial support from the Polish Ministry of Science and Higher Education (Grant No. 52807030802) and the National Science Center (Grant No. 312 469640).

## References

- Aljewicz, M., & Cichosz, G. (2015). Protective effects of *Lactobacillus* cultures in Dutch-type cheese-like products. *LWT – Food Science and Technology*, 63(1), 52–56.
- AOAC. (2005). *AOAC official methods of analysis* (18th ed.). Gaithersburg, MD, USA: AOAC International.
- Bergamini, C. V., Hynes, E. R., Palma, S. B., Sabbag, N. G., & Zalazar, C. A. (2009). Proteolytic activity of three probiotic strains in semi-hard cheese as single and mixed cultures: *Lactobacillus acidophilus*, *Lactobacillus paracasei* and *Bifidobacterium lactis*. *International Dairy Journal*, 19, 467–475.
- Bockisch, M. (1998). Fat as or in Food. In *Fats and oils handbook* (pp. 719–802). AOCS Press.
- Buriti, F. C. A., Cardarelli, H. R., Filisetti, T. M. C. C., & Saad, S. M. I. (2007). Synbiotic potential of fresh cream cheese supplemented with inulin and *Lactobacillus paracasei* in co-culture with *Streptococcus thermophilus*. *Food Chemistry*, 104, 1605–1610.
- Bzducha, A., & Obiedziński, M. W. (2007). Influence of two probiotic *Lactobacillus* strains on CLA content in model ripening cheeses. *Polish Journal of Food and Nutrition Sciences*, 57(4), 65–69.
- Coeuret, V., Gueguen, M., & Vernoux, J. P. (2004). In vitro screening of potential probiotic activities of selected lactobacilli isolated from unpasteurized milk products for incorporation into soft cheese. *Journal of Dairy Research*, 71, 451–460.
- Collins, Y. F., McSweeney, P. L. H., & Wilkinson, M. G. (2003). Lipolysis and free fatty acid catabolism in cheese: a review of current knowledge. *International Dairy Journal*, 13, 841–866.
- De Angelis, M., Di Cagno, R., Huet, C., Crechchio, C., Fox, P. F., & Gobbetti, M. (2004). Heat shock response in *Lactobacillus plantarum*. *Applied and Environmental Microbiology*, 70(3), 1336–1346.
- Desbois, A. P., & Smith, V. J. (2010). Antibacterial free fatty acids: activities, mechanisms of action and biotechnological potential. *Applied Microbiology and Biotechnology*, 85(6), 1629–1642.
- Gomes, A. M. P., Malcata, F. X., Klaver, F. A. M., & Grande, H. J. (1995). Incorporation of *Bifidobacterium* sp. strain Bo and *Lactobacillus acidophilus* strain Ki in a cheese product. *Netherlands Milk and Dairy Journal*, 49, 71–95.
- Graumann, P., Wendrich, T. M., Weber, M. H., Schroder, K., & Marahiel, M. A. (1997). A family of cold shock proteins in *Bacillus subtilis* is essential for cellular growth and for efficient protein synthesis at optimal and low temperatures. *Molecular Microbiology*, 25, 741–756.
- Hamel, F. G. (2009). Preliminary report: inhibition of cellular proteasome activity by free fatty acids. *Metabolism*, 58, 1047–1049.
- Hosseini, N. M., Hussain, M. A., & Britz, M. L. (2015). Stress responses in probiotic *Lactobacillus casei*. *Critical Reviews in Food Science and Nutrition*, 55(6), 740–749.
- Immonen, M., Karjalainen, H., Sirviö, P., & Tanskanen, J. (2008). *Identification and quantification of NSLAB from Finnish Emmental Cheese – Material of conference*. [www.cheese2008.ch](http://www.cheese2008.ch).
- ISO. (2006). *Milk products – Enumeration of presumptive Lactobacillus acidophilus on a selective medium colony-count technique at 37 °C*, ISO 20128. Geneva, Switzerland: International Organization for Standardisation.
- ISO. (2008). *Cheese – Determination of fat content – Van Gulik method*, ISO 3433. Geneva, Switzerland: International Organization for Standardisation.
- ISO. (2011). *Cheese and processed cheese – Determination of the nitrogenous fractions*, ISO 27871. Geneva, Switzerland: International Organization for Standardisation.
- Jordan, K. N., & Cogan, T. M. (1999). Heat resistance of *Lactobacillus* spp. isolated from Cheddar cheese. *Letters in Applied Microbiology*, 29(2), 136–140.
- Karimi, R., Mortazavian, A. M., & Cruz, G. A. (2011). Viability of probiotic microorganisms in cheese during production and storage: a review. *Dairy Science & Technology*, 91(3), 283–308.
- Lahtinen, S. J., Forssten, S., Aakko, J., Granlund, L., Rautonen, N., Salminen, S., et al. (2012). Probiotic cheese containing *Lactobacillus rhamnosus* HN001 and *Lactobacillus acidophilus* NCFM® modifies subpopulations of fecal lactobacilli and *Clostridium difficile* in the elderly. *Age (Dordr)*, 34(1), 133–143.
- Madureira, A. R., Soares, J. C., Pintado, M. E., Gomes, A. M. P., Freitas, A. C., & Malcata, F. X. (2008). Sweet whey cheese matrices inoculated with the probiotic strain *Lactobacillus paracasei* LAFTI® L26. *Dairy Science Technology*, 88, 649–665.
- Markiewicz, L. H., Biedrzycka, E., Wasilewska, E., & Bielecka, M. (2010). Rapid molecular identification and characterisation of *Lactobacillus* strains. *Folia Microbiologica*, 55(5), 481–488.
- Masuda, T., Yamanari, R., & Itoh, T. (2005). The trial for production of fresh cheese incorporated probiotic *Lactobacillus acidophilus* group lactic acid bacteria. *Milchwissenschaft*, 60, 167–171.
- Montanari, C., Sado-Kamdem, S. L., Serrazanetti, D. I., Etoa, F. X., & Guerzoni, M. E. (2010). Synthesis of cyclopropane fatty acids in *Lactobacillus helveticus* and *Lactobacillus sanfranciscensis* and their cellular fatty acids changes following short term acid and cold stresses. *Food Microbiology*, 27, 493–502.
- Özer, B., Kirmaci, H. A., Senel, E., Atamer, M., & Hayaloğlu, A. (2008). Improving the viability of *Bifidobacterium bifidum* BB<sup>12</sup> and *Lactobacillus acidophilus* LA-5 in White-brined cheese by microencapsulation. *International Dairy Journal*, 19, 22–29.
- PN-EN ISO. (2010). *Microbiology of food and animal feeding stuffs – Preparation of test samples, initial suspension and decimal dilutions for microbiological examination – Part 5: Specific rules for the preparation of milk and milk products*. PN-EN ISO 6887-5. PKN. Warsaw, Poland: Polski Komitet Normalizacyjny.
- Rodrigues, D., Rocha-Santos, T. A. P., Gomes, A. M., Goodfellow, B. J., & Freitas, A. C. (2012). Lipolysis in probiotic and symbiotic cheese: the influence of probiotic bacteria, prebiotic compounds and ripening time on free fatty acid profiles. *Food Chemistry*, 131, 1414–1421.
- Rodrigues, D., Rocha-Santos, T. A. P., Pereira, C. I., Gomes, A. M., Malcata, F. X., & Freitas, A. C. (2011). The potential effect of FOS and inulin upon probiotic bacterium performance in curdled milk matrices. *LWT – Food Science and Technology*, 44, 100–108.
- Sharp, M. D., McMahon, D. J., & Roadbent, J. R. (2008). Comparative evaluation of yogurt and low-fat Cheddar cheese as delivery media for probiotic *Lactobacillus casei*. *Journal of Food Science*, 73, 375–377.
- Song, Y., Kato, N., Liu, C., Matsumiya, Y., Kato, H., & Watanabe, K. (2000). Rapid identification of 11 human intestinal *Lactobacillus* species by multiplex PCR assays using groupand species-specific primers derived from the 16S-23S rRNA intergenic spacer region and its flanking 23S rRNA. *FEMS Microbiology Letters*, 187, 167–173.
- Vasiljevic, T., & Shah, N. P. (2008). Probiotics – from Metchnikoff to bioactives. *International Dairy Journal*, 18, 714–728.
- Vinderola, C. G., Mocchiutti, P., & Reinheimer, J. A. (2002). Interactions among lactic acid starter and probiotic bacteria used for fermented dairy products. *Journal of Dairy Science*, 85, 721–729.
- Wang, J., Zhang, H., Chen, X., Chen, Y., Menghebilige, & Bao, Q. (2012). Selection of potential probiotic lactobacilli for cholesterol-lowering properties and their effect on cholesterol metabolism in rats fed a high-lipid diet. *Journal of Dairy Science*, 95, 1645–1654.
- Ward, L. J., & Timmins, M. J. (1999). Differentiation of *Lactobacillus casei* *Lactobacillus paracasei* and *Lactobacillus rhamnosus* by polymerase chain reaction. *Letters in Applied Microbiology*, 29, 90–92.
- Won, S.-R., Hong, M.-J., Kim, Y.-M., Li, C. Y., Kim, J.-W., & Rhee, H.-I. (2007). Oleic acid: an efficient inhibitor of glucosyltransferase. *FEBS Letters*, 581, 4999–5002.
- Zheng, C. J., Yoo, J. S., Lee, T. G., Cho, H. Y., Kim, Y. H., & Kim, W. G. (2005). Fatty acid synthesis is a target for antibacterial activity of unsaturated fatty acids. *FEBS Letters*, 579, 5157–5162.
- Ziarno, M., Zareba, D., & Bzducha-Wróbel, A. (2002). Study on dynamics of microflora growth in probiotic rennet cheese models. *Polish Journal of Food and Nutrition Sciences*, 60(2), 127–131.



## Microbiological and physico-chemical analysis of fermented protein-fortified cassava (*Manihot esculenta* Crantz) flour



Maria U. Rosales-Soto <sup>a</sup>, Peter M. Gray <sup>a</sup>, John K. Fellman <sup>b</sup>, D. Scott Mattinson <sup>b</sup>, Gülhan Ünlü <sup>c</sup>, Kerry Huber <sup>d</sup>, Joseph R. Powers <sup>a,\*</sup>

<sup>a</sup> School of Food Science, Washington State University, Pullman, WA 99164, USA

<sup>b</sup> Department of Horticulture, Washington State University, Pullman, WA 99164, USA

<sup>c</sup> School of Food Science, University of Idaho, Moscow, ID 83844, USA

<sup>d</sup> Department of Animal and Food Science, Brigham Young University-Idaho, Rexburg, ID 83460, USA

### ARTICLE INFO

#### Article history:

Received 19 May 2015

Received in revised form

3 September 2015

Accepted 20 October 2015

Available online 23 October 2015

#### Keywords:

Cassava

Fufu

Biofortification

*Lactobacillus plantarum*

Volatiles

### ABSTRACT

*Lactobacillus plantarum* strain 6710 was used as the starter for wet fufu using protein (zeolin, sporazein, sporazein plus pro-vitamin A) and pro-vitamin A-fortified and wild-type cassava flours that were fermented with or without the addition of starter culture. Lactic acid bacteria count of the non-inoculated and inoculated wild type flours increased 4 and 1 log units in 24 h, respectively. The added strain rapidly increased titratable acidity when using wild-type cassava from 0.24 to 0.96% lactic acid at 24 h and 1.18% at 96 h. Titratable acidity also increased with sporazein, sporazein plus pro-vitamin A, and pro-vitamin A samples. A similar aroma profile was found in all samples suggesting that protein fortification does not have a detrimental effect on the aroma of fufu. This study showed that use of *L. plantarum* is feasible for production of wet fufu from protein-fortified cassava making the increased consumption of a nutritious product possible.

© 2015 Elsevier Ltd. All rights reserved.

### 1. Introduction

Cassava (*Manihot esculenta* Crantz) is a major source of calories in under-developed countries such as Ghana and Nigeria (Nweke, 2004) and ranks sixth in overall global crop production. However, a cassava-based diet does not provide complete nutrition. Cassava is cultivated mainly for its edible storage root, which contains 85% starch and only 1–2% protein (Han et al., 2001; Sheffield, Taylor, Fauquet, & Chen, 2006).

Another limitation of cassava is the potential toxicity of cassava roots due to the accumulation of the cyanogenic glycosides linamarin and lotaustralin. In Africa, improperly processed cassava is a major problem associated with cyanide-related health disorders (Maziya-Dixon, Dixon, & Adebowale, 2007). Numerous cassava processing methods have been devised, including fermentation followed by drying or roasting, to reduce toxicity while converting the highly perishable cassava into stable products (Vasconcelos, Twiddy, Westby, & Reilly, 1990).

Fufu is a fermented wet paste product, usually consumed in many parts of West Africa. For the production of fufu, cassava roots are peeled, washed, cut into pieces and submerged in water at room temperature for 5 days, but it has been found that local processors ferment cassava for different lengths of time (Oyewole & Ogundele, 2001; Ray & Sivakumar, 2009). Cassava roots release hydrogen cyanide into the soak water, reducing the pH and imparting the characteristic flavor of the retted cassava meal. Fufu is sold to consumers in wet or cooked form (Ray & Sivakumar, 2009).

Species of lactic acid bacteria (LAB) belonging to the genera *Lactobacillus*, *Leuconostoc* and *Streptococcus* are the predominant microorganisms in fufu (Ray & Sivakumar, 2009). In Africa, most food fermentations are done at the household level, and are conducted as spontaneous processes taking a relatively long time that can result in spoilage and survival of pathogens. Thus, the use of starter cultures is recommended, as rapid acidification of the product can inhibit growth of undesirable bacteria.

*Lactobacillus plantarum* has been found to have the highest acid producing ability in cassava tubers (Kostinek et al., 2007), therefore, a strain of this species was used in an attempt to reduce fermentation time that may cause the production of unacceptable aroma compounds. While traditional fufu processing involves the

\* Corresponding author.

E-mail address: [powersjr@cahnrs.wsu.edu](mailto:powersjr@cahnrs.wsu.edu) (J.R. Powers).

utilization of cassava roots, this study proposes the use of cassava flour as starting material.

Specifically, this study was undertaken to evaluate the microbiological and physico-chemical characteristics of *L. plantarum* 6710 on the course of fermentation of protein – and pro-vitamin A-fortified cassava flours in comparison to wild type flour, and their suitability to produce wet fufu.

## 2. Materials and methods

### 2.1. Cassava flours

Protein-fortified cassava flours (zeolin (Z), sporazein (S), sporazein plus pro-vitamin A (SPRO)), pro-vitamin A-fortified (PRO) and wild-type cassava (WT) flours were provided by the International Laboratory for Tropical Agricultural Biotechnology (ILTAB) (St. Louis, MO).

### 2.2. Microbiological assessment

#### 2.2.1. Microorganisms and growth conditions

*L. plantarum* BFE 6710 provided by the Max Rubner-Institut (Germany) was grown from a stab culture in Lactobacillus de Man, Rogosa and Sharpe (MRS) broth at 32 °C for 24 h under aerobic conditions. Cultures were placed in cryogenic vials with 50% glycerol (1.5:1 ratio) and stored at –72 °C. Working cultures were obtained by streaking stock culture on MRS agar, incubated at 32 °C for 48 h and a single colony transferred into MRS broth and incubated under the same conditions. The broth culture was centrifuged at 8000× g at 4 °C for 10 min. The pellet was washed twice with sterile buffered peptone water (BPW), centrifuged as noted above and resuspended in 9 mL of BPW resulting in  $7 \times 10^{10}$  CFU/mL.

#### 2.2.2. Growth of starter culture in cassava flour

All wild-type and fortified cassava flours were stored in sealed plastic containers at 4 °C. Ninety g of cassava flour samples were transferred to sterilized plastic containers. Initial inoculation by *L. plantarum* was done by transferring a cell pellet suspension of  $7 \times 10^{10}$  CFU/mL into cassava flour. Moisture content of cassava flours was adjusted to 68% with sterile water. A second set of control (non-inoculated) flours was also prepared. Non-inoculated (NF) and inoculated (LF) cassava flour samples were covered and incubated at 32 °C for 96 h.

#### 2.2.3. Monitoring lactic acid bacteria (LAB) growth

Cassava samples were removed at 0, 24, 48, 72 and 96 h of incubation and assessed as follows: 5 g sample was placed in 80-mL sterile stomacher bag and homogenized for 2 min with 45 mL of sterile BPW. One hundred  $\mu$ L of appropriate ten-fold serial dilutions of samples prepared in 0.2% peptone water were duplicate spread-plated on MRS agar for enumeration of LAB after incubation at 32 °C for 48 h.

### 2.3. Physico-chemical analyses

Fermented cassava flours (wet fufu) were removed at pre-determined incubation times and kept at –70 °C for 7 days until evaluation.

#### 2.3.1. Chemical composition

Moisture and ash of cassava flours was determined by the air oven method 925.10 and the direct method 923.03, respectively (AOAC, 2000). Soluble protein was determined in wet fufu. Samples were extracted with 100 mM Tris–HCl, pH 7.8, 200 mM NaCl, 1 mM

EDTA, 0.2% Triton X-100 with 4% 2-mercaptoethanol in a ratio of 0.1:1 (wet fufu:solvent). The homogenate was vortexed for 5 min at 2500 rpm and centrifuged at 1500× g for 10 min at 4 °C. The supernatant was analyzed by the Bradford method (CBX kit) (G-Biosciences, St. Louis, MO) according to the manufacturer's protocol. A calibration curve was constructed with bovine serum albumin. Total nitrogen content of cassava flours was determined by Approved Method 46-30.01 (AACC, 2010) with a LECO Instrument FP-528 nitrogen analyzer. Total starch of cassava flours was determined by the total starch assay procedure (amyloglucosidase/ $\alpha$ -amylase) K-TSTA (Megazyme International Ltd., Wicklow, Ireland).

#### 2.3.2. pH and titratable acidity (TA)

Modified methods 943.02, sec. 32.1.20 and 942.15, sec. 37.1.37B were used for determination of pH and titratable acidity, respectively (AOAC, 2000).

#### 2.3.3. Pasting properties

Cassava flour starch pasting properties were measured with the Newport Scientific Pty Rapid Visco Analyzer (RVA) interfaced with a personal computer equipped with Thermocline software for Windows 2.1 according to the AACC Approved Method 76-21.01 (AACC, 2000). The samples were analyzed by transferring 3.5 g (14% moisture basis) flour with 25 mL of water into an RVA canister, held at 50 °C for 1 min, heated from 50 to 95 °C in 4.42 min, held at 95 °C for 2.7 min, cooled to 50 °C in 3.82 min, and held at 50 °C for 1.06 min.

#### 2.3.4. Color evaluation

A Minolta colorimeter CM-2002 was calibrated using its white standard calibration cover. The cassava flour was placed in a plastic petri dish, slightly shaken to form a layer of 5 mm thickness, covered with the Petri dish lid and the color read on the meter. The L, a\* and b\* values were recorded and averages computed from two randomly selected points.

#### 2.3.5. Volatile analysis

An optimized method of Iyer, Mattinson, and Fellman (2010) was used. A slurry sample of wet fufu at all fermentation times (0.5 g), sodium chloride (0.98 g) and distilled water (3.0 mL) was prepared in a 10 mL headspace amber vial. Automation of the procedure was achieved using a CTC CombiPal autosampler and programmed using CycleComposer software (A.01.04). A SPME stableflex fiber coated with 65  $\mu$ m polydimethylsiloxane/divinylbenzene was conditioned for 1 h at 270 °C. The sample was stirred at 250 rpm, the fiber was exposed to the headspace of the slurry and volatile compounds were collected for 60 min.

The volatiles were thermally desorbed into the injection port of a gas chromatograph equipped with a 6890N GC split/splitless injector and a HP-5MS column (30 m × 0.248 mm × 0.25  $\mu$ m film thickness). Data were collected using Chemstation software (E.02.00.493). Helium was the carrier gas. The injector and detector temperatures were 200 °C and 250 °C, respectively. The column temperature was initially at 33 °C for 5 min before increasing to 50 °C at a rate of 2 °C/min, then to 225 °C at a rate of 5 °C/min. The sample was desorbed for 5 min in the splitless mode. Wet fufu volatile compounds were identified using a mass spectrometer MS 5975C and the MS spectra were compared against a NIST library. The quantitative data were determined by running standards and developing response factors based on water matrices. The data were reported as  $\mu$ g/mL.

### 2.4. Data analysis

Cassava flour physico-chemical data were analyzed for

significant differences using a one-way analysis of variance (ANOVA). Wet fufu physico-chemical data were analyzed using a three-way ANOVA. Tukey's HSD multiple comparisons of means were used to analyze both cassava flour and wet fufu data with XLSTAT (7.5.3) at the  $p \leq 0.05$  confidence level. The ANOVA performed on wet fufu used sample, fermentation and fermentation time as fixed effects. All tests were performed in duplicate.

### 3. Results and discussion

#### 3.1. Chemical composition

Moisture, ash, nitrogen, protein and starch were expressed on a wet weight basis. Pro-vitamin A-fortified cassava sample showed the greatest moisture ( $9.15 \pm 0.06\%$ ) and ash content ( $4.86 \pm 0.15\%$ ). No significant difference in ash content was found between WT and Z ( $p > 0.05$ ). Z had the greatest nitrogen content ( $1.28 \pm 0.09\%$ ) and the greatest soluble protein concentration ( $9.52 \pm 0.007\%$ ). No significant differences were observed among soluble protein contents of WT, SPRO and PRO fortified flours with values of  $1.41 \pm 0.001\%$ ,  $3.63 \pm 0.003\%$  and  $2.14 \pm 0.004\%$ , respectively ( $p > 0.05$ ).

While we expected high protein flours to have reduced starch contents, there were no significant differences between the WT ( $55.83 \pm 3.71\%$ ) and S ( $63.31 \pm 2.91\%$ ) samples ( $p > 0.05$ ). Also, no significant differences in starch content were found among WT, Z, SPRO and PRO cassava flours with values of  $55.83 \pm 3.71\%$ ,  $63.31 \pm 2.91\%$ ,  $50.98 \pm 1.57\%$  and  $51.56 \pm 2.55\%$ , respectively. There are several factors that influence cassava starch content such as variety, growth conditions and harvest time (Santisopasri et al. 2001).

Through the fermentation process a reduction of the soluble protein content was observed for each cassava sample (Table 1). No significant differences were observed in protein content as a function of addition of the starter culture at all fermentation times ( $p > 0.05$ ). Protein content of all fermented cassava flours decreased more than 60% after 96 h incubation. NF PRO showed the greatest reduction (78%) at 96 h fermentation. Protein content of NFWT decreased from 0.25% at the beginning of fermentation to 0.09% at 96 h. Ahaotu, Ogueke, Owuamanam, Ahaotu, and Nwosu (2011) found an increase in protein content during gari production. The cassava fermented with mixed fungi showed the greatest final amount in protein. The increased crude protein is associated with the ability of the organism to produce protein during the fermentation. Hence, the low protein content observed during fermentation was possibly due to a non-efficient utilization of the

**Table 1**

Soluble protein content (%) of fermented cassava flours with (LF) and without (NF) the addition of a starter culture during fermentation based on 100% soluble protein content at 0 h fermentation.

Cassava material <sup>a</sup>		Fermentation time (h)				
		0	24	48	72	96
NF	WT	100	56	48	44	36
	Z	100	77	38	27	23
	S	100	64	33	33	24
	SPRO	100	53	33	38	40
	PRO	100	57	41	32	22
LF	WT	100	48	52	61	35
	Z	100	52	48	32	32
	S	100	83	30	27	37
	SPRO	100	41	31	28	23
	PRO	100	68	61	29	26

<sup>a</sup> Wild-type (WT), zeolin (Z), sporazein (S), sporazein plus pro-vitamin A (SPRO) and pro-vitamin A (PRO) cassava flours.

carbohydrates in the cassava flours.

According to Westby and Twiddy (1992), LAB showed only a weak ability to hydrolyze starch during fufu processing. LAB are in general not amylolytic. According to Kostinek et al. (2005), none of the predominant LAB isolated from fermented cassava showed  $\alpha$ -amylase activity. Since cassava generally contains about 84% carbohydrates as starch, a potential energy source for LAB, this is surprising (Kostinek et al., 2007).

Table 2 shows the pH and titratable acidity (TA) of the non fermented cassava flours. All samples had a pH value between 6.31 and 6.72 with S having the greatest value. SPRO showed the greatest TA value (0.73% lactic acid). Table 3 shows the pH data of the NF and LF cassava flours at all fermentation times. The fermentation resulted in a decrease of pH and increase of acidity in the cassava mash. LF samples had the greatest values of TA (data not shown).

The Z sample showed a decrease of pH from 6.02 (0 h) to 3.25 at 96 h for NF and from 5.15 (0 h) to 3.28 (96 h) for LF (Table 3). A similar trend was observed in all samples. The lowest pH was reached at 72 h of fermentation in LF samples. These results agree with Brauman, Keleke, Malonga, Miambi, and Ampe (1996), who pointed out that LAB produced high amounts of lactic acid, leading to a rapid drop in pH to around 4.5. The environment is then selective against acid-sensitive microorganisms.

A similar pattern was observed for TA where most samples reached a maximum value at 72 h of fermentation. This increase can be attributed to the activities of the LAB on the carbohydrates of the cassava flours (Fayemi & Ojokoh, 2014). When *L. plantarum* starter culture was added, the decrease of pH and increase of TA was large after 24 h, when compared with no addition of starter. This agrees with Kostinek et al. (2005) findings who determined a high capability of the obligate homo- and facultative heterofermentative group (mostly *L. plantarum*) of lowering the pH of the medium. Acid production and the subsequent decrease in pH extends the lag phase of acid-sensitive organisms, including food-borne pathogens (Kostinek et al., 2007).

The addition of *L. plantarum* BFE 6710, rapidly decreased the pH at 24 h of fermentation (Table 3). Edward et al. (2011) determined that spontaneous fermentations generally take 96 h to obtain desired characteristics such as pH and sensory traits while there is the risk that spoilage microorganisms will outgrow desirable microorganisms. Therefore, adding starter culture notably reduces fermentation times, demonstrated here by a fast decrease in pH, and noticeable increase in acidity when compared to samples at 0 h of fermentation. This helps reduce the risk of growth of undesirable microorganisms and contributes to control over aroma, texture and flavor of the final cassava product.

Consideration must be taken in selection of the specific LAB strains to use as starter cultures. Some LAB strains associated with fermented foods degrade antinutritional factors, such as phytic acid

**Table 2**

pH and titratable acidity of cassava flours.<sup>a</sup>

Cassava material <sup>b</sup>	pH	Titratable acidity (% <sup>c</sup> )
WT	$6.60 \pm 0.03^b$	$0.37 \pm 0.01^d$
Z	$6.61 \pm 0.06^b$	$0.48 \pm 0.00^c$
S	$6.72 \pm 0.03^a$	$0.49 \pm 0.00^c$
SPRO	$6.31 \pm 0.02^c$	$0.73 \pm 0.01^a$
PRO	$6.32 \pm 0.03^c$	$0.66 \pm 0.02^b$

<sup>a</sup> Results are reported as the mean of two determinations  $\pm$  standard deviation. Means containing different letters within the same column are significantly different ( $p \leq 0.05$ ).

<sup>b</sup> Wild-type (WT), zeolin (Z), sporazein (S), sporazein plus pro-vitamin A (SPRO) and pro-vitamin A (PRO) cassava flours.

<sup>c</sup> Titratable acidity (TA) results are expressed as % lactic acid.

**Table 3**  
pH<sup>a</sup> of fermented cassava flours with (LF) and without (NF) the addition of a starter culture during fermentation.

Cassava material <sup>b</sup>		Fermentation time (h)				
		0	24	48	72	96
LF	WT	5.15 ± 0.00 <sup>Acd</sup>	3.48 ± 0.04 <sup>Bf</sup>	3.36 ± 0.00 <sup>Cf</sup>	3.07 ± 0.02 <sup>Ef</sup>	3.16 ± 0.01 <sup>Df</sup>
	Z	5.15 ± 0.01 <sup>Acd</sup>	3.61 ± 0.03 <sup>Be</sup>	3.29 ± 0.01 <sup>Cf</sup>	3.13 ± 0.01 <sup>Def</sup>	3.28 ± 0.01 <sup>Cde</sup>
	S	4.78 ± 0.03 <sup>Ae</sup>	3.71 ± 0.04 <sup>Bde</sup>	3.55 ± 0.08 <sup>Be</sup>	3.27 ± 0.01 <sup>Cd</sup>	3.33 ± 0.01 <sup>Cd</sup>
	SPRO	4.98 ± 0.03 <sup>Ad</sup>	3.79 ± 0.03 <sup>Bd</sup>	3.72 ± 0.01 <sup>Bd</sup>	3.53 ± 0.01 <sup>Cc</sup>	3.72 ± 0.02 <sup>Bbc</sup>
	PRO	5.30 ± 0.10 <sup>Ac</sup>	4.05 ± 0.01 <sup>Bc</sup>	3.91 ± 0.01 <sup>Bc</sup>	3.69 ± 0.00 <sup>Cb</sup>	3.64 ± 0.01 <sup>Cc</sup>
NF	WT	6.03 ± 0.00 <sup>Aa</sup>	4.14 ± 0.06 <sup>Bc</sup>	3.61 ± 0.00 <sup>Cde</sup>	3.16 ± 0.06 <sup>De</sup>	3.18 ± 0.07 <sup>Def</sup>
	Z	6.02 ± 0.01 <sup>Aa</sup>	4.57 ± 0.04 <sup>Ba</sup>	3.56 ± 0.00 <sup>Ce</sup>	3.36 ± 0.01 <sup>Dd</sup>	3.35 ± 0.00 <sup>Dd</sup>
	S	6.04 ± 0.09 <sup>Aa</sup>	4.44 ± 0.01 <sup>Bb</sup>	4.41 ± 0.01 <sup>Ba</sup>	4.11 ± 0.00 <sup>Ca</sup>	3.76 ± 0.02 <sup>Db</sup>
	SPRO	5.86 ± 0.06 <sup>Aab</sup>	4.55 ± 0.01 <sup>Bab</sup>	4.47 ± 0.01 <sup>Ba</sup>	4.11 ± 0.01 <sup>Ca</sup>	4.05 ± 0.01 <sup>Ca</sup>
	PRO	5.67 ± 0.01 <sup>Ab</sup>	4.63 ± 0.00 <sup>Ba</sup>	4.13 ± 0.04 <sup>Cb</sup>	3.76 ± 0.00 <sup>Db</sup>	3.66 ± 0.01 <sup>Ec</sup>

<sup>a</sup> Results are reported as the mean of three determinations ± standard deviation. Means within the same column containing different lowercase letters are significantly different ( $p \leq 0.05$ ). Means within the same row containing different uppercase letters are significantly different ( $p \leq 0.05$ ).

<sup>b</sup> Wild-type (WT), zeolin (Z), sporazein (S), sporazein plus pro-vitamin A (SPRO) and pro-vitamin A (PRO) cassava flours.

to inositol and phosphoric acid and thereby reducing its metal chelating capacity (Chen, Li, Vadlani, Madl, & Wang, 2013; Holzapfel, 2002). Incorporation of these microorganisms may help increase the nutritional value of foods. In addition, selected strains may enhance the general benefits of spontaneous fermentation such as improved protein digestibility and micronutrient bioavailability, and contribute to biological enrichment through the biosynthesis of vitamins and essential amino acids.

### 3.2. Microbial counts

A background microbial population of presumptive, indigenous LAB in non-inoculated (0 h) NFWT, NF SPRO and NF PRO samples of  $1.55 \times 10^5$ ,  $6.47 \times 10^4$  and  $9.63 \times 10^5$  CFU/g, respectively, was revealed. Brauman et al. (1996) determined that LAB accounted for more than 99% of the total microflora during cassava root fermentation. Variations of cell numbers are evident in non-inoculated and inoculated samples (i.e. NF PRO,  $1.98 \times 10^9$  and LF PRO,  $6.41 \times 10^9$ ) at 24 h fermentation. The NFZ and NFS sample counts increased 9 log in 24 h, while those of LFZ and LFS increased 1 log unit. Through the fermentation process, a greater variation was observed in the LF cassava samples after 24 h compared to NF samples. *L. plantarum* (homofermenting population), as facultatively anaerobic LAB, could proliferate from the onset of retting, when oxygen was still present in the medium, and due to their great growth rates on the fermentable sugars present (sucrose, glucose and fructose), could overcome other flora.

### 3.3. Pasting properties

Fermented cassava is usually cooked into paste before consumption. The pasting properties become important in predicting the behavior of cassava flour during and after cooking. When starch-based foods are heated in water beyond a critical temperature, the granules absorb a large amount of water and swell to many times their original size. Over a critical temperature, the starch undergoes an irreversible process known as gelatinization. When the temperature rises above the gelatinization temperature, the starch granules begin to swell and viscosity increases. The temperature at the onset of this rise in viscosity is referred to as the pasting temperature. There were significant differences in the pasting temperature among the cassava flours ( $p \leq 0.05$ ) (Table 4) that ranged from 80.23 to 90.4 °C, with WT showing the greatest value. No significant differences were found between SPRO and PRO flours ( $p > 0.05$ ). The differences in pasting temperature of cassava flour might be attributed to diverse cassava genotypes, high fiber content or other non-starch components in the flours. The

presence of neutral and water soluble substances contribute to increased starch pasting temperature (Shittu & Adedokun, 2010). In addition, low pasting temperatures such as that found for Z (80.23 °C) may be due to the partial gelatinization of starch granules during roasting while making the flour. The pasting temperatures determined that all flours can form a paste in hot water below boiling point which is translated to cost savings (Adebowale, Sanni, & Onitilo, 2008).

The trough viscosity ranged from 120 to 157.44 RVU with the lowest values obtained for S and SPRO samples. Significant differences were found for peak viscosity, breakdown viscosity and setback viscosity ( $p \leq 0.05$ ). The values for peak viscosity indicative of the strength of pastes (Aloys & Zhou, 2006) ranged from 305.78 to 471.22 RVU. Thus, WT cassava flour with the smallest peak viscosity may be the most easily handled during cooking followed by the SPRO sample. The peak viscosity values were lower compared to values found for dried fufu flour by Adebowale, Sanni, and Awonorin (2005) due to partial gelatinization of the cassava flours. The breakdown viscosity recorded for Z (313.78 RVU) was higher than WT (153.31). Thus, WT showed a greater ability to withstand breakdown during cooling followed by SPRO (222.83 RVU), an important factor for many processes that require stable paste and low retrogradation/syneresis. The greatest setback viscosity was found in the PRO sample (127.92 RVU) which means that PRO had the greatest tendency to retrograde and produce a more consistent dough after cooling (Table 4). As mentioned by Maziya-Dixon et al. (2007), a high setback is also associated with syneresis or weeping during freeze/thaw cycles. Therefore, SPRO cassava flour offered pasting characteristics near to those found for WT that will help obtain a characteristic final fufu product.

### 3.4. Color evaluation

Color was influenced by flour fortification. Cassava flour lightness ( $L^*$ ), greenness to redness ( $a^*$ ) and blueness to yellowness ( $b^*$ ) ranged from 88.01 to 91.17,  $-0.46$  to  $0.44$ , and  $8.06$  to  $15.80$ , respectively (Table 5). Cassava flours differed significantly in terms of  $L^*$  and  $a^*$  ( $p \leq 0.05$ ). However, significant differences were not found for lightness between Z and S samples. Regarding  $a^*$ , only SPRO and PRO showed low positive values indicating red on the hue axis, whereas the other cassava flours had negative  $a^*$  values (green on hue axis). All samples had positive  $b^*$  values (yellow on hue axis). The  $b^*$  values for WT and Z samples did not significantly differ ( $p > 0.05$ ). SPRO sample showed the greatest  $b^*$  value (15.80) due to the yellow color provided by the pro-vitamin A fortification followed by PRO (15.13).

Concerning color differences with respect to the WT flour, SPRO

**Table 4**  
Pasting properties<sup>a</sup> of cassava flours.

Cassava material <sup>b</sup>	Peak viscosity (RVU)	Trough (RVU)	Breakdown viscosity (RVU)	Final viscosity (RVU)	Setback viscosity (RVU)	Peak time (min)	Pasting temperature (°C)
WT	305.78 ± 1.13 <sup>e</sup>	152.47 ± 1.09 <sup>b</sup>	153.31 ± 0.24 <sup>e</sup>	268.53 ± 3.61 <sup>ab</sup>	116.06 ± 3.81 <sup>b</sup>	4.24 ± 0.08 <sup>a</sup>	90.40 ± 0.74 <sup>a</sup>
Z	471.22 ± 2.08 <sup>a</sup>	157.44 ± 1.55 <sup>a</sup>	313.78 ± 3.13 <sup>a</sup>	263.86 ± 0.83 <sup>b</sup>	106.42 ± 2.32 <sup>c</sup>	3.18 ± 0.04 <sup>d</sup>	80.23 ± 0.42 <sup>d</sup>
S	413.19 ± 1.34 <sup>b</sup>	120.00 ± 0.90 <sup>d</sup>	293.19 ± 1.88 <sup>b</sup>	194.50 ± 1.71 <sup>d</sup>	74.50 ± 1.73 <sup>e</sup>	3.62 ± 0.04 <sup>c</sup>	84.50 ± 0.39 <sup>c</sup>
SPRO	344.94 ± 4.44 <sup>d</sup>	122.11 ± 0.05 <sup>d</sup>	222.83 ± 4.39 <sup>d</sup>	212.11 ± 2.48 <sup>c</sup>	90.00 ± 2.44 <sup>d</sup>	3.93 ± 0.07 <sup>b</sup>	87.48 ± 0.60 <sup>b</sup>
PRO	389.64 ± 2.88 <sup>c</sup>	142.03 ± 2.01 <sup>c</sup>	247.61 ± 0.91 <sup>c</sup>	269.94 ± 1.05 <sup>a</sup>	127.92 ± 1.02 <sup>a</sup>	3.80 ± 0.00 <sup>b</sup>	86.20 ± 0.05 <sup>b</sup>

<sup>a</sup> Results are reported as the mean of three determinations ± standard deviation. Means containing different letters within the same column are significantly different ( $p \leq 0.05$ ).

<sup>b</sup> Wild-type (WT), zeolin (Z), sporazein (S), sporazein plus pro-vitamin A (SPRO) and pro-vitamin A (PRO) cassava flours.

**Table 5**  
Color<sup>a</sup> determination of cassava flours.

Cassava material <sup>b</sup>	L*	a*	b*	ΔE
WT <sup>c</sup>	91.17 ± 0.10 <sup>a</sup>	-0.33 ± 0.02 <sup>d</sup>	8.22 ± 0.18 <sup>d</sup>	–
Z	90.10 ± 0.08 <sup>b</sup>	-0.09 ± 0.01 <sup>c</sup>	8.06 ± 0.06 <sup>d</sup>	1.12 ± 0.11 <sup>c</sup>
S	90.32 ± 0.03 <sup>b</sup>	-0.46 ± 0.03 <sup>e</sup>	9.71 ± 0.18 <sup>c</sup>	1.73 ± 0.10 <sup>c</sup>
SPRO	88.01 ± 0.21 <sup>d</sup>	0.33 ± 0.01 <sup>b</sup>	15.80 ± 0.13 <sup>a</sup>	8.24 ± 0.26 <sup>a</sup>
PRO	88.94 ± 0.29 <sup>c</sup>	0.44 ± 0.04 <sup>a</sup>	15.13 ± 0.17 <sup>b</sup>	7.31 ± 0.44 <sup>b</sup>

<sup>a</sup> Results are reported as the mean of three determinations ± standard deviation. Means containing different letters within the same column are significantly different ( $p \leq 0.05$ ).

<sup>b</sup> Wild-type (WT), zeolin (Z), sporazein (S), sporazein plus pro-vitamin A (SPRO) and pro-vitamin A (PRO) cassava flours.

<sup>c</sup> Wild-type (WT): Reference used for computing ΔE.

showed the largest ΔE value of 8.24 and can be attributed to the pro-vitamin A fortification as cited above. However the Z flour recorded the least color difference (1.12) (Table 5) that showed a very white sample. These data suggest that the color of cassava flours can be an important quality parameter, which has a direct influence on the acceptability of the developed product that could be further tested with a consumer sensory study. Color may contribute to the depreciation of the commercial value of the final product (Aloys & Zhou, 2006).

### 3.5. Volatile compounds

The volatiles detected and quantified in cassava samples at all fermentation times varied in number and it is reasonable to presume that are direct or indirect results of the metabolic activities of microorganisms or from chemical reactions (Aloys, 2012). The majority of the compounds identified were alcohols (1-hexanol, 1-pentanol, 1-heptanol and 1-octanol). In addition, one volatile acid (acetic acid), one aldehyde (hexanal) and two ketones (2-

propanone and 2-butanone) were identified and quantified. Most of the compounds detected tended to increase at 24 h of fermentation and new compounds were formed due to the fermentation process.

The number of compounds varied depending on the cassava sample, addition of the starter culture and fermentation time. The only compound found in all samples was 2-propanone. Levels of 2-propanone in all NF samples at 0 h fermentation were below the published odor detection threshold value of 40.9 μg/mL (Stahl, 1973). At 0 h fermentation, 2-propanone was above the published threshold value in the LFWT sample. No 2-butanone was observed in the NFS sample from 0 to 48 h and 1-hexanol was found in all samples from 24 to 72 h of fermentation.

Production of acetic acid was observed at 0 h of fermentation only in the NFS and LFS samples (Table 6). Acetic acid, which imparted the characteristic odor and taste to the fermented product, was detected in all wet fufu samples from 24 to 96 h fermentation with concentrations above the threshold value of 24.3 μg/mL (Stahl, 1973) suggesting that the concentration of the acetic acid was greatly altered by the fermentation time. As cited by Chaves-López et al. (2014), during fermented cassava sour starch processing the pH of cassava starch decreases below 4, with variations depending on the fermentation type and manufacturing conditions. The microbiota present in the fermenting medium converts starch and sugars into organic acids. Most organic acids such as malic, tartaric, and acetic acids can be metabolized by *L. plantarum* resulting in the production of carbon dioxide, lactic acid and acetic acid (Todorov & Franco, 2010). Also, *L. plantarum* can produce diacetyl, acetone and carbon dioxide when grown in complex media. The presence of carbohydrates may also contribute to other reactions, as sucrose can also be used as a substrate for the formation of polysaccharides.

Contrary to the findings of Iyer et al. (2010), no compounds related to linamarin hydrolysis during the first step of cyanogenesis

**Table 6**  
Volatile compounds<sup>a</sup> detected in fermented cassava flours with (LF) and without (NF) the addition of a starter culture at 0 h of fermentation.

Cassava material <sup>b</sup>	Volatile compound concentration (μg/mL)									
	2-propanone	2-butanone	Acetic acid	Hexanal	Nonanal	Decanal	1-hexanol	2-decanol	1-octanol	1-heptanol
LF	WT	43.11 <sup>a</sup>	3.75 <sup>a</sup>	nd	0.022 <sup>b</sup>	0.006 <sup>c</sup>	nd	0.049 <sup>bc</sup>	nd	nd
	Z	7.71 <sup>b</sup>	1.11 <sup>b</sup>	nd	nd	nd	nd	nd	nd	nd
	S	40.16 <sup>ab</sup>	2.05 <sup>b</sup>	68.92 <sup>a</sup>	0.022 <sup>b</sup>	nd	nd	0.106 <sup>ab</sup>	nd	nd
	SPRO	27.68 <sup>ab</sup>	1.88 <sup>b</sup>	nd	0.043 <sup>b</sup>	0.008 <sup>c</sup>	nd	0.188 <sup>a</sup>	0.016 <sup>a</sup>	0.008 <sup>a</sup>
	PRO	10.70 <sup>ab</sup>	1.15 <sup>b</sup>	nd	0.120 <sup>b</sup>	0.031 <sup>b</sup>	nd	nd	0.017 <sup>a</sup>	nd
NF	WT	11.87 <sup>ab</sup>	1.28 <sup>b</sup>	nd	0.042 <sup>b</sup>	0.018 <sup>bc</sup>	0.004 <sup>a</sup>	nd	nd	nd
	Z	11.08 <sup>ab</sup>	1.07 <sup>b</sup>	nd	0.009 <sup>b</sup>	nd	nd	nd	nd	nd
	S	25.43 <sup>ab</sup>	nd	172.03 <sup>a</sup>	0.035 <sup>b</sup>	nd	nd	0.024 <sup>bc</sup>	nd	nd
	SPRO	16.30 <sup>ab</sup>	1.51 <sup>b</sup>	nd	0.099 <sup>b</sup>	0.011 <sup>bc</sup>	nd	nd	0.017 <sup>a</sup>	nd
	PRO	22.38 <sup>ab</sup>	1.65 <sup>b</sup>	nd	0.491 <sup>a</sup>	0.068 <sup>a</sup>	0.003 <sup>a</sup>	nd	0.016 <sup>a</sup>	0.011 <sup>a</sup>

nd: Not detectable.

<sup>a</sup> Results are reported as the mean of two determinations. Means containing different letters within the same column are significantly different ( $p \leq 0.05$ ).

<sup>b</sup> Wild-type (WT), zeolin (Z), sporazein (S), sporazein plus pro-vitamin A (SPRO) and pro-vitamin A (PRO) cassava flours.

were identified. As occurred in other cassava fermented products studied by Aloys (2012), the alcohols may originate from a chemical degradation of hydroperoxides of unsaturated fatty acids or from the microbial activity. Regarding the ketones, the operating biosynthetic pathway which leads to ketone formation seems to be via  $\beta$ -oxidative shortening of fatty acids followed by reduction of the carbonyl functional group on C4–C12 carboxylic acids (Iyer et al., 2010). According to Lauble, Miehlich, Förster, Wajant, and Effenberger (2001), the formation of 2-propanone and 2-butanone can be attributed to hydroxynitrile lyase (HNL) activity in cassava.

Fortified samples were found to be similar to wild-type cassava flour with respect to qualitative volatile composition. LFWT showed the greatest amount of acetic acid production (759.21  $\mu\text{g/mL}$ ) followed by the NFWT (324.07  $\mu\text{g/mL}$ ) and NF PRO (318.95  $\mu\text{g/mL}$ ) at 72 h, but no significant differences were found for the acetic acid concentrations among those samples ( $p > 0.05$ ). As reported by Fagbemi and Ijah (2006), an acidic odor decreases the product acceptability that should be further studied by a consumer sensory panel. A less strong aroma due to low production of acids, such as acetic acid, could be an advantage of using protein and pro-vitamin A-fortified cassava flours in fermented products.

In conclusion, protein or pro-Vitamin A-fortified cassava flours, with or without the addition of *L. plantarum* strain 6710, are suitable for fermentation to produce wet fufu. Fermentation of cassava flours with addition of *L. plantarum* is recommended due to the decrease in pH in less fermentation time (24 h). Among the cassava flours, SPRO showed similar pasting properties to the WT sample that may be a positive factor when processing cooked fufu product. Fortified cassava flours did not influence microbial growth during fermentation. Further research should include identification of the microbial flora of the initial material that may have an impact on the fermentation process and characteristics of the final product, and the consumer sensory evaluation of a cooked fufu product.

## References

- Adebowale, A. A., Sanni, L. O., & Awonorin, S. O. (2005). Effect of texture modifiers on the physicochemical and sensory properties of dried fufu. *Food Science and Technology International*, 11(5), 373–382.
- Adebowale, A. A., Sanni, L. O., & Onitilo, O. M. (2008). Chemical composition and pasting properties of tapioca grits from different cassava varieties and roasting methods. *African Journal of Food Science*, 2, 77–82.
- Ahaotu, I., Ogueke, C. C., Owuamanam, C. I., Ahaotu, N. N., & Nwosu, J. N. (2011). Protein improvement in gari by the use of pure cultures of microorganisms involved in the natural fermentation process. *Pakistan Journal of Biological Sciences*, 14, 933–938.
- Aloys, N. (2012). Volatile compounds in Ikivunde and Inyange, two Burundian cassava products. *Global Advanced Research Journal of Food Science and Technology*, 1(1), 1–7.
- Aloys, N., & Zhou, H. M. (2006). Functional and chemical properties of Ikivunde and Inyange, two traditionally processed burundian cassava flours. *Journal of Food Biochemistry*, 30(4), 429–443.
- American Association of Cereal Chemists (AACC). (2000). *Approved methods of analysis* (10th ed.). Saint Paul, MN: AACC.
- American Association of Cereal Chemists (AACC). (2010). *Approved methods of analysis* (11th ed.). Saint Paul, MN: AACC.
- Association of Official Analytical Chemists (AOAC). (2000). *Official methods of analysis* (17th ed.). Gaithersburg, MD: AOAC.
- Brauman, A., Keleke, S., Malonga, M., Miambi, E., & Ampe, F. (1996). Microbiological and biochemical characterization of cassava retting, a traditional lactic acid fermentation for foo-foo (cassava flour) production. *Applied and Environmental Microbiology*, 62, 2854–2858.
- Chaves-López, C., Serio, A., Grande-Tovar, C. D., Cuervo-Mulet, R., Delgado-Ospina, J., & Paparella, A. (2014). Traditional fermented foods and beverages from a microbiological and nutritional perspective: the Colombian Heritage. *Comprehensive Reviews in Food Science and Food Safety*, 13(5), 1031–1048.
- Chen, L., Li, L., Vadrani, P. V., Madl, R. L., & Wang, W. (2013). *Value-added products from soybean: Removal of anti-nutritional factors via bioprocessing*. INTECH Open Access Publisher.
- Edward, V. A., Huch, M., Dortu, C., Thonart, P., Egonlety, M., Van Zyl, P. J., et al. (2011). Biomass production and small-scale testing of freeze-dried lactic acid bacteria starter strains for cassava fermentations. *Food Control*, 22, 389–395.
- Fagbemi, A. O., & Ijah, U. J. J. (2006). Microbial population and biochemical changes during production of protein-enriched fufu. *World Journal of Microbiology and Biotechnology*, 22(6), 635–640.
- Fayemi, O. E., & Ojokoh, A. O. (2014). The effect of different fermentation techniques on the nutritional quality of the cassava product (fufu). *Journal of Food Processing and Preservation*, 38(1), 183–192.
- Han, Y. H., Gomez-Vasquez, R., Reilly, K., Li, H. Y., Tohme, J., Cooper, R. M., et al. (2001). Hydroxyproline-rich glycoproteins expressed during stress responses in cassava. *Euphytica*, 120, 59–70.
- Holzappel, W. H. (2002). Appropriate starter culture technologies for small-scale fermentation in developing countries. *International Journal of Food Microbiology*, 75, 197–212.
- Iyer, S., Mattinson, D., & Fellman, J. (2010). Study of the early events leading to cassava root postharvest deterioration. *Tropical Plant Biology*, 3, 151–165.
- Kostinek, M., Specht, I., Edward, V. A., Pinto, C., Egonlety, M., Sossa, C., et al. (2007). Characterization and biochemical properties of predominant lactic acid bacteria from fermenting cassava for selection as starter cultures. *International Journal of Food Microbiology*, 114, 342–351.
- Kostinek, M., Specht, I., Edward, V. A., Schillinger, U., Hertel, C., Holzappel, W. H., et al. (2005). Diversity and technological properties of predominant lactic acid bacteria from fermented cassava used for the preparation of gari, a traditional African food. *Systematic and Applied Microbiology*, 28, 527–540.
- Lauble, H., Miehlich, B., Förster, S., Wajant, H., & Effenberger, F. (2001). Mechanistic aspects of cyanogenesis from active-site mutant Ser80Ala of hydroxynitrile lyase from *Manihot esculenta* in complex with acetone cyanohydrin. *Protein Science*, 10(5), 1015–1022.
- Maziya-Dixon, B., Dixon, A. G. O., & Adebowale, A. R. A. (2007). Targeting different end uses of cassava: genotypic variations for cyanogenic potentials and pasting properties. *International Journal of Food Science and Technology*, 42, 969–976.
- Nweke, F. (2004). *New challenges in the cassava transformation in Nigeria and Ghana* (Vol. 118). Washington, D.C: International Food Policy Research Institute.
- Oyewole, O. B., & Ogundele, S. L. (2001). Effect of length of fermentation on the functional characteristics of fermented cassava 'fufu'. *Journal of Food Technology in Africa*, 6, 38–40.
- Ray, R. C., & Sivakumar, P. S. (2009). Traditional and novel fermented foods and beverages from tropical root and tuber crops: review. *International Journal of Food Science and Technology*, 44, 1073–1087.
- Santisopasri, V., Kurotjanawong, K., Chotineeranat, S., Piyachomkwan, K., Sriroth, K., & Oates, C. G. (2001). Impact of water stress on yield and quality of cassava starch. *Industrial Crops and Products*, 13, 115–129.
- Sheffield, J., Taylor, N., Fauquet, C., & Chen, S. X. (2006). The cassava (*Manihot esculenta* Crantz) root proteome: protein identification and differential expression. *Proteomics*, 6, 1588–1598.
- Shittu, T. A., & Adedokun, I. I. (2010). Comparative evaluation of the functional and sensory characteristics of three traditional fermented cassava products. *Journal of Natural Sciences Engineering and Technology*, 9, 106–116.
- Stahl, W. H. (1973). *Compilation of odor and taste threshold values data*. Philadelphia: American Society for Testing and Materials.
- Todorov, S. D., & Franco, B. D. G. D. M. (2010). *Lactobacillus Plantarum*: characterization of the species and application in food production. *Food Reviews International*, 26, 205–229.
- Vasconcelos, A. T., Twiddy, D. R., Westby, A., & Reilly, P. J. A. (1990). Detoxification of cassava during gari preparation. *International Journal of Food Science and Technology*, 25, 198–203.
- Westby, A., & Twiddy, D. R. (1992). Characterization of the gari and fufu preparation procedures in Nigeria. *World Journal of Microbiology and Biotechnology*, 8, 175–182.



## Peach polyphenol and carotenoid content as affected by frozen storage and pasteurization



Ana Oliveira<sup>a</sup>, Elisabete M.C. Alexandre<sup>a</sup>, Marta Coelho<sup>a</sup>, Rui M. Barros<sup>a</sup>, Domingos P.F. Almeida<sup>b</sup>, Manuela Pintado<sup>a,\*</sup>

<sup>a</sup> Centro de Biotecnologia e Química Fina – Laboratório Associado, Escola Superior de Biotecnologia, Universidade Católica Portuguesa/Porto, Rua Arquitecto Lobão Vital, 4202-401 Porto, Portugal

<sup>b</sup> Instituto Superior de Agronomia, Universidade de Lisboa, Tapada da Ajuda, 1349-017 Lisboa, Portugal

### ARTICLE INFO

#### Article history:

Received 30 April 2015

Received in revised form

28 August 2015

Accepted 15 October 2015

Available online 20 October 2015

#### Keywords:

Freezing

Storage

Phytochemicals

*Prunus persica*

Pasteurization

### ABSTRACT

The profile of polyphenol and carotenoid of peach were analysed on fresh fruits, immediately after freezing or after pasteurization, and during frozen storage at  $-20\text{ }^{\circ}\text{C}$  for 360 days. Freezing did not affect the concentration of polyphenols or carotenoids. Pasteurization of fresh and frozen samples induced an increase in the extractability of chlorogenic acid (38% and 24%) and of zeaxanthin (336% and 127%) and a decrease of lutein (22% and 56%) and  $\beta$ -cryptoxanthin (32 and 51%).

Total antioxidant capacity and total phenolic content changed by less than 20% after frozen storage for 360 d. However, total carotenoid content decreased 41% and 48% in unpasteurized and pasteurized samples, after the same storage period. Long term storage induced an increase in the extractability of (+)-catechin (47%) and zeaxanthin (90%) and a decrease in neochlorogenic acid (59%), chlorogenic acid (39%), quercetin-3-glucoside (21%), lutein (24%) and  $\beta$ -cryptoxanthin (40%). Pasteurization of frozen samples promoted a decrease in the concentration of neochlorogenic acid (91%), chlorogenic acid (87%) and quercetin-3-rutinoside (71%) and increase in lutein (16%),  $\beta$ -cryptoxanthin (42%) and  $\beta$ -carotene (31%).

Peach should be stored for periods no longer than 230 d, since pasteurization after that, induced a higher decrease in neochlorogenic, chlorogenic acids and quercetin-3-rutinoside content.

© 2015 Elsevier Ltd. All rights reserved.

### 1. Introduction

Freezing fruits slows down, but does not stop, the physical, chemical, and biochemical reactions that induce phytochemical deterioration. About 6–8% of peaches produced are processed as frozen peaches (Siddiq, 2006). During freezing most of the liquid water is transformed into ice, greatly reducing microbial and enzymatic activities, and oxidative processes associated with lipids (Chassagne-Berces, Fonseca, Citeau, & Marin, 2010). In fruits, phytochemicals can be located as free compounds in the cell vacuole or in chromoplasts according to their polarity. Heating or freezing can disrupt the cell membrane leading to the release of membrane-bound phytochemicals, which implies higher extractability (Leong & Oey, 2012).

According to Thane and Reddy (1997), the amount of

carotenoids was not affected by freezing, particularly rapid freezing, and deteriorative processes occur at a very low rate during storage. When studying the effect of frozen storage on the levels of carotenoids in peas Puupponen-Pimiä et al. (2003) reported 17% loss of  $\beta$ -carotene content after 18 months at  $-20\text{ }^{\circ}\text{C}$ , while in carrots the decrease varied from 27 to 75% depending upon how the products had been processed (cubes or slices) and their harvest year. The effect of vacuum-packed and freezing in air-blast freezer at  $-40\text{ }^{\circ}\text{C}$  of papaya slices was studied by M. P. Cano, de Ancos, Lobo, and Monreal (1996) and it was reported a decrease of 14–65% in carotenoids after freezing and 40% after thermal treatment for the canning process. Hong, Barrett, and Mitchell (2004) determined the levels and fate of procyanidins in frozen and canned Ross clingstone peaches. D. K. Asami, Y. J. Hong, D. M. Barrett, and A. E. Mitchell (2003) found a 30% increase in the total phenolic content of clingstone peaches after freezing.

Phenolics play a role in plant defence against insect and mammal herbivory and oxidative damage (Chang, Tan, Frankel, &

\* Corresponding author.

E-mail address: [mpintado@porto.ucp.pt](mailto:mpintado@porto.ucp.pt) (M. Pintado).

Barrett, 2000; Duval, Shetty, & Thomas, 1999). Peach carotenoids act as pigments and are also involved in the protection of plant cells against oxidative stress (Asami et al. 2003).

Many fruit is subjected to various types of processing prior to consumption which involves storage under frozen conditions ( $< -20\text{ }^{\circ}\text{C}$ ) until used in fruit formulations that generally undergo thermal treatment. Therefore the objectives of this study were to analyze the polyphenols and carotenoid patterns of peach pieces and to study the effects that the two most commonly employed processing techniques to preserve peach, freezing and pasteurization, have on these classes of phytochemicals and their potential as antioxidative agents.

## 2. Materials and methods

### 2.1. Reagents

The ABTS diammonium salt (2, 2-azinobis-3-ethylbenzothiazoline-6-sulphonic acid), formic acid, methanol, potassium sorbate and sodium carbonate were purchased from Sigma–Aldrich (Sintra, Portugal). Folin-Ciocalteu's reagent, potassium persulfate from Merck (Algés, Portugal). Standards of ascorbic acid, gallic acid, (+)-catechin, chlorogenic acid, neochlorogenic acid,  $\beta$ -carotene and quercetin-3-glucoside were obtained from Sigma–Aldrich (Sintra, Portugal), whereas lutein, zeaxanthin and  $\beta$ -cryptoxanthin were purchased from Extrasynthèse (Lyon, France).

### 2.2. Peach treatments

Peach (*Prunus persica* (L.) Batsch 'Diamond Princess') was harvested at commercial maturity in Portugal, peeled, the pit removed, and the flesh cut by hand with a sharp knife into cubes with ca. 10 mm sides. Pieces were frozen in a fluidized bed until temperature at the centre of the cubes reached  $-20\text{ }^{\circ}\text{C}$  (HD 8802 thermometer, Delta OHM, Padova, Italy).

Peach pieces were analysed fresh, after cutting into cubes ca. 10 mm sides, after storage of individually quick frozen (IQF) at  $-20\text{ }^{\circ}\text{C}$  on days 1, 15, 30, 60, 90, 180, 240, and 360 and finally, after pasteurization ( $90\text{ }^{\circ}\text{C}$  for 5 min) of frozen peach pieces (on days 1, 15, 30, 60, 90, 180, 240, and 360). To study the impact of pasteurization, the extracts were prepared after a resting period of 24 h at  $23\text{ }^{\circ}\text{C}$ .

Frozen cubes were packed in polyethylene bags containing  $100 \pm 10\text{ g}$ , sealed, and stored at  $-20 \pm 2\text{ }^{\circ}\text{C}$  for 360 d. At each sampling time (1, 15, 30, 60, 90, 180, 240, and 360 d of frozen storage), the samples were removed from individual bags to allow partial thawing and after 1 h at room temperature they were used to prepare the extracts in triplicates.

To study the impact of pasteurization, the fresh and frozen (in each frozen storage period, after partial and standing for 1 h at room temperature) samples were used to fill 50 mL glass tubes, which were then pasteurized at  $90\text{ }^{\circ}\text{C}$  for 5 min in water-bath in triplicates. After that they were cooled down in ice until reach ca.  $22\text{ }^{\circ}\text{C}$  and left 24 h at  $23\text{ }^{\circ}\text{C}$  prior to prepare the extracts.

### 2.3. Extracts preparation

Aqueous methanol (800 mL/L) was added to peach pieces; they were homogenized with ultra-turrax for 2 min (IKA Ultra-turrax T18, Wilmington, USA) and left under 300 rpm agitation for 30 min at room temperature. The slurry was centrifuged ( $4000 \times g$ , 10 min,  $4\text{ }^{\circ}\text{C}$ ) to remove debris. The supernatant was analysed for water-soluble antioxidant activity and total phenolics. A 15-mL aliquot of the extract was evaporated to dryness in a RVC 2–18

speed-vacuum evaporator (Christ.Osterode am Harz, Germany) at  $30\text{ }^{\circ}\text{C}$  and the residue dissolved in 4 mL of methanol and analysed by HPLC-DAD.

To prepare the carotenoids extracts 2.5 g of peach pieces were homogenized with 5 mL of cold ethanol for 2 min with an ultra-turrax. Hexane (4 mL) was added and the resulting slurry was mixed centrifuged and the top layer was removed to polypropylene tube. The extraction was repeated again with 2.5 mL of saturated NaCl and 4 mL hexane. Both resultant hexane fractions were combined and used for saponification with 100 g/L methanolic KOH overnight (Wright & Kader, 1997). The mixture was washed with 100 g/L NaCl and three washes with deionized water.

### 2.4. Water-soluble antioxidant assay content

This was based on the method of Gao et al. (2007). Briefly,  $\text{ABTS}^+$  radical cation was obtained by the reaction of 7 mmol/L of ABTS and 2.45 mmol/L potassium persulfate. The  $\text{ABTS}^+$  solution was diluted with water to an absorbance of  $0.70 \pm 0.02$  at 734 nm. The  $\text{ABTS}^+$  solution was read after 10  $\mu\text{L}$  sample extract react for 6 min in triplicates for each extract replica. The antioxidant capacity of sample was calculated and expressed as milligrams of ascorbic acid equivalent antioxidant capacity per g biomass.

### 2.5. Determination of the total phenolics content

The total phenolic content of peach extracts was determined according the Folin-Ciocalteu method (Singleton & Rossi, 1965). Briefly 50  $\mu\text{L}$  of methanolic extract, 50  $\mu\text{L}$  Folin-Ciocalteu reagent, 1 mL of  $\text{Na}_2\text{CO}_3$  (75 g/L) and 1.4 mL of ultra-pure water. The triplicate tubes of each extract were left 60 min in dark at room temperature. The absorbance of the sample was read at 750 nm using gallic acid (0.015–0.50 mg/mL) as a standard. Results were expressed as mg of gallic acid equivalent per g of biomass.

### 2.6. Quantitative colorimetric analysis of total carotenoids content

Carotenoids content of peach extracts were estimated in triplicates using a spectrophotometric analysis at 454 nm. The  $\beta$ -carotene ( $6.3 \times 10^{-5} - 4.0 \times 10^{-3}\text{ mg/mL}$ ) was used as standard curve. Total carotenoids content was expressed based on mg of  $\beta$ -carotene equivalents/g biomass.

### 2.7. Quantitative analysis of polyphenols and carotenoids by HPLC with DAD detector

A 50  $\mu\text{L}$  aliquot of peach hydrophilic extract was injected onto a Waters Alliance (Waters Series 600, Mildford MA, USA) high-pressure liquid chromatographer, equipped with a Waters 996 PDA detector. Separation of the polyphenols was accomplished on a reverse phase Symmetry<sup>®</sup> C18 column ( $250 \times 4.6\text{ mm i.d.}$  5  $\mu\text{m}$  particle size and 125  $\text{\AA}$  pore size) with a guard column (Symmetry<sup>®</sup> C18). Chromatograms were recorded through a diode array detector (Waters, Mildford MA, USA) at wavelengths ranging from 200 to 600 nm in 2 nm intervals. Absorbance was measured at 280 nm (flavan-3-ols), 320 nm (flavonols) and 454 nm (carotenoids).

Solvents A was water/methanol/formic acid (925:50:25 mL/mL/mL) and solvent B methanol/water (940:60 mL/mL). The elution follows a linear gradient starting with 0% solvent B which increased to 30% B in 40 min, 30–50% B in 20 min and from 50 to 0% B in 10 min at a flow rate of 0.75 mL/min.

Retention times and spectra of compounds were analysed by comparison with pure standards and quantification performed by the calibration curves of (+)-catechin, chlorogenic acid, neochlorogenic acid and quercetin-3-rutinoside and expressed as

micrograms per gram of biomass.

Carotenoids were eluted using the mobile phase composed by acetonitrile (55%), methanol (22%), dichloromethane (11.5%) and hexane (11.5%). Ammonium acetate was added at 0.02% to stabilize carotenoids under isocratic conditions at 1.0 mL/min flow rate during 20 min, at 25 °C with an injection volume of 40 µL β-Carotene, zeaxanthin, lutein, β-cryptoxanthin were quantified using a calibration curve built with pure standards and expressed as micrograms per gram of biomass. All the analysis, of each extract, were made in triplicates.

## 2.8. Statistical analysis content

Statistical analysis was performed using the software SPSS version 22. Normality of data distribution was tested by Kolmogorov–Smirnov method.

A GLM repeated measures procedure was used to measure the effect of each process, while accounting for the within-subjects effect of storage time. The test associated with sphericity assumed that the assumption about the covariance matrix is met. When the covariance matrix assumption was not met, was used the Greenhouse–Geisser test.

It also tested the homogeneity of covariance. Furthermore, one-way ANOVA with post-hoc Tukey tests were used. The overall acceptable significance level of differences for all statistical tests was set at  $P < 0.05$ .

## 3. Results and discussion

### 3.1. Effect of freezing and pasteurization on total antioxidant activity, total phenolic, total carotenoids content and individual phytochemicals

Fresh peach presented a total antioxidant activity of 0.14 mg ascorbic acid equivalents per gram of biomass which increased 7% by the process of freezing at  $-20$  °C for 24 h. It has been reported that freezing of peas and spinach reduced water-soluble antioxidant activity by 50% thereafter levels remained constant on storage at  $-20$  °C (Hunter & Fletcher, 2002). After pasteurization, the antioxidant capacity of fresh peach increased 36% and after pasteurization of frozen peach an increase of 21% was observed when compared with frozen peach (Fig. 1A). Total phenolic content

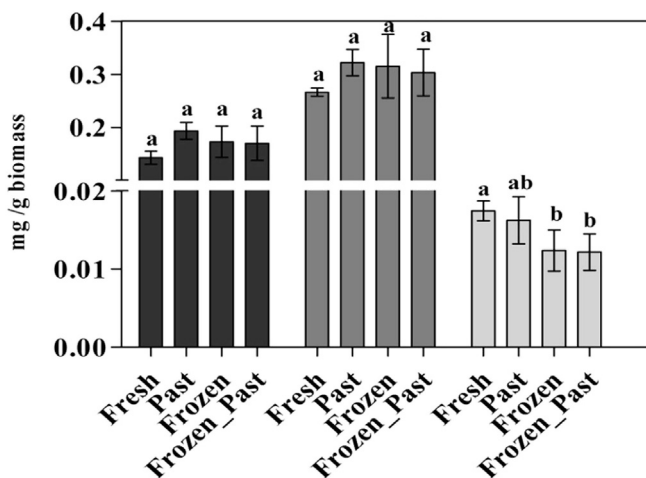


Fig. 1. Effect of pasteurization, freezing and pasteurization after freezing on total antioxidant activity (■), total phenolics (■) and total carotenoids (■) on peach. <sup>a</sup> Different letters represent significant differences between each treatment.

did not change significantly when fresh peaches were frozen and pasteurized (Fig. 1A). Total carotenoids decreased 29% after freezing, while the process of pasteurization did not change in a significant way the content of carotenoids in fresh neither in previously frozen peach (Fig. 1A).

Within individual polyphenols (+)-catechin, neochlorogenic acid and quercetin-3-rutinoside contents presented no significant differences within treatments. The effect of pasteurization was determined on fresh and frozen samples and compared with results obtained before pasteurization. Chlorogenic acid content increased 38% after pasteurization of fresh peach and after pasteurization of frozen peach increased 24%. Breaking of cell membranes by freezing release enzymes, and this could lead to the formation of other physiological compounds. Cano, Lobo, and De Ancos (1998) observed that, freezing process produces a significant increase solubility of some peroxidase fractions linked to cellular membranes such as polyphenol oxidase and peroxidase, which use chlorogenic acid as a substrate.

Within carotenoids the process of freezing for 24 h had no significant effect excepting on β-cryptoxanthin which increased 18% (Fig. 2B). The content of lutein decreased significantly ( $P < 0.05$ ) 22% after pasteurization and 56% after pasteurization of frozen samples and compared with just frozen samples (Fig. 2B). The same happened with β-cryptoxanthin which decreased 32 and 51% respectively after pasteurization of fresh and frozen samples (Fig. 2B).

Zeaxanthin presented a different behaviour, compared with the remaining carotenoids, by presenting an increase with thermal treatment. After pasteurization of fresh peach zeaxanthin increased

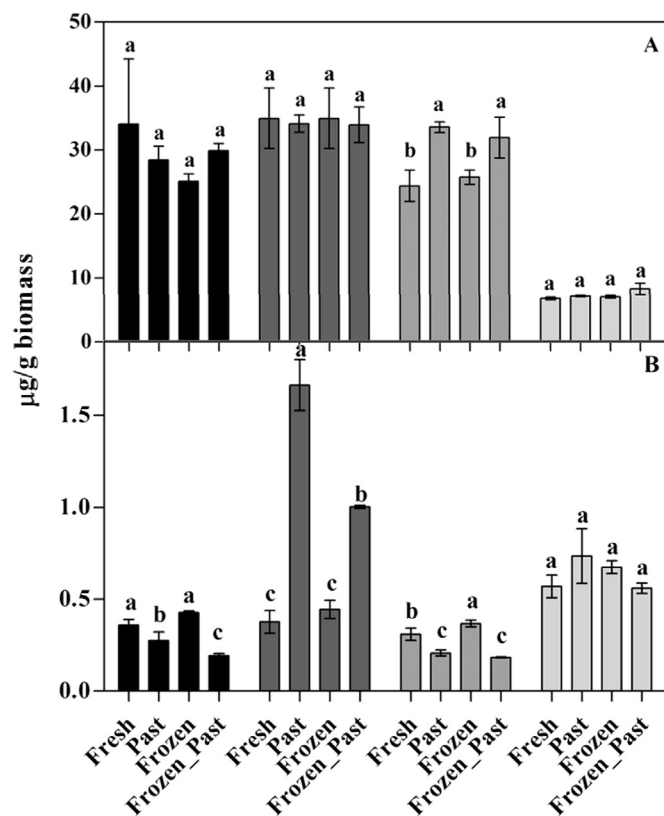


Fig. 2. Effect of pasteurization, freezing and pasteurization after freezing on A: individual phenolic compounds ((+)-catechin (■), neochlorogenic acid (■), chlorogenic acid (■) and quercetin-3-rutinoside (■)) and B: individual carotenoids (lutein (■), zeaxanthin (■), β-cryptoxanthin and β-carotene (■)) of peach. <sup>a</sup> Different letters represent significant differences between each treatment.

336% and after pasteurization of frozen samples increased 127% (Fig. 2B). The  $\beta$ -carotene was the carotenoid more stable, presenting only a significant increase of 30% after pasteurization of fresh samples (Fig. 2B). Little effect of freezing was reported by Scott and Eldridge (2005) for corn lutein content and also in  $\beta$ -cryptoxanthin and  $\beta$ -carotene from another cultivar. Zeaxanthin stability was reported by Maiani et al. (2009) on potato and a similar trend was also observed in sweet corn after a heat treatment (Updike & Schwartz, 2003). Gradual dissociation of zeaxanthin from the native protein complex stimulated by previous heat treatment may explain the observed increase (Sánchez-Moreno, Plaza, De Ancos, & Cano, 2006). Thermal treatment may be beneficial for carotenoids content through the disruption of food matrices (e.g. cell walls and membranes) facilitating the liberation (bound) and solubilisation of carotenoids (free and ester forms) resulting in an increased carotenoid bioavailability (Maiani et al., 2009).

### 3.2. Effect of storage and pasteurization on total antioxidant activity, total phenolic and total carotenoids content of frozen peach

Total antioxidant activity increased 19% after freezing for 360 d. The pasteurization promoted a decrease of 20% when day 1 and 360 were compared (Fig. 3A). However, besides the variations no significant differences were observed between samples pasteurized and unpasteurized and within storage time (Table 1). The 12-month storage at  $-20\text{ }^{\circ}\text{C}$  induced a 42% decrease in the antioxidant activity of cauliflower but storage at  $-30\text{ }^{\circ}\text{C}$  improved the antioxidant activity by 9% (Gębczyński & Kmiecik, 2007).

Total phenolic content increased between 60 and 180 d of storage and then after 360 d decreased to a similar value obtained the beginning of storage (Fig. 3B). However, during all the storage period no significant differences were detected between samples pasteurized and unpasteurized (Table 1). Asami et al. (2003) found a 30% increase in the total phenolics of clingstone peaches after 3 months storage at  $-12\text{ }^{\circ}\text{C}$ . Freezing process may result in disruption of the cellular matrix and more facilitated extraction of the phenolics. Puupponen-Pimiä et al. (2003) studied the effects of freezing on phenolic compounds of peas, carrots, cauliflower, cabbage and potatoes and they reported an average loss of 20–30% of total phenolics in most vegetables, although no change was observed in most carrot samples and a 26% increase was observed in cabbage. In the process of freeze-drying higher extraction efficiency of the total phenolics can be obtained because it can lead to the development of ice crystals within the plant matrix. Ice crystals can result in a greater rupturing of plant cell structure, allowing better solvent access and extraction (Keinänen & Julkunen-Tiitto, 1996).

In total carotenoids content time factor was significant since it decreased 41% after 360 d at  $-20\text{ }^{\circ}\text{C}$  and 48% after pasteurization (Fig. 3C) while the process was not significant (Table 1). After 12 months of storage at  $-18\text{ }^{\circ}\text{C}$ , an important decrease of total carotenoid occurred in papaya, although the carotenoid profile was unchanged (M. P. Cano et al., 1996). A decrease in total carotenoids (36%) as well  $\beta$ -carotene (51%) and lycopene (48%) was reported for tomato cubes stored 12 months at  $-20\text{ }^{\circ}\text{C}$  (Lisiewska & Kmiecik, 2000). Cauliflower stored for 12-months at  $-20\text{ }^{\circ}\text{C}$  had an insignificant (10–11%) decrease in carotenoids and polyphenols while storage at  $-30\text{ }^{\circ}\text{C}$  improved the preservation of carotenoids by 10% and of polyphenols by 6% (Gębczyński & Kmiecik, 2007).

Most of studies reported results on a wet weight basis, and the majority found carotenoid losses from 5% to 48% for freezing (Rickman, Bruhn, & Barrett, 2007).

### 3.3. Frozen storage and pasteurization effect on peach polyphenols

Within individual polyphenols the content of (+)-catechin

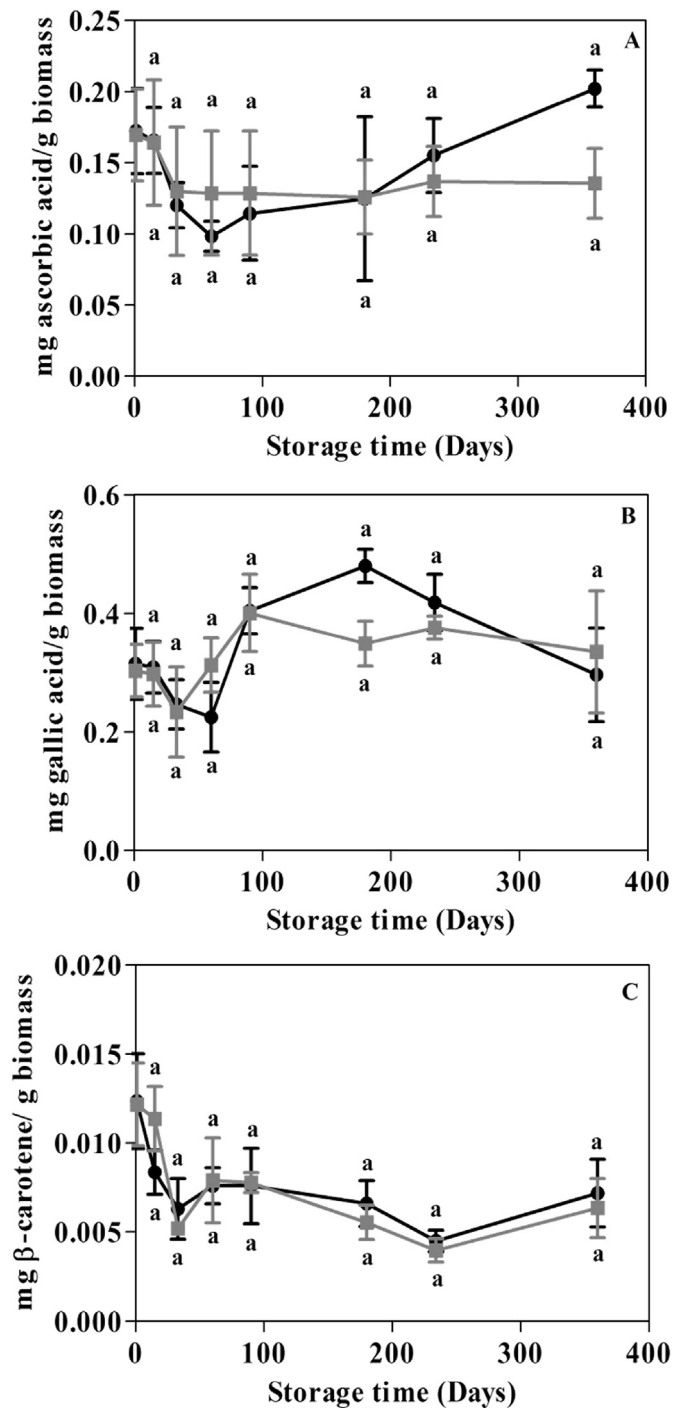


Fig. 3. Effect of 360 d storage at  $-20\text{ }^{\circ}\text{C}$  on peach (●) and after pasteurization (■) in antioxidant activity (A), total phenolics (B) and total carotenoids (C). Results are expressed as the average  $\pm$  SD ( $n = 3$ ).

increased ( $P < 0.05$ ) 47% after 360 d at  $-20\text{ }^{\circ}\text{C}$ . The higher accessibility was obtained specially from day 60 reaching the maximum of (+)-catechin content at day 234 (Fig. 4A). The process of pasteurization did not change significantly the (+)-catechin content along all the storage period (Table 1). Wang and Zhou (2004) observed higher stability in green tea catechins during freezing and frozen storage at  $-20\text{ }^{\circ}\text{C}$  for up to 9 weeks. The increase observed for (+)-catechin could be due to degradation of cell structure of fruit; therefore, they could be easily hydrolysed and

**Table 1**  
Summary about the effect of process and time for each component.

Component	Variable	p-value
Antioxidant activity	Time	0.099
	Process	0.745
Total phenolic	Time	0.000
	Process	0.420
Total carotenoids	Time	0.000
	Process	0.054
(+)-Catechin	Time	0.002
	Process	0.549
Neochlorogenic acid	Time	0.000
	Process	0.314
Chlorogenic acid	Time	0.002
	Process	0.002
Rutin	Time	0.002
	Process	0.000
Lutein	Time	0.002
	Process	0.122
Zeaxanthin	Time	0.001
	Process	0.000
β-cryptoxanthin	Time	0.007
	Process	0.000
β-carotene	Time	0.007
	Process	0.000

extracted during frozen storage (Türkben, Sariburun, Demir, & Uylaşer, 2010).

The content of neochlorogenic acid decreased 59% after 360 d at  $-20^{\circ}\text{C}$  and the pasteurization after that period of freezing promoted a decrease of 91% (Fig. 4B). Besides the difference observed in the final period of storage no significant differences between the processes of freezing storage and pasteurization were detected (Table 1).

The chlorogenic acid presented a similar behaviour to neochlorogenic acid where frozen storage for 360 d lead to a total decrease ( $P < 0.05$ ) of 39% and the pasteurization after that induced a total decrease ( $P < 0.05$ ) of 87% (Fig. 4C). Significant differences

were observed between the processes where freezing allowed to get higher accessibility than in pasteurized samples, besides that time seemed to represent a variable that affected negatively the content of chlorogenic acid (Table 1). Freeze injuries are a consequence of cell dehydration and important cell destruction caused by ice crystals forming inside parenchyma cells. These cause serious destruction of cell membranes, leading to cell death and a high oxidation of cell contents as a result of contact between enzymes and their respective substrates (Morelló, Motilva, Ramo, & Romero, 2003). The release of phytochemicals by freezing can increase the exposure to degradation by thermal treatment. Xu, Ye, Chen, and Liu (2006) observed that chlorogenic acid content of citrus peel extract decreased with heating time (30, 60 and 90 min) and temperature ( $90\text{--}150^{\circ}\text{C}$ ) which indicated that the esterified bond could be cleaved by heat treatment.

Quercetin-3-rutinoside content decreased 21% at the end of 360 d of freezing storage, and the subsequent pasteurization induced a total decrease ( $P < 0.05$ ) of 71% when compared with pasteurized samples at the beginning of storage (Fig. 4D). This compound presented a significant decrease of its content with storage time and between processes, where freezing allowed to get higher accessibility of quercetin-3-rutinoside (Table 1). Raspberry and blackberry presented an increase in quercetin after 6 months of frozen storage, where the high level of vitamin C was reported to inhibit the degradation of quercetin during frozen storage (Häkkinen, Kärenlampi, Mykkänen, Heinonen, & Törrönen, 2000).

The results revealed that are more advantageous to pasteurize peach with a maximum of 230 d of storage at  $-20^{\circ}\text{C}$ , since from this day on the decrease in the content of neochlorogenic, chlorogenic acids and quercetin-3-rutinoside was significantly higher.

#### 3.4. Effect of frozen storage and pasteurization on carotenoids content

The carotenoids identified on peach samples were lutein, zeaxanthin, β-cryptoxanthin and β-carotene. The lutein content

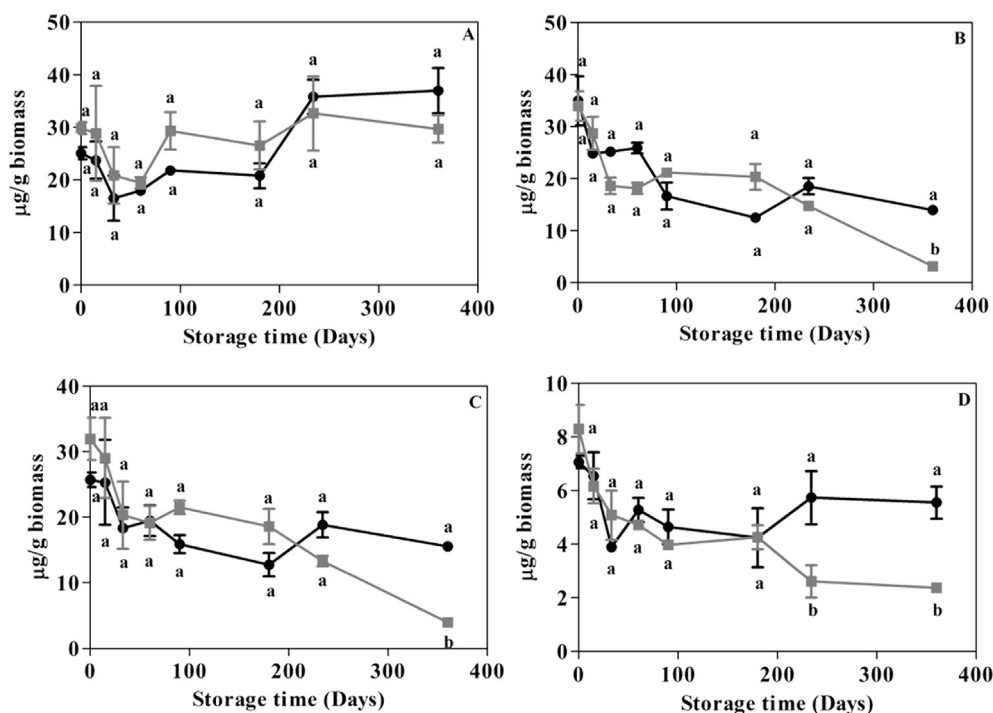


**Fig. 4.** Effect of 360 d storage at  $-20^{\circ}\text{C}$  on peach (●) and after pasteurization (■) in (+)-catechin (A), neochlorogenic acid (B), chlorogenic acid (C) and quercetin-3-rutinoside (D). Results are expressed as the average  $\pm$  SD ( $n = 3$ ).

decreased 24% after 360 d at  $-20^{\circ}\text{C}$ . The process of pasteurization in the beginning of storage promoted a decrease of 56%, when compared with unpasteurized samples and after that lutein content kept constant. During storage the lutein content was significantly lower ( $P < 0.05$ ) in pasteurized samples only on d 1, 90 and 234 (Fig. 5A). Different access to lutein depends on the type of thermal treatment applied as it was reported to tomato samples, where microwave-cooking markedly decreased lutein content, steaming only had a small negative effect, while boiling and grilling significantly increased its content (Ryan, O'Connell, O'Sullivan, Aherne, & O'Brien, 2008).

The zeaxanthin content increased 90% after 360 d of storage (Fig. 5B). The breakdown of chromoplast, by mechanical damage, improves carotenoids extraction with organic solvents, since carotenoids are fat-soluble pigments (Stinco et al., 2012). The process of freezing can disrupt the cell membrane leading to the release of membrane-bound phytochemicals, increasing their free content (Leong & Oey, 2012). Freezing process can dehydrate vegetables resulting in water weight losses (0.3%–5%) and this moisture decrease may artificially inflating the carotenoid content on a wet weight (Rickman et al., 2007).

Higher extractability was obtained after pasteurization, revealing differences between the processes tested (Table 1). The increase in carotenoid concentrations found in frozen corn was reported as a result of water loss from the kernels (Scott & Eldridge, 2005). It has been reported that the food processing which modifies the matrix structure by mechanical homogenization or heat treatment may have a beneficial impact on the bioavailability of carotenoids from different foodstuffs (Van Buggenhout et al., 2010; Yeum & Russell, 2002). Most fruits and vegetables soften during thermal treatment, which is related to pectin  $\beta$ -eliminative degradation, solubilization and consequent changes in cellular architecture: in raw products, fracture occurs through cell walls while in cooked products, fracture occurs through cells (Van Buggenhout,

Sila, Duvetter, Van Loey, & Hendrickx, 2009; Waldron, Smith, Parr, Ng, & Parker, 1997).

The  $\beta$ -cryptoxanthin content decreased 40% after 360 d of storage at  $-20^{\circ}\text{C}$  (Fig. 5C). The process of pasteurization, in the beginning of storage, induced a reduction of 50% in  $\beta$ -cryptoxanthin content, however, an increase of 42% was observed after that until the end of the 360 d of storage (Fig. 5C). In the end of storage the  $\beta$ -cryptoxanthin content was similar between samples pasteurized and unpasteurized. The increased extractability of some phytochemicals through freezing, exposed them to degradation by oxidation during prolonged storage (Desobry, Netto, & Labuza, 1998).

The  $\beta$ -carotene content was quite stable during frozen storage (Fig. 5D). Contrarily to our results, other authors reported a decrease in the  $\beta$ -carotene content and consequently the provitamin A value during frozen storage of kiwi (M. P. Cano & Marin, 1992), papaya (Jeremiah, 1996), and tomato (Lisiewska & Kmiecik, 2000), being losses mainly due to the activity of enzymes (POD, LOX and CAT), particularly during frozen storage in an oxygen environment.

Freezing produced a decrease in  $\beta$ -carotene content in all varieties of mangoes slices tested at the end of 4 months frozen storage at  $-18^{\circ}\text{C}$ . Since this pigment is fat-soluble, it is not subject to leaching losses, but it could be altered during food processing by reactions of cis-trans isomerization, epoxidation and oxidative changes (Antonia Marín, Cano, & Fuster, 1992). Lisiewska and Kmiecik (2000) showed that, after one-year of storage at  $-30^{\circ}\text{C}$ , cut tomatoes contained 40% more  $\beta$ -carotene that did the product stored at  $-20^{\circ}\text{C}$ .

The decrease in  $\beta$ -carotene was reported and supported by other studies as being most likely due to oxidation during frozen storage (Desobry et al., 1998). However the higher stability reported in our study could be related with the fact that generally  $\beta$ -carotene can form structures semi-crystalline where it binds to membranes

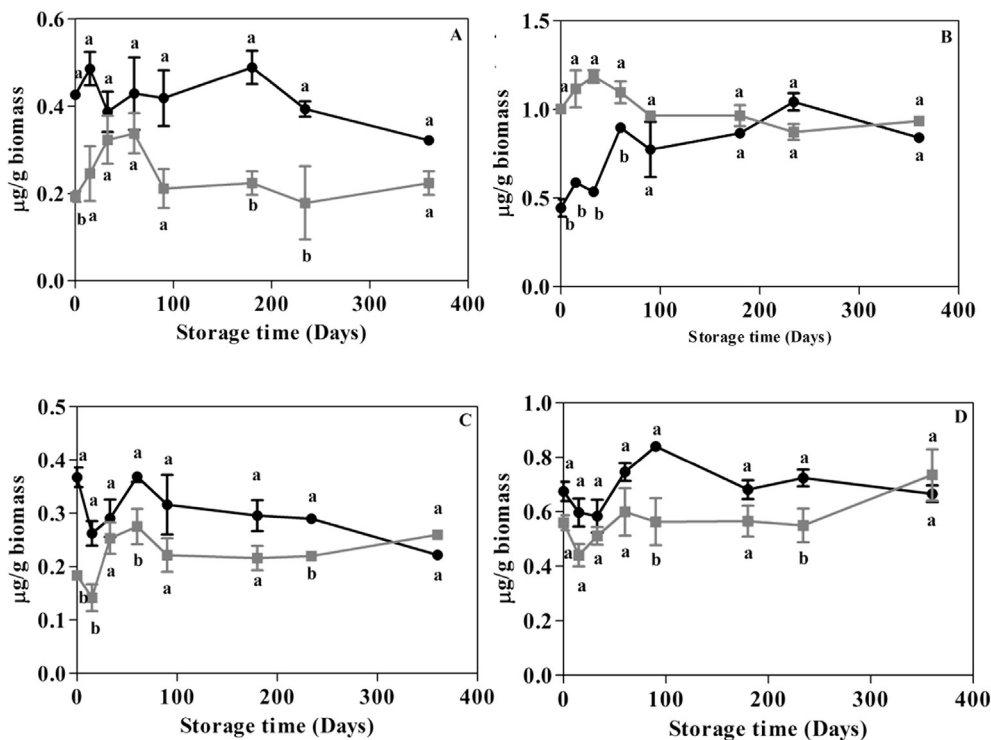


Fig. 5. Effect of 360 d storage at  $-20^{\circ}\text{C}$  on peach (●) and after pasteurization (■) in lutein (A), zeaxanthin (B),  $\beta$ -cryptoxanthin (C) and  $\beta$ -carotene (D). Results are expressed as the average  $\pm$  SD ( $n = 3$ ).

derived from plastids and can be found in association with sub-cellular lipid structures and proteins (Van Buggenhout et al., 2010) as already reported by Milicua, Juarros, De Las Rivas, Ibarrondo, and Gomez (1991) in carrots.

The pasteurization process did not promote significant changes in  $\beta$ -carotene content from stored peach. Only on days 90 and 230 of storage the quantifications were significant lower than that obtained on unpasteurized peach (Fig. 5D). Through the analysis within and between subjects, storage time and the processes presented a significant effect in  $\beta$ -carotene content (Table 1). The absolute amount of  $\beta$ -carotene that is accessible in carrot pieces increases upon thermal treatment and this effect is more pronounced as heating temperature and time are increasing (Lemmens, Colle, Van Buggenhout, Van Loey, & Hendrickx, 2011). The  $\beta$ -carotene levels in the tomato quarters, red pepper strips and courgette strips were decreased by boiling, grilling, microwave-cooking and steaming (Ryan et al., 2008).

The fact that food processing can have different impact on the extractability of different carotenoids it might be explained by their difference in their lipophilicity (Van Buggenhout et al., 2010).

#### 4. Conclusions

The pasteurization of fresh or previously frozen peach induced an increase in chlorogenic acid and zeaxanthin while for  $\beta$ -cryptoxanthin and  $\beta$ -carotene their content decreased. Storage for 360 d at  $-20^{\circ}\text{C}$  induced an increase on (+)-catechin and zeaxanthin while the remaining phenolics and carotenoids decreased. Pasteurization after 360 d frozen peach induced a decrease on neochlorogenic acid, chlorogenic acid and quercetin-3-rutinoside between days 230 and 360. In carotenoids the lutein strongly decreased and zeaxanthin content increased after pasteurization of samples stored for 60 d. The remaining carotenoids presented no significant differences between samples pasteurized and unpasteurized.

Freezing can increase phytochemicals extractability becoming more susceptible to degradation by the followed thermal treatment applied. Besides that, time seemed to be a factor preponderant, where carotenoids and (+)-catechin extractability increased with time while for the remaining phenolic compounds their content decreased in a significant way with time. The increase in phytochemicals content, namely carotenoids after processing treatments could increase further the bioaccessibility (transfer of carotenoids from digestate to micelles) of these compounds during the gastrointestinal digestion, increasing their potential availability for absorption *in vivo*.

#### Funding

The work was financially supported by Agência de Inovação, Portugal and Quadro de Referência Estratégico Nacional (QREN Portugal) through project Frutamais – Preservation of functional nutritional and organoleptic characteristic of fruits and derived food (QREN-ADI 3436), FCT – Fundação para a Ciência e a Tecnologia through project PEst-OE/EQB/LA0016/and by the PhD grant SFRH/BD/75041/2010 to A. Oliveira.

#### References

Antonia Marín, M., Cano, P., & Fuster, C. (1992). Freezing preservation of four Spanish mango cultivars (*Mangifera indica* L.): chemical and biochemical aspects. *Zeitschrift für Lebensmittel-Untersuchung und Forschung*, 194(6), 566–569.

Asami, D. K., Hong, Y.-J., Barrett, D. M., & Mitchell, A. E. (2003). Processing-induced changes in total phenolics and procyanidins in clingstone peaches. *Journal of the Science of Food and Agriculture*, 83(1), 56–63.

Cano, M. P., de Ancos, B., Lobo, G., & Monreal, M. (1996). Effects of freezing and

canning of papaya slices on their carotenoid composition. *Zeitschrift für Lebensmittel-Untersuchung und Forschung*, 202(4), 279–284.

Cano, M., Lobo, M., & De Ancos, B. (1998). Peroxidase and polyphenol oxidase in long-term frozen stored papaya slices. Differences among hermaphrodite and female papaya fruits. *Journal of the Science of Food and Agriculture*, 76(1), 135–141.

Cano, M. P., & Marin, M. A. (1992). Pigment composition and color of frozen and canned kiwi fruit slices. *Journal of Agricultural and Food Chemistry*, 40(11), 2141–2146.

Chang, S., Tan, C., Frankel, E. N., & Barrett, D. M. (2000). Low-density lipoprotein antioxidant activity of phenolic compounds and polyphenol oxidase activity in selected clingstone peach cultivars. *Journal of Agricultural and Food Chemistry*, 48(2), 147–151.

Chassagne-Berces, S., Fonseca, F., Citeau, M., & Marin, M. (2010). Freezing protocol effect on quality properties of fruit tissue according to the fruit, the variety and the stage of maturity. *LWT – Food Science and Technology*, 43(9), 1441–1449.

Desobry, S. A., Netto, F. M., & Labuza, T. P. (1998). Preservation of  $\beta$ -carotene from carrots. *Critical Reviews in Food Science and Nutrition*, 38(5), 381–396.

Duval, B., Shetty, K., & Thomas, W. H. (1999). Phenolic compounds and antioxidant properties in the snow alga *Chlamydomonas nivalis* after exposure to UV light. *Journal of Applied Phycology*, 11(6), 559–566.

Gębczyński, P., & Kmiecik, W. (2007). Effects of traditional and modified technology, in the production of frozen cauliflower, on the contents of selected antioxidative compounds. *Food Chemistry*, 101(1), 229–235.

Giao, M. S., Gonzalez-Sanjose, M. L., Rivero-Perez, M. D., Pereira, C. I., Pintado, M. E., & Malcata, F. X. (2007). Infusions of Portuguese medicinal plants: dependence of final antioxidant capacity and phenol content on extraction features. *Journal of the Science of Food Agriculture*, 87(14), 2638–2647.

Häkkinen, S. H., Kärenlampi, S. O., Mykkänen, H. M., Heinonen, I. M., & Törrönen, A. R. (2000). Ellagic acid content in berries: influence of domestic processing and storage. *European Food Research and Technology*, 212(1), 75–80.

Hong, Y.-J., Barrett, D. M., & Mitchell, A. E. (2004). Liquid chromatography/mass spectrometry investigation of the impact of thermal processing and storage on peach procyanidins. *Journal of Agricultural and Food Chemistry*, 52(8), 2366–2371.

Hunter, K. J., & Fletcher, J. M. (2002). The antioxidant activity and composition of fresh, frozen, jarred and canned vegetables. *Innovative Food Science & Emerging Technologies*, 3(4), 399–406.

Jeremiah, L. E. (1996). *Freezing effects on food quality* (Vol. 72). CRC Press.

Keinänen, M., & Julkunen-Tiitto, R. (1996). Effect of sample preparation method on birch (*Betula pendula* Roth) leaf phenolics. *Journal of Agricultural and Food Chemistry*, 44(9), 2724–2727.

Lemmens, L., Colle, I. J., Van Buggenhout, S., Van Loey, A. M., & Hendrickx, M. E. (2011). Quantifying the influence of thermal process parameters on *in vitro*  $\beta$ -carotene bioaccessibility: a case study on carrots. *Journal of Agricultural and Food Chemistry*, 59(7), 3162–3167.

Leong, S. Y., & Oey, I. (2012). Effects of processing on anthocyanins, carotenoids and vitamin C in summer fruits and vegetables. *Food Chemistry*, 133(4), 1577–1587.

Lisiewska, Z., & Kmiecik, W. (2000). Effect of storage period and temperature on the chemical composition and organoleptic quality of frozen tomato cubes. *Food Chemistry*, 70(2), 167–173.

Maiani, G., Periago Castón, M. J., Catasta, G., Toti, E., Cambrodón, I. G., Bysted, A., et al. (2009). Carotenoids: actual knowledge on food sources, intakes, stability and bioavailability and their protective role in humans. *Molecular Nutrition & Food Research*, 53(S2), S194–S218.

Milicua, J., Juarros, J., De Las Rivas, J., Ibarrondo, J., & Gomez, R. (1991). Isolation of a yellow carotenoprotein from carrot. *Phytochemistry*, 30(5), 1535–1537.

Morelló, J.-R., Motilva, M.-J., Ramo, T., & Romero, M.-P. (2003). Effect of freeze injuries in olive fruit on virgin olive oil composition. *Food Chemistry*, 81(4), 547–553.

Puupponen-Pimiä, R., Häkkinen, S. T., Aarni, M., Suortti, T., Lampi, A. M., Eurola, M., et al. (2003). Blanching and long-term freezing affect various bioactive compounds of vegetables in different ways. *Journal of the Science of Food and Agriculture*, 83(14), 1389–1402.

Rickman, J. C., Bruhn, C. M., & Barrett, D. M. (2007). Nutritional comparison of fresh, frozen, and canned fruits and vegetables II. Vitamin A and carotenoids, vitamin E, minerals and fiber. *Journal of the Science of Food and Agriculture*, 87(7), 1185–1196.

Ryan, L., O'Connell, O., O'Sullivan, L., Aherne, S., & O'Brien, N. (2008). Micellarisation of carotenoids from raw and cooked vegetables. *Plant Foods for Human Nutrition*, 63(3), 127–133.

Sánchez-Moreno, C., Plaza, L., De Ancos, B., & Cano, M. P. (2006). Impact of high-pressure and traditional thermal processing of tomato purée on carotenoids, vitamin C and antioxidant activity. *Journal of the Science of Food and Agriculture*, 86(2), 171–179.

Scott, C. E., & Eldridge, A. L. (2005). Comparison of carotenoid content in fresh, frozen and canned corn. *Journal of Food Composition and Analysis*, 18(6), 551–559.

Siddiq, M. (2006). Peach and nectarine. In *Handbook of fruits and fruit processing*, 519.

Singleton, V., & Rossi, J. A. (1965). Colorimetry of total phenolics with phosphomolybdic-phosphotungstic acid reagents. *American Journal of Enology and Viticulture*, 16(3), 144–158.

Stinco, C. M., Fernández-Vázquez, R., Escudero-Gilete, M. L., Heredia, F. J., Meléndez-Martínez, A. J., & Vicario, I. M. (2012). Effect of orange juice's processing on the

- color, particle size, and bioaccessibility of carotenoids. *Journal of Agricultural and Food Chemistry*, 60(6), 1447–1455.
- Thane, C., & Reddy, S. (1997). Processing of fruit and vegetables: effect on carotenoids. *Nutrition & Food Science*, 97(2), 58–65.
- Türkben, C., Sarıburun, E., Demir, C., & Uylaşer, V. (2010). Effect of freezing and frozen storage on phenolic compounds of raspberry and blackberry cultivars. *Food Analytical Methods*, 3(3), 144–153.
- Updike, A. A., & Schwartz, S. J. (2003). Thermal processing of vegetables increases cis isomers of lutein and zeaxanthin. *Journal of Agricultural and Food Chemistry*, 51(21), 6184–6190.
- Van Buggenhout, S., Almingier, M., Lemmens, L., Colle, I., Knockaert, G., Moelants, K., et al. (2010). In vitro approaches to estimate the effect of food processing on carotenoid bioavailability need thorough understanding of process induced microstructural changes. *Trends in Food Science & Technology*, 21(12), 607–618.
- Van Buggenhout, S., Sila, D., Duvetter, T., Van Loey, A., & Hendrickx, M. (2009). Pectins in processed fruits and vegetables: part III—texture engineering. *Comprehensive Reviews in Food Science and Food Safety*, 8(2), 105–117.
- Waldron, K. W., Smith, A. C., Parr, A. J., Ng, A., & Parker, M. L. (1997). New approaches to understanding and controlling cell separation in relation to fruit and vegetable texture. *Trends in Food Science & Technology*, 8(7), 213–221.
- Wang, R., & Zhou, W. (2004). Stability of tea catechins in the breadmaking process. *Journal of Agricultural and Food Chemistry*, 52(26), 8224–8229.
- Wright, K. P., & Kader, A. A. (1997). Effect of controlled-atmosphere storage on the quality and carotenoid content of sliced persimmons and peaches. *Postharvest Biology and Technology*, 10(1), 89–97.
- Xu, G., Ye, X., Chen, J., & Liu, D. (2006). Effect of heat treatment on the phenolic compounds and antioxidant capacity of citrus peel extract. *Journal of Agricultural and Food Chemistry*, 55(2), 330–335.
- Yeum, K.-J., & Russell, R. M. (2002). Carotenoid bioavailability and bioconversion. *Annual Review of Nutrition*, 22(1), 483–504.



## Analysis of the variability in microbial inactivation by acid treatments



Maria R. Rodríguez <sup>a</sup>, Juan S. Aguirre <sup>a, b, \*</sup>, Alexandra Lianou <sup>c</sup>, Julio Parra-Flores <sup>d</sup>, Gonzalo D. García de Fernando <sup>a</sup>

<sup>a</sup> Depto. Nutrición, Bromatología y Tecnología de los Alimentos, Facultad de Veterinaria, Universidad Complutense, Ciudad Universitaria, Madrid 28040, Spain

<sup>b</sup> Laboratorio de Microbiología y Probióticos, INTA, Universidad de Chile, Avenida El Líbano 5524, Macul, Santiago, Chile

<sup>c</sup> Laboratory of Microbiology and Biotechnology of Foods, Department of Food Science and Human Nutrition, Agricultural University of Athens, Iera Odos 75, Athens 11855, Greece

<sup>d</sup> Departamento de Nutrición y Salud Pública, Facultad de Ciencias de la Salud y de los Alimentos, Universidad del Bio Bio, Chillán, Chile

### ARTICLE INFO

#### Article history:

Received 15 July 2015

Received in revised form

23 October 2015

Accepted 23 October 2015

Available online 28 October 2015

#### Keywords:

Variability

Inactivation

Acid treatment

Acetic acid

Chicken soup

### ABSTRACT

The variability in microbial inactivation through acid treatments was evaluated in the present study. *Enterococcus faecalis*, *Listeria innocua*, *Salmonella enterica*, and *Pseudomonas fluorescens* were inoculated in buffered peptone water, chicken soup, and citrate solution, and were subjected to acid treatments of various intensities to reach a microbicidal effect of 0, 2, 3, and 4 logarithmic cycles. The variability in the number of survivors was greater in treated than in untreated samples. Furthermore, the effect of acid treatment on survival variability depended on the intensity of the acidification. More specifically, as the intensity of the applied acid treatment increased, the number of viable microorganisms, although smaller, was more variable. The results of this study indicate that the inactivation behaviour of microbial cells within a population is subject to variation; such variability must be quantified and taken into account in predictive food microbiology, and it can be valuable for risk assessment purposes when acidification of food is involved.

© 2015 Elsevier Ltd. All rights reserved.

### 1. Introduction

Given the increasing consumer demand for ready-to-eat (RTE) or minimally-processed food, the food industry has applied and continues to develop strategies aimed at providing a variety of high-quality, safe, and nutritionally balanced food products. With particular reference to the microbiological quality and safety of foods, a method that has been used extensively for food preservation is acidification through either fermentation or addition of weak acids. These organic acids (e.g., acetic, ascorbic, citric, lactic and malic), in addition to their contribution to the development of desirable organoleptic/technological traits, have been commonly used in the food industry due to their microbicidal activity (Hartwing & McDaniel, 1995).

Despite the fact of the effectiveness of the acidification, biological systems are extremely complex, particularly with regard to the application of preservation treatments where many variables

are involved. For instance, a non-homogeneous inoculum size in a product batch before its treatment will lead to a distributions of number of survivors, although many zeros will be found, units with “1, 2, 3” etc., survivors can be detected, even if it is assumed a similar initial microbial load, the survivors after a treatment is inherent not the same per each unit. This variability response depends on the intensity of the treatment (Aguirre, Pin, Rodriguez, & García Fernando, 2009). More specifically, the greater the intensity of the applied treatment, the smaller the number of viable cells, with the latter number being highly variable (Aguirre et al., 2009, Aguirre, Rodriguez, & García Fernando, 2011).

Biological variability may be associated with strain variability (Lianou, Stopforth, Yoon, Wiedmann, & Sofos, 2006) and/or intrinsic cell-to-cell variability (i.e. the variable manner in which individual cells respond to environmental conditions) (Nauta, 2000). This intrinsic variability may reflect the differential physiological states of single cells, which are affected by the environmental conditions (including potential stress conditions) that they were previously exposed to (Augustin, Carlier, & Rozier, 1998; Robinson et al., 2001; Whitell, 1942), and, such variability is expected to have a considerable impact on the kinetic behaviour of

\* Corresponding author. Laboratorio de Microbiología y Probióticos, INTA, Universidad de Chile. Avenida El Líbano 5524 Macul. Santiago, Chile.

E-mail address: [juaguirre@vet.ucm.es](mailto:juaguirre@vet.ucm.es) (J.S. Aguirre).

microorganisms, its modelling, and on the processing design to control them (Aguirre et al., 2011). The variation may be even more relevant, especially when a “minimal” treatment is applied, expecting to inactivate all the cells; for instance, in foods in which the presence of a pathogen in a determined weight (usually 25 g) is unacceptable. Knowledge of only the mean population decline is unlikely to be a sufficient basis for processing design. On the other hand, the use of the ‘worst-case’ scenario approach in food processing leads to unrealistic estimations with negative impacts on food quality (Aspridou & Koutsoumanis, 2015), although it may be desirable from a safety point of view.

Ultimately, the number of survivors and its variability will affect and determine the shelf-life of foods during storage. Given that both the variability and uncertainty of each parameter involved in overall risk estimation should be taken into account (Delignette-Muller & Rosso, 2000), characterizing the variability in microbial inactivation is expected to be useful in quantitative microbial risk assessment (QMRA) approaches. Nevertheless, although the biological variability of the number of viable bacteria has been studied with regard to inactivation caused by heat (Aguirre et al., 2009; Mackey, Kelly, Colvin, Robbins, & Fryer, 2006; Metris, George, Mackey, & Baranyi, 2008), irradiation (Aguirre et al., 2011), and high pressure (Cuevas-Muñoz et al., 2013), as well as with respect to individual cell lag phases and growth rate after acidification (Lianou & Koutsoumanis, 2011, 2013; Metris, George, & Baranyi, 2006; Rasch, Metris, Baranyi, & Bjorn Budde, 2007), heat (Metris et al., 2008), osmotic stress (Niven, Morton, Fuks, & Mackey, 2008), and irradiation (Aguirre et al., 2011), few data are available on the effect of acidification on inactivation variability.

The aim of this work was to quantify and analyse the variability in the number of survivors during inactivation through acidification of Gram-positive bacteria *Enterococcus faecalis* and *Listeria innocua*, as well as to the Gram-negative bacteria *Salmonella enterica* serovar Enteritidis, and *Pseudomonas fluorescens*. To do this, two substrates were used: buffered peptone water as a model system, and chicken soup as food system. The latter was chosen because the poultry industry has been involved in several recalls and outbreaks. Both systems were acidified using acetic acid. Citrate solution was used as a control.

## 2. Materials and methods

### 2.1. Bacterial strains and preparation of inocula

*E. faecalis* (LM24), *L. innocua* (ATCC33090), *S. enterica* serovar Enteritidis (ATCC 13076), and *P. fluorescens* (CECT 378) were kept frozen (−20 °C) in tryptic soy broth (TSB, Pronadisa, Madrid, Spain) supplemented with 10% glycerol (Panreac Chemistry S.A., Barcelona, Spain). The bacterial strains were activated and subcultured in sterilised TSB and incubated at 37 °C for 24 h, with the exception of *Pseudomonas fluorescens* which was incubated at 25 °C for 36 h. The strains' cultures were centrifuged (8000 × g for 9 min at 5 ± 1 °C) in a Sorvall RC5B refrigerated centrifuge. Pellets were washed with 10 ml of sterile saline solution (0.80% NaCl [Panreac Chemistry S.A.]), centrifuged again at the same conditions, and the pellets were resuspended in sterile saline solution (diluted in 40 ml of saline solution), resulting in a final inoculum concentration of approximately 10<sup>8</sup> cfu/ml.

### 2.2. Acid challenge trials

The acid challenge trials were undertaken in duplicate test tubes containing three different substrates: (i) sterile citrate solution (citric acid) 0.1 N (C<sub>6</sub>H<sub>8</sub>O<sub>7</sub> [Panreac Chemistry S.A.] and C<sub>6</sub>H<sub>5</sub>O<sub>7</sub>N<sub>3</sub>·2H<sub>2</sub>O [Panreac Chemistry, S.A.]), (ii) chicken soup (Don Simon™,

Almeria, Spain), and (iii) sterile buffered peptone water (Oxoid LTD., Hampshire, United Kingdom). The ingredients of the chicken soup are water, chicken, carrots, onions, parsley, olive oil, salt, corn starch, and aromas, with a composition of 0.4% fat, 0.7% carbohydrates, and 0.6% protein, as stated by the manufacturer. The pH of Chicken soup and buffered peptone water were adjusted with glacial acetic acid (Panreac Chemistry S.A.). The pH values used for acidification treatments, shown in Table 1, were determined in aliquots after sterilization. Each tube containing 9 ml of substrate was inoculated with 1-ml of the bacterial suspensions, and at regular time intervals (1–5 min) 100 µl-aliquots were removed and immediately mixed in tubes with 900 µl of sterile phosphate buffer solution 0.2 N (pH 7.0 Na<sub>2</sub>HPO<sub>4</sub> [Scharlau, Barcelona, Spain] and NaH<sub>2</sub>PO<sub>4</sub> \* H<sub>2</sub>O [Merck, Darmstadt, Germany]) in order to stop the inactivation treatment. Bacterial suspensions were surface-plated on tryptic soy agar (TSA, Pronadisa, Madrid, Spain) using a spiral platter system (model Eddy Jet, IUL Instruments, Barcelona, Spain), and surviving bacteria were enumerated, using an image analyser (model Countermath Flash, IUL Instruments, Barcelona, Spain), after incubation of the plates at 37 °C for 48 h (*L. innocua*, *E. faecalis*, *S. Enteritidis*) or at 25 °C for 72 h (*P. fluorescens*).

### 2.3. Inactivation kinetic parameters

The characterization of the inactivation kinetic behaviour of the tested organisms was based on the estimation of (i) the time required for a 1–log population reduction ( $D_{pH}$  value) and (ii) the difference in pH needed to increase or decrease the  $D_{pH}$  value by 10 times ( $z_{pH}$  value). Both of the above inactivation kinetic parameters were estimated from the inactivation curves of the bacterial strains corresponding to the different treatments applied. More specifically, the  $D_{pH}$  values were calculated as the inverse of the absolute value of the slope of the graphic representing the log of the number of survivors as a function of time. Accordingly, the  $z_{pH}$  values were estimated as the inverse of the slope of the straight line describing log  $D_{pH}$  as a function of pH.

### 2.4. Variability in inactivation

In order to quantify the variability of the number of survivors to acidification treatments, 4.5-ml portions of each one of the three substrates, contained in test tubes, were adjusted to different pH values (see Table 2), and then inoculated with 0.5-ml aliquots of the bacterial suspensions, as described above. In total, 75 tubes were used for each treatment, while 30 tubes, containing the same substrates with pH adjusted to 7.0, were used as controls. By using the  $D_{pH}$  values (Table 1), the times required to obtain from 0 to 4 logarithmic reductions in the populations of each bacterium in the above substrates were applied. When the acid treatment was completed, an aliquot of 100 µl from each tube was removed and mixed with 900 µl of sterile phosphate buffer solution 0.2 N (pH 7.0) in Eppendorf tubes in order to stop the microbicidal effects. To minimize the error due to processing a high number of samples, the order of the tubes was the same for inoculation and for sampling, and the time spent on inoculation was kept as close as possible to the time spent for sampling.

Forty microlitres of each sample (from each Eppendorf tube) was further diluted, if needed, and plated onto TSA by using a spiral platter system. The plates were incubated at 37 °C for 48 h (*L. innocua*, *E. faecalis*, *S. Enteritidis*) or at 25 °C for 72 h (*P. fluorescens*), and colonies were counted with a digital colony counter.

All experiments described in Sections 2.3–2.5 were carried out in triplicated.

**Table 1**  
Estimated  $D_{pH}$  and  $z$  values of selected bacterial species in different substrates.

Bacterium	Acid challenge medium	pH	$D$ value <sup>a</sup> (min)	SE <sup>b</sup>	$R^2$	$z$ values	SE <sup>b</sup>	$R^2$
<i>E. faecalis</i>	Peptone water/acetic acid	3.03	1.16	0.0337	0.98	0.27		
	Peptone water/acetic acid	3.49	47.39	0.0018	0.67			
	Chicken soup/acetic acid	2.59	1.55	0.0459	0.90	0.38	0.32	0.99
	Chicken soup/acetic acid	3.07	51.02	0.0009	0.86			
	Chicken soup/acetic acid	3.52	454.55	0.0009	0.10			
	Citrate solution	2.39	1.86	0.0096	1.00	0.78		
<i>L. innocua</i>	Citrate solution	3.51	6.12	0.0072	0.97			
	Peptone water/acetic acid	3.51	20.12	0.0049	0.83	0.55		
	Peptone water/acetic acid	4.00	158.73	0.0012	0.54			
	Chicken soup/acetic acid	3.09	5.69	0.0195	0.93	0.55	0.28	0.98
	Chicken soup/acetic acid	3.50	52.91	0.0005	0.99			
	Chicken soup/acetic acid	4.01	270.27	0.0006	0.68			
	Citrate solution	2.63	2.78	0.0198	0.97	0.65	0.17	0.98
	Citrate solution	3.09	7.15	0.0152	0.92			
	Citrate solution	3.55	73.53	0.0008	0.94			
<i>P. fluorescens</i>	Citrate solution	4.04	322.58	0.0006	0.57			
	Peptone water/acetic acid	3.84	4.36	0.0098	0.96	0.28		
	Peptone water/acetic acid	4.08	32.57	0.0025	0.76			
	Chicken soup/acetic acid	3.33	1.06	0.0828	0.91	0.32	0.21	1.00
	Chicken soup/acetic acid	3.51	3.22	0.0217	0.91			
	Chicken soup/acetic acid	3.82	37.04	0.0009	0.93			
	Citrate solution	3.01	3.39	0.1142	0.53	0.45	0.24	0.98
	Citrate solution	3.57	34.36	0.0007	0.97			
	Citrate solution	4.08	769.23	0.0004	0.15			
<i>S. Enteritidis</i>	Peptone water/acetic acid	3.52	6.67	0.0107	0.96	0.45		
	Peptone water/acetic acid	4.07	114.94	0.0014	0.67			
	Chicken soup/acetic acid	3.03	2.97	0.0094	1.00	0.44	0.83	0.88
	Chicken soup/acetic acid	3.57	285.71	0.0005	0.72			
	Chicken soup/acetic acid	4.06	666.67	0.0005	0.37			
	Citrate solution	2.56	5.62	0.0122	0.92	0.45	0.23	0.98
	Citrate solution	3.06	109.89	0.0007	0.91			
	Citrate solution	3.52	769.23	0.0001	0.90			

$R^2$  Coefficient of the determination.

<sup>a</sup>  $D_{pH}$  value.

<sup>b</sup> Standard error of the parameter.

### 2.5. Statistical tests

Normal distribution fitting of the numbers of survivors was carried out using the Microsoft Excel Add-in Varifit (BACANOVA, 2005), kindly donated by the programmers from the Computational Microbiology Group of the Institute of Food Research (Norwich, United Kingdom). To analyse the variability, the variances in the distributions of the concentrations of survivors were compared using the Bartlett test (Zar, 1999).

## 3. Results

### 3.1. Inactivation kinetic parameters

The estimated  $D_{pH}$  and  $z_{pH}$  values, obtained for each bacterium from the acid inactivation curves in the different substrates, are shown in Table 1. The experimental data confirmed that a decrease in the applied treatment's pH resulted in a corresponding decrease in the decimal reduction times.

Both tested Gram-positive bacteria (i.e. *L. innocua* and *E. faecalis*), as well as *S. Enteritidis* (Gram-negative) are more acid-tolerant than *P. fluorescens*, which was more susceptible to acidic pH values (Table 1). Also, the estimated  $z_{pH}$  values indicate that acetic acid holds a stronger inactivation potential than citric acid (Table 1). On the other hand, the substrate significantly affected the resistance of the microorganisms to the applied acidification treatments (Table 1). Complex substrates, such as the chicken soup, protected the organisms against the acidification.

### 3.2. Variability in inactivation

Times required to obtain various degrees of inactivation are summarized in Table 2. These times were calculated based on the  $D_{pH}$  and  $z_{pH}$  values presented in Table 1. Despite the fact that the  $D_{pH}$  values in Tables 1 and 2 should theoretically coincide, they showed, in fact, a certain degree of variability, possibly due to the difficulty of adjusting the pH to an exact value and the effect of the auto-claving on the pH.

With regard to the acid tolerance exhibited by the tested bacteria, there were remarkable differences among the substrates used. In general, for the same acidity and similar treatment times, the degree of inactivation was lower in food than that observed in peptone water and citrate solution (Table 2). Indeed, the treatment times required to attain the same degree of inactivation followed the order of magnitude chicken soup/acetic acid > peptone water/acetic acid > citrate solution (Table 2), demonstrating the well-recognized microbicidal activity of acetic acid.

The values of the standard deviation of the number of survivors in the untreated samples were always smaller than those observed in the acidified samples. In addition, as the intensity of the acid treatments increased, the number of surviving bacteria decreased and the standard deviation of the obtained distributions increased proportionally (Table 2). Table 3 shows the regression equations and the corresponding coefficients of determination ( $R^2$ ), describing the effect of the degree of inactivation on the variability in the number of survivors in terms of standard deviation, for each microorganism and substrate. Although in some cases (*E. faecalis* and *L. innocua* in chicken soup/acetic acid and *E. faecalis* and *P. fluorescens* in citrate buffer), the  $R^2$  are far from the unit, the rest

**Table 2**  
Bacterial survival after the application of various acid treatments in different substrates.

Bacterium	medium/acidulant	pH	Expected inactivation	Length of treatment (min)	N° of samples	Mean of survivors (log cfu/ml)	SD	Mean inactivation achieved (log cfu/ml)	Min <sup>a</sup>	Max <sup>b</sup>	Coefficient of variation (%) (100 × SD/mean)
<i>E. faecalis</i>	Peptone/acetic acid	3.08	0	0.0	30	7.4	0.08	0.0	7.3	7.6	1.1
			2	5.3	61	5.2	0.32	2.3	4.6	5.8	6.2
			3	7.9	63	4.6	0.37	2.9	3.8	5.3	8.0
			4	10.6	67	3.9	0.48	3.5	3.0	4.8	12.3
	Chicken soup/ acetic acid	2.80	0	0.0	24	7.6	0.07	0.0	7.4	7.7	0.9
			2	13.9	70	5.4	0.08	2.2	5.3	5.6	1.4
			3	20.9	75	4.9	0.14	2.6	4.7	5.2	2.8
			4	27.8	70	4.0	0.29	3.6	3.4	4.6	7.4
	Citrate solution	3.59	0	0.0	30	7.7	0.08	0.0	7.6	7.9	1.0
			2	13.3	68	5.6	0.44	2.1	4.7	6.5	7.9
			3	20.0	60	5.0	0.50	2.7	4.0	6.0	9.9
			4	26.7	66	4.0	0.60	3.8	2.8	5.1	15.2
<i>L. innocua</i>	Peptone/acetic acid	3.48	0	0.0	24	7.7	0.15	0.0	7.4	8.0	1.9
			2	36.6	76	5.1	0.39	2.6	4.3	5.9	7.7
			3	54.8	76	4.4	0.44	3.4	3.5	5.2	10.2
			4	73.1	76	3.7	0.60	4.0	2.5	4.9	16.2
	Chicken soup/ acetic acid	3.13	0	0.0	15	8.5	0.04	0.0	8.4	8.6	0.5
			2	16.1	75	6.5	0.10	1.9	6.3	6.7	1.6
			3	24.2	76	5.7	0.26	2.8	5.2	6.2	4.6
			4	32.3	76	4.7	0.29	3.8	4.1	5.3	6.2
	Citrate solution	2.97	0	0.0	58	7.7	0.14	0.0	7.4	7.9	1.8
			2	14.8	76	5.9	0.63	1.8	4.7	7.1	10.8
			3	22.3	76	4.9	0.69	2.8	3.5	6.2	14.2
			4	29.7	76	4.1	0.57	3.5	3.0	5.3	13.7
<i>P. fluorescens</i>	Peptone/acetic acid	4.03	0	0.0	30	6.7	0.12	0.0	6.5	7.0	1.8
			2	32.8	73	4.6	0.35	2.1	3.9	5.3	7.6
			3	49.2	75	3.3	0.37	3.4	2.6	4.0	11.3
			4	65.6	76	2.7	0.42	4.0	1.9	3.5	15.4
	Chicken soup/ acetic acid	3.80	0	0.0	11	6.7	0.07	0.0	6.5	6.8	1.0
			2	60.0	75	4.8	0.32	1.8	4.2	5.5	6.6
			3	90.1	75	3.6	0.38	3.2	2.9	4.4	10.5
			4	120.1	75	2.5	0.43	4.2	1.6	3.3	17.4
	Citrate solution	3.77	0	0.0	28	7.3	0.12	0.0	7.1	7.6	1.6
			2	189.3	69	5.1	0.55	2.3	4.0	6.1	10.9
			3	284.0	54	3.3	0.64	4.0	2.1	4.6	19.2
			4	378.7	61	2.8	0.57	5.0	1.3	3.5	20.1
<i>S. Enteritidis</i>	Peptone/acetic acid	3.80	0	0.0	11	7.2	0.13	0.0	7.0	7.5	1.8
			2	57.4	76	5.9	0.23	1.3	5.4	6.3	3.9
			3	243.5	76	3.9	0.48	4.1	2.9	4.8	12.4
			4	324.7	76	3.6	0.47	4.3	2.7	4.6	12.9

SD: Standard deviation (log cfu/ml).

<sup>a</sup> Minimum concentration in a sample (log cfu/ml).

<sup>b</sup> Maximum concentration in a sample (log cfu/ml).

of the  $R^2$  are higher than 0.91.

The increasing variability was proportional to the lethality of the acidification, as can be seen in Fig. 1, which shows the effect of the microbial inactivation on the CVs, a dimensionless parameter that considers both the mean and the standard deviation, and is independent of the unit in which the measurement has been taken. The values of the CVs of the number of bacterial survivors after the most intense treatments were between 5 and 17 times higher than those of untreated samples, particularly in the case of *P. fluorescens* in chicken soup (Table 2). Independently of the CV values, we consistently observed a positive linear relationship between CV (variability) and the intensity of the acidification treatment.

As illustrated in Fig. 2, in which the distributions of the survivors of all microorganisms in each of the tested substrates are presented, the data dispersion becomes greater as the treatment is intensified, increasing the variability of the number of surviving bacteria. Although the achieved inactivation was relatively close to that expected, this was not always the case. For example, the reduction observed in practice for *E. faecalis* in chicken soup acidified with acetic acid was lower than the theoretically expected reduction of 4 logarithmic cycles (Fig. 2B); however, in other cases, the actual reduction was greater than the expected, for instance, for *P. fluorescens* in the three substrates (Fig. 2G–I).

A Bartlett test showed that the variability in the number of viable cells was significantly smaller for the control than for any of the acid-treated organisms (Fig. 2). In most of the cases, the variances in the final bacterial concentrations were significantly different ( $p < 0.05$ ) for the different acid treatments (Fig. 2). In general, the distributions of the logarithms of the final bacterial concentrations did not show tails and the shapes were nearly symmetrical (Fig. 2). In contrast, the distributions of *E. faecalis*, *L. innocua* and *P. fluorescens* concentrations were bimodal for the most severe acid treatments in both chicken soup and peptone, which may be explained by the different acid-resistance patterns within the cell populations.

A multi-test-comparison, using the Bartlett test, showed the significant differences within and in-between intensities, substrates for the same microorganism (Table 4). In general, there were significant differences ( $p < 0.05$ ) between substrates and intensities of the treatments.

#### 4. Discussion

In this study, the effect of pH on the inactivation variability of four microorganisms relevant to food safety was investigated through the application of various acidification (pH) intensities

**Table 3**Equations of regression lines relating the standard deviation of the number of viable bacteria ( $y$ ) to the inactivation achieved ( $x$ ).

Organisms	Substrate	Equation	SE <sup>a</sup>	R <sup>2b</sup>
<i>Enterococcus faecalis</i>	Peptone/acetic acid	$y = 0.108x + 0.0789$	0.023	0.99
	Chicken soup/acetic acid	$y = 0.054x + 0.0309$	0.079	0.62
	Citrate solution	$y = 0.142x + 0.0992$	0.042	0.98
<i>Listeria innocua</i>	Peptone/acetic acid	$y = 0.104x + 0.1333$	0.045	0.96
	Chicken soup/acetic acid	$y = 0.057x + 0.1273$	0.152	0.37
	Citrate solution	$y = 0.136x + 0.2345$	0.176	0.68
<i>Pseudomonas fluorescens</i>	Peptone/acetic acid	$y = 0.072x + 0.1436$	0.046	0.92
	Chicken soup/acetic acid	$y = 0.085x + 0.1045$	0.053	0.93
	Citrate solution	$y = 0.096x + 0.2010$	0.137	0.78
<i>Salmonella</i> Enteritidis	Peptone/acetic acid	$y = 0.724x + 0.1328$	0.010	0.99
	Chicken soup/acetic acid	$y = 0.070x + 0.1615$	0.019	0.99
	Citrate solution	$y = 0.912x + 0.1042$	0.033	0.98

<sup>a</sup> Standard error of the regression.<sup>b</sup> Values of coefficient of determination.

using two acidulants (acetic acid and citrate solution) on two substrates (soup chicken and buffered peptone water). The results showed that the higher the intensity of the applied acid treatments

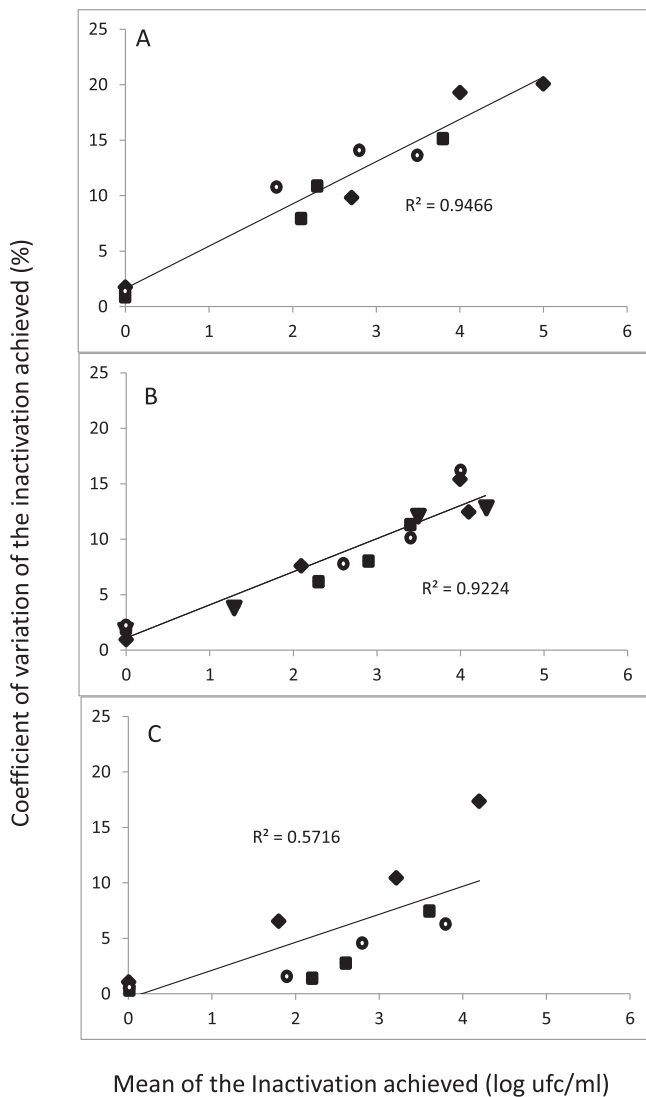


**Fig. 1.** Effect of the inactivation degree achieved through acidification on the variability (coefficient of variation) of the inactivation of *E. faecalis* (squares), *L. innocua* (circles), *Pseudomonas fluorescens* (diamonds) and *Salmonella* Enteritidis (triangles) in citrate buffer (A), peptone/acetic acid (B) and chicken soup/acetic acid (C). R<sup>2</sup> of the regression are shown.

(2, 3, and 4 log reductions), the lower the number of survivors, although number of 4 log reductions is more variable than the others. Several researchers have attempted to characterize the acid stress responses of pathogenic microorganisms, and variable results have been reported (Adams & Nicolaidis, 1997; Buchanan & Edelson, 1999; Koutsoumanis & Sofos, 2004; Lianou & Koutsoumanis, 2013; Nightingale, Thippareddi, Phebus, Marsden, & Nutsch, 2006). Despite the variability and sometimes the discrepancies between the published research findings, such data are of great value from a food quality/safety perspective. Janssen et al. (2007) observed that the inactivation of *L. innocua* with lactic acid was greater, the number of survivors was more variable, and that it may even cause (or not) inactivation of the entire population. These observations coincide with the results obtained in this study (Table 2). This fact has been found in other food conservation operations such as heat treatment (Aguirre et al., 2009) and electron beam irradiation (Aguirre et al., 2011).

Bacterial cells that survive acid treatments may adapt relatively fast to new conditions and have a high chance of recovery and multiplication under favourable conditions (Koutsoumanis & Sofos, 2004), potentially reaching high concentrations during storage of food products, thus compromising their quality (i.e. shelf life) and safety. Acid resistance data are, therefore, expected to be useful in the development of new or the adjustment of already-existing microbial control interventions for application in the food industry.

When microbial inactivation is the result of the application of organic acid treatments, then the estimation of the inactivation parameters ( $D$  and  $z$  values) is relatively complex (Valero, Carrasco, Pérez-Rodríguez, García-Gimeno, & Zurera, 2006) because classic deterministic inactivation models do not take into account heterogeneity in the resistance of individual cells to a lethal stress (Casolari, 1988) which, as in the case of growth, can be a significant source of variability in microbial inactivation during food processing (Aspridou & Koutsoumanis, 2015). In addition, there are certain methodological difficulties in acid inactivation studies that need to be taken into account, most of them stemming from the fact that even minor differences in pH may result in considerable differences in the estimated  $D$  values, as also demonstrated by the results of the present study (Table 1). Such an excessive effect can be attributed to the fact that minimal variations in extracellular pH may produce a corresponding change (increase or decrease) in cytoplasmic pH. Indeed, the cytoplasmic membrane, by comprising a barrier between the external environment and the cellular cytosol, regulates the substances entering and leaving the cell, permitting homeostasis of the cytoplasmic environment (Moat & Foster, 1995). As such, cytoplasmic membranes are both specific and selective structural entities, capable of being actively modified in response to changes in the external medium (Brown, Ross, McMeekin, &

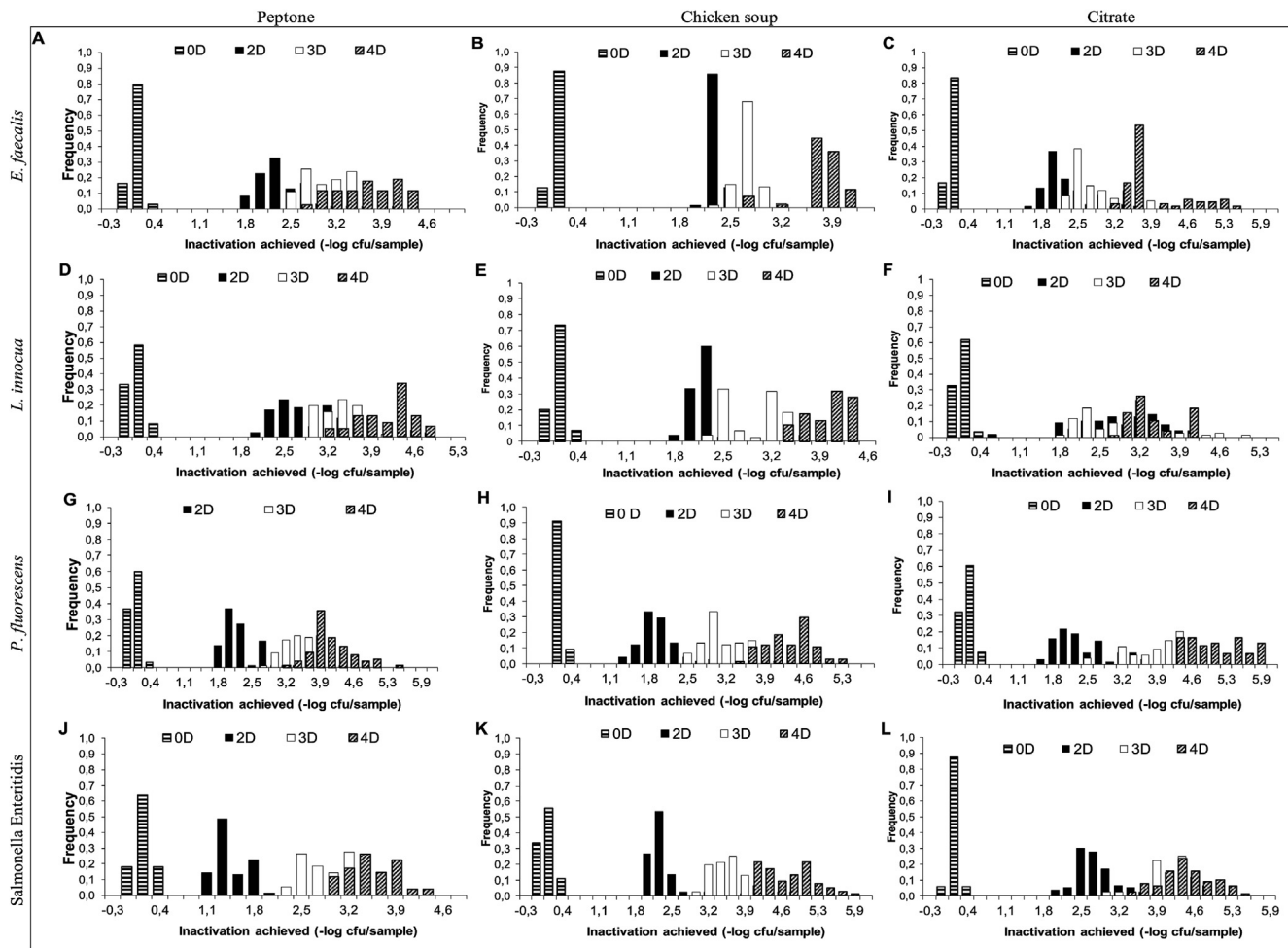


Fig. 2. Distributions of bacterial inactivation in peptone water, chicken soup and citrate solution after the application of different acid treatments. 0D–4D indicate the expected number of decimal reduction.

Nichols, 1997). Hence, increased extracellular concentrations of organic acids can result in the ample movement of the undissociated acid through the cell membrane, causing great mechanical stress to the cell wall and leading to serious cellular damage affecting bacterial survival or even to cell death (Valero et al., 2006).

The results obtained in this study indicate that the resistance intervals to pH of 4.03–2.80 follows a pattern: *E. faecalis* > *L. innocua* > *S. Enteritidis* > *P. fluorescens*, as shown in Table 2, which may be considered similar to that reported by Koutsoumanis and Sofos (2004), who observed that the bacteria with greater resistance to pH ranges of 4.0–5.5 follow this order: *Listeria monocytogenes* > *Escherichia coli* O157:H7 > *Salmonella Typhimurium*.

$D_{pH}$  values estimated in this study are not necessarily comparable to those obtained by other investigators under similar conditions, due to potential differences in the experimental protocols and procedures. According to Fernández, Álvarez-Ordóñez, López, and Bernardo (2009), a treatment time of 3.69 min was required in order to achieve a decimal reduction of 2.5  $\log_{10}$  of *Enterococcus faecium* in brain heart infusion (BHI) acidified to pH 5.0 with acetic acid ( $D$  value around 1.5 min). Álvarez-Ordóñez, Fernández, Bernardo, and López (2009) reported that *S. Typhimurium* inoculated in meat extract acidified to pH 4.5 with acetic acid, was reduced by 4 logarithmic cycles in approximately 9 min ( $D$  value around 2.25 min). These findings are quite different from ours,

where the  $D_{pH}$  value for *S. Enteritidis* at pH 3.5 was estimated at 7 min, a difference that may be ascribed to strain variability. It is well known that the inherent differences among identically treated strains of the same microbial species may constitute an important source of variability in microbiological studies (Whiting & Golden, 2002).

Observations made by other researchers showed that the rate of inactivation is dependent not only on the environmental pH, but also on the type and the concentration of the acidulants used (Buchanan & Edelson, 1999; Buchanan, Golden, & Whiting, 1993). For instance, Buchanan et al. (1993) reported that both the lag (shoulder) period and the inactivation rate of *L. monocytogenes* in BHI acidified with lactic or acetic acid depended on the pH, as well as the identity and the concentration of the acidulant. More specifically, the estimated  $D$  values were inversely related to the levels of undissociated lactic and acetic acids (Buchanan et al., 1993). However in the present study it was not possible to use both acidulants to modify pH of the substrates, so the citrate solution was used only as blank.

In addition, the type of applied acidulant may also determine the extent of variability in the number of surviving bacteria that was seen in our study was also by observed Conner, Scott, and Bernard (1990).

In addition to the pH value and the applied acidulant, another parameter that may have an important effect on the observed acid

**Table 4**

Comparison of the inactivation distributions achieved by acidification treatments using the Bartlett test. The \* in a square means that the distributions obtained with the two inactivation treatments were not significantly different ( $p > 0.05$ ).

<i>E. faecalis</i>					<i>L. innocua</i>				
Substrate	Inactivation	0	2	3	4	0	2	3	4
Peptone	0	0	2	3		0	2	3	
	2		*	4			*	4	
	3				0				0
	4								
Chicken soup	0	*				*			
	2		*			*			
	3			*			*		
	4				*				
Citrate	0	*				*			
	2								
	3			*				*	
	4				*				*

<i>Ps. fluorescens</i>					<i>S. Enteritidis</i>				
Substrate	Inactivation	0	2	3	4	0	2	3	4
Peptone	0	0	2	3		0	2	3	
	2		*	4			*	4	
	3				0				0
	4								
Chicken soup	0	*				*			
	2		*				*		
	3			*				*	
	4				*				
Citrate	0	*				*			
	2								
	3			*				*	
	4				*				*

resistance profiles of microorganisms is the composition of the substrate/food matrix under study. Waterman and Small (1998) showed that bacterial resistance to extremely acidic conditions was enhanced in food matrices with a high fat or protein content. In concordance with these findings, the  $D_{pH}$  values estimated in our study were higher in chicken soup, although its content in fat is not high, but is higher than in the other two substrates (Table 2). Such differences may be attributed to the fact that fat content of foods favour an increase in the concentration of acids in the lipid phase of the bacterial cytoplasmic membrane, limiting the availability and, thus, the antimicrobial activity of acids (Sofos & Busta, 1993). On the other hand, it has been shown that the presence of certain amino acids (e.g., arginine, lysine, and glutamic acid) in the treatment medium can also have an impact on bacterial acid resistance, enabling the activation and manifestation of acid tolerance response (ATR) systems (Castaine-Cornet & Foster, 2001; Castaine-Cornet, Penfound, Smith, Elliott, & Foster, 1999; Foster, 2004; Iyer, Williams, & Miller, 2003). Nevertheless, the peptone contains free amino acids while it is doubtful that chicken soup does.

The linear regressions of Fig. 1 show the variability of the number of survivors after different acidifying treatments. It is evident that the greater the intensity of acidification, the higher is the variability. Some researchers have explained the heterogeneity of microorganisms as a response to the acidification conditions (Brown et al., 1997; Dufourc, Smith, & Jarrell, 1984; Dunkley, Guffanti, Clejan, & Krulwich, 1991).

Variability is characterized by equations (Table 3), where  $y$  is the standard deviation and  $x$  is the degree of inactivation achieved ( $-\log$  cfu/sample). These regressions, in general, are characterized by acceptable coefficients of determination ( $R^2 > 0.91$ ), showing some similarity to other variability data;  $f$ . For instance, the inactivation of *E. faecium* through heating at 70 °C in BHI ( $R^2 = 0.86$ ) (Fernández

et al., 2009) and the irradiation of ham with electron beams irradiation of ham and TSA ( $R^2 = 0.84$ ) experimentally contaminated with *E. faecalis*, *L. innocua*, *P. fluorescens*, and *S. Enteritidis* (Aguirre et al., 2011). The increasing variation in the response of bacteria to less favourable conditions (Fig. 1) has been widely reported in the literature (Aguirre et al., 2009; Álvarez-Ordóñez et al., 2009; Buchanan et al., 1993; Koutsoumanis & Sofos, 2004). This non-homogeneous response of the microbial population to stress conditions depends on many factors, like, the environmental pH of the identity and concentration of acidulant used to modify the pH of the substrate (Buchanan et al., 1993). This heterogeneity can also be a phenotypic response to the modification of fatty acid compositions in the cell membrane, associated with acidity (Brown et al., 1997).

The microbial response in different substrates (Table 1) makes it difficult to compare with other studies; in fact, the components of the substrate, type of acid, inoculum preparation, conditions of pH, time of habituation, and other environmental conditions, make it almost impossible to compare the behaviour of organisms with other studies (Bearson, Wilson, & Foster, 1998; Foster & Hall, 1990). However, there are studies in thermal (Aguirre et al., 2009) and irradiation treatments (Aguirre et al., 2011) that showed that the variability of the number of survivors increased as the intensity of the treatments increased, which was the same tendency observed in the present study. Aguirre et al. (2011) observed  $R^2 (>0.90)$  values in irradiated samples of ham similar to those reported here (Table 3). Our study, suggests that linear equations can be used to predict the variability in the number of survivors after the application of a specific treatment and to calculate the expected frequency in bacterial load in a batch, same finding was described by Aguirre et al. (2009; 2011).

Our results indicate that the distribution of the number of

survivors depends on the severity of the treatment (Fig. 2). This leads to the idea that the inactivation times for the cells within a population are not identically distributed and that applying acid treatments of different severities allows for the survival of different subpopulations, which can explain the bimodal distributions observed at the higher acid treatment (Fig. 2). Regarding inactivation parameters, it has been reported that the resistance of the surviving bacteria and spores increases during the inactivation treatment (Augustin et al., 1998; Aspridou & Koutsoumanis, 2015; Smelt, Bos, Kort, & Brul, 2008), which explains further the heterogeneity of the cells within a population as the result of dynamic survival strategies.

The extensive quantity of data obtained in this study allows us to conclude that microbial inactivation is not constant and that more intense condition of inactivation increase the variability of the number of surviving bacteria. This enormous versatility makes a more solid knowledge of the responses of survivors microorganisms necessary, through predictive models that evaluate and subsequently adjust the shelf-life of foods and minimize microbial hazards, to ensure food safety. Furthermore, the quantification of variability in microbial inactivation is expected to improve the accuracy of risk assessment models.

## Acknowledgements

The authors gratefully acknowledge the support of the Spanish Ministry of Education and Science (projects AGL-2010-16598 and Consolider CSD2007-0016). The authors wish to thank William Chalmers for technical assistance with the manuscript.

## References

- Adams, M. R., & Nicolaides, L. (1997). Review of the sensitivity of different food borne pathogens to fermentation. *Food Control*, *8*, 227–239.
- Aguirre, J. S., Pin, C., Rodríguez, M. R., & García Fernando, G. D. (2009). Analysis of the variability in the number of viable bacteria after mild heat treatment of food. *Applied and Environmental Microbiology*, *75*, 6992–6997.
- Aguirre, J. S., Rodríguez, M. R., & García Fernando, G. D. (2011). Effects of electron beam irradiation on variability of the number of survivors and on duration of lag phase of four food-borne organisms. *International Journal of Food Microbiology*, *149*, 236–246.
- Álvarez-Ordóñez, A., Fernández, A., Bernardo, A., & López, M. (2009). Comparison of acids on the induction of an acid tolerance response in *Salmonella typhimurium*, consequences for food safety. *Meat Science*, *81*, 65–70.
- Aspridou, Z., & Koutsoumanis, K. (2015). Individual cell heterogeneity as variability source in population dynamics of microbial inactivation. *Food Microbiology*, *45*, 216–221.
- Augustin, J. C., Carlier, V., & Rozier, J. (1998). Mathematical modelling of the heat resistance of *Listeria monocytogenes*. *Journal of Applied Microbiology*, *84*, 185–191.
- BACANOVA-Consortium. (2005). *Final report on the European project QLRT-2000-01145: Optimisation of safe food processing methods based on accurate characterisation of bacterial lag time using analysis of variance techniques (BACANOVA)*. Brussels, Belgium: European Commission.
- Bearson, B. L., Wilson, L., & Foster, J. W. (1998). A low pH-inducible, PhoPQ-dependent acid tolerance response protects *Salmonella typhimurium* against inorganic acid stress. *Journal of Bacteriology*, *180*, 2409–2417.
- Brown, J. L., Ross, T., McMeekin, T. A., & Nichols, P. D. (1997). Acid habituation of *Escherichia coli* and the potential role of cyclopropane fatty acids in low pH tolerance. *International Journal of Food Microbiology*, *37*, 163–173.
- Buchanan, R. L., & Edelson, S. G. (1999). pH-dependent stationary-phase acid resistance response of enterohemorrhagic *Escherichia coli* in the presence of various acidulants. *Journal of Food Protection*, *62*, 211–218.
- Buchanan, R., Golden, M. H., & Whiting, R. C. (1993). Differentiation of effects of pH and lactic or acetic acid concentration on the kinetics of *Listeria monocytogenes* inactivation. *Journal of Food Protection*, *56*, 474–484.
- Casolari, A. (1988). Microbial death. In M. J. Bazin, & J. I. Prosser (Eds.), *Physiological models in microbiology* (pp. 1–44). Boca Raton: CRC Press.
- Castaine-Cornet, M. P., & Foster, J. W. (2001). *Escherichia coli* acid resistance: cAMP receptor protein and a 20-bp cis-acting sequence control pH and stationary-phase expression of the *gadA* and *gadBC* glutamate decarboxylase genes. *Microbiology*, *147*, 709–715.
- Castaine-Cornet, M. P., Penfound, T. A., Smith, D., Elliott, J. F., & Foster, J. W. (1999). Control of acid resistance in *Escherichia coli*. *Journal of Bacteriology*, *181*, 3525–3535.
- Conner, D. E., Scott, V. N., & Bernard, D. T. (1990). Growth, inhibition, and survival of *Listeria monocytogenes* as affected by acidic conditions. *Journal of Food Protection*, *53*, 652–655.
- Cuevas-Muñoz, M., Guevara, L., Aznar, A., Martínez, A., Periago, P. M., & Fernández, P. S. (2013). Characterization of the resistance and the growth variability of *Listeria monocytogenes* after high hydrostatic pressure treatments. *Food Control*, *29*, 409–415.
- Delignette-Muller, M. L., & Rosso, L. (2000). Biological variability and exposure assessment. *International Journal of Food Microbiology*, *58*, 203–212.
- Dufourc, E. J., Smith, I. C., & Jarrell, H. C. (1984). Role of cyclopropane moieties in the lipid properties of biological membranes: a H NMR structural and dynamical approach. *Biochemistry*, *23*, 2300–2309.
- Dunkley, E. A., Guffanti, A. A., Clejan, S., & Krulwich, T. A. (1991). Facultative alkaliophiles lack fatty acid desaturase activity and lose the ability to grow at near-neutral pH when supplemented with an unsaturated fatty acid. *Journal of Bacteriology*, *173*, 1331–1334.
- Fernández, A., Álvarez-Ordóñez, A., López, M., & Bernardo, A. (2009). Effects of organic acids on thermal inactivation of acid and cold stressed *Enterococcus faecium*. *Food Microbiology*, *26*, 497–503.
- Foster, J. W. (2004). *Escherichia coli* acid resistance: tales of an amateur acidophile. *Nature Reviews. Microbiology*, *2*, 898–907.
- Foster, J. W., & Hall, H. K. (1990). Adaptive acidification tolerance response of *Salmonella typhimurium*. *Journal of Bacteriology*, *172*, 771–778.
- Hartwing, P., & McDaniel, M. R. (1995). Flavour characteristics of lactic, malic, citric and acetic acids at various pH levels. *Journal of Food Science*, *60*, 384–388.
- Iyer, R., Williams, C., & Miller, C. (2003). Arginine-arginine antipermease in extreme acid resistance in *Escherichia coli*. *Journal of Bacteriology*, *185*, 6556–6561.
- Janssen, M., Geeraerd, A. H., Cappuyens, A., García-Gonzales, L., Schockaert, G., Van Houteghem, N., et al. (2007). Individual and combined effects of pH and lactic acid concentration on *Listeria innocua* inactivation: development of a predictive model and assessment of experimental variability. *Applied and Environmental Microbiology*, *73*, 1601–1611.
- Koutsoumanis, K. P., & Sofos, J. N. (2004). Comparative acid stress response of *Listeria monocytogenes*, *Escherichia coli* O157:H7 and *Salmonella Typhimurium* after habituation at different pH conditions. *Letters in Applied Microbiology*, *38*, 321–326.
- Lianou, A., & Koutsoumanis, K. P. (2011). Effect of the growth environment on the strain variability of *Salmonella enterica* kinetic behaviour. *Food Microbiology*, *28*, 828–837.
- Lianou, A., & Koutsoumanis, K. P. (2013). Evaluation of the strain variability of *Salmonella enterica* acid and heat resistance. *Food Microbiology*, *34*, 259–267.
- Lianou, A., Stopforth, J. D., Yoon, Y., Wiedmann, M., & Sofos, J. N. (2006). Growth and stress resistance variation in culture broth among *Listeria monocytogenes* strains of various serotypes and origins. *Journal of Food Protection*, *69*, 2640–2647.
- Mackey, B. M., Kelly, A. F., Colvin, J. A., Robbins, P. T., & Fryer, P. J. (2006). Predicting the thermal inactivation of bacteria in a solid matrix: simulation studies on the relative effects on microbial thermal resistance parameters and process conditions. *International Journal of Food Microbiology*, *107*, 295–303.
- Metris, A., George, S. M., & Baranyi, J. (2006). Use of optical density detection times to assess the effect of acetic acid on single-cell kinetics. *Applied and Environmental Microbiology*, *72*, 6674–6679.
- Metris, A., George, S. M., Mackey, B. M., & Baranyi, J. (2008). Modelling the variability of single-cell lag times for *Listeria innocua* populations after sublethal and lethal heat treatments. *Applied and Environmental Microbiology*, *74*, 6949–6955.
- Moat, A. G., & Foster, J. W. (1995). *Microbial physiology* (3rd ed., pp. 266–269). New York: Wiley-Liss, Inc.
- Nauta, M. J. (2000). Separation of uncertainty and variability in quantitative microbial risk assessment models. *International Journal of Food Microbiology*, *57*, 9–18.
- Nightingale, K. K., Thippareddi, H., Phebus, R. K., Marsden, J. L., & Nutsch, A. L. (2006). Validation of a traditional Italian-style salami manufacturing process for control of *Salmonella* and *Listeria monocytogenes*. *Journal of Food Protection*, *69*, 794–800.
- Niven, G. W., Morton, J. S., Fuks, T., & Mackey, B. M. (2008). Influence of environmental stress on distributions of times to first division in *Escherichia coli* populations, as determined by digital-image analysis of individual cells. *Applied and Environmental Microbiology*, *74*, 3757–3763.
- Rasch, M., Metris, A., Baranyi, J., & Bjorn Budde, B. (2007). The effect of reuterin on the lag time of single cells of *Listeria innocua* grown on a solid agar surface at different pH and NaCl concentrations. *International Journal of Food Microbiology*, *113*, 35–40.
- Robinson, T. P., Aboaba, O. O., Kaloti, A., Ocio, M. J., Baranyi, J., & Mackey, B. M. (2001). The effect of inoculum size on the lag phase of *Listeria monocytogenes*. *International Journal of Food Microbiology*, *70*, 163–173.
- Smelt, J. P., Bos, A. P., Kort, R., & Brul, S. (2008). Modelling the effect of sublethal heat treatment of *Bacillus subtilis* spores on germination rate and outgrowth to exponentially growing vegetative cells. *International Journal of Food Microbiology*, *128*, 34–40.
- Sofos, J. N., & Busta, E. F. (1993). Sorbic acid and sorbates. In P. M. Davidson, & A. L. Branen (Eds.), *Antimicrobials in foods* (2nd ed., pp. 49–94). New York: Marcel Dekker, Inc.
- Valero, A., Carrasco, E., Pérez-Rodríguez, F., García-Gimeno, R. M., & Zurera, G. (2006). Growth/no growth model of *Listeria monocytogenes* as a function of temperature, pH, citric acid and ascorbic acid. *European Food Research and*

- Technology*, 224, 91–100.
- Waterman, S. R., & Small, P. L. C. (1998). Acid-sensitive enteric pathogens are protected from killing under extremely acidic conditions of pH 2.5 when they are inoculated onto certain solid food sources. *Applied and Environmental Microbiology*, 64, 3882–3886.
- Whitell, E. R. (1942). The significance of the variation on shape of time-survivor curves. *Journal of Hygiene*, 42, 124–183.
- Whiting, R. C., & Golden, M. H. (2002). Variation among *Escherichia coli* O157:H7 strains relative to their growth, survival, thermal inactivation, and toxin production in broth. *International Journal of Food Microbiology*, 75, 127–133.
- Zar, J. H. (1999). *Biostatistical analysis* (4th ed.). Upper Saddle River, NJ: Prentice-Hall.



# Fatty acid ethyl esters (FAEE) in extra virgin olive oil: A case study of a quality parameter



Raquel B. Gómez-Coca <sup>a,\*</sup>, Gabriel D. Fernandes <sup>b</sup>, María del Carmen Pérez-Camino <sup>a</sup>, Wenceslao Moreda <sup>a</sup>

<sup>a</sup> Department of Characterization and Quality of Lipids, Instituto de la Grasa –CSIC, Campus of Universidad Pablo de Olavide, Building 46, Ctra. de Utrera, km 1, 41013, Sevilla, Spain

<sup>b</sup> Fat and Oil Laboratory, Faculty of Food Engineering, University of Campinas, 13083-970, Campinas, SP, Brazil

## ARTICLE INFO

### Article history:

Received 28 August 2015

Received in revised form

14 October 2015

Accepted 25 October 2015

Available online 28 October 2015

### Keywords:

Acidity

FAAE

FAME

Filtration

Volatiles

## ABSTRACT

After establishing the relationship between fatty acid alkyl esters (FAAE) in olive oil and its sensory classification, we proved the correlation between the presence of large quantities of FAAE and the oil's fermentative defects.

Nowadays the olive oil industry is facing strict demands regarding the fatty acid ethyl ester (FAEE) presence in extra virgin olive oil, since a 30 mg/kg limit must be applied to oils produced from 1st March 2016. This decision was made under the assumption that the concentration of FAEE is something fixed. Results here demonstrate otherwise. After a study under controlled storage conditions (temperature, free acidity and volatiles), it is shown that the FAEE concentration increases dramatically over time once the oil is bottled. This, in the case of extra virgin olive oils obtained from mature healthy fruits, may lead in a few month time to FAEE concentrations above the limit permitted to classify the oils as extra virgin, underlying the need of applying certain working practices systematically such as filtering prior bottling, and strict control of the storage temperature.

© 2015 Elsevier Ltd. All rights reserved.

## 1. Introduction

According to the lexicon, to characterize means to present or to describe something through its distinguishing features. It is widely accepted in the olive oil world that the special and typical organoleptic profile of EVOO is the one that will differentiate it from the rest of the oils, including olive oils from other categories.

Olive oil organoleptic assessment plays a relevant role in olive oil classification since it is included in the quality parameters required to allocate a certain oil within one of the legally recognized olive oil categories (European Commission Regulation, 1991). In this case the organoleptic evaluation is made by a trained panel

of experts (International Olive Council, 2011a; International Olive Council, 2011b) where oil's rejection is not a question of acceptance –as in the case of, e.g., preference tests focused on market research (Angerosa & Campestre, 2013)– but a more objective issue. Expert tasters will score positively features such as bitterness, pungency or fruitiness, whereas attributes such as musty, winey-vinegary or muddy sediment will be considered as defects present in the oil due to the utilization of low quality fruits in which fermentative processes have occurred (European Commission Regulation, 1991). There also exist an intermediate and above everything illicit situation in which poor quality virgin olive oils with low organoleptic defects and poor market value (but that would be perfectly accepted by most consumers) are subjected to, e.g., soft deodorization followed by blending with EVOO, in order to mask their negative flavour in front of a panel of experts and therefore to enhance its market price. This is difficult to detect and so far analytical approaches have not been successful enough to unmistakably differentiate this kind of fraud (Saba, Mazzini, Riffaelli, Mattei, & Salvadori, 2005; Serani & Piacenti, 2001; Serani, Piacenti, & Staiano, 2001). To overcome this situation the determination of the content the FAAE was proposed since it was

*Abbreviations:* C16 ET, C16 fatty acid ethyl esters; C16 ME, C16 fatty acid methyl esters; C17:0 ME, methyl heptadecanoate; C18:1, oleic acid; C18 ET, C18 fatty acid ethyl esters; C18 ME, C18 fatty acid methyl esters; EtOH, ethanol; EVOO, extra virgin olive oil; FAAE, fatty acid alkyl esters; FAEE, fatty acid ethyl esters; FAME, fatty acid methyl esters; FID, flame ionization detector; GC, gas chromatography; IOC, International Olive Council; IS, Internal Standard; MeOH, methanol; PrOH, 1-propanol; PTFE, polytetrafluoroethylene; SDr, standard deviation of the repeatability.

\* Corresponding author.

E-mail address: [raquel.coca@ig.csic.es](mailto:raquel.coca@ig.csic.es) (R.B. Gómez-Coca).

demonstrated that they were present at a certain concentration when olive fruits with fermentative alterations had been used for oil extraction (Bendini, Cerretani, Valli, Lercker, & Mazzini, 2009; Pérez-Camino, Cert, Romero-Segura, Cert-Trujillo, & Moreda, 2008). In fact a relationship between the presence of large quantities of FAEE and the sensory classification was established (Gómez-Coca, Moreda, & Pérez-Camino, 2012).

In past years Authorities introduced the FAEE determination as quality parameter that would directly differentiate between extra virgin and non-extra virgin olive oils. This would assure the maximum quality from the point of oil extraction to that of oil bottling. In this way, one had to report the sum of the contents of the FAME and the FAEE from C16 to C18 fatty acids and the total of the two. The limit was set at 75 mg/kg but higher concentrations were allowed provided that they did not exceed 150 mg/kg and that the FAEE/FAME ratio was 1.5 at the maximum (European Commission Regulation, 2011; International Olive Council, 2010).

The knowledge that EtOH was produced as metabolic by-product after alcoholic fermentation (Conte, Mariani, Gallina Toschi, & Tagliabue, 2014) drove to conclude that the presence of high concentration of both FAEE and EtOH would evidence the use of, e.g., fermented olive fruits for oil extraction. Therefore, new requirements were officially published. According to those only C16 ET and C18 ET were to be taken into account in order to decide if a certain olive oil could be classified as extra virgin. This decision was accompanied by a reduction of the maximum allowed limit to 40 mg/kg (2013–14 crop year). Additionally, it was approved to decrease such threshold by 5 mg/kg per year within the two subsequent years (European Commission Regulation, 2013; International Olive Council, 2013a) even considering a further 25 mg/kg threshold (Olimerca, 2015). These reductions represent undoubtedly a critical, although not new, situation since some virgin olive oils first declare as extra virgin will be classified as non-extra virgin. It is clear then clear: That the FAEE content determined after oil extraction will be conditioned by the maturity index of the olive fruit from which it had been extracted, being *really high* if poor quality, overripe, fermented fruits have been used; that both fruit characteristics and good manufacturing practices become crucial for oil quality (Biedermann, Bongartz, Mariani, & Grob, 2008; Mariani & Bellan, 2011); and that some parts of the olive oil obtaining process (e.g. filtering prior bottling) may have to be further optimized. However, worries may arise regarding the FAEE suitability as quality parameter when taking into account the following facts: First of all, it has been demonstrated that ethanol is not only a fermentation by-product, but that it also accumulates in *perfectly healthy fruits* during their maturation on the tree (Beltrán, Bejaoui, Jiménez, & Sánchez-Ortiz, 2015) as derivative in reactions directed to produce, e.g., aroma compounds (Pesis, 2005). Secondly, it has been proven that certain technological processes, e.g., *water addition* during the oil extraction procedure, can change the original EtOH concentration in the oil and therefore FAEE formation (Olimerca, 2015). Finally, with the decreasing limits for FAEE concentration, worries arose regarding oil's behaviour during storage, since the *slightest* FAEE formation after oil extraction when using healthy, *mature* fruits may push EVOO out of the extra virgin classification. So, taking into account the importance of FAEE as quality parameter and in order to increase our knowledge on this subject, we decided to check if EVOO would still remain in the 30 mg/kg legal limit (European Commission Regulation, 2013; International Olive Council, 2013a) after a certain time. Therefore, we carried out a study under controlled conditions (storage temperature and substrate availability), measuring FAEE (FAME and FAEE) concentrations from the moment of the extraction on. We then studied the ester formation in dependence on the substrate availability (free fatty acids and short-chain alcohols such as EtOH and MeOH).

The goal of this work is to study how good quality virgin olive oil (a product of wide scope and significance in the food market) behaves with respect to FAEE formation within the frame of the reduction of the maximum allowed limits. Needless to say that there will be other aspects of the oil, e.g., oxidative quality bound to polyphenol composition, etc., that are also affected by the experimental conditions, but such study is beyond the scope of this article.

## 2. Materials and methods

### 2.1. Chemicals

All chemical reagents were of recognized analytical quality. Water was either distilled or of equivalent purity. The standards of C17:0 ME and C18:1, phenolphthalein, potassium hydroxide, silica gel, 60–200  $\mu\text{m}$  mesh, and Sudan I (1-phenylazo-2-naphthol) were purchased from Sigma (St. Louis, MO, USA). EtOH, ethyl ether, n-hexane, n-heptane, MeOH and PrOH were from Romil Ltd. (Waterbeach, Cambridge, GB).

### 2.2. Samples

A set of 45 EVOO bottles was provided directly by producers from different geographical origins in Andalucía, Spain. These oils were referred as *coupage* oils, meaning they were the result of the fine mixing between each producer's varieties.

These samples were classified as belonging to high quality EVOO by the Official Panel of Tasters of the Instituto de la Grasa (CSIC) in Seville, Spain (International Olive Council, 2013b), as previously described (Gómez-Coca et al., 2012).

### 2.3. Sample preparation

In order to assure that there would be enough quantity of identical oils through out the study, an only starting blend was prepared by gradually adding increasing amounts from all 45 oils and mixing by magnetic stirrers. An alkyl ester analysis was performed (International Olive Council, 2012) to make sure that there were no chromatographic peaks within the retention time windows of the FAEE under study. Also the free acidity expressed as percentage of oleic acid (European Commission Regulation, 1991), and the presence of EtOH and MeOH (Gómez-Coca, Cruz-Hidalgo, Fernandes, Pérez-Camino, & Moreda, 2014) were checked. This starting sample was divided in two portions, one of them to be kept at room temperature (20 °C) and the other at 40 °C. From each portion a set of batches was prepared dividing each of them into three aliquots and spiking them with C18:1 till the free acidity was around 0.2, 0.4, and 0.7%, respectively. Subsequently, each of these aliquots was once again distributed into three equal portions, which were spiked with EtOH and MeOH at concentrations of approximately 20, 40 and 60 mg/kg, respectively. All samples were permanently protected from light. According to the described procedure each alkyl ester determination (FAME, FAEE, and FAEE) encompassed a total of 18 measurements made, at least, in duplicate. This experimental approach has the advantage of including real temperature conditions mimicking both a good storage situation and a less optimal circumstance in which samples are subjected to high temperature. The fact of spiking the EVOO samples with MeOH, EtOH, and C18:1 (see Section 2.3) instead of using virgin olive oil samples of different qualities, obeys to the goal of starting from a olive oil matrix identical in all cases, since it would be unpractical to measure the same analyte in systems with different initial background composition. The chosen volatile concentrations (20, 40, and 60 mg/kg) correspond to the standard

concentration found in EVOO, a higher concentration measured in some single-variety oils (data not shown), and the concentration mimicking accelerated experimental conditions, respectively.

#### 2.4. Analysis of fatty acid alkyl esters (FAAE)

Stock solutions of C17:0 ME were prepared by dissolving this standard in n-heptane at a concentration of 5 mg/L.

Sudan I dye was prepared at 1 mg/mL in a solution of n-hexane in ethyl ether at 990 mL/L.

Samples were prepared just before the analysis. They consisted of a mixture of 0.1 ( $\pm 0.001$ ) g oil and 1 mL C17:0 ME solution, utilized as IS; 100  $\mu$ L of the Sudan I solution were also added to check visually that the analytes were eluted properly.

A procedure recommended by the IOC was used (International Olive Council, 2012). In short: 3 g of silica gel suspended in n-hexane were introduced into the chromatographic column and made to settle homogeneously. The silica was then conditioned with 10 mL n-hexane. Thereafter, the sample prepared as described above was transferred onto the column followed by two 1 mL n-hexane rinses. Washing was made with 10 mL n-hexane. The adsorbed esters were then eluted with 30 mL of a freshly prepared solution of n-hexane in ethyl ether at 990 mL/L. The eluate was evaporated in a rotary evaporator at room temperature under vacuum until a volume of 2 mL, which was then dried under a gentle nitrogen flux, dissolved in 0.5 mL n-heptane, and analysed by GC as described in Section 2.7.

#### 2.5. Peak identification and quantitative analysis

The methyl and ethyl esters of the principal fatty acids found in olive oil (C16 ME, C16 ET, C18 ME and C18 ET, respectively) were identified following published information (Pérez-Camino, Moreda, Mateos, & Cert, 2002).

The quantification of each peak was carried out on the basis of the area corresponding to the C17:0 ME IS as described previously (Gómez-Coca et al., 2012). The results were reported as the sum of the content of the methyl and ethyl esters from C16 to C18, and the total of the two, expressed to the nearest mg/kg.

#### 2.6. Analysis of volatiles: ethanol and methanol

The determination of EtOH and MeOH was carried out according to a published procedure (Gómez-Coca et al., 2014). Summarizing: concentrated PrOH (IS) solutions were prepared in refined olive-pomace oil (2.5 mL/kg). From these concentrated solutions, diluted solutions were made by mixing 1 g concentrated solution with 24 g refined olive-pomace oil.

Samples were prepared just before the analysis in the following way: 3.00 g oil together with 300 mg diluted IS solutions were introduced into a 9 mL vial, which was immediately sealed. They were heated in a dry heat bath at 110 °C during 60 min. The vial headspace was then sampled via a thermostated stainless steel syringe (110 °C; sampling time = 30 s) and analysed by GC (see Section 2.7).

#### 2.7. Instrumentation

GC analyses of the FAAE were carried out with an Agilent 6890N Gas Chromatograph (Agilent Technologies, Santa Clara, California, USA) as described in previous publications (Gómez-Coca et al., 2012), although with some modifications. In this sense, conditions for the GC assays were: HP-5 fused silica capillary column (5% diphenyl-95% dimethylpolysiloxane; 15 m, 0.32 mm ID, 0.10  $\mu$ m film; Agilent Technologies, Santa Clara, California, USA), 2.0  $\mu$ L

injection volume, hydrogen carrier gas at 9.6 mL/min and ECP cool on-column injection. The oven temperature program was: 70 °C, rise at 10 °C/min to 180 °C, then at 5 °C/min to 220 °C, and finally at 10 °C/min to 340 °C, 10 min. The detector temperature was 350 °C.

GC analyses of the volatiles were done with an Agilent 7890B Gas Chromatograph equipped with a Tracer MHS123 2t<sup>®</sup> Head Space Sampler and FID (Agilent Technologies, Santa Clara, California, USA), as described somewhere else (Gómez-Coca et al., 2014).

#### 2.8. Determination of free fatty acids

The determination of the free fatty acids expressed as the percentage of oleic acid was carried out after the procedure published by the European Commission Regulation (1991). According to this, samples were dissolved in a mixture of equal parts by volume of diethyl ether and ethanol (950 mL/L), and titrated using a titrated 0.1 mol/L potassium hydroxide (56.11 g/mol) ethanolic solution, using phenolphthalein as indicator. The acidity was expressed as a percentage by weight and the result as the arithmetic mean of two calculations. Oleic acid molar weight (282 g/mol) was used in the calculations since this is the acid utilized to express results.

### 3. Results and discussion

FAAE concentration is a quality parameter that reflects fruit quality at the moment of the extraction. The evolution of this and other quality parameters are independent from each other and occur in different ways.

In this study olive oil samples have been spiked with short-chain alcohols and free oleic acid; furthermore, half of them have been stored at 40 °C. It is clear that not only the original FAAE content was going to be altered, but also that other quality parameters such as the peroxide content or the UV absorption were going to suffer some transformation, probably reaching limits incompatible with high quality EVOO. However, the development of a comprehensive quality study is quite beyond the scope of this paper and therefore is not going to be discussed in this work, whose only focus is FAAE as the sum of FAME and FAEE.

FAAE are formed by esterification of free fatty acids with short chain alcohols, mainly MeOH and EtOH, yielding methyl and ethyl esters, respectively. FAAE formation takes place easily in acid medium. The development of this first order reaction depends on both temperature and substrate presence. Therefore, we have followed the oil's behaviour at both normal storage conditions (around 20 °C, room temperature) and somehow more extreme situation (40 °C, accelerated conditions), at acidity values according to which the oils would be classified as extra virgin –although they wouldn't be of the same quality-, and with volatile content much higher than that typically found in EVOO of the highest quality (Gómez-Coca et al., 2014; Mariani & Bellan, 2012).

#### 3.1. Analysis of fatty acid methyl and ethyl esters: product formation

The selected chromatographic conditions lead to the separation of the individual esters according to the number of carbon atoms. In this way the gas chromatograms consist of five peaks whose retention times appear within the range from 8.0 to 10.3 min, corresponding to C16 ME, C16 ET, C17:0 ME (IS), C18 ME, and C18 ET.

Generally speaking (for every acidity degree and every volatile concentration) it has been observed that, according to the reaction kinetic, the higher the temperature, the higher the ester formation, regardless if one considers the methyl (data not shown) or ethyl ester contents (Table 1) separately, or the total alkyl ester concentration (Fig. 1). This is because the high temperature increases the

**Table 1**

Fatty acid ethyl ester (FAEE) presence in the virgin olive oil under study measured at different times. Comparison between the evolution at 20 °C and at 40 °C. Before spiking, the oil had been classified as extra virgin of the highest quality according to the existing legislation. After spiking, the oil, divided into three separated batches, had initial acidity values of 0.22%, 0.38%, and 0.77%, respectively. The initial ethanol (EtOH) concentrations are given too. The yellow highlighted figures indicate situations in which the oil is either near or passed the critical 30 mg/kg value. Each value corresponds to the average of at least two individual data. Three times the standard of the repeatability (3SDr) is also given.

Time, days	Acidity (initially) = 0.22 %											
	Initial [EtOH] = 24 mg.kg <sup>-1</sup>				Initial [EtOH] = 43 mg.kg <sup>-1</sup>				Initial [EtOH] = 68 mg.kg <sup>-1</sup>			
	FAEE, mg.kg <sup>-1</sup>	3SDr	FAEE, mg.kg <sup>-1</sup>	3SDr	FAEE, mg.kg <sup>-1</sup>	3SDr	FAEE, mg.kg <sup>-1</sup>	3SDr	FAEE, mg.kg <sup>-1</sup>	3SDr	FAEE, mg.kg <sup>-1</sup>	3SDr
0	1.72	0.42					1.92	0.15	1.49	0.36	1.29	0.25
4	2.02	0.21	1.37	0.25			1.59	0.21			1.65	0.17
12			0.97	0.11	2.41	0.23	1.05	0.15			1.26	0.19
18	3.61	0.34	2.29	0.04	2.91	0.11	3.95	0.76	3.71	0.25	3.22	0.06
27	1.92	0.17			3.92	0.32	1.26	0.23	4.78	0.68	2.35	0.23
34	5.25	0.17			3.94	0.06	2.54	0.02	5.79	0.64	3.43	0.04
48	3.74	0.19	2.15	0.49	6.92	0.40	2.15	0.36	5.85	1.25	3.37	0.04
55	5.89	0.06			7.77	1.59	2.01	0.02	12.09	1.78	3.46	0.28
71	7.14	0.36	2.16	0.30	9.16	0.08	2.69	0.17	13.98	1.80	4.40	0.11
84	7.86	1.40	2.26	0.06	11.02	0.21	2.94	0.59			4.65	0.72
91	8.41	0.93	1.80	0.08	11.25	0.30	3.77	0.08	15.52	3.16		
98	7.96	1.40	2.27	0.23	13.25	1.89	2.67	0.38	17.17	0.59	3.18	0.47
117	8.90	0.38	2.27	0.17	14.08	0.55	3.08	0.28	19.32	3.69	5.10	0.36
134	13.57	1.72	2.55	0.30	21.41	4.45	4.03	0.87	32.38	1.85	5.41	0.02
154	18.35	1.42	3.35	1.10	28.14	4.43	4.36	0.21	39.45	5.32	7.15	0.28
188	26.30	5.41	4.49	1.48	42.78	1.99	6.46	1.53	67.07	6.19	9.73	1.15
209	28.12	0.00	4.59	0.34	45.01	5.24	6.61	0.06			9.92	0.23
224	32.96	8.80	5.40	0.51	45.90	13.19	7.42	0.36	71.95	4.09	10.96	2.40
Time, days	Acidity (initially) = 0.38 %											
	Initial [EtOH] = 22 mg.kg <sup>-1</sup>				Initial [EtOH] = 44 mg.kg <sup>-1</sup>				Initial [EtOH] = 58 mg.kg <sup>-1</sup>			
	FAEE, mg.kg <sup>-1</sup>	3SDr	FAEE, mg.kg <sup>-1</sup>	3SDr	FAEE, mg.kg <sup>-1</sup>	3SDr	FAEE, mg.kg <sup>-1</sup>	3SDr	FAEE, mg.kg <sup>-1</sup>	3SDr	FAEE, mg.kg <sup>-1</sup>	3SDr
0	2.38	0.34	1.94	0.36	3.23	0.56			3.66	0.21	2.38	0.51
4	2.89	0.81	2.03	0.36	4.16	0.67	2.49	0.36	2.98	0.23	2.47	0.36
12			3.01	0.53	9.83	0.04	3.29	0.38			4.15	0.02
18	4.26	0.89	4.26	0.02	6.65	0.41	4.76	0.81	7.35	0.62	4.38	0.91
27	6.08	1.04	2.20	0.28	8.28	1.55	4.05	0.00			4.50	0.17
34	8.40	1.57	5.00	0.70	11.50	0.19	4.89	0.78	10.55	1.36	5.43	0.21
48	9.08	1.85	5.03	0.62	13.21	0.45	7.29	0.83	21.38	1.06	6.12	0.06
55	13.65	1.70	5.32	0.28	19.74	0.49	7.96	0.49	26.79	2.72		
71	14.78	3.56			22.23	1.04	6.59	0.51	30.08	4.62	8.80	0.36
84	16.48	1.19	6.41	0.11	26.47	5.58			36.76	2.88	9.03	0.64
91	16.83	1.29	5.29	0.98	27.94	0.36	6.59	0.59	41.80	15.68	8.53	0.38
98	17.59	0.51	5.05	0.21	26.24	2.21	7.48	1.91	39.44	0.28	8.99	1.29
117			6.48	0.17	32.28	1.87	7.54	0.28			10.60	1.04
134	29.15	0.21	7.81	1.76	52.42	1.08	11.57	0.45	70.49	18.65	14.37	0.30
154	33.30	0.53	10.08	1.38	50.77	8.89	15.18	1.80	73.93	3.73	18.97	4.37
188	47.80	4.14	12.38	0.57	74.72	4.39	20.75	2.50	116.32	11.96	24.00	3.56
209	44.77	4.52	12.22	0.06			17.77	0.13			23.76	0.55
224	50.32	11.31	13.47	0.17			20.71	4.31			25.08	0.72
Time, days	Acidity (initially) = 0.77 %											
	Initial [EtOH] = 20 mg.kg <sup>-1</sup>				Initial [EtOH] = 47 mg.kg <sup>-1</sup>				Initial [EtOH] = 55 mg.kg <sup>-1</sup>			
	FAEE, mg.kg <sup>-1</sup>	3SDr	FAEE, mg.kg <sup>-1</sup>	3SDr	FAEE, mg.kg <sup>-1</sup>	3SDr	FAEE, mg.kg <sup>-1</sup>	3SDr	FAEE, mg.kg <sup>-1</sup>	3SDr	FAEE, mg.kg <sup>-1</sup>	3SDr
0	2.49	0.23			3.03	0.11	2.42	0.69			3.14	0.49
4	3.14	0.47	2.51	0.57			3.31	0.25			3.19	1.00
12	7.55	1.63	3.33	0.25	11.09	4.24	3.26	0.02	6.36	2.08	3.38	1.17
18	4.45	1.02	2.96	0.21	8.57	0.78	5.21	0.98	9.68	0.04	2.92	0.28
27	6.26	1.91	3.04	0.19	11.49	1.12	5.57	1.04	13.87	1.06	5.40	0.53
34	10.33	1.48	4.89	1.06	16.63	4.79	7.45	1.42	20.62	2.38	5.77	1.17
48	16.26	0.78	5.07	1.15	27.78	2.08	8.73	0.59	28.41	2.35	8.58	0.42
55	18.32	2.78	6.55	0.08	38.77	3.71	11.04	0.47	34.33	4.09	9.05	0.02
71			5.59	0.21	46.25	7.81	12.81	1.57	52.40	2.46		
84	21.70	0.06	6.97	0.86	47.13	8.38	12.83	2.25	48.49	1.99	15.03	0.11
91	23.54	0.23	6.76	0.74	47.61	3.33	11.82	1.29	50.76	8.59	15.74	1.29
98	20.26	1.59	6.56	0.25	51.71	18.63	13.35	1.97	48.41	2.27		
117	22.72	9.76	6.78	0.95	50.77	0.11	14.54	0.32	55.57	0.21	14.41	0.95
134	37.62	0.62	10.29	1.10	88.20	4.43	23.02	4.14	99.75	20.60	17.33	1.72
154	38.01	2.31	14.00	3.50	95.11	0.98	29.42	4.01			26.79	4.43
188	51.43	5.54	18.21	0.23			38.06	2.44			34.02	3.25
209			16.08	1.46			35.44	0.68			44.92	1.70
224			17.42	3.82			36.43	4.35				

proportion of reactant molecules (substrates) whose energy is higher than the activation energy, giving rise to a higher concentration of products at a certain time.

Since the limit presently into effect only takes into account the FAEE presence, the discussion has been focused on the ethyl ester (C16 ET and C18 ET) formation, although the results are quite similar for all products and a parallel reasoning may be followed in the case of, e.g., the FFAE (Fig. 1).

Table 1 shows the numerical results for the different conditions tested. The first third of this table gives the figures corresponding to

the lowest acidity value (0.22%). As expected, the higher the substrate concentration (EtOH), the greater the product formation (FAEE). At the lowest EtOH concentration (24 mg/kg) all the samples kept at 20 °C remained within the legal range (that is, with a FAEE content below 30 mg/kg, which is the one required for the oil to be considered as extra virgin) during the time of the measurements. However, those at 40 °C presented FAEE concentrations above 30 mg/kg after seven and a half months. Actually, the moment that the presence of EtOH was more important (around 43 mg/kg) the temperature seemed to have a dramatic effect and

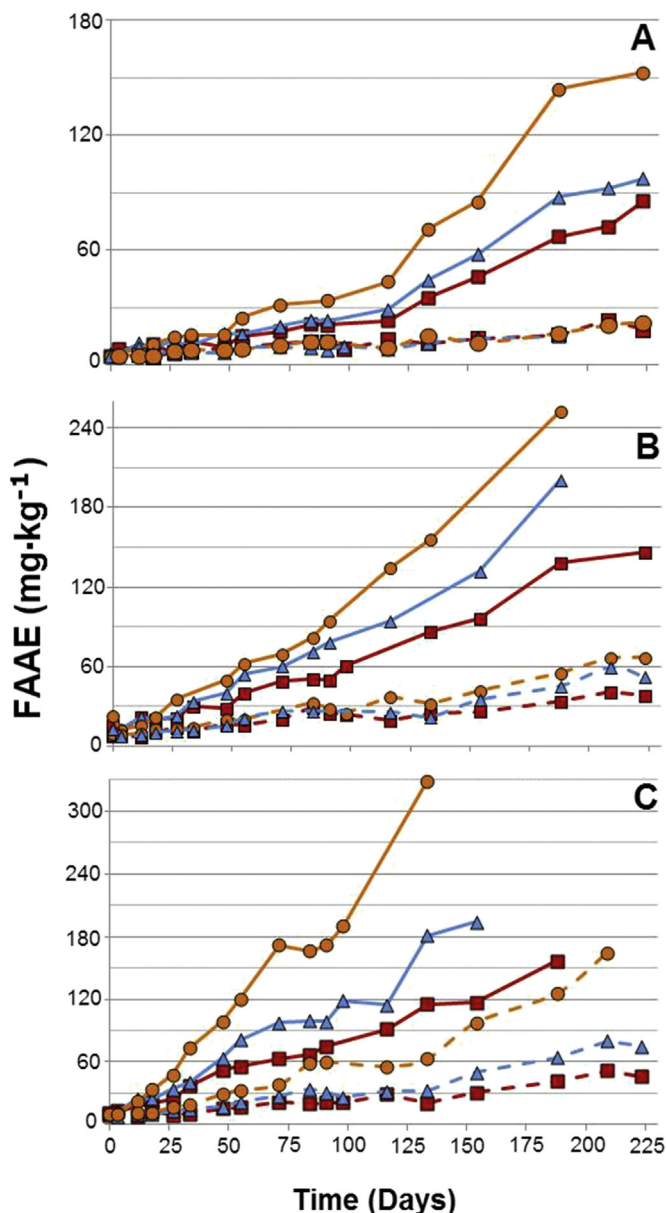


**Fig. 1.** Fatty acid alkyl ester (FAAE) presence in the virgin olive oil under study measured at different times, obtained as the sum of the contents of the fatty acid methyl esters (FAME) and the fatty acid ethyl esters (FAEE) from C16 to C18 fatty acids. Comparison between the evolution at 20 °C (dashed lines) and at 40 °C (solid lines). Before spiking, the oil had been classified as extra virgin of the highest quality according to the existing legislation. After spiking, the oil had an initial acidity value of A) 0.22%, B) 0.38%, and C) 0.77%. The initial methanol and ethanol concentrations, respectively, were: A) 42 and 68 mg/kg (circles), 23 and 43 mg/kg (triangles), and 17 and 24 mg/kg (squares); B) 52 and 58 mg/kg (circles), 37 and 44 mg/kg (triangles), and 25 and 22 mg/kg (squares); C) 86 and 55 mg/kg (circles), 25 and 47 mg/kg (triangles), and 27 and 20 mg/kg (squares).

samples kept at 40 °C were in around five-month time out of limit.

The second third of Table 1 shows homologous results at higher acidity (0.38%). Again, substrate availability enhances product formation. Attention is to be paid even at the lowest volatile concentration, since the samples kept at 40 °C were above the FAAE maximum allowed limit before five months; this period was reduced to two and a half months at the highest EtOH concentration. However, when the storage conditions were optimal (20 °C), even at the highest volatile concentrations, the 30 mg/kg limit was not exceeded.

Finally, in the case of oils with an acidity level near the 0.8% threshold (0.77%), the only samples that at the end of the study (around eight months) clearly showed a FAAE concentration below the 30 mg/kg were those with a relatively low EtOH presence, provided that they were not exposed at high temperatures (third part of Table 1).

### 3.2. Free acidity and volatile concentration: substrate availability

When we looked at how the substrate presence evolved, we verified that at 20 °C there was a reduction of both, free acidity (from 0.22 to 0.18%, from 0.38 to 0.36%, and from 0.77 to 0.53%) and EtOH concentration (decreases between 29 and 49%), which made sense since substrates were disappearing when products were formed. A similar behaviour was observed at 40 °C (EtOH concentration diminished between 33 and 65%) except for the fact that even if free fatty acids were being consumed due to FAAE formation, triglyceride hydrolysis was strong enough to raise the acidity value progressively (from 0.22 to 0.41%, from 0.38 to 0.73%, and from 0.77 to 0.92%), revealing once again the importance of controlling the storage temperature. The law of mass action states that the speed of a chemical reaction is proportional to the quantity of the reacting substances, therefore the boosted FAAE formation at 40 °C when compare with the same situation at 20 °C.

The importance of the temperature on the presence of free fatty acid and therefore on the FAAE formation is also supported by the observations made at different acidity values when comparing results from approximately the same EtOH concentration.

Consequently, at high temperature at least two factors must be considered to have an influence over the increase in FAAE formation in comparison with that at room temperature: A) The enlarged number of reacting molecules charged with enough energy as to surpass the activation energy of the reaction. B) The enhanced triglyceride hydrolysis, which provides the media with higher substrate concentration.

As far as the presumptive EtOH formation is concern, oil filtering before storage prevents the presence of water within the oil matrix, therefore possible fermentation reactions. That would explain the fact that the EtOH present in the media is just consumed and not produced. It is also important to point out that aqueous media will also enhance the presence of alcohols since it will act as media for their solution.

## 4. Final remarks and conclusions

Olive oil is a very complex food bound to a strong industry whose current world production reaches easily three million tons of oil per year (Vossen, 2013) therefore, any decision regarding the corresponding trade standards must be founded on objective data and not be biased by the desires of the different parties involved.

This work has focused on how virgin olive oil behaves with respect to FAAE formation within the frame of the reduction of the maximum allowed limits from 75 mg/kg (FAAE) to 30 mg/kg (FAEE) (European Commission Regulation, 2013; International Olive Council, 2013a).

We have shown that the presence of a certain amount of FAAE is not always indicative of poor quality. EtOH and FAAE will always be present in newly extracted oils classified as extra virgin since it was demonstrated that EtOH is not only a fermentation by-product but that it is also formed in the fruit during aroma development (Beltrán et al., 2015). Both EtOH and FAAE concentrations in oil will be low if fruits with low maturity index have been used, or somehow higher in the case of oil from mature olives. It is important to highlight that, in the opposite way, low FAAE concentrations may not be indicative of high quality, since water addition during the

extraction stage diminishes the EtOH presence (Olimerca, 2015).

To sum up: the formation of FAEE depends, in addition on technological aspects, on the occurrence of the corresponding substrates: free fatty acids and short-chain (from 1 to 4 C-atom) alcohols, mainly EtOH. The FAEE concentration is not something static. We have demonstrated that it increases with time under certain storage conditions, going above the maximum allowed limits in a few months. This evolution over time may lead, in the case of EVOO obtained from healthy, mature (therefore, not necessarily overripe) fruits, to FAEE concentrations above the limit permitted to classify the oils as extra virgin, pushing them out of the highest category in a few-month time. This will be accompanied by the consequent economic loss, being the most acute difference between the extra virgin and the refined categories (International Olive Council, 2015a).

To circumvent the presence of short-chain alcohols in the media once the oil has been extracted, filtration before storage is recommended.

As previously observed (Pérez-Camino, Moreda, & Cert, 2001), controlled temperature conditions (around 20 °C) will decrease TAG hydrolysis, diminishing substrate (free fatty acids) concentration. Besides, low temperature will also prevent such substrate from reaching the activation energy needed to turn it into product, therefore the importance of optimising the storage conditions.

Finally, the economic crisis has pressed the first stages of the production chain (olive milling), decreasing the prices that are being paid to the farmers (International Olive Council, 2015b), who in turn may look for the maximum yield harvesting at the latest (sometimes even overripe) stage of maturation. Besides, olive oil is getting a low-price image and the market loss of manufacturing brands is becoming very serious (International Olive Council, 2015b). Therefore, it may be positive to revise the current olive oil chain situation together with the knowledge of the different parts involved regarding the official limits –in the case at hand, FAEE maximum allowed concentration–, their obligatory nature, and the continuous implementation of good practices focused on getting virgin olive oil of the maximum quality consistently, economically and efficiently.

## Conflict of interest

The authors have declared no conflict of interest.

## Acknowledgements

The authors would like to thank Mss Diana Gómez Castillo for her technical assistance and to the Coordination for the Improvement of Higher Education Personnel (CAPES, Brazil) and National Council for Scientific and Technological Development (CNPq, Brazil) for financial support (Brazilian scholarship).

## References

- Angerosa, F., & Campestre, C. (2013). Sensory quality: methodology and applications. In R. Aparicio, & J. Harwood (Eds.), *Handbook of olive oil. Analysis and properties* (pp. 523–560). New York-Heidelberg-Dordrecht-London: Springer.
- Beltrán, G., Bejaoui, M. A., Jiménez, & Sánchez-Ortiz, A. (2015). Ethanol in olive fruit. Changes during ripening. *Journal of Agriculture and Food Chemistry*, 62, 5309–5312.
- Bendini, A., Cerretani, L., Valli, E., Lercker, G., & Mazzini, C. (2009). Metodi analitici per la determinazione di oli deodorati mild in oli extra vergini di oliva commerciali [Application of analytical methods to determine mildly deodorized olive oils in commercial extra virgin olive oils]. In Italian *Industrie Alimentari*, 48, 46–51.
- Biedermann, M., Bongartz, A., Mariani, C., & Grob, K. (2008). Fatty acid methyl and ethyl esters as well as wax esters for evaluating the quality of olive oils. *European Food Research and Technology*, 228, 65–74.
- Conte, L., Mariani, C., Gallina Toschi, T., & Tagliabue, S. (2014). Alchil esteri e composti correlati in oli d'oliva vergini: loro evoluzione nel tempo [Alkyl esters and related compounds in virgin olive oils: their evolution over time]. In Italian *La Rivista Italiana delle Sostanze Grasse*, 91, 21–29.
- \* European Commission Implementing Regulation. (2013). EU No 1348/2013 of 16 December 2013 amending Regulation No 2568/91/EEC on the characteristics of olive oil and olive-residue oil and on the relevant methods of analysis. *Official Journal of the European Community*, L338, 1–37.
- \* European Commission Regulation. (1991). EEC No 2568/91 of 11 July 1991 on the characteristics of olive oil and olive-residue oil and on the relevant methods of analysis, and subsequent amendments. *Official Journal of the European Community*, L248, 1–102.
- \* European Commission Regulation. (2011). EU No 61/2011 of 24 January 2011 amending Regulation No 2568/91/EEC on the characteristics of olive oil and olive-residue oil and on the relevant methods of analysis. *Official Journal of the European Community*, L23, 1–13.
- Gómez-Coca, R. B., Cruz-Hidalgo, F., Fernandes, G. D., Pérez-Camino, M. C., & Moreda, W. (2014). Analysis of methanol and ethanol in virgin olive oil. *MethodsX*, 1, e207–e211.
- Gómez-Coca, R. B., Moreda, W., & Pérez-Camino, M. C. (2012). Fatty acid alkyl esters presence in olive oil vs. organoleptic assessment. *Food Chemistry*, 135, 1205–1209.
- \* International Olive Council. (2010). Trade standard applying to olive oils and olive pomace oils. *COI/T. 15/NC No 3/Rev. 5*, 1–19.
- International Olive Council. (2011a). Guide for the selection, training and monitoring of skilled virgin olive oil tasters. *COI/T. 20/Doc. No 14/Rev. 3*, 1–13.
- International Olive Council. (2011b). Sensory analysis of olive oil. Method for the organoleptic assessment of virgin olive oil. *COI/T. 20/Doc. No 15/Rev. 4*, 1–14.
- International Olive Council. (2012). Determination of the content of waxes, fatty acid methyl esters and fatty acid ethyl esters by capillary gas chromatography using 3 grams of silica. *COI/T. 20/Doc. No 31*, 1–14.
- \* International Olive Council. (2013a). Trade standard applying to olive oils and olive-pomace oils. *COI/T. 15/Doc. No 3/Rev. 7*, 1–19.
- International Olive Council. (2013b). List of laboratories undertaking the sensory analysis of virgin olive oils recognised by the International Olive Council for the period from 1.12.2013 to 30.11.2014. *T.28/Doc. No 3/Rev. 16*, 1–15.
- International Olive Council (2015a). <http://www.internationaloliveoil.org/estaticos/view/133-eu-producer-prices>. Uploaded on August 26th.
- International Olive Council (2015b). <http://www.internationaloliveoil.org/estaticos/view/307-the-olive-oil-value-chain-in-spain>. Uploaded on August 26th.
- Mariani, C., & Bellan, G. (2011). Sul possibile aumento degli alchil esteri negli oli extra vergini di oliva [Possible increase of alkyl esters in extra virgin olive oil]. In Italian *La Rivista Italiana delle Sostanze Grasse*, 88, 3–10.
- Mariani, C., & Bellan, G. (2012). Sulla determinazione degli alcoli metilico ed etilico negli oli extra vergini di oliva [Determination of methyl and ethyl alcohols in olive oils]. In Italian *La Rivista Italiana delle Sostanze Grasse*, 39, 215–220.
- Olimerca. (2015). <http://www.olimerca.com/noticiadet/uploaded> on May 13th. In Spanish.
- Pérez-Camino, M. C., Cert, A., Romero-Segura, A., Cert-Trujillo, R., & Moreda, W. (2008). Alkyl esters of fatty acids a useful tool to detect soft deodorized olive oils. *Journal of Agriculture and Food Chemistry*, 56, 6740–6744.
- Pérez-Camino, M. C., Moreda, W., & Cert, A. (2001). Effects of olive fruit quality and oil storage practices on the diacylglycerol content of virgin olive oils. *Journal of Agriculture and Food Chemistry*, 49, 699–704.
- Pérez-Camino, M. C., Moreda, W., Mateos, R., & Cert, A. (2002). Determination of esters of fatty acids with low molecular weight alcohols in olive oils. *Journal of Agriculture and Food Chemistry*, 50, 4721–4725.
- Pesis, E. (2005). The role of anaerobic metabolites, acetaldehyde and ethanol, in fruit ripening, enhancement of fruit quality and fruit deterioration. *Postharvest Biology and Technology*, 37, 1–19.
- Saba, A., Mazzini, F., Riffaelli, A., Mattei, A., & Salvadori, P. (2005). Identification of 9(E),11(E)-18:2 fatty acid methyl ester at trace level in thermal stressed olive oils by GC coupled to acetonitrile CI-MS and CI-MS/MS, a possible marker for adulteration by addition of deodorized olive oil. *Journal of Agriculture and Food Chemistry*, 53, 4867–4872.
- Serani, A., & Piacenti, D. (2001). Sistema analitico per l'identificazione di oli deodorati in oli vergini di oliva. Nota 1 – Analisi dei pigmento clorofilliani in oli vergini di oliva [Identification of deodorized oils in virgin olive oils. Note 1 – Analysis of chlorophyll pigment in virgin olive oils]. In Italian *La Rivista Italiana delle Sostanze Grasse*, 78, 459–463.
- Serani, A., Piacenti, D., & Staiano, G. (2001). Sistema analitico per l'identificazione di oli deodorati in oli vergini di oliva. Nota 2-Cinetica di isomerizzazione dei digliceridi in oli vergini di oliva [Identification of deodorized oils in virgin olive oils. Note 2-Kinetics of diacylglycerols isomerization in virgin olive oils]. In Italian *La Rivista Italiana delle Sostanze Grasse*, 78, 525–528.
- Vossen, P. (2013). Growing olives for oil. In R. Aparicio, & J. Harwood (Eds.), *Handbook of olive oil. Analysis and properties* (pp. 19–56). New York-Heidelberg-Dordrecht-London: Springer.



# Effect of stepwise baking on the structure, browning, texture, and *in vitro* starch digestibility of cookie



Kiyoshi Kawai <sup>a, b, \*</sup>, Kana Hando <sup>b</sup>, Ratiya Thuwapanichayanan <sup>c</sup>, Yoshio Hagura <sup>a, b</sup>

<sup>a</sup> Department of Biofunctional Science and Technology, Graduate School of Biosphere Science, Hiroshima University, Hiroshima, Japan

<sup>b</sup> Faculty of Applied Biological Science, Hiroshima University, Hiroshima, Japan

<sup>c</sup> Department of Farm Mechanics, Faculty of Agriculture, Kasetsart University, Bangkok, Thailand

## ARTICLE INFO

### Article history:

Received 30 March 2015

Received in revised form

25 October 2015

Accepted 28 October 2015

Available online 2 November 2015

### Keywords:

Baking temperature

Baking time

Water evaporation rate

Melting temperature

Differential scanning calorimetry

## ABSTRACT

In order to demonstrate stepwise baking without starch melting of cookie, the effects of water content on the starch melting temperature ( $T_m$ ) and baking temperature on the water evaporation rate were investigated in cookie dough. The  $T_m$  of starch was confirmed to increase with the decrease in water content. The water evaporation rate was evaluated by first-order kinetics, and temperature dependence of the water evaporation rate was described by two Arrhenius lines intersecting at approximately 107 °C. From these results, stepwise baking set to at least 10 °C lower than the starch  $T_m$  was designed. The spread factor of the stepwise-baked cookie was lower than that of conventionally baked cookie (control). Further, browning differed minimally and no significant difference in rupture force was observed between methods. The non-hydrolyzed starch content at a given condition was much higher in the stepwise-baked cookie than in the control.

© 2015 Elsevier Ltd. All rights reserved.

## 1. Introduction

Starch is one of the major ingredients in food, and considerable interest has been focused on the reduction of starch digestibility with respect to its physiological benefits (Englyst, Englyst, Hudson, Cole, & Cummings, 1999; Lehmann & Robin, 2007). The susceptibility of starch to digestion depends on its physical state; non-melted starch (crystalline amylopectin) is more stable chemically and physically than the melted (amorphous) form, depending on the botanical source of the starch. For example, non-melted starch in cereal starch (e.g., wheat, rice, and corn) and in tuber starch (e.g., potato) usually contributes to slowly digested starch and resistant starch, respectively (Liu, Donner, Yin, Huang, & Fan, 2006; Chung, Liu, & Hoover, 2009; Fuentes-Zaragoza, Riquelme-Navarrete, Sánchez-Zapata, & Pérez-Álvarez, 2010; Themeier, Hollmann, Neese, & Lindhauer, 2005).

Since the melting temperature ( $T_m$ ) of starch increases with decreasing water content (Biliaderis, Page, Maurice, & Juliano, 1986; Roos, 1995; Tester & Debon, 2000), the melting of starch in

low-moisture starchy food products can be partially prevented, depending on the ingredients, structure, and thermal processing (Bravo, Englyst, & Hudson, 1998; Goñi, Bravo, Larrauri, & Saura Calixto, 1997; Kingman & Englyst, 1994; Lineback & Wongsrikasem, 1980; Primo-Martín, van Nieuwenhuijzen, Hamer, & van Vliet, 2007; Wootton & Chaudhry, 1980). The possibility exists that the digestibility of low-moisture starchy food products can be reduced by further dehydration prior to thermal processing (pre-dehydration). In our previous studies (Kawai, Kawai, Tomoda, Matsusaki, & Hagura, 2012a; Kawai, Matsusaki, Hando, & Hagura, 2013), the *in vitro* starch digestibility of pre-dehydrated cookie dough baked at a given condition was significantly lower than that of normal (non-dehydrated) cookie. In addition, the pre-dehydrated cookie showed a significantly reduced blood glucose peak in mice at 30 min post-administration. It is known that cookie originally contains a large amount of non-melted starch (Lineback & Wongsrikasem, 1980; Wootton & Chaudhry, 1980). As mentioned above, the degree of starch melting depends on the ingredients, structure, and thermal processing of the starchy food. Our previous results suggest that the reduction of starch digestibility can be further enhanced when starch melting is completely prevented by pre-dehydration treatment. However, cookie production does not currently involve a dehydration process, making it challenging for the food industry to produce a pre-dehydrated cookie.

\* Corresponding author. Department of Biofunctional Science and Technology, Graduate School of Biosphere Science, Hiroshima University, 1-4-4 Kagamiyama, Higashi-Hiroshima, Hiroshima 739-8528, Japan.

E-mail address: [kawai@hiroshima-u.ac.jp](mailto:kawai@hiroshima-u.ac.jp) (K. Kawai).

When cookie dough is baked at a lower temperature than the  $T_m$  of starch in cookie dough, starch melting will be completely prevented. However, under these conditions, cookie dough water evaporation would require too much time for optimal baking. Thus, it was proposed that baking without starch melting would occur during a limited period, when baking temperature was raised simultaneously with decreased water content (with increased  $T_m$  of starch). This baking process is denoted as “stepwise baking” in this paper (Fig. 1). In designing stepwise baking, the effects of water content on the starch  $T_m$  and baking temperature on the water evaporation rate were investigated in cookie dough. Subsequently, qualities (macroscopic structure, browning, texture, and *in vitro* starch digestibility) of stepwise-baked cookie were compared to conventional cookie.

## 2. Materials and methods

### 2.1. Preparation of cookie dough

Cookie dough samples were prepared according to our previous studies (Kawai et al., 2013). Foodstuffs required for the cookie preparation were purchased at a local market. The butter (80 g), whole eggs (50 g) and sugar (60 g) were mixed, and wheat flour (200 g) was then added with brief stirring. The mixture was covered with plastic wrap and kept at 4 °C for 1 h, and then the dough was formed into columns ( $\phi$  30 mm  $\times$  5 mm). The cookie dough samples were placed on a metal plate covered with a silicone baking paper, and baked using a drying oven (OFW-300S; As One Co., Osaka, Japan). In order to obtain conventionally baked cookie (control), cookie dough was baked at 180 °C for 18 min. Stepwise-baked cookie was prepared by a multiple baking processing; at 93 °C for 65.4 min, at 103 °C for 23.3 min, at 114 °C for 11.8 min, at 124 °C for 5.0 min, at 134 °C for 3.3 min, and at 144 °C for 12.2 min, details of which are given later.

### 2.2. Melting temperature of starch in cookie dough

Effect of water content on the starch  $T_m$  of the cookie dough was investigated using a differential scanning calorimetry (DSC120; Seiko Instruments Inc., Tokyo, Japan). Alumina powder was used as a reference, and the temperature and heat flow were calibrated with indium and distilled water. Cookie dough samples were dehydrated by pressure vacuum at 6.3 kPa at 40 °C for up to 6 h. Individual dehydrated cookie dough samples were homogeneously mixed before measurement. The sample (20–50 mg) was hermetically sealed in an aluminum pan. DSC measurement was performed at 5 °C/min in the temperature range between 0 °C and 200 °C. The DSC thermogram was analyzed using a software (EXSTAR6000) interfaced with the DSC. In order to identify the starch melting peak from the DSC thermogram, a polarized light microscopy study was carried out (Kawai et al., 2012a). DSC measurement was stopped at several temperatures, and the sample was removed from the DSC pan. The sample was set on a glass plate, and microscopically (BH-2 connected U-PMTVC; Olympus, Co., Tokyo, Japan) assessed for characteristic polarization crosses due to the presence of crystalline amylopectin. Water content of the samples for DSC measurement was determined gravimetrically by drying at 105 °C for 18 h. All tests were performed in duplicate and the results averaged.

### 2.3. Water evaporation rate of cookie dough

In order to understand the effect of temperature on the water evaporation rate of cookie dough samples, the water content change of the cookie dough samples was investigated at each

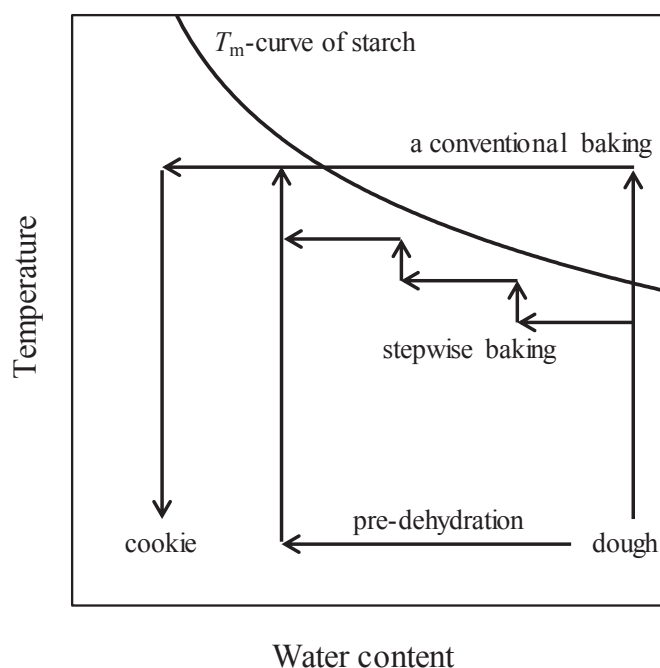


Fig. 1. Schematic representation of the pre-dehydrated baking and stepwise baking of cookie dough.

temperature. The drying oven was set in the temperature range between 90 °C and 180 °C. The cookie dough samples were placed on a metal plate covered with a silicone baking paper, and baked for up to 420 min in the oven. The cookie dough samples were removed from the oven at regular intervals, and then each sample was immediately placed into a poly-pack in order to avoid further water evaporation. The samples in the pack were cooled at room temperature. Individual samples were powdered by pounding and homogeneously mixed, and then the water content of samples was evaluated gravimetrically by drying at 105 °C for 18 h. All tests were performed in triplicate and the results averaged.

### 2.4. Temperature change of cookie dough

The temperature change of cookie dough samples during baking was recorded every second using a data logger (TC-08; Pico Technology Ltd., Cambridgeshire, UK). Thermocouples were applied to two areas; one was inserted into the center part of the cookie dough and the other was attached to the metal plate on which the cookie dough samples were placed. All measurements were performed in triplicate and the results averaged.

### 2.5. Macroscopic structure of cookie

In order to understand the macroscopic structure of the cookie samples, the spread ratio ( $D/T$ ) was investigated (Jacob & Leelavathi, 2007; Sharma, Velu, Indrani, & Singh, 2013; Singh et al., 2011). The mean diameter ( $D$ ) and thickness ( $T$ ) of cookie samples were measured with a digital caliper. Since the cookies were not always an exact round shape, the longest and shortest diameters were measured and the mean  $D$  value was determined. The  $T$  of cookie samples was measured as the length between the top and bottom of the cookie. All tests were performed in triplicate and the results averaged.

## 2.6. Browning of cookie

Browning of cookie samples was evaluated using a color-difference meter (NR-3000; Nippon Denshoku Ind., Co., Ltd., Tokyo Japan). Since browning depended on the location of the cookie, a cookie pellet was employed for the measurement. Individual cookie samples were homogeneously crushed, and the cookie powder (200 mg) was placed between stainless steel plates in a stainless steel die. The powder was compressed at 100 kgf using a hand press, and a pelleted sample (diameter = 14 mm) was obtained. The photometer was positioned to the flat surface of the pelleted samples, and brightness ( $L$ ), red to green ( $a$ ), and yellow to blue ( $b$ ) values were determined. All tests were performed in triplicate and the results averaged.

## 2.7. Rupture force of cookie

The rupture force ( $F_r$ ) of cookie samples was investigated using a rheometer (CR-150; Sun Scientific Co., Ltd., Tokyo, Japan). Two acrylic blocks (38 mm × 70 mm × 20 mm) were used to support the samples. The blocks were put on the sample stage at intervals of 15 mm, and the cookie sample was placed on the two blocks like a bridge. The center part of the cookie bridge was pushed at 1 mm/s by a front tooth plunger (contact area: 1.73 mm × 11.88 mm), and  $F_r$  (N) was then determined from the fracture point. All tests were performed in triplicate and the results averaged.

## 2.8. *In vitro* starch digestibility of cookie

*In vitro* starch digestibility of the cookie samples was evaluated using a resistant starch assay kit (Megazyme International Ireland, Wicklow, Ireland) with minor modifications according to our previous studies (Kawai et al., 2012a; Kawai et al., 2013). In brief, pancreatin (1 g) in 100 ml of 0.1 mol/l sodium maleate buffer (pH 6.0) was mixed with 1.0 ml of amyloglucosidase solution (5  $\mu$ kat/ml), and the supernatant was decanted after centrifuging at 1500 g for 10 min. Homogeneously crushed cookie sample (102.1–100.5 mg) was added to 4 ml of the decanted supernatant, and the sample was incubated in a water bath (37 °C) with continuous shaking at 200 strokes/min for 20 min and 120 min. The sample was mixed with 4 ml of ethanol using a vortex mixer, and then centrifuged at 1500 g for 10 min. The supernatant was removed, and ethanol washing was repeated once more. The obtained sediment was hydrolyzed using 2 ml of 2 mol/l KOH and a subsequent 8 ml of 1.2 mol/l sodium acetate buffer (pH 3.8) with 0.1 ml of amyloglucosidase (55  $\mu$ kat/ml). The amount of glucose in the sample was analyzed quantitatively according to the glucose oxidase/peroxidase method, and the non-hydrolyzed starch contents of the cookie samples treated for 20 min (NHS20) and 120 min (NHS120) were evaluated. All tests were performed in quadruplicate and the results averaged.

## 2.9. Statistical analysis

Statistical analysis of cookie qualities between conventionally baked cookie (control) and stepwise-baked cookie was performed using a t-test ( $p < 0.05$ ) with Kaleida Graph (Version 3.6; Synergy software, Reading, PA, USA).

## 3. Results and discussion

### 3.1. Melting temperature of starch in cookie dough

The DSC thermogram showed multiple endothermic peaks reflecting the melting of butter, egg protein, amylose–lipid

complex, a portion of the sugar, and starch (Barbut & Findlay, 1990; Kawai, Takato, Sasaki, & Kajiwara, 2012b; Ma, 1990; Roos, 1995). In order to identify the melting of starch, a polarized microscopy study was carried out, and the endothermic peak observed at the highest temperature was determined to be the starch melting of this sample. This interpretation agreed with starch melting in another type of cookie dough (Kawai et al., 2012a). The  $T_m$  of starch in cookie dough was evaluated from the onset point of the peak. The  $T_m$  values were varied in the range of  $\pm 4$  °C. The effect of water content on the  $T_m$  of starch in cookie dough is shown in Fig. 2. The solid line is provided as a visual guide ( $y = -34.99\ln(x) + 209.64$ ,  $R^2 = 0.9993$ ). It was confirmed that  $T_m$  increased with the decrease in water content of cookie dough (Biliaderis et al., 1986; Roos, 1995; Tester & Debon, 2000). For comparison,  $T_m$ -curves of starch in another type of cookie dough ( $y = -30.72\ln(x) + 183.5$ ,  $R^2 = 0.9995$ ) and in wheat flour ( $y = -3.1742x + 198.77$ ,  $R^2 = 0.9980$ ) were referenced from our previous study (Kawai et al., 2012a). The  $T_m$  values obtained in this study were much greater than the previous results. The previous cookie dough contained double the amount of sugar (120 g) used in this study. This indicates that sugar acts as a plasticizer in the cookie dough (Kalichevsky, Jaroszkievicz, & Blanshard, 1992; Kawai, Toh, & Hagura, 2014; Mathew & Dufresne, 2002; Roos, 1995) and promotes starch melting. This interpretation is also supported by the fact that the  $T_m$  values of starch in cookie dough samples were much lower than those in wheat flour. In addition, similar results can be found in some previous studies (Perry & Donald, 2002; Van Soest, Bezemer, De Wit, & Vliegenthart, 1996). For example, Perry and Donald (2002) investigated  $T_m$  of starch in starch-glucose-water mixture and in starch-glycerol-water mixture. When water content of the mixtures was 17.6 g/100 g-DM,  $T_m$  of starch in the mixtures was approximately 120 °C and 106 °C, respectively (DSC peak top temperature). At the same water content, the  $T_m$  values are much lower than wheat flour (143 °C), but are close to cookie dough (110 °C) obtained in this study. It should be noted that saccharide

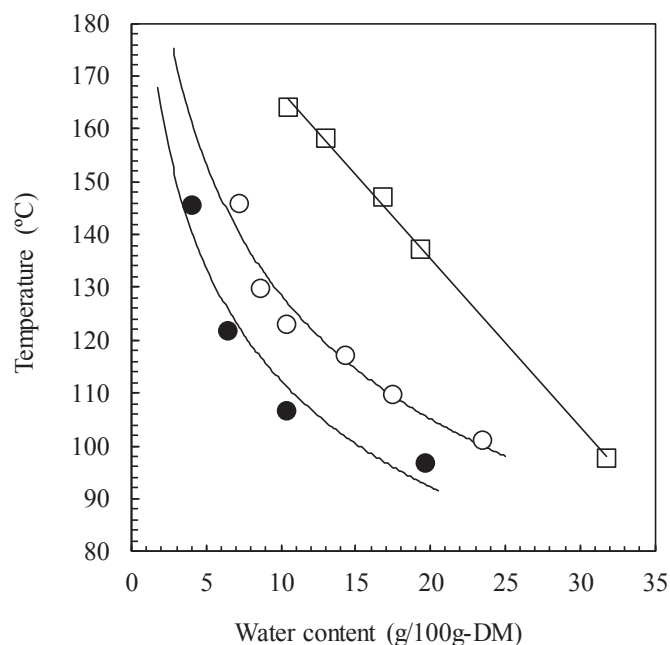


Fig. 2.  $T_m$ -curves of starch in cookie dough and wheat flour, ○: cookie dough (this study), ●: cookie dough containing double the amount of sugar used in this study (Kawai et al., 2012a), □: wheat flour (Kawai et al., 2012a). The  $T_m$  was evaluated from the onset point of the DSC peak. The solid lines are empirically provided as a visual guide.

and/or polyol can elevate the  $T_m$  of starch at a higher water content (Ahmed, 2012; Li, Li, & Gao, 2015; Perry & Donald, 2002; Van Soest et al., 1996; Sopade, Halley, & Junming, 2004). This indicates that effect of the additives on the  $T_m$  of starch is affected by water content. In an excess water system, water can strongly contribute to the starch melting. The additives which have dissolved in water reduce water activity, and thus the  $T_m$  of starch will be elevated. In a limited water system, the additives as well as water can contribute to the starch melting as plasticizer. In a comparison of molecular mobility at a same water content, starch containing the additives is more flexible than non-additive starch. Consequently, the  $T_m$  of starch will be reduced by the additives. In order to prove this suggestion, further experiment will be required.

### 3.2. Temperature dependence of the water evaporation rate

The plate ( $T_{plate}$ ) and sample-center ( $T_{center}$ ) temperatures were investigated during baking at various preset oven temperatures. The  $T_{plate}$  increased rapidly from baking onset, and reached equilibrium within 5–8 min. The equilibrium plate temperature ( $T_{Eplate}$ ) was lower than the corresponding preset oven temperature ( $T_{set}$ ), and the relationship was described experimentally as a linear function ( $T_{Eplate} = 0.9841 \times T_{set} - 1.6971$ ,  $R^2 = 0.9997$ ). The  $T_{center}$ , on the other hand, increased gradually in comparison to  $T_{plate}$ , and continued increasing gradually during baking. This is because the heat capacity of the samples decreased according to their water content. For this reason, the equilibrium  $T_{center}$  could not be determined clearly. Since the purpose of this study was to prevent starch melting during baking, it was important that the maximum sample temperature was lower than the starch  $T_m$ . The  $T_{Eplate}$  can be assumed to be the maximum temperature of the sample. Thus,  $T_{Eplate}$  was employed for the following analysis as the typical temperature at each baking condition.

The effect of baking time on the water content of cookie dough samples at various temperatures is shown in Fig. 3. The water content decreased with the increase in baking time depending on

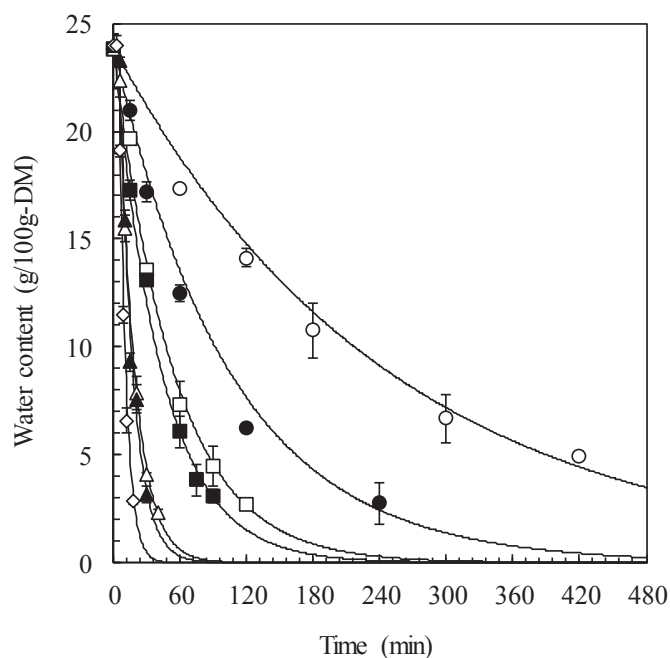


Fig. 3. Effect of baking time on the water content of cookie dough samples at each equilibrium plate temperature ( $T_{Eplate}$ ). ○: 87 °C, ●: 96 °C, □: 107 °C, ■: 116 °C, △: 137 °C, ▲: 146 °C, ◇: 175 °C. The values are expressed as mean  $\pm$  SD ( $n = 3$ ).

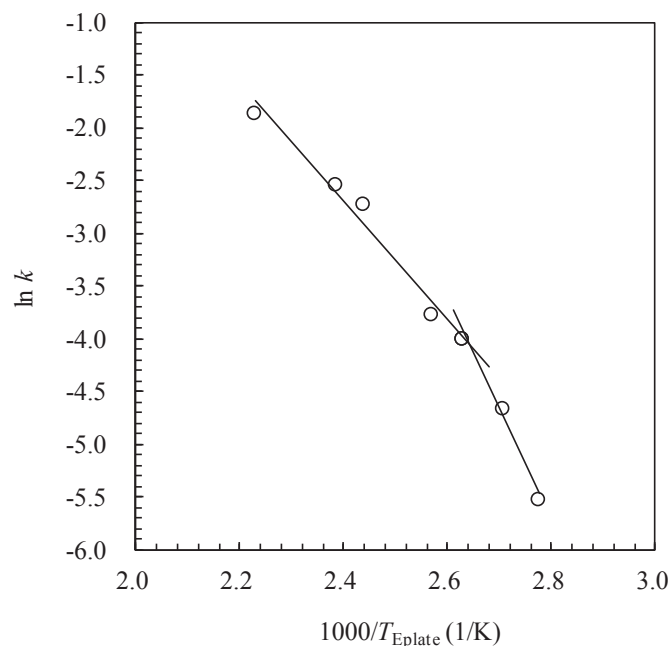


Fig. 4. Arrhenius plot for the water evaporation rate ( $k$ ) of cookie dough samples.

the temperature. This behavior can be described as first-order kinetics ( $R^2 > 0.9839$ ), and the water evaporation rate was determined at each temperature. At temperatures higher than  $T_{Eplate} = 116$  °C, first-order kinetics deviated from the experimental data at the initial stage because of heat transfer. Consequently, the initial data for up to 5 min was removed from the evaluation of water evaporation rate.

The effect of  $T_{Eplate}$  on the water evaporation rate of cookie dough samples was described as an Arrhenius plot in Fig. 4. Temperature dependence of the water evaporation rate was described by two lines intersecting at approximately 107 °C. This result suggests that there are two different mechanisms in the water evaporation. The activation energy and pre-exponential factor at temperatures below and above the crossover temperature were 86 kJ/mol and  $1 \times 10^{10}$  1/min ( $R^2 = 0.9859$ ) and 47 kJ/mol and  $5 \times 10^4$  1/min ( $R^2 = 0.9795$ ), respectively. When hydrogen bond energy is estimated to be 20 kJ/mol (Oguni, Kanke, Nagoe, & Namba, 2011), the activation energies for water evaporation at temperatures below and above the crossover temperature were approximately equivalent to the energy required to break four and two hydrogen bonds, respectively. Although water molecules form maximally four hydrogen bonds, the hydrogen bonds are partially broken at a higher temperature.

### 3.3. Design of stepwise baking

In order to design a typical stepwise baking, baking temperature was set to at least 10 °C lower than the  $T_m$  of starch in cookie dough. Since the  $T_m$  of starch in the initial cookie dough was approximately 100 °C,  $T_{Eplate}$  was set to 90 °C. When the  $T_m$  of starch was increased up to 110 °C during baking, the baking temperature was increased up to 100 °C. This process was repeated until the water content of cookie dough was reduced to the water content of control cookie (approximately 3.09 g/100 g-DM). Each  $T_{set}$  was evaluated from the linear function between  $T_{Eplate}$  and  $T_{set}$  mentioned above. The baking time at each temperature was calculated from the Arrhenius plot (Fig. 4). The result is shown as a solid line in Fig. 5. In order to demonstrate the stepwise baking, the cookie dough sample was

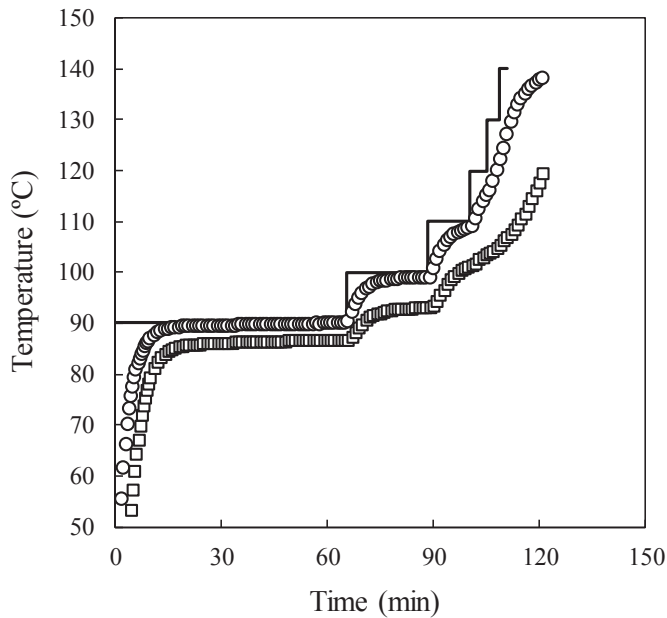


Fig. 5. Relationship between temperature and time in the stepwise baking of cookie, ○: plate temperature ( $T_{\text{plate}}$ ), □: sample-center temperature ( $T_{\text{center}}$ ). The solid line is equilibrium plate temperature ( $T_{\text{Eplate}}$ ) calculated from the Arrhenius plot (Fig. 4).

baked according to the solid line shown in Fig. 5. Time courses of  $T_{\text{plate}}$  and  $T_{\text{center}}$  during the stepwise baking are also shown in Fig. 5. From the results, it was confirmed that  $T_{\text{plate}}$  was lower than calculated  $T_{\text{Eplate}}$  at the initiation of each step. This is because the thermal output of the oven cannot be instantaneously altered according to the heating program. The  $T_{\text{center}}$  was always lower than  $T_{\text{plate}}$  because of thermal conduction in the cookie dough sample. For these reasons, the stepwise-baked cookie sample had higher water content (5.93 g/100 g-DM) than the expected value (3.09 g/100 g-DM). In order to improve the stepwise baking, a further 10 min baking was added at the final step. Then, it was confirmed that the water content of cookie samples was 3.63 g/100 g-DM. This was within the accepted water content range of cookie (Pareyt et al., 2009).

#### 3.4. Quality of stepwise-baked cookie

Spread ratio ( $D/T$ ), color values ( $L$ ,  $a$ , and  $b$ ), rupture force ( $F_r$ ), and non-hydrolyzed starch (NHS20 and NHS120) content at a given condition of control and stepwise-baked cookie are shown in Table 1.

The  $D/T$  value of stepwise-baked cookie was significantly higher than that of control. Since stepwise baking was always conducted at

a lower temperature than the  $T_m$  of starch, expansion caused by high water vapor pressure would have been suppressed. In addition, rheological property change of cookie dough during baking will have affected the  $D/T$  value. It is thought that stepwise-baked cookie dough had a lower viscosity than control because of slower water evaporation. It is suggested that the lower dough viscosity causes increased spreading during baking (Pareyt et al., 2009).

There were no significant differences in  $L$  and  $a$  of stepwise-baked cookie compared to control, whereas  $b$  was significantly higher. As browning progresses,  $L$  and  $b$  usually decrease, while  $a$  initially increases, then decreases as well (Lara, Cortés, Briones, & Perez, 2011; Purlis & Salvadori, 2009). This indicates that the stepwise-baked cookie showed slightly lower browning than control. Changes in the browning of bakery products are mainly caused by the Maillard reaction. The Maillard reaction is promoted under conditions of high temperature and low moisture content (Laguna, Salvador, Sanz, & Fiszman, 2011). Since stepwise-baked cookie was baked at a lower temperature than the  $T_m$  of starch, browning was slightly prevented.

There was no significant difference in  $F_r$  between control and stepwise-baked cookie. It is known that the hardness of cookie strongly depends on the baking temperature. For example, a biscuit sample baked at 250 °C was significantly harder than that baked at 190 °C (Lara et al., 2011). This is because the crystalline sugar, which exists partially in cookie dough, completely melts under high-temperature baking conditions, and the melted sugar strengthens the cookie structure (Chevallier, Valle, Colonna, Broyart, & Trystram, 2002; Slade & Levine, 1994). Although the control cookie showed slightly greater browning than the stepwise-baked sample, there was little contribution to the cookie hardness.

The NHS20 and NHS120 of the control cookie were 16.4% and 2.0%, respectively. These results agreed with that previously reported (16.8% and 2.6%) by our group (Kawai et al., 2013). The stepwise-baked cookie exhibited a much higher NHS20 (26.7%) than the control. This is because the baking temperature was maintained at a lower temperature than the  $T_m$  of starch in the cookie dough. Although the NHS120 drastically decreased in comparison with the NHS20, the stepwise-baked cookie maintained a significantly higher value (3.5%) than control. From these results, it is suggested that the stepwise-baked cookie contains a large amount of slowly digestible starch (Englyst et al., 1999) and contributes to a reduction in the glycemic response (Kawai et al., 2013).

In a comparison between stepwise-baked cookie and pre-dehydrated cookie reported in our previous study (Kawai et al., 2013), it was noted that the NHS20 and NHS120 of stepwise-baked cookie were significantly lower than those of pre-dehydrated cookie (32.5% and 6.0%). The  $T_m$  of starch in cookie dough was evaluated from the onset point of DSC melting peak.

Table 1  
Quality properties of control and stepwise-baked cookie samples.

	$D/T^c$	$L$	Color <sup>d</sup>		$F_r^e$ (N)	NHS20 <sup>f</sup> (%, w/w-DM)	NHS120 <sup>f</sup>
			$a$	$b$			
control <sup>a</sup>	3.6 ± 0.3	75 ± 1.5	8 ± 0.8	32 ± 1.1	59 ± 5.3	16.4 ± 0.5	2 ± 0.3
stepwise <sup>b</sup>	4.1 ± 0.0 <sup>g</sup>	77 ± 1.4	6 ± 1.1	25 ± 1.2 <sup>g</sup>	51 ± 3.1	26.7 ± 0.6 <sup>g</sup>	4 ± 1.1 <sup>g</sup>

<sup>a</sup> Conventionally baked at 180 °C for 18 min.

<sup>b</sup> Stepwise-baked at 93 °C for 65.4 min, at 103 °C for 23.3 min, at 114 °C for 11.8 min, at 124 °C for 5.0 min, at 134 °C for 3.3 min, and at 144 °C for 12.2 min.

<sup>c</sup>  $D/T$ : spread ratio. The values are expressed as mean ± SD ( $n = 3$ ).

<sup>d</sup>  $L$ : brightness value,  $a$ : red to green value,  $b$ : yellow to blue value. The values are expressed as mean ± SD ( $n = 3$ ).

<sup>e</sup>  $F_r$ : rupture force. The values are expressed as mean ± SD ( $n = 3$ ).

<sup>f</sup> NHS: non-hydrolyzed starch contents of the cookie samples treated for 20 min (NHS20) and 120 min (NHS120). The values are expressed as mean ± SD ( $n = 4$ ).

<sup>g</sup> There is a significant difference at  $p < 0.05$ .

However, there may have been a distribution of starch melting in the cookie dough, and then localized starch melting will have occurred at a lower temperature than the  $T_m$ . The stepwise-baked cookie was at least 10 °C lower than the  $T_m$  of starch in cookie dough. Pre-dehydrated cookie, on the other hand, was at least 13 °C lower than the  $T_m$  of starch in cookie dough (data not shown here). From the comparison, it is suggested that the localized starch melting occurred in stepwise-baked cookie more than in pre-dehydrated cookie. Detailed understanding of starch melting behavior in cookie dough is a subject that will be examined in follow-up studies.

#### 4. Conclusion

This study utilized stepwise baking set to at least 10 °C lower than the  $T_m$  of starch in cookie dough, and then the qualities of stepwise-baked cookie were compared to conventionally baked cookie. From the results, it was suggested that localized starch melting occurred in the stepwise-baked cookie. This will be originated from the distribution of starch  $T_m$  in cookie dough. In order to obtain some insight into the problem, it is important to understand *in vitro* starch digestibility of cookie dough held at various temperatures around  $T_m$  determined by DSC. On the other hand, it was found that the  $T_m$  values of starch in cookie dough samples were much lower than those in wheat flour. This will be because sugar acts as a plasticizer in the cookie dough. On the other hand, it is known that sugar can elevate the  $T_m$  of starch in an excess water system. This indicates that effect of sugar on the  $T_m$  of starch is affected by the water content. In order to prove the suggestion, fundamental study should be carried out systematically (e.g., DSC study on the starch melting of starch-sucrose-water system). These are next subjects of this study.

#### Acknowledgments

This work was supported by JSPS KAKENHI (Grant-in-Aid for Young Scientists B; 24780129).

#### References

- Ahmed, J. (2012). Rheometric non-isothermal gelatinization kinetics of mung bean starch slurry: effect of salt and sugar – Part 1. *Journal of Food Engineering*, 109, 321–328.
- Barbut, S., & Findlay, C. J. (1990). Thermal analysis of egg proteins. In V. R. Harwalkar, & C.-Y. Ma (Eds.), *Thermal analysis of foods* (pp. 126–148). New York: Elsevier Applied Science.
- Biliaderis, C., Page, C. M., Maurice, T. J., & Juliano, B. O. (1986). Thermal characterization of rice starches: a polymeric approach to phase transitions of granular starch. *Journal of Agricultural and Food Chemistry*, 34, 6–14.
- Bravo, L., Englyst, H. N., & Hudson, G. J. (1998). Nutritional evaluation of carbohydrates in the Spanish diet: non-starch polysaccharides and *in vitro* starch digestibility of breads and breakfast products. *Food Research International*, 31, 129–135.
- Chevallier, S., Valle, G. D., Colonna, P., Broyart, B., & Trystram, G. (2002). Structural and chemical modifications of short dough during baking. *Journal of Cereal Science*, 35, 1–10.
- Chung, H.-J., Liu, Q., & Hoover, R. (2009). Impact of annealing and heat-moisture treatment on rapidly digestible, slowly digestible and resistant starch levels in native and gelatinized corn, pea and lentil starches. *Carbohydrate Polymers*, 75, 436–447.
- Englyst, K. N., Englyst, H. N., Hudson, G. J., Cole, T. J., & Cummings, J. H. (1999). Rapidly available glucose in foods: an *in vitro* measurement that reflects the glycemic response. *American Journal of Clinical Nutrition*, 69, 448–458.
- Fuentes-Zaragoza, E., Riquelme-Navarrete, M. J., Sánchez-Zapata, E., & Pérez-Álvarez, J. A. (2010). Resistant starch as functional ingredient: a review. *Food Research International*, 43, 931–942.
- Goñi, I., Bravo, L., Larrauri, J. A., & Saura Calixto, F. (1997). Resistant starch in potatoes deep-fried in olive oil. *Food Chemistry*, 59, 269–272.
- Jacob, J., & Leelavathi, K. (2007). Effect of fat-type on cookie dough and cookie quality. *Journal of Food Engineering*, 79, 299–305.
- Kalichevsky, M. T., Jaroszkiewicz, E. M., & Blanshard, J. M. V. (1992). Glass transition of gluten. 1: Gluten and gluten-sugar mixtures. *International Journal of Biological Macromolecules*, 14, 257–266.
- Kawai, K., Kawai, H., Tomoda, Y., Matsusaki, K., & Hagura, Y. (2012a). Effect of pre-dehydration treatment on the *in vitro* digestibility of starch in cookie. *Food Chemistry*, 135, 1527–1532.
- Kawai, K., Matsusaki, K., Hando, K., & Hagura, Y. (2013). Temperature-dependent quality characteristics of pre-dehydrated cookies: structure, browning, texture, *in vitro* starch digestibility, and the effect on blood glucose levels in mice. *Food Chemistry*, 141, 223–228.
- Kawai, K., Takato, S., Sasaki, T., & Kajiwar, K. (2012b). Complex formation, thermal properties, and *in-vitro* digestibility of gelatinized potato starch–fatty acid mixtures. *Food Hydrocolloids*, 27, 228–234.
- Kawai, K., Toh, M., & Hagura, Y. (2014). Effect of sugar composition on the water sorption and softening properties of cookie. *Food Chemistry*, 145, 772–776.
- Kingman, S. M., & Englyst, H. N. (1994). The influence of food preparation methods on the *in-vitro* digestibility of starch in potatoes. *Food Chemistry*, 49, 181–186.
- Laguna, L., Salvador, A., Sanz, T., & Fiszman, S. M. (2011). Performance of a resistant starch rich ingredient in the baking and eating quality of short-dough biscuits. *LWT - Food Science and Technology*, 44, 737–746.
- Lara, E., Cortés, P., Briones, V., & Perez, M. (2011). Structural and physical modifications of corn biscuits during baking process. *LWT - Food Science and Technology*, 44, 622–630.
- Lehmann, U., & Robin, F. (2007). Slowly digestible starch – its structure and health implications: a review. *Trends in Food Science & Technology*, 18, 346–355.
- Li, Q., Li, H., & Gao, Q. (2015). The influence of different sugars on corn starch gelatinization process with digital image analysis method. *Food Hydrocolloids*, 43, 803–811.
- Lineback, D. R., & Wongsrikasem, E. (1980). Gelatinization of starch in baked products. *Journal of Food Science*, 45, 71–71.
- Liu, Q., Donner, E., Yin, Y., Huang, R. L., & Fan, M. Z. (2006). The physicochemical properties and *in vitro* digestibility of selected cereals, tubers and legumes grown in china. *Food Chemistry*, 99, 470–477.
- Ma, C.-Y. (1990). Thermal analysis of vegetable proteins and vegetable protein-based food products. In V. R. Harwalkar, & C.-Y. Ma (Eds.), *Thermal analysis of foods* (pp. 149–167). New York: Elsevier Applied Science.
- Mathew, A. P., & Dufresne, A. (2002). Plasticized waxy starch: effect of polyols and relative humidity on material properties. *Biomacromolecules*, 3, 1101–1108.
- Oguni, M., Kanke, Y., Nagoe, A., & Namba, S. (2011). Calorimetric study of water's glass transition in nanoscale confinement, suggesting a value of 210 K for bulk water. *The Journal of Physical Chemistry B*, 115, 14023–14029.
- Pareyt, B., Talhaoui, F., Kerckhofs, G., Brijs, K., Goesaert, H., Wevers, M., ... Delcour, J. A. (2009). The role of sugar and fat in sugar-snap cookies: structural and textural properties. *Journal of Food Engineering*, 90, 400–408.
- Perry, P. A., & Donald, A. M. (2002). The effect of sugars on the gelatinization of starch. *Carbohydrate Polymer*, 49, 155–165.
- Primo-Martín, C., van Nieuwenhuijzen, N. H., Hamer, R. J., & van Vliet, T. (2007). Crystallinity changes in wheat starch during the bread-making process: starch crystallinity in the bread crust. *Journal of Cereal Science*, 45, 219–226.
- Purlis, E., & Salvadori, V. O. (2009). Modeling the browning of bread during baking. *Food Research International*, 42, 865–870.
- Roos, Y. H. (1995). Food components and polymers. In Y. H. Roos (Ed.), *Phase transitions in foods* (pp. 109–155). London: Academic Press.
- Sharma, P., Velu, V., Indrani, D., & Singh, R. P. (2013). Effect of dried guduchi (*Tinospora cordifolia*) leaf powder on rheological, organoleptic and nutritional characteristics of cookies. *Food Research International*, 50, 704–709.
- Singh, G. D., Riar, C. S., Saini, C., Bawa, A. S., Sogi, D. S., & Saxena, D. C. (2011). Indian water chestnut flour- method optimization for preparation, its physicochemical, morphological, pasting properties and its potential in cookies preparation. *LWT - Food Science and Technology*, 44, 665–672.
- Slade, L., & Levine, H. (1994). Water and the glass transition – dependence of the glass transition on composition and chemical structure: special implications for flour functionality in cookie baking. *Journal of Food Engineering*, 22, 143–188.
- Sopade, P. A., Halley, P. J., & Junming, L. L. (2004). Gelatinisation of starch in mixtures of sugars. II. Application of differential scanning calorimetry. *Carbohydrate Polymers*, 58, 311–321.
- Tester, R. F., & Debon, S. J. J. (2000). Annealing of starch – a review. *International Journal of Biological Macromolecules*, 27, 1–12.
- Themeier, H., Hollmann, J., Neese, U., & Lindhauer, M. G. (2005). Structural and morphological factors influencing the quantification of resistant starch II in starches of different botanical origin. *Carbohydrate Polymers*, 61, 72–79.
- Van Soest, J. J. G., Bezemer, R. C., De Wit, D., & Vliegenthart, J. F. G. (1996). Influence of glycerol on the melting of potato starch. *Industrial Crops and Products*, 5, 1–9.
- Wootton, M., & Chaudhry, M. A. (1980). Gelatinization and *in vitro* digestibility of starch in baked products. *Journal of Food Science*, 45, 1783–1784.



## Comparison of carbonyl profiles from Czech and Spanish lagers: Traditional and modern technology



Cristina Andrés-Iglesias<sup>a,b</sup>, Jakub Nešpor<sup>a</sup>, Marcel Karabín<sup>a</sup>, Olimpio Montero<sup>c</sup>, Carlos A. Blanco<sup>b</sup>, Pavel Dostálek<sup>a,\*</sup>

<sup>a</sup> Department of Biotechnology, Faculty of Food and Biochemical Technology, University of Chemistry and Technology, Prague, Technická 5, 166 28 Prague 6-Dejvice, Czech Republic

<sup>b</sup> Departamento de Ingeniería Agrícola y Forestal (Área de Tecnología de los Alimentos), E.T.S. Ingenierías Agrarias, Universidad de Valladolid, Avda. de Madrid 44, 34004 Palencia, Spain

<sup>c</sup> Centre for Biotechnology Development (CDB), Spanish Council for Scientific Research (CSIC), Francisco Vallés 8, Boecillós Technological Park, 47151 Boecillo, Valladolid, Spain

### ARTICLE INFO

#### Article history:

Received 22 April 2015

Received in revised form

25 October 2015

Accepted 27 October 2015

Available online 30 October 2015

#### Keywords:

Beer

Carbonyl compounds

GC-MS

### ABSTRACT

Beer is one from the most popular alcoholic beverages worldwide. For consumer acceptance, a significant factor is its flavour and taste; carbonyl compounds play an important role as indicators of the deterioration of flavour and aroma in beers. The aim of this study was to characterize differences in the carbonyl profile from Czech and Spanish beers, based on tradition and modern technology, respectively.

Headspace solid-phase microextraction and gas-chromatography mass spectrometry were used to compare lager beers. The technique of on-fibre derivatization with O-(2,3,4,5,6-pentafluorobenzyl)hydroxylamine (PFBOA) was used to achieve satisfactory recovery and sensitivity.

Statistical factor analysis showed three principal components, two of them explaining more than 79% of the variability and these results were related to ANOVA-significant difference analysis based on the country of origin. These two factors were related to Strecker aldehydes and Maillard products. PCA analysis scatterplot confirmed a significant difference between the Spanish and Czech beers, particularly with regard to the content of diacetyl and (*E*)-non-2-enal.

© 2015 Elsevier Ltd. All rights reserved.

### 1. Introduction

The term beer refers to very wide range of beverages produced from different malts and brewing water, hopped by dozens of different varieties of hops and fermented using two species of yeast – top-fermenting (*Saccharomyces cerevisiae* – wheat beers, ale, stout) and bottom-fermenting (*Saccharomyces pastorianus* – lager beers) (Priest & Stewart, 2006). Part of Europe, to which the Czech Republic geographically belongs, is characterized by the production of Czech-type lager beers, which is a tradition established in Pilsen (from which the name of this beer – Pilsner - is derived) in 1842 by brewer Josef Groll (Basařová, Hlaváček, Basař, & Hlaváček, 2011). Although it is difficult to distinguish beer according to its place of origin only on the basis of clearly defined analytical characteristics, strong conservatism of Czech brewers in choosing technologies,

and the diversity of raw materials used, led to the emergence of the specific type of beer (Olsovská, Cejka, Sigler, & Honigová, 2014), so different from other lagers that it is legislatively protected by the European Union Protected Geographical Indication, “Czech beer”. This designation clearly defines the origin of the raw materials and technology used, and greatly emphasizes the unique analytical and sensory characteristics of the product (Anonymous, 2006).

The most appreciated sensory characteristics of beer is fresh flavour (Bravo et al., 2008), and flavour stability is thus an important quality criterion, and a concern for the brewing industry (Guido et al., 2004; Moreira, Meireles, Brandao, & de Pinho, 2013; Saison et al., 2010). Despite carbonyl compound concentrations being generally very low in fresh beer, these compounds make an important and mostly unwanted contribution to the flavour profile because of their particular sensory descriptors (Table 1) and low flavour thresholds (Blanco, Andrés-Iglesias, & Montero, 2014; Saison, De Schutter, Delvaux, & Delvaux, 2009a). The off-flavours that typically develop in aged beer include cardboard, sweet and toffee, but also butter notes (Guido et al., 2004), and some

\* Corresponding author.

E-mail address: [Pavel.Dostalek@vscht.cz](mailto:Pavel.Dostalek@vscht.cz) (P. Dostálek).

**Table 1**  
Carbonyl compounds studied, flavour threshold, formation in beer and flavour descriptors.

Name	Groups	Threshold (µg/l)	Formation/description	Flavour descriptors
2-Methylpropanal	Strecker aldehyde	86–1000	Produced through Strecker degradation of the amino acid valine; may be released by the oxidative degradation of isohumulones; component of aged beer and inappropriate storage of the finished beer in addition to oxygen exposure; created by insufficient boiling of wort (too little evaporation).	Grainy, Varnish, Fruity (1, 4)
2-Methylbutanal	Strecker aldehyde	45–1250	Produced through Strecker degradation of the amino acid isoleucine; increased formation at high oxygen concentrations, inappropriate storage of the finished beer (oxygen).	Almond, Apple-like, Malty (1, 4)
3-Methylbutanal	Strecker aldehyde	56–600	Produced through Strecker degradation of the amino acid leucine; component of aged beer and inappropriate storage of the finished beer, as well as oxygen exposure, indicator of thermal load.	Malty, Chocolate, Cherry, Almond (1, 4)
Benzaldehyde	Strecker aldehyde	515–2000	Increased formation with high oxygen concentrations during brewing and packaging as well as inappropriate storage of the finished beer, component in aged beer.	Almond, Cherry, Stone (1, 4)
Heptanal	Linear aldehyde	75–80	Created by the degradation (enzymatic, auto- or photooxidative) of the fatty acid oleic acid during ageing.	Aldehyde, Vinous, Bitter (2)
Octanal	Linear aldehyde	40	Created by the degradation (enzymatic, auto- or photooxidative) of the fatty acid oleic acid during ageing.	Aldehydic, Orange peel, Bitter (2, 4)
Furfural	Heterocyclic compound	15,000–150,000	Product of the Maillard reaction, formed during boiling, indicator for flavour instability in beer, component of aged beer.	Caramel, Bready, Cooked meat (1, 4)
(E)-Non-2-enal	Linear aldehyde	0.03–0.11	Can be created by auto-oxidation or an enzymatic oxidation of linoleic acid and linolenic acid with lipoxygenases during mashing and malting, also created by the reaction between heptanal and acetaldehyde, (E)-non-2-enal can be enzymatically reduced by yeast using an enzyme that acts like an aldehyde reductase; decreases significantly after 36 h of fermentation; inappropriate storage of the finished beer increases its level.	Cardboard, Papery, Cucumber (1, 2, 3, 4)
2,3-Butanedione (Diacetyl)	Ketone	100–200	From $\alpha$ -acetoxy acids that are excreted during fermentation by yeast cells to the wort where they undergo spontaneous oxidative decarboxylation to diacetyl; occurs at the end of the conventional main period of fermentation and during the maturation of beer; formation correlates to the amino acid content in wort; may be formed in packaged beer as a result of Maillard reactions or oxidation of acetoin and 2,3-butanediol; too short maturation, poor yeast vitality, too many repitches, old yeast, yeast stored too long also increases diacetyl content; can be formed by contamination with some microorganisms.	Butterscotch, Buttery, Buttermilk, Rancid (2, 3, 4, 5)
2,3-Pentanedione	Ketone	900–1000	Intermediate product during the synthesis of valine and isoleucine; can be formed by bacterial infection.	Moldy, Wood-like (5)

(1) (Baert et al., 2012); (2) (Meilgaard, 1975); (3) (Guido, Rajendram, & Barros, 2009); (4) (Saison, De Schutter, Uyttenhove, Delvaux, & Delvaux, 2009b); (5) (Krogerus & Gibson, 2013).

aldehydes and ketones have been considered to be the most important factors in the deterioration of beer flavour and the formation of off-flavours (Bueno, Zapata, & Ferreira, 2014; Gonçalves et al., 2014; Rossi, Sileoni, Perretti, & Marconi, 2014).

There are many ways in which carbonyls get into beer. These compounds can originate from a raw material, which is typical for furfural derivatives arising from Maillard reactions during kilning of the malt (Yahya, Linforth, & Cook, 2014). Malting technology and the quality of raw materials is also significant with regard to the formation of precursors of carbonyl compounds and activation of enzymatic systems, allowing their conversion at later stages of brewing. An important reaction is the activation of lipoxygenases, enabling enzymatic oxidation of unsaturated fatty acids during mashing, which, together with corresponding non-enzymatic oxidation during beer storage, is the main cause of the formation of carbonyl compounds such as hexanal, and (E)-non-2-enal (Noel et al., 1999; Yu et al., 2014). Moreover, malt and hop polyphenols inhibit the activity of reactive oxygen species (hydroxyl and hydroperoxide radicals, singlet oxygen, hydrogen peroxide, superoxide anion), which is a crucial factor in the formation of carbonyl compounds during storage of the finished beer (Mikyska, Krofta, Haskova, Culik, & Cejka, 2011; Vanderhaegen, Neven, Verachtert, & Derdelinckx, 2006) Saaz hop is known for its high content of polyphenolic compounds (Jelinek et al., 2012; Lermusieau, Liegeois,

& Collin, 2001) and its use can become an important factor affecting the sensorial quality of the product.

Decisive steps in brewing technology for changes in carbonyl content are mashing, fermentation and maturation (Briggs, Boulton, Brookes, & Stevens, 2004). In addition to fatty acid oxidation, the formation of the Strecker aldehydes 2-methylpropanal, 2-methyl butanal, 3-methylbutanal and phenyl-acetaldehyde by degradation of amino acids valine, isoleucine, leucine and phenylalanine respectively, occurs during mashing (da Costa et al., 2004). Therefore amounts of these amino acids in wort, resulting from proteolytic modification of malt (Stephan, Kusche, & Stettner, 2007), or the use of malt adjuncts, usually in the form of rice or maize (Taylor, Dlamini, & Kruger, 2013) plays an important role. Apart from economic reasons, these adjuncts became popular in recent years with respect to the production of gluten-free beer, which can be consumed by customers suffering celiac disease (Yeo & Liu, 2014). Metabolism of amino acids also plays an important role during fermentation, particularly when using modern high-volume cylindro-conical fermenters. Their gradual filling with fresh wort from multiple batches leads to intensive synthesis of the branched chain amino acids valine and isoleucine by yeast cells, and thus to the formation of vicinal diketones (diacetyl and 2,3-pentanedione) that at very low concentrations gives beer an unwanted buttery off-flavour (Krogerus & Gibson, 2013). Modern

intensified technologies are often based on shortening of fermentation and maturation times, which leads to limited re-assimilation of vicinal diketones as well as other carbonyls by yeast (Pires, Teixeira, Branyik, Brandao, & Vicente, 2015; Stewart & Murray, 2012). Unconverted carbonyl compounds are bound to sulphur dioxide produced during fermentation and the resulting adducts are degraded during transport and storage of beer. This can result in significant deterioration in the sensorial properties of the product (Dufour, Leus, Baxter, & Hayman, 1999; Ilett & Simpson, 1995).

The description above clearly shows that adherence to time-tested technologies and the use of traditional raw materials has a significant influence on the qualitative characteristics of the beer. The Czech Republic has a long tradition in the production of lagers and Czech hops are traditionally considered to be one of the finest in the world. The protected geographical indication “Czech beer” defines, in addition to analytical and organoleptic characteristics of the product, permitted varieties and growing areas of two raw materials (barley and hops) and prohibits the use of brewing adjuncts (Anonymous, 2006; Olsovska et al., 2014). It also specifies the parameters of the technological process, with an emphasis on the use of decoction mashing, sufficient length of wort boiling and the appropriate temperature during fermentation (max. 14 °C) and maturation (0–1 °C). In contrast, in countries where tradition associated with the production and consumption of beer is not so strong, local preferences of consumers can be different and efforts to intensify production and/or reduce production costs may lead to the use of significant surrogation (Goode & Arendt, 2006), high-gravity brewing (Dekoninck, Verbelen, Delvaux, Van Mulders, & Delvaux, 2012), infusion mashing, enzymatic preparations (Ma, Zhu, Zheng, Li, & Li, 2014) or shorter fermentation times, and therefore to the production of beers with significantly different analytical profiles. The content and profile of certain compounds could even become an important marker for characterizing the authenticity of beer.

In this study, HS-SPME-GC-MS, with on-fibre derivatization by PFBOA, has been successfully applied to the analysis of carbonyl compounds in Spanish and Czech beers. This methodology and statistical analysis were used to identify, quantify and compare the profile of carbonyl compounds in relation to the country of origin and/or production processes, in 28 different types of pale, dark and non-alcoholic (produced using different technologies) lager beers. While differences between lagers produced within the Czech Republic and foreign beers, in terms of general analytical parameters such as attenuation, colour or polyphenol content, has previously been demonstrated (Olsovska et al., 2014), this work is in our behalf the first that focuses on distinguishing between beers from different countries of origin based on the content of particular sensorial-active carbonyls.

## 2. Materials and methods

### 2.1. Sample and derivatization reagent preparation

Thirteen beers from Spain, including a non-alcoholic one, and fifteen Czech beers, including three non-alcoholic ones, of different commercial brands, were obtained from several local markets. Beers were purchased as fresh as possible to avoid long storage periods. The alcoholic beers contained between 3.5 and 6.7% alcohol by volume (ABV). Among the non-alcoholic beers, the Spanish one contained less than 0.01% ABV, and all Czech beers up to 0.5% ABV. Beer samples were stored at 4 °C until analysis. 250 ml of each beer were placed in 500 ml glass bottles and agitated in a shaker for 5 min to reduce the CO<sub>2</sub> content. Subsequently, for GC-MS analysis, the same number of vials with beer samples as those of derivatization reagent solution were prepared. 20 ml dark vials

sealed with PTFE-silicone septa (Supelco, USA) were used for preparation of samples and derivatization reagent.

For beer samples, vials were loaded with 2.5 g of NaCl (Penta, CZ), 10 ml of beer and 100 µl of an internal standard solution (IS) containing 52.6 ppm 3-fluorobenzaldehyde (Sigma–Aldrich, USA; ≥ 97% purity). For derivatization reagent, vials contained 2.5 g of NaCl (Penta, CZ), 10 ml of demineralized water from a Mili-Q water Milipore purification system (Milipore, Bedford, USA) and 200 µl of 5978 ppm *o*-(2,3,4,5,6-pentafluorobenzyl)hydroxylamine hydrochloride (PFBOA) (Fluka, Germany; ≥ 99% purity) solution.

All vials were stirred for 1 min to dissolve the NaCl and to homogenize the sample and derivatization reagent solution.

### 2.2. Gas chromatography-mass spectrometry (GC-MS) equipment

Carbonyl compounds were separated and detected by a gas chromatograph (Agilent GC 6890N – Agilent Technologies, USA) equipped with a quadrupole mass spectrometer detector (Agilent 5975B, Inert MSD – Agilent Technologies, USA). The gas chromatograph was coupled to a headspace solid phase microextraction (HS-SPME) autosampler (COMBI PAL CTC Analytics, CH). Chromatographic separations were performed using an HP-5MS 30 m × 0.25 mm × 0.25 µm capillary column (Agilent Technologies, USA). Derivatization, extraction and concentration of carbonyl compounds were carried out using a 50/30 µm divinylbenzene/Carboxen®/polydimethylsiloxan (DVB/CAR/PDMS) fibre (Supelco, USA).

### 2.3. Analysis of carbonyl compounds. On-fibre derivatization

The concentrations of carbonyls in beer samples were measured in triplicate. Head space solid phase microextraction of compounds was performed at 50 °C. The first step was coating of the SPME fibre with PFBOA for 20 min. The coated fibre was subsequently transferred to the head space of a vial containing degassed beer and held for 60 min. Compound desorption was achieved in the injector of the GC chromatograph in splitless mode for 5 min, and the temperature was set at 250 °C. Carrier gas was helium at a constant flow rate of 1.1 ml/min.

The oven temperature was programmed as follows: the temperature was initially set at 40 °C and increased at 10 °C/min to 140 °C, then the temperature was raised at 7 °C/min to 250 °C, this temperature was held for 14 min, and finally the temperature was increased at 20 °C/min to 300 °C and this temperature was held for 2 min.

The ionization energy was 70 eV, and detection and data acquisition were performed in scan mode from 20 to 500 Da. For identification, data obtained in the GC-MS analysis were compared with *m/z* values compiled in the spectrum library, NIST MS Search version 2.0 (National Institute of Standards and Technology, USA).

Validation of compound identification was carried out by comparison of their MS spectra and retention times with standards. Quantification was done in SIM mode using quantification ion (*m/z* = 181) and was carried out using standard calibration curves for 2-methylpropanal (≥99%), 3-methylbutanal (≥97%), (*E*)-non-2-enal (≥97%), 2,4-pentadione (≥97%) and diacetyl (≥97%) (Sigma–Aldrich, USA), 2-methylbutanal (≥97%) (Fluka, Germany), heptanal (≥97%), octanal (≥98%), furfural (≥98%) and benzaldehyde (≥98%) (Alfa Aesar, Germany). In order to eliminate instrumental variations, the peak area of each compound (single peak or double derivative, Fig. 1) was normalized to the peak area of the internal standard – 3-fluorobenzaldehyde (double derivative, Fig. 1); the normalized values were then used for statistical analysis.

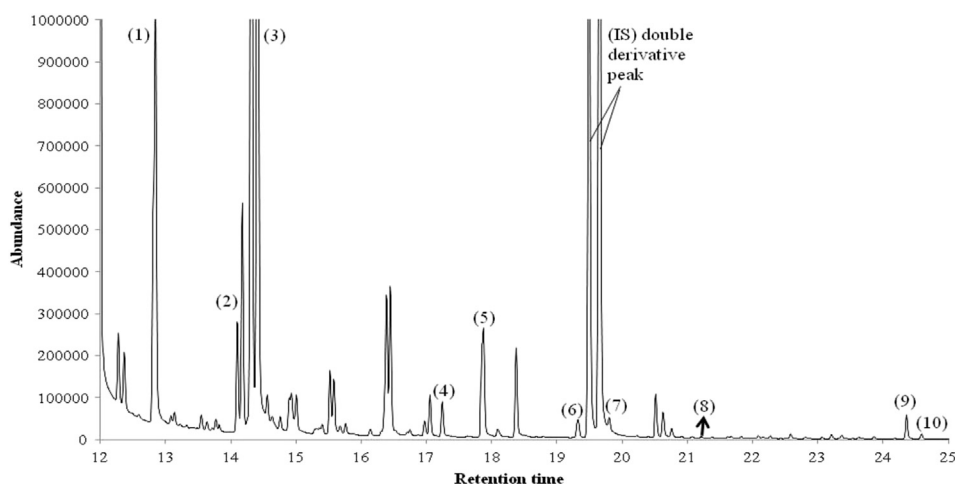


**Fig. 1.** TIC chromatogram of carbonyl compounds of a Spanish beer. (1) 2-methyl propanal, (2) 2-methyl butanal, (3) 3-methyl butanal, (4) furfural, (5) heptanal, (6) octanal, (7) benzaldehyde, (8) (*E*)-non-2-enal, (9) diacetyl, (10) pentadione.

#### 2.4. Statistical analysis

Statistical analysis of the chromatographic data was performed with Statistica 12 software (StatSoft, Inc., Tulsa, OK, USA). One-way analysis of variance (ANOVA) followed by *t*-test was used to compare the profiles of beers based on their country of origin and type (pale beers, dark beers and non-alcoholic beers). Significant differences were considered at a level of  $p < 0.05$ . Factorial analysis was used to explain differences between beers by their principal components, factors or eigenvalues that explain the maximal variability as well as the contribution of each variable to the factors.

### 3. Results and discussion

A total of 28 lager beers were analyzed, among them 13 beers were produced in Spain (samples 1 to 13) and 15 beers were of Czech origin (samples 14 to 28) (Table 2). Legislation related to the labelling of individual types of beer in the Czech Republic and in Spain varies considerable (Anonymous, 2013; BOE., 2013), so allocation of beers into individual groups is only approximate. Three samples of non-alcoholic beers from the Czech Republic were chosen, reflecting different manufacturing technologies (vacuum distillation, limited fermentation of low gravity wort and use of a special yeast strain). The carbonyl compound profile consisted of: 3 linear aldehydes ((*E*)-non-2-enal, heptanal and octanal), 4 Strecker aldehydes (2-methylpropanal, 2-methylbutanal, 3-methylbutanal and benzaldehyde), 1 heterocyclic aldehyde (furfural) and 2 ketones (2,3-butanedione and 2,3-pentadione). A typical total ion chromatogram (TIC) of carbonyl compounds of a Spanish regular lager is shown in Fig. 1. Analytical profiles based on carbonyl compound content obtained by HS-SPME-GC-MS analysis of the different types of beer are shown in Tables 3 and 4.

#### 3.1. Differences in concentration of carbonyl compounds in beers

A certain proportion of carbonyl compounds and their precursors in beer originate in the malt; others are formed during beer production and significant increases in content, being highly dependent on storage temperature, pH, oxygen level and exposure to ultraviolet light (Ochiai, Sasamoto, Daishima, Heiden, & Hoffmann, 2003), occur during ageing and storage of the product. Differences in content of these compounds, or their presence above a sensorial threshold, can therefore indicate the use of different or

low-quality raw materials, adjuncts, problems in brewing technology and/or inappropriate beer storage. A list of carbonyl compounds studied, their flavour thresholds, formation pathways and flavour descriptors are shown in Table 1.

Results (Tables 3 and 4) show that the average concentrations of 2-methylbutanal, 3-methylbutanal, benzaldehyde, furfural, heptanal, (*E*)-non-2-enal and 2,3-pentadione in Czech beers were higher than in Spanish beers. For the rest of the carbonyl compounds (2-methylpropanal, octanal and diacetyl) their concentrations were higher in Spanish beers.

Significant differences based on ANOVA were only found for (*E*)-non-2-enal and diacetyl (Table 5). The average concentration of (*E*)-non-2-enal in Czech beers was 4.25  $\mu\text{g/l}$  whereas for Spanish beers was 0.47  $\mu\text{g/l}$ . These amounts of (*E*)-non-2-enal are above the

**Table 2**

List of beers used in this study, coding, type, nationality, and % alcohol by volume (ABV).

Sample no.	Coding	Type	Country	ABV %
1	SP-1	Special lager	Spain	6.50
2	SP-2	Regular lager	Spain	3.50
3	SP-3	Premium lager	Spain	5.40
4	SP-4	Regular lager	Spain	4.80
5	SP-5	Special lager	Spain	6.40
6	SP-6	Premium lager	Spain	4.70
7	SP-7	Dark lager	Spain	4.80
8	SP-8	Regular lager	Spain	5.00
9	SP-9	Special lager	Spain	6.40
10	SP-10	Premium lager	Spain	5.50
11	SP-11	Non-alcoholic	Spain	0.01
12	SP-12	Premium lager	Spain	5.20
13	SP-13	Premium lager	Spain	5.50
14	CZ-1	Regular lager	Czech Republic	4.00
15	CZ-2	Regular lager	Czech Republic	4.00
16	CZ-3	Regular lager	Czech Republic	4.00
17	CZ-4	Premium lager	Czech Republic	4.40
18	CZ-5	Premium lager	Czech Republic	5.00
19	CZ-6	Premium lager	Czech Republic	5.10
20	CZ-7	Dark lager	Czech Republic	4.40
21	CZ-8	Premium lager	Czech Republic	5.00
22	CZ-9	Non-alcoholic	Czech Republic	0.50
23	CZ-10	Non-alcoholic	Czech Republic	0.49
24	CZ-11	Non-alcoholic	Czech Republic	0.49
25	CZ-12	Regular lager	Czech Republic	3.80
26	CZ-13	Dark lager	Czech Republic	4.70
27	CZ-14	Special lager	Czech Republic	7.50
28	CZ-15	Special semi-dark lager	Czech Republic	5.20

**Table 3**  
Concentrations of carbonyl compounds and their retention time (RT) as determined in Spanish beer samples.

No.	RT	Compounds	Spanish beers ( $\mu\text{g/l}$ )												
			SP-1	SP-2	SP-3	S-4	SP-5	SP-6	SP-7	SP-8	SP-9	SP-10	SP-11	SP-12	SP-13
1	12.340	2-Methylpropanal	2.42	8.47	14.10	4.40	5.63	11.50	229.00	19.12	17.87	12.29	1.71	30.83	10.09
2	13.673	2-Methylbutanal*	3.18	2.56	3.38	1.80	3.04	7.10	60.41	6.26	6.28	4.18	1.67	6.03	5.24
3	13.811	3-Methylbutanal*	2.30	2.18	3.79	2.51	4.45	5.01	47.23	6.68	8.22	4.56	0.97	9.91	4.03
4	16.741	Furfural	20.29	38.59	44.80	38.28	30.01	32.90	202.22	24.59	100.06	86.29	24.48	129.32	21.08
5	17.351	Heptanal	0.42	0.13	0.16	0.32	0.56	0.44	2.45	0.55	0.40	0.34	0.28	0.64	0.23
6	18.820	Octanal	0.25	0.05	0.06	0.12	0.15	0.30	0.79	0.18	0.15	0.11	0.18	0.20	0.07
7	19.294	Benzaldehyde	11.55	13.11	12.86	13.02	12.82	8.72	16.96	8.63	20.35	16.12	9.63	18.07	8.41
8	21.327	(E)-Non-2-enal	0.22	0.11	0.17	0.37	0.26	0.31	1.81	0.73	0.55	0.44	0.09	0.83	0.25
9	23.854	2-3 Butanedione (diacetyl)*	12.67	7.17	8.15	20.41	20.48	14.65	52.19	12.90	129.49	90.62	10.14	88.79	19.58
10	24.089	2,3-Pentanedione*	32.14	15.67	23.85	44.46	51.85	36.96	112.80	32.41	281.28	223.21	24.60	252.76	53.95

\*Double derivative with PFBOA.

**Table 4**  
Concentrations of carbonyl compounds and their retention time (RT) as determined in Czech beer samples.

No.	RT	Compounds	Czech beers ( $\mu\text{g/l}$ )														
			CZ-1	CZ-2	CZ-3	CZ-4	CZ-5	CZ-6	CZ-7	CZ-8	CZ-9	CZ-10	CZ-11	CZ-12	CZ-13	CZ-14	CZ-15
1	12.340	2-Methylpropanal	11.16	11.26	8.72	14.50	18.54	15.53	57.96	38.16	28.39	4.63	4.97	8.15	49.49	35.75	53.28
2	13.673	2-Methylbutanal*	4.29	6.62	4.73	9.00	6.95	8.28	34.51	9.92	15.88	3.16	3.34	3.30	25.17	10.84	29.55
3	13.811	3-Methylbutanal*	6.94	7.05	6.11	10.09	7.54	9.91	38.20	13.63	27.14	3.57	3.68	4.33	22.03	13.15	32.38
4	16.741	Furfural	42.69	100.36	78.37	48.65	53.20	46.93	174.39	97.32	90.26	13.21	45.68	31.62	85.59	81.13	84.17
5	17.351	Heptanal	0.65	0.87	0.57	0.81	0.76	0.79	1.43	1.33	1.39	0.20	0.30	0.35	0.81	1.11	1.32
6	18.820	Octanal	0.14	0.19	0.12	0.17	0.15	0.17	0.33	0.23	0.23	0.04	0.08	0.11	0.19	0.29	0.35
7	19.294	Benzaldehyde	12.81	18.59	12.74	13.66	14.25	14.19	21.76	15.03	18.85	9.77	14.96	11.61	15.91	16.13	15.50
8	21.327	(E)-Non-2-enal	3.62	5.25	3.60	3.86	4.03	4.01	6.14	4.24	5.32	2.77	4.22	3.28	4.49	4.55	4.38
9	23.854	2-3 Butanedione (diacetyl)*	3.44	5.18	4.01	3.61	4.21	4.12	14.12	5.71	8.68	2.25	4.28	6.78	8.17	14.74	16.11
10	24.089	2,3-Pentanedione	66.98	127.22	97.70	179.34	109.09	159.88	345.64	114.08	142.57	16.66	39.25	60.40	120.70	220.77	176.90

\* Double derivative with PFBOA.

flavour threshold (0.03–0.11  $\mu\text{g/l}$ , Table 1), especially in Czech beers, the highest concentration being shown for the dark beer CZ-7. This compound is considered to be a key marker for beer ageing, with a stale taste of paper or cardboard when present in concentrations above its threshold (Baert, De Clippeleer, Hughes, De Cooman, & Aerts, 2012). (E)-non-2-enal is created mainly by lipid oxidation during beer production and may also be released during beer storage; in beers stored at temperatures higher than 4 °C, the concentration of this compound is known to increase (Rossi et al., 2014) and the concentration of (E)-non-2-enal was found to exceed its flavour threshold in beer after 3 months of natural ageing (Guido et al., 2004). It is therefore possible that the higher content of this carbonyl is a result of the use of traditional materials and technologies. Brewing adjuncts, such as rice, malt extracts and corn endosperm grits, which are not used in the Czech Republic but are in other countries, may constitute up to 40% of the fermentable extract (Fumi, Galli, Lambri, Donadini, & De Faveri, 2009; Zhu, Ma, Li, & Li, 2015) and have a lower content of lipid components than barley malt (Taylor et al., 2013). Also traditional multi-step mashing procedures, necessary for amyolytic and proteolytic degradation of the malt, creates suitable conditions for the action of lipoxigenases on unsaturated fatty acids that represent about 80% of the fatty acids in barley malt (Bravi, Sensidoni, Floridi, & Perretti, 2009).

The average concentration of diacetyl was higher in Spanish beers than in Czech ones (37.48  $\mu\text{g/l}$  and 7.03  $\mu\text{g/l}$  respectively). The most representative Spanish beers, with the highest level of diacetyl, being distinct from other samples, were the special lager SP-9, with 129.49  $\mu\text{g/l}$ , and the premium lager SP-10, with 90.62  $\mu\text{g/l}$ . For SP-9, the concentration of diacetyl was above the flavour threshold (100  $\mu\text{g/l}$ , Table 1), but for the remainder of samples, it was lower. The higher concentration of diacetyl found in Spanish beers could be caused by overproduction of acetolactic acid. When a cylindro-conical fermenter is used for primary fermentation,

yeast growth is activated by a higher fermentation temperature. This procedure can cause rapid exhaustion of valine, and subsequent biosynthesis by the yeast leads to an increase in the concentration of acetolactic acid that spontaneously transforms into diacetyl (Inoue, 2009). The same effect occurs with gradual filling of the fermenter and poor aeration of the wort prior to fermentation (Briggs et al., 2004). Another possible reason for overproduction of acetolactic acid is the use of an adjunct, leading to a reduction in free amino nitrogen and especially the valine content of the wort (Kobayashi, Shimizu, & Shioya, 2008). Increased wort aeration during fermentation, elevated fermentation temperature or gentle agitation can also lead to augmentation of free diacetyl in the medium (Inoue, 2009). In order to reduce the content of diacetyl formed in the initial stages of fermentation and to shorten time- and energy-consuming fermentation, an increase in temperature (15–18 °C) for 24–48 h (diacetyl rest), followed by rapid cooling to maturation temperature is used (Krogerus & Gibson, 2013; Saerens, Verbelen, Vanbeneden, Thevelein, & Delvaux, 2008). If the diacetyl content in the fermenting wort is too high and/or fermentation is not followed by a sufficiently long maturation necessary for the reduction of diacetyl to the relatively sensorially inactive 2,3-butanediol (Stewart & Murray, 2012), this procedure may be insufficient because unreduced diacetyl, as well as other carbonyls, can create adducts with sulphur dioxide and pass into the finished beer. High concentrations of diacetyl in beer may therefore indicate incomplete fermentation and maturation, or even contamination of the wort (Rossi et al., 2014).

In non-alcoholic beers, the average concentrations of particular carbonyl compounds were lower or similar in comparison to their concentration in regular beers. SP-11, which was produced by vacuum distillation, had the lowest concentrations of 2-methylpropanal, 2-methylbutanal, 3-methylbutanal and (E)-non-2-enal in comparison with other alcohol free beers. CZ-11, produced

**Table 5**  
Analysis of variance (ANOVA) for carbonyl compounds dependent on country of origin.

Compound	Sum of squares	Degree of freedom	Mean square	F-ratio	p-value	Remarks
2-Methylpropanal	124.68	1	124.68	0.07	0.799	–
2-Methylbutanal	69.30	1	69.30	0.41	0.527	–
3-Methylbutanal	240.97	1	240.97	1.81	0.190	–
Benzaldehyde	779.28	1	779.28	0.36	0.555	–
Heptanal	0.68	1	0.68	2.73	0.111	–
Octanal	0.00	1	0.00	0.07	0.792	–
Furfural	26.63	1	26.63	2.27	0.144	–
(E)-Non-2-enal	99.40	1	99.40	204.73	0.000	Significant
Diacetyl	6458.04	1	6458.04	8.57	0.007	Significant
2,3-Pentanedione	11471.66	1	11471.66	1.48	0.235	–

by vacuum distillation, and CZ-10, produced by the special yeast *Saccharomyces ludwigii*, had similar low concentrations of carbonyl compounds, with the lowest concentrations of furfural, octanal, diacetyl and 2,3-pentanedione being shown by CZ-10. In the case of CZ-9, a non-alcoholic beer produced by short fermentation of low gravity wort at low temperature, which is the most commonly used technology for production of non-alcoholic beer in the Czech republic, the concentration of carbonyl compounds was close to that in regular beers (Tables 3 and 4). This fact could be due, at least partly, to the special wort used for the production of this beer. As for other beers studied, the concentration of (E)-non-2-enal in non-alcoholic beers was at the limit of the flavour threshold (3.10 µg/l), but in this case, the absence of ethanol and a higher level of mono and disaccharides could have intensified its undesirable flavour (Perpete & Collin, 2000).

Measured data showed significant differences between types of beers and particularly dark beers when compared with non-alcoholic, regular and premium beers. These significant differences were related to 2-methylpropanal, 2- and 3-methylbutanal, furfural, heptanal and octanal. Some beer aldehydes, such as heptanal and octanal, produced by lipooxygenases and hydroperoxide isomerases from cereal grains, are formed during the malting process (Riu-Aumatell, Miro, Serra-Cayuela, Buxaderas, & Lopez-Tamames, 2014). The higher temperatures used for the roasting of malt in dark beer production can increase the concentration of these carbonyl compounds. Maillard reactions responsible for different colours of malt most likely lead to the formation of more Maillard intermediates, namely heterocyclic furfural derivatives, which become reactive substrates during ageing of dark beers (Riu-Aumatell et al., 2014; Vanderhaegen, Delvaux, Daenen, Verachtert, & Delvaux, 2007). All of these reactions, along with the initial malt and wort used, could be responsible for the high concentrations of carbonyl compounds found in these dark beers. For dark beer SP-7, the amounts of 2-methylpropanal and 2-methylbutanal were above their flavour thresholds and for both SP-7 and CZ-7, (E)-non-2-enal was above its flavour threshold.

### 3.2. Factor and principal components analysis (PCA)

A classical factor analysis with quartimax rotation of the 10 variables (contents of carbonyl compounds) resulted in 3 principal factors that explained 93.47% of the variation in the measured

**Table 6**  
Eigenvalues, percentage of variation and percentage of cumulative variation for the three principal components of the PCA.

Factors	Eigenvalue	Variation (%)	Cumulative variation (%)
1	6.14	61.38	61.38
2	1.78	17.79	79.17
3	1.43	14.31	93.47

variables (Table 6). Table 6 shows the eigenvalues and the percentage variation of each component. The contributions of each compound (variable), positive or negative, to every component are depicted in Table 7.

Factor 1 explains 61.38% of the variation (Table 6) and loading factors ranged from 0.0929 to 0.9705. This factor represents almost all carbonyl compounds studied, including the ANOVA-significant compounds according to type of beer. The maximal contribution to this factor came from 2-methylpropanal and 2-methylbutanal; both are Strecker aldehydes and exhibited higher concentrations in dark beers.

For Factor 2, which explains 17.79% of the variation, loadings varied from –0.0388 to 0.8992. The carbonyl compounds contributing to this factor were the ketone 2,3-pentadione, followed by furfural.

Finally, Factor 3 explained 14.31% of the variation, with loading factors ranging from –0.7781 to 0.8653. The principal contributors to this factor were (E)-non-2-enal and diacetyl. This factor represents the ANOVA-significant carbonyl compounds according to country of origin; they were (E)-non-2-enal for Czech beers and diacetyl for Spanish beers.

The scatterplot resulting from PCA analysis (Fig. 2) was used to visualize beer sample groupings. Factor 1 and factor 3 show that the samples could be clearly separated in two main groups according to their carbonyl content. One group contained Spanish beers and fell on the positive side of Factor 3. Another group contained Czech beers, all of which were located on the negative side of Factor 3. It is therefore evident that both groups differ significantly and that the most relevant carbonyl compounds in the differentiation of beers by country of origin were diacetyl for Spanish beers and (E)-non-2-enal for Czech beers. SP-7 and CZ-7 were shown to be clearly separated from the respective SP and CZ groups; these dark beers were characterized by high concentrations of most of the carbonyl compounds, in particular furfural, 2,3-pentanedione and 2-methylpropanal.

**Table 7**

Main beer carbonyl compounds and their contribution to (loading) factors (principal components).

Compounds	Factor 1	Factor 2	Factor 3
2-Methylpropanal	<b>0.964676</b>	–0.029028	–0.156780
2-Methylbutanal	<b>0.970471</b>	0.079707	0.051885
3-Methylbutanal	<b>0.918157</b>	0.234333	0.187039
Benzaldehyde	<b>0.778030</b>	0.563202	–0.045207
Heptanal	<b>0.922337</b>	0.173329	0.236726
Octanal	<b>0.951691</b>	–0.038835	–0.112650
Furfural	0.404174	<b>0.853388</b>	0.116916
(E)-Non-2-enal	0.280985	0.362630	<b>0.865341</b>
Diacetyl	0.092912	0.590368	<b>–0.778098</b>
2,3-Pentanedione	0.301286	<b>0.899176</b>	0.006582

Loadings greater than 0.7000 are marked by bold type; Factor. Load (Quartimax normalized).

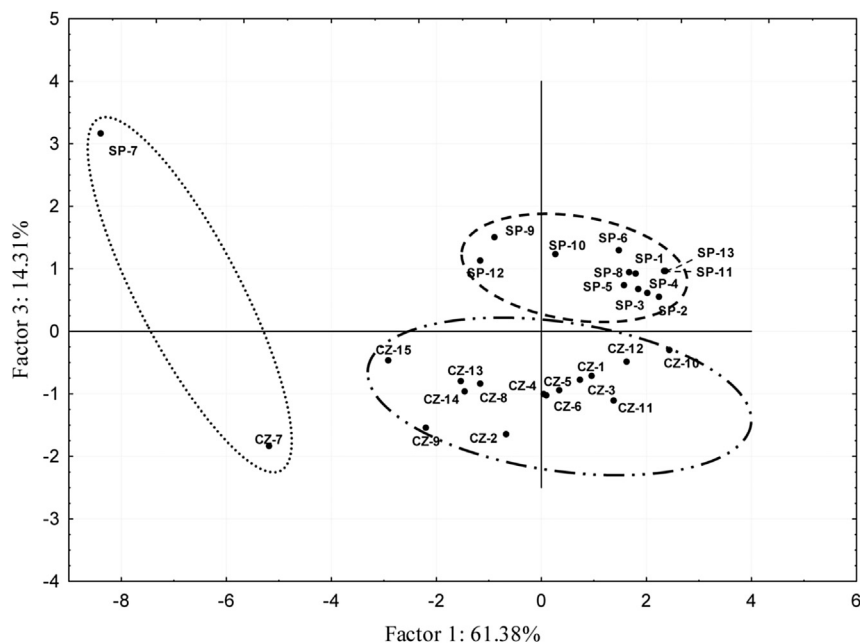


Fig. 2. PCA – scatterplot of beers sorted by their carbonyl compound content.

#### 4. Conclusions

In this study, we report a comparative analysis of carbonyl compounds in Czech and Spanish beers. Ten carbonyl compounds were identified and quantified in 28 samples of different types of *lager* beers. Results confirm that the carbonyl profiles of Czech and Spanish beers are quite different. Factor analysis showed that 3 principal components contributed to the differences between Spanish and Czech beers, each factor being mainly related to significant differences with regard to country of origin and type of beer. Two factors explained about 76% of variability and were related to Strecker aldehydes (Factor 1) and (*E*)-non-2-enal and diacetyl contents (Factor 3). Factor 2 describes the effect of Maillard products, such as furfural and 2,3-pentadione, which are present in dark beers. Differences between both groups were confirmed by PCA scatterplot, which showed that the decisive parameter was factor 3, and was mainly contributed by (*E*)-non-2-enal and diacetyl. Non-alcoholic beers had a very low content of carbonyl compounds, with the exception of a non-alcoholic Czech beer (CZ-9) that was made by arrested or limited fermentation using a mashing process that reduces fermentable sugars in the wort and a short fermentation time; this beer had a carbonyl profile closer to that of regular beers.

#### Acknowledgements

Supported by the Ministry of Education, Youth and Sports of the Czech Republic, Project No. MSM 6046137305, and Research Centre, Projects No. 1M0570.

#### References

Anonymous. (2006). Publication of an application pursuant to article 6(2) of Council regulation (EC) No 510/2006 on the protection of geographical indications and designations of origin for agricultural products and foodstuffs. *Official Journal of the European Union*, 51, 14–22.

Anonymous. (2013). *Vyhláška Ministerstva zemědělství, kterou se provádí §18 písm.a),d),h),i),j) a k) zákona č. 110/1997 Sb., o potravinách a tabákových výrobcích a o změně a doplnění některých souvisejících zákonů, pro nealkoholické nápoje a koncentráty k přípravě nealkoholických nápojů, ovocná vína, ostatní vína a*

*medovinu, pivo, konzumní líh, lihoviny a ostatní alkoholické nápoje, kvasný ocet a droždí. Sběrka zákonů ČR.*

Baert, J. J., De Clippeler, J., Hughes, P. S., De Cooman, L., & Aerts, G. (2012). On the origin of free and bound staling aldehydes in beer. *Journal of Agricultural and Food Chemistry*, 60(46), 11449–11472.

Basařová, G., Hlaváček, I., Basař, P., & Hlaváček, J. (2011). *České pivo* (3rd ed.). Prague: Havlíček Brain Team.

Blanco, C. A., Andrés-Iglesias, C., & Montero, O. (2014). Low-alcohol beers: flavour compounds, defects and improvement strategies. *Critical Reviews in Food Science and Nutrition*. <http://dx.doi.org/10.1080/10408398.2012.733979>.

BOE. (2013). *Real Decreto 53/1995, de 20 de enero, por el que se aprueba la Reglamentación técnico-sanitaria para la elaboración, circulación y comercio de la cerveza y de la malta líquida.*

Bravi, E., Sensidoni, M., Floridi, S., & Perretti, G. (2009). Fatty acids composition differences between beers made with all-malt and brewer's corn grits and malt. *Technical Quarterly – Master Brewers Association of Americas*, 46(3). <http://dx.doi.org/10.1094/TQ-46-3-0916-01>.

Bravo, A., Herrera, J. C., Scherer, E., Ju-Nam, Y., Ruebsam, H., Madrid, J., et al. (2008). Formation of alpha-dicarbonyl compounds in beer during storage of Pilsner. *Journal of Agricultural and Food Chemistry*, 56(11), 4134–4144.

Briggs, D. E., Boulton, C. A., Brookes, P. A., & Stevens, R. (2004). *Brewing: Science and practice*. Boca Raton: CRC Press.

Bueno, M., Zapata, J., & Ferreira, V. (2014). Simultaneous determination of free and bonded forms of odor-active carbonyls in wine using a headspace solid phase microextraction strategy. *Journal of Chromatography A*, 1369, 33–42.

da Costa, M. S., Gonçalves, C., Ferreira, A., Ibsen, C., de Pinho, P. G., & Ferreira, A. C. S. (2004). Further insights into the role of methional and phenylacetaldehyde in lager beer flavor stability. *Journal of Agricultural and Food Chemistry*, 52(26), 7911–7917. <http://dx.doi.org/10.1021/jf0491781>.

Dekoninck, T. M. L., Verbelen, P. J., Delvaux, F., Van Mulders, S. E., & Delvaux, F. R. (2012). The importance of wort composition for yeast metabolism during accelerated brewery fermentations. *Journal of the American Society of Brewing Chemists*, 70(3), 195–204. <http://dx.doi.org/10.1094/Asbcj-2012-0809-01>.

Dufour, J. P., Leus, M., Baxter, A. J., & Hayman, A. R. (1999). Characterization of the reaction of bisulfite with unsaturated aldehydes in a beer model system using nuclear magnetic resonance spectroscopy. *Journal of the American Society of Brewing Chemists*, 57(4), 138–144.

Fumi, M. D., Galli, R., Lambri, M., Donadini, G., & De Faveri, D. M. (2009). Impact of full-scale brewing processes on lager beer nitrogen compounds. *European Food Research and Technology*, 230(2), 209–216. <http://dx.doi.org/10.1007/s00217-009-1161-6>.

Gonçalves, J. L., Figueira, J. A., Rodrigues, F. P., Ornelas, L. P., Branco, R. N., Silva, C. L., et al. (2014). A powerful methodological approach combining headspace solid phase microextraction, mass spectrometry and multivariate analysis for profiling the volatile metabolomic pattern of beer starting raw materials. *Food Chemistry*, 160, 266–280.

Goode, D. L., & Arendt, E. K. (2006). Developments in the supply of adjunct materials for brewing. In C. Bamforth (Ed.), *Brewing: New technologies* (pp. 30–67). Cambridge: Woodhead Publishing Ltd.

Guido Carneiro, J. R., Santos, J. R., Almeida, P. J., Rodrigues, J. A., & Barros, A. A.

- (2004). Simultaneous determination of E-2-nonenal and beta-damascenone in beer by reversed-phase liquid chromatography with UV detection. *Journal of Chromatography A*, 1032(1–2), 17–22.
- Guido, L. F., Rajendram, R., & Barros, A. A. (2009). Pitching yeast and beer flavor. In V. R. Preedy (Ed.), *Beer in health and disease prevention*. London, UK: Academic Press.
- Ilett, D. R., & Simpson, W. J. (1995). Loss of sulfur-dioxide during storage of bottled and canned beers. *Food Research International*, 28(4), 393–396. [http://dx.doi.org/10.1016/0963-9969\(95\)00012-B](http://dx.doi.org/10.1016/0963-9969(95)00012-B).
- Inoue, T. (2009). Beer. In ASBC (Ed.), *Diacetyl in fermented foods and beverages* (pp. 45–75). St. Paul: American Society of Brewing Chemists.
- Jelinek, L., Doleckova, M., Karabin, M., Hudcova, T., Kotlikova, B., & Dostalek, P. (2012). Influence of growing area, plant age, and virus infection on the contents of hop secondary metabolites. *Czech Journal of Food Sciences*, 30(6), 541–547.
- Kobayashi, M., Shimizu, H., & Shioya, S. (2008). Beer volatile compounds and their application to low-malt beer fermentation. *Journal of Bioscience and Bioengineering*, 106(4), 317–323.
- Krogerus, K., & Gibson, B. R. (2013). 125th anniversary review: diacetyl and its control during brewery fermentation. *Journal of the Institute of Brewing*, 119(3), 86–97. <http://dx.doi.org/10.1002/jib.84>.
- Lermusieau, G., Liegeois, C., & Collin, S. (2001). Reducing power of hop cultivars and beer ageing. *Food Chemistry*, 72(4), 413–418. [http://dx.doi.org/10.1016/S0308-8146\(00\)00247-8](http://dx.doi.org/10.1016/S0308-8146(00)00247-8).
- Ma, T., Zhu, L. J., Zheng, F. Y., Li, Y. X., & Li, Q. (2014). Evaluation of emerging factors blocking filtration of high-adjunct-ratio wort. *Journal of Agricultural and Food Chemistry*, 62(33), 8486–8490. <http://dx.doi.org/10.1021/jf5023109>.
- Meilgaard, M. C. (1975). Flavor chemistry of beer Part II: flavor and threshold of 239 aroma volatiles. *MBAA Technical Quarterly*, 12(3), 151–168.
- Mikyska, A., Krofta, K., Haskova, D., Culik, J., & Cejka, P. (2011). The influence of hopping on formation of carbonyl compounds during storage of beer. *Journal of the Institute of Brewing*, 117(1), 47–54.
- Moreira, N., Meireles, S., Brandao, T., & de Pinho, P. G. (2013). Optimization of the HS-SPME-GC-IT/MS method using a central composite design for volatile carbonyl compounds determination in beers. *Talanta*, 117, 523–531.
- Noel, S., Liegeois, C., Lermusieau, G., Bodart, E., Badot, C., & Collin, S. (1999). Release of deuterated nonenal during beer aging from labeled precursors synthesized in the boiling kettle. *Journal of Agricultural and Food Chemistry*, 47(10), 4323–4326. <http://dx.doi.org/10.1021/jf990211r>.
- Ochiai, N., Sasamoto, K., Daishima, S., Heiden, A. C., & Hoffmann, A. (2003). Determination of stale-flavor carbonyl compounds in beer by stir bar sorptive extraction with in-situ derivatization and thermal desorption-gas chromatography-mass spectrometry. *Journal of Chromatography A*, 986(1), 101–110.
- Olsovska, J., Cejka, P., Sigler, K., & Honigova, V. (2014). The phenomenon of czech beer: a review. *Czech Journal of Food Sciences*, 32(4), 309–319.
- Perpete, P., & Collin, S. (2000). Influence of beer ethanol content on the wort flavour perception. *Food Chemistry*, 71(3), 379–385.
- Pires, E. J., Teixeira, J. A., Branyik, T., Brandao, T., & Vicente, A. A. (2015). Continuous beer fermentation – diacetyl as a villain. *Journal of the Institute of Brewing*, 121(1), 55–61. <http://dx.doi.org/10.1002/jib.205>.
- Priest, F. G., & Stewart, G. G. (2006). *Handbook of brewing* (2nd ed.). Boca Raton: CRC Press LLC.
- Riu-Aumatell, M., Miro, P., Serra-Cayuela, A., Buxaderas, S., & Lopez-Tamames, E. (2014). Assessment of the aroma profiles of low-alcohol beers using HS-SPME-GC-MS. *Food Research International*, 57, 196–202.
- Rossi, S., Sileoni, V., Perretti, G., & Marconi, O. (2014). Characterization of the volatile profiles of beer using headspace solid-phase microextraction and gas chromatography-mass spectrometry. *Journal of the Science of Food and Agriculture*, 94(5), 919–928.
- Saerens, S. M. G., Verbelen, P. J., Vanbeneden, N., Thevelein, J. M., & Delvaux, F. R. (2008). Monitoring the influence of high-gravity brewing and fermentation temperature on flavour formation by analysis of gene expression levels in brewing yeast. *Applied Microbiology and Biotechnology*, 80(6), 1039–1051. <http://dx.doi.org/10.1007/s00253-008-1645-5>.
- Saison, D., De Schutter, D. P., Delvaux, F., & Delvaux, F. R. (2009a). Determination of carbonyl compounds in beer by derivatisation and headspace solid-phase microextraction in combination with gas chromatography and mass spectrometry. *Journal of Chromatography A*, 1216(26), 5061–5068.
- Saison, D., De Schutter, D. P., Uyttenhove, B., Delvaux, F., & Delvaux, F. R. (2009b). Contribution of staling compounds to the aged flavour of lager beer by studying their flavour thresholds. *Food Chemistry*, 114(4), 1206–1215.
- Saison, D., De Schutter, D. P., Vanbeneden, N., Daenen, L., Delvaux, F., & Delvaux, F. R. (2010). Decrease of aged beer aroma by the reducing activity of brewing yeast. *Journal of Agricultural and Food Chemistry*, 58(5), 3107–3115.
- Stephan, A., Kusche, M., & Stettner, G. (2007). Influence of malt quality on the generation of odouractive strecker aldehydes during beer aging. In *Proc. Congr. – Eur. Brew. Conv., 31st, steph1/1-step1/5*.
- Stewart, G. G., & Murray, J. P. (2012). Brewing intensification – successes and failures. *Technical Quarterly – Master Brewers Association of Americas*, 49(3), 111–120. <http://dx.doi.org/10.1094/TQ-49-3-1016-01>.
- Taylor, J. R. N., Dlamini, B. C., & Kruger, J. (2013). 125th anniversary review: the science of the tropical cereals sorghum, maize and rice in relation to lager beer brewing. *Journal of the Institute of Brewing*, 119(1–2), 1–14. <http://dx.doi.org/10.1002/jib.68>.
- Vanderhaegen, B., Delvaux, F., Daenen, L., Verachtert, H., & Delvaux, F. R. (2007). Aging characteristics of different beer types. *Food Chemistry*, 103(2), 404–412.
- Vanderhaegen, B., Neven, H., Verachtert, H., & Derdelinckx, G. (2006). The chemistry of beer aging – a critical review. *Food Chemistry*, 95(3), 357–381. <http://dx.doi.org/10.1016/j.foodchem.2005.01.006>.
- Yahya, H., Linforth, R. S. T., & Cook, D. J. (2014). Flavour generation during commercial barley and malt roasting operations: a time course study. *Food Chemistry*, 145, 378–387. <http://dx.doi.org/10.1016/j.foodchem.2013.08.046>.
- Yeo, H. Q., & Liu, S. Q. (2014). An overview of selected specialty beers: developments, challenges and prospects. *International Journal of Food Science and Technology*, 49(7), 1607–1618. <http://dx.doi.org/10.1111/ijfs.12488>.
- Yu, J. H., Huang, S. X., Dong, J. J., Fan, W., Huang, S. L., Liu, J., et al. (2014). The influence of LOX-less barley malt on the flavour stability of wort and beer. *Journal of the Institute of Brewing*, 120(2), 93–98. <http://dx.doi.org/10.1002/jib.122>.
- Zhu, L. J., Ma, T., Li, Y. X., & Li, Q. (2015). Permeability analysis of high-adjunct-ratio spent grain layer in the high-gravity wort separation process. *Process Biochemistry*, 50(5), 846–852. <http://dx.doi.org/10.1016/j.procbio.2015.02.015>.



# Melting release point of encapsulated phosphates and heating rate effects on control of lipid oxidation in cooked ground meat



B. Kılıç<sup>a,\*</sup>, A. Şimşek<sup>b</sup>, J.R. Claus<sup>c</sup>, E. Atılğan<sup>a</sup>

<sup>a</sup> Suleyman Demirel University, Faculty of Engineering, Department of Food Engineering, 32260, Isparta, Turkey

<sup>b</sup> Suleyman Demirel University, Egirdir Vocational School, Department of Food Processing, Isparta, Turkey

<sup>c</sup> University of Wisconsin-Madison, Meat Science and Muscle Biology Building, 1805 Linden Drive, Madison, WI 53706, United States

## ARTICLE INFO

### Article history:

Received 10 June 2015

Received in revised form

21 October 2015

Accepted 26 October 2015

Available online 30 October 2015

### Keywords:

Encapsulated phosphate

Melting release point

Lipid oxidation

Beef

Chicken

## ABSTRACT

Lipid oxidation inhibition effects of 0.5% encapsulated (e) phosphates (sodium tripolyphosphate, STP; sodium hexametaphosphate, HMP; sodium pyrophosphate, SPP) designed with a 60 or 68 °C encapsulate melting temperature (MT) incorporated into ground meat (beef, chicken) and stored (0, 1, 7 d) after being cooked at two heating rates (HR; slow, fast) were investigated. Both a fast heating rate and eSTP resulted in lower ( $p < 0.01$ ) cooking loss (CL) compared to slow heating and STP. Encapsulated STP increased pH, whereas eSPP decreased pH ( $p < 0.05$ ). CL and pH were not affected by MT. The highest orthophosphate (OP) was obtained with eSTP, followed by eSPP and eHMP ( $p < 0.05$ ). Higher OP was determined in beef that underwent slow heating ( $p < 0.05$ ) in contrast to chicken which was not influenced by HR. Using eSTP or eSPP enhanced reduction in TBARS and lipid hydroperoxides (LPO) compared with eHMP ( $p < 0.05$ ). Higher MT resulted in lower TBARS and LPO ( $p < 0.05$ ).

© 2015 Elsevier Ltd. All rights reserved.

## 1. Introduction

Lipid oxidation is a primary cause of quality deterioration that negatively influences acceptability of ready-to-eat-meat (RTE) products. Oxidation of lipids, pigments, proteins, and vitamins in a meat system results in discoloration, drip losses, off-odor, off-flavor, texture defects, loss of nutrient value, and the production of toxic compounds (Morrissey, Sheehy, Galvin, Kerry, & Buckley, 1998). Deterioration in quality of RTE products associated with oxidation is strongly enhanced during storage.

The susceptibility of meat to lipid oxidation depends on a number of factors such as the level of polyunsaturated fatty acids in the meat, pH, disruption of the integrity of muscle membranes by grinding, mechanical deboning, restructuring, and cooking (Buckley, Morrissey, & Gray, 1995). Initiation or acceleration of lipid oxidation can occur by the action of low molecular weight metals and iron-containing heme proteins such as hemoglobin and myoglobin. The disruption of the lipid membrane system during cooking facilitates the interactions of prooxidants such as oxygen and low molecular weight metals with unsaturated fatty acids. This interaction results in the generation of free radicals and the

propagation of oxidative reactions (Asghar, Gray, Buckley, Pearson, & Booren, 1988).

Food-grade phosphates are additives having a wide application in the meat industry. Phosphates provide beneficial effects such as increasing the water holding capacity, improving shelf-life, stabilizing the texture and reducing microbial growth in meat (Fonseca et al., 2011). Phosphates also have very strong antioxidant effects against oxidation of lipids in cooked meat products during storage by binding metal ions that act as catalysts for oxidation (Cheng, Wang, & Ockerman, 2007). However, the ability to inhibit lipid oxidation by added phosphates in cooked meat products is reduced by phosphatases, which are typically found in red meat and poultry (Jones, Fletcher, & Lyon, 2002). Phosphatases in raw meats hydrolyze phosphates into small chain length phosphates which are less effective in controlling lipid oxidation (Jung, Ghoul, & de Lamballerie-Anton, 2000). Even though phosphatase activity is greatly reduced by cooking, most of the added phosphates are lost by the time meat is cooked due to phosphatase activity in the meat (Davis & Townsend, 1994; Li, Bowers, Craig, & Perng, 1993). As a result of a reduced level of added phosphates by phosphatase activity, a desired antioxidant effect is not achieved in cooked meat products during storage.

Applications utilizing ingredient encapsulation have increased in the food industry primarily because the encapsulated materials

\* Corresponding author.

E-mail addresses: [bkilic@yahoo.com](mailto:bkilic@yahoo.com), [birolkilic@sdu.edu.tr](mailto:birolkilic@sdu.edu.tr) (B. Kılıç).

can be protected from moisture, heat or other adverse conditions, thus enhancing their stability and functionality. It was previously demonstrated that encapsulation technology can be applied to polyphosphates to protect them from phosphatases in order to achieve more effective lipid oxidation inhibition in muscle foods (Kılıç, Şimşek, Claus, & Atılğan, 2014; Sickler, Claus, Marriott, Eigel, & Wang, 2013a, b). Kılıç et al. (2014) and Sickler et al. (2013a, b) have reported the only three studies related to improving the antioxidant functionality of phosphates through encapsulation with hydrogenated vegetable oils. However, the effect of melting point temperature of the encapsulate on the effectiveness of the antioxidant properties of the phosphates was not addressed in those studies. It is important to be aware of some issues when using this technology for polyphosphates. During the cooking process, if polyphosphates are released early into the meat system they could be exposed to undenatured, active phosphatases. Therefore, it is important to evaluate different melting point temperatures for releasing the encapsulated polyphosphates to further optimize the antioxidant potential.

The objective of this research was to test the hypothesis that more effective lipid oxidation inhibition in muscle foods can be accomplished by the use of phosphates encapsulated with encapsulation material possessing a higher melting point temperature. A higher temperature release point would permit the opportunity for greater thermal inactivation of the phosphatases prior to the release of the polyphosphates.

## 2. Materials and methods

### 2.1. Sample preparation

Fresh skinless, boneless broiler chicken breast meat (*Musculus superficialis*) and beef (*Musculus longissimus dorsi*) were obtained from a local slaughterhouse for each of two replications on separate production days. The meat was ground (9.5 mm), mixed in a bowl mixer and then reground (3.2 mm). All treatments contained 1.0% sodium chloride (meat weight basis, 106404; Merck, Germany) and 10% added distilled water (meat weight basis). After the first grind and initial mixing the test ingredients were incorporated using a hand mixer. Ground meat was formulated to contain 0.5% encapsulated phosphate (phosphate weight basis) at two different melting release points (60 or 68 °C) associated with the hydrogenated vegetable oil used for encapsulation. The three phosphates used (STP: Brifisol 5-1327; HMP: 7-1462; SPP: 5-1230) were obtained from a commercial supplier (BK Giulini Corporation, Simi Valley, CA, U.S.A.). Encapsulation was accomplished by a commercial coating company (Coating Place Inc., Verona, WI, U.S.A.). The encapsulate (coating) was designed to achieve a melting release point of 60 or 68 °C. A commercially available hydrogenated vegetable oil (Loders Crocklaan, Channahon, IL, U.S.A.) was selected to achieve the desired melting release point. The hydrogenated vegetable oils were hydrogenated palm oil (27 Stearine) with a supplier verified capillary melting point of 60 °C (140 °F) and hydrogenated soybean oil (17 Stearine) with a supplier verified capillary melting point of 68 °C (155 °F). Briefly, the encapsulation process entailed the use of a Wurster column (bottom spray fluid bed process). The encapsulation material (hydrogenated vegetable oil) was placed in a stainless steel vessel and heated on a hot plate to the appropriate temperature above the melt point. An electronic heat sensor (temperature probe) was placed into the vessel to monitor oil temperature. The intended ingredient (polyphosphate) was added to a clean Wurster coating unit. Heppa filtered process air was drawn through the Wurster coating unit at a rate suitable to pneumatically transport polyphosphate particles upward through a coating zone (up-bed region) to a region of reduced air velocity

(expansion chamber) where particles fell back into the fluidizing particle bed (down-bed region) that feeds back to the coating zone. The molten hydrogenated vegetable oil was pumped through heat traced liquid lines to a heated nozzle located on the fluidization plate at the base of the coating zone where it was atomized concurrently with pneumatically transported particles. Process air temperature was set to congeal spray droplets as they contacted particle surfaces during transport to the expansion chamber. The polyphosphate made multiple passes through the spraying zone with a small amount of the hydrogenated oil being applied with each pass. The coating process continued until the proper weight of encapsulation material had been applied. After desired encapsulation level (30%) was achieved, encapsulated polyphosphates were removed from the system and packaged. Thirty percent of the finished weight of the encapsulated phosphate represented the encapsulate coating.

Ground meat samples from each species were cooked in capped plastic centrifuge tubes (50 mL) eight hours after the phosphate was added. Approximately 45 g of ground meat was placed into each tube and heat processed in a water bath. To establish two different HR, the starting temperature of the water in the water bath was either 60 °C (Slow) or 85 °C (Fast). For the slower HR, after the tubes had been loaded, the water bath setting was changed to 85 °C. Samples were cooked to 74 °C endpoint temperature determined with thermocouple (TK100S, Kimo Instruments, France). Cooked samples were stored in tubes under refrigeration conditions (4 °C) and analyzed for dependent variables during storage (0, 1, 7 days).

### 2.2. pH analysis

The pH was determined using spear electrode (FC 200, Hanna Instruments, Germany) attached to a portable pH meter (HI 9024, Hanna Instruments, Germany).

### 2.3. Cooking loss

Cooking loss was calculated by the equation: Cooking loss percentage = (weight of raw ground meat – weight of cooked ground meat)/(weight of raw ground meat) \* 100.

### 2.4. Determination of soluble orthophosphates

The soluble orthophosphate was determined by the modified method of Molins, Kraft, and Olson (1985) as described by Kılıç et al. (2014). The soluble orthophosphate (expressed as µg/g) was found by multiplying the dilution factor (20) by the observed value derived from the standard curve which was prepared with potassium phosphate (104873; Merck, Germany).

### 2.5. Thiobarbituric acid reactive substances (TBARS) analysis

TBARS were determined in duplicate from each sample using the muscle extraction procedure of Lemon (1975) as described by Kılıç et al. (2014). The TBARS values were expressed as µmol TBARS per kg meat.

### 2.6. Lipid hydroperoxides analysis

The lipid hydroperoxide was determined by the method of Shantha and Decker (1994) as described by Kılıç et al. (2014). The lipid hydroperoxide was expressed as µmol LPO per kg meat.

## 2.7. Design and statistical analysis

The experimental design for statistical purposes was three phosphate types (STP, HMP, SPP)  $\times$  two MT (60, 68 °C)  $\times$  two HR (slow, fast)  $\times$  three storage times (0, 1, 7 days) as a factorial arrangement. The six phosphate treatments (phosphate type and MT combinations) used are listed in Table 1.

The data were analyzed as a  $3 \times 2 \times 2 \times 3$  factorial design with all main effects and interactions associated with the independent variable factors (phosphate treatments, HR, and storage time). The dependent variables for the analysis included pH, OP, TBARS and LPO. Cooking loss was only measured at 0 h and therefore storage time was not an independent variable.

All experiments were replicated two times. Data for the ground chicken samples were analyzed separately from ground beef sample data. The SAS MIXED procedure (SAS 9.1.3 Service Pack 3, SAS Institute Inc., Cary, NC, USA) was used to determine significance ( $p < 0.01$ ) in the model and when significance was found, means were separated using the Least Significant Difference (LSD) method. Letter assignment to individual means to enable statistical comparisons was achieved using the pdmix800 macro (Saxton, 1998).

## 3. Results and discussions

Tests of fixed effects for cooked ground beef and ground chicken with encapsulated phosphates designed with two different MT (60 or 68 °C) are presented in Table 2. The results of the dependent variables (CL, pH, OP, TBARS and LPO) with main effects and up to four way interactions containing phosphate type, MT or both are presented.

### 3.1. pH

Regardless of MT and HR differences, results compared within a meat species for samples formulated with eSTP had higher pH values (5.99 in beef, 6.24 in chicken;  $p < 0.05$ ; standard error = 0.01 for beef and chicken) than those formulated with eHMP (5.80 in beef, 6.09 in chicken) or eSPP (5.60 in beef, 5.86 in chicken). eSPP had lower ( $p < 0.05$ ) pH values compared to those of eSTP or eHMP. As a relative benchmark, pH of control group (no encapsulated phosphate) was  $6.11 \pm 0.01$  (mean  $\pm$  standard error) for ground chicken and  $5.82 \pm 0.01$  for ground beef. Effect of phosphates such as STP and SPP on the pH of meat is well established (Li et al., 1993).

It was previously reported that since phosphates were completely released from the hydrogenated vegetable oil, the encapsulated phosphates had no significant effect on the final pH of the cooked meat samples (Kılıç et al., 2014; Sickler et al., 2013a, b). In general, the initial pH of meat increased in beef and chicken samples during storage ( $p < 0.05$ ). In this study, MT was not a significant factor for controlling pH changes in both meat species. This result was anticipated as the encapsulate would be expected to completely melt and release an equivalent amount of phosphate as provided by the added unencapsulated phosphate. However, pH was affected ( $p < 0.001$ ) by HR in both chicken and beef. Slow HR resulted in a slightly higher ( $p < 0.05$ ) pH in beef (slow vs fast; 5.81, 5.78; std error, 0.004) and chicken (slow vs fast; 6.07, 6.05; std error, 0.01) samples compared with a fast HR. Lawrie (1985) reported that the pH of meat increases with increasing temperature due to the loss of free acidic groups. Thus, the slow heating rate would allow more overall thermal input to cause additional loss of some acidic groups in comparison to a fast heating rate to the same endpoint temperature.

MT  $\times$  HR interaction indicated that the fast HR in both MT resulted in lower ( $p < 0.05$ ) pH in beef samples compared with slow HR (slow vs fast; 5.81 at 60 °C, 5.82 at 68 °C; 5.79 at 60 °C, 5.77 at 68 °C; std error, 0.01). No interaction was found on pH in the chicken samples. A phosphate type and storage time interaction revealed that the use of eSTP in beef and chicken samples resulted in an increase ( $p < 0.05$ ) in pH from day 0 to day 1. However, pH did not change significantly during further storage (data not shown). In contrast to the results for eSTP, the pH started to decrease during storage in beef samples manufactured with eHMP or eSPP ( $p < 0.05$ ). A phosphate type and storage time interaction showed that chicken samples produced with eSPP had a lower ( $p < 0.05$ ) pH at day 1 (5.82) than that of day 0 (5.86) and day 7 (5.89; std error, 0.01) which were not different from each other. A phosphate type  $\times$  HR  $\times$  storage time interaction demonstrated that HR did not affect pH level in chicken samples at each storage day except in the samples which underwent a slow HR and contained eHMP had higher pH on day 7 (6.12) compared to those cooked at a fast HR (6.07; std error, 0.01). Furthermore, this interaction showed that a slow HR caused higher pH on day 0 (slow vs fast; 5.90, 5.83; std error, 0.01) and lower pH on day 1 (slow vs fast; 5.78, 5.87; std error, 0.01) in chicken samples produced with eSPP. In addition, there was a phosphate type  $\times$  MT  $\times$  storage time interaction showing no pH differences among chicken samples produced with different encapsulated phosphates and MT on each storage day.

**Table 1**  
Coding for phosphate treatments evaluated and abbreviation list.

Phosphate treatment	Phosphate type	Melting point temperature (°C)
eSTP-60	Sodium tripolyphosphate, STP	60
eSTP-68	Sodium tripolyphosphate, STP	68
eHMP-60	Sodium hexametaphosphate, HMP	60
eHMP-68	Sodium hexametaphosphate, HMP	68
eSPP-60	Sodium pyrophosphate, SPP	60
eSPP-68	Sodium pyrophosphate, SPP	68
Abbreviations	Definition	
STP	Sodium tripolyphosphate	
HMP	Sodium hexametaphosphate	
SPP	Sodium pyrophosphate	
e	Encapsulated	
MT	Encapsulate melting temperature	
HR	Heating rate	
CL	Cooking loss	
OP	Orthophosphate	
TBARS	Thiobarbituric acid reactive substances	
LPO	Lipid hydroperoxides	

**Table 2**

Tests of fixed effects (Type 3) for cooked ground beef and ground chicken with encapsulated phosphates.

Independent variables <sup>a</sup>		Dependent variables <sup>a</sup>				
		pH	Cooking loss	OP	TBARS	LPO
Beef	PT	<0.0001	<0.0001	<0.0001	<0.0001	<0.0001
	MT	0.8973	0.3529	0.0126	0.0030	0.1199
	PT*MT	0.0499	0.4845	0.1075	0.2639	0.6949
	HR	<0.0001	0.0002	0.0108	0.2297	<0.0001
	PT*HR	0.5112	0.0045	0.0236	0.0471	0.5877
	MT*HR	0.0235	0.8240	0.2773	0.1516	0.5265
	PT*MT*HR	0.1511	0.3504	0.0221	0.1035	0.7798
	CS	<0.0001		0.4128	<0.0001	<0.0001
	PT*CS	0.0019		0.3673	<0.0001	<0.0001
	MT*CS	0.2294		0.9371	0.7603	0.2725
	PT*MT*CS	0.1049		0.4901	0.9697	0.0938
	HR*CS	0.0279		<0.0001	0.3888	<0.0001
	PT*HR*CS	0.5878		0.7279	0.9128	0.0853
	MT*HR*CS	0.6431		0.7754	0.0774	0.7463
	PT*MT*HR*CS	0.4543		0.4772	0.1103	0.6011
	Chicken	PT	<0.0001	<0.0001	<0.0001	<0.0001
MT		0.3406	0.3203	0.0399	<0.0001	<0.0001
PT*MT		0.2886	0.3732	0.6863	<0.0001	<0.0001
HR		0.0138	<0.0001	0.5224	0.8329	0.0108
PT*HR		0.3557	0.0249	0.0891	0.9186	0.0013
MT*HR		0.2613	0.9066	0.7719	0.0354	<0.0001
PT*MT*HR		0.2503	0.1008	0.2914	0.0337	<0.0001
CS		0.0026		0.2029	<0.0001	<0.0001
PT*CS		0.0002		0.1394	<0.0001	<0.0001
MT*CS		0.3513		0.7883	<0.0001	<0.0001
PT*MT*CS		0.0149		0.1261	<0.0001	<0.0001
HR*CS		<0.0001		0.0191	0.3082	0.0029
PT*HR*CS		0.0176		0.7039	0.6061	0.0030
MT*HR*CS		0.7408		0.8099	0.2917	<0.0001
PT*MT*HR*CS		0.7960		0.5221	0.4154	<0.0001

<sup>a</sup> Independent variables and dependent variable abbreviations: PT: Phosphate type, MT: Melting point temperature, HR: Heating rate, CS: Cooked storage, OP: Soluble orthophosphate, TBARS: Thiobarbituric acid reactive substances, LPO: lipid hydroperoxides.

However, the use of eSPP with a 60 °C MT compared to eSPP with a 68 °C MT resulted in higher pH (5.89 and 5.84, respectively; std error, 0.01) on day 0 and lower pH (5.80 and 5.85, respectively; std error, 0.01) on day 1. No clear explanation for these interactions was evident.

### 3.2. Cooking loss

The results showed that the highest ( $p < 0.05$ ) CL was observed in samples manufactured with eSPP ( $20.57 \pm 0.22$  in beef,  $9.43 \pm 0.14$  in chicken) followed by those produced with eHMP ( $19.62 \pm 0.22$  in beef,  $9.19 \pm 0.14$  in chicken). This might be due to a greater loss of the water holding capacity of the muscle proteins at the decreased pH by sodium pyrophosphate. Among three phosphates studied, the use of eSTP resulted in the lowest ( $p < 0.05$ ) CL values in beef ( $16.45 \pm 0.22$ ) and chicken ( $5.32 \pm 0.14$ ) samples. Apart from phosphate treatments, CL of the control group was  $19.57 \pm 0.22$  for beef and  $9.64 \pm 0.93$  for chicken. Our results are in agreement with those of Craig, Bowers, and Seib (1991) who also found a decrease in CL in ground turkey meat with added STP. A decreased CL due to eSTP may partly relate to the higher meat pH than the samples with eHMP or eSPP because there is a clear tendency for the water-holding capacity to increase with increasing meat pH (Thomsen & Zeuthen, 1988). Furthermore, it was stated that more effective water-holding capacity can be accomplished by alkaline phosphates due to the increase in pH than acidic phosphates which cause a decrease in pH (Townsend & Olson, 1987). Higher pH is known to protect proteins from heat denaturation. Kılıç et al. (2014) reported that eSTP and eSPP decreased and increased CL, respectively, compared with eHMP in ground meat. However, differences in MT used in this study had no observable

effect on CL (Table 2). HR was a factor affecting CL ( $p < 0.05$ ) as demonstrated by a higher CL in beef ( $19.55 \pm 0.18$ ) and chicken ( $9.46 \pm 0.11$ ) samples that underwent a slow HR compared with a fast HR ( $18.20 \pm 0.18$  in beef,  $6.5 \pm 0.11$  in chicken). The differences in CL between HR observed in our study could be due to a difference in cooking times required for each HR. The lower CL in samples with a fast HR could be the result of less heat exposure time thereby not denaturing the meat proteins as extensively (Kılıç et al., 2014).

A phosphate type  $\times$  HR interaction indicated that the use of a slow HR for cooking the beef samples formulated with eSTP caused higher CL (17.87) compared with a fast HR (15.02; std error, 0.31). This finding was not evident for beef samples that contained eHMP or eSPP. The same interaction also indicated that slow HR resulted in higher CL values (11.25) in chicken samples formulated with eSPP compared to those determined in the samples incorporated with eHMP (10.59; std error, 0.20). But this difference was not observed in chicken samples underwent fast HR. The reason for this interaction is unknown.

### 3.3. Soluble orthophosphate content

Results of OP are presented in Fig. 1. Regardless of MT and HR, OP content of all samples was generally quite stable during the 7 d storage period. The highest ( $p < 0.05$ ) OP level was determined in the samples formulated with eSTP in ground beef ( $3457.2 \pm 18.45$ ) and ground chicken ( $5877.1 \pm 44.98$ ). The results indicated that HMP was not as susceptible to hydrolysis as STP and SPP. The lowest ( $p < 0.05$ ) OP level was determined in samples with eHMP in both meat species ( $2437.6 \pm 18.45$  in beef,  $3777.1 \pm 44.98$  in chicken). Both beef and chicken samples produced with eSPP had OP values falling between eSTP and eHMP groups ( $2907.1 \pm 18.45$  in

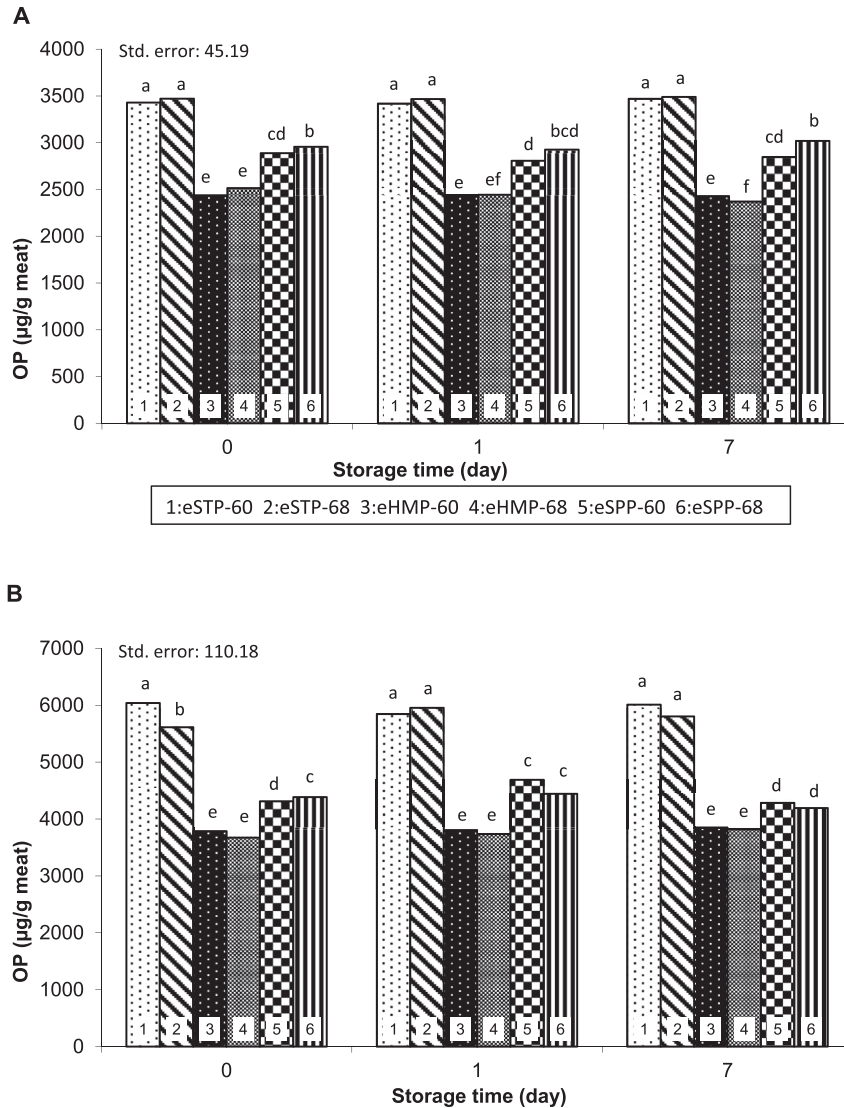


**Fig. 1.** Pooled mean results for soluble orthophosphate levels ( $\mu\text{g/g}$  of meat) associated with cooked ground chicken and ground beef. A: Beef samples, B: Chicken samples. Phosphate treatment of numbered bars; 1: eSTP-60, 2: eSTP-68, 3: eHMP-60, 4: eHMP-68, 5: eSPP-60, 6: eSPP-68. Bars with no matching letters between phosphate treatments are different ( $p < 0.05$ ). The standard error (Std. error) is associated with the three-way interaction (phosphate type  $\times$  encapsulate melting temperature  $\times$  storage time).

beef,  $4383.5 \pm 44.98$  in chicken). OP levels on the same products manufactured without phosphate added (control group) were  $2171.6 \pm 18.20$  for beef and  $3413.1 \pm 29.10$  for chicken. Our previous study (Kılıç et al., 2014) indicated that incorporation of unencapsulated or encapsulated phosphates into ground meat increased OP content in both ground chicken and beef. Molins, Kraft, and Olson (1987) reported that 100% added SPP was hydrolyzed to orthophosphate within four days of storage at  $5^\circ\text{C}$ . Li et al. (1993) also determined that all added STP was converted to orthophosphates within one day storage at  $5^\circ\text{C}$  in ground turkey meat. Awad (1968) showed that one mole of STP is hydrolyzed to one mole of orthophosphate and one mole of pyrophosphate. In the present study, higher OP content in samples containing eSTP compared to eSPP or eHMP could be related to the increased pH by eSTP. This observation is supported by the findings of Molins, Kraft, and Olson (1987) and Molins, Kraft, Walker, et al. (1987), who reported that higher orthophosphate levels in beef patties paralleled higher pH values. Awad (1968) also theorized that the ability of condensed phosphates to increase the pH of meat is related to the extent to which a particular phosphate is degraded to orthophosphate. Higher meat pH may provide more ideal conditions for phosphatase activity

(Kılıç et al., 2014). Results from the present study indicated that the higher MT resulted in higher ( $p < 0.05$ ) OP in beef samples ( $2906$  at  $60^\circ\text{C}$ ,  $2961.9$  at  $68^\circ\text{C}$ ; std error,  $15.06$ ). This result was not anticipated as it was expected more of the phosphatases would have been heat inactivated before the phosphates were released and therefore the reason for this result is not known. However, the reverse was true in chicken samples ( $4734.6$  at  $60^\circ\text{C}$ ,  $4623.8$  at  $68^\circ\text{C}$ ; std error,  $36.73$ ). In beef samples, a slow HR resulted in a higher OP ( $2962.6$ ) level compared with a fast HR ( $2905.3 \pm 15.06$ ,  $p < 0.05$ ). This indicated that the higher HR accelerated thermal inactivation of phosphatases in ground meat. A phosphate type  $\times$  MT  $\times$  HR interaction indicated that the use of a slow HR in beef samples resulted in higher OP values compared to a fast HR in samples formulated with eSTP having a  $68^\circ\text{C}$  MT (slow vs fast;  $3548.4$ ,  $3403$ ) and samples formulated with eSPP having a  $60^\circ\text{C}$  MT (slow vs fast;  $2943.3$ ,  $2751$ ; std error,  $36.90$ ). However, the use of a slow or a fast HR did not cause any significant differences on OP levels determined in samples produced with eSTP having a  $60^\circ\text{C}$  MT or eSTP having a  $68^\circ\text{C}$  MT or eHMP with a  $60$  or  $68^\circ\text{C}$  MT. In the case of chicken, a phosphate type  $\times$  MT  $\times$  HR interaction had no significant impact on OP level.

3.4. TBARS

Results of TBARS analysis (Fig. 2) illustrated that the TBARS values increased gradually during storage in all beef and chicken samples regardless of phosphate type, MT, or HR ( $p < 0.05$ ). Regardless of MT or HR, the lowest ( $p < 0.05$ ) TBARS values were determined in the samples formulated with eSTP or eSPP in beef (0.70, 0.83, respectively; std error, 0.06) and chicken (0.71, 0.59, respectively; std error, 0.12). On the other hand, the highest ( $p < 0.05$ ) TBARS were obtained in samples with eHMP in both meat species ( $2.26 \pm 0.06$  in beef,  $3.54 \pm 0.12$  in chicken). Furthermore, TBARS values of the control group were  $13.06 \pm 2.15$  for beef and  $7.99 \pm 1.3$  for chicken. Shahidi, Rubin, Diosady, Kassam Fong, and Wood (1986) reported that STP was a reasonably effective antioxidant when compared with other chelators. In addition, previous works (Kılıç et al., 2014; Sickler et al., 2013a, b) suggested that the use of eSTP was an effective strategy to reduce the formation of TBARS in precooked ground meat. Furthermore, regardless of the phosphate incorporated or HR, the study results indicated that the use of encapsulated phosphate with the higher MT (68 °C) resulted in lower ( $p < 0.05$ ) TBARS compared with

encapsulated phosphate with the lower MT (60 °C) in beef (1.37 at 60 °C, 1.16 at 68 °C; std error, 0.05) and chicken samples (2.00 at 60 °C, 1.23 at 68 °C; std error, 0.10). This was probably because higher melting points of encapsulation might have provided more time for further thermal inactivation of phosphatases during cooking, leading to more effective protection of phosphates from phosphatase activity. Thus, phosphates could contribute more to inhibition of lipid oxidation. However, there was no observable effect of HR on TBARS values of beef and chicken samples.

There was a significant interaction between phosphate type and storage time ( $p < 0.0001$ ) for TBARS. This interaction indicated that TBARS values of beef samples formulated with eHMP increased significantly ( $p < 0.05$ ) during 7 d storage (1.33 0 d; 1.86 1d; 3.59 7d; std error, 0.10). However, such significant differences among storage days in beef samples formulated with eSTP or eSPP were not evident. This interaction was thought to be the results of superior antioxidant capabilities of eSTP or eSPP compared with that of eHMP. According to a phosphate type  $\times$  HR interaction, the use of a slow HR for cooking ground beef samples containing eHMP resulted in higher ( $p < 0.05$ ) TBARS (2.41) compared with a fast HR (2.11; std error, 0.08), however, HR was not a factor creating differences in

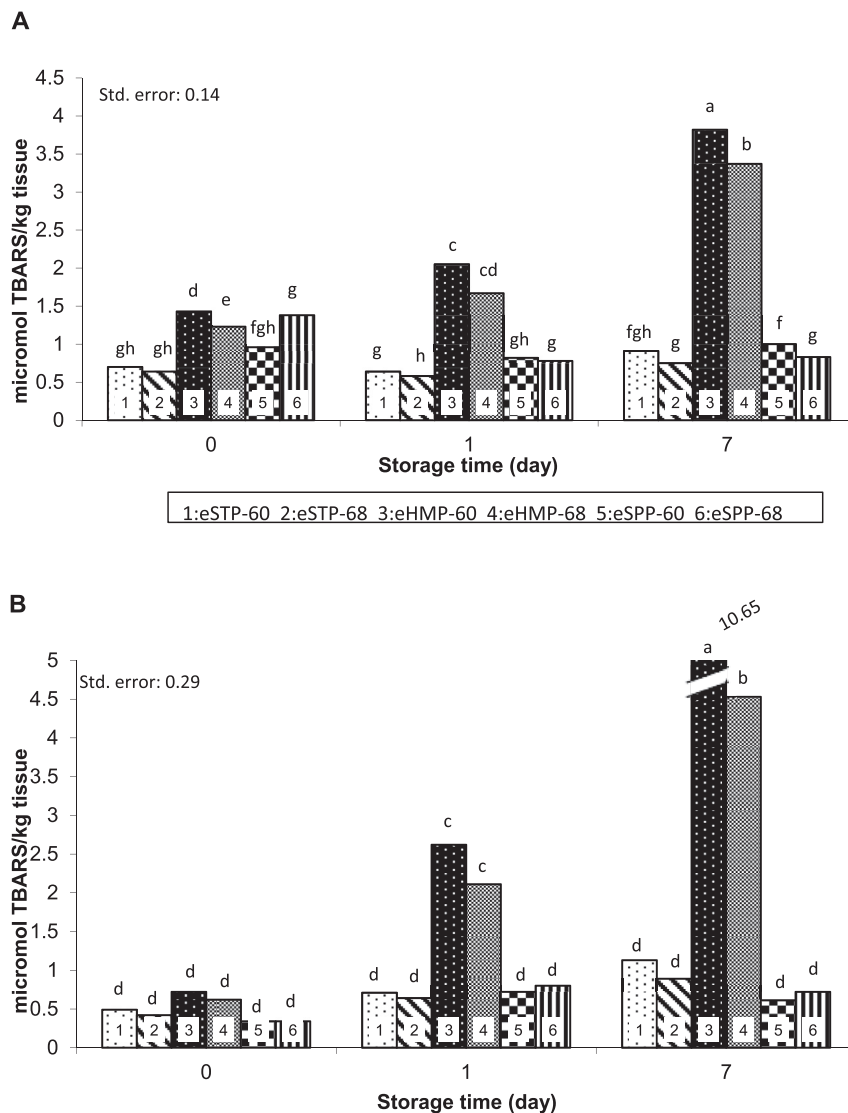


Fig. 2. Pooled mean results for TBARS values ( $\mu\text{mol/kg}$  of meat) associated with cooked ground chicken and ground beef. A: Beef samples, B: Chicken samples. Phosphate treatment of numbered bars; 1: eSTP-60, 2: eSTP-68, 3: eHMP-60, 4: eHMP-68, 5: eSPP-60, 6: eSPP-68. Bars with no matching letters between phosphate treatments are different ( $p < 0.05$ ). The standard error (Std. error) is associated with the three-way interaction (phosphate type  $\times$  encapsulate melting temperature  $\times$  storage time).

TBARS values in samples formulated with eSTP or eSPP. In the case of chicken, some 3-way interactions were found. A phosphate type  $\times$  MT  $\times$  HR interaction revealed that the use of a slow HR resulted in higher ( $p < 0.05$ ) TBARS values compared with a fast HR in chicken samples formulated with eHMP having a 60 °C MT (slow vs fast; 5.12, 4.21; std error, 0.24). However the reverse was true in the samples formulated with eHMP with 68 °C MT (slow vs fast; 2.04, 2.80; std error, 0.24). This was most likely due to the higher amount of iron released from the polyphyrin rings because of the longer cooking time to reach the targeted internal temperature of 74 °C and weaker protection provided by a lower MT for eHMP against phosphatase activity. However, the same interaction indicated that these TBARS differences observed for the use of eHMP were not determined for the use of eSTP or eSPP in the chicken. This could be the results of stronger suppression effects provided by STP or SPP on TBARS values compared with HMP. On the other hand, a phosphate type  $\times$  MT  $\times$  storage time interaction showed that the use of eHMP with a 60 °C MT in chicken samples resulted in higher ( $p < 0.05$ ) TBARS values compared with a 68 °C MT on day 1 and day 7 (60 vs 68 °C; 2.62, 2.11 1 d; 10.65, 4.53 7 d; std error, 0.29), but

these differences were not found for chicken samples containing eSTP or eSPP. This was most likely due to differences in the antioxidant capacity of the tested phosphates as described above.

### 3.5. Lipid hydroperoxides

There was a gradual increase in LPO in all samples during 7 days of storage ( $p < 0.05$ ) in beef and chicken samples (Fig. 3). Regardless of MT or HR, ground beef with eSTP resulted in the lowest ( $p < 0.05$ ) LPO values (12.64) followed by eSPP (14.21, std error, 0.53). This result was dissimilar to chicken, where the use of eSTP or eSPP inhibited LPO at the same level. On the other hand, the highest ( $p < 0.05$ ) LPO values were obtained in samples with eHMP in both meat species (26.78  $\pm$  0.53 in beef, 180.74  $\pm$  3.39 in chicken). Furthermore, LPO values of the control group were 67.01  $\pm$  11.82 for beef and 322.74  $\pm$  52.71 for chicken. It has been shown that the prooxidative activity of low molecular weight metals is in the order of: iron > copper > cobalt > magnesium (Pokorny, 1987, chap. 5, pp. 141–207). In addition, high levels of iron and copper are contained in the phospholipids of muscle foods (Pokorny, 1987). When

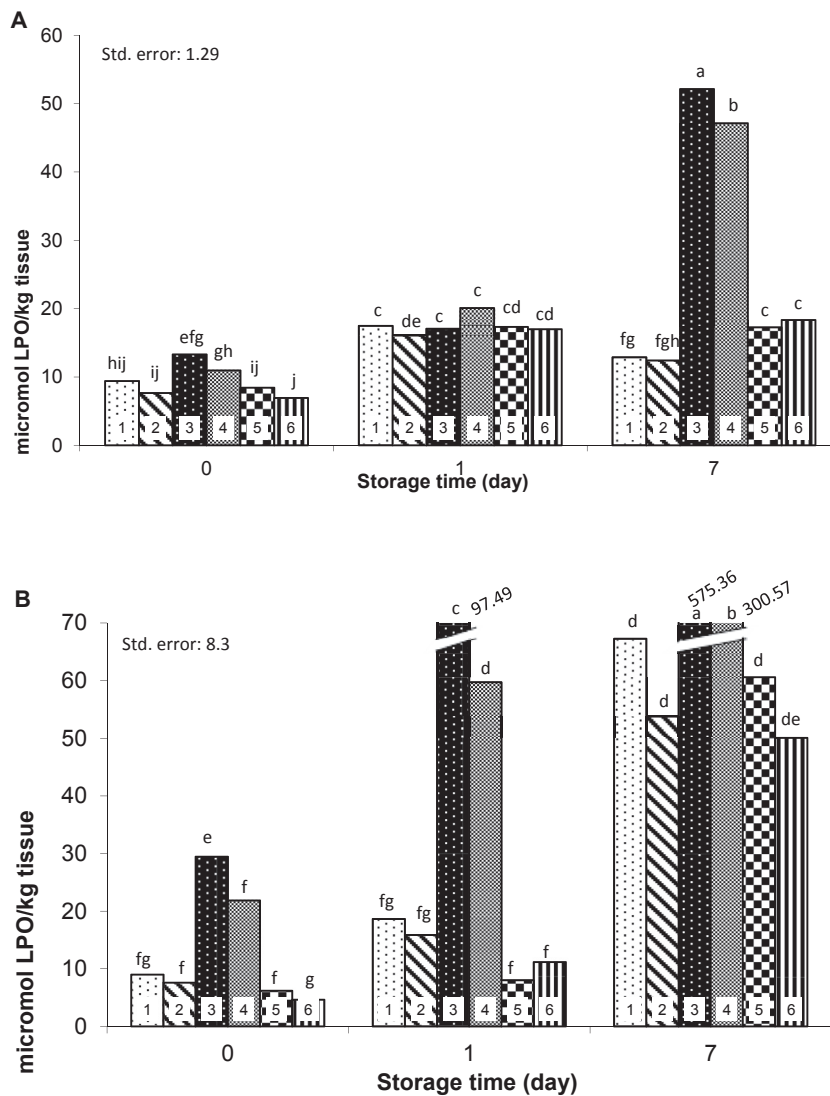


**Fig. 3.** Pooled mean results for lipid hydroperoxide values ( $\mu\text{mol/kg}$  of meat) associated with cooked ground chicken and ground beef. A: Beef samples, B: Chicken samples. Phosphate treatment of numbered bars; 1: eSTP-60, 2: eSTP-68, 3: eHMP-60, 4: eHMP-68, 5: eSPP-60, 6: eSPP-68. Bars with no matching letters between phosphate treatments are different ( $p < 0.05$ ). The standard error (Std. error) is associated with the three-way interaction (phosphate type  $\times$  encapsulate melting temperature  $\times$  storage time).

phosphates sequester metal ions, the metals are still present in meat system but are incapable of participating with any reaction. Differences in the antioxidant effect of phosphates used in this study might be the result of their sequestering capacity of various metal ions. Although, STP can be used to sequester many ions, this phosphate can effectively sequester heavy metals, such as copper and iron (Ellinger, 1972). On the other hand, sodium hexametaphosphate was reported to be the best sequestering agents for calcium and magnesium (Ellinger, 1972). In addition, regardless of phosphate incorporated or HR, it was determined that the higher MT (68 °C) resulted in lower ( $p < 0.05$ ) LPO values compared with the lower MT (60 °C) in ground chicken (90.88 at 60 °C, 58.35 at 68 °C; std error, 2.77). This was dissimilar to ground beef, where there was no observable effect of differences in MT on LPO. Although the melting point of the encapsulate material was verified by the supplier, the exact temperature release point of the encapsulated phosphate may vary in response to differences in the chemical properties (fat content, moisture, pH) between the chicken and beef. Contrary to the TBARS results, the use of a fast HR resulted in higher ( $p < 0.05$ ) LPO values in beef samples (slow vs fast; 15.87, 19.89; std error, 0.43) and ground chicken (slow vs fast; 72.36, 82.88; std error, 2.77).

There was a significant 2-way interaction between phosphate type and storage time ( $p < 0.0001$ ) for LPO in ground beef. A phosphate type and storage time interaction indicated that LPO values of beef samples formulated with eHMP increased ( $p < 0.05$ ) significantly during 7 d storage (12.13 0 d; 18.57 1d; 49.64 7d; std error, 0.91). This interaction also revealed that LPO values in beef samples containing eSTP showed an increasing trend from processing day to 1 d storage and then a decreasing trend from 1 d to 7d (8.53 0 d; 16.77 1d; 12.64 7d; std error, 0.91). As far as eSPP was concerned, the same interaction indicated there was an increasing trend in LPO values of the samples with eSPP from processing day to 1 d. However, such a differences did not exist between 1d and 7 d (7.67 0 d; 17.15 1d; 17.80 7d; std error, 0.91). In case of the chicken samples, a phosphate type  $\times$  MT  $\times$  HR  $\times$  storage time interaction was evident for LPO ( $p < 0.0001$ ). This interaction showed that the use of eHMP having a 60 °C MT in chicken samples that underwent a slow HR resulted in higher ( $p < 0.05$ ) LPO compared with the use of eHMP having a 60 °C MT in the samples cooked with a fast HR on day 7 (slow vs fast; 655.36, 495.36). However the reverse was existed in case of eHMP having a 68 °C MT for the same day (slow vs fast; 210.95, 390.20; std error, 11.74). According to the same interaction, while the higher LPO values due to fast HR were determined in the samples containing eHMP having a 60 or 68 °C MT on day 1 (slow vs fast; 47.42, 147.56 at 60 °C MT; 23.05, 96.37 at 68 °C MT; std error, 11.74), this differences did not exist on day 0. Furthermore, eSTP or eSPP incorporation in chicken samples under the same conditions described above did not created any significant differences in LPO due to HR at any days of storage.

#### 4. Conclusion

Regarding the results of TBARS and LPO, this study demonstrated that better oxidation inhibition in cooked ground beef and ground chicken during storage can be achieved by eSTP and eSPP and the antioxidant effect of these encapsulated phosphates can be enhanced with a higher MT of the encapsulate. It is suggested that the use of eSTP and eSPP with a higher MT can be an effective strategy to inhibit lipid oxidation in pre-cooked ready-to-eat meat products that require prolonged shelf life.

#### Acknowledgments

Appreciation is expressed to The Scientific and Technological Research Council of Turkey (TUBITAK) for providing financial support for this work (Project no: 111O261).

#### References

- Asghar, A., Gray, J. I., Buckley, D. J., Pearson, A. M., & Booren, A. M. (1988). Perspectives on warmed-over flavor. *Food Technology*, 42, 102–108.
- Awad, M. K. (1968). *Hydrolysis of polyphosphates added to meat*. MS. thesis. Edmonton, Alberta: The University of Alberta.
- Buckley, D. J., Morrissey, P. A., & Gray, J. I. (1995). Influence of dietary vitamin E on the oxidative stability and quality of pig meat. *Journal of Animal Science*, 73, 3122–3130.
- Cheng, J., Wang, S., & Ockerman, H. W. (2007). Lipid oxidation and color change of salted pork patties. *Meat Science*, 75, 71–77.
- Craig, J., Bowers, J. A., & Seib, P. (1991). Sodium tripolyphosphate and sodium ascorbate monophosphate as inhibitors of off-flavor development in cooked, vacuum-packaged, frozen Turkey. *Journal of Food Science*, 56, 1529–1531, 1561.
- Davis, C. E., & Townsend, W. E. (1994). Rapid fluorometric analysis of acid phosphatase activity in cooked poultry meat. *Journal of Food Protection*, 57(12), 1094–1097.
- Ellinger, R. H. (1972). Some general chemical characteristics of phosphates (Chap. 3). In *Phosphates as food ingredients*. Boca Raton, FL: CRC Press.
- Fonseca, B., Kuri, V., Zumalacárregui, J. M., Fernández-Diez, A., Salvá, B. K., Caro, I., et al. (2011). Effect of the use of a commercial phosphate mixture on selected quality characteristics of 2 spanish-style dry-ripened sausages. *Journal of Food Science*, 76, S300–S305.
- Jones, D. R., Fletcher, D. L., & Lyon, C. E. (2002). Variations in levels of acid phosphatase present in chicken whole leg meat. *Poultry Science*, 81, 1567–1570.
- Jung, S., Ghoul, M., & de Lamballerie-Anton, M. (2000). Changes in lysosomal enzyme activities and shear values of high pressure treated meat during ageing. *Meat Science*, 56, 239–246.
- Kılıç, B., Şimşek, A., Claus, J. R., & Atılğan, E. (2014). Encapsulated phosphates reduce lipid oxidation in both ground chicken and ground beef during raw and cooked meat storage with some influence on color, pH, and cooking loss. *Meat Science*, 97(1), 93–103.
- Lawrie, R. A. (1985). The storage and preservation of meat. In R. A. Lawrie (Ed.), *Meat science* (pp. 138–159). Oxford, UK: Pergamon Press.
- Lemon, D. W. (1975). *An improved TBA test for rancidity*. New Series Circular No. 51. Halifax, Nova Scotia: Halifax Laboratory.
- Li, W., Bowers, J. A., Craig, J. A., & Perng, S. K. (1993). Sodium tripolyphosphate stability and effect in ground turkey meat. *Journal of Food Science*, 58, 501–504.
- Molins, R. A., Kraft, A. A., & Olson, D. G. (1985). Adaptation of a method for the determination of soluble ortho-phosphates in cooked and uncooked pork containing acid-labile polyphosphates and pyrophosphates. *Journal of Food Science*, 50(5), 1482–1483.
- Molins, R. A., Kraft, A. A., & Olson, D. G. (1987). Insolubilization of orthophosphates in fresh or cooked ground pork. *Journal of Food Science*, 52, 1486–1489.
- Molins, R. A., Kraft, A. A., Walker, H. W., Rust, R. E., Olson, D. G., & Merkenich, K. (1987). Effect of inorganic polyphosphates on ground beef characteristics: some chemical, physical, and sensory effects on frozen beef patties. *Journal of Food Science*, 52, 50–52.
- Morrissey, P. A., Sheehy, P. J. A., Galvin, K., Kerry, J. P., & Buckley, D. J. (1998). Lipid stability in meat and meat products. *Meat Science*, 49, S73–S86.
- Pokorny, J. (1987). *Autoxidation of unsaturated lipids*. NY: Academic Press.
- Saxton, A. M. (1998). A macro for converting mean separation output to letter groupings in proc mixed. In *Proc. 23rd SAS users group intl., SAS Institute, Cary, NC* (pp. 1243–1246).
- Shahidi, F., Rubin, L. J., Diosady, L. L., Kassam Fong, L. S., & Wood, D. F. (1986). Effect of sequestering agents on lipid oxidation in cooked meats. *Food Chemistry*, 21, 145–152.
- Shantha, N. C., & Decker, E. A. (1994). Rapid, sensitive, iron-based spectrophotometric methods for determination of lipid hydroperoxides of food lipids. *Journal of AOAC International*, 77, 421–424.
- Sickler, M. L., Claus, J. R., Marriott, N. G., Eigel, W. N., & Wang, H. (2013a). Antioxidative effects of encapsulated sodium tripolyphosphate and encapsulated sodium acid pyrophosphate in ground beef patties cooked immediately after antioxidant incorporation and stored. *Meat Science*, 94(3), 285–288.
- Sickler, M. L., Claus, J. R., Marriott, N. G., Eigel, W. N., & Wang, H. (2013b). Reduction in lipid oxidation by incorporation of encapsulated sodium tripolyphosphate in ground turkey. *Meat Science*, 95(2), 376–380.
- Thomsen, H. H., & Zeuthen, P. (1988). The influence of mechanically deboned meat and pH on the water-holding capacity and texture of emulsion type meat products. *Meat Science*, 22, 189–201.
- Townsend, W. E., & Olson, D. G. (1987). Cured meats and cured meat products processing (Chap. 3 (pt. 2)). In J. F. Price, & B. S. Schweigert (Eds.), *The sci. of meat and meat prod* (3rd ed., pp. 103–114). Westport, CT: Food & Nutrition Press, Inc.



# Simultaneous inoculation of yeasts and lactic acid bacteria: Effects on fermentation dynamics and chemical composition of Negroamaro wine



Mariana Tristezza <sup>a</sup>, Luca di Feo <sup>a</sup>, Maria Tufariello <sup>a</sup>, Francesco Grieco <sup>b</sup>, Vittorio Capozzi <sup>c</sup>, Giuseppe Spano <sup>c</sup>, Giovanni Mita <sup>a</sup>, Francesco Grieco <sup>a,\*</sup>

<sup>a</sup> CNR – Institute of Sciences of Food Production (ISPA), via Prov. Lecce-Monteroni, 73100 Lecce, Italy

<sup>b</sup> CNR – Institute of Sciences of Food Production (ISPA), via G. Amendola, 122/O, 70126 Bari, Italy

<sup>c</sup> Department of the Sciences of Agriculture, Food and Environment, University of Foggia, Foggia, Italy

## ARTICLE INFO

### Article history:

Received 10 July 2015

Received in revised form

21 October 2015

Accepted 26 October 2015

Available online 31 October 2015

### Keywords:

Negroamaro wine

Yeast/bacteria coinoculation

Alcoholic fermentation

Malolactic fermentation

### Chemical compounds studied in this article:

Malic acid (PubChem CID: 525)

Glycerol (PubChem CID: 753)

Ethanol (PubChem CID: 702)

Lactic acid (PubChem CID: 612)

(R,R)-2,3-Butanediol (PubChem CID:

225936)

gamma-Butyrolactone (PubChem CID:

7302)

Isoamyl acetate (PubChem CID: 31276)

Isoamyl alcohol (PubChem CID: 31260)

2-Phenylethanol (PubChem CID: 6054)

Diethyl succinate (PubChem CID: 31249)

## ABSTRACT

Traditional vinification process is undertaken with the inoculation of the lactic acid bacteria (LAB) at the end of alcoholic fermentation (AF) to induce malolactic fermentation (MLF). MLF is an important phase during winemaking and the LAB co-inoculation with yeast starter represents a promising approach to enhance the quality and safety of wine. In this investigation we have studied: i) the effect of timing of LAB inoculation on the vinification dynamics and chemical features of Negroamaro wines; ii) the interactions between two commercial yeast and two commercial *Oenococcus oeni* strains. The fermentations dynamics were monitored by microbial counts, quantifying L-malic acid concentration and analyzing the volatile compounds contents in the obtained wines. Our results indicate that simultaneous yeasts/bacteria inoculation at the beginning of vinification reduces the processes duration and simultaneously lowers of volatile acidity. Wine obtained after co-inoculum showed a profile dominated by red and ripe fruits notes associated to esters and to buttery and creamy notes linked to diethyl succinate and ethyl lactate. Furthermore, compatibility specification between commercial yeasts and LAB strains were observed, suggesting the importance of the assessment of microbial-compatibility before their utilization in large-scale vinification.

© 2015 Elsevier Ltd. All rights reserved.

## 1. Introduction

The malolactic fermentation (MLF) is the conversion of L-malic

acid into L-lactic acid and CO<sub>2</sub> implemented by malolactic bacteria (MLB), as a result of their metabolism in wine (Zapparoli, Tosi, Azzolini, Vagnoli, & Krieger, 2009). This microbiological process causes the de-acidification of wine, since the di-carboxylic malic acid, is transformed into a mono-carboxylic acid such as lactic acid (Bartowsky, Costello, & Henschke, 2002). Associated with this decarboxylation, other transformations take place, that are important for consumer's safety and the organoleptic characteristic, such as increased stability, color changes and modifications of wine aroma and taste (Bauer & Dicks, 2004). MLF can occur spontaneously by the indigenous flora or through the use of

\* Corresponding author. National Research Council – Institute of Sciences of Food Production (ISPA), via Prov. Lecce-Monteroni, 73100 Lecce, Italy.

E-mail addresses: [mariana.tristezza@unifg.it](mailto:mariana.tristezza@unifg.it) (M. Tristezza), [delfinusmaris@gmail.com](mailto:delfinusmaris@gmail.com) (L. di Feo), [maria.tufariello@ispa.cnr.it](mailto:maria.tufariello@ispa.cnr.it) (M. Tufariello), [francescogrieco@ispa.cnr.it](mailto:francescogrieco@ispa.cnr.it) (F. Grieco), [vittorio.capozzi@gmail.com](mailto:vittorio.capozzi@gmail.com) (V. Capozzi), [giuseppe.spano@unifg.it](mailto:giuseppe.spano@unifg.it) (G. Spano), [giovanni.mita@ispa.cnr.it](mailto:giovanni.mita@ispa.cnr.it) (G. Mita), [francesco.grieco@ispa.cnr.it](mailto:francesco.grieco@ispa.cnr.it) (F. Grieco).

selected starter cultures, that usually belong to the species *Oenococcus oeni* (Capozzi et al., 2010). The advantages of induction of MLF by inoculation of selected MLB consist in the possibility to control the desired/undesired effects, in particular i) to complete degradation of malic acid; ii) to enhance the positive effect on wine bouquet, and iii) to achieve dominance of the starter culture on the undesired wild bacterial strains, often producing biogenic amines (Beneduce et al., 2010). Together with selected microbial resources, also the time of bacteria inoculation plays an important role in defining the wine sensory profile (Zapparoli et al., 2009). Generally the inoculum of the bacteria in the wine is introduced after alcoholic fermentation (AF) (sequential inoculation), when the sugars concentration is low. In fact, a possible undesirable consequence of the hetero-fermentative metabolism of MLB in must is degradation of sugars resulting in the production of acetic acid and lactic acid (Maicas, Ferrer, & Pardo, 2002) with the consequent rising of volatile acidity. However, sequential inoculations of LAB starter pose risks: MLF can be sluggish due to the elevated ethanol concentration and to the low pH of wine (Massera, Soria, Catania, Krieger, & Combina, 2009). Moreover, with sequential inoculation the antibacterial action of SO<sub>2</sub> is limited because of the decreased addition of this preservative at the end of the alcoholic fermentation (Alexandre, Costello, Remize, Guzzo, & Guilloux-Benatier, 2004), thus increasing the possibility for microorganisms such as *Brettanomyces* spp. to spoil the produced wine (Di Toro et al., 2015; Gerbaux, Briffox, Dumont, & Krieger, 2009). Therefore, early inoculation of a LAB starter together with yeast directly into the must, in order to stimulate a simultaneous MLF and AF, has been suggested to overcome these problems and to speed up wine production by reducing the time requested for MLF completion (Azzolini, Tosi, Vagnoli, Krieger, & Zapparoli, 2010; Izquierdo Cañas, Pérez-Martín, García Romero, Seseña Prieto, & Palop Herreros, 2012; Zapparoli et al., 2009). However, in spite of its many advantages on winemaking process, the co-inoculation approach and, particularly, the unpredictable interactions between *Saccharomyces cerevisiae* and *O. oeni* strains during grape must fermentation has been poorly investigated (Arnink & Henick-Kling, 2005). Moreover, strain specific yeast-bacteria interactions can also affect the dynamics of the AF, since yeast growth might even be repressed by some LAB strains (Mendoza, Merín, Morata, & Fariás, 2011).

The aim of this study was to compare the performance of four yeast/bacterium combinations when inoculated in two different approaches: simultaneously (co-inoculation), or sequential yeast followed by the bacteria when AF was close to the end. At the best of our knowledge, we report the first data about the application of a yeasts/bacteria multi-starter approach for the production of Negroamaro wines denoted by high alcohol content and high total acidity, typical of the oenological production of Southern Italy and other similar climates.

## 2. Materials and methods

### 2.1. Microorganisms

The following commercially available microorganisms were used for must inoculation: the *S. cerevisiae* strains coded as CY1 (Lallemand, USA) and CY2 (Enartis, Italy) and the commercially available *O. oeni* strains coded as CL1 (Lallemand, USA) and CL2 (Enartis, Italy). The yeast and bacterial starters have been purchased in active dried form. Rehydration and acclimatization procedures were done according to suppliers' instructions. The following codification was adopted to denote the different mixed inocula: A, CY1+CL1; B, CY1+CL2; C, CY2+CL1; D, CY2+CL2.

### 2.2. Microvinifications and wine analysis

To evaluate strain-specific fermentation performances, the starter cultures were used in micro-fermentations assays to inoculate Negroamaro grape must (20.8° Babo; 7.2 g/L total acidity; 3.44 g/L malic acid; pH 3.34; free ammonium 163.5 mg/L), following a procedure previously described (De Benedictis et al., 2011). The must was clarified by centrifugation (10 min at 8000 g), sterilized by filtration (0.45 µm membrane) and then supplemented with potassium metabisulphite (70 mg/L). One liter of must was placed in sterile Erlenmeyer 2 L flasks and then inoculated at a final concentration of 10<sup>9</sup> CFU/mL of a yeast inoculum pre-cultured in the same must. Malolactic bacteria were inoculated at a final concentration of 10<sup>7</sup> CFU/mL, as follow: i) LAB starter culture was inoculated 24 h after the yeast inoculation (Versari et al., 2015), in the case of evidence of co-inoculation or ii) bacteria starter cultures were added at the end of AF (15 days after yeast starters inoculation) in the case of traditional inoculum (Capozzi et al., 2010). The starter cultures were prepared and inoculated in the must according to the manufacturer's instructions. The ratio between yeast and MLB starter was equivalent to 100:1. In this study, we used the ratio recommended by starter manufacturers, that allowed us to mime the actual vinery conditions, as already described by several similar investigations (Antalick, Perello, & de Revel, 2013; Izquierdo Cañas et al., 2012, 2014; Versari et al., 2015). The temperature of the must at the time of inoculation was 24 °C, and it ranged between 23 °C and 26 °C during the experiments. The kinetics of the fermentations were monitored daily by gravimetric determinations, evaluating the loss of weight due to the production of CO<sub>2</sub>. Samples were weighted daily to follow the weight loss caused by CO<sub>2</sub> production. When CO<sub>2</sub> evolution stopped (i.e. at constant weight), samples were stored at -20 °C, until required for chemical analysis. Each fermentation experiment was carried out by performing three simultaneous independent repetitions.

### 2.3. Determination of microbial population

The viable count of yeasts was performed by diluting samples serially with 0.1% (wt/vol) peptone water and applying them to agar slants containing WL-agar medium (Sigma, USA) added with 0.1 g/L ampicillin. Plates were incubated at 28 °C for 48 h. Appropriate dilutions of must and wine were also plated on MRS supplemented with 2% tomato juice pH 4.8, added with 0.05 g/L nystatin. Plates were incubated at 28 °C under anaerobic conditions for 5–7 days and isolates were counted in order to quantify LAB (Capozzi et al., 2011).

### 2.4. Chemical analysis

Wines and musts were analyzed by Fourier Transform Infrared Spectroscopy (FTIR), employing the WineScan Flex (FOSS Analytical, DK). Samples were centrifuged at 8000 rpm for 10 min and then analyzed as previously described (Tristezza et al., 2012). Ethanol was routinely quantified using a specific enzymatic kit (Megazyme, Ireland). Extraction of volatile compounds in wines was carried out by means of solid phase extraction (SPE), according to Tufariello et al. (2014). SPE samples were analyzed using a gas chromatograph 6890N (Agilent Technologies, USA) equipped with DBWax column (60 m, 0.25 mm i.d., 0.25 µm film thickness, Agilent Technologies) and 5975C quadrupole mass spectrometer (Agilent Technologies). The injection was made in the splitless mode, the injector temperature was 250 °C. As regards wine volatile compounds, the temperature program was 40 °C for 3 min, 4 °C min<sup>-1</sup> to 200 °C, 20 min at maximum temperature. Carrier gas (He) flow was at 1.0 mL min<sup>-1</sup>. Spectra were recorded in the electron impact

mode (ionization energy, 70 eV) in a range of 30–500 amu at 3.2 scans/s. A solvent delay time of 10 min was used to avoid overloading the mass spectrometer with solvent. The identification of the volatile compounds was achieved by comparing mass spectra with those of the data system library (NIST 98,  $P > 90\%$ ) and retention indexes with published data, or by injection of pure standards. Concentration of each volatile compound is expressed as mg internal standard equivalents  $L^{-1}$  wine, obtained by normalizing the compound peak area to that of the internal standard and multiplying by concentration of the internal standard.

## 2.5. Statistical analysis

Significant differences among samples were determined for each chemical compound by analysis of variance (post-hoc Tukey,  $\alpha = 0.05$ ). Statistical data processing was performed using the free software package PAST (Hammer, Harper, & Ryan, 2001).

## 3. Results

### 3.1. Development of microbial populations during alcoholic fermentation

The alcoholic fermentation performance of the two *S. cerevisiae* strains, as single-, traditional- and sequential-inoculum were assessed, by the daily loss of weight of the flasks in relation to  $CO_2$  production. After 20 days, a stable ethanol concentration in all the samples indicated the end of the alcoholic fermentation. The obtained data showed that the two yeast starter cultures had a similar fermentative performance in all the produced must fermentations (Fig. 1). The presence of the bacteria in the early stages of the AF did not affect or inhibit the dynamics of yeast fermentation (Fig. 2). In fact, in the inoculated must we observed that the presence of the bacteria does not contrast the development of the yeasts population during fermentation, highlighting the ability of yeast to co-exist with bacteria and the capacity of the latter to better adapt to the environment in a co-inoculation rather than in a sequential inoculum. (Fig. 2). In the case of co-inoculation the development profile of the bacterial population shows its gradual acclimatization in the must during the increase of alcohol concentration due to yeasts (Fig. 3). However, the two commercial bacterial starter showed a different behavior in presence of the yeast strains used for co-inoculation. In fact, the CL1 strain was able to grow in the

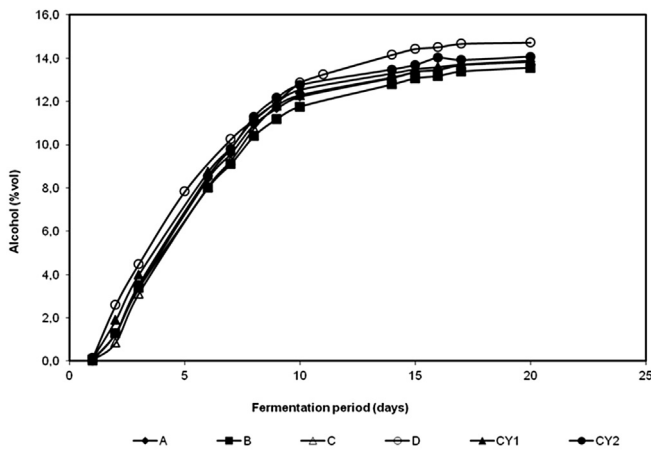


Fig. 1. Ethanol concentrations measured during fermentations of Negroamaro must inoculated with bacteria at the beginning of the alcoholic fermentation. A, CY1+CL1; B, CY1+CL2; C, CY2+CL1; D, CY2+CL2.

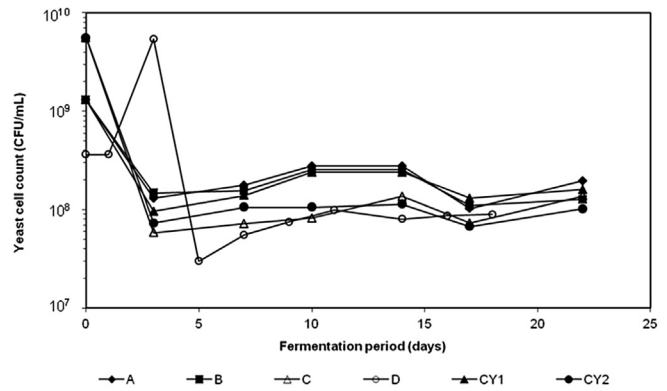


Fig. 2. Yeast populations (CFU/mL) measured during fermentations of Negroamaro must inoculated with bacteria at the beginning of the alcoholic fermentation. A, CY1+CL1; B, CY1+CL2; C, CY2+CL1; D, CY2+CL2.

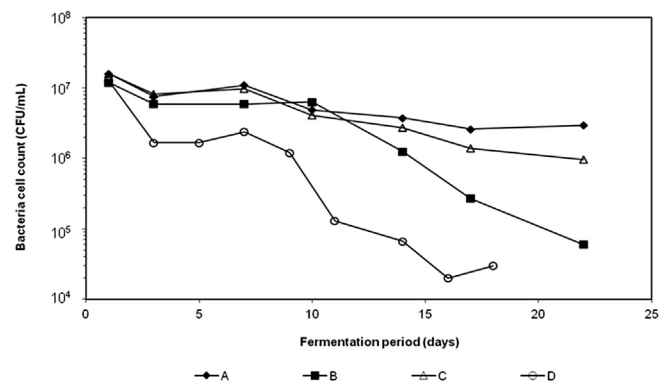


Fig. 3. Bacterial populations (CFU/mL) measured during fermentation of Negroamaro must inoculated with bacteria at the beginning of the alcoholic fermentation. A, CY1+CL1; B, CY1+CL2; C, CY2+CL1; D, CY2+CL2.

presence of both CY1 and CY2 yeast starters at similar level and they maintained a constant concentration (c.  $1 \times 10^7$  CFU/mL) during the progress of the MLF. In contrast, CL2 strain was unable to successfully grow in presence of both yeast strains, since its concentration decreased from  $1 \times 10^7$  CFU/mL to  $10^4$  CFU/mL (Fig. 3). When the bacterial inoculum was carried out at the end of the AF, the CL1 bacterial starter was able to proliferate in both wines produced with CY1 and CY2 yeast starters, showing a comparable

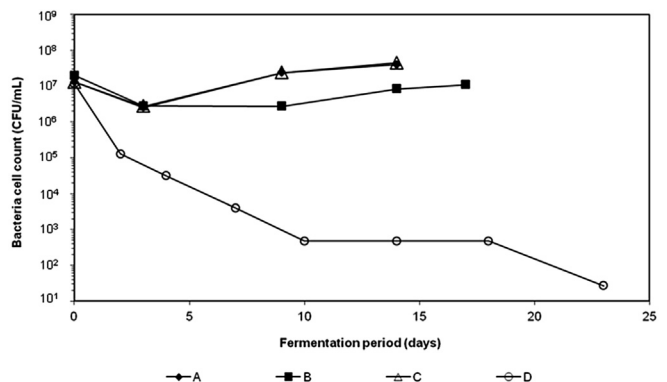


Fig. 4. Bacterial populations (CFU/mL) measured during fermentation of Negroamaro must in samples inoculated with bacteria at the end of the alcoholic fermentation. A, CY1+CL1; B, CY1+CL2; C, CY2+CL1; D, CY2+CL2.

behavior to the CL2 strain inoculated in the wine obtained by CY1 starter (Fig. 4). On the contrary when the CL2 strain was used to promote MLF in the wine obtained after CY2 fermentation, a continuous decrease in the number of bacteria during the whole period of their monitoring was observed (Fig. 4).

### 3.2. Malolactic fermentation

The dynamics of the MLF process was monitored by recording the transformation of malic acid in lactic acid. When the MLF was promoted by the co-inoculation of yeast with the LAB strains CL1 and CL2, these strains showed different performances (Fig. 4). In fact, CL1 strain was able to completely consume the malic acid in about 22 days either in presence of CY1 or of CY2 yeast starters, whereas the CL2 strain did not complete the MLF in both mixed fermentations, resulting in residual malic acid concentration of 0.69 g/L (CY1/CL2 inoculum) and 0.80 g/L (CY2/CL2 inoculum) (Fig. 5; Table 1).

The traditional inoculum was performed by adding the LAB starter culture at the end of the AF. The dynamics of MLF carried out by the CL1 strain was similar in both analyzed fermentations (CY1 and CY2), since they had a similar profile and they both resulted in the complete transformation of malic acid in lactic acid 14 days after inoculation (Fig. 6). However, the fermentative performances of CL2 strain were strictly dependent on yeast strain used to promote AF. In fact, when CL2 strain was inoculated in the wine produced with CY1 yeast starter, it was able to complete the MLF process in 22 days, whereas it was unable to successfully complete the conversion of malic in lactic acid when CY2 yeast was used, thus leaving a residual concentration of the former organic acid, corresponding to 2.05 g/L (Fig. 6; Table 1).

### 3.3. Determination of chemical parameters of fermentations

A positive effect on the volatile acidity (VA) was observed when yeasts and bacteria were co-inoculated. In particular, a decrease in acetic acid concentration was achieved, 0.30 g/L for CY1/CL1 co-inoculum and 0.31 g/L for CY2/CL1 co-inoculum, and these values were lower than those (0.49 and 0.51 g/L, respectively) detected in wines produced with the same starters in a sequential approach (Table 1). When CL2 was used as LAB starter a similar VA reduction was obtained in the wine produced by co-inoculum with yeast strain CY1 versus that produced by sequential starter inoculation (0.40 g/L versus 0.54 g/L). No significant variation in VA values was recorded in wine produced with CY2/CL2 strains by both co- and post AF inoculation. The values of citric acid, density, glycerol and

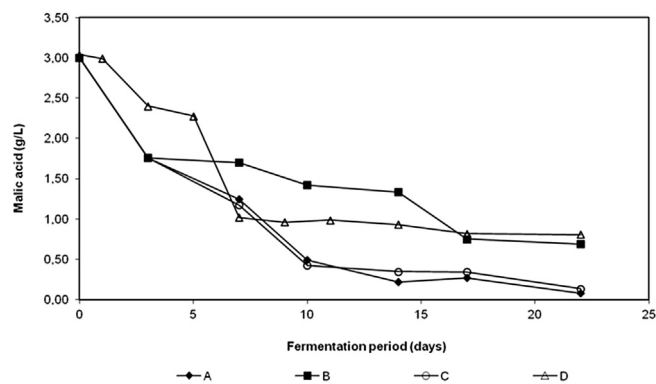


Fig. 5. L-malic acid consumption (g/L) evaluated during vinification of Negroamaro must in samples inoculated with bacteria at the beginning of the alcoholic fermentation. A, CY1+CL1; B, CY1+CL2; C, CY2+CL1; D, CY2+CL2.

pH are unchanged in the three fermentations, indicating that the technique of co-inoculation does not adversely affect the chemistry of the wine compared to the classical MLF induction technique (Table 1).

### 3.4. Analysis of volatile compounds

The different metabolism of yeast and bacteria can determine changes in volatile chemical composition of wines, including the compounds related to MLF. SPE/GC-MS analysis of the wine produced by the four combinations of yeasts/bacteria starter either sequentially or co-inoculated allowed the identification and quantification of a number of volatile compounds belonging to eight different groups that are by-products of yeast metabolism namely: alcohols, esters, acids and other compounds (Table 2). Table 2 shows the ester concentrations measured in the wine produced by co-inoculation and those obtained by sequential inoculation. The ester content was higher in wines produced by co-inoculation in all cases, 26,95 mg/L in CY1+CL1 vs 14,45 mg/L in CY1/CL1 inoculated post AF (pAF), 16,28 mg/L in CY1/CL2 vs 12,15 mg/L in CY1/CL2 pAF, 14,93 mg/L in CY2/CL1 vs 10,44 mg/L in CY2/CL1 pAF, 14,36 mg/L in CY2/CL2 vs 8,21 mg/L in CY2/CL2 pAF. The influence of co-inoculation on the chemical composition of wines was even more evident when the concentrations of alcohols and fatty acids were compared with those present in wines obtained after sequential starters inoculation. Total alcohol and acid concentrations were found to be higher in wines produced by co-inoculation and these compounds are responsible for fruity, sweet, winery and acid sensory notes in wine. Moreover, the concentration of fermentation-derived compounds (Table 2) also varied among the co-inoculated wines. All the esters and alcohols measured were found at higher concentrations in wines produced with CY1/CL1 co-inoculum compared with the other co-inoculated wines.

## 4. Discussion

One of the most important known benefit of yeasts/LAB simultaneous inoculation consists in the reduction of the total fermentation time (Abrahamse & Bartowsky, 2012). This study corroborated this statement and it is consistent with previous investigations performed on a lab-scale and with experiential winemakers' remarks (Antalick et al., 2013; Massera et al., 2009; Rosi, Fia, & Canuti, 2006). After co-inoculation, MLF can also occur when AF ended, but still in this case the length of the process is diminished, because of the adaptation of the bacterial starter to the "grape must" environment from the beginning of AF.

Specific interactions between *S. cerevisiae* and *O. oeni* are recognized to happen all through the alcoholic and malolactic fermentations, when co-inoculation of both starter cultures is chosen as strategy (Alexandre et al., 2004). In fact, definite yeasts–bacteria relations might be observed being different to those occurring in post-fermentation inoculations. In our investigation, we used two commercial yeast and two *O. oeni* strains that had been described by the producers to be highly suitable for the use as component of a mixed yeasts/bacteria co-inoculum.

Indeed, the viability of the *S. cerevisiae* starter cultures was not influenced during the simultaneous progress of AF and MLF, indicating that the exponential growth stage of the yeast starter populations was not decreased before reaching the stationary phase (Massera et al., 2009). These evidences are consistent to those obtained in a similar study on Tempranillo and Merlot wines (Izquierdo Cañas et al., 2012). When the bacterial starters were added, either simultaneously or sequentially, at the end of the AF an initial reduction in their viability was recorded. This evidence was

**Table 1**  
Chemical composition of wines at the end of MLF. A, CY1+CL1; B, CY1+CL2; C, CY2+CL1; D, CY2+CL2.

Method	Inoculum	Alcohol	Sugars	TA	VA	pH	Malic	Lactic	Tartaric	Citric	Glycerol
Coinoculation	<b>A</b>	13.89	0.58 <sup>ab</sup>	6.01 <sup>bc</sup>	0.30 <sup>b</sup>	3.44 <sup>de</sup>	0.05 <sup>b</sup>	1.59 <sup>a</sup>	2.07	0.35 <sup>bc</sup>	10.12 <sup>a</sup>
	STD	±0.16	±0.11	±0.37	±0.03	±0.01	±0.03	±0.02	±0.18	±0.00	±0.06
	<b>B</b>	13.78	0.54 <sup>ab</sup>	6.19 <sup>ab</sup>	0.40 <sup>e</sup>	3.43 <sup>ef</sup>	0.69 <sup>c</sup>	0.74 <sup>b</sup>	2.00	0.38 <sup>ac</sup>	10.28 <sup>ae</sup>
	STD	±0.16	±0.14	±0.21	±0.02	±0.00	±0.22	±0.23	±0.19	±0.02	±0.12
	<b>C</b>	13.82	0.71 <sup>a</sup>	6.07 <sup>bc</sup>	0.31 <sup>b</sup>	3.47 <sup>ac</sup>	0.04 <sup>b</sup>	1.63 <sup>a</sup>	2.03	0.38 <sup>ac</sup>	10.22 <sup>a</sup>
	STD	±0.29	±0.11	±0.13	±0.06	±0.01	±0.02	±0.01	±0.01	±0.02	±0.10
	<b>D</b>	13.91	0.55 <sup>ab</sup>	6.59 <sup>a</sup>	0.64 <sup>c</sup>	3.36 <sup>b</sup>	0.80 <sup>c</sup>	0.58 <sup>b</sup>	1.97	0.39 <sup>a</sup>	11.17 <sup>c</sup>
	STD	±0.13	±0.17	±0.15	±0.04	±0.01	±0.07	±0.02	±0.15	±0.01	±0.09
Post AF	<b>A</b>	13.82	0.60 <sup>ab</sup>	5.96 <sup>b</sup>	0.49 <sup>d</sup>	3.44 <sup>df</sup>	0.10 <sup>b</sup>	1.51 <sup>a</sup>	1.95	0.36 <sup>ac</sup>	10.37 <sup>ad</sup>
	STD	±0.16	±0.13	±0.18	±0.01	±0.00	±0.02	±0.02	±0.12	±0.02	±0.13
	<b>B</b>	13.89	0.68 <sup>a</sup>	6.05 <sup>bc</sup>	0.54 <sup>e</sup>	3.49 <sup>a</sup>	1.06 <sup>c</sup>	1.94	1.94	0.33 <sup>b</sup>	10.57 <sup>de</sup>
	STD	±0.01	±0.02	±0.01	±0.04	±0.01	±0.04	±0.00	±0.02	±0.01	±0.01
	<b>C</b>	13.87	0.54 <sup>ab</sup>	5.94 <sup>b</sup>	0.51 <sup>d</sup>	3.46 <sup>cd</sup>	0.11 <sup>b</sup>	1.54 <sup>a</sup>	1.95	0.38 <sup>ac</sup>	10.52 <sup>d</sup>
	STD	±0.16	±0.04	±0.05	±0.03	±0.00	±0.01	±0.00	±0.03	±0.00	±0.13
	<b>D</b>	14.11	0.28 <sup>b</sup>	6.48 <sup>ac</sup>	0.59 <sup>a</sup>	3.36 <sup>b</sup>	2.05 <sup>a</sup>	0.57 <sup>b</sup>	1.92	0.35 <sup>bc</sup>	11.54 <sup>b</sup>
	STD	±0.13	±0.13	±0.02	±0.05	±0.01	±0.03	±0.02	±0.09	±0.01	±0.08

TA, total acidity; VA, volatile acidity. The ethanol concentration is expressed as g/100 mL. The other values are expressed as g/L; the standard deviation values ( $\pm$ ) are indicated. Different letters indicate significant differences ( $\alpha = 0.05$ ).

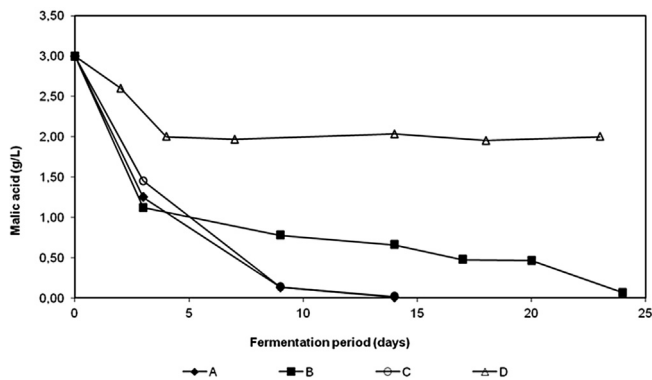


**Fig. 6.** L-malic acid consumption (g/L) evaluated during vinification of Negroamaro must in samples inoculated with bacteria at the end of the alcoholic fermentation. A, CY1+CL1; B, CY1+CL2; C, CY2+CL1; D, CY2+CL2.

already observed by King and Beelman (1986), after inoculating bacteria in synthetic grape juice and by Muñoz, Beccaria, and Abreo (2014), when they added the bacterial starter to musts in the mid of alcoholic fermentation.

The growth level of one of the two bacterial starters used in this study was affected by yeast presence, and the degree of the inhibition depended upon both yeast strain and timing of bacteria inoculation. In fact, when the CL2 bacteria were simultaneously or sequentially inoculated with the CY2 yeast strain, they showed the highest lag phase, the minimal growth and the highest residual malic acid. The yeast strain CY1 affected the growth of CL2 strain when they were early inoculated at the same time, whereas when the bacteria was added post AF a delayed MLF occurred. On the other hand the bacterial starter CL1 successfully carried out MLF process independently from yeast strain or inoculum modality. These evidences confirm the concept that the correct selection of the yeast–bacterium pair is critical for performing a concurrent AF/MLF, as the incompatibility between the two microorganisms can affect both processes (Guzzon et al., 2013; Nehme, Mathieu, & Taillandier, 2008). This study also confirmed that MLF can take place in the presence of fermentable sugars without a significant increase of acetic acid, it being an interesting findings if we consider that contrasting results were reported about the concentration of acetic acid in a co-inoculation approach (Garofalo, El Khoury et al., 2015; Knoll et al., 2012; Liu, 2012). This variability in scientific literature, in the light of our results, led us to

hypothesize that the effect of volatile acidity might be a strain-dependent character. In the experimental tests carried out, the consumption of malic acid occurred during the AF, when the population of bacteria was not in the growth phase. To further support the effectiveness of the yeast–bacteria co-inoculation, it has been considered a volatile acid content of 23% lower than that found in the wine produced by traditional inoculation, resulting in an improving effect on the organoleptic characteristics of the wine (Garofalo, El Khoury et al., 2015; Izquierdo Cañas et al., 2014).

The results reported in this study suggest that the use of co-inoculation for the management of the MLF has a positive influence on fermentation time as well as on aromatic composition of wine. In fact, the considerable effect of yeasts/LAB co-inoculation on the aromatic pattern of produced wine, compared to those obtained by sequential starters inoculation, was clearly shown. Recent investigations have highlighted the variation of the biochemical profile of wine produced by different LAB inoculation procedures (Abrahamse & Bartowsky, 2012; Izquierdo Cañas et al., 2012; Knoll et al., 2012). Our data suggested, in accordance to literature (Antalick et al., 2013), that yeast/LAB co-inoculation could enhance the fruity aroma, thereby increasing the level of esters. Twelve esters were identified and quantified, and wines produced by co-inoculation contained higher concentrations of diethyl and monoethyl succinate, ethyl lactate, 2-phenylethyl acetate and ethyl esters of fatty acids (Versari et al., 2015). Overall, for all strains tested, co-inoculation resulted in a significant change of the wine esters profile, with ethyl fatty acid esters becoming quantitatively the most representative class of esters. This procedure probably stimulates the formation of mid-chain fatty acids and, hence, the concentration of esters of fatty acids in wines. These compounds were considered to be odorant esters because they had a much higher impact on wine aroma (Fang & Qian, 2005). The presence of 2,3-butanediol indicates that in the case of co-inoculation bacteria were able to perform the degradation of diacetyl, the compound derived from the MLF with high organoleptic impact on wine (Martineau & Henick-Kling, 1995). This compound, if present in the wine at high concentrations, is able to adversely affect the bouquet of the wine conferring aromatic buttery notes that interfere with wines fruity aromas (Bartowsky & Henschke, 2004). Consequently, applying the technique of co-inoculation it will be possible to produce wines with lower hints of butter and milk, but with the sensory profiles dominated by organoleptic notes related to the grape. A bacterial-mediated modification of yeast by-products is likely to be the molecular mechanism in charge of the increase in butyrolactone

**Table 2**

Volatile compounds concentration of red wines obtained with co-inoculum and sequential. A, CY1+CL1; B, CY1+CL2; C, CY2+CL1; D, CY2+CL2.

Compounds	Co-inoculation								Sequential							
	A		B		C		D		A pAF		B pAF		C pAF		D pAF	
	Mean	±SD	Mean	±SD	Mean	±SD	Mean	±SD	Mean	±SD	Mean	±SD	Mean	±SD	Mean	±SD
<b>Esters</b>																
diethyl malate	n.d.		0.98a	0.1	0.73a	0.16	0.51a	0.47	0.84a	0.17	0.83a	0.21	n.d.		n.d.	
diethyl succinate	3.78c	0.70	1.20a	0.32	1.89b	0.18	1.27a	0.07	1.09a	0.14	1.01a	0.18	0.98a	0.2	0.53a	0.02
ethyl lactate	4.32b	0.12	5.35b	0.41	3.78b	0.29	4.74b	0.15	3.62b	1.47	2.87a	0.74	2.90a	0.03	3.37b	0.22
monoethyl succinate	10.90b	1.33	5.46a	0.47	5.06a	0.82	3.90a	0.39	4.83a	0.09	4.71a	2.34	3.55a	0.55	2.46a	0.09
2-phenylethyl acetate	1.20b	0.13	0.45a	0.12	0.48a	0.1	2.17c	0.12	0.65a	0.09	0.32a	0.06	0.38a	0.03	0.68a	0.04
3-hydroxy-ethylbutanoate	0.61	0.27	0.27	0.03	0.23	0.13	0.26	0.07	0.28	0.02	0.27	0.04	0.19	0.12	n.d.	
ethyl butanoate	0.80a	0.16	0.60a	0.05	0.76a	0.04	0.43a	0.18	0.64a	0.15	0.46a	0.24	0.57a	0.08	0.36a	0.02
ethyl decanoate	0.88b	0.24	0.19a	0.01	n.d.		0.29a	0.08	0.45b	0.2	0.27a	0.07	0.28a	0.14	0.04a	0.01
ethyl hexanoate	1.68b	0.32	0.53a	0.03	0.70a	0.06	0.43a	0.29	0.85a	0.43	0.49a	0.25	0.58a	0.16	0.50a	0.06
ethyl octanoate	1.97b	0.49	0.76a	0.16	0.98a	0.08	0.07a	0.01	0.56a	0.06	0.55a	0.18	0.75a	0.03	n.d.	
ethyl vanillate	0.06a	0.02	0.07a	0.06	0.04a	0.01	n.d.		0.07a	0.04	0.07a	0.05	0.03a	0	n.d.	
isoamyl acetate	0.75a	0.32	0.42a	0.03	0.28a	0.03	0.29a	0.01	0.57a	0.01	0.3a	0.05	0.23a	0.01	0.27a	0.02
<b>Total</b>	26.95	4.10	16.28	1.79	14.93	1.9	14.36	1.84	14.45	2.87	12.15	4.41	10.44	1.35	8.21	0.48
<b>Alcohols</b>																
1-butanol	2.28b	0.13	0.33a	0.04	0.08a	0.04	0.13a	0.06	0.46a	0.25	0.47a	0.28	0.04a	0.01	0.27a	0.02
2,3 butanediol (R,R)	1.59b	0.63	3.10c	0.56	n.d.		n.d.		3.32c	0.02	2.96c	0.41	n.d.		0.37a	0.06
2,3 butanediol (S,S)	1.41b	0.28	1.25b	0.38	0.23a	0.06	n.d.		1.20b	0.18	1.21b	0.26	n.d.		0.07a	0.03
2-phenylethanol	40.61	4.21	34.55	1.33	52.63	5.12	32.69	5.43	36.51	2.11	29.39	2.29	30.35	6.59	29.24	4.98
3-hexen-ol (E)	0.07a	0.02	0.42a	0.05	0.02a	0.01	n.d.		0.02a	0.01	0.15a	0.19	0.03a	0.01	n.d.	
3-hexen-ol (Z)	0.66b	0.18	0.73b	0.11	0.13a	0.04	0.04a	0.01	0.03a	0.01	0.03a	0.01	0.03a	0.01	0.12a	0.04
hexanol	0.35a	0.14	0.16a	0.01	0.16a	0.01	0.22a	0.03	0.15a	0.05	0.19a	0.02	0.15a	0.04	0.16a	0.05
Isoamyl alcohols	132.4	5.92	137.63	8.11	135.38	1.99	114.36	8.36	128.62	8.6	128.55	13.12	115.44	11.41	98.55	3.29
isobutanol	13.60b	3.71	8.67b	2.44	10.42b	0.37	5.01a	1.13	8.97b	0.86	6.65a	0.23	6.04a	1.64	3.53a	0.19
propanol	19.87b	3.89	12.54b	2.42	4.85a	0.62	n.d.		14.15b	2.87	19.2b	3.88	nd		3.44a	0.17
<b>Total</b>	212.86	15.22	199.38	13.03	203.90	7.61	152.45	18.02	193.44	12.09	188.81	16.81	152.09	19.71	135.75	8.83
<b>Acids</b>																
2-methylpropanoic acid	0.51b	0.22	2.12c	0.23	0.14b	0.08	0.11b	0.02	0.18b	0.08	0.17b	0.04	0.1a	0.01	0.1 a	0
3-methyl butanoic acid	1.66b	0.37	0.67a	0.02	0.51a	0.19	0.66a	0.17	0.73a	0.03	0.67a	0.05	0.46a	0.21	0.53a	0.09
benzoic acid	0.60b	0.14	0.28a	0.16	0.11a	0.01	0.13a	0.05	0.24a	0.2	0.26a	0.16	0.07a	0.03	0.07a	0.03
butanoic acid	0.15a	0.06	0.32a	0.02	0.47a	0.27	0.28a	0.08	0.58a	0.24	0.54a	0.13	0.28a	0.12	0.04a	0.02
decanoic acid	0.8c	0.28	n.d.		0.2b	0.02	0.09a	0.03	0.58a	0.18	0.25a	0.11	0.11a	0.17	0.13a	0.03
hexanoic acid	0.38a	0.16	0.42a	0.02	1.98c	0.08	0.37a	0.13	0.49a	0.05	0.63a	0.05	1.11b	0.15	0.44a	0.03
octanoic acid	0.4	0.16	0.36	0.11	0.21	0.03	0.4	0.11	0.36	0.15	0.31	0.04	0.31	0.21	0.51	0.05
phenylacetic acid	0.16a	0.05	0.18a	0.12	0.13a	0.01	0.10a	0.04	0.17a	0.03	0.18a	0.06	0.09a	0.03	n.d.	
propanoic acid	0.60a	0.24	0.23a	0.05	2.08b	0.04	n.d.		n.d.		0.05a	0.03	n.d.		n.d.	
<b>Total</b>	5.27	1.68	4.58	0.73	5.83	0.73	2.14	0.63	3.31	0.96	3.05	0.67	2.94	0.93	1.82	0.25
<b>Other Compounds</b>																
acetoin	1.52b	0.59	2.94c	0.62	1.66b	0.15	n.d.		0.43a	0.12	0.68a	0.28	n.d.		n.d.	
acetovanillone	0.08a	0.04	0.08a	0.05	0.05a	0.01	0.15a	0.07	0.07a	0.02	0.08a	0.05	0.04a	0.02	0.12a	0.04
benzaldehyde	0.38b	0.14	n.d.		0.11a	0.04	n.d.		0.20a	0.05	n.d.		n.d.		n.d.	
butyrolactone	1.84b	0.69	1.25b	0.08	0.69a	0.38	0.30a	0.06	0.91b	0.21	0.32a	0.04	0.38a	0.25	0.34a	0.08
<b>Total</b>	3.83	1.46	4.26	0.75	2.41	0.58	0.45	0.13	1.6	0.4	1.07	0.37	0.43	0.27	0.46	0.12

Nd: not detected.

Each value is expressed in mg/L, and is the mean of 3 extraction replicates ± ds (standard deviation).

concentrations in wines produced by the co-inoculation system compared to the sequential technique (Antalick et al., 2013). In fact, it has been previously demonstrated that yeasts/LAB interactions promote lactones synthesis during whisky-production process (Wanikawa, Hosoi, & Kato, 2000).

## 5. Conclusions

In addition to consistent data on the possible use of autochthonous resources from Apulian region (Cappello, Stefani, Grieco, Logrieco, & Zapparoli, 2008; Garofalo, Russo et al., 2015; Grieco et al., 2011; Tristezza et al., 2013, 2014) already published, this study provides the first report on the application of the method of co-inoculation in the winemaking conditions typical of Southern Italy (Puglia) wine production using commercial starter cultures. The present investigation highlighted the need to assess the real compatibility of commercial yeast bacteria strains, even if they are

indicated as suitable for simultaneous fermentations, before they are used for wine production. Furthermore, our data suggest that grape-cultivar-derived extrinsic factors can appreciably modify the intrinsic yeast-bacteria metabolic relation (Costello, Henschke, & Markides, 2003), even in strain that are described to have compatible interactions.

## Acknowledgment

We thank P. A. Giovanni Colella for the technical support. This research was supported by the Italian Ministry of Education, University and Research - Project S.I.Mi.S.A. - PON02\_00186\_3417512/1 and by the Regione Puglia - Project Nr. 6N7AD82 "Autochthonous2Autochthonous: risorse microbiologiche per vini in purezza da vitigni autoctoni (e per produzioni biologiche)".

## References

- Abrahamse, C. E., & Bartowsky, E. J. (2012). Timing of malolactic fermentation inoculation in Shiraz grape must and wine: influence on chemical composition. *World Journal of Microbiology and Biotechnology*, 28, 255–265.
- Alexandre, H., Costello, P. J., Remize, F., Guzzo, J., & Guilloux-Benatier, M. (2004). *Saccharomyces cerevisiae*-*Oenococcus oeni* interactions in wine: current knowledge and perspectives. *International Journal of Food Microbiology*, 93, 141–154.
- Antalick, G., Perello, M. C., & de Revel, G. (2013). Co-inoculation with yeast and LAB under winery conditions: modification of the aromatic profile of merlot wines. *South African Society for Enology & Viticulture*, 34, 223–232.
- Arnink, K., & Henick-Kling, T. (2005). Influence of *Saccharomyces cerevisiae* and *Oenococcus oeni* strains on successful malolactic conversion in wine. *American Journal of Enology & Viticulture*, 56, 228–237.
- Azzolini, M., Tosi, E., Vagnoli, P., Krieger, S., & Zapparoli, G. (2010). Evaluation of technological effects of yeast-bacterial co-inoculation in red table wine production. *Italian Journal of Food Science*, 3, 257–263.
- Bartowsky, E., Costello, P., & Henschke, P. (2002). Management of malolactic fermentation-wine flavour manipulation. *Australian & New Zealand Grape-grower & Winemaker*, 461, 10–12.
- Bartowsky, E. J., & Henschke, P. A. (2004). The 'buttery' attribute of wine – diacetyl – desirability, spoilage and beyond. *International Journal of Food Microbiology*, 96, 235–252.
- Bauer, R., & Dicks, L. M. T. (2004). Control of malolactic fermentation in wine. A review. *South African Society for Enology & Viticulture*, 25, 74–88.
- Beneduce, L., Romano, A., Capozzi, V., Lucas, P., Barnavon, L., Bach, B., et al. (2010). Biogenic amine in regional wines. Review Article *Annals of Microbiology*, 60, 573–578.
- Capozzi, V., Ladero, V., Beneduce, L., Fernández, M., Alvarez, M. A., Bach, B., et al. (2011). Isolation and characterization of tyramine-producing *Enterococcus faecium* strain from red wine. *Food Microbiology*, 28, 434–439.
- Capozzi, V., Russo, P., Beneduce, L., Weidmann, S., Grieco, F., Guzzo, J., et al. (2010). Technological properties of *Oenococcus oeni* strains isolated from typical southern Italian wines. *Letters in Applied Microbiology*, 50, 327–334.
- Cappello, M. S., Stefani, D., Grieco, F., Logrieco, A., & Zapparoli, G. (2008). Genotyping by amplified fragment length polymorphism and malate metabolism performances of indigenous *Oenococcus oeni* strains isolated from Primitivo wine. *International Journal of Food Microbiology*, 127, 241–245.
- Costello, P. J., Henschke, P. A., & Markides, A. J. (2003). Standardised methodology for testing malolactic bacteria and wine yeast compatibility. *Australian Journal of Grape and Wine Research*, 9, 127–137.
- De Benedictis, M., Bleve, G., Grieco, F., Tristezza, M., Tufariello, M., & Grieco, F. (2011). An optimized procedure for the enological selection of non-*Saccharomyces* starter cultures. *Antonie van Leeuwenhoek*, 99, 189–200.
- Di Toro, M. A., Capozzi, V., Beneduce, L., Alexandre, H., Tristezza, M., Durante, M., et al. (2015). Intraspecific biodiversity and 'spoilage potential' of *Brettanomyces bruxellensis* in Apulian wines. *LWT – Food Science and Technology*, 60, 102–108.
- Fang, Y., & Qian, M. (2005). Aroma compounds in Oregon Pinot Noir wine determined by aroma extract dilution analysis (AEDA). *Flavour and Fragrance Journal*, 20, 22–29.
- Garofalo, C., El Khoury, M., Lucas, P., Bely, M., Russo, P., Spano, G., et al. (2015). Autochthonous starter cultures and indigenous grape variety for regional wine production. *Journal of Applied Microbiology*, 118, 1395–1408.
- Garofalo, C., Russo, P., Beneduce, L., Massa, S., Spano, G., & Capozzi, V. (2015). Non-*Saccharomyces* biodiversity in wine and the 'microbial terroir': a survey on Nero di Troia wine from the Apulian region, Italy. *Annals of Microbiology*. <http://dx.doi.org/10.1007/s13213-015-1090-5>.
- Gerbaux, V., Briffox, C., Dumont, A., & Krieger, S. (2009). Influence of inoculation with malolactic bacteria on volatile phenols in wines. *American Journal of Enology & Viticulture*, 60, 233–235.
- Grieco, F., Tristezza, M., Vetrano, C., Bleve, G., Panico, E., Grieco, F., et al. (2011). Exploitation of autochthonous micro-organism potential to enhance the quality of Apulian wine. *Annals of Microbiology*, 61, 67–73.
- Guzzon, R., Roman Villega, T., Pedron, M., Malacarne, M., Nicolini, G., & Larcher, R. (2013). Simultaneous yeast–bacteria inoculum. A feasible solution for the management of oenological fermentation in red must with low nitrogen content. *Annals of Microbiology*, 63, 805–808.
- Hammer, Ø., Harper, D. A. T., & Ryan, P. D. (2001). Past: paleontological statistics software package for education and data analysis. *Palaeontologia Electronica*, 4, 9.
- Izquierdo Cañas, P. M., García Romero, E., Pérez-Martín, F., Prieto, S., & Palop Herreros, M. L. (2014). Sequential inoculation versus co-inoculation in Cabernet Franc wine fermentation. *Food Science and Technology International*, 21, 1–10.
- Izquierdo Cañas, P. M., Pérez-Martín, F., García Romero, E., Seseña Prieto, S., & Palop Herreros, M. L. (2012). Influence of inoculation time of an autochthonous selected malolactic bacterium on volatile and sensory profile of Tempranillo and Merlot wines. *International Journal of Food Microbiology*, 156, 245–254.
- King, S. W., & Beelman, R. B. (1986). Metabolic interactions between *Saccharomyces cerevisiae* and *Leuconostoc oenos* in a model grape juice/wine system. *American Journal of Enology & Viticulture*, 37, 53–60.
- Knoll, C., Fritsch, S., Schnell, S., Grossmann, M., Krieger-Weber, S., Du Toit, M., et al. (2012). Impact of different malolactic fermentation inoculation scenarios on Riesling wine aroma. *World Journal of Microbiology and Biotechnology*, 28, 1143–1153.
- Liu, S.-Q. (2012). Malolactic fermentation in wine – beyond deacidification. *Journal of Applied Microbiology*, 92, 589–601.
- Maicas, S., Ferrer, S., & Pardo, I. (2002). NAD(P)H regeneration is the key for heterolactic fermentation of hexoses in *Oenococcus oeni*. *Microbiology*, 148, 325–332.
- Martineau, B., & Henick-Kling, T. (1995). Performance and diacetyl production of commercial strains of malolactic bacteria in wine. *Journal of Applied Bacteriology*, 78, 526–536.
- Massera, A., Soria, A., Catania, C., Krieger, S., & Combina, M. (2009). Simultaneous inoculation of Malbec (*Vitis vinifera*) musts with yeast and bacteria: effects on fermentation performance, sensory and sanitary attributes of wines. *Food Technology and Biotechnology*, 47, 192–201.
- Mendoza, L., Merin, M., Morata, V., & Farías, M. (2011). Characterization of wines produced by mixed culture of autochthonous yeasts and *Oenococcus oeni* from the northwest region of Argentina. *Journal of Industrial Microbiology & Biotechnology*, 38, 1777–1785.
- Muñoz, V., Beccaria, B., & Abreo, E. (2014). Simultaneous and successive inoculations of yeasts and lactic acid fermentation of an unsulfited Tannat grape must. *Brazilian Journal of Microbiology*, 45, 59–66.
- Nehme, N., Mathieu, F., & Taillandier, P. (2008). Quantitative study of interactions between *Saccharomyces cerevisiae* and *Oenococcus oeni* strains. *Journal of Industrial Microbiology & Biotechnology*, 35, 685–693.
- Rosi, I., Fia, G., & Canuti, V. (2006). Influence of different pH values and inoculation time on the growth and malolactic activity of a strain of *Oenococcus oeni*. *Australian Journal of Grape and Wine Research*, 9, 194–199.
- Tristezza, M., Fantastico, L., Vetrano, C., Bleve, G., Corallo, D., Grieco, F., et al. (2014). Molecular and technological characterization of *Saccharomyces cerevisiae* strains isolated from natural fermentation of Susumaniello grape must in Apulia, southern Italy. *International Journal of Microbiology*, 2014. Article ID 897428, 11 pages.
- Tristezza, M., Vetrano, C., Bleve, G., Grieco, F., Tufariello, M., Quarta, A., et al. (2012). Autochthonous fermentation starters for the industrial production of Negroamaro wines. *Journal of Industrial Microbiology & Biotechnology*, 39, 81–92.
- Tristezza, M., Vetrano, C., Bleve, G., Spano, G., Capozzi, V., Logrieco, A., et al. (2013). Biodiversity and safety aspects of yeast strains characterized from vineyards and spontaneous fermentations in the Apulia Region, Italy. *Food Microbiology*, 36, 335–342.
- Tufariello, M., Chiriatti, M. A., Grieco, F., Perrotta, C., Capone, S., Rampino, P., et al. (2014). Influence of autochthonous *Saccharomyces cerevisiae* strains on volatile profile of Negroamaro wines. *LWT – Food Science and Technology*, 58, 35–48.
- Versari, A., Patrizi, C., Parpinello, G. P., Mattioli, A. U., Pasini, L., Meglioli, M., et al. (2015). Effect of co-inoculation with yeast and bacteria on chemical and sensory characteristics of commercial Cabernet Franc red wine from Switzerland. *Journal of Chemical Technology and Biotechnology*. <http://dx.doi.org/10.1002/jctb.4652>.
- Wanikawa, A., Hosoi, K., & Kato, T. (2000). Conversion of unsaturated fatty acids to precursors of gamma-lactones by lactic acid bacteria during the production of malt whisky. *Journal of the American Society of Brewing Chemists*, 58, 51–56.
- Zapparoli, G., Tosi, E., Azzolini, M., Vagnoli, P., & Krieger, S. (2009). Bacterial inoculation strategies for the achievement of malolactic fermentation in high-alcohol wines. *South African Society for Enology & Viticulture*, 30, 49–55.



# Contribution of cross-links and proteoglycans in intramuscular connective tissue to shear force in bovine muscle with different marbling levels and maturities



Fulong Wang, Yawei Zhang, Junke Li, Xiuyun Guo, Baowei Cui, Zengqi Peng\*

Key Laboratory of Meat Processing and Quality Control, Ministry of Education, National Centre of Meat Quality and Safety Control, No. 1 Weigang, Nanjing Agricultural University, Nanjing, 210095, China

## ARTICLE INFO

### Article history:

Received 3 April 2015

Received in revised form

22 October 2015

Accepted 25 October 2015

Available online 28 October 2015

### Keywords:

Shear force

Connective tissue

Cross-links

Proteoglycans

Collagen heat solubility

## ABSTRACT

To explain the factors contributing to the changes in shear force, pyridinoline cross-links and proteoglycans (decorin and glycosaminoglycans) were investigated in *longissimus thoracis* (LT) taken from Qinchuan steers. In LT muscles with different marbling levels (C, B, A, S) and the same teeth maturity (group I), the contents of cross-links, decorin and glycosaminoglycans (GAGs), as well as the shear force declined gradually with increasing marbling while the collagen heat solubility increased. In group II, the heat solubility gradually declined by 58.22% along with the teeth maturity from 0 to 8 permanent incisors at the same marbling level, whereas the shear force increased by 37.49%. The contents of cross-links, decorin and GAGs increased to 0.72  $\mu\text{mol/g}$  collagen, 34.86  $\mu\text{g/g}$  collagen and 25.46  $\text{mg/g}$  collagen respectively. Multivariate statistical results indicated that the shear force was positively correlated with the inherent intramuscular connective tissue traits (content of mature cross-links and proteoglycans) and relied more on the collagen heat solubility than on the content of total collagen. The distribution of the score plots definitely indicated that “youthful and marbled” beef had similar beef characteristics, such as high collagen heat solubility and low shear force.

© 2015 Elsevier Ltd. All rights reserved.

## 1. Introduction

Tenderness is a paramount factor in the determination of meat quality. Shear force is an objective method to evaluate meat texture. The intramuscular connective tissue (IMCT) plays a significant role in determining meat tenderness (Nishimura, 2010).

Early researches showed that shear force generally increased (Nishimura, Hattori, & Takahashi, 1996; Nishimura, Ojima, Liu, Hattori, & Takahashi, 1996) and tenderness declined with animal age due to many factors, such as collagen content and perimysium thickness (Nishimura, Hattori, & Takahashi, 1999; Purslow, 2005; Schönfeldt & Strydom, 2011). In Torrecano, Sánchez-Escalante, Giménez, Roncalés, and Beltrán (2003), a high positive correlation between the total collagen and shear force of raw beef was observed in Swiss Brown young bull (485 days). Nevertheless, in Christensen et al. (2011), there was no correlation between collagen

characteristics and the raw and cooked meat texture in *longissimus thoracis* from 15 different European breeds (15 months). Chriki et al. (2013) also concluded that total collagen was not a good predictor of overall tenderness in more than 5000 animals from 1 to 120 months of age belonging to 20 different breeds but this conclusion depended on muscle type.

Un-reducible (mature) cross-links between the collagen molecules in macromolecular fibrils provide connective tissue with the required physical-chemical properties and biomechanical stability (Lepetit, 2008; McCormick, 1999; Purslow, 2005). The known mature cross-links are hydroxylysyl pyridinoline (HP) and lysyl pyridinoline (LP). However, the exact changes that occur in IMCT and the contribution of cross-links to the tenderness during the process of maturity still require further research.

Meanwhile, fatness may play a more important role than maturity in the improvement of meat tenderness (Pflanzer & De Felicio, 2009). The decreased shear force in beef from marbled Japanese Black cattle was attributed to mechanical “disorganisation and weakening” of the IMCT structure caused by the development of adipose tissue (Nishimura et al., 1999). The honeycomb structure of the endomysium was partially broken, and the perimysium was

\* Corresponding author.

E-mail addresses: [wangf0319@163.com](mailto:wangf0319@163.com) (F. Wang), [zqpeng@njau.edu.cn](mailto:zqpeng@njau.edu.cn) (Z. Peng).

separated into thinner collagen fibres. Although collagen heat solubility was taken into account, it could not explain the primary reasons for tenderisation in highly marbled beef. Cross-links were only used to explain the slight increase in heat solubility of collagen in theory.

In addition, other principal components in IMCT are proteoglycans (PGs) (Eggen, Pedersen, Lea, & Kolset, 2001; Hannesson, Pedersen, Ofstad, & Kolset, 2003). Decorin is a major type of PG in striated muscle (Eggen, Malmström, & Kolset, 1994). A number of glycosaminoglycans (GAGs) attach to the core protein in PGs. Some studies have proposed that PGs likely interact with both collagen and non-collagen materials and play an important role in tissue function, architecture and morphogenesis (Nishimura, Futami, Taneichi, Mori, & Hattori, 2002; Nishimura, Hattori, et al., 1996; Velleman, Patterson, & Nestor, 1997). Nevertheless, there have been few reports on the contributions of PGs (decorin and GAGs) to meat texture at different marbling levels and maturities.

Thus, the objectives of the present study were (1) confirm the role of heat solubility on shear force; (2) to quantify the contributions of cross-links and PGs in IMCT to the tenderisation of highly marbled beef and the toughening of old cattle beef; and (3) investigate the content of pyridinoline cross-links, decorin, GAGs, collagen and the changes in shear force in bovine *longissimus thoracis* (LT) with different marbling levels and maturities.

## 2. Materials and methods

### 2.1. Sample preparation

According to Table 1, eighty Qinchuan steers were harvested and selected at Shaanxi Kingbull Animal Husbandry Development Co., Ltd. After 24 h of rest, the cattle were slaughtered according to halal method. The slaughter was executed by a throat cut using a sharp knife in order to bring the animal to a quick death without suffering. Carcasses were carefully selected according to GB/T29392-2012 “Beef cuts grading for high rib, ribeye, striploin, tenderloin of national beef” (AQSIQ & SAC, 2012) and NY/T676-2010 “Beef Quality Grading” (Ministry of Agriculture, 2010) in China. The number of permanent incisors was recorded by looking directly at the teeth after removal of the animal's head. The marbling was evaluated by observing a section of the ribeye (12–13th rib cross-section). In China, 36-h post-mortem is usually adopted as the content of intramuscular fat in LT muscle is less than 15%. LT muscle samples (7th to 12–13th thoracic vertebrae) were selected from the carcasses at 4 °C, and then were split into two groups. The selection scheme for LT muscle can be found in Table 1. All of the LT muscles were individually vacuum packaged and stored at –20 °C until sampling. In group I, all of the test samples were at different

marbling levels with the same number of permanent incisors. The experiments were executed to explore the changes in the inherent traits of the IMCT (mature cross-links, PGs), heat solubility and shear force at different levels of marbling in beef. In group II, all of the test muscles were at the same marbling level to observe the changes affected by maturity. The content of fat in each sample was measured according to the method described by Folch, Lees, and Sloane-Stanley (1957). The fat content of each muscle was in accordance with the corresponding marbling level described in GB29392-2012 (AQSIQ & SAC, 2012).

The whole LT muscle was cut into two segments (approximately 7–10th and 10–12th from cranial to caudal). The cranial sections were used for the quantification of total collagen, collagen heat solubility, cross-links, decorin, and GAGs. The caudal sections were arranged to measure the shear force. Before the test, muscle samples were thawed at 4 °C overnight. The cranial sections were cut into pieces of 1-cm cross-sections and then fully minced and mixed in a pulveriser. Visible fat and noticeable connective tissue were removed. The mixed samples were freeze-dried and stored at –20 °C until the next experiment. In the caudal sections, the medial central portions of the muscles were used for the analysis of shear force to avoid interferences of haemorrhagic spots, tendons, thick perimysium or epimysium, and extra fat.

### 2.2. Methods

#### 2.2.1. Measurement of shear force

Shear force was determined according to a previously published method (Xu, Zhou, Peng, Zhao, & Yao, 2009). Samples from each group were sealed in polyethylene bags and cooked in a water bath (80 °C) until the internal temperature of each sample reached 75 °C. Next, the samples were cooled to room temperature (25 °C). Muscle strips of approximately 1 cm × 1 cm were taken parallel to the fibre direction of the muscle, avoiding visible fat and IMCT. The shear force was measured with a digital meat tenderness meter (Model C-LM3B, Northeast Agricultural University, Harbin, China). Strips were sheared perpendicular to the fibre's longitudinal axis. At least three strips from each muscle specimen were sheared into 6–8 cuts.

#### 2.2.2. Total collagen and heat solubility of collagen

To estimate the total collagen content, approximately 300 mg of freeze-dried samples were randomly selected and hydrolysed in 10 mL of 6 mol/L HCl for 16 h at 110 °C. The hydroxyproline content was measured in the method described by Xu et al. (2009). The amount of hydroxyproline was determined and converted to the collagen content with a factor 7.25.

The heat solubility of collagen was determined by the procedure

**Table 1**  
Selection scheme of *longissimus thoracis* (LT) muscle according to teeth maturity and marbling level.

	Permanent incisors	8	8	8	8	/
Group I	Equivalent to animal age <sup>a</sup>	54–60 months	54–60 months	54–60 months	54–60 months	/
	Marbling level	C	B	A	S	/
	Equivalent to intramuscular fat content <sup>b</sup>	<5%	5–10%	10–15%	>15%	/
	n	10	10	10	10	/
	Permanent incisors	0	2	4	6	8
Group II	Equivalent to animal age <sup>a</sup>	<18 months	18–24 months	30–36 months	42–48 months	54–60 months
	Marbling level	B	B	B	B	B
	Equivalent to intramuscular fat content <sup>b</sup>	5–10%	5–10%	5–10%	5–10%	5–10%
	n	10	10	10	10	10

n: The number of steers.

<sup>a</sup> Equivalent to animal age described in NY/T676-2010 “Beef Quality Grading” in China.

<sup>b</sup> Equivalent to intramuscular fat content described in GB/T29392-2012 “Beef cuts grading for high rib, ribeye, striploin, tenderloin of national beef” in China.

described by Nishimura et al. (1999). Freeze-dried samples (approximately 300 mg) were suspended and homogenised with 3 mL of Ringer's solution. The homogenates were heated in a water bath (77 °C, 70 min) and centrifuged (6000 g, 20 min). The supernatant solution was decanted, and the pellet was suspended in the same solution and recentrifuged. The two supernatants were combined, and the amount of soluble collagen was determined as described above. The heat solubility of collagen was expressed as a percentage of the total amount of collagen.

### 2.2.3. Glycosaminoglycan quantification

GAG concentrations were assayed according to Farndale, Sayers, and Barrett (1982) and Velleman et al. (1997) with slight modification. A stable solution of DMB (1, 9-dimethylmethylene blue) was prepared as follows: DMB (16 mg) was stirred with 5 mL of ethanol, 2.0 g of sodium formate, and 2.0 mL of formic acid, and the volume was brought to 1 L. The reagent (A535 of approximately 0.38) was stored in a brown bottle at room temperature. Chondroitin sulphate was used as the standard in the GAG assay. A volume of 2.5 mL of DMB solution was added to 250 µL of the standard solution, and the absorbance at 535 nm was immediately determined.

The samples (approximately 300 mg) were homogenised on ice and digested at 65 °C for 4 h in a solution of papain (>800 U/mg, 500 µg/mL) in 5 mL of phosphate buffer (50 mM, pH 6.5) containing 2 mM N-acetyl cysteine and 2 mM EDTA. The samples were centrifuged at 10000 g for 40 min at 4 °C, and the recovered supernatants were used for GAG quantification. The results were expressed in mg of GAG per g of total collagen (mg/g).

### 2.2.4. Determination of cross-links and decorin

For cross-links, approximately 250 mg frozen dried muscle sample were weighed, acid hydrolysed with 4 mL of HCl (6 mol/L) in a screw-capped glass tube overnight at 110 °C and then centrifuged at 16,000 g for 5 min (Dubost, Micol, Meunier, Lethias, & Listrat, 2013). One millilitre of 6 mol/L NaOH and 1 mL of 1 mol/L Tris were added to 1 mL of the acidic supernatant. The final pH of the supernatant was adjusted to 7.0–7.2 for analysis. For decorin, approximately 500 mg of frozen sample were rinsed in ice-cold PBS (0.02 mol/L, pH 7.0–7.2) to thoroughly remove traces of blood. Minced samples were homogenized in 10 mL of PBS (pH 7.0–7.2) on ice. The resulting suspension was subjected to two freeze–thaw cycles. Next, the homogenates were centrifuged for 15 min at 1500 g. The supernatant was collected for the decorin analysis.

The amounts pyridinoline cross-links and decorin were all determined with an enzyme-linked immunoassay kit (Blue Gene Biotechnology Co., Ltd., Shanghai China) according to the manufacturers' protocol. The absorbance of the reaction product was determined (model M2e, Molecular Devices Corp., CA, USA) at 450 nm. The results were expressed in µmol of pyridinoline cross-links per g of collagen (µmol/g) and µg of decorin per g of collagen (µg/g).

### 2.3. Statistical analysis

The figures were designed by the Origin Pro SR4 (Microcal, Northampton, USA). All data were analysed using statistical package SAS (Version 8.0, SAS Inc. Institute). The data were analysed by one-way ANOVA and Duncan's multiple range tests in SAS. Differences were considered significant at  $P < 0.05$ . Data from groups I and II were analysed with stepwise regression techniques to partition the factors affecting the collagen heat solubility and shear force, respectively. The independent variables for heat solubility were cross-links, decorin, GAGs and total collagen. Combined with heat solubility, five traits were considered as partition factors that affected the shear force. The criterion for independent variable

entry into the model was a probability value of 0.05 or less. Correlation analysis was performed to study the relationships between variables. To examine the relationship among several quantitative variables and characterize the beef, principal component analysis (PCA) was performed after standardization of the variables to a mean of zero and a variance of one. PCA transformed the original variables into new axes, or principal components (PCs), which are orthogonal, so that the data presented in those axes are uncorrelated with each other. Therefore, PCA expresses as much as possible of the total variation in the data in only a few principal components and each successively derived PC expresses decreasing amounts of the variation.

## 3. Results and discussion

### 3.1. Effects of marbling levels on IMCT traits and shear force

A slight decrease in total collagen can be observed in Table 2. The lowest collagen content in level S (23.44 mg/g DM) might be attributed to deposited fat. The heat soluble collagen floated between 2.41 and 4.09 mg/g DM. The shear force significantly decreased from 74.74 to 67.15 N with intramuscular fat deposition (level B to A,  $P < 0.05$ ) in Fig. 1 while the heat solubility increased significantly ( $P < 0.05$ , level B to A). The muscles were selected according to the permanent incisors and marbling levels, which could provide a relatively objective, accurate and convenient evaluation to ensure that the carcasses in the same group were as consistent as possible. Meanwhile, muscles were sampled carefully to minimize possible interferences. Shear force was not different between level S and A, as well as between level B and C ( $P > 0.05$ ), which was partially in agreement with Moon, Yang, Park, and Joo (2006). There were also no significant differences in the shear force or collagen solubility in *longissimus* as the fat content gradually increased in Nishimura et al. (1999).

In Table 2, the content of pyridinoline cross-links gradually decreased from 0.74 to 0.58 µmol/g collagen, which might be attributed to the role of lysyl oxidase (Rucker et al., 1998) during the process of fat deposition. A similar observation was also summarized by Lu, Wang, Zhu, Wan, and Peng (2013). Reduced cross-links meant that there were not enough cross-links to join three collagen molecules (McCormick, 1999), which reduced the strength of the IMCT. A negative effect of an increased content of cross-links on tenderness was observed by Dubost, Micol, Picard et al. (2013) in muscle grilled at 55 °C.

Decorin acted as a spacer during the lateral assembly of the molecular structure of collagen and was important in maintaining normal tissue function and mechanical properties (Gillies & Lieber, 2011; Weber, Harrison, & Iozzo, 1996). In the present research, reductions were observed in decorin and GAGs during the process of fat deposition, which might be attributed to the hormonal status and feeding intensity (Eggen et al., 2001). According to the description proposed by Nishimura et al. (2002), the fibrillogenesis process and/or the maturation of the collagen fibrils into larger fibrils/fibre networks are disturbed by the reduction of decorin. The decrease in GAGs indicated that the IMCT's ability to transfer forces had been weakened without enough modifications between contiguous fibrils (Redaelli et al., 2003). Thus, the decreases in PGs would weaken the extracellular modification and probably have a negative effect on the properties of the collagen. The treatment of lyophilised IMCT incubated with chondroitinase ABC by Nishiumi, Fukuda, and Nishimura (1997) also confirmed the contribution of PGs to collagen heat solubility.

Moderate correlations were observed between PGs (decorin and GAGs) and heat solubility, and a higher correlation in cross-links and heat solubility ( $r = -0.60$ ,  $P < 0.05$ ) can be showed in

**Table 2**  
Content of cross-links, decorin, GAGs, heat soluble collagen and total collagen.

Permanent incisors/Marbling level		8C	8B	8A	8S	
Group I	Total collagen (mg/g DM)	29.39 ± 0.78ab	31.24 ± 0.86a	27.90 ± 0.90b	23.44 ± 0.69c	
	Heat soluble collagen (mg/g DM)	2.41 ± 0.074c	2.51 ± 0.048c	4.09 ± 0.17b	3.93 ± 0.23a	
	Cross-links (μmol/g collagen)	0.74 ± 0.029a	0.72 ± 0.026a	0.59 ± 0.050b	0.58 ± 0.036b	
	Decorin (μg/g collagen)	39.44 ± 1.72a	34.86 ± 0.63b	32.51 ± 0.99b	31.02 ± 2.09b	
	GAGs (mg/g collagen)	24.62 ± 1.65a	25.46 ± 0.93a	18.05 ± 1.11b	18.39 ± 0.79b	
Permanent incisors/Marbling level		0B	2B	4B	6B	8B
Group II	Total collagen (mg/g DM)	34.09 ± 1.37a	33.26 ± 1.25a	33.40 ± 1.01a	31.67 ± 1.21a	31.25 ± 0.86a
	Heat soluble collagen (mg/g DM)	6.57 ± 0.12a	6.14 ± 0.19a	5.26 ± 0.19b	3.64 ± 0.14c	2.51 ± 0.048d
	Cross-links (μmol/g collagen)	0.45 ± 0.017c	0.55 ± 0.040b	0.54 ± 0.025b	0.61 ± 0.035b	0.72 ± 0.026a
	Decorin (μg/g collagen)	25.41 ± 1.69a	26.21 ± 1.61a	28.04 ± 1.11b	33.57 ± 1.95b	34.86 ± 0.63b
	GAGs (mg/g collagen)	14.96 ± 0.71c	18.44 ± 1.06b	23.13 ± 1.84a	23.22 ± 0.89a	25.46 ± 0.93a

All of the experimental samples were from group I: samples with different marbling level (S, A, B, C) but the same teeth maturity (8 permanent incisors).

All of the test samples were from group II: samples with different teeth maturity (0, 2, 4, 6, 8) but the same marbling level B.

GAGs: glycosaminoglycans.

Each value is expressed as the mean ± s.e..

The different letters in the same row indicate significant differences ( $P < 0.05$ ).

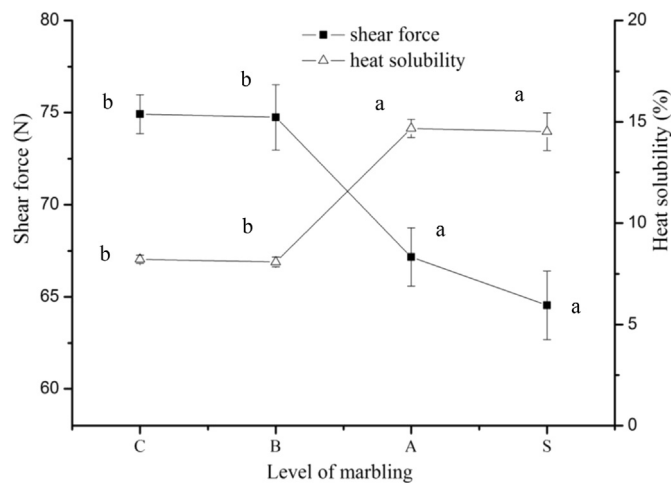


**Fig. 1.** Shear force and collagen heat solubility of samples with different marbling levels but the same teeth maturity (8 permanent incisors).

**Table 3**  
Correlation coefficients between the different variables.

Test samples		Shear force	Heat-solubility	Heat soluble collagen
Group I: samples with different marbling levels (S, A, B, C) but the same teeth maturity (8 permanent incisors)	Cross-links	0.40*	-0.60**	-0.62**
	Decorin	0.40**	-0.36**	-0.34*
	GAGs	0.39*	-0.46**	-0.40*
	Total collagen	0.49**	-0.60**	-0.20
	Shear force	-	-0.64**	-0.52**
Group II: Samples with different teeth maturity (0, 2, 4, 6, 8) but the same marbling level (B)	Cross-links	0.49**	-0.63**	-0.65**
	Decorin	0.38**	-0.56**	-0.68**
	GAGs	0.46**	-0.55**	-0.60**
	Total collagen	-0.10	0.19	0.51**
	Shear force	-	-0.72**	-0.66**

\* $P < 0.05$ , \*\* $P < 0.01$ .

GAGs: glycosaminoglycans.

**Table 3.** There was a significantly negative correlation ( $r = -0.64$ ,  $P < 0.01$ ) between heat solubility and shear force, in agreement with data reported by other authors (Chriki et al., 2013; Kong, Tang, Lin, & Rasco, 2008; Nishimura, Hattori, & Takahashi, 1995; Torrescano et al., 2003).

Stepwise regression techniques were employed to partition factors affecting heat solubility and shear force in samples with different marbling level and the same 8 permanent incisor teeth. The stepwise selection retained cross-links ( $P < 0.0001$ ), GAGs ( $P < 0.0001$ ) and total collagen ( $P < 0.0001$ ) for heat solubility and described 0.64 of the heat solubility variation (Table 4). Cross-links were the first independent variable (partial  $R^2 = 0.37$ ) selected in the model. A 1-unit decrease in cross-links was associated with approximate 0.13-unit increases in heat solubility. Regarding the model of shear force, only heat solubility was entered, describing 0.41 of the shear force variation. A 0.01-unit increase in heat solubility was associated with approximate 1.18-N decreases in shear force. Total collagen was discarded from the regression model in the present study, which was partially in agreement with no and/or weak correlations between the collagen and shear force in cattle LT muscle (Chriki et al., 2013) and in 15 primal cuts of African beef (Schönfeldt & Strydom, 2011). However, in Torrescano et al. (2003), a high positive correlation between total collagen and shear force was observed in raw beef from Swiss Brown young bull. A certain amount of variation could be explained by the total collagen in the

regression model of shear force in the *gluteus medius* muscle of beef (Girard, Bruce, Basarab, Larsen, & Aalhus, 2012). According to Chriki et al. (2013), Christensen et al. (2011) and Listrat and Hocquette (2004), LT muscle had a lower collagen content compared with *semitendinosus* (ST) muscle, which could result in the weak

**Table 4**  
Regression equations and partial R<sup>2</sup> values for heat solubility and shear force.

Test samples	Dependent	Constant	Coefficients										R <sup>2</sup>	sig
			Cross-links		Decorin		GAGs		Total collagen		Heat solubility			
			Coefficients	Partial R <sup>2</sup>	Coefficients	Partial R <sup>2</sup>	Coefficients	Partial R <sup>2</sup>	Coefficients	Partial R <sup>2</sup>	Coefficients	Partial R <sup>2</sup>		
Group I	Heat solubility	0.35	-0.13	0.37	/	/	-0.0017	0.050	-0.0040	0.23	-	-	0.64	****
	Shear force	88.84	/	/	/	/	/	/	/	/	-118.81	0.41	0.41	****
Group II	Heat solubility	0.32	-0.16	0.39	-0.026	0.10	/	/	/	/	-	-	0.49	****
	Shear force	91.07	/	/	/	/	/	/	/	/	-161.54	0.52	0.52	****
Groups I & II	Heat solubility	0.31	-0.14	0.40	-0.00018	0.093	-0.0017	0.032	/	/	-	-	0.53	****
All of the samples	Shear force	87.84	/	/	/	/	/	/	/	/	-143.80	0.48	0.48	****

Group I: samples with different marbling level (S, A, B, C) but the same teeth maturity (8 permanent incisors).

Group II: samples with different teeth maturity (0, 2, 4, 6, 8) but the same marbling level (B).

\* $P < 0.05$ ; \*\* $P < 0.01$ ; \*\*\* $P < 0.001$ ; \*\*\*\* $P < 0.0001$ .

GAGs: glycosaminoglycans.

correlation between the shear force and collagen content.

In fact, according to Abdallah (1983), Faucitano, Rivest, Daigle, Lévesque, and Gariépy (2004), Wulf, Morgan, Tatum, and Smith (1996) and Moon et al. (2006), intramuscular fat was deposited from the thoracic region to the lumbar region with maturity, and the LT marbling score was positively correlated with animal age. Meanwhile, mature cross-links increased with physiological maturity, resulting in decreased collagen solubility and tougher beef (Bosselmann, Möller, Steinhart, Kirchgessner, & Schwarz, 1995; Nishimura, 2010). Considering that the aim of this research was to explore the internal relationships between inherent IMCT characteristics (such as mature cross-links) and shear force in different maturity and marbling levels of beef, LT muscle was chosen in this study.

### 3.2. Effect of teeth maturity on shear force

In general, a gradual increase from 0.45 to 0.72  $\mu\text{mol/g}$  collagen in cross-links was observed during the process of maturity (0–8 permanent incisors, Table 2). A similar increase in total pyridinoline cross-links was also observed in bovine muscle from the age of 150–620 days (Bosselmann et al., 1995), indicating that the formation of cross-links is an essential step in growth to obtain and uphold the mechanical strength of collagen fibres. The increase in cross-links was mainly attributed to maturity, sex and feeding intensity in a previous study, which was related to the increased mechanical and chemical stability of collagen with chronological age (Nishimura, 2010). Shiba, Matsuzaki, Tsuneishi, and Iwamoto (2007) also found that the pyridinoline concentrations of collagen in goat muscle increased from 2 weeks before birth to 24 weeks of age, whereas the heat solubility decreased.

A steady rise in PGs can be observed in Table 2. The content of decorin and GAGs increased from 25.41 to 34.86  $\mu\text{g/g}$  collagen and 14.96–25.46  $\text{mg/g}$  collagen, respectively. An investigation of the decorin distribution revealed that decorin was located in the perimysium during the foetal period and in both the endomysium and perimysium in adult bovine muscle (Eggen et al., 1994; Nishimura et al., 2002), providing sufficient evidence of the “age-related” effect on decorin. In an experiment with the *semite-dinosus* and *psaos major* muscles (Pedersen, Kulseth, Kolset, Velleman, & Eggen, 2001), high decorin and mRNA levels were found in tougher muscle, but the opposite result was observed when collagen (decorin/collagen) was taken into account, which was contrary to our findings. The difference might stem from the total collagen content, which might change with differences in maturity, cut, and cattle breed. Considering the plateau at approximately 4 permanent incisors (Table 2), it might be inferred that the effect of maturity on GAGs was weakened at 30–36

months and earlier. In addition, based on image and biochemical analyses, Dubost, Micol, Meunier et al. (2013) showed that PGs were negatively correlated with structural parameters. PGs were proposed to be related to the water-holding capacity, which was likely ascribed to hydration of the negative charge in GAGs. Hydration is important in the resistance against compressive forces and might also influence the “juiciness” of meat (Dubost, Micol, Picard et al., 2013; Velleman, 2012; Velleman et al., 1997).

In Fig. 2, as the permanent incisors increased from 0 to 8, the collagen heat solubility decreased to approximately 8.21%, and the shear force increased from 56.74 to 78.01 N. The decrease in heat solubility with maturity indicated that connective tissue was more stable during heating, which had a positive impact on shear force. Weak and significant ( $P < 0.01$ ) correlations were explored between pyridinoline cross-links, decorin, GAGs and shear force (Table 3). A negative correlation between the collagen heat solubility and shear force was observed in Table 3 ( $r = -0.72$ ,  $P < 0.01$ ), whereas there was poor correlation between the total collagen content and shear force in the present research ( $r = -0.10$ ,  $P > 0.05$ ). The content of heat soluble collagen decreased from 6.57 to 2.51  $\text{mg/g}$  DM with maturity (Table 2). There was a significant correlation ( $r = 0.52$ ,  $P < 0.05$ ) between the total collagen and heat soluble collagen (Table 3).

In group II, for heat solubility, the multiple regression analysis retained cross-links ( $P < 0.0001$ ) and decorin ( $P = 0.0037$ ), which described 0.49 of the variation. Cross-links were the first independent variable (partial R<sup>2</sup> = 0.39) selected for inclusion. For shear

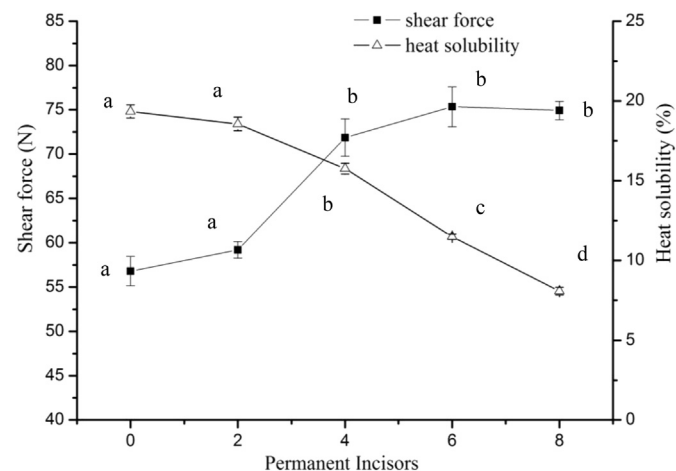


**Fig. 2.** Shear force and collagen heat solubility of samples with different teeth maturity but the same marbling level (marbling level B).

force, only heat solubility ( $P < 0.0001$ ) was retained and described 0.52 of the variation. A 0.01-unit decrease in heat solubility was associated with approximate 1.60-N increases in shear force (Table 4), indicating that the heat solubility of collagen was a better determining factor of shear force than the content of IMCT in different teeth maturity samples with the same level of marbling.

In addition, we tried to pool all of the samples to explore the contribution of the inherent traits to the heat solubility and shear force across marbling levels and teeth maturity (combining groups I and II, Table 4). Similar to the regression models in groups I and II, respectively, heat solubility was the only independent variable (0.48 of the variation,  $P < 0.0001$ ) selected to describe the variation of shear force. For heat solubility, cross-links ( $P < 0.0001$ ), decorin ( $P = 0.0003$ ) and GAGs ( $P = 0.027$ ) accounted for 0.53 of the variation. Cross-links described most (partial  $R^2 = 0.40$ ) of the variation in heat solubility across all of the test samples. The difference was that GAGs and decorin accounted for certain variations in heat solubility, potentially because the samples employed in groups I or II were insufficient.

### 3.3. Principal component analysis (PCA)

To exam the relationship among several quantitative variables, principal component analysis was performed (Destefanis, Barge, Brugiapaglia, & Tassone, 2000). The PCA showed that the first two principal components explained 71.21% of the total variance: PC1 explained 54.71% and PC2 explained 16.50% of the total variance (Table 5). Heat solubility, heat soluble collagen, shear force and inherent traits (cross-links, decorin and GAGs) resulted in even variables for PC1. PC2 was mainly characterized by total collagen. Considering the loadings in PC1 and the loading plot (Fig. 3), mature cross-links, decorin, GAGs and shear force were relatively close together and therefore positively correlated. Heat solubility was placed opposite and negatively associated to shear force. Combined with the regression results, shear force was positively correlated with the inherent IMCT traits (content of mature cross-links, decorin and GAGs) and relied more on the collagen heat solubility than on the collagen content.

The score plot (Fig. 4) shows the location of the objects in the multivariate space of the first two principal component score vectors. The scores were arranged in two groups: the first group included muscles from the 0B, 2B, 8A and 8S groups and the second included meats from the 6B, 8B and 8C groups. LT muscles from the 0B, 2B, 8A and 8S groups were higher in collagen heat solubility and lower in shear force compared with the LT muscles from 6B, 8B and 8C. As explained by Naes, Baardseth, Helgesen, and Isaksson (1996), objects that are close together (in score plots) have similar characteristics. This definitely showed that “youthful and marbled” muscle might have similar characteristics, such as low shear force and high collagen solubility, which was similar to the conclusion of Duarte et al. (2011). However, the samples in group 4B showed a heterogeneous distribution in the score plot, which made it difficult to define them on the basis of the considered variables. The reason for this might be that the characteristics of muscles in 4B were similar to those in adjacent grade samples.

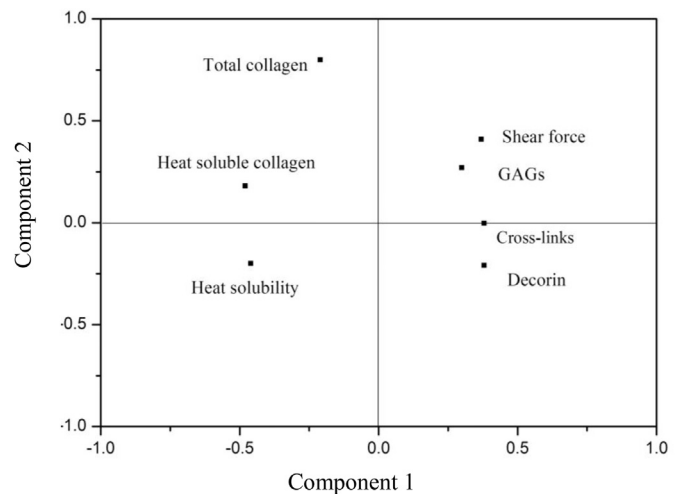


Fig. 3. Plot of the first two PC loading vectors.

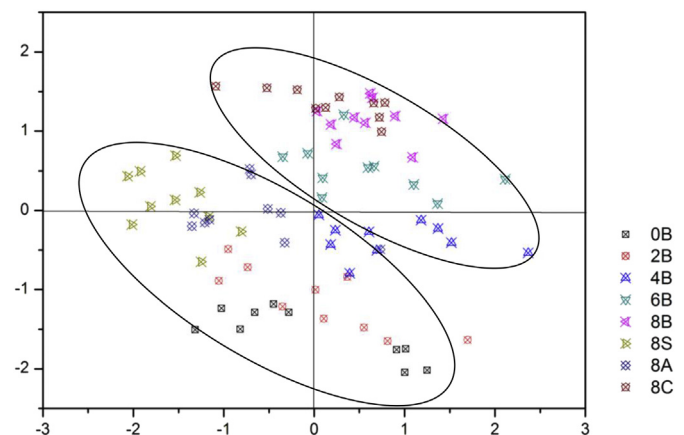


Fig. 4. Plot of the first two PC score vectors.

## 4. Conclusions

Both teeth maturity and marbling level played important roles in determining the shear force. The contents of cross-links, decorin and glycosaminoglycans (GAGs), as well as shear force, declined gradually in the muscle from marbling levels C to S with the same teeth maturity (group I), while the collagen heat solubility increased. Meanwhile, at the same marbling level, beef from samples with 0 permanent incisors had lower cross-links, decorin, GAGs and shear force and higher collagen heat solubility compared to those with 8 permanent incisors. The multivariate statistical results indicated that shear force was positively correlated with the inherent IMCT traits (content of mature cross-links and PGs) and relied more on the collagen heat solubility than on the collagen content. PCA also directly showed that “youthful and marbled” beef had similar characteristics.

Table 5

Results from the principal component analysis for the first and second principal components and the principal component loadings.

	Eigenvalues	% of variance	Cumulative variance %	Cross-links	Decorin	GAGs	Total collagen	Heat solubility	Heat soluble collagen	Shear force
PC1	3.83	54.71	54.71	0.38	0.38	0.30	-0.21	-0.46	-0.48	0.37
PC2	1.15	16.50	71.21	-0.0019	-0.21	0.27	0.80	-0.20	0.18	0.41

## Acknowledgements

This research was supported by the earmarked fund for the Modern Agro-industry Technology Research System (CARS-38) and Synergetic Innovation Center of Food Safety and Nutrition in Jiangsu province.

## References

- Abdallah, O. Y. (1983). Tissue growth patterns in the carcasses of water buffalo and Friesian crossbred cattle-part 1: individual muscles and anatomical muscle groups. *Meat Science*, 8(4), 301–315.
- AQSIQ & SAC. (2012). *National standard of the People's Republic of China. Beef cuts grading for high rib, ribeye, striploin, tenderloin of national beef (GB/T29392–2012)*. Beijing, China: China's Standard Publishing.
- Bosselmann, A., Möller, C., Steinhart, H., Kirchgessner, M., & Schwarz, F. J. (1995). Pyridinoline cross-links in bovine muscle collagen. *Journal of Food Science*, 60(5), 953–958.
- Chriki, S., Renand, G., Picard, B., Micola, D., Journaux, L., & Hocquette, J. F. (2013). Meta-analysis of the relationships between beef tenderness and muscle characteristics. *Livestock Science*, 155(2–3), 424–434.
- Christensen, M., Ertbjerg, P., Failla, S., Sañudo, C., Richardson, R. I., Nute, G. R., et al. (2011). Relationship between collagen characteristics, lipid content and raw and cooked texture of meat from young bulls of fifteen European breeds. *Meat Science*, 87(1), 61–65.
- Destefanis, G., Barge, M. T., Brugiapaglia, A., & Tassone, S. (2000). The use of principal component analysis (PCA) to characterize beef. *Meat Science*, 56, 255–259.
- Duarte, M. S., Paulino, P. V. R., Fonseca, M. A., Diniz, L. L., Cavali, J., Serão, N. V. L., et al. (2011). Influence of dental carcass maturity on carcass traits and meat quality of Nelore bulls. *Meat Science*, 88(3), 441–446.
- Dubost, A., Micol, D., Meunier, B., Lethias, C., & Listrat, A. (2013). Relationships between structural characteristics of bovine intramuscular connective tissue assessed by image analysis and collagen and proteoglycan content. *Meat Science*, 93(3), 378–386.
- Dubost, A., Micol, D., Picard, B., Lethias, C., Andueza, D., Bauchart, D., et al. (2013). Structural and biochemical characteristics of bovine intramuscular connective tissue and beef quality. *Meat Science*, 95(3), 555–561.
- Eggen, K. H., Malmstrøm, A., & Kolset, S. O. (1994). Decorin and a large dermatan sulfate proteoglycan in bovine striated muscle. *Biochimica et Biophysica Acta (BBA)-Protein Structure and Molecular Enzymology*, 1204(2), 287–297.
- Eggen, K., Pedersen, M., Lea, P., & Kolset, S. (2001). Structure and solubility of collagen and glycosaminoglycans in two bovine muscles with different textural properties. *Journal of Muscle Foods*, 12(4), 245–261.
- Farndale, R. W., Sayers, C. A., & Barrett, A. J. (1982). A direct spectrophotometric microassay for sulfated glycosaminoglycans in cartilage cultures. *Connective Tissue Research*, 9(4), 247–248.
- Faucitano, L., Rivest, J., Daigle, J. P., Lévesque, J., & Gariépy, C. (2004). Distribution of intramuscular fat content and marbling within the *longissimus* muscle of pigs. *Canadian Journal of Animal Science*, 84(1), 57–61.
- Folch, J., Lees, M., & Sloane-Stanley, G. H. (1957). A simple method for the isolation and purification of total lipids from animal tissues. *Journal of Biological Chemistry*, 226(1), 497–509.
- Gillies, A. R., & Lieber, R. L. (2011). Structure and function of the skeletal muscle extracellular matrix. *Muscle & Nerve*, 44(3), 318–331.
- Girard, I., Bruce, H., Basarab, J., Larsen, I., & Aalhus, J. (2012). Contribution of myofibrillar and connective tissue components to the Warner–Bratzler shear force of cooked beef. *Meat Science*, 92(4), 775–782.
- Hannesson, K. O., Pedersen, M. E., Ofstad, R., & Kolset, S. O. (2003). Breakdown of large proteoglycans in bovine intramuscular connective tissue early postmortem. *Journal of Muscle Foods*, 14(4), 301–318.
- Kong, F., Tang, J., Lin, M., & Rasco, B. (2008). Thermal effects on chicken and salmon muscles: tenderness, cook loss, area shrinkage, collagen solubility and microstructure. *LWT-Food Science and Technology*, 41(7), 1210–1222.
- Lepetit, J. (2008). Collagen contribution to meat toughness: theoretical aspects. *Meat Science*, 80(4), 960–967.
- Listrat, A., & Hocquette, J. F. (2004). Analytical limits of total and insoluble collagen content measurements and of type I and III collagen analysis by electrophoresis in bovine muscles. *Meat Science*, 68(1), 127–136.
- Lu, G. S., Wang, F. L., Zhu, Y., Wan, K. H., & Peng, Z. Q. (2013). Study on the relationships between pyridinoline cross-links and solubility of collagen and shear force of Qinchuan Marbling beef. *Scientia Agricultura Sinica*, 46(1), 130–135.
- McCormick, R. J. (1999). Extracellular modifications to muscle collagen: implications for meat quality. *Poultry Science*, 78(5), 785–791.
- Ministry of Agriculture. (2010). *Standard of the Ministry of Agriculture of the People's Republic of China. Beef quality grading (NY/T676–2010)*. Beijing, China: China's Standard Publishing.
- Moon, S. S., Yang, H. S., Park, G. B., & Joo, S. T. (2006). The relationship of physiological maturity and marbling judged according to Korean grading system to meat quality traits of Hanwoo beef females. *Meat Science*, 74(3), 516–521.
- Naes, T., Baardseth, P., Helgesen, H., & Isaksson, T. (1996). Multivariate techniques in the analysis of meat quality. *Meat Science*, 43(3), 135–149.
- Nishimura, T. (2010). The role of intramuscular connective tissue in meat texture. *Animal Science Journal*, 81(1), 21–27.
- Nishimura, T., Futami, E., Taneichi, A., Mori, T., & Hattori, A. (2002). Decorin expression during development of bovine skeletal muscle and its role in morphogenesis of the intramuscular connective tissue. *Cells Tissues Organs*, 171(2–3), 199–214.
- Nishimura, T., Hattori, A., & Takahashi, K. (1995). Structural weakening of intramuscular connective tissue during conditioning of beef. *Meat Science*, 39(1), 127–133 (7).
- Nishimura, T., Hattori, A., & Takahashi, K. (1996). Relationship between degradation of proteoglycans and weakening of the intramuscular connective tissue during post-mortem ageing of beef. *Meat Science*, 42(3), 251–260.
- Nishimura, T., Hattori, A., & Takahashi, K. (1999). Structural changes in intramuscular connective tissue during the fattening of Japanese black cattle: effect of marbling on beef tenderization. *Journal of Animal Science*, 77(1), 93–104.
- Nishimura, T., Ojima, K., Liu, A., Hattori, A., & Takahashi, K. (1996). Structural changes in the intramuscular connective tissue during development of bovine semitendinosus muscle. *Tissue and Cell*, 28(5), 527–536.
- Nishiumi, T., Fukuda, T., & Nishimura, T. (1997). Isolation and characterization of a small proteoglycan associated with porcine intramuscular connective tissue. *Journal of Agricultural and Food Chemistry*, 45(8), 2978–2983.
- Pedersen, M., Kulseth, M. A., Kolset, S., Velleman, S., & Eggen, K. (2001). Decorin and fibromodulin expression in two bovine muscles (*M. Semitendinosus* and *M. Psoas major*) differing in texture. *Journal of Muscle Foods*, 12(1), 1–17.
- Pfanzner, S., & De Felicio, P. (2009). Effects of teeth maturity and fatness of Nelore (*Bos indicus*) steer carcasses on instrumental and sensory tenderness. *Meat Science*, 83(4), 697–701.
- Purcell, P. P. (2005). Intramuscular connective tissue and its role in meat quality. *Meat Science*, 70(3), 435–447.
- Redaelli, A., Vesentini, S., Soncini, M., Vena, P., Mantero, S., & Montevecchi, F. (2003). Possible role of decorin glycosaminoglycans in fibril to fibril force transfer in relative mature tendons—a computational study from molecular to microstructural level. *Journal of Biomechanics*, 36(10), 1555–1569.
- Rucker, R. B., Kosonen, T., Clegg, M. S., Mitchell, A. E., Rucker, B. R., Uriu-Hare, J. Y., et al. (1998). Copper, lysyl oxidase, and extracellular matrix protein cross-linking. *The American Journal of Clinical Nutrition*, 67(5), 996S–1002S.
- Schönfeldt, H., & Strydom, P. E. (2011). Effect of age and cut on tenderness of South African beef. *Meat Science*, 87(3), 206–218.
- Shiba, N., Matsuzaki, M., Tsuneishi, E., & Iwamoto, H. (2007). Changes in the pyridinoline concentration of the *gastrocnemius* and *soleus* muscle in goats from 2 weeks prenatal to 24 weeks of age. *Small Ruminant Research*, 71(1), 144–149.
- Torrescano, G., Sánchez-Escalante, A., Giménez, B., Roncalés, P., & Beltrán, J. A. (2003). Shear values of raw samples of 14 bovine muscles and their relation to muscle collagen characteristics. *Meat Science*, 64(1), 85–91.
- Velleman, S. (2012). Meat science and muscle biology symposium: extracellular matrix regulation of skeletal muscle formation. *Journal of Animal Science*, 90(3), 936–941.
- Velleman, S. G., Patterson, R. A., & Nestor, K. E. (1997). Identification of decorin and chondroitin sulfate proteoglycans in turkey skeletal muscle. *Poultry Science*, 76(3), 506–510.
- Weber, I. T., Harrison, R. W., & Iozzo, R. V. (1996). Model structure of decorin and implications for collagen fibrillogenesis. *Journal of Biological Chemistry*, 271(50), 31767–31770.
- Wulf, D. M., Morgan, J. B., Tatum, J. D., & Smith, G. C. (1996). Effects of animal age, marbling score, calpastatin activity, subprimal cut, calcium injection, and degree of doneness on the palatability of steaks from limousin steers. *Journal of Animal Science*, 74(3), 569–576.
- Xu, S. Q., Zhou, G. H., Peng, Z. Q., Zhao, L. Y., & Yao, R. (2009). The influence of polyphosphate marination on Simmental beef shear value and ultrastructure. *Journal of Muscle Foods*, 20(1), 101–116.



# Development of a combined low-methoxyl-pectin and rice-bran-extract delivery system to improve the viability of *Lactobacillus plantarum* under acid and bile conditions<sup>☆</sup>



Arranee Chotiko<sup>a</sup>, Subramaniam Sathivel<sup>a, b, \*</sup>

<sup>a</sup> School of Nutrition and Food Sciences, Louisiana State University Agricultural Center, Baton Rouge, USA

<sup>b</sup> Department of Biological and Agricultural Engineering, Louisiana State University, Baton Rouge, USA

## ARTICLE INFO

### Article history:

Received 8 June 2015

Received in revised form

13 October 2015

Accepted 24 October 2015

Available online 28 October 2015

### Keywords:

Pectin-rice bran delivery system

*Lactobacillus plantarum*

Capsules

## ABSTRACT

A combined pectin-rice bran delivery system for *Lactobacillus plantarum* NRRL-B4496 (LP) was developed. Four pectin (PE)-rice bran extract (RB) gel solutions were prepared: (1) 2.0 g/100 mL PE with 0.5 g/100 mL RB, (2) 2.0 g/100 mL PE with 1.0 g/100 mL RB, (3) 2.0 g/100 mL PE with 2.0 g/100 mL RB, and (4) 2.0 g/100 mL PE (control). *L. plantarum* was grown in MRS broth, centrifuged, and mixed with the gel solutions. The capsules loaded with *L. plantarum* (LP/PE-RB capsules) were then prepared by ionotropic gelation. PE-RB gel solutions exhibited pseudoplastic behavior. The gel solution containing 2.0 g/100 mL RB had the highest consistency and viscosity. All LP/PE-RB capsules had similar diameter size. Both the sphericity and the encapsulation efficiency of the capsules were increased with higher RB content, while the hardness and springiness were decreased. When exposed to acidic and bile salt conditions, the viability of encapsulated cells was higher than free cells. The study demonstrated that pectin-rice bran capsules could have potential as a delivery system for *L. plantarum*.

© 2015 Elsevier Ltd. All rights reserved.

## 1. Introduction

Probiotics have been well-known for their health promoting effects. They can relieve diarrhea, reduce colonization of pathogenic bacteria and intestinal inflammation, alleviate lactose intolerance, reduce blood cholesterol, and possess anti-colon cancer effects (Ratna Sudha, Chauhan, Dixit, Babu, & Jamil, 2009; Saxelin, Tynkkynen, Mattila-Sandholm, & de Vos, 2005). The probiotic activity depends on the dose levels and the probiotic's viability in products and in gut environments (Kailasapathy & Chin, 2000). The recommended levels of live probiotic bacteria in food products is at least  $10^6$ – $10^7$  cfu/g (Floch et al., 2008). Therefore, it is necessary to maintain high levels of probiotics in products before consumption and to ensure good survival during the digestion processes to reach the sites of action with sufficient numbers and viability to provide health benefits.

<sup>☆</sup> Approved for publication by the director of the Louisiana Agricultural Experimental Station.

\* Corresponding author. School of nutrition and food sciences, 282 Knapp Hall, LSU Agricultural Center, Baton Rouge, LA, 70803, USA.

E-mail address: [Ssathivel@agcenter.lsu.edu](mailto:Ssathivel@agcenter.lsu.edu) (S. Sathivel).

Encapsulation is the packaging technology of active ingredients in small capsules that release their content at controlled rates over prolonged periods of time (Corbo, Bevilacqua, Gallo, Speranza, & Sinigaglia, 2013). Different encapsulation techniques are used for probiotics to enhance their viability and for target delivery, generally, including spray drying, freeze drying, emulsion, and extrusion (Huq, Khan, Khan, Riedl, & Lacroix, 2012). According to Krasaekoopt, Bhandari, and Deeth (2003), probiotic powder encapsulated by drying processes is released in food products. This results in loss of protection and deterioration in unfavorable environments such as during the passage through the gastrointestinal (GI) tract. de Castro-Cislaghi, Silva, Fritzen-Freire, Lorenz, and Sant'Anna (2012) found that spray dried *Bifidobacterium animalis* subsp. *lactis* Bb-12 powder with whey had greater decrease in viability at low pH and at bile conditions than free cells. On the other hand, encapsulation of probiotics in a hydrocolloid gel matrix provides protection against GI conditions. Encapsulated *B. animalis* Bb-12 in milk protein or alginate-chitosan capsules formed by gelation methods had a larger number of viable cells than free cells at GI conditions (Heidebach, Först, & Kulozik, 2009; Liserre, Ré, & Franco, 2007).

Encapsulation of probiotics in gel/bead matrix, such as sodium

alginate (Sathyabama, Ranjith Kumar, Bruntha Devi, Vijayabharathi, & Brindha Priyadarisini, 2014), carrageenan (Hernández-Rodríguez, Lobato-Calleros, Pimentel-González, & Vernon-Carter, 2014), carboxymethyl cellulose (Chitprasert, Sudsai, & Rodklongtan, 2012), and gelatin (Annan, Borza, & Hansen, 2008) has been successfully studied. However, there are few reports on encapsulation of probiotics using pectin matrix although it has been widely used in the pharmaceutical industry as a delivery vehicle for colon-specific oral drugs. Pectin is a complexly structured polysaccharide predominantly composed of homogalacturonan, a homopolymer of partially methyl-esterified (1–4)-linked  $\alpha$ -D-galacturonic acid, and a range of neutral sugars such as rhamnose, galactose, or arabinose (Maxwell, Belsshaw, Waldron, & Morris, 2012). It can form three dimensional rigid and water insoluble hydrogels by calcium-induced ionotropic gelation (Lee, Kim, Chung, & Lee, 2009). Pectin is a soluble fiber, that is resistant to GI conditions and degradable by colonic microorganisms (Cabrera, Cambier, & Cutsem, 2011). It also has prebiotic properties, enhancing the growth of *Bifidobacterium* and *Lactobacillus* sp. (Wicker et al., 2014).

Pectin has been reported to be less sensitive to chemical agents and more resistant to the GI environments than alginate. Voo, Ravindra, Tey, and Chan (2011) found that pectin based beads containing poultry probiotic cells had higher mechanical strength than alginate beads. As a result, cell release from pectin beads was less than that from alginate beads during fermentation. Viability of *Lactobacillus rhamnosus* in gastric conditions at pH 2 was improved when the cell was encapsulated with pectin (Gerez, Font de Valdez, Gigante, & Grosso, 2012). In a recent study, Gebara et al. (2013) encapsulated *Lactobacillus acidophilus* in pectin beads by ionotropic gelation. The result showed that the reduction of encapsulated cells was 1.51 log cycles after incubating in simulated gastric (pH 3) and intestinal (pH 7) juices, while a reduction of 3.54 log cycles was observed in non-encapsulated cells.

Pectin's high porosity and weak binding behavior to a crosslink agent ( $\text{Ca}^{2+}$ ) are disadvantages, limiting the use of pectin in encapsulation technology (Chan et al., 2011; Fang et al., 2008). Adding a filler agent, such as starch or rice bran was suggested to overcome the problem and to increase the protective effect for probiotic delivery. Chan et al. (2011) revealed that starch filler could improve sphericity, flowability and mechanical strength and reduce porosity of the calcium alginate beads. Viability of *Lactobacillus casei* encapsulated in the beads with starch filler was higher than the control after lyophilization and during storage. Chitprasert et al. (2012) determined that encapsulation of *Lactobacillus reuteri* in aluminum carboxymethyl cellulose–rice bran capsules helped increase microencapsulation yield and contributed to cell survival during heat exposure.

A pectin (PE) and rice bran extract (RB) delivery system may protect viable *Lactobacillus plantarum* cells under acidic and bile conditions. There are either no data or only limited information available on effects of PE and RB delivery systems containing probiotics at acidic and bile conditions. Therefore, the intention of this study was to develop and analyze pectin-rice bran extract loaded with *L. plantarum* capsules. The effects of rice bran extract on physical properties of the capsules were investigated, as well as the viability of the encapsulated cells after processing and exposure to acidic and bile conditions. The *L. plantarum* NRRL-B4496 strain used is one of the major probiotic strains in fermented food products (Fijan, 2014; Pedreschi, Campos, Noratto, Chirinos, & Cisneros-Zevallos, 2003; Upadhyay, 2014). It has the ability to inhibit the growth of some bacteria that cause digestive illness such as *Helicobacter pylori* (Apostolidis, Kwon, Shinde, Ghaedian, & Shetty, 2011) and *Listeria monocytogenes* (Upadhyay, 2014). The probiotic also reduces hypolipidemic activity (Haroun, Refaat, El-Waseif, El-Menoufy, & Amin, 2013). Additionally, it had antioxidant (Das &

Goyal, 2015) and antifungal activities (Cortés-Zavaleta, López-Malo, Hernández-Mendoza, & García, 2014).

## 2. Materials and methods

### 2.1. Cell culture preparation

*L. plantarum* NRRL B-4496 (LP) isolated from pickled cabbage was kindly provided by ARS Culture Collection (Washington DC, US). The frozen stock culture was reactivated twice in de Man Rogosa Sharpe (MRS) broth (Neogen Corporation, Lansing, MI). Twenty five milliliters of the culture was subsequently inoculated in MRS broth (500 mL) and incubated at 37 °C for 16 h to reach stationary phase. Cell pellets were harvested by centrifuging at 10,000  $\times$  g for 10 min at 4 °C (Beckman J2-HC, Beckman Coulter, Inc., Brea, CA). The pellets were washed three times and suspended in sterile distilled water (LP suspension).

### 2.2. Preparation of pectin-rice bran loaded with *L. plantarum* capsules

The preparation was performed as described by Lee et al. (2009) with some modification. First, pectin-rice bran gel solutions loaded (PE-RB gel solution) with LP were prepared by mixing a LP suspension ( $\sim 10^9$  cfu/mL) with 2 g/100 mL of low-methoxyl pectin (PE) (TIC PRETESTED<sup>®</sup> pectin LM 32 powder), provided by TIC Gums Inc (Belcamp, MD) and rice bran extract (RB), provided by Ribus Inc. (St. Louis, MO). According to the product's specifications, RB contains 17 g/100 g protein, 41 g/100 g carbohydrate, 22 g/100 g fat, 13 g/100 g ash, and 7 g/100 g water. The required concentrations of RB were 0.5 g/100 mL, 1 g/100 mL, and 2 g/100 mL. PE gel solution (without RB) containing LP was used to produce control (LP/PE) capsules. All gel solutions with LP were then stirred for 1 h, extruded through a 23G needle by a syringe pump at a flow rate of 1.2 mL/min, and dropped into calcium chloride solution ( $\text{CaCl}_2$ ) (4 g/100 mL) (Fisher Scientific Inc., Pittsburgh, PA). The PE-RB loaded with LP (LP/PE-RB) capsules were immediately formed and continuously hardened in  $\text{CaCl}_2$  solution for 30 min. The capsules were collected, washed twice, and kept at 4 °C for further analysis.

### 2.3. Rheological properties of PE-RB gel solutions

Flow behaviors of the PE-RB gel solutions without LP were measured using an AR 2000 Ex Rheometer (TA Instruments, New Castle, DE) fitted with a plate geometry (a steel plate with a 40-mm diameter, having a 200  $\mu\text{m}$  gap between the two plates). Each sample was placed on the temperature-controlled parallel plate at 25 °C. The shear stress was measured at shear rates from 1 to 100  $\text{s}^{-1}$ . The flow properties of the gel sample were characterized by the power law, shown in Eq. (1).

$$\sigma = K\gamma^n \quad (1)$$

where  $\sigma$  = shear stress (Pa),  $\gamma$  = shear rate ( $\text{s}^{-1}$ ),  $K$  = consistency index ( $\text{Pa s}^n$ ), and  $n$  = flow behavior index. A plot of  $\log \sigma$  against  $\log \gamma$  was constructed, and the magnitudes of  $K$  and  $n$  were determined from the resulting straight line intercept and slope, respectively. The mean values of  $n$ ,  $K$ , and apparent viscosity for gel solution samples were reported in triplicate.

### 2.4. Determination of LP/PE-RB capsule size and shape

Thirty capsule diameters were measured with a stereomicroscope (Zeiss SteREO Lumar.V12, Thornwood, NY) using image

analyzer software. The capsule shape was quantified by the sphericity factor (SF), shown in Eq. (2) (Chan et al., 2011).

$$SF = \frac{d_{\max} - d_{\min}}{d_{\max} + d_{\min}} \quad (2)$$

where  $d_{\max}$  is the largest diameter and  $d_{\min}$  is the smallest diameter perpendicular to  $d_{\max}$ .

### 2.5. Determination of encapsulation efficiency

The encapsulation efficiency (EE) represented a combined measure of the efficacy of entrapment and survival of viable cells during the microencapsulation procedure, calculated according to Eq. (3) (Gebara et al., 2013).

$$EE(\%) = \frac{N}{N_0} \times 100 \quad (3)$$

where EE is the encapsulation efficiency, expressed in percentage, N is the number of cells released from the beads (log CFU/g of capsules), and  $N_0$  is the number of cells in the gel solution (log CFU/g of LP suspension).

To determine the number of cells in the capsules, the encapsulated LP was released according to the method described by Sathyabama et al. (2014) with some modification. One gram of the capsules was added to 100 mL of 0.1 M phosphate buffer (pH 7.2) and stirred at 250 rpm by a shaker (Lab line incubator shaker model 3525, Fisher Scientific Inc., Pittsburgh, PA) for 30 min. The colony forming units (CFU/g) was examined by pour-plate method on MRS agar containing  $\text{CaCO}_3$  (0.6 g/100 mL). The plate was incubated at 37 °C for 24–48 h.

### 2.6. Textural properties of LP/PE-RB capsules

The LP/PE-RB capsules were analyzed for texture profile as described by Sandoval-Castilla, Lobato-Calleros, García-Galindo, Alvarez-Ramírez, and Vernon-Carter (2010) with some modification. An Instron Universal Testing Device (Model 5544, Norwood, MA) equipped with a 5 Kg-load cell was used for determination. The capsule samples (5 g) were placed on a fixed bottom plate under the probe. The contact force was controlled at 0.005 N. The samples were compressed 30%, using two compression cycles at a constant crosshead velocity of 30 mm min<sup>-1</sup>. Hardness, cohesiveness, and springiness (ratio between the areas under the compression and decompression curves) were analyzed using the software Bluehill Materials Testing Software (Bluehill 3, version 3.13, 2010, Instron).

### 2.7. Scanning electron micrographs of LP/PE-RB capsules

The LP/PE-RB capsules were incubated overnight in a mixture of ethanol, acetic acid, and formaldehyde. After that, they were rinsed and dehydrated with ethanol. Then they were dried with liquid  $\text{CO}_2$  with a critical point-dryer. The dried capsules were cut, mounted on aluminum SEM stubs, and coated with gold:palladium (60:40) in an Edwards S150 sputter coater. The capsule morphology was observed under a scanning electron microscope (JSM-6610LV, JEOL Ltd. Japan).

### 2.8. Survival of the cells in LP/PE-RB capsules under acidic and bile conditions

Acid and bile tolerance of the encapsulated cells and of free cells were determined according to the method described by Ding and

Shah (2007). One gram of capsules and 1 mL of free cells ( $\sim 10^8$  CFU/g) were inoculated into acidified MRS broth (pH 3.0) to measure acid tolerance and separately into MRS broth containing 1 g/100 mL oxgall (Sigma Aldrich, St. Louis, MO) to measure bile tolerance. They were then incubated at 37 °C for 2 h (acid) and 24 h (bile) to determine acid and bile tolerances. The encapsulated LP was released from the capsules and enumerated as in the method described in section 2.5.

### 2.9. Statistical analysis

All values were means and standard deviations of three determinations. Statistical analysis on the mean values was conducted with the SAS (Statistical Analysis System) software (version 9.4) (SAS Institute Inc., Cary, NC, USA) to test for differences among the different treatments ( $P \leq 0.05$ ).

## 3. Results and discussions

### 3.1. Rheological properties of PE-RB gel solutions

Flow behavior and apparent viscosity of the gel solutions are shown in Table 1. The results indicated that the rheological properties of gel solutions were affected by RB concentrations. All gel solutions exhibited non-Newtonian behavior, shear-thinning (pseudoplastic) fluids as evidenced by the flow index ( $n$ ), which was less than 1.0 (Paredes, Rao, & Bourne, 1989). The  $n$  obtained in the current study was  $0.968 \pm 0.014$ ,  $0.961 \pm 0.013$ ,  $0.865 \pm 0.024$ , and  $0.275 \pm 0.035$  for PE, PE-0.5RB, PE-1.0RB, and PE-2.0RB gel solutions, respectively. PE and PE-0.5RB gel solutions demonstrated a nearly Newtonian like fluid behavior. Pseudoplasticity of the gel solutions increased significantly with higher RB concentrations. As expected, the PE-2.0RB gel solution had the highest consistency ( $5.711 \pm 0.865 \text{ Pa s}^n$ ) ( $P \leq 0.05$ ). Moreover, RB concentration greatly influenced gel solution viscosity. The PE-0.5RB gel solution had significantly lower viscosity than the PE gel solution ( $0.018 \pm 0.001$  and  $0.056 \pm 0.007 \text{ Pa s}$ , respectively) ( $P \leq 0.05$ ). RB functions as a processing aid for extrusion processes, helping to reduce a product's surface irregularity and increase production rates (Hammond, 2000). In general, viscosities of polymers decrease when the proper amount of processing aid is used (Achilleos, Georgiou, & Hatzikiriakos, 2002). This could possibly explain the reduction of viscosity at low levels of RB (PE-0.5RB gel solution), followed by increased viscosity at higher RB concentrations. The PE-2.0RB gel solution had a viscosity value of  $0.213 \pm 0.007 \text{ Pa s}$ , which was significantly higher than PE-1.0RB gel solution ( $0.050 \pm 0.001 \text{ Pa s}$ ) and the PE gel solution. Some interactions between RB and PE may have occurred, causing changes to their functional properties. Our lab examined structural aspects of PE-RB powder by Fourier Transform Infrared Spectroscopy (FTIR) and found certain changes in spectra profiles of PE-RB powder, compared to PE or RB alone (results not shown). RB contains high protein and fat content. Certain functional groups of RB protein and fatty acids are mainly involved in the interaction, as reported by Chitprasert et al. (2012).

### 3.2. LP/PE-RB capsule sizes, shapes, and encapsulation efficiency

As shown in Table 2, all capsules had similar sizes ( $P \leq 0.05$ ). The sphericity factor (SF) was used to determine the shape of the capsule samples. Capsules with SF less than 0.05 are considered to be spherical beads (Lee, Ravindra, & Chan, 2013). LP/PE-2.0RB capsules had the lowest SF ( $0.03 \pm 0.02$ ), which was not different compared to LP/PR-1.0RB ( $0.05 \pm 0.03$ ). The highest SF was in LP/PE-0.5RB ( $0.07 \pm 0.05$ ) capsules, which were not significantly different than LP/PE samples ( $0.06 \pm 0.04$ ). The appearance of the

**Table 1**  
Flow behavior properties of PE-RB gel solutions at 25 °C.

Gel solutions	RB concentration (g/100 mL)	<i>n</i>	<i>K</i> (Pa s <sup>n</sup> )	Viscosity (Pa s)
PE (control)	0	0.968 ± 0.014 <sup>a</sup>	0.064 ± 0.005 <sup>b</sup>	0.056 ± 0.007 <sup>b</sup>
PE-0.5RB	0.5	0.961 ± 0.013 <sup>a</sup>	0.021 ± 0.001 <sup>c</sup>	0.018 ± 0.001 <sup>c</sup>
PE-1.0RB	1	0.865 ± 0.024 <sup>b</sup>	0.092 ± 0.009 <sup>b</sup>	0.050 ± 0.001 <sup>b</sup>
PE-2.0RB	2	0.275 ± 0.035 <sup>c</sup>	5.711 ± 0.865 <sup>a</sup>	0.213 ± 0.007 <sup>a</sup>

<sup>a-c</sup>Means ± standard deviation with different letters within the same column were significantly different ( $P \leq 0.05$ ). Gel solutions of PE, PE-0.5RB, PE-1.0RB, and PE-2.0RB were gel solution containing 2.0 g/100 mL pectin, 2.0 g/100 mL pectin with 0.5 g/100 mL rice bran extract, 2.0 g/100 mL pectin with 1.0 g/100 mL rice bran extract, and 2.0 g/100 mL pectin with 2.0 g/100 mL rice bran extract, respectively.

**Table 2**  
Diameter, sphericity factor, and encapsulation yield of LP/PE-RB capsules.

Capsules	RB concentration (g/100 mL)	Diameter of beads (mm)	Sphericity factor (SF)	Encapsulation efficiency (EE) (%)
LP/PE	0	6.54 ± 0.53 <sup>a</sup>	0.06 ± 0.04 <sup>a</sup>	83.23 ± 3.41 <sup>c</sup>
LP/PE-0.5RB	0.5	6.52 ± 0.57 <sup>a</sup>	0.07 ± 0.05 <sup>a</sup>	90.94 ± 1.98 <sup>b</sup>
LP/PE-1.0RB	1	6.23 ± 0.52 <sup>a</sup>	0.05 ± 0.03 <sup>b</sup>	93.40 ± 1.64 <sup>ab</sup>
LP/PE-2.0RB	2	6.37 ± 0.28 <sup>a</sup>	0.03 ± 0.02 <sup>b</sup>	95.44 ± 1.22 <sup>a</sup>

<sup>a-c</sup>Means ± standard deviation with different letters within the same column were significantly different ( $P \leq 0.05$ ). LP/PE = *L. plantarum* loaded in pectin capsules without rice bran extract (control); LP/PE-0.5RB, LP/PE-1.0RB, and LP/PE-2.0RB = *L. plantarum* loaded in pectin capsules containing 0.5 g/100 mL, 1.0 g/100 mL, and 2.0 g/100 mL rice bran extract, respectively.

LP/PE-RB capsules is shown in Fig. 1. The LP/PE-2.0RB capsules had spherical shapes, and were light brown in color due to the natural color of RB. LP/PE, LP/PE-0.5RB, and LP/PE-1.0RB samples were unable to form spherical particles, which may be due to insufficient RB and low concentration of pectin. These results are compatible with those of Chitprasert et al. (2012) who determined that the capsules produced from carboxymethyl cellulose became more spherical when rice bran was added. This effect may be viscosity dependent as noted by Chan et al. (2011). Lee et al. (2013) reported that spherical beads or capsules could not be formed if the gel solutions had viscosity between 60 and 150 cp. Although all gel solutions in the present study had viscosities out of this critical range, only PE-2.0RB gel solution had higher viscosity than the critical value (0.213 Pa s or 213 cp).

Table 2 demonstrated that LP/PE-RB capsules showed high encapsulation efficiency (EE) in all samples (less than one log cycle of viable cells reduction). LP/PE-RB capsules contained more than  $10^7$  CFU/g of viable cells. Mattila-Sandholm et al. (2002) suggested that for colonization, the viable population of probiotics should be

in a range of  $10^7$ – $10^9$  CFU/g. High EE would be attributed to the pectin shell. White, Budarin, and Clark (2010) have reported that pectin is categorized as a nanoporous polymer having pore size between 2 and 50 nm. As well known, bacteria size is about 0.2 μm in diameter and 2–8 μm in length. Thus, pectin has considerable capacity for cell entrapment. It was obvious that RB helped improve the EE of LP/PE-RB capsules. The EE monotonically increased with RB. LP/PE-2.0RB samples had the highest EE (95.44 ± 1.22%), followed by LP/PE-1.0RB (93.40 ± 1.64%), LP/PE-0.5RB (90.94 ± 1.98%), and LP/PE capsules (83.23 ± 3.41%). The increase of EE probably resulted from higher sphericity of the LP capsules containing RB, leading to a reduction of cell losses during the gelation process. Woo et al. (2007) have mentioned that irregular and tear shape beads could cause the release of encapsulants.

### 3.3. Textural properties of LP/PE-RB capsules

LP/PE-RB capsules were affected by RB concentration (Table 3). Hardness and springiness decreased with increasing RB content. The lowest hardness and springiness were in LP/PE-2.0RB capsules (8.61 ± 1.74 N and 0.97 ± 0.01 mm, respectively). This was not significantly different from LP/PE-1.0RB samples (11.49 ± 1.18 N and 0.99 ± 0.02 mm, respectively). Similarly, no significant differences were observed in hardness and springiness between LP/PE-0.5RB and LP/PE samples ( $P \leq 0.05$ ). All treatment samples had similar cohesiveness. The softer texture of LP/PE-1.0RB and LP/PE-2.0RB capsules possibly occurred because of protein and fat in RB. Liu, Xu, and Guo (2008) observed that protein is broken up by water and functions as a lubricant providing smoothness and softness. Similarly, fat can also act as a lubricant, changing the compression properties of a gel matrix by decreasing its breakdown forces (Pereira, Matia-Merino, Jones, & Singh, 2006). Moreover, lipids increase apparent viscosity of a gel matrix, resulting in a lower friction coefficient and consequently changing the gel's lubricant properties (Chojnicka, Sala, De Kruif, & Van De Velde, 2009). Sala, Van Vliet, Cohen Stuart, Aken, and Van De Velde (2009) noted that an increase of viscosity leads to the reduction of gel deformation which affects textural properties of the gels.

### 3.4. Morphology of LP/PE-RB capsules

Scanning electron micrographs of the external and internal structures of LP/PE-RB capsules is showed in Fig. 2. Cracks were

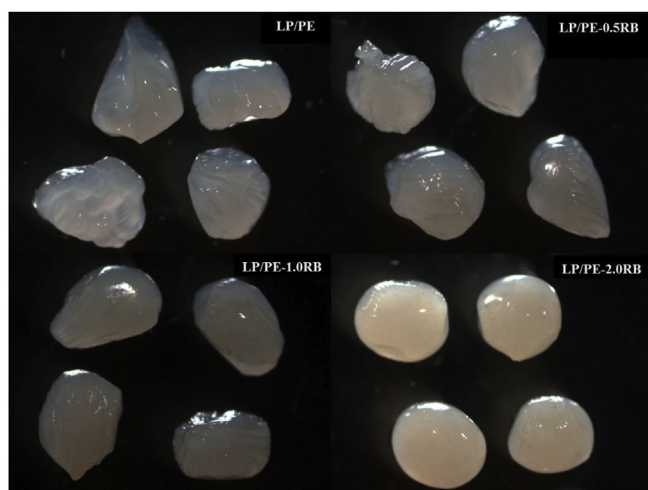


**Fig. 1.** *L. plantarum*-loaded pectin-rice bran extract capsules. LP/PE = *L. plantarum* loaded in pectin capsules without rice bran extract (control); LP/PE-0.5RB, LP/PE-1.0RB, and LP/PE-2.0RB = *L. plantarum* loaded in pectin capsules containing 0.5 g/100 mL, 1.0 g/100 mL, and 2.0 g/100 mL rice bran extract, respectively.

**Table 3**  
Textural properties of LP/PE-RB capsules.

Capsules	RB concentration (g/100 mL)	Hardness (N)	Springiness (mm)	Cohesiveness (ratio)
LP/PE	0	14.59 ± 0.75 <sup>a</sup>	1.43 ± 0.11 <sup>a</sup>	0.63 ± 0.01 <sup>a</sup>
LP/PE-0.5RB	0.5	14.90 ± 0.89 <sup>a</sup>	1.29 ± 0.19 <sup>a</sup>	0.63 ± 0.05 <sup>a</sup>
LP/PE-1.0RB	1	11.49 ± 1.18 <sup>ab</sup>	0.99 ± 0.02 <sup>b</sup>	0.63 ± 0.05 <sup>a</sup>
LP/PE-2.0RB	2	8.61 ± 1.74 <sup>b</sup>	0.97 ± 0.01 <sup>b</sup>	0.58 ± 0.01 <sup>a</sup>

<sup>a,b</sup>Means ± standard deviation with different letters within the same column were significantly different ( $P \leq 0.05$ ). LP/PE = *L. plantarum* loaded in pectin capsules without rice bran extract (control); LP/PE-0.5RB, LP/PE-1.0RB, and LP/PE-2.0RB = *L. plantarum* loaded in pectin capsules containing 0.5 g/100 mL, 1.0 g/100 mL, and 2.0 g/100 mL of the rice bran extract, respectively.

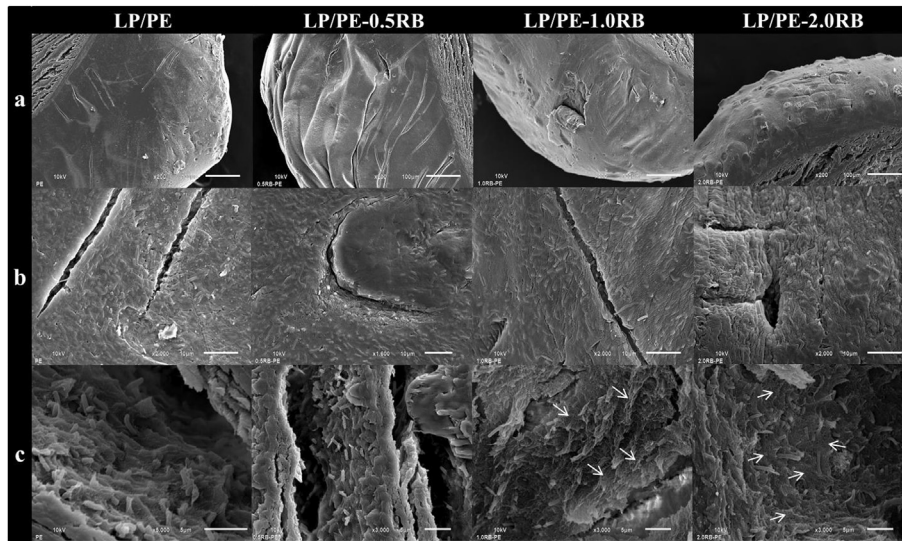


**Fig. 2.** Scanning electron micrographs of LP/PE-RB capsules illustrating capsule surface area at low magnification (a), at high magnification (b), and capsule cross sections (c); LP/PE = *L. plantarum* loaded in pectin capsules without rice bran extract (control); LP/PE-0.5RB, LP/PE-1.0RB, and LP/PE-2.0RB = *L. plantarum* loaded in pectin capsules containing 0.5 g/100 mL, 1.0 g/100 mL, and 2.0 g/100 mL of the rice bran extract, respectively.

observed on the surface of all samples (Fig. 2a). In accordance with literature, this was presumably due to loss of water and collapse of the gel matrix during sample drying (Badve, Sher, Korde, & Pawar, 2007; Jung, Arnold, & Wicker, 2013). Furthermore, it was reported that crosslinking fixatives and the base buffer used in sample preparation could weaken the integrity of hydrated capsules (Allan-Wojtas, Truelstrup Hansen, & Paulson, 2008). In the present study, cells were covered with a thin matrix and distributed under the surface (Fig. 2b); there were no cells observed on the surface. The results were similar to the microstructures recently revealed by Jiménez-Pranteda et al. (2012) and Martín, Lara-Villoslada, Ruiz, and Morales (2013). In our study, it was evident that the bacteria cells were randomly entrapped in the mesh-like network (indicated by white arrows), as illustrated in Fig. 2c. At higher concentrations of RB, a greater network was observed. This could suggest that there were some interactions or overlaps between RB and the PE matrix. In this regard, our results were in agreement with the study of Chitprasert et al. (2012). They found that it was more difficult to find *L. reuteri* entrapped in aluminum carboxymethyl cellulose capsules with added RB (AICMC-RB), than in capsules without RB. They suggested that AICMC-RB consisted of a dense matrix of RB sheets and AICMC-entrapped RB interstices.

### 3.5. Survival of the cells in LP/PE-RB capsules under acid and bile conditions

The viability of LP under acidified media (pH 3.0) is shown in Fig. 3. The results demonstrated that the cells in all samples exhibited good acid survivability after 2h incubation, which is supported by the work of Chotiko and Sathivel (2014). Regarding

reduction of the viable cells, viability of LP in all capsules, except LP/PE-0.5RB samples, had lower log reductions than free cells ( $P \leq 0.05$ ). After incubation, the free cell sample had 1.0 log CFU/g reduction. The LP/PE-1.0RB sample had the least viable cell reduction (0.4 log CFU/g), followed by LP/PE-2.0RB (0.5 log CFU/g),

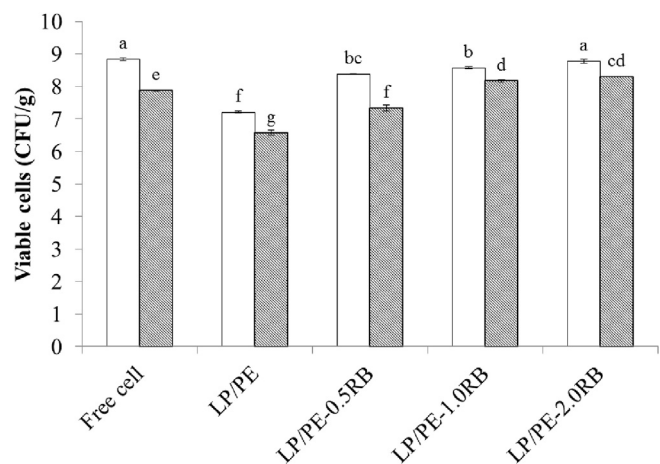


**Fig. 3.** Viability of *L. plantarum*-loaded calcium pectinate-rice bran capsules before (□) and after (■) incubating in acidified MRS at pH 3.0; Free cells = *L. plantarum* grown in MRS broth for 16 h, LP/PE = *L. plantarum* loaded in pectin capsules without rice bran extract (control); LP/PE-0.5RB, LP/PE-1.0RB, and LP/PE-2.0RB = *L. plantarum* loaded in pectin capsules containing 0.5 g/100 mL, 1.0 g/100 mL, and 2.0 g/100 mL of the rice bran extract, respectively. <sup>a–f</sup>Means ± standard deviation with different letters in different treatments before and after incubation are significantly different.

LP/PE (0.6 log CFU/g), and LP/PE-0.5RB (1.1 log CFU/g) ( $P \leq 0.05$ ). The greatest number of viable cells was found in LP/PE-2.0RB capsules (8.3 log CFU/g), which was not significantly different from the number of viable cells in LP/PE-1.0RB (8.2 log CFU/g). This indicated that pectin could protect the cell from acidic conditions and that sufficient concentrations of RB were able to enhance the protection of the encapsulated cells.

Protective effects of biopolymer encapsulation on probiotic survivability have been studied by several researchers. Their results indicated that encapsulated bacteria exhibited a significantly greater number of viable cells than free or non-encapsulated cells when were exposed to low pH conditions (Mokarram, Mortazavi, Najafi, & Shahidi, 2009; Nazzaro, Fratianni, Coppola, Sada, & Orlando, 2009; Sabikhi, Babu, Thompkinson, & Kapila, 2010; Shi et al., 2013). Recently, Gebara et al. (2013) reported that viability of *L. acidophilus* LA 5 after exposure to simulated gastric juice (pH 3.0) was increased when the cell was encapsulated with 2% amidated pectin. de Vos, Faas, Spasojevic, and Sikkema (2010) suggested that the formation of hydrogels acted as a physical barrier, delaying penetration of fluids into the cells. Sandoval-Castilla et al. (2010) found that addition of pectin to alginate beads loaded with *L. casei* slowed the diffusion rate of growth inhibition compounds, such as acids and hydrogen peroxide into the cells. In addition, our results suggest that, at low pH viability of LP in the capsules was enhanced by the presence of RB. This is possibly due to their structural stability. Regarding the effect of mechanical strength (hardness) of the gel matrix on cell viability under acidic conditions, our results were contradicted by that reported by Zhao et al. (2015). They found that viability of encapsulated cells in simulated gastric juice was positively correlated with mechanical strength of the capsules, and that greater mechanical strength led to a more integrated structure and a smaller mesh size of the network. In our study, the mechanical strength of PE capsules containing RB was lower than the capsules without RB, however, they had more mesh-like networks, as shown in Fig. 2. This could effectively help protect the cells from acid penetration. This is in agreement with the results reported by Chitprasert et al. (2012) that the addition of rice bran to carboxyl methyl cellulose beads provided a high density structure to the encapsulating matrix, which contributed to high survival rates of probiotic bacteria. Lactobacilli survive under acidic conditions when they can maintain a pH gradient between the medium and their cytoplasm (Charalampopoulos, Pandiella, & Webb, 2003). The mesh matrix formed by RB could increase the diffusion path length (Chitprasert et al., 2012), which possibly reduced the diffusion rate of acid into the encapsulated cells.

To obtain a measure of bile tolerance both encapsulated LP and free cells were exposed to media containing high oxgall concentration (1 g/100 mL). Oxgall functions as an emulsifier and fat solubilizer, hydrolyzing plasma membranes of bacteria cells, resulting in cell damage (Begley, Gahan, & Hill, 2005). In our study, encapsulated LP of all samples had higher cell viability than the free cells (Fig. 4). After 24h incubation, the number of free cells was reduced to 3.5 log CFU/g (5.4 log CFU/g reduction). A greater number of viable cells was observed for LP/PE capsules (5.8 log CFU/g) ( $P \leq 0.05$ ). These cells had undergone a reduction of 2.4 log CFU/g, indicating that a pectin matrix could protect LP from bile effects. According to Cheewatanakornkool et al. (2012), pectins have the ability to bind with bile salts, however their binding efficiency depends upon pectin sources. Many studies have reported that encapsulation of probiotic bacteria in polysaccharide matrices, such as alginate, pectin, or carrageenan successfully enhanced the survival of the bacteria during exposure to 1–3% bile salt solutions (Rokka & Rantamäki, 2010; Sandoval-Castilla et al., 2010; Shi et al., 2013).

RB also helped protect the survival of LP from bile salts. After incubation under the bile condition, the number of viable cells in

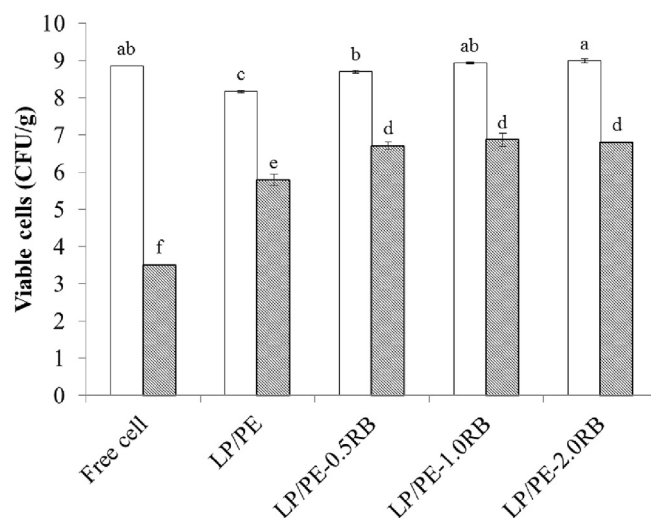


**Fig. 4.** Viability of *L. plantarum*-loaded calcium pectinate-rice bran capsules before (□) and after (■) incubating in MRS containing 1 g/100 mL oxgall; Free cells = *L. plantarum* grown in MRS broth for 16 h, LP/PE = *L. plantarum* loaded in pectin capsules without rice bran extract (control); LP/PE-0.5RB, LP/PE-1.0RB, and LP/PE-2.0RB = *L. plantarum* loaded in pectin capsules containing 0.5 g/100 mL, 1.0 g/100 mL, and 2.0 g/100 mL of the rice bran extract, respectively. <sup>a–f</sup>Means ± standard deviation with different letters in different treatments before and after incubation are significantly different.

LP/PE capsules with RB was greater than either that of capsules without RB or free cells. LP/PE-1.0RB capsules had the most viable cells (6.9 log CFU/g) after incubation, which was not significantly different from LP/PE-2.0RB (6.8 log CFU/g) and LP/PR-0.5RB (6.7 log CFU/g). Viable cells in the tested acidic condition were reduced by less than one log, therefore, approximately  $10^6$  CFU of LP/g of PE-RB capsules could survive for colonization. Compared to LP/PE-RB capsules, the greater mechanical strength of LP/PE capsules did not contribute to increase cell viability. According to Zhao et al. (2015), survivability of encapsulated cells in bile conditions were not increased when the mechanical strength of the matrix was increased. Similar to the acid tolerance study, RB possibly provided the capsules with greater networks and diffusion path lengths, reducing penetration of bile solution and consequently decreasing cell losses.

#### 4. Conclusion

The use of pectin and rice bran extract to obtain capsules loaded with *L. plantarum* NRRL-B4496 could improve encapsulation efficiency and sphericity of the capsules. Addition of 2 g/100 mL RB yielded the highest encapsulation efficiency and highest sphericity, however it reduced hardness and springiness of the capsules. The rice bran extract helped create a mesh-like network in the calcium pectinate-based capsules, contributing to enhancement of cell viability after exposure to acid and bile conditions. In summary, the pectin-rice bran extract capsules could be used as a new vehicle for probiotics bacteria. For example, the capsules could be incorporated into some food products, such as yogurt, cereal bars, or fruit juices.

#### References

- Achilleos, E. C., Georgiou, G., & Hatzikiriakos, S. G. (2002). Role of processing aids in the extrusion of molten polymers. *Journal of Vinyl and Additive Technology*, 8(1), 7–24. <http://dx.doi.org/10.1002/vnl.10340>.
- Allan-Wojtas, P., Truelstrup Hansen, L., & Paulson, A. T. (2008). Microstructural studies of probiotic bacteria-loaded alginate microcapsules using standard electron microscopy techniques and anhydrous fixation. *LWT - Food Science and*

- Technology, 41(1), 101–108. <http://dx.doi.org/10.1016/j.lwt.2007.02.003>.
- Annan, N. T., Borza, A. D., & Hansen, L. T. (2008). Encapsulation in alginate-coated gelatin microspheres improves survival of the probiotic *Bifidobacterium adolescentis* 15703T during exposure to simulated gastro-intestinal conditions. *Food Research International*, 41(2), 184–193. <http://dx.doi.org/10.1016/j.foodres.2007.11.001>.
- Apostolidis, E., Kwon, Y.-I., Shinde, R., Ghaedian, R., & Shetty, K. (2011). Inhibition of *Helicobacter pylori* by fermented milk and soy milk using select lactic acid bacteria and link to enrichment of lactic acid and phenolic content. *Food biotechnology*, 25(1), 58–76.
- Badve, S. S., Sher, P., Korde, A., & Pawar, A. P. (2007). Development of hollow/porous calcium pectinate beads for floating-pulsatile drug delivery. *European Journal of Pharmaceutics and Biopharmaceutics*, 65(1), 85–93. <http://dx.doi.org/10.1016/j.ejpb.2006.07.010>.
- Begley, M., Gahan, C. G. M., & Hill, C. (2005). The interaction between bacteria and bile. *FEMS microbiology reviews*, 29(4), 625–651.
- Cabrera, J. C., Cambier, P., & Cutsem, P. V. (2011). Drug encapsulation in pectin hydrogel beads—A systematic study of stimulated digestion media. *International Journal of Pharmacy and Pharmaceutical Sciences*, 3(5), 292–299.
- de Castro-Cislaghi, F. P., Silva, C. D. R. E., Fritzen-Freire, C. B., Lorenz, J. G., & Sant'Anna, E. S. (2012). Bifidobacterium Bb-12 microencapsulated by spray drying with whey: survival under simulated gastrointestinal conditions, tolerance to NaCl, and viability during storage. *Journal of Food Engineering*, 113(2), 186–193. <http://dx.doi.org/10.1016/j.jfoodeng.2012.06.006>.
- Chan, E.-S., Wong, S.-L., Lee, P.-P., Lee, J.-S., Ti, T. B., Zhang, Z., et al. (2011). Effects of starch filler on the physical properties of lyophilized calcium–alginate beads and the viability of encapsulated cells. *Carbohydrate Polymers*, 83(1), 225–232. <http://dx.doi.org/10.1016/j.carbpol.2010.07.044>.
- Charalampopoulos, D., Pandiella, S. S., & Webb, C. (2003). Evaluation of the effect of malt, wheat and barley extracts on the viability of potentially probiotic lactic acid bacteria under acidic conditions. *International Journal of Food Microbiology*, 82(2), 133–141. [http://dx.doi.org/10.1016/S0168-1605\(02\)00248-9](http://dx.doi.org/10.1016/S0168-1605(02)00248-9).
- Cheewatanakornkool, K., Chaidedumjorn, A., Sotanaphun, U., Limsirichaiikul, S., Wassapan, C., & Sriamornsak, P. (2012). Comparison of *in vitro* binding of bile salt by pectins from various sources. *Advanced Materials Research*, 506, 274–277.
- Chitprasert, P., Sudsai, P., & Rodklongtan, A. (2012). Aluminum carboxymethyl cellulose—rice bran microcapsules: enhancing survival of *Lactobacillus reuteri* KUB-AC5. *Carbohydrate Polymers*, 90(1), 78–86. <http://dx.doi.org/10.1016/j.carbpol.2012.04.065>.
- Chojnicka, A., Sala, G., de Kruijff, C. G., & van de Velde, F. (2009). The interactions between oil droplets and gel matrix affect the lubrication properties of sheared emulsion-filled gels. *Food Hydrocolloids*, 23(3), 1038–1046. <http://dx.doi.org/10.1016/j.foodhyd.2008.08.008>.
- Chotiko, A., & Sathivel, S. (2014). Effects of enzymatically-extracted purple rice bran fiber as a protectant of *L. plantarum* NRRL B-4496 during freezing, freeze drying, and storage. *LWT - Food Science and Technology*, 59(1), 59–64. <http://dx.doi.org/10.1016/j.lwt.2014.05.056>.
- Corbo, M. R., Bevilacqua, A., Gallo, M., Speranza, B., & Sinigaglia, M. (2013). Immobilization and microencapsulation of *Lactobacillus plantarum*: performances and *in vivo* applications. *Innovative Food Science & Emerging Technologies*, 18(0), 196–201. <http://dx.doi.org/10.1016/j.ifset.2012.12.004>.
- Cortés-Zavaleta, O., López-Malo, A., Hernández-Mendoza, A., & García, H. (2014). Antifungal activity of lactobacilli and its relationship with 3-phenyllactic acid production. *International Journal of Food Microbiology*, 173, 30–35.
- Das, D., & Goyal, A. (2015). Antioxidant activity and  $\gamma$ -aminobutyric acid (GABA) producing ability of probiotic *Lactobacillus plantarum* DM5 isolated from Marcha of Sikkim. *LWT-Food Science and Technology*, 61(1), 263–268.
- Ding, W. K., & Shah, N. P. (2007). Acid, bile, and heat tolerance of free and microencapsulated probiotic bacteria. *Journal of Food Science*, 72(9), M446–M450. <http://dx.doi.org/10.1111/j.1750-3841.2007.00565.x>.
- Fang, Y., Al-Assaf, S., Phillips, G. O., Nishinari, K., Funami, T., & Williams, P. A. (2008). Binding behavior of calcium to polyuronates: comparison of pectin with alginate. *Carbohydrate Polymers*, 72(2), 334–341. <http://dx.doi.org/10.1016/j.carbpol.2007.08.021>.
- Fijan, S. (2014). Microorganisms with claimed probiotic properties: an overview of recent literature. *International journal of environmental research and public health*, 11(5), 4745–4767.
- Floch, M. H., Walker, W. A., Guandalini, S., Hibberd, P., Gorbach, S., Surawicz, C., et al. (2008). Recommendations for probiotic Use—2008. *Journal of Clinical Gastroenterology*, 42, S104–S108. [10.1097/MCG.1090b1013e31816b31903f](http://dx.doi.org/10.1097/MCG.1090b1013e31816b31903f).
- Gebara, C., Chaves, K. S., Ribeiro, M. C. E., Souza, F. N., Grosso, C. R. F., & Gigante, M. L. (2013). Viability of *Lactobacillus acidophilus* La5 in pectin–whey protein microparticles during exposure to simulated gastrointestinal conditions. *Food Research International*, 51(2), 872–878. <http://dx.doi.org/10.1016/j.foodres.2013.02.008>.
- Gerez, C. L., Font de Valdez, G., Gigante, M. L., & Grosso, C. R. F. (2012). Whey protein coating bead improves the survival of the probiotic *Lactobacillus rhamnosus* CRL 1505 to low pH. *Letters in Applied Microbiology*, 54(6), 552–556. <http://dx.doi.org/10.1111/j.1472-765X.2012.03247.x>.
- Hammond, N. A. (2000). US Patent No. 6,054,149. Woodland, CA: US.
- Haroun, B. M., Refaat, B. M., El-Waseif, A. A., El-Menoufy, H. A., & Amin, H. A. (2013). Hypolipidemic activity of the probiotic *Lactobacillus plantarum* NRRL B-4496 and their prebiotic exopolysaccharide *in vitro* and *in vivo*. *Journal of Applied Sciences Research*, 9(1), 1015–1020.
- Heidebach, T., Först, P., & Kulozik, U. (2009). Microencapsulation of probiotic cells by means of rennet-gelation of milk proteins. *Food Hydrocolloids*, 23(7), 1670–1677. <http://dx.doi.org/10.1016/j.foodhyd.2009.01.006>.
- Hernández-Rodríguez, L., Lobato-Calleros, C., Pimentel-González, D. J., & Vernon-Carter, E. J. (2014). *Lactobacillus plantarum* protection by entrapment in whey protein isolate:  $\kappa$ -carrageenan complex coacervates. *Food Hydrocolloids*, 36(0), 181–188. <http://dx.doi.org/10.1016/j.foodhyd.2013.09.018>.
- Huq, T., Khan, A., Khan, R. A., Riedl, B., & Lacroix, M. (2012). Encapsulation of probiotic bacteria in biopolymeric system. *Critical Reviews in Food Science and Nutrition*, 53(9), 909–916. <http://dx.doi.org/10.1080/10408398.2011.573152>.
- Jiménez-Pranteda, M. L., Poncelet, D., Náder-Macias, M. E., Arcos, A., Aguilera, M., Monteoliva-Sánchez, M., et al. (2012). Stability of lactobacilli encapsulated in various microbial polymers. *Journal of Bioscience and Bioengineering*, 113(2), 179–184. <http://dx.doi.org/10.1016/j.jbiosc.2011.10.010>.
- Jung, J., Arnold, R. D., & Wicker, L. (2013). Pectin and charge modified pectin hydrogel beads as a colon-targeted drug delivery carrier. *Colloids and Surfaces B: Biointerfaces*, 104(0), 116–121. <http://dx.doi.org/10.1016/j.colsurfb.2012.11.042>.
- Kailasapathy, K., & Chin, J. (2000). Survival and therapeutic potential of probiotic organisms with reference to *Lactobacillus acidophilus* and *Bifidobacterium* spp. *Immunol Cell Biology*, 78(1), 80–88.
- Krasaekoopt, W., Bhandari, B., & Deeth, H. (2003). Evaluation of encapsulation techniques of probiotics for yoghurt. *International Dairy Journal*, 13(1), 3–13. [http://dx.doi.org/10.1016/S0958-6946\(02\)http://dx.doi.org/10.1016/S0958-6946\(02\)00155-3](http://dx.doi.org/10.1016/S0958-6946(02)http://dx.doi.org/10.1016/S0958-6946(02)00155-3).
- Lee, J.-S., Kim, E.-J., Chung, D., & Lee, H. G. (2009). Characteristics and antioxidant activity of catechin-loaded calcium pectinate gel beads prepared by internal gelation. *Colloids and Surfaces B: Biointerfaces*, 74(1), 17–22. <http://dx.doi.org/10.1016/j.colsurfb.2009.06.018>.
- Lee, B. B., Ravindra, P., & Chan, E. S. (2013). Size and shape of calcium alginate beads produced by extrusion dripping. *Chemical Engineering & Technology*, 36(10), 1627–1642. <http://dx.doi.org/10.1002/ceat.201300230>.
- Liserre, A. M., Ré, M. L., & Franco, B. D. G. M. (2007). Microencapsulation of bifidobacterium animalis subsp. Lactis in modified alginate-chitosan beads and evaluation of survival in simulated gastrointestinal conditions. *Food biotechnology*, 21(1), 1–16. <http://dx.doi.org/10.1080/0890543070191064>.
- Liu, H., Xu, X. M., & Guo, S. D. (2008). Comparison of full-fat and low-fat cheese analogues with or without pectin gel through microstructure, texture, rheology, thermal and sensory analysis. *International Journal of Food Science & Technology*, 43(9), 1581–1592. <http://dx.doi.org/10.1111/j.1365-2621.2007.01616.x>.
- Martin, M. J., Lara-Villoslada, F., Ruiz, M. A., & Morales, M. E. (2013). Effect of unmodified starch on viability of alginate-encapsulated *Lactobacillus fermentum* CECT5716. *LWT - Food Science and Technology*, 53(2), 480–486. <http://dx.doi.org/10.1016/j.lwt.2013.03.019>.
- Mattila-Sandholm, T., Myllärinen, P., Crittenden, R., Mogensen, G., Fondén, R., & Saarela, M. (2002). Technological challenges for future probiotic foods. *International Dairy Journal*, 12(2–3), 173–182. [http://dx.doi.org/10.1016/S0958-6946\(01\).http://dx.doi.org/10.1016/S0958-6946\(01\)00099-1](http://dx.doi.org/10.1016/S0958-6946(01).http://dx.doi.org/10.1016/S0958-6946(01)00099-1).
- Maxwell, E. G., Belsshaw, N. J., Waldron, K. W., & Morris, V. J. (2012). Pectin – an emerging new bioactive food polysaccharide. *Trends in Food Science & Technology*, 24(2), 64–73. <http://dx.doi.org/10.1016/j.tifs.2011.11.002>.
- Mokarram, R. R., Mortazavi, S. A., Najafi, M. B. H., & Shahidi, F. (2009). The influence of multi stage alginate coating on survivability of potential probiotic bacteria in simulated gastric and intestinal juice. *Food Research International*, 42(8), 1040–1045. <http://dx.doi.org/10.1016/j.foodres.2009.04.023>.
- Nazzaro, F., Fratianni, F., Coppola, R., Sada, A., & Orlando, P. (2009). Fermentative ability of alginate-prebiotic encapsulated *Lactobacillus acidophilus* and survival under simulated gastrointestinal conditions. *Journal of Functional Foods*, 1(3), 319–323. <http://dx.doi.org/10.1016/j.jff.2009.02.001>.
- Paredes, M. D. C., Rao, M. A., & Bourne, M. C. (1989). Rheological characterization of salad dressings 2: effect of storage. *Journal of Texture Studies*, 20(2), 235–250. <http://dx.doi.org/10.1111/j.1745-4603.1989.tb00436.x>.
- Pedreschi, R., Campos, D., Noratto, G., Chirinos, R., & Cisneros-Zevallos, L. (2003). Andean yacon root (*Smallanthus sonchifolius* Poepp. Endl) fructooligosaccharides as a potential novel source of prebiotics. *Journal of Agricultural and Food Chemistry*, 51(18), 5278–5284. <http://dx.doi.org/10.1021/jf0344744>.
- Pereira, R., Matia-Merino, L., Jones, V., & Singh, H. (2006). Influence of fat on the perceived texture of set acid milk gels: a sensory perspective. *Food Hydrocolloids*, 20(2–3), 305–313. <http://dx.doi.org/10.1016/j.foodhyd.2005.01.009>.
- Ratna Sudha, M., Chauhan, P., Dixit, K., Babu, S., & Jamil, K. (2009). Probiotics as complementary therapy for hypercholesterolemia. *Biology & Medicine*, 1(4), 1–13.
- Rokka, S., & Rantamäki, P. (2010). Protecting probiotic bacteria by microencapsulation: challenges for industrial applications. *European Food Research and Technology*, 231(1), 1–12. <http://dx.doi.org/10.1007/s00217-010-1246-2>.
- Sabikhi, L., Babu, R., Thompkinson, D. K., & Kapila, S. (2010). Resistance of microencapsulated *Lactobacillus acidophilus* LA1 to processing treatments and simulated gut conditions. *Food and Bioprocess Technology*, 3(4), 586–593. <http://dx.doi.org/10.1007/s11947-008-0135-1>.
- Sala, G., van Vliet, T., Cohen Stuart, M. A., Aken, G. A. v., & van de Velde, F. (2009). Deformation and fracture of emulsion-filled gels: Effect of oil content and deformation speed. *Food Hydrocolloids*, 23(5), 1381–1393. <http://dx.doi.org/10.1016/j.foodhyd.2008.11.016>.
- Sandoval-Castilla, O., Lobato-Calleros, C., García-Galindo, H. S., Alvarez-Ramírez, J., & Vernon-Carter, E. J. (2010). Textural properties of alginate–pectin beads and survivability of entrapped *Lb. casei* in simulated gastrointestinal conditions and in yoghurt. *Food Research International*, 43(1), 111–117. <http://dx.doi.org/10.1016/j.foodres.2010.01.006>.

- 1016/j.foodres.2009.09.010.
- Sathyabama, S., Ranjith kumar, M., Bruntha devi, P., Vijayabharathi, R., & Brindha priyadharisini, V. (2014). Co-encapsulation of probiotics with prebiotics on alginate matrix and its effect on viability in simulated gastric environment. *LWT - Food Science and Technology*, 57(1), 419–425. <http://dx.doi.org/10.1016/j.lwt.2013.12.024>.
- Saxelin, M., Tynkkynen, S., Mattila-Sandholm, T., & de Vos, W. M. (2005). Probiotic and other functional microbes: from markets to mechanisms. *Current Opinion in Biotechnology*, 16(2), 204–211. <http://dx.doi.org/10.1016/j.copbio.2005.02.003>.
- Shi, L. E., Li, Z. H., Li, D. T., Xu, M., Chen, H. Y., Zhang, Z. L., et al. (2013). Encapsulation of probiotic *Lactobacillus bulgaricus* in alginate–milk microspheres and evaluation of the survival in simulated gastrointestinal conditions. *Journal of Food Engineering*, 117(1), 99–104. <http://dx.doi.org/10.1016/j.jfoodeng.2013.02.012>.
- Upadhyay, A. (2014). *Investigating the potential of plant-derived Antimicrobials and probiotic bacteria for controlling Listeria monocytogenes*. doctoral. University of Connecticut - Storrs. Retrieved from <http://digitalcommons.uconn.edu/dissertations/326>.
- Voo, W.-P., Ravindra, P., Tey, B.-T., & Chan, E.-S. (2011). Comparison of alginate and pectin based beads for production of poultry probiotic cells. *Journal of Bioscience and Bioengineering*, 111(3), 294–299. <http://dx.doi.org/10.1016/j.jbiosc.2010.11.010>.
- de Vos, P., Faas, M. M., Spasojevic, M., & Sikkema, J. (2010). Encapsulation for preservation of functionality and targeted delivery of bioactive food components. *International Dairy Journal*, 20(4), 292–302. <http://dx.doi.org/10.1016/j.idairyj.2009.11.008>.
- White, R. J., Budarin, V. L., & Clark, J. H. (2010). Pectin-derived porous materials. *Chemistry – A European Journal*, 16(4), 1326–1335. <http://dx.doi.org/10.1002/chem.200901879>.
- Wicker, L., Kim, Y., Kim, M.-J., Thirkield, B., Lin, Z., & Jung, J. (2014). Pectin as a bioactive polysaccharide – extracting tailored function from less. *Food Hydrocolloids*, 42, Part 2(0), 251–.
- Woo, J. W., Roh, H. J., Park, H. D., Ji, C. I., Lee, Y. B., & Kim, S. B. (2007). Sphericity optimization of calcium alginate gel beads and the effects of processing conditions on their physical properties. *Food Sci. Biotechnology*, 16, 715–721.
- Zhao, M., Qu, F., Cai, S., Fang, Y., Nishinari, K., Phillips, G., et al. (2015). Microencapsulation of *Lactobacillus acidophilus* CGMCC1.2686: correlation between bacteria survivability and physical properties of microcapsules. *Food Biophysics*, 10(3), 292–299. <http://dx.doi.org/10.1007/s11483-014-9389-5259>. <http://dx.doi.org/10.1016/j.foodhyd.2014.01.002>.



# Probiotic characterization of lactic acid bacteria isolated from fermented foods and beverage of Ladakh



Kunzes Angmo, Anila Kumari, Savitri, Tek Chand Bhalla\*

Department of Biotechnology, Himachal Pradesh University, Summer Hill, Shimla 171005, India

## ARTICLE INFO

### Article history:

Received 12 February 2015

Received in revised form

7 September 2015

Accepted 24 October 2015

Available online 30 October 2015

### Keywords:

Fermented food

Beverage

Lactic acid bacteria

Probiotic

Probiotic properties

## ABSTRACT

The present research was focused on probiotic characterization of lactic acid bacteria from fermented foods and beverage of Ladakh. Twenty five lactic acid bacteria were examined *in vitro* for potential probiotic properties based on their low pH tolerance, bile-salt resistance, lysozyme tolerance, cholesterol removal, hydrophobicity, autoaggregation, production of antimicrobial substances, exopolysaccharide production,  $\beta$ -galactosidase activity and haemolytic activity. The outcome of these studied parameters was used as input data for a principal component analysis (PCA) to select the most promising isolate and ten most potential probiotic isolates were identified through 16S rDNA sequencing. On the basis of PCA, isolate 84 (*Lactobacillus plantarum* KJ722784) showed similar trend to *Lactobacillus casei* Shirota used as reference strain in terms of probiotic properties. Fermented milk sample inoculated with *L. plantarum* KJ722784 exhibited decrease in viable count during storage at 4 °C on day 28. However, the survival count is greater than 7 log CFU/ml which is higher than the requirement of 6 log CFU/ml to exhibit health benefit.

© 2015 Elsevier Ltd. All rights reserved.

## 1. Introduction

Probiotics are non-pathogenic microorganisms, which on ingested in adequate amount exert a positive health benefit on host (FAO/WHO, 2006). Consumption of probiotic have been shown to be helpful in overcome various clinical conditions ranging from infantile diarrhoea, antibiotic associated diarrhoea, relapsing *Clostridium difficile* colitis, *Helicobacter pylori* infections, inflammatory bowel disease to cancer and female uro-genital infections (Reid, Jass, Sebulsky, & McCormick, 2003). Other beneficial effects of probiotics include improving lactose intolerance, lowering serum cholesterol level, increasing utilization of nutrients and decreasing use of antibiotics (Guo, Kim, Namb, Park, & Kim, 2010). In general, log 6- log 7 of probiotic bacteria per ml or g of food has been recommended for exhibition of health benefit (Lahtinen et al., 2010).

Lactic acid bacteria (LAB) are most commonly studied probiotic for the past few decades. These are desirable microflora of the gastro intestinal tract (GIT) and are thus 'generally regarded as safe' (Tannock, 1997). Secondly they are involved in the fermentation and are dominant microflora of fermented products. They are

known to play an essential role in food preservation and inhibit spoilage microorganisms or food borne pathogens by production of lactic acid, acetic acid, H<sub>2</sub>O<sub>2</sub>, bacteriocin, diacetyl and CO<sub>2</sub> (Nur & Aslim, 2010).

Worldwide a variety of traditional fermented foods and beverages are prepared and consumed. Fermented products are associated with desired and edible microbes which are beneficial for health. Research in the field of exploring an interesting strain with probiotic potential from fermented food products as a source of new isolates are blooming. In Asia, an array of fermented foods and beverages are produced. The people of the Himalayan region of India particularly Ladakh region consume a variety of indigenous fermented foods such as *tagi khambir/skyurchuk* (brown sourdough bread), *zho* (curd), *tara* (buttermilk), *labo* (cottage cheese), *chhurphe* (dried cottage cheese), etc. (Angchok, Dwivedi, & Ahmed, 2009) and fermented vegetables and alcoholic beverages like *chhang* and *aarak* (Angmo & Bhalla, 2014). However, no work has been carried out to explore the microflora of fermented foods and beverages of Ladakh and study their proposed health attributes. Therefore present study aimed on isolation of lactic acid bacteria from traditional fermented foods and beverage of Ladakh and examination of various phenotypic characteristics, widely used in the screening and selection of probiotic bacteria.

\* Corresponding author.

E-mail address: [bhallatc@rediffmail.com](mailto:bhallatc@rediffmail.com) (T.C. Bhalla).

## 2. Materials and methods

### 2.1. Sample collection

Samples of *chhurphe* (dried cottage cheese), vegetable pickle and *chhang* (barley based beer) were collected in sterile vials from different villages (Nyemo, Saspol, Sankar, Thiksay, Zanskar) and Leh town of Ladakh, India and were used for isolation of lactic acid bacteria (LAB).

### 2.2. Isolation of lactic acid bacteria

LAB were isolated by spread plating on MRS (de Mann Rogosa Sharpe) agar (Himedia), and the plates were incubated at 30 °C for 48 h. Colonies with different morphologies on the MRS agar plate were selected and further subcultured in order to obtain a pure colony. Glycerol stock of LAB isolates were prepared and stored at –80 °C.

Provisional or tentative identification of genera was made by Gram staining, cell morphology and catalase reaction. Physiological properties such as growth at different temperature and different NaCl concentration, gas production from glucose, hydrolysis of arginine and carbohydrate fermentation were also studied.

### 2.3. Strains

Reference strain: *Lactobacillus casei* Shirota (P1) was from University of Helsinki, Finland. Test strains: *Bacillus cereus*, *Escherichia coli*, *Staphylococcus aureus*, *Shigella dysenteriae* and *Pseudomonas* sp. were obtained from Indira Gandhi Medical College (IGMC) Shimla, India and *Listeria monocytogenes* was procured from Microbial Type Culture Collection (MTCC), Institute of Microbial Technology, Chandigarh, India.

### 2.4. Evaluation of probiotic properties

#### 2.4.1. Acid and bile tolerance

The experiment for tolerance of isolate to pH 2.0, 3.0 and 7.0 (control) was performed following the method described by Yu et al. (2013).

The ability of the isolates to grow in the presence of 0.5% and 1% of bile (w/v) was determined according to the method of Vinderola and Reinheimer (2003). Resistance was evaluated by plate count on MRS agar.

#### 2.4.2. Lysozyme tolerance

Tolerance to lysozyme was assessed following the method reported by Vizoso-Pinto, Franz, Schillinger, and Holzapfel (2006).

#### 2.4.3. Cholesterol removal

Cholesterol removal was determined using o-phthalaldehyde method according to Liong and Shah (2005). Three different bile salts such as deconjugated bile (cholic acid), conjugated bile (sodium taurocholate) and mixture of conjugated (97%) and deconjugated (3%) bile (oxbile) were used in this study.

#### 2.4.4. Cell surface hydrophobicity

This assay was done by the method given by Mishra and Prasad (2005).

#### 2.4.5. Autoaggregation

Autoaggregation was carried out according to Collado, Meriluoto, and Salminen (2008) with little modifications. Overnight grown cells were suspended in PBS buffer to obtain an optical density (O.D.) of  $0.25 \pm 0.05$  at 600 nm. The bacterial suspension

(4 ml) was vortexed for 10 s and incubated at 30 °C. Samples were monitored during different time intervals (0 h, 3 h and 24 h) and autoaggregation percentage was expressed as  $[1 - A_t/A_0] \times 100$ , where  $A_t$  represents the absorbance at time t and  $A_0$  as the absorbance at t = 0.

#### 2.4.6. Antibacterial activity

Agar well diffusion method was used to test the antimicrobial activity as described by Mishra and Prasad (2005). The supernatants of 18–20 h grown LAB cells were tested against *B. cereus*, *E. coli*, *S. aureus*, *S. dysenteriae* and *Pseudomonas* sp. and *L. monocytogenes*.

#### 2.4.7. Antibiotic resistance

MRS agar plate was overlaid with 100 µl of LAB culture containing  $10^8$  CFU/ml and antibiotic discs containing penicillin G (10 units), clindamycin (2 mcg), co-trimoxazole (25 mcg), erythromycin (15 mcg), vancomycin (30 mcg) and ampicillin (10/10 mcg) were placed on inoculated plates under sterile conditions. After incubation for 24 h at 30 °C, the diameter (mm) of inhibition zone was measured.

#### 2.4.8. β-Galactosidase activity

For β-galactosidase activity, bacterial cultures were streaked on MRS agar plates containing 60 µl X-gal (5-bromo-4-chloro-3-indolyl-β-D-galactopyranoside) and 10 µl of IPTG (iso-propyl-thio-β-D galactopyranoside) solution as inducer.

#### 2.4.9. Exopolysaccharide production

Overnight cultures were streaked on the surface of plates containing ruthenium red milk (10% w/v, skim milk powder, 1% w/v, sucrose and 0.08 g/l ruthenium red, 1.5% w/v agar).

#### 2.4.10. Haemolytic activity

LAB isolates were streaked on the surface of Columbia blood agar plates (Oxoid) supplemented with 5% sheep blood. After 48 h of incubation at 30 °C the plates were examined for haemolytic reaction.

#### 2.4.11. Statistical analysis

Statistical analysis was performed on the data by SPSS 19.0 Bivariate Correlation Analysis (SPSS Inc., Chicago, Ill., U.S.A.). Principal component analysis (PCA) was conducted with XLSTAT™ software (Addinsoft, Paris, France). The results of both qualitative (antibiotic resistance, β-galactosidase activity and haemolytic) and quantitative assays (acid, bile and lysozyme tolerance, antimicrobial activity, cholesterol removal, hydrophobicity and autoaggregation) were converted into three coded values (0, 1 and 2) and used as input data.

### 2.5. Identification of the finally selected isolates by 16S rDNA sequencing

16S rDNA of the selected isolates were amplified by PCR using primers 27F (5'- AGAGTTTGATCTTGCTCAG-3') and 1492R (5'- TACGGYTACCTGTTACGACTT-3').

DNA sequencing of amplified fragments was carried out by sequencing service of Xcelris Labs Limited, Ahmedabad, India. The fragments of sequences were assembled and edited with software BioEdit 7.2.5 and consensus sequences were compared with those deposited in the GenBank DNA database using the Basic Local Alignment Search Tool (BLAST; <http://blast.ncbi.nlm.nih.gov/Blast.cgi>). A phylogenetic tree based on 16S rRNA genes was also constructed to determine the closest bacterial species by the neighbor-joining method (Saitou & Nei, 1987), using MEGA 6.06 (Tamura

et al., 2011).

## 2.6. Production of fermented milk

The LAB isolate was assessed for the production of fermented milk product. The preparation and fermentation of milk was performed according to the method of Chiu, Lu, Tseng, and Pan (2006). Skimmed milk powder was weighed and dissolved in water to obtain 4% skimmed milk (w/v), which was sterilized in an autoclave at 121 °C for 15 min and cooled to room temperature. The milk was inoculated with 2% bacterial culture and inoculated milk was incubated for fermentation (24 h) at 37 °C in sealed container. After fermentation, the fermented milk was stored at 4 °C for 28 days, and the viability of bacteria and changes in pH of fermented milk was determined at every week during the storage period.

## 3. Results

### 3.1. Isolation and physiological properties of isolates

One hundred and four isolates from fermented foods and beverage of different regions of Ladakh were isolated. Out of these isolates, twenty five isolates showing typical appearance of lactic acid bacteria on MRS medium (small pin pointed colonies) were randomly selected and assayed for physiological properties.

All the selected isolates were Gram positive, catalase negative and rod shaped bacteria. They were mesophilic and showed good growth at 1.5% and 2.5% of NaCl concentration. Seven isolates produced CO<sub>2</sub> from glucose. All the isolates hydrolyzed arginine and showed diversity in their ability to ferment different sugars (data not shown).

### 3.2. Evaluation of probiotic properties

#### 3.2.1. Acid and bile tolerance

When exposed to stimulated *in vitro* gastric juice of pH 2, the survival of LAB isolates showed a significant ( $p < 0.05$ ) variability ranging from 3.21 log CFU/ml to 6.75 log CFU/ml (Table 1). At pH 2, each isolates demonstrated progressive reduction in survival rate and isolate 45 showed maximum 4.8 log CFU/ml decline in viability. Whereas, compared to pH 2, pH 3 had little or no impact on the viability of most isolates. LAB isolates 11, 20, 40, 52, 63, 68, 72 and 75 retained same level of viability after exposure to pH 3 for 3 h. Among all LAB, isolates 40, 52, 63 and 68 had higher tolerance than reference strain, *L. casei* Shirota (P1) at pH 2.

As shown in Table 1, bile salt has a significant influence on the viability of LAB isolate. With the exception of isolate 40, all the isolates exhibited reduction in viability at 1% of bile salt. Though, survival rate of isolates 20, 27, 40, 52, 63 and 84 remained unaffected at 0.5% bile salt hence no significant ( $p < 0.05$ ) difference was found. However, isolates 11, 20, 40 and 45 showed comparatively better tolerance than strain P1 at 1% bile salt.

#### 3.2.2. Lysozyme tolerance

In lysozyme test, isolates 11, 20, 22, 40, 68 and 72 exhibited an excellent resistance to 50 mcg/ml concentration of lysozyme since no significant ( $p < 0.05$ ) differences in viability was noted after 3 h (Table 1). While all isolates consistently showed reduce tolerance towards 100 mcg/ml of lysozyme. In particular, isolates 55 and 72 in 100 mcg/ml concentration of lysozyme demonstrated similar tolerance to 50 mcg/ml of lysozyme, without any loss in viability. Strain P1 revealed 2.41 log CFU/ml reduction in viability after 3 h of incubation in 100 mcg/ml of lysozyme.

### 3.2.3. Cholesterol removal

Uptake of cholesterol in the medium containing cholic acid, oxbile and sodium taurocholate was highest, intermediate and least, respectively with majority of isolates (Fig. 1). Medium having cholic acid, the overall cholesterol removal was observed to be highest for isolates 55 and 72 (upto 38%) whereas isolates 70 and 76 showed least cholesterol removal (8.52% and 4.24% respectively). Cholesterol removal for medium containing oxbile varied from 1.14% to 19% although isolate 11 demonstrated higher cholesterol assimilation of 19.75%. Strain P1 had significantly highest cholesterol removal in cholic acid than compared to oxbile and sodium taurocholate.

### 3.2.4. Cell surface hydrophobicity and autoaggregation

Cell surface hydrophobicity of the LAB isolates tested was highly variable (<5%–47%) depending upon bacterial cell (Table 2). In general, isolates 20, 63 and 72 possessed a high percent hydrophobicity (47%, 45% and 45%, respectively) compared to other isolates investigated. Reference strain P1 had hydrophobicity of 40%. However, isolates 38, 45 and 66 had lowest percent hydrophobicity.

All isolates investigated showed higher percentages of aggregation after 24 h than at 3 h of incubation (Table 2). The most autoaggregative isolate was isolate 52 (73%) while isolates 20, 29, 40, 63 and 72 exhibited higher autoaggregation than strain P1 (60%). On the other hand, least autoaggregation ability was shown by isolates 11 and 12.

### 3.2.5. Antimicrobial activity

Isolate 40 showed an evident zone of inhibition (>5 mm) against *B. cereus*, *S. aureus* and *S. dysenteriae* whereas, isolate 11 exhibited inhibitory activity towards *S. aureus* and *S. dysenteriae* (5 mm zone of inhibition). Isolates 12, 20, 29, 38 and 55 were found to have antimicrobial activity against *B. cereus* and *L. monocytogenes*, although their inhibitory extents were variable. In addition, a few LAB isolates were observed to have weak to medium antimicrobial activity against *E. coli* (isolates 30, 45, 52 and 75) and *S. aureus* (isolates 11, 40 and 68). However, none of the isolates showed any antimicrobial activity against *Pseudomonas* sp.

### 3.2.6. Antibiotic resistance

Most of the LAB isolates were found to be susceptible to all tested antibiotics such as penicillin G, clindamycin, co-trimoxazole, erythromycin and ampicillin except vancomycin. Isolates 11, 20 and 40 were moderately resistant to penicillin G and isolates 20, 52, 55 and 63 toward ampicillin.

### 3.2.7. $\beta$ -Galactosidase activity

In qualitative  $\beta$ -galactosidase screening, isolates 11, 20, 40, 52, 55, 63, 68, 72 and 84 possessed the presence of  $\beta$ -galactosidase activity after 42 h of incubation at 30 °C.

### 3.2.8. Exopolysaccharide production

The isolates 20, 27, 30, 32, 40, 68, 72 and 84 gave ropy colonies and were positive for production of exopolysaccharide.

### 3.2.9. Haemolytic activity

All the LAB isolates studied for haemolytic activity gave negative result.

## 3.3. Principal component analysis (PCA)

Analysis of Principal component analysis (PCA) revealed that first four principal components (PCs) explaining 73.647% of total variation, while PC1 and PC2 accounting for 37.7% and 17.4% respectively. As shown in Table 4, pH2, lysozyme (100 mcg/ml),

**Table 1**  
Effect of low pH, bile salt and lysozyme on the viability of LAB isolates during 3 h incubation.

Isolate	pH tolerance			Bile tolerance			Lysozyme tolerance		
	pH 7	pH 3	pH 2	Control	0.5%	1%	Control	50 mcg/ml	100 mcg/ml
11	8.52 ± 0.17 <sup>b</sup>	8.11 ± 0.30 <sup>b</sup>	5.70 ± 0.17 <sup>a</sup>	8.50 ± 0.15 <sup>c</sup>	7.49 ± 0.08 <sup>b</sup>	6.99 ± 0.09 <sup>a</sup>	8.25 ± 0.05 <sup>b</sup>	8.10 ± 0.03 <sup>b</sup>	6.47 ± 0.23 <sup>a</sup>
12	8.42 ± 0.08 <sup>c</sup>	6.66 ± 0.12 <sup>b</sup>	4.63 ± 0.90 <sup>a</sup>	8.58 ± 0.06 <sup>c</sup>	7.26 ± 0.11 <sup>b</sup>	5.33 ± 0.07 <sup>a</sup>	8.64 ± 0.29 <sup>c</sup>	7.44 ± 0.11 <sup>b</sup>	5.78 ± 0.14 <sup>a</sup>
17	9.12 ± 0.05 <sup>c</sup>	7.95 ± 0.08 <sup>b</sup>	3.73 ± 0.12 <sup>a</sup>	8.96 ± 0.10 <sup>c</sup>	8.60 ± 0.04 <sup>b</sup>	6.10 ± 0.09 <sup>a</sup>	8.86 ± 0.11 <sup>c</sup>	7.46 ± 0.23 <sup>b</sup>	6.12 ± 0.09 <sup>a</sup>
19	9.04 ± 0.06 <sup>c</sup>	7.88 ± 0.10 <sup>b</sup>	5.08 ± 0.06 <sup>a</sup>	8.89 ± 0.03 <sup>c</sup>	7.58 ± 0.12 <sup>b</sup>	6.78 ± 0.04 <sup>a</sup>	8.93 ± 0.21 <sup>c</sup>	6.96 ± 0.17 <sup>b</sup>	5.09 ± 0.07 <sup>a</sup>
20	8.65 ± 0.10 <sup>b</sup>	8.60 ± 0.11 <sup>b</sup>	6.03 ± 0.09 <sup>a</sup>	8.40 ± 0.06 <sup>b</sup>	8.11 ± 0.05 <sup>b</sup>	7.38 ± 0.04 <sup>a</sup>	8.41 ± 0.05 <sup>b</sup>	8.15 ± 0.003 <sup>b</sup>	6.54 ± 0.21 <sup>a</sup>
22	8.50 ± 0.14 <sup>c</sup>	7.94 ± 0.08 <sup>b</sup>	4.02 ± 0.16 <sup>a</sup>	8.47 ± 0.06 <sup>c</sup>	5.29 ± 0.06 <sup>b</sup>	3.81 ± 0.07 <sup>a</sup>	8.04 ± 0.23 <sup>b</sup>	7.60 ± 0.15 <sup>b</sup>	5.01 ± 0.15 <sup>a</sup>
24	8.93 ± 0.10 <sup>c</sup>	8.44 ± 0.09 <sup>b</sup>	3.73 ± 0.12 <sup>a</sup>	8.83 ± 0.08 <sup>c</sup>	7.96 ± 0.09 <sup>b</sup>	6.59 ± 0.13 <sup>a</sup>	8.83 ± 0.08 <sup>c</sup>	7.96 ± 0.09 <sup>b</sup>	6.59 ± 0.13 <sup>a</sup>
27	8.88 ± 0.07 <sup>c</sup>	7.77 ± 0.11 <sup>b</sup>	4.97 ± 0.15 <sup>a</sup>	8.09 ± 0.04 <sup>b</sup>	7.86 ± 0.04 <sup>b</sup>	5.68 ± 0.07 <sup>a</sup>	8.69 ± 0.04 <sup>c</sup>	7.16 ± 0.04 <sup>b</sup>	5.68 ± 0.07 <sup>a</sup>
29	8.95 ± 0.05 <sup>c</sup>	7.91 ± 0.09 <sup>b</sup>	4.19 ± 0.07 <sup>a</sup>	8.84 ± 0.09 <sup>c</sup>	6.33 ± 0.06 <sup>b</sup>	4.95 ± 0.10 <sup>a</sup>	8.63 ± 0.17 <sup>c</sup>	7.35 ± 0.03 <sup>b</sup>	6.81 ± 0.17 <sup>a</sup>
30	8.70 ± 0.07 <sup>c</sup>	6.27 ± 0.07 <sup>b</sup>	3.93 ± 0.07 <sup>a</sup>	8.69 ± 0.06 <sup>c</sup>	7.99 ± 0.13 <sup>b</sup>	4.66 ± 0.05 <sup>a</sup>	8.96 ± 0.19 <sup>c</sup>	7.78 ± 0.18 <sup>b</sup>	5.85 ± 0.40 <sup>a</sup>
32	8.48 ± 0.08 <sup>c</sup>	7.73 ± 0.10 <sup>b</sup>	4.14 ± 0.07 <sup>a</sup>	8.35 ± 0.07 <sup>c</sup>	6.66 ± 0.04 <sup>b</sup>	5.36 ± 0.04 <sup>a</sup>	8.08 ± 0.07 <sup>c</sup>	6.73 ± 0.28 <sup>b</sup>	4.13 ± 0.14 <sup>a</sup>
38	8.03 ± 0.06 <sup>c</sup>	6.86 ± 0.04 <sup>b</sup>	3.04 ± 0.12 <sup>a</sup>	8.11 ± 0.11 <sup>c</sup>	7.65 ± 0.09 <sup>b</sup>	5.79 ± 0.09 <sup>a</sup>	8.23 ± 0.23 <sup>c</sup>	7.57 ± 0.12 <sup>b</sup>	6.88 ± 0.12 <sup>a</sup>
40	8.87 ± 0.08 <sup>b</sup>	8.79 ± 0.06 <sup>b</sup>	6.69 ± 0.05 <sup>a</sup>	7.19 ± 0.06 <sup>a</sup>	6.97 ± 0.15 <sup>a</sup>	6.79 ± 0.03 <sup>a</sup>	8.64 ± 0.21 <sup>b</sup>	8.30 ± 0.03 <sup>b</sup>	7.84 ± 0.12 <sup>a</sup>
44	8.88 ± 0.05 <sup>c</sup>	7.91 ± 0.04 <sup>b</sup>	5.43 ± 0.17 <sup>a</sup>	8.74 ± 0.14 <sup>c</sup>	7.06 ± 0.05 <sup>b</sup>	5.73 ± 0.12 <sup>a</sup>	8.80 ± 0.16 <sup>c</sup>	6.80 ± 0.17 <sup>b</sup>	5.42 ± 0.07 <sup>a</sup>
45	8.04 ± 0.10 <sup>c</sup>	6.87 ± 0.05 <sup>b</sup>	3.21 ± 0.04 <sup>a</sup>	8.15 ± 0.08 <sup>b</sup>	6.51 ± 0.04 <sup>a</sup>	6.48 ± 0.06 <sup>a</sup>	8.42 ± 0.21 <sup>c</sup>	7.37 ± 0.16 <sup>b</sup>	4.56 ± 0.12 <sup>a</sup>
52	8.62 ± 0.08 <sup>b</sup>	8.45 ± 0.06 <sup>b</sup>	6.54 ± 0.11 <sup>a</sup>	8.20 ± 0.06 <sup>b</sup>	7.97 ± 0.06 <sup>b</sup>	5.84 ± 0.05 <sup>a</sup>	8.35 ± 0.13 <sup>b</sup>	8.21 ± 0.22 <sup>b</sup>	6.86 ± 0.11 <sup>a</sup>
55	8.84 ± 0.05 <sup>c</sup>	7.89 ± 0.02 <sup>b</sup>	6.40 ± 0.09 <sup>a</sup>	8.63 ± 0.07 <sup>c</sup>	7.32 ± 0.09 <sup>b</sup>	5.91 ± 0.08 <sup>a</sup>	8.68 ± 0.09 <sup>c</sup>	7.01 ± 0.11 <sup>b</sup>	6.65 ± 0.24 <sup>b</sup>
63	8.52 ± 0.07 <sup>b</sup>	8.29 ± 0.17 <sup>b</sup>	6.63 ± 0.10 <sup>a</sup>	8.12 ± 0.08 <sup>b</sup>	7.80 ± 0.10 <sup>b</sup>	5.61 ± 0.07 <sup>a</sup>	8.13 ± 0.13 <sup>c</sup>	7.45 ± 0.22 <sup>b</sup>	6.23 ± 0.13 <sup>a</sup>
66	9.12 ± 0.04 <sup>c</sup>	8.76 ± 0.09 <sup>b</sup>	4.43 ± 0.11 <sup>a</sup>	8.85 ± 0.08 <sup>c</sup>	7.03 ± 0.05 <sup>b</sup>	6.68 ± 0.07 <sup>a</sup>	8.78 ± 0.16 <sup>c</sup>	7.13 ± 0.13 <sup>b</sup>	5.48 ± 0.17 <sup>a</sup>
68	8.75 ± 0.56 <sup>b</sup>	8.65 ± 0.14 <sup>b</sup>	6.75 ± 0.12 <sup>a</sup>	8.77 ± 0.09 <sup>c</sup>	7.37 ± 0.07 <sup>b</sup>	6.05 ± 0.12 <sup>a</sup>	8.47 ± 0.03 <sup>b</sup>	8.24 ± 0.04 <sup>b</sup>	7.50 ± 0.13 <sup>a</sup>
70	7.97 ± 0.04 <sup>c</sup>	6.88 ± 0.09 <sup>b</sup>	4.35 ± 0.05 <sup>a</sup>	8.10 ± 0.06 <sup>c</sup>	6.03 ± 0.07 <sup>b</sup>	4.69 ± 0.06 <sup>a</sup>	8.44 ± 0.21 <sup>c</sup>	7.83 ± 0.15 <sup>b</sup>	6.12 ± 0.13 <sup>a</sup>
72	8.95 ± 0.05 <sup>b</sup>	8.82 ± 0.10 <sup>b</sup>	6.53 ± 0.06 <sup>a</sup>	8.71 ± 0.03 <sup>c</sup>	7.69 ± 0.04 <sup>b</sup>	6.06 ± 0.05 <sup>a</sup>	8.40 ± 0.05 <sup>b</sup>	8.27 ± 0.04 <sup>ba</sup>	8.16 ± 0.04 <sup>a</sup>
75	8.36 ± 1.07 <sup>b</sup>	8.10 ± 0.10 <sup>b</sup>	4.46 ± 0.07 <sup>a</sup>	8.45 ± 0.05 <sup>c</sup>	7.37 ± 0.06 <sup>b</sup>	4.90 ± 0.07 <sup>a</sup>	8.81 ± 0.04 <sup>c</sup>	8.24 ± 0.07 <sup>b</sup>	5.12 ± 0.10 <sup>a</sup>
76	8.89 ± 0.04 <sup>c</sup>	8.29 ± 0.06 <sup>b</sup>	4.88 ± 0.06 <sup>a</sup>	8.96 ± 0.09 <sup>c</sup>	8.08 ± 0.12 <sup>b</sup>	4.98 ± 0.13 <sup>a</sup>	8.77 ± 0.11 <sup>c</sup>	6.85 ± 0.16 <sup>b</sup>	5.26 ± 0.16 <sup>a</sup>
84	8.75 ± 0.09 <sup>c</sup>	7.81 ± 0.15 <sup>b</sup>	4.94 ± 0.08 <sup>a</sup>	8.08 ± 0.08 <sup>b</sup>	7.70 ± 0.10 <sup>b</sup>	5.77 ± 0.05 <sup>a</sup>	8.33 ± 0.12 <sup>c</sup>	7.49 ± 0.17 <sup>b</sup>	5.33 ± 0.10 <sup>a</sup>
P1	8.12 ± 0.24 <sup>c</sup>	7.94 ± 0.21 <sup>b</sup>	5.69 ± 0.45 <sup>a</sup>	8.32 ± 0.09 <sup>c</sup>	7.81 ± 0.16 <sup>b</sup>	6.12 ± 0.16 <sup>a</sup>	8.75 ± 0.09 <sup>c</sup>	7.65 ± 0.13 <sup>b</sup>	6.34 ± 0.19 <sup>a</sup>

Values represented as mean ± SD; for each column, different subscripts lowercase letters indicate significantly different at  $p < 0.05$ , as measured by 2-sided Tukey's HSD; Reference strain P1 is *Lactobacillus casei* Shirota.

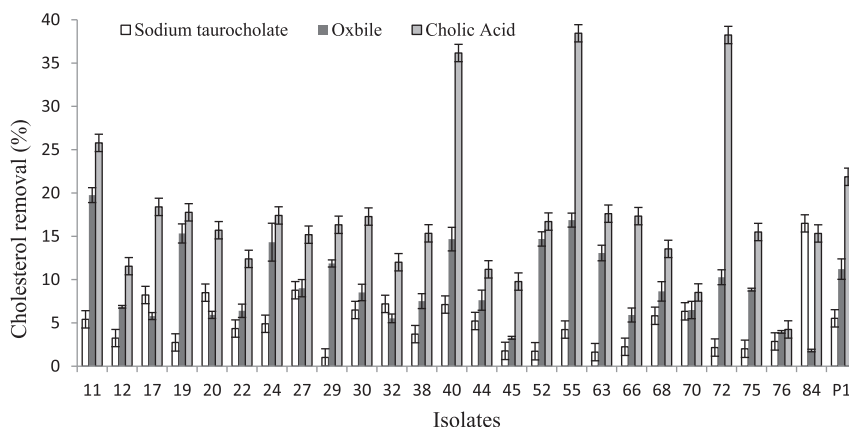


**Fig. 1.** Cholesterol removal (%) by LAB isolates.

cholic acid, n-hexadecane, *S. aureus*, *S. dysenteriae*, penicillin G and  $\beta$ -galactosidase were correlated to PC1 and PC2, suggesting that these variables are contributing for the selection of the most relevant technological isolates.

Fig. 2(a) represents the distribution plots of variables on the plane of first two principal components. Projection of LAB isolates in two-dimensional space of the PC1 and PC2 loading factors could be differentiated three main clusters (Fig. 2(b)). It can be inferred that LAB isolates present in quadrant I and IV were significant as they showed correlation with respect to variables. Isolates 11 and 40 of quadrant I was related with antimicrobial activity against *S. aureus* and *S. dysenteriae* and resistant toward penicillin G. On the other hand, isolates 29, 84, 72, 20, 63, 55 and 52 were the most potential candidate as they showed highest probiotic character. While isolate 84 demonstrated higher resemblances with strain P1 explaining the similar trend in probiotic activities of isolate 84 with

respect to reference strain. Therefore isolate 84 was selected for the preparation of milk based fermented probiotic drink.

### 3.4. Identification by 16S rDNA sequencing

All ten potential probiotic isolates (based on PCA) were identified by 16S rRNA gene sequence and PCR amplification of the 16S rRNA gene resulted in amplicon of 1300–1500 bp. Alignments were performed using the BLAST and *lactobacilli* identified were designated as PLA (Probiotic lactic acid bacteria) followed by the numbers 22 to 37.

In an effort to identify LAB isolates at the species level, molecular phylogeny analysis was conducted and phylogenetic tree was constructed based on the 16S rDNA sequences from evolutionary distances by the neighbor-joining method (Fig. 3). Analysis of the sequences depicted that the 50% of isolates clustered with 16S rRNA

**Table 2**  
Hydrophobicity and autoaggregation ability of LAB isolates.

Isolate	Hydrophobicity %		Autoaggregation %	
	n-Hexadecane		3 h	24 h
11	12.02 ± 1.70 <sup>bcde</sup>		1.84 ± 0.10 <sup>a</sup>	5.04 ± 0.10 <sup>a</sup>
12	7.44 ± 0.67 <sup>ab</sup>		1.76 ± 0.11 <sup>a</sup>	8.24 ± 0.22 <sup>b</sup>
17	16.52 ± 1.21 <sup>efg</sup>		11.54 ± 0.10 <sup>def</sup>	25.33 ± 0.10 <sup>e</sup>
19	35.93 ± 2.30 <sup>i</sup>		17.52 ± 0.10 <sup>kl</sup>	33.96 ± 0.10 <sup>gh</sup>
20	46.59 ± 2.12 <sup>kl</sup>		15.24 ± 0.11 <sup>ghij</sup>	63.25 ± 0.11 <sup>no</sup>
22	11.66 ± 0.67 <sup>bcde</sup>		5.55 ± 0.10 <sup>b</sup>	28.01 ± 0.10 <sup>f</sup>
24	8.47 ± 0.56 <sup>ab</sup>		11.80 ± 0.44 <sup>def</sup>	29.94 ± 0.11 <sup>f</sup>
27	9.70 ± 0.56 <sup>abc</sup>		13.75 ± 0.10 <sup>fghi</sup>	35.16 ± 0.10 <sup>hi</sup>
29	20.28 ± 0.45 <sup>g</sup>		16.15 ± 0.13 <sup>ijk</sup>	62.18 ± 0.13 <sup>n</sup>
30	15.74 ± 0.87 <sup>efg</sup>		13.35 ± 0.09 <sup>efghi</sup>	19.88 ± 0.09 <sup>d</sup>
32	7.59 ± 0.56 <sup>ab</sup>		6.40 ± 0.09 <sup>bc</sup>	28.98 ± 0.09 <sup>f</sup>
38	5.81 ± 0.67 <sup>a</sup>		8.89 ± 0.09 <sup>cd</sup>	33.06 ± 0.09 <sup>g</sup>
40	26.96 ± 0.88 <sup>h</sup>		18.42 ± 0.23 <sup>kl</sup>	64.71 ± 0.23 <sup>r</sup>
44	11.26 ± 0.56 <sup>abcde</sup>		10.55 ± 0.63 <sup>de</sup>	36.18 ± 0.31 <sup>i</sup>
45	5.69 ± 0.45 <sup>a</sup>		26.78 ± 0.79 <sup>m</sup>	40.23 ± 0.79 <sup>j</sup>
52	38.90 ± 0.89 <sup>i</sup>		24.56 ± 0.09 <sup>m</sup>	73.09 ± 0.18 <sup>p</sup>
55	30.47 ± 4.33 <sup>i</sup>		5.27 ± 0.25 <sup>b</sup>	24.78 ± 0.37 <sup>e</sup>
63	44.56 ± 2.33 <sup>jk</sup>		18.42 ± 0.23 <sup>kl</sup>	64.78 ± 0.11 <sup>o</sup>
66	5.96 ± 0.56 <sup>a</sup>		1.63 ± 0.11 <sup>a</sup>	16.73 ± 0.21 <sup>c</sup>
68	11.63 ± 1.10 <sup>bcde</sup>		5.68 ± 0.14 <sup>b</sup>	15.71 ± 0.29 <sup>c</sup>
70	15.34 ± 0.86 <sup>defg</sup>		12.82 ± 2.22 <sup>efgh</sup>	40.06 ± 0.11 <sup>j</sup>
72	44.74 ± 2.93 <sup>l</sup>		12.46 ± 0.13 <sup>efg</sup>	61.91 ± 1.27 <sup>mn</sup>
75	10.43 ± 1.10 <sup>abcd</sup>		19.88 ± 1.01 <sup>l</sup>	42.69 ± 1.01 <sup>k</sup>
76	13.66 ± 0.65 <sup>cde</sup>		24.01 ± 0.10 <sup>m</sup>	41.36 ± 1.07 <sup>l</sup>
84	35.74 ± 1.43 <sup>i</sup>		15.45 ± 0.18 <sup>hij</sup>	58.37 ± 0.09 <sup>q</sup>
P1	40.16 ± 1.56 <sup>ij</sup>		15.04 ± 1.58 <sup>ghij</sup>	60.00 ± 2.00 <sup>lm</sup>

Values represented as mean ± SD of triplicate analyses; for each column, different subscripts lowercase letters indicate significantly different at  $p < 0.001$  as measured by 2-sided Tukey's HSD between different strains.

**Table 3**  
Identified LAB isolates by 16S rRNA gene sequencing and their GenBank accession number.

Isolate	Species	NCBI accession No
11	<i>Lactobacillus brevis</i>	KJ722770
20	<i>Lactobacillus brevis</i>	KJ722771
29	<i>Lactobacillus brevis</i>	KJ722772
68	<i>Lactobacillus brevis</i>	KJ722773
40	<i>Lactobacillus plantarum</i>	KJ722780
63	<i>Lactobacillus brevis</i>	KJ722781
52	<i>Lactobacillus plantarum</i>	KJ722782
55	<i>Lactobacillus plantarum</i>	KJ722783
84	<i>Lactobacillus plantarum</i>	KJ722784
72	<i>Lactobacillus fermentum</i>	KJ722785

**Table 4**  
Correlation of variables to the factors of the PCA analysis based on factor loadings.

Variables	PC 1	PC 2	PC 3	PC 4
pH2	<b>0.625</b>	-0.155	<b>-0.644</b>	-0.137
Bile 1%	0.386	0.212	<b>0.736</b>	-0.259
Lysozyme 100 mcg/ml	<b>0.698</b>	-0.132	-0.043	-0.081
Oxibile	0.586	0.336	-0.082	-0.522
Cholic Acid	<b>0.712</b>	-0.091	0.063	0.165
Hexadecane	<b>0.715</b>	-0.530	0.215	-0.067
Autoaggregation 24 h	0.554	-0.513	0.337	0.079
<i>B. cereus</i>	0.595	-0.134	0.161	0.586
<i>S. aureus</i>	0.560	<b>0.738</b>	-0.186	0.072
<i>S. dysenteriae</i>	0.483	<b>0.739</b>	0.007	0.029
<i>Pseudomonas</i> sp.	0.000	0.000	0.000	0.000
Penicillin G	<b>0.634</b>	0.527	0.202	-0.023
Co-Trimoxazole	0.000	0.000	0.000	0.000
Vancomycin	0.485	0.046	-0.193	<b>0.611</b>
Ampicillin	0.540	-0.531	-0.178	-0.374
β-Galactosidase	<b>0.868</b>	-0.141	-0.142	-0.056

Values in bold within the same factor indicate the variable with the largest correlation.

sequences of *Lactobacillus brevis* while 40% isolates clustered with sequences of *Lactobacillus plantarum*, and only one isolate clustered with *Lactobacillus fermentum*. The GenBank accession numbers for the 16S rRNA gene sequence of isolates are given in Table 3.

### 3.5. Production of fermented milk

Isolate 84 (*Lactobacillus plantarum* KJ722784) was used for the preparation of milk based fermented probiotic drink. The isolate 84 and reference strain P1 grew well on sterilized milk and their count reached 8.68 log CFU/ml and 8.83 log CFU/ml, respectively after 24 h of fermentation at 30 °C (Fig. 4). During the fermentation process gradual decrease in pH was observed and after fermentation pH of sample inoculated with isolate 84 and strain P1 was 4.62 and 4.46, respectively. However, a change in the viable count of isolate during 28 day of storage at 4 °C was found. Isolate 84 and strain P1 revealed 0.98 log CFU/ml and 0.93 log CFU/ml reduction in viability during the 28 d of storage. pH of fermented milk continued to decrease and reached 4.3 (isolate 84) and 4.24 (P1) on 28 d of

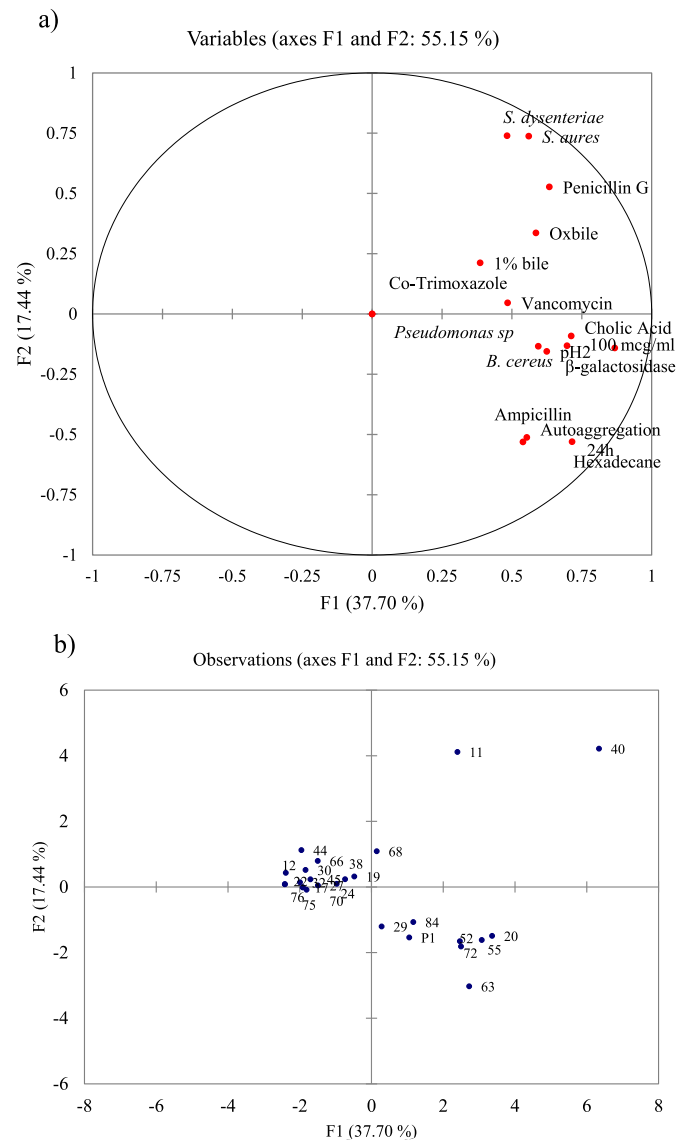


**Fig. 2.** (a). Projection of the variables on the plane formed by PC1 and PC2 analyzed by principal component analysis. (b). Projection of the LAB isolates and reference strain *L. casei* Shirota (P1) in the space of PC1 and PC2.

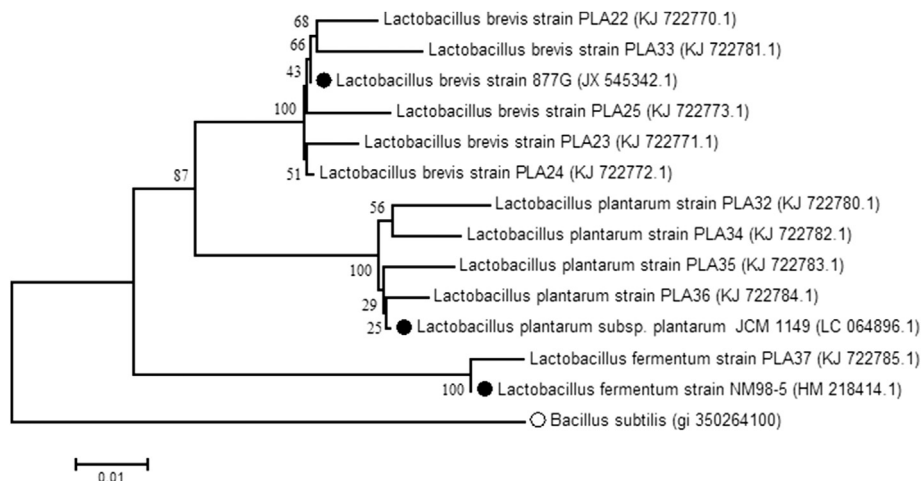


**Fig. 3.** Neighbor joining phylogenetic tree based on 16S rDNA sequences. Numbers in parentheses are accession numbers of published sequences. Filled circles are the reference strains from NCBI and empty circle is the out group used for tree construction.

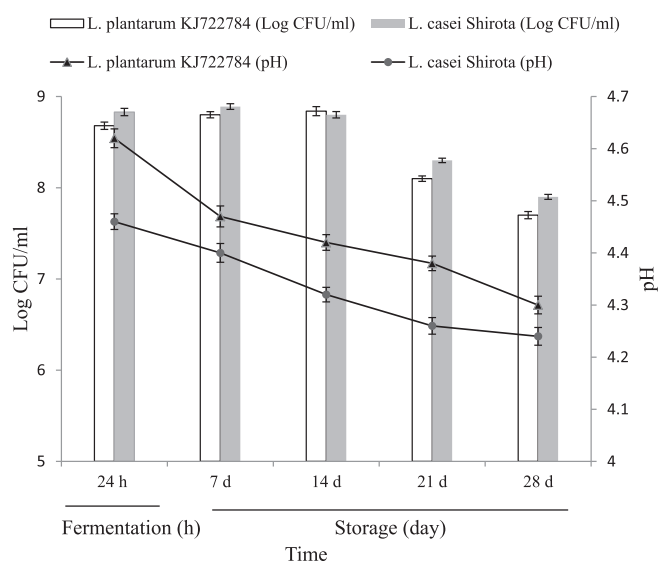


**Fig. 4.** pH and viable count of *Lactobacillus plantarum* (KJ722784) and reference strain *Lactobacillus casei* Shirota during milk fermentation (24 h at 37 °C) and cold storage (28 days at 4 °C). Error bars are standard deviations with respect to the mean values of triplicate analyses.

storage.

#### 4. Discussion

In this paper, significant effort has been made to select lactic acid bacteria originating from the indigenous Ladakhi fermented products on the basis of the most important technological criteria in order to obtain probiotic lactic acid bacteria. Indeed, it is worthwhile to isolate and identify probiotic strain from fermented products as they are safe and cause various health benefits.

Microorganisms to be applied as probiotic must overcome the inhospitable condition of human gastrointestinal tract (GIT) and subsequently colonize the intestinal tract. In order to reach active and viable enough through GIT, they should be resistant to acid, lysozyme and bile. Acid tolerance of bacteria is important not only for withstanding gastric stresses, but it also enables the strain to survive for longer periods in high acid carrier foods, such as yogurt,

without reduction in their number (Wang, Lin, Ng, & Shyu, 2010). The *in vitro* low pH tolerance study revealed that several isolates at pH 3 showed equal percent of viability as compared to pH 7 (control). However, incubation at pH 2 resulted in significant decrease in the survival rate of all LAB isolates. These results are in agreement with the finding of Guo et al. (2010). They reported that the viable counts of all lactic acid bacteria were significantly affected by the low acidity, especially at pH 2. Corcoran, Stanton, Fitzgerald, and Ross (2005) reported that resistance to low pH by *Lactobacillus* is due to the presence of F<sub>0</sub>F<sub>1</sub>-ATPase activity. Bile salts are toxic for living cells and bile salt tolerance is considered one of the essential properties required for lactic acid bacteria to survive in the small intestine (Succi et al., 2005). In this study, most of the isolates showed resistance to 0.5% bile concentration. But at 1% bile salt only isolate 40 demonstrated full tolerance. This decrease in viability caused by bile salts is implicated with its effect on cell membrane of the microorganisms (Papamanoli, Tzanetakis, Litopoulou-Tzanetaki, & Kotzekidou, 2003). The variation in bile sensitivity observed in this study is consistent with many previous reports (Jacobsen et al. 1999; Maldonado, de-Ruiz, Otero, Sesma, & Nader-Macias, 2012; Mishra & Prasad, 2005).

Another important property of probiotic is its hypocholesterolemic effect on host, however it is not essential but one of the desired quality/character of the probiotic strain. We found that overall cholesterol removal was highest in cholic acid and least in sodium taurocholate. The decrease in cholesterol suggests that a significant amount of cholesterol in the medium precipitated after addition of deconjugated bile acids (cholic acid). No or very little precipitation of cholesterol was observed in the presence of conjugated bile acids sodium taurocholate. This coprecipitation effect of cholesterol and deconjugated bile acids *vis-a-vis* reduction in cholesterol level has been reported in *Lactobacilli* and *Bifidobacterium bifidum* (Klaver & van der Meer, 1993) and *L. fermentum* KC5b (Pereira, McCartney, & Gibson, 2003).

LAB exerts their health promoting effects by several mechanisms. The property of adherence to intestinal epithelial cell is one of the mechanisms which involved different type of interaction. Several workers have reported that hydrophobicity (Botes, Loos, van Reenen, & Dicks, 2008; Duary, Rajput, Batish, & Grover, 2011) and aggregation ability (Collado et al., 2008; Jankovic, Frece, Abram, & Gobin, 2012) are correlated to cell adherence properties. With this regard, LAB isolates were examined for degree of hydrophobicity and autoaggregation ability. In our study, LAB isolates

showed wide differences in their hydrophobicity and isolates viz. 20, 63 and 72 demonstrated higher hydrophobicity toward n-hexadecane. This suggest that the complexity of the cell surface mosaic resulting from hydrophobic and hydrophilic appendages and other macromolecule components might give rise to differential hydrophobicity toward hydrocarbons. Mishra and Prasad (2005) reported that the strain NCDC17 had maximum hydrophobicity towards hexadecane while NCDC19 possesses maximum hydrophobicity for octane. In another study of assessing the adhesion of faecal isolates, *L. plantarum* Lp91 showed maximum percentage hydrophobicity for n-hexadecane and toluene which was followed by *L. plantarum* Lp9 (Duary et al., 2011). As far as aggregation is concerned, all the isolates in the present study exhibited some degree of autoaggregation. Although, autoaggregation ability was enhanced with time and was higher at 24 h of incubation than at 3 h. It can be explained that aggregation promoting factors increase self-aggregation with incubation (Goh & Klaenhammer, 2010). Similar finding was also reported by Dias, Duarte, and Schwan (2013), that the autoaggregation ability of *L. plantarum* strains improved with the increase in time of incubation.

Other important characteristics require to be screened progressively for selection of probiotic is the absence of undesirable properties (virulence factors and transmissible antibiotic resistances) and safety aspect of probiotic isolates. In this regard, the antibiotic resistance, antimicrobial activity and haemolytic activity of the isolates were assessed. Furthermore,  $\beta$ -galactosidase activity and exopolysaccharide production were also studied.

Multivariate data analysis was used for the selection of most promising probiotic potential isolates with respect to technological activities assayed. The most potential probiotic isolate was isolates 20, 52, 55 and 72 as they exhibited survival at pH 2, lysozyme (100 mcg/ml), cholesterol removal (cholic acid), antagonistic activity against *B. cereus* and  $\beta$ -galactosidase activity while isolate 63 showed autoaggregation ability (24 h), hydrophobicity and resistant toward ampicillin. However, isolate 84 provide an interesting perspective as it demonstrated same trend as reference strain and selected for the production of milk based probiotic product.

The last parameter of this study was development of milk based probiotic product presupposes the application of probiotic lactic acid bacteria which not only grows in milk but also show survival in acidic fermented milk. Meanwhile, the extent of health benefit on consumption of fermented milk containing probiotic depends upon the high viability of the probiotic microorganisms. In our study, *L. plantarum* KJ722784 was selected for the production of milk based probiotic product after its extensive characterization. The viable cell counts of *L. plantarum* KJ722784 showed decrease over the storage period, but its viable cell numbers in fermented milk remained above the legal requirement of 6 log CFU/ml to exhibit health benefit. Similar result of fermented milk containing probiotic was reported by Yerlikaya, Ender, Torunoglu, and Akbulut (2013).

## 5. Conclusions

The emerging demand for the products having health benefits beyond nutrition has provided ample opportunity to explore relatively unexplored foods and beverages for isolation of lactic acid bacteria for their potential role in probiotic research. Traditional fermented foods and beverages of Ladakh region of India have been explored for isolation of lactic acid bacteria to be used as probiotic. A promising isolate, *L. plantarum* KJ722784 having good probiotic traits has been identified as favorable candidate for the production of probiotic products. These isolates were originated from fermented products and considered safe for consumption, thus traditional foods can serve as potential source of lactic acid bacteria

to be used as probiotic. Additionally, these foods and beverages can be proposed as delivery vehicle for probiotics, leading to increased demand of these traditional foods which indirectly lead to improvement of rural economy.

## Acknowledgment

The present study was supported by Department of Biotechnology (DBT), Ministry of Science and Technology, Government of India (Grant No. DBT/JRF/14/FIN/503) and University Grants Commission, New Delhi (Grant No. F. 15-13/12 (SA-II)). The authors are thankful to Dr. R. B. Srivastava, Director, DIHAR, DRDO, Leh-Ladakh, and Dr. Tsering Stobdan, Horticulture Division, DIHAR, DRDO, Leh-Ladakh for giving permission and providing facilities to do part of research work in their Laboratory.

## References

- Angchok, D., Dwivedi, S. K., & Ahmed, Z. (2009). Traditional foods and beverages of Ladakh. *Indian Journal Traditional Knowledge*, 8(4), 551–558.
- Angmo, K., & Bhalla, T. C. (2014). Preparation of *Phabs* – an indigenous starter culture for production of traditional alcoholic beverage, *Chhang*, in Ladakh. *Indian Journal Traditional Knowledge*, 13(2), 347–351.
- Botes, M., Loos, B., van Reenen, C. A., & Dicks, L. M. T. (2008). Adhesion of the probiotic strains *Enterococcus mundtii* ST4SA and *Lactobacillus plantarum* 423 to Caco-2 cells under conditions simulating the intestinal tract, and in the presence of antibiotics and anti-inflammatory medicaments. *Archives of Microbiology*, 190, 573–584.
- Chiu, C. H., Lu, T. Y., Tseng, Y. Y., & Pan, T. M. (2006). The effects of *Lactobacillus*-fermented milk on lipid metabolism in hamsters fed on high-cholesterol diet. *Applied Microbiology and Biotechnology*, 71(2), 238–245.
- Collado, M. C., Meriluoto, J., & Salminen, S. (2008). Adhesion and aggregation properties of probiotic and pathogen strains. *European Food Research and Technology*, 226(5), 1065–1073.
- Corcoran, B. M., Stanton, C., Fitzgerald, G. F., & Ross, R. P. (2005). Survival of *Lactobacilli* in acidic environments is enhanced in the presence of metabolizable sugars. *Applied and Environmental Microbiology*, 71, 3060–3067.
- Dias, F. S., Duarte, W. F., & Schwan, R. F. (2013). Evaluation of adhesive properties of presumptive probiotic *Lactobacillus plantarum* strains. *Bioscience Journal*, 29(1), 1678–1686.
- Duary, R. K., Rajput, Y. S., Batish, V. K., & Grover, S. (2011). Assessing the adhesion of putative indigenous probiotic *lactobacilli* to human colonic epithelial cells. *Indian Journal of Medical Research*, 134, 664–671.
- FAO/WHO. (2006). *Probiotics in food, health and nutritional properties and guidelines for evaluation*. FAO Food and Nutritional Paper. No. 85 (Rome:WHO/FAO).
- Goh, Y. J., & Klaenhammer, T. R. (2010). Functional roles of aggregation promoting like factor in stress tolerance and adherence of *Lactobacillus acidophilus* NCFM. *Applied and Environmental Microbiology*, 76(15), 5005–5012.
- Guo, X. H., Kim, J. M., Namb, H. M., Park, S. Y., & Kim, J. M. (2010). Screening lactic acid bacteria from swine origins for multistrain probiotics based on *in vitro* functional properties. *Anaerobe*, 16(4), 321–326.
- Jacobsen, C. N., Rosenfeldt-Nielsen, V., Hayford, A. E., Moller, P. L., Michaelsen, K. F., Paerregaard, A. ... Jakobsen, M. (1999). Screening of probiotic activities of forty-seven strains of *Lactobacillus* spp. by *in vitro* techniques and evaluation of the colonization ability of five selected strains in humans. *Applied and Environmental Microbiology*, 65(11), 4949–4956.
- Jankovic, T., Frece, J., Abram, M., & Gobin, I. (2012). Aggregation ability of potential probiotic *Lactobacillus plantarum* strains. *International Journal of Sanitary Engineering Research*, 6, 19–24.
- Klaver, F. A., & van der Meer, R. (1993). The assumed assimilation of cholesterol by *Lactobacilli* and *Bifidobacterium bifidum* is due to their bile salt-deconjugating activity. *Applied and Environmental Microbiology*, 59(4), 1120–1124.
- Lahtinen, T., Malinen, E., Koort, J. M. K., Mertaniemi-Hannus, U., Hankimo, T., Karikoski, N. ... Palva, A. (2010). Probiotic properties of *Lactobacillus* isolates originating from porcine intestine and feces. *Anaerobe*, 16, 293–300.
- Liong, M. T., & Shah, N. P. (2005). Acid and Bile tolerance and cholesterol removal ability of *Lactobacilli* strains. *Journal of Dairy Science*, 88(1), 55–66.
- Maldonado, N. C., de-Ruiz, C. S., Otero, M. C., Sesma, F., & Nader-Macias, M. E. (2012). Lactic acid bacteria isolated from young calves – characterization and potential as probiotics. *Research in Veterinary Science*, 92(2), 342–349.
- Mishra, V., & Prasad, D. N. (2005). Application of *in vitro* methods for selection of *Lactobacillus casei* strains as potential probiotics. *International Journal of Food Microbiology*, 103(1), 109–115.
- Nur, Y. Z., & Aslim, B. (2010). Assessment of potential probiotic and starter properties of *Pediococcus* spp. isolated from Turkish-type fermented sausages (sucuk). *Journal of Microbiology Biotechnology*, 20, 161–168.
- Papamanoli, E., Tzanetakis, N., Litopoulou-Tzanetaki, E., & Kotzekidou, P. (2003). Characterization of lactic acid bacteria isolated from a Greek dry-fermented sausage in respect of their technological and probiotic properties. *Meat*

- Science, 65, 859–867.
- Pereira, D. I. A., McCartney, A. L., & Gibson, G. R. (2003). An *in vitro* study of probiotic potential of a bile salt hydrolyzing *Lactobacillus fermentum* strain and determination of its cholesterol lowering properties. *Applied and Environmental Microbiology*, 69(8), 4743–4752.
- Reid, G., Jass, J., Sebulsky, M. T., & McCormick, J. K. (2003). Potential use of probiotics in clinical practice. *Clinical Microbiology Reviews*, 16, 658–672.
- Saitou, N., & Nei, M. (1987). The neighbor-joining method: a new method for reconstructing phylogenetic trees. *Molecular Biology and Evolution*, 4, 406–425.
- Succi, M., Tremonte, P., Reale, A., Sorrentino, E., Grazia, L., Pacifico, S., ... (2005). Bile salt and acid tolerance of *Lactobacillus rhamnosus* strains isolated from Parmigiano Reggiano cheese. *FEMS Microbiology Letters*, 244(1), 129–137.
- Tamura, K., Peterson, D., Peterson, N., Stecher, G., Nei, M., & Kumar, S. (2011). MEGA5: molecular evolutionary genetics analysis using maximum likelihood, evolutionary distance, and maximum parsimony methods. *Molecular Biology and Evolution*, 28, 2731–2739.
- Tannock, G. W. (1997). Probiotic properties of lactic-acid bacteria: plenty of scope for fundamental R & D. *Trends in Biotechnology*, 15(7), 270–274.
- Vinderola, C. G., & Reinheimer, J. A. (2003). Lactic acid starter and probiotic bacteria: a comparative “in vitro” study of probiotic characteristics and biological barrier resistance. *Food Research International*, 36(9–10), 895–904.
- Vizoso-Pinto, M. G., Franz, C. M. A. P., Schillinger, U., & Holzapfel, W. H. (2006). *Lactobacillus* spp. with *in vitro* probiotic properties of human faeces and traditional fermented products. *International Journal of Food Microbiology*, 109(3), 205–214.
- Wang, C. Y., Lin, P. R., Ng, C. C., & Shyu, Y. T. (2010). Probiotic properties of *Lactobacillus* strains isolated from the feces of breast-fed infants and Taiwanese pickled cabbage. *Anaerobe*, 16, 578–585.
- Yerlikaya, O., Ender, G., Torunoglu, F., & Akbulut, N. (2013). Production of probiotic milk drink containing *Lactobacillus acidophilus*, *Bifidobacterium animalis* subsp. *lactis* and *Lactobacillus casei*. *Agro Food Industry Hi-Tech*, 24(2), 49–52.
- Yu, Z., Zhang, X., Li, S., Li, C., Li, D., & Yang, Z. (2013). Evaluation of probiotic properties of *Lactobacillus plantarum* strains isolated from Chinese sauerkraut. *World Journal of Microbiology and Biotechnology*, 29(3), 489–498.



## Microencapsulation of nisin in alginate beads by vibrating technology: Preliminary investigation



Diamante Maresca, Annachiara De Prisco, Antonietta La Storia, Teresa Cirillo, Francesco Esposito, Gianluigi Mauriello\*

Department of Agricultural Science, University of Naples Federico II, via Università 100, 80055 Portici, Naples, Italy

### ARTICLE INFO

#### Article history:

Received 17 June 2015

Received in revised form

19 October 2015

Accepted 25 October 2015

Available online 29 October 2015

#### Keywords:

Alginate

Active microcapsule units

Biopreservative

Bacteriocin

### ABSTRACT

Nisin is an antimicrobial peptide widely used as natural food preservative. Unfortunately, some factors lead to a reduction in its antimicrobial activity in food matrices. In this work nisin was microencapsulated in alginate matrix by vibrating technology with a high efficiency (75%) and microcapsules were characterized by having homogeneity in shape and surface morphology. Antimicrobial activity of microcapsules was evaluated against *Brochothrix thermosphacta* 7R1 immediately after microencapsulation process and during storage (24, 48, 72, 120, 144 and 168 h) under different conditions (i.e. 4 and 20 °C, pH 2.5, 4.5 and 6.0). We proposed a new method to evaluate the residual activity of encapsulated antimicrobial substances measured in Active Microcapsule Units per ml (AMU/ml). The test revealed that during a storage at 4 °C and pH 6.0, microcapsules retained their antimicrobial activity better than under other tested storage conditions. Furthermore, microcapsules efficiently protected nisin from the activity of protease. Resting cell experiments for the determination of antimicrobial activity of microcapsules during 120 h of storage under several conditions indicated greater activity at pH 6.0 with stirring. Nisin release from microcapsules determined by HPLC analysis showed that no trace of nisin was detected in the storage solution.

© 2015 Elsevier Ltd. All rights reserved.

### 1. Introduction

Natural antimicrobial compounds are widely applied as food preservatives to improve microbiological safety, quality and to extend the shelf-life of food products (Tiwari et al., 2009). A great number of natural compounds are attracting increased interest from researchers and food industry for their potential role as antimicrobial agents against spoilage and pathogenic microorganisms. Several bacteriocins from lactic acid bacteria (LAB) have a great potential application as “food-grade antimicrobials” and their use in various foods could be a safe alternative to the chemical preservatives widely utilized (García, Rodríguez, Rodríguez, & Martínez, 2010). Nisin is the only bacteriocin recognized as safe by FAO/WHO and Expert Committee on Food Additives and that can be used as preservative in meat, dairy products and vegetables. Nisin is a small (3353 Da) cationic polypeptide produced by several strains of *Lactococcus lactis* subsp. *lactis* and belonging to the Class I

bacteriocins, called lantibiotics (Cheigh & Pyun, 2005). It is primarily active against Gram-positive pathogenic and spoilage bacteria including food-borne pathogens such as *Clostridium botulinum* and *Listeria monocytogenes* (Field, Conno, Cotter, Hill, & Ross, 2008). Despite the large use of nisin in the food industry, a loss of antimicrobial efficacy has been demonstrated when it is incorporated in food matrices (Chi-Zhang, Yam, & Chikindas, 2004). Bacteriocins could be subjected to a rapid inactivation by binding to food components such as proteins and lipids, or degradation by proteolytic enzymes, resulting in reduced availability to act against microorganisms in food matrices (De Arauz, Jozala, Mazzola, & Vessoni Penna, 2009). It was shown that *Streptococcus thermophilus*, *Lactobacillus plantarum* and certain *Bacillus* species could produce the enzyme “nisinase”, which neutralizes the antimicrobial activity of this peptide (European Food Safety Authority, 2006). Furthermore, its ineffectiveness in food products has been attributed to poor solubility, high bacterial loads, interaction with phospholipids and non homogeneous distribution throughout the product (Galvez, Abriouel, López, & Omar, 2007). Encapsulation is a promising technology to preserve bioactive compounds from inactivation by food components as above reported. It is proposed

\* Corresponding author.

E-mail address: [giamauri@unina.it](mailto:giamauri@unina.it) (G. Mauriello).

as an effective delivery system to enhance biological activity and stability of active ingredients in foods and achieve controlled release over time. Some authors have previously described the microencapsulation of nisin using different matrices and different technologies (Huq, Riedl, Bouchard, Salmieri, & Lacroix, 2014; Khaksar et al., 2014; Narsaiah, Jha, Wilson, Mandage, & Manikantan, 2012; Xiao, Davidson, & Zhong, 2011; Xiao & Zhong, 2011). However, to the extent of our knowledge no previous works described the microencapsulation of bacteriocins by using the vibrating technology. It is a fairly new technique and its evolution during the time has been described in our previous report (De Prisco, Maresca, Ongeng, & Mauriello, 2015). Furthermore, principles, pros and cons of vibrating technology are well reported by Whelehan and Marison (2011). Undoubtedly, the main advantage of vibrating technology with respect to other techniques is the production of very regular in size and homogeneous microparticles.

An important step in the microencapsulation process is the selection of appropriate encapsulating materials. The polymers should be chemically compatible, non-reactive with the component to encapsulate and provide the desired coating properties such as strength, flexibility, impermeability and stability. Several natural polymers like alginate, pectins, guar gums or chitosan have been proposed in many foods and pharmaceutical applications. However, alginate is one of the most widely used materials for microencapsulation of many bioactive compounds. It is a food grade, cheap and biocompatible polysaccharide obtained mainly from marine algae and some bacteria (Pawar & Edgar, 2012). Due to its structure, composed of alternating block of 1,4-linked  $\alpha$ -L-guluronic acid (G) and  $\beta$ -D-mannuronic acid (M) residues, alginates form ionic hydrogels by cross-linking between the carboxylate anions of guluronic acid and divalent cations (Zarate et al., 2011). The aim of this study was to validate the vibrating technology to microencapsulate nisin in Ca-alginate matrix and to investigate the biological activity of microencapsulated nisin and its release from microcapsules. Moreover, the resistance of microencapsulated nisin towards proteolytic enzymes action was demonstrated.

## 2. Materials and methods

### 2.1. Bacterial strain and culture conditions

*Brochothrix thermosphacta* 7R1 was used as an indicator strain in the nisin bioactivity assay. It was provided by Department of Agriculture, Division of Microbiology, University of Naples Federico II. Previously isolated from fresh meat (Russo, Ercolini, Mauriello, & Villani, 2006), it was routinely cultured in Tryptone Soya Broth (TSB) supplemented with 5 g/L Yeast Extract Powder at 20 °C for 24 h. For nisin activity detection the strain was seeded in TSB agar (TSBA; TSB with addition of 7.5 g/L agar and 5 g/L Yeast Extract Powder). All media were purchased from Oxoid (Oxoid S.p.A., Milan, Italy).

### 2.2. Preparation of nisin

Bacteriocin to be microencapsulated was obtained as described in Mauriello, De Luca, La Storia, Villani, and Ercolini (2005) with some modifications. Briefly, 1.1 g of Nisin (Sigma, 2.5% of nisin) were dissolved in 10 ml of 0.02 mol/L HCl (Merck, Vimodrone, Italy) and centrifuged at 5200 g for 10 min. Pellet was treated in the same way twice and all supernatants from each round of centrifugation were mixed in a single solution. It represents the nisin solution (Nis) routinely stored at 4 °C and further used for microcapsules production.

### 2.3. Microencapsulation process

Microencapsulation of Nis was carried out by using the Encapsulator B-395 Pro (BUCHI, Switzerland) equipped with an 80  $\mu$ m nozzle and the syringe pump. A scheme of the Buchi Encapsulator is reported in De Prisco et al. (2015). The feeding solution was prepared mixing 5 ml of Nis in 20 ml of a 16 g/L alginic acid sodium salt (Sigma) solution previously degassed and sterilized by autoclaving at 121 °C for 15 min. This mixture was loaded in the syringe and forced into the pulsation chamber to be further extruded through a nozzle. The microencapsulation conditions used were: flow rate 2.91 ml/min, vibration frequency 2000 Hz, electrode voltage of 950 V. These conditions were chosen on the basis of results obtained in preliminary experiments carried out with different usage conditions of the equipment. Microcapsules containing nisin were obtained by hardening of the droplets in 100 ml of a sterile 0.5 mol/L CaCl<sub>2</sub> solution at pH 6.0 (hardening solution) continuously stirred at 300 rpm. The process was performed maintaining the hardening solution both at 4 and 20 °C to evaluate the effect of different temperatures during hardening. Suspension was recovered in batch and stored at 4 °C and 20 °C until the sedimentation of microcapsules. Finally, hardening solution was discarded to obtain a final volume of 30 ml of microcapsules. Residual nisin in the hardening solution was detected by agar diffusion assay and HPLC as described below.

### 2.4. Morphology of microcapsules

Size and surface microcapsule morphology were examined using both a Zeiss light microscope ( $\times$ 200 magnification and calibrated micrometer) and an Evo 40 Zeiss scanning electron microscope (SEM). Microcapsules from each encapsulation trial were analyzed immediately after the process and after 0 and 7 days of storage in quarter strength Ringer solution (Ringer) at 4 °C and 20 °C. For SEM analysis, microcapsules were initially rinsed three times with MilliQ water (Lichrosolv water for Chromatography) and then 10  $\mu$ l of each sample were placed on a pin type SEM specimen mount and maintained at 45 °C for 2 h in order to achieve a gentle dehydration of the microcapsules and their fixing. All samples were sputter treated in a metallizer (Agar Sputter Coater) with gold palladium to reach a thickness of coating of 100 Å and then observed by SEM in high vacuum mode (EHT, 20.00 kV).

### 2.5. Microcapsules staining

Microcapsules were stained with fluorescein isothiocyanate (FITC) as follows: 10 mg of FITC (Sigma) previously dissolved in 2 ml of Tris-HCl (BoehringerMannheim GmbH) were added to 500  $\mu$ l of microcapsules. This solution was stirred at 250 rpm for 2 h. After this time the sample was washed three times with 20 ml of isopropanol (Merck) and incubated for 24 h at room temperature. Similarly, the staining of free nisin and of empty microcapsules was carried out as control. Samples were observed by Nikon Eclipse E400 epifluorescence microscope (Nikon, Tokyo, Japan) equipped with an UV lamp and a  $\times$ 40 magnification objective. Images were captured by a Nikon Coolpix 4500 Digital Camera equipped with a microscope adapter.

### 2.6. Antimicrobial activity of free nisin solutions

Free nisin solutions were tested against *B. thermosphacta* 7R1 by an agar diffusion and critical dilution assay as described by Villani et al. (1994). Briefly, serial two-fold dilutions of bacteriocin in 0.02 mol/L HCl were prepared and 10  $\mu$ l of each dilution were spotted onto TSBA seeded with 25  $\mu$ l/ml of an overnight culture of

the indicator strain. After incubation at optimal conditions, the arbitrary units per ml (AU/ml) of bacteriocin solution were calculated as the reciprocal value of the highest dilution that gives a clear growth inhibition of the indicator strain.

### 2.7. Antimicrobial activity of microencapsulated nisin

Antimicrobial activity of encapsulated nisin was investigated in two different ways. In the first case microcapsules were disrupted by exposition to an equal volume of a 0.1 mol/L phosphate buffer solution at pH 8.8 and stirred at 200 rpm until complete alginate dissolution. Disruption of microcapsules was confirmed by microscopic observation and dissolved microcapsules were analyzed as above described for free nisin solutions. Accordingly, initial dilution 1:1 of microcapsules for their disgregation was taken into account for AU/ml calculation. This method was also used for calculation of the Encapsulation Efficiency (EE) as described below. In the other way microcapsules were tested in their whole form. They were ten fold serially diluted in Ringer and 1 ml of each dilution added in melted TSBA seeded with 25 µl/ml of an overnight culture of *B. thermosphacta* 7R1. Media was poured in Petri dishes and after an overnight incubation at 20 °C plates showed small growth inhibition haloes of the indicator strain, presumably in correspondence of nisin microcapsules. Each inhibition zone was interpreted as 1 Active Microcapsule Unit (AMU). Plates containing well isolated inhibition haloes (about 30–300 haloes) were counted and multiplied by the dilution factor, the result was expressed as Active Microcapsule Units per ml (AMU/ml). This method was used to evaluate the antimicrobial stability of microcapsules during storage as described below.

### 2.8. Evaluation of nisin concentration by HPLC

Detection of nisin was performed through HPLC system equipped with UV detector set at 220 nm. A C18 reversed-phase column (150 × 4.6 mm) was used and an isocratic elution was performed. Mobile phase was water:acetonitrile (70:30) containing 0.1% (v/v) trifluoroacetic acid. Before the analysis samples were filtered through a 0.22 µm cellulose filter. The calibration curve was determined by plotting peak area ratio against concentration using a standard solution of nisin (94.6% pure, donated by Aplin and Barret, Dorset, UK) with three replicate samples for each nisin concentration (5, 10, 20, 30, 40, and 50 ppm).  $R^2$  was equal to 0.998 and limit of detection (LOD) and limit of quantification (LOQ) were 1.40 mg/L and 4.20 mg/L, respectively. LOD was calculated as  $3.3 \times SD/S$  and LOQ as  $10 \times SD/S$ , where SD is the standard deviation of y-intercept of the calibration curve and S is the slope of the calibration curve.

### 2.9. Calculation of efficiency of microencapsulation process

The efficiency of microencapsulation process, Encapsulation Efficiency (EE), was defined as the percentage ratio between the nisin into the microcapsules and the amount of nisin in Nis. EE was calculated in terms of both protein content and residual antimicrobial activity. The amount of nisin was measured by using both HPLC and agar diffusion assay.

### 2.10. Enzymatic treatment of microcapsules

Protease treatment was carried out to evaluate the protective effect of calcium alginate microcapsules toward nisin. Briefly, 1 ml of whole or disrupted microcapsules were added to 500 µl of a 10 mg/ml protease solution (Protease from *Streptomyces griseus*, Sigma cod. P-5147) and incubated at 37 °C for 30 min. After incubation, all samples were ten fold serially diluted in Ringer and

plate-counted on TSBA seeded with 25 µl/ml of an overnight culture of indicator strain. Plates were incubated at optimal growth conditions and results were expressed as AMU/ml.

### 2.11. Residual activity of microcapsules during their storage under different conditions

Ten ml of microcapsules obtained at 4 and 20 °C were diluted 1:1 in Ringer at 4 °C and 20 °C and at different pH values (2.5, 4.5 and 6.0) adjusted with HCl 0.1 mol/L. Antimicrobial activity of microcapsules in terms of AMU/ml was evaluated at 0, 24, 48, 72, 120, 144 and 168 h. Furthermore, an aliquot of 1 ml of aqueous phase from each sample was collected after gentle mixing and used to evaluate the release of nisin during the time by both HPLC and agar diffusion assay.

### 2.12. Resting cell experiments

Nis, intact and disrupted microcapsules were added to a suspension of *B. thermosphacta* 7R1 in Ringer, adjusted at pH 4.5 and 6.0 with 0.1 M HCl to reach a nisin concentration of 50 µg/ml and a cell concentration of  $1 \times 10^4$  and  $1 \times 10^6$  CFU/ml. Solutions were analyzed immediately (time 0) and after incubation for 2, 4, 24, 48, 72 and 120 h at 4 °C both in static and stirring (1000 rpm) conditions. An aliquot of 1 ml of aqueous phase was collected at each time after gentle mixing and used for plate counting. A cell suspension without microcapsules was used as control.

### 2.13. Data analysis

Analyses were carried out in triplicate and all values were expressed as their means. A two-way Anova test and a t-test analysis (Microsoft Excel for Mac version 11.5) were performed to ascertain significant differences between averages; significance was declared at  $P < 0.05$ .

## 3. Results and discussion

### 3.1. Microscopic characterization of microcapsules

Image of microcapsules immediately after the microencapsulation process captured by using a light microscope is shown in Fig. 1. Image shows well-formed microcapsules, regular in shape and in size with an average diameter ± standard deviation of  $118 \pm 3$  µm. Microcapsules have a drop shape characterized by the presence of a small peduncle. This could be attributed to formation at the extrusion phase or at impact of alginate bead on the surface of hardening solution. According to our hypothesis, drop shape is molded during the alginate-nisin mixture extrusion and the phenomenon could be due to electrostatic interactions between nisin and alginate matrix, which prevent spherical drop formation. Furthermore, when a solution with a high surface tension is used, such as calcium chloride, the droplets can be held back briefly at the surface during entrance, resulting in the formation of non-spherical droplets, which are gelified before regaining their original shape (Whelehan & Marison, 2011). The hypothesis is confirmed by the fact that empty microcapsules showed spherical shape (data not shown).

In Fig. 2 are shown SEM images of microcapsules hardened at 4 °C (Fig. 2A) and 20 °C (Fig. 2B). As can be seen, both samples show homogeneous shape, rough surface and no apparent crack zones. Furthermore, a microcapsule's diameter smaller of that shown by light microscopy was observed; it could be reasonably a consequence of the preliminary drying treatment of samples for the SEM analysis. Therefore, no relevant morphological difference between

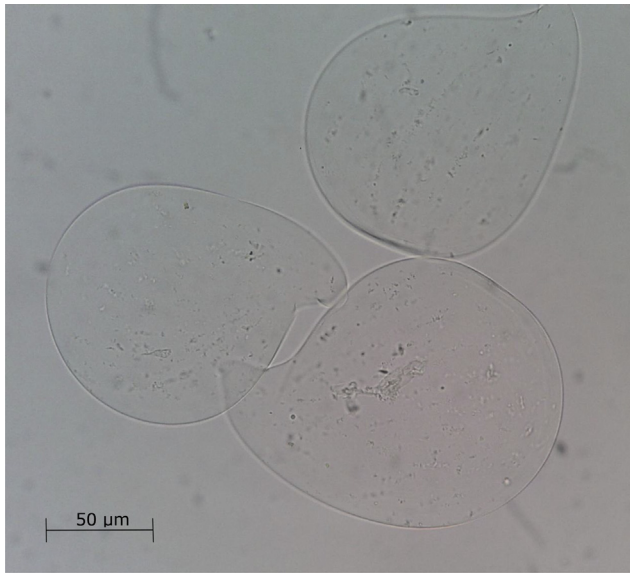


Fig. 1. Optical microscopy image of nisin microcapsules at  $\times 200$  magnification.

microcapsules hardened at two different temperatures was found. Microcapsules stored in Ringer, both at 4 °C and 20 °C, seem to retain their original morphological characteristics even after 7 days of storage (Fig. 2C and D). This result is interesting because other authors found rapid swelling and consequent degradation of Ca-

alginate microcapsules in salt solutions (Bajpai & Shubhra, 2004; Mørch, Donati, Strand, & Break, 2006). However, the conflicting results could be due to the different concentrations of alginate tested or to the interaction between alginate network and nisin, which could be involved in the stability of our microcapsules.

### 3.2. Staining of microcapsules with fluorescein isothiocyanate (FITC)

A fluorescence microscopy image of a sample stained with FITC is showed in Fig. 3. The image shows a uniformly green stained microcapsule containing nisin suggesting a uniform distribution of the bacteriocin. The isothiocyanate reactive groups of FITC bind to the primary amino groups of nisin allowing the viewing of the fluorescence at excitation and emission wavelengths of about 494 nm and 518 nm, respectively. On the other hand, empty microcapsules were not green stained (data not shown) confirming that only the protein is stained in the nisin loaded microcapsules. To the best of our knowledge no previous work describes the staining of encapsulated nisin with a fluorochrome. However, a similar approach was carried out by Kim et al. (2008), who encapsulated insulin with FITC to monitor the protein encapsulation process by using fluorescence microscopy.

### 3.3. Encapsulation efficiency (EE)

Parameters defined to evaluate the encapsulation efficiency (EE) and their values determined by using both HPLC and agar diffusion assay are summarized in Table 1. Nis showed a total content of nisin

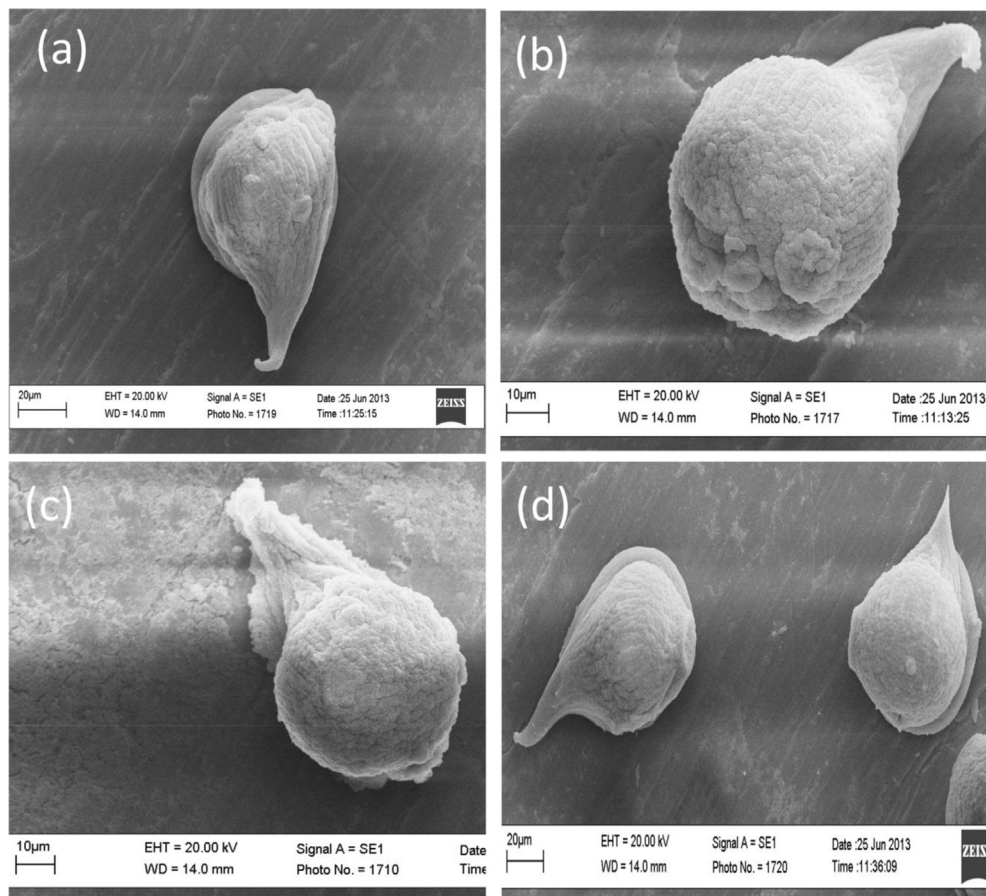
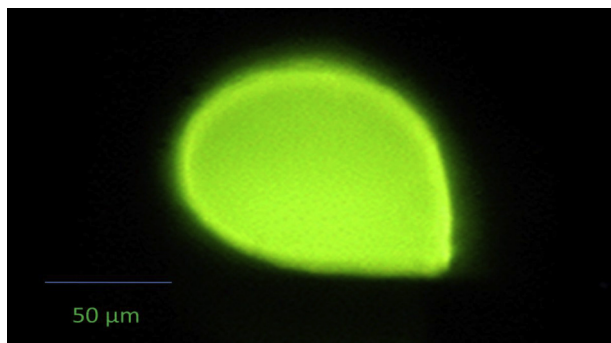


Fig. 2. SEM images of microcapsules hardened at 4 and 20 °C; immediately after production, (A) and (B), respectively, and over 7 days storage, (C) and (D), respectively.



**Fig. 3.** Fluorescence microscopy image at  $\times 400$  magnification of stained nisin with fluorescein isothiocyanate (FITC) in alginate microcapsule.

of 2.5 mg and a total activity of 128,000 AU while a low concentration and a low activity in both hardening solutions were detected. In particular, the nisin detected in the hardening solution at 4 °C was significantly lower ( $P < 0.05$ ) than that at 20 °C suggesting a higher protein retention during the process at lower temperature. Accordingly, [Dini, Islan, de Urraza, and Castro \(2012\)](#) reported that higher temperatures reduced gel matrix stability facilitating ion exchange and diffusion rate between microcapsules and media and determining a lower load of the product into the microcapsules. Because high viscosity of samples obtained after microcapsule disruption did not permit their loading in HPLC column, the total content of nisin in the microcapsules was estimated by subtracting the initial amount of that found in the hardening solution. Therefore, an EE of 76% at 4 °C and 71% at 20 °C was calculated. Interestingly, no difference in the antimicrobial activity of microcapsules between two temperatures used was found, leading to an EE in terms of activity of 75% in both conditions. Our results showed a marked improvement compared to the EE obtained by other authors ([Hosseini et al., 2014](#); [Khaksar et al., 2014](#); [Narsaiah et al., 2012](#); [Xiao et al., 2011](#)), who found lower values (35–60%) probably ascribable to the different technology and different matrix used. Furthermore, these authors probably underestimated the loaded nisin because they tested only the supernatant after

disruption of microcapsules. As a matter of fact, because the alginate is more negatively charged at higher pH ([Harnsilawat, Pongsawatmanit, & Mc Clements, 2006](#)), we supposed that in this condition  $\text{Na}^+$  of phosphate buffer is facilitated to substitute  $\text{Ca}^+$  ions of alginate network so promoting its disaggregation. Accordingly, our preliminary investigations showed that after microcapsule disruption at pH 4.0 and 7.0, the antimicrobial activity was retained both in supernatant and pellet (data not shown). Consequently, we carried out a microcapsule disruption at higher pH (i.e. pH 8.8, isoelectric point of nisin) to reach a complete dissolution of alginate. We hypothesize that at this pH both a complete dissolution of alginate network and a reduction of interaction between nisin and alginate were promoted and this facilitated bacteriocin release. Despite nisin hydrophilicity and the aqueous system in which the microencapsulation process is done, we obtained a satisfying result in terms of EE. High EE could be reasonably attributed to high affinity between polymeric matrix and active ingredient. In fact, at the pH of the feeding solution (i.e. pH 5.0) the net charge of alginate is negative, due to the anionic carboxylic groups, while that of the nisin is positive, due to the cationic amino groups. This situation could lead to a strong nisin–alginate complex formation, which could compete with the interaction between calcium ions and carboxylic residues of guluronic acid. The strong electrostatic interaction between nisin and alginate was also hypothesized by [Hosseini et al. \(2014\)](#), who corroborated their hypothesis by using Fourier-transform infrared analysis. Similarly, [Harnsilawat et al. \(2006\)](#) found strong interaction between  $\beta$ -lactoglobulin and sodium alginate.

#### 3.4. Antimicrobial activity of microcapsules during storage

In this work we propose a new method to evaluate the functional stability of microcapsules containing an antimicrobial substance. The basic idea is that the entrapped substance could lose antimicrobial activity inside the capsule or flow out from the capsule. In both cases the single microcapsule could lose or reduce its ability to inhibit the growth of microbial target. Accordingly, the method we propose in this work can show the loss of antimicrobial activity of microcapsules. In fact, well isolated inhibition halos of about  $0.1 \pm 0.02$  mm in diameter (like phage plaques), following microcapsules dilution and plating in the medium with the indicator strain, were visualized ([Fig. 4A](#)). We assumed that each halo is produced by a single microcapsule so allowing to estimate the number of microcapsules containing active nisin. In [Fig. 4B](#) is shown an image of widespread inhibition obtained with disrupted microcapsules. This result confirms that spot inhibition haloes of [Fig. 4A](#) are produced by microcapsules loaded with active nisin. Our results showed that microcapsule samples contained about  $10^5$  AMU/ml immediately after the microencapsulation process. Counting of AMU/ml performed at different times during storage at different conditions are reported in [Fig. 5](#). First of all it is interesting to observe that significant ( $P < 0.05$ ) differences were already registered at time 0 of the incubation period and a general reduction of AMU/ml according to the decrease of pH value was observed. Results show that the activity of microcapsules is very stable within 168 h of storage at 4 °C at both pH 6.0 and pH 4.5, in fact a reduction of less than 0.5 Log AMU/ml was recorded in these conditions. At pH 6.0 and 20 °C a dramatic reduction of activity starting from 72 h was observed. At pH 4.5 and 20 °C a significant ( $P < 0.05$ ) reduction was observed starting from 120 h of storage. Results of AMU/ml at pH 2.5 showed a reversed situation. In fact, a reduction of activity of about 1 Log AMU/ml was registered at 4 °C while a more stable trend was observed at 20 °C. Decrease of AMU/ml at higher temperature and higher pH is probably due to the efflux of nisin from microcapsules. However, we registered negative

**Table 1**

Nisin content along the microencapsulation process determined by HPLC analysis and agar diffusion assay.

HPLC analysis					
Samples		Parameters			
		Concentration	Volume	Total content	EE
		$\mu\text{g ml}^{-1}$	ml	mg	%
Nis		$500 \pm 0.7$	5	2.5	
Hardening solution	4 °C	$5.9 \pm 0.23$	100	0.59	
	20 °C	$7.2 \pm 0.10$	100	0.72	
Microcapsules	4 °C	n.d.	30	1.91 <sup>a</sup>	76
	20 °C	n.d.	30	1.78 <sup>a</sup>	71

Agar diffusion assay					
Samples		Parameters			
		Activity	Volume	Total activity	EE
		AU $\text{ml}^{-1}$	ml	AU	%
Nis		25,600	5	128,000	
Hardening solution	4 °C	100	100	10,000	
	20 °C	200	100	20,000	
Microcapsules	4 °C	3200	30	96,000	75
	20 °C	3200	30	96,000	75

n.d.: not determined.

<sup>a</sup> Calculated as difference between total content in Nis and hardening solution.

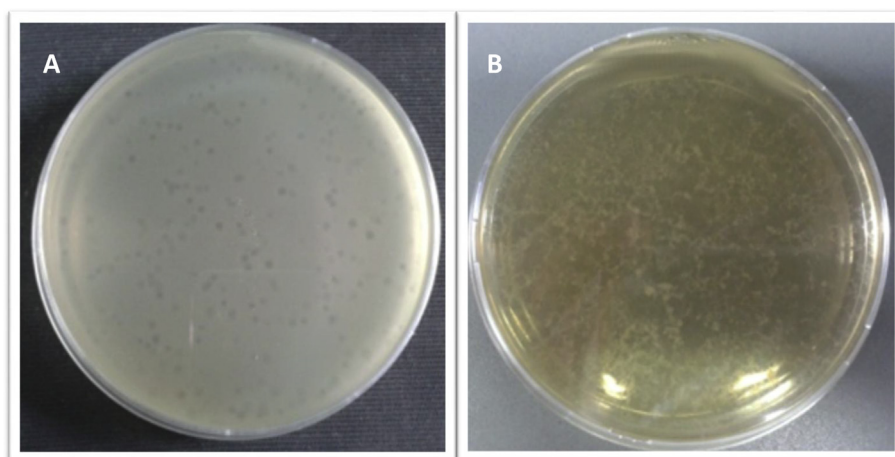


Fig. 4. Like-phage plaque and widespread growth inhibition of *Brochothrix thermosphacta* 7R1 in contact with intact (A) and disrupted (B) nisin microcapsules, respectively.

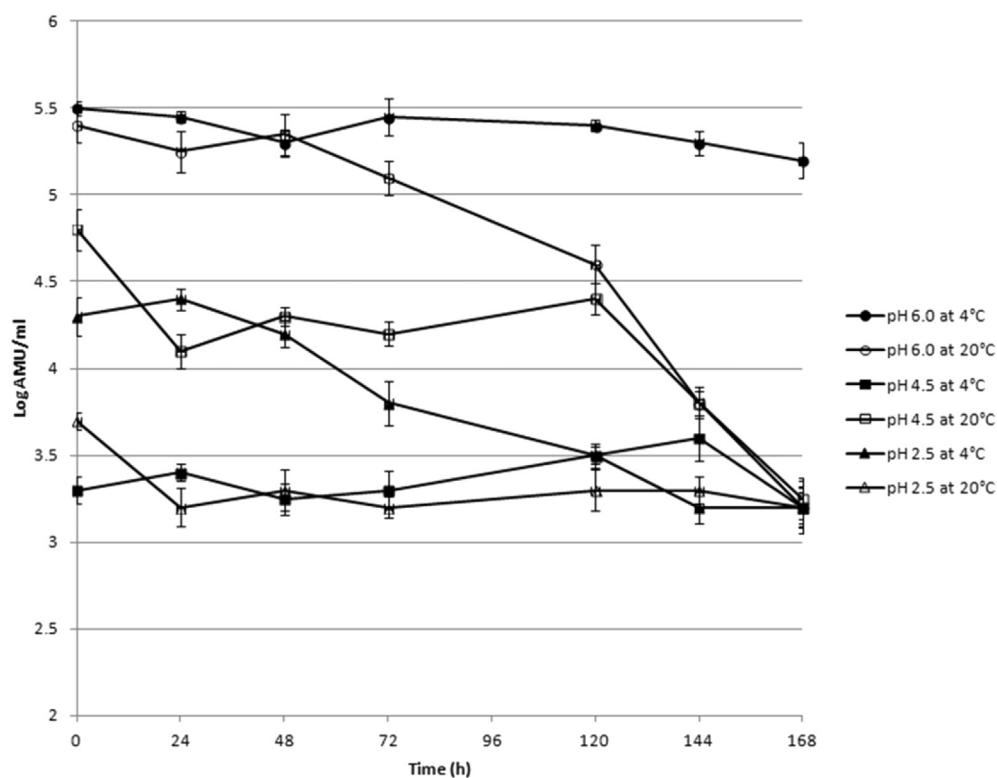


Fig. 5. Antimicrobial activity (Log AMU/ml) of nisin microcapsules during 168 h of storage under different conditions.

results when the supernatants were tested by HPLC and agar diffusion assay (data not shown). Hosseini et al. (2014) evaluated the nisin release from alginate capsules but unfortunately they did not take into account the pH condition of their experiments. In contrast with our findings, Xiao et al. (2011) reported a fast release of nisin from spray dried zein capsules at pH 2.0 compared to a sustained release at pH 6.0 and 8.0. Therefore, consistently with the chemical characteristics of the active peptide and its carrier, the retarded release could be explained by the electrostatic interactions that became stronger with increasing of pH value. Finally, we can also hypothesize that nisin does not flow from the capsules but change its activity according to pH condition. In particular, nisin solubility, and consequently its antimicrobial activity, is

compromised at pH higher than 5.5 (Liu & Hansen, 1990).

### 3.5. Protease treatment of microcapsules

Antimicrobial activity of microcapsules expressed in AMU/ml before and after protease treatment showed a significant difference ( $P < 0.05$ ) of 0.91 Log cycles. In fact, we registered a concentration of  $5.5 \pm 0.04$  and  $4.6 \pm 0.06$  Log AMU/ml before and after the enzyme treatment, respectively. On the contrary, when microcapsules were previously disrupted and then treated with protease, the antimicrobial activity totally disappeared. The protective effect of microcapsules toward nisin could be a consequence of the extensive cross-linking of alginate matrix, which inhibited the interaction

between nisin and the proteolytic enzyme. The protection against proteolytic enzymes could provide a possible technological advantage for delivery of nisin or other protease-sensitive molecules in food systems.

### 3.6. Resting cell experiments

Preliminary experiments showed that free nisin or disrupted microcapsules totally inactivated a population of  $10^5$  CFU/ml resting cells of *B. thermosphacta* 7R1 in about 1 h of contact (data not shown). On the contrary, bacterial population decreased more slowly when in contact with whole nisin microcapsules, according to the different tested settings (i.e. initial cell load, pH and static/stirring condition). Accordingly, viable counts of *B. thermosphacta* 7R1 resting cells during 120 h of contact with nisin microcapsules are reported in Fig. 6A and B for the two different initial cell loads,

respectively. In both experiments the bacterial population of control sample (without microcapsules) remained constant over the time. Results show that initial cell load affected the time needed to totally inactivate the bacterial population. In particular, unsurprisingly, shorter times were registered for the lower cell load. Both graphs show that the inactivation times of total population are sorted from shorter to longer according to the conditions pH 6.0/stirring; pH 4.5/stirring; pH 4.5/static; pH 6.0/static. It seems that pH 6.0/static is the condition in which the slower release of nisin occurs and generally the stirring reduces the time needed to reach the inactivation of bacterial population, compared to the static one. Probably, stirring promotes a faster release of nisin from alginate microcapsules and the subsequent contact between bacteriocin and cell target. Moreover, the results of pH 6.0/stirring and pH 4.5/stirring are very similar, both for  $10^4$  and  $10^6$  CFU/ml, showing a stronger influence of stirring condition with respect to pH level. On

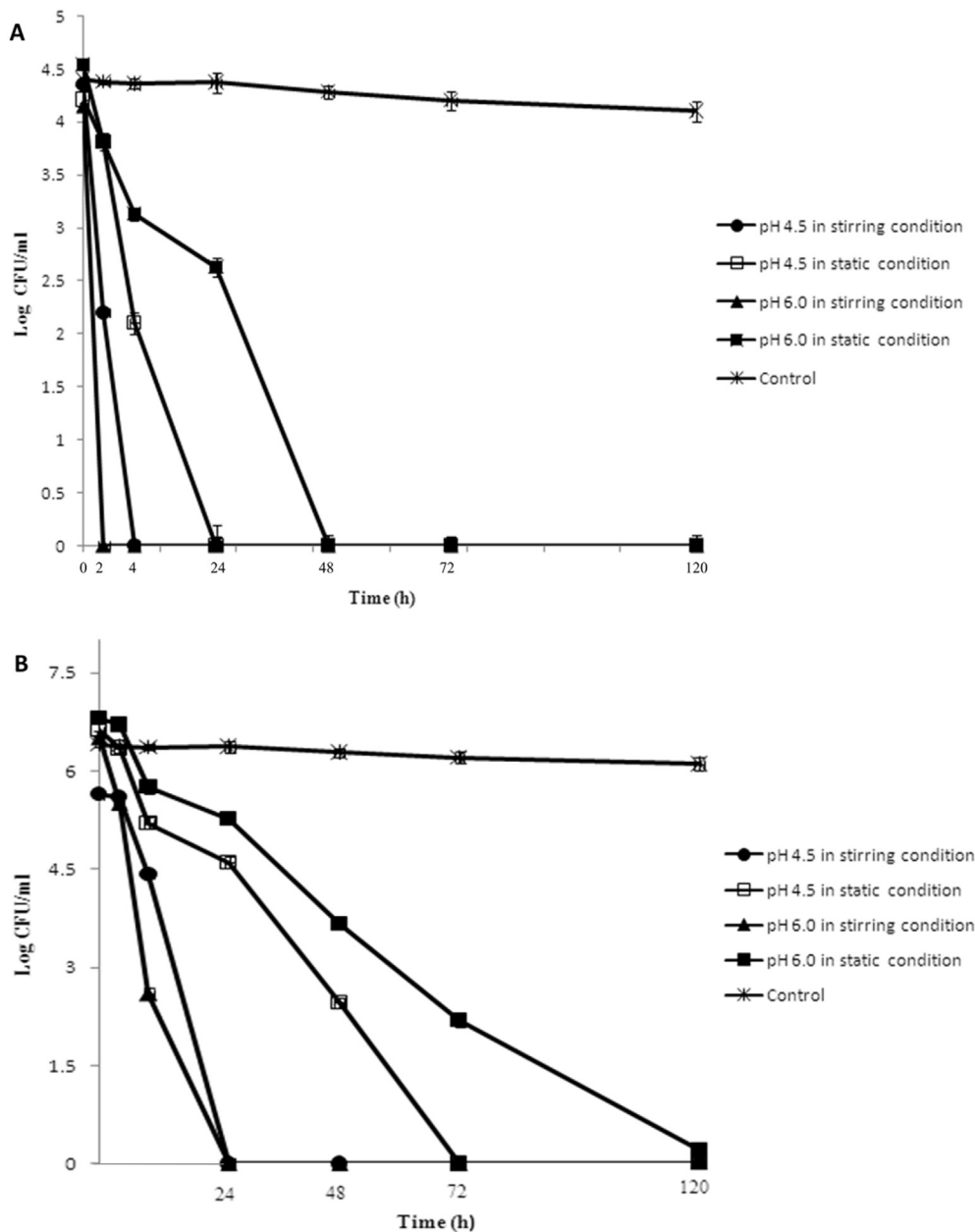


Fig. 6. Residual population (Log CFU/ml) of  $10^4$  (A) and  $10^6$  CFU/ml (B) resting cells of *Brochothrix thermosphacta* 7R1 in contact with nisin microcapsules for 120 h under different storage conditions.

the other hand, total reduction times of combination pH 4.5/static are drastically shorter than the combination pH 6.0/static, for both population levels, showing the relevant effect of pH level in static condition. It is well known that acidic pH enhances the antimicrobial activity of nisin because of its better solubility (Liu & Hansen, 1990). Our results give evidence that microencapsulation could be an effective method to obtain a prolonged bioavailability of entrapped substances. In fact, a slower release of nisin from microcapsules reduced the time of contact with some food components, which could be the reason of inactivation.

#### 4. Conclusion

Nisin was successfully microencapsulated in alginate matrix by vibrating technology as suggested by the results of encapsulation efficiency and retention capacity. Electron microscopy studies showed well-formed microcapsules, regular in shape and in size. Antimicrobial activity of each microcapsule against *B. thermosphacta* 7R1 was shown by the presence of phage plaques-like inhibition halos that called Active Microcapsule Units (AMU). Antimicrobial activity monitored during the storage of microcapsules at different conditions of temperature and pH simulating the different food environments was highly preserved at 4 °C and pH 4.5 and 6.0. The best antimicrobial performance of microcapsules was shown at pH 6.0 in stirring condition.

Alginate microcapsules were shown to protect nisin from protease, which minimally affected antimicrobial activity of bacteriocin only when this was encapsulated. Finally, to the extent of our findings, no traces of released nisin from microcapsules were detected. This study concluded that alginate microcapsules produced by vibrating technology could serve as valid system to improve nisin stability during its delivery in food matrices to overcome difficulties encountered with the use of free bacteriocin. Further research is needed to evaluate microcapsules activity in real food systems or in the developing of antimicrobial food packaging.

#### Acknowledgments

This work was supported by a grant from the “Ministero dell’Istruzione, dell’Università e della Ricerca” within the program Research and Competitiveness 2007–2013 grant number PON01\_02863. Project title: “Encapsulation of active ingredients for improving the quality and food safety”.

#### References

- Bajpai, S. K., & Sharma, S. (2004). Investigation of swelling/degradation behaviour of alginate beads crosslinked with  $\text{Ca}^{2+}$  and  $\text{Ba}^{2+}$  ions. *Reactive and Functional Polymers*, 59, 129–140.
- Cheigh, C., & Pyun, Y. (2005). Nisin biosynthesis and its properties. *Biotechnology Letters*, 27, 1641–1648.
- Chi-Zhang, Y., Yam, K. L., & Chikindas, M. L. (2004). Effective control of *Listeria monocytogenes* by combination of nisin formulated and slowly released into a broth system. *International Journal of Food Microbiology*, 90, 15–22.
- De Arauz, L. J., Jozala, A. F., Mazzola, P. G., & Vessoni Penna, T. C. (2009). Nisin biotechnological production and application: a review. *Trend in Food Science & Technology*, 20, 146–154.
- De Prisco, A., Maresca, D., Ongeng, D., & Mauriello, G. (2015). Microencapsulation by vibrating technology of the probiotic bacteria *Lactobacillus reuteri* DSM 17938 to enhance its survival in foods and gastrointestinal environment. *LWT—Food and Science Technology*, 61, 452–462.
- Dini, C., Islan, G. A., de Urraza, P. J., & Castro, G. R. (2012). Novel biopolymer matrices for microencapsulation of phages: enhanced protection against acidity and protease activity. *Macromolecular Bioscience*, 12, 1200–1208.
- European Food Safety Authority. (2006). Opinion of the scientific panel on food additives, flavourings, processing aids and materials in contact with food on a request from the commission related to the use of nisin (E 234) as a food additive. *The EFSA Journal*, 314, 1–16.
- Field, D., Conno, P. M. O., Cotter, P. D., Hill, C., & Ross, P. R. (2008). The generation of nisin variants with enhanced activity against specific Gram-positive pathogens. *Molecular Microbiology*, 61, 218–230.
- Galvez, A., Abriouel, H., López, R. L., & Omar, N. B. (2007). Bacteriocin-based strategies for food biopreservation. *International Journal of Food Microbiology*, 120, 51–70.
- García, P., Rodríguez, L., Rodríguez, A., & Martínez, B. (2010). Food biopreservation promising strategies using bacteriocins, bacteriophages and endolysin. *Trends in Food Science & Technology*, 21, 373–382.
- Harnsilawat, T., Pongsawatmanit, R., & Mc Clements, D. J. (2006). Characterization of  $\beta$ -lactoglobulin-sodium alginate interactions in aqueous solution: a calorimetry, light scattering, electrophoretic mobility and solubility study. *Food Hydrocolloids*, 20, 577–588.
- Hosseini, S. M., Hosseini, H., Mohammadifar, M. A., German, J. B., Mortazavian, A. M., Mohammadi, A., et al. (2014). Preparation and characterization of alginate and alginate-resistant starch microparticles containing nisin. *Carbohydrate Polymers*, 103, 537–580.
- Huq, T., Riedl, B., Bouchard, J., Salmieri, S., & Lacroix, M. (2014). Microencapsulation of nisin in alginate-cellulose nanocrystal (CNC) microbeads for prolonged efficacy against *Listeria monocytogenes*. *Cellulose*, 21, 4309–4321.
- Khaksar, R., Hosseini, S. M., Hosseini, H., Aliabadi, S., Mohammadifar, M. A., Mortazavian, A. M., et al. (2014). Nisin-loaded alginate-high methoxy pectin microparticles: preparation and physicochemical characterisation. *International Journal of Food Science & Technology*, 49, 2076–2082.
- Kim, B. S., Oh, J. M., Hyun, H., Kim, K. S., Lee, S. H., Kim, Y. H., et al. (2008). Insulin-loaded microcapsules for *in vivo* delivery. *Molecular Pharmaceutics*, 6, 353–365.
- Liu, W., & Hansen, J. N. (1990). Some chemical and physical properties of nisin a small-protein antibiotic produced by *Lactococcus lactis*. *Applied and Environmental Microbiology*, 56, 2551–2558.
- Mauriello, G., De Luca, E., La Stora, A., Villani, F., & Ercolini, D. (2005). Antimicrobial activity of a nisin-activated plastic film for food packaging. *Letters in Applied Microbiology*, 41, 464–469.
- Mørch, Y. A., Donati, I., Strand, L. B., & Break, G. S. (2006). Effect of  $\text{Ca}^{2+}$ ,  $\text{Ba}^{2+}$  and  $\text{Sr}^{2+}$  on alginate microbeads. *Biomacromolecules*, 7, 1471–1480.
- Narsaiah, K., Jha, S. N., Wilson, R. A., Mandage, H. M., & Manikantan, M. R. (2012). Optimizing microencapsulation of nisin with sodium alginate and guar gum. *Journal of Food Science and Technology*, 51, 4054–4059.
- Pawar, S. N., & Edgar, K. J. (2012). Alginate derivatization: a review of chemistry, properties and application. *Biomaterials*, 33, 3279–3305.
- Russo, F., Ercolini, E., Mauriello, G., & Villani, F. (2006). Behaviour of *Brochothrix thermosphacta* in presence of other meat spoilage microbial groups. *Food Microbiology*, 23, 797–802.
- Tiwari, B. K., Valdramidis, V. P., O’Donnel, C. P., Muthukumarappan, K., Bourke, P., & Cullen, P. J. (2009). Application of natural antimicrobial for food preservation. *Journal of Agricultural and food chemistry Review*, 57, 5987–6000.
- Villani, F., Pepe, O., Mauriello, G., Salzano, G., Moschetti, G., & Coppola, S. (1994). Antimicrobial activity of *Staphylococcus xylosus* from Italian sausage against *Listeria monocytogenes*. *Letters in Applied Microbiology*, 18, 159–161.
- Whelehan, M., & Marison, I. W. (2011). Microencapsulation using vibrating technology. *Journal of Microencapsulation*, 28, 669–688.
- Xiao, D., Davidson, P., & Zhong, Q. (2011). Release and antilisterial properties of nisin from zein capsules spray-dried at different temperatures. *LWT—Food science and Technology*, 44, 1977–1985.
- Xiao, D., & Zhong, Q. (2011). In vitro release kinetics of nisin as affected by Tween 20 and glycerol co-encapsulated in spray dried capsules. *Journal of Food Engineering*, 106, 65–73.
- Zarate, J., Virdis, L., Orive, G., Igartua, M., Hernández, R. M., & Pedraz, J. L. (2011). Design and characterization of calcium alginate microparticles coated with polycations as proteins delivery system. *Journal of Microencapsulation*, 28, 614–620.



Contents lists available at ScienceDirect

## LWT - Food Science and Technology

journal homepage: [www.elsevier.com/locate/lwt](http://www.elsevier.com/locate/lwt)

# Production of seafood flavour formulations from enzymatic hydrolysates of fish by-products

I. Peinado <sup>a, \*</sup>, G. Koutsidis <sup>a</sup>, J. Ames <sup>b</sup>

<sup>a</sup> Department of Biology, Food and Nutrition, Health and Life Sciences, Northumbria University, Newcastle City Campus, Ellison Place, Newcastle Upon Tyne, NE1 8ST, UK

<sup>b</sup> Centre for Research in Biosciences, Faculty of Health and Applied Sciences, The University of the West of England, Frenchay Campus, Bristol, BS16 1QY, UK

## ARTICLE INFO

## Article history:

Received 14 June 2015

Received in revised form

7 September 2015

Accepted 13 September 2015

Available online 15 September 2015

## Keywords:

Enzymatic hydrolysis

Amino acids

Volatiles

Fish by-products

Seafood flavour

## Chemical compounds studied in this article:

Glutamic acid (Pubchem CID: 611)

Aspartic acid (Pubchem CID: 424)

Leucine (Pubchem CID: 6106)

Lysine (Pubchem CID: 5962)

1-Octen-3-ol (Pubchem CID: 18827)

2,4-Heptadienal (Pubchem CID: 20307)

4-Heptenal (Pubchem CID: 71590)

1-Hepten-4-ol (Pubchem CID: 19040)

## ABSTRACT

Amino acid-rich extracts derived from fish by-products were utilised to generate flavour model systems with added glucose and/or fish oil.

Combination of endo and exo peptidases resulted in the most marked increased in free amino acids, particularly for leucine, lysine and glutamic acid ( $48.3 \pm 3.4$  to  $1423.4 \pm 59.6$ ,  $43.3 \pm 1.2$  to  $1485.4 \pm 25.6$  and  $143.6 \pm 21.7$  to  $980.9 \pm 63.6$   $\mu\text{g/g}$  respectively).

Main volatile products formed after heating the systems were 4-heptenal, 2,4-heptadienal, and some pyrazines. Increased concentrations of 1-octen-3-ol or 1-hepten-4-ol were also observed in the heated systems compared to the controls. All of these volatile compounds have been identified among the volatile profile of cooked seafood.

Conversion of low value fish derived materials such as fish powder, into more valuable products such as flavour precursors and subsequently flavour compounds might be a commercially viable proposition for the fish industry.

© 2015 Published by Elsevier Ltd.

## 1. Introduction

Traditionally, waste from the fish industry such as small catch, flesh, viscera etc. are either disposed of or utilised as fishmeal for animal feeding. Nevertheless, over the last few decades, raised awareness on the environmental impact of products and processes has led to retailers and consumers making concerted efforts to make the best use of all resources. Nowadays, there is growing interest in using food wastes as sources of materials or ingredients that are capable of providing added value to consumer products including uses in foods. Some examples of this are the extraction and recovery of different compounds of interest such as amino

acids, peptides, collagen or omega fatty acids from fish wastes (Guerard, Dufosse, Broise, & Binet, 2001). Development of novel means of processing is required to convert the wastes and by-products into forms that are safe, marketable and acceptable to the consumer.

Fish wastes have also been utilised for the production of fish powders or fish protein hydrolysates, used as nitrogen source for microbial growth and enzyme production. Autolytic process, which depends only on endogenous enzymes, is considered to be economically advantageous; however, exogenous commercial enzymes are sometimes preferred since they allow controlled hydrolysis, hence control over the properties of the resulting products. Many enzymes have attracted interest for the hydrolysis of fish proteins (e.g., papain, alcalase, neutrase, Flavourzyme<sup>®</sup>, Protamex<sup>®</sup>). Characteristics of the final hydrolysate will depend on the enzyme(s) added, but also on the substrate, which plays an

\* Corresponding author. Faculty of Science and Technology, Piazza Università, 5, 39100, Bozen-Bolzano, Italy.

E-mail addresses: [irene.peinadopardo@unibz.it](mailto:irene.peinadopardo@unibz.it), [irpeipar@gmail.com](mailto:irpeipar@gmail.com) (I. Peinado).

important role in the hydrolysis (Annadurai, Sadeeshkumar, Vijayalakshmi, & Pirithiviraj, 2012; Aspino, Horn, & Eijnsink, 2005; Ghorbel et al., 2005; Souissi, Bougatef, Triki-ellouz, & Nasri, 2007).

Flavour is an important factor to determine the quality of fish and fish derived products as well as consumer acceptance. Fishy flavour often makes products derived from fish less acceptable (Ganeko et al., 2008). This characteristic aroma is influenced by the species but also by the conditions used for its post-harvest handling, storage and cooking. Some fish such as salmon or trout, have a strong flavour while might have a relatively mild smell before cooking that becomes strong and pleasant after heating (Ganeko et al., 2008; Whitfield, Freeman, Last, Bannister, & Kennett, 1982; Whitfield, Last, Shaw, & Tindale, 1988). Important aroma compounds, characteristic of fresh fish, are lipid derived volatile compounds generated mainly by oxidative enzymatic reactions and autoxidation of lipids such as aldehydes and ketones. However, compounds derived from Maillard reaction such as pyrazines and furans, also make important contributions to the flavour and aroma of fish products after frying or grilling (Giri, Osako, & Ohshima, 2010).

The aim of this study was to demonstrate the use of by-products of the fish industry (fish powder) for the generation of fish flavour formulations after protease biocatalysis and subsequent heating in the presence of glucose and/or fish oil.

## 2. Material and methods

### 2.1. Chemicals

Proteases (Biocatalysts Ltd, UK), fish oil and fish powder (Croda International plc, UK), as well as glucose and glycerol, (Sigma–Aldrich Company Ltd, Poole, UK) used to produce the model systems were all food grade. Chemicals used for analytical determinations: disodium tetraborate decahydrate, sodium dodecyl sulphate (SDS), *o*-phthalaldehyde (OPA), dithiothreitol (DTT), serine, hydrochloric acid, *iso*-octane, C7 – C30 saturated alkanes (1000 µg/mL each component in hexane) were all analytical grade purchased from Sigma–Aldrich.

### 2.2. Hydrolysis and formation of aromas

Table 1 summarizes the characteristics of the commercial proteases as well as the composition of the fish powder used as starting materials to produce fish-like aromas. Fish powder (100 g/L in water) was hydrolysed for 15 h at constant stirring, under controlled conditions of temperature and pH (60 °C at pH 6). The reaction was terminated by heating the mixture at 95 °C for 20 min in a water bath. Each protease used was added so all mixtures had the same enzymatic activity per gram of sample. The conditions of pH, temperature and time of reaction, as well as the enzymes and their combinations were selected based on the combination of those parameters that resulted in the higher concentration of free amino acids in a preliminary experiment (data not shown). The resulting slurries were centrifuged at 8000 × g for 20 min and aliquots were analysed to determine the degree of hydrolysis (DH) and amounts of free amino acids.

Subsequent reactions to generate aroma compounds were carried out with selected slurries of the fish powder hydrolysates (FPHs) based on the degree of hydrolysis and free amino acid content. Aliquots of FPHs (0.2 mL) were mixed, homogenised with a glucose solution (0.05 mL, 80 µmol/mL) in glass reaction vials and freeze-dried. Glycerol (500 µL) was added to each freeze-dried sample to facilitate homogenisation while fish oil (1.5 g/100 g) was added to some of the samples according to the experimental design (Table 2). All samples in closed vials were then homogenised

at 60 °C for 10 min and subsequently heated at 110 °C for 30 min to promote flavour formation. Fish powder hydrolysates without addition of fish oil and before heating were used as control. All samples were prepared and analysed in triplicate.

### 2.3. Analyses

#### 2.3.1. Chemical analyses. Composition of fish powder and fish oil

The moisture, ash and extractable fat content of the fish powder were calculated according to the Association of Official Analytical Chemists (AOAC, 2000). Total protein was determined by the Kjeldahl method using a nitrogen conversion factor of 6.25 (Ortiz et al., 2006; Yaich et al., 2011).

The fatty acid composition was analysed by GC-FID after transesterification to methyl esters (FAMES) with a mixture BF<sub>3</sub> methanol at 20 °C according to the IUPAC standard method (IUPAC, 1992; Peinado, Girón, Koutsidis, & Ames, 2014; Yaich et al., 2011). Analysis of FAMES was carried out with a DANI Master GC equipped with an auto sampler, a DANI FID detector (DANI Instruments S.p.A, Italy) and an Agilent DB-23 (60 m × 0.25 mm, 0.25 µm) capillary column (Agilent Technologies, Cheshire, UK). The oven temperature was programmed from 90 °C to 240 °C at 4 °C/min and the injector and detector temperatures were set at 250 °C. The carrier gas was helium at 1.0 mL/min constant flow (split ratio 10:1). Data analysis, identification and quantification of FAMES was accomplished by comparing the retention times and areas of the peaks with those of pure standards (Supelco® 37 Component FAME Mix, Sigma–Aldrich, Poole, UK) and analysed under the same conditions. The results were expressed as a g of each fatty acid/100 g of the lipid fraction.

#### 2.3.2. Degree of hydrolysis, DH

The Degree of Hydrolysis (DH) was estimated following a modified OPA spectrophotometric method using aqueous serine, (0.1 g/L) as the reference standard (Church, Porter, Catignani, & Swaisgood, 1985; Nielsen, Petersen, & Dambmann, 2001). For the OPA reagent, disodium tetraborate decahydrate (7.620 g) and sodium dodecyl sulphate (SDS; 200 mg) were dissolved in 150 mL deionized water followed by the addition of 4 mL of *o*-phthalaldehyde (160 mg) in ethanol and dithiothreitol (176 mg, 99%, DTT). The final solution was made up to 200 mL with deionized water. For the analysis, aliquots of FPH or serine standard solution (50 µL) were placed in the wells of a 96-well micro-plate containing 150 µL of OPA-reagent and the absorbance was read at 340 nm. The DH was calculated using Equations (1)–(3) (Church et al., 1985; Nielsen et al., 2001).

$$DH = \frac{h}{h_{tot}} \cdot 100\% \quad (1)$$

$$h = \frac{(\text{serine} - \text{NH}_2) - b}{a} \quad (2)$$

$$\text{Serine} - \text{NH}_2 = \frac{\text{Abs}_{\text{sample}} - \text{Abs}_{\text{blank}}}{\text{Abs}_{\text{standard}} - \text{Abs}_{\text{blank}}} \cdot 0.9516 \cdot 0.1 \cdot \frac{100}{X} \cdot P \quad (3)$$

where  $h_{tot}$  depends on the specific raw material, and for the present study was estimated as  $h_{tot} = 8.6$ ;  $h = \text{meqv serine/g protein}$ ;  $\text{serine-NH}_2 = \text{meqv serine-NH}_2/\text{g protein}$ ;  $a$  and  $b$  depend on the specific raw material, and for the present study they were estimated as  $a = 1.00$ ,  $b = 0.4$ ;  $X = \text{g sample}$ ;  $P = \text{protein \% in the sample}$ ; 0.1 is the sample volume (L) (Nielsen et al., 2001).

**Table 1**  
Description of commercial enzymes used for the fish powder hydrolysis. Characterization of fish powder (ash, moisture, fat, protein, carbohydrates (g/100 g)). Composition of fish oil (n = 3).

Enzymes characteristics <sup>a</sup>								
Enzyme	Activity			Optimum pH	Optimum T <sup>a</sup>			
A	Flavopro Umami F825MDP			Leucine aminopeptidase	5.5–7.5			
B	Flavopro 750P			Casein peptidase	5.5–7.5			
C	Promod 144			Papain	5.0–7.6			
D	Promod 439			Casein protease	6.0–9.0			
E	Promod 671			Casein protease	5.5–8.0			
Fish powder composition (%)								
x <sup>w</sup>	Ash		Protein		Fat <sup>a</sup>		Carbohydrates	
4.67 ± 0.16	22.4 ± 0.3		60.3 ± 0.6		1.5 ± 0.4		11.1 ± 0.70	
Fat composition (g/100g total fat)								
	C14:0	C16:0	C18:0	C18:1	C18:2	C18:3	C20:5	C22:6
Fish powder fat <sup>a</sup>	4.3 ± 0.5	47.0 ± 1.3	16.3 ± 0.5	15.3 ± 0.6	0.40 ± 0.03	–	0.67 ± 0.09	0.55 ± 0.02
Fish oil	10.4 ± 0.3	29.1 ± 0.8	16.7 ± 1.8	8.2 ± 0.5	2.8 ± 0.3	3.8 ± 0.6	11.2 ± 0.7	6.5 ± 0.3

<sup>a</sup> Biocatalysts, Ltd.

### 2.3.3. Free amino acids

The free amino acid content was calculated following the same method as Elmore, Koutsidis, Dodson, Mottram, and Wedzicha (2005). Aliquots of the FPHs (500 µL) were mixed with HCl (500 µL, 0.01 mol/L) and centrifuged at 7200 × g for 15 min. Centrifuged supernatant (100 µL) was derivatized using the EZ-Faast amino acid kit (Phenomenex, Cheshire, UK), and analysed by (GC-MS). The derivatized amino acids were extracted into iso-

octane (100 µL) and analysed in electronic ionization mode at 70 eV using a 6890 GC coupled to a 5973 MSD instrument (Agilent, Palo Alto, CA). Derivatized amino acid solution (1 µL) was injected at 250 °C in split mode (10:1) onto a 10 m × 0.25 mm × 0.25 µm Zebron ZB-AAA capillary column (film composition 50% phenyl 50% dimethyl polysiloxane) (Phenomenex, Cheshire, UK). The oven temperature was 110 °C for 1 min, then increased at 30 °C/min to 320 °C, and held at 320 °C for 2 min. The transfer line was held at

**Table 2**  
Fish powder hydrolysates obtained with individual enzymes or combination of enzymes. Degree of Hydrolysis (DH %) and concentration of individual free amino acids (µg/g). Changes in the concentration of the individual free amino acids compared to the control (ΔC)<sup>a</sup>. (n = 3).

DH	(%)	Fish powder			FPH		
		Control	A	B	B + C	B + D	B + E
		7 ± 2	31 ± 1	46 ± 1	23 ± 1	21 ± 6	57 ± 5
Alanine	µg/g	235 ± 8	365 ± 4	829 ± 40	938 ± 33	655 ± 34	677 ± 19
	ΔC (%)		55 ± 2	252 ± 17	299 ± 14	178 ± 14	188 ± 8
Glycine	µg/g	155 ± 5	114 ± 3	322 ± 10	315 ± 10	371 ± 26	247 ± 6
	ΔC (%)		–27 ± 2	107 ± 6	103 ± 7	139 ± 17	59 ± 4
Valine	µg/g	47 ± 3	224 ± 15	661 ± 50	726 ± 59	448 ± 47	541 ± 16
	ΔC (%)		374 ± 31	1297 ± 106	1435 ± 123	848 ± 97	1045 ± 33
Leucine	µg/g	48 ± 3	675 ± 15	1,113 ± 51	1,423 ± 59	929 ± 47	1,025 ± 16
	ΔC (%)		12,989 ± 31	2205 ± 105	2848 ± 123	1825 ± 98	2022 ± 33
Isoleucine	µg/g	29 ± 3	227 ± 5	613 ± 50	683 ± 14	412 ± 8	522 ± 9
	ΔC (%)		670 ± 16	1981 ± 170	2218 ± 47	1299 ± 27	1674 ± 32
Threonine	µg/g	54 ± 6	194 ± 21	604 ± 29	742 ± 48	473 ± 18	541 ± 72
	ΔC (%)		260 ± 39	1023 ± 53	1280 ± 88	778 ± 33	906 ± 135
Serine	µg/g	60 ± 8	178 ± 42	616 ± 20	652 ± 34	429 ± 51	454 ± 99
	ΔC (%)		198 ± 70	927 ± 33	988 ± 57	616 ± 85	658 ± 166
Proline	µg/g	50 ± 2	60 ± 3	174 ± 2	154 ± 6	116 ± 5	130 ± 14
	ΔC (%)		19 ± 6	247 ± 5	207 ± 13	130 ± 10	158 ± 27
Aspartic acid	µg/g	51 ± 6	84 ± 2	260 ± 33	274 ± 36	181 ± 6	160 ± 13
	ΔC (%)		68 ± 4	421 ± 66	450 ± 72	262 ± 12	222 ± 25
Methionine	µg/g	11 ± 3	125 ± 8	298 ± 26	346 ± 23	239 ± 17	263 ± 6
	ΔC (%)		997 ± 63	2511 ± 224	2932 ± 204	1997 ± 147	2202 ± 54
Glutamic acid	µg/g	144 ± 23	470 ± 31	880 ± 7	981 ± 64	573 ± 86	431 ± 25
	ΔC (%)		227 ± 21	513 ± 5	583 ± 44	299 ± 60	200 ± 17
Phenylalanine	µg/g	27 ± 1	255 ± 31	360 ± 43	451 ± 15	292 ± 15	352 ± 2
	ΔC (%)		860 ± 115	1256 ± 162	1597 ± 55	997 ± 55	1227 ± 6
Lysine	µg/g	43 ± 1	369 ± 80	818 ± 157	1,485 ± 22	887 ± 101	836 ± 66
	ΔC (%)		751 ± 186	1789 ± 363	3332 ± 50	1949 ± 233	1830 ± 152
Other	µg/g	23 ± 2	138 ± 3	187 ± 14	286 ± 3	167 ± 5	229 ± 3
	ΔC (%)		687 ± 120	831 ± 206	1273 ± 271	760 ± 209	1094 ± 169

Production of Fish powder hydrolysates (FPH): fish powder (100 g/L in water) + commercial enzymes ([A, B, C, D, E], Table 1), heated overnight (15 h) at constant stirring (pH 6, and 60 °C, enzyme (10–20 g/L).

<sup>a</sup> ΔC (%) = 100 · [concentration of each free amino acid in the fish powder hydrolysates – concentration of each free amino acid in the control]/concentration of each free amino acid in the control.

320 °C, and the carrier gas was helium at a constant flow rate of 1.1 mL/min. The ion source was maintained at 320 °C. Standard mix stock solution (200 µmol/L each) of 15 non-basic amino acids (Ala, Asp, Glu, Gly, His, Ile, Leu, Lys, Met, Orn, Phe, Pro, Ser, Thr, Val) in hydrochloric acid (0.1 mol/L) and 2 basic amino acids (Asn, and Gln) in water were prepared; different dilutions (10–150 µmol/L) were derivatized, and calibration curves were plotted for each amino acid (effect of food matrix composition was studied by spiking samples). Norvaline (100 µL (0.2 mmol/L)) was used as the internal standard.

### 2.3.4. Volatiles analysis

GC/MS analyses were performed using an Agilent 7890A gas chromatograph equipped with a DB-WAX capillary column (60m × 0.25 mm i.d. × 0.25 µm FT) and coupled to a BenchToF Time of Flight Mass Spectrometer (Markes International Ltd, Llantrisant UK) and a CTC CombiPal autosampler (CTC Analytics AG, Zwingen, Switzerland). HS-SPME was performed on aqueous extracts (200 µL) in 2 mL of saturated NaCl solution. Samples were incubated at 40 °C for 40 min followed by a 1 min extraction using a CAR/PDMS/DVB SPME fibre (Supelco, Sigma–Aldrich Company Ltd, UK) and desorption at 260 °C for 5 min. The oven temperature was 40 °C (held for 5 min), 40–200 °C at 4 °C/min, then to 250 °C at 8 °C/min, held for 5 min. Helium was used as the carrier gas at a flow rate of 1 mL/min.

The volatile compounds were identified by comparing their mass spectra with spectral data from the National Institute of Standards and Technology 2008 library as well as retention indices published in the literature (Ganeko et al., 2008; Giri et al., 2010; pherobase.org). Relative retention indices were determined by injection into the column of a solution containing a series of *n*-alkanes (C7–C30, saturated alkanes (1000 µg/mL in hexane) Sigma–Aldrich Company Ltd, UK) in the same temperature programmed run as described above. Quantification of selected compounds was carried out using external calibration curves.

### 2.4. Sensory evaluation

Consumers' preferences were assessed by the Friedman Pairwise ranking analysis (Escriche, Fernández-Segovia, Serra, Andrés, & Barat, 2001; González-Tomás, Carbonell, & Costell, 2004; Peinado, Rosa, Heredia, Escriche, & Andrés, 2012). This test is used with a non-trained panel, to evaluate sets of three to six samples, considering a single attribute each time. Twenty-seven subjects constituted the panel. The samples selected were presented to each of the subjects in all possible paired combinations. The selection of the sensory attributes was based on the characteristic criteria of the samples as well as some previous experiments on similar products (Ganeko et al., 2008; Giri et al., 2010). Panellists were asked which of the two samples presented they would assess as: "stale" (smell of fish cooked for too long), "fried" (smell of fish cooked in fat or oil, usually over direct heat), "grilled" (typical fish cooked in a grill), and their overall preference.

Significant differences between the samples were established by the statistical function T-Friedman and compared with the tabulated  $\chi^2 = 7.81$  ( $\alpha = 0.05$ ) with ( $t-1$ ) degrees of freedom (Meilgaard, Civille, & Carr, 1999).

Afterwards, Tukey's honestly significant difference (HSD) was calculated to establish between which samples these differences lay (Equation (4)), (Meilgaard et al., 1999):

$$HSD = q_{\alpha,t,\infty} (p \cdot t/4)^{\frac{1}{2}} \quad (4)$$

where  $q_{\alpha,t,\infty}$  is a tabulated value,  $p$  is the number of panellists and  $t$  the number of samples ( $t = 4$ ), (Meilgaard et al., 1999).

### 2.5. Statistics

Analysis of variance (ANOVA) and the Friedman test ( $p$ -value < 0.05) were carried out using SPSS to estimate the differences in amino acid composition of the FPHs. Principal Component Analysis, PCA, (SPSS) was applied to differentiate the FPHs based on their volatile compound.

Furthermore, a correspondence analysis was performed to establish whether the selected samples and the evaluated sensory attributes map. This tool establishes the association between categorical variables (Beh, Lombardo, & Simonetti, 2011; Guerrero et al., 2010).

## 3. Results and discussion

### 3.1. Hydrolysis of fish powder

#### 3.1.1. Degree of hydrolysis (DH)

The OPA method to determine the DH is based on the specific reaction between the OPA-reagent and primary amino groups, in the presence of a thiol to form 1-alkylthio-2-alkyl-substituted isoindoles that can be quantified spectrophotometrically at 340 nm (Medina Hernández, Villanueva Camañas, Monfort Cuenca, & García Álvarez-Coque, 1990). The DH is presented in Table 2; All proteases produced a high DH compared to the control FP. Individual proteases, "A" (endo and exo peptidase activities) and "B" (exopeptidase activity) showed high degrees of hydrolysis ( $30.5 \pm 1.2\%$  and  $46.0 \pm 0.7\%$  respectively). The fact that the DH was higher with enzyme "B" indicates that having dual enzymatic activity within one enzyme does not necessarily increase the DH. The same conclusion could be achieved when enzyme "B" was combined with enzymes "C" or "D" (endopeptidases). However, the combination "B + E" produced the highest DH ( $57.4 \pm 0.9\%$ ). It is not easy to compare the hydrolysates prepared using the different proteases because they have optimal working conditions and specificities.

The individual free amino acid content of the FPHs is illustrated in Table 2 together with the changes in the concentrations for the amino acids in the FPHs compared to the control ( $\Delta C\%$ ). 17 amino acids were identified and quantified in the different FPHs. Lysine, leucine, glutamic acid and alanine, were the most abundant in most of the FPHs (235–1484 µg/g), reaching their highest concentrations for the combination "B + C" (Lys [ $1484 \pm 43$  µg/g], Leu [ $1423 \pm 48$  µg/g], Glu [ $981 \pm 142$  µg/g] and Ala [ $939 \pm 135$  µg/g]). His, Ile, Phe, Ser and Thr, were in the range of 178–742 µg/g, also with their highest concentrations for the combination "B + C"; while Gly, Pro, Asp, Met, His, Tyr and Trp, were found in smaller concentrations. Depending on the enzymes/combination of enzymes, there were significant differences in the concentration of the amino acids within the FPHs; some amino acids, such as Ala, Gly or Pro, increased their concentration, up to 3–6 fold compared to the control-FPH (regardless of their initial concentration) while some others such as Lys, Met or Leu increased their concentrations up to 23–35 fold compared to the control-FPH (Table 2).

### 3.2. Development of aromas

A total of 32 volatile compounds were identified in the heated fish powder hydrolysates (H-FPHs) (Table 3). Most of the compounds identified in the control sample (heated without the addition of external enzymes), were also identified in the H-FPHs heated with glucose with or without fish oil (Table 4).

Aldehydes significantly contribute to the overall aroma of cooked fish/seafood due to their low threshold values (Table 3). In the present study, the concentration of aldehydes increased in the

H-FPHs, being higher in those samples containing fish oil (Table 4). This increase in samples containing oil might be expected, as some aldehydes might be generated from lipid oxidation, e.g., hexanal, present in much higher concentrations in the H-FPHs containing fish oil, derives mainly from the oxidation of linoleic acid. Moreover, some other aldehydes, such as 2-methylpropanal, 4-heptenal and 2,4-heptadienal, not found in the control, were abundant in the H-FPHs. 2,4-Heptadienal, which is a degradation product of linolenic acid (Decker, Elias, & McClements, 2010), was only found in samples containing fish oil (Table 4). Some branched short chain aldehydes could result from deamination of amino acids. The major aldehyde in the H-FPHs, regardless of the incorporation of fish oil, was 3-methyl-butanal, which presence was attributed to the high concentration of leucine in the FPHs. While in some other cases aldehydes can originate from the Strecker degradation of amino acids, for instance, 2-methylbutanal, which was also in considerable concentrations in the H-FPHs, may be derived from isoleucine. Due to their low threshold values, the Strecker aldehydes including 2-methylpropanal, 2-methylbutanal and 3-methylbutanal, might impart nutty/malty nuances to the product while, some others aldehydes such as heptanal, octanal or nonanal might impart a more characteristic fishy flavour (Caprino et al., 2008; Giri et al., 2010;

Selli & Cayhan, 2009).

**Alcohols** are mainly formed by an enzymic peroxidation of the n-3 and n-6 polyunsaturated fatty acids, present in fish tissue. 1-Penten-3-ol, significantly increased in samples containing fish oil (Table 4). Although not all alcohols are likely to have an important contribution to odour, due to their relatively high odour threshold values (Table 3), unsaturated alcohols such as 1-octen-3-ol, with generally much lower threshold values than the saturated counterparts, might have a greater impact on the overall aroma (Kawai & Sakaguchi, 1996; Selli & Cayhan, 2009).

Amongst the **ketones** identified, 2-heptanone, 2-octanone, 2-nonanone and undecanone, slightly increased in the H-FPHs, regardless the addition of fish oil. However, 1-penten-3-one, not present in the control, appeared in all H-FPHs, with a significant increase in those H-FPHs containing fish oil. Due to its low odour threshold value (Table 3), this compound, which might result as a degradation product of linolenic acid, is likely to contribute pungent and fish-like notes to the aroma (Decker et al., 2010; Giri et al., 2010). Ketones are mainly produced a result of lipid-oxidation and/or amino acid degradation due to the Strecker reaction, and are associated with off-flavour (Selli & Cayhan, 2009).

**Acids** such as acetic acid, propanoic acid, 2-methyl propanoic

**Table 3**  
Retention time, retention index and odour descriptors of volatile compounds found in the different fish powder hydrolysates after heating them with or without fish oil (H-FPHs) (n = 3).

	RT	RI	Odour threshold	Identification	Odour description
<i>Aldehydes</i>					
2-Methyl propanal	6.03	647	0.1–2.3 <sup>D</sup>	MS, RI Std	Green, Pungent, Burnt, Malty, Toasted, Fruity <sup>C</sup>
2-Methyl butanal	8.42	912	1 <sup>D</sup>	MS, RI Std	Green, Almond, Strong burnt, Malty, Cocoa <sup>C</sup>
3-Methyl butanal	8.53	914	0.2–2 <sup>D</sup>	MS, RI Std	Cashew, apple <sup>A</sup> , almond-like, toasted, malty, green <sup>C</sup> Herbaceous
hexanal	16.54	1079	4.5–5 <sup>D</sup>	MS, RI Std	Fishy, grass <sup>A,B,C</sup>
Heptanal	21.60	1170	3 <sup>D</sup>	MS, RI Std	Citrus like <sup>A</sup> , dry fish <sup>B</sup> green, fatty, solvent, smoky, Rancid <sup>C</sup>
4-Heptenal	24.14	1226	0.8–10 <sup>D</sup>	MS, RI Std	Boiled potato, creamy, sweet, biscuit-like <sup>A,B,C</sup>
Octanal	26.06	1286	0.7 <sup>D</sup>	MS, RI Std	Lemon, stew-like, boiled meat-like, rancid, soapy, citrus, green, flower, fruit, orange <sup>A,B,C</sup>
Nonanal	30.03	1405	1 <sup>D</sup>	MS, RI Std	Gravy, green, fruity, gas, chlorine, floral, waxy, sweet, melon, soapy, fatty, citrus fruit <sup>A,B,C</sup>
2-Octenal	31.30	1512	3 <sup>D</sup>	MS, RI	Aromatic, oxidized oil-like <sup>A</sup> , Green <sup>C</sup>
Benzaldehyde	33.014	1539	350–3,500 <sup>D</sup>	MS, RI	Bitter almond <sup>A,C,C</sup> , Burnt sugar, Woody <sup>C</sup>
2,4-Heptadienal	33.52	1548	15–95 <sup>A</sup>	MS, RI Std	Fatty, fishy <sup>A,C</sup> , aromatic, oxidized oil-like <sup>B</sup>
<i>Alcohols</i>					
1-Penten-3-ol	20.321	1145	350–400 <sup>A,D</sup>	MS, RI Std	Burnt, meaty <sup>A</sup> , paint like chemical like <sup>B</sup> grassy-green <sup>C</sup>
4-Ethyl phenol	23.70	1213	140 <sup>D</sup>	MS, RI	Shoe polish, phenolic, leather, smoky <sup>A,B,C</sup>
1-Octen-3-ol	31.79	1519	1–1.5 <sup>A,D</sup>	MS, RI Std	Fishy, grassy <sup>A</sup> , sweet earthy <sup>C</sup>
1- heptanol	31.96	1522	3–5.4 <sup>A,D</sup>	MS, RI, Std	Fresh, light green, nutty <sup>A,B,C</sup>
4-Hepten-1-ol	33.57	1597	–	MS, RI Std	Fishy <sup>C</sup>
<i>Ketones</i>					
1-Penten-3-one	13.45	1020	1–1.3 <sup>D</sup>	MS, RI, Std	Pungent, fish-like, rotten, fruity, plastic, leather <sup>A,B,C</sup>
2-Heptanone	21.43	1167	140–3,000 <sup>D</sup>	MS, RI Std	Cured ham-like, toasted, nutty, gas, gravy, soapy, Fruity <sup>C</sup>
2-octanone	25.86	1280	50 <sup>A,D</sup>	MS, RI Std	Gas, stewed, fatty, green, fruity, cheese-apple <sup>C</sup>
2-Nonanone	29.83	1395	5–200 <sup>D</sup>	MS, RI Std	Fruity, soapy, fatty, green, earthy, baked <sup>C</sup>
Undecanone	36.79	1601	5–7 <sup>A,D</sup>	MS, RI Std	Tallow, musty <sup>A</sup> Fruity, musty, dusty, green <sup>C</sup>
<i>Acids</i>					
Butanoic acid butyl ester	23.09	1196	100 <sup>D</sup>	MS, RI	Fresh, Sweet, Fruity <sup>C</sup>
Acetic acid	32.13	1525	30–150 <sup>D</sup>	MS, RI	Sour, Vinegar, Pungent <sup>C</sup>
<i>Sulphur compounds</i>					
Dimethyl disulfide	16.01	1069	0.16–12 <sup>A,D</sup>	MS, RI	Sulphur, Cabbage, Ripened cheese, Putrid <sup>A,C</sup>
Dimethyl trisulfide	29.66	1390	0.005–0.01 <sup>D</sup>	MS, RI, Std	Rotten food, Sulphury, Fishy, Cauliflower, Cabbage, Onion <sup>A,C</sup>
<i>Furans</i>					
2-Ethyl furan	10.16	950	8 <sup>A,D</sup>	MS, RI	Rubber, Pungent, Acid, Sweet <sup>C</sup>
2-Ethyl-5-methyl furan	14.02	1031	–	MS, RI	
2-Pentyl furan	23.70	1213	6 <sup>A,D</sup>	MS, RI, Std	Buttery, Green bean-like <sup>A,C</sup>
<i>Pyrazines</i>					
Methyl pyrazine	25.01	1253	60–105,000 <sup>D</sup>	MS, RI, Std	Nutty, Roasty, Cocoa, Chocolate <sup>C</sup>
2,5-dimethyl pyrazine	27.24	1321	800–1,800 <sup>D</sup>	MS, RI, Std	Cocoa, Roasted nut, Roastbeef, Woody <sup>C</sup>
2,6-Dimethyl pyrazine	24.47	1327	200–9,000 <sup>D</sup>	MS, RI, Std	Baked potato, Nutty, Fruity <sup>C</sup>
2,3-Dimethyl pyrazine	28.18	1348	2500–35,000 <sup>D</sup>	MS, RI, Std	Nutty, musty <sup>C</sup>

<sup>A</sup>Giri et al., 2010; <sup>B</sup>Ganeko et al., 2008; <sup>C</sup>pherobase.org; <sup>D</sup><http://www.leffingwell.com/odorthre.htm>.  
Odour thresholds in water (µg/L).

**Table 4**  
Fish powder hydrolysates obtained with the enzymes or combination of enzymes. Volatile compounds associated with fish-like aroma in the different heated fish powder hydrolysates (H-FPHs) with or without addition of fish oil (1.5 g/100 g) expressed as  $\mu\text{g/mL}$ . (n = 3).

	Control		A + H-FPH		B + H-FPH		(B + C) + H-FPH		(B + D) + H-FPH		(B + E) + H-FPH	
	No-FO	1.5% FO	No-FO	1.5% FO	No-FO	1.5% FO	No-FO	1.5% FO	No-FO	1.5% FO	No-FO	1.5% FO
<b>Aldehydes</b>												
2-Methyl butanal	4 ± 2	35 ± 5	312 ± 6	270 ± 18	1361 ± 78	955 ± 120	588 ± 134	681 ± 99	436 ± 171	528 ± 230	317 ± 1	618 ± 13
3-Methyl butanal	9 ± 6	65 ± 18	1073 ± 131	1139 ± 116	1475 ± 68	1295 ± 94	1275 ± 221	1113 ± 160	1046 ± 272	881 ± 229	769 ± 20	1026 ± 172
Hexanal	0.323 ± 0.007	1.200 ± 0.651	0.524 ± 0.119	1.688 ± 0.641	0.441 ± 0.079	5 ± 1	0.358 ± 0.109	1.609 ± 0.159	0.361 ± 0.055	1.571 ± 0.128	0.285 ± 0.062	1.758 ± 0.785
Heptanal	0.174 ± 0.029	0.262 ± 0.065	0.392 ± 0.018	0.406 ± 0.002	0.329 ± 0.035	0.572 ± 0.067	0.278 ± 0.049	0.349 ± 0.109	0.181 ± 0.019	0.279 ± 0.012	0.153 ± 0.002	0.316 ± 0.016
4-Heptenal	–	0.103 ± 0.077	0.033 ± 0.012	0.239 ± 0.027	0.032 ± 0.003	0.508 ± 0.159	0.047 ± 0.028	0.211 ± 0.194	0.040 ± 0.002	0.161 ± 0.015	0.010 ± 0.005	0.240 ± 0.135
Octanal	0.017 ± 0.002	0.008 ± 0.002	0.054 ± 0.007	0.011 ± 0.005	0.038 ± 0.014	0.006 ± 0.002	0.027 ± 0.002	0.013 ± 0.009	0.024 ± 0.004	0.011 ± 0.007	0.013 ± 0.002	0.006 ± 0.001
Nonanal	3.605 ± 0.710	0.692 ± 0.140	12 ± 2	3 ± 1	8 ± 2	0.915 ± 0.088	5.192 ± 0.219	2.131 ± 1.067	3.969 ± 0.832	1.572 ± 0.999	3.371 ± 0.617	0.737 ± 0.008
2,4-Heptadienal	0	0.212 ± 0.015	0	0.215 ± 0.197	0	2 ± 1	0	0.417 ± 0.056	0	0.455 ± 0.044	0	0.501 ± 0.042
<b>Alcohols</b>												
1-Penten-3-ol	0.052 ± 0.007	4 ± 1	0.139 ± 0.036	17 ± 3	0.729 ± 0.152	44 ± 3	0.797 ± 0.132	26 ± 3	1.010 ± 0.329	17 ± 2	0.365 ± 0.006	23 ± 2
1-Octen-3-ol	0.063 ± 0.002	0.136 ± 0.051	0.120 ± 0.004	0.367 ± 0.022	0.108 ± 0.014	0.787 ± 0.260	0.101 ± 0.005	0.289 ± 0.025	0.106 ± 0.009	0.345 ± 0.266	0.102 ± 0.014	0.420 ± 0.032
4-Hepten-1-ol	0.939 ± 0.048	0.618 ± 0.177	1.353 ± 0.061	1.005 ± 0.026	1.206 ± 0.084	1.015 ± 0.051	1.094 ± 0.118	0.965 ± 0.092	1.199 ± 0.027	0.925 ± 0.316	1.132 ± 0.125	0.881 ± 0.002
<b>Pyrazines</b>												
Methyl pyrazine	1.137 ± 0.896	2.295 ± 0.340	6 ± 1	9.802 ± 0.228	8.609 ± 0.023	7.958 ± 0.356	9 ± 2	9 ± 3	7 ± 1	7.326 ± 0.614	11 ± 2	11 ± 1
2,5-Dimethyl pyrazine	3 ± 1	5 ± 1	40 ± 6	49 ± 3	27 ± 1	21 ± 1	48 ± 3	43 ± 8	46 ± 4	42.625 ± 0.216	55 ± 9	61 ± 6
2,6-Dimethyl pyrazine	3 ± 1	4 ± 1	8 ± 2	12 ± 2	7.453 ± 0.015	7.104 ± 0.252	14 ± 3	15 ± 4	36 ± 4	39 ± 3	41 ± 4	69 ± 3
2,3-Dimethyl pyrazine	0.136 ± 0.057	0.419 ± 0.112	0.582 ± 0.140	0.944 ± 0.016	1.096 ± 0.051	0.755 ± 0.043	1.133 ± 0.088	0.965 ± 0.247	3.931 ± 0.555	3 ± 1	4 ± 2	4 ± 1

Development of aroma: 1. Aliquots of FPHs (0.2 mL) mixed with a dextrose solution (0.05 mL (80  $\mu\text{mol/mL}$ )) and glycerol (500  $\mu\text{L}$ ); 2. Addition of fish oil (1.5 g/100 g); 3. Samples homogenised at 60 °C for 10 min, followed by heating at 110 °C for 30 min.

acid, butanoic acid and 3-methyl butanoic acid with relatively low threshold values (Table 3), have been reported to result from fermentation in several fish products (Giri et al., 2010). In the present study acetic acid was identified but its concentration did not differ significantly when compared to the control. These acids can derive either from lipolysis or from amino acid metabolism (deamination) (Montel, Masson, & Talon, 1998).

**Sulphur-containing compounds** dimethyl disulphide, (cooked cabbage aroma), and dimethyl trisulphide, (meaty and cooked onion aroma), increased considerably. These compounds, usually associated with deterioration of seafood, have a very strong effect on the overall food aroma even at low concentrations because of their low threshold values (Table 3) (Le Guen, Prost, & Demaimay, 2001; Selli & Cayhan, 2009). They are known to originate from the free, peptidic and proteinic sulphur amino acids, such as methionine, which concentration increased considerably after enzymatic hydrolysis (Table 2).

**Furans** Amongst the heterocyclic compounds identified, furans, which possess low odour threshold values, were present in much higher concentrations in the H-FPHs containing fish oil. They can be formed from amino acids by the Amadori rearrangement pathway, but also by the oxidation of fatty acids, i.e. the formation of 2-pentylfuran, which is one of the resulting products from the oxidation of linoleic acid (Giri et al., 2010; Taylor & Mottram, 1990; Whistler & Daniel, 1985).

**Pyrazines** characteristic compounds derived from the Maillard reaction imparting amongst other roasted and nutty flavour (Fox & Wallace, 1997; Giri et al., 2010), importantly increased in the H-FPHs. However, the fact that there were no significant differences in their concentration in the model systems with added fish oil compared to those without fish oil demonstrates that the addition of lipo-oxidation products did not contribute to the pool of carbohydrates. This might have been due to carbohydrates being in excess in the model systems (i.e. added glucose).

Fig. 1 illustrates the PCA conducted to evaluate the differences in the volatile composition of the different samples. The first three components explain 88.1% of the total variability. The first two principal components (PC1: 39.9% and PC2: 31.6%) differentiate between the H-FPHs containing additional fish oil from those without it. In the same way some of the volatile compounds such as hexanal, heptanal, 4-heptanal, 2,4,-heptadienal, 1-penten-3-ol or 1-octen-3-ol, derived from fatty acids such as linoleic and linolenic acids, are located on the right side of the plot together with the H-FPHs containing fish oil. The two H-FPHs controls (with and without fish oil) are separated from the compounds that illustrated a higher increase as a result of the addition of enzymes. These compounds include 2-methylbutanal, 3-methylbutanal, 1-hepten-4-ol and the sulphur compounds, which have also been found in the volatile profile of cooked fish or meals containing seafood (Ganeko et al., 2008; Giri et al., 2010; Selli & Cayhan, 2009). The addition of fish oil, however, did not have a significant impact on the formation of these compounds or pyrazines. The use of enzymes did produce a high DH with different concentrations of the free amino acids in the FPHs that would have been expected to have a high impact on the formation of the volatile compounds. However, the differences due to the use of these various enzymes were not significant in terms of concentrations of the Maillard reaction products including pyrazines, sulphur compounds and some aldehydes.

### 3.3. Sensory evaluation

Only enzyme B with increased amounts of fish oil was selected to carry out the sensory evaluation (Fig. 2). The selection of enzyme B was based on its high release of free amino acids. Different

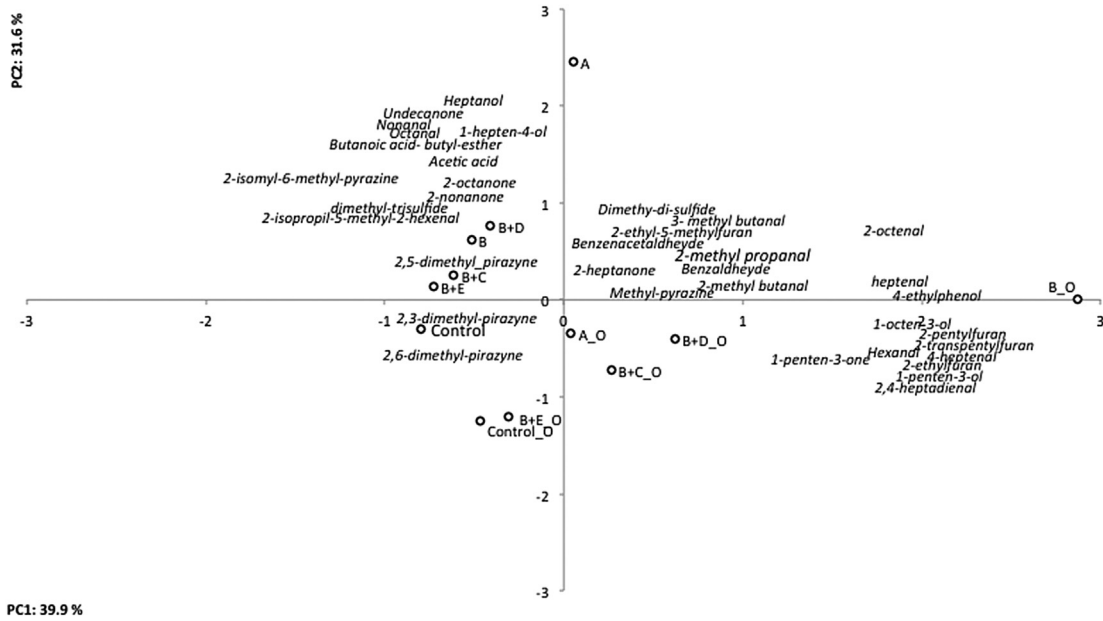


**Fig. 1.** Biplot for the different heated fish powder hydrolysates generated with the different enzymes (Control: fish powder heated without addition of enzymes; A: H-FPH-Flavopro Umami 852; B: H-FPH-Flavopro 750; B + C: H-FPH- Flavopro 750 + Promod439; B + D: H-FPH-Flavopro 750 + Promod671; B + E: H-FPH-Flavopro 750 + Promod144; \_O stands for addition of fish oil (1.5 g/100 g) and the volatile compounds obtained by the PCA. (PC1: 39.9%, PC2: 31.6%).

concentrations of fish oil (0, 1.5 and 3 g/100 g) were investigated to establish the role of fish oil on the formation of aroma, as well as its influence on sensory perception.

Panellists evaluated a total of six pairs of samples, corresponding to all the possible combinations. The statistic of Friedman test

for each sample was compared with the statistic of chi-square ( $X^2$ ) with 3 degrees of freedom (7.82,  $\alpha = 0.05$ ). A significant difference was observed for all the attributes in the samples evaluated.

Friedman test was followed by specific comparisons using Tukey's Honestly Significant Difference (HSD) multiple comparison

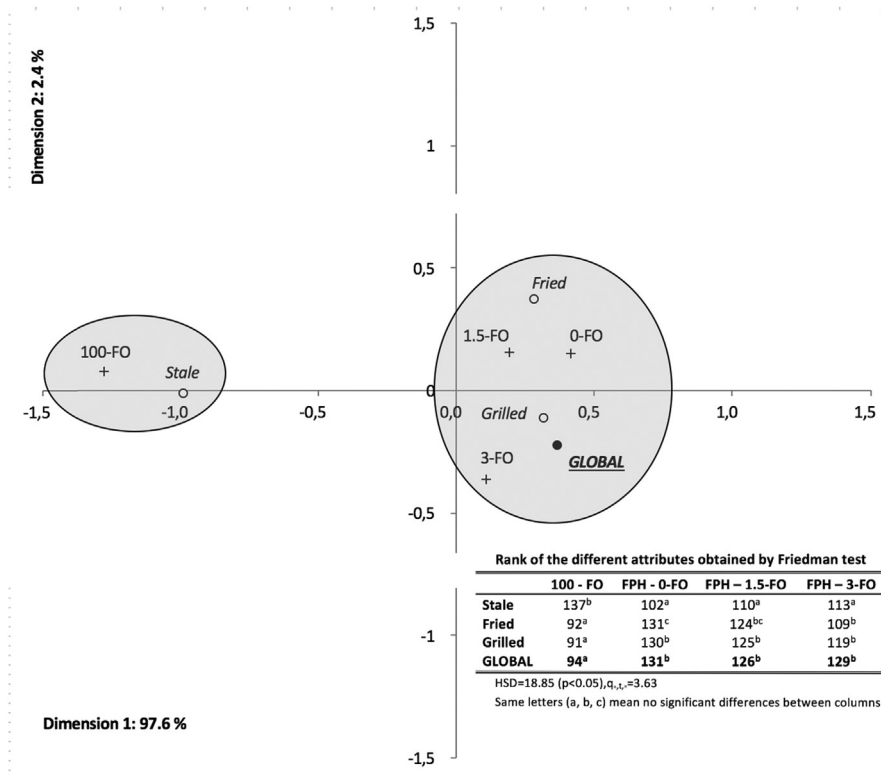


**Fig. 2.** Two-dimensional correspondence plot (99.9% of the total variance: dimension 1, 97.4%; dimension 2, 2.6%) obtained from performing the correspondence analysis for the four selected samples considering the fish powder hydrolysate obtained with enzyme A and increasing concentrations of fish oil (0, 1.5, 3 g/100 g and pure fish oil heated under the same conditions). Rank sum for the different attributes obtained by Friedman test. a, b and c Values in the same row with significant differences (95%).

post-hoc statistical test (Meilgaard et al., 1999). The value of  $q$  tabulated for 3 degrees of freedom ( $\alpha = 0.05$ ), was 3.63 and the HSD value obtained by Equation (4) was 18.85. The rank sums (addition of twice the sum of the frequencies of the columns to the sum of the frequencies of the rows for each sample (Peinado et al., 2012)) were calculated, a table of rank sum differences was prepared and the differences were compared with the value of HSD being significant when this value was exceeded (Fig. 2).

Panellist did not find significant differences between the H-FPHs samples regardless the concentration of added fish oil (0, 1.5 and 3 g/100 g) for all the attributes. However, panellists found significant differences for “stale” when “100% FO” was compared to H-FPHs without addition of fish oil. For “fried” aroma, significant differences were found when “100% FO” was compared with H-FPHs with 0 and 1.5 g/100 g of fish oil. Finally for “grilled” aroma, panellists found significant differences between “100% FO” and all the H-FPHs regardless the addition of fish oil. For the global preference the three H-FPHs had similar scores. Furthermore, Fig. 2 illustrates the two-dimensional plot of the sample scores and compound loadings obtained by the correspondence analysis. The first two dimensions explained 99.99% of the total variance (dimension 1, 97.4%; dimension 2, 2.6%). H-FPHs with different concentrations of fish oil were preferred by the panellists. “Fried” and “grilled” contributed the most to the global preference while “stale” contributed negatively to the global preference of the product. There were no differences between the three H-FPHs in terms global preference.

#### 4. Conclusions

Heating FPHs (as a source of amino acids), a source of sugar and fish oil successfully produced volatiles at a laboratory scale. Enzyme “B” (exopeptidase) on its own or in combination with endopeptidases is suggested as the starting point to liberate amino acids from fish protein while the dual activity enzyme “A” produced a lower amount of free amino acids.

The use of various enzymes produced different amounts of amino acids in the FPHs with important amounts of lysine, leucine, glutamic acid and alanine being released. These increased on free amino acids will have an influence on the characteristic compounds derived from the Maillard reaction, such as pyrazines, sulphur compounds or some aldehydes. Fish oil had a great impact on the volatile compounds associated with fish aroma; its addition enhanced the concentration of some lipid oxidation products such as hexanal, heptanal, 4-heptanal, 2,4-hexadienal, 1-penten-3-ol or 1-octen-3-ol, characteristic impact compounds in seafood, that have been previously identified in the volatile profile of cooked fish or meals containing seafood. “Grilled” and “fried” aromas, characteristics of FPHs heated with fish oil, were preferred by panellists, while fish oil on its own produced unpleasant aromas.

Future work involving different types and concentrations of fish oil together with sensory evaluation is suggested to investigate the acceptability of seafood-derived fish-like flavouring formulations based on such approaches.

#### Acknowledgements

The authors would like to thank Frutarom (UK) Ltd, Biocatalysts (UK) Ltd and the Technology Strategy Board (TSB), (UK) (101126) for the financial support given to this investigation.

#### References

Annadurai, D., Sadeeshkumar, R., Vijayalakshmi, M., & Pirithiviraj, N. (2012). Studies on growth of marine bacteria using marine fish waste medium. *International*

- Journal of Pharmaceutical & Biological Archives*, 3(4), 910–913, 0976 – 3333.
- AOAC Association of Official Analytical Chemists. (2000). *Official methods of analysis* (Washington, DC, USA).
- Aspmo, S. I., Horn, S. J., & Eijsink, V. G. H. (2005). Enzymatic hydrolysis of Atlantic cod (*Gadus morhua* L.) viscera. *Process Biochemistry*, 40(5), 1957–1966. <http://dx.doi.org/10.1016/j.procbio.2004.07.011>.
- Beh, E. J., Lombardo, R., & Simonetti, B. (2011). A European perception of food using two methods of correspondence analysis. *Food Quality and Preference*, 22(2), 226–231. <http://dx.doi.org/10.1016/j.foodqual.2010.10.001>.
- Caprino, F., Moretti, V. M., Bellagamba, F., Turchini, G. M., Busetto, M. L., Giani, I., et al. (2008). Fatty acid composition and volatile compounds of caviar from farmed white sturgeon (*Acipenser transmontanus*). *Analytica Chimica Acta*, 617(1–2), 139–147. <http://dx.doi.org/10.1016/j.aca.2008.02.005>.
- Church, F. C., Porter, D. H., Catignani, G. L., & Swaisgood, H. E. (1985). An o-phthalaldehyde spectrophotometric assay for proteinases. *Analytical Biochemistry*, 146(2), 343–348. [http://dx.doi.org/10.1016/0003-2697\(85\)90549-4](http://dx.doi.org/10.1016/0003-2697(85)90549-4).
- Decker, E., Elias, R., & McClements, D. J. (2010). *Oxidation in foods and beverages and antioxidant applications: management in different industry sectors*. Woodhead Publishing. Retrieved from <https://www.elsevier.com/books/oxidation-in-foods-and-beverages-and-antioxidant-applications/decker/978-1-84569-983-3>.
- Elmore, J. S., Koutsidis, G., Dodson, A. T., Mottram, D. S., & Wedzicha, B. L. (2005). Measurement of acrylamide and its precursors in potato, wheat, and rye model systems. *Journal of Agricultural and Food Chemistry*, 53(4), 1286–1293. <http://dx.doi.org/10.1021/jf048557b>.
- Escrive, I., Fernández-Segovia, I., Serra, J. A., Andrés, A., & Barat, J. M. (2001). Evaluación sensorial del bacalao desalado, pretratado térmicamente listo para cocinar. *Alimentaria: Revista de Tecnología E Higiene de Los Alimentos*, 322, 51–54, 0300–5755.
- Fox, P. F., & Wallace, J. M. (1997). Formation of flavor compounds in cheese. In *Advances in applied microbiology* (Vol. 45, pp. 17–85). [http://dx.doi.org/10.1016/S0065-2164\(08\)70261-2](http://dx.doi.org/10.1016/S0065-2164(08)70261-2).
- Ganek, N., Shoda, M., Hirohara, I., Bhadra, A., Ishida, T., Matsuda, H., et al. Matoba, T. (2008a). Analysis of volatile flavor compounds of sardine (*Sardinops melanosticta*) by solid phase microextraction. *Journal of Food Science*, 73(1), S83–S88. <http://dx.doi.org/10.1111/j.1750-3841.2007.00608.x>.
- Ghorbel, S., Souissi, N., Triki-Ellouz, Y., Dufosse, L., Guerdar, F., & Nasri, M. (2005). Preparation and testing of Sardinella protein hydrolysates as nitrogen source for extracellular lipase production by *Rhizopus oryzae*. *World Journal of Microbiology and Biotechnology*, 21(1), 33–38. <http://dx.doi.org/10.1007/s11274-004-1556-2>.
- Giri, A., Osako, K., & Ohshima, T. (2010). Identification and characterisation of headspace volatiles of fish miso, a Japanese fish meat based fermented paste, with special emphasis on effect of fish species and meat washing. *Food Chemistry*, 120(2), 621–631. <http://dx.doi.org/10.1016/j.foodchem.2009.10.036>.
- González-Tomás, L., Carbonell, I., & Costell, E. (2004). Influence of type, concentration and flow behaviour of hydrocolloid solutions on aroma perception. *European Food Research and Technology*, 218(3), 248–252. <http://dx.doi.org/10.1007/s00217-003-0852-7>.
- Guerdar, F., Dufosse, L., Broise, D., La, & Binet, A. (2001). Enzymatic hydrolysis of proteins from yellowfin tuna (*Thunnus albacares*) wastes using Alcalase. *Journal of Molecular Catalysis B: Enzymatic*, 11, 1051–1059. doi:1381-1177/01.
- Guerrero, L., Claret, A., Verbeke, W., Enderli, G., Zakowska-Biemans, S., Vanhonacker, F., et al. Hersleth, M. (2010). Perception of traditional food products in six European regions using free word association. *Food Quality and Preference*, 21(2), 225–233. <http://dx.doi.org/10.1016/j.foodqual.2009.06.003>.
- IUPAC (1992). [http://lipidlibrary.aocs.org/topics/ester\\_93/file.pdf](http://lipidlibrary.aocs.org/topics/ester_93/file.pdf) Accessed 20.07.13
- Kawai, T., & Sakaguchi, M. (1996). Fish flavour. *Critical Reviews in Food Science and Nutrition*, 36(3), 257–298. <http://dx.doi.org/10.1080/10408399609527725>.
- Leffingwell.com: <http://www.leffingwell.com/odorthre.htm> (Accessed 12.01.15).
- Le Guen, S., Prost, C., & Demaimay, M. (2001). Evaluation of the representativeness of the odour of cooked mussel extracts and the relationship between sensory descriptors and potent odorants. *J. Agric. Food Chem.*, 49, 1321–1327. <http://dx.doi.org/10.1021/jf000781n>.
- Medina Hernández, M. J., Villanueva Camañas, R. M., Monfort Cuenca, E., & García Alvarez-Coque, M. C. (1990). Determination of the protein and free amino acid content in a sample using o-phthalaldehyde and N-acetyl-L-cysteine. *The Analyst*, 115(8), 1125–1128. Retrieved from <http://www.ncbi.nlm.nih.gov/pubmed/2256555>.
- Meilgaard, M., Civille, G. V., & Carr, B. T. (1999). Attribute difference test III. Pairwise ranking test: Friedman analysis. In *Sensory evaluation techniques* (3rd ed., pp. 103–106). Taylor & Francis Group: CRC Press. Retrieved from <http://goo.gl/vvAjSK>.
- Montel, M. C., Masson, F., & Talon, R. (1998). Bacterial role in flavour development. *Meat Science*, 49, S111–S123. [http://dx.doi.org/10.1016/S0309-1740\(98\)90042-0](http://dx.doi.org/10.1016/S0309-1740(98)90042-0).
- Nielsen, P. M., Petersen, D., & Dambmann, C. (2001). Improved method for determining food protein degree of hydrolysis. *Food Chemistry and Toxicology*, 66(5), 642–646. <http://dx.doi.org/10.1111/j.1365-2621.2001.tb04614.x>.
- Ortiz, J., Romero, N., Robert, P., Araya, J., López-Hernández, J., Bozzo, C., et al. Rios, A. (2006). Dietary fiber, amino acid, fatty acid and tocopherol contents of the edible seaweeds *Ulva lactuca* and *Durvillaea antarctica*. *Food Chemistry*, 99, 98–104. <http://dx.doi.org/10.1016/j.foodchem.2005.07.027>.
- pherobase.com: <http://goo.gl/DjyLOB> (Accessed 10.02.15).
- Peinado, I., Girón, J., Koutsidis, G., & Ames, J. (2014). Chemical composition, antioxidant activity and sensory evaluation of five different species of brown edible seaweeds. *Food Research International*, 66, 36–44. <http://dx.doi.org/10.1016/>

- [j.foodres.2014.08.035](http://dx.doi.org/10.1016/j.foodres.2014.08.035).
- Peinado, I., Rosa, E., Heredia, A., Escriche, I., & Andrés, A. (2012). Optical, mechanical and sensorial properties of strawberry spreadable products formulated with isomaltulose. *Food and Bioprocess Technology*, 6(9), 2353–2364. <http://dx.doi.org/10.1007/s11947-012-0970-y>.
- Selli, S., & Cayhan, G. G. (2009). Analysis of volatile compounds of wild gilthead sea bream (*Sparus aurata*) by simultaneous distillation–extraction (SDE) and GC–MS. *Microchemical Journal*, 93(2), 232–235. <http://dx.doi.org/10.1016/j.microc.2009.07.010>.
- Souissi, N., Bougatef, A., Triki-ellouz, Y., & Nasri, M. (2007). Biochemical and functional properties of *Sardinella (Sardinella aurata)* by-product hydrolysates. 45(2), 187–194, 1330–9862.
- Taylor, A. J., & Mottram, D. S. (1990). Composition and odour of volatiles from autoxidised methyl arachidonate. *Journal of the Science of Food and Agriculture*, 50(3), 407–417. <http://dx.doi.org/10.1002/jsfa.2740500313>.
- Whistler, R. L., & Daniel, J. R. (1985). Carbohydrates. In O. Fennema (Ed.), *Food chemistry* (pp. 248–339). <http://dx.doi.org/10.1007/978-3-540-69934-7>.
- Whitfield, F. B., Freeman, D. J., Last, J. H., Bannister, P. A., & Kennett, B. H. (1982). Oct-1-en-3-ol and (5Z)-Octa-1,5-dien-3-ol, compounds important in the flavour of prawns and sand-lobsters. *Australian Journal of Chemistry*, 35(2), 373–383. <http://dx.doi.org/10.1071/CH9820373>.
- Whitfield, F. B., Last, J. H., Shaw, K. J., & Tindale, C. R. (1988). 2,6-Dibromophenol: the cause of an iodoform-like off-flavour in some Australian crustacea. *Journal of the Science of Food and Agriculture*, 46(1), 29–42. <http://dx.doi.org/10.1002/jsfa.2740460104>.
- Yaich, H., Garna, H., Besbes, S., Paquot, M., Blecker, C., & Attia, H. (2011). Chemical composition and functional properties of *Ulva lactuca* seaweed collected in Tunisia. *Food Chemistry*, 128(4), 895–901. <http://dx.doi.org/10.1016/j.foodchem.2011.03.114>.



# Extraction and characterization of acid-soluble collagen from scales and skin of tilapia (*Oreochromis niloticus*)



Junde Chen<sup>\*</sup>, Long Li, Ruizao Yi, Nuohua Xu, Ran Gao, Bihong Hong

Marine Biological Resource Comprehensive Utilization Engineering Research Center of the State Oceanic Administration, The Third Institute of Oceanography of the State Oceanic Administration, Xiamen 361005, China

## ARTICLE INFO

### Article history:

Received 30 June 2015  
Received in revised form  
20 October 2015  
Accepted 30 October 2015  
Available online 4 November 2015

### Keywords:

Acid-soluble collagen  
LC-MS/MS  
Characteristics  
Tilapia scales  
Fugu skin

## ABSTRACT

Acid-soluble collagen (ASC) was extracted from scales and skin of tilapia. The yields of scale collagen (SCC) and skin collagen (SKC) were 3.2 g/100 g and 27.2 g/100 g respectively, dry weight. The SDS-PAGE profile showed all collagen samples contained  $[\alpha 1(I)]_2\alpha 2(I)$  component and were characterized as type I collagen. LC-MS/MS analysis confirmed the SCC and SKC to be *Oreochromis niloticus* type I collagen. Amino acid analysis revealed the imino acid content from the SCC and SKC samples were 207 and 197 residues/1000 amino acid residues, respectively. Based on FTIR spectra and X-ray diffraction, isolation of ASC did not affect its three dimensional structure. Zeta potential studies indicated both SCC and SKC exhibited a net zero charge at pH 6.82 and 6.42, respectively. Both ASC samples exhibited high solubility in acidic pH (1–3) and lost their solubility at NaCl concentrations below 3 g/100 mL. The data collected here indicate that SCC and SKC may be suitable for use as an alternative to land-based mammalian collagen in food, nutraceuticals and pharmaceutical industries.

© 2015 Elsevier Ltd. All rights reserved.

## 1. Introduction

Collagen is the main structural protein in vertebrates, accounting for approximately 30% of the total protein in these organisms (Sinthusamran, Benjakul, & Kishimura, 2013). Currently, researchers have identified at least 29 different types of collagen from a variety of animal tissues, and each type of collagen has its own unique amino acid sequence and molecular structure (Liu, Liang, Regenstein, & Zhou, 2012). Among these various collagen proteins, type I is the most common form. It is used in food, biomedical materials, pharmaceuticals, and cosmetics industries (Sinthusamran et al., 2013). Typically, the collagen used in commercial production processes is derived from terrestrial organisms, such as cows, pigs, and chickens. However, in recent years, due to the increasing incidences and prevalence of avian flu, mad cow disease, foot and mouth disease, and other infectious diseases, collagen extraction from land animals has had an increasing risk of diseases (Jongiareonrak, Benjakul, Visessanguan, Nagai, & Tanaka, 2005). In addition, due to religions and consumer related issues,

porcine collagen use is prohibited in some regions and by various religious groups, such as Muslims and Jews (Ahmad & Benjakul, 2010). Therefore, researchers have focused on searching for new sources of collagen. In China, fish and processed fish products are some of the most important food staples. Tilapia are favorite fish foods of the Chinese people. During fish processing, a large amount of by-products are produced, including scales, skin, and bones. These by-products account for 50–70 g/100 g of total fish weight (Kittiphattanabawon, Benjakul, Visessanguan, Nagai, & Tanaka, 2005). Of these by-products, scales and skin are rich in collagen, which can be used as an alternative source for collagen traditionally harvested from land mammals. In this way, the extraction of collagen from the scales and skin from tilapia would not only improve the added value of these fish products, but also reduce environmental pollution. Currently, collagen is extracted from perch (Sinthusamran et al., 2013), striped catfish (Singh, Benjakul, Maqsood, & Kishimura, 2011), and gold shall snapper (Matmaroh, Benjakul, Prodpran, Encarnation, & Kishimura, 2011), and horse mackerel scales (Thuy, Okazaki, & Osako, 2014). However, there are few reports that systematically compare the characteristics of scale collagen (SCC) and skin collagen (SKC) from tilapia. Therefore, the purpose of this investigation was to address the extraction of acid-soluble collagen (ASC) from the scales and skin of tilapia, and to compare the characteristics of collagen derived from these two organs.

<sup>\*</sup> Corresponding author.

E-mail addresses: [jdchen@tio.org.cn](mailto:jdchen@tio.org.cn) (J. Chen), [lli@tio.org.cn](mailto:lli@tio.org.cn) (L. Li), [rzyi@tio.org.cn](mailto:rzyi@tio.org.cn) (R. Yi), [nhxu@tio.org.cn](mailto:nhxu@tio.org.cn) (N. Xu), [rgao@tio.org.cn](mailto:rgao@tio.org.cn) (R. Gao), [bhhong@tio.org.cn](mailto:bhhong@tio.org.cn) (B. Hong).

## 2. Materials and methods

### 2.1. Materials

Tilapia (*Oreochromis niloticus*) were purchased from a market in Xiamen, China and authenticated by Professor Ruizao Yi of the Xiamen, Marine Biological Resource Comprehensive Utilization Engineering Research Center, SOA. Tilapia scales and skin were manually removed from the fish and washed with water. The harvested scales and skin were stored in polyethylene bags at  $-20\text{ }^{\circ}\text{C}$  until experimentation. Sodium dodecyl sulfate (SDS), Coomassie blue R-250 and *N,N,N',N'*-tetramethylethylenediamine (TEMED) were obtained from Bio-Rad Laboratories (Hercules, CA, U.S.). Acetonitrile was HPLC grade and other chemicals and reagents were of analytical grade.

### 2.2. Preparation of ASC from the scales and skin of tilapia

ASC from the scales and skin was isolated following the protocol previously reported by Matmaroh et al. (2011), with some modifications. Thawed scales and skin were treated with 10 volumes of 0.1 mol/L  $\text{NaHCO}_3$  for 6 h to remove non-collagenous proteins and pigment. Scales and skin were then neutralized by washing with water until samples reached a pH 7. The scales were cut into small pieces. Scales and skin samples were then subjected to ASC extraction by treating samples with 0.5 mol/L acetic acid for 24 h. Next, samples were centrifuged at 20,000 g for 15 min. The supernatants of scale ASC extraction and skin ASC extraction were salted out by adding NaCl to a final concentration of 2 and 0.5 mol/L, respectively. The precipitate was collected after centrifugation at 10,000 g for 20 min. The precipitate was dissolved in 0.5 mol/L acetic acid at the ratio of 1:9 (w/v) and then dialyzed in 20 volumes of 0.1 mol/L acetic acid, followed by distilled water. All processes were carried out at  $4\text{ }^{\circ}\text{C}$ . ASC was lyophilized and then stored at  $-20\text{ }^{\circ}\text{C}$  until experimentation.

### 2.3. Yield

The yield of ASC was calculated based on the dry weight of starting material:

$$\text{Yield (g/100 g)} = (\text{Weight of lyophilized collagen}) / (\text{Weight of initial dry fish by-product}) \times 100$$

### 2.4. Analyses

#### 2.4.1. Protein sequence analysis

Collagen samples were dissolved in purified water to prepare an 8 mg/mL solution. Sample solutions were then mixed with loading buffer. The mixture was boiled for 3 min at  $100\text{ }^{\circ}\text{C}$ , and centrifuged for 5 min (8500 g) after cooling. SDS-PAGE gels were prepared using a 8% separating gel matrix and 3% concentrating gel matrix. Electrophoresis was performed at 60 V. After electrophoresis, the gels were placed in a 0.25 mol/L potassium chloride solution at  $4\text{ }^{\circ}\text{C}$  for 10 min. Next, subunit bands were excised and washed with pure water till they became transparent. The excised bands of collagen subunits were minced and 400  $\mu\text{L}$  of Solution A (1  $\mu\text{g/mL}$  PVPP and 2  $\mu\text{g/mL}$   $\beta$ -mercaptoethanol in acetone solution containing 10 mL/100 mL trifluoroacetic acid) from a PAGE gel trace protein extraction kit [Sangon Biotech (Shanghai) Co., Ltd.] was added. Samples were incubated for 18 h, next extraction samples were transferred to centrifuge tubes, and

2 mL of Solution B (Tris-HCl at pH = 8.83) was added. Samples were incubated at  $4\text{ }^{\circ}\text{C}$  for 30 min and centrifuged for 5 min (8500 g) at  $4\text{ }^{\circ}\text{C}$ . The supernatant was removed and the white precipitate was placed in a vacuum desiccator to remove moisture, and yielded isolated collagen subunits. Collagen subunits were subjected to analysis.

Liquid chromatography/mass spectrometry/mass spectrometry (LC-MS/MS) analysis was used to determine collagen protein sequences. Collagen subunits (6 mg) were dissolved in 225  $\mu\text{L}$  of 100 mmol/L ammonium bicarbonate and then 10 mmol/L DDT was added. Samples were incubated for 1 h at  $58\text{ }^{\circ}\text{C}$  and then 225  $\mu\text{L}$  of 55 mmol/L iodoacetamide was added. Next, samples were incubated in the dark for 1 h at room temperature to allow for alkylation. Finally, 100  $\mu\text{g}$  of trypsin was added and the samples were incubated at  $37\text{ }^{\circ}\text{C}$  for 20 h.

The hydrolyzed samples were separated using an Eksigent nanoLC-Ultra™ 2D LC system (AB SCIEX) equipped with a C18 column (100  $\mu\text{m} \times 3\text{ cm}$ , C18, 3  $\mu\text{m}$ , 150  $\text{\AA}$ ), with a flow rate of 4  $\mu\text{L}/\text{min}$ . For gradient elution, the samples were eluted with 5–35 mL/100 mL solvent B over 70 min, where solvent A was 5 mL/100 mL acetonitrile, containing 0.1 mL/100 mL formic acid and solvent B was 100 mL/100 mL acetonitrile, containing 0.1 mL/100 mL formic acid. A TripleTOF 5600 system (AB SCIEX), with a spray voltage of 2.5 kV, and TOF-MS was used for MS scans. The information acquisition mode used was Information Dependent Analysis (IDA) and the map data scan time was 250 ms.

All MS/MS data were analyzed using the NCBI Mascot database (Matrix Science, London, UK; PLGS v2.3). The range of allowable quality error was: Peptide Mass Tolerance  $\pm 15\text{ mg/kg}$ , Fragment Mass Tolerance  $\pm 0.15\text{ Da}$ . PLGS v23 was used to verify the protein subunit identification results. A confidence level of  $>95\%$  protein identification, assigned by the Mascot program, was considered a valid protein identification.

#### 2.4.2. Sodium dodecyl sulfate-polyacrylamide gel electrophoresis (SDS-PAGE)

SDS-PAGE was performed using the Laemmli (1970) protocol with slight modification. A mini-protein vertical slab electrophoresis system was used (Bio-Rad Laboratories, U.S.). The staining ratio of  $\alpha 1$  to  $\alpha 2$  were determined using Quantity One 4.6.0 (Bio-Rad Laboratories, U.S.).

#### 2.4.3. Amino acid composition

The amino acid compositions of samples were analyzed according to the protocol reported by Zeng et al. (2012).

#### 2.4.4. Fourier transform infrared (FTIR) spectroscopy

FTIR spectroscopy of samples were analyzed according to the protocol reported by Singh et al. (2011) with slight modification. Collagen samples were subjected to FTIR analysis using a horizontal ATR Trough plate crystal cell (PIKE technology Inc., Madison, WI, U.S.) equipped with a Bruker Model VERTEX 70 FTIR spectrometer (Bruker Co., Ettlingen, Germany). Analysis of spectral data was carried out using the OPUS 6.5 data collection software program (Bruker Co., Ettlingen, Germany).

#### 2.4.5. X-ray diffraction

The crystal structures of lyophilized collagen samples were determined using a DX-1000 X-ray diffraction instrument (Dandong Fangyuan Instrument Co., Ltd.). The X-ray source was Cu Ka, tube voltage 40 kV, tube current 25 mA, scanning range  $10^{\circ}$ – $50^{\circ}$  ( $2\theta$ ), and the scanning speed was  $0.06^{\circ}/\text{s}$ .

#### 2.4.6. Zeta potential

Zeta potential of samples were analyzed according to the

protocol described by Singh et al. (2011). Collagen samples were dissolved in 0.5 mol/L acetate to a final concentration of 0.05 g/100 g. These samples were stirred for 6 h at 4 °C. The zeta potential of the ASC samples was determined using a zeta potential analyzer (ZetaPALS, Brookhaven Instruments Co., Holtsville, NY, U.S.). Using a titration instrument (BIZTU, Brookhaven Instruments Co., Holtsville, New York, U.S.), the pH of the samples (20 mL) was adjusted across a pH range (1–11) with 1 mol/L KOH and 1 mol/L nitric acid. The isoelectric point (pI) was determined from a pH rendering a zero potential.

#### 2.4.7. Solubility

The effects of pH and NaCl on the collagen samples' solubility were done according to the protocol previously reported by Liu et al. (2012).

##### 1) Effect of pH on solubility

ASC samples were dissolved in 0.5 mol/L acetic acid at 4 °C for 12 h to obtain a final concentration of 3 mg/mL. Next, 8 mL of ASC sample solutions were adjusted, with either 6 mol/L HCl or 6 mol/L NaOH, to produce a final pH ranging from 1 to 10. The volume of the solution was brought up to 10 mL with 0.5 mol/L acetic acid previously adjusted to the same pH as the ASC samples. The solution was centrifuged at 20,000 g at 4 °C for 30 min. Protein concentration in the supernatant was determined according to a protocol previously reported (Lowry, Rosebrough, Farr, & Randall, 1951), using bovine serum albumin as a standard. Relative solubility was calculated in comparison to that obtained at the pH giving the highest solubility.

##### 2) Effect of NaCl on solubility

ASC samples were dissolved in 0.5 mol/L acetic acid at 4 °C for 12 h to produce a final concentration of 6 mg/mL. Next, 5 mL of ASC sample solutions were mixed with 5 mL of 0.5 mol/L acetic acid containing various concentrations of NaCl to obtain final concentrations of 0, 1, 2, 3, 4, 5, and 6 g/100 g. Solutions were then centrifuged at 20,000 g at 4 °C for 30 min. The protein concentration, in the supernatant, was measured as described in the previous section. Relative solubility was calculated in comparison to the control (sample without NaCl).

#### 2.4.8. Statistical analyses

Statistical calculations were performed using a SPSS software package. One-way ANOVA followed by a Dunnett's test for multiple comparisons of treatment means with a control, were used. Statistical significance was defined as  $P < 0.05$ .

### 3. Results and discussion

#### 3.1. Yield

ASCs, isolated from skin and scales, reached yield of 27.2 g/100 g and 3.2 g/100 g (dry weight), respectively. The yields of SKC were higher than those from giant red sea cucumber skin (3.4 g/100 g) but were lower than cobia skin (35.5 g/100 g) (Liu, Oliveira, & Su, 2010; Zeng et al., 2012). The yields of SCC were higher than those from spotted golden goatfish scales (0.45 g/100 g) but similar to those from rohu scales (~5 g/100 g) (Matmaroh et al., 2011; Pati, Adhikari, & Dhara, 2010). The difference in the yields of these ASCs indicated that the collagen yields might be associated with interchain cross-linking at the telopeptide region of the collagen, which makes the collagen less soluble under acidic conditions (Tamilmozhi, Anguchamy, & Arumugam, 2013). The above-

mentioned data also indicated the added-value of fish by-products may be improved by SCC and SKC isolation.

#### 3.2. SDS-PAGE profile of collagen samples

SDS-PAGE data of Collagen samples and their  $\alpha$ -chains are shown in Fig. 1. SCC and SKC samples contained two different  $\alpha$  chains ( $\alpha 1$  and  $\alpha 2$ ). The initial estimates of the staining ratio of  $\alpha 1$  to  $\alpha 2$  were 2.17 and 2.33 for SCC and SKC, respectively. The band intensity of  $\alpha 1$  was higher than that of  $\alpha 2$  by approximately 2 fold. This suggested that the collagen contained 2 identical subunits of  $\alpha 1$ . Matmaroh et al. reported that type I collagen contain 2 identical subunits of  $\alpha 1$  and one of  $\alpha 2$  (2011). Moreover, the electrophoretic positions of the chains ( $\alpha 1$ -MW 132 kDa;  $\alpha 2$ -MW 121 kDa) of SCC were slightly higher the positions observed for SKC ( $\alpha 1$ -MW 130 kDa;  $\alpha 2$ -MW 120 kDa). Type I collagen has been reported to be the primary collagen found in fish skin and scales (Tamilmozhi et al., 2013). This observation is consistent with findings that reported type I collagen from lizard fish scales ( $\alpha 1$ -MW less than 120 kDa;  $\alpha 2$ -MW less than 110 kDa) (Thuy et al., 2014), spotted golden goatfish scale ASC ( $\alpha 1$ -MW 117 kDa;  $\alpha 2$ -MW 108 kDa) (Matmaroh et al., 2011), and seafish skin ASC ( $\alpha 1$ -MW less than 122 kDa;  $\alpha 2$ -MW less than 116 kDa) (Sinthusamran et al., 2013). SKC and SCC has been reported to be type I collagen that contains, two identical  $\alpha 1$  chains and one  $\alpha 2$  chain in the molecular form of [ $\alpha 1(I)$ ]<sub>2</sub> $\alpha 2(I)$  (Liu et al., 2012). Additionally, both SCC and SKC contained high molecular weight (MW) components, including  $\beta$  chains (dimers) and  $\gamma$  chains (trimers).

#### 3.3. Protein identification

After trypsinization, protein sequences were determined using LC-MS/MS analysis. The results are shown in Table 1. Proteins were identified based on the following parameters: 1) Scores calculated from collagen subunit MS/MS fragment ion mass matches; 2) Coverage of protein sequences (%); 3) Number of collagen subunit peptides that matched peptides in the NCBI database. As shown in

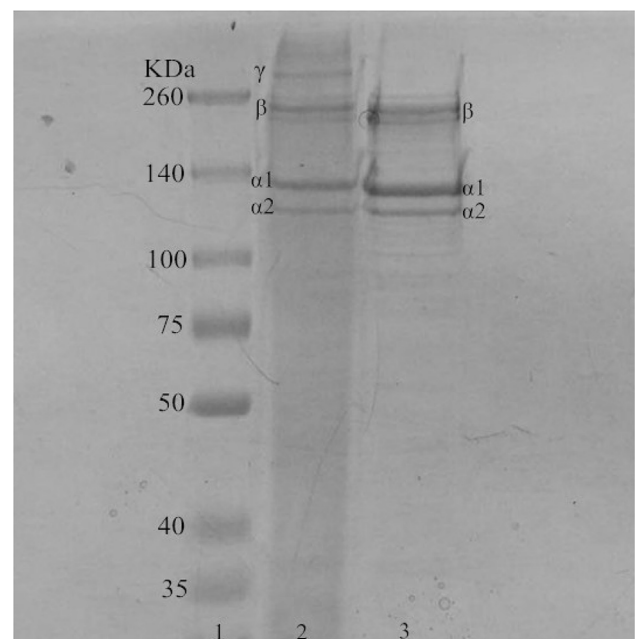


Fig. 1. SDS-PAGE profiles of SCC and SKC from fish by-products. Line 1: Standard protein marker; Line 2: Sample 1 (SCC); Line 3: Sample 2 (SKC).

**Table 1**  
Summary of LC-MS/MS analysis.

Protein	Protein description	Accession no.	Mass (Da)/PI	Coverage <sup>a</sup> (%)	Score	Peptide hits
SKC subunit $\alpha$ 1	Collagen alpha 1(I), ( <i>Oreochromis niloticus</i> )	gi 359804080	138225/5.64	10	1415	8
SKC subunit $\alpha$ 2	Collagen alpha 2(I), ( <i>Oreochromis niloticus</i> )	gi 348539636	127407/9.18	23	6654	23
SCC subunit $\alpha$ 1	Collagen alpha 1 (I), ( <i>Oreochromis niloticus</i> )	gi 359804080	138225/5.64	15	1601	15
SCC subunit $\alpha$ 2	Collagen alpha 2 (I), ( <i>Oreochromis niloticus</i> )	gi 359804082	126856/9.18	12	1023	14

<sup>a</sup> Matched peptide coverage of protein sequence.

the Table 1, the SKC subunit  $\alpha$ 1 score matching the *O. niloticus* type I collagen subunit  $\alpha$ 1 was 1415, the coverage was 10%, and contained 8 matching peptides. The SKC subunit  $\alpha$ 2 score matching the *O. niloticus* type I collagen subunit  $\alpha$ 2 was 6654, the coverage was 23%, and contained 23 matching peptides. The SCC subunit  $\alpha$ 1 score matching the *O. niloticus* type I collagen subunit  $\alpha$ 1 was 1601, the coverage was 15%, and contained 15 matching peptides. The SCC subunit  $\alpha$ 2 score matching the *O. niloticus* type I collagen subunit  $\alpha$ 2 was 1023, the coverage was 12%, and contained 14 matching peptides. These data are more robust results than the *O. niloticus* collagen identification data reported by Zeng et al. (2012). Data reported in the Zeng study were; sample collagen data and *O. niloticus* collagen subunit  $\alpha$ 1 had a match score of 93, coverage of 2%, and contained 3 matching peptides; sample collagen data and *O. niloticus* collagen subunit  $\alpha$ 2 had a match score of 117, coverage rate of 2%, and contained 3 matching peptides. Therefore, we concluded the SCC and SKC to be *O. niloticus* type I collagen.

### 3.4. Collagen amino acid composition

The amino acid composition of collagen samples were expressed as amino acid residues per 1000 total amino acid residues (Table 2). SCC and SKC samples were rich in glycine, proline, alanine, and hydroxyproline. Moreover, the samples had low concentrations of cysteine, tyrosine, and hydroxylysine. Glycine, accounted for nearly one-third of the total residues, and it occurred as every third residue in samples examined. These results were in accordance with collagens isolated from the scales and skin of other fish species, such as collagen from rohu scales, cata scales (Pati

**Table 2**  
ASC amino acid composition (residues/1000 amino acid residues).

Amino acids	SCC	SKC
Arginine	41	41
Hydroxylysine	10	9
Lysine	52	52
Alanine	137	141
Threonine	27	27
Glycine	276	287
Valine	35	33
Hydroxyproline	72	70
Serine	20	19
Proline	135	127
Isoleucine	12	11
Leucine	25	24
Methionine	12	14
Histidine	13	14
Phenylalanine	18	18
Glutamine acid	47	51
Aspartic acid	58	56
Cysteine	2	1
Tyrosine	6	5
Hydrophobic amino acids <sup>a</sup>	401	395
Imino acid <sup>b</sup>	207	197

<sup>a</sup> Hydrophobic amino acids: Alanine + Threonine + Valine + Proline + Isoleucine + Leucine + Methionine + Phenylalanine.

<sup>b</sup> Imino acid: Proline + Hydroxyproline.

et al., 2010) and collagen from ornate threadfin bream skin (Nalinanon, Benjakul, Kishimura, & Osako, 2011). SKC contained higher amounts of alanine, glycine, and glutamine acid but lower amounts of valine, hydroxyproline, proline, and aspartic acid than the SCC did. It has been reported that food-protein hydrolysates with antioxidant activity are composed of hydrophobic amino acids, leucine or valine at the N-terminus and contain histidine, tyrosine or proline in the sequence (Vercruyse, Smagghe, Beckers, & Camp, 2009). Peptides with hydrophobic amino acids (such as alanine, threonine, valine, proline, isoleucine, leucine, methionine and phenylalanine) at the C-terminal usually give rise to stronger ACE inhibitory activity because the hydrophobic properties of these peptides render them accessible the active site of ACE (Cheung, Wang, Ondetti, Sabo, & Cushman, 1980; Li, Le, Shi, & Shrestha, 2004). Both SCC and SKC, were rich in hydrophobic amino acids which indicate collagen could be used as an alternative source for antioxidant peptides and antihypertensive peptides. The imino acid content (Proline + Hydroxyproline) of SCC were 207 residues/1000 amino acid residues, which were higher than those reported for seabass scale ASC (193 residues/1000 amino acid residues) (Chuaychan, Benjakul, & Kishimura, 2015), spotted golden goatfish scale ASC (178 residues/1000 amino acid residues) (Matmaroh et al., 2011), and bighead carp scale ASC (156 residues/1000 amino acid residues) (Liu et al., 2012). Additionally, the imino acid content of SKC were 197 residues/1000 amino acid residues, which were similar to seabass skin ASC (195 residues/1000 amino acid residues) (Sinthusamran et al., 2013), but lower than those reported for striped catfish skin ASC (206 residues/1000 amino acid residues) (Singh et al., 2011), cobia skin ASC (203 residues/1000 amino acid residues) (Zeng et al., 2012). The imino acid content was used to determine the thermal stability of the collagen and the formation of junction zones via hydrogen bonding (Sinthusamran et al., 2013). The pyrrolidine rings of proline and hydroxyproline impose restrictions on the conformation of the polypeptide chain and help to strengthen the triple helix (Nalinanon et al. 2011). Thus, SCC exhibited higher thermal stability than SKC, owing to the higher content of imino acid.

### 3.5. Collagen FTIR spectra

The collagen FTIR spectra exhibited characteristic peaks of Amide A and B, as well as Amide I, II, III (Fig. 2). The major peaks in the collagen spectra were similar to those of collagen purified from other fish species (Kaewdang, Benjakul, Kaewmanee, & Kishimura, 2014; Singh et al., 2011; Zhang, Duan, Huang, Song, & Regenstein, 2014). The amide A bands of SCC and SKC were found at a wavenumbers of 3318.24 and 3321.55  $\text{cm}^{-1}$ , respectively, and associated with N–H stretching vibrations. According to Doyle, Bendit, & Blout, 1975, a free N–H stretching vibration occurs in the range of 3400–3440  $\text{cm}^{-1}$ , and when the NH group of a peptide is involved in a hydrogen bond, the position is shifted to a lower frequency (Doyle et al., 1975). The amide B bands of SCC and SKC were found at a wavenumbers of 2925.91 and 2924.26  $\text{cm}^{-1}$ , respectively, and associated with an asymmetrical stretch of  $\text{CH}_2$  (Abe & Krimm, 1972). The amide I, II, and III bands are known to be responsible

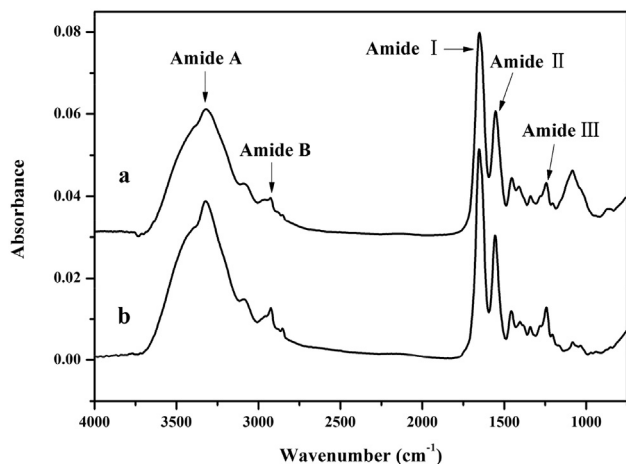


Fig. 2. FTIR spectra of SCC (a) and SKC (b).

for the degree of molecular order found in collagen, and to be involved in the formation of its triple helical structure, which results from C=O stretching, and N–H bending and C–H stretching, respectively (Muyonga, Cole, & Duodu, 2004). The amide I, II, and III bands of SKC were found at 1652.22, 1554.92, and 12442.3  $\text{cm}^{-1}$ , respectively. The amide I, II, and III bands of SCC were found at lower wavenumbers of 1651.03, 1551.91, and 1242.83  $\text{cm}^{-1}$  compared to the SKC, suggesting SCC had more and/or stronger hydrogen bonds. Increased hydrogen bonding in the triple helical structure of SCC would result in a lower degree of molecular order in the collagen. Additionally, strong C–H stretching occurred at wavenumbers of 1453.29 and 1453.87  $\text{cm}^{-1}$  for SCC and SKC, respectively. According to Plepis, Goissis, & Das-Gupta, 1996, an absorption ratio of approximately 1, between the amide III and the 1450–1454  $\text{cm}^{-1}$  band, indicates that triple helical structure is intact (Plepis et al., 1996). Radii of 0.93 and 1.10 were obtained for SKC and SCC, respectively, indicating the triple helical structures were maintained.

### 3.6. X-ray diffraction

The X-ray diffraction diagram of collagen is shown in Fig. 3. The collagens from skin and scales had three diffraction peaks. The Bragg equation  $2d\sin\theta = \lambda$  ( $\lambda = 0.154$ ) was used to describe the X-

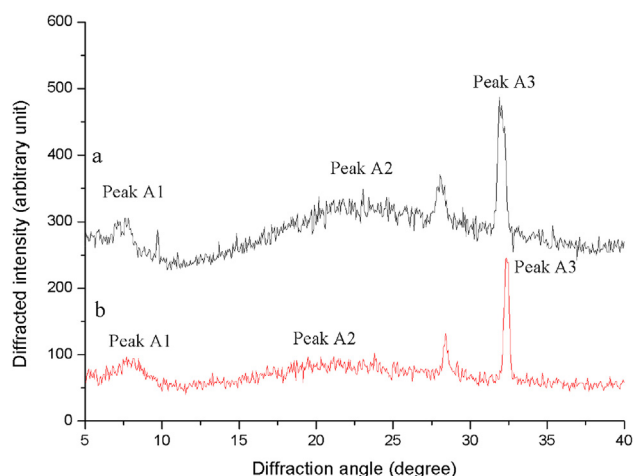


Fig. 3. X-ray diffraction diagram of SCC (a) and SKC (b).

ray diffraction results (Table 3). The first diffraction peak was found to be between 7° and 8°, and presented a relatively sharp diffraction peak (the peak labeled A1). This peak reflects the distance between the molecular chains of collagen fibers (Marie-Madeleine, Laurence, Christine, Patrick, & Daniel, 2000). The distance between the molecular chains of SCC fibers was 1.24 nm. The distance between the molecular chains of SKC fibers was 1.16 nm. The gap observed in the SKC sample was greater than the distance observed in the SKC sample, indicating scale collagen may be a better drug delivery tool than skin collagen. The second diffraction peak was found to be between 20° and 25° (the peak labeled A2), this reflects diffuse scatter caused by many structural layers of collagen fibers. The d value that corresponds to the SCC A2 peak value was slightly lower than it was for SKC. The third diffraction peak was found to be between 30° and 35° (the peak labeled A3). The d value corresponding to this peak represents the distance between adjacent amino acid residues along the central axis of its helical structure. Eyre (1980) reported that in the helical structure of collagen, every circle of the helix contained 3.3 amino acid residues ( $n = 3.3$ ) with a pitch of 0.96 nm, and along the central axis of the helix, the distance between adjacent amino acid residues was 0.29 nm. The d value that corresponds to the collagens A3 peak value were 0.29 nm, indicating the helical structure was preserved in the collagens we extracted from fish scales and skin. The crystallinity of SCC and SKC were 15.87% and 15.18%, respectively.

### 3.7. Zeta potential

The potential values of the SCC and SKC samples, at different pH values, are shown in Fig. 4. Both collagen samples were positively charged between a pH of 2–6, and negatively charged between a pH of 7–11. The Zeta potential data revealed when the SKC and SCC samples' Zeta net charge was zero, their potential values and pI values were 6.42 and 6.82, respectively. When pH values were above or below the proteins' pI values, the repulsion between the protein chains increased, resulting in a high net charge and the solubility of protein molecules. When the net charge of a protein was zero, hydrophobic–hydrophobic interactions increased, resulting in protein precipitation and aggregation (Singh et al., 2011). Collagen from various fish scraps have been shown to exhibit different pI values. For example, the pI value of collagen from striped catfish skin is 4.27 (Singh et al., 2011), collagen from spotted golden goatfish scales has a pI of 4.96 (Matmaroh et al., 2011), and the pI of bamboo shark skin collagen is 6.12 (Kittiphattanabawon, Benjakul, Visessanguan, Kishimura, & Shahidi, 2010). Collagen pI values may differ due to various amino acid sequences and distribution of amino acid residues.

### 3.8. Solubility studies

#### 3.8.1. Effect of pH

The effect of pH on the solubility of collagens is shown in Fig. 5A. All collagen samples were solubilized in an acidic pH range from 1 to 3, with the highest solubility observed at pH 3. Similar results

Table 3  
d values of X-ray diffraction peaks of ASCs.

Sample	Peak	Peak position ( $2\theta$ , °)	d values (nm)
SKC	A1	7.70	1.16
	A2	21.14	0.32
	A3	32.04	0.29
SCC	A1	7.13	1.24
	A2	22.09	0.41
	A3	31.89	0.29

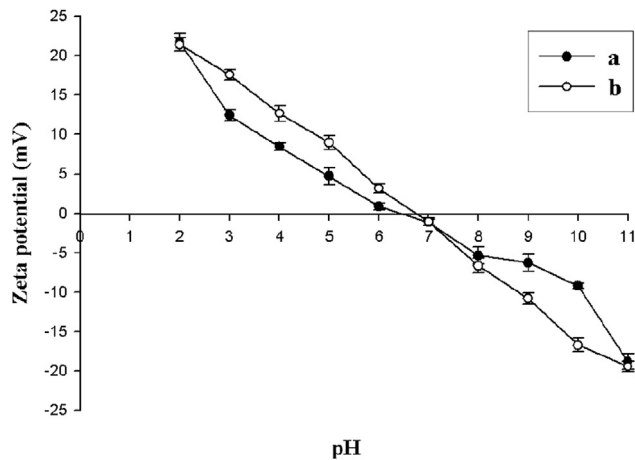


Fig. 4. Zeta potential of SKC (a) and SCC (b) at different pH levels.

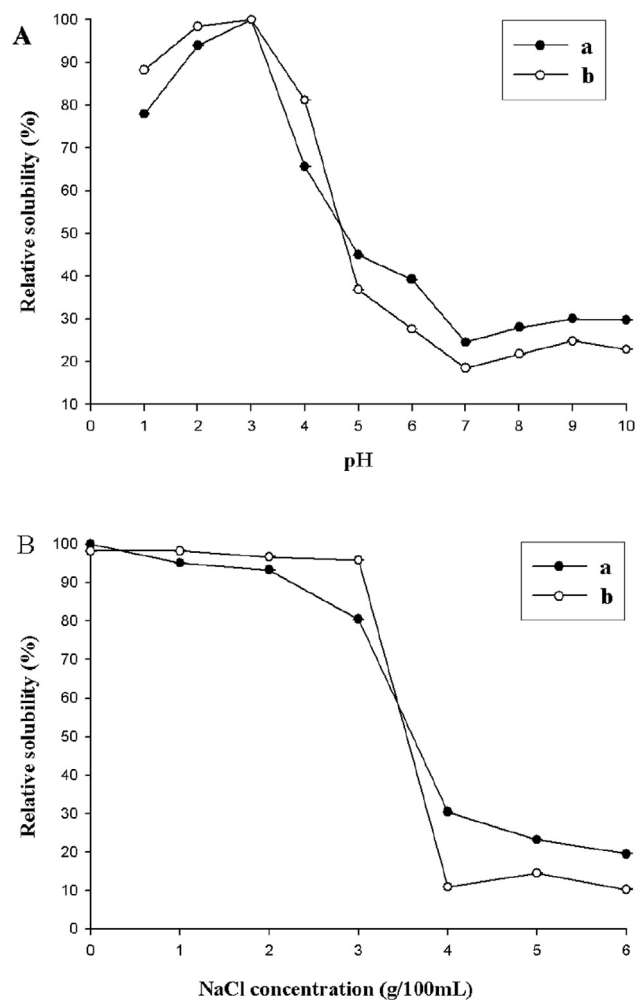


Fig. 5. Relative solubility (%) of SKC (a) and SCC (b) as affected by different pH (A) and NaCl (B) concentrations.

were reported for collagen isolated from the scales of grey mullet (Thuy et al., 2014). Low solubility was observed in neutral and alkaline pH ranges. However, the lowest collagen solubility was observed at pH 7. This result was in accordance with the reported solubility of collagen from the skin of striped catfish (Singh et al.,

2011). Differences in the solubility of collagens, at various pH values, were caused by the differences in the molecular properties and structural conformations of the collagens (Kittiphattanabawon et al., 2010).

### 3.8.2. Effect of NaCl

The effect of NaCl on collagen solubility is shown in Fig. 5B. At different concentrations of NaCl, SCC and SKC displayed similar solubility. A NaCl concentration of 0 g/100 mL was used as a blank control. When the NaCl concentration was between 1 and 3 g/100 mL, as the NaCl concentration increased, the solubility of the collagens did not change significantly ( $p > 0.05$ ). When the NaCl concentration was between 3 and 4 g/100 mL, as the NaCl concentration increased, the solubility of the collagens drastically decreased ( $p < 0.05$ ). When the NaCl concentration was  $>4$  g/100 mL, the collagens solubility remained low ( $p > 0.05$ ). This decrease in solubility may be due to a salting out effect (Bae et al., 2008). This effect occurs when the salt concentration reaches a certain level; an increase in salt concentration will lead to enhanced hydrophobic–hydrophobic interactions between protein chains and increased competition for water with salt ions, resulting in protein precipitation, thereby reducing the solubility of the protein (Damodaran, 1996). These results support the use of collagen from fish scales and skin as an alternative source of collagen for use in food, pharmaceutical and nutraceutical industries.

## 4. Conclusion

ASCs were extracted from scales and skin. The yield of SKC was approximately threefold great than that of the SCC. Both collagens were characterized as type I collagen and maintained their triple helical structure after purification. LC-MS/MS analysis confirmed the SCC and SKC were *O. niloticus* type I collagen. SCC exhibited high thermal stability as compared to that of the SKC, owing to the higher imino acid content of.

## Acknowledgment

This work was supported by grants from the Scientific and Technological Key Projects of Fujian Province (2013N0020), National Natural Science Foundation of China (41106149), Ocean Public Welfare Scientific Research Special Appropriation Project (201405017), Southern Ocean Research Center Project of Xiamen (13GYY001NF05).

## Appendix A. Supplementary data

Supplementary data related to this article can be found at <http://dx.doi.org/10.1016/j.lwt.2015.10.070>.

## References

- Abe, Y., & Krimm, S. (1972). Normal vibrations of crystalline polyglycine I. *Biopolymers*, 11(9), 1817–1839.
- Ahmad, M., & Benjakul, S. (2010). Extraction and characterisation of pepsin-solubilised collagen from the skin of unicorn leatherjacket (*Aluterus monoceros*). *Food Chemistry*, 120, 817–824.
- Bae, I., Osatomi, K., Yoshida, A., Osako, K., Yamaguchi, A., & Hara, K. (2008). Biochemical properties of acid-soluble collagens extracted from the skins of underutilised fishes. *Food Chemistry*, 108, 49–54.
- Cheung, H. S., Wang, F. L., Ondetti, M. A., Sabo, E. F., & Cushman, D. W. (1980). Binding of peptide substrates and inhibitors of angiotensin-converting enzyme. Importance of the COOH-terminal dipeptide sequence. *Journal of Biological Chemistry*, 255, 401–407.
- Chuaychan, S., Benjakul, S., & Kishimura, H. (2015). Characteristics of acid- and pepsin-soluble collagens from scale of seabass (*Lates calcarifer*). *LWT-Food Science and Technology*, 63, 71–76.
- Damodaran, S. (1996). Amino acids, peptides, and proteins. In O. R. Fennema (Ed.), *Food chemistry* (3rd ed., pp. 321–429). New York: Marcel Dekker.

- Doyle, B. B., Bendit, E. G., & Blout, E. R. (1975). Infrared spectroscopy of collagen and collagen-like polypeptides. *Biopolymers*, *14*, 937–957.
- Eyre, D. R. (1980). Collagen: molecular diversity in the body's protein scaffold. *Science*, *207*, 1315–1322.
- Jongiareonrak, A., Benjakul, S., Visessanguan, W., Nagai, T., & Tanaka, M. (2005). Isolation and characterisation of acid and pepsin-solubilised collagens from the skin of Brownstripe red snapper (*Lutjanus vitta*). *Food Chemistry*, *93*, 475–484.
- Kaewdang, O., Benjakul, A., Kaewmanee, T., & Kishimura, H. (2014). Characteristics of collagens from the swim bladders of yellowfin tuna (*Thunnus albacares*). *Food Chemistry*, *155*, 264–270.
- Kittiphattanabawon, P., Benjakul, S., Visessanguan, W., Kishimura, H., & Shahidi, F. (2010). Isolation and characterization of collagen from the skin of brownbanded bamboo shark (*Chiloscyllium punctatum*). *Food Chemistry*, *119*, 1519–1526.
- Kittiphattanabawon, P., Benjakul, S., Visessanguan, W., Nagai, T., & Tanaka, M. (2005). Characterisation of acid soluble collagen from skin and bone of bigeye snapper (*Priacanthus tayenus*). *Food Chemistry*, *89*, 363–372.
- Laemmli, U. K. (1970). Cleavage of structural proteins during the assembly of the head of bacteriophage T4. *Nature*, *227*, 680–685.
- Li, G. H., Le, G. W., Shi, Y. H., & Shrestha, S. (2004). Angiotensin I-converting enzyme inhibitory peptides derived from food proteins and their physiological and pharmacological effects. *Nutrition Research*, *24*, 469–486.
- Liu, D. S., Liang, L., Regenstein, J. M., & Zhou, P. (2012). Extraction and characterization of pepsin-solubilised collagen from fins, scales, skins, bones and swim bladders of bighead carp (*Hypophthalmichthys nobilis*). *Food Chemistry*, *133*, 1441–1448.
- Liu, Z., Oliveira, A. C. M., & Su, Y. C. (2010). Purification and characterization of pepsin-solubilized collagen from skin and connective tissue of Giant Red Sea Cucumber (*Parastichopus californicus*). *Journal of Agricultural and Food Chemistry*, *58*, 1270–1274.
- Lowry, O. H., Rosebrough, N. J., Farr, A. L., & Randall, R. J. (1951). Protein measurement with the folin phenol reagent. *Journal of Biological Chemistry*, *193*, 265–275.
- Marie-Madeleine, G.-G., Laurence, B., Christine, C., Patrick, D., & Daniel, H. (2000). Structural aspects of fish skin collagen which forms ordered arrays via liquid crystalline states. *Biomaterials*, *21*, 899–906.
- Matmaroh, K., Benjakul, S., Prodran, T., Encarnation, A. B., & Kishimura, H. (2011). Characteristics of acid soluble collagen and pepsin soluble collagen from scale of spotted golden goatfish (*Parupeneus heptacanthus*). *Food Chemistry*, *129*, 1179–1186.
- Muyonga, J. H., Cole, C. G. B., & Duodu, K. G. (2004). Characterisation of acid soluble collagen from skins of young and adult Nile perch (*Lates niloticus*). *Food Chemistry*, *85*, 81–89.
- Nalinanon, S., Benjakul, S., Kishimura, H., & Osako, K. (2011). Type I collagen from the skin of ornate threadfin bream (*Nemipterus hexodon*): characteristics and effect of pepsin hydrolysis. *Food Chemistry*, *125*, 500–507.
- Pati, F., Adhikari, B., & Dhara, S. (2010). Isolation and characterization of fish scale collagen of higher thermal stability. *Bioresource Technology*, *101*, 3737–3742.
- Plepis, A. M. D. G., Goisis, G., & Das-Gupta, D. K. (1996). Dielectric and pyroelectric characterization of anionic and native collagen. *Polymer Engineering Science*, *36*, 2932–2938.
- Singh, P., Benjakul, S., Maqsood, S., & Kishimura, H. (2011). Isolation and characterization of collagen extracted from the skin of striped catfish (*Pangasianodon hypophthalmus*). *Food Chemistry*, *124*, 97–105.
- Sinthusamran, S., Benjakul, S., & Kishimura, H. (2013). Comparative study on molecular characteristics of acid soluble collagens from skin and swim bladder of seabass (*Lates calcarifer*). *Food Chemistry*, *138*, 2435–2441.
- Tamilmozhi, S., Anguchamy, V., & Arumugam, M. (2013). Isolation and characterization of acid and pepsin-solubilized collagen from the skin of sailfish (*Istiophorus platypterus*). *Food Research International*, *54*, 1499–1505.
- Thuy, L. T. M., Okazaki, E., & Osako, K. (2014). Isolation and characterization of acid-soluble collagen from the scales of marine fishes from Japan and Vietnam. *Food Chemistry*, *149*, 264–270.
- Vercruyse, L., Smagghe, G., Beckers, T., & Camp, J. V. (2009). Antioxidative and ACE inhibitory activities in enzymatic hydrolysates of the cotton leafworm, *Spodoptera littoralis*. *Food Chemistry*, *114*, 38–43.
- Zeng, S. K., Yin, J. J., Yang, S. Q., Zhang, C. H., Yang, P., & Wu, W. L. (2012). Structure and characteristics of acid and pepsin-solubilized collagens from the skin of cobia (*Rachycentro canadum*). *Food Chemistry*, *135*, 1975–1984.
- Zhang, J. J., Duan, R., Huang, L., Song, Y. J., & Regenstein, M. J. (2014). Characterisation of acid-soluble and pepsin-solubilised collagen from jellyfish (*Cyanea nozakii* Kishinouye). *Food Chemistry*, *150*, 22–26.



# Raspberry marc extracts increase antioxidative potential, ellagic acid, ellagitannin and anthocyanin concentrations in fruit purees



Ramunė Bobinaityė<sup>a</sup>, Pranas Viškelis<sup>a</sup>, Česlovas Bobinas<sup>a</sup>, Aldona Mieželiienė<sup>b</sup>, Gitana Alenčikienė<sup>b</sup>, Petras Rimantas Venskutonis<sup>c,\*</sup>

<sup>a</sup> Institute of Horticulture, Lithuanian Research Centre for Agriculture and Forestry, Kauno st. 30, LT-54333, Babtai, Kaunas Reg., Lithuania

<sup>b</sup> Food Institute of Kaunas University of Technology, Taikos pr. 92, LT-51180, Kaunas, Lithuania

<sup>c</sup> Kaunas University of Technology, Department of Food Science and Technology, Radvilėnų pl. 19, LT-50254, Kaunas, Lithuania

## ARTICLE INFO

### Article history:

Received 6 May 2015

Received in revised form

28 October 2015

Accepted 29 October 2015

Available online 3 November 2015

### Keywords:

Fruit puree

Raspberry marc extract

Ellagitannins

Antioxidants

Sensory properties

## ABSTRACT

Two types of fruit puree consisting of (1) pears/apples/yellow cherry plums and (2) apples/black currants were enriched with raspberry marc extract containing valuable antioxidants. The addition of 2% marc extract increased total phenolic content (TPC) from 108.8 to 345.8 and from 176.1 to 396.2 mg/100 g in the puree (1) and (2), respectively. The total anthocyanin content (TAC), ellagic acid and ellagitannin concentrations as well as antioxidant capacity of purees also increased with increasing concentration of marc extract additive. The increase of free ellagic acid (up to 44%) in the purees with extract additives after preparation was related to a partial hydrolysis of ellagitannins. Higher extract concentrations resulted in the increased bitterness and astringency of the products; therefore the concentration of raspberry marc additives in purees of up to 1.6% may be recommended.

© 2015 Elsevier Ltd. All rights reserved.

## 1. Introduction

Enrichment of foods with healthy constituents is the main way in developing functional foods. Healthy phytochemicals are available in raw and processed edible plants, or may be obtained from agricultural processing by-products. Berries are the richest sources of polyphenolics; they are consumed fresh or processed, due to a limited shelf life. Pressing of berry juices results in high amounts of by-products (the pulp/peels and the seeds), which are rich sources of health-beneficial compounds (Viškelis et al., 2009). For instance, after juice separation the yield of raspberry marc may account for up to 34% of the original fruit mass (Četojević-Simin et al., 2015). Considering that the global production of raspberries is increasing (>0.55 million tons in 2011) (FAO, 2013) development of the effective processing methods of raspberry by-products may provide remarkable amounts of high value functional ingredients.

Strawberry achenes were reported to contain remarkably higher concentrations of ellagitannins and free ellagic acid than their flesh (Aaby, Wrolstad, Ekeberg, & Skrede, 2007). High ellagic acid and

ellagitannins contents were also reported in red raspberry marc (Bobinaityė, Viškelis, Šarkinas, & Venskutonis, 2013). Ellagitannins and ellagic acid exhibit a wide range of biological effects such as antioxidant, antimutagenic, anticarcinogenic, antibacterial, and antiviral, suggesting that they could have beneficial effects on human health (Landete, 2011). Therefore, it may be expected that adding raspberry marc constituents to foods might increase the levels of important phytonutrients in human diet.

Although official daily requirements for many phytonutrients have not been established it is suggested that dietary recommendations and regulations for foods enriched with polyphenols should limit their consumption to dietary reference levels and avoid mega-doses (Bohn, 2014; Williamson & Holst, 2008). The cases of severe toxicity associated with consumption of phenolic phytonutrients are very scarce; for instance, grade 4 toxicity reactions associated with consumption of green tea polyphenols and quercetin were reported (Thomasset et al., 2007). However, a number of dietary intervention studies have not revealed any negative effects for the studied polyphenols (Bhatt, Thoman, & Nanjan, 2012; Perumalla & Hettiarachchy, 2011; Thomasset et al., 2007). The more recent study demonstrated that three ellagitannin-rich pomegranate extract capsules per day (each containing 1000 mg polyphenol extract) to men with recurrent

\* Corresponding author.

E-mail address: [rimas.venskutonis@ktu.lt](mailto:rimas.venskutonis@ktu.lt) (P.R. Venskutonis).

prostate cancer did not show any adverse effect (Paller et al., 2013).

Functional ingredients may be used in foods and nutraceuticals. In our study, a wide range of raspberry marc extract concentrations was used for the enrichment of fruit purees, assuming that the addition of up to 250 mg of polyphenols, expressed in gallic acid equivalents (GAE), to 100 g puree would be potentially useful in supplementing the diet with antioxidants, and at the same time safe. Especially, considering the fact that individuals consuming recommended five portions of fruit and vegetables a day could be exposed to more than 500 mg of polyphenols (Williamson & Holst, 2008), while consumption of certain foods (cocoa, tea, coffee) could naturally increase this dose by 500–1000 mg (Bohn, 2014; Williamson & Holst, 2008).

The objectives of this study were to evaluate how much of the raspberry marc extract phenolic antioxidants are retained after being added into a food system, such as fruit puree, and what effect the extracts may have on the content of the main bioactive constituents, antiradical activity and sensory properties of purees.

## 2. Materials and methods

### 2.1. Chemicals and fruit raw material

Ethanol was from distillery AB Stumbras (Kaunas, Lithuania). HPLC grade acetonitrile and methanol, gallic acid, NaOH, anhydrous Na<sub>2</sub>CO<sub>3</sub>, ellagic acid and 2,2-diphenyl-1-picrylhydrazyl hydrate stable radical (DPPH<sup>•</sup>, 95%) were from Sigma–Aldrich (Steinheim, Germany). Folin–Ciocalteu phenol reagent and analytical grade methanol were from Fluka Chemie (Buchs, Switzerland), concentrated HCl and formic acid (98–100%) from Merck (Darmstadt, Germany).

The fruits and berries were grown in the Institute of Horticulture of Lithuanian Research Centre for Agriculture and Forestry (LRCAF IH). Raspberry marc was obtained from fresh berries of different cultivars using de-stoning/straining machine EP1000 (Vorán Maschinen, Pichl bei Wels, Austria), with changeable screen (aperture size 1 mm).

### 2.2. Preparation of raspberry marc extract and fruit purees

Raspberry marc was dried in a convection oven (Memmert GmbH, Schwabach, Germany) at 50 °C and ground in a laboratory mill Retsch ZM 200 (Retsch GmbH, Haan, Germany) using 0.5 mm sieve. Three-step batch extraction (5 h each) was carried out at 50 °C with aqueous ethanol (80% EtOH) at 5:1 (I), 3:1 (II), and 3:1 (III) solvent to marc ratios. The extracts were combined, filtered, pre-concentrated in a rotary evaporator Rotavapor R-250 (Büchi Labortechnik AG, Flawil, Switzerland), freeze-dried (iShin Europe B.V., Ede, The Netherlands) and kept in the hermetically sealed container at  $-20 \pm 2$  °C.

Fresh fruits and berries were blanched; their edible parts were separated and pureed using a de-stoning/straining machine EP1000. All purees were prepared using standardized formulae developed in LRCAF IH. Puree of pears, apples and yellow cherry plums (PACP) was prepared by blending 20% pear, 10% apple and 20% yellow cherry plum purees and adding 50% sucrose syrup (30 °Brix). Puree of apples and black currants (ABCP) was prepared by blending 50% apple and 25% black currant purees and by adding 25% sucrose syrup (30 °Brix). These recipes were selected as the most successful products, which have been commercialised and gained the popularity among the consumers. Raspberry marc extract was added to the blended purees at the concentrations of 0.0 (control), 0.2, 0.4, 0.6, 0.8, 1.0, 1.2, 1.4, 1.6, 1.8 and 2%; then they were heated up to  $85 \pm 5$  °C by stirring, poured to 500 mL glass jars, pasteurized for 20 min at  $85 \pm 2$  °C and air-tight sealed with metal covers.

### 2.3. Determination of total phenolic content (TPC) and total anthocyanin content (TAC)

The TPC of the samples was determined with Folin–Ciocalteu's phenol reagent (Slinkard & Singleton, 1977) as described in detail elsewhere (Bobinaitė, Viškelis, & Venskutonis, 2012). For TPC measurement in purees, 5 g were extracted with 50 mL methanol at ambient temperature for 1 h under shaking; the solution was filtered, and the residue was repeatedly extracted under the same conditions. The combined extracts were diluted 1:3 (v/v) with methanol.

For TPC measurement in dry extract, 200 mg of extract was dissolved in 1 mL water and 99 mL methanol and diluted 1:3 (v/v) with methanol.

The TAC was determined using the pH differential method (Giusti & Wrolstad, 2001) in the dried extract or the liquid part of the centrifuged purees and expressed in mg of cyanidin-3-glucoside in 100 g of puree or 1 g of dry extract.

### 2.4. Analysis of ellagic acid (EA) and ellagitannins (ETs) hydrolysis products

ETs were determined as EA equivalents after acidic hydrolysis (Koponen, Happonen, Mattila, & Törrönen, 2007). Two quantitatively major ETs hydrolysis products, namely methyl-sanguisorboate and ellagic acid were measured.

For ETs analysis in purees, 5 g were mixed with 50 mL of acidified methanol (8.3 mL of conc. HCl in 50 mL methanol) and refluxed for 20 h at 85 °C. After hydrolysis the samples were cooled, filtered and made up to 50 mL with methanol.

For ETs analysis in dry extract, 200 mg were dissolved in 1 mL water and 49 mL acidified methanol and hydrolysed under the same conditions as described above. The sample was cooled, filtered and made up to 100 mL with methanol.

Free EA was analysed in the samples without hydrolysis. For purees 5 g were extracted with 25 mL of 90% methanol at room temperature for 30 min under shaking. The suspension was filtered and the residue was re-extracted under the same conditions. The supernatants were combined and made up to 50 mL with methanol.

For free EA analysis in dry extract, 500 mg were dissolved in 20 mL of 99% methanol.

The extracts prepared for ETs and free EA determination were filtered and transferred into LC vials. The HPLC system consisted of a Shimadzu HPLC (Model LC-10Avp with two pumps and DGU-14A Degasser) equipped with a UV–Vis detector SPD-10AV<sub>vp</sub> (Shimadzu, Kyoto, Japan). The separation was performed on a LiChro-CART LiChrospher 100 RP-18 column, 5 μm, 125 × 4 mm (Merck, Darmstadt, Germany) as reported previously (Bobinaitė et al., 2012).

### 2.5. Evaluation of radical scavenging capacity (RSC)

The extracts of purees that were prepared for free EA determination were used for the measurement of RSC against stable DPPH<sup>•</sup> (Brand-Williams, Cuvelier, & Berset, 1995). Briefly, DPPH<sup>•</sup> methanolic solution (2 mL,  $6 \times 10^{-5}$  M) was mixed with 20 μL of prepared extract and the absorbance was measured after 30 min on a spectrometer Genesys-10 UV/Vis (Thermo Spectronic, Rochester, USA). Antiradical activity was expressed in trolox equivalents (TE) i.e., trolox quantity (μmol), which at the equal conditions possesses the same antioxidant capacity as 1 g of puree.

### 2.6. Colour measurement, determination of total soluble solids and pH

The CIE Lab values of purees were measured with a

spectrophotometer MiniScan XE Plus (Hunter Associates Laboratory, Reston, Virginia). The recorded X, Y and Z tristimulus values were converted to CIE L\* (lightness), a\* (redness(+)/greenness(-)) and b\* (yellowness(+)/blueness(-)) colour values. The chroma (C) (1.1), hue angle (h°) (1.2) and the total colour difference ( $\Delta E$ ) (1.3) between purees without extract (control) and with different percentages of extract additive were calculated using formulae;

$$C = (a^{*2} + b^{*2})^{1/2} \quad (1.1)$$

$$h^{\circ} = \arctan\left(\frac{b^{*}}{a^{*}}\right) \quad (1.2)$$

$$\Delta E = \sqrt{(\Delta L^{*})^2 + (\Delta a^{*})^2 + (\Delta b^{*})^2} \quad (1.3)$$

Colour coordinates were processed with the Universal Software V.4-10.

The total soluble solids were determined using an ATAGO PR-32 digital refractometer (Atago Co., Ltd., Tokyo, Japan). The pH was measured using an inoLab Level 1 pH meter (WTW GmbH & Co., Weilheim, Germany).

### 2.7. Sensory evaluation

Sensory evaluation was performed in the Sensory Analysis Laboratory of Food Institute of Kaunas University of Technology established in compliance with ISO 8589. In the acceptance test expert panel consisting of 11 assessors evaluated the acceptance of puree samples by using five-point hedonic scale: 5 - the highest and 1- the lowest acceptability. In addition they were asked to indicate the defect, which they had observed for the sample if 3 points or lower score was given. A sensory profiling test was performed by 6 assessors (age from 25 till 55 years), all being experienced in sensory analysis of different foods and selected and trained according to the ISO 8586-1. All sessions were conducted in a climate-controlled sensory analysis laboratory. The assessors developed a vocabulary describing sensory attributes of puree samples, and agreed on a consensus list of key sensory attributes. A continuous, unstructured scale (150 mm length) was used for evaluation of the intensity of each attribute. The left side of the scale corresponded to the lowest intensity of each attribute and the right side corresponded to the highest intensity. In the pre-test

session panellists were trained to use the selected attributes by testing samples with extreme intensity of the selected attributes. Samples were served in a randomized order. The average response over replicates and panellists for each significant attribute were used in the multivariate analyses.

### 2.8. Statistical evaluation

The results of chemical composition, antioxidant activity and colour were expressed as a mean of three replicate assays  $\pm$  standard deviation. Mean values were further compared using Turkey's test, and differences were considered to be statistically significant when  $p \leq 0.05$ . The Fizz software was used for gathering and analysis of sensory evaluation data. All results are an average of two replicate determinations, the significance of differences among means was analyzed using ANOVA and Duncan multiple comparison test. Level of significance was set for  $p \leq 0.05$ . SPSS software, version 20 was used for statistical analysis (SPSS Inc., Chicago, USA).

## 3. Results and discussion

### 3.1. Influence of raspberry marc extract on chemical composition and RSC of purees

One g of dry raspberry marc extract contained  $5.54 \pm 0.20$  mg TAC,  $121.10 \pm 1.50$  mg TPC,  $1.93 \pm 0.05$  mg free EA and  $20.65 \pm 1.10$  mg ETs; its RSC was  $496.87 \pm 10.52$   $\mu$ mol TE/g. It is interesting noting that our previous study demonstrated that the TAC of red raspberry seedless pulp extracts, depending on raspberry cultivar, was by 3–17% higher than that of the corresponding marc extracts, whereas in marc extracts the TPC, free EA and ETs contents were remarkably higher (Bobinaitė et al., 2013). The TPC of marc extracts was by 68–83% higher than that of the corresponding pulp extracts; similarly free EA content of raspberry marc extracts was by 60–84% higher and ETs content by 63–80% higher than that of the corresponding pulp extracts (Bobinaitė et al., 2013).

In the current study the initial TPC of the ABCP was by 38.2% higher than that of the PACP (Table 1). The TPC of both purees increased gradually as the concentration of marc extract increased (Fig. 1A): 2% of extract increased TPC in the PACP 3.2 times, from 108.8 to 345.8 mg/100 g, whereas in ABCP - 2.2 times, from 176.10 to 396.2 mg/100 g.

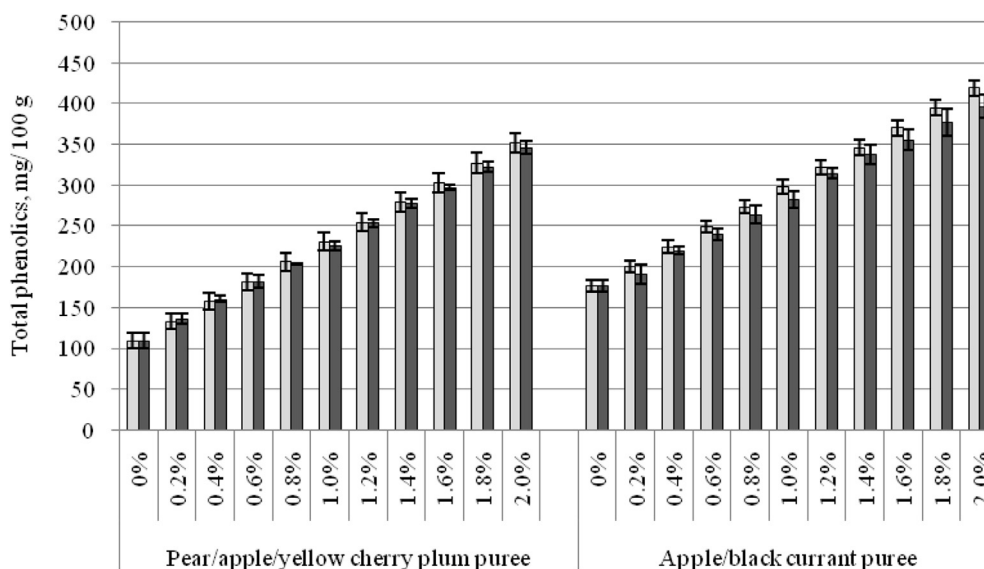
The TPC recoveries of added raspberry marc extract in purees were not significantly affected by the thermal treatment (Fig. 1A).

**Table 1**

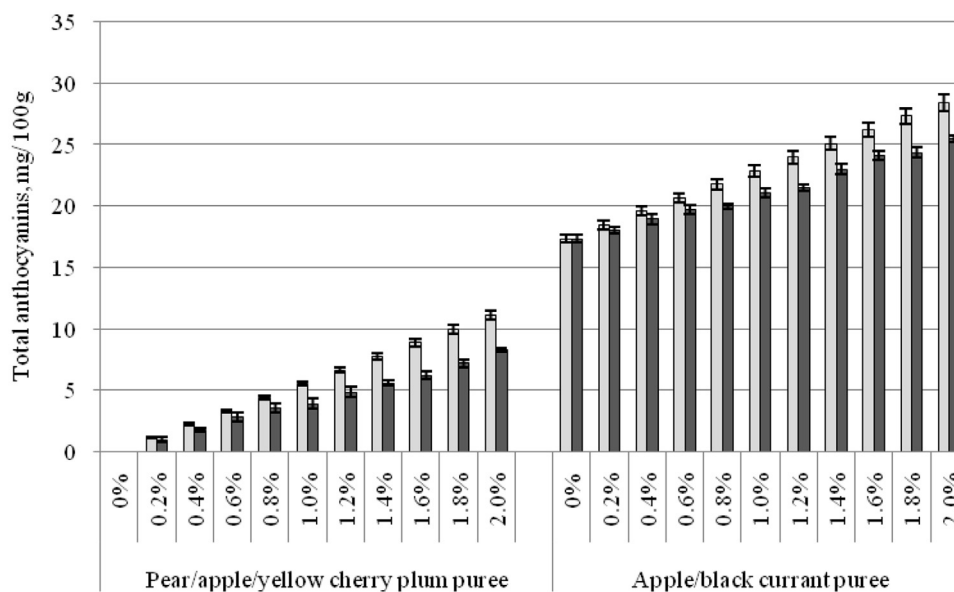
Total phenolic content (TPC), total anthocyanins content (TAC), free ellagic acid, ellagitannins contents and radical scavenging capacity (RSC) of fruit purees.<sup>a</sup>

Extract conc., %	TPC mg/100 g fresh weight	TAC	Free EA	ETs	RSC $\mu$ mol TE/g
<b>Pears, apples and yellow cherry plums (PACP)</b>					
0	108.8 $\pm$ 9.48 <sup>a</sup>	n.d.	n.d.	n.d.	3.5 $\pm$ 0.20 <sup>a</sup>
0.4	159.9 $\pm$ 4.10 <sup>b</sup>	1.8 $\pm$ 0.15 <sup>a</sup>	1.3 $\pm$ 0.08 <sup>a</sup>	7.5 $\pm$ 0.61 <sup>a</sup>	5.2 $\pm$ 0.18 <sup>b</sup>
0.8	202.9 $\pm$ 0.84 <sup>c</sup>	3.5 $\pm$ 0.34 <sup>b</sup>	2.7 $\pm$ 0.10 <sup>b</sup>	15.0 $\pm$ 1.06 <sup>b</sup>	7.0 $\pm$ 0.29 <sup>c</sup>
1.0	224.8 $\pm$ 5.20 <sup>d</sup>	3.9 $\pm$ 0.40 <sup>b</sup>	3.3 $\pm$ 0.16 <sup>c</sup>	18.7 $\pm$ 1.13 <sup>c</sup>	8.0 $\pm$ 0.47 <sup>cd</sup>
1.2	253.2 $\pm$ 4.82 <sup>e</sup>	4.9 $\pm$ 0.44 <sup>c</sup>	3.6 $\pm$ 0.14 <sup>c</sup>	22.1 $\pm$ 0.52 <sup>d</sup>	8.7 $\pm$ 0.40 <sup>d</sup>
1.6	296.9 $\pm$ 3.69 <sup>f</sup>	6.2 $\pm$ 0.30 <sup>d</sup>	4.7 $\pm$ 0.24 <sup>d</sup>	30.1 $\pm$ 1.30 <sup>e</sup>	11.3 $\pm$ 0.53 <sup>e</sup>
2.0	345.8 $\pm$ 8.00 <sup>g</sup>	8.3 $\pm$ 0.16 <sup>e</sup>	5.6 $\pm$ 0.20 <sup>e</sup>	37.4 $\pm$ 1.62 <sup>f</sup>	13.5 $\pm$ 0.33 <sup>f</sup>
<b>Apples and black currants (ABCP)</b>					
0	176.1 $\pm$ 6.88 <sup>a</sup>	17.3 $\pm$ 0.29 <sup>a</sup>	n.d.	n.d.	6.1 $\pm$ 0.47 <sup>a</sup>
0.4	219.5 $\pm$ 4.61 <sup>b</sup>	18.9 $\pm$ 0.4 <sup>b</sup>	1.2 $\pm$ 0.12 <sup>a</sup>	7.3 $\pm$ 0.68 <sup>a</sup>	8.3 $\pm$ 0.40 <sup>b</sup>
0.8	264.0 $\pm$ 11.81 <sup>c</sup>	20.0 $\pm$ 0.22 <sup>c</sup>	2.7 $\pm$ 0.15 <sup>b</sup>	15.1 $\pm$ 0.85 <sup>b</sup>	9.8 $\pm$ 0.32 <sup>c</sup>
1.0	282.1 $\pm$ 9.97 <sup>cd</sup>	21.1 $\pm$ 0.36 <sup>d</sup>	3.1 $\pm$ 0.20 <sup>b</sup>	19.0 $\pm$ 1.34 <sup>c</sup>	11.3 $\pm$ 0.25 <sup>d</sup>
1.2	314.5 $\pm$ 5.99 <sup>d</sup>	21.5 $\pm$ 0.22 <sup>d</sup>	3.6 $\pm$ 0.14 <sup>c</sup>	22.6 $\pm$ 1.40 <sup>d</sup>	11.6 $\pm$ 0.51 <sup>d</sup>
1.6	355.5 $\pm$ 12.9 <sup>f</sup>	24.1 $\pm$ 0.40 <sup>e</sup>	4.5 $\pm$ 0.18 <sup>d</sup>	30.1 $\pm$ 0.80 <sup>e</sup>	13.9 $\pm$ 0.20 <sup>e</sup>
2.0	396.2 $\pm$ 14.44 <sup>g</sup>	25.5 $\pm$ 0.23 <sup>f</sup>	5.6 $\pm$ 0.29 <sup>e</sup>	38.5 $\pm$ 1.00 <sup>f</sup>	15.9 $\pm$ 0.25 <sup>f</sup>

<sup>a</sup> Different letters in the same column indicates significant differences between the samples ( $P \leq 0.05$ ).



A



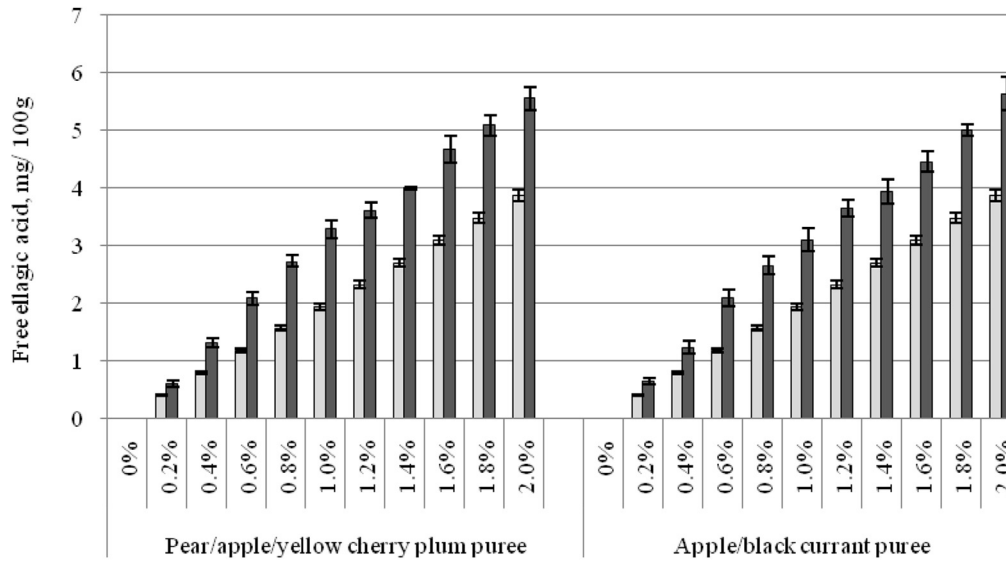
B

**Fig. 1.** TPC (A) and TAC (B) of fruit purees: the sum of the content determined in the control puree and dry extract (light grey bars □), content recovered in the product (dark grey bars ■).

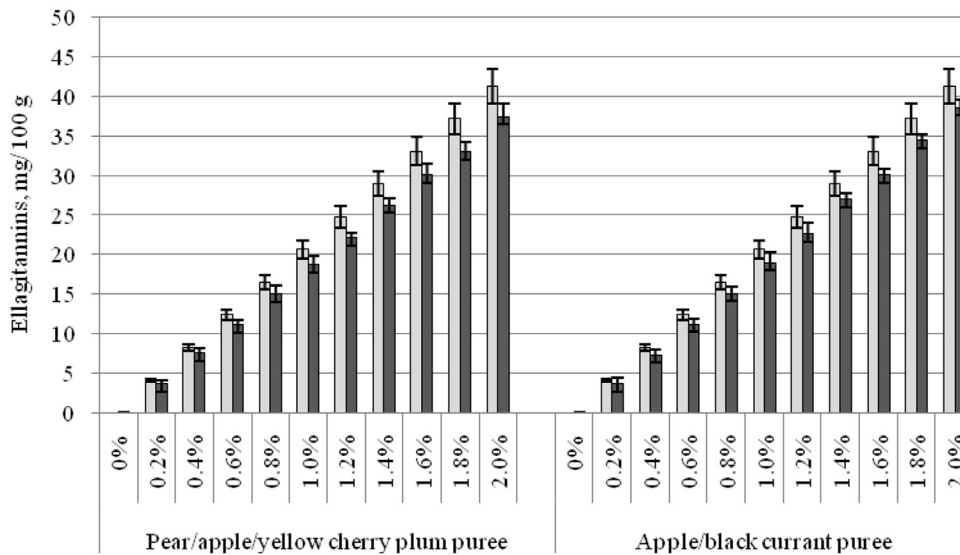
Most probably, the added polyphenolics were protected against enzymatic degradation because the enzymes present in plants that could catalyse degradation of the added polyphenols were inactivated during the blanching of fruits and berries prior to the addition of extract. It should also be noted that Folin-Ciocalteu reagent is not specific and detects all phenolic groups found in extract as well as other oxidation substrates (Everette et al., 2010); therefore, it could also react with breakdown products of polyphenols if such occurred. Furthermore, previously it was also shown that cooking had no effect on TPC of vegetables (Turkmen, Sari, & Velioglu, 2005).

Anthocyanins are unstable molecules in foods; their colour stability is strongly affected by pH, temperature, anthocyanin concentration and structure, oxygen, light, enzymes and other substances (Cavalcanti, Santos, & Meireles, 2011). The TAC in PACP was below detection limits whereas after adding 2% marc extract it was 8.3 mg/100 g (Table 1). TAC in ABCP due to the presence of anthocyanin-rich black currant was initially high, 17.3 mg/100 g and after adding 2% marc extract it further increased to 25.5 mg/100 g (Fig. 1B).

Thermal treatment of purees with extract significantly influenced anthocyanins; their recoveries in the PACP ranged from 70.1



A



B

**Fig. 2.** Free ellagic acid (A) and ellagitannins (B) content of fruit purees: the sum of the content determined in the control puree and dry extract (light grey bars □), content recovered in the product (dark grey bars ■).

to 85.7% of the content present in the raspberry marc extract (Fig. 1B). The added anthocyanins were better preserved in the ABCP with recoveries from 89.1 to 97.6% of the initial TAC in the extract. Most likely, anthocyanins initially present in the ABCP was a possible reason for a higher stability of added anthocyanins with extract. It was reported that increased anthocyanin concentration promotes their higher stability (Giusti & Wrolstad, 2003); however, in the previous study acylated anthocyanins were considered, while in our study acylated derivatives were not determined. It is known, that inter/intramolecular copigmentation and self-

association reactions may increase the stability of both acylated and nonacylated pigments in foods. For example, it was suggested interaction of nonacylated anthocyanins with plant constituents such as hydroxycinnamic acids in canned strawberries may provide copigmentation functions (Krammerer, Schillmöller, Maier, Schieber, & Reinhold, 2006).

Increasing marc extract concentration in the purees proportionally increased their RSC: 2% of extract additive increased RSC of PACP 3.9 times, while the RSC of ABCP increased 2.6 times (Table 1). The extract also enriched fruit purees with EA (Fig. 2A) and ETs

(Fig. 2B). Free EA content in the purees was by 30.4–44.1% higher than its content in the added amount of extract (Table 1). Whereas, the amount of ETs in the purees with marc extract was slightly reduced by thermal treatment (Fig. 2B). The content of ETs in purees was from 6.7 to 11.3% lower than their content in the added amount of raspberry marc extract. The increase of free EA in the purees after thermal treatment and storage may be explained by the release of hexahydroxydiphenic acid from ETs and its further transformation to EA. EA monomers most likely have higher bioavailability than high molecular weight ETs (Zafrilla, Ferreres, & Tomas-Barberan, 2001). Therefore, it may be hypothesised that the depolymerisation of ETs during processing would result in additional health benefits (Herber, 2008; Larrosa, Tomás-Barberán, & Espín, 2006).

It was observed previously that free EA content increases 2.5-fold during raspberry jam cooking (Zafrilla et al., 2001). The content of ETs in strawberry purees made with an achene-enriched fraction during 16 weeks of storage at ambient temperature decreased by 28% of their initial level, whereas the concentration of free EA in the product almost doubled at the same time (Aaby et al., 2007). Only minimal changes in the total ETs content were reported during storage of thermally processed blackberry products however, the authors reported that compositional changes indicative of ETs depolymerization were apparent (Hager, Howard, & Prior, 2010).

In general, the phenolic compounds (especially colourless phenolics) present in the raspberry marc extract were well retained during the production of purees. Enrichment of purees with such extracts can be effectively used to enhance their polyphenolic composition and to increase their antioxidant potential, thus improving functional properties of the product.

### 3.2. Influence of raspberry marc extract on puree quality characteristics

Raspberry marc extract used in this study was fine dry dark red powder; its CIELab colour parameters were as follows:  $L^* = 40.7 \pm 0.16$ ,  $a^* = 20.8 \pm 0.11$ ,  $b^* = 6.0 \pm 0.15$ ,  $C^* = 21.6 \pm 0.15$  and  $h^\circ = 16.0 \pm 0.32$ . The effect of extract on puree colour parameters is shown in Table 2. For both puree formulations, the extract reduced the lightness ( $L^*$ ) and increased the redness ( $a^*$ ); it also reduced the yellowness ( $b^*$ ) of PACP, but had no effect on the yellowness value of ABCP. The hue angle ( $h^\circ$ ) decreased with increasing extract concentration. The  $h^\circ$  value of the control PACP ( $75.4^\circ$ ) indicated that the yellowness component had the largest influence on the overall puree colour ( $90^\circ$  indicates that the puree is yellow, and  $0^\circ$  indicates that the puree is red). Increasing extract concentration gradually increased the influence of the redness component on the

overall puree colour. The  $h^\circ$  value of the ABCP was only slightly reduced with increased extract concentration in puree (from  $11.4^\circ$  to  $10.9^\circ$ ).

The colour purity ( $C^*$ ) of PACP decreased at lower extract concentrations, however when it reached 1.2%  $C^*$  started to increase (Table 2). Interestingly, this transition was reflected in the colour acceptability scores of PACP (Table 3); at 0.8 and 1% extract addition the colour was less acceptable than the control sample or purees with higher extract percentages. The  $C^*$  of ABCP slightly increased by increasing extract concentrations in purees. The total colour difference of PACP with 2% extract additive was 12.8, and the total colour difference of ABCP with the same percentage of extract was only 1.1 (Table 2). The total colour difference values between 1 and 2 indicates slight differences that are perceivable only by a person capable of distinguishing nuances of colours, while  $\Delta E$  values higher than 5 indicate large overall colour differences.

The extract additive increased soluble solids content and reduced pH of the purees. Soluble solids in PACP increased from 20.5 (control) to 22.0 °Brix (2% of extract) and in ABCP from 18.8 to 20.1 °Brix, respectively. The pH of PACP reduced from 3.45 (control) to 3.30 (2% of extract) and that of ABCP from 3.34 to 3.18, respectively.

### 3.3. Influence of raspberry marc extract on sensory properties of purees

Functional foods are an exciting trend in the food and nutrition field (Crowe & Francis, 2013). However, many plant-origin phenolics are characterised by bitterness and astringency, which are well known for eliciting negative consumer reaction at high intensities (Soares et al., 2013). Therefore, the competing demands of taste and health may pose a dilemma for the food industry. The off-taste of functional ingredients may be masked with a properly chosen (balanced) food product flavour. Considering these aspects sensory properties of fruit purees with raspberry marc extract were evaluated.

The colour, odour and texture of all tested purees were equally acceptable for the panellists (Table 3). When the additive concentration was between 0.2 and 1.2%, the colour of PACP became somewhat “muddy/dirty”, which made those samples slightly less acceptable compared to the control sample or purees with higher additive percentages (Table 3). The reduction and then following increase in colour acceptance values of PACP correlated with the changes in colour purity values  $C^*$  (Table 2). The colour of the red-coloured puree (ABCP) became slightly darker (lower  $L^*$ ) and redder (higher  $a^*$ ) with increased percentages of extract (Table 2), but this change did not influence the colour acceptance values (Table 3).

**Table 2**  
CIEL\*a\*b\* colour parameters of fruit purees.<sup>a</sup>

Extract conc., %	$L^*$	$a^*$	$b^*$	$C^*$	$h^\circ$	$\Delta E$
<b>Pears, apples and yellow cherry plums (PACP)</b>						
0	41.6 ± 0.05 <sup>e</sup>	3.7 ± 0.09 <sup>a</sup>	14.1 ± 0.10 <sup>c</sup>	14.6 ± 0.12 <sup>c</sup>	75.4 ± 0.24 <sup>f</sup>	—
0.4	38.9 ± 0.07 <sup>d</sup>	7.1 ± 0.14 <sup>b</sup>	10.7 ± 0.20 <sup>d</sup>	12.8 ± 0.24 <sup>a</sup>	56.4 ± 0.03 <sup>e</sup>	5.5 ± 0.04 <sup>a</sup>
0.8	37.4 ± 0.04 <sup>c</sup>	9.1 ± 0.10 <sup>c</sup>	9.3 ± 0.07 <sup>c</sup>	13.0 ± 0.12 <sup>ab</sup>	45.5 ± 0.10 <sup>d</sup>	8.4 ± 0.03 <sup>b</sup>
1.2	36.5 ± 0.01 <sup>b</sup>	10.4 ± 0.04 <sup>d</sup>	8.3 ± 0.12 <sup>b</sup>	13.3 ± 0.11 <sup>b</sup>	38.6 ± 0.30 <sup>c</sup>	10.3 ± 0.02 <sup>c</sup>
1.6	35.5 ± 0.14 <sup>a</sup>	11.0 ± 0.09 <sup>e</sup>	7.5 ± 0.19 <sup>a</sup>	13.3 ± 0.18 <sup>b</sup>	34.1 ± 0.45 <sup>b</sup>	11.6 ± 0.10 <sup>d</sup>
2.0	35.3 ± 0.03 <sup>a</sup>	12.5 ± 0.05 <sup>f</sup>	7.3 ± 0.09 <sup>a</sup>	14.4 ± 0.00 <sup>c</sup>	30.1 ± 0.41 <sup>a</sup>	12.8 ± 0.08 <sup>e</sup>
<b>Apples and black currants (ABCP)</b>						
0	31.2 ± 0.06 <sup>c</sup>	8.5 ± 0.16 <sup>a</sup>	1.7 ± 0.09 <sup>a</sup>	8.7 ± 0.17 <sup>a</sup>	11.4 ± 0.37 <sup>a</sup>	—
0.4	31.0 ± 0.06 <sup>c</sup>	8.7 ± 0.16 <sup>ab</sup>	1.6 ± 0.10 <sup>a</sup>	8.8 ± 0.18 <sup>ab</sup>	10.3 ± 0.45 <sup>a</sup>	0.2 ± 0.01 <sup>a</sup>
0.8	30.6 ± 0.04 <sup>b</sup>	8.6 ± 0.05 <sup>a</sup>	1.6 ± 0.14 <sup>a</sup>	8.7 ± 0.07 <sup>a</sup>	10.4 ± 0.85 <sup>a</sup>	0.6 ± 0.01 <sup>b</sup>
1.2	30.4 ± 0.19 <sup>ab</sup>	8.5 ± 0.16 <sup>a</sup>	2.0 ± 0.34 <sup>a</sup>	8.8 ± 0.08 <sup>a</sup>	13.2 ± 2.41 <sup>a</sup>	0.9 ± 0.25 <sup>bc</sup>
1.6	30.3 ± 0.10 <sup>a</sup>	9.0 ± 0.08 <sup>bc</sup>	1.6 ± 0.21 <sup>a</sup>	9.1 ± 0.14 <sup>bc</sup>	10.1 ± 1.19 <sup>a</sup>	1.0 ± 0.08 <sup>c</sup>
2.0	30.2 ± 0.01 <sup>a</sup>	9.1 ± 0.07 <sup>c</sup>	1.8 ± 0.12 <sup>a</sup>	9.3 ± 0.09 <sup>c</sup>	10.9 ± 0.65 <sup>a</sup>	1.1 ± 0.01 <sup>c</sup>

<sup>a</sup> Different letters in the same column indicates significant differences between the samples ( $P \leq 0.05$ ).

**Table 3**  
Acceptability scores of the purees.<sup>a</sup>

Extract conc., %	Pears, apples and yellow cherry plums (PACP)					Apples and black currants (ABCP)				
	Colour	Odour	Taste	Texture	Total <sup>b</sup>	Colour	Odour	Taste	Texture	Total <sup>b</sup>
0.0	4.6 <sup>a</sup>	4.8 <sup>a</sup>	5.0 <sup>d</sup>	4.2 <sup>a</sup>	4.8 <sup>d</sup>	5.0 <sup>a</sup>	5.0 <sup>a</sup>	4.5 <sup>e</sup>	4.2 <sup>a</sup>	4.5 <sup>e</sup>
0.2	4.2 <sup>a</sup>	4.7 <sup>a</sup>	4.8 <sup>d</sup>	4.2 <sup>a</sup>	4.6 <sup>cd</sup>	5.0 <sup>a</sup>	4.5 <sup>a</sup>	4.3 <sup>e</sup>	4.2 <sup>a</sup>	4.2 <sup>de</sup>
0.4	4.4 <sup>a</sup>	4.7 <sup>a</sup>	4.4 <sup>cd</sup>	4.4 <sup>a</sup>	4.6 <sup>cd</sup>	5.0 <sup>a</sup>	4.7 <sup>a</sup>	4.2 <sup>d</sup>	4.2 <sup>a</sup>	4.2 <sup>de</sup>
0.6	4.2 <sup>a</sup>	4.7 <sup>a</sup>	5.0 <sup>d</sup>	4.8 <sup>a</sup>	4.8 <sup>cd</sup>	5.0 <sup>a</sup>	4.5 <sup>a</sup>	3.3 <sup>cd</sup>	4.0 <sup>a</sup>	3.7 <sup>cde</sup>
0.8	4.0 <sup>a</sup>	4.7 <sup>a</sup>	4.4 <sup>cd</sup>	4.6 <sup>a</sup>	4.5 <sup>cd</sup>	5.0 <sup>a</sup>	4.8 <sup>a</sup>	3.3 <sup>cd</sup>	4.2 <sup>a</sup>	3.8 <sup>cde</sup>
1.0	4.0 <sup>a</sup>	4.6 <sup>a</sup>	4.1 <sup>bcd</sup>	4.6 <sup>a</sup>	4.2 <sup>bcd</sup>	5.0 <sup>a</sup>	4.7 <sup>a</sup>	2.8 <sup>bc</sup>	3.8 <sup>a</sup>	3.5 <sup>bcd</sup>
1.2	4.2 <sup>a</sup>	4.6 <sup>a</sup>	3.9 <sup>bcd</sup>	4.6 <sup>a</sup>	3.9 <sup>abcd</sup>	5.0 <sup>a</sup>	4.7 <sup>a</sup>	2.7 <sup>abc</sup>	3.8 <sup>a</sup>	3.2 <sup>abc</sup>
1.4	4.8 <sup>a</sup>	4.6 <sup>a</sup>	3.4 <sup>abc</sup>	4.4 <sup>a</sup>	3.6 <sup>abc</sup>	5.0 <sup>a</sup>	4.5 <sup>a</sup>	2.5 <sup>abc</sup>	3.8 <sup>a</sup>	2.7 <sup>ab</sup>
1.6	4.8 <sup>a</sup>	4.4 <sup>a</sup>	3.2 <sup>ab</sup>	4.4 <sup>a</sup>	3.3 <sup>ab</sup>	5.0 <sup>a</sup>	4.5 <sup>a</sup>	2.5 <sup>abc</sup>	3.8 <sup>a</sup>	2.7 <sup>ab</sup>
1.8	4.8 <sup>a</sup>	4.4 <sup>a</sup>	3.0 <sup>ab</sup>	4.6 <sup>a</sup>	2.9 <sup>a</sup>	5.0 <sup>a</sup>	4.7 <sup>a</sup>	2.2 <sup>ab</sup>	3.8 <sup>a</sup>	2.5 <sup>a</sup>
2.0	4.8 <sup>a</sup>	4.4 <sup>a</sup>	2.6 <sup>a</sup>	4.4 <sup>a</sup>	2.8 <sup>a</sup>	5.0 <sup>a</sup>	4.5 <sup>a</sup>	1.8 <sup>a</sup>	3.7 <sup>a</sup>	2.5 <sup>a</sup>

<sup>a</sup> Different letters in the same column indicates significant differences between the samples ( $P \leq 0.05$ ).

<sup>b</sup> The total taste acceptance score of the fruit puree without separating any specific taste property.

The extract most significantly influenced taste acceptance (Table 3): for PACP it did not change significantly until the extract concentration was <1.2%. However, when it exceeded 1.2%, the taste acceptance values significantly decreased and the total acceptance of puree significantly reduced when extract concentration exceeded 1.4%. Therefore, extract concentration in PACP should preferably not exceed 1.4%. According to the results, the taste of marc extract was less effectively masked in ABCP, most likely, because ABCP was initially slightly bitterer and had stronger astringent and bitter aftertaste than PACP. The most acceptable ABCP contained 0.4% of extract, while the taste acceptability reduced when extract concentration was  $\geq 1\%$ . All panellists indicated that increased bitterness and astringency were the major defects causing reduced taste acceptance of purees possessing higher percentage of extract i.e. reduced taste acceptance inversely correlated with the higher percentage of added phenolic compounds and ellagitannins in the samples. It should be also noted that extract concentration up to 0.8% did not influence the total acceptability of ABCP; however, it significantly decreased when extract concentration was  $\geq 1.2\%$  (Table 3).

The purees with 0.0 (control), 0.4, 0.8, 1.0, 1.2 and 1.6% extract concentrations were selected for the sensory profiling test. The overall odour was similarly intense in all samples tested. An acidic odour of the purees was less noticeable. However, according to the above mentioned odour properties the tested samples did not differ significantly (Table 4). The fresh and fruity odours of PACP significantly decreased with increasing extract concentrations; however,

the extract did not have a significant impact on the fresh and fruity odours of ABCP. It should be noted that the tested samples had a specific odour note, characteristic to high temperature-treated foods, which was described as a caramel/burnt. The odour intensity of PACP was directly dependent on the amount of the extract; however, marc extract did not show a significant influence on the odour properties of ABCP (Table 4).

The colour of PACP changed from light yellow (control) to brown and reddish-brown with increasing concentrations of the extract, i.e. higher percentage of anthocyanin fraction in the purees (Table 4). The brown, reddish-brown colour became particularly intense at  $\geq 1.2\%$ . The colour intensity of ABCPs did not markedly change with increased extract concentration.

The perceived overall taste intensity was similar for all samples (Table 4): they had moderately sweet and slightly less expressed acidic taste, which did not change with increasing extract concentration. Fresh and fruity taste of PACP, as well as fresh taste of ABCP decreased by increasing extract concentration.

The specific taste related to the extract (bitter and caramel/burnt) increased with increasing extract concentration for both purees (Table 4). Higher extract concentrations also increased astringent, bitter and burnt aftertastes. Such result is not surprising since both astringency and bitterness are elicited by polyphenolic compounds of which monomeric phenols are more bitter than astringent, whereas the reverse is true for larger molecular weight derivatives (Brossaud, Cheynier, & Noble, 2001). Furthermore, we assume that ellagitannins, ellagic acid and some other phenolic

**Table 4**  
The influence of extract additive (0–1.6%) on sensory profile of purees.<sup>a</sup>

Sensory properties	Pears, apples and yellow cherry plums (PACP)						Apples and black currants (ABCP)					
	0	0.4	0.8	1.0	1.2	1.6	0	0.4	0.8	1.0	1.2	1.6
Overall odour intensity	97.3 <sup>a</sup>	96.0 <sup>a</sup>	90.9 <sup>a</sup>	89.3 <sup>a</sup>	85.6 <sup>a</sup>	91.6 <sup>a</sup>	107.0 <sup>a</sup>	108.1 <sup>a</sup>	104.9 <sup>a</sup>	103.3 <sup>a</sup>	104.6 <sup>a</sup>	104.9 <sup>a</sup>
Acidic odour	72.0 <sup>a</sup>	74.9 <sup>a</sup>	63.1 <sup>a</sup>	65.2 <sup>a</sup>	66.1 <sup>a</sup>	63.8 <sup>a</sup>	77.5 <sup>a</sup>	73.6 <sup>a</sup>	68.4 <sup>a</sup>	75.1 <sup>a</sup>	70.0 <sup>a</sup>	66.3 <sup>a</sup>
Fresh odour	95.1 <sup>d</sup>	88.3 <sup>cd</sup>	75.0 <sup>bc</sup>	69.0 <sup>bc</sup>	63.8 <sup>ab</sup>	50.4 <sup>a</sup>	90.6 <sup>a</sup>	87.5 <sup>a</sup>	81.8 <sup>a</sup>	86.9 <sup>a</sup>	82.6 <sup>a</sup>	79.8 <sup>a</sup>
Fruity odour	94.3 <sup>c</sup>	89.0 <sup>bc</sup>	79.6 <sup>b</sup>	73.0 <sup>ba</sup>	65.7 <sup>a</sup>	59.3 <sup>a</sup>	90.9 <sup>a</sup>	93.5 <sup>a</sup>	90.0 <sup>a</sup>	93.8 <sup>a</sup>	89.5 <sup>a</sup>	89.0 <sup>a</sup>
Caramel/burnt odour	23.9 <sup>a</sup>	26.6 <sup>a</sup>	37.8 <sup>a</sup>	43.6 <sup>ab</sup>	59.3 <sup>b</sup>	78.4 <sup>b</sup>	40.0 <sup>a</sup>	39.0 <sup>a</sup>	43.1 <sup>a</sup>	45.0 <sup>a</sup>	42.3 <sup>a</sup>	47.9 <sup>a</sup>
Colour intensity	27.7 <sup>a</sup>	48.4 <sup>b</sup>	66.5 <sup>c</sup>	70.8 <sup>cd</sup>	82.9 <sup>d</sup>	93.6 <sup>d</sup>	110.2 <sup>a</sup>	112.5 <sup>a</sup>	115.2 <sup>a</sup>	116.9 <sup>a</sup>	117.8 <sup>a</sup>	120.8 <sup>ab</sup>
Overall taste intensity	97.4 <sup>ab</sup>	95.2 <sup>ab</sup>	93.2 <sup>a</sup>	97.9 <sup>ab</sup>	99.2 <sup>ab</sup>	106.7 <sup>b</sup>	108.5 <sup>a</sup>	106.3 <sup>a</sup>	105.8 <sup>a</sup>	106.3 <sup>a</sup>	107.6 <sup>a</sup>	108.9 <sup>a</sup>
Sweet taste	79.9 <sup>b</sup>	73.1 <sup>ab</sup>	67.7 <sup>ab</sup>	64.8 <sup>ab</sup>	63.7 <sup>ab</sup>	63.8 <sup>ab</sup>	83.4 <sup>a</sup>	82.1 <sup>a</sup>	81.6 <sup>a</sup>	77.1 <sup>a</sup>	78.1 <sup>a</sup>	72.3 <sup>a</sup>
Acidic taste	62.7 <sup>a</sup>	66.1 <sup>a</sup>	65.6 <sup>a</sup>	61.0 <sup>a</sup>	60.8 <sup>a</sup>	56.7 <sup>a</sup>	78.5 <sup>a</sup>	77.8 <sup>a</sup>	77.5 <sup>a</sup>	78.4 <sup>a</sup>	75.5 <sup>a</sup>	74.3 <sup>a</sup>
Fresh taste	90.8 <sup>b</sup>	84.5 <sup>b</sup>	76.5 <sup>b</sup>	67.2 <sup>ab</sup>	52.2 <sup>a</sup>	39.4 <sup>a</sup>	87.0 <sup>b</sup>	83.6 <sup>b</sup>	82.0 <sup>b</sup>	73.8 <sup>ab</sup>	74.3 <sup>ab</sup>	60.8 <sup>a</sup>
Bitter taste	25.1 <sup>a</sup>	33.7 <sup>a</sup>	43.0 <sup>a</sup>	48.1 <sup>ab</sup>	67.4 <sup>b</sup>	80.0 <sup>b</sup>	35.1 <sup>a</sup>	46.4 <sup>a</sup>	53.3 <sup>ab</sup>	70.3 <sup>bc</sup>	72.9 <sup>bc</sup>	89.8 <sup>c</sup>
Fruity taste	92.0 <sup>c</sup>	85.2 <sup>bc</sup>	75.5 <sup>ab</sup>	72.0 <sup>a</sup>	71.7 <sup>a</sup>	68.0 <sup>a</sup>	87.8 <sup>a</sup>	88.8 <sup>a</sup>	85.6 <sup>a</sup>	89.0 <sup>a</sup>	87.8 <sup>a</sup>	83.0 <sup>a</sup>
Caramel/burnt taste	24.0 <sup>a</sup>	28.2 <sup>a</sup>	47.4 <sup>b</sup>	52.3 <sup>b</sup>	65.4 <sup>bc</sup>	83.4 <sup>c</sup>	41.8 <sup>a</sup>	48.1 <sup>a</sup>	59.3 <sup>ab</sup>	71.5 <sup>bc</sup>	71.3 <sup>bc</sup>	84.3 <sup>c</sup>
Overall aftertaste intensity	71.0 <sup>a</sup>	70.7 <sup>a</sup>	73.7 <sup>a</sup>	76.2 <sup>a</sup>	77.0 <sup>a</sup>	85.3 <sup>a</sup>	90.8 <sup>a</sup>	90.8 <sup>a</sup>	92.3 <sup>a</sup>	95.8 <sup>a</sup>	95.9 <sup>a</sup>	104.3 <sup>a</sup>
Astringent aftertaste	24.5 <sup>a</sup>	29.0 <sup>a</sup>	40.1 <sup>ab</sup>	44.6 <sup>ab</sup>	52.1 <sup>b</sup>	61.0 <sup>b</sup>	52.8 <sup>a</sup>	56.5 <sup>a</sup>	61.0 <sup>ab</sup>	77.6 <sup>ab</sup>	76.9 <sup>ab</sup>	82.3 <sup>b</sup>
Bitter aftertaste	24.4 <sup>a</sup>	28.0 <sup>a</sup>	40.2 <sup>ab</sup>	48.4 <sup>bc</sup>	55.2 <sup>bc</sup>	67.9 <sup>c</sup>	32.4 <sup>a</sup>	50.4 <sup>ab</sup>	54.0 <sup>abc</sup>	66.8 <sup>bcd</sup>	74.9 <sup>cd</sup>	87.8 <sup>d</sup>
Caramel/burnt aftertaste	23.7 <sup>a</sup>	27.1 <sup>a</sup>	41.9 <sup>ab</sup>	47.2 <sup>bc</sup>	54.9 <sup>bc</sup>	68.1 <sup>c</sup>	36.9 <sup>a</sup>	45.9 <sup>a</sup>	50.6 <sup>ab</sup>	65.6 <sup>bc</sup>	66.9 <sup>bc</sup>	77.0 <sup>c</sup>

<sup>a</sup> The letters in the same row indicate significant differences between the samples ( $P \leq 0.05$ ).

compounds that are present in marc extract, but not anthocyanin fraction, were responsible for the increased bitterness and astringency of the purees. It was demonstrated previously that the addition of anthocyanin extract to wine had only minor effect on its astringency and no effect on bitterness (Brossaud et al., 2001). The changes of pH and the content of soluble solids may also influence sensory quality of purees. For instance, reduced pH might cause an increase in product acidity; however the relationships between pH and sensory perception in a complex food matrix are rather complicated and therefore in our case the reduction in pH by marc extract, most likely, was too low (by 0.15–0.16 units) to provide any significant changes in sensory characteristics. Regarding soluble solids, higher content of sugars might increase product sweetness; however, the effects of extract were not remarkable. Soluble solids also contain other substances such as organic acids, and from this point of view, the possibilities of complex interactions of sweet and sour taste might play some role.

According to the results of this study, the undesirable taste and aftertaste related to the raspberry marc extract were better masked in PACP than in ABCP, possibly due to the interaction of sensory attributes: sweetness and bitterness are typically mutually suppressed in the mixtures (Tokita & Boughter, 2012). As it was mentioned above, PACP had higher content of soluble solids than ABCP, which may explain why bitter taste was better masked in the former product. In addition, ABCP was initially bitterer and had lower pH than PACP. It was shown that in model wine solutions lower pH increases the astringency and the association of tannins with proteins (McRae & Kennedy, 2011).

The results of sensory profiling confirmed that puree odour, texture and colour acceptance was not influenced by the raspberry marc extract; however, they had a negative impact on the puree taste, and the samples with higher extract concentrations were less acceptable. Both purees with raspberry marc extract concentration of 1.6% and higher had a poor taste and were acknowledged as being unsuitable for consumption.

#### 4. Conclusion

The constituents of added raspberry marc extract increased the antiradical activity of fruit purees and the content of valuable polyphenolic constituents, thus improving functional properties of the products. The phenolics (especially colourless) of the raspberry marc extract were well retained during purees production process. The increase of free ellagic acid (up to 44%) in purees with extracts after thermal treatment was related to a partial hydrolysis of ellagitannins. Bitter and astringent tastes as well as aftertastes increased with increasing marc extract concentration in puree; therefore products with  $\geq 1.6\%$  of marc extract were acknowledged as being unsuitable for consumption.

#### Acknowledgement

This work was supported by the grant VP-3.1-ŠMM-10-V-02-021, Ministry of Education and Science, European Social Fund Agency, Lithuania; and Research Council of Lithuania, grant SVE01/2014.

#### References

Aaby, K., Wrolstad, R. E., Ekeberg, D., & Skrede, G. (2007). Polyphenol composition and antioxidant activity in strawberry purees; impact of achene level and storage. *Journal of Agricultural and Food Chemistry*, 55, 5156–5166.

Bhatt, J. K., Thoman, S., & Nanjan, M. J. (2012). Resveratrol supplementation improves glycemic control in type 2 diabetes mellitus. *Nutrition Research*, 32, 537–541.

Bobinaitė, R., Viskelis, P., Šarkinas, A., & Venskutonis, P. R. (2013). Phytochemical composition, antioxidant and antimicrobial properties of raspberry fruit, pulp, and marc extracts. *CyTA – Journal of Food*, 11, 334–342.

Bobinaitė, R., Viskelis, P., & Venskutonis, P. R. (2012). Variation of total phenolics, anthocyanins, ellagic acid and radical scavenging capacity in various raspberry (*Rubus* spp.) cultivars. *Food Chemistry*, 132, 1495–14501.

Bohn, T. (2014). Dietary factors affecting polyphenol bioavailability. *Nutrition Reviews*, 72, 429–452.

Brand-Williams, W., Cuvelier, M. E., & Berset, C. (1995). Use of a free radical method to evaluate antioxidant activity. *LWT-Food Science and Technology*, 28, 25–30.

Brossaud, F., Cheynier, V., & Noble, A. C. (2001). Bitterness and astringency of grape polyphenols. *Australian Journal of Grape and Wine Research*, 7, 33–39.

Cavalcanti, R. N., Santos, D. T., & Meireles, M. A. A. (2011). Non-thermal stabilization mechanisms of anthocyanins in model and food systems – an overview. *Food Research International*, 44, 499–509.

Četojević-Simin, D. D., Velićanski, A. S., Cvetković, D. D., Markov, S. L., Četković, G. S., Šaponjac, V. T. T., et al. (2015). Bioactivity of Meeker and Willamette raspberry (*Rubus idaeus* L.) pomace extracts. *Food Chemistry*, 166, 407–413.

Crowe, K. M., & Francis, C. (2013). Position of the academy of nutrition and dietetics: functional foods. *Journal of the Academy of Nutrition and Dietetics*, 113, 1096–1103.

Everette, J. D., Bryant, Q. M., Green, A. M., Abbey, Y. A., Wangila, G. W., & Walker, R. B. (2010). Thorough study of reactivity of various compound classes towards the Folin-Ciocalteu reagent. *Journal of Agricultural and Food Chemistry*, 58, 8139–8144.

FAO of UN: Economic and social Department: The Statistical Division. (2013). <http://faostat3.fao.org>.

Giusti, M. M., & Wrolstad, R. E. (2001). Anthocyanins. Characterization and measurement with UV-visible spectroscopy. In R. E. Wrolstad (Ed.), *Current protocols in food analytical chemistry (Unit F.1.2.1–F.1.2.13)*. New York: Wiley & Sons.

Giusti, M. M., & Wrolstad, R. E. (2003). Acylated anthocyanins from edible sources and their applications in food systems. *Biochemical Engineering Journal*, 14, 217–225.

Hager, T. J., Howard, L. R., & Prior, R. L. (2010). Processing and storage effects on the ellagitannin composition of processed blackberry products. *Journal of Agricultural and Food Chemistry*, 58, 11749–11754.

Herber, D. (2008). Multitargeted therapy of cancer by ellagitannins. *Cancer Letters*, 269, 262–268.

Koponen, J. M., Happonen, A. M., Mattila, P. H., & Törrönen, A. R. (2007). Contents of anthocyanins and ellagitannins in selected foods consumed in Finland. *Journal of Agricultural and Food Chemistry*, 55, 1612–1619.

Krammerer, D., Schillmüller, S., Maier, O., Schieber, A., & Reinhold, C. (2006). Colour stability of canned strawberries using black carrot and elderberry juice concentrates as natural colorants. *European Food Research and Technology*, 224, 667–669.

Landete, J. M. (2011). Ellagitannins, ellagic acid and their derived metabolites: a review about source, metabolism, functions and health. *Food Research International*, 44, 1150–1160.

Larrosa, M., Tomás-Barberán, F. A., & Espín, J. C. (2006). The dietary hydrolysable tannin punicalagin releases ellagic acid that induces apoptosis in human colon adenocarcinoma Caco-2 cells by using the mitochondrial pathway. *The Journal of Nutritional Biochemistry*, 17, 611–625.

McRae, J. M., & Kennedy, J. A. (2011). Wine and grape tannin interactions with salivary proteins and their impact on astringency: a review of current research. *Molecules*, 16, 2348–2364.

Paller, C. J., Ye, X., Wozniak, P. J., Gillespie, B. K., Sieber, P. R., Greengold, R. H., et al. (2013). A randomized phase II study of pomegranate extract for men with rising PSA following initial therapy for localized prostate cancer. *Prostate Cancer and Prostatic Diseases*, 16, 50–55.

Perumalla, A. V. S., & Hettiarachchy, N. S. (2011). Green tea and grape seed extracts - potential applications in food safety and quality. *Food Research International*, 44, 827–837.

Slinkard, K., & Singleton, V. L. (1977). Total phenol analysis: automation and comparison with manual methods. *American Journal of Enology and Viticulture*, 28, 49–55.

Soares, S., Kohl, S., Thalmann, S., Mateus, N., Meyerhof, W., & De Freitas, V. (2013). Different phenolic compounds activate distinct human bitter taste receptors. *Journal of Agricultural and Food Chemistry*, 61, 1525–1533.

Thomasset, S. C., Berry, D. P., Garcea, G., Marczylo, T., Steward, W. P., & Gescher, A. J. (2007). Dietary polyphenolic phytochemicals – promising cancer chemopreventive agents in humans? A review of their clinical properties. *International Journal of Cancer*, 120, 451–458.

Tokita, K., & Boughter, T. D., Jr. (2012). Sweet-bitter and umami-bitter taste interactions in single parabrachial neurons in C57BL/6J mice. *Journal of Neurophysiology*, 108, 2179–2190.

Turkmen, N., Sari, F., & Velioglu, Y. S. (2005). The effect of cooking methods on total phenolics and antioxidant activity of selected green vegetables. *Food Chemistry*, 93, 713–718.

Viskelis, P., Rubinskienė, M., Jasutienė, I., Šarkinas, A., Daubaras, R., & Česonienė, L. (2009). Anthocyanins, antioxidative, and antimicrobial properties of American cranberry (*Vaccinium macrocarpon* Ait.) and their press cakes. *Journal of Food Science*, 74, C157–C161.

Williamson, G., & Holst, B. (2008). Dietary reference intake (DRI) value for dietary polyphenols: are we heading in the right direction? *The British Journal of Nutrition*, 99(Suppl. 3), S55–S58.

Zafrailla, P., Ferreres, F., & Tomas-Barberan, F. A. (2001). Effect of processing and storage on the antioxidant ellagic acid derivatives and flavonoids of red raspberry (*Rubus idaeus*) jams. *Journal of Agricultural and Food Chemistry*, 49, 3651–3655.



# Malolactic fermentation before or during wine aging in barrels



P.M. Izquierdo-Cañas<sup>a, b, \*</sup>, A. Mena-Morales<sup>c</sup>, E. García-Romero<sup>a</sup>

<sup>a</sup> Instituto de la Vid y el Vino de Castilla-La Mancha, Crta. Toledo-Albacete s/n., 13700, Tomelloso, Ciudad Real, Spain

<sup>b</sup> Parque Científico-Tecnológico de Castilla-La Mancha, Paseo de la Innovación, 1, 02006, Albacete, Spain

<sup>c</sup> Instituto Regional de Investigación Científica Aplicada, Universidad de Castilla-La Mancha, Camilo José Cela, s/n., 13071, Ciudad Real, Spain

## ARTICLE INFO

### Article history:

Received 15 May 2015

Received in revised form

14 September 2015

Accepted 2 November 2015

Available online 5 November 2015

### Keywords:

Malolactic fermentation

Wine aging

Barrels

Tanks

## ABSTRACT

Malolactic fermentation (MLF) and aging in oak barrels are two oenological processes which modify the composition and sensory characteristics of the wines. However, there are few studies on the MLF in barrels.

This work compares wines in which MLF is carried out in steel tanks and then aged in oak barrels, with wines in which MLF has been carried out in barrels.

MLF occurs faster in barrels and while the fundamental structure of the wine is virtually identical, there is less color loss.

Some groups of volatile compounds vary significantly depending on whether MLF takes place in tanks prior to aging or in the oak barrels themselves. It was shown that in this latter case, wines were obtained with slightly higher concentrations of methoxy-phenols and approximately double amount of whisky-lactones and furanic compounds.

© 2015 Elsevier Ltd. All rights reserved.

## 1. Introduction

In addition to alcoholic fermentation, red winemaking also requires malolactic fermentation (MLF) and aging in barrels and/or in bottles. The main purpose of MLF is to reduce wine acidity by transforming the malic acid, into lactic acid (Moreno-Arribas, Gómez-Cordovés, & Martín-Alvarez, 2008).

Moreover, volatile compounds are also formed during this process that enrich the wine's aromatic quality while also modifying color and phenolic composition (Izquierdo-Cañas, García, Gómez, & Palop, 2008; Martínez-Pinilla, Martínez-Lapiente, Guadalupe, & Ayestarán, 2012).

When MLF is complete, the wine is subjected to different clarification and stabilization treatments and/or is stored in oak barrels for aging for a variable period of time. This practice modifies wine composition due to the compounds extracted from the wood and to the chemical reactions that take place when oxygen passes through wood pores or staves (Gómez García-Carpintero, Gómez Gallego, Sánchez-Palomo, & González Viñas, 2012).

In an attempt to obtain more complex quality wines from an

organoleptic point of view with their own distinguishing personality, another production method employed consists of carrying out the MLF process in the oak barrels where the wine is stored to age (Hernández-Orte, Peña, Pardo, Cacho, & Ferreira, 2012).

Traditional red wine production, in which MLF is carried out in tanks and aging in barrels, has been widely studied (Castro-Vázquez et al. 2011; Jarauta, Cacho, & Ferreira, 2005). However, less research has been done on MLF in barrels in which there is less control over the process and therefore entails greater risks.

Barrel MLF modifies the aromatic sensory profile of wine in varying degrees depending differences in the design of the studies performed (De Revel, Bloem, Augustin, Lonvaud-Funel, & Bertrand, 2005; Gómez García-Carpintero, Sánchez-Palomo, & González Viñas, 2014), the general consensus showing a preference for barrel MLF wines over the tank MLF variety (Vivas, Lonvaud-Funel, & Glories, 1995). However, few articles have taken a close look at the changes occurring in the concentration of the different volatile compounds when MLF takes place in barrels.

The objective of this study is to compare the chemical composition, color, volatile composition and sensory qualities of two groups of red wines aged in French oak barrels: one in which MLF was carried out in tanks and the other in barrels.

\* Corresponding author. Instituto de la Vid y el Vino de Castilla-La Mancha, Crta. Toledo-Albacete s/n, 13700, Tomelloso, Ciudad Real, Spain.

E-mail address: [pmizquierdo@jccm.es](mailto:pmizquierdo@jccm.es) (P.M. Izquierdo-Cañas).

## 2. Material and methods

### 2.1. Fermentation assays

Cabernet Franc grape variety was fermented in our experimental winery, vintage 2013. The chemical composition of the must was: ° Brix 23.00; total acidity 6.89 g/L; pH 3.24; L-malic acid 1.83 g/L. Alcoholic fermentation was carried out at  $25 \pm 2$  °C using the commercial yeast Uvaferm VN<sup>®</sup> (Lallemand Inc.) at 20 g/HL. The fermentation was monitored daily by measuring density and the wine was pressed upon reaching a density of 995 g/L marking the completion of alcoholic fermentation at room temperature.

After alcoholic fermentation, the wine was divided into two batches to carry out MLF in tanks and in barrels, by triplicate. Fifty-liter stainless-steel tanks were used for one batch and 32-L French oak barrels for the other. Upon completion of the MLF process, the wine held in the tanks was transferred to barrels for 45 days so that it would have the same contact time with the oakwood as the other batch.

A commercial Alpha strain (MBR<sup>®</sup>) at 1 g/HL was used for MLF according to the manufacturer's instructions (Lallemand Inc.) at a temperature of 22 °C.

MLF development was controlled by monitoring the L-malic acid content of the wines. When malic acid content reached values  $\leq 0.2$  g/L, the wines were sulphited until a final free SO<sub>2</sub> concentration of 30.0 mg/L.

When MLF was finished, the wines were left for a total of 45 days in barrels and were then stabilized, filtered through 0.2 μm filters and bottled.

### 2.2. Chemical analysis

The wines were analytically characterized following the official analytical methods (OIV, 2014).

Anthocyanins were determined by decoloring with sulfur dioxide (Ribereau-Gayon & Stronestreet, 1965) and total polyphenols by measuring the absorbance at 280 nm (Somers & Evans, 1976). Total flavan-3-ols were determined by reaction with dimethylaminocinnamaldehyde and measurement of the absorbance at 640 nm (Vivas, Glories, Lagune, Sancier, & Augustin, 1994), and tannins by precipitation with methylcellulose (Smith, 2005).

### 2.3. Volatile compound analysis

Volatile compounds were analyzed by GC–MS with quadrupole analyzer. A BP21 column (SGE) 50 m–0.32 mm internal diameter and 0.25 mm thick of Free Fatty Acid Phase (FFAP) (polyethylene glycol treated with nitroterephthalic acid) was used.

For the major volatile compounds, 1 μL of the samples was directly injected with 4-methyl-2-pentanol as internal standard (final concentration 20 mg/L). The chromatographic conditions were as follows: carrier helium gas (1.7 mL/min, split 1/25); injector temperature, 220 °C and oven temperature, 43 °C for 5 min, 4 °C/min to 100 °C, 20 °C/min to 190 °C, and 45 min at 190 °C.

Minor volatile compounds were extracted using the method developed by Ibarz, Ferreira, Hernández-Orte, Loscos, and Cacho (2006). Extracts were concentrated by distillation in a Vigreux column and under nitrogen stream to 100 μL and then kept at –20 °C until analysis.

Separated compounds were identified by their mass spectra and their chromatographic retention times, using commercial products as a standard. Quantification was performed by analyzing the characteristic *m/z* fragment for each compound using the internal standard method. Results for non-available compounds was expressed in concentration units (μg/L or mg/L) as internal

standard equivalents obtained by normalizing the compound peak area to that of the internal standard and multiplying by the concentration of the internal standard.

### 2.4. Sensory analysis

Sensory analyses were performed to identify the differences among the two different MLF procedures. Both triangle and descriptive tests were carried out. Wines were analyzed by a panel of expert assessors (between 25 and 50 years age) who were staff members from Institute of Wine and Vin of Castilla-La Mancha, Spain, with experience in sensory analysis. Previously, assessors were trained in descriptive sensory analysis over several sessions, using discriminative tests.

A triangular test to evaluate differences in color, aroma and taste was performed. Sets of three samples each were analyzed by 14 panelists in three sessions carried out on different days in accordance with ISO Standard 4120 (ISO, 1983).

Descriptive sensory analysis was performed by 10 selected panelists following the Sensory Profile method according to ISO Standard 11035 (ISO, 1994). The descriptors were scored on a scale of 0–5 (0 absence of the descriptor and 5 maximum intensity of the descriptor).

### 2.5. Statistical analysis

The paired Student *t* test was used to identify any significant differences between chemical analysis results and volatile compounds. SPSS 12.0 software was used for both analyses.

## 3. Result and discussion

### 3.1. Evolution of L-malic acid

Fig. 1 shows the evolution of L-malic acid from tank MLF and barrel MLF assays. The figure shows that malic acid degradation began on day 5 in the oak trials but on day 11 in the steel tank trials. MLF was completed after 18 and 21 days respectively. De Revel et al. (2005) showed that the LAB population was higher in samples containing oak heated shavings than in the controls, which would explain the quicker fermentation.

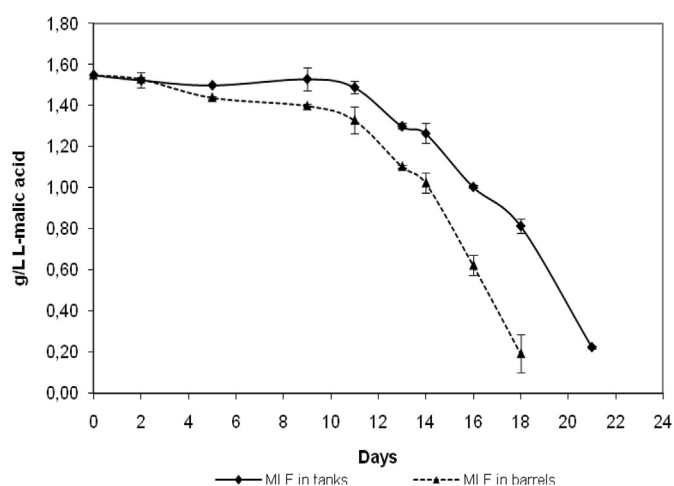


Fig. 1. Evolution of MLF.

### 3.2. General wine composition

Table 1 summarizes the mean values  $\pm$  standard deviation of the chemical parameters analyzed. The Table shows the expected transformations resulting from MLF such as lower total acidity and the corresponding rise in pH due to the disappearance of malic acid and its transformation into lactic acid. A slight rise in volatile acidity is also observed. Acetic acid concentrations exceeding 0.7 g/L give a sour and pungent aroma and a vinegar-like character to wine (Swiegers, Bartowsky, Henschke, & Pretorius, 2005), while concentrations between 0.2 and 0.7 g/L can contribute to the complexity of wine aroma (Dubois, 1994).

The MLF has not led to an increase of the volatile acidity by citric acid metabolism (Bartowsky & Henschke, 2004) given that citric acid was maintained at similar levels in the two trials. In other studies (Vivas et al. 1995) found small increments of acetic acid from the acetylated groups of the hemicellulose. This could be the cause of the higher value of the volatile acidity of wines “MLF in barrels” a fact that cannot be categorically said by the absence of statistically significant differences.

A comparison of the tank and barrel MLF trials suggests that the basic structure of the wines is virtually identical. Some statistically significant differences have been found but are unimportant from a practical point of view. The only differences that do merit attention are those related with the color. When MLF was carried out in barrels, color intensity was greater and luminosity lower. Also, Cielab  $a^*$  parameter and tonality values were slightly lower. These results could be due to two events occurring simultaneously. The rise in pH due to MLF causes a decrease in the percentage of colored anthocyanins which is why MLF typically results in a reduction in color intensity as has been reported (Ruíz-Pérez, Izquierdo-Cañas, Seseña-Prieto, García-Romero, & Palop-Herreros, 2012). Furthermore, a micro-oxygenation process takes place in barrels but not in stainless-steel tanks which may favor anthocyanin polymerization reactions compensating the loss of color described above. Oxygen in small quantities favors polymerization reactions among anthocyanins and tannins (Atanasova, Fulcrand, Cheynier, & Moutounet, 2002).

**Table 1**  
Physicochemical analysis of wines.

	Before MLF	MLF tanks	MLF barrels
Alcohol content (% v/v)	13.19	13.25 $\pm$ 0.01 <sup>b</sup>	13.21 $\pm$ 0.01 <sup>a</sup>
Total acidity (g/L)	6.83	5.80 $\pm$ 0.04	5.72 $\pm$ 0.09
pH	3.26	3.34 $\pm$ 0.01 <sup>a</sup>	3.35 $\pm$ 0.01 <sup>b</sup>
Volatile acidity (g/L)	0.39	0.41 $\pm$ 0.13	0.51 $\pm$ 0.05
l-Malic acid (g/L)	1.56	0.08 $\pm$ 0.01	0.06 $\pm$ 0.1
l-Lactic acid (g/L)	0.20	1.21 $\pm$ 0.02	1.26 $\pm$ 0.01
Citric acid (g/L)	0.22	0.16 $\pm$ 0.01 <sup>a</sup>	0.17 $\pm$ 0.01 <sup>b</sup>
Tartaric acid (g/L)	1.85	1.81 $\pm$ 0.02 <sup>a</sup>	1.90 $\pm$ 0.01 <sup>b</sup>
Succinic acid (g/L)	1.09	1.07 $\pm$ 0.09	1.13 $\pm$ 0.01
Glycerin (g/L)	8.80	9.02 $\pm$ 0.03	8.97 $\pm$ 0.05
Anthocyanins (mg/L)	551.57	544.13 $\pm$ 14.39	510.47 $\pm$ 2.74
Catechins (mg/L cat.)	114.92	121.34 $\pm$ 9.53 <sup>b</sup>	106.15 $\pm$ 0.57 <sup>a</sup>
Tannins (g/L)	0.29	0.28 $\pm$ 0.04	0.30 $\pm$ 0.21
Total polyphenols (mg/L)	34.95	35.40 $\pm$ 0.23	35.06 $\pm$ 0.49
L*	24.74	26.89 $\pm$ 0.36 <sup>b</sup>	24.74 $\pm$ 0.24 <sup>a</sup>
a*	55.98	58.10 $\pm$ 0.04 <sup>b</sup>	56.70 $\pm$ 0.35 <sup>a</sup>
b*	31.75	32.98 $\pm$ 1.10	33.16 $\pm$ 0.05
Color Intensity	6.34	5.77 $\pm$ 0.17 <sup>a</sup>	6.33 $\pm$ 0.04 <sup>b</sup>
Tonality	0.55	0.62 $\pm$ 0.01 <sup>b</sup>	0.58 $\pm$ 0.01 <sup>a</sup>

Values are the mean of triplicates.

<sup>(a,b)</sup> Denotes statistically significant differences ( $p \leq 0.05$ ) between the different MLF methods.

### 3.3. Volatile compounds

Volatile compounds were determined both before and after MLF. The compounds were grouped according to chemical similarities. Table 2 and 3 shows the results obtained for these groups of compounds.

#### 3.3.1. Compounds that do not vary depending on the type of recipient used by MLF

**Ethyl lactate** is the most important ester typically playing a role in MLF (Ruíz-Pérez et al. 2012; Ugliano & Moio, 2005), resulting from esterification of the lactate produced by lactic acid bacteria (LAB) and the ethanol produced during alcoholic fermentation (AF). Ethyl lactate concentrations rise significantly following MLF, and some authors (Ruíz-Pérez et al. 2012) have reported that concentrations reached are dependent on the strain of *Oenococcus oeni* used. It gives wines milky notes and is responsible for the volume feeling (Ugliano & Moio, 2005). Results from this study show similar concentrations of ethyl lactate in wines in which MLF was carried out in tanks and barrels coinciding with the very similar values of lactic acid produced (Table 2).

Although statistical analysis cannot be used since there are not replications of the initial wine before MLF, we did observe that there were three groups of compounds that increased after MLF but which show no differences attributable to container type.

Monoterpenes, C<sub>13</sub>-norisoprenoids, benzene derivatives and some aliphatic compounds are frequently found as D-glucopyranosides, aglycone being the volatile linked by a  $\beta$ -glycoside bond to a single D-glucopyranose or to a disaccharide, in which the glucose can be further conjugated to apiose, arabinose, rhamnose or xylose (Pérez-Martin, Izquierdo-Cañas, Seseña, García-Romero, Palop, & Li, 2015; Williams, 1993). The ability of *O. oeni* to release diverse aglycons from natural glycosylated compounds extracted from grapes (Mansfield, Zoecklein, & Whiton, 2002; McMahan, Zoecklein, Fugelsang, & Jasinski, 1999) and oakwood (Bloem, Lonvaud-Funel, & de Revel, 2008; Gagné et al. 2011) was observed.

Hernández-Orte et al. (2009) also reported increases in damascenone in wines whose MLF was by the strain *O. oeni* 5106. Boido, Lloret, Medina, Carrau, and Dellacassa (2002) reported increases of benzyl alcohol in wines inoculated with three *O. oeni* commercial strains.

All these compounds contribute substantially to the aroma of wine. Thus, the norisoprenoids provide fruity, floral or spicy notes and hence, their presence has very beneficial effects for the sensory quality of wines. Typical aroma descriptions of some important terpenes are floral, rose-like, coriander, camphoraceous, green and herbaceous (Simpson, 1979). Benzyl alcohol provides notes of blackberry, floral and sweet aroma (Selli, Canbas, Cabaroglu, Erten, & Günata, 2006).

For **terpenes**, a global increase is observed following MLF, although citronellol accounts for most of this increase as its concentration nearly doubles. Similar results were obtained by Ortega-Heras, González-San José, and González-Huerta (2008). These authors attributed this increase to the micro-oxygenation process the experimental wines underwent. In our case, the time spent in barrels also supplied the wines with oxygen but, given that the increase was also observed in the tank MLF wines we believe that this also has to do with the effect of  $\beta$ -glucosidase activity of lactic bacteria as may also occur in the research cited since their wines were subjected to MLF after micro-oxygenation.

In relation to **volatile phenols**, no significant differences were observed between the two groups of wines. In both cases, 4-ethyl phenol, 4-vinyl guaiacol and 4-vinylphenol increased after MLF whatever the process. Different studies have identified the capacity of certain LAB to produce volatile phenols (Couto, Campos,

**Table 2**  
Volatile compounds that do not vary depending on the type of recipient used by MLF.

	Units	m/z	Before MLF	MLF tanks	MLF barrels
Ethyl lactate	mg/L	75	8.09	33.46 ± 3.92	37.57 ± 2.01
Diethyl malate <sup>a</sup>	µg/L	117	79.15	59.61 ± 27.37	39.32 ± 21.99
2-Phenylethyl lactate	µg/L	104	2.39	15.00 ± 6.71	15.71 ± 7.31
3-Hydroxy-2-butanone	mg/L	45	13.55	19.95 ± 3.00	19.63 ± 2.49
Benzyl alcohol	µg/L	79	183.12	244.83 ± 91.72	228.69 ± 84.34
2-Phenylethanol	mg/L	122	45.42	62.07 ± 10.41	59.48 ± 9.19
Phenol	µg/L	94	5.46	6.37 ± 3.61	8.89 ± 4.05
Tyrosol	mg/L	107	6.84	6.79 ± 3.98	10.44 ± 4.67
<b>Benzenic alcohols</b>	mg/L		<b>52.45</b>	<b>69.12 ± 14.49</b>	<b>70.16 ± 13.95</b>
Linalool	µg/L	93	5.42	6.30 ± 0.91	6.56 ± 0.06
Citronellol	µg/L	95	27.62	49.11 ± 10.81	42.84 ± 5.45
Geraniol	µg/L	93	2.27	3.44 ± 0.75	2.82 ± 1.31
Hidroxicitronellol <sup>a</sup>	µg/L	59	3.91	5.12 ± 1.90	6.73 ± 1.68
2,7-dimethyl-4,5-octanodiol	µg/L	69	21.70	31.51 ± 5.55	29.90 ± 7.64
3,7-dimethyl-1,5-octadien-3,7-diol <sup>a</sup>	µg/L	71	2.51	2.71 ± 0.61	2.02 ± 0.94
<b>Terpenes</b>	µg/L		<b>63.43</b>	<b>98.18 ± 20.54</b>	<b>90.86 ± 16.96</b>
Damascone <sup>a</sup>	µg/L	177	1.13	0.79 ± 0.24	0.64 ± 0.35
Damascenone	µg/L	190	3.77	6.12 ± 2.66	6.05 ± 2.58
3-oxo- $\alpha$ -ionol <sup>a</sup>	µg/L	108	57.05	77.81 ± 14.28	74.26 ± 14.35
3-oxo-7,8-dihydro- $\alpha$ -ionol <sup>1</sup>	µg/L	135	0.76	0.93 ± 0.38	0.87 ± 0.52
<b>Norisoprenoids</b>	µg/L		<b>62.71</b>	<b>85.64 ± 17.56</b>	<b>81.80 ± 17.80</b>
4-Ethyl phenol	µg/L	122	0.42	0.77 ± 0.04	0.89 ± 0.32
4-Vinyl guaiacol	µg/L	150	16.41	78.72 ± 37.97	75.35 ± 23.77
4-Vinyl phenol <sup>a</sup>	µg/L	91	2.63	1.98 ± 1.24	3.75 ± 1.65
<b>Volatile phenols</b>	µg/L		<b>19.05</b>	<b>80.71 ± 39.21</b>	<b>79.10 ± 22.12</b>
<b>Acetates</b>	mg/L		<b>38.99</b>	<b>36.59 ± 4.76</b>	<b>38.67 ± 1.40</b>
<b>Ethyl esters</b>	mg/L		<b>31.87</b>	<b>32.99 ± 14.72</b>	<b>34.13 ± 6.34</b>
<b>Ethyl esters of Hydroxy acids</b>	mg/L		<b>30.93</b>	<b>32.56 ± 14.67</b>	<b>33.76 ± 6.23</b>
<b>Acids</b>	mg/L		<b>28.86</b>	<b>42.50 ± 9.47</b>	<b>38.06 ± 10.61</b>
<b>Linear Alcohols</b>	mg/L		<b>557.07</b>	<b>500.64 ± 31.53</b>	<b>493.17 ± 26.09</b>
<b>C6 Alcohols</b>	mg/L		<b>1.79</b>	<b>0.74 ± 0.24</b>	<b>0.68 ± 0.28</b>

Values are the mean of triplicates.

The total concentrations of different groups of volatile aroma compounds are in bold.

<sup>a</sup> Denote concentration expressed in µg/L or mg/L as internal standard equivalents.

Figueiredo, & Hogg, 2006; Nelson, 2008), including ethyl phenols. These compounds have an unpleasant animal odor described as leather and even as horse sweat and are a serious defect in wine when they exceed the perception threshold. In our study, no significant differences were observed in ethylphenol content between tank and barrel MLF.

Here we find all esters (acetates, ethyl esters and ethyl esters of hydroxy acids), organic acids, linear alcohols and C6 alcohols. Several authors (Hernández-Orte et al. 2012; Izquierdo-Cañas et al. 2008) failed to find any significant difference in acids or alcohols arising from MLF.

The findings published regarding ethyl esters are controversial. Some authors associate MLF with a general increase in these compounds (Swiegers et al. 2005) while others have reported significant decreases in some of them (Jeromel, Herjavec, Orlic, Redzepovic, & Wondra, 2008). The effect of MLF on concentrations of these esters in wine varies depending on esterase activity which some authors have noted with regard to some LAB (Matthews et al. 2004). Given that in our work the LAB strain was the same in the two trials. The results in Table 2 indicate that the MLF methods tried in this work did not significantly alter the initial concentration of the wine esters.

### 3.3.2. Compounds that vary depending on the type of recipient used for MLF

**Acetaldehyde** is one of the most important sensory carbonyl compounds formed during alcoholic fermentation, associated with herbaceous and oxidative notes in wines (Liu & Pilone, 2000). As reported by other authors (Osborne, Mira de Orduña, Pilone, & Liu, 2000), a decrease in acetaldehyde concentration was observed in wines after MLF, with differences depending on the malolactic

culture used (Ruiz-Pérez et al. 2012). In our study, decreases were higher when MLF was carried out in tanks. Two facts could explain these results. On the one hand by the influence of the micro-oxygenation that occurs when the MLF takes place in barrels. We must also consider which an MFL tank takes the MLF 3 days more. The presence of lactic bacteria for a few extra days in the tank wines possibly allowing for the metabolization of more acetaldehyde must also be considered. Reduction of acetaldehyde could have a positive impact on the aroma of wines given its oxidative properties (Osborne et al. 2000).

**2,3-butanedione** is another important aromatic compound produced by LAB which at low concentrations makes a positive contribution to wine aroma supplying buttery notes and adding complexity (Swiegers et al. 2005), but at high concentrations has an adverse effect on quality. It is formed as an intermediate product in the metabolism of citric acid (Bartowsky, Costello, & Henschke, 2002) and may be reduced to 3-hydroxy-2-butanone. The concentration of 2,3-butanedione in barrel MLF wines is one half that of the tank wines but 3-hydroxy-2-butanone levels are identical. According to other authors of the advantages of carrying out MLF in small volumes (225 L barrels) is the swifter reduction in carbonylic compounds due to the greater contact of the wine with the lees of the yeast and the bacteria themselves (Hernández-Orte et al. 2012).

*O. oeni* is able to break down 2-oxoglutarate producing succinate which accounts for the rise in their esters due to MFL (Van Vuuren & Dicks, 1993). Diethyl succinate also contributes to the aroma of wines, supplying fruity and melon notes to the wine and has on odor threshold of 1.2 mg/L (Peinado, Moreno, Bueno, Moreno, & Mauricio, 2004). Wines obtained from barrel MLF have higher levels of succinate derivatives except for ethyl monosuccinate.

As can be observed in Table 3, only small differences were

**Table 3**  
Volatile compounds that vary depending on the type of recipient used for MLF.

	Units	m/z	Before MLF	MLF tanks	MLF barrels
Acetaldehyde	mg/L	43	32.53	19.18 ± 3.93 <sup>a</sup>	24.58 ± 1.69 <sup>b</sup>
2,3-butanodione	mg/L	86	1.59	7.19 ± 1.34 <sup>b</sup>	3.73 ± 0.10 <sup>a</sup>
Dimethyl succinate	μg/L	115	2.05	5.22 ± 0.24 <sup>a</sup>	7.11 ± 0.81 <sup>b</sup>
Methyl-Ethyl succinate <sup>1</sup>	μg/L	115	4.45	7.76 ± 0.62 <sup>a</sup>	11.51 ± 2.43 <sup>b</sup>
Diethyl succinate	mg/L	129	1.18	1.84 ± 0.98 <sup>a</sup>	4.15 ± 1.64 <sup>b</sup>
Ethyl-Propyl succinate <sup>1</sup>	mg/L	101	2.27	16.42 ± 7.10 <sup>a</sup>	35.75 ± 12.29 <sup>b</sup>
Ethyl monosuccinate <sup>1</sup>	mg/L	128	6.48	6.85 ± 3.62	6.62 ± 2.79
Methyl monosuccinate <sup>1</sup>	μg/L	101	8.59	6.97 ± 1.85 <sup>a</sup>	13.30 ± 2.35 <sup>b</sup>
<b>Succinates</b>	mg/L		<b>9.95</b>	<b>25.13 ± 9.74<sup>a</sup></b>	<b>46.56 ± 16.74<sup>b</sup></b>
γ-butyrolactone	μg/L	86	235.30	268.42 ± 8.36 <sup>b</sup>	385.30 ± 52.54 <sup>b</sup>
γ-valerolactone	μg/L	85	253.10	101.03 ± 38.31	102.54 ± 5.25
γ-caprolactone	μg/L	85	8.17	12.83 ± 3.07	12.39 ± 2.14
γ-nonolactone	μg/L	85	7.61	9.11 ± 3.96	6.63 ± 2.94
γ-decalactone	μg/L	85	0.77	1.45 ± 0.08	1.26 ± 0.72
δ-decalactone	μg/L	99	3.18	21.44 ± 3.17 <sup>b</sup>	10.25 ± 1.27 <sup>a</sup>
δ-dodecalactone	μg/L	114	8.44	22.82 ± 0.82	25.77 ± 4.62
4-ethoxy-γ-butyrolactone <sup>1</sup>	μg/L	85	1.00	1.04 ± 0.57 <sup>a</sup>	2.40 ± 0.92 <sup>b</sup>
4-ethoxycarbonyl-γ-butyrolactone <sup>1</sup>	mg/L	85	0.58	0.57 ± 0.29	0.50 ± 0.20
4(1-Hydroxy-ethyl)-γ-butyrolactone <sup>1</sup>	μg/L	85	8.60	11.63 ± 4.29	11.22 ± 6.77
Pantolactone	μg/L	71	9.27	14.07 ± 6.52	12.23 ± 5.71
<b>Lactones</b>	mg/L		<b>1.12</b>	<b>1.14 ± 0.38</b>	<b>1.28 ± 0.24</b>
Syringaldehyde	μg/L	182	n/F	28.75 ± 7.94	27.38 ± 3.01
Acetosyringone	μg/L	196	n/F	23.08 ± 5.06 <sup>b</sup>	12.07 ± 0.82 <sup>a</sup>
Syringol	μg/L	154	6.32	34.70 ± 11.81	38.07 ± 6.46
Guaiacol	μg/L	124	29.10	40.59 ± 5.50 <sup>a</sup>	51.19 ± 7.20 <sup>b</sup>
Eugenol	μg/L	164	0.28	4.98 ± 2.63	6.47 ± 2.50
<i>t</i> -isoeugenol	μg/L	164	0.30	1.67 ± 0.76	1.24 ± 0.29
Methoxyeugenol	μg/L	194	1.57	2.78 ± 0.19	2.23 ± 0.50
Vanillin	μg/L	151	5.49	89.23 ± 25.87 <sup>b</sup>	56.78 ± 10.69 <sup>a</sup>
Ethyl vanillate <sup>1</sup>	μg/L	196	9.72	13.29 ± 2.97	13.28 ± 2.36
Methyl vanillate	μg/L	182	7.83	10.05 ± 1.29	12.15 ± 2.93
Homovanillyl alcohol	μg/L	137	2.95	25.32 ± 4.28 <sup>b</sup>	11.17 ± 4.10 <sup>a</sup>
Acetovanillone	μg/L	166	74.20	128.15 ± 25.29	110.48 ± 18.89
Propiovanillone <sup>1</sup>	μg/L	180	2.06	3.27 ± 1.29	4.17 ± 2.25
<b>Methoxyphenols</b>	μg/L		<b>139.82</b>	<b>407.84 ± 104.30</b>	<b>350.69 ± 5.88</b>
<i>t</i> -β-Methyl-γ-octalactone	μg/L	100	n/F	27.76 ± 7.22 <sup>a</sup>	91.10 ± 28.41 <sup>b</sup>
<i>c</i> -β-Methyl-γ-octalactone	μg/L	87	n/F	73.45 ± 26.64	118.82 ± 43.08
<b>Whiskylactones</b>	μg/L		<b>n/F</b>	<b>101.21 ± 33.87<sup>a</sup></b>	<b>209.92 ± 71.49<sup>b</sup></b>
5-Methyl-2-furfural	μg/L	110	0.49	27.05 ± 12.88	41.35 ± 7.32
2-Ethyl furoate	μg/L	95	2.48	15.39 ± 3.42	28.86 ± 13.43
Hydroxy methyl furfural	μg/L	97	6.79	44.26 ± 27.50 <sup>a</sup>	113.20 ± 54.33 <sup>b</sup>
Furfural	μg/L	96	0.17	46.60 ± 27.18	38.14 ± 14.22
Furfuryl alcohol	μg/L	98	n/F	10.36 ± 0.14 <sup>a</sup>	104.74 ± 27.03 <sup>b</sup>
<b>Furanic compounds</b>	μg/L		<b>9.76</b>	<b>143.67 ± 64.29<sup>a</sup></b>	<b>326.29 ± 6.97<sup>b</sup></b>

Values are the mean of triplicates.

<sup>1</sup>Denote concentration expressed in μg/L or mg/L as internal standard equivalents.

The total concentrations of different groups of volatile aroma compounds are in bold. n/F not found.

<sup>(a,b)</sup>Denotes statistically significant differences ( $p \leq 0.05$ ) between the different MLF methods.

observed in the content of the **Lactones** group between the two MLF methods. However, after MLF wines contained higher concentrations of γ-butyrolactone, δ-decalactone and δ-dodecalactone, and a lower amount of γ-valerolactone. Moreover, barrel MLF produces wines with higher levels of γ-butyrolactone, 4-ethoxy-γ-butyrolactone and a lower amount of δ-decalactone.

There are three groups of compounds that, while found in low concentrations in the initial wine, increase in concentration during the process due to their presence in barrel wood. However, if this were the only factor, and bearing in mind that both wines were in contact with the oakwood for the same period of time, the two trials should contain similar concentrations of methoxyphenols, whisky-lactones and furanic compounds. This is the case for most compounds from these groups.

After spending time in the barrel, the wines have higher concentrations of some **methoxyphenols**. This led to an improvement in the aromatic characteristics of the wines since this group of compounds contributes highly appreciated spicy aromas (Gómez García-Carpintero et al. 2012). However, in the case of MLF barrels, the concentration of acetosyringone, vanillin and homovanillyl

alcohol is lower than in steel MLF tanks but guaiacol concentration is higher.

Vanillin, together with acetovanillone, acetosyringone and propiovanillone contribute to the characteristic vanilla smell of wines aged in oak barrels. These results appeared to contradict the conclusions reached by Bloem et al. (2008) since the glycosidase activity of the bacteria must have liberated greater amounts of vanillin and methoxyphenols in general found in the form of glycosides in the oakwood. However, as these authors have demonstrated, vanillin glycosides are less polar than whisky lactone ones allowing the wine to more easily extract the latter. Also, glycosidic enzymes from the LAB would release the corresponding aglicones.

Gómez García-Carpintero et al. 2014 show higher concentrations of vanillin in wines with MLF and chips while other authors have described a decline in vanillin concentration during barrel fermentation and aging in presence of lees (Chatonnet, 1992). These declines have been attributed to the transformation of vanillin to its corresponding alcohol and subsequent conversion to vanillin ethyl ether (Spillman, Pollnitz, Liacopoulos, Skaouroumons, & Sefton, 1997). We should also consider that the cell walls of lactic

bacteria and the proteins and peptides they liberate are able to absorb methoxyphenols decreasing their concentration by means of a natural clarification process.

$\beta$ -methyl- $\delta$ -octalactones, known as **whisky-lactones** give aged wines a characteristic coconut aroma. The perception threshold of the *cis*-isomer is 4 or 5 times lower than that of the *trans*-isomer (Masson, Guichard, Fornier, & Puech, 1997).

The presence of whisky-lactones in wines is exclusively due to aging in oakwood, the barrel MLF wines had a higher concentration media of these two compounds with the particularity that there is three times more *trans*-isomer. Gómez García-Carpintero et al. (2014) also found more lactones in MLF wines with chips although in this case the duration of the contact with oak was longer during MLF than after it. De Revel et al. (2005) also observed large quantities of  $\beta$ -methyl- $\gamma$ -octalactone in barrel MLF.

The *cis/trans* whisky-lactone ratio is above 5 for American oak and around 2 for French oak (Torey & Waterhouse, 1996). However, there are a great many factors affecting this ratio such as the degree of toasting, age of the oak and duration and type of wood drying (Cadahia, Fernández de Simón, Vallejo, Sanz, & Broto, 2007). In our case we would note that the *cis/trans* ratio of the lactones extracted from the oak by the tank MLF wine is 2.6 while barrel MLF wine not only increased the amount extracted but also lowered the ratio to 1.3. A potential precursor of the lactones is the 6'-O-gallate derivate of (3S, 4S)-3-methyl-4-hydroxybutanoic acid 3-O- $\beta$ -D-glucopyranoside (Masson, Baumes, Moutounet, & Puech, 2000). The action of the glycosidic enzymes on oakwood extracts liberates these lactones, but liberates greater quantities of the *trans*-isomer (Bloem et al. 2008). Hence, the  $\beta$ -glycosidase activity of the LAB as explained in the foregoing accounts for our results.

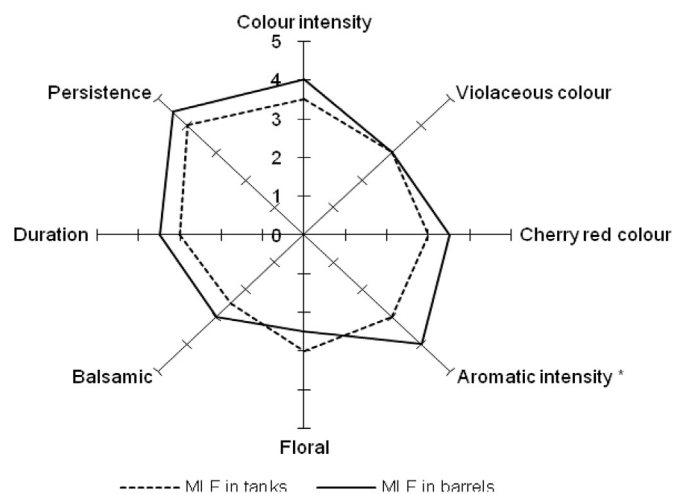
**Furanic compounds** are responsible for almond, caramel and toasted aromas in aged wines. They are generated by means of the Maillard reaction from oakwood cellulose and hemicellulose during toasting of the staves (Chatonnet, 1992). When the wine is aged in barrels, furfural and 5-methyl-2-furfural may be transformed into their corresponding alcohols and these converted into their esters (Pérez-Prieto, López-Roca, Martínez-Cutillas, Pardo-Mínguez, & Gómez-Plaza, 2003).

For short aging periods, their extraction from the wood outpaces conversion, so they tend to accumulate in the wine (Gómez García-Carpintero et al. 2012). In this work we found significant concentrations of furanic compounds (both aldehydes and alcohols) in wines after spending time in barrels. Barrel MLF wines had more than double the concentration of these compounds as compared to tank MLF wines.

The greater extraction of furanic compounds in barrel MLF could be due to two additional factors. First of all to the lower pH of the initial wine when is this barrel and second to the less oxidant atmosphere since the micro-oxygenation from the air supplied through the wood counteracts the CO<sub>2</sub> produced during MLF in these wines thus favoring the extraction of these compounds. However, the effect of LAB cannot be ignored, and the findings should be studied in more depth in future work.

### 3.4. Sensory analysis

In the triangle test, tasters detected statistically significant differences (95% probability) in the color, aroma and taste of the two types of wines. Fig. 2 shows the results from the descriptive sensory analysis. The two types of wines were very similar with only slight differences attributable to the type of MLF. Barrel MLF wines were characterized by more aromatic intensity with significant differences with regard to MLF tanks. In addition the tasters appreciated slight increases of cherry-red color, balsamic, duration and persistence in barrel MLF wines.



\* Denotes statistically significant differences ( $p \leq 0.05$ ) between the different MLF assays.

Fig. 2. Sensory descriptive analysis for MLF in tanks and MLF in barrels.

## 4. Conclusions

MLF occurs easily in large tanks simplifying control of the process producing wines with differentiating characteristics. The basic structure of the wine is essentially the same regardless of whether MLF is done in tanks and then aged in barrels or whether both processes, MLF and ageing, are done simultaneously in barrels. However, these latter wines undergo MLF faster and lose less color intensity in the process. It has also been shown that there are important variations in some volatile compounds; in general terms, fewer methoxyphenols and more whisky-lactones and furanic compounds. The effects on color and these volatile compounds both have a positive effect on the sensory profile of the wines produced.

## Acknowledgments

P. M. Izquierdo is grateful to the INCRECYT program and the European Social Fund for financial support.

## References

- Atanasova, V., Fulcrand, H., Cheynier, V., & Moutounet, M. (2002). Effect of oxygenation on polyphenol changes occurring in the course of wine-making. *Analytica Chimica Acta*, 458, 15–27.
- Bartowsky, E., Costello, P., & Henschke, P. A. (2002). Management of malolactic fermentation-wine flavour manipulation. *Australian & New Zealand Grape-grower & Winemaker*, 461, 10–12.
- Bartowsky, E., & Henschke, P. A. (2004). The “buttery” attribute of wine-diacetyl—desirability, spoilage and beyond. *International Journal of Food Microbiology*, 96, 325–352.
- Bloem, A., Lonvaud-Funel, A., & de Revel, G. (2008). Hydrolysis of glycosidically bound flavour compounds from oak wood by *Oenococcus oeni*. *Food Microbiology*, 25, 99–104.
- Boido, E., Lloret, A., Medina, K., Carrau, F., & Dellacassa, E. (2002). Effect of  $\beta$ -glucosidase activity of *Oenococcus oeni* on the glycosylated flavour precursors of Tannat wine during malolactic fermentation. *Journal of Agricultural and Food Chemistry*, 50, 2344–2349.
- Cadahia, E., Fernández de Simón, B., Vallejo, R., Sanz, M., & Broto, M. (2007). Volatile compound evolution in Spanish oak Wood (*Quercus petraea* and *Quercus pyrenaica*) during natural seasoning. *American Journal of Enology and Viticulture*, 58(2), 163–172.
- Castro-Vázquez, L., Alañón, M. E., Calvo, E., Cejudo, M. C., Díaz-Maroto, M. C., & Pérez-Coello, M. S. (2011). Volatile compounds as markers of ageing in Tempranillo red wines from La Mancha D.O. stored in oak wood barrels. *Journal of Chromatography A*, 1218, 4910–4917.
- Chatonnet, P. (1992). Les composés aromatiques de bois de chêne cédés aux vins. Influence des opérations de décahuffe en tonnellerie. En Bois et la qualité de vins et des aux-de vie. *Journal International des Sciences de la Vigne et du Vin*, 81–91.

- Couto, J. A., Campos, F. M., Figueiredo, A. R., & Hogg, T. A. (2006). Ability of lactic acid bacteria to produce volatile phenols. *American Journal of Enology and Viticulture*, 57, 166–171.
- De Revel, G., Bloem, A., Augustin, M., Lonvaud-Funel, A., & Bertrand, A. (2005). Interaction of *Oenococcus oeni* and oak wood compounds. *Food Microbiology*, 22, 569–575.
- Dubois, P. (1994). Les arômes des vins et leurs défauts. *Revue Française d'Oenologie*, 145, 27–40.
- Gagné, S., Lucas, P. M., Perello, M. C., Claisse, O., Lonvaud-Funel, A., & de Revel, G. (2011). Variety and variability of glycosidase activities in an *Oenococcus oeni* strain collection tested with synthetic and natural substrates. *Journal of Applied Microbiology*, 110, 218–228.
- Gómez García-Carpintero, E., Gómez Gallego, M. A., Sánchez-Palomo, E., & González Viñas, M. A. (2012). Impact of alternative technique to ageing using oak chips in alcoholic or in malolactic fermentation on volatile and sensory composition of red wines. *Food Chemistry*, 134, 851–863.
- Gómez García-Carpintero, E., Sánchez-Palomo, E., & González Viñas, M. A. (2014). Volatile composition of Bobal red wines subjected to alcoholic/malolactic fermentation with oak chips. *LWT-Food Science and Technology*, 55, 586–594.
- Hernández-Orte, P., Cersosimo, M., Loscos, N., Cacho, J., García-Moruno, E., & Ferreira, V. (2009). Aroma development from non-floral grape precursors by wine lactic acid bacteria. *Food Research International*, 42, 773–781.
- Hernández-Orte, P., Peña, A., Pardo, I., Cacho, J., & Ferreira, V. (2012). Amino acid and volatile compounds in wines from Cabernet Sauvignon and Tempranillo varieties subjected to malolactic fermentation in barrels. *Food Science and Technology International*, 18(2), 103–112.
- Ibarz, M., Ferreira, V., Hernández-Orte, P., Loscos, N., & Cacho, J. (2006). Optimization and evaluation of a procedure for the gas chromatographic-mass spectrometric analysis of the aromas generated by fast acid hydrolysis of flavors precursors extracted from grapes. *Journal of Chromatography A*, 1116, 217–229.
- ISO Standard 11035. (1994). *Sensory Analysis. Identification and selection of descriptors for establishing a sensory profile*.
- ISO Standard 4120. (1983). *Sensory Analysis. Methodology for triangular test*.
- Izquierdo-Cañas, P. M., García, E., Gómez, S., & Palop, M. L. L. (2008). Changes in the aromatic composition of Tempranillo wines during spontaneous malolactic fermentation. *Journal of Food Composition and Analysis*, 21, 724–730.
- Jarauta, I., Cacho, J., & Ferreira, V. (2005). Concurrent phenomena contributing to the formation of the aroma of wine during aging in oak wood: an analytical study. *Journal of Agricultural and Food Chemistry*, 53, 4166–4177.
- Jeromel, A., Herjavec, S., Orlic, S., Redzepovic, S., & Wondra, M. (2008). Changes in volatile composition of Kraljevina wines by controlled malolactic fermentation. *Journal of Central European Agriculture*, 9, 363–372.
- Liu, S. Q., & Pilone, G. J. (2000). An overview of formation and roles of acetaldehyde in winemaking with emphasis on microbiological implications. *International Journal of Food Science & Technology*, 35, 49–61.
- Mansfield, A. K., Zoecklein, B. W., & Whiton, R. S. (2002). Quantification of glycosidase activity in selected strains of *Brettanomyces bruxellensis* and *Oenococcus oeni*. *American Journal of Enology and Viticulture*, 53, 303–307.
- Martínez-Pinilla, O., Martínez-Lapuente, L., Guadalupe, Z., & Ayestarán, B. (2012). Sensory profiling and changes in colour and phenolic composition produced by malolactic fermentation in red minority varieties. *Food Research International*, 46, 286–293.
- Masson, E., Baumes, R., Moutounet, M., & Puech, J. L. (2000). The effect of kilndrying on the levels of ellagitannins and volatile compounds of European oak (*Quercus petraea* Liebl.) stave wood. *American Journal of Enology and Viticulture*, 51, 201–214.
- Masson, G., Guichard, E., Fornier, N., & Puech, J. L. (1997). Teneurs en stéréoisomères de la B-méthyl-gamma octalactone des bois de chère européens et américains. Application aux vins et aux sucres de vie. *Journal des sciences et techniques de la Tonnellerie*, 3, 1–8.
- Matthews, A., Grimaldi, A., Walker, M., Bartowsky, E., Grbin, P., & Jiranek, V. (2004). Lactic acid bacteria as a potential source of enzymes for use in vinification. *Applied and Environmental Microbiology*, 70, 5715–5731.
- McMahon, H., Zoecklein, B. W., Fugelsang, K. C., & Jasinski, Y. (1999). Quantification of glycosidase activities in selected yeast and lactic acid bacteria. *Journal of Industrial Microbiology and Biotechnology*, 23, 198–203.
- Moreno-Arribas, M. V., Gómez-Cordovés, C., & Martín-Alvarez, P. J. (2008). Evolution of red wine anthocyanins during malolactic fermentation, postfermentative treatments and ageing with lees. *Food Chemistry*, 109, 149–158.
- Nelson, L. (2008). *The production of volatile phenols by wine microorganisms*. Thesis. Private Bag X1, 7602. Matieland (Stellenbosch), South Africa: Stellenbosch University.
- OIV Organización Internacional de la Viña y el Vino. (2014). *Compendium of international methods of wine and must analysis*.
- Ortega-Heras, M., González-San José, M. L., & González-Huerta, C. (2008). Consideration of the influence of aging process, type of wine and oenological classic parameters on the level of Wood Volatile compounds present in red wines. *Food Chemistry*, 103, 1434–1448.
- Osborne, J. P., Mira de Orduña, R., Pilone, J. G., & Liu, S. Q. (2000). Acetaldehyde metabolism by wine lactic acid bacteria. *FEMS Microbiology Letters*, 91, 51–55.
- Peinado, R. A., Moreno, J., Bueno, J. E., Moreno, J. A., & Mauricio, J. C. (2004). Comparative study of aromatic compounds in two young white wines subjected to pre-fermentative cryomaceration. *Food Chemistry*, 84, 589–590.
- Pérez-Martin, F., Izquierdo-Cañas, P. M., Seseña, S., García-Romero, E., & Palop, M. L. L. (2015). Aromatic compounds released from natural precursors by selected *Oenococcus oeni* strains during malolactic fermentation. *European Food Research and Technology*, 240, 609–618.
- Pérez-Prieto, L. J., López-Roca, J. M., Martínez-Cutillas, A., Pardo-Mínguez, F., & Gómez-Plaza, E. (2003). Extraction and formation dynamic of oak-related volatile compounds from different volume barrels to wine and their behavior during bottle storage. *Journal of Agricultural and Food Chemistry*, 51, 5444–5449.
- Ribereau-Gayon, P., & Stronestreet, E. (1965). Le dosage des anthocyanes dans les vins rouges. *Bulletin de la Société de Chimie*, 9, 2649–2652.
- Ruiz-Pérez, P., Izquierdo-Cañas, P. M., Seseña-Prieto, S., García-Romero, E., & Palop-Herreros, M. L. L. (2012). Malolactic fermentation and secondary metabolite production by *Oenococcus oeni* strains in low pH wines. *Journal of Food Science*, 77(10), 579–585.
- Selli, S., Canbas, A., Cabaroglu, T., Erten, H., & Günata, Z. (2006). Aroma components of cv. Muscat of Bornova wines and influence of skin contact treatment. *Food Chemistry*, 94, 319–326.
- Simpson, R. F. (1979). Some important aroma components of white wine. *Food Technology in Australia*, 31, 516–522.
- Smith, P. A. (2005). Development of an assay to quantify tannins in grape and wine samples. *Australian Wine Research Institute Technical Review*, 154, 37–38.
- Somers, T. C., & Evans, M. E. (1976). Spectral evaluation of young red wines: anthocyanin equilibria, total phenolics, free and molecular SO<sub>2</sub>, "Chemical age". *Journal of the Science of Food and Agriculture*, 28, 279–287.
- Spillman, P. J., Pollnitz, A. P., Liacopoulos, D., Skaouroumons, G.-K., & Sefton, M. A. (1997). Accumulation of vanillin during barrel-ageing of white, red, and model wines. *Journal of Agricultural and Food Chemistry*, 45, 2584–2589.
- Swiegers, J. H., Bartowsky, E. J., Henschke, P. A., & Pretorius, I. S. (2005). Yeast and bacterial modulation of wine aroma and flavour. *Australian Journal of Grape and Wine Research*, 11, 139–173.
- Torey, J. P., & Waterhouse, A. L. (1996). The extraction of volatile compounds from French and American oak barrels in Chardonnay during the successive vintages. *American Journal of Enology and Viticulture*, 47, 163–172.
- Ugliano, M., & Moio, L. (2005). Changes in the concentration of yeast-derived volatile compounds of red wine during malolactic fermentation with four commercial starter cultures of *Oenococcus oeni*. *Journal of Agricultural and Food Chemistry*, 53, 10134–10139.
- Van Vuuren, H. J. J., & Dicks, L. M. T. (1993). *Leuconostoc oenos*: a review. *American Journal of Enology and Viticulture*, 44, 99–112.
- Vivas, N., Glories, V., Lagune, L., Sancier, C., & Augustin, M. (1994). Estimation de degré de polymérisation des procyanidines du raisin et du vin par la méthode au p-diméthylaminocinnamaldéhyde. *Journal International des Sciences de la Vigne et du Vin*, 28, 319–336.
- Vivas, N., Lonvaud-Funel, A., & Glories, Y. (1995). Observations sur l'augmentation de l'acidité volatile dans les vins rouges aux cours de leur élevage en barriques. *Journal des sciences et techniques de la Tonnellerie*, 1, 81–104.
- Williams, P. J. (1993). Hydrolytic flavor release in fruit and wines through hydrolysis of nonvolatile precursors. In T. E. Acree, & R. Teranishi (Eds.), *Flavor science—sensible principles and techniques* (pp. 287–308). Washington DC: American Chemical Society.



## Enhanced curcumin permeability by SLN formulation: The PAMPA approach



Chiara Righeschi <sup>a,1</sup>, Maria Camilla Bergonzi <sup>a,\*</sup>, Benedetta Isacchi <sup>a</sup>, Carla Bazzicalupi <sup>b</sup>, Paola Gratteri <sup>c</sup>, Anna Rita Bilia <sup>a</sup>

<sup>a</sup> Department of Chemistry "Ugo Schiff", University of Florence, Via Ugo Schiff 6, 50019, Sesto Fiorentino, Florence, Italy

<sup>b</sup> Department of Chemistry "Ugo Schiff", University of Florence, Via della Lastruccia 3-13, 50019, Sesto Fiorentino, Florence, Italy

<sup>c</sup> Department of NEUROFARBA, Pharmaceutical and Nutraceutical Section, Laboratory of Molecular Modeling Cheminformatics & QSAR, University of Florence, Via Ugo Schiff 6, 50019, Sesto Fiorentino, Florence, Italy

### ARTICLE INFO

#### Article history:

Received 28 May 2015

Received in revised form

2 November 2015

Accepted 4 November 2015

Available online 10 November 2015

#### Keywords:

Curcumin

Solid lipid nanoparticles

Parallel artificial permeability assay

*In vitro* release

Stability studies

### ABSTRACT

Curcumin health benefits are strongly limited by its poor aqueous solubility and low oral bioavailability. This work was focused on the development and characterization of solid lipid nanoparticles (SLNs) for the encapsulation of curcumin for oral administration. High shear homogenization and ultrasonication techniques were employed to prepare Compritol SLNs. The physicochemical characterization of round shaped curcumin-loaded SLNs was carried out by monitoring particle size (lower than 300 nm), zeta potential (−33 mV), drug loading capacity (1.60%), drug entrapment efficiency (80%), TEM analysis and *in vitro* drug release. Stability (4 °C) was investigated over one month. Parallel Artificial Membrane Permeability Assay (PAMPA) showed a considerable increase of curcumin permeated when formulated as SLNs. A modified release profile suggested that curcumin molecules are solubilized into the solid lipid matrix. The developed SLNs were produced without the use of solvents and all excipients were GRAS ingredients; both technology and composition were suitable for food application.

© 2015 Elsevier Ltd. All rights reserved.

## 1. Introduction

Curcumin is a yellow-colored phenolic natural constituent derived from the rhizome of the spice herb *Curcuma longa* L., widely known as turmeric. It has a broad spectrum of biological activities, principally antioxidant (Ruby, Kuttan, Babu, Rajasekharan, & Kuttan, 1995; Selvam, Subramanian, Gayathri, & Angayarkanni, 1995; Sharma, Manoharlal, Puri, & Prasad, 2010) anti-inflammatory (Menon & Sudheer, 2007; Rao, Basu, & Siddiqui, 1982), antibacterial (Negi, Jayaprakasha, Jagan Mohan Rao, & Sakariah, 1999), antifungal (Sharma, 1976). Its chemopreventive (Devasena, Rajasekaran, Gunasekaran, Viswanathan, & Venugopal, 2003; Park, 2010) activity has received considerable attention because curcumin influences multiple signaling pathways, modulating more than 30 different proteins, including thioredoxin reductase, cyclooxygenase-2 (COX-2), protein kinase C (PKC), 5-lipoxygenase, activated AMP-activated protein kinase (AMPK) and

tubulin. Other molecular targets modulated by this substance included transcription factors, growth factors and their receptors, cytokines, enzymes, and genes regulating cell proliferation and apoptosis (Aggarwal et al., 2009; Aggarwal, Kumar, & Bharti, 2003; Shishodia, Singh, & Chaturvedi, 2007).

Curcumin shows a good safety profile, no studies in either animals or humans have demonstrated any toxicity associated with its use, even at high doses (Lao et al., 2006; Shankar, Shantha, Ramesh, Murthy, & Murthy, 1980). This safe profile has been reflected by the continuous increase of preparations based on curcumin marketed as food ingredient or constituent of dietary supplements. Despite multiple health benefits, its utility is strongly limited by its poor aqueous solubility and low oral bioavailability. The latter is attributed to poor absorption, extensive intestinal and hepatic metabolism, rapid elimination and clearance from the body (Anand, Kunnumakkara, Newman, & Aggarwal, 2007; Pan, Huang, & Lin, 1999). Formulation of curcumin in effective dosage forms represented a challenge to overcome its poor physicochemical properties. Several strategies such as nanoparticles, liposomes, solid dispersions, microemulsions and complexation with phospholipids and cyclodextrins have been developed to improve the

\* Corresponding author.

E-mail address: [mc.bergonzi@unifi.it](mailto:mc.bergonzi@unifi.it) (M.C. Bergonzi).

<sup>1</sup> These authors contributed equally to this work.

bioavailability of curcumin (Bergonzi, Hamdouch, Mazzacua, Isacchi, & Bilia, 2014; Bisht et al., 2007; Chaurasia et al., 2015; Maiti, Mukherjee, Gantait, Saha, & Mukherjee, 2007; Sanoj Rejinold, Sreerekha, Chennazhi, Nair, & Jayakumar, 2011; Tiyaboonchai, Tungpradit, & Plianbangchang, 2007).

This study was focused on the preparation and characterization of solid lipid nanoparticles (SLNs) for oral administration of curcumin (Dhillon, Aggarwal, Newman, Wolff, Kunnumakkara, & Abbruzzese, 2008). Lipid-based drug delivery systems are promising formulations, since lipids are known oral drug absorption enhancers (Chakraborty, Shukla, Mishra, & Singh, 2009; Porter, Wasan, & Constantinides, 2008) and they can be developed in small particle sizes ranging from micro to nanometers (Jia, 2005; Pouton, 2006), that can increase the absorption in the hydrophilic environment of the gastrointestinal tract. SLNs combine these features: they are colloidal carriers of submicron size constituted of solid lipids at body and room temperatures. Substances used to prepare these nanoparticles are physiologic and generally recognized as safe compounds (GRAS ingredients); this aspect makes SLNs carriers without toxicity in humans (Müller, Mehnert, Lucks, Schwarz, Zur mühlen, & Meyhers, 1995). Moreover, they retain the advantages of traditional colloidal systems (Müller, Mader, & Gohla, 2000) such as enhanced physical stability, protection of drug molecules from degradation in the body, controlled drug release, organ or tissue specific targeting, biocompatibility, laboratory to industrial-scalability. SLNs, consist of a lipid core and an outer shell of amphiphilic surfactant. If drug is loaded in the outer shell and on the particle surface, it is quickly released, displaying a burst effect. On the other hand, if it is incorporated into the particle core, it is released in a prolonged way. This make possible a controlled drug release from these carriers, representing an important tool to obtain a prolonged release of the drug (Müller et al., 2000; Reddy, 2005).

A few studies concerning the development of curcumin SLNs have been reported in the literature, but only one paper is dealing SLN for oral administration (Kakkar, Singh, Singla, & Kaur, 2011). This study described the preparation of SLNs using Tween 80, soy lecithin and Compritol with microemulsion technique. *In vivo* pharmacokinetics performed in rats after oral administration of SLNs revealed significant improvement of curcumin bioavailability, but the percentage of Tween 80 in the SLNs is quite high (more than six times higher than the lipid phase). In other studies, the percentage of surfactant is the same or much higher than that of the lipid (Aditya et al., 2014; Hazzah, Farid, Nasra, EL-Massik, & Abdallah, 2015; Kakkar, Mishra, Chuttani, & Kaur, 2013; Sun et al., 2013).

In the present study, the preparation of curcumin SLNs for a suitable oral dosage form was investigated, by using 50 g/kg fat phase and a low content of surfactant (25 g/kg), very suitable for oral administration.

In addition, the development of SLNs was carried out by homogenization-ultrasonication technique without the use of the solvents, technology that can be applied also to an industrial process.

Another key aspect was the analyses by DSC and X-ray diffractometry to investigate the drug–lipid interactions and the crystallinity of both curcumin and lipids, because this aspect could influence the release. Particle size analysis is a necessary, but not a sufficient step to characterize SLN quality. Special attention must be paid to the characterization of the degree of lipid crystallinity and the modification of the lipid, because these parameters are strongly correlated with drug incorporation and release profiles. DSC uses the fact that different lipid modifications possess different melting points and melting enthalpies. By means of X-ray scattering it is possible to assess the length of the long and short spacings of the lipid lattice.

Finally, stability test, release profile and permeability assay were performed to confirm the optimized biopharmaceutical properties of the developed nanovectors. The results confirmed that the developed SLNs offer a promising delivery system for enhancing the oral absorption of curcumin, suitable either for food fortification or as dietary supplements.

## 2. Materials and methods

### 2.1. Materials

Compritol 888 ATO, a mixture of mono-, di- and triglycerides of behenic acid (C22), was a gift of Gattefossè (Milan, Italy). Curcumin, Pluronic F68 and 1,7-octadiene were purchased from Sigma Aldrich Corporation (St. Louis, MO, USA). Lecithin was kindly provided by Galeno (Comeana, Prato, Italy). Lipase from porcine pancreas, pepsin from porcine gastric mucosa, bile salts and cholesterol were analytical grade from Sigma Aldrich (Milan, Italy). 96-well Multi-Screen PAMPA filter plate were purchased from Millipore Corporation, (Tullagreen, Carrigtwohill, County Cork, Ireland). All the solvents used were HPLC grade from Merck (Darmstadt, Germany); 85% formic acid was provided by Carlo Erba (Milan, Italy). Ethanol analytical reagent grade was from Riedel-de Haen Laborchemikalien GmbH & Co. KG, (Seelze, Germany). Water was purified by a Milli-Q<sub>plus</sub> system from Millipore (Milford, MA). Phosphotungstic acid (PTA) was from Electron Microscopy Sciences (Hatfield, USA). Hydrion Buffer chemvelope pH 7.40 ± 0.02 was purchased from Micro Essential Laboratory (Brooklin, New York, USA).

### 2.2. High shear homogenization-ultrasonication method

Blank and drug loaded SLNs were prepared using hot homogenization process followed by ultrasonication (Castelli, Puglia, Sarpietro, Rizza, & Bonina, 2005). Two formulations were investigated (SLN-1 and SLN-2) loaded with two different concentrations of curcumin: 0.01 g/g and 0.02 g/g respect to the lipid phase, respectively.

Briefly, different amounts of curcumin, (respectively 75 and 150 mg) were accurately weighed and added to melted Compritol (7.5 g, 80 °C). Pluronic F68 (3.75 g) was dissolved in distilled water (138 g) and heated at 85 °C in a beaker. When a clear homogenous lipid phase was obtained, hot aqueous surfactant solution was added to hot lipid phase and homogenized at 9660 × g, by using a high-speed stirrer (Ultra Turrax T25, IKA-Werke GmbH&Co. KG, Staufen, Germany) for five minutes. The temperature was maintained at 80 °C during this step. Then, the coarse emulsion was subjected to probe sonication (Sonopuls HD 2200, 200 W power, probe MS 72, Bandelin Electronic GmbH, Berlin, Germany) for different times. Probe sonication process was suspended for 2' intervals during each cycle, to prevent increase of temperature. Temperature was monitored during the process. Sonication was applied maximum for 15 min to avoid metal contamination, by considering also previously published experimental conditions (Müller, Rühl, Runge, Schulze-Forster, & Mehnert, 1997; Nassimi, Schleh, Lauenstein, Hussein, Hoymann, & Koch, 2010; Nayak, Tiyaboonchai, Patankar, Madhusudhan, & Souto, 2010; Silva et al., 2011; Vitorino, Carvalho, Almeida, Sousa, & Pais, 2011).

Working temperature was kept at least 5 °C above the lipid melting point (85 °C) to prevent recrystallization during homogenization and ultrasonication. After ultrasonication, the obtained emulsion (O/W) was cooled in an ice bath in order to solidify the lipid matrix and to form SLNs. Blank and curcumin loaded SLNs were prepared and characterized as well. SLNs dispersions were stored at 4 °C for further analyses.

### 2.3. Particle size analysis and zeta potential measurements

Mean diameter of the population and polydispersity index (P.I.) as a measure of the width of particle size distribution together with the measure of zeta potential values were assessed by photon correlation spectroscopy (PCS) using a Zetasizer Nano ZS (Malvern Instruments, UK). Samples were prepared diluting 10  $\mu\text{L}$  of SLN suspension with 2 mL of deionized water. All measurements were done in triplicate. pH was measured prior to and after dilution, because its value could alter the zeta-potential. pH resulted 6.1 prior to dilution and 6.3 after dilution.

### 2.4. Determination of encapsulation efficiency

The percentage of curcumin entrapped in the lipid matrix was determined as follows: a fixed amount of SLNs dispersion was purified by dialysis method, using a membrane (MW = 12,400, Sigma Aldrich, Milan, Italy). Then, an amount of material retained in the bag was freeze-dried at  $-40\text{ }^{\circ}\text{C}$  for 24 h, for following stability studies. The freeze drying process was optimized to obtain a homogenous porous solid and according to TEM and light scattering analyses.

Sample was dissolved in MeOH under stirring at  $80\text{ }^{\circ}\text{C}$  for 10 min and then cooled to room temperature to preferentially precipitate the lipid (Nayak et al., 2010; Sanna, Gavini, Cossu, Rassu, & Giunchedi, 2007; Tiyaboonchai et al., 2007). The suspension was centrifuged for 30 min at  $13,148 \times g$  and the supernatant was analyzed by HPLC/DAD analysis using curcumin as external standard. Calibration curves were performed on six solutions in the concentration range 1.38–138  $\mu\text{g}/\text{mL}$ . The squared correlation coefficient was  $>0.99$ . Curcumin encapsulation efficiency was expressed as drug recovery and calculated from the following equation:

#### Drug encapsulation efficiency (%)

$$= \frac{\text{mass of active in nanoparticles}}{\text{mass of active fed to the system}} \times 100$$

The drug loading content was the ratio of incorporated drug to lipid (w/w):

$$\text{Drug loading (\%)} = \frac{\text{mass of active in nanoparticles}}{\text{weight of lipid}} \times 100$$

No lipid interference occurred during UV determination of curcumin (data not shown). Curcumin loaded concentration was assayed by HPLC/DAD analysis performed using a HP 1100 Liquid Chromatograph (Agilent Technologies, Palo Alto, CA, USA) equipped with a HP 1040 Diode Array Detector (DAD), an automatic injector, an auto sampler and a column oven and managed by a HP 9000 workstation (Agilent Technologies, Palo Alto, CA, USA). The UV–Vis spectra were recorded between 220 and 500 nm and the chromatographic profiles were registered at 420 nm. Separations were performed on a reversed phase column Luna C18 (150  $\times$  4.6 mm, 5  $\mu\text{m}$ , Phenomenex) maintained at  $27\text{ }^{\circ}\text{C}$ . The eluents were  $\text{H}_2\text{O}$  at pH 3.2 by formic acid (Solvent A) and acetonitrile (Solvent B), using a multi-step linear gradient of 32 min at a flow rate of 0.4 mL/min: 0.10 min 72% A and 18% of B; 10.0 min 56% A to 44% B; 27.0 min 52% A to 48% B; 27.0 min 52% A to 48% B; 32.0 min 20% A to 80% B.

### 2.5. Transmission electron microscopy (TEM)

The morphological characterization of the systems was obtained by using transmission electron microscopy technique (TEM, CM12 Philips, Netherlands). Samples were deposited on a *formuvar* film-

coated copper grid and then stained with one drop of 20 g/L aqueous solution of phosphotungstic acid (PTA), allowing to dry before TEM observation.

### 2.6. Differential scanning calorimetry (DSC)

DSC was carried out using a Mettler TA4000 apparatus equipped with a DSC 25 cell. Samples (about 10 mg) were accurately weighed (Mettler M3 Microbalance) directly in pierced aluminum pans and scanned between 30 and  $250\text{ }^{\circ}\text{C}$  at a heating rate of 10 K/min under static air. DSC thermograms of pure curcumin, Compritol, and curcumin-loaded SLNs were compared.

### 2.7. X-ray powder diffractometry

X-ray powder diffractograms were obtained with a Bruker D8 advance powder diffractometer, equipped with Cu K $\alpha$  radiation and operating in  $\theta$ - $2\theta$  Bragg Brentano geometry at 40 kV and 30 mA. The “SolX” solid-state detector was used. C/Ni Goebel mirrors for the incident beam were used. The samples were analyzed at ambient temperature over the  $10$ – $35^{\circ}$   $2\theta$  range at a scan rate of  $0.02\text{ deg s}^{-1}$ .

### 2.8. In vitro release studies

Dialysis bag method was applied to study the drug release using a mixture of PBS (pH 6.8) and EtOH (150 mL/L ethanol to maintain the sink conditions) or simulated intestinal fluid as dissolution media. Simulated intestinal conditions contained intestinal enzymes (lipase 0.4 mg/mL, bile salts 0.7 mg/mL and pancreatin 0.5 mg/mL) and calcium chloride solution 750 mM at pH 7.0, (Aditya et al., 2014). Release was monitored for 12 h. The dialysis bags were hydrated in PBS before use. Two milliliter of SLNs dispersion was introduced into the dialysis bag. The bag was placed in a beaker containing 200 mL of dissolution medium maintained at  $37\text{ }^{\circ}\text{C}$  under magnetic stirring (50 rpm). Aliquots of the dissolution medium were withdrawn at different time intervals and replaced with the same volume of fresh medium to maintain the sink conditions. The samples were suitably diluted and analyzed for curcumin determination. All the operations were carried out in triplicate.

### 2.9. Stability studies

Stability of curcumin SLNs was studied over 1 month. SLNs were kept at  $4 \pm 1\text{ }^{\circ}\text{C}$  and at fixed time intervals; they were assayed for their physical stability. Physical stability was checked by monitoring size, zeta potential and polydispersity of formulation.

### 2.10. Parallel artificial membrane permeability assay (PAMPA)

The PAMPA assay is a method for predicting passive intestinal absorption. The assay is carried out in a 96-well, MultiScreen-IP PAMPA (Millipore corporation) filter plate. The ability of compounds to diffuse from a donor compartment, through a PVDF membrane filter pretreated with a lipid-containing organic solvent, into an acceptor compartment is evaluated. 5  $\mu\text{L}$  of lecithin (10 g/L) and cholesterol (8 g/L) in 1,7-octadiene solution were added to the filter of each well. Immediately after the application of the artificial membrane, 150  $\mu\text{L}$  of drug containing donor solutions (free drug or curcumin-SLNs diluted in 0.05 mL/mL DMSO/PBS) were added to each well of the donor plate. In details, SLNs suspension was diluted to obtain in each donor compartment a final concentration of curcumin of 160  $\mu\text{g}$ . A saturated solution of curcumin (0.3  $\mu\text{g}$  of curcumin solubilized in the donor compartment) was used as control. 300  $\mu\text{L}$  of buffer (0.05 mL/mL DMSO/PBS, pH 7.4) were

added to each well of the acceptor plate. The acceptor plate was then placed into the donor plate, ensuring that the underside of the membrane was in contact with buffer. The plate was covered and incubated at room temperature under shaking for 24 h and permeation was evaluated at 1, 2, 4, 6, 19, 24 h.

### 3. Results and discussion

#### 3.1. Preparation of SLNs

The use of solid lipids instead of liquid oils is a very attractive idea to achieve controlled drug release, because drug mobility in a solid lipid should be considerably lower, compared with a liquid oil. SLNs are non-toxic, high biocompatible and easy to produce in large scale. SLN are drug carriers composed of a solid core suitable to target drugs to specific intestine associated systems. The nanoparticles are in the submicron size range. At room temperature the particles are in the solid state. Therefore, the mobility of incorporated drugs is reduced, which is a prerequisite for controlled drug release.

Selected SLNs consisting of a core of Compritol were stabilized with Pluronic F68. Compritol was selected because it is a mixture of mono, di and triglycerides. Moreover, Compritol in enhancing the oral bioavailability in comparison to other lipid matrices was previously highlighted (Paliwal et al., 2009).

Compritol-based nanoparticles were heterogeneous with better drug-loading and release characteristics as compared with the other formulations. Accordingly, SLNs containing lipids with highly crystalline structure can give drug expulsion. On the other hand, the imperfections (lattice defects) of the lipid structure could offer more loading space to accommodate drugs (Freitas & Müller, 1999; Mehnert & Mäder, 2012; Muller et al., 2000; Silva et al., 2011; Westesen, Bunjes, & Koch, 1997) while the use of a mixture of different oils as lipophilic can benefit the encapsulation efficiency. Compritol was also chosen as the lipid component because it gives stable dispersions with smaller particles. Two formulations with different amount of curcumin (0.01 g/g and 0.02 g/g respect to the lipid phase, SLN-1 and SLN-2 respectively) were prepared and fully characterized.

Homogenization-ultrasonication method was selected because economical, efficient and reproducible process to produce SLNs. Effect of different process variables on size, P.I., zeta potential, encapsulation efficiency was analyzed, and the results were reported on Table 1. Homogenization time was maintained constant at 10 min, time necessary to obtain a good emulsification of lipid (Das, Ng, Kanaujia, Kim, & Tan, 2011).

Sonication time (5, 10 and 15 min) showed huge influence on particle size. Sizes significantly decreased with increasing sonication time and the samples resulted always homogeneous. The best

results in terms of P.I. values were found in the formulations SLN-1 and SLN-2, when 15 min of sonication were applied.

All formulations were negatively charged, the zeta potential varied from  $-10$  to  $-45$  mV indicating a relatively good stability and dispersion of the system. The negative value of zeta potential of SLNs was attributed to the presence of behenic acid into the lipid matrix surface and also to Pluronic. This is a non-ionic surfactant used in the production of relatively stable dispersions. Although non-ionic surfactant could not interact with charging group like ionic ones, but it can influence the particle/water interface and electric double layer. Pluronic can also provide additional steric stabilization of particles (Lim & Kim, 2002; Schwarz & Mehnert, 1999).

The quantity of curcumin loaded in the system increased the dimensions of SLNs: with 2% (0.02 g/g) the sizes ranged from 415 to 270, by increasing the sonication time. Particle size slightly increased with higher drug concentration; this is probably due to the presence of curcumin inside of lipidic core.

The data in Table 1 shows that all formulations possessed high entrapment efficiency (E.E. %) ranged from  $70.7 \pm 2\%$  to  $80.2 \pm 2\%$ . Encapsulation efficiency was not significantly different among SLN-1 and SLN-2, resulting around of 70%; such values might be related to the structure of the lipid which had a great influence on drug incorporation. Lipids which form highly crystalline particles with a perfect structure lead to drug expulsion (Westesen et al., 1997), while, more complex lipids such as Compritol, being mixtures of mono-, di- and triglycerides, produce less perfect structures with many imperfections offering space to accommodate curcumin (Müller et al., 2000). Another feature of Compritol that favors the encapsulation of lipophilic curcumin was the high hydrophobicity due to the long chain fatty acids attached to the triglycerides.

The formulation selected on the basis of the best properties in terms of size, P.I. and zeta potential was SLN-2-15, loaded with 0.02 g/g of curcumin and sonicated for 15 min: it showed also an encapsulation efficiency of 80% and was selected for further investigations.

#### 3.2. TEM analysis

TEM was conducted to investigate the morphology of solid lipid nanoparticles SLN-2-15. It was evident from TEM images that nanoparticles were almost spherical with smooth morphology, appeared as black dots, well dispersed and separated (Fig. 1). This description agrees with a previous observation that the use of chemically heterogeneous lipids in combination with heterogeneous surfactants favors the formation of ideally spherical lipid nanoparticles (Mehnert & Mader, 2001). The mean diameter was in the range of 250–300 nm.

**Table 1**  
Characterization of developed blank and curcumin loaded SLNs; effect of sonication time and amount of curcumin on size, polydispersity index (P.I.), encapsulation efficiency (EE%) and drug loading (D.L.%). SLN-1, SLN-2 are solid lipid nanoparticles loaded respectively with 0.01 and 0.02 g/g of curcumin. 5, 10 and 15 indicate sonication time. Each data represent the mean  $\pm$  standard deviation of three experiments.

Formulation	Time of sonication (min)	Curcumin (g/g)	Size (nm)	P.I.	$\zeta$ potential (mV)	EE (%)	DL (%)
Blank SLN	5	–	333 $\pm$ 1	0.28 $\pm$ 0.02	$-36 \pm 3$	–	–
	10	–	254 $\pm$ 6	0.25 $\pm$ 0.01	$-24 \pm 2$	–	–
	15	–	241 $\pm$ 9	0.33 $\pm$ 0.03	$-10 \pm 1$	–	–
SLN-1-5	5	0.01	320 $\pm$ 18	0.31 $\pm$ 0.03	$-45 \pm 2$	76.4 $\pm$ 4.9	0.76
SLN-1-10	10	0.01	238 $\pm$ 4	0.31 $\pm$ 0.04	$-34 \pm 4$	74.2 $\pm$ 16	0.74
SLN-1-15	15	0.01	199 $\pm$ 23	0.26 $\pm$ 0.02	$-39 \pm 4$	76.4 $\pm$ 4.6	0.76
SLN-2-5	5	0.02	415 $\pm$ 6	0.31 $\pm$ 0.08	$-39 \pm 3$	70.7 $\pm$ 2	1.41
SLN-2-10	10	0.02	313 $\pm$ 13	0.33 $\pm$ 0.01	$-29 \pm 4$	77.8 $\pm$ 8	1.56
SLN-2-15	15	0.02	270 $\pm$ 15	0.29 $\pm$ 0.01	$-33 \pm 3$	80.2 $\pm$ 2	1.60

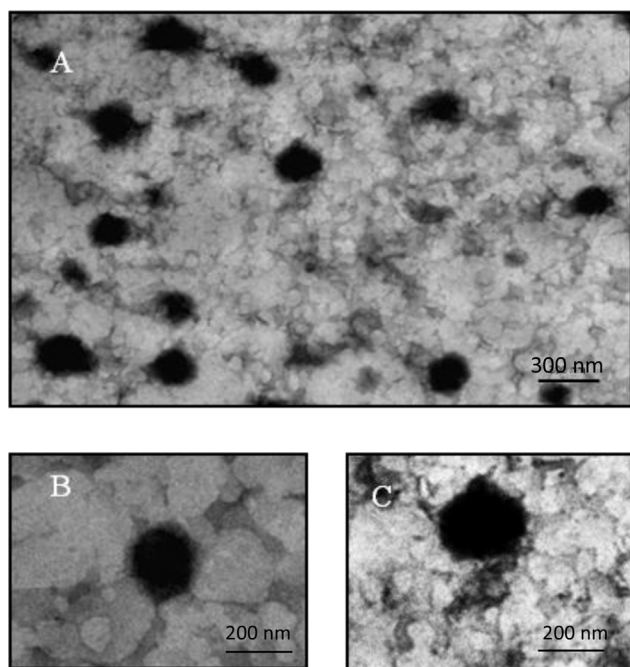


**Fig. 1.** TEM micrographs of curcumin of SLN-2-15 sample (loaded with 0.02 g/g of curcumin and obtained with 15 min of sonication) (A) with details of single SLN (B; C).

### 3.3. DSC and X-ray diffractometry assay

DSC and X-ray diffraction were performed for the assessment of the drug–lipid interactions and the crystallinity of curcumin and lipid matrices, because this aspect could influence the *in vitro* and *in vivo* release of the compound from the systems (Müller et al., 2000). Lipid crystallization is an important point for the performance of the SLN carriers. In fact, less perfect crystals with many imperfections can offer space to accommodate the drug (Müller et al., 2000) and also it can modulate the mobility of the drug during the release process (Mehnert & Mader, 2001, 2012; Silva et al., 2011). The lack of crystallinity is also highly required to avoid extrusion of drug during storage.

The following samples were analysed: pure curcumin, Compritol, unloaded and loaded SLNs SLN-2-15. Fig. 2 depicts the DSC

thermograms obtained. As Compritol is not composed of pure triacylglycerols, the observed melting peak at 72.1 °C might be due to a mixture of metastable polymorphic  $\beta$  and  $\beta'$  forms. The thermogram showed also a relatively small endothermic shoulder at around 55 °C; this small shoulder corresponds to the melting of a very unstable modification of Compritol which is the  $\alpha$  modification (Souto, Mehnert, & Müller, 2006), that clearly disappears after the nanoparticles preparation. DSC analysis of curcumin showed the melting point at 173.17 °C. In the DSC thermograms of blank SLNs (unloaded) and loaded SLNs, a small endothermic peak was observed at 50 °C. This peak indicates the presence of Pluronic either in the form of coating surrounding the nanoparticles or as residue after dialysis and lyophilization.

Curcumin melting peak was not recorded in the SLN formulation attributed to the solubility of the drug within the solid lipid matrix.

X-ray diffraction studies evidenced that diffraction pattern of bulk Compritol (Fig. 3) presents two main typical signals at 21.5° (2 $\theta$ ) and 23.5° (2 $\theta$ ), significantly modified when formulated into nanoparticles. Besides, another signal arises at 19.4° (2 $\theta$ ) after SLN preparation, corresponding to the most stable polymorphic form of triacylglycerols  $\beta$  (Souto et al., 2006). These results might indicate that the final formulation is composed of the most stable polymorphic state of Compritol: SLNs seem to lose part of their crystallinity by transforming from a mixture of  $\beta$  and  $\beta'$  polymorphs in the most stable  $\beta$  polymorph and allowing curcumin to penetrate in the molecular gaps.

### 3.4. *In vitro* release studies

The release of curcumin from SLN-2-15 formulation was tested *in vitro* in of PBS (pH 6.8) and simulated intestinal medium. Due to the poor aqueous solubility of curcumin, ethanol (150 mL/L) was used in the receptor medium to mimic sink condition, as already described in literature (Kakkar et al., 2011; Mulik, Mönkkönen, Juvonend, Mahadika, & Paradkar, 2010). Cumulative drug release percentage versus time was plotted to demonstrate the release patterns (Fig. 4). In both dissolution media a sustained/prolonged release. Curcumin reached about 40% of the amount loaded in the formulation during 12 h in PBS. This may be attributed to the curcumin released slowly from the lipidic solid matrices, through diffusion and dissolution mechanisms (Mehnert & Mäder, 2012; zur Mühlen, Schwarz, & Mehnert, 1998). Although the release rate of SLNs could be influenced by complex factors, it was reported

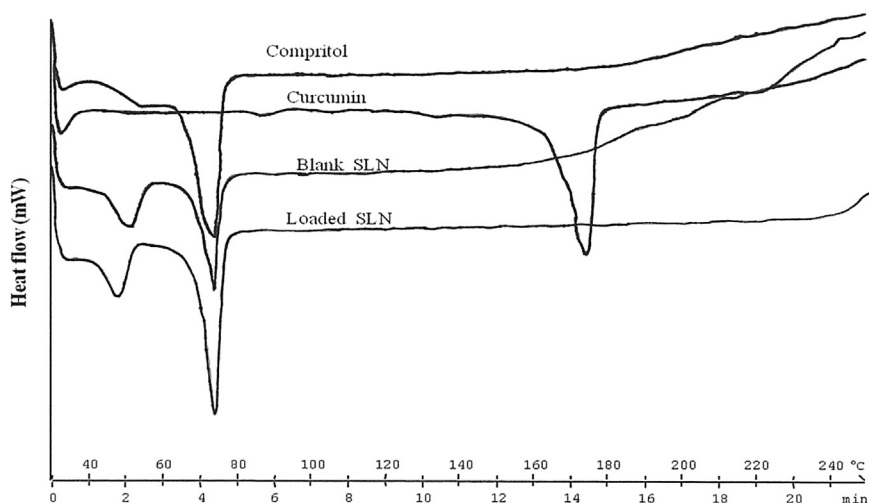


**Fig. 2.** DSC thermographs of Compritol; pure curcumin; blank and loaded solid lipid nanoparticles (SLN-2-15 sample, loaded with 0.02 g/g of curcumin and obtained with 15 min of sonication).

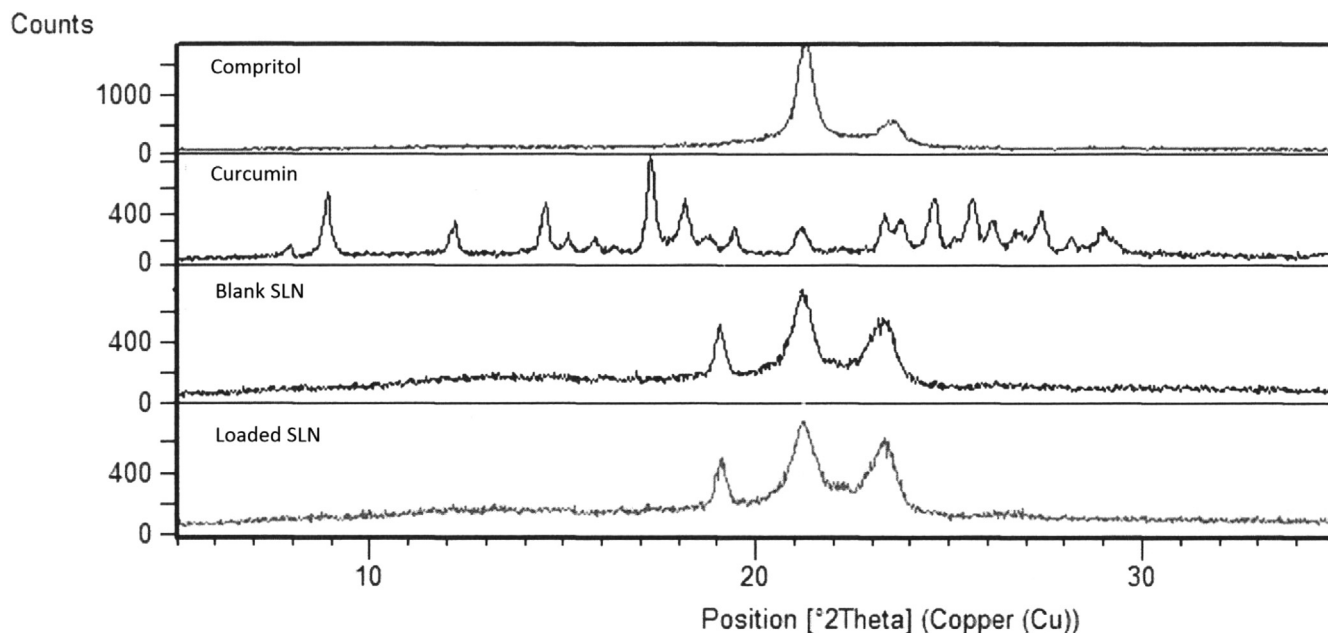


**Fig. 3.** X-ray diffraction pattern of Compritol; pure curcumin; blank and loaded solid lipid nanoparticles SLN-2-15 sample, loaded with 0.02 g/g of curcumin and obtained with 15 min of sonication).

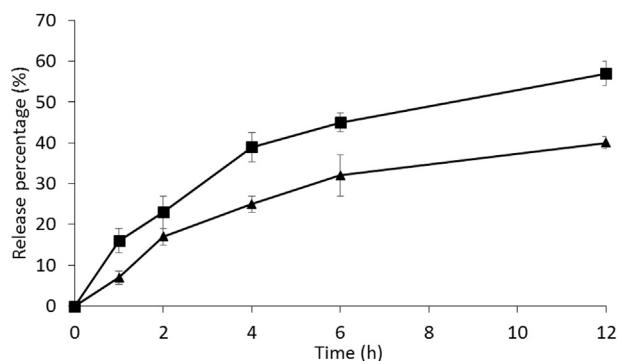


**Fig. 4.** *In vitro* release profile of curcumin from SLN-2-15 sample (loaded with 0.02 g/g of curcumin and obtained with 15 min of sonication). Close square: simulated intestinal medium; close triangle: PBS medium. Each data represent the mean  $\pm$  standard deviation of three experiments.

that among the factors, the large surface area and high diffusion coefficient due to small molecular size or low viscosity in the matrix are preponderant (zur Mühlen et al., 1998).

The release profile was similar, but more intense during the incubation of SLNs in simulated intestinal medium. After 12 h the percentage reached about 60%. The presence of enzymes and bile salts caused a pronounced release, probably due to degradation of the lipid carrier and the subsequent solubilization of curcumin in colloidal species, like mixed micelles and swollen micelles (Noack, Oidtmann, Kutza, & Mäder, 2012).

### 3.5. Stability studies

Stability of curcumin solid lipid nanoparticles was studied over 1 month. Physical stability was checked by monitoring size, zeta potential and P.I. during time, by DLS measurements. There was no modification neither of the particle size nor of the zeta potential (Fig. 5). Furthermore, polydispersity was stable over time, no

vesicle size alterations occurred over the tested period.

### 3.6. Parallel artificial membrane permeability assay (PAMPA)

An approach for rapid assessment of absorption potential include the Parallel Artificial Membrane Permeability Assay (PAMPA) (Kansy, Avdeef, & Fischer, 2004). Pampa is based on a 96-well microplate technology and allows reasonable throughput, although it lacks similarity to natural membranes because it does not possess pores or active transport mechanism. It enables fast determination of the trends in the ability of the compounds to permeate membrane by passive diffusion and it is thus suited for the screening of large libraries. Due to their small particle size, SLNs may exhibit bioadhesion properties to the gastrointestinal tract wall or enter in the intervillar spaces thus increasing their residence time in the gastrointestinal tract and releasing the active drug encapsulated. This increase in adhesion results in enhanced bioavailability.

The experiment was carried out measuring the ability of curcumin to diffuse from our SLNs suspension to a donor compartment through a PVDF membrane.

A showed a strong increase of permeated curcumin was found in the case of SLNs suspension when compared with a saturated solution of curcumin used as control (Fig. 6). In the case of SLNs, 4.2  $\mu\text{g}$ , 7.9  $\mu\text{g}$  and 9.3  $\mu\text{g}$  of curcumin permeated to the acceptor compartment after 6, 19 and 24 h, respectively; within the same timeframe, 0.03  $\mu\text{g}$ , 0.03  $\mu\text{g}$  and 0.04  $\mu\text{g}$  respectively of curcumin permeated from saturated solution. We can observe also that in the case of aqueous saturated solution, the amount of permeated curcumin remains constant during the test while, in the case of SLNs, permeated curcumin increases with time during 24 h of test.

## 4. Conclusions

In this study the poorly-soluble curcumin was incorporated into SLNs by homogenization and ultrasound technique without the use of solvents.

Compritol demonstrated good solubilization of curcumin and

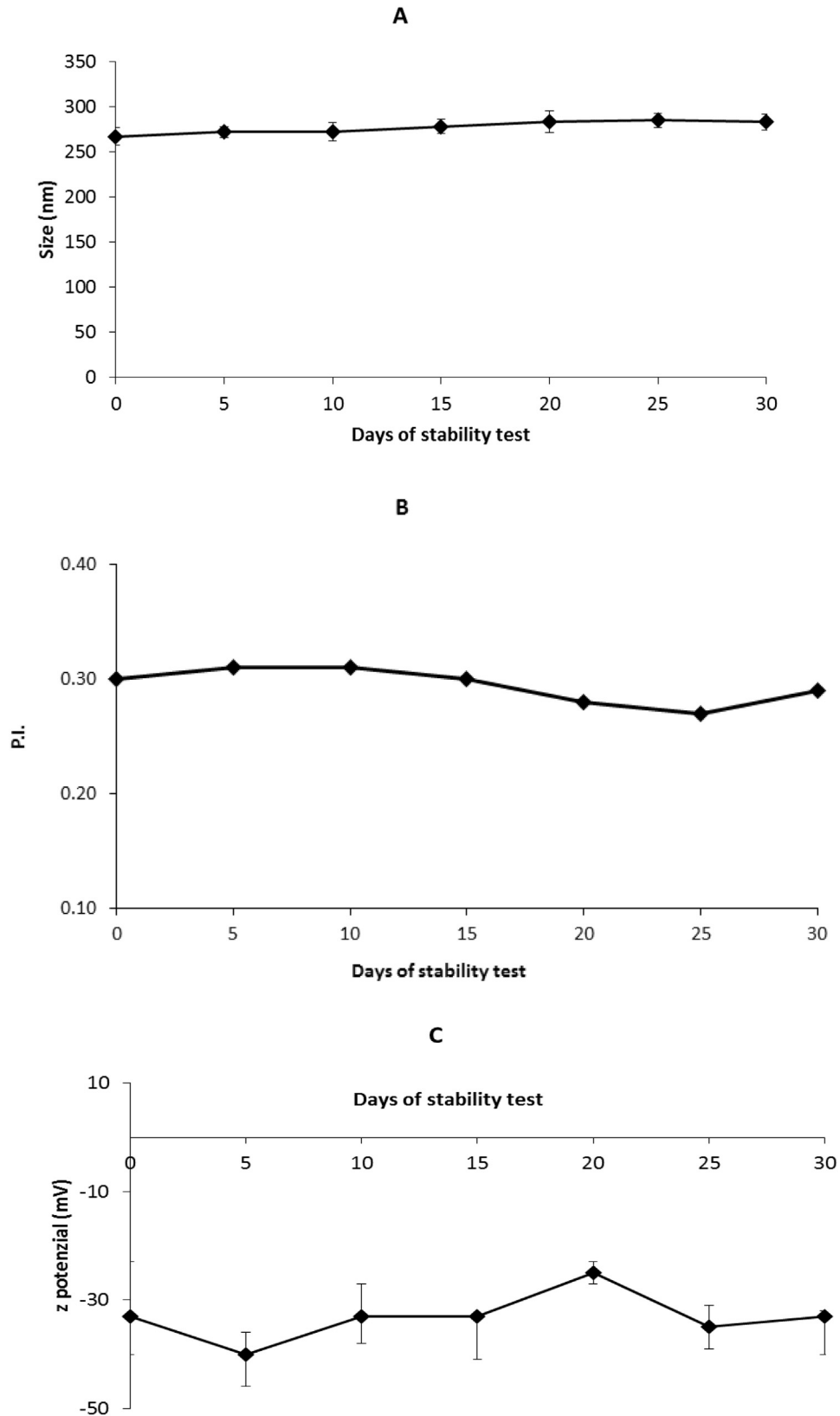


**Fig. 5.** Particle size (A), polydispersity index (P.I., B) and zeta potential (C) evolution of curcumin solid lipid nanoparticles (SLN-2-15 sample, loaded with 0.02 g/g of curcumin and obtained with 15 min of sonication) at storage conditions (30 days, 4 °C). (Mean  $\pm$  S.D.; n = 3).

formulation was obtained in terms of drug loading, surfactant percentage and sonication time. Pluronic F68 was selected as surfactant in the amount of 28 g/L of the formulation. SLN-2-15

formulation showed good values of encapsulation efficiency, size, P.I., zeta potential and stability.

These SLNs resulted round shape with homogeneous size

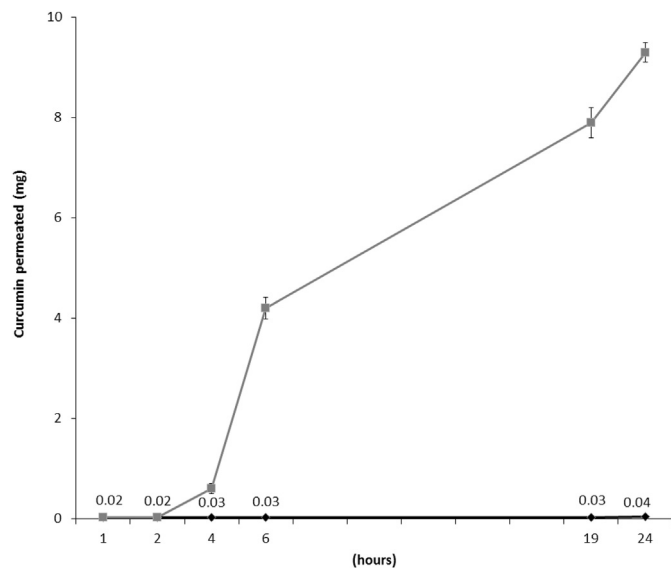


**Fig. 6.** Permeation profile of free curcumin and curcumin loaded SLNs by Parallel artificial membrane permeability assay (PAMPA). Amount of curcumin is referred to each well. Black: control; grey: SLN-2-15 sample, loaded with 0.02 g/g of curcumin and obtained with 15 min of sonication. (Mean  $\pm$  S.D.;  $n = 3$ ).

distribution, as confirmed by TEM analysis. Size of the particles is a key factor for improve oral performance of poorly soluble drugs and the average particle size of the developed nanoparticles was maintained below 300 nm, like other effective formulations, such as microemulsions or submicron emulsions. The increased permeability of curcumin loaded in SLNs was confirmed by PAMPA, a simple technique to evaluate *in vitro* passive gastrointestinal performance of innovative carriers. A prolonged release profile was observed suggesting that curcumin is solubilized into the solid lipid matrix. An increase in saturation solubility and, consequently, an increase in the release rate of the drug allows it to reach high concentrations in the gastrointestinal tract. It is expected a better *in vivo* performance of SLN because Pluronic may increase the permeability through the intestinal membrane and they may promote the bioadhesion to the GI wall. Also, the incorporation of curcumin into SLNs solid lipid matrix reduces its enzymatic degradation during the process of absorption.

SLNs are very versatile carriers, particularly for the oral administration, they can be easily transformed into powder (by spray-drying or lyophilization) and converted into solid dosage forms, such as tablets, hard gelatin capsules, pellets or powders. The obtained powders can be also dispersed in water or juice prior to administration.

## References

Aditya, N. P., Macedo, A. S., Doktorovova, S., Souto, E. B., Kim, S., Chang, P. S., et al. (2014). Development and evaluation of lipid nanocarriers for quercetin delivery: a comparative study of solid lipid nanoparticles (SLN), nanostructured lipid carriers (NLC), and lipid nanoemulsions (LNE). *LWT-Food Science and Technology*, 59, 115–121.

Aggarwal, B. B., Kuiken, V., Michelle, E., Laxmi, I. H., Kuzhuvilil, H. B., & Bokyoung, S. (2009). Molecular targets of nutraceuticals derived from dietary spices: potential role in suppression of inflammation and tumorigenesis. *Experimental Biology and Medicine*, 234, 825–849.

Aggarwal, B. B., Kumar, A., & Bharti, A. C. (2003). Anticancer potential of curcumin: preclinical and clinical studies. *Anticancer Research*, 23, 363–398.

Anand, P., Kunnumakkara, A. B., Newman, R. A., & Aggarwal, B. B. (2007). Bioavailability of curcumin: problems and promises. *Molecular Pharmacology*, 4, 807–818.

Bergonzi, M. C., Hamdouch, R., Mazzacava, F., Isacchi, B., & Bilia, A. R. (2014). Optimization, characterization and *in vitro* evaluation of curcumin microemulsions. *LWT-Food Sciences and Technology*, 59, 148–155.

Bisht, S., Feldmann, G., Soni, S., Ravi, R., Karikar, C., Maitra, A., et al. (2007). Polymeric nanoparticle-encapsulated curcumin ("nanocurcumin"): a novel strategy for human cancer therapy. *Journal of Nanobiotechnology*, 17, 5–3.

Castelli, F., Puglia, C., Sarpietro, M. G., Rizza, L., & Bonina, F. (2005). Characterization of indomethacin-loaded lipid nanoparticles by differential scanning calorimetry. *International Journal of Pharmaceutics*, 304, 231–238.

Chakraborty, S., Shukla, D., Mishra, B., & Singh, S. (2009). Lipid-an emerging platform for oral delivery of drugs with poor bioavailability. *European Journal of Pharmaceutics and Biopharmaceutics*, 73, 1–15.

Chaurasia, S., Patel, R. R., Chaubey, P., Kumar, N., Khan, G., & Mishra, B. (2015). Lipopolysaccharide based oral nanocarrier for the improvement of bioavailability and anticancer efficacy of curcumin. *Carbohydrate Polymers*, 130, 9–17.

Das, S., Ng, W. K., Kanaujia, P., Kim, S., & Tan, R. B. H. (2011). Formulation design, preparation and physicochemical characterizations of solid lipid nanoparticles containing a hydrophobic drug: effects of process variables. *Colloids and Surfaces B Biointerfaces*, 88, 483–489.

Devasena, T., Rajasekaran, K. N., Gunasekaran, G., Viswanathan, P., & Venugopal, P. (2003). Anticarcinogenic effect of bis-1,7-(2-hydroxyphenyl)-hepta-1,6-diene-3,5-dione a curcumin analog on DMH-induced colon cancer model. *Pharmacological Research*, 47, 133–140.

Dhillon, N., Aggarwal, B. B., Newman, R. A., Wolff, R. A., Kunnumakkara, A. B., Abbruzzese, J. L., et al. (2008). Phase II trial of curcumin in patients with advanced pancreatic cancer. *Clinical Cancer Research*, 14, 4491–4499.

Freitas, C., & Müller, R. H. (1999). Correlation between long-term stability of solid lipid nanoparticles (SLN) and crystallinity of the lipid phase. *European Journal of Pharmaceutics and Biopharmaceutics*, 47, 125–132.

Hazzah, H. A., Farid, R. M., Nasra, M. M. A., EL-Massik, M. A., & Abdallah, O. Y. (2015). Lyophilized sponges loaded with curcumin solid lipid nanoparticles for buccal delivery: development and characterization. *International Journal of Pharmaceutics*, 492, 248–257.

Jia, L. (2005). Nanoparticle formulation increases oral bioavailability of poorly soluble drugs: approaches experimental evidences and theory. *Current Nanoscience*, 1, 237–243.

Kakkar, V., Mishra, A. K., Chuttani, K., & Kaur, I. P. (2013). Proof of concept studies to confirm the delivery of curcumin loaded solid lipid nanoparticles (C-SLNs) to brain. *International Journal of Pharmaceutics*, 448, 354–359.

Kakkar, V., Singh, S., Singla, D., & Kaur, I. P. (2011). Exploring solid lipid nanoparticles to enhance the oral bioavailability of curcumin. *Molecular Nutrition & Food Research*, 55, 495–503.

Kansy, M., Avdeef, A., & Fischer, H. (2004). Advances in screening for membrane permeability: high-resolution PAMPA for medicinal chemists. *Drug Discovery Today: Technologies*, 4, 349–355.

Lao, C. D., Ruffin, M. T., Normolle, D., Heath, D. D., Murray, S. I., Bailey, J. M., et al. (2006). Dose escalation of a curcuminoid formulation. *BMC Complementary and Alternative Medicines*, 17, 6–10.

Lim, S. J., & Kim, C. K. (2002). Formulation parameters determining the physicochemical characteristics of solid lipid nanoparticles loaded with all-trans retinoic acid. *International Journal of Pharmaceutics*, 243, 135–146.

Maiti, K., Mukherjee, K., Gantait, A., Saha, B. P., & Mukherjee, P. K. (2007). Curcumin phospholipid complex: preparation, therapeutic evaluation and pharmacokinetic study in rats. *International Journal of Pharmaceutics*, 330, 155–163.

Mehnert, W., & Mader, K. (2001). Solid lipid nanoparticles: production, characterization and applications. *Advanced Drug Delivery Reviews*, 47, 165–196.

Mehnert, W., & Mader, K. (2012). Solid lipid nanoparticles. Production, characterization and applications. *Advanced Drug Delivery Reviews*, 64, 83–101.

Menon, V. P., & Sudheer, A. R. (2007). Antioxidant and anti-inflammatory properties of curcumin. *Advances in Experimental Medicines and Biology*, 595, 105–125.

zur Mühlen, A., Schwarz, C., & Mehnert, W. (1998). Solid lipid nanoparticles (SLN) for controlled drug delivery-drug release and release mechanism. *European Journal of Pharmaceutics and Biopharmaceutics*, 45, 149–155.

Mulik, R. S., Mönkkönen, J., Juvonend, R. O., Mahadika, K. R., & Paradkar, A. R. (2010). Transferrin mediated solid lipid nanoparticles containing curcumin: enhanced *in vitro* anticancer activity by induction of apoptosis. *International Journal of Pharmaceutics*, 5, 190–203.

Müller, R. H., Mader, K., & Gohla, S. (2000). Solid lipid nanoparticles (SLN) for controlled drug delivery – a review of the state of art. *European Journal of Pharmaceutics and Biopharmaceutics*, 50, 161–177.

Müller, R. H., Mehnert, W., Lucks, J.-S., Schwarz, C., Zur mühlen, A., Meyhers, H., et al. (1995). Solid lipid nanoparticles (SLN)-an alternative colloidal carrier system for controlled drug delivery. *European Journal of Pharmaceutics and Biopharmaceutics*, 41, 62–69.

Müller, R. H., Rühl, D., Runge, S., Schulze-Forster, K., & Mehnert, W. (1997). Cytotoxicity of solid lipid nanoparticles as a function of the lipid matrix and the surfactant. *Pharmaceutical Research*, 14, 458–462.

Nassimi, M., Schleh, C., Lauenstein, H. D., Hussein, R., Hoymann, H. G., Koch, W., et al. (2010). Toxicological evaluation of inhaled solid lipid nanoparticles used as a potential drug delivery system for the lung. *Colloids and Surfaces B: Biointerfaces*, 75, 107–116.

Nayak, A. P., Tiyafoonchai, W., Patankar, S., Madhusudhan, B., & Souto, E. B. (2010). Curcuminoids-loaded lipid nanoparticles: novel approach towards malaria treatment. *Colloids and Surfaces B: Biointerfaces*, 81, 263–273.

Negi, P. S., Jayaprakash, G. K., Jagan Mohan Rao, L., & Sakariah, K. K. (1999). Antibacterial activity of turmeric oil: a byproduct from curcumin manufacture. *Journal of Agricultural and Food Chemistry*, 47, 4297–4300.

Noack, A., Oidtmann, J., Kutza, J., & Mäder, K. (2012). *In vitro* digestion of

- curcuminoid-loaded lipid nanoparticles. *Journal of Nanoparticles Research*, 14, 1113.
- Paliwal, R., Rai, S., Vaidya, B., Khatri, K., Goyal, A. K., Mishra, N., et al. (2009). Effect of lipid core material on characteristics of solid lipid nanoparticles designed for oral lymphatic delivery. *Nanomedicine*, 5, 184–191.
- Pan, M. H., Huang, T. M., & Lin, J. K. (1999). Biotransformation of curcumin through reduction and glucuronidation in mice. *Drug Metabolism and Disposition*, 27, 486–494.
- Park, J. (2010). Anti-carcinogenic properties of curcumin on colorectal cancer. *World Journal of Gastrointestinal Oncology*, 4, 169–176.
- Porter, C. J., Wasan, K. M., & Constantinides, P. (2008). Lipid-based systems for the enhanced delivery of poorly water soluble drugs. *Advanced Drug Delivery Reviews*, 60, 615–616.
- Pouton, C. (2006). Formulation of poorly water-soluble drugs for oral administration: physicochemical and physiological issues and the lipid formulation classification system. *European Journal of Pharmaceutical Sciences*, 29, 278–287.
- Rao, T. S., Basu, N., & Siddiqui, H. H. (1982). Anti-inflammatory activity of curcumin analogues. *Indian Journal of Medical Research*, 75, 574–578.
- Reddy, L. H. (2005). Etoposide-loaded nanoparticles made from glyceride lipids: formulation, characterization, in vitro drug release, and stability evaluation. *AAPS PharmSciTech*, 6, 155–166.
- Ruby, A. J., Kuttan, G., Babu, K. D., Rajasekharan, K. N., & Kuttan, R. (1995). Antitumour and antioxidant activity of natural curcuminoids. *Cancer Letters*, 94, 79–83.
- Sanna, V., Gavini, E., Cossu, M., Rassu, G., & Giunchedi, P. (2007). Solid lipid nanoparticles (SLN) as carriers for the topical delivery of econazole nitrate: in-vitro characterization, ex-vivo and in-vivo studies. *Journal of Pharmaceutical and Pharmacology*, 59, 1057–1064.
- Sanoj Rejinold, N., Sreerekha, P. R., Chennazhi, K. P., Nair, S. V., & Jayakumar, R. (2011). Biocompatible, biodegradable and thermo-sensitive chitosan-g-poly (N-isopropylacrylamide) nanocarrier for curcumin drug delivery. *International Journal of Biological Macromolecules*, 49, 161–172.
- Schwarz, C., & Mehnert, W. (1999). Solid lipid nanoparticles (SLN) for controlled drug delivery II. Drug incorporation and physicochemical characterization. *Journal of Microencapsulation*, 16, 205–213.
- Selvam, R., Subramanian, L., Gayathri, R., & Angayarkanni, N. (1995). The anti-oxidant activity of turmeric (*Curcuma longa*). *Journal of Ethnopharmacology*, 47, 59–67.
- Shankar, T. N., Shantha, N. V., Ramesh, H. P., Murthy, I. A., & Murthy, V. S. (1980). Toxicity studies on turmeric (*Curcuma longa*): acute toxicity studies in rats, guinea pigs & monkeys. *Indian Journal of Experimental Biology*, 18, 73–75.
- Sharma, O. P. (1976). Antioxidant activity of curcumin and related compounds. *Biochemical Pharmacology*, 25, 1811–1812.
- Sharma, M., Manoharlal, R., Puri, N., & Prasad, R. (2010). Antifungal curcumin induces reactive oxygen species and triggers an early apoptosis but prevents hyphae development by targeting the global repressor TUP1 in *Candida albicans*. *Bioscience Reports*, 30, 391–404.
- Shishodia, S., Singh, T., & Chaturvedi, M. M. (2007). Modulation of transcription factors by curcumin. In B. B. Aggarwal, Y. J. Surh, & S. Shishodia (Eds.), *The molecular targets and therapeutics of curcumin in health and disease. Advances in experimental medicine and biology* (Vol. 995, pp. 127–141). New York: Springer Publication.
- Silva, A. C., González-Mira, E., García, M. L., Egea, M. A., Fonseca, J., Silva, R., et al. (2011). Preparation, characterization and biocompatibility studies on risperidone-loaded solid lipid nanoparticles (SLN): high pressure homogenization versus ultrasound. *Colloids and Surfaces B: Biointerfaces*, 86, 158–165.
- Souto, E. B., Mehnert, W., & Müller, R. H. (2006). Polymorphic behaviour of Compritol 888 ATO as bulk lipid and as SLN and NLC. *Journal of Microencapsulation*, 23, 417–433.
- Sun, J., Bi, C., Chan, H. M., Sun, S., Zhang, Q., & Zheng, Y. (2013). Curcumin-loaded solid lipid nanoparticles have prolonged in vitro antitumour activity, cellular uptake and improved in vivo bioavailability. *Colloids and Surfaces B: Biointerface*, 11, 367–375.
- Tiyaboonchai, W., Tungpradit, W., & Plianbangchang, P. (2007). Formulation and characterization of curcuminoids loaded solid lipid nanoparticles. *International Journal of Pharmaceutics*, 337, 299–306.
- Vitorino, C., Carvalho, F. A., Almeida, A. J., Sousa, J. J., & Pais, A. A. (2011). The size of solid lipid nanoparticles: an interpretation from experimental design. *Colloids and Surfaces B: Biointerfaces*, 84, 117–130.
- Westesen, K., Bunjes, H., & Koch, M. H. J. (1997). Physicochemical characterization of lipid nanoparticles and evaluation of their drug loading capacity and sustained release potential. *Journal of Controlled Release*, 48, 223–236.



## The influence of different the drying methods on chemical composition and antioxidant activity in chokeberries



Justyna Samoticha<sup>a</sup>, Aneta Wojdyło<sup>a, \*</sup>, Krzysztof Lech<sup>b</sup>

<sup>a</sup> Department of Fruit, Vegetable and Cereals Technology, Wrocław University of Environmental and Life Sciences, Chelmonskiego 37, 51-630, Wrocław, Poland

<sup>b</sup> Institute of Agricultural Engineering, Wrocław University Environmental and Life Sciences, 37/41 Chelmońskiego Street, 51-630, Wrocław, Poland

### ARTICLE INFO

#### Article history:

Received 31 August 2015

Received in revised form

25 October 2015

Accepted 31 October 2015

Available online 4 November 2015

#### Keywords:

*Aronia melanocarpa*

Phenolic compounds

Anthocyanins

Freeze-drying

Microwave

Vacuum and convective drying

Combined-

### ABSTRACT

Drying has been long known and widely used method of food preservation. The aim of this study was to determine the effect of different drying methods (by freeze-drying (FD), vacuum (VD), convective drying (CD), microwave (VMD) and combined method (CVM)) on the quality factors of chokeberry fruit, including phenolic compounds, antioxidant activity, and color. All products were characterized by water activity which determines their storage stability. The highest content of bioactive compounds and antioxidant activity were determined in freeze-dried samples, compared with fresh fruits (total phenolic in gallic acid equivalents- 8008 mg/100 g dm, anthocyanins- 3917 mg/100 g dm). The increase in air temperature during CD as well as the increase in material temperature during VMD deteriorated dried product quality in terms of the content of phenolic compounds, antioxidant activity, and color, which was correlated with anthocyanin content. A new combined CVM method allowed obtaining high quality dried material compared to the CD and VMD methods applied separately. The drying process affected changes in the appearance and brightening of color, and also increased the contribution of yellow color in the fruits. The results show that the quality of dried chokeberry depends on the method and conditions of fruit drying.

© 2015 Elsevier Ltd. All rights reserved.

### 1. Introduction

Chokeberry belongs to the family Rosaceae (*Rosaceae*), sub-family pome (*Pomoideae*). This plant is native to the North America, from where it was brought to Russia and then to other European countries, including Poland. Studies of healthy properties of chokeberry fit into the current trends and consumer interest in healthy diet and lifestyle.

Chokeberry contains a small amount of vitamin C as compared to other berries, however, is rich in polyphenols such as flavonoids (flavan-3-ols>anthocyanins>>flavonols) and phenolic acids (neochlorogenic and chlorogenic acid), with contents reaching 2000–3500 mg/100 g fresh fruit (Danielczuk, 2003). Bitter taste of the fruits is due to the presence of significant amounts of polyphenols, particularly proanthocyanidins whose oligomers have a high affinity to proteins, causing them to shear and inducing the feeling of dryness in the mouth (Oneksiak, 2000; Kolniak,

Augustyniok, & Oszmiański, 2009).

Chokeberry fruits can be classified as natural medicines due to their health properties (Kolniak et al., 2009). Chokeberry is useful in treating diseases of the cardiovascular system and of the digestive tract, owing to a high content of biologically-active compounds (Ostrowska & Rzemkowska, 1998) because its products have the highest antioxidant activity and are superior, in this regard, over blueberries, cranberries, black and red currants, raspberries, elderberries and strawberries. Wine from chokeberry has a higher antioxidant activity than the wine from grapes (Jakobek, Seruga, & Krivak, 2011). Chokeberry juice is considered a natural antibiotic and may be used in the treatment of stomach disorders, atherosclerosis, colds and food poisonings. These fruits are also helpful in obesity management due to significant amounts of polyphenolic compounds and dietary fiber. This enables blood glucose level adjustment and has a beneficial effect upon lipolysis and lipid metabolism as well as on the control of appetite (Jankowski, Niedworok, & Jankowska, 1999). In addition, compounds contained in chokeberry prevent damage of  $\beta$  cells of the pancreas which are responsible for insulin production (Oszmiański & Nowicka, 2011).

\* Corresponding author.

E-mail address: [aneta.wojdylo@up.wroc.pl](mailto:aneta.wojdylo@up.wroc.pl) (A. Wojdyło).

Due to its bitter taste, chokeberry is not consumed in the form of raw fruits, but is mainly processed into juices the tart flavor of which is less perceptible. A high content of pectin makes that chokeberry may also be processed into jams, jellies and marmalades. In turn, due to the high content of anthocyanins, chokeberry may be used to produce a natural food coloring, which is used to prepare e.g. jellies (Oneksiak, 2000; Danielczuk, 2003). Furthermore, whole chokeberry fruits may be dried to obtain snack products, additives to cereal products or tea infusions. The drying process affects the appearance of the fruit and their chemical composition. Considering consumer preferences, the appropriate method of drying should be selected, so as to ensure retention of the maximum quantity of bioactive compounds in the product. Choosing the adequate drying method and parameters of this process will provide a product with a high antioxidant activity, only slightly changed appearance compared to fresh fruit, and with a more favorable taste.

The aim of this study was to investigate the influence of different methods of drying and their parameters (freeze drying, vacuum, convection, vacuum–microwave drying and convection–vacuum–microwave) on the content of bioactive compounds, antioxidant activity and color of chokeberry fruit. The use of various drying methods was aimed at identifying which of them ensures the best preservation of these parameters.

## 2. Material and methods

### 2.1. Material

Samples of chokeberry (*Aronia melanocarpa* Elliott; 5 kg) were bought from Sady Trzebnickie near Trzebnica at processing maturity in September 2012 and were immediately brought to the University for further processing.

### 2.2. Drying experiments

Chokeberry fruits were dried with 5 methods: (i) freeze drying – FD (24 h; Alpha 1–4 LSC; Martin Christ GmbH, Osterode am Harz, Germany); (ii) vacuum drying – VD (SPT-200, ZEAMiLHoryzont, Kraków, Poland), (iii) convective drying – CD (convective drier designed and made at the Agricultural Engineering Institute of Wrocław University of Environmental and Life Sciences), (iv) vacuum–microwave drying – VMD (VM-200; Plazmatronika S.A., Wrocław, Poland), (v) and combined method: convection–vacuum–microwave drying – CVM.

During FD, the pressure was reduced to 0.960 kPa. The temperature in the drying chamber was  $-60^{\circ}\text{C}$ , while the temperature of shelves reached  $26^{\circ}\text{C}$ . Drying kinetics for CD and VMD was determined according to sample mass losses measured during drying. The process of dehydration using all the above-mentioned methods was continued until moisture content in the dried samples was 0.05 kg/kg dm. In the case of FD, the samples were kept in the drying chamber for 24 h.

Hot air temperatures during convective drying (CD) were  $50^{\circ}\text{C}$ ,  $60^{\circ}\text{C}$ , and  $70^{\circ}\text{C}$ ; air velocity was 1.2 m/s. Hot air temperatures were measured using thermocouples located close to the dried samples. The accuracy of the temperature gauge was  $0.1^{\circ}\text{C}$ . This allowed controlling air temperature to  $\pm 1^{\circ}\text{C}$  by adjusting autotransformers that supplied heating elements with electric energy.

During the vacuum–microwave drying (VMD), the initial microwave power was set to 240 W, 360 W, and 480 W. The pressure in the VMD chamber varied between 4 and 6 kPa.

Vacuum drying (VD) was conducted at  $50^{\circ}\text{C}$  and a pressure of 100 Pa, for 24 h.

In convection–vacuum–microwave drying (CVM), the fresh

material was dried first at a temperature of  $70^{\circ}\text{C}$  for 2 h or 6 h to achieve the same dry weight before further final drying. Then, the fruits were dried by vacuum–microwave with 360 W reduced to 120 W or 240 W.

### 2.3. Determination of water activity

The determination was performed on the Novasina (LabMasterav., Lachen, Switzerland) at  $20^{\circ}\text{C}$ .

### 2.4. Analysis of content of total phenolic, anthocyanins and antioxidant activity

The solvent for analysis of total polyphenols was prepared as described previously by Wojdyło, Figiel, and Oszmiański (2009). The determination was performed using the Folin-Ciocalteu method described previously by Gao, Ohlander, Jeppsson, Björk, and Trajkovski (2000). The results are given in mg of gallic acid/100 g dry matter (dm). Content of anthocyanins was measured according to Hosseinian, Li, and Beta (2008). Results are expressed in mg of anthocyanins/100 g of dm.

The ABTS<sup>+</sup>, and FRAP assay were determined as previously described by Re et al. (1999) and Benzie and Strain (1996), respectively. All antioxidant activity were expressed as millimoles of Trolox per 100 g of dm. Determinations by total phenolic, anthocyanins, ABTS and FRAP methods were performed using a UV2401 PC spectrophotometer (Shimadzu, Kyoto, Japan).

### 2.5. Color measurement

The color of chokeberry powders was determined using an A5 Chroma-Meter (Minolta CR300, Osaka, Japan), referring to color space CIE L\*a\*b\*. Determination was based on measuring the specific color parameters: L-color brightness, a\*– red parameter, b\*– participated of a yellow. Data were mean of three measurements.

### 2.6. Statistical analysis

Statistical analysis was conducted using Statistica version 10 (StatSoft, Krakow, Poland). Significant differences ( $p \leq 0.05$ ) between means were evaluated by one-way ANOVA and Duncan's multiple range test. Results of tables and figures are presented as mean  $\pm$  standard deviation of two independent technological determinations. All analyses were done in triplicate.

## 3. Results and discussion

Water activity is a factor that has a significant impact on the stability of dried fruit. A high water activity can lead to a shorter storage time of products, which is due to the possibility of adverse biochemical changes and microbial growth. To eliminate these factors, water activity in dried fruits should range from 0.600 to 0.800, but it is even better when it is below 0.600 (Barbosa-Canovas, Fontana, Schmidt, & Labuza, 2007; Cupiał, Witrowa-Rajchert, & Hankus, 2011).

Depending on the drying method applied, the dried fruits obtained were characterized by water activity ranging from 0.126 to 0.548, which is shown in Table 1. It can be assumed that the obtained products were microbiologically stable. The lowest water activity was determined in chokeberry subjected to FD. Similar results were reported by Cupiał et al. (2011), whereas Sumic, Tepic, Vidovic, Jokic, and Malbasa (2013) demonstrated that the dried sour cherry obtained by the vacuum under different conditions was characterized by  $a_w = 0.434–0.916$ . The highest result was obtained in the variant with the pressure of 300 mbar and temperature of

**Table 1**  
Effects of drying method on total phenolic content, gallic acid equivalents (mg/100 g of dry matter) and anthocyanins content (mg/100 g dry of matter) in chokeberry.

Method of drying	Drying conditions	Water activity ( $a_w$ )	Total phenolic gallic acid equivalents (mg/100 g dm)	Anthocyanins (mg/100 g dm)
Fresh	–	0.899	8008 ± 30a	3917 ± 24a
CD	50 °C	0.330	4956 ± 34f	965 ± 13i
	60 °C	0.336	5223 ± 26ef	781 ± 54i i
	70 °C	0.323	5631 ± 172d	964 ± 87 i
VMD	120 W	0.467	5597 ± 134d	1871 ± 170 defg
	240 W	0.502	5533 ± 131d	1797 ± 194 gf
	240/120 W	0.491	4954 ± 73f	1839 ± 40 efg
	360/120 W	0.474	5174 ± 238ef	1940 ± 96 defg
	360/240 W	0.463	5550 ± 186d	2076 ± 137 bcd
	480/120 W	0.635	5436 ± 549de	2005 ± 172cdef
	480/240 W	0.477	5548 ± 227d	2040 ± 77 bcde
VD	–	0.548	5443 ± 81de	1821 ± 114 fg
CVM	6h + 360/240	0.239	6338 ± 266c	1741 ± 89 g
	2h + 360/240	0.321	6425 ± 473c	2208 ± 301 cb
	6h + 360/120	0.239	5697 ± 409c	1458 ± 112 h
	2h + 360/120	0.383	6554 ± 205d	1738 ± 142 g
FD	–	0.126	7265 ± 81b	2227 ± 37 b

Values followed by the same letter, within the same column, were significantly different ( $p < 0.05$ ), according to Duncan's test.

FD freeze drying, VMD vacuum–microwave drying, VD–vacuum drying, CD convection drying CVM–convection–vacuum–microwave.

46 °C. FD chokeberries were characterized by a water activity equal to 0.126, while fruits subjected to CD at 60 °C were characterized by about twice the value determined for the product made by VMD in the variant with microwave power reduction from 480 W to 120 W, however the resulting value was not satisfactory–0.635. Dried fruits can have a reduced microbiological stability and can be exposed to the growth of osmophilic yeast, for which the limit of water activity is 0.600.

Contents of total phenolics and anthocyanins and antioxidant activity were shown in Tables 1 and 2, respectively. Polyphenols play an important protective function in the fruit (Mikulic-Petkovsek, Schmitzer, Slatnar, Stampar, & Veberic, 2012). In raw material, the content of polyphenols was measured at gallic acid equivalents at 8008 mg/100 g dm. This value was similar to the results reported by Oszmiański and Wojdyto (2005). All drying methods applied caused a 9–38% decrease of polyphenols content, which means that their final content was at gallic acid equivalents at 4954–7265 mg/100 g dm. To measure the total polyphenol

content, Folin-Ciocalteu method was used. The result may be slightly overestimated, as has been shown by Ikawa, Schaper, Dollard, and Sasner (2003) Folin-Ciocalteu phenol reagent can react with other compounds, e.g. nitrogen compounds.

FD allowed preserving the highest amounts of polyphenolic compounds in the resultant dried chokeberry (loss of 9%). In contrast, Wojdyto et al. (2009) showed a 5% loss of polyphenols in freeze-dried strawberries of Kent var., but for Elsanta var. polyphenols content after FD was statistically equivalent to that of the fresh fruits. A similar effect was observed by Horszwald, Julien, and Andlauer (2013) who determined a higher content of total polyphenols in chokeberry after oven-vacuum drying, especially at 60 °C, than after FD.

In CD, in the case of the low temperature (50 °C), destruction of polyphenolic compounds in the tested chokeberry fruit was higher than in the samples dried at 70 °C, which is associated with the drying time. At 50 °C, the fruits were dried for 23 h while at 70 °C – for 11 h. Wojdyto, Figiel, Lech & Nowicka (2013) obtained a opposite result when investigating the impact of CD on the content of polyphenols in sour cherries. The reduction in polyphenols content was smaller while the fruits were dried at 50 °C (35%) than at 60 °C and 70 °C. As a result of CD of apples at 60 and 70 °C, Fabisiak, Sheng, Stawczyk, and Witrowa-Rajchert (2005) reported approximately 35% reduction in the content of polyphenols. The greater loss of polyphenolic compounds in fruits dried at lower temperatures was explained by the authors with the longer residence time of the raw material at a temperature close to the optimum temperature of the polyphenol oxidase (40 °C). A much larger loss of polyphenols (41%) in blueberries dried at 70 °C for 10 h was found by Ścibisz and Mitek (2006). According to Borowska, Zadernowski, Markowski, and Białobrzewski (1999), in CD the losses of polyphenols are associated with enzymatic and non-enzymatic oxidation. Rapid and short heating may cause inactivation of oxidative enzymes and contribute to better preservation of phenolic compounds. According to Nowacka, Śledź, Wiktor, and Witrowa-Rajchert (2012), the application of VMD reduces the loss of polyphenols compared with CD as in the case of other fruits. Apples subjected to CD were characterized by 29% reduction of the initial content of polyphenols, while these exposed to convection microwave drying by only 20% loss of these compounds. Also Wojdyto et al. (2009) observed lesser degradation of polyphenols in strawberries when microwave techniques (240 W) were applied for drying – 10% compared to 30% in VD and CD (70 °C)– 36%. The

**Table 2**  
Effects of drying method on antioxidant activity (mmol Trolox/100 g dm) in chokeberry.

Method of drying	Drying conditions	Antioxidant activity	
		ABTS <sup>+</sup>	FRAP
Fresh	–	234.9 ± 5.8a	39.0 ± 13.5a
CD	50 °C	41.9 ± 4.2f	15.4 ± 1.5i
	60 °C	52.4 ± 35.5e	16.1 ± 1.8 h
	70 °C	75.0 ± 1.1cd	17.7 ± 1.0 hg
VMD	120 W	78.4 ± 3.5cd	18.5 ± 1.7f
	240 W	77.2 ± 5.2cd	19.1 ± 1.0ef
	240/120 W	73.2 ± 0.7cd	17.8 ± 1.4g
	360/120 W	72.3 ± 0.7d	17.5 ± 1.5g
	360/240 W	75.9 ± 0.7cd	20.7 ± 0.9e
	480/120 W	76.3 ± 1.3cd	19.3 ± 0.9ef
	480/240 W	76.2 ± 2.8cd	19.7 ± 1.7ef
VD	–	75.3 ± 5.0cd	19.5 ± 1.4ef
CVM	6h + 360/240	80.5 ± 3.9cd	22.1 ± 1.0d
	2h + 360/240	83.0 ± 2.8c	2.38 ± 1.3c
	6h + 360/120	82.7 ± 1.4cd	21.5 ± 1.7 d
	2h + 360/120	77.9 ± 1.4cd	19.3 ± 1.2e
FD	–	114.7 ± 4.5b	26.3 ± 1.7b

Values followed by the same letter, within the same column, were significantly different ( $p < 0.05$ ), according to Duncan's test.

FD freeze drying, VMD vacuum–microwave drying, VD–vacuum drying, CD convection drying CVM–convection–vacuum–microwave.

application VD resulted in 32% loss of polyphenols in the tested chokeberry, while Sumic et al. (2013) showed 14–77% lower content of these compounds in sour cherry subjected to VD, under different conditions of temperature and pressure.

The beneficial effect of polyphenolic compounds preservation was also demonstrated in the samples subjected to CVM drying. A decrease in the content of polyphenols ranged from 18 to 29%, depending on the variant of drying. A particularly advantageous effect has been achieved with the combined method with a 2 h convection drying and all variants of the final vacuum-microwave drying (CVM: 2h + 360/240 W; CVM: 2h + 360/120 W). The lowest total polyphenol content was measured in the samples dried by convection at 50 °C and dried with a reduction of microwave power from 240 W to 120 W.

Drying resulted in a significant loss (43–80%) of anthocyanins, because they are very sensitive to temperature and to the presence of oxygen. Among all drying methods applied, the greatest losses (80%) were obtained during CD at 60 °C. The shortening of the drying process, despite the higher temperature (70 °C), allowed achieving better results of anthocyanins preservation. In the samples dried at 70 °C, the content of anthocyanins decreased by 75%. Wojdyto et al. (2009) determined losses of these compounds amounting to 73% during the drying of strawberry variety Kent under the same temperature conditions. Ścibisz and Mitek (2006) reported that the loss of anthocyanins in blueberries dried at the same temperature for 10 h reached 74%. In turn Horszwald et al. (2013) showed that anthocyanins content of chokeberry fruits was the highest after oven-vacuum drying at 40 °C, compared to the drying process conducted at 60 and 80 °C.

Moreover, a greater loss of these compounds was observed by using the pre-treatment, especially during osmotic dehydration. According to Kwok, Hu, Durance, and Kitts (2004), the loss of anthocyanins in Saskatoon berries after CD (75 °C) was at 83–88%, while in the lyophilized product at 23–32%. In the case of CD of chokeberry, important is not only temperature, but also the aeration.

The smallest loss was observed for anthocyanins after FD (43% loss), and CVM (44% loss) - 2h + 360/240 W variant. Longer time (6 h) of convective pre-drying resulted in greater losses when compared to the 2 h long variants. In the VMD method, anthocyanin content reduction was achieved at a similar level and ranged from 47% to 50%. A slightly greater loss was observed only in the case of VMD conducted at the power of 240 W (54%). When analyzing dried strawberry variety Kent, Wojdyto et al. (2009) achieved only 23% losses using the microwave power of 240 W.

It is still very important to prevent losses in anthocyanins content after the drying process, because they have the strongest antioxidant properties of all biologically-active compounds of chokeberry.

The antioxidant activity determined by ABTS<sup>•+</sup> in fresh fruit was 234.9 mmol Trolox/100 g dm, and when measured by FRAP it was at 3.92 mmol Trolox/100 g dm. The drying process had a significant influence upon a decrease in the antioxidant activity of chokeberry measured by ABTS<sup>•+</sup>, i.e. 41.9–114.7 mmol Trolox/100 g depending on the drying method applied. Similarly to the content of polyphenols and anthocyanins, the FD method allowed preserving the highest antioxidant activity. However, even in this method, the losses were significant and amounted to 51%. Also the FRAP assay showed that chokeberry fruits obtained by freeze-drying and by CVM were characterized by the smallest loss of antioxidant activity, i.e. 34.4% and 42–45%, respectively. Wojdyto et al. (2009) demonstrated that a decrease in the value of this parameter in the freeze-dried strawberries equaled to 28%. The CVM method allowed for the best preservation of the ability to reduce Fe<sup>+3</sup>, in the variant of 2 h CD and final drying with VMD with the reduction of microwave

power from 360 W to 240 W (2h + 360/240 W).

A high correlation ( $r^2 = 0.83$  for ABTS<sup>•+</sup>, and  $r^2 = 0.90$  for FRAP) was observed between the decrease in the total polyphenol content and antioxidant activity, because the greatest losses (82%) were measured in the samples after CD at 50 °C. In the samples dried by the CD method at 70 °C the loss was lower (68%), but higher than that demonstrated by Ścibisz and Mitek (2006) for blueberries, analogously. These authors reported that 10 h CD of these fruits at 70 °C resulted in a decrease of the antioxidant activity by about 41%. It was observed that fruits obtained by drying at a higher temperature were characterized by a higher antioxidant activity, which can be explained by not only a shorter drying time, but also by the probability of formation of Maillard reaction products (and caramelization) which also exhibit free radical scavenging capacity (Bober & Oszmiański, 2004). Low temperature ensures better preservation of bioactive compounds and consequently a higher antioxidant activity, hence the differences in the values of the antioxidant activity measured by ABTS<sup>•+</sup> in chokeberry after freeze drying and vacuum-oven drying at 40 °C, were small. In dried sour cherry, Wojdyto, Figiel, Lech, Nowicka, and Oszmiański (2013) observed improved performance of the antioxidant activity of ABTS<sup>•+</sup> at a temperature of 50 °C compared to 60 °C and 70 °C. The reduction in the value of this parameter reached 25% at the lowest tested temperature, and 49% at the highest one. Studying dried Saskatoon berry, Kwok et al. (2004), showed the loss of the antioxidant activity of ABTS at 75–76% after CD (75 °C), and at 21–43% after FD. Also Wojdyto et al. (2013) obtained a smaller loss of the antioxidant activity by ABTS<sup>•+</sup> in dried cherry using FD (5%). The temperature of 70 °C caused a 32% reduction in the value of this parameter, which was a little more than after FD (26%). Significant losses of the antioxidant activity were determined in the VD samples (48%). The lowest decreased of the antioxidant activity measured by ABTS<sup>•+</sup> in dried chokeberry, to compare to CD and VMD, was found after CVM conducted for 2 h at the power of 360/240 W. The activity of these samples was measured at 83.0 mmol Trolox/100 g dm, which represented 35% of the initial value. Wojdyto et al. (2013) also measured the preservation of the antioxidant activity by ABTS<sup>•+</sup> in the products subjected to microwave drying process compared to the convective method.

The smaller loss (41%) of the antioxidant activity measured by FRAP in convective-dried strawberries at 70 °C was demonstrated by Wojdyto et al. (2009). However, in the sour cherries dried under the same conditions, Wojdyto et al. (2013) showed the highest reduction of the antioxidant activity at 70 °C (48%). The high temperature causes degradation of the compounds responsible for the antioxidant activity, anthocyanins in particular. Dried chokeberries obtained by the VD were characterized by a 51% reduction of the initial value of this parameter. According to Wojdyto et al. (2009), in dried strawberry the FRAP activity decreased by 44% after applying the VD method. In turn, Arancibia-Avila et al. (2012) showed that chokeberry retained its biological activity when heated at 100 °C for up to 20 min. Such short heating, despite high temperature, does not cause degradation of anthocyanins, which are largely responsible for the antioxidant properties of chokeberry.

Among the studied variants of microwave power applied, the smallest losses were observed after applying the method with power reduction from 240 W to 120 W. Samples dried with the VMD method had the highest activity as measured by FRAP assay, in the variant with microwave power reduction from 360 W to 240 W (50% reduction). During VMD, Wojdyto et al. (2013) demonstrated 23–40% loss of the antioxidant activity measured by FRAP method. To save the values of this parameter, the best conditions of VMD drying include using a power of 480 W with reduction to 120 W.

Changes in the antiradical activity of dried fruits are ambiguous.



Fig. 1. Appearance of the chokeberry fruit after drying: 1-CD 60 °C; 2- CVM 2h + 360/120 W.

High temperature and dehydration lead to the degradation of biologically-active compounds, however products of enzymatic and non-enzymatic browning formed in the course of the drying process may also exhibit antioxidant properties (Nowacka et al., 2012). However in this study in all dried chokeberry fruit after applying a high temperature, antioxidant activity significantly decreased.

Color and appearance (Fig. 1) is one of the most important stimuli recorded by human receptors, and therefore plays an important role in consumer evaluation of food quality. It may encourage to consumption by suggesting the sensation of certain flavors, or discourage by warning of the product in the state of rottenness (Cupiał et al., 2011). In chokeberry fruit, anthocyanin dyes (derivatives of cyanidin) are responsible for the color. Approximately 93% of these dyes are represented by 2 main compounds: cyanidin-3-*O*-galactose and cyanidin-3-*O*-arabinose. Anthocyanins have low resistance to external factors such as light, oxygen and temperature (Cupiał et al., 2011; Oszmiański & Wojdyło, 2005). The values of the parameters  $L^*$ ,  $a^*$   $b^*$  in fresh chokeberry amounted to 21.4, 8.9 and  $-3.7$ , respectively (Table 3).

In the tested fruits obtained by CD, VMD and FD, the  $L^*$  value was observed to increase (to the greatest extent in the convection method, in the case of drying at 70 °C), which corresponds to the brightening of product color. In all variants of the combined convection and vacuum-microwave, and in vacuum drying, the value of  $L^*$  parameter decreased, which indicates that the fruits were darker

compared to the fresh material. Horszwald et al. (2013) noted that oven-vacuum dried chokeberry fruits were darker than the dried fruits obtained by freeze-drying.

Different methods of chokeberry drying had various effects on the value of green-red coordinate  $a^*$  parameter. In the fresh material it reached 8.9, whereas its increase was recorded in freeze-drying methods, combined drying (except the variant of vacuum-microwave power of 360/120 W and convection for 2 h) and microwave drying (480/240 W, 360/240 and 360/120 W). In these dried fruits, increase was observed in the intensity of the red color. The highest percentage increase was measured in the sample subjected to combined drying (360/240 W, convection for 6 h) - 41%, which corresponds to the value of 12.5. In other dried chokeberries, an increase was observed in the contribution of green color, which was the highest in the VD samples where the value of  $a^*$  parameter was at 3.6 ( $r^2 = 0.33$  for anthocyanins, and  $r^2 = 0.40$  for total polyphenols).

In turn, the value of blue-yellow coordinate parameter increased in all obtained dried chokeberry, which represents the intensity of yellow color. The greatest increase in the value of  $b^*$  parameter was found in CVM-dried fruits (with convection for 2 h and final drying with microwave power of 360/240 W). The increase in the intensity of yellow color was 9%. The lowest value of  $b^*$  parameter was found in the sample subjected to convective drying at 50 °C.

The destruction of dyes increases with increasing heating temperature or time, and also during storage. There occurs the

Table 3  
Color parameters of chokeberry as affected by different drying methods.

Method of drying	Drying conditions	Color		
		$L^*$	$a^*$	$b^*$
Fresh	—	21.4 ± 4.7e	8.9 ± 1.7cde	-3.7 ± 5.1g
CD	50 °C	28.5 ± 0.1 abcd	5.2 ± 0.1 hi	-0.3 ± 0.6 f
	60 °C	30.3 ± 5.1 ab	7.0 ± 5.5 efgh	0.5 ± 1.1ef
	70 °C	30.6 ± 1.3 a	5.5 ± 0.5 gh	0.9 ± 0.1 def
	120 W	29.9 ± 2.8 abc	6.6 ± 1.7 fgh	1.4 ± 1.2 cde
VMD	240 W	28.7 ± 1.1 abcd	7.4 ± 1.4 efg	1.7 ± 1.0 cde
	240/120 W	28.0 ± 2.1 bcd	7.3 ± 1.6 efgh	1.2 ± 0.5 cdef
	360/120 W	28.8 ± 1.4 abcd	10.3 ± 2.2 bc	2.5 ± 0.6 bcd
	360/240 W	29.0 ± 1.3 abc	9.8 ± 2.7 bcd	1.9 ± 1.0 cde
	480/120 W	26.4 ± 1.4 d	8.0 ± 1.7 def	1.5 ± 0.5 cde
	480/240 W	27.4 ± 2.5 cd	8.9 ± 0.9 cde	1.7 ± 0.6 cde
VD	—	16.9 ± 3.7 g	3.6 ± 2.4 i	1.9 ± 0.6 cde
CVM	6h + 360/240	17.0 ± 1.5 fg	12.5 ± 1.5 a	3.9 ± 0.6 ab
	2h + 360/240	14.7 ± 2.0 g	11.7 ± 1.4 ab	4.9 ± 1.4 a
	6h + 360/120	17.5 ± 4.8 f	11.7 ± 4.2 ab	3.8 ± 1.1 ab
	2h + 360/120	17.1 ± 3.0 f	7.0 ± 1.9 efgh	2.7 ± 0.3 bc
FD	—	30 ± 1.2abc	10.9 ± 2.7abc	3.7 ± 0.8ab

Values followed by the same letter, within the same column, were significantly different ( $p < 0.05$ ), according to Duncan's test.

FD freeze drying, VMD vacuum-microwave drying, VD-vacuum drying, CD convection drying CVM-convection-vacuum-microwave.

conversion from red anthocyanin cation to colorless or yellow chalcones, and then brown polymers (Ścibisz, Kalisz, & Mitek, 2010). Analogous results were obtained in the research by Czapski and Walkowiak-Tomczak (2008), who demonstrated the effect of heating on the stability of chokeberry anthocyanins. Also, a similar dependency was observed by Ścibisz et al. (2010) in blueberries. It was found that with increasing time and temperatures, the values of parameters  $L^*$  and  $b^*$  increased as well. Thus, the brightening and increased contribution of a yellow color were observed while drying. Research conducted by Rutkowska, Adamska, Pielat, and Białek (2012) showed that lyophilized dried wild rose retained bright orange color characteristic of the fresh fruit. In contrast, the product obtained by convective drying (70 °C) was characterized by a darker color.

#### 4. Conclusions

Drying resulted in a decrease in the content of bioactive compounds (polyphenols from 9 to 38%, anthocyanins from 43 to 80%) and antioxidant activity (measured by ABTS - from 51 to 82%, by FRAP - from 34 to 62%), regardless of the method used. Among those, the greatest qualitative changes occurred during CD especially during drying at 50 °C, and the lowest after FD. In the method using the convection, at a temperature of 70 °C, dried fruits had a higher content of polyphenols and anthocyanins, and antioxidant activity than these dried at 50 °C, due to more than twice longer drying process at a lower temperature. The proposed combined method of drying -CD and VMD - allowed preserving more bioactive compounds of chokeberry than in the case of drying using these methods separately. A higher quality of the dried product was achieved using CD for 2 h than for 6 h, and then VMD with microwave power reduction from 360 to 240 W, than from 360 to 120 W.

Among all studied methods of drying, the best and therefore the least reducing the content of bioactive compounds and antioxidant activity, was freeze drying. Remarkable is also the method CVM, in particular variant 2h + 360/240 W, and at the same time it is more economical than freeze-drying. Dried chokeberry may be used in the industry as a raw material for the production of teas and infusions, as a natural food coloring, as well as a valuable addition to cakes and desserts.

#### Acknowledgments

A parts of this work was financially supported by the Ministry of Agricultural and Rural Development as the project no HORre-msz-078-9/15 (441). Publication supported by Wrocław Centre of Biotechnology, programme The Leading National Research Centre (KNOW) for years 2014–2018.

#### References

Arancibia-Avila, P., Namiesnik, J., Toledo, F., Werner, E., Martinez-Ayala, A. L., Rocha-Guzman, N. E., et al. (2012). The influence of different time durations of thermal processing on berries quality. *Food Control*, 26, 587–593.

Barbosa-Canovas, V. G., Fontana, J. A., Jr., Schmidt, J. S., & Labuza, P. T. (2007). *Water activity in foods - Fundamentals and applications*. Iowa: John Wiley & Sons.

Benzie, I. F. F., & Strain, J. J. (1996). The ferric reducing ability of plasma (FRAP) as a measure of "Antioxidant Power": the FRAP assay. *Analytical Biochemistry*, 239, 70–76.

Bober, I., & Oszmiański, J. (2004). Zastosowanie wyłoków aronii do naparów herbat

owocowych. *Acta Scientiarum Polonorum, Technologia Alimentaria*, 3, 63–72.

Borowska, J., Zadernowski, R., Markowski, M., & Białobrzeski, I. (1999). Wykorzystanie owoców krzewów mniej znanych w produkcji suszu. *Zeszyty Problemowe Postępów Nauk Rolniczych*, 46, 301–309.

Cupiał, D., Witrowa-Rajchert, D., & Hankus, M. (2011). Wybrane właściwości fizyczne mikrokapsułowanego soku z aronii. *Zeszyty problemowe postępów nauk rolniczych*, 558, 35–42.

Czapski, J., & Walkowiak-Tomczak, D. (2008). Kinetyka zmian barwy antocyjanów w czasie ogrzewania roztworów barwników aronii, czerwonych winogron i czarnego bzu. *Acta Agrophysica*, 12, 625–636.

Danielczuk, J. (2003). Aronia w przetwórstwie spożywczym- właściwości i kierunki wykorzystania. *Przemysł Fermentacyjny i Owocowo-warzywny*, 12, 26–28.

Fabisiał, A., Sheng, L., Stawczyk, J., & Witrowa-Rajchert, D. (2005). Wpływ metody i temperatury suszenia jablek na aktywność przeciwutleniającą otrzymanych z nich ekstraktów. *Żywność. Nauka. Technologia. Jakość*, 2, Supl., 318–327.

Gao, X., Ohlander, M., Jeppsson, N., Björk, L., & Trajkovski, V. (2000). Changes in antioxidant effects and their relationship to phytonutrients in fruits of sea buckthorn (*Hippophae rhamnoides* L.) during maturation. *Journal of Agricultural and Food Chemistry*, 48, 1485–1490.

Horszwald, A., Julien, H., & Andlauer, W. (2013). Characterisation of Aronia powders obtained by different drying processes. *Food Chemistry*, 141, 2858–2863.

Hosseinian, F. S., Li, W., & Beta, T. (2008). Measurement of anthocyanins and other phytochemicals in purple wheat. *Food Chemistry*, 109, 916–924.

Ikawa, M., Schaper, T. D., Dollard, C. A., & Sasner, J. J. (2003). Utilization of folin-ciocalteu phenol reagent for the detection of certain nitrogen compounds. *Journal of Agriculture and Food Chemistry*, 51, 1811–1815.

Jakobek, L., Seruga, M., & Krivak, P. (2011). The influence of interactions among phenolic compounds on the antiradical activity of chokeberries (*Aronia melanocarpa*). *International Journal of Food Sciences and Nutrition*, 64, 345–352.

Jankowski, A., Niedworok, J., & Jankowska, B. (1999). Wpływ aronii czarnaowocowej (*Aronia Melanocarpa* Elliot) na doświadczalną cukrzycę u szczurów. *Herba Polonica*, 4, 345–353.

Kolnias, J., Augustyniok, A., & Oszmiański, J. (2009). Wpływ dodatku owoców i warzyw do przecieru aroniowego na zawartość związków polifenolowych i jakość. *Przemysł Fermentacyjny i Owocowo-warzywny*, 10, 13–15.

Kwok, B. H. L., Hu, C., Durance, T., & Kitts, D. D. (2004). Dehydration techniques affect phytochemical contents and free radical scavenging activities of saskatoon berries (*Amelanchier alnifolia* Nutt.). *Journal of Food Science*, 3, 122–126.

Mikulic-Petkovek, M., Schmitzer, V., Slatnar, A., Stampar, F., & Veberic, R. (2012). Composition of sugars, organic acids, and total phenolics in 25 wild or cultivated berry species. *Journal of Food Science*, 10, 1064–1070.

Nowacka, M., Śledź, M., Wiktor, A., & Witrowa-Rajchert, D. (2012). Fizyczne i chemiczne właściwości produktów spożywczych suszonych z wykorzystaniem mikrofal. *Żywność. Nauka. Technologia. Jakość*, 6, 5–20.

Onęsiak, K. (2000). Aronia i jej żywieniowo-lecznicze znaczenie. *Żywność. Żywnienie. Prawo a zdrowie*, 3, 328–332.

Ostrowska, B., & Rzemikowska, Z. (1998). Przeciwutleniająca aktywność polifenolowych surowców roślinnych w profilaktyce i leczeniu miażdżycy. *Herba Polonica*, 4, 417–428.

Oszmiański, J., & Nowicka, P. (2011). Aronia- niedoceniony w Polsce owoc prozdrowotny w profilaktyce otyłości. *Przemysł Fermentacyjny i Owocowo-warzywny*, 7–8, 14–16.

Oszmiański, J., & Wojdyto, A. (2005). Aronia melanocarpa phenolics and their antioxidant activity. *European Food Research and Technology*, 221, 809–813.

Re, R., Pellegrini, N., Proteggente, A., Pannala, A., Yang, M., & Rice-Evans, C. (1999). Antioxidant activity applying an improved ABTS radical cation decolorization assay. *Free Radical Biology & Medicine*, 26, 1231–1237.

Rutkowska, J., Adamska, A., Pielat, M., & Białek, M. (2012). Porównanie składu i właściwości owoców dzikiej róży (*Rosa rugosa*) utrwalanych metodami liofilizacji i suszenia konwencjonalnego. *Żywność. Nauka. Technologia. Jakość*, 4, 32–43.

Ścibisz, I., Kalisz, S., & Mitek, M. (2010). Termiczna degradacja antocyjanów owoców borówki wysokiej. *Żywność. Nauka. Technologia. Jakość*, 5, 56–66.

Ścibisz, I., & Mitek, M. (2006). Aktywność przeciwutleniająca i zawartość związków fenolowych w suszach z owoców borówki wysokiej (*Vaccinium corymbosum* L.). *Żywność. Nauka. Technologia. Jakość*, 4, 68–76.

Sumic, Z., Tepic, A., Vidovic, S., Jokic, S., & Malbasa, R. (2013). Optimization of frozen sour cherries vacuum drying process. *Food Chemistry*, 136, 55–63.

Wojdyto, A., Figiel, A., Lech, K., Nowicka, P., & Oszmiański, J. (2013). Effect of convective and vacuum-microwave drying on the bioactive compounds, color, and antioxidant capacity of sour cherries. *Food and Bioprocess Technology*, 7, 829–841.

Wojdyto, A., Figiel, A., & Oszmiański, J. (2009). Effect of drying methods with the application of vacuum microwaves on the bioactive compounds, color, and antioxidant activity of strawberry fruits. *Journal of Agricultural and Food Chemistry*, 57, 1337–1343.



# Seabuckthorn as a novel prebiotic source improves probiotic viability in yogurt



Aynur Gunenc<sup>a</sup>, Christina Khoury<sup>a</sup>, Candace Legault<sup>a</sup>, Hannah Mirrashed<sup>a</sup>, Jenny Rijke<sup>b</sup>, Farah Hosseinian<sup>a, c, \*</sup>

<sup>a</sup> Food Science and Nutrition, Chemistry Department, Carleton University, Ottawa, Ontario, Canada

<sup>b</sup> Applied Human Nutrition, Guelph University, Guelph, Ontario, Canada

<sup>c</sup> Institute of Biochemistry, Carleton University, Ottawa, Ontario, Canada

## ARTICLE INFO

### Article history:

Received 11 June 2015

Received in revised form

23 October 2015

Accepted 25 October 2015

Available online 29 October 2015

### Keywords:

Microwave-extraction

Probiotic

Seabuckthorn

Selective media

## ABSTRACT

It was aimed to i) investigate if seabuckthorn whole fruit (S), and seabuckthorn purified mucilage (SP) addition into yogurt enhance bacterial viability, by measuring total bacterial counts of different yogurt trials on selective media, pH and total titratable acidity (TTA) during 28 day cold storage at 4 °C, as well as ii) measure antioxidant activities of microwave extracted seabuckthorn crude mucilage (SC) and SP using oxygen radical absorbance capacity (ORAC) and DPPH scavenging activity. After 21 days of cold storage, yogurts with S and SP maintained higher viable bacteria counts in both of probiotics, *Lactobacillus acidophilus* (9.3 log cfu/mL) and *Bifidobacterium lactis* (9.2 log cfu/mL), higher TTA (0.8%), and lower pH (5.0) compared to the controls ( $P < 0.05$ ). SC exhibited strong antioxidant activity with an ORAC value of 138.9 μmol Trolox equivalents/100 g, and a %DPPH scavenging activity value of 37.0%. Results of this study suggest S may serve as a new prebiotic source for functional foods and nutraceutical applications.

© 2015 Elsevier Ltd. All rights reserved.

## 1. Introduction

Seabuckthorn (*S*), *Hippophae rhamnoides* is a thorny, deciduous shrub, native to Europe and Asia (Upadhyay, Kumar, & Gupta, 2010). *S* has non-digestible oligosaccharides (NDOs) like prebiotics having the ability to enhance the activity of health promoting bacteria found in the human digestive system (Roberfroid, 2007). Prebiotics are substances such as carbohydrate polymers and sugars that improve host health by stimulating the growth and activity of health promoting bacteria found in the human digestive system (Santos, San Mauro, & Diaz, 2006). Probiotics are defined as live microorganisms, beneficially affect the health of the host by improving the properties of the indigenous microflora (Champagne & Gardner, 2008; Schrezenmeir & de Vrese, 2001).

To the best of our knowledge, there is no report on employing *S*, and *S*-purified mucilage (SP) into yogurt as a source of prebiotic. Hence, the objectives were to i) investigate if the addition of *S* and SP into yogurt enhance bacterial viability through measuring total

bacterial counts of different yogurt trials on selective media, pH and total titratable acidity (TTA%) during 28 days of cold storage at 4 °C, and ii) measure antioxidant activities of microwave extracted *S*-crude mucilage (SC) and SP using ORAC and DPPH scavenging activity.

## 2. Materials and Methods

### 2.1. Materials

Ethanol, methanol, and HCL were purchased from Caledon Laboratories LTC (Georgetown, ON, Canada). Trolox, mono- and di-basic potassium phosphate, fluorescein, rutin, AAPH, DPPH, and phenolphthalein were from Sigma (Oakville, ON, Canada). Sodium carbonate, sodium propionate was from Church and Dwight Canada Corp (Mississauga, ON, Canada). Protease (*Bacillus licheniformis*, EC 232-560-9) and  $\alpha$ -amylase (*Bacillus licheniformis*, EC 232-752-2) were from Sigma–Aldrich (St. Louis, Missouri, USA). Peptone, yeast extract powder, sodium acetate anhydrous, ammonium citrate, magnesium sulfate were from BioShop® Canada Inc. (Burlington, ON). *Lactobacillus delbrueckii* subsp. *bulgaricus* (B-548; USDA) and *Streptococcus salivarius* subsp. *thermophilus* (14485; ATCC), *Lactobacillus acidophilus* (B-4495; USDA) and *Bifidobacterium lactis*

\* Corresponding author. Food Science and Nutrition, Chemistry Department, Carleton University, Ottawa, Ontario, Canada.

E-mail address: [farah.hosseinian@carleton.ca](mailto:farah.hosseinian@carleton.ca) (F. Hosseinian).

(41405; USDA) were purchased from Oxoid Ltd. (Basingstoke, UK).

## 2.2. Sample preparations

### 2.2.1. S samples

Horticulture Research Center (Laval University, Quebec, Canada) has provided seabuckthorns as whole fruits upon arrival at  $-20^{\circ}\text{C}$ .

### 2.2.2. SC and SP extractions

**SC:** S was crushed using a juice processor (Black & Decker, WI, USA) and stored in Ziploc bags in the freezer at  $-20^{\circ}\text{C}$  prior to analysis. The samples (5 g) and 50 mL distilled water were added into a quartz vessel and placed into the CEM STAR System 2 microwave digestion system (CEM STAR System 2- Microwave, NC, USA) at  $90^{\circ}\text{C}$  for 30 min (Liavid, Palma, Brigui, & Barroso, 2007). The mixture was cooled and then centrifuged at 4000 rpm for 20 min (Thermo Sorval, Nepean, ON, Canada) at room temperature ( $23^{\circ}\text{C}$ ). The supernatant was collected and stored at  $-20^{\circ}\text{C}$  in the freezer until further analysis, while some extract was run through further purification. All analysis was made in triplicate.

**SP:** SC were treated with  $\alpha$ -amylase and protease (20  $\mu\text{L}/100\text{ mL}$ ) and stirred at  $37^{\circ}\text{C}$  for 24 h to eliminate proteins and starch molecules. The mixture was centrifuged at 4000 rpm for 20 min. The supernatant was heated at  $95^{\circ}\text{C}$  for 5 min to inactivate the enzymes, cooled to room temperature and re-centrifuged at  $6000\times g$  for 20 min. Then, it was dialyzed against double distilled water for 48 h and replaced with fresh distilled water every 6 h to separate polysaccharides and other materials with a molecular weight cut-off of 3500 Da (Spectra/Por, Rancho Dominguez, CA, USA).

## 2.3. Prebiotic activity

The best concentration of S and SP to be added for each yogurt trial without resulting in syneresis was preliminary determined as 2% (Agil & Hosseini, 2012). Therefore, 2% of S and SP was added to 50 mL pasteurized milk and incubated at  $42^{\circ}\text{C}$  until completion of fermentation.

### 2.3.1. Microbial cultures

Starter cultures (*Lactobacillus bulgaricus* and *Streptococcus thermophilus*) and probiotics (*L. acidophilus* and *B. lactis*) were employed and each strain was grown in 10 mL sterile aliquots of corresponding broth liquid media (MRS or M17), and incubated at  $37^{\circ}\text{C}$  for 48 h. The cultures were diluted with sterilized milk to obtain a concentration of approximately 6.5 log cell/mL. Then,

0.5 mL of each yogurt starter culture and 1.0 mL of required probiotic(s) was inoculated according to the experimental design (Table 1).

### 2.3.2. Yogurt trials

Whole milk was heated at  $85^{\circ}\text{C}$  for 15 min, and cooled to  $42^{\circ}\text{C}$  in a water bath. 50 mL portions was transferred to test tubes and inoculated with each starter cultures, probiotics, 2% S, and 2% SP. Twelve yogurt trials were divided in three groups (2% S homogenate, 2% SP, and controls). Tubes were placed in an incubator ( $42^{\circ}\text{C}$ ) and terminated once pH reached  $\sim\text{pH } 5.0$  and stored at  $4^{\circ}\text{C}$  (Espírito Santo et al., 2010). All yogurt treatments were carried out in triplicate.

### 2.3.3. Bacterial counts

Bacterial enumerations were performed during 4 week storage; *Streptococcus thermophilus* (M17, aerobic, 24 h at  $37^{\circ}\text{C}$ ) (Santos et al., 2006), *L. bulgaricus* (MRS, aerobic, 72 h,  $42^{\circ}\text{C}$ ) (Goncalves, Freitas, Nero, & Carvalho, 2009), *L. acidophilus* (T-MRS, aerobic, 48 h,  $37^{\circ}\text{C}$ ) and *B. lactis* (LP-MRS, anaerobic, 72 h,  $42^{\circ}\text{C}$  using a BBL GasPak™ System (Basingstoke, Hampshire, England) (Vinderola & Reinheimer, 1999). Colonies were counted as the log of colony forming units per microliter of sample using the following equation:

$$\text{Log} \frac{\text{CFU}}{\text{mL}} = \frac{1000 \mu\text{L} \times \frac{\text{CFU}}{\text{plate}}}{10 \mu\text{L}} \times \text{dilution factor}$$

### 2.3.4. pH and TTA

pH (Denver Instrument) and TTA were determined (Espírito Santo et al., 2010) during 4 week storage. The amount of acid produced during fermentation was expressed as TTA% (Behrad, Yusuf, Goh, & Baba, 2009).

## 2.4. Antioxidant activity

### 2.4.1. ORAC

Antioxidant activity of SC and SP was determined by ORAC assay (FLx800™ BioTek Instruments) (Hosseini et al., 2007; Huang, Ou, Hampsch-Woodill, Flanagan, & Prior, 2002) and was expressed as  $\mu\text{mol Trolox equivalents per } 100\text{ g}$  of whole S.

### 2.4.2. DPPH scavenging activity assay

200  $\mu\text{L}$  of SC and SP was mixed with 3.8 mL of DPPH (60  $\mu\text{M}$ ). The absorbance (UV–Visible Spectra–Max Plus384) of the mixture was measured at 515 nm at 60 min. DPPH was calculated as (Li, Hydamaka, Lowry, & Beta, 2009):

$$\% \text{DPPH} = \left( 1 - \left[ \frac{A_{\text{sample}}}{A_{\text{control } t=0}} \right] \right) \times 100$$

## 2.5. Statistical analyses

All experiments were conducted in triplicates. A two-way analysis of variance (ANOVA) was used by SAS (Statistical Analysis System, 9th Version, SAS Institute Inc., Cary, NC) to compare the mean differences between groups. Duncan's Multiple Range test was used when significant ( $P < 0.05$ ) mean comparison was performed.

**Table 1**

Experimental design for evaluating S and SP mucilage addition effects on microbial viability in different yogurt trials.

Yogurt trials*	Fruit	Sample coding
Y	–	Y
Y + Pro1	–	Y+1
Y + Pro2	–	Y+2
Y + Pro1&2	–	Y+1+2
YS	+	S
YS + Pro1	+	S+1
YS + Pro2	+	S+2
YS + Pro1&2	+	S+1+2
YSP	+	SP
YSP + Pro1	+	SP+1
YSP + Pro2	+	SP+2
YSP + Pro1&2	+	SP+1+2

\*S = seabuckthorn; SP = seabuckthorn purified mucilage; (–) = without S or SP; (+) = with S or SP; Y = yogurt with only starter cultures of *Lactobacillus delbrueckii* subsp. *bulgaricus* and *Streptococcus salivarius* subsp. *thermophilus*; Pro1 = probiotics of *Lactobacillus acidophilus*; Pro2 = *Bifidobacterium lactis*.

### 3. Results and discussion

#### 3.1. Probiotic activity

##### 3.1.1. Starter culture enumerations

Both of starter culture counts ( $\log \text{cfu mL}^{-1}$ ) in all yogurt trials are shown in Table 2. On day 1, *S. thermophilus* and *L. bulgaricus* counts ranged from 7.18 to 8.16  $\log \text{cfu mL}^{-1}$  and 5.33 to 7.82  $\log \text{cfu mL}^{-1}$  amongst all treatments, respectively. S and S+1 yogurts showed significantly ( $P < 0.05$ ) higher *S. thermophilus* counts than corresponding controls while there was no difference in comparison to SP yogurts. Control yogurts showed significantly lower *L. bulgaricus* counts ( $P < 0.05$ ) compared to S and SP yogurts.

On day 7, *S. thermophilus* counts in SP yogurts were significantly higher ( $P < 0.05$ ) than the Y and S yogurts. S yogurt had the highest ( $P < 0.05$ ) *L. bulgaricus* counts, with an increase of over 1  $\log \text{cfu mL}^{-1}$ .

On day 14, S and SP yogurts exhibited higher *S. thermophilus* counts than Y, Y+1, Y+2, and Y+1+2 yogurts. Also, the highest *L. bulgaricus* count was recorded on day 14 of cold storage.

On day 21, all S and SP treatments showed significantly higher counts of *S. thermophilus* ( $P < 0.05$ ) than the controls (Y, Y+1, Y+2, and Y+1+2). All S yogurts showed significantly higher *L. bulgaricus* ( $P < 0.05$ ) count in comparison to the controls by more than 1  $\log \text{cfu mL}^{-1}$ .

On day 28 *Streptococcus thermophilus* counts were higher in S and SP yogurts than the controls. S addition no longer showed any effect on *L. bulgaricus* growth. Interestingly, almost all SP yogurts presented a lower growth in comparison to the controls. Suggesting that after 28 days of cold storage SP addition may have a negative impact on *L. bulgaricus*.

Overall, *S. thermophilus* count was better compared to those of *L. bulgaricus* which was parallel to the literature (Dave & Shah,

1997; Gunenc, Fang, & Hosseinian, 2015). Therefore, S and SP addition may have benefit of increasing the growth of starter cultures. After 28 days, *L. bulgaricus* seemed to be negatively impacted by the presence of SP compared to the control. This observation may be explained by the fact that counts of *L. bulgaricus* increase initially followed by a sharp decline during the latter stages of a storage period (Dave & Shah, 1997). In the present study, counts were initially low, followed by maximum increase at day 14 and slightly decreasing by day 28. This may be explained by *L. bulgaricus* requirements for simple sugars, like sucrose and lactose for growth (Vinderola, Costa, Regenhardt, & Reinheimer, 2002). Seabuckthorn polysaccharide extract contains more complex sugars, which may not have been easily digested by the starter culture. In addition, the presence of probiotics and *S. thermophilus* in different treatments and depletion of nutrients would be expected by the end of the cold storage. Furthermore, the growth of all probiotics (Fig. 1) in the presence of S and SP flourished and in some cases grew more with SP presence. Therefore, increased microbial activity of the probiotics and lack of simple sugars in the SP extract may have negative effect on *L. bulgaricus* growth. Therefore, the addition of SP may indirectly aid probiotic viability by antagonizing the growth of *L. bulgaricus* (Vasiljevic & Shah, 2008).

##### 3.1.2. Probiotics enumerations

The viable microbial counts ( $\log \text{cfu mL}^{-1}$ ) of *L. acidophilus* and *B. lactis* in yogurt treatments during 28 days of cold storage were shown in Fig. 1A and B, respectively. On day 1, the presence of S and SP resulted in more growth ( $P < 0.05$ ) of *L. acidophilus* in S+1 and SP+1 as well as S+1+2 and SP+1+2 yogurts. For *B. lactis*, both S and SP addition increased ( $P < 0.05$ ) the growth in S+2 and SP+2 yogurts compared to the controls of Y+2 and Y+1+2 (Fig. 1B).

On day 7, the presence of S and SP revealed significantly higher ( $P < 0.05$ ) growth of *L. acidophilus* in S+1 and SP+1 as well as in S+1+2 and SP+1+2 yogurts. *B. lactis* counts were significantly higher ( $P < 0.05$ ) in S+2 and SP+2 as well as in S+1+2 and SP+1+2 yogurts in comparison to the controls (Y+2 and Y+1+2).

On day 14, *L. acidophilus* counts were significantly higher ( $P < 0.05$ ) in S, SP S+1+2, and SP+1+2 yogurts in comparison to the respective controls. Also SP addition contained the highest amount of *L. acidophilus*: 9.1  $\log \text{cfu mL}^{-1}$  in SP+1 and 9.0  $\log \text{cfu mL}^{-1}$  in SP+1+2. *B. lactis* in S and SP yogurts was significantly higher ( $P < 0.05$ ) than the controls (Y+2 and Y+1+2).

On day 21, S+1, S+1+2, and SP+1+2 yogurts showed significantly higher *L. acidophilus* growth ( $P < 0.05$ ) than the controls (Y+1 and Y+1+2). Also, S and SP yogurts had higher ( $P < 0.05$ ) *B. lactis* growth in comparison to the respective controls (Y+2 and Y+1+2). Interestingly, the yogurts containing SP (SP+2 and SP+1+2) had the highest amount ( $P < 0.05$ ) of viable *B. lactis*: 8.9  $\log \text{cfu mL}^{-1}$  in the third treatment and 9.2  $\log \text{cfu mL}^{-1}$  in the fourth treatment, which paralleled results observed of *L. acidophilus* (Fig. 1A and B).

On day 28, only SP+1 yogurt exhibited higher ( $P < 0.05$ ) *L. acidophilus* counts in comparison to the control Y+1. No differences ( $P < 0.05$ ) in *B. lactis* counts between Y+2, S+2, and SP+2 yogurts were observed. However, SP+1+2 yogurt showed significantly higher ( $P < 0.05$ ) counts of *B. lactis*.

Based on two-way ANOVA analysis, all control yogurts containing *L. acidophilus* were significantly lower than both S and SP added yogurts during the 28 days of cold storage. Yogurts containing the polysaccharide extract exhibited the highest counts of *L. acidophilus* in SP+1 and SP+1+2 yogurts. Both of S and SP additions had a positive effect, because they have substrates such as oligosaccharides; stimulating the growth of probiotic bacteria. Oligosaccharides are water-soluble low molecular carbohydrates and fermented by various strains of bifidobacteria and lactobacilli,

**Table 2**

*S. thermophilus* and *L. bulgaricus* counts ( $\log \text{cfu/mL}$ ) in yogurts with/without S and SP mucilage during 28 days cold storage at 4 °C.

<i>S. thermophilus</i>	Day 1	Day 7	Day 14	Day 21	Day 28
Y	7.83 <sup>abc</sup>	7.96 <sup>cde</sup>	8.29 <sup>c</sup>	8.55 <sup>c</sup>	8.72 <sup>bc</sup>
Y+1	7.68 <sup>bc</sup>	7.84 <sup>cde</sup>	8.46 <sup>bc</sup>	8.19 <sup>d</sup>	8.62 <sup>bc</sup>
Y+2	7.53 <sup>cd</sup>	7.49 <sup>e</sup>	7.85 <sup>d</sup>	8.64 <sup>bc</sup>	8.40 <sup>cd</sup>
Y+1+2	7.18 <sup>d</sup>	7.64 <sup>de</sup>	8.31 <sup>c</sup>	8.64 <sup>bc</sup>	8.12 <sup>d</sup>
S	7.68 <sup>bc</sup>	7.86 <sup>cde</sup>	9.18 <sup>a</sup>	9.25 <sup>a</sup>	9.04 <sup>ab</sup>
S+1	8.16 <sup>a</sup>	8.19 <sup>abcd</sup>	8.77 <sup>ab</sup>	8.94 <sup>ab</sup>	8.88 <sup>ab</sup>
S+2	7.76 <sup>abc</sup>	7.83 <sup>cde</sup>	8.95 <sup>a</sup>	9.17 <sup>a</sup>	8.87 <sup>ab</sup>
S+1+2	7.82 <sup>abc</sup>	8.14 <sup>bcd</sup>	8.85 <sup>ab</sup>	9.07 <sup>a</sup>	9.15 <sup>a</sup>
SP	7.77 <sup>abc</sup>	8.73 <sup>a</sup>	9.13 <sup>a</sup>	9.13 <sup>a</sup>	8.91 <sup>ab</sup>
SP+1	8.03 <sup>ab</sup>	8.20 <sup>abcde</sup>	9.00 <sup>a</sup>	9.22 <sup>a</sup>	8.87 <sup>ab</sup>
SP+2	7.94 <sup>abc</sup>	8.39 <sup>abc</sup>	9.05 <sup>a</sup>	9.16 <sup>a</sup>	8.75 <sup>ab</sup>
SP+1+2	7.66 <sup>bc</sup>	8.67 <sup>ab</sup>	9.15 <sup>a</sup>	9.10 <sup>a</sup>	8.67 <sup>bc</sup>
<i>L. bulgaricus</i>					
Y	5.96 <sup>b</sup>	7.27 <sup>de</sup>	8.04 <sup>d</sup>	7.68 <sup>c</sup>	8.32 <sup>ab</sup>
Y+1	5.33 <sup>b</sup>	7.25 <sup>de</sup>	9.14 <sup>ab</sup>	7.62 <sup>c</sup>	8.50 <sup>a</sup>
Y+2	6.01 <sup>b</sup>	7.22 <sup>de</sup>	8.95 <sup>abc</sup>	7.94 <sup>c</sup>	8.21 <sup>ab</sup>
Y+1+2	5.64 <sup>b</sup>	7.37 <sup>cde</sup>	9.18 <sup>ab</sup>	8.08 <sup>bc</sup>	7.80 <sup>bc</sup>
S	7.02 <sup>a</sup>	7.39 <sup>cde</sup>	9.27 <sup>a</sup>	9.16 <sup>a</sup>	8.76 <sup>a</sup>
S+1	7.31 <sup>a</sup>	7.65 <sup>abcd</sup>	9.15 <sup>ab</sup>	8.98 <sup>a</sup>	8.55 <sup>a</sup>
S+2	7.17 <sup>a</sup>	7.16 <sup>e</sup>	9.28 <sup>a</sup>	9.23 <sup>a</sup>	8.55 <sup>a</sup>
S+1+2	7.26 <sup>a</sup>	7.54 <sup>bcde</sup>	8.73 <sup>abcd</sup>	9.27 <sup>a</sup>	8.24 <sup>ab</sup>
SP	7.82 <sup>a</sup>	8.03 <sup>a</sup>	8.25 <sup>cd</sup>	7.63 <sup>c</sup>	7.10 <sup>d</sup>
SP+1	7.76 <sup>a</sup>	7.96 <sup>ab</sup>	8.75 <sup>abcd</sup>	8.83 <sup>ab</sup>	7.80 <sup>bc</sup>
SP+2	7.66 <sup>a</sup>	7.55 <sup>bcde</sup>	8.65 <sup>abcd</sup>	8.47 <sup>abc</sup>	7.51 <sup>cd</sup>
SP+1+2	7.46 <sup>a</sup>	7.73 <sup>abc</sup>	8.38 <sup>bcd</sup>	7.89 <sup>c</sup>	7.49 <sup>cd</sup>

\*S = seabuckthorn; SP = seabuckthorn purified mucilage; Y = yogurt with only starter cultures of *Lactobacillus delbrueckii* subsp. *bulgaricus* and *Streptococcus salivarius* subsp. *thermophilus*; 1 = Probiotic1(*Lactobacillus acidophilus*); 2 = Probiotic 2 (*Bifidobacterium lactis*); Different letters in columns in the same day are significantly different ( $P < 0.05$ ) in Duncan's multiple range tests.

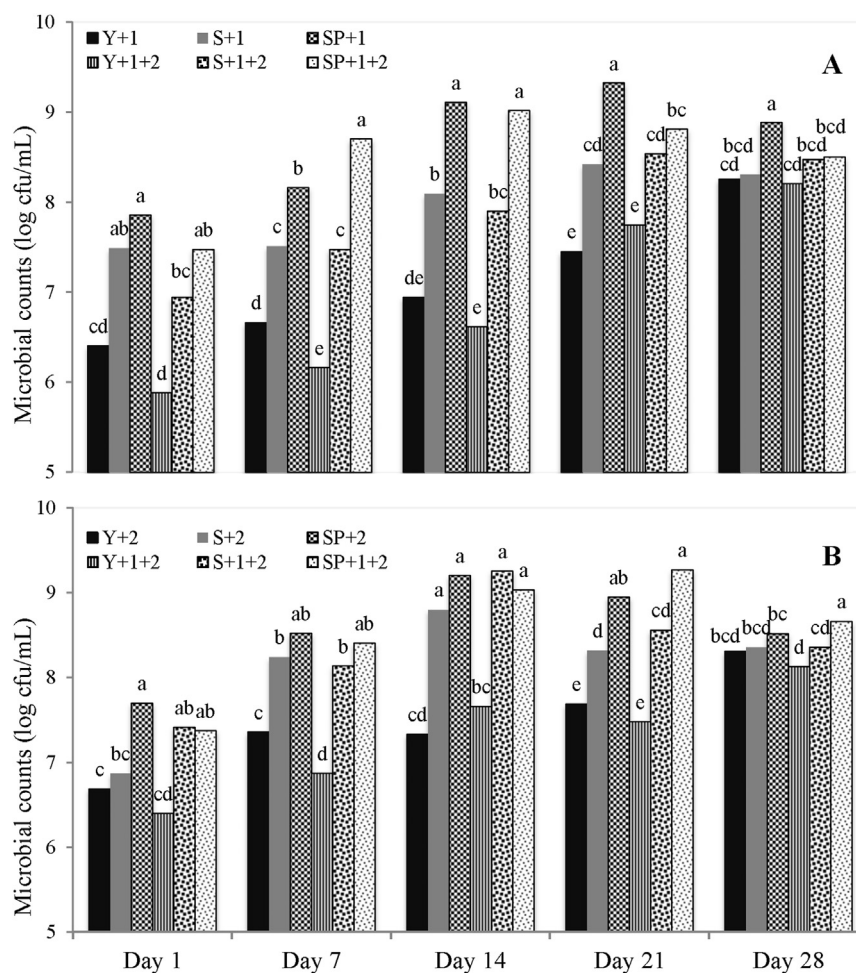


**Fig. 1.** A) Probiotic 1 (*Lactobacillus acidophilus*) counts in control (Y+1, Y+1+2), S (S+1, S+1+2) and SP (SP+1, SP+1+2) yogurts over 28 days of cold storage; B) Probiotic 2 (*Bifidobacterium lactis*) counts in control (Y+2, Y+1+2), S (S+2, S+1+2), and SP (SP+2, SP+1+2) yogurts over 28 days of cold storage. Means with different letters are significantly ( $P < 0.05$ ) different within the same day.

because they serve as a food source and S has a mixture of hydrophobic materials from the fruit and seeds, while SP contained a more potent amount of the NDOs (Mussatto & Mancilha, 2007). Therefore, SP might have a stronger effect on *L. acidophilus* than S since the higher level of polysaccharide substrates selectively stimulating microbial growth (Agil & Hosseinian, 2012). However, on day 28, *L. acidophilus* counts in SP+1+2 yogurt was  $8.4 \log \text{cfu mL}^{-1}$  and showed no difference compared to the control. Indicating that the presence of a second probiotic may have an effect on *L. acidophilus* counts due to an accumulation of cellular waste and nutrient depletion (Vasiljevic & Shah, 2008).

*B. lactis* showed a slightly different growth pattern from that of *L. acidophilus*. It was found that all control yogurts containing *B. lactis* were significantly lower than both S and SP addition throughout the 28 days of cold storage. SP yogurts exhibited the highest counts of *B. lactis* in SP+2 and SP+1+2 yogurts. S contains oligosaccharides and essential nutrients that promote viability and growth of microbes. In particular, Bifidobacteria utilizes amino acids such as valine, glycine, and histidine to support its growth (Vasiljevic & Shah, 2008). S has high quantities of valine, glycine, and histidine, with levels of 21.8 mg/100 g, 16.7 mg/100 g, and 13.7 mg/100 g, respectively (Beveridge, Li, Oomah, & Smith, 1999). Probiotic organisms have weak proteolytic activity, therefore they require these free amino acids to increase their numbers (Vasiljevic & Shah, 2008).

### 3.1.3. pH and TTA

On day 1, pH varied from 6.10 to 6.56 amongst all yogurt treatments. S and SP yogurts did not show a significant difference in pH ( $P < 0.05$ ) compared to corresponding controls (Table 3). TTA data ranged from 0.1 to 0.22 mg lactic acid  $\text{g}^{-1}$ , where TTA data showed no significant differences between S and SP yogurts.

On day 7, S yogurts showed no difference ( $P < 0.05$ ) in pH compared to the respective controls. The pH of SP yogurts was lower ( $P < 0.05$ ) than those of the controls (Y, Y+2, and Y+1+2) with the exception of SP+1. TTA was significantly higher ( $P < 0.05$ ) in the yogurts containing SP when compared to the controls without extracts and the yogurts containing S. From the S yogurts, only S+2 yogurt had higher ( $P < 0.05$ ) TTA in comparison to the control (Y+2).

After 14 days, all S and SP yogurts exhibited significantly lower pH ( $P < 0.05$ ) in comparison to the controls. Similarly, TTA data for all S and SP yogurt showed higher levels in comparison to their respective controls.

On day 21, pH ranged from 6.3 to 5.29 amongst the different treatments and it was observed that all S and SP yogurts had significantly lower pH ( $P < 0.05$ ) compared to their respective controls. In addition, only S, S+1, S+2, and S+1+2 yogurts had higher levels ( $P < 0.05$ ) of TTA in comparison to their respective controls, however SP showed no significant differences when compared to their controls.

**Table 3**  
pH and TTA values of yogurts with/without S and SP mucilage during 28 days cold storage at 4 °C.

pH	Day 1	Day 7	Day 14	Day 21	Day 28
Y	6.56 <sup>a</sup>	6.47 <sup>a</sup>	6.41 <sup>a</sup>	6.31 <sup>a</sup>	6.04 <sup>a</sup>
Y+1	6.10 <sup>a</sup>	6.02 <sup>bcde</sup>	6.30 <sup>ab</sup>	5.90 <sup>b</sup>	5.71 <sup>b</sup>
Y+2	6.43 <sup>a</sup>	6.36 <sup>ab</sup>	6.16 <sup>b</sup>	6.31 <sup>a</sup>	6.10 <sup>a</sup>
Y+1+2	6.50 <sup>a</sup>	6.47 <sup>a</sup>	6.23 <sup>b</sup>	6.48 <sup>a</sup>	6.21 <sup>a</sup>
S	6.35 <sup>a</sup>	6.11 <sup>abcd</sup>	5.73 <sup>de</sup>	5.43 <sup>c</sup>	5.13 <sup>c</sup>
S+1	6.36 <sup>a</sup>	6.22 <sup>abc</sup>	5.86 <sup>cd</sup>	5.36 <sup>c</sup>	5.11 <sup>c</sup>
S+2	6.31 <sup>a</sup>	6.10 <sup>abcd</sup>	5.73 <sup>de</sup>	5.29 <sup>c</sup>	5.01 <sup>c</sup>
S+1+2	6.39 <sup>a</sup>	6.28 <sup>abc</sup>	5.91 <sup>c</sup>	5.44 <sup>c</sup>	5.21 <sup>c</sup>
SP	6.51 <sup>a</sup>	5.72 <sup>de</sup>	5.65 <sup>ef</sup>	5.41 <sup>c</sup>	5.16 <sup>c</sup>
SP+1	6.48 <sup>a</sup>	5.89 <sup>cde</sup>	5.62 <sup>ef</sup>	5.29 <sup>c</sup>	5.25 <sup>c</sup>
SP+2	6.24 <sup>a</sup>	5.69 <sup>e</sup>	5.56 <sup>f</sup>	5.33 <sup>c</sup>	5.16 <sup>c</sup>
SP+1+2	6.41 <sup>a</sup>	5.75 <sup>de</sup>	5.59 <sup>ef</sup>	5.31 <sup>c</sup>	5.12 <sup>c</sup>
<b>TTA%</b>					
Y	0.10 <sup>b</sup>	0.17 <sup>d</sup>	0.21 <sup>c</sup>	0.38 <sup>bc</sup>	0.39 <sup>g</sup>
Y+1	0.11 <sup>b</sup>	0.17 <sup>d</sup>	0.22 <sup>c</sup>	0.37 <sup>bcd</sup>	0.38 <sup>g</sup>
Y+2	0.13 <sup>b</sup>	0.17 <sup>d</sup>	0.24 <sup>c</sup>	0.37 <sup>bc</sup>	0.39 <sup>g</sup>
Y+1+2	0.11 <sup>b</sup>	0.16 <sup>d</sup>	0.23 <sup>c</sup>	0.36 <sup>bcd</sup>	0.42 <sup>g</sup>
S	0.21 <sup>a</sup>	0.21 <sup>cd</sup>	0.33 <sup>b</sup>	0.71 <sup>a</sup>	0.74 <sup>b</sup>
S+1	0.22 <sup>a</sup>	0.22 <sup>cd</sup>	0.35 <sup>b</sup>	0.68 <sup>a</sup>	0.87 <sup>a</sup>
S+2	0.22 <sup>a</sup>	0.24 <sup>bc</sup>	0.35 <sup>b</sup>	0.65 <sup>a</sup>	0.71 <sup>bc</sup>
S+1+2	0.19 <sup>b</sup>	0.21 <sup>cd</sup>	0.31 <sup>b</sup>	0.63 <sup>a</sup>	0.69 <sup>cd</sup>
SP	0.18 <sup>a</sup>	0.26 <sup>bc</sup>	0.33 <sup>b</sup>	0.41 <sup>cd</sup>	0.57 <sup>de</sup>
SP+1	0.21 <sup>a</sup>	0.35 <sup>a</sup>	0.42 <sup>a</sup>	0.32 <sup>d</sup>	0.53 <sup>ef</sup>
SP+2	0.20 <sup>a</sup>	0.30 <sup>ab</sup>	0.38 <sup>ab</sup>	0.36 <sup>bcd</sup>	0.53 <sup>ef</sup>
SP+1+2	0.21 <sup>a</sup>	0.33 <sup>a</sup>	0.35 <sup>b</sup>	0.44 <sup>b</sup>	0.51 <sup>f</sup>

\*S = seabuckthorn; SP = seabuckthorn purified mucilage; Y = yogurt with only starter cultures of *Lactobacillus delbrueckii* subsp. *bulgaricus* and *Streptococcus salivarius* subsp. *thermophilus*; 1 = Probiotic 1 (*Lactobacillus acidophilus*); 2 = Probiotic 2 (*Bifidobacterium lactis*); Different letters in columns in the same day are significantly different ( $P < 0.05$ ) in Duncan's multiple range tests.

After 28 days, all S and SP yogurts exhibited significantly lower pH ( $P < 0.05$ ) in comparison to the respective controls. All S yogurts had higher TTA levels in comparison to the respective controls and to their equivalent SP treatments.

Fermentation was allowed to reach a range between 6.2 and 4.9 following a U.S. patent for preparing cultured dairy products (Lundstedt & Corbin, 1983). A pH of approximately six was recommended as the most active form of the enzyme  $\beta$ -galactosidase ( $\beta$ -gal), found in the bacteria *S. thermophilus* and *L. bulgaricus*, which is responsible for digesting lactose in yogurt (Martini, Kukielka, & Savaiano, 1991). This enzyme helps break down the lactose, which makes it easier for lactase-deficient people to consume yogurt. After 28 days, all S and SP samples exhibited lower pH compared to the control which coincided with the TTA results. By this time S and SP treatments showed a pH drop of ~1.2 and 1.5 respectively, while those of the controls only dropped ~0.4 units from day 1 readings. Suggesting that in the presence of S, bacteria are potentially more active, thus producing more lactic acid and consequently decreasing pH.

The TTA test was used to identify and quantify the amount of lactic acid present in the yogurt samples. Lactic acid was targeted, because it is the most prevalent acid produced by probiotic bacteria, while other acids such as butyric and propionic acids are produced in lesser amounts (Agil & Hosseini, 2012). It was observed that all yogurt treatments showed a general trend of increasing TTA levels indicating an increasing amount of bacteria activity, thus a result of growing number of bacteria (Gunenc et al., 2015). The TTA readings for both S and SP were significantly higher than the respective controls ( $P < 0.05$ ) and suggesting that in the presence of S, bacteria produce more lactic acid, which confirm the pH results. Other studies have reported similar findings of increased probiotic viability in yogurts with increased TTA levels and corresponding lower pH levels (Agil & Hosseini, 2012; Espirito Santo et al., 2010).

## 3.2. Antioxidant activity

### 3.2.1. ORAC

SC had higher antioxidant activity ( $P < 0.05$ ) compared to SP with ORAC values of  $138.95 \pm 0.99$   $\mu\text{mol TE}/100$  g of fruit and  $29.22 \pm 3.08$   $\mu\text{mol TE}/100$  g of fruit respectively (Table 4). As expected, SC showed a much higher antioxidant activity than SP. SC contained water soluble materials including proteins, flavonoids, and polysaccharides. S contains high levels of ascorbic acid; ranging from 360 to 2500 mg/100 g of berries compared to 35–56 mg/100 ml of orange juice as well as flavonoids or quercetin bound to carbohydrates such as glucose, fructose, and xylose (Bal, Meda, Naik, & Satya, 2011). These compounds are most certainly responsible for the antioxidant activity exhibited in SC extracts. Decreased antioxidant activity was observed in SP extracts, because of the purification step of dialysis. Compounds that were greater than 3500 Da were eliminated from the extraction. In addition, the enzymes  $\alpha$ -amylase and protease broke down proteins and carbohydrates conjugated to phenolic acids that are responsible for scavenging free radicals. Interestingly, polysaccharides in the purified solution showed some antioxidant activity, which may indicate that phenolic acids may be bound, such as gallic acid, a type of phenolic acid (Arimboor, Kumar, & Arumughan, 2008).

### 3.2.2. DPPH

The DPPH radical (60  $\mu\text{M}$ ) scavenging activity assay was used as an additional method to confirm antioxidant trends of seabuckthorn extracts (1 g/10 mL). SC clearly showed higher antioxidant activity ( $P < 0.05$ ) than SP, confirming ORAC results (Table 4). After 60 min, SC showed 37% DPPH scavenging activity, while SP showed 12%. These results are comparable with the literature that found DPPH radical (60  $\mu\text{M}$ ) scavenging activity after 60 min was 29.97% for seabuckthorn (1 g/15 mL) (Li et al., 2009). The antioxidant activity of this berry may be attributed to the high content of flavonoids (mainly isorhamnetin, quercetin glycosides, and kaempferol), which can be found in the amount of 100–1000 mg/100 g fruit (Uruakpa & Utioh, 2012). In another study, the anthocyanin composition and antioxidant activity of various berries were measured. The % DPPH scavenging activity of raspberry and strawberry was 46% and 25% respectively (Ogawa et al., 2008). Our findings were in close range with those above mentioned studies.

For accurate comparison among the measured antioxidant capacity of samples varies with the assay method used, pH and time of reaction and it is a function of the array of individual antioxidants present in the sample. Therefore, accurate comparison among fruit samples require that reaction times be standardized and more than one assay should be used to describe the total antioxidant activity of fruit samples (Ozgen, Reese, Tulio, Scheerens, & Miller, 2006).

## 4. Conclusion

This study indicates that S addition may selectively enhance probiotic counts in yogurt. S yogurts displayed decreased pH and

**Table 4**  
ORAC<sup>a</sup> and %DPPH<sup>b</sup> values of SC<sup>c</sup> and SP<sup>d</sup>.

Sample	ORAC ( $\mu\text{mol TE}/100$ g)	%DPPH
SC	$138.95 \pm 0.99^a$	$37 \pm 0.85^a$
SP	$29.22 \pm 3.08^b$	$12 \pm 0.98^b$

<sup>a</sup> Different letters in columns are significantly different ( $P < 0.05$ ) in Duncan's multiple range tests.

<sup>b</sup> ORAC = Oxygen radical absorbance capacity values was calculated as  $\mu\text{mole Trolox Equivalent (TE)}/100$  g of sample.

<sup>c</sup> %DPPH = 2,2-diphenyl-1-picrylhydrazyl radical.

<sup>d</sup> SC = seabuckthorn crude mucilage.

<sup>e</sup> SP = seabuckthorn purified mucilage.

increased TTA after 28 days of cold storage as well as SC showed significant antioxidant activity which is attributed to flavonoids present in solution. Further studies are needed like animal models and human clinical trials to determine the reputable health-related properties of S and additionally its use in yogurt. This study is novel in the field, because S has never been studied in a yogurt medium. S can potentially be a valuable addition in dairy products due to the promotion of probiotic bacteria. This study suggests that whole fruit or crude extract have potential to make/produce probiotic yogurt with antioxidant activity. Optimization for production of yogurt in larger scale can be done for future studies.

## Acknowledgments

Authors are grateful to Martin Trépanier at Horticulture Research Center (Laval University, Québec, Canada) for providing seabuckthorn samples.

## References

- Agil, R., & Hosseini, F. (2012). Dual functionality of triticale as a novel dietary source of prebiotics with antioxidant activity in fermented dairy products. *Plant Foods for Human Nutrition*, 67(1), 88–93.
- Arimboor, R., Kumar, K. S., & Arumugham, C. (2008). Simultaneous estimation of phenolic acids in sea buckthorn (*Hippophae rhamnoides*) using RP-HPLC with DAD [Research Support, Non-U.S. Gov't] *Journal of Pharmaceutical and Biomedical Analysis*, 47(1), 31–38. <http://dx.doi.org/10.1016/j.jpba.2007.11.045>.
- Bal, L. M., Meda, V., Naik, S. N., & Satya, S. (2011). Sea buckthorn berries: a potential source of valuable nutrients for nutraceuticals and cosmeceuticals. *Food Research International*, 44, 1718–1727.
- Behrad, S., Yusof, M. Y., Goh, K. L., & Baba, A. S. (2009). Manipulation of probiotics fermentation of yogurt by cinnamon and licorice: effects of yogurt formation and inhibition of *Helicobacter pylori* growth in vivo. *WASET*, 60, 590–594.
- Beveridge, T., Li, T. S., Oomah, B. D., & Smith, A. (1999). Sea buckthorn products: manufacture and composition. *Journal of Agricultural and Food Chemistry*, 47(9), 3480–3488.
- Champagne, C. P., & Gardner, N. J. (2008). The growth and recovery of an exopolysaccharide-producing *Lactobacillus rhamnosus* culture on growth media containing apple juice or molasses. *Journal of General and Applied Microbiology*, 54(4), 237–241.
- Dave, R. L., & Shah, N. P. (1997). Viability of yoghurt and probiotic bacteria in yoghurts made from commercial starter cultures. *International Dairy Journal*, 7(1), 31–41.
- Espírito Santo, A. P., Silva, R. C., Soares, F. A. S. M., Anjos, D., Gioielli, L. A., & Oliveira, M. N. (2010). Açai pulp addition improves fatty acid profile and probiotic viability in yoghurt. *International Dairy Journal*, 20, 415–422.
- Goncalves, M. M., Freitas, R., Nero, L. A., & Carvalho, A. F. (2009). Enumeration of starter cultures during yogurt production using Petrifilm AC plates associated with acidified MRS and M17 broths [Research Support, Non-U.S. Gov't] *Journal of Dairy Research*, 76(2), 229–233.
- Gunenc, A., Fang, S., & Hosseini, F. (2015). Raspberry and strawberry addition improves probiotic viability in yogurt and possess antioxidant activity. *Journal of Food Research*, 4(4), 47–58.
- Hosseini, F. S., Li, W., Hydamaka, A. W., Tsopmo, A., Lowry, L., Friel, J., et al. (2007). Proanthocyanidin profile and ORAC values of Manitoba berries, chokecherries, and seabuckthorn. *Journal of Agricultural and Food Chemistry*, 55(17), 6970–6976. <http://dx.doi.org/10.1021/jf071163a>.
- Huang, D., Ou, B., Hampsch-Woodill, M., Flanagan, J. A., & Prior, R. L. (2002). High-throughput assay of oxygen radical absorbance capacity (ORAC) using a multichannel liquid handling system coupled with a microplate fluorescence reader in 96-well format. *Journal of Agricultural and Food Chemistry*, 50(16), 4437–4444.
- Li, W., Hydamaka, A. W., Lowry, L., & Beta, T. (2009). Comparison of antioxidant capacity and phenolic compounds of berries, chokecherry and seabuckthorn. *Central European Journal of Biology*, 4, 499–506.
- Liazi, A., Palma, M., Brigui, J., & Barroso, C. G. (2007). Investigation on phenolic compounds stability during microwave-assisted extraction. *Journal of Chromatography A*, 1140, 29–34.
- E. Lundstedt, & E. A. Corbin Jr., Washington, DC, 4, 905, 1983, U.S. Patent & Trademark Office.
- Martini, M. C., Kukielka, D., & Savaiano, D. A. (1991). Lactose digestion from yogurt: influence of a meal and additional lactose. *The American Journal of Clinical Nutrition*, 53(5), 1253–1258.
- Mussatto, S. I., & Mancilha, I. M. (2007). Non-digestible oligosaccharides: a review. *Carbohydrate Polymers*, 68(3), 587–597.
- Ogawa, K., Sakakibara, H., Iwata, R., Ishii, T., Sato, T., Goda, T., et al. (2008). Anthocyanin composition and antioxidant activity of the crowberry (*Empetrum nigrum*) and other berries. *Journal of Agricultural and Food Chemistry*, 56(14), 4457–4462.
- Ozgen, M., Reese, R. N., Tulio, A. Z., Scheerens, J. C., & Miller, A. R. (2006). Modified 2,2'-azino-bis(3-ethylbenzothiazoline)-6-sulfonic acid (ABTS) method to measure antioxidant capacity of selected small fruits and comparison to ferric reducing antioxidant power (FRAP) and 2,2'-diphenyl-1-picrylhydrazyl (DPPH) methods. *Journal of Agricultural and Food Chemistry*, 54, 1151–1157.
- Roberfroid, M. B. (2007). Inulin-type fructans: functional food ingredients [Review] *Journal of Nutrition*, 137(11 Suppl.), 2493S–2502S.
- Santos, A., San Mauro, M., & Diaz, D. M. (2006). Prebiotics and their long-term influence on the microbial populations of the mouse bowel. *Food Microbiol*, 23(5), 498–503. <http://dx.doi.org/10.1016/j.fm.2005.07.004>.
- Schrezenmeier, J., & de Vrese, M. (2001). Probiotics, prebiotics, and synbiotics—approaching a definition [Review] *The American Journal of Clinical Nutrition*, 73(2 Suppl.), 361S–364S.
- Upadhyay, N. K., Kumar, M. S., & Gupta, A. (2010). Antioxidant, cytoprotective and antibacterial effects of Sea buckthorn (*Hippophae rhamnoides* L.) leaves [Research Support, Non-U.S. Gov't] *Food and Chemical Toxicology*, 48(12), 3443–3448. <http://dx.doi.org/10.1016/j.fct.2010.09.019>.
- Uruakpa, F. O., & Utioh, A. (2012). Seabuckthorn (*Hippophae rhamnoides* L.) and its products: a powerhouse of phytochemicals. In F. O. Uruakpa (Ed.), *Bioactive molecules in plant foods* (pp. 163–189). New York: Nova Science Publishers, Inc.
- Vasiljevic, T., & Shah, N. P. (2008). Probiotics—from Metchnikoff to bioactives. [Milestone achievements in dairy science research and their current and future industrial applications — Proceedings of a symposium marking the retirement of Professor Paul Jelen from active service at University of Alberta, Canada]. *International Dairy Journal*, 18(7), 714–728.
- Vinderola, C. G., Costa, G. A., Regenhart, S., & Reinheimer, J. A. (2002). Influence of compounds associated with fermented dairy products on the growth of lactic acid starter and probiotic bacteria. *International Dairy Journal*, 12(7), 579–589.
- Vinderola, C. G., & Reinheimer, J. A. (1999). Culture media for the enumeration of bifidobacterium bifidum and *Lactobacillus acidophilus* in the presence of yoghurt bacteria. *International Dairy Journal*, 9, 497–505.



## Effect of ultrasound treatment on physico-chemical, nutraceutical and microbial quality of strawberry



Adil Gani <sup>a,\*</sup>, Waqas N. Baba <sup>a,1</sup>, Mudasir Ahmad <sup>a</sup>, Umar Shah <sup>a</sup>, Asma Ashraf Khan <sup>a</sup>, Idrees Ahmed Wani <sup>a</sup>, F.A. Masoodi <sup>a</sup>, Asir Gani <sup>b</sup>

<sup>a</sup> Department of Food Science and Technology, University of Kashmir, Hazratbal, Srinagar, 190006, India

<sup>b</sup> Department of Food Technology, Faculty of Agro-Industry, Prince of Songkla University, Hat Yai, Songkhla, 90112, Thailand

### ARTICLE INFO

#### Article history:

Received 8 June 2015

Received in revised form

27 October 2015

Accepted 28 October 2015

Available online 2 November 2015

#### Keywords:

Minimal processing

Shelf-life

Antioxidant activity

Fruit quality

Microbial count

### ABSTRACT

Ultrasound (US) treatment (33 kHz, 60 W) was applied to freshly harvested strawberry for different time (0, 10, 20, 30, 40, 60, min) and analyzed for the storage period of 15 days at 4 °C. The pH, vitamin C, acidity & total soluble solids were better retained between 30 and 40 min, while as firmness and color of the fruit were found to be optimum between 20 and 30 min. At 40 min treatment time, the bacterial count decreased from 5.91 to 3.91 (Log<sub>10</sub> CFU g<sup>-1</sup>) and yeast and mold count decreased from 4.80 to 3.58 (Log<sub>10</sub> CFU g<sup>-1</sup>), while as the DPPH and ABTS % inhibition was increased by 14.41 and 8.53% from control, respectively on day 15. The 30–40 min US treated fruit was shelf stable for all the storage days. The higher exposure time (60 min) increased the microbial load, decreased antioxidant potential and changes the desirable quality of the fruit.

© 2015 Elsevier Ltd. All rights reserved.

### 1. Introduction

Strawberry is a highly perishable fruit and known for its nutritional and organoleptic properties. It is a rich source of vitamins, minerals and potent bioactive components such as flavonoids, anthocyanins etc. (Aaby, Skrede, & Wrolstad, 2005) and its quality is determined by sensory attributes such as flavor, texture and color, the soluble sugars, organic acids, pectin and anthocyanins are found to be responsible for these sensory attributes. Anthocyanins along with other phenolic compounds and secondary metabolites impart various health benefits such as effects on diabetic neuropathy (Anjaneyulu & Chopra, 2004), anti-inflammatory properties, antioxidant and anti-carcinogenic properties (Seeram, 2008; Zafra-Stone et al., 2007). However this fruit is quite delicate, its shelf-life is quite low and its survival is a challenging task which is further complicated by its susceptibility to fungal attacks and textural losses, for example *Grey mold rot* caused by *Botrytis cinerea* remains a major factor in limiting shelf-life of strawberries and causes up to 50% loss (Garcia, Aguilera, & Jimenez, 1996). However, the Shelf-life of strawberry can be extended to one week when

stored at low temperature, fungicides and chemical sanitizers can also be used but food safety concerns and environmental considerations limit their use (Lopez-Gomez et al., 2009). Consumer awareness about pesticide residues on foods, pathogen resistance, and nutritional losses through traditional methods of storage has increased the need to develop new methods to control postharvest diseases (Yang, Cao, Cai, & Zheng, 2011).

Researchers are now looking for the most promising and result-oriented novel techniques that can be used without causing any loss of the nutrients. In recent years, interest has been developed from thermal food preservation methods towards non-thermal technologies. Therefore, several non-thermal technologies have been introduced such as ultrasound (US), high hydrostatic pressure (HHP), high pressure homogenization (HPH), Ultraviolet (UV) and pulse electric field (PEF). The non thermal technologies can improve the quality and shelf-life of fruits and has become a potential alternative to the conventional methods (Rupasinghe & Yu, 2012). Among newer non thermal technologies, application of ultrasound is gaining considerable importance as it increases the microbial safety and prolongs the shelf-life particularly in heat sensitive foods. Ultra sound waves have the advantage of being eco-friendly and non-toxic unlike other techniques employed in food industry for enhancing shelf-life of fruits and vegetables (Kentish & Ashokkumar, 2011). Some research has been carried out on

\* Corresponding author.

E-mail address: [Adil.gani@gmail.com](mailto:Adil.gani@gmail.com) (A. Gani).

<sup>1</sup> The contribution of second author is similar to first author.

ultrasound application, on chemical and physical properties of strawberry (Cao et al., 2010). However its effect on antioxidant potential of the fruit has not been reported to the best of our knowledge. Thus study aims at studying the effect of ultrasound for different time periods on physico-chemical, microbial load and antioxidant potential of the fruit during a period of 15 days stored at 4 °C. This study was designed to suggest the most effective treatment that can retain the quality parameters and maximizes the shelf-life of the fruit.

## 2. Material and methods

### 2.1. Materials

All the chemicals and reagents used were of analytical grade and purchased from Sigma Aldrich and Hi-media laboratories.

### 2.2. Sample procurement and ultrasound treatment

Ripened strawberry (*chandler*, cultivar) were harvested from local farms of Kashmir province, India and transported within an hour to our lab. The average length and breadth of the cultivar was 4.2 cm and 3.6 cm, respectively. They were sorted to eliminate damaged and selected for color and then randomly divided according to treatment. Five hundred gram of fruit for each batch was directly immersed in a sonicator bath (Frequency 33 KHZ, Power 60 W, Jain scientific, India) and the treatment time (0, 10, 20, 30, 40 and 60 min) was varied for each batch. The surface of water (distilled) in the bath was kept at the same level during each experiment and temperature ( $25 \pm 1$  °C) of the water was kept constant using oven thermometer, whenever a slight change in the temperature was observed, fresh water was circulated to stabilize the temperature of ultrasound water bath at 25 °C. All fruits were then air-dried for approximately 20 min and then stored at 4 °C and were analyzed at an interval of 3-days for a period of 15 days from Day 1. On each experimental day, approximately 100 g of fruit was taken for analysis; some fruits were tested for color and firmness. The remaining sample (50–60 g approx.) was pulped, homogenized and centrifuged for 10 min at 5000 rpm and supernatant was collected and analyzed on the same day for measuring titratable acidity, pH, Vitamin C, total soluble solids and antioxidant activity of the fruit. The analysis was carried out in triplicates.

### 2.3. Physico-chemical analysis

#### 2.3.1. Total titratable acidity (TA) and pH

Titratable acidity (TA) was determined by titrating 20 mL strawberry pulp (supernatant) to pH 8.2 using 0.1 M NaOH and was calculated as reported by Guinness, Kravchuk, Nottingham, Arcy, and Gidley (2009). The pH was measured using HI 2215pH/ORP meter (Hanna Instruments Woonsocket RI USA).

#### 2.3.2. Total soluble solids & vitamin C

Total soluble solids (TSS) of the supernatant were determined at room temperature using a portable refractometer (Atago, Japan). Vitamin C content of the strawberries was measured using 2, 6-dichloro-indophenol titration as described by Jones and Hughes (1983). Fresh supernatant of pulp (10 mL) was mixed with 10 mL of 3% (V/V) metaphosphoric acid. The extract was made up to a volume of 100 mL and centrifuged at 3000 g for 15 min at 25 °C. The 10 mL supernatant was titrated against standard 2, 6-dichloro-indophenol, which had already been standardized against standard ascorbic acid and the results were expressed in mg/100 g fresh weight (FW).

#### 2.3.3. Color

Color of the whole Strawberry fruit was determined using Color Flex Spectrocolorimeter (Hunter Lab Colorimeter D-25, Hunter Associates Laboratory, Ruston, USA) after being standardized using Hunter Lab color standards and their Hunter L\*, a\* and b\* values were measured. The total color difference (TCD) parameter was considered for evaluation of color changes. This parameter quantifies the overall color difference of a given sample when compared to a reference being the index "0" indicative of reference untreated samples (0 min US treatment), according to the expression (DrLange, 1994)

$$\Delta E^* = [(a - a_0) + (b - b_0) + (L - L_0)]^{1/2} \quad (1)$$

### 2.4. Antioxidant activity

To prepare the fruit extracts, 2.5 g of fresh pulp was homogenized with 2.5 mL of 95% (V/V) cold ethanol and centrifuged at 10,000 rpm for 15 min, the 2.5 mL of 80% (V/V) cold ethanol was used to extract the residue. The supernatants were combined and the final volume made to 10 mL with ethanol. The ethanol extract was used for analysis of DPPH, ABTS and Total Phenols. All tests were performed in triplicate and means were calculated.

Total phenolic content was measured using Folin–Ciocalteu method described by Tezcan, Gultekin-Ozguven, Diken, Ozcelik, and Erim (2009). The final result was expressed as milligram of Gallic acid equivalents per 100 mg of Strawberry fresh weight.

DPPH (1, 1-dihpenyl-2-picrylhydrazyl) free radical scavenging activity was measured according to the method reported by Shah et al., (2015) with modifications. Briefly, 2.0 mL of 0.2 mM ethanolic DPPH solution was added in 2.0 mL juice sample. This mixture was placed in dark at room temperature for 30 min. The absorbance was determined with spectrophotometer (Hitachi) at 517 nm. The same procedure was revised for control by using ethanol instead of sample solution. Following equation was used to calculate the percent inhibition of DPPH.

$$\text{Inhibition (\%)} = (A_c - A_s/A_c) \times 100 \quad (2)$$

Where  $A_c$  is the absorbance of the control and  $A_s$  is the absorbance of the juice sample.

ABTS (2, 2'-azino-bis(3-ethylbenzthiazoline-6-sulfonic acid)) radical-scavenging assay was determined according to the method of Wang, Gan, Zhang, and Pan (2010) with slight modification. The radical-scavenging activity of the samples was expressed as scavenging capacity (SC %)

$$(\text{SC}) \% = [(A_{\text{control}} - A_{\text{test}})/A_{\text{control}}] \times 100 \quad (3)$$

Where,  $A_{\text{control}}$  is the absorbance of the control (ABTS<sup>•+</sup> solution without test sample) and  $A_{\text{test}}$  is the absorbance of the test sample (ABTS<sup>•+</sup> solution plus extract).

### 2.5. Firmness

The firmness of each ultrasound treated strawberry (0, 10, 20, 30, 40, 60 min) was carried out by the method of Alexandre, Brandao, and Silva (2012) with some modifications and it was measured using a TA.XT PLUS Texture Analyzer (Stable Micro Systems Ltd., UK) fitted with a cylinder plunger SMS-P/10 CYL Delrin probe (10 mm diameter). The whole strawberry samples were placed on heavy duty platform under the probe along the transversal axis. Tests were performed in a compression mode (1.5 mm/s velocity). Firmness of strawberries is recorded as the maximum

force in “g” observed during penetration of sample. Test was done in replicates of 20 and the average peak force is recorded as the firmness.

## 2.6. Microbiological analysis

The microbial population of the Strawberry juice sample was determined by the FDA's standard method mentioned in Bacteriological Analytical Manual (FDA, 2001). Total plate counts were determined by pour plate method using nutrient agar media and incubated for 24 h at 37 °C. Whereas, yeast and mold counts were determined using Potato Dextrose Agar media and incubated for 72 h at 28 °C. All the analysis was carried out in triplicates.

## 2.7. Stastical analysis

Analysis of variance (ANOVA) was carried out using Microsoft Excel software and Fishers least significant difference (LSD) test was used to describe means with 95% ( $p < 0.05$ ) confidence. All the tests were carried out in triplicates.

## 3. Results and discussions

### 3.1. Physico-chemical properties

#### 3.1.1. pH and titrable acidity

A significant increase in pH was seen in untreated as well as treated samples over 15 days (Table 1). On day 15, an increase of 13.84, 4.32, 3.20, 3.50, 2.93 & 13.88% was seen in samples for treatment times of 0, 10, 20, 30, 40 & 60 min respectively. Coinciding with increase in pH a decrease in total acidity was seen (Table 1) and the percentage decrease in TA showed the same pattern as that of pH. The decrease in acidity and increase in pH can be attributed to consumption of organic acids in fruit metabolism e.g. these acids may serve as substratum for respiration (Chitarra & Chitarra, 2005). The increase in pH after 60 min of ultrasound treatment may be due to interference in respiration by increased exposure of fruit to ultrasound. Jose et al., (2014) also reported the

same and concluded that ultrasound can cause deactivation of enzymes and hindered the process of decomposition of organic acids to sugars and can also interfered with the respiration process of the fruit.

#### 3.1.2. Total soluble solids (TSS) and vitamin C

Total soluble solids (TSS) represent the content of soluble sugars, organic acid and other minor constituents. During storage TSS of untreated as well as treated strawberry pulp was found to increase over a storage period of 15 days. On day 15, total soluble solids increased by 24.66, 21.43, 18.23, 17.07, 18.84 & 30.05% for US treatment of 0, 10, 20, 30, 40, & 60 min respectively. Over the storage period of 15 days greater increase in TSS values at 60 min of US treatment time can be attributed to cavitations that leads to disruption of cellular structure and formation of microscopic channels that increase dehydration (Fernandes, Gallao, & Rodrigues, 2009). Lower increase in TSS values as a result of US treatment can be attributed to decreased decomposition of organic acids and cell wall components due to decreased fruit metabolism. Aday, Temizkan, Buyukcan, and Caner (2013) also reported that with increase in power of US treatment a decrease in TSS of strawberry was seen.

Strawberry is a rich source of vitamin C, an important constituent in terms of health considerations. Vitamin C content decreased from 80.12 mg/100 g to 36.31 mg/100 g with storage in untreated samples. Thus a reduction of 54.68% in Vitamin C content was seen with storage for 15 days at refrigeration. Decrease in vitamin C content with storage was inversely proportional to treatment time. The decrease in vitamin C content was 36.68, 35.57, & 32.20% for treatment time of 10, 20, & 30 min of treatment times, respectively. However further increase in treatment time lead to a decrease in the retention of vitamin C (Table 1). Increased retention of vitamin C is due to ultrasound and ultraviolet treatment has also been reported already in strawberry (Alexandre et al., 2012), strawberry juice (Tiwari, O'Donnell, Patras, Brunton, & Cullen, 2009b), grape fruit juice (Aadil, Zeng, Han, & Sun, 2013) However the percentage decrease reported earlier varies which might be due to difference in cultivar and treatment parameters. Increase in

**Table 1**  
Physico-chemical properties of ultrasound treated strawberry.

	Treatment time (Min.)	Day 1	Day 3	Day 6	Day 9	Day 12	Day 15	
pH	0	3.36 <sup>aA</sup> ± 0.01	3.39 <sup>aB</sup> ± 0.01	3.42 <sup>aC</sup> ± 0.01	3.48 <sup>aD</sup> ± 0.01	3.52 <sup>aE</sup> ± 0.00	3.9 <sup>aF</sup> ± 0.01	
	10	3.32 <sup>bA</sup> ± 0.01	3.37 <sup>bB</sup> ± 0.01	3.39 <sup>bC</sup> ± 0.00	3.43 <sup>bD</sup> ± 0.02	3.45 <sup>bE</sup> ± 0.02	3.47 <sup>bF</sup> ± 0.01	
	20	3.32 <sup>bA</sup> ± 0.00	3.34 <sup>bB</sup> ± 0.00	3.36 <sup>bC</sup> ± 0.00	3.39 <sup>bD</sup> ± 0.01	3.41 <sup>bE</sup> ± 0.01	3.43 <sup>bF</sup> ± 0.00	
	30	3.30 <sup>bA</sup> ± 0.01	3.32 <sup>bB</sup> ± 0.02	3.33 <sup>bB</sup> ± 0.03	3.35 <sup>bC</sup> ± 0.01	3.37 <sup>bD</sup> ± 0.00	3.42 <sup>bE</sup> ± 0.01	
	40	3.31 <sup>bA</sup> ± 0.02	3.34 <sup>bB</sup> ± 0.01	3.36 <sup>bC</sup> ± 0.00	3.38 <sup>bD</sup> ± 0.00	3.40 <sup>bE</sup> ± 0.01	3.41 <sup>bE</sup> ± 0.02	
	60	3.35 <sup>aA</sup> ± 0.00	3.38 <sup>bB</sup> ± 0.01	3.43 <sup>bC</sup> ± 0.00	3.47 <sup>bD</sup> ± 0.01	3.53 <sup>bE</sup> ± 0.00	3.89 <sup>bF</sup> ± 0.02	
	TA (%)	0	0.69 <sup>aA</sup> ± 0.02	0.64 <sup>aB</sup> ± 0.02	0.60 <sup>aC</sup> ± 0.01	0.57 <sup>aD</sup> ± 0.01	0.55 <sup>aE</sup> ± 0.01	0.50 <sup>aF</sup> ± 0.02
TA (%)	10	0.73 <sup>bA</sup> ± 0.01	0.71 <sup>bB</sup> ± 0.01	0.69 <sup>bC</sup> ± 0.00	0.68 <sup>bC</sup> ± 0.01	0.65 <sup>bD</sup> ± 0.01	0.62 <sup>bE</sup> ± 0.02	
	20	0.73 <sup>bA</sup> ± 0.01	0.72 <sup>bB</sup> ± 0.01	0.70 <sup>bC</sup> ± 0.01	0.69 <sup>bD</sup> ± 0.00	0.67 <sup>bE</sup> ± 0.00	0.65 <sup>bF</sup> ± 0.01	
	30	0.74 <sup>bA</sup> ± 0.00	0.74 <sup>bA</sup> ± 0.00	0.72 <sup>bB</sup> ± 0.01	0.70 <sup>bC</sup> ± 0.01	0.69 <sup>bD</sup> ± 0.01	0.66 <sup>bE</sup> ± 0.01	
	40	0.72 <sup>bA</sup> ± 0.01	0.69 <sup>bA</sup> ± 0.01	0.68 <sup>bB</sup> ± 0.01	0.66 <sup>bC</sup> ± 0.00	0.64 <sup>bD</sup> ± 0.01	0.65 <sup>bE</sup> ± 0.02	
	60	0.65 <sup>bA</sup> ± 0.01	0.63 <sup>bB</sup> ± 0.00	0.60 <sup>bC</sup> ± 0.01	0.58 <sup>bD</sup> ± 0.01	0.55 <sup>bE</sup> ± 0.01	0.51 <sup>bF</sup> ± 0.01	
	TSS (%)	0	6.17 <sup>aA</sup> ± 0.02	6.65 <sup>aB</sup> ± 0.08	6.95 <sup>aC</sup> ± 0.02	7.25 <sup>aD</sup> ± 0.05	7.76 <sup>aE</sup> ± 0.05	8.19 <sup>aF</sup> ± 0.05
	TSS (%)	10	6.13 <sup>bA</sup> ± 0.05	6.39 <sup>bB</sup> ± 0.05	6.76 <sup>bC</sup> ± 0.05	6.92 <sup>bD</sup> ± 0.08	7.34 <sup>bE</sup> ± 0.05	7.79 <sup>bF</sup> ± 0.05
20		6.10 <sup>bA</sup> ± 0.09	6.30 <sup>bB</sup> ± 0.05	6.55 <sup>bC</sup> ± 0.08	6.73 <sup>bD</sup> ± 0.05	7.13 <sup>bE</sup> ± 0.08	7.46 <sup>bF</sup> ± 0.05	
30		6.07 <sup>bA</sup> ± 0.07	6.24 <sup>bB</sup> ± 0.08	6.33 <sup>bC</sup> ± 0.09	6.55 <sup>bD</sup> ± 0.05	6.84 <sup>bE</sup> ± 0.08	7.32 <sup>bF</sup> ± 0.05	
40		6.09 <sup>bA</sup> ± 0.005	6.27 <sup>bB</sup> ± 0.08	6.56 <sup>bC</sup> ± 0.08	6.89 <sup>bD</sup> ± 0.05	7.26 <sup>bE</sup> ± 0.05	7.43 <sup>bE</sup> ± 0.01	
60		6.56 <sup>bA</sup> ± 0.05	6.96 <sup>bB</sup> ± 0.08	7.32 <sup>bC</sup> ± 0.09	7.83 <sup>bD</sup> ± 0.05	8.24 <sup>bE</sup> ± 0.05	8.85 <sup>bF</sup> ± 0.01	
Vit. C (mg/100 g (FW))		0	80.12 <sup>aA</sup> ± 0.01	75.21 <sup>aB</sup> ± 0.01	64.21 <sup>aC</sup> ± 0.01	59.74 <sup>aD</sup> ± 0.01	43.21 <sup>aE</sup> ± 0.01	36.31 <sup>aE</sup> ± 0.01
Vit. C (mg/100 g (FW))		10	85.78 <sup>bA</sup> ± 0.00	79.61 <sup>bB</sup> ± 0.01	69.43 <sup>bC</sup> ± 0.00	65.31 <sup>bD</sup> ± 0.01	62.21 <sup>bE</sup> ± 0.00	54.31 <sup>bE</sup> ± 0.00
	20	86.21 <sup>bA</sup> ± 0.01	79.63 <sup>bB</sup> ± 0.01	70.56 <sup>bC</sup> ± 0.01	66.79 <sup>bD</sup> ± 0.00	63.21 <sup>bE</sup> ± 0.01	55.54 <sup>bE</sup> ± 0.01	
	30	85.32 <sup>bA</sup> ± 0.01	77.45 <sup>bB</sup> ± 0.01	71.56 <sup>bC</sup> ± 0.01	65.59 <sup>bD</sup> ± 0.01	62.2 <sup>bE</sup> ± 0.01	57.84 <sup>bE</sup> ± 0.00	
	40	82.45 <sup>bA</sup> ± 0.00	82.23 <sup>bB</sup> ± 0.01	80.13 <sup>bC</sup> ± 0.00	75.51 <sup>bD</sup> ± 0.00	70.01 <sup>bE</sup> ± 0.00	49.31 <sup>bE</sup> ± 0.01	
	60	78.54 <sup>bA</sup> ± 0.01	72.12 <sup>bB</sup> ± 0.01	62.61 <sup>bC</sup> ± 0.01	57.31 <sup>bD</sup> ± 0.01	45.45 <sup>bE</sup> ± 0.01	34.03 <sup>bE</sup> ± 0.01	

Values are mean ± standard deviations of three (n = 3) measurements with different small and capital superscripts in a column and a row vary significantly ( $p \leq 0.05$ ). TSS (Total soluble solids), TA (Titrable acidity), FW (Fresh Weight).

retention of vitamin C has also been reported in ultrasonicated orange juice than thermally processed juice samples and ultrasonicated grape fruit juice. Increase in retention of vitamin C content can be attributed to evacuation of entrapped oxygen due to cavitation (Tiwari et al. 2009b) or due to fruit enzyme inactivation that can cause reduction in vitamin C content as reviewed by Jose et al. (2014). However during prolonged US treatment time (60 min), retention of vitamin C content decreased which might be due to degradation of vitamin C due to excessive formation of OH<sup>•</sup> by cavitation (Lee & Feng, 2011).

### 3.1.3. Color

Color of strawberry is due to presence of anthocyanins primarily. The US treatment resulted in better retention of color during storage of strawberry samples (Table 2), however the 60 min treatment did not result in better color retention during storage. Similar, results were reported by Alexandre et al. (2012). Value of  $\Delta E^*$  increased by 4.61%, 5.25, 6.16, 7.94 and 11.29% for treatment times 10, 20, 30, 40 and 60 in comparison to the untreated sample on day 1. This change in color can be attributed to anthocyanin degradation due to cavitations as a result of increase in treatment time (Tiwari, O'Donnell, & Cullen, 2009a). Anthocyanin degradation was also reported by Tiwari, O'Donnell, Patras, and Cullen (2008), with increase in amplitude of US treatment in fruit juices. During storage period (15 days), a percentage increase of 23.30, 10.25, 7.35, 13.64, 17.29, 16.60 was seen in  $\Delta E^*$  for 0, 10, 20, 30, 40, 60 min of treatment time respectively. Over different treatment times minimum change in TCD and hence maximum color retention was seen at 10–30 min over a period of 15 days.

$L^*$  and  $a^*$  values of both untreated as well as treated strawberry samples were significantly affected during the storage period of 15 days (Table 2).

$L^*$  value significantly decreased in all the samples suggesting darkening of the product. Zavala, Wang, Wang & Aguilar (2004) found similar trend in  $L$  values of strawberry during storage at different temperatures. However, the decrease in  $L^*$  value was seen more in untreated samples (39.12%) in comparison to the treated samples. As US treatment time increased, the percentage decrease in  $L^*$  value of samples was least in 30 min (11.89%) and 40 min (11.87%) treated samples and further increase in treatment time to 60 min resulted in greater decrease (31.93%) in  $L^*$  value after the storage period of 15 days. This suggests 30–40 min US treatment

time (33 W) as most suitable for better retention of  $L$  value in strawberry. Aday et al. (2013) also reported a similar trend of better retention of  $L$  values due to US treatment at 30 W in comparison to untreated samples.

A significant increase in  $a$  values (+redness) was seen in untreated as well as treated samples upto day 12 of storage followed by a significant decrease. This increase in  $a$ -value can be due to increase in anthocyanin content during storage due to fruit metabolism. Cordenunsi and Genovese (2005) reported an increase in the anthocyanin content of three different strawberry cultivars during storage. Similarly, Tiwari et al., (2009b) reported a slight increase in the anthocyanin content of strawberry juice at lower amplitude levels and treatment times as a result of extraction of bound anthocyanins from the suspended pulp. Our results are also in accordance with Birmpa, Sfika, and Vantakar (2013), who reported that 30 W/L ultrasonication of fresh vegetables, retained bright color for treatments of 10, 20 and 30 min. Treatment time significantly affected  $a$ -value that decreased non-significantly at 10 and 20 min, followed by a significant increase at 30 and 40 min of treatment time. This increase can be due to greater release of glucosidically bound anthocyanins from sugars (Galoburda, Boc, Krupskis, & Seglina, 2014) due to this specific time and power combination of US. A Further increase in treatment time (60 min) lead to a significant decrease in ' $a$ ' value. This decrease might be due to increased degradation of anthocyanin content due to cavitation induced by US treatment with increase in treatment time (Tiwari et al., 2008).

### 3.2. Antioxidant properties

#### 3.2.1. Total phenolic content, DPPH and ABTS assays

Ultrasound treatment resulted in an increase in the total phenolic content of the samples on Day 1 as showed in Table 3. As the US treatment time increased from 0 to 40 min a significant increase (1.39–1.50 mg GAE/100 g of sample) in TPC content was seen. This was followed by a decrease (1.28 mg GAE/100 g of sample) when the treatment time was 60 min on day 1. Hence, the maximum increase in TPC (7.9%) was found in the sample, when treated with US for 40 min. Earlier, Vilkuh, Mawson, Simons, and Bates (2008) has reported an increase of 6–35% due to US treatment than conventional processing. Thus higher values of TPC can be attributed to better extraction of polyphenols at 40 min

**Table 2**  
Color analysis of US treated strawberry fruit stored for a period of 15 days at 4 °C.

		Day 1	Day 3	Day 6	Day 9	Day 12	Day 15
$L^*$	0 min	35.03 <sup>bf</sup> ± 0.41	34.86 <sup>be</sup> ± 0.21	31.18 <sup>bd</sup> ± 0.21	29.18 <sup>bc</sup> ± 0.11	27.18 <sup>bb</sup> ± 0.13	25.18 <sup>aa</sup> ± 0.16
	10 min	34.93 <sup>bd</sup> ± 0.21	34.27 <sup>bc</sup> ± 0.08	31.82 <sup>be</sup> ± 0.34	31.42 <sup>bb</sup> ± 0.21	30.62 <sup>ca</sup> ± 0.11	30.12 <sup>ba</sup> ± 0.22
	20 min	34.98 <sup>bc</sup> ± 0.11	34.21 <sup>bc</sup> ± 0.23	32.26 <sup>cb</sup> ± 0.22	31.56 <sup>bba</sup> ± 0.09	31.16 <sup>ca</sup> ± 0.12	31.02 <sup>ca</sup> ± 0.16
	30 min	35.11 <sup>be</sup> ± 0.17	34.47 <sup>bd</sup> ± 0.17	33.88 <sup>dc</sup> ± 0.27	32.98 <sup>bcb</sup> ± 0.22	32.26 <sup>db</sup> ± 0.08	31.37 <sup>ca</sup> ± 0.22
	40 min	35.15 <sup>be</sup> ± 0.22	34.58 <sup>bd</sup> ± 0.14	34.24 <sup>dd</sup> ± 0.14	33.64 <sup>cc</sup> ± 0.16	32.74 <sup>db</sup> ± 0.24	31.42 <sup>ca</sup> ± 0.23
	60 min	33.14 <sup>ad</sup> ± 0.20	31.94 <sup>ad</sup> ± 0.10	29.05 <sup>ac</sup> ± 0.17	27.85 <sup>ab</sup> ± 0.21	26.35 <sup>ab</sup> ± 0.19	25.12 <sup>aa</sup> ± 0.13
$a^*$	0 min	51.74 <sup>ca</sup> ± 0.13	51.95 <sup>ba</sup> ± 0.16	52.15 <sup>ba</sup> ± 0.12	53.35 <sup>bb</sup> ± 0.09	54.45 <sup>bc</sup> ± 0.13	53.56 <sup>bb</sup> ± 0.19
	10 min	51.95 <sup>ca</sup> ± 0.21	52.04 <sup>ba</sup> ± 0.27	52.88 <sup>bca</sup> ± 0.25	53.22 <sup>bb</sup> ± 0.25	55.56 <sup>cc</sup> ± 0.21	54.06 <sup>bb</sup> ± 0.17
	20 min	51.58 <sup>ca</sup> ± 0.17	52.45 <sup>cb</sup> ± 0.17	53.93 <sup>cdc</sup> ± 0.15	54.32 <sup>cc</sup> ± 0.12	55.19 <sup>cd</sup> ± 0.09	54.69 <sup>bcc</sup> ± 0.21
	30 min	50.72 <sup>ba</sup> ± 0.26	52.89 <sup>cb</sup> ± 0.25	53.44 <sup>cc</sup> ± 0.28	54.29 <sup>cc</sup> ± 0.16	56.14 <sup>dd</sup> ± 0.17	55.64 <sup>cdd</sup> ± 0.11
	40 min	50.59 <sup>ba</sup> ± 0.23	52.02 <sup>be</sup> ± 0.26	53.22 <sup>cc</sup> ± 0.16	54.72 <sup>cd</sup> ± 0.09	55.47 <sup>de</sup> ± 0.11	53.97 <sup>bc</sup> ± 0.16
	60 min	47.39 <sup>aa</sup> ± 0.16	49.06 <sup>abc</sup> ± 0.27	49.56 <sup>ac</sup> ± 0.31	49.01 <sup>abc</sup> ± 0.25	48.86 <sup>ab</sup> ± 0.23	48.41 <sup>ab</sup> ± 0.11
$\Delta E^*$	0 min	65.37 <sup>aa</sup> ± 0.09	67.49 <sup>ab</sup> ± 0.14	72.46 <sup>bc</sup> ± 0.12	74.74 <sup>cd</sup> ± 0.19	79.22 <sup>de</sup> ± 0.14	82.20 <sup>ef</sup> ± 0.23
	10 min	67.41 <sup>ba</sup> ± 0.19	67.57 <sup>ab</sup> ± 0.35	68.77 <sup>ab</sup> ± 0.28	70.11 <sup>bc</sup> ± 0.21	72.00 <sup>ad</sup> ± 0.07	74.30 <sup>be</sup> ± 0.19
	20 min	67.41 <sup>ba</sup> ± 0.19	67.67 <sup>ab</sup> ± 0.17	68.84 <sup>ab</sup> ± 0.26	69.18 <sup>abc</sup> ± 0.26	72.02 <sup>ac</sup> ± 0.29	73.13 <sup>bd</sup> ± 0.13
	30 min	68.46 <sup>ca</sup> ± 0.18	70.91 <sup>bb</sup> ± 0.09	72.09 <sup>bc</sup> ± 0.17	75.38 <sup>cd</sup> ± 0.23	77.71 <sup>be</sup> ± 0.31	78.78 <sup>df</sup> ± 0.16
	40 min	69.47 <sup>da</sup> ± 0.16	73.84 <sup>cb</sup> ± 0.11	75.61 <sup>cc</sup> ± 0.09	76.95 <sup>de</sup> ± 0.24	81.52 <sup>ef</sup> ± 0.18	84.39 <sup>ef</sup> ± 0.11
	60 min	72.52 <sup>ea</sup> ± 0.19	74.78 <sup>da</sup> ± 0.16	76.30 <sup>db</sup> ± 0.26	79.62 <sup>ec</sup> ± 0.16	83.94 <sup>dd</sup> ± 0.11	86.36 <sup>fe</sup> ± 0.24

Values are mean ± standard deviations of three (n = 3) measurements with different small and capital superscripts in a column and a row vary significantly (p ≤ 0.05).  $\Delta E^*$  represents total color difference.

**Table 3**  
Antioxidant activity of US treated strawberry fruit.

	US treatment (Min.)	Day 1	Day 3	Day 6	Day 9	Day 12	Day 15
DPPH (% inhibition)	0	21.75 <sup>aA</sup> ± 1.2	25.34 <sup>aB</sup> ± 1.2	26.34 <sup>aC</sup> ± 1.3	30.46 <sup>aD</sup> ± 1.1	33.53 <sup>aE</sup> ± 1.3	32.32 <sup>aF</sup> ± 1.2
	10	26.84 <sup>bA</sup> ± 1.1	30.08 <sup>bB</sup> ± 1.3	33.43 <sup>bC</sup> ± 1.2	37.26 <sup>bD</sup> ± 1.2	38.82 <sup>bE</sup> ± 1.2	33.36 <sup>bF</sup> ± 1.1
	20	32.09 <sup>cA</sup> ± 1.2	35.58 <sup>cB</sup> ± 1.2	36.67 <sup>cC</sup> ± 1.1	39.86 <sup>cD</sup> ± 1.1	40.43 <sup>cE</sup> ± 1.3	35.78 <sup>cF</sup> ± 1.1
	30	37.98 <sup>dA</sup> ± 1.1	41.23 <sup>dB</sup> ± 1.1	45.37 <sup>dC</sup> ± 1.1	49.03 <sup>dD</sup> ± 1.2	49.63 <sup>dE</sup> ± 1.1	42.03 <sup>dF</sup> ± 1.2
	40	42.35 <sup>eA</sup> ± 1.1	46.87 <sup>eB</sup> ± 1.2	49.39 <sup>eC</sup> ± 1.2	53.92 <sup>eD</sup> ± 1.1	54.06 <sup>eE</sup> ± 1.1	46.73 <sup>eF</sup> ± 1.1
	60	24.92 <sup>fA</sup> ± 1.2	27.46 <sup>fA</sup> ± 1.1	29.70 <sup>fB</sup> ± 1.1	31.48 <sup>fC</sup> ± 1.1	32.18 <sup>fC</sup> ± 1.2	30.26 <sup>fD</sup> ± 1.3
TPC (mg GAE/100 mg of sample)	0	1.39 <sup>aA</sup> ± 0.01	1.39 <sup>aA</sup> ± 0.01	1.42 <sup>aB</sup> ± 0.01	1.45 <sup>aC</sup> ± 0.01	1.45 <sup>aC</sup> ± 0.01	1.42 <sup>aB</sup> ± 0.01
	10	1.44 <sup>bA</sup> ± 0.01	1.46 <sup>bB</sup> ± 0.01	1.45 <sup>bB</sup> ± 0.01	1.47 <sup>bC</sup> ± 0.01	1.45 <sup>bB</sup> ± 0.01	1.46 <sup>bB</sup> ± 0.01
	20	1.46 <sup>cA</sup> ± 0.01	1.48 <sup>bB</sup> ± 0.01	1.50 <sup>cC</sup> ± 0.01	1.53 <sup>cD</sup> ± 0.01	1.50 <sup>cC</sup> ± 0.02	1.48 <sup>cB</sup> ± 0.01
	30	1.48 <sup>cA</sup> ± 0.01	1.50 <sup>cB</sup> ± 0.01	1.51 <sup>cB</sup> ± 0.01	1.53 <sup>cC</sup> ± 0.01	1.51 <sup>cB</sup> ± 0.01	1.48 <sup>cA</sup> ± 0.01
	40	1.50 <sup>dA</sup> ± 0.01	1.52 <sup>dB</sup> ± 0.01	1.53 <sup>dC</sup> ± 0.01	1.53 <sup>cC</sup> ± 0.01	1.56 <sup>dD</sup> ± 0.01	1.52 <sup>dB</sup> ± 0.01
	60	1.28 <sup>eB</sup> ± 0.01	1.30 <sup>eD</sup> ± 0.00	1.29 <sup>eC</sup> ± 0.00	1.30 <sup>dD</sup> ± 0.00	1.28 <sup>eB</sup> ± 0.01	1.22 <sup>eA</sup> ± 0.01
ABTS (%Scavenging Capacity)	0	9.38 <sup>aA</sup> ± 1.05	11.21 <sup>aB</sup> ± 1.05	13.19 <sup>aC</sup> ± 1.05	15.01 <sup>aD</sup> ± 1.05	16.94 <sup>aE</sup> ± 1.05	16.14 <sup>aF</sup> ± 1.05
	10	13.73 <sup>bA</sup> ± 1.05	19.49 <sup>bB</sup> ± 1.05	17.15 <sup>bC</sup> ± 1.05	18.84 <sup>bD</sup> ± 1.05	19.79 <sup>bE</sup> ± 1.05	17.83 <sup>bF</sup> ± 1.05
	20	16.14 <sup>cA</sup> ± 1.05	17.92 <sup>cB</sup> ± 1.05	19.14 <sup>cC</sup> ± 1.05	20.29 <sup>cD</sup> ± 1.05	19.98 <sup>cE</sup> ± 1.05	16.48 <sup>cF</sup> ± 1.05
	30	19.21 <sup>dA</sup> ± 1.04	20.35 <sup>dB</sup> ± 1.05	22.81 <sup>dC</sup> ± 1.05	25.01 <sup>dD</sup> ± 1.05	24.47 <sup>dE</sup> ± 1.05	21.79 <sup>dF</sup> ± 1.05
	40	23.19 <sup>eA</sup> ± 1.05	24.63 <sup>eB</sup> ± 1.05	27.25 <sup>eC</sup> ± 1.05	27.92 <sup>eD</sup> ± 1.05	29.22 <sup>eE</sup> ± 1.05	24.67 <sup>eF</sup> ± 1.05
	60	11.39 <sup>fA</sup> ± 1.05	12.92 <sup>fA</sup> ± 1.08	14.51 <sup>fB</sup> ± 1.05	17.95 <sup>fC</sup> ± 1.05	18.27 <sup>fC</sup> ± 1.05	15.88 <sup>fD</sup> ± 1.05

Values are mean ± standard deviations of three (n = 3) measurements with different small and capital superscripts in a column and a row vary significantly (p ≤ 0.05).

treatment time and a frequency of 33 KHz and 60 W powers due to greater disruption of cell wall material. An increase in phenolic content can also be attributed to hydroxylation of flavanols which will have a positive effect on antioxidant activity (Soria & Villamiel, 2010). Increase in total phenolic content of *kasturi* juice as result of sonication (25 kHz) has also been reported by Bhat, Kamaruddin, Min-Tze, and Karim (2011). Increase in TPC with increase in extraction time has also been reported in hemp, flax and canola seeds upto 20 min at 200 W followed by a decrease with further increase in extraction time (The and Birch, 2014). Golmohamadi, Moller, Powers, and Nindo (2013) reported an increase in TPC in red raspberry by increasing ultrasound power (20–1000 kHz). This increase in TPC was attributed to increase in temperature that would have facilitated release of bioactive components into the extraction solvent. Also cavitation or sonolysis leads to breakdown of cell wall and hence greater release of polyphenolic compounds into the extract. Thus a synergistic effect of sonication with time and temperature increased the extractability of total phenols.

Total phenolic content increased in both untreated as well as treated (except 60 Min.) samples with a storage time of 15 days at 4 °C (Table 3). Increase in TPC was also reported by Zavala, Wang, Wang, and Aguilar (2004) in untreated strawberry stored at 0 °C and 5 °C storage temperatures. Main phenolic compounds found in strawberry include anthocyanins, flavanols, ellagic acid and its derivatives (Sun, Liu, Yang, Slovin, & Chen, 2014). The biosynthetic pathway for anthocyanin is still operative after strawberry harvest, and storage at low temperatures does not inhibit this process (Holcroft & Kader, 1999) and the major portion of phenolic compounds in strawberry are proanthocyanidins and anthocyanins (Pallauf, Rivas-Gonzalo, Del-Castillo, Cano, & De-Pascual-Teres, 2008) and hence TPC increases. This increase was seen up to day 12 and after that TPC values decreased (Table 3). However in

samples treated for 60 min, TPC values decreased and can be due to excessive cavitation and cell disruption leading to degradation of polyphenolic compounds (Jahouach-Rabai et al., 2008).

Antioxidant activity of US treated samples increased with increase in treatment time. Both DPPH as well as ABTS showed a similar pattern. An abrupt increase was seen at 10 min treatment which was followed by a mild, but significant increase (Maximum value at 40 min) with further increase in treatment time. Higher antioxidant values than control were seen in raspberry up to 30 min of ultrasound treatment (Golmohamadi et al., 2013). Increased antioxidant activity can be attributed to higher TPC content in US treated samples due to release of bound phenolics. A positive correlation was seen between the antioxidants by DPPH & ABTS and total phenols at 30 min treatment time (r = 0.846 and r = 0.816). It has also been suggested that due to generation of hydroxyl radicals hydroxylation of food materials is increased which can increase its antioxidant activity (Ashokkumar et al., 2008). However a treatment time of 60 min showed detrimental effect on antioxidant activity which might be due to excessive damage to cell structure leading to greater chances of oxidation as well as degradation of polyphenolic compounds.

### 3.3. Fruit firmness

Fruit firmness is an important food quality attribute and a parameter, related to the cell wall strength and intercellular adhesion (Toivonen and Brummell, 2008). Fruit firmness was better retained throughout all refrigerated storage if samples had been previously sonicated (Table 4). However the untreated sample lost its firmness consistently, and by the last day of refrigerated storage only 53.77% of fruit firmness was retained. The loss of firmness, however, is most often attributed to the enzymatic breakdown of

**Table 4**  
Texture analysis of US treated strawberry fruit for a period of 15 days at 4 °C.

	Day 1	Day 3	Day 6	Day 9	Day 12	Day 15
0 min	763 <sup>aF</sup> ± 2.1	731 <sup>aE</sup> ± 3.12	687 <sup>aD</sup> ± 3.2	621 <sup>aC</sup> ± 4.8	525 <sup>aB</sup> ± 3.2	414 <sup>aA</sup> ± 5.2
10 min	762 <sup>bF</sup> ± 3.9	741 <sup>bE</sup> ± 4.1	715 <sup>bD</sup> ± 5.6	680 <sup>bC</sup> ± 2.3	615 <sup>bB</sup> ± 4.5	511 <sup>bA</sup> ± 3.5
20 min	771 <sup>dF</sup> ± 2.9	752 <sup>dE</sup> ± 4.8	731 <sup>dD</sup> ± 3.2	710 <sup>dC</sup> ± 3.5	671 <sup>eB</sup> ± 2.1	619 <sup>eA</sup> ± 4.5
30 min	772 <sup>dF</sup> ± 2.0	750 <sup>dE</sup> ± 3.9	730 <sup>dD</sup> ± 2.8	709 <sup>dC</sup> ± 3.6	672 <sup>eB</sup> ± 3.2	620 <sup>eA</sup> ± 4.1
40 min	769 <sup>cdF</sup> ± 1.6	749 <sup>ce</sup> ± 3.1	730 <sup>cdD</sup> ± 3.1	707 <sup>dc</sup> ± 2.1	667 <sup>dB</sup> ± 2.2	585 <sup>dA</sup> ± 2.5
60 min	768 <sup>cf</sup> ± 1.2	748 <sup>ce</sup> ± 2.1	723 <sup>cd</sup> ± 1.8	698 <sup>cc</sup> ± 1.5	663 <sup>cb</sup> ± 1.8	555 <sup>ca</sup> ± 3.5

Values are mean ± standard deviations of three (n = 3) measurements with different small and capital superscripts in a column and a row vary significantly (p ≤ 0.05).

**Table 5**  
Microbial analysis of US treated strawberry fruit stored for a period for 15 days 4 °C.

Microbiology	Treatment	Day1	Day3	Day6	Day 9	Day 12	Day 15
Bacterial (Log <sub>10</sub> CFU g <sup>-1</sup> )	0	3.60 <sup>aA</sup> ± 0.11	4.1 <sup>ab</sup> ± 0.08	4.5 <sup>aC</sup> ± 0.11	5.14 <sup>ad</sup> ± 0.13	5.56 <sup>ae</sup> ± 0.15	5.91 <sup>af</sup> ± 0.01
	10	3.01 <sup>bA</sup> ± 0.16	3.41 <sup>bb</sup> ± 0.27	3.81 <sup>bc</sup> ± 0.13	4.21 <sup>bd</sup> ± 0.07	4.81 <sup>be</sup> ± 0.05	5.14 <sup>cf</sup> ± 0.11
	20	2.61 <sup>cA</sup> ± 0.08	2.90 <sup>cb</sup> ± 0.09	3.21 <sup>cc</sup> ± 0.03	3.34 <sup>cd</sup> ± 0.02	4.12 <sup>de</sup> ± 0.11	4.42 <sup>df</sup> ± 0.06
	30	2.32 <sup>dA</sup> ± 0.02	2.65 <sup>db</sup> ± 0.07	3.01 <sup>dc</sup> ± 0.09	3.24 <sup>dd</sup> ± 0.05	3.82 <sup>ee</sup> ± 0.02	4.13 <sup>ef</sup> ± 0.01
	40	2.14 <sup>eA</sup> ± 0.01	2.42 <sup>eb</sup> ± 0.03	2.90 <sup>ec</sup> ± 0.03	3.11 <sup>ed</sup> ± 0.02	3.62 <sup>fe</sup> ± 0.01	3.91 <sup>ff</sup> ± 0.02
	60	2.01 <sup>fA</sup> ± 0.02	2.72 <sup>db</sup> ± 0.04	3.21 <sup>cc</sup> ± 0.02	3.94 <sup>cd</sup> ± 0.01	4.72 <sup>ce</sup> ± 0.06	5.32 <sup>bf</sup> ± 0.01
Yeast and mold (Log <sub>10</sub> CFU g <sup>-1</sup> )	0	3.52 <sup>aA</sup> ± 0.01	4.20 <sup>ab</sup> ± 0.03	3.46 <sup>aC</sup> ± 0.01	3.71 <sup>ad</sup> ± 0.01	4.64 <sup>ae</sup> ± 0.02	4.80 <sup>af</sup> ± 0.03
	10	2.91 <sup>bA</sup> ± 0.02	4.09 <sup>bb</sup> ± 0.01	3.35 <sup>bc</sup> ± 0.01	3.62 <sup>cd</sup> ± 0.03	3.92 <sup>ce</sup> ± 0.02	4.11 <sup>cf</sup> ± 0.01
	20	2.41 <sup>cA</sup> ± 0.03	2.61 <sup>cb</sup> ± 0.05	2.94 <sup>dc</sup> ± 0.02	3.43 <sup>dd</sup> ± 0.04	3.41 <sup>de</sup> ± 0.06	3.83 <sup>df</sup> ± 0.01
	30	2.26 <sup>dA</sup> ± 0.02	2.43 <sup>db</sup> ± 0.01	2.51 <sup>ec</sup> ± 0.01	3.04 <sup>ed</sup> ± 0.01	3.32 <sup>ee</sup> ± 0.01	3.67 <sup>ef</sup> ± 0.02
	40	2.24 <sup>dA</sup> ± 0.03	2.35 <sup>eb</sup> ± 0.02	2.42 <sup>fc</sup> ± 0.04	2.73 <sup>fd</sup> ± 0.06	3.03 <sup>fe</sup> ± 0.01	3.58 <sup>ff</sup> ± 0.03
	60	2.04 <sup>eA</sup> ± 0.05	2.65 <sup>cb</sup> ± 0.01	3.19 <sup>cc</sup> ± 0.03	3.59 <sup>bd</sup> ± 0.01	4.04 <sup>be</sup> ± 0.02	4.31 <sup>bf</sup> ± 0.02

Values are mean ± standard deviations of three (n = 3) measurements with different small and capital superscripts in a column and a row vary significantly (p ≤ 0.05).

the middle lamella and cell wall by pectinmethylesterase, polygalacturonase, b-galactosidase and cellulase (Ketsa and Daengkanit, 1999), the retention of texture in US treated samples could be attributed due to the inactivation of enzymes by US. Ultrasound induced various mechanical and chemical effects such as disruption of hydrogen bonding and van der Waals interactions in polypeptide chains, leading to alterations of the secondary and tertiary structures of the protein and the biological activities of enzymes are lost by these modifications (Mason, Riera, Vercet, & Lopez-Buesa, 2005; Manas, Munoz, Sanz, & Condon, 2006; Rawson, Tiwari, Tuohy, O'Donnell, & Brunton, 2011). The 20–30 min US treated samples showed maximum retention of firmness, while the minimum values were obtained at 0, 10, 40 and 60 min treatment time. The observed decrease of firmness at 40 and 60 min of sonication could be attributed to the destructive effect of prolonged exposure of ultrasound on stability of cell wall which results in cell injury and loss of water (Aday et al., 2013; Gabaldon-Leyva et al., 2007).

#### 3.4. Microbial analysis

The ultrasound treatment reduces the microbial load, due to the cavitations that damages the biological species by increasing localized temperature and pressure of the product. This creates shock waves and hydroxyl radicals, which ultimately enhances biocidal effect (Abid et al., 2013). The effect of ultrasound treatment to strawberry samples on the total plate count of bacteria, yeast and mold growth are mentioned in Table 5. The increase in US treatment time of strawberries decreased the microbial load significantly (p < 0.05) from 3.60 ± 0.11–2.01 ± 0.02 for bacteria and 3.52 ± 0.01–2.04 ± 0.05 for yeast & mold on day 1, almost similar type of results are also found by (Birmpa et al., 2013) in case of lettuce and strawberries, when Treated with UV (ultraviolet) and US. After storage of all treated samples at 4 °C for the period of 15 days, the microbial load varied significantly (p < 0.05) and the lowest Total plate count (log CFU/ml) for bacteria (3.91 ± 0.02) and yeast & mold (3.58 ± 0.03) was observed in 40 (min) US treatments. The prolonged ultrasound exposure of samples did not help in extending the shelf-life of the fruit as the results showed comparatively higher microbial load as compared to less treatment time of US; the prolonged treatment time may have caused injuries to the sample (Gabaldon-Leyva et al., 2007) that permits easy penetration of microbes deep inside the fruit and consequently showed higher microbial load.

#### 4. Conclusion

The present study indicates that application of ultrasound

waves (33 kHz) on strawberry. The ultrasound treatment helped in better retention of physicochemical parameters like TSS, titratable acidity, pH and color of the sample during its storage period for 15 days at refrigerated temperature. The treatment not only maintained the firmness of the fruit, but also enhanced antioxidant activity and reduced the microbial load. All the parameters studied were found to be commercially more acceptable when the treatment time was limited to 30–40 min. The 30–40 min treatment time extended the shelf-life up to 15 days, where 0, 10 & 60 and 20 min of US treatment limited the shelf-life up to 6, 9 and 12 days, respectively. The higher treatment time showed detrimental effect on all the parameters. It was concluded that ultrasonic waves can be used as a minimal processing technique to enhance the shelf-life and consumer acceptability of perishable fruits. The future work should be carried out to explore its application on other perishable industrial crops and food products.

#### Acknowledgments

The authors are highly thankful to Department of Biotechnology, Ministry of India.

#### References

- Aaby, K., Skrede, G., & Wroldstad, R. E. (2005). Phenolic composition and antioxidant activities in flesh and achenes of strawberries (*Fragaria ananassa*). *Journal of Agricultural and Food Chemistry*, 53, 4032–4040.
- Aadil, R. M., Zeng, X., Han, Z., & Sun, D. (2013). Effects of ultrasound treatments on quality of grapefruit juice. *Food Chemistry*, 141, 3201–3206.
- Abid, M., Jabbar, S., Wu, T., Hashim, M. M., Hu, B., & Lei, S. (2013). Effect of ultrasound on different quality parameters of apple juice. *Ultrasonics Sonochemistry*, 20, 1182–1187.
- Aday, M. S., Temizkan, R., Buyukcan, M. B., & Caner, C. (2013). An innovative technique for extending shelf-life of strawberry: ultrasound. *LWT – Food Science and Technology*, 52, 93–101.
- Alexandre, E. M. C., Brandao, T. R. S., & Silva, C. L. M. (2012). Efficacy of non-thermal technologies and sanitizer solutions on microbial load reduction and quality retention of strawberries. *Journal of Food Engineering*, 108, 417–426.
- Anjaneyulu, M., & Chopra, K. (2004). Quercetin, an anti-oxidant bioflavonoid, attenuates diabetic nephropathy in rats. *Clinical and Experimental Pharmacology and Physiology*, 31, 244–248.
- Ashokkumar, M., Sunartio, D., Kentish, S., Mawson, R., Simons, L., & Vilkuh, K. (2008). Modification of food ingredients by ultrasound to improve functionality: a preliminary study on a model system. *Innovative Food Science and Emerging Technologies*, 9, 155–160.
- Bhat, R., Kamaruddin, N. S. B. C., Min-Tze, L., & Karim, A. A. (2011). Sonication improves kasturi lime (*Citrus microcarpa*) juice quality. *Ultrasonics Sonochemistry*, 18, 1295–1300.
- Birmpa, A., Sfika, V., & Vantakar, A. (2013). Ultraviolet light and ultrasound as non-thermal treatments for inactivation of micro-organisms in fresh ready-to-eat foods. *International Journal of Food Microbiology*, 16, 96–102.
- Cao, S., Hu, Z., Pang, B., Wang, H., Xie, H., & Wu, F. (2010). Effect of ultrasound treatment on fruit decay and quality maintenance in strawberry after harvest. *Food Control*, 21, 529–532.
- Chitarra, M. I. F., & Chitarra, A. B. (2005). *Pos-colheita de frutas e hortaliças: Fisiologia e manuseio* (2. ed., p. 785). Lavras: UFLA.

- Cordenunsi, B. R., Genovese, M. I., do Nascimento, J. R. O., Hassimotto, N. M. A., dos Santos, R. J., & Lajolo, F. M. (2005). Effects of temperature on the chemical composition and antioxidant activity of three strawberry cultivars. *Food Chemistry*, *91*, 113–121.
- DrLange. (1994). *Color review. DrLange application report no. 8* (USA).
- FDA. (2001). *U.S. food and drug administration. In bacteriological analytical manual* (8th ed.). FDA Center for Food Safety and Applied Nutrition (Chap. 3).
- Fernandes, F. A. N., Gallao, M. I., & Rodrigues, S. (2009). Effect of osmosis and ultrasound on pineapple cell tissue structure during dehydration. *Journal of Food Engineering*, *90*, 186–190.
- Gabaldon-Leyva, C. A., Quintero-Ramos, A., Barnard, J., Balandrán-Quintana, R. R., Talamás-Abbud, R. T., & Jiménez-Castro, J. (2007). Effect of ultrasound on the mass transfer and physical changes in brine bell pepper at different temperature. *Journal of Food Engineering*, *81*, 374–379.
- Galoburda, R., Boc, S., Krupskis, I., & Seglina, D. (2014). *Physical and chemical parameters of strawberry puree*. Foodbalt.
- García, J. M., Aguilera, C., & Jimenez, A. M. (1996). Gray mold in and quality of strawberry fruit following postharvest heat treatment. *Horticultural Science*, *31*, 255–257.
- Golmohamadi, A., Moller, G., Powers, J., & Nindo, C. (2013). Effect of ultrasound frequency on antioxidant activity, total phenolic and anthocyanin content of red raspberry puree. *Ultrasonics Sonochemistry*, *20*, 1316–1323.
- Gunness, P., Kravchuk, O., Nottingham, S. M., Arcy, B. R., & Gidley, M. J. (2009). Sensory analysis of individual strawberry fruit and comparison with instrumental analysis. *Postharvest Biology and Technology*, *52*, 164–172.
- Holcroft, D. M., & Kader, A. A. (1999). Controlled atmosphere-induced changes in pH and organic acid metabolism may affect color of stored strawberry fruit. *Postharvest Biology and Technology*, *17*, 19–32.
- Jahouach-Rabai, W., Trabelsi, M., Van Hoed, V., Adams, A., Verhe, R., De Kimpe, N., et al. (2008). Influence of bleaching by ultrasound on fatty acids and minor compounds of olive oil. Qualitative and quantitative analysis of volatile compounds (by SPME coupled to GC/MS). *Ultrasonics Sonochemistry*, *15*, 590–597.
- Jones, E., & Hughes, R. E. (1983). Foliar ascorbic acid in some angiosperms. *Phytochemistry*, *22*, 2493–2499.
- Jose, S. J. F. B. D., Andrade, N. J. D., Ramos, A. M., Vanetti, M. C. D., Stringheta, P. C., & Chaves, J. B. P. (2014). Decontamination by ultrasound application in fresh fruits and vegetables. *Food control*, *45*, 36–50.
- Kentish, S., & Ashokkumar, M. (2011). The physical and chemical effects of ultrasound. In H. Feng, G. V. Barbosa-Cánovas, & J. Weiss (Eds.), *Ultrasound technologies for food and Bioprocessing* (pp. 1–12). London: Springer.
- Ketsa, S., & Daengkanit, T. (1999). Firmness and activities of polygalacturonase, pectinesterase, b-galactosidase and cellulase in ripening durian harvest at different stages of maturity. *Scientia Horticulturae*, *80*, 181–188.
- Lee, H., & Feng, H. (2011). Effect of power ultrasound on food quality. In H. Feng, G. V. Barbosa-Cánovas, & J. Weiss (Eds.), *Ultrasound technologies for food and Bioprocessing* (pp. 559–582). New York: Springer.
- Lopez-Gomez, P. S., Palop, F. A., Periago, P. M., Martínez-Lopez, A., Marin-Iniesta, F., & Barbosa-Cánovas, G. V. (2009). Food safety engineering: an emergent perspective. *Food Engineering Review*, *1*, 84–104.
- Manas, P., Munoz, B., Sanz, D., & Condon, S. (2006). Inactivation of lysozyme by ultrasonic waves under pressure at different temperatures. *Enzyme and Microbial Technology*, *39*, 1177–1182.
- Mason, T., Riera, E., Vercet, A., & Lopez-Buesa, P. (2005). Application of ultrasound. In D. W. Sun (Ed.), *Emerging technologies for food processing California* (pp. 323–350). Elsevier Academic Press.
- Pallauf, K., Rivas-Gonzalo, J. C., Del-Castillo, M. D., Cano, M. P., & De-Pascual-Teres, S. (2008). Characterization of the antioxidant composition of strawberry tree (*Arbutus unedo* L.) fruits. *Journal of Food Composition and Analysis*, *21*, 273–281.
- Rawson, A., Tiwari, B. K., Tuohy, M. G., O'Donnel, C. P., & Brunton, N. (2011). Effect of ultrasound and blanching pretreatments on polyacetylene and carotenoid content of hot air and freeze dried carrots discs. *Ultrasonics Sonochemistry*, *18*, 1172–1179.
- Rupasinghe, H. V., & Yu, L. J. (2012). Emerging preservation methods for fruit juices and beverages. In Y. El-Samragy (Ed.), *Food additives* (pp. 65–82). Rijeka, Croatia: InTech-Open Access Publisher.
- Seeram, N. P. (2008). Berry fruits for cancer prevention: current status and future prospects. *Journal of Agricultural Food Chemistry*, *56*, 630–635.
- Shah, A., Ahmad, M., Ashwar, B. A., Gani, A., Masoodi, F. A., Wani, I. A., et al. (2015). Effect of  $\gamma$ -irradiation on structure and nutraceutical potential of  $\beta$ -d- glucan from barley (*Hordeum vulgare*). *International Journal of Biological Macromolecules*, *72*, 1168–1175.
- Soria, A. C., & Villamiel, M. (2010). Effect of ultrasound on the technological properties and bioactivity of food: a review. *Trends in Food Science & Technology*, *21*, 323–331.
- Sun, J., Liu, X., Yang, T., Slovín, J., & Chen, P. (2014). Profiling polyphenols of two diploid strawberry (*Fragaria vesca*) inbred lines using UHPLC-HRMS. *Food Chemistry*, *146*, 289–298.
- Tezcan, F., Gultekin-Ozguven, M., Diken, T., Ozcelik, B., & Erim, F. B. (2009). Antioxidant activity and total phenolic, organic acid and sugar content in commercial pomegranate juices. *Food Chemistry*, *115*, 873–877.
- The, S., & Birch, E. J. (2014). Effect of ultrasonic treatment on the polyphenol content and antioxidant capacity of extract from defatted hemp, flax and canola seed cakes. *Ultrasonics Sonochemistry*, *21*, 346–363.
- Tiwari, B. K., O'Donnell, C. P., & Cullen, P. J. (2009a). Effect of non-thermal processing technologies on the anthocyanin content of fruit juices. *Trends in Food Science & Technology*, *20*, 137–145.
- Tiwari, B. K., O'Donnell, C. P. O., Patras, A., Brunton, N., & Cullen, P. J. (2009b). Stability of anthocyanins and ascorbic acid in sonicated strawberry juice during storage. *European Food Research Technology*, *228*, 717–724.
- Tiwari, B. K., O'Donnell, C. P., Patras, A., & Cullen, P. J. (2008). Anthocyanin and ascorbic acid degradation in sonicated strawberry juice. *Journal of Agricultural and Food Chemistry*, *56*, 10071–10077.
- Toivonen, P. M. A., & Brummell, D. A. (2008). Biochemical bases of appearance and texture changes in fresh-cut fruit and vegetables. *Postharvest Biology and Technology*, *48*, 1–14.
- Vilkhu, K., Mawson, R., Simons, L., & Bates, D. (2008). Applications and opportunities for ultrasound assisted extraction in the food industry e a review. *Innovative Food Science & Emerging Technologies*, *9*, 161–169.
- Wang, H., Gan, D., Zhang, X., & Pan, Y. (2010). Antioxidant capacity of the extracts from pulp of *Osmanthus fragrans* and its components. *LWT – Food Science and Technology*, *43*, 319–325.
- Yang, Z. F., Cao, S. F., Cai, Y. T., & Zheng, Y. H. (2011). Combination of salicylic acid and ultrasound to control postharvest blue mold caused by *Penicillium expansum* in peach fruit. *Innovative Food Science and Emerging Technologies*, *12*, 310–314.
- Zafra-Stone, S., Yasmin, T., Bagchi, M., Chatterjee, A., Vinson, J. A., & Bagchi, D. (2007). Berry anthocyanin as novel antioxidants in human health and disease prevention. *Molecular Nutrition and Food Research*, *51*, 675–683.
- Zavala, A. J. F., Wang, S. Y., Wang, C. Y., & Aguilar, G. G. A. (2004). Effect of storage temperatures on antioxidant capacity and aroma compounds in strawberry fruit. *LWT – Food Science and Technology*, *37*, 687–695.



## Effects of foam mat drying on physicochemical and microstructural properties of yacon juice powder



Talita Szlapak Franco<sup>a,\*</sup>, Camila Augusto Perussello<sup>b</sup>, Luciana Neves Ellendersen<sup>a</sup>,  
Maria Lucia Masson<sup>a</sup>

<sup>a</sup> Department of Chemical Engineering, Graduate Program in Food Engineering, Federal University of Paraná, Av. Francisco Hoffman dos Santos, s.n., CEP 81530-900 Curitiba, PR, Brazil

<sup>b</sup> Department of Industrial Engineering, University of Parma, Parco Area delle Scienze, 181/A, 43131, Parma, PR, Italy

### ARTICLE INFO

#### Article history:

Received 10 August 2015  
Received in revised form  
3 November 2015  
Accepted 4 November 2015  
Available online 10 November 2015

#### Keywords:

Temperature  
Thickness  
Hygroscopicity  
Color  
Density  
Solubility

### ABSTRACT

Yacon juice powder can be used as a highly nutritious ingredient in several food preparations. To this purpose, factors such as moisture content, density, porosity and solubility should be optimized as they are determinant to the product's ease of reconstitution, stability and sensory quality. In this work, yacon juices with two different concentrations (8°Brix and 24°Brix), both added of egg albumin as foaming agent, were subjected to foam mat drying using different temperatures (50 °C, 60 °C and 70 °C) and thicknesses of the foam layer (0.5 cm, 1.0 cm and 1.5 cm). The resulting juice powders were assessed for color, moisture, chemical composition, water activity, solubility in water, water absorption rate, absolute and bulk densities, intragranular porosity, microstructure and hygroscopicity. The drying conditions did not affect solubility index, density, microstructure and porosity of the particles, however the temperature increase reduced moisture content, water activity and, consequently, hygroscopicity. The powders of concentrate juice resulted lighter and reddish respect to the non concentrate juices, which tended to green. The highest air temperature coupled with reduced thickness for both juices was found to be the best drying condition, yielding juice powders with low water activity and satisfactory physicochemical characteristics.

© 2015 Elsevier Ltd. All rights reserved.

### 1. Introduction

The tuberous root of yacon, scientifically known as *Smallanthus sonchifolius* (Poepp. & Endl.) H. Rob., is native to the Andean foothills, where it is commonly cultivated and consumed since the time of the pre-Inca culture (Graefe, Hermann, Manrique, Golombek, & Buerkert, 2004). The global expansion of production and marketing of yacon was launched after studies reported several benefits to human health promoted by this tuber, such as the antioxidant activity associated to the phenolic compounds (Takaneka et al., 2003), reduction of blood glucose levels and prebiotic potential (Mentreddy, 2007; Valentová et al., 2008).

Another big draw is its low caloric value ascribed to its composition rich in water (above 70 g 100 g<sup>-1</sup> of wet weight).

However, the high moisture content and the presence of enzymes such as polyphenol oxidase and peroxidase render it a perishable food, hindering storage, distribution and transport (Shi, Zheng, & Zhao, 2013). Inasmuch as yacon is a seasonal crop, post harvest treatments such as drying are important to preserve its characteristics and make it available either for marketing for longer periods or for further processing (Scher, Rios, & Noreña, 2009).

The reduction of water activity attributed to the moisture removal is one of the most viable alternatives to extend this tuber's shelf life and also to add it value, increasing its market potential and availability (Yemmireddy, Chinnan, Kerr, & Hung, 2013). The foam mat drying (FMD) consists in the transformation of liquid or semi-liquid materials into a stable foam, by incorporation of air or other gases, which is subjected to drying with hot air to the extent that prevents microorganisms growth and development of chemical and/or enzymatic reactions (Falade, Adeyanju, & Uzo-Peters, 2003). It is a relatively simple and low cost method that relies on the use of agents capable of maintaining the foam stability during drying (Widyastutil & Srianta, 2011). Advantages of this method are the

\* Corresponding author.

E-mail addresses: [talitaszlapak@gmail.com](mailto:talitaszlapak@gmail.com) (T.S. Franco), [camila\\_ea@yahoo.com.br](mailto:camila_ea@yahoo.com.br) (C.A. Perussello), [lucianalsn@gmail.com](mailto:lucianalsn@gmail.com) (L.N. Ellendersen), [masson@ufpr.br](mailto:masson@ufpr.br) (M.L. Masson).

lower drying temperatures and shorter drying time ascribed to the greater surface area exposed to air, allowing higher drying rates respect to other drying techniques to obtain easy rehydration porous particles (Kudra & Ratti, 2008).

In the context of FMD, parameters such as temperature, velocity and relative humidity of the drying air as well as layer thickness and composition of the foam are determining to the quality of the resulting powder, influencing its physicochemical properties, such as moisture content, bulk density, absolute density, particle porosity, solubility and dispensability, which play an important role in both reconstitution and stability of the product (Abadio, Domingues, Borges, & Oliveira, 2004; Kadam et al., 2011).

There are few studies reporting the influence of drying conditions on the physicochemical properties and microstructure of food powders obtained by FMD, thus the main objective of this study was to evaluate the influence of drying air temperature, foam layer thickness and concentration of soluble solids of the yacon juice on color, chemical composition, water activity, solubility, water absorption index, bulk and absolute densities, intragranular porosity, microstructure and hygroscopicity of the juice powders.

## 2. Materials and methods

### 2.1. Preparation of the yacon juice

Yacon juice was obtained from processing tuberous roots of yacon purchased in the municipal market of Curitiba, Brazil, in a food centrifuge after being washed and peeled. Immediately after processing, the juice was added of sodium metabisulfite ( $0.3 \text{ g L}^{-1}$  juice) (Maia, Monteiro, & Guimarães, 2001) in order to limit the enzymatic activity. The total soluble solids (TSS) was measured with the aid of a refractometer (RL3, PZO, Brochowska, Poland). The samples were packed and stored in a freezer ( $-18 \text{ }^\circ\text{C}$ ) until preparation of the foams.

To evaluate the effect of TSS on the foam characteristics, part of the juice was freeze concentrated using the modified methodology of Wiecheteck, Nogueira, Drilleau, and Wosiacki (2005), and then was stored under the same conditions presented to the non concentrate juice. The total soluble solids content was  $8^\circ\text{Brix}$  and  $24^\circ\text{Brix}$  for the yacon juice (YJ) and concentrate yacon juice (CYJ), respectively.

### 2.2. Preparation and drying of the foams

Foams of YJ and CYJ were obtained with the addition of 200 g of egg albumin per L of juice (Cami, Mizumoto Alimentos Ltda, Gua-pirama, Paraná, Brazil). After complete homogenization, the solution was incorporated of air by stirring it in a domestic mixer (360 W) at maximum speed for 20 min. The conditions for preparing the foams were obtained in a previous research conducted by these authors (Franco, Ellendersen, Fattori, Granato, and Masson, 2015).

After stirring, the foams were placed in metal beds, not drilled, with thicknesses of 0.5, 1.0 and 1.5 cm, and then forwarded to dehydration in a convective oven (Fabbe-Primar, São Paulo, Brazil) under controlled temperature (50, 60 and  $70 \text{ }^\circ\text{C}$ ) and constant air speed (4 m/s), as measured by an anemometer (Testo 405, Testo AG, Lenzkirch, Germany). The moisture loss was determined by weighing the samples every 15 min with an electronic scale until obtaining equal masses in three consecutive weightings (Franco, Perussello, Ellendersen, and Masson, 2015).

The dry foams were then removed from the drying beds, crushed with the aid of a mortar and pestle and then sieved so that the particles were standardized between 250 and  $500 \text{ }\mu\text{m}$  to carry out further analysis (Barbosa-Cánovas, Ortega-Rivas, Juliano, & Yan,

2005). The crushed samples were packed in polyethylene bags, subjected to vacuum and stored in a home freezer ( $-6 \text{ }^\circ\text{C}$ ) until use.

### 2.3. Analysis of the dried juice

#### 2.3.1. Physicochemical characterization

Water activity was assessed by direct measurement in hygrometer (Aqualab, Pullman, United States) according to the manufacturer's specifications.

Color was determined by direct reading with a colourimeter (Color Quest II, Hunter Lab, Reston, United States) according to the international CIE (International Commission on Illumination) color coordinates  $L^*$ ,  $a^*$  and  $b^*$ :  $L^*$  represents brightness, ranging from white (100) to black (0),  $a^*$  represents the tones between green ( $-a^*$ ) and red ( $+a^*$ ), and  $b^*$ , between blue ( $-b^*$ ) and yellow ( $+b^*$ ).

The chemical composition was measured using standard methods of analysis for fruit and vegetable products, according to AOAC (2000). Proteins were quantified by the Kjeldahl digestion (Method 930.02), lipids were analyzed by continuous extraction in a Soxhlet-type apparatus (Method 920.39), ashes were determined by incineration in a muffle furnace at  $550 \text{ }^\circ\text{C}$ , and moisture content was assessed by gravimetric analysis in oven set at  $105 \text{ }^\circ\text{C}$  (Method 966.02). Total carbohydrates were calculated by difference.

#### 2.3.2. Physical properties

In order to evaluate the influence of the drying conditions on the dried juice's quality, analyses were conducted on several physical properties of the powders.

**2.3.2.1. Solubility in water.** Samples of 1 g of powder were diluted by adding 100 mL of distilled water under stirring for 5 min. The solutions were then centrifuged at 3000 g-force for 5 min and 20.0 mL aliquots of the supernatant were transferred to pre-weighed filters and dried in oven at  $105 \text{ }^\circ\text{C}$ . The weight of dried powder in the filters was used to determine the solubility in water (g of water per 100 g of powder) (Falade and Okocha, 2010).

**2.3.2.2. Water absorption index.** The water absorption capacity was determined by the method of Sharma Gujral, and Rosell (2011) adapted. A sample of 12.5 g was introduced in a centrifuge with 15 mL of water. After stirring for 30 min, the solution was centrifuged at 3000 g-force for 10 min. The supernatant liquid was collected in a tared filter and placed in oven at  $105 \text{ }^\circ\text{C}$  for 24 h, then the hydrated powder remaining in the centrifuge tube was weighed. The water absorption index (WAI) was determined from the residue of the supernatant evaporation according to Equation (1).

$$WAI = \frac{m_{rc}}{m_a - m_{re}} \quad (1)$$

where  $m_{rc}$  is the mass of the residue centrifugation (g),  $m_a$  is the sample's mass (g) and  $m_{re}$  is the mass of the residue evaporation (g).

**2.3.2.3. Bulk density.** The bulk density ( $\rho_a$ ) of the particles was measured according to the methodology of Goula and Adamopoulos (2008) adapted. Approximately 5 g of the powder was discharged in a 25 mL measuring cylinder (1 mL scale). The beaker and its content were agitated manually by repeated vertical movements to a height of  $14 \text{ cm} \pm 2 \text{ cm}$  until there was no difference in the powder volume. The bulk density was then calculated by the ratio between the known powder's mass ( $\pm 5 \text{ g}$ ) and the volume displayed in the tube (Equation (2)).

$$\rho_b = \frac{m_s}{v_s} \quad (2)$$

where  $\rho_b$  is the bulk density ( $\text{g cm}^{-3}$ ),  $m_s$  is the solid's mass (g) and  $v_s$  is the volume occupied by the solid ( $\text{cm}^3$ ).

**2.3.2.4. Absolute density.** The absolute density ( $\rho_{abs}$ ) of the yacon juice particles was calculated by the method of Caparino et al. (2012) adapted. Approximately 2.5 g of the powder were placed in an empty cylinder and the total volume was filled with a controlled amount of toluene (used for its ability to penetrate pores extremely connected to the material's surface without dissolving it). The absolute density was then calculated from Equation (3).

$$\rho_{abs} = \frac{m_s}{v_t} \quad (3)$$

where  $\rho_{abs}$  is the absolute density ( $\text{g cm}^{-3}$ ),  $m_s$  is the solid's mass (g) and  $v_t$  is the toluene's volume ( $\text{cm}^3$ ).

**2.3.2.5. Intragranular porosity.** The intragranular porosity ( $\varepsilon$ ) was determined by the ration between the particle's absolute density and bulk density using Equation (4) (Caparino et al., 2012).

$$\varepsilon = 1 - \frac{\rho_a}{\rho_p} \quad (4)$$

where  $\varepsilon$  is the intragranular porosity of the powdered juice,  $\rho_a$  its bulk density ( $\text{g cm}^{-3}$ ) and  $\rho_{abs}$  its absolute density ( $\text{g cm}^{-3}$ ).

**2.3.2.6. Hygroscopicity.** Hygroscopicity was determined according to the methodology proposed by Tonon, Brabet, and Hubinger (2008), with some modifications. Approximately 10 g of powdered juice samples were set in open containers and then triplicates of each sample were placed in three different desiccators containing aqueous saturated solution of sodium chloride (approximately  $75.5 \text{ g } 100 \text{ g}^{-1}$  moisture content), which were stored for 7 days in BOD ovens at  $25 \text{ }^\circ\text{C}$ .

The hygroscopicity (HG) of the juice powders was calculated basing on the mass of water (g) adsorbed per 100 g of dry matter ( $\text{g } 100 \text{ g}^{-1}$ ):

$$HG = \frac{\Delta m / (m + m_1)}{1 + (\Delta m / m)} \quad (5)$$

where  $\Delta m$  corresponds to the increasing of powder's weight after reaching equilibrium (g),  $m$  is the powder's initial mass (g) and  $m_1$  is the free water content of the powder before being exposed to air's humidity ( $\text{g } 100 \text{ g}^{-1}$ ).

**2.3.2.7. Microstructure.** The particles' morphology was assessed by scanning electron microscopy (SEM). The powders were set on copper supports with double-sided tape, were vacuum metalized with gold particles and then visualized with a scanning electron microscope (Vega3 LMU, Tescan Orsay Holding, Brno, Czech Republic) operating at a controlled pressure of 15 kV. Micrographs were photographed at magnifications of 250 and 1300 times.

## 2.4. Statistical analysis

To estimate the effects of air temperature and layer thickness to be dehydrated on the drying behavior of YJ and CYJ foams, a  $2^2$  design in duplicate with four replicates at the central point was performed, totaling 32 experiments (16 experiments for each one of the foams). Each experimental analysis of microstructural and physicochemical characterization was conducted in triplicate.

The comparison of the average values between treatments was conducted by one-way ANOVA with Tukey test ( $p < 0.05$ ). For evaluating the influence of the independent variables on the characteristics of the dried powder, the Response Surface Methodology (RSM) was applied when statistical differences were detected by the one-way variance analysis (ANOVA). The isolated effects of each factor, their linear interaction and their statistical significance were calculated. Equation (6) shows the relationship between the factors for each dependent variable:

$$E(y) = b_0 + b_1x_1 + b_2x_2 + b_3x_1x_2 \quad (6)$$

where  $b_0$  is a constant,  $b_1$  and  $b_2$  are the regression coefficients that represent the isolated effects of factors and  $b_3$  is the regression coefficient of the interaction between variables. Only regression coefficients that were significant when ANOVA was applied remained in the final model presented.

The statistical quality of the proposed models was assessed by the variability percentage explained by the multiple linear regression equation ( $R^2$ ), the determination coefficient adjusted to the experimental data ( $R^2_{adj}$ ) and the model's significance (p-value) (Granato, Grevink, Zielinski, Nunes, & van Ruth, 2014).

All statistical analyses were performed using the software Statistica 7.0 (StatSoft Inc. South America, Toulou, United States).

## 3. Results and discussion

### 3.1. Physicochemical characteristics

The moisture content of the juice powders (Table 1) ranged from  $6.58 \text{ g } 100 \text{ g}^{-1}$  (SY –  $1.5 \text{ cm} - 50 \text{ }^\circ\text{C}$ ) to  $3.51 \text{ g } 100 \text{ g}^{-1}$  (SY –  $0.5 \text{ cm} - 70 \text{ }^\circ\text{C}$ ), values similar to those for low moisture commercial products like soluble coffee (from  $4.18$  to  $5.25 \text{ g } 100 \text{ g}^{-1}$ ) and tomato soup powder ( $3.4$ – $4.0 \text{ g } 100 \text{ g}^{-1}$ ), indicating a very low availability of water for the occurrence of chemical reactions and microbiological growth (Jaya & Das, 2004). Pereira, Barcelos, Pereira, and Ferreira (2013) produced juices with  $8.09 \text{ g } 100 \text{ g}^{-1}$  of moisture content from grinded dehydrated slices of yacon after 96 h of drying at  $55 \text{ }^\circ\text{C}$ , a period 16 times longer than that needed for drying a  $1.5 \text{ cm}$  layer of yacon juice at  $50 \text{ }^\circ\text{C}$ , which generated powder particles with moisture content of  $6.58 \text{ g } 100 \text{ g}^{-1}$ .

The moisture content of a food is strongly linked to its stability, however it cannot be related only to water content, but mainly to the availability of water to be used for chemical reactions (Lewicki, 2004). This parameter, known as water activity ( $A_w$ ), is defined as the ratio between the water vapor pressure of the food and the vapor pressure of pure water at the same temperature (Berk, 2009). A decrease of  $A_w$  prevents from development of microorganisms, reduces the rate of enzymatic reactions and retards non-enzymatic browning (Belitz, Grosch, & Schieberle, 2009). All samples showed  $A_w$  below 0.25 (Table 1), values much lower than those of the foams ( $0.96$ – $0.98$ ), which is quite favorable to the stability of the juice powders since  $A_w$  rates between 0.2 and 0.3 minimize microbial proliferation and oxidative and enzymatic activity (Rao, Rizvi, & Datta, 2005).

The  $A_w$  determined for the yacon juice powders (Table 1) is in agreement with other studies involving FMD. For instance, guavira juice powders showed  $A_w$  in the range of  $0.2$ – $0.3$  (Breda, Sanjinez-Argandoña, & Correia, 2012) and yogurt with egg albumin foams dried at  $50$ ,  $60$  and  $70 \text{ }^\circ\text{C}$  resulted in  $A_w$  from  $0.32$  to  $0.35$  (Krasaekoopt & Bhatia, 2012).

The fixed mineral residue (or ash) is the inorganic material that remains after burning an organic matter sample, which is transformed into carbon dioxide, water and nitric oxide (Cecchi, 2009). Mineral elements are present in the form of oxides, sulfates,

**Table 1**  
Physicochemical characteristics of yacon juice (YJ) and concentrate juice (CYJ) powders obtained by foam mat drying under different conditions.

Sample	Drying condition	Physicochemical characteristics					
		Moisture (g 100 g <sup>-1</sup> )	Aw	Ashes (g 100 g <sup>-1</sup> )	Proteins (g 100 g <sup>-1</sup> )	Fats (g 100 g <sup>-1</sup> )	Carbohydrates (g 100 g <sup>-1</sup> )
YJ	0.5 cm/50 °C	6.24 ± 0.16 <sup>a</sup>	0.19 ± 0.001 <sup>a</sup>	4.53 ± 0.11 <sup>a</sup>	47.72 ± 0.09 <sup>a</sup>	0.28 ± 0.01 <sup>a</sup>	41.23 ± 0.20 <sup>a</sup>
	1.5 cm/50 °C	6.58 ± 0.04 <sup>a</sup>	0.19 ± 0.001 <sup>a</sup>	4.37 ± 0.09 <sup>a</sup>	47.50 ± 0.29 <sup>a</sup>	0.25 ± 0.01 <sup>a</sup>	41.30 ± 0.25 <sup>a</sup>
	1.0 cm/60 °C	5.50 ± 0.03 <sup>d</sup>	0.15 ± 0.001 <sup>d</sup>	4.49 ± 0.09 <sup>a</sup>	48.20 ± 0.53 <sup>a</sup>	0.2 ± 0.01 <sup>a</sup>	41.63 ± 0.45 <sup>a</sup>
	0.5 cm/70 °C	3.51 ± 0.02 <sup>b</sup>	0.10 ± 0.001 <sup>b</sup>	5.08 ± 0.31 <sup>a</sup>	49.19 ± 0.23 <sup>a</sup>	0.27 ± 0.01 <sup>a</sup>	42.06 ± 0.52 <sup>a</sup>
	1.5 cm/70 °C	4.09 ± 0.05 <sup>c</sup>	0.12 ± 0.001 <sup>c</sup>	4.63 ± 0.13 <sup>a</sup>	49.49 ± 0.15 <sup>a</sup>	0.28 ± 0.01 <sup>a</sup>	41.51 ± 0.20 <sup>a</sup>
CYJ	0.5 cm/50 °C	4.91 ± 0.09 <sup>c</sup>	0.20 ± 0.001 <sup>c</sup>	5.68 ± 0.06 <sup>a</sup>	29.37 ± 0.09 <sup>a</sup>	0.30 ± 0.01 <sup>a</sup>	59.74 ± 0.02 <sup>a</sup>
	1.5 cm/50 °C	6.19 ± 0.05 <sup>a</sup>	0.22 ± 0.001 <sup>a</sup>	5.38 ± 0.12 <sup>a</sup>	29.13 ± 0.55 <sup>a</sup>	0.28 ± 0.02 <sup>a</sup>	59.00 ± 0.62 <sup>a</sup>
	1.0 cm/60 °C	5.70 ± 0.07 <sup>b</sup>	0.21 ± 0.001 <sup>b</sup>	5.50 ± 0.14 <sup>a</sup>	30.29 ± 0.36 <sup>a</sup>	0.32 ± 0.02 <sup>a</sup>	58.19 ± 0.49 <sup>a</sup>
	0.5 cm/70 °C	4.11 ± 0.05 <sup>e</sup>	0.12 ± 0.001 <sup>e</sup>	5.67 ± 0.06 <sup>a</sup>	30.13 ± 0.61 <sup>a</sup>	0.27 ± 0.01 <sup>a</sup>	59.82 ± 0.55 <sup>a</sup>
	1.5 cm/70 °C	4.31 ± 0.14 <sup>d</sup>	0.17 ± 0.001 <sup>d</sup>	5.73 ± 0.05 <sup>a</sup>	31.03 ± 0.44 <sup>a</sup>	0.26 ± 0.01 <sup>a</sup>	58.69 ± 0.32 <sup>a</sup>

The results comprise means ± standard deviation. Each analysis was conducted three times and each experiment was composed of 4 replicates in the central point and two replicates in the levels -1 and +1 of the experimental design (see Section 2.4). For samples of the same juice, different letters in the same column indicate significant difference ( $p < 0.05$ ) between treatments according to the Tukey test.

phosphates, silicates and chlorides, depending on the conditions of incineration and food composition (Campbell-Platt, 2009). Although the fixed mineral residue (FMR) indicates the mineral content in the sample, it does not necessarily represents the same composition than the mineral matter originally present in the food as there may be loss by evaporation or some interaction between the sample's constituents (Adolfo Lutz Institute, 2008). The samples of YJ and CYJ powders showed FMR ranging from 4.37 to 5.08 g 100 g<sup>-1</sup> and 5.38 and 5.73 g 100 g<sup>-1</sup>, respectively (Table 1). Fruits, vegetables and tubers have relatively high mineral content, and yacon is especially rich in calcium and phosphorus. However, it is important to consider that egg albumin, used as foaming agent, interfere in the FMR of the powders for their average FMR is 6.0 g 100 g<sup>-1</sup> (information provided by the manufacturer).

Due to the need of adding egg albumin for forming the foam and maintaining its stability during drying, the juice powders showed significant protein contents (Table 1) that are not natural to yacon, whose average value is between 0.2 and 2.0 g 100 g<sup>-1</sup> (Valentová & Ulrichová, 2003).

The low fat content of the dried samples was influenced by the composition of both yacon and egg albumin, which are low fat foods. The average fat content is 0.35 g 100 g<sup>-1</sup> for egg albumin (information provided by the manufacturer) and between 0.1 and 0.3 g 100 g<sup>-1</sup> for yacon (Valentová & Ulrichová, 2003), so it would not be possible that the blend of these two compounds resulted in a high lipid profile product.

Powders of CYJ showed higher concentrations of carbohydrates than those of YJ (Table 1), a variation ascribed to the different TSS between juice (8°Brix) and concentrate juice (24°Brix). Forasmuch as the carbohydrate content of yacon consists essentially of inulin and FOS (40–70 g 100 g<sup>-1</sup>) (Delgado, Thomé, Gabriel, Tamashiro, & Pastore, 2012), it is important that the juice powders presents a high-carbohydrate profile as this may indicate the functionality the powders can play when consumed directly or as formulation ingredients. Nonetheless, the functionality of juice powders can only be confirmed from the determination of oligofructans, which indeed indicate the actual content of these compounds among total carbohydrates.

Results published by other researchers confirm the important role of FOS as main constituents of the yacon roots' carbohydrate fraction. Vasconcelos, Silva, Teixeira, Chaves, and Martino (2010) produced flour by convective drying yacon slices with 39.71 g 100 g<sup>-1</sup> carbohydrates, 19.43 g 100 g<sup>-1</sup> FOS and 9.84 g 100 g<sup>-1</sup> inulin. Campos et al. (2012) used yacon extract with 63.7 g 100 g<sup>-1</sup> of FOS as a substrate for fermentation by probiotic microorganisms, and Lago, Bernstein, Brandelli, and Noreña (2012) spray dried concentrate yacon juice containing 31.5 g 100 g<sup>-1</sup> inulin.

The influence of drying conditions (thickness of the foam layer and air temperature) on the physicochemical characteristics of juice powders was evaluated by the response surface methodology. The variables did not exert significant effect on ashes, lipids, proteins and carbohydrates, but influenced Aw and moisture content.

Mathematical models that represent the effect of process parameters on water activity and moisture content (Table 2) were obtained by applying SRM. The models showed R<sup>2</sup> and R<sup>2</sup>-adj greater than 0.75, that is, these models can account for over 75% of the responses variability. It is also noted that the lack of adjustment for all answers was not significant ( $p > 0.05$ ) indicating that the models have adjusted well to the experimental data and can be used for predictive purposes.

As indicated by the equations obtained for the YJ powder (Table 2), thickness and temperature influenced Aw either isolatedly or interacting one to the other for  $x_1$  is positive,  $x_2$  is negative and  $x_1x_2$  is positive. This means that Aw decreases with a higher temperature and a less thick layer. As regard to moisture content, thickness did not affect the result, in opposition to temperature and the interaction between temperature and thickness. Thus, higher drying temperatures yielded juice powders with lower moisture content, and the interaction between temperature and thickness had minor influence on moisture content respect to temperature alone, given the lower value of the coefficient attributed to it ( $x_2$ ).

For the YJC powders, an increase in temperature led to a reduction of Aw and the interaction between temperature and thickness did not influence Aw as strongly as temperature alone (Table 1). As regard to moisture content, only thickness and the interaction between thickness and temperature influenced the results: an increase in thickness increased moisture content.

The influence of drying air temperature on Aw was also verified by other authors (Lago et al., 2012; Reddy et al., 2014) for the use of higher temperatures imply a higher heat transfer rate, leading to increased evaporation of water from the product, resulting in powders with a lower Aw.

Temperature also influenced moisture content of dried powders of mango juices (Wilson, Dattatreya, Chadha, Grewal, & Sharma, 2014) and açai (Tonon et al., 2008) since a temperature rise increases the driving force for evaporation of water as a consequence of the larger temperature gradient between product and drying air.

### 3.2. Physical properties

Some quality aspects require special attention during food dehydration as partial or complete compromise of the product quality may occur (Ratti, 2009). The parameters used to assess the

**Table 2**

Mathematical models for water activity and moisture content of yacon juice (YJ) and concentrate juice (CYJ) powders as a function of foam layer thickness ( $x_1$ ) and temperature ( $x_2$ ).

Parameter	Type of powder	Mathematical model	R <sup>2</sup>	R <sup>2</sup> -adjusted	p-value
Water activity	YJ	$y = 0.4245 + 0.0323x_1 - 0.0046x_2 + 0.0006x_1 \cdot x_2$	0.9964	0.9954	$p < 0.001$
	CYJ	$y = 0.3663 - 0.0036x_2 + 0.0006x_1 \cdot x_2$	0.8912	0.8738	$p < 0.001$
Moisture content	YJ	$y = 13.0001 - 0.1380x_2 + 0.0073x_1 \cdot x_2$	0.9739	0.9696	$p < 0.001$
	CYJ	$y = 4.3069 + 4.6025x_1 - 0.0644x_1 \cdot x_2$	0.8085	0.7769	$p < 0.001$

quality of a food product may be physical, chemical and biochemical, since the water removal during drying can affect food composition and structure (Van't Land, 2012). Some physical parameters are porosity, solubility, hydration capacity, while biochemical changes include loss of vitamins and proteins, browning reactions and degradation of nutraceutical compounds (Chen & Mujumdar, 2008).

Drying processes also cause changes in the microstructure and distribution of components, influencing reconstitution and mainly affecting their function as food ingredients and the way they can be added to other foods (Chen & Mujumdar, 2008).

### 3.2.1. Solubility in water, water absorption index and hygroscopicity percentage

Solubility is an important indicator of the powder's ability to remain homogeneously mixed with water, i.e., the stability of the mixture composed by particles dissolved in liquid. Presenting percentage solubility above 80 g 100 g<sup>-1</sup>, the yacon juice powders were more soluble than mango juice powder obtained by FMD using egg albumin as foaming agent, which showed values between 51.83 and 66.65 g 100 g<sup>-1</sup> (Wilson et al., 2014), but were less soluble than inulin crystals extracted from yam roots by the same technology, showing solubility between 100 and 98.61 g 100 g<sup>-1</sup> (Harmayani, Winarti, & Nurismanto, 2011).

The solubility of the particulates produced with YJ and YCJ was not influenced by the variation in drying conditions (Table 3). Various works report similar trends: Mishra, Mishra, and Mahanta (2014) observed no interference of dehydration temperature on the solubility of atomized juice of amla (*Embllica officinalis*), Souza, Borges, Magalhães, Ricardo, and Azevedo (2008) found that drying conditions did not affect this property when working with tomato juice, as well as observed by Kha, Nguyen, and Roach (2010) for juice of gac (*Momordica cochinchinensis*). Probably there was no change in solubility because it is strongly affected by the foaming agent added (Yousefi, Emam-Djomeh, & Mousavi, 2011), a factor that has been maintained the same in all experiments.

The good solubility of the dried juice obtained in this study may be attributed to the significant amount of carbohydrates and

proteins and low level of lipids in its composition (Mishra et al., 2014), as well as the low moisture content of the powders, since the lower the moisture content, less sticky is the final product, which has in addition a higher surface area available for contact with hydration water (Fazaeli, Emam-Djomeh, Ashtari, & Omid, 2012).

The water absorption index (WAI) relates to the amount of water the dry food is capable of absorbing and is directly related to its hydration capacity (Barbosa-Cánovas et al., 2005). During rehydration, the dried material, which is submerged in water or other aqueous medium, undergoes through multiple simultaneous physicochemical changes (moisture content, total solids content, porosity, volume, gelatinization and texture). Rehydration involves several processes which occur in parallel, including liquid soaking into the dry material, transport of liquid through the pores network and subsequent distribution within the solid matrix, causing swelling of the matrix and leaching of soluble solids to the medium (Ratti, 2009).

Water absorption is an important property for applications in meat products, bread and cakes, for high WAI values may help retain moisture within them, improving handling characteristics and preventing dryness during storage (Oliveira, Pirozi, Borges, Germani, & Fontes, 2009). In addition to the applications already mentioned, powdered products with high WAI are listed as ingredients adequate for rapid preparation of products given its ability to absorb large amounts of water even at low temperatures (Clerici & El-Dash, 2008).

The water absorption capacity of the YJ and CYJ powders varied from 148.76 to 181.08 and 118.15 to 150.87, respectively, indicating good rehydration capacity (Table 3). The somewhat higher hydration capacity of the YJ powders can be explained by its composition richer in protein respect to YCJ. Harmayani et al. (2011) observed that the WAI of inulin powder was affected by the foaming agent composition (egg albumin) given the number of free hydroxyls present on egg albumin, which are able to bind to water molecules from the surrounding medium.

Considering there was significant difference ( $p < 0.5$ ) between responses of WAI, the SRM was applied for proper assessment of

**Table 3**

Physicochemical properties of yacon juice (YJ) and concentrate juice (CYJ) powders obtained by foam mat drying under different conditions.

Sample	Drying condition	Properties		
		Solubility in water(g 100 g <sup>-1</sup> )	Water absorption index	Hygroscopicity (g 100 g <sup>-1</sup> )
YJ	0.5 cm–50 °C	84.16 ± 0.40 <sup>a</sup>	181.08 ± 2.86 <sup>a</sup>	18.61 ± 0.34 <sup>c</sup>
	1.5 cm–50 °C	80.49 ± 0.13 <sup>a</sup>	170.94 ± 0.84 <sup>b</sup>	18.06 ± 0.11 <sup>c</sup>
	1.0 cm–60 °C	81.99 ± 1.48 <sup>a</sup>	162.18 ± 0.96 <sup>c</sup>	20.21 ± 0.01 <sup>b</sup>
	0.5 cm–70 °C	80.97 ± 0.40 <sup>a</sup>	150.52 ± 1.31 <sup>d</sup>	22.31 ± 0.08 <sup>a</sup>
	1.5 cm–70 °C	81.51 ± 1.27 <sup>a</sup>	148.76 ± 0.87 <sup>d</sup>	21.49 ± 0.18 <sup>a</sup>
	0.5 cm–50 °C	83.07 ± 0.13 <sup>a</sup>	150.87 ± 1.26 <sup>a</sup>	18.86 ± 0.27 <sup>b</sup>
CYJ	1.5 cm–50 °C	81.44 ± 0.20 <sup>a</sup>	152.69 ± 0.63 <sup>a</sup>	15.24 ± 0.04 <sup>c</sup>
	1.0 cm–60 °C	80.89 ± 0.32 <sup>a</sup>	139.40 ± 0.37 <sup>b</sup>	18.12 ± 0.12 <sup>b</sup>
	0.5 cm–70 °C	83.24 ± 0.24 <sup>a</sup>	118.15 ± 1.15 <sup>c</sup>	20.39 ± 0.09 <sup>a</sup>
	1.5 cm–70 °C	82.87 ± 0.51 <sup>a</sup>	118.90 ± 1.55 <sup>c</sup>	18.78 ± 0.26 <sup>b</sup>

The results comprise means ± standard deviation. Each analysis was conducted three times and each experiment was composed of 4 replicates in the central point and two replicates in the levels -1 and +1 of the experimental design (see Section 2.4). For samples of the same juice, different letters in the same column indicate significant difference ( $p < 0.05$ ) between treatments according to the Tukey test.

**Table 4**  
Mathematical models for water absorption index and hygroscopicity of yacon juice (YJ) and concentrate juice (CYJ) powders as a function of foam layer thickness ( $x_1$ ) and temperature ( $x_2$ ).

Parameter	Type of powder	Mathematical model	R <sup>2</sup>	R <sup>2</sup> -adjusted	p-value
Water absorption index	SY	$y = 272.9022 - 31.0816x_1 - 1.7376x_2 + 0.4189x_1 \cdot x_2$	0.9678	0.9590	$p < 0.001$
	SYC	$y = 235.7730 - 1.6629x_2 + 0.0005x_1 \cdot x_2$	0.9752	0.9733	$p < 0.001$
Hygroscopicity	SY	$y = 10.1282 - 0.6845x_1 + 0.1782x_2$	0.9743	0.9699	$p < 0.001$
	SYC	$y = 20.8998 - 9.9068x_1 + 0.1214x_1 \cdot x_2$	0.9721	0.9674	$p < 0.001$

the drying conditions' influence. The correspondent models are presented in Table 4. As these models could explain more than 96% of the responses variability ( $R^2 > 0.96$ ) and showed good fitting to the experimental data ( $p > 0.5$ ), they may be used for predictive purposes.

The increase in foam layer thickness ( $x_1$ ) and drying temperature ( $x_2$ ) reduced hydration capacity for the YJ powders (Table 4). With respect to the CYJ powders, in turn, only temperature caused a reduction in hydration capacity. Wilson et al. (2014) observed similar effect during FMD of mango pulp, for which there was a decrease in the water absorption rate when increasing drying temperature. This fact can be explained by the lower moisture content of powders processed at higher temperatures, forasmuch as higher moisture contents can contribute to the absorption of water, since the liquid penetrates the pores more easily, allowing a better moisture dispersion (Ghosal, Indira, & Bhattacharya, 2010).

Hygroscopicity is the ability of a food powder to absorb water from an environment with relative humidity higher than the equilibrium moisture content and it is linked to their physical, chemical and microbiological stability. The knowledge of the hygroscopic behavior of these products is essential mainly when it comes to establish drying, packaging and storage conditions (Oliveira, Clemente, & Costa, 2014).

The YJ powders showed hygroscopicity values from 18.06 (thickness 1.5 cm and drying temperature 50 °C) to 22.31 g 100 g<sup>-1</sup> (0.5 cm and 70 °C). In turn, the CYJ powders ranged from 15.24 to 20.39 g 100 g<sup>-1</sup> in the same conditions of thickness and temperature.

Our results are far above those outlined by Jaya and Das (2004) as ideal for instant products, between 5.13 g 100 g<sup>-1</sup> (instant coffee) and 9.38 g 100 g<sup>-1</sup> (tomato soup instant powder). The high values obtained are ascribed to the chemical nature of the product. It is known that in foods such as powdered fruit juices (sucrose, glucose and fructose) sugars are the main responsible for water absorption due to the ability of hydroxyl groups to form hydrogen bonds with water molecules (Jaya & Das, 2004). Regarding to the yacon juices produced in the current work, the structure of egg albumin must be

considered for its polar conformation increases the capacity of the powder to attract water molecules when in contact with surrounding air.

Another factor that must be considered is that most juice powders are produced by spray-drying and added of maltodextrin, a compound with low hygroscopicity applied as a carrier agent to prevent agglomeration of particles (Tonon et al., 2008). This feature is regarded in the work of Caparino et al. (2012), which demonstrated the effects of different drying methods on the physical properties and microstructure of mango puree powders. According to the authors, the lowest hygroscopicity ascribed to the spray-dried powder ( $16.5 \pm 0.06$  g 100 g<sup>-1</sup>) is a consequence of the addition of maltodextrin, which was not used in the other dehydration methods, drum drying ( $20.1 \pm 0.88$  g 100 g<sup>-1</sup>), lyophilization ( $18.0 \pm 0.19$  g 100 g<sup>-1</sup>) and refractive window drying ( $18.0 \pm 0.36$  g 100 g<sup>-1</sup>).

In a study comparing different drying methods applied to apple purees, Jakubczyk, Gondek, and Tambor (2011) obtained a product with 17 g 100 g<sup>-1</sup> hygroscopicity by convective dehydration, 19 g 100 g<sup>-1</sup> by lyophilization, 14 g 100 g<sup>-1</sup> when 6% maltodextrin was added to the foam to be lyophilized and 11 g 100 g<sup>-1</sup> when the concentration of maltodextrin was increased to 15%, suggesting again the maltodextrin's ability to decrease water absorption for powdered foods.

RSM was also applied to evaluate the effects of drying conditions on hygroscopicity. The models obtained (Table 4) could explain more than 97% of the variability of responses and showed good fitting to the experimental data ( $p > 0.05$ ), hence can be used for predictive purposes. The increase in thickness of the foam layer ( $x_1$ ) caused a reduction of hygroscopicity, while drying temperature ( $x_2$ ) increased this response. The influence of temperature is in agreement with the results found by Tonon et al. (2008) and Frascarelli, Silva, Tonon, and Hubinger (2012) on drying of tomato pulp, açai juice and coffee oil, respectively, but contradicts the studies of Moreira et al. (2009) on dehydration of acerola juice and Mishra et al. (2014) on amla juice. For the CYJ powders, the increase in thickness of the foam layer caused a stronger reduction in

**Table 5**  
Physical properties of yacon juice (YJ) and concentrate juice (CYJ) powders obtained by foam mat drying under different conditions.

Type of powder	Drying conditions	Properties		
		Apparent density (g cm <sup>-3</sup> )	Absolute density (g cm <sup>-3</sup> )	Intragranular porosity
YJ	0.5 cm–50 °C	0.69 ± 0.01 <sup>a</sup>	1.18 ± 0.01 <sup>a</sup>	0.413 ± 0.002 <sup>a</sup>
	1.5 cm–50 °C	0.67 ± 0.02 <sup>a</sup>	1.20 ± 0.01 <sup>a</sup>	0.442 ± 0.011 <sup>a</sup>
	1.0 cm–60 °C	0.66 ± 0.01 <sup>a</sup>	1.20 ± 0.001 <sup>a</sup>	0.445 ± 0.008 <sup>a</sup>
	0.5 cm–70 °C	0.65 ± 0.01 <sup>a</sup>	1.20 ± 0.01 <sup>a</sup>	0.461 ± 0.004 <sup>a</sup>
	1.5 cm–70 °C	0.65 ± 0.01 <sup>a</sup>	1.19 ± 0.01 <sup>a</sup>	0.450 ± 0.002 <sup>a</sup>
CYJ	0.5 cm–50 °C	0.50 ± 0.01 <sup>a</sup>	1.21 ± 0.01 <sup>a</sup>	0.588 ± 0.001 <sup>a</sup>
	1.5 cm–50 °C	0.47 ± 0.01 <sup>a</sup>	1.21 ± 0.01 <sup>a</sup>	0.606 ± 0.003 <sup>a</sup>
	1.0 cm–60 °C	0.51 ± 0.01 <sup>a</sup>	1.20 ± 0.01 <sup>a</sup>	0.577 ± 0.001 <sup>a</sup>
	0.5 cm–70 °C	0.52 ± 0.01 <sup>a</sup>	1.20 ± 0.01 <sup>a</sup>	0.567 ± 0.003 <sup>a</sup>
	1.5 cm–70 °C	0.51 ± 0.01 <sup>a</sup>	1.19 ± 0.01 <sup>a</sup>	0.567 ± 0.003 <sup>a</sup>

The results comprise means ± standard deviation. Each analysis was conducted three times and each experiment was composed of 4 replicates in the central point and two replicates in the levels -1 and +1 of the experimental design (see Section 2.4). For samples of the same juice, different letters in the same column indicate significative difference ( $p < 0.05$ ) between treatments according to the Tukey test.

**Table 6**  
Color coordinates of yacon juice (YJ) and concentrate juice (CYJ) powders obtained by foam mat drying under different conditions.

Type of powder	Drying conditions	Color coordinates		
		L*	a*	b*
YJ	0.5 cm–50 °C	77.88 ± 0.01 <sup>b</sup>	–1.89 ± 0.01 <sup>b</sup>	45.86 ± 0.05 <sup>e</sup>
	1.5 cm–50 °C	77.75 ± 0.01 <sup>b</sup>	–1.16 ± 0.01 <sup>e</sup>	47.97 ± 0.03 <sup>d</sup>
	1.0 cm–60 °C	77.69 ± 0.01 <sup>b</sup>	–2.23 ± 0.02 <sup>a</sup>	54.99 ± 0.01 <sup>a</sup>
	0.5 cm–70 °C	78.60 ± 0.02 <sup>a</sup>	–1.59 ± 0.01 <sup>c</sup>	49.04 ± 0.04 <sup>c</sup>
CYJ	1.5 cm–70 °C	75.91 ± 0.02 <sup>c</sup>	–1.31 ± 0.02 <sup>d</sup>	50.65 ± 0.09 <sup>b</sup>
	0.5 cm–50 °C	82.99 ± 0.01 <sup>b</sup>	0.54 ± 0.01 <sup>e</sup>	26.51 ± 0.01 <sup>d</sup>
	1.5 cm–50 °C	83.12 ± 0.01 <sup>a</sup>	1.30 ± 0.01 <sup>d</sup>	22.57 ± 0.01 <sup>e</sup>
	1.0 cm–60 °C	79.09 ± 0.01 <sup>c</sup>	3.09 ± 0.01 <sup>b</sup>	31.23 ± 0.01 <sup>b</sup>
	0.5 cm–70 °C	72.19 ± 0.05 <sup>d</sup>	1.45 ± 0.01 <sup>c</sup>	27.80 ± 0.02 <sup>c</sup>
	1.5 cm–70 °C	62.60 ± 0.03 <sup>e</sup>	14.72 ± 0.02 <sup>a</sup>	41.87 ± 0.07 <sup>a</sup>

The results comprise means ± standard deviation. Each analysis was conducted three times and each experiment was composed of 4 replicates in the central point and two replicates in the levels –1 and +1 of the experimental design (see Section 2.4). For samples of the same juice, different letters in the same column indicate significant difference ( $p < 0.05$ ) according to the tests of Tukey and t-Student.

hygroscopicity (highest coefficient) than the interaction between the two factors, which caused a slight increase.

The low hygroscopicity found at low temperatures and higher thicknesses can be explained by the fact that powders obtained under these conditions have higher moisture content and, as a consequence, lower moisture gradient between product and ambient.

Regarding the quality parameters of food powders, lower values of hygroscopicity, water content and water activity, and greater solubility and water absorption index are desirable characteristics for them to be used in food formulations due to the storage stability (Bakar, Muhammad, Hashim, & Adzahan, 2013).

Predominantly, all powders had satisfactory characteristics. The combination of thinner layers of foam with higher drying temperatures allowed the production of yacon juice powders with low moisture content and water activity, increasing their storage stability. All particulates were soluble in water (above 80%), factor that was not influenced by the drying conditions, and also showed good rates of water absorption, especially those dried at higher temperatures. Regarding the hygroscopicity, the particles had characteristics similar to those of many fruit juices powders. Drying temperature exerted greater influence on hygroscopicity respect to layer thickness.

### 3.2.2. Bulk density, absolute density and intragranular porosity

Physical low cost determinations such as bulk and absolute densities are useful to predict the quality of particulates (Shishir, Taip, Aziz, & Talib, 2014). Bulk density is a factor directly correlated with the ease of reconstitution, packaging, transportation and marketing of powdered foods (Marques, Borges, Mendonça, Fernandes, & Menezes, 2014). A dehydrated product with a high bulk density can be stored in smaller containers than low density products.

Bulk density varied between 0.65 and 0.69 g 100 g<sup>-1</sup> for the yacon juice powder and between 0.47 and 0.52 g 100 g<sup>-1</sup> for the concentrate juice powder. Absolute density ranged from 1.18 to 1.20 g 100 g<sup>-1</sup> and from 1.19 to 1.21 g 100 g<sup>-1</sup> for the YJ and CYJ powders. Similar results were found by Oguntunde and Adejo (1992) for the foam mat drying of whole milk and by Falade and Omojola (2010) for the dehydration of okra foams.

The large reduction in bulk density compared to absolute density may be related to the air incorporated to the juice during preparation of the foams. Similar behavior was reported by Jakubczyk et al. (2011) for apple juice powder obtained by FMD, resulting in bulk and absolute densities of 0.54 and 1.43 g 100 g<sup>-1</sup>, respectively.

The powder samples of YJ showed the highest values for bulk

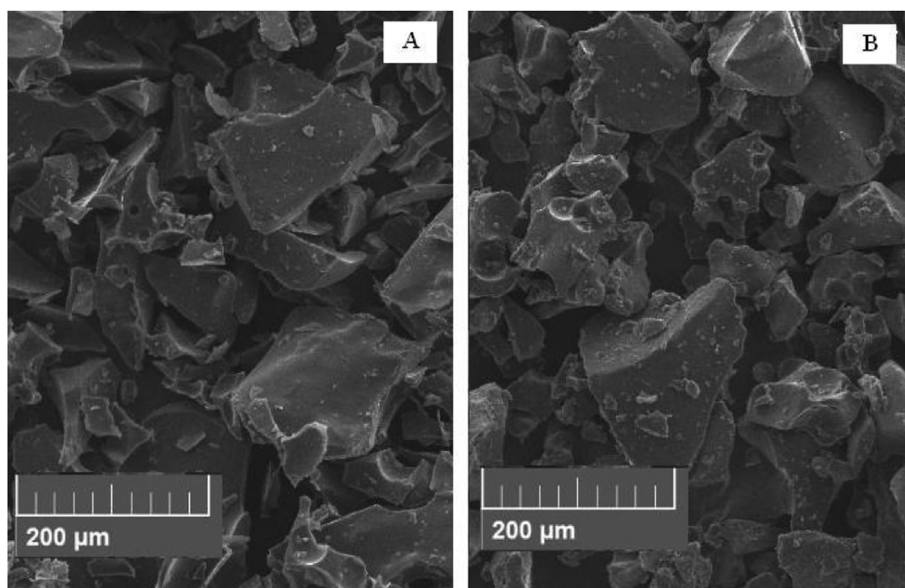


**Fig. 1.** Scan electron microscopy of powder particles of (A) yacon juice (YJ) and (B) yacon concentrate juice (YCJ) foam mat dried (width 1.0 cm and temperature 60 °C).

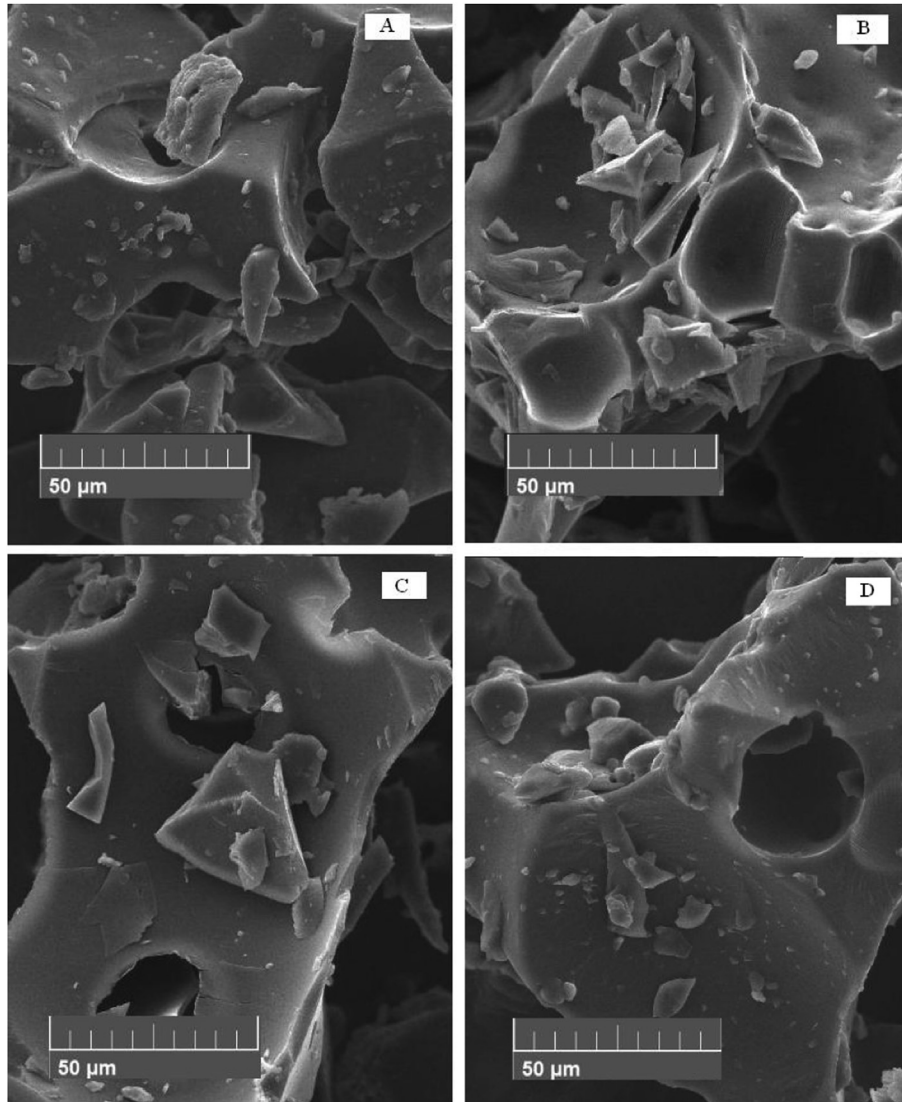


**Fig. 2.** Scan electron microscopy of powder particles of yacon juice (YJ) and yacon concentrate juice (YCJ) foam mat dried at different conditions: (A) YJ, 0.5 cm and 50 °C; (B) YJ, 1.5 cm and 70 °C; (C) YCJ, 0.5 cm and 50 °C; and (D) YCJ, 1.5 cm and 70 °C.

density. Although all samples are composed of yacon juice and egg albumin, the slight difference on the physicochemical characterization (Table 1) reflected on density. The higher density of the YJ powders in comparison to the CYJ powders can be related to their higher percentage of proteins respect to carbohydrates, as proteins have higher molecular weight (Nelson & Cox, 2004). Such behavior was also observed by Martin (2013) during spray drying of cupuaçu pulp.

The drying conditions did not influence significantly ( $p < 0.05$ ) on density for both powders (YJ and CYJ) (Table 5). This behavior differs from other studies (Fazaeli et al., 2012; Reddy et al., 2014) where higher dehydration temperatures decreased the particles' bulk density. In the current work, however, drying temperature ranges from 50 to 70 °C and higher temperatures (above 100 °C) are required so that evaporation rates are increased to the point where the removal of water causes structural breakage and fragmentation, resulting in lower density powders (Walton, 2000).

Porosity, which indicates the volume fraction of voids in a material, is an important property for particulate materials because a great number of voids implies the presence of higher amount of oxygen that may cause a fast material degradation (Ratti, 2009).

The porosity for the YJ and CYJ powders ranged between 0.413 and 0.461 and between 0.567 and 0.606, respectively, and was affected by the drying conditions employed. Very similar values were reported by Caparino et al. (2012) for the freeze drying (0.43–0.52) and spray drying (0.47) of mango juice and by Souza et al. (2009) for spray dried tomato pulp (0.5–0.59), but smaller rates were found by Jinapong, Supphantharika, and Jamnong (2008) for atomized soybean soluble extract (between 0.70 and 0.74).

The intragranular porosity is inversely proportional to density, indicating that incorporation of air into the foam induced accumulation of air within the dried particles, making them more porous and less dense (Goula & Adamopoulos, 2008).

### 3.2.3. Color

Color is one of the most important parameters in foods because it reflects their sensory attractiveness and quality. Color is influenced by many factors, including the variety of the fruit, its ripeness and mainly the impact of drying processes (Viuda-Martos et al., 2012). During dehydration, fruit pulps are subjected to high temperatures that cause enzymatic and non-enzymatic browning (Maillard reactions) and become dark at the end of the process

(Damodaran, Parkin, & Fennema, 2010).

Lightness ( $L^*$ ) in foods is related to several factors, such as concentration and type of pigments present, water content and concentration of water on the surface (Viuda-Martos et al., 2012). The juice powders showed  $L^*$  of 75.91–78.60 for YJ and 62.60–83.12 for CYJ, and the results were influenced ( $p < 0.05$ ) by the drying conditions (Table 6). Almost all YJ powders were a little less bright than the CYJ ones, which can be attributed to the drying time slightly longer needed to dry the YJ foams. Reis, Lenzi, and Masson (2012) found the same behavior during drying of yacon slices in vacuum oven:  $L^*$  decreased as drying time increased. However, all samples obtained in this work can be considered light, since within a brightness scale from 0 to 100 these exhibited  $L^* > 50$  (Vasconcelos, Minim, & Chaves, 2012).

With regard to the  $a^*$  coordinate (from green to red), the powders of YJ exhibited negative coefficients of  $-2.23$  to  $-1.16$ , representing a green tone, while the particulates of CYJ tended to red (positive coefficients), with values between 0.54 and 14.72. The drying conditions (layer thickness and air temperature) significantly influenced on the quality responses (Table 6). The sharp difference found between concentrate and non concentrate juices may have been caused by their concentration, as this coordinate is affected by the structural integrity of the food fibers, amount of pigments present and their solubility (hydro or liposoluble) (Fernández-López, Zhi, Aleson-Carbonell, Pérez-Alvarez, & Kuri, 2005).

The drying conditions also affected the yellow – blue coordinate ( $b^*$ ), with results corresponding to yellow for all samples:  $b^*$  ranged from 45.86 to 54.99 for the YJ powders and between 22.57 and 41.87 for the CYJ ones. The yellow tone may be ascribed to the presence of carotenoids in the roots of yacon.

### 3.2.4. Microstructure

Through evaluation of the food microstructure, it is possible to assess details of each component (water, starch, carbohydrates, lipids, sugars, proteins, lipids and salts) at microscopic level and their connections inside the cell at molecular level. As a food undergoes various treatments or processes, its microstructure can be preserved or destroyed for the development of new products (Ratti, 2009).

The scanning electron microscopy revealed data on the morphological and structural characteristics of powders of YJ and CYJ. In general, the particle morphology was not affected by the juice concentration or the drying conditions applied: they all presented a porous and irregular structure similar to freeze-dried mango juice (Caparino et al., 2012), which maintained structure and shape without shrinking or collapsing (Fig. 1A and B).

Forasmuch as the juices were dried after the cells of the yacon roots' tissues were ruptured, visible changes were not observed as a result of dehydration, unlike reported by Bernstein and Noreña (2014), who observed changes to macroscopic (volume and format) and microscopic (wall and cell membranes) levels in the yacon slices caused by the treatments applied.

There was a lack of uniformity for all samples. However, the SEM photomicrographs indicate that all samples had cavities in their structure derived probably from the spaces left by the air bubbles contained in the yacon foams, which contributed to the porosity of the juice powders (Fig. 2).

## 4. Conclusions

The investigation of new attributes and/or new uses from raw materials is of great relevance, given their key impact on economy, society and environment. In fact, the better use of natural resources can contribute to fight world hunger, given the globalization of the food market.

Foam mat drying proved to be an efficient alternative for the processing of yacon juice, since it allowed the development of a product with appropriate features for pure consumption or addition as a food ingredient. Although several drying technologies have been applied to yacon in the literature, there is no paper regarding the FMD. The results obtained in this paper may expand the industrialization of yacon, aiding small producers and industries to develop new yacon-based products.

The drying conditions did not affect significantly the solubility in water, bulk density, absolute density and intragranular porosity of the particles, however the temperature rise reduced moisture content and water activity of the samples. The powders obtained from yacon juice showed greater capacity of water absorption respect to the concentrate juice, which was lower for higher temperatures and lower layer thicknesses. Hygroscopicity was also positively affected by temperature. Brightness decreased with drying time and the color coordinates  $a^*$  and  $b^*$  indicated colour difference between powders of YJ (reddish) and CYJ (yellowish). The images obtained by scanning electron microscopy indicated that the morphologic characteristics of the particulates were not affected by the drying conditions: all samples presented irregular morphology and cavities that contribute to porosity.

The combination between the higher drying temperature ( $70^\circ\text{C}$ ) and the smallest thickness (0.5 cm) led to a shorter drying time and consequent lower energy demand to produce a powdered yacon juice with high stability (low moisture content and water activity). These process conditions did not affect the physical and chemical characteristics of the final product.

## Acknowledgments

The authors would like to thank CAPES – Coordination for the Improvement of Higher Education Personnel – for the financial support.

## References

- Abadio, F. D. B., Domingues, A. M., Borges, S. V., & Oliveira, V. M. (2004). Physical properties of powdered pineapple (*Ananas comosus*) juice – effect of malt dextrin concentration and atomization speed. *Journal of Food Engineering*, *64*, 285–287.
- Adolfo Lutz Institute. (2008). *Métodos físico-químicos para análise de alimentos* (4th ed.). São Paulo: Editora Instituto Adolfo Lutz (in Portuguese).
- Association of Official Analytical Chemists (AOAC). (2000). *Official methods of the association of official analytical chemists*. Washington.
- Bakar, J., Muhammad, S. C. E. K., Hashim, D. M., & Adzahan, N. (2013). Spray-drying optimization for red pitaya peel (*Hylocereus polyrhizus*). *Food and Bioprocess Technology*, *6*, 1332–1342.
- Barbosa-Cánovas, G. V., Ortega-Rivas, E., Juliano, P., & Yan, H. (2005). *Food Powders: Physical properties, processing and functionality* (1st ed.). New York: Kluwer Academic/Plenum Publishers.
- Belitz, H. D., Grosch, W., & Schieberle, P. (2009). *Food chemistry* (4th ed.). Berlin: Springer.
- Berk, Z. (2009). *Food process engineering and technology* (1st ed.). New York: Academic Press – Elsevier.
- Bernstein, A., & Noreña, C. P. Z. (2014). Study of thermodynamic, structural, and quality properties of yacon (*Smallanthus sonchifolius*) during drying. *Food and Bioprocess Technology*, *7*, 148–160.
- Breda, C. A., Sanjinez-Argandoña, E. J., & Correia, C. A. C. (2012). Shelf life of powdered *Campomanesia adamantium* pulp in controlled environments. *Food Chemistry*, *135*, 2960–2964.
- Campbell-Platt, G. (2009). *Food science and technology* (1st ed.). West Sussex: Blackwell Publishing.
- Campos, D., Betalleluz-Pallardel, I., Chirinos, R., Aguilar-Galvez, A., Noratto, G., & Pedreschi, R. (2012). Prebiotic effects of yacon (*Smallanthus sonchifolius* Poep. & Endl.), a source of fructooligosaccharides and phenolic compounds with antioxidant activity. *Food Chemistry*, *135*, 1592–1599.
- Caparino, O. A., Tang, J., Nindo, C. I., Sabiani, S. S., Powers, J. R., & Fellman, J. K. (2012). Effect of drying methods on the physical properties and microstructures of mango (Philippine 'Carabao' var.) powder. *Journal of Food Engineering*, *111*, 135–148.
- Cecchi, H. M. (2009). *Fundamentos teóricos e práticos em análise de alimentos* (2nd ed.). Campinas: Editora Unicamp (in Portuguese).

- Chen, X. D., & Mujumdar, A. S. (2008). *Drying technologies in food processing* (1st ed.). West Sussex: Blackwell Publishing.
- Clerici, M. T. P. S., & El-Dash, A. A. (2008). Características tecnológicas de farinhas de arroz pré-gelatinizadas obtidas por extrusão termoplástica. *Ciencia e Agro-tecnologia*, 32(5), 1543–1550 (in Portuguese).
- Damodaran, S., Parkin, K. L., & Fennema, O. R. (2010). *Fennema's food chemistry* (4th ed.). London: CRC Press.
- Delgado, G. T. C., Thomé, R., Gabriel, D. L., Tamashiro, W. M. S. C., & Pastore, G. M. (2012). Yacon (*Smallanthus sonchifolius*) – derived fructooligosaccharides improves the immune parameters in the mouse. *Nutrition Research*, 32(11), 884–892.
- Falade, K. O., Adeyanju, K. I., & Uzo-Peters, P. I. (2003). Foam-mat drying of cowpea (*Vigna unguiculata*) using glyceryl monostearate and egg albumin as foaming agents. *European Food Research and Technology*, 217, 486–491.
- Falade, K. O., & Okocha, J. O. (2010). Foam-mat drying of plantain and cooking banana (*Musa spp.*). *Food and Bioprocess Technology*, 5(4), 1173–1180.
- Falade, K. O., & Omojola, B. S. (2010). Effect of processing methods on physical, chemical, rheological, and sensory properties of okra (*Abelmoschus esculentus*). *Food and Bioprocess Technology*, 3, 387–394.
- Fazaeli, M., Emam-Djomeh, Z., Ashtari, A. K., & Omid, M. (2012). Effect of spray drying conditions and feed composition on the physical properties of black mulberry juice powder. *Food and Bioprocess Technology*, 90, 667–675.
- Fernández-López, J., Zhi, N., Aleson-Carbonell, L., Pérez-Alvarez, J. A., & Kuri, V. (2005). Antioxidant and antibacterial activities of natural extracts: application in beef meatballs. *Meat Science*, 69(3), 371–380.
- Franco, T. S., Ellendersen, L. S. N., Fattori, D., Granato, D., & Masson, M. L. (2015). Influence of the addition of ovalbumin and emulsifier on the physical properties and stability of yacon (*Smallanthus sonchifolius*) juice foams prepared for foam mat drying process. *Food and Bioprocess Technology*, 8(10), 2012–2026.
- Franco, T. S., Perussello, C. A., Ellendersen, L. S. N., & Masson, M. L. (2015). Foam mat drying of yacon juice: experimental analysis and computer simulation. *Journal of Food Engineering*, 158, 48–57.
- Frascareli, E. C., Silva, V. M., Tonon, R. V., & Hubinger, M. D. (2012). Effect of process conditions on the microencapsulation of coffee oil by spray drying. *Food and Bioprocess Technology*, 90(3), 413–424.
- Ghosal, S., Indira, T. N., & Bhattacharya, S. (2010). Agglomeration of a model food powder: effect of maltodextrin and gum Arabic dispersions on flow behavior and compacted mass. *Journal of Food Engineering*, 96, 222–228.
- Goula, A. M., & Adamopoulos, K. G. (2008). Effect of maltodextrin addition during spray drying of tomato pulp in dehumidified air: II. Powder Properties. *Drying Journal*, 26, 726–737.
- Graefe, S., Hermann, M., Manrique, I., Golombek, S., & Buerkert, A. (2004). Effects of post-harvest treatment on the carbohydrate composition of yacon roots in the Peruvian Andes. *Field Crops Research*, 86, 157–165.
- Granato, D., Grevink, R., Zielinski, A. A. F., Nunes, D. S., & van Ruth, S. M. (2014). Analytical strategy coupled with response surface methodology to maximize the extraction of antioxidants from green, yellow, and red teas (*Camellia sinensis* var *sinensis*). *Journal of Agricultural and Food Chemistry*, 62, 10283–10296.
- Harmayani, E., Winarti, S., & Nurismanto, R. (2011). Preparation of inulin powder from *Dioscorea Esculenta* tuber with foam mat drying method. In *Proceedings of the 12th Asian Food Conference, Bangkok* (pp. 16–18).
- Jakubczyk, E., Gondek, E., & Tambor, K. (2011). Characteristics of selected functional properties of apple powders obtained by the foam-mat drying method. In *Proceedings of the 11th International Congress on Engineering and Food, Athens* (pp. 1385–1386).
- Jaya, S., & Das, H. (2004). Effect of maltodextrin, glycerol monostearate and tricalcium phosphate on vacuum dried mango powder properties. *Journal of Food Engineering*, 63, 125–134.
- Jinapong, N., Suphantharika, M., & Jamnong, P. (2008). Production of instant soymilk powders by ultrafiltration, spray drying and fluidized bed agglomeration. *Journal of Food Engineering*, 84(2), 194–205.
- Kadam, D. M., Rai, D. R., Patil, R. T., Wilson, R. A., Kaur, S., & Kumar, R. (2011). Quality of fresh and stored foam mat dried Mandarin powder. *International Journal of Food Science & Technology*, 46, 793–799.
- Kha, T. C., Nguyen, M. H., & Roach, P. D. (2010). Effects of spray drying conditions on the physicochemical and antioxidant properties of the gac (*Momordica cochinchinensis*) fruit aril powder. *Journal of Food Engineering*, 98(3), 385–392.
- Krasaekoopt, W., & Bhatia, S. (2012). Production of yogurt powder using foam-mat drying. *AU Journal of Technology*, 15(3), 166–171.
- Kudra, T., & Ratti, C. (2008). Process and energy optimization in drying of foamed materials. *Transactions of the Tambov State Technical University*, 14(4), 812–819.
- Lago, C. C., Bernstein, A., Brandelli, A., & Noreña, C. Z. (2012). Characterization of powdered yacon (*Smallanthus sonchifolius*) juice and pulp. *Food and Bioprocess Technology*, 5, 2183–2191.
- Lewicki, P. P. (2004). Water as the determinant of food engineering properties. A review. *Journal of Food Engineering*, 61, 483–495.
- Maia, G. A., Monteiro, J. C. S., & Guimarães, A. C. L. (2001). Estudo da estabilidade físico-química e química do suco de caju com alto teor de polpa. *Ciencia e Tecnologia de Alimentos*, 21(1), 43–46 (in Portuguese).
- Marques, G. R., Borges, S. V., Mendonça, K. S., Fernandes, R. V. B., & Menezes, E. G. T. (2014). Application of maltodextrin in green corn extract powder production. *Powder Technology*, 263, 89–95.
- Mentreddy, S. R. (2007). Medicinal plant species with potential antidiabetic properties. *Journal of the Science of Food and Agriculture*, 87, 743–750.
- Mishra, P., Mishra, S., & Mahanta, C. L. (2014). Effect of maltodextrin concentration and inlet temperature during spray drying on physicochemical and antioxidant properties of amla (*Emblica officinalis*) juice powder. *Food and Bioprocess Technology*, 92, 252–258.
- Moreira, G. E. G., Costa, M. G. M., Rodriguez de Souza, A. C., Brito de, E. S., Medeiros de, M. F. D., & Azeredo de, H. M. C. (2009). Physical properties of spray dried acerola pomace extract as affected by temperature and drying aids. *LWT – Food Science and Technology*, 42, 641–645.
- Nelson, D. L., & Cox, M. M. (2004). *Lehninger principles of biochemistry* (4th ed.). New York: W. H. Freeman and Company.
- Oguntunde, A. O., & Adejojo, O. O. (1992). Foam-mat drying of fluid whole milk with glyceryl monostearate. *Nigerian Food Journal*, 10, 61–69.
- Oliveira, D. M., Clemente, E., & Costa, J. M. C. (2014). Hygroscopic behavior and degree of caking of grugru palm (*Acronomia aculeate*) powder. *Journal of Food Science and Technology*, 51(10), 2783–2789.
- Oliveira, T. M., Pirozi, M. R., Borges, J. T. S., Germani, R., & Fontes, M. P. F. (2009). Caracterização do amido de grão-de-bico. *Boletim do Centro de Pesquisa e Processamento em Alimentos*, 27(1), 27–42 (in Portuguese).
- Pereira, J. A. R., Barcelos, M. F. P., Pereira, M. C. D., & Ferreira, E. B. (2013). Studies of chemical and enzymatic characteristics of yacon (*Smallanthus sonchifolius*) and its flours. *LWT – Food Science and Technology*, 33(1), 75–83.
- Rao, M. A., Rizvi, S. S. H., & Datta, A. K. (2005). *Engineering properties of foods* (3rd ed.). Boca Raton: CRC Press.
- Ratti, C. (2009). *Advances in food dehydration* (1st ed.). Boca Raton: CRC Press.
- Reddy, R. S., Ramachandra, C. T., Hiregoudar, S., Nidoni, U., Ram, J., & Kammar, M. (2014). Influence of processing conditions on functional and reconstitution properties of milk powder made from Osmanabadi goat milk by spray-drying. *Small Ruminant Research*, 119, 130–137.
- Reis, F. R., Lenzi, M. K., & Masson, M. L. (2012). Effect of vacuum drying conditions on the quality of yacon (*Smallanthus sonchifolius*) slices: process optimization toward colour quality. *Journal of Food Processing and Preservation*, 36, 67–73.
- Scher, C. F., Rios, A. O., & Noreña, C. P. (2009). Hot air drying of yacon (*Smallanthus sonchifolius*) and its effect on sugar concentrations. *International Journal of Food Science & Technology*, 44, 2169–2175.
- Sharma, A. P., Gujral, H. S., & Rosell, C. M. R. (2011). Effects of roasting on barley  $\beta$ -glucan, thermal, textural and pasting properties. *Journal of Cereal Science*, 53, 25–30.
- Shi, Q., Zheng, Y., & Zhao, Y. (2013). Mathematical modeling on thin-layer heat pump drying of yacon (*Smallanthus sonchifolius*) slices. *Energy Conversion and Management*, 71, 208–216.
- Shishir, M. R. I., Taip, F. S., Aziz, N. A., & Talib, R. A. (2014). Physical properties of spray-dried pink guava (*Psidium guajava*) powder. *Agriculture and Agricultural Science Procedia*, 2, 74–81.
- Souza, A. S. D., Borges, S. V., Magalhães, N. F., Ricardo, H. V., & Azevedo, A. D. (2008). Spray dried tomato powder reconstitution and colour. *Brazilian Archives of Biology and Technology*, 51(4), 807–817.
- Souza, A. S., Borges, S. V., Magalhães, N. F., Ricardo, H. V., Cereda, M. P., & Daiuto, E. R. (2009). Influence of spray drying conditions on the physical properties of dried pulp tomato. *Ciencia e Tecnologia de Alimentos*, 29(2), 291–294.
- Takaneka, M., Yan, X., Ono, H., Yoshida, M., Nagata, T., & Nakanishi, T. (2003). Caffeic acid derivatives in the roots of yacon (*Smallanthus sonchifolius*). *Journal of Agricultural and Food Chemistry*, 51, 793–796.
- Tonon, R. V., Brabet, C., & Hubinger, M. D. (2008). Influence of process conditions on the physicochemical properties of açai (*Euterpe oleracea* Mart.) powder produced by spray drying. *Journal of Food Engineering*, 88, 411–418.
- Valentová, K., Stejskal, D., Bartek, J., Dvoráková, S., Kren, V., Ulřichová, J., et al. (2008). Maca (*Lepidium meyenii*) and yacon (*Smallanthus sonchifolius*) in combination with silymarin as food supplements: In vivo safety assessment. *Food and Chemical Toxicology*, 46, 1006–1013.
- Valentová, K., & Ulřichová, J. (2003). *Smallanthus sonchifolius* and *Lepidium meyenii* – Prospective andean crops for the prevention of chronic diseases. *Biomedical Papers*, 147(2), 119–130.
- Van't Land, C. M. (2012). *Drying in the process Industry* (1st ed.). New Jersey: John Wiley & Sons.
- Vasconcelos, C. M., Minim, V. P. R., & Chaves, J. B. P. (2012). Low-calorie yogurt added with yacon flour: development and physicochemical evaluation. *Revista Chilena de Nutrición*, 39(3), 65–71.
- Vasconcelos, C. M., Silva, C. O., Teixeira, L. J. Q., Chaves, J. B. P., & Martino, H. S. D. (2010). Determination of dietary soluble fibers in yacon (*Smallanthus sonchifolius*) roots and yacon flour by the enzymatic-gravimetric method and high-performance liquid chromatography. *Revista do Instituto Adolfo Lutz*, 69(2), 188–193 (in Portuguese).
- Viuda-Martos, M., Ruiz-Navajas, Y., Martín-Sánchez, A., Sánchez-Zapata, E., Fernández-López, J., Sendra, E., et al. (2012). Chemical, physico-chemical and functional properties of pomegranate (*Punica granatum* L.) bagasses powder co-product. *Journal of Food Engineering*, 110, 220–224.
- Walton, D. E. (2000). The morphology of spray-dried particles, a qualitative view. *Drying Technology*, 18, 1943–1986.
- Widjastutil, T. E. W., & Srianta, I. (2011). Development of functional drink based on foam-mat dried papaya (*Carica papaya* L.): optimization of foam-mat drying process and its formulation. *International Journal of Food, Nutrition and Public Health*, 4(2), 167–176.
- Wiecheteck, F. V., Nogueira, A., Drilleau, J. F., & Wosiacki, G. (2005). Effect of cryo-concentration in total phenolic compounds of industrial apple must. *Publicatio UEPG: Ciências Exatas e da Terra, Ciências Agrárias e Engenharias*, 11(1), 27–34.
- Wilson, R. A., Dattatreya, M. K., Chadha, S., Grewal, M. K., & Sharma, M. (2014).

- Evaluation of physical and chemical properties of foam-mat dried mango (*Mangifera indica*) powder during storage. *Journal of Food Processing and Preservation*, 38, 1866–1874.
- Yemmireddy, V. K., Chinnan, M., Kerr, W. L., & Hung, Y. C. (2013). Effect of drying method on drying time and physico-chemical properties of dried rabbit eye blueberries. *LWT – Food Science and Technology*, 50, 739–745.
- Yousefi, S., Emam-Djomeh, Z., & Mousavi, S. M. (2011). Effect of carrier type and spray drying on the physicochemical properties of powdered and reconstituted pomegranate juice (*Punica Granatum L.*). *Journal of Food Science and Technology*, 48(6), 677–684.



# Preparation of iron/zinc bound whey protein concentrate complexes and their stability



B.G. Shilpashree, Sumit Arora\*, Vivek Sharma

Dairy Chemistry Division, National Dairy Research Institute, Karnal, Haryana, 132001, India

## ARTICLE INFO

### Article history:

Received 27 August 2015

Received in revised form

1 November 2015

Accepted 3 November 2015

Available online 6 November 2015

### Keywords:

WPC

Ultrafiltration

Membrane processing

RP-HPLC

Stability

## ABSTRACT

Food fortification is the most cost effective, sustainable and optimal approach in the battle against iron and zinc deficiencies. Iron/zinc, being members of the transition metal series, are highly reactive and poses numerous challenges with respect to physicochemical stability of fortified foods. Whey proteins concentrate (WPC) produced as the principal byproduct of cheese or casein manufacturing is widely used as food ingredient. Among the various technologies explored, iron/zinc binding to milk proteins has long been understood and applied. Therefore, method for the preparation of WPC – mineral (iron/zinc) complex was standardized on the basis of maximum mineral binding ability of proteins. Method involving ultrafiltration and diafiltration (repeated washing to remove free mineral from retentate) has been standardized. Structural modification upon mineral binding was confirmed by RP-HPLC chromatograms. Both iron and zinc bound WPC complexes possessed good stability (resistance towards release of bound mineral) under different processing conditions. However, zinc bound WPC showed better heat stability and lower pH and ionic stability compared to iron bound WPC. The final protein – mineral complexes could be used as a suitable organic fortificants for various food applications with better solubility.

© 2015 Elsevier Ltd. All rights reserved.

## 1. Introduction

Iron and zinc have several functions in the human body and their deficiency lead to severe consequences which has a great impact on health and economic development of countries. Anemia affects one-fourth of the world's population, accounting for 8.8% of the total global burden of disease. Iron deficiency is the predominant cause of anemia across countries and in both sexes, with women more commonly afflicted (De Benoist, McLean, Egli, & Cogswell, 2008; Jimenez, Kuhnig-Gabsch, & Gasche, 2015; Kassebaum et al., 2014). Zinc deficiency has serious wide-ranging health consequences and is thought to be one of the most prevalent micronutrient deficiencies in the world (Wieringa, Dijkhuizen, Fiorentino, Laillou, & Berger, 2015). Strategies to combat mineral deficiency include supplementation with medicinal form as well as fortification of foods with soluble mineral salts. The major problems associated with the fortification of soluble mineral salts especially cations in food products are: chemical reactivity of the

fortificants, lack of stability under food processing and storage conditions, incompatibility of the fortificant with other food components and ensuring bioavailability of the fortificants (Ellis, Mittal, & Sugiarto, 2013). Hence, researchers are now focusing their attention on preparation of organic mineral fortificants (using proteins or carbohydrates), which are demonstrated to be efficient mineral supplements for human beings without side effects (Sharma, Shilpa Shree, Arora, & Tomar, 2015; Sugiarto, Ye, & Singh, 2009; Sugiarto, Ye, Taylor, & Singh, 2010). Milk is a poor source of iron and zinc (i.e. 0.2–0.4 mg iron/L and 2–6 mg zinc/L of milk), the addition of iron and zinc to dairy ingredient such as milk protein could be used as a potential approach to deliver these minerals to consumers. Whey proteins produced as the principal byproduct of cheese or casein manufacturing are widely used as food ingredients such as whey protein concentrate (WPC) or whey protein isolate, as they possess high nutritional value and desired functional properties (Kim, Saltmarch, & Labuze, 1989; Kinsella & Whitehead, 1989; Nakano, Goto, Nakaji, & Aoki, 2007).

Studies to determine the interactions of iron/zinc with whey proteins are lacking in the literature, although binding of iron/zinc to whey proteins has been demonstrated for experimental purposes (Sugiarto, 2004; Sugiarto et al., 2009). Preparation of

\* Corresponding author.

E-mail addresses: [shilpashreebg14@gmail.com](mailto:shilpashreebg14@gmail.com) (B.G. Shilpashree), [sumitak123@gmail.com](mailto:sumitak123@gmail.com) (S. Arora), [vishk12000@yahoo.com](mailto:vishk12000@yahoo.com) (V. Sharma).

lyophilized whey protein–iron complex involving acid precipitation (pH 3–4) (Douglas, Rainey, Wong, Edmondson, & Lacroix, 1981; El-Kholy, Osman, Gouda, & Ghareeb, 2011; Indumathi, Kaushik, Arora, & Wadhwa, 2015; Jones, Kalan, Jones & Hazel, 1972; Jones et al., 1975; Rice & McMahon, 1998; Zang & Mohoney, 1989; Zang & Mohoney, 1990) or by direct addition of iron to the concentrated whey obtained after ultrafiltration (Nakano et al., 2007) have been reported. In the former method, the final protein–iron complex was recovered by acid precipitation which confirmed that the complex was not soluble under acidic conditions. Moreover, the reports of Sugiarto (2004) and Baomy and Brule (1988) stated that cationic binding ability of whey protein reduced at pH < 5.5. As a consequence, the protein–iron complex prepared by acid precipitation may not be suitable for wide range of food application. The key purpose of protein – iron complexation was to reduce the reactivity of iron (as discussed above). However, the later method was deficient in removing of free iron form the final complex. Therefore, the present was intended to prepare mineral (iron/zinc) enriched whey protein concentrate (commercially available whey protein product) by adopting three basic processing conditions such as centrifugation (to remove the insoluble mineral content), ultrafiltration (to remove the free mineral content) and lyophilization (to facilitate protein – mineral complex in powder form). The specific objectives of this work included (i) preparation of whey protein concentrate (WPC) – mineral (iron/zinc) complex, (ii) confirmation of the structural modification of protein with respect to chromatographic behaviour using RP-HPLC and (iii) evaluation of the stability of bound iron from complex under different conditions encountered during processing.

## 2. Materials and methods

### 2.1. Materials

WPC (80 g protein/100 g) was procured from Davisco Foods International Co., Le Sueur, MN, USA. Folin and Ciocalteu's reagent, sodium carbonate, copper sulphate, potassium tartarate, bovine serum albumin, sodium hydroxide, ferrous sulphate heptahydrate (20.07 g iron content/100 g), zinc sulphate heptahydrate ( $ZnSO_4 \cdot 7H_2O$ ) (22.7 g zinc content/100 g), trifluoroacetic acid (TFA, HPLC grade) and standards of whey proteins such as  $\alpha$ -La and  $\beta$ -Lg were procured from Sigma Aldrich, St. Louis, MO, USA. Acetonitrile (HPLC grade) and water (HPLC grade) were procured from Rankem, RFCL Ltd., New Delhi, India. Triple distilled water and acid washed glassware were used throughout the experiment.

### 2.2. Methods

#### 2.2.1. Preparation of WPC – mineral complexes

The method of Sugiarto et al. (2009) was essentially followed for the preparation of WPC – mineral complexes. Protein solution was prepared by dissolving 10 g of protein in 1000 mL of triple distilled water. To this solution, iron/zinc was added slowly from the stock solution to obtain a final mineral concentration ranging from 1 to 10 mmol/L with constant stirring using magnetic stirrer. The pH of the solution was adjusted to 6.6 and was left undisturbed for 2 h at 20 °C. The mixture was then centrifuged at  $12,000 \times g$  at 20 °C for 30 min. Supernatant which contained soluble iron/zinc and protein was carefully decanted and filtered through Whatman No. 1 filter paper (mineral content in supernatant and protein solubility were analysed at this stage). The filtered supernatant was then passed through an Amicon ultrafiltration (UF) membrane centrifuge tubes (MW cut off 10 kDa) and the iron/zinc content in permeate was analysed by atomic absorption spectroscopy (AAS). Finally, iron/

zinc content was optimized (on the basis of maximum mineral binding ability of protein) and was subjected to large scale production using UF membrane processing system as follows.

**Membrane processing system:** The basic steps involved in UF membrane processing system were followed as described by Ferrer, Alexander, and Corredig (2011). Membrane with a nominal molecular weight cut-off (NMWCO) of 10 kDa hydrasart material with filtration area 0.1 m<sup>2</sup> was used for the present work. Clear filtered supernatant was concentrated using a Sartorius ultrafiltration unit (Model No. 7578, Sartorius India Pvt. Ltd. Mumbai, India) assembled with Master flex easy load pump – 7518-00 (Thermo Fisher Scientific, Mumbai, India). Pressure gauge and flow meter were connected to the inlet of the membrane and also at exit of retentate and permeate. UF was carried out by re-circulating the supernatant from feed tank. Membrane pressure and cross-flow velocity were set to 10 psi and 300 mL/min, respectively. The experiment was conducted at room temperature (~30 °C). Free iron/zinc content was completely removed from retentate by diafiltration (i.e. constant volume washing). To ensure the presence of free iron/zinc in permeate, 1 mL of 1 mol/L NaOH was added to 10 mL of permeate, followed by centrifugation at  $671 \times g/15$  min. Diafiltration was repeated until no appearance of mineral precipitate upon addition of NaOH and pellet formation upon centrifugation. Finally, retentate with no free iron/zinc was concentrated 4 times (4 $\times$ ) the original volume (e.g. 1 L to 250 mL) and freeze dried at –50 °C under 6.67 Pa pressure for 72 h.

Mineral retention in protein – mineral complex was estimated as follows:

Mineral retention (%)

$$= \frac{\text{Amount of added mineral}}{\text{Amount of obtained mineral in the complex}} \times 100$$

Total yield of protein – mineral complex was estimated as follows:

$$\text{Yield (\%)} = \frac{\text{Weight of added protein source (g)}}{\text{Weight of obtained complex (g)}} \times 100$$

#### 2.2.2. Estimation of mineral content

Mineral (iron/zinc) content of the complex was estimated by dry digestion method of AOAC (2005) using Atomic absorption spectrophotometer (AAS). 100 mg of sample was weighed and ashed at 550 °C/8 h. 10 mL of triple acid (nitric acid: perchloric acid: sulphuric acid in the ratio 3:2:1) was added to ash and heated for complete dissolution. Samples were diluted suitably and mineral content was estimated using AAS at  $\lambda_{\text{max}}$  248.3 for iron and 213.9 nm for zinc.

#### 2.2.3. Solubility

Method of Lawal, Adebowale, and Adebowale (2007) as modified by Shilpashree, Arora, Chawla, Vakkalagadda and Apurva (2015) and Mutilangi and Kilara (1985) with slight modification (i.e. centrifugation speed and time were optimized) were followed for the analysis of protein solubility. Sample solution (1 g/100 mL) was prepared in phosphate buffer (0.05 mol/L, pH 7) and the solution was adjusted to pH 7 using 0.1 mol/L NaOH. The disperse was mixed for 1 h at 30 °C using magnetic stirrer followed by centrifugation at  $18,000 \times g$  for 20 min at 4 °C. The supernatant was filtered through Whatman No. 1 filter paper and protein content was determined using the method of Lowry, Rosebrough, Farr, and Randall (1951). Determinations were carried out in triplicates and solubility (percentage) was evaluated as follows.

$$\text{Solubility (\%)} = \frac{\text{Amount of protein content in supernatant}}{\text{Amount of protein in the sample}} \times 100$$

Note: Protein solubility of supernatant obtained from protein – mineral mixtures was analysed directly by estimating the protein content in the supernatant.

#### 2.2.4. RP-HPLC

Reverse phase HPLC was used, following the method of [Yuksel and Erdem \(2010\)](#) with slight modification (i.e. sample preparation and elution sequence were standardized) to determine the elution profile of the whey proteins from WPC and its mineral complexes. Standards were dissolved in mixed solvent (solvent A and B in 70:30 ratio) to obtain the concentration of 25 and 10 mg/mL for  $\beta$ -Lg and  $\alpha$ -La, respectively. The individual standards were mixed together with equal ratio (1:1), followed by filtration through 0.22  $\mu$ m syringe filter. Protein solution (1 g/100 mL) of control (WPC without any treatment i.e. centrifugation and UF) and each sample was prepared in the solvent mixture (solvent A and B in 70:30 ratio) and centrifuged to 12,000  $\times$  g/30 min followed by filtration through 0.22  $\mu$ m syringe filter.

Chromatographic conditions: Solvent A – acetonitrile, water and TFA in a ratio 100:900:1 (mL:mL:mL); Solvent B – acetonitrile, water and TFA in a ratio 900:100:1 (mL:mL:mL); Total run time – 45 min; Column temperature – 40 °C; Detection wavelength – 220 nm (Waters 2998 Photodiode Array Detector); Injection volume – 20  $\mu$ l (CAPLUCE RC 11 injector with a 20  $\mu$ l loop); Gradient solvent delivery was achieved using Waters Pump Control Module II at a flow rate of 1 mL/min; Solvent gradient programme was initiated at 20% of solvent B and it was generated immediately after sample injection by increasing the proportion of solvent B to 60% at the end of the run. It was returned to the start conditions in 2.4 min.

#### 2.2.5. Stability of bound iron from WPC – mineral complex

Evaluation of stability of bound iron from protein complexes was carried out by essentially following the method of [Gaucheron, Famelart, and Le Graet \(1996\)](#). Sample solution (1 g/100 mL) was prepared in 0.05 mol/L phosphate buffer (pH 7) and monitored under different conditions encountered during processing such as pH (3–7), heat treatment (50–70 °C/30 min) and ionic concentration (0.1–0.5 mol/L NaCl). Further, the adjusted solutions were incubated at room temperature (~30 °C) for 24 h. The released free mineral (iron/zinc) in permeate upon UF using Amicon UF centrifuge tubes was used as an index to determine the stability of bound iron from protein – mineral complex. Control represented the retention of mineral upon UF of both WPC – iron and WPC–zinc complex solutions at its native conditions i.e. pH ~5.75 (WPC – iron) and ~6.5 (WPC – zinc), ~30 °C temperature and no change in ionic concentration.

#### Stability (%)

$$= \frac{\text{Mineral content obtained after ultrafiltration}}{\text{Mineral content originally present in the complex}} \times 100$$

#### 2.2.6. Chemical composition

Protein was estimated using Kjeldahl method as described by [AOAC \(1984\)](#). Moisture was determined using the method of [IS: 16072 \(2012\)](#). Fat, lactose and ash contents of MPC were estimated according to the methods of [IDF 127A \(1988\)](#), [IDF 106 \(1982\)](#) and [IDF 90 \(1979\)](#), respectively.

#### 2.2.7. Statistical analysis

Means and standard error mean (SEM) were calculated using Microsoft Excel, 2007 (Microsoft Corp., Redmond, WA). Significant difference between values was verified by one way analysis of variance (ANOVA) and comparison between means was made by critical difference value ([Snedecor & Cochran, 1994](#)).

### 3. Results and discussion

Addition of mineral (iron/zinc) to protein solution led to the distribution of added mineral into two different states upon centrifugation such as mineral remaining in the soluble (supernatant) and insoluble (precipitate) portion. The soluble mineral was again categorized into two forms upon UF, protein bound mineral (retentate) and free mineral (permeate). Based on this hypothesis the results were described as follows.

#### 3.1. Preparation of WPC–iron complex

##### 3.1.1. Separation of soluble protein and iron by centrifugation

Iron remaining in supernatant after centrifugation of WPC – iron solution prepared with different concentrations of ferrous sulphate is presented in [Fig. 1a](#). At low levels of added iron (1–3.6 mmol/L), approximately 16 mg of iron (80% of added iron) was associated with the soluble fraction of WPC – iron solution. Further addition of iron, markedly increased the insoluble iron portion from 3.97 to 30.29 mg of iron (19–54% of added iron) at 3.6–10 mmol/L of added iron, respectively. This could be due to the insolubility of iron rather than the insolubility of whey proteins, as addition of iron to protein solution caused only a slight decrease in the solubility of whey protein at all levels as shown in [Fig. 1b](#).

##### 3.1.2. Separation of iron bound protein by UF

Supernatant obtained after centrifugation of WPC – iron solution was subjected to UF, iron that was retained in the retentate and permeate at various levels of ferrous sulphate is presented in [Fig. 2a](#). It was observed that a small amount of iron (approximately <3 mg of iron viz. 20% of total added iron) was found in permeate as free (unbound) iron up to a concentration of around 3 mmol/L added iron. This indicated that at this concentration, most of the iron was bound to the soluble whey proteins under the present experimental conditions. It was also observed that iron concentration in retentate remained constant viz. 11.80 mg from 3 to 3.8 mmol/L and finally reduced to 5 mg iron for 10 mmol/L of added iron. These findings clearly demonstrated that maximum iron content in final complex was obtained at 3 mmol/L level without much iron loss through centrifugation and UF. Therefore, this concentration was finally selected for the production of WPC–iron complex through pilot scale membrane processing system.

#### 3.2. Preparation of WPC–zinc complex

##### 3.2.1. Separation of soluble protein and iron by centrifugation

Zinc remaining in the supernatant and sediment after centrifugation of WPC with different concentrations of added zinc sulphate is shown in [Fig. 1a](#). Most of the added zinc was soluble (>10 mg of zinc viz. 90% added zinc) up to 1.6 mmol/L zinc concentration. The relative proportions of zinc bound to soluble protein decreased with increasing zinc concentration up to 10 mmol/L. This decrease was probably due to the precipitation of the zinc and the whey proteins from the WPC – zinc solution, as addition of zinc to a WPC solution resulted in reduction in protein solubility ([Fig. 1b](#)). Zinc proved to be a better agent for lowering solubility of several plasma proteins by shifting isoelectric point of protein from acidic to alkaline pH ([Gurd & Goodman, 1952](#)). Moreover, zinc ions

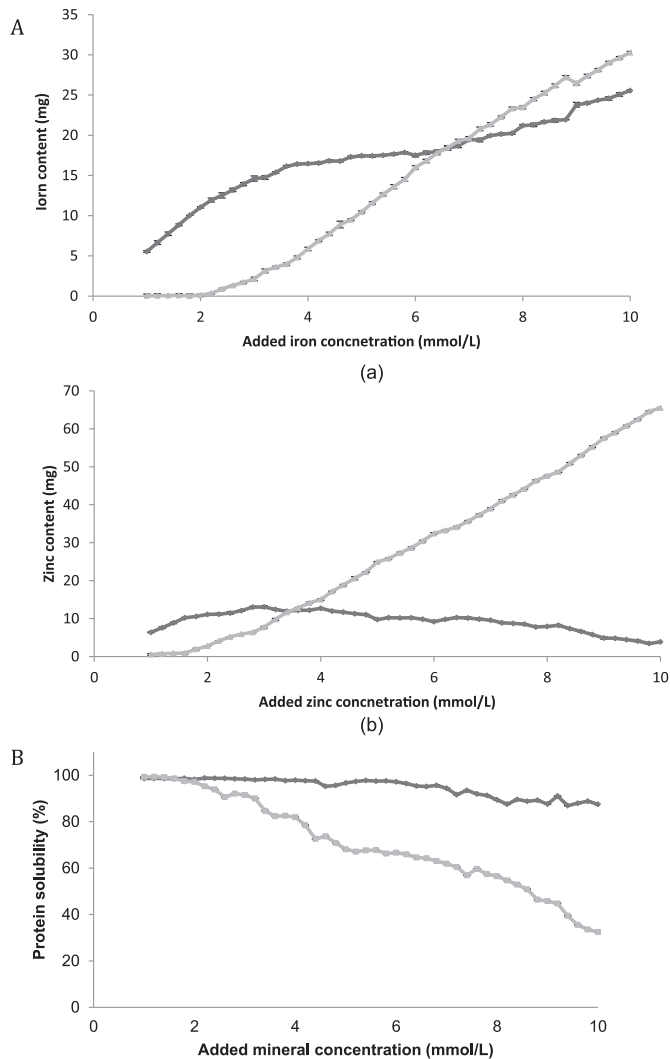


**Fig. 1.** A: Amount of mineral obtained after centrifugation of WPC – mineral mixtures; (a) WPC – iron (— iron in supernatant, — iron in sediment) and (b) WPC – zinc (— zinc in supernatant, — zinc in sediment). B: Solubility of protein as a function of added mineral concentration in WPC – mineral mixture; — WPC – iron, — WPC – zinc.

are commonly used as a direct protein precipitation and as auxiliary agent, especially during the recovery of plasma and coagulated proteins (Cohn et al., 1950; Lovrien & Matulis, 1997). Many techniques also include zinc salts for purification of proteins (Cohn et al., 1950; Gurd & Wilcox, 1956; Rothstein, 1994). Therefore, it was evident that the addition of zinc even at lower concentration (at >1.6 mmol/L) could precipitate more whey proteins as compared to iron.

### 3.2.2. Separation of iron bound protein by UF

Zinc that was retained in the retentate and permeate (after UF) at various levels of ferrous sulphate is presented in Fig. 2b. Addition of zinc from 1 to 1.6 mmol/L gradually increased zinc content in retentate viz. 6.35–10.05 mg of zinc, respectively. Relatively greater proportion of zinc in retentate implied that availability of soluble protein was higher at these levels. The findings of present study clearly demonstrated that whey proteins could bind relatively small amount of zinc compared to iron, even at low concentrations of added zinc (<2 mmol/L). Maximum zinc content in final complex was obtained at 1.6 mmol/L (10.05 mg zinc) level without much

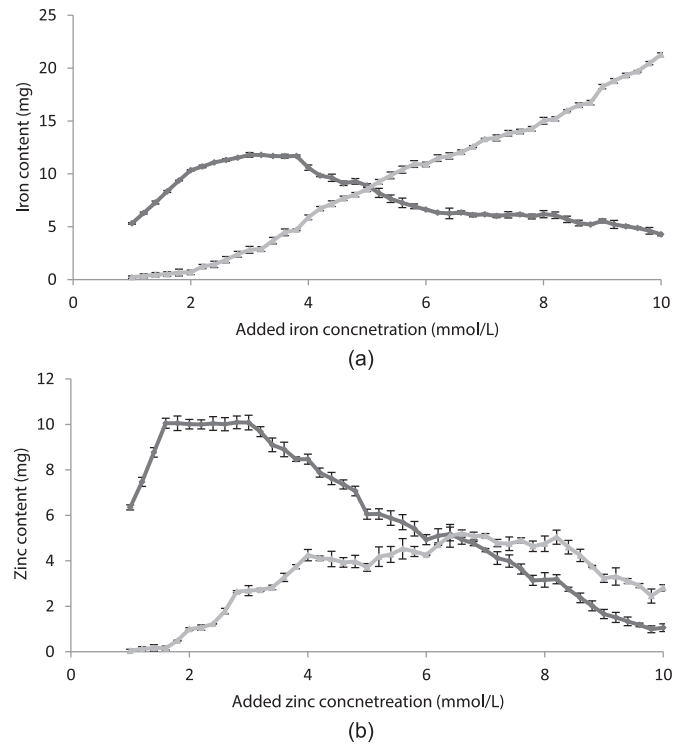


**Fig. 2.** Amount of mineral obtained after ultrafiltration of WPC – mineral supernatant; (a) WPC – iron (— iron in retentate, — iron in permeate) and (b) WPC – zinc (— zinc in retentate, — zinc in permeate).

zinc loss on centrifugation and UF. Therefore, this concentration was finally selected for the production of WPC–zinc complex through pilot scale membrane processing system.

### 3.3. Preparation of WPC – mineral complex on pilot scale

The free mineral (iron/zinc) was completely removed from retentate by diafiltration (i.e. constant volume washing) or by repeated UF steps. Initially the supernatant (obtained from optimized level of iron/zinc) was concentrated up to 2× (e.g. 1 L to 500 mL) and to this an equal amount of deionised water (500 mL) was added and then subjected to UF process. Since, iron/zinc cations forms a dirty green/white precipitate in presence of sodium hydroxide and further centrifugation leads to pellet formation (Lambert & Mohammed, 1978). The presence of free mineral in the permeate was confirmed by the addition of NaOH. Since, the supernatant obtained from WPC – iron and WPC – zinc solution released around 2.82 mg of iron and 0.16 mg of zinc (viz. 16.82% and 1.48% of added iron and zinc), respectively in permeate upon UF at its optimized concentration (Fig. 2). The former required 3× and later required 2× of washing to remove free iron/zinc content completely from retentate. Retentate obtained after diafiltration was concentrated 4× (e.g. 1 L to 250 mL) and then immediately subjected to lyophilization (freeze drying).

One of the important purpose of this research was to prepare a protein complex which should satisfy three basic requirements (i.e. it should carry sufficient amount of mineral, it should possess better solubility under physiological conditions and it should also contain maximum amount of protein, which in turn contributes towards better yield) for acceptability of both iron and zinc fortificant in wide range of food application. It was evident from Table 1 that both the complexes satisfied basic requirements. This also indicated that the conditions adopted for the membrane processing were found acceptable.

**Table 1**  
Different properties of Lyophilized powders of WPC – mineral complexes.

WPC – mineral complexes	Optimized mineral concentration (mmol/L)	Different properties			mg of mineral/g of complex
		Mineral retention (%)	Solubility (%) (pH 7.0)	Total yield (%)	
WPC – iron	3.0	70.41 ± 0.17	93.25 ± 0.13	80.60 ± 0.007	11.71 ± 0.004
WPC – zinc	1.6	90.05 ± 0.60	91.27 ± 0.21	73.42 ± 0.48	10.27 ± 0.02

Data are presented as means ± SEM (n = 3).

The composition of WPC – iron and WPC – zinc complexes along with WPC in the absence of minerals was estimated (Table 2). Preparation of iron and zinc bound WPC involved centrifugation and UF process. During centrifugation the fat portion separates out as flakes in the supernatant (therefore, supernatant was filtered before UF) and during UF, major portion of soluble components especially lactose is removed through permeate. Therefore, fat and lactose content of WPC – iron and WPC – zinc complexes reduced significantly ( $P < 0.05$ ), with subsequent increase in protein and ash content of both iron and zinc bound WPC compared to WPC in the absence of minerals.

#### 3.4. Reverse – phase HPLC profiles of protein – mineral complexes

The RP-HPLC profiles of WPC and its mineral complexes were evaluated to confirm the structural modifications and respective chromatograms are shown in Fig. 3 and different aspects of peaks are presented in Table 3. The retention time of the two important fractions of whey proteins such as  $\alpha$ -lactalbumin ( $\alpha$ -La) and  $\beta$ -lactoglobulin ( $\beta$ -Lg) were identified by running the standards (Fig. 3b). Whey proteins in WPC were separated into two main fractions  $\alpha$ -La and  $\beta$ -Lg and on the basis of chromatographic area obtained, it can be inferred that WPC contains higher amount of  $\beta$ -Lg than  $\alpha$ -La (Fig. 3c) similar to milk whey proteins composition i.e. 50 and 28% of total whey proteins, respectively (Walstra & Jenness, 1984). RP-HPLC profile of WPC – iron (Fig. 3d) and WPC – zinc (Fig. 3e) showed significant differences ( $P < 0.05$ ) in chromatographic area but non significant difference in retention time as compared to WPC.  $\alpha$ -La chromatographic area of WPC was reduced up to 75% and 90% of initial area upon complex formation with iron and zinc, respectively. Whereas,  $\beta$ -Lg chromatographic area of WPC was reduced up to 67% and 91% of initial area upon complex formation with iron and zinc, respectively. Complexation of WPC with iron resulted in greater variation in chromatographic area of both the fractions as compared to zinc. Therefore, it could be inferred that added iron forms complex mainly with  $\beta$ -Lg as compared to  $\alpha$ -La. Vaughan and Knauff (1961) also showed the relative affinity of  $Fe^{3+}$  with different milk protein fractions and reported that among the whey

proteins, iron binds mainly to  $\beta$ -Lg and then to  $\alpha$ -La. Whey protein fractions on complexation with zinc showed a slight reduction in chromatographic area of  $\alpha$ -La than  $\beta$ -Lg. These results corroborated with the findings of Baummy and Brule (1988) who reported that  $\alpha$ -La showed more affinity than  $\beta$ -Lg towards zinc binding. Therefore, it could be safely inferred that zinc forms a complex mainly with  $\alpha$ -La than  $\beta$ -Lg.

#### 3.5. Stability of bound mineral in WPC – mineral complexes

Stability of the bound mineral (iron/zinc) in the complex was defined as the amount of mineral that was retained in retentate after UF. The stability of bound mineral was expressed in terms of percentage of mineral retention obtained (Section 3.3) and results are presented in Table 4.

**WPC–iron complex:** pH adjustment from 3 to 7 of WPC–iron complex solution resulted in significant increase ( $P < 0.05$ ) in the amount of free iron in permeate which in turn reduced the stability. This could be due to the reduced iron and zinc binding ability of whey proteins at lower pH as reported by Baummy and Brule (1988). They also revealed that lower pH conditions leads to dissociation of carboxylic groups of ionic amino acids which are mainly involved in mineral binding mechanism of whey proteins. However, 92–99% of the initial iron was still bound to the proteins under this pH range. Heat treatment from 50 to 90 °C/30 min to WPC–iron complex solution resulted in significant increase ( $P < 0.05$ ) in the amount of free iron in permeate which in turn reduced the stability. However, 90% of the initial iron was still bound to the proteins even after heat treatment at 90 °C/30 min. The increase in ionic concentration of WPC–iron complex solution also resulted in significant increase ( $P < 0.05$ ) in the amount of free iron in permeate which in turn reduced the stability. Baummy and Brule (1988) also reported that an increase in ionic strength from 0.01 to 0.1 M caused a 50% decrease in the binding ability of iron for both  $\alpha$ -La and  $\beta$ -Lg. However, 92.5% of the initial iron was still bound to WPC even at 0.5 mol/L NaCl ionic concentration under present experimental conditions. Findings from the present work clearly demonstrated that iron retained in the complex was not much affected by different processing conditions.

**WPC–zinc complex:** zinc bound WPC also showed similar kind of variations in stability as compared to iron bound protein complex, but better stability under high heat treatment (~99% at 90 °C/30 min) and lower stability under lower pH values (~88% at pH 3.0) and higher ionic concentrations (~72% at 0.5 mol/L NaCl). Some reports are available regarding the effect of low pH on zinc binding ability of whey proteins. De Wit (1989) reported that  $\alpha$ -La undergoes conformational changes at around pH 4.0 and release bound  $Ca^{2+}$ , whereas this binding was tighter at higher pH. They also revealed that  $\beta$ -Lg also undergoes conformational changes from a stable dimer (at pH 6.7–5.2) to an octamer (at pH 5.2–3.5) or a monomer (below pH 3.5) which might also contribute to the zinc binding ability. Sugiarto et al. (2009) also studied the effect of pH on metal ion binding ability of WPI and reported that the change in pH affected the complex formation between metal ions and proteins, as hydrogen ions compete with

**Table 2**  
Composition of WPC and its mineral complexes.

Constituents (g/100g)	Samples			
	WPC <sup>1</sup>	WPC <sup>2</sup>	WPC – iron	WPC – zinc
Protein	80.0	79.69 ± 0.29 <sup>a</sup>	86.32 ± 0.24 <sup>b</sup>	87.21 ± 0.24 <sup>b</sup>
Lactose	8.50	8.36 ± 0.32 <sup>a</sup>	0.80 ± 0.31 <sup>b</sup>	0.75 ± 0.43 <sup>b</sup>
Fat	5.50	5.42 ± 0.17 <sup>a</sup>	2.10 ± 0.26 <sup>b</sup>	2.00 ± 0.25 <sup>b</sup>
Ash	3.00	2.80 ± 0.22 <sup>a</sup>	6.00 ± 0.22 <sup>b</sup>	5.80 ± 0.28 <sup>b</sup>
Moisture	4.60	4.52 ± 0.26 <sup>a</sup>	4.51 ± 0.28 <sup>a</sup>	4.49 ± 0.30 <sup>a</sup>

Data are presented as means ± SEM (n = 3).

<sup>a–b</sup>Means within rows with different superscripts are significantly different ( $P < 0.05$ ) from each other.

<sup>1</sup>Data obtained from Davisco Foods International Co.

<sup>2</sup>Data obtained from laboratory analysis.

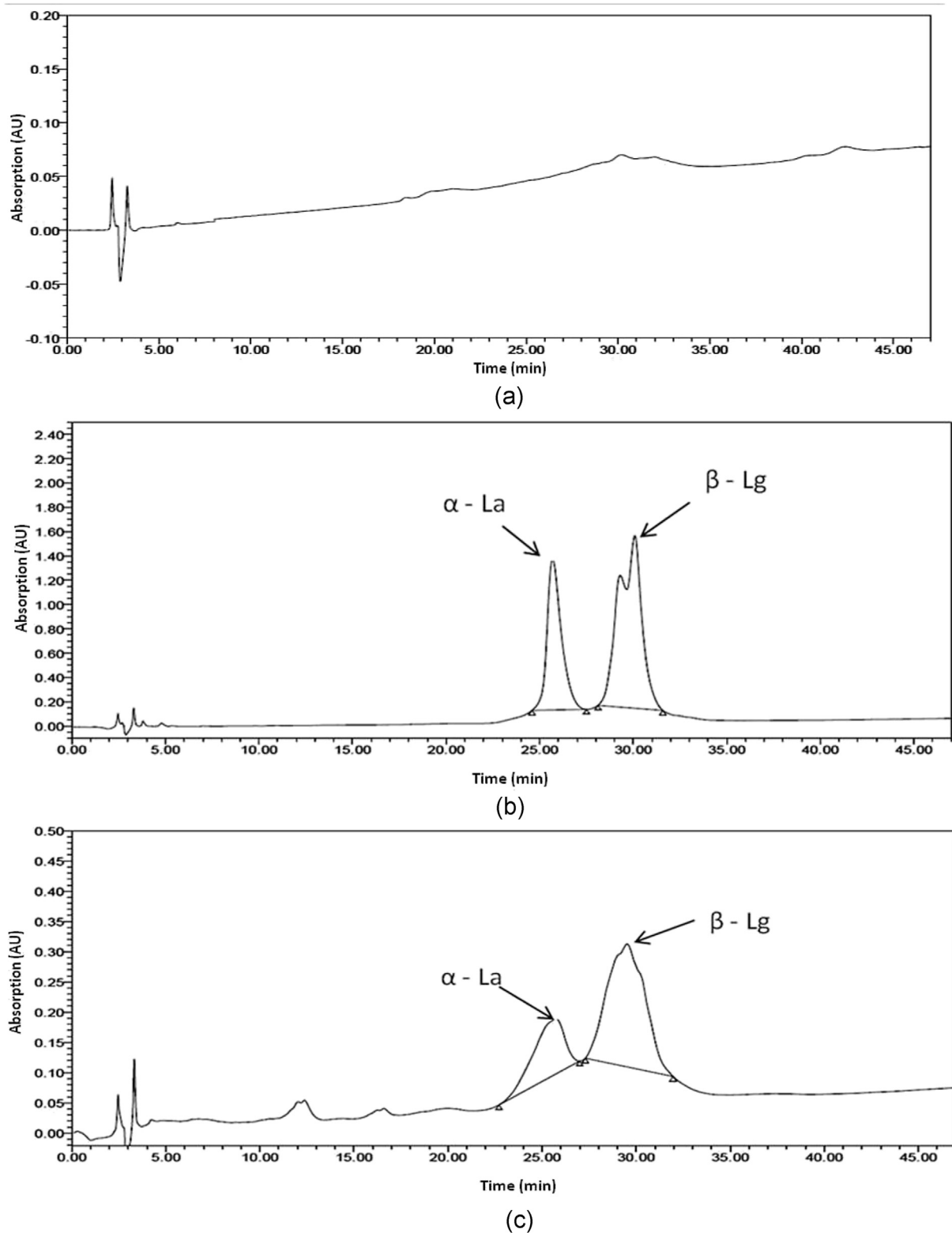


Fig. 3. RP-HPLC chromatograms of WPC and its mineral complexes: (a) Blank (b) WP standards (c) WPC (d) WPC – iron complex and (e) WPC – zinc complex.

the metal ions for binding to proteins. Therefore, it could be inferred that lower pH values (<5) decreased ionization and structural modification of  $\alpha$ -La and  $\beta$ -Lg, which in turn reduced zinc holding ability of whey proteins and hence reduced stability under this pH range.

The main intention was to determine the mineral (iron/zinc) retention stability of whey proteins in the complex under different processing conditions. Findings from the iron and zinc bound WPC complexes revealed that whey proteins bind iron more tenaciously than zinc.

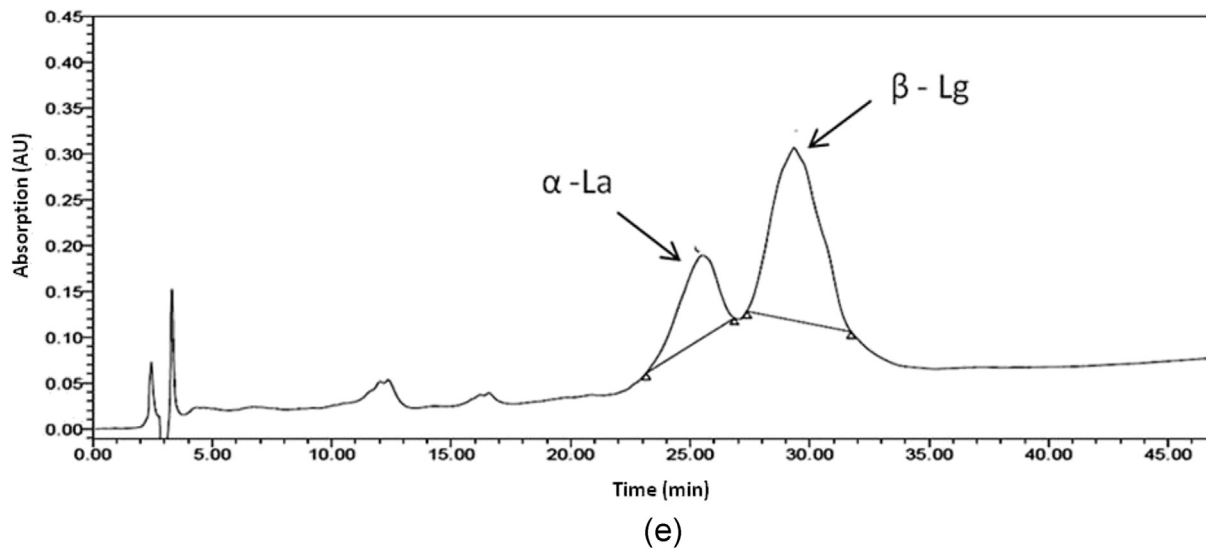
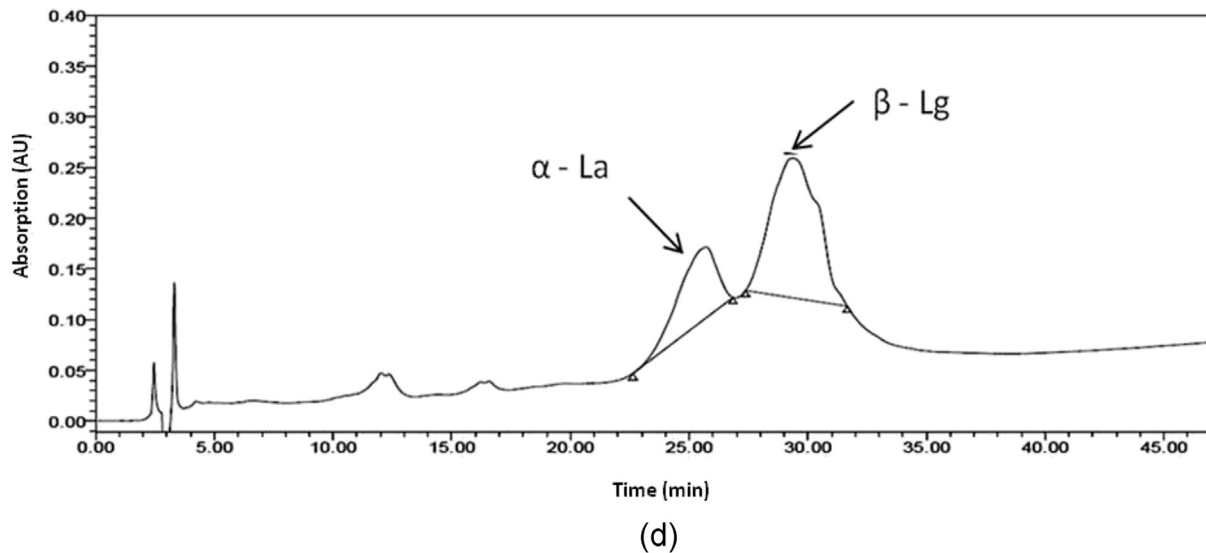


Fig. 3. (continued).

#### 4. Summary and conclusion

Method for the preparation of WPC – mineral (iron/zinc) complex has been standardized. The mineral concentration was optimized on the basis of maximum mineral binding ability of WPC and the concentrations include 3.0 mmol of iron/L and 1.6 mmol of zinc/L for WPC – iron and WPC–zinc complex, respectively. Optimized levels were further subjected to pilot scale membrane processing. The membrane processing method and diafiltration (repeated washing to remove free mineral from retentate) have

been standardized. The complexes prepared, satisfied the basic requirements such as better mineral retention, solubility and yield on the basis of weight. Fat and lactose content of WPC – iron and WPC – zinc complexes reduced significantly ( $P < 0.05$ ) with subsequent increase in protein and ash content compared to WPC in the absence of minerals. Structural modification upon binding with mineral was confirmed by RP-HPLC chromatograms, which showed variation in chromatographic area but no change in retention time of whey protein fractions. Iron and zinc bound WPC complexes possessed good stability (resistance towards release of bound

**Table 3**

Retention time and area of peaks obtained in RP-HPLC chromatograms of WPC and its mineral complexes.

Protein samples	$\alpha$ -Lactalbumin ( $\alpha$ -La)			$\beta$ -Lactoglobulin ( $\beta$ -Lg)		
	Retention time	Area	Obtained area (%) <sup>1</sup>	Retention time	Area	Obtained area (%) <sup>1</sup>
WPC	25.65 $\pm$ 0.01 <sup>a</sup>	10852309.00 $\pm$ 12.50 <sup>a</sup>	100	29.54 $\pm$ 0.03 <sup>a</sup>	28297924.00 $\pm$ 18.77 <sup>a</sup>	100
WPC – iron	25.48 $\pm$ 0.02 <sup>a</sup>	8116942.00 $\pm$ 36.06 <sup>b</sup>	75	29.40 $\pm$ 0.02 <sup>a</sup>	18973511.00 $\pm$ 31.43 <sup>b</sup>	67
WPC – zinc	25.45 $\pm$ 0.01 <sup>a</sup>	9773745.67 $\pm$ 24.03 <sup>c</sup>	90	29.36 $\pm$ 0.03 <sup>a</sup>	25905156.33 $\pm$ 29.24 <sup>c</sup>	91

Data are presented as means  $\pm$  SEM (n = 3).

<sup>a–c</sup>Means within columns with different superscripts are significantly different ( $P < 0.05$ ) from each other.

<sup>1</sup> Obtained area in comparison with control (WPC).

**Table 4**  
Effect of different processing treatments on retention of the mineral in WPC – mineral complexes.

Different processing treatments	WPC – iron		WPC – zinc		
	Amount of iron retained in retentate		Amount of zinc retained in retentate		
	(mg)	% of initial iron content	(mg)	% of initial zinc content	
Control <sup>a</sup>	11.65 ± 0.002	99.50	10.23 ± 0.04	99.57	
pH	3	10.84 ± 0.01 <sup>a</sup>	92.54	9.09 ± 0.09 <sup>a</sup>	88.48
	4	11.12 ± 0.08 <sup>b</sup>	94.93	9.19 ± 0.04 <sup>b</sup>	89.49
	5	11.46 ± 0.02 <sup>c</sup>	97.85	9.44 ± 0.01 <sup>c</sup>	91.87
	6	11.56 ± 0.09 <sup>d</sup>	98.69	9.97 ± 0.02 <sup>d</sup>	97.06
	7	11.63 ± 0.04 <sup>e</sup>	99.33	10.17 ± 0.08 <sup>e</sup>	99.02
Heat treatment (°C/30 min)	50	11.53 ± 0.08 <sup>e</sup>	98.43	10.22 ± 0.02 <sup>d</sup>	99.55
	60	11.43 ± 0.05 <sup>d</sup>	97.58	10.22 ± 0.03 <sup>d</sup>	99.49
	70	11.29 ± 0.02 <sup>c</sup>	96.44	10.20 ± 0.05 <sup>c</sup>	99.36
	80	10.96 ± 0.02 <sup>b</sup>	93.56	10.18 ± 0.02 <sup>b</sup>	99.13
	90	10.64 ± 0.06 <sup>a</sup>	90.82	10.17 ± 0.01 <sup>a</sup>	99.04
Ionic concentration (mol/L)	0.1	11.18 ± 0.02 <sup>d</sup>	95.47	9.50 ± 0.02 <sup>e</sup>	92.54
	0.2	11.02 ± 0.02 <sup>c</sup>	94.07	9.37 ± 0.02 <sup>d</sup>	91.26
	0.3	11.01 ± 0.01 <sup>c</sup>	94.01	8.51 ± 0.04 <sup>c</sup>	82.90
	0.4	10.95 ± 0.04 <sup>b</sup>	93.48	8.14 ± 0.01 <sup>b</sup>	79.22
	0.5	10.83 ± 0.01 <sup>a</sup>	92.50	7.46 ± 0.02 <sup>a</sup>	72.63

Data are presented as means ± SEM (n = 3).

<sup>a–e</sup>Means within columns with different superscripts are significantly different (P < 0.05) from each other.

<sup>a</sup> 1.0% solution of complex in phosphate buffer kept for 24 h under native conditions without any processing treatment.

mineral) during different processing conditions. However, zinc bound WPC showed better heat stability and lower pH and ionic stability compared to iron bound WPC. In conclusion, the standardized method could be adopted for the production of WPC – iron/zinc complex commercially. Since, the obtained protein – mineral complexes were rich in both protein and mineral content, the final product would be referred as mineral enriched whey protein concentrate. These complexes could also be used as an organic mineral fortificant with better solubility for various food applications.

## Acknowledgement

This study is part of the Department of Science and Technology (DST) – project financially supported by the Ministry of Science and Technology, New Delhi, India. (Project No: SERB/MOFPI/0040/2013).

## References

- AOAC. (1984). *Official methods of analysis of AOAC International* (14th ed.). Arlington, VA: The Association of Official Analytical Chemists.
- AOAC. (2005). *Official methods of analysis. The Association of Official Analytical Chemists* (18th ed., p. 481). Maryland, USA: North Fredrick Avenue Gaithersburg.
- Baumy, J. J., & Brule, G. (1988). Binding of bivalent cations to  $\alpha$ -lactalbumin and  $\beta$ -lactoglobulin: effect of pH and ionic strength. *Le Lait*, 68(1), 33–48.
- Cohn, E. J., Gurd, F. R., Surgenor, D. M., Barnes, B. A., Brown, R. K., Derouaux, G., et al. (1950). A system for separation of the components of human blood: quantitative procedures for separation of the protein components of human plasma. *Journal of American Chemical Society*, 72, 465–474.
- De Benoist, B., McLean, E., Egli, I., & Cogswell, M. (2008). *Worldwide prevalence of anaemia 1993–2005: WHO global database on anaemia*. Geneva: WHO.
- De Wit, J. N. (1989). Functional properties of whey proteins. In P. F. Fox (Ed.), *Developments in dairy chemistry* (Vol. 4, pp. 285–321). UK: Elsevier Applied Science.
- Douglas, F. W., Rainey, N. H., Wong, N. P., Edmondson, L. F., & Lacroix, D. E. (1981). Color, flavor, and iron bioavailability in iron-fortified chocolate milk. *Journal of Dairy Science*, 64(9), 1785–1793.
- El-Kholy, A. M., Osman, M., Gouda, A., & Ghareeb, W. A. (2011). Fortification of yoghurt with iron. *World Journal of Dairy & Food Sciences*, 6(2), 159–165.
- Ellis, A., Mittal, V., & Sugiarto, M. (2013). Innovation in healthy and functional foods. In D. Ghosh, S. Das, D. Bagchi, & R. B. Smarta (Eds.), *Innovation in iron fortification is the future in iron-binding milk proteins?* (pp. 249–267). New York: CRC Press, Taylor and Francis Group publication.
- Ferrer, M. A., Alexander, M., & Corredig, M. (2011). Does ultrafiltration have a lasting effect on the physico-chemical properties of the casein micelles? *Dairy Science and Technology*, 91, 151–170.
- Gaucheron, F., Famelart, M. H., & Le Graet, Y. (1996). Iron-supplemented caseins: preparation, physicochemical characterization and stability. *Journal of Dairy Research*, 63, 233–243.
- Gurd, F. R. N., & Goodman, D. S. (1952). Preparation and properties of serum and plasma proteins XXXII. The interactions of human serum albumin with zinc ion. *Journal of the American Chemical Society*, 74, 670–675.
- Gurd, F. R. N., & Wilcox, P. E. (1956). Complex formation between metallic cations and proteins, peptides and amino acids. *Advanced Concepts in Chemistry*, 11, 311–427.
- IDF 90. (1979). *Rennet caseins and caseinates – Determination of ash (reference method)*. Brussels, Belgium.
- IDF 106. (1982). *Caseins and caseinates – Determination of lactose content (reference method)*. Brussels, Belgium.
- IDF 127A. (1988). *Caseins and caseinates – Determination of fat content by gravimetric method (reference method)*. Brussels, Belgium.
- Indumathi, K. P., Kaushik, R., Arora, S., & Wadhwa, B. K. (2015). Evaluation of iron fortified Gouda cheese for sensory and physicochemical attributes. *Journal of Food Science and Technology*, 52(1), 493–499.
- IS: 16072. (2012). *Determination of moisture content in milk powder and similar products*. ManakBhawan: New Delhi: Bureau of Indian Standards.
- Jimenez, K., Kulnigg-Dabsch, S., & Gasche, C. (2015). Management of iron deficiency anemia. *Gastroenterology & Hepatology*, 11(4), 241–250.
- Jones, S. B., Kalan, E. B., Jones, T. C., & Hazel, J. F. (1972). Ferritopolyphosphate as a whey protein precipitant. *Journal of Agricultural and Food Chemistry*, 20, 229.
- Jones, S. B., Kalan, E. B., Jones, T. C., Hazel, J. F., Edmondson, L. F., Booth, A. N., et al. (1975). Ferritopolyphosphate-whey protein powders. Their potential as nutritional iron supplements. *Journal of Agricultural and Food Chemistry*, 23, 981.
- Kassebaum, N. J., Jasrasaria, R., Naghavi, M., Wulf, S. K., Johns, N., Lozano, R., et al. (2014). A systematic analysis of global anemia burden from 1990 to 2010. *Blood*, 123(5), 615–624.
- Kim, M., Salmarch, M., & Labuze, T. P. (1989). Non-enzymatic browning of hygroscopic whey powders in open versus sealed pouches. *Journal of Food Processing and Preservation*, 5, 49–57.
- Kinsella, J. E., & Whitehead, D. M. (1989). Proteins in whey: chemical, physical, and functional properties. *Advances in Food and Nutrition Research*, 33, 343–438.
- Lambert, E. N., & Mohammed, M. J. (1978). *Comprehensive qualitative analysis for advanced level chemistry*. Oxford OX2 8EJ, UK: Heinemann Educational Publishers.
- Lawal, O. S., Adebowale, K. O., & Adebowale, Y. A. (2007). Functional properties of native and chemically modified protein concentrates from bambarra groundnut. *Food Research International*, 40, 1003–1011.
- Lovrien, R. E., & Matulis, D. (1997). *Selective precipitation of proteins. Current protocols in protein science (chapter 4)*. USA: John Wiley and Sons, Inc.
- Lowry, O. H., Rosebrough, N. J., Farr, A. L., & Randall, P. J. (1951). Protein measurement with the folin – phenol reagent. *Journal of Biological Chemistry*, 193, 265–275.
- Mutilangi, W. A. M., & Kilara, A. (1985). Functional properties of heat – denatured whey protein – 1. Solubility. *Milchwissenschaft*, 40(6), 338–341.
- Nakano, T., Goto, T., Nakaji, T., & Aoki, T. (2007). Bioavailability of iron-fortified whey protein concentrate in iron-deficient rats. *Asian Australian Journal of Animal Science*, 20, 1120–1126.
- Rice, W. H., & McMahon, D. J. (1998). Chemical, physical, and sensory characteristics

- of mozzarella cheese fortified using protein-chelated iron or ferric chloride. *Journal of Dairy Science*, 81, 318–326.
- Rothstein, F. (1994). Differential precipitation of proteins. In R. G. Harrison (Ed.), *Protein purification process engineering* (pp. 115–208). New York: Marcel Dekker.
- Sharma, A., Shilpa Shree, B. G., Arora, S., & Tomar, S. K. (2015). Lactose – zinc complex preparation and evaluation of acceptability of complex in milk. *LWT – Food Science and Technology*, 64, 275–281.
- Shilpashree, B. G., Arora, S., Chawla, P., Vakkalagadda, R., & Sharma, A. (2015). Succinylation of sodium caseinate and its effect on physicochemical and functional properties of protein. *LWT – Food Science and Technology*, 64, 1270–1277.
- Snedecor, G. W., & Cochran, W. G. (1989). *Statistical methods* (8th edn.). Amer Iowa: Affiliated East-West Press, Iowa State University Press.
- Sugiarto, M. (2004). *Studies on the binding of iron and zinc to milk protein products*. Ph.D. thesis. Palmerston North: Massey University.
- Sugiarto, M., Ye, A., Taylor, W. M., & Singh, H. (2010). Milk protein – iron complexes: inhibition of lipid oxidation in an emulsion. *Dairy Science and Technology*, 90(1), 87–98.
- Sugiarto, M., Ye, A., & Singh, H. (2009). Characterisation of binding of iron to sodium caseinate and whey protein isolate. *Food Chemistry*, 114(3), 1007–1013.
- Vaughan, O. W., & Knauff, R. E. (1961). Chemical state and nutritional availability of iron in a prepared infant formula. *Journal of Dairy Science*, 44, 1650–1654.
- Walstra, P., & Jenness, R. (1984). *Dairy chemistry and physics*. New York: John Wiley and Sons. Inc.
- Wieringa, F. T., Dijkhuizen, M. A., Fiorentino, M., Laillou, A., & Berger, J. (2015). Determination of zinc status in humans: which indicator should we use? *Nature*, 7, 3252–3263.
- Yuksel, Z., & Erdem, Y. K. (2010). Detection of the milk proteins by RP-HPLC. *GIDA: Journal of Food*, 35(1), 5–11.
- Zang, D., & Mohoney, A. W. (1989). Effect of iron fortification on quality of cheddar cheese. *Journal of Dairy Science*, 72(2), 322–332.
- Zang, D., & Mohoney, A. W. (1990). Effect of iron fortification on quality of cheddar cheese. 2. Effects of aging and fluorescent light on pilot scale cheeses. *Journal of Dairy Science*, 73, 2252–2258.



## Stability and quality of a bioactive peptide fraction incorporated orange juice



Mirna G. Khairallah<sup>a</sup>, Navam S. Hettiarachchy<sup>b,\*</sup>, Srinivas J. Rayaprolu<sup>b</sup>

<sup>a</sup> Mars GCC, Jebel Ali Gate 4, PO Box 17139, Dubai, United Arab Emirates

<sup>b</sup> Food Science Department, University of Arkansas, 2650 N Young Avenue, Fayetteville, AR 72704, USA

### ARTICLE INFO

#### Article history:

Received 28 May 2015

Received in revised form

30 September 2015

Accepted 3 October 2015

Available online 10 October 2015

#### Keywords:

Rice bran

Nutraceutical

<5 kDa protein fraction

Orange juice

### ABSTRACT

The objective of this study was to evaluate the stability of a bioactive <5 kDa sized peptide fraction in orange juice and its effect on the organoleptic properties. A concentration of 3000 µg/mL of <5 kDa peptide fraction in orange juice was prepared, the samples were stored at 4 °C along with the control without hydrolysates. Samples were drawn at 0, 1, 3, 7, 10, 14, 21, 28, 35, and 42 days to monitor pH, color, total soluble solids, ascorbic acid, and peptide fraction concentration. Organoleptic properties were assessed at 0 and 14 days using a triangle test. The orange juice with the peptide fraction showed similar pH, color, and ascorbic acid content when compared to control throughout the study. The concentration of the peptide fraction in orange juice remained stable throughout the study. Analysis of sensory data showed no significant difference between the freshly prepared control and peptide fraction incorporated orange juice ( $p = 0.0583$ ). However, the orange juice stored for 14 days at 4 °C showed varying acceptance levels from the panelists which was significant. Overall, the study demonstrated that orange juice can be a potential vehicle for application of bioactive peptide fractions.

© 2015 Elsevier Ltd. All rights reserved.

### 1. Introduction

Functional foods offer consumers the added benefits beyond the essential nutritional support from the product (Gray, Armstrong, & Farley, 2003; Granato, Branco, Nazzaro, Cruz, & Faria, 2010). The global functional food market witnessed an annual growth of 6% in the last five years (Statista, 2015) and is expected to reach \$54 billion by 2017 (Bonar, 2014). The retail sales of functional beverages in the United States is approximately \$18 billion, with half of adult buyers consuming functional drinks (Statista, 2015). Hence, there is a great demand from the consumers for incorporated nutraceutical and functional ingredients in food products. Previously, scientists have studied new sources of functional ingredients, specifically proteins and peptides (Chandi & Sogi, 2007). Rice bran is a low cost by-product of rice milling industry but is rich in health beneficial components like proteins, vitamins, minerals, soluble fiber, and lipids (Hamada, 2000; Piyyaratne, Atapattu, Mendis, & Amarasinghe, 2009). Kannan, Hettiarachchy, Johnson, and Nannapaneni (2008) demonstrated that protein hydrolysates

isolated from rice bran protein have anticancer activities on multiple human cancer cells. Other researchers have demonstrated breast cancer cell inhibition by a rice bran peptide using molecular studies (Li, Hettiarachchy, & Mahadevan, 2014a, 2014b) and incorporated a nano-encapsulated peptide in fruit juice (Alessa et al., 2014). Although FDA has strict regulation for pure peptides (as biologics) under the label of 'drugs' (FDA, 2012), incorporation of hydrolyzed protein into beverages such as protein and sports drinks has become more common in the food industry (Pennings et al., 2011; Sinha, Radha, Prakash, & Kaul, 2007).

Functional ingredients added to foods or beverages become part of the system where they are prone to interact with other components and cause detrimental effect in overall product quality. The storage stability of the nutraceutical ingredient incorporated in the food product is an important attribute that influences its bioactive viability (Day, Seymour, Pitts, Konczak, & Lundin, 2009). Therefore, testing the stability and quality is a primary step while developing functional food products. The loss of one or more product constituents such as nutrients or flavors, or the formation of off-flavors are the limits that set the shelf life. Several food and beverage products, including fruit juices and health drinks have been incorporated with functional ingredients for their unique wellness promoting role along with consumer appeal and marketability (Harbourne,

\* Corresponding author. Department of Food Science & Institute of Food Engineering, 2650 N. Young Ave, Fayetteville, AR, 72704, USA.

E-mail address: [nhettiar@uark.edu](mailto:nhettiar@uark.edu) (N.S. Hettiarachchy).

Marete, Jacquier, & O'Riordan, 2013; Ron, Zimet, Bargaram, & Livney, 2010).

Fruit juices are thought to be a good medium for serving as functional beverages (Tuorila & Cardello, 2002). They are positioned as healthy products with high acceptance in the rapidly growing market which drives the beverage product design (Luckow & Delahunty, 2004; Sorenson & Bogue, 2005). Orange juice is ranked number one in the United States and is considered as a functional beverage due to the accrued health benefits (Pollack, Lin, & Allshouse, 2003; Sloan, 2014). Beverages are conducive for modifications since they have minimum interactions among their components in comparison to other solid foods (Day et al., 2009). Acidity of orange juice influences other components including added nutraceutical or functional ingredients. Ascorbic acid or Vitamin C is the vital ingredient in natural fruit juices that is considered as a potent antioxidant, but is prone to interactions during processing and storage (Choi, Kim, & Lee, 2002; Kaack & Austed, 1998). Stability of ascorbic acid, with minimum required amounts ( $\geq 200$  mg/L) in orange juice over the storage period is essential for preserving its quality (Polydera, Stoforos, & Taoukis, 2003). Several researchers have successfully demonstrated fortification of orange juice with functional ingredients for enhanced nutrition and health-promotion without deterring its quality (Biancuzzo et al., 2010; Devaraj, Jialal, & Vega-López, 2004). However, incorporation of functional protein products for enhancing the quality through value-addition has not been reported. Hence, the overall goal of the study was to develop a functional orange juice beverage using the  $<5$  kDa peptide fraction derived from rice bran, which has been previously demonstrated as a bioactive ingredient (Kannan et al., 2008). The objective was to determine the stability of the peptide fraction incorporated in orange juice over storage.

## 2. Materials and methods

### 2.1. Materials

Rice bran peptide fraction ( $<5$  kDa) was prepared in the protein research laboratory, University of Arkansas, under optimal conditions using food grade enzyme Alcalase 2.4L and fractionated using ultrafiltration columns (Kannan et al., 2008). Orange juice concentrate was provided by Southern Gardens Citrus Processing, Florida. Series 1050 of Hewlett Packard High-Performance Liquid Chromatography system (GMI Inc., Ramsey, MN) with biopore C-18 semi-preparative affinity chromatographic column (Shimadzu, Tokyo, Japan) was used to quantify the peptide fraction. An HPLC system with C-18 column (TOSOH Bioscience, King of Prussia, PA) was used to quantify Ascorbic acid in orange juice. Other instruments included a refractometer (Bausch & Lomb, Bridgewater, New Jersey) for determining the soluble solids content ("brix value") and a CR-300 Minolta Chroma meter (Minolta Inc. Osaka, Japan) for determining the color. All other materials and supplies were purchased from VWR International Inc. (Bridgeport, NJ) while the HPLC grade chemicals were purchased from Sigma (St. Louis, MO).

### 2.2. Methods

#### 2.2.1. Determination of $<5$ kDa peptide fraction concentration

The  $<5$  kDa peptide fraction was separated from other rice bran protein hydrolysates using ultrafiltration and quantified using an HPLC procedure by Kannan, Hettiarachchy, Lay, and Liyanage (2010). The standard curve for the hydrolysates was determined using solutions of peptide fraction in deionized water with the effective concentration as the median. The standards were injected (1000  $\mu$ L) into a C18 affinity chromatographic column attached to an HPLC system with a flow rate of 2 mL/min using two solvents.

Solvent A consists of 0.1% (v/v) Trifluoro Acetic acid (TFA) in deionized water and solvent B has 0.1% (v/v) TFA in 50% acetonitrile in water. Solvent gradient used was as follows: 100% solvent A for 0–5 min which was reduced to 90% from 5 to 60 min, 30% from 60 to 75 min, and 0% A from 75 to 80 min. Absorbance was monitored at 215 nm and the peak areas were used to prepare a standard curve using the three difference concentrations of the peptide fraction in water. The equation to calculate concentration based on the standard curve was:

$$\text{Concentration}(\mu\text{g}/\text{mL}) = (\text{Area} + 163006)/902.6 \quad (1)$$

#### 2.2.2. Ascorbic acid quantification in orange juice

The ascorbic acid concentration was quantified with the HPLC method as described by the procedure from TOSOH Bioscience (2011) for the HPLC column. Single solvent system with acetonitrile in water (1% v/v) + 0.1% TFA was used for running the sample for 10 min with a 10  $\mu$ L injection volume at a flow rate of 1 mL/min. The elution peaks were detected at 280 nm and a calibration curve was prepared using ascorbic acid standard obtained from Sigma (St. Louis, MO). The equation to calculate the concentration of ascorbic acid (mg/L) is:

$$\text{Ascorbic acid concentration} = (\text{Peak Area} - 21.518)/0.4453 \quad (2)$$

#### 2.2.3. Experimental design

The experiment followed the statistical model of a repeated measure over time. The between treatment effect in this experiment were tested for orange juice with and without peptide fraction. Time (days of storage) was considered as the within treatment effect as the study was conducted for 42 days. Measurements of pH, peptide concentration, color, total soluble solids, and ascorbic acid concentration were taken at 0, 1, 3, 7, 10, 14, 17, 21, 28, 35, and 42 days of storage. The triplicates of samples for HPLC analysis were randomized to minimize experimental error.

#### 2.2.4. Peptide fraction stability determination in orange juice based on physico-chemical properties

**2.2.4.1. Preparation of protein fraction ( $<5$  kDa) incorporated orange juice.** Orange juice was prepared by mixing one part juice concentrate with 6.5 parts of water to achieve a solids content of 11.8 brix, which is the recommended soluble solids for orange juice consistency according to the Code of Federal Regulations under Title 21, Part 146.145 (Johnson, 2000). The prepared orange juice was filled into 18, 1 L PET bottles for the experiment. Half the numbers (9 bottles) were incorporated with 3 g of the peptide fraction (3 mg/mL). The other nine Pet bottles with orange juice without peptide fraction were treated as controls for the study. All 18 bottles were pasteurized at 90 °C for 10 s, cooled to ambient temperature, head space was flushed with nitrogen and stored in the dark at 5 °C.

**2.2.4.2. Testing for juice quality.** Three replicates of each treatment; control orange juice and orange juice with peptide fraction were tested for the following quality attributes.

The pH meter was calibrated with standard pH buffer solutions (pH = 4.01, and pH = 7.00) and the values for the two samples were measured.

The soluble solids were determined using a refractometer.

Color was measured using a chroma-meter. The chroma-meter was calibrated using a white tile and  $L^*$ ,  $a^*$ ,  $b^*$  color attributes

were recorded in triplicates (HunterLab, 2008). To determine the grade of quantitative difference of Hue parameter with reference to grey color the chroma (Cr.) was calculated using the formula:  $Cr = (a^{*2} + b^{*2})^{1/2}$ . The hue angle  $^{\circ}H$  is the qualitative attribute of color and it defines the difference of a color compared to grey in the orange juice. This was calculated using the formula:  $^{\circ}H = \arctan(a/b)$ .

**2.2.4.3. Sample preparation for HPLC.** The HPLC system was used to measure the ascorbic acid concentration and the peptide fraction concentration in orange juice. To prepare the samples for HPLC, they were centrifuged at  $7000 \times g$  for 5 min. The supernatant was then filtered through 25  $\mu\text{m}$  syringe filter into the sample holders. The concentration of ascorbic acid remained the same after centrifugation and filtration; this was tested by comparing the concentration added and HPLC peak areas.

**2.2.4.4. Ascorbic acid content determination.** Ascorbic acid content of the orange juice samples was quantified using HPLC (Hewlett Packard system) with C-18 column using the same method described for the standard curve preparation.

**2.2.4.5. Peptide profile.** The HPLC method described earlier (Kannan et al., 2010) was used to quantify the <5 kDa peptide fraction to study its stability in the orange juice.

### 2.2.5. Sensory properties of the juice

**2.2.5.1. Sample preparation for sensory test.** The sensory tests were conducted at the Sensory Science laboratory in the Department of Food Science, University of Arkansas. Orange juice with and without peptide fraction was prepared in four 1L PET bottles. They were tested on the same day (Day 0) for the sensory attributes. A total of 36 panelists were presented with the orange juice samples (60 mL or 2oz.) for tasting. The excess orange juice was transferred to a sterile container, the head space was flushed with nitrogen gas and stored in the refrigerator at 5 °C for 14 days for the second session of the test. The process was repeated on day 14 with 36 panelists tasting the stored orange juice with and without peptides. Panelists were asked to observe and taste the sample and evaluate the sample's appearance/overall liking, color, flavor, and texture using a 9-point hedonic scale ranging from 1 to 9 for "dislike extremely" to "like extremely."

To balance the test, the six triads of sample A: orange juice; and sample B: orange juice with peptide fraction, were distributed equally among the panelists as follows: AAB, ABA, BAA, BBA, BAB, and ABB. The three samples were placed in 60 mL (2 oz.) plastic containers with a random three digit number assigned to each container. Each combination appeared 6 times throughout the test where the panelists were asked to taste from right to left and to pick the odd sample out. All 36 panelists were presented with 2 randomly numbered samples A and B and were asked to rate the attributes: overall liking, color, flavor, and texture for both samples on the 9 point hedonic.

**2.2.5.2. Statistical analysis.** The JMP 9.0 software was used to analyze the data. Statistical model tested the significant differences ( $\alpha = 0.05$ ) in pH, peptide concentration, color, total soluble solids, and ascorbic acid concentration between treatments over storage time. If significant changes were observed between treatments throughout storage, the experiment was repeated by including a contrast of the response at day 0 over the storage period for determining the reason for the change.

## 3. Results and discussion

### 3.1. Quality parameters of peptide fraction incorporated orange juice

Preliminary tests with pasteurized orange juice showed occurrence of spoilage beyond 42 days of storage at  $\geq 4$  °C in the refrigerator. Hence, 42 day storage time period was selected for the study to determine the stability of rice bran peptide fraction. The concentration of the peptide fraction in orange juice was determined based on the minimum effective concentration of 3 mg/mL for effective biological property (data not included) which was used in this study.

#### 3.1.1. Stability of orange juice based on physico-chemical parameters

The pH of the two orange juice samples remained stable during storage. Fig. 1 shows the stability of the pH in orange juice over storage time. It was observed that the pH was constant for the three different factors: over time, between treatments, and between treatments over time. The pH of the orange juice alone and with peptide fractions did not show any significant changes ( $p < 0.05$ ) over the storage period of 42 days. This also demonstrates that the peptide fraction was stable under acidic environment of the orange juice. Similar observations were reported in whey protein incorporated orange juice by Kazmerski, Agboola, and Corredig (2003).

Color is an important quality factor that provides information on the freshness of a food product. Test of brightness (L), Chroma, and Hue was conducted over the storage period to assess the color stability of the orange juice with peptide fraction and the control. Fig. 2a, b, and c show the brightness, the Chroma, and the Hue of the orange juice with and without peptide fraction respectively through 42 day storage. The brightness and Chroma values showed a drop on day 1 in both orange juice samples while the Hue value increased with highest value on day 42 (Fig. 2b). Analysis of the model showed no statistically significant differences between treatments, but the differences are significant when factoring in the storage time ( $p = 0.030$  for brightness,  $p = 0.0441$  for Chroma and  $p < 0.0001$  for Hue). Although the color attributes remained constant over the 42 days, the changes observed on day 1 can be attributed to possible instant interactions between peptide fraction and the orange juice components which remained stable throughout the study period. However, the statistical significance of differences in color cannot correlate to actual observation of orange juice samples (peptide fraction and control) with the naked eye, which were not significant ( $p < 0.05$ ).

Orange juice has total soluble solid (TSS) value of 11.8°brix (CFR 146.145) which was used to prepare the test samples. But, addition of the peptide fraction increased the TSS to 12.0°brix on day 0. Fig. 3 shows the TSS value of orange juice samples (peptide fraction and control) where TSS of the orange juice with peptide fraction was similar or higher than control on over the storage days. The statistical model showed that TSS values were not significantly different between treatments ( $p < 0.0001$ ). The brix value in orange juice with peptide fraction increased to 12.4 on day 42 which was higher than the control. This can be explained by the possible interactions between the insoluble components in orange juice that bind to the peptide fraction in solution, thereby increasing the soluble solids content of the juice.

Fig. 4 shows the stability of ascorbic acid in orange juice with peptide fraction and control. The Ascorbic acid content of both samples decreased from 200 mg/L to 20 mg/L (by 10%) in 7 days, although the orange juice with peptide fraction showed significantly higher amount of ascorbic acid in comparison to control on day 3. From days 7–42 the ascorbic acid concentration of in both

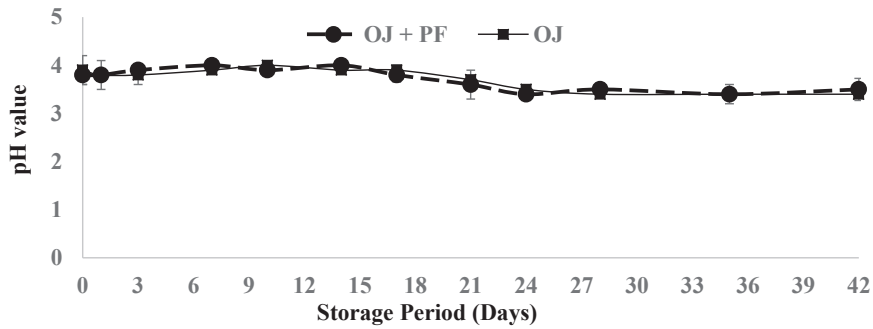


**Fig. 1.** Effect of rice bran peptide fraction incorporation on pH of orange juice during 42 day storage. Orange juice with peptide fraction = OJ + PF; Orange juice alone (control) = OJ. Values presented are means  $\pm$  standard error of the means of triplicates.

treatments remained similar ( $p < 0.0001$ ). Therefore, the study shows that variables other than the addition of peptide fraction, such as preparation conditions, storage, oxidation or other unknown factors could have contributed to the instability of ascorbic acid.

### 3.2. Stability of peptide fraction in orange juice

A two sample t-test on days 0 and 42 showed that the peptide fraction concentration (3000  $\mu\text{g}/\text{mL}$ ) was significantly different ( $p = 0.34$ ). Fig. 5 shows the concentration of the peptide fraction

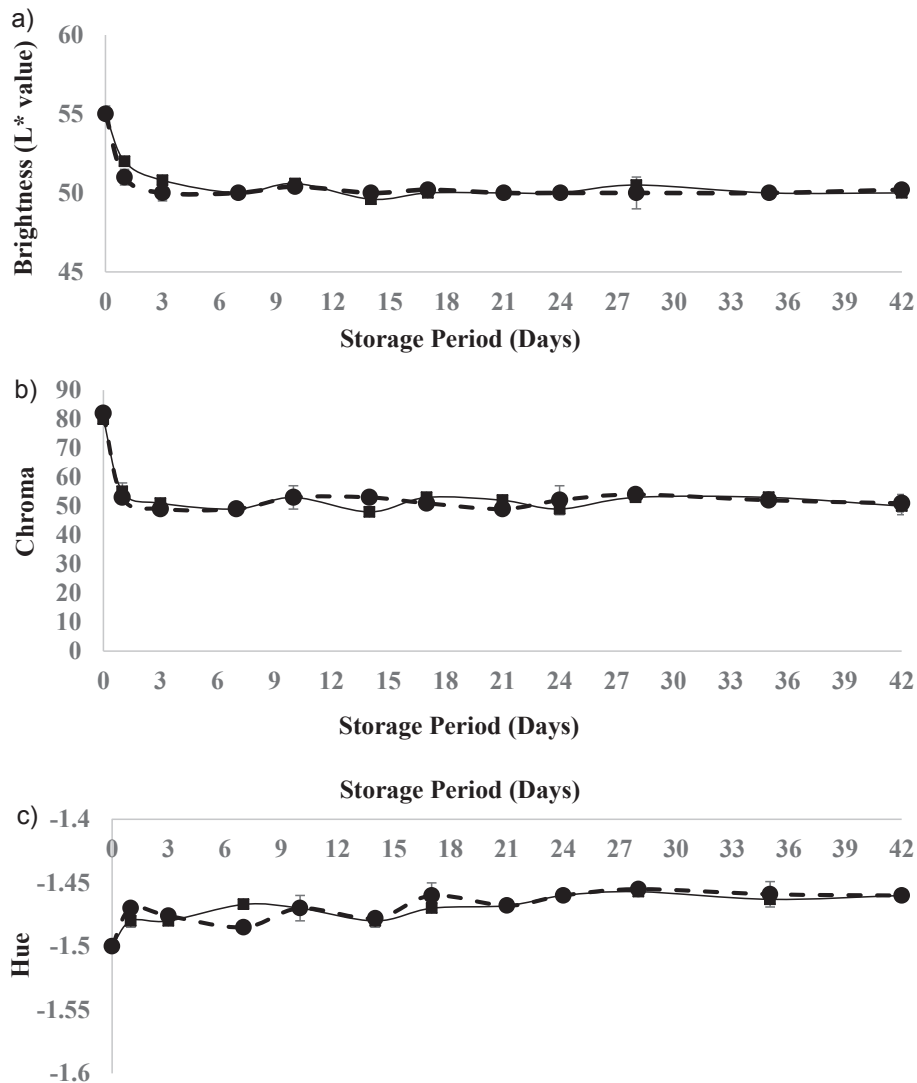


**Fig. 2.** Brightness (L), Chroma, and Hue of orange juice incorporated with rice bran peptide fraction over 42 day storage. OJ + PF (—■—) = Orange juice with peptide fraction and OJ (—●—) = Orange juice alone (control). Values presented are means  $\pm$  standard error of the means of triplicates.

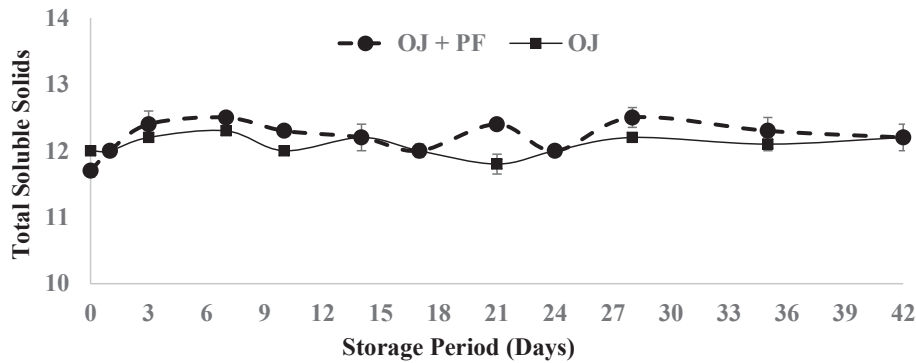


**Fig. 3.** Total soluble solids (TSS) content of orange juice incorporated with rice bran peptide fraction over the 42 day storage period. Orange juice with peptide fraction = OJ + PF; Orange juice alone (control) = OJ. Values presented are means  $\pm$  standard error of the means of triplicates.

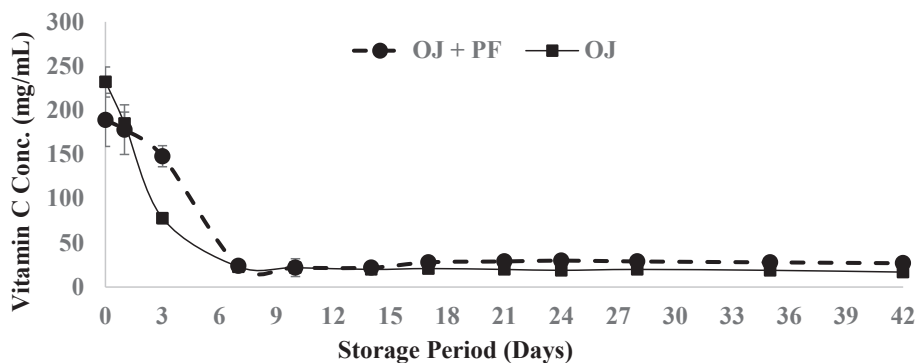


**Fig. 4.** Stability (mg/mL) of Vitamin C in orange juice incorporated with rice bran peptide fraction during 42 day storage. Orange juice with peptide fraction = OJ + PF; Orange juice alone (control) = OJ. Values presented are means  $\pm$  standard error of the means of triplicates.

in orange juice and in pH (3.5) adjusted water over storage time. From day 0–28, the peptide fraction concentration was stable in the orange juice in comparison to the control sample ( $p < 0.0001$ ). The concentration of the peptide fraction decreased with the storage progression beyond day 35 and was significantly different from control on day 42. The decrease in the peptide fraction may denote the beginning of instability and possible degradation beyond 35 day storage. The stability of the peptide in the orange juice is dependent on possible degradation factors could also affect the quality, including color, flavor, texture and sensory appeal.

### 3.3. Sensory analysis study of peptide fraction incorporated orange juice

A sensory study to determine the effect of the peptide fraction on the organoleptic properties of orange juice was conducted. The test samples contained freshly prepared orange juice (A) and freshly prepared orange juice with peptide fraction (B) on day 0. The test was repeated using orange juice samples with and without peptides that have been stored for 14 days at 4 °C. Fig. 6 shows the appeal for orange juice by the sensory panelists on test days, which was used as one of the chief criteria for selecting the test subjects.

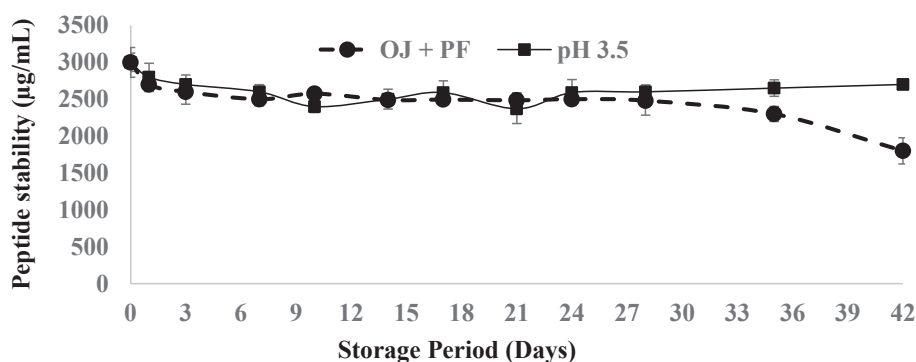


**Fig. 5.** Stability of rice bran peptide fraction ( $\mu\text{g/mL}$ ) in orange juice over the storage period. Orange juice with peptide fraction = OJ + PF; Peptide fraction in pH (3.5) adjusted water = pH 3.5 (control). Values presented are means  $\pm$  standard error of the means of triplicates.

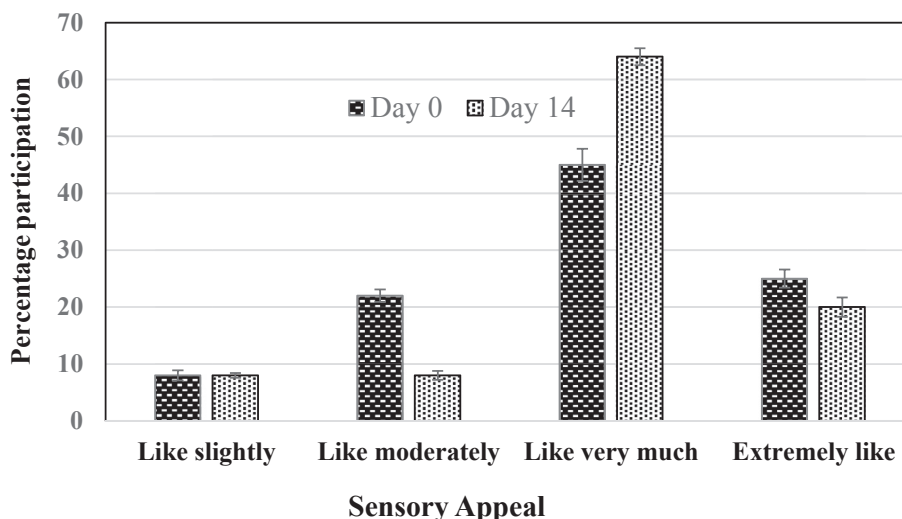


Fig. 6. Appeal of orange juice by panelist's during the study. Values presented are means  $\pm$  standard error of the means of triplicates.

Both days had the highest number of panelists who chose 'like very much' for orange juice consumption on a regular basis, although there were more panelists who selected 'extremely like' orange juice on day 0 than day 14. The sensory appeal for orange juice was vital during the selection process along with their age group distribution and consumption pattern of orange juice.

The null hypothesis for the triangle test was: samples 'A' and 'B' are dissimilar with statistically significant differences in their sensory appeal. The panelists did not discern any significant differences between A and B on day 0 ( $p = 0.0583$ ). But, during the test on day 14 the panelists distinctly identified differences between the control orange juice and the orange juice with peptide fraction ( $p = 0.00058$ ). Using the triangle test results it was inferred that panelists failed to see any difference between freshly made orange juice samples but on storage, the difference was evident. This can be due to the interaction of the peptide fraction with orange juice components over the storage period, which could have potentially led to formation of off-flavor compounds. Table 1 shows the scores from the panelists for the test samples. On a Hedonic scale of 1–9, the scores given were between 6.3 and 7.6, which is significantly high. The panelists found no significant differences between color and texture attributes of the orange juice with or without peptide over storage period. However, the panelists gave low scores for the overall liking and flavor for sample 'B' on both days.

Flavor and taste of a food product are the main attributes that appeal to consumers. Several studies have investigated the effect of the addition of functional ingredients on the liking of the product by consumers due to development of off-flavors. Researchers have found several peptides and protein hydrolysates with bioactivity to produce off-flavors and bitter taste (Möller, Scholz-Ahrens, Roos, &

Schrezenmeir, 2008). However, there is evidence that consumers could be unwilling to sacrifice taste for health if there is a significant potential in the product (Verbeke, 2006). Knowledge of a functional food product increases the rating by a consumer, but an off-flavor in a product does not play the role of an indicator that the food is functional (Tuorila & Cardello, 2002). Use of QSAR (quantitative structure-analysis relationship) technology can provide a sensory prediction ranking of bitter taste for proteins and peptides in the future (Li-Chan & Cheung, 2010). This can assist food product developers with the probable effects of proteins or peptides incorporated in food systems with information on overall flavor of the products for precise application.

#### 4. Conclusion

This study demonstrated that orange juice can be a promising vehicle for developing a potent nutraceutical beverage by incorporating rice bran peptide fractions which are effective in impeding growth of diseases like cancer. The physicochemical parameters, including pH, color, TSS and ascorbic acid content of the orange juice with the peptide fraction were not significantly different in comparison to orange juice alone over a 42 day storage. However, the sensory study showed that the peptide fraction affected the orange juice flavor when tested over 14 days. Further studies in microencapsulation or bitter masking of the peptide fraction before incorporation into the orange juice can be a novel and efficient way to extend the shelf life beyond 42 days. Encapsulation may also protect the organoleptic properties of the orange juice. This is the first time a nutraceutical beverage is developed with orange juice as the base and incorporated with a peptide fraction from rice bran.

#### References

- Alessa, F., Hettiarachchy, N., Rayaprolu, S. J., Benamara, M., Greathouse, D., & Singh, S. (2014). Stability of nano encapsulated rice bran derived bioactive pentapeptide in apple juice. *Journal of Food Processing and Technology*, 5(8).
- Biancuzzo, R. M., Young, A., Bibuld, D., Cai, M. H., Winter, M. R., Klein, E. K., et al. (2010). Fortification of orange juice with vitamin D2 or vitamin D3 is as effective as an oral supplement in maintaining vitamin D status in adults. *The American Journal of Clinical Nutrition*, 91(6), 1621–1626.
- Bonar, A. (2014). *Statistics and facts on the functional foods market in the US* Accessed at <http://www.nutraingredients.com/Markets-and-Trends/Functional-foods-market-is-expected-to-grow-25-by-2017-Leatherhead>.
- Chandi, G. K., & Sogi, D. S. (2007). Functional properties of rice bran protein concentrates. *Journal of Food Engineering*, 79(2), 592–597.
- Choi, M. H., Kim, G. H., & Lee, H. S. (2002). Effects of ascorbic acid retention on juice

Table 1

Sensory analysis using a Hedonic scale (based on scores assigned) for orange juice incorporated with peptide fraction over storage.

	Day 0		Day 14	
	Control OJ	OJ + peptide	Control OJ	OJ + peptide
Overall liking	7.1 $\pm$ 0.0 <sup>a</sup>	6.6 $\pm$ 0.3 <sup>b</sup>	7.3 $\pm$ 0.2 <sup>a</sup>	6.6 $\pm$ 0.0 <sup>b</sup>
Color	7.3 $\pm$ 0.1 <sup>a</sup>	7.3 $\pm$ 0.1 <sup>a</sup>	7.6 $\pm$ 0.1 <sup>a</sup>	7.6 $\pm$ 0.1 <sup>a</sup>
Flavor	7.1 $\pm$ 0.0 <sup>a</sup>	6.4 $\pm$ 0.1 <sup>b</sup>	7.2 $\pm$ 0.0 <sup>a</sup>	6.3 $\pm$ 0.2 <sup>b</sup>
Texture	6.9 $\pm$ 0.2 <sup>a</sup>	6.9 $\pm$ 0.0 <sup>a</sup>	7.1 $\pm$ 0.3 <sup>a</sup>	7.1 $\pm$ 0.3 <sup>a</sup>

Values are presented as means  $\pm$  standard error of mean and those connected with same letter in each row are not significantly different ( $P < 0.05$ ) for each test day.

- color and pigment stability in blood orange (*Citrus sinensis*) juice during refrigerated storage. *Food Research International*, 35(8), 753–759.
- Day, L., Seymour, R. B., Pitts, K. F., Konczak, I., & Lundin, L. (2009). Incorporation of functional ingredients into foods. *Trends in Food Science and Technology*, 20(9), 388–395.
- Devaraj, S., Jialal, I., & Vega-López, S. (2004). Plant sterol-fortified orange juice effectively lowers cholesterol levels in mildly hypercholesterolemic healthy individuals. *Arteriosclerosis, Thrombosis, and Vascular Biology*, 24(3), e25–e28.
- FDA. (2012). *Guidance for industry on biosimilars: Q & as regarding implementation of the BPCI act of 2009: Questions and answers part II. Provisions related to requirement to submit a BLA for a "biological product.* Last Updated: 02/09/2012.
- Granato, D., Branco, G. F., Nazzaro, F., Cruz, A. G., & Faria, J. A. F. (2010). Functional foods and nondairy probiotic food development: trends, concepts, and products. *Comprehensive Reviews in Food Science and Food Safety*, 9(3), 292–302.
- Gray, J., Armstrong, G., & Farley, H. (2003). Opportunities and constraints in the functional food market. *Nutrition and Food Science*, 33(5), 213–218.
- Hamada, J. S. (2000). Characterization and functional properties of Rice bran proteins modified by commercial exoproteases and endoproteases. *Journal of Food Science*, 65(2), 305–310.
- Harbourne, N., Marete, E., Jacquier, J. C., & O'Riordan, D. (2013). Stability of phytochemicals as sources of anti-inflammatory nutraceuticals in beverages—A review. *Food Research International*, 50(2), 480–486.
- HunterLab. (2008). *Hunter L, a, b color scale* Accessed at [http://www.hunterlab.com/appnotes/an08\\_96a.pdf](http://www.hunterlab.com/appnotes/an08_96a.pdf). October 13, 2011.
- Johnson, E. L. 2000. U.S. Patent No. 6,099,889. Washington, DC: U.S. Patent and Trademark office.
- Kaack, K., & Austed, T. (1998). Interaction of vitamin C and flavonoids in elderberry (*Sambucus nigra* L.) during juice processing. *Plant Foods for Human Nutrition*, 52(3), 187–198.
- Kannan, A., Hettiarachchy, N., Johnson, M. G., & Nannapaneni, R. (2008). Human colon and liver cancer cell proliferation inhibition by peptide hydrolysates derived from heat-stabilized defatted rice bran. *Journal of Agricultural Food Chemistry*, 56(24), 11643–11647.
- Kannan, A., Hettiarachchy, N. S., Lay, J. O., & Liyanage, R. (2010). Human cancer cell proliferation inhibition by a pentapeptide isolated and characterized from rice bran. *Peptides*, 31(9), 1629–1634.
- Kazmerski, M., Agboola, S., & Corredig, M. (2003). Optimizing stability of orange juice fortified with whey protein at low pH values. *Journal of Food Quality*, 26(4), 337–352.
- Li-Chan, E. C. Y., & Cheung, I. W. Y. (2010). In Y. Mine, E. Li-Chan, & B. Jiang (Eds.), *Flavor-active properties of amino acids, peptides, and proteins* (p. 341). Wiley-Blackwell.
- Li, R., Hettiarachchy, N., & Mahadevan, M. (2014a). Rice bran derived pentapeptide-induced apoptosis in human breast cancer cell models (MCF-7 and MDA-MB-231). *International Journal of Biomedical Research*, 5(10), 599–605.
- Li, R., Hettiarachchy, N., & Mahadevan, M. (2014b). Apoptotic pathways in human breast cancer cell models (MCF-7 and MDA-MB-231) induced by rice bran derived pentapeptide. *International Journal of Research in Medical and Health Sciences*, 4(5), 13–21.
- Luckow, T., & Delahunty, C. (2004). Consumer acceptance of orange juice containing functional ingredients. *Food Research International*, 37(8), 805–814.
- Möller, N. P., Scholz-Ahrens, K. E., Roos, N., & Schrezenmeir, J. (2008). Bioactive peptides and proteins from foods: indication for health effects. *European Journal of Nutrition*, 47(4), 171–182.
- Pennings, B., Boirie, Y., Senden, J. M., Gijzen, A. P., Kuipers, H., & van Loon, L. J. (2011). Whey protein stimulates postprandial muscle protein accretion more effectively than do casein and casein hydrolysate in older men. *The American Journal of Clinical Nutrition*, 93(5), 997–1005.
- Piyaratne, M., Atapattu, N., Mendis, A., & Amarasinghe, A. (2009). Effects of balancing rice bran based diets for up to four amino acids on growth performance of broilers. *Tropical Agricultural Research and Extension*, 12(2), 57–61.
- Pollack, S. L., Lin, B. H., & Allshouse, J. E. (2003). *United States. Dept. of agriculture. Economic research service. Characteristics of US orange consumption.* US Dept. of Agriculture, Economic Research Service.
- Polydera, A. C., Stoforos, N. G., & Taoukis, P. S. (2003). Comparative shelf life study and vitamin C loss kinetics in pasteurised and high pressure processed reconstituted orange juice. *Journal of Food Engineering*, 60(1), 21–29.
- Ron, N., Zimet, P., Bargarum, J., & Livney, Y. D. (2010). Beta-lactoglobulin–polysaccharide complexes as nanovehicles for hydrophobic nutraceuticals in non-fat foods and clear beverages. *International Dairy Journal*, 20(10), 686–693.
- Sinha, R., Radha, C., Prakash, J., & Kaul, P. (2007). Whey protein hydrolysate: functional properties, nutritional quality and utilization in beverage formulation. *Food Chemistry*, 101(4), 1484–1491.
- Sloan, A. E. (2014). Top ten functional food trends. *Food Technology*, 68(4).
- Sorenson, D., & Bogue, J. (2005). Market-oriented new product design of functional orange juice beverages: a qualitative approach. *Journal of Food Products Marketing*, 11(1), 57–73.
- Statista. (2015). *Statistics and facts on the functional foods market in the US* Accessed at <http://www.statista.com/topics/1321/functional-foods-market/>.
- TOSOH B. (2011 (June/6)). *Reversed phase chromatography*, 21.
- Tuorila, H., & Cardello, A. V. (2002). Consumer responses to an off-flavor in juice in the presence of specific health claims. *Food Quality and Preference*, 13(7–8), 561–569.
- Verbeke, W. (2006). Functional foods: consumer willingness to compromise on taste for health? *Food Quality and Preference*, 17(1–2), 126–131.



## Correlation between physicochemical properties of *japonica* and *indica* rice starches



Eun-Hee Jang<sup>a,1</sup>, Su-Jin Lee<sup>a,b,1</sup>, Joo-Yeon Hong<sup>a</sup>, Hyun-Jung Chung<sup>c</sup>, Young-Tack Lee<sup>d</sup>, Bo-Sik Kang<sup>a</sup>, Seung-Taik Lim<sup>a,\*</sup>

<sup>a</sup> School of Life Sciences and Biotechnology, Korea University, Seoul 136-701, Republic of Korea

<sup>b</sup> Department of Food Preparation, Suseong College, Daegu 706-711, Republic of Korea

<sup>c</sup> Division of Food and Nutrition, Chonnam National University, Gwangju 500-757, Republic of Korea

<sup>d</sup> Department of Food Science and Biotechnology, Gachon University, Gyeonggi-do 461-701, Republic of Korea

### ARTICLE INFO

#### Article history:

Received 28 July 2015

Received in revised form

8 October 2015

Accepted 1 November 2015

Available online 10 November 2015

#### Keywords:

Rice starches

Amylose content

Thermal properties

Pasting properties

Textural properties

### ABSTRACT

Rice starches isolated from different cultivars were compared in their physicochemical properties including granule size, amylose content, protein content, thermal property, pasting viscosity, and gel texture, and the relationships among those properties were determined using Pearson correlation analysis. The starch containing the greatest amount of amylose which had been isolated from a *japonica* cultivar *Goami 3* showed the highest gelatinization temperature and the greatest gel hardness among twelve rice starches tested. The *indica* starches which contained the higher amylose and protein contents and the larger granules than *japonica* starches showed the higher gelatinization and pasting temperatures with the lower pasting viscosity. Amylose content was positively correlated to pasting temperature ( $r = 0.878$ ,  $p \leq 0.01$ ), but negatively correlated to peak viscosity ( $r = -0.910$ ,  $p \leq 0.001$ ) and breakdown ( $r = -0.905$ ,  $p \leq 0.001$ ). Cohesiveness of starch gel was positively related to amylose content ( $r = 0.780$ ,  $p \leq 0.05$ ), protein content ( $r = 0.933$ ,  $p \leq 0.001$ ) and mean granule size ( $r = 0.791$ ,  $p \leq 0.05$ ).

© 2015 Elsevier Ltd. All rights reserved.

## 1. Introduction

Rice is an important staple food in many Asian countries, contributing as a major calorie source. Although most of the rice harvested in the world is consumed in the form of milled kernels, some starch is isolated from rice, and commercialized for different applications in several Asian and European countries. Its utilization is much less than other cereal starches from corn and wheat, rice starch has some desirable properties such as bland taste, white color and good digestibility. Moreover, its small granule size makes the starch advantageous in utilizing as a texture improver in a variety of foods such as sauces and puddings, or as a fat substitute in dressings and creams (Mitchell, 2009). It is hypoallergenic as it contains almost no specific proteins that cause allergic responses to human, so that infant formula would be one of the ideal products for the use of rice starch. Furthermore, rice starch containing a relatively high level of amylose was reported to display relatively

low glycemic index (Champagne, 1996), which is desirable when consumed by diabetes or obese people. These unique characteristics of rice starch make it a better option than the common corn and wheat starches, in various food applications. However, the production of rice starch is limited and its price is much higher than that of corn or wheat starch.

Rice starch is composed of amylose and amylopectin and often distinguished by its amylose content. Rice starches with amylose contents of 0–2, 5–12, 12–20, 20–25, and 25–33% have been classified as waxy, very low, low, intermediate and high amylose rice starches, respectively (Juliano, 1992). Amylose content of *indica* rice starch is generally higher than that of *japonica* rice starch (Inouchi et al., 2005; Takeda, Hizukuri, & Juliano, 1987). Physical properties of starch in pastes and gels are influenced by the amylose content, chain structure of starch, and granule size of starch. In addition to the amylose content, residual protein in starch affects the pasting characteristics of starch (Lim, Lee, Shin, & Lim, 1999). These inherent characteristics determining the physical properties of starch are usually attributed to their botanical origins (Champagne, 1996; Jane et al., 1999; Madsen & Christensen, 1996; Singh, Singh, Kaur, Sodhi, & Gill, 2003). The gelatinization and

\* Corresponding author. Tel: 82-2-3290-3435; Fax: 82-2-921-0557.

E-mail address: [limst@korea.ac.kr](mailto:limst@korea.ac.kr) (S.-T. Lim).

<sup>1</sup> Eun-Hee Jang and Su-jin Lee contributed equally.

pasting properties of starch, which are the most important characteristics for thermal processing, depend largely on the granular structure and starch composition (Bao, Shen, Sun, & Corke, 2006; Jane et al., 1999; Lim et al., 1999; Park, Ibáñez, Zhong, & Shoemaker, 2007; Vandeputte, Vermeylen, Geeroms, & Delcour, 2003; Wang et al., 2010). However, physicochemical properties of various starches from *japonica* and *indica* rice cultivars imported by different countries and statistical analysis for the relationship among those properties have not been studied. In the situation that Korean rice market must be fully opened in 2015, information on the physicochemical properties of starches from diverse rice cultivars is necessary to predict the functionality and potential application of Korean rice starches in processed food products.

The objectives of this study were to examine and compare the physicochemical characteristics such as amylose content, protein content, granule size, thermal properties, pasting viscosity, and gel textural properties of different starches from *japonica* and *indica* rice cultivars. The relationships among those properties were also determined using Pearson correlation analysis.

## 2. Materials and methods

### 2.1. Rice samples

Six non-waxy *japonica* rice cultivars (*Baegjinju 1*, *Chucheong*, *Goami 3*, *Haiami*, *Yeongan*, and *Hyangmi 1*) and three waxy *japonica* rice cultivars (*Dongjinchal*, *Aranghyangchal* and *Baekokchal*) harvested at 2011 in Korea were obtained from the National Institute of Crop Science (Suwon, Korea). Three *indica* rice cultivars were purchased from different companies: a non-waxy Chinese rice cultivar (*Jiangxi*) from Qingdao Ever-Success Trading Co., Ltd. (Qingdao, China), a non-waxy American rice cultivars (*Cop 18*) from Creative BioMart Biosciences Inc. (Shirley, NY, USA), and a waxy rice cultivar (*Remyline XS*) from BENEIO-Remy NV (Leuven-Wijgmaal, Belgium).

### 2.2. Starch isolation

Starch was isolated from rice flours by using the alkaline steeping method (Lim et al., 1999). Rice flour (100 g, db) was dispersed in a dilute sodium hydroxide solution (0.2 g/100 g, 300 mL) using a magnetic stirrer at 25 °C for 1 h. The dispersion was centrifuged (1800 × g for 10 min), and then fresh alkaline solution (0.2 g/100 g NaOH, 300 mL) was added to the precipitate to repeat the extraction process. After three cycles of extraction, starch precipitates were re-suspended in 200 mL of distilled water and neutralized to pH 7.0 by adding 0.1 mol/L HCl solution. The neutralized starch residue was washed twice with distilled water (200 mL each) and finally with 200 mL of 95 g/100 g ethanol. The starch collected by centrifugation was dried in a convection oven at 40 °C overnight.

### 2.3. Amylose and protein contents

Amylose content in rice starch samples was measured after an enzymatic debranching using a gel permeation chromatography which consisted of a pump (P2000, Spectra System, San Jose, CA, USA), an injector valve with a 0.1 mL loop (Rheodyne 7072, Cotati, CA, USA), and a refractive index detector (Shodex RI-71, Tokyo, Japan). The column used was a medium-pressure Superdex 75HR (Amersham Pharmacia Biotech, Uppsala, Sweden). The eluent was deionized water containing 0.02 g/100 g Na<sub>2</sub>S<sub>2</sub>O<sub>3</sub> that had been filtered through a 0.1-µm cellulose acetate filter (Whatman, Maidstone, UK) and degassed. The flow rate of the eluent was 0.3 mL/min.

All starch samples for amylose analysis were purified by

dissolving in 90 g/100 g DMSO and isolated by adding absolute ethanol (Jane & Chen, 1992). The purified starch (50 mg, db) was dispersed in deionized water (25 mL), and the dispersion was then autoclaved at 121 °C for 15 min for complete dissolution. Acetate buffer (0.1 mol/L, pH 3.5, 200 µL) and isoamylase (0.3 µL, 280 U/mg) were added to the starch solution, and the mixture was incubated at 45 °C for 24 h in a shaking water bath. The enzyme was inactivated by boiling the solution for 15 min. The debranched starch solution was filtered through a 5.0-µm acrylic copolymer syringe filter (Pall Gelman Science, Ann Arbor, MI, USA) before GPC analysis.

Crude protein content was determined using an auto-Kjeldahl system (AutokjelTech, Model No. 11, Tecator, Hsiganas, Sweden).

### 2.4. Particle size analysis

The particle size distribution was measured with an aqueous suspensions of starches using a laser diffraction particle size analyzer (CILAS 1064, Compagnie Industrielle des Lasers, Orléans, France). The mean diameter ( $D_{50}$ ) of rice starches was determined by the particle size distribution by volume.

### 2.5. Thermal properties

The gelatinization temperature and enthalpy of rice starches were measured using a differential scanning calorimeter (DSC6100, Seiko Instruments Inc., Chiba, Japan). The instrument was calibrated with indium and an empty aluminum pan was used as the reference. Starch sample (3.0 mg, db) and water (6.0 mg) were transferred to an aluminum DSC pan. The pan was then sealed and equilibrated at 4 °C for 2 h prior to analysis. The sample pan was heated at a speed of 5 °C/min from 20 to 130 °C. The onset ( $T_o$ ), peak ( $T_p$ ), and conclusion ( $T_c$ ) temperatures along with gelatinization enthalpy ( $\Delta H$ ) were determined from the thermograms.

### 2.6. Pasting viscosity

Pasting viscosity of the rice starches was evaluated with a Rapid Visco-Analyzer (RVA-3D, Newport Scientific, Warriewood, Australia). Starch suspensions (7 g/100 g, w/w) were heated using a programmed heating and cooling cycle: heating from 50 to 95 °C at a rate of 13 °C/min, holding at 95 °C for 3 min, cooling to 50 °C at 13 °C/min, and holding for 4 min. A constant rotating speed of the paddle (160 rpm) was used. Values of peak viscosity, breakdown, setback, final viscosity and pasting temperature were obtained from the viscograms.

### 2.7. Gel texture

Starch suspensions (13 g/100 g, w/w) were heated from 25 to 95 °C at a rate of 14 °C/min and held at 95 °C for 10 min using a Rapid Visco-Analyzer. The starch paste was transferred into petri dishes (50 mm diameter, 0.9 mm depth) taped around the edge. After cooled by leaving at room temperature for 1 h, the petri dishes were covered and then stored at 4 °C for gel formation. The texture of the starch gels was measured using a texture analyzer (TA-XT2, Stable Microsystems, Surrey, England). After the top portion above the edge was removed with a wire cheese cutter to make the gel surface smooth, the gel was compressed at a speed of 1.0 mm/s with a cylindrical plunger (20 mm diameter). The parameters analyzed included hardness, chewiness, gumminess, springiness, and cohesiveness.

### 2.8. Statistical analysis

All experiments were performed in triplicates. The data were

analyzed by one-way analysis of variance (ANOVA) using SAS software system (Version 9.2, SAS Institute Inc., Cary, NC, USA). When the difference was found among samples, Duncan's multiple comparisons were conducted to separate the means. Pearson correlation analysis was also conducted to determine the relationships among the physicochemical characteristics of the twelve rice samples. The principal component analysis (PCA) was performed using the Unscrambler, ver 9.1 (CAMO A/S, Trondheim, Norway) to summarize and visualize the differences and similarities among the twelve starches from rice cultivars on the various properties.

### 3. Results and discussion

#### 3.1. Amylose and protein contents

Amylose and protein contents in the starch samples which were isolated from *japonica* and *indica* rice cultivars are shown in Table 1. The amylose and protein contents were significantly different among the rice starches tested. The amylose contents were the lowest for *Baegjinju 1* starch and the highest for *Goami 3* starch. *Indica* rice starches such as *Jiangxi* and *Cop 18* contained the higher amylose contents than *japonica* rice starches, except *Goami 3* starch. The higher amylose content for *indica* rice than that for *japonica* rice has been reported by Singh, Okadome, Toyoshima, Isobe, and Ohtsubo (2000) and Chung, Liu, Lee, and Wei (2011). Among the *japonica* rice cultivars tested, *Baegjinju 1* could be classified as very low amylose rice and *Goami 3* was classified as intermediate amylose rice (Juliano, 1992).

Protein content was found to be highest for *Baekokchal* starch and lowest for *Dongjinchal* starch among the twelve rice starch samples. For the non-waxy starches, protein contents were relatively higher for *indica* starches than those for *japonica* starches, except for *Goami 3* starch. The differences in protein content among the rice starches tested might be attributed to genetic factors, starch isolation process, and/or plant growing environments (Singh, Kaur, Sandhu, Kaur, & Nishinari, 2006; Wang et al., 2010).

#### 3.2. Granule size

Mean granule size ( $D_{50}$ ) of the starch samples originated from different rice cultivars ranged between 4.69 and 8.74  $\mu\text{m}$ . According to Ellis et al. (1998), rice starch exists as very small granules with a mean diameter of 3–8  $\mu\text{m}$ . The lowest mean granule size (4.69  $\mu\text{m}$ ) was observed for *Dongjinchal* starch and the highest mean granule size (8.74  $\mu\text{m}$ ) for *Baekokchal* starch. Among the non-waxy rice starches, *Goami 3* starch with the greatest amylose content contained the largest granules (7.94  $\mu\text{m}$ ), whereas *Chucheong* had the

smallest granules (4.72  $\mu\text{m}$ ). *Indica* rice starches (6.69–6.96  $\mu\text{m}$ ) consisted of the larger granules than *japonica* rice starches (4.72–5.86  $\mu\text{m}$ ) except *Goami 3* starch. The granule sizes measured for the non-waxy *japonica* starches were in accordance with the results reported by Li and Yeh (2001) who studied with Taiwanese rice starches.

#### 3.3. Thermal properties

Thermal properties of the rice starch samples from different cultivars are summarized in Table 2. The temperatures ( $T_0$ ,  $T_p$ , and  $T_c$ ) and enthalpy ( $\Delta H$ ) for crystal melting of the starches varied significantly among the twelve starch samples. *Goami 3* starch, which had the highest amylose content among the rice starches tested, exhibited the highest  $T_p$  (74.4 °C) and  $T_c$  (83.7 °C), whereas *Yeongan* showed the lowest  $T_0$  (55.0 °C),  $T_p$  (61.1 °C), and  $T_c$  (70.1 °C) among the twelve samples. Among the non-waxy rice starches tested, *indica* starches including *Jiangxi* and *Cop 18* displayed the higher melting temperatures than *japonica* rice starches. Among the *indica* starches, *Remyline XS*, a waxy starch showed the lower melting temperatures ( $T_0$  58.8 °C,  $T_p$  66.3 °C, and  $T_c$  75.6 °C) than non-waxy starch samples (*Jiangxi* and *Cop 18*). This result was in agreement with that reported by Park et al. (2007) in which gelatinization temperatures ( $T_0$  and  $T_p$ ) increased with increasing amylose content in rice starches. They reported that the chain association between linear amyloses restricted the hydration of amorphous regions of starch granules and thus retarded swelling and gelatinization. Among the *japonica* rice starches, however, non-waxy *Chucheong*, *Haiami*, *Yeongan*, and *Hyangmi 1* starches exhibited lower  $T_p$  and  $T_c$  than waxy starches (*Baekokchal*, *Dongjinchal*, and *Aranghyangchal*). The waxy *japonica* starch *Baekokchal*, which contained the highest protein content and the largest granules, showed the highest  $T_0$  (59.3 °C) and  $T_p$  (66.7 °C) among the *japonica* rice starch samples except the high amylose starch *Goami 3*. *Baegjinju 1*, a non-waxy starch which had the lowest amounts of amylose (3.77 g/100 g) and protein (0.08 g/100 g) showed the melting temperatures similar to those for waxy *Dongjinchal* and *Aranghyangchal* starches. This trend indicates that the starch melting characteristics were influenced by the presences of amylose and protein.

Regarding the melting enthalpy, *japonica Baegjinju 1* and *Goami 3* starches showed the highest  $\Delta H$  (18.6 and 18.3 J/g, respectively) among the twelve rice starches tested, whereas *Baekokchal* a waxy *japonica* starch displayed the lowest value (12.0 J/g). The non-waxy *japonica* rice starches, except for *Baegjinju 1* and *Goami 3*, exhibited the lower  $\Delta H$  than waxy *Dongjinchal* and *Aranghyangchal* starches. Similar result was observed for the *indica* rice starches, showing

**Table 1**  
Amylose and protein contents, and mean granule size of starches from different rice cultivars.<sup>A</sup>

Grain types	Rice starch	Amylose content (g/100 g) <sup>***B</sup>	Protein content (g/100 g) <sup>***</sup>	Mean granule size ( $\mu\text{m}$ ) <sup>***</sup>
Non-waxy <i>indica</i> rice	<i>Jiangxi</i>	20.49 $\pm$ 2.05 <sup>ab</sup>	0.43 $\pm$ 0.12 <sup>b</sup>	6.96 $\pm$ 0.01 <sup>cd</sup>
	<i>Cop 18</i>	19.01 $\pm$ 2.73 <sup>ab</sup>	0.32 $\pm$ 0.01 <sup>c</sup>	6.69 $\pm$ 0.00 <sup>d</sup>
Non-waxy <i>japonica</i> rice	<i>Baegjinju 1</i>	3.77 $\pm$ 1.20 <sup>d</sup>	0.08 $\pm$ 0.00 <sup>ef</sup>	5.86 $\pm$ 0.02 <sup>e</sup>
	<i>Chucheong</i>	14.30 $\pm$ 2.27 <sup>c</sup>	0.14 $\pm$ 0.00 <sup>de</sup>	4.72 $\pm$ 0.01 <sup>h</sup>
	<i>Goami 3</i>	21.97 $\pm$ 0.08 <sup>a</sup>	0.36 $\pm$ 0.00 <sup>c</sup>	7.94 $\pm$ 0.05 <sup>b</sup>
	<i>Haiami</i>	16.19 $\pm$ 0.32 <sup>bc</sup>	0.14 $\pm$ 0.00 <sup>de</sup>	5.76 $\pm$ 0.09 <sup>e</sup>
	<i>Yeongan</i>	17.01 $\pm$ 0.37 <sup>bc</sup>	0.15 $\pm$ 0.00 <sup>de</sup>	5.01 $\pm$ 0.36 <sup>g</sup>
	<i>Hyangmi 1</i>	13.28 $\pm$ 2.28 <sup>c</sup>	0.14 $\pm$ 0.00 <sup>de</sup>	5.24 $\pm$ 0.31 <sup>f</sup>
Waxy <i>indica</i> rice	<i>Remyline XS</i>	–	0.21 $\pm$ 0.00 <sup>d</sup>	7.06 $\pm$ 0.00 <sup>c</sup>
Waxy <i>japonica</i> rice	<i>Dongjinchal</i>	–	0.05 $\pm$ 0.00 <sup>f</sup>	4.69 $\pm$ 0.01 <sup>h</sup>
	<i>Aranghyangchal</i>	–	0.08 $\pm$ 0.00 <sup>ef</sup>	4.93 $\pm$ 0.02 <sup>gh</sup>
	<i>Baekokchal</i>	–	1.77 $\pm$ 0.02 <sup>a</sup>	8.74 $\pm$ 0.01 <sup>a</sup>

<sup>A</sup>Values followed by the different superscripts in the same column are significantly different ( $P < 0.05$ ).

<sup>B\*\*\*</sup> Significant different at  $p = 0.001$ .

Replication:  $n = 3$ .

**Table 2**  
Thermal properties of starches from different rice cultivars.<sup>A</sup>

Grain types	Rice starch	T <sub>0</sub> (°C) <sup>***B</sup>	T <sub>p</sub> (°C) <sup>***</sup>	T <sub>c</sub> (°C) <sup>***</sup>	ΔT (T <sub>c</sub> – T <sub>0</sub> ) <sup>***</sup>	ΔH (J/g) <sup>***</sup>
Non-waxy <i>indica</i> rice	<i>Jiangxi</i>	68.0 ± 0.1 <sup>a</sup>	72.9 ± 0.0 <sup>b</sup>	78.9 ± 0.3 <sup>b</sup>	11.0 ± 0.3 <sup>h</sup>	14.6 ± 1.0 <sup>e</sup>
	<i>Cop 18</i>	67.5 ± 0.0 <sup>b</sup>	72.7 ± 0.0 <sup>c</sup>	78.9 ± 0.0 <sup>b</sup>	11.4 ± 0.0 <sup>g</sup>	15.5 ± 0.1 <sup>de</sup>
Non-waxy <i>japonica</i> rice	<i>Baegjinju 1</i>	56.5 ± 0.0 <sup>h</sup>	64.0 ± 0.0 <sup>g</sup>	73.4 ± 0.6 <sup>d</sup>	16.9 ± 0.6 <sup>b</sup>	18.6 ± 0.3 <sup>a</sup>
	<i>Chucheong</i>	56.3 ± 0.0 <sup>i</sup>	62.1 ± 0.1 <sup>i</sup>	70.4 ± 0.4 <sup>f</sup>	14.1 ± 0.4 <sup>e</sup>	16.9 ± 0.9 <sup>bcd</sup>
	<i>Goami 3</i>	67.2 ± 0.1 <sup>c</sup>	74.4 ± 0.0 <sup>a</sup>	83.7 ± 0.1 <sup>a</sup>	16.5 ± 0.1 <sup>b</sup>	18.3 ± 1.4 <sup>ab</sup>
	<i>Haiami</i>	56.1 ± 0.1 <sup>j</sup>	62.2 ± 0.1 <sup>i</sup>	71.1 ± 0.1 <sup>e</sup>	15.0 ± 0.3 <sup>d</sup>	16.8 ± 0.3 <sup>bcd</sup>
	<i>Yeongan</i>	55.0 ± 0.1 <sup>k</sup>	61.1 ± 0.1 <sup>j</sup>	70.1 ± 0.1 <sup>f</sup>	15.1 ± 0.1 <sup>d</sup>	15.9 ± 0.3 <sup>de</sup>
	<i>Hyangmi 1</i>	58.3 ± 0.2 <sup>f</sup>	63.7 ± 0.0 <sup>h</sup>	71.1 ± 0.1 <sup>e</sup>	12.8 ± 0.3 <sup>f</sup>	16.4 ± 0.1 <sup>cd</sup>
Waxy <i>indica</i> rice	<i>Remyline XS</i>	58.8 ± 0.1 <sup>e</sup>	66.3 ± 0.0 <sup>e</sup>	75.6 ± 0.3 <sup>c</sup>	16.9 ± 0.4 <sup>b</sup>	16.9 ± 0.7 <sup>bcd</sup>
Waxy <i>japonica</i> rice	<i>Dongjinchal</i>	57.8 ± 0.1 <sup>g</sup>	64.3 ± 0.1 <sup>f</sup>	73.7 ± 0.3 <sup>d</sup>	15.9 ± 0.2 <sup>c</sup>	17.8 ± 0.9 <sup>abc</sup>
	<i>Aranghyangchal</i>	56.3 ± 0.0 <sup>j</sup>	64.0 ± 0.1 <sup>g</sup>	73.8 ± 0.1 <sup>d</sup>	17.5 ± 0.1 <sup>a</sup>	17.9 ± 0.2 <sup>abc</sup>
	<i>Baekokchal</i>	59.3 ± 0.0 <sup>d</sup>	66.7 ± 0.0 <sup>d</sup>	73.4 ± 0.1 <sup>d</sup>	14.1 ± 0.1 <sup>e</sup>	12.0 ± 0.1 <sup>f</sup>

<sup>A</sup>Values followed by the different superscripts in the same column are significantly different ( $P < 0.05$ ).

T<sub>0</sub>, onset temperature; T<sub>p</sub>, peak temperature; T<sub>c</sub>, conclusion temperature; ΔT (T<sub>c</sub> – T<sub>0</sub>), melting temperature range; ΔH, enthalpy for melting.

<sup>B\*\*\*</sup> Significant different at  $p = 0.001$ .

Replication:  $n = 3$ .

that non-waxy starches (*Jiangxi* and *Cop 18*) had the lower ΔH values than the waxy starch (*Remyline XS*). The melting enthalpy (ΔH) reflects an overall measure of crystallinity and the loss of molecular (double helical) order within the granule (Cooke & Gidley, 1992; Tester & Morrison, 1990). Waxy starches have been reported to show the larger gelatinization enthalpies than non-waxy starches, reflecting the higher degrees of crystallinity due to the crystalline arrangement of amylopectin (Chung et al., 2011; Jane et al., 1999).

The ΔT value, melting temperature range, was found to be the lowest for *indica Jiangxi* (11.0 °C) and *Cop 18* (11.4 °C), starches, and the highest for waxy *japonica Aranghyangchal* starch (17.5 °C). This result was similar to the finding reported by Park et al. (2007), which was that the smaller ΔT was observed with the long grain *indica* rice starches than *japonica* rice starches. In addition, Sodhi and Singh (2003) suggested that the differences in ΔT among *indica* rice starches might be attributed to the variations in size and uniformity of starch granules.

### 3.4. Pasting viscosity

Pasting viscosity profiles of the rice starches obtained from different cultivars analyzed with a Rapid Visco-Analyzer are presented in Table 3. Pasting temperature, peak viscosity, and final viscosity ranged from 69.1 to 92.9 °C, 34 to 155 RVU, and 46 to 136 RVU, respectively. The pasting temperature of the starches was higher than the onset temperature (T<sub>0</sub>) for melting determined by DSC, indicating that the crystalline melting was usually precedent

to the viscosity increase during pasting. Non-waxy *Goami 3* starch, which contained the highest amylose content, showed the highest pasting temperature (92.9 °C) among the twelve rice starches tested, whereas waxy *Dongjinchal* starch showed the lowest pasting temperature (69.1 °C). The rice starch with the higher amylose content was reported to show the higher pasting temperature and lower peak viscosity than the starch containing the lower amylose content (Chung et al., 2011; Park et al., 2007). While amylopectin usually contributes to the swelling of starch granules, amylose tends to restrict the swelling and to keep the integrity of swollen starch granules during pasting (Tester & Morrison, 1990). Non-waxy *indica* starches exhibited the higher pasting temperatures and lower peak and final viscosities than the Korean non-waxy *japonica* starches. Among the *indica* rice starches tested, waxy *Remyline XS* starch showed the lower pasting temperature (70.4 °C) and higher peak viscosity (153 RVU) than non-waxy starches. Similar results were found for the *japonica* rice starches: the lower pasting temperatures and higher viscosities for waxy starches. Breakdown in pasting viscogram reflects the stability of starch paste against heating and mechanical shearing (Karim, Norziah, & Seow, 2000). The lower breakdown of non-waxy starches when compared to waxy starches tested indicates that the presence of amylose hinders the granular swelling and assists in stabilizing the swollen starch granules. On the other hand, a non-waxy *japonica* starch *Baegjinju 1* displayed an exceptionally high peak (155 RVU) and final viscosities (99 RVU), which were even higher than those of waxy *japonica* starches. However, the breakdown for *Baegjinju 1* was substantially higher than other starches (Table 3) indicating its

**Table 3**  
Pasting properties of starches from different rice cultivars.<sup>A</sup>

Grain types	Rice starch	Pasting temp. (°C) <sup>***B</sup>	Peak viscosity (RVU) <sup>***</sup>	Breakdown (RVU) <sup>***</sup>	Final viscosity (RVU) <sup>***</sup>	Setback (RVU) <sup>***</sup>
Non-waxy <i>indica</i> rice	<i>Jiangxi</i>	86.8 ± 0.4 <sup>d</sup>	33.9 ± 0.1 <sup>k</sup>	2.3 ± 0.1 <sup>h</sup>	45.9 ± 1.2 <sup>f</sup>	14.2 ± 1.2 <sup>h</sup>
	<i>Cop 18</i>	90.9 ± 0.4 <sup>b</sup>	34.3 ± 0.2 <sup>k</sup>	1.9 ± 0.1 <sup>h</sup>	48.2 ± 0.0 <sup>f</sup>	15.7 ± 0.2 <sup>gh</sup>
Non-waxy <i>japonica</i> rice	<i>Baegjinju 1</i>	70.3 ± 0.0 <sup>g</sup>	155.0 ± 1.2 <sup>a</sup>	78.1 ± 1.9 <sup>a</sup>	99.3 ± 1.2 <sup>c</sup>	22.1 ± 1.9 <sup>e</sup>
	<i>Chucheong</i>	77.9 ± 0.4 <sup>e</sup>	99.9 ± 0.9 <sup>f</sup>	11.5 ± 1.1 <sup>g</sup>	125.0 ± 0.4 <sup>b</sup>	37.0 ± 0.7 <sup>b</sup>
	<i>Goami 3</i>	92.9 ± 0.0 <sup>a</sup>	57.1 ± 0.7 <sup>i</sup>	14.5 ± 0.0 <sup>g</sup>	63.4 ± 0.8 <sup>e</sup>	28.3 ± 0.3 <sup>d</sup>
	<i>Haiami</i>	77.8 ± 0.4 <sup>e</sup>	103.0 ± 1.0 <sup>e</sup>	20.8 ± 0.4 <sup>f</sup>	130.0 ± 15.7 <sup>ab</sup>	40.0 ± 0.8 <sup>a</sup>
	<i>Yeongan</i>	77.9 ± 0.4 <sup>e</sup>	85.8 ± 0.4 <sup>h</sup>	12.2 ± 0.3 <sup>g</sup>	105.0 ± 0.7 <sup>c</sup>	31.5 ± 0.0 <sup>c</sup>
	<i>Hyangmi 1</i>	77.4 ± 0.1 <sup>e</sup>	117.0 ± 0.0 <sup>c</sup>	20.4 ± 1.1 <sup>f</sup>	136.0 ± 1.0 <sup>a</sup>	39.6 ± 0.0 <sup>a</sup>
Waxy <i>indica</i> rice	<i>Remyline XS</i>	70.4 ± 0.0 <sup>g</sup>	153.0 ± 1.0 <sup>b</sup>	38.5 ± 4.1 <sup>d</sup>	133.0 ± 1.6 <sup>ab</sup>	18.6 ± 1.5 <sup>f</sup>
Waxy <i>japonica</i> rice	<i>Dongjinchal</i>	69.1 ± 0.4 <sup>h</sup>	117.0 ± 0.5 <sup>c</sup>	63.5 ± 0.5 <sup>b</sup>	70.1 ± 0.1 <sup>d</sup>	16.5 ± 0.0 <sup>g</sup>
	<i>Aranghyangchal</i>	69.6 ± 0.1 <sup>h</sup>	114.0 ± 0.0 <sup>d</sup>	5.8 ± 0.9 <sup>c</sup>	71.1 ± 0.2 <sup>d</sup>	15.0 ± 0.8 <sup>gh</sup>
	<i>Baekokchal</i>	71.5 ± 0.4 <sup>f</sup>	89.5 ± 1.2 <sup>g</sup>	29.5 ± 1.9 <sup>e</sup>	70.6 ± 0.3 <sup>d</sup>	10.5 ± 0.5 <sup>i</sup>

<sup>A</sup>Values followed by the different superscripts in the same column are significantly different ( $P < 0.05$ ).

<sup>B\*\*\*</sup> Significant different at  $p = 0.001$ .

Replication:  $n = 3$ .

lower stability. The low amylose content (3.77 g/100 g), less than those in typical non-waxy starches, resulted in the high degree of granular swelling, but in the low stability of the swollen starch granules. Therefore, the exceptionally high peak viscosity eventually resulted in the high breakdown. The unique pasting behavior of *Baegjinju 1* might be attributed to the inherent characteristics of the starch besides its low amylose content, possibly including the chain structure of the starch.

Among the *japonica* starches, non-waxy starches showed the higher setback values than waxy starches, representing that the presence of amylose caused the higher degree of chain association. Among the non-waxy starches, *japonica* starches had the higher setback values than *indica* starches, possibly because of the higher amylose content in *japonica* starches. It was reported that the effect of amylose on setback was mainly from the amylose chains leached from swollen granules (Loh, 1992). Although the amylose content was highest for *Goami 3*, most of the amylose in this starch might remain inside the granules because the starch swelling was highly restricted, and thus the setback of *Goami 3* was exceptionally low. *Haiami* and *Hyangmi 1* starches which displayed the highest setback values among the non-waxy starches might have the high degree of amylose leaching during pasting. The commercial *japonica* waxy starch *Baekokchal* exhibited the lowest setback among the waxy starches tested, indicating that it had lowest tendency of association among amylopectin chains (Karim et al., 2000). Non-waxy *japonica* *Hyangmi 1* starch showed the highest final viscosity, whereas *indica* *Jiangxi* and *Cop 18* starches had the lowest viscosity among the rice starches tested. The higher final viscosity for *japonica* starches than *indica* starches suggests that *japonica* starches are more favored when used as viscosity enhancers.

### 3.5. Gel texture

Textural properties of the gels prepared with different rice starches are listed in Table 4. The textural parameters of rice starch gels varied significantly according the rice cultivars. Hardness and gumminess of *indica* starch gels were higher than those of *japonica* starch gels. It indicates that *indica* starches could retrograde more readily than *japonica* starches possibly because of the higher amount of linear amylose molecules. *Goami 3* starch which had the highest amylose content and largest granule size produced the hardest gel with the highest value in gumminess. The amount of amylose and deformability of swollen granules were important in gel formation and its strength (Lii, Tsai, & Tseng, 1996). Springiness, which represented the recovering ability against deformation, was highest for *Jiangxi indica* starch (0.91) and *Goami 3*, and lowest for

*Yeongan*, a non-waxy *japonica* starch (0.77). Gel cohesiveness, which reflected the intermolecular force in gel matrix, was higher for *indica* starches (0.83–0.90) than *japonica* starches (0.64–0.76), except *Goami 3* starch (0.88). These textural properties of starch gels from various rice cultivars appeared dependent on the amylose and protein contents.

### 3.6. Pearson correlation between physicochemical properties

Pearson correlation coefficients for the relationships between the physicochemical properties of the rice starches from different cultivars are summarized in Table 5. Protein contents in the rice starch samples were positively correlated to amylose contents ( $r = 0.806$ ,  $p \leq 0.01$ ). Hamaker, Griffin, and Moldenhauer (1991) reported that the 60 kdal protein associated with rice starch granules correlated highly with amylose content ( $r = 0.96$ ,  $p \leq 0.01$ ). Starches with the higher protein contents exhibited the larger mean granule sizes ( $r = 0.751$ ,  $p \leq 0.01$ ). Sodhi and Singh (2003) reported that *indica* rice starches with larger average granule sizes contained more amylose content than those with smaller average granule sizes, but no significant relationship between granule size and amylose content was found for the starches tested in this study. Amylose content was positively correlated to  $T_0$  ( $r = 0.681$ ,  $p \leq 0.05$ ), whereas protein content was not found to be related to the melting temperature. Contrastively, Kong, Zhu, Sui, and Bao (2015) indicated that apparent amylose content of different Chinese rice genotypes was negatively correlated with gelatinization temperatures. The melting enthalpy ( $\Delta H$ ), however, appeared negatively correlated to protein content ( $r = -0.821$ ,  $p \leq 0.001$ ). It was reported that residual protein in starch tended to restrict granule swelling during pasting (Hamaker & Griffin, 1993; Lim et al., 1999). The rice starch with the larger granules showed the higher melting temperatures:  $T_0$  ( $r = 0.602$ ,  $p \leq 0.05$ ),  $T_p$  ( $r = 0.684$ ,  $p \leq 0.01$ ), and  $T_c$  ( $r = 0.635$ ,  $p \leq 0.05$ ). The overall results indicate that not only the amylose content but the granule size are somewhat related to the thermal properties of rice starches.

In pasting profiles, amylose content was positively correlated to pasting temperature ( $r = 0.878$ ,  $p \leq 0.01$ ) and negatively correlated to peak viscosity and breakdown ( $r = -0.910$ ,  $p \leq 0.001$ ;  $r = -0.905$ ,  $p \leq 0.001$ , respectively), which was consistent with previous reports (Chung et al., 2011; Singh et al., 2003). Park et al. (2007) suggested that a starch containing more amylose required higher temperature to reach the maximum swelling because more energy was needed to break the linkages between amylose chains. For *indica* rice starches, positive correlations between amylose content and peak viscosity were reported (Singh et al., 2006). Pasting temperature was negatively correlated to peak and breakdown

**Table 4**  
Gel textural properties of starches from different rice cultivars.<sup>A</sup>

Grain types	Rice starch	Hardness (g) <sup>***B</sup>	Chewiness (g) <sup>***</sup>	Gumminess (g) <sup>***</sup>	Springiness <sup>***</sup>	Cohesiveness <sup>***</sup>
Non-waxy <i>indica</i> rice	<i>Jiangxi</i>	178 ± 16 <sup>b</sup>	146 ± 19 <sup>b</sup>	161 ± 19 <sup>b</sup>	0.91 ± 0.01 <sup>a</sup>	0.90 ± 0.03 <sup>a</sup>
	<i>Cop 18</i>	180 ± 15 <sup>b</sup>	122 ± 11 <sup>b</sup>	150 ± 17 <sup>bc</sup>	0.82 ± 0.03 <sup>b</sup>	0.83 ± 0.02 <sup>a</sup>
Non-waxy <i>japonica</i> rice	<i>Baegjinju 1</i>	—	—	—	—	—
	<i>Chucheong</i>	59 ± 1 <sup>c</sup>	38 ± 2 <sup>b</sup>	45 ± 1 <sup>c</sup>	0.84 ± 0.03 <sup>b</sup>	0.76 ± 0.03 <sup>ab</sup>
	<i>Goami 3</i>	840 ± 115 <sup>a</sup>	666 ± 114 <sup>a</sup>	736 ± 117 <sup>a</sup>	0.90 ± 0.02 <sup>a</sup>	0.88 ± 0.02 <sup>a</sup>
	<i>Haiami</i>	73 ± 7 <sup>c</sup>	41 ± 7 <sup>b</sup>	50 ± 9 <sup>c</sup>	0.82 ± 0.01 <sup>b</sup>	0.64 ± 0.14 <sup>b</sup>
	<i>Yeongan</i>	72 ± 4 <sup>c</sup>	38 ± 3 <sup>b</sup>	49 ± 3 <sup>c</sup>	0.77 ± 0.03 <sup>c</sup>	0.68 ± 0.02 <sup>b</sup>
	<i>Hyangmi 1</i>	58 ± 3 <sup>c</sup>	34 ± 1 <sup>b</sup>	41 ± 2 <sup>c</sup>	0.83 ± 0.01 <sup>b</sup>	0.71 ± 0.04 <sup>b</sup>
Waxy <i>indica</i> rice	<i>Remyline XS</i>	—	—	—	—	—
Waxy <i>japonica</i> rice	<i>Dongjinchal</i>	—	—	—	—	—
	<i>Aranghyangchal</i>	—	—	—	—	—
	<i>Baekokchal</i>	—	—	—	—	—

<sup>A</sup>Values followed by the different superscripts in the same column are significantly different ( $P < 0.05$ ).

<sup>B\*\*\*</sup> Significant different at  $p = 0.001$ .

Replication:  $n = 3$ .

**Table 5**  
Pearson correlation coefficients between physicochemical, thermal, pasting and textural properties of starches from different rice cultivars.

	Amy	Prot	Size	To	Tp	Tc	$\Delta H$	$\Delta T$	PT	PV	BD	FV	SB	Hard	Gum	Spring
Prot	0.806**															
Size	0.557	0.751**														
To	0.681*	0.187	0.602*													
Tp	0.635	0.240	0.684**	0.982												
Tc	0.590	0.112	0.635*	0.904**	0.959***	0.007										
$\Delta H$	-0.547	-0.821***	-0.540*	-0.270	-0.224	0.007	0.631*									
$\Delta T$	-0.479	-0.220	-0.194	-0.607	-0.463	-0.210	0.143	-0.610*								
PT	0.878**	-0.010	0.375	0.838***	0.775*	0.706**	0.459	0.739**	-0.868***							
PV	-0.910***	-0.237	-0.374	-0.810***	-0.735**	-0.602	0.503	0.751**	-0.796**	0.795**						
BD	-0.905***	0.170	-0.290	-0.570*	-0.458	-0.298	0.272	0.342	-0.468	0.701**	0.154					
FV	-0.554	-0.304	-0.407	-0.720**	-0.744**	-0.704*	0.344	0.055	0.087	0.195	-0.234	0.739**				
SB	-0.233	-0.437	-0.453	-0.394	-0.476	-0.454	0.598	0.456	0.725*	-0.368	0.003	-0.454	-0.195			
Hard	0.691*	0.542	0.783*	0.533	0.630	0.777*	0.583	0.439	0.734*	-0.383	0.014	-0.468	-0.211	0.999***		
Gum	0.700*	0.559	0.792*	0.548	0.644	0.788*	0.119	-0.109	0.562	-0.422	-0.206	-0.469	-0.354	0.605	0.621	
Spring	0.530	0.712*	0.681	0.636	0.658	0.674	0.119	-0.109	0.864**	-0.846**	-0.732	-0.877*	-0.565	0.583	0.749*	
Coh	0.780*	0.933***	0.791*	0.924**	0.923**	0.887**	-0.200	-0.409	0.864**	-0.846**	-0.732	-0.877*	-0.565	0.583	0.749*	

Abbreviation of variables were Amy, amylose content; Prot, protein content; Size, mean granule size; To, onset temperature; Tp, peak temperature; Tc, conclusion temperature;  $\Delta H$ , enthalpy for melting;  $\Delta T$ , melting temperature range; Hard, hardness; Chew, chewiness; Spring, springiness; Cohe, cohesiveness; PT, pasting temperature; PV, peak viscosity; BD, breakdown viscosity; FV, final viscosity; SB, setback viscosity. \*, \*\*, and \*\*\* means the correlations are significant at  $p \leq 0.05$ ,  $p \leq 0.01$  and  $p \leq 0.001$  levels, respectively.

viscosities ( $r = -0.868$ ,  $p \leq 0.001$ ;  $r = -0.796$ ,  $p \leq 0.01$ ), similar to the results in an earlier report (Singh et al., 2006). The correlation coefficient between pasting viscosity and amylose content was higher than that between pasting viscosity and protein content, or that between pasting viscosity and granule size. This result implies that amylose content plays the more significant role in determining the pasting viscosity of rice starches than protein content and granule size.

Hardness and gumminess of the starch gels were positively correlated with amylose content ( $r = 0.691$  and  $r = 0.700$ , respectively,  $p \leq 0.05$ ), mean granule size ( $r = 0.783$  and  $r = 0.792$ , respectively,  $p \leq 0.05$ ), and pasting temperature ( $r = 0.725$  and  $r = 0.734$ , respectively,  $p \leq 0.05$ ). Similarly, Bao et al. (2006), Wang et al. (2010), Chávez-Murillo, Wang, Quintero-Gutiérrez, and Bello-Pérez (2011), and Kong et al. (2015) reported that amylose content was positively related to the hardness of rice starch gels. Gel springiness was observed to be positively related with protein content ( $r = 0.712$ ,  $p \leq 0.05$ ), and cohesiveness was positively related to amylose content ( $r = 0.780$ ,  $p \leq 0.05$ ), protein content ( $r = 0.933$ ,  $p \leq 0.001$ ), and mean granule size ( $r = 0.791$ ,  $p \leq 0.05$ ). In addition, the positive correlation between gel cohesiveness and melting temperatures ( $T_o$ ,  $T_p$ , and  $T_c$ ) was significant ( $r = 0.924$ ,  $r = 0.923$ , and  $r = 0.887$ , respectively,  $p \leq 0.01$ ). These results suggest that the starch with the higher melting and pasting temperatures forms a gel with the higher cohesiveness. The amylose and mean granule size in starch raised the melting temperature, and thus increased the gel cohesiveness. The correlation analysis revealed that amylose and protein contents, as well as granule size were important factors in predicting the textural properties of rice starch gels.

Principal component analysis plots are presented in Figs. 1 and 2. The loading plot of the physicochemical properties for the twelve rice starches on first ( $x$ ) and second ( $y$ ) components is shown in Fig. 1, and the score plot of the twelve starches separated from different rice cultivars is displayed in Fig. 2. The first (PC1) and the second (PC2) principal components accounted for 67% and 19% of the variance, respectively, explaining a total of 86% of the variation. The loading plot provided the information about the correlations among the physicochemical properties of the rice starch samples (Fig. 1). Considering that characteristics near the center points are not influential characteristics for the results, characteristics located in the outer ellipses are more influential than those in the inner ellipses. Among various properties located in outer ellipses, final viscosity and setback in pasting profiles were loaded positively on PC1 and PC2, whereas peak viscosity and breakdown were loaded positively on PC1 but negatively on PC2. Amylose content, pasting temperature, and cohesiveness and springiness of gels were loaded highly and negatively on PC1 but positively on PC2. The melting temperatures ( $T_o$ ,  $T_p$ , and  $T_c$ ) were loaded negatively on PC1 and PC2. Except for the characteristics mentioned above, all of the characteristics were located inside of inner ellipses. Hardness, chewiness, and gumminess of gels, mean granule size, and protein content were loaded negatively on PC1, whereas  $\Delta H$  and  $\Delta T$  were loaded positively on PC1. The distance between the locations of any two starches on the score plot is directly proportional to the degree of difference or similarity between them (Fig. 2). Japonica Goami 3 starch and indica starches (Jiangxi and Cop 18) were located at the left of the score plot with large negative scores on PC1, whereas non-waxy japonica starches had positive scores on PC1 and PC2. Waxy starches (Dongjinchal and Aranghyangchal) and the non-waxy Baegjinju 1 starch were located at the right of the score plot with high negative scores on PC2. The waxy japonica Baekokchal and indica Remyline XS starches were located far from the other waxy starches, implying their differences in physicochemical properties.

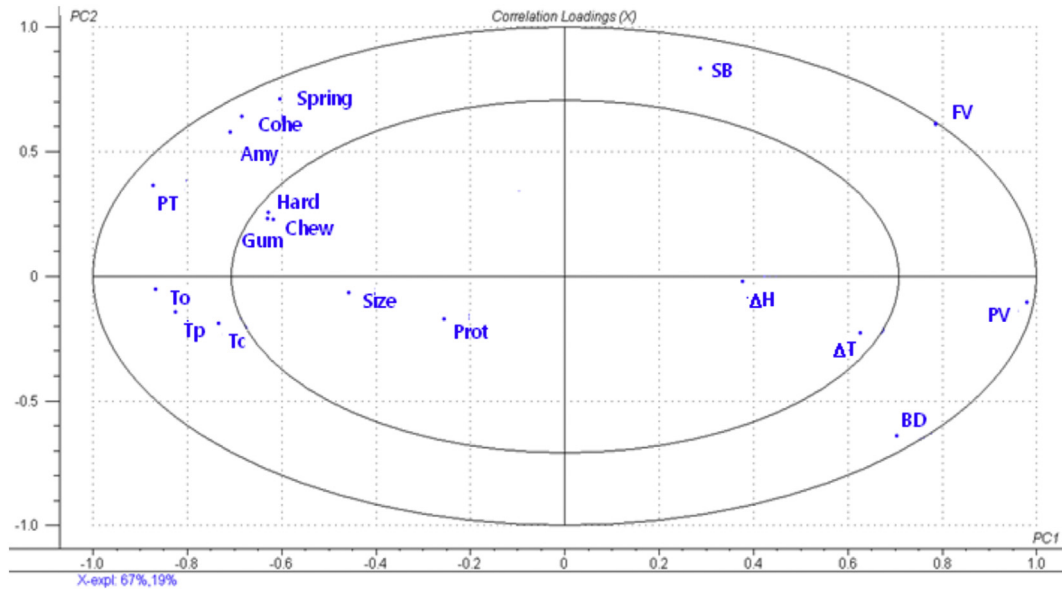


**Fig. 1.** Loading plot of physicochemical, thermal, pasting, and textural characteristics of the 12 starches from different rice cultivars in PC1 and PC2. Amy, amylose content; Prot, protein content; Size, mean granule size;  $T_0$ , onset temperature;  $T_p$ , peak temperature;  $T_c$ , conclusion temperature;  $\Delta H$ , enthalpy for melting;  $\Delta T$ , melting temperature range; Hard, hardness; Chew, chewiness; Gum, gumminess; Spring, springiness; Cohe, cohesiveness; PT, pasting temperature; PV, peak viscosity; BD, breakdown viscosity; FV, final viscosity; SB, setback viscosity.

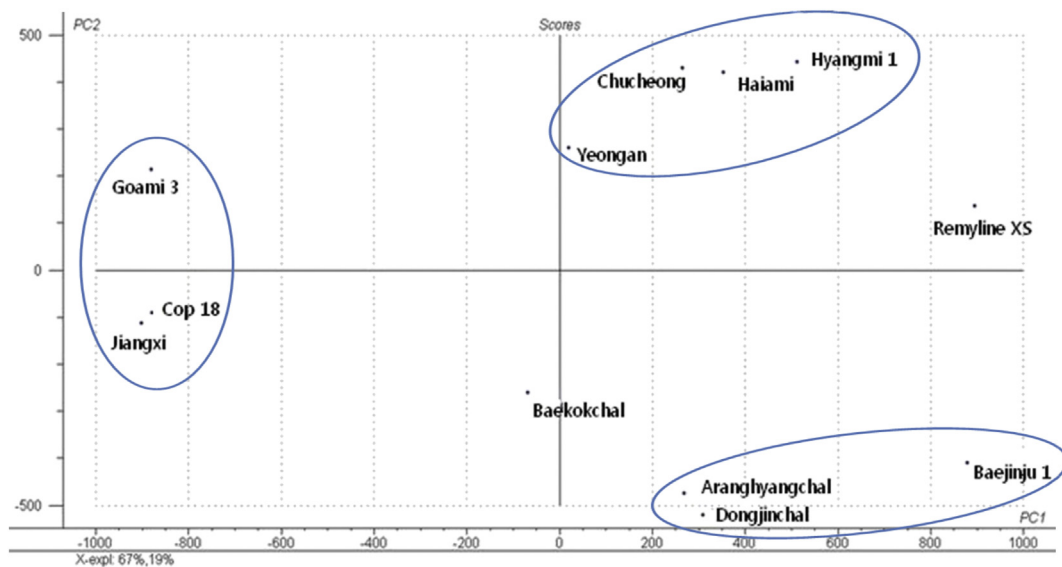


**Fig. 2.** Score plot of the 12 starches from different rice cultivars in PC1 and PC2.

The score plot indicates that the different types of rice starches used in this study can be classified into three main groups by their various properties (Group 1: non-waxy *indica* starches and non-waxy *japonica* Goami 3 starch, Group 2: non-waxy *japonica* starches, Group 3: waxy *japonica* starches and non-waxy *japonica* Baegjinju 1 starch).

#### 4. Conclusions

Amylose content of *japonica* and *indica* rice starches significantly affected their thermal, pasting, and gelling properties. The *indica* rice starches which contained the higher amylose than *japonica* rice starches showed the higher melting and pasting temperatures with the lower pasting viscosity but the higher gel

hardness. Correlation analysis showed that amylose content was the most important parameter in determining the pasting properties of various rice starches. The twelve rice starches tested could be separated into three main groups based on their thermal, pasting, and gelling properties, as revealed from the PCA score plot. The physicochemical properties for different types of starches could be used as important information for rice breeders and food processors to develop and utilize rice starches.

#### Acknowledgments

This research was supported by iPET (Korea Institute of Planning and Evaluation for Technology in Food, Agriculture, Forestry and Fisheries, under grant no: 311030-03-1-HD120), Ministry for Food,

Agriculture, Forestry and Fisheries, Republic of Korea. We also thank the Suseong College for financial support.

## References

- Bao, J., Shen, S., Sun, M., & Corke, H. (2006). Analysis of genotypic diversity in the starch physicochemical properties of nonwaxy rice: apparent amylose content, pasting viscosity and gel texture. *Starch*, *58*, 259–267.
- Champagne, E. T. (1996). Rice starch composition and characteristics. *Cereal Foods World*, *41*, 833–838.
- Chávez-Murillo, C. E., Wang, Y. J., Quintero-Gutierrez, A. G., & Bello-Pérez, L. A. (2011). Physicochemical, textural, and nutritional characterization of Mexican rice cultivars. *Cereal Chemistry*, *88*, 245–252.
- Chung, H. J., Liu, Q., Lee, L., & Wei, D. (2011). Relationship between the structure, physicochemical properties and in vitro digestibility of rice starches with different amylose contents. *Food Hydrocolloids*, *25*, 968–975.
- Cooke, D., & Gidley, M. J. (1992). Loss of crystalline and molecular order during starch gelatinization: origin of the enthalpic transition. *Carbohydrate Research*, *227*, 103–112.
- Ellis, R. P., Cochrane, M. P., Dale, M. F. B., Duffus, C. M., Lynn, A., Morrison, I. M., et al. (1998). Starch production and industrial use. *Journal of the Science of Food and Agriculture*, *77*, 289–311.
- Hamaker, B. R., & Griffin, V. K. (1993). Effect of disulfide bond-containing protein on rice starch gelatinization and pasting. *Cereal Chemistry*, *70*, 377–380.
- Hamaker, B. R., Griffin, V. K., & Moldenhauer, K. A. K. (1991). Potential influence of a starch granule-associated protein on cooked rice stickiness. *Journal of Food Science*, *356*, 1327–1330.
- Inouchi, N., Hibiu, H., Li, T., Horibata, T., Fuwa, H., & Itani, T. (2005). Structure and properties of endosperm starches from cultivated rice of Asia and other countries. *Journal of Applied Glycoscience*, *52*, 239–246.
- Jane, J., & Chen, J. (1992). Effect of amylose molecular size and amylopectin branch chain lengths on paste properties of starch. *Cereal Chemistry*, *69*, 60–65.
- Jane, J., Chen, Y. Y., Lee, L. F., McPherson, A. E., Wong, K. S., Radosavljevic, M., et al. (1999). Effects of amylopectin branch chain length and amylose content on the gelatinization and pasting properties of starch. *Cereal Chemistry*, *76*, 629–637.
- Juliano, B. O. (1992). Structure, chemistry, and function of the rice grain and its fraction. *Cereal Foods World*, *37*, 772–774.
- Karim, A. A., Norziah, M. H., & Seow, C. C. (2000). Methods for the study of starch retrogradation. *Food Chemistry*, *71*, 9–36.
- Kong, X., Zhu, P., Sui, Z., & Bao, J. (2015). Physicochemical properties of starches from diverse rice cultivars varying in apparent amylose content and gelatinization temperature combinations. *Food Chemistry*, *172*, 433–440.
- Lii, C. Y., Tsai, M. L., & Tseng, K. H. (1996). Effect of amylose content on the rheological property of rice starch. *Cereal Chemistry*, *73*, 415–420.
- Lim, S. T., Lee, J. H., Shin, D. H., & Lim, H. S. (1999). Comparison of protein extraction solutions for rice starch isolation and effects of residual protein content on starch pasting properties. *Starch*, *51*, 120–125.
- Li, J. Y., & Yeh, A. I. (2001). Relationships between thermal, rheological characteristics and swelling power for various starches. *Journal of Food Engineering*, *50*, 141–148.
- Loh, J. (1992). The effect of shear rate and strain on the pasting behavior of food starches. *Journal of Food Engineering*, *16*, 75–89.
- Madsen, M. H., & Christensen, D. H. (1996). Change in viscosity profile of potato starch during growth. *Starch*, *48*, 245–249.
- Mitchell, C. R. (2009). Rice starches: production and properties. In J. N. BeMiller, & R. L. Whistler (Eds.), *Starch: Chemistry and technology* (pp. 569–577). New York: Academic Press.
- Park, I. M., Ibáñez, A. M., Zhong, F., & Shoemaker, C. F. (2007). Gelatinization and pasting properties of waxy and non-waxy rice starches. *Starch*, *59*, 388–396.
- Singh, N., Kaur, L., Sandhu, K. S., Kaur, J., & Nishinari, K. (2006). Relationships between physicochemical, morphological, thermal, rheological properties of rice starches. *Food Hydrocolloids*, *20*, 532–542.
- Singh, V., Okadome, H., Toyoshima, H., Isobe, S., & Ohtsubo, K. (2000). Thermal and physicochemical properties of rice grain, flour and starch. *Journal of Agricultural Food and Chemistry*, *48*, 2639–2647.
- Singh, N., Singh, J., Kaur, L., Sodhi, N. S., & Gill, B. S. (2003). Morphological, thermal and rheological properties of starches from different botanical sources. *Food Chemistry*, *81*, 219–231.
- Sodhi, N. S., & Singh, N. (2003). Morphological, thermal and rheological properties of starches separated from rice cultivars grown in India. *Food Chemistry*, *80*, 99–108.
- Takeda, Y., Hizukuri, S., & Juliano, B. (1987). Structures of rice amylopectins with low and high affinities for iodine. *Carbohydrate Research*, *168*, 79–88.
- Tester, R. F., & Morrison, W. R. (1990). Swelling and gelatinization of cereal starches. I. Effect of amylopectin, amylose and lipids. *Cereal Chemistry*, *67*, 551–557.
- Vandeputte, G. E., Vermeylen, R., Geeroms, J., & Delcour, J. A. (2003). Rice starches. I. Structural aspects provide insight into crystallinity characteristics and gelatinization behaviour of granular starch. *Journal of Cereal Science*, *38*, 43–52.
- Wang, L., Xie, B., Shi, J., Xue, S., Deng, Q., Wei, Y., et al. (2010). Physicochemical properties and structure from Chinese rice cultivars. *Food Hydrocolloids*, *24*, 208–216.



## Study of two-stage microwave extraction of essential oil and pectin from pomelo peels



Qun Chen <sup>a</sup>, Zhuoyan Hu <sup>a, b</sup>, Fiona Yan-Dong Yao <sup>c</sup>, Hanhua Liang <sup>a, d, \*</sup>

<sup>a</sup> Department of Applied Biology and Chemical Technology, The Hong Kong Polytechnic University, Hung Hom, Hong Kong

<sup>b</sup> College of Food Science, South China Agricultural University, Guangzhou, China

<sup>c</sup> Hong Kong Community College, Hung Hom Campus, 8 Hung Lok Road, Hung Hom, Hong Kong

<sup>d</sup> Food Safety and Technology Research Center, The Hong Kong Polytechnic University, Hung Hom, Hong Kong

### ARTICLE INFO

#### Article history:

Received 17 July 2015

Received in revised form

6 November 2015

Accepted 9 November 2015

Available online 14 November 2015

#### Keywords:

Two-stage process

Microwave extraction

Essential oil

Pectin

Pomelo peel

### ABSTRACT

Pomelo peels were first processed by a solvent-free microwave extraction (SFME) for essential oils, then by a hot-solvent microwave extraction (HSME) for pectin. SFME was superior to the conventional hydrodistillation (HD) method for essential oil extraction and HSME was better than acidic solution method for pectin extraction in terms of extraction efficiency and yield of targeted component. Chemical composition analysis by GC–MS showed that SFME did not affect the quality of essential oils. By using the response surface methodology, the optimal conditions of HSME for pectin was found at microwave power of 520 W, solvent pH value of 1.5 and extraction time of 5.6 min. Surface view by optical microscope (OM) and cross sectional view by scanning electron microscope (SEM) of the peels suggested that microwave can enhance the extraction process by two distinct mechanisms: one attributes to the diffusion across the intact oil gland while the other involves the convection through the broken oil gland.

© 2015 Elsevier Ltd. All rights reserved.

### 1. Introduction

The pomelo (*Citrus grandis*), which commonly grows in southern China, is the largest and juiciest fruit of the citrus family. It contains large amounts of carotenoids, vitamin E, flavonoids, limonoids, phenolic compounds, polysaccharides, lignin, fiber, pectin, essential oils, and is very popular in Southeast Asia. Essential oils in pomelo peels are responsible for the typical citrus-like aroma of the fruit (Saikaew, Kaewsarn, & Saikaew, 2009). As abundant sources of terpenoids, essential oils are made up of a mixture of many volatile compounds (Baser & Buchbauer, 2010). They are obtained as by-products of citrus processing and have widespread applications around the world as aroma flavor in many food products and in the pharmaceutical industry (Başer & Demirci, 2007). Pomelo peels are also rich in pectin. As a group of complex polysaccharides, pectin is localized in the middle lamella, intercellular crevices, and primary cell walls, and is known for the possession of pharmacological, hypoglycemic, and cholesterol-lowering effects (Francis, 2000). Pectin isolated from pomelo

peels, based on their methoxyl content and degree of esterification, can be classified as low methoxyl pectin and has been applied in the manufacture of low-sugar products such as low-sugar jam and jelly (Norziah, Fang, & Abd Karim, 2000).

A traditional method of essential oil extraction is cold-press of the citrus peel (Bousbia, Vian, Ferhat, Meklati, & Chemat, 2009). Methods such as hydrodistillation (HD) and steam distillation are also popular for the extraction of volatile oils from plant materials (Lucchesi, Chemat, & Smadja, 2004). Conventionally, pectin is extracted in acidic solution at about 80–82 °C for 1 h with continuous stirring (Kratchanova, M., et al., 2004). However, these methods have disadvantages such as losses of some volatile compounds, low yield and degradation of target compounds (Lucchesi et al., 2004). Microwave extraction, a relatively novel technique that combines microwave and traditional solvent extraction, has received increasing attention over the years due to its shorter extraction time, higher yields of a target compound and less solvent consumption (Vongsangnak, Gua, Chauvatcharin, & Zhong, 2004). Solvent-free microwave extraction (SFME), one of the microwave extraction methods, combines microwave heating and dry distillation and performs in an atmospheric condition without any addition of solvent or water required (Bayramoglu, Sahin, & Sumnu, 2008). On the other hand, HSME has been successfully applied for

\* Corresponding author. Department of Applied Biology and Chemical Technology, The Hong Kong Polytechnic University, Hung Hom, Hong Kong.

E-mail address: [bchhliang@polyu.edu.hk](mailto:bchhliang@polyu.edu.hk) (H. Liang).

the extraction of pectin from apple pomace (Wang et al., 2007), orange peel (Liu, Wei, Guo, & Kennedy, 2006) and lime (Fishman, Chau, Hoagland, & Hotchkiss, 2006).

The objective of this work is to establish a two-stage microwave extraction process for pomelo peels and to study the effects of microwave power, temperature, extraction time and solvent pH on the yield of essential oil and pectin. The extraction efficiency of SFME for essential oil and HSME for pectin will be compared with that of the conventional extraction methods. The response surface methodology was applied to optimize the condition of HSME for pectin extraction. Structural changes of pomelo peels were observed by optical microscope (OM) and scanning electron microscope (SEM) after the processes of SFME and HSME. The mechanisms of mass transfer in microwave extraction were also discussed.

## 2. Materials and methods

### 2.1. Plant materials and reagents

Fresh Shatin pomelos (Teaka) were purchased from a local supermarket, then washed and peeled manually. The peel obtained was about 40 g/100 g whole fruit weight. The peel materials were cut into pieces of approximately  $5 \times 5 \times 10$  mm for immediate use in the subsequent experiments. The initial moisture content of the peels was 80.7 g/100 g total weight, as determined by a freeze-drying method (Cháfer, González-Martínez, Chiralt, & Fito, 2003) at  $-60$  °C in a freeze-dryer (Alpha 1-4 LD2 freeze dryer, Germany). All reagents were of analytical grade and purchased from a local chemical provider (Advanced Technology & Industrial Co. LTD, Hong Kong).

### 2.2. Methods for the extraction of essential oils

According to the Chinese Pharmacopoeia (Tu, 1988), conventional HD was conducted at 100 °C for 180 min in a Clevenger apparatus equipped with a heating jacket. The ratio of peel material to water was 1:6. Essential oils were collected in amber-colored vials, then dried with anhydrous sodium sulfate, and finally stored at 4 °C for further analysis. The mean yield of essential oils was expressed as ml per 100 g of fresh peels  $\pm$ S.D. (Standard Deviation). All experiments at each condition were conducted in triplicates.

SFME was performed using a focus microwave system, Model 961 (Microwave Power Consultants, VIC Australia). The power of the microwave reactor can be continuously varied up to 1000 W, and the system is equipped with a fiber-optical sensor for temperature control and measurement during extraction. Microwave is delivered from the generator to a cavity through a wave guide. The power modulation unit is equipped with the wave guide to modulate the output power levels. The power level reported in this study is the output power from the system. The same Clevenger apparatus used in HD was deployed here. 120 g fresh peels were treated during each trial without adding any solvent. Three microwave power levels, 150, 300 and 450 W, were selected to evaluate the effect of microwave energy on the extraction of essential oils. Extraction durations of 30 and 90 min were also used for studying the effect of extraction time on the yield of essential oils. The collection, treatment and storage of the obtained essential oils were the same as aforementioned HD process.

### 2.3. Methods for the extraction of pectin

The conventional hot solvent extraction for pectin was performed in a 500 mL flask by adding 10 g oil-free pomelo peels into

180 mL HCl aqueous solution at pH 2.0 and temperature 90 °C for 90 min. After extraction, the samples were hot-filtered and precipitated with 180 mL ethanol solution (95 ml/L) for 3 h. The coagulated pectin was separated and rinsed with ethanol solution (75 ml/L) and anhydrous ethanol. The treated samples were dried at 60 °C till constant weight. The pectin yield (%) was expressed in terms of gram of collected pectin per 100 g of oil-free pomelo peel.

HSME was conducted in a similar manner but performed in the same microwave system used for SFME excluding the Clevenger apparatus. In order to find the optimum condition of HSME, the response surface methodology (RSM) with the Box-Behnken experiment design was applied. Based on our previous works, only three major factors, microwave power, extraction time and solvent pH, were selected in this study. The low, middle and high levels were set as: 390, 520 and 650 W for microwave power; 3, 5 and 7 min for extraction time, and 1, 2, and 3 for solvent pH value, respectively. A total of 15 experimental trials, including 12 factorial points and three replicates at the center point, were conducted (Table 3). The pure error sum of squares was estimated by Design-Expert (Version 7.0, Stat-Ease, Inc., USA).

### 2.4. Gas chromatography-mass spectrometry identification

The composition of essential oils from the pomelo peels was analyzed by GC–MS (7890A GC system – 5975 C VLMSD with triple-axis detector, Agilent Technology, USA) equipped with a fused-silica capillary column HP-5MS (30 m  $\times$  0.25 mm  $\times$  0.25  $\mu$ m). The GC conditions were: helium carrier (gas flow rate at 1.0 ml/min; split at 0:1; injection volume of 1.0  $\mu$ l; injection temperature of 260 °C); oven temperature (programmed from 50 °C to 150 °C for 15 min, holding for 4 min, and 150 °C to 260 °C for 10 min, holding for 4 min); ionization mode (as electronic impact at 70 eV; ionization temperature of 230 °C); MSE quadrupole temperature of 150 °C; transfer line temperature of 260 °C; and solvent delay for 3 min. The components of the extracted essential oils were identified by comparing their mass spectral fragmentation patterns with those stored in the MS database (National Institute of Standards and Technology 05 libraries).

### 2.5. Stability of essential oil

A stability study was performed in order to find out the effects of microwave irradiation on essential oil. The experiments were performed by treating 1.0 ml of essential oil extracted with HD method under various processing conditions as shown in Table 1. The amounts of essential oil before and after the treatment were measured and compared.

### 2.6. Morphological analysis

After processed by HD and SFME, the microstructure of the treated pomelo peel tissues was examined using optical microscope (OM) and scanning electron microscope (SEM).

For a surface view of the tissues, samples were sliced into extremely thin layers and observed directly by an optical microscope (Olympus IX17, Japan) with a magnification of 40. For a cross-sectional view, the specimens were freeze-dried in a freeze-dryer (Alpha 1-4 LD2 freeze dryer, Germany) for 2 days, then mounted on a specimen holder with tape and coated with Au using a sputtering coater (Gatan, model 861, Japan), and examined by a field-emission SEM (Model JEOL-JSM6335F, Japan).

### 2.7. Statistical analysis

Yields of essential oil and pectin in different extraction

**Table 1**  
Processing conditions for the stability study of essential oil from pomelo peels.

Treated conditions	Microwave power (W)	Temperature (°C)	Duration (min)
1	0	100	30
2	0	100	90
3	0	106	30
4	0	106	90
5	400	100	30
6	400	100	90

**Table 2**  
Chemical composition of essential oil obtained by SFME at three power levels for 90 min and by HD.

No.	Resident time (min)	Compounds	Mol. form	Content (%) SFME at 450 W	Content (%) SFME at 300 W	Content (%) SFME at 150 W	Content (%) HD
1	3.86	$\alpha$ -Pinene	C10H16	0.28	0.67	0.43	0.45
2	4.26	$\beta$ -Phellandrene	C10H16	0.17	0.34	0.21	0.20
3	4.31	$\beta$ -Pinene	C10H16	0.35	0.65	0.36	0.53
4	4.38	$\beta$ -Myrcene	C10H16	2.07	3.69	1.53	2.49
5	4.83	Limonene	C10H16	80.70	86.53	78.06	82.58
6	4.95	Cis-ocimene	C10H16	0.39	0.55	0.39	0.46
7	5.44	Undecane	C11H24	0.27	–	3.36	–
8	5.46	$\beta$ -Linalool	C10H18O	0.46	0.78	0.85	–
9	5.73	6-Isopropenyl-3-methyl-1-cyclohexen-1-ol	C10H16O	–	–	0.08	–
10	6.31	Terpene-4-ol	C10H18O	–	–	0.06	0.14
11	6.43	$\alpha$ -Terpineol	C10H18O	0.20	0.20	0.27	–
12	6.80	(–)-Carveol	C10H16O	0.07	–	0.13	0.13
13	6.88	$\beta$ -Citral	C10H16O	0.11	0.12	–	0.46
14	7.17	$\alpha$ -Citral	C10H16O	0.14	0.13	0.07	0.41
15	7.30	Perillaldehyde	C10H14O	–	–	–	0.07
16	8.04	$\delta$ -elemene	C15H24	0.17	0.13	0.18	–
17	8.04	(+)-4-Carene	C10H16	–	–	–	0.13
18	8.25	neryl acetate	C12H20O2	0.16	0.15	0.22	0.16
19	8.52	geranyl acetate	C12H20O2	0.31	0.26	0.44	0.30
20	8.83	$\beta$ -Elemene	C15H24	–	–	0.15	0.17
21	8.88	Methyleugenol	C11H14O2	0.12	0.08	0.18	–
22	9.38	Caryophyllene	C15H24	0.22	0.17	0.29	0.24
23	10.57	Germacrene D	C15H24	–	0.15	–	0.11
24	10.60	$\beta$ -Cubebene	C15H24	0.23	–	–	–
25	10.61	2-Isopropenyl-4a,8-dimethyl-1,2,3,4,4a,5,6,7-octahydronaphthalene	C15H24	–	–	–	0.13
26	10.82	Valencene	C15H24	0.19	0.09	–	–
27	10.82	$\beta$ -Patchoulene	C15H24	–	–	–	0.31
28	10.82	$\beta$ -Panasinsene	C15H24	–	–	0.26	–
29	10.87	Selinene	C15H24	0.06	–	–	0.14
30	11.37	(–)- $\alpha$ -Panasinsen	C15H24	–	0.06	0.11	0.15
31	13.93	$\beta$ -Neoclovene;	C15H24	–	0.54	1.67	0.98
32	15.99	Solavetivone	C15H22O	–	–	0.09	–
33	16.05	Nootkatone	C15H22O	8.90	3.86	9.28	4.80
34	19.67	Osthole	C15H16O3	0.05	–	0.04	–
Sum (% in total)				95.62	99.15	98.71	95.54

**Table 3**  
Experimental setting using Box-Behnken design and the resulted yield of pectin extracted from oil-free pomelo peels by HSME.

Trail	X <sub>1</sub> microwave power (W)	X <sub>2</sub> extraction time (min)	X <sub>3</sub> pH value	Y pectin yield (%)
1	650	5	3.0	0.18
2	650	3	2.0	2.15
3	390	3	2.0	0.85
4	520	7	1.0	2.67
5	390	5	3.0	0.05
6	650	5	1.0	2.69
7	390	7	2.0	2.10
8	520	3	1.0	1.15
9	520	5	2.0	2.71
10	520	7	3.0	0.06
11	520	5	2.0	2.93
12	520	3	3.0	0.06
13	390	5	1.0	2.17
14	520	5	2.0	2.92
15	650	7	2.0	2.06

operations were statistically evaluated by analysis of variance (ANOVA) using SAS (SAS version 9.0, SAS Institute Inc., USA). The optimization and statistical analysis of HSME conditions, as well as the response surface graphs were achieved using Design-Expert.

### 3. Results and discussion

#### 3.1. Stability of essential oil

As shown in Fig. 1, there is little change in the amount of essential oil from the peels before and after treatments in conditions 1, 2, 5 and 6 as shown in Table 1. The results indicate that microwave irradiation does not affect the quantity of essential oil at the temperature of 100 °C or below and microwave power of 400 W. However, when the treatment temperature was increased to 106 °C, the amount of essential oil decreased from 1.0 ml to 0.25 ml at condition 3 and dropped to only 0.1 ml when the treatment time was prolonged from 30 min to 90 min at the same temperature (condition 4). The results confirm that thermal degradation of essential oil occurs at the extraction temperature of 106 °C or above. This finding suggests that the usage of extreme extraction condition, especially high temperature, may bring in negative effects such as thermal degradation of essential oil. As such the study on SFME was restricted within the temperature range of 100–106 °C.

#### 3.2. Extraction of essential oil by SFME

In this study, essential oil of pomelo peel was extracted by SFME at the first stage extraction. As shown in Fig. 2, SFME is obviously a better method in terms of extraction efficiency and yield of essential oil. Compared with that of HD for 180 min, the increasing yields obtained by SFME at 30 min were up to 12.6% and 25.3% at microwave power of 150 and 300 W, respectively. Moreover, increase in microwave power can cause an earlier start of the extraction, because when higher power was applied to the extraction system, more energy would be transferred to the sample matrix, thus improving yield of target compounds. However, little increase in yield was obtained when higher microwave power 450 W was applied. The results imply that over certain microwave power, further enhancement in extraction yield could not be achieved.

The study on extraction time suggests that prolonging extraction time would be helpful to complete extraction of target

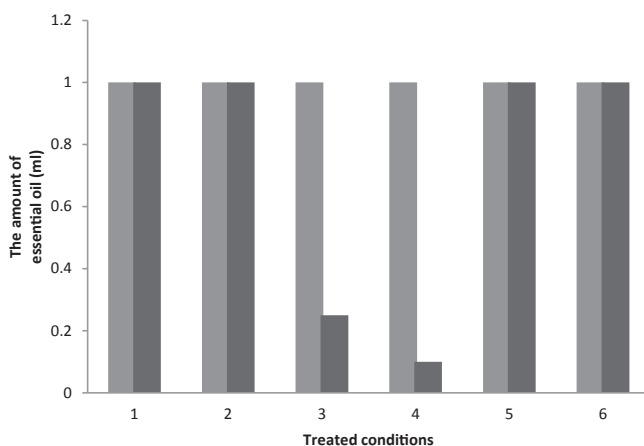


Fig. 1. Stability study of essential oil extracted from fresh pomelo peels at different treatment conditions as stated in Table 1 (■ before treatment, ■ after treatment).

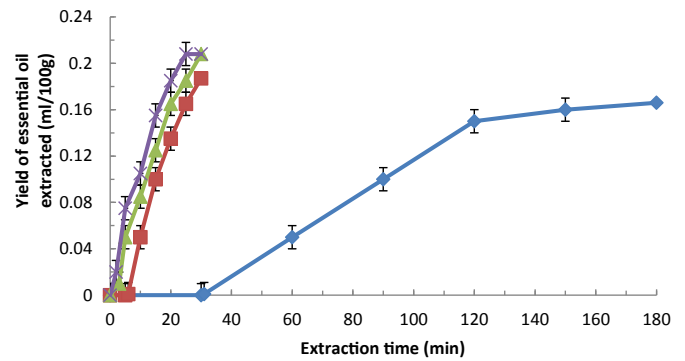


Fig. 2. Yields of essential oils extracted from pomelo peels by HD for 180 min and by SFME at different power levels for 30 min (◆ HD, ■ SFME at 150 W, ▲ SFME at 300 W, × SFME at 450 W).

compounds when microwave power remained low. As shown in Fig. 3, prolonging the extraction time to 90 min resulted in yields of essential oil that were 33.7% and 20% higher than the extraction for 30 min at microwave power of 150 and 300 W, respectively. However, when the microwave power was at 450 W the yields were the same whether the extraction time was 30 min or 90 min. Thus, the extraction conditions at microwave power of 150 W for 90 min would be appropriate for the extraction of essential oil from pomelo peels by SFME.

#### 3.3. Composition of essential oil

The chemical composition of the obtained essential oil was studied using GC–MS analysis (Table 2). The essential oil extracted from pomelo peels was mainly composed of limonene,  $\beta$ -Pinene, Linalool,  $\alpha$ -Terpineol, Nerolidol and ester compounds. Their percentage varied with different processing conditions. Limonene, a monoterpene hydrocarbon, was the most abundant component with 82.6% and 78.1–86.5% obtained by HD and SFME, respectively. The percentage of Limonene increased with increasing microwave power at low microwave power of 150 and 300 W but decreased at high microwave power of 450 W. At low microwave power (150 and 300 W) the oxygenated fraction of the essential oil obtained by SFME increased with increasing microwave power, the percentage was up to 11.9%, higher than the 6.8% by HD; but at high microwave power of 450 W, this percentage was lower than those obtained by HD. In principle, oxygenated compounds are more valuable than monoterpene hydrocarbon in terms of their contribution to the fragrance of essential oil (Wang, Ding, et al., 2006; Wang, Wang, et al., 2006). The finding suggests that SFME at low microwave power may be a promising and effective technique for the

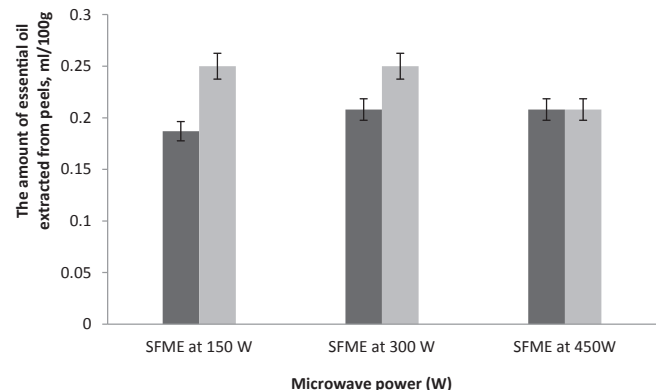
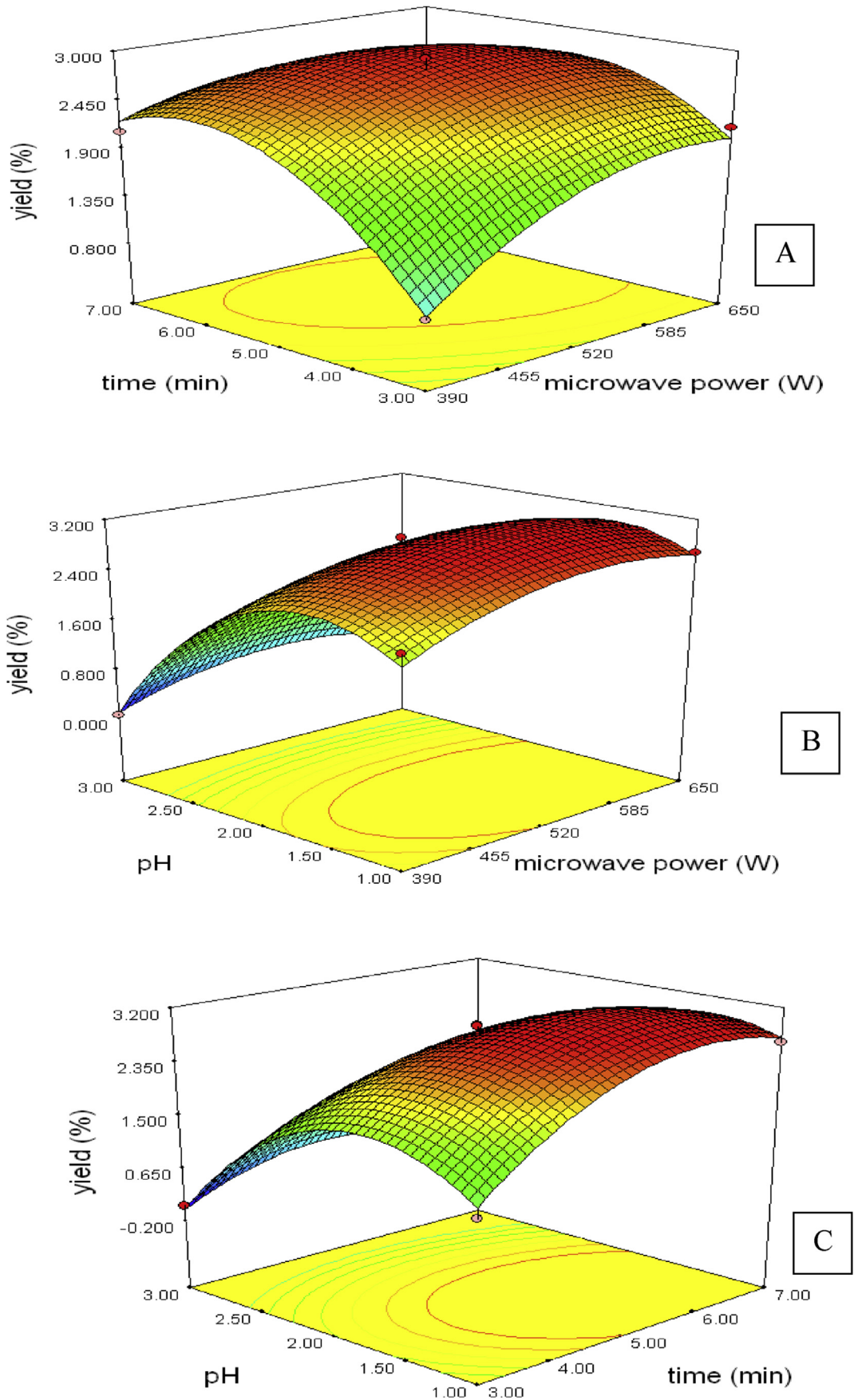


Fig. 3. Comparison of the yield of essential oil from pomelo peels by SFME at different extraction conditions (■ for 30 min, ■ for 90 min).



**Fig. 4.** Response surface for effects of: (A) microwave power level and extraction time; (B) microwave power level and pH value; (C) extraction time and pH value on pectin yield from oil-free pomelo peels.

extraction of essential oils because of its higher yield and better quality of essential oils when compared with HD. However, the problem of thermal degradation should be considered at higher microwave power.

#### 3.4. Extraction of pectin by HSME

The pectin of oil-free pomelo peel was then extracted by SFME at the second stage extraction. As aforementioned, the three factors, microwave power, extraction time and solvent pH value, were selected. Table 3 shows the experimental conditions by Box-Behnken design and the resulted pectin yield at various designed

points. The yield was found within the range of 0.05–2.93%. A second-order polynomial model was built based on the data:

$$\begin{aligned} \text{Pectin yield (\%)} = & 2.85 + 0.24x_1 + 0.34x_2 - 1.04x_3 - 0.34x_1x_2 \\ & - 0.10x_1x_3 - 0.38x_2x_3 - 0.39x_1^2 - 0.68x_2^2 \\ & - 1.19x_3^2 \end{aligned}$$

where  $x_1$  is the microwave power,  $x_2$  extraction time and  $x_3$  solvent pH value, respectively. The coefficient of determination ( $R^2$ ) of this model is 0.9887, and the lack of fit is 0.2216, which suggests a good fit, and that the regression model can reasonably represent the

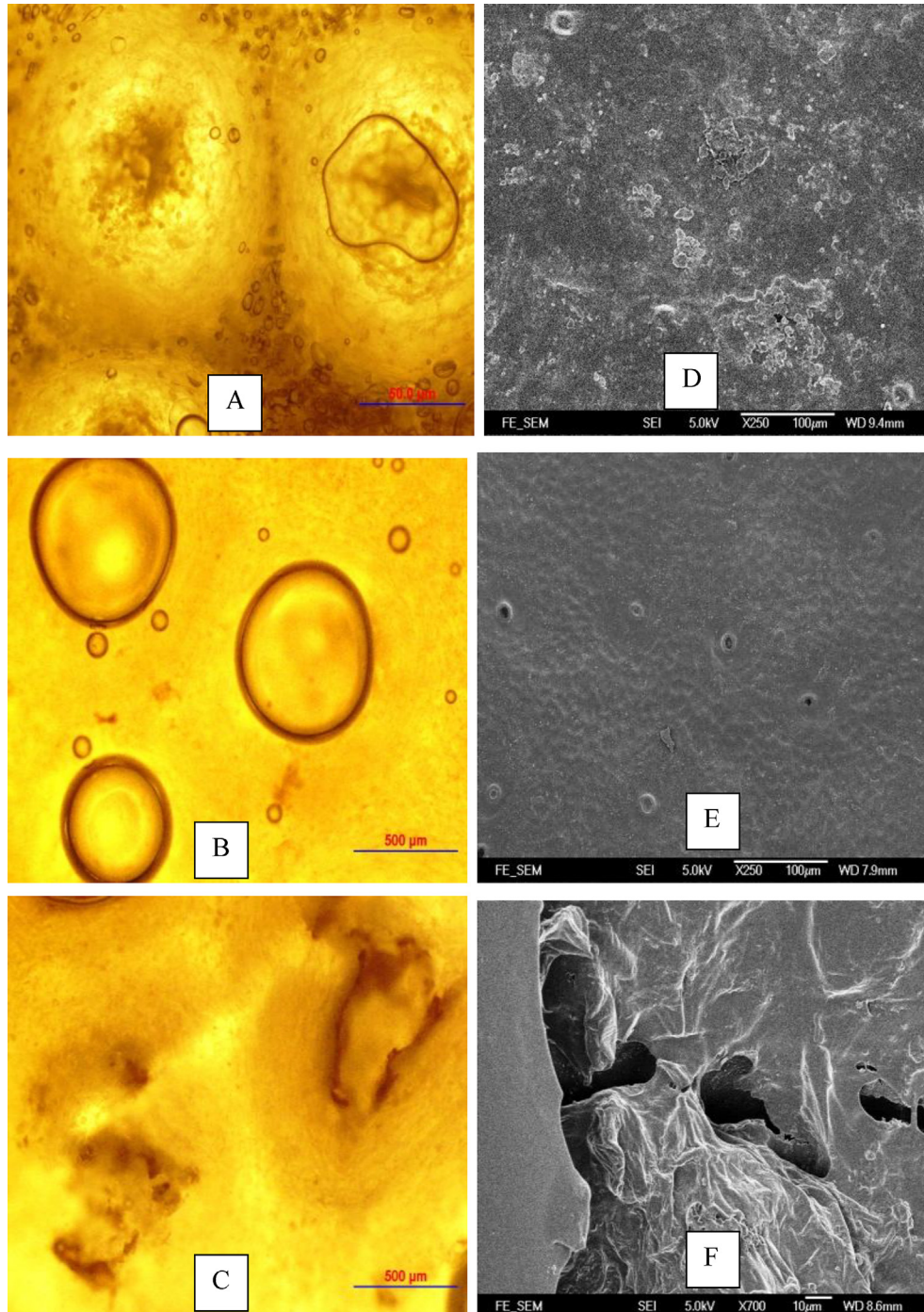


Fig. 5. Light surface view (A–C,  $\times 40$ ) and Scanning electron micrographs (D–F) of pomelo peels: Untreated (A and D); HD samples (B and E); SFME samples (C and F).

observed values. Based on the results of ANOVA, the significance of each coefficient was evaluated by *F*-test and *p*-value. The result indicated that the variables that showed extremely significant effect with  $p < 0.01$  on the pectin yield were extraction time ( $x_2$ ), pH value ( $x_3$ ) and the quadratic term of these two variables. All other variables showed significant effect with  $p < 0.05$ , except for the interaction effect of microwave power and pH value ( $x_1 \times x_3$ ) with  $p > 0.05$  as shown in Fig. 4. The pectin yield increased with increasing microwave power from 390 W to 530 W, and slightly decreased at the microwave power of 650 W. The same trend was found for the effect of extraction time and solvent pH. The results indicate that changes in pH value and extraction time had dramatic effects on pectin yield, while microwave power displayed a significant quadratic effect.

### 3.5. Optimization of HSME condition

The optimization of HSME condition for the best pectin yield was performed using the approach of graphical technique. The optimum region (shaded) was obtained by superimposing contour plots of pectin yield as functions of microwave power and extraction time (Fig. 4A), microwave power and pH value (Fig. 4B), and extraction time and pH value (Fig. 4C). The results indicate that it is possible to obtain a higher pectin yield at microwave power level of 520–585 W, extraction time of 5–6 min, and pH value of 1.3–1.7. Under these conditions, the yields were expected to be more than 3.15%. Verification experiments were carried out at the selected

optimum conditions with microwave power level of 520 W, extraction time of 5.6 min and pH value of 1.5. The resultant average yield was  $3.29 \pm 0.15\%$ , which was in good agreement with the findings obtained by graphical method. Compared with conventional acidic solution extraction, whose pectin yield was 3.11% for 90 min, HSME can be an alternative extraction method for fast extraction and better yield of pectin from oil-free pomelo peels, and shows promising industrial applications.

### 3.6. Structural changes after extraction

Fig. 5B and E presents shrunken yet still intact oil sacs after HD process at 100 °C for 180 min. However, after SFME process at microwave power 150 W for 90 min, as shown in Fig. 5C and F, intact oil sacs were not observed and a messy surface appeared due to the rupture of oil sacs. Such change is indicative of built up pressure within the oil glands exceeding their capacity for expansion, rupture readily when subjected to microwave irradiation. This implies that microwave can really affect the structure of peel tissue and cause surface changes, while the conventional extraction methods cannot.

Fig. 6 shows two types of morphological changes observable after microwave treatment. One type shows the undamaged gland wall and the other portrays the fragments of gland walls as the remaining trace of the ruptured cells. Actually, only 14–28% (by vol.) of broken glands in pomelo peels was observed for microwave power at 150 W and extraction time at 30 min. However, when the

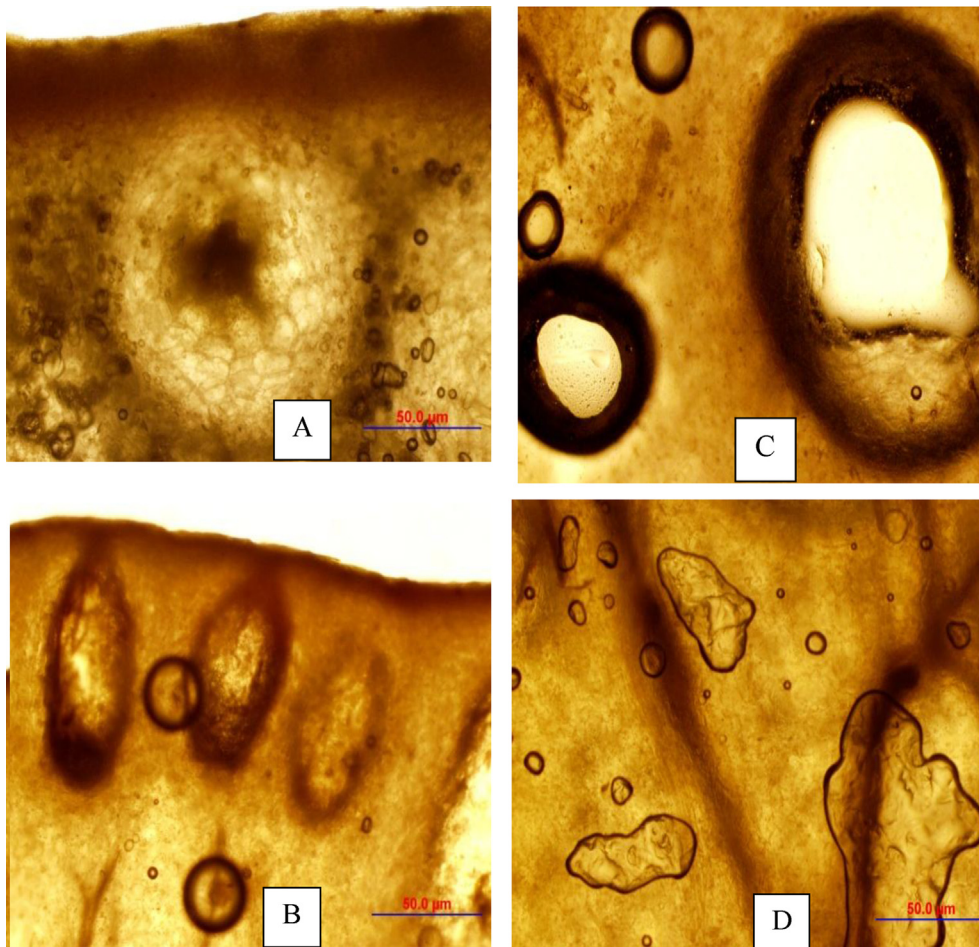


Fig. 6. Light micrographs of pomelo peels (cross section,  $\times 40$ ): untreated (A); HD samples (B); SFME samples at different views (C and D).

microwave power increased to 300 W, the percent volume of broken glands increased to 42%. Meanwhile, shrunken oil glands were also observed. The percentage of broken glands looked quite similar when the samples were treated with microwave power of 300 W or 450 W for 30 min. The observation suggests that the degree of oil sacs damage was greatly influenced by the microwave power (150–300 W) and other processing parameters. On the other hand, no further structural change occurred when microwave power was increased from 300 W to 450 W. The findings point to microwave capability of enhancing the extraction through two distinct mechanisms: improving diffusion across the intact oil gland and boosting convection from a broken oil gland.

#### 4. Conclusion

A two-stage process for microwave extraction of pomelo peels has been studied. The first stage was to employ SFME for extraction of essential oil from the fresh peels. SFME is obviously a more fitting method than HD process for the extraction of essential oils in terms of efficiency and product yield. The study on essential oil stability indicated that SFME would not affect the oil composition. The recommended operational conditions for SFME are at the microwave power of 150 W and extraction time of 90 min. The oil-free pomelo peels was then used for extraction of pectin by HSME as the second stage process. Compared with the conventional acidic solution extraction for 90 min, a higher extraction yield of 3.29% was obtained by HSME at microwave power of 520 W, pH value of 2.0 and extraction time of 5.6 min. The micrographs from OM and SEM indicated that two types of morphological changes were observed after microwave irradiation, one type showing the undamaged oil gland and the other portraying the remaining of ruptured cell walls. The proposed two-stage microwave extraction, first by SFME for essential oil then by HSME for pectin, was considered a feasible processing method for better process yield and better utilization of biomaterials for food industry.

#### Acknowledgments

The work described in this paper was substantially supported by the Research Grants Council of the Hong Kong Special Administrative Region, China (Project No.: 564507) and the Food Safety and

Technology Research Center at Hong Kong Polytechnic University (Grant Code: 4-ZZDP).

#### References

- Baser, K. H. C., & Buchbauer, G. (2010). *Handbook of essential oils science, technology and applications*. Boca Raton: Taylor & Francis.
- Başer, K. H. C., & Demirci, F. (2007). Chemistry of essential oils. In R. G. Berger (Ed.), *Flavors and fragrances: Chemistry, bioprocessing and sustainability* (pp. 43–83). Germany: Springer.
- Bayramoglu, B., Sahin, S., & Sumnu, G. (2008). Solvent-free microwave extraction of essential oil from oregano. *Journal of Food Engineering*, 88, 535–540.
- Bousbia, N., Vian, M. A., Ferhat, M. A., Meklati, B. Y., & Chemat, F. (2009). A new process for extraction of essential oil from citrus peels: microwave hydro-diffusion and gravity. *Journal of Food Engineering*, 90, 409–411.
- Châfer, M., González-Martínez, C., Chiralt, A., & Fito, P. (2003). Microstructure and vacuum impregnation response of citrus peels. *Food Research International*, 36, 35–41.
- Fishman, M. L., Chau, H. K., Hoagland, P. D., & Hotchkiss, A. T. (2006). Microwave assisted extraction of lime pectin. *Food Hydrocolloids*, 20, 1170–1177.
- Francis, J. F. (2000). *Wiley encyclopedia of food science and technology* (2nd ed.). New York: John Wiley & Sons.
- Liu, Z. D., Wei, G. H., Guo, Y. C., & Kennedy, J. F. (2006). Image study of pectin extraction from orange skin assisted by microwave. *Carbohydrate Polymers*, 64, 548–552.
- Lucchesi, M. E., Chemat, F., & Smadja, J. (2004). Solvent-free microwave extraction of essential oil from aromatic herbs: comparison with conventional hydro-distillation. *Journal of Chromatography A*, 1043, 323–327.
- Norziah, M. H., Fang, E. O., & Abd Karim, A. (2000). Extraction and characterization of pectin from pomelo fruit peels. *Gums and Stabilizers for the Food Industry*, 10, 27–36.
- Saikaew, W., Kaewsarn, P., & Saikaew, W. (2009). Pomelo peel: agricultural waste for biosorption of cadmium ions from aqueous solutions. *World Academy of Science, Engineering and Technology*, 56, 287–291.
- Tu, G. (1988). *Pharmacopoeia of the People's Republic of China* (English ed., p. A21). The People's Medical Publishing House.
- Vongsangnak, W., Gua, J., Chauvatcharin, S., & Zhong, J. J. (2004). Towards efficient extraction of notoginseng saponins from cultured cells of *Panax notoginseng*. *Biochemical Engineering Journal*, 18, 115–120.
- Wang, S. J., Chen, F., Wu, J. H., Wang, Z. F., Liao, X. J., & Hu, X. S. (2007). Optimization of pectin extraction assisted by microwave from apple pomace using response surface methodology. *Journal of Food Engineering*, 78, 693–700.
- Wang, Z., Ding, L., Li, T., Zhou, X., Wang, L., Zhang, H., et al. (2006). Improved solvent-free microwave extraction of essential oil from dried *Cuminum cyminum* L. and *Zanthoxylum bungeanum* Maxim. *Journal of Chromatography A*, 1102, 11–17.
- Wang, Z., Wang, L., Li, T., Zhou, X., Ding, L., Yu, Y., et al. (2006). Rapid analysis of the essential oil from dried *Illicium verum* Hook. f. and *Zingiber officinale* Rosc. by improved solvent-free microwave extraction with three types of microwave-absorption medium. *Analytical and Bioanalytical Chemistry*, 386, 1863–1868.



# Development and validation of ELISA technique for early detection of rhizome rot in golden spice turmeric from different agroclimatic zones



Monalisa Ray<sup>a</sup>, Swagatika Dash<sup>a</sup>, Sajad Shahbazi<sup>b</sup>, K. Gopinath Achary<sup>c</sup>, Sanghamitra Nayak<sup>a</sup>, Shikha Singh<sup>a,\*</sup>

<sup>a</sup> Centre of Biotechnology, Siksha O Anusandhan University, Bhubaneswar, Odisha, India

<sup>b</sup> Panjab University, Chandigarh, India

<sup>c</sup> Imgenex India Pvt. Ltd, E-5 Infocity, Bhubaneswar, Odisha, India

## ARTICLE INFO

### Article history:

Received 27 March 2015

Received in revised form

7 October 2015

Accepted 31 October 2015

Available online 10 November 2015

### Keywords:

Turmeric

Rhizome rot

Diagnostic kit

*Pythium aphanidermatum*

ELISA

## ABSTRACT

Early and precise diagnosis of diseases in turmeric (*Curcuma longa* L.) permits early treatment which can enhance yield and quality of Indian spices. In the present study, polyclonal antibody (pAb) raised against the protein extract from *Pythium aphanidermatum* was established for the detection of rhizome rot using serological assays. The fungal proteins were recognized by ELISA with high sensitivity (50 ng) and the proteins ranging from 15 to 95 kDa showed immuno-reactivity in Western blot using the developed pAb. Correlation coefficient between infected samples at various stages from different agroclimatic zones with antibody titres was taken as the primary endpoint for standardization of the protocol. Highest positive correlation ( $r = 0.999$ ) was observed in stage I and II infected samples of North-western zone, whereas low negative correlation ( $r = -0.284$ ) was found in stage III infected samples of Western zone with developed pAb. Linear positive correlations ( $R^2$ ) exist between antigenic proteins at all the stages of infection and the developed pAb titres. Hence, the developed pAbs could be used to detect the presence of the fungal pathogen at an early stage. These serological approaches allow us to develop a rapid, sensitive, specific and accurate diagnostic kit for early detection of rhizome rot in turmeric.

© 2015 Elsevier Ltd. All rights reserved.

## 1. Introduction

Turmeric (*Curcuma longa* L.) belonging to the family of Zingiberaceae is cultivated for its underground rhizomes. According to the market survey, the export demand of Indian turmeric has increased in the past few years due to increased food as well as non-food uses. The use of turmeric and its value added products is spreading globally so the production of turmeric has to be increased to meet up the national and international requirements (Singh, Sahoo, Dash, & Nayak, 2014).

Turmeric is vulnerable to a number of fungal diseases such as rhizome rot, leaf blotch, leaf spots, leaf blight and rhizome scale (Devasahayam & Koya, 2007; Dohroo, 2007). Among the diseases, rhizome rot is one of the most destructive diseases of turmeric, which have reduced the economic and commercial value of Indian turmeric over the last couple of years (Anusuya & Sathiyabama, 2015; Ushamalini, Nakkeeran, & Marimuthu, 2008). *Pythium*

*aphanidermatum* is the predominant organism which is actively involved in rhizome rot disease in turmeric (Anoop & Suseela Bhai, 2014; Sarathi, Kumar, Senthil Kumar, & Panneerselvam, 2014). Depending on the intensity of the disease, partial to total rotting of rhizomes may occur which would lead to death of whole plant. Rhizome rot poses a persistent threat to the cultivation and storage of turmeric. Crop loss up to 50% was reported in Telangana region where the crop is cultivated on a large scale. About 50–80% losses during storage have been reported due to this disease (Sarathi et al., 2014). The disease can easily spread out due to the dissemination of the fungal spores and would reach to the neighboring fields in a few days damaging the entire harvest. So there is an urgent need to develop a rapid detection method for early diagnosis of rhizome rot.

Beside secondary metabolites, plants also secrete polypeptides in response to fungal pathogens (Mazid, Khan, & Mohammad, 2011). Moreover, previous reports reveals effect of polypeptides on various metabolic processes like respiration, photosynthesis, proton redistribution, assimilation uptake inhibition and anthocyanin synthesis (Luini, Fleurat-Lessard, Rousseau, Roblin, & Berjeaud, 2010; Octave, Roblin, Vachaud, & Fleurat-Lessard, 2006). The

\* Corresponding author.

E-mail address: [shikhsingh@gmail.com](mailto:shikhsingh@gmail.com) (S. Singh).

polypeptides could be exploited to develop a rapid early detection method for fungal infection based on immunological assay. Previous studies have attempted this approach to detect *Eutypa lata* and *Phaeoemoniella chlamydospora* (Fleurat-Lessard, Luini, Berjeaud, & Roblin, 2010; Octave, Fleurat-Lessard, & Roblin, 2009). However, no attempt has been made so far to study early detection of rhizome rot in turmeric. Therefore, an attempt has been made (i) to describe the various steps in the development of the serological procedure for detection of *P. aphanidermatum* in infected rhizome samples collected at different stages of disease development; (ii) to evaluate the specificity and sensitivity of the developed polyclonal antibody and to determine whether ELISA based detection of *P. aphanidermatum* using the developed antibody at different stages of infection was feasible; and (iii) to compare the correlation at various stages of disease development in order to detect rhizome rot at an early stage of infection.

## 2. Materials and methods

### 2.1. Collection of infected rhizomes

*P. aphanidermatum* infected turmeric rhizomes (Pa1–Pa30) were collected from different agroclimatic regions of the states in India of Odisha, Andhra Pradesh and Tamil Nadu. The fungal pathogen, *P. aphanidermatum* was identified based on its morphological features. The isolates were categorized into three different stages of infection based on the antigen load. The concentrations of protein in *P. aphanidermatum* infected rhizomes are given in Table 1.

### 2.2. Identification of pathogen

The fungal isolates were morphologically identified using the key of Van der Plaats-Niterink (1981) and Dick (1990). Keys and descriptions by Waterhouse (1967, 1968) and Middleton (1943) and the original descriptions were also consulted for comparison or confirmation of identifications. Slides were prepared from these cultures and stained with lacto phenol cotton blue according to Parija and Prabhakar (1995) and examined under the light microscope.

### 2.3. Extraction of fungal proteins and estimation

The infected rhizomes were washed carefully with tap water to remove adhering soil and then cut into smaller sizes. The pieces were surface sterilized by immersing the sample in 70% ethanol for 1 min, rinsed three times with sterile water. The pieces were then dried on sterile filter paper for 1 h. All preparations were carried out in biosafety cabinet. The sterilized pieces were homogenized (1 g/ml) using chilled Phosphate Buffer Saline (PBS) at pH 7.4 in a mortar and pestle and transferred to centrifuge tubes. The mixture was centrifuged at 12,000 G for 20 min at 4 °C and the supernatant was collected. The protein contents were estimated by dye binding method (Bradford, 1976) using bovine serum albumin as the standard.

### 2.4. SDS-polyacrylamide gel electrophoresis of proteins

Fungal proteins ranging from 30 µg (mild) to 100 µg (chronic) were loaded into a single well of a multi-welled 10% acrylamide gel. Samples were separated by SDS-PAGE using a Bio-Rad Mini-Protean vertical electrophoresis system (Laemmli, 1970). Mixture of standard protein markers for molecular weight determination was run parallel along with the samples. Protein separation was carried out under a constant voltage of 100 V. The gels were stained with Coomassie Brilliant Blue R-250 (Sigma) to visualize the fungal

proteins and molecular weight markers.

### 2.5. Development of antibody

500 µg of fungal proteins were suspended with mineral oil and was immunized per dose per animal. The initial injection contained approximately 1 mg of the protein antigen suspension. Three subsequent booster doses were given at an interval of 15 days. Bleeding and collection of antisera were done 7 days after the 2nd and 4th immunization. The antiserum was employed for ELISA and Western blotting analysis.

### 2.6. Screening of antibody by indirect ELISA

The antiserum was tested by indirect ELISA for cross-reactivity against common fungal proteins isolated from infected rhizomes of different samples. Healthy turmeric rhizome samples were used as negative control and proteins containing *P. aphanidermatum* as positive control. The antiserum was diluted with PBS to obtain desired dilution. 1–2 µg of fungal proteins were coated per well by re-suspending in 100 µl of coating buffer (50 mM Sodium Carbonate, pH 9.6) and incubated for overnight at 4 °C. Next day the plates were washed twice with Phosphate Buffer Saline-Tween 20 (PBS-T) and blocked by 5% skimmed milk for 1 h at room temperature. 100 µl of antiserum diluted in blocking buffer at different dilutions was added to each well after washing twice with PBS-T. The plates were incubated at room temperature for 2 h. After washing three times with PBS-T, the plates were incubated with 100 µl of horseradish peroxidase-conjugated goat anti-rabbit IgG (Sigma) at a dilution of 1:5000 for 1 h at room temperature. The plates were washed with PBS-T and incubated with 100 µl of TMB (3,3', 5,5'-Tetramethylbenzidine) substrate per well for 5 min in dark for color development. The reaction was stopped by adding 50 µl of 2 N sulfuric acid to each well. The optimum density of the developed color was measured at 450 nm in a micro plate reader (Bio-Rad).

### 2.7. Assessment of developed antibody specificity by Western blotting

Fungal proteins used in the qualitative assessment were prepared by pooling equal volumes of 30 samples from each stage. The proteins separated by electrophoresis were transferred to Polyvinylidene Fluoride (PVDF) membrane (Millipore) by using Mini-Trans Blot Cell Module (Bio-Rad) as per manufacturer's instructions. Electroblooming was performed for 90 min at a constant voltage of 50 V. The membrane was stained with amidoblack (Sigma) and destained with 10% methanol and 10% acetic acid. Nonspecific sites of the PVDF strips containing the separated antigens were blocked by incubation of the membrane for 30 min at room temperature in the blocking buffer composed of Tris Buffer Saline Tween-20 (TBST: 0.02 M Tris-HCl with 0.15 M NaCl, 0.05% Tween-20, pH 8) containing 3% Bovine Serum Albumin (BSA). The strips were subsequently washed with TBST buffer and incubated with 1:100 dilution of the polyclonal antibody raised against the fungal proteins for 3 h at room temperature. Pre-immune serum was used as negative control. After incubation, the strips were again washed and immersed in a 1:5000 dilution of horseradish peroxidase-conjugated anti-rabbit IgG (Sigma) for 1 h at room temperature. The strips were washed vigorously for 15 min with TBST by an intermittent change of the wash buffer, then chemiluminescent substrate (Pierce ECL Western Blotting Substrate, Thermo Scientific) for HRP was added to the strips and bands were depicted on the Hyper-Film (Kodak) by developing in the darkroom using developer and fixer. All the above dilutions were made by

**Table 1**  
Sample wise collection from different agroclimatic locations of India and content of protein (mg/g fr. wt) in *Pythium aphanidermatum* – infected rhizomes at various stages of disease development.

State	Agro climatic zones	Districts	No. of samples collected	Sample codes	Conc. of <i>Pythium aphanidermatum</i> (mg ml <sup>-1</sup> )			
					Stage I	Stage II	Stage III	
Odisha	Eastern Ghat Highland	Koraput	3	Pa1	1.161 ± 0.019 <sup>b</sup>	4.676 ± 0.057 <sup>c</sup>	4.998 ± 0.065 <sup>c</sup>	
				Pa2	1.208 ± 0.021 <sup>c</sup>	4.833 ± 0.058 <sup>c</sup>	5.019 ± 0.068 <sup>c</sup>	
				Pa3	1.201 ± 0.016 <sup>c</sup>	4.826 ± 0.051 <sup>c</sup>	5.177 ± 0.069 <sup>c</sup>	
		Nabarangpur	2	Pa4	0.782 ± 0.014 <sup>a</sup>	2.967 ± 0.049 <sup>a</sup>	3.233 ± 0.061 <sup>a</sup>	
				Pa5	0.707 ± 0.018 <sup>a</sup>	2.718 ± 0.048 <sup>a</sup>	3.054 ± 0.060 <sup>a</sup>	
	South Eastern Ghat	Malkangiri	2	Pa6	0.856 ± 0.018 <sup>a</sup>	3.053 ± 0.044 <sup>b</sup>	3.377 ± 0.062 <sup>a</sup>	
				Pa7	0.954 ± 0.016 <sup>a</sup>	3.158 ± 0.045 <sup>b</sup>	3.613 ± 0.063 <sup>b</sup>	
		Keonjhar	2	Pa8	0.576 ± 0.015 <sup>a</sup>	2.346 ± 0.041 <sup>a</sup>	2.814 ± 0.061 <sup>a</sup>	
				Pa9	0.489 ± 0.011 <sup>a</sup>	2.247 ± 0.041 <sup>a</sup>	2.899 ± 0.060 <sup>a</sup>	
	North Eastern Ghat	Phulbani	3	Pa10	1.298 ± 0.022 <sup>c</sup>	6.125 ± 0.059 <sup>e</sup>	6.670 ± 0.079 <sup>e</sup>	
				Pa11	1.283 ± 0.021 <sup>c</sup>	5.966 ± 0.057 <sup>d</sup>	6.488 ± 0.081 <sup>d</sup>	
				Pa12	1.335 ± 0.024 <sup>d</sup>	6.239 ± 0.060 <sup>e</sup>	6.757 ± 0.080 <sup>e</sup>	
		Rayagada	2	Pa13	1.252 ± 0.022 <sup>c</sup>	5.356 ± 0.058 <sup>d</sup>	5.744 ± 0.077 <sup>d</sup>	
	Gajapati	2	Pa14	1.243 ± 0.023 <sup>c</sup>	5.310 ± 0.057 <sup>d</sup>	5.638 ± 0.078 <sup>c</sup>		
			Pa15	1.026 ± 0.019 <sup>b</sup>	3.347 ± 0.049 <sup>b</sup>	3.905 ± 0.065 <sup>b</sup>		
Ganjam		2	Pa16	1.087 ± 0.018 <sup>b</sup>	3.441 ± 0.047 <sup>b</sup>	3.858 ± 0.066 <sup>b</sup>		
			Pa17	1.102 ± 0.026 <sup>b</sup>	3.612 ± 0.048 <sup>b</sup>	3.998 ± 0.065 <sup>b</sup>		
Tamil Nadu	North-western zone	Salem	3	Pa18	1.096 ± 0.023 <sup>b</sup>	3.567 ± 0.050 <sup>b</sup>	3.913 ± 0.064 <sup>b</sup>	
				Pa19	1.189 ± 0.029 <sup>b</sup>	4.743 ± 0.051 <sup>c</sup>	5.088 ± 0.072 <sup>c</sup>	
				Pa20	1.153 ± 0.031 <sup>b</sup>	4.597 ± 0.059 <sup>c</sup>	5.113 ± 0.073 <sup>c</sup>	
	Western Zone	Coimbatore	2	Pa21	1.215 ± 0.028 <sup>c</sup>	4.849 ± 0.057 <sup>c</sup>	5.206 ± 0.072 <sup>c</sup>	
				Pa22	1.278 ± 0.032 <sup>c</sup>	5.955 ± 0.059 <sup>d</sup>	6.637 ± 0.079 <sup>e</sup>	
		Erode	2	Pa23	1.256 ± 0.030 <sup>c</sup>	5.853 ± 0.060 <sup>d</sup>	6.889 ± 0.087 <sup>e</sup>	
				Pa24	1.314 ± 0.033 <sup>d</sup>	6.237 ± 0.062 <sup>e</sup>	6.669 ± 0.084 <sup>e</sup>	
	Andhra Pradesh	North Telangana Zone	Nizamabad	3	Pa25	1.302 ± 0.033 <sup>d</sup>	6.198 ± 0.061 <sup>e</sup>	6.731 ± 0.085 <sup>e</sup>
					Pa26	1.332 ± 0.030 <sup>d</sup>	6.436 ± 0.061 <sup>e</sup>	6.842 ± 0.084 <sup>e</sup>
					Pa27	1.352 ± 0.034 <sup>d</sup>	6.746 ± 0.068 <sup>e</sup>	7.227 ± 0.088 <sup>e</sup>
Karimnagar			2	Pa28	1.367 ± 0.033 <sup>d</sup>	6.913 ± 0.069 <sup>e</sup>	7.401 ± 0.087 <sup>e</sup>	
				Pa29	1.339 ± 0.029 <sup>d</sup>	6.458 ± 0.066 <sup>e</sup>	6.989 ± 0.085 <sup>e</sup>	
				Pa30	1.321 ± 0.031 <sup>d</sup>	6.264 ± 0.063 <sup>e</sup>	6.733 ± 0.086 <sup>e</sup>	

Mean ± SD; n = 3.

Values carrying same alphabet (a–e) did not vary significantly from each other (P < 0.01).

Stages I, II and III represent stages of infection.

Stage I (Mild): The early stage of infection, which was characterized by the appearance of water soaked lesions on the roots, generally at the tips.

Stage II (Acute): The intermediate stage of infection, which was characterized by extension of root lesions and then turning into brown or dark brown color. Yellowing of young leaves was initiated during this stage.

Stage III (Chronic): The very late stage of infection, which was characterized by an increase in intensity of rotting leading to the destruction of entire root system, total yellowing of all leaves, wilting and death of the plants.

using 1% BSA in TBST buffer.

## 2.8. Statistical analysis

The experimental data were processed using Pearson's correlation coefficient method. The correlation coefficients between concentrations of *Pythium* proteins isolated from rhizome samples collected at different stages of infection with antibody titres were calculated at a significant level of P < 0.01. All experiments were done in triplicates.

## 2.9. Validation of ELISA technique

Estimation of sensitivity and specificity of the assay for diagnosis of the infected samples are the primary parameters evaluated during the validation process of the ELISA technique. Specificity and sensitivity of the technique were determined by testing the samples by the developed assay and tabulating the test results in a two way (2 × 2) table. Results of the tests on standard sera were categorized into true positive (TP) or true negative (TN) if they were in agreement with those of the “gold standard”. Alternatively, they were classified as a false positive (FP) or false negative (FN) if they disagreed with the standard. Diagnostic sensitivity was calculated as TP/(TP + FN) whereas diagnostic specificity was TN/(TN + FP); the results of both calculations were usually expressed as percentages are shown in Table 4. Table 4 is a hypothetical set of results

from which diagnostic sensitivity and diagnostic specificity estimates were obtained. Comparative examination of the data concerning the sensitivity and specificity of the test in the used approaches allows interesting observations.

## 3. Results and discussion

### 3.1. Estimation of total protein/antigenic content of infected samples

The protein content isolated from the infected turmeric rhizomes at various stages of disease development were estimated and compared with the protein content of healthy ones. The protein content of the infected rhizomes was found to be significantly

**Table 2**  
Changes in the content of total protein (mg/g fr. wt.) in healthy and *Pythium aphanidermatum* infected turmeric rhizomes at various stages of disease development.

Samples	Total proteins
Healthy rhizomes	0.253±(0.005)
Stage I infected rhizomes	1.215±(0.028)
Stage II infected rhizomes	4.849±(0.057)
Stage III infected rhizomes	5.206±(0.072)

Each value is an average triplicates samples.

Values in parenthesis indicate the standard deviation.

**Table 3**

Pearson correlation coefficient (r) between concentrations of *Pythium* proteins isolated from samples collected at different stages of infection with antibody titres based on the different agroclimatic zones of India.

State	Agro climatic zones	Conc. of stage I infected samples with antibody titres	Conc. of stage II infected samples with antibody titres	Conc. of stage III infected samples with antibody titres
Odisha	Eastern Ghat	0.991	0.994	<b>0.998</b>
	Highland			
	South Eastern Ghat	0.978	0.976	<b>0.998</b>
	North Eastern Ghat	0.934	<b>0.941</b>	<b>0.941</b>
Tamil Nadu	North-western zone	<b>0.999</b>	<b>0.999</b>	0.681
	Western Zone	0.875	<b>0.944</b>	–0.284
Andhra Pradesh	North Telangana Zone	0.900	<b>0.939</b>	0.883

Significant at  $P < 0.01$ .

Highest correlation coefficient of each agroclimatic zones are shown in bold.

**Table 4**

Diagnostic sensitivity and specificity estimates calculated from a hypothetical set of results for samples tested from known infected and non-infected populations.

		No. of reference samples	
		Infected	Non-infected
Test result	Negative	55	10
	Positive	3	132
		TP FN	FP TN
		Diagnostic sensitivity TP/(TP+FN) = 55/58 = 94.83%	Diagnostic specificity TN/(TN+FP) = 132/142 = 92.96%

higher than the healthy rhizomes (Table 2). The increase in protein content of the infected samples may be due to accumulation of nitrogenous constituents in the rhizome which can be attributed due to change in nitrogen metabolism in infected plants (Reddy, Sridevi, & Charitha Devi, 2005).

### 3.2. SDS-PAGE analysis

The methodology employed was efficient to obtain *P. aphanidermatum* proteins containing 2–7 mg/ml. The separation of proteins by SDS-PAGE followed by Coomassie blue staining allowed identification of multiple protein bands as shown in Fig. 3, with molecular masses ranging from 15 to 95 kDa (Anusuya & Sathiyabama, 2014; Ghosh, Datta, & Purkayastha, 2006). The number and intensity of bands in the antigenic protein isolated from stage III infected samples were seen to be higher in comparison to stage I and II samples.

### 3.3. ELISA analysis

In this study antiserum was tested at 1:1000, 1:2000 and 1:5000 against various fungal protein concentrations as shown in Fig. 1. It was found that antiserum was competent enough to detect up to 10 ng of fungal protein at 1:5000 dilution. From these data, standardized experimental conditions were selected for the further experiments: 1:2000 antiserum dilutions and 50 ng of antigen per well, with 0.8 absorbance unit was set as reference value. The developed antibody also showed immunological reaction with

proteins isolated from different infected rhizome samples, and the efficiency was found to be different as illustrated in Fig. 2.

### 3.4. Polyclonal antibody development and Western blot analysis

Western blot analysis of the developed polyclonal antibody against the antigens at various stages of infection showed a remarkable difference in the recognition profile. The polyclonal antibody response to antigens was mostly seen against antigens ranging from molecular weight of 15–95 kDa in all three stages. The pAb response was high against the antigens with molecular

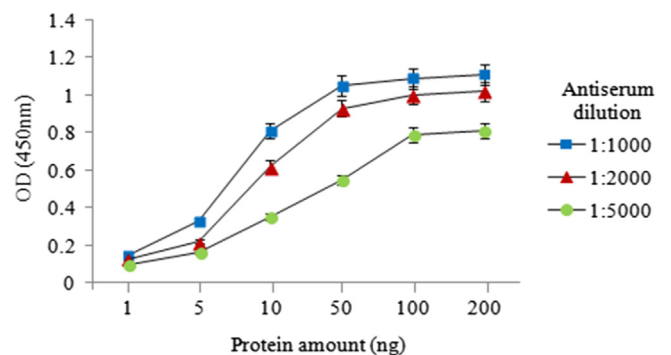


**Fig. 1.** ELISA showing the variation in absorbance at 450 nm as a function of protein amount, using various dilutions of the developed polyclonal antibody raised in rabbit as indicated. Mean ± SD; n = 3.

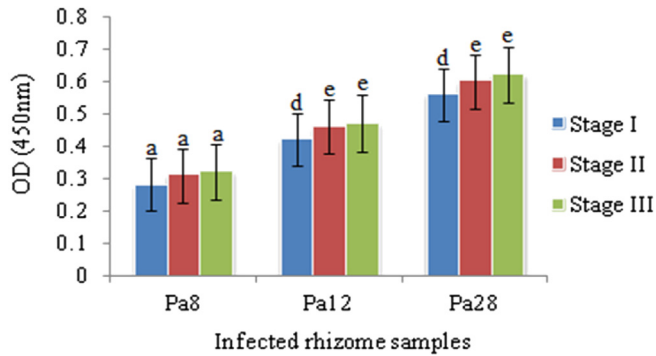


**Fig. 2.** Data of ELISA showing the variation in absorbance at 450 nm monitored in the presence of proteins isolated from three samples (Pa8, Pa12 and Pa28) at different stages of disease development. Mean  $\pm$  SD; n = 3. Values carrying same alphabet did not vary significantly from each other (P < 0.01).

weight of 65 and 45 kDa and seen additional bands of reactivity, including 95 and 25 kDa (Fig. 4).

### 3.5. Correlation of concentrations of antigenic proteins from different stages of infection and antibody titres

Correlation coefficients between concentrations of fungal proteins from different agroclimatic zones of India at different stages of infection were analyzed against antibody titres (Fig. 5). Significant positive correlations (P < 0.01) exist between concentrations of fungal proteins and antibody titres. High positive correlation ( $R^2 = 0.921$ ) was seen between the concentration of fungal antigenic proteins isolated from stage II of infected samples and polyclonal antibody titres, whereas comparatively low positive correlation ( $R^2 = 0.751$ ) was observed between the concentration of antigenic proteins isolated at stage I of infected samples and antibody titres. From the results, we can figure out though there exists a noticeable difference in the antigenic load at stage I infected samples as compared with other stages of infection, still detection can be made at an early stage in order to prevent huge loss to the plant.

### 3.6. Correlation between antigenic load from stage I (mild) infected samples and antibody titres

As evidenced from Fig. 5, at stage I rhizome rot infection, a significant positive correlation was established between the concentration of fungal antigenic proteins and polyclonal IgG antibody titres. The developed antibody showed positive correlation with the antigen concentration of stage I infected samples. A high positive correlation ( $r = 0.999$ ) was observed in infected samples collected from North-western zone with the developed antibody (Table 3). Similar high r values have been considered as positive correlation in other papers (Lau, Leong, Ismail, & Gam, 2008; Siev et al., 2011). There was a marginal variation between the samples isolated from stage I and II of infection. This minor difference might be due to changes in the mechanism of invasion of the pathogen.

### 3.7. Correlation between antigenic load from stage II (acute) infected samples and antibody titres

The concentrations of fungal antigenic proteins were positively correlated against the polyclonal IgG antibody titres at stage II of rhizome rot infection. Significantly high positive correlation ( $r = 0.999$ ) was observed in infected samples collected from North-western zone followed by Western Zone ( $r = 0.944$ ), North Eastern

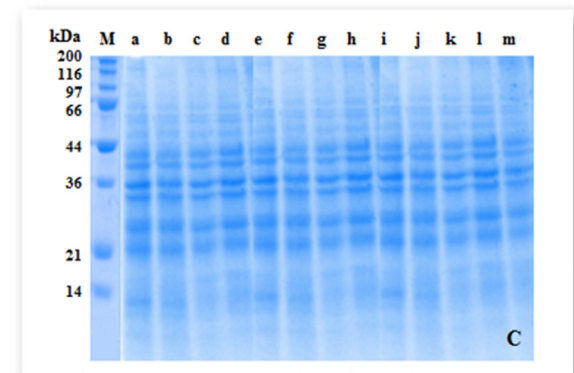
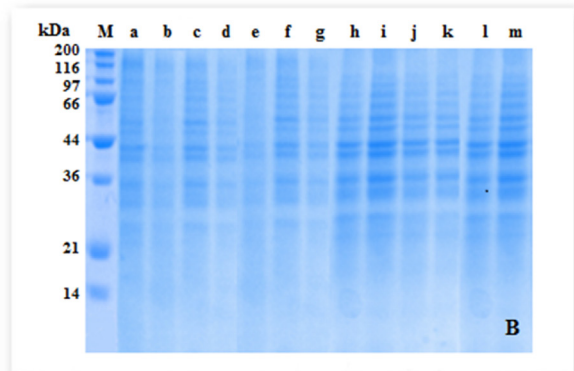
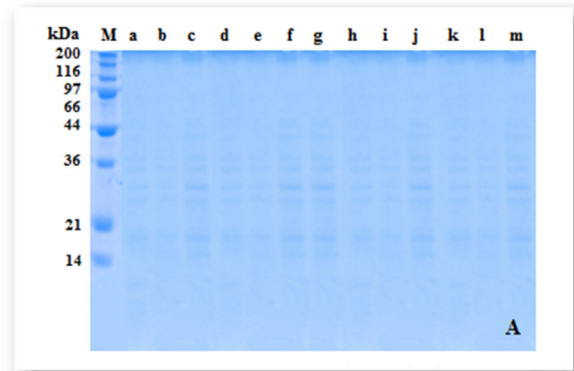


**Fig. 3.** Coomassie blue staining of *Pythium aphanidermatum* proteins separated in a 10% SDS-PAGE. (A) Proteins isolated at stage I infected samples separated by SDS-PAGE; (B) Proteins isolated at stage II infected samples separated by SDS-PAGE; and (C) Proteins isolated at stage III infected samples separated by SDS-PAGE. M-marker; Lanes a-Pa10, b-Pa11, c-Pa12, d-Pa13, e-Pa22, f-Pa23, g-Pa24, h-Pa25, i-Pa26, j-Pa27, k-Pa28, l-Pa29 and m-Pa30 best bands of the infected samples isolated at different stages. Molecular weight of standard protein is indicated on left margin.

Ghat ( $r = 0.941$ ) and North Telangana Zone ( $r = 0.939$ ). However, other agroclimatic zones possessed lesser r value in comparison with samples collected from stage III. High positive correlation in this stage was observed because these zones are prone to rhizome rot disease (Prabhakaran Nair, 2013, chap. 10) which is transmitted via infected planting material and once introduced into the soil, may persist for several years. Therefore, rotting of rhizomes in these areas gets accelerated due to early invasion of pathogens. Moreover, *P. aphanidermatum* can cause severe damage to rhizomes in warm climates (Mubeen Lodhi, Ali Khanzada, Shahzad, & Gaffar, 2013).

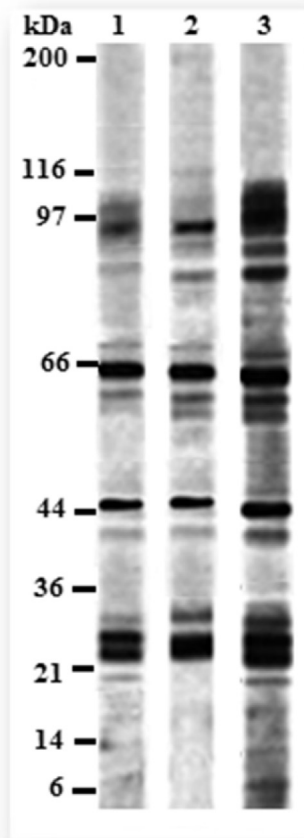


**Fig. 4.** Western blot analysis of developed polyclonal antibody to pooled *Pythium aphanidermatum* antigens from different stages of infection. SDS-PAGE separated proteins were blotted onto a PVDF membrane and incubated with rabbit serum. Lane 1, pooled antigens isolated at stage I infection; Lane 2, pooled antigens isolated at stage II infection; Lane 3, pooled antigens isolated at stage III infection. Molecular weight of standard protein is indicated on left margin.

Therefore it was observed that the antigenic load was comparatively higher in these zones.

### 3.8. Correlation between antigenic load from stage III (chronic) infected samples and antibody titres

A significant positive correlation was seen between the concentration of fungal antigenic proteins and polyclonal IgG antibody titres at stage III of rhizome rot infection. Significantly high positive correlation ( $r = 0.998$ ) was seen in samples collected from Eastern Ghat Highland and South Eastern Ghat followed by North Eastern Ghat ( $r = 0.941$ ) at  $P < 0.01$ . In contrast, the correlation between the antigenic load in the stage III infected samples collected from Western zone with developed antibody was mainly absent ( $r = -0.284$ ). Similar low negative  $r$  value ( $r = -0.12$ ) was considered to show correlation (Iqbal, Ijaz, Aleem, Rehman, & Yousaf, 2009). This low negative correlation might have attributed due to antibody response against mixed infection. At this stage the concentration of antigens is higher and the average size of antibody–antigen complexes is small, as a result of which, fewer antibody molecules are available to cross-link with the antigen molecules. This suggests that *Pythium* rhizome rot disease in the mild stage can induce a measurable effect of immunogenicity.

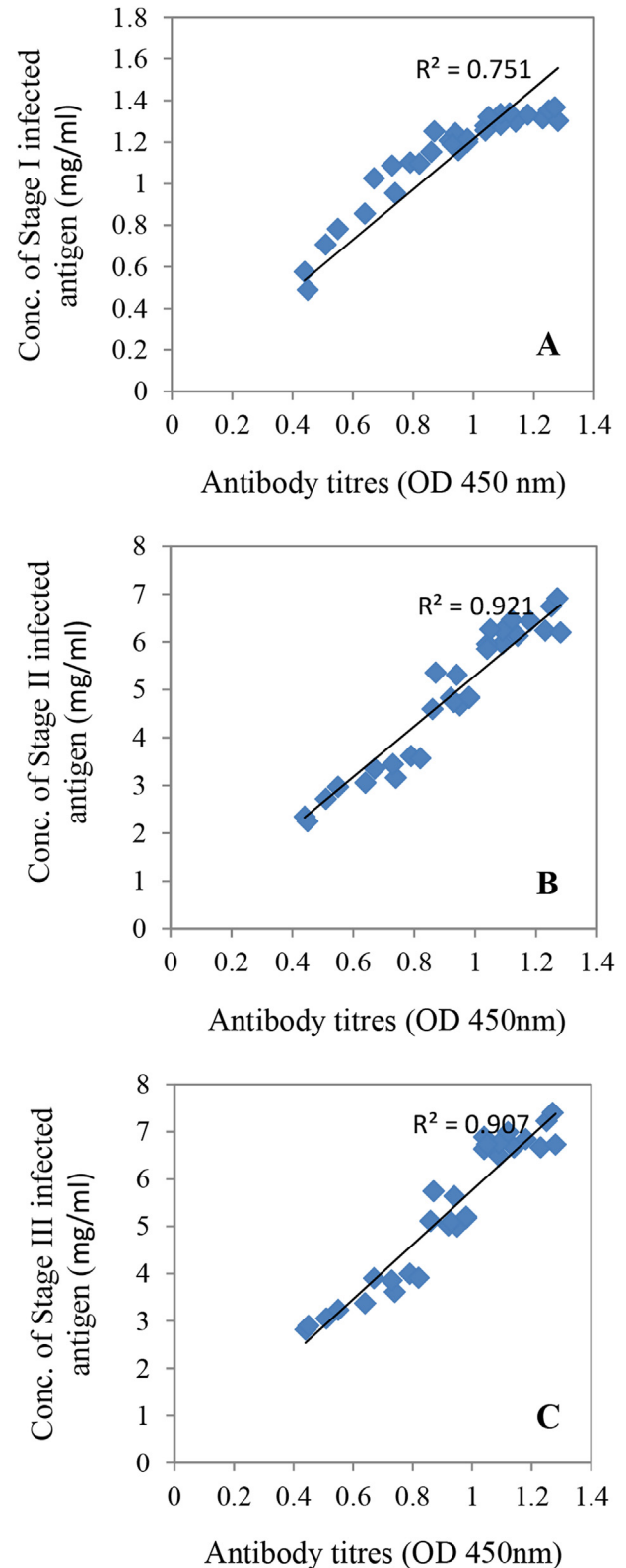


**Fig. 5.** Scatter plots showing linear correlation between concentrations of proteins (Pa1-Pa30) isolated at different stages of infection and antibody titres. A single dot represents a single sample. (A) Concentrations of proteins isolated at stage I (mild) positively correlated with antibody titres ( $R^2 = 0.751$ ,  $P < 0.01$ ) was observed by linear regression analysis. (B) A similar positive correlation concentrations of proteins isolated at stage II (acute) positively correlated with antibody titres ( $R^2 = 0.921$ ,  $P < 0.01$ ) and (C) Concentrations of proteins isolated at stage III (chronic) positively correlated with antibody titres ( $R^2 = 0.907$ ,  $P < 0.01$ ) were observed.

### 3.9. Validation of ELISA technique

The sensitivity and specificity of the diagnostic test was calculated using a hypothetical set of results from known infected and non-infected populations. The test was conducted on a sample size of 200 consisting of both infected and non-infected samples where the diagnostic sensitivity and specificity were found to be 94.83% and 92.96% respectively. Hence it was concluded that the obtained antibody raised in rabbit against *P. aphanidermatum* was highly sensitive and specific and permitted detection of signals in rhizome rot-affected rhizomes.

### 4. Conclusion

The present study demonstrated the effect of specific IgG class of polyclonal antibody upon the *P. aphanidermatum* infection. This study presented data on the detection of *P. aphanidermatum* by serological approaches, which showed that the detection is independent of antigenic load or the stages of infections. Antigens at mild stage were selected, with a minimal concentration of 50 ng having incubation time of 16–18 h for early detection using ELISA. We optimized the reaction conditions for the developed antibody in the control sera. 1:2000 dilutions with incubations for 30 min at 37 °C were chosen as the parameters for the control sera. For the enzymatic transformation, TMB (3,3', 5,5'-Tetramethylbenzidine) substrate was selected for color development. The optimum density of the developed color was measured at 450 nm. All these outcomes permitted us to develop a simple, rapid, sensitive and specific ELISA kit which can detect rhizome rot in turmeric at the mild stage of infection. Indian turmeric is of great demand because of its food uses, hence early diagnosis of infections can enhance its quality, yield and shelf-life by reducing disease losses, leading to a rise in the export value. The findings of this study will help in preventing the crop from this devastating disease. Turmeric crop is vegetatively propagated, where whole or split mother and finger rhizomes are used for planting, therefore healthy and disease-free rhizomes should be selected for further cultivation. Hence turmeric rhizome rot disease should be identified at the early stage and required action should be taken immediately to prevent major crop loss.

### Acknowledgments

The authors are grateful to Prof. (Dr.) S.C. Si, Dean, Centre of Biotechnology and Prof. (Dr.) M.R. Nayak, President, Siksha 'O' Anusandhan University for the generous financial support.

### References

- Anoop, K., & Suseela Bhai, R. (2014). Evaluation of antagonistic potential of indigenous *Trichoderma* isolates against *Pythium aphanidermatum* (Edson) Fitz. causing rhizome rot in turmeric (*Curcuma longa* L.). *Journal of Science*, 4(2), 99–105.
- Anusuya, S., & Sathiyabama, M. (2014). Effect of chitosan on rhizome rot disease of turmeric caused by *Pythium aphanidermatum*. Hindawi Publishing Corporation *ISRN Biotechnology*, 5, 305349.
- Anusuya, S., & Sathiyabama, M. (2015). Foliar application of  $\beta$ -D-glucan nanoparticles to control rhizome rot disease of turmeric. *International Journal of Biological Macromolecules*, 72, 1205–1212.
- Bradford, M. M. (1976). A rapid and sensitive method for the quantitation of microgram quantities of protein utilizing the principle of protein-dye binding. *Analytical Biochemistry*, 72, 248–254.
- Devasahayam, S., & Koya, A. K. M. (2007). Insect pests of turmeric. In P. N. Ravindran, K. N. Babu, & K. Sivaraman (Eds.), *Turmeric: the genus Curcuma medicinal and aromatic plants – Industrial profiles* (pp. 169–191). Boca Raton: CRC Press.
- Dick, M. W. (1990). *Key to Pythium* (p. 64). Whiteknights, Reading, UK: College of Estate Management.
- Dohroo, N. P. (2007). Diseases of turmeric. In P. N. Ravindran, K. N. Babu, & K. Sivaraman (Eds.), *Turmeric-the genus Curcuma* (pp. 155–167). Boca Raton: CRC Press.
- Fleurat-Lessard, P., Luini, E., Berjeaud, J. M., & Roblin, G. (2010). Diagnosis of grapevine esca disease by immunological detection of *Phaeoemoniella chlamydospora*. *Australian Journal of Grape and Wine Research*, 16, 455–463.
- Ghosh, R., Datta, M., & Purkayastha, R. P. (2006). Intraspecific strains of *Pythium aphanidermatum* induced disease resistance in ginger and response of host proteins. *Indian Journal of Experimental Biology*, 44, 68–72.
- Iqbal, M., Ijaz, A., Aleem, M., Rehman, H., & Yousaf, M. S. (2009). Assessment of Nili-Ravi buffalo (*Bubalus bubalis*) semen by MTT reduction assay. *South African Journal of Animal Science*, 39, 294–300.
- Laemmli, U. K. (1970). Cleavage of structural proteins during the assembly of the head of bacteriophage T4. *Nature*, 227(5259), 680–685.
- Lau, W. H., Leong, W. S., Ismail, Z., & Gam, L. H. (2008). Qualification and application of an ELISA for the determination of Tamm Horsfall protein (THP) in human urine and its use for screening of kidney stone disease. *International Journal of Biological Sciences*, 4(4), 215–222.
- Luini, E., Fleurat-Lessard, P., Rousseau, L., Roblin, G., & Berjeaud, J. M. (2010). Inhibitory effects of polypeptides secreted by the grapevine pathogens *Phaeoemoniella chlamydospora* and *Phaeoacremonium aleophilum* on plant cell activities. *Physiological and Molecular Plant Pathology*, 74, 403–411.
- Mazid, M., Khan, T. A., & Mohammad, F. (2011). Role of secondary metabolites in defense mechanisms of plants. *Biology and Medicine*, 3(2), 232–249.
- Middleton, J. T. (1943). The taxonomy, host range and geographic distribution of the genus *Pythium*. *Memoirs of the Torrey Botanical Club*, 20, 1–171.
- Mubeen Lodhi, A., Ali Khanzada, M., Shahzad, S., & Gaffar, A. (2013). Prevalence of *Pythium aphanidermatum* in agro-ecosystem of Sindh province of Pakistan. *Pakistan Journal of Botany*, 45(2), 635–642.
- Octave, S., Fleurat-Lessard, P., & Roblin, G. (2009). Diagnosis of *Eutypa lata* infection in grapevines by serological detection of secreted polypeptides. *Journal of Plant Pathology*, 91, 321–330.
- Octave, S., Roblin, G., Vachaud, M., & Fleurat-Lessard, P. (2006). Polypeptide metabolites secreted by the fungal pathogen *Eutypa lata* participate in *Vitis vinifera* to cell structure damage observed in *Eutypa* dieback. *Functional Plant Biology*, 33, 1–11.
- Parija, W., & Prabhakar, P. K. (1995). Evaluation of lacto-phenol cotton blue for wet mount preparation of feces. *Journal of Clinical Microbiology*, 33, 1019–1021.
- Prabhakaran Nair, K. P. (2013). *The agronomy and economy of turmeric and ginger: the invaluable medicinal spice crops* (1st ed.). Amsterdam: Elsevier Inc.
- Reddy, M. N., Sridevi, N. V., & Charitha Devi, M. (2005). Changes in the nitrogen fractions and amino acid metabolism of turmeric (*Curcuma longa* L.) roots infected with *Fusarium solani*. *Plant Pathology Bulletin*, 14, 221–226.
- Sarathi, V., Kumar, S., Senthil Kumar, R., & Panneerselvam, A. (2014). Studies on rhizome rot pathogen in *Curcuma longa*. *International Journal of Current Microbiology and Applied Sciences*, 3(8), 296–302.
- Siev, M., Yu, X., Prados-Rosales, R., Martiniuk, F. T., Casadevall, A., & Achkar, J. M. (2011). Correlation between serum and plasma antibody titers to mycobacterial antigens. *Clinical and Vaccine Immunology*, 18(1), 173–175.
- Singh, S., Sahoo, S., Dash, S., & Nayak, S. (2014). Association of growth and yield parameters with bioactive phytoconstituents in selection of promising turmeric genotypes. *Industrial Crops and Products*, 62, 373–379.
- Ushamali, C., Nakkeeran, P., & Marimuthu, T. (2008). Induction of plant defence enzymes in turmeric plants by *Trichoderma viride*. *Archives of Phytopathology and Plant Protection*, 41, 79–93.
- Van der Plaats-Niterink, A. J. (1981). Monograph of the genus *Pythium*. *Studies in Mycology*, 21, 1–244.
- Waterhouse, G. M. (1967). Key to *Pythium* Pringsheim. *Mycology Papers*, 109, 1–15.
- Waterhouse, G. M. (1968). The genus *Pythium* Pringsheim. *Mycology Papers*, 110, 1–50.



# Monitoring of spoilage and determination of microbial communities based on 16S rRNA gene sequence analysis of whole sea bream stored at various temperatures



Foteini F. Parlapani, Ioannis S. Boziaris\*

Dept. of Ichthyology and Aquatic Environment, School of Agricultural Sciences, University of Thessaly, Fitokou Street, 38446 N. Ionia, Volos, Greece

## ARTICLE INFO

### Article history:

Received 20 May 2015

Received in revised form

1 November 2015

Accepted 4 November 2015

Available online 7 November 2015

### Keywords:

Sea bream

Shelf-life

Spoilage

Sensory assessment

16S rRNA

### Chemical compounds studied in this article:

Trimethylamine (PubChem CID: 1146)

## ABSTRACT

Exploration of initial and spoilage microbiota grown on plates of whole sea bream stored aerobically at 0 (ice), 5 and 15 °C, was conducted by 16S rRNA gene sequence analysis. The course of spoilage was recorded by monitoring microbiological, sensory and chemical changes. Shelf-life of sea bream determined by sensory assessment was 16, 5 and 2 days at 0 (ice), 5 and 15 °C, respectively. *Pseudomonas* spp. was the dominant spoilage population of whole sea bream at all temperatures tested. A sum of 144 colonies were isolated from TSA (Tryptone Soy Agar) plates and identified by genotypic approach at the beginning and at the sensory rejection time points. Regarding initial microbiota, *Pseudomonas fragi* was the most abundant compared to the rest bacteria (*Pseudomonas fluorescens*, *Enterobacter hormaechei*, *Chryseobacterium carnipullorum*). *P. fragi* was also the dominant microorganism of fish stored at 0 and 5, while *P. fluorescens* at 15 °C. Concluding, genotypic approach gives accurate identification of the dominant spoilage microorganisms providing us with valuable information regarding microbiological spoilage of fish.

© 2015 Elsevier Ltd. All rights reserved.

## 1. Introduction

It is well known that fresh fish spoilage is the result of microbial activity of Specific Spoilage Organisms (SSO) (Gram & Dalgaard, 2002; Gram & Huss, 1996). *Pseudomonas* spp. have been found to be the most important spoilage microorganisms of fish from Mediterranean Sea stored aerobically at chill temperatures. In particular, sea bream spoilage occurred due to the prevailing of *Pseudomonas* species, either *Pseudomonas fragi* in whole and filleted chill-stored sea bream (Parlapani, Kormas, & Boziaris, 2015a; Parlapani, Meziti, Kormas, & Boziaris, 2013) or *Pseudomonas fluorescens* in gutted sea bream (Parlapani, Verdos, Haroutounian, & Boziaris, 2015b).

The sequence analysis of the 16S rRNA gene is currently the most common way for studying seafood microbiota that grown on plates (Alfaro & Hernandez, 2013; Broekaert, Heyndrickx, Herman, Devlieghere, & Vlaemyneck, 2011; Parlapani et al., 2015a; b; Tryfinopoulou et al., 2007). The large amount of both variable and

conserved regions within 16S rRNA gene has been established it as an excellent universal phylogenetic marker. Hence, genotypic determination based on nucleotide sequence comparison of 16S rRNA gene has become a useful tool for identification of bacteria at genus and species level (Nisiotou, Parlapani, Kormas, & Boziaris, 2014).

The exploration of dominant spoilage microbiota on whole sea bream has been already carried out (Parlapani et al., 2013) using either phenotypic characterization of colonies grown on plates or genotypic from bulk DNA (cultured independent approach). However, phenotypic determination is not accurate or reliable, while cultured independent approach does not allow the isolation of spoilage bacteria. Microorganisms grown on laboratory media can be isolated and identified using a simple colony PCR method that use bacteria cells directly as the template (Parlapani et al., 2015a; b). The genotypic identification of spoilage microbiota grown on plates (culture-dependent approach) further allows us to study the spoilage potential of the particular microorganisms that may be contribute to fish spoilage. Indeed, the isolated colonies can be used to inoculate sterile flesh or model substrate and record their metabolic activity (Parlapani, Haroutounian, & Boziaris, 2014a).

Spoilage microorganisms produce metabolites responsible for

\* Corresponding author.

E-mail address: [boziaris@uth.gr](mailto:boziaris@uth.gr) (I.S. Boziaris).

unpleasant off-flavours and off-odours, leading eventually to the sensory rejection of fish (Gram & Dalgaard, 2002). Bacterial activity leading to fish spoilage (especially *Pseudomonas* spp.) is associated with production of volatile nitrogenous compounds usually expressed as total volatile base nitrogen (TVB-N) and trimethylamine nitrogen (TMA-N) (Gram & Dalgaard, 2002; Gram & Huss, 1996; Dainty, 1996). The determination of TVB-N and TMA-N is the most commonly used chemical parameters for monitoring the microbial activity in fish (Oehlenschläger, 2014).

Gilthead sea bream (*Sparus aurata*) is one of the main fish species farmed in Greece and other Mediterranean countries. Greece is the leading producer in the world with 44.3% of the total production (FAO, 2012). The aim of the present investigation was to determine (i) the microbiological, sensory, TVB-N and TMA-N changes and shelf life and (ii) the initial and spoilage microbiota grown on plates using 16S rRNA gene sequencing analysis, of sea bream stored at various temperatures.

## 2. Materials and methods

### 2.1. Sea bream provision, storage and sampling

Two different batches of whole sea bream of approx. 350–400 g were provided from a Greek aquaculture company. Sea bream was farmed in the geographical area of Aegean Sea (FAO 37.3.1) and captured in March 2013. The fish were transferred to the laboratory within 6 h after catch, packaged in insulated boxes with melted ice. One third of the fish were stored in insulated boxes with melted ice (0 °C) in a cold room, while the ice was being replaced every 2 days. Moreover, the other two thirds of fish were stored in incubators operating at 5 and 15 °C. The temperature of 15 °C was chosen as temperature abuse challenge experiment.

At every sampling point for each storage temperature, four fish (two from each batch) were taken for analyses. From each fish 25 g and 10 g of fish tissue were used for microbiological and chemical analyses respectively. The analysis was performed in 4 replicates.

### 2.2. Sensory analysis

Sensory evaluation was conducted by 5 panelists. The panelist consisted of 2 men and 3 women between the ages of 24–52. They were postgraduate students and technicians of the department, who were trained according to ISO 8586-1 (1993). The analysis consisted of the evaluation of a list of profiling attributes concerning skin, outer slime, eyes and gills appearance and odour for determining spoilage characteristics. The overall quality rating was assigned on a 5 to 1 scale with 5, 4, 3 and 2 correspond to the categories E, A, B and C respectively according to Multilingual Guide to EU Freshness Grades for Fishery Products (Howgate, Johnston, & Whittle, 1992), while score 1 was attributed to a totally spoiled sample. Score equal to 2 (corresponding to category C) was considered as the score for rejection. According to the EU guide, the rejected criteria for fish (category C) were; skin: dull, gritty, marked bleaching and shrinkage, outer slime: yellow-brown, very clotted and thick, eyes: completely sunken, grey pupil opaque discoloured cornea, gills: brown or bleached, mucus yellowish grey and clotted, gill and internal odours: acetic, butyric, fruity, turnip, amines, sulphide, faecal.

### 2.3. Microbiological analysis

All microbiological media were obtained from LAB M (Lancashire, UK), except STAA which was supplied by Biolife Italiana srl (Milano, Italy). Iron Agar (IA) was prepared by its ingredients according to Gram, Trolle, and Huss (1987).

Twenty-five grams samples of fish flesh were transferred aseptically to stomacher bags with 225 ml MRD (Maximum Recovery Diluent, 0.1% w/v peptone, 0.85% w/v NaCl) and homogenized for 2 min using a Stomacher (Bug Mixer, Interscience, London, UK). Volumes (0.1 ml) of 10-fold serial dilutions were spread on the surface of dried media in Petri dishes for enumeration of the following (a) *Pseudomonas* spp., on cetrimide-fucidin-cephaloridine agar (CFC) and incubated at 25 °C for 48 h and (b) *Brochothrix thermosphacta*, on STAA and incubated at 25 °C for 48–72 h. Volumes (1 ml) of 10-fold serial dilutions were used for the pour plate technique for enumeration of (a) H<sub>2</sub>S producing bacteria on IA by counting only black colonies, after incubation at 25 °C for 72 h, (b) Enterobacteriaceae on Violet Red Bile Glucose agar (VRBGA), incubated at 37 °C for 24 h and (c) Lactic Acid Bacteria (LAB) on De Man, Rogosa, Sharpe agar (MRS) after incubation at 25 °C for 72 h. For aerobic plate counts (APC) and isolation of the colonies for molecular identification TSA (Tryptone Soy Agar) was used instead of PCA (Plate Count Agar) or IA (Iron Agar). TSA plates were incubated at 25 °C for 48–72 h. TSA gives almost ten-fold higher numbers of colonies compared to other agar media used for APC in sea bream (Kakasis, Parlapani, & Boziaris, 2011). TSA was also selected instead to Long & Hammer agar (L&H) due to its ability to give higher numbers and suitability for Mediterranean fish since *Photobacterium* does not exist in significant number (Koutsoumanis & Nychas, 1999; Parlapani et al., 2013).

The results were expressed as mean  $\pm$  standard deviation (log cfu g<sup>-1</sup>) of 4 replicates. The microbial population changes were fitted using Baranyi equation (Baranyi & Roberts, 1994),  $y(t) = y_{\max} - \ln[1 + (e^{-y_{\max} - y_0} - 1)e^{\mu_m A_n(t)}]$ , where:  $y(t)$  is the logarithm of population at time  $t$ ,  $y_{\max}$  is the logarithm of maximum population,  $y_0$  is the logarithm of initial population,  $\mu_m$  is the maximum specific growth rate and  $A_n(t)$  is a function related to the physiological state of the cells. DMFIT software (Institute of Food Research, Reading, UK) was used for fitting.

### 2.4. Identification of microbiota using 16S rRNA gene sequence analysis

TSA plates at the beginning of the experiment and the time of sensory rejection were taken for bacterial identification. Half of the colonies were selected randomly and were sub-cultured on TSA at 25 °C for 24–48 h.

A colony PCR method was used for the amplification of 16S rRNA gene fragments using bacteria cells directly as the template (Parlapani et al., 2015a). Approximately 900 bp of the 16S rRNA gene were amplified by PCR with universal primers 27fBAC (5'-AGAGTTTGTACMTGGCTCAG-3', M = A/C) (Lane, 1991) and 907r BAC (5'-CCCGTCAATTCCTTGGAGTTT-3') (Muyzer, Teske, Wirsén, & Jannasch, 1995) on a thermal cycler (MyCycler, Bio-Rad Inc., USA). For direct PCR amplification, the PCR mixture (20  $\mu$ l final volume) consisted of 4.0  $\mu$ l buffer 5x (Green GoTaq Flexi buffer, Promega), 2.0  $\mu$ l dNTPs (2 mM), 1.2  $\mu$ l MgCl<sub>2</sub> (25 mM, 1.2 ml), 0.1  $\mu$ l each primer (1  $\mu$ M) and 0.1  $\mu$ l Taq polymerase (GoTaq DNA polymerase, Promega). A small amount of a single colony was added to reaction mix as the DNA template by picking the colony with a sterile micropipette tip. The PCR conditions were: pre-PCR at 95 °C for 5 min, denaturation at 95 °C for 45 s, annealing at 52.5 °C for 45 s and elongation at 72 °C for 1 min and a final 10 min post-PCR elongation at 72 °C. PCR were adjusted to 28 cycles for isolated colonies of the initial and the rejection time point samples. Positive and negative controls were also included throughout the experiments. The PCR products were stained with ethidium bromide and visualized on a 1% agarose gel under UV light. NucleoSpin "R" Gel and PCR Clean-up (Macherey–Nagel, Duren, Germany) was used for purification of the PCR products according to the manufacturer's

instructions.

Sequence data were obtained by ABI Prism 3730 XL Capillary Sequencer (VBC-BIOTECH Vienna, Austria). Each sequence read was ca. 900 bp, and for each individual sample, forward and reverse reads were assembled. For the detection of closest relatives, all sequences were compared with the BLAST function (Zhang Schwartz, Wagner, & Miller, (2000), <http://www.ncbi.nlm.nih.gov/BLAST/>). Sequence data were aligned using the ClustalW2 aligning utility (<http://www.ebi.ac.uk/Tools/clustalw2/index.html>) and phylotypes were defined as sequences showing  $\geq 98\%$  homology to each other. All unique phylotypes were then compiled, along with sequences obtained from GenBank ([www.ncbi.nlm.nih.gov](http://www.ncbi.nlm.nih.gov)) and phylogenetic tree was constructed using the maximum likelihood statistical method using the MEGA6 software. Bootstrapping was performed with 1000 replicates to assign confidence levels to the tree topology. Sequences of dominant phylotypes found in this study were submitted to the GenBank with accession numbers from KR778799 to KR778804.

### 2.5. Determination of TVB-N and TMA-N

Ten grams of flesh taken from one fish were homogenized in trichloroacetic acid (TCA) 60 g/L and filtered through Whatman No.1 filter paper in a 100 ml volumetric flask. Forty ml in duplicates were used for TVB-N analysis using the steam-distillation procedure according to Vyncke, Lutén, Brünner, and Moermans (1987) and the remaining 10 ml were used for the spectrophotometric determination of trimethylamine using picric acid, according to Dyer (1945). The results were expressed as mean  $\pm$  standard deviation (mg N/100 g) of 4 replicates (4 fish, 2 from each batch). All chemicals were supplied by Sigma–Aldrich (Steinheim, Germany).

### 2.6. Statistical analysis

Differences of means in viable counts, kinetic parameters ( $\mu_m$ , Lag,  $y_{max}$ ), TVB-N, TMA-N and sensory score were statistically tested by performing Analysis of Variance followed by Tukey's significant difference test, or t-tests using STATISTICA 6.0. A probability level of  $p \leq 0.05$  was considered statistically significant.

## 3. Results

### 3.1. Sensory changes and shelf life of sea bream

Shelf-life of sea bream determined by sensory assessment was 16, 5 and 2 days at 0 °C (ice), 5 and 15 °C respectively (Fig. 1). Initially, fish freshness was excellent (grade E, score 5). Skin was bright

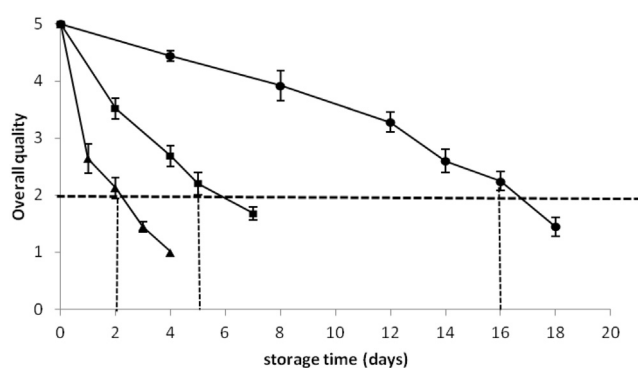


Fig. 1. Overall quality of whole sea bream stored aerobically at 0 °C (ice) (●), 5 °C (■) and 15 °C (▲). The dashed lines show the time point of organoleptic rejection.

metallic silver with thin slime, eyes with convex lens and translucent cornea, bright reddish gills and very pleasant fresh odour. Freshness was diminished gradually with time. The sensory characteristics were substantially degraded after 14, 4 and 1 day at 0 (ice), 5 and 15 °C respectively where the score was below 3 (Fig. 1). At the time point of rejection (grade C, score 2) the sensory characteristics of sea bream represented dull grayish appearance in skin, outer slime and gills with opaque red cornea while the odour was putrid.

### 3.2. Microbiological analysis

Predicted and observed parameters of total microbial population (APC) and spoilage microorganisms during storage of whole sea bream at 0 (ice), 5 and 15 °C are presented in Table 1. Initially (day 0), APC of whole sea bream was 3.54 log cfu/g. At the rejection time point, APC reached the levels of 7.86, 8.08 and 8.29 log cfu/g at 0, 5 and 15 °C, respectively (Table 1). Initial population of *Pseudomonas* spp., H<sub>2</sub>S producing bacteria and Enterobacteriaceae was 3.00, 2.34 and 2.36 log cfu/g respectively, while LAB and *B. thermosphacta* were below detection limit of 1 and 2 logs cfu/g, respectively). Spoilage microorganisms grew faster under higher temperature. The higher the temperature the higher maximum specific growth rate ( $\mu_m$ ) for all spoilage microorganisms studied (Table 1). *Pseudomonas* spp. was the fastest growing bacteria at 5 °C ( $p \leq 0.05$ ), while the growth rates were not significantly different compared to other spoilage bacteria at 0 °C ( $p > 0.05$ ). At 15 °C, Enterobacteriaceae were as fast as *Pseudomonas* spp. ( $p > 0.05$ ). *B. thermosphacta* was the slowest growing bacterium at 0 and 5 °C, while lactic acid bacteria were the slowest at 15 °C (Table 1). *B. thermosphacta* and lactic acid bacteria were also microorganisms with the longest lag phase duration at chill temperatures, while H<sub>2</sub>S producing bacteria did not exhibit any lag phase (Lag) at all temperatures tested (Table 1).

Maximum population density of *Pseudomonas* spp. ( $y_{max}$ ) was significantly higher ( $p \leq 0.05$ ) from other bacterial groups, followed by H<sub>2</sub>S producing bacteria and Enterobacteriaceae, while *B. thermosphacta* and lactic acid bacteria did not manage to reach high number especially at chill temperatures (Table 1). *Pseudomonas* spp. was the predominant spoilage microorganism. Indeed, at population level at rejection time point ( $y_{tr}$ ), pseudomonads population was significantly higher compared to other spoilage bacteria ( $p \leq 0.05$ ) (Table 1). The second highest populations were of H<sub>2</sub>S producing bacteria and Enterobacteriaceae (Table 1). *B. thermosphacta* populations were not higher than 4.5 logs cfu/g at 0 and 5 °C, but reached the level of 6.3 log cfu/g at 15 °C. LAB populations at rejection time point ( $y_{tr}$ ) were not higher than 3.5 logs cfu/g at all temperatures (Table 1).

### 3.3. Identification of microbiota using 16S rRNA gene sequence analysis

In total 144 colonies were collected from TSA medium and identified by 16S rRNA gene sequence analysis. Six different phylotypes designated as SBW-B69-d0, SBW-B32-d0, SBW-B68-d0, SBW-B67-dsp, SBW-B96-dsp and SBW-B84-dsp were detected based on a cutoff level of 98% similarity (Fig. 2). Phylotypes SBW-B69-d0, SBW-B32-d0 and SBW-B68-d0 were detected only at day 0. The phylotype SBW-B69-d0 was closely related to bacterium SBF-B5-d0 and bacterium GSB-b11, SBW-B32-d0 to *Enterobacter hormaechei* strain C7a-1m and SBW-B68-d0 to *Chryseobacterium carnipullorum* strain 9\_R23581 (Fig. 2). Phylotypes SBW-B67-dsp, SBW-B96-dsp and SBW-B84-dsp were mainly detected at spoiled sea bream and closely related to *P. fragi* strain JCM 5396, *Pseudomonas putida* strain TCA1 and *P. fluorescens* strain M-T-TSA\_84,

**Table 1**  
Initial ( $y_0$ ) and final population ( $y_{max}$ ), population at rejection time point ( $y_{tr}$ ), lag phase duration (lag) and maximum specific growth rates ( $\mu_{max}$ ) of spoilage microorganisms of whole sea bream at 0 °C, 5 °C and 15 °C. Observed data (mean  $\pm$  SD) are shown in parenthesis.

T °C	Counts	$y_0$ (log CFUg <sup>-1</sup> )	$y_{max}$ (log CFUg <sup>-1</sup> )	$y_{tr}$ (log CFUg <sup>-1</sup> )	Lag (d)	$\mu_m$ (d <sup>-1</sup> )
0	TSA	3.62 $\pm$ 0.36 <sup>aA</sup> (3.54 $\pm$ 0.32)	7.87 $\pm$ 0.17 <sup>aA</sup> (7.93 $\pm$ 0.23)	7.86 $\pm$ 0.17 <sup>aA</sup> (7.86 $\pm$ 0.11)	2.57 $\pm$ 0.68 <sup>aA</sup>	0.477 $\pm$ 0.022 <sup>aA</sup>
	CFC	3.02 $\pm$ 0.43 <sup>bA</sup> (3.00 $\pm$ 0.32)	7.35 $\pm$ 0.11 <sup>bA</sup> (7.43 $\pm$ 0.15)	7.35 $\pm$ 0.11 <sup>bA</sup> (7.34 $\pm$ 0.14)	2.55 $\pm$ 1.19 <sup>aA</sup>	0.490 $\pm$ 0.083 <sup>aA</sup>
	IA (black colonies)	2.41 $\pm$ 0.17 <sup>cA</sup> (2.34 $\pm$ 0.17)	6.73 $\pm$ 0.17 <sup>cA</sup> (6.88 $\pm$ 0.18)	6.73 $\pm$ 0.17 <sup>cA</sup> (6.69 $\pm$ 0.21)	0 <sup>bA</sup>	0.461 $\pm$ 0.021 <sup>aA</sup>
	VRBGA	2.41 $\pm$ 0.34 <sup>cA</sup> (2.36 $\pm$ 0.25)	6.63 $\pm$ 0.50 <sup>cA</sup> (6.93 $\pm$ 0.20)	6.47 $\pm$ 0.30 <sup>cA</sup> (6.29 $\pm$ 0.24)	3.69 $\pm$ 2.89 <sup>aA</sup>	0.505 $\pm$ 0.287 <sup>aA</sup>
	MRS	0.97 $\pm$ 0.01 <sup>dA</sup> (<1)	>2.90 (2.56 $\pm$ 0.75)	2.08 $\pm$ 0.66 <sup>dA</sup> (2.07 $\pm$ 0.73)	14.65 $\pm$ 3.23 <sup>cA</sup>	0.470 $\pm$ 0.073 <sup>aA</sup>
	STAA	1.99 $\pm$ 0.00 <sup>eA</sup> (<2)	>4.67 (4.46 $\pm$ 0.25)	4.15 $\pm$ 0.25 <sup>eA</sup> (4.11 $\pm$ 0.27)	4.61 $\pm$ 1.07 <sup>dA</sup>	0.188 $\pm$ 0.012 <sup>bA</sup>
5	TSA	3.54 $\pm$ 0.32 <sup>aA</sup> (3.54 $\pm$ 0.32)	8.15 $\pm$ 0.11 <sup>aB</sup> (8.17 $\pm$ 0.10)	8.14 $\pm$ 0.12 <sup>aA</sup> (8.08 $\pm$ 0.13)	0.41 $\pm$ 0.06 <sup>aB</sup>	1.330 $\pm$ 0.042 <sup>aB</sup>
	CFC	2.99 $\pm$ 0.31 <sup>bA</sup> (3.00 $\pm$ 0.32)	8.17 $\pm$ 0.09 <sup>aB</sup> (8.22 $\pm$ 0.06)	8.09 $\pm$ 0.11 <sup>bB</sup> (7.96 $\pm$ 0.30)	0.36 $\pm$ 0.07 <sup>bB</sup>	1.242 $\pm$ 0.038 <sup>aB</sup>
	IA (black colonies)	2.41 $\pm$ 0.27 <sup>cA</sup> (2.34 $\pm$ 0.17)	7.44 $\pm$ 0.13 <sup>bB</sup> (7.39 $\pm$ 0.15)	6.16 $\pm$ 0.32 <sup>cB</sup> (5.99 $\pm$ 0.31)	0 <sup>cB</sup>	0.731 $\pm$ 0.048 <sup>aB</sup>
	VRBGA	2.41 $\pm$ 0.25 <sup>cA</sup> (2.36 $\pm$ 0.25)	6.84 $\pm$ 0.26 <sup>cA</sup> (6.85 $\pm$ 0.28)	6.68 $\pm$ 0.32 <sup>cA</sup> (6.68 $\pm$ 0.31)	0 <sup>cB</sup>	0.949 $\pm$ 0.033 <sup>cB</sup>
	MRS	1.00 $\pm$ 0.02 <sup>dA</sup> (<1)	>7.30 (6.43 $\pm$ 0.57)	3.56 $\pm$ 0.56 <sup>dB</sup> (3.20 $\pm$ 0.61)	2.83 $\pm$ 0.54 <sup>dB</sup>	1.085 $\pm$ 0.097 <sup>bB</sup>
	STAA	1.99 $\pm$ 0.01 <sup>eA</sup> (<2)	6.15 $\pm$ 0.24 <sup>dA</sup> (6.13 $\pm$ 0.21)	4.32 $\pm$ 0.22 <sup>eA</sup> (4.33 $\pm$ 0.25)	2.22 $\pm$ 0.47 <sup>dB</sup>	0.791 $\pm$ 0.064 <sup>bB</sup>
15	TSA	3.61 $\pm$ 0.35 <sup>aA</sup> (3.54 $\pm$ 0.32)	8.63 $\pm$ 0.07 <sup>aC</sup> (8.80 $\pm$ 0.03)	8.58 $\pm$ 0.09 <sup>aB</sup> (8.29 $\pm$ 0.24)	0 <sup>aC</sup>	2.984 $\pm$ 0.116 <sup>aC</sup>
	CFC	3.07 $\pm$ 0.30 <sup>bA</sup> (3.00 $\pm$ 0.32)	8.07 $\pm$ 0.01 <sup>bC</sup> (8.26 $\pm$ 0.09)	8.02 $\pm$ 0.05 <sup>bB</sup> (7.73 $\pm$ 0.17)	0 <sup>aC</sup>	2.981 $\pm$ 0.275 <sup>aC</sup>
	IA (black colonies)	2.50 $\pm$ 0.31 <sup>cA</sup> (2.34 $\pm$ 0.17)	7.55 $\pm$ 0.22 <sup>cB</sup> (7.59 $\pm$ 0.22)	7.37 $\pm$ 0.30 <sup>cC</sup> (7.26 $\pm$ 0.23)	0 <sup>aB</sup>	2.629 $\pm$ 0.109 <sup>bC</sup>
	VRBGA	2.39 $\pm$ 0.21 <sup>cA</sup> (2.36 $\pm$ 0.25)	7.78 $\pm$ 0.18 <sup>cB</sup> (7.64 $\pm$ 0.16)	7.53 $\pm$ 0.11 <sup>cB</sup> (7.33 $\pm$ 0.21)	0 <sup>aB</sup>	3.113 $\pm$ 0.499 <sup>aC</sup>
	MRS	0.98 $\pm$ 0.01 <sup>dA</sup> (<1)	5.45 $\pm$ 0.11 <sup>d</sup> (5.44 $\pm$ 0.37)	3.46 $\pm$ 0.13 <sup>dB</sup> (3.41 $\pm$ 0.14)	0.43 $\pm$ 0.04 <sup>bC</sup>	1.488 $\pm$ 0.106 <sup>bC</sup>
	STAA	1.89 $\pm$ 0.12 <sup>eA</sup> (<2)	7.64 $\pm$ 0.33 <sup>cA</sup> (7.74 $\pm$ 0.25)	6.27 $\pm$ 0.15 <sup>eB</sup> (6.30 $\pm$ 0.12)	0 <sup>aC</sup>	2.184 $\pm$ 0.057 <sup>dC</sup>

Mean values with the same letter are not statistically different. The first letter (lower case) corresponds to comparisons between different bacteria and same temperature, while the second (upper case) correspond to comparisons between the same bacteria for different temperature.

Predicted values (mean  $\pm$  SD) were estimated using Baranyi equation (Baranyi & Roberts, 1994).

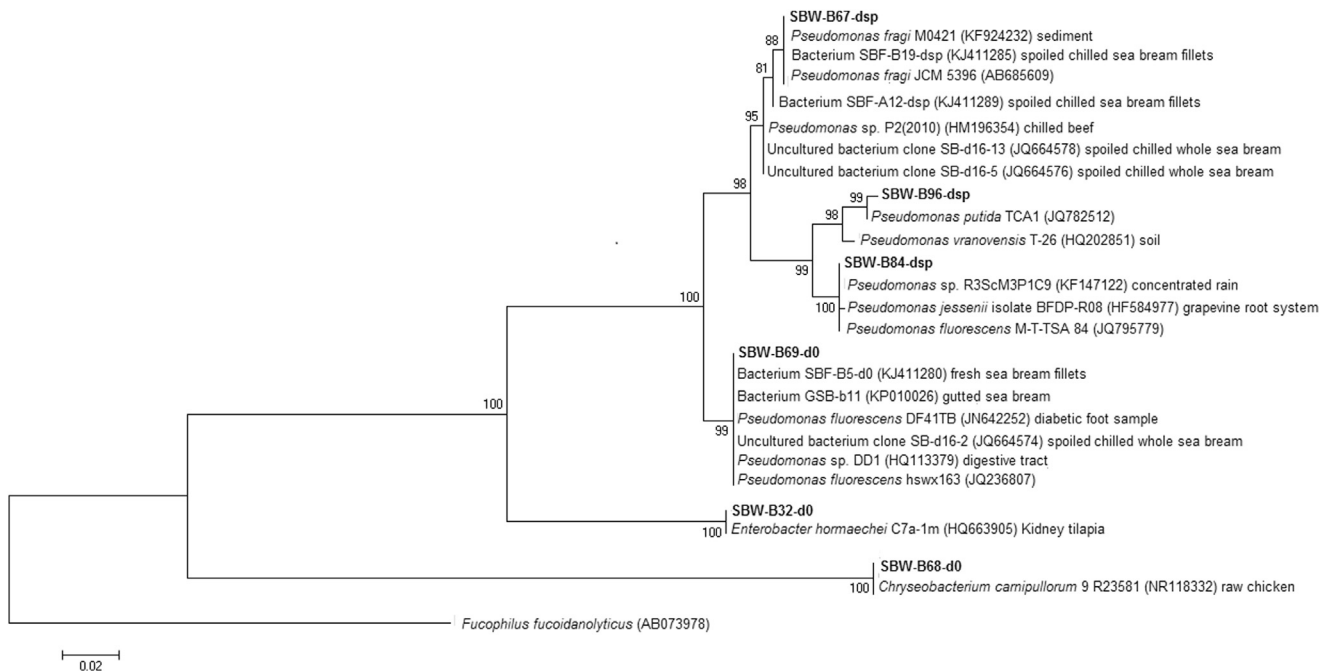


**Fig. 2.** Phylogenetic tree of the PCR-amplified bacterial 16S rRNA gene phylotypes (in bold) (ca. 900 bp) from the fresh whole sea bream and after storage at 0 °C (ice), 5 °C and 15 °C, based on the maximum likelihood method as determined by distance using Kimura's two-parameter correction (Kimura, 1980). GenBank accession numbers are shown in parentheses. One thousand bootstrap analyses (distance) were conducted, and percentages >50% are indicated at nodes. Scale bar represents 2% estimated distance.

respectively (Fig. 2). The phylotype SBW-B67-dsp was detected at both fresh and spoiled sea bream (Figs. 2 and 3). However, phylotype SBW-B67-dsp was also closely related to bacterium SBF-B19-dsp found in our previous works. For this reason, an additionally direct comparison, with cut-off level of 98% similarity in the rRNA gene sequences, of the sequences found herein and the sequences reported in our previous works was conducted. Phylotype SBW-B69-d0 found to be similar to phylotypes SBF-B5-d0 and GSB-b11, while phylotype SBW-B67-dsp to SBF-B19-dsp (Fig. 2).

Forty-eight (48) colonies were taken at day 0. *P. fragi* and *E. hormaechei* were found at higher abundances (35.5 and 30.1% of

the colonies on TSA) than other bacteria (*P. fluorescens* and *Chryseobacterium campipullorum*, 19.4 and 15.1% respectively) (Fig. 3). At rejection time point, 96 colonies (25–35 colonies for each temperature) were taken from TSA plates. For fish stored at 0 °C, *P. fragi* was the only bacterial species detected on TSA after 16 days of storage. At 5 °C, *P. fragi* was also found to predominate (52.9% of the colonies on TSA) after 5 days of storage, while *P. fluorescens* and *P. putida* were found at lower abundances (Fig. 3). Elevated temperature at 15 °C, the spoilage microbiota was found to comprise mostly by *P. fluorescens* (88.2%), while the rest was identified as *P. fragi* (Fig. 3).

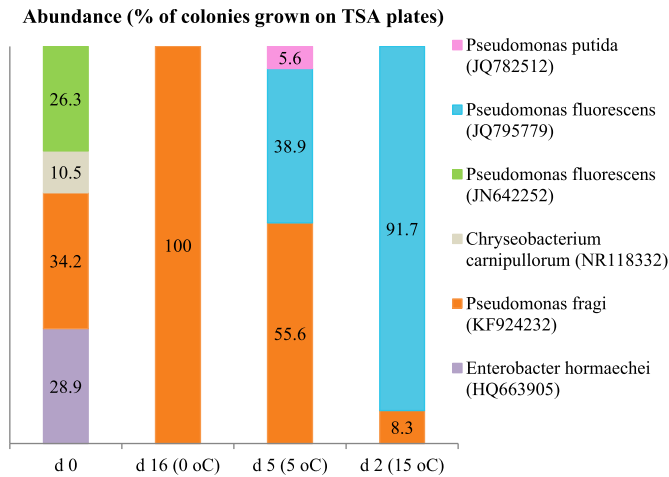


**Fig. 3.** Abundance of initial (d 0) and spoilage microbiota (end of shelf-life) of whole sea bream stored aerobically at 0 °C (ice), 5 °C and 15 °C (d 16, 5 and 2 respectively), expressed as % of colonies grown on TSA plates, determined by 16S rRNA gene sequence analysis.

#### 3.4. Determination of TVB-N & TMA-N

TVB-N changes during the storage of whole sea bream is shown in Fig. 4. Initially (day 0), TVB-N was  $12.49 \pm 1.83$  mg N/100 g fish. At the end of shelf-life at 0 °C, 5 °C and 15 °C, TVB-N amounts were  $24.20 \pm 2.43$ ,  $25.30 \pm 2.59$  and  $28.67 \pm 2.74$  mg N/100 g fish respectively.

On the other hand, initially TMA-N was  $0.76 \pm 0.03$  mg N/100 g and increased slightly reaching the levels of  $1.40 \pm 0.09$ ,  $1.20 \pm 0.05$  and  $1.28 \pm 0.10$  mg N/100 g at the end of shelf-life at 0, 5 and 15 °C, respectively (data not shown).

## 4. Discussion

In the present study the spoilage status i.e. microbiological, sensory, TVB-N, and TMA-N changes, was evaluated. Moreover, the initial and spoilage microbiota of whole sea bream stored at various temperatures was characterized by using molecular approach. The level of the initial bacterial counts (APC) usually ranges from 3 to 4 logs for fresh fish (Cakli, Kilinc, Cadun, Dincer, & Tolasa, 2007; Parlapani et al., 2013). Sea bream was rejected as spoiled when APC reached the levels of  $10^{7.5}$ – $10^{8.5}$  cfu g<sup>-1</sup>. Indeed, spoilage of

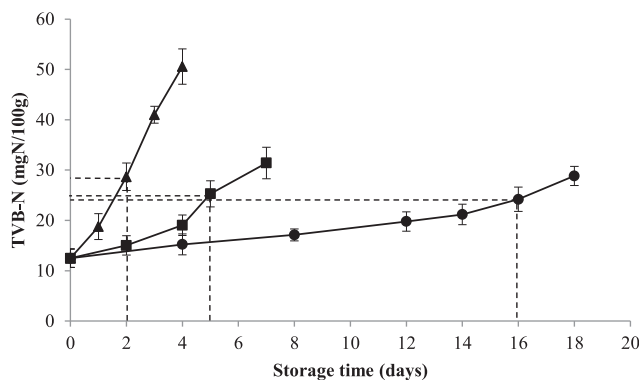


**Fig. 4.** TVB-N changes on whole sea bream stored aerobically at 0 °C (ice) (●), 5 °C (■) and 15 °C (▲). Each data point and the error bars show the mean and  $\pm$ SD of 4 replicates. The dashed lines shows the time point of organoleptic rejection.

fresh fish occurs when APC are as high as  $10^8$ – $10^9$  cfu g<sup>-1</sup> (Gram & Huss, 1996; Koutsoumanis & Nychas, 1999). Shelf-life of sea bream stored in ice varies from 14 to 18 days (Cakli et al., 2007; Kyranas, Lougovois, & Valsamis, 1997; Lougovois, Kyranas, & Kyranas, 2003; Parlapani et al., 2013). Our results are in accordance with these studies. At 5 and 15 °C, shelf-life found to be similar to this of sea bream fillets from our previous works (Parlapani, Malouchos, Haroutounian, & Boziaris, 2014b; Parlapani et al., 2015a).

*Pseudomonas* spp. are characterized as SSOs of chill-stored sea bream (Koutsoumanis & Nychas, 2000; Tryfinopoulou, Tsakalidou, & Nychas, 2002; Parlapani et al., 2013; 2014b; 2015a; b). Our results agree with these studies. *Pseudomonas* population was followed by H<sub>2</sub>S producing bacteria and Enterobacteriaceae populations in all cases. The same pattern has been also observed during spoilage of sea bream fillets (Parlapani et al., 2014b). The rest members of the microbiota i.e. LAB and *B. thermosphacta* populations remained at lower levels especially at chilling temperatures. This is in agreement with previous publications (Koutsoumanis & Nychas, 2000; Parlapani et al., 2013). Growth rates reported in this work differ from those of other studies (Koutsoumanis, 2001; Koutsoumanis, Taoukis, Drosinos, & Nychas, 2000, 2002; Parlapani et al., 2015a). Indeed, *Pseudomonas* spp., H<sub>2</sub>S producing bacteria, and *B. thermosphacta* growth rates from the present study were similar but LAB growth rates were higher than those reported on sea bream fillets stored aerobically at 0 and/or 5 °C (Parlapani et al., 2015a). On the other hand, Koutsoumanis et al. (2000, 2002) and Koutsoumanis (2001) found growth rates of *Pseudomonas* on red mullet, sea bass and sea bream respectively, almost double compare to our study. In general, the growth rates of microorganisms are not the same on different growth substrates, such as the flesh of different fish species. Additionally, different geographical locations, sea temperature, seasonal variations and processing (gutting or filleting, etc) affects the initial microbiota (Gram & Huss, 1996) which in its turn affects the observed growth rates taken by using selective media.

Only few studies have dealt with the microbial diversity of fish caught from Mediterranean Sea by using molecular approach (Tryfinopoulou et al., 2002; 2007; Parlapani et al., 2013; 2015a; b). *Pseudomonas*, *Psychrobacter*, *Acinetobacter*, *Flavobacterium*, *Shewanella* and *Macrocooccus* have been found as initial microbiota on sea bream (Parlapani et al., 2013; 2015a). In this study, the initial microbiota consisted of *P. fragi*, *P. fluorescens*, *E. hormaechei* and *Ch. carnipullorum*. *P. fragi* was found at higher abundances than *P. fluorescens* in contrast to other studies concerning gutted (Tryfinopoulou et al., 2002) and filleted sea bream (Parlapani et al., 2015a). *P. fragi* JCM 5396 has also been isolated from fillets stored aerobically at chill temperatures (Parlapani et al., 2015a), while *P. fluorescens* DF41TB from various sea bream products (Parlapani et al., 2013; 2015a; b). *E. hormaechei* C7a-1m and *Ch. carnipullorum* 9R23581 have not been isolated from sea bream in previous studies. However, *E. hormaechei* C7a-1m has also been isolated from cultured tilapia (*Oreochromis niloticus*) (Gomez-Gil, Alcaraz-Saucedo, Romalde, Balboa & Soto-Rodriguez, unpublished, GenBank), while *Ch. carnipullorum* 9R23581 from raw chicken (Charimba, Jooste, Albertyn, & Hugo, 2013).

In our study, sea bream spoilage occurred due to the prevailing either of *P. fragi* or *P. fluorescens* depended on storage temperatures. *P. fragi* JCM 5396 was the only bacterial species detected on TSA at the end of shelf life of ice-stored fish. At 5 °C, the same strain of *P. fragi* (JCM 5396) was the dominant microorganism, however, a strain of *P. fluorescens* (M-T-TSA\_84), different from this found initially (*P. fluorescens* DF41TB), was also found at high abundances (approx. 40% of the colonies on TSA). *P. fluorescens* M-T-TSA\_84 dominated at the temperature of 15 °C. This may be explained by considering that under increasing temperature *P. fragi* was

outcompeted by *P. fluorescens*. The growth parameters of *P. fragi* and *P. fluorescens* isolated from sea bream should be evaluated in a future study. *P. fluorescens* M-T-TSA\_84 has not been isolated from sea bream in our previous works, however another phylotype, similar to *P. fluorescens* hswx163 (Wei., unpublished, GenBank) and *P. fluorescens* DF41TB, has been found as the dominant microorganism in gutted sea bream stored at 2 °C (Parlapani et al., 2015b). *P. fragi* JCM 5396 has been found as the dominant microorganism isolated from fillets stored aerobically at 0 and 5 °C (Parlapani et al., 2015a). Finally, *P. fluorescens* DF41TB has been found as the dominant microorganism of initial microbiota in sea bream fillets (Parlapani et al., 2015a). The microorganisms described above seems to be key players of sea bream spoilage hence spoilage potential and activity of those isolates should be studied in single and co-culture in a future work.

TVB-N level ranges between 5 and 20 mg N/100 g for fresh fish (Connell, 1995). The initial value of  $12.49 \pm 1.83$  mg N/100 g was lower than those reported for fresh gilthead sea bream by Goulas and Kontominas (2007) (15.9 mg N/100 g) and Kyra et al. (1997) (26.0 mg N/100 g). At the end of shelf-life TVB-N value never reached amounts higher than 30–35 mg N/100 g, which is the legislation limit (EC 2074/2005). This is in agreement with other studies as well (Koutsoumanis & Nychas, 2000; Kyra et al., 1997; Parlapani et al., 2014b).

Initial TMA-N value ( $0.76 \pm 0.03$  mg N/100 g) was higher than those reported by other researchers (Goulas & Kontominas, 2007; Tejada & Huidobro, 2002). At the end of shelf-life TMA-N values were 1.20–1.40 mg N/100 g. Very low amounts of TMA-N have been also reported by other researchers (Koutsoumanis & Nychas, 2000; Kyra et al., 1997). In general TMA-N development is not pronounced in fish from Mediterranean waters as compared to other species from Northern Seas mainly due to the low amounts of the precursor compound the trimethylamine oxide found in Mediterranean fish (Kyra & Lougovois, 2002) in contrast to fish from Northern Seas e.g. *Gadus morhua* (Herland, Esaiassen, Cooper, & Olsen, 2009). Consequently, TVB-N and TMA-N were low and increased only at the late stages of storage. The same was observed for sea bream fillets and gutted sea bream (Parlapani et al., 2015a; b) making them not suitable for quality indices but only for acceptance/rejection criterion (Oehlschlager, 2014). For this reason other approaches mostly based on monitoring of volatile bacterial metabolites should be employed for exploration of useful quality/freshness indices (Soncin, Chiesa, Panseri, Biondi, & Cantoni, 2009; Parlapani et al., 2014b; 2015b).

## 5. Conclusions

Fish storage under different temperatures affected the synthesis of dominant spoilage microbiota in species and strains level. The 16S rRNA gene sequence analysis gave accurate identification of SSOs during sea bream spoilage. *P. fragi* was the dominant microorganism of fish stored at 0 and 5 °C, while *P. fluorescens* at 15 °C. *P. fragi* seems to be a key player candidate in the sea bream spoilage as it has been found both in whole (present study) and fillet samples (Parlapani et al. 2015a). Spoilage potential and activity of these isolates should be studied in a future work in order to provide us with valuable information regarding seafood spoilage mechanism. For this reason, *P. fragi* and *P. fluorescens* strains isolated from the present work should be used to contaminate sterile sea bream or fish model systems, stored under various conditions and monitor their growth and metabolic attributes based on the production of other volatile metabolites, since TVB-N and TMA-N do not seem suitable for chemical spoilage indices.

## Acknowledgements

This research has been co-financed by the European Union (European Social Fund – ESF) and Greek national funds through the Operational Program “Education and Lifelong Learning” of the National Strategic Reference Framework (NSRF) – Research Funding Program: Heracleitus II. Investing in knowledge society through the European Social Fund.

## References

- Alfaro, B., & Hernandez, I. (2013). Evolution of the indigenous microbiota in modified atmosphere packaged Atlantic horse mackerel (*Trachurus trachurus*) identified by conventional and molecular methods. *International Journal of Food Microbiology*, 167, 117–123.
- Baranyi, J., & Roberts, T. A. (1994). A dynamic approach to predicting bacterial growth in food. *International Journal of Food Microbiology*, 23, 277–294.
- Broekaert, K., Heyndrickx, M., Herman, L., Devlieghere, F., & Vlaemynck, G. (2011). Seafood quality analysis: molecular identification of dominant microbiota after ice storage on several general growth media. *Food Microbiology*, 28, 1162–1169.
- Cakli, S., Kilinc, B., Cadun, A., Dincer, T., & Tolasa, S. (2007). Quality differences of whole ungutted sea bream (*Sparus aurata*) and sea bass (*Dicentrarchus labrax*) while stored in ice. *Food Control*, 18, 391–397.
- Charimba, G., Jooste, P., Albertyn, J., & Hugo, C. (2013). *Chryseobacterium carni-pullorum* sp. nov., isolated from raw chicken. *International Journal of Systematic and Evolutionary Microbiology*, 63, 3243–3249.
- Commission Regulation (EC) No 2074/2005 of 5 December 2005. *Official Journal of the European Union L*, 338(27), (22.12.2005).
- Connell, J. J. (1995). Method of assessing and selecting for quality. In J. J. Connell (Ed.), *Control of Fish Quality* (4th ed., pp. 133–164). Fishing News Books, Ltd.
- Dainty, R. H. (1996). Chemical/biochemical detection of spoilage. *International Journal of Food Microbiology*, 33, 19–33.
- Dyer, W. J. (1945). Amines in fish muscle. I. Calorimetric determination of trimethylamine as the picrate salt. *Journal of Fisheries Research Board of Canada*, 8, 314.
- FAO. (2012). *FishStatJ – Software for fishery statistical time series*. FAO Fisheries Department, Fishery Information, Data and Statistics Unit. Version 2.0.0. Release date: March 2012.
- Goulas, A. E., & Kontominas, M. G. (2007). Combined effect of light salting, modified atmosphere packaging and oregano essential oil on the shelf-life of sea bream (*Sparus aurata*): biochemical and sensory attributes. *Food Chemistry*, 100, 287–296.
- Gram, L., & Dalgaard, P. (2002). Fish spoilage bacteria: problems and solutions. *Current Opinions in Microbiology*, 13, 262–266.
- Gram, L., & Huss, H. H. (1996). Microbiological spoilage of fish and fish products. *International Journal of Food Microbiology*, 33, 121–137.
- Gram, L., Trolle, G., & Huss, H. H. (1987). Detection of specific spoilage bacteria from fish stored at low (0 °C) and high (20 °C) temperatures. *International Journal of Food Microbiology*, 4, 65–72.
- Herland, H., Esaiassen, M., Cooper, M., & Olsen, R. L. (2009). Changes in trimethylamine oxide and trimethylamine in muscle of wild and farmed cod (*Gadus morhua*) during iced storage. *Aquaculture Research*, 41, 95–102.
- Howgate, P., Johnston, A., & Whittle, K. J. (1992). *Multilingual guide to EC freshness grades for fishery products*. Aberdeen: Marine Laboratory, Scottish Office of Agriculture, Environment and Fisheries Department.
- International Organization for Standardization (ISO) 8586-1. (1993). *Sensory analysis—General guidance for the selection, training and monitoring of assessors, Part 1: Selected assessors*. Geneva. Available at: <http://iso.org>.
- Kakasis, S., Parlapani, F. F., & Bozaris, I. S. (2011). Performance and selectivity of media used for the enumeration of bacterial populations on seafood. In *Proceedings of the 33rd Scientific Conference of Hellenic society for Biological Sciences, Edessa, Greece, may 19–21* (pp. 100–101).
- Kimura, M. (1980). A simple method for estimating evolutionary rate of base substitutions through comparative studies of nucleotide sequences. *Journal of Molecular Evolution*, 16, 111–120.
- Koutsoumanis, K. (2001). Predictive modeling of the shelf life of fish under non-isothermal conditions. *Applied and Environmental Microbiology*, 67, 1821–1829.
- Koutsoumanis, K., Giannakourou, M. C., Taoukis, P. S., & Nychas, G. J. E. (2002). Application of shelf life decision system (SLDS) to marine cultured fish quality. *International Journal of Food Microbiology*, 73, 375–382.
- Koutsoumanis, K., & Nychas, G.-J. E. (1999). Chemical and sensory changes associated with microbial flora of Mediterranean boque (*Boops boops*) stored aerobically at 0, 3, 7, a 10 °C. *Applied of Environmental Microbiology*, 65, 698–706.
- Koutsoumanis, K., & Nychas, G.-J. E. (2000). Application of a systematic experimental procedure to develop a microbial model for rapid fish shelf-life predictions. *International Journal of Food Microbiology*, 60, 171–184.
- Koutsoumanis, K. P., Taoukis, P. S., Drosinos, E. H., & Nychas, G.-J. E. (2000). Applicability of an arrhenius model for the combined effect of temperature and CO2 packaging on the spoilage Microflora of fish. *Applied and Environmental Microbiology*, 66, 3528–3534.
- Kyra, V. R., & Lougovois, V. P. (2002). Sensory, chemical and microbiological

- assessment of farm-raised European sea bass (*Dicentrarchus labrax*) stored in melting ice. *International Journal of Food Science and Technology*, 37, 319–328.
- Kyranas, V. R., Lougovois, V. P., & Valsamis, D. S. (1997). Assessment of shelf-life of maricultured gilthead sea bream (*Sparus aurata*) stored in ice. *International Journal of Food Science and Technology*, 32, 339–347.
- Lane, D. J. (1991). 16S/23S rRNA sequencing. In E. Stackenbrandt, & M. Goodfellow (Eds.), *Nucleic acid techniques in bacterial Systematics* (pp. 115–175). Chichester: John Wiley & Sons.
- Lougovois, V. P., Kyranas, E. R., & Kyranas, V. R. (2003). Comparison of selected methods of assessing freshness quality and remaining storage life of iced gilt-head sea bream (*Sparus aurata*). *Food Research International*, 36, 551–560.
- Muyzer, G., Teske, A., Wirsén, C. O., & Jannasch, H. W. (1995). Phylogenetic-relationships of Thiomicrospira species and their identification in deep-sea hydrothermal vent samples by denaturing gradient gel-electrophoresis of 16S rDNA fragments. *Archives of Microbiology*, 164, 165–172.
- Nisiotou, A., Parlapani, F. F., Kormas, K., & Boziaris, I. S. (2014). Old Targets, new weapons: food microbial communities revealed with molecular tools. In I. S. Boziaris (Ed.), *Novel food Preservation and microbial assessment techniques* (pp. 277–312). Taylor & Francis, CRC Press.
- Oehlenschläger, J. (2014). Seafood quality assessment. In I. S. Boziaris (Ed.), *IFST Advances in food Science Series Seafood processing. Technology, quality & Safety* (pp. 361–386). Wiley- Blackwell.
- Parlapani, F. F., Haroutounian, S. A., & Boziaris, I. S. (2014a). Metabolic activity of spoilage bacteria isolated from sea bream fillets. In *Abstract book, FOOD MICRO Nantes, France 1-4 September* (p. 276).
- Parlapani, F. F., Kormas, K. Ar, & Boziaris, I. S. (2015a). Microbiological changes, shelf life and identification of initial and spoilage microbiota of sea bream fillets stored under various conditions using 16S rRNA gene analysis. *Journal of the Science of Food and Agriculture*, 95, 2386–2394.
- Parlapani, F. F., Malouchos, A., Haroutounian, S. A., & Boziaris, I. S. (2014b). Microbiological spoilage and investigation of volatile profile during storage of sea bream fillets under various conditions. *International Journal of Food Microbiology*, 189, 153–163.
- Parlapani, F. F., Meziti, A., Kormas, ArK., & Boziaris, I. S. (2013). Indigenous and spoilage microbiota of farmed sea bream stored in ice identified by phenotypic and 16S rRNA gene analysis. *Food Microbiology*, 33, 85–89.
- Parlapani, F. F., Verdos, G. I., Haroutounian, S. A., & Boziaris, I. S. (2015b). The dynamics of *Pseudomonas* and volatile profile during the spoilage of gutted sea bream stored at 2°C. *Food Control*, 55, 257–265.
- Soncin, S., Chiesa, M. L., Panseri, S., Biondi, P., & Cantoni, C. (2009). Determination of volatile compounds of precooked prawn (*Penaeus vannamei*) and cultured gilthead sea bream (*Sparus aurata*) stored in ice as possible spoilage markers using solid phase microextraction and gas chromatography/mass spectrometry. *Journal of the Science of Food and Agriculture*, 89, 436–442.
- Tejada, M., & Huidobro, A. (2002). Quality of farmed gilthead seabream (*Sparus aurata*) during ice storage related to the slaughter method and gutting. *European Food Research and Technology*, 215, 1–7.
- Tryfinopoulou, P., Tsakalidou, E., & Nychas, G.-J. E. (2002). Characterization of *Pseudomonas* spp. associated with spoilage of gilt-head sea bream stored under various conditions. *Applied of Environmental Microbiology*, 68, 65–72.
- Tryfinopoulou, P., Tsakalidou, E., Vancanney, M., Hoste, B., Swings, J., & Nychas, G.-J. E. (2007). Diversity of *Shewanella* population in fish *Sparus aurata* harvested in the Aegean Sea. *Journal of Applied Microbiology*, 103, 711–721.
- Vyncke, W., Lutén, J., Brünner, K., & Moermans, R. (1987). Determination of total volatile bases in fish: a collaborative study by the West European Fish Technologists' Association (WEFTA). *Zeitschrift für Lebensmitteluntersuchung und -Forschung A*, 184, 110–114.
- Zhang, Z., Schwartz, S., Wagner, L., & Miller, W. (2000). A greedy algorithm for aligning DNA sequences. *Journal of Computational Biology*, 7, 203–214.



# Inhibitory effects of lactic and malic organic acids on autoinducer type 2 (AI-2) quorum sensing of *Escherichia coli* O157:H7 and *Salmonella* Typhimurium

Ahmad Almasoud<sup>a</sup>, Navam Hettiarachchy<sup>a,\*</sup>, Srinivas Rayaprolu<sup>a</sup>, Dinesh Babu<sup>b</sup>, Young Min Kwon<sup>c</sup>, Andy Mauromoustakos<sup>d</sup>

<sup>a</sup> Department of Food Science, University of Arkansas, Fayetteville, AR 72704, USA

<sup>b</sup> Department of Toxicology, University of Louisiana, Monroe, LA 71209, USA

<sup>c</sup> Poultry Science, University of Arkansas, Fayetteville, AR 72701, USA

<sup>d</sup> Department of Agricultural Statistics, University of Arkansas, Fayetteville, AR 72701, USA

## ARTICLE INFO

### Article history:

Received 20 May 2015

Received in revised form

5 October 2015

Accepted 8 November 2015

Available online 11 November 2015

### Keywords:

Quorum sensing

Auto inducers

Pathogenic bacteria

Produce

Organic acids

## ABSTRACT

Several organic acid based antimicrobials are reported to reduce bacterial populations but studies showing inhibition of autoinducer-2 (AI-2) activity or quorum sensing are limited. The effect of lactic and malic acids on autoinducer activity of selected strains of *Escherichia coli* O157:H7 and *Salmonella* Typhimurium is tested in this study. The strains were screened for AI-2 like activity on spinach and cantaloupe homogenates using autoinducer sensing *Vibrio harveyi* biosensor strains. The ED 14 strain of *E. coli* O157:H7 and the SD 10 strain of *Salmonella* showed highest AI-2 like activity of 55 and 53 Relative Light Units respectively. These two strains were used to evaluate the AI-2 inhibitory activities of lactic and malic acids at 1–4% concentrations (alone or in combinations). Lactic acid at 4.0% had the highest inhibition of 80% on ED 14 *E. coli* strain while the combination treatment of lactic acid + malic acid at 4.0% each had the highest inhibition of 80% on SD 10 *Salmonella* strain. Results from the study indicate that the quorum sensing ability of the *E. coli* O157:H7 and *Salmonella* Typhimurium strains can be effectively inhibited by antimicrobial organic acids.

© 2015 Elsevier Ltd. All rights reserved.

## 1. Introduction

Quorum sensing is a cell–cell signaling process used by certain bacteria to coordinate virulence gene expression and survival. During quorum sensing, certain bacteria are known to modulate the cellular functions through signaling compounds known as auto inducers (Silagyi, Kim, Lo, & Wei, 2009). Both gram-positive and gram-negative bacteria use this cell density dependent system as a response to environmental stresses such as lack of nutrients, inhibitory effects of temperature and host defense responses (Waters & Bassler, 2005). The autoinducer (AI) molecules affect the bacterial expression of various genes involved in virulence, toxicity, sporulation, plasmid transformation, antibiotic production and biofilm formation (Bainton et al., 1992; Bassler, 1999; Davies et al.,

1998; Kendall & Sperandio, 2014; Luo & Farrand, 2001; Oger & Farrand, 2002; Sperandio, Torres, Girón, & Kaper, 2001). Certain bacteria exhibit quorum-sensing behavior as a regulatory process to ensure the presence of sufficient cell density before a specific gene product is made. This process allows them to multiply exponentially and initiate to express a certain phenotype such as biofilm production. Excess concentrations of autoinducer compounds beyond a threshold within the cells are known to activate (some repress) a regulatory protein that binds to specific DNA sequence regions and activates transcription mechanism resulting in the production of biofilm (Bassler, 1999; Moriera et al., 2006). Quorum sensing bacteria such as *Escherichia coli* O157:H7 and *Salmonella* Typhimurium are known to respond to two types of auto-inducers called acylated homoserine lactones (AI-1) and furanosyl borate diester (AI-2) (Lu, Hume, & Pillai, 2005; Reading et al., 2007). Marine bacterium *Vibrio harveyi* is commonly utilized as a bioluminescent reporter strain to detect these autoinducer molecules (Fig. 1). Inhibition of autoinducer molecules or their activity may affect quorum-sensing behavior or biofilm formation by certain

\* Corresponding author. Department of Food Science & Institute of Food Engineering, University of Arkansas, 2650 N. Young Avenue, Fayetteville, AR 72704, USA.  
E-mail address: [nhettiar@uark.edu](mailto:nhettiar@uark.edu) (N. Hettiarachchy).

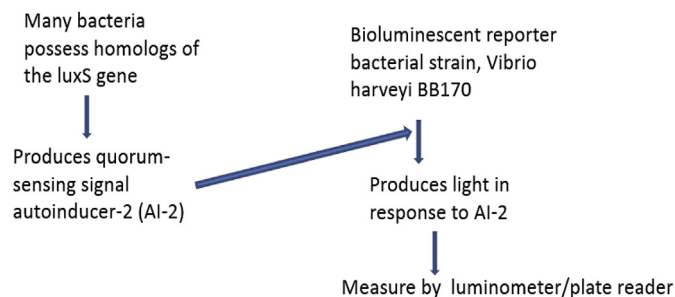


Fig. 1. Simplified scheme of the principle for detection of quorum sensing activity.

bacteria. Various natural compounds have been studied to demonstrate their role as AI-2 inhibitors. For example, fatty acids such as stearic acid, palmitic acid, oleic acid, and linoleic acids isolated from poultry meat (have shown to inhibit AI-2 activity (Widmer et al., 2007). Other examples of natural compounds that are reported to inhibit bacterial quorum sensing are vanilla extracts (Choo, Rukayadi, & Hwang, 2006) and traditional Chinese medicinal plant extracts (Koh and Tham, 2011). Pure compounds like *p*-coumaric acid have also been found to provide inhibitory effect against cell–cell communication in bacteria (Bodini, Manfredini, Epp, Valentini, & Santori, 2009). Interestingly, the antimicrobial effects of several organic acids against bacteria have been studied, but the studies on their inhibitory effects on biofilm formation and autoinducer-2 activities are limited.

Considering the importance of quorum sensing in biofilm formation by foodborne pathogens such as *E. coli* O157:H7 and *Salmonella* Typhimurium that often contaminate minimally processed produce, it would be important to inhibit the autoinducer molecules of these strains so that their survival or persistence can be hindered on these foods. In this study the effect of lactic and malic acids on autoinducer-2 (quorum sensing molecule) activity of *E. coli* O157:H7 strains on spinach and *Salmonella* Typhimurium strains on cantaloupes was demonstrated. Reporter strain, *V. harveyi* (BB170), was used to detect quorum sensing based on its ability to produce bioluminescence in response to AI-2 activity.

## 2. Materials and methods

We used the *V. harveyi* reporter strain to detect the autoinducer-2 (AI-2) activity of *E. coli* O157:H7 and *Salmonella* Typhimurium strains inoculated in minimally processed produce samples (spinach and cantaloupe). The methodology of culture preparation, inoculation and autoinducer measurements using the reporter strain are indicated below.

### 2.1. Culture preparation of *E. coli* O157:H7, *Salmonella* Typhimurium and *V. harveyi*

The procedure for this method was obtained from previous research using *V. harveyi* for detecting quorum sensing (Kim et al., 2009). The reporter strain, *V. harveyi* BB170, produces light in response to AI-2 (due to luxS gene) and is useful in biological assays for detecting and quantifying AI-2 production by bacterial cultures (Taga & Xavier, 2011). Agar slants with pure cultures of the food pathogenic bacteria *E. coli* O157:H7 and *Salmonella* Typhimurium were obtained from the University of Georgia, Center for Food Safety, Griffin, GA. The bacterial strains were; *E. coli* O157:H7 green fluorescent protein (GFP)-labeled ED 14 (CV267); ED15 (6980-2); ED16 (6982-2); MD58 (CV261), MD46 (F4546); MD47 (K4492), *Salmonella* Typhimurium -GFP-labeled SD 10 and SD 11. Working cultures from the frozen stocks (−70 °C) were prepared by

transferring aseptically to 10 mL of brain heart infusion broth media (BHI) (Becton Dickinson Microbiology Systems, Sparks, MD, U.S.A.) and incubated at 37 °C for 24 h with shaking (200-rpm) in a New Brunswick Scientific (Edison NJ, U.S.A.) agitating-incubator. Second-day inoculum of each strain was prepared by transferring 10 µl of first-day culture into 10 mL of fresh BHI and incubated for 24 h in a shaker maintained at 37 °C and this was used to inoculate ( $10^9$  log CFU/mL) spinach and cantaloupe for the study. The *V. harveyi* BB170 (ATCC BBA-1117) was used as a reporter strain to detect AI-2 molecule while *V. harveyi* BB152 (ATCC BBA-1119) that produces AI-1 and AI-2, was used as a positive control. The *Vibrio* strains were grown in the auto-inducer bioassay (AB) medium. The AB medium was prepared as follows: A solution consisting of NaCl (17.5 g/L), MgSO<sub>4</sub> (12.3 g/L), and vitamin-free cas-amino acids (2 g/L) was dissolved in 1 L of water with final pH 7.5 and sterilized by autoclaving (15 min, 121 °C). When the solution was cooled, sterile 1 M potassium phosphate solution (pH 7.0, 10 mL/L), 50% glycerol (20 mL/L) and filter-sterilized 0.1 M L-arginine (10 mL/L) were added.

### 2.2. Preparation of antimicrobial solutions

Separate stock solutions of organic acids were prepared in 10 mL of sterile water by dissolving malic acid powder and lactic acid to a concentration of 10%. The stock solutions were diluted to prepare 1.0, 2.0, 3.0, and 4.0% of both organic acid test solutions one day before the study (Massey, Hettiarachchy, Martin, & Ricke, 2013). The solutions were vacuum filtered through Whatman no. 4 filter paper to remove insoluble particles that may interfere with the spraying. Deionized water was measured (similar to the weight of the organic acid solution) and the pH was adjusted to that of the test solutions with 1 N hydrochloric acid (HCl) to prepare the control solutions for the organic acids.

### 2.3. Spinach/cantaloupe homogenate preparation for auto-inducer assay

Spinach and cantaloupe were purchased fresh from a local grocery store on the day of the experiment. Spinach leaves and cantaloupe rinds were rinsed with water, and submerged in sodium hypochlorite solution (6.25 mL/L) for 3 min to reduce the microbial background. The leaves/rinds were submerged again in sterile water for 3 min, removed and left under the biological safety cabinet for 2 h to dry. After drying, the leaves/rinds were placed in separate sterile bags and weighed. Sterile water was added at a volume of twice the weight of the sample to each bag and stomached using a lab-scale masticator (Neutec Group Inc., Farmingdale, NY) for 3 min to prepare homogenates. Ninety microliter samples of the homogenates (spinach/cantaloupe) were dispensed into separate 96-well plates (Becton Dickinson and Co. Franklin lakes, NJ) before adding 10 µl of the second day culture of *E. coli* O157:H7 or *Salmonella* Typhimurium. The 96-well plates were incubated for 24 h at 25 °C. After incubation the homogenates with the pathogen cultures were transferred to sterile 1.5 mL Eppendorf tubes and centrifuged at 3,000g for 5 min at 25 °C to separate the bacterial cells. The cell-free supernatants (CFS) were collected and stored at −20 °C for autoinducer activity assay.

### 2.4. Auto-inducer activity assay

Autoinducer (AI-2) detection assay in minimally processed produce was conducted as described previously (Silagyi et al., 2009). The overnight cultures of the *Vibrio* reporter and positive control strains were separately diluted (1:5000) in fresh AB medium and the diluted cells (90 µl) were dispensed into a 96-well plate. For the auto-inducer activity assay the CFS of spinach/

cantaloupe homogenates that were earlier exposed to *E. coli* O157:H7 or *Salmonella* Typhimurium strains, potentially containing AI-2 molecules, were added to the reporter strain cultures previously dispensed into a 96-well plate. The wells with *V. harveyi* BB152 strain were used as positive control. The plates were incubated for 3 h at 30 °C with shaking and luminescence measurements were made using a plate reader at 490 nm. This assay measured the uninhibited or the highest relative AI-2 activity among the stains of *E. coli* O157:H7 and *Salmonella* Typhimurium.

### 2.5. Assay to measure the effect of organic acids on the AI-2 activity

The inhibitory effects of malic (MA) and lactic (LA) acids on AI-2 activity by *E. coli* O157:H7 and *Salmonella* Typhimurium were tested by adding the organic acid solutions at different concentrations (1.0, 2.0, 3.0, 4.0%). As described above, the CFS of treated spinach/cantaloupe homogenates were added to 96-well plates containing the reporter strain *V. harveyi* BB170. Combinations of LA and MA (LA1% + MA1%, LA4% + MA4%) were also investigated. The plates were incubated at 30 °C for 3 h with shaking. Luminescence readings were measured at 490 nm using a plate reader.

### 2.6. Assay to measure the effect of organic acids on *V. harveyi* strain BB170 bacteria

Overnight AB medium cultures of *V. harveyi* BB170 were diluted (1:5000) with fresh AB medium. The subculture of *V. harveyi* BB170 and organic acids that showed the highest AI-2 inhibition activity were added to individual sterilized tubes at the ratio of 9:1 v/v (*V. harveyi* BB170: organic acids solution sample), and incubated at 30 °C for a similar time period as the AI-2 bioassay. Serial dilutions were made for enumeration of viable cells of *V. harveyi* BB170 on Marine agar (Becton Dickinson) and log counts were recorded.

### 2.7. Statistical analysis

The JMP 10.0 software (SAS Institute, Cary, NC) was used for one way analysis of variance to determine the effect of organic acids on AI-2 like activities, activity inhibitions, and the growth of reporter strain *V. harveyi* BB170. A factorial design was used in the study for the organic acid treatments. Analysis of variance (ANOVA) was performed and significant difference was determined at  $P < 0.05$ . Tukey HSD was used to compare means and all experiments were conducted in triplicates and repeated for reproducibility.

## 3. Results and discussion

### 3.1. Evaluation of the relative AI-2 activity by *E. coli* and *Salmonella* on spinach and cantaloupe

The pathogenic bacteria, *E. coli* and *Salmonella* were selected for study on spinach and cantaloupe respectively since they have been found to contaminate these produce causing numerous cases of illness. Quorum sensing and biofilm formation in pathogenic bacteria have been shown to enhance their survival rate while affecting the severity of the contamination problem (Annous, Fratamico, & Smith, 2009; Gandhi & Chikindas, 2007; Silagyi et al., 2009). The autoinducer molecules AI-1 and AI-2 were previously detected to induce quorum sensing (Surette & Bassler, 1998; Surette, Miller, & Bassler, 1999) and were used by researchers in studying quorum sensing and biofilm formation (Lu, Hume, & Pillai, 2004; Uckoo, Jayaprakasha, Vikram, & Patil, 2015). To investigate the quorum sensing ability of a pathogen the relative AI-2 activity was determined as the ratio of the average value of the sample against that of the negative control.

The results of relative AI-2-like activity in spinach homogenate inoculated with six stains of *E. coli* followed by incubation for 12 h are given in Table 1. The ED 14 strain produced the highest relative AI-2-like activity of 55 Relative Light Units (RLU, the units of measurement for the chemiluminescence or bioluminescence) which was significantly high in comparison to other tested strains ( $p < 0.05$ ). Hence, ED 14 strain of *E. coli* O157:H7 was selected to investigate the effect of various organic acid concentrations, alone and/or in combination. Table 2 shows the relative AI-2 activity produced by two *Salmonella* Typhimurium strains (SD 10 and SD 11) in cantaloupe homogenate after 12 h incubation, where the SD 10 strain showed higher (53%) relative AI-2 activity in comparison to SD 11 (21%). Hence, SD 10 strain was chosen to further investigate the effect of organic acids on biofilm formation mechanism.

### 3.2. Determination of the effect of organic acids on the AI-2 activity

Lactic and malic organic acids at concentrations of 1.0, 2.0, 3.0, and 4.0% (alone and in combination) were tested for their ability to inhibit AI-2 activity in spinach and cantaloupe homogenates inoculated with *E. coli* O157:H7 (ED 14) and *Salmonella* Typhimurium (SD 10) respectively. These concentrations were selected based on previous studies on effective pathogen inhibition by the organic acids on produce (Ganesh, Hettiarachchy, Griffis, Martin, & Ricke, 2012; Ganesh, Hettiarachchy, & Ravichandran, et al., 2010; Massey et al., 2013).

Inhibition of *E. coli* O157:H7, ED 14 AI-2 activity in spinach homogenate is shown in Table 3. Overall results show that lactic acid was more effective than malic acid in inhibiting AI-2 activities. At its highest concentration of 4.0%, malic acid showed 37% inhibition of AI-2 and at the same concentration, lactic acid inhibited the AI-2 activity by 80% which was significant ( $p < 0.05$ ). The combined treatment of lactic and malic acid at 1.0% and 4.0% were not significant in inhibiting AI-2 activity. The treatment LA + MA (1.0% each) resulted in 17% inhibition while LA + MA (4.0% each) inhibited the relative AI-2 activity by 25%. Hence, a combination of organic acids did not have any synergistic or additive effect on *E. coli*'s ability to produce AI-2.

Table 4 shows the inhibition of *Salmonella* Typhimurium, SD 10 strain by organic acid treatments. The combined treatment of LA + MA (4.0% each) had the highest inhibition by 80%. However, it is not significantly different from that shown by lactic acid alone at 4.0% concentration which resulted in an inhibition of 76%. These results on reduction of quorum sensing ability by organic acids can supplement previous studies which demonstrated their antimicrobial effect on produce (Ganesh et al., 2010).

These outcomes can be explained by the fact that the inhibitory properties of the organic acids is due to their concentrations, ability to penetrate the bacterial cell wall and the capacity to alter the

**Table 1**  
Relative AI-2 like activity in spinach homogenate inoculated with various stains of *E. coli* for 12 h.

Strain*	Relative AI-2 like activity (%)**
ED 14	55.0 ± 2.1 <sup>A</sup>
ED 15	28.0 ± 2.6 <sup>B</sup>
ED 16	36.1 ± 2.6 <sup>C</sup>
MD 46	15.2 ± 2.3 <sup>D</sup>
MD 47	15.3 ± 0.9 <sup>D</sup>
MD 58	14.3 ± 0.9 <sup>D</sup>

\* Strains of *E. coli* O157:H7 studied. Values provided are means ± standard deviation of triplicates and those conducted by the same letter are not significantly different ( $P < 0.05$ ). \*\*Relative AI-2 like activity was calculated as the ratio of luminescence of the test sample to the negative control (AB medium).

**Table 2**  
Relative AI-2 like in cantaloupe homogenate inoculated with stains of *Salmonella* for 12 h.

Strain*	Relative AI-2 like activity (%)**
SD 10	53.2 ± 0.9 <sup>A</sup>
SD 11	21.3 ± 0.7 <sup>B</sup>

\*Strains of *Salmonella* Typhimurium studied. Values provided are means ± standard deviation of triplicates and those connected by the same letter are not significantly different ( $P < 0.05$ ).

\*\*Relative AI-2 like activity was calculated as the ratio of luminescence by the test sample to the negative control (AB medium).

**Table 3**  
Reduction in quorum sensing activity of *E. coli* ED 14 strain based on AI-2 activity inhibition in spinach by organic acids.

Treatments (%)*	Inhibition %**
LA (1.0)	26.2 ± 1.0 <sup>E</sup>
LA 2.0	33.1 ± 0.3 <sup>CD</sup>
LA 3.0	49.5 ± 1.5 <sup>B</sup>
LA 4.0	80.2 ± 2.3 <sup>A</sup>
MA 1.0	23.4 ± 0.4 <sup>F</sup>
MA 2.0	26.9 ± 0.2 <sup>F</sup>
MA 3.0	28.0 ± 0.4 <sup>DE</sup>
MA 4.0	37.5 ± 1.4 <sup>C</sup>
LA MA 1	17.2 ± 0.3 <sup>E</sup>
LA MA 4	25.4 ± 0.8 <sup>E</sup>

Values are means ± standard deviations of triplicates and those connected by the same letter are not significantly different ( $P < 0.05$ ). \*LA: lactic acid, MA: Malic acid. \*\*Calculated in comparison to positive control (relative activity of AI-2 by *V. harveyi* BB152) values.

**Table 4**  
Reduction in quorum sensing activity of *Salmonella* Typhimurium SD 10 strain based on AI-2 activity inhibition in cantaloupe by organic acids.

Treatments (%)*	Inhibition %**
LA (1.0)	27.5 ± 0.8 <sup>F</sup>
LA 2.0	36.2 ± 0.6 <sup>DE</sup>
LA 3.0	58.0 ± 2.1 <sup>B</sup>
LA 4.0	76.6 ± 0.2 <sup>A</sup>
MA 1.0	16.1 ± 0.4 <sup>G</sup>
MA 2.0	26.3 ± 1.2 <sup>F</sup>
MA 3.0	28.8 ± 1.8 <sup>DE</sup>
MA 4.0	46.7 ± 1.4 <sup>C</sup>
LA MA 1	39.9 ± 1.7 <sup>D</sup>
LA MA 4	80.4 ± 2.9 <sup>A</sup>

Values provided are means ± standard deviation of triplicates and those connected by the same letter are not significantly different ( $P < 0.05$ ). \*LA: lactic acid, MA: Malic acid. \*\*Calculated in comparison to positive control (relative activity of AI-2 by *V. harveyi* BB152) value.

microbial cytoplasmic pH (Eswaranandam, Hettiarachchy, & Johnson, 2004; Midolo, Lambert, Hull, Luo, & Grayson, 1995). The differences in efficacy among the organic acids can be attributed to their molecular size (Ganesh et al., 2010).

### 3.3. Inhibitory effect of organic acids on the growth of *V. harveyi* BB170

The influence of organic acids on the multiplication of the reporter strain is shown in Table 5. The treatments selected for this tests were: Lactic acid 4.0%, Malic acid 4.0%, and LA + MA (4.0% each) since they caused significant inhibition of AI-2. This experiment was conducted to verify if the decline in AI-2 activity was due

**Table 5**  
Effect of organic acids on the growth of the reporter strain *V. harveyi* BB170.

Treatment*	Growth (log CFU/mL)
AB medium	5.4 ± 0.1 <sup>A</sup>
LA 4%	5.3 ± 0.2 <sup>A</sup>
MA 4%	5.3 ± 0.0 <sup>A</sup>
LA MA 4%	5.2 ± 0.2 <sup>A</sup>

Values provided are means ± standard deviation of triplicates and those connected by the same letter are not significantly different ( $P < 0.05$ ). \*AB medium: Auto-inducer bioassay medium; LA: Lactic acid; MA: Malic acid.

to the growth inhibition of the reporter strain *V. harveyi* BB170. For this purpose, a mixture of (1:9) of organic acids and the diluted reporter strain *V. harveyi* BB170 in AB medium was incubated as mentioned previously. There were no significant differences between the control (growth in AB medium) and the various treatments, suggesting that inhibition of reporter strain growth was not the basis for inhibition of AI-2 activity by the organic acids. Enumeration of the *V. harveyi* BB170 cells was conducted to determine the effect of organic acids on the report bacteria as an alternative to bioluminescence assay. This is due to the fact that organic acids may impact the redox reactions for NAD(P)H formation (energy source for bioluminescence) in the reporter bacteria there by affecting the bacterial metabolism and the response on AI-2 activity.

The AI-2 inhibition activity of the organic acids is considered to be lower in comparison to certain chemical food additives reported in the literature. As an example, turkey patties treated with sodium propionate showed inhibition of AI-2 by 99.8% (Lu et al., 2004). However, naturally occurring organic acids have greater potential for application in foods since most consumers are avoiding chemical additives and preservatives in food products. Among other organic acids such as fatty acids including palmitic acid, steric acid, oleic acid, and linoleic acid isolated from poultry meat have also shown inhibition of the AI-2 activity up to 65% (Soni et al., 2008). A mixture of steric, palmitic, oleic, and linoleic acids inhibited the AI-2 activity by 59.5% (Widmer et al., 2007). Although these results show significant AI-2 inhibition, they are not comparable to the higher inhibition levels of up to 80% shown by the naturally produced organic acids tested in this study. The overall significance of this study was the effect of organic acids in reducing quorum sensing ability of pathogenic bacteria on minimally processed produce.

## 4. Conclusion

Foodborne illness due to *E. coli* O157:H7 and *Salmonella* outbreaks on minimally processed produce are a consistent problem in the U.S. leading to economical and health consequences. These bacterial pathogens show virulence and sustained survival due to quorum sensing ability that provides a barrier against the effects of antimicrobials. For the first time, this study demonstrated the ability of natural antimicrobials like organic acids to inhibit the expression of autoinducer-2 molecule which thereby hinders the quorum sensing ability of pathogenic bacteria including *E. coli* O157:H7 and *Salmonella* Typhimurium. Lactic acid alone at 4.0%, and a combination treatment of malic acid 4.0% + lactic 4.0% were able to inhibit AI-2 activity by *E. coli* O157:H7 and *Salmonella* by 80% on spinach and cantaloupe respectively. Therefore, food protection and safety in the minimally processed produce industry, dealing with frozen or refrigerated vegetables and fruits, and salad mixes, can be enhanced using these natural antimicrobials. The

significance of the findings observed in this study lies in the potential capacity of natural antimicrobial agents which impact cell to cell signaling and potential biofilm formation by food-borne pathogens.

## Acknowledgments

The project was funded by a grant from the National Research Initiative by the United States Department of Agriculture (CSREES/NRI - 2008-35201-18855).

## References

- Annous, B. A., Fratamico, P. M., & Smith, J. L. (2009). Quorum sensing in biofilms: why bacteria behave the way they do. *Journal of Food Science*, 74(1), R1–R14.
- Bainton, N. J., Bycroft, B. W., Chhabra, S. R., Stead, P., Gledhill, L., Hill, P. J., et al. (1992). A general role for the lux autoinducer in bacterial cell signaling: control of antibiotic biosynthesis in *Erwinia*. *Gene*, 116, 87–91.
- Bassler, B. L. (1999). How bacteria talk to each other: regulation of gene expression by quorum sensing. *Current Opinion in Microbiology*, 2, 582–587.
- Bodini, S. F., Manfredini, S., Epp, M., Valentini, S., & Santori, F. (2009). Quorum sensing inhibition activity of garlic extract and *p*-coumaric acid. *Letters in Applied Microbiology*, 49, 551–555.
- Choo, J. H., Rukayadi, Y., & Hwang, J. (2006). Inhibition of bacterial quorum sensing by vanilla extract. *Letters in Applied Microbiology*, 42, 637–641.
- Davies, D. G., Parsek, M. R., Pearson, J. P., Iglewski, B. H., Costerton, J. W., & Greenberg, E. P. (1998). The involvement of cell-to-cell signals in the development of a bacterial biofilm. *Science*, 280, 295–298.
- Eswaranandam, S., Hettiarachchy, N. S., & Johnson, M. G. (2004). Antimicrobial activity of citric, lactic, malic, or tartaric acids and nisin-incorporated soy protein film against *Listeria monocytogenes*, *Escherichia coli* O157:H7, and *Salmonella gaminara*. *Journal of Food Science*, 69, 79–84.
- Gandhi, M., & Chikindas, M. L. (2007). *Listeria*: a foodborne pathogen that knows how to survive. *International Journal of Food Microbiology*, 113(1), 1–15.
- Ganesh, V., Hettiarachchy, N. S., Griffis, C. L., Martin, E. M., & Ricke, S. C. (2012). Electrostatic spraying of food-grade organic and inorganic acids and plant extracts to decontaminate *Escherichia coli* O157:H7 on spinach and iceberg lettuce. *Journal of Food Science*, 77(7), M391–M396.
- Ganesh, V., Hettiarachchy, N. S., Ravichandran, M., Johnson, M. G., Griffis, C. L., Martin, E. M., et al. (2010). Electrostatic sprays of food-grade acids and plant extracts are more effective than conventional sprays to decontaminate *Salmonella Typhimurium* on spinach. *Journal of Food Science*, 75(9), M574–M579.
- Kendall, M. M., & Sperandio, V. (2014). Cell-to-cell signaling in *E. coli* and *Salmonella*. *EcoSal Plus*. <http://dx.doi.org/10.1128/ecosalplus.ESP-0002-2013>.
- Kim, S., Silagyi, K., Lo, Y. M., & Wei, C. (2009). Production of biofilm and quorum sensing by *Escherichia coli* O157:H7 and its transfer from contact surfaces to meat, poultry, ready-to-eat deli, and produce products. *Food Microbiology*, 26(5), 514–519.
- Koh, K. H., & Tham, F. (2011). Screening of traditional Chinese medicinal plants for quorum-sensing inhibitors activity. *Journal of Microbiology, Immunology and Infection*, 44, 144–148.
- Lu, L., Hume, M. E., & Pillai, S. D. (2004). Autoinducer-2-like activity associated with foods and its interaction with food additives. *Journal of Food Protection*, 67, 1457–1462.
- Lu, L., Hume, M. E., & Pillai, S. D. (2005). Autoinducer-2-like activity on vegetable produce and its potential involvement in bacterial biofilm formation on tomatoes. *Foodborne Pathogens and Disease*, 2, 242–249.
- Luo, Z. Q., & Farrand, S. K. (2001). The *Agrobacterium tumefaciens* rnd homolog is required for TraR-mediated quorum-dependent activation of Ti plasmid *tra* gene expression. *Journal of Bacteriology*, 183, 3919–3930.
- Massey, L. M., Hettiarachchy, N. S., Martin, E. M., & Ricke, S. C. (2013). Electrostatic spray of food-grade organic acids and plant extract to reduce *Escherichia coli* O157:H7 on fresh-cut cantaloupe cubes. *Journal of Food Safety*, 33(1), 71–78.
- Midolo, P. D., Lambert, J. R., Hull, R., Luo, F., & Grayson, M. L. (1995). In vitro inhibition of *Helicobacter pylori* NCTC 11637 by organic acids and lactic acid bacteria. *Journal of Applied Bacteriology*, 79(4), 475–479.
- Moreira, C. G., Palmer, K., Whiteley, M., Sircili, M. P., Trabulsi, L. R., Castro, A. F. P., et al. (2006). Bundle-forming pili and EspA are involved in biofilm formation by enteropathogenic *Escherichia coli*. *Journal of Bacteriology*, 188, 3952–3961.
- Oger, P., & Farrand, S. K. (2002). Two opines control conjugal transfer of an *Agrobacterium* plasmid by regulating expression of separate copies of the quorum-sensing activator gene *traR*. *Journal of Bacteriology*, 184, 1121–1131.
- Reading, N. C., Torres, A. G., Kendall, M. M., Hughes, D. T., Yamamoto, K., & Sperandio, V. (2007). A novel two-component signaling system that activates transcription of an enterohemorrhagic *E. coli* (EHEC) effector involved in remodeling of host actin. *Journal of Bacteriology*, 189, 2468–2476.
- Silagyi, K., Kim, S., Lo, Y. M., & Wei, C. (2009). Production of biofilm and quorum sensing by *Escherichia coli* O157:H7 and its transfer from contact surfaces to meat, poultry, ready-to-eat deli, and produce products. *Food Microbiology*, 26, 514–519.
- Soni, K. A., Jesudhasan, P., Cepeda, M., Widmer, K., Jayaprakasha, G. K., Patil, B. S., et al. (2008). Identification of ground beef-derived fatty acid inhibitors of autoinducer-2-based cell signaling. *Journal of Food Protection*, 71, 134–138.
- Sperandio, V., Torres, A. G., Girón, J. A., & Kaper, J. B. (2001). Quorum sensing is a global regulatory mechanism in enterohemorrhagic *Escherichia coli* O157:H7. *Journal of Bacteriology*, 183, 5187–5197.
- Surette, M. G., & Bassler, B. L. (1998). Quorum sensing in *Escherichia coli* and *Salmonella typhimurium*. *Proceedings of the National Academy of Sciences*, 95(12), 7046–7050.
- Surette, M. G., Miller, M. B., & Bassler, B. L. (1999). Quorum sensing in *Escherichia coli*, *Salmonella typhimurium*, and *Vibrio harveyi*: a new family of genes responsible for autoinducer production. *Proceedings of the National Academy of Sciences*, 96(4), 1639–1644.
- Taga, M. E., & Xavier, K. B. (2011). Methods for Analysis of Bacterial Autoinducer-2 Production. *Current Protocols in Microbiology*, 23:C:1C.1.1C.1.1–1C.1.15.
- Uckoo, R. M., Jayaprakasha, G. K., Vikram, A., & Patil, B. S. (2015). Polymethoxyflavones isolated from the peel of *Miaray Mandarin* (*Citrus miaray*) have biofilm inhibitory activity in *Vibrio harveyi*. *Journal of Agricultural and Food Chemistry*, 63(32), 7180–7189.
- Waters, C. M., & Bassler, B. L. (2005). Quorum sensing: cell-to-cell communication in bacteria. *Annual Review of Cell and Developmental Biology*, 21, 319–346.
- Widmer, K. W., Soni, K. A., Hume, M. E., Beier, R. C., Jesudhasan, P., & Pillai, S. D. (2007). Identification of poultry meat-derived fatty acids functioning as quorum sensing signal inhibitors to autoinducer-2 (AI-2). *Journal of Food Science*, 72, M363–M368.



# Quality of the pre-cooked potato strips processed by Radiant Wall Oven



Bilal Kirmaci\*, Rakesh K. Singh

Department of Food Science and Technology, The University of Georgia, Athens, GA 30602, USA

## ARTICLE INFO

### Article history:

Received 24 June 2015

Received in revised form

1 October 2015

Accepted 3 November 2015

Available online 6 November 2015

### Keywords:

Color

Infrared heating

Potato strips

Sensory

Texture

## ABSTRACT

Steam processing was paired with the Radiant Wall Oven (RWO) to produce reduced-fat baked potato strips. Par-fried frozen potato strips, having  $5 \times 1 \times 1$  cm<sup>3</sup> dimensions, were pre-cooked in steam chamber for 75 or 90 s. Then, steam-processed potato strips were heated in RWO at different temperatures: 450 °C for 3 or 3.5 min, at 500 °C for 2.5 or 3 min, at 550 °C for 1.5 or 2 min. Instrumental and sensory quality characteristics of RWO processed pre-cooked potato strips were investigated and compared to deep-fat fried samples at 177 °C for 3 min. RWO baked pre-cooked potato strips at 500 °C for 3 min, regardless of steam processing time, were similar to control in terms of texture, chroma, shrinkage and yield, yet contained 86.8% less fat. A trained panel indicated that texture of the potato strips, baked in RWO at 500 °C for 3 min after steam processing for 90 s, was not significantly different than that of the control samples. Finally, consumer panel indicated 51.2% acceptability and 35% willingness to purchase the RWO-baked pre-cooked potato strips. However, acceptability of the RWO-baked pre-cooked potato strips rose to more than 75% when fat content and corresponding calories were revealed.

© 2015 Elsevier Ltd. All rights reserved.

## 1. Introduction

Potato is a staple food around the world. More than half of the processed potato crop has been utilized as frozen French fries for the last six years (USDA, 2014a). French fries are very popular and can be found at any quick serve restaurants. Fat content of French fries available at quick service restaurants is in the range of 12.5–15.5% wet basis (USDA, 2014b). Because of health issues, consumers are becoming more interested in the nutritional value of the fast food products, according to 87% of fast food operators (NRA, 2014). Lowering fat intake has been advised as it decreases cardiovascular risk in short-term, although long term effects were not known (Rees et al., 2013). Furthermore, lowering energy intake by fat reduction was found to be associated with lower body weight (Hooper et al., 2012).

In recent years, reduction of fat content of the French fries has attracted interest from consumer and food industry. French fries are produced by deep-fat frying in which potatoes gain all of the oil. Efforts to reduce fat content of the French fries have been redirected

at modifying raw material or the cooking process. Modification of the raw material for production of reduced-fat French fries has been accomplished using enzymes or outer parts of potatoes (Lisińska, Tajner-Czopek, & Kalum, 2007; Rommens, Shaky, Heap, & Fessenden, 2010). Unit operations in French fry production has also been modified to reduce fat absorption by improving blanching, pre-drying, or par-frying (Aguilar, Anzaldúa-Morales, Talamás, & Gastélum, 1997; Ahmad Tarmizi & Niranjana, 2013; van Loon et al., 2007; Tajner-Czopek, Figiel, & Carbonell-Barrachina, 2008).

Infrared (IR) heating was utilized as a dry blanching treatment of potatoes to reduce fat absorption during frying (Bingol, Zhang, Pan, & McHugh, 2012). Lloyd, Farkas, and Keener (2004) and Kirmaci, Singh, and Shewfelt (2015) investigated to replace final frying with infrared heating. While the former used quartz halogen radiant emitters, the latter used a Radiant Wall Oven (RWO). When IR electromagnetic waves hit the surface of the product, the incident radiation is absorbed, reflected and transmitted. Absorbed electromagnetic waves cause change in molecular vibrational state leading to radiative heating (Decareau, 1985). Heat transfer occurs mainly through radiation in RWO. A RWO contains a perforated conveyor belt surrounded by stainless alloy elliptical tube which is heated by natural gas combustion. The heated tube emits IR to the product.

\* Corresponding author.

E-mail address: [bkirmaci@uga.edu](mailto:bkirmaci@uga.edu) (B. Kirmaci).

Color, texture, oily mouth feel were the most important quality attributes of French fries, besides the oil content (Weaver, Reeve, & Kueneman, 1975). The light golden-brown color of French fries is a result of the reaction between reducing sugars and free amino acids during frying, known as Maillard reaction (Márquez & Anón, 1986). When not limited by lowering reducing sugar content of the raw potato, this reaction will cause excessive darkening, off-flavor and acrylamide formation (Lisińska, 1989; Rommens et al., 2010; Sahin, 2000). Texture of the French fries can be described as a mealy-like baked potato core wrapped with a porous, crisp and oily crust (Miranda & Aguilera, 2006; Pedreschi, 2009; Weaver et al., 1975).

Consumer acceptability/preference, or any affective analysis, cannot be inferred from either descriptive sensory analysis or instrumental analysis. Thus, a thorough quality analysis of a specific product requires affective consumer evaluation, in addition to the instrumental analysis. A nine-point hedonic scale has been widely used to determine the consumer acceptability (Barrett, Beaulieu, & Shewfelt, 2010). Using a three-point acceptability scale was also suggested to determine the consumer acceptability by reporting the frequency of the each response (Shewfelt, 1999).

In the previous study, RWO was used to bake potato strips at 365 °C for 6.5 min to have similar quality attributes with deep-fat fried ones (Kirmaci et al., 2015). A doubling of preparation time for French fries when compared with deep-fat frying could reduce profitability for the restaurants and cause inconvenience to the consumer. To shorten the processing time, RWO can be operated at higher temperature using precooked potato strips rather than frozen ones. We envision that a combination of steam and RWO processing improves the previously suggested new technique to bake potato strips while reducing the total processing time.

The objectives of this study were (i) to investigate the quality characteristics of RWO processed pre-cooked potato strips by both instrumental and sensory analysis in comparison with deep-fat fried counterparts, and, (ii) to determine consumer acceptability of the selected RWO processed pre-cooked potato strips based on instrumental and sensory analysis.

## 2. Materials and methods

### 2.1. Sample preparation

Total number of 127 packages of 0.9 kg par-fried frozen potato strips (Great Value - Regular Cut French Fries, Walmart Inc., Ben-

tonville, AR) were purchased from a local supermarket and stored in a walk-in freezer at -40 °C. For each treatment, 81 strips were sorted from the packages to have 1 cm × 1 cm cross-section, and cut to have 5 cm in length. Then, strips were placed in a zippered, plastic bag and stored overnight in a freezer at -20 °C in order to be processed. Moisture and fat contents of the frozen par-fried potato strips was 73.56 ± 0.32 g/100 g and 11.47 ± 0.28 g fat/100 g dry

### 2.2. Experimental design

Frozen potato strips were partially cooked in a steam chamber (Pyramid Food Processing Equipment Manufacturing Inc., Tewksbury, MA) for 75 or 90 s. The final steam chamber temperature was 99.4 ± 0.3 °C. After steaming, pre-cooked potato strips were transferred immediately to the radiant wall oven (Pyramid Food Processing Equipment Manufacturing Inc., RWO-12-36, Tewksbury, MA) and placed on a disposable aluminum foil sheet. Steam processed potato strips were heated in RWO at six different time-temperature combinations based on preliminary experiment (Table 1). To keep the processing times close to that used in deep-fat frying, the pre-cooked potato strips were processed in the RWO processing at high temperatures. As a control treatment, par-fried frozen potato strips were fried in 5 L peanut oil at 177 °C for 3 min using a deep-fat fryer (GE Model 168997, General Electric Company, Fairfield, CT). Fried potato strips were drained on a paper towel. Oil of the fryer was replaced after each 10 h of usage. Each treatment was conducted in triplicate.

Wall temperature of the RWO and oil temperature of the deep-fat fryer were monitored by Type K (XCIB-K-4-6, Omega Engineering Inc., Stamford, CT). Heating in steam chamber was also monitored by Type T thermocouples.

### 2.3. Yield

The moisture gain or loss during steam cooking and RWO processing was determined gravimetrically. Weight of the 9 frozen par-fried potato strips, steam cooked potato strips and RWO processed and deep-fat fried potato strips were measured by analytical balance in triplicate. Then, yield after steam processing and RWO baking was calculated by Equations (1) and (2), respectively:

$$Yield_{steam} = 100 - \frac{\text{Weight of frozen samples} - \text{Weight of steamed samples}}{\text{Weight of frozen samples}} \times 100 \quad (1)$$

$$Yield_{RWO} = 100 - \frac{\text{Weight of frozen samples} - \text{Weight of RWO baked samples}}{\text{Weight of frozen samples}} \times 100 \quad (2)$$

tonville, AR) were purchased from a local supermarket and stored in a walk-in freezer at -40 °C. For each treatment, 81 strips were sorted from the packages to have 1 cm × 1 cm cross-section, and cut to have 5 cm in length. Then, strips were placed in a zippered, plastic bag and stored overnight in a freezer at -20 °C in order to be processed. Moisture and fat contents of the frozen par-fried potato strips was 73.56 ± 0.32 g/100 g and 11.47 ± 0.28 g fat/100 g dry

for steam cooking and steam-RWO baked/deep-fat fried samples, respectively.

### 2.4. Shrinkage

Width and thickness of the middle of the potato strips before

and after RWO processing or deep-fat frying were measured by a caliper. Shrinkage was then calculated by percent change in total area of nine strips before and after processing, as shown in Equation (3):

$$\% \text{ Shrinkage} = \frac{\text{Total Area of frozen samples} - \text{Total Area of RWO baked samples}}{\text{Total Area of frozen samples}} \times 100 \quad (3)$$

## 2.5. Moisture and fat content

Moisture content of the frozen, steam-RWO baked and deep-fat fried potato strips was determined gravimetrically by vacuum oven method (AOAC, 1995). Baked/fried potato strips were submerged into liquid nitrogen for 20 s and stored at  $-20\text{ }^{\circ}\text{C}$  in a freezer until analysis. After homogenization under liquid nitrogen, 2–3 g samples were placed into pre-dried thimbles. Vacuum oven (Cole–Parmer Instrument Co., Vernon Hills, IL) at below 61 kPa at  $70\text{ }^{\circ}\text{C}$  for 24 h was used to dry the samples. Total fat content was determined by Soxhlet (AOAC, 1995) using petroleum ether.

## 2.6. Instrumental texture – cutting test

Cutting force of the steam-RWO baked and deep-fat fried potato strips were determined using Texture Analyzer (TA.XT2i, Stable Micro Systems Ltd., Hamilton, MA) with a 5 kg load cell. Cross arm with chisel knife blade ( $45^{\circ}$ ) attachment halved the five potato strips that were placed adjacent to each other on a slotted base. Thickness and width of the potato samples were determined by a caliper. The peak force (N) normalized by sum of the cross sectional area ( $\text{cm}^2$ ) of the five potato strips was reported as the cutting force ( $\text{N}/\text{cm}^2$ ) of the samples. The equipment was calibrated prior to the analysis. Pre-test and test speed were set at 1.5 mm/s and 2 mm/s, respectively. The experiment was repeated nine times for each treatment.

**Table 1**  
Experimental design of pre-cooking and RWO processing of potato strips.<sup>a</sup>

Treatment #	Steam processing <sup>b</sup>	RWO processing	
	Time (s)	Set point temperature <sup>c</sup> ( $^{\circ}\text{C}$ )	Time <sup>d</sup> (min)
1	75	450	3
2	90	450	3
3	75	450	3.5
4	90	450	3.5
5	75	500	2.5
6	90	500	2.5
7	75	500	3
8	90	500	3
9	75	550	1.5
10	90	550	1.5
11	75	550	2
12	90	550	2

<sup>a</sup> Potato strips were fried in a deep-fat fryer at  $177.6 \pm 1.7\text{ }^{\circ}\text{C}$  for 3 min as a control treatment.

<sup>b</sup> Steam chamber temperature increased above  $99.0 \pm 0.3\text{ }^{\circ}\text{C}$  in 23 s, and stayed at  $99.4 \pm 0.3\text{ }^{\circ}\text{C}$ .

<sup>c</sup> Mean wall temperature was  $452 \pm 3$ ,  $501 \pm 3$  and  $550 \pm 2\text{ }^{\circ}\text{C}$  for the set point temperatures of 450, 500 and  $550\text{ }^{\circ}\text{C}$ , respectively.

<sup>d</sup> Mean processing time was  $1.54 \pm 0.02$ ,  $2.07 \pm 0.01$ ,  $2.55 \pm 0.02$ ,  $3.05 \pm 0.02$  and  $3.59 \pm 0.05$  min when the belt speed was set for the processing time of 1.5, 2, 2.5, 3 and 3.5 min, respectively.

## 2.7. Instrumental texture – puncture force

Texture Analyzer (TA.XT2i, Stable Micro Systems Ltd., Hamilton, MA) was used to evaluate surface of the middle part of the potato

strip by inserting a 3 mm puncture probe. A 5 kg load cell was used to measure the maximum force (N) required to penetrate the probe into the samples for 6 mm. Pre-test and test speed was same as cutting test, and Texture Analyzer was calibrated before conducting the test. Nine potato strips were tested for each treatment and analysis was replicated three times.

## 2.8. Color

Color of the steam-RWO baked and deep-fat fried potato strips were quantified by CIE color space using a colorimeter (Model# CR-410, Konica Minolta Sensing Inc., Ramsey, NJ). Lightness (L), chroma, and hue angle were determined. Colorimeter was calibrated with a white standard prior to the analysis. Surface color in contact with the belt, and the opposing surface of the baked samples was measured and their average was reported. Color of the two opposing surfaces was measured for the deep-fat fried samples. The experiment was repeated nine times for each treatment.

## 2.9. Sensory analysis

White fluorescent lighting was used throughout the evaluation sessions and positive air flow at the sensory booths prevented any aroma circulation from the sample preparation area. Three potato strips from each treatment were placed into a 3-random digit coded paperboard food tray, and then served to the panelists immediately. Panelists were given water at room temperature and unsalted top saltine crackers and asked to cleanse their palate between samples. At the end of evaluations, panelists were given a bite-size food reward.

### 2.9.1. Trained panel

After statistically analyzing the instrumental analysis data, two RWO treatments that produced the most similar product with deep-fat fried potato strips were selected. The panel, consisting of 11 members, recruited from the individuals who like to eat French fries. The panelists were familiarized with the typical color and texture of the French fries at one of the quick serve restaurant in Athens, GA before the evaluations. The panelists evaluated one RWO processed pre-cooked potato strip and control samples in pre-determined randomized order in each evaluation session. Each RWO treatment was evaluated in duplicate.

Panelists used the unstructured 150 mm modified just about right (JAR) scale to evaluate the color and texture of the samples (Fig. 1). After evaluation, a ruler was used to convert responses to the numbers, and least square mean scores were reported with standard error.

### 2.9.2. Consumer acceptability

Consumer acceptability and willingness to purchase of the best RWO treatment, determined by trained panel, and control treatment were evaluated by 41-member consumer panel over a two-day period, as described by Kirmaci et al. (2015). Three point

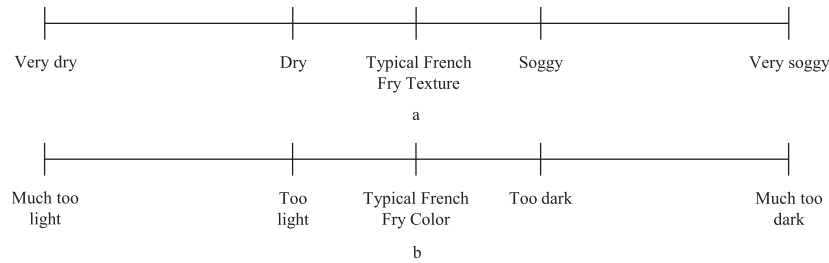


Fig. 1. Unstructured 150 mm modified just-about-right scale for the evaluation of texture (a) and color (b) of baked/fried potato strips.

acceptability scale (superior, acceptable and unacceptable) and 5-point scale (definitely would buy, probably would buy, might or might not buy, probably would not buy, and definitely would not buy) were used for each samples.

Upon completion of evaluation, fat content and corresponding calorie of the samples were revealed to the panelists. Then, each panelist was asked about the acceptability of the steam-RWO baked samples again. Consumer acceptability of samples was calculated, before and after nutritional information was revealed, as the total frequency of “superior” and “acceptable”. Willingness to purchase of samples was reported as the total frequency of “definitely would buy” and “probably would buy”.

### 2.10. Statistical analysis

Experiments were conducted in a randomized order. Time-temperature combinations were randomized, and then steam processing condition (75 or 90 s) was randomized within each combination. Data were analyzed by One-way analysis of variance (ANOVA) using SAS (9.3, SAS Institute Inc., Cary, NC). Least square means (LS-means) of the steam-RWO baked samples were compared to that of control sample by Dunnett’s test at 95% confidence level. Sensory analysis data from trained panel was analyzed using PROC MIXED procedure, since each treatment had its own variation. Sensory analysis data from consumer panel was analyzed using Microsoft Office Excel 2007 (Microsoft Corp., Redmond, WA).

## 3. Results and discussion

### 3.1. Steam and RWO processing

Temperature at the center of the potato strips after steam processing for 75 and 90 s was significantly different, and the center temperatures were  $66.8 \pm 2.7$  °C and  $77.2 \pm 1.9$  °C, respectively ( $p < 0.05$ ). Gelatinization of potato starch starts at  $61.1$ – $61.6$  °C and peaks at  $65.9$  °C (Ratnayake & Jackson, 2008; Shiotsubo, 1984). End gelatinization temperature of potato starch was reported as  $79$ – $79.4$  °C (Belitz, Grosch, & Schieberle, 2009; Ratnayake & Jackson, 2008). Ratnayake and Jackson (2008) stated that degree of gelatinization was 36% and 55% at 65 °C and 75 °C, respectively. When the effect of two steam processing treatments was analyzed by comparing the quality characteristics of the final products, the only significant difference between two treatments was the moisture content ( $p < 0.05$ ). Baked potato strips that were steamed for 90 s had higher moisture content than baked potato strips that were steamed for 75 s (data not shown). However, there were no significant differences between two treatments in terms of cutting force, puncture force, lightness, chroma, hue angle, shrinkage, yield and fat content.

Proposed total processing times (2.75–5 min) were shorter than suggested 6.5 min processing time by Kirmaci et al. (2015).

Integration of steam processing to RWO processing reduced the processing times by 22–57%. Since potato strips were already pre-cooked, RWO was operated at higher temperatures than 365 °C, used in the previous study (Kirmaci et al., 2015). As temperature increased in RWO, wavelength of the infrared electromagnetic waves decreased according to Wien’s displacement law. Therefore, RWO processing improved the color and texture of the potato strips by removal of the moisture from the surface due to low penetration depth of IR. The corresponding wavelengths of IR energy were 4, 3.74 and 3.52  $\mu\text{m}$  for the operating temperatures of 450, 500 and 550 °C, respectively. Thus, IR heating occurred at far-infrared region (FIR).

Mean wall temperatures were measured as  $452 \pm 3$ ,  $501 \pm 3$  and  $550 \pm 2$  °C for the set point temperatures of 450, 500 and 550 °C, respectively. Variation in the motor power controlling the RWO belt speed caused deviation in the processing time in the range of 0.01–0.05 min (Table 1). Potato strips in contact with the belt showed marks in the preliminary experiments. Hence, aluminum foil sheet was used to prevent those marks. At the end of baking, potato strips were transferred to a food warmer.

### 3.2. Yield

Steam processing increased the yield, as steam condensed on the potato strips during the process. However, there was no significant difference in the yield of steam processed potato strips for 75 and 90 s. The yield of the steamed potato strips was  $119.2 \pm 1.48\%$  and  $118.1 \pm 1.1\%$  for 75 and 90 s steam processing, respectively.

Deep-fat frying, in which moisture is lost by evaporation and fat is absorbed, resulted in  $74.21 \pm 1.21\%$  yield. Only yield of treatment #7 and #8 was not significantly different from that of control treatment (Table 2). All the other treatments had significantly higher yield than control treatment ( $p < 0.01$ ). Even though samples gained weight during steam processing, RWO processing caused baked samples to have less weight than their original weight.

### 3.3. Shrinkage

Shrinkage in deep fat fried and RWO processed pre-cooked potato strips was in the range of 12.6–16.3% (Table 2). However, the effect of both methods was not significantly different than each other. Kirmaci et al. (2015) reported that when only RWO used to bake the potato strips at 365 °C for 6.5 min, it caused significantly more shrinkage than deep-fat frying. In the current study, yield showed that potato strips gained 18–19% weight during steam processing. That added moisture and the moisture found in the raw material was removed during RWO processing. That might be the reason for the difference between two studies in terms of shrinkage. Taiwo and Baik (2007) investigated the effect of frying on the shrinkage of sweet potato discs. They reported that

**Table 2**

Yield, shrinkage, moisture and fat content of the RWO baked and deep-fat fried potato strips.

Treatment #	Yield <sup>1</sup> (%)	Shrinkage <sup>1</sup> (%)	Moisture content <sup>2</sup> (% wet basis)	Fat content <sup>2</sup> (% dry basis)
1	87.66 <sup>a</sup>	15.1 <sup>a</sup>	72.41 <sup>ab</sup>	3.97 <sup>bc</sup>
2	84.81 <sup>a</sup>	16.3 <sup>a</sup>	72.01 <sup>ac</sup>	4.81 <sup>bc</sup>
3	80.59 <sup>a</sup>	13.7 <sup>a</sup>	68.46 <sup>ac</sup>	5.45 <sup>bc</sup>
4	81.6 <sup>a</sup>	13.9 <sup>a</sup>	70.83 <sup>ac</sup>	5.89 <sup>bc</sup>
5	85.07 <sup>a</sup>	15.6 <sup>a</sup>	70.99 <sup>ac</sup>	5.88 <sup>bc</sup>
6	85.1 <sup>a</sup>	16.2 <sup>a</sup>	72.62 <sup>ab</sup>	4.83 <sup>bc</sup>
7	78.17 <sup>b</sup>	12.6 <sup>a</sup>	68.5 <sup>ac</sup>	5.22 <sup>bc</sup>
8	79.26 <sup>b</sup>	13.8 <sup>a</sup>	69.43 <sup>ac</sup>	4.93 <sup>bc</sup>
9	92.78 <sup>a</sup>	13.6 <sup>a</sup>	74.53 <sup>ab</sup>	5.15 <sup>bc</sup>
10	93.8 <sup>a</sup>	12.8 <sup>a</sup>	75.07 <sup>aA</sup>	4.66 <sup>bc</sup>
11	84.61 <sup>a</sup>	15.0 <sup>a</sup>	70.17 <sup>ac</sup>	4.88 <sup>bc</sup>
12	84.57 <sup>a</sup>	15.3 <sup>a</sup>	70.93 <sup>ac</sup>	4.05 <sup>bc</sup>
Control <sup>3</sup>	74.21 <sup>b</sup>	12.7 <sup>a</sup>	55.60 <sup>bc</sup>	39.53 <sup>aA</sup>
Raw material <sup>4</sup>	n/a <sup>5</sup>	n/a	73.56 <sup>ab</sup>	11.47 <sup>bb</sup>
Standard error	1.2	1.7	0.32	0.28

<sup>1</sup>: n = 3.<sup>2</sup>: n = 6.<sup>3</sup>: Deep-fat frying of potato strips at 177 °C for 3 min.<sup>4</sup>: Frozen par-fried potato strips.<sup>5</sup>: not applicable.ab: Least square means followed by same letters within same column show not significant difference with control treatment ( $p > 0.05$ ).ABC: Least square means followed by same letters within same column show not significant difference with raw material ( $p > 0.05$ ).

shrinkage in diameter of the fried sweet potato discs was in the range of 6.7–10.2%. Furthermore, the thickness of the samples was lowered by 18.3% (Taiwo & Baik, 2007).

### 3.4. Moisture and fat content

Moisture and fat content of the steam-RWO baked pre-cooked potato strips are given in Table 2. The moisture content of the treatment #10 was significantly higher than that of frozen par-fried potato strips ( $p < 0.05$ ). There was no significant difference in the moisture content of frozen par-fried potato strips and steam-RWO baked potato strips according to treatments #1, #6, and #9. The rest of the treatments #2, #3, #4, #5, #7, #8, #11, #12, and control caused potato strips to have significantly lower moisture content than that in frozen par-fried potato strips ( $p < 0.05$ ). Moisture content of the all RWO processed pre-cooked potato strips was significantly higher than that of deep-fat fried samples ( $p < 0.0001$ ).

Deep-fat fried samples had the highest fat content among all treatments. All the steam-RWO baked pre-cooked potato strips had significantly lower fat content than both deep-fat fried and frozen par-fried strips ( $p < 0.0001$ ). RWO processing of potato strips after steam processing resulted in 85.1–90% reduction of fat content as compared to deep-fat fried samples. Moreover, fat content of the steam processed steam-RWO baked potato strips was  $7.56 \pm 0.6$  g fat per 100 g dry solids, lower than the reported fat content of strips processed in only RWO at 365 °C for 6.5 min (Kirmaci et al., 2015). It was observed that some oil was released on the aluminum foil after potato strips were transferred to the RWO. Condensed moisture from steam processing was also removed during RWO processing. Higher fat reduction might also be due to extra moisture removal from the product as steam distillation is one of the methods to extract oils (Ahmad Tarmizi & Niranjana, 2013; Charles & Simon, 1990).

### 3.5. Texture

Cutting and puncture force of the baked/fried potato strips are given in Table 3. Cutting force of the potato strips, that was RWO processed at 500 °C for 3 min (treatment #7 & #8), was not significantly different than that of control treatments. It is important to note that, besides cutting force, yield of these treatments was not significantly different than yield of deep-fat frying. Even

though moisture content of the samples baked by RWO treatments #7 and #8 were significantly higher than control, cutting force of the potato strips was not significantly different. Treatments with a significantly higher yield than the control (treatments # 1–6 and # 9–12), had significantly less cutting force than that of control treatment ( $p < 0.01$ ). The moisture removal from those treatments was insufficient and caused potato strips to have softer texture.

The surface puncture force did not show any significant difference between RWO treated samples and control. The variation in the texture data of potato strips or French fries was associated with the non-uniform distribution of starch and other compounds in the potato tuber (Miranda & Aguilera, 2006). Puncture and fracture/cutting tests are the most common means of evaluating texture of French fries (Bingol et al., 2012; Lloyd et al., 2004; van Loon et al., 2007; Miranda & Aguilera, 2006; Walter Jr et al., 2002). Walter Jr et al. (2002) stated that Kramer Shear test of restructured sweet potato French fries had the lowest coefficient of variation when compared to puncture and three-point bending test. Kirmaci et al. (2015) used a 3 mm puncture probe to evaluate the surface of the steam-RWO baked potato strips, and were able to distinguish the treatments statistically. However, puncture force test with the same equipment and the same settings did not detect any textural difference between samples.

### 3.6. Color

Lightness, chroma and hue angle of RWO processed pre-cooked potato strips are given in Table 3. Lightness and hue angle of the all RWO processed pre-cooked potato strips were significantly higher than that of deep-fat fried counterparts ( $p < 0.001$ ). Whereas, chroma of the baked/fried potato strips was in the range of 35.3–37.64, and there is no significant difference in the chroma of the all RWO processed pre-cooked and deep-fat fried samples. These results are in agreement with those of Kirmaci et al. (2015) for RWO baked potato strips at 365 °C for 6.5 min. The data suggest that modification of RWO processing by addition of steam processing did not improve the product in terms of color. It should be noted that some parts of the steam-RWO baked potato strips were darker.

Results of instrumental analysis revealed that treatments #7 and #8 were most similar in quality attributes to deep-fat fried counterparts. Texture, chroma, shrinkage and yield of these

**Table 3**  
Texture and color of the RWO baked and deep-fat fried potato strips.

Treatment	Texture		Color <sup>3</sup>		
	Cutting force <sup>1</sup> (N/cm <sup>2</sup> )	Puncture force <sup>2</sup> (N)	Lightness	Chroma	Hue (°)
1	3.37 <sup>b</sup>	1.33 <sup>a</sup>	73.14 <sup>a</sup>	36.23 <sup>a</sup>	89.49 <sup>a</sup>
2	3.78 <sup>b</sup>	1.32 <sup>a</sup>	74.0 <sup>a</sup>	37.31 <sup>a</sup>	89.42 <sup>a</sup>
3	4.47 <sup>b</sup>	1.66 <sup>a</sup>	73.98 <sup>a</sup>	37.01 <sup>a</sup>	88.42 <sup>a</sup>
4	4.36 <sup>b</sup>	1.44 <sup>a</sup>	73.49 <sup>a</sup>	37.64 <sup>a</sup>	88.26 <sup>a</sup>
5	3.56 <sup>b</sup>	1.29 <sup>a</sup>	72.2 <sup>a</sup>	37.42 <sup>a</sup>	88.1 <sup>a</sup>
6	3.82 <sup>b</sup>	1.44 <sup>a</sup>	72.23 <sup>a</sup>	35.91 <sup>a</sup>	88.37 <sup>a</sup>
7	5.35 <sup>a</sup>	1.61 <sup>a</sup>	71.89 <sup>a</sup>	37.0 <sup>a</sup>	86.75 <sup>a</sup>
8	5.34 <sup>a</sup>	1.88 <sup>a</sup>	72.34 <sup>a</sup>	37.05 <sup>a</sup>	87.15 <sup>a</sup>
9	2.90 <sup>b</sup>	1.29 <sup>a</sup>	72.22 <sup>a</sup>	35.58 <sup>a</sup>	89.84 <sup>a</sup>
10	2.93 <sup>b</sup>	1.45 <sup>a</sup>	73.23 <sup>a</sup>	35.3 <sup>a</sup>	90.33 <sup>a</sup>
11	4.25 <sup>b</sup>	1.70 <sup>a</sup>	71.94 <sup>a</sup>	36.87 <sup>a</sup>	88.03 <sup>a</sup>
12	4.31 <sup>b</sup>	1.50 <sup>a</sup>	71.36 <sup>a</sup>	36.15 <sup>a</sup>	87.93 <sup>a</sup>
Control <sup>4</sup>	5.8 <sup>a</sup>	1.38 <sup>a</sup>	69.17 <sup>b</sup>	36.6 <sup>a</sup>	84.53 <sup>b</sup>
Standard error	0.24	0.15	0.35	0.35	0.24

<sup>1</sup>: Required cutting force normalized by the cross-sectional area to cut the five baked/fried potato strips (n = 9).

<sup>2</sup>: Required peak force to penetrate 3 mm diameter puncture probe into the baked/fried potato strips for 6 mm (n = 3).

<sup>3</sup>: n = 18.

<sup>4</sup>: Deep-fat frying of potato strips at 177 °C for 3 min.

<sup>ab</sup>: Least square means followed by same letters within same column show not significant difference with control treatment (p > 0.05).

samples were not significantly different than those of fried samples. Therefore, potato strips, RWO processed at 500 °C for 3 min after steam processing for 75 or 90 s, were chosen to be evaluated by a trained panel. As only chroma of the all RWO processed pre-cooked potato strips were not significantly different than that of control samples, color was not taken into account when selecting the treatments leading to the most similar quality of fried French fries. It is important to note that treatments #7 and #8 resulted in 87% and 88% fat reduction with respect to deep-fat frying. Moreover, processing time of the treatments #7 and #8 was shorter by 34% and 30% than that of previous research in which potato strips were processed in RWO for 6.5 min, respectively (Kirmaci et al., 2015).

### 3.7. Sensory analysis

Control and treatments #7 and #8, were evaluated by trained panel to determine the treatment that resulted in most similar product to deep-fat fried samples.

#### 3.7.1. Sensory descriptive analysis

Color of the potato strips from treatment #7, #8 and control was determined as  $64.9 \pm 3.0$ ,  $69.6 \pm 3.0$  and  $77.7 \pm 1.7$ , respectively, where 75.0 was labeled as “typical French fry color” and 50.0 was labeled as “too light” as shown in Fig. 1. Results of trained panel data showed that color of the RWO processed pre-cooked potato strips from treatment #7 and #8 were significantly lighter than that of control treatment as seen in the instrumental color analysis (p < 0.05).

Texture of the potato strips from treatment #7, #8 and control were determined as  $88.6 \pm 4.3$ ,  $86.8 \pm 6.5$ ,  $76.2 \pm 2.1$ , respectively, where 75.0 labeled as “typical French fry texture” and 100.0 labeled as “soggy” as shown in Fig. 1. The panel determined that the RWO processed potato strips at 500 °C for 3 min after steam processing for 75 s were soggy than the control samples (p < 0.05). However, it found no significant difference between potato strips that were RWO processed after steam processing for 90 s (treatment #8) and deep-fat fried in terms of texture. Therefore, potato strips that had 87.5% less fat than the control samples (treatment #8) were chosen to be evaluated by consumer panel.

#### 3.7.2. Consumer acceptability

The results indicated consumer acceptability of 51.2% for RWO baked potato strips at 500 °C for 3 min after steam processing for 90 s and 100% for the control samples. Results of consumer acceptability suggest that the modification of RWO processing by addition of steam processing did not improve the product. Furthermore, when only RWO was used to bake potato strips at 365 °C for 6.5 min, consumer acceptability of those samples was 65.7% (Kirmaci et al., 2015). Panelists were also asked about acceptability of the RWO processed pre-cooked samples again after the nutritional information of the samples were shared with them. Half of the panelists, who rated the product as unacceptable, prioritized the reduced-fat content, acceptability of the RWO processed pre-cooked potato strips, thus, increased to 75.6%. A similar result of consumers lowering their expectation of a product as a trade for reduced-fat product was observed previously (Kirmaci et al., 2015).

Willingness to purchase of the RWO processed pre-cooked potato strips and control samples were 35% and 82.5%, respectively. Willingness to purchase of RWO processed pre-cooked potato strips was very close to the that of RWO baked potato strips at 365 °C for 6.5 min (Kirmaci et al., 2015). Consumer panel showed that integration of steam processing to RWO processing for baking potato strips did not meet their expectation.

## 4. Conclusions

RWO baking of steam processed potato strips resulted in fat reduction drastically when compared to deep-fat frying. However, total processing time decreased by 30% as compared to that in previous research (Kirmaci et al., 2015). RWO processing at 500 °C for 3 min after steam processing for 75/90 s produced the best quality potato strips in terms of texture, chroma, shrinkage and yield. However, trained panel perceived the texture of 75 s steam processed and RWO baked potato strips at 500 °C for 3 min soggy than the control. Consumer acceptability of potato strips, that were RWO processed at 500 °C for 3 min after steam processing for 90 s, was 51.2% and 75.6% before and after revealing the nutritional information of the treatment and control samples, respectively. In contrast to rise in the consumer acceptability due to reduced-fat contents, low willingness to purchase showed that further research is needed to improve the quality of the steam-RWO baked

potato strips. The integration of steam and RWO processing to bake potato strips reduced cooking time but did not improve the product quality. Steam processing might be replaced by superheated steam processing, as the latter will not condense on the potato strips.

## Acknowledgments

The authors would like to thank Dr. Robert L. Shewfelt for helping to plan and organize the sensory analysis, and, Dr. Chi-Ching Lee and Mr. Carl Ruiz for their assistance conducting the sensory panel.

## References

- Aguilar, C. N., Anzaldúa-Morales, A., Talamás, R., & Gastélum, G. (1997). Low-temperature blanch improves textural quality of French-fries. *Journal of Food Science*, 62(3), 568–571.
- Ahmad Tarmizi, A., & Niranjana, K. (2013). Post-frying oil drainage from potato chips and French fries: a comparative study of atmospheric and vacuum drainage. *Food and Bioprocess Technology*, 6(2), 489–497.
- AOAC. (1995). *Official methods of analysis* (16th ed.). Gaithersburg: Association of Official Analytical Chemists International.
- Barrett, D. M., Beaulieu, J. C., & Shewfelt, R. L. (2010). Color, flavor, texture, and nutritional quality of fresh-cut fruits and vegetables: desirable levels, instrumental and sensory measurement, and the effects of processing. *Critical Reviews in Food Science and Nutrition*, 50(5), 369–389.
- Belitz, H., Grosch, W., & Schieberle, P. (2009). *Food chemistry*. Berlin: Springer-Verlag.
- Bingol, G., Zhang, A., Pan, Z., & McHugh, T. H. (2012). Producing lower-calorie deep fat fried French fries using infrared dry-blanching as pretreatment. *Food Chemistry*, 132(2), 686–692.
- Charles, D. J., & Simon, J. E. (1990). Comparison of extraction methods for the rapid determination of essential oil content and composition of basil. *Journal of the American Society for Horticultural Science*, 115(3), 458–462.
- Decareau, R. V. (1985). *Microwaves in the food processing industry*. Orlando, FL: Academic Press.
- Hooper, L., Abdelhamid, A., Moore, H. J., Douthwaite, W., Skeaff, C. M., & Summerbell, C. D. (2012). Effect of reducing total fat intake on body weight: systematic review and meta-analysis of randomised controlled trials and cohort studies. *BMJ: British Medical Journal*, 345.
- Kirmaci, B., Singh, R. K., & Shewfelt, R. L. (2015). Consumer acceptability and quality evaluation of potato strips baked in a radiant wall oven. *International Journal of Food Properties*, 18(8), 1829–1836.
- Lisińska, G. (1989). Manufacture of potato chips and French fries. In G. Lisińska, & W. Leszczynski (Eds.), *Potato science and technology*. London: Elsevier Science Publishers Ltd.
- Lisińska, G., Tajner-Czopek, A., & Kalum, L. (2007). The effects of enzymes on fat content and texture of French fries. *Food Chemistry*, 102(4), 1055–1060.
- Lloyd, B. J., Farkas, B. E., & Keener, K. M. (2004). Quality comparison of French fry style potatoes produced by oven heating, immersion frying and controlled dynamic radiant heating. *Journal of Food Processing & Preservation*, 28(6), 460–472.
- van Loon, W. A. M., Visser, J. E., Linssen, J. H., Somsen, D. J., Klok, H. J., & Voragen, A. G. J. (2007). Effect of pre-drying and par-frying conditions on the crispness of French fries. *European Food Research and Technology*, 225(5–6), 929–935.
- Márquez, G., & Anón, M. C. (1986). Influence of reducing sugars and amino acids in the color development of fried potatoes. *Journal of Food Science*, 51(1), 157–160.
- Miranda, M. L., & Aguilera, J. M. (2006). Structure and texture properties of fried potato products. *Food Reviews International*, 22(2), 173–201.
- NRA. (2014). *National Restaurant Association: 2014 Restaurant industry forecast*. Available at: <http://www.restaurant.org/News-Research/Research/Forecast-2014> Accessed 21.09.14.
- Pedreschi, F. (2009). Fried and dehydrated potato products. In J. Singh, & L. Kaur (Eds.), *Advances in potato chemistry and technology* (pp. 319–337). San Diego: Academic Press.
- Ratnayake, W. S., & Jackson, D. S. (2008). Chapter 5 starch gelatinization. In L. T. Steve (Ed.), *Advances in food and nutrition research* (pp. 221–268). Academic Press.
- Rees, K., Dyakova, M., Wilson, N., Ward, K., Thorogood, M., & Brunner, E. (2013). Dietary advice for reducing cardiovascular risk. *Cochrane Database Systematic Reviews*, 3.
- Rommens, C. M., Shakya, R., Heap, M., & Fessenden, K. (2010). Tastier and healthier alternatives to French fries. *Journal of Food Science*, 75(4), H109–H115.
- Sahin, S. (2000). Effects of frying parameters on the colour development of fried potatoes. *European Food Research and Technology*, 211(3), 165–168.
- Shewfelt, R. L. (1999). What is quality? *Postharvest Biology and Technology*, 15(3), 197–200.
- Shiotsubo, T. (1984). Gelatinization temperature of potato starch at the equilibrium state. *Agricultural and Biological Chemistry*, 48(1), 1–7.
- Taiwo, K. A., & Baik, O. D. (2007). Effects of pre-treatments on the shrinkage and textural properties of fried sweet potatoes. *LWT – Food Science and Technology*, 40(4), 661–668.
- Tajner-Czopek, A., Figiel, A., & Carbonell-Barrachina, Á. A. (2008). Effects of potato strip size and pre-drying method on french fries quality. *European Food Research & Technology*, 227(3), 757–766.
- USDA. (2014a). *United States Department of Agriculture Economic Research Service: Yearbook tables. Production, trade, stocks, and price for potatoes*. Available at: [http://www.ers.usda.gov/datafiles/Vegetable\\_and\\_Pulses\\_Yearbook\\_Tables/Potatoes/YRBK2014\\_Section%207\\_Potato\\_FMT.xlsx](http://www.ers.usda.gov/datafiles/Vegetable_and_Pulses_Yearbook_Tables/Potatoes/YRBK2014_Section%207_Potato_FMT.xlsx) Accessed 18.09.14.
- USDA. (2014b). *United States Department of Agriculture Agriculture Research Service: National nutrient database for standard reference national agriculture library*. Available at: <http://ndb.nal.usda.gov/ndb/> Accessed 20.09.14.
- Walter, W. M., Jr., Truong, V. D., & Espinel, K. R. (2002). Textural measurements and product quality of restructured sweetpotato French fries. *LWT – Food Science and Technology*, 35(3), 209–215.
- Weaver, M. L., Reeve, R. M., & Kueneman, R. W. (1975). Frozen French fries and other frozen potato products. In W. F. Talburt, & O. Smith (Eds.), *Potato processing*. Westport, CT: The AVI Publishing Company.



## Characterization of kefir-like beverages produced from vegetable juices



Onofrio Corona <sup>a</sup>, Walter Randazzo <sup>a</sup>, Alessandro Miceli <sup>a</sup>, Rosa Guarcello <sup>a</sup>, Nicola Francesca <sup>a</sup>, Hüseyin Erten <sup>b</sup>, Giancarlo Moschetti <sup>a</sup>, Luca Settanni <sup>a,\*</sup>

<sup>a</sup> Dipartimento Scienze Agrarie e Forestali, Università degli Studi di Palermo, Viale delle Scienze 4, 90128 Palermo, Italy

<sup>b</sup> Department of Food Engineering, Faculty of Agriculture, Cukurova University, 01330, Adana, Turkey

### ARTICLE INFO

#### Article history:

Received 8 April 2015

Received in revised form

7 September 2015

Accepted 8 November 2015

Available online 14 November 2015

#### Keywords:

Fermentation

Functional foods

Kefir-like beverages

Microorganisms

Vegetable juices

### ABSTRACT

The aim of this work was to develop new non-dairy fermented beverages using vegetable juices as fermentable substrates. Carrot, fennel, melon, onion, tomato and strawberry juices underwent back-slopping fermentations, carried out by water kefir microorganisms. Results indicated that lactic acid bacteria and yeasts were capable of growing in the juices tested. Melon juice registered the highest numbers of microorganisms. Almost all juices underwent a lactic fermentation. After fermentation, there was observance of a decrease of the soluble solid content and an increase of the number of volatile organic compounds. In particular, esters were present in high amounts after the fermentation, especially in strawberry, onion and melon, whereas carrot and fennel registered a significant increase of terpenes. The concentration of alcohols increased, while that of aldehydes decreased. Changes in colour attributes were registered. Strawberry, onion and tomato juices retained a high antioxidant activity after fermentation. The overall quality assessment indicated that carrot kefir-like beverage (KLB) was the product mostly appreciated by the judges. These findings support the further development of vegetable KLBs with additional benefits and functional properties.

© 2015 Elsevier Ltd. All rights reserved.

## 1. Introduction

In the past few years, there has been an increased awareness of the consumers towards disease concerns related to foods. Consequently, there has been a growing interest to develop new functional foods (Prado, Parada, Pandey, & Soccol, 2008). In general, yogurt represents the main probiotic food consumed worldwide. However, due to the allergy to dairy products by several people, there has recently been an intensive research addressed to non-dairy foods. Furthermore, the ongoing trend of vegetarianism, with an increasing number of vegan vegetarian, has established a massive worldwide importance of non-dairy probiotic products (Granato, Branco, Nazzaro, Cruz, & Faria, 2010). Fruit juices, desserts and cereal-based products are suitable media for delivering probiotics (Reichert, 2008). Among vegetable probiotic beverages, there have been recent proposal for beet-based drink (Yoon, Woodams, & Hang, 2005), tomato-based drink (Yoon, Woodams,

& Hang, 2004), cabbage juice (Yoon, Woodams, & Hang, 2006) and carrot juice (Nazzaro, Fratianni, Sada, & Orlando, 2008).

Since the beginning of recorded history, kefir is an ancient food attributed with exceptional health promoting and curative properties (Shavit, 2008), and in Caucasus, it is also associated with longevity (Cevikbas et al., 1994; Zourari & Anifantakis, 1988). Within non-dairy fermented beverages, water kefir is prepared with a sucrose solution with or without fruit extracts (Schneedorf, 2012) fermented by kefir grains, which consist of mainly lactic acid bacteria (LAB) and yeasts included into a polysaccharide matrix named kefiran (Rodrigues, Caputo, Carvalho, Evangelista, & Schneedorf, 2005).

Since the beginning of the third millennium, the scientific interest in kefir and the promotion of its industrial production are on the increase because of its health benefits (Anar, 2000). The concept that the foods provide not only essential nutrients needed for life but also bioactive compounds for health promotion and disease prevention is quite clear among consumers. For example, there have been demonstrations that the daily consumption of fruit and vegetables reduces the risk of stroke (He, Nowson, & MacGregor, 2006) and this medical evidence induced the change of dietary

\* Corresponding author.

E-mail address: [luca.settanni@unipa.it](mailto:luca.settanni@unipa.it) (L. Settanni).

habits of several peoples.

Based on the several positive effects of kefir products, and vegetable and fruits, on human health, this work aimed to evaluate the characteristics of kefir-like beverages obtained after the fermentation of juices extracted from vegetables with water kefir microorganisms, in order to develop new non-dairy fermented products.

## 2. Materials and methods

### 2.1. Production of kefir-like beverages

The vegetable juices (VJ) fermented in this study were obtained from carrots (*Daucus carota* L.), fennels (*Foeniculum vulgare* Mill.), melons (*Cucumis melo* L.), onions (*Allium cepa* L.), tomatoes (*Solanum lycopersicum* L.) and strawberries (*Fragaria x ananassa* Duch.). Table 1 reports the characteristics of the juices, obtained by means of a centrifugal extractor (Moulinex JU650G, Milan, Italy). The commercial water kefir microorganism preparation “kefir d’acqua fai da te” (BioNova snc, Villanova sull’Arda, Italy), containing approximately  $10^9$  CFU/g of *Lactobacillus*, *Lactococcus*, *Leuconostoc* and *Saccharomyces*, as declared by the producer, was used to carry out the fermentation. VJs were subjected to pasteurisation at 75 °C for 5 min and cooled at room temperature before processing.

Kefir-like beverages (KLBs) were produced by back-slopping. Aliquots of 50 mL of each VJ were inoculated with 0.125 g of the freeze-dried microbial mixture and incubated at 25 °C for 72 h to develop the active inoculants (Ins). Higher volumes of VJ (1 L) were then inoculated with the corresponding In (4% v/v) and the fermentation processes were performed at 25 °C for 48 h. Beverage productions were carried out in triplicate.

### 2.2. Microbiological analyses

Preparation of decimal dilutions of VJs, Ins and KLBs was in Ringer’s solution (Sigma–Aldrich, Milan, Italy). The cell suspensions were used to estimate the following microbial groups: total mesophilic count (TMC) on plate count agar (PCA), incubated

aerobically at 30 °C for 72 h; *Enterobacteriaceae* on double-layered violet red bile glucose agar (VRBGA), incubated aerobically at 37 °C for 24 h; pseudomonads on *Pseudomonas* agar base (PAB) supplemented with 10 mg/mL ceftrimide fucidin, incubated aerobically at 20 °C for 48 h; rod LAB on de Man-Rogosa-Sharpe (MRS) agar, acidified to pH 5.4 with lactic acid (5 mol/L) and incubated anaerobically at 30 °C for 48 h; coccus LAB on M17 agar, incubated anaerobically at 30 °C for 48 h; yeasts on dichloran rose Bengal chloramphenicol (DRBC) agar, incubated aerobically at 25 °C for 48 h. All media and supplements were purchased from Oxoid (Milan, Italy). Count plates were carried out in duplicate for each independent production.

### 2.3. Characterization of the commercial starter preparation

Characterization of the commercial starter culture for water kefir production was at species level. Freeze-dried preparation (1 g) was diluted and analysed for LAB and yeasts, as reported above. Four colonies of yeasts and Gram-positive (determined by KOH method) and catalase negative (determined by transferring fresh colonies from a Petri dish to a glass slide and adding 5%, w/v, H<sub>2</sub>O<sub>2</sub>) bacteria for each morphology observed were isolated from the agar media inoculated with the highest dilutions of cell suspension. Purification of the cultures to homogeneity was by successive sub-culturing in the same agar media and then propagating in the corresponding broth media.

DNA from broth cultures was extracted by Instagene Matrix kit (Bio-Rad, Hercules, CA) and used as template for PCR reactions. LAB were identified by 16S rRNA gene sequencing as described by Weisburg, Barns, Pelletier, and Lane (1991). DNA fragments of about 1600 bp were purified by QJA-quick purification kit (Qiagen S.p.a., Milan, Italy) and sequenced by PRIMM (Milan, Italy). The sequences were compared to those available in the GenBank/EMBL/DDBJ database. All yeasts were grouped by restriction fragment length polymorphism (RFLP) analysis of the region spanning the internal transcribed spacers (ITS1 and ITS2) and the 5.8S rRNA gene, as reported by Esteve-Zarzoso, Belloch, Uruburu, and Querol (1999), and then identified at species level by sequencing the D1/D2 domains of

**Table 1**  
Microbial loads (Log CFU/mL) of vegetable kefir-like beverages.

Sample		Media					
		PCA	VRBGA	PAB	MRS	M17	DRBC
Carrot	VJ	5.5 ± 0.4	< d.l.	<1	5.7 ± 0.5	5.7 ± 0.2	5.0 ± 0.5
	KLB	8.4 ± 0.5 ***	< d.l. ns	<1 ns	8.5 ± 0.2 ***	8.5 ± 0.5 ***	6.7 ± 0.4 ***
Fennel	VJ	5.4 ± 0.4	< d.l.	<1	6.1 ± 0.8	5.5 ± 0.4	4.2 ± 0.7
	KLB	8.5 ± 0.4 ***	< d.l. ns	<1 ns	8.6 ± 0.4 ***	8.1 ± 0.2 ***	5.5 ± 0.4 **
Melon	VJ	5.4 ± 0.5	< d.l.	<1	6.1 ± 0.2	5.7 ± 0.5	5.4 ± 0.4
	KLB	9.1 ± 0.7 ***	3.3 ± 0.5 ***	2.3 ± 0.4 ***	9.1 ± 0.4 ***	9.2 ± 0.5 ***	7.8 ± 0.8 ***
Onion	VJ	5.8 ± 0.3	< d.l.	<1	6.2 ± 0.7	5.2 ± 0.3	2.0 ± 0.2
	KLB	8.6 ± 0.5 ***	< d.l. ns	<1 ns	8.9 ± 0.7 ***	8.5 ± 0.4 ***	3.3 ± 0.4 **
Strawberry	VJ	5.3 ± 0.7	< d.l.	<1	5.3 ± 0.4	4.9 ± 0.7	5.1 ± 0.5
	KLB	7.8 ± 0.4 ***	< d.l. ns	<1 ns	7.7 ± 0.5 ***	6.4 ± 0.7 **	7.7 ± 0.6 ***
Tomato	VJ	5.7 ± 0.8	< d.l.	<1	5.4 ± 0.7	5.3 ± 0.5	5.1 ± 0.6
	KLB	9.0 ± 0.2 ***	< d.l. ns	<1 ns	8.9 ± 0.6 ***	8.9 ± 0.2 ***	7.1 ± 0.4 ***

Results represent mean values ± SD of six measurements (carried out in duplicate for three independent productions).

Abbreviations: PCA, plate count agar for total mesophilic counts; VRBGA, violet red bile glucose agar for *Enterobacteriaceae*; PAB, *Pseudomonas* agar base for pseudomonads; MRS, de Man-Rogosa-Sharpe agar for rod LAB; M17, medium 17 agar for mesophilic coccus LAB; DRBC, dichloran rose Bengal chloramphenicol agar for yeasts; VJ, vegetable juice after pasteurisation; KLB, kefir-like beverage; d.l., detection level.

Significant differences among vegetable juices and fermented kefir-like beverages for each vegetable sample and each microbial load: \*\*\*,  $p \leq 0.001$ , \*\*,  $p \leq 0.01$ ; \*,  $p \leq 0.05$ ; ns, not significant.

the 26S rRNA gene using the primers NL1 and NL4 (O'Donnell 1993). Yeast DNAs were sequenced by PRIMM. BlastN search against the NCBI non-redundant sequence database located at <http://www.ncbi.nlm.nih.gov> determined the identity of the sequences.

#### 2.4. Physico-chemical determinations

Physico-chemical analyses of pH, total titratable acidity (TTA) and soluble solid content (SSC) were performed according to the methodology proposed by the AOAC (2000). Total phenolic compounds (TPs) were analysed according to the Folin-Ciocalteu procedure (Slinkard & Singleton, 1977). The antioxidant activity was determined as DPPH (2,2-diphenyl-1-picrylhydrazyl) radical scavenging activity (%) (Larrauri, Sánchez-Moreno, & Saura-Calixto, 1998). The total anthocyanin content (TAC) was determined according to Fuleki and Francis (1968) with some modifications (Lee, Durst, & Wrolstad, 2005).

Ethanol, acetic and lactic acids were detected using Enzymatic BioAnalysis/Food Analysis kits (Boehringer Mannheim/R-Biopharm).

Carbon dioxide was indirectly estimated by measuring the weight loss before and after the fermentations and expressed as g/100 mL (Lombardi, Delfini, Zilio, & Tosi, 2004).

Colours of juices were measured, before and after fermentation, with a colorimeter (Chroma Metre CR-400, Minolta, Osaka, Japan) recording CIElab chromaticity coordinates ( $L^*$ ,  $a^*$ ,  $b^*$ ).

All chemicals were purchased from WWR International (Milan, Italy), except when reported differently. Five readings were taken for each replicate of each sample.

#### 2.5. Volatile organic compounds (VOCs)

VJs and KLBs were subjected to GC/MS analysis in order to identify the volatile organic compounds (VOCs). The extractions of VOCs were carried out using a SPME fibre of divinylbenzene/carboxen/polydimethylsiloxane (Supelco, Bellefonte, PA). Conditioning of the fibre was at 250 °C for 30 min. The fibre was then subjected to an exposure step for 30 min at 40 °C to the headspace of the sample vial. The GC-MS equipment, column and conditions described by Corona (2010) were used for analysis. 1-heptanol solution (35 mg/L 1-heptanol in 20% ethanol aqueous solution) was used as an internal standard. Identification of individual peaks was by comparing their retention indices to those of control samples and by comparing their mass spectra with those within the NIST/EPA/NIH Mass Spectral Library database (Version 2.0d, build 2005). Expression of volatile compounds was as  $\mu\text{g/L}$ . Determinations were carried out in triplicate for each sample.

#### 2.6. Sensory evaluation

The final products were evaluated for their sensory profiles by fifteen untrained judges (six women and 9 men, 14 Italians and one Turkish, 25–35 years old). Serving of randomised, refrigerated (10 °C) samples of 10 mL was in clear, tulip-shaped glasses with a volume of 50 mL. The glasses were marked with three digit random numbers and covered with Petri dishes. Instruction to tasters was to cleanse their palates with a plain biscuit and cold, filtered tap water before evaluating each sample. Water kefir produced with the same microbial mixture used to produce KLBs was used as control. For each product, tasters were asked to indicate a mark on a 9-point hedonic scale related to the overall quality (9 = extremely good; 1 = extremely bad). Four samples were analysed in each session and the experiment was replicated three times, i.e., there were nine sessions in total (Magalhães et al., 2011).

#### 2.7. Statistical analyses

Data were analysed using a generalized linear model (GLM). The post-hoc Tukey's method ( $P < 0.05$ ) was used to determine differences among the overall quality of KLBs. Statistical data were processed with STATISTICA software version 10 (StatSoft Inc., Tulsa, OK, USA).

### 3. Results and discussion

#### 3.1. Microbial evolution of vegetable juices and fermented beverages

The levels of the six microbial populations (TMC, *Enterobacteriaceae*, pseudomonads; rod LAB; coccus LAB and yeasts) of VJs, before pasteurization, were different. Pseudomonads were undetectable in any sample, and for melon juice, the other groups were below the detection limit by the plate count method. Characterization of onion juice was by the presence of 1.6 Log CFU/mL of TMC and strawberry juice hosted 1.0 Log CFU/mL of yeasts. Carrot, fennel and tomato juices were microbiologically complex showing the presence of consistent levels of TMC (5.2–5.7 Log CFU/mL). Both LAB groups were at  $10^4$  CFU/mL in carrot and fennel juices. Rod and coccus LAB of tomato juice were 2.5 and 4.3 Log CFU/mL, respectively. Yeasts were 1.5, 2.5 and 3.5 Log CFU/mL, while *Enterobacteriaceae* were 1.3, 2.2 and 1.5 Log CFU/mL for tomato, carrot and fennel juice, respectively. Due to their different microbial composition, there was pasteurization of the bulks in order to provide enough volume of each VJ that is stable over time. The thermal treatment reduced all microbial groups at levels below the detection limits.

At the time of addition into KLBs, there was characterization of the active inoculants of the six VJs by  $10^7$  CFU/mL of TMC. Rod LAB were in the range 7.0–8.3 Log CFU/mL, while coccus LAB were in the range 6.8–7.6 Log CFU/mL. Except onion In for which a level of 3.9 Log CFU/mL was registered, yeasts ranged between 6.1 and 7.7 for the other Ins. *Enterobacteriaceae* and pseudomonads were undetectable in any Ins.

The microbiological characteristics of the KLBs are reported in Table 1. After inoculation, all microbial groups of Ins resulted as diluted by almost two orders of magnitude. At the end of fermentation, strawberry KLB contained 7.7 and 6.4 Log CFU/mL of rod and coccus LAB, respectively: melon KLB had 9.1 and 9.2 Log CFU/mL of rod and coccus LAB, respectively, while the other products hosted levels of  $10^8$  CFU/mL of both LAB groups. Yeasts were 3.3 Log CFU/mL for onion KLB and ranged between 5.5 and 7.8 Log CFU/mL for the other fermented juices. Although *Enterobacteriaceae* and pseudomonads were undetectable in all Ins, melon KLB was characterized by their presence (3.3 and 2.3 Log CFU/mL, respectively) at the end of fermentation. This phenomenon might be due to the presence of a very few cells in Ins which were not detected through the microbiological investigation, but transferred into KLB where they developed at detectable levels. Furthermore, there was characterization of melon juice by an almost neutral pH (Table 2) that is not inhibitory to the development of *Enterobacteriaceae* and pseudomonads.

We also verified the codominance of LAB and yeasts typical of traditional milk or water kefir (Chen, Wang, & Chen, 2008) for the vegetable kefir products tested in this study. However, yeasts in onion KLB developed at very low levels not only compared to those of LAB, but also compared to the levels of yeast counts estimated for the other KLBs of the experimentation. The high levels of sulphur compounds characterizing *Allium* species (garlic and onion) explain this finding and there are reports of them inhibiting different yeast species, including *Saccharomyces cerevisiae* (Kim, Kim, & Kyung,

**Table 2**  
Physico-chemical analysis of vegetable juices and kefir-like beverages.

Sample		pH	Ethanol (% v/v)	Lactic acid (g/L)	Acetic acid (g/L)	CO <sub>2</sub> (g/100 mL)	TTA <sup>a</sup> (g/L citric acid)	SSC (°Brix)	TP (mg/L)	DPPH (%)	TAC (mg/L Cy-3-glc)	Colour					
												L*	a*	b*	Croma	Hue	ΔE
Carrot	VJ	5.3 ± 0.0	n.d.	n.d.	n.d.	n.d.	9.85 ± 0.49	8.15 ± 0.21	194.25 ± 6.36	15.49 ± 0.03	n.d.	49.28 ± 0.59	23.21 ± 0.64	39.01 ± 1.00	45.39 ± 1.18	59.25 ± 0.07	
	KLB	4.1 ± 0.0	3.00 ± 0.14	4.81 ± 0.65	1.90 ± 0.71	1.51 ± 0.18	10.23 ± 0.25	3.38 ± 0.10	206.40 ± 18.60	14.53 ± 1.67	n.d.	50.22 ± 0.38	25.33 ± 1.11	40.78 ± 1.22	48.00 ± 1.62	58.17 ± 0.37	2.94 ± 0.32
		***	***	***	***	***	ns	***	ns	ns	***	***	***	**	**	***	
Fennel	VJ	5.5 ± 0.0	n.d.	n.d.	n.d.	n.d.	6.75 ± 0.21	4.45 ± 0.07	208.07 ± 1.64	22.56 ± 0.08	n.d.	37.09 ± 0.68	-0.55 ± 0.20	2.46 ± 0.79	2.54 ± 0.74	104.08 ± 6.66	
	KLB	4.4 ± 0.0	0.63 ± 0.03	3.55 ± 0.66	0.18 ± 0.10	0.87 ± 0.13	4.47 ± 0.06	1.87 ± 0.06	101.83 ± 10.11	20.12 ± 0.11	n.d.	48.20 ± 2.15	-1.37 ± 0.14	5.02 ± 1.23	5.24 ± 1.13	107.99 ± 7.80	11.55 ± 0.46
		***	***	***	**	***	***	***	***	***	***	***	***	*	*	ns	
Melon	VJ	6.4 ± 0.1	n.d.	n.d.	n.d.	n.d.	3.60 ± 0.01	10.05 ± 0.07	185.90 ± 20.15	18.42 ± 2.80	n.d.	35.70 ± 0.69	-0.11 ± 0.04	4.02 ± 0.52	4.02 ± 0.52	91.60 ± 0.43	
	KLB	4.4 ± 0.0	2.56 ± 0.62	4.80 ± 0.52	0.59 ± 0.23	3.39 ± 0.47	5.33 ± 0.31	3.83 ± 0.06	160.03 ± 5.05	20.24 ± 0.98	n.d.	43.69 ± 2.15	-1.42 ± 0.25	7.32 ± 1.18	7.46 ± 1.20	100.95 ± 0.86	8.76 ± 0.68
		***	***	***	***	***	**	***	ns	*	***	***	***	***	***	***	
Onion	VJ	5.0 ± 0.0	n.d.	n.d.	n.d.	n.d.	2.11 ± 0.42	9.95 ± 0.07	714.55 ± 85.32	81.78 ± 9.22	37.14 ± 2.92	33.17 ± 0.18	8.35 ± 0.30	-7.86 ± 0.16	11.47 ± 0.12	316.72 ± 1.62	
	KLB	5.0 ± 0.6	0.09 ± 0.02	1.24 ± 0.56	0.03 ± 0.02	0.14 ± 0.06	1.50 ± 0.06	9.17 ± 0.15	515.94 ± 45.91	78.67 ± 0.02	9.36 ± 1.32	32.74 ± 2.01	11.39 ± 1.13	-7.78 ± 1.38	13.97 ± 1.10	324.99 ± 9.17	3.91 ± 0.24
		ns	***	***	*	*	***	ns	*	ns	**	ns	**	ns	***	ns	
Strawberry	VJ	3.2 ± 0.0	n.d.	n.d.	n.d.	n.d.	7.20 ± 0.73	5.95 ± 0.07	813.79 ± 42.69	95.27 ± 1.23	90.20 ± 2.87	42.35 ± 0.35	19.61 ± 1.61	9.99 ± 1.23	22.01 ± 1.99	26.94 ± 1.06	
	KLB	3.6 ± 0.0	2.35 ± 0.26	0.58 ± 0.02	0.10 ± 0.03	1.71 ± 0.27	8.82 ± 1.40	2.47 ± 0.06	619.86 ± 41.23	95.38 ± 0.43	24.79 ± 2.85	43.81 ± 3.12	17.60 ± 1.52	8.30 ± 1.44	19.64 ± 2.56	24.52 ± 2.75	5.47 ± 0.31
		***	***	***	**	***	*	***	*	ns	***	ns	*	ns	ns	ns	
Tomato	VJ	4.1 ± 0.0	n.d.	n.d.	n.d.	n.d.	14.55 ± 0.64	4.45 ± 0.07	248.46 ± 12.98	74.30 ± 1.80	n.d.	28.74 ± 0.35	18.99 ± 1.21	3.85 ± 0.62	19.38 ± 1.30	11.40 ± 1.14	
	KLB	4.2 ± 0.1	1.48 ± 0.10	2.41 ± 0.32	1.25 ± 0.09	1.29 ± 0.11	6.70 ± 0.21	1.97 ± 0.06	268.31 ± 19.25	78.31 ± 0.14	n.d.	31.65 ± 0.59	21.92 ± 1.83	7.42 ± 0.99	23.14 ± 2.04	18.62 ± 0.98	5.55 ± 0.16
		ns	***	***	***	***	**	***	ns	*	***	***	**	***	**	***	

Mean values of five measurements for each replicate.

Abbreviations: VJ, vegetable juice after pasteurisation; KLB, kefir-like beverage; CO<sub>2</sub>, carbon dioxide; TTA, total titratable acidity; SSC, soluble solid content; TP, total phenol (gallic acid equivalent mg/L); DPPH, 2,2-diphenyl-1-picrylhydrazyl radical scavenging activity (%); TAC, total anthocyanin content (mg/L cyanidin-3-glucoside equivalents); L\*, lightness; a\*, redness; b\*, yellowness; H°, hue angle; ΔE, colour differences; n.d., not detectable.

Significant differences among vegetable juices and fermented kefir-like beverages for each vegetable sample and each physico-chemical determination: \*\*\*, p ≤ 0.001, \*\*, p ≤ 0.01; \*, p ≤ 0.05; ns, not significant.

2004; Kyung & Fleming, 1997; Lemar et al., 2007).

LAB and TMC reached loads similar to those detected for other sugary kefir (Liu & Lin, 2000; Sabokbar & Khodaiyan, 2014). The statistical differences between the levels of cocci and rod LAB were not significant as also observed by other authors (Magalhães, Pereira, Dias, & Schwan et al., 2010). In particular, Irigoyen, Arana, Castiella, Torre, and Ibanez (2005) reported cell densities of  $10^8$  CFU/mL for lactobacilli and lactococci after two days of fermentation of milk kefir. The presence of yeasts in KLBs, except that made from onion juice, was approximately in the same levels registered for several kefir products (Liu & Lin, 2000; Sabokbar & Khodaiyan, 2014).

### 3.2. Identification of the dominant microorganisms

The results of our investigation confirmed the commercial starter preparation to contain LAB and yeasts at  $10^9$  CFU/g. Leuconostocs and lactococci belonged to a single species, specifically *Leuconostoc mesenteroides* (Acc. No. KT633927) and *Lactococcus lactis* (Acc. No. KT633921), whereas dominant lactobacilli were allotted into two species: *Lactobacillus kefir* (Acc. No. KT633919) and *Lactobacillus fermentum* (KT633923). Identification of all yeasts was as *S. cerevisiae* (Bankit 1853683). All the species identified in the starter culture are commonly found associated to kefir products (Cheirsilp, Shoji, Shimizu, & Shioya, 2003; Nambou et al., 2014; Witthuhn, Schoeman, & Britz, 2005) and were isolated from KLBs. Thus, our study demonstrated the commercial starter preparation to be suitable for the fermentation of the vegetable juices used in this study.

### 3.3. Physico-chemical parameters

The results of the chemical determinations are shown in Table 2. Melon juice displayed the highest pH (6.4). The high value can explain the high microbial counts observed for the resulting KLB.

Ethanol content ranged between 0.09 and 3.00% v/v. Onion KLB registered the lowest concentration and is a clear consequence of the scarce growth of *Saccharomyces*, in particular *S. cerevisiae* primarily responsible for alcohol production (de Melo Pereira, Ramos, Galvão, Souza Dias, & Schwan, 2010). According to the Italian legislation (GURI, 2001), due to their ethanol content above 1.2% v/v, strawberry, melon, carrot and tomato KLBs produced in this study are alcoholic beverages. The presence of ethanol is important for a kefir product because it confers the typical light alcoholic flavour (Beshkova, Simova, Frengova, Simov, & Dimitrov, 2003) and, together with the CO<sub>2</sub> mainly deriving from yeast fermentation, provides the final product with the desirable exotic notes and yeasty aroma (Guzel-Seydim, Seydim, & Greene, 2000). In this study, estimation of CO<sub>2</sub> production was as reported by several authors for different fermented matrices (Liu & Shen, 2008; Lombardi et al. 2004; Varga, Klinke, Réczey, & Thomsen, 2004), through weight loss. There was well correlation of this indirect measure with yeast development.

Detection of lactic acid was at the highest concentration for carrot (4.81 g/L) and melon (4.80 g/L) KLBs. The presence of acetic acid in all KLBs confirmed the metabolic heterogeneity (homo-fermentative and heterofermentative species) of LAB active in kefir products. Carrot KLB displayed the highest concentration of acetic acid. Acetic acid contributes to provide a pleasant taste to kefir and plays a role in the inhibition of the undesirable (spoilage and/or pathogenic) microorganisms (Puerari, Magalhães, & Schwan, 2012).

A strict correlation between the decrease of solid soluble content and the increase of ethanol, lactic and acetic acids and CO<sub>2</sub> formation was found. For carrot, melon and strawberry KLBs, the total titratable acidity increased with fermentation, while there

was characterization of the other KLBs, especially tomato, by lower values than the corresponding VJs.

In general, the total phenol content decreased after fermentation, with the most consistent reduction (49%) recorded for fennel KLB. However, carrot and tomato KLBs showed a negligible increase. There was positive correlation of the total phenol content to the antioxidant activity for all samples, before and after fermentation, a phenomenon also observed by Dani et al. (2007). Detection of anthocyanins was only in onion and strawberry juices and KLBs. A relevant antioxidant activity was registered especially for strawberry KLB. The radical scavenging activity is positively associated to the content in anthocyanins (Gil, Tomás-Barberán, Hess-Pierce, Holcroft, & Kader, 2000).

Regarding colour parameters, generally significant variations were registered between juices and KLBs, except those of strawberry. The total colour difference was calculated for each sample and ranged between 2.94 (carrot) and 11.55 (fennel). Considering the just noticeable differences limit of 2.3 (Mahy, Eycken, & Oosterlinck, 1994), all samples changed their colour, on a human perception scale, after the fermentation process. Fennel and melon KLBs registered the most noticeable changes.

### 3.4. Volatile organic compounds (VOCs) of vegetable kefir-like beverages

A total of 134 different volatile organic compounds were detected by SPME GC–MS (Table 3). KLBs were characterized by higher aromatic complexities than the corresponding VJs, because there was detection of several VOCs only after fermentation. Furthermore, there was registration of some molecules present in VJs to higher levels in KLBs. There is strong influence of the sensory profile of a fermented matrix by the active microorganisms (Arrizon, Calderón, & Sandoval, 2006). In particular, the acids increased in carrot, melon and strawberry KLBs. The last product showed a consistent increase of hexanoic and octanoic acids. Both these organic acids might be defining for the sensory evaluation of the fermented products carrying a refreshing flavour, unique aroma and texture. However, their effect depends on their amount (Duarte et al., 2010).

The fermentation increased the number and the concentration of the alcoholic molecules. Isoamylalcohol increased especially in fennel, melon, strawberry and tomato KLBs. The increase of volatile higher alcohols and the corresponding esters is a common phenomenon during kefir fermentation (Magalhães et al., 2011). In particular, the concentration of isoamylalcohol and 1-hexanol registered in this study were below 20 µg/L, the maximum concentration exerting a positive influence on the flavour of fermented beverages (Dragone, Mussatto, Oliveira, & Teixeira, 2009; Magalhães et al., 2011). Among alcohols, glycerol is the main secondary product of alcoholic fermentation led by *S. cerevisiae* (Puerari et al., 2012), but in this study, its detection was at concentrations too low to confer body and texture to KLBs (Dias, Schwan, Freire, & Seródio, 2007).

The esters increased with fermentation especially in fennel, melon, strawberry and tomato KLBs. The major esters were ethyl hexanoate, octanoate and decanoate that have strong relations with fruity/floral/green aromas and yeasts mainly produce them (Nambou et al., 2014). Moreover, esters generally have a low odour threshold in fermented alcoholic beverages such as beer and wine (Saerens, Delvaux, Verstrepen, & Thevelein, 2010).

Detection of sulphur compounds was only in onion juice before and after fermentation. This result is not surprising, since *Allium* species are known to contain these compounds. The high concentrations of sulphur compounds help to explain the low levels of yeast detected in onion KLB. Kyung and Fleming (1997) reported

**Table 3**  
Analysis of the volatile organic compounds of vegetable juices and kefir-like beverages.

Chemical compound (µg/L)	Carrot		Fennel		Melon		Onion		Strawberry		Tomato	
	VJ	KLB	VJ	KLB	VJ	KLB	VJ	KLB	VJ	KLB	VJ	KLB
<b>Acids</b>												
Acetic acid	35.31 ± 1.65	1239.85 ± 57.87	11.84 ± 0.09	236.38 ± 15.94	35.96 ± 1.55	711.86 ± 55.67	n.d.	n.d.	14.06 ± 0.32	230.27 ± 1.23	15.39 ± 0.59	490.37 ± 23.23
Propionic acid	n.d.	n.d.	n.d.	n.d.	n.d.	n.d.	n.d.	n.d.	n.d.	3.85 ± 0.87	n.d.	n.d.
Isobutyric acid	n.d.	n.d.	n.d.	n.d.	n.d.	n.d.	n.d.	n.d.	n.d.	32.12 ± 1.23	n.d.	n.d.
Hexanoic acid	n.d.	n.d.	n.d.	56.20 ± 0.56	n.d.	89.45 ± 2.43	n.d.	n.d.	17.13 ± 2.34	294.22 ± 8.72	32.27 ± 1.11	66.78 ± 4.89
Octanoic acid	n.d.	16.72 ± 0.67	n.d.	119.85 ± 9.67	n.d.	124.77 ± 2.25	n.d.	n.d.	n.d.	289.75 ± 11.34	4.77 ± 0.47	106.53 ± 4.79
Decanoic acid	0.56 ± 0.01	1.95 ± 0.06	n.d.	32.57 ± 1.34	n.d.	57.05 ± 3.43	n.d.	n.d.	n.d.	92.02 ± 4.10	n.d.	16.56 ± 0.51
Total	35.87 ± 1.66	1258.5 ± 58.60	11.84 ± 0.09	445.00 ± 27.51	35.96 ± 1.55	983.14 ± 63.78	n.d.	n.d.	31.19 ± 2.66	942.23 ± 27.49	52.43 ± 2.17	680.24 ± 33.42
<b>Alcohols</b>												
Isobutanol	n.d.	n.d.	n.d.	n.d.	n.d.	138.84 ± 11.39	n.d.	n.d.	n.d.	n.d.	n.d.	n.d.
Isoamylalcohol	n.d.	194.83 ± 12.76	n.d.	522.07 ± 4.78	0.95 ± 0.02	2210.61 ± 54.67	n.d.	n.d.	n.d.	2468.84 ± 167.54	n.d.	675.81 ± 25.37
1-pentanol	n.d.	n.d.	n.d.	n.d.	n.d.	n.d.	n.d.	n.d.	n.d.	n.d.	5.32 ± 0.59	27.88 ± 2.54
1-hexanol	1.10 ± 0.07	63.55 ± 0.43	66.23 ± 0.67	28.82 ± 1.21	n.d.	25.99 ± 1.4	n.d.	11.80 ± 0.44	2.56 ± 0.11	527.40 ± 7.41	1142.32 ± 21.50	1648.35 ± 150.23
cis-3-hexen-1-ol	n.d.	n.d.	n.d.	n.d.	n.d.	n.d.	n.d.	n.d.	n.d.	n.d.	96.75 ± 0.49	96.77 ± 5.01
trans-2-hexenol	n.d.	n.d.	n.d.	n.d.	n.d.	n.d.	n.d.	n.d.	1.95 ± 0.03	n.d.	121.40 ± 0.65	n.d.
1-octen-3-ol	n.d.	n.d.	n.d.	n.d.	n.d.	n.d.	n.d.	n.d.	n.d.	n.d.	6.19 ± 0.29	15.40 ± 0.70
5-hepten-2-ol, 6-methyl	n.d.	5.01 ± 0.34	n.d.	n.d.	n.d.	n.d.	n.d.	n.d.	n.d.	n.d.	22.04 ± 1.50	337.01 ± 11.94
2-ethylhexanol	2.47 ± 0.07	13.73 ± 0.09	n.d.	n.d.	3.32 ± 0.04	9.32 ± 0.03	n.d.	n.d.	6.25 ± 0.08	10.00 ± 0.05	2.18 ± 0.04	16.10 ± 0.99
4-hepten-1-ol	n.d.	n.d.	n.d.	n.d.	n.d.	3.70 ± 0.01	n.d.	n.d.	n.d.	3.98 ± 0.05	n.d.	6.03 ± 0.81
2,3-butanediol	n.d.	142.88 ± 2.99	19.74 ± 1.45	8.43 ± 0.23	n.d.	934.63 ± 33.67	n.d.	n.d.	n.d.	3.65 ± 0.04	n.d.	264.08 ± 19.97
1-octanol	2.65 ± 0.76	31.19 ± 2.46	n.d.	46.07 ± 3.54	n.d.	39.18 ± 2.45	n.d.	n.d.	n.d.	25.33 ± 1.56	71.88 ± 4.16	170.61 ± 12.13
Fenchyl alcohol	n.d.	n.d.	968.53 ± 77.82	2033.62 ± 87.22	n.d.	n.d.	n.d.	n.d.	n.d.	n.d.	n.d.	n.d.
Furfuryl alcohol	0.69 ± 0.01	18.75 ± 1.11	3.32 ± 0.22	58.54 ± 4.56	10.85 ± 0.88	n.d.	n.d.	n.d.	4.77 ± 0.03	20.40 ± 2.22	1.58 ± 0.21	25.57 ± 0.04
Benzyl alcohol	n.d.	n.d.	n.d.	4.47 ± 0.22	1.36 ± 0.04	175.46 ± 12.54	n.d.	n.d.	0.24 ± 0.00	6.08 ± 0.45	n.d.	12.52 ± 1.51
Phenylethylalcohol	2.35 ± 0.03	54.34 ± 0.56	3.86 ± 0.11	68.80 ± 4.31	n.d.	393.97 ± 26.43	n.d.	n.d.	n.d.	215.72 ± 4.65	n.d.	255.27 ± 15.55
6,10-dimethyl 5,9-undecadien-2-ol	n.d.	n.d.	n.d.	n.d.	n.d.	n.d.	n.d.	n.d.	n.d.	n.d.	n.d.	84.96 ± 3.34
Caryophyllene alcohol	0.71 ± 0.04	10.86 ± 0.34	n.d.	n.d.	n.d.	n.d.	n.d.	n.d.	n.d.	n.d.	n.d.	n.d.
Glycerol	n.d.	n.d.	69.98 ± 1.98	11.81 ± 0.98	5.51 ± 0.04	n.d.	n.d.	n.d.	0.99 ± 0.00	8.18 ± 0.45	2.43 ± 0.21	45.78 ± 2.82
Total	9.97 ± 0.98	535.13 ± 21.08	1131.66 ± 82.25	2782.63 ± 107.05	21.99 ± 1.02	3931.70 ± 142.59	n.d.	11.80 ± 0.44	16.76 ± 0.25	3289.58 ± 184.42	1472.09 ± 29.64	3682.14 ± 252.95
<b>Aldehydes</b>												
Hexanal	3.68 ± 0.75	3.49 ± 0.87	9.32 ± 0.98	n.d.	17.41 ± 1.22	n.d.	n.d.	n.d.	9.59 ± 0.02	n.d.	164.72 ± 2.73	41.22 ± 1.08
2-methyl-2-penten-1-al	n.d.	n.d.	n.d.	n.d.	n.d.	n.d.	1905.23 ± 22.41	978.32 ± 37.78	n.d.	n.d.	n.d.	n.d.
1-octanal	1.70 ± 0.02	4.30 ± 0.06	n.d.	n.d.	n.d.	n.d.	n.d.	n.d.	n.d.	n.d.	14.13 ± 0.25	34.21 ± 4.34
Nonanal	3.65 ± 0.04	21.45 ± 0.10	n.d.	6.16 ± 2.56	38.22 ± 0.76	63.77 ± 3.54	6.86 ± 0.34	9.20 ± 0.23	6.51 ± 0.03	52.22 ± 2.31	11.12 ± 0.38	102.68 ± 7.73
trans-2-octenal	1.55 ± 0.21	3.94 ± 0.12	n.d.	n.d.	n.d.	n.d.	n.d.	n.d.	0.56 ± 0.04	7.67 ± 0.45	68.53 ± 1.22	8.40 ± 0.32
4-methylbenzaldehyde	8.06 ± 0.16	61.25 ± 0.34	n.d.	n.d.	n.d.	n.d.	48.77 ± 3.54	180.13 ± 2.45	n.d.	n.d.	n.d.	n.d.
Decanal	n.d.	9.94 ± 1.12	n.d.	n.d.	n.d.	14.07 ± 1.11	n.d.	n.d.	1.86 ± 0.01	36.25 ± 0.92	2.46 ± 0.01	71.02 ± 4.90
Benzaldehyde	2.15 ± 0.36	6.43 ± 1.09	8.44 ± 0.76	12.52 ± 0.91	4.64 ± 0.23	18.22 ± 0.98	n.d.	n.d.	11.42 ± 0.04	45.38 ± 0.89	4.06 ± 0.19	15.88 ± 1.07
β-cyclocitral	4.71 ± 1.00	63.62 ± 3.98	n.d.	n.d.	n.d.	n.d.	n.d.	n.d.	n.d.	n.d.	17.57 ± 0.37	27.01 ± 3.29
Phenylethanal	n.d.	n.d.	n.d.	n.d.	n.d.	147.29 ± 2.23	n.d.	n.d.	n.d.	164.22 ± 22.63	38.43 ± 0.45	n.d.
Geraniol	n.d.	n.d.	n.d.	n.d.	n.d.	n.d.	n.d.	n.d.	n.d.	n.d.	23.48 ± 0.84	19.06 ± 3.20
Total	25.50 ± 2.54	174.42 ± 7.68	17.76 ± 1.74	18.68 ± 3.47	60.27 ± 2.21	243.35 ± 7.86	1960.86 ± 26.29	1167.65 ± 40.46	29.94 ± 0.14	305.74 ± 27.20	344.51 ± 6.44	319.48 ± 25.93
<b>Several functional groups</b>												
6-methoxymellein	2.66 ± 0.16	17.99 ± 0.45	n.d.	n.d.	n.d.	n.d.	n.d.	n.d.	n.d.	n.d.	n.d.	n.d.
2-pentylfuran	n.d.	n.d.	n.d.	n.d.	n.d.	n.d.	n.d.	n.d.	n.d.	n.d.	106.11 ± 3.20	19.58 ± 0.64
2-isobutylthiazole	n.d.	n.d.	n.d.	n.d.	n.d.	n.d.	n.d.	n.d.	n.d.	n.d.	221.77 ± 1.40	264.71 ± 11.39
Furfuraldehyde	1.75 ± 0.01	18.90 ± 1.34	n.d.	126.60 ± 1.23	14.94 ± 0.99	n.d.	n.d.	n.d.	9.71 ± 0.44	79.66 ± 0.67	5.66 ± 0.01	54.33 ± 0.44
5-methylfurfural	n.d.	n.d.	5.45 ± 0.38	21.70 ± 1.99	7.33 ± 0.43	n.d.	n.d.	n.d.	2.50 ± 0.12	10.16 ± 0.23	n.d.	n.d.
5-hydroxymethylfurfural	2.85 ± 0.09	46.80 ± 1.65	20.41 ± 0.98	344.95 ± 19.76	66.50 ± 2.76	3.25 ± 0.01	n.d.	n.d.	30.96 ± 1.22	165.71 ± 4.56	8.92 ± 0.32	226.38 ± 8.23
Total	7.26 ± 0.26	83.69 ± 3.44	25.86 ± 1.31	493.25 ± 22.98	88.77 ± 4.18	3.25 ± 0.01	n.d.	n.d.	43.17 ± 1.78	255.53 ± 5.46	342.46 ± 4.93	565.00 ± 20.70
<b>Esters</b>												

(continued on next page)

Table 3 (continued)

Chemical compound ( $\mu\text{g/L}$ )	Carrot		Fennel		Melon		Onion		Strawberry		Tomato	
	VJ	KLB	VJ	KLB	VJ	KLB	VJ	KLB	VJ	KLB	VJ	KLB
Isoamylacetate	3.68 $\pm$ 0.21	7.45 $\pm$ 0.46	12.58 $\pm$ 1.11	7.50 $\pm$ 0.22	204.86 $\pm$ 9.43	956.35 $\pm$ 37.56	n.d.	n.d.	1.28 $\pm$ 0.03	67.58 $\pm$ 0.55	n.d.	112.48 $\pm$ 3.31
Methylhexanoate	n.d.	n.d.	n.d.	n.d.	5.14 $\pm$ 0.29	17.50 $\pm$ 2.34	n.d.	n.d.	8.38 $\pm$ 0.44	28.02 $\pm$ 0.54	n.d.	n.d.
Ethyl hexanoate	n.d.	n.d.	n.d.	79.11 $\pm$ 1.38	7.65 $\pm$ 0.57	944.53 $\pm$ 8.65	n.d.	n.d.	2.10 $\pm$ 0.10	2217.0 $\pm$ 117.33	4.61 $\pm$ 0.01	386.90 $\pm$ 27.05
Hexyl acetate	n.d.	n.d.	n.d.	n.d.	39.25 $\pm$ 2.56	84.20 $\pm$ 4.65	n.d.	n.d.	2.35 $\pm$ 0.20	2265.0 $\pm$ 116.51	12.02 $\pm$ 0.77	1067.01 $\pm$ 81.82
cis-3-hexenyl acetate	n.d.	n.d.	n.d.	n.d.	n.d.	n.d.	n.d.	n.d.	n.d.	n.d.	0.42 $\pm$ 0.01	38.73 $\pm$ 6.77
Ethyl heptanoate	n.d.	5.56 $\pm$ 0.35	n.d.	4.13 $\pm$ 0.11	n.d.	9.34 $\pm$ 0.76	n.d.	n.d.	n.d.	96.59 $\pm$ 1.61	n.d.	20.70 $\pm$ 1.18
Ethyl lactate	0.80 $\pm$ 0.01	18.41 $\pm$ 0.09	n.d.	9.92 $\pm$ 0.32	n.d.	17.47 $\pm$ 0.05	n.d.	n.d.	n.d.	n.d.	n.d.	83.86 $\pm$ 3.88
1-Heptyl acetate	n.d.	n.d.	n.d.	n.d.	n.d.	n.d.	n.d.	n.d.	n.d.	139.89 $\pm$ 6.55	n.d.	n.d.
Methyloctanoate	n.d.	4.22 $\pm$ 0.34	n.d.	10.15 $\pm$ 0.87	n.d.	26.10 $\pm$ 0.09	n.d.	n.d.	n.d.	32.57 $\pm$ 1.61	n.d.	43.53 $\pm$ 2.06
Ethyl octanoate	100.35 $\pm$ 7.56	174.90 $\pm$ 9.98	303.35 $\pm$ 22.45	962.43 $\pm$ 13.45	25.00 $\pm$ 1.45	6271.7 $\pm$ 156.88	6.28 $\pm$ 0.08	6.79 $\pm$ 0.03	10.78 $\pm$ 1.34	13579.50 $\pm$ 550.11	26.03 $\pm$ 0.70	2564.51 $\pm$ 63.27
Isoamyl hexanoate	n.d.	n.d.	n.d.	n.d.	n.d.	n.d.	n.d.	n.d.	n.d.	60.24 $\pm$ 2.45	n.d.	n.d.
Octyl acetate	n.d.	n.d.	n.d.	n.d.	n.d.	68.02 $\pm$ 9.78	n.d.	n.d.	n.d.	62.34 $\pm$ 3.65	n.d.	25.12 $\pm$ 1.33
Ethyl nonanoate	n.d.	7.26 $\pm$ 0.45	273.47 $\pm$ 21.56	40.40 $\pm$ 2.76	n.d.	51.81 $\pm$ 3.77	n.d.	n.d.	n.d.	109.96 $\pm$ 7.23	n.d.	11.26 $\pm$ 1.01
Isobutyloctanoate	n.d.	n.d.	n.d.	n.d.	n.d.	n.d.	n.d.	n.d.	n.d.	23.13 $\pm$ 1.66	n.d.	n.d.
Isoamyl lactate	n.d.	n.d.	n.d.	n.d.	n.d.	n.d.	n.d.	n.d.	n.d.	n.d.	n.d.	8.35 $\pm$ 0.07
Methyl decanoate	n.d.	n.d.	n.d.	n.d.	n.d.	21.20 $\pm$ 1.33	n.d.	n.d.	n.d.	15.59 $\pm$ 1.11	n.d.	24.02 $\pm$ 1.35
$\gamma$ -butyrolactone	n.d.	n.d.	n.d.	9.60 $\pm$ 0.45	n.d.	n.d.	n.d.	n.d.	1.19 $\pm$ 0.09	5.11 $\pm$ 0.09	n.d.	n.d.
Ethyldecanoate	71.08 $\pm$ 3.28	109.87 $\pm$ 1.23	154.23 $\pm$ 9.45	346.78 $\pm$ 22.76	7.39 $\pm$ 0.49	3923.17 $\pm$ 231.99	n.d.	n.d.	3.30 $\pm$ 0.03	5087.62 $\pm$ 43.56	18.46 $\pm$ 0.01	1380.96 $\pm$ 93.47
Isoamyl octanoate	2.49 $\pm$ 0.16	n.d.	n.d.	n.d.	n.d.	14.00 $\pm$ 0.91	n.d.	n.d.	n.d.	79.97 $\pm$ 1.54	0.74 $\pm$ 0.02	15.06 $\pm$ 0.34
Ethyl-9-decenoate	15.54 $\pm$ 1.02	10.04 $\pm$ 0.79	n.d.	7.50 $\pm$ 0.45	n.d.	178.85 $\pm$ 1.02	n.d.	n.d.	0.62 $\pm$ 0.01	2156.25 $\pm$ 101.33	n.d.	45.51 $\pm$ 3.09
Phenylmethyl acetate	n.d.	n.d.	n.d.	n.d.	3.27 $\pm$ 0.32	81.55 $\pm$ 2.22	n.d.	n.d.	n.d.	n.d.	n.d.	n.d.
2(5H)-furanone	n.d.	n.d.	n.d.	18.81 $\pm$ 1.87	4.96 $\pm$ 0.11	n.d.	n.d.	n.d.	2.31 $\pm$ 0.02	11.44 $\pm$ 0.43	1.72 $\pm$ 0.03	n.d.
Methyl salicylate	n.d.	n.d.	n.d.	n.d.	n.d.	n.d.	n.d.	n.d.	n.d.	6.56 $\pm$ 0.45	n.d.	5.76 $\pm$ 0.04
Phenylethylacetate	2.29 $\pm$ 0.18	4.37 $\pm$ 0.35	n.d.	n.d.	n.d.	203.49 $\pm$ 13.43	n.d.	n.d.	n.d.	92.57 $\pm$ 1.88	n.d.	39.49 $\pm$ 1.71
Ethyl dodecanoate	9.97 $\pm$ 0.91	26.54 $\pm$ 3.04	67.78 $\pm$ 1.54	61.71 $\pm$ 0.92	n.d.	453.47 $\pm$ 11.09	n.d.	n.d.	2.36 $\pm$ 0.04	463.62 $\pm$ 11.33	6.02 $\pm$ 0.18	199.54 $\pm$ 15.61
Isoamyl decanoate	n.d.	n.d.	n.d.	n.d.	n.d.	6.63 $\pm$ 0.22	n.d.	n.d.	n.d.	20.79 $\pm$ 0.19	n.d.	n.d.
Ethyl dihydro-cinnamate	n.d.	n.d.	n.d.	n.d.	n.d.	n.d.	n.d.	n.d.	n.d.	6.08 $\pm$ 0.99	n.d.	n.d.
Neryl propionate	61.43 $\pm$ 4.80	144.54 $\pm$ 11.47	n.d.	n.d.	n.d.	n.d.	n.d.	n.d.	n.d.	n.d.	1.82 $\pm$ 0.04	n.d.
Ethyl tetradecanoate	1.27 $\pm$ 0.14	0.99 $\pm$ 0.02	3.33 $\pm$ 0.76	10.29 $\pm$ 0.34	n.d.	23.06 $\pm$ 0.78	n.d.	n.d.	0.67 $\pm$ 0.00	19.54 $\pm$ 1.33	2.00 $\pm$ 0.01	5.49 $\pm$ 0.18
Ethyl cinnamate	n.d.	n.d.	n.d.	n.d.	n.d.	n.d.	n.d.	n.d.	n.d.	208.43 $\pm$ 8.66	n.d.	n.d.
2-Phenylethyl hexanoate	n.d.	n.d.	n.d.	n.d.	n.d.	n.d.	n.d.	n.d.	n.d.	n.d.	n.d.	1.84 $\pm$ 0.03
Elemicin	0.51 $\pm$ 0.26	2.73 $\pm$ 0.01	1.63 $\pm$ 0.11	3.07 $\pm$ 0.01	n.d.	n.d.	n.d.	n.d.	n.d.	n.d.	n.d.	n.d.
Ethyl hexadecanoate	n.d.	n.d.	n.d.	n.d.	n.d.	36.42 $\pm$ 0.77	n.d.	n.d.	n.d.	n.d.	2.63 $\pm$ 0.29	32.16 $\pm$ 1.98
Phenylethyl octanoate	n.d.	n.d.	n.d.	n.d.	n.d.	n.d.	n.d.	n.d.	n.d.	1.91 $\pm$ 0.01	n.d.	n.d.
Coumaran	n.d.	n.d.	n.d.	n.d.	n.d.	n.d.	n.d.	n.d.	n.d.	118.87 $\pm$ 5.77	n.d.	n.d.
Total	269.41 $\pm$ 18.53	516.88 $\pm$ 28.58	816.37 $\pm$ 56.98	1571.40 $\pm$ 45.91	297.52 $\pm$ 15.22	13,388.86 $\pm$ 488.29	6.28 $\pm$ 0.08	6.79 $\pm$ 0.03	35.34 $\pm$ 2.30	26976.17 $\pm$ 988.47	76.47 $\pm$ 2.07	6112.28 $\pm$ 309.55
<b>Hydrocarbons</b>												
Undecane	2.18 $\pm$ 0.26	20.92 $\pm$ 0.88	n.d.	n.d.	n.d.	n.d.	n.d.	n.d.	n.d.	n.d.	n.d.	n.d.
Decane	n.d.	6.49 $\pm$ 0.33	n.d.	n.d.	n.d.	n.d.	n.d.	n.d.	n.d.	n.d.	n.d.	n.d.
1,3,8-p-menthatriene	5.58 $\pm$ 0.36	10.10 $\pm$ 0.98	n.d.	n.d.	n.d.	n.d.	n.d.	n.d.	n.d.	n.d.	n.d.	n.d.
Total	7.76 $\pm$ 0.62	37.51 $\pm$ 2.19	n.d.	n.d.	n.d.	n.d.	n.d.	n.d.	n.d.	n.d.	n.d.	n.d.
<b>Ketones</b>												
6-methyl-5-heptene-2-one	4.08 $\pm$ 0.83	24.22 $\pm$ 3.01	n.d.	n.d.	2.89 $\pm$ 0.01	12.91 $\pm$ 0.81	n.d.	n.d.	n.d.	8.76 $\pm$ 0.08	520.50 $\pm$ 5.62	266.79 $\pm$ 8.95
Acetoin	n.d.	26.50 $\pm$ 2.25	n.d.	n.d.	n.d.	n.d.	n.d.	n.d.	n.d.	n.d.	3.15 $\pm$ 0.04	24.14 $\pm$ 0.22
$\alpha$ -ionone	7.33 $\pm$ 1.23	55.30 $\pm$ 0.99	n.d.	n.d.	n.d.	n.d.	n.d.	n.d.	n.d.	n.d.	34.04 $\pm$ 0.34	n.d.
Geranylacetone	7.26 $\pm$ 0.23	95.15 $\pm$ 2.09	8.19 $\pm$ 0.43	20.06 $\pm$ 0.72	n.d.	n.d.	n.d.	n.d.	n.d.	n.d.	207.03 $\pm$ 11.55	220.53 $\pm$ 7.70
$\beta$ -ionone	1.97 $\pm$ 0.60	31.44 $\pm$ 2.43	n.d.	n.d.	n.d.	n.d.	n.d.	n.d.	n.d.	n.d.	15.79 $\pm$ 0.42	32.17 $\pm$ 1.72
Hydroxyacetone	1.07 $\pm$ 0.02	9.16 $\pm$ 1.98	7.62 $\pm$ 0.45	50.78 $\pm$ 1.18	19.48 $\pm$ 0.99	n.d.	n.d.	n.d.	7.42 $\pm$ 0.01	39.94 $\pm$ 0.43	n.d.	n.d.
1-(3-ethylphenyl) ethanone	4.41 $\pm$ 0.03	7.27 $\pm$ 0.91	10.44 $\pm$ 0.23	14.72 $\pm$ 1.77	4.44 $\pm$ 0.22	7.52 $\pm$ 0.88	13.14 $\pm$ 0.98	10.41 $\pm$ 0.03	2.03 $\pm$ 0.01	10.19 $\pm$ 0.31	2.46 $\pm$ 0.08	9.10 $\pm$ 0.09
Total	26.12 $\pm$ 2.94	249.04 $\pm$ 13.66	26.25 $\pm$ 1.11	85.56 $\pm$ 3.67	26.81 $\pm$ 1.22	20.43 $\pm$ 1.69	13.14 $\pm$ 0.98	10.41 $\pm$ 0.03	9.45 $\pm$ 0.02	58.89 $\pm$ 0.82	782.97 $\pm$ 18.06	552.73 $\pm$ 22.67

<b>Phenols</b>													
Phenol	4.14 ± 0.37	33.76 ± 1.45	n.d.	n.d.	n.d.	n.d.	n.d.	n.d.	n.d.	n.d.	0.84 ± 0.01	4.87 ± 0.75	
p-cresol	1.20 ± 0.11	1.34 ± 0.01	n.d.	n.d.	n.d.	n.d.	n.d.	n.d.	n.d.	n.d.	n.d.	n.d.	
Eugenol	0.49 ± 0.02	5.89 ± 0.08	n.d.	n.d.	n.d.	n.d.	n.d.	n.d.	n.d.	n.d.	n.d.	n.d.	
Tymol	n.d.	1.93 ± 0.23	n.d.	n.d.	n.d.	n.d.	n.d.	n.d.	n.d.	n.d.	2.56 ± 0.10	n.d.	
Total	5.83 ± 0.50	42.92 ± 1.77	n.d.	n.d.	n.d.	n.d.	n.d.	n.d.	n.d.	n.d.	2.56 ± 0.10	0.84 ± 0.01	4.87 ± 0.75
<b>Sulphur compounds</b>													
Methyl disulfide	n.d.	n.d.	n.d.	n.d.	n.d.	n.d.	222.79 ± 9.32	232.79 ± 2.35	n.d.	n.d.	n.d.	n.d.	
2,4-dimethylthio- phene	n.d.	n.d.	n.d.	n.d.	n.d.	n.d.	16.61 ± 1.11	15.52 ± 0.22	n.d.	n.d.	n.d.	n.d.	
Methyl propyl disulfide	n.d.	n.d.	n.d.	n.d.	n.d.	n.d.	42.81 ± 0.45	116.03 ± 5.54	n.d.	n.d.	n.d.	n.d.	
3,4-dimethyl- thiophene	n.d.	n.d.	n.d.	n.d.	n.d.	n.d.	921.42 ± 5.61	706.74 ± 6.99	n.d.	n.d.	n.d.	n.d.	
2,5-dimethyl- thiophene	n.d.	n.d.	n.d.	n.d.	n.d.	n.d.	181.11 ± 14.45	158.00 ± 2.34	n.d.	n.d.	n.d.	n.d.	
1,3-dithiane	n.d.	n.d.	n.d.	n.d.	n.d.	n.d.	3147.54 ± 271.11	2692.06 ± 176.67	n.d.	n.d.	n.d.	n.d.	
Dimethyl trisulfide	n.d.	n.d.	n.d.	n.d.	n.d.	n.d.	5686.36 ± 321.23	7369.83 ± 53.67	n.d.	n.d.	n.d.	n.d.	
Diallyl disulphide	n.d.	n.d.	n.d.	n.d.	n.d.	n.d.	76.54 ± 4.01	75.23 ± 0.99	n.d.	n.d.	n.d.	n.d.	
Total	n.d.	n.d.	n.d.	n.d.	n.d.	n.d.	10295.18 ± 627.39	11366.20 ± 248.77	n.d.	n.d.	n.d.	n.d.	
<b>Aromatic hydrocarbons</b>													
Styrene	n.d.	6.66 ± 0.43	n.d.	n.d.	n.d.	n.d.	n.d.	n.d.	n.d.	n.d.	2545.58 ± 41.11	n.d.	1.69 ± 0.01
p-cymene	120.20 ± 4.98	196.31 ± 12.89	1009.28 ± 39.51	735.27 ± 13.54	0.70 ± 0.01	n.d.	n.d.	n.d.	n.d.	n.d.	n.d.	1.76 ± 0.02	n.d.
2,5-Dimethylstyrene	46.42 ± 2.63	153.22 ± 11.37	6.43 ± 0.23	6.33 ± 0.23	n.d.	n.d.	n.d.	n.d.	n.d.	n.d.	n.d.	n.d.	n.d.
Total	166.62 ± 7.61	356.19 ± 24.69	1015.71 ± 39.74	741.60 ± 13.77	0.70 ± 0.01	n.d.	n.d.	n.d.	n.d.	n.d.	2545.58 ± 41.11	1.76 ± 0.02	1.69 ± 0.01
<b>Terpenes and terpenoids</b>													
Camphene	2.69 ± 0.76	8.76 ± 0.23	n.d.	n.d.	n.d.	n.d.	n.d.	n.d.	n.d.	n.d.	n.d.	n.d.	n.d.
β-pinene	20.04 ± 3.09	26.95 ± 0.21	11.66 ± 0.80	6.71 ± 0.23	n.d.	n.d.	n.d.	n.d.	n.d.	n.d.	n.d.	n.d.	n.d.
α-phellandrene	111.85 ± 4.11	77.77 ± 3.87	8.15 ± 0.23	77.77 ± 3.87	n.d.	n.d.	n.d.	n.d.	n.d.	n.d.	n.d.	n.d.	n.d.
Linalool	n.d.	n.d.	n.d.	n.d.	n.d.	n.d.	n.d.	n.d.	n.d.	28.43 ± 1.44	388.76 ± 13.45	n.d.	n.d.
β-myrcene	175.07 ± 8.68	270.50 ± 11.65	73.67 ± 0.90	68.60 ± 2.45	n.d.	n.d.	n.d.	n.d.	n.d.	n.d.	1586.53 ± 57.51	1.81 ± 0.03	n.d.
α-terpinene	41.44 ± 1.44	101.39 ± 11.48	n.d.	n.d.	n.d.	n.d.	n.d.	n.d.	n.d.	n.d.	n.d.	n.d.	n.d.
δ-limonene	100.25 ± 3.52	176.49 ± 11.21	3321.36 ± 88.45	4271.66 ± 83.56	n.d.	n.d.	n.d.	n.d.	n.d.	n.d.	n.d.	8.09 ± 0.04	28.26 ± 0 0.33
Terpinen-4-ol	3.61 ± 0.14	345.68 ± 10.43	n.d.	69.61 ± 2.23	n.d.	n.d.	n.d.	n.d.	n.d.	n.d.	n.d.	n.d.	n.d.
α-terpineol	1.39 ± 0.19	40.67 ± 2.78	n.d.	15.43 ± 0.99	n.d.	n.d.	n.d.	n.d.	n.d.	n.d.	7.50 ± 0.32	n.d.	n.d.
Estragole	12.15 ± 1.68	6.05 ± 0.43	396.49 ± 25.56	760.24 ± 33.45	0.80 ± 0.03	8.19 ± 1.23	n.d.	n.d.	n.d.	n.d.	n.d.	n.d.	n.d.
β-phellandrene	14.13 ± 1.13	17.14 ± 0.23	n.d.	n.d.	n.d.	n.d.	n.d.	n.d.	n.d.	n.d.	n.d.	n.d.	n.d.
γ-terpinene	110.87 ± 2.06	609.83 ± 14.49	634.46 ± 24.13	559.09 ± 45.90	n.d.	n.d.	n.d.	n.d.	n.d.	n.d.	n.d.	n.d.	n.d.
3-carene	20.00 ± 1.56	40.87 ± 3.78	n.d.	n.d.	n.d.	n.d.	n.d.	n.d.	n.d.	n.d.	n.d.	n.d.	n.d.
α-terpinolene	606.71 ± 25.03	1563.34 ± 99.32	n.d.	145.16 ± 11.33	n.d.	n.d.	n.d.	n.d.	n.d.	n.d.	n.d.	7.62 ± 0.03	n.d.
Citronellol	n.d.	n.d.	1.75 ± 0.01	7.60 ± 2.34	n.d.	n.d.	n.d.	n.d.	n.d.	n.d.	3.42 ± 0.99	6.30 ± 0.02	35.81 ± 11.64
Geraniol	6.24 ± 0.47	35.66 ± 0.47	n.d.	2.48 ± 0.05	n.d.	n.d.	n.d.	n.d.	n.d.	n.d.	n.d.	3.18 ± 0.04	14.06 ± 0.16
trans-carveol	n.d.	n.d.	44.03 ± 9.98	4.50 ± 0.08	n.d.	n.d.	n.d.	n.d.	n.d.	n.d.	n.d.	n.d.	n.d.
β-caryophyllene	679.39 ± 20.23	3778.30 ± 84.69	n.d.	n.d.	n.d.	n.d.	n.d.	n.d.	n.d.	n.d.	n.d.	56.65 ± 2.43	n.d.
Nerolidol	n.d.	n.d.	n.d.	n.d.	n.d.	n.d.	n.d.	n.d.	n.d.	41.58 ± 0.65	288.13 ± 10.23	n.d.	n.d.
β-farnesene	19.00 ± 0.31	91.33 ± 5.89	n.d.	n.d.	n.d.	n.d.	n.d.	n.d.	n.d.	n.d.	n.d.	n.d.	n.d.
Anethol	40.84 ± 1.17	155.58 ± 11.43	6092.43 ± 93.78	16628.19 ± 345.65	n.d.	80.01 ± 1.37	66.98 ± 3.45	97.42 ± 0.67	18.73 ± 0.43	99.10 ± 2.76	14.46 ± 0.82	83.54 ± 12.50	
β-himachalene	18.92 ± 0.14	12.89 ± 0.98	n.d.	n.d.	n.d.	n.d.	n.d.	n.d.	n.d.	n.d.	n.d.	n.d.	n.d.
α-zingiberene	2.53 ± 0.04	26.13 ± 0.67	n.d.	n.d.	n.d.	n.d.	n.d.	n.d.	n.d.	n.d.	n.d.	n.d.	n.d.
α-himachalene	123.90 ± 1.97	375.35 ± 14.76	n.d.	n.d.	n.d.	n.d.	n.d.	n.d.	n.d.	n.d.	n.d.	n.d.	n.d.
Myristicin	48.46 ± 1.89	146.63 ± 11.00	99.14 ± 11.12	139.02 ± 22.45	n.d.	n.d.	n.d.	n.d.	n.d.	n.d.	n.d.	n.d.	n.d.
α-cedrene	15.15 ± 0.81	25.27 ± 3.54	n.d.	n.d.	n.d.	n.d.	n.d.	n.d.	n.d.	n.d.	15.26 ± 1.44	n.d.	n.d.
δ-guaiene	864.86 ± 15.62	2699.14 ± 9.22	n.d.	n.d.	n.d.	n.d.	n.d.	n.d.	2.16 ± 1.36	40.20 ± 0.09	52.83 ± 3.45	n.d.	n.d.
Curcumene	115.61 ± 3.74	135.79 ± 11.11	n.d.	n.d.	n.d.	n.d.	n.d.	n.d.	0.32 ± 0.02	5.67 ± 0.01	5.22 ± 0.04	n.d.	n.d.
γ-bisabone	83.16 ± 3.38	334.59 ± 23.89	n.d.	n.d.	n.d.	n.d.	n.d.	n.d.	n.d.	4.03 ± 0.09	4.72 ± 0.44	n.d.	n.d.
Total	3238.26 ± 103.36	11102.10 ± 347.76	10683.14 ± 254.96	22678.29 ± 550.71	0.80 ± 0.03	88.20 ± 2.60	66.98 ± 3.45	97.42 ± 0.67	91.22 ± 3.90	2438.60 ± 86.89	160.88 ± 7.34	161.67 ± 24.63	

The chemicals are grouped per chemical class.

Results indicate mean values of three measurements ± S.D.

1-heptanol was used as internal standard.

Abbreviations: VJ, vegetable juice; KLB, kefir-like beverage; n.d. not detected.

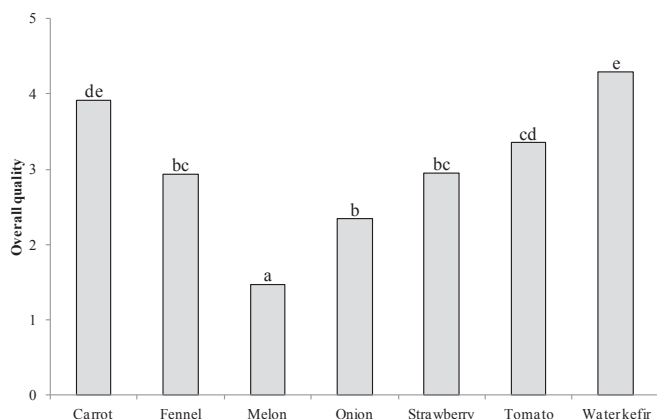


Fig. 1. Sensory evaluation of vegetable-based kefir-like beverages. Bars with the same letter are not statistically different at  $P < 0.05$  (Tukey–Kramer's multiple range test).

that the sulphur compounds derived from cabbage showed inhibitory activities against yeasts. They found that 20 ppm of dimethyl trisulfide inhibited several strains of different species, such as *S. cerevisiae* Y6, *Torulopsis etchellsii* Y24, *Hansenula mrakii* Y27 and *Pichia membranefaciens* Y20. The same authors found that dimethyl disulphide retarded the growth of *S. cerevisiae*. Other compounds of this chemical class, such as diallyl trisulfide, diallyl tetrasulfide and dimethyl trisulfide, inhibit several yeasts at concentrations ranging between 2 and 45 ppm (Kim et al., 2004). The amount of dimethyl trisulfide detected in onion KLB in this work is more than 160 folds higher than the minimum inhibitory concentration reported by Kim et al. (2004). The mechanisms of action of diallyl disulphide has been studied against *Candida*; the compound is able to trigger cell death most probably by eliciting oxidative stress as a consequence of thiol depletion and impaired mitochondrial function (Lemar et al., 2007).

Detection of terpene and terpenol compounds was in fennel and carrot KLB at very high concentrations compared to those of the corresponding VJs. Anethol increased in all samples, but consistently in fennel KLB. Strawberry KLB showed an increase of  $\beta$ -myrcene.

### 3.5. Overall quality

Fifteen untrained tasters were asked to judge the overall quality of the KLBs and Fig. 1 shows the results. A water kefir was prepared with the same microbial mixture according to the producer's instructions and used as control kefir for panellists. Only carrot KLB showed an overall quality evaluation comparable with that of water kefir. However, tomato KLB did not significantly differ from carrot KLB.

## 4. Conclusions

Taking into account the increasing complexity of the needs of different typologies of consumers, including vegan vegetarian and subjects with intolerance/allergy to dairy products, we applied an integrated technological approach in this work to obtain kefir-like beverages from an updated selection of vegetable substrates, using commercial water kefir microorganisms. Analysis were performed to address their microbial composition, physico-chemical characteristics and sensory profile, in order to evaluate the preservation of vegetable and kefir synergistic properties that exert benefits to the human health in the final beverages and test their appreciation by potential consumers.

We developed new-functional non-dairy beverages whose heterogeneous microbial characteristics reflected the same codominance of LAB and yeasts typical of traditional milk or water kefir. In addition, physico-chemical and organoleptic properties of some vegetable-based KLBs, especially carrot KLB, well met the expectations and tastes of panellists. The beverages produced in this work may help to link the gap between the actual and an ideal and innovative consumption of vegetables, recommended in human diet. Characterization of some KLBs was by the presence of molecules with antioxidant activity giving an additional benefit to the experimental products, suggesting their production at large scale as healthy products, satisfying a wider range of consumers and showing a new way of vegetable administration. The new products might represent important foods providing live microorganisms to vegan people with a limited availability of fermented products.

## References

- Anar, S. (2000). Kefir and its properties (Kefir ve ozellikleri). *Journal of Faculty of Veterinary Medicine-Uludag University-Turkey*, 19, 137–140.
- AOAC — Association of Official Analytical Chemistry. (2000). *Official methods of analysis of the association of official analytical chemistry* (17th ed.). Washington: AOAC — Association of Official Analytical Chemistry.
- Arrizon, J., Calderón, C., & Sandoval, G. (2006). Effect of different fermentation conditions on the kinetic parameters and production of volatile compounds during the elaboration of a prickly pear distilled beverage. *Journal of Industrial Microbiology and Biotechnology*, 33(11), 921–928.
- Beshkova, D. M., Simova, E. D., Frengova, G. I., Simov, Z. I., & Dimitrov, Z. P. (2003). Production of volatile aroma compounds by kefir starter cultures. *International Dairy Journal*, 13(7), 529–535.
- Cevikbas, A., Yemni, E., Ezedenn, F. W., Yardimici, T., Cevikbas, U., & Stohs, S. J. (1994). Antitumour antibacterial and antifungal activities of kefir and kefir grain. *Phytotherapy Research*, 8(2), 78–82.
- Cheirsilp, B., Shoji, H., Shimizu, H., & Shioya, S. (2003). Interactions between *Lactobacillus kefirifaciens* and *Saccharomyces cerevisiae* in mixed culture for kefir production. *Journal of Bioscience and Bioengineering*, 96(3), 279–284.
- Chen, H. C., Wang, S. Y., & Chen, M. J. (2008). Microbiological study of lactic acid bacteria in kefir grains by culture-dependent and culture-independent methods. *Food Microbiology*, 25(3), 492–501.
- Corona, O. (2010). Wine-making with protection of must against oxidation in a warm, semi-arid terroir. *South African Journal of Enology and Viticulture*, 31(1), 58–63.
- Dani, C., Oliboni, L. S., Vanderlinde, R., Bonatto, D., Salvador, M., & Henriques, J. A. P. (2007). Phenolic content and antioxidant activities of white and purple juices manufactured with organically-or conventionally-produced grapes. *Food and Chemical Toxicology*, 45(12), 2574–2580.
- Dias, D. R., Schwan, R. F., Freire, E. S., & Seródio, R. D. S. (2007). Elaboration of a fruit wine from cocoa (*Theobroma cacao* L.) pulp. *International Journal of Food Science and Technology*, 42(3), 319–329.
- Dragone, G., Mussatto, S. I., Oliveira, J. M., & Teixeira, J. A. (2009). Characterisation of volatile compounds in an alcoholic beverage produced by whey fermentation. *Food Chemistry*, 112(4), 929–935.
- Duarte, W. F., Dias, D. R., Oliveira, J. M., Teixeira, J. A., Silva, J. B. D. A., & Schwan, R. F. (2010). Characterization of different fruit wines made from cacao, cupuassu, gabiroba, jaboticaba and umbu. *LWT-Food Science and Technology*, 43(10), 1564–1572.
- Esteve-Zarzoso, B., Belloch, C., Uruburu, F., & Querol, A. (1999). Identification of yeasts by RFLP analysis of the 5.8S rRNA gene and the two ribosomal internal transcribed spacers. *International Journal of Systematic Bacteriology*, 49, 32–337.
- Fuleki, T., & Francis, F. J. (1968). Quantitative methods for anthocyanins. 4. Determination of individual anthocyanins in cranberry and cranberry products. *Journal of Food Science*, 33(5), 471–478.
- Gil, M. I., Tomás-Barberán, F. A., Hess-Pierce, B., Holcroft, D. M., & Kader, A. A. (2000). Antioxidant activity of pomegranate juice and its relationship with phenolic composition and processing. *Journal of Agricultural and Food Chemistry*, 48(10), 4581–4589.
- Granato, D., Branco, G. F., Nazzaro, F., Cruz, A. G., & Faria, J. A. (2010). Functional foods and nondairy probiotic food development: trends, concepts, and products. *Comprehensive Reviews in Food Science and Food Safety*, 9(3), 292–302.
- GURI. (2001). *Legge quadro in materia di alcol e di problemi alcolcorrelati*, Legge 125, 30 Marzo 2001, 90 p. 18). Gazzetta Ufficiale della Repubblica Italiana. Aprile 2001.
- Guzel-Seydim, Z., Seydim, A. C., & Greene, A. K. (2000). Organic acids and volatile flavor components evolved during refrigerated storage of kefir. *Journal of Dairy Science*, 83(2), 275–277.
- He, F. J., Nowson, C. A., & MacGregor, G. A. (2006). Fruit and vegetable consumption and stroke: meta-analysis of cohort studies. *The Lancet*, 367(9507), 320–326.
- Irigoyen, A., Arana, I., Castiella, M., Torre, P., & Ibanez, F. C. (2005). Microbiological,

- physicochemical, and sensory characteristics of kefir during storage. *Food Chemistry*, 90(4), 613–620.
- Kim, J. W., Kim, Y. S., & Kyung, K. H. (2004). Inhibitory activity of essential oils of garlic and onion against bacteria and yeasts. *Journal of Food Protection*, 67(3), 499–504.
- Kyung, K. H., & Fleming, H. P. (1997). Antimicrobial activity of sulfur compounds derived from cabbage. *Journal of Food Protection*, 60(1), 67–71.
- Larrauri, J. A., Sánchez-Moreno, C., & Saura-Calixto, F. (1998). Effect of temperature on the free radical scavenging capacity of extracts from red and white grape pomace peels. *Journal of Agricultural and Food Chemistry*, 46(7), 2694–2697.
- Lee, J., Durst, R. W., & Wrolstad, R. E. (2005). Determination of total monomeric anthocyanin pigment content of fruit juices, beverages, natural colorants, and wines by the pH differential method: collaborative study. *Journal of AOAC International*, 88(5), 1269–1278.
- Lemar, K. M., Aon, M. A., Cortassa, S., O'Rourke, B., Müller, C. T., & Lloyd, D. (2007). Diallyl disulphide depletes glutathione in *Candida albicans*: oxidative stress-mediated cell death studied by two-photon microscopy. *Yeast*, 24(8), 695–706.
- Liu, J. R., & Lin, C. W. (2000). Production of kefir from soymilk with or without added glucose, lactose, or sucrose. *Journal of Food Science*, 65(4), 716–719.
- Liu, R., & Shen, F. (2008). Impacts of main factors on bioethanol fermentation from stalk juice of sweet sorghum by immobilized *Saccharomyces cerevisiae* (CICC 1308). *Bioresource Technology*, 99(4), 847–854.
- Lombardi, A., Delfini, C., Zilio, F., & Tosi, E. (2004). Contributo alla valorizzazione del vino Valpolicella doc mediante l'isolamento, la caratterizzazione e il successivo impiego di lieviti specifici. *Vignevini: Rivista italiana di viticoltura e di enologia*, 31(9), 72–79.
- Magalhães, K. T., Dias, D. R., de Melo Pereira, G. V., Oliveira, J. M., Domingues, L., Teixeira, J. A., et al. (2011). Chemical composition and sensory analysis of cheese whey-based beverages using kefir grains as starter culture. *International Journal of Food Science and Technology*, 46(4), 871–878.
- Magalhães, K. T., Pereira, G. D. M., Dias, D. R., & Schwan, R. F. (2010). Microbial communities and chemical changes during fermentation of sugary Brazilian kefir. *World Journal of Microbiology and Biotechnology*, 26(7), 1241–1250.
- Mahy, M., Eycken, L., & Oosterlinck, A. (1994). Evaluation of uniform color spaces developed after the adoption of CIELAB and CIELUV. *Color Research and Application*, 19(2), 105–121.
- de Melo Pereira, G. V., Ramos, C. L., Galvão, C., Souza Dias, E., & Schwan, R. F. (2010). Use of specific PCR primers to identify three important industrial species of *Saccharomyces* genus: *Saccharomyces cerevisiae*, *Saccharomyces bayanus* and *Saccharomyces pastorianus*. *Letters in Applied Microbiology*, 51(2), 131–137.
- Nambou, K., Gao, C., Zhou, F., Guo, B., Ai, L., & Wu, Z. J. (2014). A novel approach of direct formulation of defined starter cultures for different kefir-like beverage production. *International Dairy Journal*, 34(2), 237–246.
- Nazzaro, F., Fratianni, F., Sada, A., & Orlando, P. (2008). Synbiotic potential of carrot juice supplemented with *Lactobacillus* spp. and inulin or fructooligosaccharides. *Journal of the Science of Food and Agriculture*, 88(13), 2271–2276.
- O'Donnell, K. (1993). *Fusarium and its near relatives*. In D. R. Reynolds, & J. W. Taylor (Eds.), *The fungal anamorph: mitotic, meiotic and pleomorphic speciation in fungal systematic* (pp. 225–233). Wallingford: CAB International.
- Prado, F. C., Parada, J. L., Pandey, A., & Soccol, C. R. (2008). Trends in non-dairy probiotic beverages. *Food Research International*, 41(2), 111–123.
- Puerari, C., Magalhães, K. T., & Schwan, R. F. (2012). New cocoa pulp-based kefir beverages: microbiological, chemical composition and sensory analysis. *Food Research International*, 48(2), 634–640.
- Reichert, N. (2008). *Cargill beverage concepts will address consumer demands for health, taste and texture at IFT 2008*. Available from <http://www.cargill.com/news-center/news-releases/2008/NA3007612.jsp> Accessed 03.10.15.
- Rodrigues, K. L., Caputo, L. R. G., Carvalho, J. C. T., Evangelista, J., & Schneedorf, J. M. (2005). Antimicrobial and healing activity of kefir and kefir extract. *International Journal of Antimicrobial Agents*, 25(5), 404–408.
- Sabokbar, N., & Khodaiyan, F. (2014). Characterization of pomegranate juice and whey based novel beverage fermented by kefir grains. *Journal of Food Science and Technology*, 52, 3711–3718.
- Saerens, S. M., Delvaux, F. R., Verstrepen, K. J., & Thevelein, J. M. (2010). Production and biological function of volatile esters in *Saccharomyces cerevisiae*. *Microbial Biotechnology*, 3(2), 165–177.
- Schneedorf, J. M. (2012). *Kefir D'Aqua and its probiotic properties*. INTECH Open Access Publisher.
- Shavit, E. (2008). Renewed interest in kefir, the ancient elixir of longevity. *Fungi*, 1, 14–18.
- Slinkard, K., & Singleton, V. L. (1977). Total phenol analysis: automation and comparison with manual methods. *American Journal of Enology and Viticulture*, 28(1), 49–55.
- Varga, E., Klinke, H. B., Réczey, K., & Thomsen, A. B. (2004). High solid simultaneous saccharification and fermentation of wet oxidized corn stover to ethanol. *Biotechnology and Bioengineering*, 88(5), 567–574.
- Weisburg, W., Barns, S. M., Pelletier, D. A., & Lane, D. J. (1991). 16S ribosomal DNA amplification for phylogenetic study. *Journal of Bacteriology*, 173, 697–703.
- Witthuhn, R. C., Schoeman, T., & Britz, T. J. (2005). Characterisation of the microbial population at different stages of Kefir production and Kefir grain mass cultivation. *International Dairy Journal*, 15(4), 383–389.
- Yoon, K. Y., Woodams, E. E., & Hang, Y. D. (2004). Probiotic of tomato juice by lactic acid bacteria. *Journal of Microbiology*, 42(4), 315–318.
- Yoon, K. Y., Woodams, E. E., & Hang, Y. D. (2005). Fermentation of beet juice by beneficial lactic acid bacteria. *LWT-Food Science and Technology*, 38(1), 73–75.
- Yoon, K. Y., Woodams, E. E., & Hang, Y. D. (2006). Production of probiotic cabbage juice by lactic acid bacteria. *Bioresource Technology*, 97(12), 1427–1430.
- Zourari, A., & Anifantakis, E. M. (1988). Kefir. Physico-chemical, microbiological and nutritional characters. Production technology. A review. *Le Lait*, 68, 373–392.



# Colour stability of cooked ham packed under modified atmospheres in polyamide nanocomposite blends<sup>☆</sup>



Elsa Lloret <sup>a</sup>, Pierre A. Picouet <sup>a</sup>, Raúl Trbojevič <sup>b</sup>, Avelina Fernández <sup>c,\*</sup>

<sup>a</sup> *Departament de Tecnologia Dels Aliments, Institut de Recerca i Tecnologia Agroalimentàries (IRTA), Monells, Girona, Spain*

<sup>b</sup> *Division of Biochemical Toxicology, National Center for Toxicological Research, FDA, 3900 NCTR Road, Jefferson, AR 72079, USA*

<sup>c</sup> *Instituto de Física Corpuscular (CSIC-UVEG), Parc Científic, Paterna, Valencia, Spain*

## ARTICLE INFO

### Article history:

Received 31 July 2015

Received in revised form

6 November 2015

Accepted 8 November 2015

Available online 11 November 2015

### Keywords:

Nylon

Cooked ham

Nanoclays

Oxygen permeation

Colour

Exfoliation

MAP

## ABSTRACT

Two novel blends containing a low-density polyethylene (LDPE) and a neat polyamide (PA) or a polyamide nanocomposite (PAN) layers were fabricated and their technological potential was evaluated during the refrigeration of cooked ham in modified atmospheres (MAP). Nanoclays were homogeneously distributed and nearly exfoliated, and they lowered significantly the oxygen transmission rate (OTR) of the PAN films. Due to the lower OTR, the headspace oxygen level in PAN pouches do not rise above 0.26% but it approached 2% in PA pouches at day 20. The residual oxygen levels were key for colour change during MAP storage of cooked ham. Cooked ham redness and reflectivity were stable during 27 days in PAN pouches while a strong colour deterioration took place after day 7 in PA pouches. Other parameters such as moisture content and water activity remained unaltered, and pH development was related to microbial growth and independent of the packaging polymer. The evolution of cooked ham colour in PAN was comparable to a high-barrier commercial polymer, and was acceptable for commercial sale for 27 days, showing excellent perspectives for polyamide nanocomposites in the storage of cooked ham.

© 2015 Elsevier Ltd. All rights reserved.

## 1. Introduction

Cooked ham is a highly consumed meat product across Europe due to its fine sensory properties, healthy attributes and convenience, reinforced by the effort to produce light and low-additive cooked ham varieties (Pietrasik & Gaudette, 2014). A whole range of products are much appreciated by children and elderly people, with the consumption of cooked ham in around 4.05 kg per capita in Spain (Talens, Mora, Morsy, Barbin, & Elmasry, 2013). The final quality of the product is related to the quality of the raw material, in particular pH decline post-mortem and final pH, fat content, and microbial loads, and to the effects of relatively complex mechanical processes (Casiraghi, Alamprese, & Pompei, 2007). The injection of brine is important to achieve the characteristic sensory properties and to extend the microbiological stability during refrigerated storage. The process of tumbling helps in the distribution of the

brine in the muscle fibres, and during cooking, proteins are denatured and the fibres are linked to texture retention (Casiraghi et al., 2007). Finally, the product is packaged in high barrier protecting materials to fulfil the requirements for a long shelf-life (Andersen, Bertelsen, Boeghsoerensen, Shek, & Skibsted, 1988; Singh, Wani, Saengerlaub, & Langowski, 2011). Consumer acceptability of cooked ham is strongly related to the visual appearance, of which colour, marbling and the drip loss are the most obvious parameters to be evaluated (Singh et al., 2011).

During heating, nitrosylmyoglobin Fe<sup>2+</sup> denatures to the nitrosyl-haemochrome Fe<sup>2+</sup>, which has a recognizable pink colour. When meat is exposed to light in the presence of small amounts of oxygen, this pigment turns to the characteristic grey-brown colour attributed to the oxidized nitrosyl-haemochrome Fe<sup>3+</sup> (Li, Li, Xu, & Zhou, 2012; Moeller, Jensen, Skibsted, & Bertelsen, 2000). A number of studies have been conducted to investigate the effects of packaging on the stability of cured meat products and in particular of cooked ham. Solutions from vacuum packaging combined with darkness (Haile, De Smet, Claeys, & Vossen, 2013; Li et al., 2012; Mattos, Norena, & Brandelli, 2003) to modified atmosphere packaging with low residual oxygen levels have been suggested (Haile et al. 2013). Light and residual oxygen are the critical parameters to achieve the desired colour stability (Larsen, Westad, Soerheim, &

<sup>☆</sup> Disclaimer: This article is not an official U.S. Food and Drug Administration (FDA) guidance or policy statement. No official support or endorsement by the U.S. FDA is intended or should be inferred.

\* Corresponding author.

E-mail address: [velifdez@ific.uv.es](mailto:velifdez@ific.uv.es) (A. Fernández).

Nilsen, 2006). The interactions are complex, and modified atmosphere packaging with high concentrations of carbon dioxide might have negative effects due to CO<sub>2</sub> absorption in the aqueous phase of the matrix, which often generates package shrinkage. Other solutions, such as the use of oxygen scavengers, are limited due to the imprecise legislation and the low interest shown by consumers.

To achieve the range of objectives regarding meat stability, barrier polymer blends have become common in vacuum and modified atmosphere packaging (MAP) (McMillin, 2008; Singh et al., 2011). Among the wide range of possibilities, polyamide-6 (PA6) is known to be highly resistant to abrasion, with excellent elasticity, high tensile strength and resistance to puncture (Kohno & Tamemoto, 2004). The limited barrier properties of PA6 can be considerably improved by the incorporation of nanoclays, and in particular organo-montmorillonites (Picouet, Fernandez, Realini, & Lloret, 2014; Baldi, Franceschini, Bignotti, Tieghi, & Riccò, 2009; Sadeghi, Fereydoon, & Ajji, 2013). Nano-clay fillers are not expensive and present high stability, being able to reduce the amount of polymer necessary to enhance barrier properties. Several companies have optimised them in PA6 layers. PA6 nanocomposites might be incorporated in polymer blends bringing an improvement in film barrier properties to helium, hydrogen, oxygen, and water (Picard, Gerard, & Espuche, 2008) and water vapour and oxygen (Beatrice, Branciforti, Alves, & Bretas, 2010; Fasihi & Abolghasemi, 2011; Sadeghi et al., 2013). By compression moulding, intercalated or exfoliated structures can be produced, which are more effective in reducing the permeability (Alexandre et al., 2009). The addition of nanoclays to PA6 also produces an increase in viscosity during elongation (Baldi et al., 2009), and a more shear-thinning behaviour (Tung, Gupta, Simon, Edward, & Bhattacharya, 2005).

Nanoclays enhance the mechanical and barrier properties of non-renewable plastics and in particular of polyamide-6, but research on technological applications of those films is scarce (Picouet et al., 2014). The objective of this study was to fabricate a multilayer containing a PA6 layer reinforced with nanoclays and to determine the effects of this novel nanocomposite blend on relevant quality attributes of cooked-ham during retail display resembling commercial conditions. Development of headspace composition, water activity, moisture content, pH, colour and microbial loads of cooked ham during 27 days in a nanocomposite polymer packaging were studied in detail; and they were compared to a commercial packaging polymer and an equivalent blend free of nanoclays.

## 2. Materials and methods

### 2.1. Fabrication of nanocomposites

Two blends with an A/B/C structure were fabricated with a thickness of approximately 100 microns. The internal layer C contained low-density polyethylene (LDPE Dow 410E). The B layer was a linear low density polyethylene tie-resin (Plexar 3236) for flexible packaging. The external layer A contained standard polyamide PA-6 (Ultramid B36LN, BASF, Ludwigshafen, Germany) or, as an alternative, a nanoclay modified polyamide PA-6 (commercial name not given). The films were fabricated by a cast film co-extrusion process at 85 rpm for the LDPE, 18 or 20 rpm for PA or PAN, and 8 rpm for the adhesive. Two films (160 m long and 300 mm width) were obtained. One blend has an external layer composed of standard polyamide (PA) and the other with a nanocomposite polyamide (PAN).

As control material, a coextruded multilayer commercial barrier bag was used, named internally OSB (OSB3050, OTR 20 cc/m<sup>2</sup>/24 h/bar 23 °C, 0% HR, ASTM D-3985, from Cryovac Sealed Air Packaging SL, Milano, Italy).

### 2.2. Characterization of the packaging materials

#### 2.2.1. Transmission Electron Microscope micrographs

The morphology of the films was characterized using a Transmission Electron Microscope (TEM) TEM-EDS JEOL JEM-2100F (JEOL USA, Peabody, MA) with field emission gun and optional EDAX EDS for X-ray spectroscopy. Plastic nanocomposites were inserted in an epoxy resin and cut in ultrafine sections, ~40 nm thick. Observations were made at 80 KV.

#### 2.2.2. Thickness

A micrometre (293-240, Mitutoyo Corporation, Tokyo, Japan) with an accuracy of ±1 µm was used to measure film thickness. Results were calculated from the average of ten repetitions for each material.

#### 2.2.3. Oxygen permeability

Oxygen Transmission Rate (OTR) of the fabricated films was characterised following the ASTM D3985 method (2010). Data were taken at 23 °C at 0% relative humidity with an OX-TRAN model 2/21 (MOCON, Mineapolis, USA). Three measurements were carried out for the two multilayer films PA and PAN, and results were expressed in cm<sup>3</sup>/m<sup>2</sup>/day/bar. In the commercial film OSB, available OTR values with the same experimental conditions were taken from the technical data sheet.

#### 2.2.4. X-ray scattering

The X-ray scattering analysis (XRD) were performed with a Bruker D2 Phaser X-ray Diffraction System. Scans of intensity versus scattering angle (2 theta) were recorded between 2–30° at room temperature. The scanning rate was 1°/min using Cu Kα radiation with identical instrument setting for both films (control and clay). The λ of the radiation used was 1.54 Å with an operating voltage of 40 KV and a current of 30 mA.

### 2.3. Cooked ham

The cured-cooked meat product was produced at the IRTA facility. The ingredients and additives for the cooked ham product were leg muscles (12 kg), and water (18% w/w) containing sodium chloride (18 g/kg), sodium tripolyphosphate (3 g/kg), carrageenan (1 g/kg), sodium ascorbate (0.5 g/kg) and sodium nitrite (0.1 g/kg).

The meat was grinded through a 3-hole kidney plate, the brine was added and the mixture was tumbled for 2 h to achieve a good brine distribution before stuffing into high barrier cook-in bags HT3050 (Cryovac Sealed air Packaging SL, Milano, Italy). The hams were heated at 70 °C during approximately 6 h to a core temperature of 68 °C and cooled to 3 °C for 24 h before slicing and packaging.

### 2.4. Packaging of cooked ham slices

Cooked hams were sliced in 150 × 110 × 10 mm thick slices and were MAP packaged (70% N<sub>2</sub>:30% CO<sub>2</sub>; Carbuos Metalicos, Barcelona, Spain) with a gas-to-meat-ratio ~3, using a Tecnotrip EV-13 packaging machine (Tecnotrip, S.A., Terrassa, Barcelona) placed in a clean room. The slices were packed in different pouches (PA or PAN) or with the commercial material OSB.

After MAP packaging, samples were displayed for 1, 7, 13, 20, and 27 days, with 12 h of darkness and 12 h under commercial fluorescence light using a display case Euro Lx334, (ISA S.r.l., Italy) with a fluorescence light intensity of 900 Lux (Osram L35W/54 Cool Daylight Germany) and 5 ± 2 °C. Three repetitions were carried out at each condition for each sampling day.

#### 2.4.1. Headspace evolution

During storage in modified atmospheres, oxygen (O<sub>2</sub>) of the headspace of packaging was analysed at days 1, 7, 13, 20 and 27 using a Checkmate II O<sub>2</sub>/CO<sub>2</sub> gas analyser from PBI Dansensor (PBI Dansensor, Denmark). The equipment had a sensor accuracy of ±0.1% for O<sub>2</sub>. Detection limit was 0.0001% for O<sub>2</sub> content. The gas content was analysed in duplicate in each sample.

#### 2.4.2. Physicochemical parameters

The water activity (a<sub>w</sub>) was measured at 25 °C ± 0.3 with an AquaLab CX-2 instrument (Decagon Devices Inc., Washington, USA) with a resolution of 0.003. After measuring a<sub>w</sub>, the water content of the samples was immediately determined by drying at 103 °C ± 2 until reaching constant weight (AOAC method 950.46, 1990).

The pH was measured using a Crison pH-metre (Crison PH 25, Crison Instruments S.A., Barcelona, Spain) with a resolution of 0.01 in combination with a Crison puncture electrode Crison pH 5053 (Crison Instruments S.A., Barcelona, Spain).

#### 2.4.3. Colour measurements

The colour changes were quantified with the CIELAB colour space coordinates (L\*, a\*, and b\*) obtained by a Minolta CM-2002 spectrophotometer (Minolta, Tokyo, Japan), using a C illuminant, with a 2° observation angle and 4 mm aperture diameter. The equipment was calibrated with standard black and white tiles. Coordinate values were measured at days 1, 7, 13, 20 and 27. In parallel, spectra between 360 and 740 nm were recorded and the reflectivity ratio I<sub>660</sub>/I<sub>500</sub> was calculated to evaluate differences of sample reflectivity. Measurements were carried out in triplicate for each sample. The samples were not moved during storage time. Colour coordinates were measured at the illuminated front and at the dark back to observe differences due to light exposition.

#### 2.4.4. Microbiology

The total mesophilic aerobic counts were plate counted after decimal serial dilutions on Plate Count Agar (PCA, Oxoid, Unipath, Basingstoke, UK) plates and incubated for 72 h at 30 °C (UNE-EN ISO4833-2: 2013). Enterobacteriaceae spp. and *E. coli* were analysed on Rebecca agar (with supplement) plates and incubated at 37 °C for 24 h (UNE-EN ISO16140:2003).

Each type of sample was analysed in triplicate for each microbial group. The data were fitted using the Gompertz equation proposed by Lanciotti, Corbo, Gardini, Sinigaglia, and Guerzoni (1999).

$$\text{Log}(N) = \text{Log}(N_0) + Pr_1 \times \exp \left\{ - \exp \left[ Pr_2 \times \frac{e}{Pr_1} \times (L - t) + 1 \right] \right\}$$

where N<sub>0</sub> is the microbial load at day 0, pr1 is the maximal growth at the stationary phase, pr2 is the maximal growth rate, and L is the lag time in days. Root mean square deviations were calculated:

$$RMSE = \sqrt{\frac{1}{(M-1)} \times \sum_{i=1}^{i=M} (De_i - Df_i)^2}$$

where De<sub>i</sub> is the experimental microbial load N<sub>i</sub> in log, Df<sub>i</sub> is the microbial load N<sub>i</sub> calculated by the Gompertz equation in log and M the number of samples.

#### 2.4.5. Sensory evaluation

The visual evaluation was performed by a panel of 5 experienced laboratory members. The panellists were familiar with meat colour measurements, and prior to the experiment they were trained on cooked ham samples with different

discolouration and the application of the colour scale. The colour of the ham in the different packaging materials was evaluated through the OSB, PA and PAN bags. A 5-point colour scale was used including: 5 = bright pink, 4 = pink, 3 = slightly pink (still marketable), 2 = slightly grey (not marketable), and 1 = extremely grey (not marketable).

#### 2.5. Statistical analysis

The study was designed to block all the variables related to anatomical or geometrical parts of cooked ham pieces. A one-way analysis of variance (ANOVA) was carried out using the XLSTAT-Pro statistical package (Addinsoft SARL, Paris, France). Differences were analysed by the Tukey's Range test.

### 3. Results and discussion

#### 3.1. Characterization of the packaging materials

Morphological and oxygen barrier properties of the fabricated multilayers were analysed and compared to a commercial high barrier polymer. Two films were fabricated as an A/B/C configuration. The A layer in PA contained standard PA6. The A layer in PAN contained PA6 with dispersed nanoclays. The fabricated PA and PAN nanocomposites had total thicknesses between 100 and 104 microns (Table 1). More precisely, in PA, the polyamide layer was 17 microns ±4.0; in PAN, the polyamide nanocomposite layer had 12 microns ±2.2 and was considerably thinner than in PA. TEM micrographs demonstrated an excellent clay distribution within the PA6 polymer matrix (Fig. 1). The clay was oriented parallel to the film surface, was not agglomerated and nearly exfoliated (Fig. 1b and c) into thin layers or in a pile of a few layers, presenting a morphology comparable to polyamide-6 mixed with organically modified montmorillonite by twin-screw extrusion (Beatrice et al., 2010). X-ray diffraction results must be interpreted considering the combined effects of the three layers. Diffractograms of PA (Fig. 2) revealed six diffraction peaks located at 2θ = 9.5°, 12.7°, 21.5°, 23.7°, 26.6° and 36.2°. For PAN samples, four diffraction peaks were observed located at 2θ = 12.2°, 21.5°, 23.8° and 36.3°. Organoclays such as cloisite and montmorillonite have prominent peaks below 2θ = 9° (Ophir, Dotan, Belinsky, & Kenig, 2010). However, in PAN no strong diffraction was observed in the region 2θ = 2°–10° confirming that the clay is well intercalated and acceptably exfoliated in the PA6 matrix, as suggested by Picard et al. (2008) and Sadeghi et al. (2013). The peaks at 2θ = 21.5°, 23.7° and 36.2° were likely associated to α and γ crystalline phases of polyamide and the crystalline unit cells of polyethylene (Lafrance, Pezolet, & Prud'homme, 1991). Peak intensities were similar, meaning that the thermodynamically more stable γ-phase of polyamide was not increased (Sadeghi et al., 2013).

In concordance with the excellent level of nanoclay intercalation and acceptable exfoliation achieved, the nanoclays in PAN created a

**Table 1**  
Thickness and oxygen transmission (OTR) in PA, PAN and OSB films.

Films	Thickness (μm)	OTR (cm <sup>3</sup> /m <sup>2</sup> day bar)
PR > F	0.013	<0.0001
PAN	104 ± 2 <sup>a</sup>	44 ± 1 <sup>b</sup>
PA	100 ± 3 <sup>a</sup>	96 ± 3 <sup>a</sup>
OSB	102 ± 2 <sup>a</sup>	20 <sup>*</sup>

\*Values from technical data sheet. OTR (23 °C/0% HR). PAN, multilayer nanocomposite polyamide film; PA, multilayer polyamide film; OSB, commercial high barrier film. Different superscripts indicate significantly different in the same column (P ≤ 0.05).

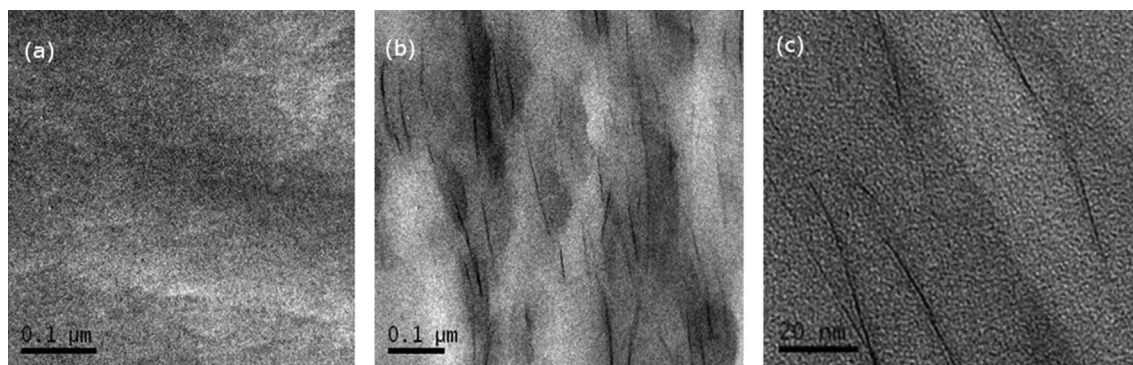


**Fig. 1.** TEM images of nanoclay modified PA6 layers in nanocomposite blends. a) PA, control blend without nanoclays; b and c) PAN, modified blend with nanoclays.

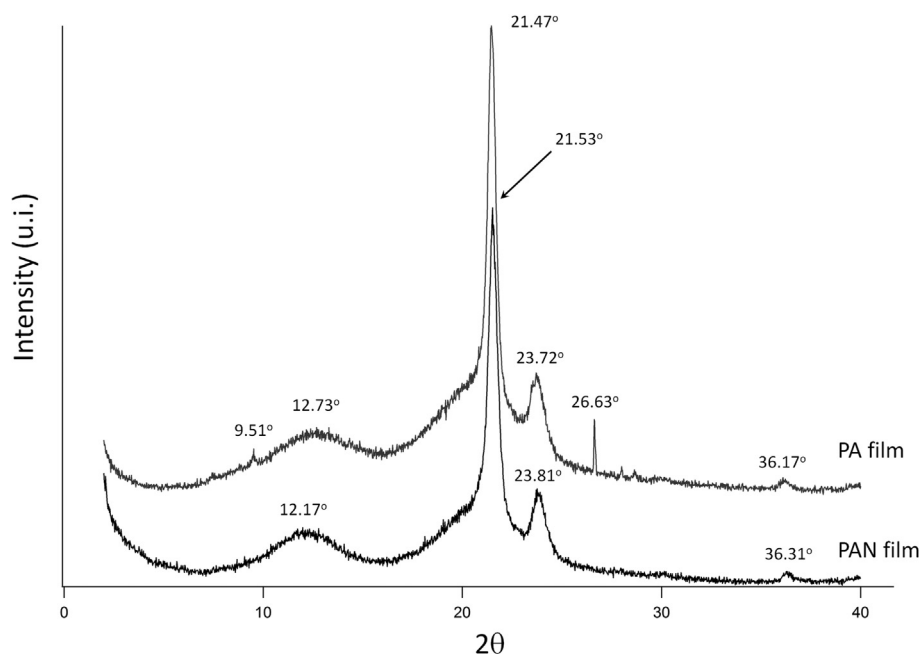


**Fig. 2.** X-ray diffraction pattern for the control blend without nanoclays (PA, black) and the modified blend with nanoclays (PAN, grey).

tortuous pathway for oxygen through the packaging material. As a result, the oxygen transmission rate (OTR) of PAN nanocomposites was about 54% lower than determined for the neat PA multilayer (Table 1) obtaining a remarkable enhancement of barrier properties as previously described by Sadeghi et al. (2013), Fasihi and Abolghasemi (2011), Picard et al. (2008) and Picouet et al. (2014) for similar polyamide nanocomposites. Furthermore, additional 30% savings in polyamide thickness could be achieved with the incorporation of nanoclays, which might also have an economic impact.

Consequently, and according to the classification of packaging barrier films (ultra-high-barrier  $\text{OTR} < 10 \text{ cm}^3/\text{m}^2/\text{day}/\text{bar}$ , high barrier  $10 < \text{OTR} < 100 \text{ cm}^3/\text{m}^2/\text{day}/\text{bar}$ , and medium barrier  $\text{OTR} > 100 \text{ cm}^3/\text{m}^2/\text{day}/\text{bar}$ ), PA, PAN and OSB could be considered high barrier polymers (Table 1), being PA closer to the properties of medium barrier packaging films.

### 3.2. Storage of sliced cooked ham in modified atmospheres

#### 3.2.1. Evolution of the headspace

The correct gas composition in modified atmosphere packaging combined with high barrier packaging materials may prolong the

shelf-life of meat products. Lack of  $\text{O}_2$  prevents aerobic microbial growth and  $\text{CO}_2$  has bacteriostatic effects on microorganisms (McMillin, 2008). However, headspace gas composition changes during meat storage. At the beginning, the concentration of  $\text{CO}_2$  decreases rapidly due to the absorption in the meat aqueous phase and small amounts of  $\text{O}_2$  are released from the tissue. In packed cooked ham, atmospheres containing mixtures of 20–40%  $\text{CO}_2$ , 60–80%  $\text{N}_2$  and extreme low residual levels of  $\text{O}_2$  show the best performances to retain the quality of the meat and to prolong the shelf-life (Moeller et al., 2000). In this study, a mixture containing 30%  $\text{CO}_2$  and 70%  $\text{N}_2$  was tested and the effects of packaging barrier properties on the evolution of oxygen were studied during 27 days MAP packaging of cooked ham.

Data shown in Fig. 3 clearly indicate that the increase in headspace oxygen is the lowest in packages with the lowest OTR (Table 1). In the OSB material,  $\text{O}_2$  did almost not vary during 27 days refrigerated storage and the concentration increased only slightly, reaching the maximum 0.08% at day 13. Afterwards, microbial growth was responsible for the slight decrease observed in the headspace concentration of  $\text{O}_2$ . PAN also proved to have excellent barrier properties, although not as good as OSB. In the PAN pouches,  $\text{O}_2$  headspace composition achieved the maximum 0.26% at day 20

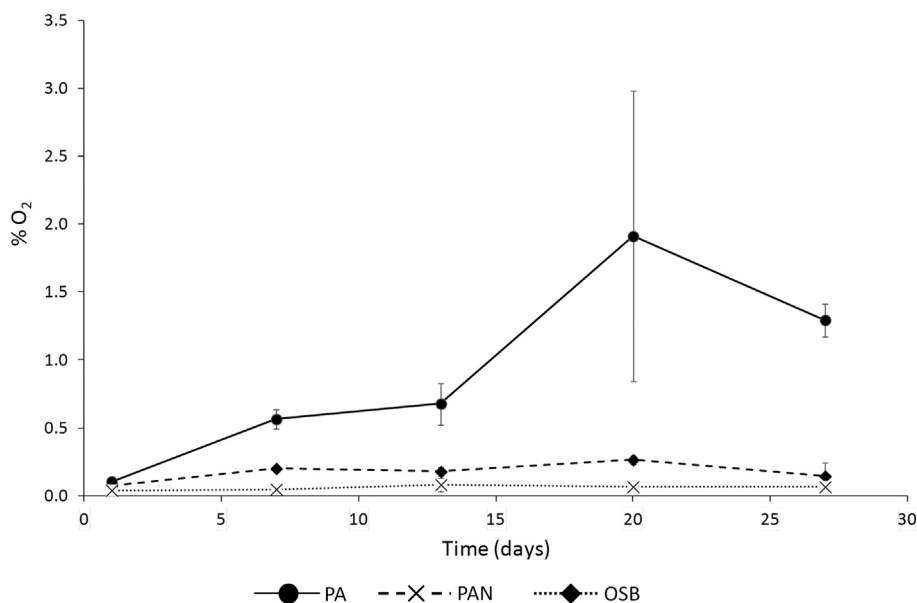


Fig. 3. Development of O<sub>2</sub> in the headspace of cooked ham packaged in modified atmospheres.

and thereafter it decreased slightly due to microbial growth. On the other hand, the composition of O<sub>2</sub> increased rapidly in PA pouches in concordance with the inferior material barrier properties. O<sub>2</sub> in PA pouches reached 1.91% at day 20 showing a non-negligible level of gas transfer through the blend, even higher than initially expected at the view of OTR instrumental results (Table 1). Thereafter, the influence of microbial metabolism on gas composition was also evident in PA pouches.

During MAP storage of cooked ham, small changes in headspace oxygen concentration are known to have strong consequences on quality parameters and therefore they might influence product shelf-life and consumer acceptability. According to Moeller et al. (2000), the O<sub>2</sub> concentrations reached in both OSB and PAN pouches were clearly below the critical level that shows an effect on cooked ham quality and microbial loads (0.5% O<sub>2</sub>). In PA pouches, however, the headspace oxygen concentration was above 0.5% after day 7 and likely had a negative influence on the quality parameters of cooked ham (Moeller et al., 2000; Larsen et al., 2006).

### 3.2.2. Quality parameters of modified atmosphere packed sliced cooked ham

Injection, tumbling, and cooking are the key processes for the final quality of cooked ham. Water activity and moisture are directly related to the brine injection level and brine composition (Casiraghi et al., 2007). Salt enhances the flavour and solubilizes myofibrillar proteins while inhibiting the growth of spoilage microorganisms by lowering the water activity. Salt also provides better texture and fat binding. In this work, no significant differences were observed in water activity (average:  $0.982 \pm 0.001$ ; maximum 0.984, minimum 0.980,  $P > 0.05$ ) or moisture content (Table 2) during 27 days of storage in any of the packaging materials, indicating the positive effects of processing and an adequate moisture control by the fabricated multilayers. The pH (Table 2) is not directly influenced by the brine and should drop in the meat surface due to the dissolution of CO<sub>2</sub>. Between day 1 and day 20, pH remained above 5.95. Subsequently, a decrease in pH was observed to values between 5.85 and 5.72 likely due to the production of lactic acid by lactic acid bacteria (LAB). This decrease falls in the range of observations made by other authors for similar products

and can be considered an indication of lactic acid metabolism (Kreyenschmidt et al., 2010).

Consumer acceptability and wholesomeness perception of cured meat products correlates particularly well with the red colour (Andersen et al., 1988). The colour is related to the quality of the raw meat, and the final attributes might be enhanced during processing. During storage of cooked ham, the fading of red colour is mainly due to a combination of light and oxygen, which are able to cause the photo-oxidation of the nitrosylmyochromogen (Andersen et al., 1988; Haile et al., 2013). In this study, the gas-to-product ratio (~3) was relatively low and all the products were stored under the same illumination conditions. Therefore, differences between samples could be mainly associated with oxygen concentration and the interaction between light and oxygen. In PA packages, O<sub>2</sub> concentrations markedly above the critical 0.5% (Fig. 3) stated by Moeller et al. (2000) accelerated the red colour fading of cooked ham (Table 3) and caused detectable differences in reflectivity (Table 5). In those packages a significant decrease in redness (CIE  $a^*$ ) was observed after 7 days storage in parallel with a significant increase in yellowness (CIE  $b^*$ ) (Table 4). Andersen et al. (1988) concluded that the CIE  $a^*$  value (redness) gives the best correlation with the visual evaluation of ham colour and Larsen et al. (2006) found that a visually acceptable cooked ham corresponded to a redness value of 8 or superior. Here the  $a^*$  value in PA packages was clearly below 8 after day 13, which originated a perceptible defect in the colour that was noticed by the panellists with scores below 2 (slightly grey) in the 5-point colour scale (Fig. 4). The grey pigment could be attributed to the oxidized nitrosyl-haemochrome Fe<sup>3+</sup> (Li et al., 2012; Moeller et al., 2000) produced by exposure to light and oxygen. A strong negative correlation between  $a^*$  values and oxygen concentration has been previously reported (Larsen et al., 2006) being samples with  $a^*$  values below 4 extremely grey. In contrast, in the backside of the product in PA packages, the colour of cooked ham was stable and only a slight discolouration and reflectivity change could be observed after day 20 (respectively, Tables 3 and 5), pointing for the strong effect of light and oxygen exposure on colour fading.

The samples kept in PAN and OSB films were considerably more stable than in PA, and no fading of redness or yellowness were evident during 27 days of storage (Tables 3 and 4). In concordance

**Table 2**

Development of moisture content (%) and pH during storage of cooked ham in modified atmosphere packaging.

Physico-chemical	Polymer type	Day 1	Day 7	Day 13	Day 20	Day 27
Moisture (%)	PA	75.9 ± 0.91 <sup>a</sup>	75.8 ± 0.83 <sup>a</sup>	75.7 ± 0.91 <sup>a</sup>	76.3 ± 0.53 <sup>a</sup>	76.0 ± 0.36 <sup>a</sup>
	PAN	76.0 ± 0.57 <sup>a</sup>	76.3 ± 3.12 <sup>a</sup>	75.6 ± 0.95 <sup>a</sup>	76.2 ± 0.36 <sup>a</sup>	76.2 ± 0.36 <sup>a</sup>
	OSB	76.0 ± 0.69 <sup>a</sup>	76.4 ± 0.76 <sup>a</sup>	75.6 ± 0.63 <sup>a</sup>	76.2 ± 0.31 <sup>a</sup>	76.1 ± 0.35 <sup>a</sup>
pH	PA	5.96 ± 0.01 <sup>a</sup>	5.98 ± 0.02 <sup>a</sup>	5.97 ± 0.03 <sup>a</sup>	5.96 ± 0.02 <sup>a</sup>	5.85 ± 0.05 <sup>abc</sup>
	PAN	5.96 ± 0.01 <sup>a</sup>	6.00 ± 0.04 <sup>a</sup>	5.95 ± 0.01 <sup>a</sup>	5.93 ± 0.02 <sup>ab</sup>	5.72 ± 0.19 <sup>bc</sup>
	OSB	5.94 ± 0.01 <sup>a</sup>	6.02 ± 0.02 <sup>a</sup>	5.94 ± 0.02 <sup>a</sup>	5.95 ± 0.00 <sup>a</sup>	5.76 ± 0.11 <sup>c</sup>

PAN, multilayer nanocomposite polyamide film; PA, multilayer polyamide film; OSB, commercial high barrier film. Different superscripts indicate significantly different ( $P \leq 0.05$ ); moisture and pH analysed independently. Moisture: RMSE = 0.7;  $Pr > F < 0.980$ ;  $F = 0.347$ ;  $R^2 = 0.139$ ; pH: RMSE = 0.06;  $Pr > F < 0.0001$ ;  $F = 6.014$ ;  $R^2 = 0.737$ .

**Table 3**CIE  $a^*$  colour coordinates of cooked ham stored in modified atmospheres during 27 days. Measurements at the front and the back when exposed in an illuminated cabinet.

Light exposure	Polymer type	Day 1	Day 7	Day 13	Day 20	Day 27
Lightness	PA	9.5 ± 0.5 <sup>ab</sup>	7.9 ± 0.9 <sup>bc</sup>	7.0 ± 0.7 <sup>c</sup>	4.4 ± 1.2 <sup>d</sup>	2.7 ± 1.5 <sup>e</sup>
	PAN	9.3 ± 0.4 <sup>ab</sup>	9.4 ± 0.1 <sup>ab</sup>	9.4 ± 0.2 <sup>ab</sup>	9.5 ± 0.2 <sup>ab</sup>	8.3 ± 0.5 <sup>ab</sup>
	OSB	9.4 ± 0.3 <sup>ab</sup>	9.0 ± 0.2 <sup>ab</sup>	9.7 ± 0.3 <sup>a</sup>	9.5 ± 0.2 <sup>ab</sup>	9.5 ± 0.3 <sup>ab</sup>
Darkness	PA	9.6 ± 0.7 <sup>a</sup>	9.3 ± 0.3 <sup>ab</sup>	9.5 ± 0.2 <sup>ab</sup>	9.2 ± 0.4 <sup>ab</sup>	8.6 ± 0.0 <sup>ab</sup>
	PAN	9.6 ± 0.1 <sup>a</sup>	9.3 ± 0.1 <sup>ab</sup>	9.6 ± 0.3 <sup>a</sup>	9.7 ± 0.1 <sup>a</sup>	9.1 ± 0.2 <sup>ab</sup>
	OSB	9.7 ± 0.3 <sup>a</sup>	9.4 ± 0.1 <sup>ab</sup>	9.7 ± 0.2 <sup>a</sup>	9.4 ± 0.2 <sup>ab</sup>	9.6 ± 0.2 <sup>a</sup>

PAN, multilayer nanocomposite polyamide film; PA, multilayer polyamide film; OSB, commercial high barrier film. Different superscripts indicate significantly different ( $P \leq 0.05$ ). RMSE = 0.5;  $Pr > F < 0.0001$ ;  $F = 30.290$ ;  $R^2 = 0.937$ .

**Table 4**CIE  $b^*$  colour coordinates of cooked ham stored in modified atmospheres during 27 days. Measurements at the front and the back when exposed in an illuminated cabinet.

Light exposure	Polymer type	Day 1	Day 7	Day 13	Day 20	Day 27
Lightness	PA	6.2 ± 0.2 <sup>cd</sup>	6.9 ± 0.7 <sup>bc</sup>	7.5 ± 0.6 <sup>ab</sup>	7.4 ± 0.4 <sup>ab</sup>	8.3 ± 1.1 <sup>a</sup>
	PAN	5.8 ± 0.2 <sup>cd</sup>	5.6 ± 0.1 <sup>d</sup>	5.8 ± 0.3 <sup>cd</sup>	5.8 ± 0.3 <sup>cd</sup>	5.3 ± 0.2 <sup>d</sup>
	OSB	5.6 ± 0.2 <sup>d</sup>	5.5 ± 0.2 <sup>d</sup>	5.7 ± 0.2 <sup>d</sup>	5.3 ± 0.2 <sup>d</sup>	5.1 ± 0.3 <sup>d</sup>
Darkness	PA	6.2 ± 0.6 <sup>cd</sup>	6.0 ± 0.2 <sup>cd</sup>	6.0 ± 0.4 <sup>cd</sup>	5.5 ± 0.2 <sup>d</sup>	5.7 ± 0.2 <sup>d</sup>
	PAN	5.9 ± 0.2 <sup>cd</sup>	5.7 ± 0.1 <sup>cd</sup>	5.9 ± 0.2 <sup>cd</sup>	5.4 ± 0.1 <sup>d</sup>	5.7 ± 0.2 <sup>d</sup>
	OSB	6.0 ± 0.2 <sup>cd</sup>	5.7 ± 0.1 <sup>d</sup>	6.0 ± 0.2 <sup>cd</sup>	5.3 ± 0.2 <sup>d</sup>	5.3 ± 0.4 <sup>d</sup>

PAN, multilayer nanocomposite polyamide film; PA, multilayer polyamide film; OSB, commercial high barrier film. Different superscripts indicate significantly different ( $P \leq 0.05$ ). RMSE = 0.4;  $Pr > F < 0.0001$ ;  $F = 11.949$ ;  $R^2 = 0.855$ .

**Table 5**

Reflectivity of cooked ham stored in modified atmospheres during 27 days. Measurements at the front and the back when exposed in an illuminated cabinet.

Reflectivity	Polymer type	Day 1	Day 7	Day 13	Day 20	Day 27
Lightness	PA	1.63 ± 0.03 <sup>a</sup>	1.56 ± 0.05 <sup>ab</sup>	1.50 ± 0.03 <sup>b</sup>	1.37 ± 0.08 <sup>c</sup>	1.31 ± 0.05 <sup>c</sup>
	PAN	1.59 ± 0.02 <sup>ab</sup>	1.60 ± 0.01 <sup>ab</sup>	1.61 ± 0.01 <sup>ab</sup>	1.64 ± 0.02 <sup>a</sup>	1.55 ± 0.02 <sup>ab</sup>
	OSB	1.59 ± 0.03 <sup>ab</sup>	1.55 ± 0.01 <sup>ab</sup>	1.62 ± 0.02 <sup>a</sup>	1.60 ± 0.02 <sup>ab</sup>	1.60 ± 0.04 <sup>ab</sup>
Darkness	PA	1.64 ± 0.04 <sup>a</sup>	1.62 ± 0.03 <sup>a</sup>	1.62 ± 0.03 <sup>a</sup>	1.62 ± 0.04 <sup>a</sup>	1.53 ± 0.09 <sup>ab</sup>
	PAN	1.62 ± 0.02 <sup>a</sup>	1.60 ± 0.02 <sup>ab</sup>	1.62 ± 0.01 <sup>a</sup>	1.64 ± 0.01 <sup>a</sup>	1.62 ± 0.03 <sup>a</sup>
	OSB	1.62 ± 0.01 <sup>a</sup>	1.60 ± 0.01 <sup>ab</sup>	1.63 ± 0.02 <sup>a</sup>	1.61 ± 0.02 <sup>ab</sup>	1.64 ± 0.02 <sup>a</sup>

PAN, multilayer nanocomposite polyamide film; PA, multilayer polyamide film; OSB, commercial high barrier film. Different superscripts indicate significantly different ( $P \leq 0.05$ ). RMSE = 0.033;  $Pr > F < 0.0001$ .  $F = 14.543$ ;  $R^2 = 0.875$ .

with those results, PAN and OSB obtained visual scores above 4 (bright pink) during 27 days (Fig. 4) and the reflectivity remained stable (Table 5). Therefore the increment in  $O_2$  up to 0.26% in PAN packages did not originate significant changes in parameters  $a^*$  or  $b^*$  or reflectivity, which was corroborated by panellists scores during 27 days. Such results are in good agreement with Moeller et al. (2000) who studied the influence of residual oxygen and light in MAP packaging of cooked ham and reported 0.5% residual oxygen as critical for cooked ham quality at gas-to-meat ratios around 3. Many parameters may influence the extent of photo-oxidation, such as the nature of the light, the gas-to-product ratio, the quality of the raw product, the processing conditions, and the nitrite content (Moeller et al., 2000; Moeller et al., 2003; Dineen et al., 2000). Moeller et al. (2000) and Larsen et al. (2006) studied

headspace gas-to-product ratios between 4.1 and 2.6 and concluded that they might have a significant influence in the oxidation rates and colour deterioration, with gas-to-product ratios below 3 better for keeping redness at low  $O_2$  concentrations.

Microbial results should correlate with the sensory perception and according to Kreyenschmidt et al. (2010) a value around 7 log [cfu/g] would already indicate the end of shelf-life in cooked-ham. In these samples, microbial growth could be accurately described using the modified Gompertz function (Lanciotti et al., 1999). Microbial loads were low at the beginning of storage, and storage time had a significant effect on bacterial growth after day 20 (Fig. 5). The growth of total colony forming units was comparable in all the samples, the levels achieved were in the range reported by Moeller et al. (2000) and close to the end of product

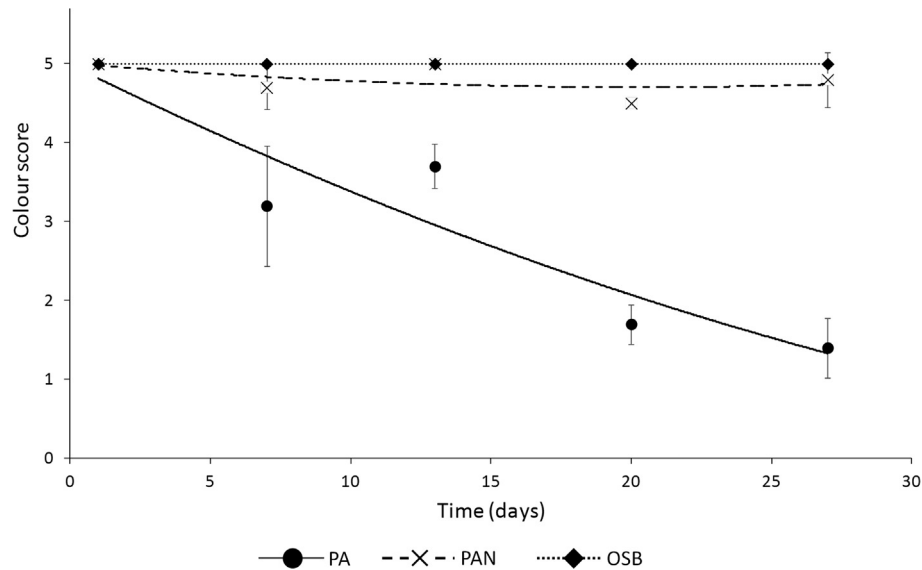


Fig. 4. Colour scores in a 5 point colour-scale of cooked ham during storage in modified atmosphere packaging.

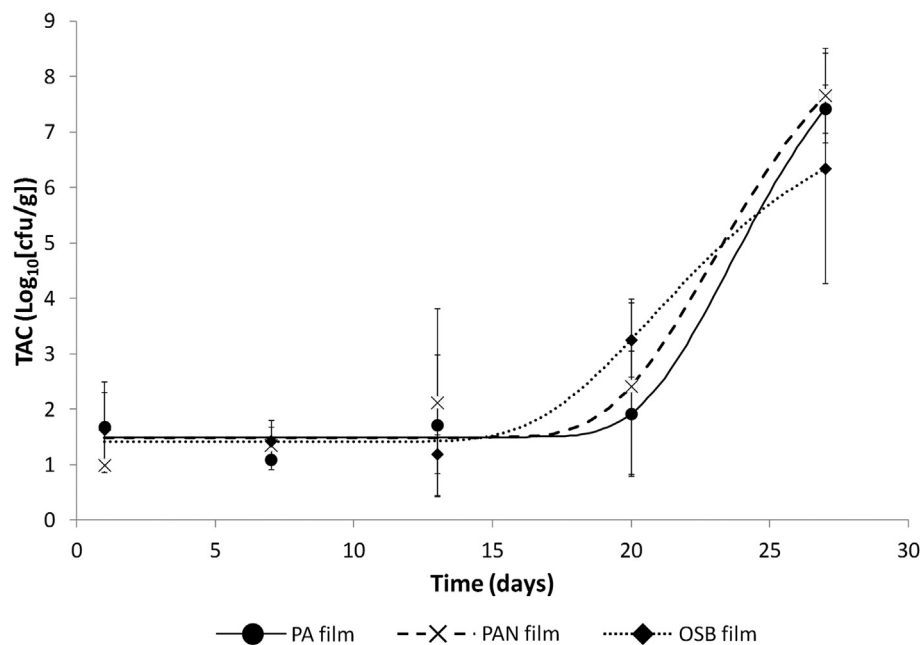


Fig. 5. Development of total viable counts during storage of cooked ham in modified atmosphere packaging.

shelf-life at day 27. At the investigated MAP conditions, the growth of microorganisms was independent of the residual oxygen or the product-to-headspace volume ratio, and an increased level of residual oxygen would have contributed to the development of mostly microaerophilic species (Moeller et al., 2000). *Enterococci* and *E. coli* were not detected in any of the samples ( $\text{cfu/g} < 1$ ). Microbial growth, and in particular the increase in lactic acid metabolism, would explain the pH drop (Table 2) after day 20, indicating that lactic acid bacteria were predominant in those samples. In MAP packaged cooked ham, the number of LAB becomes predominant during storage and the total viable counts and LAB counts are nearly identical (Kreyenschmidt et al., 2010). In fact, lactic acid bacteria (LAB) cannot be completely eradicated in raw meat and they are associated with the spoilage of cooked ham

under vacuum or modified atmosphere packaging (Arvanitoyannis & Stratakos, 2012). Contrary to this, the colour remained fairly stable in OSB and PAN samples over 27 days and has not fully agreed with microbiology results which indicated samples were approximating the end of shelf-life.

#### 4. Conclusion

A novel polyamide nanocomposite blend (PAN) was fabricated with nanoclays homogeneously distributed and nearly exfoliated. They lowered the oxygen transmission rate of PAN films. The oxygen barrier generated by PAN was adequate to slow down the colour deterioration in cooked ham and to extend the visual shelf-life of the product up to 27 days. Comparable results were achieved

with a commercial high barrier polymer. For the contrary, a polyamide blend (PA) without nanoclays showed considerably higher oxygen transmission and consequently, a strong colour deterioration took place in cooked ham after day 7. PAN showed properties comparably as good as a commercial high barrier polymer bringing excellent perspectives for this type of packaging polymer in future applications in the storage of cooked meat products.

### Acknowledgements

Financial support from the Spanish Comisión Interministerial de Ciencia y Tecnología (Ministerio de Ciencia e Innovación) under contract AGL07-65936-C02 is acknowledged. R. Trbojevich is grateful to project #E0736801 from the National Center for Toxicological Research and U.S. Food and Drug Administration. Authors are grateful to Dr. Frederick Beland and Dr. Matthew Bryant for assistance in the review of this manuscript.

### References

- Alexandre, B., Langevin, D., Mederic, P., Aubry, T., Couderc, H., Nguyen, Q. T., et al. (2009). Water barrier properties of polyamide 12/montmorillonite nanocomposite membranes: structure and volume fraction. *Journal of Membrane Science*, 328, 186–204.
- Andersen, H. J., Bertelsen, G., Boeghsoerensen, L., Shek, C. K., & Skibsted, L. H. (1988). Effect of light and packaging conditions on the colour stability of sliced ham. *Meat Science*, 22, 283–292.
- AOAC 950.46. (1990). *Official methods of analysis* (15th ed.). Arlington, VA: AOAC International.
- Arvanitoyannis, I. S., & Stratakos, A. C. H. (2012). Application of modified atmosphere packaging and active/smart technologies to red meat and poultry: a review. *Food and Bioprocess Technology*, 5, 1423–1446.
- Baldi, F., Franceschini, A., Bignotti, F., Tieghi, G., & Riccò, T. (2009). Rheological behaviour of nano-composites based on polyamide 6 under shear and elongational flow at high strain rates. *Rheological Acta*, 48, 73–88.
- Beatrice, C. A. G., Branciforti, M. C., Alves, R. M. V., & Bretas, R. E. S. (2010). Rheological, mechanical, optical, and transport properties of blown films of polyamide 6/residual monomer/montmorillonite nanocomposites. *Journal of Applied Polymer Science*, 116, 3581–3592.
- Casiraghi, E., Alamprese, C., & Pompei, C. (2007). Cooked ham classification on the basis of brine injection level and pork breeding country. *LWT-Food Science and Technology*, 40, 164–169.
- Dineen, N. M., Kerry, J. P., Lynch, P. B., Buckley, D. J., Morrissey, P. A., & Arendt, E. K. (2000). Reduced nitrite levels and dietary alpha-tocopherol acetate supplementation: effects on the colour and oxidative stability of cooked hams. *Meat Science*, 55, 475–482.
- Fasihi, M., & Abolghasemi, M. R. (2011). Oxygen barrier and mechanical properties of masterbatch-based PA6/nanoclay composite films. *Journal of Applied Polymer Science*, 125, 2–8.
- Haiile, D. M., De Smet, S., Claeys, E., & Vossen, E. (2013). Effect of light, packaging condition and dark storage durations on colour and lipid oxidative stability of cooked ham. *Journal of Food Science and Technology*, 50, 239–247.
- Kohno, M., & Tamemoto, K. (2004). Properties of biaxially oriented nylon 66 film. *Polymer Engineering and Science*, 27, 558–561.
- Kreyenschmidt, J., Hübner, A., Beierle, E., Chonsch, L., Scherer, A., & Petersen, B. (2010). Determination of the shelf life of sliced cooked ham based on the growth of lactic acid bacteria in different steps of the chain. *Journal of Applied Microbiology*, 108, 510–520.
- Lafrance, C. P., Pezolet, M., & Prud'homme, R. E. (1991). Study of the distribution of molecular orientation in highly oriented polyethylene by X-ray diffraction. *Macromolecules*, 24, 4948–4956.
- Lanciotti, R., Corbo, M. R., Gardini, F., Sinigaglia, M., & Guerzoni, M. E. (1999). Effect of hexanal on the shelf-life of fresh Apple slices. *Journal of Agricultural and Food Chemistry*, 47, 4769–4776.
- Larsen, H., Westad, F., Soerheim, O., & Nilsen, L. H. (2006). Determination of critical oxygen level in packages for cooked sliced ham to prevent colour fading during illuminated retail display. *Journal of Food Science*, 71, 407–413.
- Li, H., Li, C. B., Xu, X. L., & Zhou, G. H. (2012). Effects of illumination and packaging on non-heme iron and colour attributes of sliced ham. *Meat Science*, 91, 521–526.
- Mattos, E. C., Norena, C. P. Z., & Brandelli, A. (2003). Kinetics of pigment degradation in sliced cooked ham. *Journal of Muscle Foods*, 14, 221–231.
- McMillin, K. W. (2008). Where is map going? A review and future potential of modified atmosphere packaging for meat. *Meat Science*, 80, 43–65.
- Moeller, J. K. S., Jakobsen, M., Weber, C. J., Martinussen, T., Skibsted, L. H., & Bertelsen, G. (2003). Optimization of colour stability of cured ham during packaging and retail display by a multifactorial design. *Meat Science*, 63, 169–175.
- Moeller, J. K. S., Jensen, J. S., Skibsted, L. H., & Bertelsen, G. (2000). Effect of residual oxygen on colour stability during chill storage of sliced, pasteurized ham packaged in modified atmospheres. *Meat Science*, 54, 399–405.
- Ophir, A., Dotan, A., Belinsky, I., & Kenig, S. (2010). Barrier and mechanical properties of nanocomposites based on polymer blends and organoclays. *Journal of Applied Polymer Science*, 116, 72–83.
- Picard, E., Gerard, J. F., & Espuche, E. (2008). Water transport properties of polyamide 6 based nanocomposites prepared by melt blending: on the importance of the clay dispersion state on the water transport properties at high water activity. *Journal of Membrane Science*, 313, 284–295.
- Picouet, P. A., Fernandez, A., Realini, C. E., & Lloret, E. (2014). Influence of PA6 nanocomposite films on the stability of vacuum-aged beef loins during storage in modified atmospheres. *Meat Science*, 96, 574–580.
- Pietrasik, Z., & Gaudette, N. J. (2014). The impact of salt replacers and flavor enhancer on the processing characteristics and consumer acceptance of restructured cooked hams. *Meat Science*, 96, 1165–1170.
- Sadeghi, F., Fereydoon, A., & Aiji, A. (2013). Rheological, mechanical and barrier properties of multilayer nylon/clay nanocomposite film. *Advances in Polymer Technology*, 32, 53–64.
- Singh, P., Wani, A. A., Saengerlaub, S., & Langowski, H.-C. (2011). Understanding critical factors for the quality and shelf-life of MAP fresh meat: a review. *Critical Reviews in Food Science and Nutrition*, 51, 146–177.
- Talens, P., Mora, L., Morsy, N., Barbin, D. F., & Elmasry, T. (2013). Prediction of water and protein contents and quality classification of Spanish cooked ham using NIR hyperspectral imaging. *Journal of Food Engineering*, 117, 272–280.
- Tung, J., Gupta, R. K., Simon, G. P., Edward, G. H., & Bhattacharya, S. N. (2005). Rheological and mechanical comparative study of in situ polymerized and melt-blended nylon 6 nanocomposites. *Polymer*, 46, 10405–10418.
- UNE-EN ISO 16140. (2003). *Microbiology of food and animal feeding stuffs-protocol for the validation of alternative methods*.
- UNE-EN ISO 4833-2. (2013). *Microbiology of the food chain – Horizontal method for the enumeration of microorganisms – Part 2: Colony count at 30 degrees C by the surface plating technique*.



# Influence of microcrystalline cellulose on the microrheological property and freeze-thaw stability of soybean protein hydrolysate stabilized curcumin emulsion



Duoxia Xu, Jinjing Zhang, Yanping Cao\*, Jing Wang, Junsong Xiao

School of Food & Chemical Engineering, Beijing Engineering and Technology Research Center of Food Additives, Beijing Higher Institution Engineering Research Center of Food Additives and Ingredients, Beijing Key Laboratory of Flavor Chemistry, Beijing Laboratory for Food Quality and Safety, Beijing Technology & Business University, Beijing, China

## ARTICLE INFO

### Article history:

Received 27 June 2015

Received in revised form

27 October 2015

Accepted 2 November 2015

Available online 6 November 2015

### Keywords:

Microcrystalline cellulose (MCC)

SPI hydrolysate (SPIH)

Curcumin emulsion

Microrheological property

Freeze-thaw stability

## ABSTRACT

The impact of microcrystalline cellulose (MCC) on the physical stability, microrheological property and freeze-thaw stability of papain hydrolysate of soybean isolate protein (SPIH) stabilized curcumin emulsion was studied. Curcumin emulsions were prepared by Microfluidizer containing SPIH and various concentrations of MCC. The curcumin emulsions were assessed by zeta potential, average particle size through dynamic light scattering technique (DLS), stability index by Turbiscan and microrheological behavior through diffusive wave spectroscopy (DWS) technique. With addition of MCC, the negative charge of the droplets was increased, which indicated that the negatively charged fraction from MCC interacted with the protein at the interface. An increase in droplet size and decrease in TSI were noted with increasing MCC concentration. It demonstrated that enough MCC changed microrheological property of curcumin emulsions from purely viscous to viscoelastic over the range of decorrelation times, indicating that the droplets were not free to move due to the droplets network interaction. Freeze-thaw stability analysis demonstrated that MCC brought about a remarkable improvement, which can be attributed to the enhancement of repulsive steric forces between the curcumin droplets. It demonstrated that combined enzymatic hydrolysate of protein and addition of polysaccharide MCC could be an effective method for protecting bioactive compound in emulsions.

© 2015 Elsevier Ltd. All rights reserved.

## 1. Introduction

In recent years, curcumin is now widely used as a pigment in food processing and a number of studies have suggested that curcumin may have beneficial effects on human health including a number of bioactivities, such as antioxidant, anti-inflammatory, antiproliferative and antiangiogenic effects (Anand, Sundaram, Jhurani, Kunnumakkara, & Aggarwal, 2008). These findings have increased consumers' interest in curcumin-containing food products and generated new applications for curcumin-containing food ingredients. However, the instability of curcumin negatively influences the product quality and consumer acceptance leading to the potential rejection of curcumin fortified foods (Anand, Kunnumakkara, Newman, & Aggarwal, 2007).

Since curcumin is highly hydrophobic and lipid-soluble, it can be incorporated into foods in the oil phase of oil-in-water (O/W) emulsions (Li, Ma, & Cui, 2014; Tippetts & Martini, 2012). The emulsion is formed by small curcumin droplets dispersed in an aqueous continuous phase, and each curcumin droplet is surrounded by emulsifier molecules. It has been suggested that protein and polysaccharide have significant effects on the physicochemical properties of emulsions (Dickinson, 2011; Liu, Hou, Lei, Chang, & Gao, 2012). Many proteins can act as emulsifiers because of their ability to absorb at the oil-water interface and to increase emulsion stability (McClements, 2004). Most polysaccharides behave as emulsion stabilizers by forming an extended network in the continuous phase which thus becomes highly viscous (Bouyer, Mekhloufi, Rosilio, Grossiord, & Agnely, 2012; Dickinson, 2009).

In searching food-grade materials to emulsify curcumin, we focused on soy protein isolate (SPI). SPI is a highly refined and concentrated protein fraction produced from soybean. SPI is composed almost exclusively of two globular protein fractions

\* Corresponding author. No. 11, Fucheng Road, Beijing 100048, China.  
E-mail address: [xdxbtbu@126.com](mailto:xdxbtbu@126.com) (Y. Cao).

called 7S ( $\beta$ -conglycinin) and 11S (glycinin). Soy proteins are used extensively in food manufacturing, because of their functional properties, low cost and high nutritional value. SPI has been widely studied as emulsifying agents (Tapal & Tiku 2012). Modifications of soy proteins by enzymatic hydrolysis to improve functionalities are a well accepted and safe method (Chen, Chen, Ren, & Zhao, 2011). Our previous study showed that controlled papain hydrolysate of SPI (SPIH) could improve its emulsifying capability and emulsion stabilization against creaming during storage, which was mainly due to its higher protein solubility and random coil content (Ci, Cao, Xu, & Wang, 2013).

Microcrystalline cellulose (MCC) is cellulose derivative that has been approved for use in food as fiber additive (Ghanbarzadeh, Almasi, & Entezamin, 2010). The properties of MCC depend on the depolymerization process which often involves application of mechanical forces to generate cellulose crystals of specific sizes (Schuh et al., 2013). MCC is an anionic biopolymer that has many potential applications in the food, cosmetic, and pharmaceutical industries because of its unique nutritional and physicochemical properties (Lavoine, Desloges, Dufresne, & Bras, 2012). Especially, MCC can be used in beverage and juice as thickener due to its high viscosity. To the best of our knowledge, there are no published works related to combined protein hydrolysates with MCC to stabilize functional compound emulsions. Freeze-thaw processing is the most destructive and representative experiments to the stability of the emulsion.

Therefore, the purpose of this study was to investigate the influence of MCC on the physical stability of SPIH stabilized curcumin emulsion through microfluidization. The physical stability was assessed by average particle size through dynamic light scattering technique (DLS), zeta potential, stability index by a recently developed optical analyzer (Turbiscan) and microrheological behavior through diffusing wave spectroscopy technique (DWS). The emulsion stability to freeze-thaw processing was also evaluated to determine whether MCC could be used to protect bioactive compound in emulsions. Ultimately our goal is to use protein hydrolysates-polysaccharide to protect bioactive components and to extend the application of bioactive components in the food industry.

## 2. Materials and methods

### 2.1. Materials

Papain (EC 3.4.22.2), specified as 100,000 U/g protein, was purchased from Sigma Chemicals (St. Louis, MO, USA). SPI was purchased from Gushen Biological Technology Group Co., Ltd. (Shandong, China). MCC was supplied by Davisco Foods International Inc. (Le Sueur, MN, USA). Curcumin was purchased from Shanghai Yousi Biological Technology Group Co., Ltd. (Shanghai, China). All other chemicals were of analytical grade.

### 2.2. Preparation of SPIH

SPI was suspended in phosphate buffer (10 mmol L<sup>-1</sup>, pH 7.0) at a concentration of 20 g kg<sup>-1</sup>, and allowed to hydrate at 30 °C for 2 h with constant stirring. Papain was added at a concentration of 1.5 g kg<sup>-1</sup> and the suspension was incubated at 50 °C for 30 min with constant stirring based on our previous study (Ci et al., 2013). After the hydrolysis, the SPI hydrolysates (SPIH) were heated at 95 °C for 10 min to inactivate the enzymes. The suspensions were allowed to cool down to room temperature for the following emulsion preparation. It was found that the emulsifying activity of SPI was increased by 19.4% after hydrolysis (Ci et al., 2013).

### 2.3. Preparation of curcumin emulsion

MCC was dispersed in phosphate buffer (10 mmol L<sup>-1</sup>, pH 7.0) at different concentrations ranging from 0 to 24 g kg<sup>-1</sup>. The solutions were stirred at a speed of 200 rpm for 3 h to ensure complete dispersion and dissolution.

Curcumin emulsions were firstly prepared with 100 g kg<sup>-1</sup> medium-chain triacylglycerol (MCT) oil containing curcumin (0.2 g kg<sup>-1</sup>) as the dispersed phase and 900 g kg<sup>-1</sup> of the aqueous phase solution with SPIH (20 g kg<sup>-1</sup>) at room temperature. The mixture was then pre-homogenized using a two-speed hand-held biohomogenizer (Biospec Products Inc., Bartlesville, OK) for 3 min to form coarse emulsion, which was subsequently homogenized using Microfluidizer processor (Microfluidics 110-PS, Newton, MA) at the operational pressure of 50 MPa for a total of three passes.

The final emulsion was prepared by slow addition of the SPIH stabilized curcumin emulsion to a solution of MCC (0–24 g kg<sup>-1</sup>) at pH 7.0 using pre-homogenized and Microfluidizer processor treatment accordance with the above condition, respectively. All the final emulsions contained 9 g kg<sup>-1</sup> SPIH, 0.1 g kg<sup>-1</sup> curcumin, 50 g kg<sup>-1</sup> MCT and 0–12 g kg<sup>-1</sup> MCC. Sodium azide (0.1 g kg<sup>-1</sup>) was added as an antimicrobial agent.

### 2.4. Measurement of zeta potential

Zeta potential of the curcumin droplets was then determined by a particle electrophoresis instrument using a Zetasizer Nano-ZS90 (Malvern Instruments, Worcestershire, UK). Prior to analysis the curcumin emulsions were diluted to 0.4 g kg<sup>-1</sup> using buffer solution (10 mmol L<sup>-1</sup> phosphate, pH 7.0). Diluted emulsions were then injected into the measurement chamber of a particle electrophoresis instruments. The zeta potential was determined by measuring the direction and velocity of droplet movement in the applied electric field. The zeta potential measurements were reported as the average of measurements for two freshly samples, with five readings record of each sample.

### 2.5. Determination of droplet size

The average droplet size of the curcumin emulsions was determined by dynamic light scattering using a Zetasizer Nano-ZS90 (Malvern Instruments, Worcestershire, UK) at a fixed detector angle of 90°. Emulsions were diluted using buffer solution (10 mmol L<sup>-1</sup> phosphate buffer, pH 7.0) to minimize multiple scattering effects prior to each measurement. The measured time correlation functions were analyzed by Automatic Program equipped with the correlator. The averaged droplets size was obtained by a CONTIN mode analysis. Results were described as cumulants mean diameter (size, nm) for droplet size.

### 2.6. Evaluation of emulsion stability by turbiscan

Emulsion stability (the aggregation tendency of droplets in the emulsions) was evaluated using a Turbiscan instrument (Formulation, France). The principle underlying the operation of this instrument was detailed by Lemarchand, Couvreur, and Vauthier (2003). Briefly, the emulsion sample was transferred to a cylindrical glass cell and analyzed by a light beam emitted in near infrared (880 nm) wavelength which scanned the sample cell from the bottom to the top. Two synchronous optical sensors received respectively the light transmitted through the sample and the light backscattered by the sample. By scanning the sample at preset intervals, a pattern of the light flux backscattering as a function of the sample height was obtained, giving a macroscopic fingerprint of the sample at a given time, so that the stability of the emulsion

could be evaluated by turbiscan stability index (TSI). TSI was calculated with the special computer program Turbiscan Easy Soft with the following formula:

$$TSI = \sum_i \frac{\sum_h |scan_i(h) - scan_{i-1}(h)|}{H} \quad (1)$$

where:  $scan_i(h)$  – average backscattering for each time (i) of measurement,  $scan_{i-1}(h)$  – average backscattering for the i-1 time of measurement, H – the sample height. The changes in the emulsion stability were monitored for 7200 s. As is clear from Eq. (1) the TSI takes into account all single scans during an experiment and its value is obtained from their averaging. The lower the TSI value, the more stable the system is (Wiśniewska, Urban, Nosal-Wiercińska, Zarko, & Gunko, 2014).

### 2.7. Microrheological behavior

The microrheometer Rheolaser Lab (Formulation, France) used for the measurements of the microrheology of curcumin emulsions is based on Diffusing Wave Spectroscopy (DWS). It corresponds to dynamic light scattering in concentrated media and measures the particles Brownian motion which depends on the viscoelastic structure of the emulsion. A microrheology test of 2 h was carried out on each sample of SPIH stabilized curcumin emulsions containing different concentrations of MCC. The instrument measures the Brownian motion of the particles as the particles Mean Square Displacement (MSD) versus time. Elasticity Index (EI) and Macroscopic Viscosity Index (MVI) parameters of the samples were obtained from the software RheoSoft Master 1.4.0.0.

### 2.8. Freeze-thaw treatment

Curcumin emulsion samples were transferred into cryogenic test tubes, which were incubated in a  $-18\text{ }^{\circ}\text{C}$  freezer for 22 h and then thawed by placing them in a water bath at  $40\text{ }^{\circ}\text{C}$  for 2 h (Xu et al., 2010). The freeze-thaw cycle was designed from 0 to 3 times and its effect on the droplet size and stability of the emulsion were evaluated after each cycle. The average droplet size of the curcumin emulsions was determined by dynamic light scattering using a Zetasizer Nano-ZS90 and the stability of the curcumin emulsions was evaluated by Turbiscan.

### 2.9. Statistical analysis

All emulsions were prepared in duplicate, and all measurements were performed three times. Data were subjected to analysis of variance (ANOVA) using the software package SPSS 12.0 for Windows (SPSS Inc., Chicago, IL).

## 3. Results and discussion

### 3.1. Zeta-potential

Fig. 1 shows the influence of MCC concentration ( $0\text{--}12\text{ g kg}^{-1}$ ) on the zeta-potential of SPIH-stabilized curcumin emulsions. In the absence of MCC, the net charge on the SPIH coated droplets was about  $-35.5 \pm 0.7\text{ mV}$ . The isoelectric point of SPIH is around pH 5.0 (Cui, Zhao, Yuan, Zhang, & Ren, 2013), hence the SPIH stabilized curcumin droplets was negatively charged at pH 7.0. The net charge on the curcumin droplets became more negative as the MCC concentration was increased. A small amount of MCC decreased slightly the zeta-potential of the curcumin droplet. At higher concentrations of MCC ( $4\text{ g kg}^{-1}$ ), the emulsion droplets showed the

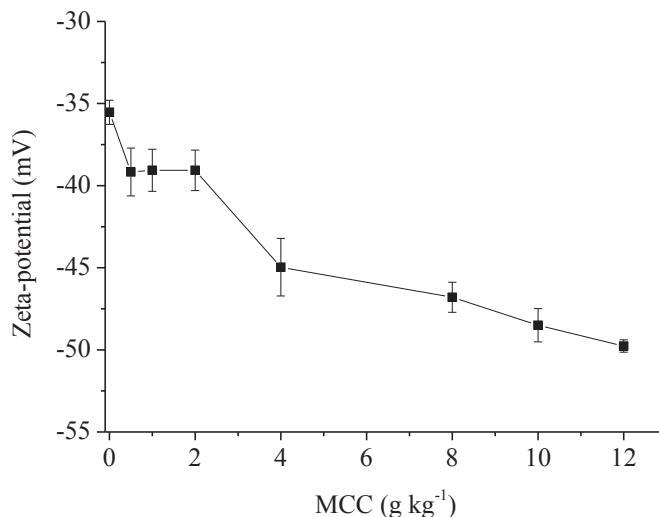


Fig. 1. Effect of the concentration of microcrystalline cellulose (MCC) on the zeta-potential of curcumin emulsions in  $10\text{ mmol L}^{-1}$  phosphate buffer at pH 7.0 with  $9\text{ g kg}^{-1}$  papain hydrolysate of soybean isolate protein (SPIH),  $50\text{ g kg}^{-1}$  medium chain triacylglycerol (MCT),  $0.1\text{ g kg}^{-1}$  curcumin and different concentrations of MCC. Error bars are standard deviations of mean values.

zeta-potential of about  $-44.9 \pm 1.7\text{ mV}$ . Eventually, the net charge on the droplets reached a high negative value ( $-49.7 \pm 0.3\text{ mV}$ ) when the MCC concentration was  $12\text{ g kg}^{-1}$ .

The change in zeta-potential was the result that negatively charged MCC adsorbed onto the surface of SPIH-stabilized curcumin droplets. It indicated that the anionic MCC molecule adsorbed to the surface layer of the cationic part of the SPIH-coated emulsion droplets and there was associative electrostatic interaction at the interface between the two polymers. The ability of charged polyelectrolytes to adsorb onto the surface of same charged colloidal particles has been well evaluated in the literature (Dickinson, 2013). With further addition of MCC ( $>8\text{ g kg}^{-1}$ ), the net charge on the droplets did not show significant difference, indicating an excess of MCC present in the emulsion continuous system.

### 3.2. Droplet size

Fig. 2 depicts the influence of MCC concentration ( $0\text{--}12\text{ g kg}^{-1}$ ) on the mean droplet size of SPIH-stabilized curcumin emulsions measured by DLS. It was found that the mean droplet size of SPIH-stabilized emulsion was about  $236.7 \pm 9.4\text{ nm}$ . At lower MCC concentrations ( $0.5\text{ g kg}^{-1}$  and  $1\text{ g kg}^{-1}$ ), there were no significant increases of the mean droplet size. When the MCC concentration was above  $4\text{ g kg}^{-1}$ , there was a large increase in the mean droplet size. The maximum level of droplet size occurred at a MCC concentration of about  $10\text{ g kg}^{-1}$ . With the further addition of MCC, the mean droplet size of the emulsion decreased and reached a value of  $892.9 \pm 3.6\text{ nm}$  at a MCC concentration of  $12\text{ g kg}^{-1}$ . The increase in droplet size was a clear indication of the interaction of the MCC with the SPIH-stabilized curcumin droplets and corresponded directly to the differences in the droplet zeta-potential described in Fig. 1.

The results could be explained by the fact that when the polysaccharide concentration was relatively low, MCC was interacting strongly with the SPIH at the surface of the droplet, thereby leading to a small increase of the droplet size. But it was insufficient to cover the entire droplet in the emulsion. Thus, it may act as a bridge to interact with protein molecules between the surfaces of the curcumin droplets by attractive electrostatic forces. When the

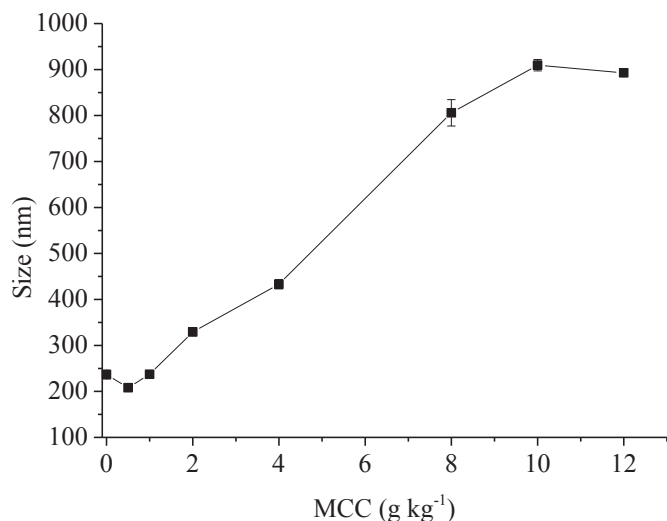


**Fig. 2.** Effect of the concentration of microcrystalline cellulose (MCC) on the average droplet size of curcumin emulsions in 10 mmol L<sup>-1</sup> phosphate buffer at pH 7.0 with 9 g kg<sup>-1</sup> papain hydrolysate of soybean isolate protein (SPIH), 50 g kg<sup>-1</sup> medium-chain triacylglycerol (MCT), 0.1 g kg<sup>-1</sup> curcumin and different concentrations of MCC. Error bars are standard deviations of mean values.

concentration of MCC increased, it would be sufficient to cover the particles and form a thick double layer on the curcumin droplets. Therefore, the flocculation would be inhibited by the strong electrostatic repulsion and the stereospecific blockade between droplets. The increased droplet size in the case of higher concentration of MCC curcumin emulsions also indicated excess of MCC present in the aqueous phase and the formation of gel. Similar phenomena were also found in the preparation of sodium caseinate and κ-carrageenan stabilized multilayer emulsions (Perrechil & Cunha, 2013). Previous studies showed that MCC can interact with proteins through physical (e.g., electrostatic) interactions to form either soluble or insoluble complexes (Schuh et al., 2013). Besides, it was demonstrated that the stability of emulsions prepared by small molecule surfactants (SDS, lecithin) could be improved by the adsorption of MCC onto the oil droplet surface.

### 3.3. Physical stability analyzed by Turbiscan

The effect of MCC concentration on the stability of curcumin emulsions was evaluated by Turbiscan based on the backscattering technology. As shown in Fig. 3, the addition of MCC to the SPIH stabilized curcumin emulsion led to a more stable system with a smaller TSI than the emulsion without MCC. It was evident that the stability behaviors of the curcumin emulsions were quite different with low MCC concentrations. Emulsions with MCC concentrations of 0–4 g kg<sup>-1</sup> were very unstable and they exhibited a remarkable increase in the TSI due to creaming and flocculation. When the MCC concentration was above 8 g kg<sup>-1</sup>, the emulsion became stable, as there was very little change in the integral backscattering. Meanwhile, the zeta potential results demonstrated that the negative charge of the curcumin emulsion droplets was sufficient to prevent droplet flocculation through electrostatic repulsion. Therefore, curcumin emulsion stabilized by 8 g kg<sup>-1</sup> MCC was preferred in the subsequent experiments.

It can be concluded that when the MCC concentration was too low (<4 g kg<sup>-1</sup>), the curcumin droplets could not be fully covered, leading to a greater degree of flocculation. The lower degree of droplet aggregation produced by increasing initial MCC concentration, could also be attributed to a greater number of MCC

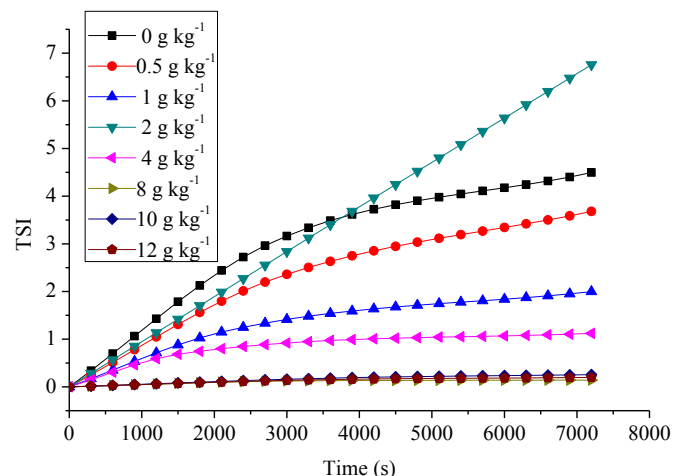


**Fig. 3.** Effect of microcrystalline cellulose (MCC) concentration on the physical stability (TSI) of papain hydrolysate of soybean isolate protein (SPIH)-curcumin emulsions (9 g kg<sup>-1</sup> SPIH, 50 g kg<sup>-1</sup> MCT – medium chain triacylglycerol, 0.1 g kg<sup>-1</sup> curcumin, pH 7.0).

molecules adsorbed onto the SPIH interface, thus promoting an increased repulsion, both electrostatic (Fig. 1) and steric, between the curcumin droplets. Some studies consider that higher concentrations of polysaccharide would promote a greater degree of depletion flocculation (McClements, 2000; Perrechil & Cunha, 2013). Nevertheless, curcumin emulsions prepared with higher concentration of MCC presented a better stability presumably also because of the viscosity increment in the continuous phase when increasing polysaccharide concentration according to the Stokes theory. The kinetic stability of emulsions is controlled by the structural organization of the curcumin droplets and by the viscosity parameters mainly involved in the Stokes' law equation of terminal velocity (McClements, 2005). The increased viscosity effect of MCC emulsified sausages has been reported by Schuh et al. (2013) as well. It was also probably that the curcumin emulsion contained MCC at higher concentration was stabilized by gel formation. As a result, more stable systems were obtained with MCC addition at higher MCC concentration.

### 3.4. Microrheological properties

The classical mechanical rheology technique has been reported to induce structural breakdown, leading to droplet deflocculation (Batista, Raymundo, Sousa, & Empis, 2006). Therefore, a non-destructive technique is needed to determine the rheological properties of emulsion. The Rheolaser lab technique as a method of monitoring the Brownian motion of droplets does not provide any kind of modification of the emulsion (Corredig & Alexander, 2008). Therefore, the influence of MCC on the microrheological properties of SPIH stabilized curcumin emulsions were measured using the Rheolaser lab.

Microrheology typically measures the motion of emulsion droplets and traces the particles interactions. The Mean Square Displacement (MSD) of droplets in the curcumin emulsions with different concentrations of MCC was measured as a function of time (Fig. 4). The MSD of the droplets is a direct measure of the dynamic properties of curcumin droplets and SPIH-MCC in which they are embedded. The collection of MSD curves was dependent on MCC concentrations studied. At lower concentrations of MCC (<8 g kg<sup>-1</sup>), the curcumin emulsions were purely viscous over the range of decorrelation times, giving a MSD that scaled linearly with decorrelation time. At higher concentrations of MCC (>8 g kg<sup>-1</sup>),

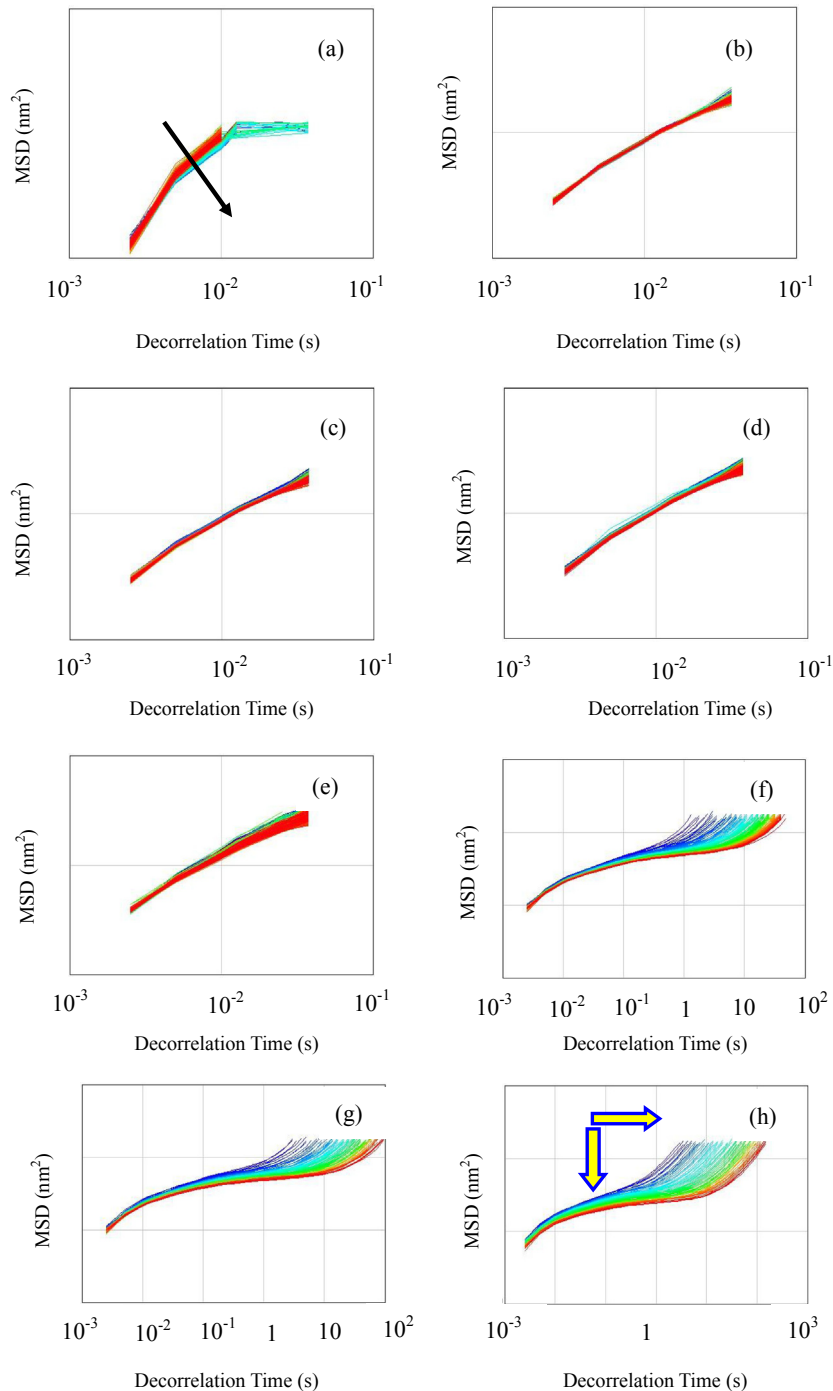


**Fig. 4.** Typical examples of the Mean Square Displacement (MSD) vs time curves for papain hydrolysate of soybean isolate protein (SPIH) stabilized curcumin emulsions ( $9 \text{ g kg}^{-1}$  SPIH,  $50 \text{ g kg}^{-1}$  MCT,  $0.1 \text{ g kg}^{-1}$  curcumin, pH 7.0) as a function of microcrystalline cellulose (MCC) concentrations (a, without MCC – medium chain triacylglycerol; b,  $0.5 \text{ g kg}^{-1}$  MCC; c,  $1 \text{ g kg}^{-1}$  MCC; d,  $2 \text{ g kg}^{-1}$  MCC; e,  $4 \text{ g kg}^{-1}$  MCC; f,  $8 \text{ g kg}^{-1}$  MCC; g,  $10 \text{ g kg}^{-1}$  MCC; h,  $12 \text{ g kg}^{-1}$  MCC). Different colors and arrows refer to different scanning time of MSD analysis. (For interpretation of the references to color in this figure legend, the reader is referred to the web version of this article.)

the MSD of all the samples were not linear indicating that SPIH-MCC stabilized curcumin emulsions were viscoelastic and the droplets were not free to move due to the curcumin droplets network interaction. It ranged from no obvious interactions detectable at very low concentration of MCC, to long range interactions at high concentration of MCC which affected the spatial arrangement of the droplets.

The Elasticity Index (EI) value represents the elasticity strength of the curcumin emulsions. It corresponds to the inverse

of the distance traveled by the particles before to interact with the network (inverse of the MSD level at the elastic plateau). The Macroscopic Viscosity Index (MVI) value quantifies the macroscopic viscosity at zero-shear. It corresponds to the inverse of the speed of the particles for long times (inverse of the linear slope of the MSD for long times). Table 1 shows the effect of different MCC concentrations on the EI and MVI values (obtained from the MSD curves) of SPIH stabilized curcumin emulsion at  $25 \text{ }^\circ\text{C}$ . There existed a remarkable increase in the EI and MVI of the

**Table 1**

The Macroscopic Viscosity Index (MVI) and Elasticity Index (EI) value for papain hydrolysate of soybean isolate protein (SPIH) stabilized curcumin emulsions ( $9 \text{ g kg}^{-1}$  SPIH,  $50 \text{ g kg}^{-1}$  MCT – medium chain triacylglycerol,  $0.1 \text{ g kg}^{-1}$  curcumin, and pH 7.0) as a function of microcrystalline cellulose (MCC) concentrations.

The concentrations of MCC ( $\text{g kg}^{-1}$ )	MVI ( $10^{-6}$ )	EI ( $10^{-3}$ )
0	$0.41 \pm 0.005$	$0.49 \pm 0.001$
0.5	$2.39 \pm 0.006$	$1.09 \pm 0.003$
1	$2.37 \pm 0.009$	$1.08 \pm 0.008$
2	$1.95 \pm 0.011$	$0.91 \pm 0.001$
4	$1.69 \pm 0.023$	$0.17 \pm 0.002$
8	$3903.02 \pm 2.349$	$3.10 \pm 0.015$
10	$7673.84 \pm 3.464$	$3.12 \pm 0.018$
12	$11,181.36 \pm 2.155$	$5.76 \pm 0.047$

curcumin emulsion with the increase of MCC concentration ( $>8 \text{ g kg}^{-1}$ ). It was typically attributed to higher interdroplet resistance force (Bouyer et al., 2011). The increase in MVI and EI for SPIH-MCC stabilized curcumin emulsions could be attributed to the fact that the presence of MCC resulted in dense gel network formation and spatial rearrangement of the curcumin droplets. It proved that the addition of MCC helped the stabilization of the emulsion due to an increase in viscosity of the aqueous phase and changing the nature of the inter-droplet interactions.

### 3.5. Influence of freeze-thaw cycling on the droplet size

The effect of freeze-thaw cycling on the droplet size of curcumin emulsions stabilized with SPIH and SPIH-MCC (MCC,  $8 \text{ g kg}^{-1}$ ) was evaluated (Fig. 5). Before freeze-thaw cycling, the droplet size of the initial emulsion stabilized with SPIH was  $236.7 \pm 9.4 \text{ nm}$ . After three freeze-thaw cycling, the droplet sizes of the SPIH emulsions were  $799 \pm 6.2$ ,  $971.8 \pm 5.4$ ,  $1521.6 \pm 10.1 \text{ nm}$ , respectively. It showed that appreciable increases in the droplet size occurred after freeze-thaw cycles. And, there was a dependence of the droplet size of the SPIH stabilized curcumin emulsion on the number of freeze-thaw cycles in the absence of MCC. It was agreed to other reports that freeze-thaw treatment resulted in an appreciable increase in the droplet size of the samples stabilized with protein alone, which

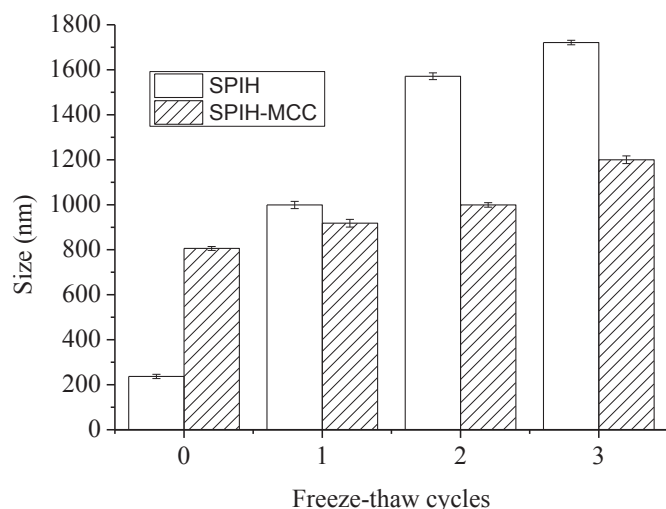


**Fig. 5.** Dependence of the average droplet size of papain hydrolysate of soybean isolate protein (SPIH) and SPIH-MCC (microcrystalline cellulose) stabilized curcumin emulsions ( $9 \text{ g kg}^{-1}$  SPIH,  $8 \text{ g kg}^{-1}$  MCC,  $50 \text{ g kg}^{-1}$  MCT – medium chain triacylglycerol,  $0.1 \text{ g kg}^{-1}$  curcumin, pH 7.0) on the number of freeze-thaw cycles.

was indicative of extensive droplet flocculation or coalescence (Gu, Decker, & McClements, 2007). It was mainly because the interfacial layers surrounding the curcumin droplets were relatively thin, curcumin crystals could probably easily penetrate through it from one droplet to another, thereby promoting partial coalescence. The freeze-thaw treatment induced denaturation of proteins may have occurred at low temperatures which could lead to a loss of protein emulsifying property when the emulsion was freeze-thawed (Kim, Decker, & McClements, 2002). It indicated that only hydrolysate of protein could not resist to the emulsion unstability of freeze-thaw treatment.

Compared with SPIH stabilized curcumin emulsion, there was a much less increase in the droplet size of curcumin emulsion with the addition of MCC, from  $805.8 \pm 8.8 \text{ nm}$  to  $818.2 \pm 7.8$ ,  $899.9 \pm 10.4$ ,  $900.3 \pm 7.7 \text{ nm}$  before and after 3 freeze-thaw cycles (Fig. 5). It indicated that emulsions stabilized with SPIH-MCC had better stability to curcumin droplet aggregation after freeze-thaw cycling than stabilized with SPIH alone. It might be expected that the SPIH-MCC should provide a thicker interfacial layer caused by the attachment of the MCC molecule, and therefore improved the SPIH curcumin emulsion freeze-thaw stability. It was also attributed to the ability of MCC to increase the amount of the fraction of unfrozen water present in the curcumin emulsions (Aoki, Decker, & McClements, 2005). The presence of MCC in the aqueous phase of the emulsions may have depressed the freezing point of the aqueous phase, thereby altering the kinetics and mechanisms of both ice crystal nucleation and growth. The MCC molecules and unfrozen water might form hydrogen bonds with the adsorbed SPIH molecules, thereby preventing them from becoming dehydration and reducing the tendency for emulsifier molecules adsorbed onto different droplets from associating with each other. The resistance to denaturation of SPIH was also expected to increase, due to the MCC moiety and this could be attributed to a shielding effect of the MCC chain bound to SPIH. Additionally, the presence of MCC increased the viscosity of the unfrozen aqueous phase and the fraction of unfrozen water present in the emulsions, which slowed down the diffusion of curcumin droplets and then inhibit the increase of the droplet size during the freeze-thaw treatment (Xu et al., 2010).

### 3.6. Influence of freeze-thaw cycling on the stability index

The emulsion stability to freeze-thaw processing was evaluated to determine whether MCC could be used to protect bioactive compound in emulsions. The freeze-thaw cycling stability of curcumin emulsions stabilized with SPIH and SPIH-MCC was also analyzed by Turbiscan, separately. Compared with other optical analytical methods, such as microscopy, particle size and zeta potential, turbiscan analysis has the advantage of being a non-destructive method (no sample dilution). The change of the TSI during 2 h as a function of freeze-thaw cycles was shown in Fig. 6 (a, before freeze-thaw; b, 1 cycle; c, 2 cycles; d, 3 cycles). It was observed that the TSI of the SPIH and SPIH-MCC emulsions showed a variation after each freeze-thaw treatment. For the original SPIH and SPIH-MCC stabilized curcumin emulsions, the TSI were 3.7 and 0.35, respectively. During the 3 freeze-thaw cycles, the TSI of SPIH and SPIH-MCC emulsions reached the values of 40.4 and 20.4 for the first freeze-thaw treatment, followed by a slight increase to 42.4 and 22.9 for the second freeze-thaw cycle and finally followed by 42.5 and 28.6 after the third freeze-thaw cycle, respectively. It indicated that droplet aggregation occurred in emulsions during freeze-thaw treatment. It revealed that coalescence was taking place after freeze-thaw treatments. This destabilization was due to the relatively thin adsorbed layers of

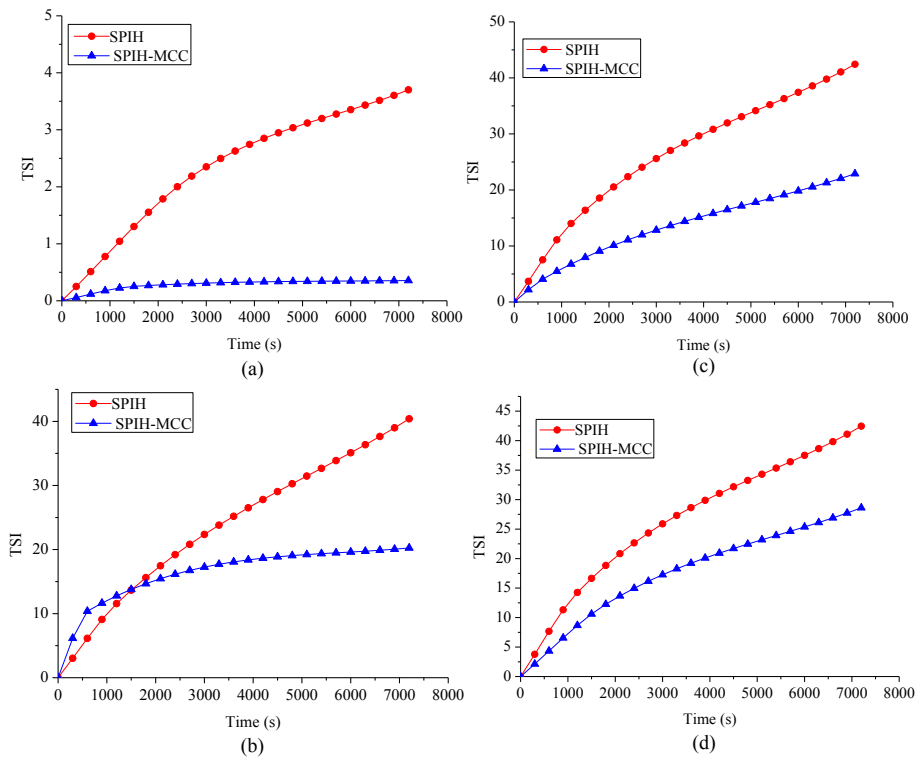


**Fig. 6.** The freeze-thaw stability (TSI – turbiscan stability index) of curcumin emulsions ( $9 \text{ g kg}^{-1}$  SPIH – papain hydrolysate of soybean isolate protein,  $8 \text{ g kg}^{-1}$  MCC – microcrystalline cellulose,  $50 \text{ g kg}^{-1}$  MCT – medium chain triacylglycerol,  $0.1 \text{ g kg}^{-1}$  curcumin, pH 7.0) stabilized with SPIH and SPIH-MCC before and after three freeze-thaw cycles (from zero to three), before freeze-thaw (a), 1 cycle (b), 2 cycles (c), 3 cycles (d).

the droplet. It was reported that the hydrophobic surface interactions between the subunits led to more intensive protein aggregation and droplet flocculation formation during freeze-thaw treatment.

As expected, the SPIH-MCC emulsion showed much lower TSI than SPIH emulsion after freeze-thaw cycling. Consequently, the freeze-thaw stability of the curcumin emulsions could be appreciably improved by the addition of MCC. In the presence of MCC, the stability of the resulting emulsions against freeze-thaw induced-aggregation increased markedly, suggesting that the presence of MCC molecules at the droplet surface inhibited the interaction between the aggregated proteins at the continuous phase with the droplet surface membrane.

The turbiscan data, therefore, supported the particle size data discussed earlier, but it provided more insight into the nature of the aggregation formed in the emulsions. Creaming instability was observed after freeze-thaw cycles in the SPIH alone stabilized emulsions. In the case of emulsions prepared with the SPIH-MCC which showed the remarkable stability against freeze-thaw aggregation. These results supported the hypothesis that the proper addition of polysaccharide and emulsifiers that form thicker interfacial membranes are more effective in preventing partial coalescence. This could be attributed to a very low droplet mobility and subsequently low degree of creaming. Results demonstrated that MCC brought about a remarkable improvement in freeze-thaw stabilizing properties when compared with SPIH which can be attributed to the increment of viscosity and enhancement of repulsive steric forces between the oil droplets as a result of MCC overlapping the thicker interfacial coatings surrounding the curcumin droplets. It was also possible because that the formation of the gel network induced by MCC enhanced the freeze-thaw stability of the curcumin emulsion.

#### 4. Conclusion

This study aimed at investigating the behavior of MCC when mixed with SPIH-stabilized curcumin emulsion droplets. The results demonstrated the interaction and attachment of MCC onto the surface of SPIH due to electrostatic interaction between the oppositely charged molecules part. Up to  $8 \text{ g kg}^{-1}$  concentration of MCC, no visual phase separation and low TSI was observed, demonstrating the kinetic stability of the curcumin emulsions. The addition of MCC led to a dramatic enhancement of the curcumin emulsion stability against freeze-thaw cycling compared with SPIH alone. It might be due to a shielding effect of the MCC chain bound to SPIH of the curcumin droplet. Additionally, the presence of MCC increased the viscosity of the emulsions and the formation of the gel network, which slowed down the diffusion of curcumin droplets and then improved the freeze-thaw stability of the emulsions.

#### Acknowledgments

This research was funded by the National Natural Science Foundation of China (31501486), Beijing Natural Science – SANYUAN jointly Foundation (15S00016), Cultivation of Excellent Talents in Beijing City (2014000020124G032), National Natural Science Foundation of China (31371722) and Development of Innovative Teams and Teachers' Occupation Advancement Project of Beijing Municipal Universities and Colleges (IDHT20130506).

#### References

- Anand, P., Kunnumakkara, A. B., Newman, R. A., & Aggarwal, B. B. (2007). Bioavailability of curcumin: problems and promises. *Molecular Pharmaceutics*, 4, 807–818.

- Anand, P., Sundaram, C., Jhurani, S., Kunnumakkara, A. B., & Aggarwal, B. B. (2008). Curcumin and cancer: an “old-age” disease with an “age-old” solution. *Cancer Letters*, 267, 133–164.
- Aoki, T., Decker, E. A., & McClements, D. J. (2005). Influence of environmental stresses on stability of O/W emulsions containing droplets stabilized by multilayered membranes produced by a layer-by-layer electrostatic deposition technique. *Food Hydrocolloids*, 19(2), 209–220.
- Batista, A. P., Raymundo, A., Sousa, I., & Empis, J. (2006). Rheological characterization of coloured oil in-water food emulsions with lutein and phycocyanin added to the oil and aqueous phases. *Food Hydrocolloids*, 20, 44–52.
- Bouyer, E., Mekhloufi, G., Potier, I. L., Kerdaniel, T., Grossiord, J., Rosilio, V., et al. (2011). Stabilization mechanism of oil-in-water emulsions by  $\beta$ -lactoglobulin and gum Arabic. *Journal of Colloid and Interface Science*, 354, 467–477.
- Bouyer, E., Mekhloufi, G., Rosilio, V., Grossiord, J., & Agnely, F. (2012). Proteins, polysaccharides, and their complexes used as stabilizers for emulsions: alternatives to synthetic surfactants in the pharmaceutical field? *International Journal of Pharmaceutics*, 436, 359–378.
- Chen, L., Chen, J., Ren, J., & Zhao, M. (2011). Effects of ultrasound pretreatment on the enzymatic hydrolysis of soy protein isolates and on the emulsifying properties of hydrolysates. *Journal of Agricultural and Food Chemistry*, 59, 2600–2609.
- Ci, F., Cao, Y., Xu, D., & Wang, B. (2013). The effect of modified papain on the emulsifying properties of soy protein. *Food and Fermentation Industries*, 39, 59–62.
- Corredig, M., & Alexander, M. (2008). Food emulsions studied by DWS: recent advances. *Trends in Food Science & Technology*, 19, 67–75.
- Cui, C., Zhao, M., Yuan, B., Zhang, Y., & Ren, J. (2013). Effect of pH and pepsin limited hydrolysis on the structure and functional properties of soybean protein hydrolysates. *Journal of Food Science*, 78, 1871–1877.
- Dickinson, E. (2009). Hydrocolloids as emulsifiers and emulsion stabilizers. *Food Hydrocolloids*, 23, 1473–1482.
- Dickinson, E. (2011). Mixed biopolymers at interfaces: competitive adsorption and multilayer structures. *Food Hydrocolloids*, 25, 1966–1983.
- Dickinson, E. (2013). Stabilising emulsion-based colloidal structures with mixed food ingredients. *Journal of the Science of Food and Agriculture*, 93, 710–721.
- Ghanbarzadeh, B., Almasi, H., & Entezamin, A. A. (2010). Physical properties of edible modified starch/carboxymethyl cellulose films. *Innovative Food Science & Emerging Technologies*, 11(4), 697–702.
- Gu, Y. S., Decker, E. A., & McClements, D. J. (2007). Application of multi-component biopolymer layers to improve the freeze-thaw stability of oil-in-water emulsions:  $\beta$ -lactoglobulin- $\iota$ -carrageenan-gelatin. *Journal of Food Engineering*, 80, 1246–1254.
- Kim, H. J., Decker, E. A., & McClements, D. J. (2002). Role of postadsorption conformation changes of  $\beta$ -lactoglobulin on its ability to stabilize oil droplets against flocculation during heating at neutral pH. *Langmuir*, 18, 7577–7583.
- Lavoine, N., Desloges, I., Dufresne, A., & Bras, J. (2012). Microfibrillated cellulose – its barrier properties and applications in cellulosic materials: a review. *Carbohydrate Polymers*, 90, 735–764.
- Lemarchand, C., Couvreur, P., & Vauthier, C. (2003). Study of emulsion stabilization by graft copolymers using the optical analyzer Turbiscan. *International Journal of Pharmaceutics*, 254, 77–82.
- Li, M., Ma, Y., & Cui, J. (2014). Whey-protein-stabilized nanoemulsions as a potential delivery system for water-insoluble curcumin. *LWT-Food Science and Technology*, 59, 49–58.
- Liu, Y., Hou, Z., Lei, F., Chang, Y., & Gao, Y. (2012). Investigation into the bio-accessibility and microstructure changes of  $\beta$ -carotene emulsions during in vitro digestion. *Innovative Food Science & Emerging Technologies*, 15, 86–95.
- McClements, D. J. (2000). Comments on viscosity enhancement and depletion flocculation by polysaccharides. *Food Hydrocolloids*, 14, 173–177.
- McClements, D. J. (2004). Protein-stabilized emulsions. *Current Opinion in Colloid & Interface Science*, 9, 305–313.
- Perrechil, F. A., & Cunha, R. L. (2013). Stabilization of multilayered emulsions by sodium caseinate and k-carrageenan. *Food Hydrocolloids*, 30, 606–613.
- Schuh, V., Allard, K., Herrmann, K., Gibis, M., Kohlus, R., & Weiss, J. (2013). Impact of carboxymethyl cellulose (CMC) and microcrystalline cellulose (MCC) on functional characteristics of emulsified sausages. *Meat Science*, 93, 240–247.
- Tapal, A., & Tiku, P. K. (2012). Complexation of curcumin with soy protein isolate and its implications on solubility and stability of curcumin. *Food Chemistry*, 130(4), 960–965.
- Tippetts, M., & Martini, S. (2012). Influence of iota-carrageenan, pectin, and gelatin on the physicochemical properties and stability of milk protein-stabilized emulsions. *Journal of Food Science*, 77, C253–C260.
- Wiśniewska, M., Urban, T., Nosal-Wiercińska, A., Zarko, V., & Gunko, V. M. (2014). Comparison of stability properties of poly (acrylic acid) adsorbed on the surface of silica, alumina and mixed silica-alumina nanoparticles – application of turbidimetry method. *European Journal of Chemistry*, 12, 476–479.
- Xu, D., Yuan, F., Wang, X., Li, X., Hou, Z., & Gao, Y. (2010). The effect of whey protein isolate-dextran conjugates on the freeze-thaw stability of oil-in-water emulsions. *Journal of Dispersion Science and Technology*, 32, 77–83.



# Effect of ovalbumin on the quality of gluten-free rice flour bread made with soymilk



Masaaki Nozawa <sup>a</sup>, Seiko Ito <sup>b</sup>, Eiko Arai <sup>b,\*</sup>

<sup>a</sup> Graduate School of Integrated Pharmaceutical and Nutritional Sciences, University of Shizuoka, 52-1 Yada, Suruga-ku, Shizuoka 422-8526, Japan

<sup>b</sup> School of Food and Nutritional Sciences, University of Shizuoka, 52-1 Yada, Suruga-ku, Shizuoka 422-8526, Japan

## ARTICLE INFO

### Article history:

Received 21 April 2015

Received in revised form

2 November 2015

Accepted 6 November 2015

Available online 11 November 2015

### Keywords:

Gluten-free

Ovalbumin

Rice flour bread

Soymilk

## ABSTRACT

The use of soymilk instead of water affects the rising of gluten-free rice flour bread into the shape of a muffin. However, when baking bread into a loaf, gas cells at the center of the crust, where thermal conduction is lowest, collect to form a hollow in the loaf. The goal of this study was to assess the components that affect the quality of gluten-free rice flour bread made with soymilk. Adding more than 1.25% of ovalbumin (OVA) to the rice flour prevented formation of this hollow. In addition, OVA levels greater than 2.5% helped the bread rise further through oven spring, which increased specific loaf volume. These improvements resulted from an increase in thermal coagulation of gas cell membranes and an increase in batter viscosity due to interactions between soy globulins and OVA that promoted starch granule aggregation. Thus, even though OVA levels greater than 2.5% increased the specific loaf volume, they also made the crust harder. As a result, the optimum OVA level is 1.25% of the rice flour.

© 2015 Elsevier Ltd. All rights reserved.

## 1. Introduction

Gluten is a fundamental component for making bread dough (Wieser, 2007; Barak, Mudgil, & Khatkar, 2013), but genetic factors or excessive intake can lead to health problems such as celiac disease (Biesiekierski, Muir, & Gibson, 2013; Sabatino & Corazza, 2009), baker's asthma (Salcedo, Quirce, & Diaz-Perales, 2011; Wang et al., 2010), and gluten sensitivity (Fasano et al., 2008). Concern over these diseases has created the need for diets with reduced or no gluten (Cosnes et al., 2008; Gallagher, Gormley, & Arendt, 2004; Norström, Sandström, Lindholm, & Ivarsson, 2012).

Variants of gluten-free rice bread, made with rice flour instead of wheat flour, have been developed, but usually require the addition of thickeners such as xanthan gum (Demirkesen et al., 2014; Lazaridou, Duta, Papageorgiou, Belc, & Biliaderis, 2007), guar gum (Schwarzlaff, Johnson, Barbeau, & Duncan, 1996), or hydroxypropyl methylcellulose (Cornejo & Rosell, 2015; De La Hera, Rosell, & Gomez, 2014; Mariotti, Ambrogina, & Lucisano, 2013) to trap the CO<sub>2</sub> released by the yeast in the batter. All of these thickeners are approved food additives in many countries. Thus, developing a rice flour bread that rises properly using approved food ingredients is beneficial.

A previous study (Nozawa, Ito, & Arai, 2014) reported that replacing water with soymilk in the dough was an effective way to produce gluten-free rice flour bread that would rise properly without the use of thickeners. Replacing the water in the rice flour batter with the same weight of soymilk reduced the water content of the batter to 90% of the original amount, increasing the batter viscosity. The sucrose in the soymilk also stimulated yeast fermentation, which increased the amount of CO<sub>2</sub>. These effects created more gas cells (CO<sub>2</sub>) in the soymilk batter compared to batter with water, and significantly increased the volume after fermentation. Additionally, glycinin and β-conglycinin contained in the soymilk formed a membrane that prevented gas cells from escaping the batter or joining together. The gas cells remained intact, even during the baking process, allowing the bread to rise significantly more compared to bread made from batter containing water.

These results, however, were achieved by baking a small amount of batter in a muffin mold. For gluten-free rice flour bread to be a useful replacement for wheat flour bread, the bread must be able to form loaves similar to those of wheat flour bread. Marston and Wannan (1976) reported that the temperature increase at the center of a wheat flour loaf at the start of heating is significantly slower than that at or near the sides of the loaf when baking. During baking of a loaf of bread made from batter containing soymilk, gas cells at the center of the loaf, where the heat transfer is

\* Corresponding author.

E-mail address: [earai@u-shizuoka-ken.ac.jp](mailto:earai@u-shizuoka-ken.ac.jp) (E. Arai).

slowest, need to remain stable.

Earlier studies on gluten-free bread have used rice flour as the main ingredient with the addition of soy protein isolates and dried egg white solids (Crockett, Ie, & Vodovotz, 2011). However, in most of these studies, hydrochlorides were used as additives. Consequently, the contribution of soybean and egg proteins to the formation and stabilization of gas cells in gluten-free bread has not yet been clarified.

The objective of the present study was to investigate the ability of albumin (which has a high capacity for thermal coagulation among dietary proteins) to improve gas cell stability and increase the leavening ability of the bread by preventing the breakdown and merging of gas cells formed by soy globulin during baking. Three types of albumin with different thermal denaturation temperatures were used: ovalbumin, bovine serum albumin, and lactalbumin. The effect of albumin addition on the quality of gluten-free rice flour bread made with soymilk also was determined.

## 2. Material and methods

### 2.1. Materials

Gluten-free bread was made using rice flour (powder rice type D; Niigata Seifun Co., Ltd., Niigata, Japan; Koshihikari cultivar; mean particle size, approximately 55  $\mu\text{m}$ ), organic soymilk (Marusan-AI Co., Ltd., Aichi, Japan; protein, fat, ash, and water contents were 4.6%, 2.8%, 0.5%, and 90.7%, respectively), granulated sugar (Fuji Nihon Seito Corporation, Tokyo, Japan), refined salt (Salt Industry Center of Japan, Tokyo, Japan), freeze-dried instant yeast (Nisshin Foods Inc., Tokyo, Japan), ovalbumin (OVA, Wako Pure Chemical Industries, Ltd., Osaka, Japan), bovine serum albumin (BSA, Nacalai Tesque, Inc., Kyoto, Japan), and bovine  $\alpha$ -lactalbumin (BLA, LKT Laboratories, Inc., Minnesota, US). Other components included soybean (*Glycine max* L., Hukuyutaka cultivar) seeds and non-glutinous rice starch (Joetsu Starch Co. Ltd., Niigata, Japan).

### 2.2. Methods

#### 2.2.1. Bread-making procedure

Gluten-free rice flour bread using was prepared in a muffin mold as described previously (Nozawa et al., 2014). Preparation of bread using a half-loaf mold was performed according to a modified muffin mold method. The batter ingredients were: 200 g rice flour (baker's percentage of 100%), 220 g soymilk or water (110%), 4 g sugar (2%), 2.5 g salt (1.25%), 2.5 g yeast (1.25%), and 1.25, 2.5, 5.0, or 10 g albumin (0.625%, 1.25%, 2.5%, or 5%, respectively). After adjusting the temperature of the ingredients to a batter temperature of 10 °C, the ingredients were placed in a bowl with ice water and mixed for 5 min with an electric mixer (THM 26M; Tescom Co. Ltd., Tokyo, Japan) at a mixing rate of 800 rpm. The resulting batter was poured in 300-g portions into a half-loaf mold made of aluminum (length, 95 mm; width, 95 mm; height, 95 mm) and yeast-fermented at 38 °C with 80% RH for 120 min in an incubator. After yeast fermentation, the batter was baked at 170 °C in a household electric oven (RE-WB30-S; Sharp Corporation, Tokyo, Japan) for 40 min. After baking, the bread was removed and cooled in an incubator at 20 °C and 60% RH for 2 h.

#### 2.2.2. Rate of batter volume increase

A 50-g portion of batter was added to a graduated cylinder (200 mL) and yeast-fermented at 38 °C with 50% RH for 80 min. The rate of volume increase (%) of the batter was calculated using the formula: [volume after fermentation (mL)/volume before fermentation (mL)]  $\times$  100.

#### 2.2.3. Specific loaf volume (SLV)

Bread using the half-loaf mold was weighed and the volume measured using a rapeseed displacement method. The SLV ( $\text{cm}^3/\text{g}$ ) value and the ratio of the volume ( $\text{cm}^3$ ) to the mass of the bread (g) also were calculated.

#### 2.2.4. Thermal coagulation of soymilk foam with added albumin

Soymilk (220 g) with added OVA, BSA, or BLA (10 g, in the same ratio as for bread-making with 5% albumin) was mixed for 5 min with an electric mixer at a rate of 800 rpm to produce soymilk foam. The foam was added to a Pyrex glass cup (diameter, 75 mm; height, 57 mm; content, 150 mL), and heated at 170 °C in a household electric oven for 10 min. After heating, an image of the soymilk foam was obtained using a digital camera.

#### 2.2.5. Differential scanning calorimetry (DSC) measurements

DSC measurements were obtained using an EXSTAR 6000 calorimeter (Seiko Instruments Inc., Chiba, Japan). Prior to the DSC measurements, 10 mg of protein (glycinin, OVA, BSA, or BLA) was placed in a silver cell (70  $\mu\text{L}$ ) and 30  $\mu\text{L}$  of distilled water was added, while the reference cell contained 50  $\mu\text{L}$  of distilled water. Glycinin was prepared from soybean seeds using a method described previously (Nozawa et al., 2014). After sealing, the sample was scanned at temperatures from 20 to 150 °C at a heating rate of 5 °C/min. The thermo compensation curves were evaluated using the software package provided with the equipment (Muse, Seiko Instruments Inc., Chiba, Japan) to calculate parameters, including peak temperature (PT) and enthalpy ( $\Delta\text{H}$ ).

#### 2.2.6. Viscosity of gelatinized rice flour-soymilk slurry

The viscosity of a gelatinized rice flour-soymilk slurry was measured using a Rapid Visco Analyzer (RVA-4, Newport Scientific, Inc., Warriewood, Australia). Rice flour (3.06 g) was transferred into a canister and water (24.94 g) or soymilk (27.49 g) was added. The amount of soymilk used was equal that of the amount of water added to the rice flour. Then, OVA, BSA, or BLA was added to the slurry in the proportions to rice flour of 0% (no additive), 0.625% (19 mg), 1.25% (38 mg), 2.5% (76 mg), and 5% (152 mg). The slurry obtained was held at 50 °C for 1 min, heated to 95 °C in 3.8 min, and then held at 95 °C for 2.5 min. The slurry then was cooled to 50 °C in 3.8 min and held at 50 °C for 1.4 min. The paddle rotation speed was 960 rpm for the first 10 s and then was reduced to 160 rpm throughout the remainder of the experiment. The peak viscosity was obtained from the Rapid Visco Analyzer (RVA) curve.

#### 2.2.7. Fractionation of soy globulin from soybean seeds and preparation of soy globulin solution

Soybean seeds were powdered with a grinder mill (IFM-720G-W/Y; Iwatani Corporation, Tokyo, Japan) and then soaked in hexane at 20 °C for 3 h. The residue was filtered and air dried (defatted soybean powder). Glycinin and  $\beta$ -conglycinin were fractionated from the defatted soybean powder using the method described by Thanh and Shibasaki (1976). The glycinin fraction, which precipitated at pH 6.4, and the  $\beta$ -conglycinin fraction, which precipitated at pH 4.2, were mixed, suspended in 60 mM Tris-HCl buffer (pH 6.4), and adjusted to pH 7.8 with sodium hydroxide. The solutions were dialyzed against water at 4 °C for 48 h and freeze-dried using a lyophilizer. The soy globulin solution was prepared by dissolving the lyophilizates in water at a concentration equivalent to the protein content of soymilk (4.6 g/100 g). The composition of proteins in the glycinin and  $\beta$ -conglycinin fractions was confirmed by SDS-PAGE (Laemmli, 1970) using a 5–20% gradient acrylamide gel (E-T/R/D5201, ATTO Corp., Tokyo, Japan). Samples used for electrophoresis were prepared by dialysis of the precipitates of the glycinin and  $\beta$ -conglycinin fractions before they were combined,

followed by freeze-drying. For comparison, a sample was prepared by defatting soymilk with hexane, followed by dialysis and freeze-drying. Then, all of the samples were subjected to electrophoresis using the AE-1440 EzStandard (ATTO Corp., Tokyo, Japan) molecular weight marker. Based on analysis of the band areas using electrophoresis image analysis software (CS Analyzer 3 for Windows, ATTO Corp., Tokyo, Japan), relative percentages of the acidic and alkaline subunits in the glycinin fraction, as well as the relative percentages of the  $\alpha$ ,  $\alpha'$ , and  $\beta$  subunits in the  $\beta$ -conglycinin fraction, were calculated (purity).

#### 2.2.8. Particle size distribution and microscopy of gelatinized rice starch

Four slurries were prepared: non-glutinous rice starch (3.08 g) with added water (24.92 g), water and OVA (0.154 g), soy globulin solution (26.11 g), and soy globulin solution and OVA (0.154 g). These were transferred into canisters for RVA. An amount of soy globulin solution was chosen that was equivalent to the amount of water added to the rice flour. The slurry was heated until it reached peak viscosity, followed by immediate collection of the gelatinized slurry. The entire volume of the gelatinized slurry collected was poured onto a stainless steel tray covered with plastic film, and then the slurry was spread out with a spatula to a thickness of about 5 mm. The slurry was placed in an ultra-low temperature freezer (PMDF-U442, Panasonic Healthcare Co. Ltd., Tokyo, Japan) at  $-85\text{ }^{\circ}\text{C}$  and frozen. After 24 h, the gelatinized slurry was freeze-dried and the lyophilized sample crushed in a grinder mill. The lyophilized samples were suspended in water and sonicated for 120 s. Particle size distribution was obtained using a laser diffraction particle-size analyzer (LS 13 320, Beckman Coulter, Inc., California, US). The lyophilized samples used for obtaining the particle-size distributions were observed at a magnification of 800 times with an optical microscope (VH-8000, Keyence Corporation, Osaka, Japan).

#### 2.2.9. Measurement of crust hardness

To assess crust hardness, the bread loaves were sliced horizontally in half 2 h after baking, and four sample cubes, 20 mm on a side, were obtained from the bottom of each loaf with an ultrasonic cutter (USC-3305, Yamaden Co., Ltd., Tokyo, Japan). Hardness was measured using a creep meter (RE2-33005s, Yamaden Co., Ltd., Tokyo, Japan) with a cylindrical plunger (diameter, 40 mm) at a rate of 1 mm/s and 50% compression. Hardness was calculated by dividing the maximum force obtained during compression by the contact area of plunger and bread ( $400\text{ mm}^2$ ).

#### 2.2.10. Statistical analysis

All measurements were performed in triplicate or more and each value expressed as mean  $\pm$  standard deviation (SD). Correlation coefficients between the amount of albumin added and specific loaf volume or peak viscosity of slurry were calculated using Pearson's correlation coefficient. The results for crust hardness were evaluated using ANOVA, and the means compared by Tukey's tests with a significance of  $p < 0.05$ . The calculations were performed using SPSS 19 (IBM, NY, US).

### 3. Results and discussion

#### 3.1. Hollow formation in bread crusts due to increased batter

The size of the bread loaves was increased by preparing them using a half-loaf mold (batter weight: 300 g) that was larger than a muffin mold (batter weight: 40 g). Then, the fermentation states of the batter and extent of bread rise after baking were compared. The results indicated no significant difference in fermentation between

the different weights of batter. However, there was significant hollowing in the top center of the loaf baked in a half-loaf mold (Fig. 1).

In wheat flour bread, a disulfide (SS) bond is created between the gliadin and glutenin, which leads to a starch-gluten matrix that forms the gas cell walls (Mills, Wilde, Salt, & Skeggs, 2003). This prevents gas cells from merging during the baking process. For bread made from batter using soymilk and rice flour, the gas cell membrane is formed mainly by the glycinin in the soymilk, as reported previously (Nozawa et al., 2014). The heat-induced denaturation temperature for glycinin is approximately  $90\text{ }^{\circ}\text{C}$  (Hermansson, 1978). Therefore, water is lost and the gas cell membranes become thinner before the glycinin at the center of the batter made with soymilk can thermally coagulate (Weaire & Hutzler, 1999). This allows adjacent gas cells to merge and a large hollow to form (Gan, Ellist, & Schofield, 1995). To prevent hollowing of the crust, adding a protein with thermal coagulation properties superior to glycinin was expected to hasten the formation of more robust gas cell membranes. Thus, the addition of albumin was investigated.

#### 3.2. Effect of albumin on bread interior and rising

Three different types of albumin were investigated. Up to 5% albumin was added to the rice flour, followed by measurement of the amount of hollowing within the baked bread. Before baking, the effects of the addition of albumin on fermentation of the batter were investigated. The percentage increase in the volume of fermentation of the batter was measured upon addition of 1.25% of each albumin. With no added albumin, the percentage increase was  $280 \pm 6\%$ . However, addition of OVA resulted in an increase of  $282 \pm 4\%$ , with BSA the increase was  $256 \pm 1\%$ , and with BLA the increase was  $262 \pm 6\%$ . The differences between no added albumin and with added BSA and BLA were significant. Although the addition of OVA did not affect fermentation of the batter, addition of BSA and BLA did inhibit fermentation.

For OVA, the amount of hollowing decreased as the OVA ratio increased, with hollowing completely eliminated at OVA ratios greater than 1.25% (Fig. 2). Ratios greater than 2.5% resulted in additional bread rising due to oven spring. A significant positive correlation between SLV and added OVA was found, which was greater for higher levels of OVA and SLV (Fig. 3;  $r = 0.922$ ,  $p < 0.05$ ). In contrast, increases in the amount of added BSA had no effect on the size of the hollowing. Added BLA reduced the size of the hollow, but also reduced the amount of bread rising compared to loaves made with OVA. These results demonstrated that OVA addition at levels greater than 1.25% improved the internal structure of the bread, while addition of 2.5% OVA improved bread rising.

#### 3.3. Improvement in thermal coagulation of gas cell membranes with albumin

The elimination of crust hollowing due to OVA addition improved the thermal coagulation of the gas cell membrane. To investigate the effect of albumin addition on the thermal coagulation of gas cell membranes, 5% OVA, BSA, or BLA was added to soymilk for bread making. These mixtures were whipped and the resulting foam transferred to a glass cup, heated, and then observed.

When soymilk without added albumin was heated, gas cells were completely eliminated and the soymilk returned to liquid form (Fig. 4). In soymilk with added OVA, gas cells merged and increased in size during heating, but coagulated while maintaining the shape of a gas cell. When BSA was added to the soymilk, gas cells on the surface merged and sheet-like membranes were

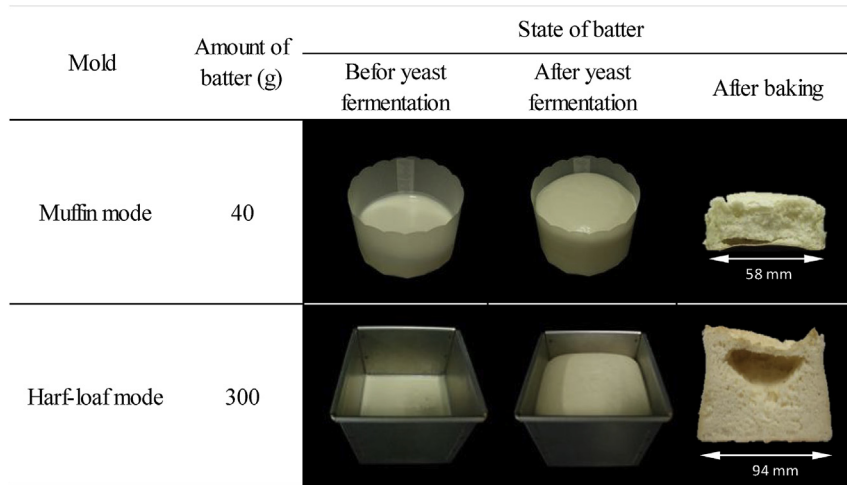


Fig. 1. Characteristics of bread batter after baking, using a muffin mold and a half-loaf mold.

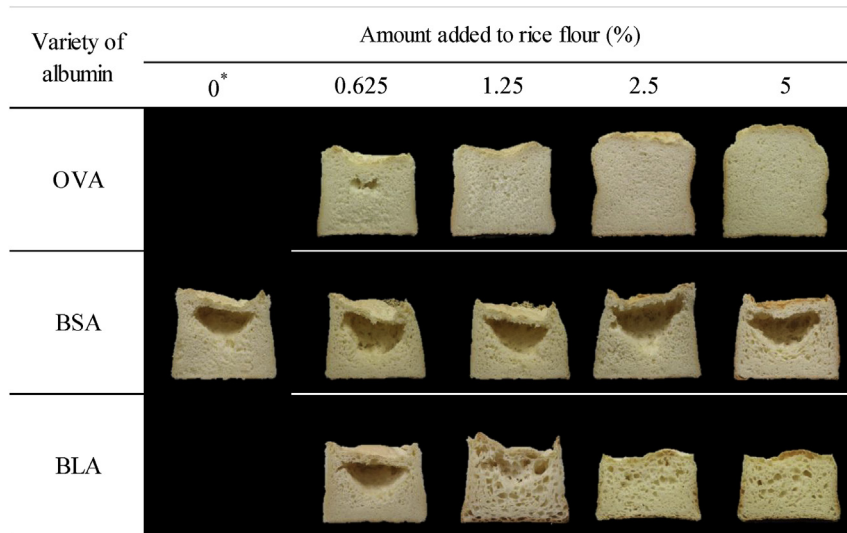


Fig. 2. Effect of adding different types and amounts of albumin on hollowing of bread crust and rising. \*Same as the image for Fig. 1.

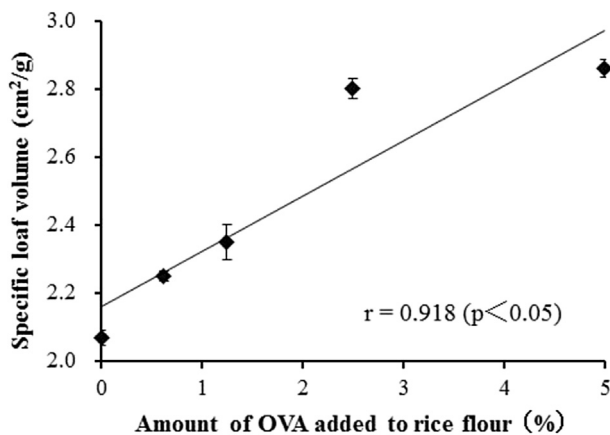
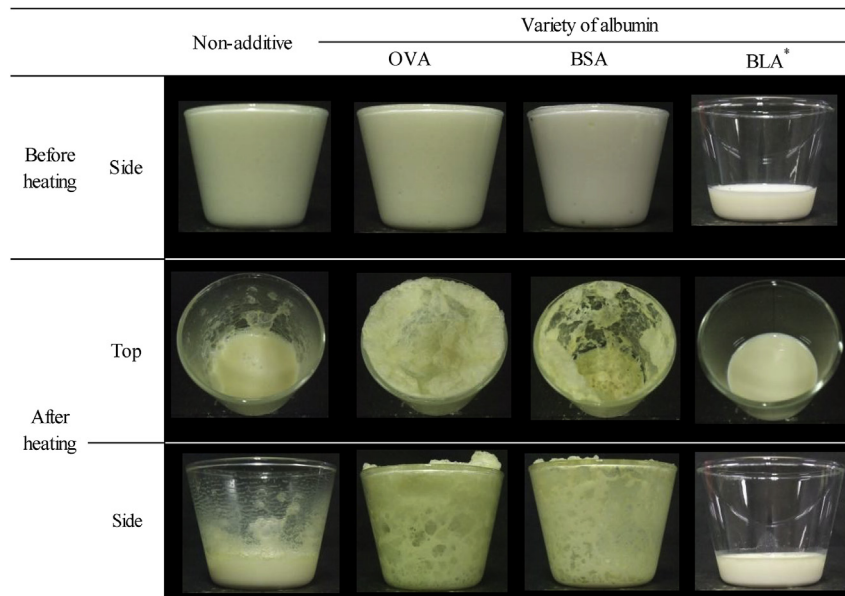


Fig. 3. Effect of OVA amount on specific loaf volume (values represent the average of 5 measurements).

formed during the initial phase of heating, but these membranes later collapsed, and, after heating, soymilk had adhered to the bottom and side of a glass cup in a semi-solid form. Soymilk with added BLA did not form gas cells, even when agitated; therefore, after the liquid was placed in a glass cup and heated, it remained liquid. These results demonstrated that adding OVA to soymilk greatly improved the thermal coagulation of the gas cell membranes compared to soymilk without added albumin, as well as soymilk with added BSA or BLA.

To clarify the manner by which OVA markedly improved the thermal coagulation of gas cell membranes, DSC analysis of the thermal behavior of glycinin, the main structural component of gas cell membranes, and three types of albumin was conducted (Fig. 5). Results showed that the peak thermal denaturation temperature for OVA was 84.4 °C; lower than the temperature of 89.8 °C found for glycinin. The OVA had a heat-induced denaturation temperature lower than that of glycinin (Du, Prokop, & Tanner, 2002). Thus, in batter with OVA, the OVA was assumed to form a gas cell membrane together with glycinin and other soy proteins that promoted



**Fig. 4.** Characteristics of soymilk foam after heating (170 °C for 10 min) with different types of albumin†. †Albumin (10 g) was added to soymilk (220 g) and mixed for 5 min with an electric mixer. \*Soymilk with added BLA did not cell.

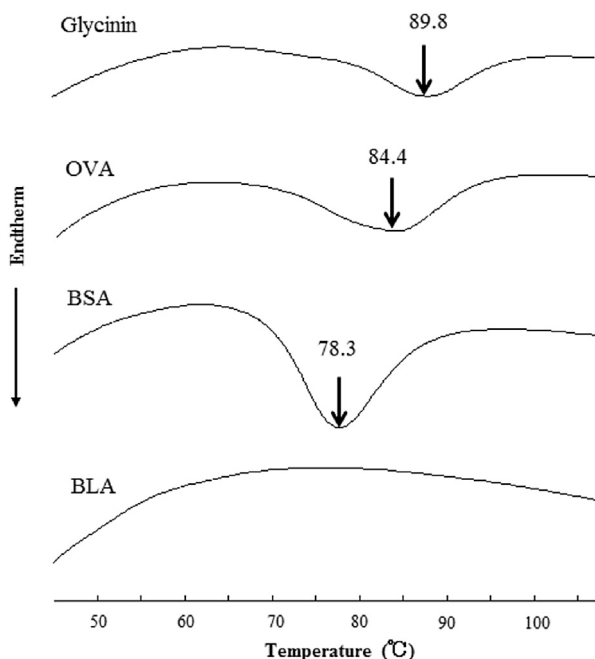


**Fig. 5.** DSC thermograms of glycinin, OVA, BSA, and BLA†. †The sample (10 mg) and distilled water (30  $\mu$ L) were placed in a silver cell (70  $\mu$ L); the reference cell contained distilled water (50  $\mu$ L). The sample was scanned from 20 to 150 °C at a heating rate of 5 °C/min. Values of peak temperature are the average of 3 measurements.

thermal coagulation of gas cell membranes in the center of the batter, preventing merging of adjacent gas cells (Gan, Ellist, & Schofield, 1995).

In contrast, the peak thermal denaturation temperature for BSA (79.3 °C) was approximately 5 °C lower than that for OVA, but upon addition to soymilk, the BSA did not improve thermal coagulation of the gas cell membranes as much as did OVA. The endothermic enthalpy ( $\Delta H$ ) required for molecular unfolding of BSA was  $9.01 \pm 0.76$  mJ/mg, greater than that for OVA ( $7.64 \pm 0.38$  mJ/mg). Therefore, the increase in BSA interactions with glycinin during

thermal coagulation of gas cell membranes was assumed to be too small to prevent the occurrence of crust hollowing because the BSA molecules were not as readily unfolded by heating as those of OVA. Furthermore, an endothermic peak was not detected for BLA, which had greater thermal stability than glycinin, OVA, or BSA, presumably because BLA contains eight cysteines, each of which forms an SS-bond in the molecule (Walstra & Jenness, 1984). Moreover, as shown in Fig. 2, an increase in the amount of added BLA caused the gas cells of the crust to merge and enlarge, decreasing the rising ability of the bread. Consequently, addition of BLA did not improve the thermal coagulation of gas cell membranes; on the contrary, it weakened the gas cell membrane.

#### 3.4. Improvement in batter viscosity with OVA

Increasing batter viscosity during baking prevents gas cells from merging (Schober, 2010). Goel, Singhal, and Kulkarni (1999) reported that proteins contain many hydrophilic groups, all of which are capable of forming crosslinks with starch; these crosslinks may be responsible for the greater paste viscosity as compared to cassava starch paste. Moreover, Hamada, Suzuki, Aoki, and Suzuki (2013) showed that the rice protein in batter of gluten-free rice flour bread made from malted rice is partially broken down by *Aspergillus oryzae* protease. Through these proteins, the rice starch granules form aggregates that reduce the fluidity of the batter. This indicates that soy proteins or albumin may have an effect on batter fluidity during the baking process. Therefore, a slurry was prepared with an amount of added albumin equivalent to the amount in bread made with rice flour and soymilk or water. The gelatinization viscosity was measured through RVA, and peak viscosity was used to indicate batter liquidity during the baking process.

With no added albumin (Fig. 6, 0%), peak viscosity of the slurry made with soymilk was lower than that of the slurry made from water, likely due to inhibition of swelling and gelatinization of the rice starch granule by the soymilk components. However, a significant positive correlation was obtained between the peak viscosity and OVA (●) or BSA (▲) level as the peak viscosity increased (i.e., as more OVA or BSA was added to the soymilk slurry) (OVA,  $r = 0.996$ ,  $p < 0.01$ ; BSA,  $r = 0.989$ ,  $p < 0.01$ ). Although the peak

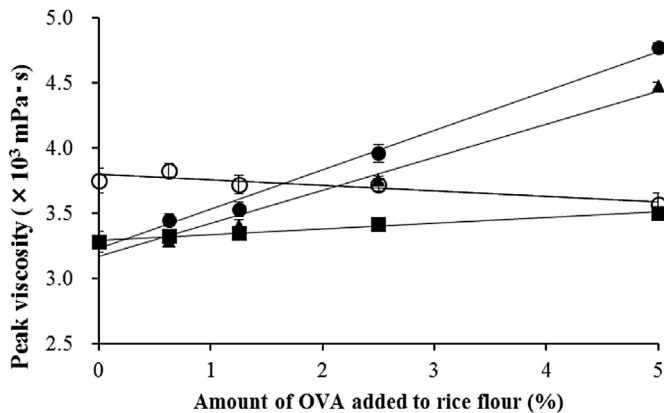


**Fig. 6.** Effects of albumin amount and dispersion liquid on peak viscosity (measured using RVA) of rice flour slurry (values represent the average of 5 measurements)<sup>†</sup>. <sup>†</sup>Rice flour (3.06 g) and soymilk (27.49 g) or water (24.94 g) were mixed. Albumin was added to the slurry in the proportions of rice flour of 0% (no additive), 0.625% (19 mg), 1.25% (38 mg), 2.5% (76 mg), and 5% (152 mg).

viscosity also increased with the amount of added BLA (■,  $r = 0.988$ ,  $p < 0.01$ ), the trend was not as evident as it was with OVA or BSA.

The major increase in the peak viscosity of soymilk slurry that occurred upon the addition of albumin, especially OVA, was caused by interactions between OVA and soymilk components. Thus, OVA was added to a water slurry (○), and the change in viscosity compared to that of soymilk (●). Results showed that viscosity decreased as the amount of OVA added to the water slurry increased ( $r = -0.890$ ,  $p < 0.05$ ), presumably because the amount of protein increased and free water was adsorbed in the protein, which suppressed swelling and gelatinization of the starch. Thus, OVA and the soymilk components aggregated with gelatinized starch particles to form larger particles. Additionally, peak viscosity of the soymilk slurry was greater than that of the water slurry when added OVA was greater than 2.5%. The amount added was consistent with the amount that produced oven spring in bread. Thus, oven spring in bread can be attributed to the increase in viscosity of the batter.

### 3.5. Formation of rice starch granule aggregates due to soy proteins and OVA

The gelatinization viscosity of soymilk and rice flour batter increased upon addition of OVA because the soy proteins and OVA promoted the aggregation of rice starch granules, resulting in larger particle diameters. To confirm this, rice flour was replaced with non-glutinous rice starch and soymilk was replaced with soy globulin solution to study the effect of soy proteins and OVA on rice starch granule size.

Prior to conducting measurements, SDS-PAGE (Laemmli, 1970) was performed to investigate the composition of the proteins in the glycinin and β-conglycinin fractions used to prepare the soy globulin solution (Fig. 7). In the glycinin fraction, alkaline and acidic subunits (Adachi, Takenak, Gidamis, Mikami, & Utsuni, 2000) were detected (purity, 60.9%), while in the β-conglycinin fraction α, α', and β subunits (Maruyama et al., 1998) were detected (purity, 62.3%). In contrast, detection of these bands in soymilk confirmed that the soy globulin solution contained the main globulins in soymilk.

When heating starch in water, the particle size distribution showed two peaks for particle diameter (Fig. 8A), one at 10 μm,

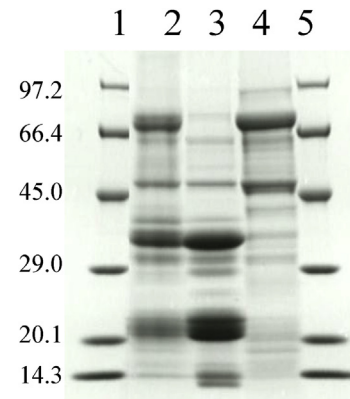


**Fig. 7.** Photograph of the SDS-PAGE pattern of proteins contained in soymilk, and the glycinin and β-conglycinin fractions: Lane 1 and 5, marker; lane 2, soymilk; lane 3, glycinin fraction; lane 4, β-conglycinin fraction.

assumed to be due to single starch granules (Cai et al., 2015; Dhital, Butardo, Jobling, & Gidley, 2015), and another at 40 μm, assumed to be due to compound starch granules. When OVA was added to water and heated, the same peak diameters were detected (B), but the volume percentage of single starch granules was lower, while the volume percentage of compound starch granules increased by the same amount. Some larger aggregates of ca. 110 μm also were detected in small numbers. In contrast, heating the soy globulin solution did not result in any peaks for single or compound starch granules (C). Instead, a single peak was identified at ca. 110 μm. Furthermore, addition of OVA to the soy globulin solution with heating increased the size of the peak attributed to particle size aggregation over that of the soy globulin solution, and also slightly increased the volume ratio (D). Additionally, the median diameter for all particles was greatest in the soy globulin solution with added OVA.

Observation of the particles by optical microscopy indicated that single and compound starch granules formed in starch heated in water (Fig. 8A) and in water with OVA (B). However, compound starch granules were formed, including even larger aggregates, when starch was heated in soy globulin solution (C) or in soy globulin solution with OVA (D).

These results indicate that slurry peak viscosity increased for rice flour and soymilk upon addition of OVA because the OVA caused single starch granules to form compound starch granules, and the soy globulin caused the compound starch granules to merge and form aggregations. Addition of OVA increased batter viscosity by creating a greater number of large starch granules, which prevented gas cells from merging. However, the proteins used in soy globulin solution were in a native form, unlike soymilk that underwent heat treatment. In the present study, although interactions between OVA and starch and soy globulin were confirmed, the effect of the state of aggregation, caused by heating soy globulin, on the viscosity of the batter is unknown and will be investigated in the future.

Adding OVA to soymilk increased gas cell membrane thermal coagulation, and produced gelatinization viscosity greater than that of batter made with water and rice flour. This may inhibit the merging of gas cells in the center of the batter and prevent hollowing of the crust. Furthermore, in soymilk batter with greater than 2.5% added OVA, oven spring was believed to occur as the increase in viscosity reduced the amount of water escaping from the batter, which in turn raised the water vapor pressure within the batter.

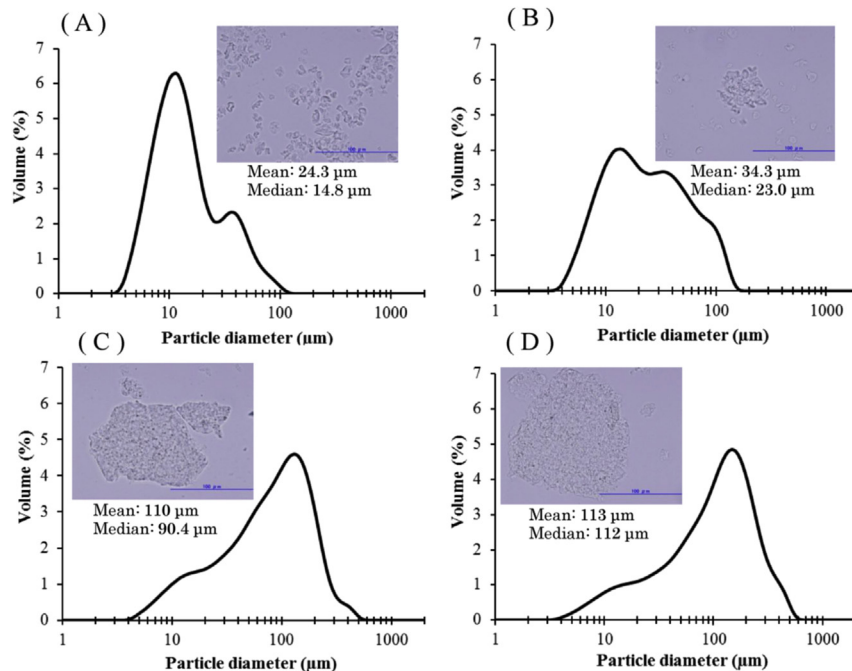


**Fig. 8.** Particle size distribution and optical microscopy images of non-glutinous rice starch lyophilizates gelatinized in water or soy globulin solution with OVA:<sup>†</sup> (A) water, (B) water + OVA, (C) soy globulin solution, (D) soy globulin solution + OVA. <sup>†</sup>5% OVA was added to rice flour. Values of mean and median diameter in the figure are the average of 3 measurements.

### 3.6. Bread crust hardness and optimum OVA addition level

Based on the experimental results, the addition of OVA to batter made from rice flour and soymilk improved the interior of the bread and the ability of the batter to rise. The crumb hardness also was investigated to determine the optimum OVA level.

At levels up to 1.25%, the crust hardness decreased as OVA levels increased (Fig. 9,  $p < 0.05$ ), due to prevention of gas cell merging by OVA, and prevention of gas cell crushing at the bottom of the crust. However, as shown in Fig. 2, OVA levels greater than 1.25% increased SLV, but also made the crust harder because high levels of OVA promoted thermal coagulation, which hardened the gas cell membranes, leading to a harder crust. Thus, OVA addition of 1.25% was optimal.

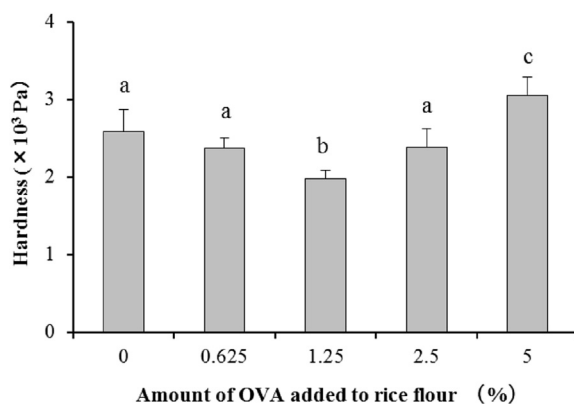


**Fig. 9.** Effect of OVA amount on crust hardness<sup>†</sup>. <sup>†</sup>Crust hardness was measured on a cube 20 mm per side using a creep meter with a 40-mm cylindrical plunger at a rate of 1 mm/s and 50% compression. Values of hardness represent the average of 12 measurements. Entries with different letters were significantly different ( $p < 0.05$ ).

### 4. Conclusions

Addition of OVA to gluten-free rice flour batter made with soymilk improved the quality of the bread by promoting gas cell membrane thermal coagulation and increasing batter viscosity. This methodology makes large-scale manufacture of these breads feasible, and enables the preparation of gluten-free rice flour bread in shapes and sizes similar to those of wheat flour bread. However, bread made with OVA cannot be consumed by people with egg allergies; therefore, work is continuing to find a suitable substitute for OVA.

### References

- Adachi, M., Takenak, Y., Gidamis, A. B., Mikami, B., & Utsuni, S. (2000). Crystal structure of soybean proglycinin A1aB1b homotrimer. *The Journal of Biological Chemistry*, 305, 291–305.
- Barak, S., Mudgil, D., & Khatkar, B. S. (2013). Relationship of gliadin and glutenin proteins with dough rheology, flour pasting and bread making performance of wheat varieties. *LWT—Food Science and Technology*, 51, 211–217.
- Biesiekierski, J. R., Muir, J. G., & Gibson, P. R. (2013). Is gluten a cause of gastrointestinal symptoms in people without celiac disease? *Current Allergy Asthma Reports*, 13, 631–638. <http://dx.doi.org/10.1007/s11882-013-0386-4>.
- Cai, J., Man, J., Huang, J., Liu, Q., Wei, W., & Wei, C. (2015). Relationship between structure and functional properties of normal rice starches with different amylose contents. *Carbohydrate Polymers*, 125, 35–44.
- Cornejo, F., & Rosell, C. M. (2015). Physicochemical properties of long rice grain varieties in relation to gluten free bread quality. *LWT—Food Science and Technology*, 62, 1203–1210.
- Cosnes, J., Cellier, C., Viola, S., Colombel, J.-F., Michaud, L., Sarles, J., et al. (2008). Incidence of autoimmune diseases in celiac disease: protective effect of the gluten-free diet. *Clinical Gastroenterology and Hepatology*, 6, 753–758.
- Crockett, R., le, P., & Vodovotz, Y. (2011). Effects of soy protein isolate and egg white solids on the physicochemical properties of gluten-free bread. *Food Chemistry*, 129, 84–91.
- De La Hera, E., Rosell, C. M., & Gomez, M. (2014). Effect of water content and flour particle size on gluten-free bread quality and digestibility. *Food Chemistry*, 151, 526–531.
- Demirkesen, I., Kelkar, S., Campanella, O. H., Sum, G., Sahin, S., & Okos, M. (2014). Characterization of structure of gluten-free breads by using X-ray microtomography. *Food Hydrocolloids*, 36, 37–44.
- Dhital, S., Butardo, V. M., Jobling, S. A., & Gidley, M. J. (2015). Rice starch granule

- amylolysis-Differentiating effects of particle size, morphology, thermal properties and crystalline polymorph. *Carbohydrate Polymers*, 115, 305–316.
- Du, L., Prokop, A., & Tanner, R. D. (2002). Effect of denaturation by preheating on the foam fractionation behavior of ovalbumin. *Journal of Colloid and Interface Science*, 248, 487–492.
- Fasano, A., Araya, M., Bhatnagar, S., Cameron, D., Catassi, C., Dirks, M., et al. (2008). Federation of International Societies of Pediatric Gastroenterology, Hepatology, and Nutrition consensus report on celiac disease. *Journal of Pediatric Gastroenterology and Nutrition*, 47, 214–219.
- Gallagher, E., Gormley, T. R., & Arendt, E. K. (2004). Recent advances in the formulation of gluten-free cereal-based products. *Trends in Food & Technology*, 15, 143–152.
- Gan, Z., Ellist, P. R., & Schofield, J. D. (1995). Gas cell stabilization and gas retention in wheat bread dough. *Journal of Cereal Science*, 21, 215–230.
- Goel, P. K., Singhal, R. S., & Kulkarni, R. P. R. (1999). Studies on interactions of corn starch with casein and casein hydrolysates. *Food Chemistry*, 64, 383–389.
- Hamada, S., Suzuki, K., Aoki, N., & Suzuki, Y. (2013). Improvements in the qualities of gluten-free bread after using a protease obtained from *Aspergillus oryzae*. *Journal of Cereal Science*, 57, 91–97.
- Hermansson, A. M. (1978). Physico-chemical aspects of soy proteins structure formation. *Journal of Texture Studies*, 9, 33–58.
- Laemmli, U. K. (1970). Cleavage of structural proteins during the assembly of the head of bacteriophage T4. *Nature*, 227, 680–685.
- Lazaridou, A., Duta, D., Papageorgiou, M., Belc, N., & Biliaderis, C. G. (2007). Effects of hydrocolloids on dough rheology and bread quality parameters in gluten-free formulations. *Journal of Food Engineering*, 79, 1033–1047.
- Mariotti, M., Ambrogina, P. M., & Lucisano, M. (2013). The role of buckwheat and HPMC on the breadmaking properties of some commercial gluten-free bread mixtures. *Food Hydrocolloids*, 30, 393–400.
- Marston, P. E., & Wannan, T. L. (1976). Bread baking, the transformation from dough to bread. *Baker's Digest*, 50, 24–28, 49.
- Maruyama, N., Katsube, T., Wada, Y., Oh, M. H., Rosa, A. P. B. D., Okuda, E., et al. (1998). The roles of N-linked glycans and extension regions of soybean  $\beta$ -conglycinin in folding, assembly and structural features. *European Journal of Biochemistry*, 258, 854–862.
- Mills, E. N. C., Wilde, P. J., Salt, L. J., & Skeggs, P. (2003). Cell formation and stabilization in bread dough. *Chemical Engineering Research and Design*, 81, 189–193.
- Norström, F., Sandström, O., Lindholm, L., & Ivarsson, A. (2012). A gluten-free diet effectively reduces symptoms and health care consumption in Swedish celiac disease population. *BMC Gastroenterology*, 12, 125.
- Nozawa, M., Ito, S., & Arai, E. (2014). Effects of soymilk on rising of gluten-free rice flour bread. *Food Science and Technology Research*, 20, 1063–1070.
- Sabatino, A. D., & Corazza, G. R. (2009). Coeliac disease. *The Lancet*, 373, 1480–1493.
- Salcedo, G., Quirce, S., & Diaz-Perales, A. (2011). Wheat allergens associated with baker's asthma. *Journal of Investigational Allergology and Clinical Immunology*, 21, 81–92.
- Schober, T. J. (2010). Manufacture of gluten-free specialty breads and confectionery products. In E. Gallagher (Ed.), *Gluten-free food science and technology* (pp. 135–143). Iowa: John Wiley & Sons, Inc.
- Schwarzlaff, S. S., Johnson, J. M., Barbeau, W. E., & Duncan, S. (1996). Guar and locust bean gums as partial replacers of all-purpose flour in bread: an objective and sensory evaluation. *Journal of Food Quality*, 19, 217–229.
- Thanh, V. H., & Shibasaki, K. (1976). Major protein of soybean seeds. A straightforward fractionation and their characterization. *Journal of Agricultural and Food Chemistry*, 24, 1117–1121.
- Walstra, P., & Jenness, R. (1984). *Dairy chemistry and physics* (1st ed.). New York: John Wiley & Sons, Inc. (Chapter 6).
- Wang, J.-R., Wei, Y.-M., Fedak, G., Liu, Z.-G., Jiang, Q.-T., Pu, Z.-E., et al. (2010). Molecular characterization of major allergens associated with baker asthma in wheat flour. *Food Science and Technology Research*, 16, 341–346.
- Weaire, D., & Hutzler, S. (1999). *The physics of foams* (1st ed.). New York: Oxford University Press Inc. (Chapter 12).
- Wieser, H. (2007). Chemistry of gluten proteins. *Food Microbiology*, 24, 115–119.



# Preparation of a coated Ti anode for producing acidic electrolyzed oxidizing water



Wenwei Tang<sup>a,\*,1</sup>, Yanfei Li<sup>b,1</sup>, Weihao Li<sup>c</sup>, Xuejin Chen<sup>b,\*\*</sup>, Xiping Zeng<sup>d,\*\*\*</sup>

<sup>a</sup> Department of Chemistry, Shanghai Key Laboratory of Chemical Assessment and Sustainability, Tongji University, 1239 Siping Road, Shanghai, 200092, China

<sup>b</sup> School of Medicine, Shanghai Jiao Tong University, South Chongqing Road, Shanghai, 200025, China

<sup>c</sup> Handan Municipal Centre for Disease Control and Prevention, Handan, 056000, China

<sup>d</sup> School of Life Science and Technology, Tongji University, Shanghai, 200092, China

## ARTICLE INFO

### Article history:

Received 11 May 2015

Received in revised form

5 September 2015

Accepted 25 October 2015

Available online 30 October 2015

### Keywords:

Acidic electrolyzed oxidizing water

RuO<sub>2</sub>–SnO<sub>2</sub>–TiO<sub>2</sub>

Electrochemical properties

Disinfection effect

## ABSTRACT

Coated Ti anodes have been prepared for producing acidic electrolyzed oxidizing water (AEOW). To improve the performance of anodes, the influence factors (sintering temperature, heat treatment time and dip-coating times) were systematically explored. The results show that the optimum sterilizing effect of AEOW is obtained in the case of sintering at 450 °C for 1 h with as many dip-coatings as possible. The sintering temperature is a critical factor. A lower temperature leads to better reaction selectivity, whereas a higher temperature results in a longer lifetime. A short heat treatment time leads to inadequate coating oxidation, a long heat treatment time prolongs the lifetime but results in high SEC. Increasing the number of dip-coatings could enhance the coating-substrate adhesion, thus extending the anode lifetime. The electrode prepared by optimization could replace the platinized Ti anode to produce AEOW. AEOW could be used as an effective disinfectant for eliminating *Escherichia coli* and *Staphylococcus aureus*. The sterilization ability is based on the combined effect of active chlorine concentration (ACC), low pH and high oxidation–reduction potential (ORP).

© 2015 Elsevier Ltd. All rights reserved.

## 1. Introduction

In recent years, large amounts of infectious diseases and drug-resistant bacteria have emerged due to globalization, deteriorating environment and anti-biotic abuse, and are striking people frequently by sudden and severe epidemic diseases. Therefore, we must implement highly effective disinfection systems in the food industry to guarantee food safety, prevent infectious diseases and create a healthy living environment.

Acidic electrolyzed oxidizing water (AEOW) has a high oxidation–reduction potential (ORP) of over 1100 mV, a low pH of 2–3, and an active chlorine concentration (ACC) of 30–100 mg/L and is characterized by its high efficiency, broad spectrum antimicrobial activity, low cost and high-level security (Udompijitkul, Daeschel, &

Zhao, 2007). AEOW is currently applied in various fields (Arealos-Sánchez et al., 2013; Wang et al., 2014; Zhang et al., 2011). It can effectively kill common bacteria, such as *Salmonella*, *Escherichia coli*, *Vibrio parahaemolyticus*, and *Listeria monocytogenes* in food sterilization (Ding, Rahman, Purev, & Deog-Hwan, 2010; Issa-Zacharia, Kamitani, Miwa, Muhimbula, & Iwasaki, 2011; Xie, Sun, Pan, & Zhao, 2012), reduce the rate of bacterial infection and control the probability of food decay in food storage and preservation (Audenaert et al., 2012; Jadeja, Hung, & Bosilevac, 2013), and improve livestock's immunity and antiviral ability in farm disinfecting (Fasenko, Christopher, & McMullen, 2009; McCarthy & Burkhardt, 2012).

However, the application of AEOW is still limited due to its high production cost. To solve this problem, it is necessary to develop an inexpensive and effective process to prepare qualified electrode to replace the traditional expensive Pt-plated Ti electrode. Recently, a low-cost Ru/Ti-coated Ti electrode was developed to produce AEOW with similar performance as that of Pt-plated Ti electrode (Cheng, Zhang, & Cui, 2007). Zeng et al. (Zeng, Chen, Wu, Wang, & Soowohn, 2007) studied the effect of IrO<sub>2</sub> loading on RuO<sub>2</sub>–TiO<sub>2</sub> anodes. These studies improved the performance of electrodes and

\* Corresponding author.

\*\* Corresponding author.

\*\*\* Corresponding author.

E-mail addresses: [tangww@tongji.edu.cn](mailto:tangww@tongji.edu.cn) (W. Tang), [chenxuejin@shsmu.edu.cn](mailto:chenxuejin@shsmu.edu.cn) (X. Chen), [zengxp@tongji.edu.cn](mailto:zengxp@tongji.edu.cn) (X. Zeng).

<sup>1</sup> These authors contributed equally to this work.

were helpful to the development of RuO<sub>2</sub>–SnO<sub>2</sub>–TiO<sub>2</sub> electrodes used in AEW generation. As reported (Cui, Feng, & Liu, 2009; Depauli & Trasatti, 1995; Smith & Okinaka, 1983), introducing Sn into coated Ti electrodes can refine the coating grains and improve the coating-substrate adhesion and stability of the active elements. In addition, the partial replacement of precious metals such as Ru and Ir by Sn, can significantly reduce the cost of anodes. A series of nano-scale RuO<sub>2</sub>–SnO<sub>2</sub>–TiO<sub>2</sub>-coated anodes, determined as an optimum formula of Ru<sub>25</sub>Sn<sub>7</sub>Ti<sub>68</sub> (Zeng, Zhao, Tang, & Zheng, 2011b; Zeng et al., 2012) have been prepared in our laboratory by using the sol–gel method with n-butyl titanate as the raw material and using the modified Pechini sol–gel method with RuCl<sub>3</sub>·3H<sub>2</sub>O and SnCl<sub>4</sub>·5H<sub>2</sub>O as the raw materials.

To achieve improved electrochemical performance (low chlorine evolution, low oxygen evolution potential, low specific energy consumption and long lifetime) and develop a less expensive nanoscale RuO<sub>2</sub>–SnO<sub>2</sub>–TiO<sub>2</sub>-coated anode, further studies on the preparation conditions of coated Ti anodes, including the sintering temperature, heat treatment time and number of dip-coatings, have been conducted based on the optimum formula in this paper. The process parameters were confirmed by means of chlorine evolution potential test, cyclic voltammetry test, accelerated life and the performance of AEW produced by the coated Ti anode. The disinfection capacity, and effect of AEW on *Escherichia coli* and *Staphylococcus aureus* (*E. coli* and *S. aureus*) was examined by suspension quantitative germicidal test. Furthermore, the membrane permeability of *S. aureus* was investigated by fluorescence microscopy.

## 2. Materials and methods

### 2.1. Preparation of the coated Ti anode

#### 2.1.1. Pretreatment of the Ti substrate

The electrode was prepared with a 20 × 20 × 1 mm titanium plate (Shanxi Ti Company, China) as the substrate. The polished titanium plates were degreased in detergent (0.1%, v/v) and acetone (5%, v/v) for 15 min with ultrasound, respectively. Then they were immersed in sulfuric acid/nitric acid (1:1, v/v) for 2 h. After that, the plates were etched with boiling oxalic acid (10%, w/w) for 2 h. Finally, the pretreated Ti plate was stored in ethyl alcohol after cleaning in distilled water (Song, Zhan, & He, 2010; Yang, Zou, Huo, Cai, & Xiao, 2009).

#### 2.1.2. Preparation of the coating materials

A TiO<sub>2</sub> sol was prepared as follows: 10 mL tetra-n-butyl titanate (TBTA) was dissolved in 5 mL isopropanol, and 3 mL acetylacetone was added as inhibitor. After vigorous stirring for 0.5 h, the solution was marked as solution A. A mixture of 2 mL distilled water, 2.5 mL isopropanol and a small amount of acetic acid was denoted as solution B. And solution C was composed of PEG-4000 (5%, w/w) and 2.5 mL isopropanol. Solution B was added dropwise into solution C under stirring, then solution A was also added dropwise. TiO<sub>2</sub> sol was obtained by stirring the mixture for 0.5 h and aging overnight.

RuO<sub>2</sub> and SnO<sub>2</sub> sols were prepared by a modified Pechini sol–gel method. The precursor solution was prepared by dissolving citric acid (CA) in ethyl alcohol. RuCl<sub>3</sub>·3H<sub>2</sub>O and SnCl<sub>4</sub>·5H<sub>2</sub>O were added to the precursor solution in a CA: Ru (Sn) molar ratio of 3:1.

The RuO<sub>2</sub> and SnO<sub>2</sub> sols were added to the TiO<sub>2</sub> sol to improve the stability and to form a homogeneous sol.

#### 2.1.3. Depositing of the Ti substrate

A Ti sheet was dipped vertically into the previously formed sol solution and elevated at a slow speed, then dried under an infrared lamp for 15 min. After the 5 dip-coatings, the sheet was annealed at

450 °C for 10 min in a muffle furnace to oxidize the coating layer completely. By repeating this process, a series of Ti substrates with different oxide coatings was obtained after placing the substrates in the muffler for 1 h at 450 °C.

### 2.2. Characterization of the coated Ti anode

#### 2.2.1. Chlorine evolution potential test

All electrochemical tests were conducted with an AUTOLAB model PGSTAT30.

A three-electrode testing system featuring a Luggin capillary with a salt bridge filled with a saturated KCl solution was constructed. A saturated calomel electrode served as the reference electrode, the prepared electrode as the anode and a Pt electrode as the cathode. Electrochemical tests were conducted in an H-type electrobath with a saturated NaCl solution. The fast linear scanning method was employed over a potential range of 0–1.5 V at a scanning speed of 50 mV s<sup>-1</sup>.

#### 2.2.2. Oxygen evolution potential test

Using a saturated calomel electrode as the reference electrode, a double salt bridge was constructed using a saturated KCl solution and a 0.5 mol L<sup>-1</sup> K<sub>2</sub>SO<sub>4</sub> solution. The salt bridge featured a Luggin capillary, and a three-electrode testing system was built as previously described. The H-type electrobath was filled with a 0.5 mol L<sup>-1</sup> H<sub>2</sub>SO<sub>4</sub> solution. The testing parameters were identical to those used in the chlorine evolution potential test.

#### 2.2.3. Cyclic voltammetry test

The tests were conducted in a saturated NaCl solution and a 0.5 mol L<sup>-1</sup> H<sub>2</sub>SO<sub>4</sub> solution, respectively, over a potential range of –0.25 to –1.3 V, at scanning speeds of 10, 20, 50, 100 and 200 mv s<sup>-1</sup>.

#### 2.2.4. Accelerated lifetime test

Using a 1.0 mol L<sup>-1</sup> H<sub>2</sub>SO<sub>4</sub> solution as the testing solution, a pure Ti plate as cathode, and the prepared electrode as anode, the electrolysis was conducted under a constant current of 2 A cm<sup>2</sup> at 40 °C, and the inter-plate distance was set at 1.5 cm. The accelerated lifetime of the electrode was then recorded when a 10 V elevation over the initial bath voltage was reached.

### 2.3. Generation and specific energy consumption (SEC) of AEW

An 8.0 g L<sup>-1</sup> NaCl solution was added to the self-made static cell (500 mL, made by polytetrafluoroethylene), then was electrolyzed at 8.0 V. The prepared electrodes worked as anode and cathode with a spacing of 5 mm. The ORP, pH and SEC of the AEW were tested and determined.

SEC is defined as the energy consumption of an electrolysis system that produces a unit mass of total oxidative substance (measured by ACC), calculated as follows:

$$SEC(\text{kW} \cdot \text{h}/\text{kg}) = \frac{UIt}{cV} \times 1000 \quad (1)$$

*U* – Average voltage of electrolysis (V); *I* – Average current of electrolysis (A); *t* – Electrolysis time (h); *c* – Concentration of the total oxidative substance (mg L<sup>-1</sup>); *V* – Volume of electrolyte (L).

### 2.4. Measurement of ACC (or TOS)

The iodometric method was used to measure TOS or ACC as follows: 10.00 mL disinfectant was added to a 150.00 mL conical beaker, and then 10.00 mL KI solution (10%) and 10.00 mL H<sub>2</sub>SO<sub>4</sub>

(20%) were added. The mixture was kept in the dark for 10 min, and then 20.00 mL distilled water was added. A  $\text{Na}_2\text{S}_2\text{O}_3$  solution ( $0.01 \text{ mol L}^{-1}$ ) was used for titration until the treated sample turned pale yellow, and then a starch solution ( $10.00 \text{ g L}^{-1}$ ) was added. The sample then turned blue. The  $\text{Na}_2\text{S}_2\text{O}_3$  titration was continued until the sample turned to achromatic color. A blank control test was conducted by replacing the disinfectant with 10.00 mL distilled water. The concentration of ACC was calculated using following equation:

$$\text{ACC} = \frac{(V_2 - V_1) \times c_{\text{Na}_2\text{S}_2\text{O}_3} \times M}{V_E} \quad (2)$$

where  $c_{\text{Na}_2\text{S}_2\text{O}_3}$  represents the concentration of the  $\text{Na}_2\text{S}_2\text{O}_3$  titrating solution (mol/L)

$V_2$  represents the volume of the  $\text{Na}_2\text{S}_2\text{O}_3$  titrating solution consumed in the treated sample (mL)

$V_1$  represents volume of the  $\text{Na}_2\text{S}_2\text{O}_3$  titrating solution consumed in the blank sample (mL)

$V_E$  represents the volume of AEW (mL)

$M$  represents the molar mass of chlorine (35,453 mg/mol)

## 2.5. Suspension quantitative germicidal test

Test strains of *E. coli* (ATCC 8099) and *S. aureus* (ATCC 6538) were obtained from the China General Microbiological Culture Collection Center.

Tests were conducted according to the Technical Standard for Disinfection (Technical Standard for Disinfection, Ministry of Health, People's Republic of China, 2002) and the literature (Dziewonski & Grzeszczuk, 2009). 1.00 mL bacteria suspension was mixed thoroughly with 4.00 mL AEW for a predetermined disinfection time. Then, 1.00 mL of neutralizer, containing 5.00 g  $\text{L}^{-1}$  sodium thiosulfate and 0.03 mol/L phosphate buffered saline (pH 7.2–7.4), was added. After a 10-min of neutralizing, the mixture was taken as the treated sample for further analysis. The control sample was prepared by replacing AEW with 4.00 mL of tryptone physiological saline.

1.00 mL of the treated sample or the control sample was inoculated and cultivated for 48 h. The number of living bacteria was determined by the viable count method. The killing logarithm (KL) value and the disinfection rate were obtained as follows:

$$\text{KL} = N_0 - N_x \quad (3)$$

$$\text{Disinfection rate(\%)} = \left(1 - 10^{N_x} / 10^{N_0}\right) \times 100 \quad (4)$$

where  $N_x$  denotes the logarithm value of the average number of living bacteria in the treatment group, and  $N_0$  denotes that in the control group.

## 2.6. Fluorescence microscopy detection

0.50 mL propidium iodide (PI,  $0.1 \text{ mg mL}^{-1}$ ) was added to an analytical sample with the same volume. After staining for 10 min, the sample was examined with a fluorescence microscope.

## 2.7. Statistical analyses

Each experiment had been repeated three time, results are expressed as mean  $\pm$  standard error (SD) of triplicate experiments.

## 3. Results and discussions

### 3.1. Effect of sintering temperature on the anode performance

The electrochemical performance was analyzed at 350, 400, 450, 500, 550 and 600 °C for 1.0 h with the formula of  $\text{Ru}_{25}\text{Sn}_7\text{Ti}_{68}$ .

#### 3.1.1. Values of the chlorine and oxygen evolution potentials

The chlorine evolution potential (Fig. 1A(a)) reached its minimum value at 350 °C and maximum value at 600 °C and was not significantly affected from 400 to 550 °C, fluctuating around 1.12 V. In the case of oxygen evolution potential (Fig. 1A(b)), a maximum value at 350 °C and a minimum value at 600 °C were obtained, and around 1.3 V of fluctuation could be seen from 400 to 550 °C. It can be seen that at higher temperature the difference between chlorine and oxygen evolution potential was reduced, whereas the reaction selectivity of the electrode weakened. Thus, anodes prepared at a lower temperature exhibited better selectivity.

#### 3.1.2. Cyclic voltammetry analysis

Voltammetric charge ( $q^*$ ), one of the important parameters for evaluating the electrochemical active surface area of oxide electrodes, was measured by a graphical integration of the cyclic voltammogram over the range of the double layer charging potential before reaching the chlorine or oxygen evolution potential (Kim, Lee, & Kim, 2001; Zhou, Ye, Hua, Zou, & Dong, 2011).

In the NaCl solution (Fig. 1B(a)), the  $q^*$  value increased first and reached the maximum at 400 °C, then decreased with the rise of sintering temperature, indicating that the greatest number of catalytic reactive sites toward chlorine evolution had been formed on the surface of the anode. In the  $\text{H}_2\text{SO}_4$  solution, a similar change trend of the  $q^*$  value was observed and its maximum can be seen at 450 °C (Fig. 1B(b)).

#### 3.1.3. Accelerated life test of the anode

By analyzing the XRD patterns and SEM images of the coated Ti anode prepared at different sintered temperature (Zeng et al., 2011b), we can see that the higher temperature resulted in more completely growth of the rutile structure. However, the higher temperature also led to the decomposition of solid solution, the separating out of Ru elementary substance and the increase of cracks on the anode coating. Consequently we summarized that sintering temperature between 450 and 500 °C is the critical factor to improve the properties of anode. As shown in Fig. 1C, the accelerated lifetime was prolonged with increasing sintering temperature, probably because of the improvement development of the rutile structure, thus improving the adhesion between coating and substrate. However, when sintering temperature was higher than 500 °C, Ru precipitation occurred due to overheating, the Ti substrate was over oxidized and more cracks appeared on the coating (Depauli & Trasatti, 1995; Zeng et al., 2011b).

In summary, the sintering temperature should be within 400–450 °C to ensure desirable electrode performance.

### 3.2. Effect of heat treatment time on the anode performance

Based on our preliminary work, grain size of rutile, and separation and morphology of Ru metal under different heating time, it is preliminary believed that the appropriate heating time is 1 h. So the performance of the fabricated  $\text{Ru}_{25}\text{Sn}_7\text{Ti}_{68}$  anodes was analyzed at 0.5, 1.0, 1.5, 2.0 and 3.0 h at a sintering temperature of 450 °C.

#### 3.2.1. Values of the chlorine and oxygen evolution potentials

The chlorine evolution potential (Fig. 2A(a)) achieved its minimum value at 2 h and its maximum value at 3 h, and was not

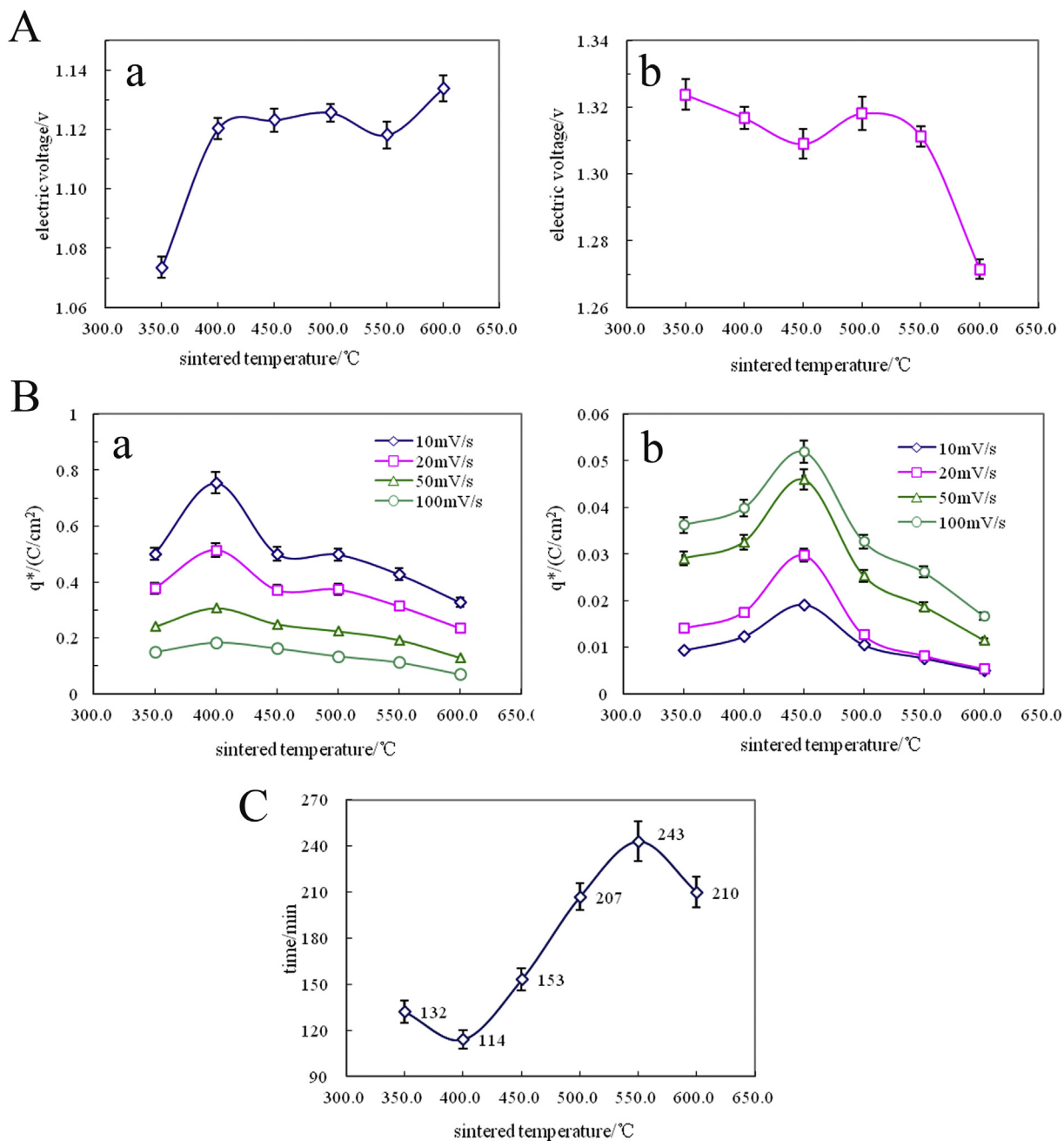


**Fig. 1.** (A) Chlorine evolution potentials and oxygen evolution potentials of the coated Ti anodes at different sintering temperatures. (a) chlorine evolution potentials, (b) oxygen evolution potentials; (B)  $q^*$  values of the coated Ti anodes at different sintering temperatures. (a) in saturated NaCl solution, (b) in  $0.5 \text{ mol L}^{-1} \text{ H}_2\text{SO}_4$  solution; (C) Accelerated lifetime of the coated Ti anodes at different sintering temperatures.

significantly influenced from 0.5 to 1.5 h, fluctuating around 1.07 V. However, the oxygen evolution potential (Fig. 2A(b)) showed the opposite trend. A maximum value at 0.5 h and a minimum value at 3 h were obtained, and only around 1.29 V of fluctuation could be seen from 1 to 2 h. The difference between chlorine and oxygen reached the most ideal value between 1 and 1.5 h.

### 3.2.2. Cyclic voltammetry analysis

In NaCl or  $\text{H}_2\text{SO}_4$  (Fig. 2B(a) and (b)), the both  $q^*$  values increased first and reached the maximum at 1.0 h, then decreased with increasing heat treatment time from 0.5 to 1.5 h. From 1.5 to 3.0 h, the  $q^*$  value reached the peak at 2.5 h in the NaCl solution. Whereas in the  $\text{H}_2\text{SO}_4$  solution, the  $q^*$  value increased with the heat

treatment time. Overall, the anodes demonstrated an increased number of surface sites catalytically reactive toward chlorine evolution.

### 3.2.3. Accelerated lifetime test of the anode

As shown in Fig. 2C, the lifetime of the coating increased overall with heat treatment time, except for the minimum reached at 1.5 h, probably owing to its poor adhesion to the substrate caused by the large size of the grains (Depauli & Trasatti, 1995; Zeng et al., 2011b). The coating could not be fully oxidized at an excessively short heat treatment time. Whereas over-prolonging the heat treatment time resulted in a longer life for the anode, but metallic Ti evolution occurred (Depauli & Trasatti, 1995; Zeng et al., 2011b), which would

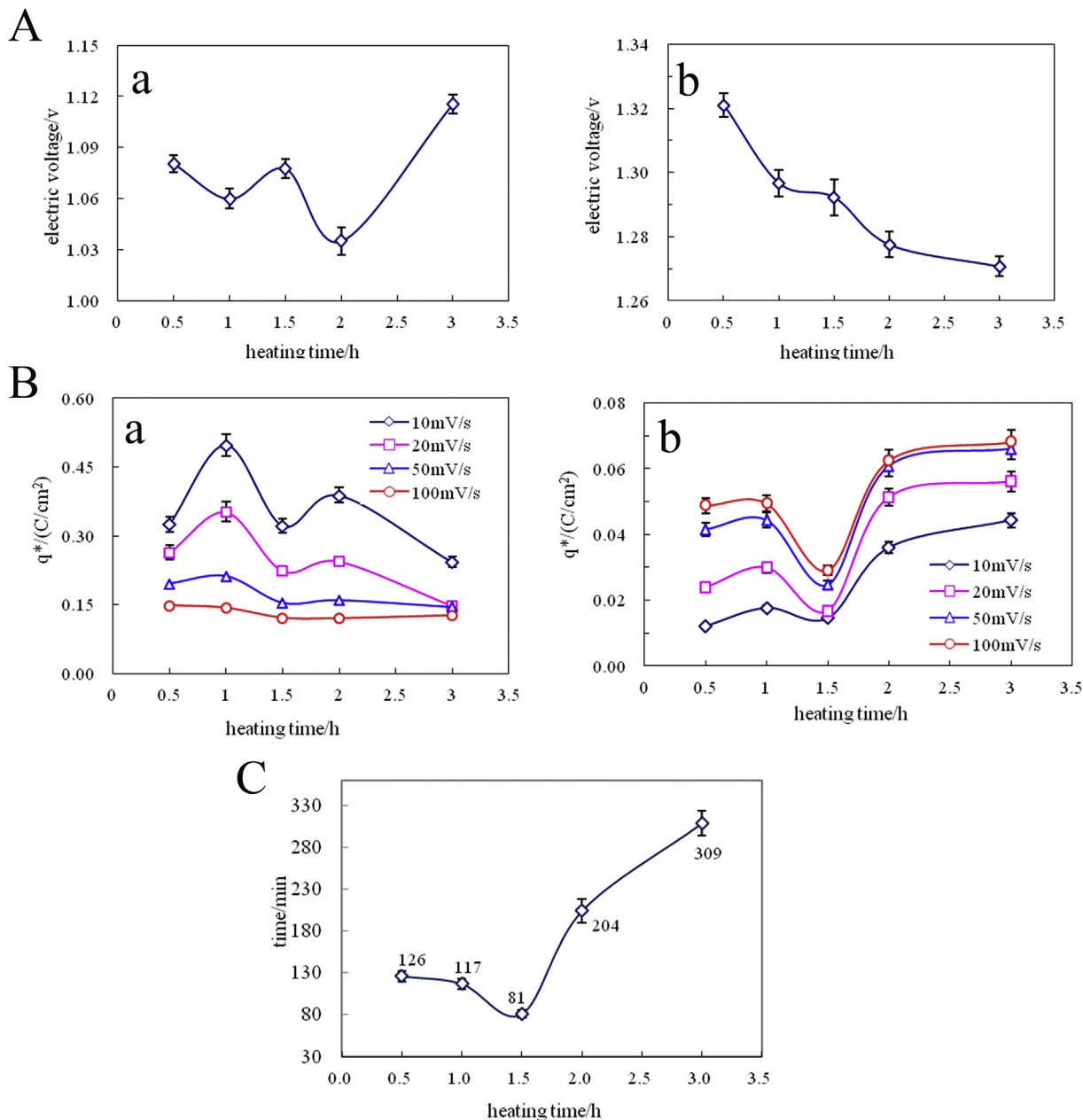


**Fig. 2.** (A) Chlorine evolution potentials and oxygen evolution potentials of the coated Ti anodes processed for different heat treatment times. (a) chlorine evolution potentials, (b) oxygen evolution potentials; (B)  $q^*$  values of the coated Ti anodes processed for different heat treatment times. (a) in saturated NaCl solution, (b) in 0.5 mol L<sup>-1</sup> H<sub>2</sub>SO<sub>4</sub> solution; (C) Accelerated lifetime of the coated Ti anodes processed for different heat treatment times.

decrease the activity of the coating and consume more energy.

Taking all the aforementioned factors into account, the heat treatment time should be set at 1 h to ensure desirable performance of the coated anode.

### 3.3. Effect of dip-coating times on the anode performance

Under the conditions of a formula of Ru<sub>25</sub>Sn<sub>7</sub>Ti<sub>68</sub> and a sintering temperature of 450 °C for 1 h, different dip-coating times of 10, 13, 15, 16 and 18 were employed to determine its effect on the anode performance.

#### 3.3.1. Values of the chlorine and oxygen evolution potentials

The results (Fig. 3A(a) and (b)) showed that the oxygen

evolution potential fluctuated slightly between 1.30 and 1.33 V with an increase in the number of dip-coating, and the chlorine evolution potential fluctuated between 1.03 and 1.09 V, with a minimum value reached at a dip-coating time of 16 dip-coatings.

#### 3.3.2. Cyclic voltammetry analysis

In most cases, the  $q^*$  value increased with the number of dip-coatings in both NaCl and H<sub>2</sub>SO<sub>4</sub> solutions (Fig. 3B(a) and (b)). The chlorine evolution activity reached a peak at 15 dip-coating times, whereas the  $q^*$  value was larger in the H<sub>2</sub>SO<sub>4</sub> solution when the number of dip-coatings exceeded 15.

#### 3.3.3. Accelerated lifetime test of the anode

As seen in Fig. 3C, a large number of dip-coatings indicated a

high level of oxidation for all components, firmer adhesion between coating and substrate, and a longer lifetime. However, in practice, the loss of the coating sol was inevitable because of solvent volatilization. Because the coating sol formulation is constant, as the number of dip-coatings increases, more coating is lost and more labor is required for processing. Therefore, the number of dip-coatings should be optimized by considering improvements in coating performance, reductions in coating sol loss and increases in labor.

In conclusion, the appropriate preparation conditions should be as follows: a sintering temperature of 450 °C, a heat treatment time of 1 h and as many dip-coatings as possible.

### 3.4. Characteristics of the generated AEW

When ACC reached approximately 100 mg L<sup>-1</sup>, the generation of AEW ceased. The characteristics of the AEW generated by the anodes under different preparation conditions were shown in Table 1.

The results showed that the sintering temperature was the most critical factor affecting the SEC when producing AEW, followed by the heat treating time and dip-coating times. The optimal preparation conditions for AEW are in line with the optimum conditions previously obtained (sintering temperature at 450 °C for 1 h and dip-coating times as many as possible), at which anodes could

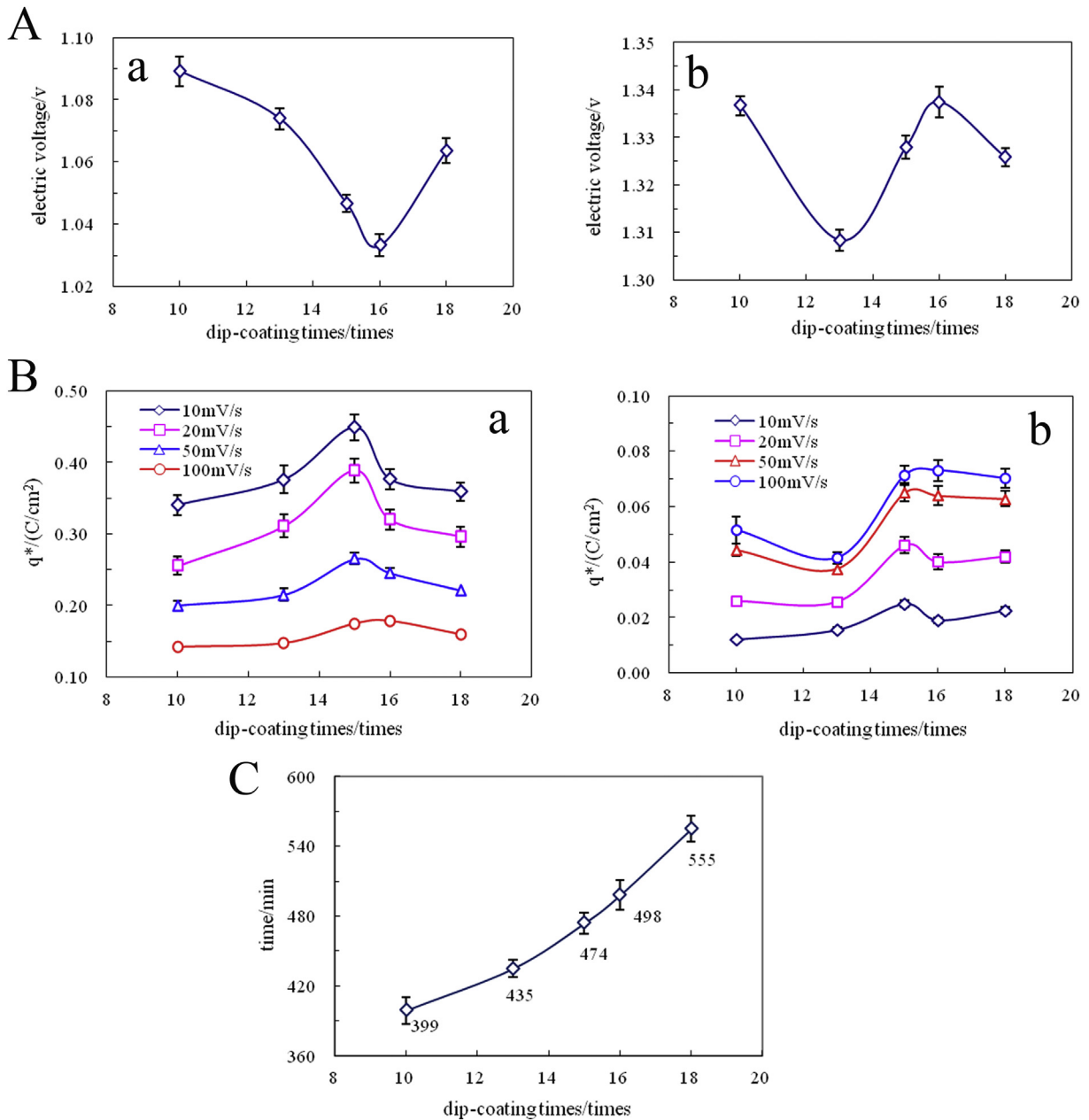


**Fig. 3.** (A) Chlorine evolution potentials and oxygen evolution potentials of the coated Ti anodes with different numbers of dip-coatings. (a) chlorine evolution potentials, (b) oxygen evolution potentials; (B) q\* values of the coated Ti anodes with different numbers of dip-coatings. (a) in saturated NaCl solution, (b) in 0.5 mol L<sup>-1</sup> H<sub>2</sub>SO<sub>4</sub> solution; (C) Accelerated lifetime of the coated Ti anodes with different numbers of dip-coatings.

**Table 1**  
Physicochemical parameters of AEOW generated by anodes prepared and analysis of the significant factors about specific energy consumption.

Experiment number	Preparation processes			Physicochemical parameters			
	A: sintering temperature (°C)	B: heat treatment time (h)	C: dip-coating times (times)	pH	ORP (mV)	ACC (mg L <sup>-1</sup> )	Specific energy consumption (kW h kg <sup>-1</sup> )
1	400	0.5	13	3.93	698	98.5	11.63
2	400	1	15	3.43	897	102.7	6.76
3	400	1.5	17	2.78	1028	99.7	5.96
4	400	2.0	19	2.89	1007	97.4	6.13
5	450	0.5	15	3.39	913	102.3	6.43
6	450	1	13	2.89	1106	102.5	2.63
7	450	1.5	19	2.64	1141	99.8	4.90
8	450	2.0	17	2.76	1109	102.3	5.56
9	500	0.5	17	3.05	975	98.6	6.69
10	500	1.0	19	2.82	1072	99.6	5.87
11	500	1.5	13	3.01	1014	98.2	6.49
12	500	2.0	15	3.26	1005	101.8	6.84
13	550	0.5	19	3.53	829	97.7	9.13
14	550	1.0	17	3.48	863	102.9	8.87
15	550	1.5	15	3.65	811	97.3	10.13
16	550	2.0	13	4.67	679	99.1	12.57
K1	30.48	33.88	33.32				
K2	19.52	24.13	30.16				
K3	25.89	27.48	27.08				
K4	40.70	31.10	26.03				
k1	7.62	8.47	8.33				
k2	4.88	6.03	7.54				
k3	6.47	6.87	6.77				
k4	10.17	7.78	6.51				
Extreme difference	5.29	2.44	1.82				
Optimum scheme	A2	B2	C4				

**Table 2**  
Sterilization effect of AEOW on *E. coli* and *S. aureus* with different ACC.

Number	pH	ORP (mV)	ACC (mg L <sup>-1</sup> )	KL			
				<i>E. coli</i>		<i>S. aureus</i>	
				1 min	2 min	1 min	3 min
1	2.97	1071	16.3	4.35 ± 0.19	4.81 ± 0.21	3.03 ± 0.13	3.49 ± 0.17
2	2.88	1097	36.2	6.16 ± 0.23	7.93 ± 0.18	3.68 ± 0.27	5.17 ± 0.20
3	2.70	1122	56.5	7.93 ± 0.20	7.93 ± 0.24	7.93 ± 0.18	7.93 ± 0.14
4	2.61	1141	75.1	7.93 ± 0.25	7.93 ± 0.31	7.93 ± 0.22	7.93 ± 0.21
5	2.55	1155	93.6	7.93 ± 0.28	7.93 ± 0.17	7.93 ± 0.26	7.93 ± 0.27

generate qualified AEOW. Therefore, it is appropriate to use these anodes to replace the platinized Ti anodes to produce AEOW, which greatly reduce the cost of preparation of AEOW.

### 3.5. Disinfection effect and its influencing factors of AEOW

#### 3.5.1. Influence of ACC on the sterilization effect

Table 2 displays the water quality of AEOW and the sterilization

effects on *E. coli* and *S. aureus*. It shows that AEOW has efficient sterilization ability and ACC played an important role in the high sterilization ability. For *E. coli* (ACC:16.3 mg L<sup>-1</sup>, 2 min, KL = 4.81) and *S. aureus* (ACC:36.2 mg L<sup>-1</sup>, 3 min, KL = 5.17), the AEOW could achieve a 100% sterilization. The sterilization effect was enhanced with increasing of ACC and treatment time. For different pathogenic bacteria, the sterilization ability of AEOW varied as follows: *E. coli* > *S. aureus*. Disinfection effects are related to the bacterial structures. The cell wall of *E. coli* (G<sup>-</sup>) is thinner than that of

**Table 3**  
Sterilization effect of AEOW and NaClO on *E. coli* and *S. aureus* at different pH and ORP.

Disinfectant	pH	ORP (mV)	ACC (mg L <sup>-1</sup> )	KL	
				<i>E. coli</i>	<i>S. aureus</i>
AEOW	2.58	1147	54.5	8.08 ± 0.24	7.77 ± 0.21
	6.01	939	56.3	5.68 ± 0.27	5.29 ± 0.25
	12.12	411	60.5	0.56 ± 0.031	0.31 ± 0.019
NaClO	2.56	1130	55.6	7.91 ± 0.25	7.53 ± 0.28
	5.98	953	58.1	5.41 ± 0.20	5.13 ± 0.22
	12.15	408	61.4	0.47 ± 0.019	0.28 ± 0.011

Note: The disinfection time is 1 min.

**Table 4**  
Influence of sterilization effect on *E. coli* and *S. aureus* at different active oxygen with a certain concentration of NaClO.

H <sub>2</sub> O <sub>2</sub> (mg L <sup>-1</sup> )	KL	
	<i>E. coli</i>	<i>S. aureus</i>
0.00	0.44 ± 0.023	0.25 ± 0.014
51.7	0.49 ± 0.027	0.29 ± 0.020
102.6	0.52 ± 0.031	0.32 ± 0.019
205.3	0.57 ± 0.029	0.38 ± 0.023

Note: The ACC of NaClO is 52.5 mg L<sup>-1</sup> and the disinfection time is 1 min.

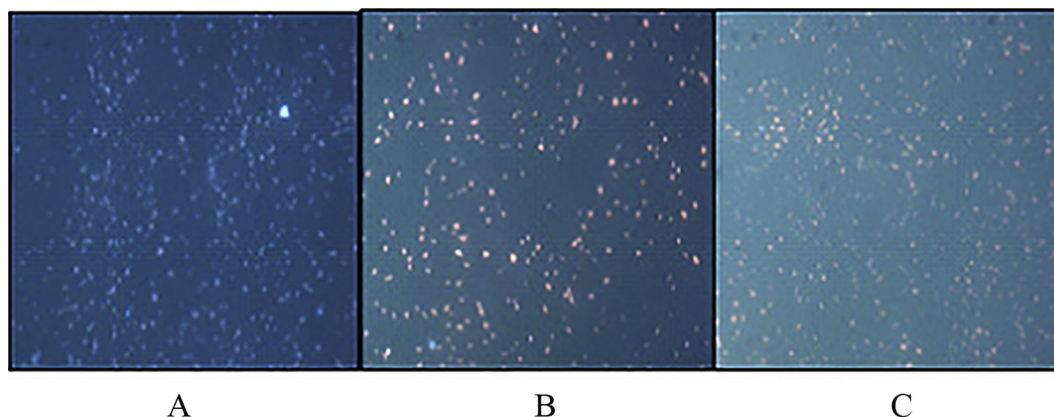


**Fig. 4.** Fluorescence images of *S. aureus* (ACC = 60.4 mg L<sup>-1</sup>, ORP = 1148, pH = 2.53, scale bar = 50 μm). (A) without treatment by AEOW, (B) treated by AEOW for 0.5 min, (C) treated by AEOW for 1 min.

*S. aureus* (G<sup>+</sup>) and the former has weaker mechanical intensity, so AEOW has better disinfection effect on *E. coli* than on *S. aureus* (Han & Fu, 2004; Liu, Tu, & Wang, 1994; Zeng et al., 2010; Zeng et al., 2011a).

### 3.5.2. Influence of pH and ORP on the sterilization effect

For AEOW and NaClO, the lower the pH level was (or the higher the ORP), the better the sterilization effect on *E. coli* and *S. aureus* became (Table 3). In addition, after adjusting the pH, the sterilization effects of NaClO and AEOW showed only slight difference when their ACC contents were similar. Thus, a low pH (high ORP) plays an important role in promoting sterilization.

### 3.5.3. Influence of active oxygen on the sterilization effect

Different concentrations of hydrogen peroxide with a certain concentration of NaClO were used as diluents. The disinfection results are shown in Table 4.

The results show that the existence of reactive oxygen species is not the main reason for strong sterilization ability of AEOW. When H<sub>2</sub>O<sub>2</sub> with a high reactive oxygen species (205.3 mg L<sup>-1</sup>) was applied to treat *E. coli* and *S. aureus* for 1 min, the KL was only 0.57 or 0.38, respectively. Meanwhile the combination of NaClO and H<sub>2</sub>O<sub>2</sub> almost did not show synergistic effects, for *E. coli*, the maximum of KL is 0.57, the minimum of KI is 0.44.

As a result, the sterilization ability of AEOW was the result of a combined effect of three factors, ACC, low pH and high ORP.

### 3.6. Fluorescence microscopy analysis

The fluorescent dye PI cannot completely penetrate the membranes of living cells. However, when the membranes are damaged, monomolecular PI can be inserted in every five base pairs of DNA, causing the nucleus turns into stained red, and the extent to which the cell membrane is destroyed can be measured by fluorescence microscopy. In Fig. 4A, PI could hardly penetrate *S. aureus* to stain the DNA without AEOW's treatment. Almost no cells were stained red, except for several incipient apoptotic individuals. As AEOW treatment (Fig. 4B and C), the number of stained cells increased, and almost all of the cells were stained red after 1 min, indicating that the cell membrane was one of the targets of AEOW. These findings indicate that AEOW can destroy the cell-membrane integrity of *S. aureus*, which confirms that AEOW has an effective sterilization ability.

## 4. Conclusions

The anodes fabricated in this study showed improved reaction selectivity at low sintering temperature but a longer lifetime at higher temperature, and the optimum sintering temperature was determined to be 450 °C. A short heat treatment time caused insufficient oxidation of the coating, whereas a long treatment time increased the lifetime of the anode, though with the evolution of metallic Ru and a waste of energy. A 1-h heat treatment time was determined to be suitable. Increasing the number of dip-coatings could improve the oxidation of all components, enhance the adhesion between coating and substrate, and prolong the lifetime of the anodes. The optimized preparation electrode could replace the platinized Ti anode and the produced AEOW could be used as an effective disinfectant for eliminating *E. coli* and *S. aureus*. The sterilization ability of AEOW is the result of a combined effect of three factors, ACC, low pH and high ORP.

## Acknowledgments

This work was supported by the National Natural Science Foundation of China (No. 21277098) and Shanghai Science and Technology Commission (14DZ2261100).

## References

- Arevalos-Sánchez, M., Regalado, C., Martín, S. E., Meas-Vong, Y., Cadena-Moreno, E., & García-Almendárez, B. E. (2013). Effect of neutral electrolyzed water on lux-tagged *Listeria monocytogenes* EGDe biofilms adhered to stainless steel and visualization with destructive and non-destructive microscopy techniques. *Food Control*, 34, 472–477.
- Audenaert, K., Monbaliu, S., Deschuyffeleer, N., Maene, P., Vekeman, F., Haesaert, G., et al. (2012). Neutralized electrolyzed water efficiently reduces *Fusarium spp.* in vitro and on wheat kernels but can trigger deoxynivalenol (DON) biosynthesis. *Food Control*, 23, 515–521.
- Cheng, H. Y., Zhang, J. H., & Cui, J. (2007). Research and development on electrolytic cell of ion-water generator. *Materials Research and Application*, 2, 154–157.
- Cui, Y. H., Feng, Y. J., & Liu, Z. Q. (2009). Influence of rare earths doping on the platinum and electro-catalytic performance of Ti/Sb–SnO<sub>2</sub> electrodes. *Electrochimica Acta*, 54, 4903–4909.
- Depauli, C. P., & Trasatti, S. (1995). Electrochemical surface characterization of IrO<sub>2</sub>+SnO<sub>2</sub> mixed oxide electrocatalysts. *Journal of Electroanalytical Chemistry*, 396, 161–168.
- Ding, T., Rahman, S. M. E., Purev, U., & Deog-Hwan, O. (2010). Modelling of *Escherichia coli* O157:H7 growth at various storage temperatures on beef treated with electrolyzed oxidizing water. *Journal of Food Engineering*, 97, 497–503.
- Dziewonski, P. M., & Grzeszczuk, M. (2009). Deposition of thin TiO<sub>2</sub> layers on platinum by means of cyclic voltammetry of selected complex Ti (IV) media leading to anatase. *Electrochimica Acta*, 54, 4045–4055.
- Fasenko, G. M., Christopher, E. E., & McMullen, L. M. (2009). Spraying hatching eggs with electrolyzed oxidizing water reduces eggshell microbial load without compromising broiler production parameters. *Poultry Science*, 88, 1121–1127.

- Han, Y. P., & Fu, J. L. (2004). The application of  $\text{ClO}_2$  as a disinfectant in drinking water disposal. *Journal of Beijing Union University*, 18, 71–75.
- Issa-Zacharia, A., Kamitani, Y., Miwa, N., Muhimbula, H., & Iwasaki, K. (2011). Application of slightly acidic electrolyzed water as a potential non-thermal food sanitizer for decontamination of fresh ready-to-eat vegetables and sprouts. *Food Control*, 22, 601–607.
- Jadeja, R., Hung, Y., & Bosilevac, J. (2013). Resistance of various shiga toxin-producing *Escherichia coli* to electrolyzed oxidizing water. *Food Control*, 30, 580–584.
- Kim, K. W., Lee, E. H., & Kim, J. S. (2001). Study on the electro-activity and non-stoichiometry of a Ru-based mixed oxide electrode. *Electrochimica Acta*, 46, 915–921.
- Liu, X. L., Tu, Y., & Wang, Q. M. (1994). Effects of chlorine dioxide on ultrastructure and permeability of *Escherichia coli*. *Chinese Journal of Public Health*, 13, 159–161.
- McCarthy, S., & Burkhardt, W. (2012). Efficacy of electrolyzed oxidizing water against *Listeria monocytogenes* and *Morganella morganii* on conveyor belt and raw fish surfaces. *Food Control*, 24, 214–219.
- Smith, C. G., & Okinaka, Y. (1983). High speed gold plating: anodic bath degradation and search for stable low polarization anodes. *International Journal of the Electrochemical Society*, 130, 2149–2157.
- Song, S., Zhan, L. Y., & He, Z. Q. (2010). Mechanism of the anodic oxidation of 4-chloro-3-methyl phenol in aqueous solution using Ti/SnO<sub>2</sub>-Sb/PbO<sub>2</sub> electrodes. *Journal of Hazardous Materials*, 175, 614–621.
- Technical Standard for Disinfection. (2002). *Ministry of health*. People's Republic of China, Beijing (pp. 15–61).
- Udompijitkul, P., Daeschel, M. A., & Zhao, Y. (2007). Antimicrobial effect of electrolyzed oxidizing water against *Escherichia coli* O157:H7 and *Listeria monocytogenes* on fresh strawberries (*Fragaria × ananassa*). *Journal of Food Science*, 72, M397–M406.
- Wang, J. J., Lin, T., Li, J. B., Liao, C., Pan, Y. J., & Zhao, Y. (2014). Effect of acidic electrolyzed water ice on quality of shrimp in dark condition. *Food Control*, 35(1), 207–212.
- Xie, J., Sun, X. H., Pan, Y. J., & Zhao, Y. (2012). Combining basic electrolyzed water pretreatment and mild heat greatly enhanced the efficacy of acidic electrolyzed water against *Vibrio parahaemolyticus* on shrimp. *Food Control*, 23, 320–324.
- Yang, X. P., Zou, R. Y., Huo, F., Cai, D. C., & Xiao, D. (2009). Preparation and characterization of Ti/SnO<sub>2</sub>-Sb<sub>2</sub>O<sub>3</sub>-Nb<sub>2</sub>O<sub>5</sub>/PbO<sub>2</sub> thin film as electrode material for the degradation of phenol. *Journal of Hazardous Materials*, 164, 367–373.
- Zeng, Y., Chen, K. N., Wu, W., Wang, J. R., & Soowohn, L. (2007). Effect of IrO<sub>2</sub> loading on RuO<sub>2</sub>-IrO<sub>2</sub>-TiO<sub>2</sub> anodes: a study of microstructure and working life for the chlorine evolution reaction. *Ceramics International*, 33, 1087–1091.
- Zeng, X. P., Tang, W. W., Ye, G. Y., Ouyang, T., Tian, L., Ni, Y. M., et al. (2010). Studies on disinfection mechanism of electrolyzed oxidizing water on *E. coli* and *Staphylococcus aureus*. *Journal of Food Science*, 75, M253–M260.
- Zeng, X. P., Ye, G. Y., Tang, W. W., Ouyang, T., Tian, L., Ni, Y. M., et al. (2011a). Fungicidal efficiency of electrolyzed oxidizing water on *Candida albicans* and its biochemical mechanism. *Journal of Bioscience and Bioengineering*, 112, 86–91.
- Zeng, X. P., Zhang, M., Wang, X. D., Chen, X. Y., Su, X. Z., & Tang, W. W. (2012). Effects of Sn content on Ti/RuO<sub>2</sub>-SnO<sub>2</sub>-TiO<sub>2</sub> anodes used in the generation of electrolyzed oxidizing water. *Journal of Electroanalytical Chemistry*, 677–680, 133–138.
- Zeng, X. P., Zhao, Y. S., Tang, W. W., & Zheng, C. Y. (2011b). Preparation process of coating Ti anode for generation electrolyzed oxidizing water and its effects. *Journal of Tongji University (Social Science Section)*, 39, 1318–1323.
- Zhang, C., Lu, Z., Li, Y., Shang, Y., Zhang, G., & Cao, W. (2011). Reduction of *Escherichia coli* O157:H7 and *Salmonella enteritidis* on mung bean seeds and sprouts by slightly acidic electrolyzed water. *Food Control*, 22(5), 792–796.
- Zhou, X. L., Ye, Z. G., Hua, X. Z., Zou, A. H., & Dong, Y. H. (2011). Electrocatalytic activity and stability of Ti/IrO<sub>2</sub>+MnO<sub>2</sub> anode in 0.5 M NaCl solution. *Journal of Solid State Electrochemistry*, 14, 1213–1219.



## Short communication

# Determination of phenolic acid decarboxylase produced by lactic acid bacteria isolated from shalgam (şalgam) juice using green analytical chemistry method



Gozde Okcu <sup>a</sup>, Kamuran Ayhan <sup>a,\*</sup>, Evrim Gunes Altuntas <sup>b</sup>, Nilufer Vural <sup>c</sup>, Ender Sinan Poyrazoglu <sup>d</sup>

<sup>a</sup> Ankara University, Faculty of Engineering, Food Engineering Department, Diskapi, Ankara 06110, Turkey

<sup>b</sup> Ankara University, Biotechnology Institute, Central Laboratory, Tandogan, Ankara 06100, Turkey

<sup>c</sup> Ankara University, Faculty of Engineering, Chemistry Engineering Department, Tandogan, Ankara 06100, Turkey

<sup>d</sup> Siirt University, Faculty of Engineering and Architecture, Food Engineering Department, Siirt, Turkey

## ARTICLE INFO

## Article history:

Received 5 June 2015

Received in revised form

28 October 2015

Accepted 31 October 2015

Available online 14 November 2015

## Keywords:

Lactic acid bacteria

Phenolic acid decarboxylase (PAD)

Phenolic compounds

Şalgam

HPLC

## ABSTRACT

Lactic acid bacteria were isolated from Şalgam (Şalgam) juice samples and phenolic acid decarboxylase activity of the strains were examined by HPLC method. The isolates were identified with biochemical tests and according to the results a significant number of the strains were determined as *Lactobacillus plantarum*. The abilities of 21 selected isolates to decarboxylate p-coumaric, caffeic, ferulic, o-coumaric, gallic and sinapic acids were determined. Six isolates were detected to have phenolic acid decarboxylase activity. The strains GK1, GK3, GK5, GK11 and GK13 reduced both p-coumaric and caffeic acid, and all the strains except GK3 and GK12 could metabolize gallic acid to p-coumaric acid. Our results demonstrate that some important phenolics were produced by different lactic strains during Şalgam fermentation process and these strains could be declared as potential starter cultures. In this study phenolic acid decarboxylase (PAD) activity of lactic acid bacteria were also determined by HPLC method in which ethanol was used as a component of the mobile phase to avoid deleterious environmental side effects associated with acetonitrile. Accordingly, ethanol can be used as a component of the mobile phase instead of acetonitrile in the HPLC method for the determination of phenolics.

© 2015 Elsevier Ltd. All rights reserved.

## 1. Introduction

Lactic acid bacteria (LAB) are industrially important organisms used in the fermentation of food products of plant origin due to their GRAS (Generally Recognized as Safe) status. These bacteria not only produce lactic acid but also preserve nutrients, vitamins of fruits and vegetables and are used as starter cultures to convert sugars into lactic acid and other end products which give the typical flavour to fermented products (Carr, Chill, & Maida, 2002; Leroy & De Vuyst, 2004; Madigan, Martinko, & Parker, 2003, Chap. 12; Ray & Panda, 2007, Chap. 5).

Phenolic compounds, important constituents of fermented vegetable products, are directly related to sensory characteristics of

foods. The most important phenolic acids produced by several *Lactobacillus brevis* strains isolated from different origins were p-coumaric, ferulic and caffeic acids (Curiel, Rodriguez, Landete, De las Rivas, & Munoz, 2010). These compounds are also beneficial to health due to their chemopreventive activities. Şalgam juice (Şalgam/turnip) is a fermented drink with health benefits attributed to its high antioxidant capacity and rich mineral and vitamin content. Şalgam juice is made with black carrot, wheat flour (setik), yeast, sourdough, turnip, rock salt (unrefined salt), spices and flavoured with çelem obtained by lactic acid fermentation. It is a red coloured, cloudy and sour soft drink mainly consumed in southern Turkey (Canbaş & Fenercioğlu, 1984; Erten, Tangüler, & Canbaş, 2008; Kabak & Dobson, 2011; Tanguler & Erten, 2012).

In recent years, several studies have been conducted on phenolics, which are known as beneficial compounds to health due to their antioxidant activities (Curiel et al., 2010; Öztan, 2006; Rodriguez et al., 2009; Erginkaya & Hammes, 1992). Phenolics are also known to play an important role in the prevention of cancer,

\* Corresponding author. Ankara University, Engineering Faculty, Food Engineering Department, Diskapi Campus, 06110, Diskapi/Ankara, Turkey. Tel.: +90 312 2033300x3609.

E-mail address: [kayhan@ankara.edu.tr](mailto:kayhan@ankara.edu.tr) (K. Ayhan).

**Table 1**  
The retention times of phenolic compounds at 280 nm.

Phenolic compound	Retention time (minute)
Gallic acid	8,92
Caffeic acid	29
p-Coumaric acid	33,5
Sinapic acid	41
Ferulic acid	43,5
o-Coumaric acid	61

cardiovascular and some other degenerative diseases (Tangüler, 2010). However, there is a lack of knowledge pertaining to the efficacy of phenolic compounds on the growth of *Lactobacillus plantarum* and the other lactic acid bacteria.

The techniques used in the determination of phenolic compounds or the phenolic acid decarboxylase mostly depend on chromatographic methods. Among them HPLC is the most preferred method. In recent years, the field of energy has been heavily impacted by the use of green technology (De la Guardia & Garrigues, 2012, Chap. 1). The novel branch of analytical chemistry known as Green Analytical Chemistry (GAC) is also in demand recently as it provides inherent safety, non-toxicity, and environmental protection (Vaher & Kaljurand, 2012). Thus, there is an increased interest on the green methods in HPLC as well as to find alternative solvents and reagents which do not have persistent biocumulative and toxic effects (De la Guardia & Armenta, 2012). In analytical processes like HPLC assays, solvents are of vital importance because of their unique characteristics. Many studies have been focused on green solvents and their contribution to provide environmental safety. When selecting a green solvent, solute solubility, viscosity, compatibility and also cost are some of the factors that should be considered (De la Guardia & Armenta, 2012; De la Guardia & Garrigues, 2012; Vaher & Kaljurand, 2012; Young &

Raynie, 2011). To date while we know the beneficial health effect of Şalgam, we do not have any commercial LAB starter cultures. While Şalgam is a traditional Turkish beverage, other fermented vegetable juice samples exists in the world. The studies conducted on this topic showed that *Lb. plantarum* is a significant potential starter culture for fermented juices. This strain also contributes some nutritional properties to end product during fermentation process [3, 18]. The aims of this study were: 1) to isolate LAB from Şalgam juice samples 2) to identify the strains isolated from Şalgam juice samples with biochemical and API 50 CHL test 3) to analyse the phenolic acids decarboxylase activity of isolated strains by HPLC. Additionally, ethanol as a component of the mobile phase was used in order to provide a green analytical alternative, as a replacement for acetonitrile. In this respect, this is one of the first studies conducted on using ethanol as a green solvent in HPLC analysis.

## 2. Material and methods

### 2.1. Isolation and identification of LAB strains

Nine commercial Şalgam samples were purchased from local markets and a total of 38 samples were taken from fermentation processes at two different Şalgam juice plants located in Mersin region. For this purpose, Şalgam juice samples were carried aseptically from factories to laboratory and 2.5 mL of the Şalgam samples were inoculated into 5 mL MRS broth (de Man Rogosa Sharpe Medium, Merck, Germany) and incubated 24 h at 30 °C. The proportion of 0.1 mL from growth cultures was transferred into MRS agar plates and incubated at the same conditions. (Harrigan & McCane, 1996). Typical colonies were randomly picked from MRS agar plates and transferred into MRS broth (Merck, Germany) medium for phenotypic characterization. These strains were

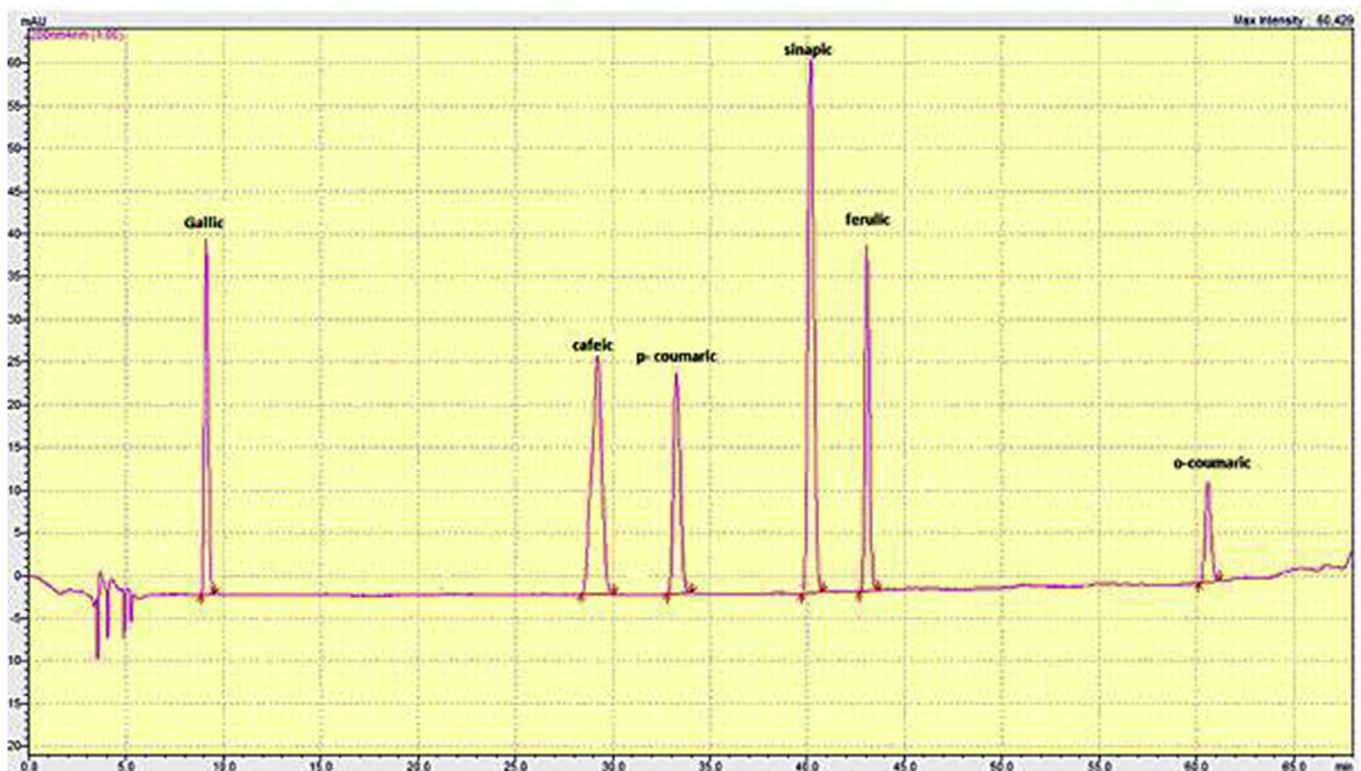


**Fig. 1.** The phenolic acid standard chromatogram at 280 nm and the retention times of the phenolic acids used in this study.

identified by using 12 different biochemical tests (motility, Gram reaction, catalase test, oxidase test, CO<sub>2</sub> production from glucose, carbohydrate (saccharose) fermentation, arginine hydrolyse, growth temperature, growth pH, salt concentration of the medium, Voges Proskauer, metil red) and named on the basis of the groups in *Bergey's Manual of Systematic Bacteriology* (1984). Afterward the isolates were identified with API 50 CHL test according to manufacturer instructions (Biomerieux, France).

## 2.2. Extraction of phenolic compounds of the lactic cultures

Strains of lactic acid bacteria were grown in duplicate in MRS broth (Merck, Germany) supplemented at 1 mM final concentration with the phenolic acid which was previously filter-sterilized (Sartorius, Germany). The 21 strains of lactic acid bacteria inoculated media were incubated at 30 °C in dark, without shaking, for 10 days. Incubated media with cells and without phenolic acids, and incubated media without cells and with the phenolic acids, were used as controls. From the supernatants, the phenolic compounds were extracted by a standard protocol involving two extraction steps with one third of the reaction volume of ethyl acetate (Curriel et al., 2010).

## 2.3. High-performance liquid chromatography (HPLC) analysis

Shimadzu SCL-10AVP was used for HPLC analysis equipped with the column Inertsil ODS-3.5 μm (4.6 × 250 mm). Samples of 20 μL were injected into the column and eluted with a gradient comprising for the mobile phase acetonitrile (Pump A) and 0.1% glacial acetic acid/water (Pump B) were used. The 6 phenolic acids analysed in this study were p-coumaric, o-coumaric, caffeic, ferulic, sinapic and gallic acids (Sigma, USA). The following gradient was at 86% B at 0–10 min, 74% B after 32 min, 20% B for 35–38 min, and 86% B for 40–43 min. Flow rate was 1 mL/min, and column temperature was 40 °C. Detection was performed by scanning from 200 to 540 nm and the quantitative analysis was done at 280 nm.

Table 1 and Fig. 1 shows the retention times of the phenolic acids used in this study.

HPLC analysis was also performed by using 100% ethanol (Pump A) and 0.1% glacial acetic acid/water (Pump B) as mobile phase (De la Guardia & Garrigues, 2012). The monitoring wavelength was 310 nm. Detection was performed by scanning from 280 to 380 nm. Tentative identification of degradation products was carried out by comparing the retention times and spectral data of each peak with those of standards from commercial suppliers (except for vinylphenol and vinylcatechol). Vinyl derivatives, 4-vinylphenol (256 nm, 37.82 min), 4-vinylcatechol and 4-vinylguaicol (258 nm, 32.33 min), were determined by using reference data (Degrassi, De Laureto, & Bruschi, 1995).

## 3. Results and discussion

### 3.1. The identification results of the LAB strains

Fermented food product quality is certainly related to the composition of food microbiota. If spontaneous fermentations are chosen then the desired properties will be changed by the dominant microorganisms. Furthermore, spontaneous process may result in spoilage or the survival of some pathogens. In industry these reasons have oriented the firms to use starter cultures in order to obtain standard products at each production time (Rodriguez et al., 2009; Ayhan, Durlu-Ozkaya, & Tunail, 2005). One of our aim was to detect appropriate starter strains as many scientific researches focused on selecting potential starter cultures.

In this study, twenty one lactic acid bacteria were isolated from

**Table 2**  
The biochemical identification test results of the strains isolated from Şalgam juice samples.<sup>a</sup>

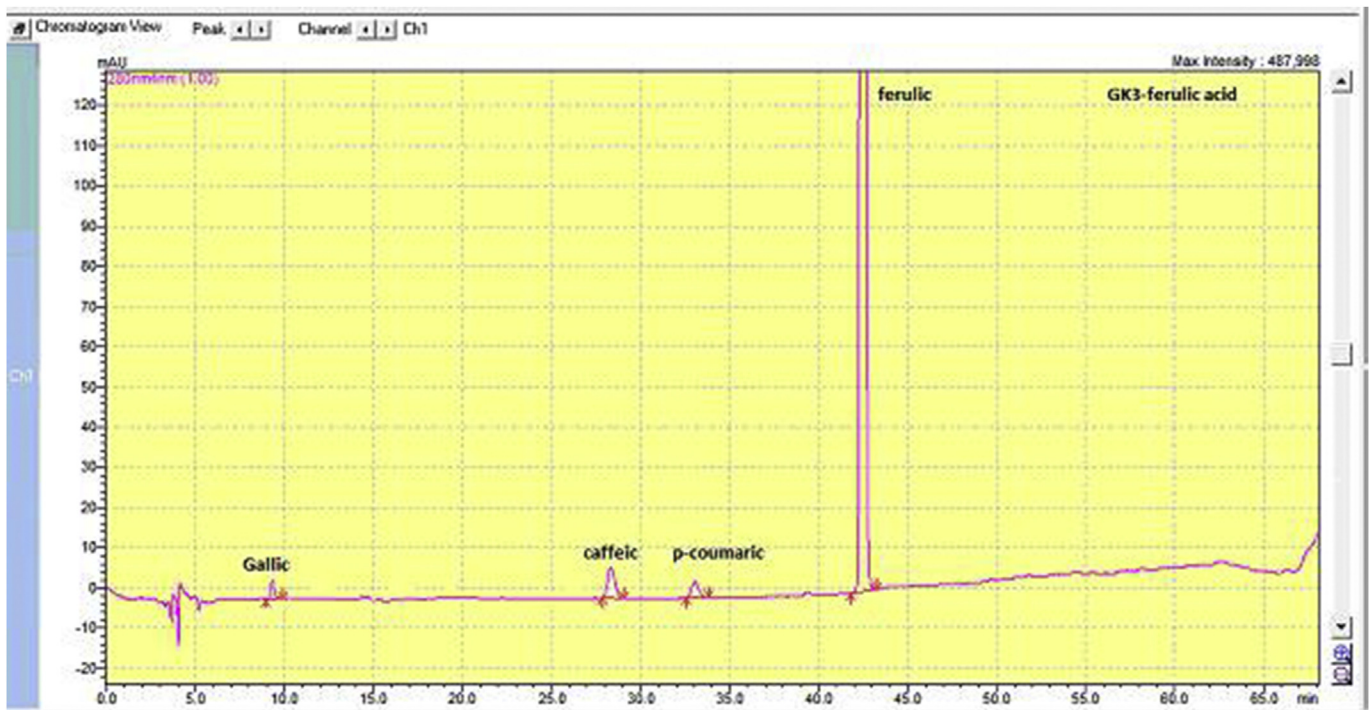
Strain number	Cell morphology	Motility	Gram reaction	Catalase test	Oxydase test	CO <sub>2</sub> production from glucose	Carbohydrate (saccharose) fermentation	Arginin hydrolyse	Growth temperature		Growth pH			Salt concentration	Voges Proskauer	Metil red
									10 °C	45 °C	4,4	9,6	4%			
1	Coccus	-	+	-	-	-	+	-	-	-	+	+	+	-	+	+
2	Coccus	-	+	-	-	-	+	-	-	-	+	+	+	-	+	+
3	Coccus	-	+	-	-	-	+	+	-	-	+	+	+	-	+	+
4	Coccus	-	+	-	-	-	+	-	-	-	+	+	+	-	+	+
5	Coccus	-	+	-	-	-	+	-	-	-	+	+	+	-	+	+
6	Coccus	-	+	-	-	-	+	-	-	-	+	+	+	-	+	+
7	Coccus	-	+	-	-	-	+	-	-	-	+	+	+	-	+	+
8	Coccus	-	+	-	-	-	+	-	-	-	+	+	+	-	+	+
9	Coccus	-	+	-	-	-	+	-	-	-	+	+	+	-	+	+
10	Coccus	-	+	-	-	-	+	-	-	-	+	+	+	-	+	+
11	Coccus	-	+	-	-	-	+	-	-	-	+	+	+	-	+	+
12	Bacil	-	+	-	-	-	+	Nd	-	-	+	+	+	-	+	+
13	Bacil	-	+	-	-	-	+	-	-	-	+	+	+	-	+	+
14	Bacil	-	+	-	-	-	+	-	-	-	+	+	+	-	+	+
15	Bacil	-	+	-	-	-	+	-	-	-	+	+	+	-	+	+
16	Bacil	-	+	-	-	-	+	-	-	-	+	+	+	-	+	+
17	Bacil	-	+	-	-	-	+	-	-	-	+	+	+	-	Nd	Nd
18	Bacil	-	+	-	-	-	+	-	-	-	+	+	+	-	Nd	Nd
19	Bacil	-	+	-	-	-	+	-	-	-	+	+	+	-	+	+
20	Coccus	-	+	-	-	-	+	-	-	-	+	+	+	-	+	+
21	Bacil	-	+	-	-	-	+	-	-	-	+	+	+	-	+	+

<sup>a</sup> +: Positive reaction, -: negative reaction. Nd: Not determined.

**Table 3**

The decarboxylation profile of the strains; observed phenolic acids after decarboxylation are indicated as positive.

Strain number	Decarboxylated phenolic acids	Phenolic acids occurred after decarboxylation					
		Gallic acid	Caffeic acid	p-Coumaric acid	Ferulic acid	Sinapic acid	o-Coumaric acid
GK1	Gallic acid	+		+			
	Caffeic acid	+	+	+	+		+
	p-Coumaric acid	+	+	+			
	Ferulic acid		+	+			
	Sinapic acid	+	+	+	+		+
	o-Coumaric acid		+	+			+
GK3	Gallic acid	+					
	Caffeic acid	+	+		+		
	p-Coumaric acid	+	+	+			
	Ferulic acid	+	+	+	+		
	Sinapic acid	+			+	+	
	o-Coumaric acid	+	+	+			
GK5	Gallic acid	+		+			
	Caffeic acid	+	+	+	+		
	p-Coumaric acid	+	+	+			
	Ferulic acid	+	+	+	+		
	Sinapic acid	+	+	+		+	
	o-Coumaric acid	+	+	+			+
GK11	Gallic acid	+		+			
	Caffeic acid	+	+	+	+		
	p-Coumaric acid	+	+	+			
	Ferulic acid	+	+	+	+		
	Sinapic acid	+	+	+		+	
	o-Coumaric acid	+	+	+			+
GK12	Gallic acid	+		+			
	Caffeic acid						
	p-Coumaric acid						
	Ferulic acid	+		+	+		
	Sinapic acid	+		+	+		
	o-Coumaric acid						+
GK13	Gallic acid	+		+			
	Caffeic acid	+	+	+	+		
	p-Coumaric acid	+	+	+			
	Ferulic acid	+	+	+			
	Sinapic acid	+		+		+	
	o-Coumaric acid					+	+

**Fig. 2.** The chromatogram of ferulic acid decarboxylation by GK3 strain at 280 nm.

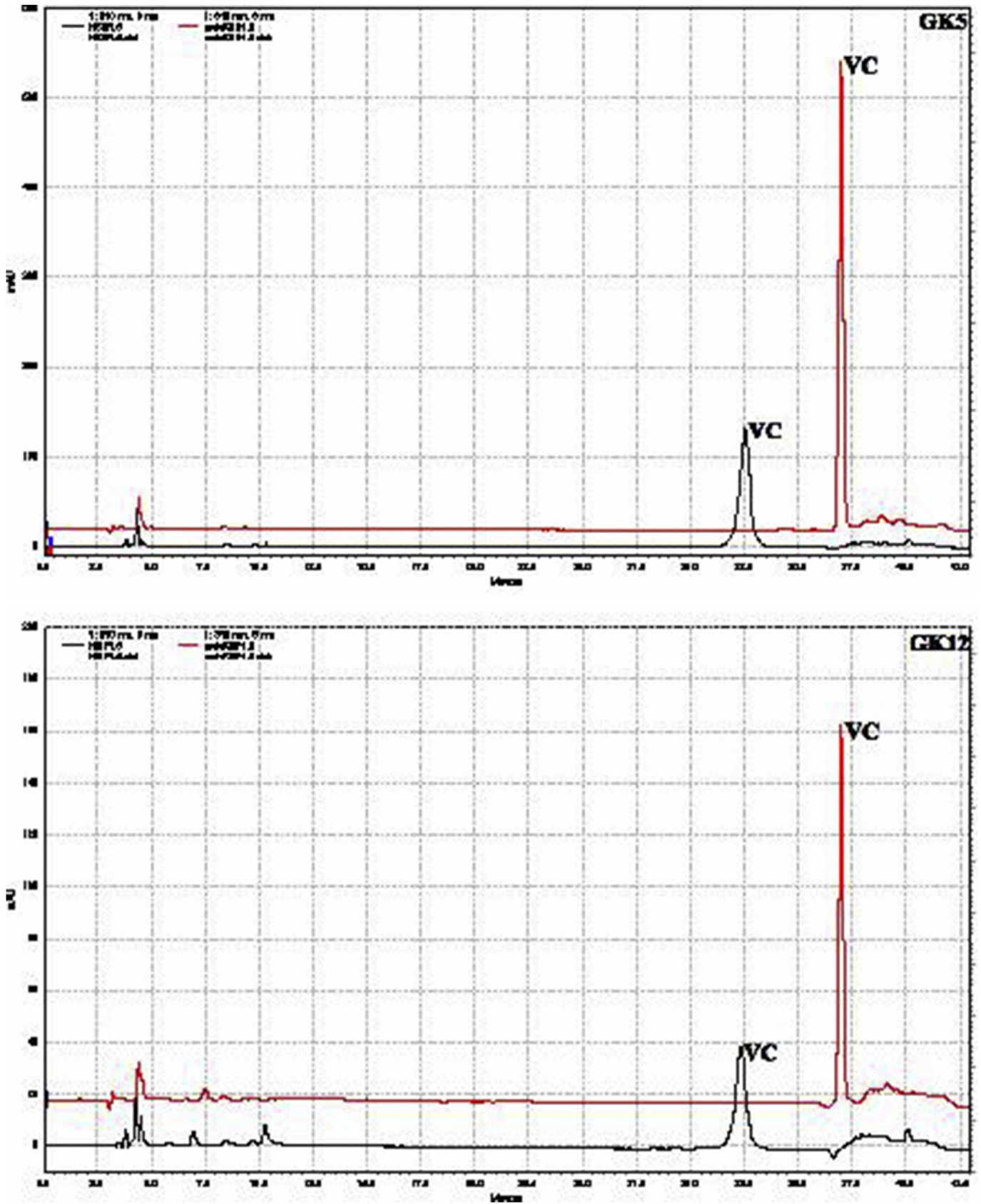


Fig. 3. HPLC chromatograms of the metabolism of caffeic acid by GK5 and GK12 strains and the production of vinylcatechol (VC): supernatants from GK5 and GK12 grown for 5 days in presence of caffeic acid. Line in black indicates that acetonitrile was used as mobile phase. Line in red indicates that ethanol was used as mobile phase. The chromatogram was recorded at 310 nm. (For interpretation of the references to colour in this figure legend, the reader is referred to the web version of this article).

41 şalgam juice samples and then identified by using 12 different biochemical tests. According to biochemical tests four of these isolates (19.05%) were *Leuconostoc mesenteroides*, six of them (28.57%) were *Lb. plantarum*, one of them was *Lactobacillus helveticus* – *Lactobacillus acidophilus*, one of them was *Lb. plantarum* – *Lb. acidophilus* and finally, one of them was *Lactobacillus casei* – *Lactobacillus paracasei* (Table 2).

The results of biochemical identification test performed with API 50 CHL kit showed that the strains numbered as GK3 and GK5 are *Leu. mesenteroides* spp. *mesenteroides/dextranicum* 2 with 96% and 97.8% similarity rates, respectively. The GK12 and GK13 strains are identified as *Lb. plantarum* with 98% and 99.9% similarity rates.

Our findings on isolation and identification of LAB are in agreement with those reported by Erginkaya and Hammes (1992). These authors isolated LAB strains (*Lb. plantarum* subsp. *arabinosus*, *Lb. fermentum* ve *Lb. brevis*) from Şalgam juice samples. Additionally, Tangüler (2010) reported that most of the strains from Şalgam juice samples purchased from the local markets were identified as *Lb. plantarum*.

### 3.2. Phenolic acid decarboxylase activity of the LAB strains

Phenolics are the secondary metabolites which affect host physiology by acting as antioxidants. The richest sources of phenolics are cranberries, grapes, tea, red wine, cabbage, onion, sorghum, peas, legumes etc. It is known that if the diet contains phenolic phytochemicals rich, the risk of some diseases such as cardiovascular disease, diabetes and some cancer forms can be reduced (Ankolekar, 2013). Due to these properties, Şalgam juice consumption is increasing in Turkey. On the other hand, today, the producers do not have a commercial LAB starter cultures for a standard Şalgam production processes (Tanguler & Erten, 2012).

A comprehensive study conducted by Leroy and De Vuyst (2004) reported that LAB are good options for the fermentation processes due to being functional. In the same study, *Lactococcus lactis* subsp. *lactis* presented as an appropriate starter culture for dairy industry. Similarly LAB (*Lb. curvatus*, *Lb. sakei*, *Pediococcus acidilactici*, *Enterococcus faecium*) are the main microorganisms used in fermented meat products. *Lb. plantarum* is offered for fermented vegetables especially for fermented olives. Gardner, Savard, Obermeier, Caldwell, and Champagne (2001) studied on determination of the most convenient starter culture for a mixed vegetable juice made by using carrot, cabbage, beet and onion. The growth of 15 cultures (including *Lb. plantarum*, *Lb. brevis*, *Lb. casei*, *P. acidilactici*, *Leu. mesenteroides*) in the vegetable juice medium was characterized by automated spectrophotometry. It was seen that the number of LAB of the juice samples added LAB as starter culture was approximately 100 times more than the native flora.

Phenolic compounds do not always exhibit beneficial effect on foods. These compounds can precipitate proteins and affect on vitamin or mineral utilization. In recent years, their preventive effect against some diseases masked their adverse health effects (Rodriguez et al., 2009). The phenolic and anthocyanin content of Şalgam juice is mostly related to black carrot. Bayram, Erdogan, Esin, Saracoglu, and Kaya (2014) explained that if the proportion of black carrot is high then the phenolics and also anthocyanin content of şalgam will increase.

In our study, HPLC analysis performed to detect phenolic acid decarboxylase activity of the isolates indicated that the strains *Lb. plantarum* GK1 and *Pediococcus pentosaceus* GK5 are able to decarboxylate all phenolic acids used in the assay. The strain *Lb. plantarum* GK3 was able to decarboxylate all phenolic acids except gallic acid and GK11 was able to decarboxylate all acids except ferulic acid. All the details on decarboxylation of the phenolic acids by the isolates are given in Table 3. Additionally, the HPLC

chromatogram showing the decarboxylation of ferulic acid by GK3 at 280 nm is available in Fig. 2.

Rodriguez, Landete, de las Rivas, and Munoz (2008) conducted a study to assess the ability of *Lb. plantarum* CECT 748T to metabolize 19 food phenolic acids. Among the hydroxycinnamic acids studied, only p-coumaric, caffeic, ferulic and m-coumaric acids were metabolized by *Lb. plantarum*.

In a study performed by Curiel et al. (2010) the aim was to show the potential to degrade 15 food phenolic acids using several *Lb. brevis* strains isolated from different sources. The researchers reported that all the strains analysed in this study showed a similar metabolism on phenolic acids. Among the benzoic acids analysed, only gallic and protocatechuic acids were modified by *Lb. brevis* strains. Both acids were decarboxylated to pyrogallol and catechol, respectively. Among the cinnamic acids assayed, only p-coumaric, ferulic and caffeic acids were metabolized by the *Lb. brevis* strains and these acids were decarboxylated to produce their corresponding vinyl derivatives.

*Lb. plantarum* is a plant origin starter culture used in the fermentation processes. This strain has ability to degrade phenolic compounds which will cause to increase antioxidant activity and influence food aroma. As it is expected, we identified the GK1, GK3, GK12 and GK13 strains as *Lb. plantarum*. Considering their decarboxylase enzyme activities these strains may be the potential starter cultures for Şalgam juice.

Lastly, phenolic acid decarboxylase activity of LAB isolates were determined by HPLC method in which ethanol was used as component of the mobile phase to avoid deleterious environmental side effects associated with acetonitrile as described by De la Guardia and Garrigues (2012). We found that when ethanol is used instead of acetonitrile as the mobile phase, peak symmetry and separation were enhanced (Fig. 3).

## 4. Conclusions

The results indicated that phenolics which could increase food antioxidant properties were produced by different lactic acid bacteria strains during Şalgam fermentation process. The *P. pentosaceus* GK5 strain and *Lb. plantarum* GK1, *Lb. plantarum* GK3, *Lb. plantarum* GK12 and *Lb. plantarum* GK13 strains which were isolated from şalgam juice samples and determined as phenolic acid decarboxylase producer could be reported as potential starter cultures. The novel isolates may contribute to sensory and nutritional characteristics of foods. Further studies on genotypically identification of 6 strains producing PAD enzymes with 16S rRNA as well as determination of the highest level of phenolics produced by those strains is warranted. Finally based on this study, ethanol can be used as a component of the mobile phase instead of acetonitrile in the HPLC method for the determination of phenolics.

## Acknowledgement

This study was a part of a Master Thesis of Gozde Okcu (Ankara University, Science Institute, Food Engineering Department) and also supported by Project Supporting Unit (BAP) of Ankara University (Project Number: 12B4343005).

## References

- Ankolekar, C. R. (2013). *Lactic acid bacteria mediated phenolic bioactive modulation from fruit systems for health benefits*. Doctor of Philosophy Thesis submitted to Department of Food Science at University of Massachusetts-Amherst. Dissertations. Paper 678.
- Ayhan, K., Durlu-Ozkaya, F., & Tunail, F. (2005). Commercially important characteristics of Turkish origin domestic strains of *Streptococcus thermophilus* and *Lactobacillus delbrueckii* spp. *bulgaricus*. *International Journal of Dairy*

- Technology*, 58(3), 150–157.
- Bayram, M., Erdogan, S., Esin, Y., Saracoglu, O., & Kaya, C. (2014). Farklı siyah havuç miktarlarının şalgam suyunun bileşimine ve duyuşal özellikleri üzerine etkisi. *Academic Food Journal*, 12(1), 29–34.
- Bergey's Manual of Systematic Bacteriology. (1984). *Bacteriological analytical manual* (8th ed.). Virginia, USA: Published and Distributed by Association of Official Analytical Chemist Suite. Revision A.
- Canbaş, A., & Fenercioglu, H. (1984). Şalgam suyu üzerinde bir araştırma. *Gıda*, 9(5), 299–286.
- Carr, F. J., Chill, D., & Maida, N. (2002). The lactic acid bacteria: a literature survey. *Critical Reviews in Microbiology*, 28(4), 281–370.
- Curiel, J. A., Rodriguez, H., Landete, J. M., De las Rivas, B., & Munoz, R. (2010). Ability of *Lactobacillus brevis* strains to degrade food phenolic acids. *Food Chemistry*, 120, 225–229.
- Degrassi, G., De Laureto, P. P., & Bruschi, C. V. (1995). Purification and characterization of ferulate and p-coumarate decarboxylase from *Bacillus pumilus*. *Applied and Environmental Microbiology*, 61(1), 326–332.
- De la Guardia, M., & Armenta, S. (2012). Green analytical methods. *Analytical and Bioanalytical Chemistry*, 404, 625–626.
- De la Guardia, M., & Garrigues, S. (2012). The concept of green analytical chemistry. In M. De la Guardia, & S. Garrigues (Eds.), *Handbook of green analytical chemistry* (pp. 3–29). West Sussex, UK: Wiley Publishing, 546 pages.
- Erginkaya, Z., & Hammes, W. P. (1992). Şalgam suyu fermentasyonu sırasında mikroorganizmaların gelişimi ve izole edilen laktik asit bakterilerinin tanımlanmaları üzerine bir araştırma. *Gıda*, 17(5), 311–314.
- Erten, H., Tangüler, H., & Canbaş, A. A. (2008). Traditional turkish lactic acid fermented beverage: shalgam (salgam). *Food Reviews International*, 24, 352–359.
- Gardner, N. J., Savard, T., Obermeier, P., Caldwell, G., & Champagne, C. P. (2001). Selection and characterization of mixed starter cultures for lactic acid fermentation of carrot, cabbage, beet and onion vegetable mixtures. *International Journal of Food Microbiology*, 64, 261–275.
- Harrigan, W. F., & McCane, M. E. (1996). *Laboratory methods in food and dairy microbiology*. London: Academic Press.
- Kabak, B., & Dobson, A. D. W. (2011). An introduction to the traditional fermented foods and beverages of Turkey. *Critical Reviews of Food Science and Nutrition*, 51, 248–260.
- Leroy, F., & De Vuyst, L. (2004). Lactic acid bacteria as functional starter cultures for the food fermentation industry. *Trends in Food Science and Technology*, 15, 67–78.
- Madigan, M. T., Martinko, J. M., & Parker, J. (2003). Evolutionary microbiology and microbial diversity. In *Brock biology of microorganisms* (10th ed., p. 1019). USA: Prentice Hall. pp: 353–404.
- Öztaş, T. (2006). *Mor havuç, konsantresi, şalgam suyu, nar suyu ve nar ekşisi ürünlerinde antioksidan aktivitesi tayini ve fenolik madde profilinin belirlenmesi*. MSc thesis submitted to İstanbul Teknik University, Science Institute, İstanbul, 92 p. (unpublished).
- Ray, R. C., & Panda, S. H. (2007). Lactic acid fermentation of fruits and vegetables—an overview. In V. P. Marta (Ed.), *Food microbiology research trends* (p. 261). New York: Nova Science Publishers, Inc. pp: 155–188.
- Rodriguez, H., Curiel, J. A., Landete, J. M., de las Rivas, B., Lopez de Felipe, F., Gomez-Cordoves, C., ... Munoz, R. (2009). Food phenolics and lactic acid bacteria. *International Journal of Food Microbiology*, 132, 79–90.
- Rodriguez, H., Landete, J. M., de las Rivas, B., & Munoz, R. (2008). Metabolism of food phenolic acids by *Lactobacillus plantarum* CECT 748T. *Food Chemistry*, 107, 1393–1398.
- Tangüler, H. (2010). *Şalgam suyu üretiminde etkili olan laktik asit bakterilerinin belirlenmesi ve şalgam suyu üretim tekniğinin geliştirilmesi*. PhD thesis submitted to Çukurova University, Science Institute, 367 s. (unpublished).
- Tanguler, H., & Erten, H. (2012). Occurrence and growth of lactic acid bacteria species during the fermentation of shalgam (salgam), a traditional Turkish fermented beverage. *LWT – Food Science and Technology*, 46, 36–41.
- Vaher, M., & Kaljurand, M. (2012). The development of paper microzone-based green analytical chemistry methods for determining the quality of wines. *Analytical and Bioanalytical Chemistry*, 404, 627–633.
- Young, J. L., & Raynie, D. E. (2011). Replacement of hazardous solvents and reagents in analytical chemistry. In M. de la Guardia, & S. Garrigues (Eds.), *Challenges in green analytical chemistry*. Cambridge, UK: Published by Royal Society of Chemistry.



# Study of the effect of microwave power coupled with hot air drying on orange peel by dielectric spectroscopy



Clara Talens <sup>a</sup>, Marta Castro-Giraldez <sup>b</sup>, Pedro J. Fito <sup>b,\*</sup>

<sup>a</sup> AZTI - Food Research, Parque Tecnológico de Bizkaia, Astondo Bidea, Edificio 609, 48160, Derio Bizkaia, Spain

<sup>b</sup> Instituto Universitario de Ingeniería de Alimentos para el Desarrollo, Universidad Politécnica de Valencia, Camino de Vera s/n, 46022 Valencia, Spain

## ARTICLE INFO

### Article history:

Received 3 June 2015

Received in revised form

9 October 2015

Accepted 8 November 2015

Available online 14 November 2015

### Keywords:

Permittivity

GAB model

Isotherms

Orange peel

Hot air–microwave drying

## ABSTRACT

Monitoring moisture and water activity during drying is crucial for process optimization, avoiding inadequate uses of energy. The main objective of this work was to study the dielectric properties of orange peel during hot air drying at 55 °C (HAD) and microwave power coupled with hot air drying at different power intensities (2 W/g, 4 W/g and 6 W/g). At 5, 15, 40, 60 and 120 min mass,  $a_w$ , moisture, and permittivity were measured in fresh and dried samples. Results allowed developing a dielectric isotherm technique by adapting the GAB model to predict  $a_w$  in dried orange peel by using  $\epsilon'$  (20 GHz). The physical meaning of the dielectric isotherm parameters ( $\epsilon'_0$  and  $C_d$ ) was studied. The value of  $\epsilon'_0$  at 20 GHz ( $\gamma$ -dispersion) represents the induction effect of the minimum quantity of adsorbed water or the monomolecular moisture layer. The parameter  $C_d$  is related with isosteric heat, as well as the C parameter of the GAB model. The application of MW power produced an increase of isosteric heat or adsorption energy of the monomolecular layer, improving surface tension of samples and thus the hygroscopicity, explaining the reduction of the  $\epsilon'_0$  independently of the quantity of the water molecules adsorbed.

© 2015 Elsevier Ltd. All rights reserved.

## 1. Introduction

Drying costs are a major issue in most valorisation processes, especially when the water content of the material is as high as citrus by-products (85%), being critical for their economic feasibility. Therefore, moisture monitoring plays a key role in food processing operations such as drying. However, water interaction with air and food depends more on water activity than on moisture, because the reactivity and the mobility of water are directly related with the water activity. The most common and faster tool to obtain the water activity from the moisture is the sorption isotherm. Sorption isotherms relate water activity to water content of a food product at a certain temperature and pressure. The sorption isotherms have an important role in the quantitative approach to the prediction of shelf-life of dried foods, due to their sensitivity to moisture and water activity changes.

On the other hand, the research of electrical properties of food systems has received tremendous attention in the recent years due to the increased development and application in the range of Hz to

THz (radiofrequency, microwaves and infrared) for heating, drying or process monitoring in the food industry. The physical properties that define the heating capability of any material are permittivity for the photon electric interactions and permeability for the photon magnetic interactions (Pozar, 2012). They are affected by many different factors, depending on the range of frequency of the photon flux emitted (Castro-Giraldez, Balaguer, Hinarejos, & Fito, 2014), such as amount of water, temperature, structure (i.e. charge conformation of proteins) and chemical composition (i.e. electrolytes), especially on the presence of mobile ions (Castro-Giraldez, 2010). In the case of electric properties, the permittivity must be explained as a vector number, polar or complex. Permittivity explained as a complex number has two parameters, the dielectric constant  $\epsilon'$  and the loss factor  $\epsilon''$ , being the real and imaginary terms of permittivity ( $\epsilon$ ), respectively. The dielectric constant is related to the material ability to absorb and store electric energy, and the loss factor is related to the dissipation of the electric energy in other energies such as thermal energy.

In the range of microwaves, the interaction of the photon flux with biological tissue produces two main dispersions,  $\gamma$ -dispersion and ionic conductivity. The  $\gamma$ -dispersion is due to the dipolar molecules orientation and induction, producing electric storage

\* Corresponding author.

E-mail address: [pedfsu@tal.upv.es](mailto:pedfsu@tal.upv.es) (P.J. Fito).

and dissipation of the electric energy in other energies such as mechanical and thermal energies. The main dipolar molecule of plant tissue is water (Castro-Giraldez, Fito, Chenoll, & Fito, 2010; Castro-Giraldez, Fito, Dalla Rosa, & Fito, 2011; Castro-Giraldez, Fito, & Fito, 2011). The other important effect in microwave range is ionic conductivity. It affects only to the loss factor, because it only produces a repulsion of charged molecules, transforming electric energy into others.

Dielectric spectroscopy has been used for many applications as non-destructive technique for monitoring different processes: pork meat salting (Castro-Giraldez, Fito, & Fito, 2010; Kent, Peymann, Gabriel, & Knight, 2002; Lyng, Zhang, & Brunton, 2005), brewing (Velázquez-Varela, Castro-Giraldez, & Fito, 2013), dehydration (Feng, Tang, & Cavalieri, 2002) and osmotic dehydration of apple (Castro-Giraldez, Fito, & Fito, 2011) and kiwi (Castro-Giraldez, Fito, Dalla Rosa, et al., 2011) and also for determination of apple maturity (Castro-Giraldez, Fito, Chenoll, et al., 2010). Traffano-Schiffo, Castro-Giraldez, Colom, and Fito (2015) analyze the viability of monitoring drying meat processes by using dielectric properties measurements at microwaves frequencies. The authors showed that there was a direct relationship between the dielectric loss factor with respect to sample surface and the number of water molecules at 20 GHz, obtaining also the desorption isotherm. This relationship can also be used for determining food product composition by applying dielectric spectroscopy. Iaccheri et al. (2015) studied water features in green and roasted coffee beans by dielectric spectroscopy.

Talens, Castro-Giraldez, and Fito (2015) analyzed the dielectric loss factor at 2.45 GHz (most commonly used MW frequency in Europe) of orange peel dried by hot air-microwave drying in order to quantify the amount of microwave energy that was absorbed and transformed into heating energy. This calorific energy was absorbed by the water molecules because at 2.45 GHz the relaxations phenomena were caused by the induction of polar molecules like

water. Fava et al. (2013) also applied microwave drying to citrus by-products in order to dehydrate the final product for further conversion into dietary fiber with optimal microbial, sensory and technological properties.

In microwave assisted drying processes, the knowledge of dielectric properties and parameters that affect their values allows to predict moisture content, water activity and drying kinetics (Barba & d'Amore, 2012). The aim of this work was to develop and to determine dielectric tools to predict the moisture and water activity by using dielectric spectroscopy and sorption isotherms of orange peel dried by microwave power coupled with hot air drying.

## 2. Materials and methods

Oranges (*Citrus sinensis* (L.) Osbeck var Washington Navel) were bought from a local supermarket in Valencia (Spain). Orange peels were used for the experiments. 60 orange peel cylinders (20 mm diameter and 3 mm thickness) were cut with a core borer. A diagram of the experimental procedure is shown in Fig. 1.

Samples were subjected to hot air drying (HAD) and microwave assisted air drying (HAD + MW) (Fig. 2), using a specially designed MW-air drying oven (Martín, Martínez-Navarrete, Chiralt, & Fito, 2003) with maximum output 2000 W at 2450 MHz, connected to a computer where temperature of ambient air and hot air, relative humidity of ambient air and incident and reflected microwave energy could be registered. In order to measure incident and reflected energy a directional coupler with power meter was also connected to the computer. The modified microwave oven presents two parallel connected lines (diameter = 105 mm), one for the application of hot air and another for the generation and application of the microwaves. Drying chamber has a Teflon chamber (edge = 100 mm) and a mode stirrer to ensure a homogeneous microwave distribution. Different variables were measured in drying chamber for process control: hot air temperature by a Pt100

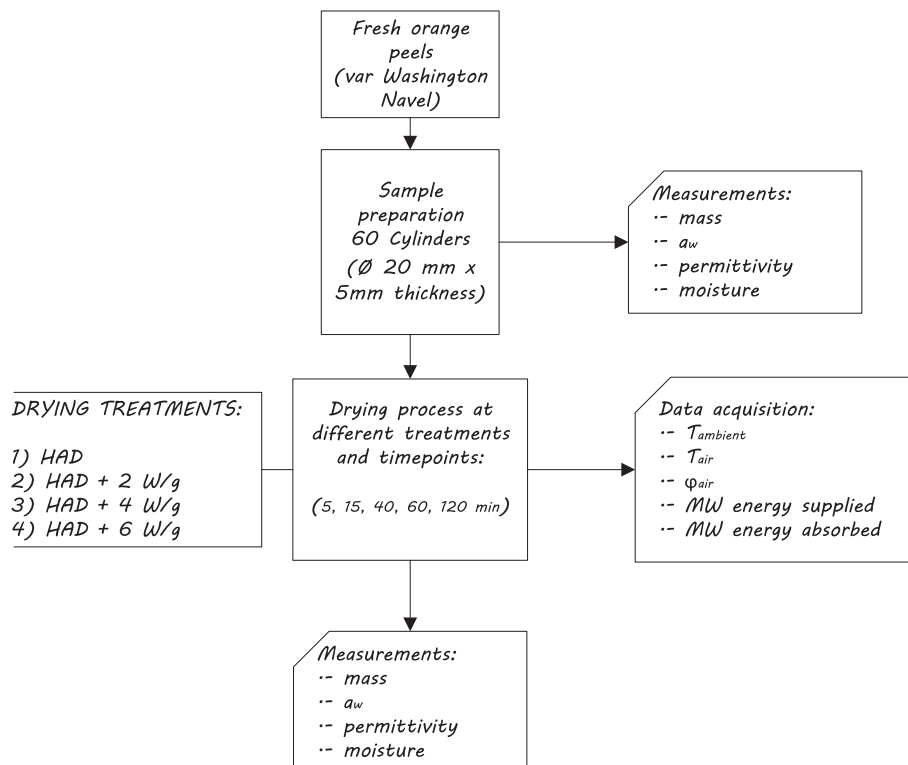


Fig. 1. Schematic diagram of the experimental procedure.

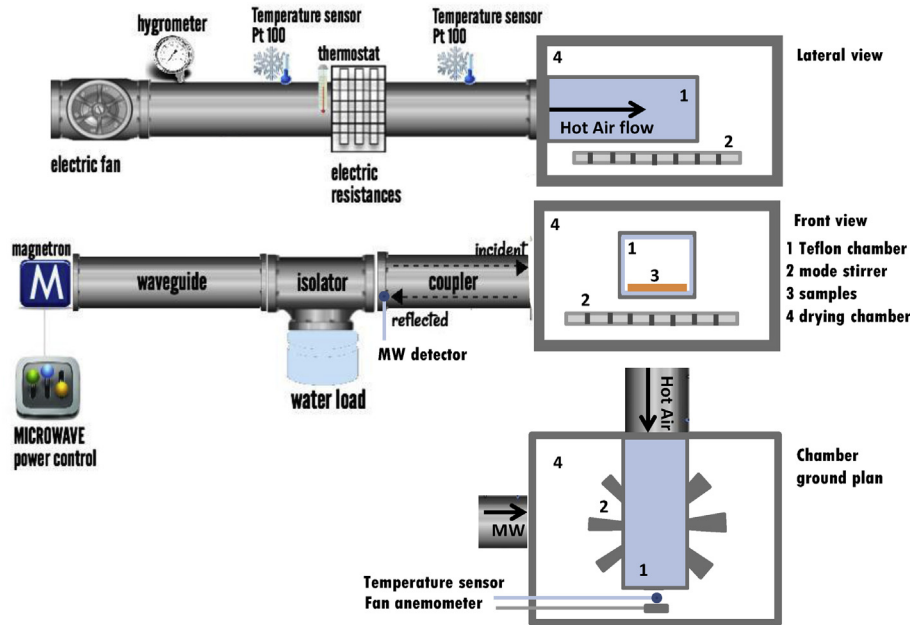


Fig. 2. Schematic description of the laboratory equipment used to dry samples.

thermocouple and air velocity by a fan anemometer.

For the experiments, air velocity was 2.5 m/s, air temperature 55 °C and the MW energy was 0, 2, 4 or 6 W/g. The MW power (W/g) was referred to the initial mass of sample. The microwave energy applied (determined by using the IEC-test) was selected such that samples did not burn during drying.

Orange peel samples were placed with flavedo side up on the dryer grid to facilitate mass transfer. Four drying experiments were carried out (HAD, HAD + 2 W/g, HAD + 4 W/g and HAD + 6 W/g). Three orange peels samples were used for each drying time (5, 15, 40, 60 and 120 min) per treatment. These 3 samples were removed at each time point and were equilibrated at 25 °C for 5 h in aqua-lab® disposable sample cups sealed with parafilm®, in order to eliminate the concentration profiles in samples. The next three samples were then placed in the drier.

Samples weight was determined by a precision balance Mettler Toledo AB304-S (precision  $\pm 0.001$  g). Surface water activity was determined by a dew point hygrometer Decagon Aqualab®, series 3 TE (precision  $\pm 0.003$ , dimensionless) (Decagon Devices Inc., Washington, USA). Measurements were done in structured samples

(not minced), thus  $a_w$  obtained was considered surface  $a_w$ . Water content of representative fresh orange peels and 120 min dried samples was determined by drying in a vacuum oven at 60 °C until constant weight was reached (AOAC method 934.06, 2000). The moisture content of the sample at intermediate drying stages was calculated from the weigh lost during drying.

The permittivity was measured with an Agilent 85070E open-ended coaxial probe connected to an Agilent E8362B Vector Network Analyser. The system was calibrated by using three different types of loads: air, short-circuit and 25 °C ultra pure (Milli®-Q) water. Once the calibration was made, 25 °C ultra pure (Milli®-Q) water was measured again to check calibration suitability. Permittivity was measured by placing the probe on the surface of the samples. All determinations were made from 500 MHz to 20 GHz. The measurements were made in triplicate.

The desorption isotherm was fitted following the GAB model using Equation (1) (van den Berg & Bruin, 1981):

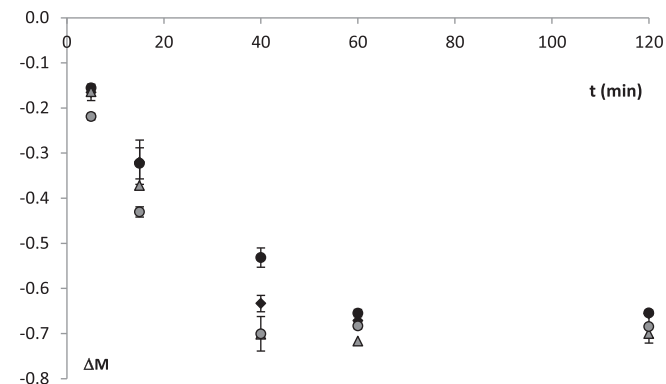


Fig. 3. Mass variation of orange peel treated by different drying treatments: ● HAD, ◆ HAD + 2 W/g, ▲ HAD + 4 W/g, ● HAD + 6 W/g. Data represent means and standard deviation of experiments performed in triplicate.

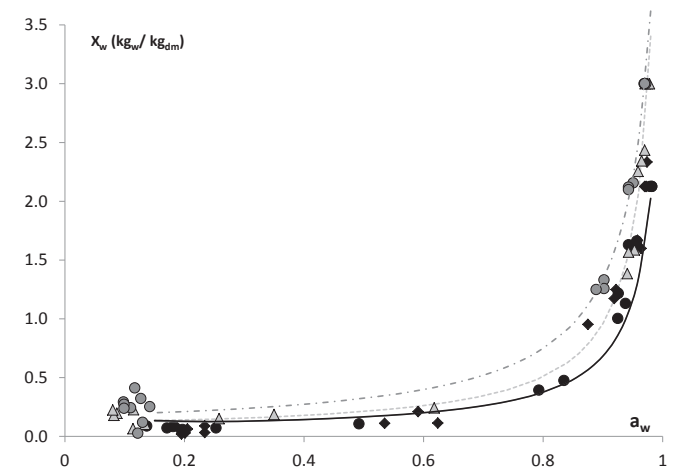


Fig. 4. Sorption isotherm of orange peel treated by different drying treatments: experimental points ● HAD, ◆ HAD + 2 W/g, ▲ HAD + 4 W/g, ● HAD + 6 W/g; and GAB model — HAD, - - HAD + 2 W/g, - · - HAD + 4 W/g, · · · HAD + 6 W/g.

**Table 1**

Estimated GAB parameters ( $X_{W0}$ , C and K) and correlated coefficient ( $R^2$ ) of GAB model for desorption isotherms of orange peel dried by hot air (HAD) and hot air coupled with microwaves (HAD + MW).

Drying treatment	GAB Parameters			$R^2$
	$X_{W0}$ (kg <sub>w</sub> /kg <sub>dm</sub> )	C	K	
HAD	0.080	22.33	0.98	0.9342
HAD + 2 W/g	0.080	18.90	0.98	0.9182
HAD + 4 W/g	0.105	70.33	0.99	0.9197
HAD + 6 W/g	0.165	153.04	0.97	0.8493

$$X_W = \frac{X_{W0} C a_w}{(1 - K a_w)(1 + (C - 1)a_w)} \quad (1)$$

Where:  $X_w$  corresponds to the orange peel moisture (kg<sub>w</sub>/kg<sub>dm</sub>),  $X_{W0}$  is the monomolecular moisture layer (kg<sub>w</sub>/kg<sub>dm</sub>), C is the energy constant and K is an empirical parameter, both dimensionless (Maroulis, Tsami, Marinou-Kouris, & Saravacos, 1988).

GAB model was using a non-linear regression with the Statgraphics Centurion XVI Software (Statgraphics, Virginia, U.S.A.).

### 3. Results and discussion

Mass variation of samples during the drying process can be obtained by the following equation:

$$\Delta M = \frac{M^t - M^0}{M^0} \quad (2)$$

Where M represents the mass of the sample (kg), the superscript t represents the process time, being 0 the initial time. The mass variation can be observed in Fig. 3.

A faster mass reduction can be observed in microwave drying treatments increasing with microwave energy. At 5 and 15 min, very significant differences ( $p \leq 0.01$ ) were found between

HAD + 6 W/g and the rest of the treatments. At 40 min, significant differences ( $p \leq 0.05$ ) were appreciated among HAD and 2 W/g and the rest of the treatments. No differences between 4 and 6 W/g were appreciated mainly because a low level of mass was reached caused by water loss; the low level of moisture reached decreases the effect of MW power. After 60 min of drying, treatments converged to the threshold of the thermodynamic properties of dry air ( $\Delta\mu_w^i = 0$  or  $a_w^{\text{sample}} \approx \phi^{\text{air}}$ ).

Fig. 4 shows the sorption isotherms obtained for each drying treatment (experimental points) and the GAB model applied for each treatment. GAB parameters are shown in Table 1.

In order to explain the variation of the GAB parameters with physical sense in the different drying treatments, the permittivity in range of the microwaves was analyzed.

Permittivity in microwave range was measured in fresh and treated samples after 5, 15, 40, 60 and 120 min of drying. In Fig. 5 it can be observed the dielectric spectra of the fresh and dried orange peels treated at different microwave power energies.

In the range of microwaves, the interaction of the electric field with biological tissue produces two main dispersions,  $\gamma$ -dispersion and ionic conductivity. The first one mainly represents the induction and orientation phenomena of water, and the second one, represents the conductivity of the electrolytes and weak organic acids. In this figure it is possible to observe at high frequencies (above 1 GHz) the common shape of samples with liquid phase, decreasing the permittivity values with the water losses throughout the treatment. Below 1 GHz, in fresh samples, a negative slope of loss factor shows the low ionic strength of the weak organic acids. Ionic conductivity decreases with the drying treatment caused by the limitation of the movement of weak organic acids due to the loss of liquid phase.

Since there is a progressive loss of liquid phase during the drying process, the dielectric loss factor decreases with time. Therefore it is possible to relate the permittivity at high frequency (dipolar effect) with the quantity of water molecules in equilibrated samples (Traffano-Schiffo et al., 2015). The water molecules can be calculated with the following equation (Eq. (3)).

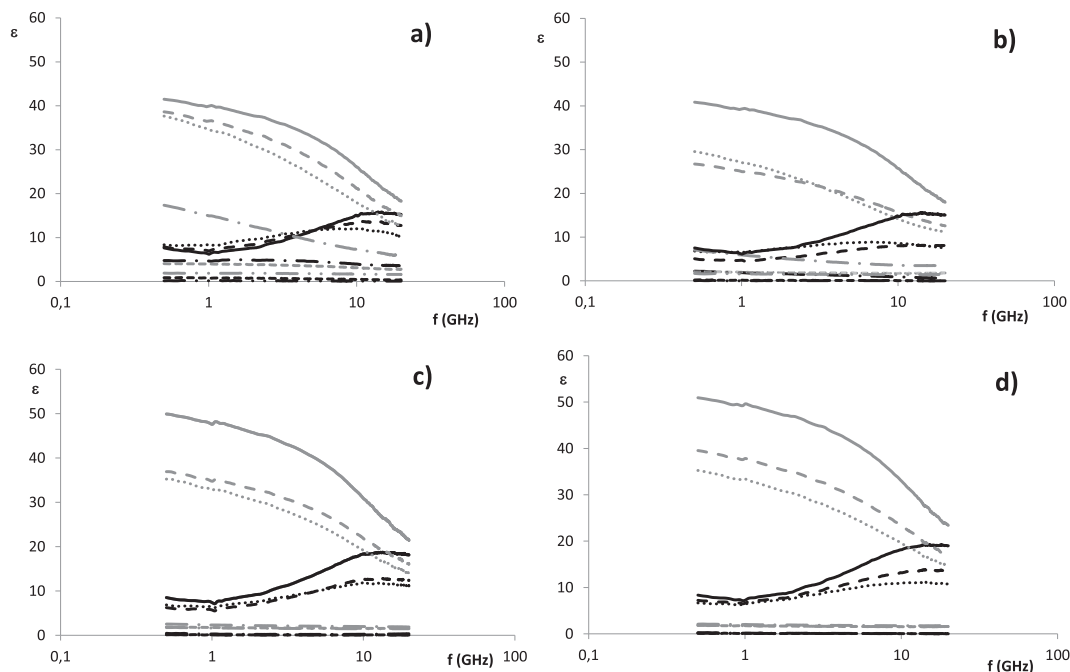


**Fig. 5.** Permittivity ( $\epsilon$ ) spectra of orange peels after 0 min —, 5 min ---, 15 min ···, 40 min -·-, 60 min □□ and 120 min -·-·- of drying by different treatments (a) HAD, (b) HAD + 2 W/g, (c) HAD + 4 W/g, (d) HAD + 6 W/g. Gray lines represent the dielectric constant ( $\epsilon'$ ) and black lines represent the loss factor ( $\epsilon''$ ).

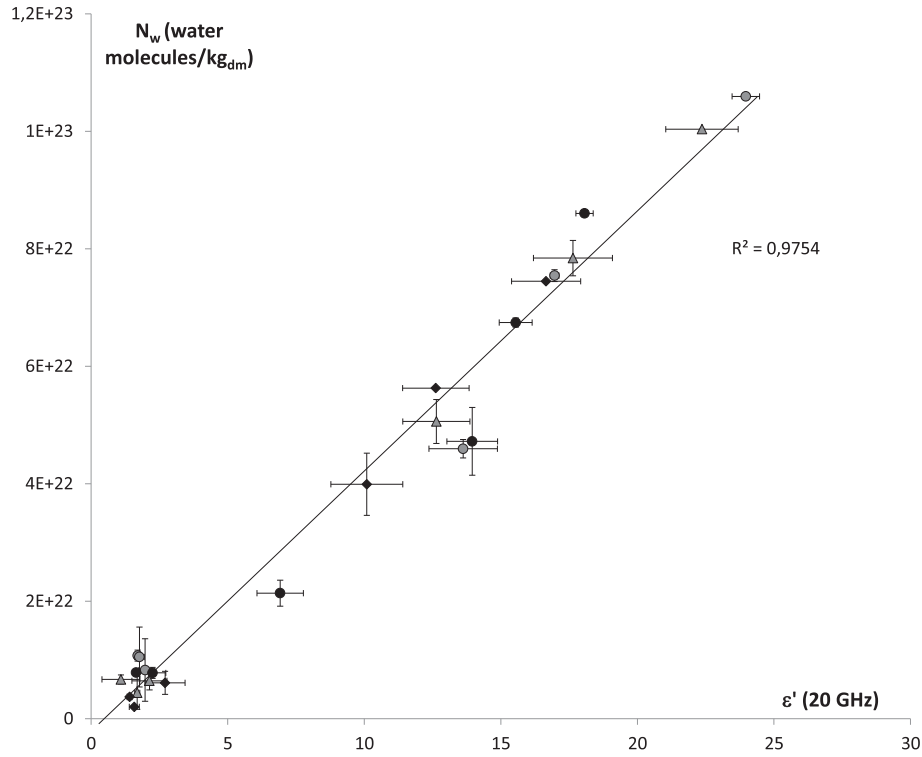


Fig. 6. Relation between number of water molecules ( $N_w$ ) and the dielectric constant at 20 GHz of orange peels dried by different hot air-microwave treatments. Where: ● HAD, ◆ HAD + 2 W/g, ▲ HAD + 4 W/g, ● HAD + 6 W/g.

$$N_w = \frac{X_w N_A}{Mr_w} \quad (3)$$

Where  $N_w$  represents the water molecules (number of water molecules in dry basis),  $X_w$  is the moisture in dry basis ( $\text{kg}_w/\text{kg}_{dm}$ ),  $N_A$  the Avogadro constant ( $6.022 \cdot 10^{23} \text{ mol}^{-1}$ ) and  $Mr_w$  the molar mass of water ( $18 \text{ kg}_w/\text{kmol}_w$ ).

Fig. 6 shows the linear relation between number of water molecules related with the dry matter (water molecules/ $\text{kg}_{dm}$ ) and the dielectric constant at 20 GHz, frequency close to the dipolar relaxation effect.

If the moisture in dry basis explains the dielectric constant, it is possible to develop a dielectric isotherm to predict the water

activity in dried samples using equation (4) adapted from GAB model, where  $\epsilon'$  (20 GHz) represents the dielectric constant at 20 GHz, close to the water relaxation frequency,  $\epsilon'_0$  is the minimum value of the dielectric constant and  $C_d$  and  $K_d$  are empirical constants (dimensionless).

$$\epsilon'(20\text{GHz}) = \frac{\epsilon'_0 C_d a_w}{(1 - K_d a_w)(1 + (C_d - 1)a_w)} \quad (4)$$

Fig. 7 shows the dielectric isotherms obtained by adapting the GAB model to dielectric approach previously explained. This figure shows that the dielectric isotherm of HAD treatment is above the rest of treatments. The dielectric isotherm equation (equation (4)) applied to the different treatments obtained well fittings (for HAD a  $R^2$  0.8960 for HAD + 2 W/g a  $R^2$  0.9494, for HAD + 4 W/g a  $R^2$  0.8833 and for HAD + 6 W/g a  $R^2$  0.9988).

The  $K_d$  parameters were similar in all treatments and the average value was  $0.95 \pm 0.02$ . In order to compare the dielectric

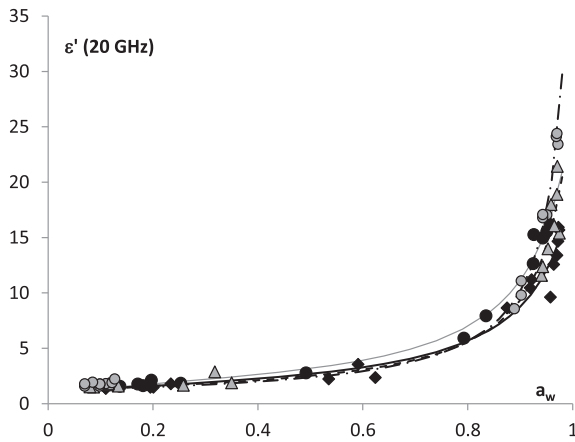


Fig. 7. Dielectric isotherm at 20 GHz of orange peel treated by different drying treatments: experimental timepoints ● HAD, ◆ HAD + 2 W/g, ▲ HAD + 4 W/g, ● HAD + 6 W/g and calculated model — HAD, — HAD + 2 W/g, - - - HAD + 4 W/g, - - - HAD + 6 W/g.

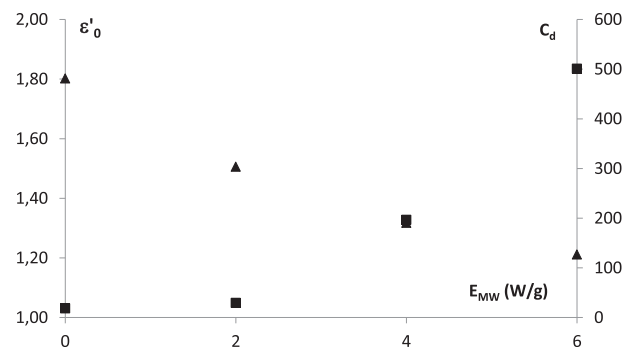


Fig. 8. Dielectric isotherm parameters (adapted to GAB model) of orange peels dried by different hot air-microwave treatments:  $\epsilon'_0$  ▲ and  $C_d$  ■.

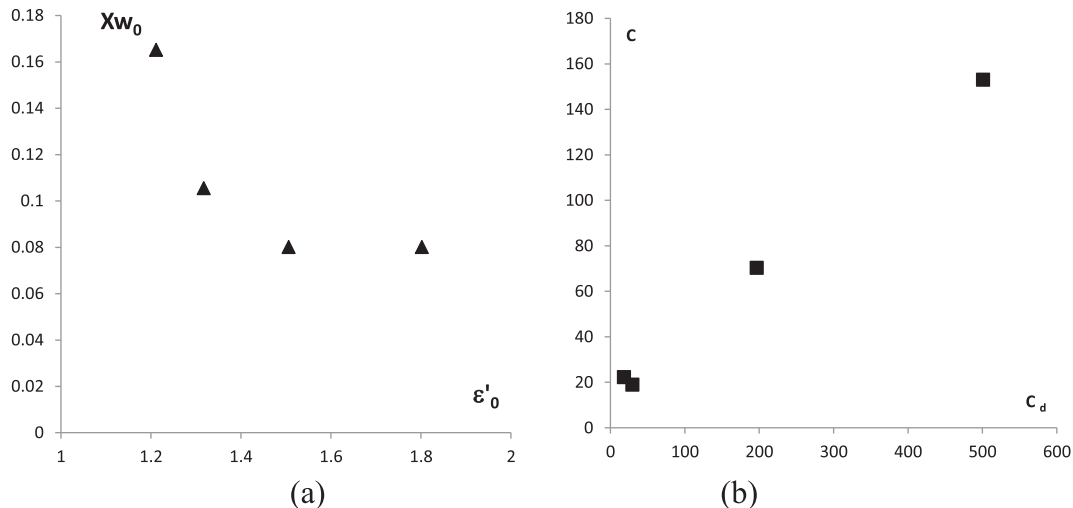


Fig. 9. Comparison of the GAB parameters and dielectric isotherm parameters. (a) Relation between  $X_{w0}$  and  $\epsilon'_0$  and (b) Relation between C and  $C_d$  parameters.

isotherms, the parameters of equation (4) have been compared in Fig. 8.

Fig. 8 relates in primary axis the minimum dielectric constant with the treatments, where it is possible to observe a homogeneous decrease with the MW power. Minimum value of dielectric constant at 20 GHz ( $\gamma$ -dispersion) represents the induction effect of the minimum quantity of adsorbed water or the monomolecular moisture layer. Therefore, the application of MW power in the dehydration process produces a decrease in the induction of the adsorbed water molecules ( $\epsilon'_0$ ). This decrease could be caused by the diminution of the  $X_{w0}$  (reduction of molecules adsorbed) or the increase of the isosteric heat (increase in the adsorption energy). Fig. 8 shows, in secondary axis, the parameter  $C_d$  with the treatments. The parameter  $C_d$  is a modification of the C parameter of the GAB model, this parameter explains the isosteric heat or the adsorption energy of the monomolecular moisture layer. In this figure, parameter  $C_d$  increases with MW power.

Fig. 9a and b relate the GAB parameters with the dielectric isotherm parameters. Fig. 9a shows the relation between the  $X_{w0}$  and the  $\epsilon'_0$ , where it is possible to observe that the minimum value of  $X_{w0}$  corresponds with the maximum value of  $\epsilon'_0$ , in opposite sense the Fig. 9b shows the linear relation between C and  $C_d$ , increasing together with the MW power. Therefore, during a drying process, the application of MW power produces an increase of the isosteric heat or adsorption energy of the monomolecular layer, improving the surface tension of samples and thus the hygroscopicity, explaining the reduction of the  $\epsilon'_0$  independently of the quantity of the water molecules adsorbed.

#### 4. Conclusions

It was possible to develop a dielectric isotherm technique by adapting the GAB model to predict the water activity in dried orange peel by using  $\epsilon'$  (20 GHz). The physical meaning of the dielectric isotherm parameters ( $\epsilon'_0$  and  $C_d$ ) was studied. The value of  $\epsilon'_0$  at 20 GHz ( $\gamma$ -dispersion) represents the induction effect of the minimum quantity of adsorbed water or the monomolecular moisture layer. The parameter  $C_d$  is related with isosteric heat or the adsorption energy of the monomolecular moisture layer, as well as the C parameter of the GAB model. The application of MW power produced an increase of the isosteric heat or adsorption energy of the monomolecular layer, improving the surface tension of samples and thus the hygroscopicity, explaining the reduction of the  $\epsilon'_0$

independently of the quantity of the water molecules adsorbed.

#### Acknowledgments

The authors would like to acknowledge the Basque Government for the financial support of the project (LasaiFood). The author Marta Castro-Giráldez wants to thanks to the UPV Postdoctoral Program (PAID-10-14) from Universidad Politécnica de Valencia for their support. The authors acknowledge the financial support from the Spanish Ministerio de Ciencia e Innovación throughout the project AGL2011-30096.

#### References

- Barba, A. A., & d'Amore, M. (2012). *Relevance of dielectric properties in microwave assisted processes, microwave materials characterization*. In I. Prof. S. Costanzo (Ed.).
- van den Berg, C., & Bruin, S. (1981). *Water activity and its estimation in food systems: theoretical aspects*. In L. B. R. F. Stewart (Ed.), *Water activity: influences on food quality* (pp. 1–61). Academic Press.
- Castro-Giraldez, M. (2010). *Estudio de los espectros dieléctricos para el control de calidad de alimentos*. Thesis, Universidad Politécnica de Valencia. (UPV3351).
- Castro-Giraldez, M., Balaguer, N., Hinarejos, E., & Fito, P. J. (2014). Thermodynamic approach of meat freezing process. *Innovative Food Science & Emerging Technologies*, 23(0), 138–145. <http://dx.doi.org/10.1016/j.ifset.2014.03.007>.
- Castro-Giraldez, M., Fito, P. J., Chenoll, C., & Fito, P. (2010). Development of a dielectric spectroscopy technique for the determination of apple (Granny Smith) maturity. *Innovative Food Science & Emerging Technologies*, 11(4), 749–754. <http://dx.doi.org/10.1016/j.ifset.2010.08.002>.
- Castro-Giraldez, M., Fito, P. J., Dalla Rosa, M., & Fito, P. (2011). Application of microwaves dielectric spectroscopy for controlling osmotic dehydration of kiwifruit (*Actinidia deliciosa* cv Hayward). *Innovative Food Science & Emerging Technologies*, 12(4), 623–627. <http://dx.doi.org/10.1016/j.ifset.2011.06.013>.
- Castro-Giraldez, M., Fito, P. J., & Fito, P. (2010). Application of microwaves dielectric spectroscopy for controlling pork meat (*Longissimus dorsi*) salting process. *Journal of Food Engineering*, 97(4), 484–490. <http://dx.doi.org/10.1016/j.jfoodeng.2009.11.005>.
- Castro-Giraldez, M., Fito, P. J., & Fito, P. (2011). Application of microwaves dielectric spectroscopy for controlling long time osmotic dehydration of parenchymatic apple tissue. *Journal of Food Engineering*, 104(2), 227–233. <http://dx.doi.org/10.1016/j.jfoodeng.2010.10.034>.
- Fava, F., Zanzaroli, G., Vannini, L., Guerzoni, E., Bordoni, A., Viaggi, D., & Brendle, H.-G. (2013). New advances in the integrated management of food processing by-products in Europe: sustainable exploitation of fruit and cereal processing by-products with the production of new food products (NAMASTE EU). *New Biotechnology*, 30(6), 647–655. <http://dx.doi.org/10.1016/j.nbt.2013.05.001>.
- Feng, H., Tang, J., & Cavalieri, R. P. (2002). Dielectric properties of dehydrated apples as affected by moisture and temperature. *Transactions of the Asae*, 45(1), 129–135.
- Iaccheri, E., Laghi, L., Cevoli, C., Berardinelli, A., Ragni, L., Romani, S., et al. (2015). Different analytical approaches for the study of water features in green and roasted coffee beans. *Journal of Food Engineering*, 146(0), 28–35. <http://dx.doi.org/10.1016/j.jfoodeng.2015.05.001>.

- [org/10.1016/j.jfoodeng.2014.08.016](http://dx.doi.org/10.1016/j.jfoodeng.2014.08.016).
- Kent, M., Peymann, A., Gabriel, C., & Knight, A. (2002). Determination of added water in pork products using microwave dielectric spectroscopy. *Food Control*, 13(3), 143–149. [http://dx.doi.org/10.1016/S0956-7135\(01\)00066-4](http://dx.doi.org/10.1016/S0956-7135(01)00066-4).
- Lyng, J. G., Zhang, L., & Brunton, N. P. (2005). A survey of the dielectric properties of meats and ingredients used in meat product manufacture. *Meat Science*, 69(4), 589–602. <http://dx.doi.org/10.1016/j.meatsci.2004.09.011>.
- Maroulis, Z. B., Tsami, E., Marinos-Kouris, D., & Saravacos, G. D. (1988). Application of the GAB model to the moisture sorption isotherms for dried fruits. *Journal of Food Engineering*, 7(1), 63–78. [http://dx.doi.org/10.1016/0260-8774\(88\)90069-6](http://dx.doi.org/10.1016/0260-8774(88)90069-6).
- Martín, M. E., Martínez-Navarrete, N., Chiralt, A., & Fito, P. (2003). Diseño y construcción de una instalación experimental para el estudio de la cinética de secado combinado por aire caliente y microondas. *Alimentación equipos y tecnología*, 22(181), 101–107.
- Pozar, D. M. (2012). *Microwave engineering: wiley India*.
- Talens, C., Castro-Giraldez, M., & Fito, P. (June 16–18, 2015). *Thermodynamic modeling of orange peel dried by Hot Air-Microwave*. 49th Annual Microwave Power Symposium (IMPI 49), book of Proceedings (p. 36). San Diego, California, USA.
- Traffano-Schiffo, M. V., Castro-Giraldez, M., Colom, R. J., & Fito, P. J. (2015). Study of the application of dielectric spectroscopy to predict the water activity of meat during drying process. *Journal of Food Engineering*, 166, 285–290.
- Velázquez-Varela, J., Castro-Giraldez, M., & Fito, P. J. (2013). Control of the brewing process by using microwaves dielectric spectroscopy. *Journal of Food Engineering*, 119(3), 633–639. <http://dx.doi.org/10.1016/j.jfoodeng.2013.06.03>.



## Release of thymol from poly(lactic acid)-based antimicrobial films containing kenaf fibres as natural filler



Intan S.M.A. Tawakkal<sup>a</sup>, Marlene J. Cran<sup>b,\*</sup>, Stephen W. Bigger<sup>b</sup>

<sup>a</sup> College of Engineering and Science, Victoria University, PO Box 14428, Melbourne, 8001, Australia

<sup>b</sup> Institute for Sustainability and Innovation, Victoria University, PO Box 14428, Melbourne, 8001, Australia

### ARTICLE INFO

#### Article history:

Received 7 July 2015

Received in revised form

6 November 2015

Accepted 7 November 2015

Available online 11 November 2015

#### Keywords:

Active packaging

Antimicrobial

Thymol

Migration

Poly(lactic acid)

### ABSTRACT

The migration of thymol, a natural antimicrobial (AM) substance, from poly(lactic acid) (PLA) films containing 300 g/kg kenaf fibres into food simulants is reported. Neat PLA and PLA/kenaf films containing 100 g/kg thymol were prepared *via* melt blending and heat pressing and were placed in contact with 150 mL/L and 950 mL/L ethanol/water mixtures at different temperatures. First-order kinetics, diffusion modelling and Fick's law modelling were used to describe the release. The release rate of thymol into 950 mL/L ethanol/water at different temperatures displays Fickian behavior with diffusion coefficient values between 1 and  $100 \times 10^{-11} \text{ m}^2 \text{ s}^{-1}$  with close to 100% of thymol being released. The release rate of thymol is temperature dependent and is affected by the percentage of ethanol in the simulant. In the case of neat PLA and PLA/kenaf films, a faster release occurred in 950 mL/L ethanol/water than in 150 mL/L ethanol/water with the composite film exhibiting a higher diffusion coefficient in each case.

© 2015 Elsevier Ltd. All rights reserved.

### 1. Introduction

Controlled release systems in food packaging have experienced considerable growth recently due to developments in active packaging concepts such as the integration of antioxidant (AOX) and/or antimicrobial (AM) substances into packages in order to improve the quality and safety of food products. In these systems, low molecular mass compounds and/or substances are released from the package in a slow and controlled manner to maintain an adequate concentration of the substance in the packed food for a certain period of time. The release of substances that involve migration is the result of diffusion, dissolution and equilibrium processes (Crank, 1979). There are various factors that influence the migration of a substance from the packaging material including the film fabrication method, the volatility and polarity of the substance, the chemical interaction between the substance and polymer chains, hydrophobicity and hydrophilicity of the polymer as well as food properties and composition (Suppakul, Miltz, Sonneveld, & Bigger, 2003).

Poly(lactic acid) (PLA) is a polyester synthesized from the renewable, bio-derived, monomer lactic acid and can be used as AM

films and/or membranes for a different range of applications (Auras, Harte, & Selke, 2004; Karami, Rezaeian, Zahedi, & Abdollahi, 2013). This GRAS (Generally Recognized As Safe) grade polymer can be used in contact with food and fabricated *via* conventional processing procedures (Jamshidian, Tehrani, Imran, Jacquot, & Desobry, 2010). The use of fillers in combination with PLA has been widely studied with aims to improve physicomechanical properties, reduce production costs and enhance biodegradability. Naturally derived additives or fillers such as starch and cellulose can be combined with PLA and other active agents such as AM and AOX compounds. For example, Hwang *et al.* (2013) studied the migration of  $\alpha$ -tocopherol and resveratrol from poly(L-lactic acid) (PLLA)/starch blend films into ethanol and found that the neat PLLA containing  $\alpha$ -tocopherol had a lower release rate than the PLLA/starch blend films at 43 °C in 100% ethanol simulant with diffusivity coefficients of  $89 \times 10^{-11}$  and  $282 \times 10^{-11} \text{ cm}^2 \text{ s}^{-1}$  respectively. A similar trend was observed for resveratrol, a non-volatile AOX compound with diffusion rate of  $25 \times 10^{-11} \text{ cm}^2 \text{ s}^{-1}$  in neat PLLA and  $40 \times 10^{-11} \text{ cm}^2 \text{ s}^{-1}$  in the PLA/starch films. Fortunati *et al.* (2012) prepared PLA AM films with 50 g/kg microcrystalline cellulose (MCC) and 10 g/kg silver nanoparticles by extrusion and injection molding techniques. The PLA films with silver nanoparticles and MCC had greater AM activity against *Escherichia coli* due to the presence of MCC; however, it had less AM activity than PLA films with silver nanoparticles. Although there are examples of

\* Corresponding author.

E-mail address: [marlene.cran@vu.edu.au](mailto:marlene.cran@vu.edu.au) (M.J. Cran).

the controlled release of AM and AOX substances from PLA materials (Busolo & Lagaron, 2013; Fernandez, Soriano, Hernandez-Munoz, & Gavara, 2010; Hwang et al., 2013; Iniguez-Franco et al., 2012; Llana-Ruiz-Cabello et al., 2015), few reports have combined PLA with natural fibres in order to control the release of active substances from composite films.

Antimicrobial packaging systems can be categorised as either migratory or non-migratory systems. In the former, AM substances migrate from the packaging material into the headspace of the package and onto the food surface, whereas in the latter, AM substances are immobilised onto the packaging material which is placed in direct contact with the foodstuff to facilitate its activity (Han, 2003). The integration of PLA with AM substances has been investigated by a number of researchers (Del Nobile et al., 2009; Jin, 2010; Qin et al., 2015; Rhim, Hong, & Ha, 2009). Of the reported studies, many have investigated the inhibition of targeted microorganisms with little attention having been devoted to studying the release rate from the active systems. This might be due to the preponderance of non-volatile and/or immobilised AM substances (e.g. nisin, chitosan, lysozyme and peptide) incorporated into PLA films rather than volatile AM substances (Green, Fulghum, & Nordhaus, 2011; Rhim, 2013; Tawakkal, Cran, Miltz, & Bigger, 2014b). Several AM substances have been incorporated directly into polymers including a range of volatile plant extracts such as basil, thymol, linalool, methyl cinnamate and cava-crol (Cran, Rupika, Sonneveld, Miltz, & Bigger, 2010; Del Nobile, Conte, Incoronato, & Panza, 2008; Fernández-Pan, Maté, Gardrat, & Coma, 2015; Rubilar et al., 2013; Suppakul, 2004; Suppakul, Sonneveld, Bigger, & Miltz, 2011; Tawakkal, Cran, & Bigger, 2015).

Thymol, an essential oil extract that has GRAS status, can be used in contact with food products and like other volatile AM substances, the migration of this substance into real food products is complex. In some studies, active AM films containing thymol were evaluated *in vitro* and *in vivo* against a wide spectrum of microorganisms such as bacteria, mould and yeast (Kuorwel, Cran, Sonneveld, Miltz, & Bigger, 2011; Wu et al., 2014). In a recent study by Petchwattana and Naknaen (2015), extruded films of poly(-butylene succinate) (PBS) containing thymol demonstrated AM activity against *E. coli* and *Staphylococcus*. Moreover, the release rate of thymol from the PBS films into 950 mL/L ethanol/water was found to be  $5.9 \times 10^{-14} \text{ m}^2 \text{ s}^{-1}$ . Ramos, Beltrán, Peltzer, Valente, and Garrigós (2014a) reported that the migration of thymol from polypropylene (PP) films into 950 mL/L ethanol at 40 °C conformed to Fick's law with a diffusion coefficient of  $1.0 \times 10^{-14} \text{ m}^2 \text{ s}^{-1}$ . In general, an AM substance can be released into a food simulant by swelling-controlled release with three main steps involved: (i) the absorption of fluid (penetrant) from the food simulant which leads to the swelling effect of the polymer, (ii) the active substance molecule being dissolved or dispersed in the polymeric matrix and (iii) the active substance migrating to the food simulant (Del Nobile & Conte, 2013).

The quantification of volatile AM substances in active films is an important consideration given that high pressure, shear forces and temperatures are required for film processing. According to Raouche, Mauricio-Iglesias, Peyron, Guillard, and Gontard (2011), a higher temperature of ca. 160–190 °C was needed to process PLA using extrusion which may easily degrade and evaporate the volatile AM substance during thermal processing. The retention of volatile additives such as thymol in PLA film was found to be approximately 70–80% after thermal fabrication (Tawakkal et al., 2015). Such retention percentages were significantly higher than those found in polyolefin film systems containing similar volatile additives. For example, Ramos, Jiménez, Peltzer, and Garrigós (2012) reported much lower retention of thymol and carvacrol (ca. 25–45% respectively) in PP formulations. The marked

reduction in the retention of these additives in polyolefin films upon thermal processing may result from the reduced compatibility between the polymer matrix and the natural additives as well as the processing parameters such as temperature, time and screw rotation (Del Nobile et al., 2009).

There are clearly many examples of the release of a wide range of AM substances from homopolymers such as PLA. However, little attention has been devoted to evaluating the release of AM agents from ternary composite systems, particularly taking into account the possible swelling of polymeric materials immersed in food simulants as well as the effects of natural fillers on the release rate. Moreover, the release of volatile AM substances from polymeric materials also has been restricted to mainly hydrophobic and moderate hydrophilic polymeric matrices (Buonocore, Del Nobile, Panizza, Corbo, & Nicolais, 2003; Herath, 2009). The aim of the current work was therefore to investigate the release of a naturally derived AM agent from a novel ternary system comprised of PLA, kenaf fibers and thymol. In particular, the release of thymol from PLA and PLA/kenaf composite and its diffusion kinetics were studied.

## 2. Experimental section

### 2.1. Materials

Poly(lactic acid) (7001D Ingeo™; specific gravity 1.24; melting temperature 152.5 °C (Tawakkal, Cran, & Bigger, 2014a)) was obtained from NatureWorks LLC, USA. Mechanically separated kenaf fibre (bast) was purchased from Ecofibre Industries, Australia. Thymol (T0501, purity of 99.5%) was purchased from Sigma Aldrich Pty. Ltd., Australia. Sodium hydroxide and acetic acid were purchased from Merck Chemicals, Australia. Un-denatured ethanol was purchased from Chem-Supply Pty Ltd., Australia. Isooctane (2,2,4-trimethylpentane, 36006) was purchased from Sigma Aldrich, Australia.

### 2.2. Production of PLA/kenaf/thymol films

Kenaf fibres were soaked in 0.05 g/mL sodium hydroxide for 2 h at room temperature. The fibres were then filtered and washed with distilled water prior to acid treatment to affect neutralization by adding a few drops of acetic acid. The fibres were then filtered, washed and rinsed with distilled water to remove the acetic acid, the latter being confirmed using a pH meter (inoLab® pH7110, WTW GmbH, Germany). Finally, the fibres were dried overnight in an oven at 105 °C. Prior to mixing, PLA resin and kenaf fibres were further dried in an oven at 60 °C overnight before mixing with thymol at 100 g/kg concentration.

The film samples were prepared firstly by melt-blending the components in an internal mixer (Haake PolyLab OS, Germany) at 155 °C for 8 min and 50 rpm followed by heat pressing, according to a method previously reported by Tawakkal, Cran, and Bigger (2014a). The PLA was added to the mixer first and the kenaf and thymol were introduced once the polymer was molten in order to avoid unnecessary loss of thymol. In the current study, a 300 g/kg loading of kenaf fibres was used to produce the PLA/kenaf composite that has moderate flexibility as well as high strength and stiffness compared with unfilled PLA which is more suitable for the production of rigid packaging applications (Tawakkal, Cran, & Bigger, 2014a). In a second step, a laboratory press (L0003, IDM Instrument Pty. Ltd., Australia) was used to prepare films. The samples were preheated at 150 °C for 3 min without applying pressure until the material melted, and then pressed at the same temperature for 2 min under a force of 20 kN before quench cooling to 30 °C under pressure. The average thicknesses of the pressed

neat PLA and PLA/kenaf films incorporated with thymol were  $0.19 \pm 0.03$  and  $0.25 \pm 0.05$  mm respectively. The film thickness was measured using a hand-held micrometer (Hahn & Kolb, Stuttgart, Germany).

### 2.3. Quantification of thymol in PLA and PLA/Kenaf films

One gram of film sample was cut into pieces ( $0.25 \text{ cm}^2$ ) and immersed in a round bottom flask containing 150 mL of isooctane for solid–liquid extraction. Isooctane was used as it promotes the swelling of the polymer and a typical reflux extraction was performed at  $100^\circ\text{C}$  for 4–5 h to extract thymol from the films. The quantification was achieved with a gas chromatography (GC) instrument (Varian 8200C<sub>x</sub>) equipped with a fused silica capillary column (DB5;  $30 \text{ m} \times 0.25 \text{ mm}$  i.d.; thickness  $0.25 \mu\text{m}$ ; J & W Scientific, USA). The conditions applied in the GC instrument were as follows: injected volume:  $1.0 \mu\text{L}$ , initial column temperature:  $80^\circ\text{C}$ ; heating rate:  $5^\circ\text{C min}^{-1}$  up to  $120^\circ\text{C}$ , held at this temperature for an additional 5 min; injector temperature:  $250^\circ\text{C}$ ; FID detector temperature:  $300^\circ\text{C}$ ; flow rate:  $2 \text{ mL min}^{-1}$ ; splitting; carrier gas: nitrogen. Standard solutions of thymol in isooctane at concentrations from  $0.05$  to  $1.0 \text{ mg mL}^{-1}$  were prepared and used to produce a calibration curve. The experiments were performed in triplicate. The retention of thymol in the neat PLA and PLA/kenaf films following thermal processing was 73% and 62% respectively as reported by Tawakkal et al. (2015). The loss of thymol observed in the present study for composite films seems to be at an acceptable level compared to petroleum-based (polyolefin) films containing volatile additives.

### 2.4. Migration of thymol into food simulants

The release of thymol from neat PLA and PLA/kenaf films into aqueous food simulants was studied at different temperatures. The release was examined via a total immersion migration test (EC, 1997) using 950 and 150 mL/L ethanol/water. Ethanol is commonly used as food simulant to investigate the migration of AM substances from the PLA matrix. The 950 and 150 mL/L ethanol/water simulants are fatty and aqueous food simulants respectively. The sorption of ethanol by the PLA matrix may lead to the creation of voids and/or swelling of the matrix where it can penetrate the PLA chains and promote the migration of the active substance (Mascheroni, Guillard, Nalin, Mora, & Piervigiovanni, 2010). In the case of the 950 mL/L ethanol/water simulant the experiments were performed at 30, 40, 50 and  $60^\circ\text{C}$  and for the 150 mL/L ethanol/water simulant experiments were performed at 60, 65, 75 and  $83^\circ\text{C}$ . In the latter experiments, the test temperatures were higher than recommended in the standard methods (EC, 1997) in order to accelerate the migration of thymol. Studying the release rates of thymol from the neat PLA and PLA/kenaf films by using fatty and aqueous food simulants is important in order to assess the *in vitro* and *in vivo* AM activity of these systems against targeted microorganisms.

Samples of film weighing ca. 0.5–0.6 g were immersed in 100 mL of simulant in a three-neck round bottom flask with the ratio of simulant volume per area film being ca.  $2.7\text{--}4.7 \text{ mL cm}^{-2}$ . The flask was immersed in an oil bath that was placed on a magnetic stirrer heating plate and the simulant was gently agitated using magnetic stirring at 60 rpm. The flask was connected to a condenser and the stirring speed and temperature were fixed and monitored throughout the experiment. The amount of AM agent released from the films was monitored until equilibrium was attained. A 0.2 mL sample of the simulant solution was collected periodically during the experiment and  $1 \mu\text{L}$  aliquots were injected into the GC. The quantification of thymol in all simulants was

performed using the same method and calibration curve described in the previous section. The thymol quantification was performed in triplicate.

### 2.5. Data analysis

The migration of thymol from the PLA and PLA/kenaf composite films was analysed using three data analysis treatments: (i) overall kinetics, (ii) diffusion models in accordance with Cran et al. (2010) and Kuorwel, Cran, Sonneveld, Miltz, and Bigger (2013) and (iii) Fick's diffusion law model.

#### 2.5.1. Overall kinetics analysis

By considering the overall diffusion process to be a single process that obeys first-order kinetics, equations describing the migration of an additive from a polymeric film into simulant with time have been described by Miltz (1987) and Crank (1979). The release of the AM agent into the simulant was initially analysed for its fit to a first order kinetics model. In the case of a first-order system, Equation (1) applies:

$$\ln\left(1 - \frac{m_t}{m_\infty}\right) = -k_1 t \quad (1)$$

where  $m_t$  is the mass of additive released from the film at time  $t$ ,  $m_\infty$  is the amount of additive released from the film at equilibrium ( $t = \infty$ ) and  $k_1$  is the first-order rate constant. From Equation (1), a plot of  $\ln(1 - m_t/m_\infty)$  versus time should be a straight line with a slope of  $-k_1$ . The apparent first-order rate constants were calculated using Equation (1) and the initial release rates,  $v_0$ , of the AM agent were calculated using Equation (2) (Kuorwel et al., 2013):

$$v_0 = m_\infty k_1 \quad (2)$$

#### 2.5.2. Diffusion model

In the diffusion model, the release of the AM agent from the film into the simulant is considered in two stages, namely the short-term and the long-term (Crank, 1979; Miltz, 1987). This diffusion model is based on a geometry whereby the release is considered to occur from both sides of the film. The diffusion data were analysed using Equation (3) for short-term migration and the corresponding rate constants were calculated using Equation (4) for long-term migration.

Short-term migration is defined as the time for which  $m_t/m_\infty < 0.6$ :

$$\frac{m_t}{m_\infty} = 4 \left( \frac{Dt}{\pi l^2} \right)^{\frac{1}{2}} \quad (3)$$

where  $D$  is the diffusion coefficient and  $l$  is the thickness of the film. A plot of  $m_t/m_\infty$  versus  $t^{1/2}$  should yield a straight line from which the diffusion coefficient can be obtained.

For long-term migration  $m_t/m_\infty > 0.6$  and Equation (4) applies:

$$\frac{m_t}{m_\infty} = 1 - \left( \frac{8}{\pi^2} \right) \exp\left( -\frac{\pi^2 Dt}{l^2} \right) \quad (4)$$

#### 2.5.3. Fick's law model

The diffusion coefficient of the AM agent can be determined from its release versus time data, by fitting these data to Fick's second law. Equation (5) can be derived from Fick's second law in the case of one dimensional diffusion from a limited volume of film that is in contact with an infinite volume of solution (Crank, 1979).

$$\frac{m_t}{m_\infty} = 1 - \frac{8}{\pi^2} \sum_{m=0}^{\infty} \frac{1}{(2m+1)^2} \exp\left[\frac{-D(2m+1)^2\pi^2 t}{l^2}\right] \quad (5)$$

#### 2.5.4. Diffusion activation energy

The effect of temperature on the release rate of the AM agent was modeled in accordance with the Arrhenius equation (Suppakul 2004):

$$D = D_0 \exp\left(\frac{E_a}{RT}\right) \quad (6)$$

where  $D$  is the diffusion coefficient,  $D_0$  is the pre-exponential factor,  $E_a$  is the activation energy for the diffusion process,  $R$  is the ideal gas constant, and  $T$  is the absolute temperature.

### 3. Results and discussion

#### 3.1. Release of thymol into simulants

Fig. 1(a) and (b) show plots of the mass fraction  $m_t/m_\infty$  versus time,  $t$  and the overall kinetic analysis for the release of thymol from neat PLA and PLA/kenaf films into 950 mL/L ethanol/water at the four temperatures studied. The thymol release reached equilibrium within ca. 9 h at the lowest temperature of 30 °C (Fig. 1(a)). A similar observation was found for PLA containing resveratrol where the system achieved equilibrium after ca. 14 h using the same food simulant at 33 °C (Soto-Valdez, Auras, & Peralta, 2011). In comparison, the times required to achieve the equilibrium concentration of thymol in different polymeric systems with the same food simulant at 40 °C were found to be 50 h for PBS/thymol films and 150 h for PP/thymol films (Ployetchara, Suppakul, Atong, & Pechyen, 2014; Ramos, Beltrán, Peltzer, Valente, et al., 2014a) and 2 h for starch/thymol films in isoctane at 35 °C (Kuorwel et al.,

2013). In the current work, it was found that increasing the temperature to say 60 °C, increases the release rate of thymol and equilibrium was attained within 1.4 h. At the end of these experiments, ca. 87–100% and 82–95% of the thymol was released from the neat PLA and PLA/kenaf films respectively into 950 mL/L ethanol/water over the temperature range of 30–60 °C.

The initial release rates and the overall rate constants for the release of thymol that were calculated from the data in Fig. 1(b) are presented in Table 1. For both neat PLA and PLA/kenaf films, the initial release rates and the overall rate constants for thymol release into 950 mL/L ethanol/water consistently increased with an increase in temperature from 30 to 60 °C. This is consistent with the findings of Kuorwel et al. (2013) where an increase in temperature was found to have a significant effect on the migration of the additive from the film. From the results in Table 1 a similar observation can also be made in the case of the 150 mL/L ethanol/water simulant over the range of the four temperatures studied. However, in the latter case the rates are significantly lower compared with the 950 mL/L ethanol/water case. The experimental results were further analyzed by using the diffusion model in which the short-term and the long-term migration periods were considered.

Fig. 2(a) and (b) show the respective plots of  $m_t/m_\infty$  versus  $t^{1/2}$  for the short-term release of thymol and  $\ln(1 - m_t/m_\infty)$  versus  $t$  for the long-term release of thymol from the neat PLA and PLA/kenaf films into 950 mL/L ethanol/water at 30 °C. A similar behavior was observed at each of the temperatures that were studied and the linearity of the plots suggests that the data conform well to the diffusion model given in Equation (3) for short-term release. Values of the apparent diffusion coefficient at each of the various temperatures were determined from the gradients of these plots and are also presented in Table 1. For the long-term release, the linearity of the  $\ln(1 - m_t/m_\infty)$  versus  $t$  plots also confirms the data reliably fit the model presented in Equation (4). Indeed, all results exhibited good linear correlation with correlation coefficients ( $r^2$  values)

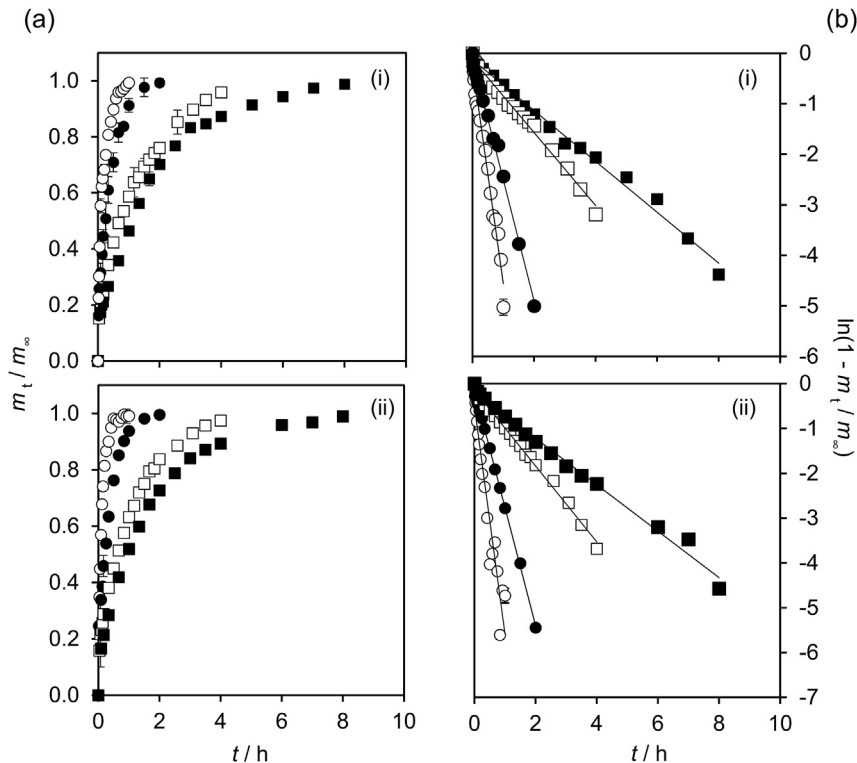
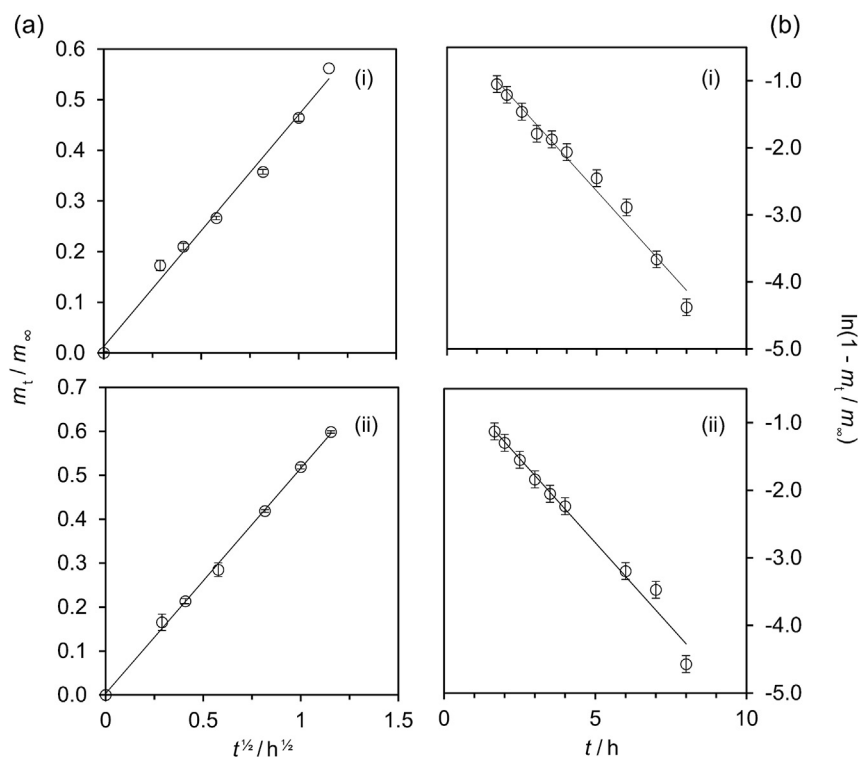


Fig. 1. Plots of: (a) the mass fraction  $m_t/m_\infty$  versus  $t$ , and (b)  $\ln(1 - m_t/m_\infty)$  versus  $t$  for the release of thymol from: (i) PLA and (ii) PLA/kenaf films into 950 mL/L ethanol/water at: ■ 30 °C, □ 40 °C, ● 50 °C and ○ 60 °C where  $m_t$  is the mass of thymol released from the film at time  $t$  and  $m_\infty$  is the amount of thymol released from the film at equilibrium ( $t = \infty$ ).

**Table 1**  
Kinetic and the diffusion analyses for the release of thymol from PLA and PLA/kenaf composite films.

	Temperature/ $^{\circ}\text{C}$	First order kinetic analysis			Diffusion analysis				Fickian diffusion		
				SSE <sup>a</sup>	Short term		SSE	Long term		SSE	SSE
		$v_0 \times 10^5/\text{g s}^{-1}$	$k_1 \times 10^5/\text{s}^{-1}$		$D \times 10^{12}/\text{m}^2 \text{s}^{-1}$			$k_2 \times 10^5/\text{s}^{-1}$			
950 mL/L ethanol/water											
PLA	30	5.2	14.0	0.220	41	0.003	13.7	0.197	0.29	0.010	
	40	7.3	20.1	0.111	93	0.002	20.0	0.057	0.60	0.060	
	50	30.2	66.6	0.147	236	0.004	69.2	0.082	1.63	0.099	
	60	49.9	119.6	0.569	1124	0.002	117.8	0.451	5.75	0.373	
PLA/kenaf	30	5.4	14.4	0.254	90	0.001	13.8	0.194	0.56	0.001	
	40	7.9	23.5	0.100	162	0.003	24.1	0.060	1.14	0.079	
	50	38.8	73.2	0.036	443	0.002	73.2	0.009	3.10	0.065	
	60	46.1	141.0	3.686	1340	0.000	124.4	2.720	10.05	0.498	
150 mL/L ethanol/water											
PLA	60	0.8	4.8	0.086	28	0.001	5.2	0.053	0.17	0.006	
	65	2.7	9.3	0.089	43	0.010	8.9	0.066	0.24	0.026	
	75	12.3	46.0	0.325	132	0.003	45.9	0.248	0.66	0.072	
	83	15.4	58.8	0.486	255	0.004	61.1	0.048	2.62	0.278	
PLA/kenaf	60	1.8	7.0	0.395	75	0.002	7.2	0.327	0.40	0.010	
	65	2.6	9.6	0.392	102	0.001	9.6	0.329	0.52	0.022	
	75	10.0	36.7	0.460	195	0.001	35.9	0.373	0.90	0.098	
	83	14.1	57.3	0.101	454	0.004	67.1	0.004	3.39	0.189	

<sup>a</sup> SSE: Sum of squared errors.



**Fig. 2.** Plots of: (a) mass fraction  $m_t/m_{\infty}$  versus  $t^{1/2}$  and (b)  $\ln(1 - m_t/m_{\infty})$  versus  $t$  for the release of thymol from: (i) PLA and (ii) PLA/kenaf films into 950 mL/L ethanol/water at  $30^{\circ}\text{C}$  where  $m_t$  is the mass of thymol released from the film at time  $t$  and  $m_{\infty}$  is the amount of thymol released from the film at equilibrium ( $t = \infty$ ).

greater than 0.97.

The results in Table 1 confirm that the diffusion coefficients of thymol from the neat PLA and PLA/kenaf films into the 950 mL/L ethanol/water increase with increasing temperature. As expected, the diffusion rates of the composite films are higher than those obtained for the neat PLA films. This may be attributed in part to the presence of the kenaf fibre filler in the polymer matrix that creates voids thereby enabling the release of thymol from the film. These findings are consistent with the result obtained for the retention of thymol in a previous study whereby following processing the

composite films were found to retain less thymol than neat PLA film (Tawakkal et al., 2015). It is important to note that the values of the  $D$  parameter found for the neat PLA and PLA/kenaf films containing thymol are one order of magnitude higher than those observed for active low-density polyethylene (LDPE), PBS and PP containing a similar AM agent and using 950 mL/L ethanol/water simulant (Cran et al., 2010; Ploypetchara et al., 2014; Ramos, Beltrán, Peltzer, Valente, et al., 2014a). Moreover, and as expected, active PLA films containing a non-volatile and thermally stable agent (i.e. resveratrol) prepared by Soto-Valdez et al. (2011) exhibit diffusion

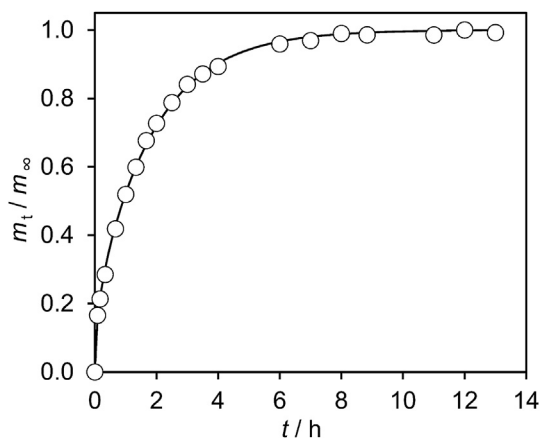


**Fig. 3.** Plot of the mass fraction  $m_t/m_\infty$  versus  $t$  for the release of thymol from the PLA film into 950 mL/L ethanol/water at 30 °C fitted using the Fick's law model where  $m_t$  is the mass of thymol released from the film at time  $t$ , and  $m_\infty$  is the amount of thymol released from the film at equilibrium ( $t = \infty$ ).

coefficients that are one order of magnitude lower than those of PLA films containing a volatile AM agent such as thymol. Similar trends in the diffusion coefficients of thymol were observed for the neat PLA and PLA/kenaf films when immersed in the 150 mL/L ethanol/water simulant. However, the diffusion coefficients for the films immersed in the 150 mL/L ethanol/water simulant were consistently lower than those pertaining to the 950 mL/L ethanol/water simulant. The observed decrease in the diffusivity may be explained by the lack of affinity between thymol and water that leads to the limited solubility of thymol in water. Moreover, PLA is a hydrophobic polymer but ethanol is sufficiently non-polar to facilitate the swelling of the PLA matrix (Sato, Gondo, Wada, Kanehashi, & Nagai, 2013), dissolve the thymol and release it into the bulk of the simulant. According to Manzanarez-López, Soto-Valdez, Auras, and Peralta (2011), ethanol is also an aggressive solvent for PLA which can penetrate into PLA chains and release the active substance.

The lower concentration of ethanol in the 150 mL/L ethanol/water simulant may lead to a slight extent of swelling as well as hydrolysis of the PLA (Manzanarez-López et al., 2011). Interestingly this slight swelling of the PLA matrix appears to be more significant than the swelling effect of the kenaf fibres. The PLA/kenaf composites are semi-hydrophilic materials due to the presence of kenaf fibres that act as a hydrophilic filler. One may therefore expect the rate of diffusion of thymol from these composite systems (PLA/kenaf films) to increase as the water content of the simulant increases. Taib, Ramarad, Mohd Ishak, and Todo (2009) prepared PLA/kenaf composites containing polyethylene glycol (PEG) and reported that when the composite was immersed into the water, the fibres absorb water leading to expansion of the fibres. Such an effect may create internal stress in the adjacent matrix and resulting in the formation of microcracks. However, the rate of diffusion of thymol from the PLA/kenaf films was in fact found to be lower in the 150 mL/L ethanol/water simulant than in the 950 mL/L ethanol/water simulant. It can therefore be suggested that a complex and strong interaction exists between the kenaf, PLA and thymol in the composite systems. The PLA matrix may act as a coating agent to the kenaf fibre filler, preventing the water from swelling the kenaf fibres and releasing thymol that is associated with the fibres. Such an interaction between the PLA, kenaf fibre and thymol was reported previously where these composite systems were studied using Fourier transform infrared (FTIR) spectroscopic and thermogravimetric (TG) analyses (Tawakkal et al., 2015). In that study, the activation energy for the thermal release of thymol, using a 3D

diffusion kinetic model, was found to be 46 kJ mol<sup>-1</sup> in the case of neat PLA containing thymol and 65 kJ mol<sup>-1</sup> for the PLA/kenaf composite system.

Fick's second law model was also used to calculate the diffusion coefficient by minimizing the sum of the squared errors (SSE) of the measured and calculated value (see Table 1). To determine the fit of the experimental data, Equation (5) was used and a non-linear regression function was applied to the data. Fig. 3 shows plots of  $m_t/m_\infty$  versus  $t$  for the diffusion of thymol from PLA/kenaf film into 950 mL/L ethanol/water at 30 °C where the data have been fitted using the Fick's second law model. The satisfactory fit of the experimental data suggests that the diffusion kinetics of thymol into 950 mL/L ethanol/water from the composite can also be adequately described by Fick's model. The SSE values for all the release models studied are also presented in Table 1. In general, the short-term diffusion model presents the best fit for the release kinetics with the lowest SSE values for all systems studied. This is followed by the Fickian diffusion model, with the first order model and long-term diffusion models showing some higher SSE values for some systems.

Using the diffusion coefficients obtained from the diffusion model, the effect of temperature on the diffusion coefficient for the release of thymol into 950 and 150 mL/L ethanol/water was determined and Arrhenius plots of the data are shown in Fig. 4. The activation energy for the diffusion process,  $E_a$ , was calculated from the slope of the  $\ln(D)$  versus  $1/T$  plot in each case (see Fig. 4) in accordance with the Arrhenius equation (see Equation (6)). The activation energies for the release of thymol from the neat PLA and PLA/kenaf films were found to be: 90.6 and 76.2 kJ mol<sup>-1</sup> in 950 mL/L ethanol/water and 98.7 and 84.8 kJ mol<sup>-1</sup> in 150 mL/L ethanol/water respectively. Significant differences were therefore found to exist amongst the  $E_a$  values for these active neat PLA and PLA/kenaf films immersed in the 950 and 150 mL/L ethanol/water simulants.

The  $E_a$  values for the neat PLA films are significantly higher than those found for PLA/kenaf films and this is attributed mainly to the strong interaction between the PLA and thymol that presumably is not as strong in the presence of the kenaf filler. Furthermore, the  $E_a$  values increase with an increase in water content of the simulant and this is consistent with the observations made in relation to the diffusion coefficients discussed above (see Table 1). The  $E_a$  values obtained in the present study are all considerably lower than those reported elsewhere for the diffusion of butylated hydroxytoluene (BHT) from PLA/BHT films into 950 mL/L ethanol/water which was 164.7 kJ mol<sup>-1</sup> (Ortiz-Vazquez, Shin, Soto-Valdez, & Auras, 2011). This significant difference may be explained by the difference in molecular interaction and hydrogen bonding that exists between the polymeric matrix and the AM additive in these systems (Kuorwel et al., 2013). As expected, the trend in  $E_a$  values for the various systems when calculated using the Fick's law model are consistent with those calculated by the diffusion model given that the latter model has been derived from the former model. The activation energies using the Fick's law model for the release of thymol from the neat PLA and PLA/kenaf films were found to be: 83.3 and 80.9 kJ mol<sup>-1</sup> in 950 mL/L ethanol/water and 118.5 and 96.3 kJ mol<sup>-1</sup> in 150 mL/L ethanol/water respectively. These slight differences in the  $E_a$  values that were obtained using the different models might be due to the use of the diffusion coefficients derived from the short-term experimental data in the construction of the Arrhenius plot.

### 3.2. Film appearance

Fig. 5 shows the images of neat PLA and PLA/kenaf films after the release of thymol into 150 and 950 mL/L ethanol/water at the different temperatures studied. A considerable change in color for

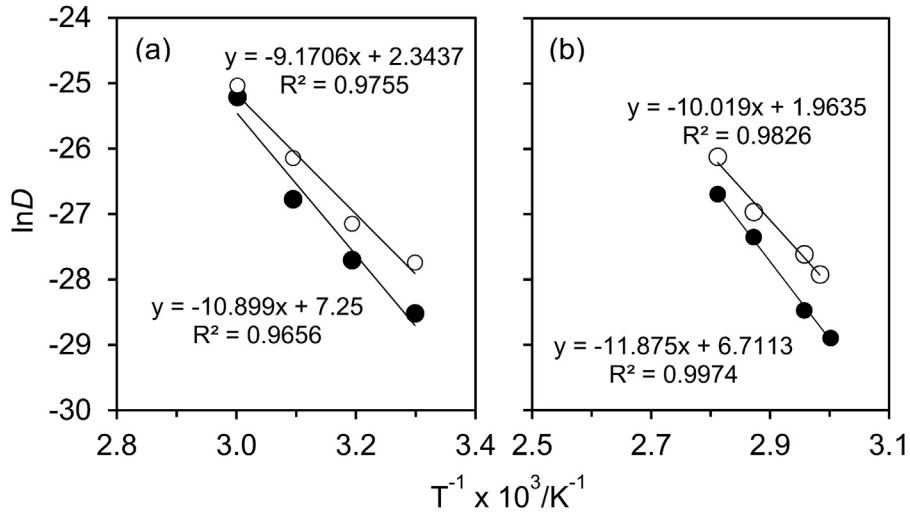


**Fig. 4.** Arrhenius plots of  $\ln(D)$  versus  $1/T$  for the release of thymol into: (a) 950 mL/L ethanol/water and (b) 150 mL/L ethanol/water from: ● PLA film and ○ PLA/kenaf film where  $D$  is the diffusion coefficient and  $T$  is the absolute temperature.

the neat PLA and PLA/kenaf films was observed after the release experiments. These color changes are due to the effects of temperature as well as the presence of water in the simulants. The color is observed to change from clear to opaque for the neat PLA immersed in 150 mL/L ethanol/water with an increase in opacity with increasing temperature. A similar observation was made in the case of the 950 mL/L ethanol/water simulant. The opacity of materials may be attributed to a polymer hydrolytic degradation

process which can be related to crystallization of the PLA matrix as well as moisture absorption. The water molecules diffuse through the films, promoting hydrolysis leading to the formation of low molecular weight degradation by-products (Ramos, Beltrán, Peltzer, Dominici, et al., 2014b). In addition, color changes from brown to light brown are also observed for the composites immersed in 150 and 950 mL/L ethanol/water. For the PLA/kenaf composites immersed in 150 mL/L ethanol/water, the PLA

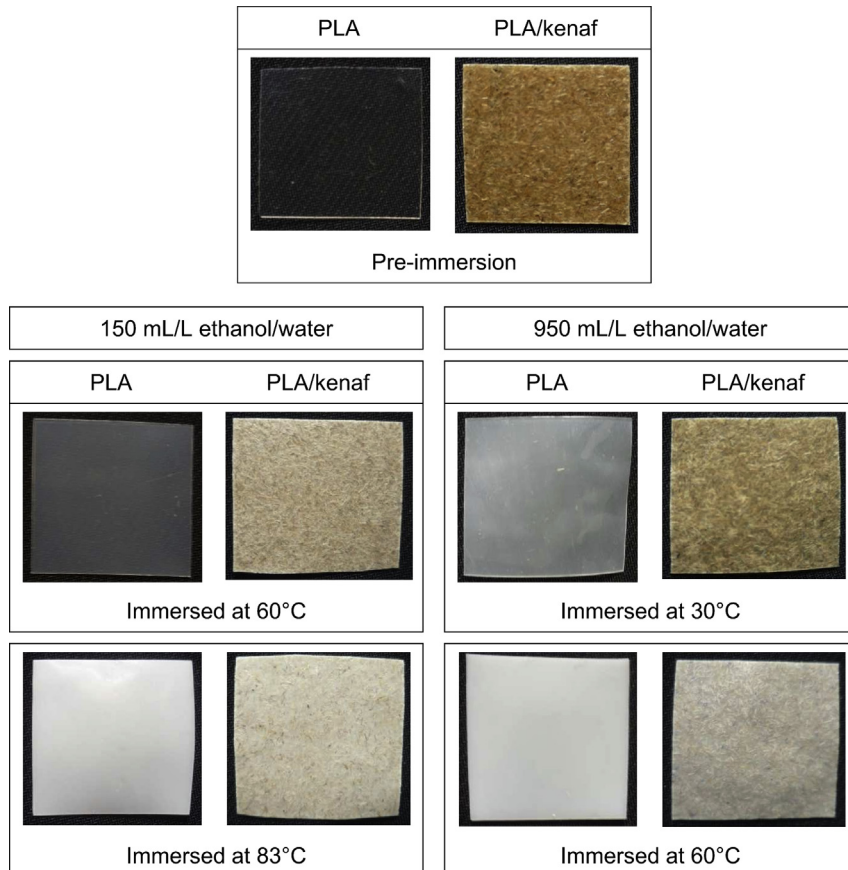


**Fig. 5.** Images of PLA and PLA/kenaf films after the release of thymol into 150 and 950 mL/L ethanol/water simulants at different temperatures.

surrounding the fibres dissolved or delaminated from the film surface revealing the kenaf fibers and this effect was less apparent in the 950 mL/L ethanol/water simulant.

#### 4. Conclusions

The results of this study suggest that thymol is readily released from neat PLA and PLA/kenaf films into 150 and 950 mL/L ethanol/water simulants and the process can be described by an overall first-order kinetics model that can be used to determine the initial release rate. The short- and long-term diffusion models also adequately describe the release of thymol from these systems and the results are consistent with those obtained using a Fick's law analysis approach. The diffusion coefficient data suggest that the addition of the kenaf filler to the PLA matrix facilitates the release of thymol from the matrix and that the diffusion follows an Arrhenius relationship with temperature. Furthermore, an increase in polarity of the simulant that results from an increase in its water content decreases the propensity of thymol to be released from the composite system. Nonetheless, it is apparent that active PLA/kenaf composites containing natural AM agents such as thymol are potential candidates to be explored further for use as active packaging systems. Such systems have the advantage of being derived from natural sources, contain a naturally-derived AM agent and, as such, are expected to be more susceptible to biodegradation than their synthetically-based counterparts.

#### Acknowledgments

The authors gratefully acknowledge the Ministry of Education Malaysia and Universiti Putra Malaysia (UPM) for providing the PhD scholarship for Intan S. M. A. Tawakkal. We would like to acknowledge Mr. Mike Allan and the technical staff from the Royal Melbourne Institute Technology, Melbourne for their invaluable assistance with the preparation of the composite samples.

#### References

- Auras, R., Harte, B., & Selke, S. (2004). An overview of polylactides as packaging materials. *Macromolecular Bioscience*, 4(9), 835–864.
- Buonocore, G. G., Del Nobile, M. A., Panizza, A., Corbo, M. R., & Nicolais, L. (2003). A general approach to describe the antimicrobial agent release from highly swellable films intended for food packaging applications. *Journal of Controlled Release*, 90(1), 97–107.
- Busolo, M. A., & Lagaron, J. M. (2013). Antimicrobial biocomposites of melt-compounded polylactide films containing silver-based engineered clays. *Journal of Plastic Film and Sheeting*, 29(3), 290–305.
- Crank, J. (1979). *The mathematics of diffusion*. London: Oxford University Press.
- Cran, M. J., Rupika, L. A., Sonneveld, K., Miltz, J., & Bigger, S. W. (2010). Release of naturally derived antimicrobial agents from LDPE films. *Journal of Food Science*, 75(2), 126–133.
- Del Nobile, M. A., & Conte, A. (2013). *Bio-based packaging materials for controlled release of active compounds packaging for food preservation*. pp. 91–107. Springer.
- Del Nobile, M. A., Conte, A., Buonocore, G. G., Incoronato, A. L., Massaro, A., & Panza, O. (2009). Active packaging by extrusion processing of recyclable and biodegradable polymers. *Journal of Food Engineering*, 93(1), 1–6.
- Del Nobile, M. A., Conte, A., Incoronato, A. L., & Panza, O. (2008). Antimicrobial efficacy and release kinetics of thymol from zein films. *Journal of Food Engineering*, 89(1), 57–63.
- EC. (1997). Commission directive 97/48/EC of 29 July 1997 amending for the second time council directive 82/711/EEC laying down the basic rules necessary for testing migration of the constituents of plastic materials and articles intended to come into contact with foodstuffs (97/48/EC). *Official Journal of the European Communities*, L, 222, 210–215.
- Fernández-Pan, I., Maté, J. I., Gardrat, C., & Coma, V. (2015). Effect of chitosan molecular weight on the antimicrobial activity and release rate of carvacrol-enriched films. *Food Hydrocolloids*, 51, 60–68.
- Fernandez, A., Soriano, E., Hernandez-Munoz, P., & Gavara, R. (2010). Migration of antimicrobial silver from composites of polylactide with silver zeolites. *Journal of Food Science*, 75(3), 186–193.
- Fortunati, E., Armentano, I., Iannoni, A., Barbale, M., Zaccheo, S., Scavone, M., ... Kenny, J. M. (2012). New multifunctional poly(lactide acid) composites: mechanical, antibacterial, and degradation properties. *Journal of Applied Polymer Science*, 124(1), 87–98.
- Green, J.-B. D., Fulghum, T., & Nordhaus, M. A. (2011). A review of immobilized antimicrobial agents and methods for testing. *Biointerphases*, 6(4), MR13–MR28.
- Han, J. H. (2003). Antimicrobial food packaging. In R. Ahvenainen (Ed.), *Novel food packaging techniques* (pp. 50–65). Cambridge: Woodhead Publishing Ltd.
- Herath, L. A. S. R. (2009). *Development and evaluation of low density polyethylene-based antimicrobial food packaging films containing natural agents*. PhD Dissertation. Melbourne: Victoria University.
- Hwang, S. W., Shim, J. K., Selke, S., Soto-Valdez, H., Matuana, L., Rubino, M., et al. (2013). Migration of  $\alpha$ -tocopherol and resveratrol from poly(L-lactic acid)/starch blends films into ethanol. *Journal of Food Engineering*, 116(4), 814–828.
- Iniguez-Franco, F., Soto-Valdez, H., Peralta, E., Ayala-Zavala, J. F., Auras, R., & Gamez-Meza, N. (2012). Antioxidant activity and diffusion of catechin and epicatechin from antioxidant active films made of poly(l-lactic acid). *Journal of Agricultural and Food Chemistry*, 60(26), 6515–6523.
- Jamshidian, M., Tehrani, E. A., Imran, M., Jacquot, M., & Desobry, S. (2010). Poly-lactic acid: production, applications, nanocomposites, and release studies. *Comprehensive Review Food Science and Food Safety*, 9(5), 552–571.
- Jin, T. (2010). Inactivation of *Listeria monocytogenes* skim milk and liquid egg white by antimicrobial bottle coating with polylactic acid and nisin. *Journal of Food Science*, 75(2), 83–88.
- Karami, Z., Rezaei, I., Zahedi, P., & Abdollahi, M. (2013). Preparation and performance evaluations of electrospun poly( $\epsilon$ -caprolactone), poly(lactic acid), and their hybrid (50/50) nanofibrous mats containing thymol as an herbal drug for effective wound healing. *Journal of Applied Polymer Science*, 129(2), 756–766.
- Kuorwel, K. K., Cran, M. J., Sonneveld, K., Miltz, J., & Bigger, S. W. (2011). Antimicrobial activity of natural agents against *Saccharomyces cerevisiae*. *Packaging Technology and Science*, 24(5), 299–307.
- Kuorwel, K. K., Cran, M. J., Sonneveld, K., Miltz, J., & Bigger, S. W. (2013). Migration of antimicrobial agents from starch-based films into a food simulant. *LWT – Food Science and Technology*, 50(2), 432–438.
- Llana-Ruiz-Cabello, M., Pichardo, S., Baños, A., Núñez, C., Bermúdez, J. M., Guillamón, E., ... Cameán, A. M. (2015). Characterisation and evaluation of PLA films containing an extract of *Allium* spp. to be used in the packaging of ready-to-eat salads under controlled atmospheres. *LWT – Food Science and Technology*, 64(2), 1354–1361.
- Manzanarez-López, F., Soto-Valdez, H., Auras, R., & Peralta, E. (2011). Release of  $\alpha$ -tocopherol from poly(lactic acid) films, and its effect on the oxidative stability of soybean oil. *Journal of Food Engineering*, 104(4), 508–517.
- Mascheroni, E., Guillard, V., Nalin, F., Mora, L., & Piergiovanni, L. (2010). Diffusivity of propolis compounds in polylactic acid polymer for the development of antimicrobial packaging films. *Journal of Food Engineering*, 98(3), 294–301.
- Miltz, J. (1987). *Migration of low molecular weight species from packaging materials: Theoretical and practical considerations food product package Compatibility*. pp. 30–43.
- Ortiz-Vazquez, H., Shin, J., Soto-Valdez, H., & Auras, R. (2011). Release of butylated hydroxytoluene (BHT) from Poly(lactic acid) films. *Polymer Testing*, 30(5), 463–471.
- Petchwattana, N., & Naknaen, P. (2015). Utilization of thymol as an antimicrobial agent for biodegradable poly(butylene succinate). *Materials Chemistry and Physics*, 163, 369–375.
- Ploypetchara, N., Suppakul, P., Atong, D., & Pechyen, C. (2014). Blend of polypropylene/poly(lactic acid) for medical packaging application: physicochemical, thermal, mechanical, and barrier properties. *Energy Procedia*, 56, 201–210.
- Qin, Y., Liu, D., Wu, Y., Yuan, M., Li, L., & Yang, J. (2015). Effect of PLA/PCL/cinnamaldehyde antimicrobial packaging on physicochemical and microbial quality of button mushroom *Agaricus bisporus*. *Postharvest Biology and Technology*, 99, 73–79.
- Ramos, M., Beltrán, A., Peltzer, M., Valente, A. J. M., & Garrigós, M. D. C. (2014a). Release and antioxidant activity of carvacrol and thymol from polypropylene active packaging films. *LWT – Food Science and Technology*, 58(2), 470–477.
- Ramos, M., Fortunati, E., Peltzer, M., Dominici, F., Jiménez, A., Garrigós, M. D. C., et al. (2014b). Influence of thymol and silver nanoparticles on the degradation of poly(lactic acid) based nanocomposites: Thermal and morphological properties. *Polymer Degradation and Stability*, 108, 158–165.
- Ramos, M., Jiménez, A., Peltzer, M., & Garrigós, M. C. (2012). Characterization and antimicrobial activity studies of polypropylene films with carvacrol and thymol for active packaging. *Journal of Food Engineering*, 109(3), 513–519.
- Raouche, S., Mauricio-Iglesias, M., Peyron, S., Guillard, V., & Gontard, N. (2011). Combined effect of high pressure treatment and anti-microbial bio-sourced materials on microorganisms' growth in model food during storage. *Innovative Food Science and Emerging Technologies*, 12(4), 426–434.
- Rhim, J. W. (2013). Preparation and characterization of vacuum sputter silver coated PLA film. *LWT – Food Science and Technology*, 54(2), 477–484.
- Rhim, J. W., Hong, S. I., & Ha, C. S. (2009). Tensile, water vapor barrier and antimicrobial properties of PLA/nanoclay composite films. *LWT – Food Science and Technology*, 42(2), 612–617.
- Rubilar, J. F., Cruz, R. M. S., Silva, H. D., Vicente, A. A., Khmelinskii, I., & Vieira, M. C. (2013). Physico-mechanical properties of chitosan films with carvacrol and grape seed extract. *Journal of Food Engineering*, 115, 466–474.
- Sato, S., Gondo, D., Wada, T., Kanehashi, S., & Nagai, K. (2013). Effects of various liquid organic solvents on solvent-induced crystallization of amorphous poly(lactic acid) film. *Journal of Applied Polymer Science*, 129(3), 1607–1617.
- Soto-Valdez, H., Auras, R., & Peralta, E. (2011). Fabrication of poly(lactic acid) films

- with resveratrol and the diffusion of resveratrol into ethanol. *Journal of Applied Polymer Science*, 121(2), 970–978.
- Suppakul, P. (2004). *Study of antimicrobial polymeric packaging films containing basil extracts*. Melbourne: Victoria University of Technology. PhD dissertation.
- Suppakul, P., Miltz, J., Sonneveld, K., & Bigger, S. W. (2003). Active packaging technologies with an emphasis on antimicrobial packaging and its applications. *Journal of Food Science*, 68(2), 408–420.
- Suppakul, P., Sonneveld, K., Bigger, S. W., & Miltz, J. (2011). Diffusion of linalool and methylchavicol from polyethylene-based antimicrobial packaging films. *LWT – Food Science and Technology*, 44(9), 1888–1893.
- Taib, R. M., Ramarad, S., Ishak, Z. A. M., & Todo, M. (2009). Properties of kenaf fiber/poly(lactic acid) biocomposites plasticized with polyethylene glycol. *Polymer Composites*, 31(7), 1213–1222.
- Tawakkal, I. S. M. A., Cran, M. J., & Bigger, S. W. (2014a). Effect of kenaf fibre loading and thymol concentration on the mechanical and thermal properties of PLA/kenaf/thymol composites. *Industrial Crops and Products*, 61, 74–83.
- Tawakkal, I. S. M. A., Cran, M. J., & Bigger, S. W. (2015). Interaction and quantification of thymol in active PLA-based materials containing natural fibers. *Journal of Applied Polymer Science*, 132, 42160.
- Tawakkal, I. S. M. A., Cran, M. J., Miltz, J., & Bigger, S. W. (2014b). A review of poly(lactic acid)-based materials for antimicrobial packaging. *Journal of Food Science*, 79(8), R1477–R1490.
- Wu, Y., Qin, Y., Yuan, M., Li, L., Chen, H., Cao, J., et al. (2014). Characterization of an antimicrobial poly(lactic acid) film prepared with poly( $\epsilon$ -caprolactone) and thymol for active packaging. *Polymers for Advanced Technologies*, 25(9), 948–954.



# Morphological and *in vitro* antibacterial efficacy of quercetin loaded nanoparticles against food-borne microorganisms



V. Dinesh Kumar, Priya Ranjan Prasad Verma\*, Sandeep Kumar Singh

Department of Pharmaceutical Sciences and Technology, Birla Institute of Technology, Mesra, Ranchi, Jharkhand, India

## ARTICLE INFO

### Article history:

Received 10 August 2015

Received in revised form

12 October 2015

Accepted 2 November 2015

Available online 10 November 2015

### Keywords:

Quercetin

Nanoparticles

Percent retardation

Atomic force microscopy

## ABSTRACT

Biodegradable nanoparticles have been used regularly as drug delivery carriers owing to its bioavailability augmentation, better entrapment, sustained release and biocompatibility. The present study aimed to compare the antibacterial efficacy of quercetin loaded nanoparticles (QLNs) with free quercetin against *Bacillus subtilis*, *Escherichia coli*, *Staphylococcus aureus*, and *Salmonella typhimurium* (food-borne microorganisms). Stability study confirmed insignificant variation in particle size, zeta potential and encapsulation efficiency over a period of 90 days of storage. High resolution-transmission electron microscopy (HR-TEM) showed the formation of spherical nanoparticles with smooth surface. The antibacterial activity of free quercetin and QLNs were evaluated for zone of inhibition, percentage retardation of bacterial growth, kinetic measurement, minimum inhibitory concentration and minimum bactericidal concentration studies. The results indicated that QLNs were more efficient than free quercetin owing to control release of quercetin from nanoparticles. The mechanism of antibacterial activity of QLNs was investigated by atomic force microscopy and scanning electron microscopy. Microscopic study revealed the adsorption of nanoparticles on bacterial cell surface followed by increased cell permeability causing cell lysis.

© 2015 Elsevier Ltd. All rights reserved.

## 1. Introduction

The presence and growth of microorganisms in food may encompass spoilage of food quality or cause infection and illness (Celiktas et al., 2007). The emergence of resistance to antimicrobial agents and side-effects of synthetic chemical preservatives are a cause of increasing global concern with reference to food-borne diseases (Janovska, Kubikova, & Kokoska, 2003). The growing need of safe and new antimicrobial agents from the natural origin seems to be imperative to curtail the menace of bacterial resistance (Goni et al., 2009). Plant-derived compounds from the natural origin have been employed as traditional medicine/preservatives since ancient times.

Polyphenols are among the most desirable plant derived compounds because of their various benefits, encompassing antimicrobial properties against pathogens and spoilage microbes (Stojković et al., 2013). Quercetin (3, 3', 4', 5, 7-penta hydroxy flavone) is a most popular dietary flavonoid found in various fruits, vegetables and beverages (Hertog, Hollman, Katan, & Kromhout,

1993). It has been associated with antibacterial (Formica & Regelson, 1995; Nijveldt et al., 2001) and various pharmacological activities like, anti-oxidant (Bischoff, 2008), anti-viral (Ohnishi & Bannai, 1993), anti-proliferative (Hirpara, Aggarwal, Mukherjee, Joshi, & Burman, 2009), anti-inflammatory (Boots, Haenen, & Bast, 2008), and anti-leishmaniasis (Kumar, Verma, & Singh, 2014; Silva, Maquaveli, & Magalhaes, 2012). Furthermore, quercetin has also been indicated in the treatment of cardiovascular diseases and also in cancer therapy (Russo, Spagnuolo, Tedesco, Bilotto, & Russo, 2012). The Clinical application of quercetin is restricted due to limited bioavailability (<17% in rats and ~1% in humans) owing to low aqueous solubility (Day et al., 2001; Li et al., 2009; Mullen, Boitier, Stewart, & Crozier, 2004). To overcome the problems of poor solubility and low bioavailability, nanoparticle based drug delivery approaches such as vesicular drug delivery (liposomes) (Gang et al., 2012), nanocrystals (Sahoo et al., 2011), nanoparticles (Pool et al., 2012), solid dispersion (Costa et al., 2011) and phospholipid complexes (Singh, Rawat, Semalty, & Semalty, 2012) have been described. Biodegradable nanoparticles are widely utilized to improve the therapeutic properties of various drugs and bioactive compounds. Nano-encapsulation protects the drugs from degradation, improves their solubility, and endorses controlled drug release and drug targeting (Dinesh Kumar, Verma,

\* Corresponding author. Department of Pharmaceutical Sciences and Technology, Birla Institute of Technology, Mesra, Ranchi, Jharkand, 835215, India.

E-mail address: [prpverma@bitmesra.ac.in](mailto:prpverma@bitmesra.ac.in) (P.R.P. Verma).

& Singh, 2015). Polymeric nanoparticles present a smart prime approach for drug delivery owing to their biodegradability, biocompatibility, non-toxicity, non-immunogenicity, physico-chemical stability (Coelho et al., 2010). Additionally, the polymeric nanoparticles in food processing may potentially increase the quality of food matrices, limit nutritional losses during processing, add new flavor or mask bad taste, add new texture, offer aroma release for longer period of time, or to improve the stability, absorption and functionalities of active components. However these applications of polymeric nanoparticles in foods will require a thorough study to enable to understanding of polymeric nanoparticles interaction in body, most importantly their safety (Sabliov, Chen & Yada, 2015). Several bioactive molecules like nisin (encapsulated in nanocomposite i.e. chitosan, sodium alginate and pluronic F68, which are permitted for use in food) (Bernela, Kaur, Chopra, & Thakur, 2014),  $\alpha$ -tocopherol (encapsulated in poly ( $\epsilon$  caprolactone)) (Byun et al., 2011) are successfully encapsulated to improve bioavailability, bioactivity and control delivery. Recent research confirm that polymeric nanoparticles loaded with antibiotics, provides long-lasting antimicrobial activity by controlled release, reduced toxicity, prolonged half-life and altered tissue distribution (Chiellini, Piras, Errico, & Chiellini, 2008; Coelho et al., 2010). In previous study (Dinesh Kumar, Verma & Singh, 2015), we have used nano-precipitation method to prepare quercetin loaded biodegradable polymeric nanoparticles that showed enhanced physicochemical stability, uniform particle size, good encapsulation efficiency, and controlled release (~48 h).

The objective of the present study was to investigate the anti-bacterial activity of quercetin loaded nanoparticles (QLNs). To achieve the goal, we compared the antibacterial efficiency of free quercetin and QLN against four food-borne microorganisms (*Bacillus subtilis*, *Escherichia coli*, *Staphylococcus aureus* and *Salmonella typhimurium*). Antibacterial activities of QLN and free quercetin were quantified by percentage retardation study and time-dependent bacterial growth kinetics using microtiter plate method. Furthermore, antibacterial mechanism of QLN was elucidated by morphological investigation using scanning electron microscopy (SEM) and atomic force microscopy (AFM).

## 2. Material and methods

### 2.1. Materials

Quercetin (95%), poly ( $\epsilon$  caprolactone; PCL) (MW, 14, 000) and resazurin were purchased from Sigma–Aldrich, India. Pluronic F127 was supplied by Ranbaxy Laboratory, India. Microtiter plate and Petri plates were obtained from Tarsons Products Pvt. Ltd., India.

### 2.2. Preparation of quercetin-loaded nanoparticles

The QLN were prepared using the nano-precipitation method as described previously (Dinesh Kumar, Verma, Singh & Viswanathan, 2015). Briefly, PCL (125.19 mg) and quercetin (10 mg) were dissolved in acetone at 30 °C using a water bath. The organic solution was then slowly added to an aqueous phase containing the hydrophilic surfactant (Pluronic F-127, 407.1 mg) under moderate magnetic stirring, using a syringe. The acetone and water were then evaporated at 40 °C under reduced pressure, using a rotary evaporator (IKA, RV-10, Germany) for 12 h. The nano-suspension was then centrifuged at 20,000 RPM using ultracentrifuge (Optima MAX-XP, Beckman Coulter, USA) for 20 min at 4 °C. The resulting pellets were re-suspended in distilled water and frozen at –20 °C for 12 h and, subsequently, frozen nanoparticles dispersion was freeze dried at –70 °C for 48 h using the freeze dryer (Heto Power Dry LL3000, Thermo Scientific, Czech Republic). The

freeze-dried nanoparticles were stored at 4 °C until further use for anti-bacterial studies. The stability samples were stored at 5 °C  $\pm$  3 °C and 25 °C  $\pm$  2 °C as discussed in section 2.3.

### 2.3. Stability study

The stability of nanoparticles was analyzed at predetermined time intervals (0, 30, 60, and 90 days) by monitoring the changes in particle size, zeta potential and encapsulation efficiency as a function of storage time at 5 °C  $\pm$  3 °C (refrigerator) and 25 °C  $\pm$  2 °C (Room temperature). All measurements were performed in triplicate.

#### 2.3.1. Particle size and zeta potential analysis

Particle size and zeta potential were elucidated by photon correlation spectroscopy (PCS) using a Zetasizer (Nano ZS, Malvern Instruments, Worcestershire, UK). The measurement conditions were: He–Ne Red laser, 4.0 mW, 633 nm; temperature, 25 °C  $\pm$  2 °C; refractive index, 1.333; zeta potential ranging from –120 to 120 mV. Samples were suitably diluted with Millipore water (pH 7.0) to avoid multiple scattering.

#### 2.3.2. Encapsulation efficiency

Encapsulation efficiency was determined using a solvent extraction method (Dinesh Kumar, Verma & Singh, 2015; Dinesh Kumar, Verma, Singh & Viswanathan, 2015). Dried nanoparticles (10 mg) equivalent to 2 mg of drug was dispersed and vortexed (10 min) in dichloromethane: methanol (1:9) to extract quercetin followed by centrifugation at 5000 rpm for 15 min. The drug concentration was measured at 371 nm by UV–Vis spectrophotometer (UV 1800, Shimadzu, Japan) by diluting with methanol. Encapsulation efficiency (%) was determined using equation (1):

$$\text{Encapsulation Efficiency (\%)} = \frac{\text{Weight of quercetin determined (mg)}}{\text{Weight of quercetin added (mg)}} \times 100 \quad (1)$$

### 2.4. High resolution-transmission electron microscopy

The morphology of QLN was investigated by high-resolution transmission electron microscopy (HR-TEM) (JEM-2100, JEOL Ltd., Akishima-shi, Japan). A drop of QLN was spread over carbon-coated copper grids followed by solvent evaporation under vacuum. A drop of phosphotungstic acid (1.0% w/v) was added to the grids. The grids were allowed to stand for 20 s followed by removal of excess stain using filter paper. The grids were air-dried at ambient temperature before loading in the microscope (Verma, Singh, Verma, & Ahsan, 2014).

### 2.5. Antibacterial activity

#### 2.5.1. Bacterial strains and cultures

The anti-microbial activity of quercetin and QLN were tested against *B. subtilis* (G+) MTCC 1790, *S. aureus* (G+) MTCC-3160, *S. typhimurium* (G–) MTCC 3224, and *E. coli* (G–) MTCC-1678, obtained from the Institute of Microbial Technology, Chandigarh, India. Muller-Hinton broth medium was used for culturing the test bacteria.

#### 2.5.2. Determination of zone of inhibition

Inocula from bacterial suspensions (McFarland 0.5 standard) were spread over solidified Mueller-Hinton agar plates. Four wells were created by well borer under the aseptic condition on agar

plates. Fifty  $\mu\text{L}$  of QLN dispersion (equivalent to 100  $\mu\text{g}/\text{mL}$  of quercetin), free quercetin (100  $\mu\text{g}/\text{mL}$ ), blank formulation and solvent (20% v/v DMSO) was added to each of the wells. The plates were incubated at 37 °C for 24 h. The antibacterial activity was evaluated by measuring the zone of inhibition around the well present on agar plates.

### 2.5.3. Microtiter bioassay

Percentage of growth retardation of free quercetin and QLN was determined by a microtiter well plate method (Langfield et al., 2004). Fifty  $\mu\text{L}$  of samples (equivalent to 1.0 mg/mL of quercetin concentration) were added to the wells of a 96-well microtiter plate. To each well 50  $\mu\text{L}$  of a Muller-Hinton broth medium and 5  $\mu\text{L}$  of test organism inoculum (McFarland 0.5 standard) was added. Positive (50  $\mu\text{L}$  of Muller Hinton Broth medium + 5  $\mu\text{L}$  bacterial suspension) and negative (Sterile Muller Hint Broth medium 50  $\mu\text{L}$ ) control wells were included in each assay. In this method, samples were analyzed by the microplate reader (Mindray-MR-96A, China) at OD<sub>625nm</sub> for 48 h.

**2.5.3.1. Percentage retardation of growth.** Antibacterial activities of QLN were determined by calculating percentage of growth retardation (Jaiswal, Duffy, Jaiswal, Stobie, & McHale, 2010) using equation (2):

$$R (\%) = \frac{(C_{48} - C_0) - (T_{48} - T_0)}{(C_{48} - C_0)} \times 100 \quad (2)$$

where R is the percentage retardation of growth, C<sub>48</sub> and C<sub>0</sub> indicate optical density (OD<sub>625</sub>) value of control samples for testing microorganisms (without treatment) at 48 h and 0 h. T<sub>48</sub> and T<sub>0</sub> indicate optical density (OD<sub>625</sub>) value of test samples at 48 h and 0 h. The plates were automatically shaken for 30 s prior to each OD reading.

**2.5.3.2. Bacterial growth kinetics.** Bacterial concentrations in the presence of free quercetin and QLN were determined by measuring the OD<sub>625</sub> for respective time intervals (up to 48 h). Kinetic measurement of bacterial growth was analyzed graphically as reported by Jaiswal et al. (2010).

**2.5.4. Determination of minimum inhibitory concentration (MIC) (Resazurin microtiter plate method) and minimum bactericidal concentration of quercetin**

The MIC value of the free quercetin and QLN was evaluated using a modified microdilution method, which is approved by the Clinical and Laboratory Standards Institute method (Li-Puma et al., 2009; NCCLS, 2006). Resazurin (7-hydroxy-3H-phenoxazin-3-one 10-oxide) is used as an oxidation–reduction indicator in the cell viability studies. It is a blue (weakly fluorescent) and non-toxic dye that turns to pink or colorless when reduced to resorufin by oxidoreductases within viable cells (Bueno et al., 2002). A sterile 96 well plate was used to determine the minimum inhibitory concentration (MIC) for estimating anti-bacterial activity. The first step of the assay was conducted by adding 50  $\mu\text{L}$  of sample A (quercetin loaded nanoparticles equivalent to a concentration of 1 mg/mL of quercetin in 20% v/v DMSO) and sample B (free quercetin in 20% v/v DMSO at a concentration of 1 mg/mL) in first well of first and second row respectively. Fifty  $\mu\text{L}$  of Sample C (standard; Ciprofloxacin, 1 mg/mL) was added to the first well of the third row. Blank formulation (Sample D) and solvent used for dispersion of samples (20% v/v DMSO; Sample E) was added to the first well of fourth and fifth rows of 96-well plates, while last two rows served as a positive (to assure viability of bacterial culture, without samples) and negative control (to confirm sterility of working

conditions and solutions). The second step was accomplished by adding 50  $\mu\text{L}$  of Muller-Hinton broth medium, followed by serial dilutions until all the wells contained 50  $\mu\text{L}$  of the solutions under examination in descending concentrations (450, 225, 112.5, 56.25, 28.12, 14.06, 7.03, 3.51, 1.75 ppm). Then, 5  $\mu\text{L}$  of resazurin indicator solution were added to each well, followed by the addition of 5  $\mu\text{L}$  of bacterial suspension (McFarland 0.5 standard). The Microplates were properly wrapped with foil to prevent from contamination; plates were prepared in triplicate and incubated at 37 °C for 24 h. The color changes were observed by visual inspection. Blue colors indicate the absence of microorganism while pink or colorless indicates the growth of the microorganism. The lowest concentration showing color change from blue to pink was considered as MICs (LiPuma et al., 2009; Ivanova, Pancevska, & Kungulovski, 2013; Sarker, Nahar, & Kumarasamy, 2007). The minimum bactericidal concentrations (MBCs) were determined by sub-culturing all broths used for MIC determination (10.0  $\mu\text{L}$  was removed from each well) over agar plates. Colonies were counted after an incubation period. MBCs are the lowest concentration of a drug resulting in killing 99.9% of the bacterial inoculum.

## 2.6. Morphological studies

### 2.6.1. Atomic force microscopy (AFM)

Bacterial cultures of the mid-exponential growth phase were diluted with nutrient broth medium to get appropriate cell density (McFarland 0.5 standard). The bacterial cells were harvested by centrifugation at 3000 g for 10.0 min and washed twice with 0.1 M phosphate buffer solution (PBS, pH 7.4), followed by suspending in 5.0 mL of PBS. The suspended bacterial cultures were treated with 1.0 mL of free quercetin (*B. subtilis*, 56.25 ppm; *S. aureus*, 28.12 ppm; *E. Coli*, 112.5 ppm; and *S. typhimurium*, 56.25 ppm.) and QLN (*B. subtilis*, 14.06 ppm; *S. aureus*, 7.03 ppm; *E. Coli*, 28.12 ppm; and *S. typhimurium* 14.06 ppm) at MIC. Untreated and QLN treated bacterial samples were incubated for 3.0 h at 37 °C. Finally, the samples were applied to coverslips (previously treated with poly-L-lysine). Microscopy was performed with an NT MDT Solver Pro 47 (NT MDT, Russia) microscope in non-contact mode at 0.85 Hz scan rate, using commercial silicon nitride probes with cantilevers having a length of 100 nm, spring constants of 420 N/m and a nominal tip curvature radius of 5–10 nm (Singh, Verma, Singh, & Verma, 2015).

### 2.6.2. Scanning electron microscopy

Bacterial samples for SEM analysis (Singh, Verma, Singh, & Verma, 2014) were prepared, as described in AFM study. Cell pellets (control and QLN treated cells) were fixed with 2.5% (v/v) glutaraldehyde for 2 h before the SEM examination (JEOL, JSM-6390LV, Japan). Platinum was sputtered on the sample to render them electrically active.

## 3. Results

### 3.1. Stability study of QLN

The stability of the QLN were assessed by measuring the particle size, zeta potential and entrapment efficiency at varying time intervals at different storage conditions (5 °C  $\pm$  3 °C and 25 °C  $\pm$  2 °C) (Fig. 1). Freeze dried nanoparticles (n = 3) were reconstituted and were analyzed for particle size, zeta potential and entrapment efficiency at 0, 30, 60, and 90 days. Mean particle size of QLN at different time intervals ranged from 251.25 nm to 267.76 nm and 251.63 nm–262.60 nm when stored at 5 °C  $\pm$  3 °C and 25 °C  $\pm$  2 °C, respectively. Similarly, the zeta potential ranged between –11.56 mV and –11.83 mV and –11.50 mV to –11.83 mV when stored at 5 °C  $\pm$  3 °C and 25 °C  $\pm$  2 °C, respectively. The encapsulation

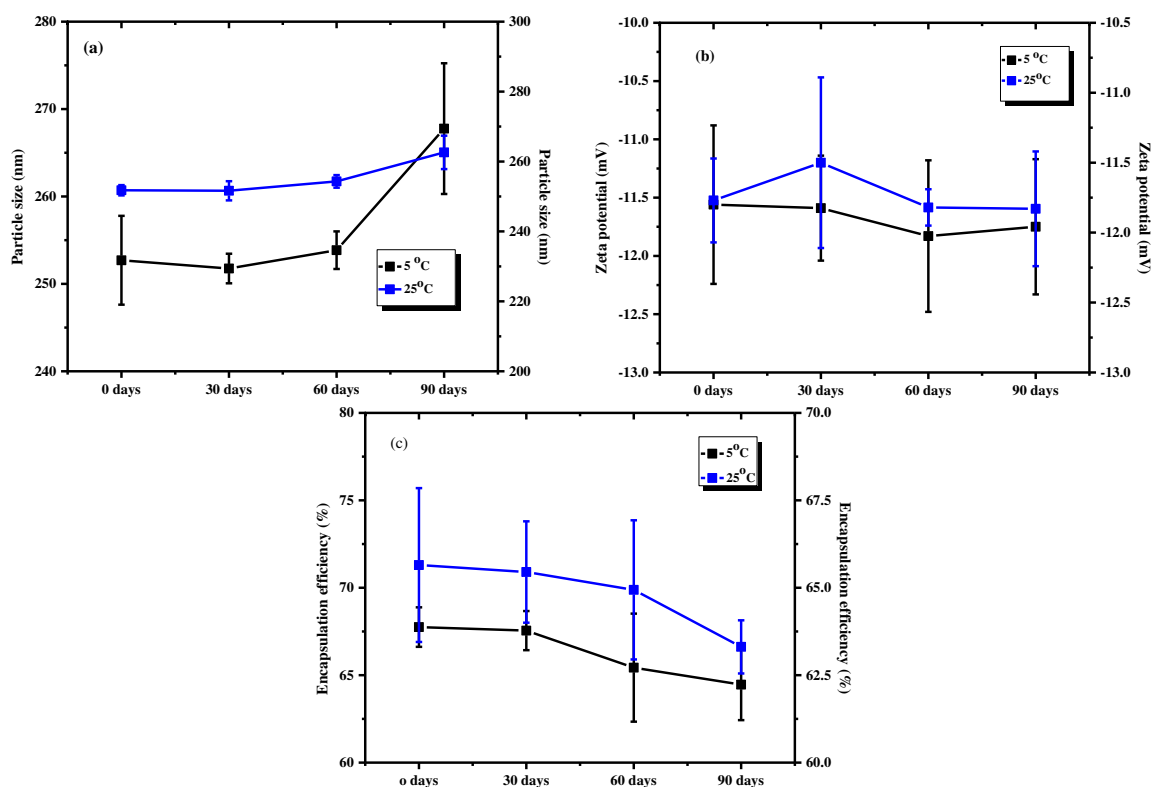


**Fig. 1.** Stability study of quercetin loaded nanoparticles stored at 5 °C ± 3 °C and 25 °C ± 2 °C with reference to particle size, nm (a); zeta potential, mV (b); and encapsulation efficiency, % (c).

efficiency ranged between 64.46% to 67.75% and 63.31%–65.65% when stored at 5 °C ± 3 °C and 25 °C ± 2 °C, respectively. QLN did not show any significant variance ( $P < 0.05$ ) with respect to particle size, zeta potential, and entrapment efficiency, after 90 days of storage condition, construing stability of QLN.

### 3.2. High resolution transmission electron microscopy

The HR-TEM images of QLN, initial and after 90 days of storage at 5 °C ± 3 °C and 25 °C ± 2 °C are portrayed in Fig. 2a–c, respectively. The representative HR-TEM images at different storage condition depicted the presence of discrete, uniform, and spherical nanoparticles (Fig. 2a–c). No signs of coalescence/aggregation of QLN were observed, indicating stability of the formulation. The particle size of QLN obtained from HR-TEM is in agreement with the mean particle size obtained from PCS.

### 3.3. Antibacterial activity

#### 3.3.1. Zone of inhibition studies

The antibacterial activity of free quercetin and QLN was tested against two Gram-Positive (*B. subtilis* and *S. aureus*) and two Gram-Negative (*E. coli* and *S. typhimurium*) bacteria by zone of inhibition and minimum inhibitory concentration (MIC) studies. The QLN showed inhibitory action (Zone of Inhibition) against all bacteria under test, and the results are summarized in Supplementary Table 1. The zone of inhibition of free quercetin and QLN against all bacteria ranged between 6.13–10.06 mm and 11.93–17.16 mm, respectively.

#### 3.3.2. Percentage retardation of growth

The antibacterial effect of free quercetin and QLN, (450, 225, 112.5, 56.25, 28.12, 14.06, 7.03, 3.51, 1.75, 0.87, 0.43, 0.21 ppm of free

quercetin and equivalent free quercetin in QLN), were also evaluated by comparing the percent retardation of bacterial growth (Fig. 3). QLN displayed significantly greater antibacterial activity ( $P < 0.05$ ) against *B. subtilis*, *S. aureus*, *E. coli* and *S. typhimurium* than free quercetin.

The percent retardation of QLN (equivalent to 14.06 ppm of quercetin) treated *B. subtilis* was 83.57% *vis-a-vis* no retardation with free quercetin. *E. coli* was 84.49% inhibited by QLN at a quercetin concentration of 56.25 ppm compared to 24.51% retardation by free quercetin. Percent retardation of QLN (14.06 ppm) against *S. aureus* was found to be 80.42% as compared to zero percent inhibition by free quercetin. QLN (56.25 ppm) showed 88.46% inhibition against *S. typhimurium* as compared to 32.40% inhibition observed by free quercetin.

#### 3.3.3. Kinetic measurement of bacterial growth

Fig. 4 portrays the time-dependent inhibitory effect of QLN and free quercetin against four food-borne microorganisms (*B. subtilis*, *E. coli*, *S. aureus*, and *S. typhimurium*). QLN delayed the growth of *B. subtilis* for 48 h compared with free quercetin (9 h). In case of *E. coli*, QLN delayed the growth by 48 h, when compared with free quercetin (3 h). The QLN exhibited excellent antibacterial activity against *S. aureus* that completely inhibited growth at 48 h as compared free quercetin that showed inhibition up to 2 h. Furthermore, QLN also delayed the growth of *S. typhimurium* for 48 h, compared with free quercetin (5 h). Although, free quercetin showed antibacterial activity against food-borne microorganisms, entrapment and controlled release of quercetin from polymeric nanoparticles significantly ( $P < 0.05$ ) prolonged the antibacterial effect.

#### 3.3.4. Effect of quercetin loaded nanoparticles on its MIC and MBC

Measurement of MIC was carried out by resazurin-microtiter plate method (Supplementary Table 2). The MIC of QLN for

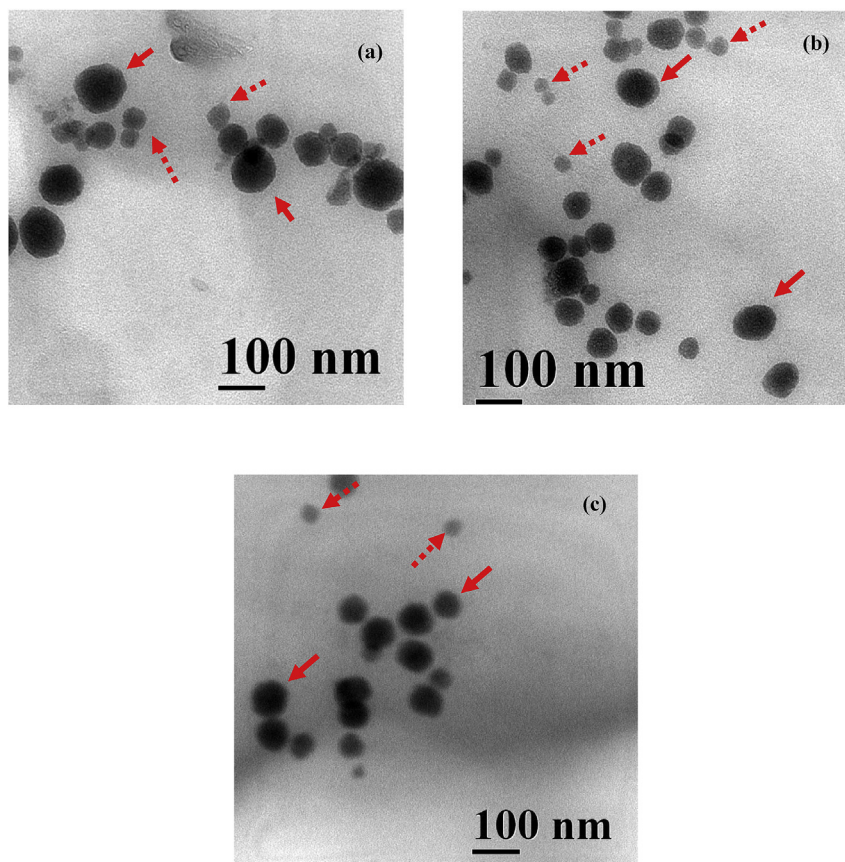


**Fig. 2.** HR-TEM images of quercetin loaded nanoparticles of initial at day 0 (a); 90 days of preparation stored at, 5 °C ± 3 °C (b) and 25 °C ± 2 °C (c). Red arrows indicate drug loaded nanoparticles and dotted red arrows indicate unloaded nanoparticles. (For interpretation of the references to color in this figure caption, the reader is referred to the web version of this article.)

*B. subtilis* (Supplementary Fig. S1), *S. aureus* (Supplementary Fig. S2), *E. coli* (Supplementary Fig. S3), and *S. typhimurium* (Supplementary Fig. S4) was 14.06 ppm, 7.03 ppm, 28.12 ppm, and 14.06 ppm, respectively, compared to 56.25 ppm, 28.12 ppm, 112.5 ppm, and 56.25 ppm of free quercetin.

The MBCs was determined by subculturing the broths used for MIC determination on agar plates. MBCs of QLNs were 56.25 ppm, 112.5 ppm, 56.25 ppm, 112.5 ppm for *B. subtilis*, *S. aureus*, *E. coli*, and *S. typhimurium*, respectively, compared to 225 ppm, 225 ppm, 450 ppm, and 225 ppm for free quercetin.

### 3.4. Morphological studies

#### 3.4.1. Atomic force microscopy

The AFM has emerged as a valuable tool to investigate microbial surfaces at high resolution. Morphological characterization of untreated cells showed smooth and uniform surface without any ostensible damage while QLNs treated cells showed a detrimental effect on bacterial topography.

*B. subtilis* cells imaged by AFM (2D, 3D and dimensional analysis), showed rod shaped contour with a smooth surface (Fig. 5a, c, e). The QLNs treated *B. subtilis* portrays damaging effects on the cell. Fig. 5b, d depicts the presence of grooves or depression on the cell surface with fragmented cellular parts (shown by dotted square) at the vicinity of cell demonstrating the bactericidal effects by QLNs. Furthermore, the dimensional analysis (Fig. 5f) also confirmed the irregular shape with pore formation (shown by an arrow). The average root means square (RMS) roughness of the untreated *B. subtilis* was  $4.85 \pm 0.49$  nm,

while the RMS of treated bacteria was increased to  $21.56 \pm 1.46$ , suggesting the exposure of rough peptidoglycan layers, due to the interaction of QLN with the cell wall of the bacteria.

Fig. 6 portrays the AFM images of control, and QLNs treated *E. coli*. The morphological representations (2D, 3D and dimensional analysis) of untreated cells showed rod-shaped bacteria with the smooth surface and no apparent cell damage (Fig. 6a, c, e). In contrast, QLNs treated cells had damaging effects, illustrated by cell-wall erosion accompanied by cell flattening. The cell flattening could be due to leakage of cellular contents (shown within dotted square) (Fig. 6b, d, g). The dimensional analysis, further confirms the irregular shape of treated cells (Fig. 6f). The average root mean square (RMS) roughness of the untreated *E. coli* was  $1.28 \pm 0.64$  nm while RMS of treated cell was increased to  $13.07 \pm 1.45$  nm illustrating the bactericidal effect of QLN.

Fig. 7 shows the images (2D, 3D and dimensional analysis) of *S. aureus* before and after treatment. The 2D and 3D images of an untreated cell showed grape like a cluster form of cocci of nearly spherical shape, and it was rare to find isolated cells (Fig. 7a, c). From the dimensional analysis, the surface of untreated bacteria indicates smooth surface without any crevices (Fig. 7e) (RMS:  $3.96 \pm 2.48$  nm). In contrast, QLNs treated cells showed surface alterations like depressions and pore formation as shown by arrows (RMS:  $25.30 \pm 3.42$  nm) (Fig. 7f). Furthermore, QLNs treated *S. aureus* also showed the presence of intermingled cellular content of collapsed neighboring cells (shown in dotted square) (Fig. 7b, d, g).

AFM analysis of *S. typhimurium* non-treated cells indicated rod-shaped with a relatively smooth surface (RMS:  $3.3 \pm 1.12$  nm)

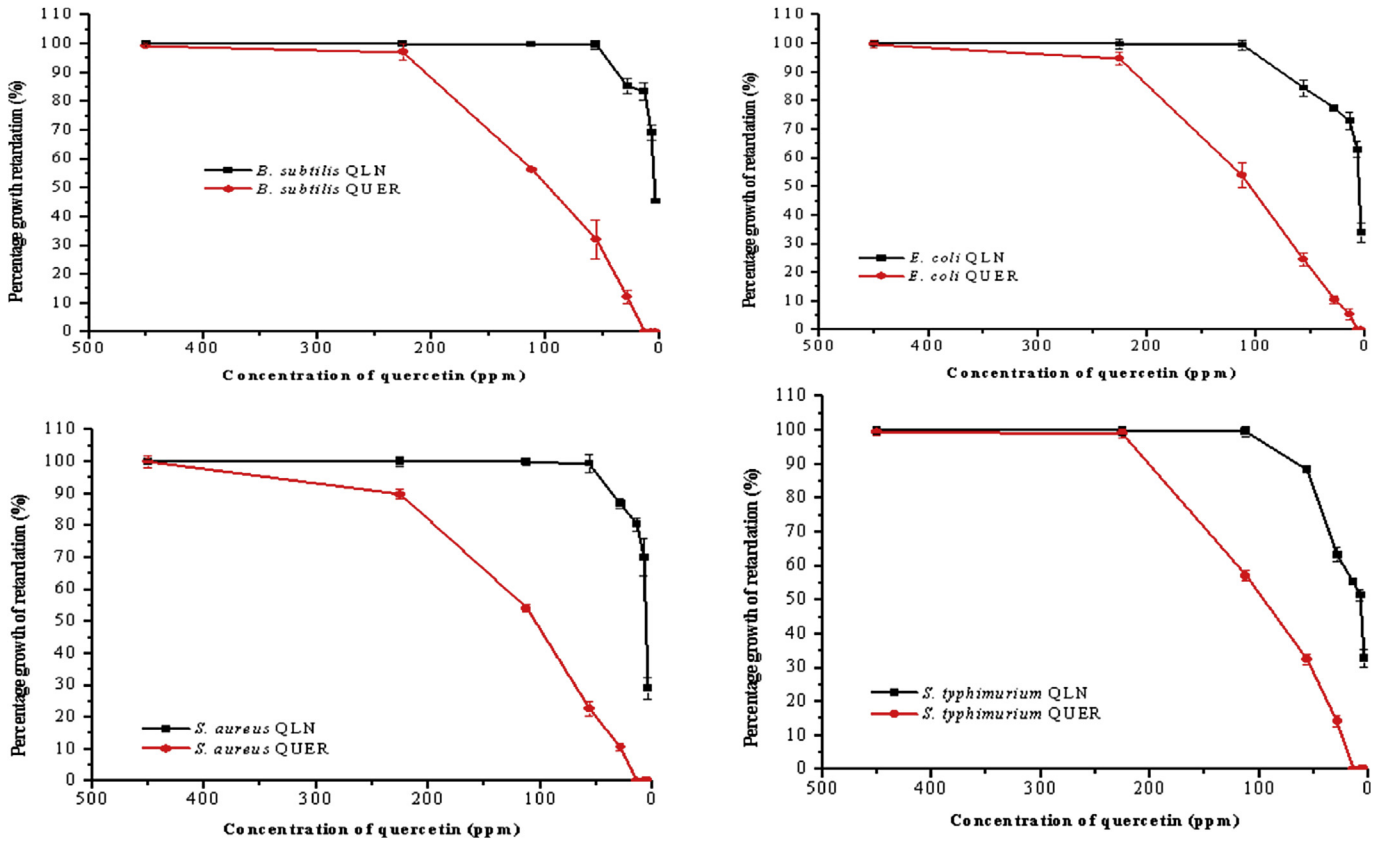


Fig. 3. Percent retardation of foodborne pathogens (*B. subtilis*, *E. coli*, *S. aureus*, and *S. typhimurium*) when treated with quercetin loaded nanoparticles and free quercetin.

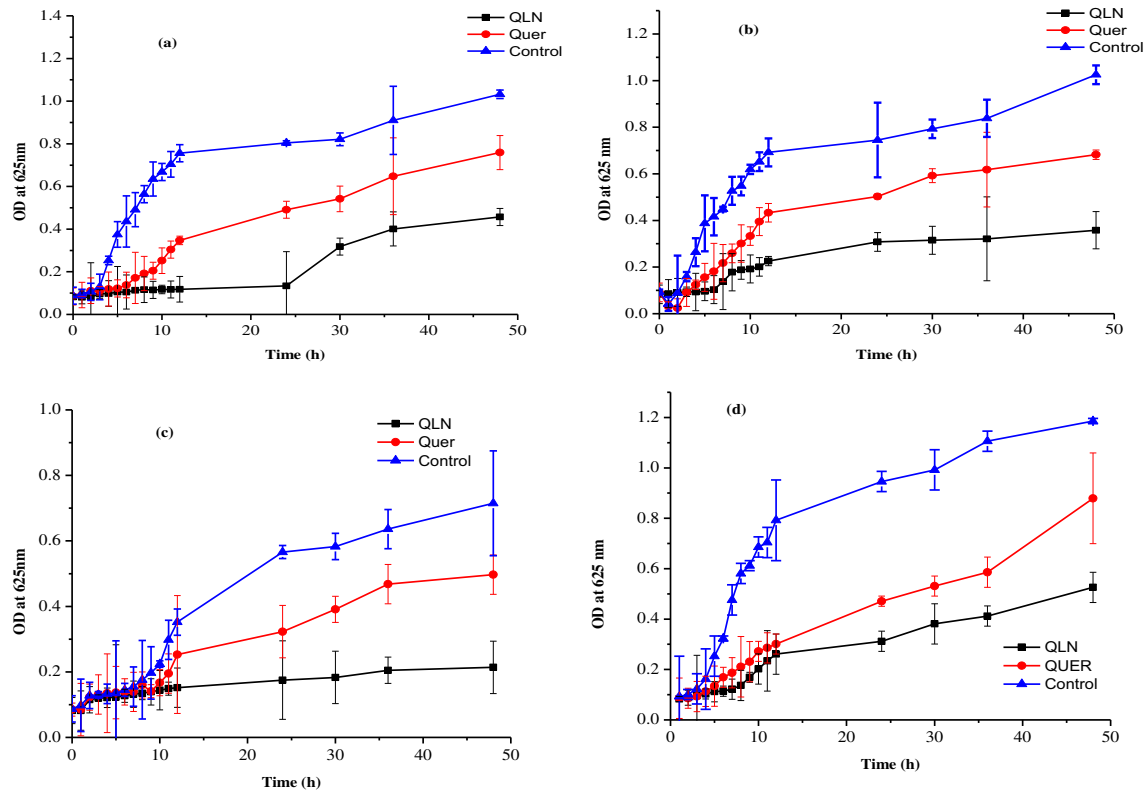
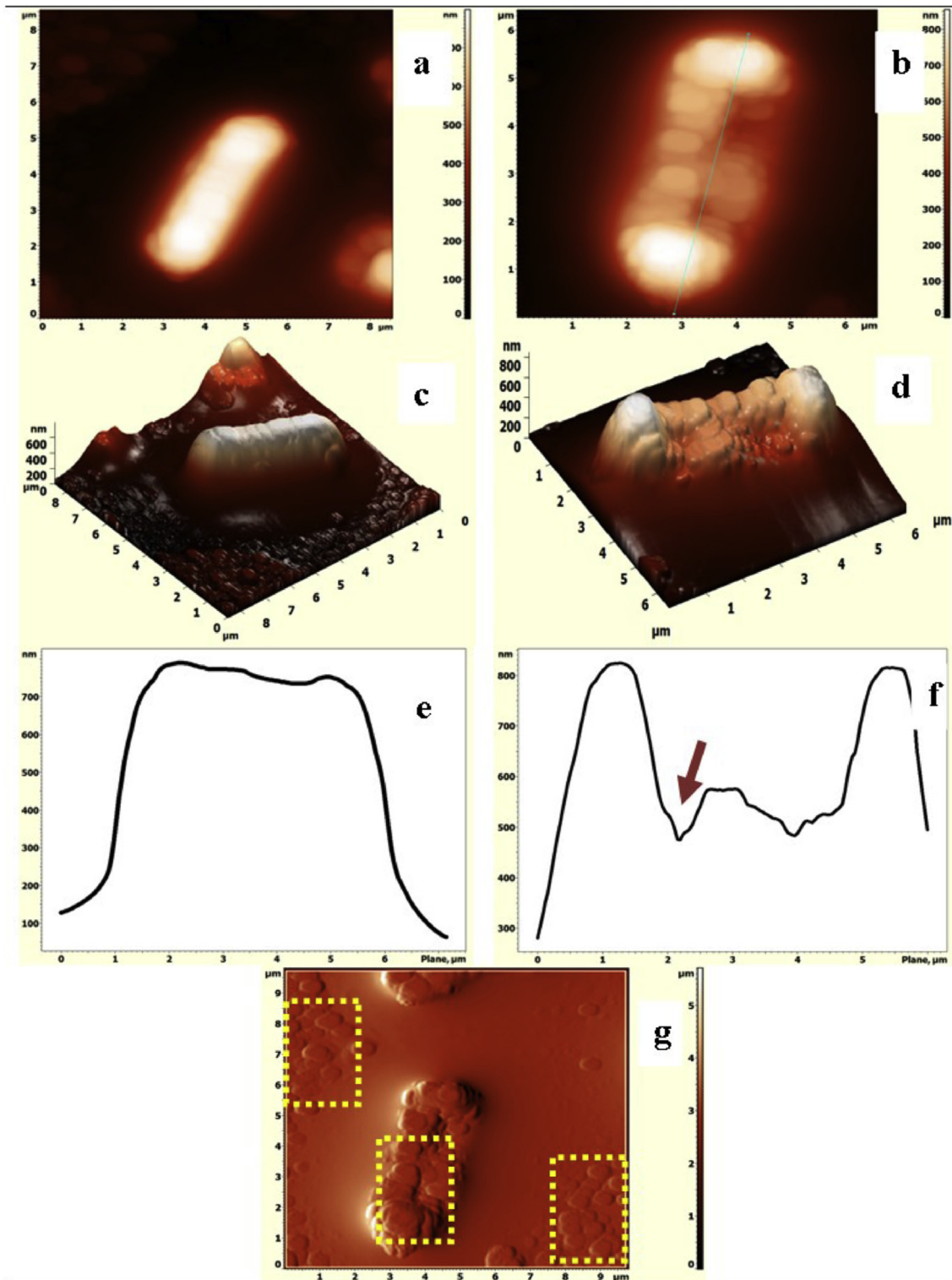


Fig. 4. The time-dependent inhibitory effect of quercetin loaded nanoparticles and free quercetin against (a) *B. subtilis* (b) *E. coli* (c) *S. aureus* (d) *S. typhimurium*.



**Fig. 5.** Atomic force microscopic images of untreated (a, c, and e) and QLN treated *B. subtilis* cell (b, d, f and g). Brown arrow indicates pore formations. The exudations of essential cytoplasmic contents are shown within yellow dotted box. (For interpretation of the references to color in this figure caption, the reader is referred to the web version of this article.)

(Fig. 8a, c, e), with no apparent cellular damages. In contrast, QLN treated cells portray the pore formation (shown by arrows) (Fig. 8f) with enhanced RMS roughness ( $18.31 \pm 2.22$  nm), followed by leakage of cellular materials (shown in dotted square) and cell fragmentations leading to cell death (Fig. 8b, d, g).

#### 3.4.2. Scanning electron microscopy (SEM)

The AFM investigations of bacterial lysis were further confirmed by SEM studies. Various authors have reported the mechanism of antimicrobial activity of quercetin like, inhibition of DNA gyrase that controls the shape of DNA (Ohemeng, Schwender, Fu, &

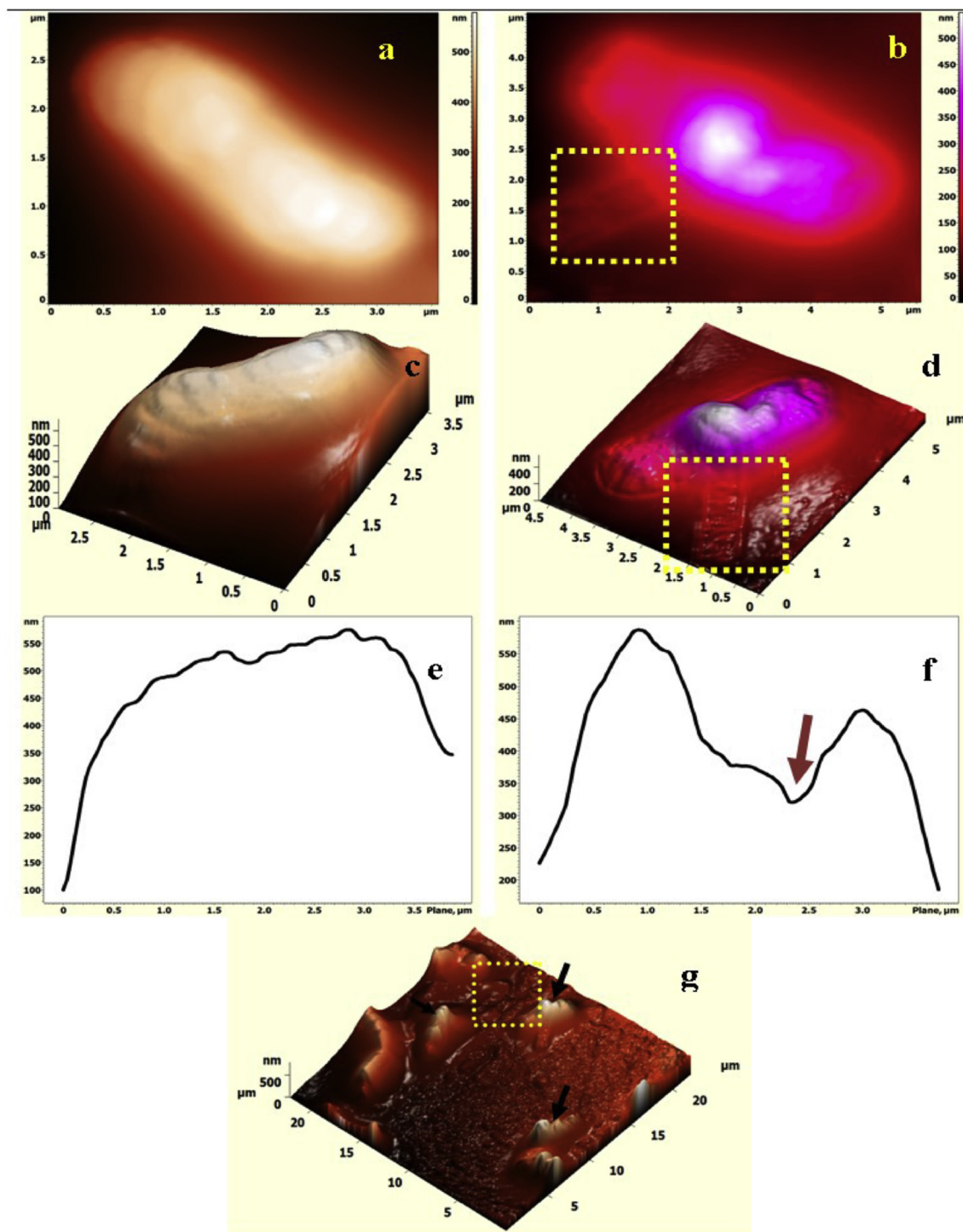


**Fig. 6.** Atomic force microscopic images of untreated (a, c, and e) and QLN treated *E. coli* cell (b, d, f and g). Brown arrow indicates pore formations. The leakages of cellular contents are shown within yellow dotted box. (For interpretation of the references to color in this figure caption, the reader is referred to the web version of this article.)

Barrett, 1993), inhibition of enzyme ATPase activity (Plaper et al., 2003), increase in membrane permeability, and inhibition of bacterial motility (Mirzoeva, Grishanin, & Calder, 1997). The electron micrographs of both untreated and treated microbial cells are presented in Fig. 9. The electron microscope illustrates the smooth, intact and undamaged bacterial cells (untreated) of *B. subtilis* (rod), *S. aureus* (spherical), *S. typhimurium* (rod), *E. coli* (rod). In contrast, QLN showed detrimental effects on the morphology of bacterial cell membranes (*B. subtilis*, *S. aureus*, *S. typhimurium*, *E. coli*) as

represented in Fig. 9. Micrograph observations suggest accumulation and penetration of QLN into the cell membrane followed by disruption of cell integrity and killing the bacterial cell.

#### 4. Discussion

From our previous study, quercetin was successfully entrapped in biodegradable polymeric nanoparticles that controlled the release of drug for 48 h, by quality design by approach (Dinesh

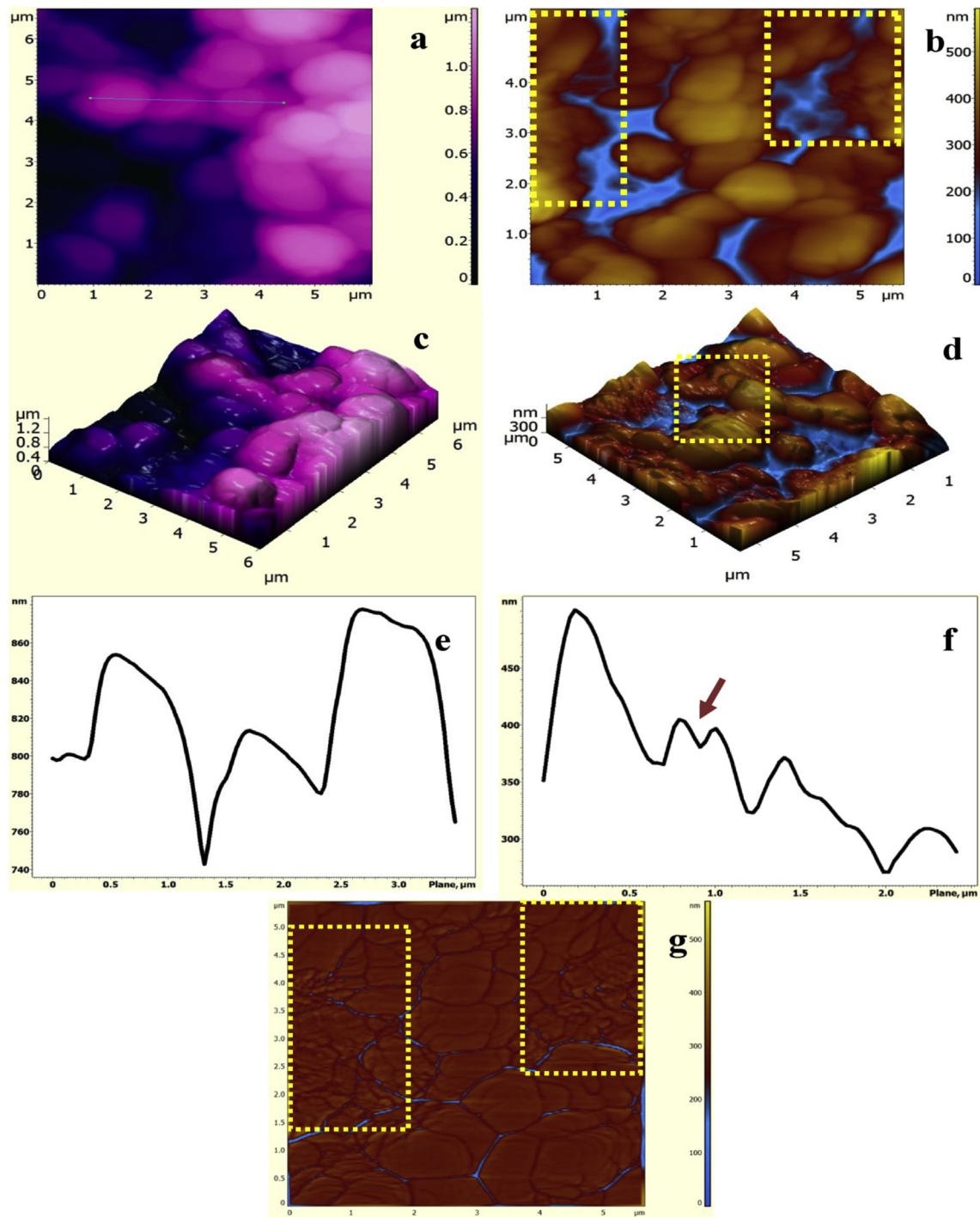


**Fig. 7.** Atomic force microscopic images of untreated (a, c, and e) and QLN treated *S. aureus* cell (b, d, f, and g). Brown arrow indicates pore formations. The leakages of cellular contents are shown within yellow dotted box. (For interpretation of the references to color in this figure caption, the reader is referred to the web version of this article.)

Kumar, Verma & Singh, 2015). In this study, Optimized formulation of QLN was employed for prolonged antibacterial activity against *B. subtilis*, *E. coli*, *S. aureus*, and *S. typhimurium*.

The purpose of stability testing is to provide evidence on time dependent integrity of drug in dosage forms under the influence of varied temperatures. QLN were stable at  $5\text{ }^{\circ}\text{C} \pm 3\text{ }^{\circ}\text{C}$  and  $25\text{ }^{\circ}\text{C} \pm 2\text{ }^{\circ}\text{C}$ , and there was no significant variance ( $P < 0.05$ ) in particle size, zeta potential, and entrapment efficiency, after 90 days of storage condition. The mean particle size remained almost constant for 90 days, indicating no effect of temperature on particle

size. The negative zeta potential of QLN may be due to the presence of terminal carboxylic groups in the polymer molecule (Mora-Huertas, Fessi, & Elaissari, 2011). The high zeta potential values are indicative of a stable QLN dispersion. Furthermore, no significant changes in the zeta potential as a function of time (up to 90 days) was observed suggesting electrostatic repulsion between negatively charged QLN. The chemical stability of QLN is another fundamental aspect of the overall stability evaluation. The insignificant change in encapsulation efficiency of QLN (for 90 days), confirms no eventual leakage of the drug from the nanoparticles

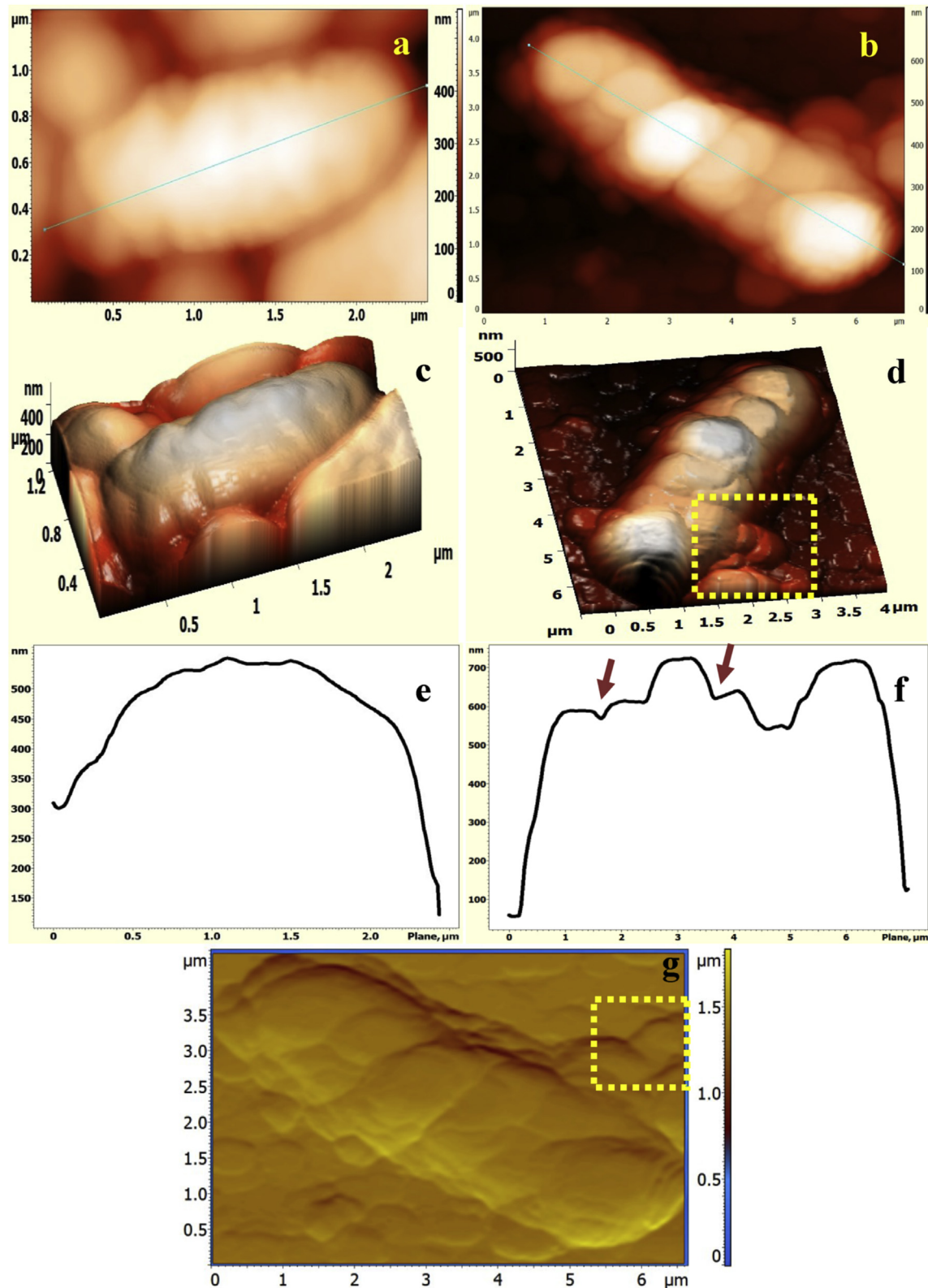


**Fig. 8.** Atomic force microscopic images of untreated (a, c, and e) and QLN treated *S. typhi* cell (b, d, f, and g). Brown arrow indicates pore formations. The leakages of cellular contents are shown within yellow dotted box. (For interpretation of the references to color in this figure caption, the reader is referred to the web version of this article.)

during storage demonstrating the structural integrity of QLN. These studies construed the stability of QLN in group I–IV geographical region at the varied temperature (WHO, 2009). The stability of QLN was further assessed by HR-TEM. It was apparent that the

nanoparticles retained the spherical shape, at different storage conditions with no aggregate formation. The finding supports the zeta potential studies that showed mutual repulsion amongst neighboring particle and hence no aggregations. Also, drug crystals

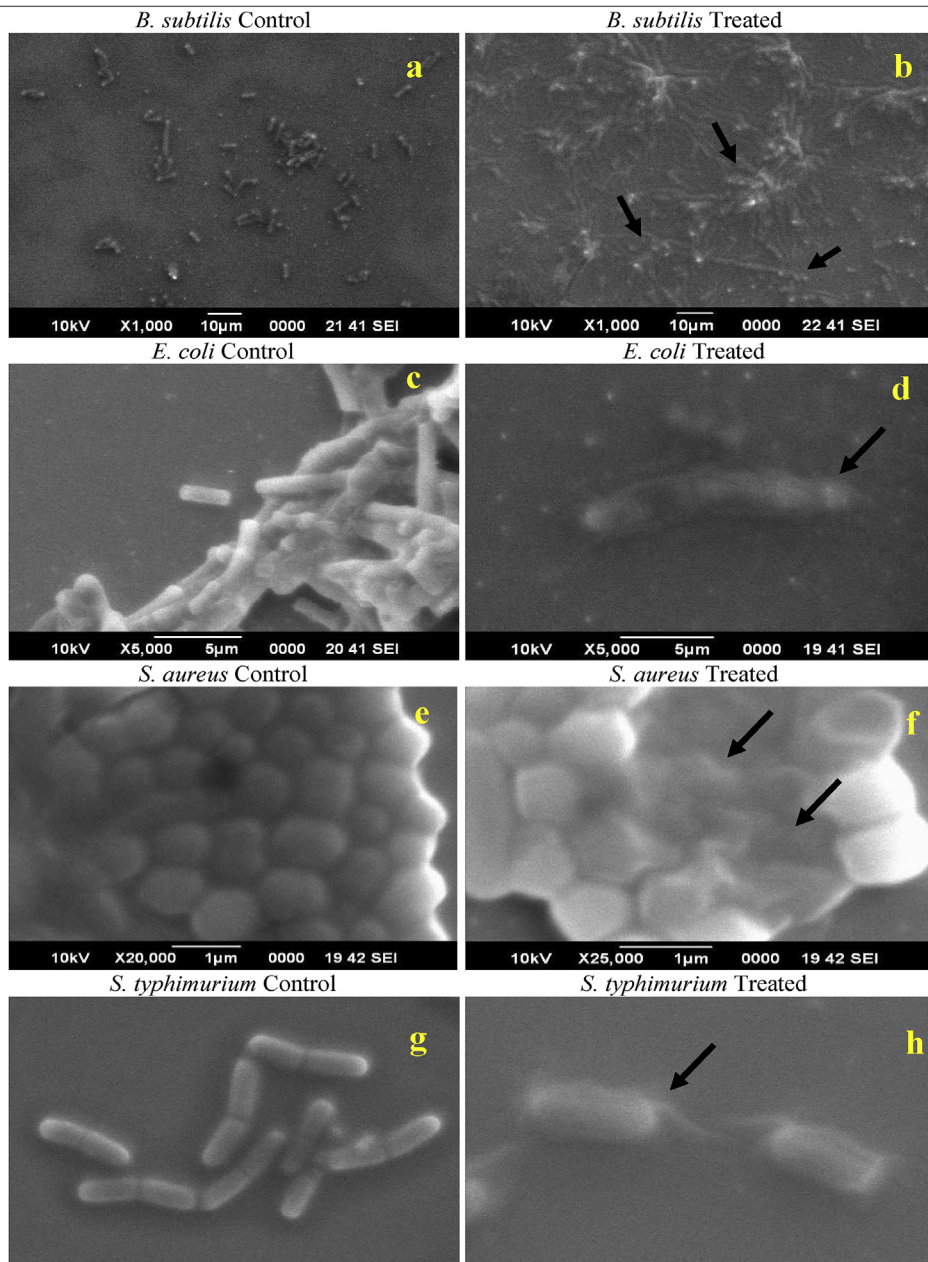


**Fig. 9.** Scanning electron microscopic images of untreated *B. subtilis* (a), *E. coli* (c), *S. aureus* (e), and *S. typhimurium* (g) and QLN treated *B. subtilis* (b), *E. coli* (d), *S. aureus* (f), and *S. typhimurium* (h).

were not observed, which further supports the non-leakage of entrapped drug due to an intact nature of QLNs. The detailed analysis of HR-TEM illustrates the presence of both loaded and unloaded nanoparticles. Fig. 2 portrays more numbers of loaded nanoparticles (electron dense nanoparticles shown by arrows), as compared to unloaded nanoparticles (lesser dense nanoparticles shown by dotted arrows). It has been reported that the dense region of nanoparticles is linked to an assembly of numerous inter-lamellar attachments in Glyceryl monooleate (GMO) based nanoparticles (Rangelov, Momekova, & Almgren, 2010). The finding is in compliance with encapsulation efficiency (~67.75%).

The effect of nanoparticles on antibacterial activity was determined by comparing the percentage retardation of bacterial growth by QLNs and free quercetin. QLNs displayed significantly ( $P < 0.05$ ) greater antibacterial activity against four food-borne pathogens

than free quercetin. Kinetics study showed the sustained release of quercetin from nanoparticles that inhibited the growth of test microorganisms over 48 h, as compared to less than 2–9 h for free quercetin. The free quercetin loses its antibacterial effect after 2–9 h (against all test microorganisms), which may facilitate the escaped bacteria to multiply at a faster rate under favorable conditions. Therefore, a controlled release formulation of QLNs will contain the growth of bacteria for the extended period, causing the complete lysis of bacteria. Similar findings were also described by Misra, Acharya, Dilnawaz, & Sahoo (2009). The bactericidal effects of QLNs against four food-borne microorganisms were in compliance with various results described by different authors. Nanoparticles entrapped with antibiotics have been explored for their bactericidal activity. In a study, azithromycin loaded nanoparticles showed more antibacterial effect than free azithromycin against

*S. typhimurium* (Mohammadi et al., 2010). The antimicrobial activity of nisin loaded nanoparticles showed an inhibitory effect against *M. luteus*, *P. aeruginosa*, *S. enterica* and *Escherichia aerogenes* for 20 days, compared to free nisin that showed antibacterial activity for six days (Bernela et al., 2014). The sustained release profile of levofloxacin from polymeric nanoparticles showed higher antibacterial efficacy against *E. coli* than the free levofloxacin (Cheow, Chang & Hadinoto, 2010). Furthermore, the antibacterial activity of nisin loaded solid lipid nanoparticles showed sustained effect against *Listeria monocytogenes* and *Lactobacillus plantarum* for 20 and 15 days, respectively, compared to <3 days for free nisin (Prombutara, Kulwatthanasal, Supaka, Sramala, & Chareonpornwattana, 2012).

We used the resazurin-microplate assay to compare the antibacterial activity of QLN and free quercetin. As reported earlier (Casey, O'Cleirigh, Walsh, & O'Shea, 2004), this method has certain advantages over the agar disk diffusion method in the determination of MIC, with reference to its sensitivity, cost-effectiveness, reproducibility, and the elimination of spectrophotometric plate reader. From the results of MIC and ZI, QLN showed better activity compared to free quercetin. It may be due to reduced particle size, which is responsible for better penetration and high uptake by the cells. Moreover, the results suggest that gram-positive bacteria (*B. subtilis* and *S. aureus*) was more sensitive than the gram-negative bacteria (*E. coli* and *S. typhimurium*), with respect to antibacterial action of QLN. It is well established that gram-positive bacteria consists of an external peptidoglycan coat while gram-negative bacteria consist of an outer lipopolysaccharide coat, both of which undergo various kinds of conversion when interacted with quercetin. Similar findings were reported by Bhawana, Basniwal, Buttar, Jain, Jain (2011). Furthermore, the MBCs values were greater than the MIC value, suggesting a higher concentration required to kill completely the bacterial populations. The *in-vitro* antibacterial assay clearly indicates that conversion to the nano form significantly improves the efficiency of quercetin as an antibacterial agent. To further illustrate the antibacterial mechanism of QLN against selected bacterial strains, AFM, and SEM studies were carried out.

The antibacterial activity of the prepared QLN was confirmed by AFM and SEM observations. QLN treated gram-positive bacteria (*B. subtilis*, and *S. aureus*) at its MIC value revealed various levels of cell disintegration, illustrated by (a) development of indentation on the surface of the cell; (b) shrinkage of cells; (c) exudation of cellular contents; and (d) loss of structural integrity. The probable mechanism might be due to direct interaction and binding of QLN to peptidoglycan layer. In the first stage, initial structural changes may occur due to the formation of indentation on bacterial surfaces followed by perturbation of the protective outer membrane and thus exposing the peptidoglycan layer beneath it. This disrupted layer might have been less protective leading to shrinkage of cells. Finally, cellular contents ooze out from bacteria causing cell lyses. In the final stage, bacteria lose its structural integrity (fragmented cellular parts) entirely leading to cell death. Similar findings were also reported by Neethirajan & DiCicco (2014) and Singh et al. (2014). At a MIC concentration of QLN, the gram-negative bacteria (*E. coli*, and *S. typhimurium*), showed morphological changes such as the formation of grooves as well as cellular debris around the damaged cells, suggesting cell lysis. Additionally, QLN treated bacterial cells showed collapsed and flattened structures indicating the leakage of cytoplasm and leaving behind the ghost cells. The results of roughness analysis further confirm the sensitivity of QLN to gram-positive bacteria (*B. subtilis* and *S. aureus*) than gram-negative bacteria (*E. coli* and *S. typhimurium*). In fact, gram-positive bacteria showed increased RMS roughness, compared to gram-negative microorganism. It could be hypothesized that QLN

have better anchoring and permeation into gram-positive cell wall leading to enhanced exposure of peptidoglycan layer followed by cell lysis.

The SEM further corroborated the mechanism of antibacterial activity of QLN. After treatment with QLN, structurally intact bacterial cell appears to be damaged. Both gram-positive bacteria and gram-negative bacteria cells were ruptured and shrunken followed by exudation of intracellular contents leading to cell lysis. SEM micrograph of treated cells elucidates adhesion and, or fusion process. The intimate contact between QLN and bacterial cells (due to high surface to volume ratio) with subsequent transfer of the entrapped drug through the polymer matrix lead to bacterial lyses.

## 5. Conclusion

The antibacterial study confirms that the QLN are more stable and more efficient in controlling the growth kinetics of tested microorganisms compared with free quercetin. It may be owing to the controlled release of the quercetin from the polymer matrix (nanoparticles) and thus, have a more profound antibacterial effect. The possible mechanism of enhanced antibacterial activity after loading the quercetin in polymeric nanoparticles is mainly due to alteration in membrane permeability, adsorption, and adhesion of nanoparticles with possible fusion with the cell membrane. Conclusively, the developed QLN may be used in the food industry to restrain the food spoilage owing to its profound anti-bacterial activity against food microorganisms.

The investigations of this research recommend that these polymeric nanoparticles might have various favorable applications within the food industry such as, encapsulation of various bioactive compounds for the progression of functional foods, enhancement of food production, and act as smart packaging material. Furthermore, it can also be used to extend the shelf life of food materials during storage.

## Acknowledgment

Dinesh Kumar V is thankful to UGC for the financial support as UGC-BSR (Grant No. F.4-1/2006 (BSR)/7-36/2007(BSR)). The authors are thankful to CIF, BIT Mesra (India) for SEM, AFM, DLS analysis. The authors are also thankful to BIT Mesra (India), for providing necessary facilities for this project.

## Appendix A. Supplementary data

Supplementary data related to this article can be found at <http://dx.doi.org/10.1016/j.lwt.2015.11.004>.

## References

- Bernela, M., Kaur, P., Chopra, M., & Thakur, R. (2014). Synthesis, characterization of nisin loaded alginate-chitosan-pluronic composite nanoparticles and evaluation against microbes. *LWT-Food Science and Technology*, 59, 1093–1099.
- Bhawana, Basniwal, R. K., Buttar, H. S., Jain, V. K., & Jain, N. (2011). Curcumin nanoparticles: preparation, characterization and antimicrobial study. *Journal of Agriculture and Food Chemistry*, 59, 2056–2061.
- Bischoff, S. C. (2008). Quercetin: potentials in the prevention and therapy of disease. *Current Opinion in Clinical Nutrition and Metabolic Care*, 11, 733–740.
- Boots, A. W., Haenen, G. R., & Bast, A. (2008). Health effects of quercetin: from antioxidant to nutraceutical. *European Journal of Pharmacology*, 585, 325–337.
- Bueno, C., Villegas, M. L., Bertolotti, S. G., Previtali, C. M., Neumann, M. G., & Encinas, M. V. (2002). The excited-state interaction of resazurin with amines in aqueous solutions: photophysics and photochemical reaction. *Photochemistry and Photobiology*, 76, 385–390.
- Byun, Y., Hwang, J. B., Bang, S. H., Darby, D., Cooksey, K., Dawson, P. L., et al. (2011). Formulation and characterization of  $\alpha$ -tocopherol loaded poly 3-caprolactone (PCL) nanoparticles. *LWT - Food Science and Technology*, 44, 24–28.
- Casey, J. T., O'Cleirigh, C., Walsh, P. K., & O'Shea, D. G. (2004). Development of a robust microtiter plate based assay method for assessment of bioactivity.

- Journal of Microbiological Methods*, 58, 327–334.
- Celiktas, O. Y., Kocabas, E. E. H., Bedir, H., Sukan, F. V., Ozek, T., & Baser, K. H. C. (2007). Antimicrobial activities of methanol extracts and essential oils of *Rosmarinus officinalis*, depending on location and seasonal variations. *Food Chemistry*, 100, 553–559.
- Cheow, W. S., Chang, M. W., & Hadinoto, K. (2010). Antibacterial efficacy of inhalable levofloxacin-loaded polymeric nanoparticles against *E. coli* biofilm cells: the effect of antibiotic release profile. *Pharmaceutical Research*, 27, 1597–1609.
- Chiellini, F., Piras, A. M., Errico, C., & Chiellini, E. (2008). Micro/nanostructured polymeric systems for biomedical and pharmaceutical applications. *Nanomedicine*, 3, 367–393.
- Coelho, J. F., Ferreira, P. C., Alves, P., Cordeiro, R., Fonseca, A. C., Góis, J. R., et al. (2010). Drug delivery systems: advanced technologies potentially applicable in personalized treatments. *The EPMA Journal*, 1, 164–209.
- Costa, A. R. M., Marquafavel, F. S., Vaz, M. M. O. L. L., Rocha, B. A., Bueno, P. C. P., Amaral, P. L. M., et al. (2011). Quercetin-PVP K25 solid dispersions. *Journal of Thermal Analysis and Calorimetry*, 104, 273–278.
- Day, A. J., Mellon, F., Barron, D., Sarrazin, G., Morgan, M. R. A., & Williamson, G. (2001). Human metabolism of dietary flavonoids: identification of plasma metabolites of quercetin. *Free Radical Research*, 35, 941–952.
- Dinesh Kumar, V., Verma, P. R. P., & Singh, S. K. (2015). Development and evaluation of biodegradable polymeric nanoparticles for the effective delivery of quercetin using a quality by design approach. *LWT – Food Science and Technology*, 61, 330–338.
- Dinesh Kumar, V., Verma, P. R. P., Singh, S. K., & Viswanathan, S. (2015). LC-ESI-MS/MS analysis of quercetin in rat plasma after oral administration of biodegradable nanoparticles. *Biomedical Chromatography*. <http://dx.doi.org/10.1002/bmc.3486>
- Formica, J. V., & Regelson, W. (1995). Review of the biology of quercetin and related bioflavonoids. *Food and Chemical Toxicology*, 33, 1061–1080.
- Gang, W., Jie, W. J., Ping, Z. L., Ming, D. S., Ying, L. J., Lei, W., et al. (2012). Liposomal quercetin: evaluating drug delivery *in vitro* and bio-distribution *in vivo*. *Expert Opinon on Drug Delivery*, 9, 599–613.
- Goñi, P., López, P., Sánchez, C., Gómez-Lus, R., Becerril, R., & Nerin, C. (2009). Antimicrobial activity in the vapour phase of a combination of cinnamon and clove essential oils. *Food Chemistry*, 116, 982–989.
- Hertog, M. G. L., Hollman, P. C. H., Katan, M. B., & Kromhout, D. (1993). Intake of potentially anticarcinogenic flavonoids and their determinants in adults in the Netherlands. *Nutrition and Cancer*, 20, 21–29.
- Hirpara, K. V., Aggarwal, P., Mukherjee, A. J., Joshi, N., & Burman, A. C. (2009). Quercetin and its derivatives: synthesis, pharmacological uses with special emphasis on anti-tumor properties and prodrug with enhanced bio-availability. *Anticancer Agents in Medicinal Chemistry*, 9, 138–161.
- Ivanova, E., Pancevska, N. A., & Kungulovski, D. (2013). Antimicrobial activities of laboratory produced essential oil solutions against five selected fungal strains. *Matica Srpska Journal of Natural Sciences*, 124, 171–183.
- Jaiswal, S., Duffy, B., Jaiswal, A. K., Stobie, N., & McHale, P. (2010). Enhancement of the antibacterial properties of silver nanoparticles using beta-cyclodextrin as a capping agent. *International Journal of Antimicrobial Agents*, 36, 280–283.
- Janovska, D., Kubikova, K., & Kokoska, L. (2003). Screening for antimicrobial activity of some medicinal plants species of traditional Chinese medicine. *Czech Journal of Food Science*, 21, 107–110.
- Kumar, V. D., Verma, P. R. P., & Singh, S. K. (2014). New insights into the diagnosis and chemotherapy for visceral leishmaniasis. *Current Drug Delivery*, 11, 200–213.
- Langfield, R. D., Scarano, F. J., Heitzman, M. E., Kondo, M., Hammond, G. B., & Neto, C. C. (2004). Use of a modified microplate bioassay method to investigate antibacterial activity in the Peruvian medicinal plant *Peperomia galioides*. *Journal of Ethnopharmacology*, 94, 279–281.
- LiPuma, J. J., Rathinavelu, S., Foster, B. K., Keoleian, J. C., Makidon, P. E., Kalikin, L. M., et al. (2009). *In vitro* activities of a novel nanoemulsion against Burkholderia and other multidrug-resistant cystic fibrosis-associated bacterial species. *Antimicrobial Agents and Chemotherapy*, 53, 249–255.
- Li, H., Zhao, X., Ma, Y., Zhai, G., Li, L., & Lou, H. (2009). Enhancement of gastrointestinal absorption of quercetin by solid lipid nanoparticles. *Journal of Controlled Release*, 133, 238–244.
- Mirzoeva, O. K., Grishanin, R. N., & Calder, P. C. (1997). Antimicrobial action of propolis and some of its components: the effects on growth, membrane potential and motility of bacteria. *Microbiological Research*, 152, 239–246.
- Misra, R., Acharya, S., Dilnawaz, F., & Sahoo, S. K. (2009). Sustained antibacterial activity of doxycycline-loaded poly(D,L-lactide-co-glycolide) and poly(epsilon-caprolactone) nanoparticles. *Nanomedicine*, 4, 519–530.
- Mohammadi, G., Valizadeh, H., Barzegar-Jalali, M., Lotfipour, F., Adibkia, K., Milani, M., et al. (2010). Development of azithromycin-PLGA nanoparticles: physicochemical characterization and antibacterial effect against *Salmonella typhi*. *Colloids and Surfaces B: Biointerfaces*, 80, 34–39.
- Mora-Huertas, C. E., Fessi, H., & Elaissari, A. (2011). Influence of process and formulation parameters on the formation of submicron particles by solvent displacement and emulsification-diffusion methods critical comparison. *Advances in Colloid Interface Science*, 163, 90–122.
- Mullen, W., Boitier, A., Stewart, A. J., & Crozier, A. (2004). Flavonoid metabolites in human plasma and urine after the consumption of red onions: analysis by liquid chromatography with photodiode array and full scan tandem mass spectrometric detection. *Journal of Chromatography A*, 1058, 163–168.
- NCCLS. (2006). *Methods for dilution antimicrobial susceptibility tests for bacteria that grow aerobically. Approved standard M7–A7*. Wayne, PA, USA: Clinical and laboratory Standards Institute.
- Neethirajan, S., & DiCicco, M. (2014). Atomic force microscopy study of the antibacterial effect of fosfomycin on methicillin-resistant staphylococcus pseudintermedius. *Applied Nanoscience*, 4, 703–709.
- Nijveldt, R. J., Van Nood, E., Van Hoorn, D. E., Boelens, P. G., Van Norren, K., & Van Leeuwen, P. A. (2001). Flavonoids: a review of probable mechanisms of action and potential applications. *American Journal of Clinical Nutrition*, 74, 418–425.
- Ohemeng, K. A., Schwender, C. F., Fu, K. P., & Barrett, J. F. (1993). DNA gyrase inhibitory and antibacterial activity of some flavones (1). *Bioorganic and Medicinal Chemistry Letters*, 3, 225–230.
- Ohnishi, E., & Bannai, H. (1993). Quercetin potentiates TNF-induced antiviral activity. *Antiviral Research*, 22, 327–331.
- Plaper, A., Golob, M., Hafner, I., Oblak, M., Solmajer, T., & Jerala, R. (2003). Characterization of quercetin binding site on DNA gyrase. *Biochemical and Biophysical Research Communications*, 306, 530–536.
- Pool, H., Quintanar, D., Figueroa, J. D., Bechara, J. E. H., Clements, D. J., & Mendoza, S. (2012). Polymeric nanoparticles as oral delivery systems for encapsulation and release of polyphenolic compounds: impact on quercetin antioxidant activity & bioaccessibility. *Food Biophysics*, 7, 276–288.
- Prombutara, P., kulwatthanasal, Y., Supaka, N., Sramala, I., & Chareonpornwattana, S. (2012). Production of nisin loaded solid lipid nanoparticles for sustained antimicrobial activity. *Food Control*, 24, 184–190.
- Rangelov, S., Momekova, D., & Almgren, M. (2010). Structural characterization of lipid based colloidal dispersions using cryogenic transmission electron microscopy. *Microscopy: Science, Technology, Applications and Education*, 1724–1734.
- Russo, M., Spagnuolo, C., Tedesco, I., Bilotta, S., & Russo, G. L. (2012). The flavonoid quercetin in disease prevention and therapy: facts and fancies. *Biochemical Pharmacology*, 83, 6–15.
- Sabliov, C., Chen, H., & Yada, R. (Eds.). (2015). *Nanotechnology and functional foods: effective delivery of bioactive ingredients*. UK: John Wiley and Sons Ltd.. pp. 285.
- Sahoo, N. G., Kakran, M., Shaal, L. A., Li, L., Muller, R. H., Pal, M., et al. (2011). Preparation and characterization of quercetin nanocrystals. *Journal of Pharmaceutical Science*, 100, 2379–2390.
- Sarker, S. D., Nahar, L., & Kumarasamy, Y. (2007). Microtitre plate-based antibacterial assay incorporating resazurin as an indicator of cell growth, and its application in the *in vitro* antibacterial screening of phytochemicals. *Methods*, 42, 321–324.
- Silva, E. R., Maquiaveli, C. C., & Magalhaes, P. P. (2012). The leishmanicidal flavonols quercetin and quercitrin target Leishmania (Leishmania) amazonensis arginase. *Experimental Parasitology*, 130, 183–188.
- Singh, D., Rawat, M. S. M., Semalty, A., & Semalty, M. (2012). Quercetin-phospholipid complex: an amorphous pharmaceutical system in herbal drug delivery. *Current Drug Discovery Technologies*, 9, 17–24.
- Singh, N., Verma, S. M., Singh, S. K., & Verma, P. R. P. (2014). Consequences of lipidic nanoemulsions on membrane integrity and ultrastructural morphology of *Staphylococcus aureus*. *Material Research Express*, 1, 1–23.
- Singh, N., Verma, S. M., Singh, S. K., & Verma, P. R. P. (2015). Antibacterial action of lipidic nanoemulsions using atomic force microscopy and scanning electron microscopy on *Escherichia coli*. *Journal of Experimental Nanoscience*, 10, 1–11.
- Stojković, D., Petrović, J., Soković, M., Glamočlija, J., Kukić-Marković, J., & Petrović, S. (2013). *In situ* antioxidant and antimicrobial activities of naturally occurring caffeic acid, p-coumaric acid and rutin, using food systems. *Journal of the Science of Food and Agriculture*, 93, 3205–3208.
- Verma, S., Singh, S. K., Verma, P. R. P., & Ahsan, M. N. (2014). Formulation by design of felodipine loaded liquid and solid self nanoemulsifying drug delivery systems using Box–Behnken design. *Drug Development and Industrial Pharmacy*, 40, 1358–1370.
- World Health Organization (WHO). (2009). *Guidelines for stability testing of pharmaceutical products*. Geneva. Available from: [http://www.gmp-compliance.org/guidemgr/files/WHO\\_TRS\\_953\\_ANNEX2.PDF](http://www.gmp-compliance.org/guidemgr/files/WHO_TRS_953_ANNEX2.PDF).



# Physical decontamination of lupin (*Lupinus angustifolius*) protein isolates, seeds and flakes: Effects on microbiological status and micellar protein yield



Denise Melde<sup>\*</sup>, Claudia Wiacek, Peggy Gabriele Braun

Institute of Food Hygiene, Leipzig University, An den Tierkliniken 1, 04103 Leipzig, Germany

## ARTICLE INFO

### Article history:

Received 26 September 2015  
Received in revised form  
10 November 2015  
Accepted 17 November 2015  
Available online 22 November 2015

### Keywords:

Seed decontamination  
Total viable count  
Micellar lupin protein yield  
Ultraviolet radiation  
Dry heat

## ABSTRACT

Plant seeds are important food sources. Because of inevitable soil contact seeds harbor a large number of microorganisms, especially spore-forming bacteria who are able to germinate in food products. Micellar lupin (*Lupinus angustifolius*) protein isolates, suitable as fat replacers in foods, may include these bacteria and therefore represent a risk for consumers. To guarantee safe food, these protein isolates were pasteurized (60–80 °C, 2.5–30 min), leading to a 4-log reduction of the microbial count. Nevertheless spore-forming microorganisms remained. To inactivate these bacteria whole lupin seeds and processed raw materials (dehulled seeds, flakes) were decontaminated before protein extraction by physical methods: Ultraviolet (UVC) radiation (20, 60 min), dry heat (60 min, 110–140 °C) and wet heat (autoclaving: 115 °C, 20 min). Protein yield and decontamination performance were investigated. Autoclaving turned out to be unsuitable (up to 50% decrease of protein yield) whereas dry heat at 110 °C and 120 °C resulted in a significant increase for all raw materials. Best results concerning protein yield and decontamination performance were obtained by a dry heat treatment (130 °C) for dehulled seeds and flakes and by UVC radiation (60 min) for whole seeds, dehulled seeds and full-fat flakes.

© 2015 Elsevier Ltd. All rights reserved.

## 1. Introduction

Legumes play an increasing role in human nutrition. Especially sweet lupins become more and more interesting due to their high protein (~40%, thereof 85% globulins and 15% albumins in *Lupinus angustifolius* (Belski, 2012)) and low starch content (Hedley, 2001). Moreover they are not genetically modified and low in alkaloids (Hudson, 1979). Numerous publications deal with functional properties of lupin protein isolates (>85% protein content) and concentrates (>60% protein content; Kroll, Krause, & Rawel, 2007), like gel formation, oil and water absorption, solubility, emulsification and foaming characteristics (Bader, Oviedo, Pickardt, & Eisner, 2011; Berghout, Boom, & van der Goot, 2015; El-Adawy, Rahma, El-Bedawey, & Gafar, 2001; King, Aguirre, & Depablo, 1985; Rodríguez-Ambriz, Martínez-Ayala, Millán, & Dávila-Ortíz, 2005). These

functional properties are strongly influenced by the extraction procedure and extraction parameters.

The micellisation, for instance, produces a protein isolate which mainly consists of globulins (El-Adawy et al., 2001). This method is initiated by a salt-induced extraction and terminated by a dilutive precipitation. There are no process steps with disruptive effects on the protein structure, like strong heat or chemicals. The micellisation results in a native protein isolate with a creamy and fat-like mouthfeel, which makes it suitable as an excellent fat replacer in foods (Muranyi, Otto, Pickardt, Koehler, & Schweiggert-Weisz, 2013; Sussmann, Halter, Pickardt, Schweiggert-Weisz, & Eisner, 2013a).

For such an application the microbiological status is important for the purposes of product and consumer safety. A total viable count (TVC) of about  $10^4$  cfu g<sup>-1</sup> was constituted to be the guide level, approximated to the declaration of commercial available soy protein isolates (D'Agostina et al. 2006). Generally the raw material, lupin seeds, and the derived defatted flakes have microbial loads of  $10^3$ – $10^5$  cfu g<sup>-1</sup> which are composed of 80–100% spore-forming bacteria e. g. *Bacillus cereus*. (D'Agostina et al. 2006; Melde, Koenig, Sussmann, Pickardt, & Braun, 2011). Only limited

Abbreviations: TVC, total viable count; MPI, micellar protein isolate; UVC, ultraviolet.

<sup>\*</sup> Corresponding author.

E-mail addresses: [melde@vetmed.uni-leipzig.de](mailto:melde@vetmed.uni-leipzig.de) (D. Melde), [claudia.wiacek@vetmed.uni-leipzig.de](mailto:claudia.wiacek@vetmed.uni-leipzig.de) (C. Wiacek), [pbraun@vetmed.uni-leipzig.de](mailto:pbraun@vetmed.uni-leipzig.de) (P.G. Braun).

information is available concerning the inactivation of bacterial spores on seeds, but without treatments these bacteria most likely would be concentrated leading to a higher microbial load of the protein isolate.

Most studies deal with decontamination treatments inactivating pathogen gram-negative bacteria, such as *Salmonella* spp. and *Escherichia coli*, without a loss in germination capacity in order to produce sprouts (Olaimat & Holley, 2012). Methods applied were for example chemical solutions, hot water, dry heat treatment, ultrasonication or microbial DNA injuring ultraviolet radiation (Chiu & Sung, 2014; Erdogdu & Ekiz, 2011; Hidaka & Kubota, 2006; Nei, Bari, & Enomoto, 2013).

The application of these methods is suitable for lupin seeds and flakes, but not for the micellar lupin protein isolate (MPI), since the harsh conditions will result in protein denaturation and loss of MPI's functional properties (Sirtori, Resta, Brambilla, Zacherl, & Arnoldi, 2010). Pasteurization might be an alternative for MPI treatment.

The aim of the present study is the examination and comparison of MPI pasteurizations and different decontamination methods for lupin seeds and flakes (UVC-radiation, dry heat treatment, autoclaving) concerning their effect on the resulting microbial load as well as the quantification of the extractable protein yield after decontamination of seeds and flakes.

We analyzed and characterized, based on lupin seeds as raw material, the microbial load of all intermediate (flakes) and final products (MPI) produced on a pilot plant scale, before and after decontamination treatments, to get information at which process steps recontamination occurs.

## 2. Materials and methods

### 2.1. Raw materials and chemicals

Whole and dehulled lupin seeds and full-fat and defatted (n-hexane) flakes from *L. angustifolius* cv Vitabor were used for the decontamination treatments. Seeds were obtained from Saat-zucht Steinach (Steinach, Germany), and dehulling, flaking and oil removal were performed at the Fraunhofer IVV (Institute for Process Engineering and Packaging) Freising.

For microbiological analysis culture media from Oxoid (Oxoid Deutschland GmbH, Wesel, Germany) were used. Nutrient Broth I was purchased from Sifin (Sifin Diagnostics GmbH, Berlin, Germany), NaCl-peptone was prepared from 1 g L<sup>-1</sup> peptone ex casein (Carl Roth GmbH & Co. KG, Karlsruhe, Germany) and 8.5 g L<sup>-1</sup> sodium chloride (Carl Roth). All chemicals were of analytical grade.

### 2.2. Micellar protein isolation procedure

Whole and dehulled seeds were milled (2–4 × 10 s, 10,000 rpm) by a knife mill (GRINDOMIX GM 200, Retsch GmbH, Haan, Germany). The micellar proteins (globulin fraction) were extracted according to the method of Sussmann, Pickardt, Schweiggert, and Eisner (2013b). From a microbial point of view the extraction temperature was determined to 50 °C. Preheated 0.5 M NaCl solution and lupin flakes were mixed in a ratio of 7:1, stirred 60 min at 500 rpm (RET basic safety control with contact thermometer ETS-D5, IKA®-Werke GmbH & Co. KG, Staufen, Germany) and separated through a sieve with 1.2 mm mesh width. After centrifugation (20 °C, 10 min, 3300 g) of the eluate the supernatant was filtered through a woven rayon–polyester filter (Miracloth, Merck KGaA, Darmstadt, Germany). The dilution precipitation was initiated by adding two parts of deionized water to one part of the extract. The precipitated protein was recovered after sedimentation (4 °C, 18 h) by centrifugation (20 °C, 10 min, 3300 g) and subsequently washed

with deionized water at a ratio of 1:3.

### 2.3. Pasteurization of micellar protein isolate

MPI from defatted lupin flakes was poured into an Erlenmeyer flask and heated in a water bath. The water temperature was set five degree above the pasteurization temperature (60 °C/10 min; 65 °C/5 and 30 min; 70 °C/5 min; 75 °C/2.5 and 5 min; 80 °C/2.5 and 5 min). The samples were stirred continuously and time stopped as soon as the protein reached the set temperature, which was measured with a digital contact thermometer in a reference. At least five replications were performed.

### 2.4. Methods of seed and flake decontamination

All treatments were realized at least in triplicate with 100 g of seeds or flakes.

#### 2.4.1. Dry heat treatment

Seeds and flakes were placed on stainless steel tablets (every seed or flake side by side) in a heating oven (Binder GmbH, Tuttlingen, Germany) on the middle rack and heated at different temperatures (110–140 °C) for 60 min.

#### 2.4.2. Wet heat treatment (autoclaving)

Seeds and flakes were autoclaved (vertical, floor-standing autoclave Systec VX-120) at 115 °C for 20 min.

#### 2.4.3. UVC radiation

Seeds and flakes were placed into beakers (filling level: max. 2 cm) on a magnetic stirrer (RET basic safety control) and deposited under UV-lamps at a distance of 20 cm (UV irradiance: 5 W m<sup>-2</sup>). The samples were radiated (2 germicidal lamps: Osram Puritec HNS 15W G13 OFR; 254 nm; ozone free) with stirring (500 rpm) for 20 and 60 min.

#### 2.4.4. Microbiological analysis

For sterility-testing 0.5 g of treated or untreated seeds and flakes were mixed with 5 ml of Nutrient Broth I and incubated 20 h at 37 °C. 100 µl of the solution were plated on blood agar (Oxoid, PB5039A) and incubated again 20 h at 37 °C. Seeds and flakes were defined to be sterile if no growth was detectable. Additionally 10 g of treated or untreated seeds and flakes were mixed with 90 ml of NaCl-peptone and 1 ml was plated on 3 Plate Count Agar (Oxoid, PO5013A) to determine the TVC after incubation at 30 °C for 72 h.

For pasteurization trials 10 g pasteurized MPI were blended (Stomacher® 400 Circulator, Seward, UK) with 90 ml of NaCl-peptone. Subsequently 1 ml of the mixture was diluted (1:10) with NaCl-peptone, plated on PC agar and incubated 72 h at 30 °C.

### 2.5. Statistical analysis

Results are expressed as mean ± standard deviation. Kruskal–Wallis test with Dunn's Multiple Comparison post test was performed for all microbial counts, one-way ANOVA with Bonferroni's post test was performed for protein yields, both using GraphPad Prism version 4.00 for Windows (GraphPad Software, San Diego California USA, [www.graphpad.com](http://www.graphpad.com)).

Protein yield was calculated by dividing extracted protein amount [g] by initial weight of raw material for the extraction [g]. The result was expressed as percentage.

### 3. Results and discussion

#### 3.1. Pasteurization of micellar lupin protein isolate

The untreated MPI had a microbial load of  $1.9 \times 10^7$  cfu g<sup>-1</sup> (Fig. 1). 95% of these bacteria, were gram-positive cocci, the remaining were gram-positive (non spore-forming, spore-forming) and gram-negative rod-shaped bacteria.

The decontamination by pasteurization was carried out by different time-temperature-combinations. A significant ( $P < 0.05$ ) reduction of microorganisms up to  $5.9 \times 10^4$  cfu g<sup>-1</sup> at first was detected at 65 °C for 30 min. Compared to the untreated MPI no alteration of the species distribution was determined. The highest microbial reductions were achieved at 75 °C for 5 min and 80 °C for 2.5 min. A further time prolongation with lower temperatures did not improve the reduction. The TVC was reduced below  $10^4$  cfu g<sup>-1</sup> whereas primarily cocci (40%) followed by spore forming rods (30%) and gram-negative rods (30%) survived. Yoshie-Stark, Bez, and Wäsche (2006) reported a satisfying bacterial reduction after 65 °C and 16.7 min for an acid insoluble/neutral pH soluble protein isolate; unfortunately they did not mention the resulting count.

There were no obvious differences between pasteurized and untreated protein isolates up to 75 °C. However, the samples treated at 80 °C exhibited a bit crumbly texture, which was classified as a signal of denaturation. Sirtori et al. (2010) investigated the thermal denaturation of another native lupin globulin isolate, mainly consisting of the vicilin-like  $\beta$ -conglutin (7S) and the legumin-like  $\alpha$ -conglutin (11S).  $\beta$ -conglutin was denatured starting at 71.49 °C followed by  $\alpha$ -conglutin at 90.92 °C for the untreated protein isolate. Sirtori et al. (2010) described a possible heat treatment of the protein isolate at 100 °C for 5 min that did not result in denaturation of  $\beta$ -conglutin, as longer times or higher temperatures did. Regarding this, heat inactivation of bacterial spores will not be achievable with such a gentle treatment and the native fat-like protein structure will be destroyed.

The TVC as well as the remaining  $2.0 \times 10^3$  cfu g<sup>-1</sup> spore-forming microorganisms of the 75 °C/5 min-sample correspond approximately to the microbial count of lupin seeds and flakes, which is mainly composed of spore-forming bacteria (95% in whole seeds, 83% in defatted flakes, chapter 3.2). Consequently our results indicate that pasteurization at 75 °C for 5 min could be a suitable method for the reduction of bacteria carried in during the process of protein isolation.

#### 3.2. Lupin seed and flake decontamination and influence on extractable MPI yield

In terms of consumer protection even surviving spore-forming microorganisms should be inactivated, in order to avoid

germination and spoilage of MPI containing food. For this purpose whole lupin seeds, dehulled seeds, full-fat flakes and defatted flakes were decontaminated by three different methods: UVC radiation (20, 60 min), dry heat (110–140 °C for 1 h) and wet heat (autoclaving at 115 °C for 20 min).

The whole seeds had an initial microbial load of  $6.1 \times 10^2$  cfu g<sup>-1</sup>, comprising 95% spore-forming bacteria. UVC radiation (60 min), autoclaving and dry heat treatments at 130 °C and 140 °C resulted in a significant reduction ( $P < 0.05$ ) of the TVC, whereby a dry heat treatment at 140 °C for 60 min as well as autoclaving led to a complete inactivation (Fig. 2a), which was verified by sterility-tests. Regarding the protein yield, strong variations were observed. Autoclaving and the 1 h dry heat treatments at 130 °C and 140 °C significantly ( $P < 0.05$ ) reduced the extracted amount of MPI from 12.0% (untreated) up to 7.5% (autoclaved) respectively 3.0% (130 °C). After the 140 °C treatment no protein was extractable. In contrast UVC radiation (60 min) and dry heat treatment with lower temperatures (110–120 °C) resulted in the opposite effect; a significant increase in extractable MPI up to 16.7% in the case of the 110 °C-sample.

Dehulling of the seeds already entailed a slight decline in the TVC up to  $2.1 \times 10^2$  cfu g<sup>-1</sup> (untreated dehulled seeds), comprising 34% spore-forming microorganisms. As Fig. 2b illustrates, seed sterility was obtained by autoclaving and dry heating starting from 130 °C. A significant ( $P < 0.05$ ) reduction of the microbial count was also achieved due to the UVC treatments (up to  $2.5 \times 10^0$  cfu g<sup>-1</sup>). A similar value ( $3.3 \times 10^0$  cfu g<sup>-1</sup>) was obtained after dry heating at 140 °C, however it is not significant because of the small number of replications ( $n = 3$ ), as with the 110 °C and 120 °C trials. The protein yield was 19.8% in the case of untreated dehulled seeds and declined significantly up to 9.7% if the heating temperature exceeded 130 °C as well as by autoclaving (12.5%). Dry heat treatments at 110–130 °C resulted in a slight increase of protein yield (22.6–26.7%), UVC treatments had no influence on the protein yield. Whole seeds contain a large amount of hulls, and the least amount extractable micellar protein. Generally, the higher micellar protein yield of dehulled seeds than of whole seeds was caused by the lower hull content, whereas the protein content of the hulls is negligibly low (Hove, 1974).

The microbial load, composition and decontamination results of the full-fat flakes (Fig. 2c) were similar to those of the dehulled seeds, since they contain the same small amount of hulls. Also the percentage of spore-forming microorganisms was comparable with the dehulled seeds. This indicates a contamination of raw materials during the dehulling. Product sterility was achieved by UVC treatment (60 min), autoclaving and dry heating at 130 and 140 °C. Regarding the protein yield, best results were obtained from full-fat flakes, compared to the other raw materials, whereby 25.3% MPI was extractable of untreated full-fat flakes. This corresponds to the

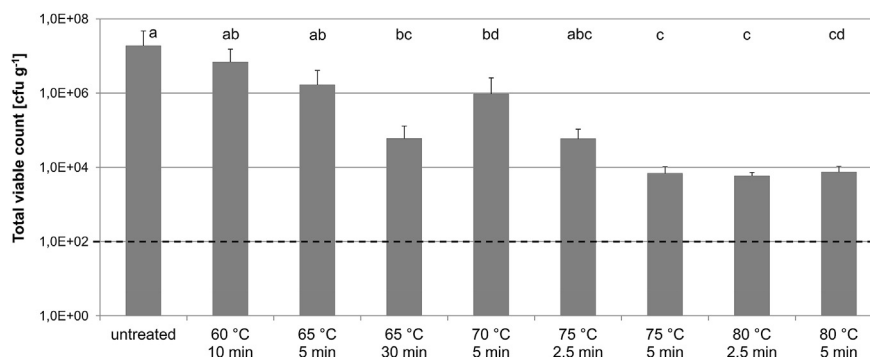


Fig. 1. TVC of micellar protein isolates before and after several heat treatments (Different letters indicate significant differences ( $P < 0.05$ ); – detection limit).

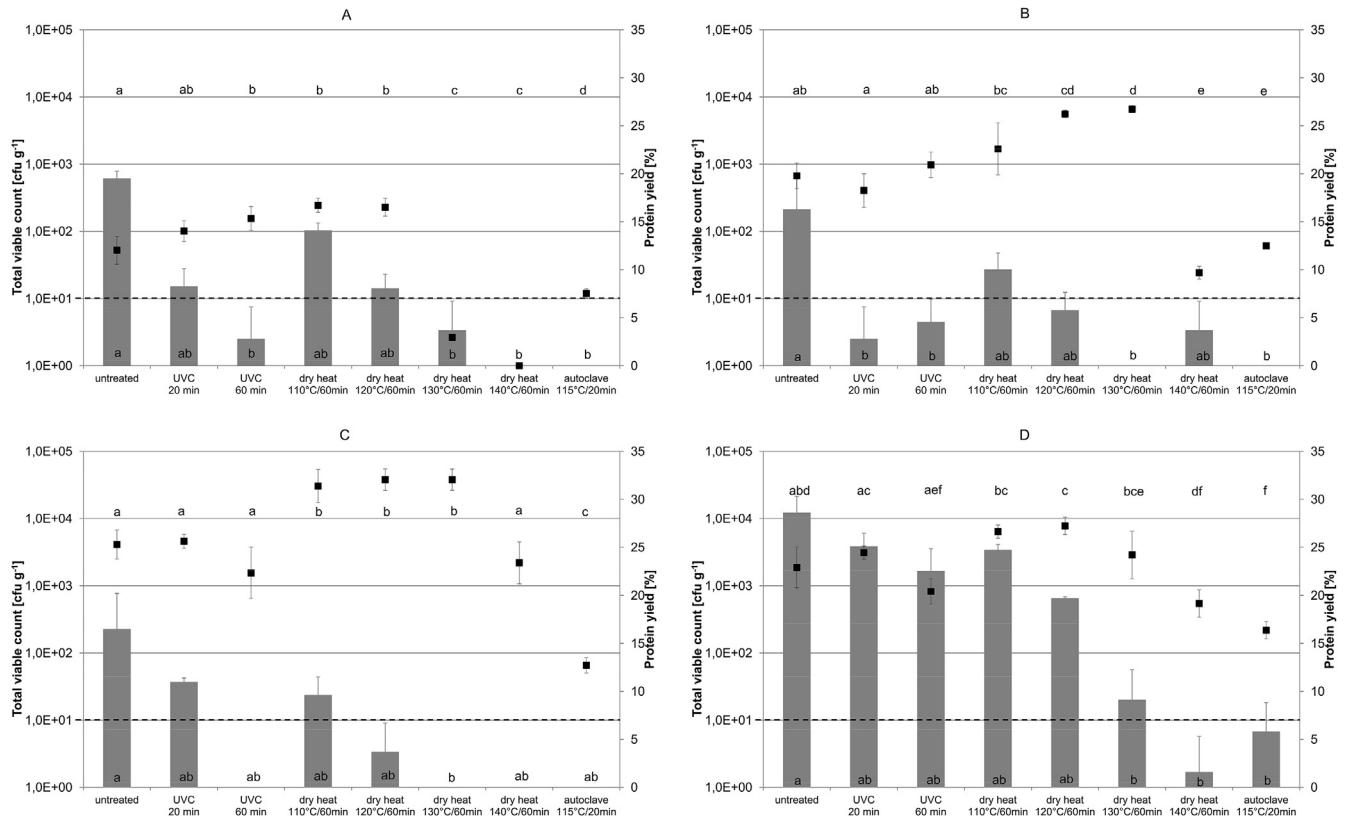


Fig. 2. Total viable count (bar) of raw materials (left y-axis) and protein yield (■) after extraction (right y-axis) of untreated and differently treated A) whole lupin seeds, B) dehulled lupin seeds, C) full-fat lupin flakes, D) defatted lupin flakes (Different letters indicate significant differences ( $P < 0.05$ ); – detection limit).

findings of [Sussmann et al. \(2013a\)](#). Only autoclaving resulted in a significant ( $P < 0.05$ ) loss of protein yield up to 12.7%. Dry heated ( $< 140$  °C) full-fat flakes exhibited a significant larger quantity of extractable MPI, up to 32.1% in the case of full-fat flakes treated at 120 and 130 °C. UVC radiation and dry heating at 140 °C did not change the protein yields.

Protein yields of defatted flakes closely resembled those of the full-fat flakes, whereas the microbial load ( $1.2 \times 10^4$  cfu  $g^{-1}$ , 83% spore-forming bacteria) differed at a high rate ([Fig. 2d](#)). Contemporaneous seed preparation (dehulling, flaking, oil removal) as a single process allows the conclusion that there is an additional bacterial contamination or growth during the de-oiling. A significant reduction ( $P < 0.05$ ) to around  $10^1$  cfu  $g^{-1}$  was only achieved by a dry heat treatment above 120 °C and autoclaving.

[Table 1](#) represents the deviation of micellar protein yield of decontaminated raw materials from micellar protein yield of untreated raw materials. Whole seeds had the highest sensitivity to

dry heat treatment at 130 and 140 °C (75.4 and 100% loss of protein yield). In addition the percental impact of all treatments on protein yield was highest for the whole seeds (maximum protein yield drift values) and lowest for the defatted flakes. The highest percentage loss of protein yield by autoclaving was observed for the full-fat flakes (49.7%).

It seems that there is an increase of protein yield after dry heat treatment at 110–120 °C for all raw materials (14.1–38.9%), additionally at 130 °C in the case of dehulled (35.1%) and flaked (5.7–26.7%) lupin seeds. Greatest loss of protein yield generally was detected after dry heating at 140 °C and autoclaving. A markedly reduction (nearly 50%) of the globulin fraction after dry heat processing (160 °C, 10–20 min) of African breadfruit seed was also observed by [Giami, Adindu, Hart, and Denenu \(2001\)](#). Unlike increasing protein yield after 110 °C or 120 °C dry heat treatment in the present study, it may be assumed that there is a higher sensitivity of lupin seed proteins to wet heat versus dry heat. [Samadi and](#)

**Table 1**  
Drift of protein yield after extraction of differently treated raw materials.

Treatment	Drift of protein yield [%] <sup>a</sup>			
	Whole seeds	Dehulled seeds	Full-fat flakes	Defatted flakes
UVC 20 min	16.6 ± 9.1	−7.8 ± 8.8	1.3 ± 2.9	6.7 ± 3.0
UVC 60 min	27.5 ± 10.3	5.8 ± 6.7	−11.7 ± 10.6	−10.9 ± 5.8
dry heat 110 °C/60 min	38.9 ± 6.1	14.1 ± 13.8	24.0 ± 6.9	16.3 ± 3.0
dry heat 120 °C/60 min	37.3 ± 7.7	32.5 ± 2.0	26.7 ± 4.5	18.9 ± 3.9
dry heat 130 °C/60 min	−75.4 ± 2.2	35.1 ± 1.9	26.7 ± 4.4	5.7 ± 10.8
dry heat 140 °C/60 min	−100.0 ± 0.0	−51.1 ± 3.4	−7.5 ± 8.6	−16.4 ± 6.2
autoclaving 115 °C/20 min	−37.4 ± 4.0	−36.9 ± 1.4	−49.7 ± 3.2	−28.5 ± 4.0

<sup>a</sup> Amount of MPI extracted after decontamination treatment related to amount of MPI of untreated seeds and flakes; negative values signify a decrease, positive values an increase of protein yield,  $n = 3-8$ .

Yu (2011) and Peng, Khan, Wang, and Yu (2014) came to the same conclusion for soybean and camelina seeds after 1 h dry heat treatment as compared to autoclaving at 120 °C concerning protein structure and nutritional profile.

Based on the fact that the hulls of lupin seeds are very impermeable to water (Karaguzel, Cakmakci, Ortacesme, & Aydinoglu, 2004), the wet heat sensitivity could be a possible reason for the high sensitivity of whole seeds to dry heat at 130 °C and 140 °C: If there is a delayed entry of water through the hulls into the seeds, it may be the same if water tries to leave the hull from inside the seed. Water could accumulate below the hull for a short time and the process becomes similar to a wet heat treatment.

Sousa, Mitchell, Ledward, Hill, and da Costa (1995) investigated lupin globulins by means of differential scanning calorimetry (DSC). The authors concluded an increasing thermal stability of these globulins with decreasing moisture content during the DSC measurement. This fact may also be a reason for the higher stability of micellar (globulin) proteins extractable after dry heat treatments at 110–120 °C and in some extent at 130 °C. However no reason for the increasing protein yield could be concluded.

By comparing the protein yields of dry heated full-fat and defatted flakes the proteins of the full-fat flakes seemed to be more heat-stable. It is possible, that the lipids of the full-fat flakes provide a protective effect on the lupin globulins, like it is known for the whey protein  $\beta$ -lactoglobulin after addition of hydrophobic compounds like lecithin and fatty acids (Wijayanti, Bansal, & Deeth, 2014).

Regarding reduction of the TVCs and only minimal drifts in protein yield UVC radiation appears as a potential method for seed decontamination. This confirms a statement of the National Advisory Committee on Microbiological Criteria for Foods (1999). UVC treatment reduced the TVCs about 68–99% within 20 min and 86–100% within 60 min, whereas the lower values belong to the defatted flakes. As expected UVC decontamination of defatted flakes would be more difficult because of the higher initial bacterial load. Additionally seed preparation (dehulling, flaking, oil removal) may have an influence on surface structure and topography and therefore on the results of the UVC treatment, since the surface character can influence the efficacy of UV light decontamination (Koutchma, 2008). Otherwise in the case of full-fat flakes a reduction of the TVC of 86 and 100% after 20 and 60 min UVC treatment could be achieved. This allows the presumption that besides the surface structure, the initial bacterial count also plays an important role for the efficacy of UVC radiation.

Compared to the results of Hidaka and Kubota (2006), who attained a 90% sterilization rate for wheat total bacterial count after a 6.3 h UVC treatment (97 W m<sup>-2</sup> UV irradiance), our decontamination performance is very adequate. Erdogdu and Ekiz (2011) gave a description on UVC treatment of cumin seeds with initial counts of total mesophilic aerobic bacteria of 10<sup>4.6</sup>–10<sup>5.6</sup> cfu g<sup>-1</sup>. A 60 min UVC treatment (105 W m<sup>-2</sup>) resulted in a 0.6 log reduction of bacterial count. Increasing treatment time (2 h) only influenced the number of coliform and fecal coliform bacteria, which were completely inactivated.

In principle all presented raw materials are suitable for extraction of micellar lupin protein isolate. Nevertheless there are some advantages and disadvantages. Whole seeds should be dehulled before milling, to increase protein yield. From the microbiological point of view these two steps are possible sources of contamination. Thus, it should be considered whether the decontamination of flakes could be more sensible, although the reduction of microbial counts of whole and dehulled seeds in certain cases is easier, especially in comparison to the defatted flakes. In case of the flakes it might be preferable to use defatted before full-fat flakes, since the legume-like flavor can be reduced by means of a de-oiling process

(Bader et al., 2011).

#### 4. Conclusions

It is generally known that spores are able to germinate in food products under specific conditions. The European Food Safety Authority (2005) reported on a potential hazard given by small counts of *B. cereus*. Since the micellar lupin protein isolation procedure is gentle, it is not to be expected that the isolate will be spore-free, even if a pasteurization step is included. As a result spore-forming bacteria could induce food spoilage or foodborne diseases, if the conditions are feasible.

Physical decontamination of lupin seeds and flakes resulted in a strong decrease (between 68%–100%) in total microbial counts, that were most of all composed of spore-forming microorganisms. In terms of UVC radiation, the reduction strongly depended on the method of seed preparation (dehulling, flaking, oil removal) as well as initial TVC. The most successful decontamination methods were UVC radiation (60 min), dry heat treatments (all for 60 min) at temperatures at 130 °C and 140 °C, and autoclaving (115 °C, 20 min). Increased protein yields were observed after dry heat treatments at 110–120 °C for all raw materials (up to 33% for full-fat flakes) and at 130 °C in the case of dehulled seeds (up to 32%) and flakes (up to 27%). There were only minimal drifts in protein yield after UVC radiation. The protein yield depended on protein disruptive effects of the particular decontamination method. Thus, taking into account both, protein yield and decontamination performance, the method of choice for whole seeds was 60 min UVC radiation, in case of dehulled seeds and full-fat flakes additionally dry heat treatment at 130 °C and for defatted flakes solely the last mentioned. Autoclaving resulted in a strong loss of protein yield up to 50% and was deemed as unsuitable for this purpose. Dry heat treatment at 140 °C (60 min) also decreased the amount of extractable micellar protein up to 51% in the case of the dehulled seeds. In case of the whole seeds no micellar protein was extractable with identical settings. Lupin seeds and flakes seemed to be more sensitive to wet heat than dry heat in the same temperature range.

To avoid a possible recontamination of raw materials, the use of defatted flakes could be more useful because of the exclusion of a new contamination (by dehulling, flaking or de-oiling) of the raw materials prior to micellar protein extraction.

In case of a bacterial recontamination during the extraction process, the protein isolate can be pasteurized at 75 °C for 5 min to reduce most of the microorganisms except the spore-forming bacteria.

It is to be considered how the decontamination treatments also affect the protein isolate itself.

#### Acknowledgment

This research project was financially sponsored by the Federal Ministry of Economics and Technology BMWi (project: InnoNet 16IN0642).

#### References

- Bader, S., Oviedo, J. P., Pickardt, C., & Eisner, P. (2011). Influence of different organic solvents on the functional and sensory properties of lupin (*Lupinus angustifolius* L.) proteins. *LWT-Food Science and Technology*, 44, 1396–1404.
- Belski, R. (2012). Fiber, protein, and lupin-enriched foods: role for improving cardiovascular health. *Advances in Food and Nutrition Research*, 66, 147–215.
- Berghout, J. A. M., Boom, R. M., & van der Goot, A. J. (2015). Understanding the differences in gelling properties between lupin protein isolate and soy protein isolate. *Food Hydrocolloids*, 43, 465–472.
- Chiu, K. Y., & Sung, J. M. (2014). Use of ultrasonication to enhance pea seed germination and microbial quality of pea sprouts. *International Journal of Food*

- Science and Technology*, 49, 1699–1706.
- D'Agostina, A., Antonioni, C., Resta, D., Arnoldi, A., Bez, J., Knauf, U., et al. (2006). Optimization of a pilot-scale process for producing lupin protein isolates with valuable technological properties and minimum thermal damage. *Journal of Agricultural and Food Chemistry*, 54, 92–98.
- El-Adawy, T. A., Rahma, E. H., El-Bedawey, A. A., & Gafar, A. F. (2001). Nutritional potential and functional properties of sweet and bitter lupin seed protein isolates. *Food Chemistry*, 74, 455–462.
- Erdogdu, S. B., & Ekiz, H. I. (2011). Effect of ultraviolet and far infrared radiation on microbial decontamination and quality of cumin seeds. *Journal of Food Science*, 76, M284–M292.
- European Food Safety Authority. (2005). Opinion of the scientific panel on biological hazards on *Bacillus cereus* and other *Bacillus* spp in foodstuffs. *The EFSA Journal*, 175, 1–48.
- Giami, S. Y., Adindu, M. N., Hart, A. D., & Denenu, E. O. (2001). Effect of heat processing on in vitro protein digestibility and some chemical properties of African breadfruit (*Treculia africana* Decne) seeds. *Plant Foods for Human Nutrition*, 56, 117–126.
- Hedley, C. L. (2001). Introduction. In C. L. Hedley (Ed.), *Carbohydrates of grain legumes. Improving nutritional quality and agronomic characteristics* (pp. 1–13). Wallingford: CABI Publishing.
- Hidaka, Y., & Kubota, K. (2006). Study on the sterilization of grain surface using UV radiation – Development and evaluation of UV irradiation equipment. *Jarq-Japan Agricultural Research Quarterly*, 40, 157–161.
- Hove, E. L. (1974). Composition and protein quality of sweet lupin seed. *Journal of the Science of Food and Agriculture*, 25, 851–859.
- Hudson, B. J. F. (1979). The nutritional quality of lupinseed. *Qualitas Plantarum-Plant Foods for Human Nutrition*, 29, 245–251.
- Karaguzel, O., Cakmakci, S., Ortacesme, V., & Aydinoglu, B. (2004). Influence of seed coat treatments on germination and early seedling growth of *Lupinus varius* L. *Pakistan Journal of Botany*, 36, 65–74.
- King, J., Aguirre, C., & Depablo, S. (1985). Functional-properties of lupin protein isolates (*Lupinus albus* cv Multolupa). *Journal of Food Science*, 50, 82–87.
- Koutchma, T. (2008). UV light for processing foods. *Ozone-Science & Engineering*, 30, 93–98.
- Kroll, J., Krause, J. P., & Rawel, H. M. (2007). Rapssamenproteine – Struktur, eigenschaften, gewinnung und modifizierung. *Deutsche Lebensmittel-Rundschau*, 103, 109–118.
- Melde, D., Koenig, K., Sussmann, D., Pickardt, C., & Braun, P. G. (2011). Methoden der mikrobiologischen Stabilisierung pflanzlicher Fettaustauschstoffe. In 52. Arbeitstagung des arbeitsgebietes lebensmittelhygiene der DVG (p. 177). Dreiländertagung.
- Muranyi, I. S., Otto, C., Pickardt, C., Koehler, P., & Schweiggert-Weisz, U. (2013). Microscopic characterisation and composition of proteins from lupin seed (*Lupinus angustifolius* L.) as affected by the isolation procedure. *Food Research International*, 54, 1419–1429.
- National Advisory Committee on Microbiological Criteria for Foods. (1999). Microbiological safety evaluations and recommendations on sprouted seeds. *International Journal of Food Microbiology*, 52, 123–153.
- Nei, D., Bari, M. L., & Enomoto, K. (2013). Validation of hot water and chlorine treatments to inactivate pathogens inoculated on mung bean seeds: Influence of the seed production area. *Food Control*, 32, 186–189.
- Olaimat, A. N., & Holley, R. A. (2012). Factors influencing the microbial safety of fresh produce: a review. *Food Microbiology*, 32, 1–19.
- Peng, Q. H., Khan, N. A., Wang, Z. S., & Yu, P. Q. (2014). Moist and dry heating-induced changes in protein molecular structure, protein subfractions, and nutrient profiles in camelina seeds. *Journal of Dairy Science*, 97, 446–457.
- Rodríguez-Ambriz, S. L., Martínez-Ayala, A. L., Millán, F., & Dávila-Ortiz, G. (2005). Composition and functional properties of *Lupinus campestris* protein isolates. *Plant Foods for Human Nutrition*, 60, 99–107.
- Samadi, & Yu, P. (2011). Dry and moist heating-induced changes in protein molecular structure, protein subfraction, and nutrient profiles in soybeans. *Journal of Dairy Science*, 94, 6092–6102.
- Sirtori, E., Resta, D., Brambilla, F., Zacherl, C., & Arnoldi, A. (2010). The effects of various processing conditions on a protein isolate from *Lupinus angustifolius*. *Food Chemistry*, 120, 496–504.
- Sousa, I. M. N., Mitchell, J. R., Ledward, D. A., Hill, S. E., & da Costa, M. L. B. (1995). Differential scanning calorimetry of lupin and soy proteins. *Zeitschrift für Lebensmittel-Untersuchung und -Forschung*, 201, 566–569.
- Sussmann, D., Halter, T., Pickardt, C., Schweiggert-Weisz, U., & Eisner, P. (2013a). An optimization approach for the production of fatlike protein isolates from different leguminous seeds using response surface methodology. *Journal of Food Process Engineering*, 36, 715–730.
- Sussmann, D., Pickardt, C., Schweiggert, U., & Eisner, P. (2013b). Influence of different processing parameters on the isolation of lupin (*Lupinus angustifolius* L.) protein Isolates: a preliminary study. *Journal of Food Process Engineering*, 36, 18–28.
- Wijayanti, H. B., Bansal, N., & Deeth, H. C. (2014). Stability of whey proteins during thermal processing: a review. *Comprehensive Reviews in Food Science and Food Safety*, 13, 1235–1251.
- Yoshie-Stark, Y., Bez, J., & Wäsche, A. (2006). Effect of different pasteurization conditions on bioactivities of *Lupinus albus* protein isolates. *LWT-Food Science and Technology*, 39, 118–123.



# Estimation of amino acids profile and escolar fish consumption risks due to biogenic amines content fluctuations in vacuum skin packaging/VSP during cold storage



Dani Đorđević<sup>a,\*</sup>, Hana Buchtová<sup>a</sup>, Ivana Borkovcová<sup>b</sup>

<sup>a</sup> Department of Meat Hygiene and Ecology, Faculty of Veterinary Hygiene and Ecology, University of Veterinary and Pharmaceutical Sciences, Palackého tř. 1/3, 612 42 Brno, Czech Republic

<sup>b</sup> Department of Milk Hygiene and Ecology, Faculty of Veterinary Hygiene and Ecology, University of Veterinary and Pharmaceutical Sciences, Palackého tř. 1/3, 612 42 Brno, Czech Republic

## ARTICLE INFO

### Article history:

Received 3 June 2015

Received in revised form

12 September 2015

Accepted 11 November 2015

Available online 19 November 2015

### Keywords:

Escolar fish

Amino acids profile

Biogenic amines

### pubchem:

Histamine (pubchem CID: 774)

2-phenyl-ethylamine (pubchem CID: 1001)

putrescine (pubChem CID: 1045)

cadaverine (pubChem CID: 273) tyramine

(pubChem CID: 5610)

spermidine (pubChem CID: 1102)

spermine (pubChem CID: 1102)

omega-3 fatty acids (pubChem CID:

56842239)

omega-6 fatty acids (pubChem CID:

56842208)

essential amino acids (pubChem CID:

56842238)

## ABSTRACT

The aim of the study was to establish quantitative and qualitative composition of proteins (amino acids profile), digestible lipids (fatty acids profile of triacylglycerols) and to monitor biogenic amines (especially histamine) content of escolar fish (*Lepidocybium flavobrunneum*) in vacuum and vacuum skin packaging (VSP) during 9 days of storage at  $+2 \pm 2$  °C. *L. flavobrunneum* Fillets packed in vacuum were used for comparison as control samples. The obtained results from our research showed that escolar fish contains higher amount of essential amino acids ( $70.63 \pm 3.61$  mg/kg) and good ratio between essential and non essential amino acids ( $0.95 \pm 0.09$ ). Oleic and lauric fatty acids were the most abundantly present in our samples ( $28.115 \pm 4.44\%$ ). Initial values of biogenic amines sum were low but they increased significantly ( $p < 0.05$ ) after 9 days of storage at  $+2 \pm 2$  °C, and consequently VSP and vacuum packaging can be recommended for storage at  $+2 \pm 2$  °C during 7 days, but not for 9 days of storage, due to higher histamine content (after 7 days VSP: 21.31 mg/kg; after 9 days VSP: 376.96 mg/kg).

© 2015 Elsevier Ltd. All rights reserved.

## 1. Introduction

Escolar (*Lepidocybium flavobrunneum*) fish used to be by-catch during tuna and swordfish fishing but harvesting of escolar fish has been increasing significantly since 1991 (11,1 metric tons) to 2013 (67,8 metric tons), meaning that deep sea fishing is in increment (Brendtro, McDowell, & Graves, 2008; NOAA, 2015; Suseno, Permata, Hayati, Nugraha, & Saraswati, 2013). Deep sea fish

species are starting to be consumed more often due to less availability of more popular fish species and due to consumers' curiosity to try something new.

Escolar fish belongs to controversial fish species (belonging to *Perciformes* order, *Gempylidae* family, *Ruvettus pretiosus* and *L. flavobrunneum*) because on one side it contains higher amount of proteins (>18%) and taurine but on the other side its fat content is composed mainly out of wax esters (20% of body weight is composed out of fatty acids esters with long chain fatty alcohols). After consumption, wax ester can lead to diarrhea and other gastrointestinal disturbances (called keriorrhea), but it is not

\* Corresponding author.

E-mail address: [dani\\_dordevic@yahoo.com](mailto:dani_dordevic@yahoo.com) (Đ. Đorđević).

possible to establish upper intake limit of escolar fish because reports indicate different sensitivity between individuals. Oppositely, among some indigenous cultures escolar fish is considered medical purgative (Zarza, Gutierrez, & Bravo, 1993; Hwang et al., 2012; EFSA, 2004; Leask, Yankos, & Ferson, 2004).

Beside wax ester content of escolar fish, potential higher content of biogenic amines can represent another disadvantage of escolar fish consumption. There is a higher chance for the formation of histamine in escolar due to higher content of histidine in muscle. The manipulation and storage of escolar is very important after catching because if it undergoes higher temperatures than +4 °C during storage or manipulation histamine content can increase to hazardous amounts (over 2000 ppm) which can be even life threatening. Biogenic amines in escolar fish can be underlined as major reason for food poisoning because in the majority of incidents none of intoxicated people experienced only gastrointestinal problems which are signs for exceed intake of wax esters (Feldman et al., 2005; Hwang et al., 2012; Leask et al., 2004).

*L. flavobrunneum* fillets are sold in the Czech Republic usually in defrosted vacuum packaging. These fillets are very popular among consumers due to their attractive “buttery” appearance and delicious taste. Sensory evaluation of marinated samples of *Lepidocybium flavobrunneum* showed high acceptance among respondents, even escolar steaks without marinades were positively evaluated (Buchtová, Dordević, Kočárek, & Chomát, 2015). There is a need for more discussions concerning benefits and risks of escolar fish meat consumption due to not entirely unambiguous assessment of its impact on human health. This paper covers very important parts concerning escolar fish consumption which are amino acids/fatty acids profile of escolar fillets and possible formation of biogenic amines during storage period. The aim of the study was to quantitatively and qualitatively establish composition of proteins (amino acids profile), digestible lipids (fatty acids profile of triacylglycerols) and to monitor biogenic amines (especially histamine) content of escolar fish (*L. flavobrunneum*) in vacuum and vacuum skin packaging (VSP) under presumably conditions (9 days of storage at +2 ± 2 °C).

## 2. Materials and methods

The study was carried out by using 6 skinless fillets (A, B, C, D, E, F) of Escolar fish (*L. flavobrunneum*), which were purchased on the market as vacuum packaged thawed product (vendor: Seafood AG, Prague, Czech Republic). The average weight of fillets was 2658.33 ± 864.65 g. The country of origin of fish was Vietnam, the fishing area Pacific Ocean FAO 71 (month/year of fish harvest/freeze: 03/2013; month/year of thawing: 10/2013; freezing time before thawing in the Czech Republic: 7 months; defrosting conditions: thawing in air at max. +12 °C for 12–16 h, temperature after thawing: max. 2 °C). Shelf-life period provided by the vendor was nine days from the date of packaging when stored at +2 ± 2 °C. Further processing (cutting), vacuum and VSP, storage at +2 ± 2 °C (98% vacuum), and laboratory analysis were conducted at the Department of Meat Hygiene and Technology (Faculty of Veterinary Hygiene and Ecology, Veterinary and Pharmaceutical University in Brno). Easy-open, microwavable package for a quick and easy preparation was used as vacuum skin packaging (SIMPLE STEPS® VSP PACKAGE FOR PRODUCE, 2014). The packaging consisted of CRYOVAC® DARFRESH® base web structure (RSB 03x56; thickness 280 µm; base weight 305 g/m<sup>2</sup>) and top film CRYOVAC® DARFRESH® top web (TC201; thickness 100 µm; basis weight 95.5 g/m<sup>2</sup>). VSP is recognized as advanced packaging in comparison with vacuum packaging, and it provides longer shelf-life of packed products. Bacterial proliferation in VSP is slower because this technique prohibits the formation of wrinkles and air spaces which

are often present in vacuum packaging (Li, Lindahl, Zamaratskaia, & Lundstrom, 2012). Cranial part (behind the head) with a thickness of 2.5 cm from each fillet (separated from the rest of fillet cross section) was analysed on the day of purchase in order to determine the input values of monitored parameters (Initial data). The remaining muscle of each fillet was cut transversally in cranio-caudal direction and portioned in 8 parts (each with a thickness of about 2.5 cm). In this manner, from each fillet were formed anatomically identical samples for vacuum packaging (1st, 3rd, 5th, 7th), and for VSP (2nd, 4th, 6th, 8th). Anatomically identical parts, obtained from two different fillets, were packed together in each type of packaging e.g. 1. mixed sample after 2 days of storage experiment; vacuum packaging: 1. cut from fillets A + B, C + D, E + F, VSP: 2. cut from fillets A + B, C + D, E + F etc. In that way were formed 24 mixed samples (12 samples for vacuum and 12 for VSP), which were analysed after 2, 4, 7, and 9 days of storage at +2 ± 2 °C (3 mixed samples for each type of packaging and for each day of storage).

The determination of the quantitative and qualitative composition of amino acids was performed using HPLC. Samples were homogenized (homogenization: Moulinex ILLICO Y92, Group SEB ČR, s.r.o., Praha, Czech Republic) and from each mixed sample was taken 0.500 g (PRECISA 240 A, France). The samples were prepared using acid hydrolysis (HCl = 6 mol/l) for 24 h at 110 °C. The amino acid assay was performed on an AAA 400 automatic amino acid analyser (INGOS a.s. Praha, Czech Republic). For their separation, sodium – citrate elution buffers in a chromatographic column with catex (OSTION LG ANB, Czech Republic) were used. After colour reaction with the ninhydrin, separated amino acids were detected in a flow photometer. AMIK software 3.0. (Czech Republic) was used to calculate retention times and areas of individual amino acid peaks, and to process data. Reagents necessary for the preparation of samples, buffers and AAA operation were supplied by the amino analyser manufacturer. Solutions of standard amino acid mixtures also supplied by the AAA manufacturer were used as external amino acid standards.

The lipids of raw samples were extracted into hexan-isopropanol extract (Hara & Radin, 1978). The determination of fatty acids composition was performed by gas chromatography using GC – 2010 (Shimadzu, Japan) apparatus with flame ionization detector (FID) and capillary column VB WAX (60 m × 0.32 mm × 0.25 µm). The optimum temperature gradient was 140 °C–240 °C (5 °C/min). The injector temperature was 280 °C, the FID temperature was 300 °C. Helium was used as the carrier gas.

Biogenic amines (tryptamine, 2-phenylethylamine, cadaverine, histamine and tyramine) and polyamines (putrescine, spermidine and spermine) were determined by the method of Paulsen, Bauer, and Vali (1997). Biogenic amines and polyamines were extracted from the sample with 10% trichloroacetic acid and subsequently derivatised and detected as dansyl derivatives. Analysis was performed by the RP-HPLC method with gradient elution and fluorescence and PDA detection.

The samples were analysed on an Alliance 2695 chromatograph (Waters, USA) with PDA 2996 and fluorescence 2495 detectors and separated on Zorbax Eclipse XDB C18, 150 × 4.6 mm, 5 µm chromatographic column (Agilent, USA). Gradient elution at a flow rate of 1 ml/min was used. Mobile phase A consisted of a mixture of 0.1 M acetic acid and acetonitrile (90:10), mobile phase B of a mixture of 0.1 M acetic acid, acetonitrile and methanol (10:45:45). The injection volume was 10 µl. Fluorescence detection was performed at  $\lambda_{ex}/\lambda_{em} = 330/500$  nm, detection within the UV region at 254 nm. Each sample was analysed in at least two parallel tests, with a blank sample in each series. The separated biogenic amines and polyamines were identified and quantified by an external standard method. Measurements were evaluated with the help of

Empower 2 software (Waters, USA).

Statistical significance at  $p < 0.05$  was evaluated using *t*-test (finding difference between vacuum and VSP samplings), one-way ANOVA analysis of variance, and post hoc Tukey test for finding differences within the same packaging type during different storage periods. Six samples for each time period was analysed and compared between different packaging and different storage periods. SPSS 20 statistical software (IBM Corporation, Armonk, USA) was used.

### 3. Results and discussion

#### 3.1. Chemical composition of *L. flavobrunneum*

Chemical composition (in g/kg) of *L. flavobrunneum* used samples is shown in Table 1. The results are taken from previous study, Buchtová et al. (2015), where are shown contents of dry matter/moisture ( $378.20 \pm 22.80/621.80 \pm 22.80$ ), crude protein ( $169.78 \pm 10.83$ , lipid ( $194.07 \pm 23.90$ ) and ash ( $8.21 \pm 0.561$ ).

#### 3.2. Amino acids profile of escolar fish

Amino acids profile of escolar fish is shown in Table 2. Total amino acids E/N ratio in escolar fish was  $0.95 \pm 0.09$  which is higher than in raw squid,  $0.59 \pm 0.0032$ . The major amino acids in escolar fish were glutamic, histidine, lysine and aspartic acid. Escolar fish sensory properties good acceptance can be explained by its amino acids profile due to glutamic and aspartic acids which are responsible for stronger umami taste (Buchtová et al., 2015; Deng, Luo, Wanga, & Zhao, 2015).

According to results of authors (Suseno et al., 2013), the major non essential amino acid in escolar meat was glutamic acid (20.94 g/kg) and among essential amino acids the most dominant was lysine (12.1 g/kg). These results don't differ much from our results but in the same study total amino acids content (117.8 g/kg) and total amino acids essential/nonessential (E/N) ratio (0.75) were much lower in comparison with our results (total amino acids content:  $145.70 \pm 7.41$ ; total amino acids ratio E/N: 0.95). Histidine ( $14.03 \pm 0.40$  g/kg), lysine ( $14.60 \pm 0.98$  g/kg), tyrosine ( $6.67 \pm 0.21$  g/kg), arginine ( $10.30 \pm 0.98$  g/kg) contents were higher in comparison with their study. Escolar fish can be considered a good source of essential amino acids when their contents are compared with daily requirements for essential amino acids. Especially branched-chain amino acids (BCAA – leucine, isoleucine, valine) content in 100 g escolar fillets (Table 2: leucine: 1150 mg; isoleucine: 697 mg; valine: 737 mg) satisfied almost 50% of daily required amounts, while histidine content exceeds daily requirements for adults weighing 80 kg (Rajkmur, Preedy, Patel, 2015, Chap. 1).

#### 3.3. The contents of biogenic amines in escolar fish

The concentrations of biogenic amines in escolar fish during 9 days of storage in vacuum and vacuum skin packaging (VSP) at  $+2 \pm 2$  °C are shown in Figs. 1–8.

2-phenyl-ethylamine content after 9 days of storage was higher in vacuum packaging (2.66 mg/kg) than in VSP (1.67 mg/kg), while contents of other investigated biogenic amines (putrescine,

cadaverine, histamine, tyramine, spermidine, spermine) were higher in VSP. These 2-Phenyl-ethylamine values are under 3 mg what is estimated as causative amount of migraine (EFSA, 2004). Values after 2 (vacuum: 0.15 mg/kg; VSP: 0.00 mg/kg) and 7 days (vacuum: 0.25 mg/kg; VSP: 0.16 mg/kg) of storage are significantly lower than after 9 days of storage in both type of packaging. There was also found that escolar fish packed in VSP had significantly lower 2-phenyl-ethylamine content than in vacuum packaging after 4 days of storage.

The content of putrescine didn't change significantly during 9 days of storage, and it was far below 170 mg/kg which is maximum tolerable putrescine level for fish (Rauscher-Gabering et al., 2012).

Statistical significance was found between cadaverine content after 9 days of storage and after 2, 4, 7 days of storage in both type of packaging, the same trend occurred with histamine and cadaverine contents. Still cadaverine contents in vacuum (5.77 mg/kg) and VSP (10.44 mg/kg) packaging after 9 days of storage at  $+2 \pm 2$  °C were much lower than estimated tolerable level for fish (510 mg/kg) (Rauscher-Gabering et al., 2012).

The biggest concern out of biogenic amines is histamine content and according to Commission Regulation (EU) No 1019/2013 it should not exceed 200 mg/kg for fishery products and 400 mg/kg for those which have undergone enzyme maturation treatment in brine. Elevated histamine content can lead to symptoms such as peppery taste, numbness of the tongue, headache, flushing and sweating, dizziness, nausea, diarrhoea, and shortness of breath. Though, histamine content can vary a lot in different parts of the same fish and that could be one of the reasons why some people get histamine intoxication symptoms and some not after the consumption of same seafood. Fish with higher level of histamine may have “honeycomb appearance” of its meat, but it is not a rule (Feldman et al., 2005). Histamine content after 9 days of storage at  $+2 \pm 2$  °C (vacuum: 223.50 mg/kg; VSP: 376.96 mg/kg) was significantly higher in both type of packaging than on previously measured times. Oppositely, after 2 days of storage histamine was not detectable in both type of packaging. In comparison with measurement after 7 days of storage (vacuum: 20.11 mg/kg; VSP: 21.31 mg/kg) histamine content increased by 10 folds after 9 days of storage (vacuum: 223.50 mg/kg; VSP: 376.96 mg/kg). After 9 days of storage, histamine content exceeded limit of 50 mg/kg for scombroid and/or product purposed by US Food and Drug Administration (Hwang et al., 2012). Emborg, Laursen, Rathjen, and Dalgaard (2002) and Dalgaard, Madsen, Samieian, and Emborg (2006) found that the formation of histamine, tyramine, cadaverine and agmatine is slower in thawed fish samples, meaning in previously frozen samples, due to inactivation of bacteria capable to decarboxylate free amino acids, than in only chilled garfish and salmon samples. This finding is suggesting that the formation of histamine in fresh only chilled escolar fish fillets would be even greater than in thawed samples, resulting in the assumption of lesser storage period. In case study was found that fish samples which caused histamine food incidence had histamine content more than 2000 mg/kg (Leask et al., 2004). Samples of escolar fish were stored in vacuum packaging at  $+2 \pm 2$  °C, and for histamine formation could not be responsible mesophilic bacteria (such as: *Photobacterium damsela* subsp. *damsela*, *Morganella morganii*) but psychrophilic bacteria (such as: *Photobacterium phosphoreum*, *Morganella psychrotolerans*) which are also able to decarboxylate

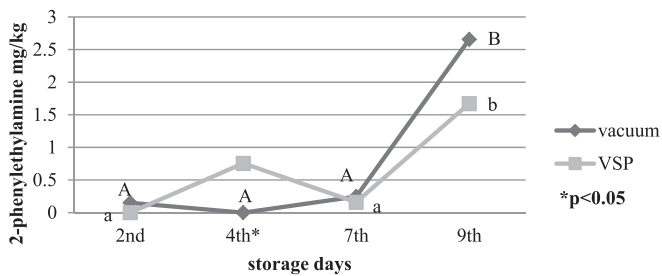
**Table 1**  
Chemical composition (g/kg) of *Lepidocybium flavobrunneum* fillets (middle part).

Dry matter/moisture	Crude protein	Lipid	Ash
$378.20 \pm 22.80/621.80 \pm 22.80$	$169.78 \pm 10.83$	$194.07 \pm 23.90$	$8.21 \pm 0.561$

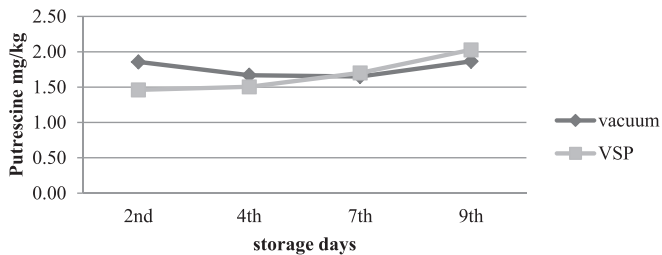
Source: Buchtová et al. (2015).

**Table 2**Amino acids composition of proteins of defrosted fillets of *Lepidocybium flavobrunneum* (initial data).

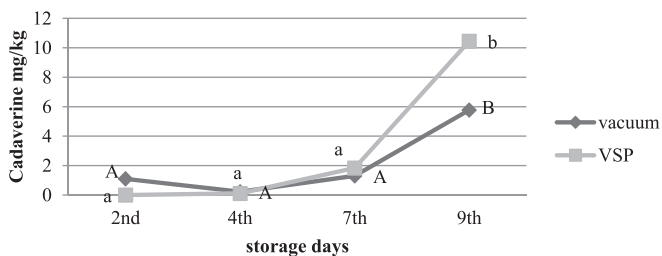
	Amino acids profile in	Mean $\pm$ s.d. (g/kg) n = 6
Essential amino acids	Threonine	6.47 $\pm$ 0.40
	Valine	7.37 $\pm$ 0.47
	Methionine	4.47 $\pm$ 0.31
	Isoleucine	6.97 $\pm$ 0.35
	leucine	11.50 $\pm$ 0.60
	Phenylalanine	5.23 $\pm$ 0.32
	Histidine	14.03 $\pm$ 0.40
	Lysine	14.60 $\pm$ 0.98
	Total essential amino acids (E)	70.63 $\pm$ 3.61
	Non-essential amino acids	Aspartic
Serine		5.53 $\pm$ 0.42
Glutamic		19.07 $\pm$ 1.26
Proline		6.23 $\pm$ 0.75
Glycine		6.43 $\pm$ 0.71
Alanine		8.17 $\pm$ 0.57
Tyrosine		6.67 $\pm$ 0.21
Arginine		10.30 $\pm$ 0.98
Total non-essential amino acids content (N)		75.07 $\pm$ 6.24
Total amino acids content		145.70 $\pm$ 7.41
Total amino acids E/N ratio	0.95 $\pm$ 0.09	



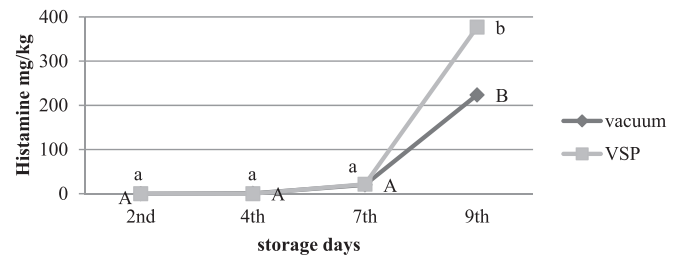
**Fig. 1.** 2-Phenyl-ethylamine content in escolar fish during 9 days of storage at  $+2 \pm 2$  °C. Parameters values **a, b, c / A, B, C, D** are indicators for statistical significance at  $p < 0.05$  for vacuum / VSP samples in dependence on day of storage; lowercase letters indicate the lower values of the particular parameter \*t-test  $p < 0.05$ .



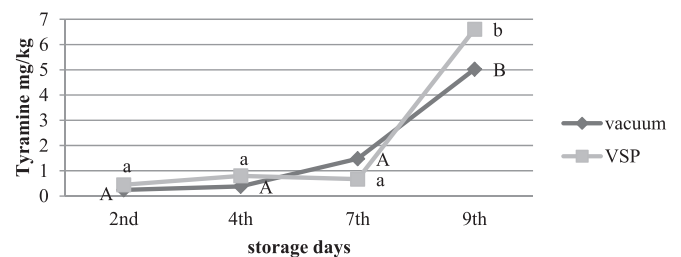
**Fig. 2.** Putrescine content in escolar fish during 9 days of storage at  $+2 \pm 2$  °C. Parameters values **a, b, c / A, B, C, D** are indicators for statistical significance at  $p < 0.05$  for vacuum / VSP samples in dependence on day of storage; lowercase letters indicate the lower values of the particular parameter



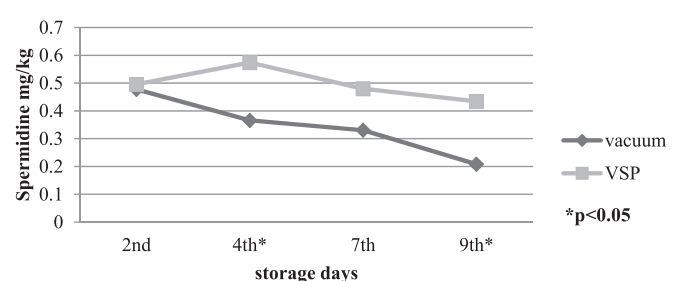
**Fig. 3.** Cadaverine content in escolar fish during 9 days of storage at  $+2 \pm 2$  °C. Parameters values **a, b, c / A, B, C, D** are indicators for statistical significance at  $p < 0.05$  for vacuum / VSP samples in dependence on day of storage; lowercase letters indicate the lower values of the particular parameter



**Fig. 4.** Histamine content in escolar fish during 9 days of storage at  $+2 \pm 2$  °C. Parameters values **a, b, c / A, B, C, D** are indicators for statistical significance at  $p < 0.05$  for vacuum / VSP samples in dependence on day of storage; lowercase letters indicate the lower values of the particular parameter



**Fig. 5.** Tyramine content in escolar fish during 9 days of storage at  $+2 \pm 2$  °C. \*t-test  $p < 0.05$

\*t-test  $p < 0.05$ 

**Fig. 6.** Spermidine content in escolar fish during 9 days of storage at  $+2 \pm 2$  °C.

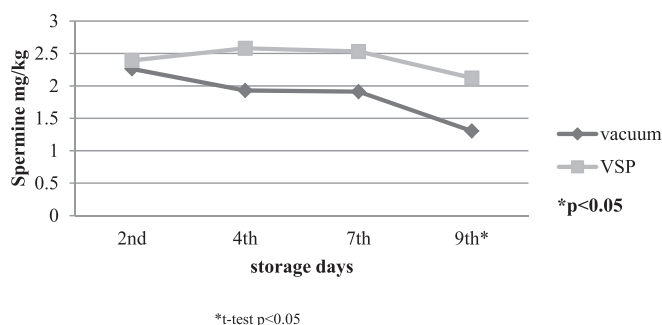


Fig. 7. Spermine content in escolar fish during 9 days of storage at +2 ± 2 °C.

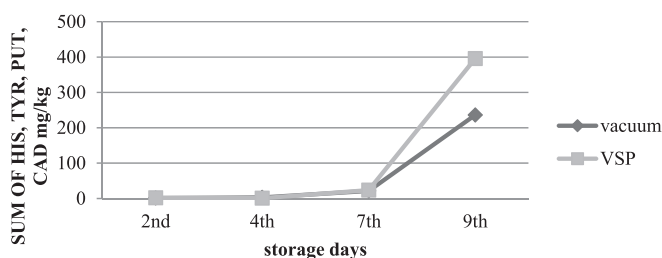


Fig. 8. The sum of histamine, tyramine, putrescine and cadaverine in escolar fish during 9 days of storage at +2 ± 2 °C.

free histidine in fish meat and produce histamine. Contamination with psychrophilic bacteria could occur at retail stores where fish was defrosted and where psychrophilic bacteria are usually present (Torido et al., 2014).

Tyramine content increased gradually during 9 days of storage and at the end of the experiment it was 5.02 mg/kg in vacuum packaging and 6.61 mg/kg in VSP. When compare tyramine contents in the samples of escolar fish used for our experiment it is possible to see that tyramine content after 9 days of storage was lower than mean values of tyramine in some raw seafood, such as: indian anchovy (46.9 mg/kg), sardine (16.3 mg/kg), pacific herring (23.3 mg/kg), pacific mackerel (40.3 mg/kg), blue scad (29.6 mg/kg) and pacific saury (21.2 mg/kg) (Visciano, Schirone, Tofalo, & Suzzi, 2012).

During experiment, spermidine and spermine contents didn't change significantly after 9 days of storage (vacuum spermidine: 0.21 mg/kg; VSP spermidine: 0.43 mg/kg; vacuum spermine: 1.30 mg/kg; VSP spermine: 2.12 mg/kg). There was statistical significance between spermidine content in vacuum and VSP after 4 and 9 days of storage. Spermine content in VSP was significantly higher in comparison with vacuum packaging after 9 days of storage.

Oppositely, VSP showed better protection against oxidative stress in comparison with vacuum packaging (Dordevic & Buchtová, 2015). These values are far below spermidine revealed in canned tuna in the study done by Zarei, Najafzadeh, Enayati, and Pashmforoush (2011), where spermidine content was 32.41 mg/kg. Spermidine detection in food is very important because it can together with putrescine, spermine and cadaviren react with nitrite

Table 3

Fatty acids composition of digestible lipids (triacylglycerols) of defrosted fillets of *Lepidocybium flavobrunneum* (initial data). Total lipid content in fillets was 194.07 ± 23.90 g kg<sup>-1</sup> (Buchtová et al., 2015).

Fatty acids profile in % of total fatty acid investigated		Mean ± s.d. n = 6		
Saturated fatty acids (SFA)	Lauric	C12:0	0.003 ± 0.00	
	Tridecane	C13:0	0.005 ± 0.00	
	Myristic	C14:0	0.040 ± 0.01	
	Palmitic	C16:0	0.416 ± 0.23	
	Heptadecane	C17:0	0.037 ± 0.01	
	Stearic	C18:0	0.219 ± 0.06	
	Arachidic	C20:0	0.004 ± 0.00	
	Tricosane	C23:0	0.061 ± 0.01	
	Lignoceric	C24:0	0.758 ± 0.38	
	<b>Σ SFA</b>		<b>1.543 ± 0.08</b>	
	Monounsaturated fatty acids (MUFA)	Myristoleic	C14:1	0.008 ± 0.00
		Palmitoleic	C16:1	0.513 ± 0.11
		cis-10-Heptadecane	C17:1	0.010 ± 0.00
<b>Σ MUFA</b>			<b>0.532 ± 0.04</b>	
Oleic/elaidic		C18:1n9t + C18:1n9c	28.115 ± 4.44	
cis-11-Eicosenoic		C20:1n9	2.321 ± 1.48	
<b>Σ MUFA<sub>n9</sub></b>			<b>30.436 ± 2.96</b>	
Polyunsaturated fatty acids (PUFA)	<b>Σ MUFA + MUFA<sub>n9</sub></b>		<b>30.968 ± 1.21</b>	
	Linoleic/linoelaidic	C18:2n6c + C18:2n6t	0.169 ± 0.13	
	γ-linolenic	C18:3n6	0.008 ± 0.00	
	cis-11,14 eicosadienic	C20:2n6	0.051 ± 0.01	
	cis -8,11,14 -eicosatrienic	C20:3n6	0.016 ± 0.01	
	Arachidonic	C20:4n6	0.292 ± 0.09	
	Docosatetraenic	C22:4n6	0.063 ± 0.01	
	<b>Σ PUFA<sub>n6</sub></b>		<b>0.599 ± 0.04</b>	
	α-linolenic	C18:3n3	0.016 ± 0.01	
	cis -11,14,17-eicosatrienic	C20:3n3	0.029 ± 0.03	
	cis-5,8,11,14,17-Eicosapentaenoic	C20:5n3	0.256 ± 0.23	
	cis-4,7,10,13,16,19-Docosahexaenoic	C22:6n3	0.542 ± 0.06	
	Docosapentaenoic	C22:5n3	0.097 ± 0.10	
	<b>Σ PUFA<sub>n3</sub></b>		<b>0.940 ± 0.09</b>	
	<b>Σ PUFA<sub>n6</sub> + PUFA<sub>n3</sub></b>		<b>1.539 ± 0.06</b>	
<b>Ratio PUFA<sub>n3/n6</sub></b>		<b>1.584 ± 0.60</b>		
<b>Total FA (Σ SFA + MUFA + MUFA<sub>n9</sub> + PUFA<sub>n3</sub> + PUFA<sub>n6</sub>)</b>		<b>34.050 ± 0.31</b>		
FAs undetectable under the conditions of the experiment e.g. in wax esters, phospholipids, sterols.		65.950 ± 4.03		

and form carcinogenic nitrosamines (Sagratini et al., 2012).

Sum of histamine, tyramine, putrescine and cadaverine increased gradually during storage period and after 7 days of storage at  $+2 \pm 2$  °C it was under 50 mg/kg, (vacuum: 21.41 mg/kg; VSP: 23.82 mg/kg), which is limit value for tuna acceptance (Visciano et al., 2012). After 9 days of storage tenfold increment occurred in the sum (vacuum: 236.16 mg/kg; VSP: 396.03 mg/kg) but it was still under estimated mean values for fish sauce (582 mg/kg – 588 mg/kg) (EFSA, 2011).

### 3.4. Fatty acids profile of escolar fish

The fatty acids profile in the samples of escolar fish is shown in Table 3. Total fatty acids content ( $34.050 \pm 0.31\%$ ) consisted of saturated fatty acids (SFA:  $1.543 \pm 0.08\%$ ), monounsaturated fatty acids (MUFA:  $30.968 \pm 1.21\%$ ) and polyunsaturated fatty acids (PUFA:  $1.539 \pm 0.06\%$ ). It means that  $65.950 \pm 4.03\%$  of fatty acids were undetectable under conditions used in method, probably due to the fact that fat content of escolar fish is 18–21%, out of which is more than 90% of wax esters. Wax esters naturally occur in the diet of escolar fish but this fish species is not able to metabolize them, and as consequence it stores them equally in the body (Brimer, 2011, Chap. 7; Karl & Rehbein, 2004). Among detectable fatty acids the most abundantly present fatty acids were oleic and elaidic

fatty acids ( $28.115 \pm 4.44\%$ ). Fatty acids profile obtained by other authors is given in Table 4. Nichols, Mooney, and Elliott (2001) determined fatty alcohols in the samples of *L. flavobrunneum* and *R. pretiosus*, using transmethylation method by which they provided the mixture of fatty acids methyl esters and fatty alcohols. Out of fatty acids methyl esters mixture and fatty alcohols can be seen that the majority of fatty acids belong to saturated fatty acids, while our results and results of Ruiz-Gutierrez, Perez-Zarza, Muri-ana, and Bravo (1997) and Schwartz (1997) are indicating that main fatty acids in escolar fish are monounsaturated fatty acids. These differences probably occurred due to specific oil composition of escolar fish and different method used for the escolar fish fatty acids profile estimation. More similar results to our obtained Suseno et al. (2013) by fatty acids profile analysis of escolar (*L. flavobrunneum*), finding monounsaturated fatty acids (oleic acid: 35.16%) as the major fatty acids in the samples of escolar fish. Suseno et al. (2013) also found total fatty acids amount of 48.88%, meaning that more than 50% of fatty acids could not be detected. Similarly,  $65.950 \pm 4.03\%$  of fatty acids in our study were not detectable.

### 4. Conclusions

The consumption of fish like escolar (*L. flavobrunneum*) has been

**Table 4**  
Lipid profile in *Lepidocybium flavobrunneum* and *Ruvettus pretiosus*.

Lipid profile	<i>Lepidocybium flavobrunneum</i> *	<i>Ruvettus pretiosus</i> *	<i>Ruvettus pretiosus</i> **		<i>Lepidocybium flavobrunneum</i>
	Mean $\pm$ s.d. n = 2	Mean $\pm$ s.d. n = 3	Mean $\pm$ s.d. n = 6	Mean $\pm$ s.d. n = 2	***
C14:0	2.65 $\pm$ 0.35	2.93 $\pm$ 0.42	–	–	***unpublished data (Schwartz, 1997)
aC15:0	0.10 $\pm$ 0.00	0.17 $\pm$ 0.06	–	–	
C15:0	0.95 $\pm$ 0.07	1.07 $\pm$ 0.15	–	–	
i C16:0	0.00 $\pm$ 0.00	0.10 $\pm$ 0.17	–	–	
C16:1(n2 9)	0.30 $\pm$ 0.14	0.80 $\pm$ 0.36	–	–	
C16:1(n2 7)	3.10 $\pm$ 0.42	3.80 $\pm$ 0.52	–	–	
C16:1(n2 5)	0.45 $\pm$ 0.21	0.50 $\pm$ 0.17	–	–	
C16:0	52.55 $\pm$ 0.92 <sup>b</sup>	47.77 $\pm$ 0.87 <sup>a</sup>	2.70 $\pm$ 3.18	2.30 $\pm$ 0.21	
C16:1n7	–	–	3.06 $\pm$ 0.97	2.35 $\pm$ 0.05	
C16:1n9	–	–	0.95 $\pm$ 0.03	0.73 $\pm$ 0.19	
C16:4n3	–	–	3.07 $\pm$ 0.36	3.19 $\pm$ 0.43	
i C17:0	0.40 $\pm$ 0.00	0.60 $\pm$ 0.20	–	–	
a C17:0	1.05 $\pm$ 0.07	1.20 $\pm$ 0.10	–	–	
C17:0	1.05 $\pm$ 0.07	1.10 $\pm$ 0.10	–	–	
i C18:0	0.35 $\pm$ 0.21	0.40 $\pm$ 0.10	–	–	
C18:1(n2 9)	21.25 $\pm$ 0.21 <sup>a</sup>	26.27 $\pm$ 0.42 <sup>b</sup>	–	–	
C18:1(n2 7)	3.30 $\pm$ 0.14	3.63 $\pm$ 0.12	–	–	
C18:1(n2 5)	0.35 $\pm$ 0.07	0.27 $\pm$ 0.06	–	–	
C18:0	8.85 $\pm$ 0.78	6.73 $\pm$ 0.85	1.93 $\pm$ 0.34	2.36 $\pm$ 0.08	
C18:1n9	–	–	45.21 $\pm$ 0.75	47.68 $\pm$ 3.10	
C18:2n6	–	–	1.76 $\pm$ 0.16	1.20 $\pm$ 0.45	
C18:3n3	–	–	4.68 $\pm$ 0.03	4.40 $\pm$ 0.59	
C20:2	0.35 $\pm$ 0.07	0.30 $\pm$ 0.17	–	–	
C20:1(n2 9)	2.50 $\pm$ 0.13	1.87 $\pm$ 0.55	–	–	
C20:1(n2 7)	0.15 $\pm$ 0.07	0.13 $\pm$ 0.06	–	–	
C20:0	0.30 $\pm$ 0.14	0.27 $\pm$ 0.06	–	–	
C20:1n11	–	–	6.40 $\pm$ 0.42	8.37 $\pm$ 2.32	
C20:3n3	–	–	0.52 $\pm$ 0.05	0.38 $\pm$ 0.01	
C20:4n6	–	–	1.15 $\pm$ 0.07	1.02 $\pm$ 0.06	
C20:5n3	–	–	3.58 $\pm$ 0.23	3.21 $\pm$ 0.64	
C22:1	0.00 $\pm$ 0.00	0.10 $\pm$ 0.17	–	–	
C22:1n-11	–	–	0.47 $\pm$ 0.06	0.86 $\pm$ 0.36	
C22:5n3	–	–	2.37 $\pm$ 0.09	1.90 $\pm$ 0.53	
C22:6n3	–	–	9.64 $\pm$ 0.84	7.90 $\pm$ 2.64	
$\Sigma$ SFA	68.25 $\pm$ 0.21 <sup>b</sup>	62.33 $\pm$ 0.60 <sup>a</sup>	6.53 $\pm$ 0.44	7.42 $\pm$ 0.38	2.75
$\Sigma$ MUFA	31.40 $\pm$ 0.14 <sup>a</sup>	37.37 $\pm$ 0.61 <sup>b</sup>	62.05 $\pm$ 1.47	66.85 $\pm$ 6.14	78.7
$\Sigma$ PUFA	0.35 $\pm$ 0.07	0.30 $\pm$ 0.17	28.86 $\pm$ 1.27	24.15 $\pm$ 6.12	17.72

\*Nichols et al. (2001).

\*\*Ruiz-Gutierrez et al. (1997).

\*\*\*Schwartz (1997).

Parameters values a, b are indicators for statistical significance at *Lepidocybium flavobrunneum* and *Ruvettus pretiosus* (results obtained by Nichols et al., 2001).

in increment due to higher exploitation of deep fishes and consumers' preferences. Escolar fish belongs to controversial fish species which can cause health problems for consumers because of high content of wax esters but its amino acids profile (higher content of essential amino acids and good ratio between essential and non essential amino acids) and sensory properties are acceptable. Fatty acids analysis showed that it is hard to obtain results in compliance with other studies, probably due to wax ester content in *L. flavobrunneum*. The study emphasized that maximum storage period under these conditions ( $+2 \pm 2$  °C) for this product and these packaging (vacuum, vacuum skin packaging) is 7 days and that the content of biogenic amines (especially histamine) can increase significantly after 9 days of storage. Vacuum packaging turned out to be slightly better option for escolar storage than vacuum skin packaging, though not significantly. Out of our results can be observed that both types of packaging (vacuum and VSP) used in the experiment are suitable for 7 days storage of escolar fish fillets at  $+2 \pm 2$  °C, but these packaging are not the solution for longer storage periods (9 days of storage at  $+2 \pm 2$  °C). Our work is emphasizing the importance of appropriate manipulation of fish before selling and the length of storage period should be reconsidered.

## References

- Brendtro, K. S., McDowell, J. R., & Graves, J. E. (2008). Population genetic structure of escolar (*Lepidocybium flavobrunneum*). *Marine Biology*, 155, 11–22.
- Brimer, L. (2011). *Chemical food safety. Modular texts*. Wallingford: Oxfordshire: CABI.
- Buchtová, H., Dorđević, D., Kočárek, S., & Chomát, P. (2015). Analysis of chemical and sensory parameters in different kinds of escolar (*Lepidocybium flavobrunneum*) products. *Czech Journal of Food Sciences*, 33, 346–353.
- Commission Regulation (EU) No 1019/2013 of 23 October 2013 amending Annex I to Regulation (EC) No 2073/2005 as regards histamine in fishery products.
- Dalgaard, P., Madsen, H. L., Samieian, N., & Emborg, J. (2006). Biogenic amine formation and microbial spoilage in chilled garfish (*Belone belone belone*) – effect of modified atmosphere packaging and previous frozen storage. *Journal of Applied Microbiology*, 101, 80–95.
- Deng, Y., Luo, Y., Wang, Y., & Zhao, Y. (2015). Effect of different drying methods on the myosin structure, amino acid composition, protein digestibility and volatile profile of squid fillets. *Food Chemistry*, 171, 168–176.
- Dorđević, D., & Buchtová, H. (2015). Freshness indicators of defrosted fillets of *Lepidocybium flavobrunneum* in vacuum skin packaging/VSP packaging during cold storage. *Acta Alimentaria*. <http://dx.doi.org/10.1556/AAlim.2015.0015>.
- EFSA. (2004). Opinion of the scientific panel on contaminants in the food Chain on a request from the commission related to the toxicity of fishery products belonging to the family of Gempylidae. *The EFSA Journal*, 92, 1–5.
- EFSA. (2011). Scientific Opinion on risk based control of biogenic amine formation in fermented foods. *EFSA Journal*, 9, 1–93.
- Emborg, J., Laursen, B. G., Rathjen, T., & Dalgaard, P. (2002). Microbial spoilage and formation of biogenic amines in fresh and thawed modified atmosphere-packed salmon (*Salmo salar*) at 2°C. *Journal of Applied Microbiology*, 92, 790–799.
- Feldman, K. A., Werner, S. B., Cronan, S. B., Hernandez, M., Horvath, A. R., Lea, C. S., ... Vugia, D. J. (2005). A large outbreak of scombroid fish poisoning associated with eating escolar fish (*Lepidocybium flavobrunneum*). *Epidemiology and Infection*, 133, 29–33.
- Hara, A., & Radin, N. S. (1978). Lipid extraction of tissues with a low-toxicity solvent. *Analytical Biochemistry*, 90, 420–426.
- Hwang, C. C., Lin, C. M., Huang, C. Y., Huang, Y. L., Kang, F. C., Hwang, D. F., et al. (2012). Chemical characterisation, biogenic amines contents, and identification of fish species in cod and escolar steaks, and salted escolar roe products. *Food Control*, 25415–25420.
- Karl, H., & Rehbein, H. (2004). Butterfish on the German market. *Dtsch Lebenscm – Rundsc. Journal of Bio Science*, 100, 34–42.
- Leask, A., Yankos, P., & Ferson, M. J. (2004). Fish, so foul! foodborne illness caused by combined fish histamine and way ester poisoning. *Communicable Diseases Intelligence*, 28, 83–85.
- Li, X., Lindahl, G., Zamaratskaia, K., & Lundstrom, K. (2012). Influence of vacuum skin packaging on color stability of beef longissimus lumborum compared with vacuum and high-oxygen modified atmosphere packaging. *Meat Science*, 92, 604–609.
- Nichols, P. D., Mooney, B. D., & Elliott, N. G. (2001). Unusually high levels of non-saponifiable lipids in the fishes escolar and rudderfish. Identification by gas and thin-layer chromatography. *Journal of Chromatography A*, 936, 183–191.
- NOAA. (2015). *National marine fisheries service annual landings*. [http://www.st.nmfs.noaa.gov/pls/webpls/MF\\_ANNUAL\\_LANDINGS.RESULTS](http://www.st.nmfs.noaa.gov/pls/webpls/MF_ANNUAL_LANDINGS.RESULTS) Accessed 15.01.15.
- Paulsen, P., Bauer, F., & Vali, S. (1997). Biogene Amine in Rohwürsten. 1. Methodische Aspekte zur Bestimmung biogener Amine. *Fleischwirtschaft*, 77, 450–452.
- Rajkumar, R., Preeedy, V. R., & Patel, V. B. (2015). *Branched chain amino acids in clinical nutrition. Nutrition and health*. New York: Humana Press.
- Rauscher-Gabering, E., Gabering, R., Brueller, W., Grossgut, R., Bauer, F., & Paulsen, P. (2012). Dietary exposure assessment of putrescine and cadaverine and derivation of tolerable levels in selected foods consumed in Austria. *European Food Research and Technology*. <http://dx.doi.org/10.1007/s00217-012-1748-1>.
- Ruiz-Gutierrez, V., Perez-Zarza, M. C., Muriana, F. J. G., & Bravo, L. (1997). Lipid and fatty acid composition of muscle and internal organs from *Ruvettus pretiosus*. *Journal of Fish Biology*, 50, 1353–1357.
- Sagrati, G., Fernandez-Franzon, M., De Berardinis, F., Font, G., Vittori, S., & Manes, J. (2012). Simultaneous determination of eight underivatized biogenic amines in fish by solid phase extraction and liquid chromatography–tandem mass spectrometry. *Food Chemistry*, 132, 537–543.
- Schwartz, F. J. (1997). Size, body component weights, and fatty acid profiles of the escolar, *Lepidocybium flavobrunneum* (Pisces, Gempylidae) caught in the Atlantic ocean off the mid-south east coast USA. *The Journal of the Elisha Mitchell Scientific Society*, 113, 9–15.
- Simple steps vsp package for produce. (2014). *Cryovac® simple Steps® package for Produce*. N.P., n.d. [on line: 2014-11-25]. Available at: <http://www.cryovac.com/NA/EN/food-packaging-products/simple-steps-vsp-produce.aspx>.
- Suseno, S. H., Permata, R. R. T. F., Hayati, S., Nugraha, R., & Saraswati. (2013). Fatty acids composition and steroid content of selected deep sea fishes escolar (*Lepidocybium flavobrunneum*) and deep sea lobster (*Linuparus somniosus*) from Southern Java Ocean-Indonesia. In *2nd International conference on ecological, environmental and bio-sciences*, Dec, 20–21 pp. 13–16.
- Torido, Y., Ohshima, C., Takahashi, H., Miya, S., Iwakawa, A., Kuda, T., et al. (2014). Distribution of psychrophilic and mesophilic histamine-producing bacteria in retail fish in Japan. *Food Control*, 46, 338–342.
- Visciano, P., Schirone, M., Tofalo, R., & Suzzi, G. (2012). Biogenic amines in raw and processed seafood. *Frontiers in Microbiology*, 3, 1–10.
- Zarei, M., Najafzadeh, H., Enayati, A., & Pashmforoush, M. (2011). Biogenic amines content of canned tuna fish marketed in Iran. *American-Eurasian Journal of Toxicological Sciences*, 3, 190–193.
- Zarza, M. C. P., Gutierrez, V. R., & Bravo, L. (1993). Composición lipídica de dos peces laxantes: *Ruvettus pretiosus* y *Lepidocybium flavobrunneum*. *Grasas y Aceites*, 44, 47–52.



## Modelling the kinetics of *Listeria monocytogenes* in refrigerated fresh beef under different packaging atmospheres



C. Saraiva <sup>a,\*,1</sup>, M.C. Fontes <sup>a,1</sup>, L. Patarata <sup>a,1</sup>, C. Martins <sup>a,1</sup>, V. Cadavez <sup>b</sup>,  
U. Gonzales-Barron <sup>b</sup>

<sup>a</sup> School of Agrarian and Veterinary Sciences, DCV, CECAV, Centro de Ciência Animal e Veterinária, Universidade de Trás-os-Montes e Alto Douro, Quinta de Prados, 5000-801, Vila Real, Portugal

<sup>b</sup> CIMO Mountain Research Centre, School of Agriculture, Polytechnic Institute of Bragança, Campus de Santa Apolónia, Apartado 1172, 5301-854, Bragança, Portugal

### ARTICLE INFO

#### Article history:

Received 6 June 2015

Received in revised form

6 October 2015

Accepted 17 November 2015

Available online 22 November 2015

#### Keywords:

Modified atmosphere packaging (MAP)

Vacuum packaging

Weibull

Survival

Predictive microbiology

### ABSTRACT

The objective of this study was to model the fate of *Listeria monocytogenes* inoculated in beef at two concentrations (2.5 and 4.0 log CFU/g), packaged under air, vacuum and three modified atmospheres MAP: 70%O<sub>2</sub>/20%CO<sub>2</sub>/10%N<sub>2</sub>, 50%O<sub>2</sub>/40%CO<sub>2</sub>/10%N<sub>2</sub> and 30%O<sub>2</sub>/60%CO<sub>2</sub>/10%N<sub>2</sub>, and refrigerated at a normal temperature (4 °C) and at a mild abusive temperature (9 °C). The experimental design produced a total of 20 environmental conditions. An omnibus model based on the Weibull equation proved statistically that *L. monocytogenes* survives better in vacuum (VP) than in aerobic conditions, although without significant difference in its ability to survive in the temperature range between 4 °C and 9 °C. Furthermore, regardless of the refrigeration temperature, the presence of CO<sub>2</sub> in the package atmosphere exerted a bactericidal effect on *L. monocytogenes* cells, being approximately 1.5 log of reduction when storage time reached 10 days. Since the pathogen can survive in VP/MAP beef, there is a need of maintaining its numbers below 100 CFU/g before packaging by placing efforts on the implementation of control measures during processing.

© 2015 Elsevier Ltd. All rights reserved.

## 1. Introduction

*Listeria monocytogenes* is a Gram-positive anaerobic facultative food-borne pathogen capable to survive in environments with pH between 4.0 and 9.6 (optimum 6.0–8.0), and at water activity ( $a_w$ ) levels as low as 0.90 (Farber & Peterkin, 1991). Moreover, this pathogen can survive at temperatures below freezing, and can grow from 1 °C to 45 °C. As a consequence, because of this bacterium's ability to proliferate under chilled temperatures, some types of food products have recurrently exhibited more susceptibility to *L. monocytogenes* contamination. In particular, refrigerated meats, ready-to-eat meat (RTE) foods, milk and cheeses, smoked fish and seafood, have been implicated in isolated cases of listeriosis (EFSA, 2015; Martins & Germano, 2011). As *L. monocytogenes* is a microorganism of ubiquitous nature, meat products may become

contaminated with this pathogen through raw materials, processing environment and at retail markets (Sofos & Geornaras, 2010).

In 2013, EU reported 1763 confirmed human cases of listeriosis, which represented an 8.6% increase compared to 2012. It was also concluded that there was a statistically significant increasing trend of listeriosis in the EU over the period 2009–2013 (EFSA, 2015). A recent meta-analysis on the incidence of pathogens in Portuguese meats revealed that incidence average of *L. monocytogenes* in beef meat is 17.6%, and in meat products is 8.8% (Xavier, Gonzales-Barron, Paula, Estevinho, & Cadavez, 2014). Although the concentrations are unknown, and may as well be low, these high prevalence estimates may represent a considerable risk due to the common practice among consumers of eating rare meat. Other malpractices resulting in higher *L. monocytogenes* levels, such as cross contamination and storage at abusive temperatures, may also exacerbate the risk for consumers, especially for immunocompromised people (Swaminathan & Gerner-smidt, 2007). According to Santos, Correia, Cunha, Saraiva, and Novais (2005), the limit of 2.0 log CFU/g of RTE was considered unacceptable or potentially dangerous for public health. This limit must not be exceeded at the end of the shelf-life (Commission European Communities, 2008).

\* Corresponding author. Departamento das Ciências Veterinárias, CECAV, Universidade de Trás-os-Montes e Alto Douro, Apartado 1013, 5001-911, Vila Real, Portugal.

E-mail address: [crisarai@utad.pt](mailto:crisarai@utad.pt) (C. Saraiva).

<sup>1</sup> [www.utad.pt](http://www.utad.pt).

Among the parameters affecting the growth of microorganisms in packaged raw meat, it is assumed that the final pH and the gaseous composition of the packaging have an important role (Zakrys, Hogan, O'Sullivan, Allen, & Kerry, 2008). In red meat packaging, the most common methods are vacuum packaging (VP) and modified atmosphere packaging (MAP). It is well known that the composition of modified atmosphere systems can be an effective way to restrict the growth of spoilage aerobic organisms (McMillin, 2008; Tsigarida, Skandamis, & Nychas, 2000); but their effectiveness strongly depends on storage temperature and film permeability (McMillin, 2008). Nevertheless, the extended shelf-life of refrigerated meats under VP and MAP conditions has raised concerns about the survival dynamics of *L. monocytogenes*. At present, in the literature, there are a series of contradictions related to the effect of VP and MAP on the growth/survival of this pathogen in meats and meat products (Arvanitoyannis & Kotsanopoulos, 2012, Chap. 3; Arvanitoyannis & Stratakis, 2012, Chap. 5; García-de-Fernando, Nychas, Peck, & Ordóñez, 1995; Lyver, Smith, Tarte, Farber, & Nattress, 1998; Uppal et al., 2012). In addition, in the references above, no efforts have been directed to developing a predictive microbiology model that can estimate the dynamics of *L. monocytogenes* in refrigerated packaged meat. Within this context, the objective of this work was to assess, by means of predictive microbiology modelling, the effect of packaging (air, vacuum and three gas compositions of MAP) on the dynamics of *L. monocytogenes* inoculated at low and high level in beef meat stored at a normal refrigeration temperature (4 °C) and a mild abusive temperature (9 °C).

## 2. Material and methods

### 2.1. Preparation of meat samples

Samples of *Longissimus dorsi* (LD) muscle were obtained from eight Portuguese bulls aged 9–11 months old, having carcass weights between 90 and 150 kg. LD was excised from the carcasses, between the 6th thoracic and the 2nd lumbar vertebra 24 h *post mortem*. The pH was measured directly in the muscle using a combined glass electrode with a pH-metre (Crison Instruments, Spain) (ISO 2917, 1999). Only muscles whose pH were below or equal to 5.8 were used. The activity of water ( $a_w$ ) was measured with a rotronic-Hygroskop DT at 25 °C according to ISO 21807 (2004). The  $a_w$  of muscles were  $0.97 \pm 0.01$ . Muscles were cut into pieces of approximately 200 g and two samples of each piece were immediately (24 h *post mortem*) investigated for the presence of *L. monocytogenes* according to ISO 11290-1 (1996). If at least one positive-sample from each muscle were detected in one meat cut, all piece cuts of the whole muscle were totally excluded from the inoculation experiments. Meat cuts were then packed in vacuum, and kept at –80 °C during 15 days before the experiment. For the experiments, meat was left to defrost overnight at 2 °C. Meat samples were then prepared by removing a layer of ~1 cm from the meat surface, and aseptically cut in small meat pieces (0.5 cm thick, surface  $2 \times 2.5$  cm) of a weight of ~5 g.

### 2.2. Preparation of inoculum and inoculation procedure

*L. monocytogenes* (ATCC 7973) stock culture was cultured on tryptone soy agar (TSA, England) slants at 4 °C, which were replaced every 30 days. During the course of the study, this bacteria was sub-cultured by transferring a single colony from the slants into 10 ml Brain Heart Infusion (BHI) broth (Oxoid CM225, England) for 24 h at 37 °C, followed by a second activation step in BHI (37 °C, 18 h) to achieve a viable cell population of 9 log CFU/ml.

The culture was then transferred to a sterile centrifuge bottle

and centrifuged at  $10,000 \times g$  for 10 min at 4 °C. The supernatant was decanted and the sediment suspended in 0.1% peptone water (Merck, Germany). The washing step was repeated twice. The suspension of washed cells was diluted in a sterile 0.1% peptone solution to obtain an optical density of 0.5 (600 nm, 10 mm). Serial (10-fold) dilutions were performed to yield approximately 2.5 or 4 log CFU/g.

On the day of the experiment, each piece of beef was placed into an individual package and inoculated with 20 µl bacterial suspension of *L. monocytogenes* in the sample's centre. The entire procedure was repeated to obtain a low inoculation level (2.5 log CFU/g) and a high inoculation level (4.0 log CFU/g). Each bag of beef was massaged manually and then bags were heat-sealed. Duplicate beef samples (5 g) inoculated with 20 µl of 0.1% (w/v) sterile peptone water served as negative controls and the bags were heat-sealed.

To verify the number of viable *L. monocytogenes* in the suspension, each inoculum was enumerated by making appropriate dilutions in peptone water (0.1%, w/v; PW) in duplicate, and plating onto TSA plates to obtain the initial population densities. Plates were incubated at 37 °C for 24 h before enumeration.

### 2.3. Packaging

Inoculated samples were packed in 5 different packaging types, namely: air (A), vacuum (V) and modified atmosphere packaging 70%O<sub>2</sub>/20%CO<sub>2</sub>/10%N<sub>2</sub> (MAP<sub>70/20</sub>), 50%O<sub>2</sub>/40%CO<sub>2</sub>/10%N<sub>2</sub> (MAP<sub>50/40</sub>) and 30%O<sub>2</sub>/60%CO<sub>2</sub>/10%N<sub>2</sub> (MAP<sub>30/60</sub>). For air-packaged samples, meat cuts were accommodated in a tray and overwrapped with polyethylene film, while for vacuum-packaged samples, meat cuts were individually packaged in COMBITHERM bags (WIPAK Walsrode, HAFRI) of 0.09 mm thickness, oxygen transmission rate (OTR) of  $63 \text{ cm}^3 \text{ m}^{-2} \text{ day}^{-1}$  at 23 °C/0% RH, and water vapour transmission (WVT) of  $1 \text{ g m}^{-2} \text{ day}^{-1}$  at 23 °C/85%RH. For modified-atmosphere packaged samples, meat cuts were individually placed in COMBITHERM XX bags (WIPAK Walsrode, HAFRI) of 0.115 mm thickness, a very low O<sub>2</sub>-permeable film (OTR of  $1 \text{ cm}^3 \text{ m}^{-2} \text{ day}^{-1}$  at 23 °C/0% RH) with a WVT of  $1 \text{ g m}^{-2} \text{ day}^{-1}$  at 23 °C/85%RH. The meat samples were packaged either in modified atmosphere or vacuum using a SAMMIC V-420 SGA machine, with a final gas-to-meat ratio of ~3:1. Individual samples were then stored at  $4 \pm 0.5$  °C and  $9 \pm 0.5$  °C, and examined for *L. monocytogenes* counts (ISO 11290-2, 1998) at days 1 (2 h after packaging), 3, 7, 10, 14, 21 and 28, depending on the packaging system.

### 2.4. Microbiological analysis

At each time point, two samples were prepared for microbiological analysis. The meat cuts were homogenised with 20-ml sterile buffered peptone water (BPW) in a stomacher (IUL, Barcelona, Spain) during 90 ss at room temperature. Serial decimal dilutions were prepared in BPW, and duplicate 0.1 ml samples were then plated onto Compass *L. monocytogenes* agar (Biokar BM06508). After incubation at 37 °C for 48 h, typical colonies were counted and results were expressed as log CFU/g.

Serial decimal dilutions of control samples were also prepared in BPW, and duplicate 1 ml samples were plated onto selective CFC (Cetrimide, Fucidin, Cephaloridine) Agar (OXOID CM0559) with CFC selective supplement (OXOID SR0103) for *Pseudomonas* spp. (25 °C for 48 h, NF V04–503, 1988) and 1 ml samples were plated on double layer on MRS agar (OXOID CM361) for LAB counts (37 °C, 24 h) (NF V04–504, 1998).

The enumeration of *Pseudomonas* spp. (NF V04–503, 1988) was completed by biochemical test in KLIGLER (OXOID CM0033) and oxidase test. Results were expressed as log CFU/g. In case the microorganism counts were below to the detection limit, the result

was considered to be zero for statistical purposes.

### 2.5. Modelling the survival of *L. monocytogenes*

The survival of *L. monocytogenes* in inoculated beef meat of normal pH was modelled using the Weibull exponential decay function as the primary predictive microbiology model (i.e., a model describing microbial concentration as a function of time). The three-parameter Weibull model is defined as,

$$\log N(t) = \log N_0 - \left(\frac{t}{\chi}\right)^\beta \quad (1)$$

with  $\chi$  representing the scale parameter and  $\beta$  the shape parameter. Although the Weibull model is basically of empirical nature, Van Boekel (2002) suggested that  $\beta < 1$  (i.e., concave curves) presumes that the surviving microorganisms have the capacity to adapt to the applied stress, whereas  $\beta > 1$  (convex curves) indicates that the remaining cells become increasingly susceptible to heat. The dependent variable  $\log N(t)$  used is the logarithm base 10 ( $\log$ ) of the number of cells at time  $t$ .  $\log N_{res}$  is the residual log number of microorganisms, which is in fact a parameter associated with the tailing effect, and  $\log N_0$  is the initial logarithmic number of microorganisms.  $\log N_0$  was considered to be a model parameter and not the first observation when  $t = 0$  as it is preferable for a kinetics model to describe the absolute population and not the population relative to the initial population (Geeraerd, Herremans, & Van Impe, 2000).

The experimental design of the survival study was of the type  $2^2 \times 5^1$  for two factors (inoculation level and storage temperature) consisting of two levels each, and one factor (packaging) consisting of five levels. This produced a total of 20 conditions or treatments which were replicated twice (i.e., yielding 40 survival curves). Hence, since the survival experiments were conducted under three different factors, secondary models were developed in order to assess the effects of each of those factors on the primary model's parameters ( $\chi$ ,  $\beta$  and  $\log N_0$ ). A more informative and neat way to adjust the primary and secondary models is by means of an omnibus or global model (Juneja, Gonzales-Barron, Butler, Yadav, & Friedman, 2013; Pradhan et al., 2012), which is a type of model fitting that jointly estimates the parameters of the primary and secondary models using all the experimental curves. Thus, the omnibus model based on the Weibull equation assumed that its parameters ( $\chi$ ,  $\beta$  and  $\log N_0$ ) could be expressed as a function of the three following categorical variables: (i) the factor packaging type defined as "Pack" comprising five levels: air (A), vacuum (V) and modified atmosphere packaging MAP<sub>70/20</sub>, MAP<sub>50/40</sub> and MAP<sub>30/60</sub>; (ii) the factor inoculation level "Inoc" consisting of a high level (4.0 log CFU/g) and a low level (2.5 log CFU/g), and (iii) the storage temperature "T" encompassing an optimal refrigeration temperature (4 °C) and a temperature of mild abuse (9 °C).

The concentration  $\log N_{ijk}$  of *L. monocytogenes* in beef with the level of inoculum  $i$ , packaged under the gaseous composition  $j$  and stored at the refrigeration temperature  $k$  was estimated as,

$$\begin{aligned} \log N_{ijk} &= \log N_{0i} - \left(\frac{t}{\chi_{jk}}\right)^{\beta_j} + \varepsilon_{ijk} \\ \ln \chi_{jk} &= a_1 \text{Pack}_j + a_2 T_k \\ \ln \beta_j &= b \text{Pack}_j \\ \log N_{0i} &= c \text{Inoc}_i \end{aligned} \quad (2)$$

where  $\varepsilon_{ijk}$  are the residuals which are assumed to follow a normal distribution with mean zero and standard deviation  $\sigma$ . The factor

"Inoc" was removed as a predictor of  $\ln \chi$  and  $\ln \beta$  as it did not have any significant effect. Similarly, the temperature "T" did not significantly affect  $\ln \beta$ . However, the initial microbial concentration (parameter  $\log N_0$ ) could only be modelled as a function of the level of inoculum "Inoc", and hence neither "Pack" nor "T" was placed in the equation of  $\log N_0$ . The factors "Inoc", "Pack" and "T" predicting the Weibull model's parameters were added to the omnibus model one by one while assessing the improvement in the goodness-of-fit measures (log-likelihood, Akaike Information Criterion [AIC] and BIC) and the behaviour of the residuals. The model was adjusted in R version 2.14.2 (R Development Core Team) using the "nlme" package and the "glns" function.

### 3. Results and discussion

The survival studies showed overall that the population numbers of *L. monocytogenes* decreased during storage of raw beef at refrigeration temperature (Fig. 1), suggesting that the packaging environment, product characteristics and, eventually, interactions with other competitive microbiota were not favourable for the growth of this pathogen. The Weibull model was able to closely represent the experimental survival curves of inoculated *L. monocytogenes* in beef for each of the twenty environmental conditions. The omnibus regression evidenced that the level of inoculum did not affect the parameter values of the Weibull model (viz. notice the absence of "Inoc" as predictor of  $\chi$  or  $\beta$  in Table 1), meaning that, regardless of the level of inoculation, the shape of the survivors' curve remains with the same tendency. Mathematically, this implies that, keeping  $\chi$  and  $\beta$  constant, a lower or higher level of contamination will merely shift the survival curve down- or upwards, respectively (Notice in Fig. 1 that for a fixed packaging condition and temperature, the increase or decrease in the level of inoculum does not affect the shape of the fitted curve). Biologically, this may indicate that, within such low levels of inoculum (2.5–4.0 log CFU/g), there is no appreciable change in the possible effect of other meat microbiota on the dynamics of *L. monocytogenes*. For example, it could have been argued that, at a lower pathogen's population, the survival or death rate becomes faster prompted by the predominance of other microbiota in proportionally higher numbers (Fig. 3). However, seemingly this did not occur as there was no significant change in the shape of the survivors' curves between the two inoculum levels. Conversely, as expected, the level of inoculum determined ( $P < .0001$ ) the value of the fitted initial microbial concentration ( $\log N_0$ ) of a survival curve. The estimated means of  $\log N_0$  for the high (4.045; Table 1) and low (2.560) inoculum corresponded closely to the target concentrations of *L. monocytogenes* inoculated (~4.0 and 2.5 log CFU/g) in the experiments.

With regards to the scale parameter  $\chi$ , both storage temperature and packaging type influenced its value (Table 1). Since the scale parameter  $\chi$  can be interpreted as the time to attain the first decimal reduction (Van Boekel, 2002) a lower intercept estimate of the packaging type will lead to a lower  $\ln \chi$  (Eq. (2)); suggesting hence a greater microbial inhibition for the same storage time. The omnibus model inferred that the survival of *L. monocytogenes* in vacuum packaging (Pack.V intercept of 2.625 in Table 1) was significantly better than in aerobic conditions (Pack.A = 2.142). In other words, oxygen restriction via vacuum showed consistently less reduction in inoculated *L. monocytogenes* populations than air packaging (Fig. 2). Comparable findings were reported by Uppal et al. (2012), who observed that VP treatment was less effective in reducing *L. monocytogenes* in turkey tenders. It is not surprising that, because of its facultative anaerobic character, *L. monocytogenes* in vacuum may behave more competitively than other microbiota, as earlier suggested by Duffy, Vanderlinde, and

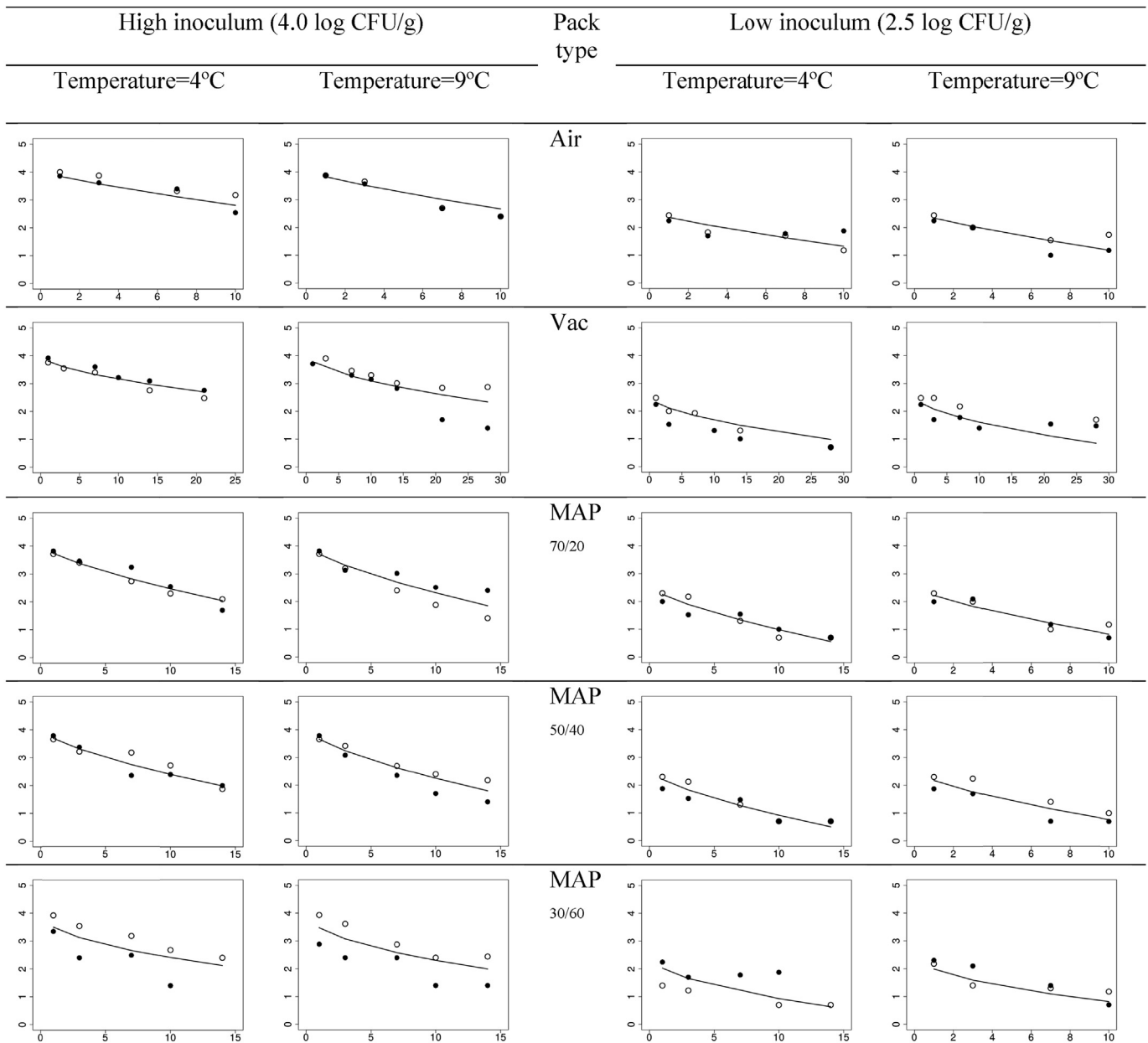


**Fig. 1.** Survival curves of *L. monocytogenes* inoculated in beef for the different combinations of packaging type, temperature and level of inoculum, as modelled by a Weibull-based omnibus regression. Same markers represent observations from the same experiment; and x-axis represents time (day) while y-axis represents microbial concentration (log CFU/g) (° experiment 1; ● experiment 2).

Grau (1994). Indeed, in VP, there is a shift from Gram-negative aerobic microbiota towards Gram-positive bacteria (Nychas, Drosinos, & Board, 1998). Specific spoilage bacteria have in air packaging better environmental conditions with the usual production of metabolites that hinders the ability of *L. monocytogenes* to survive. This may explain, to some extent, why *L. monocytogenes* populations decreased in air-packaged meat. However, results of Tsigarida et al. (2000) demonstrated that under aerobic conditions, pseudomonads in refrigerated beef predominated by yielding maximum levels of 10 log CFU/g, while *L. monocytogenes* had a slight growth. In our study, the greater survival of this pathogen in vacuum than in air-packaged samples may be also related to the  $O_2$  permeability of the packaging film used for VP ( $OTR = 63.0 \text{ cm}^3 \text{ m}^2 \text{ day}^{-1}$ ), which may not inhibit the *L. monocytogenes* development so efficiently, and the very low concentration of  $CO_2$  in VP

which renders a more favourable condition for the pathogen's survival. The effective inhibition of *L. monocytogenes* in raw meats by  $CO_2$  has been pointed out by several authors (Bennik, Smid, Rombouts, & Gorris, 1995; Fraqueza, Ferreira, & Barreto, 2006; Nissen, Alvseike, Bredholt, Holck, & Nesbakken, 2000; Stanbridge & Davies, 1998).

To this respect, the omnibus regression model confirmed that the reduction of *L. monocytogenes* in any of the MAP treatments was significantly greater than in the air-packaged meat samples (Fig. 2). Furthermore, the intercept estimates for MAP<sub>70/20</sub> (1.771; Table 1), MAP<sub>50/40</sub> (1.666) and MAP<sub>30/60</sub> (1.395) decreased progressively because a higher  $CO_2$  concentration had a greater effect on decreasing the *L. monocytogenes* population in packaged raw beef (Fig. 2); and this occurred regardless of the refrigeration temperature evaluated. This can also be associated to the resistance of LAB

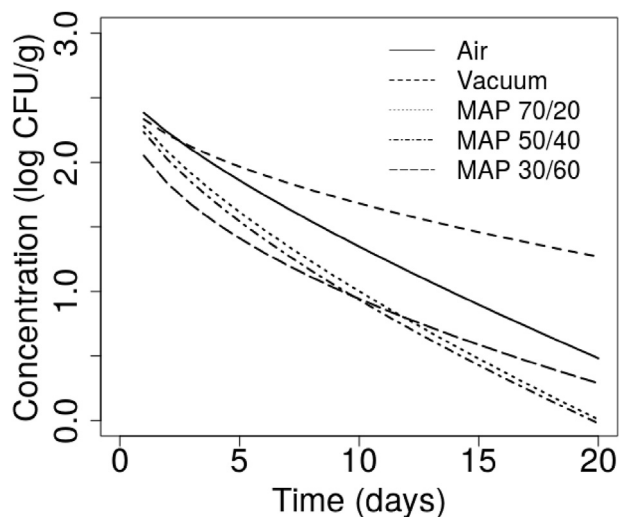


Fig. 2. Fitted survival curves of low-inoculum *L. monocytogenes* in beef under different packaging systems stored at 4 °C.

Table 1

Parameter estimates of the omnibus model based on the Weibull exponential function predicting the non-log-linear decline of *L. monocytogenes* in inoculated beef meat as a function of packaging type (Pack), storage temperature (T) and level of inoculum (Inoc).

Parameters	Mean*	Standard error	Pr >  t	AIC/BIC
<i>Predictors of Ln <math>\chi</math></i>				
T	-0.026	0.013	0.053	118/166
Pack.A	2.142 <sup>b</sup>	0.235	<0.0001	
Pack.V	2.625 <sup>a</sup>	0.324	0.0001	
Pack. MAP <sub>70/20</sub>	1.771 <sup>c</sup>	0.267	<0.0001	
Pack. MAP <sub>50/40</sub>	1.666 <sup>cd</sup>	0.278	<0.0001	
Pack. MAP <sub>30/60</sub>	1.395 <sup>d</sup>	0.356	0.0001	
<i>Predictors of Ln <math>\beta</math></i>				
Pack.A	-0.222 <sup>c</sup>	0.303	0.465	
Pack.V	-0.569 <sup>ab</sup>	0.240	0.019	
Pack. MAP <sub>70/20</sub>	-0.338 <sup>c</sup>	0.195	0.085	
Pack. MAP <sub>50/40</sub>	-0.401 <sup>b</sup>	0.185	0.032	
Pack. MAP <sub>30/60</sub>	-0.724 <sup>a</sup>	0.182	0.0001	
<i>Predictors of Log <math>N_0</math></i>				
Inoc.High (log CFU/g)	4.045 <sup>a</sup>	0.145	<0.0001	
Inoc.Low (log CFU/g)	2.560 <sup>b</sup>	0.146	<0.0001	
<i>Residuals</i>				
$\sigma$ (log CFU/g)	0.234			

\*Within each Weibull parameter, different superscript letters indicate significant differences ( $P < .05$ ).

to CO<sub>2</sub> effect (Fig. 3), with the eventual production of substances with inhibitory effect against to *L. monocytogenes*. Earlier, Nissen et al. (2000) observed that for very high CO<sub>2</sub> concentrations (60%), the development of *L. monocytogenes* in MAP beef was inhibited at 4 °C, while Fraqueza et al. (2006) obtained similar results when they packaged turkey meat in both modified atmospheres 50%CO<sub>2</sub>/50%N<sub>2</sub> and 50%CO<sub>2</sub>/50%Air, and stored it at both 0° and 7 °C. According to Phillips (1996) storing bovine meat of normal pH in a CO<sub>2</sub> atmosphere efficiently inhibits *L. monocytogenes*. Even with a brief exposition of the fresh meat of 3 h to the gas, he verified a delay of the lag-phase for longer than 74 h Bennik, Smid, and Rombouts (1995) explained that, when *L. monocytogenes* is exposed to high concentrations of CO<sub>2</sub>, inhibition takes place because of two mechanisms: acidification of the food matrix and a direct inhibitory effect. Diffusion of H<sub>2</sub>CO<sub>3</sub> through the bacterial cell membrane causes alterations in the intracellular pH, affecting enzymatic activity. High concentrations

of CO<sub>2</sub> can inhibit the decarboxylation reactions by which CO<sub>2</sub> is released through feedback mechanisms. The CO<sub>2</sub> effect on *Pseudomonas* spp. growth is no effective at higher temperature (9 °C) as can be observed in Fig. 3.

The first decimal reduction time  $\chi$  was not only affected by the packaging type ( $P < .0001$ ) but also by the storage temperature, although to a lesser extent as attested by its higher P-value (0.053 in Table 1). The influence of temperature on the kinetics of *L. monocytogenes* may have not been as high as that of the gaseous atmosphere because the temperature range tested was small (from 4° to 9 °C), and at such interval the pathogen may equally survive with only a slight variation in its dynamics. Notice in Fig. 1, that for a fixed inoculum level and packaging type, the effect of the temperature in the curve decay is weak, and this is reflected on the very low estimate of the temperature effect (-0.026 in Table 1). The negative value of the estimate only reflects the inverse relationship; this is, the higher the temperature, the lower the first decimal reduction time (i.e., the higher the survival of the pathogen).

The intercept estimates predicting Ln  $\beta$  (the shape factor) for all packaging types were negative (Table 1) because the shape of the survival curves were in all cases concave. The concavity or phenomenon of tailing arises as a manifestation of the natural adaptation of the bacteria to the stress-causing factor(s); in this case, low temperatures, gaseous atmospheres and competitive microbiota. It is known that, in a Weibull decay model depicting concavity, the parameters  $\chi$  and  $\beta$  are normally correlated (i.e., a lower  $\chi$  is associated to a lower  $\beta$ ). This happens because when inactivation occurs at a quicker pace, the first decimal reduction time  $\chi$  (which can be understood as the inverse of the slope) becomes lower, and at the same time, the curve acquires a greater concavity (i.e., a lower  $\beta$ ). Hence, as occurred for the intercept estimates of the packaging types predicting Ln  $\chi$ , the intercept estimates for MAP<sub>70/20</sub> (-0.338; Table 1), MAP<sub>50/40</sub> (-0.401) and MAP<sub>30/60</sub> (-0.724) predicting Ln  $\beta$  also decreased in the same order due to the greater inhibitory effect from increasing the CO<sub>2</sub> concentration. Yet, at a storage time of 10 days, a higher proportion of CO<sub>2</sub> in the package – from 40% in MAP<sub>50/40</sub> to 60% in MAP<sub>30/60</sub> – provided the same level of reduction in *L. monocytogenes* of ~1.5 log CFU/g (Fig. 2).

The dynamics of *L. monocytogenes* in packaged raw meats has been the subject of numerous studies with controversial findings related to the inhibitory effect of VP/MAP. It has been said that this pathogen can still grow in VP/MAP at refrigeration temperatures (Barakat & Harris, 1999; Sheridan et al., 1995; Tsigarida et al., 2000), while other studies concluded that *L. monocytogenes* can effectively be inhibited by VP/MAP (Fraqueza et al., 2006; Hudson, Mott, & Penney, 1994). However, it is not unexpected that, in some instances, the outcomes and conclusions from the different studies be barely comparable among themselves; given the many factors creating a unique ecosystem that affect the dynamics of *L. monocytogenes* in packaged meat. Among other factors, the effectiveness of the packaging systems to inhibit *L. monocytogenes* would strongly depend upon pathogen's strain and physiological status, storage temperature, temperature fluctuations, meat composition and pH, atmosphere composition and O<sub>2</sub>/CO<sub>2</sub> ratio, packaging film properties such as thickness and permeability, meat-to-air volume ratio within the package, initial concentrations of the microbiota, interrelationships with other bacterial groups such as pseudomonad and lactic acid bacteria, competition and effects of their metabolic end-products.

Thus, while other researchers reported inhibition in the sense of absence of growth of *L. monocytogenes* in refrigerated meat packaged in VP/MAP (Mano et al., 1995; Sheridan et al., 1995; Tsigarida et al., 2000), in this work, there was a decrease in *L. monocytogenes* numbers during refrigerated storage. For instance, after 10 days of storage at 4 °C, initial populations of 2.5 log CFU/g of

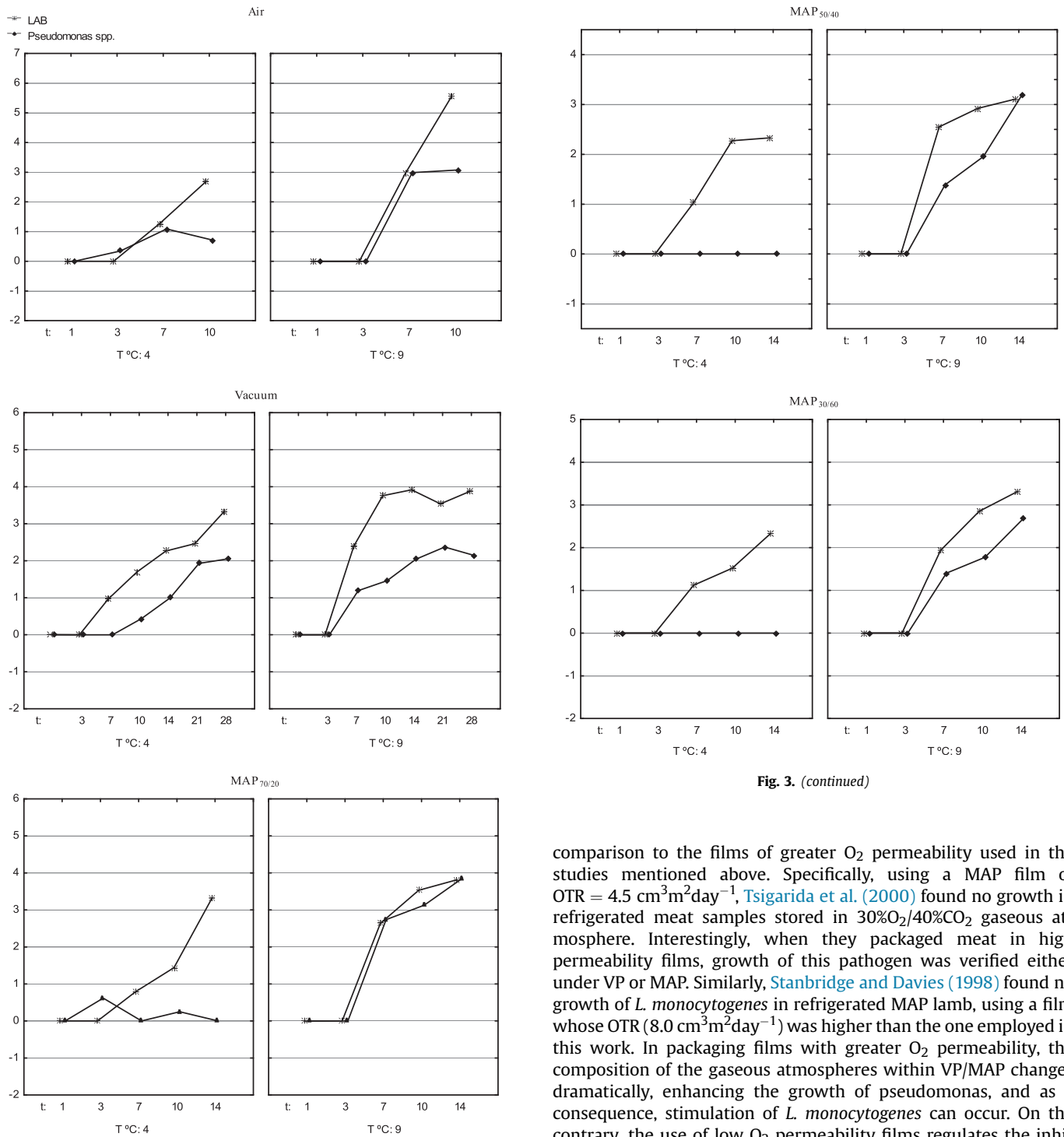


Fig. 3. (continued)

**Fig. 3.** Microbial evolution of spoilage microorganisms in beef for the different combinations of packaging type and temperature. X-axis represents time (day) while y-axis represents microbial concentration in average (log CFU/g) of Lactic Acid Bacteria (LAB) and *Pseudomonas* spp..

*L. monocytogenes* in beef may be reduced by  $\sim 1.0$  log in vacuum packaging and by  $\sim 1.5$  log on average in the MAPs (Fig. 2). One of the factors that may have contributed to the progressive reduction of *L. monocytogenes* in MAP, as opposed to the absence of growth previously reported (Sheridan et al., 1995; Tsigarida et al., 2000) may have been the lower oxygen transmission rate (OTR =  $1.0 \text{ cm}^3 \text{ m}^2 \text{ day}^{-1}$ ) of the packaging film used in this work for MAP, in

comparison to the films of greater  $\text{O}_2$  permeability used in the studies mentioned above. Specifically, using a MAP film of  $\text{OTR} = 4.5 \text{ cm}^3 \text{ m}^2 \text{ day}^{-1}$ , Tsigarida et al. (2000) found no growth in refrigerated meat samples stored in  $30\% \text{O}_2/40\% \text{CO}_2$  gaseous atmosphere. Interestingly, when they packaged meat in high permeability films, growth of this pathogen was verified either under VP or MAP. Similarly, Stanbridge and Davies (1998) found no growth of *L. monocytogenes* in refrigerated MAP lamb, using a film whose  $\text{OTR}$  ( $8.0 \text{ cm}^3 \text{ m}^2 \text{ day}^{-1}$ ) was higher than the one employed in this work. In packaging films with greater  $\text{O}_2$  permeability, the composition of the gaseous atmospheres within VP/MAP changes dramatically, enhancing the growth of pseudomonas, and as a consequence, stimulation of *L. monocytogenes* can occur. On the contrary, the use of low  $\text{O}_2$  permeability films regulates the inhibition of *L. monocytogenes* throughout the storage period (Tsigarida et al., 2000). Furthermore, our results are in agreement to those of Fraqueza et al. (2006) who verified a slight decrease in *L. monocytogenes* inoculated in raw turkey meat when packaged also in low  $\text{O}_2$ -permeability film under MAP  $50\% \text{N}_2/50\% \text{CO}_2$  and stored at  $0^\circ \text{C}$ . In this particular work, other factors that may have contributed to the decrease in *L. monocytogenes* observed in VP/MAP could have been the high gas-to-meat ratio (3:1) for the small meat sample used in the package ( $\sim 5 \text{ g}$ ). Generally, under anaerobic MAP, lactic acid bacteria have shown to be effective in inhibiting the growth of pathogenic bacteria such as *L. monocytogenes* in meat (Phillips, 1996). Nychas et al. (1998) showed that the availability of

ecological determinants ( $O_2$  tension, type of available substrates and temperature) strongly affects the end-products formation by lactic acid bacteria and *Brochothrix thermosphacta*. Bacteriocins,  $H_2O_2$ , lactate, acetate and formate are among these products, which could also contribute further to the reduction in *L. monocytogenes* numbers in VP/MAP beef. Finally, the omnibus model based on the Weibull decay function is a working model that can be used to estimate the decrease in the counts of *L. monocytogenes* in beef meat packaged in VP/MAP at any time point during refrigerated storage at 4° and 9 °C.

#### 4. Conclusions

The omnibus regression model proved that vacuum packaging was significantly less efficient than MAP in reducing *L. monocytogenes* numbers in raw beef, while higher  $CO_2$  concentrations in MAP exerted a greater bactericidal effect regardless of the refrigeration temperature, with MAP<sub>50/40</sub> being as effective as MAP<sub>30/60</sub> when storage time reached 10 days (~1.5 log reduction). Yet, the effect of the temperature ( $P = .05$ ) on *L. monocytogenes* inhibition was lower than the effect of the gaseous atmosphere ( $P < .0001$ ), implying that there is little difference in the ability of *L. monocytogenes* to survive either at 4 °C or at 9 °C. The pathogen survived significantly better in vacuum than in aerobic conditions, which can be due to its facultative anaerobic nature, and to the better development of spoilage bacteria in air packaging. Because vacuum and MAP systems may at most reduce the numbers of *L. monocytogenes* by ~1.0 and ~1.5 log, respectively, after 10 days of refrigerated storage, they cannot be regarded as a sole hurdle for pathogen reduction, but instead strict control measures should be placed during beef processing stages. Nonetheless, to attain greater inhibition and reduction of *L. monocytogenes* at the packaging stage, the use of microbial- or plant-based antimicrobial substances should be considered as combined hurdles of VP/MAP.

#### Conflict of interest

The authors declare no conflict of interest.

#### Acknowledgements

The authors would like to thank CECAV-UTAD and the research is supported by national funds by FCT- Portuguese Foundation for Science and Technology, under the PEst-OE/AGR/UI0772/2014. Dr. Gonzales-Barron wishes to acknowledge the financial support provided by the Portuguese Foundation for Science and Technology (FCT) through the award of a five-year Investigator Fellowship (IF) in the mode of Development Grants (IF/00570).

#### References

- Arvanitoyannis, I. S., & Kotsanopoulos, K. (2012). Safety and quality control of MAP products. In I. S. Arvanitoyannis (Ed.), *Modified atmosphere and active packaging technologies* (pp. 61–78). USA: CRC Press, Taylor and Francis GROUP.
- Arvanitoyannis, I. S., & Stratakos. (2012). A. Ch. Fresh and processed meat and meat products. In I. S. Arvanitoyannis (Ed.), *Modified atmosphere and active packaging technologies* (pp. 223–224). USA: CRC Press, Taylor and Francis Group.
- Barakat, R. K., & Harris, L. J. (1999). Growth of *Listeria monocytogenes* and *Yersinia enterocolitica* on cooked modified-atmosphere poultry in the presence and absence of a naturally occurring microbiota. *Applied and Environmental Microbiology*, 65, 342–345.
- Bennik, M. H. J., Smid, E. J., Rombouts, F. M., & Gorris, L. G. M. (1995). Growth of psychrotrophic foodborne pathogens in a solid surface model system under the influence of carbon dioxide and oxygen. *Food Microbiology*, 12, 509–519.
- Commission of the European Communities. (2008). *Commission staff working document. Guidance document SANCO/1628/2008*.
- Duffy, L. L., Vanderlinde, P. B., & Grau, F. H. (1994). Growth of *Listeria monocytogenes* on vacuum-packed cooked meats: effects of pH, aw, nitrite and ascorbate. *International Journal of Food Microbiology*, 23, 377–390.
- European Food Safety Authority (EFSA). (2015). The European Union summary report on trends and sources of zoonoses, zoonotic agents and foodborne outbreaks in 2013. *EFSA Journal*, 13(1), 3991.
- Farber, J. M., & Peterkin, P. I. (1991). *Listeria monocytogenes*, a food-borne pathogen. *Microbiological Reviews*, 55, 476–511.
- Fraqueza, M. J., Ferreira, M. C., & Barreto, A. S. (2006). *Listeria monocytogenes* in turkey meat under modified atmosphere packaging with gas mixtures of argon or carbon monoxide. *Revista Portuguesa de Zootecnia*, 13, 19–35.
- García-de-Fernando, G. D., Nychas, G. J. E., Peck, M. W., & Ordóñez, J. A. (1995). Growth/Survival of psychrotrophic pathogens on meat packaged under modified atmospheres. *International Journal of Food Microbiology*, 28, 221–231.
- Geeraerd, A. H., Herremans, C. H., & Van Impe, J. F. (2000). Structural model requirements to describe microbial inactivation during a mild heat treatment. *International Journal of Food Microbiology*, 59, 185–209.
- Hudson, J. A., Mott, S. J., & Penney, N. (1994). Growth of *Listeria monocytogenes*, *Aeromonas hydrophila* and *Yersinia enterocolitica* on vacuum and saturated carbon dioxide controlled atmosphere-packaged sliced roast beef. *Journal of Food Protection*, 57, 204–208.
- ISO 11290-1. (1996). *Microbiology of food and animal feeding stuffs—horizontal method for the detection and enumeration of Listeria monocytogenes – Part 1: Detection method*. Geneva: International Organization for Standardization.
- ISO 11290-2. (1998). *Microbiology of food and animal feeding stuffs—horizontal method for the detection and enumeration of Listeria monocytogenes – Part 2: Enumeration method*. Geneva: International Organization for Standardization.
- ISO 21807. (2004). *International Organization for Standardization (2004). Microbiology of food and animal feeding stuffs – Determination of water activity*.
- ISO 2917. (1999). *International Organization for Standardization (2004). Meat and meat products – Measurement of pH - Reference method*.
- Juneja, V. K., Gonzales-Barron, U., Butler, F., Yadav, A., & Friedman, M. (2013). Predictive thermal inactivation model for the combined effect of temperature, cinnamaldehyde and carvacrol on starvation-stressed multiple *Salmonella* serotypes in ground chicken. *International Journal of Food Microbiology*, 165, 184–199.
- Lyver, A., Smith, J. P., Tarte, I., Farber, J. M., & Nattress, F. N. (1998). Challenge studies with *Listeria monocytogenes* in a value-added seafood product stored under modified atmospheres. *Food Microbiology*, 15, 379–389.
- Mano, S. B., García de Fernando, G. D., López, D., Selgas, M. D., García, M. L., Cambero, M. I., et al. (1995). Growth/survival of natural flora and *Listeria monocytogenes* on refrigerated uncooked pork and turkey packaged under modified atmospheres. *Journal of Food Safety*, 15, 305–319.
- Martins, E. A., & Germano, P. M. L. (2011). *Listeria monocytogenes* in ready-to-eat, sliced, cooked ham and salami products, marketed in the city of São Paulo, Brazil: occurrence, quantification and serotyping. *Food Control*, 22, 297–302.
- McMillin, K. W. (2008). Where is MAP Going? a review and future potential of modified atmosphere packaging for meat. *Meat Science*, 80, 43–65.
- NF V04–503 (AFNOR). (1988). *Viandes et produits à base des viande – Dénombrement des Bactéries lactiques*.
- NF V04–504 (AFNOR). (1998). *Viandes et produits à base des viande – Dénombrement de Pseudomonas spp.*
- Nissen, H., Alvsøike, O., Bredholt, S., Holck, A., & Nesbakken, T. (2000). Comparison the growth of *Yersinia enterocolitica*, *Listeria monocytogenes*, *Escherichia coli* O157:H7 and *Salmonella* spp. in ground beef packed by three commercially used packaging techniques. *International Journal of Food Microbiology*, 59, 211–220.
- Nychas, G. J. E., Drosinos, E., & Board, R. G. (1998). Chemical changes in stored meat. In R. G. Board, & A. R. Davies (Eds.), *The microbiology of meat and poultry* (pp. 288–326). London: Blackie Academic and Professional.
- Phillips, C. A. (1996). Review: modified atmosphere packaging and its effects on the microbiological quality and safety produce. *International Journal of Food Science & Technology*, 31, 463–479.
- Pradhan, A. K., Li, M., Li, Y., Kelso, L. C., Costello, T. A., & Johnson, M. G. (2012). A modified Weibull model for growth and survival of *Listeria innocua* and *Salmonella* Typhimurium in chicken breasts during refrigerated and frozen storage. *Poultry Science*, 91, 1482–1488.
- Santos, M., Correia, C., Cunha, M., Saraiva, M., & Novais, M. (2005). Valores Guia para avaliação da qualidade microbiológica de alimentos prontos a comer preparados em estabelecimentos de restauração. *Revista da Ordem dos Farmacêuticos*, 64, 66–68.
- Sheridan, J. J., Doherty, A., Allen, P., McDowell, D. A., Blair, L. S., & Harrington, D. (1995). Investigations on the growth of *Listeria monocytogenes* on lamb under modified atmospheres. *Food Microbiology*, 12, 259–266.
- Sofos, J. N., & Geornaras, I. (2010). Overview of current meat hygiene and safety risks and summary of recent studies on biofilms, and control of *Escherichia coli* O157:H7 in nonintact, and *Listeria monocytogenes* in ready-to-eat, meat products. *Meat Science*, 86, 2–14.
- Stanbridge, L. H., & Davies, A. R. (1998). The microbiology of chill-stored meat. In R. G. Board, & A. R. Davies (Eds.), *The microbiology of meat and poultry* (pp. 174–219). London: Blackie Academic and Professional.
- Swaminathan, B., & Gerner-smidt, P. (2007). The epidemiology of human listeriosis. *Microbes and Infection*, 9, 1236–1243.
- Tsigarida, E., Skandamis, P., & Nychas, G. J. E. (2000). Behaviour of *Listeria monocytogenes* and autochthonous flora on meat stored under aerobic, vacuum and modified atmosphere packaging conditions with or without the presence of oregano essential oil at 5 °C. *Journal of Applied Microbiology*, 89, 901–909.
- Uppal, K. K., Getty, K. J. K., Boyle, E. A. E., Harper, N. M., Lobaton-Sulabo, A. S. S., &

- Barry, B. (2012). Effect of packaging and storage time on survival of *Listeria monocytogenes* on kippered beef steak and turkey tenders. *Journal of Food Science*, 71, 57–60.
- Van Boekel, M. A. J. S. (2002). On the use of the Weibull model to describe thermal inactivation of microbial vegetative cells. *International Journal of Food Microbiology*, 74, 139–159.
- Xavier, C., Gonzales-Barron, U., Paula, V., Estevinho, L., & Cadavez, V. (2014). Meta-analysis of the incidence of food-borne pathogens in Portuguese meats and their products. *Food Research International*, 55, 311–323.
- Zakrys, P. I., Hogan, S. A., O'Sullivan, M. G., Allen, P., & Kerry, J. P. (2008). Effects of oxygen concentration on the sensory evaluation and quality indicators of beef muscle packed under modified atmosphere. *Meat Science*, 79, 648–655.



## Biocontrol of *Listeria monocytogenes* in fish by enterocin AS-48 and *Listeria* lytic bacteriophage P100



Alberto Baños<sup>b</sup>, José David García-López<sup>b</sup>, Cristina Núñez<sup>b</sup>, Manuel Martínez-Bueno<sup>a, c</sup>, Mercedes Maqueda<sup>a</sup>, Eva Valdivia<sup>a, c, \*</sup>

<sup>a</sup> Departamento de Microbiología, Facultad de Ciencias, Universidad de Granada, Fuente Nueva s/n, 18071 Granada, Spain

<sup>b</sup> Departamento de Microbiología y Biotecnología, DMC Research Center, Camino de Jayena s/n, 18620 Granada, Spain

<sup>c</sup> Instituto de Biotecnología, Universidad de Granada, 18071 Granada, Spain

### ARTICLE INFO

#### Article history:

Received 18 June 2015

Received in revised form

23 October 2015

Accepted 17 November 2015

Available online 22 November 2015

#### Keywords:

Enterocin AS-48

Phage P100

*Listeria monocytogenes*

Raw fish

Smoked salmon

### ABSTRACT

The purpose of this study was to determine the ability of enterocin AS-48 to control *Listeria monocytogenes* in fish during storage at 4 °C. AS-48 (0.37 µg/cm<sup>2</sup>) was tested singly and in combination with phage P100 (2.3 × 10<sup>7</sup> PFU/cm<sup>2</sup>) on a cocktail of 10<sup>3</sup> CFU/cm<sup>2</sup> *L. monocytogenes* strains inoculated in fillet tissues of raw hake and salmon and in smoked salmon. In raw fish, AS-48 alone reduced listeria with respect to the untreated control by 1.68, 2.79, 2.9, and 3.13 log CFU/cm<sup>2</sup> (in hake) and by 1.9, 2.55, 2.8, and 2.8 (in salmon) at 1, 2, 3, and 7 d, respectively. Phage P100 treatment also yields significant reductions (but lower than AS-48) in listeria counts in both raw fishes. A combined treatment of AS-48/P100 eliminated listeria from hake and salmon fillets from 2 and 1 days respectively. In smoked salmon, AS-48 reduced listeria by 2, 3.4, 4.5, 4.25, and 4.25 log CFU/cm<sup>2</sup> with respect to the control at 1, 5, 10, 15, and 30 d, respectively. P100 treatment also reduced listeria counts but in lesser quantities than AS-48. A combined treatment of AS-48/P100 reduced listeria below detection levels from 1 to 15 d; afterwards, a slight listeria reactivation was detected.

© 2015 Elsevier Ltd. All rights reserved.

## 1. Introduction

Several authors have reported a high prevalence of *Listeria monocytogenes* in raw and processed fish and seafood, leading to a definitive identification of these foods as carriers of *L. monocytogenes* (Jami, Ghanbari, Zunabovic, Domig, & Kneifel, 2014). However, since these foods initially carry low concentrations of *L. monocytogenes*, the risk of contamination is frequently caused by storage in conditions favouring the growth of this bacterium. *L. monocytogenes* has been isolated on the surface and intestines of fish and seafood, but the flesh is usually free of the pathogen unless it is contaminated from a different source (Jami et al., 2014). Common routes for contamination of fish with *Listeria* are its spread from the intestinal contents to other tissues, cross-contamination through contact with other food surfaces or with the processing equipment (conveyor belts, trays, skinning and slicing machines, etc.), and storage (Gudmundsdottir,

Gudbjornsdottir, Einarsson, Kristinsson, & Kristjansson, 2006).

Current intervention strategies for *L. monocytogenes* control in fish and seafood include chemical treatments such as chlorinated products, ozone, and electrolysed oxidizing water (Norhana, Poole, Deeth, & Dykes, 2010; Wang et al., 2011). In addition, physical treatments such as steam application or pulsed light exposure have also been evaluated for *L. monocytogenes* control (Bremer, Monk, Osborne, Hills, & Butler, 2002; Hierro, Ganán, Barroso, & Fernández, 2012).

One strategy in food preservation, designed as biopreservation, is based on the use of microorganisms and/or their natural products. The use of lytic bacteriophages (phages) and antimicrobial peptides produced by LAB, known as bacteriocins, may provide an effective alternative for decontaminating fish and seafood that can contain various bacterial pathogens such as *L. monocytogenes*. Phages are specific obligate parasites that infect bacterial cells. In the absence of a host bacterium, phages exist in a metabolically inert state. Furthermore, their safe nature (due to the inherent specificity for its bacterial host) makes them excellent tools for food safety applications (Mahony, Auliffe, Ross, & Van Sinderen, 2010). In 2007, the U.S. Food and Drug Administration approved phage

\* Corresponding author. Departamento de Microbiología, Facultad de Ciencias, Universidad de Granada, Fuente Nueva s/n, 18071 Granada, Spain.

E-mail address: [evavm@ugr.es](mailto:evavm@ugr.es) (E. Valdivia).

LISTEX P100 for use for all raw and ready-to-eat foods and LISTEX™ has been accepted as GRAS (Generally Recognised as Safe) by the FDA (GRAS 198) and USDA (GRAS 218) and can be used as a processing aid in all food products susceptible to *L. monocytogenes* contamination. The application of LAB bacteriocins in food technology is currently intended for use in combination with physical and chemical treatments (Gálvez, Abriouel, Lucas-López, & Ben Omar, 2007; Khan, Flint, & Yu, 2010). This approach may resolve major current challenges for the food industry, mitigating economic losses due to food spoilage and avoiding the transmission of microbial pathogens through the food chain. At the same time, it has the potential of satisfying the growing consumer demand for foods that are ready-to-eat, fresh-tasting, nutrient and vitamin rich, low in fat and salt, and minimally processed.

Enterocin AS-48 is a cationic circular bacteriocin produced by *Enterococcus faecalis* S-48 with broad bactericidal activity against most Gram-positive bacteria, including pathogens such as *L. monocytogenes*, *Staphylococcus aureus*, *Mycobacterium* spp., *Bacillus cereus*, and some Gram-negative bacteria such as some *Escherichia coli* and *Salmonella typhimurium* strains (Gálvez, Maqueda, Martínez-Bueno, & Valdivia, 1989). The target of AS-48 is the bacterial cell membrane in which the bacteriocin inserts and destabilizes membrane potential, thus leading to pore formation and cell leakage (Sánchez-Barrena et al., 2003). The features of AS-48, a broad spectrum of antimicrobial activity, stability across a wide range of temperatures and pH, and sensitivity to digestive proteases, (Gálvez, Maqueda, Valdivia, Quesada, & Montoya, 1986) make it a promising alternative to chemical preservatives for use as a biopreservative in foods. AS-48 has been shown to be effective in the control of various food-borne pathogens in meat, vegetable and dairy products (Ananou et al., 2010; Cobo Molinos et al., 2008; Muñoz et al., 2007) and also against several spoilage bacteria in meat products and vegetable-derived foods (Baños et al., 2012; Grande et al., 2007). The purpose of the present work was to test the efficacy of AS-48, applied alone or in combination with phage P100 in the control of *L. monocytogenes* in different fish systems. Due to the increasing consumption of these foodstuffs at home and the growing popularity of trendy Japanese-like restaurants, a higher interest in the safety of these products has been paid by consumers and authorities.

## 2. Materials and methods

### 2.1. Bacterial strains and culture conditions

*E. faecalis* UGRA10 (Cebrián et al., 2012) was used as AS-48 producer. *E. faecalis* S-47 (from our collection) was used as the standard indicator strain for bacteriocin activity assays. Enterococci were grown in BHI Brain Heart Infusion broth (BHI, Difco™, Becton, Dickinson and Co., Le Pont de Claix, France) at 37 °C for 18 h. For fish inoculation, a total of five *L. monocytogenes* strains isolated from different fish industries were used to obtain more detailed information about the anti-listeria activity of AS-48, given the well-known resistance shown by some *L. monocytogenes* strains. *L. monocytogenes* CECT 4032 was used for phage P100 titration. *L. monocytogenes* strains were grown overnight on brain heart infusion (BHI) at 37 °C, washed in a sterile saline solution, and then inoculated in fillet tissue samples at the selected concentration. All bacterial cultures were maintained at 4 °C on BHI-agar slants.

### 2.2. Bacteriophage titration

The bacteriophage Listex™ P100, based on listeriophage P100 (Hagens & Loessner, 2014), approved by the U.S. Food and Drug Administration and the U.S. Department of Agriculture, was used in

this work. This bacteriophage is strictly lytic and reportedly active against multiple serovars of *L. monocytogenes* (Carlton, Noordman, Biswas, de Meester, & Loessner, 2005). It was obtained from MICREOS BV (Wageningen, The Netherlands).

The phage titre was determined using a soft agar overlay assay according to Soni and Nannapaneni (2010) with *L. monocytogenes* CECT 4032 as the host. The phage counts were expressed as plaque-forming units (PFU) per milliliter or square centimetre, as applicable.

### 2.3. Preparation of bacteriocin AS-48

AS-48 was produced by culturing the strain *E. faecalis* UGRA10 in a food-grade whey-derived substrate (Esprión 300, DMV Int., Veghel, Netherland), supplemented with 1% glucose (as described by Ananou et al., 2008). AS-48 was recovered from cultures by cation exchange chromatography on carboxymethyl Sephadex CM-25 (as in Abriouel, Valdivia, Martínez-Bueno, Maqueda, & Gálvez, 2003). Eluted fractions were tested for bacteriocin activity against the indicator strain S-47 by the agar well diffusion method (Gálvez et al., 1986). The approximate concentration of AS-48 (in µg/ml) in the preparation was estimated by comparing the diameter of inhibition halo around the well with a titration curve obtained with purified bacteriocin. Before use, the eluted fractions were dialysed at 4 °C against distilled water through a 2000-Da cut-off membrane to eliminate NaCl and then sterilized by filtration (0.22 µm, Millipore, Belford, MA, USA).

### 2.4. Fish fillet tissue preparation and treatment

Challenge test assays were performed according Soni and Nannapaneni (2010). Raw hake fillets, raw salmon fillets and smoked filleted salmon were purchased from a local retail. Fish pieces of approximately 100 cm<sup>2</sup> were cut into slices using a sterile knife. For *Listeria* inoculation, three samples for each treatment and sampling time were placed in sterile polystyrene dishes with the skin face down. Fish samples were then inoculated on the flesh side with a cocktail suspension of five strains of *L. monocytogenes* ( $5 \times 10^5$  CFU/ml) to yield a final *Listeria* level of approx.  $1 \times 10^3$  CFU/cm<sup>2</sup> using a manual spray gun. We have selected this initial level of contamination ( $10^3$  CFU/cm<sup>2</sup>) since is a middle value with respect to those found in contaminated foods responsible for *L. monocytogenes* outbreak reports, such as of the Center for Food Safety and Applied Nutrition, (2003). The amount of listeria suspension necessary to cover by complete the fillet surface (100 cm<sup>2</sup>) was previously determined. Samples were then air dried for 30 min to allow the attachment of pathogen cells. Afterwards, the different treatments were sprayed using an automated spray system (AUTOJET 1550, Spraying System Co.). The first treatment was a physiological saline preparation of phage P100 applied to yield an approximate final concentration of  $2.3 \times 10^7$  PFU/cm<sup>2</sup>. The second treatment was an AS-48 solution (50 µg/ml) applied to yield an approximate final concentration of 0.37 µg/cm<sup>2</sup>. Finally, the third treatment consisted of a combination of phage P100 ( $2.3 \times 10^7$  PFU/cm<sup>2</sup>) and AS-48 (50 µg/ml). For the untreated controls, each sample received the same amount of saline solution. The different samples were placed in polystyrene dishes (135 × 180 mm, BANDESUR, Alcalá la Real, Spain) with excellent barrier properties against water, oil, fat and oxygen. Then, samples were immediately sealed in Ziplock bags and stored in cool room at 4 °C. Two independent complete experiments were carried out for each food system for statistical analysis. In each experiment we have used 3 subsamples (fillets) for each experimental condition and sampling time.

### 2.5. Microbiological sampling and *Listeria monocytogenes* determination

Samples (100 cm<sup>2</sup>) from each treatment were withdrawn in triplicate at selected times to determine viable counts of *L. monocytogenes* and mixed (1/10, w/v) with a dilution medium (0.1% peptone, 0.85% NaCl). Homogenization was performed in a Masticator blender (IUL, Barcelona, Spain) for 1 min followed by serial 10-fold dilution and plating on chromogenic selective agar COMPASS *Listeria* Agar (Biokar Diagnostics, Pantin, France). All plates were inoculated with 100 µL of the corresponding dilution with the exception of 10<sup>-1</sup> dilution which was inoculated at 500 µL/plate. Therefore, the detection level was 10 CFU/cm<sup>2</sup>. Bacterial cultures were incubated at 37 ± 2 °C for 24–48 h before counting the colonies.

### 2.6. Determination of phage P100 stability during storage at 4 °C

To determine the stability of phage P100, 100 cm<sup>2</sup> of raw hake fillet tissue were surface-treated with phage P100 to yield a final concentration of approx. 2.3 × 10<sup>7</sup> PFU/cm<sup>2</sup> and stored at 4 °C. Phages were counted at 0, 1, 4, and 7 days. Ten grams of fillet sample were homogenized in 90 mL of peptone water, and 1 mL of the homogenate was sterilized by filtration through a 0.22 µm low protein-binding syringe filter. The filtrate was then tested for PFU counts as described in Subsection 2.2. Two independent complete experiments were carried out.

### 2.7. Determination of enterocin AS-48 stabilities during storage at 4 °C

Bacteriocin AS-48 was applied to fillet tissue of raw hake and extracted as described by Garriga, Aymerich, Costa, Monfort, and Hugas (2002). Briefly, 100 cm<sup>2</sup> of fillet tissue was sprayed with an AS-48 solution (50 µg/mL, final concentration on a fillet surface of approx. 0.37 µg/cm<sup>2</sup>). At selected times, samples were homogenized (1:10) in sodium acetate 50 mM, EDTA 100 mM, and Triton X100 0.2% at pH 5 in a blender for 1 min, boiled for 10 min, cooled, and filtered through a filter paper. The bacteriocin in the liquid phase was precipitated with 300 g/L ammonium sulphate, and the pellet was dissolved in phosphate buffer (50 mM, pH 7.2). The sample was heated at 80 °C for 10 min and then the bacteriocin titre of extracts was determined as in Subsection 2.3 and expressed as µg/cm<sup>2</sup>. Two complete independent experiments were carried out.

### 2.8. Statistical analyses

The statistics were made from the results of two independent experiments. In each experiment we have used 3 subsamples (fillets) for each experimental condition and sampling time. The average data ± standard deviations were determined with Excel software (Microsoft Corp., USA). Statistical analyses were performed using the SPSS-PC 15.0 software (SPSS, Chicago, Ill. USA). Data on microbiological counts were subjected to ANOVA, using the presence of AS-48, the presence of phage P100, or a combination of both as factors. Categories include untreated control fish fillet tissue, fish fillet tissue with added enterocin, fish fillet tissue with phage P100, and fish fillet tissue with both AS-48 and phage.

## 3. Results and discussion

### 3.1. Stability of phage P100 in raw fish fillet tissue stored at 4 °C

Fig. 1 shows the stability of phage P100 at 4 °C throughout the 7 d storage of the raw hake fillets. As can be seen, the phage P100

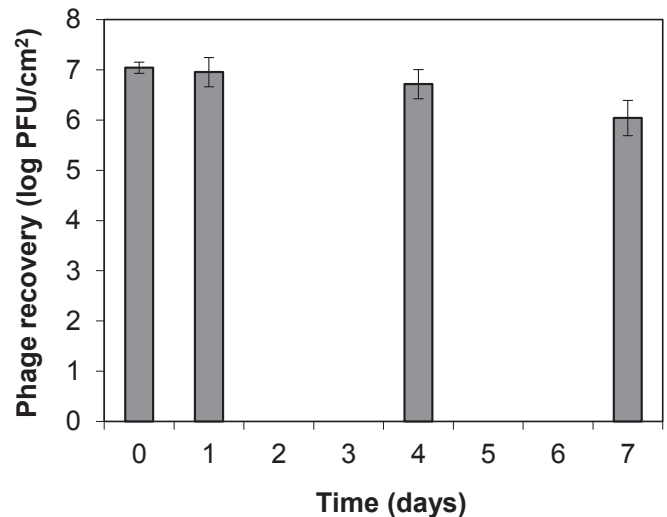


Fig. 1. Stability of bacteriophage P100 in raw hake fillets after application at a concentration of approx. 10<sup>7</sup> PFU/cm<sup>2</sup>, determined as phage recovered at selected times from the food matrix. Values are the average ± SD (error bars) of two independent experiments.

titre was quite stable in hake fillet tissue since, out of the initial approx. 7 log PFU/cm<sup>2</sup> applied to food, there was only a slight decrease in the phage P100 titre (1 log PFU/cm<sup>2</sup>) at the end of storage.

The stability of phages in foods has been described as being dependent on the food in which is applied. Soni and Nannapaneni (2010), for instance, reported a recovery for P100 in raw salmon similar to the one described by us. Leverentz et al. (2003) found that the titre of a mixture of anti-*Listeria* phages remained between 3.9 and 5.4 log PFU on melon slices, increasing 1 log over a period of 7 days, but declined rapidly to non detectable levels on apple slices within 30 min after application.

### 3.2. Stability of enterocin AS-48 in raw fish fillet tissue stored at 4 °C

Bacteriocin extraction from the raw hake fillet tissue was performed at time 0 and throughout storage. At time 0, we recovered all of the 0.37 µg/cm<sup>2</sup> of AS-48 applied. Afterwards, recovery gradually declined to 0.35, 0.27, and 0.22 µg/cm<sup>2</sup> at 1, 4, and 7 d, respectively (Fig. 2). We also detected an even greater decrease in the recovery of AS-48 during storage in other food model systems such as sausages and cooked ham (Ananou et al., 2005, 2010). This reduction in the detection of AS-48 may be due to the inactivation of enterocin by components (e.g. proteases) present in the fish tissue and/or to adsorption onto the food matrix. The adsorption issue, as well as its irregular distribution in food, have been reported as two of the main causes negatively influencing antimicrobial efficacy of bacteriocins in foods (Cleveland, Montville, Nes, & Chikindas, 2001). Therefore, the more complex the food matrix is and the greater its content in fat and protein, the higher the adsorption/retention of bacteriocin molecules to them and the less homogeneous its distribution in the food. Reinforcing this hypothesis is the fact that we noted greater effectiveness of AS-48 in fruit juices than in fruits, probably due to the more homogeneous distribution of the enterocin in the liquid food matrix (Cobo Molinos et al., 2008).

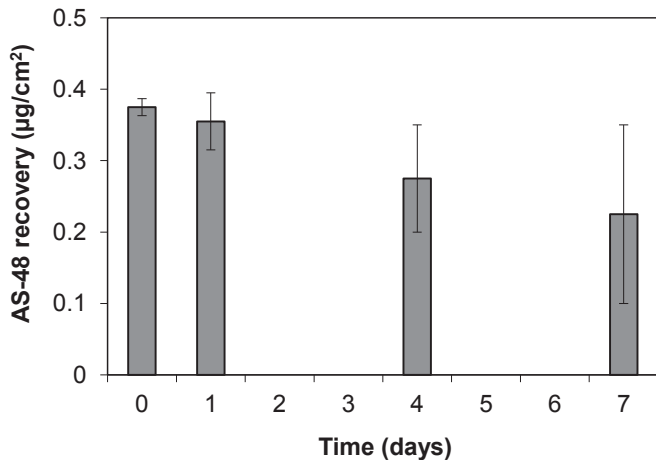


Fig. 2. Recovery of enterocin AS-48 from raw hake after spraying at a final concentration of  $0.37 \mu\text{g}/\text{cm}^2$ . Values are the average  $\pm$  SD (error bars) of two independent experiments.

### 3.3. Effect of enterocin AS-48 alone or combined with phage P100 in the control of *Listeria monocytogenes* in fillet tissue of raw hake and salmon and in smoked salmon

*L. monocytogenes* was able to grow in the fish fillet of both raw fishes at  $4^\circ\text{C}$  and reached maximum levels of  $4.78 \log \text{CFU}/\text{cm}^2$  in hake (Fig. 3A) and  $4.30 \log \text{CFU}/\text{cm}^2$  in salmon at the end of storage (Fig. 3B). AS-48 by itself significantly reduced ( $P < 0.01$ ) the viable listeria counts from day 1 of storage in both types of raw fillets. In hake, the counts were 1.68, 2.79, 2.9, and  $3.13 \log \text{CFU}/\text{cm}^2$  lower than the untreated control at 1, 2, 3, and 7 d, respectively. In AS-48-treated raw salmon fillets, listeria counts were 1.9, 2.55, 2.8, and  $2.05 \log \text{CFU}/\text{cm}^2$  lower than the respective values in untreated samples. Phage P100 also had a relevant effect on *Listeria* growth. Although significant ( $P < 0.05$ ), this anti-listeria effect was less than that achieved by AS-48 when applied in solitary. Thus, in batches of phage-treated hake fillets, the reductions in viable counts were 1.2, 1.85, 2.02, and  $1.7 \log \text{CFU}/\text{cm}^2$  at 1, 2, 3, and 7 days, respectively (Fig. 3A). In raw salmon fillets, the reductions achieved by treatment with P100 were 0.85, 1.25, 1.0, and  $1.06 \log \text{CFU}/\text{cm}^2$  at 1, 2, 3, and 7 days (Fig. 3B). The combination of AS-48 with phage P100 had a significant effect ( $P < 0.01$ ) for the control of *L. monocytogenes* in fillets of both types of fish. In these conditions, *Listeria* counts remained below detectable levels ( $10 \text{CFU}/\text{cm}^2$ ) from the first and second days of storage in raw hake and salmon respectively (Fig. 3A and B).

In fillets of smoked salmon, the listeria counts reached  $6.15 \log \text{CFU}/\text{cm}^2$  at the end of storage (Fig. 4). Spraying with an AS-48 solution had a significant effect ( $P < 0.01$ ) as the treated samples showed reductions of 2, 3.4, 4.5, 4.25, and  $4.25 \log \text{CFU}/\text{cm}^2$  with respect to the untreated control at 1, 5, 10, 15, and 30 d, respectively. This effect was particularly remarkable at 10 d, when *Listeria* counts remained below detection levels (Fig. 4). Although overgrowth of *Listeria* was observed after 10–15 days, the counts at 30 d of storage were significantly lower ( $4.25 \log$ ,  $P < 0.01$ ) than in control batches. Application of phage P100 alone reduced the viable counts of *Listeria* by 0.85, 2.4, 2.75, 2.34, and  $1.58 \log \text{CFU}/\text{cm}^2$  relative to the untreated control at 1, 5, 10, 15, and 30 d (significantly different from control at  $P < 0.05$ ). Combined treatment with AS-48 and phage P100 produced a drastic effect from the first day of storage since the listeria population was kept below detection levels at least between days 1 and 15. A slight regrowth was observed in samples treated with AS-48 and phage P100 from 15 d to 30 d, and the listeria achieved counts of  $0.78 \log \text{CFU}/\text{cm}^2$  at the end of storage.

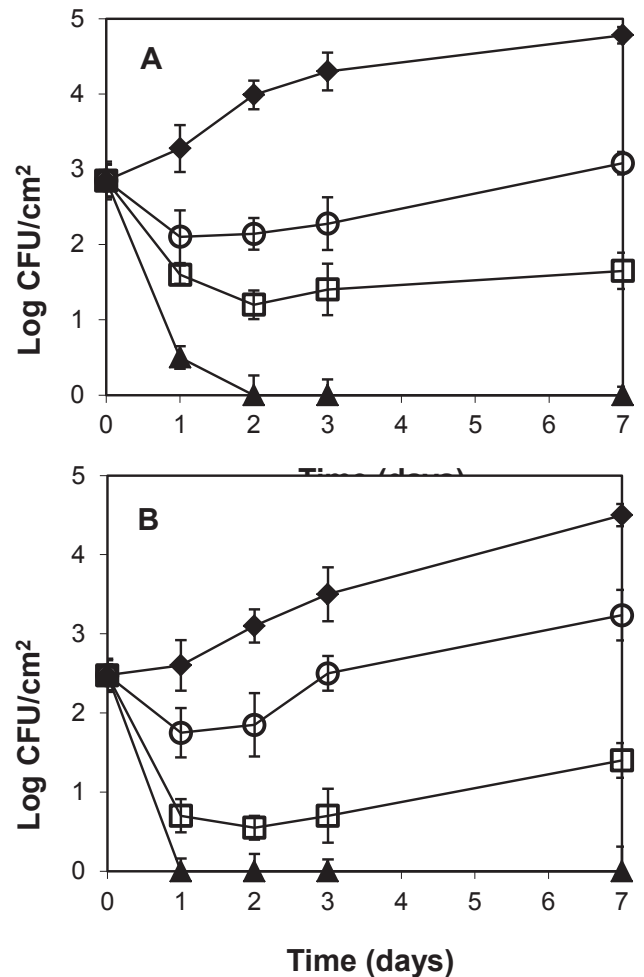
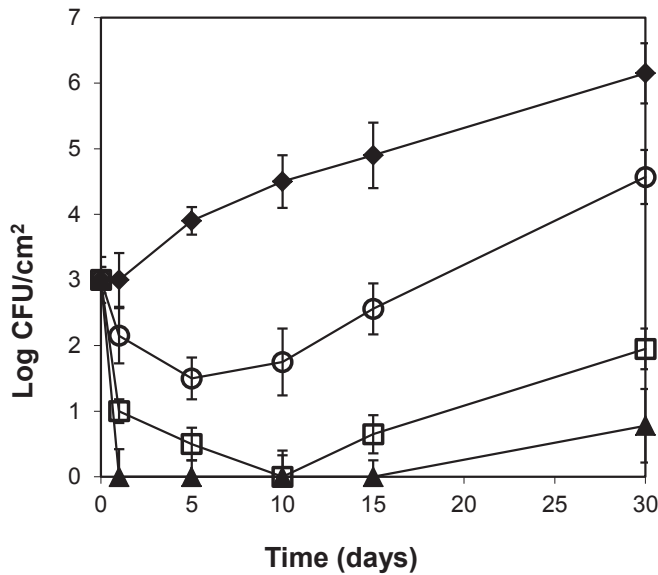


Fig. 3. Effect of treatments with enterocin AS-48 ( $0.37 \mu\text{g}/\text{cm}^2$ ) and/or phage P100 ( $2.3 \times 10^7 \text{PFU}/\text{cm}^2$ ) on the viability of *Listeria monocytogenes* in raw fish models stored at  $4^\circ\text{C}$ . A) Raw hake. B) Raw salmon. control (◆); containing AS-48 (□); containing phage P100 (○); containing AS-48 and phage P100 (▲). Values are the average  $\pm$  SD (error bars) of two independent experiments.

The regrowth in listeria populations in all samples of smoked salmon and that observed in samples of raw fish treated with AS-48 or phage by separate at the end of storage can be attributed to the inactivation of the bacteriocin, the adsorption to the food matrix, and to the recovery of sublethally damaged listeria (Donnelly, 2002). The implementation of two or more hurdles, such heat, organic acids or nitrate, acting on different cell targets can suppress or diminish the reactivation of sublethally injured bacteria (Leistner, 2000), as it has been found when AS-48 was applied in conjunction with phage P100 (Figs. 3 and 4) in salmon and hake or with nitrate/nitrite, pentasodium triphosphate, and pyrophosphate and/or heat in cooked ham (Ananou et al., 2010).

The results presented here indicate the ability of the two biological antimicrobials, enterocin AS-48 and phage P100, to control *L. monocytogenes* in raw and smoked fish products. Separately, AS-48 ( $0.37 \mu\text{g}/\text{cm}^2$ ) and P100 ( $3.2 \times 10^7 \text{PFU}/\text{cm}^2$ ) produced remarkable reductions in viable listeria counts in all foods tested. Although the dosages cannot be compared due to the marked differences in the nature of the two biological preservatives, AS-48 was much more effective in listeria control. Nevertheless, at the concentrations used for the two anti-listerials, the complete elimination of the pathogen was not achieved in either case, and it was necessary to apply a combination of enterocin and phage to accomplish this goal. The effective dose of phage P100 has been reported as 7–8 log



**Fig. 4.** Effect of treatments with enterocin AS-48 ( $0.37 \mu\text{g}/\text{cm}^2$ ) and or phage P100 ( $2.3 \times 10^7$  PFU/ $\text{cm}^2$ ) on the viability of *Listeria monocytogenes* in smoked salmon stored at  $4^\circ\text{C}$ . control (◆); containing AS-48 (□); containing phage P100 (○); containing AS-48 and phage P100 (▲). Values are the average  $\pm$  SD (error bars) of two independent experiments.

PFU/g, depending on the food tested (Carlton et al., 2005; Soni & Nannapaneni, 2010). Nevertheless, the antilisterial effect of phage P100 is dependent on the environ in which it is applied. Soni and Nannapaneni (2010) claimed that P100 was much more effective in listeria control in a broth model system than in raw salmon fillet tissue. Moreover, Leverentz et al. (2003) found that P100 stability seems to depend on the environ. The causes for this behaviour could be similar to those presented in Subsection 3.2 for bacteriocins. In this respect, we have found that the effect of enterocin AS-48 in food is also greatly affected by physical conditions and chemical compositions (e.g. contents in fat or protein) of foods. In a previous work, for instance, we demonstrated that *L. monocytogenes* CECT 4032 was highly susceptible to AS-48 in BHI broth, with a minimum bactericidal concentration (MBC) of  $0.1 \mu\text{g}/\text{mL}$  for a listeria population of  $8 \log \text{CFU}/\text{mL}$  (Mendoza, Maqueda, Gálvez, Martínez-Bueno, & Valdivia, 1999). Further experiments carried out by immersion of vegetable foods in solutions containing AS-48 showed that concentrations of  $12.5$ – $25 \mu\text{g}/\text{mL}$  of the enterocin were necessary (alone or even better in combination with chemical preservatives) to achieve effective control of listeria and that the anti-listerial effect of enterocin varied according to the type of vegetable (Cobo Molinos et al., 2005). Even when AS-48 was applied in a cooked ham model at a concentration of  $40 \mu\text{g}/\text{g}$ , additional hurdles such as nitrate/nitrite, pentasodium tripolyphosphate, and pyrophosphate and/or heat were needed to provide effective protection against *L. monocytogenes* (Ananou et al., 2010).

We would like to stress the good results achieved, despite the low AS-48 concentration of  $0.37 \mu\text{g}/\text{cm}^2$  used in this work, to protect raw and smoked fish foods against listeria. This fact makes AS-48, alone or combined with phage P100, a promising tool to improve the hygienic quality of raw and smoked fish, particularly with the concern of *L. monocytogenes* contamination.

## Acknowledgements

This work was supported by Grant (P07-AGR-02539) from the Junta de Andalucía. We would also like to acknowledge the work of Christine Laurin in editing the text.

## References

- Abriouel, H., Valdivia, E., Martínez-Bueno, M., Maqueda, M., & Gálvez, A. (2003). A simple method for semi-preparative-scale production and recovery of enterocin AS-48 derived from *Enterococcus faecalis* subsp. *liquefaciens* A-48-32. *Journal of Microbiological Methods*, *55*, 599–605.
- Ananou, S., Baños, A., Maqueda, M., Martínez-Bueno, M., Gálvez, A., & Valdivia, E. (2010). Effect of combined physico-chemical treatments based on enterocin AS-48 on the control of *Listeria monocytogenes* and *Staphylococcus aureus* in a model cooked ham. *Food Control*, *21*, 478–486.
- Ananou, S., Garriga, M., Hugas, M., Maqueda, M., Martínez-Bueno, M., Gálvez, A., et al. (2005). Control of *Listeria monocytogenes* in model sausages by enterocin AS-48. *International Journal of Food Microbiology*, *103*, 179–190.
- Ananou, S., Muñoz, A., Gálvez, A., Martínez-Bueno, M., Maqueda, M., & Valdivia, E. (2008). Optimization of enterocin AS-48 production on a whey-based substrate. *International Dairy Journal*, *18*, 923–927.
- Baños, A., Ananou, S., Martínez-Bueno, M., Gálvez, A., Maqueda, M., & Valdivia, E. (2012). Prevention of spoilage by enterocin AS-48 combined with chemical preservatives, under vacuum, or modified atmosphere in a cooked ham model. *Food Control*, *24*, 15–22.
- Bremer, P. J., Monk, I., Osborne, C. M., Hills, S., & Butler, R. (2002). Development of a steam treatment to eliminate *Listeria monocytogenes* from king salmon (*Oncorhynchus tshawytscha*). *Journal of Food Science*, *67*, 2282–2287.
- \* Carlton, R. M., Noordman, W. H., Biswas, B., de Meester, E. D., & Loessner, M. J. (2005). Bacteriophage P100 for control of *Listeria monocytogenes* in foods: genome sequence, bioinformatic analyses, oral toxicity study, and application. *Regulatory Toxicology and Pharmacology*, *43*, 301–312. Provides a broad view of basic aspects of phage P100 and its application in *Listeria* control.
- Cebrián, R., Baños, A., Valdivia, E., Pérez-Pulido, R., Martínez-Bueno, M., & Maqueda, M. (2012). Characterization of functional, safety, and probiotic properties of *Enterococcus faecalis* UGRA10, a new AS-48-producer strain. *Food Microbiology*, *30*, 59–67.
- Center for Food Safety and Applied Nutrition, Food and Drug Administration, United States Department of Health and Human Services, Food Safety and Inspection Service, & United States Department of Agriculture. (2003). Quantitative assessment of relative risk to public health from foodborne *Listeria monocytogenes* among selected categories of ready-to-eat foods. *United States Food and Drug Administration*, 46–47. <http://www.fda.gov/Food/FoodScienceResearch/RiskSafetyAssessment/ucm183966.htm>.
- Cleveland, J., Montville, T. J., Nes, I. F., & Chikindas, M. L. (2001). Bacteriocins: safe, natural antimicrobials for food preservation. *International Journal of Food Microbiology*, *71*, 1–2.
- Cobo Molinos, A., Abriouel, H., Ben Omar, N., Lucas, R., Valdivia, E., & Gálvez, A. (2008). Inactivation of *Listeria monocytogenes* in raw fruits by enterocin AS-48. *Journal of Food Protection*, *71*, 2460–2467.
- Cobo Molinos, A., Abriouel, H., Ben Omar, N., Valdivia, E., Lucas, R., Maqueda, M., et al. (2005). Effect of immersion solutions containing enterocin AS-48 on *Listeria monocytogenes* in vegetable foods. *Applied and Environmental Microbiology*, *71*, 7781–7787.
- Donnelly, C. W. (2002). Detection and isolation of *Listeria monocytogenes* from food samples: implications of sublethal injury. *Journal of AOAC International*, *85*, 495–500.
- \* Gálvez, A., Abriouel, H., Lucas-López, R., & Ben Omar, N. (2007). Bacteriocin-based strategies for food biopreservation. *International Journal of Food Microbiology*, *120*, 51–70 (It is a very complete review on the applications of bacteriocins in foods).
- Gálvez, A., Maqueda, M., Martínez-Bueno, M., & Valdivia, E. (1989). Bactericidal and bacteriolytic action of peptide antibiotic AS-48 against gram-positive and gram negative bacteria and other organisms. *Research in Microbiology*, *140*, 57–68.
- Gálvez, A., Maqueda, M., Valdivia, E., Quesada, A., & Montoya, E. (1986). Characterization and partial purification of a broad spectrum antibiotic AS-48 produced by *Streptococcus faecalis*. *Canadian Journal of Microbiology*, *32*, 765–771.
- Garriga, M., Aymerich, M. T., Costa, S., Monfort, J. M., & Hugas, M. (2002). Bactericidal synergism through bacteriocins and high pressure in meat model system during storage. *Food Microbiology*, *19*, 509–518.
- Grande, M. J., Abriouel, H., Lucas López, R., Valdivia, E., Ben Omar, N., Martínez-Cañamero, M., et al. (2007). Efficacy of enterocin AS-48 against bacilli in ready-to-eat vegetable soups and purees. *Journal of Food Protection*, *70*, 2339–2345.
- Gudmundsdottir, S., Gudbjornsdottir, B., Einarsson, H., Kristinsson, K. G., & Kristjansson, M. (2006). Contamination of cooked peeled shrimp (*Pandalus borealis*) by *Listeria monocytogenes* during processing at two processing plants. *Journal of Food Protection*, *69*, 1304–1311.
- Hagens, S., & Loessner, M. J. (2014). Phages of *Listeria* offer novel tools for diagnostics and biocontrol. *Frontiers in Microbiology*, *5*, 159.
- Hierro, E., Ganán, M., Barroso, E., & Fernández, M. (2012). Pulsed light treatment for the inactivation of selected pathogens and the shelf-life extension of beef and tuna carpaccio. *International Journal of Food Microbiology*, *158*, 42–48.
- \* Jami, M., Ghanbari, M., Zunabovic, M., Domig, K. J., & Kneifel, W. (2014). *Listeria monocytogenes* in aquatic food products — a review. *Comprehensive Reviews in Food Science and Food Safety*, *13*, 798–813 (A review on the incidence of *L. monocytogenes* in aquatic products and the routes of contamination).
- Khan, H., Flint, S., & Yu, P. L. (2010). Enterocins in food preservation. *International Journal of Food Microbiology*, *141*, 1–10.
- Leistner, L. (2000). Basic aspects of food preservation by hurdle technology.

- International Journal of Food Microbiology*, 55, 181–186.
- Leverentz, B., Conway, W. S., Camp, M. J., Janisiewicz, W. J., Abuladze, T., Yang, M., et al. (2003). Biocontrol of *Listeria monocytogenes* on fresh-cut produce by treatment with lytic bacteriophages and a bacteriocin. *Applied and Environmental Microbiology*, 69, 4519–4526.
- Mahony, J., Auliffe, O. M., Ross, R. P., & Van Sinderen, D. (2010). Bacteriophages as biocontrol agents of food pathogens. *Current Opinion in Biotechnology*, 22, 1–7.
- \* Mendoza, F., Maqueda, M., Gálvez, A., Martínez-Bueno, M., & Valdivia, E. (1999). Antilisterial activity of peptide AS-48 and study of changes induced in the cell envelope properties of an AS-48-adapted strain of *Listeria monocytogenes*. *Applied and Environmental Microbiology*, 65, 618–625. Here we describe the high susceptibility of *L. monocytogenes* to AS-48.
- Muñoz, A., Ananou, S., Gálvez, A., Martínez-Bueno, M., Rodríguez, A., Maqueda, M., et al. (2007). Inhibition of *Staphylococcus aureus* in dairy products by enterocin AS-48 produced in situ and ex situ: bactericidal synergism with heat. *International Dairy Journal*, 17, 760–769.
- Norhana, W. M. N., Poole, S. E., Deeth, H. C., & Dykes, G. A. (2010). The effects of temperature, chlorine and acids on the survival of *Listeria* and *Salmonella* strains associated with uncooked shrimp carapace and cooked shrimp flesh. *Food Microbiology*, 27, 250–256.
- \* Sánchez-Barrena, M. J., Martínez-Ripoll, M., Gálvez, A., Valdivia, E., Maqueda, M., Cruz, V., et al. (2003). Structure of bacteriocin AS-48: from soluble state to membrane bound state. *Journal of Molecular Biology*, 334, 541–549. This reference is important to learn about the molecular mechanism of action of AS-48.
- Soni, K. A., & Nannapaneni, R. (2010). Bacteriophage significantly reduces *Listeria monocytogenes* on raw salmon fillet tissue. *Journal of Food Protection*, 73, 32–38.
- Wang, F., Jiang, L., Yang, Q. R., Han, F. F., Chen, S. Y., Pu, S. H., et al. (2011). Prevalence and antimicrobial susceptibility of major foodborne pathogens in imported seafood. *Journal of Food Protection*, 74, 1451–1461.



# Nutritional improvement and physicochemical evaluation of liver pâté formulations



A.M. Terrasa<sup>a</sup>, Marina Dello Staffolo<sup>b,\*</sup>, M.C. Tomás<sup>b</sup>

<sup>a</sup> Facultad de Ciencias Veterinarias, Universidad Nacional de La Plata, La Plata 1900, Argentina

<sup>b</sup> CIDCA, CONICET CCT-La Plata, Facultad de Ingeniería and Facultad de Ciencias Exactas, Universidad Nacional de La Plata, La Plata, Argentina

## ARTICLE INFO

### Article history:

Received 13 August 2015

Received in revised form

13 October 2015

Accepted 8 November 2015

Available online 14 November 2015

### Keywords:

Chicken liver pâté

Physicochemical properties

Refrigerated storage

## ABSTRACT

Pâté formulations composed of chicken liver, a by-product of poultry industry, have been produced by replacing pork back fat with sunflower oil and reducing fat content. The characterization of these products was performed, while the oxidative stability, microstructure, texture, colour, and hygienic quality were determined throughout refrigerated storage. The hardness of pâtés with sunflower oil was lower than the other ones. Different microstructures regarding protein matrix, fat globules and pores, were associated with fat type and content. The storage time, fat type and content influenced the colour parameters. In terms of the oxidative stability, no reduction in the product quality was found during the refrigerated storage. Pâtés with 28% w/w of sunflower oil were the most suitable formulation to increase the nutritional value for this kind of meat products.

© 2015 Elsevier Ltd. All rights reserved.

## 1. Introduction

Meat products are essential components of the human diet. However, these products contain high levels of fat, cholesterol, and low (polyunsaturated fatty acids/saturated fatty acids) PUFAs/SFAs ratios, linked with development of obesity, hypercholesterolemia and cardiovascular diseases (Arihara, 2006). Currently, many consumers demand low-fat foods with healthy ingredients. Some vegetable oils are an important source of PUFAs as well as minor components such as phytosterols and tocopherols. They have been employed as saturated fat replacers in meat products (Martin, Ruiz, Kivikari, & Puolanne, 2008; Pennisi Forell, Ranalli, Zaritzky, Andrés, & Califano, 2010). However, the reduction and substitution of lipids can affect the physicochemical characteristics of high fat foods like sausages, burgers and pâtés (Delgado-Pando, Cofrades, Rodríguez-Salas, & Jiménez-Colmenero, 2011). Moreover, in these products development of rancidity could affect quality attributes (odour, taste, colour, texture) reducing nutritional value (Estévez & Cava, 2006). Protein oxidation might produce a loss of essential amino acids (Lund, Hviid, & Skibsted, 2007). Besides, the stages of processing and preserving (cooking, refrigerating, freezing, etc.) could release the iron from hem proteins decreasing its bioavailable content and modifying the colour (Estevez & Cava, 2004).

Liver pâté is a traditional food manufactured using liver from pig or calf, porcine back-fat and other characteristic ingredients. It is consumed all over the world, especially in European countries and is generally considered an added value product with high nutritional and sensory qualities (Estévez, Ramírez, Ventanas, & Cava, 2007). In recent years, there has been a very important increase in the production and consumption of poultry meat around the world (USDA, 2014). However, the poultry industry generates by-products which are generally underutilized, for example chicken liver.

The aim of this work was to produce chicken liver pâtés in order to obtain healthy products and to study the influence of fat type and its content on their physicochemical characteristics during refrigerated storage time.

## 2. Materials and methods

### 2.1. Manufacturing of liver pâtés

Pork back fat (BF), chicken breasts and livers were obtained from the local market and sunflower oil (SO) was supplied from Aceitera General Deheza (Argentina). Four formulations of pâtés (BF40, BF28, SO40 and SO28) were prepared by replacing pork with chicken liver with different type of fat (BF, SO) and content (40 or 28% w/w). These fat levels were selected according to the traditional formulations and a 30% reduction of lipid phase to obtain healthy products. Other ingredients were added at the same concentration for all formulations (Table 1).

\* Corresponding author. CIDCA, 47 esquina 116, La Plata, Argentina.

E-mail address: [marinadellostaffolo@gmail.com](mailto:marinadellostaffolo@gmail.com) (M. Dello Staffolo).

The manufacturing process is shown in Fig. 1. BF was cut into cubes of about 15 mm side and scalding at 65 °C for 30 min. Liver and muscle free of connective tissue were also cut into cubes and then, washed with chlorinated water and mixed with NaCl, NaNO<sub>2</sub> and ascorbic acid to achieve tissue nitrification. The purpose of this step is to preserve, flavour and colour the pâtés. Scalded BF and SO were pre-emulsified with sodium caseinate dissolved in distilled water at 75 °C. The batters were filled in glass flasks of 40 mm diameter and 60 mm height with about 80 g of mixture (or 40 mm height) which were subjected to a heat treatment in a stainless steel autoclave. In the core of the pâtés, temperature remained constant at 80 ± 2 °C for 30 min being monitored with a Cu-Constantan type T thermocouple. Subsequently, the flasks were cooled to room temperature and stored in the dark at 4 ± 1 °C for 150 days. Samples were taken to perform the assays every 30 d. The procedure was repeated twice for each formulation.

## 2.2. Chemical composition

### 2.2.1. Proximate analysis and energy content

Moisture, ash, and protein contents were determined according to AOAC (1984) methods: 24.002, 24.009 and 24.027, respectively. Lipid content was determined by the Soxhlet method (AOAC, 1984, 24.005) using ethyl ether as extraction solvent which was evaporated using a Rotavapor R-114 (Büchi, Flawil, Switzerland). Lipid content was expressed as g fat/100 g pâté. All determinations were performed in triplicate with freshly manufactured pâtés. Caloric value (Kcal/100 g pâté) was calculated using the Atwater coefficients corresponding to lipids (9.00 kcal/g), proteins (4.02 kcal/g) and carbohydrates (3.87 kcal/g).

### 2.2.2. Fatty acid profile

Total lipid extraction from pâtés was performed by method of Folch, Lees, and Sloane-Stanley (1957). Fatty acid methyl esters (FAMES) were prepared by acid esterification using 10% BF<sub>3</sub> in methanol (AOAC, 1990; official method 969.33). FAMES were analysed using a Hewlett Packard, mod. HP-5890A, gas chromatograph, equipped with a flame ionization detector (FID) and a capillary column Supelco Omega wax 11090-02A (30 m × 0.25 mm internal diameter and 0.1 mm thick). The temperature program was set from 175 to 220 °C at 3 °C/min. The identification of peaks was performed by comparison with retention times of reference fatty acids (Nu Check Prep, Inc., USA). The fatty acid analysis was carried out in duplicate throughout refrigerated storage. In addition, back fat, sunflower oil, chicken muscle and liver were individually analysed to know the influence of these ingredients on the pâté fatty-acid profiles. Composition results were expressed as percentage of total fatty acids.

### 2.2.3. Determination of tocopherols

Tocopherol content in pork back fat and sunflower oil was

**Table 1**

Ingredients (in per cent) used for manufacture the different pâté formulations.

Ingredient (%)	BF40	BF28	SO40	SO28
Liver	28.00	40.00	28.00	40.00
Back fat	40.00	28.00	–	–
Sunflower oil	–	–	40.00	28.00
Chicken breast	5.00	5.00	5.00	5.00
Water	22.62	22.62	22.62	22.62
Sodium caseinate	2.00	2.00	2.00	2.00
Sodium chloride	2.00	2.00	2.00	2.00
Sodium phosphate	0.30	0.30	0.30	0.30
Sodium nitrite	0.03	0.03	0.03	0.03
Ascorbic acid	0.05	0.05	0.05	0.05

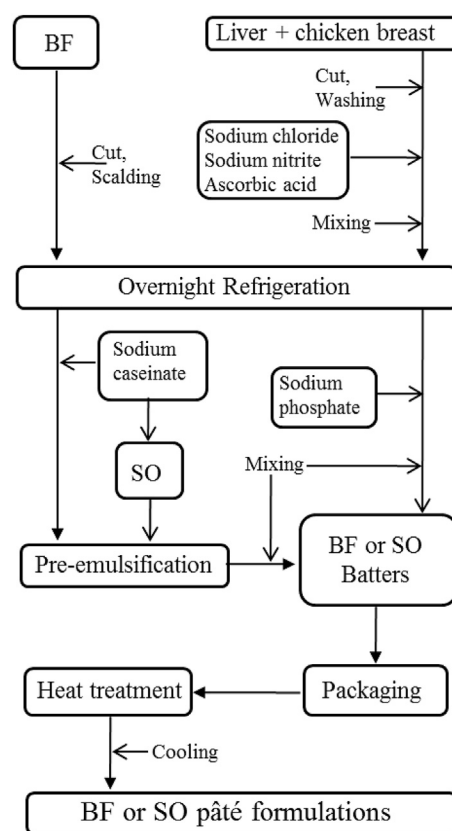


**Fig. 1.** Flow sheet of chicken liver pâté manufacturing.

determined in duplicate by a chromatographic technique based on IUPAC rules 2432 (1992) and AOCS Ce8-89 (1998). Lipids were extracted from adipose tissue using the Soxhlet method with n-hexane. This solvent was removed by a rotary evaporator R-114 (Büchi, Flawil, Switzerland) under vacuum at 40 °C. Subsequently, the extracted lipids were dissolved in n-hexane for quantification by HPLC with fluorescence detection ( $\lambda$  excitation: 290 nm,  $\lambda$  emission: 330 nm). A Hewlett Packard HPLC Series 1050 chromatograph equipped with a Lichrosorb normal phase column Si-60 (250 mm × 4 mm and 5  $\mu$ m particle size) was used. Operating conditions were: mobile phase isopropanol: hexane (0.5:99.5 v/v), a flow rate of 1.5 mL/min and 20  $\mu$ l of injection volume.

## 2.3. Assessment of quality attributes throughout refrigerated storage

### 2.3.1. Texture Measurement

Penetration test was performed on pâté formulations in their flasks with a TA-XT2i texture analyser (Stable Micro Systems, Godalming, UK) at room temperature. Force in compression was measured with a 12.7 mm diameter cylinder probe (P/R 0.5 Delrin) which penetrated the sample to a depth of 15 mm at a constant cross head speed of 1 mm/s. The hardness (maximum force required to penetrate the sample in N) were obtained from the force–time curves recorded in triplicate for each pâté formulation.

### 2.3.2. Microstructure

Microstructures of pâté formulations were observed by Scanning Electron Microscopy. Samples were fixed with 2.5% glutaraldehyde in sodium phosphate buffer 0.1 M (pH 7.2). Then, they were dehydrated with acetone and dried by critical point technique with CO<sub>2</sub> POLARON equipment. Furthermore, the samples were coated

with a gold layer by Pelco equipment 91000 and were observed in a microscope JEOL 35 CF (Tokyo, Japan).

### 2.3.3. Colour

Colour parameters on the surface of the pâté formulations were measured at room temperature in triplicate. CIE-LAB parameters: Lightness ( $L^*$ ), redness ( $a^*$ ) and yellowness ( $b^*$ ) were determined using a Chroma Meter CR-400 colorimeter (Minolta Co., Osaka, Japan).

### 2.3.4. Sanitary condition of pâtés

Microbiological analyses were performed in duplicate to evaluate sanitary condition of the pâtés from 0 to 150 d. Every 30 d, 20 g of each pâté formulation was aseptically removed from each package, transferred into sterile stomacher bags, homogenized with 80 mL of 0.1% of sterile peptone solution and blended in stomacher (West Sussex, UK) for 60 s. Decimal progressive dilutions were prepared. Mesophilic aerobic and Psychrotrophic microorganisms were evaluated on plate count agar (PCA Oxoid, Hampshire, UK), by pour plates aerobic incubation at 30 °C for 48 h and 4 °C for 7 d, respectively. *Enterobacteriaceae* microorganisms were enumerated on violet red bile agar (Merck, KGaA, Darmstadt, Germany) by spread plates aerobic incubation at 37 °C for 24 h. Sulphite-reducing Clostridium microorganisms were enumerated in differential clostridia agar (Britania, Argentina) and incubated at 37 °C for 48 h in anaerobic condition. Results were expressed as the average colony forming units per gram (CFU/g).

## 2.4. Oxidative stability

### 2.4.1. Lipid and protein oxidation

Lipid oxidation was evaluated by the 2-thiobarbituric acid reactive substances (TBARS) test in duplicate during storage time. TBARS values were determined in duplicate on pâtés according to Rosmini et al. (1996). Results were expressed as mg malonaldehyde (MDA)/kg product. The levels of oxidative modified proteins were determined in duplicate according to Oliver, Ahn, Moerman, Goldstein, and Stadtman (1987). Carbonyl compounds concentration was expressed as nmol/mg protein.

### 2.4.2. Hem iron content

Hem iron content was measured in duplicate by spectrophotometry as described Lombardi-Boccia, Martínez-Domínguez, Aguzzi, and Rincón-León (2002). Hematin concentration expressed as mg/mL was determined at 640 nm using a calibration curve with pork hematin. The concentration of hem iron was calculated using the conversion factor of 0.082  $\mu\text{g Fe}/\mu\text{g hematin}$ . Hem iron content was expressed in  $\mu\text{g Fe Hem/g pâté}$ .

## 2.5. Experimental design and statistical analysis

A full factorial randomized experimental design was used and the factors studied were: type of fat (two levels: BF and SO), fat content (two levels: 28% w/w and 40% w/w), refrigerated storage time (six levels: 0, 30, 60, 90, 120 and 150 d) and their interactions. Means and SEM (standard error of the mean values) were presented for all assays. Analysis of variance was applied to evaluate the influence of the variables using the SYSTAT software (SYSTAT Inc., USA). For simultaneous pairwise comparisons, Fisher's test was chosen. Differences in means and F-tests were considered significant when  $p < 0.05$ .

## 3. Results and discussion

### 3.1. Chemical composition

#### 3.1.1. Proximate analysis and energy content

Total lipid content was constituted essentially by the fat used as well as from the liver and muscle to a lesser extent. In SO formulations lipid content is greater than the amount of oil added and the BF formulations had a lower fat percentage when compared to the amount of BF added (Table 2). These facts are related to the composition of SO and BF used in the manufacturing process. SO has 99.90% of lipids and BF is a tissue composed mainly by fat with proteins and moisture in smaller proportions. Proteins are provided by meat ingredients, essentially muscle and liver, sodium caseinate and by the BF. SO28 and BF28 pâtés presented higher protein contents than SO40 and BF40 since the reduction in fat content was replaced with a higher content of liver. This procedure also influenced the moisture content because SO40 and BF40 formulations had lower moisture values than SO28 and BF28 pâtés. The main contribution to ash content is given by the additives and the different liver/fat ratio used, principally due to the iron supply by liver tissue. Pâtés with a low caloric value for both types of fat utilized were obtained by the reduction of the fat content.

#### 3.1.2. Fatty acid composition

Table 3 shows the fatty acid profiles of the different chicken liver pâtés studied. It was possible to observe that BF40 pâtés had oleic acid as the most abundant fatty acid, which represented 50.49%, followed by palmitic, linoleic and stearic acids and very low levels of other ones. The reduction of the fat content in BF28 pâtés was accompanied by a decrease in the oleic acid, the main fatty acid provided by the back fat. However, SFAs and PUFAs were more abundant in BF28 pâtés which could be associated with the increased contribution of hepatic tissue rich in those fatty acids (data not shown). SO formulations were constituted by linoleic, oleic, stearic and palmitic acids. Particularly, linoleic acid quadrupled BF pâté contents. However, SFAs and oleic acid contents in SO pâtés were lower than those made with BF. Therefore, replacing back fat with sunflower oil resulted in pâtés with a high proportion ( $p < 0.05$ ) of PUFAs. These types of fatty acids accounted for over 50% of the total fatty acids in SO pâtés, improving its nutritional value due to the contribution of an essential fatty acid such as linoleic acid. Throughout storage no significant changes in the fatty acids contents were observed. However, only 20:2n-6 fatty acid declined significantly ( $p = 0.021$ ) which could be attributed to lipid oxidation.

### 3.2. Quality attributes

#### 3.2.1. Textural analysis

Pâté is considered a finely comminuted meat product composed of a mixture of proteins (soluble and insoluble proteins with particles of muscle fibres and connective tissue), fat globules, water, salt and spices which are mixed into a fairly homogeneous mass. This mixture has a paste-like texture in the raw state but gradually changes into a more rigid structure by gelation of proteins throughout the cooking process. The structure is formed when the proteins start to denature and participate in protein–protein interactions (Barbut, Gordon, & Smith, 1996).

Fig. 2 shows the hardness of chicken liver pâté formulations. The type of fat was a significant factor that affected the texture of samples. SO pâtés exhibited significantly lower hardnesses ( $p = 0.001$ ) than those made with back fat due to the replacement of saturated for unsaturated fats. This effect was also observed by Martin et al. (2008) in pâtés with partial replacement of pork fat by

**Table 2**  
Proximate analysis (g/100 g) and total calories (kcal/100 g) of chicken liver pâté formulations.

	Formulations				SEM	p		
	BF40	BF28	SO40	SO28		T	C	TxC
Lipids	37.40 <sup>c</sup>	27.46 <sup>a</sup>	42.71 <sup>d</sup>	30.80 <sup>b</sup>	2.23	<0.001	0.048	<0.001
Proteins	8.79 <sup>b</sup>	10.33 <sup>c</sup>	7.95 <sup>a</sup>	10.21 <sup>c</sup>	0.38	0.002	0.006	<0.001
Ashes	2.61 <sup>b</sup>	2.84 <sup>c</sup>	2.51 <sup>a</sup>	2.59 <sup>b</sup>	0.05	<0.001	0.005	<0.001
Moisture	50.32 <sup>b</sup>	58.75 <sup>d</sup>	46.44 <sup>a</sup>	56.19 <sup>c</sup>	1.83	<0.001	0.021	<0.001
Total Calories	371.70 <sup>c</sup>	288.49 <sup>a</sup>	416.19 <sup>d</sup>	318.04 <sup>b</sup>	18.60	<0.001	0.045	<0.001

<sup>a, b, c, d</sup> Means with different letters in the same row indicate significant differences ( $p < 0.05$ ).

Abbreviations: T, type of fat; C, fat content; TxC, second level interaction between T and C.

**Table 3**  
Fatty acid profile (% of total fatty acids) of the pâté formulations ( $n = 2$ ).

	Formulations				SEM	p		
	BF40	BF28	SO40	SO28		T	C	TxC
Miristic	1.27 <sup>a</sup>	2.02 <sup>b</sup>	n.d.	n.d.	0.13	<0.001	0.004	0.004
Palmitic	20.80	24.83	6.53	8.34	1.24	<0.001	0.048	0.183
Palmitoleic	2.14	2.30	n.d.	n.d.	0.19	<0.001	0.142	0.142
Stearic	8.90	9.32	3.10	4.57	0.41	<0.001	0.004	0.240
Oleic	50.49 <sup>c</sup>	39.51 <sup>b</sup>	28.74 <sup>a</sup>	30.28 <sup>a</sup>	1.13	<0.001	0.002	<0.001
Linoleic	14.18 <sup>a</sup>	16.90 <sup>a</sup>	61.63 <sup>c</sup>	56.82 <sup>b</sup>	3.25	<0.001	0.048	<0.001
Linolenic	0.50 <sup>a</sup>	1.09 <sup>b</sup>	n.d.	n.d.	0.06	<0.001	0.001	0.001
20:00	1.11	0.88	n.d.	n.d.	0.05	<0.001	0.310	0.310
20:2n-6	0.64	0.73	n.d.	n.d.	0.06	<0.001	0.148	0.148
Arachidonic	0.47	0.32	n.d.	n.d.	0.05	<0.001	0.001	0.001
SFA	32.07	37.05	9.63	12.91	1.82	<0.001	0.011	0.340
MUFA	52.62 <sup>c</sup>	44.25 <sup>b</sup>	28.74 <sup>a</sup>	30.28 <sup>a</sup>	1.40	<0.001	0.018	<0.001
PUFA	15.78 <sup>a</sup>	19.03 <sup>b</sup>	61.63 <sup>d</sup>	56.82 <sup>c</sup>	3.10	<0.001	0.003	<0.001
Total Unsat	68.40	63.27	90.37	87.10	1.83	<0.001	0.049	0.268
PUFA/SFA	0.49	0.51	6.39	4.40	0.47	<0.001	<0.001	0.004

n.d.: not detected.

<sup>a-d</sup> Different superscripts within the same row indicate that average values differ significantly ( $p < 0.05$ ).

Abbreviations: T, type of fat; C, fat content; T × C, second level interaction between T and C; SFA, saturated fatty acids; MUFA, monounsaturated fatty acids; PUFA, polyunsaturated fatty acids.

olive oil. The fat content significantly modified the hardness of pâtés. The presence of high amounts of sunflower oil (SO40) resulted in soft pâtés ( $p = 0.014$ ) and the reduction of back fat content produced the opposite effect (Fig. 2). The storage time did not influence the hardness of pâtés ( $p > 0.05$ ).

### 3.2.2. Microstructure

Micrographs for pâté formulations show a microstructure constituted by a matrix of proteins with the inclusion of fat globules and pores (Fig. 3). The matrix is composed of proteins from chicken liver, muscle and sodium caseinate. This protein network consists of both fibrous proteins (collagen, elastin, reticulin, actin and myosin) and globular proteins (cytoplasmic proteins of liver tissue, sarcoplasmic myoglobin and haemoglobin). According to Tornberg (2005), fibrous proteins are denatured by heat, acquire random configurations and are associated with globular proteins forming the matrix. Also, the presence of holes of different size can be observed in these images. The holes were identified as the spaces where fat was placed in the gel matrix; this fat disappears with the preparation of the samples. In addition, a large number of small pores distributed in the gel network were seen in Fig. 3b, c and d. These small pores could be associated with water or air incorporated throughout the homogenization step in the preparation of the pâté formulations.

The microstructure of pâtés formulations varied with fat type and content. BF pâtés (Fig. 3a and b) showed larger fat globules with more defined shape than SO pâtés (Fig. 3c and d). BF40 formulation (Fig. 3a) exhibited a continuous protein matrix and packed structure that may be associated with increasing instrumental hardness (Fig. 2), while BF28 and SO pâtés revealed a more aggregated structure of gels (Fig. 3b, c and d). In addition, the

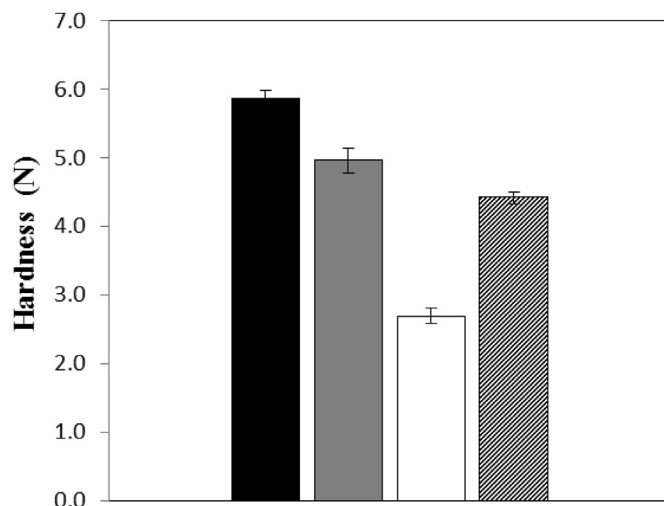


**Fig. 2.** Hardness (N) of different chicken liver pâtés. ■BF40; ▨BF28; □SO40; ▩SO28. The bars correspond to standard error of mean values.

reduction of fat content (with a liver-content increase) caused an increase in the number of pores due to the increase of moisture content (Fig. 3b and d, Table 2). This behaviour is in accordance with findings presented by Totosaus and Pérez-Chabela (2009). Moreover, a growth in connective-tissue liver proteins must be related to water retention contributing also, to raise the number of pores. On the other hand, the storage time did not affect the microstructure of the pâtés.

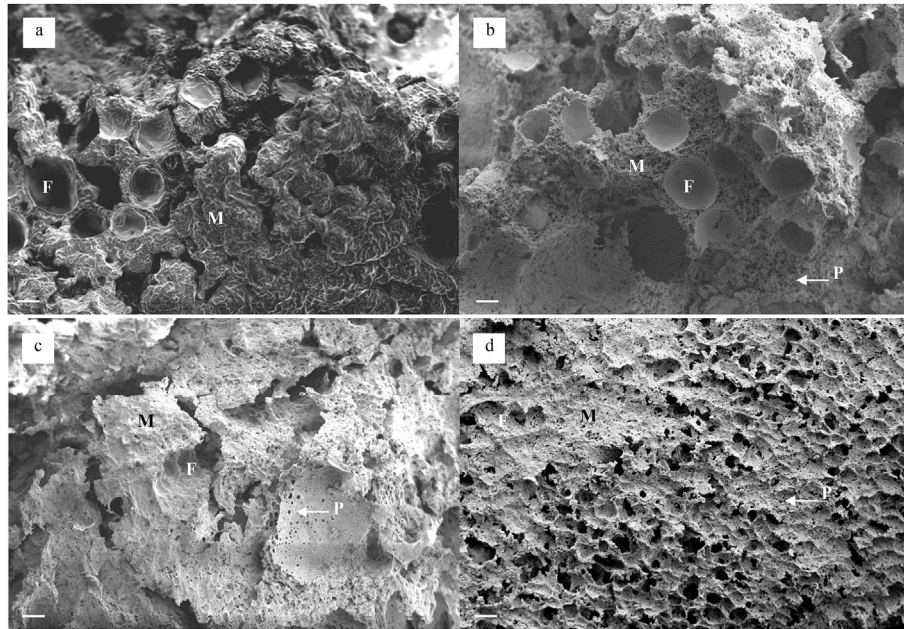


**Fig. 3.** Scanning electron micrographs ( $\times 345$  magnification) of chicken liver pâtés, a) BF40; b) BF28, c) SO40 and d) SO28. F = fat globules, M = protein matrix, P = pores. The scale bars are 50  $\mu\text{m}$  in length.

### 3.2.3. Colour

Table 4 exposes the evolution of surface colour parameters ( $L^*$ ,  $a^*$  and  $b^*$ ) of pâtés with different fat composition throughout storage. The SO pâtés oil presented higher  $L^*$  values than BF pâtés which could attribute to a milky appearance imparted by the oil emulsion. Similar results were obtained by Pennisi Forell et al. (2010) in burgers with high oleic sunflower oil due to the high refractive index of this oil. BF40 and SO40 gave higher  $L^*$  values than BF28 and SO28 pâtés ( $p < 0.01$ ), that were in agreement with the study in low-fat sausages (Crehan, Hughes, Troy, & Buckley, 2000). The storage time produced an increase ( $p < 0.01$ ) in lightness of the pâtés, similar to that reported by Estevez and Cava (2004).

The redness showed an increase ( $p < 0.01$ ) during storage time (Table 4). This fact was attributed to the formation of nitrosohaemoglobin and red nitrosomyoglobin as Bozkurt (2006) observed in fermented and cured sausages. Moreover, D'Arrigo et al. (2004) related this behaviour with the exposure to air and surface water loss of samples. The BF pâtés presented lower values than those made with sunflower oil ( $p < 0.01$ ). BF28 and SO28 exhibited the highest values for this parameter ( $p < 0.01$ ). In this sense, a significant negative correlation was found between  $a^*$  values and fat content for the pâté formulations throughout the storage time ( $r \geq -0.87$ ;  $p \leq 0.003$ ). The increase in  $a^*$  with the decrease of fat percentage can be attributed to the high hem proteins content supplied by the liver, which provide an enhanced reddish tint. Estévez, Ventanas, Cava, and Puolanne (2005) studied the physicochemical properties of pork liver pâté with different fat contents (45, 40 and 35% w/w) reporting similar results.

Statistical analysis of the values obtained for the  $b^*$  parameter (Table 4) revealed that pâtés which include back fat in their formulation were less yellow than those prepared with sunflower oil ( $p < 0.01$ ). This behaviour was observed by other researchers when fat was replaced by oil producing yellower meat products (Youssef & Barbut, 2009). BF40 and SO40 pâtés gave higher  $b^*$  values than BF28 and SO28 pâtés ( $p < 0.01$ ). The storage time produced an increase ( $p < 0.01$ ) in yellowness of pâté formulations. Fernández-López, Sayas-Barberá, Sendra, and Pérez-Alvarez (2004) observed that both oxidation and oxygenation of myoglobin could

generated increments in the  $b^*$  parameter. Considering that the third level interaction was significant ( $p < 0.05$ ), the modifications in lightness, redness and yellowness produced by storage time depended on the combination of fat type and content.

### 3.2.4. Sanitary condition of pâtés

No sulphite-reducing Clostridium was noted in any sample throughout the storage period. The microbial counts did not exceed 60 CFU/g for the other groups of microorganisms analysed: mesophilic aerobic, psychrotrophic and *Enteriobacteriaceae* at final storage time. These results indicated that the heat treatment and the application of low temperatures during the storage time were appropriate operations to maintain safe sanitary conditions for all pâté formulations.

### 3.3. Oxidative stability

Fat content and refrigerated storage time were significant factors ( $p < 0.05$ ) that influenced lipid oxidation in the pâtés. TBARS values in BF28 and SO28 pâtés presented a significant increase while SO40 pâtés showed a slight increase (Table 5). These behaviours might be explained considering that high moisture content in BF28 and SO28 may promote lipid oxidation. TBARS values in BF40 remained steady during storage time. SO40 pâtés presented the highest TBARS value (0.65 mg MDA/Kg) at initial storage time, possibly because its high content of PUFAs produces an increase in the susceptibility to lipid oxidation in pâté manufacturing steps (disruption of tissues and subsequent heat treatment).

No influence of fat type in TBA values ( $p > 0.05$ ) was observed in statistical analysis. SO pâtés exhibited the TBA values lower than expected, taking into account their fatty acid composition rich in PUFAs (Table 5). This behaviour could be attributed to the high Vitamin E content in sunflower oil. Thus, total tocopherol level in this oil was  $502 \pm 21 \mu\text{g/g}$ , with  $\alpha$ -tocopherol being the major component ( $498 \pm 20 \mu\text{g/g}$ ) followed by  $\beta$ -tocopherol ( $4 \pm 1 \mu\text{g/g}$ );  $\gamma$  and  $\delta$  vitamers were not detected. Muguerza, Ansorena, and Astiasarán (2003) also observed the influence of the natural antioxidants present in vegetable oils on lipid oxidation when back fat is replaced with soybean oil in Pamplona chorizo. Besides, the total

**Table 4**Evolution of surface color parameters ( $L^*$ ,  $a^*$  and  $b^*$ ) of pâtés with different compositions during refrigerated ( $4 \pm 1$  °C) storage time.

	Storage [d]						SEM
	0	30	60	90	120	150	
$L^*$							
BF40	60.23 <sup>a,b,z</sup>	62.70 <sup>c,β,γ</sup>	60.64 <sup>a,z</sup>	63.95 <sup>b,γ</sup>	61.48 <sup>a,z,β</sup>	62.46 <sup>a,β,γ</sup>	0.27
BF28	59.19 <sup>a,z</sup>	59.77 <sup>a,z,β</sup>	59.86 <sup>a,z,β</sup>	61.95 <sup>a,γ</sup>	61.16 <sup>a,β,γ</sup>	61.33 <sup>a,β,γ</sup>	0.26
SO40	61.58 <sup>b,z</sup>	60.81 <sup>a,b,z</sup>	64.60 <sup>b,γ</sup>	63.75 <sup>b,β,γ</sup>	62.32 <sup>a,z,β</sup>	65.17 <sup>b,γ</sup>	0.31
SO28	61.45 <sup>b,z</sup>	61.45 <sup>b,c,z</sup>	63.55 <sup>b,β</sup>	62.44 <sup>a,b,z,β</sup>	61.63 <sup>a,z</sup>	60.89 <sup>a,z</sup>	0.20
$a^*$							
BF40	2.74 <sup>a,z</sup>	2.39 <sup>a,z</sup>	4.37 <sup>a,β</sup>	3.81 <sup>a,z,β</sup>	5.97 <sup>a,γ</sup>	5.23 <sup>b,β,γ</sup>	0.25
BF28	6.70 <sup>c,β</sup>	6.07 <sup>c,z</sup>	6.35 <sup>b,z,β</sup>	7.74 <sup>c,β</sup>	9.16 <sup>b,γ</sup>	8.57 <sup>c,β,γ</sup>	0.21
SO40	2.18 <sup>a,z</sup>	3.98 <sup>b,β</sup>	6.71 <sup>a,b,γ</sup>	6.59 <sup>b,γ</sup>	6.85 <sup>a,γ</sup>	4.04 <sup>a,β</sup>	0.34
SO28	5.22 <sup>b,z</sup>	6.67 <sup>d,β</sup>	7.96 <sup>c,γ</sup>	8.93 <sup>d,γ</sup>	8.53 <sup>b,γ</sup>	8.01 <sup>c,γ</sup>	0.19
$b^*$							
BF40	15.77 <sup>a,z</sup>	17.14 <sup>b,β</sup>	15.34 <sup>a,z</sup>	16.53 <sup>a,b,z,β</sup>	16.38 <sup>a,z,β</sup>	16.52 <sup>a,z,β</sup>	0.17
BF28	15.10 <sup>a,z</sup>	15.69 <sup>a,β</sup>	16.17 <sup>a,γ</sup>	16.04 <sup>a,γ</sup>	15.79 <sup>a,b,β,γ</sup>	15.94 <sup>a,β,γ</sup>	0.21
SO40	17.81 <sup>b,β</sup>	18.61 <sup>c,z,β</sup>	19.24 <sup>c,β</sup>	18.87 <sup>c,β</sup>	19.22 <sup>c,β</sup>	21.45 <sup>c,γ</sup>	0.26
SO28	17.48 <sup>b,z</sup>	17.54 <sup>b,z</sup>	17.94 <sup>b,z</sup>	17.27 <sup>b,z</sup>	17.86 <sup>b,z,β</sup>	18.56 <sup>b,β</sup>	0.12

a,b,c,d Different letters within the same column indicate significant differences ( $p < 0.05$ ).z,β,γ Different letters within the same row indicate significant differences ( $p < 0.05$ ).**Table 5**Evolution of TBARS values (mg MDA/kg), carbonyl compounds (nmol/mg proteins) and hem iron content ( $\mu\text{g/g}$  pâté) in chicken liver pâté formulations during refrigerated storage time.

	Storage [d]						SEM
	0	30	60	90	120	150	
TBARS							
BF40	0.47 <sup>b,z</sup>	0.51 <sup>a,z</sup>	0.57 <sup>a,z</sup>	0.57 <sup>a,z</sup>	0.50 <sup>a,z</sup>	0.50 <sup>a,z</sup>	0.02
BF28	0.31 <sup>a,z</sup>	0.59 <sup>a,β</sup>	0.60 <sup>a,β</sup>	0.74 <sup>b,β,γ</sup>	0.70 <sup>b,β</sup>	0.95 <sup>c,β,γ</sup>	0.03
SO40	0.65 <sup>c,z,β</sup>	0.59 <sup>a,z</sup>	0.62 <sup>a,z,β</sup>	0.55 <sup>a,z</sup>	0.54 <sup>a,z</sup>	0.71 <sup>b,β</sup>	0.03
SO28	0.40 <sup>a,b,z</sup>	0.47 <sup>a,z</sup>	0.66 <sup>a,β</sup>	0.65 <sup>a,b,β</sup>	0.72 <sup>b,β</sup>	0.63 <sup>a,β</sup>	0.02
Carbonyl compounds							
BF40	5.27 <sup>c,z</sup>	4.62 <sup>b,c,z</sup>	6.73 <sup>b,β</sup>	4.75 <sup>a,z</sup>	5.14 <sup>a,z</sup>	6.18 <sup>b,z,β</sup>	0.29
BF28	2.25 <sup>a,z</sup>	3.22 <sup>a,z,β</sup>	3.99 <sup>a,β</sup>	5.69 <sup>a,b,β,γ</sup>	4.51 <sup>a,β,γ</sup>	7.13 <sup>c,δ</sup>	0.35
SO40	4.17 <sup>b,c,z</sup>	4.69 <sup>c,z</sup>	5.45 <sup>b,z,β</sup>	6.43 <sup>b,β</sup>	4.95 <sup>a,z</sup>	5.37 <sup>a,z,β</sup>	0.26
SO28	3.22 <sup>a,b,z</sup>	3.26 <sup>a,b,z</sup>	4.46 <sup>a,z,β</sup>	4.36 <sup>a,z,β</sup>	4.60 <sup>a,z,β</sup>	5.74 <sup>a,b,β</sup>	0.23
Fe Hem							
BF40	6.30 <sup>a,b,β,γ</sup>	4.63 <sup>a,β</sup>	4.81 <sup>a,β</sup>	4.15 <sup>b,β</sup>	1.81 <sup>a,z</sup>	2.23 <sup>a,z</sup>	0.41
BF28	7.46 <sup>b,β</sup>	6.33 <sup>b,z</sup>	6.32 <sup>b,z</sup>	7.08 <sup>c,z,β</sup>	7.00 <sup>c,z,β</sup>	6.02 <sup>b,z</sup>	0.17
SO40	5.65 <sup>a,β</sup>	4.73 <sup>a,β</sup>	5.14 <sup>a,b,β</sup>	2.42 <sup>a,z</sup>	3.24 <sup>a,z,β</sup>	2.14 <sup>a,z</sup>	0.32
SO28	5.53 <sup>a,z,β</sup>	4.51 <sup>a,z</sup>	6.51 <sup>b,β</sup>	5.91 <sup>b,c,z,β</sup>	5.34 <sup>b,z,β</sup>	4.61 <sup>b,z</sup>	0.24

a, b, c Different letters within the same column indicate significant differences ( $P < 0.05$ ).z, β, γ, δ Different letters within the same row indicate significant differences ( $P < 0.05$ ).

tocopherol content in back fat was also considerable ( $350 \pm 20$   $\mu\text{g/g}$ ), with  $\alpha$ -tocopherol as the only vitamer found.

Protein oxidation is considered to be linked to lipid oxidation. In the presence of oxidized lipids, the protein oxidation is produced by free radical chain reactions similar to those for lipid oxidation (Faustman, Sun, Mancini, & Suman, 2010). The carbonyl compounds content of pâté formulations significantly changed ( $p < 0.05$ ) with refrigerated storage time (Table 4). In this case, BF28 and SO28 increased significantly; while BF40 and SO40 fluctuated mildly probably due to the by-products of lipid oxidation could have interacted with proteins. Besides, the fat content was a significant factor since the pâtés with 40% w/w fat content had significantly higher levels of carbonyl compounds than pâtés with 28% w/w fat. On the other hand, the statistical evaluation showed that the type of fat did not significantly affect ( $p > 0.05$ ) the protein oxidation, similar to the case of the TBA test.

Hem iron is another parameter to evaluate oxidative damage in fatty meat products. Greater concentrations of iron and myoglobin are associated with greater rates of lipid oxidation (Faustman et al., 2010). In this work, the hem iron content was affected significantly ( $p < 0.01$ ) by refrigerated storage time. BF40 and SO40 showed a hem iron decrease while BF28 and SO28 pâtés varied around 6.50 and 5.50  $\mu\text{g/g}$  pâté, respectively (Table 5). The fat type and its

content significantly affected ( $p < 0.01$ ) the hem iron values obtained. BF pâtés presented higher hem iron contents than those SO pâtés. Furthermore, BF40 and SO40 pâtés showed significantly lower values of hem iron than BF28 and SO28 pâtés, probably due to their higher fat/liver ratios, since liver is the main component that provides iron in BF28 and SO28 formulations. The third level interaction was also significant ( $p < 0.05$ ), indicating that changes produced in TBARS, carbonyl compounds and hem iron levels by the storage time depended on the combination of fat type and content.

Liver pâtés contain high amounts of fat and iron, and therefore, oxidative deterioration of liver pâtés during refrigeration was expected. Georgantelis, Blekas, Katikou, Ambrosiadis, and Fletouris (2007) reported that the rancid flavour is detected in meat products with TBARS values higher than 0.6 mg MDA/kg, while Campo et al. (2006) considered that the limiting threshold for the acceptability of oxidized beef is around 2.0 mg MDA/kg. In this work, all pâté formulations presented TBARS levels below 1 mg MDA/kg after 150 d of storage at  $4 \pm 1$  °C. Moreover, the carbonyl compounds contents were lower than those found in traditional liver pâtés from pork during refrigerated storage by Estevez and Cava (2004). In addition, the decreases in the hem iron contents in BF40 and SO40 pâtés were also lower than those reported by Fernández-López et al. (2003).

The physicochemical evaluation the shelf life of the healthy chicken liver pâtés indicated that the lipid and protein oxidation levels were lower than those observed for traditional formulations. No substantial reduction of quality attributes was recorded as a function of refrigerated storage. Hence, the developed chicken liver pâtés would be suitable formulations to diversify the poultry industry.

#### 4. Conclusions

This study allowed the global characterization of chicken liver pâtés with a reduction and replacement of the traditional back fat by refined sunflower oil. SO pâtés were obtained with a fatty acid profile healthier than BF pâtés, increasing the PUFAs/MUFAs ratio. Regarding the quality attributes, BF pâtés presented higher hardness values ( $p < 0.05$ ) than those made with sunflower oil. Micrographs of pâtés revealed variations in the protein matrix, distribution pattern of the fat globules and pores with fat type and content. Thus, SO pâtés exhibited a greater number of pores than the others which could be related to a more spreadability for these formulations. Storage time, the type and concentration of the fat phase mildly modified the colour parameters. Microbiological analyses indicated an adequate hygienic quality for all pâté formulations throughout refrigerated storage. In terms of oxidative stability, changes observed in TBARS, carbonyl compounds and hem iron contents were satisfactory considering liver pâtés contain high amounts of fat and iron. Therefore, taking into account chemical composition, quality attributes and oxidative stability, the chicken liver pâté with 28% w/w of sunflower oil was the most adequate formulation to increase the nutritional value for this kind of meat products.

#### Acknowledgements

Authors acknowledged M. García (INIBIOLP), S. Nolasco (UNCPBA) and V. Sorrivás (CCTBB) for technical assistance and financial support of CONICET.

#### References

- AOAC. (1984). *Official methods of analysis* (14th ed.). Washington, DC: Association of Official Analytical Chemists.
- AOAC. (1990). Methyl esters of fatty acids in oils and fats. In K. Helrich (Ed.), *Official methods of analysis* (pp. 963–964). Arlington, USA: Association of Official Analytical Chemists.
- AOCS. (1998). *Official Methods and Recommended Practices of the American Oil Chemists' Society*. Champaign, USA: AOCS Press.
- Arihara, K. (2006). Strategies for designing novel functional meat products. *Meat Science*, 74, 219–222.
- Barbut, S., Gordon, A., & Smith, A. (1996). Effect of cooking temperature on the microstructure of meat batters prepared with salt and phosphate. *Lebensmittel-Wissenschaft und -Technologie*, 29, 475–480.
- Bozkurt, H. (2006). Utilization of natural antioxidants: green tea extract and Thymbraspicata oil in Turkish dry-fermented sausage. *Meat Science*, 73, 442–450.
- Campo, M. M., Nute, G. R., Hughes, S. I., Enser, M., Wood, J. D., & Richardson, R. I. (2006). Flavour perception of oxidation in beef. *Meat Science*, 72, 303–311.
- Crehan, C. M., Hughes, E., Troy, D. J., & Buckley, D. J. (2000). Effects of fat level and maltodextrin on the functional properties of frankfurters formulated with 5, 12 and 30 % fat. *Meat Science*, 55, 463–469.
- Delgado-Pando, G., Cofrades, S., Rodríguez-Salas, I., & Jiménez-Colmenero, F. (2011). A healthier oil combination and konjac gel as functional ingredients in low-fat pork liver pâté. *Meat Science*, 88, 241–248.
- D'Arrigo, M., Hoz, L., Cambero, I., López-Bote, C. J., Pin, C., & Ordóñez, J. A. (2004). Production of n-3 fatty acid enriched pork liver pâté. *Lebensmittel-Wissenschaft und -Technologie*, 37, 585–591.
- Estevez, M., & Cava, R. (2004). Lipid and protein oxidation, release of iron from heme molecule and colour deterioration during refrigerated storage of liver pâté. *Meat Science*, 68, 551–558.
- Estevez, M., & Cava, R. (2006). Effectiveness of rosemary essential oil as an inhibitor of lipid and protein oxidation: contradictory effects in different type of frankfurters. *Meat Science*, 72, 348–355.
- Estevez, M., Ramírez, R., Ventanas, S., & Cava, R. (2007). Sage and rosemary essential oils versus BHT for the inhibition of lipid oxidative reactions in liver pâté. *Lebensmittel-Wissenschaft und -Technologie*, 40, 58–65.
- Estevez, M., Ventanas, J., Cava, R., & Puolanne, E. (2005). Characterization of a traditional Finnish liver sausage and different types of Spanish liver pâtés: a comparative study. *Meat Science*, 71, 657–669.
- Faustman, C., Sun, Q., Mancini, R., & Suman, S. P. (2010). Myoglobin and lipid oxidation interactions: mechanistic bases and control. *Meat Science*, 86, 86–94.
- Fernández-López, J., Sayas-Barberá, E., Sendra, E., & Pérez-Alvarez, J. A. (2004). Quality characteristics of ostrich liver pâté. *Journal of Food Science*, 69, 85–91.
- Fernández-López, J., Sevilla, I., Sayas-Barberá, E., Navarro, C., Marín, F., & Pérez-Alvarez, J. A. (2003). Evaluation of the antioxidant potential of hyssop (*Hyssopus officinalis* L.) and rosemary (*Rosmarinus officinalis* L.) extracts in cooked pork meat. *Journal of Food Science*, 68, 660–664.
- Folch, J., Lees, M., & Sloane-Stanley, G. M. (1957). A simple method for the isolation and purification of total lipids from animal tissue. *Journal of Biological Chemistry*, 226, 497–508.
- Georgantelis, D., Blekas, G., Katikou, P., Ambrosiadis, I., & Fletouris, D. J. (2007). Effect of rosemary extract, chitosan and  $\alpha$ -tocopherol on lipid oxidation and colour stability during frozen storage of beef burgers. *Meat Science*, 75, 256–264.
- IUPAC. (1992). Standard methods for the analysis of oils, fats and derivatives. In C. Paquot, & A. Hautfenne (Eds.), *International Union of Pure and Applied Chemistry* (7th ed.). Oxford, UK: Backwell Scientific Publications Inc.
- Lombardi-Boccia, G., Martínez-Domínguez, B., Aguzzi, A., & Rincón-León, F. (2002). Optimization of heme iron analysis in raw and cooked red meat. *Food Chemistry*, 78, 505–510.
- Lund, M. N., Hviid, M. S., & Skibsted, L. H. (2007). The combined effect of antioxidants and modified atmosphere packaging on protein and lipid oxidation in beef patties during chill storage. *Meat Science*, 76, 226–233.
- Martin, D., Ruiz, J., Kivikari, R., & Puolanne, E. (2008). Partial replacement of pork fat by conjugated linoleic acid and/or olive oil in liver pâtés: effect on physicochemical characteristics and oxidative stability. *Meat Science*, 80, 496–504.
- Muguerza, E., Ansorena, D., & Astiasarán, I. (2003). Improvement of nutritional properties of Chorizo de Pamplona by replacement of pork back fat with soy oil. *Meat Science*, 65, 1361–1367.
- Oliver, C. N., Ahn, B. W., Moerman, E. J., Goldstein, S., & Stadtman, E. R. (1987). Age-related changes in oxidized proteins. *The Journal of Biological Chemistry*, 262, 5488–5491.
- Pennisi Forell, S. C., Ranalli, N., Zaritzky, N. E., Andrés, S. C., & Califano, A. N. (2010). Effect of type of emulsifiers and antioxidants on oxidative stability, colour and fatty acid profile of low-fat beef burgers enriched with unsaturated fatty acids and phytosterols. *Meat Science*, 86, 364–370.
- Rosmini, M. R., Perlo, F., Pérez-Alvarez, J. A., Pagan-Moreno, M. J., Gago-Gago, A., López-Santovenia, F., ... Aranda-Catalá, V. (1996). TBA test by an extractive method applied to pâté. *Meat Science*, 42, 103–110.
- Tornberg, E. (2005). Effects of heat on meat proteins—Implications on structure and quality of meat products. *Meat Science*, 70, 493–508.
- Totosaus, A., & Pérez-Chabela, M. L. (2009). Textural properties and microstructure of low-fat and sodium-reduced meat batters formulated with gellan gum and dicationic salts. *LWT-Food Science and Technology*, 42, 563–569.
- USDA. (2014). [http://apps.fas.usda.gov/psdonline/circulars/livestock\\_poultry.pdf](http://apps.fas.usda.gov/psdonline/circulars/livestock_poultry.pdf).
- Youssef, M. K., & Barbut, S. (2009). Effects of protein level and fat/oil on emulsion stability, texture, microstructure and color of meat batters. *Meat Science*, 82, 228–233.



# Hyperspectral imaging for real-time monitoring of water holding capacity in red meat



Mohammed Kamruzzaman<sup>a, b, \*</sup>, Yoshio Makino<sup>a, \*\*,</sup>, Seiichi Oshita<sup>a</sup>

<sup>a</sup> Graduate School of Agricultural and Life Sciences, The University of Tokyo, Japan

<sup>b</sup> Department of Food Technology and Rural Industries, Faculty of Agricultural Engineering & Technology, Bangladesh Agricultural University, Mymensingh, 2202, Bangladesh

## ARTICLE INFO

### Article history:

Received 30 June 2015

Received in revised form

14 September 2015

Accepted 11 November 2015

Available online 19 November 2015

### Keywords:

Hyperspectral imaging

Multispectral imaging

Red meat

Multivariate analysis

Water holding capacity

## ABSTRACT

A hyperspectral imaging system was investigated for determination of feature wavelengths to be used in a design of a multispectral system for real-time monitoring of water holding capacity (WHC) in red meat. Hyperspectral images of different red meat samples were acquired in the spectral range of 400–1000 nm and partial least-squares regression (PLSR) and least square support vector machine (LS-SVM) models were developed. Feature wavelengths were selected using regression coefficients (RCs) and competitive adaptive reweighted sampling (CARS). The best set of feature wavelengths was determined using RCs and the best calibration model obtained was based on RCs-LS-SVM. The model obtained an  $R^2_p$  of 0.93 and RPD of 4.09, indicating that the model is adequate for analytical purposes. An image processing algorithm was developed to transfer this model to each pixel in the image. The results showed that instead of selecting different sets of wavelengths for beef, lamb, and pork, a subset of feature wavelengths can be used for convenient industrial application for the determination of WHC in red meat. The pixel wise visualization of WHC obtained with the aid of image processing was another advantage of using hyperspectral imaging that cannot be obtained with either imaging or conventional spectroscopy.

© 2015 Elsevier Ltd. All rights reserved.

## 1. Introduction

Water holding capacity (WHC), defined as the ability of fresh meat to retain its water during processing, storage, and cooking, is one of the most important technological quality attributes of red meat that can affect consumer preferences. The WHC has a great influence on the appearance of fresh meat in retail and might affect the sensory properties of cooked meat (Pedersen, Morel, Andersen, & Engelsen, 2003). Poor WHC owing to high drip loss is an undesirable quality of meat, and thus reduces consumer acceptability. If WHC is properly managed, many other operational variables will consequently improve, which will result in greater consumer satisfaction with products. From an economic outlook, high WHC (less drip loss) is extremely desirable because meat is sold by

weight (Hoving-Bolink et al., 2005). Therefore, controlling WHC is very important for the meat industry to maximize yield and quality. Practically, WHC can be determined by three fundamentally different principles such as drip loss, filter paper test, and cooking loss (Prevolnik, Čandek-Potokar, & Škorjanc, 2010). These techniques are time consuming and involve destructive sampling and therefore, are not optimally suitable for on-line industrial applications.

Recently, hyperspectral imaging has emerged as one of the most efficient and advanced tools for non-destructive evaluation for a variety of applications (Kamruzzaman, Makino, & Oshita, 2015b). Hyperspectral imaging is a combination of both imaging and spectroscopy in a single instrument to acquire both spatial and spectral information simultaneously from an object. Although it was originally developed for remote sensing applications, hyperspectral imaging has now found its way into many diverse applications (ElMasry, Kamruzzaman, Sun & Allen, 2012). Considerable research has proved the potential of hyperspectral imaging in meat quality assessment (Barbin, ElMasry, Sun, & Allen, 2012a; ElMasry, Sun & Allen, 2011; Iqbal, Sun, & Allen, 2013; Kamruzzaman, ElMasry, Sun, & Allen, 2011; Park et al., 2011). However, the

\* Corresponding author. Department of Food Technology and Rural Industries, Faculty of Agricultural Engineering & Technology, Bangladesh Agricultural University, Mymensingh, 2202, Bangladesh.

\*\* Corresponding author.

E-mail addresses: [mohammed.kamruzzaman@bau.edu.bd](mailto:mohammed.kamruzzaman@bau.edu.bd) (M. Kamruzzaman), [amakino@mail.ecc.u-tokyo.ac.jp](mailto:amakino@mail.ecc.u-tokyo.ac.jp) (Y. Makino).

technology is not yet suitable for routine online monitoring due to the challenges in analyzing a vast amount of hyperspectral image data. The time spent in the image acquisition and analysis is high. On the other side, spectra contain not only useful information but also redundant and irrelevant information (i.e., noise) and collinearity between wavelength variables. Indeed, the redundant and irrelevant information in the spectra complicates the model, leading to inaccurate prediction. Removing uninformative variables and extracting informative variables not only reduces the computational load but also produces stronger and more stable prediction models (Burger & Gowen, 2011). Therefore, it is very important to select appropriate wavelengths from hyperspectral data analyzes for designing multispectral real-time monitoring systems. If the spectral bands are properly selected to facilitate the design of multispectral imaging systems, which usually operate on ten wavelengths or less, the technology would certainly be an improvement on existing technology for process monitoring and real-time inspection (Qin, Chao, Kim, Lu, & Burks, 2013). The acquisition time, complexity, and cost of these systems will generally be quite low compared to hyperspectral imaging (Park et al., 2011; Pu, Kamruzzaman, & Sun, 2015). Hence, multispectral imaging with selected feature wavelengths is an alternative and promising approach for online screening in the industry.

Recently, various studies have investigated hyperspectral imaging for selecting effective wavelengths aimed at encouraging the manufacture of online multispectral imaging instruments for beef (ElMasry et al., 2011), lamb (Kamruzzaman, Barbin, ElMasry, Sun, & Allen, 2012; Kamruzzaman, ElMasry, Sun & Allen, 2013; Kamruzzaman, Sun, ElMasry & Allen, 2013), and pork (Barbin et al., 2012a; Tao, Peng, Li, Chao, & Dhakal, 2012). In particular, one research group investigated near infrared (NIR) hyperspectral imaging (900–1700 nm) and proposed feature wavelengths for designing a multispectral imaging system for online monitoring of various quality attributes of beef (ElMasry, Sun & Allen, 2012; ElMasry et al., 2011), pork (Barbin, ElMasry, Sun & Allen, 2012b; Barbin et al., 2012a), and lamb (Kamruzzaman, ElMasry, Sun, & Allen, 2012a, 2012b). Although all these studies were performed using a common system with an identical reference and data analysis method, surprisingly different combinations of optimum wavelengths were selected for the same constituent in different types of red meat. This implies that to develop a multispectral system, different combinations of wavelengths need to be used to determine the same attribute in different types of red meat, which is not convenient and feasible for the processors. Therefore, for convenient industrial application, comprehensive research should be conducted combining all types of red meat to select a subset of feature wavelengths for multispectral prediction for a particular application.

Currently, both VIS/NIR (400–1000 nm) and NIR (900–1700 nm) hyperspectral imaging systems are widely used for meat quality assessment due to their respective benefits and drawbacks. However, the VIS/NIR range is industrially advantageous because of the wide availability and low cost of charge-coupled device (CCD) detectors compared to the indium gallium arsenide (InGaAs) detectors used in the NIR region (Qin et al., 2013). Therefore, the key aim of this study was to use a VIS/NIR hyperspectral imaging system (400–1000 nm) for selecting some important feature wavelengths to develop a real-time multispectral imaging system for monitoring of WHC in red meat for the meat industry. The specific objectives were to (a) establish quantitative relationships between spectral data and reference WHC values using PLSR and LS-SVM, (b) select some feature wavelengths to design a multispectral imaging system for real-time monitoring of WHC in red meat (c), and (d) develop image processing algorithms to generate distribution maps of WHC.

## 2. Material and methods

### 2.1. Sample collection and measurements of reference WHC

Fresh beef, lamb, and pork samples from *M. longissimus dorsi* (LD) were collected from a local slaughter house in Tokyo, Japan. Each muscle (2 cm thickness) was individually labeled and transported to laboratories of Bioprocess Engineering, The University of Tokyo, Japan. Each muscle was first scanned by the hyperspectral imaging system as described by Kamruzzaman et al. (2015a), Kamruzzaman Makino, Oshita (2016) and the reference WHC value for each muscle was then determined by using the drip loss method (Honikel, 1998). It is necessary to include a large number of samples representing a wide variation in WHC for the development of a calibration model (Berzaghi & Riovanto, 2009). In this study, it was done by including samples from different geographical origin, different quality grades, and different slaughter batches. Thereafter, some frozen samples from different geographical origin were collected (Australia, Canada, Mexico, New Zealand, and USA) to obtain a wide variation in WHC measurements to ensure that the model is representative both locally and globally as well as to ensure the credibility and reliability of wavelength selection to design a multispectral online imaging system. The frozen samples were thawed overnight at 4 °C before image acquisition. Within the drip loss method, the loss of water was determined as a percentage of weight loss from a 2.5 cm × 2.5 cm × 2.0 cm (length × width × thickness) cut slice suspended in a plastic jar for 48 h storage at 4 °C. Measurements were conducted in duplicate in each muscle and averaged to express drip loss for each muscle. In total, 120 samples, incorporating 40 samples from each red meat type were used for the investigation. These samples were systematically divided into a calibration and prediction set. To ensure that both groups appropriately covered a similar range of reference values, samples were first sorted in descending order with respect to the reference WHC for each red meat type, following which every third sample was selected to compose a prediction set. In this way, 39 samples incorporating 13 samples from each red meat type were selected as a prediction set, whereas the remaining 81 samples including beef (27), lamb (27), and pork (27) were used as a calibration set. The statistics such as mean, standard deviation (SD) and range of these samples are shown in Table 1. The complete procedures for selecting feature wavelengths for the design of online multispectral systems are depicted in Fig. 1.

### 2.2. Image acquisition and image correction

The image acquisition was conducted in a dark room to avoid any undesired stray light, and at a controlled temperature and humidity of 20 °C and 65%, respectively. Hyperspectral images were acquired in the spectral range of 400–1000 nm with 5 nm intervals between contiguous bands with 121 spectral bands. The acquired raw images were corrected with two reference images using the following equation:

$$R = \frac{R_0 - D}{W - D} \quad (1)$$

where R is the relative reflectance image of the sample,  $R_0$  is the raw image of the sample, W is the white reference image acquired from a uniform, stable, and high reflectance, ceramic tile (~99% reflectance), and D is the dark current image acquired by completely covering the camera lens with its non-reflective opaque black cap.

**Table 1**  
Descriptive statistics of reference WHC measured by drip loss (%).

Type	Calibration set (n = 81)			Validation set (n = 39)		
	Mean $\pm$ SD	Minimum	Maximum	Mean $\pm$ SD	Minimum	Maximum
Beef	2.23 $\pm$ 2.44	0.49	7.22	2.17 $\pm$ 2.42	0.54	7.02
Lamb	2.11 $\pm$ 0.74	1.03	3.85	2.16 $\pm$ 0.74	1.33	3.77
Pork	2.65 $\pm$ 3.16	0.50	9.63	2.55 $\pm$ 3.17	0.54	8.87
All	2.33 $\pm$ 2.33	0.49	9.63	2.29 $\pm$ 2.29	0.54	8.87

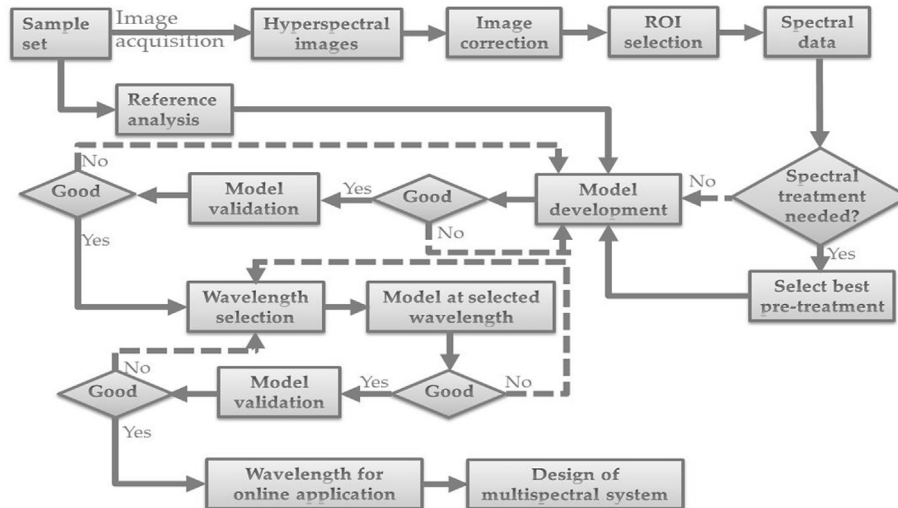


**Fig. 1.** The whole steps to select feature wavelength to design multispectral imaging system for real-time monitoring of WHC in red meat.

### 2.3. Selection of the region of interest and extraction of spectral data

The selection of the region of interest (ROI) is a very important task required for extracting spectral data from the tested objects. In the current study, each hyperspectral image was segmented to isolate the lean meat from the background and fat part of the sample. Initially, a binary mask image was created which is called full mask by thresholding the image at 625 nm (provided good contrast between meat sample and background). Once again, a binary image of fat pixels was created by thresholding the image at 475 nm (provided good contrast between lean and fat). Finally, the lean portion was isolated by subtracting fat pixels from the full mask containing both lean and fat portions to produce the final mask containing only the lean part in a black background. Morphological operations were also applied to the masked image to exclude any regions (if any) that could interfere with the spectra extracted. The isolated lean portion was then treated as the main ROI to be used for extracting spectral data from the hyperspectral image. The reflectance spectrum from the ROI was calculated by averaging the spectral value of all pixels in the ROI to produce only one mean value (spectrum) for each muscle. The same procedure was repeated to obtain the spectrum from all hyperspectral images of all tested muscles. Segmentation and extraction of spectral data from hyperspectral images were programmed in Matlab (The Mathworks Inc., Mass, USA).

### 2.4. Model development and evaluation

In this study, one multivariate linear model such as partial least-squares regression (PLSR) and one non-linear model such as least square support vector machines (LS-SVM) were used for

developing calibration models. The developed calibration models were then validated using the independent prediction set. The optimal number of latent variables (LVs) to be included in the PLSR model was determined at the minimum value of prediction residual error sum of squares (PRESS). The radial basis function (RBF) kernel was used as the kernel function of LS-SVM. A grid search and cross-validation were applied to optimize the important parameters such as the regularization parameter  $\gamma$  and the RBF kernel function parameter  $\sigma_2$  for the LS-SVM calibration model. For each combination of  $\gamma$  and  $\sigma_2$ , the root mean square error of cross-validation (RMSECV) was calculated. The optimum parameters were selected when they produced the smallest RMSECV. LS-SVM was executed in Matlab (The MathWorks, Inc., Mass, USA) using the LS-SVM toolbox (LS-SVM v. 1.5, Suykens, Leuven, Belgium) to derive all LS-SVM models (Suykens, Vandewalle, & De Moor, 2001). Performance of the regression models was evaluated using statistical criteria for the data in the validation set. These were the coefficient of determination ( $R^2$ ), the root mean square error of prediction (RMSEP), the ratio of percentage deviation (RPD), and the ratio of error range (RER). RPD is often used to evaluate how well a calibration model can predict in new validation samples. RPD is defined as the ratio of standard deviation of the reference data in the prediction set to the RMSEP and RER is defined as the ratio of the reference values in the prediction set to the RMSEP.

### 2.5. Selection of important wavelengths and visualization of WHC

Two popular and widely used variable selection strategies such as regression coefficients (RCs) (Barbin et al., 2012b; ElMasry et al. 2011; Iqbal et al., 2013; Kamruzzaman et al., 2012a) and competitive adaptive reweighted sampling (CARS) (He, Sun, & Wu, 2014; Wu & Sun, 2013) were used to choose feature wavelengths to

predict WHC. Calibration models were built based on selected feature wavelengths and the best model was applied to each pixel of the image to obtain the prediction map of WHC. The prediction map is displayed with a linear color scale, in which the spatial distribution of the predicted WHC values is easily interpretable. All steps involved in visualization purposes were implemented with a program developed using Matlab (The Mathworks Inc., Mass, USA).

### 3. Results and discussion

#### 3.1. Spectral signatures of red meats

The average spectral signatures extracted from the tested beef, lamb, and pork samples as well as the fat spectrum are shown in Fig. 2a. It was clear that the fat spectrum had a distinct spectral

profile compared to the spectra of lean meat irrespective of red meat types. A very sharp peak, related to fat absorption band of C–H third overtone, was observed at 940 nm in the fat spectrum. The spectral information extracted from the red meat species had similar spectral pattern, but it shows different in the magnitude of reflectance values for each red meat type. It was clear to discover that pork samples had higher reflectance values (lower absorbance) in the whole spectral range followed by beef and lamb samples. This tendency is in agreement with the reference drip loss value of beef, lamb and pork as demonstrated in Table 1. The pork samples had the highest mean value of drip loss (2.65%) followed by beef (2.23%) and lamb (2.11%). The difference observed in reflectance could be attributed to the difference in color reflectance ( $L^*$ ) values between the samples. This is in agreement with the real  $L^*$  values of beef, lamb and pork. In this study, the pork samples had higher  $L^*$

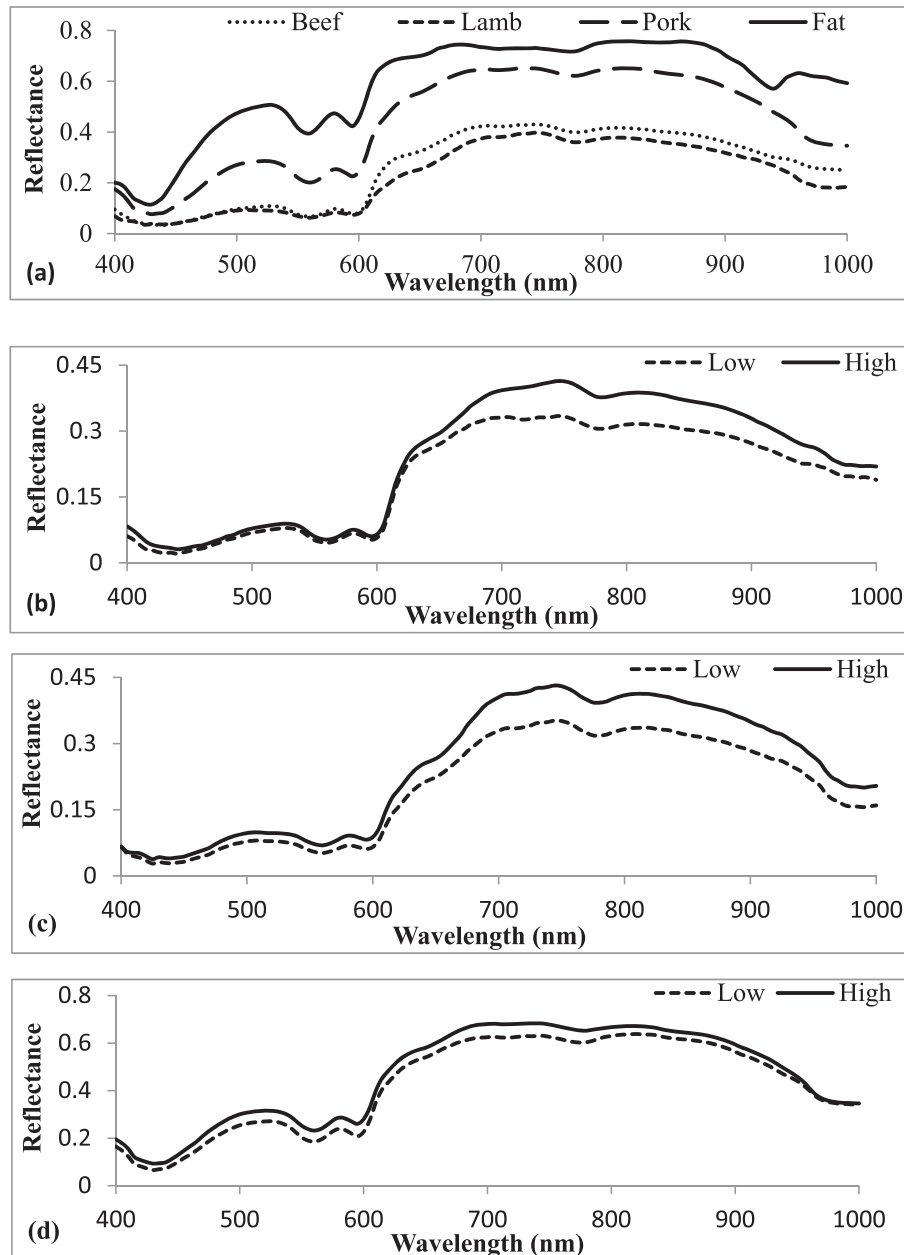


Fig. 2. Mean reflectance spectral profiles of (a) beef, lamb and pork and the mean spectra of ten samples having the lowest and highest drip loss for (b) beef, (c) lamb and (d) pork in the spectral range of 400–1000 nm.

values followed by beef and lamb samples (data not shown). By observing spectra as shown in Fig. 2a, it was observed that the major absorption occurred at 515, 505, 650, 780, and 980 nm. The absorption bands in the visible region (i.e., 515, 595, and 650 nm) are primarily associated with myoglobin, oxymyoglobin, metmyoglobin, and deoxymyoglobin, responsible for the color of meat (Mamani-Linares, Gallo, & Alomar, 2012). Absorption bands in the NIR range are related to overtones and combinations of fundamental vibrations of C–H, N–H, O–H, and S–H functional groups. Since organic samples have a very complex composition, the absorption bands in the NIR region tend to be broad and generally overlap in various parts over the NIR region. Only two subtle absorption bands were observed in the NIR region at 780 and 980 nm. These bands were related to water absorption bands, corresponding to the third and second overtones of O–H stretching, respectively (Cozzolino & Murray, 2004; Mamani-Linares et al., 2012).

The average reflectance spectra of 10 samples having the lowest (dotted line) and highest (solid line) drip loss values are shown in Fig. 2b–d for beef, lamb, and pork, respectively. It is clear that samples with high drip loss have higher reflectance values than those with low drip loss samples throughout the entire spectral pattern for all red meat. The results are in accordance with previous studies with beef (ElMasry et al., 2012a, 2012b) and pork (Barbin et al., 2012a). Those authors reported that samples with high drip loss values have high reflectance (i.e., low absorbance), and vice versa.

### 3.2. Calibration models based on full spectra

The statistical parameters of both PLSR and LS-SVM models for the prediction of WHC in red meat for calibration and prediction are shown in Table 2. The PLSR model based on 121 variables showed a good capability for predicting WHC with coefficients determination ( $R^2$ ) values of 0.94, and 0.92, as well as RMSEs of 0.52%, and 0.63% for calibration and validation, respectively. The developed PLSR models displayed good performances in predicting WHC for both calibration and prediction as the statistical criteria of calibration and validation sets were very similar along with high values of the coefficients of determination and low values of RMSEs, as well as small difference between RMSEC and RMSEP. The predictability of the PLSR model obtained in this study was higher than those reported previously by the various studies working with WHC in beef (ElMasry et al., 2011), lamb (Kamruzzaman et al., 2012a), and pork (Barbin et al., 2012b). Using the same NIR hyperspectral imaging system (900–1700 nm) with the same protocol (i.e., PLSR), these authors predicted WHC with the coefficients of determination ( $R^2_{cv}$ ) of 0.89, 0.77, and 0.88 for beef, lamb, and pork, respectively.

LS-SVM revealed a good ability for predicting WHC based on full spectra (121 variables) with the highest  $R^2$  of 0.97 and 0.94 as well

as the lowest RMSEs of 0.36% and 0.50% obtained for calibration and validation, respectively. Better performances were obtained using LS-SVM compared to PLSR. The developed models were also evaluated based on the RPD and RER. The RPD values in the range 1.8–2.0 indicate good model and/or predictions, 2.0–2.5 implies very good model and/or predictions, and >2.5 denote excellent model and/or predictions (Rossel, Taylor, & McBratney, 2007). The RER values in the range 4–8 indicate the possibility of discriminating between high and low response values, 8–12 indicate the adequate prediction of quantitative data and >12 indicate good predictability (Malley, Yesmin, & Eilers, 2002). In the current study, the obtained RPD values were 3.63 and 4.58, whereas the RER values were 13.23 and 16.67 for PLSR and LS-SVM, respectively. The higher the RPD and RER values, the greater the ability of the model to predict the reference values precisely in new and similar samples. In the current study, the higher values of RPD and RER could result from a wide range of the reference values along with the variability in the reference data and/or from smaller RMSEP. Overall, the results obtained from PLSR and LS-SVM models were encouraging and confirm the suitability of hyperspectral imaging for predicting WHC in red meat in a rapid and non-destructive way.

### 3.3. Selection of feature wavelengths for WHC

A total of eight different feature wavelengths were selected using both RCs (545, 610, 705, 765, 805, 900, 940, and 970 nm) and CARS (85, 545, 640, 670, 705, 765, 770, and 800 nm) for predicting WHC in red meat. The distribution of these selected feature wavelengths is shown in Fig. 3. Although, there were other wavelengths such as 425, 485, and 670 nm that also showed high values of RCs as observed in Fig. 3, these wavelengths did not enhance the predictability of the model when considered with the selected eight wavelengths. Therefore, these eight wavelengths were considered as the feature wavelengths to predict WHC in red meat. It is clear that CARS identifies relevant wavelengths in the spectral range up to 800 nm whereas RCs tend to spread relevant wavelengths across the entire spectral range. New calibration models can be created using only these selected feature wavelengths to properly ascertain the predictive ability of the selected feature wavelengths over the models developed from the full wavelength range. If the accuracy of the new models at selected feature wavelengths is unchanged or tolerably degraded over the model developed using full wavelengths, then a more robust multispectral imaging system could be established using these feature wavelengths, which can be used for real-time monitoring of WHC in red meat.

### 3.4. Calibration models based on selected feature wavelengths

On the basis of selected feature wavelengths, PLSR, and LS-SVM, were developed for predicting WHC. These models are denoted as RCs-PLSR, CARS-PLSR, RCs-LS-SVM, and CARS-LS-SVM, and the results are presented in Table 2. Although, the number of wavelengths/variables was substantially reduced from 121 to 8, the results tabulated in Table 2 reveal that performances of the new models at selected feature wavelengths were tolerably degraded to those models developed using the full spectral range of 121 variables, indicating that the methods for wavelength selection using RCs and CARS were efficient. The performance of the RCs-PLSR model was equivalent to the CARS-PLSR model to predict WHC at reduced spectra. Although both PLSR and LS-SVM models obtained good results based on reduced spectra in both calibration and prediction conditions for predicting WHC in red meat, it was confirmed that the LS-SVM models displayed a better performance than that of PLSR models. Therefore, the best LS-SVM model (RCs-

**Table 2**

Calibration and prediction statistics for predicting WHC using PLSR and LS-SVM based on full wavelengths range (121 variables) and feature wavelengths selected by RCs (545, 610, 705, 765, 805, 900, 940, and 970 nm) and CARS (485, 545, 640, 670, 705, 765, 770 and 800 nm). The best model indicated in bold for both full and selected wavelengths.

Model	LVs	Calibration		Validation			
		$R^2_c$	RMSEC (%)	$R^2_p$	RMSEP (%)	RPD	RER
PLSR	10	0.94	0.52	0.92	0.63	3.63	13.23
<b>LS-SVM</b>	/	<b>0.97</b>	<b>0.36</b>	<b>0.94</b>	<b>0.50</b>	<b>4.58</b>	<b>16.67</b>
CARS-PLSR	5	0.91	0.67	0.89	0.74	3.09	11.26
CARS-LS-SVM	/	0.93	0.56	0.91	0.63	3.63	13.63
RCs-PLSR	7	0.90	0.68	0.90	0.72	3.18	11.57
<b>RCs-LS-SVM</b>	/	<b>0.94</b>	<b>0.53</b>	<b>0.93</b>	<b>0.56</b>	<b>4.09</b>	<b>14.88</b>

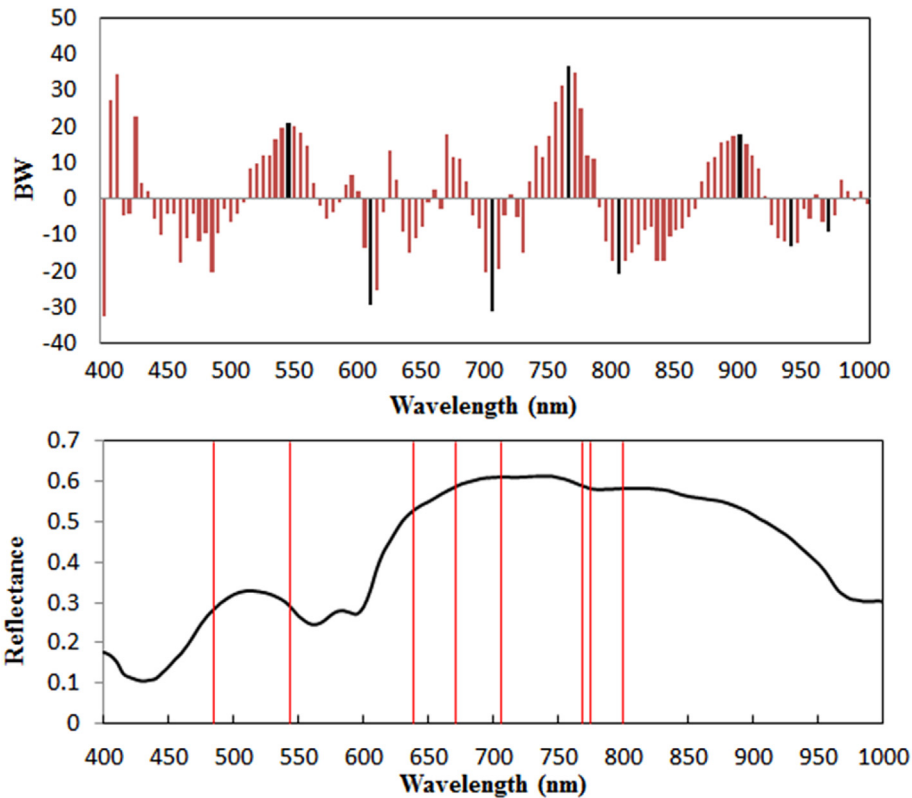


**Fig. 3.** Selection of feature wavelengths using RCs (top) and CARS (bottom). In CARS, the selected feature wavelengths are indicated by vertical lines on top of a representative spectrum. In the RCs process, the black vertical line indicates the selected feature wavelengths.

LS-SVM) was subsequently applied to each pixel in the image to obtain prediction maps of WHC.

### 3.5. Prediction maps

The RCs-LS-SVM was applied to the unfolded hyperspectral image at selected wavelengths, providing WHC values for each pixel in the image. In the prediction image (so called distribution map), pixels having similar spectral features were produced with the same predicted value of WHC. The variation in WHC values within the image was assigned with a linear color (in the web version) scale. Fig. 4 displays some distribution maps of the tested samples. Although it was difficult to identify the difference in WHC from pixel to pixel by the naked eye, the spatial variation of WHC within the different samples, even within the same sample, could be visualized from the distribution maps. Fat pixels were also easily recognized in the resulting distribution map with high predicted values. This observation is not surprising because the spectra of fat

pixels always had a higher reflectance than those of lean meat (Fig. 2a), and high reflectance is associated with high drip loss values, as shown in Fig. 2b–d and by previous studies (Barbin et al., 2012b; ElMasry et al., 2011). The distribution maps created in the current study motivate to a great extent the effectiveness of hyperspectral imaging to predict the quality attributes in red meat, not only in spectral domain, but also to visualize in the spatial domain. By merging both spatial and spectral features in one single system, hyperspectral imaging has the advantage of being effective for the rapid, precise, and non-destructive measurements of samples without any particular sample preparation. Indeed, the non-destructive nature of this technique is very promising for fast analysis in online, off-line, or at-line inspections, not only in meat processing but also in other agro-food processing industries.

## 4. Conclusion

In the current study, a hyperspectral imaging technique in the

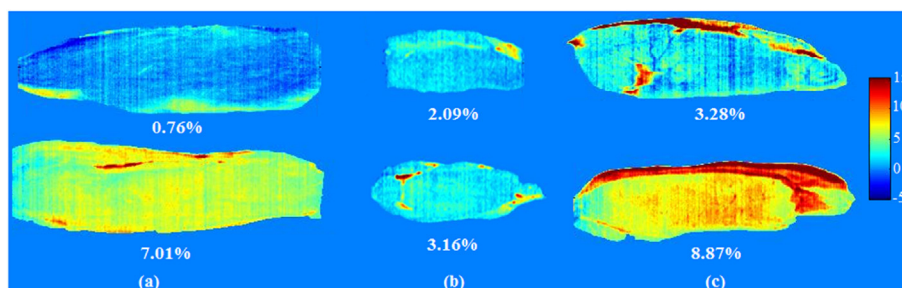


**Fig. 4.** Prediction maps of WHC for (a) beef, (b) lamb, and (c) pork. The value in the bottom of each prediction map represents the average value of WHC of the sample.

VIS/NIR region was tested to investigate the ability of the technique to determine WHC in red meat in a real-time application. The investigation was accompanied with multivariate analysis by identifying dominant feature wavelengths related to WHC. The current study demonstrated that hyperspectral imaging can be utilized to select some feature wavelengths to design an optimized multispectral imaging system to detect WHC in red meat for a real-time practical application. Instead, of selecting different sets of feature wavelengths for different red meat, only eight wavelengths (545, 610, 705, 765, 805, 900, 940, and 970 nm) were selected to be used to design a multispectral system for convenient industrial application for red meat. Instead, of using a spectrograph, these wavelengths can then be used as band pass filters within a multi-band camera. The cameras with a few wavebands will not significantly differ from conventional RGB (red–green–blue) cameras in speed and cost, and will boost the development of online multispectral imaging technology in the future.

### Acknowledgments

The authors would like to acknowledge the financial support provided by The Japan Society for the Promotion of Science (NO. P13395) and a Grant-in-Aid for Scientific Research (JSPS NO. 13F03395).

### References

- Barbin, D., ElMasry, G., Sun, D.-W., & Allen, P. (2012a). Predicting quality and sensory attributes of pork using near-infrared hyperspectral imaging. *Analytica Chimica Acta*, *719*, 30–42.
- Barbin, D., ElMasry, G., Sun, D.-W., & Allen, P. (2012b). Non-destructive determination of chemical composition in intact and minced pork by near-infrared hyperspectral imaging. *Food Chemistry*, *138*, 1162–1171.
- Berzaghi, P., & Riovanto, R. (2009). Near infrared spectroscopy in animal science production: principles and applications. *Italian Journal of Animal Science*, *8*, 39–62.
- Burger, J., & Gowen, A. (2011). Data handling in hyperspectral image analysis. *Chemometrics and Intelligent Laboratory Systems*, *108*, 13–22.
- Cozzolino, D., & Murray, I. (2004). Identification of animal meat muscles by visible and near infrared reflectance spectroscopy. *LWT – Food Science & Technology*, *37*, 447–452.
- ElMasry, G., Kamruzzaman, M., Sun, D.-W., & Allen, P. (2012). Principles and applications of hyperspectral imaging in quality evaluation of agro-food products, a review. *Critical Review in Food Science & Nutrition*, *52*, 999–1023.
- ElMasry, G., Sun, D.-W., & Allen, P. (2011). Non-destructive determination of water-holding capacity in fresh beef by using NIR hyperspectral imaging. *Food Research International*, *44*, 2624–2633.
- ElMasry, G., Sun, D.-W., & Allen, P. (2012). Chemical-free assessment and mapping of major constituents in beef using hyperspectral imaging. *Journal of Food Engineering*, *117*, 235–246.
- He, H.-J., Sun, D.-W., & Wu, D. (2014). Rapid and real-time prediction of lactic acid bacteria (LAB) in farmed salmon flesh using near-infrared (NIR) hyperspectral imaging combined with chemometric analysis. *Food Research International*, *62*, 476–483.
- Honikel, K. O. (1998). Reference methods for the assessment of physical characteristics of meat. *Meat Science*, *49*, 447–457.
- Hoving-Bolink, A. H., Vedder, H. W., Merks, J. W. M., de Klein, W. J. H., Reimert, H. G. M., Frankhuizen, R., et al. (2005). Perspective of NIRS measurements early post mortem for prediction of pork quality. *Meat Science*, *69*, 417–423.
- Iqbal, A., Sun, D.-W., & Allen, P. (2013). Prediction of moisture, color and pH in cooked, pre-sliced turkey hams by NIR hyperspectral imaging system. *Journal of Food Engineering*, *117*, 42–51.
- Kamruzzaman, M., Barbin, D., ElMasry, G., Sun, D.-W., & Allen, P. (2012). Potential of hyperspectral imaging and pattern recognition for categorization and authentication of red meat. *Innovative Food Science & Emerging Technologies*, *16*, 316–325.
- Kamruzzaman, M., ElMasry, G., Sun, D.-W., & Allen, P. (2011). Application of NIR hyperspectral imaging for discrimination of lamb muscles. *Journal of Food Engineering*, *104*, 332–340.
- Kamruzzaman, M., ElMasry, G., Sun, D.-W., & Allen, P. (2012a). Prediction of some quality attributes of lamb meat using near infrared hyperspectral imaging and multivariate analysis. *Analytica Chimica Acta*, *714*, 57–67.
- Kamruzzaman, M., ElMasry, G., Sun, D.-W., & Allen, P. (2012b). Non-destructive prediction and visualization of chemical composition in lamb meat using NIR hyperspectral imaging and multivariate regression. *Innovative Food Science & Emerging Technologies*, *16*, 218–226.
- Kamruzzaman, M., ElMasry, G., Sun, D.-W., & Allen, P. (2013b). Non-destructive assessment of instrumental and sensory tenderness of lamb meat using NIR hyperspectral imaging. *Food Chemistry*, *141*, 389–396.
- Kamruzzaman, M., Makino, Y., & Oshita, S. (2015b). Non-invasive analytical technology for the detection of contamination, adulteration, and authenticity of meat, poultry, and fish: a review. *Analytica Chimica Acta*, *853*, 19–29.
- Kamruzzaman, M., Makino, Y., & Oshita, S. (2016). Rapid and non-destructive detection of chicken adulteration in minced beef using visible near-infrared hyperspectral imaging and machine learning. *Journal of Food Engineering*, *170*, 8–15. <http://dx.doi.org/10.1016/j.jfoodeng.2015.08.02>.
- Kamruzzaman, M., Makino, Y., Oshita, S., et al. (2015). Assessment of visible near-infrared hyperspectral imaging as a tool for detection of horsemeat adulteration in minced beef. *Food and Bioprocess Technology*, *8*, 1054–1062.
- Kamruzzaman, M., Sun, D.-W., ElMasry, G., & Allen, P. (2013a). Fast detection and visualization of minced lamb meat adulteration using NIR hyperspectral imaging and multivariate image analysis. *Talanta*, *103*, 130–136.
- Mamani-Linares, L. W., Gallo, C., & Alomar, D. (2012). Identification of cattle, llama and horse meat by near infrared reflectance or transmittance spectroscopy. *Meat Science*, *90*, 378–385.
- Malley, D. F., Yesmin, L., & Eilers, R. G. (2002). Rapid analysis of hog manure and manure-amended soils using near infrared spectroscopy. *Soil Science Society of America Journal*, *66*, 1677–1686.
- Park, B., Yoon, S.-C., Windham, W., Lawrence, K., Kim, M., & Chao, K. (2011). Line-scan hyperspectral imaging for real-time in-line poultry fecal detection. *Sensing & Instrumentation in Food Quality & Safety*, *5*, 25–32.
- Pedersen, D. K., Morel, S., Andersen, H. J., & Engelsen, S. B. (2003). Early prediction of water-holding capacity in meat by multivariate vibrational spectroscopy. *Meat Science*, *65*, 581–592.
- Prevolnik, M., Čandek-Potokar, M., & Škorjanc, D. (2010). Predicting pork water-holding capacity with NIR spectroscopy in relation to different reference methods. *Journal of Food Engineering*, *98*, 347–352.
- Pu, H., Kamruzzaman, M., & Sun, D.-W. (2015). Selection of feature wavelengths for developing multispectral imaging systems for quality, safety and authenticity of muscle foods—a review. *Trends in Food Science & Technology*, *45*, 86–104.
- Qin, J., Chao, K., Kim, M. S., Lu, R., & Burks, T. F. (2013). Hyperspectral and multispectral imaging for evaluating food safety and quality—a review. *Journal of Food Engineering*, *118*, 157–171.
- Rossel, R. A. V., Taylor, H. J., & McBratney, A. B. (2007). Multivariate calibration of hyperspectral gamma-ray energy spectra for proximal soil sensing. *European Journal Soil Science*, *58*, 343–353.
- Suykens, J. A., Vandewalle, J., & De Moor, B. (2001). Optimal control by least squares support vector machines. *Neural Networks*, *14*, 23–35.
- Tao, F., Peng, Y., Li, Y., Chao, K., & Dhakal, S. (2012). Simultaneous determination of tenderness and *Escherichia coli* contamination of pork using hyperspectral scattering technique. *Meat Science*, *90*, 851–857.
- Wu, D., & Sun, D.-W. (2013). Potential of time series-hyperspectral imaging (TS-HSI) for non-invasive determination of microbial spoilage of salmon flesh. *Talanta*, *111*, 39–46.

Contents lists available at [ScienceDirect](http://www.sciencedirect.com)

# LWT - Food Science and Technology

journal homepage: [www.elsevier.com/locate/lwt](http://www.elsevier.com/locate/lwt)

## Calendar

Events	Date and Venue	Details from
2nd Food Structure and Functionality Forum Symposium	28 February-2 March 2016 <i>Singapore</i>	Internet: <a href="http://www.foodstructuresymposium.com">www.foodstructuresymposium.com</a>
IDF International Symposium on Cheese Science and Technology & the IDF Symposium on Concentration	11-13 April 2016 <i>Dublin, Ireland</i>	Internet: <a href="http://www.idfingredientsandcheese2016.com">www.idfingredientsandcheese2016.com</a>
2nd Asian Sensory and Consumer Research Symposium - SenseAsia	15-17 May 2016 <i>Shanghai, China</i>	Internet: <a href="http://www.senseasia.elsevier.com">www.senseasia.elsevier.com</a>
13th International Hydrocolloids Conference	16-20 May 2016 <i>Guelph, Ontario, Canada</i>	Email: <a href="mailto:stevevcui@gmail.com">stevevcui@gmail.com</a> or <a href="mailto:dgoff@uoguelph.ca">dgoff@uoguelph.ca</a> Internet: <a href="http://www.international-hydrocolloids-conference.com/">http://www.international-hydrocolloids-conference.com/</a>
4th International ISEKI Food Conference	6-8 July 2016 <i>Vienna, Austria</i>	Internet: <a href="http://www.isekiconferences.com/vienna2016">www.isekiconferences.com/vienna2016</a>
IFT Annual Meeting and Food Expo	16-19 July 2016 <i>Chicago, USA</i>	Internet: <a href="http://www.ift.org">www.ift.org</a>
13th Sensometrics Conference	26-29 July 2016 <i>Brighton, UK</i>	Internet: <a href="http://www.sensometrics2016.com">www.sensometrics2016.com</a>
IUFoST 2016 - 18th World Congress of Food Science and Technology	21-25 August 2016 <i>Dublin, Ireland</i>	Internet: <a href="http://www.iufost2016.com">www.iufost2016.com</a>
EuroSense 2016 - 7th European Conference on Sensory and Consumer Research	11-14 September 2016 <i>Dijon, France</i>	Internet: <a href="http://www.eurosense.elsevier.com">www.eurosense.elsevier.com</a>
IDF World Dairy Summit 2016	16-21 October 2016 <i>Rotterdam, the Netherlands</i>	Internet: <a href="http://www.idfwds2016.com">www.idfwds2016.com</a>

*LWT—Food Science and Technology* is an international journal that publishes innovative papers in the fields of food chemistry, biochemistry, microbiology, technology and nutrition. The work described should be innovative either in the approach or in the methods used. The significance of the results either for the science community or for the food industry must also be specified. Contributions written in English are welcomed in the form of review articles, short reviews, research papers, and research notes. Papers featuring animal trials are outside the scope of the journal and will not be considered for publication.

---

## Editor-in-Chief:

**Rakesh K. Singh**

University of Georgia, Food Science Building  
Athens, GA 30602, USA

## Editors:

**Sam Chang**

Food Science, Nutrition and Health Promotion,  
Mississippi State University, Starkville, MS 39762, USA

**Emma Chiavaro**

Department of Food Science, University of Parma, 43124 Parma, Italy

**Ursula Gonzales Barron**

CIMO Mountain Research Centre, School of Agriculture,  
Polytechnic Institute of Braganza, Bragança, Portugal

**Vijay K. Juneja**

Eastern Regional Research Center,  
USDA-Agricultural Research Service, Wyndmoor, PA 19038, USA

# LWT

**Catherine M.G.C. Renard**

Sécurité et Qualité des Produits d'Origine Végétale  
INRA Centre d'Avignon, Avignon, France

**Mingyong Xie**

State Key Laboratory of Food Science and Technology,  
Nanchang 330031, China

## Reviews Editor:

**Shridhar Sathe**

Department of Nutrition, Food and Exercise Sciences,  
Florida State University, Tallahassee, FL 32306-1493, USA

---

## Editorial Board:

**R. Amarowicz**

Polish Academy of Sciences, Olsztyn, Poland

**V. Balasubramaniam**

Ohio State University, Columbus, USA

**R. Buckow**

CSIRO, Werribee, Australia

**J. Chirife**

University of Buenos Aires, Buenos Aires, Argentina

**J-M. Chobert**

INRA, Nantes, France

**E. Choe**

Inha University, Incheon, Korea

**H. Corke**

University of Hong Kong, Hong Kong

**R.M.S. Cruz**

University of Algarve, Faro, Portugal

**D. De Beer**

ARC Infruitec-Nietvoorbij, Stellenbosch, South Africa

**F. Escher**

Swiss Federal Institute of Technology, Zürich, Switzerland

**P. Gélinas**

Agriculture and Agri-Food Canada, Saint-Hyacinthe, Canada

**R. Gormley**

The National Food Centre, Dublin, Ireland

**J. Hinrichs**

Universität Hohenheim, Stuttgart, Germany

**D. Hoover**

University of Delaware, Newark, USA

**W. Kerr**

University of Georgia, Athens, USA

**W. Kneifel**

University of Agricultural Sciences, Vienna, Austria

**U. Kulozik**

Technische Universität München, Freising-Weihenstephan, Germany

**C. Lacroix**

Swiss Federal Institute of Technology, Zürich, Switzerland

**A. van Loey**

Centre for Food and Microbial Technology, Heverlee, Belgium

**K. Lorenz**

Colorado State University, Colorado, USA

**H. N. Mishra**

Indian Institute of Technology, Kharagpur, India

**M.P. Montero**

Institute of Food Science, Technology and Nutrition (ICTAN),  
Madrid, Spain

**L. Nyström**

Swiss Federal Institute of Technology, Zürich, Switzerland

**S.Y. Quek**

The University of Auckland, Auckland, New Zealand

**R. Reddy**

U.S. Food and Drug Administration, Summit-Argo, USA

**Y. Roos**

University College, Cork, Ireland

**C.M. Rosell**

Institute of Agrochemistry and Food Technology, Valencia, Spain

**P. Schieberle**

Technische Universität München, Garching, Germany

**M. Schreiner**

BOKU, Vienna, Austria

**J. Shi**

Guelph Food Research Center, Agriculture and Agri-Food Canada,  
Guelph, Canada

**H. Singh**

Massey University, Palmerston North, New Zealand

**W. Spiess**

Federal Research Center for Nutrition, Karlsruhe, Germany

**C. C. Tadini**

Sao Paulo University, Sao Paulo, Brazil

**D. Topping**

CSIRO, Adelaide, Australia

**H. Tuorila**

University of Helsinki, Helsinki, Finland

**M. Venkatachalam**

The Hershey Company, Hershey, USA

**S. Wang**

Tianjin University of Science and Technology, Tianjin, China

**H. Watzke**

Nestlé Research Centre, Lausanne, Switzerland

**L. Yu**

University of Maryland, Adelphi, USA

**F. Zhong**

Jiangnan University, Wuxi, China